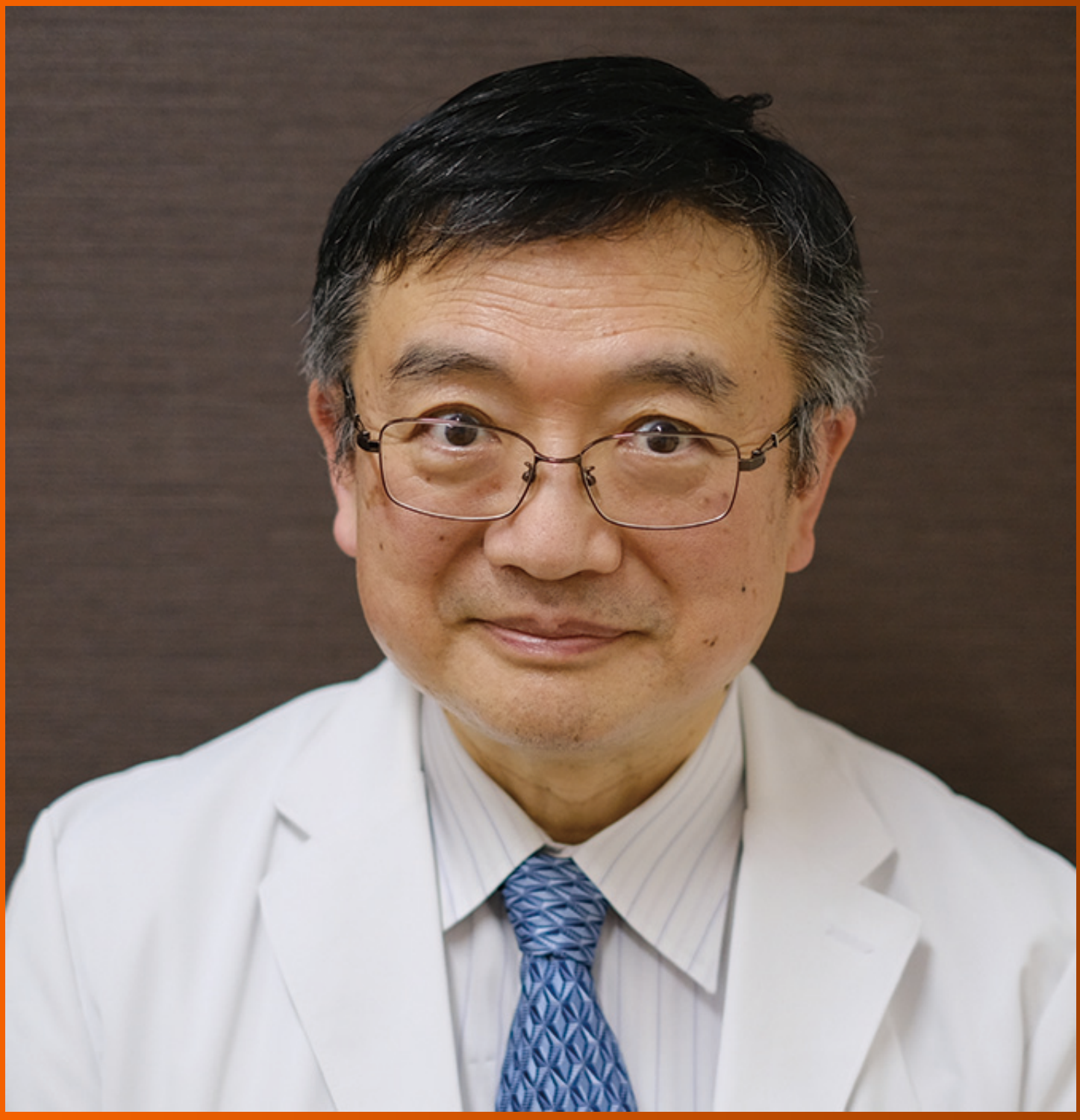
ISSN 1007-9327 (print)
ISSN 2219-2840 (online)

World Journal of *Gastroenterology*

World J Gastroenterol 2023 July 7; 29(25): 3932-4098



Published by Baishideng Publishing Group Inc

World Journal of Gastroenterology

Contents

Weekly Volume 29 Number 25 July 7, 2023

REVIEW

3932 Glycogen storage diseases: An update

Gümüş E, Özen H

3964 Past, present, and future of long-term treatment for hepatitis B virus

Broquetas T, Carrión JA

3984 Impact of gut microbiome in the development and treatment of pancreatic cancer: Newer insights

Bangolo AI, Trivedi C, Jani I, Pender S, Khalid H, Alqinai B, Intisar A, Randhawa K, Moore J, De Deugd N, Faisal S, Suresh SB, Gopani P, Nagesh VK, Proverbs-Singh T, Weissman S

MINIREVIEWS

3999 Insulin resistance and adipose tissue interactions as the cornerstone of metabolic (dysfunction)-associated fatty liver disease pathogenesis

Pal SC, Méndez-Sánchez N

4009 Recent advances and current challenges in endoscopic resection with the full-thickness resection device

Mun EJ, Wagh MS

4021 Dynamic contrast enhanced ultrasound in gastrointestinal diseases: A current trend or an indispensable tool?

Paratore M, Garcovich M, Ainora ME, Riccardi L, Gasbarrini A, Zocco MA

4036 Fractal nature of human gastrointestinal system: Exploring a new era

Grizzi F, Spadaccini M, Chiriva-Internati M, Hegazi MAAA, Bresalier RS, Hassan C, Repici A, Carrara S

ORIGINAL ARTICLE

Basic Study

4053 Molecular profiling reveals potential targets in cholangiocarcinoma

Liu D, Shi Y, Chen H, Nisar MA, Jabara N, Langwinski N, Mattson S, Nagaoka K, Bai X, Lu S, Huang CK

Retrospective Study

4072 Non-invasive model for predicting high-risk esophageal varices based on liver and spleen stiffness

Yang LB, Gao X, Li H, Tantai XX, Chen FR, Dong L, Dang XS, Wei ZC, Liu CY, Wang Y

Observational Study

4085 Real-world effectiveness and safety of direct-acting antivirals in hepatitis C virus patients with mental disorders

Dybowska D, Zarębska-Michaluk D, Rzymski P, Berak H, Lorenc B, Sitko M, Dybowski M, Mazur W, Tudrujek-Zdunek M, Janocha-Litwin J, Janczewska E, Klapaczyński J, Parfieniuk-Kowerda A, Piekarska A, Sobala-Szczygieł B, Dobrowolska K, Pawłowska M, Flisiak R

ABOUT COVER

Editorial board member of *World Journal of Gastroenterology*, Kazuaki Inoue, MD, PhD, Professor, Departemnt of Gastroenterology, International University Health and Welfare Narita Hospital, 852 Hatakeda Narita, Chiba 286-8520, Japan. kazuaki-inoue@iuhw.ac.jp

AIMS AND SCOPE

The primary aim of *World Journal of Gastroenterology* (*WJG*, *World J Gastroenterol*) is to provide scholars and readers from various fields of gastroenterology and hepatology with a platform to publish high-quality basic and clinical research articles and communicate their research findings online. *WJG* mainly publishes articles reporting research results and findings obtained in the field of gastroenterology and hepatology and covering a wide range of topics including gastroenterology, hepatology, gastrointestinal endoscopy, gastrointestinal surgery, gastrointestinal oncology, and pediatric gastroenterology.

INDEXING/ABSTRACTING

The *WJG* is now abstracted and indexed in Science Citation Index Expanded (SCIE, also known as SciSearch®), Current Contents/Clinical Medicine, Journal Citation Reports, Index Medicus, MEDLINE, PubMed, PubMed Central, Scopus, Reference Citation Analysis, China National Knowledge Infrastructure, China Science and Technology Journal Database, and Superstar Journals Database. The 2023 edition of Journal Citation Reports® cites the 2022 impact factor (IF) for *WJG* as 4.3; IF without journal self cites: 4.1; 5-year IF: 5.3; Journal Citation Indicator: 0.82; Ranking: 32 among 93 journals in gastroenterology and hepatology; and Quartile category: Q2. The *WJG*'s CiteScore for 2021 is 8.3 and Scopus CiteScore rank 2022: Gastroenterology is 22/149.

RESPONSIBLE EDITORS FOR THIS ISSUE

Production Editor: *Hua-Ge Yu*; **Production Department Director:** *Xiang Li*; **Editorial Office Director:** *Jia-Ru Fan.*

NAME OF JOURNAL
World Journal of Gastroenterology

ISSN
ISSN 1007-9327 (print) ISSN 2219-2840 (online)

LAUNCH DATE
October 1, 1995

FREQUENCY
Weekly

EDITORS-IN-CHIEF
Andrzej S Tarnawski

EDITORIAL BOARD MEMBERS
http://www.wjgnet.com/1007-9327/editorialboard.htm

PUBLICATION DATE
July 7, 2023

COPYRIGHT
© 2023 Baishideng Publishing Group Inc

INSTRUCTIONS TO AUTHORS
https://www.wjgnet.com/bpg/gerinfo/204

GUIDELINES FOR ETHICS DOCUMENTS
https://www.wjgnet.com/bpg/GerInfo/287

GUIDELINES FOR NON-NATIVE SPEAKERS OF ENGLISH
https://www.wjgnet.com/bpg/gerinfo/240

PUBLICATION ETHICS
https://www.wjgnet.com/bpg/GerInfo/288

PUBLICATION MISCONDUCT
https://www.wjgnet.com/bpg/gerinfo/208

ARTICLE PROCESSING CHARGE
https://www.wjgnet.com/bpg/gerinfo/242

STEPS FOR SUBMITTING MANUSCRIPTS
https://www.wjgnet.com/bpg/GerInfo/239

ONLINE SUBMISSION
https://www.f6publishing.com

© 2023 Baishideng Publishing Group Inc. All rights reserved. 7041 Koll Center Parkway, Suite 160, Pleasanton, CA 94566, USA
E-mail: bpgoffice@wjgnet.com https://www.wjgnet.com

World Journal of Gastroenterology

Submit a Manuscript: https://www.f6publishing.com

World J Gastroenterol 2023 July 7; 29(25): 3932-3963

DOI: 10.3748/wjg.v29.i25.3932

ISSN 1007-9327 (print) ISSN 2219-2840 (online)

REVIEW

Glycogen storage diseases: An update

Ersin Gümüş, Hasan Özen

Specialty type: Gastroenterology and hepatology

Provenance and peer review: Unsolicited article; Externally peer reviewed.

Peer-review model: Single blind

Peer-review report's scientific quality classification

Grade A (Excellent): A
Grade B (Very good): B
Grade C (Good): C, C
Grade D (Fair): 0
Grade E (Poor): 0

P-Reviewer: El-Shabrawi MH, Egypt; Rathnaswami A, India; Yao G, China

Received: December 28, 2022
Peer-review started: December 28, 2022
First decision: February 1, 2023
Revised: February 15, 2023
Accepted: April 30, 2023
Article in press: April 30, 2023
Published online: July 7, 2023

Ersin Gümüş, Hasan Özen, Department of Pediatric Gastroenterology, Hepatology and Nutrition, Hacettepe University Faculty of Medicine, Ihsan Dogramaci Children's Hospital, Ankara 06230, Turkey

Corresponding author: Hasan Özen, MD, Professor, Department of Pediatric Gastroenterology, Hepatology and Nutrition, Hacettepe University Faculty of Medicine, Ihsan Dogramaci Children's Hospital, Gevher Nesibe Cad., Ankara 06230, Turkey. haozen@hacettepe.edu.tr

Abstract

Glycogen storage diseases (GSDs), also referred to as glycogenoses, are inherited metabolic disorders of glycogen metabolism caused by deficiency of enzymes or transporters involved in the synthesis or degradation of glycogen leading to aberrant storage and/or utilization. The overall estimated GSD incidence is 1 case per 20000-43000 live births. There are over 20 types of GSD including the subtypes. This heterogeneous group of rare diseases represents inborn errors of carbohydrate metabolism and are classified based on the deficient enzyme and affected tissues. GSDs primarily affect liver or muscle or both as glycogen is particularly abundant in these tissues. However, besides liver and skeletal muscle, depending on the affected enzyme and its expression in various tissues, multiorgan involvement including heart, kidney and/or brain may be seen. Although GSDs share similar clinical features to some extent, there is a wide spectrum of clinical phenotypes. Currently, the goal of treatment is to maintain glucose homeostasis by dietary management and the use of uncooked cornstarch. In addition to nutritional interventions, pharmacological treatment, physical and supportive therapies, enzyme replacement therapy (ERT) and organ transplantation are other treatment approaches for both disease manifestations and long-term complications. The lack of a specific therapy for GSDs has prompted efforts to develop new treatment strategies like gene therapy. Since early diagnosis and aggressive treatment are related to better prognosis, physicians should be aware of these conditions and include GSDs in the differential diagnosis of patients with relevant manifestations including fasting hypoglycemia, hepatomegaly, hypertransaminasemia, hyperlipidemia, exercise intolerance, muscle cramps/pain, rhabdomyolysis, and muscle weakness. Here, we aim to provide a comprehensive review of GSDs. This review provides general characteristics of all types of GSDs with a focus on those with liver involvement.

Key Words: Glycogen storage disease; Liver; Muscle; Hypoglycemia

©The Author(s) 2023. Published by Baishideng Publishing Group Inc. All rights reserved.

Core Tip: Glycogen storage diseases are multisystemic diseases that can present at any age. Primarily affected organs are liver and skeletal muscle, but heart, central nervous system, kidneys, intestines, and other organs may also be affected. As the initial presenting symptoms can occur in adulthood, it is a group of rare diseases that should be recognized and managed by not only pediatricians but also physicians taking care of adults.

Citation: Gümüş E, Özen H. Glycogen storage diseases: An update. *World J Gastroenterol* 2023; 29(25): 3932-3963
URL: https://www.wjgnet.com/1007-9327/full/v29/i25/3932.htm
DOI: https://dx.doi.org/10.3748/wjg.v29.i25.3932

INTRODUCTION

Glycogen storage diseases (GSDs), also referred to as glycogenoses, are inherited metabolic disorders of glycogen metabolism caused by deficiency of enzymes or transporters involved in the synthesis or degradation of glycogen[1]. Disturbances in glycogen metabolism result in aberrant storage and/or utilization of glycogen. Both glycogen formation and breakdown involve several enzymatic reactions and are strictly dependent on hormone regulation (Figure 1)[2]. After a meal, insulin stimulates glycogen storage in muscle and liver by simultaneously promoting glycogen synthesis and inhibiting glycogen breakdown. During exercise or between meals, glucagon and cathecolamines inhibit glycogen synthesis while promoting glycogen breakdown[3]. Hepatic glycogen serves as a depot source of glucose to maintain euglycemia during fasting periods while glycogen in muscle provides glucose to produce necessary energy during high-intensity exertion.

GSDs are multisystemic diseases that can present at any age from the neonatal period to adulthood. The overall GSD incidence is approximately 1 case per 20000-43000 live births and 80% of hepatic GSDs are caused by types I, III, and IX[4,5]. This heterogeneous group of rare diseases represents inborn errors of carbohydrate metabolism and are classified based on the deficient enzyme and affected tissues (Table 1). GSDs primarily affect liver or muscle or both as glycogen is particularly abundant in these tissues. However, besides liver and skeletal muscle, depending on the affected enzyme and its expression in various tissues, multiorgan involvement including heart, kidney and/or brain may be seen[6]. Although GSDs share similar clinical features to some extent, there is a wide spectrum of clinical phenotypes. Hypoglycemia is the hallmark of hepatic GSDs. Hepatomegaly is also a cardinal manifestation of GSDs with liver involvement except for GSD-0. Muscle GSDs, on the other hand, may present with exercise intolerance, muscle cramps/pain, rhabdomyolysis, and muscle weakness and in the case of cardiac involvement, cardiomyopathy[7]. Since the initial presenting symptoms can occur in adulthood, it is a group of rare diseases that should be recognized and managed by not only pediatricians but also physicians taking care of adults. Being multisystemic diseases, GSDs are best managed by a cross-disciplinary approach to achieve good metabolic control, improve the quality of life of patients, and reduce morbidity and mortality[7]. It is recommended that a medical professional with expertise in treating such conditions (*e.g.*, a metabolic disorders specialist, a biochemical geneticist, an endocrinologist, or a hepatologist) should lead and coordinate the patient's care together with a metabolic dietician. Nephrologists, hematologists, genetic counselors, cardiologists, gastroenterologists, neurologists, physical therapists, social workers, and transplant specialists may also be required in the management of a GSD depending on the specific manifestations, complications, and type of the disease. In this article, we aim to update the review published in 2007[1] based on new data and provide a comprehensive review of GSDs. This review provides general characteristics of all types of GSDs with a focus on those with liver involvement.

GSDS INVOLVING LIVER

GSD-0; glycogen synthase deficiency

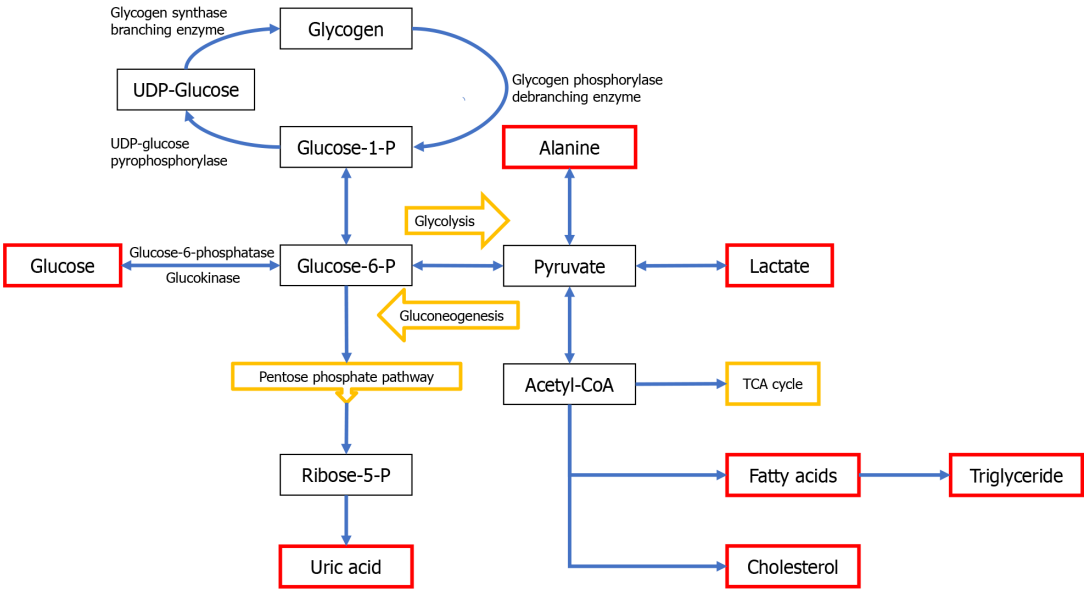
There are two types of glycogen synthase (GYS) encoded at different genetic loci; muscle GYS (*GYS1*; 19q13.33) and liver GYS (*GYS2*; 12p12.1)[8]. In 1963, GSD-0 was initially reported as glycogen synthetase deficiency in the liver[9]. GSD-0 is distinct from other hepatic GSDs due to the marked decrease in liver glycogen content, thereby making its classification questionable as a genuine GSD. However, since the disease exhibits a phenotype like that of the classic glycogenoses due to unavailability of glycogen during periods of fasting, it is classified as a GSD. GSD-0 is an autosomal recessive genetic disease[10]. The disease is caused by homozygous or compound heterozygous mutations in the *GYS2* gene which was mapped to 12p12.2 in 1994[11]. Liver GYS, the hepatic isoform, is responsible for catalyzing the

Table 1 Overview of glycogen storage diseases

GSD type (eponym)	OMIM#	Defective enzyme or transporter	Gene/inheritance	Gene location	Primary tissue involvement	Distinctive features
GSD-0	GSD-0a: 240600	Liver glycogen synthase	GYS2/AR	12p12.1	Liver	No hepatomegaly. Postprandial hyperglycemia, glycosuria, and hyperlactatemia. Extremely low amount of glycogen in liver tissue
	GSD-0b: 611556	Muscle glycogen synthase	GYS1/AR	19q13.33	Muscle	Cardiac involvement, risk of sudden cardiac arrest
GSD-I (von Gierke)	GSD-Ia: 232200	Glucose-6-phosphatase	G6PC/AR	17q.21	Liver	Coagulopathy, anemia, osteopenia, osteoporosis, renal dysfunction, HA, HCC
	GSD-Ib: 232220	Glucose-6-phosphatase transporter	SLC37A4/AR	11q23.3	Liver	Neutropenia, neutrophil dysfunction, recurrent infections, oral and intestinal mucosal ulcers, IBD, autoimmunity
GSD-II (Pompe)	232300	Acid α-glucosidase	GAA/AR	17q25.3	Muscle	Cardiomyopathy, infantile-onset form. Muscle weakness, late-onset form
Danon disease (formerly GSD-IIb)	300257	Lysosome-associated membrane protein-2	LAMP2/XLD	Xq24	Muscle	Skeletal and cardiac myopathy, arrhythmia, intellectual disability
GSD of heart	600858	AMP-activated protein kinase, γ-2 regulatory subunit	PRKAG2/AD	7q36.1	Muscle	Severe ventricular hypertrophy. Electrocardiographic preexcitation and conduction system disease. Premature sudden cardiac death (< 40 yr)
GSD of heart, lethal congenital	261740	AMP-activated protein kinase, γ-2 noncatalytic subunit	PRKAG2/AD	7q36.1	Muscle	Some mutations (R531Q, R384T) cause more severe phenotype. Fetal onset, extreme cardiomegaly, death in infancy
GSD-III (Cori/Forbes)	IIIa/IIIb: 232400	Glycogen debrancher enzyme	AGL/AR	1p21.2	IIIa: Liver + muscle; IIIb: Liver	Liver fibrosis, cirrhosis, HA, HCC (as a complication of cirrhosis). IIIa: Elevated CK, motor developmental delay, myopathy, cardiomyopathy
GSD-IV (Andersen)	232500	Glycogen branching enzyme	GBE1/AR	3p12.2	Liver	Classical hepatic form (rapidly progressive liver disease, HSM, cirrhosis, HCC). Non-progressive hepatic form. Neuromuscular presentation (perinatal, congenital, childhood and adult forms). Myopathy, cardiomyopathy, neuropathy, CNS involvement, APBD. Amylopectin aggregations in liver
GSD-V (McArdle)	232600	Muscle glycogen phosphorylase	PYGM/AR	11q13.1	Muscle	Exercise intolerance, muscle cramps, rhabdomyolysis, myoglobinuria, "second wind" phenomenon
GSD-VI (Hers)	232700	Liver glycogen phosphorylase	PYGL/AR	14q22.1	Liver	Phenotypic variability (overlap with GSD-IX). Severe hepatic involvement reported. Mild hypotonia and cardiopathy reported. Excessive glycogen accumulation with structurally normal glycogen in liver tissue. Enzyme deficiency in erythrocytes, leukocytes
GSD-VII (Tarui)	232800	Muscle phosphofructokinase	PFKM/AR	12q13.11	Muscle	Exertional myopathy, exercise intolerance, muscle cramps, hemolytic anemia. Rapidly progressive infantile form (multisystem involvement, seizures, cardiomyopathy)
GSD-IX	GSD-IXa1 (XLG-1): 306000	Phosphorylase kinase, α-subunit, liver	PHKA2/XLR	Xp22.13	Liver	The most common subtype. Symptomatic female carriers due to X chromosome inactivation. Clinical symptoms and laboratory abnormalities gradually disappear with age. Severe phenotypes reported
	GSD-IXb: 261750	Phosphorylase kinase, β-subunit	PHKB/AR	16q12.1	Liver	Marked accumulation of glycogen in both liver and muscle. Muscle symptoms are generally mild or absent
	GSD-IXc: 613027	Phosphorylase kinase, γ-subunit	PHKG2/AR	16p11.2	Liver	More severe phenotype with increased risk for liver fibrosis and cirrhosis
	GSD-IXd: 300559	Phosphorylase kinase, α-subunit, muscle	PHKA1/XLR	Xq13.1	Muscle	Muscle weakness and muscle cramps during exercise. Mostly in adults

GSD-X	261670	Muscle phosphoglycerate mutase	PGAM2/AR	7p13	Muscle	Exercise intolerance, muscle cramps and pain, rhabdomyolysis, myoglobinuria
Fanconi-Bickel syndrome (formerly GSD-XI)	227810	Glucose transporter 2	SLC2A2/AR	3q26.2	Liver	Hepatorenal involvement. Proximal renal tubular dysfunction. Osteoporosis/rickets. Different patterns of dysglycemia. Postprandial hyperglycemia and hypergalactosemia
GSD-XI	612933	Lactate dehydrogenase A	LDHA/AR	11p15.1	Muscle	Exertional myoglobinuria, easy fatigability, exercise induced myalgia, erythematosquamous skin lesions on the extensor surfaces of the extremities
GSD-XII	611881	Fructose-1,6-bisphosphate aldolase A	ALDOA/AR	16p11.2	Muscle	Rhabdomyolysis induced by fever and/or exercise, hemolytic anemia with or without myopathy or cognitive dysfunction
GSD-XIII	612932	Enolase 3 (β-enolase)	ENO3/AR	17p13.2	Muscle	Exercise intolerance, exercise induced myalgia, muscle weakness
GSD-XV	613507	Glycogenin-1	GYG1/AR	3q24	Muscle	Ventricular arrhythmogenic cardiomyopathy, progressive muscle weakness

GSD: Glycogen storage disease; HA: Hepatic adenoma; HCC: Hepatocellular carcinoma; AR: Autosomal recessive; XLR: X-linked recessive; XLD: X-linked dominant; CK: Creatinine kinase; CNS: Central nervous system; APBD: Adult polyglucosan body disease: IBD: Inflammatory bowel disease.



DOI: 10.3748/wjg.v29.i25.3932 **Copyright** ©The Author(s) 2023.

Figure 1 Simplified pathway of glycogen synthesis and degradation in hepatocytes. Glucose and glycogen convert into one another *via* synthesis or degradation (glycogenolysis) through various steps. The liver plays a central role in maintaining normoglycemia. During the fasting state, the liver maintains glucose homeostasis *via* a metabolic shift from synthesizing glycogen to endogenous glucose production by glycogenolysis and gluconeogenesis. Specific enzyme or transporter defects in these pathways are associated with clinical and biochemical manifestations including hepatomegaly, hypoglycemia, hyperlipidemia, hypertriglyceridemia, hyperlactatemia, and hyperuricemia. GSD: Glycogen storage disease; UDP-Glucose: Uridine diphosphate glucose; Glucose-1-P: Glucose 1-phosphate; Glucose-6-P: Glucose-6-phosphate; Acetyl-CoA: Acetyl coenzyme A; TCA: Tricarboxylic acid.

rate-limiting step in hepatic glycogen synthesis. GYS deficiency in liver leads to a marked reduction in hepatic glycogen stores. The inability to synthase glycogen inevitably leads to conversion of dietary carbohydrate to lactate rather than being stored as glycogen in the liver. Postprandial hyperglycemia, glycosuria, and lactic acidemia are replaced by ketotic hypoglycemia during fasting[12]. There is often ketosis after a routine overnight fast.

There are wide phenotypical variations[13]. Fasting hypoglycemia usually manifests in late infancy when overnight feedings are discontinued. Hypoglycemia typically occurs early in the morning prior to having breakfast. Hypoglycemia is responsible for the symptoms observed in GSD-0, which encompasses lethargy, pallor, nausea, vomiting, and, in some cases, seizures. Although some children may display developmental delay, most are neurologically normal. Some patients may remain asymptomatic or experience only mild symptoms[14]. Notably, liver enlargement is not a feature of GSD-0. GSD-0 is the only hepatic GSD that is not typically associated with hepatomegaly[15]. Short

stature and osteopenia are frequently observed in GSD-0, but other long-term complications commonly seen in other GSDs have not been documented[16]. Hyperglycemia and glycosuria are rare presentations in GSD-0 but may pose diagnostic difficulties when observed[17]. Postprandial hyperglycemia and glycosuria when taken together with a normal sized liver may mistakenly indicate early stages of diabetes. GSD-0 is underdiagnosed due to the lack of physical findings and milder phenotype[16,18].

Symptoms in GSD-0 are rapidly alleviated by frequent intake of protein-rich meals and bedtime consumption of uncooked cornstarch (UCCS), a slow-release glucose source. The preservation of gluconeogenesis and fatty acid oxidation pathways explains the less severe clinical course of GSD-0 compared to other types of hepatic GSDs. Increased protein intake during meals provides necessary substrates for gluconeogenesis and shows a protective effect against overweight/obesity and insulin resistance[19]. Extended periods of fasting can result in severe hyperketonemia and elevated plasma free fatty acid levels, which in turn leads to the inhibition of alanine release from skeletal muscle causing a reduction in the availability of gluconeogenic substrates, thereby exacerbating hypoglycemia [16]. While fasting is associated with hypoglycemia, hyperketonemia, and low alanine concentrations, feeding causes hyperglycemia and hyperlactatemia. Simple carbohydrates should be limited, and low-glycemic-index complex carbohydrates should be included in the diet to minimize postprandial hyperglycemia and hyperlactatemia. Patients are generally fed more frequently during the daytime to prevent hypoglycemia.

The administration of glucose or galactose to patients with GSD-0 results in elevated levels of serum lactate and lipids and can be used as a diagnostic test[2,17]. Traditional methods of diagnosis, such as liver biopsy to confirm extremely low hepatic glycogen levels and low to absent GYS activity, have been replaced by non-invasive mutation analysis of the *GYS2* gene.

Browner *et al*[20] discovered that muscle GYS, which is distinct from liver GYS, is expressed in both muscle and heart. The defect may be inherited or acquired. Enzyme activity is decreased in patients with type 2 diabetes. Muscle GYS deficiency causes cardiomyopathy and exercise intolerance in affected patients[8]. Histologic examination of muscle shows lack of glycogen and mitochondrial proliferation.

GSD-I; von Gierke disease; hepatorenal glycogenosis

The disease was first described by Gierke[21] in 1929 based on autopsy results showing excessive glycogen storage in the livers and kidneys of two patients. In 1952, Cori and Cori[22] discovered the deficiency of glucose-6-phosphatase (G6Pase) as the causative defect in patients with similar disease phenotype. After more than two decades, in 1978, Narisawa *et al*[23] described the deficiency of glucose-6-phosphate translocase (G6PT), the transporter protein of G6Pase complex (G6PC).

The deficiency of either G6Pase or G6PT activity causes GSD type I (GSD-I). The G6PT/G6PC functions as a multicomponent system and is responsible for glucose production by catalyzing the terminal step of both the glycogenolysis and gluconeogenesis pathways[24]. G6PT translocates G6P into the endoplasmic reticulum, wherein G6Pase converts G6P into free glucose and inorganic phosphate [25]. Two major subtypes of GSD-I are defined according to which part of the complex is defective. Deficiency of the catalytic subunit of G6Pase causes GSD-Ia while deficiency of G6PT activity results in GSD-Ib. Approximately 80% of cases with GSD-I are type Ia while the remaining 20% are type Ib. The presence of further subtypes (GSD-Ic and GSD-Id) is controversial. The majority, if not all, of typical cases of GSD-I are attributed to mutations in the genes encoding G6Pase and G6PT. Additionally, it has been noted that only two subtypes of GSD-I (namely, GSD-Ia and GSD-Ib) have been confirmed in clinical practice, and the existence of other forms of GSD-I requires further substantiation. Because both glycogenolysis and gluconeogenesis are affected due to inability in converting G6P to free glucose the main metabolic derangement of both subtypes is fasting hypoglycemia.

GSD-I is inherited in an autosomal recessive manner. The overall incidence of the disease is approximately 1:100000[26]. The estimated carrier rate in the general population is 1:150. The disease may be more prevalent in people of Ashkenazi Jewish (c.247C>T), Mexican-Hispanic (c.379_380dupTA) and Japanese heritage (c.648G>T) due to the increased frequency of mentioned pathogenic variants. The carrier frequency for the c.247C>T variant among Ashkenazi Jews has been reported to be as high as 1:63[27].

GSD-Ia; G6Pase deficiency

In 1952, Cori and Cori[22] identified the first specific enzyme deficiency associated with an inherited disorder through demonstration of G6Pase deficiency. Subsequently, in 1995, the gene that encodes the catalytic subunit of the G6PC was identified on chromosome 17q21[28]. Later, its molecular and biochemical characteristics were described in detail[29].

While some neonates may exhibit severe hypoglycemia and lactic acidosis, infants who do not receive any treatment typically present between 3-6 mo of age (at a median age of 6 mo) coinciding with prolonged feeding intervals, increased sleeping time through the night or onset of an intercurrent illness disrupting normal patterns of feeding[30]. The onset of symptoms can be soon after birth, and episodes typically remain unresponsive to glucagon therapy. Symptoms mainly include difficulties with feeding, tremors, pallor, excessive sweating, hyperventilation, cyanosis, apnea, irritability, seizures, somnolence, and cerebral edema/dysfunction, with exacerbations typically occurring in the morning or prior to feedings. Severe episodes of ketotic hypoglycemia, if untreated, may eventually lead to coma and

sudden infant death[31]. Older infants may exhibit certain physical characteristics, such as doll-like facies with full cheeks and relatively thin extremities along with frequent lethargy, difficulty in waking from sleep, tremors, an insatiable appetite, growth retardation, and a prominent abdomen resulting from pronounced enlargement of the liver and kidneys. In some cases, xanthomas may appear on extensor surfaces, such as the elbows, knees, or buttocks. During an infection, symptoms of severe hypoglycemia are more prevalent owing to diminished appetite and/or gastrointestinal symptoms (*e.g.*, vomiting and diarrhea) both preventing adequate oral intake. Delayed motor development can be seen but cognitive development is generally normal unless there is cerebral damage due to prolonged or recurrent neuroglycopenia[1,32].

Impaired platelet function, especially in individuals with inadequate metabolic control predisposes patients to nose bleeding[33]. Diminished glucose uptake into platelets due to chronic hypoglycemia and subsequent intracellular ATP deficiency have been proposed as potential causes of platelet dysfunction in GSD-Ia[34]. Additionally, decreased plasma concentration of von Willebrand factor antigen indicating an acquired von Willebrand disease was reported for patients with GSD-Ia[35]. In addition, epistaxis, easy bruising, menorrhagia, intrahepatic adenoma hemorrhage, and excessive bleeding during surgical procedures can also occur[36,37].

Patients with GSD-I have hypovitaminosis D despite adequate supplementation[38]. Low bone mineral density is a long-term complication of GSD-I particularly in those with poor metabolic control [39,40]. Osteoporosis may arise as a consequence of poor nutrition, chronic lactic acidosis and hypogonadism[41]. Anemia is a common complication in both subtypes of GSD-I with a reported prevalence ranging from 17% to 60% across different age groups[30]. The etiology of anemia in GSD-I is complex and involves various factors, including the restrictive nature of the diet, altered iron absorption due to excessive intake of UCCS, chronic lactic acidosis, chronic kidney disease, bleeding diathesis, chronic illness, suboptimal metabolic control, hepatic adenomas, and inflammatory bowel disease. The prevalence and pathophysiology appear to differ in individuals with GSD-Ia and those with GSD-Ib. A multicenter study involving 202 subjects with GSD-I (Ia/Ib: 163/39 subjects) showed that anemia is more common in patients with GSD-Ib compared to GSD-Ia (71.8% *vs* 41.7%, respectively). In addition, the prevalence of severe anemia is also increased in GSD-Ib in comparison to patients with GSD-Ia (41% *vs* 4.9%, respectively)[42]. Severe anemia in GSD-Ia appears to be related to large hepatic adenomas, while in GSD-Ib it is often associated with enterocolitis[42]. Development of severe anemia during the course of the disease warrants further evaluation for hepatic adenomas and inflammatory bowel disease in GSD-Ia and GSD-Ib, respectively.

Patients diagnosed with GSD-Ia or GSD-Ib may experience intermittent diarrhea which seems to deteriorate with age[43]. Diarrhea was reported in 35% of the GSD-Ia and in 55% of the GSD-Ib patients [30]. However, the cause of diarrhea remains unknown. Intolerance to UCCS and inflammatory bowel disease are possible causes of diarrhea in this population. Inflammatory bowel disease is a well characterized feature in individuals with GSD-Ib. Neutropenia and impaired neutrophil function are the underlying causes of inflammatory bowel disease in GSD-Ib[44]. However, inflammatory bowel disease was also recently reported in adult patients with GSD-Ia as a new, long-term complication of the disease [45]. The prevalence of symptomatic inflammatory bowel disease in adults with GSD-Ia also seems to be higher than the general population[45]. The authors speculated that inflammatory bowel disease in GSD-Ia may be caused by chronic UCCS therapy, which could be altering the microbiota of the gastrointestinal tract leading to inflammation. More recently, very early onset inflammatory bowel disease was reported in a child with GSD-Ia at the age of 42 mo[46].

A notable finding among the majority of patients with this condition during childhood is growth retardation, while short stature is commonly observed in affected adults[5,47,48]. In the absence of effective treatment, a range of long-term complications may arise in individuals with GSD-I, including delayed puberty, liver adenomas, hepatocellular carcinoma, renal dysfunction, chronic kidney disease, chronic renal failure, urolithiasis, arterial and pulmonary hypertension, osteopenia/osteoporosis, polycystic ovary syndrome, and gout. Cognitive delay and epilepsy due to repeated or severe hypoglycemic events may occur[31]. Hyperlipidemia may cause xanthomas, pancreatitis, and cholelithiasis[30,49]. Acute pancreatitis may develop secondary to very high serum triglycerides in GSD-I and necessitate plasmapheresis[50].

Systemic metabolic perturbations and glycogen deposition in the kidneys result in glomerular and proximal and distal renal tubular injury. Renal manifestations may occur in childhood but often are not noticed without proper diagnostic work-up. The prevalence of renal involvement tends to rise as patients age[51]. Glomerular hyperfiltration, whose underlying mechanism is not yet fully understood, is typically the initial manifestation of renal involvement. Possible etiologies have been suggested including activation of the renin-angiotensin system, persistent oxidative stress, profibrotic cytokines such as transforming growth factor-β, and changes in energy reserves of renal tubular epithelial cells[52-54]. Glomerular hyperfiltration then progresses to microalbuminuria, proteinuria, glomerular scarring and interstitial fibrosis, and end-stage renal disease in adult patients[48,55]. Hypercalciuria and hypocitraturia due to proximal and distal tubular dysfunction cause nephrocalcinosis and/or urolithiasis[56,57]. This may increase the risk of urinary tract infections causing further renal parenchymal damage. Hypertension and hematuria are other findings[55,56]. Systemic hypertension may develop early in childhood but is seen more often in adults with GSD-I[58]. Renal cysts have also been described in

individuals with GSD-I[59]. Gout can develop due to persistent hyperuricemia as gouty attacks, gouty tophi, and kidney stones.

In GSD-Ia patients, various types of liver lesions, including hepatic adenoma, hepatocellular carcinoma, hepatoblastoma, focal fatty infiltration, focal fatty sparing, peliosis hepatis, and focal nodular hyperplasia have been reported, with hepatic adenomas being the most prevalent among them[37]. The prevalence of hepatic adenomas was reported to vary between 22% to 75%, and they usually manifest during or after puberty, particularly in the second or third decade of life. The median age of adenoma presentation is 15 years[30]. Although the prevalence of hepatic adenomas increases with age in GSD-I, they may be seen in younger children[60]. Progression in size and/or number of hepatic adenomas occurs in half of patients[30]. Inadequate metabolic control appears to play a central role in hepatic adenoma formation. The degree of hyperlipidemia is associated with development of hepatic adenomas [61]. However, the pathophysiological mechanisms are yet to be fully understood and factors other than metabolic control may also be responsible for adenoma formation. In a recent study by Cho *et al*[62], in addition to mitochondrial dysfunction and metabolic alterations caused by G6Pase deficiency, persistent autophagy impairment and activation of multiple tumor-promoting pathways were reported as contributing factors to hepatic adenoma/hepatocellular carcinoma development in GSD-I. Chromosomal and genetic alterations may also play a role in hepatocellular carcinoma associated with GSD-I[63]. Hepatic adenomas have the potential to transform into hepatocellular carcinoma over an extended period, with reports of malignant transformation occurring as long as 28 years after initial diagnosis[64,65]. A rapid increase in size or number of adenomas is associated with an increased risk of adenoma to hepatocellular carcinoma transformation and should be evaluated carefully.

The link between GSD-I and risk for cardiovascular disease is controversial. Although GSD-Ia patients have elevated levels of triglycerides, very low density lipoprotein and low density lipoprotein, the occurrence of endothelial vascular dysfunction and atherosclerosis is uncommon. It has been suggested that the increased serum levels of apoE may offset the elevated risk of atherosclerosis associated with dyslipidemia[66]. Moreover, the reduced von Willebrand factor antigen and density of individual oligomers found in 60% of GSD-Ia patients may also contribute to protection against vascular complications[35]. In addition, an increase in serum levels of antioxidative factors may contribute as a protective mechanism[67,68]. There are conflicting data regarding whether patients with GSD-I are at increased risk for atherosclerosis[69,70]. Pulmonary hypertension is a rare long-term complication of GSD-I with few cases reported. Patients with a concomitant predisposing condition for pulmonary arterial hypertension are at increased risk[37].

The main neurological impact of GSD is related to hypoglycemia. Patients with GSD-I may suffer from brain damage, which may be caused by recurrent severe hypoglycemia[71]. Studies have found a significant correlation between the frequency of hospital admissions for hypoglycemia and abnormalities in both performance ability tests and brainstem auditory evoked potentials. In addition, electroencephalography abnormalities were found to be correlated with dietary compliance. The magnetic resonance imaging abnormalities observed in GSD-I patients were the dilatation of occipital horns and/or hyperintensity of subcortical white matter in the occipital lobes[71]. Brain imaging abnormalities were more frequent among GSD-I patients with early symptom onset, frequent and longer hospital admissions, and poor metabolic control including elevated levels of uric acid, lactate, and triglyceride[32,72].

Some females may have polycystic ovaries and irregular menstrual cycles with normal fertility[73]. Women with GSD-Ia may have pregnancies and deliveries without complications[74]. In consideration of the risk of development of hepatic adenomas in GSD-I patients, estrogen-containing contraceptives should be avoided whenever possible[75]. In addition to hypoglycemia, the most prominent laboratory abnormalities observed in patients with GSD-I include lactic acidosis, hyperlipidemia (especially hypertriglyceridemia but also hypercholesterolemia), and hyperuricemia (Figure 1). Mild elevation in transaminase levels is usually detected[30]. Ultrasonographic examination may reveal enlarged kidneys in affected patients of all ages. Serum biotinidase activity is increased in GSD-Ia patients[76-79]. Biotinidase activity was reported to be positively correlated with hypertriglyceridemia in subjects with GSD-I while severe fibrosis and cirrhosis were related to reduced enzyme activity[80]. There may also be hypercalciuria[5]. There is little or no increase in blood glucose concentration in response to administration of glucagon and this may even lead to worsening of the metabolic acidosis. Histopathological examination of the liver in patients with GSD-Ia typically reveals a mosaic pattern with pale-staining and swollen hepatocytes. Other observed features include steatosis and nuclear hyperglycogenation. Periodic acid-Schiff (PAS)-positive and diastase sensitive glycogen is evenly dispersed throughout the cytoplasm. Glycogen accumulation may be within the normal range or exhibit only a mild increase. While fibrosis is not as prominent in GSD-I as in GSD types III, IV, and VI, it may still be present in some affected individuals[5,81-83]. GSD-Ia is usually suspected based on a set of clinical (*e.g.*, hepatomegaly) and biochemical features (*e.g.*, hypoglycemia, lactic acidosis, hypercholesterolemia, hypertriglyceridemia, and hyperuricemia). The definitive diagnosis is confirmed by a mutation analysis or a liver biopsy and an enzyme assay. If a liver biopsy is performed, diagnosis can be confirmed by measuring G6Pase enzyme activity on a liver biopsy specimen; however, it should be kept in mind that measurement of G6Pase enzyme activity will not detect GSD-Ib. When the specific mutation in the index case is known, prenatal diagnosis *via* chorionic villus sampling can be performed for GSD-I[84].

The mainstay of treatment is to prevent hypoglycemia by avoiding prolonged fasting[85]. Continuously providing a dietary supply of glucose during the day and night by frequent feedings, frequent ingestion of UCCS or nocturnal enteral tube feeding are possible feeding strategies. Infants and children should be fed frequently, not allowing fasting periods longer than 3-4 h. In adolescents and adults, fasting more than 5-6 h should be avoided. Small, frequent meals with balanced macronutrient content and use of UCCS are recommended. Continuous intragastric feeding through a nasogastric or gastrostomy tube can be used overnight allowing the patients to sleep through the night[37]. To ensure adequate glucose supply, a glucose infusion rate of 8-10 mg/kg/min should be maintained for infants, while a rate of 4-8 mg/kg/min is recommended for older children. UCCS can be introduced as early as 6-12 mo of age. For the administration of UCCS in GSD-I patients, the recommended dose is 1-1.5 g of UCCS per kilogram of ideal body weight every 3-4 h for young children and 1.5-2 g of UCCS per kilogram of body weight every 4-5 h for older children, adolescents, and adults[85]. Digestion of UCCS is slow, enabling a sustained release of glucose, thereby achieving a more stable glycemic profile over an extended duration, in contrast to other carbohydrate sources. The administration of UCCS has been shown to achieve adequate glycemia for a median duration of 4.25 h (ranging between 2.5-6 h)[86]. Glycosade®, a modified, waxy maize extended-release cornstarch, is available as a single-dose overnight treatment[87].

In GSD-I, intake of fructose and galactose, which cannot be metabolized to glucose *via* G6P, further contributes to the metabolic derangement. Lactose (galactose and glucose), fructose and sucrose (fructose and glucose) should be restricted in all age groups. Restricting the intake of fruits, vegetables, juices, and dairy products renders the diet inadequate. Micronutrients, vitamins, and minerals should be supplemented to avoid nutritional deficiencies. The recommended dietary plan is to provide 60%-70% of calories from complex carbohydrates, such as whole-grain breads, pastas, legumes, and rice, with a portion of the carbohydrates coming from cornstarch. Additionally, 10%-15% of calories should come from protein and 25%-30% from fat. Effective dietary management is essential to minimize the metabolic derangement associated with GSD-I and to reduce the development of long-term complications[37,85]. However, caution must be exercised to avoid overtreatment. Overtreatment with UCCS has many consequences including obesity, increased glycogen storage in the liver, worsening lactic acidosis, increased gastrointestinal disturbances, hyperinsulinemia, and insulin resistance[88].

If there is anemia, the causes must be evaluated (*e.g.*, nutritional deficiencies, liver adenomas, enterocolitis, menorrhagia in females, and occult blood loss from the gastrointestinal tract) and appropriate treatment should be started. In the case of severe anemia, hepatic adenomas in GSD-Ia and enterocolitis in GSD-Ib should be investigated[42]. To prevent gout in the presence of hyperuricemia, allopurinol is typically administered at a dosage of 10 mg/kg/d, divided into three doses. If acidosis is present, indicated by a blood base excess of less than -5 mmol/L or a blood bicarbonate level below 20 mmol/L, bicarbonate or potassium citrate should be prescribed, with a recommended dose of 1 to 2 mmol/kg/d divided into four doses and 5 to 10 mEq every 8-12 h, respectively[85]. Angiotensin converting enzyme inhibitors or angiotensin receptor blockers should be used to delay the progression of renal damage[53,89-91]. Evidence of hyperfiltration (sustained estimated glomerular filtration rate > 140 mL/min/1.73 m^2), persistent microalbuminuria and frank proteinuria should prompt initiation of angiotensin converting enzyme inhibitors or angiotensin receptor blockers[37]. If serum triglyceride levels remain high despite optimizing dietary treatment, the administration of lipid-lowering drugs, such as 3-hydroxy-3-methylglutaryl-coenzyme A reductase inhibitors and fibrates, may be necessary to decrease the risk of atherosclerosis, cholelithiasis, and pancreatitis. For adults with persistently elevated cholesterol levels, statins may be considered as a treatment option[85]. The positive effect of medium-chain triglycerides on lowering serum cholesterol and triglyceride levels has been reported[92,93].

Recommendations regarding perioperative management of patients with GSD-I are available[37,94]. Close monitoring of blood glucose, electrolytes, and lactate levels is crucial during the peri-operative period. The patient should be admitted to the hospital 24 h before the surgery, continuous intravenous supply with 10% dextrose should be provided and continued until oral feeding is re-established. The administration of Ringer lactate solution should be avoided in GSD-I patients, as it may exacerbate lactic acidosis and worsen metabolic decompensation[37]. Bleeding time must be normalized before elective surgical interventions by 24-h continuous gastric drip feeding for one week or by intravenous glucose infusion over 24 to 48 h[85].

GSD-Ib; G6PT deficiency

In 1968, after realizing that *in vitro* G6Pase activity was normal despite glucose not being released from G6P *in vivo*, a second subtype of GSD-I was identified[95]. In 1975, it was elucidated that a transport system specific to G6P exists and is responsible for transporting G6P from the cytoplasm to the endoplasmic reticulum[96]. The responsible gene, *SLC37A4* (the solute carrier family 37 member 4), has been cloned and located on chromosome 11q23[97,98].

GSD-Ib is characterized by distinctive features such as recurrent infections, neutropenia, and neutrophil dysfunction, in addition to the clinical symptoms and findings observed in GSD-Ia. While not all GSD-Ib patients have neutropenia and neutrophil dysfunction, these conditions are common and predispose patients to severe infections and inflammatory bowel disease[44]. Patients with GSD-Ib may have normal neutrophil counts in the first year of life. *G6PT* gene, unlike *G6Pase*, is also expressed in

hematopoietic progenitor cells, which may be responsible for neutropenia and recurrent infections in GSD-Ib[99]. The neutrophil dysfunction in GSD-Ib includes both impaired motility and respiratory burst[100,101]. Impaired glucose transport across the cell membrane of polymorphonuclear leukocytes may be responsible for neutrophil dysfunction in GSD-Ib. Microsomal transport of G6P has a potential role in the antioxidant protection of neutrophils. Dysfunction of this transporter due to genetic defects in *G6PT* may impair cellular functions and induce apoptosis, contributing to the neutrophil dysfunction seen in GSD-Ib[102]. Some individuals with GSD-Ib do not develop neutropenia. It has been suggested that this could be due to residual transporter activity of some *G6PT* mutations[103]. GSD-Ib patients with neutropenia and neutrophil/monocyte dysfunction are at an increased risk for severe infectious complications due to impaired immune function. Young children with GSD-Ib may experience frequent otitis, gingivitis, periodontal disease, dental caries, and skin abscesses. Oral and genital ulcerations and intestinal mucosal ulcers may occur[43,104]. Individuals with GSD-Ib may experience recurrent episodes of diarrhea. The underlying cause of this symptom appears to be inflammation of the intestinal mucosa, as evidenced by elevated fecal α1-antitrypsin excretion and colonic inflammation in colonoscopic biopsies[44]. There is no established association between the specific genetic mutations causing GSD-Ib and the occurrence of neutropenia, bacterial infections, and other systemic complications in affected individuals[105]. Patients with GSD-Ib may require liver transplantation. Although hypoglycemia, lactic acidosis and dyslipidemia improve after liver transplantation, neutropenia generally continues to be present as it is primarily attributable to an intrinsic defect in the neutrophils [106-108].

Another characteristic clinical finding of GSD-Ib is the occurrence of Crohn disease-like colitis[109, 110]. The enterocolitis observed in GSD-Ib patients has been found to have histological features similar to those seen in inflammatory bowel disease/Crohn disease, characterized by transmural inflammatory changes and the formation of granulomas[111]. Accompanying findings and symptoms include fever, diarrhea, and perioral and anal ulcers. Interestingly, the severity of the primary disorder does not appear to be correlated with the occurrence or severity of intestinal symptoms[109,110]. Manifestations of inflammatory bowel disease may improve with granulocyte colony-stimulating factor (G-CSF) treatment[112]. Enteral nutrition with a polymeric formula enriched in the anti-inflammatory cytokine transforming growth factor-β is recommended as a first-line treatment of digestive complications in GSD-Ib[113]. Inflammatory bowel disease may require treatment with anti-inflammatory and immunosuppressive medications[113]. Successful treatment of inflammatory bowel disease with biologics including infliximab and adalimumab in GSD-Ib patients refractory to conventional treatment has been reported[114,115].

GSD-Ib is characterized by an increased risk for developing autoimmune disorders like thyroid autoimmunity and myasthenia gravis[116]. GSD-Ib patients have a higher likelihood of developing thyroid autoimmunity and hypothyroidism, while GSD-Ia patients show little indication of thyroid pathologies[117,118]. Based on the slightly elevated levels of thyrotropin, even in patients with overt hypothyroidism, it could be postulated that there is concomitant damage occurring at the hypothalamus or pituitary gland[118]. Recently, predisposition to autoimmunity in GSD-Ib patients was linked with a profound defect in conventional T cells and regulatory T cells caused by defective engagement of glycolysis in T cells due to G6PT deficiency[119]. Although a rare outcome of GSD-Ib, patients may develop terminal kidney disease, which may necessitate kidney transplantation[106].

Nutritional management of GSD-Ib is similar to that of GSD-Ia. Neutropenic patients with GSD-Ib should be treated with G-CSF. G-CSF therapy may normalize the number of neutrophils and restore myeloid functions[120-122]. The implementation of a combined therapeutic approach including both dietary management and G-CSF treatment improves the prognosis of patients by significantly mitigating metabolic and myeloid abnormalities. G-CSF administration is associated with not only an elevation of peripheral neutrophil counts, but also a reduction in the incidence of febrile episodes and infections, as well as improvement in enterocolitis in patients with GSD-Ib[123]. In conjunction with other therapies (aminosalicylates, mesalamine, and corticosteroids), G-CSF ameliorates inflammatory bowel disease symptoms[124]. To prevent complications such as splenomegaly, hypersplenism, hepatomegaly, and bone pain, it is recommended that the lowest effective dose of G-CSF is used. Caution must be exercised regarding the development of splenomegaly and myeloid malignancy[124,125]. Vitamin E has been reported to be effective in reducing the frequency of infections and improving neutropenia [126].

Liver transplantation is the ultimate therapy for hepatic metabolic disease related to GSD-I. There is no possibility of the recurrence of GSD-I within the allograft. Liver transplantation is warranted in various situations, such as hepatic adenomas with a high risk of malignant transformation, rapid progression in size and/or number of hepatic adenomas, development of hepatocellular carcinoma, poor metabolic control despite medical therapy, and growth failure[127]. Liver transplantation corrects all liver related biochemical abnormalities including hypoglycemia, lactic acidosis, hyperuricemia, and hyperlipidemia, but its potential to reverse and/or prevent renal disease remains uncertain[107,128-130]. Recently, an unusual post-transplant finding of two siblings with persistent hyperuricemia requiring allopurinol treatment has been reported[131]. Moreover, chronic renal failure is a well-known complication that may arise as a consequence of liver transplantation in individuals with GSD-Ia, and progression to renal failure within a few years of transplantation was reported[128]. It is uncertain

whether post-transplantation renal failure is related to disease progression, toxicity from immunosuppressants used after liver transplantation, a secondary reaction to poor metabolic control, or a combination of these factors. Renal transplantation in GSD-I, on the other hand, corrects only renal abnormalities[132]. Conflicting results have been reported in different studies regarding whether catch-up growth is achieved or not following liver transplantation in children with GSD-I[133,134].

Despite improved survival and growth, long-term complications of GSD-I like progressive renal failure and development of hepatic adenomas do not respond completely to dietary treatment. Although liver transplantation corrects metabolic derangement and improves the quality of life of these patients, it is not without complications[128]. These findings suggest that novel therapeutic approaches with higher success and lower complication rates are warranted. A recent advance in the treatment of neutropenia and neutrophil dysfunction in individuals with GSD-Ib is repurposing empagliflozin, a sodium-glucose co-transporter-2 (SGLT2) inhibitor that is approved to treat type 2 diabetes in adults, to improve neutrophil number and function. A study conducted by Veiga-Da-Cunha *et al*[135] revealed the crucial function of glucose-6-phosphate transporter in neutrophils, which clarifies the pathophysiology of neutropenia in GSD-Ib patients. In addition to G6P, G6PT transports the G6P structural analog 1,5-anhydroglucitol-6-phosphate (1,5AG6P). Neutrophils lacking G6PT activity cannot transport 1,5AG6P from the cytosol into the endoplasmic reticulum, where it is normally dephosphorylated by G6PC3, a phosphatase in the membrane of the endoplasmic reticulum. Cytosolic accumulation of 1,5AG6P inhibits glucose phosphorylation by hexokinases that catalyzes the first step of glycolysis. As glycolysis is the sole energy source for mature neutrophils, depletion of intracellular G6P leads to a deficit in energy production which in turn results in neutrophil dysfunction and subsequent apoptosis. Empagliflozin inhibits renal SGLT2 leading to increased urinary excretion of 1,5AG. This leads to a reduction in the concentration of 1,5AG in the blood, thereby decreasing the cellular accumulation of toxic 1,5AG6P in neutrophils[136]. Following the first report of successful repurposing of empagliflozin to treat neutropenia and neutrophil dysfunction in 4 patients with GSD-Ib, several case reports and case series have shown beneficial effects of this treatment approach on neutrophil number and function, inflammatory bowel disease, recurrent infections[137-139], oral and urogenital mucosal lesions, skin abscesses, anemia, wound healing, and dose reduction or even cessation of G-CSF therapy in GSD-Ib patients[140-144]. A recent international multicenter study examining the clinical experience of 112 patients with GSD-Ib treated with empagliflozin reported improvements in neutrophil counts in the majority of patients, leading to the cessation of regular G-CSF injections in 55% of the participants[145]. Despite a favorable safety profile in patients with GSD-Ib, there is a risk of hypoglycemia with SGLT2 inhibitors. A low dose at treatment initiation with careful titration to optimal dosing is recommended [141]. Growing evidence suggests that empagliflozin is a candidate for first-line treatment of neutropenia and neutrophil dysfunction related symptoms in GSD-Ib patients.

Another promising novel therapeutic strategy is gene therapy by using recombinant adeno-associated virus vectors. The use of a viral vector to administer G6Pase and hepatocyte transplantation are being investigated as potential treatments for GSD-I. Various animal models have shown an increase in hepatic G6Pase and G6PT activity, as well as improvements in metabolic parameters[146-150]. Multiple approaches have been explored for the integration of the G6Pase transgene into the host genome[151, 152]. The successful correction of metabolic imbalances in animal models through gene therapy shows promising potential for future applications of gene therapy in humans. A phase I/II clinical trial using a recombinant adeno-associated virus vector expressing a codon-optimized human G6Pase-α or G6PC for treatment of human GSD-Ia (NCT 03517085) has just been completed and the results are pending.

GSD-III; Cori disease; Forbes disease; limit dextrinosis; amylo-1,6-glucosidase deficiency; glycogen debrancher deficiency

Glycogen debrancher enzyme has two independent catalytic activities; alpha-glucanotransferase and amylo-1,6-glucosidase, with the two catalytic sites being separated on the same polypeptide. Both catalytic activities are required for complete debranching enzyme activity[153]. Deficient activity of these catalytic sites results in accumulation of glycogen with short outer chains, previously defined as limit-dextrins. Deficiency in glycogen debranching enzyme due to biallelic pathogenic variants in the *AGL* gene results in the harmful accumulation of abnormal glycogen in hepatocytes. The *AGL* gene was mapped to the chromosomal locus 1p21, and its nucleotide sequence was determined, revealing the existence of multiple tissue-specific isoforms[154,155]. GSD-III is inherited in an autosomal recessive manner.

GSD-III makes up about 24% of all GSDs, and its estimated incidence is approximately 1 case per 83000 live births in Europe, and 1 in 100000 live births in North America[156]. Certain populations have an increased prevalence due to a founder effect. The highest known GSD-III prevalence occurs in Inuit population in Nunavik (about 1:2500, c.4456delT variant), the Faroese population of the Faroe Islands (about 1:3600, c.1222C>T variant) and North African Jews from Israel (about 1:5400, c.4456delT variant) [156-158]. There is currently limited evidence supporting a correlation between disease severity and pathogenic variants in the *AGL* gene, except for specific exon 3 variants (c.18_19delGA and c.16C>T) which have been found to be associated with GSD-IIIb (liver involvement only). It was suggested that in muscle isoforms of the *AGL* gene, alternative exon or translation initiation may not require exon 3,

thereby resulting in normal enzyme activity in the muscle tissues of patients with GSD-IIIb who harbor an exon 3 deletion[159,160]. Recent evidence suggests that the presence of frameshift, nonsense, and splice site variants may lead to severe phenotypes. Differences in tissue expression of the deficient enzyme is responsible for the phenotypic variability observed in GSD-III patients[153].

GSD-III is characterized by heterogeneous involvement of the liver, skeletal muscle, and cardiac muscle, leading to variable clinical presentations. Various subtypes are defined by the extent of tissue involvement. Two major subtypes of GSD-III have been identified. GSD-IIIa affects both the liver and the muscle (skeletal and cardiac) and is the most prevalent subtype accounting for approximately 85% of cases. Meanwhile, GSD-IIIb primarily affects only the liver and comprises approximately 15% of all GSD-III cases[48,159]. In a limited number of cases, it has been demonstrated that there is a selective loss of either glucosidase activity (resulting in muscle involvement, referred to as GSD-IIIc) or transferase activity (resulting in both muscle and liver involvement, referred to as GSD-IIId)[161,162].

Hepatomegaly, ketotic hypoglycemia, growth retardation and dyslipidemia (hypertriglyceridemia) are the dominant features of hepatic involvement in infancy and childhood. As gluconeogenesis is intact in GSD-III, fasting hypoglycemia tends to be milder than that seen in GSD-I. During infancy, serum hepatic transaminases are markedly elevated. Uric acid and lactate concentrations are relatively normal [163]. Symptoms and laboratory findings related with liver involvement often improve with age and usually disappear after puberty[164,165]. However, liver disease can also be progressive resulting in liver fibrosis, cirrhosis, hepatic failure, and end-stage liver disease[107,165]. Hepatic fibrosis may occur as early as 1 year of age[166]. Overt liver cirrhosis is not common and occurs rarely[153,165]. Hepatocellular carcinoma can develop as a long-term complication of liver cirrhosis, rather than transformation of an adenoma to carcinoma, as seen in GSD-I[167,168]. The prevalence of hepatic adenomas has been reported to range from 4% to as high as 25%[169]. A recent descriptive, retrospective, international, multi-center cohort study revealed that the overall prevalence of severe hepatic complications (hepatic cirrhosis, hepatic adenomas and/or hepatocellular carcinoma) was 11%[170]. Liver transplantation for cirrhosis and/or hepatocellular carcinoma have been reported[107,168]. Children with failure to thrive often catch-up in height in adulthood with optimized, individualized dietary management.

Muscle symptoms associated with GSD-III can manifest concurrently with liver disease or long after hepatic disorders or even after the resolution of hepatic symptoms during childhood. An elevation in creatine kinase (CK) level is observed in 81% to 94% of cases with muscle involvement, serving as a useful indicator of muscle pathology[171]. Nonetheless, a normal CK level does not entirely exclude the possibility of an underlying muscular disease[172,173]. The median age of onset of CK elevation was reported to be 10 years[170]. Although muscle involvement becomes clinically more obvious later in life, mild muscle weakness on physical examination, motor developmental delay (delayed sitting, delayed standing upright, delayed onset of walking), exercise intolerance, and hypotonia were reported in the majority of pediatric patients with GSD-III[174-176]. Muscle weakness and wasting may slowly progress and become severe by the third or fourth decade of life[165,173].

In a subset of adult patients with GSD-III, muscle symptoms can present in the absence of any clinical or previous evidence of liver dysfunction[165,177]. Muscle weakness, although minimal during childhood, is slowly progressive in nature and may become the predominant feature with significant permanent muscle weakness in adults with type IIIa disease[171]. Although myopathy generally progresses slowly and is not severely debilitating, some patients may have severe muscle involvement leading to loss of ambulation[170]. Myopathy can be proximal, distal, or more generalized. Exercise intolerance with muscle fatigue, cramps and pain are evident in more than half of patients[170,174,175]. Bulbar or respiratory dysfunctions are rarely seen in GSD-III patients while no clinical involvement of facial or ocular muscles has been described in the literature[178].

Cardiac involvement in GSD-III is variable. Cardiac involvement is present in most patients, with varying degrees of severity ranging from ventricular hypertrophy detected on electrocardiography to clinically apparent cardiomegaly[179]. Left ventricular hypertrophy, right ventricular hypertrophy, interventricular septal hypertrophy, QT prolongation, sinus tachycardia, and pulmonary hypertension were among electrocardiographic and/or echocardiographic findings of cardiac involvement[170,180]. According to International Study on Glycogen Storage Disease data presented by Sentner *et al*[170], 58% of patients with GSD-IIIa showed cardiac hypertrophy mostly presented by electrocardiographic and/or echocardiographic signs of left ventricular hypertrophy. In the same cohort, only 15% of all patients developed hypertrophic cardiomyopathy. Mogahed *et al*[175] reported that cardiac muscle involvement is less common and mostly subclinical in the pediatric age group. However, a more recent study reported that 91% of patients showed cardiac involvement at a median age of 2.6 years, 86% of cases being under 2 years of age[181]. Moreover, 56% of the patients presented with a symptomatic cardiomyopathy at some point during the follow-up period indicating a more severe cardiac phenotype especially in those on a diet with insufficient caloric and protein intake and suboptimal UCCS treatment [181]. Cardiomyopathy usually presents with asymptomatic left ventricular hypertrophy but can progress to hypertrophic cardiomyopathy with decreased left ventricular function and/or arrhythmias, severe cardiac dysfunction, or congestive heart failure[181,182]. Sudden death has occasionally been reported[183].

Patients with GSD-III may exhibit facial abnormalities such as indistinct philtral pillars, bow-shaped lips with a thin vermillion border, a depressed nasal bridge and a broad upturned nasal tip, and deep-set eyes, particularly in younger patients[184]. Some individuals with GSD-III may have an increased risk of developing osteoporosis with reduced bone mineral density which, in part, may be due to suboptimal nutrition, the effects of metabolic abnormalities and muscle weakness[41,185,186]. Bone fractures due to osteopenia and osteoporosis were reported in patients with GSD-III[170]. Polycystic ovary disease has been reported in women with GSD-III with no significant effect on fertility[187]. Type 2 diabetes may occur during the course of the disease in adulthood[188]. Michon *et al*[189] reported global cognitive impairment in adult GSD-III patients as an underlying cause of psychological and attention deficits seen in this patient group.

Liver histology shows uniform distension of hepatocytes secondary to glycogen accumulation. There is often septal formation, periportal and reticular fibrosis, fine microsteatosis, and less frequently, micronodular cirrhosis without inflammation or interface hepatitis. Skeletal muscle shows subsarcolemmal glycogen accumulation[12]. The diagnosis of GSD-III is made by identification of biallelic *AGL* pathogenic variants on molecular genetic testing. If the diagnosis cannot be established by genetic analysis, demonstrating enzyme deficiency in peripheral leukocytes or erythrocytes, cultured skin fibroblasts or in the liver or muscle tissue samples is necessary.

A practice guideline was published by the American College of Medical Genetics and Genomics in 2010 providing recommendations on the diagnosis and management of the complications of GSD-III [176]. The mainstay of GSD-III treatment is dietary intervention, which aims to maintain normal blood glucose levels while balancing macronutrient and total caloric intake. This is achieved by the avoidance of fasting, frequent meals enriched in complex carbohydrates and use of UCCS. Continuous enteral feeding may be needed in some cases. Sucrose, fructose, and lactose are not contraindicated unlike GSD-I. UCCS can be used as early as the first year of life to prevent hypoglycemia. As an alternative, Glycosade®, an extended-release cornstarch, can also be used[87]. Caution must be exercised to avoid overtreating with cornstarch or carbohydrates, which may lead to excessive storage of glycogen in the liver and weight gain. In patients with myopathy, along with managing hypoglycemia, a high-protein diet is recommended as it prevents muscle protein breakdown during glucose deprivation, thereby preserving skeletal and cardiac muscle[176]. A ketogenic diet (alone or in combination with high protein and ketone bodies) was also shown to ameliorate cardiomyopathy[190,191]. It has been shown that a high-fat, low-calorie and high-protein diet can reduce cardiomyopathy in individuals with GSD-III[192, 193]. The beneficial effects on cardiac or skeletal muscle function of these ketogenic or high-fat diets are possibly related to the increased ketone bodies or fats as fuel sources, or reduced glycogen accumulation through decreased carbohydrate intake. Whether long-term muscular, cardiac, or even liver complications can be prevented by these dietary approaches warrants further studies[194].

Liver transplantation corrects all liver related biochemical abnormalities but does not correct myopathy or cardiomyopathy[107,133,195]. Cirrhosis, liver dysfunction, and/or hepatocellular carcinoma are the main indications for liver transplantation. Detailed information about surveillance recommendations on hepatic, metabolic, musculoskeletal, cardiac, nutritional, and endocrine aspects of the disease can be found elsewhere[176]. Gene therapy and gene-based therapeutic approaches are in development.

GSD-IV; Andersen disease; brancher deficiency; amylopectinosis; glycogen branching enzyme deficiency

The disease was described by Andersen[196] in 1956 as "familial cirrhosis of the liver with storage of abnormal glycogen" and, in 1966, amylo-1,4 to 1,6-transglucosidase [glycogen branching enzyme (GBE)] deficiency was reported[197]. Branching of the chains is essential to pack a very large number of glycosyl units into a relatively soluble spherical molecule. Without GBE, abnormal glycogen with fewer branching points and longer outer chains resembling an amylopectin-like structure (polyglucosan) accumulates in various tissues including hepatocytes and myocytes[198]. The mapping of the *GBE1* gene to chromosome 3p12.2 was first accomplished in 1993[199]. Notably, mutations in the same gene are also responsible for adult polyglucosan body disease. GSD-IV accounts for only 0.3% of all GSDs and follows an autosomal recessive inheritance pattern[200]. This rare disorder has a prevalence of 1:600000 to 1:800000[201].

GSD-IV exhibits significant clinical heterogeneity and phenotypic variability, partly due to variations in tissue involvement, which may be influenced by the presence of tissue-specific isozymes[198,200]. The liver is the primary organ affected, with the classical hepatic form appearing normal at birth but progressing rapidly to cirrhosis in early life, leading to liver failure and death between 3 to 5 years of age[196]. Children with GSD-IV experience growth failure, hepatomegaly and/or splenomegaly, and cirrhosis within the first 18 mo of life. Besides the complications of progressive cirrhosis including portal hypertension, ascites and esophageal varices, the development of hepatocellular carcinoma was also reported[202]. In rare cases, the hepatic disease in GSD-IV may not progress or progress slowly[203]. Patients with the non-progressive hepatic form may present with hepatosplenomegaly and mildly elevated liver transaminases, and experience normal growth. Liver size and transaminase levels may return to normal[203]. Patients with the non-progressive hepatic form usually survive into adulthood.

GSD-IV can present with multiple system involvement, with the enzyme deficiency in both liver and muscle[204]. This form of the disease can manifest as peripheral myopathy with or without cardiomyopathy, neuropathy, and liver cirrhosis. Onset of the disease can be from the neonatal period to adulthood[205]. The neuromuscular presentation can be divided into four groups based on age at onset [206]. In the perinatal (fetal) form, which can lead to hydrops fetalis and polyhydramnios, arthrogryposis develops due to akinesia[207]. Detection of cervical cystic hygroma during pregnancy may indicate the disease[200]. Prenatal diagnosis can be performed by determining enzyme activity in cultured amniocytes or chorionic villi samples. Genetic studies can complement uncertain enzyme activity studies, such as equivocal results in prenatal fetal samples and in patients with higher levels of residual enzyme activity that overlap heterozygote levels[208]. Mortality is unavoidable in the neonatal period. Liver cirrhosis or liver failure has not been reported. Severe hypotonia, hyporeflexia, cardiomyopathy, depressed respiration, and neuronal involvement are features of the congenital form of the disease[198,209-211]. Liver disease is not severe, and the child dies in early infancy due to other reasons. The childhood neuromuscular form may start at any age with either myopathy or cardiomyopathy[206, 212]. Presenting symptoms mainly include exercise intolerance, exertional dyspnea, and congestive heart failure in advanced stages. The disease can be confined to muscular tissue and serum CK level can be within the normal range. In the adult form, there is isolated myopathy or a multisystemic disease called adult polyglucosan body disease. Onset of symptoms can occur at any age during adulthood, usually after the age of 50, and may exhibit a resemblance to muscular dystrophies. Symptomatology includes progressive gait difficulty and proximal muscle weakness, which is more pronounced in the arms as compared to the legs. Both upper and lower motor neurons are affected in the disorder. The disease may manifest as pyramidal tetraparesis, peripheral neuropathy, early onset of neurogenic bladder, extrapyramidal symptoms, seizures, and cognitive dysfunction leading to dementia[210]. The diagnosis can be established by enzyme activity assay in erythrocytes[213]. Amylopectin-like inclusions are detected through ultrastructural examination of the central nervous system and skeletal muscle. These inclusions are intensely PAS-positive and diastase-resistant, both in neurons and muscular fibers [214]. Magnetic resonance imaging shows white matter abnormalities[215].

Liver biopsy can be diagnostic in patients with hepatic involvement[216]. The histopathological evaluation of the liver reveals abnormal hepatocellular glycogen deposits in the form of PAS-positive, diastase-resistant inclusions. Ultrastructural examination with electron microscopy reveals accumulation of fibrillar aggregations that are typical of amylopectin. Typically, enzyme deficiency can be documented through diagnostic assays performed on hepatocytes, leukocytes, erythrocytes, and fibroblasts. However, patients with cardioskeletal myopathy may exhibit normal leukocyte enzyme activity[198]. The diagnosis of GSD-IV can be confirmed through histopathological examination, detection of enzyme deficiency, and mutation analysis of the *GBE1* gene. Genetic confirmation is recommended whenever possible in patients with suspected GSD-IV to provide more data for genotype-phenotype correlations in this extremely rare disease. The genotype-phenotype correlation remains unclear for GSD-IV and the same genetic defect may cause different clinical presentations in unrelated patients[217]. Mutation analysis can also provide crucial diagnostic information in cases with equivocal results of biochemical analyses[218]. Mutations with significant preservation of enzyme activity may be related with milder (*e.g.*, non-progressive hepatic form) and late-onset (*e.g.*, adult polyglucosan body disease) phenotypes of the disease.

Hypoglycemia has traditionally been considered a late manifestation and generally develops due to hepatocellular dysfunction caused by progressive cirrhosis. At this stage of the disease, the biochemical profile of the patients is representative of what is observed in other causes of liver cirrhosis. However, a recent study has reported that fasting intolerance, as indicated by a thorough medical history, along with the presence of hypoglycemia and/or ketosis, can be observed in patients even in the absence of detectable liver injury or dysfunction based on biochemical or radiological assessment[201].

No specific dietary and pharmacological treatments are available for GSD-IV. There is a lack of established guidelines based on either evidence or expert consensus for the dietary management of GSD-IV. Improvement in clinical, anthropometric, and laboratory parameters was reported with a high-protein and low-carbohydrate diet[219,220]. Derks *et al*[201] recently reported improved clinical and biochemical outcomes after dietary interventions including a late evening meal, continuous nocturnal intragastric drip feeding, restriction of mono- and disaccharides, the addition of UCCS, and protein enrichment in patients with GSD-IV. Individual dietary plans should also aim to avoid hyperglycemia to minimize glycogen accumulation in the liver.

At present, there is no effective therapeutic approach other than liver transplantation for GSD-IV patients who are affected by progressive liver disease. However, anecdotal reports indicate that liver transplantation may not alter the extrahepatic progression of GSD-IV[217]. The presence of extrahepatic involvement, especially amylopectin storage in the myocardium, may lead to fatal complications following liver transplantation[221-223]. Careful assessment of cardiac function even in the absence of clinical decompensation or consideration of combined liver-heart transplantation is warranted for patients with GSD-IV[224]. Liver transplantation may provide beneficial effects not only for patients with liver disease but also for those affected by muscular involvement in GSD-IV[107,225,226]. This may be explained by systemic microchimerism (donor cells presenting in various tissues of the liver recipient) after liver allotransplantation and amelioration of pancellular enzyme deficiencies resulting in

a decrease in amylopectin in other organ systems[12]. It has been suggested that the donor cells can transfer enzyme to the native enzyme-deficient cells[226].

In recent years, animal studies have been conducted to prevent glycogen and polyglucosan body accumulation in GSD-IV patients, and GYS inhibitor guaiacol and 144DG11 are promising in this regard [227,228]. The molecular target of 144DG11 is the lysosomal membrane protein lysosome-associated membrane protein 1 (LAMP1), which enhances autolysosomal degradation of glycogen and lysosomal acidification. In the adult polyglucosan body disease mouse model, 144DG11 reduced polyglucosan and glycogen in brain, liver, heart, and peripheral nerve[228].

GSD-VI; Hers disease; liver glycogen phosphorylase deficiency

GSD-VI was first reported by Hers[229] in three patients with hepatomegaly, mild hypoglycemia, an increased glycogen content and deficient activity of glycogen phosphorylase in the liver in 1959. GSD-VI is a rare autosomal recessive genetic disease caused by deficiency of hepatic glycogen phosphorylase. At least three human glycogen phosphorylases exist including muscle, liver, and brain isoforms[230]. In response to hypoglycemia, liver glycogen phosphorylase catalyzes the cleavage of glucosyl units from glycogen which results in the release of glucose-1-phosphate. The glucose-1-phosphate is subsequently converted to glucose-6-phosphate. The *PYGL* gene is currently the only known genetic locus associated with the development of GSD-VI and was mapped to chromosome 14q21-q22 in 1987[231]. Incidence of the disease is estimated to be 1:100000 and believed to be underestimated due to nonspecific and variable phenotypes, and a paucity of cases confirmed by genetic testing[232]. GSD-VI is more prevalent among the Mennonite community, with a prevalence of 1 in 1000, representing the only known population at higher risk for the disease[232].

GSD-VI is a disorder with broad clinical heterogeneity[232]. Infants with liver phosphorylase deficiency mainly present with hepatomegaly and growth retardation. The condition typically has a benign course, and symptoms tend to improve as the child grows[229]. Hepatomegaly usually normalizes by the second decade of life[233]. The child shows mild to moderate ketotic hypoglycemia related to prolonged fasting, illness, or stressful conditions[232]. As gluconeogenesis is intact in GSD-VI, hypoglycemia is usually mild. Despite gross hepatomegaly, the patient may be largely asymptomatic without hypoglycemia. However, there is a range of clinical severity in GSD-VI, with some patients experiencing severe and potentially life-threatening hypoglycemia. There is generally mild ketosis, growth retardation, abdominal distension due to marked hepatomegaly and mildly elevated levels of serum transaminases, triglycerides, and cholesterol. However, in patients with high residual enzyme activity, biochemical investigations may be normal[234,235]. Hypertriglyceridemia may persist despite treatment[108]. A few patients showing mild muscular hypotonia, muscle weakness or developmental impairment were observed, but otherwise, no neurological symptoms were reported in the literature [232]. Sleep difficulties and overnight irritability are common[236]. In contrast to GSD-I, serum levels of lactic acid and uric acid are generally within the normal range[15]. However, in a recent clinical study including 56 GSD-VI patients, hyperuricemia was reported as a complication in adolescent and adult patients with GSD-VI, which indicates the need for long-term monitoring of uric acid in older GSD-VI patients[237]. CK concentration is usually normal. In some patients, severe and recurrent hypoglycemia, pronounced hepatomegaly, and postprandial lactic acidosis have been reported[238]. Recently, children with GSD-VI have been reported to present with only ketotic hypoglycemia as the sole manifestation of the disease, without the characteristic hepatomegaly[239]. Mild cardiopathy has also been described for GSD-VI[233].

The clinical picture of GSD-VI virtually overlaps with phosphorylase kinase (PHK) deficiency (GSD-IX) and the differential diagnosis includes other forms of GSDs associated with hepatomegaly and hypoglycemia, especially GSD-I and GSD-III[236]. It is not possible to distinguish between GSD-VI and GSD-IX based on clinical or laboratory findings alone[232].

Mutation analysis is the suggested method for the diagnosis of GSD-VI. A liver biopsy is not recommended to establish the diagnosis to avoid an invasive procedure. Excessive glycogen accumulation with structurally normal glycogen in the liver biopsy is consistent with GSD-VI. Fibrosis, mild steatosis, lobular inflammatory activity and periportal copper binding protein staining have also been reported in GSD-VI patients. Although it is possible to document glycogen phosphorylase deficiency in frozen liver biopsy tissue or blood cells including leukocytes and erythrocytes, normal *in vitro* residual enzyme activity may be seen and prevents establishment of a definitive diagnosis by an enzyme assay alone in some patients[234,235].

In GSD-VI, nutrition therapy aims to improve metabolic control and prevent primary manifestations such as hypoglycemia, ketosis, and hepatomegaly, as well as secondary complications including delayed puberty, short stature, and cirrhosis. Frequent meals, a high-protein diet providing 2-3 g protein/kg body weight/d, limitation but not prohibition of simple sugars such as sucrose, fructose, lactose, a late evening meal and use of UCCS are the main recommendations in GSD-VI patients[236]. The aim of the therapeutic approach is to achieve euglycemia and normoketosis by administration of the appropriate doses of cornstarch. The target level for blood glucose should be within 70-100 mg/dL, while the optimal range for blood ketones is 0.0-0.2 mmol/L[236]. An extended-release corn starch derived from waxy maize, marketed as Glycosade®, has been found to have a positive impact in delaying overnight hypoglycemia in children over 5 years of age and adults[87]. Some individuals with

GSD-VI may not require any treatment.

GSD-VI usually has a benign disease course. However, focal nodular hyperplasia, fibrosis, cirrhosis, and a degeneration to hepatocellular carcinoma have been reported in some patients[240-242]. Cirrhosis has been reported in patients as young as preschool age, even within the second year of life[242]. Based on these findings, aggressive treatment of GSD-VI has recently been suggested to maintain optimal metabolic control and prevent long-term complications[243]. Long-term monitoring of hepatic function is also recommended[236].

GSD-IX; PHK deficiency

Glucagon and epinephrine play a critical role in the regulation of glycogenolysis by activation of adenylate cyclase which leads to an increase in the cytosolic concentration of cyclic adenosine monophosphate (cAMP). The increased level of cAMP activates cAMP-dependent protein kinase which activates PHK. In the next step, PHK, a serine/threonine-specific protein kinase, functionally activates glycogen phosphorylase in the liver. PHK is a heterotetramer composed of 4 different subunits (α, β, γ, and δ). Each subunit is encoded by different genes that are located on different chromosomes and differentially expressed in a variety of tissues[244]. α and β subunits have regulatory functions, the γ subunit contains the catalytic site, and δ is a calmodulin protein[245]. PHK has a wide tissue distribution with multiple tissue-specific isoforms.

The α subunit has two isoforms, a muscle isoform, and a liver isoform, which are encoded by two different genes (*PHKA1* and *PHKA2*, respectively) on the X chromosome[244]. The genetic loci of other subunits are mapped to autosomal chromosomes. The γ subunit also has muscle and liver isoforms, each of which is encoded by a distinct gene (*PHKG1* and *PHKG2*, respectively). There is only one gene encoding the β-subunit (*PHKB*). However, *PHKB* is expressed in both muscle and liver[246,247].

Liver PHK deficiency (liver GSD-IX) can be classified according to the involved gene, the X-linked form (GSD-IXa, X-linked glycogenosis) and autosomal recessive forms (GSD-IXb and GSD-IXc). GSD-IXa (*PHKA2*-related GSD-IX) is caused by pathogenic variants in the *PHKA2* gene on X chromosome. GSD-IXb (*PHKB*-related GSD-IX) and GSD-IXc (*PHKG2*-related GSD-IX) are inherited in an autosomal recessive manner and caused by mutations in *PHKB* and *PHKG2* genes, respectively (Table 1). GSD-IXa is further classified into subtypes XLG-I (formerly GSD-VIII) with no enzyme activity in liver or erythrocytes, and XLG-II with no enzyme activity in liver, but normal activity in erythrocytes[248,249].

GSD-IX is one of the most common forms of GSDs. Approximately 25% of all GSDs can be attributed to PHK deficiency[249]. The frequency of liver PHK deficiency was estimated to be 1:100000[15]. GSD-IXa, the most common subtype of liver PHK deficiency, accounts for 75% of all GSD-IX cases. On the X chromosome, there are two enzyme loci; one for the alpha subunit of muscle PHK, and one for the alpha subunit of liver PHK. In 1992, the liver PHK gene was located to Xp22.2-p22.1[244]. GSD-IXa is more common in males due to the X-linked inheritance pattern. Female carriers may become symptomatic due to X chromosome inactivation[250].

Hepatomegaly, growth retardation, delayed motor development, mild hypotonia, significantly elevated serum transaminase levels, hyperlipidemia, fasting hyperketosis, and hypoglycemia are the main symptoms and findings[251-254]. Rarely described clinical features include splenomegaly, liver cirrhosis, doll-like facies, osteoporosis, neurologic involvement, high serum lactate levels, metabolic acidosis, and renal tubular acidosis[233]. With increasing age, there is a gradual resolution of both clinical symptoms and laboratory abnormalities. Although puberty may be delayed, eventual attainment of normal height and complete sexual development is still possible[253]. Most adult patients are asymptomatic[252]. Unusual presentations including asymptomatic hepatomegaly and isolated ketotic hypoglycemia without hepatomegaly have been reported in affected male children underscoring the importance of screening for GSD-IXa in male patients who are suspected of having GSD with atypical features[239,255]. More severe phenotypes including severe recurrent hypoglycemia and liver cirrhosis have also been reported[243,256,257]. Recent findings suggest that GSD-IXa is not a benign condition as is often reported in the literature and patients may have fibrosis even at the time of diagnosis[258].

GSD-IXc is caused by autosomal recessive mutations in the *PHKG2* gene. There are two isoforms, encoded by different genes, for the gamma subunit: The muscle form (*PHKG1* gene) and the testis/liver form (*PHKG2* gene)[259]. The genetic locus of the liver form was located to 16p12.1-p11.2. The presence of *PHKG2* mutations has been linked to more severe clinical and biochemical abnormalities, such as an elevated risk for liver fibrosis and cirrhosis[260-262]. Liver cirrhosis can develop in infancy[263]. Cirrhosis related esophageal varices and splenomegaly, liver adenomas, renal tubulopathy and significant hypocalcemia were other reported clinical findings[236]. Patients with this condition commonly present with severe hypoglycemia requiring overnight feeding, show very low PHK activity in the liver, and exhibit highly elevated serum transaminase levels. A wide range of clinical symptoms can be observed, including hypoglycemia during fasting, hepatomegaly, elevated levels of transaminases, hepatic fibrosis, cirrhosis, muscle weakness, hypotonia, delayed motor development, growth retardation, and fatigue[264].

The genetic cause of GSD-IXb is attributed to mutations in the *PHKB* gene, which is located on 16q12-q13 and encodes the beta subunit of PHK[265]. The main features of the disease include marked hepatomegaly, increased glycogen content in both liver and muscle, and the development of hypoglycemic

symptoms after physical activity or several hours of fasting[265]. Patients with liver fibrosis, adenoma-like mass, mild cardiopathy and interventricular septal hypertrophy were reported[233]. The muscle symptoms are generally mild or absent, affecting virtually only the liver. Distinction between GSD-IXb and individuals with pathogenic variants in *PHKA2* or *PHKG2* cannot be carried out based on clinical findings alone.

Genetic analysis is the preferred first-line diagnostic test in suspected patients. An approach using next-generation sequencing panels is advised due to the involvement of multiple genes. Liver biopsy can be a valuable diagnostic tool for confirming the diagnosis in cases where there are variants of unknown significance. Histopathological assessment of liver involvement is superior to biochemical parameters[266]. It is important to keep in mind that PHK enzyme activity can be normal in blood cells and even in liver tissue of affected patients. On the other hand, a reduction in PHK enzyme activity can also occur secondary to other metabolic defects such as pathogenic variants in *GLUT2* in Fanconi-Bickel syndrome (FBS), PRKAG2 cardiomyopathy syndrome, or mitochondrial complex 1 deficiency[236].

In patients with GSD-IX, close monitoring of long-term liver and cardiac complications is recommended[233]. Aggressive structured dietary treatment with UCCS and relatively high protein intake was associated with considerable improvement in growth velocity, energy, biochemical abnormalities, hepatomegaly, and overall well-being of patients with GSD-IX. Radiographic features of fibrosis were also reported to be improved with early and aggressive dietary management[243]. General nutritional recommendations for GSD-IX are similar to those for GSD-VI and have recently been published[236].

FBS (formerly GSD-XI)

The primary defect in FBS is deficiency of glucose transporter 2 (GLUT2), a monosaccharide carrier that is responsible for the transport of both glucose and galactose across the membranes in hepatocytes, pancreatic β-cells, enterocytes, and renal tubular cells. Utilization of both glucose and galactose is impaired in FBS[267]. Hepatorenal glycogen accumulation and proximal renal tubular dysfunction are the characteristic features of this rare disease[268,269]. FBS follows an autosomal recessive inheritance pattern. The responsible gene, *GLUT2* gene (solute carrier family 2 member 2, *SLC2A2*), was localized to 3q26.1-q26.3 in 1988[270,271]. Since the first patient reported by Fanconi and Bickel in 1949, over 100 cases of FBS with various *SLC2A2* mutations including missense, nonsense, frameshift/insertion-deletion, intronic, and compound heterozygous mutations have been reported[272].

Infants with FBS typically present between the ages of 3 to 10 mo. In addition to hepatorenal glycogen accumulation and proximal renal tubular dysfunction, FBS is characterized by fasting hypoglycemia, postprandial hyperglycemia and hypergalactosemia, rickets and marked growth retardation. Patients have entirely normal mental development. In older patients, dwarfism is the most notable finding. Puberty is significantly delayed, with other remarkable observations including a distended abdomen caused by hepatomegaly, deposition of fat on the abdomen and shoulders, and a moon-shaped face [273]. Some patients may not exhibit hepatomegaly during the early stages of the disease[269,274]. Hyperlipidemia and hypercholesterolemia are prominent and may cause acute pancreatitis. The development of generalized osteopenia occurs early and may result in fractures. Hypophosphatemic rickets and osteoporosis are characteristics of the disease that emerge later in life[275]. Tubular nephropathy is characterized by excessive glucosuria, moderate hyperphosphaturia along with persistent hypophosphatemia, hyperuricemia, hyperaminoaciduria, and intermittent albuminuria, collectively referred to as renal Fanconi syndrome[267,268]. Hypercalciuria is also evident. Due to increased renal losses, there is a frequent tendency towards hyponatremia and hypokalemia. Polyuria may develop due to high urinary osmotic load[276]. Progression to renal failure is not the case. Nephrocalcinosis was also reported in one third of the patients in a recent retrospective study[277]. There may be mild metabolic hyperchloremic acidosis with normal anion gap due to renal loss of bicarbonate[267]. Cataracts, a frequently documented consequence of hypergalactosemia, are only present in a small number of patients[278].

Laboratory findings include fasting hypoglycemia and ketonuria, hyperglycemia and hypergalactosemia in the postabsorptive state, hypercholesterolemia, hyperlipidemia, moderately elevated alkaline phosphatase, mildly elevated transaminases, normal hepatic synthetic function, hypophosphatemia, hyperaminoaciduria, glucosuria, galactosuria, proteinuria, normal activity of enzymes involved in galactose and glycogen metabolism, normal fructose metabolism, and normal endocrinologic results[267]. FBS patients develop different patterns of dysglycemia, ranging from fasting hypoglycemia, postprandial hyperglycemia, glucose intolerance, to transient neonatal diabetes to gestational diabetes and frank diabetes mellitus[279]. The exact molecular mechanisms underlying the occurrence of dysglycemia in individuals with FBS are not yet fully understood. Sharari *et al*[272] recently suggested that *SLC2A2* mutations cause dysglycemia either by a direct effect on *GLUT2* expression and/or activity or, indirectly, by the dysregulated expression of microRNAs implicated in glucose homeostasis. Impaired renal glucose reabsorption, as well as the accumulation of glucose within the hepatocytes, which stimulates glycogen synthesis and inhibits gluconeogenesis and glycogenolysis, result in fasting ketotic hypoglycemia and hepatic glycogen deposition. Postprandial findings of hyperglycemia and hypergalactosemia are caused by impaired hepatic uptake and diminished insulin response[279]. Glycated hemoglobin A1c is usually within the normal range due to recurrent

hypoglycemia episodes[280]. Accumulation of glycogen and free glucose in renal tubular cells leads to general impairment in proximal renal tubular function. Histological evaluation of liver biopsy indicates an excessive buildup of glycogen along with steatosis. Due to the presence of galactose intolerance, newborn screening for galactosemia can sometimes identify patients with FBS[281]. The diagnosis is ultimately confirmed by genetic analysis of *SLC2A2* gene.

The management of symptoms involves measures to stabilize glucose homeostasis and compensate for the renal loss of water and various solutes. Patients typically require replacement of water, electrolytes, and vitamin D, while also restricting galactose intake and adhering to a diabetes mellitus-like diet. Frequent small meals with adequate caloric intake and administration of UCCS are important components of symptomatic treatment. In cases of renal tubular acidosis, it may be required to administer alkali to maintain acid-base balance. Catch-up growth was reported to be induced by UCCS [282]. Continuous nocturnal gastric drip feeding may be indicated in some cases with growth failure [283]. With these measures, the prognosis is good. However, a recent retrospective study reported poor outcome despite adequate metabolic management emphasizing the importance of early genetic diagnosis and facilitating prompt nutritional interventions[277].

GSDS INVOLVING MUSCLE

GSD-II; Pompe disease; acid alpha-glucosidase deficiency; acid maltase deficiency; alpha-1,4-glucosidase deficiency

Pompe disease is a typical example of a lysosomal storage disease. The clinical manifestations of Pompe disease are variable, predominantly due to the varying amounts of residual acid alpha-glucosidase (GAA) activity linked with distinct mutations in the causative gene (*GAA*). *GAA* gene is mapped to chromosome 17q25.2-q25.3[284]. Enzyme deficiency results in intra-lysosomal storage of glycogen especially in skeletal and cardiac muscles. There is no genotype-phenotype correlation, but DD genotype in the angiotensin converting enzyme gene and XX genotype in the alpha actinin 3 gene are significantly associated with an earlier age of onset of the disease[285].

There are mainly two types of GSD-II according to age of onset: Infantile-onset and late-onset Pompe disease. Patients with disease onset before the age of 12 mo without cardiomyopathy and all patients with disease onset after 12 mo of age are included in the late-onset form[286]. The combined frequency of infantile onset and late onset GSD-II varies between 1:14000 and 1:100000 depending on ethnicity and geographic region. In the infantile-onset form, cardiomyopathy and muscular hypotonia are the cardinal features and patients die around 1 year of age. The enzyme activity is less than 1% of normal controls, and the enzyme is deficient in all tissues. Patients also have feeding difficulties, macroglossia, failure to thrive, hearing impairment and respiratory distress due to muscle weakness. The liver is rarely enlarged unless there is heart failure. Hypoglycemia and acidosis do not occur[286]. In the late-onset form, involvement of skeletal muscles dominates the clinical picture, and cardiac involvement is generally clinically insignificant depending on the age of onset. Enzyme activity is partially deficient (2% to 40% of normal controls)[286]. Glycogen accumulation in vascular smooth muscle may cause the formation and subsequent rupture of an aneurysm[287]. Both severe infantile and asymptomatic adult forms of the disease were observed in two generations of the same family[288]. Although women with GSD-II do not have an increased risk of pregnancy or delivery complications, pregnancy may worsen muscle weakness and respiratory complications[289]. As a rule, there is an inverse correlation between the age at disease onset and the severity of clinical manifestations with the level of residual enzyme activity[286].

Laboratory testing reveals nonspecific elevations in CK, aldolase, aminotransferases, and lactate dehydrogenase. Elevated urinary tetrasaccharide is highly sensitive but not specific. To establish the final diagnosis, the measurement of enzyme activity in skin fibroblasts or muscle tissue or the demonstration of the responsible mutation is required[286].

Although it is not curative, ERT has changed the course of Pompe disease since its first use in 2001 [290]. Alglucosidase alfa, a lysosomal glycogen-specific recombinant enzyme, was approved by the European Medicines Agency (EMA) in 2006 in the European Union and by the Food and Drug Administration (FDA) in 2010 in the United States. The indication criteria were as follows: ≥ 8 years and absence of cardiac hypertrophy (https://www.accessdata.fda.gov/drugsatfda_docs/Label/2010/125291Lbl.pdf; accessed on November 5, 2022). Based on data from later studies, treatment initiation was shifted to the neonatal period. The recommended dosage is 20 mg/kg body weight every two weeks by intravenous administration. A new formulation of GAA enzyme, avalglucosidase alfa, improves the delivery of the enzyme to target cells and has 15 times higher cellular uptake when compared with alglucosidase alfa. The FDA and EMA approved avalglucosidase in 2021 and in 2022, respectively, for the treatment of patients who are one year of age and older with late-onset Pompe disease[291]. Ongoing studies show that avalglucosidase is generally well tolerated in patients with infantile-onset Pompe disease[291]. The recommended dose is 5 to 20 mg/kg every 2 wk[291]. Criteria for starting and stopping ERT in adult patients with GSD-II are similar in different countries. While a confirmed diagnosis and being symptomatic are general criteria for starting ERT, patient wish, severe infusion

associated reactions, noncompliance with treatment, and lack of effect are criteria for stopping ERT [292]. Another way to increase the effectiveness of ERT is to use antibodies as an intracellular delivery vehicle. The 3E10 anti-nuclear antibody, that penetrates cells and localizes to the cell nucleus, has been used for this purpose. VAL-1221 is a fusion protein consisting of 3E10 antibody and GAA complex. The presence of 3E10 increases the delivery of GAA to both lysosomal and extra-lysosomal storage of glycogen within cells[293]. The earlier ERT is started, the better its effectiveness. Therefore, it is recommended that ERT is started before irreversible clinical symptoms begin. This concept has led to the development of screening programs for Pompe disease[294]. Recently, it has been shown that in utero alglucosidase alfa treatment, which was started at 24 wk 5 d of gestation and given 6 times at 2-wk intervals through the umbilical vein, was successful[295].

Although antibodies against the enzyme may develop, a recent study showed that the development of antibodies did not affect the clinical course[296]. Whether additional treatments such as oral supplementation of L-alanine is beneficial is being investigated[297]. As an alternative to ERT, studies on gene therapy have also commenced[298].

Danon disease

Although Danon disease was previously classified as a variant of GSD-II with normal alpha-glucosidase activity, it is still controversial whether it is a real GSD. A lysosomal structural protein, LAMP2, is deficient in Danon disease. LAMP2 is involved in autophagosome maturation. Disruption of autophagy leads to accumulation of glycogen granules and autophagic vacuoles[299]. It is an X-linked (Xq24) dominant hereditary disease affecting both skeletal and cardiac muscles, and characterized by skeletal and cardiac myopathy, proximal muscle weakness and intellectual disability. Female patients have a milder disease predominantly involving cardiac muscle[300]. There is currently no treatment for Danon disease. There are ongoing studies evaluating the efficacy and safety of gene therapy[300].

AMP-activated protein kinase deficiency

Another glycogen storage cardiomyopathy results from *PRKAG2* (the gene encoding gamma-2 non-catalytic subunit of adenosine monophosphate-activated protein kinase) mutations on chromosome 7q36.1. The disease is characterized by left ventricular hypertrophy due to altered glycogen metabolism and glycogen storage in cardiac muscle, similar to Danon disease[301-303]. It is inherited in an autosomal dominant pattern. *PRKAG2* gene variants cause a syndrome characterized by cardiomyopathy, conduction disease, and ventricular pre-excitation[302]. It may cause atrial fibrillation/flutter or conduction abnormalities that may cause sudden cardiac death and severe heart failure typically in the third and fourth decade[301,302]. Mutations in the gamma-2 non-catalytic subunit of AMP-activated protein kinase may cause lethal congenital storage disease of the heart, and death in the first year of life [303]. It is important to differentiate the clinical picture related to *PRKAG2* mutations from Danon disease, as management and prognosis are different.

GSD-V; McArdle disease; myophospharylase deficiency; muscle glycogen phosphorylase deficiency

GSD-V is caused by mutations in *PYGM* gene which is the gene encoding the muscle isoform of glycogen phosphorylase. The *PYGM* gene is located on 11q13.1[304]. In a recently published European registry for patients with muscle glycogenosis, 95% of all patients had GSD-V[305]. The clinical manifestations generally occur during early adulthood with physical activity intolerance and muscle cramps characterized by muscle fatigue and pain, contracture, tachypnea, tachycardia, ptosis, and retinal dystrophy. Most of the patients are symptomatic at pediatric age (< 18 years)[306]. An improvement of exercise induced symptoms, named the "second wind phenomenon", characterized by the improvement of exercise tolerance after 8 to 10 min of aerobic exercise, is observed[306,307]. Exercise induced rhabdomyolysis can cause transient myoglobinuria, leading to acute renal failure. Hyperuricemia, gout development and thyroid dysfunction are not uncommon[306]. Many patients are diagnosed with an incidental finding of abnormal serum CK levels[307].

Echaniz-Laguna *et al*[308] studied a family of 13 affected members with adult-onset muscle weakness, and reported a phenotype caused by a dominant myophosphorylase gene mutation (p.Asp639His). The first signs of the disease occurred after 40 years of age with proximal leg weakness, followed by proximal arm weakness. In contrast to McArdle disease, the patients did not have exercise intolerance, second wind phenomenon, markedly increased CK levels, or rhabdomyolysis. The authors concluded that specific *PYGM* mutations can cause either dominant or recessive GSDs[308].

GSD-VII; Tarui disease; muscle phosphofructokinase deficiency; GSD of muscle

The responsible gene is located on chromosome 12q13.3[309]. Exercise induced muscle cramps and myoglobinuria are the main characteristics of GSD-VII. Neurological examination does not reveal any abnormalities at rest. Muscle weakness and stiffness invariably occur in muscle groups that are subjected to intense or prolonged exertion. The ischemic exercise test is characterized by the absence of an increase in venous lactate level. Myoglobinuria may develop following exercise. Nausea and vomiting, icterus, elevated CK, hyperuricemia and reticulosis may also be observed[307]. In contrast to GSD-V, glucose intake prior to exercise worsens exercise capacity due to blocked use of both muscle

glycogen and blood glucose[307].

GSD-IXd; X-linked muscle PHK alpha-1 subunit deficiency

The gene is located on chromosome Xq13.1, and the disease is inherited recessively[310]. In most patients, clinical findings appear in adulthood and are characterized by muscle weakness and muscle cramps during exercise. Elevated serum CK level and myopathic findings on electromyography may guide the diagnosis[311].

GSD-X; muscle phosphoglycerate mutase deficiency

The last steps of glycogenolysis are abnormal. The disease is inherited in an autosomal recessive manner and characterized by exercise induced muscle cramps, myalgia, rhabdomyolysis and myoglobinuria. Serum CK level is increased between episodes[312].

GSD-XI; lactate dehydrogenase a deficiency

GSD-XI was first described by Kanno *et al*[313] in 1980 and characterized by easy fatigue, increase in serum CK, myoglobin, lactate, and pyruvate levels immediately after ischemic work. The gene locus is on chromosome 11p15.1[314].

GSD-XII; aldolase deficiency

GSD-XII is a very rare disease resulting from aldolase A deficiency and characterized by muscle glycogen accumulation, crisis of rhabdomyolysis induced by fever and/or exercise and hemolytic anemia with or without myopathy or cognitive dysfunction[315]. It is an autosomal recessive disorder, and the gene is located on chromosome 16p11.2[316].

GSD-XIII; muscle enolase 3 deficiency

GSD-XIII was first described by Comi *et al*[317] in 2001 in a 47-year-old man with severe deficiency of muscle enolase activity. The patient had recurrent exercise induced myalgia without cramps. Serum CK concentration was elevated while serum lactate level was normal following ischemic forearm exercise. The related gene is located on chromosome 17p13.2[317].

GSD-XV; glycogenin deficiency

Similar to Danon disease and *PRKAG2* variants, glycogenin deficiency may cause left ventricular arrhythmogenic cardiomyopathy. Patients present with chest pain, progressive weakness, and vague presyncope spells[318].

CONCLUSION

There have been significant changes and improvements in the classification, diagnosis, and treatment of GSDs in recent years. We are now more aware that many GSDs, which were previously identified as childhood diseases, may present first in adulthood. Diagnosis can be challenging, especially for GSDs with milder phenotypes and those with only skeletal and/or cardiac muscle involvement. As early diagnosis and aggressive treatment is related to better prognosis, physicians should be aware of these conditions and include GSDs in the differential diagnosis of pediatric and adult patients with not only liver related manifestations but also skeletal and/or cardiac muscle, central nervous system, and multisystemic involvement.

FOOTNOTES

Author contributions: Both authors contributed all parts of the study.

Conflict-of-interest statement: All the authors report no relevant conflicts of interest for this article.

Open-Access: This article is an open-access article that was selected by an in-house editor and fully peer-reviewed by external reviewers. It is distributed in accordance with the Creative Commons Attribution NonCommercial (CC BY-NC 4.0) license, which permits others to distribute, remix, adapt, build upon this work non-commercially, and license their derivative works on different terms, provided the original work is properly cited and the use is non-commercial. See: https://creativecommons.org/Licenses/by-nc/4.0/

Country/Territory of origin: Turkey

ORCID number: Ersin Gümüş 0000-0002-2280-9789; Hasan Özen 0000-0002-9063-3893.

S-Editor: Wang JJ
L-Editor: Webster JR
P-Editor: Zhao S

REFERENCES

1 **Ozen H**. Glycogen storage diseases: new perspectives. *World J Gastroenterol* 2007; **13**: 2541-2553 [PMID: 17552001 DOI: 10.3748/wjg.v13.i18.2541]
2 **Roach PJ**, Depaoli-Roach AA, Hurley TD, Tagliabracci VS. Glycogen and its metabolism: some new developments and old themes. *Biochem J* 2012; **441**: 763-787 [PMID: 22248338 DOI: 10.1042/BJ20111416]
3 **Ellingwood SS**, Cheng A. Biochemical and clinical aspects of glycogen storage diseases. *J Endocrinol* 2018; **238**: R131-R141 [PMID: 29875163 DOI: 10.1530/JOE-18-0120]
4 **Chen YT**, Kishnani PS, Koeberl D. Glycogen Storage Diseases. *OMMBID* 2019 [DOI: 10.1036/ommbid.380]
5 **Saltik IN**, Ozen H, Ciliv G, Koçak N, Yüce A, Gürakan F, Dinler G. Glycogen storage disease type Ia: frequency and clinical course in Turkish children. *Indian J Pediatr* 2000; **67**: 497-501 [PMID: 10957834 DOI: 10.1007/BF02760476]
6 **Kanungo S**, Wells K, Tribett T, El-Gharbawy A. Glycogen metabolism and glycogen storage disorders. *Ann Transl Med* 2018; **6**: 474 [PMID: 30740405 DOI: 10.21037/atm.2018.10.59]
7 **Burda P**, Hochuli M. Hepatic glycogen storage disorders: what have we learned in recent years? *Curr Opin Clin Nutr Metab Care* 2015; **18**: 415-421 [PMID: 26001652 DOI: 10.1097/MCO.0000000000000181]
8 **Kollberg G**, Tulinius M, Gilljam T, Ostman-Smith I, Forsander G, Jotorp P, Oldfors A, Holme E. Cardiomyopathy and exercise intolerance in muscle glycogen storage disease 0. *N Engl J Med* 2007; **357**: 1507-1514 [PMID: 17928598 DOI: 10.1056/NEJMoa066691]
9 **Lewis GM**, Spencer-Peet J, Stewart KM. Infantile Hypoglycaemia due to Inherited Deficiency of Glycogen Synthetase in Liver. *Arch Dis Child* 1963; **38**: 40-48 [PMID: 21032403 DOI: 10.1136/adc.38.197.40]
10 **Orho M**, Bosshard NU, Buist NR, Gitzelmann R, Aynsley-Green A, Blümel P, Gannon MC, Nuttall FQ, Groop LC. Mutations in the liver glycogen synthase gene in children with hypoglycemia due to glycogen storage disease type 0. *J Clin Invest* 1998; **102**: 507-515 [PMID: 9691087 DOI: 10.1172/JCI2890]
11 **Nuttall FQ**, Gannon MC, Kubic VL, Hoyt KJ. The human liver Glycogen synthase isozyme gene is located on the short arm of chromosome 12. *Genomics* 1994; **19**: 404-405 [PMID: 8188280 DOI: 10.1006/geno.1994.1086]
12 **Hicks J**, Wartchow E, Mierau G. Glycogen storage diseases: a brief review and update on clinical features, genetic abnormalities, pathologic features, and treatment. *Ultrastruct Pathol* 2011; **35**: 183-196 [PMID: 21910565 DOI: 10.3109/01913123.2011.601404]
13 **Kamenets EA**, Gusarova EA, Milovanova NV, Itkis YS, Strokova TV, Melikyan MA, Garyaeva IV, Rybkina IG, Nikitina NV, Zakharova EY. Hepatic glycogen synthase (GYS2) deficiency: seven novel patients and seven novel variants. *JIMD Rep* 2020; **53**: 39-44 [PMID: 32395408 DOI: 10.1002/jmd2.12082]
14 **Laberge AM**, Mitchell GA, van de Werve G, Lambert M. Long-term follow-up of a new case of liver glycogen synthase deficiency. *Am J Med Genet A* 2003; **120A**: 19-22 [PMID: 12794686 DOI: 10.1002/ajmg.a.20110]
15 **Wolfsdorf JI**, Weinstein DA. Glycogen storage diseases. *Rev Endocr Metab Disord* 2003; **4**: 95-102 [PMID: 12618563 DOI: 10.1023/a:1021831621210]
16 **Weinstein DA**, Correia CE, Saunders AC, Wolfsdorf JI. Hepatic glycogen synthase deficiency: an infrequently recognized cause of ketotic hypoglycemia. *Mol Genet Metab* 2006; **87**: 284-288 [PMID: 16337419 DOI: 10.1016/j.ymgme.2005.10.006]
17 **Bachrach BE**, Weinstein DA, Orho-Melander M, Burgess A, Wolfsdorf JI. Glycogen synthase deficiency (glycogen storage disease type 0) presenting with hyperglycemia and glucosuria: report of three new mutations. *J Pediatr* 2002; **140**: 781-783 [PMID: 12072888 DOI: 10.1067/mpd.2002.124317]
18 **Kasapkara ÇS**, Aycan Z, Açoğlu E, Senel S, Oguz MM, Ceylaner S. The variable clinical phenotype of three patients with hepatic glycogen synthase deficiency. *J Pediatr Endocrinol Metab* 2017; **30**: 459-462 [PMID: 28245189 DOI: 10.1515/jpem-2016-0317]
19 **Tagliaferri F**, Massese M, Russo L, Commone A, Gasperini S, Pretese R, Dionisi-Vici C, Maiorana A. Hepatic glycogen storage diseases type 0, VI and IX: description of an italian cohort. *Orphanet J Rare Dis* 2022; **17**: 285 [PMID: 35854365 DOI: 10.1186/s13023-022-02431-5]
20 **Browner MF**, Nakano K, Bang AG, Fletterick RJ. Human muscle glycogen synthase cDNA sequence: a negatively charged protein with an asymmetric charge distribution. *Proc Natl Acad Sci U S A* 1989; **86**: 1443-1447 [PMID: 2493642 DOI: 10.1073/pnas.86.5.1443]
21 **Gierke EV**. Hepato-nephro-megalia-glycogenica (Glykogenspeicherkrankheit der Leber und Nieren). *Beitr Pathol Anat* 1929; **82**: 497-513
22 **Cori GT**, Cori CF. Glucose-6-phosphatase of the liver in glycogen storage disease. *J Biol Chem* 1952; **199**: 661-667 [PMID: 13022673]
23 **Narisawa K**, Igarashi Y, Otomo H, Tada K. A new variant of glycogen storage disease type I probably due to a defect in the glucose-6-phosphate transport system. *Biochem Biophys Res Commun* 1978; **83**: 1360-1364 [PMID: 212064 DOI: 10.1016/0006-291x(78)91371-2]
24 **van Schaftingen E**, Gerin I. The glucose-6-phosphatase system. *Biochem J* 2002; **362**: 513-532 [PMID: 11879177 DOI: 10.1042/0264-6021:3620513]
25 **Chou JY**, Jun HS, Mansfield BC. Type I glycogen storage diseases: disorders of the glucose-6-phosphatase/glucose-6-phosphate transporter complexes. *J Inherit Metab Dis* 2015; **38**: 511-519 [PMID: 25288127 DOI: 10.1007/s10545-014-9772-x]

26 **Ekstein J**, Rubin BY, Anderson SL, Weinstein DA, Bach G, Abeliovich D, Webb M, Risch N. Mutation frequencies for glycogen storage disease Ia in the Ashkenazi Jewish population. *Am J Med Genet A* 2004; **129A**: 162-164 [PMID: 15316959 DOI: 10.1002/ajmg.a.30232]

27 **Scott SA**, Edelmann L, Liu L, Luo M, Desnick RJ, Kornreich R. Experience with carrier screening and prenatal diagnosis for 16 Ashkenazi Jewish genetic diseases. *Hum Mutat* 2010; **31**: 1240-1250 [PMID: 20672374 DOI: 10.1002/humu.21327]

28 **Brody LC**, Abel KJ, Castilla LH, Couch FJ, McKinley DR, Yin G, Ho PP, Merajver S, Chandrasekharappa SC, Xu J. Construction of a transcription map surrounding the BRCA1 locus of human chromosome 17. *Genomics* 1995; **25**: 238-247 [PMID: 7774924 DOI: 10.1016/0888-7543(95)80131-5]

29 **Yang Chou J**, Mansfield BC. Molecular Genetics of Type 1 Glycogen Storage Diseases. *Trends Endocrinol Metab* 1999; **10**: 104-113 [PMID: 10322403 DOI: 10.1016/s1043-2760(98)00123-4]

30 **Rake JP**, Visser G, Labrune P, Leonard JV, Ullrich K, Smit GP. Glycogen storage disease type I: diagnosis, management, clinical course and outcome. Results of the European Study on Glycogen Storage Disease Type I (ESGSD I). *Eur J Pediatr* 2002; **161** Suppl 1: S20-S34 [PMID: 12373567 DOI: 10.1007/s00431-002-0999-4]

31 **Derks TGJ**, Rodriguez-Buritica DF, Ahmad A, de Boer F, Couce ML, Grünert SC, Labrune P, López Maldonado N, Fischinger Moura de Souza C, Riba-Wolman R, Rossi A, Saavedra H, Gupta RN, Valayannopoulos V, Mitchell J. Glycogen Storage Disease Type Ia: Current Management Options, Burden and Unmet Needs. *Nutrients* 2021; **13** [PMID: 34836082 DOI: 10.3390/nu13113828]

32 **Aydemir Y**, Gürakan F, Saltık Temizel İN, Demir H, Oğuz KK, Yalnızoğlu D, Topçu M, Özen H, Yüce A. Evaluation of central nervous system in patients with glycogen storage disease type 1a. *Turk J Pediatr* 2016; **58**: 12-18 [PMID: 27922231 DOI: 10.24953/turkjped.2016.01.002]

33 **Czapek EE**, Deykin D, Salzman EW. Platelet dysfunction in glycogen storage disease type I. *Blood* 1973; **41**: 235-247 [PMID: 4350560]

34 **Hutton RA**, Macnab AJ, Rivers RP. Defect of platelet function associated with chronic hypoglycaemia. *Arch Dis Child* 1976; **51**: 49-55 [PMID: 942229 DOI: 10.1136/adc.51.1.49]

35 **Mühlhausen C**, Schneppenheim R, Budde U, Merkel M, Muschol N, Ullrich K, Santer R. Decreased plasma concentration of von Willebrand factor antigen (VWF:Ag) in patients with glycogen storage disease type Ia. *J Inherit Metab Dis* 2005; **28**: 945-950 [PMID: 16435187 DOI: 10.1007/s10545-005-0184-9]

36 **Austin SL**, El-Gharbawy AH, Kasturi VG, James A, Kishnani PS. Menorrhagia in patients with type I glycogen storage disease. *Obstet Gynecol* 2013; **122**: 1246-1254 [PMID: 24201678 DOI: 10.1097/01.AOG.0000435451.86108.82]

37 **Kishnani PS**, Austin SL, Abdenur JE, Arn P, Bali DS, Boney A, Chung WK, Dagli AI, Dale D, Koeberl D, Somers MJ, Wechsler SB, Weinstein DA, Wolfsdorf JI, Watson MS; American College of Medical Genetics and Genomics. Diagnosis and management of glycogen storage disease type I: a practice guideline of the American College of Medical Genetics and Genomics. *Genet Med* 2014; **16**: e1 [PMID: 25356975 DOI: 10.1038/gim.2014.128]

38 **Banugaria SG**, Austin SL, Boney A, Weber TJ, Kishnani PS. Hypovitaminosis D in glycogen storage disease type I. *Mol Genet Metab* 2010; **99**: 434-437 [PMID: 20060350 DOI: 10.1016/j.ymgme.2009.12.012]

39 **Jacoby JT**, Bento Dos Santos B, Nalin T, Colonetti K, Farret Refosco L, F M de Souza C, Spritzer PM, Poloni S, Hack-Mendes R, Schwartz IVD. Bone Mineral Density in Patients with Hepatic Glycogen Storage Diseases. *Nutrients* 2021; **13** [PMID: 34578865 DOI: 10.3390/nu13092987]

40 **Minarich LA**, Kirpich A, Fiske LM, Weinstein DA. Bone mineral density in glycogen storage disease type Ia and Ib. *Genet Med* 2013; **14**: 737-741 [PMID: 22481133 DOI: 10.1038/gim.2012.36]

41 **Cabrera-Abreu J**, Crabtree NJ, Elias E, Fraser W, Cramb R, Alger S. Bone mineral density and markers of bone turnover in patients with glycogen storage disease types I, III and IX. *J Inherit Metab Dis* 2004; **27**: 1-9 [PMID: 14970741 DOI: 10.1023/B:BOLI.0000016632.13234.56]

42 **Wang DQ**, Carreras CT, Fiske LM, Austin S, Boree D, Kishnani PS, Weinstein DA. Characterization and pathogenesis of anemia in glycogen storage disease type Ia and Ib. *Genet Med* 2012; **14**: 795-799 [PMID: 22678084 DOI: 10.1038/gim.2012.41]

43 **Visser G**, Rake JP, Kokke FT, Nikkels PG, Sauer PJ, Smit GP. Intestinal function in glycogen storage disease type I. *J Inherit Metab Dis* 2002; **25**: 261-267 [PMID: 12227456 DOI: 10.1023/a:1016572706488]

44 **Visser G**, Rake JP, Fernandes J, Labrune P, Leonard JV, Moses S, Ullrich K, Smit GP. Neutropenia, neutrophil dysfunction, and inflammatory bowel disease in glycogen storage disease type Ib: results of the European Study on Glycogen Storage Disease type I. *J Pediatr* 2000; **137**: 187-191 [PMID: 10931410 DOI: 10.1067/mpd.2000.105232]

45 **Lawrence NT**, Chengsupanimit T, Brown LM, Derks TG, Smit GP, Weinstein DA. Inflammatory Bowel Disease in Glycogen Storage Disease Type Ia. *J Pediatr Gastroenterol Nutr* 2017; **64**: e52-e54 [PMID: 25304890 DOI: 10.1097/MPG.0000000000000592]

46 **Hannah WB**, Ong RC, Moreno MN, Pendyal S, Abdelmalak M, Kelsen J, McGreal NM, Kishnani PS. Very early-onset inflammatory bowel disease: Novel description in glycogen storage disease type Ia. *Mol Genet Metab Rep* 2022; **31**: 100848 [PMID: 35242580 DOI: 10.1016/j.ymgmr.2022.100848]

47 **Smit GP**. The long-term outcome of patients with glycogen storage disease type Ia. *Eur J Pediatr* 1993; **152** Suppl 1: S52-S55 [PMID: 8319726 DOI: 10.1007/BF02072089]

48 **Talente GM**, Coleman RA, Alter C, Baker L, Brown BI, Cannon RA, Chen YT, Crigler JF Jr, Ferreira P, Haworth JC, Herman GE, Issenman RM, Keating JP, Linde R, Roe TF, Senior B, Wolfsdorf JI. Glycogen storage disease in adults. *Ann Intern Med* 1994; **120**: 218-226 [PMID: 8273986 DOI: 10.7326/0003-4819-120-3-199402010-00008]

49 **Ai J**, He W, Huang X, Wu Y, Lei Y, Yu C, Görgülü K, Diakopoulos KN, Lu N, Zhu Y. A case report of acute pancreatitis with glycogen storage disease type IA in an adult patient and review of the literature. *Medicine (Baltimore)* 2020; **99**: e22644 [PMID: 33080702 DOI: 10.1097/MD.0000000000022644]

50 **Rivers E**, Reynolds BC, Bunn S, Leech NJ, Straker J, Lambert HJ. Acute Pancreatitis Secondary to Severe Hypertriglyceridaemia in a Patient with Type 1a Glycogen Storage Disease: Emergent Use of Plasmapheresis. *JIMD Rep* 2018; **42**: 1-4 [PMID: 29030854 DOI: 10.1007/8904_2017_64]

51 **Chen YT**, Coleman RA, Scheinman JI, Kolbeck PC, Sidbury JB. Renal disease in type I glycogen storage disease. *N Engl J Med* 1988; **318**: 7-11 [PMID: 3422104 DOI: 10.1056/NEJM198801073180102]

52 **Urushihara M**, Kagami S, Ito M, Yasutomo K, Kondo S, Kitamura A, Takahashi A, Kuroda Y. Transforming growth factor-beta in renal disease with glycogen storage disease I. *Pediatr Nephrol* 2004; **19**: 676-678 [PMID: 15064941 DOI: 10.1007/s00467-004-1456-6]

53 **Martens DH**, Rake JP, Navis G, Fidler V, van Dael CM, Smit GP. Renal function in glycogen storage disease type I, natural course, and renopreservative effects of ACE inhibition. *Clin J Am Soc Nephrol* 2009; **4**: 1741-1746 [PMID: 19808227 DOI: 10.2215/CJN.00050109]

54 **Yiu WH**, Mead PA, Jun HS, Mansfield BC, Chou JY. Oxidative stress mediates nephropathy in type Ia glycogen storage disease. *Lab Invest* 2010; **90**: 620-629 [PMID: 20195241 DOI: 10.1038/labinvest.2010.38]

55 **Reitsma-Bierens WC**. Renal complications in glycogen storage disease type I. *Eur J Pediatr* 1993; **152** Suppl 1: S60-S62 [PMID: 8319728 DOI: 10.1007/BF02072091]

56 **Restaino I**, Kaplan BS, Stanley C, Baker L. Nephrolithiasis, hypocitraturia, and a distal renal tubular acidification defect in type 1 glycogen storage disease. *J Pediatr* 1993; **122**: 392-396 [PMID: 8441093 DOI: 10.1016/s0022-3476(05)83422-5]

57 **Lin CC**, Tsai JD, Lin SP, Lee HC. Renal sonographic findings of type I glycogen storage disease in infancy and early childhood. *Pediatr Radiol* 2005; **35**: 786-791 [PMID: 15906024 DOI: 10.1007/s00247-005-1478-7]

58 **Bhowmik E**, Ghosh M, Sabui TK, Mondal R. Glycogen Storage Disease Type I Presenting with Hypertension During Infancy. *Indian J Pediatr* 2015; **82**: 767 [PMID: 25735438 DOI: 10.1007/s12098-015-1732-4]

59 **Gjorgjieva M**, Raffin M, Duchampt A, Perry A, Stefanutti A, Brevet M, Tortereau A, Dubourg L, Hubert-Buron A, Mabille M, Pelissou C, Lassalle L, Labrune P, Mithieux G, Rajas F. Progressive development of renal cysts in glycogen storage disease type I. *Hum Mol Genet* 2016; **25**: 3784-3797 [PMID: 27436577 DOI: 10.1093/hmg/ddw224]

60 **Bianchi L**. Glycogen storage disease I and hepatocellular tumours. *Eur J Pediatr* 1993; **152** Suppl 1: S63-S70 [PMID: 8391447 DOI: 10.1007/BF02072092]

61 **Wang DQ**, Fiske LM, Carreras CT, Weinstein DA. Natural history of hepatocellular adenoma formation in glycogen storage disease type I. *J Pediatr* 2011; **159**: 442-446 [PMID: 21481415 DOI: 10.1016/j.jpeds.2011.02.031]

62 **Cho JH**, Lee YM, Bae SH, Chou JY. Activation of tumor-promoting pathways implicated in hepatocellular adenoma/carcinoma, a long-term complication of glycogen storage disease type Ia. *Biochem Biophys Res Commun* 2020; **522**: 1-7 [PMID: 31735334 DOI: 10.1016/j.bbrc.2019.11.061]

63 **Kishnani PS**, Chuang TP, Bali D, Koeberl D, Austin S, Weinstein DA, Murphy E, Chen YT, Boyette K, Liu CH, Li LH. Chromosomal and genetic alterations in human hepatocellular adenomas associated with type Ia glycogen storage disease. *Hum Mol Genet* 2009; **18**: 4781-4790 [PMID: 19762333 DOI: 10.1093/hmg/ddp441]

64 **Lee P**, Mather S, Owens C, Leonard J, Dicks-Mireaux C. Hepatic ultrasound findings in the glycogen storage diseases. *Br J Radiol* 1994; **67**: 1062-1066 [PMID: 7820397 DOI: 10.1259/0007-1285-67-803-1062]

65 **Franco LM**, Krishnamurthy V, Bali D, Weinstein DA, Arn P, Clary B, Boney A, Sullivan J, Frush DP, Chen YT, Kishnani PS. Hepatocellular carcinoma in glycogen storage disease type Ia: a case series. *J Inherit Metab Dis* 2005; **28**: 153-162 [PMID: 15877204 DOI: 10.1007/s10545-005-7500-2]

66 **Trioche P**, Francoual J, Capel L, Odièvre M, Lindenbaum A, Labrune P. Apolipoprotein E polymorphism and serum concentrations in patients with glycogen storage disease type Ia. *J Inherit Metab Dis* 2000; **23**: 107-112 [PMID: 10801051 DOI: 10.1023/a:1005605513534]

67 **Wittenstein B**, Klein M, Finckh B, Ullrich K, Kohlschütter A. Radical trapping in glycogen storage disease 1a. *Eur J Pediatr* 2002; **161** Suppl 1: S70-S74 [PMID: 12373576 DOI: 10.1007/s00431-002-1008-7]

68 **Wittenstein B**, Klein M, Finckh B, Ullrich K, Kohlschütter A. Plasma antioxidants in pediatric patients with glycogen storage disease, diabetes mellitus, and hypercholesterolemia. *Free Radic Biol Med* 2002; **33**: 103-110 [PMID: 12086688 DOI: 10.1016/s0891-5849(02)00863-8]

69 **Ubels FL**, Rake JP, Slaets JP, Smit GP, Smit AJ. Is glycogen storage disease 1a associated with atherosclerosis? *Eur J Pediatr* 2002; **161** Suppl 1: S62-S64 [PMID: 12373574 DOI: 10.1007/s00431-002-1006-9]

70 **Bernier AV**, Correia CE, Haller MJ, Theriaque DW, Shuster JJ, Weinstein DA. Vascular dysfunction in glycogen storage disease type I. *J Pediatr* 2009; **154**: 588-591 [PMID: 19101686 DOI: 10.1016/j.jpeds.2008.10.048]

71 **Melis D**, Parenti G, Della Casa R, Sibilio M, Romano A, Di Salle F, Elefante R, Mansi G, Santoro L, Perretti A, Paludetto R, Sequino L, Andria G. Brain damage in glycogen storage disease type I. *J Pediatr* 2004; **144**: 637-642 [PMID: 15127000 DOI: 10.1016/j.jpeds.2004.02.033]

72 **Muzetti JH**, do Valle DA, Santos MLSF, Telles BA, Cordeiro ML. Neurological Characteristics of Pediatric Glycogen Storage Disease. *Front Endocrinol (Lausanne)* 2021; **12**: 685272 [PMID: 34093448 DOI: 10.3389/fendo.2021.685272]

73 **Sechi A**, Deroma L, Lapolla A, Paci S, Melis D, Burlina A, Carubbi F, Rigoldi M, Di Rocco M. Fertility and pregnancy in women affected by glycogen storage disease type I, results of a multicenter Italian study. *J Inherit Metab Dis* 2013; **36**: 83-89 [PMID: 22562700 DOI: 10.1007/s10545-012-9490-1]

74 **Ryan IP**, Havel RJ, Laros RK Jr. Three consecutive pregnancies in a patient with glycogen storage disease type IA (von Gierke's disease). *Am J Obstet Gynecol* 1994; **170**: 1687-90; discussion 1690 [PMID: 8203427]

75 **Mairovitz V**, Labrune P, Fernandez H, Audibert F, Frydman R. Contraception and pregnancy in women affected by glycogen storage diseases. *Eur J Pediatr* 2002; **161** Suppl 1: S97-101 [PMID: 12373581 DOI: 10.1007/s00431-002-1013-x]

76 **Angaroni CJ**, Giner-Ayala AN, Hill LP, Guelbert NB, Paschini-Capra AE, Dodelson de Kremer R. Evaluation of the biotinidase activity in hepatic glycogen storage disease patients. Undescribed genetic finding associated with atypical enzymatic behavior: an outlook. *J Inherit Metab Dis* 2010; **33**: S289-S294 [PMID: 20532819 DOI: 10.1007/s10545-010-9139-x]

77 **Paesold-Burda P**, Baumgartner MR, Santer R, Bosshard NU, Steinmann B. Elevated serum biotinidase activity in hepatic glycogen storage disorders--a convenient biomarker. *J Inherit Metab Dis* 2007; **30**: 896-902 [PMID: 17994282 DOI: 10.1007/s10545-007-0734-4]

78 **Wolf B**, Freehauf CL, Thomas JA, Gordon PL, Greene CL, Ward JC. Markedly elevated serum biotinidase activity may indicate glycogen storage disease type Ia. *J Inherit Metab Dis* 2003; **26**: 805-809 [PMID: 14739685 DOI: 10.1023/B:BOLI.0000009949.65855.4c]

79 **Saltik IN**, Ozen H, Koçak N, Yüce A, Gürakan F. High biotinidase activity in type Ia glycogen storage disease. *Am J Gastroenterol* 2000; **95**: 2144 [PMID: 10950092 DOI: 10.1111/j.1572-0241.2000.02222.x]

80 **El-Gharbawy A**, Tolun AA, Halaby CA, Austin SL, Kishnani PS, Bali DS. Beyond predicting diagnosis: Is there a role for measuring biotinidase activity in liver glycogen storage diseases? *Mol Genet Metab Rep* 2022; **31**: 100856 [PMID: 35782603 DOI: 10.1016/j.ymgmr.2022.100856]

81 **Baertling F**, Mayatepek E, Gerner P, Baba HA, Franzel J, Schlune A, Meissner T. Liver cirrhosis in glycogen storage disease Ib. *Mol Genet Metab* 2013; **108**: 198-200 [PMID: 23357201 DOI: 10.1016/j.ymgme.2013.01.003]

82 **Göğüş S**, Koçak N, Ciliv G, Karabulut E, Akçören Z, Kale G, Cağlar M. Histologic features of the liver in type Ia glycogen storage disease: comparative study between different age groups and consecutive biopsies. *Pediatr Dev Pathol* 2002; **5**: 299-304 [PMID: 12007023 DOI: 10.1007/s10024-001-0139-6]

83 **Karhan AN**, Hizarcioglu-Gulsen H, Gumus E, Akçören Z, Demir H, Saltik-Temizel İN, Orhan D, Özen H. Distinctive Features of Hepatic Steatosis in Children: Is It Primary or Secondary to Inborn Errors of Metabolism? *Pediatr Gastroenterol Hepatol Nutr* 2021; **24**: 518-527 [PMID: 34796096 DOI: 10.5223/pghn.2021.24.6.518]

84 **Qu Y**, Abdenur JE, Eng CM, Desnick RJ. Molecular prenatal diagnosis of glycogen storage disease type Ia. *Prenat Diagn* 1996; **16**: 333-336 [PMID: 8734807 DOI: 10.1002/(SICI)1097-0223(199604)16:4<333::AID-PD861>3.0.CO;2-G]

85 **Rake JP**, Visser G, Labrune P, Leonard JV, Ullrich K, Smit GP; European Study on Glycogen Storage Disease Type I (ESGSD I). Guidelines for management of glycogen storage disease type I - European Study on Glycogen Storage Disease Type I (ESGSD I). *Eur J Pediatr* 2002; **161** Suppl 1: S112-S119 [PMID: 12373584 DOI: 10.1007/s00431-002-1016-7]

86 **Lee PJ**, Dixon MA, Leonard JV. Uncooked cornstarch--efficacy in type I glycogenosis. *Arch Dis Child* 1996; **74**: 546-547 [PMID: 8758135 DOI: 10.1136/adc.74.6.546]

87 **Ross KM**, Brown LM, Corrado MM, Chengsupanimit T, Curry LM, Ferrecchia IA, Porras LY, Mathew JT, Weinstein DA. Safety and Efficacy of Chronic Extended Release Cornstarch Therapy for Glycogen Storage Disease Type I. *JIMD Rep* 2016; **26**: 85-90 [PMID: 26303612 DOI: 10.1007/8904_2015_488]

88 **Bhattacharya K**. Dietary dilemmas in the management of glycogen storage disease type I. *J Inherit Metab Dis* 2011; **34**: 621-629 [PMID: 21491105 DOI: 10.1007/s10545-011-9322-8]

89 **Monteillet L**, Labrune P, Hochuli M, Do Cao J, Tortereau A, Miliano AC, Ardon-Zitoun C, Duchampt A, Silva M, Verzieux V, Mithieux G, Rajas F. Cellular and metabolic effects of renin-angiotensin system blockade on glycogen storage disease type I nephropathy. *Hum Mol Genet* 2022; **31**: 914-928 [PMID: 34617103 DOI: 10.1093/hmg/ddab297]

90 **Melis D**, Parenti G, Gatti R, Casa RD, Parini R, Riva E, Burlina AB, Dionisi Vici C, Di Rocco M, Furlan F, Torcoletti M, Papadia F, Donati A, Benigno V, Andria G. Efficacy of ACE-inhibitor therapy on renal disease in glycogen storage disease type 1: a multicentre retrospective study. *Clin Endocrinol (Oxf)* 2005; **63**: 19-25 [PMID: 15963056 DOI: 10.1111/j.1365-2265.2005.02292.x]

91 **Ozen H**, Ciliv G, Koçak N, Saltik IN, Yüce A, Gürakan F. Short-term effect of captopril on microalbuminuria in children with glycogen storage disease type Ia. *J Inherit Metab Dis* 2000; **23**: 459-463 [PMID: 10947200 DOI: 10.1023/a:1005608113270]

92 **Nagasaka H**, Hirano K, Ohtake A, Miida T, Takatani T, Murayama K, Yorifuji T, Kobayashi K, Kanazawa M, Ogawa A, Takayanagi M. Improvements of hypertriglyceridemia and hyperlacticemia in Japanese children with glycogen storage disease type Ia by medium-chain triglyceride milk. *Eur J Pediatr* 2007; **166**: 1009-1016 [PMID: 17206455 DOI: 10.1007/s00431-006-0372-0]

93 **Das AM**, Lücke T, Meyer U, Hartmann H, Illsinger S. Glycogen storage disease type 1: impact of medium-chain triglycerides on metabolic control and growth. *Ann Nutr Metab* 2010; **56**: 225-232 [PMID: 20357432 DOI: 10.1159/000283242]

94 **Mollet-Boudjemline A**, Hubert-Buron A, Boyer-Neumann C, Aldea R, Franco D, Trioche-Eberschweiller P, Mas AE, Mabille M, Labrune P, Gajdos V. Perioperative management of hemostasis for surgery of benign hepatic adenomas in patients with glycogen storage disease type ia. *JIMD Rep* 2011; **1**: 97-106 [PMID: 23430835 DOI: 10.1007/8904_2011_23]

95 **Senior B**, Loridan L. Functional differentiation of glycogenoses of the liver with respect to the use of glycerol. *N Engl J Med* 1968; **279**: 965-970 [PMID: 4300573 DOI: 10.1056/NEJM196810312791803]

96 **Arion WJ**, Wallin BK, Lange AJ, Ballas LM. On the involvement of a glucose 6-phosphate transport system in the function of microsomal glucose 6-phosphatase. *Mol Cell Biochem* 1975; **6**: 75-83 [PMID: 235736 DOI: 10.1007/BF01732001]

97 **Ihara K**, Kuromaru R, Hara T. Genomic structure of the human glucose 6-phosphate translocase gene and novel mutations in the gene of a Japanese patient with glycogen storage disease type Ib. *Hum Genet* 1998; **103**: 493-496 [PMID: 9856496 DOI: 10.1007/s004390050856]

98 **Annabi B**, Hiraiwa H, Mansfield BC, Lei KJ, Ubagai T, Polymeropoulos MH, Moses SW, Parvari R, Hershkovitz E, Mandel H, Fryman M, Chou JY. The gene for glycogen-storage disease type 1b maps to chromosome 11q23. *Am J Hum Genet* 1998; **62**: 400-405 [PMID: 9463334 DOI: 10.1086/301727]

99 **Ihara K**, Nomura A, Hikino S, Takada H, Hara T. Quantitative analysis of glucose-6-phosphate translocase gene expression in various human tissues and haematopoietic progenitor cells. *J Inherit Metab Dis* 2000; **23**: 583-592 [PMID: 11032333 DOI: 10.1023/a:1005677912539]

100 **Kim GY**, Lee YM, Kwon JH, Jun HS, Chou J. Glycogen storage disease type Ib neutrophils exhibit impaired cell adhesion and migration. *Biochem Biophys Res Commun* 2017; **482**: 569-574 [PMID: 27864142 DOI: 10.1016/j.bbrc.2016.11.075]

101 **Chou JY**, Jun HS, Mansfield BC. Neutropenia in type Ib glycogen storage disease. *Curr Opin Hematol* 2010; **17**: 36-42 [PMID: 19741523 DOI: 10.1097/MOH.0b013e328331df85]

102 **Leuzzi R**, Bánhegyi G, Kardon T, Marcolongo P, Capecchi PL, Burger HJ, Benedetti A, Fulceri R. Inhibition of microsomal glucose-6-phosphate transport in human neutrophils results in apoptosis: a potential explanation for neutrophil

dysfunction in glycogen storage disease type 1b. *Blood* 2003; **101**: 2381-2387 [PMID: 12424192 DOI: 10.1182/blood-2002-08-2576]

103 **Kure S**, Hou DC, Suzuki Y, Yamagishi A, Hiratsuka M, Fukuda T, Sugie H, Kondo N, Matsubara Y, Narisawa K. Glycogen storage disease type Ib without neutropenia. *J Pediatr* 2000; **137**: 253-256 [PMID: 10931421 DOI: 10.1067/mpd.2000.107472]

104 **Dababneh R**, Shawabkeh A, Gharaibeh S, Khouri ZA, Amayreh W, Bissada NF. Periodontal Manifestation of Type Ib Glycogen Storage Disease: A Rare Case Report. *Clin Adv Periodontics* 2020; **10**: 150-154 [PMID: 33460318 DOI: 10.1002/cap.10112]

105 **Melis D**, Fulceri R, Parenti G, Marcolongo P, Gatti R, Parini R, Riva E, Della Casa R, Zammarchi E, Andria G, Benedetti A. Genotype/phenotype correlation in glycogen storage disease type 1b: a multicentre study and review of the literature. *Eur J Pediatr* 2005; **164**: 501-508 [PMID: 15906092 DOI: 10.1007/s00431-005-1657-4]

106 **Martin AP**, Bartels M, Schreiber S, Buehrdel P, Hauss J, Fangmann J. Successful staged kidney and liver transplantation for glycogen storage disease type Ib: A case report. *Transplant Proc* 2006; **38**: 3615-3619 [PMID: 17175348 DOI: 10.1016/j.transproceed.2006.10.160]

107 **Matern D**, Starzl TE, Arnaout W, Barnard J, Bynon JS, Dhawan A, Emond J, Haagsma EB, Hug G, Lachaux A, Smit GP, Chen YT. Liver transplantation for glycogen storage disease types I, III, and IV. *Eur J Pediatr* 1999; **158** Suppl 2: S43-S48 [PMID: 10603098 DOI: 10.1007/pl00014320]

108 **Aeppli TR**, Rymen D, Allegri G, Bode PK, Häberle J. Glycogen storage disease type VI: clinical course and molecular background. *Eur J Pediatr* 2020; **179**: 405-413 [PMID: 31768638 DOI: 10.1007/s00431-019-03499-1]

109 **Saltik-Temizel IN**, Koçak N, Ozen H, Yüce A, Gürakan F, Demir H. Inflammatory bowel disease-like colitis in a young Turkish child with glycogen storage disease type 1b and elevated platelet count. *Turk J Pediatr* 2005; **47**: 180-182 [PMID: 16052862]

110 **Roe TF**, Thomas DW, Gilsanz V, Isaacs H Jr, Atkinson JB. Inflammatory bowel disease in glycogen storage disease type Ib. *J Pediatr* 1986; **109**: 55-59 [PMID: 3459848 DOI: 10.1016/s0022-3476(86)80572-8]

111 **Dieckgraefe BK**, Korzenik JR, Husain A, Dieruf L. Association of glycogen storage disease 1b and Crohn disease: results of a North American survey. *Eur J Pediatr* 2002; **161** Suppl 1: S88-S92 [PMID: 12373579 DOI: 10.1007/s00431-002-1011-z]

112 **Visser G**, Rake JP, Labrune P, Leonard JV, Moses S, Ullrich K, Wendel U, Groenier KH, Smit GP. Granulocyte colony-stimulating factor in glycogen storage disease type 1b. Results of the European Study on Glycogen Storage Disease Type 1. *Eur J Pediatr* 2002; **161** Suppl 1: S83-S87 [PMID: 12373578 DOI: 10.1007/s00431-002-1010-0]

113 **Wicker C**, Roda C, Perry A, Arnoux JB, Brassier A, Castelle M, Servais A, Donadieu J, Bouchereau J, Pigneur B, Labrune P, Ruemmele FM, de Lonlay P. Infectious and digestive complications in glycogen storage disease type Ib: Study of a French cohort. *Mol Genet Metab Rep* 2020; **23**: 100581 [PMID: 32300528 DOI: 10.1016/j.ymgmr.2020.100581]

114 **Gong YZ**, Zhong XM, Zou JZ. Infliximab treatment of glycogenosis Ib with Crohn's-like enterocolitis: A case report. *World J Clin Cases* 2021; **9**: 5280-5286 [PMID: 34307579 DOI: 10.12998/wjcc.v9.i19.5280]

115 **Davis MK**, Rufo PA, Polyak SF, Weinstein DA. Adalimumab for the treatment of Crohn-like colitis and enteritis in glycogen storage disease type Ib. *J Inherit Metab Dis* 2008; **31** Suppl 3: 505-509 [PMID: 18172743 DOI: 10.1007/s10545-007-0774-9]

116 **Melis D**, Balivo F, Della Casa R, Romano A, Taurisano R, Capaldo B, Riccardi G, Monsurrò MR, Parenti G, Andria G. Myasthenia gravis in a patient affected by glycogen storage disease type Ib: a further manifestation of an increased risk for autoimmune disorders? *J Inherit Metab Dis* 2008; **31** Suppl 2: S227-S231 [PMID: 18437526 DOI: 10.1007/s10545-008-0810-4]

117 **Melis D**, Della Casa R, Balivo F, Minopoli G, Rossi A, Salerno M, Andria G, Parenti G. Involvement of endocrine system in a patient affected by glycogen storage disease 1b: speculation on the role of autoimmunity. *Ital J Pediatr* 2014; **40**: 30 [PMID: 24646511 DOI: 10.1186/1824-7288-40-30]

118 **Melis D**, Pivonello R, Parenti G, Della Casa R, Salerno M, Lombardi G, Sebastio G, Colao A, Andria G. Increased prevalence of thyroid autoimmunity and hypothyroidism in patients with glycogen storage disease type I. *J Pediatr* 2007; **150**: 300-305, 305.e1 [PMID: 17307551 DOI: 10.1016/j.jpeds.2006.11.056]

119 **Melis D**, Carbone F, Minopoli G, La Rocca C, Perna F, De Rosa V, Galgani M, Andria G, Parenti G, Matarese G. Cutting Edge: Increased Autoimmunity Risk in Glycogen Storage Disease Type 1b Is Associated with a Reduced Engagement of Glycolysis in T Cells and an Impaired Regulatory T Cell Function. *J Immunol* 2017; **198**: 3803-3808 [PMID: 28389590 DOI: 10.4049/jimmunol.1601946]

120 **Schroten H**, Roesler J, Breidenbach T, Wendel U, Elsner J, Schweitzer S, Zeidler C, Burdach S, Lohmann-Matthes ML, Wahn V. Granulocyte and granulocyte-macrophage colony-stimulating factors for treatment of neutropenia in glycogen storage disease type Ib. *J Pediatr* 1991; **119**: 748-754 [PMID: 1719175 DOI: 10.1016/s0022-3476(05)80290-2]

121 **Schroten H**, Wendel U, Burdach S, Roesler J, Breidenbach T, Schweitzer S, Zeidler C, Welte K. Colony-stimulating factors for neutropenia in glycogen storage disease Ib. *Lancet* 1991; **337**: 736-737 [PMID: 1706047 DOI: 10.1016/0140-6736(91)90324-i]

122 **Roe TF**, Coates TD, Thomas DW, Miller JH, Gilsanz V. Brief report: treatment of chronic inflammatory bowel disease in glycogen storage disease type Ib with colony-stimulating factors. *N Engl J Med* 1992; **326**: 1666-1669 [PMID: 1375344 DOI: 10.1056/NEJM199206183262504]

123 **Alsultan A**, Sokol RJ, Lovell MA, Thurman G, Ambruso DR. Long term G-CSF-induced remission of ulcerative colitis-like inflammatory bowel disease in a patient with glycogen storage disease Ib and evaluation of associated neutrophil function. *Pediatr Blood Cancer* 2010; **55**: 1410-1413 [PMID: 20830779 DOI: 10.1002/pbc.22706]

124 **Dale DC**, Bolyard AA, Marrero T, Kelley ML, Makaryan V, Tran E, Leung J, Boxer LA, Kishnani PS, Austin S, Wanner C, Ferrecchia IA, Khalaf D, Maze D, Kurtzberg J, Zeidler C, Welte K, Weinstein DA. Neutropenia in glycogen storage disease Ib: outcomes for patients treated with granulocyte colony-stimulating factor. *Curr Opin Hematol* 2019; **26**: 16-21 [PMID: 30451720 DOI: 10.1097/MOH.0000000000000474]

125 **Li AM**, Thyagu S, Maze D, Schreiber R, Sirrs S, Stockler-Ipsiroglu S, Sutherland H, Vercauteren S, Schultz KR.

Prolonged granulocyte colony stimulating factor use in glycogen storage disease type 1b associated with acute myeloid leukemia and with shortened telomere length. *Pediatr Hematol Oncol* 2018; **35**: 45-51 [PMID: 29652549 DOI: 10.1080/08880018.2018.1440675]

126 **Melis D**, Della Casa R, Parini R, Rigoldi M, Cacciapuoti C, Marcolongo P, Benedetti A, Gaudieri V, Andria G, Parenti G. Vitamin E supplementation improves neutropenia and reduces the frequency of infections in patients with glycogen storage disease type 1b. *Eur J Pediatr* 2009; **168**: 1069-1074 [PMID: 19066956 DOI: 10.1007/s00431-008-0889-5]

127 **Reddy SK**, Austin SL, Spencer-Manzon M, Koeberl DD, Clary BM, Desai DM, Smith AD, Kishnani PS. Liver transplantation for glycogen storage disease type Ia. *J Hepatol* 2009; **51**: 483-490 [PMID: 19596478 DOI: 10.1016/j.jhep.2009.05.026]

128 **Boers SJ**, Visser G, Smit PG, Fuchs SA. Liver transplantation in glycogen storage disease type I. *Orphanet J Rare Dis* 2014; **9**: 47 [PMID: 24716823 DOI: 10.1186/1750-1172-9-47]

129 **Faivre L**, Houssin D, Valayer J, Brouard J, Hadchouel M, Bernard O. Long-term outcome of liver transplantation in patients with glycogen storage disease type Ia. *J Inherit Metab Dis* 1999; **22**: 723-732 [PMID: 10472532 DOI: 10.1023/a:1005544117285]

130 **Liu PP**, de Villa VH, Chen YS, Wang CC, Wang SH, Chiang YC, Jawan B, Cheung HK, Cheng YF, Huang TL, Eng HL, Chuang FR, Chen CL. Outcome of living donor liver transplantation for glycogen storage disease. *Transplant Proc* 2003; **35**: 366-368 [PMID: 12591443 DOI: 10.1016/s0041-1345(02)03951-9]

131 **Yuen WY**, Quak SH, Aw MM, Karthik SV. Long-term outcome after liver transplantation in children with type 1 glycogen storage disease. *Pediatr Transplant* 2021; **25**: e13872 [PMID: 33044776 DOI: 10.1111/petr.13872]

132 **Emmett M**, Narins RG. Renal tranplantation in type 1 glycogenosis. Failure to improve glucose metabolism. *JAMA* 1978; **239**: 1642-1644 [PMID: 204806]

133 **Iyer SG**, Chen CL, Wang CC, Wang SH, Concejero AM, Liu YW, Yang CH, Yong CC, Jawan B, Cheng YF, Eng HL. Long-term results of living donor liver transplantation for glycogen storage disorders in children. *Liver Transpl* 2007; **13**: 848-852 [PMID: 17539004 DOI: 10.1002/Lt.21151]

134 **Shimizu S**, Sakamoto S, Horikawa R, Fukuda A, Uchida H, Takeda M, Yanagi Y, Irie R, Yoshioka T, Kasahara M. Longterm Outcomes of Living Donor Liver Transplantation for Glycogen Storage Disease Type 1b. *Liver Transpl* 2020; **26**: 57-67 [PMID: 31587472 DOI: 10.1002/lt.25649]

135 **Veiga-da-Cunha M**, Chevalier N, Stephenne X, Defour JP, Paczia N, Ferster A, Achouri Y, Dewulf JP, Linster CL, Bommer GT, Van Schaftingen E. Failure to eliminate a phosphorylated glucose analog leads to neutropenia in patients with G6PT and G6PC3 deficiency. *Proc Natl Acad Sci U S A* 2019; **116**: 1241-1250 [PMID: 30626647 DOI: 10.1073/pnas.1816143116]

136 **Wortmann SB**, Van Hove JLK, Derks TGJ, Chevalier N, Knight V, Koller A, Oussoren E, Mayr JA, van Spronsen FJ, Lagler FB, Gaughan S, Van Schaftingen E, Veiga-da-Cunha M. Treating neutropenia and neutrophil dysfunction in glycogen storage disease type Ib with an SGLT2 inhibitor. *Blood* 2020; **136**: 1033-1043 [PMID: 32294159 DOI: 10.1182/blood.2019004465]

137 **Hexner-Erlichman Z**, Veiga-da-Cunha M, Zehavi Y, Vadasz Z, Sabag AD, Tatour S, Spiegel R. Favorable outcome of empagliflozin treatment in two pediatric glycogen storage disease type 1b patients. *Front Pediatr* 2022; **10**: 1071464 [PMID: 36507137 DOI: 10.3389/fped.2022.1071464]

138 **Makrilakis K**, Barmpagianni A, Veiga-da-Cunha M. Repurposing of Empagliflozin as a Possible Treatment for Neutropenia and Inflammatory Bowel Disease in Glycogen Storage Disease Type Ib: A Case Report. *Cureus* 2022; **14**: e27264 [PMID: 36039216 DOI: 10.7759/cureus.27264]

139 **Bidiuk J**, Gaciong ZA, Sobieraj P. The overall benefits of empagliflozin treatment in adult siblings with glycogen storage disease type Ib: one year experience. *Arch Med Sci* 2022; **18**: 1095-1099 [PMID: 35982912 DOI: 10.5114/aoms/150029]

140 **Grünert SC**, Rosenbaum-Fabian S, Schumann A, Selbitz AC, Merz W, Gieselmann A, Spiekerkoetter U. Two successful pregnancies and first use of empagliflozin during pregnancy in glycogen storage disease type Ib. *JIMD Rep* 2022; **63**: 303-308 [PMID: 35822091 DOI: 10.1002/jmd2.12295]

141 **Halligan RK**, Dalton RN, Turner C, Lewis KA, Mundy HR. Understanding the role of SGLT2 inhibitors in glycogen storage disease type Ib: the experience of one UK centre. *Orphanet J Rare Dis* 2022; **17**: 195 [PMID: 35549996 DOI: 10.1186/s13023-022-02345-2]

142 **Boulanger C**, Stephenne X, Diederich J, Mounkoro P, Chevalier N, Ferster A, Van Schaftingen E, Veiga-da-Cunha M. Successful use of empagliflozin to treat neutropenia in two G6PC3-deficient children: Impact of a mutation in SGLT5. *J Inherit Metab Dis* 2022; **45**: 759-768 [PMID: 35506446 DOI: 10.1002/jimd.12509]

143 **Mikami M**, Arai A, Mizumoto H. Empagliflozin ameliorated neutropenia in a girl with glycogen storage disease Ib. *Pediatr Int* 2021; **63**: 1394-1396 [PMID: 34378838 DOI: 10.1111/ped.14629]

144 **Grünert SC**, Elling R, Maag B, Wortmann SB, Derks TGJ, Hannibal L, Schumann A, Rosenbaum-Fabian S, Spiekerkoetter U. Improved inflammatory bowel disease, wound healing and normal oxidative burst under treatment with empagliflozin in glycogen storage disease type Ib. *Orphanet J Rare Dis* 2020; **15**: 218 [PMID: 32838757 DOI: 10.1186/s13023-020-01503-8]

145 **Grünert SC**, Derks TGJ, Adrian K, Al-Thihli K, Ballhausen D, Bidiuk J, Bordugo A, Boyer M, Bratkovic D, Brunner-Krainz M, Burlina A, Chakrapani A, Corpeleijn W, Cozens A, Dawson C, Dhamko H, Milosevic MD, Eiroa H, Finezilber Y, Moura de Souza CF, Garcia-Jiménez MC, Gasperini S, Haas D, Häberle J, Halligan R, Fung LH, Hörbe-Blindt A, Horka LM, Huemer M, Uçar SK, Kecman B, Kilavuz S, Kriván G, Lindner M, Lüsebrink N, Makrilakis K, Mei-Kwun Kwok A, Maier EM, Maiorana A, McCandless SE, Mitchell JJ, Mizumoto H, Mundy H, Ochoa C, Pierce K, Fraile PQ, Regier D, Rossi A, Santer R, Schuman HC, Sobieraj P, Spenger J, Spiegel R, Stepien KM, Tal G, Tanšek MZ, Torkar AD, Tchan M, Thyagu S, Schrier Vergano SA, Vucko E, Weinhold N, Zsidegh P, Wortmann SB. Efficacy and safety of empagliflozin in glycogen storage disease type Ib: Data from an international questionnaire. *Genet Med* 2022; **24**: 1781-1788 [PMID: 35503103 DOI: 10.1016/j.gim.2022.04.001]

146 **Chou JY**, Mansfield BC. Recombinant AAV-directed gene therapy for type I glycogen storage diseases. *Expert Opin Biol Ther* 2011; **11**: 1011-1024 [PMID: 21504389 DOI: 10.1517/14712598.2011.578067]

147 **Kwon JH**, Lee YM, Cho JH, Kim GY, Anduaga J, Starost MF, Mansfield BC, Chou JY. Liver-directed gene therapy for murine glycogen storage disease type Ib. *Hum Mol Genet* 2017; **26**: 4395-4405 [PMID: 28973635 DOI: 10.1093/hmg/ddx325]

148 **Chou JY**, Cho JH, Kim GY, Mansfield BC. Molecular biology and gene therapy for glycogen storage disease type Ib. *J Inherit Metab Dis* 2018; **41**: 1007-1014 [PMID: 29663270 DOI: 10.1007/s10545-018-0180-5]

149 **Lee YM**, Conlon TJ, Specht A, Coleman KE, Brown LM, Estrella AM, Dambska M, Dahlberg KR, Weinstein DA. Long-term safety and efficacy of AAV gene therapy in the canine model of glycogen storage disease type Ia. *J Inherit Metab Dis* 2018; **41**: 977-984 [PMID: 29802554 DOI: 10.1007/s10545-018-0199-7]

150 **Yiu WH**, Pan CJ, Allamarvdasht M, Kim SY, Chou JY. Glucose-6-phosphate transporter gene therapy corrects metabolic and myeloid abnormalities in glycogen storage disease type Ib mice. *Gene Ther* 2007; **14**: 219-226 [PMID: 17006547 DOI: 10.1038/sj.gt.3302869]

151 **Landau DJ**, Brooks ED, Perez-Pinera P, Amarasekara H, Mefferd A, Li S, Bird A, Gersbach CA, Koeberl DD. In Vivo Zinc Finger Nuclease-mediated Targeted Integration of a Glucose-6-phosphatase Transgene Promotes Survival in Mice With Glycogen Storage Disease Type IA. *Mol Ther* 2016; **24**: 697-706 [PMID: 26865405 DOI: 10.1038/mt.2016.35]

152 **Zhang L**, Lee C, Arnaoutova I, Anduaga J, Starost MF, Mansfield BC, Chou JY. Gene therapy using a novel G6PC-S298C variant enhances the long-term efficacy for treating glycogen storage disease type Ia. *Biochem Biophys Res Commun* 2020; **527**: 824-830 [PMID: 32430177 DOI: 10.1016/j.bbrc.2020.04.124]

153 **Shen JJ**, Chen YT. Molecular characterization of glycogen storage disease type III. *Curr Mol Med* 2002; **2**: 167-175 [PMID: 11949933 DOI: 10.2174/1566524024605752]

154 **Bao Y**, Yang BZ, Dawson TL Jr, Chen YT. Isolation and nucleotide sequence of human liver glycogen debranching enzyme mRNA: identification of multiple tissue-specific isoforms. *Gene* 1997; **197**: 389-398 [PMID: 9332391 DOI: 10.1016/s0378-1119(97)00291-6]

155 **Bao Y**, Dawson TL Jr, Chen YT. Human glycogen debranching enzyme gene (AGL): complete structural organization and characterization of the 5' flanking region. *Genomics* 1996; **38**: 155-165 [PMID: 8954797 DOI: 10.1006/geno.1996.0611]

156 **Parvari R**, Moses S, Shen J, Hershkovitz E, Lerner A, Chen YT. A single-base deletion in the 3'-coding region of glycogen-debranching enzyme is prevalent in glycogen storage disease type IIIA in a population of North African Jewish patients. *Eur J Hum Genet* 1997; **5**: 266-270 [PMID: 9412782]

157 **Santer R**, Kinner M, Steuerwald U, Kjaergaard S, Skovby F, Simonsen H, Shaiu WL, Chen YT, Schneppenheim R, Schaub J. Molecular genetic basis and prevalence of glycogen storage disease type IIIA in the Faroe Islands. *Eur J Hum Genet* 2001; **9**: 388-391 [PMID: 11378828 DOI: 10.1038/sj.ejhg.5200632]

158 **Rousseau-Nepton I**, Okubo M, Grabs R; FORGE Canada Consortium, Mitchell J, Polychronakos C, Rodd C. A founder AGL mutation causing glycogen storage disease type IIIa in Inuit identified through whole-exome sequencing: a case series. *CMAJ* 2015; **187**: E68-E73 [PMID: 25602008 DOI: 10.1503/cmaj.140840]

159 **Shen J**, Bao Y, Liu HM, Lee P, Leonard JV, Chen YT. Mutations in exon 3 of the glycogen debranching enzyme gene are associated with glycogen storage disease type III that is differentially expressed in liver and muscle. *J Clin Invest* 1996; **98**: 352-357 [PMID: 8755644 DOI: 10.1172/JCI118799]

160 **Goldstein JL**, Austin SL, Boyette K, Kanaly A, Veerapandiyan A, Rehder C, Kishnani PS, Bali DS. Molecular analysis of the AGL gene: identification of 25 novel mutations and evidence of genetic heterogeneity in patients with Glycogen Storage Disease Type III. *Genet Med* 2010; **12**: 424-430 [PMID: 20648714 DOI: 10.1097/GIM.0b013e3181d94eaa]

161 **Ding JH**, de Barsy T, Brown BI, Coleman RA, Chen YT. Immunoblot analyses of glycogen debranching enzyme in different subtypes of glycogen storage disease type III. *J Pediatr* 1990; **116**: 95-100 [PMID: 2295969 DOI: 10.1016/s0022-3476(05)81652-x]

162 **Van Hoof F**, Hers HG. The subgroups of type 3 glycogenosis. *Eur J Biochem* 1967; **2**: 265-270 [PMID: 5235982 DOI: 10.1111/j.1432-1033.1967.tb00134.x]

163 **Derks TG**, van Rijn M. Lipids in hepatic glycogen storage diseases: pathophysiology, monitoring of dietary management and future directions. *J Inherit Metab Dis* 2015; **38**: 537-543 [PMID: 25633903 DOI: 10.1007/s10545-015-9811-2]

164 **Bernier AV**, Sentner CP, Correia CE, Theriaque DW, Shuster JJ, Smit GP, Weinstein DA. Hyperlipidemia in glycogen storage disease type III: effect of age and metabolic control. *J Inherit Metab Dis* 2008; **31**: 729-732 [PMID: 18709545 DOI: 10.1007/s10545-008-0919-5]

165 **Coleman RA**, Winter HS, Wolf B, Chen YT. Glycogen debranching enzyme deficiency: long-term study of serum enzyme activities and clinical features. *J Inherit Metab Dis* 1992; **15**: 869-881 [PMID: 1293383 DOI: 10.1007/BF01800225]

166 **Halaby CA**, Young SP, Austin S, Stefanescu E, Bali D, Clinton LK, Smith B, Pendyal S, Upadia J, Schooler GR, Mavis AM, Kishnani PS. Liver fibrosis during clinical ascertainment of glycogen storage disease type III: a need for improved and systematic monitoring. *Genet Med* 2019; **21**: 2686-2694 [PMID: 31263214 DOI: 10.1038/s41436-019-0561-7]

167 **Siciliano M**, De Candia E, Ballarin S, Vecchio FM, Servidei S, Annese R, Landolfi R, Rossi L. Hepatocellular carcinoma complicating liver cirrhosis in type IIIa glycogen storage disease. *J Clin Gastroenterol* 2000; **31**: 80-82 [PMID: 10914784 DOI: 10.1097/00004836-200007000-00020]

168 **Demo E**, Frush D, Gottfried M, Koepke J, Boney A, Bali D, Chen YT, Kishnani PS. Glycogen storage disease type III-hepatocellular carcinoma a long-term complication? *J Hepatol* 2007; **46**: 492-498 [PMID: 17196294 DOI: 10.1016/j.jhep.2006.09.022]

169 **Labrune P**, Trioche P, Duvaltier I, Chevalier P, Odièvre M. Hepatocellular adenomas in glycogen storage disease type I and III: a series of 43 patients and review of the literature. *J Pediatr Gastroenterol Nutr* 1997; **24**: 276-279 [PMID: 9138172 DOI: 10.1097/00005176-199703000-00008]

170 **Sentner CP**, Hoogeveen IJ, Weinstein DA, Santer R, Murphy E, McKiernan PJ, Steuerwald U, Beauchamp NJ, Taybert J, Laforêt P, Petit FM, Hubert A, Labrune P, Smit GPA, Derks TGJ. Glycogen storage disease type III: diagnosis, genotype, management, clinical course and outcome. *J Inherit Metab Dis* 2016; **39**: 697-704 [PMID: 27106217 DOI: 10.1007/s10545-016-9932-2]

171 **Lucchiari S**, Pagliarani S, Salani S, Filocamo M, Di Rocco M, Melis D, Rodolico C, Musumeci O, Toscano A, Bresolin N, Comi GP. Hepatic and neuromuscular forms of glycogenosis type III: nine mutations in AGL. *Hum Mutat* 2006; **27**:

600-601 [PMID: 16705713 DOI: 10.1002/humu.9426]
172 **Lee P**, Burch M, Leonard JV. Plasma creatine kinase and cardiomyopathy in glycogen storage disease type III. *J Inherit Metab Dis* 1995; **18**: 751-752 [PMID: 8750616 DOI: 10.1007/BF02436768]
173 **Coleman RA**, Winter HS, Wolf B, Gilchrist JM, Chen YT. Glycogen storage disease type III (glycogen debranching enzyme deficiency): correlation of biochemical defects with myopathy and cardiomyopathy. *Ann Intern Med* 1992; **116**: 896-900 [PMID: 1580445 DOI: 10.7326/0003-4819-116-11-896]
174 **Ben Chehida A**, Ben Messaoud S, Ben Abdelaziz R, Ben Ali N, Boudabous H, Ben Abdelaziz I, Ben Ameur Z, Sassi Y, Kaabachi N, Abdelhak S, Abdelmoula MS, Fradj M, Azzouz H, Tebib N. Neuromuscular Involvement in Glycogen Storage Disease Type III in Fifty Tunisian Patients: Phenotype and Natural History in Young Patients. *Neuropediatrics* 2019; **50**: 22-30 [PMID: 30308687 DOI: 10.1055/s-0038-1669786]
175 **Mogahed EA**, Girgis MY, Sobhy R, Elhabashy H, Abdelaziz OM, El-Karaksy H. Skeletal and cardiac muscle involvement in children with glycogen storage disease type III. *Eur J Pediatr* 2015; **174**: 1545-1548 [PMID: 25948107 DOI: 10.1007/s00431-015-2546-0]
176 **Kishnani PS**, Austin SL, Arn P, Bali DS, Boney A, Case LE, Chung WK, Desai DM, El-Gharbawy A, Haller R, Smit GP, Smith AD, Hobson-Webb LD, Wechsler SB, Weinstein DA, Watson MS; ACMG. Glycogen storage disease type III diagnosis and management guidelines. *Genet Med* 2010; **12**: 446-463 [PMID: 20631546 DOI: 10.1097/GIM.0b013e3181e655b6]
177 **Momoi T**, Sano H, Yamanaka C, Sasaki H, Mikawa H. Glycogen storage disease type III with muscle involvement: reappraisal of phenotypic variability and prognosis. *Am J Med Genet* 1992; **42**: 696-699 [PMID: 1632441 DOI: 10.1002/ajmg.1320420514]
178 **Berling É**, Laforêt P, Wahbi K, Labrune P, Petit F, Ronzitti G, O'Brien A. Narrative review of glycogen storage disorder type III with a focus on neuromuscular, cardiac and therapeutic aspects. *J Inherit Metab Dis* 2021; **44**: 521-533 [PMID: 33368379 DOI: 10.1002/jimd.12355]
179 **Moses SW**, Wanderman KL, Myroz A, Frydman M. Cardiac involvement in glycogen storage disease type III. *Eur J Pediatr* 1989; **148**: 764-766 [PMID: 2792130 DOI: 10.1007/BF00443106]
180 **Vertilus SM**, Austin SL, Foster KS, Boyette KE, Bali DS, Li JS, Kishnani PS, Wechsler SB. Echocardiographic manifestations of Glycogen Storage Disease III: increase in wall thickness and left ventricular mass over time. *Genet Med* 2010; **12**: 413-423 [PMID: 20526204 DOI: 10.1097/GIM.0b013e3181e0e979]
181 **Ben Chehida A**, Ben Messaoud S, Ben Abdelaziz R, Mansouri H, Boudabous H, Hakim K, Ben Ali N, Ben Ameur Z, Sassi Y, Kaabachi N, Abdelhak S, Abdelmoula MS, Azzouz H, Tebib N. A lower energetic, protein and uncooked cornstarch intake is associated with a more severe outcome in glycogen storage disease type III: an observational study of 50 patients. *J Pediatr Endocrinol Metab* 2018; **31**: 979-986 [PMID: 30110253 DOI: 10.1515/jpem-2018-0151]
182 **Austin SL**, Proia AD, Spencer-Manzon MJ, Butany J, Wechsler SB, Kishnani PS. Cardiac Pathology in Glycogen Storage Disease Type III. *JIMD Rep* 2012; **6**: 65-72 [PMID: 23430941 DOI: 10.1007/8904_2011_118]
183 **Focardi M**, Bosco A, Bugelli V, Defraia B, Donati MA, Pinchi V. "On air" diagnosis of sudden cardiac death with dynamic Holter ECG in glycogen storage disease type III young female. *Minerva Pediatr* 2020; **72**: 142-144 [PMID: 32441908 DOI: 10.23736/S0026-4946.19.05496-3]
184 **Cleary MA**, Walter JH, Kerr BA, Wraith JE. Facial appearance in glycogen storage disease type III. *Clin Dysmorphol* 2002; **11**: 117-120 [PMID: 12002141 DOI: 10.1097/00019605-200204000-00008]
185 **Mundy HR**, Williams JE, Lee PJ, Fewtrell MS. Reduction in bone mineral density in glycogenosis type III may be due to a mixed muscle and bone deficit. *J Inherit Metab Dis* 2008; **31**: 418-423 [PMID: 18392743 DOI: 10.1007/s10545-008-0830-0]
186 **Melis D**, Rossi A, Pivonello R, Del Puente A, Pivonello C, Cangemi G, Negri M, Colao A, Andria G, Parenti G. Reduced bone mineral density in glycogen storage disease type III: evidence for a possible connection between metabolic imbalance and bone homeostasis. *Bone* 2016; **86**: 79-85 [PMID: 26924264 DOI: 10.1016/j.bone.2016.02.012]
187 **Lee PJ**, Patel A, Hindmarsh PC, Mowat AP, Leonard JV. The prevalence of polycystic ovaries in the hepatic glycogen storage diseases: its association with hyperinsulinism. *Clin Endocrinol (Oxf)* 1995; **42**: 601-606 [PMID: 7634500 DOI: 10.1111/j.1365-2265.1995.tb02686.x]
188 **Spengos K**, Michelakakis H, Vontzalidis A, Zouvelou V, Manta P. Diabetes mellitus associated with glycogen storage disease type III. *Muscle Nerve* 2009; **39**: 876-877 [PMID: 19334047 DOI: 10.1002/mus.21201]
189 **Michon CC**, Gargiulo M, Hahn-Barma V, Petit F, Nadaj-Pakleza A, Herson A, Eymard B, Labrune P, Laforet P. Cognitive profile of patients with glycogen storage disease type III: a clinical description of seven cases. *J Inherit Metab Dis* 2015; **38**: 573-580 [PMID: 25388549 DOI: 10.1007/s10545-014-9789-1]
190 **Valayannopoulos V**, Bajolle F, Arnoux JB, Dubois S, Sannier N, Baussan C, Petit F, Labrune P, Rabier D, Ottolenghi C, Vassault A, Broissand C, Bonnet D, de Lonlay P. Successful treatment of severe cardiomyopathy in glycogen storage disease type III With D,L-3-hydroxybutyrate, ketogenic and high-protein diet. *Pediatr Res* 2011; **70**: 638-641 [PMID: 21857385 DOI: 10.1203/PDR.0b013e318232154f]
191 **Francini-Pesenti F**, Tresso S, Vitturi N. Modified Atkins ketogenic diet improves heart and skeletal muscle function in glycogen storage disease type III. *Acta Myol* 2019; **38**: 17-20 [PMID: 31309177]
192 **Kumru Akin B**, Ozturk Hismi B, Daly A. Improvement in hypertrophic cardiomyopathy after using a high-fat, high-protein and low-carbohydrate diet in a non-adherent child with glycogen storage disease type IIIa. *Mol Genet Metab Rep* 2022; **32**: 100904 [PMID: 36046398 DOI: 10.1016/j.ymgmr.2022.100904]
193 **Sentner CP**, Caliskan K, Vletter WB, Smit GP. Heart Failure Due to Severe Hypertrophic Cardiomyopathy Reversed by Low Calorie, High Protein Dietary Adjustments in a Glycogen Storage Disease Type IIIa Patient. *JIMD Rep* 2012; **5**: 13-16 [PMID: 23430911 DOI: 10.1007/8904_2011_111]
194 **Derks TG**, Smit GP. Dietary management in glycogen storage disease type III: what is the evidence? *J Inherit Metab Dis* 2015; **38**: 545-550 [PMID: 25164784 DOI: 10.1007/s10545-014-9756-x]
195 **Davis MK**, Weinstein DA. Liver transplantation in children with glycogen storage disease: controversies and evaluation of the risk/benefit of this procedure. *Pediatr Transplant* 2008; **12**: 137-145 [PMID: 18307661 DOI:

10.1111/j.1399-3046.2007.00803.x]
196 **Andersen DH**. Familial cirrhosis of the liver with storage of abnormal glycogen. *Lab Invest* 1956; **5**: 11-20 [PMID: 13279125]
197 **Brown BI**, Brown DH. Lack of an alpha-1,4-glucan: alpha-1,4-glucan 6-glycosyl transferase in a case of type IV glycogenosis. *Proc Natl Acad Sci U S A* 1966; **56**: 725-729 [PMID: 5229990 DOI: 10.1073/pnas.56.2.725]
198 **Moses SW**, Parvari R. The variable presentations of glycogen storage disease type IV: a review of clinical, enzymatic and molecular studies. *Curr Mol Med* 2002; **2**: 177-188 [PMID: 11949934 DOI: 10.2174/1566524024605815]
199 **Thon VJ**, Khalil M, Cannon JF. Isolation of human glycogen branching enzyme cDNAs by screening complementation in yeast. *J Biol Chem* 1993; **268**: 7509-7513 [PMID: 8463281]
200 **L'herminé-Coulomb A**, Beuzen F, Bouvier R, Rolland MO, Froissart R, Menez F, Audibert F, Labrune P. Fetal type IV glycogen storage disease: clinical, enzymatic, and genetic data of a pure muscular form with variable and early antenatal manifestations in the same family. *Am J Med Genet A* 2005; **139A**: 118-122 [PMID: 16278887 DOI: 10.1002/ajmg.a.30945]
201 **Derks TGJ**, Peeks F, de Boer F, Fokkert-Wilts M, van der Doef HPJ, van den Heuvel MC, Szymańska E, Rokicki D, Ryan PT, Weinstein DA. The potential of dietary treatment in patients with glycogen storage disease type IV. *J Inherit Metab Dis* 2021; **44**: 693-704 [PMID: 33332610 DOI: 10.1002/jimd.12339]
202 **de Moor RA**, Schweizer JJ, van Hoek B, Wasser M, Vink R, Maaswinkel-Mooy PD. Hepatocellular carcinoma in glycogen storage disease type IV. *Arch Dis Child* 2000; **82**: 479-480 [PMID: 10833181 DOI: 10.1136/adc.82.6.479]
203 **Greene HL**, Brown BI, McClenathan DT, Agostini RM Jr, Taylor SR. A new variant of type IV glycogenosis: deficiency of branching enzyme activity without apparent progressive liver disease. *Hepatology* 1988; **8**: 302-306 [PMID: 3162725 DOI: 10.1002/hep.1840080219]
204 **Schröder JM**, May R, Shin YS, Sigmund M, Nase-Hüppmeier S. Juvenile hereditary polyglucosan body disease with complete branching enzyme deficiency (type IV glycogenosis). *Acta Neuropathol* 1993; **85**: 419-430 [PMID: 7683169 DOI: 10.1007/BF00334454]
205 **Servidei S**, Riepe RE, Langston C, Tani LY, Bricker JT, Crisp-Lindgren N, Travers H, Armstrong D, DiMauro S. Severe cardiopathy in branching enzyme deficiency. *J Pediatr* 1987; **111**: 51-56 [PMID: 3474393 DOI: 10.1016/s0022-3476(87)80341-4]
206 **Bruno C**, van Diggelen OP, Cassandrini D, Gimpelev M, Giuffrè B, Donati MA, Introvini P, Alegria A, Assereto S, Morandi L, Mora M, Tonoli E, Mascelli S, Traverso M, Pasquini E, Bado M, Vilarinho L, van Noort G, Mosca F, DiMauro S, Zara F, Minetti C. Clinical and genetic heterogeneity of branching enzyme deficiency (glycogenosis type IV). *Neurology* 2004; **63**: 1053-1058 [PMID: 15452297 DOI: 10.1212/01.wnl.0000138429.11433.0d]
207 **Alegria A**, Martins E, Dias M, Cunha A, Cardoso ML, Maire I. Glycogen storage disease type IV presenting as hydrops fetalis. *J Inherit Metab Dis* 1999; **22**: 330-332 [PMID: 10384399 DOI: 10.1023/a:1005568507267]
208 **Akman HO**, Karadimas C, Gyftodimou Y, Grigoriadou M, Kokotas H, Konstantinidou A, Anninos H, Patsouris E, Thaker HM, Kaplan JB, Besharat I, Hatzikonstantinou K, Fotopoulos S, Dimauro S, Petersen MB. Prenatal diagnosis of glycogen storage disease type IV. *Prenat Diagn* 2006; **26**: 951-955 [PMID: 16874838 DOI: 10.1002/pd.1533]
209 **Zellweger H**, Mueller S, Ionasescu V, Schochet SS, McCormick WF. Glycogenosis. IV. A new cause of infantile hypotonia. *J Pediatr* 1972; **80**: 842-844 [PMID: 4502299 DOI: 10.1016/s0022-3476(72)80144-6]
210 **McMaster KR**, Powers JM, Hennigar GR Jr, Wohltmann HJ, Farr GH Jr. Nervous system involvement in type IV glycogenosis. *Arch Pathol Lab Med* 1979; **103**: 105-111 [PMID: 284761]
211 **Giuffrè B**, Parini R, Rizzuti T, Morandi L, van Diggelen OP, Bruno C, Giuffrè M, Corsello G, Mosca F. Severe neonatal onset of glycogenosis type IV: clinical and laboratory findings leading to diagnosis in two siblings. *J Inherit Metab Dis* 2004; **27**: 609-619 [PMID: 15669676 DOI: 10.1023/b:boli.0000042980.45692.bb]
212 **Reusche E**, Aksu F, Goebel HH, Shin YS, Yokota T, Reichmann H. A mild juvenile variant of type IV glycogenosis. *Brain Dev* 1992; **14**: 36-43 [PMID: 1375445 DOI: 10.1016/s0387-7604(12)80277-4]
213 **Shin YS**, Steigüber H, Klemm P, Endres W, Schwab O, Wolff G. Branching enzyme in erythrocytes. Detection of type IV glycogenosis homozygotes and heterozygotes. *J Inherit Metab Dis* 1988; **11** Suppl 2: 252-254 [PMID: 2972882 DOI: 10.1007/BF01804250]
214 **Ferguson IT**, Mahon M, Cumming WJ. An adult case of Andersen's disease--Type IV glycogenosis. A clinical, histochemical, ultrastructural and biochemical study. *J Neurol Sci* 1983; **60**: 337-351 [PMID: 6579239 DOI: 10.1016/0022-510x(83)90144-2]
215 **Lossos A**, Barash V, Soffer D, Argov Z, Gomori M, Ben-Nariah Z, Abramsky O, Steiner I. Hereditary branching enzyme dysfunction in adult polyglucosan body disease: a possible metabolic cause in two patients. *Ann Neurol* 1991; **30**: 655-662 [PMID: 1763891 DOI: 10.1002/ana.410300505]
216 **Mizuochi T**, Kimura A, Nishiura H, Inomata Y, Okajima H, Sugie H, Mitsubuchi H, Yagi M, Kage M. Liver biopsy is an important procedure in the diagnosis of glycogen storage disease type IV. *Pediatr Int* 2011; **53**: 129-130 [PMID: 21342345 DOI: 10.1111/j.1442-200X.2010.03282.x]
217 **Willot S**, Marchand V, Rasquin A, Alvarez F, Martin SR. Systemic progression of type IV glycogen storage disease after liver transplantation. *J Pediatr Gastroenterol Nutr* 2010; **51**: 661-664 [PMID: 20531024 DOI: 10.1097/MPG.0b013e3181d29780]
218 **Li SC**, Chen CM, Goldstein JL, Wu JY, Lemyre E, Burrow TA, Kang PB, Chen YT, Bali DS. Glycogen storage disease type IV: novel mutations and molecular characterization of a heterogeneous disorder. *J Inherit Metab Dis* 2010; **33** Suppl 3: S83-S90 [PMID: 20058079 DOI: 10.1007/s10545-009-9026-5]
219 **Goldberg T**, Slonim AE. Nutrition therapy for hepatic glycogen storage diseases. *J Am Diet Assoc* 1993; **93**: 1423-1430 [PMID: 8245377 DOI: 10.1016/0002-8223(93)92246-t]
220 **Szymańska E**, Szymańska S, Truszkowska G, Ciara E, Pronicki M, Shin YS, Podskarbi T, Kępka A, Śpiewak M, Płoski R, Bilińska ZT, Rokicki D. Variable clinical presentation of glycogen storage disease type IV: from severe hepatosplenomegaly to cardiac insufficiency. Some discrepancies in genetic and biochemical abnormalities. *Arch Med Sci* 2018; **14**: 237-247 [PMID: 29379554 DOI: 10.5114/aoms.2018.72246]

221 **Rosenthal P**, Podesta L, Grier R, Said JW, Sher L, Cocjin J, Watanabe F, Vasiliauskas E, van de Velde R, Makowka L. Failure of liver transplantation to diminish cardiac deposits of amylopectin and leukocyte inclusions in type IV glycogen storage disease. *Liver Transpl Surg* 1995; **1**: 373-376 [PMID: 9346615 DOI: 10.1002/Lt.500010607]

222 **Sokal EM**, Van Hoof F, Alberti D, de Ville de Goyet J, de Barsy T, Otte JB. Progressive cardiac failure following orthotopic liver transplantation for type IV glycogenosis. *Eur J Pediatr* 1992; **151**: 200-203 [PMID: 1601012 DOI: 10.1007/BF01954384]

223 **Choi SY**, Kang B, Choe JY, Lee Y, Jang HJ, Park HD, Lee SK, Choe YH. A Case of Glycogen Storage Disease IV with Rare Homozygous Mutations in the Glycogen Branching Enzyme Gene. *Pediatr Gastroenterol Hepatol Nutr* 2018; **21**: 365-368 [PMID: 30345254 DOI: 10.5223/pghn.2018.21.4.365]

224 **Liu M**, Sun LY. Liver Transplantation for Glycogen Storage Disease Type IV. *Front Pediatr* 2021; **9**: 633822 [PMID: 33681109 DOI: 10.3389/fped.2021.633822]

225 **Selby R**, Starzl TE, Yunis E, Brown BI, Kendall RS, Tzakis A. Liver transplantation for type IV glycogen storage disease. *N Engl J Med* 1991; **324**: 39-42 [PMID: 1984162 DOI: 10.1056/NEJM199101033240107]

226 **Starzl TE**, Demetris AJ, Trucco M, Ricordi C, Ildstad S, Terasaki PI, Murase N, Kendall RS, Kocova M, Rudert WA. Chimerism after liver transplantation for type IV glycogen storage disease and type 1 Gaucher's disease. *N Engl J Med* 1993; **328**: 745-749 [PMID: 8437594 DOI: 10.1056/NEJM199303183281101]

227 **Kakhlon O**, Ferreira I, Solmesky LJ, Khazanov N, Lossos A, Alvarez R, Yetil D, Pampou S, Weil M, Senderowitz H, Escriba P, Yue WW, Akman HO. Guaiacol as a drug candidate for treating adult polyglucosan body disease. *JCI Insight* 2018; **3** [PMID: 30185673 DOI: 10.1172/jci.insight.99694]

228 **Kakhlon O**, Vaknin H, Mishra K, D'Souza J, Marisat M, Sprecher U, Wald-Altman S, Dukhovny A, Raviv Y, Da'adoosh B, Engel H, Benhamron S, Nitzan K, Sweetat S, Permyakova A, Mordechai A, Akman HO, Rosenmann H, Lossos A, Tam J, Minassian BA, Weil M. Alleviation of a polyglucosan storage disorder by enhancement of autophagic glycogen catabolism. *EMBO Mol Med* 2021; **13**: e14554 [PMID: 34486811 DOI: 10.15252/emmm.202114554]

229 **Hers HG**. [Enzymatic studies of hepatic fragments; application to the classification of glycogenoses]. *Rev Int Hepatol* 1959; **9**: 35-55 [PMID: 13646331]

230 **Newgard CB**, Hwang PK, Fletterick RJ. The family of glycogen phosphorylases: structure and function. *Crit Rev Biochem Mol Biol* 1989; **24**: 69-99 [PMID: 2667896 DOI: 10.3109/10409238909082552]

231 **Newgard CB**, Fletterick RJ, Anderson LA, Lebo RV. The polymorphic locus for glycogen storage disease VI (liver glycogen phosphorylase) maps to chromosome 14. *Am J Hum Genet* 1987; **40**: 351-364 [PMID: 2883891]

232 **Grünert SC**, Hannibal L, Spiekerkoetter U. The Phenotypic and Genetic Spectrum of Glycogen Storage Disease Type VI. *Genes (Basel)* 2021; **12** [PMID: 34440378 DOI: 10.3390/genes12081205]

233 **Roscher A**, Patel J, Hewson S, Nagy L, Feigenbaum A, Kronick J, Raiman J, Schulze A, Siriwardena K, Mercimek-Mahmutoglu S. The natural history of glycogen storage disease types VI and IX: Long-term outcome from the largest metabolic center in Canada. *Mol Genet Metab* 2014; **113**: 171-176 [PMID: 25266922 DOI: 10.1016/j.ymgme.2014.09.005]

234 **Tang NL**, Hui J, Young E, Worthington V, To KF, Cheung KL, Li CK, Fok TF. A novel mutation (G233D) in the glycogen phosphorylase gene in a patient with hepatic glycogen storage disease and residual enzyme activity. *Mol Genet Metab* 2003; **79**: 142-145 [PMID: 12809646 DOI: 10.1016/s1096-7192(03)00068-4]

235 **Burwinkel B**, Bakker HD, Herschkovitz E, Moses SW, Shin YS, Kilimann MW. Mutations in the liver glycogen phosphorylase gene (PYGL) underlying glycogenosis type VI. *Am J Hum Genet* 1998; **62**: 785-791 [PMID: 9529348 DOI: 10.1086/301790]

236 **Kishnani PS**, Goldstein J, Austin SL, Arn P, Bachrach B, Bali DS, Chung WK, El-Gharbawy A, Brown LM, Kahler S, Pendyal S, Ross KM, Tsilianidis L, Weinstein DA, Watson MS; ACMG Work Group on Diagnosis and Management of Glycogen Storage Diseases Type VI and IX. Diagnosis and management of glycogen storage diseases type VI and IX: a clinical practice resource of the American College of Medical Genetics and Genomics (ACMG). *Genet Med* 2019; **21**: 772-789 [PMID: 30659246 DOI: 10.1038/s41436-018-0364-2]

237 **Luo X**, Duan Y, Fang D, Sun Y, Xiao B, Zhang H, Han L, Liang L, Gong Z, Gu X, Yu Y, Qiu W. Diagnosis and follow-up of glycogen storage disease (GSD) type VI from the largest GSD center in China. *Hum Mutat* 2022; **43**: 557-567 [PMID: 35143115 DOI: 10.1002/humu.24345]

238 **Beauchamp NJ**, Taybert J, Champion MP, Layet V, Heinz-Erian P, Dalton A, Tanner MS, Pronicka E, Sharrard MJ. High frequency of missense mutations in glycogen storage disease type VI. *J Inherit Metab Dis* 2007; **30**: 722-734 [PMID: 17705025 DOI: 10.1007/s10545-007-0499-9]

239 **Brown LM**, Corrado MM, van der Ende RM, Derks TG, Chen MA, Siegel S, Hoyt K, Correia CE, Lumpkin C, Flanagan TB, Carreras CT, Weinstein DA. Evaluation of glycogen storage disease as a cause of ketotic hypoglycemia in children. *J Inherit Metab Dis* 2015; **38**: 489-493 [PMID: 25070466 DOI: 10.1007/s10545-014-9744-1]

240 **Manzia TM**, Angelico R, Toti L, Cillis A, Ciano P, Orlando G, Anselmo A, Angelico M, Tisone G. Glycogen storage disease type Ia and VI associated with hepatocellular carcinoma: two case reports. *Transplant Proc* 2011; **43**: 1181-1183 [PMID: 21620082 DOI: 10.1016/j.transproceed.2011.01.129]

241 **Ogawa A**, Ogawa E, Yamamoto S, Fukuda T, Sugie H, Kohno Y. Case of glycogen storage disease type VI (phosphorylase deficiency) complicated by focal nodular hyperplasia. *Pediatr Int* 2010; **52**: e150-e153 [PMID: 20723115 DOI: 10.1111/j.1442-200X.2010.03073.x]

242 **Lu SQ**, Feng JY, Liu J, Xie XB, Lu Y, Abuduxikuer K. Glycogen storage disease type VI can progress to cirrhosis: ten Chinese patients with GSD VI and a literature review. *J Pediatr Endocrinol Metab* 2020; **33**: 1321-1333 [PMID: 32892177 DOI: 10.1515/jpem-2020-0173]

243 **Tsilianidis LA**, Fiske LM, Siegel S, Lumpkin C, Hoyt K, Wasserstein M, Weinstein DA. Aggressive therapy improves cirrhosis in glycogen storage disease type IX. *Mol Genet Metab* 2013; **109**: 179-182 [PMID: 23578772 DOI: 10.1016/j.ymgme.2013.03.009]

244 **Davidson JJ**, Ozçelik T, Hamacher C, Willems PJ, Francke U, Kilimann MW. cDNA cloning of a liver isoform of the phosphorylase kinase alpha subunit and mapping of the gene to Xp22.2-p22.1, the region of human X-linked liver

glycogenosis. *Proc Natl Acad Sci U S A* 1992; **89**: 2096-2100 [PMID: 1372435 DOI: 10.1073/pnas.89.6.2096]

245 **Brushia RJ**, Walsh DA. Phosphorylase kinase: the complexity of its regulation is reflected in the complexity of its structure. *Front Biosci* 1999; **4**: D618-D641 [PMID: 10487978 DOI: 10.2741/brushia]

246 **Burwinkel B**, Moses SW, Kilimann MW. Phosphorylase-kinase-deficient liver glycogenosis with an unusual biochemical phenotype in blood cells associated with a missense mutation in the beta subunit gene (PHKB). *Hum Genet* 1997; **101**: 170-174 [PMID: 9402963 DOI: 10.1007/s004390050608]

247 **Wüllrich-Schmoll A**, Kilimann MW. Structure of the human gene encoding the phosphorylase kinase beta subunit (PHKB). *Eur J Biochem* 1996; **238**: 374-380 [PMID: 8681948 DOI: 10.1111/j.1432-1033.1996.0374z.x]

248 **Hendrickx J**, Coucke P, Hors-Cayla MC, Smit GP, Shin YS, Deutsch J, Smeitink J, Berger R, Lee P, Fernandes J. Localization of a new type of X-linked liver glycogenosis to the chromosomal region Xp22 containing the liver alpha-subunit of phosphorylase kinase (PHKA2). *Genomics* 1994; **21**: 620-625 [PMID: 7959740 DOI: 10.1006/geno.1994.1322]

249 **Hidaka F**, Sawada H, Matsuyama M, Nunoi H. A novel mutation of the PHKA2 gene in a patient with X-linked liver glycogenosis type 1. *Pediatr Int* 2005; **47**: 687-690 [PMID: 16354226 DOI: 10.1111/j.1442-200x.2005.02131.x]

250 **Cho SY**, Lam CW, Tong SF, Siu WK. X-linked glycogen storage disease IXa manifested in a female carrier due to skewed X chromosome inactivation. *Clin Chim Acta* 2013; **426**: 75-78 [PMID: 24055370 DOI: 10.1016/j.cca.2013.08.026]

251 **Schimke RN**, Zakheim RM, Corder RC, Hug G. Glycogen storage disease type IX: benign glycogenosis of liver and hepatic phosphorylase kinase deficiency. *J Pediatr* 1973; **83**: 1031-1034 [PMID: 4518931 DOI: 10.1016/s0022-3476(73)80544-x]

252 **Willems PJ**, Gerver WJ, Berger R, Fernandes J. The natural history of liver glycogenosis due to phosphorylase kinase deficiency: a longitudinal study of 41 patients. *Eur J Pediatr* 1990; **149**: 268-271 [PMID: 2303074 DOI: 10.1007/BF02106291]

253 **Schippers HM**, Smit GP, Rake JP, Visser G. Characteristic growth pattern in male X-linked phosphorylase-b kinase deficiency (GSD IX). *J Inherit Metab Dis* 2003; **26**: 43-47 [PMID: 12872839 DOI: 10.1023/a:1024071328772]

254 **Burwinkel B**, Amat L, Gray RG, Matsuo N, Muroya K, Narisawa K, Sokol RJ, Vilaseca MA, Kilimann MW. Variability of biochemical and clinical phenotype in X-linked liver glycogenosis with mutations in the phosphorylase kinase PHKA2 gene. *Hum Genet* 1998; **102**: 423-429 [PMID: 9600238 DOI: 10.1007/s004390050715]

255 **Kim JA**, Kim JH, Lee BH, Kim GH, Shin YS, Yoo HW, Kim KM. Clinical, Biochemical, and Genetic Characterization of Glycogen Storage Type IX in a Child with Asymptomatic Hepatomegaly. *Pediatr Gastroenterol Hepatol Nutr* 2015; **18**: 138-143 [PMID: 26157701 DOI: 10.5223/pghn.2015.18.2.138]

256 **Johnson AO**, Goldstein JL, Bali D. Glycogen storage disease type IX: novel PHKA2 missense mutation and cirrhosis. *J Pediatr Gastroenterol Nutr* 2012; **55**: 90-92 [PMID: 21857251 DOI: 10.1097/MPG.0b013e31823276ea]

257 **Rodríguez-Jiménez C**, Santos-Simarro F, Campos-Barros Á, Camarena C, Lledín D, Vallespín E, Del Pozo Á, Mena R, Lapunzina P, Rodríguez-Nóvoa S. A new variant in PHKA2 is associated with glycogen storage disease type IXa. *Mol Genet Metab Rep* 2017; **10**: 52-55 [PMID: 28116244 DOI: 10.1016/j.ymgmr.2017.01.003]

258 **Fernandes SA**, Cooper GE, Gibson RA, Kishnani PS. Benign or not benign? Deep phenotyping of liver Glycogen Storage Disease IX. *Mol Genet Metab* 2020; **131**: 299-305 [PMID: 33317799 DOI: 10.1016/j.ymgme.2020.10.004]

259 **Maichele AJ**, Burwinkel B, Maire I, Søvik O, Kilimann MW. Mutations in the testis/liver isoform of the phosphorylase kinase gamma subunit (PHKG2) cause autosomal liver glycogenosis in the gsd rat and in humans. *Nat Genet* 1996; **14**: 337-340 [PMID: 8896567 DOI: 10.1038/ng1196-337]

260 **Bali DS**, Goldstein JL, Fredrickson K, Rehder C, Boney A, Austin S, Weinstein DA, Lutz R, Boneh A, Kishnani PS. Variability of disease spectrum in children with liver phosphorylase kinase deficiency caused by mutations in the PHKG2 gene. *Mol Genet Metab* 2014; **111**: 309-313 [PMID: 24389071 DOI: 10.1016/j.ymgme.2013.12.008]

261 **Albash B**, Imtiaz F, Al-Zaidan H, Al-Manea H, Banemai M, Allam R, Al-Suheel A, Al-Owain M. Novel PHKG2 mutation causing GSD IX with prominent liver disease: report of three cases and review of literature. *Eur J Pediatr* 2014; **173**: 647-653 [PMID: 24326380 DOI: 10.1007/s00431-013-2223-0]

262 **Burwinkel B**, Shiomi S, Al Zaben A, Kilimann MW. Liver glycogenosis due to phosphorylase kinase deficiency: PHKG2 gene structure and mutations associated with cirrhosis. *Hum Mol Genet* 1998; **7**: 149-154 [PMID: 9384616 DOI: 10.1093/hmg/7.1.149]

263 **Burwinkel B**, Tanner MS, Kilimann MW. Phosphorylase kinase deficient liver glycogenosis: progression to cirrhosis in infancy associated with PHKG2 mutations (H144Y and L225R). *J Med Genet* 2000; **37**: 376-377 [PMID: 10905889 DOI: 10.1136/jmg.37.5.376]

264 **Waheed N**, Saeed A, Ijaz S, Fayyaz Z, Anjum MN, Zahoor Y, Cheema HA. Variability of clinical and biochemical phenotype in liver phosphorylase kinase deficiency with variants in the phosphorylase kinase (PHKG2) gene. *J Pediatr Endocrinol Metab* 2020; **33**: 1117-1123 [PMID: 32697758 DOI: 10.1515/jpem-2019-0603]

265 **Burwinkel B**, Maichele AJ, Aagenaes O, Bakker HD, Lerner A, Shin YS, Strachan JA, Kilimann MW. Autosomal glycogenosis of liver and muscle due to phosphorylase kinase deficiency is caused by mutations in the phosphorylase kinase beta subunit (PHKB). *Hum Mol Genet* 1997; **6**: 1109-1115 [PMID: 9215682 DOI: 10.1093/hmg/6.7.1109]

266 **Degrassi I**, Deheragoda M, Creegen D, Mundy H, Mustafa A, Vara R, Hadzic N. Liver histology in children with glycogen storage disorders type VI and IX. *Dig Liver Dis* 2021; **53**: 86-93 [PMID: 32505569 DOI: 10.1016/j.dld.2020.04.017]

267 **Manz F**, Bickel H, Brodehl J, Feist D, Gellissen K, Geschöll-Bauer B, Gilli G, Harms E, Helwig H, Nützenadel W. Fanconi-Bickel syndrome. *Pediatr Nephrol* 1987; **1**: 509-518 [PMID: 3153325 DOI: 10.1007/BF00849262]

268 **FANCONI G**, BICKEL H. [Chronic aminoaciduria (amino acid diabetes or nephrotic-glucosuric dwarfism) in glycogen storage and cystine disease]. *Helv Paediatr Acta* 1949; **4**: 359-396 [PMID: 15397919]

269 **Saltik-Temizel IN**, Coşkun T, Yüce A, Koçak N. Fanconi-Bickel syndrome in three Turkish patients with different homozygous mutations. *Turk J Pediatr* 2005; **47**: 167-169 [PMID: 16052858]

270 **Fukumoto H**, Seino S, Imura H, Seino Y, Eddy RL, Fukushima Y, Byers MG, Shows TB, Bell GI. Sequence, tissue distribution, and chromosomal localization of mRNA encoding a human glucose transporter-like protein. *Proc Natl Acad Sci U S A* 1988; **85**: 5434-5438 [PMID: 3399500 DOI: 10.1073/pnas.85.15.5434]

271 **Santer R**, Schneppenheim R, Dombrowski A, Götze H, Steinmann B, Schaub J. Mutations in GLUT2, the gene for the liver-type glucose transporter, in patients with Fanconi-Bickel syndrome. *Nat Genet* 1997; **17**: 324-326 [PMID: 9354798 DOI: 10.1038/ng1197-324]

272 **Sharari S**, Kabeer B, Mohammed I, Haris B, Pavlovski I, Hawari I, Bhat AA, Toufiq M, Tomei S, Mathew R, Syed N, Nisar S, Maacha S, Grivel JC, Chaussabel D, Ericsson J, Hussain K. Understanding the Role of GLUT2 in Dysglycemia Associated with Fanconi-Bickel Syndrome. *Biomedicines* 2022; **10** [PMID: 36140215 DOI: 10.3390/biomedicines10092114]

273 **Mohandas Nair K**, Sakamoto O, Jagadeesh S, Nampoothiri S. Fanconi-Bickel syndrome. *Indian J Pediatr* 2012; **79**: 112-114 [PMID: 21327337 DOI: 10.1007/s12098-011-0373-5]

274 **Aperia A**, Bergqvist G, Linné T, Zetterström R. Familial Fanconi syndrome with malabsorption and galactose intolerance, normal kinase and transferase activity. A report on two siblings. *Acta Paediatr Scand* 1981; **70**: 527-533 [PMID: 6274135 DOI: 10.1111/j.1651-2227.1981.tb05735.x]

275 **Afroze B**, Chen M. Fanconi-Bickel Syndrome: Two Pakistani Patients Presenting with Hypophosphatemic Rickets. *J Pediatr Genet* 2016; **5**: 161-166 [PMID: 27617158 DOI: 10.1055/s-0036-1584360]

276 **Massese M**, Tagliaferri F, Dionisi-Vici C, Maiorana A. Glycogen storage diseases with liver involvement: a literature review of GSD type 0, IV, VI, IX and XI. *Orphanet J Rare Dis* 2022; **17**: 241 [PMID: 35725468 DOI: 10.1186/s13023-022-02387-6]

277 **Govindarajan S**, Khandelwal P, Sharma S, Agarwala A, Sinha A, Hari P, Bagga A. Clinical Features and Genetic Sequencing of Children with Fanconi-Bickel Syndrome. *Indian J Pediatr* 2023; **90**: 178-180 [PMID: 36324017 DOI: 10.1007/s12098-022-04372-0]

278 **Furlan F**, Santer R, Vismara E, Santus F, Sersale G, Menni F, Parini R. Bilateral nuclear cataracts as the first neonatal sign of Fanconi-Bickel syndrome. *J Inherit Metab Dis* 2006; **29**: 685 [PMID: 16906471 DOI: 10.1007/s10545-006-0385-x]

279 **Sharari S**, Abou-Alloul M, Hussain K, Ahmad Khan F. Fanconi-Bickel Syndrome: A Review of the Mechanisms That Lead to Dysglycaemia. *Int J Mol Sci* 2020; **21** [PMID: 32877990 DOI: 10.3390/ijms21176286]

280 **Demirbilek H**, Galcheva S, Vuralli D, Al-Khawaga S, Hussain K. Ion Transporters, Channelopathies, and Glucose Disorders. *Int J Mol Sci* 2019; **20** [PMID: 31137773 DOI: 10.3390/ijms20102590]

281 **Müller D**, Santer R, Krawinkel M, Christiansen B, Schaub J. Fanconi-Bickel syndrome presenting in neonatal screening for galactosaemia. *J Inherit Metab Dis* 1997; **20**: 607-608 [PMID: 9266402 DOI: 10.1023/a:1005375629820]

282 **Lee PJ**, Van't Hoff WG, Leonard JV. Catch-up growth in Fanconi-Bickel syndrome with uncooked cornstarch. *J Inherit Metab Dis* 1995; **18**: 153-156 [PMID: 7564233 DOI: 10.1007/BF00711753]

283 **Pennisi A**, Maranda B, Benoist JF, Baudouin V, Rigal O, Pichard S, Santer R, Romana Lepri F, Novelli A, Ogier de Baulny H, Dionisi-Vici C, Schiff M. Nocturnal enteral nutrition is therapeutic for growth failure in Fanconi-Bickel syndrome. *J Inherit Metab Dis* 2020; **43**: 540-548 [PMID: 31816104 DOI: 10.1002/jimd.12203]

284 **Haines JL**, Ozelius LJ, McFarlane H, Menon A, Tzall S, Martiniuk F, Hirschhorn R, Gusella JF. A genetic linkage map of chromosome 17. *Genomics* 1990; **8**: 1-6 [PMID: 2081586 DOI: 10.1016/0888-7543(90)90218-j]

285 **De Filippi P**, Saeidi K, Ravaglia S, Dardis A, Angelini C, Mongini T, Morandi L, Moggio M, Di Muzio A, Filosto M, Bembi B, Giannini F, Marrosu G, Rigoldi M, Tonin P, Servidei S, Siciliano G, Carlucci A, Scotti C, Comelli M, Toscano A, Danesino C. Genotype-phenotype correlation in Pompe disease, a step forward. *Orphanet J Rare Dis* 2014; **9**: 102 [PMID: 25103075 DOI: 10.1186/s13023-014-0102-z]

286 **Leslie N**, Bailey L. Pompe Disease. 2007 Aug 31. In: GeneReviews® [Internet]. Seattle (WA): University of Washington, Seattle; 1993– [PMID: 20301438]

287 **Makos MM**, McComb RD, Hart MN, Bennett DR. Alpha-glucosidase deficiency and basilar artery aneurysm: report of a sibship. *Ann Neurol* 1987; **22**: 629-633 [PMID: 3322184 DOI: 10.1002/ana.410220512]

288 **Amartino H**, Painceira D, Pomponio RJ, Niizawa G, Sabio Paz V, Blanco M, Chamoles N. Two clinical forms of glycogen-storage disease type II in two generations of the same family. *Clin Genet* 2006; **69**: 187-188 [PMID: 16433701 DOI: 10.1111/j.1399-0004.2005.00557.x]

289 **Karabul N**, Berndt J, Kornblum C, Kley RA, Wenninger S, Tiling N, Mengel E, Plöckinger U, Vorgerd M, Deschauer M, Schoser B, Hanisch F. Pregnancy and delivery in women with Pompe disease. *Mol Genet Metab* 2014; **112**: 148-153 [PMID: 24726296 DOI: 10.1016/j.ymgme.2014.03.010]

290 **Amalfitano A**, Bengur AR, Morse RP, Majure JM, Case LE, Veerling DL, Mackey J, Kishnani P, Smith W, McVie-Wylie A, Sullivan JA, Hoganson GE, Phillips JA 3rd, Schaefer GB, Charrow J, Ware RE, Bossen EH, Chen YT. Recombinant human acid alpha-glucosidase enzyme therapy for infantile glycogen storage disease type II: results of a phase I/II clinical trial. *Genet Med* 2001; **3**: 132-138 [PMID: 11286229]

291 **Dhillon S**. Avalglucosidase alfa: First Approval. *Drugs* 2021; **81**: 1803-1809 [PMID: 34591286 DOI: 10.1007/s40265-021-01600-3]

292 **van der Ploeg AT**, Kruijshaar ME, Toscano A, Laforêt P, Angelini C, Lachmann RH, Pascual Pascual SI, Roberts M, Rösler K, Stulnig T, van Doorn PA, Van den Bergh PYK, Vissing J, Schoser B; European Pompe Consortium. European consensus for starting and stopping enzyme replacement therapy in adult patients with Pompe disease: a 10-year experience. *Eur J Neurol* 2017; **24**: 768-e31 [PMID: 28477382 DOI: 10.1111/ene.13285]

293 **Zhou Z**, Austin GL, Shaffer R, Armstrong DD, Gentry MS. Antibody-Mediated Enzyme Therapeutics and Applications in Glycogen Storage Diseases. *Trends Mol Med* 2019; **25**: 1094-1109 [PMID: 31522955 DOI: 10.1016/j.molmed.2019.08.005]

294 **Umapathysivam K**, Whittle AM, Ranieri E, Bindloss C, Ravenscroft EM, van Diggelen OP, Hopwood JJ, Meikle PJ. Determination of acid alpha-glucosidase protein: evaluation as a screening marker for Pompe disease and other lysosomal storage disorders. *Clin Chem* 2000; **46**: 1318-1325 [PMID: 10973860]

295 **Cohen JL**, Chakraborty P, Fung-Kee-Fung K, Schwab ME, Bali D, Young SP, Gelb MH, Khaledi H, DiBattista A, Smallshaw S, Moretti F, Wong D, Lacroix C, El Demellawy D, Strickland KC, Lougheed J, Moon-Grady A, Lianoglou BR, Harmatz P, Kishnani PS, MacKenzie TC. In Utero Enzyme-Replacement Therapy for Infantile-Onset Pompe's

Disease. *N Engl J Med* 2022; **387**: 2150-2158 [PMID: 36351280 DOI: 10.1056/NEJMoa2200587]

296 **van Kooten HA**, Ditters IAM, Hoogeveen-Westerveld M, Jacobs EH, van den Hout JMP, van Doorn PA, Pijnappel WWMP, van der Ploeg AT, van der Beek NAME. Antibodies against recombinant human alpha-glucosidase do not seem to affect clinical outcome in childhood onset Pompe disease. *Orphanet J Rare Dis* 2022; **17**: 31 [PMID: 35109913 DOI: 10.1186/s13023-022-02175-2]

297 **Rovelli V**, Zuvadelli J, Piotto M, Scopari A, Dionigi AR, Ercoli V, Paci S, Cefalo G, Salvatici E, Banderali G. L-alanine supplementation in Pompe disease (IOPD): a potential therapeutic implementation for patients on ERT? A case report. *Ital J Pediatr* 2022; **48**: 48 [PMID: 35346323 DOI: 10.1186/s13052-022-01249-y]

298 **Ronzitti G**, Collaud F, Laforet P, Mingozzi F. Progress and challenges of gene therapy for Pompe disease. *Ann Transl Med* 2019; **7**: 287 [PMID: 31392199 DOI: 10.21037/atm.2019.04.67]

299 **Nascimbeni AC**, Fanin M, Angelini C, Sandri M. Autophagy dysregulation in Danon disease. *Cell Death Dis* 2017; **8**: e2565 [PMID: 28102838 DOI: 10.1038/cddis.2016.475]

300 **Cenacchi G**, Papa V, Pegoraro V, Marozzo R, Fanin M, Angelini C. Review: Danon disease: Review of natural history and recent advances. *Neuropathol Appl Neurobiol* 2020; **46**: 303-322 [PMID: 31698507 DOI: 10.1111/nan.12587]

301 **Komurcu-Bayrak E**, Kalkan MA, Coban N, Ozsait-Selcuk B, Bayrak F. Identification of the pathogenic effects of missense variants causing PRKAG2 cardiomyopathy. *Arch Biochem Biophys* 2022; **727**: 109340 [PMID: 35787834 DOI: 10.1016/j.abb.2022.109340]

302 **Wilkins JL**. Challenges and Opportunities Created by the COVID-19 Pandemic. *J Nutr Educ Behav* 2020; **52**: 669-670 [PMID: 32646596 DOI: 10.1016/j.jneb.2020.05.005]

303 **Akman HO**, Sampayo JN, Ross FA, Scott JW, Wilson G, Benson L, Bruno C, Shanske S, Hardie DG, Dimauro S. Fatal infantile cardiac glycogenosis with phosphorylase kinase deficiency and a mutation in the gamma2-subunit of AMP-activated protein kinase. *Pediatr Res* 2007; **62**: 499-504 [PMID: 17667862 DOI: 10.1203/PDR.0b013e3181462b86]

304 **Lebo RV**, Anderson LA, DiMauro S, Lynch E, Hwang P, Fletterick R. Rare McArdle disease locus polymorphic site on 11q13 contains CpG sequence. *Hum Genet* 1990; **86**: 17-24 [PMID: 1701414 DOI: 10.1007/BF00205166]

305 **Scalco RS**, Lucia A, Santalla A, Martinuzzi A, Vavla M, Reni G, Toscano A, Musumeci O, Voermans NC, Kouwenberg CV, Laforêt P, San-Millán B, Vieitez I, Siciliano G, Kühnle E, Trost R, Sacconi S, Stemmerik MG, Durmus H, Kierdaszuk B, Wakelin A, Andreu AL, Pinós T, Marti R, Quinlivan R, Vissing J; EUROMAC Consortium. Data from the European registry for patients with McArdle disease and other muscle glycogenoses (EUROMAC). *Orphanet J Rare Dis* 2020; **15**: 330 [PMID: 33234167 DOI: 10.1186/s13023-020-01562-x]

306 **Pizzamiglio C**, Mahroo OA, Khan KN, Patasin M, Quinlivan R. Phenotype and genotype of 197 British patients with McArdle disease: An observational single-centre study. *J Inherit Metab Dis* 2021; **44**: 1409-1418 [PMID: 34534370 DOI: 10.1002/jimd.12438]

307 **Lucia A**, Martinuzzi A, Nogales-Gadea G, Quinlivan R, Reason S; International Association for Muscle Glycogen Storage Disease study group. Clinical practice guidelines for glycogen storage disease V & VII (McArdle disease and Tarui disease) from an international study group. *Neuromuscul Disord* 2021; **31**: 1296-1310 [PMID: 34848128 DOI: 10.1016/j.nmd.2021.10.006]

308 **Echaniz-Laguna A**, Lornage X, Laforêt P, Orngreen MC, Edelweiss E, Brochier G, Bui MT, Silva-Rojas R, Birck C, Lannes B, Romero NB, Vissing J, Laporte J, Böhm J. A New Glycogen Storage Disease Caused by a Dominant PYGM Mutation. *Ann Neurol* 2020; **88**: 274-282 [PMID: 32386344 DOI: 10.1002/ana.25771]

309 **Howard TD**, Akots G, Bowden DW. Physical and genetic mapping of the muscle phosphofructokinase gene (PFKM): reassignment to human chromosome 12q. *Genomics* 1996; **34**: 122-127 [PMID: 8661033 DOI: 10.1006/geno.1996.0250]

310 **Wehner M**, Clemens PR, Engel AG, Kilimann MW. Human muscle glycogenosis due to phosphorylase kinase deficiency associated with a nonsense mutation in the muscle isoform of the alpha subunit. *Hum Mol Genet* 1994; **3**: 1983-1987 [PMID: 7874115 DOI: 10.1093/hmg/3.11.1983]

311 **Huang K**, Duan HQ, Li QX, Luo YB, Bi FF, Yang H. Expanding the clinicopathological-genetic spectrum of glycogen storage disease type IXd by a Chinese neuromuscular center. *Front Neurol* 2022; **13**: 945280 [PMID: 36034300 DOI: 10.3389/fneur.2022.945280]

312 **Nayab A**, Alam Q, Alzahrani OR, Khan R, Sarfaraz S, Albaz AA, Rafeeq MM, Sain ZM, Waqas A, Umair M. Targeted exome sequencing identified a novel frameshift variant in the PGAM2 gene causing glycogen storage disease type X. *Eur J Med Genet* 2021; **64**: 104283 [PMID: 34237446 DOI: 10.1016/j.ejmg.2021.104283]

313 **Kanno T**, Sudo K, Takeuchi I, Kanda S, Honda N, Nishimura Y, Oyama K. Hereditary deficiency of lactate dehydrogenase M-subunit. *Clin Chim Acta* 1980; **108**: 267-276 [PMID: 7449146 DOI: 10.1016/0009-8981(80)90013-3]

314 **Maekawa M**, Sudo K, Kanno T, Li SS. Molecular characterization of genetic mutation in human lactate dehydrogenase-A (M) deficiency. *Biochem Biophys Res Commun* 1990; **168**: 677-682 [PMID: 2334430 DOI: 10.1016/0006-291x(90)92374-9]

315 **Santoro L**, Pjetraj D, Velmishi V, Campana C, Catassi C, Dionisi-Vici C, Maiorana A. A new phenotype of aldolase a deficiency in a 14 year-old boy with epilepsy and rhabdomyolysis - case report. *Ital J Pediatr* 2022; **48**: 39 [PMID: 35246226 DOI: 10.1186/s13052-022-01228-3]

316 **Kukita A**, Yoshida MC, Fukushige S, Sakakibara M, Joh K, Mukai T, Hori K. Molecular gene mapping of human aldolase A (ALDOA) gene to chromosome 16. *Hum Genet* 1987; **76**: 20-26 [PMID: 3570299 DOI: 10.1007/BF00283044]

317 **Comi GP**, Fortunato F, Lucchiari S, Bordoni A, Prelle A, Jann S, Keller A, Ciscato P, Galbiati S, Chiveri L, Torrente Y, Scarlato G, Bresolin N. Beta-enolase deficiency, a new metabolic myopathy of distal glycolysis. *Ann Neurol* 2001; **50**: 202-207 [PMID: 11506403 DOI: 10.1002/ana.1095]

318 **Moslemi AR**, Lindberg C, Nilsson J, Tajsharghi H, Andersson B, Oldfors A. Glycogenin-1 deficiency and inactivated priming of glycogen synthesis. *N Engl J Med* 2010; **362**: 1203-1210 [PMID: 20357282 DOI: 10.1056/NEJMoa0900661]

World Journal of Gastroenterology

Submit a Manuscript: https://www.f6publishing.com

World J Gastroenterol 2023 July 7; 29(25): 3964-3983

DOI: 10.3748/wjg.v29.i25.3964

ISSN 1007-9327 (print) ISSN 2219-2840 (online)

REVIEW

Past, present, and future of long-term treatment for hepatitis B virus

Teresa Broquetas, José A Carrión

Specialty type: Gastroenterology and hepatology

Provenance and peer review: Invited article; Externally peer reviewed.

Peer-review model: Single blind

Peer-review report's scientific quality classification

Grade A (Excellent): A
Grade B (Very good): B
Grade C (Good): 0
Grade D (Fair): 0
Grade E (Poor): 0

P-Reviewer: Gupta T, India; Korkmaz P, Turkey

Received: March 27, 2023
Peer-review started: March 27, 2023
First decision: May 12, 2023
Revised: May 22, 2023
Accepted: June 6, 2023
Article in press: June 6, 2023
Published online: July 7, 2023

Teresa Broquetas, José A Carrión, Liver Section, Gastroenterology Department, Hospital del Mar, Barcelona 08003, Spain

Teresa Broquetas, José A Carrión, Institut Hospital del Mar D'Investigacions Mèdiques, PSMAR, Barcelona 08003, Spain

José A Carrión, Universitat Pompeu Fabra, Facultat de Ciències de la Salut i de la Vida, Barcelona 08003, Spain

Corresponding author: José A Carrión, Doctor, MD, PhD, Assistant Professor, Liver Section, Gastroenterology Department, Hospital del Mar, 25-29 Passeig Marítim, Barcelona 08003, Spain. jcarrion@psmar.cat

Abstract

The estimated world prevalence of hepatitis B virus (HBV) infection is 316 million. HBV infection was identified in 1963 and nowadays is a major cause of cirrhosis and hepatocellular carcinoma (HCC) despite universal vaccination programs, and effective antiviral therapy. Long-term administration of nucleos(t)ide analogues (NA) has been the treatment of choice for chronic hepatitis B during the last decades. The NA has shown a good safety profile and high efficacy in controlling viral replication, improving histology, and decreasing the HCC incidence, decompensation, and mortality. However, the low probability of HBV surface antigen seroclearance made necessary an indefinite treatment. The knowledge, in recent years, about the different phases of the viral cycle, and the new insights into the role of the immune system have yielded an increase in new therapeutic approaches. Consequently, several clinical trials evaluating combinations of new drugs with different mechanisms of action are ongoing with promising results. This integrative literature review aims to assess the knowledge and major advances from the past of hepatitis B, the present of NA treatment and withdrawal, and the future perspectives with combined molecules to achieve a functional cure.

Key Words: Hepatitis B; Therapy; Antigen; Functional cure; Antiviral agents; Drug development

©The Author(s) 2023. Published by Baishideng Publishing Group Inc. All rights reserved.

Core Tip: Treatment for chronic hepatitis B has been used for decades, showing a good safety profile and high virological and clinical efficacy, decreasing hepatocellular carcinoma, clinical decompensation, and mortality. However, the low probability of hepatitis B virus surface antigen seroclearance with therapy made necessary indefinite treatment in a majority of patients. With the new insights about the immune system role in hepatitis B virus infection and the knowledge of the viral cycle phases, there has been in recent years increased activity in new therapeutic approaches. This review focuses on the past, present, and future of chronic hepatitis B therapy.

Citation: Broquetas T, Carrión JA. Past, present, and future of long-term treatment for hepatitis B virus. *World J Gastroenterol* 2023; 29(25): 3964-3983
URL: https://www.wjgnet.com/1007-9327/full/v29/i25/3964.htm
DOI: https://dx.doi.org/10.3748/wjg.v29.i25.3964

INTRODUCTION

The hepatitis B virus (HBV) was identified in 1963 when the modern research history of viral hepatitis began. The Nobel Prize winner Baruch S. Blumberg (1925-2011) discovered, 60 years ago, an enigmatic serum protein named "Australia" antigen (AuAg)[1]. Some years later, the recognition of the HBV surface antigen (HBsAg) allowed for the first-time screening of blood donors. The HBsAg was the first marker assessed by a highly sensitive immune analysis, the HBV genome the first identified by deoxyribonucleic acid (DNA), the antibody against HBV core (anti-HBc) the first evaluated by the anti-μ capture technique, and the HBV vaccine the first produced by gene technology[2].

Infection by HBV may lead to acute or chronic hepatitis. Chronic hepatitis B (CHB) infection is defined as HBsAg serum detection for at least six months. The estimated world prevalence of CHB was 316 million in 2019, a major cause of cirrhosis and hepatocellular carcinoma (HCC)[3]. The treatment of choice during the last decades has been the long-term administration of nucleos(t)ide analogues (NA) with a high barrier to resistance. However, the low probability of HBsAg seroclearance made necessary an indefinite therapy.

This integrative literature review aims to review the major advances from the past of hepatitis B, the present of NA treatment and withdrawal, and the future perspectives for the new combined molecules to achieve a functional cure.

PAST

Virus detection: The "Australia" antigen and "Dane" particle

In the 1960s, virology was a young science, and techniques for the diagnosis of most viral diseases were complicated and suboptimal. The most often used method was the complement fixation reaction, which required four complex biological component mixtures from four different animal species. The first hint came from the American physician and geneticist Baruch S. Blumberg who used an immunological approach in 1967[1]. Blumberg's co-worker, Harvey J. Alter, discovered a new antigen in Australian aborigines named the AuAg.

Dane *et al*[4] were inspecting AuAg immune complexes under the electron microscope and identified virus-like particles of 42 nm in size. In 1971, Almeida *et al*[5] were able to free the core particles from the "Dane" particle and showed that patients formed, against this core antigen (HBcAg), antibodies (anti-HBc) suggesting that the Dane particle was the cause of hepatitis B, and the AuAg was the surface antigen of the HBV envelope (HBsAg)[5].

Many scientists, including Blumberg, recognized that the HBsAg did not allow to assess the severity of the disease. Magnius *et al*[6] discovered an additional marker when looking for HBsAg subtypes, the HB e antigen (HBeAg), which helped to distinguish highly infectious from less infectious HBV carriers. However, direct detection of the nucleic acid within HBV was not possible at that time since the HBV still could not be grown in cell cultures, and patient sera contained a few nanograms of Dane particles/mL. It was in 1974 when Robinson *et al*[7] identified the polymerase activity, and the HBV-DNA. The nucleic acid of HBV was a small circular double-stranded DNA but not covalently closed such as the polyoma- or papillomaviruses. Therefore, the ability of the HBV-DNA polymerase to transcribe both RNA and DNA was similar to retroviruses[2,8].

After more than half a century, current international guidelines have recommended using these three viral markers, HBsAg, HBeAg, and HBV-DNA for characterizing HBV infection[9-11].

Hepadnaviral life cycle: The journey of Dane particle

HBV is a partially double-stranded virus that belongs to the *Hepadnaviridae* family[12]. The virus replicates in the host's hepatocytes. The first step is viral cell entry *via* the bile acid transporter sodium taurocholate cotransporting polypeptide (NTCP)[13,14]. The HBV is transported to the nucleus to release the relaxed circular DNA (rcDNA) genome[15] and becomes a covalently closed circular DNA (cccDNA) that uses the host-cell DNA repair mechanism and can serve as a template for all viral transcripts that are translated into viral proteins. The HBV genome can be integrated into the host genome with the risk of hepatocyte transformation and carcinogenesis[16]. The pre-genomic RNA (pgRNA) is packaged and reversely transcribed to begin replication. The pgRNA is also enveloped and secreted. The HBV-integrated DNA encodes three HBsAg proteins: Large (L), middle (M), and small (S) HBs which are especially important in HBeAg-negative patients[17]. The viral capsids will be enveloped with the HBsAg and released as infectious virions, non-infectious sub-viral spherical or filamentous particles[18], empty virions (HBsAg and core proteins), and RNA virions[19]. The role of subviral particles in the pathogenesis of chronic HBV infection is not fully understood, but they could act as an immune evasion mechanism by blocking the host's neutralizing antibodies (anti-HBs) and promoting the spread and persistence of the infection[20,21].

Pathogenesis and phases of HBV infection

The first step in HBV infection is a highly replicative phase before immune recognition begins, after weeks or months of delay. A vigorous cellular immune response suppresses viral replication and eliminates most of the HBV-infected hepatocytes resulting in acute hepatitis. During acute hepatitis B, HBsAg disappears within six months. If HBsAg persist longer than this period, is considered a CHB infection. CHB is a dynamic interaction between HBV and the host's immune system.

Infection of newborns or infants results in a persistent infection because of an ineffective immune response. After a long anergic phase, immune defense emerges and leads to the selection of escape mutants. The cellular immune responses against HBcAg appear and HBeAg loses its immunomodulatory function. Therefore, the HBeAg-positive chronic infection usually occurs in younger patients during the first years. Patients have a high viral load with normal liver function tests. The HBeAg-negative chronic infection is characterized by low levels of HBV-DNA with normal liver function and without significant fibrosis. Generally, treatment is not recommended in these two phases, but guidelines advocate treating older than 30-40 years HBeAg-positive patients[9-11]. Chronic hepatitis, defined by the elevation of transaminases and high viral load, induces liver fibrosis progression to cirrhosis and risk of developing HCC, being antiviral treatment recommended in these phases (Figure 1).

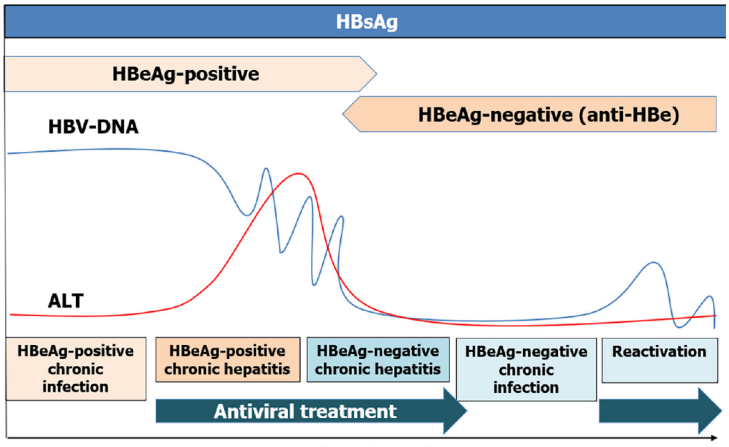
Antiviral treatments: Interferon and nucleos(t)ide analogues

In 1976, William Robinson and Thomas Merigan reported that interferon alpha suppressed HBV replication and cured some patients suffering from CHB[22]. However, further clinical studies showed that only a minority of the patients achieved the clearance of HBsAg while the majority showed a viral breakthrough under treatment or a relapse after the end of therapy (EoT). Conventional interferon alpha was approved in 1992 and one year later Wong *et al*[23] demonstrated an HBeAg loss rate of 33%. Efficacy in HBeAg-negative patients was very limited and only 15% to 25% showed a sustained biochemical response after 12 mo of treatment[24]. In 2005, pegylated interferon (Peg-IFN) replaced the standard form due to its improved pharmacokinetics and prolonged half-life. In HBeAg-positive patients, 12 mo of therapy achieved the sustained response (HBeAg loss with HBV-DNA < 2000 IU/mL, 6 mo after therapy) in 20% to 30% and the HBsAg loss in 3% to 7%[25]. The Peg-IFN therapy has important disadvantages, its high variability of response and its unfavorable safety profile with a significant number of patients ineligible or unwilling.

In 1995, Benhamou *et al*[26] reported that HIV-co-infected patients with HBV who received the HIV drug named lamivudine (LAM) lost their HBV-DNA and improved their hepatitis (Figure 2). The same year Jules Dienstag showed the efficacy and safety of LAM in HBV-mono-infected patients[27]. LAM was well tolerated, but resistance soon developed in cases with high replication. After 5 years of therapy, 75% of the LAM-treated patients developed resistant HBV variants. The acyclic nucleotide analog adefovir (ADV) was approved in 2002 for LAM-resistant CHB patients. Unfortunately, its activity was relatively low and was rapidly replaced by the newer drug named tenofovir (TDF). This very similar drug was approved in 2001 for HIV and in 2008 for HBV[28]. The guanosine analog entecavir (ETV) was originally developed against the herpes simplex virus. In 1997, ETV showed its strong activity against HBV in the HepG2.2.15 cell line. In 2001, showed its efficacy in LAM-resistant CHB patients, and in 2005, it was approved over LAM[29]. In 2006, a synthetic thymidine nucleoside analogue named telbivudine (LdT) was approved but its activity was relatively low and was rapidly replaced. In 2015, the prodrug of TDF, tenofovir alafenamide (TAF), was approved for older patients with lower eGFR or lower bone mineral density[30,31].

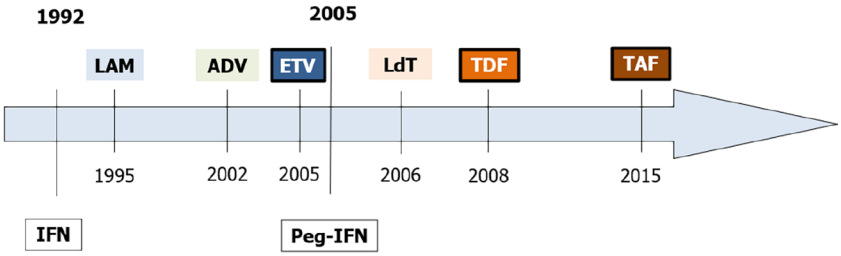
Safety of long-term treatments

The safety profile of NA is very good even in HBV-infected patients with decompensated liver disease,



DOI: 10.3748/wjg.v29.i25.3964 **Copyright** ©The Author(s) 2023.

Figure 1 Phases of hepatitis B virus infection. The persistence of hepatitis B virus surface antigen longer than six months is considered a marker for chronic hepatitis B infection. The HB e antigen (HBeAg)-positive chronic infection occurs in younger patients with high viral load and normal liver function tests. In contrast, HBeAg-negative chronic infection is characterized by low levels of hepatitis B virus-DNA with normal liver function and without fibrosis. Generally, treatment is not recommended in these two phases. Chronic hepatitis is defined by the presence of transaminases and high viral load that can induce liver fibrosis and risk of developing hepatocellular carcinoma, being antiviral treatment recommended[9-11]. HBV: Hepatitis B virus; HBeAg: Hepatitis B e antigen; ALT: Alanine aminotransferase.



DOI: 10.3748/wjg.v29.i25.3964 **Copyright** ©The Author(s) 2023.

Figure 2 Hepatitis B virus antiviral treatment history. The figure shows the United States Food and Drug Administration approval dates for hepatitis B virus drugs. IFN: Interferon; Peg-IFN: Pegylated interferon; LAM: Lamivudine; ADV: Adefovir; TDF: Tenofovir; ETV: Entecavir; LdT: Telbivudine; TAF: Tenofovir alafenamide.

liver transplants, extrahepatic manifestations, acute hepatitis, or severe exacerbation[32,33]. However, NA inhibits the HBV polymerase activity only during the time of administration. Long-term therapy with NA can produce a decline in bone mineral density and renal tubular dysfunction[34].

TDF and ETV have renal metabolism and must be adjusted if patients have an estimated glomerular filtration rate (eGFR) of less than 50 mL/min per 1.73 m^2. A multicenter retrospective study including 6189 CHB patients treated with TDF (n = 2482) or ETV (n = 3707) showed that TDF was associated with a higher risk of worsening renal function (adjusted HR 1.26, 95%CI 1.11-1.43)[35]. A systematic review and meta-analysis showed that TDF and ETV can affect renal function and patients with cirrhosis under TDF had a higher risk of renal damage and hypophosphatemia[36]. The effects of TDF on bone mineral density are suspected to be related to an increased tubular phosphate metabolism, but with few clinical implications as they appear to be reversible after withdrawal[34]. Recently, it has been shown an improvement in bone density and renal function in patients previously treated with TDF after switching to TAF[37]. However, TAF is not approved in very low eGFR (below 15 mL/min per 1.73 m^2).

Even if side effects of NA are scarce, CHB patients usually start treatment at young ages, and with NA treatment, they may be treated for decades. Therefore, questions on NA treatment duration and withdrawal have been gaining interest in recent years.

PRESENT

Monitoring HBV infection: Quantification of HBsAg levels

Classically, three viral markers have been used to characterize HBV infection: (1) The qualitative HBsAg; (2) the HBeAg; and (3) the HBV-DNA. However, most patients under NA treatment have

undetectable HBV-DNA and normal alanine aminotransferase (ALT). Therefore, other biomarkers are needed to monitor antiviral activity. The quantified HBsAg is one of the most extensively studied biomarkers because HBsAg negativization, spontaneously or with treatment, has been related to a good prognosis[38]. It has been shown that the decline in HBsAg levels during NA therapy is very slow (around 0.1 Log IU/mL per year)[39-41] suggesting that it would take decades, even long life, to achieve the HBsAg loss[42,43]. Importantly, some patients have shown a faster and larger HBsAg decline during NA therapy achieving low HBsAg levels[41,43]. Importantly, low HBsAg levels after NA withdrawal (below 1000 in Caucasian and below 100 in Asian patients) can be predictors of HBsAg seroclearance[44-47].

Efficacy of long-term antiviral therapy

The NA can be classified as low (LAM, ADV, and LdT) or high (ETV, TDF, and TAF) barrier of resistance. Current international guidelines recommend the use of NA with a high barrier of resistance to prevent the progression of liver disease, decompensation of cirrhosis, the need for liver transplantation, the development of HCC and to improve survival[9-11].

The suppression of HBV-DNA to undetectable levels (virological response) is normally associated with a normalization of transaminases (biochemical response) and an improvement in survival. In the presence of cirrhosis, all patients with detectable HBV-DNA should be treated[9-11]. Indications for HBeAg-positive and HBeAg-negative CHB patients' treatment are generally based on the combination of three main criteria: Liver disease severity, HBV-DNA units, and ALT levels[9-11].

In HBeAg-positive CHB patients, long-term NA therapy can induce HBeAg loss and seroconversion, leading to a low replicative phase with partial immune control[9-11]. In these patients, antiviral treatment with ETV has demonstrated a 5 years cumulative probability with a virological response of 99%, HBeAg loss of 53%, but HBsAg loss of only 1.4%[48]. Similarly, TDF for 10 years has demonstrated an HBeAg loss of 52% but only a 4.9% of HBsAg loss[33].

In HBeAg-negative patients, the 5-year cumulative probability with ETV of virological response was 96%, although HBsAg loss was only achieved in 4.6%[32]. In the TDF registry study with patients treated for 10 years, 100% achieved a virological response, and 83% biochemical response, but only 3.4% succeeded in the HBsAg loss[33].

Similar rates of virological response have been described for TAF in HBeAg-positive[30] and HBeAg-negative patients[31].

This high efficacy in controlling viral replication causes histological and elastographic improvement. The long-term treatment with NA has shown a significant regression of liver fibrosis and even cirrhosis. A study with paired liver biopsies, after a median time of 6 years, in 57 patients receiving ETV[49] showed histological improvement (decrease ≥ 2 points in the Knodell necroinflammatory score) in 96% of patients, and fibrosis improvement (decrease ≥ 1 point in the Ishak fibrosis score) in 88% of them. In a trial with TDF[50], including 348 patients with paired liver biopsies (at baseline and week 240), 87% showed histological improvement and 51% fibrosis regression (decrease ≥ 1 point in the Ishak fibrosis score). Among the 96 patients with cirrhosis at baseline, 74% achieved some degree of fibrosis regression.

A decrease in liver stiffness measurement (LSM) after long-term treatment with NA has been described[51]. After treatment initiation, the LSM decline is faster mainly related to the improvement in necroinflammatory activity. After 6 mo of therapy, the following LSM decrease is slower and could be associated with a true improvement of fibrosis[52,53].

The most important outcome of antiviral therapy is to improve survival. Studies comparing untreated and ETV-treated patients demonstrated that antiviral therapy reduced the incidence of liver-related complications, HCC, and mortality[54,55]. Similarly, a multicenter study in TDF-treated patients with cirrhosis showed a reduced risk of developing, clinical decompensation, HCC or liver transplantation, and death compared to untreated patients[56]. However, patients treated with NA, are still in danger of developing HCC, and high-risk patients stratified by risk scores such as REACH-B or PAGE-B, should continue HCC surveillance[57].

In recent years there has been a debate about the effect of the two main NA on HCC risk. Some data suggest that TDF is associated with significantly lower HCC risk compared to ETV in Asian patients [58]. A Chinese study including 29350 patients, showed a reduced HCC incidence in patients receiving TDF. However, there were differences in HCC risk factors between groups: TDF-treated patients were younger, and more frequently HBeAg-positive, females, without cirrhosis, and without diabetes. Thus, only 1% of patients with cirrhosis had received TDF[59]. Similarly, a recent meta-analysis of individual data including 42939 patients receiving TDF (n = 6979) or ETV (n = 35960) monotherapy, showed a lower risk of HCC with TDF, especially in patients older ≥ than 50, males, HBeAg-positive, and non-diabetic subgroups[60]. In contrast, other studies have failed to demonstrate this association[61,62]. A large study including 1935 Caucasian patients from the PAGE-B cohort did not find differences in 5-year cumulative HCC incidence between ETV (5.4%) or TDF (6.0%) after a median follow-up of 7.5 years[62].

Benefits of functional cure

The "functional" cure defined as the HBsAg loss, with or without seroconversion of antibody against HBsAg (anti-HBs), is considered the optimal goal for antiviral treatments[10,38]. However, even if third-

generation NA are drugs with a high barrier to HBV resistance, and high efficacy, achieving in most patients a virological and biochemical response, the HBsAg seroclearance is anecdotic[63,64]. Table 1 summarizes the efficacy of available treatments to achieve the HBsAg loss.

In patients without advanced fibrosis, the HBsAg loss is associated with an improvement in survival, and minimal risk of developing cirrhosis, decompensation, or HCC[38]. A recent study of 1972 patients with HBsAg loss, showed an HCC annual incidence of 0.38 per 100 person-years (median follow-up of 5.6 years). The study did not show differences between patients who achieved the functional cure spontaneously or with NA[65]. A systematic review showed lower HCC incidence in patients with functional cure (1.86%) compared to those who did not achieve it (6.56%) ($P < 0.001$). Cirrhosis, age ≥ 50, and male gender were the major risks for developing HCC after HBsAg seroclearance[66]. However, the 10-year HBsAg loss rate described in a large multicenter cohort ($n = 4769$) treated with ETV or TDF was only 2.1% with an annual incidence of 0.22%[64].

Rules to consider before treatment withdrawal

International guidelines of the main scientific societies recommend different treatment duration with NA. In non-cirrhotic HBeAg-positive CHB patients, NA treatment can be discontinued when HBeAg seroconversion is achieved and after one year of consolidation[9-11]. However, in non-cirrhotic HBeAg-negative patients, the NA treatment duration has been a matter of debate in recent years[39-43,67].

In 2008 the APASL guideline suggested the possibility of discontinuing NA therapy in HBeAg-negative patients after at least 2 years with undetectable HBV-DNA documented on three separate occasions 6 mo apart[68]. This approach in Asian patients was mostly driven by economics and reimbursement policies. Despite this, in 2012, Hadziyannis *et al*[69] reported in 33 Caucasian patients a high rate of HBsAg seroclearance after stopping ADV (39% at 5.5 years after withdrawal). In 2017, the first randomized controlled trial, the FINITE study, confirmed that the strategy of stopping therapy increased the HBsAg loss rate compared to continuing treatment (19% *vs* 0%)[70]. Based on these studies, in 2017 EASL guideline introduced the possibility of treatment withdrawal in non-cirrhotic HBeAg-negative CHB patients after 3 years of viral suppression[10]. In the last years, several studies have evaluated this strategy with different results (Table 1). Studies in Asian patients have shown a lower HBsAg loss rate compared to Caucasians. The different distribution of HBV-genotypes (especially genotype D), the inclusion or not of patients with advanced liver disease, and the different retreatment rules could explain these dissimilar results[45,71-73].

One of the important points to be considered before stopping treatment is the selection of the best candidates. The initial stopping rules proposed were based on the duration of treatment and virological suppression[9,10]. It has been suggested that NA withdrawal can be successful, only if the transcriptional activity of cccDNA has been silenced during treatment[74]. Additionally, it has been reported that long-term suppression of HBV-DNA can improve CD8 + T cell functions and restore the capacity of immune control by decreasing NK cell killing of HBV-specific T cells and increasing serum cytokines[44,75-77]. This immune restoration can exert control of viral replication after treatment discontinuation, and a large proportion of patients remain as inactive carriers. Moreover, the recurrence of HBV replication after NA discontinuation can represent a trigger for the immune response[78] that can induce an accelerated HBsAg decline and may be beneficial to eradicate residual cccDNA-containing hepatocytes. Our group has recently observed that HBsAg decline was faster during the first year after NA cessation compared to the on-treatment decline[46].

HBsAg and hepatitis B core-related antigen (HBcrAg) levels have been evaluated as surrogate markers to select the patients with a better outcome after NA cessation. It has been shown that not only HBsAg levels at the EoT but also on-treatment HBsAg kinetics are good predictors of HBsAg loss[79,80]. In a study performed by our group, we showed that on-treatment HBsAg kinetics had a high accuracy to predict the HBsAg loss one year after withdrawal[46]. Patients with an HBsAg decline > 1 Log IU/mL during treatment had a probability of 50% of achieving HBsAg loss one year after discontinuation. A large multicenter multiethnic study ($n = 1552$), the RETRACT-B study, showed different cut-offs of HBsAg at EoT in Asian and Caucasian patients. HBsAg levels at EoT < 100 IU/mL in Asian and < 1000 IU/mL in Caucasian patients were associated with a 4-year HBsAg loss probability of 33% and 41%, respectively[47]. Regarding levels of HBcrAg, the CREATE study, including 572 patients with NA discontinuation, showed lower HBcrAg levels at EoT in those with a virological response and HBsAg loss. Patients with undetectable HBcrAg (< 2 Log U/mL) at EoT showed a higher virological response and HBsAg loss rates one year after withdrawal (65% and 12%, respectively). The same group confirmed in 1216 patients that non-Asian ethnicity, HBsAg levels < 100 IU/mL, and undetectable HBcrAg were associated with the highest HBsAg loss rate[81].

Another important point is to define standardized re-treatment criteria. Some authors recommend delaying retreatment, to allow patients with a "beneficial" flare to achieve a functional cure[82]. However, other authors suggested that re-treatment should be initiated in response to significant increases in serum HBV-DNA, regardless of other liver parameters as cases of fulminant hepatitis have been reported[83]. Table 1 summarizes the efficacy of NA withdrawal to achieve the HBsAg loss[84-93].

Table 1 Efficacy of available antiviral treatments and nucleos(t)ide analogues withdrawal to achieve hepatitis B virus surface antigen loss

Ref.	Treatment (duration)	HBeAg	Ethnicity	Follow-up	HBsAg loss (%)
Current antiviral treatments					
Lau *et al*[84], 2005	Peg-IFNα (1 yr)	+	Mainly Asian	6 mo	2.9
Marcellin *et al*[85], 2013	Peg-IFNα (1 yr)	-	Asian	60 mo	12.0
Chang *et al*[48], 2010	ETV (5 yr)	+	Asian	-	1.4
Ahn *et al*[32], 2016	ETV (5 yr)	-	Mixed	-	4.6
Marcellin *et al*[33], 2019	TDF (10 yr)	+	Mixed	-	4.9
Marcellin *et al*[33], 2019	TDF (10 yr)	-	Mixed	-	3.4
Chan *et al*[30], 2016	TAF (3 yr)	+	Mixed	-	4.0
Buti *et al*[31], 2016	TAF (3 yr)	-	Mixed	-	3.0
Combined treatments					
Marcellin *et al*[86], 2016	Peg-IFN + TDF (1 yr)	+/-	Mixed	18 mo	9.1
Bourlière *et al*[87], 2017	ETV, TDF, ADV, and LAM (1 yr)	-	Caucasian	12 mo	7.8
Lim *et al*[88], 2022	NA add-on Peg-IFN (1 yr)	+/-	Asian	6 mo	12.1
Mo *et al*[89], 2022	NAs (HBsAg < 1500 IU/mL, 1 yr)	-	Asian	48 mo	33.2
Lim *et al*[88], 2022	NA switch to Peg-IFN (1 yr)	+/-	Asian	6 mo	9.7
NA discontinuation					
Chen *et al*[90], 2018	2.7 yr	+	Asian	96 mo	19.6
Song *et al*[91], 2021	2.9 yr	+	Asian	73 mo	9.5
Kuo *et al*[92], 2019	3.1 yr	+	Asian	24 mo	4.7 (ETV); 0 (TDF)
Jeng *et al*[72], 2018	2.9 yr	-	Asian	36 mo	13
Chen *et al*[90], 2018	2.9 yr	-	Asian	96 mo	33.1
Kuo *et al*[92], 2019	3.1 yr	-	Asian	36 mo	10 (ETV); 15 (TDF)
Chen *et al*[93], 2020	3.2 yr	-	Asian	58 mo	20.8
Song *et al*[91], 2021	2.7 yr	-	Asian	73 mo	14.6
Hirode *et al*[47], 2022	3.0 yr	-	Mixed	17 mo	15.0

Only studies with more than 100 patients have been included. HBsAg: Hepatitis B virus surface antigen; HBeAg: Hepatitis B e antigen; Peg-IFN: Pegylated interferon; LAM: Lamivudine; ADV: Adefovir; TDF: Tenofovir; ETV: Entecavir; TAF: Tenofovir alafenamide.

Risks of treatment withdrawal

The safety of treatment withdrawal is under discussion because on one hand hepatitis flare after NA cessation can induce hepatic decompensation but on the other hand early initiation of NA retreatment can inhibit the beneficial effect of flare-associated immune activation[47,72,94,95]. A study from Taiwan including 691 patients (44.6% with cirrhosis) showed a clinical relapse in 60.6% (7 developed a hepatic decompensation and 3 died)[72]. Similarly, the RETRACT-B study showed hepatic decompensation in only 1.22% (4.3% in patients with cirrhosis and 0.8% in those without cirrhosis; $P < 0.01$)[47]. In this study, 7 patients died (0.45%) by hepatic decompensation and 4 (0.25%) due to hepatitis B-associated flare.

Another important issue is the risk of developing HCC. The study of Jeng *et al*[72] included patients with (n = 308) and without cirrhosis (n = 383). The HCC incidence at 1, and 3 years after treatment discontinuation (0.15% and 1.00% for non-cirrhotic *vs* 1.30% and 4.00% for patients with cirrhosis) was similar to those during NA therapy (0.08% and 0.30% for non-cirrhotic *vs* 1.50% and 3.40% for patients with cirrhosis). Similarly, in the RETRACT-B study, the HCC incidence at 48 mo after NA withdrawal was 2.2% in patients with cirrhosis and 0.7% in those without cirrhosis[47]. Therefore, NA withdrawal does not seem to increase HCC rates. However, the tolerable level of circulating HBV DNA during long-term follow-up post-NA withdrawal has not been yet elucidated.

The evidence of increased HBsAg loss rates after NA cessation in some HBeAg-negative CHB patients must be balanced with safety. NA withdrawal should be performed only in centers with expertise in CHB management and in adherent patients willing stricter control after carefully discussing the pros and cons[74,96,97].

FUTURE

The need of expanding antiviral treatment criteria

Some recent studies have evaluated, with contradictory results, the use of NA in patients who do not meet strict criteria for treatment. On one hand, two retrospective studies in HBeAg-positive HBV-infected patients from Korea showed a lower risk of HCC and cirrhosis in those treated compared to untreated controls, suggesting a benefit of starting NA treatment at earlier phases[98,99]. Similarly, another Asian study including "minimally active" carriers showed a high risk of HCC (HR 9.9; 95%CI, 1.239-76.923; P = 0.031) when compared to inactive carriers[100]. But, the study included HBeAg-positive patients and those with a LSM > 9 kPa[101].

On the other hand, some European studies have not demonstrated significant benefits. A study from Italy, including patients without treatment with normal ALT and DNA < 20000 IU/mL, showed a benign course during a follow-up longer than 4 years[102]. Another study including Caucasian patients with HBeAg-negative chronic infection showed a high rate of HBsAg loss (15%) and low transition to CHB (6.3%) in patients with normal ALT and DNA < 2000 IU/mL or in the "grey zone" (HBV-DNA < 2000 IU/mL and ALT 40-80 U/L or, HBV-DNA 2000-20000 IU/mL and ALT < 40 U/L or ALT 40-80 U/L) after a median follow-up of 8.2 years[103]. However, a recent study from the United States has shown that patients without treatment indications, according to AASLD guidelines, had twice the risk of developing cirrhosis and/or HCC when compared to treated patients[104].

Simplifying indications for treatment initiation could be cost-effective and associated with survival improvement[105]. Therefore, it is plausible that antiviral treatment criteria will be expanded in the coming years to achieve the Global Hepatitis Elimination Goals, especially when new therapies with higher HBsAg loss rates will be available[106].

New HBV biomarkers to monitor antiviral therapy

The persistence of the cccDNA in the hepatocytes perpetuates HBV infection. So, detection and measurement of cccDNA levels would be the most precise tool to recognize HBV eradication. However, cccDNA can only be measured in liver biopsy samples by non-standardized or semi-automated techniques[107]. In recent years, there has been an effort to identify new biomarkers that could serve as cccDNA transcriptional activity surrogate markers.

The hepatitis B virus core-related antigen (HBcrAg) is an interesting biomarker composed of the hepatitis B core antigen (HBcAg), the HBeAg, and the 22-KDa pre-core protein (p22cr)[108]. These protein components are translated from cccDNA transcripts reflecting the cccDNA transcriptional activity. The HBcrAg is detected by automated chemiluminescence techniques using specific monoclonal antibodies with a limited sensitivity of 3.0 Log U/mL. The HBcrAg kinetics has been analyzed during NA therapy in a cohort of 222 CHB patients (132 HBeAg-negative and 90 HBeAg-positive) receiving ETV[109]. The decline of HBcrAg levels was 0.244 Log U/mL per year. HBcrAg levels were lower in HBeAg-negative patients compared to HBeAg-positive, but no differences were found between TDF or ETV[109,110]. On the other hand, the persistence of detectable HBcrAg at EoT has been related to severe aminotransferase flares after NA treatment cessation[111]. The main limitations of HBcrAg are its low sensitivity and its low levels after a long-treatment period in HBeAg-negative patients. Therefore, a great proportion of treated HBeAg-negative patients can show undetectable HBcrAg[112]. Recently, a new ultrasensitive assay has been described to improve the HBcrAg sensitivity, but further studies are needed to consider it in clinical practice[113].

The HBV-RNA is a newer marker under evaluation. The pgRNA is packaged in nucleocapsids and serves as the template for reverse transcription to HBV-DNA. In patients not receiving antiviral therapy, serum HBV-RNA levels are much lower than serum HBV-DNA levels. It can be detected in serum samples as pgRNA and spliced pgRNA variants produced by transcription of cccDNA as a marker of intrahepatic cccDNA transcriptional activity[114]. However, serum HBV-RNA is usually quantified by in-house assays and there are no commercial tests available for routine clinical practice. During NA therapy, reverse transcription of pgRNA to HBV-DNA is blocked, but cccDNA transcription to pgRNA persists, and HBV-RNA may be detected in the serum of patients with undetectable HBV-DNA. Therefore, the HBV-RNA could be useful to monitor NA-treated patients[115,116]. Recently, it has been shown that serum HBV-RNA reduced after treatment initiation from 1.46 Logs at week 48 to 1.77 Logs at week 96[117]. On one hand, serum pgRNA levels at wk 4 after NA initiation were correlated with low HBsAg levels (≤ 100 IU/mL) and seroclearance during follow-up[118]. On the other hand, high levels of pgRNA have been associated with viral relapse after NA withdrawal[119].

The recognition of HBsAg composition could be an interesting tool for following CHB patients because it changes across the stages of HBV infection. The main HBsAg component is S-HBs. The L-HBs and M-HBs proportion is lower in the inactive carrier stage compared to those in HBeAg-negative or HBeAg-positive CHB patients[120,121]. Interestingly, L-HBs and M-HBs proportions decrease prior to total HBsAg loss in patients receiving antiviral treatment[122].

Nowadays, the quantitative HBsAg is the most used and widely available biomarker as a consequence of its standardized and commercial tests. It includes the HBsAg produced not only from cccDNA but also by the integrated DNA that is the main source of the HBsAg in HBeAg-negative CHB patients, being more representative of the transcriptional activity. Moreover, quantitative HBsAg has shown a better predictive capacity compared to HBrcAg and HBV-RNA[123].

However, despite the potential utility of these new biomarkers for monitoring NA treatment, their usefulness should still be established for monitoring the new treatment strategies.

New drugs in development

After several years without major advances in novel therapies for CHB, currently, a multitude of new molecules are emerging, individually or in combination, as future treatment strategies. The last part of this review summarizes the main groups of evolving molecules evaluated in clinical trials (Table 2) and the combinations that are showing higher rates of sustained HBsAg loss (Table 3).

Several drugs are being evaluated in phase II clinical trials. These new molecules can be classified into two main groups according to their mechanism of action: (1) Molecules targeting different steps in the HBV life cycle; and (2) those acting as immunomodulators.

Molecules targeting HBV life cycle

Molecules targeting different steps in the HBV life cycle are summarized according to their treatment class, mechanism of action, and type in Table 2[124-143].

HBV entry inhibitors

HBV entry inhibitors protect naïve hepatocytes from infection. However, they do not directly target cccDNA. The recent identification of liver-specific bile acid transporter, the NTCP, has allowed exploring new therapeutics to block viral entry and reduce viral spread[144]. Bulevirtide consists of the preS1 domain of the large surface protein, which inhibits NTCP and prevents viral entry. In the phase 2 study, Bulevirtide monotherapy was evaluated in patients with CHB co-infected with the hepatitis D virus (HDV)[124]. HBV-DNA declined by > 1 Log in 32% of patients, although HBsAg was not affected. Its low effect on HBsAg levels made most studies focus on long-term treatment for HBV/HDV co-infected patients.

Capsid assembly modulators

The primary mechanism of action of nucleocapsid assembly modulators (CAMs) is to drive the nucleocapsid misassemble. These molecules interfere with capsid formation and disrupt the encapsidation of pgRNA. They have been classified into two main families (Class I and Class II). These agents have been shown to decrease serum HBV-DNA and RNA levels, although declines in HBsAg levels are negligible. Moreover, it has been shown HBV-RNA and HBcrAg rebounded after discontinuation of treatment [126]. Due to these limitations, to date, the role of CAMs in future treatments for CHB must be defined.

Post-transcriptional control inhibitors (small interfering RNA and antisense oligonucleotides)

RNA molecules, both pgRNA, and mRNAs encoding viral proteins, are essential for HBV replication. Small interfering RNA (SiRNA) is a specific post-transcriptional gene silencing mechanism that can inhibit the translation of viral proteins needed for cccDNA formation. SiRNA is 21-23 nucleotide duplexes processed from large double-stranded RNAs[145]. Chemically synthesized short RNA duplexes were shown to be capable of gene silencing *in vitro* without inducing an interferon response [146]. Different anti-HBV siRNA are being tested in clinical trials. Available clinical data are promising and show that siRNAs are safe and well-tolerated[127]. A study of siRNA therapy that targeted the common 3′ ends of all HBV transcripts showed that while the treatment markedly reduced HBsAg levels in HBeAg-positive patients, it had minimal effects in HBeAg-negative patients[128].

Antisense nucleotides (ASOs) are single-stranded DNAs (8-10 nucleotides) that target HBV mRNA sequences, forming a DNA-RNA hybrid that is rapidly degraded by cytoplasmic ribonuclease-H[147]. Early results of ASOs, alone or in combination, have shown a profound HBsAg decline[130]. The B-Clear Study, a phase 2b clinical trial evaluating bepirovirsen 300 mg subcutaneously once weekly for 24 wk, showed undetectable HBsAg in 9% of patients who received bepirovirsen plus NA and in 10% who received bepirovirsen alone[131].

HBsAg release inhibitors: Nucleic acid polymers

HBsAg plays a major role in HBV infection and is the most abundant HBV antigen. Therefore, blocking its release could potentially prevent the release of new virions, decline the number of subviral particles and restore the HBV-specific immune response[148]. Nucleic acid polymers (NAPs) are amphipathic

Table 2 Mechanisms of action of the new drugs under development

Treatment class	Mechanism of action	Types
Drugs targeting HBV life cycle		
Entry inhibitors	Blockage of liver-specific bile acid transporter (NTCP)	Inhibitors of NTCP[124]; NMAb[125]
Capsid assembly modulators	Interfere with capsid formation and disrupt the encapsidation of pgRNA	CAMs[126]
Post-transcriptional control inhibitors	Post-transcriptional gene silencing by inhibition of the translation of viral proteins	SiRNA[127-129]; ASOs[130,131]
HBsAg release inhibitors	Intracellular degradation of HBsAg *via* proteasomal and lysosomal degradation	NAPs[132,133]
Immunomodulators		
Innate immune activator	Stimulation of innate immunity through TLRs and RIG-I	TLRs agonist[134-137]; RIG-I agonists[138, 139]
Adaptive immune activator	Blocking the PD-1/PD-L1 pathway to reverse T-cell exhaustion; stimulation of host's immune response to generate CD4 and CD8 HBV-specific T cells	Checkpoint inhibitors[140,141]; therapeutic vaccines[142,143]

HBV: Hepatitis B virus; NTCP: Sodium taurocholate co-transporting polypeptide; NMAb: Neutralizing monoclonal antibodies; CAMs: Nucleocapsid assembly modulators; SiRNA: Small interfering RNA; ASO: Antisense oligonucleotides; NAP: Nucleic acid polymers; TLRs: Toll-like receptors; RIG-I: Retinoic acid-inducible gene-1; PD-1: Programmed death receptor 1; PD-L1: Programmed cell death ligand 1; HBsAg: Hepatitis B virus surface antigen; HBeAg: Hepatitis B e antigen.

phosphorothioate oligonucleotides. The antiviral effect of NAPs against HBV infection is the inhibition of HBsAg release, although the exact mechanism is unknown, resulting in rapid clearance of HBsAg [132]. In clinical studies, NAP monotherapy was accompanied by rapid HBsAg decline and seroconversion. Recently, NAP-based combination therapy with TDF and Peg-IFN achieved a functional cure in 35% of patients[133] Interestingly, in HBeAg-negative patients, HBsAg produced by integrated DNA was lost. However, more than 90% of patients experienced immune-mediated transaminase flares during therapy[132].

Immunomodulators

Immunomodulator molecules are summarized according to their treatment class, mechanism of action, and type in Table 2.

Immunomodulatory targets including therapeutic vaccines

The impaired immune response is one of the main barriers to eliminating HBV. T cell immune exhaustion due to the presence of high amounts of HBsAg and a defective response of the innate immune response has a role in HBV persistence. Thus, treatment strategies to restore HBV-specific immune responses with immunomodulatory therapies have been evaluated to achieve viral clearance.

Pegylated interferon: A "second life" for an old friend

Interferon was the first drug approved for CHB treatment. Despite the long use of this treatment, the exact mechanism of action is still unclear. It has been suggested that Peg-IFN has two main effects, acting on the transcriptional activity of cccDNA and also an immunomodulatory effect, enhancing both innate and adaptive immunity[149,150]. Due to its hypothetical immunomodulatory effects, the synergistic effects of combination with NA and Peg-IFN have been evaluated.

A recent meta-analysis found that NA and Peg-IFN combination improved HBsAg seroclearance rates (RR: 4.52, 95%CI: 1.95-10.47 for adding-on and RR: 12.15, 95%CI 3.99-37.01 for switching-to) compared to NA monotherapy. One of the strongest predictors of HBsAg seroclearance was the HBsAg level at the start of IFN therapy[151]. Our group also showed that the addition of Peg-IFN to NA produced a faster and larger decrease in HBsAg levels compared to NA monotherapy, especially in those patients with IL28CC polymorphism[112]. A better Peg-IFN response in patients with IL28CC polymorphism has been described especially in those infected with genotype D[152,153]. More recently, a Chinese real-world study (n = 3988), the Everest Project (NCT04035837), has reported that the addition of Peg-IFN alpha 2b to NA in HBeAg-negative patients achieved a 4-year HBsAg loss rate of 33%[89].

The main concerns on the use of Peg-IFN are side effects, poor tolerability, and major contraindication such as decompensated cirrhosis. These explain the preference to use NA in routine clinical practice. However, in selected patients with good tolerance, the adding-on or switching-to strategy may improve the HBsAg seroclearance. Indeed, some of the phase 2 trials evaluating new antivirals, have included concomitant treatment with Peg-IFN and have shown better outcomes.

Table 3 Efficacy of drug combinations to achieve sustained hepatitis B virus surface antigen loss

Drug class	Drug	Patients	Time therapy (wk)	Efficacy	Safety
NA +/- CAM	NA *vs* NA + JNJ-6379 (bersacapavir)	232	24-48	HBsAg decline 0.25 log IU/mL *vs* 0.41 log IU/mL	No major AE
SiRNA +/- NA	AB-729 *vs* NA + AB-729	43	8	HBsAg decline 2.03 log IU/mL monotherapy *vs* 2.16 log IU/mL combination	Injection site reactions; ALT flares
ASO + NA	ASO-GSK3228836 (bepirovirsen) ± NA	457	12-24	HBsAg < LoQ in 28%-29% and HBsAg loss in 9%-10% after 24 wk of EoT	Injection site reactions; few cases of grade 3-4 ALT flares
Inhibitor of NTCP + Peg-IFN	Bulevirtide + Peg-IFN in HDV-HBV co-infection	90	48	HBsAg loss 26.7% in one arm *vs* 0% in the other	Related to Peg-IFN; injection site reactions
NA + TLR agonists	NA + TLR7 agonist (vesatolimod, GS-9620)	162	24	No changes in HBsAg	Some grade 3 AE with higher doses (few treatment discontinuations)
NA + TLR agonists	NA + TLR8 agonist (selgantolimod)	48	24	HBsAg loss 5% at week 48	Mild and transient gastrointestinal AE
NA + checkpoint inhibitors	NA + PD-1 inhibitor (nivolumab)	12	1 dose (24 follow-up)	HBsAg reduction 0.48 log IU/mL (HBsAg loss in 5%)	No major AE
NA + checkpoint inhibitors	NA + PD-L1 inhibitor (ASC22, Menvafolimab)	48	24	HBsAg decline 0.38 log IU/mL (HBsAg loss in 19%)	Grade 1 and 2 ALT flares
NA + SiRNA +/- CAM	NA + JNJ-3989 (siRNA) + NA ± JNJ-6379 (CAM)	117	48	HBsAg decline 2.1 log IU/mL in double *vs* 1.8 log IU/mL in triple combination	No major AE
NAP + NA + Peg-IFN	REP2139 or REP 2165 + NA + Peg-IFN	40	48	HBsAg loss in 35% and HBsAg < 100 IU/mL in 75%	Related to Peg-IFN
SiRNA + NA +/- Peg-IFN	VIR 2218 (siRNA) + NA +/- Peg-IFN	80	24	HBsAg decline 2.03 log IU/mL in dual arm *vs* 2.55 log IU/mL in triple arm (HBsAg < 100 IU/mL in 95% and HBsAg < 10 IU/mL in 55%)	Related to Peg-IFN

CAM: Nucleocapsid assembly modulator; HBV: Hepatitis B virus; SiRNA: Small interfering RNA; NTCP: Sodium taurocholate co-transporting polypeptide; ASO: Antisense oligonucleotides; NAP: Nucleic acid polymers; TLRs: Toll-like receptors; RIG-I: Retinoic acid-inducible gene-1; PD-1: Programmed death receptor 1; PD-L1: Programmed cell death ligand 1; HBsAg: Hepatitis B virus surface antigen; HBeAg: Hepatitis B e antigen; ALT: Alanine aminotransferase; LoQ: Limit of quantification; EoT: End of therapy; AE: Adverse events.

Toll-like receptor and retinoic acid-inducible gene-1 agonists

HBV can be recognized by receptors such as toll-like receptors (TLRs)[154] and retinoic acid-inducible gene-1 (RIG-1)[155] TLRs are receptors that initiated intracellular pathways and induce antiviral molecules such as interferons, and cytokines. It has been reported that the activation of TLR-mediated pathways results in the suppression of HBV replication. An oral TLR 7 (TLR7) agonist, GS9620, has shown a decrease in serum HBV-DNA and HBsAg in chimpanzees[134]. However, a phase IIb trial in humans, showed a minimal decrease in HBsAg levels, despite the increase in cytokines and NK cell activity[135,136]. A more recent trial has shown that the combination of selgantolimod, a TLR8 agonist, with a NA resulted in a minimal reduction of HBsAg levels[137]. RIG-I constitutes an intracytoplasmic receptor that interacts with RNA viruses. Once activated, it leads to signal transduction through protein kinase complexes and activation of transcription factors that migrate to the nucleus and activate interferon-stimulable genes leading to the production of IFN[138]. Inarigivir activates the RIG-I pathway. Although early studies reported a reduction in HBV-DNA levels, there were cases of severe hepatotoxicity, with multiple cases of acute liver failure and one death, that lead to its discontinuation [139].

Checkpoint inhibitors

The immune system of HBV-infected patients shows high levels of programmed death receptor 1 (PD-1)-expressing CD8 T cells and high levels of programmed cell death ligand 1 (PD-L1) expression. This suggests that PD-L1 blockade could be a suitable strategy to treat chronic HBV infection. Furthermore, anti-PD-L1 blockade increases the number of IFN-γ-producing T-cells and the amount of IFN-γ produced per cell[156]. Checkpoint inhibitors against PD-1 and PD-L1 have been shown to be effective in several malignancies by reversing T-cell exhaustion and restoring immunity. However, the efficacy to achieve HBsAg clearance has been disappointing. In the CheckMate 040 trial, nivolumab increased

HBV-DNA 1 Log from baseline in 10% of HBsAg-positive patients[140]. PD-1 blockade showed limited antiviral activity, and no patient exhibited HBsAg seroconversion[141].

Monoclonal antibodies

HBV entry can be interrupted by small compounds such as neutralizing monoclonal antibodies (NMAb). In a phase 2 study, it has been evaluated the combination of NMAb VIR-3434 with small interfering RNA (SiRNA) VIR-2218 for up to 20 wk. Combination treatment was generally well tolerated with no serious adverse events. The majority of patients achieved low levels of HBsAg (< 10 IU/mL) but any patient lost the HBsAg during the study[125].

Therapeutic vaccines

These immunogenic molecules are developed to stimulate the host immune response generating CD4 and CD8 HBV-specific T cells to suppress viral replication and HBsAg loss. Early studies in humans showed a small decline in HBsAg[142]. However, several new therapeutic vaccines are in development probably to be used in combination with other drugs such as SiRNA[143].

Other immunomodulatory approaches

In recent years, a better understanding of the immune response to HBV has emerged with new therapeutic possibilities. T cell receptor (TCR)- redirected T cell and chimeric antigen receptor (CAR) T cell involve genetic engineering to confer specificity in front of HBV. CAR-T cells are transduced with an antibody-like receptor to recognize HBsAg on the surface of infected hepatocytes whereas TCR-redirected T cells respond to HBV peptides[157]. However, the investigation in this field is still under development and is being tested in Phase I studies evaluating HBV-infected patients with HCC[158, 159].

Combinations of drugs in development

None of the new previously described molecules can achieve significant sustained HBsAg loss if used alone. Therefore, the most advisable strategy seems to be the combination of molecules with different mechanisms of action[160]. Table 3 summarizes the efficacy of the evolving combinations to achieve sustained HBsAg loss.

CONCLUSION

Long-term treatment for CHB has been used for decades, showing a good safety profile and high efficacy in controlling viral replication, improving histology, and decreasing the incidence of HCC, clinical decompensation, and mortality. However, the persistence of cccDNA and the low probability of HBsAg seroclearance with NA therapy made necessary indefinite treatment in a vast majority of patients. With the new insights into the role of the immune system in HBV infection persistence and the knowledge of the different viral cycle phases, there has been an increase in new therapeutic approaches in recent years. Moreover, several clinical trials evaluating new drugs with different mechanisms of action are ongoing with promising results. It is expected that in the coming years, there will be a paradigm shift in the treatment of CHB, as we have already seen in chronic hepatitis C, and functional cure in an important number of patients seems closer than ever. Meanwhile, an effort to improve diagnostic rates, and to assure access to treatment for all patients who need it must be urgently done.

FOOTNOTES

Author contributions: Broquetas T contributed to the acquisition of data, interpretation, drafting, critical revision, and final approval; Carrión JA contributed to conception and design, acquisition of data, interpretation, drafting, critical revision, and final approval.

Conflict-of-interest statement: The authors declare that they have no conflict of interest.

Open-Access: This article is an open-access article that was selected by an in-house editor and fully peer-reviewed by external reviewers. It is distributed in accordance with the Creative Commons Attribution NonCommercial (CC BY-NC 4.0) license, which permits others to distribute, remix, adapt, build upon this work non-commercially, and license their derivative works on different terms, provided the original work is properly cited and the use is non-commercial. See: https://creativecommons.org/Licenses/by-nc/4.0/

Country/Territory of origin: Spain

ORCID number: Teresa Broquetas 0000-0002-5935-3076; José A Carrión 0000-0001-7191-6081.

S-Editor: Chen YL
L-Editor: A
P-Editor: Yu HG

REFERENCES

1 **Millman I**, Loeb LA, Bayer ME, Blumberg BS. Australia antigen (a hepatitis-associated antigen): purification and physical properties. *J Exp Med* 1970; **131**: 1190-1199 [PMID: 4246140 DOI: 10.1084/jem.131.6.1190]
2 **Gerlich WH**. Medical virology of hepatitis B: how it began and where we are now. *Virol J* 2013; **10**: 239 [PMID: 23870415 DOI: 10.1186/1743-422X-10-239]
3 **GBD 2019 Hepatitis B Collaborators**. Global, regional, and national burden of hepatitis B, 1990-2019: a systematic analysis for the Global Burden of Disease Study 2019. *Lancet Gastroenterol Hepatol* 2022; **7**: 796-829 [PMID: 35738290 DOI: 10.1016/S2468-1253(22)00124-8]
4 **Dane DS**, Cameron CH, Briggs M. Virus-like particles in serum of patients with Australia-antigen-associated hepatitis. *Lancet* 1970; **1**: 695-698 [PMID: 4190997 DOI: 10.1016/s0140-6736(70)90926-8]
5 **Almeida JD**, Rubenstein D, Stott EJ. New antigen-antibody system in Australia-antigen-positive hepatitis. *Lancet* 1971; **2**: 1225-1227 [PMID: 4143591 DOI: 10.1016/s0140-6736(71)90543-5]
6 **Magnius LO**, Espmark A. A new antigen complex co-occurring with Australia antigen. *Acta Pathol Microbiol Scand B Microbiol Immunol* 1972; **80**: 335-337 [PMID: 4624538 DOI: 10.1111/j.1699-0463.1972.tb00167.x]
7 **Robinson WS**, Clayton DA, Greenman RL. DNA of a human hepatitis B virus candidate. *J Virol* 1974; **14**: 384-391 [PMID: 4847328 DOI: 10.1128/JVI.14.2.384-391.1974]
8 **lumberg BS**. Hepatitis B: The Hunt for a Killer Virus: Princeton: Princeton University Press, 2003
9 **Sarin SK**, Kumar M, Lau GK, Abbas Z, Chan HL, Chen CJ, Chen DS, Chen HL, Chen PJ, Chien RN, Dokmeci AK, Gane E, Hou JL, Jafri W, Jia J, Kim JH, Lai CL, Lee HC, Lim SG, Liu CJ, Locarnini S, Al Mahtab M, Mohamed R, Omata M, Park J, Piratvisuth T, Sharma BC, Sollano J, Wang FS, Wei L, Yuen MF, Zheng SS, Kao JH. Asian-Pacific clinical practice guidelines on the management of hepatitis B: a 2015 update. *Hepatol Int* 2016; **10**: 1-98 [PMID: 26563120 DOI: 10.1007/s12072-015-9675-4]
10 **European Association for the Study of the Liver**. EASL 2017 Clinical Practice Guidelines on the management of hepatitis B virus infection. *J Hepatol* 2017; **67**: 370-398 [PMID: 28427875 DOI: 10.1016/j.jhep.2017.03.021]
11 **Terrault NA**, Lok ASF, McMahon BJ, Chang KM, Hwang JP, Jonas MM, Brown RS Jr, Bzowej NH, Wong JB. Update on prevention, diagnosis, and treatment of chronic hepatitis B: AASLD 2018 hepatitis B guidance. *Hepatology* 2018; **67**: 1560-1599 [PMID: 29405329 DOI: 10.1002/hep.29800]
12 **Yuen MF**, Chen DS, Dusheiko GM, Janssen HLA, Lau DTY, Locarnini SA, Peters MG, Lai CL. Hepatitis B virus infection. *Nat Rev Dis Primers* 2018; **4**: 18035 [PMID: 29877316 DOI: 10.1038/nrdp.2018.35]
13 **Colpitts CC**, Verrier ER, Baumert TF. Targeting Viral Entry for Treatment of Hepatitis B and C Virus Infections. *ACS Infect Dis* 2015; **1**: 420-427 [PMID: 27617925 DOI: 10.1021/acsinfecdis.5b00039]
14 **Verrier ER**, Colpitts CC, Sureau C, Baumert TF. Hepatitis B virus receptors and molecular drug targets. *Hepatol Int* 2016; **10**: 567-573 [PMID: 26979861 DOI: 10.1007/s12072-016-9718-5]
15 **Rabe B**, Vlachou A, Panté N, Helenius A, Kann M. Nuclear import of hepatitis B virus capsids and release of the viral genome. *Proc Natl Acad Sci U S A* 2003; **100**: 9849-9854 [PMID: 12909718 DOI: 10.1073/pnas.1730940100]
16 **Levrero M**, Zucman-Rossi J. Mechanisms of HBV-induced hepatocellular carcinoma. *J Hepatol* 2016; **64**: S84-S101 [PMID: 27084040 DOI: 10.1016/j.jhep.2016.02.021]
17 **Tong S**, Revill P. Overview of hepatitis B viral replication and genetic variability. *J Hepatol* 2016; **64**: S4-S16 [PMID: 27084035 DOI: 10.1016/j.jhep.2016.01.027]
18 **Seeger C**, Mason WS. Molecular biology of hepatitis B virus infection. *Virology* 2015; **479-480**: 672-686 [PMID: 25759099 DOI: 10.1016/j.virol.2015.02.031]
19 **Hu J**, Liu K. Complete and Incomplete Hepatitis B Virus Particles: Formation, Function, and Application. *Viruses* 2017; **9** [PMID: 28335554 DOI: 10.3390/v9030056]
20 **Zoulim F**, Testoni B, Lebossé F. Kinetics of intrahepatic covalently closed circular DNA and serum hepatitis B surface antigen during antiviral therapy for chronic hepatitis B: lessons from experimental and clinical studies. *Clin Gastroenterol Hepatol* 2013; **11**: 1011-1013 [PMID: 23602824 DOI: 10.1016/j.cgh.2013.04.010]
21 **Lebossé F**, Testoni B, Fresquet J, Facchetti F, Galmozzi E, Fournier M, Hervieu V, Berthillon P, Berby F, Bordes I, Durantel D, Levrero M, Lampertico P, Zoulim F. Intrahepatic innate immune response pathways are downregulated in untreated chronic hepatitis B. *J Hepatol* 2017; **66**: 897-909 [PMID: 28043874 DOI: 10.1016/j.jhep.2016.12.024]
22 **Greenberg HB**, Pollard RB, Lutwick LI, Gregory PB, Robinson WS, Merigan TC. Effect of human leukocyte interferon on hepatitis B virus infection in patients with chronic active hepatitis. *N Engl J Med* 1976; **295**: 517-522 [PMID: 950957 DOI: 10.1056/NEJM197609022951001]
23 **Wong DK**, Cheung AM, O'Rourke K, Naylor CD, Detsky AS, Heathcote J. Effect of alpha-interferon treatment in patients with hepatitis B e antigen-positive chronic hepatitis B. A meta-analysis. *Ann Intern Med* 1993; **119**: 312-323 [PMID: 8328741 DOI: 10.7326/0003-4819-119-4-199308150-00011]
24 **Manesis EK**, Hadziyannis SJ. Interferon alpha treatment and retreatment of hepatitis B e antigen-negative chronic hepatitis B. *Gastroenterology* 2001; **121**: 101-109 [PMID: 11438498 DOI: 10.1053/gast.2001.25524]
25 **Sonneveld MJ**, Hansen BE, Piratvisuth T, Jia JD, Zeuzem S, Gane E, Liaw YF, Xie Q, Heathcote EJ, Chan HL, Janssen HL. Response-guided peginterferon therapy in hepatitis B e antigen-positive chronic hepatitis B using serum hepatitis B surface antigen levels. *Hepatology* 2013; **58**: 872-880 [PMID: 23553752 DOI: 10.1002/hep.26436]

26 **Benhamou Y**, Dohin E, Lunel-Fabiani F, Poynard T, Huraux JM, Katlama C, Opolon P, Gentilini M. Efficacy of lamivudine on replication of hepatitis B virus in HIV-infected patients. *Lancet* 1995; **345**: 396-397 [PMID: 7845151 DOI: 10.1016/s0140-6736(95)90388-7]

27 **Dienstag JL**, Perrillo RP, Schiff ER, Bartholomew M, Vicary C, Rubin M. A preliminary trial of lamivudine for chronic hepatitis B infection. *N Engl J Med* 1995; **333**: 1657-1661 [PMID: 7477217 DOI: 10.1056/NEJM199512213332501]

28 **van Bömmel F**, Wünsche T, Mauss S, Reinke P, Bergk A, Schürmann D, Wiedenmann B, Berg T. Comparison of adefovir and tenofovir in the treatment of lamivudine-resistant hepatitis B virus infection. *Hepatology* 2004; **40**: 1421-1425 [PMID: 15565615 DOI: 10.1002/hep.20464]

29 **Petersen J**, Buti M. Considerations for the long-term treatment of chronic hepatitis B with nucleos(t)ide analogs. *Expert Rev Gastroenterol Hepatol* 2012; **6**: 683-93; quiz 694 [PMID: 23237254 DOI: 10.1586/egh.12.52]

30 **Chan HL**, Fung S, Seto WK, Chuang WL, Chen CY, Kim HJ, Hui AJ, Janssen HL, Chowdhury A, Tsang TY, Mehta R, Gane E, Flaherty JF, Massetto B, Gaggar A, Kitrinos KM, Lin L, Subramanian GM, McHutchison JG, Lim YS, Acharya SK, Agarwal K; GS-US-320-0110 Investigators. Tenofovir alafenamide versus tenofovir disoproxil fumarate for the treatment of HBeAg-positive chronic hepatitis B virus infection: a randomised, double-blind, phase 3, non-inferiority trial. *Lancet Gastroenterol Hepatol* 2016; **1**: 185-195 [PMID: 28404091 DOI: 10.1016/S2468-1253(16)30024-3]

31 **Buti M**, Gane E, Seto WK, Chan HL, Chuang WL, Stepanova T, Hui AJ, Lim YS, Mehta R, Janssen HL, Acharya SK, Flaherty JF, Massetto B, Cathcart AL, Kim K, Gaggar A, Subramanian GM, McHutchison JG, Pan CQ, Brunetto M, Izumi N, Marcellin P; GS-US-320-0108 Investigators. Tenofovir alafenamide versus tenofovir disoproxil fumarate for the treatment of patients with HBeAg-negative chronic hepatitis B virus infection: a randomised, double-blind, phase 3, non-inferiority trial. *Lancet Gastroenterol Hepatol* 2016; **1**: 196-206 [PMID: 28404092 DOI: 10.1016/S2468-1253(16)30107-8]

32 **Ahn J**, Lee HM, Lim JK, Pan CQ, Nguyen MH, Ray Kim W, Mannalithara A, Trinh H, Chu D, Tran T, Min A, Do S, Te H, Reddy KR, Lok AS. Entecavir safety and effectiveness in a national cohort of treatment-naïve chronic hepatitis B patients in the US - the ENUMERATE study. *Aliment Pharmacol Ther* 2016; **43**: 134-144 [PMID: 26510638 DOI: 10.1111/apt.13440]

33 **Marcellin P**, Wong DK, Sievert W, Buggisch P, Petersen J, Flisiak R, Manns M, Kaita K, Krastev Z, Lee SS, Cathcart AL, Crans G, Op den Brouw M, Jump B, Gaggar A, Flaherty J, Buti M. Ten-year efficacy and safety of tenofovir disoproxil fumarate treatment for chronic hepatitis B virus infection. *Liver Int* 2019; **39**: 1868-1875 [PMID: 31136052 DOI: 10.1111/liv.14155]

34 **Casado JL**, Santiuste C, Vazquez M, Bañón S, Rosillo M, Gomez A, Perez-Elías MJ, Caballero C, Rey JM, Moreno S. Bone mineral density decline according to renal tubular dysfunction and phosphaturia in tenofovir-exposed HIV-infected patients. *AIDS* 2016; **30**: 1423-1431 [PMID: 26919733 DOI: 10.1097/QAD.0000000000001067]

35 **Mak LY**, Hoang J, Jun DW, Chen CH, Peng CY, Yeh ML, Kim SE, Huang DQ, Jeong JY, Yoon E, Oh H, Tsai PC, Huang CF, Ahn SB, Trinh H, Xie Q, Wong GLH, Enomoto M, Shim JJ, Lee DH, Liu L, Kozuka R, Cho YK, Jeong SW, Kim HS, Trinh L, Dao A, Huang R, Hui RW, Tsui V, Quek S, Khine HHTW, Ogawa E, Dai CY, Huang JF, Cheung R, Wu C, Chuang WL, Lim SG, Yu ML, Yuen MF, Nguyen MH. Longitudinal renal changes in chronic hepatitis B patients treated with entecavir versus TDF: a REAL-B study. *Hepatol Int* 2022; **16**: 48-58 [PMID: 34822056 DOI: 10.1007/s12072-021-10271-x]

36 **Han Y**, Zeng A, Liao H, Liu Y, Chen Y, Ding H. The efficacy and safety comparison between tenofovir and entecavir in treatment of chronic hepatitis B and HBV related cirrhosis: A systematic review and Meta-analysis. *Int Immunopharmacol* 2017; **42**: 168-175 [PMID: 27915131 DOI: 10.1016/j.intimp.2016.11.022]

37 **Fong TL**, Lee BT, Tien A, Chang M, Lim C, Ahn A, Bae HS. Improvement of bone mineral density and markers of proximal renal tubular function in chronic hepatitis B patients switched from tenofovir disoproxil fumarate to tenofovir alafenamide. *J Viral Hepat* 2019; **26**: 561-567 [PMID: 30576085 DOI: 10.1111/jvh.13053]

38 **Anderson RT**, Choi HSJ, Lenz O, Peters MG, Janssen HLA, Mishra P, Donaldson E, Westman G, Buchholz S, Miller V, Hansen BE. Association Between Seroclearance of Hepatitis B Surface Antigen and Long-term Clinical Outcomes of Patients With Chronic Hepatitis B Virus Infection: Systematic Review and Meta-analysis. *Clin Gastroenterol Hepatol* 2021; **19**: 463-472 [PMID: 32473348 DOI: 10.1016/j.cgh.2020.05.041]

39 **Boglione L**, D'Avolio A, Cariti G, Gregori G, Burdino E, Baietto L, Cusato J, Ghisetti V, De Rosa FG, Di Perri G. Kinetics and prediction of HBsAg loss during therapy with analogues in patients affected by chronic hepatitis B HBeAg negative and genotype D. *Liver Int* 2013; **33**: 580-585 [PMID: 23311449 DOI: 10.1111/liv.12091]

40 **Zoulim F**, Carosi G, Greenbloom S, Mazur W, Nguyen T, Jeffers L, Brunetto M, Yu S, Llamoso C. Quantification of HBsAg in nucleos(t)ide-naïve patients treated for chronic hepatitis B with entecavir with or without tenofovir in the BE-LOW study. *J Hepatol* 2015; **62**: 56-63 [PMID: 25176615 DOI: 10.1016/j.jhep.2014.08.031]

41 **Broquetas T**, Garcia-Retortillo M, Hernandez JJ, Puigvehí M, Cañete N, Coll S, Cabrero B, Giménez MD, Solà R, Carrión JA. Quantification of HBsAg to predict low levels and seroclearance in HBeAg-negative patients receiving nucleos(t)ide analogues. *PLoS One* 2017; **12**: e0188303 [PMID: 29190670 DOI: 10.1371/journal.pone.0188303]

42 **Chevaliez S**, Hézode C, Bahrami S, Grare M, Pawlotsky JM. Long-term hepatitis B surface antigen (HBsAg) kinetics during nucleoside/nucleotide analogue therapy: finite treatment duration unlikely. *J Hepatol* 2013; **58**: 676-683 [PMID: 23219442 DOI: 10.1016/j.jhep.2012.11.039]

43 **Seto WK**, Wong DK, Fung J, Huang FY, Lai CL, Yuen MF. Reduction of hepatitis B surface antigen levels and hepatitis B surface antigen seroclearance in chronic hepatitis B patients receiving 10 years of nucleoside analogue therapy. *Hepatology* 2013; **58**: 923-931 [PMID: 23468172 DOI: 10.1002/hep.26376]

44 **García-López M**, Lens S, Pallett LJ, Testoni B, Rodríguez-Tajes S, Mariño Z, Bartres C, García-Pras E, Leonel T, Perpiñán E, Lozano JJ, Rodríguez-Frías F, Koutsoudakis G, Zoulim F, Maini MK, Forns X, Pérez-Del-Pulgar S. Viral and immune factors associated with successful treatment withdrawal in HBeAg-negative chronic hepatitis B patients. *J Hepatol* 2021; **74**: 1064-1074 [PMID: 33278456 DOI: 10.1016/j.jhep.2020.11.043]

45 **Sonneveld MJ**, Chiu SM, Park JY, Brakenhoff SM, Kaewdech A, Seto WK, Tanaka Y, Carey I, Papatheodoridi M, van Bömmel F, Berg T, Zoulim F, Ahn SH, Dalekos GN, Erler NS, Höner Zu Siederdissen C, Wedemeyer H, Cornberg M,

Yuen MF, Agarwal K, Boonstra A, Buti M, Piratvisuth T, Papatheodoridis G, Chen CH, Maasoumy B; CREATE study group. Probability of HBsAg loss after nucleo(s)tide analogue withdrawal depends on HBV genotype and viral antigen levels. *J Hepatol* 2022; **76**: 1042-1050 [PMID: 35092743 DOI: 10.1016/j.jhep.2022.01.007]

46 **Broquetas T**, Hernandez JJ, Garcia-Retortillo M, Canillas L, Puigvehí M, Cañete N, Coll S, Viu A, Garrido E, Mico M, Bessa X, Carrión JA. On-therapy HBsAg kinetics can predict HBsAg loss after nucleos(t)ide analogues interruption in HBeAg-negative patients. The cup is half full and half empty. *Dig Liver Dis* 2022; **54**: 1044-1051 [PMID: 35063365 DOI: 10.1016/j.dld.2021.12.017]

47 **Hirode G**, Choi HSJ, Chen CH, Su TH, Seto WK, Van Hees S, Papatheodoridi M, Lens S, Wong G, Brakenhoff SM, Chien RN, Feld J, Sonneveld MJ, Chan HLY, Forns X, Papatheodoridis GV, Vanwolleghem T, Yuen MF, Hsu YC, Kao JH, Cornberg M, Hansen BE, Jeng WJ, Janssen HLA; RETRACT-B Study Group. Off-Therapy Response After Nucleos(t)ide Analogue Withdrawal in Patients With Chronic Hepatitis B: An International, Multicenter, Multiethnic Cohort (RETRACT-B Study). *Gastroenterology* 2022; **162**: 757-771.e4 [PMID: 34762906 DOI: 10.1053/j.gastro.2021.11.002]

48 **Chang TT**, Lai CL, Kew Yoon S, Lee SS, Coelho HS, Carrilho FJ, Poordad F, Halota W, Horsmans Y, Tsai N, Zhang H, Tenney DJ, Tamez R, Iloeje U. Entecavir treatment for up to 5 years in patients with hepatitis B e antigen-positive chronic hepatitis B. *Hepatology* 2010; **51**: 422-430 [PMID: 20049753 DOI: 10.1002/hep.23327]

49 **Chang TT**, Liaw YF, Wu SS, Schiff E, Han KH, Lai CL, Safadi R, Lee SS, Halota W, Goodman Z, Chi YC, Zhang H, Hindes R, Iloeje U, Beebe S, Kreter B. Long-term entecavir therapy results in the reversal of fibrosis/cirrhosis and continued histological improvement in patients with chronic hepatitis B. *Hepatology* 2010; **52**: 886-893 [PMID: 20683932 DOI: 10.1002/hep.23785]

50 **Marcellin P**, Gane E, Buti M, Afdhal N, Sievert W, Jacobson IM, Washington MK, Germanidis G, Flaherty JF, Aguilar Schall R, Bornstein JD, Kitrinos KM, Subramanian GM, McHutchison JG, Heathcote EJ. Regression of cirrhosis during treatment with tenofovir disoproxil fumarate for chronic hepatitis B: a 5-year open-label follow-up study. *Lancet* 2013; **381**: 468-475 [PMID: 23234725 DOI: 10.1016/S0140-6736(12)61425-1]

51 **Facciorusso A**, Garcia Perdomo HA, Muscatiello N, Buccino RV, Wong VW, Singh S. Systematic review with meta-analysis: Change in liver stiffness during anti-viral therapy in patients with hepatitis B. *Dig Liver Dis* 2018; **50**: 787-794 [PMID: 29807871 DOI: 10.1016/j.dld.2018.05.005]

52 **Dong XQ**, Wu Z, Li J, Wang GQ, Zhao H; China HepB-Related Fibrosis Assessment Research Group. Declining in liver stiffness cannot indicate fibrosis regression in patients with chronic hepatitis B: A 78-week prospective study. *J Gastroenterol Hepatol* 2019; **34**: 755-763 [PMID: 30290019 DOI: 10.1111/jgh.14498]

53 **Kong Y**, Sun Y, Zhou J, Wu X, Chen Y, Piao H, Lu L, Ding H, Nan Y, Jiang W, Xu Y, Xie W, Li H, Feng B, Shi G, Chen G, Zheng H, Cheng J, Wang T, Liu H, Lv F, Shao C, Mao Y, Sun J, Chen T, Han T, Han Y, Wang L, Ou X, Zhang H, Jia J, You H. Early steep decline of liver stiffness predicts histological reversal of fibrosis in chronic hepatitis B patients treated with entecavir. *J Viral Hepat* 2019; **26**: 576-585 [PMID: 30624000 DOI: 10.1111/jvh.13058]

54 **Wong GL**, Chan HL, Mak CW, Lee SK, Ip ZM, Lam AT, Iu HW, Leung JM, Lai JW, Lo AO, Chan HY, Wong VW. Entecavir treatment reduces hepatic events and deaths in chronic hepatitis B patients with liver cirrhosis. *Hepatology* 2013; **58**: 1537-1547 [PMID: 23389810 DOI: 10.1002/hep.26301]

55 **Su TH**, Hu TH, Chen CY, Huang YH, Chuang WL, Lin CC, Wang CC, Su WW, Chen MY, Peng CY, Chien RN, Huang YW, Wang HY, Lin CL, Yang SS, Chen TM, Mo LR, Hsu SJ, Tseng KC, Hsieh TY, Suk FM, Hu CT, Bair MJ, Liang CC, Lei YC, Tseng TC, Chen CL, Kao JH; C-TEAM study group and the Taiwan Liver Diseases Consortium. Four-year entecavir therapy reduces hepatocellular carcinoma, cirrhotic events and mortality in chronic hepatitis B patients. *Liver Int* 2016; **36**: 1755-1764 [PMID: 27634134 DOI: 10.1111/liv.13253]

56 **Liu K**, Choi J, Le A, Yip TC, Wong VW, Chan SL, Chan HL, Nguyen MH, Lim YS, Wong GL. Tenofovir disoproxil fumarate reduces hepatocellular carcinoma, decompensation and death in chronic hepatitis B patients with cirrhosis. *Aliment Pharmacol Ther* 2019; **50**: 1037-1048 [PMID: 31524304 DOI: 10.1111/apt.15499]

57 **Papatheodoridis G**, Dalekos G, Sypsa V, Yurdaydin C, Buti M, Goulis J, Calleja JL, Chi H, Manolakopoulos S, Mangia G, Gatselis N, Keskin O, Savvidou S, de la Revilla J, Hansen BE, Vlachogiannakos I, Galanis K, Idilman R, Colombo M, Esteban R, Janssen HL, Lampertico P. PAGE-B predicts the risk of developing hepatocellular carcinoma in Caucasians with chronic hepatitis B on 5-year antiviral therapy. *J Hepatol* 2016; **64**: 800-806 [PMID: 26678008 DOI: 10.1016/j.jhep.2015.11.035]

58 **Choi J**, Kim HJ, Lee J, Cho S, Ko MJ, Lim YS. Risk of Hepatocellular Carcinoma in Patients Treated With Entecavir vs Tenofovir for Chronic Hepatitis B: A Korean Nationwide Cohort Study. *JAMA Oncol* 2019; **5**: 30-36 [PMID: 30267080 DOI: 10.1001/jamaoncol.2018.4070]

59 **Yip TC**, Wong VW, Chan HL, Tse YK, Lui GC, Wong GL. Tenofovir Is Associated With Lower Risk of Hepatocellular Carcinoma Than Entecavir in Patients With Chronic HBV Infection in China. *Gastroenterology* 2020; **158**: 215-225.e6 [PMID: 31574268 DOI: 10.1053/j.gastro.2019.09.025]

60 **Choi WM**, Yip TC, Wong GL, Kim WR, Yee LJ, Brooks-Rooney C, Curteis T, Cant H, Chen CH, Chen CY, Huang YH, Jin YJ, Jun DW, Kim JW, Park NH, Peng CY, Shin HP, Shin JW, Yang YH, Lim YS. Hepatocellular carcinoma risk in patients with chronic hepatitis B receiving tenofovir- vs. entecavir-based regimens: Individual patient data meta-analysis. *J Hepatol* 2023; **78**: 534-542 [PMID: 36572349 DOI: 10.1016/j.jhep.2022.12.007]

61 **Lee SW**, Kwon JH, Lee HL, Yoo SH, Nam HC, Sung PS, Nam SW, Bae SH, Choi JY, Yoon SK, Han NI, Jang JW. Comparison of tenofovir and entecavir on the risk of hepatocellular carcinoma and mortality in treatment-naïve patients with chronic hepatitis B in Korea: a large-scale, propensity score analysis. *Gut* 2020; **69**: 1301-1308 [PMID: 31672838 DOI: 10.1136/gutjnl-2019-318947]

62 **Papatheodoridis GV**, Dalekos GN, Idilman R, Sypsa V, Van Boemmel F, Buti M, Calleja JL, Goulis J, Manolakopoulos S, Loglio A, Papatheodoridi M, Gatselis N, Veelken R, Lopez-Gomez M, Hansen BE, Savvidou S, Kourikou A, Vlachogiannakos J, Galanis K, Yurdaydin C, Esteban R, Janssen HLA, Berg T, Lampertico P. Similar risk of hepatocellular carcinoma during long-term entecavir or tenofovir therapy in Caucasian patients with chronic hepatitis B. *J Hepatol* 2020; **73**: 1037-1045 [PMID: 32553667 DOI: 10.1016/j.jhep.2020.06.011]

63 **Grossi G**, Viganò M, Loglio A, Lampertico P. Hepatitis B virus long-term impact of antiviral therapy nucleot(s)ide analogues (NUCs). *Liver Int* 2017; **37** Suppl 1: 45-51 [PMID: 28052621]

64 **Hsu YC**, Yeh ML, Wong GL, Chen CH, Peng CY, Buti M, Enomoto M, Xie Q, Trinh H, Preda C, Liu L, Cheung KS, Yeo YH, Hoang J, Huang CF, Riveiro-Barciela M, Kozuka R, Istratescu D, Tsai PC, Accarino EV, Lee DH, Wu JL, Huang JF, Dai CY, Cheung R, Chuang WL, Yuen MF, Wong VW, Yu ML, Nguyen MH. Incidences and Determinants of Functional Cure During Entecavir or Tenofovir Disoproxil Fumarate for Chronic Hepatitis B. *J Infect Dis* 2021; **224**: 1890-1899 [PMID: 33999179 DOI: 10.1093/infdis/jiab241]

65 **Choi J**, Yoo S, Lim YS. Comparison of Long-Term Clinical Outcomes Between Spontaneous and Therapy-Induced HBsAg Seroclearance. *Hepatology* 2021; **73**: 2155-2166 [PMID: 33131063 DOI: 10.1002/hep.31610]

66 **Kuang XJ**, Jia RR, Huo RR, Yu JJ, Wang JJ, Xiang BD, Li LQ, Peng Z, Zhong JH. Systematic review of risk factors of hepatocellular carcinoma after hepatitis B surface antigen seroclearance. *J Viral Hepat* 2018; **25**: 1026-1037 [PMID: 29624821 DOI: 10.1111/jvh.12905]

67 **Wong DK**, Seto WK, Fung J, Ip P, Huang FY, Lai CL, Yuen MF. Reduction of hepatitis B surface antigen and covalently closed circular DNA by nucleos(t)ide analogues of different potency. *Clin Gastroenterol Hepatol* 2013; **11**: 1004-10.e1 [PMID: 23376799 DOI: 10.1016/j.cgh.2013.01.026]

68 **Liaw YF**, Leung N, Kao JH, Piratvisuth T, Gane E, Han KH, Guan R, Lau GK, Locarnini S; Chronic Hepatitis B Guideline Working Party of the Asian-Pacific Association for the Study of the Liver. Asian-Pacific consensus statement on the management of chronic hepatitis B: a 2008 update. *Hepatol Int* 2008; **2**: 263-283 [PMID: 19669255 DOI: 10.1007/s12072-008-9080-3]

69 **Hadziyannis SJ**, Sevastianos V, Rapti I, Vassilopoulos D, Hadziyannis E. Sustained responses and loss of HBsAg in HBeAg-negative patients with chronic hepatitis B who stop long-term treatment with adefovir. *Gastroenterology* 2012; **143**: 629-636.e1 [PMID: 22659218 DOI: 10.1053/j.gastro.2012.05.039]

70 **Berg T**, Simon KG, Mauss S, Schott E, Heyne R, Klass DM, Eisenbach C, Welzel TM, Zachoval R, Felten G, Schulze-Zur-Wiesch J, Cornberg M, Op den Brouw ML, Jump B, Reiser H, Gallo L, Warger T, Petersen J; FINITE CHB study investigators [First investigation in stopping TDF treatment after long-term virological suppression in HBeAg-negative chronic hepatitis B]. Long-term response after stopping tenofovir disoproxil fumarate in non-cirrhotic HBeAg-negative patients - FINITE study. *J Hepatol* 2017; **67**: 918-924 [PMID: 28736139 DOI: 10.1016/j.jhep.2017.07.012]

71 **Papatheodoridis G**, Vlachogiannakos I, Cholongitas E, Wursthorn K, Thomadakis C, Touloumi G, Petersen J. Discontinuation of oral antivirals in chronic hepatitis B: A systematic review. *Hepatology* 2016; **63**: 1481-1492 [PMID: 27100145 DOI: 10.1002/hep.28438]

72 **Jeng WJ**, Chen YC, Chien RN, Sheen IS, Liaw YF. Incidence and predictors of hepatitis B surface antigen seroclearance after cessation of nucleos(t)ide analogue therapy in hepatitis B e antigen-negative chronic hepatitis B. *Hepatology* 2018; **68**: 425-434 [PMID: 29108132 DOI: 10.1002/hep.29640]

73 **Chien RN**, Liaw YF. Re-treatment for severe hepatitis flare in HBeAg-negative chronic hepatitis B: An appraisal with combined HBsAg/ALT kinetics. *J Viral Hepat* 2020; **27**: 544-547 [PMID: 31868280 DOI: 10.1111/jvh.13253]

74 **Berg T**, Lampertico P. The times they are a-changing - A refined proposal for finite HBV nucleos(t)ide analogue therapy. *J Hepatol* 2021; **75**: 474-480 [PMID: 33957187 DOI: 10.1016/j.jhep.2021.04.040]

75 **Boni C**, Laccabue D, Lampertico P, Giuberti T, Viganò M, Schivazappa S, Alfieri A, Pesci M, Gaeta GB, Brancaccio G, Colombo M, Missale G, Ferrari C. Restored function of HBV-specific T cells after long-term effective therapy with nucleos(t)ide analogues. *Gastroenterology* 2012; **143**: 963-73.e9 [PMID: 22796241 DOI: 10.1053/j.gastro.2012.07.014]

76 **Höner Zu Siederdissen C**, Rinker F, Maasoumy B, Wiegand SB, Filmann N, Falk CS, Deterding K, Port K, Mix C, Manns MP, Herrmann E, Wedemeyer H, Kraft AR, Cornberg M. Viral and Host Responses After Stopping Long-term Nucleos(t)ide Analogue Therapy in HBeAg-Negative Chronic Hepatitis B. *J Infect Dis* 2016; **214**: 1492-1497 [PMID: 27609808 DOI: 10.1093/infdis/jiw412]

77 **Rivino L**, Le Bert N, Gill US, Kunasegaran K, Cheng Y, Tan DZ, Becht E, Hansi NK, Foster GR, Su TH, Tseng TC, Lim SG, Kao JH, Newell EW, Kennedy PT, Bertoletti A. Hepatitis B virus-specific T cells associate with viral control upon nucleos(t)ide-analogue therapy discontinuation. *J Clin Invest* 2018; **128**: 668-681 [PMID: 29309050 DOI: 10.1172/JCI92812]

78 **Rinker F**, Zimmer CL, Höner Zu Siederdissen C, Manns MP, Kraft ARM, Wedemeyer H, Björkström NK, Cornberg M. Hepatitis B virus-specific T cell responses after stopping nucleos(t)ide analogue therapy in HBeAg-negative chronic hepatitis B. *J Hepatol* 2018; **69**: 584-593 [PMID: 29758333 DOI: 10.1016/j.jhep.2018.05.004]

79 **Chen CH**, Lu SN, Hung CH, Wang JH, Hu TH, Changchien CS, Lee CM. The role of hepatitis B surface antigen quantification in predicting HBsAg loss and HBV relapse after discontinuation of lamivudine treatment. *J Hepatol* 2014; **61**: 515-522 [PMID: 24798617 DOI: 10.1016/j.jhep.2014.04.029]

80 **Liu J**, Li T, Zhang L, Xu A. The Role of Hepatitis B Surface Antigen in Nucleos(t)ide Analogues Cessation Among Asian Patients With Chronic Hepatitis B: A Systematic Review. *Hepatology* 2019; **70**: 1045-1055 [PMID: 30561829 DOI: 10.1002/hep.30474]

81 **Sonneveld MJ**, Park JY, Kaewdech A, Seto WK, Tanaka Y, Carey I, Papatheodoridi M, van Bömmel F, Berg T, Zoulim F, Ahn SH, Dalekos GN, Erler NS, Höner Zu Siederdissen C, Wedemeyer H, Cornberg M, Yuen MF, Agarwal K, Boonstra A, Buti M, Piratvisuth T, Papatheodoridis G, Maasoumy B; CREATE Study Group. Prediction of Sustained Response After Nucleo(s)tide Analogue Cessation Using HBsAg and HBcrAg Levels: A Multicenter Study (CREATE). *Clin Gastroenterol Hepatol* 2022; **20**: e784-e793 [PMID: 33309804 DOI: 10.1016/j.cgh.2020.12.005]

82 **van Bömmel F**, Berg T. Risks and Benefits of Discontinuation of Nucleos(t)ide Analogue Treatment: A Treatment Concept for Patients With HBeAg-Negative Chronic Hepatitis B. *Hepatol Commun* 2021; **5**: 1632-1648 [PMID: 34558833 DOI: 10.1002/hep4.1708]

83 **Agarwal K**, Lok J, Carey I, Shivkar Y, Biermer M, Berg T, Lonjon-Domanec I. A case of HBV-induced liver failure in the REEF-2 phase II trial: Implications for finite treatment strategies in HBV 'cure'. *J Hepatol* 2022; **77**: 245-248 [PMID: 35358614 DOI: 10.1016/j.jhep.2022.03.006]

84 **Lau GK**, Piratvisuth T, Luo KX, Marcellin P, Thongsawat S, Cooksley G, Gane E, Fried MW, Chow WC, Paik SW,

Chang WY, Berg T, Flisiak R, McCloud P, Pluck N; Peginterferon Alfa-2a HBeAg-Positive Chronic Hepatitis B Study Group. Peginterferon Alfa-2a, lamivudine, and the combination for HBeAg-positive chronic hepatitis B. *N Engl J Med* 2005; **352**: 2682-2695 [PMID: 15987917 DOI: 10.1056/NEJMoa043470]

85 **Marcellin P**, Bonino F, Yurdaydin C, Hadziyannis S, Moucari R, Kapprell HP, Rothe V, Popescu M, Brunetto MR. Hepatitis B surface antigen levels: association with 5-year response to peginterferon alfa-2a in hepatitis B e-antigen-negative patients. *Hepatol Int* 2013; **7**: 88-97 [PMID: 23518903 DOI: 10.1007/s12072-012-9343-x]

86 **Marcellin P**, Ahn SH, Ma X, Caruntu FA, Tak WY, Elkashab M, Chuang WL, Lim SG, Tabak F, Mehta R, Petersen J, Foster GR, Lou L, Martins EB, Dinh P, Lin L, Corsa A, Charuworn P, Subramanian GM, Reiser H, Reesink HW, Fung S, Strasser SI, Trinh H, Buti M, Gaeta GB, Hui AJ, Papatheodoridis G, Flisiak R, Chan HL; Study 149 Investigators. Combination of Tenofovir Disoproxil Fumarate and Peginterferon α-2a Increases Loss of Hepatitis B Surface Antigen in Patients With Chronic Hepatitis B. *Gastroenterology* 2016; **150**: 134-144.e10 [PMID: 26453773 DOI: 10.1053/j.gastro.2015.09.043]

87 **Bourlière M**, Rabiega P, Ganne-Carrie N, Serfaty L, Marcellin P, Barthe Y, Thabut D, Guyader D, Hezode C, Picon M, Causse X, Leroy V, Bronowicki JP, Carrieri P, Riachi G, Rosa I, Attali P, Molina JM, Bacq Y, Tran A, Grangé JD, Zoulim F, Fontaine H, Alric L, Bertucci I, Bouvier-Alias M, Carrat F; ANRS HB06 PEGAN Study Group. Effect on HBs antigen clearance of addition of pegylated interferon alfa-2a to nucleos(t)ide analogue therapy versus nucleos(t)ide analogue therapy alone in patients with HBe antigen-negative chronic hepatitis B and sustained undetectable plasma hepatitis B virus DNA: a randomised, controlled, open-label trial. *Lancet Gastroenterol Hepatol* 2017; **2**: 177-188 [PMID: 28404133 DOI: 10.1016/S2468-1253(16)30189-3]

88 **Lim SG**, Yang WL, Ngu JH, Chang J, Tan J, Ahmed T, Dan YY, Lim K, Lee YM, Lee GH, Tan PS, Wai KL, Phyo WW, Khine HHTW, Lee C, Tay A, Chan E. Switching to or Add-on Peginterferon in Patients on Nucleos(t)ide Analogues for Chronic Hepatitis B: The SWAP RCT. *Clin Gastroenterol Hepatol* 2022; **20**: e228-e250 [PMID: 33895361 DOI: 10.1016/j.cgh.2021.04.031]

89 **Mo Z**, Xie D, Fu L, Zhang W, Wei J, Li G, Yang J, Chen X, Li J, Shang J, Guan Y, Jiang Y, Guo Y, Zeng Y, Chang J, Peng Y, Lin M, Huang G, Gu S, Geng J, Gao Z. Functional cure based on pegylated interferon α-2b therapy in nucleoside analog-suppressed HBeAg negative chronic hepatitis B: a multicenter real-world study (Everest Project in china)-4 years data update. *Hepatology* 2022; **76**: S24-25

90 **Chen CH**, Hung CH, Wang JH, Lu SN, Hu TH, Lee CM. Long-term incidence and predictors of hepatitis B surface antigen loss after discontinuing nucleoside analogues in noncirrhotic chronic hepatitis B patients. *Clin Microbiol Infect* 2018; **24**: 997-1003 [PMID: 29288020 DOI: 10.1016/j.cmi.2017.12.013]

91 **Song DS**, Jang JW, Yoo SH, Kwon JH, Nam SW, Bae SH, Choi JY, Yoon SK. Improving the Prediction of Relapse After Nucleos(t)ide Analogue Discontinuation in Patients With Chronic Hepatitis B. *Clin Infect Dis* 2021; **73**: e892-e903 [PMID: 33417679 DOI: 10.1093/cid/ciab007]

92 **Kuo MT**, Hu TH, Hung CH, Wang JH, Lu SN, Tsai KL, Chen CH. Hepatitis B virus relapse rates in chronic hepatitis B patients who discontinue either entecavir or tenofovir. *Aliment Pharmacol Ther* 2019; **49**: 218-228 [PMID: 30484881 DOI: 10.1111/apt.15053]

93 **Chen CH**, Hu TH, Wang JH, Lai HC, Hung CH, Lu SN, Peng CY. Comparison of HBsAg changes between HBeAg-negative patients who discontinued or maintained entecavir therapy. *Hepatol Int* 2020; **14**: 317-325 [PMID: 31650509 DOI: 10.1007/s12072-019-09991-y]

94 **Seto WK**, Hui AJ, Wong VW, Wong GL, Liu KS, Lai CL, Yuen MF, Chan HL. Treatment cessation of entecavir in Asian patients with hepatitis B e antigen negative chronic hepatitis B: a multicentre prospective study. *Gut* 2015; **64**: 667-672 [PMID: 24833635 DOI: 10.1136/gutjnl-2014-307237]

95 **Liaw YF**, Jeng WJ, Chang ML. HBsAg Kinetics in Retreatment Decision for Off-Therapy Hepatitis B Flare in HBeAg-Negative Patients. *Gastroenterology* 2018; **154**: 2280-2281 [PMID: 29746811 DOI: 10.1053/j.gastro.2018.03.066]

96 **Liaw YF**. Finite nucleos(t)ide analog therapy in HBeAg-negative chronic hepatitis B: an emerging paradigm shift. *Hepatol Int* 2019; **13**: 665-673 [PMID: 31559604 DOI: 10.1007/s12072-019-09989-6]

97 **Chien RN**, Liaw YF. Current Trend in Antiviral Therapy for Chronic Hepatitis B. *Viruses* 2022; **14** [PMID: 35216027 DOI: 10.3390/v14020434]

98 **Chang Y**, Choe WH, Sinn DH, Lee JH, Ahn SH, Lee H, Shim JJ, Jun DW, Park SY, Nam JY, Cho EJ, Yu SJ, Lee DH, Lee JM, Kim YJ, Kwon SY, Paik SW, Yoon JH. Nucleos(t)ide Analogue Treatment for Patients With Hepatitis B Virus (HBV) e Antigen-Positive Chronic HBV Genotype C Infection: A Nationwide, Multicenter, Retrospective Study. *J Infect Dis* 2017; **216**: 1407-1414 [PMID: 29029102 DOI: 10.1093/infdis/jix506]

99 **Kim GA**, Lim YS, Han S, Choi J, Shim JH, Kim KM, Lee HC, Lee YS. High risk of hepatocellular carcinoma and death in patients with immune-tolerant-phase chronic hepatitis B. *Gut* 2018; **67**: 945-952 [PMID: 29055908 DOI: 10.1136/gutjnl-2017-314904]

100 **Lee HW**, Kim SU, Baatarkhuu O, Park JY, Kim DY, Ahn SH, Han KH, Kim BK. Progression of Untreated Minimally Active Chronic HBV Infection Compared to Inactive Infection. *Clin Gastroenterol Hepatol* 2019; **17**: 2808-2810.e2 [PMID: 30639778 DOI: 10.1016/j.cgh.2019.01.002]

101 **Bonacci M**, Forns X, Lens S. The HBeAg-Negative "Gray Zone" Phase: A Frequent Condition With Different Outcomes in Western and Asian Patients? *Clin Gastroenterol Hepatol* 2020; **18**: 263-264 [PMID: 31858983 DOI: 10.1016/j.cgh.2019.05.024]

102 **Oliveri F**, Surace L, Cavallone D, Colombatto P, Ricco G, Salvati N, Coco B, Romagnoli V, Gattai R, Salvati A, Moriconi F, Yuan Q, Bonino F, Brunetto MR. Long-term outcome of inactive and active, low viraemic HBeAg-negative-hepatitis B virus infection: Benign course towards HBsAg clearance. *Liver Int* 2017; **37**: 1622-1631 [PMID: 28296013 DOI: 10.1111/liv.13416]

103 **Bonacci M**, Lens S, Mariño Z, Londoño MC, Rodríguez-Tajes S, Mas A, García-López M, Pérez-Del-Pulgar S, Sánchez-Tapias JM, Forns X. Anti-viral therapy can be delayed or avoided in a significant proportion of HBeAg-negative Caucasian patients in the Grey Zone. *Aliment Pharmacol Ther* 2018; **47**: 1397-1408 [PMID: 29577350 DOI: 10.1111/apt.14613]

104 **Huang DQ**, Lee DH, Le MH, Le A, Yeo YH, Trinh HN, Chung M, Nguyen V, Johnson T, Zhang JQ, Wong C, Li J, Cheung R, Nguyen MH. Liver Complications in Untreated Treatment-Ineligible versus Treated Treatment-Eligible Patients with Hepatitis B. *Dig Dis* 2023; **41**: 115-123 [PMID: 36070707 DOI: 10.1159/000526933]

105 **Lim YS**, Ahn SH, Shim JJ, Razavi H, Razavi-Shearer D, Sinn DH. Impact of expanding hepatitis B treatment guidelines: A modelling and economic impact analysis. *Aliment Pharmacol Ther* 2022; **56**: 519-528 [PMID: 35614532 DOI: 10.1111/apt.17052]

106 **Jeng WJ**, Lok AS. Should Treatment Indications for Chronic Hepatitis B Be Expanded? *Clin Gastroenterol Hepatol* 2021; **19**: 2006-2014 [PMID: 32434068 DOI: 10.1016/j.cgh.2020.04.091]

107 **Xia Y**, Stadler D, Ko C, Protzer U. Analyses of HBV cccDNA Quantification and Modification. *Methods Mol Biol* 2017; **1540**: 59-72 [PMID: 27975308 DOI: 10.1007/978-1-4939-6700-1_6]

108 **Testoni B**, Lebossé F, Scholtes C, Berby F, Miaglia C, Subic M, Loglio A, Facchetti F, Lampertico P, Levrero M, Zoulim F. Serum hepatitis B core-related antigen (HBcrAg) correlates with covalently closed circular DNA transcriptional activity in chronic hepatitis B patients. *J Hepatol* 2019; **70**: 615-625 [PMID: 30529504 DOI: 10.1016/j.jhep.2018.11.030]

109 **Lam YF**, Seto WK, Wong D, Cheung KS, Fung J, Mak LY, Yuen J, Chong CK, Lai CL, Yuen MF. Seven-Year Treatment Outcome of Entecavir in a Real-World Cohort: Effects on Clinical Parameters, HBsAg and HBcrAg Levels. *Clin Transl Gastroenterol* 2017; **8**: e125 [PMID: 29072673 DOI: 10.1038/ctg.2017.51]

110 **Mak LY**, Wong DK, Cheung KS, Seto WK, Fung J, Yuen MF. First-line oral antiviral therapies showed similar efficacies in suppression of serum HBcrAg in chronic hepatitis B patients. *BMC Gastroenterol* 2021; **21**: 123 [PMID: 33731023 DOI: 10.1186/s12876-021-01711-x]

111 **Carey I**, Gersch J, Wang B, Moigboi C, Kuhns M, Cloherty G, Dusheiko G, Agarwal K. Pregenomic HBV RNA and Hepatitis B Core-Related Antigen Predict Outcomes in Hepatitis B e Antigen-Negative Chronic Hepatitis B Patients Suppressed on Nucleos(T)ide Analogue Therapy. *Hepatology* 2020; **72**: 42-57 [PMID: 31701544 DOI: 10.1002/hep.31026]

112 **Broquetas T**, Garcia-Retortillo M, Micó M, Canillas L, Puigvehí M, Cañete N, Coll S, Viu A, Hernandez JJ, Bessa X, Carrión JA. Hepatitis B surface antigen and hepatitis B core-related antigen kinetics after adding pegylated-interferon to nucleos(t)ids analogues in hepatitis B e antigen-negative patients. *World J Hepatol* 2020; **12**: 1076-1088 [PMID: 33312431 DOI: 10.4254/wjh.v12.i11.1076]

113 **Inoue T**, Kusumoto S, Iio E, Ogawa S, Suzuki T, Yagi S, Kaneko A, Matsuura K, Aoyagi K, Tanaka Y. Clinical efficacy of a novel, high-sensitivity HBcrAg assay in the management of chronic hepatitis B and HBV reactivation. *J Hepatol* 2021; **75**: 302-310 [PMID: 33762167 DOI: 10.1016/j.jhep.2021.02.017]

114 **Giersch K**, Allweiss L, Volz T, Dandri M, Lütgehetmann M. Serum HBV pgRNA as a clinical marker for cccDNA activity. *J Hepatol* 2017; **66**: 460-462 [PMID: 27826059 DOI: 10.1016/j.jhep.2016.09.028]

115 **van Bömmel F**, Bartens A, Mysickova A, Hofmann J, Krüger DH, Berg T, Edelmann A. Serum hepatitis B virus RNA levels as an early predictor of hepatitis B envelope antigen seroconversion during treatment with polymerase inhibitors. *Hepatology* 2015; **61**: 66-76 [PMID: 25132147 DOI: 10.1002/hep.27381]

116 **Butler EK**, Gersch J, McNamara A, Luk KC, Holzmayer V, de Medina M, Schiff E, Kuhns M, Cloherty GA. Hepatitis B Virus Serum DNA andRNA Levels in Nucleos(t)ide Analog-Treated or Untreated Patients During Chronic and Acute Infection. *Hepatology* 2018; **68**: 2106-2117 [PMID: 29734472 DOI: 10.1002/hep.30082]

117 **Mak LY**, Cloherty G, Wong DK, Gersch J, Seto WK, Fung J, Yuen MF. HBV RNA Profiles in Patients With Chronic Hepatitis B Under Different Disease Phases and Antiviral Therapy. *Hepatology* 2021; **73**: 2167-2179 [PMID: 33159329 DOI: 10.1002/hep.31616]

118 **Mak LY**, Wong D, Kuchta A, Hilfiker M, Hamilton A, Chow N, Mao X, Seto WK, Yuen MF. Hepatitis B virus pre-genomic RNA and hepatitis B core-related antigen reductions at week 4 predict favourable hepatitis B surface antigen response upon long-term nucleos(t)ide analogue in chronic hepatitis B. *Clin Mol Hepatol* 2023; **29**: 146-162 [PMID: 35989092 DOI: 10.3350/cmh.2022.0172]

119 **Wang J**, Shen T, Huang X, Kumar GR, Chen X, Zeng Z, Zhang R, Chen R, Li T, Zhang T, Yuan Q, Li PC, Huang Q, Colonno R, Jia J, Hou J, McCrae MA, Gao Z, Ren H, Xia N, Zhuang H, Lu F. Serum hepatitis B virus RNA is encapsidated pregenome RNA that may be associated with persistence of viral infection and rebound. *J Hepatol* 2016; **65**: 700-710 [PMID: 27245431 DOI: 10.1016/j.jhep.2016.05.029]

120 **Pfefferkorn M**, Böhm S, Schott T, Deichsel D, Bremer CM, Schröder K, Gerlich WH, Glebe D, Berg T, van Bömmel F. Quantification of large and middle proteins of hepatitis B virus surface antigen (HBsAg) as a novel tool for the identification of inactive HBV carriers. *Gut* 2018; **67**: 2045-2053 [PMID: 28951526 DOI: 10.1136/gutjnl-2017-313811]

121 **Peiffer KH**, Kuhnhenn L, Jiang B, Mondorf A, Vermehren J, Knop V, Susser S, Walter D, Dietz J, Carra G, Finkelmeier F, Zeuzem S, Sarrazin C, Hildt E. Divergent preS Sequences in Virion-Associated Hepatitis B Virus Genomes and Subviral HBV Surface Antigen Particles From HBV e Antigen-Negative Patients. *J Infect Dis* 2018; **218**: 114-123 [PMID: 29528436 DOI: 10.1093/infdis/jiy119]

122 **Pfefferkorn M**, Schott T, Böhm S, Deichsel D, Felkel C, Gerlich WH, Glebe D, Wat C, Pavlovic V, Heyne R, Berg T, van Bömmel F. Composition of HBsAg is predictive of HBsAg loss during treatment in patients with HBeAg-positive chronic hepatitis B. *J Hepatol* 2021; **74**: 283-292 [PMID: 32931877 DOI: 10.1016/j.jhep.2020.08.039]

123 **Lim SG**, Phyo WW, Ling JZJ, Cloherty G, Butler EK, Kuhns MC, McNamara AL, Holzmayer V, Gersch J, Yang WL, Ngu JH, Chang J, Tan J, Ahmed T, Dan YY, Lee YM, Lee GH, Tan PS, Huang DQ, Khine HTW, Lee C, Tay A, Chan E. Comparative biomarkers for HBsAg loss with antiviral therapy shows dominant influence of quantitative HBsAg (qHBsAg). *Aliment Pharmacol Ther* 2021; **53**: 172-182 [PMID: 33159496 DOI: 10.1111/apt.16149]

124 **Bogomolov P**, Alexandrov A, Voronkova N, Macievich M, Kokina K, Petrachenkova M, Lehr T, Lempp FA, Wedemeyer H, Haag M, Schwab M, Haefeli WE, Blank A, Urban S. Treatment of chronic hepatitis D with the entry inhibitor myrcludex B: First results of a phase Ib/IIa study. *J Hepatol* 2016; **65**: 490-498 [PMID: 27132170 DOI: 10.1016/j.jhep.2016.04.016]

125 **Gane E**, Jucov A, Dobryanska M, Yoon KT, Lim TH, Arizpe A, Cloutier D, L Shen, Gupta SV, Lau AH, Hwang C, Lim YS. Safety, tolerability, and antiviral activity of the siRNA VIR-2218 in combination with the investigational neutralizing

monoclonal antibody VIR-3434 for the treatment of chronic hepatitis B virus infection: preliminary results from the Phase 2 MARCH trial. *Hepatology* 2022; **76**: S18

126 **Taverniti V**, Ligat G, Debing Y, Kum DB, Baumert TF, Verrier ER. Capsid Assembly Modulators as Antiviral Agents against HBV: Molecular Mechanisms and Clinical Perspectives. *J Clin Med* 2022; **11** [PMID: 35268440 DOI: 10.3390/jcm11051349]

127 **Hui RW**, Mak LY, Seto WK, Yuen MF. RNA interference as a novel treatment strategy for chronic hepatitis B infection. *Clin Mol Hepatol* 2022; **28**: 408-424 [PMID: 35172540 DOI: 10.3350/cmh.2022.0012]

128 **Wooddell CI**, Yuen MF, Chan HL, Gish RG, Locarnini SA, Chavez D, Ferrari C, Given BD, Hamilton J, Kanner SB, Lai CL, Lau JYN, Schluep T, Xu Z, Lanford RE, Lewis DL. RNAi-based treatment of chronically infected patients and chimpanzees reveals that integrated hepatitis B virus DNA is a source of HBsAg. *Sci Transl Med* 2017; **9** [PMID: 28954926 DOI: 10.1126/scitranslmed.aan0241]

129 **Ghany MG**, Lok AS. Functional cure of hepatitis B requires silencing covalently closed circular and integrated hepatitis B virus DNA. *J Clin Invest* 2022; **132** [PMID: 36106633 DOI: 10.1172/JCI163175]

130 **Yuen MF**, Heo J, Kumada H, Suzuki F, Suzuki Y, Xie Q, Jia J, Karino Y, Hou J, Chayama K, Imamura M, Lao-Tan JY, Lim SG, Tanaka Y, Xie W, Yoon JH, Duan Z, Kurosaki M, Park SJ, Labio ME, Kumar R, Kweon YO, Yim HJ, Tao Y, Cremer J, Elston R, Davies M, Baptiste-Brown S, Han K, Campbell FM, Paff M, Theodore D. Phase IIa, randomised, double-blind study of GSK3389404 in patients with chronic hepatitis B on stable nucleos(t)ide therapy. *J Hepatol* 2022; **77**: 967-977 [PMID: 35714812 DOI: 10.1016/j.jhep.2022.05.031]

131 **Yuen MF**, Lim SG, Plesniak R, Tsuji K, Janssen HLA, Pojoga C, Gadano A, Popescu CP, Stepanova T, Asselah T, Diaconescu G, Yim HJ, Heo J, Janczewska E, Wong A, Idriz N, Imamura M, Rizzardini G, Takaguchi K, Andreone P, Arbune M, Hou J, Park SJ, Vata A, Cremer J, Elston R, Lukić T, Quinn G, Maynard L, Kendrick S, Plein H, Campbell F, Paff M, Theodore D; B-Clear Study Group. Efficacy and Safety of Bepirovirsen in Chronic Hepatitis B Infection. *N Engl J Med* 2022; **387**: 1957-1968 [PMID: 36346079 DOI: 10.1056/NEJMoa2210027]

132 **Boulon R**, Blanchet M, Lemasson M, Vaillant A, Labonté P. Characterization of the antiviral effects of REP 2139 on the HBV lifecycle in vitro. *Antiviral Res* 2020; **183**: 104853 [PMID: 32585322 DOI: 10.1016/j.antiviral.2020.104853]

133 **Bazinet M**, Pântea V, Placinta G, Moscalu I, Cebotarescu V, Cojuhari L, Jimbei P, Iarovoi L, Smesnoi V, Musteata T, Jucov A, Dittmer U, Krawczyk A, Vaillant A. Safety and Efficacy of 48 Weeks REP 2139 or REP 2165, Tenofovir Disoproxil, and Pegylated Interferon Alfa-2a in Patients With Chronic HBV Infection Naïve to Nucleos(t)ide Therapy. *Gastroenterology* 2020; **158**: 2180-2194 [PMID: 32147484 DOI: 10.1053/j.gastro.2020.02.058]

134 **Lanford RE**, Guerra B, Chavez D, Giavedoni L, Hodara VL, Brasky KM, Fosdick A, Frey CR, Zheng J, Wolfgang G, Halcomb RL, Tumas DB. GS-9620, an oral agonist of Toll-like receptor-7, induces prolonged suppression of hepatitis B virus in chronically infected chimpanzees. *Gastroenterology* 2013; **144**: 1508-1517, 1517.e1 [PMID: 23415804 DOI: 10.1053/j.gastro.2013.02.003]

135 **Janssen HLA**, Brunetto MR, Kim YJ, Ferrari C, Massetto B, Nguyen AH, Joshi A, Woo J, Lau AH, Gaggar A, Subramanian GM, Yoshida EM, Ahn SH, Tsai NCS, Fung S, Gane EJ. Safety, efficacy and pharmacodynamics of vesatolimod (GS-9620) in virally suppressed patients with chronic hepatitis B. *J Hepatol* 2018; **68**: 431-440 [PMID: 29104121 DOI: 10.1016/j.jhep.2017.10.027]

136 **Boni C**, Vecchi A, Rossi M, Laccabue D, Giuberti T, Alfieri A, Lampertico P, Grossi G, Facchetti F, Brunetto MR, Coco B, Cavallone D, Mangia A, Santoro R, Piazzolla V, Lau A, Gaggar A, Subramanian GM, Ferrari C. TLR7 Agonist Increases Responses of Hepatitis B Virus-Specific T Cells and Natural Killer Cells in Patients With Chronic Hepatitis B Treated With Nucleos(T)Ide Analogues. *Gastroenterology* 2018; **154**: 1764-1777.e7 [PMID: 29378197 DOI: 10.1053/j.gastro.2018.01.030]

137 **Gane EJ**, Kim HJ, Visvanathan K, Kim YJ, Nguyen AH, Wallin JJ, Chen DY, McDonald C, Arora P, Tan SK, Gaggar A, Roberts SK, Lim YS. Safety, Pharmacokinetics, and Pharmacodynamics of the Oral TLR8 Agonist Selgantolimod in Chronic Hepatitis B. *Hepatology* 2021; **74**: 1737-1749 [PMID: 33704806 DOI: 10.1002/hep.31795]

138 **Alexopoulou A**, Vasilieva L, Karayiannis P. New Approaches to the Treatment of Chronic Hepatitis B. *J Clin Med* 2020; **9** [PMID: 33019573 DOI: 10.3390/jcm9103187]

139 **Yuen MF**, Chen CY, Liu CJ, Jeng WJ, Elkhashab M, Coffin CS, Kim W, Greenbloom S, Ramji A, Lim YS, Kim YJ, Fung SK, Kim DJ, Jang JW, Lee KS, Iyer RP, Macfarlane C, Jackson K, Locarnini SA, Chan HLY, Afdhal NH. A phase 2, open-label, randomized, multiple-dose study evaluating Inarigivir in treatment-naïve patients with chronic hepatitis B. *Liver Int* 2023; **43**: 77-89 [PMID: 36300646 DOI: 10.1111/liv.15465]

140 **Yau T**, Hsu C, Kim TY, Choo SP, Kang YK, Hou MM, Numata K, Yeo W, Chopra A, Ikeda M, Kuromatsu R, Moriguchi M, Chao Y, Zhao H, Anderson J, Cruz CD, Kudo M. Nivolumab in advanced hepatocellular carcinoma: Sorafenib-experienced Asian cohort analysis. *J Hepatol* 2019; **71**: 543-552 [PMID: 31176752 DOI: 10.1016/j.jhep.2019.05.014]

141 **El-Khoueiry AB**, Sangro B, Yau T, Crocenzi TS, Kudo M, Hsu C, Kim TY, Choo SP, Trojan J, Welling TH Rd, Meyer T, Kang YK, Yeo W, Chopra A, Anderson J, Dela Cruz C, Lang L, Neely J, Tang H, Dastani HB, Melero I. Nivolumab in patients with advanced hepatocellular carcinoma (CheckMate 040): an open-label, non-comparative, phase 1/2 dose escalation and expansion trial. *Lancet* 2017; **389**: 2492-2502 [PMID: 28434648 DOI: 10.1016/S0140-6736(17)31046-2]

142 **Lok AS**, Pan CQ, Han SH, Trinh HN, Fessel WJ, Rodell T, Massetto B, Lin L, Gaggar A, Subramanian GM, McHutchison JG, Ferrari C, Lee H, Gordon SC, Gane EJ. Randomized phase II study of GS-4774 as a therapeutic vaccine in virally suppressed patients with chronic hepatitis B. *J Hepatol* 2016; **65**: 509-516 [PMID: 27210427 DOI: 10.1016/j.jhep.2016.05.016]

143 **Michler T**, Kosinska AD, Festag J, Bunse T, Su J, Ringelhan M, Imhof H, Grimm D, Steiger K, Mogler C, Heikenwalder M, Michel ML, Guzman CA, Milstein S, Sepp-Lorenzino L, Knolle P, Protzer U. Knockdown of Virus Antigen Expression Increases Therapeutic Vaccine Efficacy in High-Titer Hepatitis B Virus Carrier Mice. *Gastroenterology* 2020; **158**: 1762-1775.e9 [PMID: 32001321 DOI: 10.1053/j.gastro.2020.01.032]

144 **Stieger B**. The role of the sodium-taurocholate cotransporting polypeptide (NTCP) and of the bile salt export pump (BSEP) in physiology and pathophysiology of bile formation. *Handb Exp Pharmacol* 2011; 205-259 [PMID: 21103971 DOI: 10.1007/978-3-642-14541-4_5]

145 **van den Berg F**, Limani SW, Mnyandu N, Maepa MB, Ely A, Arbuthnot P. Advances with RNAi-Based Therapy for Hepatitis B Virus Infection. *Viruses* 2020; **12** [PMID: 32759756 DOI: 10.3390/v12080851]

146 **Elbashir SM**, Harborth J, Lendeckel W, Yalcin A, Weber K, Tuschl T. Duplexes of 21-nucleotide RNAs mediate RNA interference in cultured mammalian cells. *Nature* 2001; **411**: 494-498 [PMID: 11373684 DOI: 10.1038/35078107]

147 **Wong GLH**, Gane E, Lok ASF. How to achieve functional cure of HBV: Stopping NUCs, adding interferon or new drug development? *J Hepatol* 2022; **76**: 1249-1262 [PMID: 35589248 DOI: 10.1016/j.jhep.2021.11.024]

148 **Phillips S**, Jagatia R, Chokshi S. Novel therapeutic strategies for chronic hepatitis B. *Virulence* 2022; **13**: 1111-1132 [PMID: 35763282 DOI: 10.1080/21505594.2022.2093444]

149 **Lucifora J**, Xia Y, Reisinger F, Zhang K, Stadler D, Cheng X, Sprinzl MF, Koppensteiner H, Makowska Z, Volz T, Remouchamps C, Chou WM, Thasler WE, Hüser N, Durantel D, Liang TJ, Münk C, Heim MH, Browning JL, Dejardin E, Dandri M, Schindler M, Heikenwalder M, Protzer U. Specific and nonhepatotoxic degradation of nuclear hepatitis B virus cccDNA. *Science* 2014; **343**: 1221-1228 [PMID: 24557838 DOI: 10.1126/science.1243462]

150 **Nishio A**, Bolte FJ, Takeda K, Park N, Yu ZX, Park H, Valdez K, Ghany MG, Rehermann B. Clearance of pegylated interferon by Kupffer cells limits NK cell activation and therapy response of patients with HBV infection. *Sci Transl Med* 2021; **13** [PMID: 33790025 DOI: 10.1126/scitranslmed.aba6322]

151 **Liu J**, Wang T, Zhang W, Cheng Y, He Q, Wang FS. Effect of combination treatment based on interferon and nucleos(t)ide analogues on functional cure of chronic hepatitis B: a systematic review and meta-analysis. *Hepatol Int* 2020; **14**: 958-972 [PMID: 33185803 DOI: 10.1007/s12072-020-10099-x]

152 **Lampertico P**, Viganò M, Cheroni C, Facchetti F, Invernizzi F, Valveri V, Soffredini R, Abrignani S, De Francesco R, Colombo M. IL28B polymorphisms predict interferon-related hepatitis B surface antigen seroclearance in genotype D hepatitis B e antigen-negative patients with chronic hepatitis B. *Hepatology* 2013; **57**: 890-896 [PMID: 22473858 DOI: 10.1002/hep.25749]

153 **Boglione L**, Cusato J, Allegra S, Esposito I, Patti F, Cariti G, Di Perri G, D'Avolio A. Role of IL28-B polymorphisms in the treatment of chronic hepatitis B HBeAg-negative patients with peginterferon. *Antiviral Res* 2014; **102**: 35-43 [PMID: 24316030 DOI: 10.1016/j.antiviral.2013.11.014]

154 **Du K**, Liu J, Broering R, Zhang X, Yang D, Dittmer U, Lu M. Recent advances in the discovery and development of TLR ligands as novel therapeutics for chronic HBV and HIV infections. *Expert Opin Drug Discov* 2018; **13**: 661-670 [PMID: 29772941 DOI: 10.1080/17460441.2018.1473372]

155 **Chan YK**, Gack MU. Viral evasion of intracellular DNA and RNA sensing. *Nat Rev Microbiol* 2016; **14**: 360-373 [PMID: 27174148 DOI: 10.1038/nrmicro.2016.45]

156 **Ferrando-Martinez S**, Huang K, Bennett AS, Sterba P, Yu L, Suzich JA, Janssen HLA, Robbins SH. HBeAg seroconversion is associated with a more effective PD-L1 blockade during chronic hepatitis B infection. *JHEP Rep* 2019; **1**: 170-178 [PMID: 32039367 DOI: 10.1016/j.jhepr.2019.06.001]

157 **Maini MK**, Burton AR. Restoring, releasing or replacing adaptive immunity in chronic hepatitis B. *Nat Rev Gastroenterol Hepatol* 2019; **16**: 662-675 [PMID: 31548710 DOI: 10.1038/s41575-019-0196-9]

158 **Meng F**, Zhao J, Tan AT, Hu W, Wang SY, Jin J, Wu J, Li Y, Shi L, Fu JL, Yu S, Shen Y, Liu L, Luan J, Shi M, Xie Y, Zhou CB, Wong RW, Lu-En W, Koh S, Bertoletti A, Wang T, Zhang JY, Wang FS. Immunotherapy of HBV-related advanced hepatocellular carcinoma with short-term HBV-specific TCR expressed T cells: results of dose escalation, phase I trial. *Hepatol Int* 2021; **15**: 1402-1412 [PMID: 34850325 DOI: 10.1007/s12072-021-10250-2]

159 **Yang F**, Zheng X, Koh S, Lu J, Cheng J, Li P, Du C, Chen Y, Chen X, Yang L, Chen W, Wong RW, Wai LE, Wang T, Zhang Q. Messenger RNA electroporated hepatitis B virus (HBV) antigen-specific T cell receptor (TCR) redirected T cell therapy is well-tolerated in patients with recurrent HBV-related hepatocellular carcinoma post-liver transplantation: results from a phase I trial. *Hepatol Int* 2023 [PMID: 37067675 DOI: 10.1007/s12072-023-10524-x]

160 **Lim SG**, Baumert TF, Boni C, Gane E, Levrero M, Lok AS, Maini MK, Terrault NA, Zoulim F. The scientific basis of combination therapy for chronic hepatitis B functional cure. *Nat Rev Gastroenterol Hepatol* 2023; **20**: 238-253 [PMID: 36631717 DOI: 10.1038/s41575-022-00724-5]

World Journal of Gastroenterology

Submit a Manuscript: https://www.f6publishing.com

World J Gastroenterol 2023 July 7; 29(25): 3984-3998

DOI: 10.3748/wjg.v29.i25.3984

ISSN 1007-9327 (print) ISSN 2219-2840 (online)

REVIEW

Impact of gut microbiome in the development and treatment of pancreatic cancer: Newer insights

Ayrton I Bangolo, Chinmay Trivedi, Ishan Jani, Silvanna Pender, Hirra Khalid, Budoor Alqinai, Alina Intisar, Karamvir Randhawa, Joseph Moore, Nicoleta De Deugd, Shaji Faisal, Suchith Boodgere Suresh, Parva Gopani, Vignesh K Nagesh, Tracy Proverbs-Singh, Simcha Weissman

Specialty type: Gastroenterology and hepatology

Provenance and peer review: Invited article; Externally peer reviewed.

Peer-review model: Single blind

Peer-review report's scientific quality classification

Grade A (Excellent): 0
Grade B (Very good): B, B
Grade C (Good): C
Grade D (Fair): 0
Grade E (Poor): 0

P-Reviewer: Gazouli M, Greece; Imai Y, Japan, Sitkin S, Russia

Received: May 15, 2023
Peer-review started: May 15, 2023
First decision: May 23, 2023
Revised: May 24, 2023
Accepted: June 12, 2023
Article in press: June 12, 2023
Published online: July 7, 2023

Ayrton I Bangolo, Chinmay Trivedi, Ishan Jani, Silvanna Pender, Hirra Khalid, Budoor Alqinai, Alina Intisar, Karamvir Randhawa, Joseph Moore, Nicoleta De Deugd, Shaji Faisal, Suchith Boodgere Suresh, Parva Gopani, Vignesh K Nagesh, Simcha Weissman, Department of Internal Medicine, Palisades Medical Center, North Bergen, NJ 07047, United States

Tracy Proverbs-Singh, Department of Gastrointestinal Malignancies, John Theurer Cancer Center, Hackensack, NJ 07601, United States

Corresponding author: Ayrton I Bangolo, MBBS, MD, Doctor, Department of Internal Medicine, Palisades Medical Center, 7600 River Road, North Bergen, NJ 07047, United States. ayrtonbangolo@yahoo.com

Abstract

The gut microbiome plays an important role in the variation of pharmacologic response. This aspect is especially important in the era of precision medicine, where understanding how and to what extent the gut microbiome interacts with drugs and their actions will be key to individualizing therapy. The impact of the composition of the gut microbiome on the efficacy of newer cancer therapies such as immune checkpoint inhibitors and chimeric antigen receptor T-cell treatment has become an active area of research. Pancreatic adenocarcinoma (PAC) has a poor prognosis even in those with potentially resectable disease, and treatment options are very limited. Newer studies have concluded that there is a synergistic effect for immunotherapy in combination with cytotoxic drugs, in the treatment of PAC. A variety of commensal microbiota can affect the efficacy of conventional chemotherapy and immunotherapy by modulating the tumor microenvironment in the treatment of PAC. This review will provide newer insights on the impact that alterations made in the gut microbial system have in the development and treatment of PAC.

Key Words: Pancreatic cancer; Gut microbiome; Chemotherapy; Dysbiosis; Intratumoral microbiome; Gut flora

©The Author(s) 2023. Published by Baishideng Publishing Group Inc. All rights reserved.

Core Tip: Pancreatic cancer (PC) remains of on the most dismal in terms of prognosis. Treatment options are limited and even after complete surgical resection, the prognosis remains poor. The gut microbiome has been incriminated in the past for the development of certain cancers. Our review found that observation to be true as well for PC. Furthermore, we also found that it plays a role in efficacy and tolerance of certain regimens used to treat PC.

Citation: Bangolo AI, Trivedi C, Jani I, Pender S, Khalid H, Alqinai B, Intisar A, Randhawa K, Moore J, De Deugd N, Faisal S, Suresh SB, Gopani P, Nagesh VK, Proverbs-Singh T, Weissman S. Impact of gut microbiome in the development and treatment of pancreatic cancer: Newer insights. *World J Gastroenterol* 2023; 29(25): 3984-3998
URL: https://www.wjgnet.com/1007-9327/full/v29/i25/3984.htm
DOI: https://dx.doi.org/10.3748/wjg.v29.i25.3984

INTRODUCTION

Pancreatic cancer (PC) usually refers to ductal pancreatic adenocarcinoma (PAC) (including its subtypes), which represents 85 to 90 percent of all pancreatic neoplasms. PC ranks fourth among cancer related mortality in the United States, only behind lung, colorectal, and prostate cancers in males, and lung, breast, and colorectal cancers in females. Although the incidence of PC has been relatively stable over time, the increasing use of imaging techniques such as endoscopic ultrasound and helical (spiral) abdominal computed tomography (CT) scans has revealed an increasing number of incidentally found cases of PC[1,2].

PC can run in some families, and approximately 10 percent of individuals with PC have a family history of the disease[3,4]. There are two broad categories of hereditary risk for PC which are inherited genetic predisposition syndromes associated with PC and familial PC (FPC), which is defined as a family with a pair of affected first-degree relatives who do not meet criteria for a known PC-associated genetic predisposition syndrome[5].

The major gene causing most cases of hereditary PC remains unknown. Pathogenic germline variants (PGVs) in the breast cancer associated (BRCA) 1 and 2 genes are the most commonly associated mutations, occurring in 13 to 19 percent of FPC families[6]. Next generation sequencing helped uncover other genes causing hereditary pancreatic ductal adenocarcinoma: The partner and localizer of BRCA2 (PALB2) gene and the ataxia-telangiectasia mutated (ATM) gene[7,8]. PGVs are especially common in individuals with early onset PC (*i.e.*, developing before age 50)[6]. Cigarette smoking contributes to the risk of PC in patients with hereditary pancreatitis and FPC and is associated with an earlier PC diagnosis by approximately 20 years[9].

In recent years, the role of gut microbiome in the development and treatment of several cancers, including PC, has been an area of active research. *Porphyromonas gingivalis* (*P. gingivalis*), *Aggregatibacter actinomycetemcomitans* (*A. actinomycetemcomitans*) and even *Helicobacter Pylori* (*H. Pylori*) are linked to an increased risk of PC[10,11]. Probiotics have been shown to be effective in reducing pancreaticoduodenectomy complications, by directly suppressing the growth of cancer cells. Postbiotics have been shown to have selective cytotoxicity against tumor cells. Prior literature revealed that fecal microbiota transplantation led to a reduction in tumor size for PC[12].

Carcinoembryonic antigen-related cell adhesion molecule 7 (CEACAM-7), also known as CGM2, is a glycoprotein expressed on the luminal surface of epithelial cells near the mouth of colonic crypts and on pancreatic ductal epithelial cells[13]. Most recently it has been shown that CEACAM7-directed chimeric antigen receptor (CAR) T cells can effectively mediate remission of late-stage patient-derived PAC xenograft tumors[13].

This review will provide a concise and up to date overview of the impact of commensal gut microbiota in the development and management of PAC. Furthermore, we will focus on the pathophysiology and pathogenesis by which the gut flora can gain oncogenetic attributes and to what extent their alteration can affect the treatment and outcome of PAC.

DIAGNOSIS OF PC

Recent advances in imaging techniques have elevated the diagnostic acumen for PC. Abdominal ultrasound (US) is a non-invasive approach, which can detect pancreatic masses with an accuracy of 50%-70%[14]. Although there are no tell-tale characteristic signs of different pancreatic masses, a hypoechoic mass, pancreatic and/or biliary duct dilation could point towards an ominous pathology[14,15]. If a contrast enhanced US is available, the diagnostic accuracy could be significantly enhanced as hypovascularity of a mass point towards PAC whereas endocrine cell tumor is hyper vascularized and any pancreatitis associated mass is usually iso-vascularized[14,16].

CT with contrast is perhaps the most widely used-in detection and staging of PC. Hypovascularity, increased fibrous stroma, and decreased enhancement compared to surrounding tissue points towards PAC[17]. In hypoattenuating lesions and in instances where CT is equivocal, multi-detector row CT can be helpful as it provides three dimensional images and various phases of contrast enhancement-parenchymal, portal venous, and arterial-leading to earlier detection and accurate staging of the cancer [18-20]. Enhanced magnetic resonance imaging (MRI), due to better soft tissue visualization, has been shown to be equal or superior to CT imaging for blood vessel invasion and local extent, however, it is poor in detecting the involvement of portal venous system or duodenum[21-23]. The most accurate and sensitive method for detection of even the smallest tumors with or without vascular invasion is EUS-superior to MRI, CT, or US. It is also an excellent modality for diagnosis when combined with biopsy and has incredibly high sensitivity to detect metastasis to the lymph nodes as well as vascular invasion [24-27]. The biggest challenge in diagnosis is differentiating between chronic pancreatitis and PAC, this is when EUS with biopsy comes in handy.

STAGING OF PC

The staging of PC at the time of diagnosis is pivotal for prognosis and treatment planning as the aggressive or palliative care approach could be applied based on the stage. The role of CT imaging with contrast is pivotal in determining the stage, however, sometimes, sophisticated modalities such as enhanced MRI, EUS, or fluorodeoxyglucose-positron emission tomography could be needed. The tumor size, location in the pancreas, surrounding structures involvement-with or without vascular involvement, and spread to surrounding lymph nodes or metastasis are the components involved in staging for PC.

The T (tumor), N (Node), and M (Metastasis) is the widely accepted staging systems for PC as per The American Joint Committee for Cancer[28]. The T stage is classified based on the tumor size within the pancreas and/or involvement of vascular structures. The N and M stage is classified based on the involvement of regional lymph nodes and sites of metastasis, if any. Subsequently, based on the imaging, cancer is characterized as resectable, borderline resectable, locally advanced, or metastatic disease. Stages I and II do not involve any major blood vessels, stage III is a localized tumor but with involvement of a major blood vessel, whereas Stage IV is metastatic disease[28].

The National Comprehensive Cancer Network stages PC primarily based on tumor extent. This is primarily in the absence of metastatic disease and resection options are localized advanced/unresectable, borderline resectable, and resectable disease. Locally advanced/unresectable disease is predominantly when the tumor involves major vascular structures such as aorta, superior mesenteric or portal vein (unreconstructable), or > 180 degrees of tumor contact with the Superior mesenteric artery or celiac artery. Resectable disease or borderline resectable is defined as no involvement of any vascular structures mentioned above or ≤ 180 degrees of involvement[29].

PC-MODALITIES OF TREATMENT

Depending on the staging of PC, there are various modalities which are employed for the treatment. Surgical resection is always desirable, however, due to the relatively silent clinical course of PC, only 1/5th of patients have resectable tumors at the time of diagnosis[30,31]. The most utilized surgical procedures are total pancreatectomy, distal pancreatectomy, and Whipple's procedure depending on the staging of the cancer[32]. Previously, in patients presenting with jaundice, preoperative biliary stenting was considered if there was a tumor on the head of the pancreas causing biliary obstruction, however, recent studies have shown that this modality is associated with increased time to surgery, increased rates of infection, and complications; preoperative biliary stenting is as a result, no longer recommended for head of the pancreas tumors which have not metastasized and can be easily resected [33,34]. However, preoperative stenting can be considered in patients who are undergoing neoadjuvant chemotherapy, if surgery is postponed by logistical constraints, or have severe jaundice[33,34].

In patients who present with PC s of 'borderline resectability', neoadjuvant therapy prior to surgical resection is a consideration. However, data is conflicting. While there is some evidence on increased survival amongst borderline resectable tumors with neoadjuvant gemcitabine-based chemotherapy, there are also studies which suggest an increased postoperative stay and increased surgical challenges in locally resectable tumor patients who received neoadjuvant chemotherapy[35-37]. Also, it is important to note that histological diagnosis is mandatory prior to starting the chemotherapy, which may further delay the time to surgery.

The overall prognosis of PC is abysmal, even post complete surgical resection. As a result, 5-Fluorouracil (with Leucovorin) or Gemcitabine adjuvant chemotherapy is frequently employed post-surgical resection. Which agent is better though, does remain a topic of discussion. Studies are equivocal with some showing no difference between the two whereas others favor gemcitabine[38]. In patients with metastatic disease, the armamentarium consists of psychosocial support, chemotherapy, treating a

variety of other comorbid conditions, and targeted therapy. As far as chemotherapy is concerned in such a setting, Gemcitabine has been shown to be superior, by far and remains the first line standard of care[39]. Arguably, Conroy *et al*[40] have proven that FOLFIRINOX can super side Gemcitabine, as patients on FOLFIRINOX demonstrated not only a better response rate, but also improved one year, progression free, and overall survival[40]. In patients who are non-tolerant to first line gemcitabine, second line treatment consisting of oxaliplatin with fluoropyrimidines have demonstrated some clinical benefit[41,42]. Furthermore, if FOLFIRINOX was used as the first line, gemcitabine-based therapy should be tried as second line and has some clinical evidence of being beneficial[40].

Newer modalities of treatment include but are not limited to the use of epidermal growth factor receptor (EGFR) inhibitors. Medications like Cetuximab and Erlotinib which target the EGFR have been developed recently for targeted therapy and have been shown to be effective in many clinical trials. A combination of gemcitabine with Erlotinib is shown to increase overall survival rates and decrease the progression of PC[43]. PC cells are notorious to adapt in order to decrease the drug delivery to them by production of desmoplastic stroma and lead to resistance to chemotherapeutic agents[44]. Several therapies have recently been developed to decrease this stromal tissue and improve drug penetration despite the desmoplastic stroma, including nab-paclitaxel[45].

Radiation therapy has a somewhat beneficial role alongside surgery and chemotherapy. Neoadjuvant radiation therapy for PC has been described in prior literature. Pisters *et al*[46] demonstrated that minimal toxicity and a very small recurrence rate can be obtained with preoperative fractionation chemoradiation based on 5-Fluorouracil, Whipple's procedure, and intraoperative radiation[46]. In another study, utilizing a similar strategy for treatment but replacing 5-Fluorouracil with paclitaxel-based chemotherapy, the results were similar, however, the toxicity levels were higher[47].

To improve the patient's overall prognosis, radiation therapy is frequently being utilized for management of PC alongside chemotherapy. In the United States, adjuvant radiation therapy is a common norm after the Gastrointestinal Tumor Study Group's prospective study in 1985. Patients with resectable PC were enrolled in this trial and were found to have a significantly longer and medial survival rate when treated with adjuvant chemoradiation[48]. Owing to this trial, adjuvant chemoradiation, the most commonly used adjuvant treatment for patients with resectable PC, is being practiced to date in the United States.

Novel techniques like stereotactic body radiotherapy have also been developed in recent years for targeted delivery of radiation. However, it has only been shown to slow local progression of the disease but has no effect on overall survival rates as the majority of mortality in PC patients is secondary to systemic and distant metastasis[49-51]. As PC is genetically a heterogeneous malignancy, there have also been baby steps in personalized chemotherapeutic regimen based on the patient's genome to significantly increase the rates of chemotherapeutic efficacy by decreasing the resistance and making the response to chemotherapy consistent across all individuals. However, further research is needed on this novel therapeutic approach.

GUT MICROBIOTA AND PC

Mechanisms via which microbes regulate pancreatic oncogenesis

The gut microbiome, which refers to microbes naturally present in the human mucosal surfaces, has shown, when altered, to lead to oncogenesis and to some extent affect the response to therapy of several cancers, among which PAC[52]. The exact mechanisms by which oral and intestinal microbiota reach the pancreas remains unknown, but the proposed mechanisms involve the translocation *via* biliary/pancreatic ducts or through the blood circulation[52]. A summary can be found in Table 1.

P. gingivalis, which is a bacterium mainly found in the mouth and associated with periodontal diseases, has shown the ability to disseminate and affect immune response. *P. gingivalis* infection has shown an involvement of toll-like receptors (TLRs) including TLR4, involved in protective immunity. TLR signaling, especially TLR4, has been shown to play an important role in human pancreatic tumors [53]. Furthermore, periodontal diseases, such as the ones caused by *P. gingivalis* can lead to an increased production of nitrosamines[54]. Nitrosamines can be metabolized by Cytochrome P450 and produce electrophiles that can effectively interact with the DNA and lead to the formation of DNA adducts that have a carcinogenic potential if not repaired[55]. Porphyromonas Peptidyl Arginine Deaminase (PPAD) is a protein produced by *P. gingivalis* that has been associated with cancer development by the way of P53 activity and KRAS (Kirsten-ras) mutation[52]. P53, which is a tumor suppressor gene, if mutated can lead impairment of cell cycle arrest and decrease of apoptosis increasing the risk of malignancy. KRAS, which is an oncogene with hydrolyzing effect on guanosine triphosphate, can lead uncontrolled and inappropriate cell proliferation, thus increasing the risk of malignancy[52]. P53 is a transcription factor that can activate the transcription of numerous genes, including the Cyclin-dependent kinase (CDK) inhibitor p21.

P53 is rapidly degraded and therefore not detectable within the cell. Mutation of the P53 gene results in a protein that fails to bind DNA effectively. Therefore, expression of the CDK inhibitor P21 gene is decreased, and P21 protein production is decreased. P21 protein is not available to stop the entry of the

Table 1 Gut microbiota associated with Pancreatic oncogenesis

Bacteria	Primary site	Potential mechanism	Subsequent effect	Ref.
Porphyromonas gingivalis	Mouth	TLR signaling disruption; Nitrosamines production; PPAD production	Loss of protective immunity; DNA adducts formation; P53 overactivity (loss of apoptosis); KRAS mutation (cellular overproliferation)	[52-55]
Aggregatibacter actinomycetemcomitans	Mouth	Nitrosamine production; DNA double-strand breaks; CagE production	DNA adducts formation; genome instabilities; dysregulation of DNA methylation expression	[52, 58,59]
Fusobacterium nucleatum	Mouth	FadA production; Fap2 production	activation of the Wnt/β-catenin pathway; suppression of the cytotoxic effects of NK cells and lymphocytes	[59, 61-63]
Helicobacter Pylori	Stomach	cagA, cag PAI and vacA production	Disruption of host intracellular signaling pathways	[64]
Bacteroides fragilis, Bacteroides vulgatus, Listeria monocytogenes, Clostridium, Lactobacillus, Bifidobacterium	Large bowel	Transformation of primary bile acids to secondary bile acids	Reduction of susceptibility to apoptosis, induction of inflammatory mediators, and perturbation of membranes and cellular movement	[76]
Escherichia coli	Large bowel	Polyamines production	Polyamines upregulation	[81-83]

TLR: Toll-like receptor; PPAD: Porphyromonas Peptidyl Arginine Deaminase; CagE: Cytotoxin-associated gene E; NK: Natural killer; PAI: Pathogenicity island; cagA: Cytotoxin-associated gene A.

cell into S phase, again resulting in unregulated cell cycle progression, potentially leading to carcinogenesis[56]. The KRAS gene, an oncogene, is one of the most frequently mutated genes in PC. This gene is the human homolog of a transforming gene isolated from the Kirsten rat sarcoma virus, hence the name KRAS. Mutations in this gene, the vast majority of which are at codon 12, are activating, leading to abnormal activation of the protein product of the gene[57].

A. actinomycetemcomitans is also an oral microbiome that has been incriminated in PAC[52]. Similar to *P. gingivalis*, it can lead to periodontal infections and lead to increased nitrosamine production[54]. *A. actinomycetemcomitan* can also induce DNA double-strand breaks in host cells, independently of apoptosis, and cause the risk of genome instabilities and subsequently increase the risk of carcinogenesis[58]. Furthermore, the bacteria can produce the cytotoxin-associated gene E (CagE). CagE may have helicase activity, and its role in regulating DNA methylation expression is considered as possible mechanisms of tumorigenesis. CagE gene has been widely expressed in various cancer cell lines and cancer tissues including PC[59]. *Fusobacterium nucleatum* (*F. nucleatum*), which is another oral microbiome produces Fusobacterium adhesin A (FadA), that showed capacity of binding to host cells and is also the most characteristic virulence factor of *F. nucleatum*[59]. The host receptors for FadA are members of the cadherin family, mainly E-cadherin and vascular endothelial (VE) cadherin (CDH5) [60]. FadA binds to E-cadherin of epithelial cells, leading to phosphorylation and internalization of E-cadherin on the membrane; afterwards, canonical Wnt pathway is activated, accompanied by decreased phosphorylation of β-catenin, which accumulates in the cytoplasm and translocate to the nucleus[59]. Increase in Wnt signaling activity and subsequent activation of the Wnt/β-catenin pathway, has shown to be essential in the initiation of PC[61,62]. Furthermore, FadA binds VE-cadherin on VE cells, increasing endothelial penetrability[59]. Therefore, FadA not only directly invades host cells but also allows dissemination of itself and other bacteria into blood by increasing endothelial permeability[59]. *F. nucleatum* can produce a protein called familial adenomatous polyposis 2, which binds and interacts to human inhibitory receptor T cell immunoreceptor on natural killer (NK) cells and lymphocytes. Thus, suppressing the cytotoxic effects of NK cells and lymphocytes, leading to protection of tumors from the immune system and fostering a flourishing inflammatory context[63]. By a mechanism similar to *P. gingivalis*, *F. nucleatum* can be involved with the TLRs and lead to carcinogenesis as discussed previously [53].

H. Pylori is notorious for its association with gastric cancer and yields various virulence factors that may disrupt host intracellular signaling pathways and lower the threshold for neoplastic transformation. Of all virulence factors, cytotoxin-associated gene A and its pathogenicity island (cag PAI) and vacuolating cytotoxin A are the major pathogenic factors[64]. Whether *H. Pylori* infection is associated with PAC remains controversial with conflicting data in the literature. A study by Kumar *et al*[65] showed a very low incidence of *H. Pylori* among patients with PAC, whereas studies by Hirabayashi *et al*[66], and Nilsson *et al*[67] found an association.

Several members of the gut microbial community (especially of the large bowel), including *Bacteroides fragilis*, *Bacteroides vulgatus*, *Listeria monocytogenes*, *Clostridium*, *Lactobacillus*, *Bifidobacterium*, and *Escherichia*, are involved in the transformation of primary bile acids to secondary bile acids, either by

deconjugation, oxidation, dehydroxylation, or epimerization[68-70]. Bile acids have multiple nuclear receptors, including farnesoid-X-receptor (FXR), liver-X receptor, CAR, vitamin D receptor (VDR), pregnane X receptor (PXR), and a non-nuclear receptor Takeda G Protein-Coupled Receptor 5/G-protein-coupled bile acid receptor (TGR5), that may impact carcinogenesis[71,72]. Secondary bile acids can behave as both pro- and anti-carcinogens, depending on the cancer concerned and the concentration of the bile acid present[71-73]. Furthermore, bile acids can modulate the composition of the microbiome and facilitate bacterial translocation into tissues, which is a key step in the carcinogenesis of PAC[74]. Bile acid levels have been shown to be elevated in PAC[75]. Bile acids can also affect risk factors for PAC such as pancreatitis and bile acid efflux disorders, type II diabetes, obesity, and hyperlipidemia; and they can reduce susceptibility to apoptosis, induce inflammatory mediators, and may perturb membranes and cellular movement[76]. A secondary bile acid, deoxycholic acid can bind to TGR5 and activate EGFR, mitogen-activated protein kinase, and signal transducer and activator of transcription 3 signaling in PAC cells, inducing cell cycle progression[77]. Other bile acid receptors such as VDR, FXR and PXR are also found to be highly expressed in PAC tissues compared to normal tissues[78-80].

Polyamines can be produced, accumulated, or used by the following gut bacteria *Escherichia coli* (*E. coli*), *Enterococcus faecalis* (*E. faecalis*), Staphylococcus aureus, Haemophilus influenzae, Neisseria flava, Pseudomonas aeruginosa, Campylobacter jejuni, Yersinia pestis, Vibrio cholerae, Bacteroides dorei, Bacteroides thetaiotaomicron, *Bacteroides fragilis*, Bacillus subtilis, and Proteus mirabilis[81,82]. A mouse study revealed that bacterial polyamine biosynthetic capacity was upregulated and aggravated by tumor progression in PAC and there was a correlated elevated serum level of polyamines[83].

As evidence by the work of Riquelme *et al*[84], Fecal Microbiotal Transplant from human subjects to mice, yielded from PC long term murine survivors, showed a significant reduction in tumor growth, however, that effect was lost with the use of antibiotics altering the fecal microbiota[84,85]. Furthermore, it was found that long term survivor mice that did not receive antibiotics were rich in CD8+ T-cell, enhancing the tumor immune cell infiltration. On the other hand, mice that were treated with antibiotics, thus altering the fecal microbiota, showed an increased number of CD4+FOXP3+ T-regs and myeloid derived suppressor cells which are well known to lower the immune system, thus promoting tumor growth[84,85].

NK cells are a group of cells that play an important role by mediating tumor initiation and progression. NK cells are often found in the circulation, preventing tumor cells from metastasizing[86,87]. When a patient is NK cells depleted, tumor escape and growth may ensue[86]. NK cells having the ability to inhibit CD8+ T cell responses during chronic infections, it has been hypothesized that NK cells can facilitate solid tumors infiltration, among which PC[86].

Hepatotropic viruses such as hepatitis B virus (HBV) and hepatitis C virus (HCV) have been incriminated in pancreatic oncogenesis. HBV and HCV have the ability to delay host immune system clearance of the virus by integrating the DNA, modifying tissue viscoelasticity, and modulating the PI3K/AKT signaling pathway, which promotes metabolism, proliferation, cell survival, growth and angiogenesis in response to extracellular signals, *via* the HBV X protein, thus leading to oncogenesis[87].

It has been shown that fungal microbiota including *Candida*, *Saccharomyces*, *Aspergillus* or *Malassezia* spp. are involved in pancreatic oncogenesis. One proposed mechanism is that ligation of mannose-binding lectin, which binds to glycans of the fungal wall may lead to activation of the complement cascade and oncogenic progression[88].

Short-chain fatty acids (SCFA) which are metabolites from the gut microbiota and cathelicidin-related antimicrobial peptides secreted by normal pancreatic β-cells protect against tissue inflammation and control pancreatic bacterial overgrowth[89,90]. It has been shown that patients with PC have an abundance of a higher abundance of lipopolysaccharide-producing bacteria, and a reduction in beneficial microbes, such as butyrate-producing bacteria[91]. Butyrate, which is a SCFA produced by certain bacteria of gut possesses anti-inflammatory and anti-neoplastic properties in regard to PC by the means of "pro-differentiation, anti-proliferation, anti-invasion, pro-apoptosis" and chemo-sensitization effects[91]. Another SCFA from the gastrointestinal (GI) microbiota, acetate, induces insulin secretion *via* the microbiome-brain β-cell axis controlling pancreatic bacterial overgrowth[92,93]. Tryptophan metabolism can serve as an immunomodulatory factor by overexpression of indoleamine2,3-dioxygenase1 which inhibits the maturation of CD11c and dendritic cells, and T-cell proliferation and by high expression of Kyn which leads to induction and activation of the aryl hydrocarbon receptor, leading to upregulation of programmed cell death protein 1 expression; enhancing the efficacy of antitumor adoptive T-cell therapy and reducing the rate of migration and invasion in both tumor-bearing mice and patients with PC[94-96].

IMPACT OF GUT MICROBIOME ALTERATION ON THE TREATMENT OF PC

PAC is only resectable in approximately 15% to 20% of cases at the time of diagnosis, however, surgical resection offers the only chance of cure. PAC carries a dismal prognosis even after surgical resection with negative margins given its high rate of recurrence. Therefore, systemic chemotherapy, radiation therapy, and combined approaches (chemoradiotherapy) have been used both prior to and following

surgical resection in an effort to improve cure rates[97]. More recently, immunotherapy and CAR T-cell therapy have gained favor for use in the treatment of PAC[13]. The gut microbiome has been shown to interact with those treatment modalities and affect their efficacy[13,42]. Furthermore, the gut microbiome has also shown some cytotoxic effect in PAC[42].

E. coli and *Staphylococcus aureus* strains have the potential to produce Cytolysin A (ClyA), which is a pore-forming cytotoxin that possesses anticancer properties[98]. ClyA exerts its cytotoxicity, by creating multimeric pores and imposing cell death in the eukaryotic membrane by the caspase-dependent pathway[99]. *E. coli*, *A. actinomycetemcomitans*, Campylobacter and Helicobacter are known to produce Cytolethal distending toxin (CDT)[100]. CDT is known to have genotoxic attributes by DNase activity which creates DNA double stranded breaks, leading to cell cycle arrest and cytotoxicity[49]. Streptococcus pyogenes secretes streptolysin O which is implicated in cytolysis and apoptosis[101].

Prebiotics are defined as nutrients that are degraded by gut microbiota and may affect not only the intestinal microenvironment but also distant organs. In a mice study by Trivieri *et al*[102] using xenograft mice model confronted with PC gene expression dataset (GSE16515) and investigating the impact of high levels of prebiotic resistant starch diet (RSD) on miRNA expression profiles in tumor tissues, RSD was associated with dysregulation of 19 miRNAs genes expression in comparison to control. subsequent analysis revealed that part of genes participating in the regulation of processes such as the development of carcinoma, inflammatory response, abdominal cancer, metabolic disease, growth, invasion, and metastasis were downregulated in a group of mice fed with RSD in comparison to control. Furthermore, genes participating in the synthesis of carbohydrates, glucose metabolism disorder, and cell death of cancer cell lines were significantly upregulated in mice fed with RSD. Thus, the authors concluded that there is prolonged overall survival and beneficial value of RSD in PAC[103].

Lactobacillus casei is a probiotic that can produce Ferrichrome, which has the potential to suppress the growth of refractory PC cells by inhibiting cancer cells progression and dysregulating cell cycle by activating P53[102,103]. Next-generation probiotics such as *Akkermansia muciniphila* (*A. muciniphila*), are identified using next-generation sequencing and bioinformatics tools. *A. muciniphila* has been shown to inhibit the proliferative activity of INS-1 (rat pancreatic islet cell tumor cells) in a mouse model[104].

FOLFIRINOX, which is a commonly used regimen in PAC is composed of leucovorin calcium (folinic acid), fluorouracil, irinotecan hydrochloride, and oxaliplatin. Oxaliplatin has an immunomodulatory effect as well, potentiating tumoricidal T-cell immunity. In a mice model, a group with a defective TLR signaling pathway, demonstrated no response to oxaliplatin treatment[105]. Agonistic TLR molecules from microbial membranes were reported to help stimulate the immune system and increase reactive oxygen species production, thus enhancing the tumoricidal activity of oxaliplatin[105]. Irinotecan is characterized by common GI side effects limiting the dose and effectiveness of treatment. Those side effects can be modulated by enzymatic activity of the gut microbiome, with some bacteria improving the side effects profile, while others may worsen the side effects. The β-glucuronidase enzyme produced by intestinal bacteria cleaves the active irinotecan metabolite SN-38G into a toxic form that damages the colonic mucosa and causes GI side effects. The literature revealed that antibiotics or modification of gut microbiomes significantly alleviated the GI toxicity in cancer patients[106]. Furthermore, reduced risk of developing irinotecan toxicity has been shown with the use of indigestible fibers, using appropriate probiotics and adequate butyrate intake[107].

Several animal studies showed that mice housed in germ-free conditions and animals treated with broad-spectrum antibiotics showed reduced effects of immunotherapy by a combination of TLR-9 antagonist and anti-interleukin-10 antibody. Furthermore, the ineffectiveness of cancer immunotherapy directed against the major negative regulator of T cell activation cytotoxic T-lymphocyte-associated protein 4 (CTLA-4) was observed when applied to antibiotic-treated animals or germ-free mice[108]. Monoclonal antibodies that neutralize CTLA-4 have been shown to rely on the intestinal microbiota, in particular, Bacteroidales and Burkholderiales[108]. A recent study used a gut microbe-derived metabolite trimethylamine N-oxide (TMAO) that showed enhanced anti-tumor immunity to PAC. TMAO was delivered either intraperitoneally or *via* a dietary choline supplement to orthotopic PAC bearing mice, and lead to reduced tumor growth and associated with an immunostimulatory tumor-associated macrophage phenotype and activated effector T cell response in the tumor microenvironment. The combination of TMAO and immune checkpoint inhibitors (ICI) such as programmed cell death 1, in a mouse model of PAC, proved to be superior in reducing tumor burden and improving survival compared to either therapy alone[109].

CAR T-cell therapy has shown tremendous results in hematologic malignancies. Only recently, it was tried on non-hematologic malignancies with promising preliminary data. CAR T-cell therapy of solid tumors faces a major issue in that commonly targeted tumor antigens are expressed at low levels in normal tissues, leading to on-target off-tumor toxicity. CEACAM7, which has low to undetectable expression in all normal tissues and with strong surface expression on a subset of primary human PAC tumors was identified as a potential target antigen for CAR T-cell therapy of PAC. CAR T-cells targeting CEACAM7 were generated in a study by Raj *et al*[13] and showed significant antitumor activity against patient-derived PAC tumor cultures both *in vitro* and *in vivo*[13]. A brief summary can be found in Table 2.

Oncolytic adenoviruses have been engineered to replicate in cancer cells and controlling tumor progression. Oncolytic adenovirus AdNuPARmE1A with miR-222 binding sites, are made to withdraw

Table 2 Impact of gut microbiota in the treatment of Pancreatic cancer

Bacteria	Primary site	Potential mechanism	Subsequent effect	Ref.
Escherichia coli	Large bowel	Cytolysin A production; Cytolethal distending toxin production	Imposing cell death in the eukaryotic membrane by the caspase-dependent pathway; DNA double stranded breaks, leading to cell cycle arrest and cytotoxicity	[49, 86,87]
Staphylococcus aureus	Variable	Cytolysin A production	Imposing cell death in the eukaryotic membrane by the caspase-dependent pathway	[86]
Streptococcus pyogenes	Variable	Streptolysin O production	Increase in apoptosis and cytolysis	[88]
Aggregatibacter actinomycetem-comitans, Campylobacter and Helico-bacter	Mouth, stomach, large bowel	Cytolethal distending toxin production	DNA double stranded breaks, leading to cell cycle arrest and cytotoxicity	[87]
Lactobacillus casei	Mouth and small intestine	P53 activation	Upregulation of apoptosis	[90]
Bacteroidales, Burkholderiales	Large bowel	CTLA-4 upregulation	Enhancing activity of monoclonal antibody against CTLA-4	[95]

CTLA-4: Cytotoxic T-lymphocyte-associated protein 4.

the miRNA from the cellular environment. AdNuPAR-E-miR222-S mediated-decrease of miR-222 expression in pancreatic cancer cells was shown to strongly improve the viral yield and enhance the adenoviral cytotoxic effects[110].

INTRATUMORAL MICROBIOME IN PANCREATIC CA

Intratumoral microbiome is derived from 3 basic mechanisms; (1) Sloughing of the mucosal barrier; (2) Adjacent normal tissues; and (3) Hematogenous spread[111]. Interestingly, Nejman *et al*[112] demonstrated that amongst the tumors that they studied, every tumor was associated with a completely different microbiome composition[112]. The pancreas is traditionally thought to be a 'bacteria-free' organ. However, bacterial DNA belonging to the Proteobacteria phylum was very abundantly found in pancreatic cancer[112]. Another study which confirmed increased amounts of bacterial DNA in pancreatic cancer *vs* normal pancreatic tissue was the study by Geller *et al*[113]. Bacterial ribosomal DNA was detected *via* FISH technique in 76% of patients with PAC *vs* 15% of patients with normal pancreatic tissue[88]. Similarly, by using the FISH technique, Aykut *et al*[88] demonstrated that *Pseudomonadota*, *Bacillota*, and *Bacteroides* were the most abundant bacteria found intratumorally in pancreatic cancer patients[88]. Interestingly, the fungal mycobiome in pancreatic tissue samples obtained from patients with PAC was also found to be very distinct from healthy individuals with a high prevalence of Malassezia[88].

MICROBIOME IMBALANCE AND PANCREATIC CA

Dysbiosis or imbalance in the microbiome has been shown to impact the inflammatory cascade in a non-physiological way and in turn, contribute to the development of cancer[114]. The known risk factors for pancreatic carcinoma are smoking, advancing age, type 2 diabetes mellitus, chronic pancreatitis, and obesity. Interestingly, many of these risk factors have been recently found to be associated with an imbalance in the microbiome, which may increase the risk of PAC[115-118]. A meta-analysis by Maisonnuevve demonstrated a positive correlation between periodontal disease and PAC[119]. This may be related to an imbalance in the oral microbiome. Oral microbiomes have been shown to be associated with carcinogenesis *via* inducing systemic inflammation, and the most important being Porphyromonas Gingivalis[120-122]. A case control study demonstrated that the risk of PAC was 2-fold higher in patients with a higher level of antibodies against a specific strain of *P. Gingivalis*, whereas higher levels of antibodies against commensal oral microbiome were actually protective against PAC, with an almost 50% lower risk of the cancer in patients who had these antibodies[123]. In-vivo studies have shown that *P. gingivalis* enhances the proliferation of pancreatic tumor cells, regardless of the concentration of TLR-4. Furthermore, the concentration and proliferation of *P. gingivalis* is greatly increased in PAC tissue secondary to hypoxia, which is very prevalent in the cancer microenvironment[124]. Furthermore, bacteria that cause periodontitis are also found to cause K-ras and p53 mutations, and those have in turn been associated with poor prognosis in patients with pancreatic cancer[125]. They also demonstrated that the number of cases of pancreatic cancer were higher in patients who had GI infections from *H.*

Pylori, Enterobacter, and Enterococcus species[125].

This prior literature leads us into sensibly concluding that possibly, an imbalance in the oral microbiome is associated with an increased risk of PAC, however, reverse causation is an important factor that needs to be excluded before exploring this aspect further. One study evaluated this and found that 2 oral bacteria-*P. gingivalis* and Aggregatibacter actinomycetemcomitans are associated with an increased risk whereas *Leptotrichia* genus of *Fusobacterium* species was associated with a reduced risk of PAC. Interestingly, even after excluding patients who developed the cancer within 2 years from the date of sample collection, the risks remained elevated[10]. This significantly reduces the likelihood of reverse causation. Another significant study going in favor of a causality between *E. faecalis*, and pancreatic cancer is the one by Maekawa *et al*[126], wherein the level of antibodies against *E. faecalis* capsular polysaccharide were found to be increased in the serum of pancreatic cancer patients[126]. However, larger cohort studies are needed on the subject to conclusively establish causation.

CONCLUSION

Despite advances in medicine and the discovery of newer anticancer therapies, the prognosis of pancreatic cancer remains dismal. By the way of this review, we found that a prebiotic resistant starch diet has been associated with better overall survival in PAC. We also found that periodontal diseases increase the risk of developing PAC. This is especially important as periodontal diseases should be avoided and promptly treated in patients with a family history of PAC, other risk factors for PAC, and those with known/suspected genetic mutations susceptible for the development of PAC. Furthermore, we found that the use of concomitant antibiotics can positively or negatively affect treatment of PAC. Some gut microbiomes can enhance the effect of therapy and improve tolerance to therapy as well. Thus, neutropenic diet can be avoided in select patients meeting the requirements. Newer therapeutics such as ICI and CAR T-cell therapies can play a major role in the outcome of PAC, however, most promising studies are done in animal models. We hope that in the near future, there will be more clinical trials in human subjects replicating the promising results from animal studies which will possibly offer newer ways to handle this very deadly malignancy.

FOOTNOTES

Author contributions: Bangolo AI, Trivedi C, and Nagesh VK searched the literature, wrote, and revised the manuscript; Jani I, Pender S, Khalid H, Alqinai B, Intisar A, Randhawa K, Moore J, De Deugd N, Faisal S, Suresh SB, and Gopani P revised and edited the manuscript; Bangolo AI, Proverbs-Singh T and Weissman S revised and approved the final version of the article and are the article's guarantors; All authors certify that they contributed sufficiently to the intellectual content and data analysis. Each author has reviewed the final version of the manuscript and approved it for publication.

Conflict-of-interest statement: No potential conflict of interest was reported by the authors.

Open-Access: This article is an open-access article that was selected by an in-house editor and fully peer-reviewed by external reviewers. It is distributed in accordance with the Creative Commons Attribution NonCommercial (CC BY-NC 4.0) license, which permits others to distribute, remix, adapt, build upon this work non-commercially, and license their derivative works on different terms, provided the original work is properly cited and the use is non-commercial. See: https://creativecommons.org/Licenses/by-nc/4.0/

Country/Territory of origin: United States

ORCID number: Ayrton I Bangolo 0000-0002-2133-2480; Simcha Weissman 0000-0002-0796-6217.

S-Editor: Fan JR
L-Editor: A
P-Editor: Fan JR

REFERENCES

1 **Siegel RL**, Miller KD, Fuchs HE, Jemal A. Cancer statistics, 2022. *CA Cancer J Clin* 2022; **72**: 7-33 [PMID: 35020204 DOI: 10.3322/caac.21708]
2 **Klimstra DS**. Nonductal neoplasms of the pancreas. *Mod Pathol* 2007; **20** Suppl 1: S94-112 [PMID: 17486055 DOI: 10.1038/modpathol.3800686]
3 **Klein AP**. Genetic susceptibility to pancreatic cancer. *Mol Carcinog* 2012; **51**: 14-24 [PMID: 22162228 DOI: 10.1002/mc.20855]

4 **Klein AP**, Brune KA, Petersen GM, Goggins M, Tersmette AC, Offerhaus GJ, Griffin C, Cameron JL, Yeo CJ, Kern S, Hruban RH. Prospective risk of pancreatic cancer in familial pancreatic cancer kindreds. *Cancer Res* 2004; **64**: 2634-2638 [PMID: 15059921 DOI: 10.1158/0008-5472.can-03-3823]

5 **Gardiner A**, Kidd J, Elias MC, Young K, Mabey B, Taherian N, Cummings S, Malafa M, Rosenthal E, Permuth JB. Pancreatic Ductal Carcinoma Risk Associated With Hereditary Cancer-Risk Genes. *J Natl Cancer Inst* 2022; **114**: 996-1002 [PMID: 35445726 DOI: 10.1093/jnci/djac069]

6 **Hahn SA**, Greenhalf B, Ellis I, Sina-Frey M, Rieder H, Korte B, Gerdes B, Kress R, Ziegler A, Raeburn JA, Campra D, Grützmann R, Rehder H, Rothmund M, Schmiegel W, Neoptolemos JP, Bartsch DK. BRCA2 germline mutations in familial pancreatic carcinoma. *J Natl Cancer Inst* 2003; **95**: 214-221 [PMID: 12569143 DOI: 10.1093/jnci/95.3.214]

7 **Jones S**, Hruban RH, Kamiyama M, Borges M, Zhang X, Parsons DW, Lin JC, Palmisano E, Brune K, Jaffee EM, Iacobuzio-Donahue CA, Maitra A, Parmigiani G, Kern SE, Velculescu VE, Kinzler KW, Vogelstein B, Eshleman JR, Goggins M, Klein AP. Exomic sequencing identifies PALB2 as a pancreatic cancer susceptibility gene. *Science* 2009; **324**: 217 [PMID: 19264984 DOI: 10.1126/science.1171202]

8 **Roberts NJ**, Jiao Y, Yu J, Kopelovich L, Petersen GM, Bondy ML, Gallinger S, Schwartz AG, Syngal S, Cote ML, Axilbund J, Schulick R, Ali SZ, Eshleman JR, Velculescu VE, Goggins M, Vogelstein B, Papadopoulos N, Hruban RH, Kinzler KW, Klein AP. ATM mutations in patients with hereditary pancreatic cancer. *Cancer Discov* 2012; **2**: 41-46 [PMID: 22585167 DOI: 10.1158/2159-8290.CD-11-0194]

9 **Yeo TP**, Hruban RH, Brody J, Brune K, Fitzgerald S, Yeo CJ. Assessment of "gene-environment" interaction in cases of familial and sporadic pancreatic cancer. *J Gastrointest Surg* 2009; **13**: 1487-1494 [PMID: 19459017 DOI: 10.1007/s11605-009-0923-6]

10 **Fan X**, Alekseyenko AV, Wu J, Peters BA, Jacobs EJ, Gapstur SM, Purdue MP, Abnet CC, Stolzenberg-Solomon R, Miller G, Ravel J, Hayes RB, Ahn J. Human oral microbiome and prospective risk for pancreatic cancer: a population-based nested case-control study. *Gut* 2018; **67**: 120-127 [PMID: 27742762 DOI: 10.1136/gutjnl-2016-312580]

11 **Stolzenberg-Solomon RZ**, Blaser MJ, Limburg PJ, Perez-Perez G, Taylor PR, Virtamo J, Albanes D; ATBC Study. Helicobacter pylori seropositivity as a risk factor for pancreatic cancer. *J Natl Cancer Inst* 2001; **93**: 937-941 [PMID: 11416115 DOI: 10.1093/jnci/93.12.937]

12 **Sobocki BK**, Kaźmierczak-Siedlecka K, Folwarski M, Hawryłkowicz V, Makarewicz W, Stachowska E. Pancreatic Cancer and Gut Microbiome-Related Aspects: A Comprehensive Review and Dietary Recommendations. *Nutrients* 2021; **13** [PMID: 34959977 DOI: 10.3390/nu13124425]

13 **Raj D**, Nikolaidi M, Garces I, Lorizio D, Castro NM, Caiafa SG, Moore K, Brown NF, Kocher HM, Duan X, Nelson BH, Lemoine NR, Marshall JF. CEACAM7 Is an Effective Target for CAR T-cell Therapy of Pancreatic Ductal Adenocarcinoma. *Clin Cancer Res* 2021; **27**: 1538-1552 [PMID: 33479048 DOI: 10.1158/1078-0432.CCR-19-2163]

14 **Rickes S**, Unkrodt K, Neye H, Ocran KW, Wermke W. Differentiation of pancreatic tumours by conventional ultrasound, unenhanced and echo-enhanced power Doppler sonography. *Scand J Gastroenterol* 2002; **37**: 1313-1320 [PMID: 12465731 DOI: 10.1080/003655202761020605]

15 **Karlson BM**, Ekbom A, Lindgren PG, Källskog V, Rastad J. Abdominal US for diagnosis of pancreatic tumor: prospective cohort analysis. *Radiology* 1999; **213**: 107-111 [PMID: 10540649 DOI: 10.1148/radiology.213.1.r99oc25107]

16 **Kitano M**, Kudo M, Maekawa K, Suetomi Y, Sakamoto H, Fukuta N, Nakaoka R, Kawasaki T. Dynamic imaging of pancreatic diseases by contrast enhanced coded phase inversion harmonic ultrasonography. *Gut* 2004; **53**: 854-859 [PMID: 15138213 DOI: 10.1136/gut.2003.029934]

17 **Miura F**, Takada T, Amano H, Yoshida M, Furui S, Takeshita K. Diagnosis of pancreatic cancer. *HPB (Oxford)* 2006; **8**: 337-342 [PMID: 18333085 DOI: 10.1080/13651820500540949]

18 **Catalano C**, Laghi A, Fraioli F, Pediconi F, Napoli A, Danti M, Reitano I, Passariello R. Pancreatic carcinoma: the role of high-resolution multislice spiral CT in the diagnosis and assessment of resectability. *Eur Radiol* 2003; **13**: 149-156 [PMID: 12541123 DOI: 10.1007/s00330-002-1473-4]

19 **Prokesch RW**, Chow LC, Beaulieu CF, Nino-Murcia M, Mindelzun RE, Bammer R, Huang J, Jeffrey RB Jr. Local staging of pancreatic carcinoma with multi-detector row CT: use of curved planar reformations initial experience. *Radiology* 2002; **225**: 759-765 [PMID: 12461258 DOI: 10.1148/radiol.2253010886]

20 **Vargas R**, Nino-Murcia M, Trueblood W, Jeffrey RB Jr. MDCT in Pancreatic adenocarcinoma: prediction of vascular invasion and resectability using a multiphasic technique with curved planar reformations. *AJR Am J Roentgenol* 2004; **182**: 419-425 [PMID: 14736675 DOI: 10.2214/ajr.182.2.1820419]

21 **Ichikawa T**, Sou H, Araki T, Arbab AS, Yoshikawa T, Ishigame K, Haradome H, Hachiya J. Duct-penetrating sign at MRCP: usefulness for differentiating inflammatory pancreatic mass from pancreatic carcinomas. *Radiology* 2001; **221**: 107-116 [PMID: 11568327 DOI: 10.1148/radiol.2211001157]

22 **Schima W**, Függer R, Schober E, Oettl C, Wamser P, Grabenwöger F, Ryan JM, Novacek G. Diagnosis and staging of pancreatic cancer: comparison of mangafodipir trisodium-enhanced MR imaging and contrast-enhanced helical hydro-CT. *AJR Am J Roentgenol* 2002; **179**: 717-724 [PMID: 12185052 DOI: 10.2214/ajr.179.3.1790717]

23 **Romijn MG**, Stoker J, van Eijck CH, van Muiswinkel JM, Torres CG, Laméris JS. MRI with mangafodipir trisodium in the detection and staging of pancreatic cancer. *J Magn Reson Imaging* 2000; **12**: 261-268 [PMID: 10931589 DOI: 10.1002/1522-2586(200008)12:2<261::aid-jmri8>3.0.co;2-r]

24 **Müller MF**, Meyenberger C, Bertschinger P, Schaer R, Marincek B. Pancreatic tumors: evaluation with endoscopic US, CT, and MR imaging. *Radiology* 1994; **190**: 745-751 [PMID: 8115622 DOI: 10.1148/radiology.190.3.8115622]

25 **Legmann P**, Vignaux O, Dousset B, Baraza AJ, Palazzo L, Dumontier I, Coste J, Louvel A, Roseau G, Couturier D, Bonnin A. Pancreatic tumors: comparison of dual-phase helical CT and endoscopic sonography. *AJR Am J Roentgenol* 1998; **170**: 1315-1322 [PMID: 9574609 DOI: 10.2214/ajr.170.5.9574609]

26 **Rosewicz S**, Wiedenmann B. Pancreatic carcinoma. *Lancet* 1997; **349**: 485-489 [PMID: 9040589 DOI: 10.1016/s0140-6736(96)05523-7]

27 **Chang KJ**, Nguyen P, Erickson RA, Durbin TE, Katz KD. The clinical utility of endoscopic ultrasound-guided fine-needle aspiration in the diagnosis and staging of pancreatic carcinoma. *Gastrointest Endosc* 1997; **45**: 387-393 [PMID:

9165320 DOI: 10.1016/s0016-5107(97)70149-4]
28 **Byrd DR**, Carducci MA, Compton CC, Fritz A, Greene F. AJCC cancer staging manual. Edge SB, editor. New York: Springer; 2010
29 **NCCN Clinical Practice Guidelines in Oncology (NCCN Guidelines) Pancreatic Adenocarcinoma**. National Comprehensive Cancer Network, 2017. [cited 22 June 2017]. Available from: https://www.nccn.org/professionals/physician_gls/pdf/pancreatic.pdf
30 **Li D**, Xie K, Wolff R, Abbruzzese JL. Pancreatic cancer. *Lancet* 2004; **363**: 1049-1057 [PMID: 15051286 DOI: 10.1016/S0140-6736(04)15841-8]
31 **Wagner M**, Redaelli C, Lietz M, Seiler CA, Friess H, Büchler MW. Curative resection is the single most important factor determining outcome in patients with pancreatic adenocarcinoma. *Br J Surg* 2004; **91**: 586-594 [PMID: 15122610 DOI: 10.1002/bjs.4484]
32 **Hidalgo M**. Pancreatic cancer. *N Engl J Med* 2010; **362**: 1605-1617 [PMID: 20427809 DOI: 10.1056/NEJMra0901557]
33 **van der Gaag NA**, Rauws EA, van Eijck CH, Bruno MJ, van der Harst E, Kubben FJ, Gerritsen JJ, Greve JW, Gerhards MF, de Hingh IH, Klinkenbijl JH, Nio CY, de Castro SM, Busch OR, van Gulik TM, Bossuyt PM, Gouma DJ. Preoperative biliary drainage for cancer of the head of the pancreas. *N Engl J Med* 2010; **362**: 129-137 [PMID: 20071702 DOI: 10.1056/NEJMoa0903230]
34 **Jinkins LJ**, Parmar AD, Han Y, Duncan CB, Sheffield KM, Brown KM, Riall TS. Current trends in preoperative biliary stenting in patients with pancreatic cancer. *Surgery* 2013; **154**: 179-189 [PMID: 23889947 DOI: 10.1016/j.surg.2013.03.016]
35 **Lemmens VE**, Bosscha K, van der Schelling G, Brenninkmeijer S, Coebergh JW, de Hingh IH. Improving outcome for patients with pancreatic cancer through centralization. *Br J Surg* 2011; **98**: 1455-1462 [PMID: 21717423 DOI: 10.1002/bjs.7581]
36 **Gillen S**, Schuster T, Meyer Zum Büschenfelde C, Friess H, Kleeff J. Preoperative/neoadjuvant therapy in pancreatic cancer: a systematic review and meta-analysis of response and resection percentages. *PLoS Med* 2010; **7**: e1000267 [PMID: 20422030 DOI: 10.1371/journal.pmed.1000267]
37 **Kim HJ**, Czischke K, Brennan MF, Conlon KC. Does neoadjuvant chemoradiation downstage locally advanced pancreatic cancer? *J Gastrointest Surg* 2002; **6**: 763-769 [PMID: 12399067 DOI: 10.1016/s1091-255x(02)00017-3]
38 **Neoptolemos JP**, Stocken DD, Bassi C, Ghaneh P, Cunningham D, Goldstein D, Padbury R, Moore MJ, Gallinger S, Mariette C, Wente MN, Izbicki JR, Friess H, Lerch MM, Dervenis C, Oláh A, Butturini G, Doi R, Lind PA, Smith D, Valle JW, Palmer DH, Buckels JA, Thompson J, McKay CJ, Rawcliffe CL, Büchler MW; European Study Group for Pancreatic Cancer. Adjuvant chemotherapy with fluorouracil plus folinic acid vs gemcitabine following pancreatic cancer resection: a randomized controlled trial. *JAMA* 2010; **304**: 1073-1081 [PMID: 20823433 DOI: 10.1001/jama.2010.1275]
39 **Burris HA 3rd**, Moore MJ, Andersen J, Green MR, Rothenberg ML, Modiano MR, Cripps MC, Portenoy RK, Storniolo AM, Tarassoff P, Nelson R, Dorr FA, Stephens CD, Von Hoff DD. Improvements in survival and clinical benefit with gemcitabine as first-line therapy for patients with advanced pancreas cancer: a randomized trial. *J Clin Oncol* 1997; **15**: 2403-2413 [PMID: 9196156 DOI: 10.1200/JCO.1997.15.6.2403]
40 **Conroy T**, Desseigne F, Ychou M, Bouché O, Guimbaud R, Bécouarn Y, Adenis A, Raoul JL, Gourgou-Bourgade S, de la Fouchardière C, Bennouna J, Bachet JB, Khemissa-Akouz F, Péré-Vergé D, Delbaldo C, Assenat E, Chauffert B, Michel P, Montoto-Grillot C, Ducreux M; Groupe Tumeurs Digestives of Unicancer; PRODIGE Intergroup. FOLFIRINOX versus gemcitabine for metastatic pancreatic cancer. *N Engl J Med* 2011; **364**: 1817-1825 [PMID: 21561347 DOI: 10.1056/NEJMoa1011923]
41 **Custodio A**, Puente J, Sastre J, Díaz-Rubio E. Second-line therapy for advanced pancreatic cancer: a review of the literature and future directions. *Cancer Treat Rev* 2009; **35**: 676-684 [PMID: 19758760 DOI: 10.1016/j.ctrv.2009.08.012]
42 **Boeck S**, Ankerst DP, Heinemann V. The role of adjuvant chemotherapy for patients with resected pancreatic cancer: systematic review of randomized controlled trials and meta-analysis. *Oncology* 2007; **72**: 314-321 [PMID: 18187951 DOI: 10.1159/000113054]
43 **Moore MJ**, Goldstein D, Hamm J, Figer A, Hecht JR, Gallinger S, Au HJ, Murawa P, Walde D, Wolff RA, Campos D, Lim R, Ding K, Clark G, Voskoglou-Nomikos T, Ptasynski M, Parulekar W; National Cancer Institute of Canada Clinical Trials Group. Erlotinib plus gemcitabine compared with gemcitabine alone in patients with advanced pancreatic cancer: a phase III trial of the National Cancer Institute of Canada Clinical Trials Group. *J Clin Oncol* 2007; **25**: 1960-1966 [PMID: 17452677 DOI: 10.1200/JCO.2006.07.9525]
44 **Neesse A**, Michl P, Frese KK, Feig C, Cook N, Jacobetz MA, Lolkema MP, Buchholz M, Olive KP, Gress TM, Tuveson DA. Stromal biology and therapy in pancreatic cancer. *Gut* 2011; **60**: 861-868 [PMID: 20966025 DOI: 10.1136/gut.2010.226092]
45 **Von Hoff DD**, Ramanathan RK, Borad MJ, Laheru DA, Smith LS, Wood TE, Korn RL, Desai N, Trieu V, Iglesias JL, Zhang H, Soon-Shiong P, Shi T, Rajeshkumar NV, Maitra A, Hidalgo M. Gemcitabine plus nab-paclitaxel is an active regimen in patients with advanced pancreatic cancer: a phase I/II trial. *J Clin Oncol* 2011; **29**: 4548-4554 [PMID: 21969517 DOI: 10.1200/JCO.2011.36.5742]
46 **Pisters PW**, Abbruzzese JL, Janjan NA, Cleary KR, Charnsangavej C, Goswitz MS, Rich TA, Raijman I, Wolff RA, Lenzi R, Lee JE, Evans DB. Rapid-fractionation preoperative chemoradiation, pancreaticoduodenectomy, and intraoperative radiation therapy for resectable pancreatic adenocarcinoma. *J Clin Oncol* 1998; **16**: 3843-3850 [PMID: 9850029 DOI: 10.1200/JCO.1998.16.12.3843]
47 **Krishnan S**, Rana V, Evans DB, Varadhachary G, Das P, Bhatia S, Delclos ME, Janjan NA, Wolff RA, Crane CH, Pisters PW. Role of adjuvant chemoradiation therapy in adenocarcinomas of the ampulla of vater. *Int J Radiat Oncol Biol Phys* 2008; **70**: 735-743 [PMID: 17980502 DOI: 10.1016/j.ijrobp.2007.07.2327]
48 **Kalser MH**, Ellenberg SS. Pancreatic cancer. Adjuvant combined radiation and chemotherapy following curative resection. *Arch Surg* 1985; **120**: 899-903 [PMID: 4015380 DOI: 10.1001/archsurg.1985.01390320023003]
49 **Schellenberg D**, Kim J, Christman-Skieller C, Chun CL, Columbo LA, Ford JM, Fisher GA, Kunz PL, Van Dam J, Quon A, Desser TS, Norton J, Hsu A, Maxim PG, Xing L, Goodman KA, Chang DT, Koong AC. Single-fraction stereotactic

body radiation therapy and sequential gemcitabine for the treatment of locally advanced pancreatic cancer. *Int J Radiat Oncol Biol Phys* 2011; **81**: 181-188 [PMID: 21549517 DOI: 10.1016/j.ijrobp.2010.05.006]

50 **Didolkar MS**, Coleman CW, Brenner MJ, Chu KU, Olexa N, Stanwyck E, Yu A, Neerchal N, Rabinowitz S. Image-guided stereotactic radiosurgery for locally advanced pancreatic adenocarcinoma results of first 85 patients. *J Gastrointest Surg* 2010; **14**: 1547-1559 [PMID: 20839073 DOI: 10.1007/s11605-010-1323-7]

51 **Rwigema JC**, Heron DE, Parikh SD, Zeh HJ 3rd, Moser JA, Bahary N, Ashby K, Burton SA. Adjuvant stereotactic body radiotherapy for resected pancreatic adenocarcinoma with close or positive margins. *J Gastrointest Cancer* 2012; **43**: 70-76 [PMID: 20809393 DOI: 10.1007/s12029-010-9203-7]

52 **Doocey CM**, Finn K, Murphy C, Guinane CM. The impact of the human microbiome in tumorigenesis, cancer progression, and biotherapeutic development. *BMC Microbiol* 2022; **22**: 53 [PMID: 35151278 DOI: 10.1186/s12866-022-02465-6]

53 **Michaud DS**, Izard J. Microbiota, oral microbiome, and pancreatic cancer. *Cancer J* 2014; **20**: 203-206 [PMID: 24855008 DOI: 10.1097/PPO.0000000000000046]

54 **Shapiro KB**, Hotchkiss JH, Roe DA. Quantitative relationship between oral nitrate-reducing activity and the endogenous formation of N-nitrosoamino acids in humans. *Food Chem Toxicol* 1991; **29**: 751-755 [PMID: 1761254 DOI: 10.1016/0278-6915(91)90183-8]

55 **Li Y**, Hecht SS. Metabolic Activation and DNA Interactions of Carcinogenic N-Nitrosamines to Which Humans Are Commonly Exposed. *Int J Mol Sci* 2022; **23** [PMID: 35562949 DOI: 10.3390/ijms23094559]

56 **Li H**, Kern JA. Genetic and Molecular Changes in Lung Cancer: Prospects for a Personalized Pharmacological Approach to Treatment. In: Grippi MA, Elias JA, Fishman JA, Kotloff RM, Pack AI, Senior RM, et al, editors. Fishman's Pulmonary Diseases and Disorders, 5e. New York, NY: McGraw-Hill Education, 2015

57 **Hruban RH**, van Mansfeld AD, Offerhaus GJ, van Weering DH, Allison DC, Goodman SN, Kensler TW, Bose KK, Cameron JL, Bos JL. K-ras oncogene activation in adenocarcinoma of the human pancreas. A study of 82 carcinomas using a combination of mutant-enriched polymerase chain reaction analysis and allele-specific oligonucleotide hybridization. *Am J Pathol* 1993; **143**: 545-554 [PMID: 8342602]

58 **Teshima R**, Hanada K, Akada J, Kawano K, Yamaoka Y. Aggregatibacter actinomycetemcomitans infection causes DNA double-strand breaks in host cells. *Genes Cells* 2018; **23**: 264-273 [PMID: 29441648 DOI: 10.1111/gtc.12570]

59 **Sun Z**, Xiong C, Teh SW, Lim JCW, Kumar S, Thilakavathy K. Mechanisms of Oral Bacterial Virulence Factors in Pancreatic Cancer. *Front Cell Infect Microbiol* 2019; **9**: 412 [PMID: 31867287 DOI: 10.3389/fcimb.2019.00412]

60 **Fardini Y**, Wang X, Témoin S, Nithianantham S, Lee D, Shoham M, Han YW. Fusobacterium nucleatum adhesin FadA binds vascular endothelial cadherin and alters endothelial integrity. *Mol Microbiol* 2011; **82**: 1468-1480 [PMID: 22040113 DOI: 10.1111/j.1365-2958.2011.07905.x]

61 **Rubinstein MR**, Wang X, Liu W, Hao Y, Cai G, Han YW. Fusobacterium nucleatum promotes colorectal carcinogenesis by modulating E-cadherin/β-catenin signaling *via* its FadA adhesin. *Cell Host Microbe* 2013; **14**: 195-206 [PMID: 23954158 DOI: 10.1016/j.chom.2013.07.012]

62 **Zhang Y**, Morris JP 4th, Yan W, Schofield HK, Gurney A, Simeone DM, Millar SE, Hoey T, Hebrok M, Pasca di Magliano M. Canonical wnt signaling is required for pancreatic carcinogenesis. *Cancer Res* 2013; **73**: 4909-4922 [PMID: 23761328 DOI: 10.1158/0008-5472.CAN-12-4384]

63 **Gur C**, Ibrahim Y, Isaacson B, Yamin R, Abed J, Gamliel M, Enk J, Bar-On Y, Stanietsky-Kaynan N, Coppenhagen-Glazer S, Shussman N, Almogy G, Cuapio A, Hofer E, Mevorach D, Tabib A, Ortenberg R, Markel G, Miklić K, Jonjic S, Brennan CA, Garrett WS, Bachrach G, Mandelboim O. Binding of the Fap2 protein of Fusobacterium nucleatum to human inhibitory receptor TIGIT protects tumors from immune cell attack. *Immunity* 2015; **42**: 344-355 [PMID: 25680274 DOI: 10.1016/j.immuni.2015.01.010]

64 **Ahn HJ**, Lee DS. Helicobacter pylori in gastric carcinogenesis. *World J Gastrointest Oncol* 2015; **7**: 455-465 [PMID: 26690981 DOI: 10.4251/wjgo.v7.i12.455]

65 **Kumar S**, Metz DC, Kaplan DE, Goldberg DS. The association of Helicobacter pylori with pancreatic cancer. *GastroHep* 2020; **2**: 157-164 [PMID: 33692655 DOI: 10.1002/ygh2.398]

66 **Hirabayashi M**, Inoue M, Sawada N, Saito E, Abe SK, Hidaka A, Iwasaki M, Yamaji T, Shimazu T, Tsugane S. Helicobacter pylori infection, atrophic gastritis, and risk of pancreatic cancer: A population-based cohort study in a large Japanese population: the JPHC Study. *Sci Rep* 2019; **9**: 6099 [PMID: 30988344 DOI: 10.1038/s41598-019-42365-w]

67 **Nilsson HO**, Stenram U, Ihse I, Wadstrom T. Helicobacter species ribosomal DNA in the pancreas, stomach and duodenum of pancreatic cancer patients. *World J Gastroenterol* 2006; **12**: 3038-3043 [PMID: 16718784 DOI: 10.3748/wjg.v12.i19.3038]

68 **Gérard P**. Metabolism of cholesterol and bile acids by the gut microbiota. *Pathogens* 2013; **3**: 14-24 [PMID: 25437605 DOI: 10.3390/pathogens3010014]

69 **Ridlon JM**, Harris SC, Bhowmik S, Kang DJ, Hylemon PB. Consequences of bile salt biotransformations by intestinal bacteria. *Gut Microbes* 2016; **7**: 22-39 [PMID: 26939849 DOI: 10.1080/19490976.2015.1127483]

70 **Hirano S**, Masuda N, Mukai H, Hirakawa K, Imamura T. [Transformation of bile acids by Bacteroides fragilis strains isolated from the human intestine (author's transl)]. *Nihon Saikingaku Zasshi* 1979; **34**: 403-411 [PMID: 490901]

71 **Mikó E**, Vida A, Kovács T, Ujlaki G, Trencsényi G, Márton J, Sári Z, Kovács P, Boratkó A, Hujber Z, Csonka T, Antal-Szalmás P, Watanabe M, Gombos I, Csoka B, Kiss B, Vígh L, Szabó J, Méhes G, Sebestyén A, Goedert JJ, Bai P. Lithocholic acid, a bacterial metabolite reduces breast cancer cell proliferation and aggressiveness. *Biochim Biophys Acta Bioenerg* 2018; **1859**: 958-974 [PMID: 29655782 DOI: 10.1016/j.bbabio.2018.04.002]

72 **Kovács P**, Csonka T, Kovács T, Sári Z, Ujlaki G, Sipos A, Karányi Z, Szeőcs D, Hegedűs C, Uray K, Jankó L, Kiss M, Kiss B, Laoui D, Virág L, Méhes G, Bai P, Mikó E. Lithocholic Acid, a Metabolite of the Microbiome, Increases Oxidative Stress in Breast Cancer. *Cancers (Basel)* 2019; **11** [PMID: 31461945 DOI: 10.3390/cancers11091255]

73 **Luu TH**, Bard JM, Carbonnelle D, Chaillou C, Huvelin JM, Bobin-Dubigeon C, Nazih H. Lithocholic bile acid inhibits lipogenesis and induces apoptosis in breast cancer cells. *Cell Oncol (Dordr)* 2018; **41**: 13-24 [PMID: 28993998 DOI: 10.1007/s13402-017-0353-5]

74 **Slocum MM**, Sittig KM, Specian RD, Deitch EA. Absence of intestinal bile promotes bacterial translocation. *Am Surg* 1992; **58**: 305-310 [PMID: 1622012]

75 **Rees DO**, Crick PJ, Jenkins GJ, Wang Y, Griffiths WJ, Brown TH, Al-Sarireh B. Comparison of the composition of bile acids in bile of patients with adenocarcinoma of the pancreas and benign disease. *J Steroid Biochem Mol Biol* 2017; **174**: 290-295 [PMID: 29031685 DOI: 10.1016/j.jsbmb.2017.10.011]

76 **Feng HY**, Chen YC. Role of bile acids in carcinogenesis of pancreatic cancer: An old topic with new perspective. *World J Gastroenterol* 2016; **22**: 7463-7477 [PMID: 27672269 DOI: 10.3748/wjg.v22.i33.7463]

77 **Nagathihalli NS**, Beesetty Y, Lee W, Washington MK, Chen X, Lockhart AC, Merchant NB. Novel mechanistic insights into ectodomain shedding of EGFR Ligands Amphiregulin and TGF-α: impact on gastrointestinal cancers driven by secondary bile acids. *Cancer Res* 2014; **74**: 2062-2072 [PMID: 24520077 DOI: 10.1158/0008-5472.CAN-13-2329]

78 **Hummel D**, Aggarwal A, Borka K, Bajna E, Kállay E, Horváth HC. The vitamin D system is deregulated in pancreatic diseases. *J Steroid Biochem Mol Biol* 2014; **144** Pt B: 402-409 [PMID: 25090635 DOI: 10.1016/j.jsbmb.2014.07.011]

79 **Chen XL**, Xie KX, Yang ZL, Yuan LW. Expression of FXR and HRG and their clinicopathological significance in benign and malignant pancreatic lesions. *Int J Clin Exp Pathol* 2019; **12**: 2111-2120 [PMID: 31934033]

80 **Koutsounas I**, Giaginis C, Alexandrou P, Zizi-Serbetzoglou A, Patsouris E, Kouraklis G, Theocharis S. Pregnane X Receptor Expression in Human Pancreatic Adenocarcinoma: Associations With Clinicopathologic Parameters, Tumor Proliferative Capacity, Patients' Survival, and Retinoid X Receptor Expression. *Pancreas* 2015; **44**: 1134-1140 [PMID: 26355550 DOI: 10.1097/MPA.0000000000000405]

81 **Sittipo P**, Shim JW, Lee YK. Microbial Metabolites Determine Host Health and the Status of Some Diseases. *Int J Mol Sci* 2019; **20** [PMID: 31653062 DOI: 10.3390/ijms20215296]

82 **Goodwin AC**, Destefano Shields CE, Wu S, Huso DL, Wu X, Murray-Stewart TR, Hacker-Prietz A, Rabizadeh S, Woster PM, Sears CL, Casero RA Jr. Polyamine catabolism contributes to enterotoxigenic Bacteroides fragilis-induced colon tumorigenesis. *Proc Natl Acad Sci U S A* 2011; **108**: 15354-15359 [PMID: 21876161 DOI: 10.1073/pnas.1010203108]

83 **Mendez R**, Kesh K, Arora N, Di Martino L, McAllister F, Merchant N, Banerjee S. Microbial dysbiosis and polyamine metabolism as predictive markers for early detection of pancreatic cancer. *Carcinogenesis* 2020; **41**: 561-570 [PMID: 31369062 DOI: 10.1093/carcin/bgz116]

84 **Riquelme E**, Zhang Y, Zhang L, Montiel M, Zoltan M, Dong W, Quesada P, Sahin I, Chandra V, San Lucas A, Scheet P, Xu H, Hanash SM, Feng L, Burks JK, Do KA, Peterson CB, Nejman D, Tzeng CD, Kim MP, Sears CL, Ajami N, Petrosino J, Wood LD, Maitra A, Straussman R, Katz M, White JR, Jenq R, Wargo J, McAllister F. Tumor Microbiome Diversity and Composition Influence Pancreatic Cancer Outcomes. *Cell* 2019; **178**: 795-806.e12 [PMID: 31398337 DOI: 10.1016/j.cell.2019.07.008]

85 **Merali N**, Chouari T, Kayani K, Rayner CJ, Jiménez JI, Krell J, Giovannetti E, Bagwan I, Relph K, Rockall TA, Dhillon T, Pandha H, Annels NE, Frampton AE. A Comprehensive Review of the Current and Future Role of the Microbiome in Pancreatic Ductal Adenocarcinoma. *Cancers (Basel)* 2022; **14** [PMID: 35205769 DOI: 10.3390/cancers14041020]

86 **Lang PA**, Lang KS, Xu HC, Grusdat M, Parish IA, Recher M, Elford AR, Dhanji S, Shaabani N, Tran CW, Dissanayake D, Rahbar R, Ghazarian M, Brüstle A, Fine J, Chen P, Weaver CT, Klose C, Diefenbach A, Häussinger D, Carlyle JR, Kaech SM, Mak TW, Ohashi PS. Natural killer cell activation enhances immune pathology and promotes chronic infection by limiting CD8+ T-cell immunity. *Proc Natl Acad Sci U S A* 2012; **109**: 1210-1215 [PMID: 22167808 DOI: 10.1073/pnas.1118834109]

87 **Yu Q**, Xiu Z, Jian Y, Zhou J, Chen X, Chen C, Chen H, Yang S, Yin L, Zeng W. microRNA-497 prevents pancreatic cancer stem cell gemcitabine resistance, migration, and invasion by directly targeting nuclear factor kappa B 1. *Aging (Albany NY)* 2022; **14**: 5908-5924 [PMID: 35896012 DOI: 10.18632/aging.204193]

88 **Aykut B**, Pushalkar S, Chen R, Li Q, Abengozar R, Kim JI, Shadaloey SA, Wu D, Preiss P, Verma N, Guo Y, Saxena A, Vardhan M, Diskin B, Wang W, Leinwand J, Kurz E, Kochen Rossi JA, Hundeyin M, Zambrinis C, Li X, Saxena D, Miller G. The fungal mycobiome promotes pancreatic oncogenesis *via* activation of MBL. *Nature* 2019; **574**: 264-267 [PMID: 31578522 DOI: 10.1038/s41586-019-1608-2]

89 **Chen Y**, Bai X, Zhang Q, Wen L, Su W, Fu Q, Sun X, Lou Y, Yang J, Zhang J, Chen Q, Wang J, Liang T. The hepatitis B virus X protein promotes pancreatic cancer through modulation of the PI3K/AKT signaling pathway. *Cancer Lett* 2016; **380**: 98-105 [PMID: 27339327 DOI: 10.1016/j.canlet.2016.06.011]

90 **Nista EC**, Del Gaudio A, Del Vecchio LE, Mezza T, Pignataro G, Piccioni A, Gasbarrini A, Franceschi F, Candelli M. Pancreatic Cancer Resistance to Treatment: The Role of Microbiota. *Biomedicines* 2023; **11** [PMID: 36672664 DOI: 10.3390/biomedicines11010157]

91 **Attebury H**, Daley D. The Gut Microbiome and Pancreatic Cancer Development and Treatment. *Cancer J* 2023; **29**: 49-56 [PMID: 36957973 DOI: 10.1097/PPO.0000000000000647]

92 **Bastos AR**, Pereira-Marques J, Ferreira RM, Figueiredo C. Harnessing the Microbiome to Reduce Pancreatic Cancer Burden. *Cancers (Basel)* 2023; **15** [PMID: 37174095 DOI: 10.3390/cancers15092629]

93 **Chai Y**, Huang Z, Shen X, Lin T, Zhang Y, Feng X. Microbiota Regulates Pancreatic Cancer Carcinogenesis through Altered Immune Response. *Microorganisms* 2023; **11**: 1240

94 **Binda C**, Gibiino G, Sbrancia M, Coluccio C, Cazzato M, Carloni L, Cucchetti A, Ercolani G, Sambri V, Fabbri C. Microbiota in the Natural History of Pancreatic Cancer: From Predisposition to Therapy. *Cancers (Basel)* 2022; **15** [PMID: 36611999 DOI: 10.3390/cancers15010001]

95 **Yang T**, Li QQ, Liu YM, Yang B. T cells in pancreatic cancer stroma: Tryptophan metabolism plays an important role in immunoregulation. *World J Gastroenterol* 2023; **29**: 2701-2703 [PMID: 37213408 DOI: 10.3748/wjg.v29.i17.2701]

96 **Tintelnot J**, Xu Y, Lesker TR, Schönlein M, Konczalla L, Giannou AD, Pelczar P, Kylies D, Puelles VG, Bielecka AA, Peschka M, Cortesi F, Riecken K, Jung M, Amend L, Bröring TS, Trajkovic-Arsic M, Siveke JT, Renné T, Zhang D, Boeck S, Strowig T, Uzunoglu FG, Güngör C, Stein A, Izbicki JR, Bokemeyer C, Sinn M, Kimmelman AC, Huber S, Gagliani N. Microbiota-derived 3-IAA influences chemotherapy efficacy in pancreatic cancer. *Nature* 2023; **615**: 168-174 [PMID: 36813961 DOI: 10.1038/s41586-023-05728-y]

97 **Sohal DP**, Mangu PB, Khorana AA, Shah MA, Philip PA, O'Reilly EM, Uronis HE, Ramanathan RK, Crane CH,

Engebretson A, Ruggiero JT, Copur MS, Lau M, Urba S, Laheru D. Metastatic Pancreatic Cancer: American Society of Clinical Oncology Clinical Practice Guideline. *J Clin Oncol* 2016; **34**: 2784-2796 [PMID: 27247222 DOI: 10.1200/JCO.2016.67.1412]

98 **Wai SN**, Lindmark B, Söderblom T, Takade A, Westermark M, Oscarsson J, Jass J, Richter-Dahlfors A, Mizunoe Y, Uhlin BE. Vesicle-mediated export and assembly of pore-forming oligomers of the enterobacterial ClyA cytotoxin. *Cell* 2003; **115**: 25-35 [PMID: 14532000 DOI: 10.1016/s0092-8674(03)00754-2]

99 **Sawant SS**, Patil SM, Gupta V, Kunda NK. Microbes as Medicines: Harnessing the Power of Bacteria in Advancing Cancer Treatment. *Int J Mol Sci* 2020; **21** [PMID: 33066447 DOI: 10.3390/ijms21207575]

100 **Bezine E**, Vignard J, Mirey G. The cytolethal distending toxin effects on Mammalian cells: a DNA damage perspective. *Cells* 2014; **3**: 592-615 [PMID: 24921185 DOI: 10.3390/cells3020592]

101 **Yang WS**, Park SO, Yoon AR, Yoo JY, Kim MK, Yun CO, Kim CW. Suicide cancer gene therapy using pore-forming toxin, streptolysin O. *Mol Cancer Ther* 2006; **5**: 1610-1619 [PMID: 16818521 DOI: 10.1158/1535-7163.MCT-05-0515]

102 **Trivieri N**, Panebianco C, Villani A, Pracella R, Latiano TP, Perri F, Binda E, Pazienza V. High Levels of Prebiotic Resistant Starch in Diet Modulate a Specific Pattern of miRNAs Expression Profile Associated to a Better Overall Survival in Pancreatic Cancer. *Biomolecules* 2020; **11** [PMID: 33383727 DOI: 10.3390/biom11010026]

103 **Kita A**, Fujiya M, Konishi H, Tanaka H, Kashima S, Iwama T, Ijiri M, Murakami Y, Takauji S, Goto T, Sakatani A, Ando K, Ueno N, Ogawa N, Okumura T. Probioticderived ferrichrome inhibits the growth of refractory pancreatic cancer cells. *Int J Oncol* 2020; **57**: 721-732 [PMID: 32705165 DOI: 10.3892/ijo.2020.5096]

104 **Liu MN**, Zhang L, Dong XY, Liu M, Cheng G, Zhang XL, He F, Wang GQ. [Effects of Akkermansia muciniphila on the Proliferation, Apoptosis and Insulin Secretion of Rat Islet Cell Tumor Cells]. *Sichuan Da Xue Xue Bao Yi Xue Ban* 2020; **51**: 13-17 [PMID: 31950783 DOI: 10.12182/20200160202]

105 **Iida N**, Dzutsev A, Stewart CA, Smith L, Bouladoux N, Weingarten RA, Molina DA, Salcedo R, Back T, Cramer S, Dai RM, Kiu H, Cardone M, Naik S, Patri AK, Wang E, Marincola FM, Frank KM, Belkaid Y, Trinchieri G, Goldszmid RS. Commensal bacteria control cancer response to therapy by modulating the tumor microenvironment. *Science* 2013; **342**: 967-970 [PMID: 24264989 DOI: 10.1126/science.1240527]

106 **Wallace BD**, Wang H, Lane KT, Scott JE, Orans J, Koo JS, Venkatesh M, Jobin C, Yeh LA, Mani S, Redinbo MR. Alleviating cancer drug toxicity by inhibiting a bacterial enzyme. *Science* 2010; **330**: 831-835 [PMID: 21051639 DOI: 10.1126/science.1191175]

107 **Lin XB**, Farhangfar A, Valcheva R, Sawyer MB, Dieleman L, Schieber A, Gänzle MG, Baracos V. The role of intestinal microbiota in development of irinotecan toxicity and in toxicity reduction through dietary fibres in rats. *PLoS One* 2014; **9**: e83644 [PMID: 24454707 DOI: 10.1371/journal.pone.0083644]

108 **Vétizou M**, Pitt JM, Daillère R, Lepage P, Waldschmitt N, Flament C, Rusakiewicz S, Routy B, Roberti MP, Duong CP, Poirier-Colame V, Roux A, Becharef S, Formenti S, Golden E, Cording S, Eberl G, Schlitzer A, Ginhoux F, Mani S, Yamazaki T, Jacquelot N, Enot DP, Bérard M, Nigou J, Opolon P, Eggermont A, Woerther PL, Chachaty E, Chaput N, Robert C, Mateus C, Kroemer G, Raoult D, Boneca IG, Carbonnel F, Chamaillard M, Zitvogel L. Anticancer immunotherapy by CTLA-4 blockade relies on the gut microbiota. *Science* 2015; **350**: 1079-1084 [PMID: 26541610 DOI: 10.1126/science.aad1329]

109 **Mirji G**, Worth A, Bhat SA, El Sayed M, Kannan T, Goldman AR, Tang HY, Liu Q, Auslander N, Dang CV, Abdel-Mohsen M, Kossenkov A, Stanger BZ, Shinde RS. The microbiome-derived metabolite TMAO drives immune activation and boosts responses to immune checkpoint blockade in pancreatic cancer. *Sci Immunol* 2022; **7**: eabn0704 [PMID: 36083892 DOI: 10.1126/sciimmunol.abn0704]

110 **Raimondi G**, Gea-Sorlí S, Otero-Mateo M, Fillat C. Inhibition of miR-222 by Oncolytic Adenovirus-Encoded miRNA Sponges Promotes Viral Oncolysis and Elicits Antitumor Effects in Pancreatic Cancer Models. *Cancers (Basel)* 2021; **13** [PMID: 34203557 DOI: 10.3390/cancers13133233]

111 **Xie Y**, Xie F, Zhou X, Zhang L, Yang B, Huang J, Wang F, Yan H, Zeng L, Zhou F. Microbiota in Tumors: From Understanding to Application. *Adv Sci (Weinh)* 2022; **9**: e2200470 [PMID: 35603968 DOI: 10.1002/advs.202200470]

112 **Nejman D**, Livyatan I, Fuks G, Gavert N, Zwang Y, Geller LT, Rotter-Maskowitz A, Weiser R, Mallel G, Gigi E, Meltser A, Douglas GM, Kamer I, Gopalakrishnan V, Dadosh T, Levin-Zaidman S, Avnet S, Atlan T, Cooper ZA, Arora R, Cogdill AP, Khan MAW, Ologun G, Bussi Y, Weinberger A, Lotan-Pompan M, Golani O, Perry G, Rokah M, Bahar-Shany K, Rozeman EA, Blank CU, Ronai A, Shaoul R, Amit A, Dorfman T, Kremer R, Cohen ZR, Harnof S, Siegal T, Yehuda-Shnaidman E, Gal-Yam EN, Shapira H, Baldini N, Langille MGI, Ben-Nun A, Kaufman B, Nissan A, Golan T, Dadiani M, Levanon K, Bar J, Yust-Katz S, Barshack I, Peeper DS, Raz DJ, Segal E, Wargo JA, Sandbank J, Shental N, Straussman R. The human tumor microbiome is composed of tumor type-specific intracellular bacteria. *Science* 2020; **368**: 973-980 [PMID: 32467386 DOI: 10.1126/science.aay9189]

113 **Geller LT**, Barzily-Rokni M, Danino T, Jonas OH, Shental N, Nejman D, Gavert N, Zwang Y, Cooper ZA, Shee K, Thaiss CA, Reuben A, Livny J, Avraham R, Frederick DT, Ligorio M, Chatman K, Johnston SE, Mosher CM, Brandis A, Fuks G, Gurbatri C, Gopalakrishnan V, Kim M, Hurd MW, Katz M, Fleming J, Maitra A, Smith DA, Skalak M, Bu J, Michaud M, Trauger SA, Barshack I, Golan T, Sandbank J, Flaherty KT, Mandinova A, Garrett WS, Thayer SP, Ferrone CR, Huttenhower C, Bhatia SN, Gevers D, Wargo JA, Golub TR, Straussman R. Potential role of intratumor bacteria in mediating tumor resistance to the chemotherapeutic drug gemcitabine. *Science* 2017; **357**: 1156-1160 [PMID: 28912244 DOI: 10.1126/science.aah5043]

114 **Helmink BA**, Khan MAW, Hermann A, Gopalakrishnan V, Wargo JA. The microbiome, cancer, and cancer therapy. *Nat Med* 2019; **25**: 377-388 [PMID: 30842679 DOI: 10.1038/s41591-019-0377-7]

115 **Rogers CJ**, Prabhu KS, Vijay-Kumar M. The microbiome and obesity-an established risk for certain types of cancer. *Cancer J* 2014; **20**: 176-180 [PMID: 24855004 DOI: 10.1097/PPO.0000000000000049]

116 **Qin J**, Li Y, Cai Z, Li S, Zhu J, Zhang F, Liang S, Zhang W, Guan Y, Shen D, Peng Y, Zhang D, Jie Z, Wu W, Qin Y, Xue W, Li J, Han L, Lu D, Wu P, Dai Y, Sun X, Li Z, Tang A, Zhong S, Li X, Chen W, Xu R, Wang M, Feng Q, Gong M, Yu J, Zhang Y, Zhang M, Hansen T, Sanchez G, Raes J, Falony G, Okuda S, Almeida M, LeChatelier E, Renault P, Pons N, Batto JM, Zhang Z, Chen H, Yang R, Zheng W, Yang H, Wang J, Ehrlich SD, Nielsen R, Pedersen O, Kristiansen K. A

metagenome-wide association study of gut microbiota in type 2 diabetes. *Nature* 2012; **490**: 55-60 [PMID: 23023125 DOI: 10.1038/nature11450]

117 **Brubaker L**, Luu S, Hoffman K, Wood A, Navarro Cagigas M, Yao Q, Petrosino J, Fisher W, Van Buren G. Microbiome changes associated with acute and chronic pancreatitis: A systematic review. *Pancreatology* 2021; **21**: 1-14 [PMID: 33376062 DOI: 10.1016/j.pan.2020.12.013]

118 **Larsen N**, Vogensen FK, van den Berg FW, Nielsen DS, Andreasen AS, Pedersen BK, Al-Soud WA, Sørensen SJ, Hansen LH, Jakobsen M. Gut microbiota in human adults with type 2 diabetes differs from non-diabetic adults. *PLoS One* 2010; **5**: e9085 [PMID: 20140211 DOI: 10.1371/journal.pone.0009085]

119 **Maisonneuve P**, Amar S, Lowenfels AB. Periodontal disease, edentulism, and pancreatic cancer: a meta-analysis. *Ann Oncol* 2017; **28**: 985-995 [PMID: 28453689 DOI: 10.1093/annonc/mdx019]

120 **Hayashi C**, Gudino CV, Gibson FC 3rd, Genco CA. Review: Pathogen-induced inflammation at sites distant from oral infection: bacterial persistence and induction of cell-specific innate immune inflammatory pathways. *Mol Oral Microbiol* 2010; **25**: 305-316 [PMID: 20883220 DOI: 10.1111/j.2041-1014.2010.00582.x]

121 **Coussens LM**, Werb Z. Inflammation and cancer. *Nature* 2002; **420**: 860-867 [PMID: 12490959 DOI: 10.1038/nature01322]

122 **Mantovani A**, Allavena P, Sica A, Balkwill F. Cancer-related inflammation. *Nature* 2008; **454**: 436-444 [PMID: 18650914 DOI: 10.1038/nature07205]

123 **Michaud DS**, Izard J, Wilhelm-Benartzi CS, You DH, Grote VA, Tjønneland A, Dahm CC, Overvad K, Jenab M, Fedirko V, Boutron-Ruault MC, Clavel-Chapelon F, Racine A, Kaaks R, Boeing H, Foerster J, Trichopoulou A, Lagiou P, Trichopoulos D, Sacerdote C, Sieri S, Palli D, Tumino R, Panico S, Siersema PD, Peeters PH, Lund E, Barricarte A, Huerta JM, Molina-Montes E, Dorronsoro M, Quirós JR, Duell EJ, Ye W, Sund M, Lindkvist B, Johansen D, Khaw KT, Wareham N, Travis RC, Vineis P, Bueno-de-Mesquita HB, Riboli E. Plasma antibodies to oral bacteria and risk of pancreatic cancer in a large European prospective cohort study. *Gut* 2013; **62**: 1764-1770 [PMID: 22990306 DOI: 10.1136/gutjnl-2012-303006]

124 **Gnanasekaran J**, Binder Gallimidi A, Saba E, Pandi K, Eli Berchoer L, Hermano E, Angabo S, Makkawi HA, Khashan A, Daoud A, Elkin M, Nussbaum G. Intracellular Porphyromonas gingivalis Promotes the Tumorigenic Behavior of Pancreatic Carcinoma Cells. *Cancers (Basel)* 2020; **12** [PMID: 32824786 DOI: 10.3390/cancers12082331]

125 **Wei MY**, Shi S, Liang C, Meng QC, Hua J, Zhang YY, Liu J, Zhang B, Xu J, Yu XJ. The microbiota and microbiome in pancreatic cancer: more influential than expected. *Mol Cancer* 2019; **18**: 97 [PMID: 31109338 DOI: 10.1186/s12943-019-1008-0]

126 **Maekawa T**, Fukaya R, Takamatsu S, Itoyama S, Fukuoka T, Yamada M, Hata T, Nagaoka S, Kawamoto K, Eguchi H, Murata K, Kumada T, Ito T, Tanemura M, Fujimoto K, Tomita Y, Tobe T, Kamada Y, Miyoshi E. Possible involvement of Enterococcus infection in the pathogenesis of chronic pancreatitis and cancer. *Biochem Biophys Res Commun* 2018; **506**: 962-969 [PMID: 30401562 DOI: 10.1016/j.bbrc.2018.10.169]

World Journal of Gastroenterology

Submit a Manuscript: https://www.f6publishing.com

World J Gastroenterol 2023 July 7; 29(25): 3999-4008

DOI: 10.3748/wjg.v29.i25.3999

ISSN 1007-9327 (print) ISSN 2219-2840 (online)

MINIREVIEWS

Insulin resistance and adipose tissue interactions as the cornerstone of metabolic (dysfunction)-associated fatty liver disease pathogenesis

Shreya C Pal, Nahum Méndez-Sánchez

Specialty type: Gastroenterology and hepatology

Provenance and peer review: Invited article; Externally peer reviewed.

Peer-review model: Single blind

Peer-review report's scientific quality classification

Grade A (Excellent): 0
Grade B (Very good): B
Grade C (Good): C, C
Grade D (Fair): 0
Grade E (Poor): 0

P-Reviewer: Geng TY, China; Li PF, China; Ulasoglu C, Turkey

Received: December 6, 2022
Peer-review started: December 6, 2022
First decision: January 22, 2023
Revised: February 9, 2023
Accepted: March 20, 2023
Article in press: March 20, 2023
Published online: July 7, 2023

Shreya C Pal, Nahum Méndez-Sánchez, Faculty of Medicine, National Autonomous University of Mexico, Mexico City 04510, Mexico

Shreya C Pal, Nahum Méndez-Sánchez, Liver Research Unit, Medica Sur Clinic & Foundation, Mexico City 04510, Mexico

Corresponding author: Nahum Méndez-Sánchez, FAASLD, AGAF, FACG, MD, MSc, PhD, Researcher, Liver Research Unit, Medica Sur Clinic & Foundation, Puente de Piedra 150, Col. Toriello Guerra, Mexico City 04510, Mexico. nmendez@medicasur.org.mx

Abstract

The relationship between metabolic derangements and fatty liver development are undeniable, since more than 75% of patients with type 2 diabetes mellitus present with fatty liver. There is also significant epidemiological association between insulin resistance (IR) and metabolic (dysfunction)-associated fatty liver disease (MAFLD). For little more than 2 years, the nomenclature of fatty liver of non-alcoholic origin has been intended to change to MAFLD by multiple groups. While a myriad of reasons for which MAFLD is thought to be of metabolic origin could be exposed, the bottom line relies on the role of IR as an initiator and perpetuator of this disease. There is a reciprocal role in MAFLD development and IR as well as serum glucose concentrations, where increased circulating glucose and insulin result in increased *de novo* lipogenesis by sterol regulatory element-binding protein-1c induced lipogenic enzyme stimulation; therefore, increased endogenous production of triglycerides. The same effect is achieved through impaired suppression of adipose tissue (AT) lipolysis in insulin-resistant states, increasing fatty acid influx into the liver. The complementary reciprocal situation occurs when liver steatosis alters hepatokine secretion, modifying fatty acid metabolism as well as IR in a variety of tissues, including skeletal muscle, AT, and the liver. The aim of this review is to discuss the importance of IR and AT interactions in metabolic altered states as perhaps the most important factor in MAFLD pathogenesis.

Key Words: Metabolic (dysfunction)-associated fatty liver disease; Insulin resistance; Adipose tissue; Fatty liver; Metabolic syndrome; Adipokine

©The Author(s) 2023. Published by Baishideng Publishing Group Inc. All rights reserved.

Core Tip: In this review, we outline the main arguments that support the importance of insulin resistance (IR) in fatty liver pathogenesis, stressing its role in metabolic dysfunction. IR and other genetic and molecular mechanisms play a pivotal role not only in metabolic dysfunction–associated fatty liver disease development but also in some of its complications and comorbidities, such as chronic kidney disease.

Citation: Pal SC, Méndez-Sánchez N. Insulin resistance and adipose tissue interactions as the cornerstone of metabolic (dysfunction)-associated fatty liver disease pathogenesis. *World J Gastroenterol* 2023; 29(25): 3999-4008
URL: https://www.wjgnet.com/1007-9327/full/v29/i25/3999.htm
DOI: https://dx.doi.org/10.3748/wjg.v29.i25.3999

INTRODUCTION

The term non-alcoholic fatty liver disease (NAFLD) was initially used by Klatskin and colleagues in 1979[1], while Ludwig coined the term non-alcoholic steatohepatitis after witnessing similar clinical features in patients with liver steatosis[2]. Even though this nomenclature has been used for almost four decades, in 2020 a group of experts suggested a change of nomenclature from NAFLD to metabolic (dysfunction)-associated fatty liver disease (MAFLD) due to the large multifactorial basis for the disease and the fact that non-alcoholic does not accurately describe the disease pathogenesis[3-5]. By contrast, metabolic dysfunction accounts for a great deal of the pathogenesis of fatty liver whenever large alcohol consumption amounts are not present. MAFLD diagnosis is based on the presence of hepatic steatosis in addition to one of the following: obesity or overweight, type 2 diabetes mellitus (T2DM), or metabolic dysregulation. Metabolic dysfunction (in this context) accounts for the following conditions: increased waist circumference, systemic hypertension, dyslipidemia, prediabetes and insulin resistance (IR) (measured through the homeostatic model assessment [HOMA] > 2.5).

The development of MAFLD is linked to dyslipidemia, obesity, and IR. These are also the main features of metabolic syndrome (MetS). MetS constitutes a cluster of metabolic abnormalities which stem from IR and chronic low grade inflammation and on the long run increase the risk for cardiovascular disease (CVD) and T2DM[6]. The criteria for diagnosing MetS have changed since they were first established by the World Health Organization in 1988[7], evolving since the knowledge of the pathogenesis and its implications expanded. The criteria include the presence of visceral adiposity, IR, atherogenic dyslipidemia, and endothelial dysfunction, among others[8].

On a very important note, the change of nomenclature to MAFLD is very well justified by the sole fact that about 90% of NAFLD patients have one or more MetS component[9]. Furthermore, Marchesini *et al*[10] showed that the presence of MetS among patients with hepatic steatosis carry a significantly increased risk of developing steatohepatitis and fibrosis, with odds ratios of 3.2 and 3.5, respectively [10]. Also, MetS is a useful index for the prediction of the severity of obesity-related fatty liver[11].

One way in which we can argue in favor of IR's importance in MAFLD pathogenesis is by analyzing the causes of the established items in the metabolic risk abnormalities checklist. Another way is by refuting the counterarguments for the use of this new term. In this review, we will cover both issues.

One of the most valid points involves the fact that given MAFLD is a heterogeneous and complex disease, considering a single postulation to explain is pathogenesis is absurd. We agree that MAFLD is a multifactorial disease, and similar to diabetes, systemic hypertension and many more involve genetic and environmental mechanisms. In fact, there is progressively more data proving the influence of different environmental factors on fatty liver genesis, including air pollution and cigarette smoke. However, in MAFLD as a multifactorial disease, there is one specific overarching concept that accounts for most of the cases and pathogenesis of MAFLD, which is metabolic dysfunction.

To give an educated opinion on the subject, we must first understand what IR is, how it manifests on different endocrine organs, how it influences triglyceride (TG) metabolism in the liver, and its role in metabolic dysfunction.

IR: The basis

Insulin is the main anabolic hormone in the body, primordial for glucose homeostasis as well as other functions in tissue growth and development. Glucose homeostasis is maintained by regulating gluconeogenesis and glycogenolysis in the liver, as well as by inducing insulin-mediated glucose uptake in skeletal and cardiac muscle, as well as in adipose tissue (AT)[12]. IR refers to the impaired response of target tissues to insulin stimulation. This abnormality can be a result of altered number of receptors, or malfunction of the existing ones. In reality, there is not a single cause for IR development; instead

multiple factors together lead to this metabolic abnormality. These include the mentioned receptor abnormalities, as well as defects in the insulin signaling cascade, negative regulation of the cascade by inhibitors, or the presence of a proinflammatory internal milieu. There has even been a proposal regarding the induction of IR by fatty acids, which because of their abnormal metabolism lead to lipid accumulation in the muscle and liver. In any given case, whenever there is a decreased sensitivity of a hormonal stimulus, the result is a positive feedback loop that increases the concentration of the effect-lacking hormone (in this case, insulin). Increased insulin serum concentrations have a variety of effects due to its trophic effects on various tissues. Insulin serum concentrations are the basis for determining the presence of IR in an individual, principally through the use of the HOMA.

During the past decade, the "glucocentric" view of IR has shifted to the "lipocentric" view, regarding its pathogenesis and associated mechanisms. We can appreciate how much the focus of IR effect on glucose metabolism prevailed before the year 2000 in any scientific literature, even if we don't look in depth. For instance, IR had been included within a concept denominated the "IR syndrome", which considered the presence of dyslipidemia, hypertension and impaired glucose tolerance as factors leading to increased cardiovascular risk, however, that's the farthest lipids' involvement got[13]. Chronic hyperglycemia leads to glucotoxicity, directly inducing IR and the IR degree is one of the strongest predictors for T2DM onset in populations at risk[14,15]. While all of this is a fact, the role of fatty acid metabolism had been overlooked since in 1965 Randle and colleagues first suggested increased serum free fatty acids (FFAs) as one of the primary causes for decreased glucose oxidation and IR development[16]. The last decade has had an increased body of research supporting this fact, centering the role of lipids, along with that of glucose, in the development of fatty liver.

IR is present in a variety of metabolic disorders, such as MetS and T2DM. IR in the liver presents as increased gluconeogenesis and decreased hepatic glycogenesis, resulting in increased glucose production and release[17].

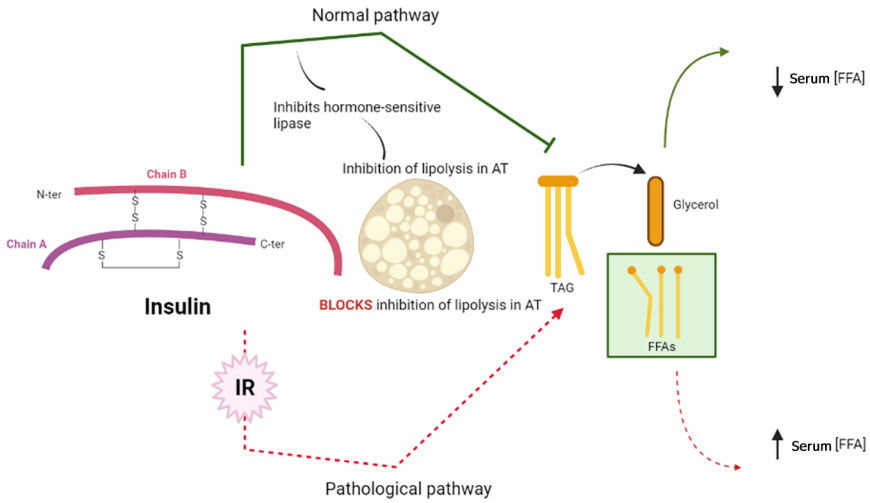
Adipose tissue IR-Which came first: The resistance or the fat?

AT has long been known to be an endocrine organ, both by releasing hormones such as leptin and adiponectin (adipokines), and by regulating proinflammatory mediator secretion and metabolic processes. AT IR refers to the impaired suppression of lipolysis in the presence of high insulin serum levels (Figure 1). One of the key hormones involved in AT-IR is adiponectin, which contributes to the development of obesity-related IR and CVD[18]. While in this case adiponectin levels are lower, other adipokines such as leptin are increased[19], the former one acting as a protective factor for hepatic steatosis development[20].

Whenever IR ensues, there is a disinhibition of lipolysis in the AT, which results in higher breakdown of stored triglycerides in AT and higher release of FFA into the blood. The circulating FFAs lead to activation of the proinflammatory nuclear factor kappa-light-chain-enhancer of activated B cells (NF-κB) pathway in the liver, ultimately resulting in lipotoxicity. Lipotoxicity, however, is not the end result of a single pathway, but rather the combination of the role of FFAs, TGs, biliary acids (BAs), free cholesterol, ceramides, and lysophosphatidyl cholines[21].

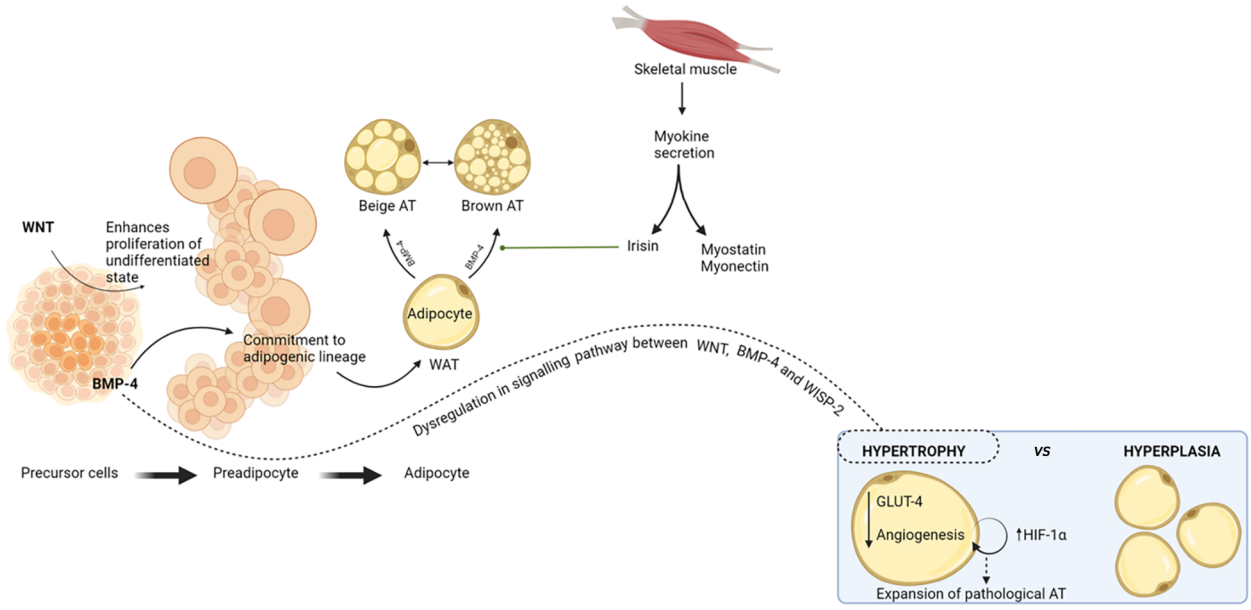
When it comes to metabolic health, AT is the major determinant given the ability of subcutaneous AT (SAT) to store excess fat (through adipocyte *de novo* lipogenesis [DNL] instead of allowing it to deposit in the non-fatty tissues, otherwise known as "ectopic" deposition of fat. Whenever this ability becomes impaired, aberrant adipocyte tissue develops, where the adipocytes undergo hypertrophy along with decreased number of glucose transporter-4 (GLUT-4) receptors. Under physiologic conditions, adipocytes carry out recruitment of adipogenic precursor cells, along with adequate angiogenesis. Dysregulation of the signaling pathway between the wingless-related integration site (WNT) and the bone morphogenetic protein 4 (BMP-4) results in alterations in the recruitment, proliferation and differentiation of the precursors. BMP-4 has also been found to contribute to "browning" of white AT in mice, where brown AT (BAT) tallies to the oxidative phenotype of lipid-storing adipocytes[22]. The alteration in AT expansion means that not only do pathologic adipocytes have decreased number of GLUT-4 receptors but they also have altered blood supply, leading to hypoxia and consequently to activation of hypoxia-inducible factor 1 alpha (HIF-1α). By having a reduced number of GLUT-4 receptors, glucose influx is impaired, which in turn limits DNL. The induction of HIF-1α factor in this pathological AT state increases systemic inflammatory conditions. Transcriptome analysis of AT macrophages in obese mice revealed rewiring of the metabolic pathways within these macrophages with increased glycolysis and oxidative phosphorylation, rendering them as inflammatory macrophages[23]. Macrophage HIF-1α is involved in the formation of crown-like structures, which lead to maintenance of inflammatory processes and inhibition of angiogenesis in preadipocytes, leading to a vicious circle of added hypoxia and expansion of the aberrant AT[24] (Figure 2). Pathologic expansion of AT leads to systemic IR, as mentioned throughout this review.

Briefly expanding upon the importance of BAT, a 2011 paper proved how cold-induced browning of AT in rats controlled TG rich lipoprotein metabolism by boosting their turnover and channeling lipids into AT browning[25]. There has been a number of studies proving that the presence of BAT in adulthood is independently associated with lower probability of developing liver steatosis[26,27], for which multiple mechanisms have been uncovered. For instance, the uncoupling protein 1 (UCP-1) expressed specifically in BAT reverses obesity and also antagonizes liver inflammation and pathology



DOI: 10.3748/wjg.v29.i25.3999 **Copyright** ©The Author(s) 2023.

Figure 1 Effect of insulin resistance on adipose tissue lipolysis. Under normal circumstances, insulin inhibits lipolysis in adipose tissue by inducing the hormone sensitive lipase, thus decreasing the release of excessive free fatty acids (FFAs) into the serum. However, in an insulin resistance state, inhibition of lipolysis is blocked, increasing serum FFAs, which eventually increase the influx of lipids into the liver. All the figures were created using BioRender. AT: Adipose tissue; IR: Insulin resistance.



DOI: 10.3748/wjg.v29.i25.3999 **Copyright** ©The Author(s) 2023.

Figure 2 Adipose tissue dysfunction in metabolic dysfunction–associated fatty liver disease. Adipocyte precursor cells undergo initial proliferation through the wingless-related integration site (WNT) signaling pathway and thereafter commitment to the adipogenic lineage by bone morphogenetic protein 4 (BMP-4) stimulus, until its conversion to preadipocytes and later on to mature adipocytes. White adipose tissue can undergo beiging or browning under the influence of two main stimuli: BMP-4 and irisin. Browning of adipose tissue (AT) implies higher catabolic and oxidation rates, In the case of WNT, BMP-4, and WNT-1 inducible signaling pathway protein 2 pathway dysregulation, there is hypertrophy of AT. Physiologically, hyperplasia through the proliferation process mentioned is the appropriate mechanism for AT expansion. Pathologically, however, hypertrophy of AT leads to decreased levels of intracellular glucose transporter 4 and limited angiogenesis. Limited angiogenesis stimulates the hypoxia inducible factor 1 alpha (HIF-1a), stimulating further AT hypertrophy, creating a vicious cycle in the expansion of pathological AT. WAT: White adipose tissue; WISP-2: WNT-1 inducible signaling pathway protein 2; GLUT-4: Glucose transporter 4.

[28]. Interestingly, uric acid transporters have been seen to influence fatty liver[19]; a study carried out by Tanaka *et al*[29] found that the use of dotinurad (urate reabsorption inhibitor) showed amelioration of IR in rats by reducing liver steatosis and promoting rebrowning of AT[29].

Novel discovery of a group of lipids known as the fatty acid esters of hydroxy fatty acids (FAHFAs) released from the AT when appropriate levels of GLUT-4 and adipogenesis are present shed light to another pathway through which AT, and specially SAT, regulates systemic IR and inflammation[30]. FAHFAs induce metabolic health by stimulating insulin-dependent glucose transport in various tissues, as well as glucagon-like peptide 1 and insulin release from the gut enteroendocrine cells and the

pancreatic β-cells, respectively. Important anti-inflammatory effects have also been shown by studying docosahexaenoic acid (DHA)-derived FAHFAs' effects in cultured human hepatoma-derived cells, finding potent activation of nuclear factor erythroid 2-related factor 2 with tenable antioxidant function [31].

The answer to the question "what came first: the resistance or the fat?" could go both ways, *i.e.* liver fat build-up could be attributed to some degree to IR and hyperinsulinemia or directly from excessive FFA availability, which consequently brings about IR. Amount of AT, hepatic steatosis, and low-grade subacute inflammation are all correlated with the development of IR and MetS[32]. For this reason, the interaction between fat and IR is not causal, but rather reciprocal.

Skeletal muscle IR

Skeletal and cardiac muscle play important roles in glucose metabolism. Studies in humans have shown that it is the principal insulin-stimulated glucose uptake site (about 75% of postprandial serum glucose), whereas AT presents with relatively lower uptake[33]. Similar to hepatic IR, one of the ways skeletal muscle IR develops is by increased FFA supply, which cannot be processed by the tissue.

The association between skeletal muscle dysfunction and the progression of MAFLD has been widely recognized. There are several muscular conditions that are directly related to fatty liver, such as myosteatosis and sarcopenic obesity. We briefly touched upon the fact that AT releases adipokines key to metabolic regulatory systems. However, skeletal muscle also has the capacity to release hormonally active molecules termed myokines, which exert their function in an autocrine, paracrine, or endocrine fashion[34]. There are hundreds of myokines and the specific function of most has not been fully elucidated; however, many have shown effects in a multisystemic manner, including cognition, bone composition, AT "browning," as well as lipid and glucose metabolism. Myostatin, myonectin, irisin and a series of interleukins are among the most important myokines. Myostatin has a negative effect on MAFLD progression, given that it enhances liver inflammation and fibrogenesis by hepatic stellate cell stimulation[35]. Irisin, on the other hand, has the opposite effect by stimulating white AT browning and UCP-1 expression reducing adipose IR. This is key, given that one of the hallmarks of treatment for MAFLD is physical exercise. Irisin, among others, is an exercise-inducible myokine; this represents one of the few pathways through which moderate or rigorous exercise can reduce progression in MAFLD by targeting IR in the liver and AT (Figure 2). An additional feature of irisin is FFA oxidation, which is a method for lipid removal from ectopic tissue; this will later be explained in the intrahepatic triglyceride content section. Lastly, myonectin plays a role in FFA oxidation in the AT and the liver, as well as thermogenesis. Therefore, we already see how different myokines can have both beneficial or detrimental effects on metabolic health depending on the collective organ characteristics. A specific phenotype based on lifestyle characteristics defines the myokines that will be released, *e.g.*, irisin, and therefore the IR in other tissues that affects the development of liver steatosis.

Lean MAFLD

The absence of overt metabolic dysfunction in the lean population with MAFLD does not exclude the presence of metabolic abnormalities at cellular level. An important measurement of our hypothesis would be measuring the presence or absence of overt IR (*e.g.*, as per international criteria, mainly the HOMA) in a follow-up period of the population.

IR causes fatty liver from the inside out and not the other way around. In other words, cellular level alterations can, on their own, cause increased TG accumulation in the liver, even if obesity, acanthosis nigricans or even HOMA are not present or are within out of normal range in the latter case.

Individuals with normal body mass index (BMI) also develop MAFLD, and many studies (mainly in non-Caucasian populations) have shown a lack of IR in patients with MAFLD. A study conducted by Ahmed *et al*[27] studied the presence of NAFLD in patients with different BMI (non-obese, overweight, and obese) and evaluated whether these NAFLD individuals presented with IR. The results showed that a significant number of individuals without IR had NAFLD; however, there was no analysis of whether the NAFLD individuals without IR had non-obese BMI. This small aspect could be quite significant, given that we claim that the two main contributors to MAFLD development are IR and AT dysfunction. Furthermore, regarding lean MAFLD, it is known that IR unrelated to obesity can occur in various hyperglycemic states.

It is important to establish that IR drives DNL in the liver. Fatty liver diagnosis is defined based on the total amount of intrahepatic TG (IHTG). A recent study showed that hepatic DNL is an important regulator of IHTG content, concluded after correcting for the potential confounding contribution of AT in DNL. It was also noted that increases in serum glucose and insulin stimulate hepatic DNL. Glucose and insulin promote DNL by inducing the carbohydrate response element binding protein, as well as the sterol regulatory element binding protein 1c (SREBP 1c) and the acetyl CoA carboxylase, respectively[36]. Increased serum insulin is a compensatory mechanism during IR when there is appropriate endocrine pancreas activity, by having increased insulin release, DNL is stimulated further.

Thus, one of the most important arguments in favor of IR as the base of pathogenesis is the fact that it directly stimulates DNL. The question here would be: can DNL alone be contribution enough to increase IHTG up to MAFLD levels? The answer is no, even though DNL contributes about 26% to total IHTG content, while most of it originates from increased influx of FFA and their esterification in the

liver, accounting for 59% of total lipid content[37]. A smaller percentage, 15%, is attributable to diet TG consumption, as shown by Donnelly *et al*[37].

Mechanisms of IHTG accumulation

Increased lipid content in the liver originates from an imbalance between FFA uptake by the liver, DNL, lipid oxidation, and hepatic very low density lipoprotein (VLDL) export rate[38]. TG synthesis and lysis are the main ways in which the liver regulates the storage of FFA in serum when levels are high, whereas in the case of energy expenditure, it releases VLDL particles containing FFA to the muscle and fat tissue[39]. There was a previous misconception on the role of hepatic TG storage as a cause of lipotoxicity; it is now known that TG storage and secretion of VLDL particles are protective mechanisms against FFA-induced lipotoxicity. An elegant study by Listenberg *et al*[40] proved that through unsaturated fatty acid supplementation in CHO an 25RA cells, a protective effect against lipotoxicity through TG synthesis induction was achieved[40].

TG storage in the liver is carried out through the conversion of FFAs into glycerol-3-phosphate. TGs, along with cholesterol esters are neutral lipid particles which can be stably stored in the liver or can be released as VLDL particles[41]. There are a number of mechanisms involved in FFA oxidation and lipid metabolism. As we briefly touched upon, irisin is one of hundreds of exercise-induced myokines secreted by skeletal muscle, which plays an important role in the AT-muscle-liver axis. It also regulates the adenosine monophosphate-activated protein kinase signaling pathway, thus increasing FFA oxidation in myocytes[42].

Another mechanism that helps keep the balance between the IHTG is fatty acid β-oxidation in the mitochondria or peroxisomes. This process leads to the production of adenosine triphosphate or in the case of excess FFAs, the production of ketone bodies[43]. Alterations in β-oxidation contribute to the development of hepatic steatosis. For instance, downregulation in peroxisome proliferator-activated receptor alpha (PPAR-α), which serves as an FFA sensor, leads to decreased fatty acid catabolism and intrahepatic lipid accumulation. These alterations also determine the severity to which steatosis will develop depending on the nutritional status of an individual[44]. Stimulation of PPAR-α in mice enhances the expression of cytochrome P450 4A and enhances lipid turnover in the liver, decreasing the risk of developing dietary steatohepatitis[45]. Furthermore, PPAR-α activation increases peroxisomal fatty acid β-oxidation by inducing acyl-coenzyme A oxidase (Acox1), the rate-limiting enzyme in the oxidation of very long-chain fatty acids[46,47]. Acox1 is also associated with spontaneous liver damage in humans, as well as spontaneous steatosis, steatohepatitis, and hepatocellular carcinoma development in mice[46]. Despite what we discussed, alterations in PPAR-α are not the only ones leading to hepatic steatosis. Instead, a number of altered function in nuclear receptors such as the pregnane and xenobiotic receptors, the liver X receptor, and the farnesoid X receptor (FXR) contribute to the pathogenesis of MAFLD[48].

What about the comorbidities in MAFLD? Let's not forget CKD: The multiple effects of gene mutations

We have already discussed two primordial concepts in the understanding of MAFLD: AT dysfunction and IR. Even though these attributes explain a great deal of the pathogenic mechanisms involved in MAFLD, saying that overseeing genetic alterations involved is a mistake would hardly be an overstatement.

As it has been already reviewed in multiple studies and around a number of countries, there is a significant amount of genetic mutations that highly predispose populations to MAFLD. Even though there are multiple genetic mutations, the most common involves the gene patatin-like phospholipase domain-containing protein 3 (PNPLA3), which encodes for a protein called adiponutrin that exerts lipolytic action on TGs and reduces DNL within the liver. The PNPLA3 gene is present in many tissues in the body; however, it is most highly expressed in the liver and the kidney.

MAFLD is known for its large range of associated comorbidities; it is not only the hepatic manifestation of MetS but is a rather multisystemic disease on its own. A recent meta-analysis evaluated the risk of having NAFLD (previous nomenclature) and the risk of developing chronic kidney disease (CKD). In total, the data from more than a million patients were analyzed, and the study concluded that pre-existing NAFLD is associated with about a 1.45-fold increased risk of incident CKD stage ≥ 3[49]. The same team carried out a meta-analysis in 2017 showing 40% increased risk of CKD in patients with NAFLD[50]. Another group of researchers reached the same conclusions, showing that the presence and severity of NAFLD are associated with an increased risk and severity of CKD[51]. However, another group concluded that the association was not because of a causal relationship between MAFLD and CKD but was due to shared risk factors between them, namely diabetes, age, hypertension, and hyperuricemia[52]. This recent cross sectional study from The National Health and Nutrition Examination Survey 2017-2018 showed that MAFLD and CKD were not independently related after propensity score matching[52].

We propose an explanation for this, which might account for the high prevalence of CKD in people with MAFLD, and also shed light on the reason why these two diseases, even when highly correlated, are not independently related.

As previously mentioned, the PNPLA3 gene is most highly expressed in two tissues: the liver and kidney. Mutations in the PNPLA3 gene, especially the PNPLA3 I148M variant, leads to CKD in a similar pattern as how the mutation predisposes to MAFLD. Montovani and his team followed this line of thought and by studying 157 patients with T2DM, found that the presence of this mutation (especially in the podocytes on the renal cortex) was associated with lower glomerular filtration rates (GFR) and higher risk of CKD, 63.6% *vs* 24.2% risk in people without homozygous mutation[53]. It is important to establish that the association between the PNPLA3 I148M variant and the risk of lower GFR and CKD development is independent of liver disease severity as well as other factors[53]. This association has also been found among children with MAFLD, where the PNPLA3 G/G genotype leads to decreased kidney function and increased 24-h proteinuria[54].

By having established this, we can understand the multifactorial nature of MAFLD and its comorbidities, as in this case, CKD's. Whether or not MAFLD predisposes to kidney malfunction could be studied in a group of patients who develop both entities but lack mutations in the PNPLA3 gene.

While PNPLA3 gene mutations might be a common factor in the predisposition for both CKD and MAFLD, there are a number of nuclear transcription factors that contribute to the pathogenesis of both diseases. These factors include the peroxisome proliferator-activated receptor (PPAR) family, FXR, and SREBP2, which modify their respective molecular pathways and influence the progression of both CKD and hepatic steatosis[55]. For instance, the downregulation of PPAR-α, PPAR-δ, and PPAR-γ causes a myriad of cellular alterations in the nephron, including increased podocyte apoptosis leading to altered glomerular barrier integrity, increased mesangial cell hypertrophy and enhanced matrix deposition, as well as NF-κB activation with consequent proinflammatory cytokine secretion in the glomerular endothelium[56]. These same factors under physiologic circumstances suppress fibrogenesis by inhibiting the transforming growth factor β in stellate cells, lower the M1/M2 Kupffer cell phenotype ratio (thus decreasing inflammatory stimulus in the liver) and increases catalase activity in hepatocytes, among other functions. It is clear how downregulation of the PPAR family of factors hinders these protective mechanisms in the liver and promotes the development of fatty liver, as well as CKD. The same situation of multiorgan damage comes about with decreased expression of FXR and upregulation of SREBP-2, given that FXR inhibits SREBP-1c-mediated DNL in hepatocytes while decreasing reactive oxygen species formation in mesangial cells and increasing endothelial nitric oxide synthase in the glomerular epithelium[55]. Finally, SREBP-2 upregulation leads to increased cholesterol synthesis and decreased excretion in both liver and renal cells[57,58]. With this brief compilation of the molecular pathway similarities between CKD and fatty liver development, it would be of no surprise to find in the near future novel discoveries on further overlapping mechanisms and genetic predisposition for both diseases.

CONCLUSION

In conclusion, although MAFLD pathogenesis is multifactorial and complex, we consider IR to be the basis for the development of the disease, the abnormal metabolic profile in patients, and disease complications. Further research is required to fully understand and test this hypothesis along with others that may develop. Understanding the basis of the disease and the many variables that play a role in its development will lead to appropriate targeted therapies for MAFLD.

FOOTNOTES

Author contributions: Pal SC contributed to manuscript writing, data analysis, and critical revision; Méndez-Sánchez N contributed to conceptualization, manuscript design, critical revision, and supervision.

Conflict-of-interest statement: All the authors report no relevant conflicts of interest for this article.

Open-Access: This article is an open-access article that was selected by an in-house editor and fully peer-reviewed by external reviewers. It is distributed in accordance with the Creative Commons Attribution NonCommercial (CC BY-NC 4.0) license, which permits others to distribute, remix, adapt, build upon this work non-commercially, and license their derivative works on different terms, provided the original work is properly cited and the use is non-commercial. See: https://creativecommons.org/Licenses/by-nc/4.0/

Country/Territory of origin: Mexico

ORCID number: Shreya C Pal 0000-0002-2464-8499; Nahum Méndez-Sánchez 0000-0001-5257-8048.

S-Editor: L Li
L-Editor: Filipodia
P-Editor: L Li

REFERENCES

1 **Reuben A**. Leave gourmandising. *Hepatology* 2002; **36**: 1303-1306 [PMID: 12395350 DOI: 10.1002/hep.510360543]

2 **Speliotes EK**, Yerges-Armstrong LM, Wu J, Hernaez R, Kim LJ, Palmer CD, Gudnason V, Eiriksdottir G, Garcia ME, Launer LJ, Nalls MA, Clark JM, Mitchell BD, Shuldiner AR, Butler JL, Tomas M, Hoffmann U, Hwang SJ, Massaro JM, O'Donnell CJ, Sahani DV, Salomaa V, Schadt EE, Schwartz SM, Siscovick DS; NASH CRN; GIANT Consortium; MAGIC Investigators, Voight BF, Carr JJ, Feitosa MF, Harris TB, Fox CS, Smith AV, Kao WH, Hirschhorn JN, Borecki IB; GOLD Consortium. Genome-wide association analysis identifies variants associated with nonalcoholic fatty liver disease that have distinct effects on metabolic traits. *PLoS Genet* 2011; **7**: e1001324 [PMID: 21423719 DOI: 10.1371/journal.pgen.1001324]

3 **Eslam M**, Newsome PN, Sarin SK, Anstee QM, Targher G, Romero-Gomez M, Zelber-Sagi S, Wai-Sun Wong V, Dufour JF, Schattenberg JM, Kawaguchi T, Arrese M, Valenti L, Shiha G, Tiribelli C, Yki-Järvinen H, Fan JG, Grønbæk H, Yilmaz Y, Cortez-Pinto H, Oliveira CP, Bedossa P, Adams LA, Zheng MH, Fouad Y, Chan WK, Mendez-Sanchez N, Ahn SH, Castera L, Bugianesi E, Ratziu V, George J. A new definition for metabolic dysfunction-associated fatty liver disease: An international expert consensus statement. *J Hepatol* 2020; **73**: 202-209 [PMID: 32278004 DOI: 10.1016/j.jhep.2020.03.039]

4 **Mendez-Sanchez N**, Arrese M, Gadano A, Oliveira CP, Fassio E, Arab JP, Chávez-Tapia NC, Dirchwolf M, Torre A, Ridruejo E, Pinchemel-Cotrim H, Castellanos Fernández MI, Uribe M, Girala M, Diaz-Ferrer J, Restrepo JC, Padilla-Machaca M, Dagher L, Gatica M, Olaechea B, Pessôa MG, Silva M. The Latin American Association for the Study of the Liver (ALEH) position statement on the redefinition of fatty liver disease. *Lancet Gastroenterol Hepatol* 2021; **6**: 65-72 [PMID: 33181118 DOI: 10.1016/S2468-1253(20)30340-X]

5 **Méndez-Sánchez N**, Bugianesi E, Gish RG, Lammert F, Tilg H, Nguyen MH, Sarin SK, Fabrellas N, Zelber-Sagi S, Fan JG, Shiha G, Targher G, Zheng MH, Chan WK, Vinker S, Kawaguchi T, Castera L, Yilmaz Y, Korenjak M, Spearman CW, Ungan M, Palmer M, El-Shabrawi M, Gruss HJ, Dufour JF, Dhawan A, Wedemeyer H, George J, Valenti L, Fouad Y, Romero-Gomez M, Eslam M; Global multi-stakeholder consensus on the redefinition of fatty liver disease. Global multi-stakeholder endorsement of the MAFLD definition. *Lancet Gastroenterol Hepatol* 2022; **7**: 388-390 [PMID: 35248211 DOI: 10.1016/S2468-1253(22)00062-0]

6 **Fahed G**, Aoun L, Bou Zerdan M, Allam S, Bouferraa Y, Assi HI. Metabolic Syndrome: Updates on Pathophysiology and Management in 2021. *Int J Mol Sci* 2022; **23** [PMID: 35054972 DOI: 10.3390/ijms23020786]

7 **Reaven GM**. Banting lecture 1988. Role of insulin resistance in human disease. *Diabetes* 1988; **37**: 1595-1607 [PMID: 3056758 DOI: 10.2337/diab.37.12.1595]

8 **Huang PL**. A comprehensive definition for metabolic syndrome. *Dis Model Mech* 2009; **2**: 231-237 [PMID: 19407331 DOI: 10.1242/dmm.001180]

9 **Almeda-Valdes P**, Aguilar-Olivos N, Uribe M, Méndez-Sánchez N. Common features of the metabolic syndrome and nonalcoholic fatty liver disease. *Rev Recent Clin Trials* 2014; **9**: 148-158 [PMID: 25514910 DOI: 10.2174/1574887109666141216103908]

10 **Marchesini G**, Bugianesi E, Forlani G, Cerrelli F, Lenzi M, Manini R, Natale S, Vanni E, Villanova N, Melchionda N, Rizzetto M. Nonalcoholic fatty liver, steatohepatitis, and the metabolic syndrome. *Hepatology* 2003; **37**: 917-923 [PMID: 12668987 DOI: 10.1053/jhep.2003.50161]

11 **Méndez-Sánchez N**, Chávez-Tapia NC, Medina-Santillán R, Villa AR, Sánchez-Lara K, Ponciano-Rodríguez G, Ramos MH, Uribe M. The efficacy of adipokines and indices of metabolic syndrome as predictors of severe obesity-related hepatic steatosis. *Dig Dis Sci* 2006; **51**: 1716-1722 [PMID: 17203555 DOI: 10.1007/s10620-006-9093-5]

12 **Sesti G**. Pathophysiology of insulin resistance. *Best Pract Res Clin Endocrinol Metab* 2006; **20**: 665-679 [PMID: 17161338 DOI: 10.1016/j.beem.2006.09.007]

13 **Rao G**. Insulin resistance syndrome. *Am Fam Physician* 2001; **63**: 1159-1163, 1165 [PMID: 11277552]

14 **Mota M**, Banini BA, Cazanave SC, Sanyal AJ. Molecular mechanisms of lipotoxicity and glucotoxicity in nonalcoholic fatty liver disease. *Metabolism* 2016; **65**: 1049-1061 [PMID: 26997538 DOI: 10.1016/j.metabol.2016.02.014]

15 **Haffner SM**. Risk factors for non-insulin-dependent diabetes mellitus. *J Hypertens Suppl* 1995; **13**: S73-S76 [PMID: 8576792 DOI: 10.1097/00004872-199508001-00011]

16 **Randle PJ**, Garland PB, Newsholme EA, Hales CN. The glucose fatty acid cycle in obesity and maturity onset diabetes mellitus. *Ann N Y Acad Sci* 1965; **131**: 324-333 [PMID: 5216972 DOI: 10.1111/j.1749-6632.1965.tb34800.x]

17 **Santoleri D**, Titchenell PM. Resolving the Paradox of Hepatic Insulin Resistance. *Cell Mol Gastroenterol Hepatol* 2019; **7**: 447-456 [PMID: 30739869 DOI: 10.1016/j.jcmgh.2018.10.016]

18 **Méndez-Sánchez N**, Chavez-Tapia NC, Zamora-Valdés D, Uribe M. Adiponectin, structure, function and pathophysiological implications in non-alcoholic fatty liver disease. *Mini Rev Med Chem* 2006; **6**: 651-656 [PMID: 16787375 DOI: 10.2174/138955706777435689]

19 **Pal SC**, Eslam M, Mendez-Sanchez N. Detangling the interrelations between MAFLD, insulin resistance, and key hormones. *Hormones (Athens)* 2022; **21**: 573-589 [PMID: 35921046 DOI: 10.1007/s42000-022-00391-w]

20 **Mendez-Sanchez N**, Chavez-Tapia NC, Villa AR, Sanchez-Lara K, Zamora-Valdes D, Ramos MH, Uribe M. Adiponectin as a protective factor in hepatic steatosis. *World J Gastroenterol* 2005; **11**: 1737-1741 [PMID: 15793855 DOI: 10.3748/wjg.v11.i12.1737]

21 **Mendez-Sanchez N**, Cruz-Ramon VC, Ramirez-Perez OL, Hwang JP, Barranco-Fragoso B, Cordova-Gallardo J. New Aspects of Lipotoxicity in Nonalcoholic Steatohepatitis. *Int J Mol Sci* 2018; **19** [PMID: 30011790 DOI: 10.3390/ijms19072034]

22 **Qian SW**, Tang Y, Li X, Liu Y, Zhang YY, Huang HY, Xue RD, Yu HY, Guo L, Gao HD, Sun X, Li YM, Jia WP, Tang QQ. BMP4-mediated brown fat-like changes in white adipose tissue alter glucose and energy homeostasis. *Proc Natl Acad Sci U S A* 2013; **110**: E798-E807 [PMID: 23388637 DOI: 10.1073/pnas.1215236110]

23 **Boutens L**, Hooiveld GJ, Dhingra S, Cramer RA, Netea MG, Stienstra R. Unique metabolic activation of adipose tissue

macrophages in obesity promotes inflammatory responses. *Diabetologia* 2018; **61**: 942-953 [PMID: 29333574 DOI: 10.1007/s00125-017-4526-6]

24 **Takikawa A**, Mahmood A, Nawaz A, Kado T, Okabe K, Yamamoto S, Aminuddin A, Senda S, Tsuneyama K, Ikutani M, Watanabe Y, Igarashi Y, Nagai Y, Takatsu K, Koizumi K, Imura J, Goda N, Sasahara M, Matsumoto M, Saeki K, Nakagawa T, Fujisaka S, Usui I, Tobe K. HIF-1α in Myeloid Cells Promotes Adipose Tissue Remodeling Toward Insulin Resistance. *Diabetes* 2016; **65**: 3649-3659 [PMID: 27625023 DOI: 10.2337/db16-0012]

25 **Bartelt A**, Bruns OT, Reimer R, Hohenberg H, Ittrich H, Peldschus K, Kaul MG, Tromsdorf UI, Weller H, Waurisch C, Eychmüller A, Gordts PL, Rinninger F, Bruegelmann K, Freund B, Nielsen P, Merkel M, Heeren J. Brown adipose tissue activity controls triglyceride clearance. *Nat Med* 2011; **17**: 200-205 [PMID: 21258337 DOI: 10.1038/nm.2297]

26 **Yilmaz Y**, Ones T, Purnak T, Ozguven S, Kurt R, Atug O, Turoglu HT, Imeryuz N. Association between the presence of brown adipose tissue and non-alcoholic fatty liver disease in adult humans. *Aliment Pharmacol Ther* 2011; **34**: 318-323 [PMID: 21631560 DOI: 10.1111/j.1365-2036.2011.04723.x]

27 **Ahmed BA**, Ong FJ, Barra NG, Blondin DP, Gunn E, Oreskovich SM, Szamosi JC, Syed SA, Hutchings EK, Konyer NB, Singh NP, Yabut JM, Desjardins EM, Anhê FF, Foley KP, Holloway AC, Noseworthy MD, Haman F, Carpentier AC, Surette MG, Schertzer JD, Punthakee Z, Steinberg GR, Morrison KM. Lower brown adipose tissue activity is associated with non-alcoholic fatty liver disease but not changes in the gut microbiota. *Cell Rep Med* 2021; **2**: 100397 [PMID: 34622234 DOI: 10.1016/j.xcrm.2021.100397]

28 **Mills EL**, Harmon C, Jedrychowski MP, Xiao H, Garrity R, Tran NV, Bradshaw GA, Fu A, Szpyt J, Reddy A, Prendeville H, Danial NN, Gygi SP, Lynch L, Chouchani ET. UCP1 governs liver extracellular succinate and inflammatory pathogenesis. *Nat Metab* 2021; **3**: 604-617 [PMID: 34002097 DOI: 10.1038/s42255-021-00389-5]

29 **Tanaka Y**, Nagoshi T, Takahashi H, Oi Y, Yoshii A, Kimura H, Ito K, Kashiwagi Y, Tanaka TD, Yoshimura M. URAT1-selective inhibition ameliorates insulin resistance by attenuating diet-induced hepatic steatosis and brown adipose tissue whitening in mice. *Mol Metab* 2022; **55**: 101411 [PMID: 34863940 DOI: 10.1016/j.molmet.2021.101411]

30 **Yore MM**, Syed I, Moraes-Vieira PM, Zhang T, Herman MA, Homan EA, Patel RT, Lee J, Chen S, Peroni OD, Dhaneshwar AS, Hammarstedt A, Smith U, McGraw TE, Saghatelian A, Kahn BB. Discovery of a class of endogenous mammalian lipids with anti-diabetic and anti-inflammatory effects. *Cell* 2014; **159**: 318-332 [PMID: 25303528 DOI: 10.1016/j.cell.2014.09.035]

31 **B Gowda SG**, Tsukui T, Fuda H, Minami Y, Gowda D, Chiba H, Hui SP. Docosahexaenoic Acid Esters of Hydroxy Fatty Acid Is a Novel Activator of NRF2. *Int J Mol Sci* 2021; **22** [PMID: 34299218 DOI: 10.3390/ijms22147598]

32 **Cai D**, Yuan M, Frantz DF, Melendez PA, Hansen L, Lee J, Shoelson SE. Local and systemic insulin resistance resulting from hepatic activation of IKK-beta and NF-kappaB. *Nat Med* 2005; **11**: 183-190 [PMID: 15685173 DOI: 10.1038/nm1166]

33 **DeFronzo RA**. Lilly lecture 1987. The triumvirate: beta-cell, muscle, liver. A collusion responsible for NIDDM. *Diabetes* 1988; **37**: 667-687 [PMID: 3289989 DOI: 10.2337/diab.37.6.667]

34 **Severinsen MCK**, Pedersen BK. Muscle-Organ Crosstalk: The Emerging Roles of Myokines. *Endocr Rev* 2020; **41**: 594-609 [PMID: 32393961 DOI: 10.1210/endrev/bnaa016]

35 **Yndestad A**, Haukeland JW, Dahl TB, Bjøro K, Gladhaug IP, Berge C, Damås JK, Haaland T, Løberg EM, Linnestad P, Birkeland K, Konopski Z, Halvorsen B, Berge RK, Aukrust P. A complex role of activin A in non-alcoholic fatty liver disease. *Am J Gastroenterol* 2009; **104**: 2196-2205 [PMID: 19532130 DOI: 10.1038/ajg.2009.318]

36 **Ferré P**, Foufelle F. Hepatic steatosis: a role for de novo lipogenesis and the transcription factor SREBP-1c. *Diabetes Obes Metab* 2010; **12** Suppl 2: 83-92 [PMID: 21029304 DOI: 10.1111/j.1463-1326.2010.01275.x]

37 **Donnelly KL**, Smith CI, Schwarzenberg SJ, Jessurun J, Boldt MD, Parks EJ. Sources of fatty acids stored in liver and secreted *via* lipoproteins in patients with nonalcoholic fatty liver disease. *J Clin Invest* 2005; **115**: 1343-1351 [PMID: 15864352 DOI: 10.1172/JCI23621]

38 **Ress C**, Kaser S. Mechanisms of intrahepatic triglyceride accumulation. *World J Gastroenterol* 2016; **22**: 1664-1673 [PMID: 26819531 DOI: 10.3748/wjg.v22.i4.1664]

39 **Alves-Bezerra M**, Cohen DE. Triglyceride Metabolism in the Liver. *Compr Physiol* 2017; **8**: 1-8 [PMID: 29357123 DOI: 10.1002/cphy.c170012]

40 **Listenberger LL**, Han X, Lewis SE, Cases S, Farese RV Jr, Ory DS, Schaffer JE. Triglyceride accumulation protects against fatty acid-induced lipotoxicity. *Proc Natl Acad Sci U S A* 2003; **100**: 3077-3082 [PMID: 12629214 DOI: 10.1073/pnas.0630588100]

41 **Kawano Y**, Cohen DE. Mechanisms of hepatic triglyceride accumulation in non-alcoholic fatty liver disease. *J Gastroenterol* 2013; **48**: 434-441 [PMID: 23397118 DOI: 10.1007/s00535-013-0758-5]

42 **Xin C**, Liu J, Zhang J, Zhu D, Wang H, Xiong L, Lee Y, Ye J, Lian K, Xu C, Zhang L, Wang Q, Liu Y, Tao L. Irisin improves fatty acid oxidation and glucose utilization in type 2 diabetes by regulating the AMPK signaling pathway. *Int J Obes (Lond)* 2016; **40**: 443-451 [PMID: 26403433 DOI: 10.1038/ijo.2015.199]

43 **Nguyen P**, Leray V, Diez M, Serisier S, Le Bloc'h J, Siliart B, Dumon H. Liver lipid metabolism. *J Anim Physiol Anim Nutr (Berl)* 2008; **92**: 272-283 [PMID: 18477307 DOI: 10.1111/j.1439-0396.2007.00752.x]

44 **Hashimoto T**, Cook WS, Qi C, Yeldandi AV, Reddy JK, Rao MS. Defect in peroxisome proliferator-activated receptor alpha-inducible fatty acid oxidation determines the severity of hepatic steatosis in response to fasting. *J Biol Chem* 2000; **275**: 28918-28928 [PMID: 10844002 DOI: 10.1074/jbc.M910350199]

45 **Ip E**, Farrell GC, Robertson G, Hall P, Kirsch R, Leclercq I. Central role of PPARalpha-dependent hepatic lipid turnover in dietary steatohepatitis in mice. *Hepatology* 2003; **38**: 123-132 [PMID: 12829994 DOI: 10.1053/jhep.2003.50307]

46 **Moreno-Fernandez ME**, Giles DA, Stankiewicz TE, Sheridan R, Karns R, Cappelletti M, Lampe K, Mukherjee R, Sina C, Sallese A, Bridges JP, Hogan SP, Aronow BJ, Hoebe K, Divanovic S. Peroxisomal β-oxidation regulates whole body metabolism, inflammatory vigor, and pathogenesis of nonalcoholic fatty liver disease. *JCI Insight* 2018; **3** [PMID: 29563328 DOI: 10.1172/jci.insight.93626]

47 **Huang J**, Jia Y, Fu T, Viswakarma N, Bai L, Rao MS, Zhu Y, Borensztajn J, Reddy JK. Sustained activation of PPARα by endogenous ligands increases hepatic fatty acid oxidation and prevents obesity in ob/ob mice. *FASEB J* 2012; **26**: 628-

638 [PMID: 22009939 DOI: 10.1096/fj.11-194019]
48 **Cave MC**, Clair HB, Hardesty JE, Falkner KC, Feng W, Clark BJ, Sidey J, Shi H, Aqel BA, McClain CJ, Prough RA. Nuclear receptors and nonalcoholic fatty liver disease. *Biochim Biophys Acta* 2016; **1859**: 1083-1099 [PMID: 26962021 DOI: 10.1016/j.bbagrm.2016.03.002]
49 **Mantovani A**, Petracca G, Beatrice G, Csermely A, Lonardo A, Schattenberg JM, Tilg H, Byrne CD, Targher G. Non-alcoholic fatty liver disease and risk of incident chronic kidney disease: an updated meta-analysis. *Gut* 2022; **71**: 156-162 [PMID: 33303564 DOI: 10.1136/gutjnl-2020-323082]
50 **Mantovani A**, Zaza G, Byrne CD, Lonardo A, Zoppini G, Bonora E, Targher G. Nonalcoholic fatty liver disease increases risk of incident chronic kidney disease: A systematic review and meta-analysis. *Metabolism* 2018; **79**: 64-76 [PMID: 29137912 DOI: 10.1016/j.metabol.2017.11.003]
51 **Musso G**, Gambino R, Tabibian JH, Ekstedt M, Kechagias S, Hamaguchi M, Hultcrantz R, Hagström H, Yoon SK, Charatcharoenwitthaya P, George J, Barrera F, Hafliðadóttir S, Björnsson ES, Armstrong MJ, Hopkins LJ, Gao X, Francque S, Verrijken A, Yilmaz Y, Lindor KD, Charlton M, Haring R, Lerch MM, Rettig R, Völzke H, Ryu S, Li G, Wong LL, Machado M, Cortez-Pinto H, Yasui K, Cassader M. Association of non-alcoholic fatty liver disease with chronic kidney disease: a systematic review and meta-analysis. *PLoS Med* 2014; **11**: e1001680 [PMID: 25050550 DOI: 10.1371/journal.pmed.1001680]
52 **Deng Y**, Zhao Q, Gong R. Association Between Metabolic Associated Fatty Liver Disease and Chronic Kidney Disease: A Cross-Sectional Study from NHANES 2017-2018. *Diabetes Metab Syndr Obes* 2021; **14**: 1751-1761 [PMID: 33911888 DOI: 10.2147/DMSO.S292926]
53 **Mantovani A**, Taliento A, Zusi C, Baselli G, Prati D, Granata S, Zaza G, Colecchia A, Maffeis C, Byrne CD, Valenti L, Targher G. PNPLA3 I148M gene variant and chronic kidney disease in type 2 diabetic patients with NAFLD: Clinical and experimental findings. *Liver Int* 2020; **40**: 1130-1141 [PMID: 32125756 DOI: 10.1111/liv.14419]
54 **Targher G**, Mantovani A, Alisi A, Mosca A, Panera N, Byrne CD, Nobili V. Relationship Between PNPLA3 rs738409 Polymorphism and Decreased Kidney Function in Children With NAFLD. *Hepatology* 2019; **70**: 142-153 [PMID: 30912854 DOI: 10.1002/hep.30625]
55 **Musso G**, Cassader M, Cohney S, De Michieli F, Pinach S, Saba F, Gambino R. Fatty Liver and Chronic Kidney Disease: Novel Mechanistic Insights and Therapeutic Opportunities. *Diabetes Care* 2016; **39**: 1830-1845 [PMID: 27660122 DOI: 10.2337/dc15-1182]
56 **Gao J**, Gu Z. The Role of Peroxisome Proliferator-Activated Receptors in Kidney Diseases. *Front Pharmacol* 2022; **13**: 832732 [PMID: 35308207 DOI: 10.3389/fphar.2022.832732]
57 **Kandasamy N**, Ashokkumar N. Renoprotective effect of myricetin restrains dyslipidemia and renal mesangial cell proliferation by the suppression of sterol regulatory element binding proteins in an experimental model of diabetic nephropathy. *Eur J Pharmacol* 2014; **743**: 53-62 [PMID: 25240712 DOI: 10.1016/j.ejphar.2014.09.014]
58 **Musso G**, Gambino R, Cassader M. Cholesterol metabolism and the pathogenesis of non-alcoholic steatohepatitis. *Prog Lipid Res* 2013; **52**: 175-191 [PMID: 23206728 DOI: 10.1016/j.plipres.2012.11.002]

World Journal of Gastroenterology

Submit a Manuscript: https://www.f6publishing.com

World J Gastroenterol 2023 July 7; 29(25): 4009-4020

DOI: 10.3748/wjg.v29.i25.4009

ISSN 1007-9327 (print) ISSN 2219-2840 (online)

MINIREVIEWS

Recent advances and current challenges in endoscopic resection with the full-thickness resection device

Elijah J Mun, Mihir S Wagh

Specialty type: Gastroenterology and hepatology

Provenance and peer review: Invited article; Externally peer reviewed.

Peer-review model: Single blind

Peer-review report's scientific quality classification

Grade A (Excellent): 0
Grade B (Very good): 0
Grade C (Good): C, C
Grade D (Fair): 0
Grade E (Poor): 0

P-Reviewer: Lin L, China; Nagata J, Japan

Received: February 10, 2023
Peer-review started: February 10, 2023
First decision: March 15, 2023
Revised: March 27, 2023
Accepted: June 5, 2023
Article in press: June 5, 2023
Published online: July 7, 2023

Elijah J Mun, Division of Gastroenterology, University of Colorado School of Medicine, Aurora, CO 80045, United States

Mihir S Wagh, Interventional Endoscopy, Division of Gastroenterology, University of Colorado School of Medicine, Aurora, CO 80045, United States

Corresponding author: Mihir S Wagh, FACG, FASGE, MD, Professor, Interventional Endoscopy, Division of Gastroenterology, University of Colorado School of Medicine, 1635 Aurora Court, F735, Aurora, CO 80045, United States. mihir.wagh@cuanschutz.edu

Abstract

Endoscopic full-thickness resection (EFTR) has emerged as a viable technique in the management of mucosal and subepithelial lesions of the gastrointestinal tract (GIT) not amenable to conventional therapeutic approaches. While various devices and techniques have been described for EFTR, a single, combined full-thickness resection and closure device (full-thickness resection device, FTRD system, Ovesco Endoscopy AG, Tuebingen, Germany) has become commercially available in recent years. Initially, the FTRD system was limited to use in the colorectum only. Recently, a modified version of the FTRD has been released for EFTR in the upper GIT as well. This review provides a broad summary of the FTRD, highlighting recent advances and current challenges.

Key Words: Endoscopic full-thickness resection; Full-thickness resection device; Colorectal neoplasm; Subepithelial lesions; Scarred non-lifting polyps

©The Author(s) 2023. Published by Baishideng Publishing Group Inc. All rights reserved.

Core Tip: Endoscopic full-thickness resection (EFTR) is an emerging technique for tissue resection of lesions in the gastrointestinal tract (GIT) not amenable to conventional resection approaches. The novel full-thickness resection device (FTRD) is a combined full-thickness resection and closure device that allows for EFTR of lesions in the GIT. EFTR with FTRD is feasible, safe, and efficacious and should be considered as a viable option for resection of select lesions in the lower and upper GIT.

Citation: Mun EJ, Wagh MS. Recent advances and current challenges in endoscopic resection with the full-thickness resection device. *World J Gastroenterol* 2023; 29(25): 4009-4020
URL: https://www.wjgnet.com/1007-9327/full/v29/i25/4009.htm
DOI: https://dx.doi.org/10.3748/wjg.v29.i25.4009

INTRODUCTION

Traditionally, flexible endoscopic removal of gastrointestinal neoplasms has been accomplished by standard polypectomy, endoscopic mucosal resection (EMR), or endoscopic submucosal dissection (ESD). More recently, endoscopic full-thickness resection (EFTR) has emerged as a complementary resection technique for the removal of colorectal lesions, particularly for lesions that are scarred or non-lifting, early cancers with deeper invasion, and subepithelial lesions, where resection *via* standard endoscopic techniques is difficult or not possible[1,2]. EFTR also has the potential added benefit of decreasing procedural time and providing a minimally-invasive organ-sparing alternative approach, obviating need for surgery. As its name implies, EFTR refers to the technique whereby a lesion is resected endoscopically in its entirety including all layers of the gastrointestinal wall[1]. The two main techniques for EFTR include the "resect and close" method, where the full-thickness resection is performed first exposing the peritoneal cavity, followed by complete closure of the defect, and "close and resect" method, where approximation of the wall layers deep to the lesion is performed first followed by full-thickness resection without exposure and contamination of the peritoneum. Various strategies and devices have been developed to accomplish EFTR, including but not limited to needle-knives, ESD knives, nylon loop accompanied by standard through-the-scope clips, omental patches, endoscopic plicating and suturing devices, and endoscopic staplers[3-9]. These methods will not be covered in this review.

Recently, a single, combined full-thickness resection and closure device referred to as the full-thickness resection device (FTRD system, Ovesco Endoscopy AG, Tuebingen, Germany) has become available and is quickly being adopted across centers worldwide to accomplish EFTR. Its appeal over other strategies includes the ability to perform resection and closure with a single device integrating an over-the-scope clip (OTSC) and electrosurgical snare. It can offer a safe and nonsurgical alternative for removal of lesions that may be challenging to resect with conventional endoscopic methods and might otherwise require surgery. Main indications for the FTRD include non-lifting or scarred polyps, partially resected or residual polyps with submucosal fibrosis, early cancers, subepithelial lesions, and diagnostic EFTR for pathologic assessment of the gut wall. It is approved for use in the colorectum, and recently, received additional approval from the U.S. Food and Drug Administration for use in the upper gastrointestinal tract (GIT)[10].

This review article will provide a summary of the major studies on FTRD, highlighting recent advances and current challenges, in the hopes that practicing endoscopists will be better equipped to understand the role and limitations of, and potentially utilize, this novel and important resection technique.

DEVICE

The FTRD system, a combined full-thickness resection and closure device, was first made available in Europe in 2014[11]. It has since been approved for use in the United States for colorectal EFTR in 2017 and gastroduodenal EFTR in 2020[12].

The FTRD system is based on the principle of "close and resect" for EFTR. It uses the well-established OTSC system (Ovesco Endoscopy AG, Tuebingen, Germany), which allows for full-thickness tissue apposition deeper to the lesion first, followed by full-thickness resection above the clip, thereby performing EFTR without exposure of the peritoneal cavity[13]. The FTRD system (Figure 1) consists of a clear, plastic distal attachment cap that has a mounted ready-for-use 14 mm nickel titanium alloy (Nitinol) clip, integrated 14 mm monofilament snare and thread, thread retriever, endoscope sleeve with fixation tapes, and a hand wheel. Separately, an FTRD Marking Probe (Figure 2A) and FTRD Grasper (Figure 2B) are provided as part of the FTRD set. These individual instruments can be advanced through the working channel for marking and mobilization of the target lesion, respectively. The FTRD system is suitable for use for endoscopes having a diameter of 11.5-13.2 mm and a working channel diameter of 3.2 mm. The cap diameter is 21 mm and the cap depth is 23 mm.

The initial FTRD system was fashioned for use in the colorectum and is now marketed as the colonic FTRD©. With recent advances demonstrating the role of the FTRD in the upper GIT, an additional FTRD system called the gastroduodenal FTRD© has now become available. The gastroduodenal FTRD system is smaller in caliber and additionally comes with an insertion balloon and guide wire to help facilitate passage of the FTRD through the upper esophageal sphincter and pylorus (Figure 2C). A

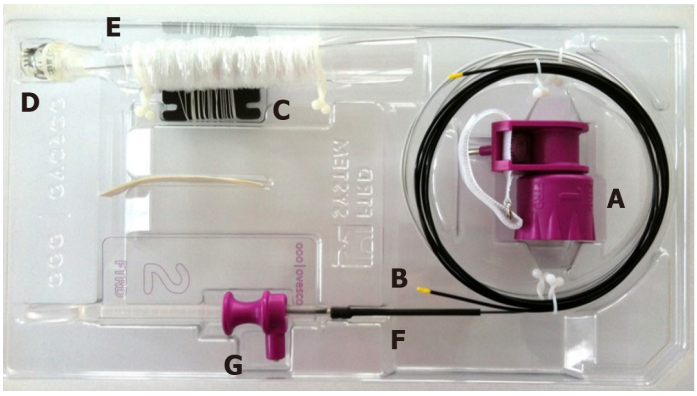


Figure 1 The colonic full-thickness resection device system. A: Hand wheel; B: Thread Retriever; C: Thread; D: Distal attachment cap with affixed over-the-scope-clip; E: Endoscope sleeve; F: Integrated snare; G: Snare lock. Images provided by Ovesco Endoscopy.

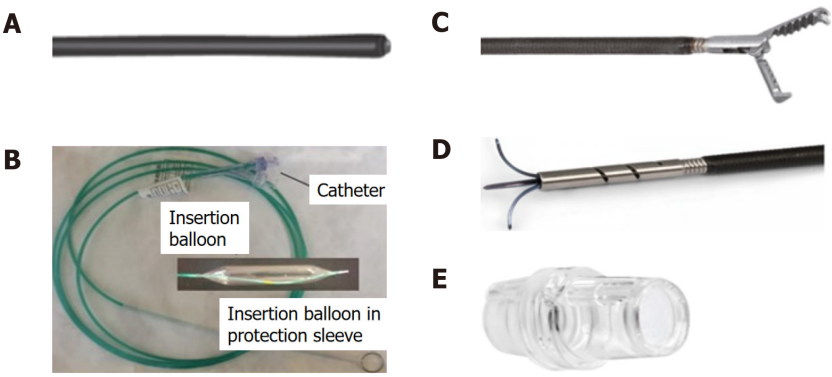


Figure 2 Full-thickness resection device separately included items. A: Marking probe; B: Grasper; C: Guidewire and balloon (diagram) — for gastroduodenal full-thickness resection device (FTRD)®; D: Modified anchor — for gastroduodenal FTRD®; E: prOVE cap. Images courtesy of Ovesco Endoscopy.

separate modified Anchor (Figure 2D) is also available to allow for better tissue mobilization (*i.e.*, for subepithelial lesions). The gastroduodenal FTRD is suitable for endoscopes having a diameter of 10.5-12.0 mm and a working channel diameter of 3.7 mm. The cap diameter is 19.5 mm and the cap depth is 23 mm.

Recently, a third FTRD system called the diagnostic FTRD© was made available for use in the colorectum for diagnostic resection, or full-thickness biopsy. This system is nearly identical to the colonic FTRD system but is smaller in size allowing for full-thickness resection of lesser tissue volume when desired for diagnostic purposes. The diagnostic FTRD system can also be applied to a pediatric colonoscope allowing for increased flexibility and mobility. The diagnostic FTRD system is suitable for endoscopes having a diameter of 10.5-12.0 mm and a working channel diameter of 3.2 mm. The cap diameter is 19.5 mm and the cap depth is 23 mm.

TECHNIQUE

Once a target lesion in the GIT is identified, its margins are delineated with the FTRD Marking Probe ensuring a margin of normal surrounding tissue (Figure 3A). The endoscope is then withdrawn from the patient. It is often cumbersome to advance the endoscope (with the attached stiff FTRD cap) to the lesion (especially lesions located in the right colon), and sometimes difficult to grasp and bring a scarred lesion into the cap. Hence many endoscopists will first attach a test cap — the FTRD prOVE cap (a "blank" cap similar to the FTRD cap but without the mounted clip or snare; see Figure 2E) — to the endoscope to perform a "test run" without using the FTRD, which may otherwise be wasted if unable to be advanced to the lesion. Once it is confirmed that the endoscope with the attached prOVE cap can be advanced to the lesion and the lesion able to be brought inside the cap, the endoscope is withdrawn and fitted with the "real" FTRD system. The hand wheel (Figure 1A) is first inserted into the working channel of the endoscope. The thread retriever (Figure 1B) is then inserted into the working channel and used to retrieve the thread (Figure 1C) allowing for attachment of the plastic attachment cap (Figure 1D) onto the distal end of the endoscope. The distal attachment cap has a preloaded clip attached to the thread that runs inside the working channel of the endoscope and attaches to the hand wheel, as well as

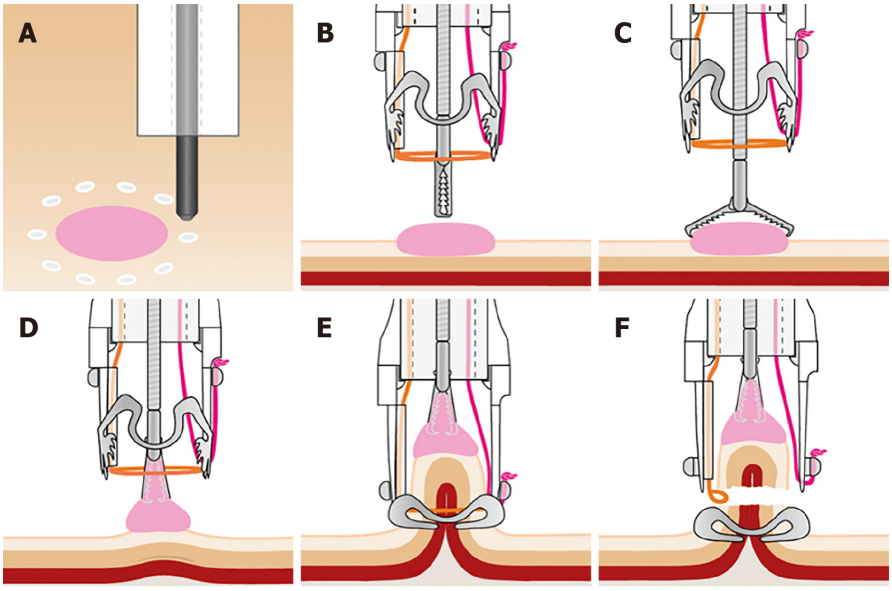


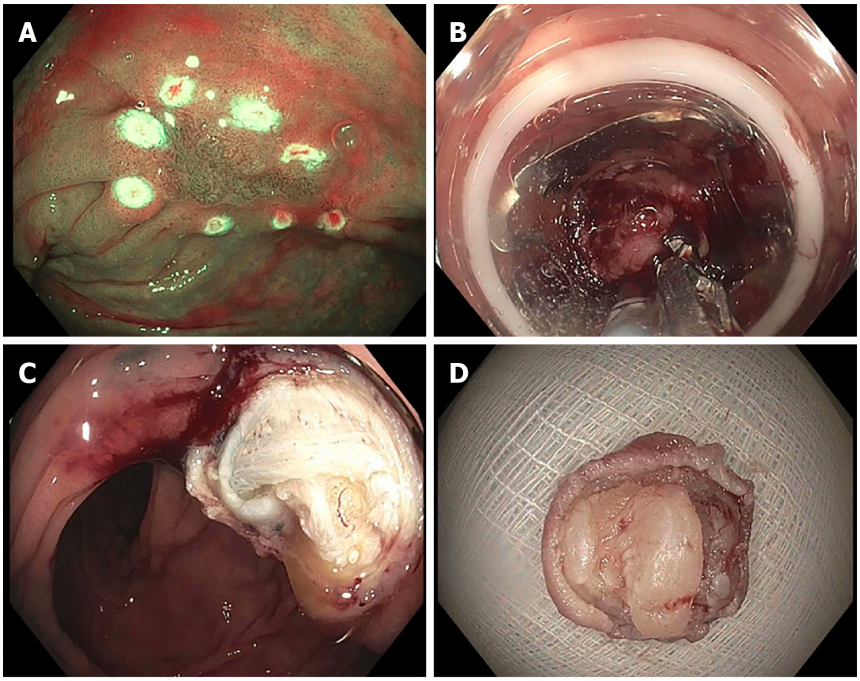
Figure 3 Technique for accomplishing endoscopic full-thickness resection using the full-thickness resection device. A: Borders of target lesion marked using full-thickness resection device (FTRD) Marking Probe; B: FTRD Grasper positioned over target lesion; C: FTRD Grasper opened over target lesion; D: Target lesion grasped and pulled into cap; E: Over-the-scope-clip deployed; F: Specimen resected with electrosurgical snare. Images provided by Ovesco Endoscopy.

a preloaded snare that runs outside of the endoscope. The accompanying endoscope sleeve (Figure 1E) and adhesion tapes help affix the snare (Figure 1F) to the outside of the endoscope and prevent inadvertent twisting of the snare around the endoscope or entrapment of tissue between the snare and the endoscope. Turning of the hand wheel allows for adjusting tension on the thread, and eventually, deployment of the clip. A snare lock (Figure 1G) helps prevent inadvertent snare opening and can be removed to "unlock" the snare once ready for use. The endoscope with the attached FTRD system is then re-inserted into the GIT to the target lesion. Next, with the tip of the cap appropriately positioned over the lesion (Figure 3B), the FTRD Grasper is used to grasp (Figure 3C) and mobilize the lesion completely within the cap (Figure 3D). All markings made by the FTRD Marking Probe should be visible inside the cap. Suction should not be used to draw the lesion into the cap as this may bring in extraluminal structures (*e.g.*, small bowel) into the cap causing significant injury to adjacent organs and structures. Finally, the clip is deployed (Figure 3E) by turning the hand wheel, and the lesion immediately resected with the snare using an electrosurgical current (Figure 3F) while being firmly grasped with the Grasper. It should be noted that once the lesion is brought into the cap, these steps should be performed quickly and sequentially in this specific order to prevent perforation and/or the lesion slipping out of the cap. The resected specimen is retrieved by withdrawing the endoscope with the lesion held by the Grasper. The endoscope without the attached FTRD is then reinserted to inspect the resection site for complete resection and confirm the absence of adverse events (AEs) (Figure 4).

PROOF OF CONCEPT AND PRECLINICAL DATA

Earlier studies established efficacy and safety of the OTSC system for endoscopic closure of gastrointestinal perforations and surgical anastomotic leaks and fistulas[14,15]. Following these data, several observational experiences and case series were described using an OTSC-assisted method for resection of gastrointestinal lesions, whereby the OTSC system was used to deploy the clip deep to a lesion prior to snare resection[16-18]. Based on these experiences, the basis for the FTRD system — a combined device containing an OTSC system plus a preloaded snare — was developed.

An early preclinical study using the FTRD in an animal (porcine) model demonstrated safety and efficacy[11]. The FTRD was used for resection of the colon wall in 11 pigs, and 7 and 28-d follow up study sessions were performed to evaluate the clip application site. Clips were still present in all but one case at 28 d and adherent stool and fibrin were found on the clips. There were mild inflammatory reactions seen histologically at day 7, but no acute inflammation was noted on day 28. The underlying tissue at the clip bed showed no signs of dehiscence or ischemia. Manometric pressure tests demonstrated no leak. Histology assessments revealed successful full-thickness resection (mucosa to serosa) in all cases.



DOI: 10.3748/wjg.v29.i25.4009 **Copyright** ©The Author(s) 2023.

Figure 4 Endoscopic images of full-thickness resection device. A: Full-thickness resection device (FTRD) Marking Probe used to mark the target lesion (non-lifting polyp); B: FTRD Grasper used to grasp the lesion and pull into the cap followed by successful clip deployment; C: Resection site after FTRD; D: Resected specimen. Images courtesy of Dr. Wagh MS.

CURRENT APPLICATIONS AND CLINICAL DATA

Study search and inclusion criteria

A summary of the major studies investigating the FTRD are included below. The keywords "endoscopic full thickness resection", "full thickness resection device," and "FTRD" were used for the initial query on PubMed. Studies published within a 10-year period from January 1, 2011-December 31, 2021, were considered for inclusion. To be considered for inclusion in this review, studies had to be original research studies using the Ovesco Endoscopy FTRD (other devices described for EFTR were not included) and be designed as prospective or retrospective studies. Observational studies, case reports, preclinical animal studies and proof of concept studies were not included. Studies that did not report the type of lesion, technical success rates, R0 resection rates, full-thickness resection rates, and rates of AEs were also not included.

Colorectal FTRD

The first clinical experience using the FTRD was published in 2015[19]. In this retrospective, two-center European study, 24 patients who underwent resection of colorectal lesions with the FTRD were identified. Indications included recurrent or incompletely resected adenomas with a non-lifting sign (n = 11), appendiceal adenomas (n = 5), untreated adenomas with a non-lifting sign (n = 2), incomplete resection of T1 carcinoma (n = 2), submucosal tumors (n = 2), adenoma within diverticulum (n = 1), flat adenoma in a coagulopathic patient (n = 1), and diagnostic resection in a patient with suspected Hirschsprung's disease (n = 1). Technical success (complete *en bloc* resection) was achieved in 20/24 (83.3%) patients and R0 resection (histologically complete resection with tumor-free margins) in 18/24 (75.0%) patients. Two patients developed post-polypectomy syndrome and required antibiotics, but there were no other reported AEs including no perforations or major bleeding events.

This study has been followed by numerous retrospective and prospective studies demonstrating safety and efficacy of FTRD in the colon and rectum (see Table 1 for summary of major clinical studies with current applications of FTRD for EFTR)[12,20-27]. In the largest, prospective multicenter study to date, 181 patients were recruited to receive EFTR with the FTRD system[25]. Indications for EFTR included "difficult" adenomas (n = 143), early carcinomas (n = 15), and subepithelial tumors (n = 23). "Difficult" adenomas included adenomas with a non-lifting sign, adenomas at the appendiceal orifice, and adenomas at a diverticulum. Technical success was achieved in 89.5% of cases and R0 resection in 76.9% of cases. AEs were noted in 18/181 (9.9%) patients and included bleeding (4/18), post-polypectomy syndrome (3/18), perforation (6/18), acute appendicitis (3/18), abdominal pain without clear etiology on laboratory and radiographic work-up (1/18), and enterocolonic fistula formation (1/18). All four patients with bleeding were treated conservatively and did not require transfusion of blood

Table 1 Summary of major clinical studies with current applications of full-thickness resection device for endoscopic full-thickness resection

	Ref.	Study type	Total FTRD cases, *n*	Site (s)	Type of lesion	Technical success, %	R0 resection, %	Full-thickness resection, %	Adverse events, %
1	Schmidt *et al* [19]	Retrospective	24	Colon; Rectum	Non-lifting polyps (*n* = 13); Appendiceal polyps (*n* = 5); Diagnostic (*n* = 3); Subepithelial tumor (*n* = 2); Polyp involving diverticulum (*n* = 1)	83.3	75.0	87.5	8.3
2	Schmidt *et al* [25]	Prospective	181	Colon; Rectum	Difficult adenomas (79.0%); Cancer (8.3%); Subepithelial tumor (12.7%)	89.5	76.9	81.0	9.9
3	Meier *et al* [12]	Retrospective	1178	Colon; Rectum	Difficult adenomas (67.1%); Cancer (18.4%); Subepithelial tumor (6.8%); Diagnostic (1.3%)	88.2	80.0	89.9	12.1
4	Boger *et al* [23]	Retrospective	68	Colon; Rectum	Non-lifting polyps (*n* = 29); Cancer (*n* = 13); Subepithelial tumor (*n* = 9); Polyps in appendix or diverticulum (*n* = 17)	88.2	76.8	NA	5.9
5	Hajifathalian *et al*[37]	Retrospective	56	Stomach; Duodenum	Mesenchymal neoplasm including GIST (*n* = 26); Diagnostic (*n* = 10), NET (*n* = 9); Adenomas (*n* = 6); Adenocarcinoma (*n* = 5)	93.0	68.0	NA	21.0
6	Meier *et al* [39]	Prospective	29	Stomach	Subepithelial tumor (*n* = 29)	89.7	76.0	65.5	31.0
7	Ichkhanian *et al*[20]	Retrospective	66	Colon/appendiceal orifice	Polyps involving appendiceal orifice	89.0	93.0	91.0	17.0
8	Zwager *et al* [28]	Prospective	367	Colon; Rectum	Difficult polyps (*n* = 133); T1 cancer (*n* = 71); Incomplete resection (*n* = 150); Subepithelial tumors (*n* = 13)	83.9	82.4	83.2	9.3
9	Zwager *et al* [29]	Retrospective	330	Colon; Rectum	Primary resection of T1 cancer (*n* = 132); Secondary resection of T1 cancer (*n* = 198)	87.0	85.6	NA	2.2

FTRD: Full-thickness resection device; GIST: Gastrointestinal stromal tumors; NA: Not available; NET: Neuroendocrine tumor.

products. Emergency surgery was required in 3/181 (2.2%) patients.

The results of a recent large retrospective analysis using the German colonic FTRD registry (*n* = 1178) reported similar findings, corroborating the previously reported findings of smaller studies[12]. Indications included difficult adenomas, early carcinomas, subepithelial tumors, and diagnostic resection. The technical success rate was 88.2% and R0 resection rate 80.0. The AE rate was 12.1% with 3.1% being major AEs. A similar but smaller retrospective study from the UK FTRD registry (*n* = 68) reported similar outcomes[23] with technical success rate 88.2%, R0 resection rate 76.8%, and AE rate 5.9%. This has since been further replicated in a larger Dutch FTRD registry (*n* = 367) with technical success rate 83.9%, R0 resection rate 82.4%, full-thickness resection rate 83.2%, and AE rate 9.3%[28].

Colorectal FTRD for early cancer, lesions at the appendix, and subepithelial lesions

Studies have reported slight variations (albeit with comparable success) in outcomes for FTRD depending on the indication for EFTR. Regarding FTRD use for early cancer, a recent study of 156 patients with a histologically proven diagnosis of adenocarcinoma showed FTRD to have a technical success rate of 92.3% and R0 resection rate of 71.8%. Serious AEs were reported in 3.9% of patients[24]. In a subgroup analysis from the previously mentioned retrospective study using the German colonic FTRD registry by Meier *et al*[12], 217 cases of FTRD in early cancers were identified. Technical success was reported to be 84.6% and R0 resection in 82.8% of cases. In a separate analysis by Schmidt *et al*[25], 29 cases of FTRD for early carcinomas were identified (14 harbored unsuspected cancer and 15 were known cancers). R0 resection was achieved in 72.4% of cases, but curative resection could only be achieved in 44.8% of cases. Similarly, a study from the Dutch FTRD registry showed overall technical

success, R0 resection, and AE rates of 87.0%, 85.6%, and 2.2%. However, the curative resection rate was only 60.3% with a curative resection rate of 23.7% for primary resection of T1 cancers[29]. Hence, given these low curative resection rates, there is some uncertainty regarding the role of FTRD as primary use for early cancers.

For lesions at the appendiceal orifice, a recent study of 66 patients demonstrated a technical success rate of 89% and R0 resection rate of 79%[20] using FTRD. Of note, 17.2% of patients developed appendicitis and 10.3% of patients (60% of those who developed appendicitis) required surgical appendectomy. Factors associated with risk of appendicitis included male sex (odds ratio: 1.2, $P = 0.03$) and failure to achieve histologic full-thickness resection (odds ratio: 1.5, $P = 0.04$)[20]. The high rates of appendicitis for this indication have raised concerns regarding the use of FTRD for appendiceal lesions. Further highly powered studies are needed to clarify the safety of FTRD for these lesions.

There is a lack of highly powered studies investigating FTRD for subepithelial tumors. A recent study of 40 patients with rectal neuroendocrine tumors (NETs) did report a technical success rate of 100%, R0 resection rate of 100%, and no AEs[21]. While these outcomes should be interpreted cautiously in the setting of a small sample size, the reported success is nonetheless encouraging and in line with the success reported in other FTRD studies[12,22,23,25]. In a subgroup analysis using the German colonic FTRD registry by Meier *et al*[12], 80 cases of FTRD for subepithelial tumors were identified. The technical success rate was 97.3% and R0 resection rate was 97%. R0 resection was significantly higher for subepithelial tumors compared with that for other lesions in the German FTRD registry (77.2% for difficult adenomas, 82.8% for early cancers). Data regarding AE rates within the subgroup analysis were not available. In a separate subgroup analysis from Schmidt *et al*[25], 23 cases of FTRD for indication of subepithelial lesions were identified, with R0 resection rate of 87%. Overall, FTRD for subepithelial lesions seems to be very effective, with greater technical success and R0 resection than FTRD for other lesions.

Subgroup analyses have also been performed in studies to determine whether differences in outcomes may be related to other factors such as lesion location, lesion size, and prior treatment. Findings have varied[12,25], though by and large, there does not appear to be convincing evidence of any significant differences in technical success and other outcomes based on lesion location, size, or prior treatment[12]. Further studies may help better clarify what factors independently predict these outcomes of success.

Similar technical success and R0 resection rates have been reported for EMR and ESD[30,31]. ESD has been associated with greater R0 resection rates than EMR, but is also associated with greater rates of AEs like perforation and major bleeding. Direct comparisons of technical success and R0 resection between EMR/ESD and FTRD are difficult to make, as the majority of indications for FTRD currently are for lesions deemed difficult or challenging to resect *via* EMR or ESD. Few studies have reported on the efficacy of salvage ESD (ESD performed for residual or locally recurrent non-lifting lesions), which would likely be a better comparator group for FTRD, but these few small studies do appear to suggest comparable rates of success[32,33]. Similar AE rates have been reported for ESD and FRTD[31]. However, procedural time for ESD is considerably longer than FTRD[31].

Overall, EFTR with the FTRD system in the colorectum appears to be safe and efficacious. Common indications for FTRD in the lower GIT include select lesions difficult to resect by more conventional approaches (*i.e.*, non-lifting adenomas, adenomas at appendiceal orifice, adenomas at diverticulum), early cancers, subepithelial lesions, and diagnostic resection. Very large lesions > 3 cm may not be appropriate for FTRD.

Gastroduodenal FTRD

Recently, a newer and smaller caliber FTRD, the gastroduodenal FTRD©, has become available for use in the upper GIT.

Prior to the development of the newer gastroduodenal FTRD system, experiences using the traditional FTRD system (now known as the colonic FTRD©) in the upper GIT were reported[34-36]. These were primarily case reports and small case series dating as far back as 2014 (when the FTRD first became available in Europe) reporting safe and successful use of the FTRD in the stomach and duodenum in patients with malignant or large, nonmalignant subepithelial lesions who were deemed unsuitable for surgery[34-36]. Several retrospective analyses have followed demonstrating safety and efficacy of FTRD in the UGIT[37,38]. The largest of these was an international multicenter trial of 56 patients across 13 centers[37]. Common indications included gastrointestinal stromal tumors (GIST), adenomas, hamartomas, and adenocarcinomas. Results showed a technical success rate of 77% and R0 resection rate of 68%. The AE rate was 21%, though none were classified as severe AEs. Common AEs included intraprocedural and delayed bleeding. No perforations were reported.

Recently, a prospective multicenter pilot study (RESET trial) investigated the new gastroduodenal FTRD in the upper GIT[39]. 29 patients underwent EFTR with the gastroduodenal FTRD in this trial for gastric subepithelial tumors, which included leiomyomas, lipomas, schwannomas, ectopic pancreas, GISTs, and NETs. The technical success rate was 89% and the R0 resection rate was 76%. Minor bleeding occurred in 31% of cases and was able to be managed intraprocedurally in all cases. No transfusion of blood products was required nor was any further bleeding observed. No other AEs were reported. The success rates and AE rates reported here are similar to those reported with FTRD in the lower GIT.

To our knowledge, there is only one single report on the use of the FTRD in the esophagus[37]. However, this was reported as part of a larger multicenter study, and it is not evident whether this case was technically successful or associated with any AEs.

Similar to FTRD in the lower GIT, various subgroup analyses have been performed to ascertain whether outcomes of FTRD in the upper GIT are associated with other variables. Thus far, variables such as indication, lesion size, lesion location, prior treatment, participating center, or number of FTRD cases performed by the endoscopist have not been clearly associated with technical success and other success outcomes[37,39]. Further studies are needed to help delineate the impact of these individual factors on gastroduodenal FTRD outcomes.

Overall, early data suggests that FTRD in the upper GIT appears to be feasible, safe, and efficacious. Common indications include gastric and duodenal subepithelial lesions, adenomas, and early cancer. However, given the paucity of data of FTRD in the upper GIT compared to the lower GIT, further studies are needed to further clarify the indications, especially for the indication of early cancer, as well as clarify overall safety and efficacy.

EMERGING APPLICATIONS

Hybrid FTRD

In cases with lesions > 3 cm or where *en bloc* EFTR appears challenging for other reasons, various hybrid techniques have been proposed. These have been referred to by varying names including Hybrid FTRD, EMR + FTRD, and ESD + FTRD. In general, these hybrid techniques refer to using either piecemeal EMR or ESD followed by FTRD of scarred areas or residual abnormal appearing tissue. Hybrid techniques have shown some promise in small case series[40-44]. However, further evaluation in larger scale studies is needed to draw conclusions on their routine use.

TECHNICAL CHALLENGES

Several limitations of the FTRD have been reported. One technical challenge is the difficulty in resecting larger lesions. With a cap diameter of 21 mm and cap depth of 23 mm for the standard colonic FTRD (and smaller for the gastroduodenal FTRD and diagnostic FTRD), it is often difficult to adequately grasp large lesions (> 3 cm) to accomplish *en bloc* resection. In addition, these lesions are often scarred and fixed to the colon wall, and therefore may be difficult to grasp and bring into the cap even if they are smaller than 3 cm. The length and stiffness of the plastic cap can also interfere with visualization and flexibility at the scope tip, thereby making it quite cumbersome to advance the colonoscope with the FTRD across a tortuous sigmoid and especially to the right colon. As described earlier, a proprietary test cap called the FTRD prOVE Cap© is available to help circumvent some of these issues and to determine whether a target lesion can be reached and might be suitable for resection with FTRD. The long plastic sheath that wraps around the scope shaft can increase friction of the device and also make advancement of the scope through tight or tortuous anatomic locations difficult. Some endoscopists leave a guidewire in the colon after the diagnostic colonoscopy is performed. The colonoscope with the attached FTRD is then advanced alongside the guidewire, following the guidewire to the lesion, overcoming the limited visualization and maneuverability with the FTRD cap. Device failure (failure of the clip to fully cinch down or complete malfunction of the clip or snare's opening and closing functions) and premature clip deployment leading to immediate perforation or incomplete resection have been reported[12]. Risk factors for incomplete or partial resection include tissue fibrosis, right-sided colonic lesions, and size > 3 cm[25]. It should be emphasized that clip placement must be immediately followed by prompt snare resection, often requiring good communication and teamwork between the endoscopist and assistants handling the snare and grasper. It is important to have the endoscopist fire the clip and have two separate assistants operate the grasper and snare. Delay in snare resection after clip placement, slippage of the lesion from the grasper, or inadvertently performing snare resection before firing the clip can result in incomplete resection or immediate perforation. As with other endoscopic devices and techniques, EFTR with the FTRD requires adequate training and endoscopic skill. Completion of mandatory training is required prior to the purchase and use of FTRD.

FUTURE DIRECTIONS

Currently, there is a lack of direct comparison between FTRD and other standard resection approaches such as EMR and ESD. Direct comparisons between FTRD and more standard approaches are needed to further clarity the role of FTRD, whether it is merely adjunctive to standard approaches or may be a suitable primary or "standard" approach itself. Cost-effectiveness studies may help further clarify this role as well. Recently, laparoscopic and endoscopic cooperative surgery (LECS) has been described as a

less invasive approach to resecting lesions in the GIT, such as GIST[45]. Prospective studies comparing FTRD with LECS and other similar novel minimally-invasive surgical techniques will help clarify the advantage of FTRD over these novel surgical approaches. Studies investigating longer term outcomes are also needed, especially regarding AEs and the ability to perform adequate endoscopic examination of the full-thickness resection site during follow-up and surveillance. This may be challenging if the FTRD clip is still in place and not fallen off. There are still concerns regarding AEs with EFTR with FTRD, especially for resection of lesions at the appendiceal orifice and with regards to delayed perforation. Long term data are needed on specific outcomes such as the development of an appendiceal mucocele or delayed appendicitis after using FTRD in this location. It is also tempting to consider whether there might be safe applications for the FTRD in the esophagus, particularly in the treatment of early carcinomas or subepithelial lesions. Future studies may help clarify this and other expanded roles of FTRD.

CONCLUSION

EFTR can be successfully and safely accomplished with the FTRD system. The role of FTRD has expanded in recent years and the FTRD is currently available for use in the lower and upper GIT. EFTR with FTRD is a crucial addition to the endoscopic armamentarium for resection of gastrointestinal lesions and reducing need for more invasive surgery. Common indications for its use include resection of lesions difficult to resect with conventional techniques like EMR and ESD, such as scarred or non-lifting polyps, early cancers, subepithelial lesions, and diagnostic resection for evaluation of various neuromuscular or entero-infiltrative conditions (*e.g.*, Hirschsprung disease, gastrointestinal amyloidosis). EFTR with FTRD has a high technical success and R0 resection rate, and AE rates are acceptable, especially when used as a less invasive option for lesions not amenable for standard endoscopic resection. Common AEs include bleeding and perforation, and further long-term data on unique complications such as post-polypectomy syndrome, delayed perforation, acute appendicitis, and enterocolonic fistula are needed. Several technical challenges exist and endoscopists should be adequately trained on the FTRD system prior to use in clinical practice. FTRD, used in its proper context, has the ability to be a major advancement in endoscopic resection for populations felt to be too high risk for traditional resection techniques and surgery (*e.g.*, elderly patients, patients at high risk of bleeding, high risk for anesthesia).

FOOTNOTES

Author contributions: Mun EJ contributed drafting of the manuscript; Wagh MS contributed critical review of the manuscript and endoscopic image acquisition.

Conflict-of-interest statement: Dr. Mun discloses no conflict of interest for this article; Dr. Wagh is consultant for Boston Scientific, Olympus, Medtronic, Fujifilm and ConMed.

Open-Access: This article is an open-access article that was selected by an in-house editor and fully peer-reviewed by external reviewers. It is distributed in accordance with the Creative Commons Attribution NonCommercial (CC BY-NC 4.0) license, which permits others to distribute, remix, adapt, build upon this work non-commercially, and license their derivative works on different terms, provided the original work is properly cited and the use is non-commercial. See: https://creativecommons.org/Licenses/by-nc/4.0/

Country/Territory of origin: United States

ORCID number: Elijah J Mun 0000-0001-6613-7518; Mihir S Wagh 0000-0003-2145-272X.

Corresponding Author's Membership in Professional Societies: American Society for Gastrointestinal Endoscopy, No. 101273.

S-Editor: Gao CC
L-Editor: A
P-Editor: Xu ZH

REFERENCES

1 **Rajan E**, Wong Kee Song LM. Endoscopic Full Thickness Resection. *Gastroenterology* 2018; **154**: 1925-1937.e2 [PMID: 29486198 DOI: 10.1053/j.gastro.2018.02.020]
2 **Schmidt A**, Meier B, Caca K. Endoscopic full-thickness resection: Current status. *World J Gastroenterol* 2015; **21**: 9273-

9285 [PMID: 26309354 DOI: 10.3748/wjg.v21.i31.9273]
3 **ASGE Technology Committee**, Aslanian HR, Sethi A, Bhutani MS, Goodman AJ, Krishnan K, Lichtenstein DR, Melson J, Navaneethan U, Pannala R, Parsi MA, Schulman AR, Sullivan SA, Thosani N, Trikudanathan G, Trindade AJ, Watson RR, Maple JT. ASGE guideline for endoscopic full-thickness resection and submucosal tunnel endoscopic resection. *VideoGIE* 2019; **4**: 343-350 [PMID: 31388606 DOI: 10.1016/j.vgie.2019.03.010]
4 **ASGE Technology Committee**, Maple JT, Abu Dayyeh BK, Chauhan SS, Hwang JH, Komanduri S, Manfredi M, Konda V, Murad FM, Siddiqui UD, Banerjee S. Endoscopic submucosal dissection. *Gastrointest Endosc* 2015; **81**: 1311-1325 [PMID: 25796422 DOI: 10.1016/j.gie.2014.12.010]
5 **Stavropoulos SN**, Modayil R, Friedel D, Brathwaite CE. Endoscopic full-thickness resection for GI stromal tumors. *Gastrointest Endosc* 2014; **80**: 334-335 [PMID: 25034842 DOI: 10.1016/j.gie.2014.05.300]
6 **Ye LP**, Yu Z, Mao XL, Zhu LH, Zhou XB. Endoscopic full-thickness resection with defect closure using clips and an endoloop for gastric subepithelial tumors arising from the muscularis propria. *Surg Endosc* 2014; **28**: 1978-1983 [PMID: 24619327 DOI: 10.1007/s00464-014-3421-1]
7 **Mönkemüller K**, Sarker S, Baig KR. Endoscopic creation of an omental patch with an over-the-scope clip system after endoscopic excavation and resection of a large gastrointestinal stromal tumor of the stomach. *Endoscopy* 2014; **46** Suppl 1 UCTN: E451-E452 [PMID: 25314189 DOI: 10.1055/s-0034-1377495]
8 **ASGE Technology Committee**, Banerjee S, Barth BA, Bhat YM, Desilets DJ, Gottlieb KT, Maple JT, Pfau PR, Pleskow DK, Siddiqui UD, Tokar JL, Wang A, Song LM, Rodriguez SA. Endoscopic closure devices. *Gastrointest Endosc* 2012; **76**: 244-251 [PMID: 22658920 DOI: 10.1016/j.gie.2012.02.028]
9 **Kaehler G**, Grobholz R, Langner C, Suchan K, Post S. A new technique of endoscopic full-thickness resection using a flexible stapler. *Endoscopy* 2006; **38**: 86-89 [PMID: 16429361 DOI: 10.1055/s-2005-921181]
10 **U. S. Food and Drug Administration**. Center for Devices and Radiological Health. Gastroduodenal FTRD Set K200684 approval letter, June 2, 2020. [cited 7 December 2020]. In: U.S. Food and Drug Administration [Internet]. Available from: https://www.accessdata.fda.gov/cdrh_docs/pdf20/K200684.pdf
11 **Schurr MO**, Baur FE, Krautwald M, Fehlker M, Wehrmann M, Gottwald T, Prosst RL. Endoscopic full-thickness resection and clip defect closure in the colon with the new FTRD system: experimental study. *Surg Endosc* 2015; **29**: 2434-2441 [PMID: 25318369 DOI: 10.1007/s00464-014-3923-x]
12 **Meier B**, Stritzke B, Kuellmer A, Zervoulakos P, Huebner GH, Repp M, Walter B, Meining A, Gutberlet K, Wiedbrauck T, Glitsch A, Lorenz A, Caca K, Schmidt A. Efficacy and Safety of Endoscopic Full-Thickness Resection in the Colorectum: Results From the German Colonic FTRD Registry. *Am J Gastroenterol* 2020; **115**: 1998-2006 [PMID: 32833733 DOI: 10.14309/ajg.0000000000000795]
13 **Kirschniak A**, Kratt T, Stüker D, Braun A, Schurr MO, Königsrainer A. A new endoscopic over-the-scope clip system for treatment of lesions and bleeding in the GI tract: first clinical experiences. *Gastrointest Endosc* 2007; **66**: 162-167 [PMID: 17591492 DOI: 10.1016/j.gie.2007.01.034]
14 **Weiland T**, Fehlker M, Gottwald T, Schurr MO. Performance of the OTSC System in the endoscopic closure of iatrogenic gastrointestinal perforations: a systematic review. *Surg Endosc* 2013; **27**: 2258-2274 [PMID: 23340813 DOI: 10.1007/s00464-012-2754-x]
15 **Arezzo A**, Verra M, Reddavid R, Cravero F, Bonino MA, Morino M. Efficacy of the over-the-scope clip (OTSC) for treatment of colorectal postsurgical leaks and fistulas. *Surg Endosc* 2012; **26**: 3330-3333 [PMID: 22580885 DOI: 10.1007/s00464-012-2340-2]
16 **Fähndrich M**, Sandmann M. Endoscopic full-thickness resection for gastrointestinal lesions using the over-the-scope clip system: a case series. *Endoscopy* 2015; **47**: 76-79 [PMID: 25221859 DOI: 10.1055/s-0034-1377975]
17 **Sarker S**, Gutierrez JP, Council L, Brazelton JD, Kyanam Kabir Baig KR, Mönkemüller K. Over-the-scope clip-assisted method for resection of full-thickness submucosal lesions of the gastrointestinal tract. *Endoscopy* 2014; **46**: 758-761 [PMID: 24830398 DOI: 10.1055/s-0034-1365513]
18 **Mönkemüller K**, Peter S, Toshniwal J, Popa D, Zabielski M, Stahl RD, Ramesh J, Wilcox CM. Multipurpose use of the 'bear claw' (over-the-scope-clip system) to treat endoluminal gastrointestinal disorders. *Dig Endosc* 2014; **26**: 350-357 [PMID: 23855514 DOI: 10.1111/den.12145]
19 **Schmidt A**, Bauerfeind P, Gubler C, Damm M, Bauder M, Caca K. Endoscopic full-thickness resection in the colorectum with a novel over-the-scope device: first experience. *Endoscopy* 2015; **47**: 719-725 [PMID: 25763833 DOI: 10.1055/s-0034-1391781]
20 **Ichkhanian Y**, Barawi M, Seoud T, Thakkar S, Kothari TH, Halabi ME, Ullah A, Edris W, Aepli P, Kowalski T, Shinn B, Shariaha RZ, Mahadev S, Mosko JD, Andrisani G, Di Matteo FM, Albrecht H, Giap AQ, Tang SJ, Naga YM, van Geenen E, Friedland S, Tharian B, Irani S, Ross AS, Jamil LH, Lew D, Nett AS, Farha J, Runge TM, Jovani M, Khashab MA. Endoscopic full-thickness resection of polyps involving the appendiceal orifice: a multicenter international experience. *Endoscopy* 2022; **54**: 16-24 [PMID: 33395714 DOI: 10.1055/a-1345-0044]
21 **Meier B**, Albrecht H, Wiedbrauck T, Schmidt A, Caca K. Full-thickness resection of neuroendocrine tumors in the rectum. *Endoscopy* 2020; **52**: 68-72 [PMID: 31614372 DOI: 10.1055/a-1008-9077]
22 **Ichkhanian Y**, Vosoughi K, Diehl DL, Grimm IS, James TW, Templeton AW, Hajifathalian K, Tokar JL, Samarasena JB, Chehade NEH, Lee J, Chang K, Mizrahi M, Barawi M, Irani S, Friedland S, Korc P, Aadam AA, Al-Haddad MA, Kowalski TE, Novikov A, Smallfield G, Ginsberg GG, Oza VM, Panuu D, Fukami N, Pohl H, Lajin M, Kumta NA, Tang SJ, Naga YM, Amateau SK, Brewer GOI, Kumbhari V, Sharaiha R, Khashab MA. A large multicenter cohort on the use of full-thickness resection device for difficult colonic lesions. *Surg Endosc* 2021; **35**: 1296-1306 [PMID: 32180001 DOI: 10.1007/s00464-020-07504-9]
23 **Boger P**, Rahman I, Hu M, Ayaru L, Bhandari P, Chedgy F, Green S, Hayat M, Hopper AD, Ishaq S, Martin J, McCallum I, Phull P, Pugh S, Russo E, Suzuki N, Thomas-Gibson S, Zeino Z, Patel P. Endoscopic full thickness resection in the colorectum: outcomes from the UK Registry. *Eur J Gastroenterol Hepatol* 2021; **33**: 852-858 [PMID: 33136721 DOI: 10.1097/MEG.0000000000001987]
24 **Kuellmer A**, Mueller J, Caca K, Aepli P, Albers D, Schumacher B, Glitsch A, Schäfer C, Wallstabe I, Hofmann C,

Erhardt A, Meier B, Bettinger D, Thimme R, Schmidt A; FTRD study group. Endoscopic full-thickness resection for early colorectal cancer. *Gastrointest Endosc* 2019; **89**: 1180-1189.e1 [PMID: 30653939 DOI: 10.1016/j.gie.2018.12.025]

25 **Schmidt A**, Beyna T, Schumacher B, Meining A, Richter-Schrag HJ, Messmann H, Neuhaus H, Albers D, Birk M, Thimme R, Probst A, Faehndrich M, Frieling T, Goetz M, Riecken B, Caca K. Colonoscopic full-thickness resection using an over-the-scope device: a prospective multicentre study in various indications. *Gut* 2018; **67**: 1280-1289 [PMID: 28798042 DOI: 10.1136/gutjnl-2016-313677]

26 **Andrisani G**, Pizzicannella M, Martino M, Rea R, Pandolfi M, Taffon C, Caricato M, Coppola R, Crescenzi A, Costamagna G, Di Matteo FM. Endoscopic full-thickness resection of superficial colorectal neoplasms using a new over-the-scope clip system: A single-centre study. *Dig Liver Dis* 2017; **49**: 1009-1013 [PMID: 28539229 DOI: 10.1016/j.dld.2017.04.015]

27 **Backes Y**, Kappelle WFW, Berk L, Koch AD, Groen JN, de Vos Tot Nederveen Cappel WH, Schwartz MP, Kerkhof M, Siersema PD, Schröder R, Tan TG, Lacle MM, Vleggaar FP, Moons LMG; T1 CRC Working Group. Colorectal endoscopic full-thickness resection using a novel, flat-base over-the-scope clip: a prospective study. *Endoscopy* 2017; **49**: 1092-1097 [PMID: 28753696 DOI: 10.1055/s-0043-114730]

28 **Zwager LW**, Bastiaansen BAJ, Bronzwaer MES, van der Spek BW, Heine GDN, Haasnoot KJC, van der Sluis H, Perk LE, Boonstra JJ, Rietdijk ST, Wolters HJ, Weusten BLAM, Gilissen LPL, Ten Hove WR, Nagengast WB, Bekkering FC, Schwartz MP, Terhaar Sive Droste JS, Vlug MS, Houben MHMG, Rando Munoz FJ, Seerden TCJ, Beaumont H, de Ridder R, Dekker E, Fockens P; Dutch eFTR Group. Endoscopic full-thickness resection (eFTR) of colorectal lesions: results from the Dutch colorectal eFTR registry. *Endoscopy* 2020; **52**: 1014-1023 [PMID: 32498100 DOI: 10.1055/a-1176-1107]

29 **Zwager LW**, Bastiaansen BAJ, van der Spek BW, Heine DN, Schreuder RM, Perk LE, Weusten BLAM, Boonstra JJ, van der Sluis H, Wolters HJ, Bekkering FC, Rietdijk ST, Schwartz MP, Nagengast WB, Ten Hove WR, Terhaar Sive Droste JS, Rando Munoz FJ, Vlug MS, Beaumont H, Houben MHMG, Seerden TCJ, de Wijkerslooth TR, Gielisse EAR, Hazewinkel Y, de Ridder R, Straathof JA, van der Vlugt M, Koens L, Fockens P, Dekker E; Dutch eFTR Group. Endoscopic full-thickness resection of T1 colorectal cancers: a retrospective analysis from a multicenter Dutch eFTR registry. *Endoscopy* 2022; **54**: 475-485 [PMID: 34488228 DOI: 10.1055/a-1637-9051]

30 **Hassan C**, Repici A, Sharma P, Correale L, Zullo A, Bretthauer M, Senore C, Spada C, Bellisario C, Bhandari P, Rex DK. Efficacy and safety of endoscopic resection of large colorectal polyps: a systematic review and meta-analysis. *Gut* 2016; **65**: 806-820 [PMID: 25681402 DOI: 10.1136/gutjnl-2014-308481]

31 **Fujiya M**, Tanaka K, Dokoshi T, Tominaga M, Ueno N, Inaba Y, Ito T, Moriichi K, Kohgo Y. Efficacy and adverse events of EMR and endoscopic submucosal dissection for the treatment of colon neoplasms: a meta-analysis of studies comparing EMR and endoscopic submucosal dissection. *Gastrointest Endosc* 2015; **81**: 583-595 [PMID: 25592748 DOI: 10.1016/j.gie.2014.07.034]

32 **Azzolini F**, Camellini L, Sassatelli R, Sereni G, Biolchini F, Decembrino F, De Marco L, Iori V, Tioli C, Cavina M, Bedogni G. Endoscopic submucosal dissection of scar-embedded rectal polyps: a prospective study (Esd in scar-embedded rectal polyps). *Clin Res Hepatol Gastroenterol* 2011; **35**: 572-579 [PMID: 21640691 DOI: 10.1016/j.clinre.2011.04.013]

33 **Hurlstone DP**, Shorthouse AJ, Brown SR, Tiffin N, Cross SS. Salvage endoscopic submucosal dissection for residual or local recurrent intraepithelial neoplasia in the colorectum: a prospective analysis. *Colorectal Dis* 2008; **10**: 891-897 [PMID: 18355372 DOI: 10.1111/j.1463-1318.2008.01510.x]

34 **Roberts JR**, Koro K, Yeh MM, Saunders MD, Templeton AW. Endoscopic resection of gastric adenocarcinoma by use of a full-thickness resection device. *VideoGIE* 2018; **3**: 244-246 [PMID: 30128404 DOI: 10.1016/j.vgie.2018.05.002]

35 **Schmidt A**, Meier B, Cahyadi O, Caca K. Duodenal endoscopic full-thickness resection (with video). *Gastrointest Endosc* 2015; **82**: 728-733 [PMID: 26077454 DOI: 10.1016/j.gie.2015.04.031]

36 **Andrisani G**, Di Matteo FM. Endoscopic full-thickness resection of duodenal lesions (with video). *Surg Endosc* 2020; **34**: 1876-1881 [PMID: 31768725 DOI: 10.1007/s00464-019-07269-w]

37 **Hajifathalian K**, Ichkhanian Y, Dawod Q, Meining A, Schmidt A, Glaser N, Vosoughi K, Diehl DL, Grimm IS, James T, Templeton AW, Samarasena JB, Chehade NEH, Lee JG, Chang KJ, Mizrahi M, Barawi M, Irani S, Friedland S, Korc P, Aadam AA, Al-Haddad M, Kowalski TE, Smallfield G, Ginsberg GG, Fukami N, Lajin M, Kumta NA, Tang SJ, Naga Y, Amateau SK, Kasmin F, Goetz M, Seewald S, Kumbhari V, Ngamruengphong S, Mahdev S, Mukewar S, Sampath K, Carr-Locke DL, Khashab MA, Sharaiha RZ. Full-thickness resection device (FTRD) for treatment of upper gastrointestinal tract lesions: the first international experience. *Endosc Int Open* 2020; **8**: E1291-E1301 [PMID: 33015330 DOI: 10.1055/a-1216-1439]

38 **Bauder M**, Schmidt A, Caca K. Endoscopic full-thickness resection of duodenal lesions-a retrospective analysis of 20 FTRD cases. *United European Gastroenterol J* 2018; **6**: 1015-1021 [PMID: 30228889 DOI: 10.1177/2050640618773517]

39 **Meier B**, Schmidt A, Glaser N, Meining A, Walter B, Wannhoff A, Riecken B, Caca K. Endoscopic full-thickness resection of gastric subepithelial tumors with the gFTRD-system: a prospective pilot study (RESET trial). *Surg Endosc* 2020; **34**: 853-860 [PMID: 31187233 DOI: 10.1007/s00464-019-06839-2]

40 **Zimmer V**. Hybrid precutting EMR-EFTR resection for a tricky rectal adenoma recurrence with high-grade fibrosis. *Dig Liver Dis* 2020; **52**: 681-682 [PMID: 32345493 DOI: 10.1016/j.dld.2020.03.016]

41 **Meier B**, Caca K, Schmidt A. Hybrid endoscopic mucosal resection and full-thickness resection: a new approach for resection of large non-lifting colorectal adenomas (with video). *Surg Endosc* 2017; **31**: 4268-4274 [PMID: 28281119 DOI: 10.1007/s00464-017-5461-9]

42 **Lupu A**, Jacques J, Rivory J, Saurin JC, Rostain F, Ponchon T, Pioche M. Hybrid endoscopic submucosal dissection using a full-thickness resection device allows en bloc resection of a large adenoma deeply invading the appendix. *Endoscopy* 2018; **50**: E296-E298 [PMID: 30089323 DOI: 10.1055/a-0651-0393]

43 **Andrisani G**, Di Matteo FM. Hybrid resection with endoscopic submucosal dissection and full-thickness resection device of a large cecal laterally spreading tumor involving the appendix. *VideoGIE* 2020; **5**: 372-374 [PMID: 32817928 DOI: 10.1016/j.vgie.2020.03.019]

44 **Andrisani G**, Di Matteo FM. Hybrid resection with ESD and FTRD: Could this be a rescue treatment in the presence of

severe submucosal fibrosis? *Dig Liver Dis* 2019; **51**: 607-609 [PMID: 30686714 DOI: 10.1016/j.dld.2019.01.003]
45 **Hiki N**, Nunobe S, Matsuda T, Hirasawa T, Yamamoto Y, Yamaguchi T. Laparoscopic endoscopic cooperative surgery. *Dig Endosc* 2015; **27**: 197-204 [PMID: 25394216 DOI: 10.1111/den.12404]

World Journal of Gastroenterology

Submit a Manuscript: https://www.f6publishing.com

World J Gastroenterol 2023 July 7; 29(25): 4021-4035

DOI: 10.3748/wjg.v29.i25.4021

ISSN 1007-9327 (print) ISSN 2219-2840 (online)

MINIREVIEWS

Dynamic contrast enhanced ultrasound in gastrointestinal diseases: A current trend or an indispensable tool?

Mattia Paratore, Matteo Garcovich, Maria Elena Ainora, Laura Riccardi, Antonio Gasbarrini, Maria Assunta Zocco

Specialty type: Gastroenterology and hepatology

Provenance and peer review: Invited article; Externally peer reviewed.

Peer-review model: Single blind

Peer-review report's scientific quality classification

Grade A (Excellent): 0
Grade B (Very good): B
Grade C (Good): C
Grade D (Fair): 0
Grade E (Poor): 0

P-Reviewer: Aydin S, Turkey; Lu Q, China

Received: March 26, 2023
Peer-review started: March 26, 2023
First decision: May 13, 2023
Revised: May 24, 2023
Accepted: June 5, 2023
Article in press: June 5, 2023
Published online: July 7, 2023

Mattia Paratore, Matteo Garcovich, Maria Elena Ainora, Laura Riccardi, Medicina Interna e Gastroenterologia, CEMAD Digestive Disease Center, Fondazione Policlinico Universitario A. Gemelli IRCCS, Rome 00168, Italy

Antonio Gasbarrini, Maria Assunta Zocco, Medicina Interna e Gastroenterologia, CEMAD Digestive Disease Center, Università Cattolica del Sacro Cuore, Fondazione Policlinico Universitario A. Gemelli IRCCS, Rome 00168, Italy

Corresponding author: Matteo Garcovich, MD, PhD, Research Scientist, Staff Physician, Medicina Interna e Gastroenterologia, CEMAD Digestive Disease Center, Fondazione Policlinico Universitario A. Gemelli IRCCS, Largo A. Gemelli 8, Rome 00168, Italy.
matteogarcovich@yahoo.it

Abstract

Contrast enhanced ultrasound (CEUS) has been widely implemented in clinical practice because of the enormous quantity of information it provides, along with its low cost, reproducibility, minimal invasiveness, and safety of the second-generation ultrasound contrast agents. To overcome the limitation of CEUS given by the subjective evaluation of the contrast enhancement behaviour, quantitative analysis of contrast kinetics with generation of time-intensity curves has been introduced in recent years. The quantification of perfusion parameters [named as dynamic-CEUS (D-CEUS)] has several applications in gastrointestinal neoplastic and inflammatory disorders. However, the limited availability of large studies and the heterogeneity of the technologies employed have precluded the standardisation of D-CEUS, which potentially represents a valuable tool for clinical practice in management of gastrointestinal diseases. In this article, we reviewed the evidence exploring the application of D-CEUS in gastrointestinal diseases, with a special focus on liver, pancreas, and inflammatory bowel diseases.

Key Words: Quantitative perfusion analysis; Gastrointestinal diseases; Time-intensity curve; Multiparametric ultrasound

©The Author(s) 2023. Published by Baishideng Publishing Group Inc. All rights reserved.

Core Tip: Contrast-enhanced ultrasound (CEUS) has been widely implemented in clinical practice in recent years. Despite its several advantages, the qualitative evaluation of this exam and the lack of objectivity could lead to variability between different operators and ultrasound equipments. Dynamic-CEUS (D-CEUS) with the measurement of perfusion parameters is aimed at overcoming this important limitation. The purpose of this review is to explore the usefulness of D-CEUS in gastroenterological diseases.

Citation: Paratore M, Garcovich M, Ainora ME, Riccardi L, Gasbarrini A, Zocco MA. Dynamic contrast enhanced ultrasound in gastrointestinal diseases: A current trend or an indispensable tool? *World J Gastroenterol* 2023; 29(25): 4021-4035
URL: https://www.wjgnet.com/1007-9327/full/v29/i25/4021.htm
DOI: https://dx.doi.org/10.3748/wjg.v29.i25.4021

INTRODUCTION

Contrast enhanced ultrasound (CEUS) has been widely implemented in clinical practice as a result of the enormous quantity of information it provides, along with its low cost, reproducibility, minimal invasiveness, and safety of the second-generation ultrasound contrast agents (UCAs)[1-4]. Despite its numerous advantages, one of the most significant limitations of CEUS is the subjective evaluation of contrast enhancement related behaviour of the explored tissues[5]. In recent years, dynamic-CEUS (D-CEUS) has been explored to overcome this limitation.

D-CEUS represents the quantitative analysis of UCA-kinetics in a specific region of interest (ROI)[6]. This technique allows two types of analysis in the examined tissue: Disruption-replenishment analysis and wash-in/wash out analysis[7]. The first analysis consists in the evaluation of microbubbles replacement after destroying them with high mechanical index. Requiring the continuous intravenous infusion over five to twenty minutes of UCA, the disruption-replenishment analysis are infrequently used due of their complex methodology[8]. Consequently, the second form of analysis is more frequently employed in clinical practice. It consists of measuring the average intensity of a ROI following a bolus injection of UCA and generating a time-intensity curve (TIC). Hence, multiple parameters are derived from the TIC to quantitatively characterize the different stages of the wash-in and wash-out phases. The fundamental parameters derived from TIC are summarized in Table 1[9,10] and a schematic representation of TIC is shown in Figure 1. Generally, these parameters are obtained from different softwares and might consequently have varying nomenclature but can be divided into two categories: Amplitude parameters and time parameters. These criteria reflect various vascularization features: Amplitude parameters are mainly related to blood volume in the ROI, while blood flow is mostly correlated with time parameters[11]. Tracking microbubbles circulation provides the spatial representation of blood flow patterns and the derivation of parametric values of tissue perfusion since microbubbles strictly remain within the vasculature compartment[12].

Examining the pros and cons, D-CEUS is a widely accessible, radiation-free, non-nephrotoxic and cost-effective technique that allows objective enhancement quantification, image comparison, real-time evaluation of the microcirculation perfusion by a strictly intravascular blood pool agent. This is crucial after the introduction of updated response evaluation criteria in solid tumor (RECIST) criteria based on tumour perfusion as D-CEUS potentially enables the monitoring of changes in vascularization even shortly after tumor treatment[13,14]. According to current European Federation for Ultrasound in Medicine and Biology recommendations, D-CEUS is useful for quantifying tumor enhancement objectively, to characterize focal lesions and evaluate the therapeutic response[7]. In contrast, D-CEUS should ideally be uniform regardless of the ultrasound equipment, data collecting, and analysis software, as different approaches and technical issues may influence the results' validity. Lastly, the technical limitations of the method must be addressed, particularly in the abdomen, where intestinal, respiratory, and probe motion artefacts could make this exam challenging, as well as the patient's ability to accomplish the instructions based on his mental and physical state[15].

The first D-CEUS examination was performed on oncological renal illness more than two decades ago [16]. Since then, this technique has spread to several medical specialties, especially in the gastroenterological setting and not only for oncological diseases. In this review we summarize the evidence exploring the application of D-CEUS in gastrointestinal diseases.

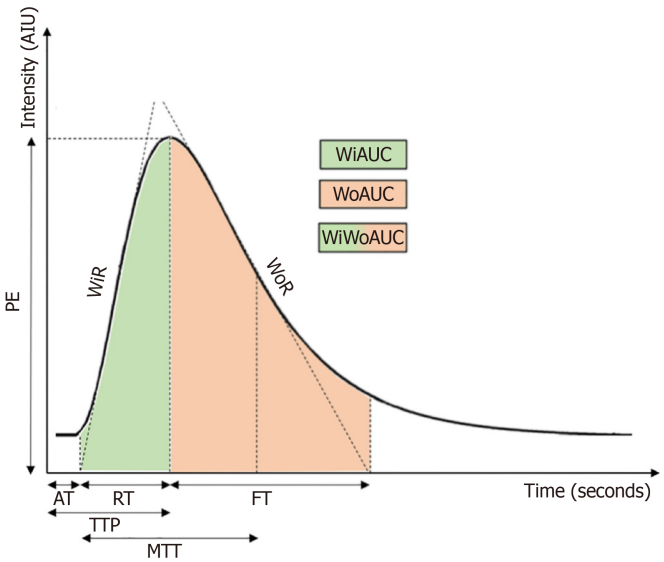
LIVER DISEASES

In liver diseases, D-CEUS has been explored primarily for its usefulness in characterizing focal liver lesions (FLLs). Several applications of D-CEUS in predicting biological behaviour, differential diagnosis, and prognosis have been explored. These studies are summarized in Table 2, and Figure 2 illustrates the

Table 1 Dynamic contrast-enhanced ultrasound parameters in time-intensity curve

Abbreviation	Parameter	Definition	Unit
AT	Arrival time	Time from administration of UCA to the beginning of the curve	s
AUC or WiWoAUC	Area under the curve or wash-in and wash-out area under the curve		AIU
FT	Fall time	Time from PE to point where tangent of descending curve across x-axis	s
IMAX or MI	Maximum intensity	Maximum intensity of the curve	AIU
MTT	Mean transit time	Mean time taken by contrast to pass through the ROI	s
PE	Peak enhancement	Maximum intensity of the curve	AIU
PI	Peak intensity	Maximum intensity of the curve	AIU
Pw	Slope coefficient of wash-in	Coefficient of the enhancement wash-in slope	AIU × s
RT	Rise time	Time from PE to point where tangent of ascending curve across x-axis	s
TPI or TTP or TP	Time to peak	Time from the beginning of the curve to peak	s
WiAUC	Wash-in area under the curve	AUC from the beginning of the curve to PE	AIU × s
WoAUC	Wash-out area under the curve	AUC from the PE to the end of the curve	AIU × s
WiR	Wash-in rate	Tangent at the ascending part of the curve	AIU × s
WoR	Wash-out rate	Tangent at the descending part of the curve	AIU × s

AIU: Absolute intensity unit; ROI: Region of interest; UCA: Ultrasound contrast agent.



DOI: 10.3748/wjg.v29.i25.4021 **Copyright** ©The Author(s) 2023.

Figure 1 Time-intensity curve and derived parameters. AIU: Absolute intensity unit; AT: Arrival time; FT: Fall time; MTT: Mean transit time; PE: Peak enhancement; s: Second; TTP: Time to peak; WiAUC: Wash-in area under the curve; WiR: Wash-in rate; WiWoAUC: Wash-in and wash-out area under the curve; WoAUC: Wash-out area under the curve; WoR: Wash-out rate; RT: Rise time.

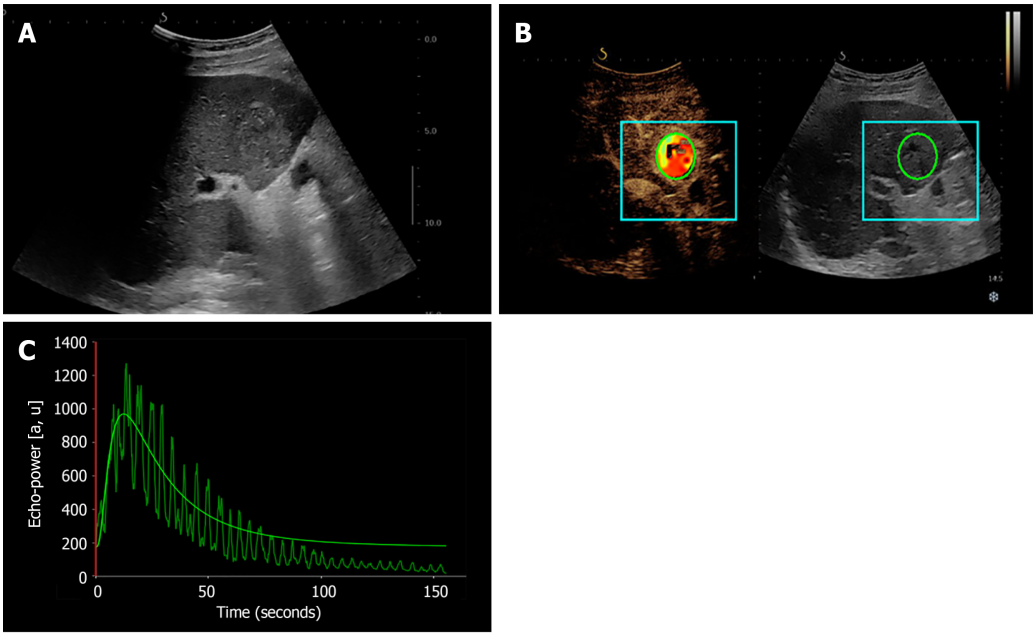
use of D-CEUS to characterize liver lesions.

Table 2 Dynamic contrast-enhanced ultrasound and liver diseases

Ref.	Study design/number of patients	Object of D-CEUS	Population/groups	Machine/UCA/software	Significant results ($P < 0.05$)
Wildner *et al*[31], 2022	Prospective/17	Melanoma liver metastasis	Patients with melanoma liver metastasis treated with sorafenib/Responders' *vs* non-responders	Sequoia 512/SonoVue/Qontrast	Increase of MTT and TTP is associated with response to treatment and prognosis
Gu *et al*[30], 2022	Retrospective/97	HCC	Patients with HCC underwent thermal ablation	Acuson Sequoia, Phillip EpiQ7/SonoVue/VueBox	WiAUC, WoAUC, and WiWoAUC ratios between HCC and surrounding parenchyma before ablation were predictors of survival
Huang *et al*[18], 2022	Prospective/120	HCC	Patients with HCC underwent biopsy/Low-Ki-67 *vs* high-Ki-67	Logiq E9/Sonazoid/NovoUltrasound Kit	PE difference between HCC and distal liver parenchyma was different in the Kupffer phase
Li *et al*[22], 2022	Retrospective/31	HCC	Patients with HCC underwent surgery/MVI-positive *vs* MVI-negative	Phillip EpiQ7/Sonazoid/built-in auto contrast software	None of the D-CEUS parameters was related to MVI
Zocco *et al*[28], 2013	Prospective/46	Liver parenchyma	Cirrhotic patient underwent HVPG/clinically significant portal hypertension *vs* severe portal hypertension	iU22/SonoVue/QLAB	Negative correlation between PI, Pw and HVPG. Positive correlation with MTT. AUROC of 1.00 for PI < 23.3 AIU to predict clinically significant portal hypertension
Dong *et al*[21], 2021	Retrospective/16	HCC	Patients with HCC underwent surgery/MVI-positive *vs* MVI-negative	Acuson Oxana, Logiq E9, Siemens Acuson Sequoia/SonoVue, Lumason/VueBox	WiAUC and WoAUC were higher in MVI positive group
Schwarz *et al*[24], 2021	Retrospective/139	Focal liver lesion	Patients with diagnosed focal liver lesion/malignant versus benign	Acuson Sequoia, S2000 or S3000 and Phillip EpiQ7/SonoVue/VueBox	RT and late phase ratio were different between malignant and benign liver lesion
Xuan *et al*[19], 2021	Retrospective/128	HCC	Patients with HCC underwent biopsy or surgery/highly-differentiated *vs* moderate-differentiated *vs* poorly-differentiated	-/SonoVue/-	RT and MTT increased from poorly- to moderate- to highly-differentiated. Enhancement rates decreased from poorly- to moderate- to highly-differentiated
Amadori *et al*[32], 2018	Prospective/37	CRC Liver metastasis	Patients underwent chemotherapy/chemotherapy *vs* chemotherapy plus bevacizumab	iU22 vision 2008/SonoVue/QLAB	Reduction of PI and AUC and increase of TPI correlated with higher PFS in chemotherapy plus bevacizumab group
Wildner *et al*[25], 2019	Prospective/148	Focal liver lesion	Patients with focal liver lesion and subsequent final diagnosis/HCC, CCC, PCA, CRC, BC, MM, FNH	Sequoia 512/SonoVue/VueBox	Higher PE and WiWoAUC in HCC than CRC. Lower Relative intensity signal for PCA and CRC compared to HCC at 30 and 120 s after PE
Mogensen *et al*[33], 2017	Prospective/12	CRC liver metastasis	Patients underwent chemotherapy/chemotherapy *vs* chemotherapy plus bevacizumab	Logiq E9/SonoVue/VueBox	Early changes of PE correlate with tumor shrinkage at CT scan
Zocco *et al*[28], 2013	Prospective/28	HCC	Patients treated with sorafenib/Responders' *vs* non-responders	iU22/SonoVue/QLAB	PI, Pw and AUC 10% decrease correlate with response to therapy. AUC 10% decrease and increased/unchanged TPI and MTT are associated with longer survival. Decrease of Pw is associated with PFS
Zhan *et al*[20], 2019	Prospective/35	HCC	Patients with HCC underwent microwaves ablation	Acuson Sequia/Sonovue/SonoLiver	Positive correlation between MVD, VEGF and IMAX; negative correlation

					between MVD and TTP. TTP was an independent predictor of OS
Wildner *et al*[26], 2014	Prospective/43	HCC, ICC	Patient with proven HCC and ICC	Acuson Sequoia 512/SonoVue/VueBox	FT and MTT were lower in ICC than HCC. Relative signal intensity was lower in ICC than HCC in all time point after PE
Frampas *et al*[69], 2013	Prospective/19	HCC	Patients with HCC treated with sorafenib or sunitinib/RECIST progressor *vs* non-progressor	Aplio XV/SonoVue/Vascular Recognition Imaging" mode	AUC decrease ≥ 40% correlated with RECIST non-progression
Lassau *et al* [29], 2011	Prospective/42	HCC	Patients with HCC treated with Bevacizumab	Aplio scanner/SonoVue/Contrast Harmonic Imaging-Quantification software	AUC, WiAUC, WoAUC and TPI decrease correlate with tumor response. TPI decrese correlate with PFS. AUC and WoAC decrease correlate with OS

AIU: Arbitrary intensity unit; AUC: Area under the curve; AUROC: Area under the receiver operating characteristic; BC: Breast cancer; CCC: Cholangiocarcinoma; CRC: Colorectal cancer; CT: Computed tomography; D-CEUS: Dynamic contrast-enhanced ultrasound; FNH: Focal nodular hyperplasia; HCC: Hepatocellular carcinoma; HVPG: Hepatic vein portal pressure; MM: Malignant melanoma; MTT: Mean transit time; MVD: Microvascular density; MVI: Microvascular invasion; OS: Overall survival; PCA: Pancreatic adenocarcinoma; PE: Peak enhancement; PFS: Progression free survival; PI: Peak intensity; Pw: Slope coefficient of wash-in; RECIST: Response evaluation criteria in solid tumors; RT: Rise time; TPI: Time to peak intensity; TTP: Time to peak; UCA: Ultrasound contrast agent; WiAUC: Wash-in area under the curve; WoAUC: Wash-out area under the curve; WiWoAUC: Wash-in and wash-out area under the curve.



DOI: 10.3748/wjg.v29.i25.4021 **Copyright** ©The Author(s) 2023.

Figure 2 Dynamic contrast-enhanced ultrasound and time-intensity curves of the liver. A: Hypoechoic mass (hepatocellular carcinoma) of IV liver segment visualized in B-mode ultrasound; B and C: Contrast-enhanced ultrasound with corresponding time-intensity curve of the liver mass.

Biological behaviour

The vascular structure of a tumour lesion is closely associated with microscopic features such as the degree of differentiation, the proliferation index and growth rate, the presence of necrosis, the angiogenesis and the vascular invasion[17]. Therefore, the analysis of vascularization parameters could be different according to each of the aforementioned characteristics.

Huang *et al*[18] investigated the correlation between perfusion parameters and Ki-67 in hepatocellular carcinoma (HCC) patients. Prospective analysis of one hundred twenty patients showed that the peak enhancement (PE) difference between HCC and distal liver parenchyma in the Kupffer phase was significantly higher in low Ki-67 (< 10%) group compared to high Ki-67 (≥ 10%) group, probably due to lower concentration of Kupffer cells in poorly differentiated neoplasms[18]. Supporting this, differences in D-CEUS parameters were found among HCC differentiation classes. Specifically, rise time (RT) and time to peak (TTP) demonstrated a significant positive correlation with differentiation degree, whereas

enhancement rate was significantly higher in lesions with less differentiation[19].

Regarding the pure vascular features of tumors, Zhan *et al*[20] demonstrated that histological determined microvessel density and vascular endothelial grow factor stain positively correlated with maximum intensity (MI), while microvessel density negative correlated with TTP[20]. This suggested that D-CEUS parameters could provide a reliable characterization of the microvascular scaffold of lesions. In another study Dong *et al*[21] perform a retrospective analysis of D-CEUS characteristics of HCC to investigate the capability to predict microvascular invasion in a cohort of 16 patients who underwent subsequent surgery. They found that wash-in area under the curve (WiAUC) and wash-out area under the curve (WoAUC) were significantly higher in microvascular invasion positive group ($P < 0.05$), especially when the ROI was positioned in the marginal area of the lesion. This phenomenon is likely to be attributed to the formation of arteriovenous fistulas during vascular invasion, which leads to an increase in blood flow[21]. In contrast, using different UCA, Li *et al*[22] found no correlation between quantitative parameters and microvascular invasion in thirty-one resected HCCs[22]. One of the most significant differences between second-generation UCAs is their resistance to US wave pressure, which could explain this apparent contradiction in results[23].

This evidence suggests that D-CEUS may serve as a biomarker of the biological behaviour and microscopic characteristics of HCC, detecting the abnormal vascularization characteristics that developed as the disease progressed.

Differential diagnosis

Quantitative analysis of perfusion parameters demonstrated a promising potential to distinguish between benign and malignant FLLs. In a retrospective study including one hundred and thirty-nine FLLs of which forty-four benign and ninety-five malignant, benign lesions showed a significantly higher late-phase ratio (ratio between signal intensities of lesion and surrounding tissue in late phase, LPR) compared to malignant counterpart, showing an area under the curve (AUC) of 0.9, with maximal sensitivity (100%) but low specificity (56.8%). Interestingly, the difference in LPR remains significant also comparing hypoechoic haemangiomas to malignant lesions, suggesting the ability to distinguish a real wash-out from other phenomena. Although RT demonstrated a lower AUC (0.58) for distinguishing benign from malignant lesions, it demonstrated outstanding accuracy (AUC: 0.91) when applied to the distinction between haemangioma and malignancy. Furthermore, considering only benign lesions, haemangioma and adenoma displayed longer mean RT values than other benign lesions[24]. This suggests that quantitative analysis could increase the diagnostic accuracy between benign liver lesions and in challenging situations, such as benign lesions with moderate hyperenhancement (*e.g.*, thrombosed haemangioma) or modest hypoenhancement in late phase (*e.g.*, certain subtypes of hepatic adenoma).

D-CEUS might be helpful to differentiate hypervascular tumours like HCC from other malignant liver lesions that are predominantly necrotic and hypovascular. Wildner *et al*[25], analysing D-CEUS parameters in HCC and different secondary liver lesions showed that PE normalized for parenchyma signal and wash-in-wash-out area under the curve (WiWoAUC) were significantly higher in HCC compared to colorectal cancer (CRC) metastasis and relative signal intensity at 30 and 120 s after PE was significantly lower for pancreatic adenocarcinoma and CRC liver metastasis compared to HCC[25]. These results clearly suit to the hypervascular nature of HCC in contrast to the more necrotic and weakly centrally vascularized secondary liver lesions of other primitive cancers. While arterial phase parameters are significantly different between HCC and CRC metastatic liver masses, their applicability to differentiate HCC from other primary intrahepatic malignancies is unfitted. Previously, the same authors had investigated the differences between HCC and intrahepatic cholangiocellular carcinoma (ICC) showing no significant differences in arterial phase parameters while ICC group showed lower values of mean transit time (MTT) and fall time in portal and venous phase. Furthermore, relative signal intensity was significantly lower in ICC compared to HCC in all time points after PE at 40 s, 80 s, 100 s and 120 s[26]. Actually, the main difference between HCC and ICC at CEUS is the early and marked wash-out in portal phase for ICC[4]. Objective quantification of the wash-out phenomenon using D-CEUS could improve the diagnostic accuracy of differentiating lesions with similar portal and late phase hypoenhancement.

Prognosis prediction

One of the most promising applications of D-CEUS is the assessment of liver tumour response to treatment, particularly in HCC where chemotherapy regimens are mostly based on vascular-targeting agents[27]. To this purpose, Zocco *et al*[28] investigated the role of D-CEUS to early detect vascular changes in HCC patients treated with sorafenib and to predict response to therapy and prognosis. The results showed that a decrease in AUC, peak intensity (PI), and slope of wash-in (Pw) between T0 (baseline) and T1 (after fifteen days of therapy) was significantly associated with response to therapy assessed with RECIST criteria after two months of treatment. Furthermore, 10% decrease in AUC was significantly associated with longer survival as increased/unchanged of time to PI (Tp) and MTT, while a Pw reduction was significantly associated with progression-free survival (PFS)[28]. Similar results were obtained by Lassau *et al*[29] considering patients with advanced HCC treated with bevacizumab. D-CEUS was performed before treatment and at days 3, 7, 14, and 60 after treatment; and every 2 mo

thereafter. Interestingly, the results showed that very early changes in D-CEUS characteristics correlated with response to therapy and prognosis. Particularly, the decreases in AUC, AUC during wash in, AUC during washout, and time to PI (TPI) at day 3 were significantly associated with RECIST response at 2 mo. Furthermore, PI, AUC and AUC during washout changes at day 3 were correlated with PFS and overall survival (OS)[29]. These results suggest that effects of antiangiogenetic treatments can be early assessed quantifying the perfusion parameters and could allow for a tempestive intervention when relative prognosis is unfavourable.

D-CEUS could also have a role in predicting the prognosis of HCC patients who received loco-regional treatments. In HCC patients undergoing microwave ablation, TTP evaluated before the procedure was confirmed as an independent predictor of OS[20]. Similarly, the WiAUC, the WoAUC and the WiWoAUC ratio between HCC lesion and surrounding liver parenchyma evaluated before thermal ablation were significantly associated with survival[30]. As a consequence, quantitative perfusion evaluation might provide additional information useful to plan treatment procedures.

Considering non-HCC malignant liver lesions, different studies evaluated D-CEUS modifications to predict early response to therapies. In patients with liver metastasis of melanoma treated with sorafenib, TTP and MTT increased significantly in responders group at 15 and 56 d assessment[31]. Furthermore, CRC-metastatic patients treated with chemotherapy plus bevacizumab showed changes in derived PI, TPI and AUC at day 15 that were significantly correlated with PFS, however these modifications were not related with tumor response or survival[32]. In contrast, Mogensen *et al*[33] observed a significant association between PE early variation and computed tomography (CT) dimensional tumour decrease in patients treated with chemotherapy plus bevacizumab[33]. Variability in these results could be explained by limitations of 2-dimensional imaging techniques used in all the discussed studies. In the future, 3-dimensional D-CEUS might provide a more accurate evaluation of entire tumor features[34].

Non-oncological hepatic application of D-CEUS

Despite most studies primarily focused on neoplastic liver disease, the application of quantitative analysis of perfusion parameters has also been explored in chronic liver disease. The TICs of the liver parenchyma can provide information's of intrahepatic blood flow and, indirectly, of portal vein pressure, either that could be altered by liver fibrosis.

In the past, different studies evaluated transit time between vessels to estimate the intrahepatic blood flow and to assess liver fibrosis stage. It was showed that hepatic vein transit time decreased as severity of histologically proved chronic hepatopathy increased, thus allowing diagnosis of severe fibrosis with an accuracy of 79%[35,36]. In addition, hepatic vein arrival time and intrahepatic transit time were correlated with hepatic venous pressure gradient (HVPG), with an area under the receiver operating characteristic (AUROC) of 0.97 for HVPG > 10 mmHg and 0.94 for HVPG > 12 mmHg, respectively[37, 38].

Recently, perfusion parameters analysis of liver parenchyma showed a decrease of amplitude-parameters and an increase of time-dependent parameters according to grade of portal pressure assessed with HVPG. Interestingly, PI resulted significantly negative correlated with portal hypertension and showed high accuracy (100% for both specificity and sensitivity) to predict clinical significant portal hypertension using a cut-off of 23.3 dB in patients with liver cirrhosis[39].

PANCREATIC DISEASES

Existing evidence about the usefulness of D-CEUS for pancreatic diseases is very limited and is resumed in Table 3. Characterization and differential diagnosis of benign and malignant pancreatic lesions are the focus of the available research. Figure 3 depicts an example of D-CEUS in pancreatic disease.

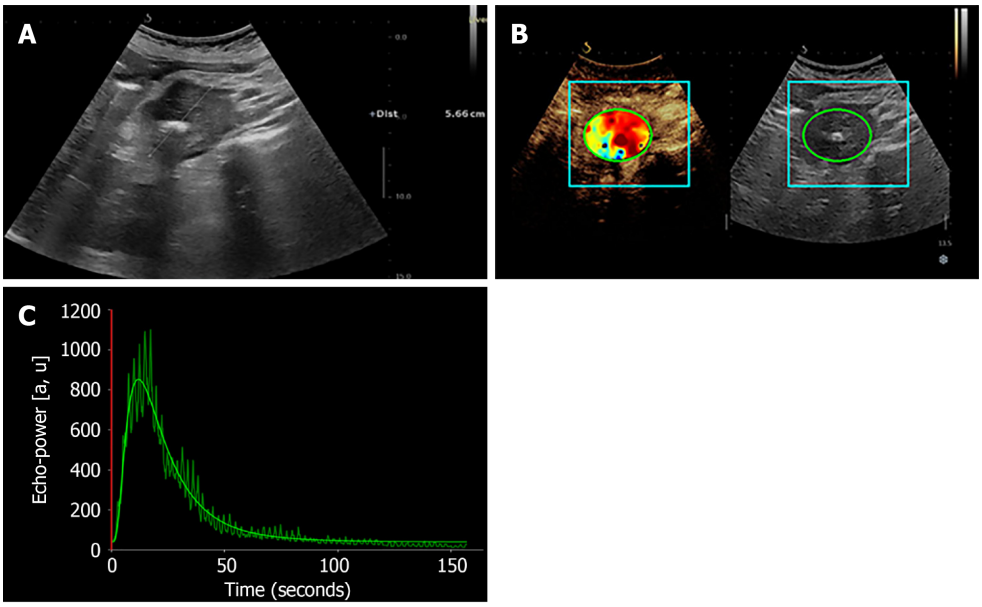
One of the first studies regarding the perfusion analysis of pancreatic cancer was conducted by D'Onofrio *et al*[40]. Prospectively, ten patients with suspected pancreatic ductal adenocarcinoma (PDAC) (as confirmed by histology) underwent CEUS with subsequent quantitative perfusion analysis. The results showed a significant difference in PE and ascending curve between PDAC and normal pancreatic parenchyma, providing an objective quantification of enhancement for the assessment of pancreatic lesion[40].

Chronic pancreatitis (CP), localized autoimmune pancreatitis (AIP), and paraduodenal pancreatitis can present CT and magnetic resonance imaging abnormalities identical to PDAC and, vice versa, potentially resectable malignant lesions can be misdiagnosed due to their similarities with benign masses[41]. In such instances, D-CEUS may reveal the pathophysiological differences between highly vascularized inflammatory lesions and essentially necrotic malignant masses, enabling a correct differentiation between benign lesions and cancer. To compare CP to PDAC, Kersting *et al*[42] performed D-CEUS in sixty undetermined pancreatic lesions that were histologically characterized as PDAC (fourty-five) or inflammatory lesion in CP (fifteen). The grouped analysis of TICs showed that TTP and arrival time were significantly prolonged in PDAC compared to CP. On the contrary, no differences were detected in MI and AUC between the two pathological conditions[42]. Regarding AIP, D-CEUS with quantitative analysis has the potential to make pre-operative differential diagnosis between focal-type

Table 3 Dynamic contrast-enhanced ultrasound and pancreatic diseases

Ref.	Study design/number of patients	Object of D-CEUS	Population/groups	Machine/UCA/Software	Significant results ($P < 0.05$)
Yang *et al* [47], 2023	Retrospective/42	pNET	Patients with histopathologically proved pNET/G1, G2, G3, pNEC	Acuson Sequoia, Acuson Oxana2/SonoVue/VueBox	rPE, rMTT and rAUC were higher in pNETs G1/G2 than G3/pNECs
Zhang *et al* [45], 2020	Prospective/11	LAPC	Patient with LAPC underwent chemoradiotherapy	Acuson Oxana2/SonoVue/SonoLiver	MI decreased after chemoradiotherapy
Vitali *et al* [43], 2015	Prospective/20	PC, focal AIP	Patients with diagnosis of AIP *vs* histologically proved PC	Acuson Sequoia 512, S200/SonoVue/VueBox	The difference in PE (dPE) between lesion and surrounding parenchyma in AIP was lower compared to dPE in PC
D'Onofrio *et al*[40], 2014	Prospective/10	Suspected PDAC	Patients with suspected and then histologically proved PDAC	Acuson S2000/SonoVue/VueBox	PE and ascending curve values were different between lesion and adjacent parenchyma
Kersting *et al* [42], 2009	Prospective/60	Undefined pancreatic lesion	Patients with undefined pancreatic lesion underwent biopsy/PDAC *vs* CP	Sonoline Elegra/SonoVue/Axius ACQ	TTP and AT were longer in PDAC compared to focal masses in CP

AIP: Autoimmune pancreatitis; AT: Arrival time; CP: Chronic pancreatitis; D-CEUS: Dynamic contrast-enhanced ultrasound; LAPC: Local advanced pancreatic cancer; MI: Maximum intensity; PC: Pancreatic cancer; PDAC: Pancreatic ductal adenocarcinoma; PE: Peak enhancement; pNET: Pancreatic neuroendocrine tumor; pNEC: Pancreatic neuroendocrine carcinoma; rAUC: Relative area under the curve; rMTT: Relative mean transit time; rPE: Relative peak enhancement; TTP: Time to peak; UCA: Ultrasound contrast agent.



DOI: 10.3748/wjg.v29.i25.4021 **Copyright** ©The Author(s) 2023.

Figure 3 Dynamic contrast-enhanced ultrasound and time-intensity curves of the pancreas. A: Hypoechoic mass (adenocarcinoma) of pancreatic head in B-mode ultrasound; B and C: Contrast-enhanced ultrasound with corresponding time-intensity curve of the pancreatic lesion.

AIP and PDAC non-invasively. Vitali *et al*[43] compared D-CEUS parameters of three patients with focal AIP with seventeen PDAC patients. Specifically, the difference between PE of PDAC and circumjacent normal parenchyma was significantly lower as compared to AIP. Significant was also the difference between wash in index perfusion (WiPI = WiAUC/RT) of PC and AIP[43]. In another study, TICs of AIP lesions showed delayed and higher enhancement compared to PDAC. Among all CEUS perfusion parameters, ratio of PE, WiAUC, wash-in rate (WiR), WiPI, WoAUC, WiWoAUC, and wash-out rate (WoR) between pancreatic lesion and surrounding normal pancreatic tissue were significantly higher in AIP lesions than PDAC lesions[44]. In cases of diffuse AIP, quantitative perfusion analysis is not suggested since there is no healthy parenchyma for comparison, which is necessary to enhance the

comparability of the results regardless of exam- or patient-related factors[42].

Similarly to perfusion analysis for malignant liver lesions, D-CEUS could be considered to evaluate the response to therapies in PDAC. Recently, Zhang *et al*[45] investigated the role of D-CEUS to monitor the response to chemoradiotherapy in eleven patients with local advanced pancreatic cancer. They performed D-CEUS at baseline and after four weeks of therapy and analyzed the variation of TICs and related parameters. The rising and falling slope rates of TICs diminished after four weeks, and the percentage of MI decreased significantly compared to the surrounding normal parenchyma[45]. Since MI is related to tumour microvascular density, its reduction is coupled with a decrease in lesion blood perfusion, and the quantification of this consequence might reflect the objective efficacy of chemotherapy.

Lastly, D-CEUS could provide information in other types of pancreatic tumors. It has been proven that pancreatic neuroendocrine tumors (pNETs) with different histopathological grades have differences in tumor microvascular perfusion[46], therefore Yang *et al*[47] analyzed the correlation between perfusion analysis and histopathological grades of pNETs. In forty-two patients, the TICs shape of grade 1 (G1)/grade (G2) lesions were significantly different compared to TICs of grade 3 (G3)/pancreatic neuroendocrine carcinomas (pNECs). Significant differences were revealed at relative RT, relative MTT and relative AUC which were higher in G1/G2 than G3/pNECs. ROC analysis showed that relative AUC had the higher accuracy to distinguish the two groups[47]. The D-CEUS analysis and quantitative parameters have the potential value to non-invasively predict the biological behaviour of pNETs.

INFLAMMATORY BOWEL DISEASES

Table 4 summarizes the evidence regarding the role of D-CEUS in inflammatory bowel diseases, and Figure 4 depicts a TIC derived from intestinal wall examination. These studies are mainly focused on Crohn's disease (CD).

D-CEUS and inflammatory/fibrotic disease

TICs represent the perfusion of a tissue, and we would expect a difference in perfusion parameters not only when comparing fibrosis to inflammation, but also when considering various degrees of inflammation.

Girlich *et al*[48] described for the first time the difference in perfusion parameters between CD and healthy gut. As expected, the differences were substantially with significantly higher PE and regional blood volume, and longer TTP of thickness bowel wall of CD patients[48]. In another study, the same authors investigated the correlation between perfusion parameters and histopathological characteristics of the gut wall in surgically treated CD patients, confirming that TTP was negatively correlated with the histological inflammatory score[49]. Similarly, a higher PE, regional blood flow and regional blood volume, and shorter TTP were significantly correlated with high vascular density defined as the presence of more than two hundred sixty five vessels per field on histological examination[50]. On the contrary, Ripollés *et al*[51] showed a non-significant association of TTP with inflammatory or fibrosis histological score, however they used different histological scores and had longer time between CEUS and surgery (34.5 ± 17.3 *vs* 4.7 ± 4.7 d)[51].

To assess the differences between fibrotic or inflammatory CD, Nylund *et al*[52] compared sixteen patients with fibrotic disease undergoing surgery to seventeen patients with medically treated active inflammatory disease. In inflammatory disease, the blood volume and blood flow were significantly higher compared to fibrotic disease, while MTT was not significantly different between the two groups. Interestingly, blood volume/bowel wall thickness ratio showed a high accuracy to predict surgery[52]. Similarly, Quaia *et al*[53] found a significant difference in blood volume related parameters (PE, AUC, WiAUC, WoAUC, WiR and, WiPI) between fibrotic strictures and inflammatory strictures among patients with CD, with the latter having higher values. However, TTP showed no significant differences between the two groups[53]. These findings imply that D-CEUS can detect the microvascular differences between fibrotic and inflammatory tissue and allows non-invasive differentiation of CD phenotypes.

Regarding ulcerative colitis (UC), only one prospective study investigated the relationship between perfusion parameters and histopathological findings. In this study, TTP/Peak(%) showed a strong negative correlation with histopathological inflammatory activity score[54].

D-CEUS and clinical outcomes

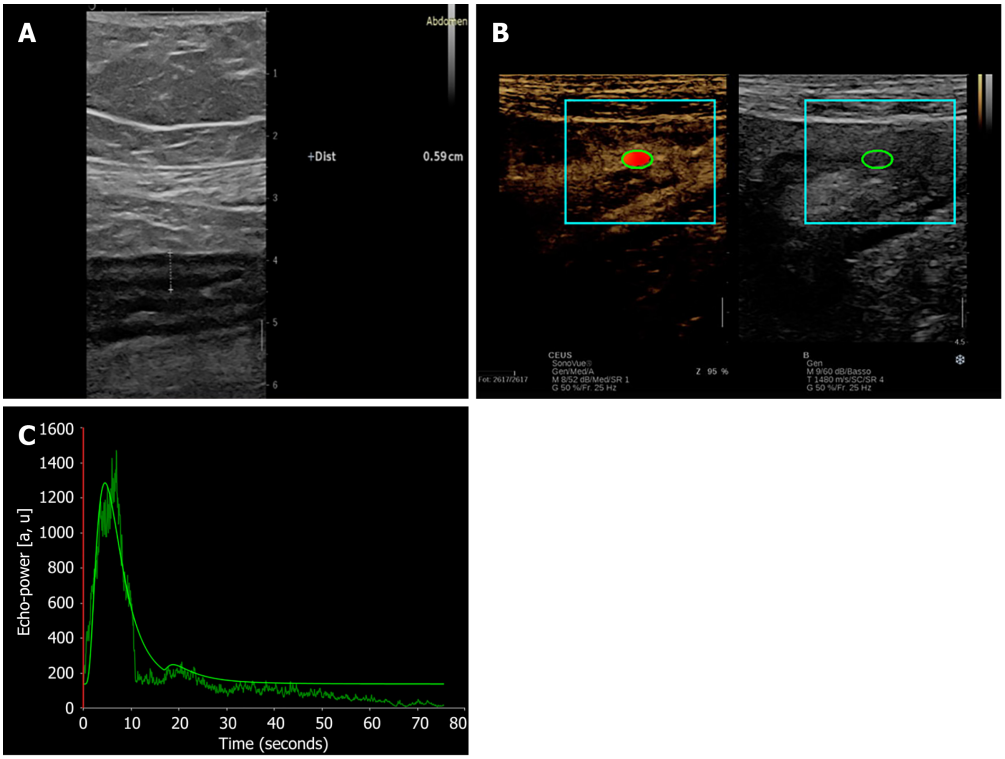
Given the negative correlation with inflammation, Peak% > 40.5% and TTP < 35 seconds had a high positive predictive value (94%) and a high negative predictive value (92.3%) for active disease, respectively[50].

It has also been shown that the evaluation of PE and AUC is a useful tool to assessing the severity of CD when the ultrasound global assessment and colorDoppler imaging criteria are indeterminate. Particularly, PE > 23 dB showed a sensitivity and specificity of 90% and 89.5%, respectively, to distinguish moderate from severe disease[55]. Using this cut-off to identify patients with severe disease, Wilkens *et*

Table 4 Dynamic contrast-enhanced ultrasound and inflammatory bowel diseases

Ref.	Study design/number of patients	Object of D-CEUS	Population/groups	Machine/UCA/Software	Significant results ($P < 0.05$)
Laterza *et al* [60], 2021	Prospective/44	CD	Patients with CD treated with anti-TNFα/responders *vs* non-responders	iU22/SonoVue/QLAB	Correlation between decrease in PI, AUC, Pw, and MTT and response to therapy
Goertz *et al* [57], 2018	Prospective/18	CD and UC	Patients with CD or UC treated with vedolizumab/responders *vs* non-responders	Acuson S2000/SonoVue/VueBox	WiR was lower in responders' group after 14 wk
Wilkens *et al* [56], 2018	Retrospective/104	CD	Patients with severe CD underwent CEUS/normal *vs* atypical intensity decline on CEUS	iU22/Definity/QLAB	AUC, wash-out time, and intensity at 60s and 120s were higher in atypical decline group and this correlated with bad outcomes
Quaia *et al*[53], 2017	Prospective/65	CD	Patients with CD with terminal ileal loop stricture histologically characterized/inflammatory *vs* fibrostenotic disease	iU22/SonoVue/VueBox	PE, WiR, WiPI, AUC, WiAUC and WoAUC were higher in inflammatory group compared to fibrostenotic gruoup. TTP was not different between the two groups
Medellin-Kowalewski *et al*[55], 2016	Retrospective/127	CD	Patients with CD underwent US and CEUS	iU22/Definity/QLAB	PE correlate with wall thickness
Quaia *et al*[61], 2016	Prospective/50	CD	Patient with CD underwent medical treatment/responders *vs* non-responders	iU22/SonoVue/VueBox	Changes in PE, WiR, WoR, WiPI, AUC, WiAUC, and WoAUC from baseline to six weeks after therapy differed between responders and non-responses
Socaciu *et al* [58], 2015	Prospective/38	CD and UC	Patients with CD or CU candidate for medical treatment	Logiq 7/SonoVue/SonoLiver	Logarithm of AUC correlated with endoscopic improvement in both diseases
Saevik *et al* [59], 2014	Prospective/14	CD	Patients with CD started medical treatment/remission *vs* treatment failure	Logiq E9/SonoVue/VueBox	PE, WiR, WoR, and WiAUC were different between two groups at 1 mo of treatment
Romanini *et al* [50], 2014	Prospective/33	CD	Patients with CD undergoing colonoscopy and biopsy	Sequoia 512/SonoVue/Qontrast	Correlation between high vascular density and Peak% and regional blood flow
Ripollés *et al* [51], 2013	Prospective/25	CD	Patients with CD undergoing elective bowel resection/inflammatory *vs* fibrostenotic disease	Aplio 80/SonoVue/Software in Aplio 80 system	The percentage of increase in contrast enhancement of the bowel wall in inflammatory lesions was greater than fibrotic lesions
Nylund *et al* [52], 2013	Prospective/33	CD	Patient with CD underwent surgery or medical treatment/inflammatory *vs* fibrostenotic disease	Logiq E9/SonoVue/Custom software	Blood flow and blood volume were higher in the medical group compared to surgery group
Girlich *et al* [54], 2012	Prospective/11	UC	Patients with UC undergoing endoscopy	Logiq E9/SonoVue/Qontrast	Negative correlation between TTP/Peak% and histopathological score
Girlich *et al* [49], 2011	Prospective/20	CD		Logiq 9/SonoVue/Qontrast	Negative correlation between TTP and histopathological score. Positive correlation with single items of the score
Girlich *et al* [48], 2009	Prospective/20	CD	Patients with active CD *vs* healthy volunteers	Logiq 9/SonoVue/Qontrast	Higher PE and regional blood volume and shorter TTP in CD

AUC: Area under the curve; CD: Crohn's disease; CEUS: Contrast-enhanced ultrasound; D-CEUS: Dynamic contrast-enhanced ultrasound; MTT: Mean transit time; PE: Peak enhancement; PI: Peak intensity; Pw: Slope coefficient of wash-in; TNF-α: Tumor necrosis factor-α; TTP: Time to peak; UC: Ulcerative colitis; UCA: Ultrasound contrast agent; US: Ultrasound; WiAUC: Wash-in area under the curve; WiPi: Wash-in ratio index; WiR: Wash-in rate; WoR: Wash-out rate.



DOI: 10.3748/wjg.v29.i25.4021 **Copyright** ©The Author(s) 2023.

Figure 4 Dynamic contrast-enhanced ultrasound and time-intensity curves of the bowel wall. A: B-mode ultrasound features of ileal bowel wall thickening in Crohn's disease; B and C: Contrast-enhanced ultrasound with corresponding time-intensity curve of the bowel wall thickening.

al[56] investigated the clinical outcomes in twenty patients with severe disease in whom they observed an atypical, prolonged intestinal washout due to the stuck bubble phenomenon (AUC > 20000 AIU) compared to patient with severe disease and AUC < 20000 AIU (control group). They found a significative higher rate of surgery and a trend toward more combination therapies in study group. Interestingly, they ascribed the stuck bubbles phenomena to the attachment of microbubbles to active leukocytes on the endothelium; if confirmed, this might be utilized as a tool for targeted therapy[56].

Assessment of perfusion parameters is important for identifying disease status, as well as monitoring and predicting the efficacy of therapies. Indeed, D-CEUS measurements changed significantly between clinical- and endoscopic-assessed responders and non-responders with CD and UC following treatments[57,58]. In a prospective study, Saevik *et al*[59] included fourteen patients with acute CD who started treatment with steroids or tumor necrosis factor-α (TNF-α) inhibitors. CEUS was performed before starting therapy and at one, three and twelve months. At one month, the differences between patients who achieved clinical remission and those who had treatment failure during the follow-up period were significant. Particularly, PE, WiAUC, WiR and WoR was significantly lower in effective treatment group[59]. The reduction in perfusion parameters could be related to a decrease in inflammation and, thus, a treatment response. Recently, it was demonstrated that the reduction in PI, AUC, Pw, and MTT was higher in patients responding to anti-TNF-α therapy after two weeks than in patients who relapsed within six months of treatment initiation, who displayed not only a lower early reduction in perfusion parameters but also an increase in PI after twelve weeks[60]. Changes in quantitative perfusion analysis parameters between baseline and six weeks after therapy initiation distinguished responders from non-responders defined by clinical and endoscopic evaluation at twelve weeks[61]. This highlights the potential for D-CEUS to detect therapy-induced modifications in the pathologic bowel wall and support clinicians in disease management.

OTHER GASTROINTESTINAL DISEASES

The investigation of perfusion parameters with D-CEUS could be an informative tool in the diagnosis and prognosis of other gastrointestinal diseases, such as gastric cancer[62]. In a prospective study including forty-three patients with advanced gastric cancer, Joo *et al*[63] showed a good feasibility of CEUS (88.4%) and a significant difference in PI and AUC according to differentiation status of the tumor. Localization in the upper stomach and an ulcerated phenotype were the limiting variables for D-CEUS feasibility[63]. Regarding the CRC, the difference in AUC was significantly related with tumor

necrosis and T stage[64], suggesting a possible role of D-CEUS in predicting tumor microenvironment characteristics and behavior. Furthermore, dynamic contrast enhanced endoscopic ultrasound (D-CE-EUS) showed a significant correlation between RT and vessel density in patients with left side colonic tumors[65], indicating that perfusion analysis might be useful to predict outcomes of antiangiogenic treatment as Lassau *et al*[66] has showed in a multicentric study including over one thousand D-CEUS evaluations in more than five hundred patients with solid tumor treated with antiangiogenic therapy [66]. In particular, D-CEUS blood volume related parameters showed significant early changes in gastrointestinal stromal tumours treated with masitinib, predicting positron emission tomography-CT outcome[67].

Concerning non-neoplastic bowel diseases, different studies described the CEUS aspects of various inflammatory bowel diseases, including abscesses, acute appendicitis, diverticulitis, vascular bowel disease, such as intestinal ischemia, and graft *vs* host disease[68]. To the best of our knowledge, no specific study employing D-CEUS in the aforementioned conditions has been published yet; however, it would be desirable to investigate the potential usefulness of quantitative perfusion analysis in predicting pathological features and prognosis also in this field.

CONCLUSION

The quantification of perfusion parameters in CEUS has several applications in gastrointestinal neoplastic and inflammatory disorders. Everything that is visible with ultrasound can be measured, and this has allowed D-CEUS to be employed within the pancreas and digestive system in addition to the liver evaluation. The objective assessment of tissue perfusion is crucial for the evaluation of all disorders in which the vascular component plays a key pathophysiological role, such as malignant tumours and inflammatory bowel disease. However, the limited availability of large studies and the heterogeneity of the technologies employed have precluded the standardization of this approach which potentially represents a valuable tool for clinical practice in management of gastrointestinal diseases.

FOOTNOTES

Author contributions: Paratore M, Garcovich M and Zocco MA contributed to conceptualization, review of the literature and collection of data, writing first draft, review and editing; Ainora ME, Riccardi L and Gasbarrini A contributed to conceptualization, supervision, review, and editing; all authors revised the manuscript critically for intellectual content and have approved the final version.

Conflict-of-interest statement: Authors declare no conflict of interests for this article.

Open-Access: This article is an open-access article that was selected by an in-house editor and fully peer-reviewed by external reviewers. It is distributed in accordance with the Creative Commons Attribution NonCommercial (CC BY-NC 4.0) license, which permits others to distribute, remix, adapt, build upon this work non-commercially, and license their derivative works on different terms, provided the original work is properly cited and the use is non-commercial. See: https://creativecommons.org/Licenses/by-nc/4.0/

Country/Territory of origin: Italy

ORCID number: Mattia Paratore 0000-0002-7546-8041; Matteo Garcovich 0000-0002-5805-7953; Maria Elena Ainora 0000-0001-5847-1065; Laura Riccardi 0000-0001-6249-0314; Antonio Gasbarrini 0000-0003-4863-6924; Maria Assunta Zocco 0000-0002-0814-9542.

S-Editor: Fan JR
L-Editor: A
P-Editor: Xu ZH

REFERENCES

1 **Braden B**, Ignee A, Hocke M, Palmer RM, Dietrich C. Diagnostic value and clinical utility of contrast enhanced ultrasound in intestinal diseases. *Dig Liver Dis* 2010; **42**: 667-674 [PMID: 20598952 DOI: 10.1016/j.dld.2010.05.018]
2 **Chung YE**, Kim KW. Contrast-enhanced ultrasonography: advance and current status in abdominal imaging. *Ultrasonography* 2015; **34**: 3-18 [PMID: 25342120 DOI: 10.14366/usg.14034]
3 **Sidhu PS**, Cantisani V, Dietrich CF, Gilja OH, Saftoiu A, Bartels E, Bertolotto M, Calliada F, Clevert DA, Cosgrove D, Deganello A, D'Onofrio M, Drudi FM, Freeman S, Harvey C, Jenssen C, Jung EM, Klauser AS, Lassau N, Meloni MF, Leen E, Nicolau C, Nolsoe C, Piscaglia F, Prada F, Prosch H, Radzina M, Savelli L, Weskott HP, Wijkstra H. The EFSUMB Guidelines and Recommendations for the Clinical Practice of Contrast-Enhanced Ultrasound (CEUS) in Non-

Hepatic Applications: Update 2017 (Long Version). *Ultraschall Med* 2018; **39**: e2-e44 [PMID: 29510439 DOI: 10.1055/a-0586-1107]

4 **Dietrich CF**, Nolsøe CP, Barr RG, Berzigotti A, Burns PN, Cantisani V, Chammas MC, Chaubal N, Choi BI, Clevert DA, Cui X, Dong Y, D'Onofrio M, Fowlkes JB, Gilja OH, Huang P, Ignee A, Jenssen C, Kono Y, Kudo M, Lassau N, Lee WJ, Lee JY, Liang P, Lim A, Lyshchik A, Meloni MF, Correas JM, Minami Y, Moriyasu F, Nicolau C, Piscaglia F, Saftoiu A, Sidhu PS, Sporea I, Torzilli G, Xie X, Zheng R. Guidelines and Good Clinical Practice Recommendations for Contrast-Enhanced Ultrasound (CEUS) in the Liver-Update 2020 WFUMB in Cooperation with EFSUMB, AFSUMB, AIUM, and FLAUS. *Ultrasound Med Biol* 2020; **46**: 2579-2604 [PMID: 32713788 DOI: 10.1016/j.ultrasmedbio.2020.04.030]

5 **Chiorean L**, Tana C, Braden B, Caraiani C, Sparchez Z, Cui XW, Baum U, Dietrich CF. Advantages and Limitations of Focal Liver Lesion Assessment with Ultrasound Contrast Agents: Comments on the European Federation of Societies for Ultrasound in Medicine and Biology (EFSUMB) Guidelines. *Med Princ Pract* 2016; **25**: 399-407 [PMID: 27318740 DOI: 10.1159/000447670]

6 **Fröhlich E**, Muller R, Cui XW, Schreiber-Dietrich D, Dietrich CF. Dynamic contrast-enhanced ultrasound for quantification of tissue perfusion. *J Ultrasound Med* 2015; **34**: 179-196 [PMID: 25614391 DOI: 10.7863/ultra.34.2.179]

7 **Dietrich CF**, Averkiou MA, Correas JM, Lassau N, Leen E, Piscaglia F. An EFSUMB introduction into Dynamic Contrast-Enhanced Ultrasound (DCE-US) for quantification of tumour perfusion. *Ultraschall Med* 2012; **33**: 344-351 [PMID: 22843433 DOI: 10.1055/s-0032-1313026]

8 **Arditi M**, Frinking PJ, Zhou X, Rognin NG. A new formalism for the quantification of tissue perfusion by the destruction-replenishment method in contrast ultrasound imaging. *IEEE Trans Ultrason Ferroelectr Freq Control* 2006; **53**: 1118-1129 [PMID: 16846144 DOI: 10.1109/tuffc.2006.1642510]

9 **Leen E**, Averkiou M, Arditi M, Burns P, Bokor D, Gauthier T, Kono Y, Lucidarme O. Dynamic contrast enhanced ultrasound assessment of the vascular effects of novel therapeutics in early stage trials. *Eur Radiol* 2012; **22**: 1442-1450 [PMID: 22302501 DOI: 10.1007/s00330-011-2373-2]

10 **Dietrich CF**, Dong Y, Froehlich E, Hocke M. Dynamic contrast-enhanced endoscopic ultrasound: A quantification method. *Endosc Ultrasound* 2017; **6**: 12-20 [PMID: 28218195 DOI: 10.4103/2303-9027.193595]

11 **Lassau N**, Chebil M, Chami L, Bidault S, Girard E, Roche A. Dynamic contrast-enhanced ultrasonography (DCE-US): a new tool for the early evaluation of antiangiogenic treatment. *Target Oncol* 2010; **5**: 53-58 [PMID: 20379790 DOI: 10.1007/s11523-010-0136-7]

12 **Saini R**, Hoyt K. Recent developments in dynamic contrast-enhanced ultrasound imaging of tumor angiogenesis. *Imaging Med* 2014; **6**: 41-52 [PMID: 25221623 DOI: 10.2217/iim.13.74]

13 **Lencioni R**, Llovet JM. Modified RECIST (mRECIST) assessment for hepatocellular carcinoma. *Semin Liver Dis* 2010; **30**: 52-60 [PMID: 20175033 DOI: 10.1055/s-0030-1247132]

14 **Hudson JM**, Williams R, Tremblay-Darveau C, Sheeran PS, Milot L, Bjarnason GA, Burns PN. Dynamic contrast enhanced ultrasound for therapy monitoring. *Eur J Radiol* 2015; **84**: 1650-1657 [PMID: 26231046 DOI: 10.1016/j.ejrad.2015.05.013]

15 **Schäfer S**, Nylund K, Sævik F, Engjom T, Mézl M, Jiřík R, Dimcevski G, Gilja OH, Tönnies K. Semi-automatic motion compensation of contrast-enhanced ultrasound images from abdominal organs for perfusion analysis. *Comput Biol Med* 2015; **63**: 229-237 [PMID: 25453358 DOI: 10.1016/j.compbiomed.2014.09.014]

16 **Escudier B**, Lassau N, Couanet D, Angevin E, Mesrati F, Leborgne S, Garofano A, Leboulaire C, Dupouy N, Laplanche A. Phase II trial of thalidomide in renal-cell carcinoma. *Ann Oncol* 2002; **13**: 1029-1035 [PMID: 12176780 DOI: 10.1093/annonc/mdf213]

17 **Santhakumar C**, Gane EJ, Liu K, McCaughan GW. Current perspectives on the tumor microenvironment in hepatocellular carcinoma. *Hepatol Int* 2020; **14**: 947-957 [PMID: 33188512 DOI: 10.1007/s12072-020-10104-3]

18 **Huang Z**, Zhou P, Li S, Li K. Prediction of the Ki-67 marker index in hepatocellular carcinoma based on Dynamic Contrast-Enhanced Ultrasonography with Sonazoid. *Insights Imaging* 2022; **13**: 199 [PMID: 36536262 DOI: 10.1186/s13244-022-01320-6]

19 **Xuan Z**, Wu N, Li C, Liu Y. Application of contrast-enhanced ultrasound in the pathological grading and prognosis prediction of hepatocellular carcinoma. *Transl Cancer Res* 2021; **10**: 4106-4115 [PMID: 35116708 DOI: 10.21037/tcr-21-1264]

20 **Zhan Y**, Zhou F, Yu X, Luo F, Liu F, Liang P, Cheng Z, Han Z, Yu J. Quantitative dynamic contrast-enhanced ultrasound may help predict the outcome of hepatocellular carcinoma after microwave ablation. *Int J Hyperthermia* 2019; **35**: 105-111 [PMID: 30300039 DOI: 10.1080/02656736.2018.1483533]

21 **Dong Y**, Qiu Y, Yang D, Yu L, Zuo D, Zhang Q, Tian X, Wang WP, Jung EM. Potential application of dynamic contrast enhanced ultrasound in predicting microvascular invasion of hepatocellular carcinoma. *Clin Hemorheol Microcirc* 2021; **77**: 461-469 [PMID: 33459703 DOI: 10.3233/CH-201085]

22 **Li X**, Han X, Li L, Su C, Sun J, Zhan C, Feng D, Cheng W. Dynamic Contrast-Enhanced Ultrasonography with Sonazoid for Diagnosis of Microvascular Invasion in Hepatocellular Carcinoma. *Ultrasound Med Biol* 2022; **48**: 575-581 [PMID: 34933756 DOI: 10.1016/j.ultrasmedbio.2021.11.005]

23 **Barr RG**, Huang P, Luo Y, Xie X, Zheng R, Yan K, Jing X, Xu H, Fei X, Lee JM. Contrast-enhanced ultrasound imaging of the liver: a review of the clinical evidence for SonoVue and Sonazoid. *Abdom Radiol (NY)* 2020; **45**: 3779-3788 [PMID: 32424608 DOI: 10.1007/s00261-020-02573-9]

24 **Schwarz S**, Clevert DA, Ingrisch M, Geyer T, Schwarze V, Rübenthaler J, Armbruster M. Quantitative Analysis of the Time-Intensity Curve of Contrast-Enhanced Ultrasound of the Liver: Differentiation of Benign and Malignant Liver Lesions. *Diagnostics (Basel)* 2021; **11** [PMID: 34359327 DOI: 10.3390/diagnostics11071244]

25 **Wildner D**, Schellhaas B, Strack D, Goertz RS, Pfeifer L, Fiessler C, Neurath MF, Strobel D. Differentiation of malignant liver tumors by software-based perfusion quantification with dynamic contrast-enhanced ultrasound (DCEUS). *Clin Hemorheol Microcirc* 2019; **71**: 39-51 [PMID: 29865043 DOI: 10.3233/CH-180378]

26 **Wildner D**, Pfeifer L, Goertz RS, Bernatik T, Sturm J, Neurath MF, Strobel D. Dynamic contrast-enhanced ultrasound (DCE-US) for the characterization of hepatocellular carcinoma and cholangiocellular carcinoma. *Ultraschall Med* 2014;

35: 522-527 [PMID: 25202903 DOI: 10.1055/s-0034-1385170]
27 **European Association for the Study of the Liver**. EASL Clinical Practice Guidelines: Management of hepatocellular carcinoma. *J Hepatol* 2018; **69**: 182-236 [PMID: 29628281 DOI: 10.1016/j.jhep.2018.03.019]
28 **Zocco MA**, Garcovich M, Lupascu A, Di Stasio E, Roccarina D, Annicchiarico BE, Riccardi L, Ainora ME, Ponziani F, Caracciolo G, Rapaccini GL, Landolfi R, Siciliano M, Pompili M, Gasbarrini A. Early prediction of response to sorafenib in patients with advanced hepatocellular carcinoma: the role of dynamic contrast enhanced ultrasound. *J Hepatol* 2013; **59**: 1014-1021 [PMID: 23811306 DOI: 10.1016/j.jhep.2013.06.011]
29 **Lassau N**, Koscielny S, Chami L, Chebil M, Benatsou B, Roche A, Ducreux M, Malka D, Boige V. Advanced hepatocellular carcinoma: early evaluation of response to bevacizumab therapy at dynamic contrast-enhanced US with quantification--preliminary results. *Radiology* 2011; **258**: 291-300 [PMID: 20980447 DOI: 10.1148/radiol.10091870]
30 **Gu DY**, Zhang Y, Hu JX, Qin HY, Lu X, He GB, Shang L. The value of contrast-enhanced ultrasound quantitative parameters in the prognosis prediction of hepatocellular carcinoma after thermal ablation: a retrospective cohort study. *J Gastrointest Oncol* 2022; **13**: 2522-2531 [PMID: 36388675 DOI: 10.21037/jgo-22-919]
31 **Wildner D**, Heinzerling L, Scheulen ME, Kaempgen E, Schuler G, Strobel D, Janka R, Neurath MF, Sturm J, Knieling F. Assessment of sorafenib induced changes in tumor perfusion of uveal melanoma metastases with dynamic contrast-enhanced ultrasound (DCE-US). *J Cancer Res Clin Oncol* 2022; **148**: 955-965 [PMID: 34050396 DOI: 10.1007/s00432-021-03666-8]
32 **Amadori M**, Barone D, Scarpi E, Oboldi D, Amadori E, Bandi G, Rossi A, Ferroni F, Ragazzini A, Casadei Gardini A, Frassineti GL, Gavelli G, Passardi A. Dynamic contrast-enhanced ultrasonography (D-CEUS) for the early prediction of bevacizumab efficacy in patients with metastatic colorectal cancer. *Eur Radiol* 2018; **28**: 2969-2978 [PMID: 29417252 DOI: 10.1007/s00330-017-5254-5]
33 **Mogensen MB**, Hansen ML, Henriksen BM, Axelsen T, Vainer B, Osterlind K, Nielsen MB. Dynamic Contrast-Enhanced Ultrasound of Colorectal Liver Metastases as an Imaging Modality for Early Response Prediction to Chemotherapy. *Diagnostics (Basel)* 2017; **7** [PMID: 28604623 DOI: 10.3390/diagnostics7020035]
34 **El Kaffas A**, Sigrist RMS, Fisher G, Bachawal S, Liau J, Wang H, Karanany A, Durot I, Rosenberg J, Hristov D, Willmann JK. Quantitative Three-Dimensional Dynamic Contrast-Enhanced Ultrasound Imaging: First-In-Human Pilot Study in Patients with Liver Metastases. *Theranostics* 2017; **7**: 3745-3758 [PMID: 29109773 DOI: 10.7150/thno.20329]
35 **Lim AK**, Patel N, Eckersley RJ, Goldin RD, Thomas HC, Cosgrove DO, Taylor-Robinson SD, Blomley MJ. Hepatic vein transit time of SonoVue: a comparative study with Levovist. *Radiology* 2006; **240**: 130-135 [PMID: 16720867 DOI: 10.1148/radiol.2401041517]
36 **Staub F**, Tournoux-Facon C, Roumy J, Chaigneau C, Morichaut-Beauchant M, Levillain P, Prevost C, Aubé C, Lebigot J, Oberti F, Galtier JB, Laumonier H, Trillaud H, Bernard PH, Blanc JF, Sironneau S, Machet F, Drouillard J, de Ledinghen V, Couzigou P, Foucher P, Castéra L, Tranquard F, Bacq Y, d'Altéroche L, Ingrand P, Tasu JP. Liver fibrosis staging with contrast-enhanced ultrasonography: prospective multicenter study compared with METAVIR scoring. *Eur Radiol* 2009; **19**: 1991-1997 [PMID: 19259683 DOI: 10.1007/s00330-009-1313-x]
37 **Kim MY**, Suk KT, Baik SK, Kim HA, Kim YJ, Cha SH, Kwak HR, Cho MY, Park HJ, Jeon HK, Park SY, Kim BR, Hong JH, Jo KW, Kim JW, Kim HS, Kwon SO, Chang SJ, Baik GH, Kim DJ. Hepatic vein arrival time as assessed by contrast-enhanced ultrasonography is useful for the assessment of portal hypertension in compensated cirrhosis. *Hepatology* 2012; **56**: 1053-1062 [PMID: 22473911 DOI: 10.1002/hep.25752]
38 **Jeong WK**, Kim TY, Sohn JH, Kim Y, Kim J. Severe portal hypertension in cirrhosis: evaluation of perfusion parameters with contrast-enhanced ultrasonography. *PLoS One* 2015; **10**: e0121601 [PMID: 25798930 DOI: 10.1371/journal.pone.0121601]
39 **Simon R**. Complications After Pancreaticoduodenectomy. *Surg Clin North Am* 2021; **101**: 865-874 [PMID: 34537148 DOI: 10.1016/j.suc.2021.06.011]
40 **D'Onofrio M**, Canestrini S, Crosara S, De Robertis R, Pozzi Mucelli R. Contrast enhanced ultrasound with quantitative perfusion analysis for objective characterization of pancreatic ductal adenocarcinoma: A feasibility study. *World J Radiol* 2014; **6**: 31-35 [PMID: 24765238 DOI: 10.4329/wjr.v6.i3.31]
41 **Schima W**, Böhm G, Rösch CS, Klaus A, Függer R, Kopf H. Mass-forming pancreatitis versus pancreatic ductal adenocarcinoma: CT and MR imaging for differentiation. *Cancer Imaging* 2020; **20**: 52 [PMID: 32703312 DOI: 10.1186/s40644-020-00324-z]
42 **Kersting S**, Konopke R, Kersting F, Volk A, Distler M, Bergert H, Saeger HD, Grützmann R, Bunk A. Quantitative perfusion analysis of transabdominal contrast-enhanced ultrasonography of pancreatic masses and carcinomas. *Gastroenterology* 2009; **137**: 1903-1911 [PMID: 19715694 DOI: 10.1053/j.gastro.2009.08.049]
43 **Vitali F**, Pfeifer L, Janson C, Goertz RS, Neurath MF, Strobel D, Wildner D. Quantitative perfusion analysis in pancreatic contrast enhanced ultrasound (DCE-US): a promising tool for the differentiation between autoimmune pancreatitis and pancreatic cancer. *Z Gastroenterol* 2015; **53**: 1175-1181 [PMID: 26480053 DOI: 10.1055/s-0041-103847]
44 **Qiu YJ**, Zhao GC, Shi SN, Zuo D, Zhang Q, Dong Y, Lou WH, Wang WP. Application of dynamic contrast enhanced ultrasound in distinguishing focal-type autoimmune pancreatitis from pancreatic ductal adenocarcinoma. *Clin Hemorheol Microcirc* 2022; **81**: 149-161 [PMID: 35253737 DOI: 10.3233/CH-221390]
45 **Zhang Q**, Wu L, Yang D, Qiu Y, Yu L, Dong Y, Wang WP. Clinical application of dynamic contrast enhanced ultrasound in monitoring the treatment response of chemoradiotherapy of pancreatic ductal adenocarcinoma. *Clin Hemorheol Microcirc* 2020; **75**: 325-334 [PMID: 31985457 DOI: 10.3233/CH-190786]
46 **Khanna L**, Prasad SR, Sunnapwar A, Kondapaneni S, Dasyam A, Tammisetti VS, Salman U, Nazarullah A, Katabathina VS. Pancreatic Neuroendocrine Neoplasms: 2020 Update on Pathologic and Imaging Findings and Classification. *Radiographics* 2020; **40**: 1240-1262 [PMID: 32795239 DOI: 10.1148/rg.2020200025]
47 **Yang DH**, Cheng J, Tian XF, Zhang Q, Yu LY, Qiu YJ, Lu XY, Lou WH, Dong Y, Wang WP. Prediction of Pathological Grades of Pancreatic Neuroendocrine Tumors Based on Dynamic Contrast-Enhanced Ultrasound Quantitative Analysis. *Diagnostics (Basel)* 2023; **13** [PMID: 36673048 DOI: 10.3390/diagnostics13020238]
48 **Girlich C**, Jung EM, Iesalnieks I, Schreyer AG, Zorger N, Strauch U, Schacherer D. Quantitative assessment of bowel

wall vascularisation in Crohn's disease with contrast-enhanced ultrasound and perfusion analysis. *Clin Hemorheol Microcirc* 2009; **43**: 141-148 [PMID: 19713608 DOI: 10.3233/CH-2009-1228]

49 **Girlich C**, Jung EM, Huber E, Ott C, Iesalnieks I, Schreyer A, Schacherer D. Comparison between preoperative quantitative assessment of bowel wall vascularization by contrast-enhanced ultrasound and operative macroscopic findings and results of histopathological scoring in Crohn's disease. *Ultraschall Med* 2011; **32**: 154-159 [PMID: 20449794 DOI: 10.1055/s-0029-1245398]

50 **Romanini L**, Passamonti M, Navarria M, Lanzarotto F, Villanacci V, Grazioli L, Calliada F, Maroldi R. Quantitative analysis of contrast-enhanced ultrasonography of the bowel wall can predict disease activity in inflammatory bowel disease. *Eur J Radiol* 2014; **83**: 1317-1323 [PMID: 24908589 DOI: 10.1016/j.ejrad.2014.05.012]

51 **Ripollés T**, Rausell N, Paredes JM, Grau E, Martínez MJ, Vizuete J. Effectiveness of contrast-enhanced ultrasound for characterisation of intestinal inflammation in Crohn's disease: a comparison with surgical histopathology analysis. *J Crohns Colitis* 2013; **7**: 120-128 [PMID: 22483566 DOI: 10.1016/j.crohns.2012.03.002]

52 **Nylund K**, Jirik R, Mezl M, Leh S, Hausken T, Pfeffer F, Ødegaard S, Taxt T, Gilja OH. Quantitative contrast-enhanced ultrasound comparison between inflammatory and fibrotic lesions in patients with Crohn's disease. *Ultrasound Med Biol* 2013; **39**: 1197-1206 [PMID: 23643057 DOI: 10.1016/j.ultrasmedbio.2013.01.020]

53 **Quaia E**, Gennari AG, van Beek EJR. Differentiation of Inflammatory from Fibrotic Ileal Strictures among Patients with Crohn's Disease through Analysis of Time-Intensity Curves Obtained after Microbubble Contrast Agent Injection. *Ultrasound Med Biol* 2017; **43**: 1171-1178 [PMID: 28385471 DOI: 10.1016/j.ultrasmedbio.2017.01.024]

54 **Girlich C**, Schacherer D, Jung EM, Klebl F, Huber E. Comparison between quantitative assessment of bowel wall vascularization by contrast-enhanced ultrasound and results of histopathological scoring in ulcerative colitis. *Int J Colorectal Dis* 2012; **27**: 193-198 [PMID: 21847545 DOI: 10.1007/s00384-011-1300-y]

55 **Medellin-Kowalewski A**, Wilkens R, Wilson A, Ruan J, Wilson SR. Quantitative Contrast-Enhanced Ultrasound Parameters in Crohn Disease: Their Role in Disease Activity Determination With Ultrasound. *AJR Am J Roentgenol* 2016; **206**: 64-73 [PMID: 26700336 DOI: 10.2214/AJR.15.14506]

56 **Wilkens R**, Wilson A, Burns PN, Ghosh S, Wilson SR. Persistent Enhancement on Contrast-Enhanced Ultrasound Studies of Severe Crohn's Disease: Stuck Bubbles? *Ultrasound Med Biol* 2018; **44**: 2189-2198 [PMID: 30076030 DOI: 10.1016/j.ultrasmedbio.2018.06.018]

57 **Goertz RS**, Klett D, Wildner D, Atreya R, Neurath MF, Strobel D. Quantitative contrast-enhanced ultrasound for monitoring vedolizumab therapy in inflammatory bowel disease patients: a pilot study. *Acta Radiol* 2018; **59**: 1149-1156 [PMID: 29345146 DOI: 10.1177/0284185117752032]

58 **Socaciu M**, Ciobanu L, Diaconu B, Hagiu C, Seicean A, Badea R. Non-Invasive Assessment of Inflammation and Treatment Response in Patients with Crohn's Disease and Ulcerative Colitis using Contrast-Enhanced Ultrasonography Quantification. *J Gastrointestin Liver Dis* 2015; **24**: 457-465 [PMID: 26697572 DOI: 10.15403/jgld.2014.1121.244.chr]

59 **Saevik F**, Nylund K, Hausken T, Ødegaard S, Gilja OH. Bowel perfusion measured with dynamic contrast-enhanced ultrasound predicts treatment outcome in patients with Crohn's disease. *Inflamm Bowel Dis* 2014; **20**: 2029-2037 [PMID: 25185684 DOI: 10.1097/MIB.0000000000000159]

60 **Laterza L**, Ainora ME, Garcovich M, Galasso L, Poscia A, Di Stasio E, Lupascu A, Riccardi L, Scaldaferri F, Armuzzi A, Rapaccini GL, Gasbarrini A, Pompili M, Zocco MA. Bowel contrast-enhanced ultrasound perfusion imaging in the evaluation of Crohn's disease patients undergoing anti-TNFα therapy. *Dig Liver Dis* 2021; **53**: 729-737 [PMID: 32900648 DOI: 10.1016/j.dld.2020.08.005]

61 **Quaia E**, Sozzi M, Angileri R, Gennari AG, Cova MA. Time-Intensity Curves Obtained after Microbubble Injection Can Be Used to Differentiate Responders from Nonresponders among Patients with Clinically Active Crohn Disease after 6 Weeks of Pharmacologic Treatment. *Radiology* 2016; **281**: 606-616 [PMID: 27192460 DOI: 10.1148/radiol.2016152461]

62 **Li T**, Lu M, Song J, Wu P, Cheng X, Zhang Z. Improvement to ultrasonographical differential diagnosis of gastric lesions: The value of contrast enhanced sonography with gastric distention. *PLoS One* 2017; **12**: e0182332 [PMID: 28783738 DOI: 10.1371/journal.pone.0182332]

63 **Joo I**, Kim SH, Lee DH, Han JK. Dynamic Contrast-Enhanced Ultrasound of Gastric Cancer: Correlation with Perfusion CT and Histopathology. *Korean J Radiol* 2019; **20**: 781-790 [PMID: 30993929 DOI: 10.3348/kjr.2018.0273]

64 **Zhuang H**, Yang ZG, Wang ZQ, Wang XD, Chen HJ, Zhang YC, Luo Y. Features of time-intensity curve parameters of colorectal adenocarcinomas evaluated by double-contrast enhanced ultrasonography: initial observation. *Eur J Radiol* 2012; **81**: 677-682 [PMID: 21316889 DOI: 10.1016/j.ejrad.2011.01.075]

65 **Malmstrøm ML**, Săftoiu A, Riis LB, Hassan H, Klausen TW, Rahbek MS, Gögenur I, Vilmann P. Dynamic contrast-enhanced EUS for quantification of tumor perfusion in colonic cancer: a prospective cohort study. *Gastrointest Endosc* 2018; **87**: 1530-1538 [PMID: 29329991 DOI: 10.1016/j.gie.2018.01.001]

66 **Lassau N**, Bonastre J, Kind M, Vilgrain V, Lacroix J, Cuinet M, Taieb S, Aziza R, Sarran A, Labbe-Devilliers C, Gallix B, Lucidarme O, Ptak Y, Rocher L, Caquot LM, Chagnon S, Marion D, Luciani A, Feutray S, Uzan-Augui J, Coiffier B, Benastou B, Koscielny S. Validation of dynamic contrast-enhanced ultrasound in predicting outcomes of antiangiogenic therapy for solid tumors: the French multicenter support for innovative and expensive techniques study. *Invest Radiol* 2014; **49**: 794-800 [PMID: 24991866 DOI: 10.1097/RLI.0000000000000085]

67 **Lassau N**, Chami L, Koscielny S, Chebil M, Massard C, Benatsou B, Bidault S, Cioffi A, Blay JY, Le Cesne A. Quantitative functional imaging by dynamic contrast enhanced ultrasonography (DCE-US) in GIST patients treated with masatinib. *Invest New Drugs* 2012; **30**: 765-771 [PMID: 21136137 DOI: 10.1007/s10637-010-9592-2]

68 **Medellin A**, Merrill C, Wilson SR. Role of contrast-enhanced ultrasound in evaluation of the bowel. *Abdom Radiol (NY)* 2018; **43**: 918-933 [PMID: 29260278 DOI: 10.1007/s00261-017-1399-6]

69 **Frampas E**, Lassau N, Zappa M, Vullierme MP, Koscielny S, Vilgrain V. Advanced Hepatocellular Carcinoma: early evaluation of response to targeted therapy and prognostic value of Perfusion CT and Dynamic Contrast Enhanced-Ultrasound. Preliminary results. *Eur J Radiol* 2013; **82**: e205-e211 [PMID: 23273822 DOI: 10.1016/j.ejrad.2012.12.004]

World Journal of Gastroenterology

Submit a Manuscript: https://www.f6publishing.com

World J Gastroenterol 2023 July 7; 29(25): 4036-4052

DOI: 10.3748/wjg.v29.i25.4036

ISSN 1007-9327 (print) ISSN 2219-2840 (online)

MINIREVIEWS

Fractal nature of human gastrointestinal system: Exploring a new era

Fabio Grizzi, Marco Spadaccini, Maurizio Chiriva-Internati, Mohamed A A A Hegazi, Robert S Bresalier, Cesare Hassan, Alessandro Repici, Silvia Carrara

Specialty type: Gastroenterology and hepatology

Provenance and peer review: Invited article; Externally peer reviewed.

Peer-review model: Single blind

Peer-review report's scientific quality classification

Grade A (Excellent): A
Grade B (Very good): B, B
Grade C (Good): 0
Grade D (Fair): D
Grade E (Poor): 0

P-Reviewer: Jennane R, France; Paparoupa M, Germany; Vieth M, Germany

Received: March 28, 2023
Peer-review started: March 28, 2023
First decision: May 4, 2023
Revised: May 26, 2023
Accepted: June 13, 2023
Article in press: June 13, 2023
Published online: July 7, 2023

Fabio Grizzi, Mohamed A A A Hegazi, Department of Immunology and Inflammation, IRCCS Humanitas Research Hospital, Rozzano 20089, Milan, Italy

Fabio Grizzi, Cesare Hassan, Alessandro Repici, Department of Biomedical Sciences, Humanitas University, Pieve Emanuele 20072, Milan, Italy

Marco Spadaccini, Cesare Hassan, Alessandro Repici, Silvia Carrara, Division of Gastroenterology and Digestive Endoscopy, Department of Gastroenterology, IRCCS Humanitas Research Hospital, Rozzano 20089, Milan, Italy

Maurizio Chiriva-Internati, Robert S Bresalier, Departments of Gastroenterology, Hepatology & Nutrition, Division of Internal Medicine, The University of Texas MD Anderson Cancer Center, Houston, TX 77030, United States

Corresponding author: Fabio Grizzi, PhD, Senior Scientist, Head Histology Core, Department of Immunology and Inflammation, IRCCS Humanitas Research Hospital, 56 Via Manzoni, Rozzano 20089, Milan, Italy. fabio.grizzi@humanitasresearch.it

Abstract

The morphological complexity of cells and tissues, whether normal or pathological, is characterized by two primary attributes: Irregularity and self-similarity across different scales. When an object exhibits self-similarity, its shape remains unchanged as the scales of measurement vary because any part of it resembles the whole. On the other hand, the size and geometric characteristics of an irregular object vary as the resolution increases, revealing more intricate details. Despite numerous attempts, a reliable and accurate method for quantifying the morphological features of gastrointestinal organs, tissues, cells, their dynamic changes, and pathological disorders has not yet been established. However, fractal geometry, which studies shapes and patterns that exhibit self-similarity, holds promise in providing a quantitative measure of the irregularly shaped morphologies and their underlying self-similar temporal behaviors. In this context, we explore the fractal nature of the gastrointestinal system and the potential of fractal geometry as a robust descriptor of its complex forms and functions. Additionally, we examine the practical applications of fractal geometry in clinical gastroenterology and hepatology practice.

Key Words: Fractals; Geometry; Gastroenterology; Esophagus; Stomach; Colon; Pancreas;

Liver; Time-series; Shape; Behavior

©The Author(s) 2023. Published by Baishideng Publishing Group Inc. All rights reserved.

Core Tip: Utilizing fractal analysis to estimate the fractal dimension is a potent tool for investigating the geometrical properties of the gastrointestinal system. This approach has the potential to improve diagnostic and prognostic rates, leading to better patient care and a deeper understanding of the underlying pathophysiological mechanisms.

Citation: Grizzi F, Spadaccini M, Chiriva-Internati M, Hegazi MAAA, Bresalier RS, Hassan C, Repici A, Carrara S. Fractal nature of human gastrointestinal system: Exploring a new era. *World J Gastroenterol* 2023; 29(25): 4036-4052
URL: https://www.wjgnet.com/1007-9327/full/v29/i25/4036.htm
DOI: https://dx.doi.org/10.3748/wjg.v29.i25.4036

INTRODUCTION

"In One Dimension, did not a moving Point produce a Line with two terminal points? In Two Dimensions, did not a moving Line produce a Square with four terminal points? In Three Dimensions, did not a moving Square produce-did not this eye of mine behold it-that blessed Being, a Cube, with eight terminal points? And in Four Dimensions shall not a moving Cube-alas, for Analogy, and alas for the Progress of Truth, if it be not so-shall not, I say, the motion of a divine Cube result in a still more divine Organization with sixteen terminal points? Behold the infallible confirmation of the Series, 2, 4, 8, and 16 is not this a Geometrical Progression? Is not this-if I might quote my Lord's own words-strictly according to Analogy?" From Flatland: A romance of many dimensions, Edwin A. Abbott.

The complexity of nature, characterized by its various degrees of irregularity and diverse physical properties[1], is a challenging topic. The Scottish biologist and mathematician D'Arcy Wentworth Thompson (1860-1948) proposed that the form of an anatomical entity can be identified through its dimensions and contour. However, Euclidean-based morphometric analyses, which involve measurements like area, perimeter, and form factor, fall short in accurately describing natural, including anatomical, entities due to their irregular shapes that cannot be quantified by means of the classical Euclidean geometry, which is only able to describe regular geometrical objects. Mandelbrot[2] (1924-2010) introduced the notion of fractal geometry[3] and coined the term "fractal" to describe spatial or temporal irregular patterns[4,5]. Fractal geometry has been suggested as an instrument to define the geometry of various natural entities, such as mountains, coastlines, clouds, trees, molecular structures, and an array of forms within anatomical systems along with their underlying dynamic processes[6]. The gastrointestinal or digestive system is a complex network of organs including the mouth, pharynx, esophagus, stomach, small and large intestines, rectum, and anus, as well as the salivary glands, liver, gallbladder, and pancreas. The morphological intricacy of the gastrointestinal system, both in its natural state and under pathological conditions, is mainly characterized by its irregularity and self-similarity across varying scales[7]. Classical examples of irregularly-shaped histological entities that defy Euclidean geometric principles include gastric pits, which are indentations in the stomach signifying entrances to tubular gastric glands, and villi, which are finger-like structures that significantly increase the surface area of the small intestine[8]. The human stomach is known to have millions of these pits across the surface of its lining epithelium. The adult small intestine, with an average inner surface area of around 30 m^2[9,10], necessitates such a large surface for effective metabolism and nutrient absorption. This is achieved by forming unique irregularly-shaped structures like villi and microvilli. The functional efficiency of epithelia is enhanced by their fractal organization, which expands the surface area for processes like absorption or sensory reception, thereby enabling more efficient interaction with the external environment[11]. This level of surface area and functional efficiency would be unattainable if the colonic mucosa were to be represented by a two-dimensional Euclidean plane. However, the fractal-like characteristics observed in epithelial tissues, which line organ surfaces and body structures, are not universal but rather specific to certain instances. The liver development, commonly described as a fractal-like phenomenon, involves intricate processes and interactions among various cell types. During embryonic development, a bud-like structure known as the hepatic diverticulum, which emerges from the endodermal layer of the early gut tube, forms the liver. The hepatic diverticulum then undergoes branching morphogenesis, leading to a complex network of interconnected structures that enable liver tissue expansion and development of bile ducts, blood vessels, and functional units like lobes or lobules. Similarly, pancreas development is a regulated process involving growth and branching. While the developing liver and pancreas' branching patterns may superficially resemble fractal structures, it's

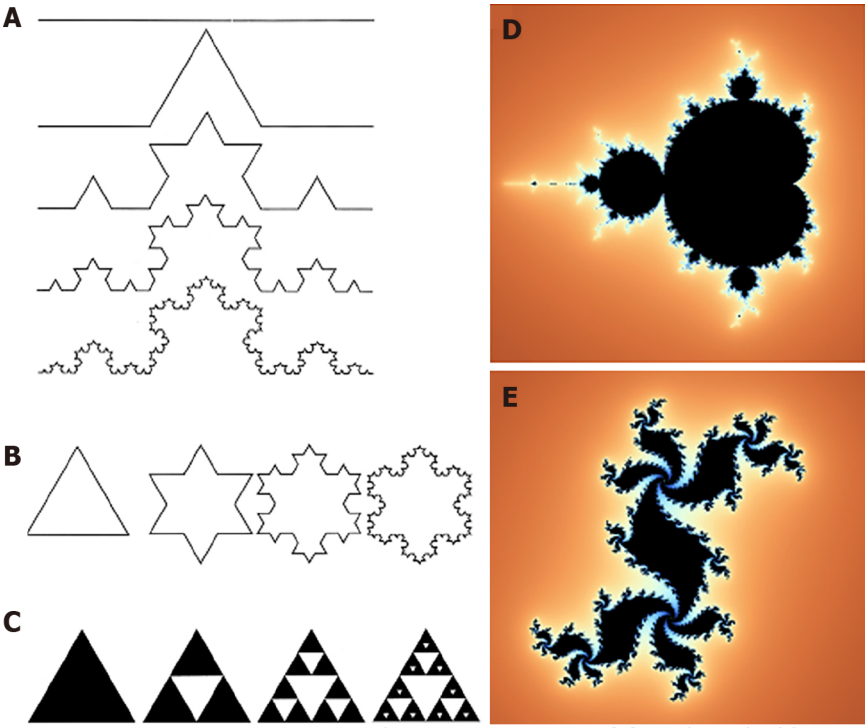
crucial to acknowledge that true fractals display self-similarity across multiple scales, a trait not precisely seen in liver development. Fractal geometry has been used to describe pathological entities within the gastrointestinal system as well. The irregularity in the shape of the interface between epithelial and connective tissues is a recognized characteristic of malignant and pre-malignant epithelial lesions. However, efforts to objectively assess this have been sparse. Landini and Rippin[12] have applied fractal geometry as an instrument for evaluating this irregular epithelial-connective tissue interface[13]. Intestinal polyps, characterized by abnormal tissue overgrowth within the intestinal lining, can display varying shapes and structures based on factors like the type of polyp (*i.e.*, adenomatous polyps, hyperplastic polyps), their location, and size. Some polyps, such as villous adenomas, appear to exhibit a self-similar form, hinting at a possible fractal structure within a specific magnification range. The fractal dimension has been leveraged to quantify these polyps, proving to be a more effective discriminator between diagnostic groups than Euclidean measures like area or perimeter length[14]. Several studies suggest that fractal estimation could offer a novel method for examining the nonlinear dynamics of the gastrointestinal system. This approach sheds light on the complexity and unevenness of colonic pressure activity during different periods, providing potential applications for understanding gastrointestinal system functions. As fractal analysis becomes increasingly prevalent in biomedical research, it serves to quantify the irregularities of anatomical entities, their generation patterns, and their physiological and pathological processes. In this context, we delve into the potential of fractal geometry as a tool for understanding the gastrointestinal system and its possible applications in clinical practice.

FRACTAL GEOMETRY: BASIC PRINCIPLES

Fractals, whether anatomical or natural, are characterized by four primary attributes: (1) Irregularity in shape; (2) self-similarity in structure; (3) non-integer or fractal dimension; and (4) scaling. Scaling indicates that the measured features of a fractal depend on the scale at which they are observed[15]. The most significant characteristic of fractal objects is their ability to display similar patterns at different scales, resulting in the component parts having a form that is similar to the whole in all dimensions. Complex curves such as coastline shapes serve as typical examples of this property, where each segment can be regarded as a smaller version of the complete structure in a statistical sense (Figure 1). The term "self-similarity" refers to a property of fractals that can be either geometric or statistical. Geometric self-similarity occurs when every smaller piece of an object is an exact replica of the whole object. For instance, the "snowflake" and the "curve", both described by Swedish mathematician Niels Fabian Helge von Koch (1870-1924) in 1904, are examples of geometrically self-similar figures[16]. Another geometrically self-similar figure is the "Sierpinski triangle", originally described by Polish mathematician Waclaw Sierpinski (1882-1969) in 1915. In contrast, statistical self-similarity pertains to biological objects, including natural objects (Figure 2) and anatomical forms (Figure 3). While small components of anatomical systems are not typically exact replicas of the entire system, they still exhibit self-similarity. For instance, if we examine a segment of a tree branch or vascular vessel, it may not look identical to the entire tree or vessel, but it still displays self-similarity. Many anatomical structures have been identified as statistical self-similar entities, including the circulatory system, the biliary tree of the liver, the dendritic structure of neuronal cells, the ductal system of glands, the cell membrane, and the extracellular matrix (ECM) in cases of chronic liver disease[17].

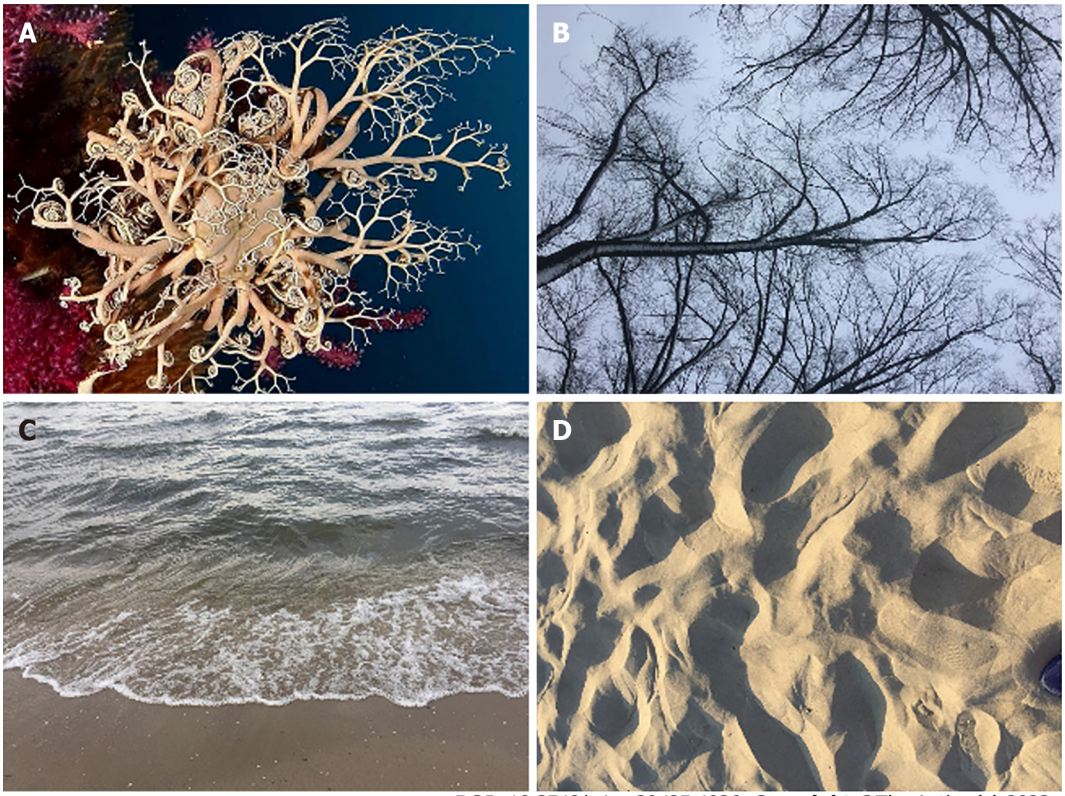
The concept of "dimension" is a fundamental aspect of fractals and represents a characteristic value of the object. There are two definitions of dimension: the first is the "topological dimension", introduced by Austrian mathematician Karl Menger (1902-1985), which assigns an integer number to each point in three-dimensional Euclidean space (E3). For example, a "point" is assigned a dimension of 0, a "straight line" a dimension of 1, a "plane surface"a dimension of 2, and a "three-dimensional figure" a dimension of 3. The second definition was introduced by Felix Hausdorff (1868-1942) and Abram Besicovitch (1891-1970), who assigned a "real number" between the topological dimension and 3 to every natural object in E3. Mandelbrot designated Menger's dimension with the symbol D_γ and Hausdorff and Besicovitch's dimension with the symbol D. For all Euclidean figures, D_γ and D are equivalent ($D_\gamma = D$). However, this equality does not apply to all fractal natural objects, as the inequality $D > D_\gamma$ is true. Many methods have been proposed to estimate the fractal dimension, with the "box-counting method" being the most widely used in biomedical sciences to estimate the space-filling properties of anatomical objects in two-dimensional and three-dimensional space.

It applies the following formula: $D = \lim \varepsilon \to 0 [\log N(\varepsilon)/\mathrm{Log}(1/\varepsilon)]$, where D is the box-counting fractal dimension of the object, ε is the side length of the box, and N(ε) is the smallest number of boxes of side ε required to cover the outline or the surface of the object completely. Because the zero limit cannot be applied to natural objects, the dimension was estimated by the formula D = d, where d is the slope of the graph of Log N(ε) against Log (1/ε). The linear segments of these graphs were identified using the least-squares method of regression, and the gradients of these segments are assessed using an iterative resistant-line method[15,18-25].



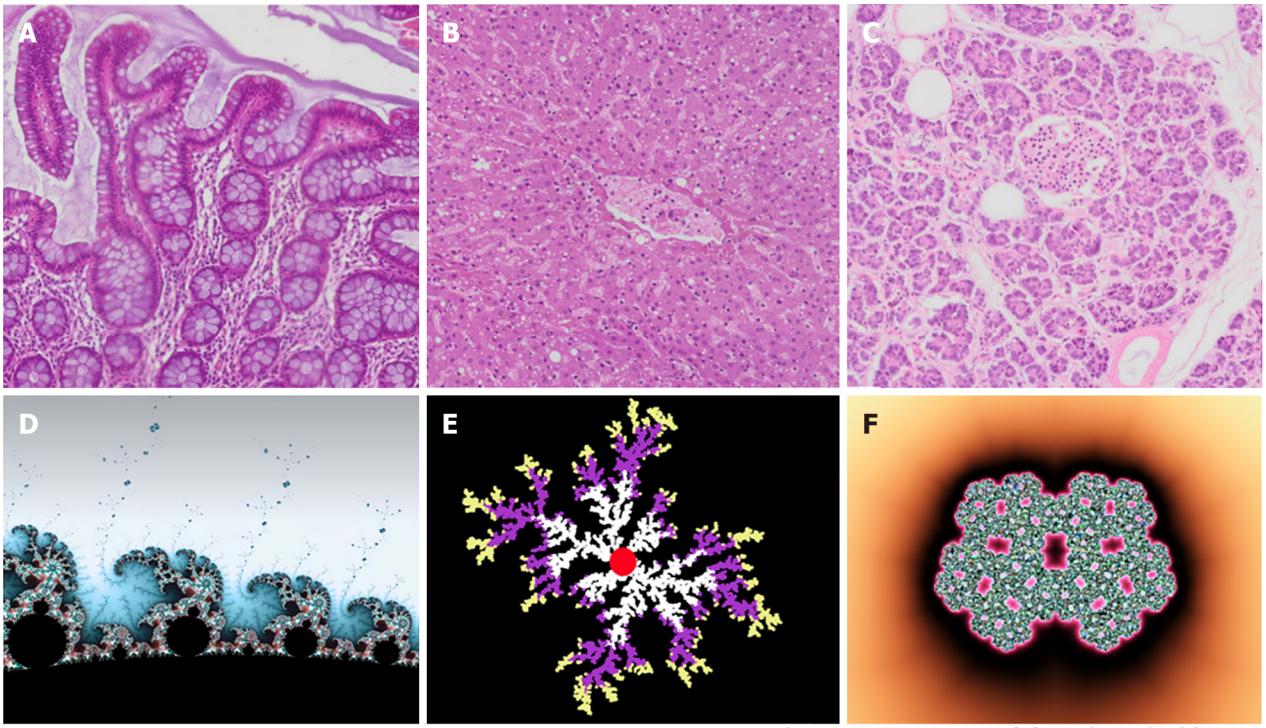
DOI: 10.3748/wjg.v29.i25.4036 **Copyright** ©The Author(s) 2023.

Figure 1 Examples of geometrical self-similar objects. A: "Curve" from Niels Fabian Helge von Koch; B: "Snowflake" from Niels Fabian Helge von Koch; C: "Sierpinski triangle"; D: Mandelbrot set; E: Julia set named after the studies on the geometrical complexity by the French mathematicians Gaston Julia e Pierre Fatou.



DOI: 10.3748/wjg.v29.i25.4036 **Copyright** ©The Author(s) 2023.

Figure 2 Examples of natural statistical self-similar structures resembling mathematical fractals. A: Marine invertebrates corals; B: Tree branches; C: Water breaking waves; D: Sand dunes.



DOI: 10.3748/wjg.v29.i25.4036 **Copyright** ©The Author(s) 2023.

Figure 3 Some self-similar tissues in the gastrointestinal system and their corresponding idealized mathematical fractals. A: Intestine villi; B: Liver; C: Pancreatic Langerhans islet; D: Mandelbrot set; E: Diffusion-limited aggregation model; F: Julia fractal islet.

The fractal esophagus

Wax *et al*[26] conducted a quantitative analysis of nuclear morphometry in epithelial cells using an animal model of esophageal carcinogenesis in 2003. They observed changes in the size and texture of cell nuclei caused by neoplastic transformation and chemopreventive action[26]. However, the fractal dimension did not enhance the diagnostic ability of the technique for classifying neoplasia[26]. Instead, the increase in fractal dimension observed in dysplastic tissues corresponded with changes in the texture of cell nuclei observed in histological images, where clumped and grainy cell nuclei are typical of dysplasia. The authors concluded that the increased fractal dimension resulted from alterations in the organization of chromatin and proteins within the nucleus, as demonstrated by the changes in the visual appearance of cell nuclei in histological images[26]. A framework for creating a two-dimensional, globally interconnected map to simulate epithelium dynamics has been proposed by Hosseini and Hashemi Golpayegani[27]. The aim of this model was to facilitate early-stage dysplasia detection using microscopic imagery from endoscopic biopsies. Their findings suggested a potential direct correlation between the system's structural complexity and the unpredictability of its dynamics[27]. Textural analysis of positron emission tomography (PET) and other imaging techniques is gaining interest in measuring intra-tumoral heterogeneity.

Studies have demonstrated that measuring tumor heterogeneity through textural analysis in 18F-fluorodeoxy glucose PET can provide predictive and prognostic information. In a study by Doumou *et al*[28], sixty-four patients with adenocarcinoma of the lower esophagus underwent 18F-FDG PET/CT imaging for clinical staging before surgery. Using in-house software implemented under MATLAB (The MathWorks Inc.) and calculating 57 textural features, including fractal indexes, they discovered that altering the "bin width" produced poor agreement for most second- and high-order features, with less impact on fractal parameters. The authors concluded that fractal analysis features were relatively resistant to changes in smoothing, segmentation, and bin width. In 2005, Gardner *et al*[29] noted that in normal subjects, patients with gastroesophageal reflux disease (GERD), and individuals with GERD treated with a proton pump inhibitor, both esophageal and gastric pH reflect an underlying stochastic process that generates a fractal pattern over time. The authors hypothesized that the fractal pattern of esophageal pH and gastric pH, along with the statistical association of sequential pH values for up to 2 h, encodes information regarding gastric acidity. They proposed that depending on the value of gastric acidity, gastroesophageal reflux causes the esophagus to signal the stomach to alter gastric acidity by influencing gastric secretion of acid or bicarbonate[29]. The authors subsequently confirmed their hypothesis by investigating 26 healthy adults with no history of gastrointestinal disease or symptoms and 27 adult subjects with a history of GERD who experienced heartburn at least four times per week for at least 6 mo[30] Their findings suggest that the esophagus can signal the stomach to alter gastric acidity, depending on the value of gastric pH, and that this ability is impaired in subjects with GERD.

Thus, the self-similar, fractal pattern encodes information about gastric acidity that the esophagus can decode and, when necessary, signal the stomach to reduce gastric pH.

The fractal stomach

In 1994, Demling and Ell[31] conducted a study titled "Fractal stomach ulcer. A new measurement parameter for benign and malignant changes for the future", proposing that fractal geometry could be beneficially applied for the spatial and temporal analysis of the stomach. Abdominal sound analysis is known to aid in the diagnosis of gastrointestinal diseases, and bowel sounds originating from the stomach and intestine are highly variable over time. They are described as loose successions or clusters of sudden bursts. Realistic recordings of abdominal sounds are contaminated with noise and artifacts that must be differentiated from the bowel sounds. More recently, Kölle *et al*[32] suggested a method of intrinsic mode function-fractal dimension filtering based on a multivariate empirical mode decomposition approach. The intrinsic mode function-fractal dimension filtering method has been applied to a realistic, contaminated dataset, with close to 100% of manually labeled bowel sounds correctly identified[32]. In a novel approach, West *et al*[33] analyzed fluctuations in human myoelectric gastric activity noninvasively measured from the surface of the abdomen. They estimated the "scaling index" in 17 healthy individuals and found it to be statistically different from a set of surrogate data. The authors also demonstrated that the dynamical pattern of the gastric rate variability time series was significantly reduced in systemic sclerosis patients compared to healthy individuals, indicating a decrease in complexity of the underlying gastrointestinal control system. In terms of clinical relevance, employing fractal image analysis to model the conduction patterns of slow waves (SWs) through detailed networks of interstitial cells of Cajal can enhance our comprehension of the principles driving gastrointestinal myoelectric activity, as well as the diseases linked to its malfunction[34]. Interstitial cells of cajal (ICC) are specialized pacemaker cells in the gastrointestinal system responsible for generating and propagating SWs of depolarization throughout the muscularis propria. These SWs regulate the motility of the gastrointestinal system tract, which is essential for digestion, nutrient absorption, and waste elimination. By using a combined approach based on image analysis and fractal geometry of detailed ICC networks, researchers have demonstrated that modeling SW conduction patterns can aid in improving our understanding of the mechanisms underlying gastrointestinal system myoelectric activity and the diseases associated with its dysfunction[35,36].

Watanabe *et al*[37] applied fractal analysis to contrast-enhanced computed tomography (CT) images to estimate structural abnormality in gastric tumors and evaluated its biomarker value for predicting survival in surgically treated gastric cancer patients. The authors found that high fractal dimension values of tumors were significantly associated with high T stage and high pathological stage. Moreover, in Kaplan-Meier analysis, patients with higher fractal dimension tumors had significantly worse disease-specific survival, indicating that contrast-enhanced CT fractal analysis could be a useful biomarker for gastric cancer patients, reflecting clinic-pathologic features and survival.

In a study by Liliac *et al*[38], the pattern of E-cadherin at the cell membrane level was analyzed using fractal dimension analysis on fluorescence immunohistochemistry samples labeled with E-cadherin in gastric well/moderate and solid gastric adenocarcinoma from patients without any associated chemotherapeutic treatment or radiotherapy. The images were binarized using a fixed threshold of the E-cadherin fluorescence channel, and the fractal dimension of the binarized image outlines was calculated to assess the ruggedness of the cellular membranes. The study demonstrated that the morphological analysis of a simple marker for the cell membrane can identify and distinguish tumor cells.

The fractal colon

Cross *et al*[14] suggested that colorectal polyps have a self-similar structure that may contain fractal elements, and that the fractal dimension could be a useful morphometric discriminator. The authors estimated the fractal dimensions of images from hematoxylin and eosin-stained sections of 359 colorectal polyps, including 214 tubulovillous adenomas, 41 tubular adenomas, 29 villous adenomas, 68 metaplastic polyps, and 7 inflammatory polyps, and found that colorectal polyps exhibit a fractal structure within a defined range of magnification[14]. They concluded that fractal dimension can provide a new method of estimating polyp shape and serve as a useful morphometric discriminator between diagnostic categories[14].

It is clear that the invasive front of colorectal cancers (CRCs) can vary in complexity, ranging from smooth to highly complex when the front breaks up into small cell clusters or single cancer cells[39]. Currently, the degree of complexity is estimated visually and/or semi-quantitatively. Franzén *et al*[39] compared the visual estimation of CRC invasive front irregularity to different quantitative image analytical techniques and developed a "complexity index" for the invasive margin. They analyzed cytokeratin 8-stained tissue sections from 29 CRCs and found that the fractal dimension and tumor cell clusters provided the best correlation to visual grading using discriminant analysis. Moreover, the fractal dimension separated tumors up to a certain level of complexity, while tumor cell cluster counting distinguished cells above and beyond the fractal dimension when the tumor front fragmented into small cell clusters. These results suggest that the fractal dimension could be a valid index for objectively quantifying the complexity of tumor invasive fronts. In another study, Hahn-Strömberg *et al*[40]

correlated the complexity of colon carcinoma invasive fronts with cell adhesion protein expression and polymorphisms in their genes. They constructed a "complexity index" using computer-assisted morphometry to estimate fractal dimension and tumor cell clusters, followed by tree analysis, for 32 colon carcinomas. Hahn-Strömberg *et al*[40] found that adhesion protein distribution was significantly altered in most carcinomas, but no correlation was observed between the complexity of the invasive border and protein distribution or genetic alterations. These findings indicate that the complexity of CRC invasion is not solely dependent on genetic derangements in adhesion protein genes or protein distribution, but also on aberrations in the function of other proteins related to adhesive proteins.

In their research, Ştefănescu *et al*[41] utilized fractal analysis and neural network modeling of colon mucosa images generated by confocal laser endomicroscopy to develop an automatic diagnosis algorithm for CRCs. They examined 1035 images of normal mucosa and tumor regions, processed using a computer-aided imaging system to achieve an automatic diagnosis. The researchers found that non-malignant colon mucosa has polyhedral crypt structures while malignant colon mucosa has irregular and interrupted crypts. They estimated seven parameters for each image, with only contrast, homogeneity and feature number showing significant differences between natural and cancer images. Their findings suggest that computed aided diagnosis through fractal analysis of glandular structures can be used in combination with traditional histological and minimally invasive imaging methods[41]. Another study by Shaleve *et al*[42] used the fractal dimension to predict clinically significant post-endoscopic bleeding (CSPEB) by analyzing blood vessel morphology within post-colonic endoscopic mucosal resection (EMR) mucosal defects. They introduced the fractal dimension estimate as a measure of the complexity of blood vessel contour, and on multivariate analysis, found that fractal dimension and four other independent variables correlated with CSPEB. This suggests that the morphometric characteristics of blood vessels in post-EMR defects can be used to predict delayed bleeding following colonic EMR. Ren *et al*[43] measured curvature, fractal dimension, and volumetric feature maps to assist radiologists in reducing interpretation time and improving detection results in computed tomographic colonography.

In their study, Mah *et al*[34] investigated the use of fractal dimension to distinguish between healthy and cancerous colon images and to examine the relationship between fractal dimension and traditional texture analysis features. They found a highly significant difference between the groups using fractal analysis. Interestingly, they also reported that micro-architectural analysis of the histologically examined colon mucosa provided unprecedented sensitivity for early detection of CRC[34]. They observed significant alterations in spectral slope, fractal dimension, and principal component 3 in mouse mucosa at the earliest time points, and these alterations increased over time, indicating the micro-architectural underpinnings of subsequent tumorigenesis.

Additionally, these indexes spatially correlated with future adenoma development. The concept of "deformability" has been introduced as a hallmark of the CRC process leading to metastatic spread.

Furthermore, Streba *et al*[44] used fractal analysis to estimate elements obtained from images taken from pathological and immunohistochemical investigations of colonic biopsy fragments in patients who underwent surgery for previously diagnosed CRC. They introduced the concept of "deformability" as a hallmark of the CRC process leading to metastatic spread. The authors performed a fractal analysis using an in-house tool.

Streba *et al*[44] found that the fractal dimensions were significantly different between adenocarcinomas and other types of colonic cancers, but no significant differences were found between most types of CRCs. They also reported a significant statistical difference when comparing well-differentiated tumors with all other stages. The authors concluded that fractal analysis is a novel and interesting tool for determining the pathologic diagnosis of CRCs, and may further improve diagnostic and prognostic rates, thus enhancing patient care.

Several initial studies have suggested that the novel agent polyethylene glycol (PEG) may have the necessary chemopreventive properties for widespread clinical use[45]. Despite reports attesting to its remarkable efficacy, the mechanisms of action of PEG remain largely unexplored. To determine the stage of carcinogenesis that PEG targets, Roy *et al*[45] assessed fractal dimension, one of the earliest markers of neoplastic transformation of the colon, in fresh colonic tissue using four-dimensional elastic light-scattering fingerprinting.

Studies have shown that PEG can suppress morphologic variables and restore micro-architectural organization, as indicated by the fractal dimension estimate. Changes in fractal dimension have been observed prior to the development of aberrant crypt foci in azoxymethane-treated rats and adenomas in mouse models, making fractal dimension a sensitive early marker in cancer prevention. Short-term treatment with PEG has been shown to completely normalize fractal dimension, indicating that PEG can reverse the earliest changes of colon carcinogenesis.

Strauss *et al*[46] assessed the impact of quantitative parameters on the differentiation of primary CRCs from normal colon tissue. They applied compartment and non-compartment modeling to dynamic PET data in 22 patients with CRCs prior to surgery, five of whom also had liver metastases at the time of the PET study. The non-compartment modeling was used to calculate the fractal dimension of the time-activity data. The study found that using quantitative data had the advantage of not being primarily dependent on the individual assessment and experience of the physician visually evaluating the FDG PET data. Additionally, the analysis of dynamic PET data of the corresponding primary tumor

could predict the presence of metastatic lesions.

Strauss *et al*[46] found that the fractal dimension, standardized uptake value, influx, and k3 were the most important single parameters for lesion differentiation[46]. The study also demonstrated that the highest accuracy for lesion differentiation was achieved with the fractal dimension[46]. The use of quantitative data has the advantage that the detection of CRC is not solely dependent on the individual assessment and experience of the physician visually evaluating the FDG-PET data. Quantitative FDG-PET studies provide accurate data for differentiating primary CRCs from natural tissue, and most of these studies conclude that the presence of metastatic lesions can be predicted by analyzing the dynamic PET data of the corresponding primary tumor[46,47].

Studies have found that 18F-FDG kinetics are primarily dependent on the expression of genes associated with glucose transporters and hexokinases, but may also be modulated by other genes. Strauss *et al*[47] investigated the dependency of 18F-FDG kinetics on angiogenesis-related gene expression. They evaluated a series of 25 patients with primary CRCs using PET and 18F-FDG within 2 d before surgery.

During surgery, tissue specimens were obtained from the tumor and adjacent non-tumoral colon, and gene expression was assessed using gene arrays. Strauss *et al*[47] identified 23 angiogenesis-related genes with a tumor-to-normal ratio exceeding 1.50, and found a significant correlation between k1 and vascular endothelial growth factor, as well as between fractal dimension and angiopoietin-2. They also noted a negative correlation between k3 and VEGF-B, and a positive correlation for angiopoietin-like 4 gene. In a recent study, Goh *et al*[48] evaluated the feasibility of using fractal analysis to assess the spatial pattern of CRC perfusion at dynamic contrast-enhanced CT (perfusion CT).

Twenty CRC patients who underwent a 65-second perfusion CT study. A perfusion parametric map was generated using validated commercial software. The tumor was identified by an experienced radiologist, segmented *via* thresholding, and fractal analysis was applied using in-house software. Fractal dimension, abundance, and lacunarity were assessed for the entire outlined tumor, as well as for selected representative areas within the tumor of low and high perfusion.

The study by Goh *et al*[48] concluded that fractal values were higher in cancer than in normal colon, and that fractal values were lower in areas of high perfusion compared to low perfusion areas. Lacunarity curves were shifted to the right for cancer compared to normal colon. The results suggest that CRCs mapped by perfusion CT demonstrate fractal properties, and thus fractal analysis is feasible, potentially providing a quantitative measure of the spatial pattern of tumor perfusion.

Lętowska-Andrzejewicz *et al*[49] have investigated the effects of 5-fluorouracil, interferon, and dexamethasone, on the healing of colon anastomosis by assessing morphometric and fractal parameters of the colonic wall. Lętowska-Andrzejewicz *et al*[49] performed an experimental anastomosis of the ascending colon in 60 male Wistar rats and subsequently randomly assigned them to four groups. On the second to sixth post-operative days, the rats were administered 5-fluorouracil, interferon-α, dexamethasone, or 0.9% NaCl solution as a control. The healing of the anastomosis was assessed through macroscopic, histomorphometric, and microbiological evaluations. The histomorphometric parameter changes were most evident on the seventh and fourteenth post-operative days in all treatment groups. Connective tissue fractal dimension significantly decreased in those animals treated with interferon and dexamethasone. All three pharmaceutical agents impaired healing of the anastomosis and promoted infection in the anastomosis and skin wound sites. Dexamethasone was considered the most detrimental in this study, as it induced both morphometric and macroscopic alterations.

The inability of cytotoxic anticancer therapies to effectively treat tumors may lead to changes in their morphology and increased tissue invasion. This effect is more prominent in cancer cells with strong metastatic capabilities. Researchers, Pasqualato *et al*[50], have established a clear correlation between alterations in cell shape and the development of a more aggressive phenotype in colon cancer cells that are resistant to 5-FU treatment, specifically HCT-8FUres.

The observed changes in cell shape were strongly associated with an increase in the speed of cellular movement. Pasqualato *et al*[50] developed a method to quantitatively measure the shape of both wild-type and chemoresistant HCT-8 cells during a wound healing assay. They assessed various shape descriptors such as the area/perimeter ratio, circularity, roundness, fractal dimension, and solidity to characterize the biological behavior of these two cell lines. Solidity was identified as the most effective parameter for distinguishing between the chemoresistant and wild-type cells. Moreover, this parameter was found to capture the differences in cell shape at each time point of the migration process. Furthermore, a negative correlation was observed between solidity and motility speed.

The fractal pancreas

Studies that attempt to quantitatively analyze the growth and development of pancreatic islets in both normal and pathological conditions have encountered significant challenges in terms of methodology and conceptualization. To address these challenges, Hastings *et al*[51] conducted a study that utilized the "geometry of random fractals" to investigate the regeneration of islets in guinea pigs that had been treated with alloxan.

The authors of the aforementioned study have since demonstrated that the power-law distribution of pancreatic islets is consistent across various mammalian species and is maintained throughout ontogenetic development in guinea pigs[52]. This suggests that islet formation adheres to an iterative or fractal pattern that is common among mammals. The islets of Langerhans, which are responsible for regulating blood glucose levels, are known to be unevenly distributed throughout the pancreas. In fact, it has been reported that there exists a universal power-law that governs the fractal spatial distribution of islets in two-dimensional pancreatic sections[52].

In a study conducted by Jo *et al*[53], the three-dimensional spatial distribution of islets in intact mouse pancreata was examined using optical projection tomography. The results showed a power law distribution with a fractal dimension of 2.1. The authors also analyzed two-dimensional pancreatic sections from human autopsies and found that the distribution of human islets followed a universal power law with a fractal dimension of 1.5 in adult pancreata. This value is consistent with previous findings in smaller mammalian pancreas sections. Finally, the authors developed a growth model to explain the development of islet distribution and suggested that the fractal nature of the spatial islet distribution may be due to self-avoidance in the branching process of vascularization in the pancreas[53].

Pancreatic cancer is a highly aggressive disease with a poor prognosis, despite surgical intervention. To improve patient outcomes and avoid unnecessary laparotomies, it is crucial to identify reliable factors that can predict the resectability of pancreatic tumors. Vasilescu *et al*[54] conducted a study to determine if nuclear morphometry and fractal dimension of pancreatic nuclear features could serve as preoperative indicators for assessing pancreatic resectability. The study involved sixty-one patients diagnosed with pancreatic cancer, who were divided into two groups: those with resectable cancer and those with non-resectable pancreatic cancer. The authors evaluated several morphometric parameters, including nuclear area, length of minor and major axes, and nuclear shape and chromatin distribution of pancreatic tumor cells, which were estimated using fractal dimension analysis. The morphometric analysis conducted by Vasilescu *et al*[54] revealed significant differences in the nuclear area between the resectable and non-resectable groups. The non-resectable group was also found to have a higher value of fractal dimension in both nuclear outlines and chromatin distribution. Based on these findings, the authors suggested that objective measurements should be utilized to enhance risk assessment and treatment decision-making for pancreatic cancer. Additionally, they proposed that the fractal dimension of nuclear shape and chromatin distribution could be a valuable tool for conventional pathological analysis. In another study, fractal analysis was used to demonstrate that ghrelin administration increased structural complexity and tissue disorder in rat exocrine pancreas[55].

The study involved 40 male Wistar rats, where pancreas tissue sections were stained with hematoxylin and eosin and visualized through light microscopy. The average values of tissue fractal dimension, lacunarity, and co-occurrence matrix texture parameters were determined for each animal using computer-aided image analysis. The authors found that regardless of age, administration of ghrelin increased the fractal dimension and textural entropy of the exocrine pancreas, while decreasing its lacunarity. This is the first study to examine the effects of ghrelin on the morphological properties of pancreatic tissue and the first to utilize fractal and textural analysis methods to quantify the architecture of exocrine pancreas tissue.

According to Metze[56], fractal characteristics of chromatin have been identified through light or electron microscopy in the past 20 years. These features can be easily estimated from digitized microscopic images and are useful for cancer diagnosis and prognosis. Studies have shown that an increase in the fractal dimension of stained nuclei occurs during carcinogenesis and tumor progression in various cancers, including pancreatic cancer. Researchers have also reported potential connections between changes in chromatin organization during carcinogenesis and tumor progression and an increase in the fractal dimension of stained chromatin.

The fractal dimension of chromatin in routine histological or cytological preparations has been found to increase during various stages of tumor development, including from pre-neoplastic stages to cancer, and from initial cancer stages to advanced stages. Additionally, higher fractal dimensions are associated with poor prognosis, while lower fractal dimensions are observed in patients with a better prognosis. Al-Mrabeh *et al*[57] conducted a study to determine whether the low volume and irregular border of the pancreas in patients with type-2 diabetes could be normalized following the reversal of diabetes.

The study conducted by Al-Mrabeh *et al*[57] utilized three-dimensional volume-rendering and fractal dimension analysis of MRI-acquired images, along with three-point Dixon imaging to measure fat content. The results indicated no change in pancreas volume six months after diabetes reversal compared to baseline. However, the reversal of diabetes was associated with an increase in the irregularity of pancreas borders between baseline and eight weeks, followed by a decrease at six months. In contrast, no changes in fractal dimension were observed in the non-reversed group. The authors concluded that combining three-dimensional volume segmentation of the pancreas with fractal dimension analysis could provide a promising mathematical definition of the pancreas border morphology.

Fractal dimension analysis revealed a significant increase in pancreas complexity after acute weight loss in the responder group, followed by a significant decrease resulting in a smoother pancreas border by the end of the study. Conversely, no changes in the pancreas border were observed in the non-responder group. Although the effect of insulin on the endocrine pancreas has been extensively studied,

there have been few quantitative morphometric investigations of the exocrine pancreas. Recently, Pajevic *et al*[58] conducted a study to investigate the effect of acute and chronic insulin administration on the morphology of rat pancreas acini. The results showed that acute insulin treatment, regardless of the applied doses, increased the fractal dimension of the pancreas acini while decreasing their lacunarity.

The study showed that chronic low-dose insulin treatment decreased the fractal dimension and increased the lacunarity of pancreas acini, whereas high-dose insulin had the opposite effect. These findings suggest that fractal analysis could be used to detect fine architectural changes in acini, making it a potential alternative or addition to routine stereology.

In recent years, endoscopic ultrasound (EUS) elastography has been demonstrated as a useful technique for characterizing solid pancreatic lesions (SPLs). Carrara *et al*[59] introduced a combined analysis using EUS elastography (strain ratio) and fractal analysis to characterize the morphology of SPLs. A total of 102 SPLs from 100 patients were analyzed, and the results showed that both the parenchymal strain ratio (pSR) and wall strain ratio (wSR) were significantly higher in malignant SPLs than benign ones during elastography.

Fractal analysis revealed a significant difference in mean surface fractal dimensions between malignant lesions and neuroendocrine tumors, suggesting that combining EUS elastography with pSR and fractal-based analysis is a promising method for quantitatively characterizing SPLs[60].

It is widely accepted that the desmoplastic reaction is a hallmark of pancreatic cancer, although its impact on tumor behavior remains debated. Grizzi *et al*[61] recently developed a computer-aided method for quantifying the amount of pancreatic collagenic ECM, its spatial distribution pattern, and its degradation process.

The study conducted by Grizzi *et al*[61] demonstrated a progressive increase in pancreatic collagenic ECM from normal to inflammatory and pancreatic ductal adenocarcinoma. The two-dimensional fractal dimension revealed a significant difference in the spatial complexity of collagenic ECM between normal and inflammatory and pancreatic ductal adenocarcinoma. Moreover, a significant difference was observed when comparing the number of cycles required to degrade pancreatic collagenic ECM in normal *vs* inflammatory and pancreatic ductal adenocarcinoma. The mean velocity of collagenic ECM degradation was also found to be faster in inflammatory and pancreatic ductal adenocarcinoma than in normal. These findings highlight the potential of computer-aided methods and fractal analysis in quantifying the pancreatic ECM and its role in pancreatic diseases.

The study has demonstrated that inflammatory and pancreatic ductal adenocarcinomas are characterized by an increased amount of pancreatic collagenic ECM, as well as changes in its spatial complexity and degradation. These findings define new features of the pancreatic collagenic ECM and provide a basis for further investigations into the clinical behavior of pancreatic ductal adenocarcinoma and the development of therapeutic strategies. Overall, the study highlights the potential of computer-aided methods and fractal analysis in quantifying the pancreatic ECM and its role in pancreatic diseases, ultimately contributing to improved diagnostic and therapeutic approaches for patients with pancreatic cancer.

Recently, researchers investigated the relationship between ductal morphometry and ramification patterns in the submandibular gland and pancreas to confirm their shared fractal dimension[62]. The study found that while the length of the intraglandular submandibular duct and the main pancreatic duct were correlated, other morphometric features of the ducts were not. This suggests a more intricate relationship between the two digestive glands beyond a simple shared fractal dimension.

Fractal analysis offers maps of the FD, which allows for a more dependable and size-independent measurement utilizing gross pathology or multi-parametric MRI as reference standards[63]. This approach quantifies perfusion chaos, the underlying pathophysiological principle, and can differentiate the more chaotic tumor rim from the tumor core and nearby non-tumorous pancreatic tissue.

Abdominal CT biomarkers, both inside and outside the pancreas, have the potential to diagnose type 2 diabetes mellitus. Tallam *et al*[64] conducted a study on a large clinical dataset using fully automated deep learning to investigate abdominal CT biomarkers for type 2 diabetes mellitus. Their findings revealed that the most accurate predictors of type 2 diabetes mellitus include intrapancreatic fat percentage, pancreatic fractal dimension, plaque severity between the L1 and L4 vertebra levels, average liver CT attenuation, and BMI.

The fractal liver

In 1989, Dioguardi[65-67] (1921-2019) proposed the liver as a composite system comprised of a set of operative microunits that receive a continuous flow of matter, energy, and information. The development of mathematical models for non-Euclidean geometry has led to the creation of models for highly complex natural phenomena[68]. In developmental biology, branching morphogenesis has been explained through self-similar iterative branching rules that have helped to elucidate branch patterns observed in various tissue types. However, in solid viscera, the issue of geometry is more complex, as there is no readily available marker for geometry in parenchymal tissue. The mosaic pattern provides such a marker for studying solid viscera.

The patches observed in mosaic liver have been shown to exhibit fractal properties, indicating that the pattern may have arisen from a self-similar process in which small areas are representative of, although not necessarily identical to, the whole object. This observation provides a new analytical approach to the study of biological structure in organogenesis[68]. It is well-established that partial hepatectomy induces compensatory, non-neoplastic growth and regeneration in mammalian liver[69]. Previous experimental evidence has suggested that compensatory liver growth occurs uniformly, without focal centers of proliferation. Given this information, fractal analysis was used to test various hypothesized patterns of regenerative growth in the liver. The results of this analysis indicate that the mosaic pattern does not change significantly during the regenerative process. The area and perimeter of patches (the area occupied by or perimeter around cells of like lineage) increase during compensatory liver growth in chimeric rats without altering the geometric complexity of patch boundaries (the boundaries around cells of like lineage). These tissue findings are consistent with previously reported computer models of growth in which repetitive application of simple decisions assuming uniform growth created complex mosaic patterns.

These findings support the idea that an iterating, self-similar cell division program is sufficient for the regeneration of liver tissue following partial hepatectomy. Such programs are important because they suggest a way in which complex patterns, or morphogenesis, can be efficiently created from a small amount of stored information. In geometrical terms, liver fibrosis is an example of self-similar natural fractal structure[70].

To evaluate the usefulness of a reliable and reproducible mathematical scoring system based on fractal geometry for quantifying the irregular pattern in fibrosis commonly seen in liver biopsy specimens from chronic liver diseases, Dioguardi *et al*[70] investigated 26 liver biopsy sections obtained from patients with chronic hepatitis C virus-related liver disease. The degree of fibrosis in each section was estimated using a quantitative scoring system based on the computer-assisted evaluation of both the fractal and spectral dimensions of deposited collagen. The findings indicated that the fractional dimension of its irregular shape defines fibrosis as a natural fractal structure.

The study by Dioguardi *et al*[70] proposed a method for quantifying irregular patterns in liver tissue using fractal geometry. The method is based on a quantitative scoring system that evaluates the fractal and spectral dimensions of collagen deposited in liver biopsy sections obtained from patients with chronic hepatitis C virus-related liver disease. The results showed that the fractional dimension of the irregular shape of fibrosis defines it as a natural fractal structure, and a single numerical score can be used to quantify the complex distribution of collagenous components. The method is reproducible, rapid, and inexpensive, and eliminates subjectivity and external factors that can influence staging and classification. The method uses a rectified meter implemented in a computer-assisted planar image analysis system to give metric measures of irregular outlines and surfaces, which can be used to produce an index that quantifies the typical wrinkledness of biologic objects[71]. A computer-aided morphometric method employing fractal geometry and Delaunay triangulation was introduced to quantify the necro-inflammatory phase in liver biopsy specimens. The method was applied to two-micrometer thick sections from 78 chronic hepatitis C virus-infected patients, immunohistochemically treated to identify inflammatory cells[62]. An automatic image analysis system was used to define the inflammatory cell network based on Delaunay triangulation, and the cells were categorized geometrically into clusters or irregular distributions within the tissue. This automatic method is fast and objective, producing accurate results represented by scalar numbers and allowing the organ's condition to be represented by Hurst's exponent with an error of no more than 12%. The availability of precise measurements and a reasonably representative assessment of the organ's overall state raises questions about revising the indications for hepatic biopsy, taking into account its invasiveness and subjective interpretation. A computer-aided method utilizing fractal principles was applied to digitized histological biopsy sections from 209 patients with varying degrees of chronic hepatitis C virus-related fibrosis or cirrhosis[72]. This model offers the first metric evaluations of fibrosis's geometric properties and quantitative liver tissue architectural changes[72]. To evaluate the sampling variability of computer-aided, fractal-corrected fibrosis measurements in liver biopsies, Grizzi *et al*[73] examined samples from different liver parts removed from 12 patients with clinically and histologically proven cirrhosis who underwent orthotopic liver transplantation. A computer-aided image analysis system automatically measured fibrosis surface, perimeter, fractal surface and dimensions, wrinkledness, and Hurst coefficient in Sirius red-stained sections. High inter-sample variability was found in fibrosis surface and wrinkledness measurements, while Hurst's exponent variability was low. The study suggests that Hurst's exponent is a valuable histological estimate of fibrosis in the entire organ for clinical use, emphasizing the crucial role biopsy sections play in qualitatively diagnosing chronic hepatitis and quantitatively estimating architectural changes in liver tissue.

A technique for analyzing liver biopsy samples was proposed, which involves the use of the "Dioguardi Histological Metriser" machine to automatically measure various parameters related to liver health, including residual hepatocyte mass, inflammation, fibrosis, and loss of liver tissue tectonics[74]. This technique was validated by analyzing digitized images of liver biopsy sections from 398 patients and comparing the results to a semi-quantitative scoring system. The method provides measurements for the extent of hepatocyte mass, including abnormal lipid accumulation; the size of the inflammation basin and the number of leukocytes within it; the degree of collagen islets, which are classified into three

magnitudes; and the tectonic index, which quantifies the degree of liver tissue organization disorders.

The findings of the proposed technique represent the first standardized method for measuring the geometric properties of liver tissue, including parenchyma, inflammation, fibrosis, and tectonics of biopsy sections. Other authors have also reported on the accuracy and feasibility of using fractal analysis to measure liver fibrosis. A study involving 77 rats, including 10 sham, 46 with fibrosis due to bile duct ligation, and 21 with fibrosis resulting from CCl_4 intoxication, was conducted to investigate various measurements, such as the fractal dimension of Kolmogorov, histologic lesions, the area of fibrosis by image analysis, liver hydroxyproline content, messenger RNA fibronectin, serum hyaluronate level, and portal pressure[75]. The results showed that the fractal dimension of Kolmogorov was correlated with other markers of fibrosis, including the area of fibrosis, hydroxyproline content, serum hyaluronate level, and portal pressure.

The study found that the fractal dimension of Kolmogorov was significantly different between the two fibrosis models, unlike the area of fibrosis, and this relationship was independent of other histologic lesions. These results suggest that fractal analysis is an appropriate technique for analyzing liver fibrosis and has excellent reproducibility. In fact, this method is the only quantitative morphometric approach that can distinguish between different fibrosis models and is sensitive enough to detect pharmacologically-induced changes in liver fibrosis. Meanwhile, Fibroscan is a widely used technique for assessing liver fibrosis in chronic hepatitis C by measuring liver stiffness. However, it remains unclear how liver steatosis, which is a common feature of chronic hepatitis C and other chronic liver diseases, affects the accuracy of liver stiffness evaluation (LSE).

A quantitative morphometric analysis was conducted on 650 patients with chronic hepatitis C who underwent liver biopsy and LSE. The liver specimens were evaluated using both optical analysis (Metavir F and A, steatosis grading) and computerized morphometry to determine the area and fractal dimension of liver fibrosis and steatosis. The precise evaluation of liver histology using computerized morphometry revealed that liver stiffness measured by Fibroscan was associated with liver fibrosis, activity, and steatosis. In cases of high levels of steatosis, Fibroscan measurements may result in misinterpretation of liver fibrosis. Meanwhile, Nielsen *et al*[76] used a polygonization-based method to estimate the fractal dimension and other scalar lacunarity features from digitized transmission electron micrographs of mouse liver cell nuclei.

The aim of Nielsen *et al*[76] was to determine whether a small set of fractal features could differentiate between natural liver samples, hyperplastic nodules, and hepatocellular carcinomas (HCC). They found that several single fractal features estimated from the periphery of the cell nuclei could distinguish between samples from hyperplastic nodules and HCC and those from normal liver tissue. Recent studies suggest that the cellular environment's mechanical influences can have significant effects on gene activity, cell differentiation, and proliferation, in addition to chemical factors[77]. These mechanisms involve a tissue matrix system that includes the ECM, nuclear matrix, and cytoskeleton. As hepatocytes during fetal development are a useful model for studying such variations, Vassy *et al*[77] investigated hepatocyte differentiation from fetal to adult livers using computerized quantitative image analysis of cytokeratin 8 immunofluorescent localization.

Vassy *et al*[77] investigated a set of line features, including the number and length of lines, orientation of lines, and the fractal dimension of the filament network, to analyze hepatocyte differentiation from fetal to adult livers. The study found highly significant differences in the features studied throughout liver development, including an increase in the total amount of cytokeratin filaments, demonstrating the feasibility of objective and quantitative analysis of the differences in the pattern of the cytokeratin filament network. Meanwhile, the organization of the hepatic microvascular network has been widely studied in recent years, particularly in cirrhosis. A quantitative mathematical approach based on fractal and Fourier analyses performed on photomicrographs has been used to recognize the distinctive vascular patterns in cirrhotic livers compared to natural livers[78]. The study found that the natural hepatic sinusoidal network had higher complexity than the cirrhotic network, with more significant morphological changes observed in rats with bile duct-ligation cirrhosis than those with CCl_4-induced cirrhosis. These findings could provide insight into the pathophysiological alterations of the liver and may have diagnostic value in future clinical research. Additionally, aging-related modifications have been shown to cause marked changes in both the structure of the liver sinusoidal endothelial cell and liver perfusion[79]. Fractal and Fourier analyses and micro-CT showed that age did not affect sinusoidal dimensions, sinusoidal density, or dispersion number, but there were changes in the geometry and complexity of the sinusoidal network as determined by fractal dimension and degree of anisotropy.

Small age-related changes in the architecture of the liver sinusoidal network can influence hepatic function and may reflect broader aging changes in the microcirculation. Fractal analysis has been applied to HCC as well[80-83]. The fractal dimension has been investigated as a quantifier of non-Euclidean two-dimensional vascular geometry in a series of paired specimens of primary HCC and surrounding non-tumoral tissue. Blood vessels had a higher fractal dimension in primary tumors compared to liver metastasis, and this approach allowed for differentiation between primary liver tumors with and without neurodifferentiation. Fractal geometry has also been used to investigate alpha-fetoprotein behavior in patients with HCC waiting for liver transplant[84]. Furthermore, it has been shown that the chromatin of mouse hepatocytes exhibits age-related reduction of fractal dimension, suggesting that this index can be a potential indicator of age-associated changes in chromatin structure

[83].

The study of fractal architecture in various organs and structures has expanded the possibilities for determining their functioning and structural arrangement, leading to the development of new approaches to diagnostics and therapeutic interventions. Recently, Azmaiparashvili *et al*[85] investigated the spatial geometry of the biliary tree and assessed the significance of both its fractal and Euclidean characteristics for developing approaches that provide a comprehensive description of intrahepatic biliary tract architecture. This configuration of the biliary bed is essential for ensuring the smooth implementation of the physiological function of the liver and its adaptation to different pathologies accompanied by biliary hypertension. Furthermore, the findings could be considered in the diagnosis and assessment of ductular reaction, biliary regeneration, and/or carcinogenesis.

There is a growing interest among researchers in employing fractal geometry-based algorithms for modeling, monitoring, and treating hepatitis B virus infections, as comprehending the intricate relationships between pathogens, immune systems, and overall liver function is of vital importance[86].

Recently, fractal geometry has been employed to model portal hypertension[87]. Specifically, the model encompasses the entire process of blood flow, starting from the sinusoids and culminating in the portal vein. It can be adjusted to account for the diagnosis of portal hypertension caused by thrombosis and liver cirrhosis. Moreover, this approach offers a novel way to detect portal vein pressure noninvasively from a biomechanical perspective. Furthermore, the combination of qualitative MRI features with fractal analysis has enabled the identification of subtypes of hepatocellular adenomas HCCs in patients with non-cirrhotic livers[88]. This approach also enhances the differentiation of lesions with a high-risk of malignant transformation from those with a low-risk[88]. Liver and tumor segmentation from CT scans plays a critical role in hepatic surgical planning. As manual segmentation is both time-consuming and labor-intensive, a fully automated approach is highly sought after. Chen *et al*[89] introduced an automatic two-step liver and tumor segmentation method. Full-field optical coherence tomography (FF-OCT) has been recognized for its label-free subcellular imaging capabilities. Recently, Zhu *et al*[90] demonstrated the promise of their classifier using FF-OCT images for label-free, quantified tumor detection. This suggests that a fractal dimension-based classifier could potentially assist clinicians in identifying tumor boundaries for surgical resection in the future.

CONCLUSION

Irregularity and self-similarity under scale changes are the main attributes of the morphologic complexity of cells and tissues, either normal or pathologic. Fractal analysis is used in biomedical studies for the exact characterization of the complexity of analyzed structures. Fractal analysis has been demonstrated as a suitable method for quantifying heterogeneity from histological, endoscopic, radiological, and nuclear medicine images under a variety of conditions and in different organs. The application of nontraditional mathematics models to GI tract oncology may represent a comprehensive way to interpret the physical and biological nature of tumors opening new windows in the field of knowledge. Further research is required to exploit physiologically proven fractal behavior in the clinical setting. It is encouraging to see mathematicians, biologists, and clinicians collaborating towards a common quantitative understanding of anatomical complexity. This interdisciplinary approach has the potential to clarify concepts, interpret new and old experimental data, identify alternative experiments, and categorize acquired knowledge based on similarities and shared behaviors of different types of anatomical entities.

ACKNOWLEDGEMENTS

The Authors express their gratitude to Dr. Lorenzo Mottadelli for granting permission to feature his personally photographed Figure 2A as a representative illustration of an underwater natural fractal organism. The Authors are also grateful to Teri Fields for her assistance in editing this manuscript.

FOOTNOTES

Author contributions: Grizzi F and Carrara S contributed to study conception and design; Grizzi F, and Carrara S contributed to writing of article; Spadaccini M, Chiriva-Internati M, Hegazi AAAM, Hassan C, Bresalier RS, and Repici A critically reviewed the manuscript; all the authors contributed to editing, reviewing and final approval of article.

Conflict-of-interest statement: The Authors have no conflict of interest to declare.

Open-Access: This article is an open-access article that was selected by an in-house editor and fully peer-reviewed by external reviewers. It is distributed in accordance with the Creative Commons Attribution NonCommercial (CC BY-

NC 4.0) license, which permits others to distribute, remix, adapt, build upon this work non-commercially, and license their derivative works on different terms, provided the original work is properly cited and the use is non-commercial. See: https://creativecommons.org/Licenses/by-nc/4.0/

Country/Territory of origin: Italy

ORCID number: Fabio Grizzi 0000-0003-0925-742X; Marco Spadaccini 0000-0003-3909-9012; Maurizio Chiriva-Internati 0000-0002-4180-5046; Mohamed A A A Hegazi 0000-0001-7810-5011; Robert S Bresalier 0000-0002-9740-281X; Cesare Hassan 0000-0001-7167-1459; Alessandro Repici 0000-0002-1621-6450; Silvia Carrara 0000-0003-4206-9463.

S-Editor: Chen YL
L-Editor: A
P-Editor: Yu HG

REFERENCES

1 **Nia HT**, Munn LL, Jain RK. Physical traits of cancer. *Science* 2020; **370** [PMID: 33122355 DOI: 10.1126/science.aaz0868]
2 **Mandelbrot BB**. Stochastic models for the Earth's relief, the shape and the fractal dimension of the coastlines, and the number-area rule for islands. *Proc Natl Acad Sci U S A* 1975; **72**: 3825-3828 [PMID: 16578734 DOI: 10.1073/pnas.72.10.3825]
3 **Giles J**. Benoit Mandelbrot: father of fractals. *Nature* 2004; **432**: 266-267 [PMID: 15549068 DOI: 10.1038/432266a]
4 **King RB**, Weissman LJ, Bassingthwaighte JB. Fractal descriptions for spatial statistics. *Ann Biomed Eng* 1990; **18**: 111-121 [PMID: 2350059 DOI: 10.1007/BF02368424]
5 **Di Ieva A**, Grizzi F, Ceva-Grimaldi G, Russo C, Gaetani P, Aimar E, Levi D, Pisano P, Tancioni F, Nicola G, Tschabitscher M, Dioguardi N, Baena RR. Fractal dimension as a quantitator of the microvasculature of normal and adenomatous pituitary tissue. *J Anat* 2007; **211**: 673-680 [PMID: 17784937 DOI: 10.1111/j.1469-7580.2007.00804.x]
6 **Grizzi F**, Chiriva-Internati M. The complexity of anatomical systems. *Theor Biol Med Model* 2005; **2**: 26 [PMID: 16029490 DOI: 10.1186/1742-4682-2-26]
7 **Mehran YZ**, Nasrabadi AM, Golpayegani MR. An investigation on chaotic approach to detect functional gastrointestinal disorders. *Annu Int Conf IEEE Eng Med Biol Soc* 2007; **2007**: 2000-2003 [PMID: 18002377 DOI: 10.1109/IEMBS.2007.4352711]
8 **Walton KD**, Freddo AM, Wang S, Gumucio DL. Generation of intestinal surface: an absorbing tale. *Development* 2016; **143**: 2261-2272 [PMID: 27381224 DOI: 10.1242/dev.135400]
9 **Helander HF**, Fändriks L. Surface area of the digestive tract - revisited. *Scand J Gastroenterol* 2014; **49**: 681-689 [PMID: 24694282 DOI: 10.3109/00365521.2014.898326]
10 **Kwon O**, Han TS, Son MY. Intestinal Morphogenesis in Development, Regeneration, and Disease: The Potential Utility of Intestinal Organoids for Studying Compartmentalization of the Crypt-Villus Structure. *Front Cell Dev Biol* 2020; **8**: 593969 [PMID: 33195268 DOI: 10.3389/fcell.2020.593969]
11 **Linares V**, Aguilar-de-Leyva Á, Casas M, Caraballo I. 3D Printed Fractal-like Structures with High Percentage of Drug for Zero-Order Colonic Release. *Pharmaceutics* 2022; **14** [PMID: 36365117 DOI: 10.3390/pharmaceutics14112298]
12 **Landini G**, Rippin JW. Fractal dimensions of the epithelial-connective tissue interfaces in premalignant and malignant epithelial lesions of the floor of the mouth. *Anal Quant Cytol Histol* 1993; **15**: 144-149 [PMID: 8318129]
13 **Guerrero-Sánchez Y**, Gómez García F, Chamorro-Petronacci CM, Suárez-Peñaranda JM, Pérez-Sayáns M. Use of the Fractal Dimension to Differentiate Epithelium and Connective Tissue in Oral Leukoplakias. *Cancers (Basel)* 2022; **14** [PMID: 35681677 DOI: 10.3390/cancers14112697]
14 **Cross SS**, Bury JP, Silcocks PB, Stephenson TJ, Cotton DW. Fractal geometric analysis of colorectal polyps. *J Pathol* 1994; **172**: 317-323 [PMID: 8207612 DOI: 10.1002/path.1711720406]
15 **Grizzi F**, Russo C, Colombo P, Franceschini B, Frezza EE, Cobos E, Chiriva-Internati M. Quantitative evaluation and modeling of two-dimensional neovascular network complexity: the surface fractal dimension. *BMC Cancer* 2005; **5**: 14 [PMID: 15701176 DOI: 10.1186/1471-2407-5-14]
16 **Losa GA**. The fractal geometry of life. *Riv Biol* 2009; **102**: 29-59 [PMID: 19718622]
17 **Losa GA**, Nonnenmacher TF. Self-similarity and fractal irregularity in pathologic tissues. *Mod Pathol* 1996; **9**: 174-182 [PMID: 8685210]
18 **Obert M**, Pfeifer P, Sernetz M. Microbial growth patterns described by fractal geometry. *J Bacteriol* 1990; **172**: 1180-1185 [PMID: 2106504 DOI: 10.1128/jb.172.3.1180-1185.1990]
19 **Cross SS**, Start RD, Silcocks PB, Bull AD, Cotton DW, Underwood JC. Quantitation of the renal arterial tree by fractal analysis. *J Pathol* 1993; **170**: 479-484 [PMID: 8410497 DOI: 10.1002/path.1711700412]
20 **Chung HW**, Chu CC, Underweiser M, Wehrli FW. On the fractal nature of trabecular structure. *Med Phys* 1994; **21**: 1535-1540 [PMID: 7869984 DOI: 10.1118/1.597263]
21 **Cross SS**, McDonagh AJ, Stephenson TJ, Cotton DW, Underwood JC. Fractal and integer-dimensional geometric analysis of pigmented skin lesions. *Am J Dermatopathol* 1995; **17**: 374-378 [PMID: 8600802 DOI: 10.1097/00000372-199508000-00012]
22 **Paun MA**, Nichita MV, Paun VA, Paun VP. Fractal analysis in the quantification of medical imaging associated with multiple sclerosis pathology. *Front Biosci (Landmark Ed)* 2022; **27**: 66 [PMID: 35227009 DOI: 10.31083/j.fbl2702066]

23 **Lyu X**, Jajal P, Tahir MZ, Zhang S. Fractal dimension of retinal vasculature as an image quality metric for automated fundus image analysis systems. *Sci Rep* 2022; **12**: 11868 [PMID: 35831401 DOI: 10.1038/s41598-022-16089-3]

24 **Lookian PP**, Chen EX, Elhers LD, Ellis DG, Juneau P, Wagoner J, Aizenberg MR. The Association of Fractal Dimension with Vascularity and Clinical Outcomes in Glioblastoma. *World Neurosurg* 2022; **166**: e44-e51 [PMID: 35772703 DOI: 10.1016/j.wneu.2022.06.073]

25 **Di Ieva A**, Grizzi F, Sherif C, Matula C, Tschabitscher M. Angioarchitectural heterogeneity in human glioblastoma multiforme: a fractal-based histopathological assessment. *Microvasc Res* 2011; **81**: 222-230 [PMID: 21192955 DOI: 10.1016/j.mvr.2010.12.006]

26 **Wax A**, Yang C, Müller MG, Nines R, Boone CW, Steele VE, Stoner GD, Dasari RR, Feld MS. In situ detection of neoplastic transformation and chemopreventive effects in rat esophagus epithelium using angle-resolved low-coherence interferometry. *Cancer Res* 2003; **63**: 3556-3559 [PMID: 12839941]

27 **Hosseini ZS**, Hashemi Golpayegani SMR. Esophageal epithelium modeling based on globally coupled map: an approach toward precancerous lesion diagnosis. *Med Biol Eng Comput* 2020; **58**: 1297-1308 [PMID: 32239347 DOI: 10.1007/s11517-020-02151-7]

28 **Doumou G**, Siddique M, Tsoumpas C, Goh V, Cook GJ. The precision of textural analysis in (18)F-FDG-PET scans of oesophageal cancer. *Eur Radiol* 2015; **25**: 2805-2812 [PMID: 25994189 DOI: 10.1007/s00330-015-3681-8]

29 **Gardner JD**, Young W, Sloan S, Robinson M, Miner PB Jr. The fractal nature of human gastro-oesophageal reflux. *Aliment Pharmacol Ther* 2005; **22**: 823-830 [PMID: 16225491 DOI: 10.1111/j.1365-2036.2005.02665.x]

30 **Lu L**, Mu JC, Sloan S, Miner PB, Gardner JD. Exploring the physiologic role of human gastroesophageal reflux by analyzing time-series data from 24-h gastric and esophageal pH recordings. *Physiol Rep* 2014; **2** [PMID: 25347850 DOI: 10.14814/phy2.12051]

31 **Demling L**, Ell C. [Fractal stomach ulcer. A new measurement parameter for benign and malignant changes for the future]. *Fortschr Med* 1994; **112**: 315-316 [PMID: 7959498]

32 **Kölle K**, Aftab MF, Andersson LE, Fougner AL, Stavdahl Ø. Data driven filtering of bowel sounds using multivariate empirical mode decomposition. *Biomed Eng Online* 2019; **18**: 28 [PMID: 30894187 DOI: 10.1186/s12938-019-0646-1]

33 **West BJ**, Maciejewski A, Latka M, Sebzda T, Swierczynski Z, Cybulska-Okolow S, Baran E. Wavelet analysis of scaling properties of gastric electrical activity. *J Appl Physiol (1985)* 2006; **101**: 1425-1431 [PMID: 16794018 DOI: 10.1152/japplphysiol.01364.2004]

34 **Mah SA**, Avci R, Du P, Vanderwinden JM, Cheng LK. Deciphering Stomach Myoelectrical Slow Wave Conduction Patterns *via* Confocal Imaging of Gastric Pacemaker Cells and Fractal Geometry. *Annu Int Conf IEEE Eng Med Biol Soc* 2022; **2022**: 3514-3517 [PMID: 36085915 DOI: 10.1109/EMBC48229.2022.9870891]

35 **Al-Mrabeh A**, Hollingsworth KG, Shaw JAM, McConnachie A, Sattar N, Lean MEJ, Taylor R. 2-year remission of type 2 diabetes and pancreas morphology: a post-hoc analysis of the DiRECT open-label, cluster-randomised trial. *Lancet Diabetes Endocrinol* 2020; **8**: 939-948 [PMID: 33031736 DOI: 10.1016/S2213-8587(20)30303-X]

36 **Mah SA**, Du P, Avci R, Vanderwinden JM, Cheng LK. Analysis of Regional Variations of the Interstitial Cells of Cajal in the Murine Distal Stomach Informed by Confocal Imaging and Machine Learning Methods. *Cell Mol Bioeng* 2022; **15**: 193-205 [PMID: 35401841 DOI: 10.1007/s12195-021-00716-6]

37 **Watanabe H**, Hayano K, Ohira G, Imanishi S, Hanaoka T, Hirata A, Kano M, Matsubara H. Quantification of Structural Heterogeneity Using Fractal Analysis of Contrast-Enhanced CT Image to Predict Survival in Gastric Cancer Patients. *Dig Dis Sci* 2021; **66**: 2069-2074 [PMID: 32691383 DOI: 10.1007/s10620-020-06479-w]

38 **Liliac IM**, Sacerdoțianu MV, Ungureanu BS, Mogoantă L, Mărgăritescu C, Pirici D, Săftoiu A, Crisan AE. Subtle Immunoreactivity Differences in the Fractal Patterns of Membrane E-Cadherin in Gastric Adenocarcinoma. *Curr Health Sci J* 2022; **48**: 303-310 [PMID: 36815089 DOI: 10.12865/CHSJ.48.03.08]

39 **Franzén LE**, Hahn-Strömberg V, Edvardsson H, Bodin L. Characterization of colon carcinoma growth pattern by computerized morphometry: definition of a complexity index. *Int J Mol Med* 2008; **22**: 465-472 [PMID: 18813853]

40 **Hahn-Strömberg V**, Edvardsson H, Bodin L, Franzén L. Disturbed expression of E-cadherin, beta-catenin and tight junction proteins in colon carcinoma is unrelated to growth pattern and genetic polymorphisms. *APMIS* 2008; **116**: 253-262 [PMID: 18397460 DOI: 10.1111/j.1600-0463.2008.00894.x]

41 **Ştefănescu D**, Streba C, Cârțână ET, Săftoiu A, Gruionu G, Gruionu LG. Computer Aided Diagnosis for Confocal Laser Endomicroscopy in Advanced Colorectal Adenocarcinoma. *PLoS One* 2016; **11**: e0154863 [PMID: 27144985 DOI: 10.1371/journal.pone.0154863]

42 **Shaleve Y**, Sabo E, Bourke MJ, Klein A. Computerized image analysis of blood vessels within mucosal defects for the prediction of delayed bleeding following colonic endoscopic mucosal resection: a pilot study. *Endoscopy* 2021; **53**: 837-841 [PMID: 32898919 DOI: 10.1055/a-1258-8992]

43 **Ren Y**, Ma J, Xiong J, Chen Y, Lu L, Zhao J. Improved False Positive Reduction by Novel Morphological Features for Computer-Aided Polyp Detection in CT Colonography. *IEEE J Biomed Health Inform* 2019; **23**: 324-333 [PMID: 29994459 DOI: 10.1109/JBHI.2018.2808199]

44 **Streba L**, ForȚofoiu MC, Popa C, Ciobanu D, Gruia CL, Mogoantă SȘ, Streba CT. A pilot study on the role of fractal analysis in the microscopic evaluation of colorectal cancers. *Rom J Morphol Embryol* 2015; **56**: 191-196 [PMID: 25826505]

45 **Roy HK**, Kunte DP, Koetsier JL, Hart J, Kim YL, Liu Y, Bissonnette M, Goldberg M, Backman V, Wali RK. Chemoprevention of colon carcinogenesis by polyethylene glycol: suppression of epithelial proliferation *via* modulation of SNAIL/beta-catenin signaling. *Mol Cancer Ther* 2006; **5**: 2060-2069 [PMID: 16928827 DOI: 10.1158/1535-7163.MCT-06-0054]

46 **Strauss LG**, Klippel S, Pan L, Schönleben K, Haberkorn U, Dimitrakopoulou-Strauss A. Assessment of quantitative FDG PET data in primary colorectal tumours: which parameters are important with respect to tumour detection? *Eur J Nucl Med Mol Imaging* 2007; **34**: 868-877 [PMID: 17219134 DOI: 10.1007/s00259-006-0319-8]

47 **Strauss LG**, Koczan D, Klippel S, Pan L, Cheng C, Willis S, Haberkorn U, Dimitrakopoulou-Strauss A. Impact of angiogenesis-related gene expression on the tracer kinetics of 18F-FDG in colorectal tumors. *J Nucl Med* 2008; **49**: 1238-

1244 [PMID: 18632818 DOI: 10.2967/jnumed.108.051599]
48 **Goh V**, Sanghera B, Wellsted DM, Sundin J, Halligan S. Assessment of the spatial pattern of colorectal tumour perfusion estimated at perfusion CT using two-dimensional fractal analysis. *Eur Radiol* 2009; **19**: 1358-1365 [PMID: 19190914 DOI: 10.1007/s00330-009-1304-y]
49 **Lętowska-Andrzejewicz K**, Torres A, Torres K, Dobrowolski P, Piersiak T, Maciejewski R, Gawron A, Staśkiewicz G, Plewa Z. The use of morphometric and fractal parameters to assess the effects of 5-fluorouracil, interferon and dexamethasone treatment on colonic anastomosis healing: an experimental study in rats. *Folia Histochem Cytobiol* 2011; **49**: 80-89 [PMID: 21526493 DOI: 10.5603/fhc.2011.0012]
50 **Pasqualato A**, Lei V, Cucina A, Dinicola S, D'Anselmi F, Proietti S, Masiello MG, Palombo A, Bizzarri M. Shape in migration: quantitative image analysis of migrating chemoresistant HCT-8 colon cancer cells. *Cell Adh Migr* 2013; **7**: 450-459 [PMID: 24176801 DOI: 10.4161/cam.26765]
51 **Hastings HM**, Schneider BS, Schreiber MA, Gorray K, Maytal G, Maimon J. Statistical geometry of pancreatic islets. *Proc Biol Sci* 1992; **250**: 257-261 [PMID: 1362994 DOI: 10.1098/rspb.1992.0157]
52 **Schneider BS**, Hastings HM, Maytal G. The spatial distribution of pancreatic islets follows a universal power law. *Proc Biol Sci* 1996; **263**: 129-131 [PMID: 8587894 DOI: 10.1098/rspb.1996.0020]
53 **Jo J**, Hörnblad A, Kilimnik G, Hara M, Ahlgren U, Periwal V. The fractal spatial distribution of pancreatic islets in three dimensions: a self-avoiding growth model. *Phys Biol* 2013; **10**: 036009 [PMID: 23629025 DOI: 10.1088/1478-3975/10/3/036009]
54 **Vasilescu C**, Giza DE, Petrisor P, Dobrescu R, Popescu I, Herlea V. Morphometrical differences between resectable and non-resectable pancreatic cancer: a fractal analysis. *Hepatogastroenterology* 2012; **59**: 284-288 [PMID: 22260836 DOI: 10.5754/hge11277]
55 **Pantic I**, Nesic D, Stevanovic D, Starcevic V, Pantic S, Trajkovic V. Effects of ghrelin on the structural complexity of exocrine pancreas tissue architecture. *Microsc Microanal* 2013; **19**: 553-558 [PMID: 23628379 DOI: 10.1017/S1431927613000524]
56 **Metze K**. Fractal dimension of chromatin: potential molecular diagnostic applications for cancer prognosis. *Expert Rev Mol Diagn* 2013; **13**: 719-735 [PMID: 24063399 DOI: 10.1586/14737159.2013.828889]
57 **Al-Mrabeh A**, Hollingsworth KG, Steven S, Taylor R. Morphology of the pancreas in type 2 diabetes: effect of weight loss with or without normalisation of insulin secretory capacity. *Diabetologia* 2016; **59**: 1753-1759 [PMID: 27179658 DOI: 10.1007/s00125-016-3984-6]
58 **Pajevic M**, Aleksic M, Golic I, Markelic M, Otasevic V, Jankovic A, Stancic A, Korac B, Korac A. Fractal and stereological analyses of insulin-induced rat exocrine pancreas remodelling. *Folia Morphol (Warsz)* 2018; **77**: 478-484 [PMID: 29131278 DOI: 10.5603/FM.a2017.0106]
59 **Carrara S**, Di Leo M, Grizzi F, Correale L, Rahal D, Anderloni A, Auriemma F, Fugazza A, Preatoni P, Maselli R, Hassan C, Finati E, Mangiavillano B, Repici A. EUS elastography (strain ratio) and fractal-based quantitative analysis for the diagnosis of solid pancreatic lesions. *Gastrointest Endosc* 2018; **87**: 1464-1473 [PMID: 29329992 DOI: 10.1016/j.gie.2017.12.031]
60 **Spadaccini M**, Koleth G, Emmanuel J, Khalaf K, Facciorusso A, Grizzi F, Hassan C, Colombo M, Mangiavillano B, Fugazza A, Anderloni A, Carrara S, Repici A. Enhanced endoscopic ultrasound imaging for pancreatic lesions: The road to artificial intelligence. *World J Gastroenterol* 2022; **28**: 3814-3824 [PMID: 36157539 DOI: 10.3748/wjg.v28.i29.3814]
61 **Grizzi F**, Fiorino S, Qehajaj D, Fornelli A, Russo C, de Biase D, Masetti M, Mastrangelo L, Zanello M, Lombardi R, Domanico A, Accogli E, Tura A, Mirandola L, Chiriva-Internati M, Bresalier RS, Jovine E, Leandri P, Di Tommaso L. Computer-aided assessment of the extra-cellular matrix during pancreatic carcinogenesis: a pilot study. *J Transl Med* 2019; **17**: 61 [PMID: 30819202 DOI: 10.1186/s12967-019-1817-3]
62 **Stimec BV**, Ignjatovic D, Lobrinus JA. Establishing correlations between normal pancreatic and submandibular gland ducts. *BMC Gastroenterol* 2022; **22**: 362 [PMID: 35906544 DOI: 10.1186/s12876-022-02443-2]
63 **Michallek F**, Haouari MA, Dana O, Perrot A, Silvera S, Dallongeville A, Dewey M, Zins M. Fractal analysis improves tumour size measurement on computed tomography in pancreatic ductal adenocarcinoma: comparison with gross pathology and multi-parametric MRI. *Eur Radiol* 2022; **32**: 5053-5063 [PMID: 35201407 DOI: 10.1007/s00330-022-08631-8]
64 **Tallam H**, Elton DC, Lee S, Wakim P, Pickhardt PJ, Summers RM. Fully Automated Abdominal CT Biomarkers for Type 2 Diabetes Using Deep Learning. *Radiology* 2022; **304**: 85-95 [PMID: 35380492 DOI: 10.1148/radiol.211914]
65 **Dioguardi N**. The liver as a self-organizing system. I. Theoretics of its representation. *Ric Clin Lab* 1989; **19**: 281-299 [PMID: 2699067 DOI: 10.1007/BF02871818]
66 **Dioguardi N**, Kasangian S. Liver system. II. A categorical coarse model for its autoisodiasostasis. *Ric Clin Lab* 1989; **19**: 301-305 [PMID: 2633297]
67 **Dioguardi N**. Liver system. IV. More on the liver micro-unit: physics and geometry of its action. *Ric Clin Lab* 1991; **21**: 41-68 [PMID: 1866575 DOI: 10.1007/BF02919113]
68 **Iannaccone PM**. Fractal geometry in mosaic organs: a new interpretation of mosaic pattern. *FASEB J* 1990; **4**: 1508-1512 [PMID: 2307328 DOI: 10.1096/fasebj.4.5.2307328]
69 **Ng YK**, Iannaccone PM. Fractal geometry of mosaic pattern demonstrates liver regeneration is a self-similar process. *Dev Biol* 1992; **151**: 419-430 [PMID: 1601177 DOI: 10.1016/0012-1606(92)90182-g]
70 **Dioguardi N**, Grizzi F, Bossi P, Roncalli M. Fractal and spectral dimension analysis of liver fibrosis in needle biopsy specimens. *Anal Quant Cytol Histol* 1999; **21**: 262-266 [PMID: 10560501]
71 **Dioguardi N**, Franceschini B, Aletti G, Russo C, Grizzi F. Fractal dimension rectified meter for quantification of liver fibrosis and other irregular microscopic objects. *Anal Quant Cytol Histol* 2003; **25**: 312-320 [PMID: 14714297]
72 **Dioguardi N**, Grizzi F, Franceschini B, Bossi P, Russo C. Liver fibrosis and tissue architectural change measurement using fractal-rectified metrics and Hurst's exponent. *World J Gastroenterol* 2006; **12**: 2187-2194 [PMID: 16610019 DOI: 10.3748/wjg.v12.i14.2187]
73 **Grizzi F**, Russo C, Franceschini B, Di Rocco M, Torri V, Morenghi E, Fassati LR, Dioguardi N. Sampling variability of

computer-aided fractal-corrected measures of liver fibrosis in needle biopsy specimens. *World J Gastroenterol* 2006; **12**: 7660-7665 [PMID: 17171796 DOI: 10.3748/wjg.v12.i47.7660]

74 **Dioguardi N**, Grizzi F, Fiamengo B, Russo C. Metrically measuring liver biopsy: a chronic hepatitis B and C computer-aided morphologic description. *World J Gastroenterol* 2008; **14**: 7335-7344 [PMID: 19109867 DOI: 10.3748/wjg.14.7335]

75 **Moal F**, Chappard D, Wang J, Vuillemin E, Michalak-Provost S, Rousselet MC, Oberti F, Calès P. Fractal dimension can distinguish models and pharmacologic changes in liver fibrosis in rats. *Hepatology* 2002; **36**: 840-849 [PMID: 12297831 DOI: 10.1053/jhep.2002.35533]

76 **Nielsen B**, Albregtsen F, Danielsen HE. The use of fractal features from the periphery of cell nuclei as a classification tool. *Anal Cell Pathol* 1999; **19**: 21-37 [PMID: 10661622 DOI: 10.1155/1999/986086]

77 **Vassy J**, Beil M, Irinopoulou T, Rigaut JP. Quantitative image analysis of cytokeratin filament distribution during fetal rat liver development. *Hepatology* 1996; **23**: 630-638 [PMID: 8617446 DOI: 10.1002/hep.510230331]

78 **Gaudio E**, Chaberek S, Montella A, Pannarale L, Morini S, Novelli G, Borghese F, Conte D, Ostrowski K. Fractal and Fourier analysis of the hepatic sinusoidal network in normal and cirrhotic rat liver. *J Anat* 2005; **207**: 107-115 [PMID: 16050897 DOI: 10.1111/j.1469-7580.2005.00436.x]

79 **Warren A**, Chaberek S, Ostrowski K, Cogger VC, Hilmer SN, McCuskey RS, Fraser R, Le Couteur DG. Effects of old age on vascular complexity and dispersion of the hepatic sinusoidal network. *Microcirculation* 2008; **15**: 191-202 [PMID: 18386215 DOI: 10.1080/10739680701600856]

80 **Gheonea DI**, Streba CT, Vere CC, Şerbănescu M, Pirici D, Comănescu M, Streba LA, Ciurea ME, Mogoantă S, Rogoveanu I. Diagnosis system for hepatocellular carcinoma based on fractal dimension of morphometric elements integrated in an artificial neural network. *Biomed Res Int* 2014; **2014**: 239706 [PMID: 25025042 DOI: 10.1155/2014/239706]

81 **Hayano K**, Lee SH, Yoshida H, Zhu AX, Sahani DV. Fractal analysis of CT perfusion images for evaluation of antiangiogenic treatment and survival in hepatocellular carcinoma. *Acad Radiol* 2014; **21**: 654-660 [PMID: 24703479 DOI: 10.1016/j.acra.2014.01.020]

82 **Hayano K**, Yoshida H, Zhu AX, Sahani DV. Fractal analysis of contrast-enhanced CT images to predict survival of patients with hepatocellular carcinoma treated with sunitinib. *Dig Dis Sci* 2014; **59**: 1996-2003 [PMID: 24563237 DOI: 10.1007/s10620-014-3064-z]

83 **Streba CT**, Pirici D, Vere CC, Mogoantă L, Comănescu V, Rogoveanu I. Fractal analysis differentiation of nuclear and vascular patterns in hepatocellular carcinomas and hepatic metastasis. *Rom J Morphol Embryol* 2011; **52**: 845-854 [PMID: 21892528]

84 **Lai Q**, Levi Sandri GB, Lerut J. Selection tool alpha-fetoprotein for patients waiting for liver transplantation: How to easily manage a fractal algorithm. *World J Hepatol* 2015; **7**: 1899-1904 [PMID: 26244064 DOI: 10.4254/wjh.v7.i15.1899]

85 **Azmaiparashvili E**, Patarashvili L, Bebiashvili I, Tsomaia K, Gvidiani S, Tananashvili D, Kakabadze M, Gusev S, Kordzaia D. Spatial architecture of biliary tree in mammals: Fractal and Euclidean geometric features. *J Anat* 2021; **239**: 682-692 [PMID: 33817796 DOI: 10.1111/joa.13441]

86 **Qurashi MA**, Rashid S, Jarad F. A computational study of a stochastic fractal-fractional hepatitis B virus infection incorporating delayed immune reactions *via* the exponential decay. *Math Biosci Eng* 2022; **19**: 12950-12980 [PMID: 36654030 DOI: 10.3934/mbe.2022605]

87 **Xie C**, Li X, Qu W, Ji R, Wang J, Song H. Numerical prediction of portal hypertension by a hydrodynamic blood flow model combing with the fractal theory. *J Biomech* 2023; **150**: 111504 [PMID: 36871430 DOI: 10.1016/j.jbiomech.2023.111504]

88 **Michallek F**, Sartoris R, Beaufrère A, Dioguardi Burgio M, Cauchy F, Cannella R, Paradis V, Ronot M, Dewey M, Vilgrain V. Differentiation of hepatocellular adenoma by subtype and hepatocellular carcinoma in non-cirrhotic liver by fractal analysis of perfusion MRI. *Insights Imaging* 2022; **13**: 81 [PMID: 35482151 DOI: 10.1186/s13244-022-01223-6]

89 **Chen Y**, Zheng C, Hu F, Zhou T, Feng L, Xu G, Yi Z, Zhang X. Efficient two-step liver and tumour segmentation on abdominal CT *via* deep learning and a conditional random field. *Comput Biol Med* 2022; **150**: 106076 [PMID: 36137320 DOI: 10.1016/j.compbiomed.2022.106076]

90 **Zhu Y**, Gao W, Guo Z, Zhou Y. Liver tissue classification of en face images by fractal dimension-based support vector machine. *J Biophotonics* 2020; **13**: e201960154 [PMID: 31909553 DOI: 10.1002/jbio.201960154]

World Journal of Gastroenterology

Submit a Manuscript: https://www.f6publishing.com

World J Gastroenterol 2023 July 7; 29(25): 4053-4071

DOI: 10.3748/wjg.v29.i25.4053

ISSN 1007-9327 (print) ISSN 2219-2840 (online)

ORIGINAL ARTICLE

Basic Study

Molecular profiling reveals potential targets in cholangiocarcinoma

Dan Liu, Yang Shi, Hongze Chen, Muhammad Azhar Nisar, Nicholas Jabara, Noah Langwinski, Sophia Mattson, Katsuya Nagaoka, Xuewei Bai, Shaolei Lu, Chiung-Kuei Huang

Specialty type: Gastroenterology and Hepatology

Provenance and peer review: Unsolicited article; Externally peer reviewed.

Peer-review model: Single blind

Peer-review report's scientific quality classification

Grade A (Excellent): 0
Grade B (Very good): B, B
Grade C (Good): C
Grade D (Fair): 0
Grade E (Poor): 0

P-Reviewer: Amin A, United Arab Emirates; Han J, China; Wang CY, Taiwan

Received: January 21, 2023
Peer-review started: January 21, 2023
First decision: February 1, 2023
Revised: February 16, 2023
Accepted: May 23, 2023
Article in press: May 23, 2023
Published online: July 7, 2023

Dan Liu, Yang Shi, Department of Gastroenterology, The First Affiliated Hospital of Zhengzhou University, Zhengzhou 450052, Henan Province, China

Hongze Chen, Muhammad Azhar Nisar, Nicholas Jabara, Noah Langwinski, Sophia Mattson, Chiung-Kuei Huang, Pathology and Laboratory Medicine, Tulane University School of Medicine, New Orleans, LA 70112, United States

Katsuya Nagaoka, Xuewei Bai, Department of Medicine, Rhode Island Hospital and the Alpert Medical School of Brown University, Providence, RI 02903, United States

Shaolei Lu, Department of Pathology, Alpert Medical School of Brown University, Providence, RI 02903, United States

Corresponding author: Chiung-Kuei Huang, PhD, Assistant Professor, Pathology and Laboratory Medicine, Tulane University School of Medicine, 1430 Tulane Ave, New Orleans, LA 70112, United States. chuang17@tulane.edu

Abstract

BACKGROUND

Cholangiocarcinoma (CCA) is a devastating malignancy and has a very poor prognosis if tumors spread outside the liver. Understanding the molecular mechanisms underlying the CCA progression will likely yield therapeutic approaches toward treating this deadly disease.

AIM

To determine the molecular pathogenesis in CCA progression.

METHODS

In silico analysis, *in vitro* cell culture, CCA transgenic animals, histological, and molecular assays were adopted to determine the molecular pathogenesis.

RESULTS

The transcriptomic data of human CCA samples were retrieved from The Cancer Genome Atlas (TGCA, CHOL), European Bioinformatics Institute (EBI, GAD-00001001076), and Gene Expression Omnibus (GEO, GSE107943) databases. Using Gene set enrichment analysis, the cell cycle and Notch related pathways were demonstrated to be significantly activated in CCA in TCGA and GEO datasets. We, through differentially expressed genes, found several cell cycle and notch associated genes were significantly up-regulated in cancer tissues when compared

with the non-cancerous control samples. The associated genes, *via* quantitative real-time PCR and western blotting assays, were further examined in normal human cholangiocytes, CCA cell lines, mouse normal bile ducts, and mouse CCA tumors established by specifically depleting P53 and expressing $Kras^{G12D}$ mutation in the liver. Consistently, we validated that the cell cycle and Notch pathways are up-regulated in CCA cell lines and mouse CCA tumors. Interestingly, targeting cell cycle and notch pathways using small molecules also exhibited significant beneficial effects in controlling tumor malignancy. More importantly, we demonstrated that several cell cycle and Notch associated genes are significantly associated with poor overall survival and disease-free survival using the Log-Rank test.

CONCLUSION

In summary, our study comprehensively analyzed the gene expression pattern of CCA samples using publicly available datasets and identified the cell cycle and Notch pathways are potential therapeutic targets in this deadly disease.

Key Words: Bile duct cancer; Notch; Cell cycle; Liver cancer; Therapeutic target

©The Author(s) 2023. Published by Baishideng Publishing Group Inc. All rights reserved.

Core Tip: Molecular profiling of cholangiocarcinoma (CCA) has been conducted using various cohorts. However, the identified targets vary among different cohorts. In the current study, we combined different cohorts of CCA RNA sequencing datasets and refined the potential therapeutic targets in human CCA malignancy. We validated the findings using human CCA cell lines, the $Kras^{G12D}$ and P53 mutation transgenic mouse model, and human CCA clinical data, thus supporting the potential of targeting the identified pathways in clinical trials.

Citation: Liu D, Shi Y, Chen H, Nisar MA, Jabara N, Langwinski N, Mattson S, Nagaoka K, Bai X, Lu S, Huang CK. Molecular profiling reveals potential targets in cholangiocarcinoma. *World J Gastroenterol* 2023; 29(25): 4053-4071

URL: https://www.wjgnet.com/1007-9327/full/v29/i25/4053.htm

DOI: https://dx.doi.org/10.3748/wjg.v29.i25.4053

INTRODUCTION

Cholangiocarcinoma (CCA) is a devastating malignancy with "silent" clinical manifestations, genetically heterogeneous, anatomically distinct, but limited treatment options[1]. CCA can be classified as three subtypes depending on the origin of anatomical site, including intrahepatic (iCCA), perihilar (pCCA) and distal (dCCA) CCA[2]. If CCAs are diagnosed at the early stage, surgical resection may be a treatment option. However, CCA tumors are generally diagnosed at advanced stages due to lack of symptoms. Therefore, it is urgent to develop early detection markers and effective therapies for CCA patients. Understanding the molecular pathogenesis of CCAs may help identify early detection markers and potential therapies for this deadly disease.

Advances in whole-exome and transcriptome sequencing have paved the way for precision medicine in patients with advanced-stage or unresectable lesions[3-5]. Several genetic mutations have been identified in CCA patients[6]. Among them, IDH1 mutations have been well studied and the IDH1 mutation specific inhibitor has been developed for targeting malignant tumors with this mutation. In the ClarIDHy clinical trial, it was found that Ivosidenib-IDH1 mutation inhibitor could improve CCA patient overall survival (OS) and progression free survival[7,8], which eventually led to the FDA approval of Ivosidenib use in CCA patients with IDH1 mutation. Nevertheless, the 5-year survival of these patients treated with Ivosidenib is not significantly improved[7,8]. Besides, there is no effective therapy for those CCA patients with wild-type IDH1, despite that cisplatin and gemcitabine could extend the median OS for 3.6 mo but is not curative. Therefore, there is still an unmet need for identifying effective therapies in CCA patients.

In the current study, we utilized the transcriptomic profiling of CCA to explore the oncogenic driver events, analyzed the relevant genes expression, and identified the feasibility of target therapies with respect to those tumorigenic lesions.

MATERIALS AND METHODS

Human data

A total of 2 archival tissue blocks from patients with eCCA were retrieved from the First Affiliated Hospital of Zhengzhou University (Zhengzhou, Henan Province, China) and the specimens were independently diagnosed by two hepatobiliary pathologists. This study was conducted in accordance with the Declaration of Helsinki, and approved by the Institutional Review Board of the same institution (Approval No. 2022-KY-1514-002). Informed consents were obtained from all patients.

Cell Lines and reagents

Human CCA cell lines, including H1 (OCUCh-LM1-H1)[9], HuCCT1[10], SSP-25[11], and ETK1[12] cell lines were kindly provided by Dr. Jack Wands. TFK-1 and RBE were purchased from RIKEN Cell Bank (Tsukuba, Japan). The non-malignant human bile duct cells hBD was purchased from Celprogen Inc (Torrance, CA, United States, Catalog Number: 36755-12). CCA cell lines were cultured in RPMI-1640 supplemented with 10% fetal bovine serum (FBS; Gibco™, Thermo Scientific, Waltham, MA, United States; Cat# 10099141C), 100 μg/mL streptomycin, and 100 U/mL penicillin (HyClone™, Logan, UT, United States). The hBD cell line was grown in DMEM containing 10% FBS, 100 μg/mL strep. All cell lines were authenticated by STR and were negative for contamination of mycoplasma recently. Arcyriaflavin A, Flavopiridol, Roscovitine, and γ-secretase inhibitor, DAPT (N-[N-(3, 5-difluorophenacetyl)-l-alanyl]-s-phenylglycinet-butyl ester) were all purchased from Cayman Chemical (Ann Arbor, MI, United States).

Data collection

RNA-Seq, DNA methylation, and clinicopathological data of 36 patients with cholangiocarcinoma (liver/normal bile duct = 9, iCCA = 30, pCCA = 4, dCCA = 2) were retrieved from The Cancer Genome Atlas (TCGA) database. The Genomic Data Commons mRNA quantifications were calculated by STAR [13], and then annotated by the reference gene model GENCODE v36. iCCA and the related para-cancerous normal livers from 30 patients, and their survival information were employed (GSE107943) [14]. Fastq files of RNA-Seq from 162 samples of CCA (iCCA = 122, pCCA = 14, dCCA = 26) and the associated survival status of patients were fetched from the European Genome-phenome Archive[15].

Survival analysis

The Kaplan-Meier analysis was performed to evaluate the OS and disease-free survival (DFS) of patients from GEO and EBI cohorts. The optimal cutoff point for two groups was estimated based on maximally selected rank statistics[16], and then significance of survival analysis was calculated using log-rank test between the two groups.

Gene set enrichment analyses

Gene set enrichment analysis (GSEA) was conducted using R package "Pi"[17]. Hallmark (H) and KEGG subset of Canonical Pathways (CP) gene sets were selected for GSEA[18].

Tumor-infiltrating immune cell analysis

Single-sample GSEA was performed to analyze the tumor-infiltrating lymphocytes (TILs) based on the 28 immune cell types[19]. Correlations between the indicated genes expression and each infiltrating immune cells levels were calculated based on Spearman correlation (ρ).

Genetically engineered mouse

All protocols were approved by the Institutional Animal Care and Use Committee (IACUC) at Rhode Island Hospital, and all experiments were conducted in accordance with the guidelines of this IACUC. The specifical $Kras^{G12D}$ (LSL-$Kras^{G12D}$), floxed-p53 (p53L/L), and albumin-Cre mutants strains were purchased from the Jackson Laboratory (Bar Harbor, ME, United States). They were intercrossed to achieve the mutant mice as indicated in the results section. The specific primers and genotyping protocol were performed following the instruction suggested by the Jackson Laboratory. Mice were bred in a pathogen-free environment and provided with free access to food and sterilized water Ad Libitum. Animals within experimental cohorts were monitored until the appearance of illness, including diminished activity, abdominal bloating, and cachexia, followed by full necropsy and the subsequent histopathological analysis.

MTT cell growth assay

Three CCA cell lines, including HuCCT1, H1, RBE, were seeded at 2×10^3 cells/well into 96-well plate in six replicates. And then the above-mentioned cells were treated with small molecular inhibitors targeting cell cycle (Arcyriaflavin a, Flavopiridol, and Roscovitine) and Notch (DAPT) pathways 24 h post-seeding, respectively. The treatments were changed as indicated at days 1, 3, 5, and 7. Cell proliferation was measured using MTT at the following day (day 0 and day 1) and every 48 h after (up to day

7). Absorbance at OD570 nm and 650 nm were read and then normalized to vehicle control (0.1% DMSO or the corresponding medium). The relative cell proliferation rates were calculated as OD570-OD650.

RNA extraction and real-time quantitative PCR

Total RNA was extracted from CCA cell lines using TRIzol™ (Invitrogen, Thermo Scientific; Cat# 15596026) according to the manufacturer's protocol. 1 μg of total RNA was used to reverse transcription using iScript™ Reverse Transcription Supermix (Bio-Rad, Hercules, CA, United States, Cat#1708840). The qRT-PCR was conducted using SYBR® Green Realtime PCR Master Mix (Bio-Rad, Cat#1725270) by QuantStudio™ 5 Real-Time PCR System (Applied Biosystems). The relative mRNA expression was calculated based on $2^{-\Delta\Delta Ct}$ protocol. All primers were listed in Supplementary Table 1.

Western blotting

Whole-cell protein extractions was acquired using RIPA Lysis and Extraction Buffer (Thermo Fisher Scientific, Cat# 89901), supplemented with protease inhibitor (Thermo Fisher Scientific, Cat#78430). The concentration of protein was quantified using Pierce BCA Protein Assay Kit (Thermo Fisher Scientific, Cat# J63283.QA) before mixed with protein loading buffer (3×). Then the protein samples were separated by 10% SDS-PAGE, and the detailed procedures conducted as previously described[20].

Antibodies including α-Tubulin, GAPDH, Cyclin D1, P21, PCNA, E2F1, CDK2, CDK4, CDK6, RB1, JAG1, JAG2, Caspase 8, BAX, XIAP, BCL-2L12, ATR, ATM, Rad50, Mre11, PIK3C3, LC3A/B, and ULK1 were purchased from Cell Signaling Technology (Danvers, MA, United States) and Santa Cruz Biotechnology (Dallas, TX, United States).

Statistical analysis

Statistical analyses were performed using STATA software 16.0 (StataCorp, College Station, TX, United States) and R software (version 4.2.0). Statistical analysis was performed using unpaired Student's *t* and Mann-Whitney *U* test with respect to Gaussian distribution or not, respectively, unless otherwise indicated. Kruskal-wallis test was performed to compare the expression of genes examined by PCR, and the *post-hoc* tests within two groups were adjusted by Holm's correction. Spearman correlation coefficient (ρ) is used to evaluate the correlations between DNA methylation levels of CpG islands and the associated genes expression. Wilcoxon signed-rank test was utilized to compare the expression level of cell cycle and Notch related genes between iCCA and its corresponding normal tissues. Two-way repeated measures Anova was utilized to compare optical densities of CCA cell lines treated with the serial gradient concentration of drugs, which measured more than once. Then simple effect at day 7 was calculated when there were interaction effects between time and dosages. *P* values were shown as: $^{a}P < 0.05$, $^{b}P < 0.01$, and $^{c}P < 0.001$.

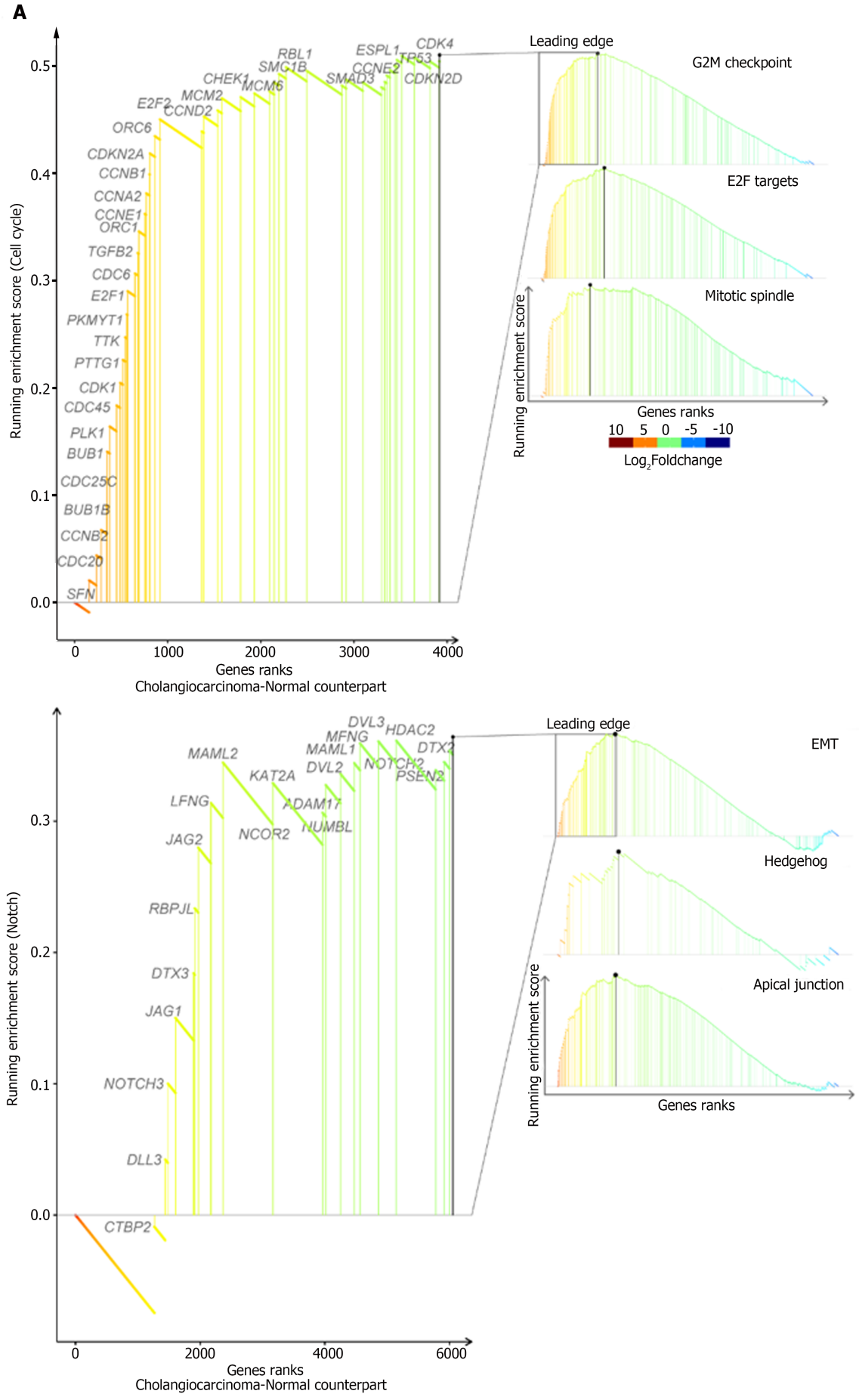
RESULTS

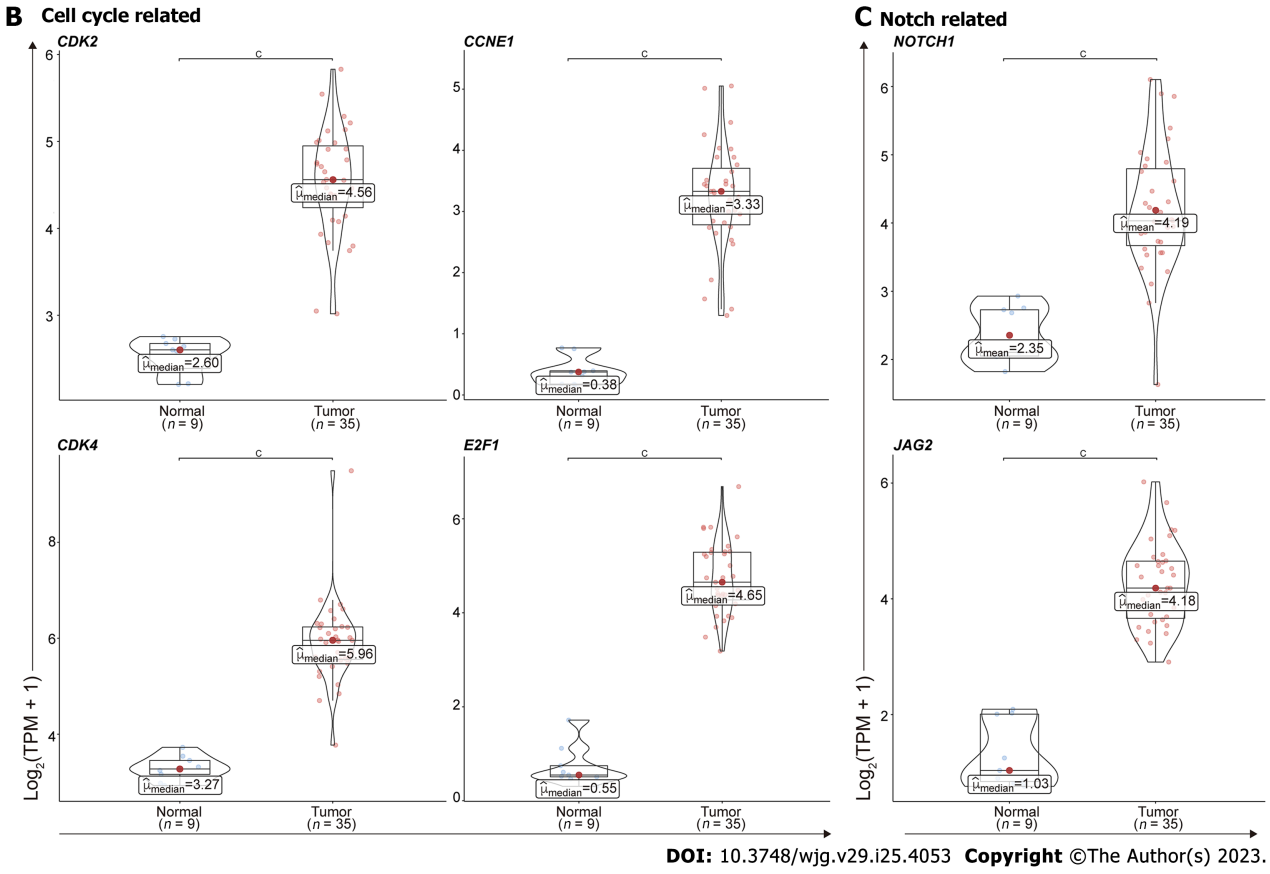
CCA oncogenesis is highly associated with elevated cell cycle and Notch associated pathways

To determine what molecular events are up-regulated in cholangiocarcinogenesis, we downloaded the transcriptomic data of CHOL from the TCGA database. We performed the GSEA and found that cell cycle associated pathways were preferentially activated in tumors compared with the normal samples, such as genes involved in G2M checkpoint, E2F Targets, and Mitotic spindle (Figure 1A, upper). Besides, the pathways related with Notch were also induced in tumors, *e.g.*, genes implicated in epithelial mesenchymal transition (EMT), Hedgehog, and Apical Junction (Figure 1A, lower). We retrieved the leading edge gene sets from those pathways, which drive the enrichment score and dominate the tumorigenicity of those pathways. Consistently, the genes from those leading edges are distinctly up-regulated in tumors compared with the normal samples, in line with the oncogenic properties (Figure 1B and C). Together, through the analysis of GSEA and differentially expressed genes, we found cell cycle and Notch pathways are up-regulated in CCA patients compared to non-malignant patient controls.

Cell cycle and Notch associated pathways were found upregulated in CCA cell lines compared to normal biliary epithelial cells

To facilitate the application of identified genes in preclinical studies, we must validate if these findings are reproducible in established normal biliary epithelial cells and CCA cells. In this case, we would be able to evaluate whether these pathways can be targeted using the *in vitro* cell culture system. Thus, we examined several leading-edge genes associated with these pathways in normal biliary epithelial cells and several CCA cell lines. The results suggest that several cell cycles associated genes were up-regulated in CCA cancer lines, including *PCNA*, *E2F1*, *CDK2*, *CDK4*, and *CDK6* (Figure 2A). Besides, *JAG1* and *JAG2* which serve as the Notch ligand also substantially increased in CCA cell lines when compared with normal biliary epithelial cells (Figure 2B). We also examined several genes involved in autophagy, cell death, and DNA damage pathways since we wanted to illustrate if cell cycle associated


A
Running enrichment score (Cell cycle)
0.5
0.4
0.3
0.2
0.1
0.0
RBL1
SMG1B
CHEK1
MCM6
MCM2
E2F2
CCND2
ORC6
CDKN2A
CCNB1
CCNA2
CCNE1
ORC1
TGFB2
CDC6
E2F1
PKMYT1
TTK
PTTG1
CDK1
CDC45
PLK1
BUB1
CDC25C
BUB1B
CCNB2
CDC20
SFN
ESPL1
TP53
CDK4
CCNE2
SMAD3
CDKN2D
0
1000
2000
3000
4000
Genes ranks
Cholangiocarcinoma-Normal counterpart
Leading edge
G2M checkpoint
E2F targets
Mitotic spindle
Running enrichment score
Genes ranks
10 5 0 -5 -10
Log2Foldchange
Running enrichment score (Notch)
0.3
0.2
0.1
0.0
DVL3
MFNG
HDAC2
MAML2
MAML1
DTX2
KAT2A
DVL2
NOTCH2
PSEN2
LFNG
ADAM17
NCOR2
NUMBL
JAG2
RBPJL
DTX3
JAG1
NOTCH3
DLL3
CTBP2
0
2000
4000
6000
Genes ranks
Cholangiocarcinoma-Normal counterpart
Leading edge
EMT
Hedgehog
Apical junction
Running enrichment score
Genes ranks



DOI: 10.3748/wjg.v29.i25.4053 **Copyright** ©The Author(s) 2023.

Figure 1 Cholangiocarcinogenesis driven by cell cycle and Notch associated pathways. A: Rank-based gene set enrichment analysis of genes preferentially activated in tumors identified the tumorigenic pathways, cell cycle and Notch from Hallmark gene sets, in CHOL transcriptome from TCGA database. Upper: Cell cycle associated pathways, including G2M checkpoint, E2F Targets, and Mitotic spindle gene sets; Lower: Notch associated pathways, including epithelial mesenchymal transition, Hedgehog, and apical junction gene sets. The mRNA expression levels from the leading edges of cell cycle (B) and Notch (C) associated pathways were analyzed in human normal bile ducts (n = 9) and CCA samples (n = 35) using TCGA database, suggesting up-regulation of cell cycle and Notch associated genes in CCA samples. TPM: Transcripts per kilobase million; Red: Cholangiocarcinoma (iCCA/eCCA), Blue: Normal bile ducts and/or para-cancerous liver; EMT: Rpithelial mesenchymal transition. $^{c}P < 0.001$ when compared with the normal control.

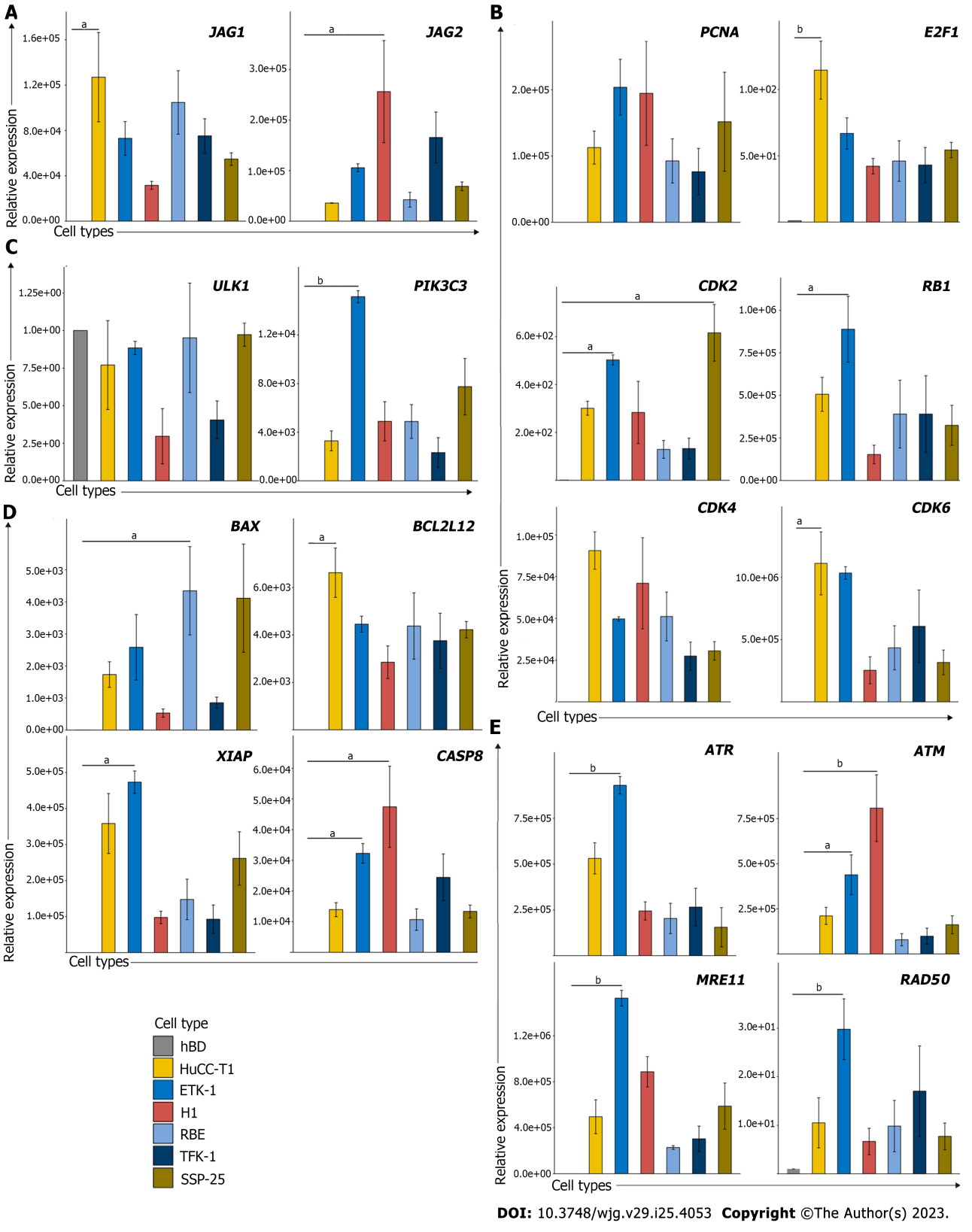
pathways play a dominant role or cell death pathways dominate the CCA tumorigenesis. Interestingly, we found several up-regulated genes that are associated with DNA damage and cell death pathways, but not autophagy (Figure 2C-E). Moreover, the negative correlations between the methylation status (β value) and its expression of those genes suggested that the aberrant expression might be attributed to the hyper- or hypomethylation (Supplementary Figure 1).

Up-regulated cell cycle and Notch associated gene expression levels were correlated with protein expression profiles in CCA cell lines

To determine if the identified genes have increased protein expression levels or promote other protein expression levels of the same pathway in CCA cell lines compared with the control biliary epithelial cells, we decided to examine protein expression of several major representative genes in each pathway (Figure 3, Supplementary Figure 2). As shown, several cell cycles associated genes were up-regulated in CCA cell lines when compared with the control biliary epithelial cells, including CDK2, CDK4, CDK6, and E2F1. Unexpectedly, several cyclins which include cyclin D1 and cyclin E1 were found decreased (Figure 3A). When we examined Notch ligands which include JAG1 and JAG2, we found JAG1 and JAG2 were all significantly increased in CCA cell lines compared to the biliary epithelial cells (Figure 3B). We further examined autophagy associated proteins and found no significant difference in autophagy between normal and malignant cells based on the autophagy definition (Figure 3C)[21]. In line with the mRNA change data, several apoptosis and DNA damage associated genes that were identified elevated in CCA cell lines were found increased as well (Figure 3D and E). Together, the mRNA and protein profile data demonstrated that it is feasible to identify potential target genes through mining public datasets and validating through *in vitro* human CCA cell lines.

Validation of the identified genes in a triple transgenic CCA mouse model

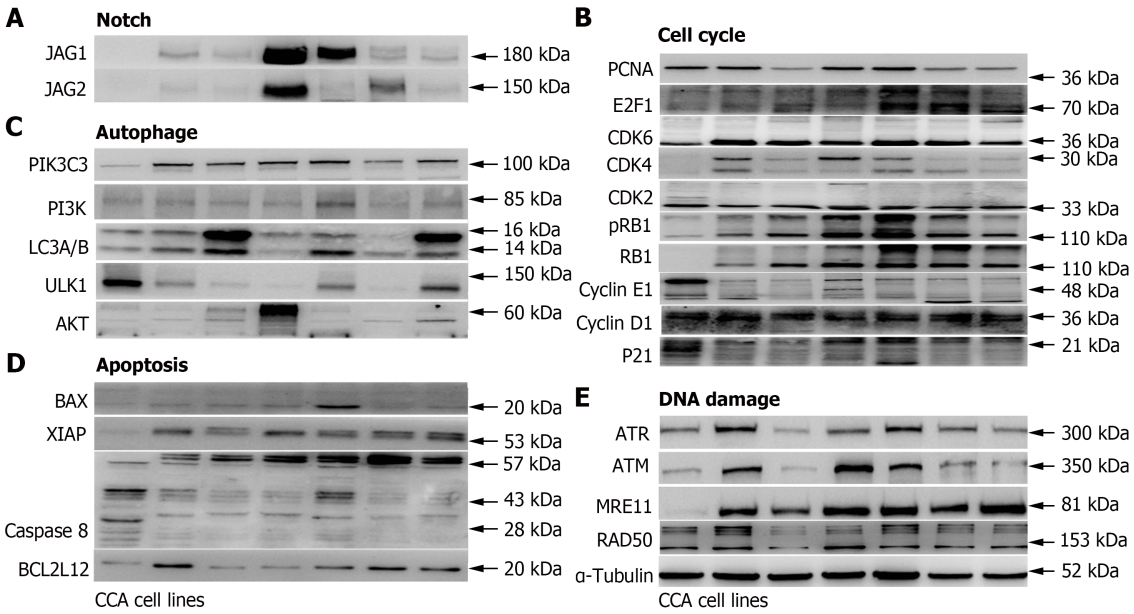
It has been well characterized that *KRAS* and *P53* are two of the most mutant genes in human CCA tumor samples[22]. Thus, a previous study has established the CCA transgenic mouse model by



DOI: 10.3748/wjg.v29.i25.4053 **Copyright** ©The Author(s) 2023.

Figure 2 Cell cycle and Notch associated pathways are increased in cholangiocarcinoma cell lines *in vitro*. The mRNA expression levels of leading-edge genes from (A) Notch, (B) cell cycle, (C) autophagy, (D) cell death, and (E) DNA damage were examined in cholangiocarcinoma (CCA) cell lines compared to normal biliary epithelial cells (hBD), indicating up-regulation of these genes in CCA tumor samples. CCA tumor cell lines including HuCCT1, ETK-1, H1, RBE, TFK-1 and SSP25. Data are relative to hBD cell line and normalized to 18S rRNA.

conditionally activating Kras^{G12D} and depleting P53 (either P53 homozygous or P53 heterozygous knockout) in mouse liver using the Albumin promoter driven cre recombinase[23]. We also established the CCA transgenic mouse (Figure 4A) as evidenced by the genotyping data showing positive cre, Kras^{G12D}, and heterozygous floxed P53 genes (Figure 4B). The gross images of representative mouse



DOI: 10.3748/wjg.v29.i25.4053 **Copyright** ©The Author(s) 2023.

Figure 3 The cell cycle and Notch pathway associated protein expression levels are up-regulated in cholangiocarcinoma cell lines compared to the normal human bile duct cells. The protein expression levels of leading-edge genes from (A) Notch, (B) cell cycle, (C) autophagy, (D) cell death, and (E) DNA damage were determined in cholangiocarcinoma (CCA) cell lines compared to hBD. Several cell cycle and Notch associated genes, including CDK4, CDK6, E2F1, JAG1, and JAG2, were up-regulated in CCA cell lines. CCA tumor cell lines including HuCCT1, ETK-1, H1, RBE, TFK-1 and SSP25. α-Tubulin served as the loading control.

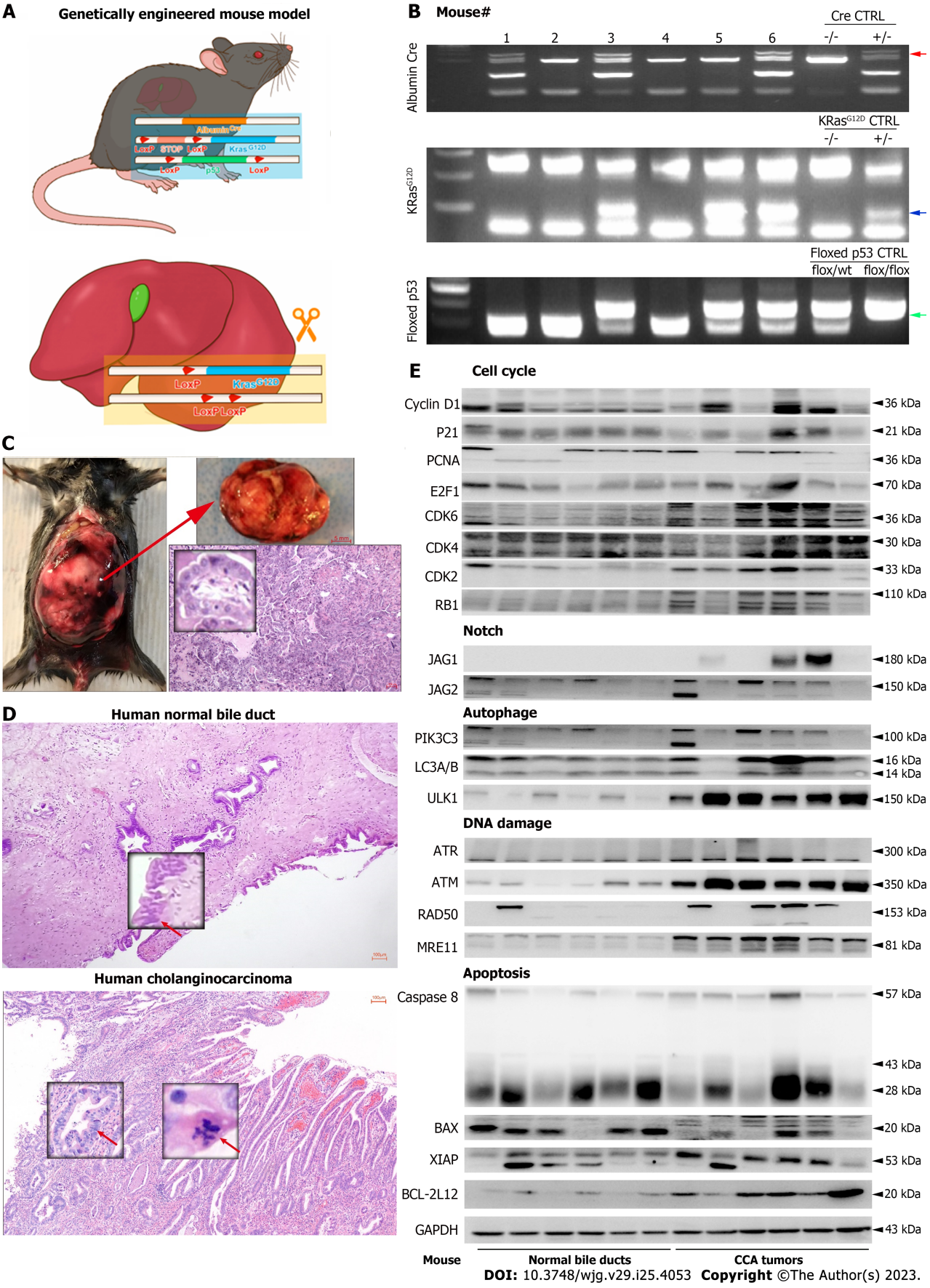
tumor were showed (Figure 4C). When comparing with human non-malignant bile duct and CCA tumor samples, the mouse CCA tumors present almost identical CCA histology to human CCA tumor samples (Figure 4C and D). To further determine whether mouse CCA and human CCA tumors have similar molecular profiles, we examined the genes that we identified using public human CCA dataset and validated using normal biliary epithelial cells and human CCA cell lines. Intriguingly, mouse and human CCA both have highly elevated genes associated with cell cycles and Notch, including CDK2, CDK4, CDK6, JAG1, and JAG2 (Figure 4E and Supplementary Figure 3). In line with CCA cell line data, several DNA damage genes, including RAD50 and MRE11, were found increased in mouse CCA tumor samples as well (Figure 4E). Given all these facts, our data demonstrated that the CCA tumors derived from the CCA transgenic mouse model have very high similarity to human CCA tissues and cell lines. Besides, the results of CCA transgenic mouse tumor data further demonstrated that refining the public human RNA sequencing data would help identify dysregulated pathways which may be druggable.

Targeting cell cycle and Notch pathways inhibited cell growth of human CCA cell lines

As we have found that cell cycle and Notch associated pathways are highly elevated in human CCA tumor samples and validated these findings in CCA cell lines, we proposed to determine whether targeting these pathways using small molecular inhibitors could achieve therapeutic potential in CCA cell lines, including H1, HuCCT1 (Kras and P53 mutations), and RBE (IDH1 mutation). It was found that the D1-dependent CDK4 inhibitor Arcyriaflavin a significantly suppressed cell growth in HuCCT1 and RBE CCA cell lines, but to a less extent in H1 (Figure 5A). The pan-CDK inhibitor Flavopiridol and the selected CDK inhibitor Roscovitine, which targets multiple CDKs, both displayed substantial growth inhibition in H1, HuCCT1, and RBE CCA cell lines (Figure 5B and C). It was noted that RBE CCA cells with IDH1 mutation are very vulnerable upon the treatments of CDK inhibitors (Figure 5A-C). Regarding the treatment using a Notch inhibitor, a γ-secretase inhibitor-DAPT was used to challenge these CCA cell lines. Although the Notch inhibitor could exert anti-tumor effects in CCA cell lines, the suppressive effects are not as strong as CDK inhibitors. Furthermore, the close relationships between the levels of TILs and those genes expressed indicated that cell cycle related pathways are associated with immune check point therapies (Supplementary Figure 4). Taken together, our results suggested that targeting cell cycle and/or Notch pathways could be considered as alternative modalities for patients with CCA.

Validation of identified cell cycle and Notch related pathways in other datasets

It is essential to verify whether our findings are applicable to other datasets. Thus, we utilized another dataset (GSE107943) to validate the oncogenic traits of cell cycle and Notch related pathways in CCA. Consistently, the leading edge of GSEA showed pathways pertaining to cell cycle (Figure 6A, upper) and Notch (Figure 6A, lower) were significantly activated in tumors compared with the normal



DOI: 10.3748/wjg.v29.i25.4053 **Copyright** ©The Author(s) 2023.

Figure 4 Validation of the identified cell cycle and Notch associated genes in the triple transgenic cholangiocarcinoma mouse model. A: The cartoon diagram of the genetically engineered mouse modeling (GEM) strategies. Triple transgenic mice bearing Albumin-Cre transgene, LSL-Kras^{G12D}, and floxed-p53 were conditionally activated KrasG12D and heterozygous knocked out P53 in the liver. B: The genotyping data presenting positive Cre (red triangle),

KrasG12D (blue triangle), and homozygous floxed P53 genes (green triangle). C: The gross image of representative tumor (upper right, scale bar = 5 mm), and the corresponding histopathology (lower right, scale bar = 100 μm) with inset showing glandular appearance (arrow, scale bar = 20 μm). D: Histology of human bile duct (upper, scale bar = 100 μm) with inset showing biliary epithelium (arrow, scale bar = 20 μm), and cholangiocarcinoma (lower, scale bar = 100 μm) with inset showing mitotic figure (arrowhead, scale bar = 20 μm) and glandular appearance (arrow, scale bar = 20 μm). E: The protein expression levels of leading-edge genes from cell cycle and Notch associated pathways, and genes involved in autophagy, cell death and DNA damage in CCA tumor tissues from the GEM (50 wk) compared to the normal bile ducts of control mice (50 wk). GAPDH was used as the loading control.

samples. Besides, the analysis of differentially expressed genes also revealed that upregulation of cell cycle related genes, including *CDK2*, *CDK4*, *CCNE1*, and *E2F1*, were observed in human CCA tumor samples compared with the adjacent normal liver tissues. Similarly, several Notch associated genes, including *NOTCH1* and *JAG2*, were found up-regulated in CCA tumor samples as well (Figure 6C). Together, with the validation data derived from another dataset, it is therefore suggested that our findings are applicable to other clinical human CCA tumor samples.

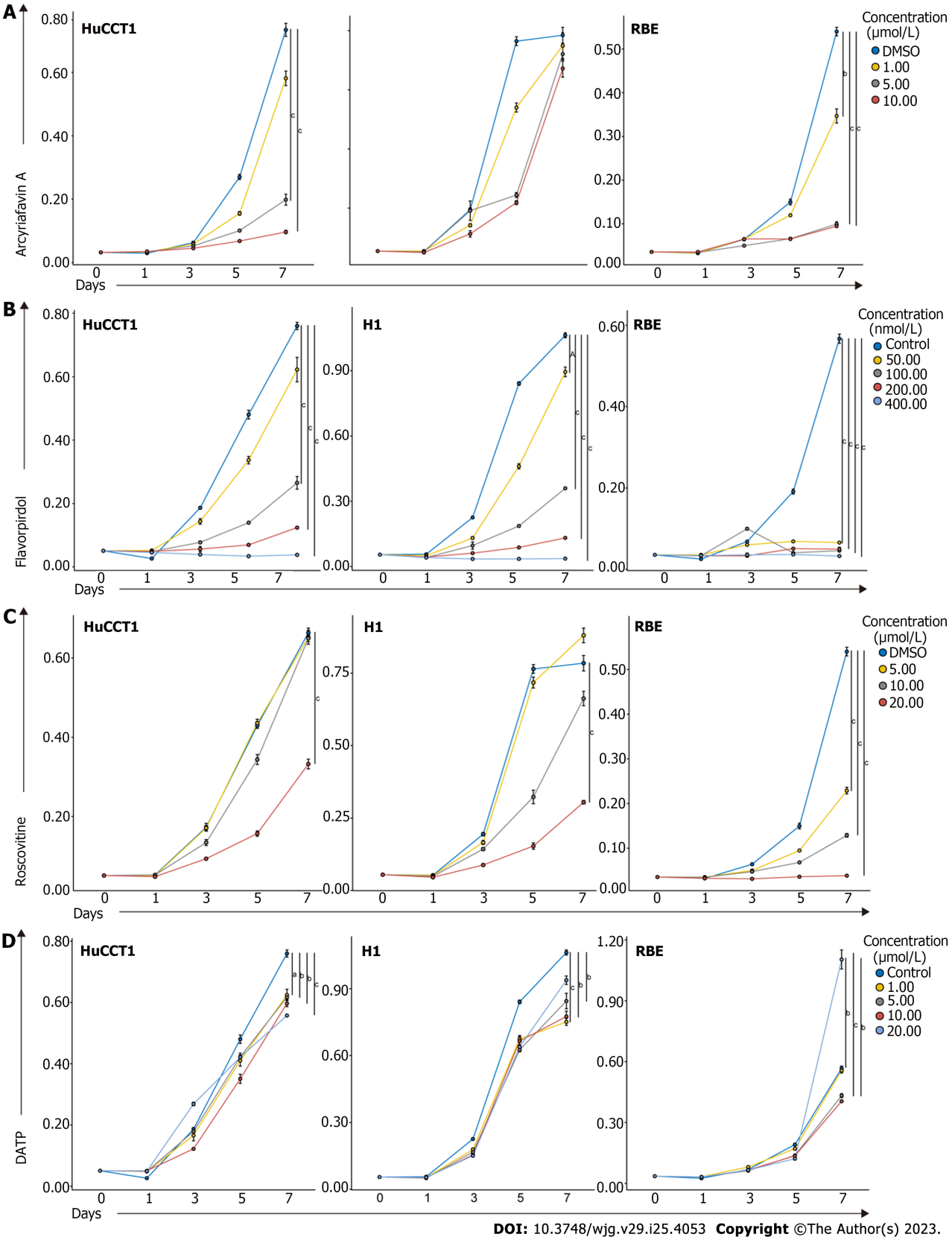
Cell cycle and Notch associated genes were correlated with poor prognosis in CCA patients

The cell cycle and Notch pathways were refined from the analysis of GSEA. These genes were found up-regulated in CCA tumor samples as well when compared with adjacent normal liver tissues. As we have found that targeting these pathways significantly suppressed CCA cell growth *in vitro*, we speculated that high expression of these genes may correlate with poor prognosis. To determine the correlation of these genes and CCA patient prognosis, we conducted the Kaplan-Meier survival analysis using the cell cycle and Notch pathways associated genes in CCA patients derived from two datasets, including GSE107943 and EBI (EGAD00001001076). It was found that high expression of cell cycle genes, including *CDK2*, *CDK6*, *CCNE1*, and *E2F1*, were negatively correlated with OS of CCA patients derived from the EBI database (EGAD00001001076) (Figure 7A). Similarly, high expression of Notch related genes, including *NOTCH1* and *JAG2*, were associated with poor prognosis in these patients (Figure 7B). These findings were further validated using the GSE107943 database. Consistently, high *CDK2*, *CDK4*, *CCNE1*, and *E2F1* were correlated with poor OS of CCA patients (Figure 7C). High *NOTCH1* expression was associated with poor OS and DFS in these patients as well (Figure 7D). Collectively, these data demonstrated that refining the signaling pathways associated with tumorigenesis of human CCA using bioinformatics approach could identify potential therapeutic targets for patients with this deadly disease (Figure 8).

DISCUSSION

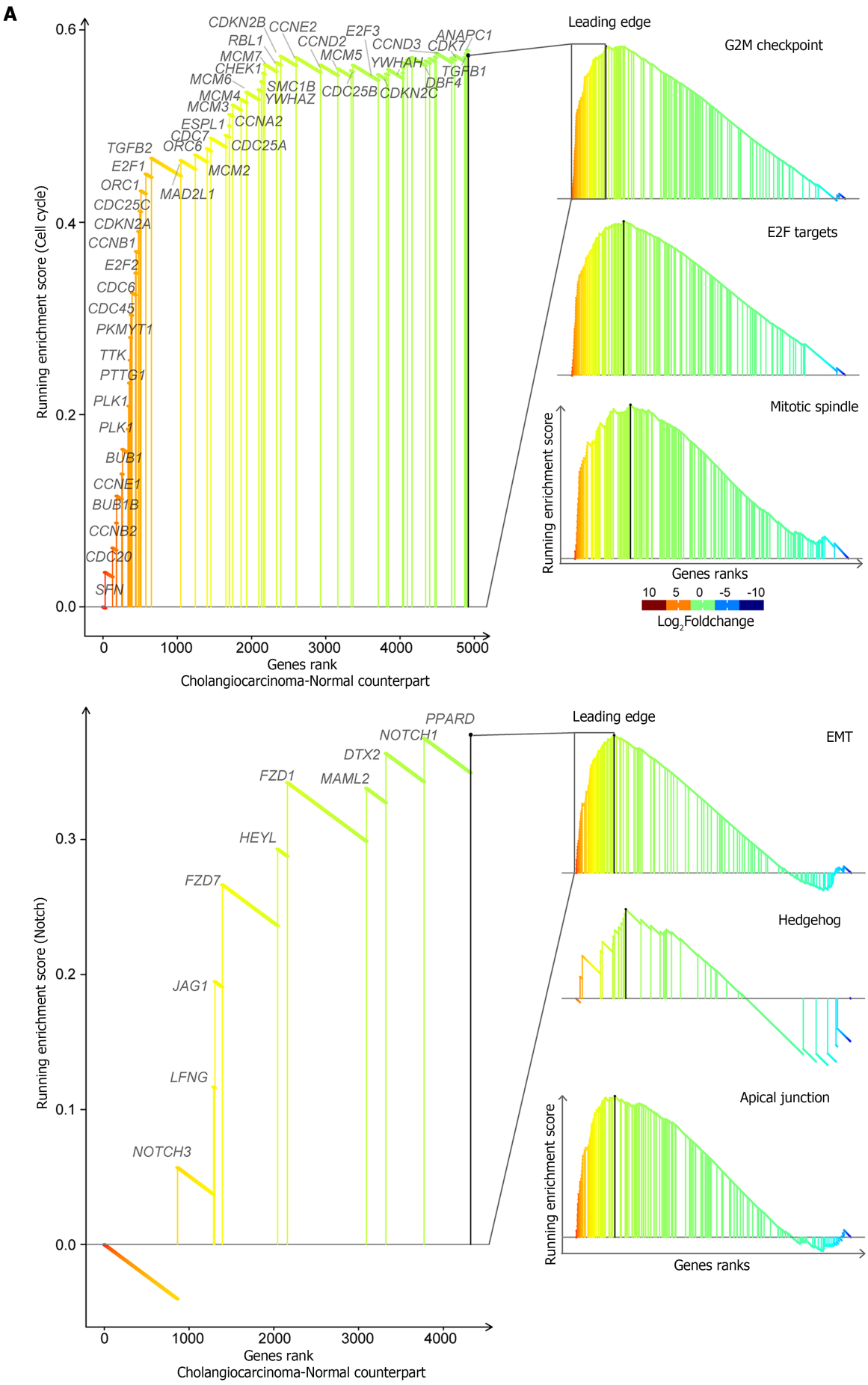
The current study demonstrated that cell cycle and notch associated pathways are elevated in human CCA patients compared with adjacent normal tissues. These findings were verified using human biliary epithelial cells and CCA cell lines. Consistently, cell cycle and Notch associated genes were found increased in CCA cell lines compared with non-malignant human biliary epithelial cells. As it has not been investigated if the cell cycle and Notch associated pathways are up-regulated in the CCA transgenic mice, our studies therefore disclose the similar but novel findings in the transgenic CCA mouse model. Cell cycle and Notch associated genes were up-regulated in mouse CCA tumors when compared with age-matched mouse normal bile ducts. Besides, we demonstrated that targeting cell cycle and Notch pathways could inhibit cell growth in human CCA cell lines. Furthermore, we validated the GSEA findings using another dataset. Most importantly, we demonstrated that high expression of several cell cycle and Notch associated genes are highly associated with poor prognosis in human CCA patients in two databases.

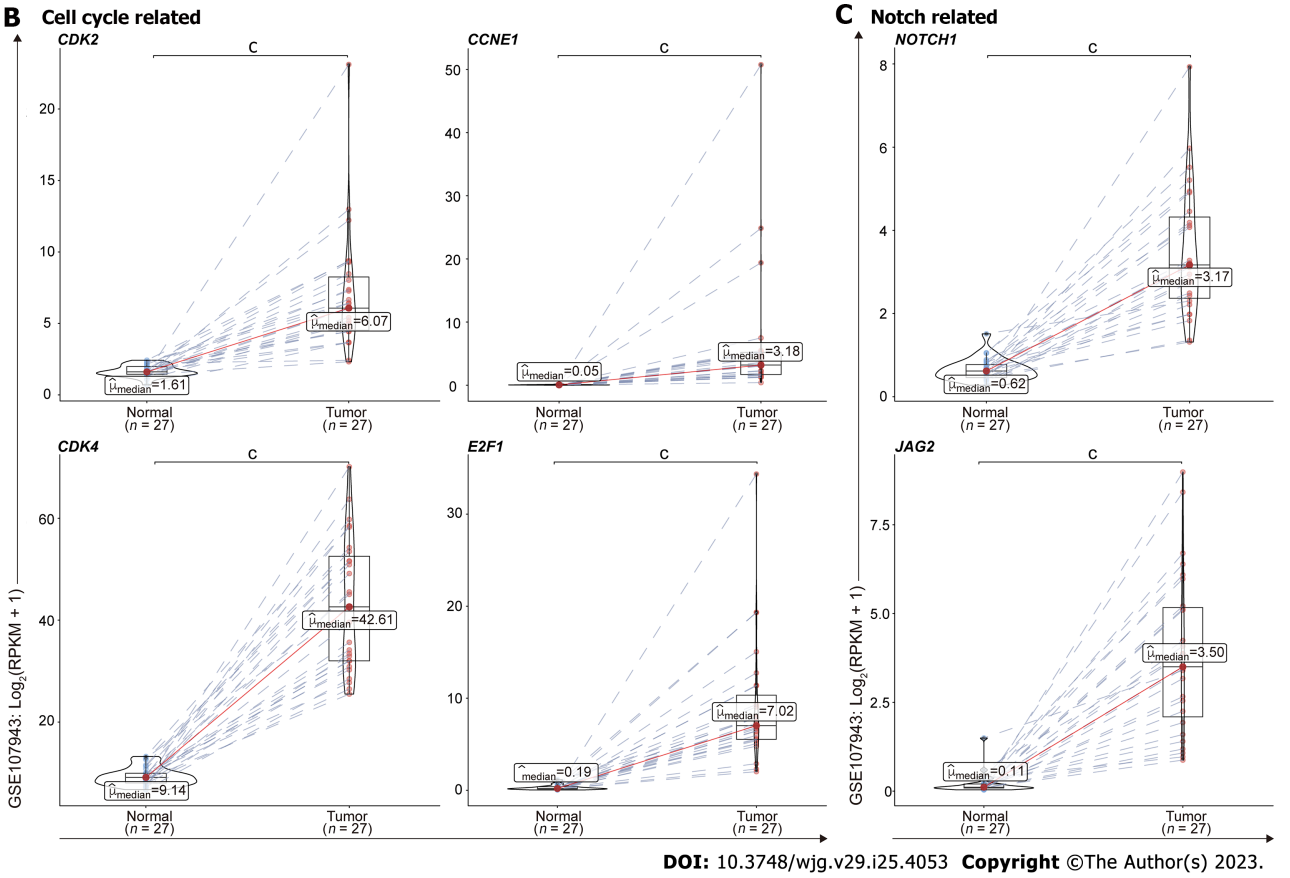
Refining RNA sequencing results have been well studied in liver malignancy, including hepatocellular carcinoma and CCA[3,4,24,25]. By combining whole genomic sequencing and RNA sequencing data, it was previously suggested that intrahepatic CCA could be classified as inflammation and proliferation groups which have different clinical outcomes, specifically worse prognosis in the proliferation group[26]. Recently, it was also suggested that extrahepatic CCA could be classified as immune, mesenchymal, metabolic, and proliferation groups. Further analysis revealed specific potential therapeutic targets correspondent to different groups, *i.e.*, PD1/PD-L1 inhibitors were suggested to be potential therapies for the immune group of extrahepatic CCA patients[4]. Nevertheless, these potential therapeutic approaches have not been evaluated in preclinical models due to the possible reasons that no preclinical models could represent the individual group specifically. However, the recent study investigated the microenvironment-based classification of intrahepatic CCA and identified the inflammatory stroma class of intrahepatic CCA with T cell exhaustion and KRas mutation. Thus, they evaluated if the combination of KRas inhibitor and PD1 antibody could inhibit the malignant progression of CCA tumors established by using tail vein hydrodynamic injection of SB13 transposase, CRISPR/Cas9-sg-p19, pCaggs-KrasG12D. The model has high similarity to the inflammatory stroma intrahepatic CCA group. Their findings demonstrated that Kras inhibitor and PD1 antibody could



DOI: 10.3748/wjg.v29.i25.4053 **Copyright** ©The Author(s) 2023.

Figure 5 Targeting cell cycle and Notch pathways inhibited cell growth of human cholangiocarcinoma cell lines. Growth curves of three cholangiocarcinoma cell lines with different genetic background, *e.g.*, HuCCT1 (KRAS and P53 mutations), RBE (IDH1 mutation), and H1, treated with cell cycle and Notch inhibitors, respectively. For targeting cell cycle pathways, (A) D1-dependent CDK4 inhibitor Arcyriaflavin a, (B) pan-CDK inhibitor Flavopiridol, (C) selected CDK inhibitor Roscovitine were utilized, and (D) the γ-secretase inhibitor (DAPT) was used against Notch pathway. Absorbance at OD570 nm and 650 nm analyzed by MTT, and then normalized to vehicle control (0.1% DMSO or the corresponding medium; n = 6 wells/dose point). The relative cell proliferation rates were calculated as OD570 - OD650. $^{a}P < 0.05$, $^{b}P < 0.01$, and $^{c}P < 0.001$ when compared with the vehicle control at day 7.


A
Running enrichment score (Cell cycle)
Genes rank
Cholangiocarcinoma-Normal counterpart
Leading edge
G2M checkpoint
E2F targets
Mitotic spindle
Running enrichment score
Genes ranks
Log2Foldchange
Running enrichment score (Notch)
Genes rank
Cholangiocarcinoma-Normal counterpart
Leading edge
EMT
Hedgehog
Apical junction
Running enrichment score
Genes ranks



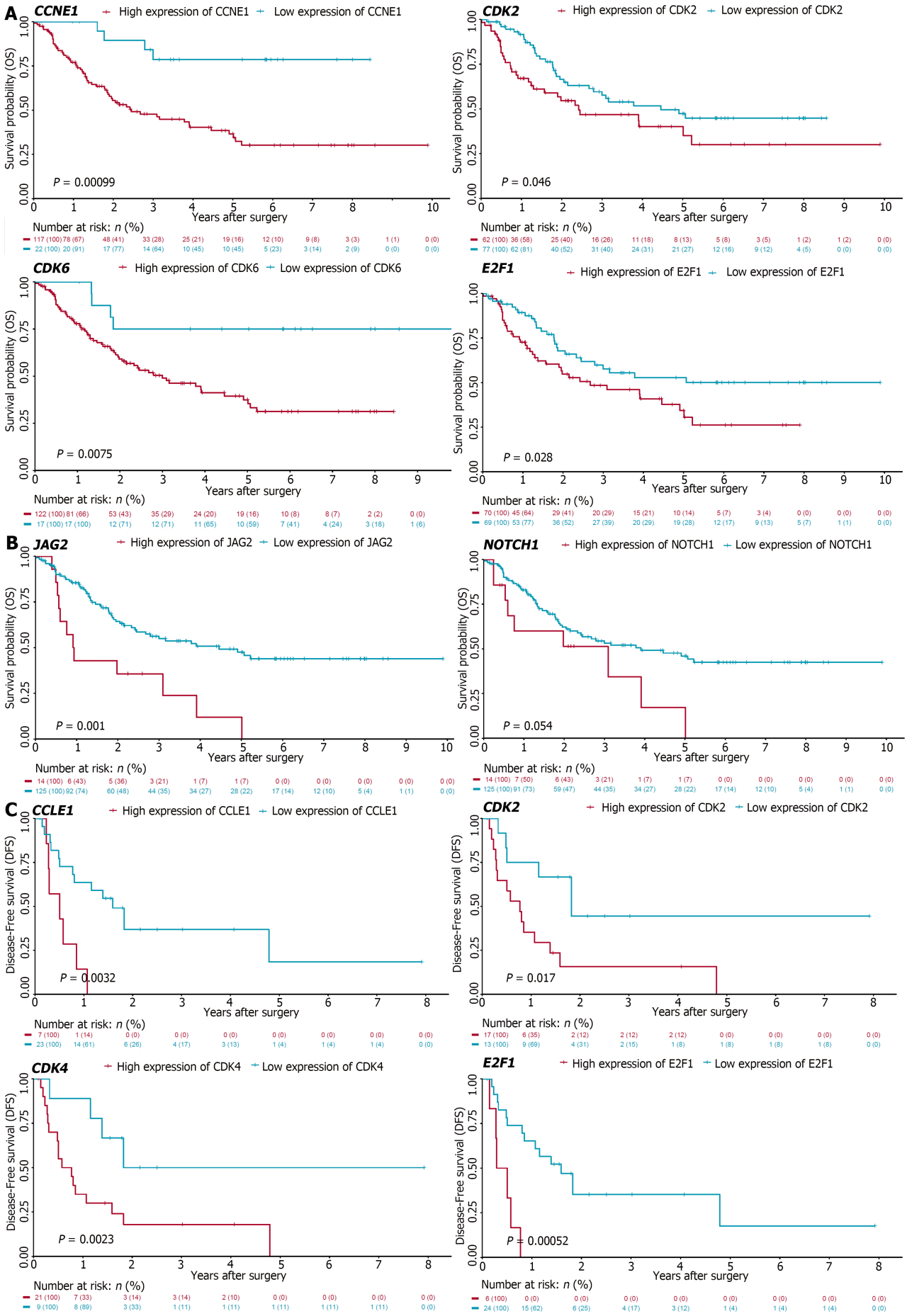
DOI: 10.3748/wjg.v29.i25.4053 **Copyright** ©The Author(s) 2023.

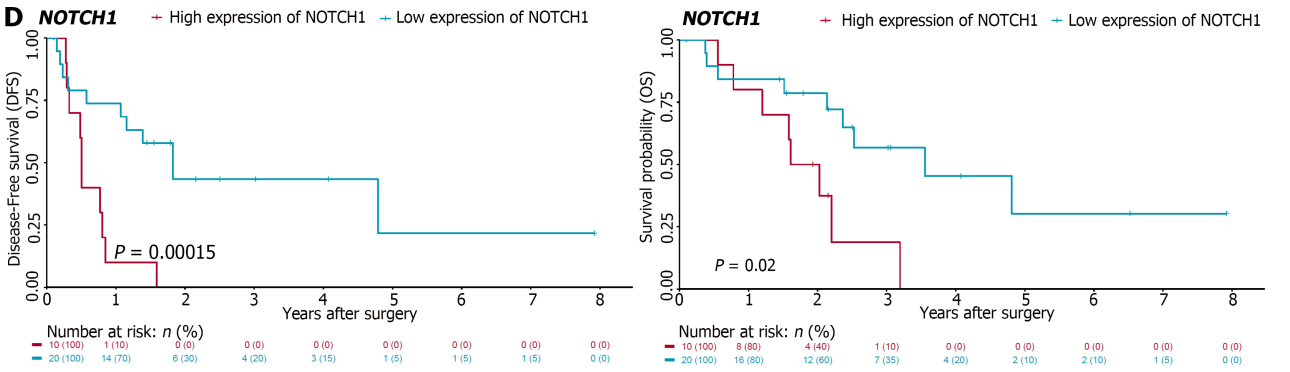
Figure 6 The generalizable oncogenic traits of cell cycle and Notch associated pathways in cholangiocarcinoma. GSEA identified cell cycle and Notch associated pathways significantly activated in tumors compared to the corresponding adjacent normal livers from GEO database (GSE107943) (A). Upper: Cell cycle associated pathways, including G2M checkpoint, E2F Targets, and Mitotic spindle gene sets; lower: Notch associated pathways, including epithelial mesenchymal transition, Hedgehog, and apical junction gene sets. The mRNA expression levels from the leading edges of cell cycle (B) and Notch (C) associated pathways were analyzed in CCA samples compared to the corresponding adjacent normal livers (pairs = 27). RPKM: Reads per kilobase million; Red: Intrahepatic cholangiocarcinoma; Blue: Para-cancerous normal liver; $^{c}P < 0.001$ when compared with the relevant normal control.

substantially inhibit tumor malignant progression[3]. Taken together, it is very likely to identify potential therapeutic targets by refining publicly available RNA sequencing datasets.

By using this approach, we found that Notch and cell cycle associated pathways are potential therapeutic targets in CCA tumors. It has been previously demonstrated that specific overexpression of intracellular domain of Notch 1 could lead to CCA development possibly through cyclin E1[27]. The Notch1 Ligand, JAG1 could activate Notch1 signaling cascade to initiate cyclin D1 transcriptional expression[28]. Both JAG1 and Notch1 contain the epidermal growth factor like domain[29] which could be hydroxylated by aspartate beta-hydroxylase[30-32]. Indeed, previous studies have demonstrated that aspartate beta-hydroxylase could promote CCA progression through the Notch1-mediated cyclin D1 pathway[33]. Cell cycle is tightly controlled by the tumor suppressor retinoblastoma protein (RB1)[34]. Although RB1 mutation is not a common event in CCA patients[35], dysregulated cell cycle regulating genes are often found in these patients. Dysregulated cell cycle control would lead to cancer cell proliferation. As discussed, intrahepatic CCA patients could be classified as proliferative and inflammatory groups[26]. Previous studies also demonstrated the therapeutic potential of targeting CCA tumors by using the specific inhibitor targeting cyclin dependent kinases 4 and 6[36,37] which are important mediator controlling RB1 phosphorylation. Phosphorylation of RB1 prevents its binding from the E2F1 transcriptional factor, which finely modulates cell cycle regulating genes[38]. Thus, phosphorylation of RB1 would lead to inactivation of RB1 tumor suppressor function, in turn promoting cell cycle progression. It was previously reported that aspartate beta-hydroxylase could promote RB1 phosphorylation to disrupt cell cycle regulation in CCA tumors[39]. Interestingly, aspartate beta-hydroxylase was reported to be highly expressed in CCA but barely detectable in normal bile duct tissues[39], suggesting the linkage of identified Notch1 and cell cycle associated pathways to aspartate beta-hydroxylase.

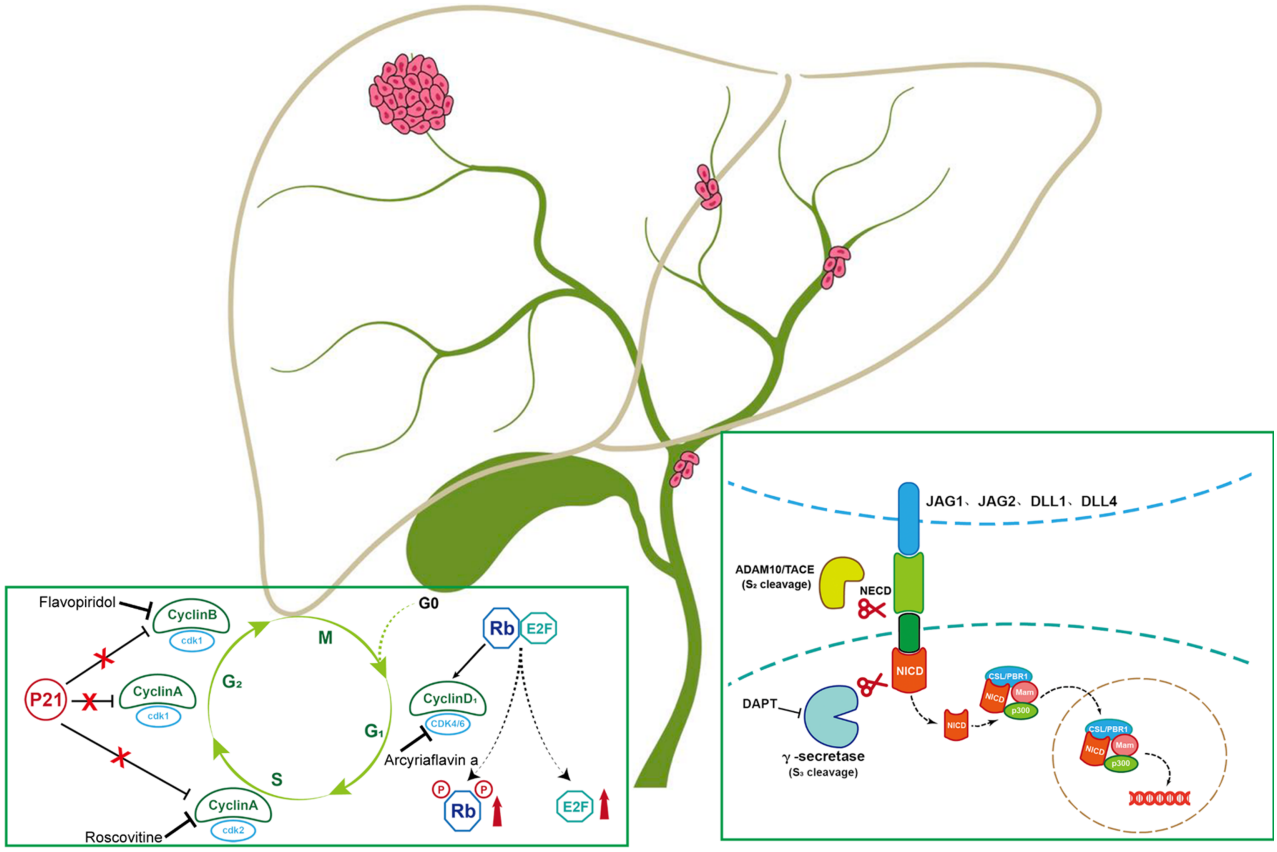
The current study has several limitations. (1) We did not evaluate if targeting Notch1 and cell cycle pathways could inhibit CCA progression using preclinical models. Actually, the previous studies have demonstrated that Notch1 inhibitor could be a potential therapeutic approach[27] and that targeting cell cycle with CDK4/6 inhibitors could suppress CCA progression[36,37]. Although the current study was


A
CCNE1
High expression of CCNE1
Low expression of CCNE1
Survival probability (OS)
P = 0.00099
Years after surgery
Number at risk: n (%)
CDK2
High expression of CDK2
Low expression of CDK2
P = 0.046
CDK6
High expression of CDK6
Low expression of CDK6
P = 0.0075
E2F1
High expression of E2F1
Low expression of E2F1
P = 0.028
B
JAG2
High expression of JAG2
Low expression of JAG2
P = 0.001
NOTCH1
High expression of NOTCH1
Low expression of NOTCH1
P = 0.054
C
CCLE1
High expression of CCLE1
Low expression of CCLE1
Disease-Free survival (DFS)
P = 0.0032
CDK2
High expression of CDK2
Low expression of CDK2
P = 0.017
CDK4
High expression of CDK4
Low expression of CDK4
P = 0.0023
E2F1
High expression of E2F1
Low expression of E2F1
P = 0.00052



DOI: 10.3748/wjg.v29.i25.4053 **Copyright** ©The Author(s) 2023.

Figure 7 Cell cycle and Notch associated genes correlate with dismal survival in patients with cholangiocarcinoma. Kaplan-Meier analysis of cholangiocarcinoma patients in EBI-EGAD00001001076 (A and B) and GSE107943 (C and D) database. The optimal cutoff of genes from the leading edges of cell cycle (A and C) and Notch (B and D) associated pathways was calculated by maximally selected rank statistics. And then the difference between two groups was analyzed by log-rank test. Red: Higher expression of the indicated genes, Blue: Lower expression of indicated genes; DFS: Disease-free survival, OS: Overall survival.



DOI: 10.3748/wjg.v29.i25.4053 **Copyright** ©The Author(s) 2023.

Figure 8 The summary of dysregulated cell cycle and Notch pathways in cholangiocarcinoma progression. The cholangiocarcinogenesis driven by aberrant cell cycle and Notch pathways, which may be targeted by small molecular inhibitors.

initiated from a different angle by using transcriptomic analysis, it ended up with similar findings that Notch1 and cell cycle pathways could be potential targets in CCA patients; (2) We did not separate intrahepatic and extrahepatic CCA patients. We pooled the available data by combining intrahepatic and extrahepatic transcriptomic datasets due to the limited datasets publicly available; and (3) our studies did not investigate if elevation of cell cycle and Notch associated pathways may be used as early detection markers. Future studies will be needed to further determine potential therapeutic approaches specifically for intrahepatic and extrahepatic CCA patients, respectively.

CONCLUSION

In conclusion, our data, through mRNA and protein profiling, identified very high similarity between CCA tumors derived from the CCA transgenic mice and human CCA tumors, thus providing a potential preclinical CCA model for investigating the CCA tumorigenesis. Besides, our data suggested that cell cycle and Notch associated pathways could be potential therapeutic targets in CCA patients.

ARTICLE HIGHLIGHTS

Research background

The molecular pathogenesis of cholangiocarcinoma (CCA) remains largely unknown. Investigating the molecular mechanisms underlying CCA progression will potentially yield results toward identifying therapeutic targets.

Research motivation

Several mRNA sequencing (Seq) datasets in CCA samples are publicly available, but it remains unclear if the data can be validated in CCA cell lines, the transgenic CCA mouse model, and human CCA samples.

Research objectives

To summarize the mRNA Seq results and validate the findings in CCA cell lines, the transgenic CCA mouse model, and human CCA samples.

Research methods

Bioinformatic analysis, cell culture studies, transgenic mouse model, human CCA samples, and molecular strategies were used to determine molecular pathogenesis of CCA.

Research results

Through bioinformatic analysis, we found that cell cycle and Notch associated pathways are up-regulated in human CCA samples, compared to the non-tumor controls. We validated the findings in human CCA cell lines and the transgenic CCA mouse model.

Research conclusions

Our data, through mRNA and protein profiling, identified very high similarity between CCA tumors derived from the CCA transgenic mice and human CCA tumors, thus providing a potential preclinical CCA model for investigating CCA tumorigenesis. Besides, our data suggested that cell cycle and Notch associated pathways could be potential therapeutic targets in CCA patients.

Research perspectives

Systemic chemotherapy, gemcitabine and cisplatin, is recommended for CCA patients. However, the 5-year survival of CCA patients has not been significantly improved, suggesting an urgent need to develop novel therapeutic approaches.

FOOTNOTES

Author contributions: Huang CK contributed to the study concept and design; Liu D, Shi Y, Chen H, Nisar MA, Jabara N, Langwinski N, Mattson S, Nagaoka K, Bai X and Huang CK contributed to the acquisition of data; Liu D, Shi Y, Bai X, Huang CK and Lu S contributed to analysis and interpretation of data; Liu D, Lu S, Jabara N, Nagaoka K, Chen H and Nisar MA contributed to the technical support; Lu S contributed to the material support; Huang CK and Lu S obtained the funding; Liu D, Shi Y, Huang CK, Lu S and Nisar MA drafted the manuscript; Shi Y, Nisar MA, Huang CK, Lu S, Jabara N, Langwinski N and Mattson S revised the manuscript. Liu D and Shi Y contributed equally.

Supported by 2017 AASLD Pinnacle Research Career Development Award.

Institutional review board statement: All protocols were approved by the Institutional Animal Care and Use Committee (IACUC) at Rhode Island Hospital (CMTT # 5051-18), and all experiments were conducted in accordance with the guidelines of this IACUC.

Conflict-of-interest statement: The authors declare that they have no known competing financial interests or personal relationships that could have appeared to influence the work reported in this paper.

Data sharing statement: No additional data are available.

ARRIVE guidelines statement: The authors have read the ARRIVE Guidelines, and the manuscript was prepared and revised according to the ARRIVE Guidelines.

Open-Access: This article is an open-access article that was selected by an in-house editor and fully peer-reviewed by external reviewers. It is distributed in accordance with the Creative Commons Attribution NonCommercial (CC BY-NC 4.0) license, which permits others to distribute, remix, adapt, build upon this work non-commercially, and license their derivative works on different terms, provided the original work is properly cited and the use is non-commercial. See: https://creativecommons.org/Licenses/by-nc/4.0/

Country/Territory of origin: United States

ORCID number: Dan Liu 0000-0001-8313-4343; Chiung-Kuei Huang 0000-0001-6331-7898.

S-Editor: Chang KL
L-Editor: A
P-Editor: Cai YX

REFERENCES

1 **Banales JM**, Marin JJG, Lamarca A, Rodrigues PM, Khan SA, Roberts LR, Cardinale V, Carpino G, Andersen JB, Braconi C, Calvisi DF, Perugorria MJ, Fabris L, Boulter L, Macias RIR, Gaudio E, Alvaro D, Gradilone SA, Strazzabosco M, Marzioni M, Coulouarn C, Fouassier L, Raggi C, Invernizzi P, Mertens JC, Moncsek A, Rizvi S, Heimbach J, Koerkamp BG, Bruix J, Forner A, Bridgewater J, Valle JW, Gores GJ. Cholangiocarcinoma 2020: the next horizon in mechanisms and management. *Nat Rev Gastroenterol Hepatol* 2020; **17**: 557-588 [PMID: 32606456 DOI: 10.1038/s41575-020-0310-z]

2 **Banales JM**, Cardinale V, Carpino G, Marzioni M, Andersen JB, Invernizzi P, Lind GE, Folseraas T, Forbes SJ, Fouassier L, Geier A, Calvisi DF, Mertens JC, Trauner M, Benedetti A, Maroni L, Vaquero J, Macias RI, Raggi C, Perugorria MJ, Gaudio E, Boberg KM, Marin JJ, Alvaro D. Expert consensus document: Cholangiocarcinoma: current knowledge and future perspectives consensus statement from the European Network for the Study of Cholangiocarcinoma (ENS-CCA). *Nat Rev Gastroenterol Hepatol* 2016; **13**: 261-280 [PMID: 27095655 DOI: 10.1038/nrgastro.2016.51]

3 **Martin-Serrano MA**, Kepecs B, Torres-Martin M, Bramel ER, Haber PK, Merritt E, Rialdi A, Param NJ, Maeda M, Lindblad KE, Carter JK, Barcena-Varela M, Mazzaferro V, Schwartz M, Affo S, Schwabe RF, Villanueva A, Guccione E, Friedman SL, Lujambio A, Tocheva A, Llovet JM, Thung SN, Tsankov AM, Sia D. Novel microenvironment-based classification of intrahepatic cholangiocarcinoma with therapeutic implications. *Gut* 2023; 72: 736-748 [PMID: 35584893 DOI: 10.1136/gutjnl-2021-326514]

4 **Montal R**, Sia D, Montironi C, Leow WQ, Esteban-Fabró R, Pinyol R, Torres-Martin M, Bassaganyas L, Moeini A, Peix J, Cabellos L, Maeda M, Villacorta-Martin C, Tabrizian P, Rodriguez-Carunchio L, Castellano G, Sempoux C, Minguez B, Pawlik TM, Labgaa I, Roberts LR, Sole M, Fiel MI, Thung S, Fuster J, Roayaie S, Villanueva A, Schwartz M, Llovet JM. Molecular classification and therapeutic targets in extrahepatic cholangiocarcinoma. *J Hepatol* 2020; **73**: 315-327 [PMID: 32173382 DOI: 10.1016/j.jhep.2020.03.008]

5 **Nelson DR**, Hrout AA, Alzahmi AS, Chaiboonchoe A, Amin A, Salehi-Ashtiani K. Molecular Mechanisms behind Safranal's Toxicity to HepG2 Cells from Dual Omics. *Antioxidants (Basel)* 2022; **11** [PMID: 35740022 DOI: 10.3390/antiox11061125]

6 **Chan-On W**, Nairismägi ML, Ong CK, Lim WK, Dima S, Pairojkul C, Lim KH, McPherson JR, Cutcutache I, Heng HL, Ooi L, Chung A, Chow P, Cheow PC, Lee SY, Choo SP, Tan IB, Duda D, Nastase A, Myint SS, Wong BH, Gan A, Rajasegaran V, Ng CC, Nagarajan S, Jusakul A, Zhang S, Vohra P, Yu W, Huang D, Sithithaworn P, Yongvanit P, Wongkham S, Khuntikeo N, Bhudhisawasdi V, Popescu I, Rozen SG, Tan P, Teh BT. Exome sequencing identifies distinct mutational patterns in liver fluke-related and non-infection-related bile duct cancers. *Nat Genet* 2013; **45**: 1474-1478 [PMID: 24185513 DOI: 10.1038/ng.2806]

7 **Abou-Alfa GK**, Macarulla T, Javle MM, Kelley RK, Lubner SJ, Adeva J, Cleary JM, Catenacci DV, Borad MJ, Bridgewater J, Harris WP, Murphy AG, Oh DY, Whisenant J, Lowery MA, Goyal L, Shroff RT, El-Khoueiry AB, Fan B, Wu B, Chamberlain CX, Jiang L, Gliser C, Pandya SS, Valle JW, Zhu AX. Ivosidenib in IDH1-mutant, chemotherapy-refractory cholangiocarcinoma (ClarIDHy): a multicentre, randomised, double-blind, placebo-controlled, phase 3 study. *Lancet Oncol* 2020; **21**: 796-807 [PMID: 32416072 DOI: 10.1016/S1470-2045(20)30157-1]

8 **Zhu AX**, Macarulla T, Javle MM, Kelley RK, Lubner SJ, Adeva J, Cleary JM, Catenacci DVT, Borad MJ, Bridgewater JA, Harris WP, Murphy AG, Oh DY, Whisenant JR, Lowery MA, Goyal L, Shroff RT, El-Khoueiry AB, Chamberlain CX, Aguado-Fraile E, Choe S, Wu B, Liu H, Gliser C, Pandya SS, Valle JW, Abou-Alfa GK. Final Overall Survival Efficacy Results of Ivosidenib for Patients With Advanced Cholangiocarcinoma With IDH1 Mutation: The Phase 3 Randomized Clinical ClarIDHy Trial. *JAMA Oncol* 2021; **7**: 1669-1677 [PMID: 34554208 DOI: 10.1001/jamaoncol.2021.3836]

9 **Yamada N**, Chung YS, Arimoto Y, Sawada T, Seki S, Sowa M. Establishment of a new human extrahepatic bile duct carcinoma cell line (OCUCh-LM1) and experimental liver metastatic model. *Br J Cancer* 1995; **71**: 543-548 [PMID: 7880737 DOI: 10.1038/bjc.1995.107]

10 **Miyagiwa M**, Ichida T, Tokiwa T, Sato J, Sasaki H. A new human cholangiocellular carcinoma cell line (HuCC-T1) producing carbohydrate antigen 19/9 in serum-free medium. *In Vitro Cell Dev Biol* 1989; **25**: 503-510 [PMID: 2544546

DOI: 10.1007/BF02623562]
11 **Enjoji M**, Sakai H, Nawata H, Kajiyama K, Tsuneyoshi M. Sarcomatous and adenocarcinoma cell lines from the same nodule of cholangiocarcinoma. *In Vitro Cell Dev Biol Anim* 1997; **33**: 681-683 [PMID: 9358283 DOI: 10.1007/s11626-997-0125-z]
12 **Enjoji M**, Nakashima M, Honda M, Sakai H, Nawata H. Hepatocytic phenotypes induced in sarcomatous cholangiocarcinoma cells treated with 5-azacytidine. *Hepatology* 1997; **26**: 288-294 [PMID: 9252136 DOI: 10.1002/hep.510260206]
13 **Dobin A**, Davis CA, Schlesinger F, Drenkow J, Zaleski C, Jha S, Batut P, Chaisson M, Gingeras TR. STAR: ultrafast universal RNA-seq aligner. *Bioinformatics* 2013; **29**: 15-21 [PMID: 23104886 DOI: 10.1093/bioinformatics/bts635]
14 **Ahn KS**, O'Brien D, Kang YN, Mounajjed T, Kim YH, Kim TS, Kocher JA, Allotey LK, Borad MJ, Roberts LR, Kang KJ. Prognostic subclass of intrahepatic cholangiocarcinoma by integrative molecular-clinical analysis and potential targeted approach. *Hepatol Int* 2019; **13**: 490-500 [PMID: 31214875 DOI: 10.1007/s12072-019-09954-3]
15 **Nakamura H**, Arai Y, Totoki Y, Shirota T, Elzawahry A, Kato M, Hama N, Hosoda F, Urushidate T, Ohashi S, Hiraoka N, Ojima H, Shimada K, Okusaka T, Kosuge T, Miyagawa S, Shibata T. Genomic spectra of biliary tract cancer. *Nat Genet* 2015; **47**: 1003-1010 [PMID: 26258846 DOI: 10.1038/ng.3375]
16 **Wright MN**, Dankowski T, Ziegler A. Unbiased split variable selection for random survival forests using maximally selected rank statistics. *Stat Med* 2017; **36**: 1272-1284 [PMID: 28088842 DOI: 10.1002/sim.7212]
17 **Fang H**; ULTRA-DD Consortium, De Wolf H, Knezevic B, Burnham KL, Osgood J, Sanniti A, Lledó Lara A, Kasela S, De Cesco S, Wegner JK, Handunnetthi L, McCann FE, Chen L, Sekine T, Brennan PE, Marsden BD, Damerell D, O'Callaghan CA, Bountra C, Bowness P, Sundström Y, Milani L, Berg L, Göhlmann HW, Peeters PJ, Fairfax BP, Sundström M, Knight JC. A genetics-led approach defines the drug target landscape of 30 immune-related traits. *Nat Genet* 2019; **51**: 1082-1091 [PMID: 31253980 DOI: 10.1038/s41588-019-0456-1]
18 **Subramanian A**, Tamayo P, Mootha VK, Mukherjee S, Ebert BL, Gillette MA, Paulovich A, Pomeroy SL, Golub TR, Lander ES, Mesirov JP. Gene set enrichment analysis: a knowledge-based approach for interpreting genome-wide expression profiles. *Proc Natl Acad Sci U S A* 2005; **102**: 15545-15550 [PMID: 16199517 DOI: 10.1073/pnas.0506580102]
19 **Charoentong P**, Finotello F, Angelova M, Mayer C, Efremova M, Rieder D, Hackl H, Trajanoski Z. Pan-cancer Immunogenomic Analyses Reveal Genotype-Immunophenotype Relationships and Predictors of Response to Checkpoint Blockade. *Cell Rep* 2017; **18**: 248-262 [PMID: 28052254 DOI: 10.1016/j.celrep.2016.12.019]
20 **Huang CK**, Lee SO, Lai KP, Ma WL, Lin TH, Tsai MY, Luo J, Chang C. Targeting androgen receptor in bone marrow mesenchymal stem cells leads to better transplantation therapy efficacy in liver cirrhosis. *Hepatology* 2013; **57**: 1550-1563 [PMID: 23150236 DOI: 10.1002/hep.26135]
21 **Mizushima N**, Yoshimori T. How to interpret LC3 immunoblotting. *Autophagy* 2007; **3**: 542-545 [PMID: 17611390 DOI: 10.4161/auto.4600]
22 **Farshidfar F**, Zheng S, Gingras MC, Newton Y, Shih J, Robertson AG, Hinoue T, Hoadley KA, Gibb EA, Roszik J, Covington KR, Wu CC, Shinbrot E, Stransky N, Hegde A, Yang JD, Reznik E, Sadeghi S, Pedamallu CS, Ojesina AI, Hess JM, Auman JT, Rhie SK, Bowlby R, Borad MJ; Cancer Genome Atlas Network, Zhu AX, Stuart JM, Sander C, Akbani R, Cherniack AD, Deshpande V, Mounajjed T, Foo WC, Torbenson MS, Kleiner DE, Laird PW, Wheeler DA, McRee AJ, Bathe OF, Andersen JB, Bardeesy N, Roberts LR, Kwong LN. Integrative Genomic Analysis of Cholangiocarcinoma Identifies Distinct IDH-Mutant Molecular Profiles. *Cell Rep* 2017; **18**: 2780-2794 [PMID: 28297679 DOI: 10.1016/j.celrep.2017.02.033]
23 **O'Dell MR**, Huang JL, Whitney-Miller CL, Deshpande V, Rothberg P, Grose V, Rossi RM, Zhu AX, Land H, Bardeesy N, Hezel AF. Kras(G12D) and p53 mutation cause primary intrahepatic cholangiocarcinoma. *Cancer Res* 2012; **72**: 1557-1567 [PMID: 22266220 DOI: 10.1158/0008-5472.CAN-11-3596]
24 **Craig AJ**, Garcia-Lezana T, Ruiz de Galarreta M, Villacorta-Martin C, Kozlova EG, Martins-Filho SN, von Felden J, Ahsen ME, Bresnahan E, Hernandez-Meza G, Labgaa I, D'Avola D, Schwartz M, Llovet JM, Sia D, Thung S, Losic B, Lujambio A, Villanueva A. Transcriptomic characterization of cancer-testis antigens identifies MAGEA3 as a driver of tumor progression in hepatocellular carcinoma. *PLoS Genet* 2021; **17**: e1009589 [PMID: 34166362 DOI: 10.1371/journal.pgen.1009589]
25 **Montironi C**, Castet F, Haber PK, Pinyol R, Torres-Martin M, Torrens L, Mesropian A, Wang H, Puigvehi M, Maeda M, Leow WQ, Harrod E, Taik P, Chinburen J, Taivanbaatar E, Chinbold E, Solé Arqués M, Donovan M, Thung S, Neely J, Mazzaferro V, Anderson J, Roayaie S, Schwartz M, Villanueva A, Friedman SL, Uzilov A, Sia D, Llovet JM. Inflamed and non-inflamed classes of HCC: a revised immunogenomic classification. *Gut* 2023; **72**: 129-140 [PMID: 35197323 DOI: 10.1136/gutjnl-2021-325918]
26 **Sia D**, Hoshida Y, Villanueva A, Roayaie S, Ferrer J, Tabak B, Peix J, Sole M, Tovar V, Alsinet C, Cornella H, Klotzle B, Fan JB, Cotsoglou C, Thung SN, Fuster J, Waxman S, Garcia-Valdecasas JC, Bruix J, Schwartz ME, Beroukhim R, Mazzaferro V, Llovet JM. Integrative molecular analysis of intrahepatic cholangiocarcinoma reveals 2 classes that have different outcomes. *Gastroenterology* 2013; **144**: 829-840 [PMID: 23295441 DOI: 10.1053/j.gastro.2013.01.001]
27 **Zender S**, Nickeleit I, Wuestefeld T, Sörensen I, Dauch D, Bozko P, El-Khatib M, Geffers R, Bektas H, Manns MP, Gossler A, Wilkens L, Plentz R, Zender L, Malek NP. A critical role for notch signaling in the formation of cholangiocellular carcinomas. *Cancer Cell* 2013; **23**: 784-795 [PMID: 23727022 DOI: 10.1016/j.ccr.2013.04.019]
28 **Cohen B**, Shimizu M, Izrailit J, Ng NF, Buchman Y, Pan JG, Dering J, Reedijk M. Cyclin D1 is a direct target of JAG1-mediated Notch signaling in breast cancer. *Breast Cancer Res Treat* 2010; **123**: 113-124 [PMID: 19915977 DOI: 10.1007/s10549-009-0621-9]
29 **Bicker F**, Vasic V, Horta G, Ortega F, Nolte H, Kavyanifar A, Keller S, Stankovic ND, Harter PN, Benedito R, Lutz B, Bäuerle T, Hartwig J, Baumgart J, Krüger M, Radyushkin K, Alberi L, Berninger B, Schmidt MHH. Neurovascular EGFL7 regulates adult neurogenesis in the subventricular zone and thereby affects olfactory perception. *Nat Commun* 2017; **8**: 15922 [PMID: 28656980 DOI: 10.1038/ncomms15922]
30 **Jia S**, McGinnis K, VanDusen WJ, Burke CJ, Kuo A, Griffin PR, Sardana MK, Elliston KO, Stern AM, Friedman PA. A

fully active catalytic domain of bovine aspartyl (asparaginyl) beta-hydroxylase expressed in Escherichia coli: characterization and evidence for the identification of an active-site region in vertebrate alpha-ketoglutarate-dependent dioxygenases. *Proc Natl Acad Sci U S A* 1994; **91**: 7227-7231 [PMID: 8041771 DOI: 10.1073/pnas.91.15.7227]

31 **Jia S**, VanDusen WJ, Diehl RE, Kohl NE, Dixon RA, Elliston KO, Stern AM, Friedman PA. cDNA cloning and expression of bovine aspartyl (asparaginyl) beta-hydroxylase. *J Biol Chem* 1992; **267**: 14322-14327 [PMID: 1378441]

32 **Stenflo J**, Holme E, Lindstedt S, Chandramouli N, Huang LH, Tam JP, Merrifield RB. Hydroxylation of aspartic acid in domains homologous to the epidermal growth factor precursor is catalyzed by a 2-oxoglutarate-dependent dioxygenase. *Proc Natl Acad Sci U S A* 1989; **86**: 444-447 [PMID: 2492106 DOI: 10.1073/pnas.86.2.444]

33 **Huang CK**, Iwagami Y, Aihara A, Chung W, de la Monte S, Thomas JM, Olsen M, Carlson R, Yu T, Dong X, Wands J. Anti-Tumor Effects of Second Generation β-Hydroxylase Inhibitors on Cholangiocarcinoma Development and Progression. *PLoS One* 2016; **11**: e0150336 [PMID: 26954680 DOI: 10.1371/journal.pone.0150336]

34 **Giacinti C**, Giordano A. RB and cell cycle progression. *Oncogene* 2006; **25**: 5220-5227 [PMID: 16936740 DOI: 10.1038/sj.onc.1209615]

35 **Zou S**, Li J, Zhou H, Frech C, Jiang X, Chu JS, Zhao X, Li Y, Li Q, Wang H, Hu J, Kong G, Wu M, Ding C, Chen N, Hu H. Mutational landscape of intrahepatic cholangiocarcinoma. *Nat Commun* 2014; **5**: 5696 [PMID: 25526346 DOI: 10.1038/ncomms6696]

36 **Sitthithumcharee G**, Suppramote O, Vaeteewoottacharn K, Sirisuksakun C, Jamnongsong S, Laphanuwat P, Suntiparpluacha M, Matha A, Chusorn P, Buraphat P, Kakanaporn C, Charngkaew K, Silsirivanit A, Korphaisarn K, Limsrichamrern S, Tripatara P, Pairojkul C, Wongkham S, Sampattavanich S, Okada S, Jirawatnotai S. Dependency of Cholangiocarcinoma on Cyclin D-Dependent Kinase Activity. *Hepatology* 2019; **70**: 1614-1630 [PMID: 31077409 DOI: 10.1002/hep.30704]

37 **Song X**, Liu X, Wang H, Wang J, Qiao Y, Cigliano A, Utpatel K, Ribback S, Pilo MG, Serra M, Gordan JD, Che L, Zhang S, Cossu A, Porcu A, Pascale RM, Dombrowski F, Hu H, Calvisi DF, Evert M, Chen X. Combined CDK4/6 and Pan-mTOR Inhibition Is Synergistic Against Intrahepatic Cholangiocarcinoma. *Clin Cancer Res* 2019; **25**: 403-413 [PMID: 30084835 DOI: 10.1158/1078-0432.CCR-18-0284]

38 **Nevins JR**. The Rb/E2F pathway and cancer. *Hum Mol Genet* 2001; **10**: 699-703 [PMID: 11257102 DOI: 10.1093/hmg/10.7.699]

39 **Huang CK**, Iwagami Y, Zou J, Casulli S, Lu S, Nagaoka K, Ji C, Ogawa K, Cao KY, Gao JS, Carlson RI, Wands JR. Aspartate beta-hydroxylase promotes cholangiocarcinoma progression by modulating RB1 phosphorylation. *Cancer Lett* 2018; **429**: 1-10 [PMID: 29733964 DOI: 10.1016/j.canlet.2018.04.041]

World Journal of Gastroenterology

Submit a Manuscript: https://www.f6publishing.com

World J Gastroenterol 2023 July 7; 29(25): 4072-4084

DOI: 10.3748/wjg.v29.i25.4072

ISSN 1007-9327 (print) ISSN 2219-2840 (online)

ORIGINAL ARTICLE

Retrospective Study

Non-invasive model for predicting high-risk esophageal varices based on liver and spleen stiffness

Long-Bao Yang, Xin Gao, Hong Li, Xin-Xing Tantai, Fen-Rong Chen, Lei Dong, Xu-Sheng Dang, Zhong-Cao Wei, Chen-Yu Liu, Yan Wang

Specialty type: Gastroenterology and hepatology

Provenance and peer review: Unsolicited article; Externally peer reviewed.

Peer-review model: Single blind

Peer-review report's scientific quality classification

Grade A (Excellent): 0
Grade B (Very good): B
Grade C (Good): C, C
Grade D (Fair): 0
Grade E (Poor): 0

P-Reviewer: El-Shabrawi MH, Egypt; Ullah K, Pakistan

Received: April 23, 2023
Peer-review started: April 23, 2023
First decision: May 15, 2023
Revised: May 20, 2023
Accepted: June 2, 2023
Article in press: June 2, 2023
Published online: July 7, 2023

Long-Bao Yang, Xin Gao, Hong Li, Xin-Xing Tantai, Fen-Rong Chen, Lei Dong, Zhong-Cao Wei, Chen-Yu Liu, Yan Wang, Department of Gastroenterology, The Second Affiliated Hospital of Xi'an Jiaotong University, Xi'an 710004, Shaanxi Province, China

Xu-Sheng Dang, Department of Emergency, The Second Affiliated Hospital of Xi'an Jiaotong University, Xi'an 710004, Shaanxi Province, China

Corresponding author: Yan Wang, MD, Assistant Professor, Department of Gastroenterology, The Second Affiliated Hospital of Xi'an Jiaotong University, No. 157 of Xiwu Road, Xi'an 710004, Shaanxi Province, China. sarrye@163.com

Abstract

BACKGROUND

Acute bleeding due to esophageal varices (EVs) is a life-threatening complication in patients with cirrhosis. The diagnosis of EVs is mainly through upper gastrointestinal endoscopy, but the discomfort, contraindications and complications of gastrointestinal endoscopic screening reduce patient compliance. According to the bleeding risk of EVs, the Baveno VI consensus divides varices into high bleeding risk EVs (HEVs) and low bleeding risk EVs (LEVs). We sought to identify a non-invasive prediction model based on spleen stiffness measurement (SSM) and liver stiffness measurement (LSM) as an alternative to EVs screening.

AIM

To develop a safe, simple and non-invasive model to predict HEVs in patients with viral cirrhosis and identify patients who can be exempted from upper gastrointestinal endoscopy.

METHODS

Data from 200 patients with viral cirrhosis were included in this study, with 140 patients as the modelling group and 60 patients as the external validation group, and the EVs types of patients were determined by upper gastrointestinal endoscopy and the Baveno VI consensus. Those patients were divided into the HEVs group (66 patients) and the LEVs group (74 patients). The effect of each parameter on HEVs was analyzed by univariate and multivariate analyses, and a non-invasive prediction model was established. Finally, the discrimination ability,

calibration ability and clinical efficacy of the new model were verified in the modelling group and the external validation group.

RESULTS

Univariate and multivariate analyses showed that SSM and LSM were associated with the occurrence of HEVs in patients with viral cirrhosis. On this basis, logistic regression analysis was used to construct a prediction model: Ln [P/(1-P)] = -8.184 -0.228 × SSM + 0.642 × LSM. The area under the curve of the new model was 0.965. When the cut-off value was 0.27, the sensitivity, specificity, positive predictive value and negative predictive value of the model for predicting HEVs were 100.00%, 82.43%, 83.52%, and 100%, respectively. Compared with the four prediction models of liver stiffness-spleen diameter to platelet ratio score, variceal risk index, aspartate aminotransferase to alanine aminotransferase ratio, and Baveno VI, the established model can better predict HEVs in patients with viral cirrhosis.

CONCLUSION

Based on the SSM and LSM measured by transient elastography, we established a non-invasive prediction model for HEVs. The new model is reliable in predicting HEVs and can be used as an alternative to routine upper gastrointestinal endoscopy screening, which is helpful for clinical decision making.

Key Words: Cirrhosis; High-risk esophageal varices; Non-invasive prediction model; Spleen stiffness measurement; Liver stiffness measurement; Upper gastrointestinal endoscopy

©The Author(s) 2023. Published by Baishideng Publishing Group Inc. All rights reserved.

Core Tip: The non-invasive prediction model for predicting high risk esophageal varices (HEVs) in patients with viral cirrhosis was successfully established based on the spleen stiffness measurement and liver stiffness measurement. It is a novel model that has not been reported. The model was shown to be better than previous prediction models. The new model is reliable in predicting HEVs and can be used as an alternative to routine upper gastrointestinal endoscopy screening, which is helpful for clinical decision making.

Citation: Yang LB, Gao X, Li H, Tantai XX, Chen FR, Dong L, Dang XS, Wei ZC, Liu CY, Wang Y. Non-invasive model for predicting high-risk esophageal varices based on liver and spleen stiffness. *World J Gastroenterol* 2023; 29(25): 4072-4084

URL: https://www.wjgnet.com/1007-9327/full/v29/i25/4072.htm

DOI: https://dx.doi.org/10.3748/wjg.v29.i25.4072

INTRODUCTION

Liver cirrhosis is the end stage of chronic liver disease. When hepatic venous pressure gradient (HVPG) ≥ 10 mmHg is defined as clinically significant portal hypertension (CSPH), the patients who meet this criteria may suffer from complications such as esophageal variceal bleeding, ascites, hepatic encephalopathy, and jaundice due to portal hypertension and liver insufficiency[1,2]. Rupture of esophageal varices (EVs) is a common and life-threatening complication in patients with liver cirrhosis. The incidence of EVs bleeding is approximately 5%-15% per year, the re-bleeding rate within 6 wk after EVs rupture bleeding is 30% to 40%, and the mortality rate is 15%-25%[3-5]. The severity of liver cirrhosis, the size of EVs and the presence or absence of the red sign (RS) are related indicators of EVs bleeding [6]. For routine assessment of the above indicators, the Baveno VI consensus recommends that patients with cirrhosis need to undergo regular screening upper gastrointestinal endoscopy so that appropriate preventive treatment can be administered to prevent variceal bleeding events[7]. To date, HPVG and upper gastrointestinal endoscopy are considered the gold standards for the assessment of PH and EVs, respectively[6]. However, the prevalence of varicose veins requiring treatment (VNT), as defined by the Baveno VI guidelines, is very low in Compensated advanced chronic liver disease (cACLD) patients who are detected at an early stage[8]. HPVG and EGD are invasive procedures and expensive, and the patient compliance associated with them is poor[9,10]. Therefore, in clinical practice, it is necessary to develop a safe, non-invasive and patient-acceptable prediction model that can not only prevent frequent HPVG or gastrointestinal endoscopy examinations but also better predict HEVs in patients with viral cirrhosis. With the development of transient elastography (TE), studies have shown that liver stiffness

(LS) and spleen stiffness (SS) detected by TE are associated with liver fibrosis, significant portal hypertension, and EVs. SS is increased in patients with viral hepatitis, and SS is positively correlated with HVPG, which has good predictive performance for CSPH and EVs in patients with cACLD[11-13].

At present, in addition to ultrasound, CT, MRI, and other imaging methods, there are also several common prediction models[14,15]. The LS-spleen diameter to platelet (PLT) ratio score (LSPS), variceal risk index (VRI), aspartate aminotransferase (AST) to alanine aminotransferase (ALT) ratio (AAR) and Baveno VI model have all achieved good clinical effects in predicting HEVs[16-19]. In addition, the Baveno VI consensus states that LS measurement (LSM) combined with PLT helps to exclude HEVs[8, 19,20]. To initially predict HEVs in patients with viral cirrhosis, the aim of this study is to establish a non-invasive prediction model that can predict HEVs based on SS measurement (SSM) and LSM and to evaluate the accuracy of the new model in identifying HEVs in patients with viral cirrhosis who can be exempted from upper gastrointestinal endoscopy.

MATERIALS AND METHODS

Patients and study design

The study was authorized by the Ethics Committee of the Second Affiliated Hospital of Xi'an Jiaotong University (Xi'an, Shaanxi Province, China). As a retrospective study; therefore, the Ethics Committee waived the informed consent. This study retrospectively analyzed the data of patients with viral cirrhosis who were admitted to the Second Affiliated Hospital of Xi'an Jiaotong University and underwent upper abdominal computed tomography (CT) examination from March 2020 to November 2022. The inclusion criteria were: (1) Age > 18 years old; (2) patients with hepatitis B and hepatitis C cirrhosis; (3) patients who underwent endoscopy, upper abdominal CT, and laboratory examinations with complete results; and (4) the interval between two examinations was not more than 3 mo. Exclusion criteria: (1) Other liver injury factors, such as alcoholic liver disease, autoimmunity, metabolic liver disease, occult liver cirrhosis, *etc*; (2) suspicious liver tumor; (3) history of liver resection, liver transplantation or splenectomy; (4) frequent use of proton pump inhibitors; (5) other diseases that may impact the haemodynamics of the splenic vein or portal vein, such as cavernous degeneration, thrombosis, embolism; (6) cirrhotic patients with moderate or massive ascites; (7) previous treatment of portal hypertension, such as splenectomy, transjugular intrahepatic portosystemic shunt, endoscopic therapy, and nonselective β-blocker therapy; (8) diseases may affect the liver or spleen size, such as cysts, leukaemia, thrombocytopenic purpura, haemolytic anaemia, multiple myeloma, *etc*; (9) patients with a history of esophageal bleeding undergoing endoscopic or surgical treatment; (10) severe malnutrition or weight loss; (11) unreliable LSM: Quartile range/median > 0.3, success rate < 60%, or the number of effective measurements < 10; or (12) other conditions affecting LSM, such as body mass index > 35 kg/m^2.

A total of 140 patients who met the inclusion criteria were selected as the modelling group. According to the results of upper gastrointestinal endoscopy and the Baveno VI criteria, the patients were divided into the HEVs group and the LEVs group; 66 patients were HEVs patients, and 74 patients were LEVs patients. In addition, 60 patients who met the inclusion criteria were used as the validation group. The patient's data were collected when the model was established, and the data collection procedure and the model application did not interfere with each other.

Definition of EVs

Patients with liver cirrhosis were graded and scored using the Child-Pugh scoring system[21]. According to Baveno VI criteria, HEVs were defined as EVs with a diameter ≥ 5 mm, EVs with a diameter ≤ 5 mm and a positive RS, EVs in patients with Child grade C, and EVs that did not meet these criteria were LEVs with a low risk of bleeding[22,23].

CT scan-based liver and spleen volume measurement

The CT examinations were conducted by a multislice spiral CT scanner (GE 128-slice spiral CT scanner; Linux Medical System, United States) with a 5 mm reconstructed layer thickness, and the time interval was 5 s.

Actual liver volume measured by CT (CTLV), actual spleen volume measured by CT (CTSV), portal vein diameter (PVD) and spleen long diameter (SLD) were simultaneously measured by experienced radiologists who did not know the basic information of the patients. CTLV and CTSV were obtained by manually tracing the surface area of the liver and spleen at each level and multiplying by the layer thickness. The entire measurement process requires active avoidance of large blood vessels, gallbladder, and fissure. The SLD was defined as the length of the superior pole to the inferior line of the spleen at the plane of maximum surface area. The PVD needs to be measured at the midpoint between the portal vein bifurcation site and the vein confluence site[24].

Laboratory examination

For each patient, data on age, sex, height, weight, medical history, medication use, the presence or absence of ascites, and Child-Pugh score were collected. The white blood cell count, red blood cell count, PLT, ALT, AST, total bilirubin (TBil), alkaline phosphatase (ALP), glutamine transferase (GGT), albumin (ALB), total cholesterol (TCHO), prothrombin time (PT), international prothrombin ratio (INR), and prothrombin activity (PTA) of all patients included in the study were collected. The blood test was tested by an XN-9000 analyser (Xisen Meikang Medical Electronics Co. Ltd., Shanghai, China), and the coagulation function was tested by a Sysmex CO-CS-1500 system (SYSMEX Co., Ltd, Kobe, Japan) and the liver function test was performed using a Cobas 8000 analyser (Roche Diagnostics, Mannheim, Germany).

Liver and SS measurements by TE

LSM and SSM were measured in all patients using FibroScan (Echosens, Paris, France) and FibroTouch (Hai's Medical Technology Center, Beijing, China). The LSM was assessed by a trained and experienced operator after at least 4 h of fasting, and the SSM was performed on the same day as the LSM assessment. All measurements were obtained by experienced operators who had performed at least 300 tests in patients with chronic liver disease. The TE results of the patients were collected retrospectively, and the obtained results were expressed in kilopascals (kPa). The interquartile range (IQR) was defined as the intrinsic variation index between the 25th and 75th percentiles of the LS results containing 50% of the valid measurements. Therefore, LSM and SSM values were considered to be reliable when at least 10 valid measurements were obtained and the results were reliable, with an overall success rate of more than 60% and IQR/median ≤ 0.3[25,26].

Upper gastrointestinal endoscopy

Upper gastrointestinal endoscopy was performed by an endoscopic operator who was experienced in the assessment of patients with cirrhosis (with a minimum of 500 endoscopic procedures). Endoscopic examinations were performed to determine whether the patients had EVs, and if so, the EVs were graded according to the location (L), shape and size (F), colour (C), and presence or absence of RS of the lesion.

Non-invasive score of EVs

The non-invasive prediction models we choose to compare were as shown blow: LSPS = [LSM (KPa) × SLD (cm)]/PLT (× 10^9/L)[16]; VRI = -4.364 + 0.538 × SLD-0.049 × PLT-0.044 × LSM + 0.001 × (LSM × PLT)[17]; AAR = AST/ALT[18] and the Baveno VI criteria proposed by the consensus conference. The Baveno VI criteria were defined as LSM < 20 kPa and platelet count > 150 × 10^9/L. The extended Baveno VI criteria were defined as LSM < 25 kPa and platelet count > 110 × 10^9/L[8,27]. The results of upper gastrointestinal endoscopy were used as the gold standard. The receiver operating characteristic (ROC) curves of LSPS, VRI, AAR and Baveno VI were drawn, and the area under the ROC curve (AUC), sensitivity, specificity and Youden index were calculated to evaluate the performance of the new model and the previous four models in identifying HEVs. The point with the largest sum of sensitivity and specificity was selected as the best cut-off value for the diagnosis of HEVs.

EVs saluation of new prediction models

The discrimination ability of the new model was assessed by the ROC curves in the modelling group and the external validation group. The *Z* test was used to evaluate differences in ROC curves. If there was no significant difference in the ROC between the two groups and AUC > 0.7, the model was considered to have good discrimination ability. The calibration ability of the prediction model was evaluated by the Hosmer-Lemeshow test and the two sets of calibration scatter plots. Decision curve analysis (DCA) was performed to evaluate the clinical efficacy of the new model.

Statistical analysis

SPSS 26.0 and R software (IBM SPSS, Chicago, IL, United States) were used for statistical analysis. Data are presented as the mean ± SD. The chi-square test was used to compare the measurement data between the HEVs group and the LEVs group. The Mann-Whitney *U* test was used for univariate analysis of continuous variable measurement data, and WALD backwards regression analysis was used for multivariate analysis. SPSS 26.0 software was used to draw the ROC curve and calculate the AUC to evaluate the diagnostic performance of the model. The maximum corresponding point of the Youden index was selected as the best cut-off value, and a positive prediction result was defined as equal to or greater than the best cut-off value. The best discrimination probability threshold, sensitivity, specificity and predictive value were calculated, and the diagnostic accuracy was compared. The higher the Youden index (1% or 100%), the more effective the correlation. Hosmer-Lemeshow test results, calibration charts and DCA were obtained using R software. All statistical tests were two-sided, with an alpha value of 0.05 and a statistical significance threshold of $P < 0.05$.

RESULTS

Baseline characteristics of the patients

Tables 1 and 2 List the baseline characteristics of the modelling group and the external validation group, respectively. In the LEVs group, the mean age was 50.88 years ± 11.6 years, 43 (58.1%) were male, and 61 (82.4%) had hepatitis B. The age of the HEVs patients was 55.36 years ± 11.1 years old, 37 (56.1%) were male, and 53 (80.3%) had hepatitis B. In the modelling group, there was a significant difference in age between the HEVs group and the LEVs group ($P < 0.05$) but no significant difference in sex or hepatitis type ($P > 0.05$), and the two groups were comparable. In the external validation group, there was no significant difference in sex, age or hepatitis type ($P > 0.05$).

Univariate analysis of HEVs

T tests and non-parametric rank sum tests were used for the univariate analysis. The summarized results are shown in Table 3. There were significant differences in SSM, PLT, LSM, ALT, AST, GGT, SLD, PT, INR, PTA, PVD, CTLV, and CTSV between the HEVs group and the LEVs group ($P < 0.05$). There were no significant differences in ALP, TBil, and TCHO between the two groups ($P > 0.05$).

Multivariate analysis of HEVs

The parameters shown in Table 3 with statistically significant differences between the HEVs and LEVs groups were analyzed by multivariate analysis using backwards WALD regression analysis. As shown in Table 4, the SSM and LSM between the HEVs group and LEVs group were significantly different ($P < 0.05$). There were no significant differences in PLT, ALT, AST, GGT, SLD, PT, INR, PTA, PVD, CTLV, and CTSV ($P > 0.05$).

Establishment of a non-invasive prediction model

Based on the results of the multivariate analysis, the parameters with no statistically significant difference between the two groups were excluded, and the parameters with statistically significant differences, including SSM and LSM, were used to establish a non-invasive prediction model. The logistic regression analysis showed that SSM and LSM were independent factors affecting the occurrence of HEVs and were statistically significant ($P < 0.05$). As shown in Table 5, the model was as follows: Ln [P/(1-P)] = -8.184 - 0.228 × SSM + 0.642 × LSM. HEVs in patients with viral cirrhosis were negatively correlated with SSM and positively correlated with LSM.

Comparison of non-invasive prediction models

The new model was compared with other models reported to predict EVs in patients with liver cirrhosis, namely, the LSPS, VRI, AAR, and Baveno VI models. The sensitivity, specificity and AUC of the new model based on the SSM and LSM and LSPS, VRI, AAR and Baveno VI models were calculated. The cut-off value of the model was defined as the maximum value of the sum of the specificity and sensitivity. Patients were considered to have HEVs when the P value calculated by the established formula was greater than the cut-off value. As shown in Figure 1A and Table 6, the AUC of this model was 0.965, while the AUCs of LSPS, VRI, AAR and Baveno VI were 0.835, 0.744, 0.641, and 0.675, respectively. The AUC > 0.7 indicated the good discrimination power of the model. The higher the AUC is, the better the discriminative power of the model, so the new model has good discriminative power.

Diagnostic accuracy of non-invasive tests for predicting HEVs

The accuracy, positive predictive value and negative predictive value of LSPS, VRI, ARR, Baveno VI, and the new model of 140 patients in the modelling group were calculated according to the calculation formula. As shown in Table 7, the non-invasive prediction model shown in this study had an accuracy of 89.30% and a positive predictive value of 83.52%. The accuracy and positive predictive values suggest the likelihood that the new model can correctly diagnose HEVs, with higher values indicating a more correct diagnosis.

Discriminating ability edicting HEVs

Evaluation of the ability of the non-invasive model was performed by drawing the ROC curve of the established new model in the external validation group and using the Z test to compare the AUC curve between the modelling group and the external validation group and to evaluate the discriminative power of the new model. The AUC of the new model for predicting HEVs in the modelling group was 0.965, which was higher than that of the LSPS, VRI, AAR, and Baveno VI models. The AUC of the new model in the external validation group was 1. The Z test result was 0.896, and the *P* value was 0.37, indicating that there was no significant difference between the modelling group and the external validation group. The ROC curve of the external validation group is shown in Figure 1B.

EVs saluation of the calibration ability of the new model

The Hosmer-Lemeshow test was used to calculate the χ^2 value of the modelling group and the external

Table 1 Comparison of general characteristics in the modelling group

Parameter	Patients with LEVs, *n* = 74	Patients with HEVs, *n* = 66	*T* value/χ^2 value	*P* value
Age in yr	50.88 ± 11.60	55.36 ± 11.10	-2.333	0.021
Male (%)	43 (58.1%)	37 (56.1%)	0.060	0.807
Etiology, HBV/HCV	61/13	53/13	0.105	0.746

P < 0.05 is considered statistically significant. HEVs: High-risk esophageal varices; LEVs: Low-risk esophageal varices; HBV: Hepatitis B virus; HCV: Hepatitis C virus.

Table 2 Comparison of general characteristics in the external validation group

Parameter	Patients with LEVs, *n* = 28	Patients with HEVs, *n* = 32	*T* value/χ^2 value	*P* value
Age in yr	52.54 ± 13.70	54.97 ± 10.40	-0.780	0.438
Male (%)	15 (53.6%)	14 (43.8%)	0.577	0.448
Etiology, HBV/HCV	25/3	30/2	0.024	0.876

P < 0.05 is considered statistically significant. HEVs: High-risk esophageal varices; LEVs: Low-risk esophageal varices; HBV: Hepatitis B virus; HCV; Hepatitis C virus.

Table 3 Univariate analysis of parameters of patients with high-risk esophageal varices and low-risk esophageal varices

Parameter	Patients with LEVs, *n* = 74	Patients with HEVs, *n* = 66	*t*/*Z*	*P* value
SSM, KPa	22.70 ± 6.00	19.06 ± 4.90	3.880	< 0.001
PLT, × 10^9/L	108.55 ± 68.10	62.53 ± 29.00	5.096	< 0.001
LSM, KPa	14.90 ± 5.10	24.83 ± 4.30	-12.354	< 0.001
ALT, IU/L	37.50 (26.00, 49.50)	23.00 (16.00, 35.00)	-4.278	< 0.001
AST, IU/L	43.00 (31.75, 69.00)	34.50 (27.75, 45.25)	-2.796	0.005
ALP, IU/L	108.00 (81.25, 137.25)	93.50 (78.00, 128.75)	-1.012	0.311
GGT, IU/L	60.50 (28.00, 114.00)	33.00 (19.75, 58.75)	-3.609	< 0.001
SLD, mm	13.58 ± 3.10	15.10 ± 3.30	-2.806	0.006
TBIL, μmol/L	22.63 (16.01, 34.96)	27.80 (18.05, 39.65)	-0.960	0.337
ALB, g/dL	37.16 ± 8.30	36.02 ± 5.80	0.935	0.351
TCHO, mmol/L	3.57 ± 1.40	3.18 ± 0.90	1.981	0.050
PT, s	12.45 ± 2.20	13.34 ± 2.50	-2.284	0.024
INR	1.13 ± 0.20	1.21 ± 0.20	-2.175	0.031
PTA, %	82.15 ± 20.80	75.09 ± 16.10	2.228	0.028
PVD, mm	12.20 ± 1.90	13.64 ± 2.30	-4.024	< 0.001
CTLV, cm^3	1031.88 ± 361.20	920.85 ± 241.50	2.111	0.037
CTSV, cm^3	558.11 ± 338.70	808.25 ± 409.90	-3.951	< 0.001

P < 0.05 is considered statistically significant. HEVs: High-risk esophageal varices; LEVs: Low-risk esophageal varices; SSM: Spleen stiffness measurement; LSM: Liver stiffness measurement; ALT: Alanine aminotransferase; AST: Aspartate aminotransferase; ALP: Alkaline phosphatase; GGT: Glutamine transferase; SLD: Spleen long diameter; TBIL: Total bilirubin; ALB: Albumin; TCHO: Total cholesterol; PT: Prothrombin time; INR: International prothrombin ratio; PTA: Prothrombin activity; PVD: Portal vein diameter; CTLV: Actual liver volume measured by computed tomography; CTSV: Actual spleen volume measured by computed tomography.

Table 4 Multivariate analysis of parameters of patients with high-risk esophageal varices and low-risk esophageal varices

Parameter	Patients with LEVs, *n* = 74	Patients with HEVs, *n* = 66	*t*/*Z*	*P* value
SSM, KPa	22.70 ± 6.00	19.06 ± 4.90	3.880	0.009
PLT, × 10^9/L	108.55 ± 68.10	62.53 ± 29.00	5.096	0.606
LSM, KPa	14.90 ± 5.10	24.83 ± 4.30	-12.354	< 0.001
ALT, IU/L	37.50 (26.00, 49.50)	23.00 (16.00, 35.00)	-4.278	0.669
AST, IU/L	43.00 (31.75, 69.00)	34.50 (27.75, 45.25)	-2.796	0.125
	60.50 (28.00, 114.00)	33.00 (19.75, 58.75)	-3.609	0.790
SLD, mm	13.58 ± 3.10	15.10 ± 3.30	-2.806	0.952
PT, s	12.45 ± 2.20	13.34 ± 2.50	-2.284	0.883
INR	1.13 ± 0.20	1.21 ± 0.20	-2.175	0.777
PTA, %	82.15 ± 20.80	75.09 ± 16.10	2.228	0.920
PVD, mm	12.20 ± 1.90	13.64 ± 2.30	-4.024	0.220
CTLV, cm^3	1031.88 ± 361.10	920.85 ± 241.50	2.111	0.892
CTSV, cm^3	558.11 ± 338.70	808.25 ± 409.90	-3.951	0.713

P < 0.05 is considered statistically significant. HEVs: High-risk esophageal varices; LEVs: Low-risk esophageal varices; SSM: Spleen stiffness measurement; LSM: Liver stiffness measurement; ALT: Alanine aminotransferase; AST: Aspartate aminotransferase; SLD: Spleen long diameter; PT: Prothrombin time; INR: International prothrombin ratio; PTA: Prothrombin activity; PVD: Portal vein diameter; CTLV: Actual liver volume measured by computed tomography; CTSV: Actual spleen volume measured by computed tomography.

Table 5 Parameters used to establish the non-invasive prediction model

Parameter	B	S.E.	Wald	*P*	Exp (B)	95%CI of exp (B)
SSM	-0.228	0.074	9.647	0.002	0.796	0.689-0.919
LSM	0.642	0.123	27.245	< 0.001	1.900	1.493-2.418
Constant	-8.184	2.300	12.659	< 0.001	0.000	-

SSM: Spleen stiffness measurement; LSM: Liver stiffness measurement; CI: Confidence interval.

Table 6 Comparison of various parameters of each model

	Area	SE	*P*	95%CI of exp (B)
LSPS	0.835	0.033	< 0.001	0.771-0.900
VRI	0.744	0.041	< 0.001	0.663-0.824
AAR	0.641	0.046	0.004	0.550-0.732
Baveno VI	0.675	0.045	< 0.001	0.586-0.764
The new model	0.965	0.015	< 0.001	0.936-0.995

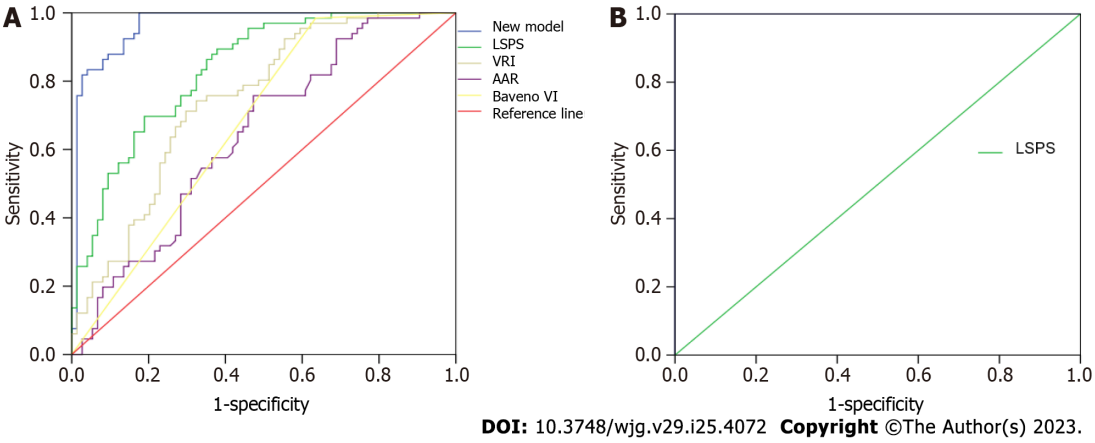
LSPS: Liver stiffness-spleen diameter to platelet ratio score; VRI: Variceal risk index; AAR: Aspartate aminotransferase/alanine aminotransferase ratio; BavenoVI: Baveno VI criteria were defined as liver stiffness measurement < 20 kPa and platelet count > 150 × 10^9 /L; CI: Confidence interval.

validation group to evaluate the calibration ability of the new model. The results showed that χ^2 was -10.39 in the modelling group and 0.03 in the external validation group. The P values were 0.999 and 1.000, respectively. Both the groups' P value were greater than 0.05, indicating that the model could predict HEVs accurately. The calibration scatter plots of the two groups were shown in Figure 2. As seen from the figure, all scatter points fluctuated around the baseline without significant deviation because the *P* values of both groups were greater than 0.05 and the difference between the groups was not statistically significant. The results showed that the HEVs patients who were predicted to have viral

Table 7 Comparison of various parameters of each model

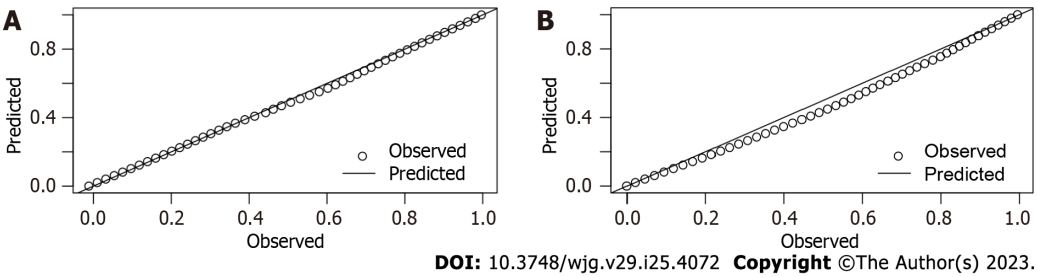
	Sensitivity	Specificity	Accuracy, %	Positive predictive value, %	Negative predictive value, %	Cutoff value
LSPS	89.39	62.16	74.30	67.78	86.81	3.12
VRI	74.24	67.57	69.30	67.09	74.66	0.03
AAR	75.76	52.70	57.90	58.78	70.95	1.27
Baveno VI[1]	98.48	36.49	65.70	57.99	96.42	-
The new model	100.00	82.43	89.30	83.52	100.00	0.27

[1]Baveno VI criteria were defined as liver stiffness measurement < 20 kPa and platelet count > 150 × 10^9 /L.
LSPS: Liver stiffness-spleen diameter to platelet ratio score; VRI: Variceal risk index; AAR: Aspartate aminotransferase/alanine aminotransferase ratio.



DOI: 10.3748/wjg.v29.i25.4072 Copyright ©The Author(s) 2023.

Figure 1 Area under the curve of various models in predicting high-risk esophageal varices of patients. A: Modelling group; B: External validation group. The area under the curve of the new model in predicting high-risk esophageal varices of patients was 0.965 in the modelling group, which was higher than that of liver stiffness-spleen diameter to platelet ratio score, variceal risk index, aspartate aminotransferase/alanine aminotransferase ratio and Baveno VI; and it was 1 in the external validation group. LSPS: Liver stiffness-spleen diameter to platelet ratio score; VRI: Variceal risk index; AAR: Aspartate aminotransferase/alanine aminotransferase ratio.



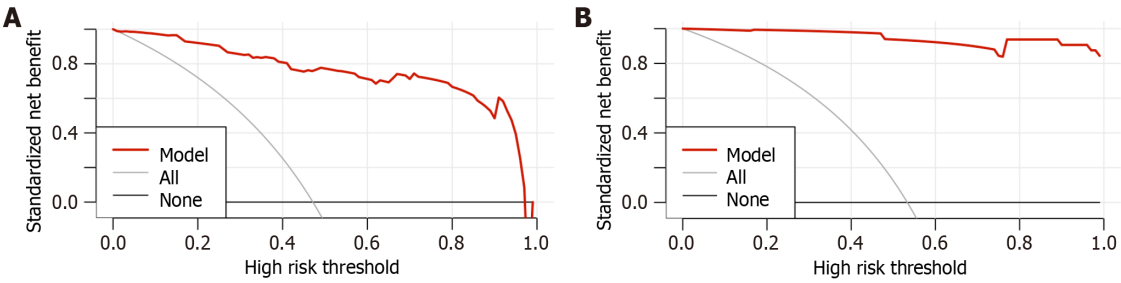
DOI: 10.3748/wjg.v29.i25.4072 Copyright ©The Author(s) 2023.

Figure 2 Calibration scatter plot of data of patients. A: Modelling group; B: External validation group. In predicting patients in the modelling group and external validation group, the scattered points fluctuated around the reference line without significant deviations.

cirrhosis by using the new model were in good agreement with the actual HEVs patients.

EVs salvation of the clinical efficacy of the new model

DCA was plotted against the probability of actual HEVs occurrence by predicting the probability of the modelling group and the external validation group by the new model. The DCA of the two groups is shown in Figure 3. In the DSA curve, the two dashed lines represent the two extreme cases, and the black line indicates that the new model predicts there was no HEVs, and a net clinical benefit of zero. The other grey line with a negative slope indicates that the new model predicts HEVs in all patients with viral cirrhosis, and the net clinical benefit is a back-slope with a negative slope[28]. The red line is the new model's DCA. As the DCA curve shown, the red line was higher than the black and grey lines, indicating that when the new model was applied to the modelling group and the external validation group, both groups of patients could benefit, so the new model had certain clinical efficacy.



DOI: 10.3748/wjg.v29.i25.4072 **Copyright** ©The Author(s) 2023.

Figure 3 Adjusted decision curve analysis of data of patients. A: Modelling group; B: External validation group. The black line indicates that in extreme cases, the new model predicted that there were no high-risk esophageal varices in all patients with viral cirrhosis, and the clinical net benefit was 0. The gray curve indicates that in extreme cases, the new model predicts there are high-risk esophageal varices in all patients with viral cirrhosis, the clinical net benefit is the negative slope. The red line indicates that the new model has a clinical net benefit. The red line is higher than the black and gray lines, indicating that patients in the modelling group can benefit from the new model.

DISCUSSION

Long-term chronic viral hepatitis can lead to liver cirrhosis and is associated with high morbidity and mortality; therefore, it is a public health concern that deserves attention[29-31]. EVs rupture and bleeding are common causes of death in patients with liver cirrhosis. Clinical guidelines recommend the use of upper gastrointestinal endoscopy in screening and periodic reexamination of patients with cirrhosis regardless of the disease cause[9]. According to the results of upper gastrointestinal endoscopy and the Baveno VI criteria, EVs were divided by the low bleeding risk EVs (LEVs) and the high bleeding risk EVs (HEVs). For patients with HEVs, early precation measures can significantly reduce the esophageal variceal bleeding risk[22,32]. However, the invasiveness of upper gastrointestinal endoscopy, the high price, and the risk of anaesthesia make the compliance of patients to upper gastrointestinal endoscopy very low[9,10]. Considering that many patients do not have EVs in the early stage of liver cirrhosis, there is a need for non-invasive, simple, and safe means to identify liver cirrhosis patients with HEVs. In addition to upper gastrointestinal endoscopy, a variety of imaging methods, such as ultrasound, CT, and MRI, can be used to predict HEVs. However, these three methods cannot visually observe EVs, and the accuracy of identifying HEVs is poor[33]. A number of non-invasive models have been developed to predict HEVs, and several studies have shown that the LSPS, VRI, AAR, and Baveno VI models have achieved good results in predicting HEVs. Measurement of LS and SS by TE (using FibroScan) is a fast, non-invasive, easy to perform and reproducible procedure for predicting the presence of clinically significant EVs and PH, so LS and SS were measured by TE in this study[34]. In this study, to ensure the homogeneity of aetiology, we included patients with cirrhosis and HBV/HCV infection. Our study showed that LSM and SSM were two independent variables associated with the presence of HEVs. The results of our study are similar to those of several studies. LSM is associated with PH, and LSM combined with other indicators can predict HEVs[35,36]. Splenomegaly is common in patients with chronic viral cirrhosis, and splenic blood flow enters the portal vein system through the splenic vein. Therefore, SSM can simultaneously reflect static resistance fibrosis of the liver (LSM can also reflect) and dynamically capture PH-related visceral hypoperfusion, changes in spleen results, changes in blood flow, and PH-induced splenic fibrosis[37].

In this study, we constructed a non-invasive prediction model including LSM and SSM. The AUC of the new model was 0.965, the accuracy was 89.30%, which was better than that of the LSPS, VRI, AAR, and Baveno VI models, and the new model showed good diagnostic performance. When the optimal cut-off value was 0.27, the sensitivity and negative predictive value (NPV) of the new model in the modelling group were both 100%, and due to the Baveno VI criteria and other models, the new model could best identify non-HEVs patients so that these patients could be spared from undergoing upper gastrointestinal endoscopy. Morishita *et al*[38] used a similar approach in 135 patients with HCV-related cirrhosis to predict the presence of HEVs in patients with viral cirrhosis using a single indicator of LSM, and their results showed that the AUC of LSM for predicting the presence of HEVs was 0.868. The sensitivity, specificity, positive predictive value and negative predictive value were 81%, 82%, 69%, and 89%, respectively[38]. Similarly, in another study, Stefanescu *et al*[5] used a single-indicator SSM to assess the presence of HEVs, selecting an SSM@50 Hz with a 95% sensitivity for the best cut-off value [5]. Moreover, many studies have shown that when the HVPG value is ≥ 12 mmHg, LSM alone cannot reliably diagnose or exclude the risk grade of varices because of the poor correlation of extrahepatic factors. However, SSM can evaluate the severity of PH, the presence of EVs and the risk of bleeding but cannot predict the grade of EVs[39]. Therefore, this study developed and validated whether a non-invasive prediction model based on the combination of SSM and LSM indicators can be used as a useful tool to assess the severity of EVs and the risk of upper gastrointestinal bleeding (UGIB). These results of our study suggest that in the majority of patients with viral cirrhosis evaluated, the new model can

accurately exclude patients with HEVs, thereby allowing these patients to avoid endoscopy or prophylactic therapy. Furthermore, the higher NPV and sensitivity, regardless of the cirrhosis severity, suggest that use of the new model may be more cost-effective, as endoscopic screening of patients with both compensated and decompensated cirrhosis proved to be cost-effective[40]. In addition, a second independent dataset was used to externally validate the clinical utility of the new model, and the results showed that the new model had high discrimination power. In addition, DCA was cited to illustrate the clinical benefit of the new model, and both the modelling group and the external validation group could benefit from the new model. In addition, the included indicators in the new model can be obtained by TE and B-ultrasound, which are non-invasive, inexpensive, do not require radiation, are highly feasible in clinical practice, and are easy to popularize in clinical work.

Generally speaking, we have successfully developed a non-invasive prediction model using LSM and SSM indicators to predict the presence of HEVs in patients with viral cirrhosis, which has not been reported in the literature. Compared with other models LSPS, VRI, AAR, and Baveno VI, the new model has a good diagnostic performance, a high discrimination ability, calibration ability and a clinical application value. In addition, we enrolled patients with viral cirrhosis, which provided good consistency while minimizing bias in the results. However, this retrospective study has limitations. First, the sample size of this study is relatively small, and more data need to be collected for evaluation. Second, the patients in this study were all Chinese, and it is unclear whether this model can be applied in other ethnic groups. Additionally, because the patients in this study were all patients with viral cirrhosis and because changes in liver and spleen volume can vary with cirrhosis from different causes, it is unclear whether the new model can be applied to cirrhosis from other causes.

In conclusion, the new model based on SSM and LSM indicators, ln [P/(1-P)] = -8.184 - 0.228 × SSM + 0.642 × LSM, can effectively rule out the presence of HEVs in patients with viral cirrhosis, and this model needs to be further verified in prospective trials. This model helps physicians recognize the presence of HEVs in patients with viral cirrhosis, make more informed decisions, and provide appropriate preventive treatment.

CONCLUSION

The new model can effectively rule out the presence of HEVs in patients with viral cirrhosis and can be used as an alternative to routine upper gastrointestinal endoscopy screening.

ARTICLE HIGHLIGHTS

Research background

Acute bleeding due to esophageal varices (EVs) is a life-threatening complication in patients with cirrhosis. The diagnosis of EVs is mainly through upper gastrointestinal endoscopy, but the discomfort, contraindications and complications of gastrointestinal endoscopic screening reduce patient compliance.

Research motivation

To develop a safe, simple and non-invasive model to predict high risk EVs (HEVs) in patients with viral cirrhosis and identify patients who can be exempted from upper gastrointestinal endoscopy.

Research objectives

To establish a non-invasive prediction model based on spleen stiffness measurement (SSM) and live stiffness measurement (LSM) as an alternative to EVs screening.

Research methods

Two hundred Chinese adults, from March 2020 to November 2022, were included at the Second Affiliated Hospital of Xi'an Jiaotong University. Required data were collected by the medical records, and the EVs types of patients were determined by upper gastrointestinal endoscopy and the Baveno VI consensus. The effect of each parameter on HEVs was analyzed by univariate and multivariate analyses, and a non-invasive prediction model was established, and then the effect of each parameter on HEVs was analyzed by univariate and multivariate analyses, and a non-invasive prediction model was established.

Research results

After univariate and multivariate analyses, SSM and LSM were used to established a prediction model. The new non-invasive model was better than other four models to predict HEVs in patients with viral cirrhosis.

Research conclusions

The new model is reliable in predicting HEVs and can be used as an alternative to routine upper gastrointestinal endoscopy screening, which is helpful for clinical decision making.

Research perspectives

In the future, we will try to apply the new model to predict HEVs in patients with viral cirrhosis.

ACKNOWLEDGEMENTS

We thank all the participants in this study.

FOOTNOTES

Author contributions: Yang LB and Gao X contributed equally to this work; Li H, Dong L, and Dang XS designed the research study; Liu CY and Gao X performed the research; Tantai XX and Wei ZC contributed new reagents and analytic tools; Yang LB, Wang Y, and Chen FR analyzed the data and wrote the manuscript; and all authors have read and approve the final manuscript.

Supported by the Shaanxi Provincial Key Research and Development Plan, No. 2020SF-159.

Institutional review board statement: The study was reviewed and approved by the Ethics Committee of the Second Affiliated Hospital of Xi'an Jiaotong University (approval No. 2017-445).

Informed consent statement: This study is a retrospective study; thus, the ethics committee has exempted the informed consent of the patients.

Conflict-of-interest statement: There was no any interests conflicts.

Data sharing statement: No additional data are available.

Open-Access: This article is an open-access article that was selected by an in-house editor and fully peer-reviewed by external reviewers. It is distributed in accordance with the Creative Commons Attribution NonCommercial (CC BY-NC 4.0) license, which permits others to distribute, remix, adapt, build upon this work non-commercially, and license their derivative works on different terms, provided the original work is properly cited and the use is non-commercial. See: https://creativecommons.org/Licenses/by-nc/4.0/

Country/Territory of origin: China

ORCID number: Yan Wang 0000-0002-1127-9102.

S-Editor: Chen YL
L-Editor: A
P-Editor: Zhao S

REFERENCES

1 **Camilleri M**, Parkman HP, Shafi MA, Abell TL, Gerson L; American College of Gastroenterology. Clinical guideline: management of gastroparesis. *Am J Gastroenterol* 2013; **108**: 18-37; quiz 38 [PMID: 23147521 DOI: 10.1038/ajg.2012.373]
2 **de Franchis R**, Dell'Era A. Invasive and noninvasive methods to diagnose portal hypertension and esophageal varices. *Clin Liver Dis* 2014; **18**: 293-302 [PMID: 24679495 DOI: 10.1016/j.cld.2013.12.002]
3 **Liang H**, Si H, Liu M, Yuan L, Ma R, Zhang G, Yang J, Mo Z, Zhao Q. Non-Invasive Prediction Models for Esophageal Varices and Red Signs in Patients With Hepatitis B Virus-Related Liver Cirrhosis. *Front Mol Biosci* 2022; **9**: 930762 [PMID: 35911970 DOI: 10.3389/fmolb.2022.930762]
4 **Yu S**, Chen W, Jiang Z. Platelet count/spleen volume ratio has a good predictive value for esophageal varices in patients with hepatitis B liver cirrhosis. *PLoS One* 2021; **16**: e0260774 [PMID: 34855845 DOI: 10.1371/journal.pone.0260774]
5 **Stefanescu H**, Marasco G, Calès P, Fraquelli M, Rosselli M, Ganne-Carrié N, de Ledinghen V, Ravaioli F, Colecchia A, Rusu C, Andreone P, Mazzella G, Festi D. A novel spleen-dedicated stiffness measurement by FibroScan® improves the screening of high-risk oesophageal varices. *Liver Int* 2020; **40**: 175-185 [PMID: 31444849 DOI: 10.1111/liv.14228]
6 **Sebastiani G**, Tempesta D, Fattovich G, Castera L, Halfon P, Bourliere M, Noventa F, Angeli P, Saggioro A, Alberti A. Prediction of oesophageal varices in hepatic cirrhosis by simple serum non-invasive markers: Results of a multicenter, large-scale study. *J Hepatol* 2010; **53**: 630-638 [PMID: 20615567 DOI: 10.1016/j.jhep.2010.04.019]

7 **Augustin S**, Pons M, Maurice JB, Bureau C, Stefanescu H, Ney M, Blasco H, Procopet B, Tsochatzis E, Westbrook RH, Bosch J, Berzigotti A, Abraldes JG, Genescà J. Expanding the Baveno VI criteria for the screening of varices in patients with compensated advanced chronic liver disease. *Hepatology* 2017; **66**: 1980-1988 [PMID: 28696510 DOI: 10.1002/hep.29363]

8 **Gaete MI**, Díaz LA, Arenas A, González K, Cattaneo M, Fuster F, Henríquez R, Soza A, Arrese M, Barrera F, Arab JP, Benítez C. Baveno VI and Expanded Baveno VI criteria successfully predicts the absence of high-risk gastro-oesophageal varices in a Chilean cohort. *Liver Int* 2020; **40**: 1427-1434 [PMID: 31916360 DOI: 10.1111/liv.14373]

9 **Wickremeratne T**, Turner S, O'Beirne J. Systematic review with meta-analysis: ultra-thin gastroscopy compared to conventional gastroscopy for the diagnosis of oesophageal varices in people with cirrhosis. *Aliment Pharmacol Ther* 2019; **49**: 1464-1473 [PMID: 31059160 DOI: 10.1111/apt.15282]

10 **La Mura V**, Garcia-Guix M, Berzigotti A, Abraldes JG, García-Pagán JC, Villanueva C, Bosch J. A Prognostic Strategy Based on Stage of Cirrhosis and HVPG to Improve Risk Stratification After Variceal Bleeding. *Hepatology* 2020; **72**: 1353-1365 [PMID: 31960441 DOI: 10.1002/hep.31125]

11 **Singh S**, Eaton JE, Murad MH, Tanaka H, Iijima H, Talwalkar JA. Accuracy of spleen stiffness measurement in detection of esophageal varices in patients with chronic liver disease: systematic review and meta-analysis. *Clin Gastroenterol Hepatol* 2014; **12**: 935-45.e4 [PMID: 24055985 DOI: 10.1016/j.cgh.2013.09.013]

12 **Hu X**, Huang X, Hou J, Ding L, Su C, Meng F. Diagnostic accuracy of spleen stiffness to evaluate portal hypertension and esophageal varices in chronic liver disease: a systematic review and meta-analysis. *Eur Radiol* 2021; **31**: 2392-2404 [PMID: 32974686 DOI: 10.1007/s00330-020-07223-8]

13 **Manatsathit W**, Samant H, Kapur S, Ingviya T, Esmadi M, Wijarnpreecha K, McCashland T. Accuracy of liver stiffness, spleen stiffness, and LS-spleen diameter to platelet ratio score in detection of esophageal varices: Systemic review and meta-analysis. *J Gastroenterol Hepatol* 2018; **33**: 1696-1706 [PMID: 29736946 DOI: 10.1111/jgh.14271]

14 **de Alcantara RV**, Yamada RM, Cardoso SR, de Fátima M, Servidoni CP, Hessel G. Ultrasonographic predictors of esophageal varices. *J Pediatr Gastroenterol Nutr* 2013; **57**: 700-703 [PMID: 23941999 DOI: 10.1097/MPG.0b013e3182a7bc2e]

15 **Lipp MJ**, Broder A, Hudesman D, Suwandhi P, Okon SA, Horowitz M, Clain DJ, Friedmann P, Min AD. Detection of esophageal varices using CT and MRI. *Dig Dis Sci* 2011; **56**: 2696-2700 [PMID: 21380758 DOI: 10.1007/s10620-011-1660-8]

16 **Kim BK**, Han KH, Park JY, Ahn SH, Kim JK, Paik YH, Lee KS, Chon CY, Kim DY. A liver stiffness measurement-based, noninvasive prediction model for high-risk esophageal varices in B-viral liver cirrhosis. *Am J Gastroenterol* 2010; **105**: 1382-1390 [PMID: 20087336 DOI: 10.1038/ajg.2009.750]

17 **Berzigotti A**, Seijo S, Arena U, Abraldes JG, Vizzutti F, García-Pagán JC, Pinzani M, Bosch J. Elastography, spleen size, and platelet count identify portal hypertension in patients with compensated cirrhosis. *Gastroenterology* 2013; **144**: 102-111.e1 [PMID: 23058320 DOI: 10.1053/j.gastro.2012.10.001]

18 **Wang JH**, Chuah SK, Lu SN, Hung CH, Chen CH, Kee KM, Chang KC, Tai WC, Hu TH. Transient elastography and simple blood markers in the diagnosis of esophageal varices for compensated patients with hepatitis B virus-related cirrhosis. *J Gastroenterol Hepatol* 2012; **27**: 1213-1218 [PMID: 22432969 DOI: 10.1111/j.1440-1746.2012.07132.x]

19 **Marot A**, Trépo E, Doerig C, Schoepfer A, Moreno C, Deltenre P. Liver stiffness and platelet count for identifying patients with compensated liver disease at low risk of variceal bleeding. *Liver Int* 2017; **37**: 707-716 [PMID: 27862856 DOI: 10.1111/liv.13318]

20 **Bae J**, Sinn DH, Kang W, Gwak GY, Choi MS, Paik YH, Lee JH, Koh KC, Paik SW. Validation of the Baveno VI and the expanded Baveno VI criteria to identify patients who could avoid screening endoscopy. *Liver Int* 2018; **38**: 1442-1448 [PMID: 29495113 DOI: 10.1111/Liv.13732]

21 **Edeline J**, Blanc JF, Johnson P, Campillo-Gimenez B, Ross P, Ma YT, King J, Hubner RA, Sumpter K, Darby S, Evans J, Iwuji C, Swinson D, Collins P, Patel K, Muazzam I, Palmer DH, Meyer T. A multicentre comparison between Child Pugh and Albumin-Bilirubin scores in patients treated with sorafenib for Hepatocellular Carcinoma. *Liver Int* 2016; **36**: 1821-1828 [PMID: 27214151 DOI: 10.1111/liv.13170]

22 **Abraldes JG**, Bureau C, Stefanescu H, Augustin S, Ney M, Blasco H, Procopet B, Bosch J, Genesca J, Berzigotti A; Anticipate Investigators. Noninvasive tools and risk of clinically significant portal hypertension and varices in compensated cirrhosis: The "Anticipate" study. *Hepatology* 2016; **64**: 2173-2184 [PMID: 27639071 DOI: 10.1002/hep.28824]

23 **Lee E**, Kim YJ, Goo DE, Yang SB, Kim HJ, Jang JY, Jeong SW. Comparison of hepatic venous pressure gradient and endoscopic grading of esophageal varices. *World J Gastroenterol* 2016; **22**: 3212-3219 [PMID: 27003998 DOI: 10.3748/wjg.v22.i11.3212]

24 **Patel M**, Tann M, Liangpunsakul S. CT-scan Based Liver and Spleen Volume Measurement as a Prognostic Indicator for Patients with Cirrhosis. *Am J Med Sci* 2021; **362**: 252-259 [PMID: 33947583 DOI: 10.1016/j.amjms.2020.10.031]

25 **Boursier J**, Zarski JP, de Ledinghen V, Rousselet MC, Sturm N, Lebail B, Fouchard-Hubert I, Gallois Y, Oberti F, Bertrais S, Calès P; Multicentric Group from ANRS/HC/EP23 FIBROSTAR Studies. Determination of reliability criteria for liver stiffness evaluation by transient elastography. *Hepatology* 2013; **57**: 1182-1191 [PMID: 22899556 DOI: 10.1002/hep.25993]

26 **Rigamonti C**, Cittone MG, Manfredi GF, Sorge A, Moia R, Patriarca A, Donato MF, Gaidano G, Pirisi M, Fraquelli M. High reproducibility of spleen stiffness measurement by vibration-controlled transient elastography with a spleen-dedicated module. *Hepatol Commun* 2022; **6**: 3006-3014 [PMID: 36082990 DOI: 10.1002/hep4.2070]

27 **Zheng KI**, Liu C, Li J, Zhao L, Zheng MH, Wang F, Qi X. Validation of Baveno VI and expanded Baveno VI criteria to identify high-risk varices in patients with MAFLD-related compensated cirrhosis. *J Hepatol* 2020; **73**: 1571-1573 [PMID: 32972730 DOI: 10.1016/j.jhep.2020.06.042]

28 **Vickers AJ**, Holland F. Decision curve analysis to evaluate the clinical benefit of prediction models. *Spine J* 2021; **21**: 1643-1648 [PMID: 33676020 DOI: 10.1016/j.spinee.2021.02.024]

29 **Leoni S**, Casabianca A, Biagioni B, Serio I. Viral hepatitis: Innovations and expectations. *World J Gastroenterol* 2022; **28**:

517-531 [PMID: 35316960 DOI: 10.3748/wjg.v28.i5.517]

30 **Xiang Z**, Li J, Lu D, Wei X, Xu X. Advances in multi-omics research on viral hepatitis. *Front Microbiol* 2022; **13**: 987324 [PMID: 36118247 DOI: 10.3389/fmicb.2022.987324]

31 **Razavi H**. Global Epidemiology of Viral Hepatitis. *Gastroenterol Clin North Am* 2020; **49**: 179-189 [PMID: 32389357 DOI: 10.1016/j.gtc.2020.01.001]

32 **Reiberger T**, Püspök A, Schoder M, Baumann-Durchschein F, Bucsics T, Datz C, Dolak W, Ferlitsch A, Finkenstedt A, Graziadei I, Hametner S, Karnel F, Krones E, Maieron A, Mandorfer M, Peck-Radosavljevic M, Rainer F, Schwabl P, Stadlbauer V, Stauber R, Tilg H, Trauner M, Zoller H, Schöfl R, Fickert P. Austrian consensus guidelines on the management and treatment of portal hypertension (Billroth III). *Wien Klin Wochenschr* 2017; **129**: 135-158 [PMID: 29063233 DOI: 10.1007/s00508-017-1262-3]

33 **Zardi EM**, Di Matteo FM, Pacella CM, Sanyal AJ. Invasive and non-invasive techniques for detecting portal hypertension and predicting variceal bleeding in cirrhosis: a review. *Ann Med* 2014; **46**: 8-17 [PMID: 24328372 DOI: 10.3109/07853890.2013.857831]

34 **Roccarina D**, Rosselli M, Genesca J, Tsochatzis EA. Elastography methods for the non-invasive assessment of portal hypertension. *Expert Rev Gastroenterol Hepatol* 2018; **12**: 155-164 [PMID: 28856972 DOI: 10.1080/17474124.2017.1374852]

35 **Kim BK**, Kim DY, Han KH, Park JY, Kim JK, Paik YH, Lee KS, Chon CY, Ahn SH. Risk assessment of esophageal variceal bleeding in B-viral liver cirrhosis by a liver stiffness measurement-based model. *Am J Gastroenterol* 2011; **106**: 1654-1662, 1730 [PMID: 21691339 DOI: 10.1038/ajg.2011.160]

36 **Berger A**, Ravaioli F, Farcau O, Festi D, Stefanescu H, Buisson F, Nahon P, Bureau C, Ganne-Carrié N, Berzigotti A, de Ledinghen V, Petta S, Calès P; multicenter groups Varices œsophagiennes - Vidéo-capsule œsophagienne, Agence Nationale de Recherches sur le Sida et les Hépatites Virales, Cohort 12 Cirrhoses Virales, M116, and Validation of Expanded Baveno VI Criteria. Including Ratio of Platelets to Liver Stiffness Improves Accuracy of Screening for Esophageal Varices That Require Treatment. *Clin Gastroenterol Hepatol* 2021; **19**: 777-787.e17 [PMID: 32562889 DOI: 10.1016/j.cgh.2020.06.022]

37 **Reiberger T**. The Value of Liver and Spleen Stiffness for Evaluation of Portal Hypertension in Compensated Cirrhosis. *Hepatol Commun* 2022; **6**: 950-964 [PMID: 34904404 DOI: 10.1002/hep4.1855]

38 **Morishita N**, Hiramatsu N, Oze T, Harada N, Yamada R, Miyazaki M, Yakushijin T, Miyagi T, Yoshida Y, Tatsumi T, Kanto T, Takehara T. Liver stiffness measurement by acoustic radiation force impulse is useful in predicting the presence of esophageal varices or high-risk esophageal varices among patients with HCV-related cirrhosis. *J Gastroenterol* 2014; **49**: 1175-1182 [PMID: 24005957 DOI: 10.1007/s00535-013-0877-z]

39 **Buechter M**, Kahraman A, Manka P, Gerken G, Jochum C, Canbay A, Dechêne A. Spleen and Liver Stiffness Is Positively Correlated with the Risk of Esophageal Variceal Bleeding. *Digestion* 2016; **94**: 138-144 [PMID: 27756066 DOI: 10.1159/000450704]

40 **Takuma Y**, Nouso K, Morimoto Y, Tomokuni J, Sahara A, Toshikuni N, Takabatake H, Shimomura H, Doi A, Sakakibara I, Matsueda K, Yamamoto H. Measurement of spleen stiffness by acoustic radiation force impulse imaging identifies cirrhotic patients with esophageal varices. *Gastroenterology* 2013; **144**: 92-101.e2 [PMID: 23022955 DOI: 10.1053/j.gastro.2012.09.049]

World Journal of Gastroenterology

Submit a Manuscript: https://www.f6publishing.com

World J Gastroenterol 2023 July 7; 29(25): 4085-4098

DOI: 10.3748/wjg.v29.i25.4085

ISSN 1007-9327 (print) ISSN 2219-2840 (online)

ORIGINAL ARTICLE

Observational Study

Real-world effectiveness and safety of direct-acting antivirals in hepatitis C virus patients with mental disorders

Dorota Dybowska, Dorota Zarębska-Michaluk, Piotr Rzymski, Hanna Berak, Beata Lorenc, Marek Sitko, Michał Dybowski, Włodzimierz Mazur, Magdalena Tudrujek-Zdunek, Justyna Janocha-Litwin, Ewa Janczewska, Jakub Klapaczyński, Anna Parfieniuk-Kowerda, Anna Piekarska, Barbara Sobala-Szczygieł, Krystyna Dobrowolska, Malgorzata Pawłowska, Robert Flisiak

Specialty type: Gastroenterology and hepatology

Provenance and peer review: Invited article; Externally peer reviewed.

Peer-review model: Single blind

Peer-review report's scientific quality classification

Grade A (Excellent): 0
Grade B (Very good): B
Grade C (Good): C
Grade D (Fair): 0
Grade E (Poor): 0

P-Reviewer: Isakov V, Russia; Liu CH, Taiwan

Received: March 23, 2023
Peer-review started: March 23, 2023
First decision: March 28, 2023
Revised: April 1, 2023
Accepted: April 28, 2023
Article in press: April 28, 2023
Published online: July 7, 2023

Dorota Dybowska, Malgorzata Pawłowska, Department of Infectious Diseases and Hepatology, Faculty of Medicine, Nicolaus Copernicus University, Bydgoszcz 85-030, Poland

Dorota Zarębska-Michaluk, Department of Infectious Diseases and Allergology, Jan Kochanowski University, Kielce 25-317, Poland

Dorota Zarębska-Michaluk, Department of Infectious Diseases, Provincial Hospital, Kielce 25-317, Poland

Piotr Rzymski, Department of Environmental Medicine, University of Medical Sciences, Poznań 60-806, Poland

Piotr Rzymski, Integrated Science Association, Universal Scientific Education and Research Network, Poznań 60-806, Poland

Hanna Berak, Outpatient Clinic, Hospital for Infectious Diseases in Warsaw, Warsaw 01-201, Poland

Beata Lorenc, Pomeranian Center of Infectious Diseases, Medical University, Gdańsk 80-214, Poland

Marek Sitko, Department of Infectious and Tropical Diseases, Jagiellonian University, Kraków 31-088, Poland

Michał Dybowski, Utrecht University School of Economics, Utrecht University, Utrecht 3584 EC, Netherlands

Włodzimierz Mazur, Clinical Department of Infectious Diseases, Medical University of Silesia, Chorzów 41-500, Poland

Magdalena Tudrujek-Zdunek, Department of Infectious Diseases, Medical University of Lublin, Lublin 20-059, Poland

Justyna Janocha-Litwin, Department of Infectious Diseases and Hepatology, Medical University of Wrocław, Wrocław 50-367, Poland

Ewa Janczewska, Department of Basic Medical Sciences, Faculty of Public Health in Bytom,

Medical University of Silesia, Katowice 40-007, Poland

Jakub Klapaczyński, Department of Internal Medicine and Hepatology, Central Clinical Hospital of the Ministry of Internal Affairs and Administration, Warsaw 00-241, Poland

Anna Parfieniuk-Kowerda, Robert Flisiak, Department of Infectious Diseases and Hepatology, Medical University of Białystok, Białystok 15-089, Poland

Anna Piekarska, Department of Infectious Diseases and Hepatology, Medical University of Łódź, Łódź 91-347, Poland

Barbara Sobala-Szczygieł, Department of Infectious Diseases and Hepatology, Medical University of Silesia, Bytom 41-902, Poland

Krystyna Dobrowolska, Collegium Medicum, Jan Kochanowski University, Kielce 25-317, Poland

Corresponding author: Dorota Zarębska-Michaluk, PhD, Assistant Professor, Professor, Department of Infectious Diseases and Allergology, Jan Kochanowski University, Żeromskiego 5, Kielce 25-317, Poland.
dorota1010@tlen.pl

Abstract

BACKGROUND

It is estimated that 58 million people worldwide are infected with the hepatitis C virus (HCV). Patients with severe psychiatric disorders could not be treated with previously available interferon-based therapies due to their unfavorable side effect profile. This has changed with the introduction of direct-acting antivirals (DAA), although their real-life tolerance and effectiveness in patients with different psychiatric disorders remain to be demonstrated.

AIM

To evaluate the effectiveness and safety of DAA in patients with various mental illnesses.

METHODS

This was a retrospective observational study encompassing 14272 patients treated with DAA for chronic hepatitis C in 22 Polish hepatology centers, including 942 individuals diagnosed with a mental disorder (anxiety disorder, bipolar affective disorder, depression, anxiety-depressive disorder, personality disorder, schizophrenia, sleep disorder, substance abuse disorder, and mental illness without a specific diagnosis). The safety and effectiveness of DAA in this group were compared to those in a group without psychiatric illness (n = 13330). Antiviral therapy was considered successful if serum ribonucleic acid (RNA) of HCV was undetectable 12 wk after its completion [sustained virologic response (SVR)]. Safety data, including the incidence of adverse events (AEs), serious AEs (SAEs), and deaths, and the frequency of treatment modification and discontinuation, were collected during therapy and up to 12 wk after treatment completion. The entire study population was included in the intent-to-treat (ITT) analysis. Per-protocol (PP) analysis concerned patients who underwent HCV RNA evaluation 12 wk after completing treatment.

RESULTS

Among patients with mental illness, there was a significantly higher percentage of men, treatment-naive patients, obese, human immunodeficiency virus and hepatitis B virus-coinfected, patients with cirrhosis, and those infected with genotype 3 (GT3) while infection with GT1b was more frequent in the population without psychiatric disorders. The cure rate calculated PP was not significantly different in the two groups analyzed, with a SVR of 96.9% and 97.7%, respectively. Although patients with bipolar disorder achieved a significantly lower SVR, the multivariate analysis excluded it as an independent predictor of treatment non-response. Male sex, GT3 infection, cirrhosis, and failure of previous therapy were identified as independent negative predictors. The percentage of patients who completed the planned therapy did not differ between groups with and without mental disorders. In six patients, symptoms of mental illness (depression, schizophrenia) worsened, of which two discontinued treatments for this reason. New episodes of sleep disorders occurred significantly more often in patients with mental disorders. Patients with mental illness were more frequently lost to follow-up (4.2% *vs* 2.5%).

CONCLUSION

DAA treatment is safe and effective in HCV-infected patients with mental disorders. No specific

psychiatric diagnosis lowered the chance of successful antiviral treatment.

Key Words: Hepatitis C; Mental disorders; Direct-acting antivirals

©The Author(s) 2023. Published by Baishideng Publishing Group Inc. All rights reserved.

Core Tip: In the population of patients with mental illness, the prevalence of hepatitis C virus infection is many times higher than in the general population. In the era of interferon-based therapy, these patients had minimal access to antiviral treatment due to contraindications to interferon with the risk of exacerbation of psychiatric diseases. Their situation has improved with the introduction of direct-acting antivirals, but data from real-world studies are scarce. This retrospective analysis carried out in clinical practice confirmed that the good safety profile and treatment effectiveness are not inferior to those obtained in a population without mental disorders.

Citation: Dybowska D, Zarębska-Michaluk D, Rzymski P, Berak H, Lorenc B, Sitko M, Dybowski M, Mazur W, Tudrujek-Zdunek M, Janocha-Litwin J, Janczewska E, Klapaczyński J, Parfieniuk-Kowerda A, Piekarska A, Sobala-Szczygieł B, Dobrowolska K, Pawłowska M, Flisiak R. Real-world effectiveness and safety of direct-acting antivirals in hepatitis C virus patients with mental disorders. *World J Gastroenterol* 2023; 29(25): 4085-4098

URL: https://www.wjgnet.com/1007-9327/full/v29/i25/4085.htm

DOI: https://dx.doi.org/10.3748/wjg.v29.i25.4085

INTRODUCTION

Hepatitis C virus (HCV) infection, currently affecting approximately 58 million individuals worldwide, still poses a severe global issue[1]. It remains a major cause of chronic liver disease worldwide, liable to progress to cirrhosis and hepatocellular carcinoma, and can lead to various extrahepatic manifestations [2]. The prevalence of HCV infection is significantly increased (3-fold to 20-fold) in individuals with mental disorders compared to the general population. This includes patients with depression, bipolar disorder, schizophrenia, and personality disorders. In patients with substance abuse, particularly with intravenous drug use, the reported percentage of HCV infection is as high as 60%-70%[3,4]. In addition, preexisting mental illness may complicate HCV treatment by adversely affecting treatment adherence[5-7]. Moreover, HCV infection itself can further exacerbate or accelerate psychiatric symptoms[6,8].

In the past, treatment of patients with severe psychiatric disorders infected with HCV was highly challenging due to neuropsychiatric side effects (*e.g.*, anxiety, affective, cognitive, and psychotic symptoms) of previously used interferon (IFN)-based therapies[9]. Their situation has improved with the introduction of direct-acting antivirals (DAA), which are well tolerated and easier to dose[10]. Whether they are also effective in different mental disorders requires further studies. Observations from the IFN-era period indicate that these disorders were not necessarily associated with a worse sustained viral response (SVR) rate[11-13]. However, the observations encompassing the period when DAA were introduced are scarce, include small study groups, only particular diseases (*e.g.*, depression), or treat them collectively as mental disorders[14-17]. The results of one multicenter study evaluating a single DAA regimen among psychiatric patients by type of mental disorder have recently been published, but evidence is still needed from large populations of real-world experience that discriminate between individual psychiatric diseases treated with different DAA options and compare the results to the group without mental disorders while controlling for confounding variables[18].

To this end, the present study aimed to evaluate the effectiveness and safety of DAA in patients with various mental illnesses: Anxiety, anxiety-depressive disorder, bipolar disorder, depression, personality disorder, schizophrenia, sleep disorder, substance abuse, and mental illness without a specific diagnosis. In order to achieve this goal, a retrospective, real-world analysis of the Polish population of HCV-infected patients treated with DAA between 2015 and 2022 was conducted.

MATERIALS AND METHODS

Data collection

The data of 14272 patients treated with DAA for chronic hepatitis C (CHC) from 1 July 2015 to 30 December 2022, included in the EpiTer-2 observational study database, were analyzed. This study was conducted under the auspices of the Polish Association of Epidemiologists and Infectiologists and

included data from 22 Polish hepatology centers on treating CHC in everyday practice. The choice of CHC therapy was at the physician's discretion and followed the existing recommendations of the Polish Group of Experts for HCV and the recommendations of the National Health Fund. The data were collected retrospectively and included age, sex, body mass index, the severity of liver disease, HCV genotype (GT), human immunodeficiency virus (HIV) and/or hepatitis B virus (HBV) coinfection, previous and current CHC treatment, presence of hepatocellular carcinoma, HCV viral load, alanine transaminase activity, albumin, hemoglobin, creatinine, and platelets level.

Assessment of mental disorders

The patients were divided into two groups: 942 patients with concomitant mental illness (group A) and 13330 without psychiatric disorders (group B). Mentally ill patients were under the care of psychiatrists, who diagnosed their mental illness, prescribed and monitored psychiatric treatment.

Assessment of liver disease severity

The severity of liver disease was assessed using non-invasive methods of fibrosis assessment: Transient elastography or shear-wave elastography with an Aixplorer device (SuperSonic Imagine, Aix-en-Provence, France) or transient FibroScan. Based on the METAVIR score, according to the guidelines of the European Association for the Study of the Liver, the cutoff value of 13 kPa was used to predict individuals considered to be cirrhotic[19]. These patients were evaluated for the presence of decompensation of liver function (in the past and at the beginning of antiviral therapy) and were assessed on the Child-Pugh (CP) scale. Patients scored as B or C on the CP scale were considered to be decompensated. Data were also collected on the past diagnosis of HCC and liver transplantation.

Effectiveness assessment

Antiviral therapy was considered successful if ribonucleic acid of the virus (HCV RNA) in serum was undetectable 12 wk after its completion, meaning that the patient achieved a sustained virologic response (SVR). Patients with detectable viral load at this time point were considered virologic failures, while those lost to follow-up without HCV RNA evaluation 12 wk after the end of therapy were recognized as non-virological failures and not included in the PP analysis.

Safety assessment

An analysis of potential drug-drug interactions was carried out before the start of DAA therapy using an online tool on the University of Liverpool website[20]. The results of this analysis influenced the choice of DAA regimen or modification of psychiatric therapy. Safety data, including the incidence of adverse events (AEs), serious AEs (SEAs), and deaths, as well as the frequency of treatment modification and discontinuation, were collected during therapy and up to 12 wk after treatment completion.

Ethics

The data were originally collected not for scientific purposes but to evaluate the effectiveness and safety of real-world treatment with registered drugs. Patients were not exposed to any experimental interventions. According to local law (Law of 6 September 2001, Pharmaceutical Law, Article 37al), non-interventional studies do not require ethics committee approval. Due to the retrospective design of the analysis, the requirement for patient consent was not necessary. Patient data were collected and analyzed in accordance with applicable data protection rules.

Statistical analysis

Statistical analyses were performed using Statistica v. 13 (StatSoft, Tulsa, OK, United States) and MedCalc v. 15.8 (MedCalc Software Ltd, Ostend, Belgium). The entire study population was included in the ITT analysis. The PP analysis concerned patients who underwent HCV RNA evaluation 12 wk after completing treatment. Differences in frequencies of events between groups with and without mental disorders were assessed with χ^2 Pearson's test or Fisher exact test (when the number of observations was < 10). The differences in data expressed on the interval scale were evaluated with a non-parametric Mann-Whitney U test because they did not meet the Gaussian assumption (Shapiro-Wilk's test, $P < 0.05$). Multiple logistic regression was used to predict the odds of no response to HCV treatment for mental disorders (for which a lower frequency of SVR was observed) while controlling for known factors affecting the chance of SVR in the IFN and IFN-free era: male sex, obesity, GT3, cirrhosis, history of HCV treatment failure, HIV coinfection, HBV coinfection, and three antiviral combinations: asunaprevir (ASV) and daclatasvir (DCV), sofosbuvir (SOF) and velpatasvir (VEL), and SOF/VEL with ribavirin (RBV)[21-24]. A P value below 0.05 was deemed statistically significant.

RESULTS

Characteristics of the studied groups

The demographic characteristics of the groups are summarized in Table 1. Group A included 503 patients who had depression (55.6%), 121 with schizophrenia (12.8%), 36 with mental illness without a specific diagnosis (3.8%), 26 with anxiety-depressive disorders (2.8%), 24 with bipolar affective disorder (2.6%), 21 with anxiety disorders (2.2%), 16 with personality disorders (1.7%), and 6 with sleep disorders (0.6%). Substance abuse disorder was diagnosed in 159 cases (16.9%). Moreover, in 30 patients (3.2%), substance abuse and other mental illness coexisted: Depression in 21 patients (2.2%), personality disorders in 4 (0.4%), schizophrenia in 2 (0.2%), anxiety disorders in 2 (0.2%), and an anxiety-depressive disorder in 1 patient (0.1%).

The mean age of patients in both groups was comparable. Group A included a higher percentage of men, obese individuals, patients with more advanced liver fibrosis, and a higher percentage of CP class B and C patients. Similar to group B, the GT1b prevailed, although its frequency was lower, while the higher percentage of HCV-infections with GTs 3 and 4 were noted. Coinfections with HIV and/or HBV were also more common in the group of patients with mental disorders (Table 2).

This group was also characterized by a higher baseline HCV viral load. Most patients in group A (80.6%) were treatment-naïve, while 16.7% (n = 157) of the cases had previously been treated with IFN. Of these, 34 patients discontinued IFN-based therapy due to AEs. During current therapy, 12/34 (35%) had mild AEs, the most common of which was headache (n = 3), and one patient in this group experienced increased insomnia. All patients in this group completed therapy as planned, 31 achieved SVR, and 1 patient was lost to follow-up. Patients with mental illnesses were more often treated with pangenotypic therapy for CHC (Table 3).

Treatment effectiveness

There were no statistically significant differences in the achievement of SVR in groups A and B in both the ITT (92.8% *vs* 95.3%, respectively) and PP (96.9% *vs* 97.7%) analyses (Figure 1A). A significantly lower percentage of SVR was observed in patients with bipolar disorder (Figure 1B). In multivariate analyses, a lower chance of SVR was associated with male sex, GT3, cirrhosis, history of previous HCV-treatment failure, and two DAA regimens: ASV + DCV and SOF + VEL + RBV (Table 4).

Treatment safety

Patients with mental illness more often belonged to the group lost to follow-up (4.2% *vs* 2.5%). In six patients symptoms of mental illness (depression - 5, schizophrenia - 1) worsened during antiviral therapy, of which two permanently discontinued treatment for this reason. New episodes of sleep disorders occurred significantly more often in group A during DAA therapy. In group B, one patient experienced an episode of schizophrenia, and six were diagnosed with depression. In both groups, a similar percentage of patients completed the planned treatment. There were no statistically significant differences in discontinued and modified treatments (Table 5).

Modification of therapy concerned only a change in the dose of RBV. Possible drug interactions were analyzed prior to antiviral therapy. Patients in group A were treated with neuroleptics, anticonvulsants, antidepressants, sedatives, anxiolytics, and methadone. Only carbamazepine could have clinically relevant interactions. This drug was used in 3 patients in group A and in 12 patients in group B. All patients with mental diseases using carbamazepine completed the treatment as planned without AEs, and all achieved SVR.

DISCUSSION

By documenting the high rate of SVR in patients with mental diseases, our study proves that this patient population does not differ in their response to DAA treatment from those with CHC not affected by psychiatric conditions supporting the findings of a recently published multicenter analysis[18]. Thus, there is no rationale for considering these patients as a difficult-to-treat population in terms of virologic response to therapy, as they were previously recognized in the era of IFN-based regimens. Antiviral therapy for mentally ill patients has been a challenge due to contraindications to the use of IFN and the side effects of this cytokine[9,25]. Neuropsychiatric disorders of various caliber during IFN therapy have been widely reported[26-28]. Most were mild in severity and transient in nature, but severe psychosis and suicide attempts have also been described as a reason for discontinuing therapy. Such side effects of therapy have been described even in patients with no prior mental disorders[29]. Due to the risk of exacerbating psychiatric conditions, many patients with a diagnosed mental illness were not eligible for treatment. The mental state of those included in therapy had to be closely monitored, requiring cooperation with the patient's attending psychiatrist[30]. This was the only way to keep the patient in therapy and in the event of exacerbation of mental disorders, to react swiftly and to modify or discontinue antiviral treatment, if necessary for safety reasons[5,31]. At the same time, this was a population of patients in whom successful antiviral therapy offered a chance for mental improvement

Table 1 Baseline characteristics of chronic hepatitis C patients with (group A) and without (group B) psychiatric disorders, %, *n*

Parameter	All patients (*n* = 14272)	Group A (*n* = 942)	Group B (*n* = 13330)	*P* value
Age, mean (min-max yr)	51.2 (18-92)	50.8 (19-90)	51.2 (18-92)	0.599 (*U* = 6216478)
Men/women	49.3/50.7 (7035/7237)	54.9/45.1, 507/435	49.0/51.0, 6528/6802	0.004 (χ^2 = 8.3)
BMI, mean (SD)	26.2 (4.5)	26.9 (5.1)	26.1 (4.5)	0.0001 (*U* = 5811710)
BMI ≥ 30	17.4 (2486)	23.9 (225)	17.0 (2261)	< 0.0001 (χ^2 = 29.4)
Comorbidities				
Hypertension	32.0 (4567)	34.4 (324)	31.8 (4243)	0.103 (χ^2 = 2.6)
Diabetes	11.3 (1614)	13.0 (122)	11.2 (1492)	0.100 (χ^2 = 0.5)
Renal disease	3.8 (543)	3.4 (32)	3.8 (511)	0.498 (χ^2 = 0.5)
Autoimmune disease	2.1 (304)	2.0 (19)	2.1 (285)	0.803 (χ^2 = 0.06)
Non-HCC tumor	2.0 (279)	2.1 (20)	1.9 (259)	0.700 (χ^2 = 0.15)
ALT (IU/L), median (IQR)	58.0 (37.0-97.0)	59.0 (36.0-96.0)	58.0 (37.0-97.0)	0.581 (*U* = 6204221)
Albumin (g/dL), median (IQR)	4.1 (3.8-4.4)	4.1 (3.8-4.4)	4.1 (3.8-4.4)	0.633 (*U* = 6222478)
Bilirubin (mg/dL), median (IQR)	0.6 (0.5-0.9)	0.6 (0.5-0.9)	0.6 (0.5-0.9)	0.060 (*U* = 6050856)
Hemoglobin (g/dL), median (IQR)	14.5 (13.4-15.5)	14.4 (13.4-15.4)	14.5 (13.4-15.6)	0.307 (*U* = 6120464)
Platelets (× 1000/μL), median (IQR)	197.0 (146.0-244.0)	190.0 (136.0-240.0)	197.0 (146.0-244.0)	0.01 (*U* = 597757)
Creatinine (mg/dL), median (IQR)	0.8 (0.7-0.9)	0.8 (0.7-0.9)	0.8 (0.7-0.9)	0.798 (*U* = 6101372)
HCV RNA, × 10^6 IU/mL, median (IQR)	0.97 (0.32-2.53)	1.17 (0.38-3.0)	0.96 (0.31-2.48)	0.0005 (*U* = 5856849)

The reported *P* value relates to Pearson's chi-square test (or Fisher's exact test if the number of observations in a category was less than 10) or the Mann-Whitney *U* test. BMI: Body mass index; ALT: Alanine transaminase; HCC: Hepatocellular carcinoma; IQR: Interquartile range; HCV: Hepatitis C virus; RNA: Ribonucleic acid.

[32]. In addition to causing liver disease, HCV can potentially induce extrahepatic manifestations, *i.e.*, disorders of other organs and systems that are pathogenetically associated with infection[33]. One of them is the central nervous system, whose involvement results in neurological and psychiatric disorders [6,7,34]. The mechanism of the virus's impact on the nervous system is complex and includes both a direct cytopathic effect related to the infection of nerve cells, as well as the impact of the immune response triggered by the HCV and the effects of psychogenic stressors[8,34,35].

The frequent co-occurrence of CHC and psychiatric disorders was confirmed by numerous studies analyzing this issue in Real World Evidence (RWE) populations[36,37]. The estimated frequency of active mental illness in patients with CHC assessed in the large cohort of American Veterans was as high as one-third, while in our analysis, the percentage of patients was 6.6%[38]. Among them, depression, addiction, and schizophrenia were the most common. On the other hand, the pooled prevalence of HCV infection among patients with severe psychiatric diseases evaluated in a meta-analysis that included papers from 1989-2020 was 8%, which is several times higher compared to the general population[38,39]. However, the fact that patients with mental illnesses are disproportionately affected by HCV is also influenced by other factors beyond the pathogenetic relationship. One that seems to be historical is exposure to infection through frequent contact with healthcare facilities, and it cannot be overlooked that hospitalizations for mental illness are very long. Another factor contributing to the higher prevalence of HCV infections in this population, the importance of which persists to the present day, is that persons diagnosed with mental disorders are much more likely to abuse substances, including injection drugs and needle sharing used for intravenous drug administration is the most common route of HCV transmission[17]. This was also documented in our analysis. Moreover, the population of HCV-infected patients with mental diseases, which was underserved in the era of IFN, has gained its opportunity in the time of DAA therapy. The much shorter course of treatment and the lack of contraindications to the drugs has enabled patients with psychiatric disorders to access therapy on the same principles as for other HCV-infected individuals and has provided a basis for predicting HCV microelimination in this population[18]. In the current analysis, we found no statistically significant differences in the course of treatment in mentally ill patients compared to others. The percentage of those who had their therapy modified or discontinued was comparable; the modification

Table 2 Characteristics of liver disease in patients with chronic hepatitis C with (group A) and without (group B) psychiatric disorders, %, *n*

Parameters	All patients (*n* = 14272)	Group A (*n* = 942)	Group B (*n* = 13330)	*P* value
Genotype				
1a	4.4 (633)	4.1 (39)	4.5 (594)	0.649 (χ^2 = 0.2)
1b	77.3 (11029)	67.8 (639)	77.9 (10390)	< 0.0001 (χ^2 = 51.2)
1	2.1 (303)	2.4 (23)	2.1 (280)	0.483 (χ^2 = 0.5)
2	0.2 (29)	0.2 (2)	0.2 (27)	> 0.948 (χ^2 = 0.004)
3	11.1 (1580)	17.5 (165)	10.6 (1415)	< 0.0001 (χ^2 = 42.6)
4	4.9 (695)	8.0 (74)	4.7 (621)	< 0.0001 (χ^2 = 19.4)
5	0.007 (1)	0.0 (0)	0.007 (1)	1.0
6	0.01 (2)	(0.0) 0	0.01 (2)	1.012
Liver fibrosis				
F0	2.5 (361)	1.4 (13)	2.6 (348)	0.02 (χ^2 = 5.4)
F1	40.8 (5831)	34.8 (328)	41.3 (5503)	< 0.0001 (χ^2 = 15.2)
F2	19.2 (2743)	21.0 (198)	19.1 (2545)	0.147 (χ^2 = 2.1)
F3	13.5 (1925)	13.2 (124)	13.5 (1801)	0.763 (χ^2 = 0.09)
F4	23.9 (3412)	29.6 (279)	23.5 (3133)	< 0.0001 (χ^2 = 18.1)
Child-Pugh				
Child-Pugh-B	2.8 (398)	4.4 (41)	2.7 (357)	0.003 (χ^2 = 9.1)
Child-Pugh-C	0.2 (23)	0.4 (4)	0.1 (19)	0.061
HCC history	1.3 (191)	1.2 (11)	1.3 (180)	0.637 (χ^2 = 0.2)
Coinfection				
HIV	5.9 (848)	9.1 (86)	5.7 (762)	< 0.0001 (χ^2 = 18.4)
HBV	13.5 (1933)	17.5 (165)	13.3 (1768)	0.0002 (χ^2 = 13.6)
HIV/HBV	1.6 (225)	3.4 (32)	1.4 (193)	< 0.0001 (χ^2 = 21.6)

The reported *P* value relates to Pearson's chi-square test or Fisher's exact test if the number of observations in the category was less than 10. HCC: Hepatocellular carcinoma; HIV: Human immunodeficiency virus; HBV: Hepatitis B virus.

in both groups concerned only RBV dose reduction according to the label. The safety profile was also comparable with the percentage of patients experiencing SEAs and deaths. Similar conclusions on the good tolerability of DAA can be drawn from the observations of other researchers in RWE cohorts[40,41]. When analyzing psychiatric complications occurring during therapy, we found a significantly higher percentage of sleep disorders in patients with psychiatric diseases than in those without mental conditions. Other researchers evaluating the quality of sleep in patients with mental disorders did not find any significant differences during DAA therapy compared to the baseline, demonstrating that DAA regimens are free of mental side effects regardless of current and/or past psychiatric history[14,15].

In our analysis, however, in six patients, the underlying disease (five cases of depression and one of schizophrenia) worsened during antiviral therapy, which in 2 cases was the reason for discontinuing treatment. However, we cannot exclude the potential influence of other factors. It should be noted that the cited analyses were prospective, while ours is a retrospective study with limitations in data collection. Interestingly, another prospective study reported some degree of neuropsychiatric impairment associated with IFN-free treatment in 10 cirrhotic patients, suggesting their susceptibility to mild DAA neurotoxicity[42].

Despite the significant change in access to treatment, there are still some challenges for a group of patients with mental illness. These are related to potential drug interactions. For this reason, this is carefully reviewed before therapy, and if there are contraindications to combining medications, psychiatric drugs are modified to allow the patient to receive antiviral treatment. This is not always possible; in our study, three patients were on carbamazepine, which could not be discontinued as it was the only drug that stabilized their mental state. Although this drug is not recommended in combination with DAA because it can reduce their levels below therapeutic levels, all patients completed the

Table 3 Treatment characteristics in chronic hepatitis C patients with (group A) and without (group B) psychiatric disorders, %, *n*

Parameter	All patients (*n* = 14272)	Group A (*n* = 942)	Group B (*n* = 13330)	*P* value
History of antiviral treatment				
Treatment-naïve	78.7 (11238)	80.6 (760)	78.6 (10478)	0.132 (χ^2 = 2.2)
Nonresponder to IFN-based regimens	19.6 (2791)	16.7 (157)	19.8 (2634)	0.02 (χ^2 = 5.3)
Nonresponder to IFN-free regimens	1.7 (247)	2.7 (25)	1.6 (222)	0.02 (χ^2 = 5.1)
Current treatment regimen				
Pangenotypic regimens	35.2 (5028)	43.0 (405)	34.7 (4619)	< 0.0001 (χ^2 = 26.0)
Genotype-specific regimens	64.8 (9248)	57.0 (537)	65.3 (8711)	
Current-RBV-containing regimens	16.2 (2308)	16.5 (155)	16.1 (2153)	0.807 (χ^2 = 0.05)
Genotype-specific treatment regimens				
ASV + DCV	0.8 (118)	1.3 (12)	0.8 (106)	0.117 (χ^2 = 2.5)
SOF/LDV ± RBV	19.6 (2795)	21.8 (205)	19.4 (2590)	0.081 (χ^2 = 3.1)
OBV/PTV/r ± DSV ± RBV	25.4 (3626)	14.1 (133)	26.2 (3493)	< 0.0001 (χ^2 = 67.8)
GZR/EBR ± RBV	16.8 (2400)	16.3 (154)	16.8 (2246)	0.691 (χ^2 = 0.1)
Other SOF ± SMV ± DCV ± RBV, SMV ± DCV ± RBV	2.2 (305)	3.2 (33)	2.1 (272)	0.02 (χ^2 = 5.7)
Pangenotypic regimens				
GLE/PIB	20.6 (2940)	20.6 (194)	20.6 (2746)	0.997 (χ^2 = 0.0)
GLE/PIB + SOF + RBV	0.05 (6)	0.0 (0)	0.05 (6)	1.0
SOF/VEL ± RBV	14.4 (2058)	22.2 (209)	13.9 (1849)	< 0.0001 (χ^2 = 49.3)
SOF/VEL/VOX	0.2 (24)	0.2 (2)	0.2 (22)	0.670

The reported *P* value relates to Pearson's chi-square test or Fisher's exact test if the number of observations in the category was less than 10. CHC: Chronic hepatitis C; IFN: Interferon; RBV: Ribavirin; ASV: Asunaprevir; DCV: Daclatasvir; LDV: Ledipasvir; SOF: Sofosbuvir; OBV: Ombitasvir; PTV: Paritaprevir; r: Ritonavir; DSV: Dasabuvir; GZR: Grazoprevir; EB: Elbasvir; SMV: Simeprevir; GLE: Glecaprevir; PIB: Pibrentasvir; VEL: Velpatasvir; VOX: Voxilaprevir.

treatment as planned without AEs and achieved SVR. It should be emphasized that a possible modification in psychiatric treatment in case of expected drug interactions, as well as monitoring the mental state of the patient, requires the cooperation of a hepatologist and a psychiatrist. However, the scope of supervision is significantly smaller than in the case of IFN-based therapy[17,43]. The issue we highlighted in our analysis was the significantly higher percentage of patients lost to follow-up without SVR evaluation in the population of patients with mental illness compared to those without mental disorders, 4.2% *vs* 2.5%, respectively. The problem with adherence, concerning not only the use of drugs which was not evaluated in our study but, as in this case, keeping the dates of follow-up visits, is also raised by other authors[18]. However, some analyses did not report the difference in adherence between mentally ill patients (including those with substance abuse disorder) and the general HCV-infected population[3,40,44].

In patients with available SVR, we did not observe significant differences in the effectiveness of DAA therapy depending on the diagnosis of mental illness, which is consistent with reports from other RWE cohorts[40,45]. A 96.9% cure rate was achieved in the mentally affected group compared to 97.7% in the patients without psychiatric disorders, despite a higher proportion of men, those with liver cirrhosis, and a higher prevalence of GT3 infection in this population, which are considered negative predictors of SVR in HCV-infected patients treated with DAA[21]. Significantly lower SVR rates have been documented in patients with bipolar disorder, which is consistent with the results of the analysis by Wedemeyer *et al*[18]. However, this multicenter study did not control for potential confounders, while in our research, the multivariate analysis clearly excluded bipolar disorder as an independent predictor of non-response to treatment. The identified independent negative predictors included the presence of liver cirrhosis, GT3 infection, history of prior therapy failure, and male gender, which is in line with available data concerning the general HCV-infected population[21,46]. However, apart from the abovementioned factors, administration of the ASV + DCV regimen or SOF/(VEL + RBV) combination was also associated with a lower chance of SVR. The ASV + DCV option was registered only for patients with GT1b infection and used until 2018. Due to its cumulative efficacy of 85%, evaluated in a meta-analysis of 9 clinical trials, it was considered suboptimal[23]. The SOF/(VEL + RBV) regimen is

Table 4 Logistic multiple regression results on the association between lack of sustained viral response, bipolar disorder (for which lower frequency of sustained viral response was observed in the present study), and known risk factors of non-response to antiviral treatment in the studied cohort (*n* = 14272)

Parameter	OR	95%CI	*P* value
Bipolar disorder	3.52	0.76-16.34	0.109
Male sex	1.93	1.51-2.45	< 0.0001
Obesity (BMI > 30 kg/m^2)	1.08	0.82-1.43	0.579
GT3	3.26	2.50-4.27	< 0.0001
Cirrhosis	2.55	2.01-3.22	< 0.0001
HIV-coinfection	1.37	0.88-2.13	0.165
HBV-coinfection	0.85	0.61-1.18	0.323
History of HCV-treatment failure	1.46	1.14-1.87	0.003
ASV+DCV	4.97	2.60-9.55	< 0.0001
SOF/VEL	0.86	0.61-1.20	0.371
SOF/VEL+RBV	2.37	1.34-4.17	0.003

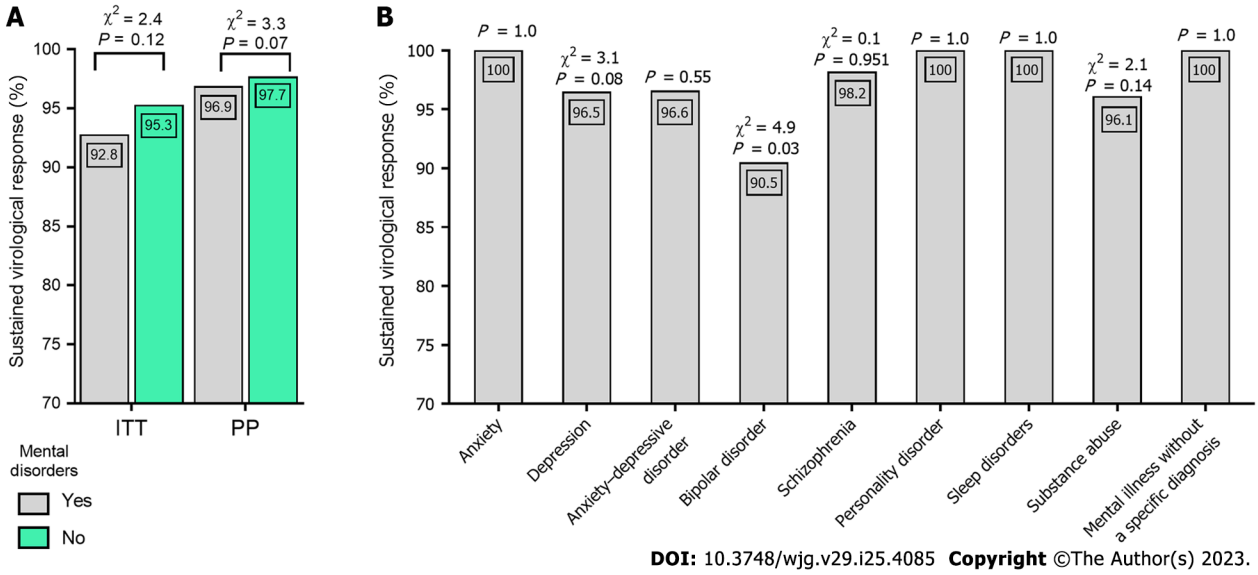
BMI: Body mass index; GT: Genotype; HIV: Human immunodeficiency virus; HBV: Hepatitis B virus; HCV: Hepatitis C virus; ASV: Asunaprevir; DCV: Daclatasvir; SOF: Sofosbuvir; VEL: Velpatasvir; RBV: Ribavirin; OR: Odds ratio; CI: Confidence interval.

Table 5 Safety of direct-acting antiviral treatment in chronic hepatitis C patients with (group A) and without (group B) psychiatric disorders, %, *n*

Parameter	All patients (*n* = 14272)	Group A (*n* = 942)	Group B (*n* = 13330)	*P* value
Treatment course				
According to schedule	97.5 (13848)	96.8 (907)	97.6 (12941)	0.164 (χ^2 = 1.9)
Therapy discontinuation	1.1 (157)	1.4 (13)	1.1 (144)	0.394 (χ^2 = 0.7)
Therapy modification	1.4 (194)	1.8 (17)	1.3 (177)	0.222 (χ^2 = 1.5)
No data	0.5 (73)	0.5 (5)	0.5 (68)	0.813
Death	0.5 (71)	0.4 (4)	0.5 (67)	1.0
SAE	1.0 (145)	1.6 (15)	0.97 (130)	0.068 (χ^2 = 3.3)
Psychiatric complications				
New incidence of depression	0.1 (8)	0.2 (2)	0.05 (6)	0.093
New incidence of schizophrenia	0.0 (1)	0.0 (0)	0.0 (1)	1.0
New incidence of sleep disorders	1.8 (262)	3.3 (31)	1.7 (231)	0.001 (χ^2 = 10.4)
New incidence of anxiety	0.0 (1)	0.1 (1)	0.0 (0)	1.0
Drinking binge	0.0 (1)	0.1 (1)	0.0 (0)	1.0
Exacerbation of psychiatric disease		0.6 (6)		
Depression		0.5 (5)		
Schizophrenia		0.1 (1)		

The reported *P* value relates to Pearson's chi-square test or Fisher's exact test if the number of observations in the category was less than 10. SAEs: Serious adverse events.

registered in patients with decompensated cirrhosis, and its efficacy in a randomized clinical trial was 83%[47]. In our analysis, 23/26 (88.5%) patients with mental disorders responded to this type of treatment. There are no papers evaluating this regimen exclusively in patients with mental illness, so we cannot relate our results to another study.



DOI: 10.3748/wjg.v29.i25.4085 **Copyright** ©The Author(s) 2023.

Figure 1 The sustained virological response rate in the group with mental disorders compared to the control group in intention-to-treat and per protocol analyses and calculated per protocol analysis in the population with mental disorders. A: The sustained virological response rate (SVR) in the group with mental disorders (n = 942) compared to the control group (n = 13330) in intention-to-treat and per protocol analyses; B: SVR calculated per protocol analysis in the population with mental disorders considering the type of the psychiatric illness in comparison to the control group. All statistical comparisons were performed with Pearson's chi-square or Fisher's exact test. ITT: Intention-to-treat; PP: Per protocol.

Our study has some limitations which we wish to stress. This is a retrospective study with all its consequences, such as incomplete data, including information on side effects, data entry errors, and possible bias. The database includes information from baseline to 12 wk after the end of therapy, and there are no data on the number of patients who had their psychiatric treatment modified before treatment, as well as the nature of these modifications. Additionally, no data were collected on the adjustment of psychiatric treatment during DAA therapy. Another limitation is the lack of systematic monitoring of the patient's mental state, such as with appropriate questionnaires. The main strength of the current study is the large group of patients from different centers in our country treated in routine clinical practice, which affects the quality of the results and the possibility of generalizing conclusions. To the best of our knowledge, this is the first study to address the problem of treating CHC with various DAA regimens in patients with mental disorders, highlighting the differences in specific psychiatric illnesses.

CONCLUSION

This study provides real-world evidence for the effectiveness and safety of DAA treatment of HCV infection in patients with preexisting psychiatric disorders. As shown, most of these patients achieve SVR. No specific psychiatric diagnosis lowered the chance of successful DAA treatment. Negative predictors of virologic response do not differ for these patients compared to the general HCV-infected population and include cirrhosis, GT3 infection, male gender, and failure of previous therapy.

ARTICLE HIGHLIGHTS

Research background

In the era of interferon (IFN)-based therapies, patients with psychiatric disorders had limited access to therapy due to their unfavorable safety profile. This changed with the introduction of direct-acting antiviral (DAA) drugs.

Research motivation

We aimed to evaluate the tolerability and effectiveness of IFN-free therapies in patients with various psychiatric disorders and to identify predictors of virologic response in this patient population.

Research objectives

Data of 14272 patients treated with IFN-free regimens for chronic hepatitis C included in the EpiTer-2 database were analyzed. The patients were divided into two groups: 942 patients with mental disorders and 13330 without psychiatric diseases.

Research methods

The effectiveness and safety of antiviral treatment were compared between both populations. Effectiveness was assessed by the percentage of patients with sustained virologic response (SVR). Multiple logistic regression was used to predict the odds of no SVR in patients with mental illness. Safety data were collected through the treatment period and 12 wk of follow-up.

Research results

The cure rate was not significantly different in the two groups analyzed, with an SVR of 96.9% in patients with psychiatric disorders and 97.7% without psychiatric disorders. Patients with bipolar disorder achieved a lower SVR (90.5%), but multivariate analysis excluded it as an independent predictor of treatment non-response. Male gender, genotype 3 infection, cirrhosis and failure of previous therapy were identified as independent negative predictors. The percentage of patients who completed the planned therapy did not differ between the groups with and without mental disorders. In six patients, symptoms of mental illness (depression, schizophrenia) worsened, of which two discontinued treatment for this reason. New episodes of sleep disorders occurred significantly more often in patients with mental disorders. Patients with mental illness were more frequently lost to follow-up (4.2% *vs* 2.5%).

Research conclusions

DAA treatment is safe and effective in hepatitis C virus (HCV)-infected patients with mental disorders. No specific psychiatric diagnosis lowered the chance of successful antiviral treatment.

Research perspectives

The data obtained provide real-world evidence of the effectiveness and safety of DAA for HCV infection in patients with mental disorders, indicating that there are no differences compared with the general HCV-infected population.

FOOTNOTES

Author contributions: Dybowska D, Zarębska-Michaluk D, Rzymski P, Pawłowska M and Flisiak R conceived the study design; Dybowska D and Dybowski M cured data and prepared data for analysis; Dybowska D and Rzymski P analyzed and interpreted the data; Rzymski P performed the statistical analysis; Rzymski P prepared tables and figures; Dybowska D, Zarębska-Michaluk, Rzymski P, Pawłowska M, and Flisiak R drafted the manuscript; Dobrowolska K prepared the manuscript for submission; Berak H, Lorenc B, Sitko M, Dybowski M, Mazur W, Tudrujek-Zdunek M, Janocha-Litwin J, Janczewska E, Klapaczyński J, Parfieniuk-Kowerda A, Piekarska A, Sobala-Szczygieł Barbara, Dobrowolska K, and Pawłowska M acquired the data and approved the final version of the manuscript.

Institutional review board statement: According to local law (Pharmaceutical law of 6th September 2001, art.37al), non-interventional studies do not require ethics committee approval.

Informed consent statement: All study participants provided informed consent for antiviral treatment and processing of personal data according to the requirements of the therapeutic program.

Conflict-of-interest statement: All the authors report no relevant conflicts of interest for this article.

Data sharing statement: Dataset available upon reasonable request to the corresponding author at dorota1010@tlen.pl.

STROBE statement: The authors have read the STROBE Statement-checklist of items, and the manuscript was prepared and revised according to the STROBE Statement-checklist of items.

Open-Access: This article is an open-access article that was selected by an in-house editor and fully peer-reviewed by external reviewers. It is distributed in accordance with the Creative Commons Attribution NonCommercial (CC BY-NC 4.0) license, which permits others to distribute, remix, adapt, build upon this work non-commercially, and license their derivative works on different terms, provided the original work is properly cited and the use is non-commercial. See: https://creativecommons.org/Licenses/by-nc/4.0/

Country/Territory of origin: Poland

ORCID number: Dorota Dybowska 0000-0002-1961-8519; Dorota Zarębska-Michaluk 0000-0003-0938-1084; Piotr Rzymski 0000-0002-4713-0801; Hanna Berak 0000-0002-0844-9158; Beata Lorenc 0000-0002-6319-9278; Marek Sitko 0000-0003-3078-8604; Włodzimierz Mazur 0000-0001-9023-2670; Magdalena Tudrujek-Zdunek 0000-0002-5640-5432; Justyna Janocha-Litwin 0000-0002-6072-4559; Ewa Janczewska 0000-0002-5406-4603; Jakub Klapaczyński 0000-0003-0209-1930; Anna Parfieniuk-Kowerda 0000-0002-3815-3745; Anna Piekarska 0000-0002-7188-4881; Barbara Sobala-Szczygieł 0000-0001-5937-9711; Malgorzata Pawłowska 0000-0002-6044-0425; Robert Flisiak 0000-0003-3394-1635.

S-Editor: Wang JJ
L-Editor: Webster JR
P-Editor: Zhao S

REFERENCES

1 **Centers for Disease Control and Prevention**. Global Viral Hepatitis: Millions of People are Affected. [cited 8 March 2023]. Available from: https://www.cdc.gov/hepatitis/global/index.htm
2 **Lavanchy D**. Evolving epidemiology of hepatitis C virus. *Clin Microbiol Infect* 2011; **17**: 107-115 [PMID: 21091831 DOI: 10.1111/j.1469-0691.2010.03432.x]
3 **Gutiérrez-Rojas L**, de la Gándara Martín JJ, García Buey L, Uriz Otano JI, Mena Á, Roncero C. Patients with severe mental illness and hepatitis C virus infection benefit from new pangenotypic direct-acting antivirals: Results of a literature review. *Gastroenterol Hepatol* 2023; **46**: 382-396 [PMID: 35718017 DOI: 10.1016/j.gastrohep.2022.06.001]
4 **Roncero C**, Littlewood R, Vega P, Martinez-Raga J, Torrens M. Chronic hepatitis C and individuals with a history of injecting drugs in Spain: population assessment, challenges for successful treatment. *Eur J Gastroenterol Hepatol* 2017; **29**: 629-633 [PMID: 28230562 DOI: 10.1097/MEG.0000000000000855]
5 **Rifai MA**, Gleason OC, Sabouni D. Psychiatric care of the patient with hepatitis C: a review of the literature. *Prim Care Companion J Clin Psychiatry* 2010; **12** [PMID: 21494349 DOI: 10.4088/PCC.09r00877whi]
6 **Faccioli J**, Nardelli S, Gioia S, Riggio O, Ridola L. Neurological and psychiatric effects of hepatitis C virus infection. *World J Gastroenterol* 2021; **27**: 4846-4861 [PMID: 34447230 DOI: 10.3748/wjg.v27.i29.4846]
7 **Adinolfi LE**, Nevola R, Lus G, Restivo L, Guerrera B, Romano C, Zampino R, Rinaldi L, Sellitto A, Giordano M, Marrone A. Chronic hepatitis C virus infection and neurological and psychiatric disorders: an overview. *World J Gastroenterol* 2015; **21**: 2269-2280 [PMID: 25741133 DOI: 10.3748/wjg.v21.i8.2269]
8 **Mathew S**, Faheem M, Ibrahim SM, Iqbal W, Rauff B, Fatima K, Qadri I. Hepatitis C virus and neurological damage. *World J Hepatol* 2016; **8**: 545-556 [PMID: 27134702 DOI: 10.4254/wjh.v8.i12.545]
9 **Davoodi L**, Masoum B, Moosazadeh M, Jafarpour H, Haghshenas MR, Mousavi T. Psychiatric side effects of pegylated interferon-α and ribavirin therapy in Iranian patients with chronic hepatitis C: A meta-analysis. *Exp Ther Med* 2018; **16**: 971-978 [PMID: 30116347 DOI: 10.3892/etm.2018.6255]
10 **McGlynn EA**, Adams JL, Kramer J, Sahota AK, Silverberg MJ, Shenkman E, Nelson DR. Assessing the Safety of Direct-Acting Antiviral Agents for Hepatitis C. *JAMA Netw Open* 2019; **2**: e194765 [PMID: 31173117 DOI: 10.1001/jamanetworkopen.2019.4765]
11 **Niederau C**, Mauss S, Schober A, Stoehr A, Zimmermann T, Waizmann M, Moog G, Pape S, Weber B, Isernhagen K, Sandow P, Bokemeyer B, Alshuth U, Steffens H, Hüppe D. Predictive factors for sustained virological response after treatment with pegylated interferon α-2a and ribavirin in patients infected with HCV genotypes 2 and 3. *PLoS One* 2014; **9**: e107592 [PMID: 25238535 DOI: 10.1371/journal.pone.0107592]
12 **Schäfer A**, Scheurlen M, Weissbrich B, Schöttker K, Kraus MR. Sustained virological response in the antiviral therapy of chronic hepatitis C: is there a predictive value of interferon-induced depression? *Chemotherapy* 2007; **53**: 292-299 [PMID: 17496415 DOI: 10.1159/000102584]
13 **Elsherif O**, Bannan C, Keating S, McKiernan S, Bergin C, Norris S. Outcomes from a large 10 year hepatitis C treatment programme in people who inject drugs: No effect of recent or former injecting drug use on treatment adherence or therapeutic response. *PLoS One* 2017; **12**: e0178398 [PMID: 28636638 DOI: 10.1371/journal.pone.0178398]
14 **Fabrazzo M**, Zampino R, Vitrone M, Sampogna G, Del Gaudio L, Nunziata D, Agnese S, Santagata A, Durante-Mangoni E, Fiorillo A. Effects of Direct-Acting Antiviral Agents on the Mental Health of Patients with Chronic Hepatitis C: A Prospective Observational Study. *Brain Sci* 2020; **10** [PMID: 32726940 DOI: 10.3390/brainsci10080483]
15 **Sundberg I**, Lannergård A, Ramklint M, Cunningham JL. Direct-acting antiviral treatment in real world patients with hepatitis C not associated with psychiatric side effects: a prospective observational study. *BMC Psychiatry* 2018; **18**: 157 [PMID: 29843679 DOI: 10.1186/s12888-018-1735-6]
16 **Janjua NZ**, Wong S, Darvishian M, Butt ZA, Yu A, Binka M, Alvarez M, Woods R, Yoshida EM, Ramji A, Feld J, Krajden M. The impact of SVR from direct-acting antiviral- and interferon-based treatments for HCV on hepatocellular carcinoma risk. *J Viral Hepat* 2020; **27**: 781-793 [PMID: 32187430 DOI: 10.1111/jvh.13295]
17 **Sockalingam S**, Sheehan K, Feld JJ, Shah H. Psychiatric care during hepatitis C treatment: the changing role of psychiatrists in the era of direct-acting antivirals. *Am J Psychiatry* 2015; **172**: 512-516 [PMID: 26029803 DOI: 10.1176/appi.ajp.2015.14081041]
18 **Wedemeyer H**, Di Marco V, Garcia-Retortillo M, Teti E, Fraser C, Morano Amado LE, Rodriguez-Tajes S, Acosta-López S, O'Loan J, Milella M, Buti M, Guerra-Veloz MF, Ramji A, Fenech M, Martins A, Borgia SM, Vanstraelen K, Mertens M, Hernández C, Ntalla I, Ramroth H, Milligan S. Global Real-World Evidence of Sofosbuvir/Velpatasvir as a Highly Effective Treatment and Elimination Tool in People with Hepatitis C Infection Experiencing Mental Health Disorders. *Viruses* 2022; **14** [PMID: 36423102 DOI: 10.3390/v14112493]
19 **European Association for the Study of the Liver**. Clinical Practice Guidelines Panel: Chair:; EASL Governing Board

representative:; Panel members:. EASL recommendations on treatment of hepatitis C: Final update of the series(☆). *J Hepatol* 2020; **73**: 1170-1218 [PMID: 32956768 DOI: 10.1016/j.jhep.2020.08.018]

20 **University of Liverpool**. Liverpool HEP Interactions. [cited 8 March 2023]. Available from: https://www.hep-druginteractions.org/

21 **Pabjan P**, Brzdęk M, Chrapek M, Dziedzic K, Dobrowolska K, Paluch K, Garbat A, Błoniarczyk P, Reczko K, Stępień P, Zarębska-Michaluk D. Are There Still Difficult-to-Treat Patients with Chronic Hepatitis C in the Era of Direct-Acting Antivirals? *Viruses* 2022; **14**: 96 [PMID: 35062302 DOI: 10.3390/v14010096]

22 **Brzdęk M**, Zarębska-Michaluk D, Rzymski P, Lorenc B, Kazek A, Tudrujek-Zdunek M, Janocha-Litwin J, Mazur W, Dybowska D, Berak H, Parfieniuk-Kowerda A, Klapaczyński J, Sitko M, Sobala-Szczygieł B, Piekarska A, Flisiak R. Changes in characteristics of patients with hepatitis C virus-related cirrhosis from the beginning of the interferon-free era. *World J Gastroenterol* 2023; **29**: 2015-2033 [PMID: 37155527 DOI: 10.3748/wjg.v29.i13.2015]

23 **Nguyen Thi Thu P**, Ngo Thi Quynh M, Pham Van L, Nguyen Van H, Nguyen Thanh H. Determination of Risk Factors Associated with the Failure of 12 Weeks of Direct-Acting Antiviral Therapy in Patients with Hepatitis C: A Prospective Study. *Biomed Res Int* 2022; **2022**: 6054677 [PMID: 35572735 DOI: 10.1155/2022/6054677]

24 **Xie J**, Xu B, Wei L, Huang C, Liu W. Effectiveness and Safety of Sofosbuvir/Velpatasvir/Voxilaprevir as a Hepatitis C Virus Infection Salvage Therapy in the Real World: A Systematic Review and Meta-analysis. *Infect Dis Ther* 2022; **11**: 1661-1682 [PMID: 35749010 DOI: 10.1007/s40121-022-00666-0]

25 **Ho SB**, Nguyen H, Tetrick LL, Opitz GA, Basara ML, Dieperink E. Influence of psychiatric diagnoses on interferon-alpha treatment for chronic hepatitis C in a veteran population. *Am J Gastroenterol* 2001; **96**: 157-164 [PMID: 11197246 DOI: 10.1111/j.1572-0241.2001.03468.x]

26 **Trask PC**, Esper P, Riba M, Redman B. Psychiatric side effects of interferon therapy: prevalence, proposed mechanisms, and future directions. *J Clin Oncol* 2000; **18**: 2316-2326 [PMID: 10829053 DOI: 10.1200/JCO.2000.18.11.2316]

27 **Juszczyk J**, Baka-Cwierz B, Beniowski M, Berak H, Bolewska B, Boroń-Kaczmarska A, Cianciara J, Cieśla A, Dziambor A, Gasiorowski J, Gietka A, Gliwińska E, Gładysz A, Gonciarz Z, Halota W, Horban A, Inglot M, Janas-Skulina U, Janczewska-Kazek E, Jaskowska J, Jurczyk K, Knysz B, Kryczka W, Kuydowicz J, Lakomy EA, Logiewa-Bazger B, Lyczak A, Mach T, Mazur W, Michalska Z, Modrzewska R, Nazzal K, Pabjan P, Piekarska A, Piszko P, Sikorska K, Szamotulska K, Sliwińska M, Swietek K, Tomasiewicz K, Topczewska-Staubach E, Trocha H, Wasilewski M, Wawrzynowicz-Syczewska M, Wrodycki W, Zarebska-Michaluk D, Zejc-Bajsarowicz M. [Pegylated interferon-alfa 2a with ribavirin in chronic viral hepatitis C (final report)]. *Przegl Epidemiol* 2005; **59**: 651-660 [PMID: 16433307]

28 **Raison CL**, Borisov AS, Broadwell SD, Capuron L, Woolwine BJ, Jacobson IM, Nemeroff CB, Miller AH. Depression during pegylated interferon-alpha plus ribavirin therapy: prevalence and prediction. *J Clin Psychiatry* 2005; **66**: 41-48 [PMID: 15669887 DOI: 10.4088/jcp.v66n0106]

29 **Drozdz W**, Borkowska A, Wilkosc M, Halota W, Dybowska D, Rybakowski JK. Chronic paranoid psychosis and dementia following interferon-alpha treatment of hepatitis C: a case report. *Pharmacopsychiatry* 2007; **40**: 146-148 [PMID: 17694476 DOI: 10.1055/s-2007-984390]

30 **Lotrich F**. Management of Psychiatric Disease in Hepatitis C Treatment Candidates. *Curr Hepat Rep* 2010; **9**: 113-118 [PMID: 20871787 DOI: 10.1007/s11901-010-0035-5]

31 **Quelhas R**, Lopes A. Psychiatric problems in patients infected with hepatitis C before and during antiviral treatment with interferon-alpha: a review. *J Psychiatr Pract* 2009; **15**: 262-281 [PMID: 19625882 DOI: 10.1097/01.pra.0000358313.06858.ea]

32 **Goñi Esarte S**, Juanbeltz R, Martínez-Baz I, Castilla J, San Miguel R, Herrero JI, Zozaya JM. Long-term changes on health-related quality of life in patients with chronic hepatitis C after viral clearance with direct-acting antiviral agents. *Rev Esp Enferm Dig* 2019; **111**: 445-452 [PMID: 31066286 DOI: 10.17235/reed.2019.6063/2018]

33 **Zarebska-Michaluk DA**, Lebensztejn DM, Kryczka WM, Skiba E. Extrahepatic manifestations associated with chronic hepatitis C infections in Poland. *Adv Med Sci* 2010; **55**: 67-73 [PMID: 20371429 DOI: 10.2478/v10039-010-0009-4]

34 **Yarlott L**, Heald E, Forton D. Hepatitis C virus infection, and neurological and psychiatric disorders - A review. *J Adv Res* 2017; **8**: 139-148 [PMID: 28149649 DOI: 10.1016/j.jare.2016.09.005]

35 **Więdłocha M**, Marcinowicz P, Sokalla D, Stańczykiewicz B. The neuropsychiatric aspect of the HCV infection. *Adv Clin Exp Med* 2017; **26**: 167-175 [PMID: 28397449 DOI: 10.17219/acem/37787]

36 **Perry W**, Hilsabeck RC, Hassanein TI. Cognitive dysfunction in chronic hepatitis C: a review. *Dig Dis Sci* 2008; **53**: 307-321 [PMID: 17703362 DOI: 10.1007/s10620-007-9896-z]

37 **Butt AA**, Khan UA, McGinnis KA, Skanderson M, Kent Kwoh C. Co-morbid medical and psychiatric illness and substance abuse in HCV-infected and uninfected veterans. *J Viral Hepat* 2007; **14**: 890-896 [PMID: 18070293 DOI: 10.1111/j.1365-2893.2007.00885.x]

38 **el-Serag HB**, Kunik M, Richardson P, Rabeneck L. Psychiatric disorders among veterans with hepatitis C infection. *Gastroenterology* 2002; **123**: 476-482 [PMID: 12145801 DOI: 10.1053/gast.2002.34750]

39 **Braude MR**, Phan T, Dev A, Sievert W. Determinants of Hepatitis C Virus Prevalence in People With Serious Mental Illness: A Systematic Review and Meta-Analysis. *J Clin Psychiatry* 2021; **83** [PMID: 34905666 DOI: 10.4088/JCP.21r14079]

40 **Fiore V**, De Vito A, Colpani A, Manca V, Maida I, Madeddu G, Babudieri S. Viral Hepatitis C New Microelimination Pathways Objective: Psychiatric Communities HCV Free. *Life (Basel)* 2022; **12** [PMID: 36431008 DOI: 10.3390/life12111873]

41 **de Gennaro N**, Diella L, Monno L, Angarano G, Milella M, Saracino A. Efficacy and tolerability of DAAs in HCV-monoinfected and HCV/HIV-coinfected patients with psychiatric disorders. *BMC Infect Dis* 2020; **20**: 196 [PMID: 32138757 DOI: 10.1186/s12879-020-4922-2]

42 **Volpato S**, Montagnese S, Zanetto A, Turco M, De Rui M, Ferrarese A, Amodio P, Germani G, Senzolo M, Gambato M, Russo FP, Burra P. Neuropsychiatric performance and treatment of hepatitis C with direct-acting antivirals: a prospective study. *BMJ Open Gastroenterol* 2017; **4**: e000183 [PMID: 29333276 DOI: 10.1136/bmjgast-2017-000183]

43 **Chasser Y**, Kim AY, Freudenreich O. Hepatitis C Treatment: Clinical Issues for Psychiatrists in the Post-Interferon Era.

Psychosomatics 2017; **58**: 1-10 [PMID: 27871760 DOI: 10.1016/j.psym.2016.09.004]

44 **DiMatteo MR**, Lepper HS, Croghan TW. Depression is a risk factor for noncompliance with medical treatment: meta-analysis of the effects of anxiety and depression on patient adherence. *Arch Intern Med* 2000; **160**: 2101-2107 [PMID: 10904452 DOI: 10.1001/archinte.160.14.2101]

45 **Back D**, Belperio P, Bondin M, Negro F, Talal AH, Park C, Zhang Z, Pinsky B, Crown E, Mensa FJ, Marra F. Efficacy and safety of glecaprevir/pibrentasvir in patients with chronic HCV infection and psychiatric disorders: An integrated analysis. *J Viral Hepat* 2019; **26**: 951-960 [PMID: 30977945 DOI: 10.1111/jvh.13110]

46 **Wang HL**, Lu X, Yang X, Xu N. Effectiveness and safety of daclatasvir plus asunaprevir for hepatitis C virus genotype 1b: Systematic review and meta-analysis. *J Gastroenterol Hepatol* 2017; **32**: 45-52 [PMID: 27597318 DOI: 10.1111/jgh.13587]

47 **Curry MP**, O'Leary JG, Bzowej N, Muir AJ, Korenblat KM, Fenkel JM, Reddy KR, Lawitz E, Flamm SL, Schiano T, Teperman L, Fontana R, Schiff E, Fried M, Doehle B, An D, McNally J, Osinusi A, Brainard DM, McHutchison JG, Brown RS Jr, Charlton M; ASTRAL-4 Investigators. Sofosbuvir and Velpatasvir for HCV in Patients with Decompensated Cirrhosis. *N Engl J Med* 2015; **373**: 2618-2628 [PMID: 26569658 DOI: 10.1056/NEJMoa1512614]



Published by **Baishideng Publishing Group Inc**
7041 Koll Center Parkway, Suite 160, Pleasanton, CA 94566, USA
Telephone: +1-925-3991568
E-mail: bpgoffice@wjgnet.com
Help Desk: https://www.f6publishing.com/helpdesk
https://www.wjgnet.com



© 2023 Baishideng Publishing Group Inc. All rights reserved.

ISSN 1007-9327 (print)
ISSN 2219-2840 (online)

World Journal of *Gastroenterology*

World J Gastroenterol 2023 July 14; 29(26): 4099-4221



Published by Baishideng Publishing Group Inc

World Journal of Gastroenterology

Contents

Weekly Volume 29 Number 26 July 14, 2023

REVIEW

4099 Impact of COVID-19 in individuals with and without pre-existent digestive disorders with a particular focus on elderly patients

Papa A, Covino M, De Lucia SS, Del Gaudio A, Fiorani M, Polito G, Settanni CR, Piccioni A, Franceschi F, Gasbarrini A

4120 Irritable bowel syndrome: Epidemiology, overlap disorders, pathophysiology and treatment

Huang KY, Wang FY, Lv M, Ma XX, Tang XD, Lv L

4136 Peroxisome proliferator-activated receptors as targets to treat metabolic diseases: Focus on the adipose tissue, liver, and pancreas

Souza-Tavares H, Miranda CS, Vasques-Monteiro IML, Sandoval C, Santana-Oliveira DA, Silva-Veiga FM, Fernandes-da-Silva A, Souza-Mello V

MINIREVIEWS

4156 Schistosomal (bilharzial) polyps: Travel through the colon and beyond

Emara MH, Mahros AM, Rasheda AMA, Radwan MI, Mohamed B, Abdelrazik O, Elazab M, Elbatae H

4166 Mortality from chronic liver disease: Recent trends and impact of the COVID-19 pandemic

Fedeli U, Barbiellini Amidei C, Casotto V, Grande E, Saia M, Zanetto A, Russo FP

4174 Progress in immunotherapy for neuroendocrine neoplasm of the digestive system

Pan WX, Zhang XM, Hao SL, Han W

ORIGINAL ARTICLE

Retrospective Study

4186 Radiomics model based on contrast-enhanced computed tomography to predict early recurrence in patients with hepatocellular carcinoma after radical resection

Li SQ, Su LL, Xu TF, Ren LY, Chen DB, Qin WY, Yan XZ, Fan JX, Chen HS, Liao WJ

Clinical Trials Study

4200 Raf kinase inhibitor protein combined with phosphorylated extracellular signal-regulated kinase offers valuable prognosis in gastrointestinal stromal tumor

Qu WZ, Wang L, Chen JJ, Wang Y

CASE REPORT

4214 Value of contrast-enhanced ultrasound in deep angiomyxoma using a biplane transrectal probe: A case report

Zhang Q, Yan HL, Lu Q, Luo Y

ABOUT COVER

Editorial Board Member of *World Journal of Gastroenterology*, Zoltán Rakonczay Jr, DSc, MD, PhD, Professor, Department of Pathophysiology, University of Szeged, Szeged 6701, Hungary. rakonczay.zoltan@med.u-szeged.hu

AIMS AND SCOPE

The primary aim of *World Journal of Gastroenterology* (*WJG*, *World J Gastroenterol*) is to provide scholars and readers from various fields of gastroenterology and hepatology with a platform to publish high-quality basic and clinical research articles and communicate their research findings online. *WJG* mainly publishes articles reporting research results and findings obtained in the field of gastroenterology and hepatology and covering a wide range of topics including gastroenterology, hepatology, gastrointestinal endoscopy, gastrointestinal surgery, gastrointestinal oncology, and pediatric gastroenterology.

INDEXING/ABSTRACTING

The *WJG* is now abstracted and indexed in Science Citation Index Expanded (SCIE, also known as SciSearch®), Current Contents/Clinical Medicine, Journal Citation Reports, Index Medicus, MEDLINE, PubMed, PubMed Central, Scopus, Reference Citation Analysis, China National Knowledge Infrastructure, China Science and Technology Journal Database, and Superstar Journals Database. The 2023 edition of Journal Citation Reports® cites the 2022 impact factor (IF) for *WJG* as 4.3; IF without journal self cites: 4.1; 5-year IF: 5.3; Journal Citation Indicator: 0.82; Ranking: 33 among 93 journals in gastroenterology and hepatology; and Quartile category: Q2. The *WJG*'s CiteScore for 2021 is 8.3 and Scopus CiteScore rank 2022: Gastroenterology is 22/149.

RESPONSIBLE EDITORS FOR THIS ISSUE

Production Editor: *Ying-Yi Yuan*; **Production Department Director:** *Xu Guo*; **Editorial Office Director:** *Jia-Ru Fan.*

NAME OF JOURNAL
World Journal of Gastroenterology

ISSN
ISSN 1007-9327 (print) ISSN 2219-2840 (online)

LAUNCH DATE
October 1, 1995

FREQUENCY
Weekly

EDITORS-IN-CHIEF
Andrzej S Tarnawski

EDITORIAL BOARD MEMBERS
http://www.wjgnet.com/1007-9327/editorialboard.htm

PUBLICATION DATE
July 14, 2023

COPYRIGHT
© 2023 Baishideng Publishing Group Inc

INSTRUCTIONS TO AUTHORS
https://www.wjgnet.com/bpg/gerinfo/204

GUIDELINES FOR ETHICS DOCUMENTS
https://www.wjgnet.com/bpg/GerInfo/287

GUIDELINES FOR NON-NATIVE SPEAKERS OF ENGLISH
https://www.wjgnet.com/bpg/gerinfo/240

PUBLICATION ETHICS
https://www.wjgnet.com/bpg/GerInfo/288

PUBLICATION MISCONDUCT
https://www.wjgnet.com/bpg/gerinfo/208

ARTICLE PROCESSING CHARGE
https://www.wjgnet.com/bpg/gerinfo/242

STEPS FOR SUBMITTING MANUSCRIPTS
https://www.wjgnet.com/bpg/GerInfo/239

ONLINE SUBMISSION
https://www.f6publishing.com

© 2023 Baishideng Publishing Group Inc. All rights reserved. 7041 Koll Center Parkway, Suite 160, Pleasanton, CA 94566, USA

E-mail: bpgoffice@wjgnet.com https://www.wjgnet.com

World Journal of Gastroenterology

Submit a Manuscript: https://www.f6publishing.com

World J Gastroenterol 2023 July 14; 29(26): 4099-4119

DOI: 10.3748/wjg.v29.i26.4099

ISSN 1007-9327 (print) ISSN 2219-2840 (online)

REVIEW

Impact of COVID-19 in individuals with and without pre-existent digestive disorders with a particular focus on elderly patients

Alfredo Papa, Marcello Covino, Sara Sofia De Lucia, Angelo Del Gaudio, Marcello Fiorani, Giorgia Polito, Carlo Romano Settanni, Andrea Piccioni, Francesco Franceschi, Antonio Gasbarrini

Specialty type: Gastroenterology and hepatology

Provenance and peer review: Invited article; Externally peer reviewed.

Peer-review model: Single blind

Peer-review report's scientific quality classification

Grade A (Excellent): 0
Grade B (Very good): B, B
Grade C (Good): 0
Grade D (Fair): 0
Grade E (Poor): 0

P-Reviewer: Sharma V, India; Shrestha MR, Nepal

Received: November 27, 2022
Peer-review started: November 27, 2022
First decision: December 27, 2022
Revised: January 10, 2023
Accepted: March 20, 2023
Article in press: March 20, 2023
Published online: July 14, 2023

Alfredo Papa, Sara Sofia De Lucia, Angelo Del Gaudio, Marcello Fiorani, Giorgia Polito, Antonio Gasbarrini, CEMAD, Center for Diagnosis and Treatment of Digestive Diseases, Fondazione Policlinico Universitario A. Gemelli, IRCCS, Roma 00168, Italy

Alfredo Papa, CEMAD, Università Cattolica del Sacro Cuore, Roma 00168, Italy

Marcello Covino, Department of Emergency, Università Cattolica del Sacro Cuore - Fondazione Policlinico Universitario A. Gemelli, IRCCS, Rome 00168, Italy

Marcello Covino, Emergency Medicine, Università Cattolica del Sacro Cuore, Roma 00168, Italy

Carlo Romano Settanni, Digestive Disease Center, Fondazione Policlinico Universitario A. Gemelli IRCCS - Università Cattolica del Sacro Cuore, Rome 00168, Italy

Andrea Piccioni, Francesco Franceschi, Department of Emergency, Fondazione Policlinico Universitario A. Gemelli, IRCCS, Roma 00168, Italy

Francesco Franceschi, Department of Emergency, Università Cattolica del Sacro Cuore, Roma 00168, Italy

Corresponding author: Marcello Covino, MD, PhD, Assistant Professor, Department of Emergency, Università Cattolica del Sacro Cuore - Fondazione Policlinico Universitario A. Gemelli, IRCCS, Largo A. Gemelli 1, Rome 00168, Italy.
marcello.covino@policlinicogemelli.it

Abstract

Coronavirus disease 2019 (COVID-19) has several extrapulmonary symptoms. Gastrointestinal (GI) symptoms are among the most frequent clinical manifestations of COVID-19, with severe consequences reported in elderly patients. Furthermore, the impact of COVID-19 on patients with pre-existing digestive diseases still needs to be fully elucidated, particularly in the older population. This review aimed to investigate the impact of COVID-19 on the GI tract, liver, and pancreas in individuals with and without previous digestive diseases, with a particular focus on the elderly, highlighting the distinctive characteristics observed in this population. Finally, the effectiveness and adverse events of the anti-COVID-19 vaccination in patients with digestive disorders and the peculiarities found in the elderly are discussed.

Key Words: COVID-19; Elderly; Inflammatory bowel disease; Liver disease; Cirrhosis; Pancreatic disease

©The Author(s) 2023. Published by Baishideng Publishing Group Inc. All rights reserved.

Core Tip: Gastrointestinal symptoms are frequent in coronavirus disease 2019 (COVID-19), with more severe consequences reported in elderly patients. Patients with pre-existing liver disease are at an increased risk for worse outcomes, while no definitive conclusions can be drawn regarding patients with inflammatory bowel disease or pancreatic diseases. Elderly patients with digestive disorders, although the available data are limited, have no worse COVID-19 outcomes than those without these diseases.

Citation: Papa A, Covino M, De Lucia SS, Del Gaudio A, Fiorani M, Polito G, Settanni CR, Piccioni A, Franceschi F, Gasbarrini A. Impact of COVID-19 in individuals with and without pre-existent digestive disorders with a particular focus on elderly patients. *World J Gastroenterol* 2023; 29(26): 4099-4119
URL: https://www.wjgnet.com/1007-9327/full/v29/i26/4099.htm
DOI: https://dx.doi.org/10.3748/wjg.v29.i26.4099

INTRODUCTION

Severe acute respiratory syndrome coronavirus 2 (SARS-CoV-2) is responsible for the ongoing pandemic of coronavirus disease 2019 (COVID-19). Since its first report in December 2019 in Wuhan, China[1], COVID-19 has quickly spread worldwide with 635229101 confirmed cases, including 6602552 deaths according to the World Health Organization (WHO) at the moment of writing[2]. Although symptomatic COVID-19 patients exhibit various signs and symptoms, the typical clinical presentation has been predominantly respiratory[3]. The most common symptoms include cough (60%-86%), shortness of breath (53%-80%), and taste and smell alteration (64%-80%)[4-6]. However, as caseloads rise, many extrapulmonary effects have been observed, affecting the cardiovascular, neurologic, gastrointestinal (GI), and dermatologic systems. Liver and pancreatic impairment may also occur, especially in critically ill patients[7]. Although their exact prevalence is still the subject of debate, GI symptoms are more and more frequently reported[8]. However, it is impossible to exclude a bias thriving from the increased awareness of GI manifestations[9]. Some authors reported a prevalence of GI involvement of around 31.9%[10,11], while others up to 61%[12]. Regarding the impact of SARS-CoV-2 infection on older age, more severe outcomes are described [13,14]. The reason is the various age-related changes and the higher number of comorbidities typical of these patients. However, increasing evidence suggests that age is the most significant risk factor for worse outcomes[15]. Immunosenescence, the age-associated decline of immune system function, is the primary reason for the increased susceptibility to viral infection[16,17].

Methods

Considering a broad topic such as SARS-CoV-2 infection, this narrative review aimed to provide an overview of current knowledge of its impact on the GI tract, liver, and pancreas, with a particular interest in the elderly population. First, we created a list of keywords related to our research question. Articles were searched in the PubMed, Scopus, and EMBASE databases using the following search terms: "COVID-19", "SARS-CoV2 infection", "Elderly people", "Elderly population", "Old people", "Gerontal population", "Extrapulmonary manifestations", "Gastrointestinal symptoms", "Gastrointestinal bleeding (GIB)", "Inflammatory bowel disease (IBD) ", "Liver injury", "Liver dysfunction", "Chronic liver disease", "Drug liver injury", "Pancreatic involvement", "Acute pancreatitis" and "COVID-19 vaccination". We then synthesized, analyzed, and critically evaluated the related data to identify trends and patterns, in theory, debates, conflicts, and, most of all, persistent gaps in the existing knowledge.

Mechanisms of GI involvement in COVID-19

It is well known that SARS-CoV-2 enters cells using angiotensin-converting enzyme 2 (ACE2)[8,18]. In addition to the respiratory tract, ACE2 has also been found in the GI tract, especially in the tongue, esophageal, gastric, and rectal mucosa[19]. Mechanisms underlying the probable pathological effect of SARS-CoV-2 are varied. First, the virus's entry into cells may lead to a direct cytopathic effect[20]. SARS-CoV-2 infection emphasizes inflammatory pathways determining the "cytokine storm", which is characterized by the overproduction of mediators such as interleukin-2 (IL-2), IL-7, tumor necrosis factor (TNF) and granulocyte monocyte colony-stimulating factors[21]. This condition could generate diarrhea due to the alteration of gut motility and GI flora[22]. Notably, gut microbiota alterations have been found in these patients, probably due to factors such as exposition to antimicrobial agents or expression of viral proinflammatory mediators. Moreover, ACE2 seems to be involved in the antimicrobial peptide secretion through target of rapamycin activity; an aberrant functioning of this pathway has been described during COVID-19[23]. In addition to this mechanism, disorders of the gut-lung axis may be involved in the pathophysiology of GI symptoms. For example, it has been reported that lung flora alteration can correlate with intestinal microbiota modifications, probably due to increased recruitment of lung-derived CCR9+CD4+T cells into the bowel[24,25]. Regarding nausea and vomiting, these symptoms are likely

related to SARS-CoV-2 infection of the vagus nerve and a cytokine-mediated stimulation of the central and autonomic nervous systems[26]. Moreover, anorexia might be related to nausea and vomiting or associated with acute viral prodrome and cytokine storm[27]. Some studies have identified a lower prevalence of GI symptoms in the elderly population. This finding could be related to differences in gene expression of the ACE2, which seems to be directly correlated with age[9,28,29]. Older patients showed higher intestinal ACE2 mRNA expression, which could modify susceptibility to GI symptoms by influencing intestinal immunity and microbiota composition[29,30]. However, studies on this relation are few and with uncertain results.

GI symptoms in patients with COVID-19

In one-third of patients with COVID, GI symptoms occur as the first presentation. Nausea and vomiting may be present in up to two-thirds, diarrhea in up to 50%, loss of appetite in approximately 40%, and less than 10% present abdominal pain[7]. Moreover, extreme cases, such as the autoptic finding of segmental dilatation and stenosis of the small intestine in an 85-year-old man with COVID-19, have been reported in the literature[31]. However, the causal role of SARS-CoV-2 has yet to be established.

GI manifestations in elderly patients with COVID-19

Anorexia and diarrhea were the most frequent symptoms reported in the elderly, with variable frequencies depending on the study. In a large Brazilian cohort of 9807 patients, low frequencies of GI symptoms were reported, with diarrhea being registered only in 2% of patients[32]. Marziliano *et al*[33] reported a prevalence of GI symptoms of near 9% in a population of older adults (65 years and older). Ramos-Rincon *et al*[34] reported that very old patients (age > 80 years old) had higher frequencies of GI symptoms, with diarrhea presenting in 14% and vomiting in 5%, and anorexia in nearly 21% of patients. In the studies mentioned above, GI symptomatology did not impact mortality. Other studies pointed out an inverse correlation between age and the prevalence of GI symptoms[9,28]. Aroniadis *et al*[9] reported that older COVID-19 patients were less likely to exhibit digestive symptoms. A lower prevalence of GI symptoms was reported in 70 and older patients compared with those < 70 years (32% *vs* 41%). This potential age-related protective effect is found in a dysregulation of the immune system activation and a different expression of the ACE2 receptor in the digestive system [28]. Surprisingly, some studies highlighted a possible protective role of GI symptoms in COVID-19. Belgian research observed a prevalence of 30% of GI symptoms in frail older patients (aged over 80 years) and a positive correlation between their presence and patients' survival[35]. These results were also aligned with those of Vrillon *et al*[36], who described a positive outcome in older people presenting with GI symptoms, whereas younger adults with digestive symptoms had a higher prevalence of complications. On the contrary, Atalla *et al*[37] in their retrospective study, revealed a higher incidence of loss of appetite (83.3% *vs* 44.4%) and diarrhea (50% *vs* 28.6%) in the deceased patients than in those who survived. However, the onset of diarrhea during hospitalization was not necessarily related to SARS-CoV-2 infection, and the etiological analyses are not presented in the article[37]. Patients with SARS-CoV-2 infection are also at risk of other potential causes of diarrhea, such as Clostridium difficile infection and antibiotic-associated diarrhea due to frequent antimicrobic therapy and hospitalization. These could be confounding factors that alter the analysis of GI symptoms during SARS-Cov-2 infection, especially when they appear during infection and not at onset[18,24]. GI bleeding (GIB) in COVID-19 patients can represent a fatal complication. In the literature, a rate of GIB between 1.1% and 13% during SARS-CoV-2 infection has been reported[38]. However, the actual incidence and prevalence of GIB in COVID-19 patients are extremely difficult to assess. The underlying mechanisms for GI hemorrhage in COVID-19 patients could involve conditions that increase the risk of thromboembolism, such as dehydration, which may follow fever or diarrhea[39]. Anticoagulation drugs prescribed for preventing thrombotic events should be considered additional risk factors[40]. Although Ion *et al*[41] sustained that the use of anticoagulation or antiplatelet agents was not a risk factor for GIB, at least in hospitalized COVID-19 patients. Stress ulcers may be another major cause of bleeding unrelated to SARS-COV-2[41]. Furthermore, assisted ventilation techniques could cause stress ulceration and generate GIB[42]. However, rates of thrombosis and bleeding related to COVID-19 were congruent to those reported in hospitalized patients with comparable grades of critical illness. Except for case reports, no elective studies on the elderly population are available in the literature[43]. An overview of the analyzed studies is shown in Table 1.

COVID-19 in inflammatory bowel disease patients

Due to the immunosuppressive therapies, malnutrition, and chronic inflammation, patients affected by inflammatory bowel disease (IBD) are potentially at augmented risk for SARS-CoV-2 infections and complications due to the immunosuppressive therapies, malnutrition, and chronic inflammation[44,45]. However, various studies have investigated the incidence of COVID-19 in IBD patients, concluding that it is not increased compared to the general population [46-48]. Interestingly, COVID-19 in IBD patients has a clinical presentation similar to the general population. A recent meta-analysis found that the most common symptoms in these patients are extraintestinal, such as fever and cough[49]. However, GI manifestations appear more common than in the general population. Diarrhea can occur in 27.2% of patients, followed by abdominal pain, nausea, and vomiting, with a pooled prevalence rate of 13%, 10%, and 8.8%, respectively, and sporadically GI symptoms can be the only clinical presentation, which could be challenging to differentiate from IBD reactivation[49]. The prognosis of COVID-19 patients affected by IBD is not different from that of the general population. A recent meta-analysis observed that IBD was not correlated with augmented risk of death, intensive care unit (ICU) admission, or hospitalization related to COVID-19, and the pooled odds ratios were 0.67 [95% confidence interval (CI): 0.32-1.42], 1.09 (95%CI: 0.27-4.47), and 0.58 (95%CI: 0.28-1.18), respectively[50]. On the other hand, another meta-analysis found that in IBD patients affected by COVID-19, the risk ratio (RR) of adverse outcomes was increased (RR = 1.32; 95%CI: 1.06-1.66) compared to patients without IBD[51]. The risk factors for worse outcomes of COVID-19,

Table 1 Overview of studies evaluating the course of gastrointestinal symptoms during severe acute respiratory syndrome coronavirus 2 infection in the elderly population

Ref.	*n*	Age (yrs)	GI symptoms	Diarrhoea	Nausea/vomiting	Anorexia	Abdominal pain	Outcomes
de Souza *et al* [32]	9807	70.21 ± 8	-	2%	-	-	-	No association
Ramos-Rincon *et al* [34]	2772	86.3 ± 3	-	14%	5%	22%	-	No association
Marziliano *et al*[33]	4961	77 ± 8	9%	-	-	-	-	No association
Atalla *et al* [37]	111	87.0 median (IQR: 77.0-92.0)		7% (38% all ages)	2%	17% (61% all ages)	-	Mortality was associated with a disease course beginning with a loss of appetite, and the incidence of diarrhea was more frequent in the deceased
Lanthier *et al* [35]	50	88 median (IQR: 83-92)	30%	24%	6%	10%	6%	Digestive symptoms were associated with a favorable outcome
Aroniadis *et al*[9]	434	Age > 70	31%	19%	-	-	-	Older patients were less likely to exhibit gastrointestinal symptoms
Zhan *et al*[23]	39	Age > 75	36%	-	-	-	-	No association
Vrillon *et al* [36]	76	90 median (IQR: 86-92)	22%	-	-	-	-	Digestive symptoms were associated with a favorable outcome

The sample's age was expressed either by the mean or the median in the studies analyzed. For some non-specific studies performed on older people, only the characteristics of the population mentioned above have been shown in the table. However, some of these have yet to express a category-specific significant trend measure. For example, the relationship between the course of the infection and the outcome was reported in the last column. SD: Standard deviation; IQR: Interquartile range; GI: Gastrointestinal.

such as age, male sex, and comorbidities, are the same as observed in the general population. In IBD patients with COVID-19, an active disease was considered a risk factor for poor outcome[52,53], and in a cohort of 79 patients with IBD and COVID-19, active IBD, especially in elderly patients, was correlated with worse outcomes such as pneumonia, hospitalization, respiratory support, and death[52]. Another study reported that the correlation between IBD activity and the risk of severe COVID-19 appears to vary with age and is more relevant in younger patients[53]. The impact of IBD medications on the course of COVID-19 is still under investigation. A meta-analysis by Tripathi *et al*[54] has shown that the therapy with TNF-α antagonists is associated with favorable hospitalization and mortality outcomes, while the use of mesalamine was correlated with worse outcomes in terms of hospitalization, ICU admissions, and death. Another recent study, including 6144 patients, found that systemic corticosteroids were associated with severe COVID-19, while mesalamine and sulfasalazine were not associated with adverse outcomes[55]. In addition, combination therapy with TNF-α antagonists plus thiopurines was correlated with an augmented risk of hospitalization or death, but not the combination with methotrexate. Moreover, biologics were not associated with worse COVID-19 outcomes and could have a protective effect without differences when comparing biologic classes such as TNF-α, IL-12/23, or integrin antagonists [56]. Therefore, the correct management of IBD therapy is relevant because SARS-CoV-2 is not correlated with the risk of IBD relapse. Conversely, the discontinuation or delay of the IBD therapy, regardless of SARS-CoV-2 infection, is significantly associated with the disease activity[55,56] (Table 2).

COVID-19 in elderly patients with IBD

Elderly-onset IBD is defined as onset at 60 years or older[57], and up to 30% of the IBD population is older than 60 years, while 15% of IBD patients have been diagnosed after age 65. It has been observed that in elderly-onset IBD, there is a different natural history and disease phenotype. The disease outcomes are less influenced by genetics, while frailty, immunosenescence, and dysbiosis have a more significant role[58]. In IBD patients, as in the general population, age and comorbidities increase the risk of severe COVID-19 and disease-related mortality[45,59]. A prospective observational study that included 482 patients confirmed that age over 60 years was correlated with severe COVID-19 [odds ratio (OR) = 4.59, 95%CI: 1.3-15.9] and was an independent risk factor related to death (OR = 7.1, 95%CI: 1.8-27.4), as to have two or more comorbidities (OR = 3.9, 95%CI: 1.3-11.6)[60]. Wetwittayakhlang *et al*[61] examined a cohort of 3516 IBD patients, of whom 82 were diagnosed with COVID-19 infection, and they observed that age over 55 years was an independent risk factor for developing severe COVID-19. The study by Brenner *et al*[59], through an extensive international registry, corroborates these observations, finding that advanced age [adjusted OR (aOR) = 1.04; 95%CI: 1.01-1.06] and having at

Table 2 Risk of severe coronavirus disease 2019 in elderly inflammatory bowel disease patients

Ref.	Total number of IBD patients	Number of COVID-19-positive IBD patients	Age threshold considered (yrs)	Risk of severe COVID-19
Ludvigsson *et al*[45]	67292	179 (hospitalized patients)	60	HR = 1.42; 95%CI: 0.94-2.13
Brenner *et al*[59]	SECURE-IBD database	525	Increasing age on multivariable analysis	OR = 1.04; 95%CI: 1.01-1.06
Zabana *et al*[60]	53682	482	60	OR = 4.59, 95%CI: 1.3-15.9, *P* = 0.02
Wetwittayakhlang *et al*[61]	3516	82	55	OR = 11.09, 95%CI: 1.81-68.09, *P* = 0.02

OR: Odds ratio; CI: Confidence interval; IBD: Inflammatory bowel disease; COVID-19: Coronavirus disease 2019; HR: Hazard ratio.

least two comorbidities (categorized into lung disease, cardiovascular disease, hypertension, history of stroke, cancer, liver disease, kidney disease, and diabetes) (aOR = 2.9; 95%CI: 1.1-7.8) were positively associated with severe COVID-19.

Regarding the risk of SARS-CoV-2 infection, a study by Gubatan *et al*[62] observed that IBD patients older than 66 years have an augmented risk of acquiring SARS-CoV-2 infection compared to younger patients. On the other hand, a retrospective cohort study by Calafat *et al*[63] that included 418 IBD patients over 65 years of age, of whom 32 were diagnosed with COVID-19, found that the incidence of COVID-19 in elderly IBD patients is similar to that reported in the age-adjusted general population. Furthermore, the incidence of COVID-19 was not influenced by the use of immunosuppressants, but the authors observed a worse prognosis among the patients who did not use immunosuppressants. Medication use in older patients with IBD differs from younger ones since they are treated less often with biological agents and immunosuppressants. However, corticosteroid use is similar[63,64], and it is possible to hypothesize that these differences could have a role in the course of SARS-CoV-2 infection. Overall, in the elderly population, IBD does not seem to increase the risk of SARS-CoV-2 infection or severe COVID-19[65] (Table 2).

LIVER MANIFESTATIONS ASSOCIATED WITH COVID-19

Introduction

Among the extrapulmonary manifestations of SARS-CoV-2, abnormal liver function reflecting hepatocellular and cholangiocellular injury is often reported[12,66]. COVID-19-associated liver injury includes any liver abnormality due to the disease course or the treatment. Indeed, it is not always possible to determine whether the liver injury is due to the infection or other concomitant conditions, such as the co-administration of hepatotoxic agents or ischemic hepatitis from severe and prolonged hypotension. Moreover, the cytokines storm observed in the severe forms of COVID-19 and caused by systemic hyper-inflammation may result in multiple severe organs injury and, in turn, it represents another cause of liver damage[67]. However, the frequency of liver dysfunction in COVID-19 infection has not yet been well understood [68].

Liver test abnormalities

Among abnormal liver function, liver test abnormalities have often been described. The incidence of elevated liver transaminases, alanine transaminase (ALT), and aspartate aminotransferase (AST) in COVID-19 patients range from 2.5% to 76.3%[69]. A systemic review pointed out that elevated liver chemistries occurred in 23.1% of adult patients with COVID-19 at initial presentation[66]. In comparison, 24.4% develop elevated liver chemistries during the illness, and up to 10.7% have severe liver injury[66]. In detail, the pooled incidence of AST and ALT elevation at initial presentation of COVID-19 was 22.5% and 17.9%, respectively[66]. The incidence of hyperbilirubinemia at the onset of symptoms was 13.4%, while the incidence of alkaline phosphatase (ALP) and gamma-glutamyltransferase (gamma-gt) was 6.1% and 21.1%, respectively[66]. In addition, hypoalbuminemia ranged from 1.1% to 45.8% in non-severely infected patients, reaching 72.9% in those severely infected[66].

The cause of the elevated liver enzymes in COVID-19 patients without pre-existent liver diseases still needs to be well elucidated. In the study of Kulkarni *et al*[66], only 3.6% of the analyzed patients had underlying chronic liver disease (CLD), suggesting that liver damage might be directly caused by the viral infection of liver cells. It is believed that SARS-CoV-2 could penetrate the liver cells thanks to the ACE2 receptor, which is expressed in the liver and bile duct cells[70]. Recent data show that ACE2 is expressed in 2.6% of hepatocytes and 59.7% of cholangiocytes. The level of ACE2 expression in cholangiocytes was similar to type 2 alveolar cells of the lungs. Therefore, liver dysfunction may result from SARS-CoV-2 attachment to ACE2 on cholangiocytes[71]. Of note, studies on both mice and humans reveal an increased ACE2 expression in hepatocytes when liver fibrotic/cirrhotic conditions are present[69]. This finding leads us to believe that preexisting liver injury could exacerbate SARS-CoV-2 hepatic tropism. Although COVID-19 may contribute to liver dysfunction directly through an inflammatory response, postmortem pathological findings of the liver suggest that COVID-19-related liver dysfunction may be mainly caused by secondary liver damage by respiratory distress syndrome-induced hypoxia, multiple organ failure, and the use of potentially hepatotoxic drugs[72]. Microscopically, the most

significant findings in postmortem hepatic tissue of patients with COVID-19 were microvesicular steatosis and mild lobular inflammation[73]. Zhao *et al*[72] presented unique findings, such as platelet-fibrin microthrombi in hepatic sinusoids, central vein or portal vein, histolytic hyperplasia in portal tracts, and megakaryocytic in sinusoids.

Liver test abnormalities and COVID-19 outcomes

Liver test abnormalities can predict the severity of COVID-19 disease[74]. Patients with abnormal liver tests at admission or during hospitalization, classified as hepatocyte type or mixed type, had significantly higher risks of progressing to severe COVID-19 and mortality when compared to patients with normal liver tests[66,75]. Elevated liver enzyme levels are linked to adverse manifestations such as shock, admission to an ICU, and mechanical ventilation. Although, Săbiescu *et al*[76] proved that only elevation over five times the upper limit is strongly correlated with high mortality risk. Also, hypoalbuminemia is a strong predictor of severe COVID-19 course and, in combination with AST or total bilirubin (TBIL), has a remarkable association with mortality[77], even in patients without chronic illness[78]. Furthermore, Da *et al*[79] reported a correlation between ALT levels and levels of inflammatory markers such as C-reactive protein, D-dimers, ferritin, and IL-6.

It appears evident that liver injury in COVID-19 patients is linked to the severity of the hyperinflammatory response, thus, reinforcing the hypothesis that the entity of liver damage is related to the severe forms of SARS-CoV-2 infection. Pazgan-Simon *et al*[80] reported that liver injury in patients with COVID-19 with no underlying liver disease did not correlate with higher mortality. On the other hand, patients with preexisting liver disease, particularly those with cirrhosis, have a higher risk of death than those without any known liver pathology[81].

Impact of SARS-CoV-2 infection on patients with CLD

Wang *et al*[82] showed an increased risk of COVID-19 infection in patients with a recent diagnosis of CLD. A multicentric retrospective study revealed that nearly one-fifth of hospitalized COVID-19 patients had CLD[82]. However, the elevated aminotransferases on admission were higher in patients with CLD than those without CLD. On the contrary, during hospitalization, the aminotransferase level did not differ between patients with or without CLD. Iavarone *et al*[83] described the impact of SARS-CoV-2 infection on ALT levels in cirrhotic patients, revealing that acute liver injury was observed in almost 50% of patients with previously average ALT values. However, more data are necessary to clarify the impact of an ALT increase on the natural history of cirrhosis and COVID-19. It has been described that CLD can negatively influence the clinical outcomes of patients with COVID-19[84,85]. The overall mortality rate of COVID-19 is estimated at 0%-2% in these patients[86]. However, currently, there is no convincing evidence that patients with stable CLD without advanced fibrosis/cirrhosis, primary biliary cholangitis, or primary sclerosing cholangitis have increased susceptibility to severe COVID-19 infection[87]. Contradictory data exist on the risk of developing severe illnesses of non-alcoholic fatty liver disease (NAFLD)[88]. Patients with NAFLD often suffer from metabolic comorbidities such as diabetes, hypertension, and obesity and, for this reason, present an increased risk of a severe course of COVID-19[89]. However, Sachdeva *et al*[90] affirmed that NAFLD might represent a predictor of severe COVID-19, even after adjusting to the presence of confounding factors. The risk of a worse prognosis of COVID-19 is directly related to the severity of the liver disease, and cirrhosis may appear independently associated with an increased risk of death in patients hospitalized with COVID-19[91]. A large multinational cohort study determined that baseline liver disease severity is the primary determinant of SARS-CoV-2 infection outcome[92]. This study resulted in a mortality of 32% in patients with cirrhosis compared to only 8% of those with CLD without cirrhosis. In addition, patients with CLD without cirrhosis appear to have a similar risk of SARS-CoV-2 infection-related mortality compared to patients without liver disease. Furthermore, since only 19% of cirrhosis patients' mortality was related to liver complications, the leading cause of death remained COVID-19-related lung injury. Patients with cirrhosis may also have underlying complications such as hepato-pulmonary syndrome, porto-pulmonary hypertension, or hepatic hydrothorax, which can increase the risk of respiratory failure[93]. On the contrary, a Korean cohort study showed no significant association between developing severe complications from COVID-19, including mortality, or the presence of liver cirrhosis[94]. A possible explanation could be attributed to the different etiologies of cirrhosis in the patients analyzed. In particular, chronic hepatitis B is responsible for more than 70% of cirrhosis cases in Korea[95], and NAFLD and alcoholic liver disease are the most common etiologies of liver cirrhosis in Europe and North America. Consequently, the different etiologies of cirrhosis may play a critical role in developing severe complications from COVID-19. For example, a United States multicentric study pointed out that, among patients with CLD, those with decompensated cirrhosis, alcohol-related liver disease, and hepatocellular carcinoma (HCC) were more vulnerable to adverse outcomes from COVID-19. These patients also had a higher risk for all-cause mortality from COVID-19[96] (Table 3).

Drug-induced liver injury caused by COVID-19 treatment

Liver injury can be caused by several medications used in the treatment of COVID-19. Drug metabolites can cause cellular stress that can lead to apoptosis or necrosis of liver cells[97]. Since most of these drugs cause an elevation of liver enzymes alone, it is important to correctly define acute liver injury to avoid withdrawing this medication improperly[98]. Drug-induced liver injury (DILI) is defined as an increased level of ALT ≥ 5-times upper limit of normal (ULN), or increased level of ALP ≥ 2-times ULN (in the absence of bone pathology), or a simultaneous increase of ALT ≥ 3-times ULN and TBIL concentration > 2-times ULN. While analyzing the different medications used for COVID-19 infection, liver-related adverse effects were more common in patients who used hydroxychloroquine and azithromycin and those who did not receive any targeted therapy[99]. In contrast, drugs, including lopinavir/ritonavir (LPV/v), were associated with 4 × higher odds of liver injury[75]. According to another study, no apparent side effects were found in the LPV/r group, except for transient ALT elevation (< 125 U/L)[96]. A meta-analysis revealed that the incidence of DILI in patients treated

Table 3 Summary of studies on the relationship between liver disease and coronavirus disease 2019 in elderly patients

Ref.	Outcome considered	Results
Khateri *et al* [108]	Incidence of acute liver injury in patients affected by COVID-19	Acute liver injury has no relationship with age
Metawea *et al* [110]	Mortality of patients with hepatocellular carcinoma infected with COVID-19	Age is associated with poorer outcomes and higher mortality
Ji *et al*[111]	Severe COVID-19 in patients affected by NAFLD	Associated in patients older than 60 yr
Zhou *et al* [112]	Severe COVID-19 in patients affected by NAFLD	Associated in patients younger than 60 yr
Hartl *et al* [113]	Liver-related death due to COVID-19 between different age groups	More frequent in the 40-69 years old group than in the over 70 years old group (6.5% *vs* 2.2%)
Ioannou *et al* [115]	Predictors of mortality among patients with cirrhosis and SARS-CoV-2 infection	Advanced age was one of the main risk factors for mortality among patients with cirrhosis and SARS-CoV-2 infection
Brozat *et al* [116]	The case fatality rate in patients with cirrhosis and SARS-CoV-2 infection	The case fatality rate in cirrhotic patients and SARS-CoV-2 infection aged 65 yr and older was nearly three times that in patients younger than 65 yr (43.6% *vs* 16.1%)

SARS-CoV-2: Severe acute respiratory syndrome coronavirus 2; COVID-19: Coronavirus disease 2019; NAFLD: Non-alcoholic fatty liver disease.

with remdesivir was 15.2%, while the incidence of DILI in patients treated with LPV/v was 37.2%[66]. Although some extensive reviews concluded that remdesivir does not affect liver function[100], AST and ALT elevations have been described in a cohort of patients treated with remdesivir. However, in most cases, elevated levels of AST and ALT do not progress to severe liver injury[101]. Hepatotoxicity is documented among the possible Tocilizumab-related side effects. In registration trials, serum aminotransferase elevations occurred in up to 40% of patients receiving tocilizumab. After its licensure, it has been linked to several instances of clinically apparent liver injury with jaundice. Also, liver failure and transplantation may occur in patients treated with tocilizumab[102]. Interestingly, the median age of COVID-19 patients with DILI ranged from 54.3 to 56 years; therefore, age does not appear to significantly influence the risk of developing DILI[103]. Although animal studies have demonstrated changes in hepatic physiology that affect drug metabolism in the aging liver, there is no evidence that this leads to any appreciable deterioration of liver function in healthy elder patients. Moreover, several large international DILI registries do not support elder age as an independent risk factor for developing hepatic injury[104]. On the contrary, it has been described that age does affect the incidence rates of liver injury in COVID-19 patients. Older patients have a higher incidence of liver injury. In addition, impaired liver function in the elderly increases the drug concentrations in their livers. The decline in liver function also explains the higher incidence of DILI in the elderly[105]. Therefore, intensive liver function monitoring should be considered for patients treated with drugs such as remdesivir, LPV/v, and tocilizumab.

COVID-19 liver manifestations in elderly patients

It has been debated if age may represent a risk factor in developing severe complications of SARS-CoV-2 infection in patients with CLD. Several studies demonstrated that older patients are more susceptible to developing severe COVID-19 [106] but are also more likely to develop liver function abnormalities[68]. However, advanced age as a risk factor for more severe forms of COVID-19 has not yet been well assessed. Older patients with COVID-19 have a higher risk of liver injury [107]. Indeed, Khateri *et al*[108] have revealed that the prevalence of acute liver injury has no relationship with age. Spearman *et al*[109] have pointed out that age represents one of the main risk factors for adverse outcomes in individuals with CLD and COVID-19. In patients with HCC infected with COVID-19, age is considered one of the factors responsible for poorer outcomes and higher mortality[109,110]. In a Chinese retrospective study of patients with COVID-19, NAFLD and age over 60 years were associated with a more severe course of COVID-19[111]. On the contrary, Zhou *et al*[112] demonstrated that the association between metabolic-associated fatty liver disease and the development of severe COVID-19 was significant in patients aged less than 60 years. The higher prevalence of severe COVID-19 in patients aged under 60 years with NAFLD compared to those without NAFLD may be attributed to hepatic and systemic immune responses caused by NAFLD, which may increase the severity of the cytokine storm in younger patients with COVID-19. Hartl *et al*[113] analyzed the frequency and the predictive role of abnormal liver chemistries in different age groups. Interestingly, the study revealed that patients aged 40-69 years had a significant risk for COVID-19-associated liver injury. The median levels of hepatocellular injury were highest in patients aged between 40 and 69 years, while cholestatic liver injury was similar within both groups (40-69 years and > 70 years). However, the patients aged over 70 had the highest risk of COVID-19-related mortality; liver-related death due to COVID-19 occurred significantly more often in 40-69-year-old patients than those aged over 70 years (6.5% *vs* 2.2%)[113]. Moreover, this study revealed that increased AST levels were linked to a shorter survival time in patients older than 70, while elevated AST seems to predict a severe course of COVID-19 in all age strata[113]. Of all patients with liver-related death, only 1.7% had no preexisting liver disease. Another study pointed out that among patients with CLD, the highest risk of death was found in their eighth decade of life[92]. Age was associated with higher 30-d mortality in patients with cirrhosis and SARS-CoV-2 infection compared with patients without SARS-CoV-2 infection[114]. Ioannou *et al*[115] also highlighted that higher age, decompensation,

and high model for end-stage liver disease scores were mortality predictors. Also, a more recent study pointed out that older age > 65 and Child-Pugh class C were associated with a high mortality rate[116]. In contrast, Marjot *et al*[92] revealed that mortality in patients with cirrhosis was more evenly distributed across age categories, including a high mortality rate under age 40. A multicentric retrospective Italian study confirmed that the outcomes of cirrhosis patients with COVID-19 were poor. According to a previous study, cirrhotic patients had a higher mortality rate and lower age at death[83].

In summary, COVID-19 is frequently associated with liver function abnormality. However, liver dysfunction may predict a severe form of COVID-19. Therefore, special attention should be paid to older patients, especially those with preexisting CLD and after using hepatotoxic agents. Lastly, cirrhotic patients deserve special attention because they have a high risk of liver function deterioration and mortality with COVID-19 infection, regardless of age (Table 3).

Pancreatic manifestations associated with COVID-19 in elderly patients

The pancreatic involvement of COVID-19, both in terms of clinical implications and underlying mechanisms, is highly manifold and individual-specific[97]. Clinical presentations may range from asymptomatic increases in pancreatic enzyme levels to episodes of acute pancreatitis (AP) and its related complications included pseudocyst formation, peripancreatic fluid collection, pancreatic necrosis, and walled-off necrosis[97,117-119]. Several studies also reported the impact of COVID-19 on metabolic and endocrinologic pancreatic function; manifestations include the development of glucose intolerance and the exacerbation of hyperglycemia, both leading to the development of new-onset diabetes[120, 121].

COVID-19 and AP: Examining the causality

The mechanisms underlying COVID-induced pancreatic damage can be direct, due to the cytopathic effect of local SARS-CoV-2 replication, or indirect, caused by the infection's systemic inflammatory and immune response. Moreover, drug-induced pancreatic injury resulting from antipyretics, anti-inflammatories, and corticosteroids, should also be considered as an additional risk factor[122,123]. However, despite several proposed explanations, no comprehensive theory of COVID-induced pancreatic impairment is universally accepted. The most accredited theory views the engagement of several complexes and interrelated processes. For example, whether the pancreatic injury is caused by SARS-CoV-2 or is just an epiphenomenon is often unclear.

Incidence of COVID-induced pancreatic impairment

From an analysis of the present literature, it can be inferred that the range of incidence of COVID-19-caused pancreatic damage is susceptible to the definition of pancreatic impairment itself. Studies accounting for amylase or lipase serum level increases as an index of pancreatic involvement report an incidence level of 8.5%-17.3%[122,124]. When the more stringent Atlanta criteria are considered, lower incidence values of 1.7%-1.8% are reported[125-127]. An example of this can be found in McNabb-Baltar *et al*[128]'s work; who pointed out that despite mild hyperlipasemia being observed in 9 out of 71 patients (12.1%), only 2 of those (2.8%) had levels more than three times higher than the ULN and that none of them showed any characteristic imaging findings of AP. Similar conclusions are supported by the works of Bansal *et al* [129], Rasch *et al*[130], Barlass *et al*[131], and Bacaksiz *et al*[132], all of which call out for caution when addressing the interrelation between the alteration of pancreatic enzymes and COVID-induced pancreatic impairment. Despite the increase in pancreatic biomarkers typical of COVID-19 patients, no direct correlation to pancreatic impairment is established, as these imbalances could result from concurrent clinical conditions[86,133].

On the other hand, many authors have recognized and described a significant prognostic role of amylase and lipase levels in poor outcomes in COVID-19. Liu *et al*[125] reported a pancreatic enzyme alteration incidence about nine times higher in patients with severe COVID conditions compared to those with non-severe disease (17.4% *vs* 1.85%). Barlass *et al*[131] showed an association between lipase elevation and worse disease outcomes, especially in terms of the need for intensive care (92.9% in patients with elevated lipase levels *vs* 32.8% in those with lower levels) and rate of intubation (78.6% *vs* 23.5%). Ultimately, the multicenter retrospective cohort study by Singh *et al*[134] played a vital role in strengthening this theory, and if its findings are confirmed, serum lipase can be utilized as a marker of disease severity in patients with COVID-19.

Prevalence and outcomes of acute and chronic pancreatitis in COVID-19

After carefully examining the existing literature, a bidirectional relationship between COVID-19 disease and AP can be inferred, at least in terms of outcomes. As part of their retrospective observational cohort study, Inamdar *et al*[135] reported the point prevalence, risk factors, and outcomes among hospitalized patients with pancreatitis with or without COVID-19. This work illustrated a point prevalence of pancreatitis of 0.27%, a higher need for intensive care (mechanical ventilation), and a longer length of hospital stay (OR = 5.65 and OR = 3.22, respectively) among COVID-19 patients. Comparable data were obtained in the works of Karaali and Topal[136], Dirweesh *et al*[137], and from the COVID PAN collaborative study[138], the last of which reported longer length of hospital-stay, persistent organ failure, and higher 30-d mortality in patients with SARS-CoV-2 co-infection. As clearly described by Ye *et al*[139], COVID-19 patients with comorbidities had worse clinical outcomes and greater risk of adverse events proportionally to the number of comorbidities. Focusing on AP, only two studies have compared outcomes in COVID-19 patients with and without pancreatic impairment. Mirò *et al*[140] found comparable results for these two groups, except for the former, being more frequently in need of hospitalization. Similarly, Akarsu *et al*[141] reported that COVID-19 patients who suffered from pancreatitis were more likely to have higher hospitalization and mortality rates. Gubatan *et al*[62] were the first to evaluate the prevalence and outcomes of COVID-19 among patients with a history of pancreatitis. As thoroughly

described by Huang *et al*[142], preexisting pancreas condition was associated with an increased risk of COVID-19 hospitalization and mortality compared to pancreatitis-free patients. Specifically, the highest hospitalization and ICU admission rates were registered in those with a history of chronic pancreatitis. Multicenter research by Hadi *et al*[143] have confirmed that COVID-19 patients with convalescent plasma (CP) bear higher hospitalization rates despite showing no difference in mortality and critical care need. A plausible explanation looks at the higher pancreatic fibrosis grade and the lower inflammatory state, typical of these patients, as predisposing agents to the burden of comorbidities and worse COVID-19 outcomes (Tables 4 and 5).

Distinctive features of COVID-19-associated AP in elderly patients

Focusing on the elderly population, it seems that AP has some particular clinical features that lead to a clinically severe evolution, systemic complications, and, therefore, higher mortality rates[145]. AP has been increasing globally because of an aging population. However, it is worth noting that even if the WHO's definition of elderly is over > 65 years, the age cut-off used for "elderly" in AP prevalence studies differs. In detail, the highest prevalence was found in subjects between 55 and 65 years of age[145-147]. The non-specific presentation and the last occurrence of the symptoms typical of elderly patients make the clinical assessment more difficult for physicians. For example, the typical abdominal pain radiating to the back is absent or mild in 53.8% of cases[148]. For these reasons and the overlap of coexisting comorbidities, AP is often clinically indistinguishable from other clinical conditions in this population. Márta *et al*[149] reported that aging greatly influenced AP's outcome. Their work demonstrated a direct relationship between age and the mortality rate with mortality increase of 0.08% per year between the ages of 20 and 59 and up to 0.76% per year between 59 and 70[149]. These findings, suggesting the involvement of additional deteriorating factors in the elderly population, led the way to other/further studies. COVID-19-induced AP in the elderly population is increasingly reported. Unfortunately, no studies account for only COVID-19 elderly patients with pancreatic impairment, and the few data available are insufficient to draw general conclusions. In Wang *et al*[122]'s work, which describes the incidence of comorbidities in a COVID-19-affected population, the nine patients with pancreatic damage had an average age of 55 years, ranging from 25 to 71 years. Similar data are reported in Inamdar *et al*[135]'s (average age of 54 years), Bruno *et al*[124]'s (average age of 56), and Bulthuis *et al*[150]'s work (60 years). Moreover, a systematic review of case reports and case series pointed out that COVID-19-associated AP affected primarily females with a median age of 53.5 years[144]. The average age of all these study populations aligns with the definition mentioned above of elderly in AP, but the range does not[145]. Conversely, from what was stated before about geriatric patients solely affected by AP[142], 11 case reports of AP in COVID-19-affected elderly patients showed the typical clinical presentation with all the patients experiencing abdominal pain radiating to the back[151-160]. However, these findings are insufficient to suggest a direct or, most likely, indirect effect of SARS-CoV-2 infection on AP's clinical presentation. Therefore, further studies are necessary to establish a causative role. As previously reported, aging is considered a risk factor for a worse outcome not only in COVID-19 disease[161] but also in pancreatitis[149]. Advancing age is one of the 8 modified Glasgow Imrie severity Criteria for AP [162]. Three or more positive criteria, generally assessed within 48 h from admission, are indicative of severe pancreatitis and may require transfer to an intensive care unit[163]. Three of the 11 case reports had to be excluded from the analysis for insufficient data availability. Half of the remaining reports showed a result equal to or higher than three, suggesting severe pancreatitis. However, it is essential to highlight that due to the intrinsic limitation of retrospective analysis, information about the specific timings of the blood test is missing. To the authors' knowledge, no studies evaluating the isolated impact of age as a risk factor for severe prognosis exist for specific subgroups of patients like COVID-19 and AP. Moreover, in the aforementioned prognostic studies[136-138], the demographic composition of the age of the analyzed groups was so similar that no meaningful information could be inferred on the topic.

Impact of SARS-CoV-2 vaccines on patients with IBD

Initially, SARS-CoV-2 vaccines caused hesitancy in the IBD, mainly due to fear of poor response and safety concerns. IBD represents impaired immune function due to the disease and the therapies used to control this illness[60]. Jena *et al*[164] in a systematic review and meta-analysis, analyzed the response to complete vaccination in IBD patients. They reported positive seroconversion rates (95%), although these rates were slightly lower than non-IBD controls (98%). However, if considering only mRNA vaccines, the seroconversion data overlapped between the two populations. Similar results are reported by Bhurwal *et al*[165], which confirmed the adequate response to vaccination in the IBD population (96%), again showing improved outcomes with mRNA vaccines. Moreover, these two meta-analyses found no significant difference in seroconversion concerning the therapy administered (anti-TNF alone, vedolizumab, ustekinumab, or JAK inhibitors), in contrast to other studies which found lower responses to vaccination during anti-TNF alpha and JAK inhibitors therapy [166,167]. In addition, the analysis of breakthrough infections suggests an overall frequency similar to the general population. Nevertheless, a more rapid decline in antibody titers is described in IBD patients, particularly those treated with anti-TNF, immunomodulators, or a combination of these drugs[164]. Another parameter used to assess the efficacy of vaccination is the T cellular response, which plays an essential role in preventing disease progression[168]. Patients with IBD maintain this response even when receiving immune-targeted therapies, confirming that the immunocompromised state does not necessarily prevent a response to vaccination[169,170]. Interestingly, the T cellular response appears to be increased in patients taking anti-TNF-α due to unclear mechanisms[170]. Regarding the safety of vaccinations, several studies have observed similar side effect frequencies between the IBD population and the general population. However, no worsening or flare-up of the disease following vaccination has been proved. Thus, vaccines are considered a safe and well-tolerated strategy for IBD patients[171,172].

Focusing on the elderly population, it is well known that the response to vaccines may be lower than in young people [173], which may also occur with SARS-CoV-2 vaccines. This is probably the result of immune-senescence phenomena, which leads to quantitative and qualitative alterations in the immune system, including a reduction in naive T

Table 4 Evidence regarding pancreatic involvement in coronavirus disease 2019 patients

Ref.	Study design	No. of patients with pancreatic injury/total no. of patients	Remarks
Wang *et al*[122]	CHS	9/52 (4.68%)	Potential mild pancreatic involvement in patients with COVID-19 pneumonia
Bruno *et al*[124]	CHS	6/70 (8.5%)	Pancreatic involvement in hospitalized patients with documented COVID-19
Liu *et al*[125]	RS	13/121 (10.74%)	Pancreatic enzyme alteration incidence was higher in patients with severe COVID-19-related conditions than those with the non-severe disease. However, only a minority of patients with pancreatic enzyme alteration had a confirmed diagnosis of AP as defined by the AC
Stephens *et al*[126]	RS	158/234 (67.5%)	Raised serum amylase in patients with COVID-19 may not be associated with pancreatitis
Akkus *et al*[127]	RS	127/309 (15.7%)	Pancreatic injuries or AP are frequent during COVID-19 infection, especially in those with pre-existing DM
McNabb-Baltar *et al*[128]	RS	9/71 (12.1%)	Although a mild elevation in serum lipase was observed in some patients with COVID-19, acute clinical pancreatitis was not seen, according to the AC
Bansal *et al*[129]	RS	14/42 (33%), 7/29 patients (24.1%)	Pancreatic injury showed no statistically significant relation to the severity or outcome of COVID-19
Rasch *et al*[130]	CHS	22/38 (57.8%)	Patients with lipasemia needed more extended periods of mechanical ventilation than patients with COVID-19-associated ARDS
Barlass *et al*[131]	CCS	14/83 (16.8%)	Elevated lipase is associated with worse disease outcomes and increased ICU admission and intubation
Bacaksiz *et al*[132]	RS	316/1378 (23%)	Hyperamilasemia was significantly associated with COVID-19 severity
Magro *et al*[86]	Review	NA	Increased amylase or lipase levels might not be associated with AP in COVID-19 and may be a consequence of concurrent clinical conditions
Hunt *et al*[133]	Review	NA	No direct correlation between COVID-19 and pancreatic impairment could be established
Singh *et al*[134]	MS	1406/435731 (0.32%)	Worse clinical outcomes
Inamdar *et al*[135]	MS	189/11.883 (0.01%)	COVID-19 patients with pancreatitis were more likely to require mechanical ventilation and had a more extended hospital stay than patients without COVID-19
Karaali and Topal[136]	RS	189/562 (33.6%)	COVID-19 patients with AP had a higher rate of severe AP and a higher need for ICU admission
Dirweesh *et al*[137]	RS	75/339 (22.1%)	Higher mortality, MOF, and POF rates were registered in patients with AP and coexisting COVID-19
Pandanaboyana *et al*[138]	CHS	149/1777 (8.3%)	SARS-CoV-2 infection in acute pancreatitis increases 30-d mortality and disease severity
Mirò *et al*[140]	MS	45/63.822 (0.0007%)	Higher need for hospitalisation in COVID-19 patients with pancreatitis
Akarsu *et al*[141]	CCS	40/316 (12.6%)	Higher mortality rate and increased need for hospitalisation in COVID-19 patients with pancreatitis
Gubatan *et al*[62]	RS	100% total population 14235	Patients with a history of pancreatitis may be more susceptible to COVID-19
Huang *et al*[142]	RCS	4706/326993 (1.4%)	Pre-existing pancreatitis was associated with an increased risk of COVID-19–related hospitalisation and mortality
Hadi *et al*[143]	CS	2/3 (66.6%)	COVID-19 patients with CP bear higher hospitalisation rates
Georgakopoulou *et al*[144]	RS	100%	COVID-19-associated acute pancreatitis affected primarily females with a median age of 53.5 yr

CS: Case series; CR: Case reports; RS: Retrospective studies; RCS: Retrospective cohort study; MS: Multicentric study; CCS: Case-control study; CHS: Cohort study; CSS: Cross-sectional study; NA: Not available; SARS-CoV-2: Severe acute respiratory syndrome coronavirus 2; COVID-19: Coronavirus disease 2019; AC: Atlanta criteria; CP: Convalescent plasma; ICU: Intensive care unit; MOF: Multiple-organ failure; POF: Persistent organ failure; ARDS: Acute respiratory distress syndrome.

lymphocytes available to respond to a vaccine, a significant decrease in CD8 T cells, and a reduction in the T helper follicular cell response[174-176]. Unfortunately, there are currently no studies evaluating vaccination efficacy and safety in elderly patients with IBD. However, in many studies, older age has been associated with attenuated responses, with an earlier decline of the antibody title and reduction differences in the overall strength of the T-cell, although in most of

Table 5 Case reports regarding pancreatic involvement in old coronavirus disease 2019 patients

Ref.	Study design	Age (yrs)	Remarks
Meyers *et al* [151]	CR	67	COVID-19 can cause clinical AP. Typical abdominal pain radiating to the back. Increase lipase serum level. Evidence of AP in abdominal CT scan. Glasgow Acute Pancreatitis Score: NA
Karimzadeh *et al*[152]	CR	65	COVID-19 presents as mild AP. Typical abdominal pain radiating to the back. Increase lipase serum level. Negative abdominal CT scan. Glasgow Acute Pancreatitis Score: 1 point
Gadiparthi *et al* [153]	CR	74	AP in a patient with COVID-19 with SARS-CoV-2 as the possible etiological agent. Typical abdominal pain radiating to the back. Increase lipase serum level. Evidence of AP in abdominal CT scan. Glasgow Acute Pancreatitis Score: 1 point
Wifi *et al*[154]	CR	72	Emphasises the importance of measuring serum amylase and lipase in patients with COVID-19. Typical abdominal pain radiating to the back. Increase lipase and amylase serum levels. Negative abdominal CT scan. Glasgow Acute Pancreatitis Score: 3 points
Gonzalo-Voltas *et al*[155]	CR	76	A case of AP that could be related to COVID-19 infection. Typical abdominal pain radiating to the back. Increase amylase serum level. Evidence of AP in abdominal CT scan. Glasgow Acute Pancreatitis Score: NA
Reick-Mitrisin *et al*[156]	CR	71	AP should be considered in differential abdominal pain in patients with active or recent SARS-CoV-2 infection. Typical abdominal pain. Increase lipase serum level. Evidence of AP in abdominal CT scan. Glasgow Acute Pancreatitis Score: 3 points
Brikman *et al* [163]	CR	61	Unresolved abdominal pain occurring late during COVID-19 warrants a thorough workup. Typical abdominal pain. Increase lipase serum level. Evidence of AP in abdominal CT scan. Glasgow Acute Pancreatitis Score: 2 points
Acherjya *et al* [157]	CR	57	Pay attention to the atypical presentations of SARS-CoV-2, including AP. Typical abdominal pain radiating to the back. Increase lipase serum level. Evidence of AP in abdominal CT scan. Glasgow Acute Pancreatitis Score: 4 points
Alves *et al*[158]	CR	56	Physicians should be aware that asymptomatic or mildly gastrointestinal symptomatic patients with COVID-19 require pancreatic enzymes and even abdomen imaging to diagnose pancreatitis. Typical abdominal pain. Increase lipase and amylase serum levels. Evidence of AP in abdominal CT scan. Glasgow Acute Pancreatitis Score: 3 points
Shinohara *et al* [159]	CR	58	Extrapulmonary clinical characteristics of COVID-19 remain unclear. Typical abdominal pain. Increase amylase serum level. Evidence of AP in abdominal CT scan. Glasgow Acute Pancreatitis Score: NA
Kumaran *et al* [160]	CR	67	Importance of considering COVID-19 as a potential cause in patients presenting with idiopathic pancreatitis. Typical abdominal pain. Increase amylase serum level. Evidence of AP in abdominal CT scan. Glasgow Acute Pancreatitis Score: 2 points

AP: Acute pancreatitis; CR: Case reports; CT: Computed tomography; NA: Not available; SARS-CoV-2: Severe acute respiratory syndrome coronavirus 2.

them, the presence of IBD does not influence these findings[169,170,177,178].

In conclusion, most of the studies mentioned above agree on the potential benefit of a further vaccine booster dose in patients with IBD, especially if elderly or on specific immunosuppressive therapies, such as anti-TNF alpha or JAK inhibitors. To date, studies reporting response rates with additional doses of COVID-19 vaccine in IBD are limited; however, current data suggest a significant boost in antibody binding levels from a third vaccine dose, even during immunosuppressive therapies, but patients receiving infliximab or tofacitinib show a lower response than healthy controls[179].

Impact of SARS-CoV-2 vaccines on patients with CLD

As mentioned above, cirrhotic patients are at high risk of severe COVID-19 infection. Therefore, vaccination against SARS-CoV-2 represents a significant protective measure in patients with CLD, which must be administered as early as possible[180,181]. Moreover, due to vaccinations, patients should not discontinue any of their medications for liver disease or delay any local or regional treatments for HCC[182]. Current COVID-19 vaccines are safe, but a rare vaccine-triggered immune-mediated hepatitis is reported after COVID-19 vaccination. These events are described in the literature in association with mRNA platforms, but cases have also been described for vector-based vaccines. These cases of liver injury are sporadic and respond to corticosteroid treatment. Therefore, liver injury after vaccination should not represent a limit to further vaccination[183]. Furthermore, a Chinese multi-centric study analyzed the safety and immunogenicity of inactivated SARS-CoV-2 vaccines in patients with CLDs[184]. These vaccines are safe in patients with CLD, as there was no significant difference in adverse reactions among the non-cirrhotic CLD, compensated cirrhosis, and decompensated cirrhosis subgroups. Pain was the most common local adverse reaction, while fever was the most commonly systematic adverse reaction reported. Among laboratory findings, only three patients of 437 with CLD had significant aminopherase elevation with ALT levels > 5 ULN, all of which had elevated aminopherase at baseline. Only one of the three patients required hospitalization. Nevertheless, it is impossible to attribute his adverse reaction to the vaccine for certainty since this patient had a history of discontinuing anti-hepatitis B virus therapy before the SARS-CoV-2 vaccination. In addition, patients with CLD often present an inadequate immune response, which may cause an incomplete immediate and long-term protective response[185]. Therefore, although these vaccines are safe in patients with CLD, they do not guarantee such patients equal antibody levels if compared to healthy controls. However, the difference in the positive rate of SARS-CoV-2 neutralizing antibodies between patients with CLD and healthy control groups is statistically significant (77.3% *vs*

90.3%) despite the adjustment for age, gender, and body mass index[184]. While there was no significant difference in positive rate between non-cirrhotic CLD patients (76.8%), compensated cirrhosis patients (78.9%), and decompensated cirrhosis patients (76.7%). Chen *et al*[186] confirmed in their study that inactivated SARS-CoV-2 vaccines are safe and well tolerated in patients with severe liver disease (such as cirrhosis or HCC). However, they also stressed the necessity to assign priority to vaccine patients with severe liver disease, which may have worse antibody responses than those with non-severe CLDs. Thuluvath *et al*[187] instead, analyzed the antibody response in CLD patients after administration of 2 doses of mRNA vaccines or a single dose of viral vector vaccine. This study revealed that only 24% of patients with CLDs had poor antibody responses. More in detail, 15.8% of patients who received the vector vaccine Johnson & Johnson had a good response, and the mRNA Moderna vaccine showed a better response than the mRNA Pfizer vaccine (76.4% *vs* 64.4%). Moreover, analyzing patients' characteristics, it emerged that those with undetectable antibodies (< 0.4 U/mL) had the highest mean age (64.8 years). In line with Thuluvath *et al*[187], Bakasis *et al*[188] highlighted that CLD was not associated with mRNA vaccine hypo-responsiveness. Only 4% of patients with CLD did not respond to SARS-CoV-2 vaccination, with statistically significant differences between cirrhotic and non-cirrhotic patients. The presence of liver disease showed no correlation with antibody titers or neutralizing activity, while age was negatively correlated with neutralizing activity. According to Willuweit *et al*[189], up to 96% of patients with liver cirrhosis presented an antibody response after receiving two doses of the mRNA-based vaccine. Unfortunately, antibody titers remained relatively stable in the control group while showing a rapid and significant decrease in patients with liver cirrhosis, with any differences stratifying cirrhotic patients according to age. The studies mentioned above do not focus on the differences between safety and efficacy among age (patients under 65 and over 65 years old or following stratification of groups according to age). Moreover, the studies conducted to evaluate the safety and efficacy of SARS-CoV-2 vaccination include a limited number of older adults[190]. Therefore, considering that older adults are more inclined to develop vaccine-related adverse events[191] and the lack of older adults in specific SARS-CoV-2 vaccination studies, further research is recommended to evaluate the safety and efficacy of COVID-19 vaccines in older people.

COVID-19 vaccines and pancreatic involvement

To the best of our knowledge, no published work evaluates the COVID-19 vaccination response in older adults suffering from pancreatic diseases. On the other hand, according to Pfizer's data, only 2 cases of AP as an adverse reaction (among 38000 participants) were reported during the clinical trial of the COVID-19 mRNA vaccine[192]. Since the Pfizer-BioNTech mRNA vaccine was approved for COVID-19 infection, AP has been reported in a few case reports[193-201]. Data inferred from United Kingdom databases (up to November 2022) for the same vaccine report 21 cases of pancreatitis, 19 cases of AP, and 3 cases of necrotizing pancreatitis[202]. The National Agency for the Safety of Medicines and Health Products reports 164 cases of pancreatitis up to February 10, 2022[203]. Data released from VigiBase, the WHO's global database, show 1093 cases of pancreatitis[204]. Currently, there is no evidence supporting a direct relationship between the vaccine and AP; even assuming the existence of vaccine-related pancreatic injury, its mechanism would still be unclear[194]. Moreover, considering the high rate of idiopathic pancreatitis[205], the available data are even more challenging to analyze. Considering the higher vaccination prevalence, fewer cases of AP following vaccination may suggest the involvement of different mechanisms in developing a vaccine-related pancreatic injury[196]. The benefits of vaccination against COVID-19 are unquestionable and not disputed in this paper. However, by reporting this evidence, we aim to make all healthcare workers aware of these possible adverse effects and to highlight the importance of not underestimating any abdominal pain after vaccination. As far as we know, the current literature does not include studies evaluating the safety and efficacy of SARS-CoV-2 vaccines in patients with CP. As mentioned above[142,143], CP may be associated with an increased risk of complications from COVID-19 infection leading to worse outcomes. Thus, reducing that risk by having the vaccine would be advisable.

CONCLUSION

Literature data confirm that the digestive manifestations of COVID-19 are frequent and often impact the clinical course of affected patients. In particular, patients with pre-existing liver disease, including cirrhosis or HCC, are at increased risk for worse outcomes. On the contrary, no definitive conclusions can be drawn for patients with IBD or pancreatic diseases. As for elderly patients with digestive disorders, although the available data are limited and extrapolated from studies not designed for this specific issue, there seems to be no evidence of worse COVID-19 outcomes than those without digestive diseases. As expected, this review confirms that age represents one of the main risk factors for poorer outcomes and higher mortality for COVID-19. Moreover, considering the under-representation of older adults in SARS-CoV-2 vaccination studies, further studies are necessary to evaluate better the safety and efficacy of COVID-19 vaccines, especially in frail older people with chronic digestive diseases.

FOOTNOTES

Author contributions: Papa A and Covino M contributed to the conception and design of this study, analysis and interpretation of data; De Lucia SS, Del Gaudio A, Fiorani M, Polito G, and Settanni CR were involved in the acquisition and collection of data; Papa A, Covino M, De Lucia SS, Del Gaudio A, Fiorani M, Polito G, Settanni CR, Franceschi F, and Gasbarrini A drafted the paper or revised it critically for intellectual content; and all authors approved the final version of the manuscript to be published.

Conflict-of-interest statement: All the authors report no relevant conflicts of interest for this article.

Open-Access: This article is an open-access article that was selected by an in-house editor and fully peer-reviewed by external reviewers. It is distributed in accordance with the Creative Commons Attribution NonCommercial (CC BY-NC 4.0) license, which permits others to distribute, remix, adapt, build upon this work non-commercially, and license their derivative works on different terms, provided the original work is properly cited and the use is non-commercial. See: https://creativecommons.org/Licenses/by-nc/4.0/

Country/Territory of origin: Italy

ORCID number: Marcello Covino 0000-0002-6709-2531; Andrea Piccioni 0000-0001-5703-8737; Francesco Franceschi 0000-0001-6266-445X.

S-Editor: Wang JJ
L-Editor: Ma JY
P-Editor: Wang JJ

REFERENCES

1 **Liu YC**, Kuo RL, Shih SR. COVID-19: The first documented coronavirus pandemic in history. *Biomed J* 2020; **43**: 328-333 [PMID: 32387617 DOI: 10.1016/j.bj.2020.04.007]
2 **World Health Organization**. WHO Coronavirus (COVID-19) Dashboard. [cited 17 October 2022]. Available from: https://covid19.who.int/?gclid=CjwKCAiAlNf-
3 **Wiersinga WJ**, Rhodes A, Cheng AC, Peacock SJ, Prescott HC. Pathophysiology, Transmission, Diagnosis, and Treatment of Coronavirus Disease 2019 (COVID-19): A Review. *JAMA* 2020; **324**: 782-793 [PMID: 32648899 DOI: 10.1001/jama.2020.12839]
4 **Struyf T**, Deeks JJ, Dinnes J, Takwoingi Y, Davenport C, Leeflang MM, Spijker R, Hooft L, Emperador D, Domen J, Tans A, Janssens S, Wickramasinghe D, Lannoy V, Horn SRA, Van den Bruel A; Cochrane COVID-19 Diagnostic Test Accuracy Group. Signs and symptoms to determine if a patient presenting in primary care or hospital outpatient settings has COVID-19. *Cochrane Database Syst Rev* 2022; **5**: CD013665 [PMID: 35593186 DOI: 10.1002/14651858.CD013665.pub3]
5 **Chua AJ**, Charn TC, Chan EC, Loh J. Acute Olfactory Loss Is Specific for COVID-19 at the Emergency Department. *Ann Emerg Med* 2020; **76**: 550-551 [PMID: 32410763 DOI: 10.1016/j.annemergmed.2020.05.015]
6 **Carpenter CR**, Mudd PA, West CP, Wilber E, Wilber ST. Diagnosing COVID-19 in the Emergency Department: A Scoping Review of Clinical Examinations, Laboratory Tests, Imaging Accuracy, and Biases. *Acad Emerg Med* 2020; **27**: 653-670 [PMID: 32542934 DOI: 10.1111/acem.14048]
7 **Long B**, Carius BM, Chavez S, Liang SY, Brady WJ, Koyfman A, Gottlieb M. Clinical update on COVID-19 for the emergency clinician: Presentation and evaluation. *Am J Emerg Med* 2022; **54**: 46-57 [PMID: 35121478 DOI: 10.1016/j.ajem.2022.01.028]
8 **D'Amico F**, Baumgart DC, Danese S, Peyrin-Biroulet L. Diarrhea During COVID-19 Infection: Pathogenesis, Epidemiology, Prevention, and Management. *Clin Gastroenterol Hepatol* 2020; **18**: 1663-1672 [PMID: 32278065 DOI: 10.1016/j.cgh.2020.04.001]
9 **Aroniadis OC**, Wang X, Gong T, Forbes N, Yang JY, Canakis A, Elmunzer BJ, Yadav D; North American Alliance for the Study of Digestive Manifestations of Covid-19. Factors Associated with the Development of Gastrointestinal Symptoms in Patients Hospitalized with Covid-19. *Dig Dis Sci* 2022; **67**: 3860-3871 [PMID: 34751837 DOI: 10.1007/s10620-021-07286-7]
10 **Cholankeril G**, Podboy A, Aivaliotis VI, Tarlow B, Pham EA, Spencer SP, Kim D, Hsing A, Ahmed A. High Prevalence of Concurrent Gastrointestinal Manifestations in Patients With Severe Acute Respiratory Syndrome Coronavirus 2: Early Experience From California. *Gastroenterology* 2020; **159**: 775-777 [PMID: 32283101 DOI: 10.1053/j.gastro.2020.04.008]
11 **Wang Y**, Li Y, Zhang Y, Liu Y. Are gastrointestinal symptoms associated with higher risk of Mortality in COVID-19 patients? A systematic review and meta-analysis. *BMC Gastroenterol* 2022; **22**: 106 [PMID: 35255816 DOI: 10.1186/s12876-022-02132-0]
12 **Gupta A**, Madhavan MV, Sehgal K, Nair N, Mahajan S, Sehrawat TS, Bikdeli B, Ahluwalia N, Ausiello JC, Wan EY, Freedberg DE, Kirtane AJ, Parikh SA, Maurer MS, Nordvig AS, Accili D, Bathon JM, Mohan S, Bauer KA, Leon MB, Krumholz HM, Uriel N, Mehra MR, Elkind MSV, Stone GW, Schwartz A, Ho DD, Bilezikian JP, Landry DW. Extrapulmonary manifestations of COVID-19. *Nat Med* 2020; **26**: 1017-1032 [PMID: 32651579 DOI: 10.1038/s41591-020-0968-3]
13 **Zheng Z**, Peng F, Xu B, Zhao J, Liu H, Peng J, Li Q, Jiang C, Zhou Y, Liu S, Ye C, Zhang P, Xing Y, Guo H, Tang W. Risk factors of critical & mortal COVID-19 cases: A systematic literature review and meta-analysis. *J Infect* 2020; **81**: e16-e25 [PMID: 32335169 DOI: 10.1016/j.jinf.2020.04.021]
14 **Mueller AL**, McNamara MS, Sinclair DA. Why does COVID-19 disproportionately affect older people? *Aging (Albany NY)* 2020; **12**: 9959-9981 [PMID: 32470948 DOI: 10.18632/aging.103344]
15 **Goodman KE**, Magder LS, Baghdadi JD, Pineles L, Levine AR, Perencevich EN, Harris AD. Impact of Sex and Metabolic Comorbidities on Coronavirus Disease 2019 (COVID-19) Mortality Risk Across Age Groups: 66 646 Inpatients Across 613 U.S. Hospitals. *Clin Infect Dis* 2021; **73**: e4113-e4123 [PMID: 33337474 DOI: 10.1093/cid/ciaa1787]
16 **Chen Y**, Klein SL, Garibaldi BT, Li H, Wu C, Osevala NM, Li T, Margolick JB, Pawelec G, Leng SX. Aging in COVID-19: Vulnerability, immunity and intervention. *Ageing Res Rev* 2021; **65**: 101205 [PMID: 33137510 DOI: 10.1016/j.arr.2020.101205]
17 **Channappanavar R**, Perlman S. Age-related susceptibility to coronavirus infections: role of impaired and dysregulated host immunity. *J Clin Invest* 2020; **130**: 6204-6213 [PMID: 33085654 DOI: 10.1172/JCI144115]
18 **Papa A**, Covino M, Pizzolante F, Miele L, Lopetuso LR, Bove V, Iorio R, Simeoni B, Vetrone LM, Tricoli L, Mignini I, Schepis T, D'Alessandro A, Coppola G, Nicoletti T, Visconti E, Rapaccini G. Gastrointestinal symptoms and digestive comorbidities in an Italian cohort of patients with COVID-19. *Eur Rev Med Pharmacol Sci* 2020; **24**: 7506-7511 [PMID: 32706091 DOI: 10.26355/eurrev_202007_21923]
19 **Zou X**, Chen K, Zou J, Han P, Hao J, Han Z. Single-cell RNA-seq data analysis on the receptor ACE2 expression reveals the potential risk of different human organs vulnerable to 2019-nCoV infection. *Front Med* 2020; **14**: 185-192 [PMID: 32170560 DOI: 10.1007/s11684-020-0754-0]

20 **Lin L**, Jiang X, Zhang Z, Huang S, Fang Z, Gu Z, Gao L, Shi H, Mai L, Liu Y, Lin X, Lai R, Yan Z, Li X, Shan H. Gastrointestinal symptoms of 95 cases with SARS-CoV-2 infection. *Gut* 2020; **69**: 997-1001 [PMID: 32241899 DOI: 10.1136/gutjnl-2020-321013]

21 **Selva KJ**, Chung AW. Insights into how SARS-CoV2 infection induces cytokine storms. *Trends Immunol* 2022; **43**: 417-419 [PMID: 35537983 DOI: 10.1016/j.it.2022.04.007]

22 **Villapol S**. Gastrointestinal symptoms associated with COVID-19: impact on the gut microbiome. *Transl Res* 2020; **226**: 57-69 [PMID: 32827705 DOI: 10.1016/j.trsl.2020.08.004]

23 **Zhan T**, Tang Y, Han Z, Zhu Q, Tan J, Liu M, Cai Y, Huang M, Chen X, Cheng X, Deng J, Huang X, Tian X. Clinical Characteristics of 195 Cases of COVID-19 with Gastrointestinal Symptoms COVID-19 with Gastrointestinal Symptoms. *Turk J Gastroenterol* 2021; **32**: 148-154 [PMID: 33960938 DOI: 10.5152/tjg.2021.20379]

24 **Perisetti A**, Goyal H, Gajendran M, Boregowda U, Mann R, Sharma N. Prevalence, Mechanisms, and Implications of Gastrointestinal Symptoms in COVID-19. *Front Med (Lausanne)* 2020; **7**: 588711 [PMID: 33195352 DOI: 10.3389/fmed.2020.588711]

25 **Papadakis KA**, Prehn J, Nelson V, Cheng L, Binder SW, Ponath PD, Andrew DP, Targan SR. The role of thymus-expressed chemokine and its receptor CCR9 on lymphocytes in the regional specialization of the mucosal immune system. *J Immunol* 2000; **165**: 5069-5076 [PMID: 11046037 DOI: 10.4049/jimmunol.165.9.5069]

26 **Babic T**, Browning KN. The role of vagal neurocircuits in the regulation of nausea and vomiting. *Eur J Pharmacol* 2014; **722**: 38-47 [PMID: 24184670 DOI: 10.1016/j.ejphar.2013.08.047]

27 **Fang D**, Ma J, Guan J, Wang M, Song Y, Tian D, Li P. Manifestations of digestive system of hospitalized patients with coronavirus disease 2019 in Wuhan, China: a single-center descriptive study. *Chin J Digestion* 2020; 151-156

28 **Jiménez E**, Fontán-Vela M, Valencia J, Fernandez-Jimenez I, Álvaro-Alonso EA, Izquierdo-García E, Lazaro Cebas A, Gallego Ruiz-Elvira E, Troya J, Tebar-Martinez AJ, Garcia-Marina B, Peña-Lillo G, Abad-Motos A, Macaya L, Ryan P, Pérez-Butragueño M; COVID@HUIL Working Group; COVID@HUIL Working Group. Characteristics, complications and outcomes among 1549 patients hospitalised with COVID-19 in a secondary hospital in Madrid, Spain: a retrospective case series study. *BMJ Open* 2020; **10**: e042398 [PMID: 33172949 DOI: 10.1136/bmjopen-2020-042398]

29 **Vuille-Dit-Bille RN**, Liechty KW, Verrey F, Guglielmetti LC. SARS-CoV-2 receptor ACE2 gene expression in small intestine correlates with age. *Amino Acids* 2020; **52**: 1063-1065 [PMID: 32627059 DOI: 10.1007/s00726-020-02870-z]

30 **Hashimoto T**, Perlot T, Rehman A, Trichereau J, Ishiguro H, Paolino M, Sigl V, Hanada T, Hanada R, Lipinski S, Wild B, Camargo SM, Singer D, Richter A, Kuba K, Fukamizu A, Schreiber S, Clevers H, Verrey F, Rosenstiel P, Penninger JM. ACE2 links amino acid malnutrition to microbial ecology and intestinal inflammation. *Nature* 2012; **487**: 477-481 [PMID: 22837003 DOI: 10.1038/nature11228]

31 **Liu Q**, Wang RS, Qu GQ, Wang YY, Liu P, Zhu YZ, Fei G, Ren L, Zhou YW, Liu L. Gross examination report of a COVID-19 death autopsy. *Fa Yi Xue Za Zhi* 2020; **36**: 21-23 [PMID: 32198987 DOI: 10.12116/j.issn.1004-5619.2020.01.005]

32 **de Souza CD**, de Arruda Magalhães AJ, Lima AJ, Nunes DN, de Fátima Machado Soares É, de Castro Silva L, Santos LG, Dos Santos Cardoso VI, Nobre YV, do Carmo RF. Clinical manifestations and factors associated with mortality from COVID-19 in older adults: Retrospective population-based study with 9807 older Brazilian COVID-19 patients. *Geriatr Gerontol Int* 2020; **20**: 1177-1181 [PMID: 33111433 DOI: 10.1111/ggi.14061]

33 **Marziliano A**, Burns E, Chauhan L, Liu Y, Makhnevich A, Zhang M, Carney MT, Dbeis Y, Lindvall C, Qiu M, Diefenbach MA, Sinvani L. Patient Factors and Hospital Outcomes Associated With Atypical Presentation in Hospitalized Older Adults With COVID-19 During the First Surge of the Pandemic. *J Gerontol A Biol Sci Med Sci* 2022; **77**: e124-e132 [PMID: 34279628 DOI: 10.1093/gerona/glab171]

34 **Ramos-Rincon JM**, Buonaiuto V, Ricci M, Martín-Carmona J, Paredes-Ruíz D, Calderón-Moreno M, Rubio-Rivas M, Beato-Pérez JL, Arnalich-Fernández F, Monge-Monge D, Vargas-Núñez JA, Acebes-Repiso G, Mendez-Bailon M, Perales-Fraile I, García-García GM, Guisado-Vasco P, Abdelhady-Kishta A, Pascual-Pérez MD, Rodríguez-Fernández-Viagas C, Montaño-Martínez A, López-Ruiz A, Gonzalez-Juarez MJ, Pérez-García C, Casas-Rojo JM, Gómez-Huelgas R; SEMI-COVID-19 Network. Clinical Characteristics and Risk Factors for Mortality in Very Old Patients Hospitalized With COVID-19 in Spain. *J Gerontol A Biol Sci Med Sci* 2021; **76**: e28-e37 [PMID: 33103720 DOI: 10.1093/gerona/glaa243]

35 **Lanthier N**, Mahiat C, Henrard S, Stärkel P, Gilard I, De Brauwer I, Cornette P, Boland B. Gastro-intestinal symptoms are associated with a lower in-hospital mortality rate in frail older patients hospitalized for COVID-19. *Acta Gastroenterol Belg* 2021; **84**: 135-136 [PMID: 33639706 DOI: 10.51821/84.1.824]

36 **Vrillon A**, Hourregue C, Azuar J, Grosset L, Boutelier A, Tan S, Roger M, Mourman V, Mouly S, Sène D, François V, Dumurgier J, Paquet C; for LRB COVID Group. COVID-19 in Older Adults: A Series of 76 Patients Aged 85 Years and Older with COVID-19. *J Am Geriatr Soc* 2020; **68**: 2735-2743 [PMID: 33045106 DOI: 10.1111/jgs.16894]

37 **Atalla E**, Zhang R, Shehadeh F, Mylona EK, Tsikala-Vafea M, Kalagara S, Henseler L, Chan PA, Mylonakis E. Clinical Presentation, Course, and Risk Factors Associated with Mortality in a Severe Outbreak of COVID-19 in Rhode Island, USA, April-June 2020. *Pathogens* 2020; **10** [PMID: 33374131 DOI: 10.3390/pathogens10010008]

38 **González González R**, Jacob J, Miró Ò, Llorens P, Jiménez S, González Del Castillo J, Burillo-Putze G, Martín A, Martín-Sánchez FJ, Lamberechts JG, Alquézar-Arbé A, Higa-Sansone L, Gayoso Martín S, Carbajosa V, Beddar Chaib F, Salido M, Marchena González MJ, Calvo López R, González Martínez F, Pavón Monzo J, Velarde Herrera DM, Niembro Valdés AP, Quero Motto E, Ferreras Amez JM, Piñera-Salmerón P; Spanish Investigators on Emergency Situations TeAm (SIESTA) Network. Incidence, Clinical Characteristics, Risk Factors, and Outcomes of Upper Gastrointestinal Bleeding in Patients With COVID-19: Results of the UMC-19-S12. *J Clin Gastroenterol* 2022; **56**: e38-e46 [PMID: 33252555 DOI: 10.1097/MCG.0000000000001465]

39 **Zhai Z**, Li C, Chen Y, Gerotziafas G, Zhang Z, Wan J, Liu P, Elalamy I, Wang C; Prevention Treatment of VTE Associated with COVID-19 Infection Consensus Statement Group. Prevention and Treatment of Venous Thromboembolism Associated with Coronavirus Disease 2019 Infection: A Consensus Statement before Guidelines. *Thromb Haemost* 2020; **120**: 937-948 [PMID: 32316065 DOI: 10.1055/s-0040-1710019]

40 **Tiwari NR**, Khatib KI, Dixit SB, Rathore PK, Melinkeri S, Ganapule A, Borawake KS, Mhatre U. Anticoagulation in COVID - 19: An Update. *J Crit Care Med (Targu Mures)* 2020; **6**: 217-223 [PMID: 33200092 DOI: 10.2478/jccm-2020-0033]

41 **Ion D**, Gherghinescu M, Andronic O, Andreescu CV, Păduraru DN, Bolocan A, Russu C, Aprodu S, Mationi G, Nicolescu C, Popa D. Prognosis Evaluation for Patients with Abdominal Trauma Using Usual Biological Parameters. *Chirurgia (Bucur)* 2021; **116**: 737-747 [PMID: 34967718 DOI: 10.21614/chirurgia.116.6.737]

42 **Dioscoridi L**, Giannetti A, Massad MT, Forti E, Pugliese F, Cintolo M, Bonato G, Rosa R, Mutignani M. A "double-hit" damage mechanism can explain self-limited GI bleeding in COVID-19 pneumonia. *Gastrointest Endosc* 2021; **93**: 1192-1193 [PMID: 33875144 DOI: 10.1016/j.gie.2020.12.022]

43 **Al-Samkari H**, Karp Leaf RS, Dzik WH, Carlson JCT, Fogerty AE, Waheed A, Goodarzi K, Bendapudi PK, Bornikova L, Gupta S, Leaf DE, Kuter DJ, Rosovsky RP. COVID-19 and coagulation: bleeding and thrombotic manifestations of SARS-CoV-2 infection. *Blood* 2020; **136**: 489-500 [PMID: 32492712 DOI: 10.1182/blood.2020006520]

44 **Ojetti V**, Saviano A, Covino M, Acampora N, Troiani E, Franceschi F; GEMELLI AGAINST COVID-19 group. COVID-19 and intestinal inflammation: Role of fecal calprotectin. *Dig Liver Dis* 2020; **52**: 1231-1233 [PMID: 33060042 DOI: 10.1016/j.dld.2020.09.015]

45 **Ludvigsson JF**, Axelrad J, Halfvarson J, Khalili H, Larsson E, Lochhead P, Roelstraete B, Simon TG, Söderling J, Olén O. Inflammatory bowel disease and risk of severe COVID-19: A nationwide population-based cohort study in Sweden. *United European Gastroenterol J* 2021; **9**: 177-192 [PMID: 33704918 DOI: 10.1002/ueg2.12049]

46 **Amiot A**, Rahier JF, Baert F, Nahon S, Hart A, Viazis N, Biancone L, Domenech E, Reenears C, Peyrin-Biroulet L, Beaugerie L, Burisch J; I-CARE collaborator group. The Impact of COVID-19 on Patients with IBD in a Prospective European Cohort Study. *J Crohns Colitis* 2023; **17**: 37-48 [PMID: 35767639 DOI: 10.1093/ecco-jcc/jjac091]

47 **Maconi G**, Bosetti C, De Monti A, Boyapati RK, Shelton E, Piazza N, Carvalhas Gabrielli AM, Lenti MV, Bezzio C, Ricci C, Greco S, Romeo S, Giangregorio F, Gridavilla D, Tagliani F, Massari A, Pastorelli L, Di Sabatino A, Saibeni S, Alicante S, Ferretti F, Rizzardini G, Galli M, Ardizzone S. Risk of COVID 19 in patients with inflammatory bowel diseases compared to a control population. *Dig Liver Dis* 2021; **53**: 263-270 [PMID: 33483259 DOI: 10.1016/j.dld.2020.12.013]

48 **Papa A**, Gasbarrini A, Tursi A. Epidemiology and the Impact of Therapies on the Outcome of COVID-19 in Patients With Inflammatory Bowel Disease. *Am J Gastroenterol* 2020; **115**: 1722-1724 [PMID: 32826572 DOI: 10.14309/ajg.0000000000000830]

49 **Singh AK**, Jena A, Kumar-M P, Jha DK, Sharma V. Clinical presentation of COVID-19 in patients with inflammatory bowel disease: a systematic review and meta-analysis. *Intest Res* 2022; **20**: 134-143 [PMID: 33440918 DOI: 10.5217/ir.2020.00108]

50 **Lee MH**, Li HJ, Wasuwanich P, Kim SE, Kim JY, Jeong GH, Park S, Yang JW, Kim MS, Yon DK, Lee SW, Koyanagi A, Jacob L, Kim EY, Cheon JH, Shin JI, Smith L. COVID-19 susceptibility and clinical outcomes in inflammatory bowel disease: An updated systematic review and meta-analysis. *Rev Med Virol* 2022; e2414 [PMID: 36504172 DOI: 10.1002/rmv.2414]

51 **Chen L**, Hu K, Cheng C, Hu Q, Zhang L, An T, Guo Y, Chen S, Duan G. Risk of adverse outcomes in inflammatory bowel disease patients infected with SARS-CoV-2: a systematic review and meta-analysis. *Int J Colorectal Dis* 2022; **37**: 2277-2289 [PMID: 36271206 DOI: 10.1007/s00384-022-04265-w]

52 **Bezzio C**, Saibeni S, Variola A, Allocca M, Massari A, Gerardi V, Casini V, Ricci C, Zingone F, Amato A, Caprioli F, Lenti MV, Viganò C, Ascolani M, Bossa F, Castiglione F, Cortelezzi C, Grossi L, Milla M, Morganti D, Pastorelli L, Ribaldone DG, Sartini A, Soriano A, Manes G, Danese S, Fantini MC, Armuzzi A, Daperno M, Fiorino G; Italian Group for the Study of Inflammatory Bowel Disease (IG-IBD). Outcomes of COVID-19 in 79 patients with IBD in Italy: an IG-IBD study. *Gut* 2020; **69**: 1213-1217 [PMID: 32354990 DOI: 10.1136/gutjnl-2020-321411]

53 **Ricciuto A**, Lamb CA, Benchimol EI, Walker GJ, Kennedy NA, Kuenzig ME, Kaplan GG, Kappelman MD, Ungaro RC, Colombel JF, Brenner EJ, Agrawal M, Reinisch W, Griffiths AM, Sebastian S. Inflammatory Bowel Disease Clinical Activity is Associated with COVID-19 Severity Especially in Younger Patients. *J Crohns Colitis* 2022; **16**: 591-600 [PMID: 34570886 DOI: 10.1093/ecco-jcc/jjab172]

54 **Tripathi K**, Godoy Brewer G, Thu Nguyen M, Singh Y, Saleh Ismail M, Sauk JS, Parian AM, Limketkai BN. COVID-19 and Outcomes in Patients With Inflammatory Bowel Disease: Systematic Review and Meta-Analysis. *Inflamm Bowel Dis* 2022; **28**: 1265-1279 [PMID: 34718595 DOI: 10.1093/ibd/izab236]

55 **Bezzio C**, Fiorino G, Ribaldone DG, Armuzzi A, Saibeni S; IG-IBD COVID-19 Study Group. IBD Flare in the COVID-19 Pandemic: Therapy Discontinuation Is to Blame. *Inflamm Bowel Dis* 2022 [PMID: 35972338 DOI: 10.1093/ibd/izac173]

56 **Papa A**, Papa V, Lopetuso LR, Gasbarrini A, Tursi A. Covid-19 and the management of patients with inflammatory bowel disease: a practical decalogue for the post-pandemic phase. *Therap Adv Gastroenterol* 2020; **13**: 1756284820968747 [PMID: 33149764 DOI: 10.1177/1756284820968747]

57 **Sturm A**, Maaser C, Mendall M, Karagiannis D, Karatzas P, Ipenburg N, Sebastian S, Rizzello F, Limdi J, Katsanos K, Schmidt C, Jeuring S, Colombo F, Gionchetti P. European Crohn's and Colitis Organisation Topical Review on IBD in the Elderly. *J Crohns Colitis* 2017; **11**: 263-273 [PMID: 27797918 DOI: 10.1093/ecco-jcc/jjw188]

58 **Hong SJ**, Katz S. The elderly IBD patient in the modern era: changing paradigms in risk stratification and therapeutic management. *Therap Adv Gastroenterol* 2021; **14**: 17562848211023399 [PMID: 34276809 DOI: 10.1177/17562848211023399]

59 **Brenner EJ**, Ungaro RC, Gearry RB, Kaplan GG, Kissous-Hunt M, Lewis JD, Ng SC, Rahier JF, Reinisch W, Ruemmele FM, Steinwurz F, Underwood FE, Zhang X, Colombel JF, Kappelman MD. Corticosteroids, But Not TNF Antagonists, Are Associated With Adverse COVID-19 Outcomes in Patients With Inflammatory Bowel Diseases: Results From an International Registry. *Gastroenterology* 2020; **159**: 481-491.e3 [PMID: 32425234 DOI: 10.1053/j.gastro.2020.05.032]

60 **Zabana Y**, Marín-Jiménez I, Rodríguez-Lago I, Vera I, Martín-Arranz MD, Guerra I, P Gisbert J, Mesonero F, Benítez O, Taxonera C, Ponferrada-Díaz Á, Piqueras M, J Lucendo A, Caballol B, Mañosa M, Martínez-Montiel P, Bosca-Watts M, Gordillo J, Bujanda L, Manceñido N, Martínez-Pérez T, López A, Rodríguez-Gutiérrez C, García-López S, Vega P, Rivero M, Melcarne L, Calvo M, Iborra M, Barreiro de Acosta M, Sicilia B, Barrio J, Pérez Calle JL, Busquets D, Pérez-Martínez I, Navarro-Llavat M, Hernández V, Argüelles-Arias F, Ramírez Esteso F, Meijide S, Ramos L, Gomollón F, Muñoz F, Suris G, Ortiz de Zarate J, Huguet JM, Llaó J, García-Sepulcre MF, Sierra M, Durà M, Estrecha S, Fuentes Coronel A, Hinojosa E, Olivan L, Iglesias E, Gutiérrez A, Varela P, Rull N, Gilabert P, Hernández-Camba A, Brotons A, Ginard D, Sesé E, Carpio D, Aceituno M, Cabriada JL, González-Lama Y, Jiménez L, Chaparro M, López-San Román A, Alba C, Plaza-Santos R, Mena R, Tamarit-Sebastián S, Ricart E, Calafat M, Olivares S, Navarro P, Bertoletti F, Alonso-Galán H, Pajares R, Olcina P, Manzano P, Domènech E, Esteve M, On Behalf Of The Eneida Registry Of Geteccu. Risk Factors for COVID-19 in Inflammatory Bowel Disease: A National, ENEIDA-Based Case-Control Study (COVID-19-EII). *J Clin Med* 2022; **11** [PMID: 36556155 DOI: 10.3390/jcm11247540]

61 **Wetwittayakhlang P**, Albader F, Golovics PA, Hahn GD, Bessissow T, Bitton A, Afif W, Wild G, Lakatos PL. Clinical Outcomes of COVID-19 and Impact on Disease Course in Patients with Inflammatory Bowel Disease. *Can J Gastroenterol Hepatol* 2021; **2021**: 7591141 [PMID: 34858891 DOI: 10.1155/2021/7591141]

62 **Gubatan J**, Levitte S, Patel A, Balabanis T, Sharma A, Jones E, Lee B, Manohar M, Swaminathan G, Park W, Habtezion A. Prevalence, risk factors and clinical outcomes of COVID-19 in patients with a history of pancreatitis in Northern California. *Gut* 2021; **70**: 440-441 [PMID: 32493828 DOI: 10.1136/gutjnl-2020-321772]

63 **Calafat M**, González-Muñoza C, Fortuny M, Roig C, Calm A, Mombiela A, Cañete F, Bertoletti F, González-González L, Teller-Martín M, Gordillo J, Mañosa M, Garcia-Planella E, Domènech E. Impact of immunosuppressants on SARS-CoV-2 infection in elderly patients with inflammatory bowel disease. *Aging Clin Exp Res* 2021; **33**: 2355-2359 [PMID: 34164799 DOI: 10.1007/s40520-021-01917-9]

64 **Geisz M**, Ha C, Kappelman MD, Martin CF, Chen W, Anton K, Sandler RS, Long MD. Medication Utilization and the Impact of Continued

Corticosteroid Use on Patient-reported Outcomes in Older Patients with Inflammatory Bowel Disease. *Inflamm Bowel Dis* 2016; **22**: 1435-1441 [PMID: 26978725 DOI: 10.1097/MIB.0000000000000747]

65 **Bernstein CN**, Singh H, Murthy SK, Nguyen GC, Benchimol EI, Bitton A, Kuenzig ME, Huang JG, Jones JL, Lee K, Targownik LE, Windsor JW, Mukhtar MS, Tandon P, Kaplan GG. Crohn's and Colitis Canada's 2021 Impact of COVID-19 and Inflammatory Bowel Disease in Canada: Seniors With IBD. *J Can Assoc Gastroenterol* 2021; **4**: S34-S39 [PMID: 34755037 DOI: 10.1093/jcag/gwab025]

66 **Kulkarni AV**, Kumar P, Tevethia HV, Premkumar M, Arab JP, Candia R, Talukdar R, Sharma M, Qi X, Rao PN, Reddy DN. Systematic review with meta-analysis: liver manifestations and outcomes in COVID-19. *Aliment Pharmacol Ther* 2020; **52**: 584-599 [PMID: 32638436 DOI: 10.1111/apt.15916]

67 **Mehta P**, McAuley DF, Brown M, Sanchez E, Tattersall RS, Manson JJ; HLH Across Speciality Collaboration, UK. COVID-19: consider cytokine storm syndromes and immunosuppression. *Lancet* 2020; **395**: 1033-1034 [PMID: 32192578 DOI: 10.1016/S0140-6736(20)30628-0]

68 **Li S**, Li J, Zhang Z, Tan L, Shao T, Li M, Li X, Holmes JA, Lin W, Han M. COVID-19 induced liver function abnormality associates with age. *Aging (Albany NY)* 2020; **12**: 13895-13904 [PMID: 32721928 DOI: 10.18632/aging.103720]

69 **Nardo AD**, Schneeweiss-Gleixner M, Bakail M, Dixon ED, Lax SF, Trauner M. Pathophysiological mechanisms of liver injury in COVID-19. *Liver Int* 2021; **41**: 20-32 [PMID: 33190346 DOI: 10.1111/liv.14730]

70 **Hamming I**, Timens W, Bulthuis ML, Lely AT, Navis G, van Goor H. Tissue distribution of ACE2 protein, the functional receptor for SARS coronavirus. A first step in understanding SARS pathogenesis. *J Pathol* 2004; **203**: 631-637 [PMID: 15141377 DOI: 10.1002/path.1570]

71 **Kumar P**, Sharma M, Kulkarni A, Rao PN. Pathogenesis of Liver Injury in Coronavirus Disease 2019. *J Clin Exp Hepatol* 2020; **10**: 641-642 [PMID: 32837092 DOI: 10.1016/j.jceh.2020.05.006]

72 **Zhao CL**, Rapkiewicz A, Maghsoodi-Deerwester M, Gupta M, Cao W, Palaia T, Zhou J, Ram B, Vo D, Rafiee B, Hossein-Zadeh Z, Dabiri B, Hanna I. Pathological findings in the postmortem liver of patients with coronavirus disease 2019 (COVID-19). *Hum Pathol* 2021; **109**: 59-68 [PMID: 33307078 DOI: 10.1016/j.humpath.2020.11.015]

73 **Xu Z**, Shi L, Wang Y, Zhang J, Huang L, Zhang C, Liu S, Zhao P, Liu H, Zhu L, Tai Y, Bai C, Gao T, Song J, Xia P, Dong J, Zhao J, Wang FS. Pathological findings of COVID-19 associated with acute respiratory distress syndrome. *Lancet Respir Med* 2020; **8**: 420-422 [PMID: 32085846 DOI: 10.1016/S2213-2600(20)30076-X]

74 **Ibrahim N**, Hosri J, Bteich Y, Dib A, Abou Rached A. COVID-19 and Liver Dysfunction. *Cureus* 2022; **14**: e21302 [PMID: 35186564 DOI: 10.7759/cureus.21302]

75 **Cai Q**, Huang D, Yu H, Zhu Z, Xia Z, Su Y, Li Z, Zhou G, Gou J, Qu J, Sun Y, Liu Y, He Q, Chen J, Liu L, Xu L. COVID-19: Abnormal liver function tests. *J Hepatol* 2020; **73**: 566-574 [PMID: 32298767 DOI: 10.1016/j.jhep.2020.04.006]

76 **Săbiescu DM**, Kamal AM, Kamal CK, Alexandru DO, Mitruț P. Liver damage in the context of SARS-CoV-2. Covid-19 treatment and its effects on the liver. *J Med Life* 2022; **15**: 727-734 [PMID: 35928369 DOI: 10.25122/jml-2022-0177]

77 **Tokarczyk U**, Kaliszewski K, Kopszak A, Nowak Ł, Sutkowska-Stępień K, Sroczyński M, Sępek M, Dudek A, Diakowska D, Trocha M, Gajecki D, Gawryś J, Matys T, Maciejiczek J, Kozub V, Szalast R, Madziarski M, Zubkiewicz-Zarębska A, Letachowicz K, Kiliś-Pstrusińska K, Matera-Witkiewicz A, Pomorski M, Protasiewicz M, Sokołowski J, Adamik B, Kujawa K, Doroszko A, Madziarska K, Jankowska EA. Liver Function Tests in COVID-19: Assessment of the Actual Prognostic Value. *J Clin Med* 2022; **11** [PMID: 35956107 DOI: 10.3390/jcm11154490]

78 **Phipps MM**, Barraza LH, LaSota ED, Sobieszczyk ME, Pereira MR, Zheng EX, Fox AN, Zucker J, Verna EC. Acute Liver Injury in COVID-19: Prevalence and Association with Clinical Outcomes in a Large U.S. Cohort. *Hepatology* 2020; **72**: 807-817 [PMID: 32473607 DOI: 10.1002/hep.31404]

79 **Da BL**, Kushner T, El Halabi M, Paka P, Khalid M, Uberoi A, Lee BT, Perumalswami PV, Rutledge SM, Schiano TD, Friedman SL, Saberi B. Liver Injury in Patients Hospitalized with Coronavirus Disease 2019 Correlates with Hyperinflammatory Response and Elevated Interleukin-6. *Hepatol Commun* 2021; **5**: 177-188 [PMID: 33230491 DOI: 10.1002/hep4.1631]

80 **Pazgan-Simon M**, Serafińska S, Kukla M, Kucharska M, Zuwała-Jagiełło J, Buczyńska I, Zielińska K, Simon K. Liver Injury in Patients with COVID-19 without Underlying Liver Disease. *J Clin Med* 2022; **11** [PMID: 35054003 DOI: 10.3390/jcm11020308]

81 **Singh S**, Khan A. Clinical Characteristics and Outcomes of Coronavirus Disease 2019 Among Patients With Preexisting Liver Disease in the United States: A Multicenter Research Network Study. *Gastroenterology* 2020; **159**: 768-771.e3 [PMID: 32376408 DOI: 10.1053/j.gastro.2020.04.064]

82 **Wang Q**, Davis PB, Xu R. COVID-19 risk, disparities and outcomes in patients with chronic liver disease in the United States. *EClinicalMedicine* 2021; **31**: 100688 [PMID: 33521611 DOI: 10.1016/j.eclinm.2020.100688]

83 **Iavarone M**, D'Ambrosio R, Soria A, Triolo M, Pugliese N, Del Poggio P, Perricone G, Massironi S, Spinetti A, Buscarini E, Viganò M, Carriero C, Fagiuoli S, Aghemo A, Belli LS, Lucà M, Pedaci M, Rimondi A, Rumi MG, Invernizzi P, Bonfanti P, Lampertico P. High rates of 30-day mortality in patients with cirrhosis and COVID-19. *J Hepatol* 2020; **73**: 1063-1071 [PMID: 32526252 DOI: 10.1016/j.jhep.2020.06.001]

84 **Mallet V**, Beeker N, Bouam S, Sogni P, Pol S; Demosthenes research group. Prognosis of French COVID-19 patients with chronic liver disease: A national retrospective cohort study for 2020. *J Hepatol* 2021; **75**: 848-855 [PMID: 33992699 DOI: 10.1016/j.jhep.2021.04.052]

85 **Mohammed A**, Paranji N, Chen PH, Niu B. COVID-19 in Chronic Liver Disease and Liver Transplantation: A Clinical Review. *J Clin Gastroenterol* 2021; **55**: 187-194 [PMID: 33394628 DOI: 10.1097/MCG.0000000000001481]

86 **Magro F**, Nuzzo A, Abreu C, Libânio D, Rodriguez-Lago I, Pawlak K, Hollenbach M, Brouwer WP, Siau K. COVID-19 in gastroenterology: Where are we now? Current evidence on the impact of COVID-19 in gastroenterology. *United European Gastroenterol J* 2021; **9**: 750-765 [PMID: 34190413 DOI: 10.1002/ueg2.12115]

87 **Ekpanyapong S**, Bunchorntavakul C, Reddy KR. COVID-19 and the Liver: Lessons Learnt from the EAST and the WEST, A Year Later. *J Viral Hepat* 2022; **29**: 4-20 [PMID: 34352133 DOI: 10.1111/jvh.13590]

88 **Hoffmann C**, Gerber PA, Cavelti-Weder C, Licht L, Kotb R, Al Dweik R, Cherfane M, Bornstein SR, Perakakis N. Liver, NAFLD and COVID-19. *Horm Metab Res* 2022; **54**: 522-531 [PMID: 35468630 DOI: 10.1055/a-1834-9008]

89 **Boettler T**, Newsome PN, Mondelli MU, Maticic M, Cordero E, Cornberg M, Berg T. Care of patients with liver disease during the COVID-19 pandemic: EASL-ESCMID position paper. *JHEP Rep* 2020; **2**: 100113 [PMID: 32289115 DOI: 10.1016/j.jhepr.2020.100113]

90 **Sachdeva S**, Khandait H, Kopel J, Aloysius MM, Desai R, Goyal H. NAFLD and COVID-19: a Pooled Analysis. *SN Compr Clin Med* 2020; **2**: 2726-2729 [PMID: 33173850 DOI: 10.1007/s42399-020-00631-3]

91 **Berenguer J**, Ryan P, Rodríguez-Baño J, Jarrín I, Carratalà J, Pachón J, Yllescas M, Arriba JR; COVID-19@Spain Study Group; Fundación SEIMC-GESIDA; Hospital General Universitario Gregorio Marañón; Hospital Universitario La Paz; Hospital Infanta Leonor; Complejo

Hospitalario Virgen de la Salud; Hospital Universitario Rafael Méndez; Hospital Universitario de Cruces; Hospital de Melilla; Hospital San Eloy de Barakaldo; Hospital Universitario Central de Asturias; Hospital General Universitario de Alicante; Hospital Virgen de la Victoria; Hospital Universitario Puerto Real; EOXI Pontevedra e Salnés; Hospital de Figueres; Hospital Sant Jaume de Calella; Hospital del Mar; Hospital Virgen de la Arrixaca; Hospital de Can Misses; Hospital de Sagunto; Hospital Clínico San Cecilio; Hospital Universitario Príncipe de Asturias; Parc Sanitari Sant Joan de Déu; Hospital Nuestra Señora de Gracia; HC Marbella Internacional Hospital; Hospital La Princesa; Hospital Josep Trueta; Hospital Dos de Maig; Hospital Arnau de Vilanova-Lliria; Hospital General Universitario de Elche; Hospital Clínico Universitario de Valencia; Complejo Asistencial de Ávila; Hospital Comarcal de Alcañiz; Hospital Universitario Marqués de Valdecilla; Hospital Quiron-Salud de Torrevieja; Hospital Universitario Miguel Servet; SCIAS, Hospital de Barcelona; Fundación Hospital Universitario Alcorcón; Hospital Álvaro Cunqueiro; Complejo Asistencial Universitario de Salamanca; Hospital Universitario Severo Ochoa; Hospital CIMA-Sanitas; Hospital HLA Inmaculada; Hospital Universitario Rio Hortega; Hospital de Guadalajara; Hospital Universitario Infanta Sofía; Hospital Comarcal de Blanes; Hospital Universitari de Tarragona Joan XXIII; Hospital Universitario Basurto; Hospital Universitario de Canarias; Hospital Universitario de Gran Canaria Dr Negrín; Hospital Son Espases; Hospital Universitario de Móstoles; Complejo Hospitalario Universitario A Coruña; Hospital Costa del Sol; Hospital Clínico Universitario Lozano Blesa; Hospital Mutua de Terrassa; Hospital de la Plana; Hospital Virgen de la Concha–Complejo Asistencial de Zamora; Complejo Hospitalario Universitario Insular Materno-Infantil; Hospital de la Marina Baixa; Hospital Universitario Virgen Macarena; Hospital Universitari de Bellvitge; Hospital Universitario y Politécnico la Fe; Hospital Universitario del Vinalopó; Hospital de Sabadell (Parc Tauli); Hospital Clinic de Barcelona; Hospital Universitario de la Ribera; Fundación Jiménez Díaz; Hospital Clínico Universitario de Valladolid; Hospital Clínico San Carlos; Hospital Santa Creu i Sant Pau; Clínica Universitaria de Navarra–Campus Madrid; Hospital Son Llatzer; Hospital General de la Defensa Gómez Ulla; Hospital Universitario de Álava; Hospital Santos Reyes; Hospital Dr José Molina Orosa; Hospital Vall d'Hebrón; Hospital Universitario Rey Juan Carlos; Complejo Hospitalario Universitario Santa Lucía; Hospital Santa Bárbara; Complejo Hospitalario Universitario de Ferrol; Hospital de l'Esperit Sant; Hospital Universitario los Arcos del Mar Menor; Hospital HLA Universitario Moncloa; Hospital Virgen del Puerto; Hospital Marina Salud de Dénia; Hospital Universitario de Jerez; Hospital Reina Sofía de Tudela; Hospital Clínico Universitario de Santiago de Compostela; Hospital Universitario del Henares; Hospital Universitario Lucus Augusti; Hospital de Donostia; Hospital de Urduliz Alfredo Espinosa; Hospital de Mendaro; Hospital Juan Ramón Jiménez; Hospital de Tortosa Virgen de la Cinta; Hospital Riotinto; Hospital Vega Baja; Hospital Puerta de Hierro; Hospital Universitario de Getafe; Hospital General de la Palma; Hospital El Bierzo; Fundación Hospital de Calahorra; Hospital Alto Deba; Hospital Universitario San Juan de Alicante; Hospital de Guadarrama; Hospital Universitario de Jaén; Hospital de Mataró; Hospital de Palamós; Hospital Universitario de Valme; Clínica Universitaria de Navarra–Campus Navarra; Hospital Clínica Benidorm; Hospital Doce de Octubre; Hospital Universitario Virgen del Rocío; Hospital Universitario Ramón y Cajal; Hospital Universitario San Pedro; Hospital Quirón A Coruña; HM Sanchinarro; Hospital Francesc de Borja; Complejo Hospitalario Universitario Nuestra Señora de La Candelaria; Hospital Universitario HM Montepríncipe; Hospital Universitario HM Puerta del Sur; Hospital Universitario HM Torrelodones; Hospital Universitario HM Madrid; Hospital Don Benito-Villanueva de la Serena; Hospital de Viladecans; Centro Nacional de Epidemiología. Characteristics and predictors of death among 4035 consecutively hospitalized patients with COVID-19 in Spain. *Clin Microbiol Infect* 2020; **26**: 1525-1536 [PMID: 32758659 DOI: 10.1016/j.cmi.2020.07.024]

92 **Marjot T**, Moon AM, Cook JA, Abd-Elsalam S, Aloman C, Armstrong MJ, Pose E, Brenner EJ, Cargill T, Catana MA, Dhanasekaran R, Eshraghian A, García-Juárez I, Gill US, Jones PD, Kennedy J, Marshall A, Matthews C, Mells G, Mercer C, Perumalswami PV, Avitabile E, Qi X, Su F, Ufere NN, Wong YJ, Zheng MH, Barnes E, Barritt AS 4th, Webb GJ. Outcomes following SARS-CoV-2 infection in patients with chronic liver disease: An international registry study. *J Hepatol* 2021; **74**: 567-577 [PMID: 33035628 DOI: 10.1016/j.jhep.2020.09.024]

93 **Karcz M**, Bankey B, Schwaiberger D, Lachmann B, Papadakos PJ. Acute respiratory failure complicating advanced liver disease. *Semin Respir Crit Care Med* 2012; **33**: 96-110 [PMID: 22447264 DOI: 10.1055/s-0032-1301738]

94 **Jeon D**, Son M, Choi J. Impact of liver cirrhosis on the clinical outcomes of patients with COVID-19: a nationwide cohort study of Korea. *Korean J Intern Med* 2021; **36**: 1092-1101 [PMID: 34399573 DOI: 10.3904/kjim.2020.486]

95 **Choi J**, Han S, Kim N, Lim YS. Increasing burden of liver cancer despite extensive use of antiviral agents in a hepatitis B virus-endemic population. *Hepatology* 2017; **66**: 1454-1463 [PMID: 28628942 DOI: 10.1002/hep.29321]

96 **Kim D**, Adeniji N, Latt N, Kumar S, Bloom PP, Aby ES, Perumalswami P, Roytman M, Li M, Vogel AS, Catana AM, Wegermann K, Carr RM, Aloman C, Chen VL, Rabiee A, Sadowski B, Nguyen V, Dunn W, Chavin KD, Zhou K, Lizaola-Mayo B, Moghe A, Debes J, Lee TH, Branch AD, Viveiros K, Chan W, Chascsa DM, Kwo P, Dhanasekaran R. Predictors of Outcomes of COVID-19 in Patients With Chronic Liver Disease: US Multi-center Study. *Clin Gastroenterol Hepatol* 2021; **19**: 1469-1479.e19 [PMID: 32950749 DOI: 10.1016/j.cgh.2020.09.027]

97 **Ghazanfar H**, Kandhi S, Shin D, Muthumanickam A, Gurjar H, Qureshi ZA, Shaban M, Farag M, Haider A, Budhathoki P, Bhatt T, Ghazanfar A, Jyala A, Patel H. Impact of COVID-19 on the Gastrointestinal Tract: A Clinical Review. *Cureus* 2022; **14**: e23333 [PMID: 35464519 DOI: 10.7759/cureus.23333]

98 **Olry A**, Meunier L, Délire B, Larrey D, Horsmans Y, Le Louët H. Drug-Induced Liver Injury and COVID-19 Infection: The Rules Remain the Same. *Drug Saf* 2020; **43**: 615-617 [PMID: 32514859 DOI: 10.1007/s40264-020-00954-z]

99 **Kelly M**, O'Connor R, Townsend L, Coghlan M, Relihan E, Moriarty M, Carr B, Melanophy G, Doyle C, Bannan C, O'Riordan R, Merry C, Clarke S, Bergin C. Clinical outcomes and adverse events in patients hospitalised with COVID-19, treated with off-label hydroxychloroquine and azithromycin. *Br J Clin Pharmacol* 2021; **87**: 1150-1154 [PMID: 32687645 DOI: 10.1111/bcp.14482]

100 **Zhai G**, Li M, Wang Y, Wu J. Drug-Induced Liver Disturbance During the Treatment of COVID-19. *Front Pharmacol* 2021; **12**: 719308 [PMID: 34483929 DOI: 10.3389/fphar.2021.719308]

101 **Zampino R**, Mele F, Florio LL, Bertolino L, Andini R, Galdo M, De Rosa R, Corcione A, Durante-Mangoni E. Liver injury in remdesivir-treated COVID-19 patients. *Hepatol Int* 2020; **14**: 881-883 [PMID: 32725454 DOI: 10.1007/s12072-020-10077-3]

102 **Serviddio G**, Villani R, Stallone G, Scioscia G, Foschino-Barbaro MP, Lacedonia D. Tocilizumab and liver injury in patients with COVID-19. *Therap Adv Gastroenterol* 2020; **13**: 1756284820959183 [PMID: 33101458 DOI: 10.1177/1756284820959183]

103 **Teschke R**, Méndez-Sánchez N, Eickhoff A. Liver Injury in COVID-19 Patients with Drugs as Causatives: A Systematic Review of 996 DILI Cases Published 2020/2021 Based on RUCAM as Causality Assessment Method. *Int J Mol Sci* 2022; **23** [PMID: 35563242 DOI: 10.3390/ijms23094828]

104 **Stine JG**, Sateesh P, Lewis JH. Drug-induced liver injury in the elderly. *Curr Gastroenterol Rep* 2013; **15**: 299 [PMID: 23250699 DOI: 10.1007/s11894-012-0299-8]

105 **Gao S**, Yang Q, Wang X, Hu W, Lu Y, Yang K, Jiang Q, Li W, Song H, Sun F, Cheng H. Association Between Drug Treatments and the Incidence of Liver Injury in Hospitalized Patients With COVID-19. *Front Pharmacol* 2022; **13**: 799338 [PMID: 35387350 DOI: 10.3389/fphar.2022.799338]

106 **Sargiacomo C**, Sotgia F, Lisanti MP. COVID-19 and chronological aging: senolytics and other anti-aging drugs for the treatment or prevention of corona virus infection? *Aging (Albany NY)* 2020; **12**: 6511-6517 [PMID: 32229706 DOI: 10.18632/aging.103001]

107 **Yadav DK**, Singh A, Zhang Q, Bai X, Zhang W, Yadav RK, Zhiwei L, Adhikari VP, Liang T. Involvement of liver in COVID-19: systematic review and meta-analysis. *Gut* 2021; **70**: 807-809 [PMID: 32669289 DOI: 10.1136/gutjnl-2020-322072]

108 **Khateri S**, Mohammadi H, Khateri R, Moradi Y. The Prevalence of Underlying Diseases and Comorbidities in COVID-19 Patients; an Updated Systematic Review and Meta-analysis. *Arch Acad Emerg Med* 2020; **8**: e72 [PMID: 33134968]

109 **Spearman CW**, Aghemo A, Valenti L, Sonderup MW. COVID-19 and the liver: A 2021 update. *Liver Int* 2021; **41**: 1988-1998 [PMID: 34152690 DOI: 10.1111/liv.14984]

110 **Metawea MI**, Yousif WI, Moheb I. COVID 19 and liver: An A-Z literature review. *Dig Liver Dis* 2021; **53**: 146-152 [PMID: 32988758 DOI: 10.1016/j.dld.2020.09.010]

111 **Ji D**, Qin E, Xu J, Zhang D, Cheng G, Wang Y, Lau G. Non-alcoholic fatty liver diseases in patients with COVID-19: A retrospective study. *J Hepatol* 2020; **73**: 451-453 [PMID: 32278005 DOI: 10.1016/j.jhep.2020.03.044]

112 **Zhou YJ**, Zheng KI, Wang XB, Sun QF, Pan KH, Wang TY, Ma HL, Chen YP, George J, Zheng MH. Metabolic-associated fatty liver disease is associated with severity of COVID-19. *Liver Int* 2020; **40**: 2160-2163 [PMID: 32573883 DOI: 10.1111/liv.14575]

113 **Hartl L**, Haslinger K, Angerer M, Jachs M, Simbrunner B, Bauer DJM, Semmler G, Scheiner B, Eigenbauer E, Strassl R, Breuer M, Kimberger O, Laxar D, Trauner M, Mandorfer M, Reiberger T. Age-adjusted mortality and predictive value of liver chemistries in a Viennese cohort of COVID-19 patients. *Liver Int* 2022; **42**: 1297-1307 [PMID: 35412018 DOI: 10.1111/liv.15274]

114 **Ge J**, Pletcher MJ, Lai JC; N3C Consortium. Outcomes of SARS-CoV-2 Infection in Patients With Chronic Liver Disease and Cirrhosis: A National COVID Cohort Collaborative Study. *Gastroenterology* 2021; **161**: 1487-1501.e5 [PMID: 34284037 DOI: 10.1053/j.gastro.2021.07.010]

115 **Ioannou GN**, Liang PS, Locke E, Green P, Berry K, O'Hare AM, Shah JA, Crothers K, Eastment MC, Fan VS, Dominitz JA. Cirrhosis and Severe Acute Respiratory Syndrome Coronavirus 2 Infection in US Veterans: Risk of Infection, Hospitalization, Ventilation, and Mortality. *Hepatology* 2021; **74**: 322-335 [PMID: 33219546 DOI: 10.1002/hep.31649]

116 **Brozat JF**, Hanses F, Haelberger M, Stecher M, Dreher M, Tometten L, Ruethrich MM, Vehreschild JJ, Trautwein C, Borgmann S, Vehreschild MJGT, Jakob CEM, Stallmach A, Wille K, Hellwig K, Isberner N, Reuken PA, Geisler F, Nattermann J, Bruns T; LEOSS study group. COVID-19 mortality in cirrhosis is determined by cirrhosis-associated comorbidities and extrahepatic organ failure: Results from the multinational LEOSS registry. *United European Gastroenterol J* 2022; **10**: 409-424 [PMID: 35482663 DOI: 10.1002/ueg2.12232]

117 **Kandasamy S**. An unusual presentation of COVID-19: Acute pancreatitis. *Ann Hepatobiliary Pancreat Surg* 2020; **24**: 539-541 [PMID: 33234760 DOI: 10.14701/ahbps.2020.24.4.539]

118 **Schepis T**, Larghi A, Papa A, Miele L, Panzuto F, De Biase L, Annibale B, Cattani P, Rapaccini GL. SARS-CoV2 RNA detection in a pancreatic pseudocyst sample. *Pancreatology* 2020; **20**: 1011-1012 [PMID: 32498972 DOI: 10.1016/j.pan.2020.05.016]

119 **Aday U**, Gedik E, Kafadar MT, Özbek E. Acute Necrotizing Pancreatitis and Coronavirus Disease-2019 (COVID-19). *Korean J Gastroenterol* 2021; **78**: 353-358 [PMID: 34955513 DOI: 10.4166/kjg.2021.131]

120 **Tsai PH**, Lai WY, Lin YY, Luo YH, Lin YT, Chen HK, Chen YM, Lai YC, Kuo LC, Chen SD, Chang KJ, Liu CH, Chang SC, Wang FD, Yang YP. Clinical manifestation and disease progression in COVID-19 infection. *J Chin Med Assoc* 2021; **84**: 3-8 [PMID: 33230062 DOI: 10.1097/JCMA.0000000000000463]

121 **Khunti K**, Del Prato S, Mathieu C, Kahn SE, Gabbay RA, Buse JB. COVID-19, Hyperglycemia, and New-Onset Diabetes. *Diabetes Care* 2021; **44**: 2645-2655 [PMID: 34625431 DOI: 10.2337/dc21-1318]

122 **Wang F**, Wang H, Fan J, Zhang Y, Zhao Q. Pancreatic Injury Patterns in Patients With Coronavirus Disease 19 Pneumonia. *Gastroenterology* 2020; **159**: 367-370 [PMID: 32247022 DOI: 10.1053/j.gastro.2020.03.055]

123 **Samanta J**, Gupta R, Singh MP, Patnaik I, Kumar A, Kochhar R. Coronavirus disease 2019 and the pancreas. *Pancreatology* 2020; **20**: 1567-1575 [PMID: 33250089 DOI: 10.1016/j.pan.2020.10.035]

124 **Bruno G**, Fabrizio C, Santoro CR, Buccoliero GB. Pancreatic injury in the course of coronavirus disease 2019: A not-so-rare occurrence. *J Med Virol* 2021; **93**: 74-75 [PMID: 32497298 DOI: 10.1002/jmv.26134]

125 **Liu F**, Long X, Zhang B, Zhang W, Chen X, Zhang Z. ACE2 Expression in Pancreas May Cause Pancreatic Damage After SARS-CoV-2 Infection. *Clin Gastroenterol Hepatol* 2020; **18**: 2128-2130.e2 [PMID: 32334082 DOI: 10.1016/j.cgh.2020.04.040]

126 **Stephens JR**, Wong JLC, Broomhead R, Stümpfle R, Waheed U, Patel P, Brett SJ, Soni S. Raised serum amylase in patients with COVID-19 may not be associated with pancreatitis. *Br J Surg* 2021; **108**: e152-e153 [PMID: 33793756 DOI: 10.1093/bjs/znaa168]

127 **Akkus C**, Yilmaz H, Mizrak S, Adibelli Z, Akdas O, Duran C. Development of pancreatic injuries in the course of COVID-19. *Acta Gastroenterol Belg* 2020; **83**: 585-592 [PMID: 33321015]

128 **McNabb-Baltar J**, Jin DX, Grover AS, Redd WD, Zhou JC, Hathorn KE, McCarty TR, Bazarbashi AN, Shen L, Chan WW. Lipase Elevation in Patients With COVID-19. *Am J Gastroenterol* 2020; **115**: 1286-1288 [PMID: 32496339 DOI: 10.14309/ajg.0000000000000732]

129 **Bansal P**, Margekar SL, Suman V, Sud R, Meena S, Sharma AK, Islam SY, Gurtoo A, Agrawal A, Pangtey GS, Prakash A. Pancreatic Injury in COVID-19 Patients. *J Assoc Physicians India* 2020; **68**: 58-60 [PMID: 33247644]

130 **Rasch S**, Herner A, Schmid RM, Huber W, Lahmer T. High lipasemia is frequent in Covid-19 associated acute respiratory distress syndrome. *Pancreatology* 2021; **21**: 306-311 [PMID: 33277183 DOI: 10.1016/j.pan.2020.11.023]

131 **Barlass U**, Wiliams B, Dhana K, Adnan D, Khan SR, Mahdavinia M, Bishehsari F. Marked Elevation of Lipase in COVID-19 Disease: A Cohort Study. *Clin Transl Gastroenterol* 2020; **11**: e00215 [PMID: 32764201 DOI: 10.14309/ctg.0000000000000215]

132 **Bacaksız F**, Ebik B, Ekin N, Kılıc J. Pancreatic damage in COVID-19: Why? *Int J Clin Pract* 2021; **75**: e14692 [PMID: 34331821 DOI: 10.1111/ijcp.14692]

133 **Hunt RH**, East JE, Lanas A, Malfertheiner P, Satsangi J, Scarpignato C, Webb GJ. COVID-19 and Gastrointestinal Disease: Implications for the Gastroenterologist. *Dig Dis* 2021; **39**: 119-139 [PMID: 33040064 DOI: 10.1159/000512152]

134 **Singh RR**, Chhabra P, Kumta NA. Does Hyperlipasemia Predict Worse Clinical Outcomes in COVID-19? A Multicenter Retrospective Cohort Study. *J Clin Gastroenterol* 2022; **56**: e227-e231 [PMID: 34294655 DOI: 10.1097/MCG.0000000000001590]

135 **Inamdar S**, Benias PC, Liu Y, Sejpal DV, Satapathy SK, Trindade AJ; Northwell COVID-19 Research Consortium. Prevalence, Risk Factors, and Outcomes of Hospitalized Patients With Coronavirus Disease 2019 Presenting as Acute Pancreatitis. *Gastroenterology* 2020; **159**: 2226-2228.e2 [PMID: 32860787 DOI: 10.1053/j.gastro.2020.08.044]

136 **Karaali R**, Topal F. Evaluating the effect of SARS-Cov-2 infection on prognosis and mortality in patients with acute pancreatitis. *Am J Emerg*

Med 2021; **49**: 378-384 [PMID: 34246968 DOI: 10.1016/j.ajem.2021.06.045]
137 **Dirweesh A**, Li Y, Trikudanathan G, Mallery JS, Freeman ML, Amateau SK. Clinical Outcomes of Acute Pancreatitis in Patients With Coronavirus Disease 2019. *Gastroenterology* 2020; **159**: 1972-1974 [PMID: 32721439 DOI: 10.1053/j.gastro.2020.07.038]
138 **Pandanaboyana S**, Moir J, Leeds JS, Oppong K, Kanwar A, Marzouk A, Belgaumkar A, Gupta A, Siriwardena AK, Haque AR, Awan A, Balakrishnan A, Rawashdeh A, Ivanov B, Parmar C, M Halloran C, Caruana C, Borg CM, Gomez D, Damaskos D, Karavias D, Finch G, Ebied H, K Pine J, R A Skipworth J, Milburn J, Latif J, Ratnam Apollos J, El Kafsi J, Windsor JA, Roberts K, Wang K, Ravi K, V Coats M, Hollyman M, Phillips M, Okocha M, Sj Wilson M, A Ameer N, Kumar N, Shah N, Lapolla P, Magee C, Al-Sarireh B, Lunevicius R, Benhmida R, Singhal R, Balachandra S, Demirli Atıcı S, Jaunoo S, Dwerryhouse S, Boyce T, Charalampakis V, Kanakala V, Abbas Z, Nayar M; COVID PAN collaborative group. SARS-CoV-2 infection in acute pancreatitis increases disease severity and 30-day mortality: COVID PAN collaborative study. *Gut* 2021; **70**: 1061-1069 [PMID: 33547182 DOI: 10.1136/gutjnl-2020-323364]
139 **Ye C**, Zhang S, Zhang X, Cai H, Gu J, Lian J, Lu Y, Jia H, Hu J, Jin C, Yu G, Zhang Y, Sheng J, Yang Y. Impact of comorbidities on patients with COVID-19: A large retrospective study in Zhejiang, China. *J Med Virol* 2020; **92**: 2821-2829 [PMID: 32543710 DOI: 10.1002/jmv.26183]
140 **Miró Ò**, Llorens P, Jiménez S, Piñera P, Burillo-Putze G, Martín A, Martín-Sánchez FJ, Lamberechts J, Alquézar-Arbé A, Jacob J, Noceda J, Cano Cano MJ, Fortuny Bayarri MJ, Marín Porrino JM, Meléndez N, Pérez García C, Brasó Aznar JV, Ponce MC, Díaz Fernández E, Ejarque Martínez L, Peiró Gómez A, Tost J, Domínguez MJ, Teigell Muñoz FJ, González Del Castillo J; Spanish Investigators on Emergency Situations TeAm (SIESTA) network. A case-control emergency department-based analysis of acute pancreatitis in Covid-19: Results of the UMC-19-S(6). *J Hepatobiliary Pancreat Sci* 2021; **28**: 953-966 [PMID: 33259695 DOI: 10.1002/jhbp.873]
141 **Akarsu C**, Karabulut M, Aydin H, Sahbaz NA, Dural AC, Yegul D, Peker KD, Ferahman S, Bulut S, Dönmez T, Asar S, Yasar KK, Adas GT. Association between Acute Pancreatitis and COVID-19: Could Pancreatitis Be the Missing Piece of the Puzzle about Increased Mortality Rates? *J Invest Surg* 2022; **35**: 119-125 [PMID: 33138658 DOI: 10.1080/08941939.2020.1833263]
142 **Huang BZ**, Sidell MA, Wu BU, Setiawan VW, Chen Z, Xiang AH. Pre-Existing Pancreatitis and Elevated Risks of COVID-19 Severity and Mortality. *Gastroenterology* 2022; **162**: 1758-1760.e3 [PMID: 35149034 DOI: 10.1053/j.gastro.2022.02.005]
143 **Hadi Y**, Shah-Khan SM, Sohail AH, Jannat FRU, Syed A, Humphries CE, Daum TL, Malik A, Krafft MR, Bilal M, Thakkar S, Singh S. Su1270: Chronic pancreatitis and COVID-19: Incidence and outcomes. A multicenter research network analysis. *Gastroenterology* 2022; **162**: S564-S565
144 **Georgakopoulou VE**, Gkoufa A, Garmpis N, Makrodimitri S, Papageorgiou CV, Barlampa D, Garmpi A, Chiapoutakis S, Sklapani P, Trakas N, Damaskos C. COVID-19 and Acute Pancreatitis: A Systematic Review of Case Reports and Case Series. *Ann Saudi Med* 2022; **42**: 276-287 [PMID: 35933608 DOI: 10.5144/0256-4947.2022.276]
145 **Xin MJ**, Chen H, Luo B, Sun JB. Severe acute pancreatitis in the elderly: etiology and clinical characteristics. *World J Gastroenterol* 2008; **14**: 2517-2521 [PMID: 18442198 DOI: 10.3748/wjg.14.2517]
146 **Kara B**, Olmez S, Yalcın MS, Tas A, Ozturk NA, Sarıtaş B. Update on the effect of age on acute pancreatitis morbidity: a retrospective, single-center study. *Prz Gastroenterol* 2018; **13**: 223-227 [PMID: 30302167 DOI: 10.5114/pg.2018.75677]
147 **Quero G**, Covino M, Fiorillo C, Rosa F, Menghi R, Simeoni B, Potenza A, Ojetti V, Alfieri S, Franceschi F. Acute pancreatitis in elderly patients: a single-center retrospective evaluation of clinical outcomes. *Scand J Gastroenterol* 2019; **54**: 492-498 [PMID: 30905212 DOI: 10.1080/00365521.2019.1588369]
148 **Yu B**, Li N, Li J, Wan J, He W, Zhu Y, Lu N. The Clinical Characteristics of Acute Pancreatitis in Gerontal Patients: A Retrospective Study. *Clin Interv Aging* 2020; **15**: 1541-1553 [PMID: 32982192 DOI: 10.2147/CIA.S259920]
149 **Márta K**, Lazarescu AM, Farkas N, Mátrai P, Cazacu I, Ottóffy M, Habon T, Erőss B, Vincze À, Veres G, Czakó L, Sarlós P, Rakonczay Z, Hegyi P. Aging and Comorbidities in Acute Pancreatitis I: A Meta-Analysis and Systematic Review Based on 194,702 Patients. *Front Physiol* 2019; **10**: 328 [PMID: 31001131 DOI: 10.3389/fphys.2019.00328]
150 **Bulthuis MC**, Boxhoorn L, Beudel M, Elbers PWG, Kop MPM, van Wanrooij RLJ, Besselink MG, Voermans RP. Acute pancreatitis in COVID-19 patients: true risk? *Scand J Gastroenterol* 2021; **56**: 585-587 [PMID: 33715577 DOI: 10.1080/00365521.2021.1896776]
151 **Meyers MH**, Main MJ, Orr JK, Obstein KL. A Case of COVID-19-Induced Acute Pancreatitis. *Pancreas* 2020; **49**: e108-e109 [PMID: 33122538 DOI: 10.1097/MPA.0000000000001696]
152 **Karimzadeh S**, Manzuri A, Ebrahimi M, Huy NT. COVID-19 presenting as acute pancreatitis: Lessons from a patient in Iran. *Pancreatology* 2020; **20**: 1024-1025 [PMID: 32576441 DOI: 10.1016/j.pan.2020.06.003]
153 **Gadiparthi C**, Mohapatra S, Kanna S, Vykuntam V, Chen W. Acute pancreatitis in a patient with COVID-19: a case report. *Transl Gastroenterol Hepatol* 2021; **6**: 65 [PMID: 34805587 DOI: 10.21037/tgh-20-234]
154 **Wifi MN**, Nabil A, Awad A, Eltatawy R. COVID-induced pancreatitis: case report. *Egypt J Intern Med* 2021; **33**: 10 [PMID: 33716498 DOI: 10.1186/s43162-021-00039-y]
155 **Gonzalo-Voltas A**, Uxia Fernández-Pérez-Torres C, Baena-Díez JM. Acute pancreatitis in a patient with COVID-19 infection. *Med Clin (Engl Ed)* 2020; **155**: 183-184 [PMID: 32835111 DOI: 10.1016/j.medcle.2020.05.010]
156 **Reick-Mitrisin V**, Mukhtar K, Khan ZH. Acute Pancreatitis in a Patient With Recent History of SARS-CoV-2 Infection. *Cureus* 2022; **14**: e29032 [PMID: 36237820 DOI: 10.7759/cureus.29032]
157 **Acherjya GK**, Rahman MM, Islam MT, Alam AS, Tarafder K, Ali M, Deb SR. Acute pancreatitis in a COVID-19 patient: An unusual presentation. *Clin Case Rep* 2020; **8**: 3400-3407 [PMID: 33363941 DOI: 10.1002/ccr3.3412]
158 **Alves AM**, Yvamoto EY, Marzinotto MAN, Teixeira ACS, Carrilho FJ. SARS-CoV-2 leading to acute pancreatitis: an unusual presentation. *Braz J Infect Dis* 2020; **24**: 561-564 [PMID: 32961108 DOI: 10.1016/j.bjid.2020.08.011]
159 **Shinohara T**, Otani A, Yamashita M, Wakimoto Y, Jubishi D, Okamoto K, Kanno Y, Ikeda M, Ishigaki K, Nakai Y, Harada S, Okugawa S, Koike K, Moriya K. Acute Pancreatitis During COVID-19 Pneumonia. *Pancreas* 2020; **49**: e106-e108 [PMID: 33122537 DOI: 10.1097/MPA.0000000000001695]
160 **Kumaran NK**, Karmakar BK, Taylor OM. Coronavirus disease-19 (COVID-19) associated with acute necrotising pancreatitis (ANP). *BMJ Case Rep* 2020; **13** [PMID: 32900752 DOI: 10.1136/bcr-2020-237903]
161 **Chen T**, Dai Z, Mo P, Li X, Ma Z, Song S, Chen X, Luo M, Liang K, Gao S, Zhang Y, Deng L, Xiong Y. Clinical Characteristics and Outcomes of Older Patients with Coronavirus Disease 2019 (COVID-19) in Wuhan, China: A Single-Centered, Retrospective Study. *J Gerontol A Biol Sci Med Sci* 2020; **75**: 1788-1795 [PMID: 32279081 DOI: 10.1093/gerona/glaa089]
162 **Imrie CW**. Prognosis of acute pancreatitis. *Ann Ital Chir* 1995; **66**: 187-189 [PMID: 7668494]

163 **Brikman S**, Denysova V, Menzal H, Dori G. Acute pancreatitis in a 61-year-old man with COVID-19. *CMAJ* 2020; **192**: E858-E859 [PMID: 32719021 DOI: 10.1503/cmaj.201029]

164 **Jena A**, James D, Singh AK, Dutta U, Sebastian S, Sharma V. Effectiveness and Durability of COVID-19 Vaccination in 9447 Patients With IBD: A Systematic Review and Meta-Analysis. *Clin Gastroenterol Hepatol* 2022; **20**: 1456-1479.e18 [PMID: 35189387 DOI: 10.1016/j.cgh.2022.02.030]

165 **Bhurwal A**, Mutneja H, Bansal V, Goel A, Arora S, Attar B, Minacapelli CD, Kochhar G, Chen LA, Brant S, Seril D. Effectiveness and safety of SARS-CoV-2 vaccine in Inflammatory Bowel Disease patients: a systematic review, meta-analysis and meta-regression. *Aliment Pharmacol Ther* 2022; **55**: 1244-1264 [PMID: 35355306 DOI: 10.1111/apt.16913]

166 **Kennedy NA**, Lin S, Goodhand JR, Chanchlani N, Hamilton B, Bewshea C, Nice R, Chee D, Cummings JF, Fraser A, Irving PM, Kamperidis N, Kok KB, Lamb CA, Macdonald J, Mehta S, Pollok RC, Raine T, Smith PJ, Verma AM, Jochum S, McDonald TJ, Sebastian S, Lees CW, Powell N, Ahmad T; Contributors to the CLARITY IBD study. Infliximab is associated with attenuated immunogenicity to BNT162b2 and ChAdOx1 nCoV-19 SARS-CoV-2 vaccines in patients with IBD. *Gut* 2021; **70**: 1884-1893 [PMID: 33903149 DOI: 10.1136/gutjnl-2021-324789]

167 **Lin S**, Kennedy NA, Saifuddin A, Sandoval DM, Reynolds CJ, Seoane RC, Kottoor SH, Pieper FP, Lin KM, Butler DK, Chanchlani N, Nice R, Chee D, Bewshea C, Janjua M, McDonald TJ, Sebastian S, Alexander JL, Constable L, Lee JC, Murray CD, Hart AL, Irving PM, Jones GR, Kok KB, Lamb CA, Lees CW, Altmann DM, Boyton RJ, Goodhand JR, Powell N, Ahmad T; CLARITY IBD study. Antibody decay, T cell immunity and breakthrough infections following two SARS-CoV-2 vaccine doses in inflammatory bowel disease patients treated with infliximab and vedolizumab. *Nat Commun* 2022; **13**: 1379 [PMID: 35296643 DOI: 10.1038/s41467-022-28517-z]

168 **McMahan K**, Yu J, Mercado NB, Loos C, Tostanoski LH, Chandrashekar A, Liu J, Peter L, Atyeo C, Zhu A, Bondzie EA, Dagotto G, Gebre MS, Jacob-Dolan C, Li Z, Nampanya F, Patel S, Pessaint L, Van Ry A, Blade K, Yalley-Ogunro J, Cabus M, Brown R, Cook A, Teow E, Andersen H, Lewis MG, Lauffenburger DA, Alter G, Barouch DH. Correlates of protection against SARS-CoV-2 in rhesus macaques. *Nature* 2021; **590**: 630-634 [PMID: 33276369 DOI: 10.1038/s41586-020-03041-6]

169 **Xu AM**, Li D, Ebinger JE, Mengesha E, Elyanow R, Gittelman RM, Chapman H, Joung S, Botwin GJ, Pozdnyakova V, Debbas P, Mujukian A, Prostko JC, Frias EC, Stewart JL, Horizon AA, Merin N, Sobhani K, Figueiredo JC, Cheng S, Kaplan IM, McGovern DPB, Merchant A, Melmed GY, Braun J. Differences in SARS-CoV-2 Vaccine Response Dynamics Between Class-I- and Class-II-Specific T-Cell Receptors in Inflammatory Bowel Disease. *Front Immunol* 2022; **13**: 880190 [PMID: 35464463 DOI: 10.3389/fimmu.2022.880190]

170 **Li D**, Xu A, Mengesha E, Elyanow R, Gittelman RM, Chapman H, Prostko JC, Frias EC, Stewart JL, Pozdnyakova V, Debbas P, Mujukian A, Horizon AA, Merin N, Joung S, Botwin GJ, Sobhani K, Figueiredo JC, Cheng S, Kaplan IM, McGovern DPB, Merchant A, Melmed GY, Braun J. The T-Cell Response to SARS-CoV-2 Vaccination in Inflammatory Bowel Disease is Augmented with Anti-TNF Therapy. *Inflamm Bowel Dis* 2022; **28**: 1130-1133 [PMID: 35397000 DOI: 10.1093/ibd/izac071]

171 **Tabesh E**, Soheilipour M, Rezaeisadrabadi M, Zare-Farashbandi E, Mousavi-Roknabadi RS. Comparison the effects and side effects of Covid-19 vaccination in patients with inflammatory bowel disease (IBD): a systematic scoping review. *BMC Gastroenterol* 2022; **22**: 393 [PMID: 35987619 DOI: 10.1186/s12876-022-02460-1]

172 **Botwin GJ**, Li D, Figueiredo J, Cheng S, Braun J, McGovern DPB, Melmed GY. Adverse Events After SARS-CoV-2 mRNA Vaccination Among Patients With Inflammatory Bowel Disease. *Am J Gastroenterol* 2021; **116**: 1746-1751 [PMID: 34047304 DOI: 10.14309/ajg.0000000000001342]

173 **Derhovanessian E**, Pawelec G. Vaccination in the elderly. *Microb Biotechnol* 2012; **5**: 226-232 [PMID: 21880118 DOI: 10.1111/j.1751-7915.2011.00283.x]

174 **Soiza RL**, Scicluna C, Thomson EC. Efficacy and safety of COVID-19 vaccines in older people. *Age Ageing* 2021; **50**: 279-283 [PMID: 33320183 DOI: 10.1093/ageing/afaa274]

175 **Collier DA**, Ferreira IATM, Kotagiri P, Datir RP, Lim EY, Touizer E, Meng B, Abdullahi A; CITIID-NIHR BioResource COVID-19 Collaboration, Elmer A, Kingston N, Graves B, Le Gresley E, Caputo D, Bergamaschi L, Smith KGC, Bradley JR, Ceron-Gutierrez L, Cortes-Acevedo P, Barcenas-Morales G, Linterman MA, McCoy LE, Davis C, Thomson E, Lyons PA, McKinney E, Doffinger R, Wills M, Gupta RK. Age-related immune response heterogeneity to SARS-CoV-2 vaccine BNT162b2. *Nature* 2021; **596**: 417-422 [PMID: 34192737 DOI: 10.1038/s41586-021-03739-1]

176 **Karamese M**, Tutuncu EE. The effectiveness of inactivated SARS-CoV-2 vaccine (CoronaVac) on antibody response in participants aged 65 years and older. *J Med Virol* 2022; **94**: 173-177 [PMID: 34427924 DOI: 10.1002/jmv.27289]

177 **Kappelman MD**, Weaver KN, Zhang X, Dai X, Watkins R, Adler J, Dubinsky MC, Kastl A, Bousvaros A, Strople JA, Cross RK, Higgins PDR, Ungaro RC, Bewtra M, Bellaguarda EA, Farraye FA, Boccieri ME, Firestine A, Chun KY, Fernando M, Bastidas M, Zikry M, Long MD. Factors Affecting Initial Humoral Immune Response to SARS-CoV-2 Vaccines Among Patients With Inflammatory Bowel Diseases. *Am J Gastroenterol* 2022; **117**: 462-469 [PMID: 35029167 DOI: 10.14309/ajg.0000000000001619]

178 **Classen JM**, Muzalyova A, Nagl S, Fleischmann C, Ebigbo A, Römmele C, Messmann H, Schnoy E. Antibody Response to SARS-CoV-2 Vaccination in Patients with Inflammatory Bowel Disease: Results of a Single-Center Cohort Study in a Tertiary Hospital in Germany. *Dig Dis* 2022; **40**: 719-727 [PMID: 34915480 DOI: 10.1159/000521343]

179 **Alexander JL**, Liu Z, Muñoz Sandoval D, Reynolds C, Ibraheim H, Anandabaskaran S, Saifuddin A, Castro Seoane R, Anand N, Nice R, Bewshea C, D'Mello A, Constable L, Jones GR, Balarajah S, Fiorentino F, Sebastian S, Irving PM, Hicks LC, Williams HRT, Kent AJ, Linger R, Parkes M, Kok K, Patel KV, Teare JP, Altmann DM, Goodhand JR, Hart AL, Lees CW, Boyton RJ, Kennedy NA, Ahmad T, Powell N; VIP study investigators. COVID-19 vaccine-induced antibody and T-cell responses in immunosuppressed patients with inflammatory bowel disease after the third vaccine dose (VIP): a multicentre, prospective, case-control study. *Lancet Gastroenterol Hepatol* 2022; **7**: 1005-1015 [PMID: 36088954 DOI: 10.1016/S2468-1253(22)00274-6]

180 **Cornberg M**, Buti M, Eberhardt CS, Grossi PA, Shouval D. EASL position paper on the use of COVID-19 vaccines in patients with chronic liver diseases, hepatobiliary cancer and liver transplant recipients. *J Hepatol* 2021; **74**: 944-951 [PMID: 33563499 DOI: 10.1016/j.jhep.2021.01.032]

181 **Fix OK**, Blumberg EA, Chang KM, Chu J, Chung RT, Goacher EK, Hameed B, Kaul DR, Kulik LM, Kwok RM, McGuire BM, Mulligan DC, Price JC, Reau NS, Reddy KR, Reynolds A, Rosen HR, Russo MW, Schilsky ML, Verna EC, Ward JW, Fontana RJ; AASLD COVID-19 Vaccine Working Group. American Association for the Study of Liver Diseases Expert Panel Consensus Statement: Vaccines to Prevent Coronavirus Disease 2019 Infection in Patients With Liver Disease. *Hepatology* 2021; **74**: 1049-1064 [PMID: 33577086 DOI: 10.1002/hep.31751]

182 **Sripongpun P**, Pinpathomrat N, Bruminhent J, Kaewdech A. Coronavirus Disease 2019 Vaccinations in Patients With Chronic Liver Disease

and Liver Transplant Recipients: An Update. *Front Med (Lausanne)* 2022; **9**: 924454 [PMID: 35814781 DOI: 10.3389/fmed.2022.924454]

183 **Marjot T**, Eberhardt CS, Boettler T, Belli LS, Berenguer M, Buti M, Jalan R, Mondelli MU, Moreau R, Shouval D, Berg T, Cornberg M. Impact of COVID-19 on the liver and on the care of patients with chronic liver disease, hepatobiliary cancer, and liver transplantation: An updated EASL position paper. *J Hepatol* 2022; **77**: 1161-1197 [PMID: 35868584 DOI: 10.1016/j.jhep.2022.07.008]

184 **Ai J**, Wang J, Liu D, Xiang H, Guo Y, Lv J, Zhang Q, Li J, Zhang X, Li Q, Liang J, Guo X, Feng Y, Liu L, Qin W, Wang X, Rao W, Tian Q, Zhang Y, Xie F, Jiang S, Yan Y, Qiu Y, Wu H, Hou Z, Zhang N, Zhang A, Ji J, Yang J, Huang J, Zhao Z, Gu Y, Bian L, Zhang Z, Zou S, Ji H, Ge G, Du X, Hou A, Zhu Y, Cong Q, Xu J, Zu H, Wang Y, Yan Z, Yan X, BianBa Y, Ci Q, Zhang L, Yang S, Gao X, Zhong L, He S, Liu C, Huang Y, Liu Y, Xu D, Zhu Q, Xu X, Lv M, Zhang W, Qi X. Safety and Immunogenicity of SARS-CoV-2 Vaccines in Patients With Chronic Liver Diseases (CHESS-NMCID 2101): A Multicenter Study. *Clin Gastroenterol Hepatol* 2022; **20**: 1516-1524.e2 [PMID: 34942370 DOI: 10.1016/j.cgh.2021.12.022]

185 **Noor MT**, Manoria P. Immune Dysfunction in Cirrhosis. *J Clin Transl Hepatol* 2017; **5**: 50-58 [PMID: 28507927 DOI: 10.14218/JCTH.2016.00056]

186 **Chen Z**, Zhang Y, Song R, Wang L, Hu X, Li H, Cai D, Hu P, Shi X, Ren H. Waning humoral immune responses to inactivated SARS-CoV-2 vaccines in patients with severe liver disease. *Signal Transduct Target Ther* 2022; **7**: 174 [PMID: 35654782 DOI: 10.1038/s41392-022-01032-9]

187 **Thuluvath PJ**, Robarts P, Chauhan M. Analysis of antibody responses after COVID-19 vaccination in liver transplant recipients and those with chronic liver diseases. *J Hepatol* 2021; **75**: 1434-1439 [PMID: 34454993 DOI: 10.1016/j.jhep.2021.08.008]

188 **Bakasis AD**, Bitzogli K, Mouziouras D, Pouliakis A, Roumpoutsou M, Goules AV, Androutsakos T. Antibody Responses after SARS-CoV-2 Vaccination in Patients with Liver Diseases. *Viruses* 2022; **14** [PMID: 35215801 DOI: 10.3390/v14020207]

189 **Willuweit K**, Frey A, Passenberg M, Korth J, Saka N, Anastasiou OE, Möhlendick B, Schütte A, Schmidt H, Rashidi-Alavijeh J. Patients with Liver Cirrhosis Show High Immunogenicity upon COVID-19 Vaccination but Develop Premature Deterioration of Antibody Titers. *Vaccines (Basel)* 2022; **10** [PMID: 35335009 DOI: 10.3390/vaccines10030377]

190 **Voysey M**, Clemens SAC, Madhi SA, Weckx LY, Folegatti PM, Aley PK, Angus B, Baillie VL, Barnabas SL, Bhorat QE, Bibi S, Briner C, Cicconi P, Collins AM, Colin-Jones R, Cutland CL, Darton TC, Dheda K, Duncan CJA, Emary KRW, Ewer KJ, Fairlie L, Faust SN, Feng S, Ferreira DM, Finn A, Goodman AL, Green CM, Green CA, Heath PT, Hill C, Hill H, Hirsch I, Hodgson SHC, Izu A, Jackson S, Jenkin D, Joe CCD, Kerridge S, Koen A, Kwatra G, Lazarus R, Lawrie AM, Lelliott A, Libri V, Lillie PJ, Mallory R, Mendes AVA, Milan EP, Minassian AM, McGregor A, Morrison H, Mujadidi YF, Nana A, O'Reilly PJ, Padayachee SD, Pittella A, Plested E, Pollock KM, Ramasamy MN, Rhead S, Schwarzbold AV, Singh N, Smith A, Song R, Snape MD, Sprinz E, Sutherland RK, Tarrant R, Thomson EC, Török ME, Toshner M, Turner DPJ, Vekemans J, Villafana TL, Watson MEE, Williams CJ, Douglas AD, Hill AVS, Lambe T, Gilbert SC, Pollard AJ; Oxford COVID Vaccine Trial Group. Safety and efficacy of the ChAdOx1 nCoV-19 vaccine (AZD1222) against SARS-CoV-2: an interim analysis of four randomised controlled trials in Brazil, South Africa, and the UK. *Lancet* 2021; **397**: 99-111 [PMID: 33306989 DOI: 10.1016/S0140-6736(20)32661-1]

191 **Liang CK**, Lee WJ, Peng LN, Meng LC, Hsiao FY, Chen LK. COVID-19 Vaccines in Older Adults: Challenges in Vaccine Development and Policy Making. *Clin Geriatr Med* 2022; **38**: 605-620 [PMID: 35868676 DOI: 10.1016/j.cger.2022.03.006]

192 **US Food Drug Aaministration**. Vaccines and Related Biological Products Advisory Committee. [cited 15 October 2022]. Available from: https://www.fda.gov/advisory-committees/blood-vaccines-and-other-biologics/vaccines-and-related-biological-products-advisory-committee

193 **Parkash O**, Sharko A, Farooqi A, Ying GW, Sura P. Acute Pancreatitis: A Possible Side Effect of COVID-19 Vaccine. *Cureus* 2021; **13**: e14741 [PMID: 34084669 DOI: 10.7759/cureus.14741]

194 **Dey RK**, Ilango H, Bhatta S, Shaheed A, Dole S, Zooshan A, Faisham M, Murad M. Acute pancreatitis in pregnancy following COVID-19 vaccine: a case report. *J Med Case Rep* 2022; **16**: 354 [PMID: 36175940 DOI: 10.1186/s13256-022-03607-0]

195 **Ozaka S**, Kodera T, Ariki S, Kobayashi T, Murakami K. Acute pancreatitis soon after COVID-19 vaccination: A case report. *Medicine (Baltimore)* 2022; **101**: e28471 [PMID: 35029194 DOI: 10.1097/MD.0000000000028471]

196 **Cacdac R**, Jamali A, Jamali R, Nemovi K, Vosoughi K, Bayraktutar Z. Acute pancreatitis as an adverse effect of COVID-19 vaccination. *SAGE Open Med Case Rep* 2022; **10**: 2050313X221131169 [PMID: 36313269 DOI: 10.1177/2050313X221131169]

197 **Kantar A**, Seminara M, Odoni M, Dalla Verde I. Acute Mild Pancreatitis Following COVID-19 mRNA Vaccine in an Adolescent. *Children (Basel)* 2021; **9** [PMID: 35053654 DOI: 10.3390/children9010029]

198 **Kalra RK**, Jayadeep S, Ball AL. Acute Pancreatitis in an Adolescent Following COVID Vaccination. *Clin Pediatr (Phila)* 2022; **61**: 236-240 [PMID: 35081801 DOI: 10.1177/00099228211067678]

199 **Patel AH**, Amin R, Lalos AT. Acute liver injury and IgG4-related autoimmune pancreatitis following mRNA-based COVID-19 vaccination. *Hepatol Forum* 2022; **3**: 97-99 [PMID: 36177105 DOI: 10.14744/hf.2022.2022.0019]

200 **Walter T**, Connor S, Stedman C, Doogue M. A case of acute necrotising pancreatitis following the second dose of Pfizer-BioNTech COVID-19 mRNA vaccine. *Br J Clin Pharmacol* 2022; **88**: 1385-1386 [PMID: 34423463 DOI: 10.1111/bcp.15039]

201 **Cieślewicz A**, Dudek M, Krela-Kaźmierczak I, Jabłecka A, Lesiak M, Korzeniowska K. Pancreatic Injury after COVID-19 Vaccine-A Case Report. *Vaccines (Basel)* 2021; **9** [PMID: 34205898 DOI: 10.3390/vaccines9060576]

202 COVID-19 mRNA Pfizer- BioNTech vaccine analysis print. [cited 15 October 2022]. Available from: https://assets.publishing.service.gov.uk/government/uploads/system/uploads/attachment_data/file/1072043/COVID-19_mRNA_Pfizer-_BioNTech_vaccine_analysis_print.pdf

203 Enquête de pharmacovigilance du vaccin Pfizer-BioNTech Comirnaty. [cited 15 October 2022]. Available from: https://ansm.sante.fr/uploads/2021/10/22/20211021-covid-19-vaccins-pfizer-focus-1-2.pdf

204 **World Health Organization**. VigiAccess. [cited 17 October 2022]. Available from: https://www.vigiaccess.org/

205 **Guda NM**, Trikudanathan G, Freeman ML. Idiopathic recurrent acute pancreatitis. *Lancet Gastroenterol Hepatol* 2018; **3**: 720-728 [PMID: 30215363 DOI: 10.1016/S2468-1253(18)30211-5]

World Journal of Gastroenterology

Submit a Manuscript: https://www.f6publishing.com

World J Gastroenterol 2023 July 14; 29(26): 4120-4135

DOI: 10.3748/wjg.v29.i26.4120

ISSN 1007-9327 (print) ISSN 2219-2840 (online)

REVIEW

Irritable bowel syndrome: Epidemiology, overlap disorders, pathophysiology and treatment

Kai-Yue Huang, Feng-Yun Wang, Mi Lv, Xiang-Xue Ma, Xu-Dong Tang, Lin Lv

Specialty type: Gastroenterology and hepatology

Provenance and peer review: Invited article; Externally peer reviewed.

Peer-review model: Single blind

Peer-review report's scientific quality classification

Grade A (Excellent): 0
Grade B (Very good): B
Grade C (Good): C
Grade D (Fair): 0
Grade E (Poor): 0

P-Reviewer: Ertan A, United States; Garg P, India

Received: April 17, 2023
Peer-review started: April 17, 2023
First decision: May 12, 2023
Revised: May 19, 2023
Accepted: June 11, 2023
Article in press: June 11, 2023
Published online: July 14, 2023

Kai-Yue Huang, Feng-Yun Wang, Mi Lv, Xiang-Xue Ma, Xu-Dong Tang, Lin Lv, Institute of Digestive Diseases, Xiyuan Hospital of China Academy of Chinese Medical Sciences, Beijing 100091, China

Kai-Yue Huang, Feng-Yun Wang, Mi Lv, Xiang-Xue Ma, Xu-Dong Tang, Lin Lv, Institute of Digestive Diseases, Beijing Institute of Spleen and Stomach Disease of Traditional Chinese Medicine, Beijing 100091, China

Corresponding author: Lin Lv, MD, Associate Chief Physician, Institute of Digestive Diseases, Xiyuan Hospital of China Academy of Chinese Medical Sciences, No. 1 Xiyuan Playground, Haidian District, Beijing 100091, China. lushangshitou@qq.com

Abstract

Irritable bowel syndrome (IBS) is a common chronic gastrointestinal disease with a significant impact on patients' quality of life and a high socioeconomic burden. And the understanding of IBS has changed since the release of the Rome IV diagnosis in 2016. With the upcoming Rome V revision, it is necessary to review the results of IBS research in recent years. In this review of IBS, we can highlight future concerns by reviewing the results of IBS research on epidemiology, overlap disorders, pathophysiology, and treatment over the past decade and summarizing the latest research.

Key Words: Irritable bowel syndrome; Overlap; Pathophysiology; Treatment

©The Author(s) 2023. Published by Baishideng Publishing Group Inc. All rights reserved.

Core Tip: Irritable bowel syndrome (IBS) is a physical and mental illness that is becoming more prevalent, and its impact on society is expanding. Understanding of IBS has changed since the release of the Rome IV diagnosis in 2016, and this paper reviews the literature from the past decade to find that research around the brain-gut axis, diet, and gut microbiota are at the forefront of IBS. Moreover, as the research on the physiopathology of IBS has advanced, the treatment model has become more refined, which has important clinical implications.

Citation: Huang KY, Wang FY, Lv M, Ma XX, Tang XD, Lv L. Irritable bowel syndrome: Epidemiology, overlap disorders, pathophysiology and treatment. *World J Gastroenterol* 2023; 29(26): 4120-4135
URL: https://www.wjgnet.com/1007-9327/full/v29/i26/4120.htm
DOI: https://dx.doi.org/10.3748/wjg.v29.i26.4120

INTRODUCTION

Irritable bowel syndrome (IBS) is a chronic functional disease, and the changes that it causes in bowel function and abdominal pain seriously affect the patient's normal life and work. It mainly affects young and female individuals, and it tends to overlap with other functional gastrointestinal diseases (FGIDs) and cause a huge burden to life and society's economy[1,2]. Prevalence varies greatly between countries because of differences in food, culture, and diagnosis. The Rome Foundation Global Study[3] coverage across the country reported that the overall prevalence of IBS was 3.8% in Rome IV and 10.1% in Rome III. The Rome IV criteria, based on symptoms that have undergone a change in dynasty, suggest that the pathogenesis of IBS is associated with gut-brain interactions, which may be an overlapping pathogenesis between FGIDs. Based on the results of Rome IV, many studies have been performed, so it is necessary to summarize their findings. The aim of this study is to summarize IBS from the perspectives of epidemiology, disease overlap, pathological mechanisms, diagnosis, and treatment, focusing on disease overlap, pathological mechanisms, and treatment.

REGIONALIZATION SHOULD BE EMPHASIZED IN EPIDEMIOLOGY

The prevalence of IBS varies widely between different countries. In 2017, the Rome Foundation working group reviewed related work and showed that the prevalence of IBS varied from 1.1% (France and Iran) to 35.5% (Mexico), and the prevalence in Asia is also uneven[4-6]. It might be that many previous surveys did not use uniform diagnostic criteria or the same methodology, with geography, culture, and population being the reasons for different prevalences, and thus the included studies were heterogeneous. The goal of determining the global prevalence of IBS is still inaccurate[7]. Therefore, we discuss the epidemiology of IBS in different continents in recent years.

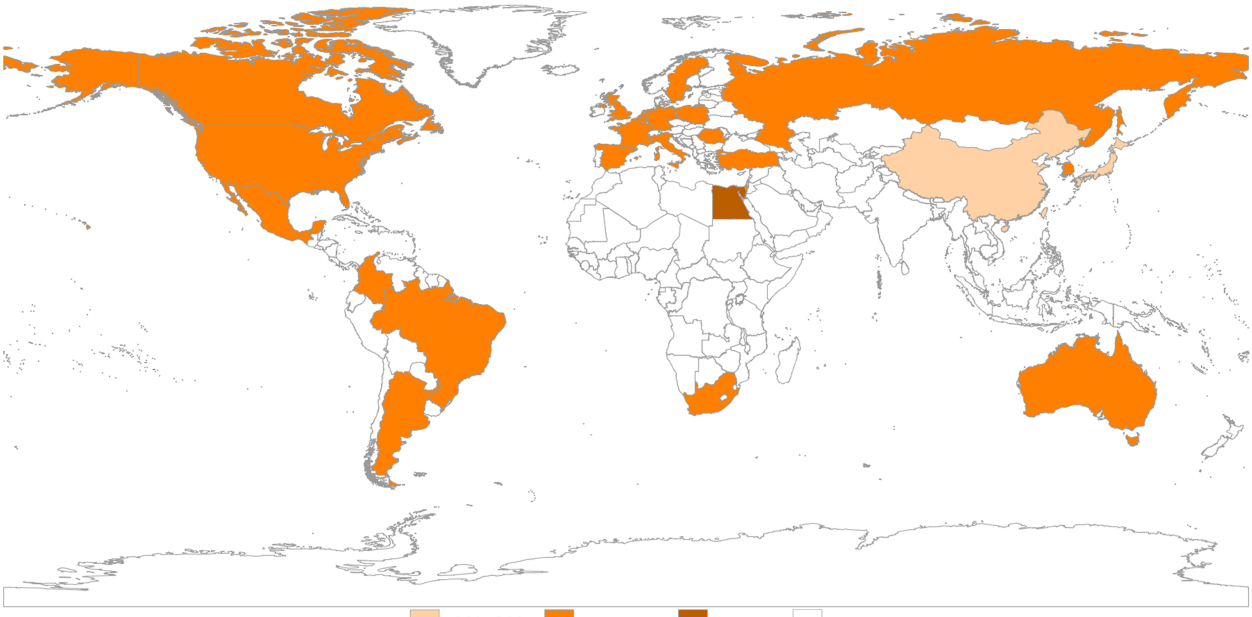
The Rome Foundation Global Epidemiological Study organized a study using Rome IV in 33 countries and Our analysis discovered that the prevalence rates in Europe and the United States were comparable, while those in Asia and Australia were marginally lower[7] (Figure 1). Egypt had the highest prevalence rate of internet surveyed countries[8]. As well as that, representative researches have also been carried out in various countries in recent years and reported that the prevalence of IBS was 5.2% (Rome IV), 5.9% (Rome III), and 6.98% (Rome IV) in Gibraltar, the United Kingdom[9], Hangzhou, China[10] and Latin America[11], respectively. Based on population survey data in the United States, Canada, and the United Kingdom, the results revealed the Rome III IBS rate was roughly twice as high as the Rome IV rate[12]. Overall, there is a clear predominance in the prevalence in Africa, and the prevalence based on Rome IV diagnosis is similar in the United States and Europe. However, prevalence varies widely between Europe and Asia, especially in Asian countries surveyed by using the internet and questionnaires. In the past, most studies have shown a higher prevalence of IBS in women[13]. Interestingly, IBS is equally common in men and women in Asia[14-16]. The highest prevalence was observed in the educated, the wealthy, students and younger individuals[17]. It also declined with age[1,18,19]. Through years of research and analysis, it was determined that estimating a pooled global prevalence of IBS was unlikely to be feasible, so regionalization should be emphasized in future research.

NEW INSIGHTS INTO THE OVERLAP OF IBS

Rome criteria for IBS based on symptoms were the most recognized, and the overlap of FGIDs was gradually valued by Roman criteria over time (Figure 2). Now, Rome IV suggests that the pathologies exist in the gastrointestinal tract on a continuum instead of as separate disorders, and overlap may be a natural clinical symptom of FGIDs[20]. Likewise, 54127 adults from 26 countries participated in an internet survey and discovered that 68.3% had symptom overlap in both gastrointestinal regions and 2.3% had esophageal, gastroduodenal, bowel, and anorectal overlap[21]. Overall, by reviewing the overlap of IBS and other diseases, it was found that there was obvious overlap between IBS and FGIDs, and anxiety and depression were their common characteristics, which verified the vital position of the central nervous system and brain-gut axis in the pathological mechanism of FGIDs. Therefore, the overlapping pattern and pathology of FGIDs are something that should be studied in depth.

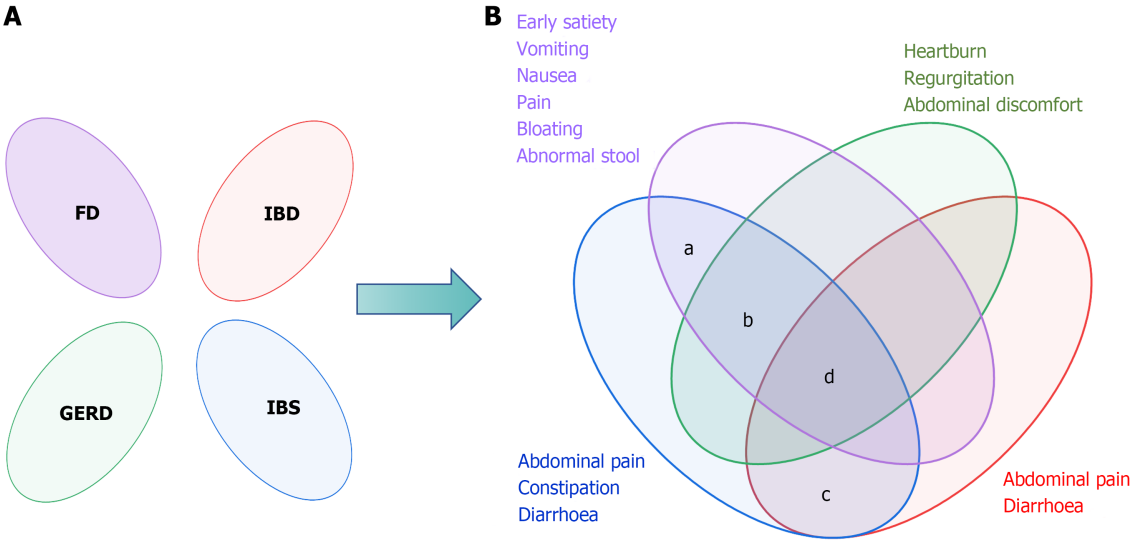
Functional dyspepsia

Functional dyspepsia (FD) and IBS are the most prevalent FGIDs, postprandial fullness, early satiation, epigastric pain, and epigastric burning are the main symptoms of FD. The global prevalence of FD varies from 10%-20%[22]. Clinical studies have identified not only overlap between FD and IBS[23-25], but also the most common overlapping characteristics. In the overlap between FD and IBS-D (diarrhea), abdominal pain, bloating, and diarrhea are prominent. However, in the overlap between FD and IBS-C (constipation), abdominal fullness and constipation are prominent.



DOI: 10.3748/wjg.v29.i26.4120 **Copyright** ©The Author(s) 2023.

Figure 1 Prevalence of irritable bowel syndrome by Rome IV. Prevalence of an Internet survey conducted by the Rome Foundation in multiple centers worldwide based on Rome IV. Asia, 1.3%-4.7%; Europe, 3.5%-5.9%; America, 3.5%-5.3%; Australia, 3.5%; Egypt, 7.6%; and South Africa, 5.9%.



DOI: 10.3748/wjg.v29.i26.4120 **Copyright** ©The Author(s) 2023.

Figure 2 The Rome Foundation's views on the overlap of functional gastrointestinal diseases. A: Rome I considered the functional bowel disorders to be independent diseases; B: Rome II and Rome III recognized there was overlap between functional gastrointestinal diseases. a: The prevalence of overlap between irritable bowel syndrome (IBS) and functional dyspepsia was 55.3%; b: The overlap between IBS and gastroesophageal reflux disease ranged from 3%-79% in the questionnaire and 10%-74% when diagnosed by endoscopy; c: A 2020 meta-analysis showed that the pooled prevalence of IBS-type symptoms was 32.5%; d: Only 2.3% had esophageal, gastroduodenal, bowel, and anorectal overlap. FD: Functional dyspepsia; IBD: Inflammatory bowel diseases; GERD: Gastroesophageal reflux disease; IBS: Irritable bowel syndrome.

In a longitudinal follow-up study published in 2022, 807 individuals (Rome IV) were included, 446 (55.3%) of whom had overlapping IBS and FD, which showed that patients with overlapping IBS and FD had more severe symptoms and were more likely to have depression and anxiety[26,27]. Furthermore, a prospective study in South Korea in 2019-2020 reported the same conclusion; moreover, women with overlap of IBS and FD experienced more severe gastrointestinal and depression symptoms than men. Interestingly, an Australian study showed no relationship between gender and overlap[25,28]. There seems to be a distinct overlap between IBS, FD, and gastroesophageal reflux disease (GERD), in which it is easier to merge psychological morbidity and sleep disturbance[29]. Although age, gender, and IBS subtype were not correlated with overlap[25], the pathogenesis analysis of IBS and FD indicates that psychological factors are linked to the overlap of IBS and FD. Therefore, the diagnosis of IBS or FD should be considered in terms of each other,

especially when encountering some anxious, severe symptoms.

GERD

GERD is a condition in which stomach contents reflux and cause uncomfortable symptoms[30], which present with regurgitation, heartburn, or being asymptomatic. Then, GERD is divided into three phenotypic presentations: Nonerosive reflux disease, erosive esophagitis (RE), and Barrett's esophagus (BE), with prevalence rates of 60%-70%, 30%, and 6%-8%, respectively[31]. Before Rome IV, a small number of studies had shown overlap between GERD and FGIDs[32], and IBS is a risk factor for GERD[33]. But now, the Rome Foundation considers overlap between FGIDs to be a trend. In patients with overlapping GERD and IBS, acid reflux and heartburn may present with abdominal pain or discomfort, and visceral hypersensitivity and gastrointestinal motility disorders may be coexisting mechanisms. However, the prevalence of patients with GERD and IBS (different criteria) varies greatly, and the overlap between IBS and GERD ranges from 3% to 79% based on the questionnaire and 10% to 74% when diagnosed by endoscopy[34]. In 2016, an Italian study with 697 heartburn patients found that cases of IBS overlapping with GERD/hypersensitive esophagus (HE) and overlapping functional heartburn (FH) were 147/454 (33%) and 187/243 (77%), respectively[35]. Besides, there is a higher risk of possible overlap between FGIDs.

Inflammatory bowel disease

Crohn's disease (CD) and ulcerative colitis (UC) are common inflammatory bowel diseases (IBDs). CD is characterized by chronic or nocturnal diarrhea, abdominal pain, and weight loss, whereas UC is characterized by bloody diarrhea with rectal urgency and tenesmus[36,37]. Although some biomarkers are used to distinguish between IBS and IBD, there is also overlap between them. Patients with overlapping IBD and IBS are prone to diarrhea and abdominal pain, which can be serious. Besides, a 2020 meta-analysis showed that the pooled prevalence of IBS-type symptoms among patients with IBD was 32.5%[38]. IBS-D is related to gut infections, and the gut microbiome and the intestinal barrier are bridges that connect them. Thus, IBS-D is a common diagnosis in patients with chronic diarrhea following chronic infection[39,40]. Overall, IBD and IBS can be different stages of the same disease. Therefore, the overlapping disease characteristics of IBS and IBD should not be ignored when the patient has a history of intestinal infection. At the same time, it is necessary to prevent IBS when diagnosing IBD.

Other

A follow-up study in the US performed an analysis of data from 655 adults to compare the degree of overlap between chronic overlapping pain conditions (COPCs). Surprisingly, IBS is the most common COPC other than headache. Furthermore, 63% of IBS cases have one or more COPCs, and 53% of IBS cases reported pain in ≥ 3 non abdominal areas [41]. Therefore, when there is chronic physical and abdominal pain, IBS overlap should not be ignored[42]. It was observed that IBS and nonceliac gluten sensitivity had significant symptom overlap, and their physiology and pathology were not clear[43]. Moreover, there is overlap between adolescents with endometriosis and IBS[44], and the overlap between IBS and endometriosis may have the same pathogenesis; specific mechanisms need to be further explored.

PATHOPHYSIOLOGY

In the past, IBS was thought to be a functional disorder that could not be explained by organic disease or a clear etiology [45]. With the increasing research on IBS and the update of the Rome criteria, the view on the pathophysiological mechanisms of IBS has changed from functional to brain-gut interaction. The aim of this article is to review the pathophysiology from clinical studies and basic research on IBS after Rome IV.

Clinical studies

Recurrent abdominal discomfort, abdominal pain, and altered bowel habits are the core clinical symptoms of patients with IBS, and clinical studies on pathogenesis show that the microbiome, gastrointestinal endocrine cells, visceral hypersensitivity, and gastrointestinal motility disorders , are observed in IBS patients and are the direct causes of abdominal discomfort, abdominal pain, or diarrhea. It was discovered through experiments that the levels of colonic mucosal Takeda G protein-coupled receptor 5 protein expression, short-chain fatty acid (SCFA), fecal bile acids (FBA)[46, 47], tryptophan (aryl hydrocarbon receptor kynurenine pathways), and methane gas production[47,48] were higher in patients with IBS than in healthy control (HC), and metabolites such as SCFA and bile acids are mainly associated with gastrointestinal malabsorption; there are differences between IBS subtypes, and neurotransmitters cause abdominal pain through the brain-gut axis and center. DuPont *et al*[49], recorded intestinal transport in 46 patients with IBS using a wireless pH/pressure recording capsule and found a delayed gastric emptying time in 35/46 (76%) IBS patients. And abnormal colonic transit and disorders of evacuation are important physiopathologies in patients with IBS, leading to constipation, bloating, and abdominal pain. Furthermore, abnormal oroanal transit time (OATT) was associated with hydrogen and methane concentrations, and more rapid OATT was associated with a higher severity of abdominal discomfort, rumbling, and nausea[48]. In addition, gut endocrine cells are scattered throughout the gastrointestinal tract and have sensory microvilli that sense gut pressure and gut contents[50-52], and when the gut lumen is stimulated by food[53], and microbial metabolism, the cells release hormones into the lamina propria to act mainly through paracrine and afferent and efferent synaptic transmission[54-56]. And studies found that histamine, 5-HT, glutamate, and noradrenalin strengthen visceral pain, and γ-aminobutyric acid reduces gastrointestinal motility.

Abdominal pain in IBS patients has been shown to be associated with structural features of the brain. Rectal stimulation seems to activate the anterior cingulate cortex, prefrontal cortex, insula, thalamus, and cerebellum, and is higher in patients with IBS[57]. A study[58] of female IBS patients included 216 female IBS patients and 138 women serving as HC. In comparison to HC, patients with IBS had an increase in gray matter volume and cortical thickness in the primary and secondary somatosensory cortex and subcortical regions; however, the volume, surface, and cortical thickness of the gray matter in the posterior insula and superior frontal gyrus were reduced. Moreover, abdominal pain caused by rectal dilation is linked to the thicker left primary somatosensory cortex (Figure 3).

Animal experiments

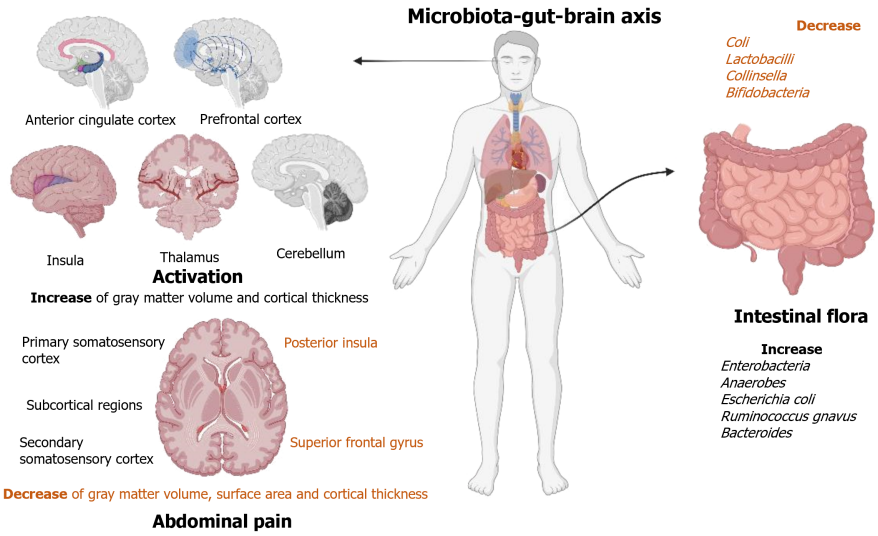
Visceral hypersensitivity and gut barrier disruption have been shown to be mediated *via* corticotropin-releasing factor (CRF)-Toll-like receptor 4 (TLR4)-proinflammatory cytokine signaling in animal experiments[59,60]. In addition, Nozu *et al*[61] conducted experiments based on IBS model rats and discovered that apelin activates CRF and TLR4, which may create a vicious cycle of proinflammatory cytokine signaling, which is a key pathway for the pathological mechanism of IBS. Then, the disruption of the gut barrier leads to an increase in lipopolysaccharides (LPS) and proinflammatory cytokines, which is a vital pathological mechanism that causes abdominal pain in patients with IBS[62]. And there are some new developments, such as a study using NanoString mRNA measurement of colonic neuroimmune gene expression and founding that the expression of the gene Trpv1 was higher in Gnotobiotic mice from patients with IBS and comorbid anxiety; moreover, it was associated with visceral hypersensitivity and anxiety[63]. Besides, decreasing miR-199 caused visceral hypersensitivity and augmented visceral pain in patients with IBS through translational upregulation of TRPV1[64]. Both activating BDNF-TrkB-PKMζ signaling in the thoracolumbar spinal cord of rats to increase synaptic activity and activating TLR4 trigger the release of pro-inflammatory cytokine afferent nerves and can cause visceral hypersensitivity[65,66]. Moreover, recent studies have shown that abnormal mast cell structure or function is a potential mechanism for visceral hypersensitivity in IBS[67], and post-IBS with gut microbial disorders leading to IBS and signaling pathways are also associated with visceral hypersensitivity[67,68]. In addition, an excellent review by Tozlu *et al*[69]. indicated that the number of mucosal eosinophils increased substantially more in patients with post-IBD IBS-D than in patients with active IBD, there was a reaction to the removal of allergic foods during treatment, and intestinal inflammation in patients with IBS was associated with food allergic reactions. Peptide YY (PYY) is localized in endocrine cells and regulates gut motility and visceral sensitivity by releasing and modulating serotonin[70] (Figure 4).

Microbiome

Koloski *et al*[71,72] discovered that higher baseline levels of anxiety and depression were significant predictors of developing IBS, and two prospective studies found that functional gastrointestinal symptoms preceded the mood disorder in two-thirds of patients. Dinan *et al*[73,74] have suggested that disturbances in the gut microbiota can affect brain function, behavior, and cognition, and the theory has developed into the microbiota-gut-brain axis, which is an important basis for the influence of gut microbes as well as neurotransmitters on IBS. The microbial diversity and abundance of stool in patients with IBS were altered compared to those in HC, with a decrease in *Coli*, *Lactobacilli*, *Collinsella*, and *Bifidobacteria* and an increase in *Enterobacteria*, *Coli*, anaerobes, *Escherichia coli*, *Ruminococcus gnavus*, and Bacteroides in patients with IBS. And a higher proportion of Bacteroides and *Allisonella* in patients with IBS-M[75,76]. In addition a study[77] used 16S rRNA metagenomic sequencing and performed phylogenetic investigation of communities by reconstruction of unobserved states to analyze fecal samples from control (n = 12) and IBS-D patients (n = 7) and reported that in patients with IBS, the abundances of *Sutterellaceae*, *Acidaminococcaceae,* and *Desulfovibrionaceae* were significantly increased, and those of *Clostridiaceae, Leuconostocaceae, Enterococcaceae, Peptostreptococcaceae*, and *Lachnospiraceae* were significantly decreased; moreover, secondary bile acid biosynthesis was decreased, and the citrate cycle was increased. Moreover, a study[78] used proton nuclear magnetic resonance spectroscopy and shotgun metagenomic sequencing to analyze fecal metabolites and the gut microbiome (IBS patients =142 and HC =120). It reported that the gut microbial diversity of IBS (Simpson's evenness metric) was drastically lower than that of HC, and metabolomics found that the mechanism of IBS was related to 5-HT.

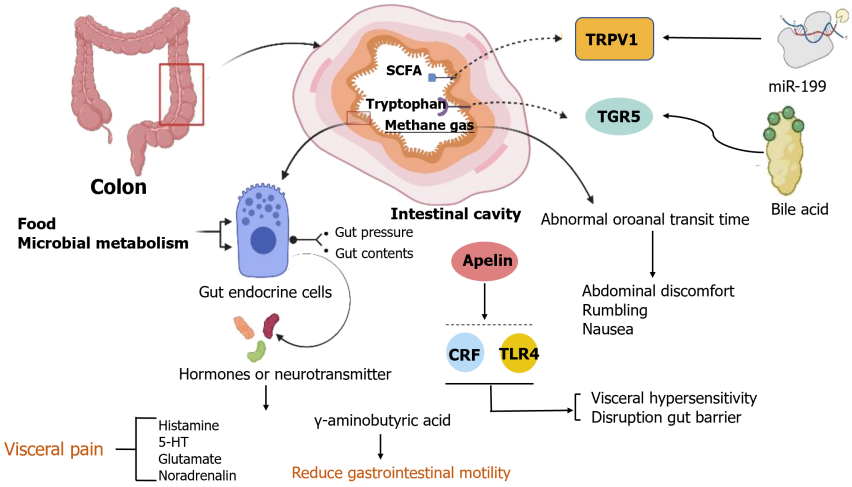
TREATMENTS

The diagnosis of IBS is based on symptoms ranging from the Manning criteria to the Rome criteria, and the most widely used diagnostic criteria are the Rome IV[79]. Research around Rome IV has revealed that there are many important biomarkers that guide the differential diagnosis and symptomatic treatment of IBS that may be taken into account. According to Vijayvargiya *et al*[80], FBA and fecal fat are potential biomarkers for IBS-D and IBS-C. Total FBA, chenodeoxycholic acid (CDCA), cholic acid (CA), and primary bile acids were significantly higher in patients with IBS-D than in healthy patients or patients with IBS-C. In contrast, deoxycholic acid (DCA) and combined DCA and CDCA (secretory) bile acids were significantly lower in patients with IBS-C than in HC and patients with IBS-D. Combining fasting serum 7α-hydroxy-4-cholesten-3-one and primary bile acids or fecal bile acid concentrations in stool samples is a simple, low-cost diagnostic for bile acid diarrhea (BAD). Circulating resolvin D1 (RvD1) and c-reactive protein (CRP) are inflammatory markers in patients with IBS-C; patients with IBS-C have higher CRP and lower RvD1 concentrations than HC[81]. Furthermore, radiopaque markers and scintigraphy can be used to assess transit function, and rectal sensation to balloon distension can be used to assess visceral hypersensitivity[82]. All of the ancillary tests listed above can be used to further identify the cause and guide medication use if the first-line medication is ineffective.



DOI: 10.3748/wjg.v29.i26.4120 **Copyright** ©The Author(s) 2023.

Figure 3 Research progresses on the mechanism of action of the microbiota-gut-brain axis. Brain changes in patients with irritable bowel syndrome (IBS) are associated with abdominal pain. They have higher activation of the anterior cingulate cortex, prefrontal cortex, insula, thalamus, and cerebellum. They also mainly showed an increase of gray matter volume and cortical thickness in the primary somatosensory cortex, secondary somatic sensory cortex, and subcortical regions and a decrease of gray matter volume, surface area, and cortical thickness in the posterior insula and superior frontal gyrus. Specific changes in the intestinal flora of patients with IBS. The number of *Coli*, *Lactobacilli*, *Collinsella*, and *Bifidobacteria* in IBS patients decreased, while the number of *Enterobacteria*, *Anaerobes*, *Escherichia coli*, *Ruminococcus gnavus*, and *Bacteroides* increased.



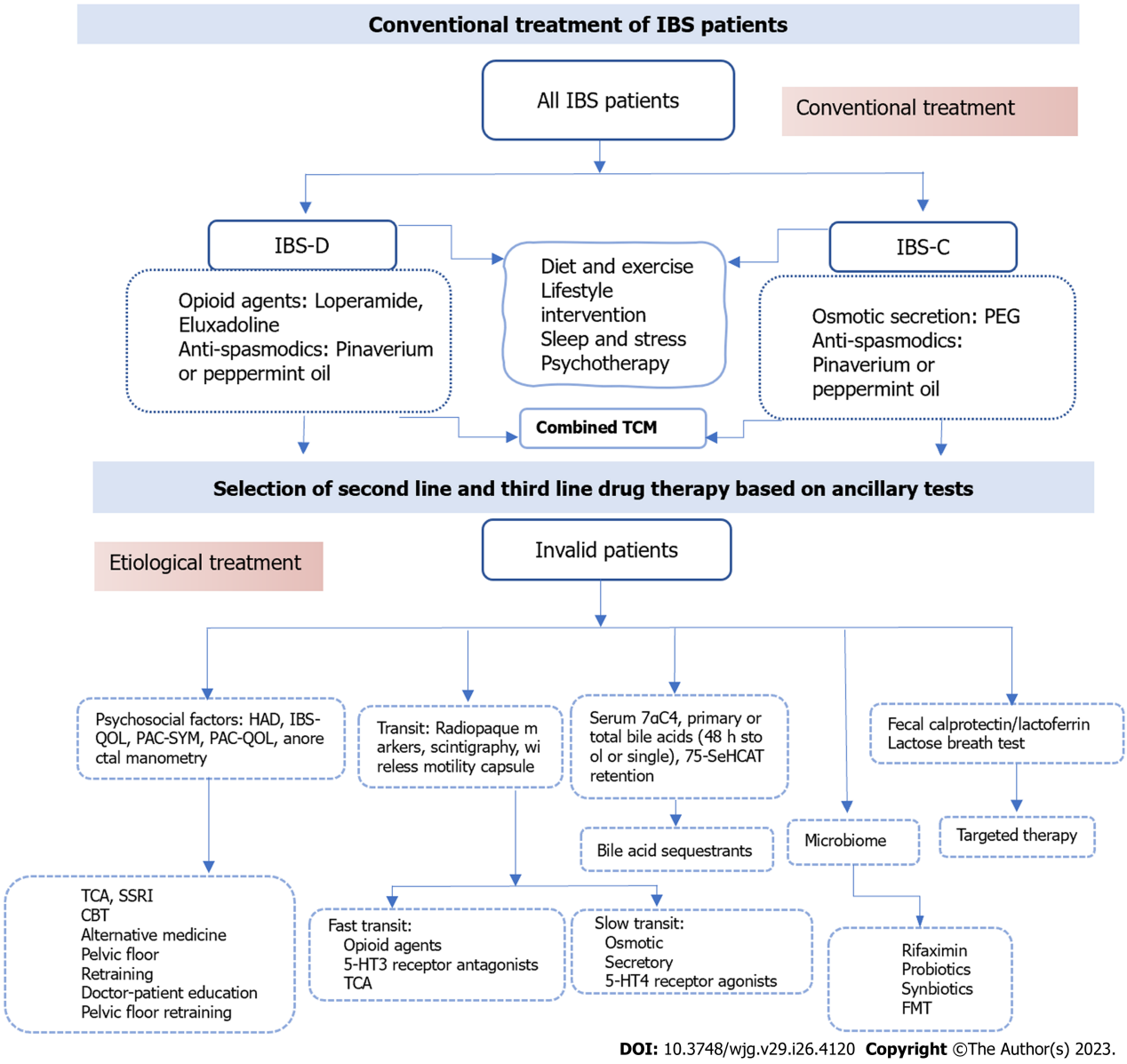
DOI: 10.3748/wjg.v29.i26.4120 **Copyright** ©The Author(s) 2023.

Figure 4 Pathology of irritable bowel syndrome in the intestinal. Food and microbial metabolism stimulate the gut's endocrine cells to release hormones and neurotransmitters, leading to visceral pain and reducing gastrointestinal motility. Apelin, corticotropin-releasing factor, and Toll-like receptor 4-proinflammatory cytokine signaling lead to visceral hypersensitivity and disruption of the gut barrier. The concentrations of hydrogen and methane are related to abnormal oroanal transit time (OATT), and a more rapid OATT was associated with a higher severity of abdominal discomfort, rumbling, and nausea. Decreasing miR-199 caused visceral hypersensitivity and augmented visceral pain in patients with irritable bowel syndrome (IBS) through translational upregulation of TRPV1. Colonic mucosal protein expression and faecal bile acids were correlated with the symptom severity of IBS-D patients. CRF: Corticotropin-releasing factor; TLR4: Toll-like receptor 4.

Patients with mild IBS first choose education, diet, and lifestyle interventions as prerequisites, combined with first-line therapeutic drugs. If first-line treatment is ineffective, clinical judgment combined with ancillary tests is required to select appropriate second-line drugs and non-pharmacological interventions (Figure 5). Furthermore, patients with psychological problems can be assessed using psychological questionnaires, emphasizing doctor-patient communication for emotional relief, and using tricyclic antidepressant (TCA) or selective serotonin reuptake inhibitor (SSRI) medications.

Lifestyle intervention therapy

Stress reduction, appropriate exercise, and a special diet are the main non-pharmacological treatments for preventing induction; likewise, the publication of the British Gastroenterological Society guidelines[83] in 2021 and the updated guidelines from the American College of Gastroenterology (ACG) in 2022 emphasized that dietary counseling should be regarded as a first-line treatment option. A low-FODMAP (fermentable oligosaccharides, disaccharides, monosac-



DOI: 10.3748/wjg.v29.i26.4120 **Copyright** ©The Author(s) 2023.

Figure 5 The conventional treatment and further treatment of irritable bowel syndrome patients. TCM: Traditional Chinese treatment; CBT: Cognitive behavioral treatment; HAD: Hospital Anxiety and Depression scale; IBS-QOL: Irritable Bowel Syndrome-Quality of Life Questionnaire; PAC-QOL: Patient Assessment of Constipation-Quality of Life Questionnaire; PAC-SYM: PAC-Symptoms Questionnaire; 7αC4: 7α-hydroxy-4-cholesten-3-one; 75-SeHCAT: 75-selenium homocholic acid taurine; TCA: Tricyclic Antidepressants; SSRI: Selective Serotonin Reuptake Inhibitors; IBS: Irritable bowel syndrome; IBS-C: IBS-constipation; IBS-D: IBS-diarrhea.

charides, and polyols, LFD) diet is currently the most recommended and effective diet for IBS intervention[84]. And FODMAP induces symptom generation in IBS based on the gut-brain axis[85]. The ACG suggests that the LFD diet be implemented in three steps: (1) A period of strict restriction (lasting no longer than 4-6 wk); (2) reintroduction of FODMAP foods; and (3) personalization based on reintroduction results[86]. The short-term efficacy and safety of LFD compared to a Western diet and conventional diet in relieving IBS patients are definite[87]; of course, a regular diet is the foundation. Gluten-free foods and dietary fiber are other currently approved diets for patients with IBS[88,89]. IBS-D patients benefit more from LFD than IBS-C patients, while fiber diets such as psyllium fiber are more effective in IBS-C patients[90]. Garg[91], professor, proposed the "FEED" method, in which ample daily psyllium fiber (25 g) and sufficient water (500 mL), along with elevation of the feet and exercises of the abdominal muscles while sitting on the toilet, can help IBS-D symptoms. In contrast, lactose, sorbitol, fructose, xylitol, mannitol, fat, alcohol, insoluble fibers, and fizzy drinks increase pain and flatulence and should be avoided by patients with IBS[92-94].

Cognitive behavioral treatment

Since IBS is a gastrointestinal physical disorder that often fluctuates with stress, the Rome working team strongly recommends brain-gut axis behavior therapies as part of the treatment of DGBI disorders such as IBS[95]. Including hypnotherapy, dynamic psychotherapy, and relaxation therapy[96] can improve abdominal pain, standard of living, and psychological symptoms in patients with IBS and can reduce health care costs. Although some patients are unable to

receive psychotherapy, recent studies have shown that cognitive behavioral treatment (CBT) of hypnotherapy is a potential and affordable treatment. A study included 436 patients with IBS (Rome III) who were followed up at 2 wk and 3, 6, 9 and 12 mo after the end of specific CBT treatment, and the results showed that not only did CBT improve symptoms, but the improvement usually extended up to 12 mo after treatment[97,98]. Additionally, gut-directed hypnotherapy (GHT) can also improve the symptoms of IBS by affecting gastrointestinal motility and visceral sensitivity [99,100]. Overall, most views support the ideal that it works because it is based on the brain-gut axis. GHT is beneficial in directly reducing the discomfort of IBS and refractory IBS as well as improving quality of life and health, and the efficacy is sustained. Moreover, it can reduce anxiety and depression, but its mechanism is largely unclear[101]. The mechanism of hypnotherapy is related to the brain-gut axis, but current research on the microbiome has not provided definitive results[102]. What is certain is that hypnotherapy works by regulating the autonomic nervous system (ANS). The vagus nerve is related to the brain-gut axis and can coordinate gastrointestinal functions, and there seems to be potential in studying the role of the vagus nerve[102,103].

Pharmacological treatment

IBS-D: The ACG published guidelines for IBS-D conditional recommendations in 2022[104] include the three drugs eluxadoline, rifaximin, and alosetron (moderate certainty), which can relieve or assist abdominal pain and stools, but there are adverse effects and contraindications. Loperamide (very low certainty) can relieve diarrhea, but there is no evidence that it improves abdominal discomfort. TCA and antispasmodics have low certainty. Moreover, SSRIs are recommended against use (low certainty) (Table 1).

IBS-C: The first-line therapy for IBS-C are bulking agents and osmotic laxatives. The ACG published guidelines for IBS-C [105] and recommended them in 2022, including a strong recommendation for linaclotide (high certainty) and conditional recommendations for tenapanor, plecanatide, tegaserod, and lubiprostone (moderate certainty); polyethylene glycol laxatives, TCA, and antispasmodics have low certainty. The panel made a conditional recommendation against the use of SSRIs (low certainty). Chloride channel activators and guanylate cyclase activators are recommended for global IBS with constipation symptoms[106]. However, adverse effects of diarrhea may occur (Table 1).

Pain: Antispasmodics, including anticholinergic and calcium-blocking drugs, which can relieve pain and improve bowel movements, remain the first choice for abdominal pain in IBS[107]. Such as cimetropium/dicyclomine, peppermint oil, pinaverium, and trimebutine have clear benefits on abdominal pain and symptom scores[108]. By reviewing relevant RCTs[109-112], it was shown that most samples were small and of moderate quality. Overall, limited to short-term treatment Antidepressants can improve pain through central nervous system action, but clinical trials are scarce and the limitation of adverse events is uncertain. Although pinaverium was the most commonly used drug for the treatment of abdominal pain with a rapid onset of action and the improvement in abdominal pain was greater than that of bowel movements, its efficacy was less significant than that of placebo after one week. Whereas otilonium bromide (OB) significantly has a longer onset of action than pinaverium but is more suitable for patients with diarrhea. Moreover, drotaverine has a slow onset of action and is more suitable for the later stages of IBS. Although peppermint oil has been shown to be effective, it has many adverse events (heartburn or GERD symptoms, belching, headache, *etc.*). Finally, TCA and SSRIs have been shown to be effective, but SSRI adverse events are more numerous, and TCA is recommended for patients with significant anxiety or abdominal pain[113,114] (Table 1).

Traditional Chinese treatment

Traditional Chinese treatment: Traditional Chinese treatment (TCM) prescriptions Traditional Chinese medicine treatments, including prescriptions, acupuncture, and moxibustion, are the main treatments for IBS, although they are still complementary treatments that have been found to have great potential through research. Its possible mechanisms of action are mainly through regulating the enteric nervous system, improving gastrointestinal motility, reducing visceral hypersensitivity, regulating intestinal flora, and regulating the immune system to alleviate IBS[115].

A RCT designed in China, enrolling 216 patients with IBS who were assigned to the control group that took the Chang'an I Recipe or placebo group, reported that the Chang'an I Recipe outperformed the placebo in the treatment of IBS-D with no major side effects[116]. Furthermore, 60 IBS patients were enrolling in a study and were divided into the control group (n = 20) and the treatment group (n = 40), which were given oral pinaverium bromide tablets and Tongxie Yaofang decoction on the basis of conventional treatment, respectively. And the results reported that the flavored Tongxie Yaofang had a significant effect on the symptoms of patients with IBS-D[117], and improving the gut microbiome, alleviating visceral hypersensitivity, regulating 5-HT level in patients, and inhibiting colonic contraction are mechanisms for the treatment of IBS[118-120]. Moreover, Tongxie Anchang Decoction improves IBS by reducing visceral hypersensitivity, reversing mast cell infiltration, and regulating 5-HT[118,121]. And Xiang Sha Liu Jun Zi Decoction reduced the mean diarrhea score of IBS patients[122]. Finally, the Fuzi-Lizhong pill can impact bacterial diversity in the gut and regulate inflammation and immune system to treat IBS-D[123].

Acupuncture and moxibustion: The therapeutic effects of acupuncture are recognized worldwide, although its mechanisms of action are still being further explored. Acupuncture has a bright future in IBS and FGIDs, yet there remain controversies that need to be further explored. A randomized trial of 344 patients with IBS in the acupuncture group and 175 in the pinaverium bromide group reported that the acupuncture group was more effective than the control group, and the effect lasted up to 12 wk[124]. Besides, 126 patients with IBS-D (liver stagnation and spleen deficiency) were randomly assigned to one of three groups: A herb-separated moxibustion group (n = 42, applied to Jinsuo (GV 8)-eight-diagram points), a Western medication group (n = 42), and a Chinese herbal medication group (n = 42), and the results

Table 1 Summary of irritable bowel syndrome medications

Type	Mechanism of action	Example	Appearing dose	Efficient	
IBS-D					
Opioid agents	Inhibits secretion, transit	Loperamide	4 mg tid	Unknown for IBS; effective for diarrhea	First-line
		Eluxadoline	75 mg or 100 mg bid	Effective for FDA composite: 100 mg: OR, 0.87 (95%CI: 0.83-0.91); 75 mg: OR, 0.89 (95%CI: 0.84-0.94). RCTs: Effective for diarrhea and composite diarrhea + pain; not pain alone	
Bile acid sequestrants	Bind to bile acids	Cholestyramine	4 g bid	Unknown: effective in open-label studies; ineffective in 1, single-center RCT	
		Colestipol	-		
		Colesevelam	32 mg bid		
Antibiotic	Anti-inflammatory	Rifaximin	550 mg tid	Effective: In 2012 SRMA: Global: OR 1.57 (1.22 to 2.01); Bloating: OR 1.55 (1.23 to 1.96); In 2020 SRMA: FDA composite: OR: 0.92 (0.86 to 0.98) Global OR: 0.91 (0.77, 1.07)	Second-line
5-HT3 Receptor antagonists	Delays colonic transit and reduces visceral pain	Alosetron	0.5-1 mg qd or 1 mg bid	Effective: Global RR 1.60 (1.49 to 1.72); Pain RR 1.30 (1.22 to 1.39); FDA composite: OR 0.69 (0.60 to 0.80)	Third-line
		Ramosetron	2.5 μg qd		
IBS-C					
Osmotic	Osmotic secretion	PEG3350	-	Effective: improves SBMs, CSBMs, consistency straining but not pain, bloating or incomplete evacuation	First-line
Secretory	Increased Cl- and water secretion	Lubiprostone	8 μg bid	Effective: Lubiprostone 8 μg RR: 0.85 (0.78 to 0.96) for FDA endpoint	Second-line
		Linaclotide	290 mg qd	Effective: Adequate relief IBS: RR 1.95 (1.3 to 2.9); Abdo pain: RR 1.58 (1.02 to 2.46) RR 0.81 (0.76 to 0.86) for 290 μg for FDA endpoint	
		Plecanatide	3 mg/6 mg qd	Effective: Using FDA endpoint 6 mg: RR 0.87 (0.81 to 0.94); 3 mg RR 0.88 (0.82 to 0.94)	
Anti-absorptive	NHE3 inhibitor stimulates Na+, water secretion	Tenapanor	15mg bid	Effective at 50 mg 2/d; NNT, 7-9 for complete SBM and combined complete SBM ≥ 30% pain reduction; 11 for abdominal pain reduction > 30% alone	Third-line
Pain					
Anti-spasmodics	Inhibition of muscarinic Ach receptors or block Ca++ channels, relaxation of GI smooth muscle	Pinaverium	50 mg tid	May be effective: OR, 0.68 (95%CI: 0.57-0.71); overall NNT, 5	First-line
		Otilonium	20/40/80 mg tid		
		Hyoscine	-		
		Peppermint Oil	182 mg	Effective: OR, 0.43 (95%CI: 0.32-0.59); Global: RR 2.23 (95%CI: 1.78-2.81); overall NNT, 2.5; RCT of sustained release formulation: decrease pain, bloat, urgency but not total IBS scores	
Antidepressants	Psychological, acting on the CNS	TCA	-	Effective: OR, 0.67 (95%CI: 0.58-0.77); for global: OR, 0.62 (95%CI: 0.43-0.88); NNT, 4 for abdominal pain	Second-line
		SSRI	-		

Adapted from Camilleri *et al*[82]. Ach: Acetylcholine; 5-HT3: Serotonin type 3; IBS: Irritable bowel syndrome; IBS-C: Constipation; IBS-D: Diarrhea; IBS-M: Mixed symptoms; NHE3: Sodium-hydrogen exchanger 3; OR: Odds ratio; PEG 3350: Polyethylene glycol 3350; RCT: Randomized clinical trial; RR: Relative risk; Rx: Prescription; SSRI: Selective serotonin reuptake inhibitor; SBM: Spontaneous bowel movement; SRMA: Systematic review and meta-analysis; TCA: Tricyclic antidepressant.

showed that the TCM symptom score, gastrointestinal symptom score, and IBS-SSS score were significantly reduced in the moxibustion group[125]. Overall, Pishu (BL 20), Zhongwan (RN 12), and Zusanli (ST 36) are acupuncture points commonly used in clinical practice, and acupuncture and moxibustion have few side effects[93].

Microbial therapy

Probiotics: Probiotics can relieve bloating, intestinal gas, and IBS symptoms, and in addition, studies have shown that probiotics (*Lactobacillus*, *Bifidobacterium*, *Escherichia coli*, and *Streptococcus*) can significantly relieve the overall symptoms of diarrhea and IBS-D[126,127]. However, the role of probiotics is controversial; a small number of studies have discovered that probiotics have no effect on bloating or abdominal pain[128,129]. A RCT included 389 patients with IBS. The control group was treated with oral probiotics for 6 wk. The final results showed that the treatment effect of probiotics was not superior to placebo when all IBS subtypes were included, but the analysis found a higher percentage of sustained responders in the probiotic group than in the placebo group in IBS-D[130]. Although there is a contradiction in the current evidence, analyzing it objectively resolved the contradictions and also demonstrated that probiotics have great potential for the treatment of IBS, especially in patients with IBS-D[131].

Prebiotics and synbiotics: Prebiotics and synbiotics, the collaboration of prebiotics and probiotics, become synbiotics, which have beneficial effects on the gastrointestinal tract by regulating the diversity and activity of intestinal microorganisms and protecting the integrity of the intestinal mucosa[132,133]. A RCT reported, that compared to placebo, synbiotics treatment over an 8-wk period (*Lactobacillus* and *Bifidobacterium* probiotic strains and short-chain fructooligosaccharides; colony-forming units (CFU) per sachet was five billion, bid) significantly improved overall symptoms of IBS, flatulence (P = 0.028), and bowel habits (P = 0.028). It is recommended to try probiotics for 12 wk and observe the efficacy[83], have benefits in improving IBS-D.

Fecal microbiota transplantation: Fecal microbiota transplantation (FMT) for *Clostridium difficile* infection has shown good efficacy in improving intestinal flora[134], and although studies on FMT for IBS are scarce and results remain controversial, the overall results suggest a positive trend for FMT for IBS. A RCT included 135 IBS patients randomly assigned to receive their own stool, 30 g FMT, or 60 g FMT, with response rates of 23.6%, 76.9%, and 89.1%, respectively [135]. Moreover, a recent study has found that FMT not only improves the symptoms of IBS patients but also improves depression and anxiety[93]. However, the studies of Madsen, A.M.A. *et al*[136] and Browne *et al*[137] reported that FMT capsules have no clinical benefit on abdominal pain, stool frequency, or stool form in IBS patients and have no benefit. Therefore, the clinical practice and clinical effect of FMT in the field of gut microbiomes and IBS need to be further verified and explored.

CONCLUSION

IBS-related studies have shown a downward trend in IBS dysfunction, and the brain-gut axis is gradually becoming more prominent in IBS research by reviewing the related research of the last decade. With the help of convenient laboratory tests, a new diagnosis and treatment model was formed based on the complex etiology and clinical combination of IBS, and the above has positive implications for a new understanding of IBS.

It is concluded that a pooled global prevalence of IBS is unlikely to be meaningful and that future research should focus more on regionalization. The definition of IBS has been updated with the discovery of overlapping symptoms and advances in research on IBS pathogenesis, and its definition tends to suggest that FGIDs are a group of disorders with the same pathogenesis, such as the brain-gut axis and visceral hypersensitivity. Therefore, in the future, we should pay more attention to the influence of the brain-gut axis and the central nervous system on the entire gastrointestinal tract and understand FGIDs as a whole. IBS is a dysfunctional disease, but in the absence of simple and inexpensive screening tests for many biological markers, patients such as those with BAD are still included in IBS-D. These technologies still need further validation and dissemination. It is possible that an updated Rome criteria will exclude them from the IBS diagnosis as technology advances. Furthermore, studies of IBS-related dietary interventions, such as LFD, special diets for IBS-C, and foods with gastrointestinal allergies, as well as the gut microenvironment and the brain-gut axis, are the hot spots of research on gut inflammation and the gut barrier.

Long-term treatment brings economic pressure and psychological burden, and for patients for whom conventional treatment is ineffective, further search for etiology should be done with the help of adjuvant examinations, and appropriate second-line treatment or psychotherapy should be chosen. In recent years, non-pharmacological treatment and Chinese medicine have been favored by IBS patients, but the current treatment should be further improved in order to facilitate the development of alternative medicine, with lifestyle, diet, and acupressure as routine interventions. It is important to note that lifestyle and CBT only relieve the symptoms and frequency of IBS; they do not improve the quality of life. Moreover, the involvement of microbiota in the brain-gut axis is widely recognized and studied, and RCTs related to intestinal flora have yielded encouraging results. However, current studies of microbiota are mostly related to IBS-D and have limitations. Let's look forward to more clarity on the treatment and management of IBS.

FOOTNOTES

Author contributions: Huang KY reviewed the literature and wrote the first draft of the paper; Wang FY contributed to searching the literature and edited it; Lv M and Ma XX contributed to revising the paper and wrote it; and Tang XD conceived the idea and edited it; Lv L contributed to writing the paper, completed Figures 3 and 4, and edited it extensively.

Supported by National Natural Science Foundation of China, No. 81873297; the Fundamental Research Funds for the Central Public

Welfare Research Institutes, China, No. ZZ13-YQ-006; and Innovation Fund of Chinese Academy of Chinese Medical Sciences, China, No. CI2021A01003.

Conflict-of-interest statement: Dr. LV reports grants from National Natural Science Foundation of China, grants from The Fundamental Research Funds for the Central Public Welfare Research Institutes, China, and grants from Innovation Fund of Chinese Academy of Chinese Medical Sciences, outside the submitted work.

Open-Access: This article is an open-access article that was selected by an in-house editor and fully peer-reviewed by external reviewers. It is distributed in accordance with the Creative Commons Attribution NonCommercial (CC BY-NC 4.0) license, which permits others to distribute, remix, adapt, build upon this work non-commercially, and license their derivative works on different terms, provided the original work is properly cited and the use is non-commercial. See: https://creativecommons.org/Licenses/by-nc/4.0/

Country/Territory of origin: China

ORCID number: Kai-Yue Huang 0000-0001-6535-8466; Feng-Yun Wang 0000-0002-4058-7905; Mi Lv 0000-0002-1715-8643; Xu-Dong Tang 0000-0002-0875-3491; Lin Lv 0000-0003-4474-1938.

S-Editor: Yan JP
L-Editor: A
P-Editor: Cai YX

REFERENCES

1 **Yang W**, Yang X, Cai X, Zhou Z, Yao H, Song X, Zhao T, Xiong P. The Prevalence of Irritable Bowel Syndrome Among Chinese University Students: A Systematic Review and Meta-Analysis. *Front Public Health* 2022; **10**: 864721 [PMID: 35493361 DOI: 10.3389/fpubh.2022.864721]
2 **Roisinblit KC**. Irritable bowel syndrome in women. *J Midwifery Womens Health* 2013; **58**: 15-24; quiz 116 [PMID: 23279011 DOI: 10.1111/j.1542-2011.2012.00200.x]
3 **Sperber AD**, Bangdiwala SI, Drossman DA, Ghoshal UC, Simren M, Tack J, Whitehead WE, Dumitrascu DL, Fang X, Fukudo S, Kellow J, Okeke E, Quigley EMM, Schmulson M, Whorwell P, Archampong T, Adibi P, Andresen V, Benninga MA, Bonaz B, Bor S, Fernandez LB, Choi SC, Corazziari ES, Francisconi C, Hani A, Lazebnik L, Lee YY, Mulak A, Rahman MM, Santos J, Setshedi M, Syam AF, Vanner S, Wong RK, Lopez-Colombo A, Costa V, Dickman R, Kanazawa M, Keshteli AH, Khatun R, Maleki I, Poitras P, Pratap N, Stefanyuk O, Thomson S, Zeevenhooven J, Palsson OS. Worldwide Prevalence and Burden of Functional Gastrointestinal Disorders, Results of Rome Foundation Global Study. *Gastroenterology* 2021; **160**: 99-114.e3 [PMID: 32294476 DOI: 10.1053/j.gastro.2020.04.014]
4 **Black CJ**, Ford AC. Global burden of irritable bowel syndrome: trends, predictions and risk factors. *Nat Rev Gastroenterol Hepatol* 2020; **17**: 473-486 [PMID: 32296140 DOI: 10.1038/s41575-020-0286-8]
5 **Sperber AD**, Dumitrascu D, Fukudo S, Gerson C, Ghoshal UC, Gwee KA, Hungin APS, Kang JY, Minhu C, Schmulson M, Bolotin A, Friger M, Freud T, Whitehead W. The global prevalence of IBS in adults remains elusive due to the heterogeneity of studies: a Rome Foundation working team literature review. *Gut* 2017; **66**: 1075-1082 [PMID: 26818616 DOI: 10.1136/gutjnl-2015-311240]
6 **Rahman MM**, Mahadeva S, Ghoshal UC. Epidemiological and clinical perspectives on irritable bowel syndrome in India, Bangladesh and Malaysia: A review. *World J Gastroenterol* 2017; **23**: 6788-6801 [PMID: 29085223 DOI: 10.3748/wjg.v23.i37.6788]
7 **Sperber AD**. Epidemiology and Burden of Irritable Bowel Syndrome: An International Perspective. *Gastroenterol Clin North Am* 2021; **50**: 489-503 [PMID: 34304784 DOI: 10.1016/j.gtc.2021.04.001]
8 **Galica AN**, Galica R, Dumitrascu DL. Epidemiology of Irritable Bowel Syndrome in Albania. *J Gastrointestin Liver Dis* 2021; **30**: 334-338 [PMID: 34551031 DOI: 10.15403/jgld-3828]
9 **Kovács DB**, Szekely A, Hubai AG, Palsson O. Prevalence, epidemiology and associated healthcare burden of Rome IV irritable bowel syndrome and functional dyspepsia in the adult population of Gibraltar. *BMJ Open Gastroenterol* 2022; **9** [PMID: 35953148 DOI: 10.1136/bmjgast-2022-000979]
10 **Long Y**, Huang Z, Deng Y, Chu H, Zheng X, Yang J, Zhu Y, Fried M, Fox M, Dai N. Prevalence and risk factors for functional bowel disorders in South China: a population based study using the Rome III criteria. *Neurogastroenterol Motil* 2017; **29** [PMID: 27412422 DOI: 10.1111/nmo.12897]
11 **Pontet Y**, Olano C. [Irritable bowel syndrome prevalence in Latin America]. *Rev Gastroenterol Peru* 2021; **41**: 144-149 [PMID: 34978550]
12 **Palsson OS**, Whitehead W, Törnblom H, Sperber AD, Simren M. Prevalence of Rome IV Functional Bowel Disorders Among Adults in the United States, Canada, and the United Kingdom. *Gastroenterology* 2020; **158**: 1262-1273.e3 [PMID: 31917991 DOI: 10.1053/j.gastro.2019.12.021]
13 **Lovell RM**, Ford AC. Effect of gender on prevalence of irritable bowel syndrome in the community: systematic review and meta-analysis. *Am J Gastroenterol* 2012; **107**: 991-1000 [PMID: 22613905 DOI: 10.1038/ajg.2012.131]
14 **Gwee KA**, Lu CL, Ghoshal UC. Epidemiology of irritable bowel syndrome in Asia: something old, something new, something borrowed. *J Gastroenterol Hepatol* 2009; **24**: 1601-1607 [PMID: 19788601 DOI: 10.1111/j.1440-1746.2009.05984.x]
15 **Gwee KA**. Irritable bowel syndrome in developing countries--a disorder of civilization or colonization? *Neurogastroenterol Motil* 2005; **17**: 317-324 [PMID: 15916618 DOI: 10.1111/j.1365-2982.2005.00627.x]
16 **Ghoshal UC**, Singh R. Frequency and risk factors of functional gastro-intestinal disorders in a rural Indian population. *J Gastroenterol Hepatol* 2017; **32**: 378-387 [PMID: 27262283 DOI: 10.1111/jgh.13465]
17 **Husain N**, Chaudhry IB, Jafri F, Niaz SK, Tomenson B, Creed F. A population-based study of irritable bowel syndrome in a non-Western population. *Neurogastroenterol Motil* 2008; **20**: 1022-1029 [PMID: 18492027 DOI: 10.1111/j.1365-2982.2008.01143.x]

18 **Devanarayana NM**, Rajindrajith S, Pathmeswaran A, Abegunasekara C, Gunawardena NK, Benninga MA. Epidemiology of irritable bowel syndrome in children and adolescents in Asia. *J Pediatr Gastroenterol Nutr* 2015; **60**: 792-798 [PMID: 26000888 DOI: 10.1097/MPG.0000000000000714]

19 **AlButaysh OF**, AlQuraini AA, Almukhaitah AA, Alahmdi YM, Alharbi FS. Epidemiology of irritable bowel syndrome and its associated factors in Saudi undergraduate students. *Saudi J Gastroenterol* 2020; **26**: 89-93 [PMID: 32031159 DOI: 10.4103/sjg.SJG_459_19]

20 **Drossman DA**. Functional Gastrointestinal Disorders: History, Pathophysiology, Clinical Features and Rome IV. *Gastroenterology* 2016 [PMID: 27144617 DOI: 10.1053/j.gastro.2016.02.032]

21 **Sperber AD**, Freud T, Aziz I, Palsson OS, Drossman DA, Dumitrascu DL, Fang X, Fukudo S, Ghoshal UC, Kellow J, Khatun R, Okeke E, Quigley EMM, Schmulson M, Simren M, Tack J, Whitehead WE, Whorwell P, Bangdiwala SI. Greater Overlap of Rome IV Disorders of Gut-Brain Interactions Leads to Increased Disease Severity and Poorer Quality of Life. *Clin Gastroenterol Hepatol* 2022; **20**: e945-e956 [PMID: 34052391 DOI: 10.1016/j.cgh.2021.05.042]

22 **Madisch A**, Andresen V, Enck P, Labenz J, Frieling T, Schemann M. The Diagnosis and Treatment of Functional Dyspepsia. *Dtsch Arztebl Int* 2018; **115**: 222-232 [PMID: 29669681 DOI: 10.3238/arztebl.2018.0222]

23 **Agréus L**, Svärdsudd K, Nyrén O, Tibblin G. Irritable bowel syndrome and dyspepsia in the general population: overlap and lack of stability over time. *Gastroenterology* 1995; **109**: 671-680 [PMID: 7657095 DOI: 10.1016/0016-5085(95)90373-9]

24 **Whitehead WE**, Gibbs NA, Li Z, Drossman DA. Is functional dyspepsia just a subset of the irritable bowel syndrome? *Baillieres Clin Gastroenterol* 1998; **12**: 443-461 [PMID: 9890081 DOI: 10.1016/s0950-3528(98)90017-3]

25 **von Wulffen M**, Talley NJ, Hammer J, McMaster J, Rich G, Shah A, Koloski N, Kendall BJ, Jones M, Holtmann G. Overlap of Irritable Bowel Syndrome and Functional Dyspepsia in the Clinical Setting: Prevalence and Risk Factors. *Dig Dis Sci* 2019; **64**: 480-486 [PMID: 30368683 DOI: 10.1007/s10620-018-5343-6]

26 **Barberio B**, Yiannakou Y, Houghton LA, Black CJ, Savarino EV, Ford AC. Overlap of Rome IV Irritable Bowel Syndrome and Functional Dyspepsia and Effect on Natural History: A Longitudinal Follow-Up Study. *Clin Gastroenterol Hepatol* 2022; **20**: e89-e101 [PMID: 33839276 DOI: 10.1016/j.cgh.2021.04.011]

27 **Choi YJ**, Kim N, Yoon H, Shin CM, Park YS, Kim JW, Kim YS, Lee DH, Jung HC. Overlap between irritable bowel syndrome and functional dyspepsia including subtype analyses. *J Gastroenterol Hepatol* 2017; **32**: 1553-1561 [PMID: 28160607 DOI: 10.1111/jgh.13756]

28 **Nam K**, Kim N, Song HJ, Baik GH, Choi SC, Kim HJ, Lee JY, Park KS, Park SY, Park SJ. Gender difference in the overlap of irritable bowel syndrome and functional dyspepsia: a prospective nationwide multicenter study in Korea. *J Gastroenterol* 2021; **56**: 537-546 [PMID: 33687537 DOI: 10.1007/s00535-021-01775-2]

29 **Jones MP**, Shah A, Walker MM, Koloski NA, Holtmann G, Talley NJ. Overlap of heartburn, functional dyspepsia, and irritable bowel syndrome in a population sample: Prevalence, temporal stability, and associated comorbidities. *Neurogastroenterol Motil* 2022; **34**: e14349 [PMID: 35293084 DOI: 10.1111/nmo.14349]

30 **Vakil N**, van Zanten SV, Kahrilas P, Dent J, Jones R; Global Consensus Group. The Montreal definition and classification of gastroesophageal reflux disease: a global evidence-based consensus. *Am J Gastroenterol* 2006; **101**: 1900-20; quiz 1943 [PMID: 16928254 DOI: 10.1111/j.1572-0241.2006.00630.x]

31 **Fass R**, Boeckxstaens GE, El-Serag H, Rosen R, Sifrim D, Vaezi MF. Gastro-oesophageal reflux disease. *Nat Rev Dis Primers* 2021; **7**: 55 [PMID: 34326345 DOI: 10.1038/s41572-021-00287-w]

32 **Rasmussen S**, Jensen TH, Henriksen SL, Haastrup PF, Larsen PV, Søndergaard J, Jarbøl DE. Overlap of symptoms of gastroesophageal reflux disease, dyspepsia and irritable bowel syndrome in the general population. *Scand J Gastroenterol* 2015; **50**: 162-169 [PMID: 25525975 DOI: 10.3109/00365521.2014.983157]

33 **Lovell RM**, Ford AC. Prevalence of gastro-esophageal reflux-type symptoms in individuals with irritable bowel syndrome in the community: a meta-analysis. *Am J Gastroenterol* 2012; **107**: 1793-801; quiz 1802 [PMID: 23032982 DOI: 10.1038/ajg.2012.336]

34 **de Bortoli N**, Tolone S, Frazzoni M, Martinucci I, Sgherri G, Albano E, Ceccarelli L, Stasi C, Bellini M, Savarino V, Savarino EV, Marchi S. Gastroesophageal reflux disease, functional dyspepsia and irritable bowel syndrome: common overlapping gastrointestinal disorders. *Ann Gastroenterol* 2018; **31**: 639-648 [PMID: 30386113 DOI: 10.20524/aog.2018.0314]

35 **de Bortoli N**, Frazzoni L, Savarino EV, Frazzoni M, Martinucci I, Jania A, Tolone S, Scagliarini M, Bellini M, Marabotto E, Furnari M, Bodini G, Russo S, Bertani L, Natali V, Fuccio L, Savarino V, Blandizzi C, Marchi S. Functional Heartburn Overlaps With Irritable Bowel Syndrome More Often than GERD. *Am J Gastroenterol* 2016; **111**: 1711-1717 [PMID: 27644732 DOI: 10.1038/ajg.2016.432]

36 **Torres J**, Mehandru S, Colombel JF, Peyrin-Biroulet L. Crohn's disease. *Lancet* 2017; **389**: 1741-1755 [PMID: 27914655 DOI: 10.1016/S0140-6736(16)31711-1]

37 **Glick LR**, Cifu AS, Feld L. Ulcerative Colitis in Adults. *JAMA* 2020; **324**: 1205-1206 [PMID: 32857108 DOI: 10.1001/jama.2020.11583]

38 **Fairbrass KM**, Costantino SJ, Gracie DJ, Ford AC. Prevalence of irritable bowel syndrome-type symptoms in patients with inflammatory bowel disease in remission: a systematic review and meta-analysis. *Lancet Gastroenterol Hepatol* 2020; **5**: 1053-1062 [PMID: 33010814 DOI: 10.1016/S2468-1253(20)30300-9]

39 **Müller M**, Willén R, Stotzer PO. Colonoscopy and SeHCAT for investigation of chronic diarrhea. *Digestion* 2004; **69**: 211-218 [PMID: 15205569 DOI: 10.1159/000079150]

40 **Klem F**, Wadhwa A, Prokop LJ, Sundt WJ, Farrugia G, Camilleri M, Singh S, Grover M. Prevalence, Risk Factors, and Outcomes of Irritable Bowel Syndrome After Infectious Enteritis: A Systematic Review and Meta-analysis. *Gastroenterology* 2017; **152**: 1042-1054.e1 [PMID: 28069350 DOI: 10.1053/j.gastro.2016.12.039]

41 **Slade GD**, Greenspan JD, Fillingim RB, Maixner W, Sharma S, Ohrbach R. Overlap of Five Chronic Pain Conditions: Temporomandibular Disorders, Headache, Back Pain, Irritable Bowel Syndrome, and Fibromyalgia. *J Oral Facial Pain Headache* 2020; **34**: s15-s28 [PMID: 32975538 DOI: 10.11607/ofph.2581]

42 **Üçüncü MZ**, Çoruh Akyol B, Toprak D. The early diagnosis of fibromyalgia in irritable bowel syndrome patients. *Med Hypotheses* 2020; **143**: 110119 [PMID: 32721811 DOI: 10.1016/j.mehy.2020.110119]

43 **Rej A**, Sanders DS. The overlap of irritable bowel syndrome and noncoeliac gluten sensitivity. *Curr Opin Gastroenterol* 2019; **35**: 199-205 [PMID: 30762700 DOI: 10.1097/MOG.0000000000000517]

44 **DiVasta AD**, Zimmerman LA, Vitonis AF, Fadayomi AB, Missmer SA. Overlap Between Irritable Bowel Syndrome Diagnosis and Endometriosis in Adolescents. *Clin Gastroenterol Hepatol* 2021; **19**: 528-537.e1 [PMID: 32184183 DOI: 10.1016/j.cgh.2020.03.014]

45 **Holtmann GJ**, Ford AC, Talley NJ. Pathophysiology of irritable bowel syndrome. *Lancet Gastroenterol Hepatol* 2016; **1**: 133-146 [PMID:

28404070 DOI: 10.1016/S2468-1253(16)30023-1]
46 **Waseem MR**, Shin A, Siwiec R, James-Stevenson T, Bohm M, Rogers N, Wo J, Waseem L, Gupta A, Jarrett M, Kadariya J, Xu H. Associations of Fecal Short Chain Fatty Acids With Colonic Transit, Fecal Bile Acid, and Food Intake in Irritable Bowel Syndrome. *Clin Transl Gastroenterol* 2023; **14**: e00541 [PMID: 36227781 DOI: 10.14309/ctg.0000000000000541]
47 **Wei W**, Wang H, Zhang Y, Niu B, Chen S, Zhang W, Yao S. Faecal bile acids and colonic bile acid membrane receptor correlate with symptom severity of diarrhoea-predominant irritable bowel syndrome: A pilot study. *Dig Liver Dis* 2021; **53**: 1120-1127 [PMID: 34053874 DOI: 10.1016/j.dld.2021.04.022]
48 **Algera JP**, Colomier E, Melchior C, Hreinsson JP, Midenfjord I, Clevers E, Simrén M, Törnblom H. Associations between postprandial symptoms, hydrogen and methane production, and transit time in irritable bowel syndrome. *Neurogastroenterol Motil* 2023; **35**: e14482 [PMID: 36221245 DOI: 10.1111/nmo.14482]
49 **DuPont AW**, Jiang ZD, Harold SA, Snyder N, Galler GW, Garcia-Torres F, DuPont HL. Motility abnormalities in irritable bowel syndrome. *Digestion* 2014; **89**: 119-123 [PMID: 24503633 DOI: 10.1159/000356314]
50 **Sandström O**, El-Salhy M. Ageing and endocrine cells of human duodenum. *Mech Ageing Dev* 1999; **108**: 39-48 [PMID: 10366038 DOI: 10.1016/s0047-6374(98)00154-7]
51 **Lee J**, Cummings BP, Martin E, Sharp JW, Graham JL, Stanhope KL, Havel PJ, Raybould HE. Glucose sensing by gut endocrine cells and activation of the vagal afferent pathway is impaired in a rodent model of type 2 diabetes mellitus. *Am J Physiol Regul Integr Comp Physiol* 2012; **302**: R657-R666 [PMID: 22160540 DOI: 10.1152/ajpregu.00345.2011]
52 **Cani PD**, Everard A, Duparc T. Gut microbiota, enteroendocrine functions and metabolism. *Curr Opin Pharmacol* 2013; **13**: 935-940 [PMID: 24075718 DOI: 10.1016/j.coph.2013.09.008]
53 **Mazzawi T**, El-Salhy M. Effect of diet and individual dietary guidance on gastrointestinal endocrine cells in patients with irritable bowel syndrome (Review). *Int J Mol Med* 2017; **40**: 943-952 [PMID: 28849091 DOI: 10.3892/ijmm.2017.3096]
54 **Gershon MD**, Tack J. The serotonin signaling system: from basic understanding to drug development for functional GI disorders. *Gastroenterology* 2007; **132**: 397-414 [PMID: 17241888 DOI: 10.1053/j.gastro.2006.11.002]
55 **Bertrand PP**, Bertrand RL. Serotonin release and uptake in the gastrointestinal tract. *Auton Neurosci* 2010; **153**: 47-57 [PMID: 19729349 DOI: 10.1016/j.autneu.2009.08.002]
56 **Bertrand PP**. The cornucopia of intestinal chemosensory transduction. *Front Neurosci* 2009; **3**: 48 [PMID: 20582275 DOI: 10.3389/neuro.21.003.2009]
57 **Nisticò V**, Rossi RE, D'Arrigo AM, Priori A, Gambini O, Demartini B. Functional Neuroimaging in Irritable Bowel Syndrome: A Systematic Review Highlights Common Brain Alterations With Functional Movement Disorders. *J Neurogastroenterol Motil* 2022; **28**: 185-203 [PMID: 35189600 DOI: 10.5056/jnm21079]
58 **Grinsvall C**, Ryu HJ, Van Oudenhove L, Labus JS, Gupta A, Ljungberg M, Törnblom H, Mayer EA, Simrén M. Association between pain sensitivity and gray matter properties in the sensorimotor network in women with irritable bowel syndrome. *Neurogastroenterol Motil* 2021; **33**: e14027 [PMID: 33174312 DOI: 10.1111/nmo.14027]
59 **Nozu T**, Okumura T. Corticotropin-releasing factor receptor type 1 and type 2 interaction in irritable bowel syndrome. *J Gastroenterol* 2015; **50**: 819-830 [PMID: 25962711 DOI: 10.1007/s00535-015-1086-8]
60 **Nozu T**, Miyagishi S, Nozu R, Takakusaki K, Okumura T. Lipopolysaccharide induces visceral hypersensitivity: role of interleukin-1, interleukin-6, and peripheral corticotropin-releasing factor in rats. *J Gastroenterol* 2017; **52**: 72-80 [PMID: 27075754 DOI: 10.1007/s00535-016-1208-y]
61 **Nozu T**, Miyagishi S, Ishioh M, Takakusaki K, Okumura T. Peripheral apelin mediates visceral hypersensitivity and impaired gut barrier in a rat irritable bowel syndrome model. *Neuropeptides* 2022; **94**: 102248 [PMID: 35526468 DOI: 10.1016/j.npep.2022.102248]
62 **Dlugosz A**, Nowak P, D'Amato M, Mohammadian Kermani G, Nyström J, Abdurahman S, Lindberg G. Increased serum levels of lipopolysaccharide and antiflagellin antibodies in patients with diarrhea-predominant irritable bowel syndrome. *Neurogastroenterol Motil* 2015; **27**: 1747-1754 [PMID: 26387872 DOI: 10.1111/nmo.12670]
63 **Constante M**, De Palma G, Lu J, Jury J, Rondeau L, Caminero A, Collins SM, Verdu EF, Bercik P. Saccharomyces boulardii CNCM I-745 modulates the microbiota-gut-brain axis in a humanized mouse model of Irritable Bowel Syndrome. *Neurogastroenterol Motil* 2021; **33**: e13985 [PMID: 32955166 DOI: 10.1111/nmo.13985]
64 **Zhou Q**, Yang L, Larson S, Basra S, Merwat S, Tan A, Croce C, Verne GN. Decreased miR-199 augments visceral pain in patients with IBS through translational upregulation of TRPV1. *Gut* 2016; **65**: 797-805 [PMID: 25681400 DOI: 10.1136/gutjnl-2013-306464]
65 **Nozu T**, Miyagishi S, Nozu R, Ishioh M, Takakusaki K, Okumura T. EMA401, an angiotensin II type 2 receptor antagonist blocks visceral hypersensitivity and colonic hyperpermeability in rat model of irritable bowel syndrome. *J Pharmacol Sci* 2021; **146**: 121-124 [PMID: 34030794 DOI: 10.1016/j.jphs.2021.04.001]
66 **Fan F**, Tang Y, Dai H, Cao Y, Sun P, Chen Y, Chen A, Lin C. Blockade of BDNF signalling attenuates chronic visceral hypersensitivity in an IBS-like rat model. *Eur J Pain* 2020; **24**: 839-850 [PMID: 31976585 DOI: 10.1002/ejp.1534]
67 **Hasler WL**, Grabauskas G, Singh P, Owyang C. Mast cell mediation of visceral sensation and permeability in irritable bowel syndrome. *Neurogastroenterol Motil* 2022; **34**: e14339 [PMID: 35315179 DOI: 10.1111/nmo.14339]
68 **Chen Z**, Liu Y, Wu X, Lin W, Liu Z, Huang Y, Chen Y, Tang Y, Chen A, Lin C. Spinal CircKcnk9 Regulates Chronic Visceral Hypersensitivity of Irritable Bowel Syndrome. *J Pain* 2023; **24**: 463-477 [PMID: 36257575 DOI: 10.1016/j.jpain.2022.10.007]
69 **Tozlu M**, Cash B, Younes M, Ertan A. Dilemma in post-IBD patients with IBS-D symptoms: A 2020 overview. *Expert Rev Gastroenterol Hepatol* 2021; **15**: 5-8 [PMID: 32990090 DOI: 10.1080/17474124.2021.1829469]
70 **El-Salhy M**, Hatlebakk JG, Hausken T. Possible role of peptide YY (PYY) in the pathophysiology of irritable bowel syndrome (IBS). *Neuropeptides* 2020; **79**: 101973 [PMID: 31727345 DOI: 10.1016/j.npep.2019.101973]
71 **Koloski NA**, Jones M, Kalantar J, Weltman M, Zaguirre J, Talley NJ. The brain--gut pathway in functional gastrointestinal disorders is bidirectional: a 12-year prospective population-based study. *Gut* 2012; **61**: 1284-1290 [PMID: 22234979 DOI: 10.1136/gutjnl-2011-300474]
72 **Koloski NA**, Jones M, Talley NJ. Evidence that independent gut-to-brain and brain-to-gut pathways operate in the irritable bowel syndrome and functional dyspepsia: a 1-year population-based prospective study. *Aliment Pharmacol Ther* 2016; **44**: 592-600 [PMID: 27444264 DOI: 10.1111/apt.13738]
73 **Dinan TG**, Cryan JF. Gut-brain axis in 2016: Brain-gut-microbiota axis - mood, metabolism and behaviour. *Nat Rev Gastroenterol Hepatol* 2017; **14**: 69-70 [PMID: 28053341 DOI: 10.1038/nrgastro.2016.200]

74 **Dinan TG**, Cryan JF. Brain-Gut-Microbiota Axis and Mental Health. *Psychosom Med* 2017; **79**: 920-926 [PMID: 28806201 DOI: 10.1097/PSY.0000000000000519]

75 **Sabo CM**, Dumitrascu DL. Microbiota and the irritable bowel syndrome. *Minerva Gastroenterol (Torino)* 2021; **67**: 377-384 [PMID: 34515452 DOI: 10.23736/S2724-5985.21.02923-5]

76 **Mishima Y**, Ishihara S. Molecular Mechanisms of Microbiota-Mediated Pathology in Irritable Bowel Syndrome. *Int J Mol Sci* 2020; **21** [PMID: 33212919 DOI: 10.3390/ijms21228664]

77 **Lee SM**, Kim N, Yoon H, Kim YS, Choi SI, Park JH, Lee DH. Compositional and Functional Changes in the Gut Microbiota in Irritable Bowel Syndrome Patients. *Gut Liver* 2021; **15**: 253-261 [PMID: 32457278 DOI: 10.5009/gnl19379]

78 **Mujagic Z**, Kasapi M, Jonkers DM, Garcia-Perez I, Vork L, Weerts ZZRM, Serrano-Contreras JI, Zhernakova A, Kurilshikov A, Scotcher J, Holmes E, Wijmenga C, Keszthelyi D, Nicholson JK, Posma JM, Masclee AA. Integrated fecal microbiome-metabolome signatures reflect stress and serotonin metabolism in irritable bowel syndrome. *Gut Microbes* 2022; **14**: 2063016 [PMID: 35446234 DOI: 10.1080/19490976.2022.2063016]

79 **Mearin F**, Lacy BE, Chang L, Chey WD, Lembo AJ, Simren M, Spiller R. Bowel Disorders. *Gastroenterology* 2016 [PMID: 27144627 DOI: 10.1053/j.gastro.2016.02.031]

80 **Vijayvargiya P**, Camilleri M, Burton D, Busciglio I, Lueke A, Donato LJ. Bile and fat excretion are biomarkers of clinically significant diarrhoea and constipation in irritable bowel syndrome. *Aliment Pharmacol Ther* 2019; **49**: 744-758 [PMID: 30740753 DOI: 10.1111/apt.15106]

81 **Karatay E**, Utku ÖG. Serum resolvin D1 levels as a marker of inflammation in constipation dominant irritable bowel syndrome. *Turk J Gastroenterol* 2020; **31**: 113-119 [PMID: 32141819 DOI: 10.5152/tjg.2020.19751]

82 **Camilleri M**, Boeckxstaens G. Irritable bowel syndrome: treatment based on pathophysiology and biomarkers. *Gut* 2023; **72**: 590-599 [PMID: 36307180 DOI: 10.1136/gutjnl-2022-328515]

83 **Vasant DH**, Paine PA, Black CJ, Houghton LA, Everitt HA, Corsetti M, Agrawal A, Aziz I, Farmer AD, Eugenicos MP, Moss-Morris R, Yiannakou Y, Ford AC. British Society of Gastroenterology guidelines on the management of irritable bowel syndrome. *Gut* 2021; **70**: 1214-1240 [PMID: 33903147 DOI: 10.1136/gutjnl-2021-324598]

84 **Black CJ**, Staudacher HM, Ford AC. Efficacy of a low FODMAP diet in irritable bowel syndrome: systematic review and network meta-analysis. *Gut* 2022; **71**: 1117-1126 [PMID: 34376515 DOI: 10.1136/gutjnl-2021-325214]

85 **Wu J**, Masuy I, Biesiekierski JR, Fitzke HE, Parikh C, Schofield L, Shaikh H, Bhagwanani A, Aziz Q, Taylor SA, Tack J, Van Oudenhove L. Gut-brain axis dysfunction underlies FODMAP-induced symptom generation in irritable bowel syndrome. *Aliment Pharmacol Ther* 2022; **55**: 670-682 [PMID: 35166384 DOI: 10.1111/apt.16812]

86 **Chey WD**, Hashash JG, Manning L, Chang L. AGA Clinical Practice Update on the Role of Diet in Irritable Bowel Syndrome: Expert Review. *Gastroenterology* 2022; **162**: 1737-1745.e5 [PMID: 35337654 DOI: 10.1053/j.gastro.2021.12.248]

87 **Schumann D**, Klose P, Lauche R, Dobos G, Langhorst J, Cramer H. Low fermentable, oligo-, di-, mono-saccharides and polyol diet in the treatment of irritable bowel syndrome: A systematic review and meta-analysis. *Nutrition* 2018; **45**: 24-31 [PMID: 29129233 DOI: 10.1016/j.nut.2017.07.004]

88 **Zannini E**, Arendt EK. Low FODMAPs and gluten-free foods for irritable bowel syndrome treatment: Lights and shadows. *Food Res Int* 2018; **110**: 33-41 [PMID: 30029704 DOI: 10.1016/j.foodres.2017.04.001]

89 **Ford AC**, Moayyedi P, Chey WD, Harris LA, Lacy BE, Saito YA, Quigley EMM; ACG Task Force on Management of Irritable Bowel Syndrome. American College of Gastroenterology Monograph on Management of Irritable Bowel Syndrome. *Am J Gastroenterol* 2018; **113**: 1-18 [PMID: 29950604 DOI: 10.1038/s41395-018-0084-x]

90 **Di Rosa C**, Altomare A, Terrigno V, Carbone F, Tack J, Cicala M, Guarino MPL. Constipation-Predominant Irritable Bowel Syndrome (IBS-C): Effects of Different Nutritional Patterns on Intestinal Dysbiosis and Symptoms. *Nutrients* 2023; **15** [PMID: 37049488 DOI: 10.3390/nu15071647]

91 **Garg P**. Inflammation in Irritable Bowel Syndrome (IBS): Role of Psyllium Fiber Supplementation in Decreasing Inflammation and Physiological Management of IBS. *Turk J Gastroenterol* 2021; **32**: 108-110 [PMID: 33893774 DOI: 10.5152/tjg.2020.20229]

92 **Saha L**. Irritable bowel syndrome: pathogenesis, diagnosis, treatment, and evidence-based medicine. *World J Gastroenterol* 2014; **20**: 6759-6773 [PMID: 24944467 DOI: 10.3748/wjg.v20.i22.6759]

93 **Bonetto S**, Fagoonee S, Battaglia E, Grassini M, Saracco GM, Pellicano R. Recent advances in the treatment of irritable bowel syndrome. *Pol Arch Intern Med* 2021; **131**: 709-715 [PMID: 34463082 DOI: 10.20452/pamw.16067]

94 **Sunderland R**. Irritable bowel syndrome in adults: symptoms, treatment and management. *Nurs Stand* 2017; **31**: 52-63 [PMID: 28224836]

95 **Keefer L**, Ballou SK, Drossman DA, Ringstrom G, Elsenbruch S, Ljótsson B. A Rome Working Team Report on Brain-Gut Behavior Therapies for Disorders of Gut-Brain Interaction. *Gastroenterology* 2022; **162**: 300-315 [PMID: 34529986 DOI: 10.1053/j.gastro.2021.09.015]

96 **Ford AC**, Lacy BE, Harris LA, Quigley EMM, Moayyedi P. Effect of Antidepressants and Psychological Therapies in Irritable Bowel Syndrome: An Updated Systematic Review and Meta-Analysis. *Am J Gastroenterol* 2019; **114**: 21-39 [PMID: 30177784 DOI: 10.1038/s41395-018-0222-5]

97 **Lackner JM**, Jaccard J, Radziwon CD, Firth RS, Gudleski GD, Hamilton F, Katz LA, Keefer L, Krasner SS, Ma CX, Sitrin MD, Brenner DM. Durability and Decay of Treatment Benefit of Cognitive Behavioral Therapy for Irritable Bowel Syndrome: 12-Month Follow-Up. *Am J Gastroenterol* 2019; **114**: 330-338 [PMID: 30429592 DOI: 10.1038/s41395-018-0396-x]

98 **Lalouni M**, Ljótsson B, Bonnert M, Ssegonja R, Benninga M, Bjureberg J, Högström J, Sahlin H, Simrén M, Feldman I, Hedman-Lagerlöf E, Serlachius E, Olén O. Clinical and Cost Effectiveness of Online Cognitive Behavioral Therapy in Children With Functional Abdominal Pain Disorders. *Clin Gastroenterol Hepatol* 2019; **17**: 2236-2244.e11 [PMID: 30502501 DOI: 10.1016/j.cgh.2018.11.043]

99 **Prior A**, Colgan SM, Whorwell PJ. Changes in rectal sensitivity after hypnotherapy in patients with irritable bowel syndrome. *Gut* 1990; **31**: 896-898 [PMID: 2387513 DOI: 10.1136/gut.31.8.896]

100 **Whorwell PJ**, Houghton LA, Taylor EE, Maxton DG. Physiological effects of emotion: assessment *via* hypnosis. *Lancet* 1992; **340**: 69-72 [PMID: 1352012 DOI: 10.1016/0140-6736(92)90394-i]

101 **Peter J**, Fournier C, Keip B, Rittershaus N, Stephanou-Rieser N, Durdevic M, Dejaco C, Michalski M, Moser G. Intestinal Microbiome in Irritable Bowel Syndrome before and after Gut-Directed Hypnotherapy. *Int J Mol Sci* 2018; **19** [PMID: 30453528 DOI: 10.3390/ijms19113619]

102 **De Benedittis G**. Hypnobiome: A New, Potential Frontier of Hypnotherapy in the Treatment of Irritable Bowel Syndrome-A Narrative Review of the Literature. *Int J Clin Exp Hypn* 2022; **70**: 286-299 [PMID: 35792903 DOI: 10.1080/00207144.2022.2094269]

103 **DeBenedittis G**, Cigada M, Bianchi A, Signorini MG, Cerutti S. Autonomic changes during hypnosis: a heart rate variability power spectrum analysis as a marker of sympatho-vagal balance. *Int J Clin Exp Hypn* 1994; **42**: 140-152 [PMID: 8200716 DOI: 10.1080/00207149408409347]

104 **Lembo A**, Sultan S, Chang L, Heidelbaugh JJ, Smalley W, Verne GN. AGA Clinical Practice Guideline on the Pharmacological Management of Irritable Bowel Syndrome With Diarrhea. *Gastroenterology* 2022; **163**: 137-151 [PMID: 35738725 DOI: 10.1053/j.gastro.2022.04.017]

105 **Chang L**, Sultan S, Lembo A, Verne GN, Smalley W, Heidelbaugh JJ. AGA Clinical Practice Guideline on the Pharmacological Management of Irritable Bowel Syndrome With Constipation. *Gastroenterology* 2022; **163**: 118-136 [PMID: 35738724 DOI: 10.1053/j.gastro.2022.04.016]

106 **Lacy BE**, Pimentel M, Brenner DM, Chey WD, Keefer LA, Long MD, Moshiree B. ACG Clinical Guideline: Management of Irritable Bowel Syndrome. *Am J Gastroenterol* 2021; **116**: 17-44 [PMID: 33315591 DOI: 10.14309/ajg.0000000000001036]

107 **Qin D**, Tao QF, Huang SL, Chen M, Zheng H. Eluxadoline Versus Antispasmodics in the Treatment of Irritable Bowel Syndrome: An Adjusted Indirect Treatment Comparison Meta-analysis. *Front Pharmacol* 2022; **13**: 757969 [PMID: 35281934 DOI: 10.3389/fphar.2022.757969]

108 **Ruepert L**, Quartero AO, de Wit NJ, van der Heijden GJ, Rubin G, Muris JW. Bulking agents, antispasmodics and antidepressants for the treatment of irritable bowel syndrome. *Cochrane Database Syst Rev* 2011; **2011**: CD003460 [PMID: 21833945 DOI: 10.1002/14651858.CD003460.pub3]

109 **Zheng L**, Lai Y, Lu W, Li B, Fan H, Yan Z, Gong C, Wan X, Wu J, Huang D, Wang Y, Mei Y, Li Z, Jiang Z, Liu X, Ye J, Yang Y, Huang H, Xiao J. Pinaverium Reduces Symptoms of Irritable Bowel Syndrome in a Multicenter, Randomized, Controlled Trial. *Clin Gastroenterol Hepatol* 2015; **13**: 1285-1292.e1 [PMID: 25632806 DOI: 10.1016/j.cgh.2015.01.015]

110 **Zheng L**, Lu W, Xiao Q, Lai Y, Fan H, Sun Y, Huang D, Wang Y, Li Z, Jiang Z, Liu X, Zhang L, Zuo D, Shou Z, Tang Q, Huang H, Yang Y, Tang Z, Xiao J. Assessing the post-treatment therapeutic effect of pinaverium in irritable bowel syndrome: a randomized controlled trial. *Sci Rep* 2021; **11**: 13894 [PMID: 34230526 DOI: 10.1038/s41598-021-92990-7]

111 **Chmielewska-Wilkoń D**, Reggiardo G, Egan CG. Otilonium bromide in irritable bowel syndrome: a dose-ranging randomized double-blind placebo-controlled trial. *World J Gastroenterol* 2014; **20**: 12283-12291 [PMID: 25232263 DOI: 10.3748/wjg.v20.i34.12283]

112 **Rai RR**, Nijhawan S. Comparative evaluation of efficacy and safety of drotaverine versus mebeverine in irritable bowel syndrome: A randomized double-blind controlled study. *Saudi J Gastroenterol* 2021; **27**: 136-143 [PMID: 33642357 DOI: 10.4103/sjg.SJG_266_20]

113 **Weerts ZZRM**, Masclee AAM, Witteman BJM, Clemens CHM, Winkens B, Brouwers JRBJ, Frijlink HW, Muris JWM, De Wit NJ, Essers BAB, Tack J, Snijkers JTW, Bours AMH, de Ruiter-van der Ploeg AS, Jonkers DMAE, Keszthelyi D. Efficacy and Safety of Peppermint Oil in a Randomized, Double-Blind Trial of Patients With Irritable Bowel Syndrome. *Gastroenterology* 2020; **158**: 123-136 [PMID: 31470006 DOI: 10.1053/j.gastro.2019.08.026]

114 **Xie C**, Tang Y, Wang Y, Yu T, Jiang L, Lin L. Efficacy and Safety of Antidepressants for the Treatment of Irritable Bowel Syndrome: A Meta-Analysis. *PLoS One* 2015; **10**: e0127815 [PMID: 26252008 DOI: 10.1371/journal.pone.0127815]

115 **Chen GR**, Xie XF, Peng C. Treatment of Irritable Bowel Syndrome by Chinese Medicine: A Review. *Chin J Integr Med* 2023; **29**: 377-384 [PMID: 34546535 DOI: 10.1007/s11655-021-3521-4]

116 **Tang XD**, Lu B, Li ZH, Wei W, Meng LN, Li BS, Tang ZP, Gao R, Wang FY, Lu F, Bian LQ, Zhao YP, Wang P, Zhang YQ. Therapeutic Effect of Chang'an I Recipe (I) on Irritable Bowel Syndrome with Diarrhea: A Multicenter Randomized Double-Blind Placebo-Controlled Clinical Trial. *Chin J Integr Med* 2018; **24**: 645-652 [PMID: 27487786 DOI: 10.1007/s11655-016-2596-9]

117 **He S**, Lin Q, Huang J, Zheng L, Lai J, Chen C. Effect and Mechanism of Flavored Tongxie Yaofang Decoction for Diarrheal Irritable Bowel Syndrome under Intestinal Microecology. *Evid Based Complement Alternat Med* 2022; **2022**: 3904571 [PMID: 35966738 DOI: 10.1155/2022/3904571]

118 **Tan X**, Pei W, Xie C, Wang Z, Liu J, Cheng Y, Mao T, Shi L, Zhao X, Lu Q, Sun Z, Kou F, Jiang H, Li J. Tongxie Anchang Decoction Relieves Visceral Hypersensitivity in Diarrhea-Predominant Irritable Bowel Syndrome Rats by Regulating the NGF/TrkA Signaling Pathway. *Evid Based Complement Alternat Med* 2021; **2021**: 6679348 [PMID: 34239591 DOI: 10.1155/2021/6679348]

119 **Yang C**, Zhang SS, Li XL, Wang ZF, Zhao LQ. Inhibitory effect of TongXie-YaoFang formula on colonic contraction in rats. *World J Gastroenterol* 2015; **21**: 2912-2917 [PMID: 25780288 DOI: 10.3748/wjg.v21.i10.2912]

120 **Li J**, Cui H, Cai Y, Lin J, Song X, Zhou Z, Xiong W, Zhou H, Bian Y, Wang L. Tong-Xie-Yao-Fang Regulates 5-HT Level in Diarrhea Predominant Irritable Bowel Syndrome Through Gut Microbiota Modulation. *Front Pharmacol* 2018; **9**: 1110 [PMID: 30323765 DOI: 10.3389/fphar.2018.01110]

121 **Tan X**, Pei W, Xie C, Wang Z, Mao T, Zhao X, Kou F, Lu Q, Sun Z, Xue X, Li J. Network Pharmacology Identifies the Mechanisms of Action of Tongxie Anchang Decoction in the Treatment of Irritable Bowel Syndrome with Diarrhea Predominant. *Evid Based Complement Alternat Med* 2020; **2020**: 2723705 [PMID: 33281910 DOI: 10.1155/2020/2723705]

122 **Shih YS**, Tsai CH, Li TC, Lai HC, Wang KT, Liao WL, Hsieh CL. The effect of Xiang-Sha-Liu-Jun-Zi tang (XSLJZT) on irritable bowel syndrome: A randomized, double-blind, placebo-controlled trial. *J Ethnopharmacol* 2019; **238**: 111889 [PMID: 31009707 DOI: 10.1016/j.jep.2019.111889]

123 **Zhen Z**, Xia L, You H, Jingwei Z, Shasha Y, Xinyi W, Wenjing L, Xin Z, Chaomei F. An Integrated Gut Microbiota and Network Pharmacology Study on Fuzi-Lizhong Pill for Treating Diarrhea-Predominant Irritable Bowel Syndrome. *Front Pharmacol* 2021; **12**: 746923 [PMID: 34916934 DOI: 10.3389/fphar.2021.746923]

124 **Pei L**, Geng H, Guo J, Yang G, Wang L, Shen R, Xia S, Ding M, Feng H, Lu J, Li J, Liu L, Shu Y, Fang X, Wu X, Wang X, Weng S, Ju L, Chen X, Shen H, Sun J. Effect of Acupuncture in Patients With Irritable Bowel Syndrome: A Randomized Controlled Trial. *Mayo Clin Proc* 2020; **95**: 1671-1683 [PMID: 32499125 DOI: 10.1016/j.mayocp.2020.01.042]

125 **Hao LJ**, Shi ZM. [Therapeutic effect of herb-separated moxibustion at Jinsuo (GV 8)-eight-diagram points on diarrhea-type irritable bowel syndrome of liver stagnation and spleen deficiency]. *Zhongguo Zhen Jiu* 2020; **40**: 702-706 [PMID: 32648391 DOI: 10.13703/j.0255-2930.20190621-k0007]

126 **Ki Cha B**, Mun Jung S, Hwan Choi C, Song ID, Woong Lee H, Joon Kim H, Hyuk J, Kyung Chang S, Kim K, Chung WS, Seo JG. The effect of a multispecies probiotic mixture on the symptoms and fecal microbiota in diarrhea-dominant irritable bowel syndrome: a randomized, double-blind, placebo-controlled trial. *J Clin Gastroenterol* 2012; **46**: 220-227 [PMID: 22157240 DOI: 10.1097/MCG.0b013e31823712b1]

127 **Dai C**, Zheng CQ, Jiang M, Ma XY, Jiang LJ. Probiotics and irritable bowel syndrome. *World J Gastroenterol* 2013; **19**: 5973-5980 [PMID: 24106397 DOI: 10.3748/wjg.v19.i36.5973]

128 **Sun YY**, Li M, Li YY, Li LX, Zhai WZ, Wang P, Yang XX, Gu X, Song LJ, Li Z, Zuo XL, Li YQ. The effect of Clostridium butyricum on symptoms and fecal microbiota in diarrhea-dominant irritable bowel syndrome: a randomized, double-blind, placebo-controlled trial. *Sci Rep* 2018; **8**: 2964 [PMID: 29445178 DOI: 10.1038/s41598-018-21241-z]

129 **Wang Y**, Chen N, Niu F, Li Y, Guo K, Shang X, E F, Yang C, Yang K, Li X. Probiotics therapy for adults with diarrhea-predominant irritable bowel syndrome: a systematic review and meta-analysis of 10 RCTs. *Int J Colorectal Dis* 2022; **37**: 2263-2276 [PMID: 36251040 DOI: 10.1007/s00384-022-04261-0]

130 **Mack I**, Schwille-Kiuntke J, Mazurak N, Niesler B, Zimmermann K, Mönnikes H, Enck P. A Nonviable Probiotic in Irritable Bowel Syndrome: A Randomized, Double-Blind, Placebo-Controlled, Multicenter Study. *Clin Gastroenterol Hepatol* 2022; **20**: 1039-1047.e9 [PMID: 34214682 DOI: 10.1016/j.cgh.2021.06.028]

131 **Jung K**, Kim A, Lee JH, Cho D, Seo J, Jung ES, Kang HJ, Roh J, Kim W. Effect of Oral Intake of Lactiplantibacillus plantarum APsulloc 331261 (GTB1(TM)) on Diarrhea-Predominant Irritable Bowel Syndrome: A Randomized, Double-Blind, Placebo-Controlled Study. *Nutrients* 2022; **14** [PMID: 35631156 DOI: 10.3390/nu14102015]

132 **Gu Q**, Yin Y, Yan X, Liu X, Liu F, McClements DJ. Encapsulation of multiple probiotics, synbiotics, or nutrabiotics for improved health effects: A review. *Adv Colloid Interface Sci* 2022; **309**: 102781 [PMID: 36209686 DOI: 10.1016/j.cis.2022.102781]

133 **You S**, Ma Y, Yan B, Pei W, Wu Q, Ding C, Huang C. The promotion mechanism of prebiotics for probiotics: A review. *Front Nutr* 2022; **9**: 1000517 [PMID: 36276830 DOI: 10.3389/fnut.2022.1000517]

134 **Kelly CR**, Khoruts A, Staley C, Sadowsky MJ, Abd M, Alani M, Bakow B, Curran P, McKenney J, Tisch A, Reinert SE, Machan JT, Brandt LJ. Effect of Fecal Microbiota Transplantation on Recurrence in Multiply Recurrent Clostridium difficile Infection: A Randomized Trial. *Ann Intern Med* 2016; **165**: 609-616 [PMID: 27547925 DOI: 10.7326/M16-0271]

135 **El-Salhy M**, Hatlebakk JG, Gilja OH, Bråthen Kristoffersen A, Hausken T. Efficacy of faecal microbiota transplantation for patients with irritable bowel syndrome in a randomised, double-blind, placebo-controlled study. *Gut* 2020; **69**: 859-867 [PMID: 31852769 DOI: 10.1136/gutjnl-2019-319630]

136 **Madsen AMA**, Halkjær SI, Christensen AH, Günther S, Browne PD, Kallemose T, Hansen LH, Petersen AM. The effect of faecal microbiota transplantation on abdominal pain, stool frequency, and stool form in patients with moderate-to-severe irritable bowel syndrome: results from a randomised, double-blind, placebo-controlled study. *Scand J Gastroenterol* 2021; **56**: 761-769 [PMID: 34000958 DOI: 10.1080/00365521.2021.1915375]

137 **Browne PD**, Cold F, Petersen AM, Halkjær SI, Christensen AH, Günther S, Hestbjerg Hansen L. Engraftment of strictly anaerobic oxygen-sensitive bacteria in irritable bowel syndrome patients following fecal microbiota transplantation does not improve symptoms. *Gut Microbes* 2021; **13**: 1-16 [PMID: 34074214 DOI: 10.1080/19490976.2021.1927635]

World Journal of Gastroenterology

Submit a Manuscript: https://www.f6publishing.com

World J Gastroenterol 2023 July 14; 29(26): 4136-4155

DOI: 10.3748/wjg.v29.i26.4136

ISSN 1007-9327 (print) ISSN 2219-2840 (online)

REVIEW

Peroxisome proliferator-activated receptors as targets to treat metabolic diseases: Focus on the adipose tissue, liver, and pancreas

Henrique Souza-Tavares, Carolline Santos Miranda, Isabela Macedo Lopes Vasques-Monteiro, Cristian Sandoval, Daiana Araujo Santana-Oliveira, Flavia Maria Silva-Veiga, Aline Fernandes-da-Silva, Vanessa Souza-Mello

Specialty type: Biochemistry and molecular biology

Provenance and peer review: Invited article; Externally peer reviewed.

Peer-review model: Single blind

Peer-review report's scientific quality classification

Grade A (Excellent): 0
Grade B (Very good): B
Grade C (Good): C
Grade D (Fair): 0
Grade E (Poor): 0

P-Reviewer: Morozov S, Russia; Wu QN, China

Received: April 21, 2023
Peer-review started: April 21, 2023
First decision: May 15, 2023
Revised: May 26, 2023
Accepted: June 13, 2023
Article in press: June 13, 2023
Published online: July 14, 2023

Henrique Souza-Tavares, Carolline Santos Miranda, Isabela Macedo Lopes Vasques-Monteiro, Daiana Araujo Santana-Oliveira, Flavia Maria Silva-Veiga, Aline Fernandes-da-Silva, Vanessa Souza-Mello, Department of Anatomy, Rio de Janeiro State University, Rio de Janeiro 20551030, Brazil

Cristian Sandoval, Escuela de Tecnología Médica, Facultad de Salud, Universidad Santo Tomás, Osorno 5310431, Chile

Cristian Sandoval, Departamento de Ciencias Preclínicas, Universidad de la Frontera, Temuco 4780000, Chile

Corresponding author: Vanessa Souza-Mello, PhD, Associate Professor, Department of Anatomy, Rio de Janeiro State University, Blvd. 28 de setembro 87, fundos, Rio de Janeiro 20551030, Brazil. souzamello.uerj@gmail.com

Abstract

The world is experiencing reflections of the intersection of two pandemics: Obesity and coronavirus disease 2019. The prevalence of obesity has tripled since 1975 worldwide, representing substantial public health costs due to its comorbidities. The adipose tissue is the initial site of obesity impairments. During excessive energy intake, it undergoes hyperplasia and hypertrophy until overt inflammation and insulin resistance turn adipocytes into dysfunctional cells that send lipotoxic signals to other organs. The pancreas is one of the organs most affected by obesity. Once lipotoxicity becomes chronic, there is an increase in insulin secretion by pancreatic beta cells, a surrogate for type 2 diabetes mellitus (T2DM). These alterations threaten the survival of the pancreatic islets, which tend to become dysfunctional, reaching exhaustion in the long term. As for the liver, lipotoxicity favors lipogenesis and impairs beta-oxidation, resulting in hepatic steatosis. This silent disease affects around 30% of the worldwide population and can evolve into end-stage liver disease. Although therapy for hepatic steatosis remains to be defined, peroxisome proliferator-activated receptors (PPARs) activation copes with T2DM management. Peroxisome PPARs are transcription factors found at the intersection of several metabolic pathways, leading to insulin resistance relief, improved thermogenesis, and expressive hepatic steatosis mitigation by increasing mitochondrial beta-oxidation. This review aimed to update the potential of PPAR agonists as targets to treat meta-

bolic diseases, focusing on adipose tissue plasticity and hepatic and pancreatic remodeling.

Key Words: Obesity; Insulin resistance; Peroxisome proliferator-activated receptors; Pancreas; Hepatic steatosis; Adipose tissue

©The Author(s) 2023. Published by Baishideng Publishing Group Inc. All rights reserved.

Core Tip: The world faces a pandemic of obesity and metabolic diseases. Peroxisome proliferator-activated receptors' (PPARs') target genes regulate several metabolic pathways, alleviating obesity and its metabolic impairments. PPARα exerts relevant anti-inflammatory, anti-steatotic, and pro-thermogenic effects, collaborating with weight loss and insulin resistance alleviation. PPARγ is useful for glycemic management, albeit with caution due to side effects after its total activation. PPAR β/δ is not clinically used owing to a pro-tumorigenic profile. However, Pan-PPAR or dual-PPAR agonists can retain PPARβ /δ or partial PPARγ activation benefits and configure promising approaches to treat metabolic diseases alone or in combination with other drug classes.

Citation: Souza-Tavares H, Miranda CS, Vasques-Monteiro IML, Sandoval C, Santana-Oliveira DA, Silva-Veiga FM, Fernandes-da-Silva A, Souza-Mello V. Peroxisome proliferator-activated receptors as targets to treat metabolic diseases: Focus on the adipose tissue, liver, and pancreas. *World J Gastroenterol* 2023; 29(26): 4136-4155
URL: https://www.wjgnet.com/1007-9327/full/v29/i26/4136.htm
DOI: https://dx.doi.org/10.3748/wjg.v29.i26.4136

INTRODUCTION

The unprecedented obesity rates have become an immense public health problem due to increased costs to treat comorbidities like diabetes, cancer, osteoarticular diseases, and cardiovascular events[1]. Most obesity cases stem from a chronic positive energy balance, where surplus energy intake surpasses the energy expenditure (EE), sending excessive energy to the adipose tissue[2,3].

The white adipose tissue (WAT) is a buffer against excess energy from the diet and first undergoes hyperplasia and hypertrophy and preserves its different types of cell composition[4,5]. As this process continues, preadipocytes become rare, and hypertrophy predominates until the adipocyte reaches its maximal capacity to enlarge, parallel to a rarefaction of vascularization and the high amount of proinflammatory immune cells within the stromal vascular fraction of the WAT[6,7]. At this stage, inflammation and insulin resistance activates lipolysis to allow the storage of the continuing excessive energy from the diet at the expense of diverting the non-esterified fatty acids (NEFAs) from lipolysis to organs not specialized to store lipids like the liver and the pancreas (lipotoxicity), triggering steatosis[8,9].

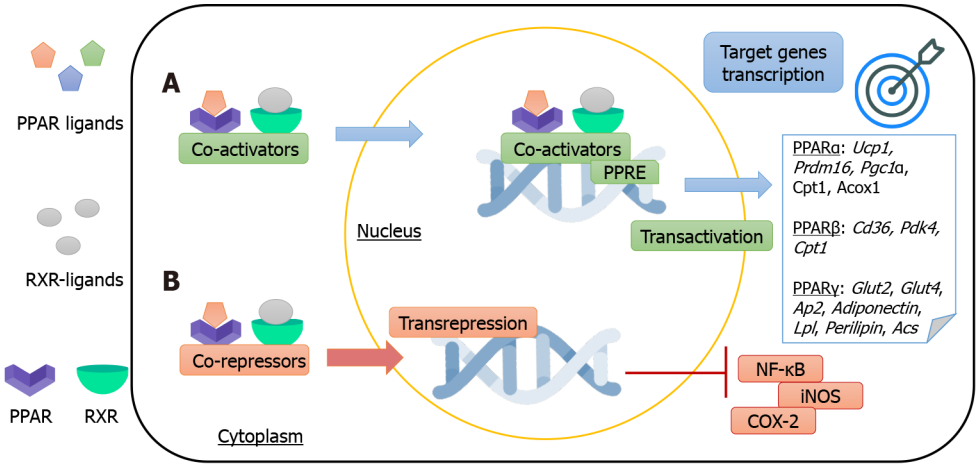
Hepatic and pancreatic steatosis compromises the physiology of these organs, collaborating with the progression to end-stage liver diseases and diabetes[10-12]. Thus, the scientific community seeks for strategies to mitigate the deleterious effects of obesity and its comorbidities, which affects the worldwide population regardless of economic income or age. The peroxisome proliferator-activated receptors (PPARs) are a family of transcription factors linked to the cellular metabolism of lipids, carbohydrates, proteins, and cell proliferation, existing in three isoforms: PPARα, PPARβ/δ, and PPARγ and emerged in recent decades as a strategy to treat obesity and its complications[13].

PPARs are binding-dependent transcription factors that regulate gene expression by specifically binding to PPAR-responsive elements (PPREs). Each receptor heterodimerizes with the retinoid X receptor (RXR, where X can be α, β/δ, or γ) and binds to its respective PPRE, forming a structure that will recognize specific DNA sequences (AGGTCA) for the transcription of their target genes. This PPAR mechanism of action is known as trans-activation. Moreover, PPARs can regulate gene expression independently of binding to PPREs, through the mechanism of trans-repression. There is a crosstalk between PPARs and other transcription factors that regulate their gene expression, and most of the anti-inflammatory effects of PPARs stem from this mechanism[14,15]. Figure 1 summarizes PPARs mechanisms of action.

PPARs regulate countless metabolic pathways after activation by endogenous ligands, such as fatty acids and their derivatives or synthetic agonists, which trigger a conformational change to interact with transcriptional coactivators[16,17]. The PPARα isoform expression is high in the liver, muscle, and heart, and its activation, according to previous studies, suggests that this receptor participates in lipid metabolism. PPARγ is mainly expressed in white and brown adipose tissue (BAT), being responsible, among other functions, for adipogenesis. Finally, PPARβ/δ has a wide body distribution with described roles in fatty acids oxidation in muscle and general energy regulation[13].

PPARs exert their physiological activities by activating the transcription of their target genes and, in this way, regulate lipid metabolism, glucose homeostasis, cell differentiation, obesity, and cancer. Furthermore, PPARs may directly participate in immune responses and inflammation mechanisms[18].

Considering that PPARs are found at the intersection of several metabolic pathways, influencing glucose homeostasis, adiposity, and mitochondrial function in the liver, this review aimed to update the potential of PPAR agonists as targets to treat metabolic diseases, focusing on adipose tissue plasticity, hepatic, and pancreatic remodeling.



DOI: 10.3748/wjg.v29.i26.4136 **Copyright** ©The Author(s) 2023.

Figure 1 Peroxisome proliferator-activated receptors mechanisms of action. Proliferator-activated receptors (PPARs) are ligand-activated transcription factors that regulate gene expression through two different mechanisms. A: PPAR-retinoid X receptor heterodimers bind to DNA-specific sequences called peroxisome proliferator-response elements to trigger target genes transcription (transactivation). PPARs' target genes include thermogenic [*Ucp1*, *PPAR-gamma coactivator 1 alpha* (*Pgc1α*), and *PR domain containing 16* (*Prdm16*)], mitochondrial and peroxisomal [*carnitine palmitoyltransferase I (Cpt1)*, peroxisomal acyl-coenzyme A oxidase (*Acox*), and pyruvate dehydrogenase kinase 4 (*Pdk4*)], anti-inflammatory (*Adiponectin*), insulin-sensitizing [glucose transporter 2 (*Glut2*), *Glut4*], and adipocyte metabolism [*Cd36*, adipocyte protein 2 (*Ap2*), lipoprotein lipase (*Lpl*), *Perilipin*, and acetyl CoA synthetase (*Acs*)] genes; B: PPARs regulate gene expression through transrepression, a DNA-independent mechanism. For example, PPARs inhibits the activity of nuclear factor kappa b and enzymes, yielding anti-inflammatory effects. Abbreviations: Uncoupling protein 1, *Pgc1α*, *Prdm16*, *Cpt1*, peroxisomal *Acox*, *Pdk4*, *Glut*, *Ap2*, *Lpl*, and *Acs*, inducible nitric oxide synthase, nuclear factor kappa B, and ciclooxigenase-2. PPARs: Peroxisome proliferator-activated receptors; RXR: Retinoid X receptor; PPRE: PPAR-responsive elements; NF-κB: Nuclear factor kappa B; iNOS: Inducible nitric oxide synthase; COX-2: Ciclooxigenase-2.

ADIPOSE TISSUE PHYSIOLOGY AND PLASTICITY

In mammals, the adipose organ comprises two types of tissues: WAT and BAT. Depending on the adipose tissue origin (for example, gonadal or subcutaneous), differences occur in its lipolytic or lipogenic capacity[19].

The white adipocytes are the only cells specialized in storing lipids without compromising their functional integrity. They have the necessary enzymatic machinery to synthesize triacylglycerol (TAG) when the energy supply is abundant and to mobilize them through lipolysis when there is an energy deficit[20].

The autonomic nervous system acts directly on the adipose tissue. The sympathetic nervous system promotes catabolic actions (lipolysis) *via* adrenergic stimulation, which activates the hormone-sensitive lipase (HSL) enzyme[21]. Conversely, the parasympathetic nervous system yields anabolism by stimulating insulin secretion, increasing glucose uptake, and activating lipogenesis[22].

Regarding the mature white adipocyte characteristics, it stores TAG in a single large lipid droplet that occupies the central portion of the cell, promoting displacement of the nucleus to the periphery and its consequent flattening. The single lipid droplet occupies 85%-95% of the cell volume, characterizing the white adipocyte as unilocular[23,24].

WAT, described as the chief energy reservoir in mammals, has a mesenchymal origin and is composed of adipocytes and the stromal vascular fraction (the main constituent of pre-adipocytes, immune cells, and fibroblasts); together, adipocytes and the stromal vascular fraction produce the extracellular matrix to maintain the structural and functional integrity of the tissue[25,26].

For a long time, the WAT was a secondary structure whose characteristic was the reservoir of large amounts of fat in the form of TAG. There was a lack of attention to its participation in body weight and food intake control. As a result of the discovery of the ability of WAT to secrete substances with biological effects like leptin in 1994, known collectively as adipokines, WAT emerged as a major endocrine organ[27,28].

Conversely, BAT has a smaller adipocyte than WAT, exhibiting several cytoplasmic lipid droplets of different sizes (multilocular), relatively abundant cytoplasm, spherical and slightly eccentric nucleus, and numerous mitochondria that produce energy by oxidizing acids[29]. The brownish BAT coloration stems from its high mitochondrial content, whose uncoupling protein 1 (UCP1) is one of the primary markers for brown adipocyte identification[30,31].

The brown adipocytes specialize in performing nonshivering thermogenesis (NST), by which the UCP1 acts as an alternative channel in the inner mitochondrial membrane to the proton gradient in the intermembrane space return to the mitochondrial matrix without resulting in ATP synthesis. Instead, the chemical energy is released as heat, enhancing the body temperature and EE, a promising target to treat obesity through negative energy balance[32,33].

Brown adipocytes originate from myocyte progenitor cells (myogenic lineage) and express the myogenic factor 5. *Prdm16* controls a bidirectional cell fate switching between skeletal myoblasts and brown adipose cells. Loss of the PR domain containing 16 (*Prdm16*) in brown fat precursors causes loss of brown fat characteristics and promotes muscle differentiation[34]. *Prdm16* induces a complete program of brown fat differentiation, including the expression of PPAR-gamma coactivator 1α (*Pgc-1α*) and *Ucp-1*. *Pgc-1α* is an essential transcriptional coactivator for NST and mitochondrial biogenesis[35].

Although BAT total mass in mammals is small, previous research has already shown that its adequate stimulation (cold exposure, specific drugs, some food compounds, or physical activity) could quadruple the EE of an animal, parallel to an increase in tissue perfusion[36-38]. Thus, understanding the damage obesity causes to BAT morphology and physiology can help to develop strategies to treat obesity.

Recently, experimental studies reported that diet-induced obesity (DIO) results in glucose intolerance, functional BAT hypoxia, and structural whitening. Brown adipocytes in obese animals reduce their thermogenic capacity and assume a white phenotype, becoming unilocular[39,40]. The molecular mechanisms that lead to reduced BAT activity in obesity and its physiological implications are under investigation, and altered PPAR expression may have a role in the whitening phenomenon as *Pparα* expression declines in whitened BAT[41]. Compared to WAT, BAT is more extensively vascularized, and vascular endothelial growth factor-A (VEGFA)-dependent angiogenesis is pivotal for the thermogenic response[42]. The hypoxic microenvironment in BAT, due to obesity, has been shown to lead to an accelerated loss of mitochondria, and as oxidative capacity is lost, lipid droplets accumulate, generating the white phenotype[39].

Since obesity is a public health problem in developed and developing countries, the world urges us to find new approaches to treat or prevent this metabolic disease and its comorbidities. WAT plasticity towards an intermediary adipocyte between white and brown, the beige adipocyte, may emerge as a suitable strategy to fight the obesity pandemic [43].

Beige adipocytes are found in the subcutaneous WAT (sWAT) and exhibit a brown-like adipocyte phenotype (multilocular). In the basal state, beige adipocytes act like white adipocytes, but under the right stimulus, they can acquire intermediate mitochondrial content and perform thermogenesis, a process called browning[44]. *Prdm16* is essential to the browning phenomenon once its down-regulation turns a beige adipocyte into a white one, showing that browning is reversible and morphophysiological changes rely on adequate PRDM16 expression and active mitochondrial biogenesis machinery to increase mitochondrial content and thermogenic capacity[45,46].

Beige adipocytes originate from mature white adipocytes [low expression of the cluster of differentiation 137 (*Cd137*)], which under specific stimulation, acquire a brown-like phenotype, or even from a beige pre-adipocyte (high *Cd137*), which differentiates into a multilocular cell capable of performing thermogenesis. The latter originates from a lineage different from the WAT[47,48]. Although the beige adipocytes have a lower thermogenic activity than the brown adipocytes, their presence is linked to a metabolically healthy phenotype in humans[49], reducing the chances of developing type 2 diabetes mellitus (T2DM), hepatic steatosis, and other metabolic constraints.

The metabolic benefits of beige/brown adipocytes presence also stem from their endocrine role in secreting the batokines. Like the adipokines from the WAT, batokines act in autocrine, paracrine, and endocrine fashions to provide increased neurovascular supply to BAT, favoring thermogenesis and inhibiting whitening besides exerting anti-inflammatory effects, favoring browning, and influencing glucose homeostasis[50]. Figure 2 depicts white and BAT plasticity under obesogenic and thermogenic stimuli.

The recent literature suggests that less than 100 g of adipose tissue in an adult human with thermogenic activity can prevent 4 kg of fat accumulation per year[51], stimulating the search for drugs that trigger browning while inhibiting whitening, relevant for metabolic disease control.

PPARS ROLE IN THE ADIPOSE TISSUE PLASTICITY

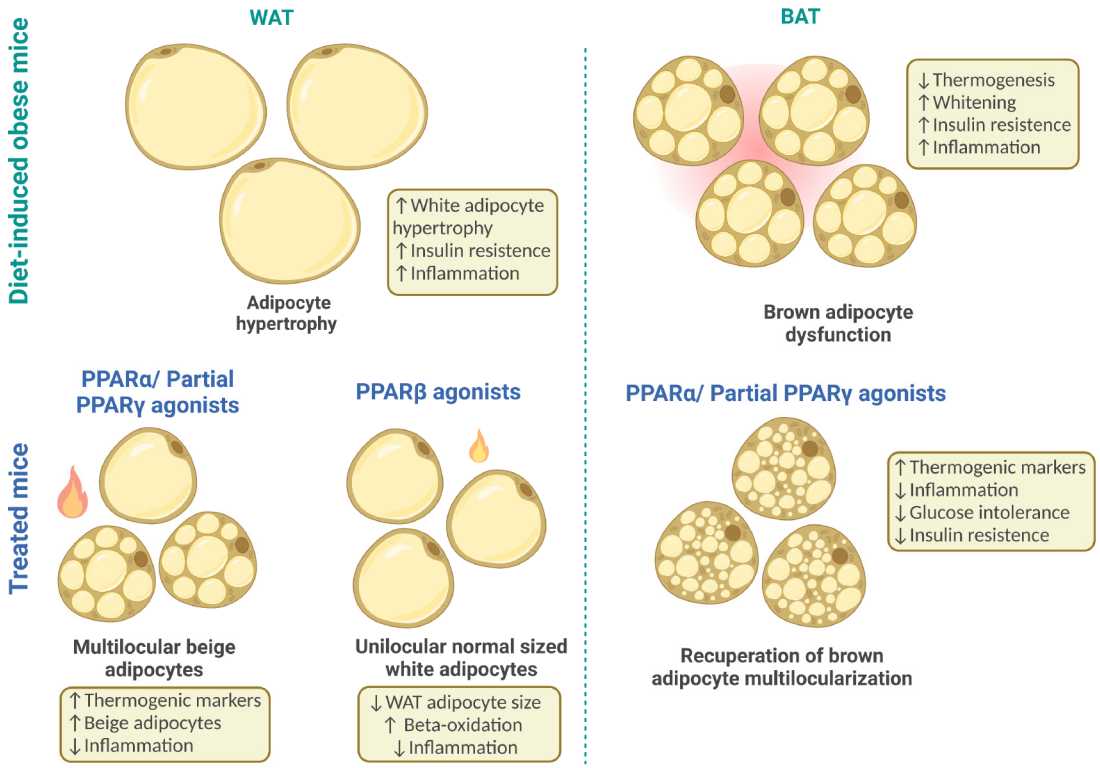
PPARα was the first receptor discovered, mapped to chromosome 22q12-13.1 in humans, found in metabolically active tissues such as the liver, kidney, heart, skeletal muscle, and brown fat[52,53]. PPARα has polyunsaturated fatty acids and leukotrienes as natural ligands, which are inflammatory mediators; as pharmacological ligands, the family of hypolipidemic drugs, fibrates, is considered an accessible PPARα agonist[54].

The participation of PPARα in the thermogenic pathway involves directing NEFAs, generated after adrenergic stimulation, to the β-oxidation instead of cellular efflux. β-adrenergic stimulus mobilizes most of NEFA in normal conditions, and this mobilization is related to the inflammatory response and the reduction of cell function in the long term. The chronic stimulation of the beta-3 adrenergic receptor upregulates PPARα expression, increasing adipocytes' oxidative capacity[55].

Natural or pharmacological ligands mainly control the expression of genes involved in lipid metabolism. If the concentration of fatty acids increases, PPARα is activated and absorbs the oxidized forms of these acids. During the influx of fatty acids, the transcription of PPARα-regulated genes increases, and the systems are activated[55,56]. Thus, PPARα functions as a lipid sensor and controls energy combustion.

A previous study showed that treatment with WY14643 (PPARα agonist) exerted lipolytic effects with reduced fat mass and increased whole-body fat oxidation. These results demonstrate a novel role for PPARα activation in beta-adrenergic regulation of adipose tissue lipolysis[57]. In addition, treatment with WY-14643 has already shown effects in reducing hepatic steatosis, serum insulin, and inflammation in adipose tissue, and these changes are generally observed in obesity onset[58,59].

In BAT, PPARα stimulates lipid oxidation and thermogenesis in synergy with PGC1α[60]. In this scenario, a study demonstrated that the activation of PPARα by a pharmacological agent (fenofibrate) activated NST (and mitochondrial biogenesis in the BAT of obese mice fed a high-fat diet[61]. Subsequently, the chronic intake of a high-fat diet caused BAT whitening, and the treatment with WY14643 mitigated this morphophysiological impairment through anti-inflammatory signals and enhanced VEGFA, resulting in increased thermogenesis. In the same experiment, the high-fructose diet did not trigger whitening, but the WY14643 also attenuated the histological changes caused by excessive dietary fructose[62].



DOI: 10.3748/wjg.v29.i26.4136 **Copyright** ©The Author(s) 2023.

Figure 2 Adipose tissue plasticity and peroxisome proliferator-activated receptor effects. Under an obesogenic diet, the white adipocytes undergo hypertrophy and profound change in adipokine profile release, leading to growing insulin resistance and low-grade inflammation. Conversely, under adequate stimuli [peroxisome proliferator-activated receptors α (PPARα) and dual PPARα/γ], the subcutaneous white adipose tissue can also undergo browning and form beige adipocytes, an intermediate between white and brown adipocytes with lower thermogenic capacity than brown adipocytes but whose presence points to metabolic homeostasis. Finally, the brown adipose tissue, which has the most potent thermogenic capacity, can express a whitened phenotype when exposed to a lipotoxic milieu. Whitening entails decreased vascularization and pro-inflammatory signals characterizing brown adipocyte dysfunction. In contrast, PPARα and dual PPARα/γ treatments counter whitening, increasing thermogenesis through anti-inflammatory and proangiogenic effects. Made with Biorender (www.biorender.com). PPARs: Peroxisome proliferator-activated receptors; WAT: White adipose tissue; BAT: Brown adipose tissue. Created by BioRender.

PPARα is the isoform that induces the browning of sWAT more abundantly. Fenofibrate has yielded expressive browning in DIO mice, with an irisin-*Pgc1α*-*Prdm16* interaction driven by PPARα stimulating thermogenesis and mitigating insulin resistance and inflammation, countering obesity[63]. Confirming these results, the PPARα agonist WY14643 yielded *Cd137*/*Prdm16*/*Ucp1*+ beige adipocytes, whereas the PPARβ/δ agonist GW0742 reduced sWAT adipocyte size and increased beta-oxidation without browning induction[59]. PPARβ/δ activation by GW501516 countered adipocyte hypertrophy through suppression of angiotensin-converting enzyme (ACE)/angiotensin II receptor type 1 (AT1r) axis and downstream potent anti-inflammatory effects[64].

PPARγ received much attention since the mid-1990s as the molecular target of thiazolidinediones (TZDs) or glitazones, a class of insulin-sensitizing and antidiabetic drugs[65]. PPARγ, a transcription factor from the nuclear receptor family, plays a significant role in lipid and glucose metabolism regulation[66]. WAT and BAT, large intestine, and spleen express PPARγ. However, its expression is much higher in adipocytes[67,68].

Ligand-activated PPARγ induces adipocyte differentiation, stimulates mitochondrial biogenesis, and inhibits the production of pro-inflammatory mediators[68]. In addition, PPARγ activated in adipocytes ensures a balanced and adequate secretion of adipokines (adiponectin and leptin), mediators of insulin action in peripheral tissues[69].

In WAT, PPARγ is pivotal to lipid accumulation. In contrast, PPARγ activation in BAT induces the expression of genes related to the thermogenic program, including *Pgc1α* and *Ucp1*. PPARγ is crucial for brown adipocyte differentiation, but additional transcription factors, including PRDM16, are required to activate the thermogenic program[70].

The PPARγ1 isoform is expressed in almost all cells, while PPARγ2 is mainly limited to adipose tissue. However, PPARγ2 is a more potent transcriptional activator[71]. Both PPARγ1 and PPARγ2 are essential for adipogenesis and insulin sensitivity control. However, PPARγ2 is the isoform upregulated in response to nutrient intake and obesity[72,73].

TZDs, synthetic PPARγ ligands, are antidiabetic drugs with potent insulin-sensitizing effects that confer long-term glycemic control[74]. However, its clinical use has been contested due to side effects such as weight gain, edema, and bone fractures[75]. The increase in body weight after TZDs administration is due to PPARγ-dependent WAT expansion [76] and fluid retention caused by PPARγ activation in the renal collecting ducts[77].

TZDs improve peripheral insulin sensitivity and have a spectrum of anti-inflammatory properties, including a reduction in plasma inflammatory markers and adipose tissue macrophages[72,78]. In WAT, TZDs promote adipocyte differentiation, insulin action, and the formation of beige adipocytes[66]. In BAT, TZDs activate thermogenic activity[79].

The dual PPARα/γ agonist tesaglitazar reversed iBAT whitening through gut dysbiosis and ultrastructure improvements[80]. Intestinal PPARα activation suppresses postprandial hyperlipidemia by increasing the fatty acid oxidation of intestinal epithelial cells[81]. In addition, intestinal PPARα activation reduces cholesterol esterification, suppresses chylomicron production, and increases enterocytes' HDL synthesis[82]. These observations pave a new way to treat metabolic diseases through the modulation of gut microbiota by PPARs and the consequent gut-adipose tissue stimulation of thermogenesis due to anti-inflammatory, angiogenic, and high beta-adrenergic signaling[80]. Figure 2 shows the main PPAR effects on the adipose tissue.

PANCREAS MORPHOPHYSIOLOGY AND OBESITY OUTCOMES

The human pancreas is a mixed gland made up of five anatomical divisions: Head (fitted with the duodenum), uncinate process, neck, body, and tail (nearby the spleen); measures 15-25 cm in length; and weighs 100 g to 150 g in a healthy adult[83]. The inferior pancreaticoduodenal artery, the superior pancreaticoduodenal artery, and the splenic artery are responsible for its perfusion, and the pancreatic plexus, celiac ganglia, and vagus nerve innervate this gland[84,85].

The pancreas has endocrine and exocrine functions, encompassing four structural components: The exocrine portion, constituted by acinar and ductal cells; the endocrine region formed by the islet cells; the blood vessels; and the extracellular space[84]. The exocrine portion corresponds to 85% of the pancreas volume, comprehending a ductal system like a bunch of grapes with a blinded end. Each acinus corresponds to a grape and secretes pancreatic juice enzymes that flow into bicarbonate-secreting ductal epithelial cells[83,84]. After passing through accessory ducts, these enzymes reach the main pancreatic duct that connects with the bile duct in the ampulla of Vater in the duodenum. The exocrine pancreatic secretion (amylase, lipase, and zymogens) helps to digest proteins, fats, and carbohydrates, being secreted by the autonomic nervous system stimulation in the presence of food in the duodenum and the consequent release of secretin, cholecystokinin, and other hormones by the enteroendocrine cells[83].

The endocrine portion of the pancreas comprises mini-organs called islets of Langerhans, corresponding to 1%-2% of the total pancreatic volume. Pancreatic islets have a spherical shape and secrete hormones related to glucose homeostasis. There are five islet cell types: Alpha cells (α cells, produce glucagon), beta cells (β cells, insulin), delta cells (δ cells, somatostatin), PP cells (also known as F cells, pancreatic polypeptide-containing cells), and epsilon cells (ε cells, ghrelin). Neuroendocrine, endocrine, paracrine, and endocrine mechanisms influence islet secretion. Therefore, overactivation or inactivation of their regulatory pathways can drastically impact the metabolism, causing metabolic diseases[86-88].

The most prevalent cell types in pancreatic islets are alpha and beta cells. In mice, alpha cells are restricted to the islet periphery, while the beta cells found in the core of the islet are vastly innervated and comprehend 60%-80% of the total islet mass. In humans, alpha and beta cells are interspersed all around the islets, with beta cells comprising 50%-75% of the islet mass with a sparse innervation. The remaining islet cell types do not differ significantly between men and mice. Even though there are cytoarchitectural differences regarding the islets of these species, the dynamics of islet remodeling in obesity and T2DM are similar and propitiates relevant translational studies[87].

Obesity entails an impaired glucose-stimulated insulin secretion (GSIS) triggered by the adipoinsular axis deregulation due to increased demand for insulin release. The resistance to insulin action relates to hyperleptinemia, prompted by the inflamed hypertrophied WAT[89,90]. Under an insulin-resistant state, the glucose fails to enter the pancreatic beta cell, resulting in a high demand for insulin to keep euglycemia. Islet hypertrophy and hypersecretion are commonplace features in DIO mice as the expansion of alpha and beta cell masses cope with normal glycemic levels maintenance at the beginning of glucose homeostasis impairments[91-93].

Insulin resistance (IR) precedes the T2DM diagnosis by around ten years[94]. Initially, the compensatory hyperinsulinemia prompts normal fasting glucose levels (IR). As adiposity evolves, hyperinsulinemia cannot cope with adequate glycemic control. At this point, raised plasma insulin and glucose concentrations coexist, characterizing glucose intolerance[91,95]. Glucose-intolerant mice exhibit hyperglycemia, alpha cells infiltrated to the islet core, besides a disrupted GSIS, with endoplasmic reticulum (ER) stress and loss of beta cell polarity, compromising its secretion and threatening islet survival[96,97].

Glucotoxicity (hyperglycemia) elicits ER stress, which leads to proinsulin misfolding and accumulation, a hallmark of beta cell dysfunction and T2DM onset[98]. Beta cell dysfunction originates from continuing islet hypertrophy and hypersecretion (lipotoxicity), impaired GSIS, beta cell ER stress (glucolipotoxicity), and downregulation of proliferative markers like the pancreatic duodenal homeobox-1 (PDX1)[96,99]. Compromised beta cell proliferation, increased apoptosis rate, and dedifferentiation result in beta cell failure[100]. T2DM is linked to a decreased beta cell mass (-22%-63%) and begins when beta cell mass cannot compensate for the high demand for insulin to sustain glucose homeostasis [101].

As a multi-hormonal disease, T2DM entails decreased beta cell mass coupled with the loss of incretin effect. Incretins are gut-derived hormones that enhance insulin secretion and sensitivity after meal ingestion, participating in the glycemic control at the postprandial state. Chronic high-fat diets lead to loss of the incretin glucagon-like peptide-1 (GLP-1) capacity to enhance beta cell responsiveness to glucose and proliferation, resulting in beta cell exhaustion[102,103]. Loss of incretin effect occurs even with normal GLP-1 and gastric inhibitory polypeptide levels in obese subjects, suggesting a possible resistance to their actions like described for insulin and leptin[104].

To avoid the progression of IR towards T2DM onset, therapies that could promote pancreatic alpha cell transdifferentiation into beta cells to maintain glycemic control are promising approaches to tackle beta cell exhaustion and reduced beta cell mass[105]. In this context, PPARs may be therapeutic targets for glycemic homeostasis.

PPARS EFFECTS ON PANCREATIC REMODELING AND ISLET PRESERVATION

PPARs regulate the expression of several target genes and allow the proper functioning of pathways linked to energy metabolism. An imbalance of these pathways can lead to the development of T2DM and other disorders[106,107]. Thus, PPARs are relevant therapeutic targets for the clinical management of diabetes.

Numerous drugs have been used and developed for the treatment of hyperlipidemia and T2DM such as PPARα agonists (fibrates, *e.g.*, fenofibrate, bezafibrate and clofibrate) and PPARγ agonists (TZDs, *e.g.*, troglitazone, rosiglitazone, pioglitazone and ciglitazone). PPARβ/δ does not have a role well-established in glucose metabolism, but it is known to improve insulin sensitivity by facilitating fatty acid oxidation in some tissues and reducing glucose oxidation[108,109].

PPARα plays an essential role in glucose homeostasis and regulates enzymes and proteins involved in glucose synthesis in the fasting state[110]. In addition, it stimulates pancreatic beta cells and increases fatty acid oxidation and GSIS[111]. Fenofibrate and fish oil countered islet hypertrophy and increased adiponectin levels in diabetic KK mice [112], mitigating lipotoxicity-induced beta cell dysfunction by inhibiting the nuclear factor kappa B (NF-κB) and reducing macrophage migration[113]. In agreement, fenofibrate exerted anti-inflammatory and antiapoptotic effects besides enhancing islet innervation in young non-obese diabetic mice, providing adequate glucose handling, and preventing diabetes-associated diseases[114].

Conversely, Fenofibrate long-term use (12 wk, 100 mg/kg) disrupted beta cell function due to increased NF-κB and inducible nitric oxide synthase islet expression in monosodium glutamate-induced obese rats[115]. An *in vitro* study showed that PPARα activation by WY14643 or bezafibrate (pan-PPAR agonist) enhances GSIS. However, long-term treatments contribute to beta cell dysfunction owing to overstimulation[116]. In a clinical study, bezafibrate showed that parameters related to insulin resistance were attenuated during the follow-up period, while the placebo group showed an increase in this parameter over two years[117].

PPARγ, in turn, controls glucose homeostasis as it increases glucose transporter (GLUT4) expression and its translocation in adipocytes, causing adipose remodeling by reducing visceral fat deposits while selectively increasing sWAT, resulting in a possible insulin sensitization scenario[118,119]. Furthermore, studies have shown that PPARγ activation increases adipocytes' fatty acid uptake, reducing lipotoxic damage to insulin-sensitive tissues[120], increasing glucose uptake by skeletal muscle, and consequent peripheral reduction[120,121].

PPARγ agonists are the most developed antidiabetic and insulin-sensitizing agents to date. Studies have shown that TZDs (or glitazones) bind specifically to the ligand binding domain (LBD) of recombinant PPARγ but not to PPARα or PPARβ/δ. These agents also selectively stimulate the activity of the PPARγ gene promoter and modulate the expression of several of its target genes[122]. TZDs class increases glucose catabolism and reduces its hepatic production[123,124], sensitizes cells to insulin, improves insulin sensitivity and action[125,126], and promotes pre-adipocyte differentiation along with lipogenesis, which favors a reduction in NEFAs concentrations, attributed to increased glucose utilization and reduced gluconeogenesis.

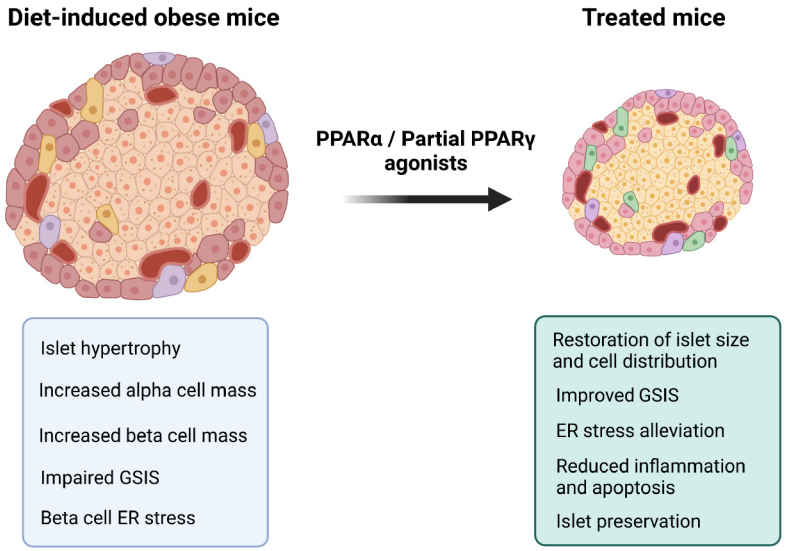
Human and animal studies indicate that the TZDs (total PPARγ agonists) rosiglitazone and pioglitazone improve hyperglycemia by reversing insulin resistance and improving insulin sensitivity. In addition, both agents also show significant effects on plasma lipoprotein lipids in humans, although pioglitazone results in a relatively better lipid profile than rosiglitazone[127,128]. Of note, the clinical use of rosiglitazone was discouraged owing to the unwanted effects of fluid retention, arterial vasodilation, endothelial alterations[129,130], increased risk of bone fracture and congestive heart failure[131], and weight gain in both animal models and humans due to the master regulatory role of PPARγ in adipogenesis[66].

Pioglitazone (15 mg/kg per mouse) yielded healthy pancreatic islets in db/db mice, enhancing insulin and NK6 homeobox 1 expression and restoring islet function in this mice model[132]. The islet preservation due to PPARγ activation by pioglitazone encompasses anti-inflammatory effects and alleviation of ER stress[133]. Pioglitazone and vildagliptin (DPP-4 inhibitor) combination maximized pioglitazone's effects on suppressed inflammation and oxidative stress in male rats[134]. In agreement with this, pioglitazone plus sitagliptin enhanced alpha and beta cell functions at the postprandial state in T2DM subjects[135].

Telmisartan, a partial PPARγ agonist and angiotensin receptor blocker, reduces serum insulin levels and mitigates insulin resistance without affecting serum adiponectin levels[136]. The experimental background shows that telmisartan reduced islet hypertrophy, with adequate glycemic control and normalized alpha and beta cell mass in DIO mice. These effects were maximized by telmisartan combination with sitagliptin, reverting oral glucose intolerance and normalizing body mass in this DIO model[93]. Telmisartan combination with linagliptin promoted islet preservation by suppressing oxidative stress[137].

The beneficial effects of telmisartan on islet cytoarchitecture featured ultrastructural remodeling, with polarized cells and mature insulin granules reestablished after the treatment[97]. Telmisartan elicited enhanced islet vascularization, enhanced PDX1 and GLP-1 islet expression plasma concentrations, ameliorating GSIS and preserving pancreatic islets through reduced apoptosis rate and macrophage infiltration[96]. Due to improved islet proliferation capacity, telmisartan might be a candidate for beneficial islet cell transdifferentiation to slow insulin resistance to T2DM onset progression. Figure 3 summarizes the main effects of PPARα and partial PPAR γ agonists on the endocrine pancreas.

Drugs with specificity for at least two PPAR isoforms (*e.g.*, dual PPARα/γ or pan-PPAR agonists) could be more effective and have relatively fewer undesirable side effects compared with currently used agonists with specificity for a single PPAR isoform[138]. In this context, a series of dual PPARα/γ agonists, named glitazars, was designed to combine total PPARα and partial PPARγ activation, retaining the insulin-sensitizing property of PPARγ target genes with the beneficial effects of PPARα activation on energy metabolism[139,140]. However, muraglitazar showed many of the same side effects (weight gain and edema) in patients[141,142], having glitazars development halted due to safety concerns.



DOI: 10.3748/wjg.v29.i26.4136 **Copyright** ©The Author(s) 2023.

Figure 3 Beneficial effects of Peroxisome proliferator-activated receptor agonist on islet remodelling. Diet-induced obese mice exhibit enlarged pancreatic islets, with are prone to exhaustion in the long run due to glucolipotoxicity. Peroxisome proliferator-activated receptor α (PPARα) and partial PPARγ activation are promising targets to counter glucolipotoxicity, yielding islet preservation. Made with Biorender (www.biorender.com). PPARs: Peroxisome proliferator-activated receptors; GSIS: Glucose-stimulated insulin secretion; ER: Endoplasmic reticulum. Created by BioRender.

Research is ongoing to develop new PPAR agonists without side effects. Since PPARs orchestrate many physiological processes, agonists may play beneficial or non-beneficial effects. So, PPAR actions on pancreatic islets need elucidation to support the development of new drugs with more assertive outcomes.

LIVER MORPHOPHYSIOLOGY AND OBESITY IMPLICATIONS

The liver is a complex organ that concentrates on several physiological processes as macronutrient metabolism, immune system support, fatty acid, and cholesterol homeostasis, besides the degradation of xenobiotic compounds and many medications[143]. It is the largest solid glandular organ in the body. With versatile endocrine and exogenous functions, the liver is considered paramount for metabolic activities[144]. It has a remarkably uniform anatomical structure composed of the regular arrangement of lobules that are the functional unit of the liver. The base of the lobule is composed of hepatocytes, the most prevalent cells of the liver[145]. Hepatocytes arranged between the sinusoids along the portal-central axis demonstrate heterogeneity concerning their biochemical and physiological functions[146]. Additional cell types within the liver include cholangiocytes, Kupffer cells, stellate cells, and endothelial cells, with specialized functions[147].

The liver is enriched with cell organelles to fulfill its metabolic functions. It is one of the organs with the highest number and density of mitochondria, which interact with other organelles such as ER, lipid deposits (LDs), and lysosomes[148,149]. In the gastrointestinal tract, food digestion generates metabolic substrates (glucose, fatty acids, and amino acids) that are absorbed by the bloodstream and conducted to the liver through the portal vein circulation system. In the postprandial state, glucose forwards to glycogen storage, and the excess undergoes *de novo* lipogenesis (DNL) in the liver. DNL forms new TAG from acetyl-CoA or malonyl-CoA[150,151].

In mammals, acetyl-CoA carboxylase (ACC) and fatty acid synthase (FAS)-an enzyme intricately regulated by several nuclear receptors (NRs, *e.g.*, PPARα, PPARγ, and the bile acid receptor/farnesoid X receptor) catalyze fatty acid production. NRs are also relevant mediators of insulin signaling, whereas DNL occurs under anabolic conditions, linking glucose and lipid metabolism. Further support of this link encompasses insulin stimulation of FAS expression. In hepatocytes, NEFAs are esterified with glycerol-3-phosphate to synthesize TAG. TAG is stored in LDs within hepatocytes or secreted into the circulation as very low-density lipoprotein (VLDL) particles. In the fasted state or during exercise, fuel substrates (glucose and TAG) are delivered from the liver into the circulation and metabolized by muscle, adipose tissue, and other extrahepatic tissues[150,151]. However, the increased intake of dietary lipids, associated with upregulated DNL process, causes lipotoxicity and the abnormal accumulation of lipids, often consistent with insulin resistance in steatotic livers, which is related to disturbed ER protein folding homeostasis in hepatocytes[152,153].

The ER in hepatocytes can adapt to extracellular and intracellular changes, allowing the maintenance of essential hepatic metabolic functions. However, several alterations can disturb the ER homeostasis of hepatocytes, contributing to the dysregulation of hepatic lipid metabolism and liver diseases. Consequently, ER includes a progressively conserved pathway called unfolded protein response (UPR) to control liver protein and lipid homeostasis[154]. UPR decreases secretory protein quantity, increases ER protein folding (chaperone and foldase transcription), and enhances deletion capacity by stimulating autophagy and ER-related degradation[152]. Thus, ER stress is a cellular stress in which the demand for folding newly synthesized proteins exceeds ER capacity to fold or to correct it through UPR, generating

unfolded protein accumulation[155].

The existence of three transmembrane-ER proteins is understood to reveal and transduce the ER stress response: Protein kinase RNA-like ER kinase (PERK), inositol-requiring protein-1α (IRE-1α) and activating transcription factor 6 (ATF6). Activation of ATF6 and PERK elicit the expression of the C/EBP homologous protein (CHOP), whereas IRE-1α induces the activation of the N-terminal C-Jun kinase and also generates an improved form of X-box binding protein-1 (XBP1), the spliced XBP1, which attempts to the depletion of misfolded ER proteins through chaperone, folding proteins, and ERAD components encoding[156].

However, when ER stress is intense to the point that damage is irreversible, the ER cannot restore its function. Hence, inflammatory responses trigger cell death pathways[157]. There is strong communication between ER homeostasis perturbations and mitochondrial dysfunction in the onset of obesity and metabolic syndrome. The mitochondrion organelle plays an essential role in hepatic cellular redox, lipid metabolism, and cell death regulation[158], and genes related to mitochondrial fatty acid β-oxidation are mostly transcriptionally regulated by PPARα[159]. Fatty acids input into the mitochondria requires carnitine palmitoyltransferase 1a (*Cpt1a*) (a PPARα target gene), located in the outer mitochondrial membrane. PPARα activation leads to the transcription of *Cpt1a*, associated with fatty acid oxidation in mitochondria, peroxisomes (acyl-CoA oxidase, ACOX), and cytochrome P450 4A family[160].

Mitochondrial dysfunction is associated with acute and chronic liver diseases, and relevant information indicates that mitophagy, a selective form of autophagy (catabolic process, which manifests itself by selective sequestration of mitochondria by autophagosomes, phagophores, a double membrane that isolates autophagic components)[161] of dysfunctional/excessive mitochondria, plays a pivotal role in liver physiology and pathophysiology[158]. There are specificities and mechanisms mediating mitophagy, many of them mediated by the FUN14 domain containing 1 (FUNDC1), a mitochondrial outer membrane protein tightly regulated at transcriptional and post-transcriptional levels. NRF1 (nuclear respiratory factor 1) and PGC1α, the major transcription factor and related cofactor in mitochondrial biogenesis, beneficially adjust FUNDC1 expression and enhance mitophagy[162]. Therefore, mitophagy favors mitochondrial remodeling, and PPARs are implicated in this pathway[163]. Figure 4 summarizes liver alterations under lipotoxicity in obesity.

PPARS IN THE LIVER

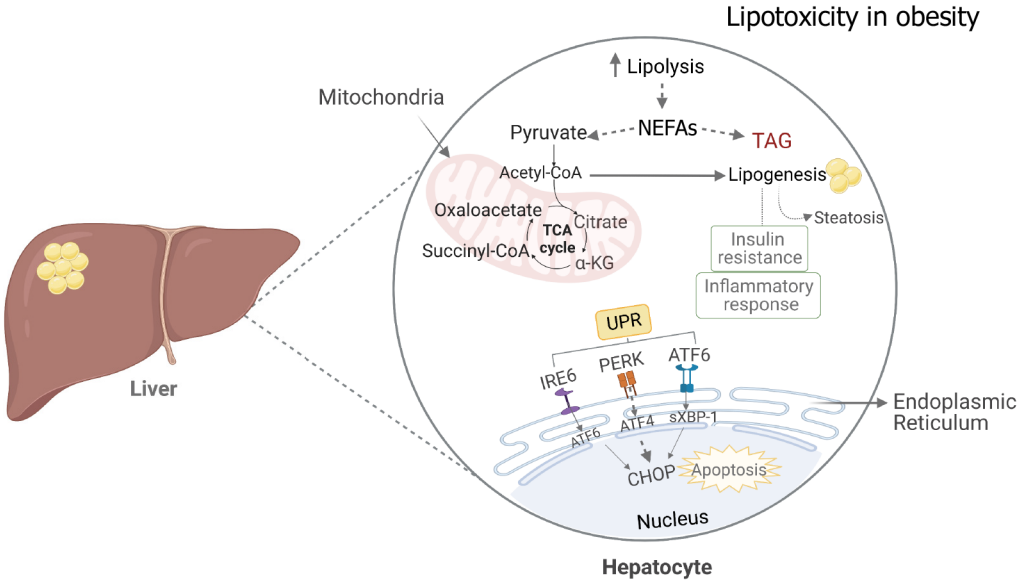
Functional studies have demonstrated that PPARα governs hepatic expression of genes involved in nearly all aspects of lipid metabolism, including fatty acid uptake, elongation and desaturation, activation and binding of intracellular fatty acids, formation and degradation of TGs and lipid droplets, and metabolism from plasma lipoproteins[164,165]. The constitutive activity of mitochondrial β-oxidation was significantly reduced in the liver of mice lacking the *Pparα* gene (*Pparα* null mice)[166]. *Pparα* knockout mice fed a high-fat diet increased markers of oxidative stress, inflammation, and cell death[167].

Thus, PPARα has been the target of hypolipidemic drugs from the fibrate family, under investigation for treating non-alcoholic fatty liver disease (NAFLD). PPARα upregulates fatty acid β-oxidation and lipolysis, upregulating the expression of several genes involved in lipid metabolism (*Pgc1α* and *Cpt1a*), leading to less fat accumulation in NAFLD [168]. *Pgc1α* modulates the expression of key metabolic enzymes involved in gluconeogenesis, fatty acid oxidation, and oxidative phosphorylation in the liver through their functional interaction with PPARα[169]. Mitochondrial β-oxidation of long-chain fatty acids is regulated by CPT1a, an enzyme physiologically inhibited by malonyl-CoA, a glucose-derived metabolite and an intermediate in DNL synthesis[170].

Administration of Wy-14643, one of the most potent PPARα agonists, decreased serum insulin, rescued hyperglycemia, and suppressed carbohydrate response element binding protein (ChREBP), mitigating steatosis and hepatic damage. The reductions in ChREBP and FAS activity likely reflect the diminished stimulatory effects of glucose on ChREBP and as a substrate (AcylCoA) for fatty acid synthesis[171]. Moreover, WY-14643 markedly reduced hepatic steatosis in high-fat-fed C57BL/6 mice by augmenting the volume density of mitochondria per area of liver tissue and downregulating hepatic gluconeogenesis and DNL[58]. More recently, WY-14643 treated gut dysbiosis in high-fat and high-fructose-fed-mice, exerting antisteatotic effects through diminished endotoxemic inflammatory inputs to the liver, showing that PPARα mitigates liver steatosis by acting on multiple hits that trigger this outcome[172,173].

Fibrates are a less potent but clinically relevant class of PPARα agonists compared to Wy-14643, which have also been evaluated in experimental models and human studies[174]. *In vivo* experiments, treatment with pemafibrate, a selective PPARα agonist, identify PPARα as a pharmacological, sexually dimorphic target primarily related to related gene functions to lipid homeostasis, with the female liver being much more responsive to pemafibrate than the male liver[175]. The potency of synthetic PPARα agonists may differ from receptor to species as measured using the PPARα-GAL4 transactivation system, *i.e.*, fenofibrate (mouse receptor, EC50 = 18000 nM *vs* human receptor, EC50 = 30000 nM), bezafibrate (EC50 = 90000 nM *vs* 50000 nM, respectively) and Wy14643 (EC50 = 630 nM *vs* 5000 nM, respectively)[176].

In contrast, several studies have provided evidence that hepatic PPARγ expression markedly increases in many models of obesity (lipoatrophy and hyperphagic obesity), insulin resistance, and diabetes with varying degrees of steatosis[177]. PPARγ expression in the liver is low under healthy conditions but increases as steatosis develops in rodents[178]; this effect is not seen in humans[75,179]. They have tremendous potential in patients with NAFLD because they promote preadipocyte differentiation into adipocytes and may induce fat redistribution from visceral sites such as the liver and muscle to peripheral subcutaneous adipose tissue, increase circulating adiponectin levels, and improve insulin sensitivity [180].



DOI: 10.3748/wjg.v29.i26.4136 **Copyright** ©The Author(s) 2023.

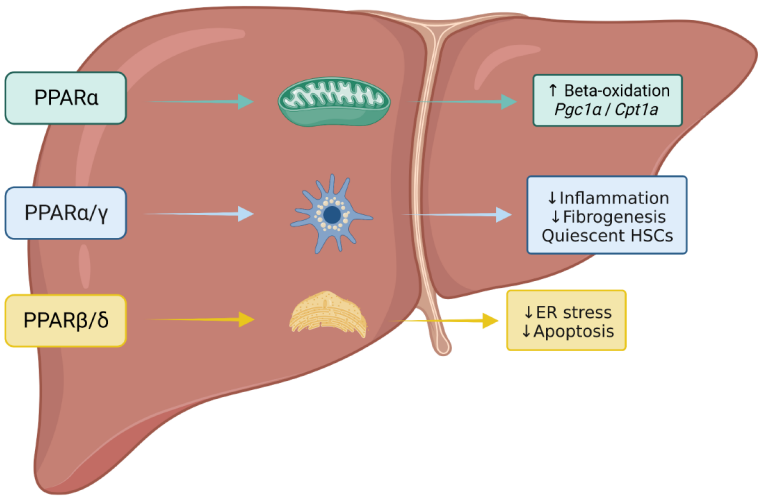
Figure 4 Schematic illustrates hepatic lipotoxicity caused by obesity. There is an increase in lipolysis, which triggers the intracellular accumulation of fatty acids (FAs) within hepatocytes, resulting in a delay in mitochondrial beta-oxidation followed by an increase in lipogenesis, favoring the deposition of lipid droplets in the hepatic parenchyma, culminating in hepatic steatosis. Concomitantly, there is a reduction in insulin signaling, potentiating inflammation, and endoplasmic reticulum (ER) stress. ER stress is detected by the unfolded protein response-IRE1, PERK, and activating transcription factor 6 (ATF6) in the ER membrane. If it is impossible to reverse the unfolded proteins, ATF4 promotes transcription of the C/element binding protein homologous protein, a transcription factor that induces apoptosis. Made with Biorender (www.biorender.com). TAG: Triacylglycerol; UPR: Unfolded protein response; UPR: Unfolded protein response; PERK: Protein kinase RNA-like ER kinase; ATF: Activating transcription factor 6; IRE6: CHOP: C/EBP homologous protein; NEFAs: Non-esterified fatty acids. Created by BioRender.

PPARγ agonists, such as the TZDs, stimulate genes that favor the storage of TAG, thus lowering circulating free fatty acid concentrations[181]. In humans, one-year treatment with pioglitazone (at low dosage) significantly improved liver steatosis, inflammation, and systemic and local adipose tissue insulin resistance in patients with T2D. A decrease in sterol regulatory element-binding transcription factor 1c (SREBP-1c) expression by pioglitazone has a primary effect in reducing hepatic steatosis[182]. Pooled results suggest that acetaldehyde produced from ethanol metabolism may increase the synthesis of the mature SREBP-1 protein, which increases hepatic lipogenesis, thus leading to the development of fatty liver[183,184].

Administration of the PPARγ agonist rosiglitazone (5 mg/kg, daily, gavage) accelerated regression of liver fibrosis as associated with increased expression of PPARγ in mice, with similar findings in human hepatic stellate cells (HSCs). Furthermore, *in vitro*, GATA binding protein 6 (GATA6)-deficient HSCs exhibit a defect in inactivation, suggesting that GATA6 and PPARγ agonists can be used to drive the inactivation of HSCs/myofibroblasts and could compose a combination strategy to halt liver fibrosis in patients[185]. On the other hand, some studies associate TZD therapy with an average weight gain of 4 kg to 5 kg[186,187]. Weight gain combines adiposity and fluid retention as the increased peripheral edema observed during the pre-marketing clinical trials of pioglitazone and rosiglitazone. Increased vascular permeability through high vascular endothelial growth factor secretion and decreased systemic vascular resistance are non-kidney factors that contribute to this edema[188,189].

Recently, dual PPAR-α/γ agonists emerged as a strategy to lessen undesirable side effects related to PPAR-γ agonism. In a randomized controlled clinical trial, Saroglitazar (PPAR-α/γ agonist, 4 mg) significantly improved alanine transaminase, liver fat content, insulin resistance, and atherogenic dyslipidemia in participants with NAFLD/nonalcoholic steatohepatitis (NASH)[190]. In an *in vitro* study on HepG2 cells, saroglitazar prevented HSC activation from quiescent cells to highly proliferative and fibrogenic cells. Pro-inflammatory cytokines, upregulated in NAFLD, can activate hepatic stellate cells, causing increased collagen deposition that initiates fibrogenesis. In turn, the use of saroglitazar reduced the expression of pro-inflammatory [tumor necrosis factor-alpha (*Tnfα*), interleukin (IL)-1β, and IL-6] and pro-fibrogenic (monocyte chemoattractant protein-1, transforming growth factor beta, collagen type I alpha 1 chain, and α-smooth muscle actin) genes in HSC[191]. Evidence is growing in favor of dual PPARα/γ agonism as a candidate for the treatment of NAFLD/NASH due to findings of improvements in all components responsible for these conditions.

In agreement with PPARα beneficial effects on the liver, PPARβ/δ possesses anti-inflammatory effects in the liver by inhibiting NF-κB activity by directly binding to its subunit p65[192-195]. The PPAR-β/δ agonist GW0742 Led to the modulation of the inflammatory response induced by NF-κB in rats, reducing the release of pro-inflammatory cytokines and neutrophils infiltration into the liver[193,196]. During the induction of inflammatory responses, the inactivated PPAR β/δ participates in the activation of NF-κB p65. Activation by ligand PPARβ/δ results in a lack of this cooperation, and consequently, activation of PPARβ/δ interferes with the function of NF-κB p65. As a result, inflammatory responses caused by a high concentration of glucose, activation of the receptor for TNF-α, IL-1β, or activation of TLR4 are reduced [197]. Along with the anti-inflammatory effects, GW0742 has recently mitigated hepatic steatosis through attenuating



DOI: 10.3748/wjg.v29.i26.4136 **Copyright** ©The Author(s) 2023.

Figure 5 Beneficial effects of Peroxisome proliferator-activated receptor activation on the liver. Peroxisome proliferator-activated receptor α (PPARα) activation mitigates hepatic steatosis through the activation of genes related to mitochondrial biogenesis and beta-oxidation, such as *Pgc1α* and *Cpt1a*. Dual PPARα/γ agonists emerge as promising candidates to treat nonalcoholic steatohepatitis once this approach reduces hepatic stellate cells activation, keeping their quiescent stage and impeding fibrogenesis. PPARβ/δ/δ activation entails antisteatotic effects through alleviating the hepatic endoplasmic reticulum stress, inflammation, and apoptosis. Made with Biorender (www.biorender.com). PPAR: Peroxisome proliferator-activated receptor; *Pgc1α*: Peroxisome proliferator-activated receptor gamma coactivator-1 alpha; *Cpt1a*: Carnitine palmitoyltransferase 1a; HSC: Hepatic stellate cell; ER: Endoplasmic reticulum. Created by BioRender.

hepatic ER stress (reduced p-eIF2α/ATF4/CHOP expression), yielding anti-apoptotic signals and favored beta-oxidation over lipogenesis in high-fat-fed mice[198].

Despite this, the contribution of PPARβ/δ to hepatic lipid metabolism is still controversial. PPAR-β/δ null mice on a high-fat diet showed an increased rate of hepatic VLDL production and an increase in the plasma VLDL apoB48, apoE, apoAI, and apoAII levels, as well as a reduction in hepatic lipid stores[178]. However, the other potent PPARβ/δ agonist, GW501516, increased the expression of the lipogenic enzyme ACC2 and consequently increased the hepatic TAG content in db/db mice[192,199]. The role that PPAR-β/δ has on liver metabolism is not defined as there is not a PPAR-β/δ agonist available to the population[200]. Figure 5 depicts the beneficial effects of PPAR activation on the liver. Table 1 shows the main mechanisms and endpoints of PPAR agonists on experimental, *in vitro*, and clinical backgrounds.

CONCLUSION

Overall, there is no doubt that PPARs are promising therapeutic targets for metabolic syndrome, insulin resistance, dyslipidemia, and NAFLD/NASH. However, more research, improvement, and testing are needed to apply PPAR-targeted agents to human metabolic diseases with increased safety and efficacy. Much as PPARs agonists are widely prescribed to treat dyslipidemia, hypertension, and T2DM, dual agonists are promising in the context of obesity due to the combination of anti-inflammatory, lipid oxidation, insulin-sensitizing, and thermogenesis activation, which prevails from one of the isoforms actions and might be highlighted with suitable modulation of their combined activation. Considering that the jury is still out on defined drug therapy for obesity and NAFLD (one of obesity's more prevalent comorbidity), PPARs entail a potent target to reach adequate control of the glucolipotoxicity that trigger metabolic diseases, whether as part of a combination of different PPARs isoforms or combined with agents from other drug classes.

Table 1 Summary of evidence on PPARs agonists on metabolic outcomes in clinical and experimental studies

Model	PPAR agonist	Effect/mechanism	Ref.
HF diet fed C57BL/6 mice (14 wk)	WY14643 (3.0 mg/kg BM)	Decreased body mass and increased hepatic beta-oxidation	Barbosa-da-Silva *et al* [57], 2015
HF diet fed C57BL/6 mice (14 wk)	WY14643 (2.5 mg/kg BM)	Decreased insulin, hepatic steatosis, and enhanced mitochondria per area of liver tissue	Veiga *et al*[58], 2017
HF diet fed C57BL/6 mice (14 wk)	WY14643 (2.5 mg/kg BM)	Browning of subcutaneous WAT, increased thermogenesis	Rachid *et al*[59], 2018
HF diet or high-fructose-fed C57BL/6 mice (17 wk)	WY14643 (3.5 mg/kg BM)	Reduced whitening in HF-fed mice *via* increased VEGFA and reduced inflammation	Miranda *et al*[62], 2020

HF diet fed C57BL/6 mice (15 wk)	Fenofibrate (100.0 mg/kg BM)	Increased irisin-*Pgc1α*-*Prdm16* and induced thermogenic beige adipocytes	Rachid *et al*[63], 2015
High-fructose diet-fed C57BL/6 mice (11 wk)	GW501516 (3.0 mg/kg/d)	Potent anti-inflammatory effects that reversed adipocyte hypertrophy	Magliano *et al*[64], 2015
Knockout mice for *Pparγ* in collecting duct	Rosiglitazone (320.0 mg/kg diet)	PPARγ regulates sodium transport in the collecting ducts and mediates the rosiglitazone-induced edema	Zhang *et al*[77], 2005
Human subcutaneous white adipose tissue biopsy	Pioglitazone (45 mg daily for two months)	Pioglitazone reduced CD68 and MCP-1 expression in adipose tissue, improving insulin sensitivity	Di Gregorio *et al*[78], 2005
HF diet fed C57BL/6 mice (16 wk)	Tesaglitazar (4 mg/kg BM)	PPARα/γ synergism treated dysbiosis and favored thermogenesis	Miranda *et al*[80], 2023
Human jejunal biopsies	Cells treated with GW7647 (600 nM) or GFT505 (1 μM) for 18 h	Intestinal PPARα activation induces HDL production	Colin *et al*[82], 2013
Knockout mice	25.0% fish oil in the diet	Increased adiponectin, improved glucose metabolism, and islet hypertrophy	Nakasatomi *et al*[112], 2018
Non-obese diabetic mice	0.1% fenofibrate in the diet	Anti-inflammatory, antiapoptotic effects, and enhanced islet innervation, ameliorating glucose handling	Holm *et al*[114], 2019
Monosodium glutamate induced obese rats	100 mg/kg fenofibrate for 12 wk	Long-term treatment disrupted beta cell function due to increased NF-κB and iNOS expression	Liu *et al*[115], 2011
Rat pancreatic islets *in vitro*	300 microM bezafibrate for 8 h	Bezafibrate enhanced GSIS through *Pparα* activation in short-term culture. Long-term culture caused beta cell dysfunction due to overstimulation	Yoshikawa *et al*[116], 2001
Diabetic subjects	400 mg bezafibrate for two years	Bezafibrate avoided the progressive decline of beta cell function and insulin resistance increase	Tenenbaum *et al*[117], 2007
Subjects diagnosed with type 2 diabetes and dyslipidemia	Pioglitazone 30 mg/d for 12 wk and 45 mg/d for additional 12 wk; rosiglitazone 4 mg/d for 12 wk and 8 mg/d for additional 12 wk	Pioglitazone had better effects regarding improvements in triglycerides, HDL cholesterol, LDL particle concentration, and LDL particle size	Goldberg *et al*[127], 2005
db/db mice	Pioglitazone 15 mg/kg BM for 18 d	Restoration of pancreatic islet function with increased expression of insulin and NK6 Homeobox 1 expression	Collier *et al*[132], 2021
Knockout-Ay mice	High-fat diet plus pioglitazone 0.02% for 6 wk	Islet preservation through ER stress and inflammation alleviation	Hong *et al*[133], 2018
Diabetic Wistar rats (low streptozotocin dose)	10 mg/kg pioglitazone or vildagliptin or their combination for 4 wk	Vildagliptin maximized pioglitazone effects on inflammation and oxidative stress attenuation	Refaat *et al*[134], 2016
Type 2 diabetic patients	Sitagliptin 100 mg/d or Pioglitazone 30 mg/d or their combination for 12 wk	Both drugs exerted complementary effects on blood glucose control	Alba *et al*[135], 2013
Non-diabetic hypertensive subjects	Telmisartan (80 mg/d) for 6 wk	Telmisartan enhanced insulin sensitivity in hypertensive patients independent of adiponectin induction	Benndorf *et al*[136], 2006
High-fat diet-fed mice (16 wk)	Telmisartan (5 mg/kg BM) alone or in combination with sitagliptin (1 g/kg BM) or metformin (300 mg/kg BM)	Treated animals exhibited marked mitigation of hepatic steatosis and islet hypertrophy; telmisartan combination with sitagliptin normalized alpha and beta cell mass	Souza-Mello *et al*[93], 2010; Souza-Mello *et al*[97], 2011
High-fat diet-fed mice (15 wk)	Telmisartan (10 mg/kg)	Amelioration of endocrine pancreas structure and function, with enhanced islet vascularization and reduced apoptosis rate	Graus-Nunes *et al*[96], 2017
db/db mice	Telmisartan (3 mg/kg BM), linagliptin (3 mg/kg BM) or their combination for eight weeks	Combined therapy provided better results than the monotherapies on glucose homeostasis, islet cell functions, and structure *via* reduced oxidative stress	Zhao *et al*[137], 2016
High-fat-fed foz/foz obese/diabetic mice for 16 wk	WY14643 (0.1% w/w) for 10 d or 20 d	PPARα activation mitigated steatosis, and hepatocyte ballooning, besides reducing NF-κB and JNK activation. Persistent adipose-derived MCP1 enhanced levels may limit its property to treat NASH	Larter *et al*[171], 2012
High-fructose diet-fed mice (17 wk)	WY14643 (3.5 mg/kg BM) or linagliptin (15.0 mg/kg BM) or their combination	The WY14643 monotherapy or its combination with linagliptin-treated dysbiosis, controlling endotoxemia and mitigating liver steatosis	Silva-Veiga *et al*[173], 2020
Type 2 diabetic patients	Metformin 2 g/d + Pioglitazone (15 mg/d, 30 mg/d, or 45 mg/d)	All pioglitazone doses exerted similar effects, with mitigation of liver steatosis and inflammation, with improved systemic insulin resistance	Della Pepa *et al*[182], 2021
CCl4-injured mice	Rosiglitazone (5 mg/kg BM) for two weeks	Rosiglitazone blocked liver fibrosis progression through the down-regulation of fibrogenic genes and HSCs inactivation	Liu *et al*[185], 2020
Patients with	Saroglitazar 1 mg, 2 mg, or 4 mg for 16	Saroglitazar 4 mg significantly mitigated insulin resistance	Gawrieh *et al*[190],

NAFLD/NASH	wk	and atherogenic dyslipidemia	2021
HF diet fed mice (14 wk)	GW0742 (1 mg/kg BM) for four weeks	PPARβ/δ mitigated hepatic steatosis through improved insulin resistance and ER stress alleviation	Silva-Veiga *et al* [198], 2018

HF: High-fructose; NAFLD: Non-alcoholic fatty liver disease; NASH: Nonalcoholic steatohepatitis; PPAR: Peroxisome proliferator-activated receptors; WAT: White adipose tissue; ER: Endoplasmic reticulum; NF-κB: Noncanonical nuclear factor-kappaB; HSCs: Hepatic stellate cells; iNOS: Inducible nitric oxide synthase; GSIS: Glucose-stimulated insulin secretion; HDL: High-density cholesterol; LDL: Low-density cholesterol.

FOOTNOTES

Author contributions: Souza-Mello V and Souza-Tavares H conceived the idea for the manuscript; Souza-Tavares H, Miranda CS, Vasques-Monteiro IML, Sandoval C, Santana-Oliveira DA, Silva-Veiga FM, Fernandes-da-Silva A, and Souza-Mello V performed the literature search and drafted the manuscript; Santana-Oliveira DA, Silva-Veiga FM, and Souza-Mello V designed the figures; Souza-Mello V critically revised the work; and all authors read and approved the final version of the manuscript.

Supported by the Conselho Nacional de Desenvolvimento Científico e Tecnológico (Brazil), No. 303785/2020-9; and Fundação Carlos Chagas Filho de Amparo à Pesquisa do Estado do Rio de Janeiro, No. E-26/200.984/2022 for V.S-M.

Conflict-of-interest statement: The authors declare that they have no conflict of interest.

Open-Access: This article is an open-access article that was selected by an in-house editor and fully peer-reviewed by external reviewers. It is distributed in accordance with the Creative Commons Attribution NonCommercial (CC BY-NC 4.0) license, which permits others to distribute, remix, adapt, build upon this work non-commercially, and license their derivative works on different terms, provided the original work is properly cited and the use is non-commercial. See: https://creativecommons.org/Licenses/by-nc/4.0/

Country/Territory of origin: Brazil

ORCID number: Henrique Souza-Tavares 0000-0001-79314384; Carolline Santos Miranda 0000-0001-5488-0179; Isabela Macedo Lopes Vasques-Monteiro 0000-0003-1729-3201; Cristian Sandoval 0000-0003-3184-6482; Daiana Araujo Santana-Oliveira 0000-0002-2474-5846; Flavia Maria Silva-Veiga 0000-0002-3320-5825; Aline Fernandes-da-Silva 0000-0002-6369-0235; Vanessa Souza-Mello 0000-0002-2510-9569.

S-Editor: Chen YL
L-Editor: A
P-Editor: Yuan YY

REFERENCES

1 **GBD 2015 Obesity Collaborators**, Afshin A, Forouzanfar MH, Reitsma MB, Sur P, Estep K, Lee A, Marczak L, Mokdad AH, Moradi-Lakeh M, Naghavi M, Salama JS, Vos T, Abate KH, Abbafati C, Ahmed MB, Al-Aly Z, Alkerwi A, Al-Raddadi R, Amare AT, Amberbir A, Amegah AK, Amini E, Amrock SM, Anjana RM, Ärnlöv J, Asayesh H, Banerjee A, Barac A, Baye E, Bennett DA, Beyene AS, Biadgilign S, Biryukov S, Bjertness E, Boneya DJ, Campos-Nonato I, Carrero JJ, Cecilio P, Cercy K, Ciobanu LG, Cornaby L, Damtew SA, Dandona L, Dandona R, Dharmaratne SD, Duncan BB, Eshrati B, Esteghamati A, Feigin VL, Fernandes JC, Fürst T, Gebrehiwot TT, Gold A, Gona PN, Goto A, Habtewold TD, Hadush KT, Hafezi-Nejad N, Hay SI, Horino M, Islami F, Kamal R, Kasaeian A, Katikireddi SV, Kengne AP, Kesavachandran CN, Khader YS, Khang YH, Khubchandani J, Kim D, Kim YJ, Kinfu Y, Kosen S, Ku T, Defo BK, Kumar GA, Larson HJ, Leinsalu M, Liang X, Lim SS, Liu P, Lopez AD, Lozano R, Majeed A, Malekzadeh R, Malta DC, Mazidi M, McAlinden C, McGarvey ST, Mengistu DT, Mensah GA, Mensink GBM, Mezgebe HB, Mirrakhimov EM, Mueller UO, Noubiap JJ, Obermeyer CM, Ogbo FA, Owolabi MO, Patton GC, Pourmalek F, Qorbani M, Rafay A, Rai RK, Ranabhat CL, Reinig N, Safiri S, Salomon JA, Sanabria JR, Santos IS, Sartorius B, Sawhney M, Schmidhuber J, Schutte AE, Schmidt MI, Sepanlou SG, Shamsizadeh M, Sheikhbahaei S, Shin MJ, Shiri R, Shiue I, Roba HS, Silva DAS, Silverberg JI, Singh JA, Stranges S, Swaminathan S, Tabarés-Seisdedos R, Tadese F, Tedla BA, Tegegne BS, Terkawi AS, Thakur JS, Tonelli M, Topor-Madry R, Tyrovolas S, Ukwaja KN, Uthman OA, Vaezghasemi M, Vasankari T, Vlassov VV, Vollset SE, Weiderpass E, Werdecker A, Wesana J, Westerman R, Yano Y, Yonemoto N, Yonga G, Zaidi Z, Zenebe ZM, Zipkin B, Murray CJL. Health Effects of Overweight and Obesity in 195 Countries over 25 Years. *N Engl J Med* 2017; **377**: 13-27 [PMID: 28604169 DOI: 10.1056/NEJMoa1614362]

2 **Betz MJ**, Enerbäck S. Human Brown Adipose Tissue: What We Have Learned So Far. *Diabetes* 2015; **64**: 2352-2360 [PMID: 26050667 DOI: 10.2337/db15-0146]

3 **Tseng YH**, Cypess AM, Kahn CR. Cellular bioenergetics as a target for obesity therapy. *Nat Rev Drug Discov* 2010; **9**: 465-482 [PMID: 20514071 DOI: 10.1038/nrd3138]

4 **Gustafson B**, Hedjazifar S, Gogg S, Hammarstedt A, Smith U. Insulin resistance and impaired adipogenesis. *Trends Endocrinol Metab* 2015; **26**: 193-200 [PMID: 25703677 DOI: 10.1016/j.tem.2015.01.006]

5 **Gustafson B**, Smith U. Regulation of white adipogenesis and its relation to ectopic fat accumulation and cardiovascular risk. *Atherosclerosis* 2015; **241**: 27-35 [PMID: 25957567 DOI: 10.1016/j.atherosclerosis.2015.04.812]

6 **Cildir G**, Akıncılar SC, Tergaonkar V. Chronic adipose tissue inflammation: all immune cells on the stage. *Trends Mol Med* 2013; **19**: 487-500 [PMID: 23746697 DOI: 10.1016/j.molmed.2013.05.001]

7 **Gustafson B**, Hammarstedt A, Hedjazifar S, Smith U. Restricted adipogenesis in hypertrophic obesity: the role of WISP2, WNT, and BMP4. *Diabetes* 2013; **62**: 2997-3004 [PMID: 23970518 DOI: 10.2337/db13-0473]

8 **DeFronzo RA**. Dysfunctional fat cells, lipotoxicity and type 2 diabetes. *Int J Clin Pract Suppl* 2004; 9-21 [PMID: 16035392 DOI: 10.1111/j.1368-504x.2004.00389.x]

9 **Longo M**, Zatterale F, Naderi J, Parrillo L, Formisano P, Raciti GA, Beguinot F, Miele C. Adipose Tissue Dysfunction as Determinant of Obesity-Associated Metabolic Complications. *Int J Mol Sci* 2019; **20** [PMID: 31085992 DOI: 10.3390/ijms20092358]

10 **Polyzos SA**, Kountouras J, Mantzoros CS. Adipose tissue, obesity and non-alcoholic fatty liver disease. *Minerva Endocrinol* 2017; **42**: 92-108 [PMID: 27711029 DOI: 10.23736/S0391-1977.16.02563-3]

11 **Poitout V**, Robertson RP. Minireview: Secondary beta-cell failure in type 2 diabetes--a convergence of glucotoxicity and lipotoxicity. *Endocrinology* 2002; **143**: 339-342 [PMID: 11796484 DOI: 10.1210/endo.143.2.8623]

12 **Saponaro C**, Gaggini M, Carli F, Gastaldelli A. The Subtle Balance between Lipolysis and Lipogenesis: A Critical Point in Metabolic Homeostasis. *Nutrients* 2015; **7**: 9453-9474 [PMID: 26580649 DOI: 10.3390/nu7115475]

13 **Harrington WW**, S Britt C, G Wilson J, O Milliken N, G Binz J, C Lobe D, R Oliver W, C Lewis M, M Ignar D. The Effect of PPARalpha, PPARdelta, PPARgamma, and PPARpan Agonists on Body Weight, Body Mass, and Serum Lipid Profiles in Diet-Induced Obese AKR/J Mice. *PPAR Res* 2007; **2007**: 97125 [PMID: 17710237 DOI: 10.1155/2007/97125]

14 **Li M**, Pascual G, Glass CK. Peroxisome proliferator-activated receptor gamma-dependent repression of the inducible nitric oxide synthase gene. *Mol Cell Biol* 2000; **20**: 4699-4707 [PMID: 10848596 DOI: 10.1128/mcb.20.13.4699-4707.2000]

15 **Delerive P**, De Bosscher K, Besnard S, Vanden Berghe W, Peters JM, Gonzalez FJ, Fruchart JC, Tedgui A, Haegeman G, Staels B. Peroxisome proliferator-activated receptor alpha negatively regulates the vascular inflammatory gene response by negative cross-talk with transcription factors NF-kappaB and AP-1. *J Biol Chem* 1999; **274**: 32048-32054 [PMID: 10542237 DOI: 10.1074/jbc.274.45.32048]

16 **Dubois V**, Eeckhoute J, Lefebvre P, Staels B. Distinct but complementary contributions of PPAR isotypes to energy homeostasis. *J Clin Invest* 2017; **127**: 1202-1214 [PMID: 28368286 DOI: 10.1172/JCI88894]

17 **Corrales P**, Vidal-Puig A, Medina-Gómez G. PPARs and Metabolic Disorders Associated with Challenged Adipose Tissue Plasticity. *Int J Mol Sci* 2018; **19** [PMID: 30037087 DOI: 10.3390/ijms19072124]

18 **Moraes LA**, Piqueras L, Bishop-Bailey D. Peroxisome proliferator-activated receptors and inflammation. *Pharmacol Ther* 2006; **110**: 371-385 [PMID: 16168490 DOI: 10.1016/j.pharmthera.2005.08.007]

19 **Fonseca-Alaniz MH**, Takada J, Alonso-Vale MI, Lima FB. Adipose tissue as an endocrine organ: from theory to practice. *J Pediatr (Rio J)* 2007; **83**: S192-S203 [PMID: 17989837 DOI: 10.2223/JPED.1709]

20 **Ahima RS**, Flier JS. Adipose tissue as an endocrine organ. *Trends Endocrinol Metab* 2000; **11**: 327-332 [PMID: 10996528 DOI: 10.1016/s1043-2760(00)00301-5]

21 **Pénicaud L**, Cousin B, Leloup C, Lorsignol A, Casteilla L. The autonomic nervous system, adipose tissue plasticity, and energy balance. *Nutrition* 2000; **16**: 903-908 [PMID: 11054595 DOI: 10.1016/s0899-9007(00)00427-5]

22 **Kreier F**, Fliers E, Voshol PJ, Van Eden CG, Havekes LM, Kalsbeek A, Van Heijningen CL, Sluiter AA, Mettenleiter TC, Romijn JA, Sauerwein HP, Buijs RM. Selective parasympathetic innervation of subcutaneous and intra-abdominal fat--functional implications. *J Clin Invest* 2002; **110**: 1243-1250 [PMID: 12417562 DOI: 10.1172/jci15736]

23 **Giralt M**, Villarroya F. White, brown, beige/brite: different adipose cells for different functions? *Endocrinology* 2013; **154**: 2992-3000 [PMID: 23782940 DOI: 10.1210/en.2013-1403]

24 **Lidell ME**, Betz MJ, Enerbäck S. Two types of brown adipose tissue in humans. *Adipocyte* 2014; **3**: 63-66 [PMID: 24575372 DOI: 10.4161/adip.26896]

25 **Wronska A**, Kmiec Z. Structural and biochemical characteristics of various white adipose tissue depots. *Acta Physiol (Oxf)* 2012; **205**: 194-208 [PMID: 22226221 DOI: 10.1111/j.1748-1716.2012.02409.x]

26 **Divoux A**, Clément K. Architecture and the extracellular matrix: the still unappreciated components of the adipose tissue. *Obes Rev* 2011; **12**: e494-e503 [PMID: 21366833 DOI: 10.1111/j.1467-789X.2010.00811.x]

27 **Frederich RC**, Hamann A, Anderson S, Löllmann B, Lowell BB, Flier JS. Leptin levels reflect body lipid content in mice: evidence for diet-induced resistance to leptin action. *Nat Med* 1995; **1**: 1311-1314 [PMID: 7489415 DOI: 10.1038/nm1295-1311]

28 **Lee MW**, Lee M, Oh KJ. Adipose Tissue-Derived Signatures for Obesity and Type 2 Diabetes: Adipokines, Batokines and MicroRNAs. *J Clin Med* 2019; **8** [PMID: 31208019 DOI: 10.3390/jcm8060854]

29 **Nedergaard J**, Bengtsson T, Cannon B. Unexpected evidence for active brown adipose tissue in adult humans. *Am J Physiol Endocrinol Metab* 2007; **293**: E444-E452 [PMID: 17473055 DOI: 10.1152/ajpendo.00691.2006]

30 **Langin D**. Recruitment of brown fat and conversion of white into brown adipocytes: strategies to fight the metabolic complications of obesity? *Biochim Biophys Acta* 2010; **1801**: 372-376 [PMID: 19782764 DOI: 10.1016/j.bbalip.2009.09.008]

31 **Cannon B**, Nedergaard J. Brown adipose tissue: function and physiological significance. *Physiol Rev* 2004; **84**: 277-359 [PMID: 14715917 DOI: 10.1152/physrev.00015.2003]

32 **Lowell BB**, Spiegelman BM. Towards a molecular understanding of adaptive thermogenesis. *Nature* 2000; **404**: 652-660 [PMID: 10766252 DOI: 10.1038/35007527]

33 **Nedergaard J**, Golozoubova V, Matthias A, Asadi A, Jacobsson A, Cannon B. UCP1: the only protein able to mediate adaptive non-shivering thermogenesis and metabolic inefficiency. *Biochim Biophys Acta* 2001; **1504**: 82-106 [PMID: 11239487 DOI: 10.1016/s0005-2728(00)00247-4]

34 **Timmons JA**, Wennmalm K, Larsson O, Walden TB, Lassmann T, Petrovic N, Hamilton DL, Gimeno RE, Wahlestedt C, Baar K, Nedergaard J, Cannon B. Myogenic gene expression signature establishes that brown and white adipocytes originate from distinct cell lineages. *Proc Natl Acad Sci U S A* 2007; **104**: 4401-4406 [PMID: 17360536 DOI: 10.1073/pnas.0610615104]

35 **Seale P**, Kajimura S, Yang W, Chin S, Rohas LM, Uldry M, Tavernier G, Langin D, Spiegelman BM. Transcriptional control of brown fat determination by PRDM16. *Cell Metab* 2007; **6**: 38-54 [PMID: 17618855 DOI: 10.1016/j.cmet.2007.06.001]

36 **Nedergaard J**, Bengtsson T, Cannon B. Three years with adult human brown adipose tissue. *Ann N Y Acad Sci* 2010; **1212**: E20-E36 [PMID: 21375707 DOI: 10.1111/j.1749-6632.2010.05905.x]

37 **Smith RE**, Hock RJ. Brown fat: thermogenic effector of arousal in hibernators. *Science* 1963; **140**: 199-200 [PMID: 13989560 DOI: 10.1126/science.140.3563.199]

38 **Smith RE**. Thermoregulatory and adaptive behavior of brown adipose tissue. *Science* 1964; **146**: 1686-1689 [PMID: 14224520 DOI: 10.1126/science.146.3652.1686]

39 **Shimizu I**, Aprahamian T, Kikuchi R, Shimizu A, Papanicolaou KN, MacLauchlan S, Maruyama S, Walsh K. Vascular rarefaction mediates

whitening of brown fat in obesity. *J Clin Invest* 2014; **124**: 2099-2112 [PMID: 24713652 DOI: 10.1172/JCI71643]

40 **Roberts-Toler C**, O'Neill BT, Cypess AM. Diet-induced obesity causes insulin resistance in mouse brown adipose tissue. *Obesity (Silver Spring)* 2015; **23**: 1765-1770 [PMID: 26242777 DOI: 10.1002/oby.21134]

41 **Rangel-Azevedo C**, Santana-Oliveira DA, Miranda CS, Martins FF, Mandarim-de-Lacerda CA, Souza-Mello V. Progressive brown adipocyte dysfunction: Whitening and impaired nonshivering thermogenesis as long-term obesity complications. *J Nutr Biochem* 2022; **105**: 109002 [PMID: 35346828 DOI: 10.1016/j.jnutbio.2022.109002]

42 **Xue Y**, Petrovic N, Cao R, Larsson O, Lim S, Chen S, Feldmann HM, Liang Z, Zhu Z, Nedergaard J, Cannon B, Cao Y. Hypoxia-independent angiogenesis in adipose tissues during cold acclimation. *Cell Metab* 2009; **9**: 99-109 [PMID: 19117550 DOI: 10.1016/j.cmet.2008.11.009]

43 **Concha F**, Prado G, Quezada J, Ramirez A, Bravo N, Flores C, Herrera JJ, Lopez N, Uribe D, Duarte-Silva L, Lopez-Legarrea P, Garcia-Diaz DF. Nutritional and non-nutritional agents that stimulate white adipose tissue browning. *Rev Endocr Metab Disord* 2019; **20**: 161-171 [PMID: 31020455 DOI: 10.1007/s11154-019-09495-y]

44 **Wu J**, Boström P, Sparks LM, Ye L, Choi JH, Giang AH, Khandekar M, Virtanen KA, Nuutila P, Schaart G, Huang K, Tu H, van Marken Lichtenbelt WD, Hoeks J, Enerbäck S, Schrauwen P, Spiegelman BM. Beige adipocytes are a distinct type of thermogenic fat cell in mouse and human. *Cell* 2012; **150**: 366-376 [PMID: 22796012 DOI: 10.1016/j.cell.2012.05.016]

45 **Harms MJ**, Ishibashi J, Wang W, Lim HW, Goyama S, Sato T, Kurokawa M, Won KJ, Seale P. Prdm16 is required for the maintenance of brown adipocyte identity and function in adult mice. *Cell Metab* 2014; **19**: 593-604 [PMID: 24703692 DOI: 10.1016/j.cmet.2014.03.007]

46 **Spiegelman BM**. Banting Lecture 2012: Regulation of adipogenesis: toward new therapeutics for metabolic disease. *Diabetes* 2013; **62**: 1774-1782 [PMID: 23704518 DOI: 10.2337/db12-1665]

47 **Sanchez-Gurmaches J**, Guertin DA. Adipocyte lineages: tracing back the origins of fat. *Biochim Biophys Acta* 2014; **1842**: 340-351 [PMID: 23747579 DOI: 10.1016/j.bbadis.2013.05.027]

48 **Long JZ**, Svensson KJ, Tsai L, Zeng X, Roh HC, Kong X, Rao RR, Lou J, Lokurkar I, Baur W, Castellot JJ Jr, Rosen ED, Spiegelman BM. A smooth muscle-like origin for beige adipocytes. *Cell Metab* 2014; **19**: 810-820 [PMID: 24709624 DOI: 10.1016/j.cmet.2014.03.025]

49 **Min SY**, Kady J, Nam M, Rojas-Rodriguez R, Berkenwald A, Kim JH, Noh HL, Kim JK, Cooper MP, Fitzgibbons T, Brehm MA, Corvera S. Human 'brite/beige' adipocytes develop from capillary networks, and their implantation improves metabolic homeostasis in mice. *Nat Med* 2016; **22**: 312-318 [PMID: 26808348 DOI: 10.1038/nm.4031]

50 **Martins FF**, Souza-Mello V, Aguila MB, Mandarim-de-Lacerda CA. Brown adipose tissue as an endocrine organ: updates on the emerging role of batokines. *Horm Mol Biol Clin Investig* 2022 [PMID: 36288452 DOI: 10.1515/hmbci-2022-0044]

51 **Virtanen KA**, Lidell ME, Orava J, Heglind M, Westergren R, Niemi T, Taittonen M, Laine J, Savisto NJ, Enerbäck S, Nuutila P. Functional brown adipose tissue in healthy adults. *N Engl J Med* 2009; **360**: 1518-1525 [PMID: 19357407 DOI: 10.1056/NEJMoa0808949]

52 **Sher T**, Yi HF, McBride OW, Gonzalez FJ. cDNA cloning, chromosomal mapping, and functional characterization of the human peroxisome proliferator activated receptor. *Biochemistry* 1993; **32**: 5598-5604 [PMID: 7684926 DOI: 10.1021/bi00072a015]

53 **Braissant O**, Foufelle F, Scotto C, Dauça M, Wahli W. Differential expression of peroxisome proliferator-activated receptors (PPARs): tissue distribution of PPAR-alpha, -beta, and -gamma in the adult rat. *Endocrinology* 1996; **137**: 354-366 [PMID: 8536636 DOI: 10.1210/endo.137.1.8536636]

54 **Vamecq J**, Latruffe N. Medical significance of peroxisome proliferator-activated receptors. *Lancet* 1999; **354**: 141-148 [PMID: 10408502 DOI: 10.1016/s0140-6736(98)10364-1]

55 **Li P**, Zhu Z, Lu Y, Granneman JG. Metabolic and cellular plasticity in white adipose tissue II: role of peroxisome proliferator-activated receptor-alpha. *Am J Physiol Endocrinol Metab* 2005; **289**: E617-E626 [PMID: 15941786 DOI: 10.1152/ajpendo.00010.2005]

56 **Rösch S**, Ramer R, Brune K, Hinz B. Prostaglandin E2 induces cyclooxygenase-2 expression in human non-pigmented ciliary epithelial cells through activation of p38 and p42/44 mitogen-activated protein kinases. *Biochem Biophys Res Commun* 2005; **338**: 1171-1178 [PMID: 16256948 DOI: 10.1016/j.bbrc.2005.10.051]

57 **Barbosa-da-Silva S**, Souza-Mello V, Magliano DC, Marinho Tde S, Aguila MB, Mandarim-de-Lacerda CA. Singular effects of PPAR agonists on nonalcoholic fatty liver disease of diet-induced obese mice. *Life Sci* 2015; **127**: 73-81 [PMID: 25748419 DOI: 10.1016/j.lfs.2015.02.003]

58 **Veiga FMS**, Graus-Nunes F, Rachid TL, Barreto AB, Mandarim-de-Lacerda CA, Souza-Mello V. Anti-obesogenic effects of WY14643 (PPAR-alpha agonist): Hepatic mitochondrial enhancement and suppressed lipogenic pathway in diet-induced obese mice. *Biochimie* 2017; **140**: 106-116 [PMID: 28711683 DOI: 10.1016/j.biochi.2017.07.003]

59 **Rachid TL**, Silva-Veiga FM, Graus-Nunes F, Bringhenti I, Mandarim-de-Lacerda CA, Souza-Mello V. Differential actions of PPAR-α and PPAR-β/δ on beige adipocyte formation: A study in the subcutaneous white adipose tissue of obese male mice. *PLoS One* 2018; **13**: e0191365 [PMID: 29351550 DOI: 10.1371/journal.pone.0191365]

60 **Seale P**. Transcriptional Regulatory Circuits Controlling Brown Fat Development and Activation. *Diabetes* 2015; **64**: 2369-2375 [PMID: 26050669 DOI: 10.2337/db15-0203]

61 **Rachid TL**, Penna-de-Carvalho A, Bringhenti I, Aguila MB, Mandarim-de-Lacerda CA, Souza-Mello V. PPAR-α agonist elicits metabolically active brown adipocytes and weight loss in diet-induced obese mice. *Cell Biochem Funct* 2015; **33**: 249-256 [PMID: 25959716 DOI: 10.1002/cbf.3111]

62 **Miranda CS**, Silva-Veiga F, Martins FF, Rachid TL, Mandarim-De-Lacerda CA, Souza-Mello V. PPAR-α activation counters brown adipose tissue whitening: a comparative study between high-fat- and high-fructose-fed mice. *Nutrition* 2020; **78**: 110791 [PMID: 32682271 DOI: 10.1016/j.nut.2020.110791]

63 **Rachid TL**, Penna-de-Carvalho A, Bringhenti I, Aguila MB, Mandarim-de-Lacerda CA, Souza-Mello V. Fenofibrate (PPARalpha agonist) induces beige cell formation in subcutaneous white adipose tissue from diet-induced male obese mice. *Mol Cell Endocrinol* 2015; **402**: 86-94 [PMID: 25576856 DOI: 10.1016/j.mce.2014.12.027]

64 **Magliano DC**, Penna-de-Carvalho A, Vazquez-Carrera M, Mandarim-de-Lacerda CA, Aguila MB. Short-term administration of GW501516 improves inflammatory state in white adipose tissue and liver damage in high-fructose-fed mice through modulation of the renin-angiotensin system. *Endocrine* 2015; **50**: 355-367 [PMID: 25854303 DOI: 10.1007/s12020-015-0590-1]

65 **Lehmann JM**, Moore LB, Smith-Oliver TA, Wilkison WO, Willson TM, Kliewer SA. An antidiabetic thiazolidinedione is a high affinity ligand for peroxisome proliferator-activated receptor gamma (PPAR gamma). *J Biol Chem* 1995; **270**: 12953-12956 [PMID: 7768881 DOI: 10.1074/jbc.270.22.12953]

66 **Ahmadian M**, Suh JM, Hah N, Liddle C, Atkins AR, Downes M, Evans RM. PPARγ signaling and metabolism: the good, the bad and the future. *Nat Med* 2013; **19**: 557-566 [PMID: 23652116 DOI: 10.1038/nm.3159]

67 **Stuhlmeier KM**, Kao JJ, Bach FH. Arachidonic acid influences proinflammatory gene induction by stabilizing the inhibitor-kappaBalpha/nuclear factor-kappaB (NF-kappaB) complex, thus suppressing the nuclear translocation of NF-kappaB. *J Biol Chem* 1997; **272**: 24679-24683 [PMID: 9305938 DOI: 10.1074/jbc.272.39.24679]

68 **Korbecki J**, Baranowska-Bosiacka I, Gutowska I, Chlubek D. Cyclooxygenase pathways. *Acta Biochim Pol* 2014; **61**: 639-649 [PMID: 25343148]

69 **Lawrence T**, Natoli G. Transcriptional regulation of macrophage polarization: enabling diversity with identity. *Nat Rev Immunol* 2011; **11**: 750-761 [PMID: 22025054 DOI: 10.1038/nri3088]

70 **Inagaki T**, Sakai J, Kajimura S. Transcriptional and epigenetic control of brown and beige adipose cell fate and function. *Nat Rev Mol Cell Biol* 2016; **17**: 480-495 [PMID: 27251423 DOI: 10.1038/nrm.2016.62]

71 **Consoli A**, Devangelio E. Thiazolidinediones and inflammation. *Lupus* 2005; **14**: 794-797 [PMID: 16218490 DOI: 10.1191/0961203305lu2223oa]

72 **Staels B**, Fruchart JC. Therapeutic roles of peroxisome proliferator-activated receptor agonists. *Diabetes* 2005; **54**: 2460-2470 [PMID: 16046315 DOI: 10.2337/diabetes.54.8.2460]

73 **Fritsche K**. Fatty acids as modulators of the immune response. *Annu Rev Nutr* 2006; **26**: 45-73 [PMID: 16848700 DOI: 10.1146/annurev.nutr.25.050304.092610]

74 **Kahn SE**, Haffner SM, Heise MA, Herman WH, Holman RR, Jones NP, Kravitz BG, Lachin JM, O'Neill MC, Zinman B, Viberti G; ADOPT Study Group. Glycemic durability of rosiglitazone, metformin, or glyburide monotherapy. *N Engl J Med* 2006; **355**: 2427-2443 [PMID: 17145742 DOI: 10.1056/NEJMoa066224]

75 **Gross B**, Pawlak M, Lefebvre P, Staels B. PPARs in obesity-induced T2DM, dyslipidaemia and NAFLD. *Nat Rev Endocrinol* 2017; **13**: 36-49 [PMID: 27636730 DOI: 10.1038/nrendo.2016.135]

76 **Lefterova MI**, Haakonsson AK, Lazar MA, Mandrup S. PPARγ and the global map of adipogenesis and beyond. *Trends Endocrinol Metab* 2014; **25**: 293-302 [PMID: 24793638 DOI: 10.1016/j.tem.2014.04.001]

77 **Zhang H**, Zhang A, Kohan DE, Nelson RD, Gonzalez FJ, Yang T. Collecting duct-specific deletion of peroxisome proliferator-activated receptor gamma blocks thiazolidinedione-induced fluid retention. *Proc Natl Acad Sci U S A* 2005; **102**: 9406-9411 [PMID: 15956187 DOI: 10.1073/pnas.0501744102]

78 **Di Gregorio GB**, Yao-Borengasser A, Rasouli N, Varma V, Lu T, Miles LM, Ranganathan G, Peterson CA, McGehee RE, Kern PA. Expression of CD68 and macrophage chemoattractant protein-1 genes in human adipose and muscle tissues: association with cytokine expression, insulin resistance, and reduction by pioglitazone. *Diabetes* 2005; **54**: 2305-2313 [PMID: 16046295 DOI: 10.2337/diabetes.54.8.2305]

79 **Nedergaard J**, Petrovic N, Lindgren EM, Jacobsson A, Cannon B. PPARgamma in the control of brown adipocyte differentiation. *Biochim Biophys Acta* 2005; **1740**: 293-304 [PMID: 15949696 DOI: 10.1016/j.bbadis.2005.02.003]

80 **Miranda CS**, Silva-Veiga FM, Fernandes-da-Silva A, Guimarães Pereira VR, Martins BC, Daleprane JB, Martins FF, Souza-Mello V. Peroxisome proliferator-activated receptors-alpha and gamma synergism modulate the gut-adipose tissue axis and mitigate obesity. *Mol Cell Endocrinol* 2023; **562**: 111839 [PMID: 36581062 DOI: 10.1016/j.mce.2022.111839]

81 **Kimura R**, Takahashi N, Goto T, Murota K, Kawada T. Activation of peroxisome proliferator-activated receptor-α (PPARα) in proximal intestine improves postprandial lipidemia in obese diabetic KK-Ay mice. *Obes Res Clin Pract* 2013; **7**: e353-e360 [PMID: 24455763 DOI: 10.1016/j.orcp.2013.05.005]

82 **Colin S**, Briand O, Touche V, Wouters K, Baron M, Pattou F, Hanf R, Tailleux A, Chinetti G, Staels B, Lestavel S. Activation of intestinal peroxisome proliferator-activated receptor-α increases high-density lipoprotein production. *Eur Heart J* 2013; **34**: 2566-2574 [PMID: 22843443 DOI: 10.1093/eurheartj/ehs227]

83 **Leung PS**. Overview of the pancreas. *Adv Exp Med Biol* 2010; **690**: 3-12 [PMID: 20700834 DOI: 10.1007/978-90-481-9060-7_1]

84 **Atkinson MA**, Campbell-Thompson M, Kusmartseva I, Kaestner KH. Organisation of the human pancreas in health and in diabetes. *Diabetologia* 2020; **63**: 1966-1973 [PMID: 32894306 DOI: 10.1007/s00125-020-05203-7]

85 **Bornman P**. The Pancreas: An Integrated Textbook of Basic Science, Medicine and Surgery. 2nd Ed. Oxford: Oxford University Press, 2008

86 **Cabrera O**, Berman DM, Kenyon NS, Ricordi C, Berggren PO, Caicedo A. The unique cytoarchitecture of human pancreatic islets has implications for islet cell function. *Proc Natl Acad Sci U S A* 2006; **103**: 2334-2339 [PMID: 16461897 DOI: 10.1073/pnas.0510790103]

87 **Steiner DJ**, Kim A, Miller K, Hara M. Pancreatic islet plasticity: interspecies comparison of islet architecture and composition. *Islets* 2010; **2**: 135-145 [PMID: 20657742 DOI: 10.4161/isl.2.3.11815]

88 **Noguchi GM**, Huising MO. Integrating the inputs that shape pancreatic islet hormone release. *Nat Metab* 2019; **1**: 1189-1201 [PMID: 32694675 DOI: 10.1038/s42255-019-0148-2]

89 **Vickers MH**, Reddy S, Ikenasio BA, Breier BH. Dysregulation of the adipoinsular axis -- a mechanism for the pathogenesis of hyperleptinemia and adipogenic diabetes induced by fetal programming. *J Endocrinol* 2001; **170**: 323-332 [PMID: 11479129 DOI: 10.1677/joe.0.1700323]

90 **Martínez-Sánchez N**. There and Back Again: Leptin Actions in White Adipose Tissue. *Int J Mol Sci* 2020; **21** [PMID: 32839413 DOI: 10.3390/ijms21176039]

91 **Cerf ME**. High fat diet modulation of glucose sensing in the beta-cell. *Med Sci Monit* 2007; **13**: RA12-RA17 [PMID: 17179917]

92 **Cerf ME**. Beta Cell Physiological Dynamics and Dysfunctional Transitions in Response to Islet Inflammation in Obesity and Diabetes. *Metabolites* 2020; **10** [PMID: 33182622 DOI: 10.3390/metabo10110452]

93 **Souza-Mello V**, Gregório BM, Cardoso-de-Lemos FS, de Carvalho L, Aguila MB, Mandarim-de-Lacerda CA. Comparative effects of telmisartan, sitagliptin and metformin alone or in combination on obesity, insulin resistance, and liver and pancreas remodelling in C57BL/6 mice fed on a very high-fat diet. *Clin Sci (Lond)* 2010; **119**: 239-250 [PMID: 20415664 DOI: 10.1042/CS20100061]

94 **Pennings N**, Jaber J, Ahiawodzi P. Ten-year weight gain is associated with elevated fasting insulin levels and precedes glucose elevation. *Diabetes Metab Res Rev* 2018; **34**: e2986 [PMID: 29392827 DOI: 10.1002/dmrr.2986]

95 **Janikiewicz J**, Hanzelka K, Kozinski K, Kolczynska K, Dobrzyn A. Islet β-cell failure in type 2 diabetes--Within the network of toxic lipids. *Biochem Biophys Res Commun* 2015; **460**: 491-496 [PMID: 25843796 DOI: 10.1016/j.bbrc.2015.03.153]

96 **Graus-Nunes F**, Marinho TS, Barbosa-da-Silva S, Aguila MB, Mandarim-de-Lacerda CA, Souza-Mello V. Differential effects of angiotensin receptor blockers on pancreatic islet remodelling and glucose homeostasis in diet-induced obese mice. *Mol Cell Endocrinol* 2017; **439**: 54-64 [PMID: 27780713 DOI: 10.1016/j.mce.2016.10.021]

97 **Souza-Mello V**, Gregório BM, Relvas-Lucas B, da Silva Faria T, Aguila MB, Mandarim-de-Lacerda CA. Pancreatic ultrastructural enhancement due to telmisartan plus sitagliptin treatment in diet-induced obese C57BL/6 mice. *Pancreas* 2011; **40**: 715-722 [PMID: 21602737 DOI: 10.1097/MPA.0b013e3182153922]

98 **Fernandes-da-Silva A**, Miranda CS, Santana-Oliveira DA, Oliveira-Cordeiro B, Rangel-Azevedo C, Silva-Veiga FM, Martins FF, Souza-Mello V. Endoplasmic reticulum stress as the basis of obesity and metabolic diseases: focus on adipose tissue, liver, and pancreas. *Eur J Nutr* 2021; **60**: 2949-2960 [PMID: 33742254 DOI: 10.1007/s00394-021-02542-y]

99 **Sun J**, Cui J, He Q, Chen Z, Arvan P, Liu M. Proinsulin misfolding and endoplasmic reticulum stress during the development and progression of diabetes. *Mol Aspects Med* 2015; **42**: 105-118 [PMID: 25579745 DOI: 10.1016/j.mam.2015.01.001]

100 **Cerf ME**. High fat programming of beta-cell failure. *Adv Exp Med Biol* 2010; **654**: 77-89 [PMID: 20217495 DOI: 10.1007/978-90-481-3271-3_5]

101 **Cho JH**, Kim JW, Shin JA, Shin J, Yoon KH. β-cell mass in people with type 2 diabetes. *J Diabetes Investig* 2011; **2**: 6-17 [PMID: 24843456 DOI: 10.1111/j.2040-1124.2010.00072.x]

102 **Nauck MA**, Meier JJ. The incretin effect in healthy individuals and those with type 2 diabetes: physiology, pathophysiology, and response to therapeutic interventions. *Lancet Diabetes Endocrinol* 2016; **4**: 525-536 [PMID: 26876794 DOI: 10.1016/S2213-8587(15)00482-9]

103 **Holst JJ**, Knop FK, Vilsbøll T, Krarup T, Madsbad S. Loss of incretin effect is a specific, important, and early characteristic of type 2 diabetes. *Diabetes Care* 2011; **34** Suppl 2: S251-S257 [PMID: 21525464 DOI: 10.2337/dc11-s227]

104 **Knop FK**, Aaboe K, Vilsbøll T, Vølund A, Holst JJ, Krarup T, Madsbad S. Impaired incretin effect and fasting hyperglucagonaemia characterizing type 2 diabetic subjects are early signs of dysmetabolism in obesity. *Diabetes Obes Metab* 2012; **14**: 500-510 [PMID: 22171657 DOI: 10.1111/j.1463-1326.2011.01549.x]

105 **Katahira T**, Miyatsuka T, Miura M, Suzuki L, Himuro M, Nishida Y, Satoh H, Watada H. Conversion of pancreatic α cells into insulin-producing cells modulated by β-cell insufficiency and supplemental insulin administration. *Biochem Biophys Res Commun* 2020; **521**: 178-183 [PMID: 31653346 DOI: 10.1016/j.bbrc.2019.10.100]

106 **Fruchart JC**. Peroxisome proliferator-activated receptor-alpha (PPARalpha): at the crossroads of obesity, diabetes and cardiovascular disease. *Atherosclerosis* 2009; **205**: 1-8 [PMID: 19386311 DOI: 10.1016/j.atherosclerosis.2009.03.008]

107 **Jay MA**, Ren J. Peroxisome proliferator-activated receptor (PPAR) in metabolic syndrome and type 2 diabetes mellitus. *Curr Diabetes Rev* 2007; **3**: 33-39 [PMID: 18220654 DOI: 10.2174/157339907779802067]

108 **Gilde AJ**, van der Lee KA, Willemsen PH, Chinetti G, van der Leij FR, van der Vusse GJ, Staels B, van Bilsen M. Peroxisome proliferator-activated receptor (PPAR) alpha and PPARbeta/delta, but not PPARgamma, modulate the expression of genes involved in cardiac lipid metabolism. *Circ Res* 2003; **92**: 518-524 [PMID: 12600885 DOI: 10.1161/01.Res.0000060700.55247.7c]

109 **Planavila A**, Laguna JC, Vázquez-Carrera M. Nuclear factor-kappaB activation leads to down-regulation of fatty acid oxidation during cardiac hypertrophy. *J Biol Chem* 2005; **280**: 17464-17471 [PMID: 15728586 DOI: 10.1074/jbc.M414220200]

110 **Patsouris D**, Mandard S, Voshol PJ, Escher P, Tan NS, Havekes LM, Koenig W, März W, Tafuri S, Wahli W, Müller M, Kersten S. PPARalpha governs glycerol metabolism. *J Clin Invest* 2004; **114**: 94-103 [PMID: 15232616 DOI: 10.1172/JCI20468]

111 **Lefebvre P**, Chinetti G, Fruchart JC, Staels B. Sorting out the roles of PPAR alpha in energy metabolism and vascular homeostasis. *J Clin Invest* 2006; **116**: 571-580 [PMID: 16511589 DOI: 10.1172/jci27989]

112 **Nakasatomi M**, Kim H, Arai T, Hirako S, Shioda S, Iizuka Y, Sakurai K, Matsumoto A. Fish oil and fenofibrate inhibit pancreatic islet hypertrophy, and improve glucose and lipid metabolic dysfuntions with different ways in diabetic KK mice. *Obes Res Clin Pract* 2018; **12**: 29-38 [PMID: 27130153 DOI: 10.1016/j.orcp.2016.03.012]

113 **Zheng S**, Ren X, Han T, Chen Y, Qiu H, Liu W, Hu Y. Fenofibrate attenuates fatty acid-induced islet β-cell dysfunction and apoptosis *via* inhibiting the NF-κB/MIF dependent inflammatory pathway. *Metabolism* 2017; **77**: 23-38 [PMID: 28941594 DOI: 10.1016/j.metabol.2017.09.001]

114 **Holm LJ**, Haupt-Jorgensen M, Giacobini JD, Hasselby JP, Bilgin M, Buschard K. Fenofibrate increases very-long-chain sphingolipids and improves blood glucose homeostasis in NOD mice. *Diabetologia* 2019; **62**: 2262-2272 [PMID: 31410530 DOI: 10.1007/s00125-019-04973-z]

115 **Liu SN**, Liu Q, Li LY, Huan Y, Sun SJ, Shen ZF. Long-term fenofibrate treatment impaired glucose-stimulated insulin secretion and up-regulated pancreatic NF-kappa B and iNOS expression in monosodium glutamate-induced obese rats: is that a latent disadvantage? *J Transl Med* 2011; **9**: 176 [PMID: 21999347 DOI: 10.1186/1479-5876-9-176]

116 **Yoshikawa H**, Tajiri Y, Sako Y, Hashimoto T, Umeda F, Nawata H. Effects of bezafibrate on beta-cell function of rat pancreatic islets. *Eur J Pharmacol* 2001; **426**: 201-206 [PMID: 11527545 DOI: 10.1016/s0014-2999(01)01204-3]

117 **Tenenbaum H**, Behar S, Boyko V, Adler Y, Fisman EZ, Tanne D, Lapidot M, Schwammenthal E, Feinberg M, Matas Z, Motro M, Tenenbaum A. Long-term effect of bezafibrate on pancreatic beta-cell function and insulin resistance in patients with diabetes. *Atherosclerosis* 2007; **194**: 265-271 [PMID: 16970952 DOI: 10.1016/j.atherosclerosis.2006.08.005]

118 **Semple RK**, Chatterjee VK, O'Rahilly S. PPAR gamma and human metabolic disease. *J Clin Invest* 2006; **116**: 581-589 [PMID: 16511590 DOI: 10.1172/jci28003]

119 **Berthiaume M**, Sell H, Lalonde J, Gélinas Y, Tchernof A, Richard D, Deshaies Y. Actions of PPARgamma agonism on adipose tissue remodeling, insulin sensitivity, and lipemia in absence of glucocorticoids. *Am J Physiol Regul Integr Comp Physiol* 2004; **287**: R1116-R1123 [PMID: 15256367 DOI: 10.1152/ajpregu.00339.2004]

120 **Armoni M**, Harel C, Bar-Yoseph F, Milo S, Karnieli E. Free fatty acids repress the GLUT4 gene expression in cardiac muscle *via* novel response elements. *J Biol Chem* 2005; **280**: 34786-34795 [PMID: 16096283 DOI: 10.1074/jbc.M502740200]

121 **Panunti B**, Fonseca V. Effects of PPAR gamma agonists on cardiovascular function in obese, non-diabetic patients. *Vascul Pharmacol* 2006; **45**: 29-35 [PMID: 16777491 DOI: 10.1016/j.vph.2005.11.013]

122 **Tontonoz P**, Spiegelman BM. Fat and beyond: the diverse biology of PPARgamma. *Annu Rev Biochem* 2008; **77**: 289-312 [PMID: 18518822 DOI: 10.1146/annurev.biochem.77.061307.091829]

123 **Nagashima K**, Lopez C, Donovan D, Ngai C, Fontanez N, Bensadoun A, Fruchart-Najib J, Holleran S, Cohn JS, Ramakrishnan R, Ginsberg HN. Effects of the PPARgamma agonist pioglitazone on lipoprotein metabolism in patients with type 2 diabetes mellitus. *J Clin Invest* 2005; **115**: 1323-1332 [PMID: 15841215 DOI: 10.1172/JCI23219]

124 **Rhee EJ**, Oh KW, Lee WY, Kim SY, Oh ES, Baek KH, Kang MI, Kim SW. Effects of two common polymorphisms of peroxisome proliferator-activated receptor-gamma gene on metabolic syndrome. *Arch Med Res* 2006; **37**: 86-94 [PMID: 16314192 DOI: 10.1016/j.arcmed.2005.04.008]

125 **Barnett AH**. Redefining the role of thiazolidinediones in the management of type 2 diabetes. *Vasc Health Risk Manag* 2009; **5**: 141-151 [PMID: 19436665 DOI: 10.2147/vhrm.s4664]

126 **Jandeleit-Dahm KA**, Calkin A, Tikellis C, Thomas M. Direct antiatherosclerotic effects of PPAR agonists. *Curr Opin Lipidol* 2009; **20**: 24-29 [PMID: 19133407 DOI: 10.1097/mol.0b013e32831f1b18]

127 **Goldberg RB**, Kendall DM, Deeg MA, Buse JB, Zagar AJ, Pinaire JA, Tan MH, Khan MA, Perez AT, Jacober SJ; GLAI Study Investigators. A comparison of lipid and glycemic effects of pioglitazone and rosiglitazone in patients with type 2 diabetes and dyslipidemia. *Diabetes Care* 2005; **28**: 1547-1554 [PMID: 15983299 DOI: 10.2337/diacare.28.7.1547]

128 **Deeg MA**, Buse JB, Goldberg RB, Kendall DM, Zagar AJ, Jacober SJ, Khan MA, Perez AT, Tan MH; GLAI Study Investigators. Pioglitazone and rosiglitazone have different effects on serum lipoprotein particle concentrations and sizes in patients with type 2 diabetes and dyslipidemia. *Diabetes Care* 2007; **30**: 2458-2464 [PMID: 17595355 DOI: 10.2337/dc06-1903]

129 **Nesto RW**, Bell D, Bonow RO, Fonseca V, Grundy SM, Horton ES, Le Winter M, Porte D, Semenkovich CF, Smith S, Young LH, Kahn R; American Heart Association; American Diabetes Association. Thiazolidinedione use, fluid retention, and congestive heart failure: a consensus statement from the American Heart Association and American Diabetes Association. October 7, 2003. *Circulation* 2003; **108**: 2941-2948 [PMID: 14662691 DOI: 10.1161/01.Cir.0000103683.99399.7e]

130 **Sotiropoulos KB**, Clermont A, Yasuda Y, Rask-Madsen C, Mastumoto M, Takahashi J, Della Vecchia K, Kondo T, Aiello LP, King GL. Adipose-specific effect of rosiglitazone on vascular permeability and protein kinase C activation: novel mechanism for PPARgamma agonist's effects on edema and weight gain. *FASEB J* 2006; **20**: 1203-1205 [PMID: 16672634 DOI: 10.1096/fj.05-4617fje]

131 **Yang T**, Soodvilai S. Renal and vascular mechanisms of thiazolidinedione-induced fluid retention. *PPAR Res* 2008; **2008**: 943614 [PMID: 18784848 DOI: 10.1155/2008/943614]

132 **Collier JJ**, Batdorf HM, Merrifield KL, Martin TM, White U, Ravussin E, Burk DH, Cooley CR, Karlstad MD, Burke SJ. Pioglitazone Reverses Markers of Islet Beta-Cell De-Differentiation in db/db Mice While Modulating Expression of Genes Controlling Inflammation and Browning in White Adipose Tissue from Insulin-Resistant Mice and Humans. *Biomedicines* 2021; **9** [PMID: 34572374 DOI: 10.3390/biomedicines9091189]

133 **Hong SW**, Lee J, Cho JH, Kwon H, Park SE, Rhee EJ, Park CY, Oh KW, Park SW, Lee WY. Pioglitazone Attenuates Palmitate-Induced Inflammation and Endoplasmic Reticulum Stress in Pancreatic β-Cells. *Endocrinol Metab (Seoul)* 2018; **33**: 105-113 [PMID: 29589392 DOI: 10.3803/EnM.2018.33.1.105]

134 **Refaat R**, Sakr A, Salama M, El Sarha A. Combination of Vildagliptin and Pioglitazone in Experimental Type 2 Diabetes in Male Rats. *Drug Dev Res* 2016; **77**: 300-309 [PMID: 27520857 DOI: 10.1002/ddr.21324]

135 **Alba M**, Ahrén B, Inzucchi SE, Guan Y, Mallick M, Xu L, O'Neill EA, Williams-Herman DE, Kaufman KD, Goldstein BJ. Sitagliptin and pioglitazone provide complementary effects on postprandial glucose and pancreatic islet cell function. *Diabetes Obes Metab* 2013; **15**: 1101-1110 [PMID: 23782502 DOI: 10.1111/dom.12145]

136 **Benndorf RA**, Rudolph T, Appel D, Schwedhelm E, Maas R, Schulze F, Silberhorn E, Böger RH. Telmisartan improves insulin sensitivity in nondiabetic patients with essential hypertension. *Metabolism* 2006; **55**: 1159-1164 [PMID: 16919533 DOI: 10.1016/j.metabol.2006.04.013]

137 **Zhao S**, Chan LK, Chen L, Cheng TW, Klein T, Leung PS. Combination of Telmisartan and Linagliptin Preserves Pancreatic Islet Cell Function and Morphology in db/db Mice. *Pancreas* 2016; **45**: 584-592 [PMID: 26495783 DOI: 10.1097/MPA.0000000000000505]

138 **Willson TM**, Brown PJ, Sternbach DD, Henke BR. The PPARs: from orphan receptors to drug discovery. *J Med Chem* 2000; **43**: 527-550 [PMID: 10691680 DOI: 10.1021/jm990554g]

139 **Wallenius K**, Kjellstedt A, Thalén P, Löfgren L, Oakes ND. The PPAR α / γ Agonist, Tesaglitazar, Improves Insulin Mediated Switching of Tissue Glucose and Free Fatty Acid Utilization In Vivo in the Obese Zucker Rat. *PPAR Res* 2013; **2013**: 305347 [PMID: 24285952 DOI: 10.1155/2013/305347]

140 **Harrity T**, Farrelly D, Tieman A, Chu C, Kunselman L, Gu L, Ponticiello R, Cap M, Qu F, Shao C, Wang W, Zhang H, Fenderson W, Chen S, Devasthale P, Jeon Y, Seethala R, Yang WP, Ren J, Zhou M, Ryono D, Biller S, Mookhtiar KA, Wetterau J, Gregg R, Cheng PT, Hariharan N. Muraglitazar, a novel dual (alpha/gamma) peroxisome proliferator-activated receptor activator, improves diabetes and other metabolic abnormalities and preserves beta-cell function in db/db mice. *Diabetes* 2006; **55**: 240-248 [PMID: 16380499]

141 **Sun Y**, Alexander SP, Kendall DA, Bennett AJ. Cannabinoids and PPARalpha signalling. *Biochem Soc Trans* 2006; **34**: 1095-1097 [PMID: 17073758 DOI: 10.1042/BST0341095]

142 **Mittra S**, Sangle G, Tandon R, Sharma S, Roy S, Khanna V, Gupta A, Sattigeri J, Sharma L, Priyadarsiny P, Khattar SK, Bora RS, Saini KS, Bansal VS. Increase in weight induced by muraglitazar, a dual PPARalpha/gamma agonist, in db/db mice: adipogenesis/or oedema? *Br J Pharmacol* 2007; **150**: 480-487 [PMID: 17211457 DOI: 10.1038/sj.bjp.0707000]

143 **Trefts E**, Gannon M, Wasserman DH. The liver. *Curr Biol* 2017; **27**: R1147-R1151 [PMID: 29112863 DOI: 10.1016/j.cub.2017.09.019]

144 **Mahadevan V**. Anatomy of the liver. *Surgery (Oxford)* 2020; **38**: 427-431 [DOI: 10.1016/j.mpsur.2014.10.004]

145 **Gebhardt R**, Matz-Soja M. Liver zonation: Novel aspects of its regulation and its impact on homeostasis. *World J Gastroenterol* 2014; **20**: 8491-8504 [PMID: 25024605 DOI: 10.3748/wjg.v20.i26.8491]

146 **Jungermann K**, Sasse D. Heterogeneity of liver parenchymal cells. *Trends Biochem Sci* 1978; **3**: 198-202 [DOI: 10.1016/S0968-0004(78)91764-4]

147 **Vasconcellos R**, Alvarenga ÉC, Parreira RC, Lima SS, Resende RR. Exploring the cell signalling in hepatocyte differentiation. *Cell Signal* 2016; **28**: 1773-1788 [PMID: 27555287 DOI: 10.1016/j.cellsig.2016.08.011]

148 **Wang M**, Kaufman RJ. Protein misfolding in the endoplasmic reticulum as a conduit to human disease. *Nature* 2016; **529**: 326-335 [PMID: 26791723 DOI: 10.1038/nature17041]

149 **Nassir F**. NAFLD: Mechanisms, Treatments, and Biomarkers. *Biomolecules* 2022; **12** [PMID: 35740949 DOI: 10.3390/biom12060824]

150 **Rui L**. Energy metabolism in the liver. *Compr Physiol* 2014; **4**: 177-197 [PMID: 24692138 DOI: 10.1002/cphy.c130024]

151 **Bechmann LP**, Hannivoort RA, Gerken G, Hotamisligil GS, Trauner M, Canbay A. The interaction of hepatic lipid and glucose metabolism in liver diseases. *J Hepatol* 2012; **56**: 952-964 [PMID: 22173168 DOI: 10.1016/j.jhep.2011.08.025]

152 **Lebeaupin C**, Vallée D, Hazari Y, Hetz C, Chevet E, Bailly-Maitre B. Endoplasmic reticulum stress signalling and the pathogenesis of non-alcoholic fatty liver disease. *J Hepatol* 2018; **69**: 927-947 [PMID: 29940269 DOI: 10.1016/j.jhep.2018.06.008]

153 **Magliano DC**, Bargut TC, de Carvalho SN, Aguila MB, Mandarim-de-Lacerda CA, Souza-Mello V. Peroxisome proliferator-activated receptors-alpha and gamma are targets to treat offspring from maternal diet-induced obesity in mice. *PLoS One* 2013; **8**: e64258 [PMID: 23700465 DOI: 10.1371/journal.pone.0064258]

154 **Walter P**, Ron D. The unfolded protein response: from stress pathway to homeostatic regulation. *Science* 2011; **334**: 1081-1086 [PMID: 22116877 DOI: 10.1126/science.1209038]

155 **Oyadomari S**, Araki E, Mori M. Endoplasmic reticulum stress-mediated apoptosis in pancreatic beta-cells. *Apoptosis* 2002; **7**: 335-345 [PMID: 12101393 DOI: 10.1023/a:1016175429877]

156 **Malhi H**, Kaufman RJ. Endoplasmic reticulum stress in liver disease. *J Hepatol* 2011; **54**: 795-809 [PMID: 21145844 DOI: 10.1016/j.jhep.2010.11.005]

157 **Kim YS**, Kim SG. Endoplasmic reticulum stress and autophagy dysregulation in alcoholic and non-alcoholic liver diseases. *Clin Mol Hepatol* 2020; **26**: 715-727 [PMID: 32951410 DOI: 10.3350/cmh.2020.0173]

158 **Ma X**, McKeen T, Zhang J, Ding WX. Role and Mechanisms of Mitophagy in Liver Diseases. *Cells* 2020; **9** [PMID: 32244304 DOI: 10.3390/cells9040837]

159 **Su Q**, Baker C, Christian P, Naples M, Tong X, Zhang K, Santha M, Adeli K. Hepatic mitochondrial and ER stress induced by defective PPAR α signaling in the pathogenesis of hepatic steatosis. *Am J Physiol Endocrinol Metab* 2014; **306**: E1264-E1273 [PMID: 24735884 DOI: 10.1152/ajpendo.00438.2013]

160 **Badmus OO**, Hillhouse SA, Anderson CD, Hinds TD, Stec DE. Molecular mechanisms of metabolic associated fatty liver disease (MAFLD): functional analysis of lipid metabolism pathways. *Clin Sci (Lond)* 2022; **136**: 1347-1366 [PMID: 36148775 DOI: 10.1042/CS20220572]

161 **Zhang T**, Liu Q, Gao W, Sehgal SA, Wu H. The multifaceted regulation of mitophagy by endogenous metabolites. *Autophagy* 2022; **18**: 1216-1239 [PMID: 34583624 DOI: 10.1080/15548627.2021.1975914]

162 **Liu L**, Li Y, Wang J, Zhang D, Wu H, Li W, Wei H, Ta N, Fan Y, Liu Y, Wang X, Pan X, Liao X, Zhu Y, Chen Q. Mitophagy receptor FUNDC1 is regulated by PGC-1α/NRF1 to fine tune mitochondrial homeostasis. *EMBO Rep* 2021; **22**: e50629 [PMID: 33554448 DOI: 10.15252/embr.202050629]

163 **Ke PY**. Mitophagy in the Pathogenesis of Liver Diseases. *Cells* 2020; **9** [PMID: 32235615 DOI: 10.3390/cells9040831]

164 **Kersten S**. Integrated physiology and systems biology of PPARα. *Mol Metab* 2014; **3**: 354-371 [PMID: 24944896 DOI: 10.1016/j.molmet.2014.02.002]

165 **Kersten S**, Stienstra R. The role and regulation of the peroxisome proliferator activated receptor alpha in human liver. *Biochimie* 2017; **136**: 75-84 [PMID: 28077274 DOI: 10.1016/j.biochi.2016.12.019]

166 **Aoyama T**, Peters JM, Iritani N, Nakajima T, Furihata K, Hashimoto T, Gonzalez FJ. Altered constitutive expression of fatty acid-metabolizing enzymes in mice lacking the peroxisome proliferator-activated receptor alpha (PPARalpha). *J Biol Chem* 1998; **273**: 5678-5684 [PMID: 9488698 DOI: 10.1074/jbc.273.10.5678]

167 **Abdelmegeed MA**, Yoo SH, Henderson LE, Gonzalez FJ, Woodcroft KJ, Song BJ. PPARalpha expression protects male mice from high fat-induced nonalcoholic fatty liver. *J Nutr* 2011; **141**: 603-610 [PMID: 21346097 DOI: 10.3945/jn.110.135210]

168 **Yoo J**, Jeong IK, Ahn KJ, Chung HY, Hwang YC. Fenofibrate, a PPARα agonist, reduces hepatic fat accumulation through the upregulation of TFEB-mediated lipophagy. *Metabolism* 2021; **120**: 154798 [PMID: 33984335 DOI: 10.1016/j.metabol.2021.154798]

169 **Lin J**, Wu PH, Tarr PT, Lindenberg KS, St-Pierre J, Zhang CY, Mootha VK, Jäger S, Vianna CR, Reznick RM, Cui L, Manieri M, Donovan MX, Wu Z, Cooper MP, Fan MC, Rohas LM, Zavacki AM, Cinti S, Shulman GI, Lowell BB, Krainc D, Spiegelman BM. Defects in adaptive energy metabolism with CNS-linked hyperactivity in PGC-1alpha null mice. *Cell* 2004; **119**: 121-135 [PMID: 15454086 DOI: 10.1016/j.cell.2004.09.013]

170 **Weber M**, Mera P, Casas J, Salvador J, Rodríguez A, Alonso S, Sebastián D, Soler-Vázquez MC, Montironi C, Recalde S, Fucho R, Calderón-Domínguez M, Mir JF, Bartrons R, Escola-Gil JC, Sánchez-Infantes D, Zorzano A, Llorente-Cortes V, Casals N, Valentí V, Frühbeck G, Herrero L, Serra D. Liver CPT1A gene therapy reduces diet-induced hepatic steatosis in mice and highlights potential lipid biomarkers for human NAFLD. *FASEB J* 2020; **34**: 11816-11837 [PMID: 32666604 DOI: 10.1096/fj.202000678R]

171 **Larter CZ**, Yeh MM, Van Rooyen DM, Brooling J, Ghatora K, Farrell GC. Peroxisome proliferator-activated receptor-α agonist, Wy 14,643, improves metabolic indices, steatosis and ballooning in diabetic mice with non-alcoholic steatohepatitis. *J Gastroenterol Hepatol* 2012; **27**: 341-350 [PMID: 21929649 DOI: 10.1111/j.1440-1746.2011.06939.x]

172 **Silva-Veiga FM**, Miranda CS, Vasques-Monteiro IML, Souza-Tavares H, Martins FF, Daleprane JB, Souza-Mello V. Peroxisome proliferator-activated receptor-alpha activation and dipeptidyl peptidase-4 inhibition target dysbiosis to treat fatty liver in obese mice. *World J Gastroenterol* 2022; **28**: 1814-1829 [PMID: 35633911 DOI: 10.3748/wjg.v28.i17.1814]

173 **Silva-Veiga FM**, Miranda CS, Martins FF, Daleprane JB, Mandarim-de-Lacerda CA, Souza-Mello V. Gut-liver axis modulation in fructose-fed mice: a role for PPAR-alpha and linagliptin. *J Endocrinol* 2020; **247**: 11-24 [PMID: 32698143 DOI: 10.1530/JOE-20-0139]

174 **Liss KH**, Finck BN. PPARs and nonalcoholic fatty liver disease. *Biochimie* 2017; **136**: 65-74 [PMID: 27916647 DOI: 10.1016/j.biochi.2016.11.009]

175 **Dille M**, Nikolic A, Wahlers N, Fahlbusch P, Jacob S, Hartwig S, Lehr S, Kabra D, Klymenko O, Al-Hasani H, Kotzka J, Knebel B. Long-term adjustment of hepatic lipid metabolism after chronic stress and the role of FGF21. *Biochim Biophys Acta Mol Basis Dis* 2022; **1868**: 166286 [PMID: 34624498 DOI: 10.1016/j.bbadis.2021.166286]

176 **Pawlak M**, Lefebvre P, Staels B. Molecular mechanism of PPARα action and its impact on lipid metabolism, inflammation and fibrosis in non-alcoholic fatty liver disease. *J Hepatol* 2015; **62**: 720-733 [PMID: 25450203 DOI: 10.1016/j.jhep.2014.10.039]

177 **Han L**, Shen WJ, Bittner S, Kraemer FB, Azhar S. PPARs: regulators of metabolism and as therapeutic targets in cardiovascular disease. Part II: PPAR-β/δ and PPAR-γ. *Future Cardiol* 2017; **13**: 279-296 [PMID: 28581362 DOI: 10.2217/fca-2017-0019]

178 **Gavrilova O**, Haluzik M, Matsusue K, Cutson JJ, Johnson L, Dietz KR, Nicol CJ, Vinson C, Gonzalez FJ, Reitman ML. Liver peroxisome proliferator-activated receptor gamma contributes to hepatic steatosis, triglyceride clearance, and regulation of body fat mass. *J Biol Chem* 2003; **278**: 34268-34276 [PMID: 12805374 DOI: 10.1074/jbc.M300043200]

179 **Francque S**, Verrijken A, Caron S, Prawitt J, Paumelle R, Derudas B, Lefebvre P, Taskinen MR, Van Hul W, Mertens I, Hubens G, Van Marck E, Michielsen P, Van Gaal L, Staels B. PPARα gene expression correlates with severity and histological treatment response in patients with non-alcoholic steatohepatitis. *J Hepatol* 2015; **63**: 164-173 [PMID: 25703085 DOI: 10.1016/j.jhep.2015.02.019]

180 **Mundi MS**, Velapati S, Patel J, Kellogg TA, Abu Dayyeh BK, Hurt RT. Evolution of NAFLD and Its Management. *Nutr Clin Pract* 2020; **35**: 72-84 [PMID: 31840865 DOI: 10.1002/ncp.10449]

181 **Janani C**, Ranjitha Kumari BD. PPAR gamma gene--a review. *Diabetes Metab Syndr* 2015; **9**: 46-50 [PMID: 25450819 DOI: 10.1016/j.dsx.2014.09.015]

182 **Della Pepa G**, Russo M, Vitale M, Carli F, Vetrani C, Masulli M, Riccardi G, Vaccaro O, Gastaldelli A, Rivellese AA, Bozzetto L. Pioglitazone even at low dosage improves NAFLD in type 2 diabetes: clinical and pathophysiological insights from a subgroup of the

TOSCA.IT randomised trial. *Diabetes Res Clin Pract* 2021; **178**: 108984 [PMID: 34311022 DOI: 10.1016/j.diabres.2021.108984]

183 **Ahn HY**, Kim HH, Hwang JY, Park C, Cho BY, Park YJ. Effects of Pioglitazone on Nonalcoholic Fatty Liver Disease in the Absence of Constitutive Androstane Receptor Expression. *PPAR Res* 2018; **2018**: 9568269 [PMID: 30363699 DOI: 10.1155/2018/9568269]

184 **You M**, Matsumoto M, Pacold CM, Cho WK, Crabb DW. The role of AMP-activated protein kinase in the action of ethanol in the liver. *Gastroenterology* 2004; **127**: 1798-1808 [PMID: 15578517 DOI: 10.1053/j.gastro.2004.09.049]

185 **Liu X**, Xu J, Rosenthal S, Zhang LJ, McCubbin R, Meshgin N, Shang L, Koyama Y, Ma HY, Sharma S, Heinz S, Glass CK, Benner C, Brenner DA, Kisseleva T. Identification of Lineage-Specific Transcription Factors That Prevent Activation of Hepatic Stellate Cells and Promote Fibrosis Resolution. *Gastroenterology* 2020; **158**: 1728-1744.e14 [PMID: 31982409 DOI: 10.1053/j.gastro.2020.01.027]

186 **Richter B**, Bandeira-Echtler E, Bergerhoff K, Clar C, Ebrahim SH. Rosiglitazone for type 2 diabetes mellitus. *Cochrane Database Syst Rev* 2007; **2007**: CD006063 [PMID: 17636824 DOI: 10.1002/14651858.CD006063.pub2]

187 **Richter B**, Bandeira-Echtler E, Bergerhoff K, Clar C, Ebrahim SH. Pioglitazone for type 2 diabetes mellitus. *Cochrane Database Syst Rev* 2006; **2006**: CD006060 [PMID: 17054272 DOI: 10.1002/14651858.CD006060.pub2]

188 **Lebovitz HE**. Thiazolidinediones: the Forgotten Diabetes Medications. *Curr Diab Rep* 2019; **19**: 151 [PMID: 31776781 DOI: 10.1007/s11892-019-1270-y]

189 **Horita S**, Nakamura M, Satoh N, Suzuki M, Seki G. Thiazolidinediones and Edema: Recent Advances in the Pathogenesis of Thiazolidinediones-Induced Renal Sodium Retention. *PPAR Res* 2015; **2015**: 646423 [PMID: 26074951 DOI: 10.1155/2015/646423]

190 **Gawrieh S**, Noureddin M, Loo N, Mohseni R, Awasty V, Cusi K, Kowdley KV, Lai M, Schiff E, Parmar D, Patel P, Chalasani N. Saroglitazar, a PPAR-α/γ Agonist, for Treatment of NAFLD: A Randomized Controlled Double-Blind Phase 2 Trial. *Hepatology* 2021; **74**: 1809-1824 [PMID: 33811367 DOI: 10.1002/hep.31843]

191 **Jain MR**, Giri SR, Bhoi B, Trivedi C, Rath A, Rathod R, Ranvir R, Kadam S, Patel H, Swain P, Roy SS, Das N, Karmakar E, Wahli W, Patel PR. Dual PPARα/γ agonist saroglitazar improves liver histopathology and biochemistry in experimental NASH models. *Liver Int* 2018; **38**: 1084-1094 [PMID: 29164820 DOI: 10.1111/Liv.13634]

192 **Wang Y**, Nakajima T, Gonzalez FJ, Tanaka N. PPARs as Metabolic Regulators in the Liver: Lessons from Liver-Specific PPAR-Null Mice. *Int J Mol Sci* 2020; **21** [PMID: 32192216 DOI: 10.3390/ijms21062061]

193 **Zingarelli B**, Piraino G, Hake PW, O'Connor M, Denenberg A, Fan H, Cook JA. Peroxisome proliferator-activated receptor {delta} regulates inflammation *via* NF-{kappa}B signaling in polymicrobial sepsis. *Am J Pathol* 2010; **177**: 1834-1847 [PMID: 20709805 DOI: 10.2353/ajpath.2010.091010]

194 **Alvarez-Guardia D**, Palomer X, Coll T, Serrano L, Rodríguez-Calvo R, Davidson MM, Merlos M, El Kochairi I, Michalik L, Wahli W, Vázquez-Carrera M. PPARβ/δ activation blocks lipid-induced inflammatory pathways in mouse heart and human cardiac cells. *Biochim Biophys Acta* 2011; **1811**: 59-67 [PMID: 21070867 DOI: 10.1016/j.bbalip.2010.11.002]

195 **Wahli W**, Michalik L. PPARs at the crossroads of lipid signaling and inflammation. *Trends Endocrinol Metab* 2012; **23**: 351-363 [PMID: 22704720 DOI: 10.1016/j.tem.2012.05.001]

196 **Botta M**, Audano M, Sahebkar A, Sirtori CR, Mitro N, Ruscica M. PPAR Agonists and Metabolic Syndrome: An Established Role? *Int J Mol Sci* 2018; **19** [PMID: 29662003 DOI: 10.3390/ijms19041197]

197 **Korbecki J**, Bobiński R, Dutka M. Self-regulation of the inflammatory response by peroxisome proliferator-activated receptors. *Inflamm Res* 2019; **68**: 443-458 [PMID: 30927048 DOI: 10.1007/s00011-019-01231-1]

198 **Silva-Veiga FM**, Rachid TL, de Oliveira L, Graus-Nunes F, Mandarim-de-Lacerda CA, Souza-Mello V. GW0742 (PPAR-beta agonist) attenuates hepatic endoplasmic reticulum stress by improving hepatic energy metabolism in high-fat diet fed mice. *Mol Cell Endocrinol* 2018; **474**: 227-237 [PMID: 29580823 DOI: 10.1016/j.mce.2018.03.013]

199 **Lee CH**, Olson P, Hevener A, Mehl I, Chong LW, Olefsky JM, Gonzalez FJ, Ham J, Kang H, Peters JM, Evans RM. PPARdelta regulates glucose metabolism and insulin sensitivity. *Proc Natl Acad Sci U S A* 2006; **103**: 3444-3449 [PMID: 16492734 DOI: 10.1073/pnas.0511253103]

200 **Souza-Mello V**. Peroxisome proliferator-activated receptors as targets to treat non-alcoholic fatty liver disease. *World J Hepatol* 2015; **7**: 1012-1019 [PMID: 26052390 DOI: 10.4254/wjh.v7.i8.1012]

World Journal of Gastroenterology

Submit a Manuscript: https://www.f6publishing.com

World J Gastroenterol 2023 July 14; 29(26): 4156-4165

DOI: 10.3748/wjg.v29.i26.4156

ISSN 1007-9327 (print) ISSN 2219-2840 (online)

MINIREVIEWS

Schistosomal (bilharzial) polyps: Travel through the colon and beyond

Mohamed H Emara, Aya M Mahros, Abdelrahman M Ahmed Rasheda, Mohamed I Radwan, Besher Mohamed, Osama Abdelrazik, Mostafa Elazab, Hassan Elbatae

Specialty type: Gastroenterology and hepatology

Provenance and peer review: Invited article; Externally peer reviewed.

Peer-review model: Single blind

Peer-review report's scientific quality classification

Grade A (Excellent): A
Grade B (Very good): B
Grade C (Good): 0
Grade D (Fair): 0
Grade E (Poor): 0

P-Reviewer: Gao F, China; Khefacha F, Tunisia

Received: December 24, 2022
Peer-review started: December 24, 2022
First decision: January 14, 2023
Revised: January 18, 2023
Accepted: March 29, 2023
Article in press: March 29, 2023
Published online: July 14, 2023

Mohamed H Emara, Aya M Mahros, Mostafa Elazab, Hassan Elbatae, Department of Hepatology, Gastroenterology and Infectious Diseases, Kafrelsheikh University, Kafr-Elshikh 33516, Egypt

Abdelrahman M Ahmed Rasheda, Department of Internal Medicine, Gastroenterology Unit, Security Forces Hospital, Ryiadh 11481, Saudi Arabia

Mohamed I Radwan, Department of Tropical Medicine, Zagazig University, Zagazig 44519, Egypt

Besher Mohamed, Department of Gastroenterology, Surrey and Sussex Hospitals NHS Trust, Surrey RH1 5RH, United Kingdom

Osama Abdelrazik, Department of Hepato-Gastroenterology and Infectious Diseases, Al-Azhar University, Cairo 11651, Egypt

Corresponding author: Mohamed H Emara, MD, MSc, Professor, Department of Hepatology, Gastroenterology and Infectious Diseases, Kafrelsheikh University, Ageish Street, Kafr-Elshikh 33516, Egypt. emara_20007@yahoo.com

Abstract

Schistosomiasis (bilharziasis) is a major neglected tropical disease. It is endemic in many tropical and subtropical communities. Schistosomal polyps (S. polyps) are not uncommon presentation of this infection. Although the colon is the most commonly affected organ, many other organs are affected. S. polyps are associated with a variable range of morbidity independent of the Schistosomal infection. S. polyps are frequently described in endemic areas and increasingly reported in non-endemic areas mainly among immigrants and visitors to the endemic areas. This review aimed to increase awareness of practitioners, especially gastroenterologists, for this peculiar type of polyps caused by this neglected infection hence improving patient outcomes. Web-based search of different databases was conducted for the literature focusing the development of S. polyps in the colon and other organs with analysis of the clinical manifestations, diagnosis and treatment. The following key words were used in the search, "Schistosomiasis" OR "Bilharziasis" AND "Polyps" OR "Polyp" AND "Colon" OR "Small intestine" OR " Duodenum" OR " Stomach" OR "Esophagus" OR " Gallbladder" OR" Pharynx" OR "Larynx" OR "Trachea" OR "Urinary bladder" OR " Ureter" OR "Renal Pelvis" OR "Urethra". All publication types including case reports, case series, original research, and review articles were retrieved and analyzed. S.

polyps are not infrequent presentation of acute or chronic Schistosomal infection. S. polyps are described in many organs including the bowel, genitourinary tract, skin, gallbladder and the larynx. Presentation of S. polyps is variable and depends on the site, number as well as the polyp size. The relationship of *S. polyps* to malignant transformation is a matter of discussion. Presence of S. polyps is sometimes the only manifestation of Schistosomiasis. Small polyps can be treated medically with praziquantel, while large accessible polyps are amendable for endoscopic excision through different polyp resection techniques. However, huge, complicated, non-accessible and suspicious polyps are indicated for surgical management or advanced endoscopic resection when appropriate. Clinicians and endoscopists should be aware about these facts when treating patients living in, immigrated from or visiting endemic areas.

Key Words: Schistosomiasis; Bilharziasis; *Schistosomal polyps*; Colon; Praziquantel

©The Author(s) 2023. Published by Baishideng Publishing Group Inc. All rights reserved.

Core Tip: Schistosomiasis is associated with a wide range of pathological lesions including development of polyps. Colon is the commonest site for polyp development, however polyps are reported in many organs including urinary bladder, ureters, larynx, duodenum, small intestine, gallbladder, anus, uterine cervix and external genitalia. Schistosomal polyps are associated with a wide range of morbidity according to the polyp site, size and number. The malignant potential of these polyps is a hot point of discussion. Although small sized polyps can regress with medical therapy using praziquantel, large accessible polyps can be retrieved endoscopically. Complicated, huge and inaccessible polyps can be treated surgically.

Citation: Emara MH, Mahros AM, Rasheda AMA, Radwan MI, Mohamed B, Abdelrazik O, Elazab M, Elbatae H. Schistosomal (bilharzial) polyps: Travel through the colon and beyond. *World J Gastroenterol* 2023; 29(26): 4156-4165
URL: https://www.wjgnet.com/1007-9327/full/v29/i26/4156.htm
DOI: https://dx.doi.org/10.3748/wjg.v29.i26.4156

INTRODUCTION

Schistosomiasis is a major neglected tropical disease. It is endemic in many geographical regions mainly in Africa, Latin America and Asia**.** Many data have been published from endemic areas and also from areas where the infection is not likely to occur with diverse clinical presentations. In non-endemic areas the infection is reported among immigrants or visitors to endemic areas[1,2].

This parasitic infestation was described in early human history, with evidence of infection reported in the ancient Egyptian papers and probably other old civilizations. The infection was characterized in the 19th century by the German pathologist Theodor Bilharz; that is why it is named after him as "Bilharziasis". There are many species of the parasite. Human infection is likely caused by five species, namely *Schistosoma Mansoni, S. Haematobium, S. Japonicum, S. Intercalatum and S. Mekongi*[1]. It is obvious that, the infection is linked to water supplies because of the snail intermediate host settles in the water canals and hence agricultural communities are the ultimate victims of the infestations, although persons who came in contact with infected water are prone also to catch the infection.

The clinical manifestation of this infection is either acute or chronic. The acute manifestations are related to the invasion of the human body by the cercarial invading stage through the skin, migration within the body and the early stage of ovi-position. Chronic manifestations are related to the establishment of adult worms and trapping of the deposited ova within the tissues and consequently granuloma formation[1]. The acute presentations include constitutional manifestations with fever, myalgia, urticarial rashes and with ovi-position the manifestations will change to hematuria (urinary Schistosomiasis), diarrhea with blood (intestinal Schistosomiasis), and chronic blood loss; manifested as anemia[1,3]. In chronic cases, development of fibrosis is the hallmark of the disease and this results in devastating sequelae including portal hypertension, hepatic peri-portal fibrosis, and splenomegaly for intestinal Schistosomiasis, while urinary Schistosomiasis is associated with obstructive lesions, increased incidence of stone formation, chronic urinary tract infections, and urinary bladder malignancy[4].

The current review aimed to increase awareness of practitioners, especially gastroenterologists, for this peculiar type of polyps caused by this neglected infection and hence improve patient outcomes.

LITERATURE SEARCH

Web-based search of different databases was conducted, including PubMed/MEDLINE, Cochrane library, Web of Science, Ovid, Science Direct, Scopus, Directory of Open Access Journals, EBSCO HOST, ProQuest, Institute for Scientific Information, EBESCO, Egyptian knowledge bank, Google scholar, *Reference Citation Analysis* (https://www.referencecitationanalysis.com/) and the Research Gate, for relevant articles focusing on the development of Schistosomal polyps (S.

polyps) in the colon and other organs with analysis of the clinical manifestations, diagnosis and treatment. The following key words were used in the search, "Schistosomiasis" OR "Bilharziasis" AND "Polyps" OR "Polyp" AND " Colon" OR "Small intestine" OR " Duodenum" OR " Stomach" OR "Esophagus" OR " Gallbladder" OR" Pharynx" OR "Larynx" OR "Trachea" OR "Urinary bladder" OR " Ureter" OR "Renal Pelvis" OR "Urethra". All publication types including case reports, case series, original research, and review articles were retrieved and analyzed.

PATHOGENESIS OF S. POLYPS

The development of polyps in general is linked to hollow organs or organs with contact to space; this enables external growth. Consequently, polyps are frequently reported in the bowel rather than other organs. The final shelters for adults Schistosomes are the intestinal and pelvic venous plexuses whatever the species are and hence the development of S. polyps in the hollow organs drained by this plexuses is not strange, *e.g.*, colon and urinary bladder, while development of polyps in other organs, *e.g.*, skin is considered ectopic. Furthermore, S. polyps may develop in atypical sites, *e.g.*, duodenum, that are not drained by the intestinal or pelvic veins.

The development of polyps in different stages

Stage of ova deposition and trapping: The eggs laid by the adult parasite had a characteristic spine that helps it to dig and find way out, *e.g.*, through the colon mucosa to be released with the stool. The initial step in polyp formation starts when Bilharzial eggs are deposited and trapped within the superficial layers of submucosa. The submucosal connective tissue is delicate and not superficially bound by firmer tissue. Consequently, accumulation of large amounts of eggs, reactive cellular debris and vascular granulation tissue do occur. In the submucosa, the trapped ova produce a TH2 cell-mediated inflammatory response with many cellular and chemical elements being recruited to the area and granuloma formation begins. The hallmark of the granuloma is infiltration by eosinophils (eosinophilic granuloma)[1], however, during this exudative stage of granuloma formation, other inflammatory cells are seen including the epithelioid macrophages and mononuclear cells[1,5].

Stage of proliferation: Within the granuloma necrosis occur[5]. Healing of the developed necrotic foci is associated with fibrous connective tissue formation. Furthermore, the adjacent muscularis mucosa becomes hypertrophied[1,5]. The fibrous tissue in the submucosa and the hypertrophied muscularis mucosa form a barrier hindering the ova transit from the veins to the lumen, hence more ova are entrapped. Sometimes, the adult worms either alone or matted are seen lodged and obstructing small venules within the polyp[5].

Stage of growth and protrusion: The granuloma formation is the basic pathology unit of chronic Schistosomiasis. Ova entrapment induces a foreign body reaction with progressive inflammation and fibrosis (chronic granuloma). As this process continues, a nodule is formed that elevates the hypertrophied muscularis mucosa and mucosa to form the polyp [6]. The polyp's mucosa harbors many goblet cells which secrete large amounts of mucus and this matches the abdominal pain and passage of mucus with stool seen among those patients. Furthermore, the delicate, and highly vascular nature of the polyp facilitates bleeding with the passage of stools[1,5-7].

This previously described mechanism of fibrosis and ova entrapment explain why the Schistosomal eggs are concentrated within the polyps more frequently than in the surrounding mucosa and submucosa[8]. Furthermore, non-inflammatory polyps associated with Schistosomiasis including adenomatous, hamartomatous, and hyperplastic polyps have been reported[1,9].

Stage of fibrosis: When the infection became chronic, the developed granulomas are infiltrated with fibroblasts, and fibrosis does occur[2,10]. Consequently, the polyps may become fibrotic. Small polyps especially when medically treated with praziquantel (PZQ) can then regress in size[11].

SCHISTOSOMAL COLONIC POLYPS

Site

The most common site for the development of S. polyps is the left colon, mainly recto-sigmoid region[3,12] because mesenteric (especially inferior mesenteric) and pelvic venous plexuses are the final habitat of the adult parasite. However, no part of the colon is immune against development of S. polyps. The polyps were described in all parts of the colon mainly in the rectosigmoid[12], but also were described in the caecum[13], ileocaecal valve[14], appendix[15], ascending colon[16], transverse colon[17] as well as the descending colon[12], some reports documented the distribution of S. polyps all through the large bowel starting from the caecum up to the anus during the course of heavy infestations in endemic areas[18].

Number

Schistosomiasis in the endemic areas, is associated with development of multiple polyps and multiplicity correlates with the density of infection[3,18]. However, there are many reports that Schistosomiasis can manifest by single colon polyp discovered either incidentally during colonoscopy or complicated[13,16,19] even without any clinical manifestations suggestive of Schistosomal infection.

Size

Schistosomiasis is usually associated with small-sized polyps[1,3,12]. However, large-sized S. polyps have been described in many case reports[12,16,18,19]. We reported earlier[20] that, no part of the colon was immune against development of large S. polyps. Many cases presented with solitary S. polyps[13,16,19,21] even in absence of any Schistosomiasis-related colon inflammation[9,13,16,19,21].

Atypical presentations and complications

Schistosomal colonic polyps had a wide range of atypical presentations. Elbatee *et al*[19], Alyhari *et al*[7], and Al-Zubaidi *et al*[22], described colo-rectal cancer (CRC) like presentation due to huge polyp size, abnormal polyp morphology or both, respectively. Furthermore, Smith *et al*[23], described diffuse colonic polypoid masses with dysensteric features, a picture endoscopically indistinguishable from familial polyposis and severe ulcerative colitis. Polyp-like lesion in the appendix manifestated as acute appendicitis was reported in a Chinese woman by Zhu *et al*[15], while pan-colonic inflammation and polyposis were described in Kenia by Bosire *et al*[18].

S. POLYPS BEYOND THE COLON

Urinary bladder polyps due to *S. Haematobium* have long been described and development of polyps correlates with heaviness of the infection in endemic areas[23]. Urinary bladder S. polyps were also reported among visitors to endemic areas[24]. Urinary S. polyps are not limited to urinary bladder, they were described within the ureters with a prevalence of 5.9% (30/511) in a large Egyptian study[25]. Due to the anatomical constraints, ureteric S. polyps tend to be small[25].

The atypical sites of S. polyps (Table 1) were described not infrequently in the literature. As early as in 1951, Gilges [26], described a skin polyp in the clitoris area of an African child. Furthermore, Schistosomal vulvual polyps have been described as vulvual swelling in 9- and 11-year-old girls from endemic areas in Senegal[27] and Nigera[28] respectively.

An ectopic cervical polyp was reported in Puerto Rico by File *et al*[29], despite the light Schistosomal infection. While Eladl *et al*[30] reported an endocervical polyp containing granulomas rich in viable eggs of *S. Hematobium* in a 43-year-old Egyptian woman who manifested with vaginal bleeding.

A slowly growing anal polyp containing Schistosomal ova as well as adult worms was described in a young Brazilian adult by Raso *et al*[5], the parasites probably migrated to the anus through the veins of hemorrhoidal plexus and it was associated with troublesome mass lesion with intense pruritus.

Duodenal polyps due to schistosomiasis have been reported in the literature although not common. In the duodenum it is discovered during endoscopic evaluation for obscure anemia and/or abdominal pain. The described duodenal S. polyps are either small, multiple and sessile[31] or solitary and large[32]. One case of dull abdominal pain was diagnosed in the United States with Schistosomiasis complicating a huge duodenal Peutz-Jeghers hamartomatous polyp[9].

The small intestine is infrequently affected with S. polyps and due to its narrow lumen, which is usually characterized by obstructive manifestations and diagnosis is established either at laparotomy or more frequently retrograde through histopathologic assessment. Small bowel obstruction due to huge polyp/polypoid mass at the ileocaecl valave[14] was described among visitors as well as residents of endemic areas[33] and small bowel obstruction is the usual presentation of such cases.

Gallbladder S. polyps are infrequently reported in the literature, the developed polyps are usually small in size and grew in the fundus, hence obstructive presentation is not likely and it is usually manifest (if any) as right upper quadrant pain. Both urinary (*S. Haematobium*) and intestinal Schistosomiasis (*S. Mansoni* and *S. Japonicum*) have been associated with gallbladder Schistosomiasis[34,35].

Larynx is less commonly affected during the course of Schistosomiasis. Toppozada described S. polyp involving the right vocal cord of a 25-year-old Egyptian male presented with 5-mo progressive hoarseness of voice, surgical microscopic excision and pathological examination showed granuloma with terminal sine ova[36].

S. POLYPS AND MALIGNANT TRANSFORMATION

The malignant potential of S. polyps is debatable. Although the relationship of urinary Schistosomiasis to malignancy is well established, the direct tumorigenic impact of intestinal S. polyps is questionable.

The bowel S. polyps have been implicated in the development of CRC and liver (HCC) cancers. The evidence supporting the malignant potential of intestinal Schistosomiasis is in favor of *S. Japonicum* rather than *S. Mansoni*. The chronic inflammatory state induced by ovi-position in the submucosa and other tissues have been proposed as the potential mechanism linking *S. Japonicum* in the Far East to the development of CRC and liver cancer[37].

So far the link between *S. Mansoni* and CRC has been viewed as no more than an epidemiological association and most published literatures deny the precancerous potential of the *S. Mansoni*-associated lesions including the polyps[38]. However, the mood of clinicians is spoiled by the emerging evidence incriminating *S. Mansoni* as a potential carcinogen. A large Egyptian study proposed an association between *S. Mansoni* infection and CRC relying on the increased levels of carcinoembryonic antigen within Bilharzial polyps' tissue[39]. In addition, one case report[40] retrieved Schistosome ova from the CRC specimens during histologic examination. Parasitism is associated with DNA repair defects with resultant genome instability, a commonly reported anomaly in CRC[38]. Furthermore, an emerging evidence through biomolecular mechanisms suggests an association between *S. Mansoni* and human carcinogenesis mainly for HCC and CRC and this is

Table 1 Summary of atypical and ectopic schistosomal polyps

Ref.	Site	Size	Presentation	Source
Raso *et al*[5], 2013	Anus	Large (2.5 cm)	Swelling with pain and intense pruritus	Endemic area
Gilges[26], 1951	External genitalia (clitoris)	Not mentioned	Mass like	Report from endemic area
Eladl *et al*[30], 2012	Cervix	Large sized (3 mc)	Vaginal bleeding	Endemic area
File *et al*[29], 1998	Cervix	Large	Gynecologic	Common area of spread. Adult worms within the polyp
Dioussé *et al*[27], 2016	Vulva	Large	Mass like	Endemic area
Sahabi and Rabiu [28], 2017	Vulva	Large	Mass like	Endemic area
Gonzalez *et al*[9], 2021	Duodenum	Huge (≥ 4 cm)	Dull abdominal pain	Resident of non-endemic area with a history of travel to endemic areas
Altonbary *et al*[31], 2014	Duodenum	Diminutive (≤ 4 mm)	Abdominal pain and generalized lymphadenopathy	Endemic area
Thatcher *et al*[32], 1984	Duodenum	Large	Isolated polyp	Non-endemic area
Lamyman *et al*[14], 2006	Ileocaecal valve area	Large	Intestinal obstruction	Visitor to endemic areas
Ali *et al*[34], 2021	Gallbladder fundus	Small 6 mm	Vague Abdominal pain	Patient from endemic area
Ghimire *et al*[35], 2020	Gallbladder fundus	Diminutive 3 mm	Right hypochndrial pain	Non-endemic areas
Toppozada[36], 1985	Larynx, right vocal cord	Large	Hoarseness of voice	Endemic area

likely through many egg-related agents and Th2-immune mechanisms[41]. A single recent report described for the first time a concomitant infection with *S. Mekongi* and rectal cancer[42].

The association of *S. Haematobium* and the urinary bladder squamous cell cancer is well established[43] and that is why *S. Haematobium* is classified as group 1 definitive biological carcinogenic. This association is probable with all forms of urinary bladder- induced Schistosomal pathology including chronic bladder wall inflammation and irritation by the deposited ova, the induced ulcers, sandy patches and also to the developed S. polyps[44]. There is no clear evidence in the literature linking intestinal Schistosomiasis to bladder tumors and vice versa[9].

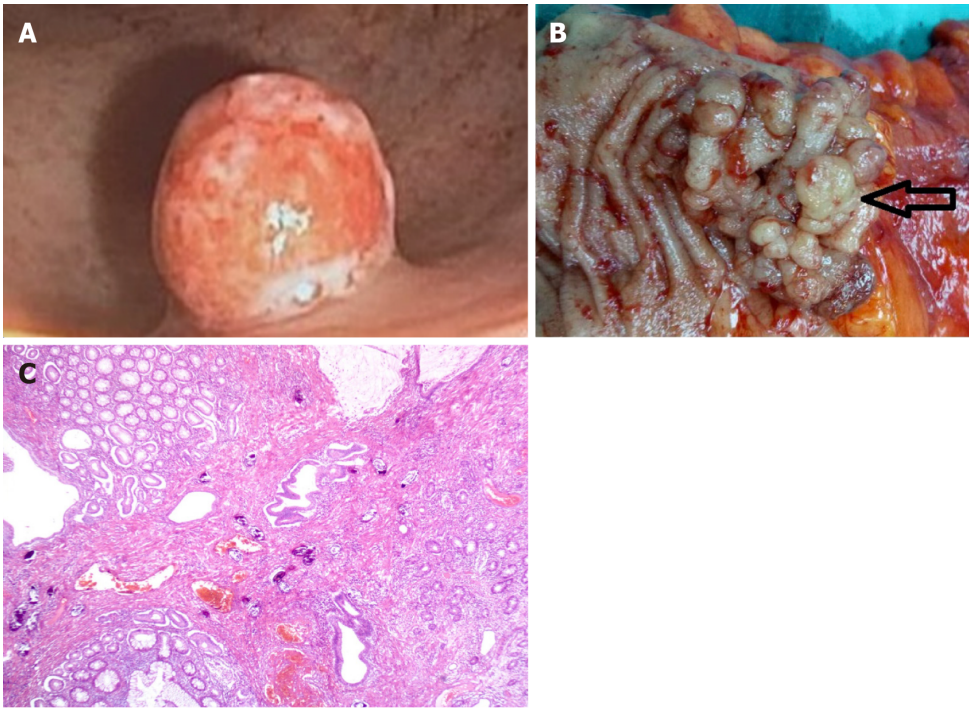
DIFFERENTIAL DIAGNOSIS

The severe forms of intestinal Schistosomiasis are characterized by the presence of multiple variable sized polyps against a background of diffuse mucosal affection showing mucosal erythema, and ulcerations, a picture mistaken with inflammatory bowel disease[3]. S. polyps of the colon are usually located in the recto-sigmoid region[12] and tend to be small[3, 12] (Figure 1A) and dark grey in color with surface ulceration, however other conditions with multiple colonic polyps should be considered in the differential diagnosis.

The solitary forms of S. polyps should be differentiated from other polyps according to the location. In fact, there is no characteristic morphology for S. polyps[45]. The huge polyps are commonly mistaken as malignant polyps (Figure 1B) and in such cases diagnosis is achieved through histopathology either by biopsy or after excision[19,21,22].

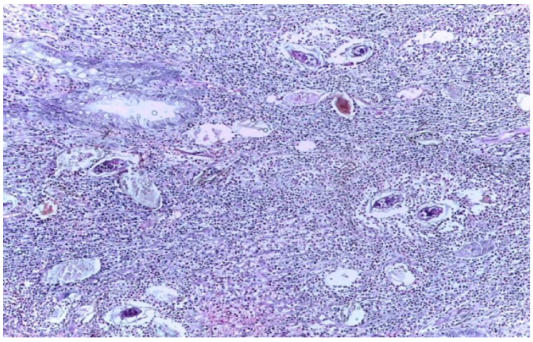
DIAGNOSIS

Diagnosis of polyps of the Schistosomal origin is sometimes challenging. There are no peculiar endoscopic morphologic features of S. polyps in comparison to other types of polyps and high index of suspicion is required especially in endemic areas. However, most cases are diagnosed either through endoscopic biopsy from the polyps or retrograde upon histopathology examination of removed polyps where the characteristic eosinophilic granulomas with the pathogenomic ova (Figure 2) of the parasite are seen [12-19,22] and infrequently the mature parasites may also be seen embedded within the background tissue of the excised polyps[22,29] or is seen lodged within thrombosed veins inside the polyp[5].



DOI: 10.3748/wjg.v29.i26.4156 **Copyright** ©The Author(s) 2023.

Figure 1 Schistosomal polyp. A: Small Schistosomal polyp located in the rectum. Note its dark red color with minute surface ulcerations; B: Surgical specimen of huge lobulated Schistosomal polyp morphologically and radiological confused with colo-rectal cancer; C: Schistosomal polyp with noticeable mucoid hyperplasia.



DOI: 10.3748/wjg.v29.i26.4156 **Copyright** ©The Author(s) 2023.

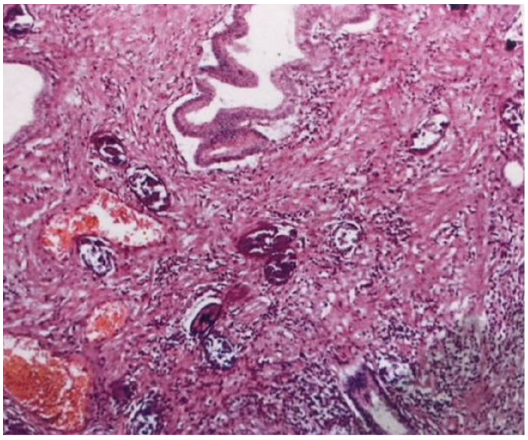
Figure 2 Active schistosomal granuloma; multiple schistosomal eggs in the submucosa surrounded by cellular infiltrate composed of eosinophils, lymphocytes, plasma cells and macrophages.

Linking the developed polyps, whatever its location, with active intestinal or urinary Schistosomiasis is not always achievable. In many cases described in the literature, identification of Bilharzial ova in fresh stool or urine samples taken from the same cases was not possible[9,16,31]. Furthermore, S. polyps may be the only clue of a Bilharzial infection[19,31].

Barium enema was used frequently to diagnose Bilharzial polyps of the bowel[46] in endemic areas before the era of endoscopy. However, currently the role of contrast study in diagnosis of intestinal or urinary Schistosomiasis is not likely to replace the standard methods for direct ova detection in stool or urine samples or detection of the ova with its characteristic granuloma on endoscopic or surgical specimens due to low sensitivity and specificity of these contrast studies[47].

Upon histologic examination, the polyp had a stalk of fibrous connective tissue that project from the submucosa into the lumen and is covered with mucosa. The overlying mucosa harbor distorted glands showing variable degrees of mucoid activity (Figure 1C), mucinous degeneration, and adenomatous hyperplasia. The covering mucosa frequently had focal areas of ulceration. Larger areas of ulceration may be replaced by granulation tissue. Mononuclear cells, eosinophils, and few polymorphonuclear leucocytes infiltrate the mucosa[48].

The peculiar granuloma had a centrally located ova (viable and/or nonviable) surrounded by cellular infiltrate characteristically with eosinophils, mononuclear cells and multinucleated histiocytes (Figure 2)[1,5], chronic granulomas are surrounded by fibroblasts (Figure 3). The supporting tissue is composed of fibrous connective tissue and muscle derived from the muscularis mucosa. Blood vessels may be present in large numbers but diminish with progression of fibrosis [48].



DOI: 10.3748/wjg.v29.i26.4156 **Copyright** ©The Author(s) 2023.

Figure 3 Schistosomal granuloma infiltrated by fibroblasts with dense submucosal fibrosis.

TREATMENT

Medical treatment

Currently, PZQ is the recommended first-line medical therapy for Schistosomiasis. The drug is active and effective in treatment of all Schistosome species with no reports of resistance[49]. Small-sized polyps can be cured with PZQ therapy alone. The dose is 40-60 mg/kg, it is given as a single dose after a meal[1] and can be divided over one day[3,9], and can be repeated[7]. The side effects associated with PZQ are usually mild and include nausea, vomiting, abdominal cramps and allergic reactions. S. polyps are exceptional types of polyps that can regress with medical treatment[11] especially when they are small and are not associated with manifestations necessitating excision. All cases associated with large or ectopic polyps after being excised either endoscopically or surgically were followed by treatment with PZQ irrespective of the patients' active intestinal or urinary Schistosomiasis state[9,13,19,34].

Endoscopic treatment

Large polyps are indicated for excision. Endoscopic excision for S. polyps have been reported thoroughly in the literature as early as the 80s of the last century[50,51] with the early time of endoscopy. S. polyps were excised with different techniques including cold snare for small polyps, standard direct hot polypectomy for larger polyps whatever the site is the duodenum[9], or the colon[3]. Hot polypectomy after application of endoloop[52], or clips[13] has been associated with good outcomes. While advanced endoscopic resection techniques including endoscopic mucosal resection[21,22] and endoscopic submucosal dissection[53] were also used for endoscopic removal of large S. polyps. All endoscopic resection techniques were used with accepted safety profile. The adverse events reported were not different from those reported with other types of polyps[3,9,13,16,22]. Resection of S. polyps combined with medical treatment using PZQ was successful [3,9,13,16,22,48]. Endoscopic resection of urinary S. polyps is less frequently performed in comparison to bowel and was associated with acceptable success rates[24].

Surgical treatment

Surgical excision is not the standard of care in treatment of S. polyps. However, surgery is usually the ultimate solution for challenging situations including cases presented with bowel obstruction[14,33], or when the lesion is morphologically or radiologically suspected to be malignant[7,12,19] and also for lesions in ectopic areas including the anus[5], cervix[30] and the external genitalia[27,28]. Atypical sites of S. polyps may require special surgical approaches, *e.g.*, in the larynx, the surgical microscope is essential to excise the polyp[36], while in other situations, *e.g.*, gallbladder, the organ is excised with the polyp en bloc[34]. All cases managed by surgery, similar to endoscopic management, should be followed by PZQ therapy.

Outcomes of treatment

The outcome of S. polyps achieved by the above mentioned treatments depend on many factors. First, the number of lesions detected. For single lesions excision (either endoscopic or surgical) is usually curative, while multiple lesions may require more rounds of excision[3]. Second, patients' residency; patients residing in endemic areas are susceptible to re-infection and hence should follow the general preventive measures together with PZQ therapy that sometimes given as chemoprophylaxis or as mass treatment campaigns even without testing for the presence of the parasite[54], while patients out of the endemic areas a single course of PZQ is usually sufficient for treatment. Third, the location of the polyps, some polyps are accessible for endoscopic treatment, such as polyps in the colon, and urinary bladder, while other lesions, *e.g.*, gallbladder are not. Last, presentation of the lesions, such as lesions presented with acute manifestations including bowel obstruction, surgery usually the corner stone of treatment and in such cases diagnosis is often achieved retrograde[14,33].

CONCLUSION

Schistosomiasis is a neglected tropical disease and its prevalence is no more limited to endemic areas. S. polyps are not infrequent presentation of acute or chronic Schistosomal infection. S. polyps are described in many organs including the bowel, genitourinary tract, skin, gallbladder and the larynx. Presentation of S. polyps is variable and depends on the site, number as well as the polyp size. The relationship of S. polyps to malignant transformation is a matter of discussion. Small polyps can be treated medically with PZQ, while large accessible polyps are amendable for endoscopic excision through different polyp resection techniques. However, huge, complicated and suspicious polyps are indicated for surgical management or advanced endoscopic resection if appropriate. Clinicians and endoscopists should be aware about these facts when treating patients living in, immigrated from or visiting endemic areas.

FOOTNOTES

Author contributions: Emara MH, Mahros AM, Radwan MI, and Rasheda AMA developed concept of the study, and retrieved the evidence; Elbatae H, Emara MH, Abdelrazik O, and Elazab M searched the literature; Elbatae H, Emara MH, Abdelrazik O, Elazab M, Mahros AM, and Radwan MI analyzed the evidence; Emara MH, Rasheda AMA, Elazab M, and Mahros AM drafted the article; All authors revised the article.

Conflict-of-interest statement: All the authors report no relevant conflicts of interest for this article.

Open-Access: This article is an open-access article that was selected by an in-house editor and fully peer-reviewed by external reviewers. It is distributed in accordance with the Creative Commons Attribution NonCommercial (CC BY-NC 4.0) license, which permits others to distribute, remix, adapt, build upon this work non-commercially, and license their derivative works on different terms, provided the original work is properly cited and the use is non-commercial. See: https://creativecommons.org/Licenses/by-nc/4.0/

Country/Territory of origin: Egypt

ORCID number: Mohamed H Emara 0000-0002-1504-7851; Aya M Mahros 0000-0002-6849-4065; Hassan Elbatae 0000-0001-7804-8424.

Corresponding Author's Membership in Professional Societies: Egyptian Association for Research and Training in Hepatogastroenterology.

S-Editor: Fan JR
L-Editor: Ma JY
P-Editor: Zhang XD

REFERENCES

1 **Elbaz T**, Esmat G. Hepatic and intestinal schistosomiasis: review. *J Adv Res* 2013; **4**: 445-452 [PMID: 25685451 DOI: 10.1016/j.jare.2012.12.001]
2 **Hams E**, Aviello G, Fallon PG. The schistosoma granuloma: friend or foe? *Front Immunol* 2013; **4**: 89 [PMID: 23596444 DOI: 10.3389/fimmu.2013.00089]
3 **Abd El-Latif N**, Bedewy E. Bilharzial Colonic Polyps: Case Presentation. *Afro-Egyptian J Infect Endemic Dis* 2020; **10**: 233-236 [DOI: 10.21608/aeji.2020.29738.1079]
4 **Barsoum RS**. Urinary schistosomiasis: review. *J Adv Res* 2013; **4**: 453-459 [PMID: 25685452 DOI: 10.1016/j.jare.2012.08.004]
5 **Raso P**, Sander EM, Raso LA, Andrade Filho Jde S. Anal polyp caused by Schistosoma mansoni. *Rev Soc Bras Med Trop* 2013; **46**: 252-254 [PMID: 23740071 DOI: 10.1590/0037-8682-1681-2013]
6 **Mostafa I**. Schistosomal colonic polyposis. *Gastrointest Endosc* 1997; **46**: 584-587 [PMID: 9434242]
7 **Alyhari Q**, Ahmed F, Al Shaibani H, Al Kubati M, Alhadi A. Huge Colonic Granuloma of Schistosomiasis Mimicked Cancer in a 10-Years-Old Child: A Case Report. *Int Med Case Rep J* 2022; **15**: 379-384 [PMID: 35903496 DOI: 10.2147/IMCRJ.S372186]
8 **Cao J**, Liu WJ, Xu XY, Zou XP. Endoscopic findings and clinicopathologic characteristics of colonic schistosomiasis: a report of 46 cases. *World J Gastroenterol* 2010; **16**: 723-727 [PMID: 20135720 DOI: 10.3748/wjg.v16.i6.723]
9 **Gonzalez A**, Gupta K, Rodriguez S, Wadhwa V, Bejarano P, Charles R. Unique Case of a Hamartomatous Duodenal Polyp Associated With Intestinal Schistosomiasis. *ACG Case Rep J* 2021; **8**: e00485 [PMID: 33532510 DOI: 10.14309/crj.0000000000000485]
10 **Pesce JT**, Ramalingam TR, Mentink-Kane MM, Wilson MS, El Kasmi KC, Smith AM, Thompson RW, Cheever AW, Murray PJ, Wynn TA. Arginase-1-expressing macrophages suppress Th2 cytokine-driven inflammation and fibrosis. *PLoS Pathog* 2009; **5**: e1000371 [PMID: 19360123 DOI: 10.1371/journal.ppat.1000371]
11 **Nebel OT**, el-Masry NA, Castell DO, Farid Z, Fornes MF, Sparks HA. Schistosomal disease of the colon: a reversible form of polyposis. *Gastroenterology* 1974; **67**: 939-943 [PMID: 4426495]
12 **Ahmed MH**, Emara MH, Elfert AA, El-Saka AM, Abd-Elsalam S, Yousef M. Persistent Colonic Schistosomiasis among Symptomatic Rural Inhabitants in the Egyptian Nile Delta. *Mediterr J Hematol Infect Dis* 2021; **13**: e2021033 [PMID: 34007421 DOI: 10.4084/MJHID.2021.033]
13 **Orare K**, Mohamed A, Thakkar M, Rajula A, Gatheru J. Colonic polyps: a rare clinical manifestation of schistosomiasis (a case report). *Pan Afr Med J* 2022; **42**: 187 [PMID: 36212935 DOI: 10.11604/pamj.2022.42.187.34227]
14 **Lamyman MJ**, Noble DJ, Narang S, Dehalvi N. Small bowel obstruction secondary to intestinal schistosomiasis. *Trans R Soc Trop Med Hyg* 2006; **100**: 885-887 [PMID: 16443245 DOI: 10.1016/j.trstmh.2005.10.013]

15 **Zhu XL**, Song JZ, Yu WY, Hua LQ, Zhang ML. Intestinal schistosomiasis masquerading as intestinal polyps. *BMC Infect Dis* 2021; **21**: 434 [PMID: 33964884 DOI: 10.1186/s12879-021-06125-4]

16 **Issa I**, Osman M, Aftimos G. Schistosomiasis manifesting as a colon polyp: a case report. *J Med Case Rep* 2014; **8**: 331 [PMID: 25296942 DOI: 10.1186/1752-1947-8-331]

17 **Lin CT**, Chen CY, Jao SW, Wu CC. An unusual pedunculated polyp of the transverse colon associated with schistosomiasis. *Endoscopy* 2010; **42** Suppl 2: E160 [PMID: 20556713 DOI: 10.1055/s-0029-1244142]

18 **Bosire F**, Orwa I, Mwachiro M, Parker R, Whit R. Schistosoma Mansoni Proctocolitis with Polyposis. *Ann African Sury* 2018; **15**: 81-85

19 **Elbatee HE**, Emara MH, Zaghloul MS, Ahmed MH, Radwan MI, Seif AS, Elmoghazy MB, Elkashef WF. Huge bilharzial polyp mimicking colon cancer. *JGH Open* 2020; **4**: 280-283 [PMID: 32280778 DOI: 10.1002/jgh3.12181]

20 **Emara MH**, Ahmed MH, Mahros AM, Amer IF, Elkerdawy MA. No part of the colon is immune from large Bilharzial polyps. *Eur J Gastroenterol Hepatol* 2020; **32**: 896-897 [PMID: 32472818 DOI: 10.1097/MEG.0000000000001727]

21 **Farooq A**, Hussain A, Singh C, Kadkhodayan K, Arain M, Hasan MK, Yang D. Large Colon Polyp as the Only Manifestation of Chronic Schistosomiasis Infection. *ACG Case Rep J* 2022; **9**: e00889 [PMID: 36237280 DOI: 10.14309/crj.0000000000000889]

22 **Al-Zubaidi AM**, Bashanfer GA, Alqannas MH, Al Atawi AS. Colonic Polyps an Unusual Manifestation of Schistosomiasis. *Am J Case Rep* 2020; **21**: e923177 [PMID: 32764533 DOI: 10.12659/AJCR.923177]

23 **Smith JH**, Torky H, Kelada AS, Farid Z. Schistosomal polyposis of the urinary bladder. *Am J Trop Med Hyg* 1977; **26**: 85-88 [PMID: 842788 DOI: 10.4269/ajtmh.1977.26.85]

24 **Dessyn JF**, Duquenne S, Hoarau G. Incidental pseudolymphomatous bladder inflammatory polyp revealing urinary schistosomiasis. *Int J Infect Dis* 2016; **53**: 39-40 [PMID: 27810520 DOI: 10.1016/j.ijid.2016.10.022]

25 **Saad SM**, Hanafy HM. Bilharzial (schistosomal) polypi of ureter. *Urology* 1974; **4**: 85-89 [PMID: 21322991 DOI: 10.1016/0090-4295(74)90114-9]

26 **Gilges W**. Skin polyp-only symptom of bilharzia infection. *East Afr Med J* 1951; **28**: 288 [PMID: 14872783]

27 **Dioussé P**, Dione H, Bammo M, Dial C, Thiam M, Diamé AA, Diop BM, Ka MM. Vulvar bilharzia on nine-year old girl: A case report. *Int J Case Rep Images* 2016; **7**: 724-728

28 **Sahabi MS**, Rabiu FA. Unusual presentation of schistosomiasis as vulval polyp. *Obs Gyne Review: J Obstet Gynecol* 2017; **3**: 33-37 [DOI: 10.17511/joog.2017.i04.01]

29 **File S**, Francheschini AB, Fernandez-Santiago A. Short report: A case of ectopic schistosomiasis in Puerto Rico with some observations on the biology of the parasite. *Am J Trop Med Hyg* 1998; **58**: 671-672 [PMID: 9598459 DOI: 10.4269/ajtmh.1998.58.671]

30 **Eladl AE**, Shebl AM, Elkashef WF, Zalata KR. Bilharzial endocervical polyp. *Indian J Pathol Microbiol* 2012; **55**: 377-378 [PMID: 23032837 DOI: 10.4103/0377-4929.101750]

31 **Altonbary A**, Bahgat M, Elkashef W. Bilharzial granuloma of the duodenum. *OA Case Rep* 2014; **3**: 62

32 **Thatcher BS**, Fleischer D, Rankin GB, Petras R. Duodenal schistosomiasis diagnosed by endoscopic biopsy of an isolated polyp. *Am J Gastroenterol* 1984; **79**: 927-929 [PMID: 6507419]

33 **Gul R**, Khalid K, Al-Rajhi MF, Bismar HA. Acute small bowel obstruction due to bilharziasis. *Saudi Med J* 2005; **26**: 1624-1626 [PMID: 16228068]

34 **Ali GA**, Goravey W, Al-Bozom I, Al Maslamani MA, Abdel Hadi H. Schistosoma gallbladder polyp masquerading as a neoplasm: Rare case report and literature review. *Clin Case Rep* 2021; **9**: e04420 [PMID: 34267906 DOI: 10.1002/ccr3.4420]

35 **Ghimire PG**, Ghimire P. Gallbladder schistosomiasis - a rare presentation as gallbladder polyp: a case report. *Radiol Case Rep* 2020; **15**: 1394-1397 [PMID: 32636981 DOI: 10.1016/j.radcr.2020.06.013]

36 **Toppozada HH**. Laryngeal bilharzia. *J Laryngol Otol* 1985; **99**: 1039-1041 [PMID: 4056583 DOI: 10.1017/s0022215100098145]

37 **Hamid HKS**. Schistosoma japonicum-Associated Colorectal Cancer: A Review. *Am J Trop Med Hyg* 2019; **100**: 501-505 [PMID: 30560774 DOI: 10.4269/ajtmh.18-0807]

38 **H Salim OE**, Hamid HK, Mekki SO, Suleiman SH, Ibrahim SZ. Colorectal carcinoma associated with schistosomiasis: a possible causal relationship. *World J Surg Oncol* 2010; **8**: 68 [PMID: 20704754 DOI: 10.1186/1477-7819-8-68]

39 **Abdulla H**, Khalil RY, Ibrahim MS, Elaish N, Abdulaziz A. The relationship between colonic Bilharzial polyposzs and colorectal cancer, Sci. *Med J ESCME* 1996; **8**: 129-140

40 **Herman AM**, Kishe A, Babu H, Shilanaiman H, Tarmohamed M, Lodhia J, Amsi P, Pyuza J, Mremi A, Mwasamwaja A, Nyindo M, Chilonga K, Msuya D. Colorectal cancer in a patient with intestinal schistosomiasis: a case report from Kilimanjaro Christian Medical Center Northern Zone Tanzania. *World J Surg Oncol* 2017; **15**: 146 [PMID: 28768520 DOI: 10.1186/s12957-017-1217-1]

41 **von Bülow V**, Lichtenberger J, Grevelding CG, Falcone FH, Roeb E, Roderfeld M. Does Schistosoma Mansoni Facilitate Carcinogenesis? *Cells* 2021; **10** [PMID: 34440754 DOI: 10.3390/cells10081982]

42 **Burky M**, Trembath D, Bookhout C. Rectal carcinoma arising in a patient with intestinal and hepatic schistosomiasis due to Schistosoma mekongi. *IDCases* 2022; **27**: e01383 [PMID: 35036322 DOI: 10.1016/j.idcr.2022.e01383]

43 **Mostafa MH**, Sheweita SA, O'Connor PJ. Relationship between schistosomiasis and bladder cancer. *Clin Microbiol Rev* 1999; **12**: 97-111 [PMID: 9880476 DOI: 10.1128/CMR.12.1.97]

44 **Ishida K**, Hsieh MH. Understanding Urogenital Schistosomiasis-Related Bladder Cancer: An Update. *Front Med (Lausanne)* 2018; **5**: 223 [PMID: 30159314 DOI: 10.3389/fmed.2018.00223]

45 **Ye C**, Tan S, Jiang L, Li M, Sun P, Shen L, Luo H. Endoscopic characteristics and causes of misdiagnosis of intestinal schistosomiasis. *Mol Med Rep* 2013; **8**: 1089-1093 [PMID: 23969514 DOI: 10.3892/mmr.2013.1648]

46 **El-Masry NA**, Farid Z, Kilpatrick ME, Watten RH. Role of the barium enema in schistosomal colonic polyposis. *East Afr Med J* 1982; **59**: 465-468 [PMID: 7160324]

47 **Shebel HM**, Elsayes KM, Abou El Atta HM, Elguindy YM, El-Diasty TA. Genitourinary schistosomiasis: life cycle and radiologic-pathologic findings. *Radiographics* 2012; **32**: 1031-1046 [PMID: 22786992 DOI: 10.1148/rg.324115162]

48 **Mostafa IM**, Zakaria S, Khalil A, El-Kaluoby A. The effect of medical treatment and endoscopic polypectomy on clinicopathological, immunological and endoscopic aspects of schistosomal colonic polyposis in Egypt. In: Proceedings of the world congresses of gastroenterology 1990. Australia: Sydney; 1990: 1260

49 **Vale N**, Gouveia MJ, Rinaldi G, Brindley PJ, Gärtner F, Correia da Costa JM. Praziquantel for Schistosomiasis: Single-Drug Metabolism Revisited, Mode of Action, and Resistance. *Antimicrob Agents Chemother* 2017; **61** [PMID: 28264841 DOI: 10.1128/AAC.02582-16]

50 **Thakeb F**, El-Kalouby AH, Ibrahim IM, Hunter S, Zakaria S. Colonoscopic polypectomy in management of schistosomal colonic polyposis. *Egypt J Bilh* 1980; **7**: 49-56

51 **Bessa SM**, Helmy I, El-Kharadly Y. Colorectal schistosomiasis. Endoscopic polypectomy. *Dis Colon Rectum* 1983; **26**: 772-774 [PMID: 6641458 DOI: 10.1007/BF02554745]

52 **Ahmed S**, Babiker F, Elshafie A, Alhedaithy M, Yousif OE, Toulaymat M. Unusual Presentations of Intestinal Schistosomiasis. *Dr. Sulaiman Al Habib Med J* 2020; **2**: 33-37

53 **Probst A**, Schaller T, Ebigbo A, Messmann H. Colonic schistosomiasis and early rectal cancer: coincidence or causal relationship? *Endoscopy* 2014; **46** Suppl 1: E671 [PMID: 25526419 DOI: 10.1055/s-0034-1390863]

54 **Kabuyaya M**, Chimbari MJ, Mukaratirwa S. Efficacy of praziquantel treatment regimens in pre-school and school aged children infected with schistosomiasis in sub-Saharan Africa: a systematic review. *Infect Dis Poverty* 2018; **7**: 73 [PMID: 29986763 DOI: 10.1186/s40249-018-0448-x]

World Journal of Gastroenterology

Submit a Manuscript: https://www.f6publishing.com

World J Gastroenterol 2023 July 14; 29(26): 4166-4173

DOI: 10.3748/wjg.v29.i26.4166

ISSN 1007-9327 (print) ISSN 2219-2840 (online)

MINIREVIEWS

Mortality from chronic liver disease: Recent trends and impact of the COVID-19 pandemic

Ugo Fedeli, Claudio Barbiellini Amidei, Veronica Casotto, Enrico Grande, Mario Saia, Alberto Zanetto, Francesco Paolo Russo

Specialty type: Gastroenterology and hepatology

Provenance and peer review: Invited article; Externally peer reviewed.

Peer-review model: Single blind

Peer-review report's scientific quality classification

Grade A (Excellent): 0
Grade B (Very good): B, B, B
Grade C (Good): 0
Grade D (Fair): 0
Grade E (Poor): 0

P-Reviewer: Goja S, India; Wang D, Thailand; Zhang XF, China

Received: April 14, 2023
Peer-review started: April 14, 2023
First decision: May 23, 2023
Revised: May 26, 2023
Accepted: June 12, 2023
Article in press: June 12, 2023
Published online: July 14, 2023

Ugo Fedeli, Claudio Barbiellini Amidei, Veronica Casotto, Epidemiological Department, Azienda Zero, Veneto Region, Padova 35132, Italy

Enrico Grande, Integrated System for Health, Social Assistance and Welfare, National Institute of Statistics, Rome 00184, Italy

Mario Saia, Clinical Governance, Azienda Zero, Veneto Region, Padova 35132, Italy

Alberto Zanetto, Francesco Paolo Russo, Department of Surgery Oncology and Gastroenterology, University of Padua, Padova 35128, Italy

Alberto Zanetto, Francesco Paolo Russo, Gastroenterology and Multivisceral Transplant Unit, Azienda Ospedale-Università di Padova, Padova 25128, Italy

Corresponding author: Ugo Fedeli, MD, Senior Scientist, Epidemiological Department, Azienda Zero, Veneto Region, 35 Via Avanzo, Padova 35132, Italy. ugo.fedeli@azero.veneto.it

Abstract

Prepandemic time trends in mortality from chronic liver disease (CLD) differed according to specific cause of death (decreasing for liver cirrhosis, stable or increasing for liver cancer), etiology (increasing for nonalcoholic fatty liver disease, generally decreasing for other etiologies), and world region (decreasing in areas with the highest burden of hepatitis B virus, increasing in Eastern Europe and other countries). The coronavirus disease 2019 (COVID-19) pandemic affected mortality of patients with CLD both directly, with a higher risk for severe illness and death depending on age, stage and etiology of the disease, and indirectly, through social isolation and loss of support, harmful drinking, and difficulties in access to care. Nevertheless, only sparse data are available on variations in CLD as a cause of death during the pandemic. In the USA, in 2020-2021 a growth in mortality was registered for all liver diseases, more marked for alcoholic liver disease, especially among young people aged 25-44 years and in selected ethnic groups. COVID-19 related deaths accounted only for a minor part of the excess. Further data from mortality registers of other countries are warranted, preferably adopting the so-called multiple cause-of-death approach, and extended to deaths attributed to viral hepatitis and liver cancer.

Key Words: Mortality; Multiple causes of death; COVID-19; Chronic liver disease; Liver

cirrhosis; Liver cancer

©The Author(s) 2023. Published by Baishideng Publishing Group Inc. All rights reserved.

Core tip: Preliminary data on causes of death during the coronavirus disease 2019 pandemic suggest that mortality from chronic liver disease (CLD) increased especially in countries where the alcoholic etiology was predominant, or with a prepandemic growing trend in mortality from alcoholic liver disease. Population-based studies on the direct and indirect effects of the pandemic on CLD mortality are strongly warranted. Analyses adopting the multiple cause-of-death approach might be better suited to fully investigate the impact of the pandemic on complex long-term pre-existing trends.

Citation: Fedeli U, Barbiellini Amidei C, Casotto V, Grande E, Saia M, Zanetto A, Russo FP. Mortality from chronic liver disease: Recent trends and impact of the COVID-19 pandemic. *World J Gastroenterol* 2023; 29(26): 4166-4173
URL: https://www.wjgnet.com/1007-9327/full/v29/i26/4166.htm
DOI: https://dx.doi.org/10.3748/wjg.v29.i26.4166

INTRODUCTION

According to a systematic analysis of the Global Burden of Disease (GBD) Study 2017, deaths from cirrhosis and other chronic liver diseases (CLDs) were estimated at 1.32 million in 2017, compared to 889 000 in 1990. However, the corresponding age-standardized rate decreased from 21.0 to 16.5 per 100000 population. Rates decreased or remained constant in all regions except for Eastern Europe and Central Asia. Globally, age-standardized death rates associated to all main etiologies (alcohol, hepatitis B, and hepatitis C) declined, except for nonalcoholic steatohepatitis[1].

However, interpretation of mortality data on CLD poses several challenges. Cirrhosis mortality captures only a limited fraction of deaths due to CLD. In the USA, by adopting the standard definition for CLD mortality, a 38% decrease in rates was observed from 1979 to 2008; if other liver-related causes of death including viral hepatitis and liver cancer were examined, rates remained essentially unchanged[2]. Liver cirrhosis mortality dropped, whereas death rates for primary liver cancer were stable in Northeastern Italy in 1995-2010[3], and increased in China in 1987-2016[4]. A more comprehensive assessment on mortality from CLD can also be achieved by analyses not limited to the underlying cause of death, but extended to all conditions mentioned in death certificates. The so-called multiple cause-of-death approach can unveil rapidly changing trends limited to specific etiologies within selected birth cohorts. As an example, a rise in mortality related to hepatitis C virus (HCV) was registered in the USA in 2003-2013; most deaths were confined to the 1945-1965 birth cohort, affected by the highest prevalence of HCV infection[5]. A similar growth in HCV-related mortality within a specific birth cohort was observed in Northern Italy[6]. After 2014, time trends in the USA changed and mortality related to HCV started to decline, whereas death rates related to alcoholic liver disease and nonalcoholic fatty liver disease (NAFLD) were on the rise[7].

In the most recent years, patients with CLD represented a vulnerable population during the coronavirus disease 2019 (COVID-19) pandemic due to immune dysregulation and coagulopathy among those with advanced disease, and coexisting comorbidity, including obesity, diabetes and cardiovascular diseases. Notably, baseline liver disease stage and alcoholic liver disease were demonstrated to be independent risk factors for death from COVID-19[8]. Nevertheless, to date, population-based data on trends in CLD as a cause of death during the pandemic are lacking, except for an increase in mortality from liver cirrhosis reported from the USA already in its early phases[9]. We review here the available evidence on the impact of the pandemic on pre-existing time trends in mortality from CLD.

MORTALITY TRENDS BEFORE THE PANDEMIC

In 2017, there were 2.14 million estimated liver-related deaths; liver cirrhosis and liver cancer accounted for 61.7% and 38.3%, respectively. Between 2012 and 2017 the global age-standardized death rate increased (annual percent change, APC = 0.51%, 0.05%-0.98%) for liver cancer and decreased (APC = 0.70%, 1.01% to 0.40%) for liver cirrhosis. In Asia, the most common cause was hepatitis B virus (HBV) infection (highest in East Asia), whereas HCV was the most common cause in high-income Asia Pacific and Middle East and North Africa (MENA), and alcohol-related liver disease in Central Asia. Incidence and mortality associated with NAFLD increased globally, and this increase was recorded in almost every region worldwide[10].

Hepatitis B is the leading etiology for liver cancer mortality and the third largest contributor to deaths from cirrhosis. HBV-related diseases resulted in 555 000 global deaths in 2019; the number of HBV-related deaths increased between 1990 and 2019. By contrast, age-standardized death rates declined globally and in all world regions. Meanwhile, there was a 31.3% decrease in the prevalence of HBV at all ages[11]. Mortality trends related to hepatitis C are less pronounced; in 2010-2019 the decline in mortality was larger for acute hepatitis C than for HCV-related cirrhosis, with no significant change for HCV-related liver cancer[12].

A number of studies addressed global trends in liver cancer incidence and mortality. According to the GBD 2015 study, globally, HBV accounted for 33% of a total of 810 000 liver cancer deaths, alcohol for 30%, and HCV for 21%. The highest share for HBV was observed in Western sub-Saharan Africa, East Asia, and Andean Latin America; that for HCV in high-income Asia Pacific, MENA, Central and Southern Latin America, and Western Europe; and that for alcohol in Central and Eastern Europe. From 1999 to 2015, age-standardized mortality rates declined substantially in regions with high liver cancer burden such as East Asia and sub-Saharan Africa, probably due to the effect of primary liver cancer prevention through HBV vaccination[13]. These trends parallel those in liver cancer incidence. The burden in highly endemic regions has been partially alleviated due to improved control of viral hepatitis, especially among young and middle-aged people. By contrast, an unfavorable trend was observed in most developed countries and in older populations[14]. In fact, the most significant increases in incidence were generally observed in countries with a high sociodemographic index, including the UK and the USA[15]. Nevertheless, chronic HBV and HCV remain important risk factors for liver cancer. Based on the GLOBOCAN database, the overall increasing trend in incidence and mortality from liver cancer was confirmed among older male subjects, and in countries with a higher prevalence of HCV-related liver cancer. The increasing prevalence of alcohol consumption and obesity may have contributed to this epidemiological scenario in high-income countries[16].

As regards mortality from liver cirrhosis, analyses of the GBD 2017 study showed that deaths due to cirrhosis constituted 2.4% of total deaths globally. Central Asia had the highest age-standardized death rate, followed by Sub-Saharan Africa. Central Asia and Eastern Europe were the only two regions in which mortality rates significantly increased during 1990-2017; in both, prevalent cases were predominantly caused by alcohol-related liver disease. At the national level, the highest mortality rate was registered in Egypt, whereas the steepest growth was observed in Lithuania. Deaths from cirrhosis in males were mostly attributed to hepatitis B (31.5%), alcohol (27.3%), and hepatitis C (25.5%); the corresponding percentages in females were 24.0%, 20.6%, and 26.7%[1].

In view of the above, prepandemic global patterns in CLD mortality differed according to cause of death (liver cirrhosis or liver cancer), etiology, and world region (Figure 1). Furthermore, even within a single country, different patterns of mortality could be registered according to complex interactions between demographic characteristics (sex, age group, ethnicity, and socioeconomic status) and etiology of liver disease. Mortality from CLD overall, and especially that from alcoholic liver disease, is in fact strongly associated with socioeconomic status[17]. Different trends in CLD mortality by etiology have been investigated in the USA by means of the multiple cause-of-death approach. Overall, an increase in mortality from cirrhosis and hepatocellular carcinoma has been registered in the prepandemic period[18]. However, drastically different trends were observed according to etiology. HCV-related mortality increased from 2007 to 2014 and sharply declined in 2014-2016, after the introduction of direct-acting antiviral therapies; meanwhile, a decrease in HBV-related mortality, and an increase in alcoholic liver disease and NAFLD mortality was observed in 2007-2016. Minorities were disproportionately affected, especially non-Hispanic blacks by HCV-related mortality and Asians by HBV-related mortality[7]. An increase in mortality related to NAFLD was confirmed by other authors in the same period, especially among older subjects, females, non-Hispanic whites, and American Indian/Alaskan Natives[19].

CLD AND COVID-19

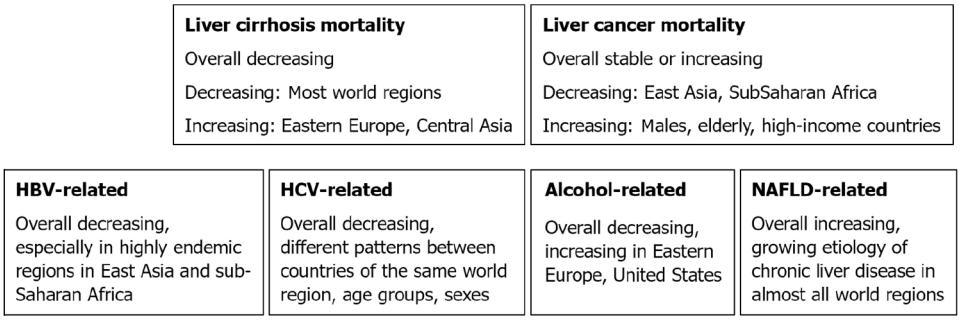
Although COVID-19 primarily affects the respiratory system, causing pneumonia and acute respiratory distress syndrome in severe cases, it can also result in multiple extrapulmonary complications. The pathogenesis of extrapulmonary damage in patients with COVID-19 is probably multifactorial, involving both the direct effects of SARS-CoV-2 and the indirect mechanisms associated with the host inflammatory response[20]. Research has shown that COVID-19 can cause liver injury due to inflammation, which can lead to liver damage or failure, particularly in people with pre-existing liver conditions such as cirrhosis. People with COVID-19 who have pre-existing liver conditions may be at a higher risk for severe illness and death[21]. For these reasons, they should always continue to follow their treatment plan and keep in close contact with their healthcare provider.

Etiology of liver disease and COVID-19 impact

It is reported that liver diseases of viral etiology are not associated *per se* with the severity or outcome of COVID-19, and this finding has been consistent across Asia, Europe and the USA. According to recent data from the European Reference Network for Rare Liver Diseases, autoimmune liver diseases and the related immunosuppressive therapy do not represent a specific risk factor for COVID-19, and the risk, as with other etiologies, is determined by the stage of cirrhosis [22]. Several studies highlighted the presence of severe complications in patients with SARS-CoV-2 infection and metabolic-syndrome-associated comorbidities, including NAFLD. The shared genetic influence between COVID-19 susceptibility and NAFLD, the sex-linked and the liver single-cell differential expression level of diverse transcripts and biological pathways might uncover shared disease mechanisms that explain the severe complications and increased in-hospital mortality risk associated with comorbidities, including NAFLD[23]. Lockdown, economic hardship, and the psychological impact of the pandemic all had a detrimental effect on people with liver disease, including poorer metabolic control in people with metabolic syndrome and fatty liver disease. This likely had deleterious consequences on the liver and cardiovascular outcomes of people with NAFLD, particularly those with advanced liver disease. Mortality has been shown to increase in people with alcohol-associated liver disease[24].

The role of cirrhosis

Prospective data from multicenter studies confirmed that patients with cirrhosis, particularly those who are



DOI: 10.3748/wjg.v29.i26.4166 **Copyright** ©The Author(s) 2023.

Figure 1 Trends in mortality from liver diseases before the pandemic, by cause of death and etiology. HBV: Hepatitis B virus; HCV: Hepatitis C virus; NAFLD: Nonalcoholic fatty liver disease.

decompensated, are at a higher risk of hospitalization, ventilation and death than those without CLD. Older age and cirrhosis severity, as assessed by Child-Pugh class, are the most important predictors of mortality[25]. Overall mortality in patients with cirrhosis following SARS-CoV-2 infection was 32% in a large registry cohort of 729 predominantly hospitalized patients with CLD across 29 countries, with case-fatality rates incrementally increasing with each Child-Pugh class (CLD without cirrhosis 8%; class A 19%; class B 35%; class C 51%). The multivariable analysis of factors associated with death demonstrated persisting positive associations with age [odds ratio (OR) 1.02; 95% confidence interval (CI) 1.01-1.04; $P = 0.011$], the different stages of cirrhosis compared with CLD without cirrhosis (Child-Pugh class A, OR 1.90; 95%CI: 1.03-3.52; $P = 0.040$; class B, OR 4.14; 95%CI: 2.4-7.65; $P < 0.001$; and class C, OR 9.32; 95%CI: 4.80-18.08; $P < 0.001$), and alcoholic liver disease (OR 1.79; 95%CI: 1.03-3.13; $P = 0.040$)[8].

Patients with CLD and especially cirrhosis, have multiple mechanisms of immune dysfunction that can lead to increased susceptibility to infection and an aberrant inflammatory response during infection, collectively known as cirrhosis-associated immune dysfunction[26]. This immune dysfunction includes reduced components of the complement system, macrophage activation, impaired lymphocyte and neutrophil function, Toll-like receptor upregulation, and intestinal dysbiosis[27].

The role of vaccination

By April 2022, more than half of the world's population had received at least one vaccine dose, with real-world data showing that vaccination is generally safe and significantly reduces mortality. However, the initial high efficacy against infection has decreased following the emergence of new SARS-CoV-2 variants. Vaccine efficacy is particularly low against the Omicron variant, although fortunately it still confers considerable protection against severe COVID-19[28,29]. Although vaccines and previous infections largely protect against severe clinical courses of COVID-19, particularly in the current phase of the pandemic, which is dominated by sublineages of the SARS-CoV-2 Omicron variant, there is still a significant unmet medical need for therapeutics to treat severe disease in unvaccinated or older patients and patients with chronic disease conditions[30]. The impact of liver disease severity on vaccine efficacy should be convened to patients, so that they are aware of their increased risk and continue to take personal protective measures[31].

CLD AS A CAUSE OF DEATH DURING THE COVID-19 PANDEMIC

Between 2012 and 2019, rates of alcohol-specific deaths in the UK remained stable, whereas during the pandemic years, they rose from 11.8 per 100000 in 2019 to 14.8 in 2021. Alcoholic liver disease accounted for 78% of alcohol-specific mortality: the number of registered deaths grew from 5840 in 2019 to 7518 in 2021. This rise was attributed to increased alcohol consumption during the pandemic. Although alcoholic liver disease takes many years to develop, a further increase in alcohol intake among high-risk consumers can lead to rises in mortality in a short period of time, from what is known as acute-on-chronic liver failure[32].

In Minnesota, USA, an increase in both alcoholic liver disease and cirrhosis/other CLD as the underlying cause of death was registered in 2020 with respect to 2018-2019[33]. The growth in deaths from alcoholic liver disease as the underlying cause was confirmed at the national level[34]. According to analyses of national US multiple cause-of-death data, during the first year of the COVID-19 pandemic, the pre-existing growing trend in alcoholic liver disease mortality further accelerated, with the quarterly increase rising from 1.1% to 11.2%. Similarly, the quarterly increase in NAFLD grew from 1.9% to 6.6%. Mortality related to HBV and HCV, previously declining in the prepandemic period, remained stable[35]. Similar analyses were extended to 2021 data from the USA, confirming the increase through the second year of the pandemic for all liver diseases. This was more marked for alcoholic liver disease, especially among the young population aged 25-44 years and in selected ethnic groups such as American Indian/Alaskan Natives. The decline in HCV-related mortality observed since 2014 slowed down[36]. Years of potential life lost from premature deaths (< 65 years) attributable to cirrhosis listed as one of the causes of death in US certificates grew by 20.7% in 2020 and by 29.5% in 2021. COVID-19-related deaths accounted only for a minor part of such excess. Again, the increase was more pronounced for the alcoholic etiology, consistent with growing alcohol sales in the USA during the pandemic[37]. Patients with

alcoholic liver disease might have disproportionally suffered from a surge in harmful drinking, social isolation, and loss of familial and social support, along with barriers to access to outpatient clinics and rehabilitation services. Another study of US national multiple cause-of-death data reported a marked increase in mortality from CLD and/or cirrhosis among decedents with mention of diabetes, specifically associated with increased mortality from NAFLD and alcohol-related liver diseases[38].

By contrast in Spain, no major change in the number of deaths from CLD in 2020 compared to the 2018-2019 average was observed, based both on the underlying cause of death (0.9%) and on multiple cause-of-death data (+3.1%)[39].

In view of the paucity of published evidence outside the USA, we retrieved mortality rates for liver cirrhosis (International Classification of Diseases-10th Revision codes K70 and K74) from the World Health Organization (WHO) mortality database (https://platform.who.int/mortality). Table 1 shows countries with data updated at least until 2020; few had data available for the year 2021. In 2020 a large increase was registered in the USA (+18% with respect to 2019) and the UK (+16%). Among the other most populous countries, rates in the Americas were almost unchanged (Mexico, Brazil and Argentina) or declined (Peru and Colombia). European countries showed no increase (Spain) or only a limited mortality increase (Germany and Poland). Rates decreased in Malaysia and showed only minor growth in other Asian countries (Kazakhstan, Japan and Korea) and in Australia. Among less populous countries, a marked increase was registered in some Eastern European countries: Estonia, Lithuania, and in 2021 Latvia, Czechia and North Macedonia. A more comprehensive evaluation will however be possible when complete 2021 data become available, in consideration of how the pandemic involved different world regions in subsequent phases (*e.g.*, Central and Eastern Europe were more severely affected in 2021 compared to 2020). Additional nationwide data not included in the WHO database can be retrieved from institutional websites. As an example, in Italy age-adjusted mortality rates from liver cirrhosis, fibrosis and chronic hepatitis in 2020 showed a 3% reduction with respect to 2019, which is consistent with the decreasing trend observed in recent years (http://dati.istat.it/). Mortality from liver cirrhosis more closely parallels mortality from alcoholic liver disease with respect to that associated with other etiologies, and analyses including codes for viral hepatitis and liver cancer are warranted[3]. Lastly, also due to coding rules set by WHO[40], COVID-19 itself may have acted as a competing condition for the selection as the underlying cause of death in patients affected by pre-existing chronic diseases[35].

CONCLUSION

A large variation in trends of mortality from CLD was observed at the global level before 2020. Based on the few available published reports, the COVID-19 pandemic had a different impact depending on the local epidemiological context. Probably, mortality from CLD increased, especially in areas where the alcoholic etiology was predominant, or where a growing trend in mortality from alcoholic liver disease was already in place. Therefore, population-based studies on the direct and the indirect effects of the COVID-19 pandemic on CLD mortality are strongly warranted. Analyses adopting the multiple cause-of-death approach, and extended to deaths attributed to viral hepatitis and liver cancer, might be better suited to fully investigate the impact of the pandemic on complex long-term pre-existing trends.

Table 1 Age-standardized mortality rates (×100000) from cirrhosis, World Health Origination mortality database

	2021	2020	2019	2018	2017	2016	2015	2014	2013	2012
Antigua-Barbuda		3.4	2.7	4.5	3.6	0.9	2.9	6.8	1.9	10.1
Argentina		6.7	6.6	7.0	7.2	8.3	7.9	6.8	6.5	6.5
Armenia	10.9	12.2	10.6	12.0	16.0	19.5	16.6	17.1	14.9	16.5
Australia	4.6	4.3	4.1	4.0	4.0	3.7	4.1	3.9	3.9	3.3
Austria	8.6	8.5	8.1	7.9	8.4	9.0	9.5	9.4	9.9	10.7
Bosnia-Herzegovina		5.4	5.0	4.8	5.1	5.6		5.9		
Brazil		8.0	8.1	8.4	8.8	9.2	9.3	9.4	9.8	10.0
Bulgaria		15.6	15.8	14.3	14.5	14.8	14.4	13.4	13.1	13.8
Chile		9.7	9.4	9.9	11.3	12.4	11.7	11.8	12.3	13.5
Colombia		4.6	5.1	5.1	5.1	5.4	5.2	5.1	4.8	4.8
Costa Rica		5.2	6.9	6.2	6.3	6.3	6.5	6.1	6.2	5.2
Croatia		11.4	13.0		12.5	12.1	12.4	13.7	13.3	14.8
Cuba		10.8	10.5	10.0	9.8	9.0	8.9	8.5	8.2	7.9
Cyprus		3.6	3.9	3.2	3.2	2.7	3.2	3.6	4.0	2.8
Czechia	13.8	12.4	12.4	12.0	11.8	10.7	11.2	11.2	11.5	11.5

Denmark		6.7	7.2	6.5	7.2	7.1	6.7	7.6	7.6	8.4
Ecuador	12.5	11.8	13.2	13.7	14.0	14.6	14.5	13.3	13.1	13.7
Estonia	24.9	22.0	17.1	16.1	14.7	15.3	15.8	14.0	13.4	12.4
Finland		13.7	12.5	11.9	11.4	12.5	12.1	13.7	14.4	14.3
Georgia	7.2	7.0	7.0	7.5	5.6	5.5	7.4	8.0	6.0	6.4
Germany		9.2	8.7	8.9	9.1	9.3	9.1	9.0	9.5	9.3
Greece		3.3	3.3	3.1	3.5	3.6	3.6	3.7	4.1	3.8
Grenada	1.4	6.3	3.7	7.1	6.4	8.4	9.9	10.1	7.2	7.0
Guatemala		29.5	29.6	29.4	28.3	32.7	31.8	31.2	29.0	29.2
Iceland	2.7	1.8	1.4	1.9	2.5	1.6	2.7	1.5	1.7	1.4
Israel		2.0	2.5	2.4	2.3	2.5	2.7	2.3	2.7	2.8
Japan		4.9	4.7	4.7	4.7	4.4	4.4	4.5	4.7	4.7
Kazakhstan	38.6	40.2	38.5	38.5	41.4	46.4	50.5	55.2	57.9	
Latvia	18.9	12.4	12.1	13.6	11.5	13.6	12.8	12.5	12.6	12.4
Lebanon	2.6	2.1	1.9							
Lithuania	20.6	19.6	15.3	15.9	16.4	19.1	18.7	19.7	22.8	21.2
Luxemburg	7.0	7.8	7.2	8.0	7.2	8.9	6.7	8.0	7.5	9.1
Malaysia		1.7	2.0	2.0	1.8	1.8	2.0	1.9	1.8	1.7
Mauritius	10.9	10.7	8.6	7.9	8.0	8.8	8.9	8.9	10.3	9.7
Mexico		25.5	24.5	24.4	25.3	26.1	24.2	24.1	25.4	26.0
Mongolia	25.9	24.5	27.2	28.9	31.0	35.6				
Netherlands		3.0	2.7	2.8	2.9	2.9	2.8	2.7	2.6	2.9
Nicaragua		15.4	15.6	19.9	19.8	23.0	20.7	23.0	22.0	19.1
North Macedonia	6.9	5.0	4.9	4.7	6.0	5.2	5.9		6.3	5.4
Oman	1.5	1.5	2.0	1.5	2.6	2.2		1.6		
Paraguay		6.4	8.1	8.4	7.4	8.2	7.5	7.1	6.3	6.6
Peru		12.1	13.2	14.2	12.6	11.1	12.4	11.9	11.4	12.8
Poland		14.5	13.5	13.3	12.3	11.6	10.7	10.4	11.2	12.0
Qatar	1.6	2.1	1.2		2.9	1.8	0.6	1.7	1.2	2.1
Republic of Korea		7.1	6.8	7.3	7.5	7.8	8.1	8.0	8.3	8.8
Saint Lucia		3.7	3.6	6.2	4.2	5.9	8.9	12.1	7.9	9.1
Saint Vincent	3.1	4.5	5.6	6.9	5.7	4.9	2.5	5.4	7.0	7.2
Serbia	6.3	5.8	5.8	5.2	5.7	5.5	5.7	5.7	5.6	5.9
Singapore		1.7	2.2	2.2	2.3	2.4	2.2	2.6	2.5	2.4
Slovenia		9.9	10.2	10.9	9.6	9.9	11.4	13.5	16.2	17.9
Spain	4.6	4.4	4.5	4.6	4.9	4.9	5.4	5.3	5.6	5.8
Switzerland		3.6	3.8	3.9	3.9	4.1	4.4	4.4	4.5	5.0
United Arab Emirates		1.8	1.9	0.0						
UK		9.4	8.1	8.2	8.5	8.4	8.2	8.1	8.1	8.0
USA		10.9	9.2	9.0	8.9	8.7	8.8	8.5	8.2	8.0
Uruguay		3.3	3.0	3.3	3.3	3.7	4.3	4.4	3.8	3.9

FOOTNOTES

Author contributions: Fedeli U designed the outline, coordinated the writing of the paper, prepared figures/tables; Barbiellini Amidei C,

Casotto V, Grande E, Saia M, Zanetto A, and Russo FP collected the relevant bibliography and wrote the sections of the review; Barbiellini Amidei C and Casotto V contributed to "trends before the pandemic"; Zanetto A and Russo FP contributed to "COVID-19 and CLD"; Grande E and Saia M contributed to "CLD as a cause of deaths during the pandemic"; and all authors contributed to revising the first draft and approved the final version of the manuscript.

Conflict-of-interest statement: The authors declare they have no conflict of interest.

Open-Access: This article is an open-access article that was selected by an in-house editor and fully peer-reviewed by external reviewers. It is distributed in accordance with the Creative Commons Attribution NonCommercial (CC BY-NC 4.0) license, which permits others to distribute, remix, adapt, build upon this work non-commercially, and license their derivative works on different terms, provided the original work is properly cited and the use is non-commercial. See: https://creativecommons.org/Licenses/by-nc/4.0/

Country/Territory of origin: Italy

ORCID number: Ugo Fedeli 0000-0002-9939-3398.

S-Editor: Chen YL
L-Editor: Kerr C
P-Editor: Cai YX

REFERENCES

1 **GBD 2017 Cirrhosis Collaborators**. The global, regional, and national burden of cirrhosis by cause in 195 countries and territories, 1990-2017: a systematic analysis for the Global Burden of Disease Study 2017. *Lancet Gastroenterol Hepatol* 2020; **5**: 245-266 [PMID: 31981519 DOI: 10.1016/S2468-1253(19)30349-8]

2 **Asrani SK**, Larson JJ, Yawn B, Therneau TM, Kim WR. Underestimation of liver-related mortality in the United States. *Gastroenterology* 2013; **145**: 375-82.e1 [PMID: 23583430 DOI: 10.1053/j.gastro.2013.04.005]

3 **Fedeli U**, Avossa F, Guzzinati S, Bovo E, Saugo M. Trends in mortality from chronic liver disease. *Ann Epidemiol* 2014; **24**: 522-526 [PMID: 24861431 DOI: 10.1016/j.annepidem.2014.05.004]

4 **Sun Y**, Chang J, Liu X, Liu C. Mortality trends of liver diseases in mainland China over three decades: an age-period-cohort analysis. *BMJ Open* 2019; **9**: e029793 [PMID: 31712333 DOI: 10.1136/bmjopen-2019-029793]

5 **Ly KN**, Hughes EM, Jiles RB, Holmberg SD. Rising Mortality Associated With Hepatitis C Virus in the United States, 2003-2013. *Clin Infect Dis* 2016; **62**: 1287-1288 [PMID: 26936668 DOI: 10.1093/cid/ciw111]

6 **Fedeli U**. Increasing mortality associated with the more recent epidemic wave of hepatitis C virus infection in Northern Italy. *J Viral Hepat* 2018; **25**: 996-998 [PMID: 29532570 DOI: 10.1111/jvh.12893]

7 **Kim D**, Li AA, Gadiparthi C, Khan MA, Cholankeril G, Glenn JS, Ahmed A. Changing Trends in Etiology-Based Annual Mortality From Chronic Liver Disease, From 2007 Through 2016. *Gastroenterology* 2018; **155**: 1154-1163.e3 [PMID: 30009816 DOI: 10.1053/j.gastro.2018.07.008]

8 **Marjot T**, Moon AM, Cook JA, Abd-Elsalam S, Aloman C, Armstrong MJ, Pose E, Brenner EJ, Cargill T, Catana MA, Dhanasekaran R, Eshraghian A, García-Juárez I, Gill US, Jones PD, Kennedy J, Marshall A, Matthews C, Mells G, Mercer C, Perumalswami PV, Avitabile E, Qi X, Su F, Ufere NN, Wong YJ, Zheng MH, Barnes E, Barritt AS 4th, Webb GJ. Outcomes following SARS-CoV-2 infection in patients with chronic liver disease: An international registry study. *J Hepatol* 2021; **74**: 567-577 [PMID: 33035628 DOI: 10.1016/j.jhep.2020.09.024]

9 **Kim D**, Bonham CA, Konyn P, Cholankeril G, Ahmed A. Mortality Trends in Chronic Liver Disease and Cirrhosis in the United States, Before and During COVID-19 Pandemic. *Clin Gastroenterol Hepatol* 2021; **19**: 2664-2666.e2 [PMID: 34256143 DOI: 10.1016/j.cgh.2021.07.009]

10 **Paik JM**, Golabi P, Younossi Y, Mishra A, Younossi ZM. Changes in the Global Burden of Chronic Liver Diseases From 2012 to 2017: The Growing Impact of NAFLD. *Hepatology* 2020; **72**: 1605-1616 [PMID: 32043613 DOI: 10.1002/hep.31173]

11 **GBD 2019 Hepatitis B Collaborators**. Global, regional, and national burden of hepatitis B, 1990-2019: a systematic analysis for the Global Burden of Disease Study 2019. *Lancet Gastroenterol Hepatol* 2022; **7**: 796-829 [PMID: 35738290 DOI: 10.1016/S2468-1253(22)00124-8]

12 **Veracruz N**, Gish RG, Cheung R, Chitnis AS, Wong RJ. Global incidence and mortality of hepatitis B and hepatitis C acute infections, cirrhosis and hepatocellular carcinoma from 2010 to 2019. *J Viral Hepat* 2022; **29**: 352-365 [PMID: 35274406 DOI: 10.1111/jvh.13663]

13 **Global Burden of Disease Liver Cancer Collaboration**, Akinyemiju T, Abera S, Ahmed M, Alam N, Alemayohu MA, Allen C, Al-Raddadi R, Alvis-Guzman N, Amoako Y, Artaman A, Ayele TA, Barac A, Bensenor I, Berhane A, Bhutta Z, Castillo-Rivas J, Chitheer A, Choi JY, Cowie B, Dandona L, Dandona R, Dey S, Dicker D, Phuc H, Ekwueme DU, Zaki MS, Fischer F, Fürst T, Hancock J, Hay SI, Hotez P, Jee SH, Kasaeian A, Khader Y, Khang YH, Kumar A, Kutz M, Larson H, Lopez A, Lunevicius R, Malekzadeh R, McAlinden C, Meier T, Mendoza W, Mokdad A, Moradi-Lakeh M, Nagel G, Nguyen Q, Nguyen G, Ogbo F, Patton G, Pereira DM, Pourmalek F, Qorbani M, Radfar A, Roshandel G, Salomon JA, Sanabria J, Sartorius B, Satpathy M, Sawhney M, Sepanlou S, Shackelford K, Shore H, Sun J, Mengistu DT, Topór-Mądry R, Tran B, Ukwaja KN, Vlassov V, Vollset SE, Vos T, Wakayo T, Weiderpass E, Werdecker A, Yonemoto N, Younis M, Yu C, Zaidi Z, Zhu L, Murray CJL, Naghavi M, Fitzmaurice C. The Burden of Primary Liver Cancer and Underlying Etiologies From 1990 to 2015 at the Global, Regional, and National Level: Results From the Global Burden of Disease Study 2015. *JAMA Oncol* 2017; **3**: 1683-1691 [PMID: 28983565 DOI: 10.1001/jamaoncol.2017.3055]

14 **Liu Z**, Suo C, Mao X, Jiang Y, Jin L, Zhang T, Chen X. Global incidence trends in primary liver cancer by age at diagnosis, sex, region, and etiology, 1990-2017. *Cancer* 2020; **126**: 2267-2278 [PMID: 32201944 DOI: 10.1002/cncr.32789]

15 **Liu Z**, Jiang Y, Yuan H, Fang Q, Cai N, Suo C, Jin L, Zhang T, Chen X. The trends in incidence of primary liver cancer caused by specific etiologies: Results from the Global Burden of Disease Study 2016 and implications for liver cancer prevention. *J Hepatol* 2019; **70**: 674-683 [PMID: 30543829 DOI: 10.1016/j.jhep.2018.12.001]

16 **Huang J**, Lok V, Ngai CH, Chu C, Patel HK, Thoguluva Chandraseka V, Zhang L, Chen P, Wang S, Lao XQ, Tse LA, Xu W, Zheng ZJ, Wong MCS. Disease Burden, Risk Factors, and Recent Trends of Liver Cancer: A Global Country-Level Analysis. *Liver Cancer* 2021; **10**:

330-345 [PMID: 34414121 DOI: 10.1159/000515304]
17 **Fedeli U**, Avossa F, Goldoni CA, Caranci N, Zambon F, Saugo M. Education level and chronic liver disease by aetiology: A proportional mortality study. *Dig Liver Dis* 2015; **47**: 1082-1085 [PMID: 26315625 DOI: 10.1016/j.dld.2015.07.154]
18 **Kim D**, Li AA, Perumpail BJ, Gadiparthi C, Kim W, Cholankeril G, Glenn JS, Harrison SA, Younossi ZM, Ahmed A. Changing Trends in Etiology-Based and Ethnicity-Based Annual Mortality Rates of Cirrhosis and Hepatocellular Carcinoma in the United States. *Hepatology* 2019; **69**: 1064-1074 [PMID: 30014489 DOI: 10.1002/hep.30161]
19 **Paik JM**, Henry L, De Avila L, Younossi E, Racila A, Younossi ZM. Mortality Related to Nonalcoholic Fatty Liver Disease Is Increasing in the United States. *Hepatol Commun* 2019; **3**: 1459-1471 [PMID: 31701070 DOI: 10.1002/hep4.1419]
20 **Ning Q**, Wu D, Wang X, Xi D, Chen T, Chen G, Wang H, Lu H, Wang M, Zhu L, Hu J, Liu T, Ma K, Han M, Luo X. The mechanism underlying extrapulmonary complications of the coronavirus disease 2019 and its therapeutic implication. *Signal Transduct Target Ther* 2022; **7**: 57 [PMID: 35197452 DOI: 10.1038/s41392-022-00907-1]
21 **Dufour JF**, Marjot T, Becchetti C, Tilg H. COVID-19 and liver disease. *Gut* 2022; **71**: 2350-2362 [PMID: 35701093 DOI: 10.1136/gutjnl-2021-326792]
22 **Williamson EJ**, Walker AJ, Bhaskaran K, Bacon S, Bates C, Morton CE, Curtis HJ, Mehrkar A, Evans D, Inglesby P, Cockburn J, McDonald HI, MacKenna B, Tomlinson L, Douglas IJ, Rentsch CT, Mathur R, Wong AYS, Grieve R, Harrison D, Forbes H, Schultze A, Croker R, Parry J, Hester F, Harper S, Perera R, Evans SJW, Smeeth L, Goldacre B. Factors associated with COVID-19-related death using OpenSAFELY. *Nature* 2020; **584**: 430-436 [PMID: 32640463 DOI: 10.1038/s41586-020-2521-4]
23 **Pirola CJ**, Sookoian S. COVID-19 and non-alcoholic fatty liver disease: Biological insights from multi-omics data. *Liver Int* 2023; **43**: 580-587 [PMID: 36593576 DOI: 10.1111/Liv.15509]
24 **Rivera-Esteban J**, Manzano-Nuñez R, Broquetas T, Serra-Matamala I, Bassegoda O, Soriano-Varela A, Espín G, Castillo J, Bañares J, Carrión JA, Ginès P, Graupera I, Pericàs JM. Impact of the COVID-19 pandemic on the care and outcomes of people with NAFLD-related cirrhosis. *JHEP Rep* 2022; **4**: 100574 [PMID: 36061511 DOI: 10.1016/j.jhepr.2022.100574]
25 **Russo FP**, Burra P, Zanetto A. COVID-19 and liver disease: where are we now? *Nat Rev Gastroenterol Hepatol* 2022; **19**: 277-278 [PMID: 35301465 DOI: 10.1038/s41575-022-00607-9]
26 **Zanetto A**, Pelizzaro F, Campello E, Bulato C, Balcar L, Gu W, Gavasso S, Saggiorato G, Zeuzem S, Russo FP, Mandorfer M, Reiberger T, Trebicka J, Burra P, Simioni P, Senzolo M. Severity of systemic inflammation is the main predictor of ACLF and bleeding in individuals with acutely decompensated cirrhosis. *J Hepatol* 2023; **78**: 301-311 [PMID: 36150575 DOI: 10.1016/j.jhep.2022.09.005]
27 **Marjot T**, Webb GJ, Barritt AS 4th, Moon AM, Stamataki Z, Wong VW, Barnes E. COVID-19 and liver disease: mechanistic and clinical perspectives. *Nat Rev Gastroenterol Hepatol* 2021; **18**: 348-364 [PMID: 33692570 DOI: 10.1038/s41575-021-00426-4]
28 **Andrews N**, Stowe J, Kirsebom F, Toffa S, Rickeard T, Gallagher E, Gower C, Kall M, Groves N, O'Connell AM, Simons D, Blomquist PB, Zaidi A, Nash S, Iwani Binti Abdul Aziz N, Thelwall S, Dabrera G, Myers R, Amirthalingam G, Gharbia S, Barrett JC, Elson R, Ladhani SN, Ferguson N, Zambon M, Campbell CNJ, Brown K, Hopkins S, Chand M, Ramsay M, Lopez Bernal J. Covid-19 Vaccine Effectiveness against the Omicron (B.1.1.529) Variant. *N Engl J Med* 2022; **386**: 1532-1546 [PMID: 35249272 DOI: 10.1056/NEJMoa2119451]
29 **Russo FP**, Izzy M, Rammohan A, Kirchner VA, Di Maira T, Belli LS, Berg T, Berenguer MC, Polak WG. Global impact of the first wave of COVID-19 on liver transplant centers: A multi-society survey (EASL-ESOT/ELITA-ILTS). *J Hepatol* 2022; **76**: 364-370 [PMID: 34653592 DOI: 10.1016/j.jhep.2021.09.041]
30 **Schmitt CA**, Tchkonia T, Niedernhofer LJ, Robbins PD, Kirkland JL, Lee S. COVID-19 and cellular senescence. *Nat Rev Immunol* 2023; **23**: 251-263 [PMID: 36198912 DOI: 10.1038/s41577-022-00785-2]
31 **Simão AL**, Palma CS, Izquierdo-Sanchez L, Putignano A, Carvalho-Gomes A, Posch A, Zanaga P, Girleanu I, Henrique MM, Araújo C, Degre D, Gustot T, Sahuco I, Spagnolo E, Carvalhana S, Moura M, Fernandes DA, Banales JM, Romero-Gomez M, Trifan A, Russo FP, Stauber R, Berenguer M, Moreno C, Gonçalves J, Cortez-Pinto H, Castro RE. Cirrhosis is associated with lower serological responses to COVID-19 vaccines in patients with chronic liver disease. *JHEP Rep* 2023; **5**: 100697 [PMID: 36844943 DOI: 10.1016/j.jhepr.2023.100697]
32 **Office for National statistics**. Alcohol-specific deaths in the UK: registered in 2021. December 8, 2022. [cited 23 May 2023]. Available from: https://www.nisra.gov.uk/news/annual-alcohol-specific-deaths-statistics-2021#:~:text=Key%20points%201%20The%20total%20number%20of%20alcohol-specific,all%20alcohol-specific%20deaths%20registered%20in%202021.%20More%20items
33 **McCoy RG**, Campbell RL, Mullan AF, Bucks CM, Clements CM, Reichard RR, Jeffery MM. Changes in all-cause and cause-specific mortality during the first year of the COVID-19 pandemic in Minnesota: population-based study. *BMC Public Health* 2022; **22**: 2291 [PMID: 36474190 DOI: 10.1186/s12889-022-14743-z]
34 **Deutsch-Link S**, Jiang Y, Peery AF, Barritt AS, Bataller R, Moon AM. Alcohol-Associated Liver Disease Mortality Increased From 2017 to 2020 and Accelerated During the COVID-19 Pandemic. *Clin Gastroenterol Hepatol* 2022; **20**: 2142-2144.e2 [PMID: 35314353 DOI: 10.1016/j.cgh.2022.03.017]
35 **Kim D**, Alshuwaykh O, Dennis BB, Cholankeril G, Ahmed A. Trends in Etiology-based Mortality From Chronic Liver Disease Before and During COVID-19 Pandemic in the United States. *Clin Gastroenterol Hepatol* 2022; **20**: 2307-2316.e3 [PMID: 35811045 DOI: 10.1016/j.cgh.2022.05.045]
36 **Gao X**, Lv F, He X, Zhao Y, Liu Y, Zu J, Henry L, Wang J, Yeo YH, Ji F, Nguyen MH. Impact of the COVID-19 pandemic on liver disease-related mortality rates in the United States. *J Hepatol* 2023; **78**: 16-27 [PMID: 35988691 DOI: 10.1016/j.jhep.2022.07.028]
37 **Zhao Y**, Yeo YH, Samaan J, Lv F, He X, Gao N, Park J, Yang JD, Ayoub W, Odden MC, Ji F, Nguyen MH. Most excess years of potential life loss among individuals with cirrhosis during the pandemic were not related to COVID-19. *Gut* 2022 [PMID: 36282906 DOI: 10.1136/gutjnl-2022-328188]
38 **Kim D**, Alshuwaykh O, Dennis BB, Cholankeril G, Knowles JW, Ahmed A. Chronic liver disease-related mortality in diabetes before and during the COVID-19 in the United States. *Dig Liver Dis* 2023; **55**: 3-10 [PMID: 36182570 DOI: 10.1016/j.dld.2022.09.006]
39 **Spijker JJA**, Trias-Llimós S. Cause-specific mortality in Spain during the pandemic: educational differences and its impact on life expectancy. *Eur J Public Health* 2023; **33**: 543-549 [PMID: 36944099 DOI: 10.1093/eurpub/ckad036]
40 **World Health Organization**. International Guidelines for Certification and Classification (Coding) of COVID-19 as Cause of Death. April 20, 2020. [cited 23 May 2023]. Available from: https://www.who.int/publications/m

World Journal of Gastroenterology

Submit a Manuscript: https://www.f6publishing.com

World J Gastroenterol 2023 July 14; 29(26): 4174-4185

DOI: 10.3748/wjg.v29.i26.4174

ISSN 1007-9327 (print) ISSN 2219-2840 (online)

MINIREVIEWS

Progress in immunotherapy for neuroendocrine neoplasm of the digestive system

Wei-Xuan Pan, Xin-Mu Zhang, Shao-Long Hao, Wei Han

Specialty type: Oncology

Provenance and peer review: Unsolicited article; Externally peer reviewed.

Peer-review model: Single blind

Peer-review report's scientific quality classification

Grade A (Excellent): 0
Grade B (Very good): B, B
Grade C (Good): 0
Grade D (Fair): 0
Grade E (Poor): 0

P-Reviewer: Forns X, Spain; Klapper W, Germany

Received: May 4, 2023
Peer-review started: May 4, 2023
First decision: May 19, 2023
Revised: May 29, 2023
Accepted: June 13, 2023
Article in press: June 13, 2023
Published online: July 14, 2023

Wei-Xuan Pan, Shao-Long Hao, Wei Han, Department of General Surgery, Beijing Luhe Hospital, Capital Medical University, Beijing 101100, China

Xin-Mu Zhang, Department of Liver Surgery, State Key Laboratory of Complex Severe and Rare Diseases, Peking Union Medical College Hospital, Chinese Academy of Medical Sciences and Peking Union Medical College, Beijing 100730, China

Corresponding author: Wei Han, MD, Chief Doctor, Director, Professor, Department of General Surgery, Beijing Luhe Hospital, Capital Medical University, No. 28 South Xinhua Road, Tongzhou District, Beijing 101100, China. dr-han1972@mail.ccmu.edu.cn

Abstract

Neuroendocrine neoplasms (NENs) are rare heterogeneous tumors that can develop in almost any organ, with the digestive organs, including the gastrointestinal tract and pancreas being the most commonly affected sites. Despite the fact that advances in initial therapies have progressed, there is presently no recognized effective treatment for advanced NEN. Immune checkpoint inhibitors (ICIs) have shown superior efficacy in treating several types of solid tumors. Despite their successful role in the treatment of partial NENs, such as small cell lung cancer, and Merkel cell carcinoma, the role of ICIs in most of the NENs remains limited. Nevertheless, due to their specific anti-tumor mechanisms and acceptable safety profile, ICIs are a promising avenue for further study in NENs therapy. Recent clinical trials have illustrated that combination therapy with ICI is more efficient than monotherapy, and multiple clinical trials are constantly ongoing to evaluate the efficacy and safety of these combination therapies. Therefore, the purpose of this review is to provide a comprehensive summary of the clinical progress of immunotherapy in NENs affecting the digestive system, with a specific emphasis on the application of programmed cell death protein 1/programmed death receptor ligand 1 inhibitor. Furthermore, this review has an exploration of the potential beneficiary population and the inherent value of utilizing immunotherapy in the management of NENs.

Key Words: Immunotherapy; PD-1 inhibitor; Neuroendocrine neoplasm; Neuroendocrine tumor; Neuroendocrine carcinoma; Gastrointestinal; Pancreatic

©The Author(s) 2023. Published by Baishideng Publishing Group Inc. All rights reserved.

Core Tip: The application of immune checkpoint inhibitor (ICI) in neuroendocrine neoplasm (NEN) is regulated by the latest clinical practice guidelines. However, immunotherapy has achieved some breakthroughs for high-grade or advanced NENs of the digestive system, for which there is currently no effective drug therapy. In this regard, we investigated the causes of the heterogeneous efficacy of ICI in NEN with different grades, differentiation, and primary organs. This review summarizes the state-of-the-art progress and trend of clinical trials for different ICI-containing regimens in NENs of the digestive system, which will aid in the conduct of subsequent clinical trials and research of related mechanisms.

Citation: Pan WX, Zhang XM, Hao SL, Han W. Progress in immunotherapy for neuroendocrine neoplasm of the digestive system. *World J Gastroenterol* 2023; 29(26): 4174-4185
URL: https://www.wjgnet.com/1007-9327/full/v29/i26/4174.htm
DOI: https://dx.doi.org/10.3748/wjg.v29.i26.4174

INTRODUCTION

Neuroendocrine Neoplasms (NENs) are a group of rare and heterogeneous neoplasms that may originate from cells throughout the endocrine system[1]. These tumors express neuroendocrine markers and can occur in any part of the body, with a particular prevalence in the digestive system, such as the gastrointestinal (GI) tract and hepatopancreato-biliary organs. The majority of NENs are sporadic, and the exact etiology is still unknown[2]. However, less than 5% of gastroenteropancreatic (GEP) NENs occur as hereditary neoplastic syndromes, associated with gene deletions or alterations, including multiple endocrine neoplasia type 1 associated with duodenopancreatic NENs[3,4], and the von Hippel-Lindau syndrome associated with pancreatic NENs[5].

NENs of the digestive system consist of a range of tumor types, including well-differentiated neuroendocrine tumors (NETs), poorly differentiated neuroendocrine carcinomas (NECs), and mixed neuroendocrine-non-neuroendocrine neoplasms (MiNENs), which based on the degree of NEN malignancy according to the World Health Organization (WHO) classification of tumors of the digestive system (5th edition, 2019)[6]. NETs can be further classified and graded into three categories: Neuroendocrine tumors grade 1 (NET G1; low grade), NET G2 (intermediate grade), and NET G3 (high grade). This classification is determined based on the Ki-67 proliferation index and the number of mitotic figures per 2 mm^2. NECs include large cell-type NEC (LCNEC) and small cell-type NEC (SCNEC), both of which are considered as high grades. MiNENs exhibit varying degrees of differentiation and grades because they possess both neuroendocrine and non-neuroendocrine components in a single patch of neoplastic tissue, with each component accounting for ≥ 30%.

In recent years, with widespread improvements in clinical diagnosis and treatment, including endoscopy and imaging, there has been a noticeable worldwide upward trend in the detection of early-stage and non-functioning NENs from the digestive system. NEN incidence increased 6.4 times between 1973 (1.09/100000) and 2012 (6.98/100000), according to an analysis published in 2017 and based on 64971 NEN cases from the Surveillance Epidemiology and End Results database of the National Cancer Institute[7]. According to statistics from England, the incidence of NENs was about 9/100000 in 2018, and the incidences of pancreatic and rectal NENs have increased significantly[8]. Similarly, based on Taiwanese data, the incidence of NENs in digestive organs increased from 0.15 per 100000 people in 1996 to 2.36 per 100000 people in 2015[9].

The most prevalent primary sites have also been shown to vary across different regions. In the United Kingdom, the order of frequency among all primary sites of GEP-NETs, was as follows: Small intestine (25.6%), appendix (23.6%), pancreas (17.7%), colon (9.8%), stomach (9.8%), and rectum (7.8%)[10]. In China, however, the order was different, with the pancreas (31.5%), rectum (29.6%), and stomach (27.0%) being the common sites. The small intestine (5.6%) and colon (3.0%) accounted for relatively small proportions of NENs in this region[11]. Compared with others, gallbladder NENs are more scarce and account for only 0.5% of all NENs[12]. NETs are prone to metastasis to the liver; however, the liver itself is rarely the primary site of NENs, accounting for only 0.46% of primary liver tumors[13]. Owing to the rarity of the diagnosis and a lack of valid statistics for relevant cases, the quality of published data is limited, and the epidemiology of patients with digestive MiNENs remains unknown[14].

Immune checkpoint inhibitors (ICIs) have potent, strong anti-tumor activity in the management of various cancer types. These inhibitors, which target programmed cell death protein 1 (PD-1) or programmed death receptor ligand 1 (PD-L1), are profoundly researched and widely used in tumor immunotherapy. Both PD-1 and PD-L1 targeted antibodies relieve the functional inhibition of T cells and reactivate the immune response against cancer cells. Several α-PD-1 (*e.g.*, palivizumab, nivolumab, and toripalimab) and α-PD-L1 antibodies (*e.g.*, atezolizumab and durvalumab) have been licensed by the Food and Drug Administration (FDA) for the treatment of multiple forms of tumor owing to their efficacy in clinical trials. More than 10 different cancer types have been authorized for therapy with single-agent PD-1 or PD-L1 monoclonal antibodies, with objective response rates (ORR) ranging from 15%-20%[15]. However, the PD-1 or PD-L1 axis is not the only signaling access that contributes to tumor immunosuppression, and the inhibition of this pathway alone is insufficient to effectively elicit anti-tumor immunity. Consequently, several combination immunotherapies, such as PD-1/PD-L1 antibodies combined with chemotherapy, radiotherapy, angiogenesis inhibitors, other ICIs, gut microbiota transplantation, and metabolic modulators, may improve the overall anti-tumor activity and raise the response rates (RRs) of NENs of the digestive system[16].

Herein, we comprehensively summarize the clinical application status and research progress of immunotherapy drugs, mainly PD-1 and PD-L1 inhibitors, for the treatment regimen of NENs of the digestive system, which might provide more potent and widely applicable regimens as well as direction for subsequent studies.

IMMUNOTHERAPY AND NENS OF THE DIGESTIVE SYSTEM

The use of immunotherapy to treat NENs of the digestive system is still in the clinical exploration phase and is not yet recommended as the preferred regimen. This is because available clinical trials have demonstrated low ORRs to immunotherapy using PD-1 or PD-L1 inhibitors. Currently, several immunotherapeutic strategies for NENs are undergoing clinical trials, including ICI monotherapy, dual ICI therapy, anti-angiogenesis with ICIs, and chemotherapy with ICI. Table 1 provides a summary of relevant data from the clinical trials mentioned below.

Application status of ICIs in NENs of the digestive system

According to the National Comprehensive Cancer Network Clinical Practice Guidelines of Neuroendocrine and Adrenal Tumors (version 2.2022), ICIs are not currently available as a preferred regimen for the systemic treatment of patients with unresectable locally advanced or distant metastases from NEN. In the preferred regimen, the molecularly targeted drug everolimus is more effective in advanced G1 or G2 NET. In phase III clinical research, mPFS in the everolimus group was longer than in the placebo group (11 *vs* 3.9 mo; $P < 0.00001$) and decreased recurrence rate as well as mortality by 52%[17]. Somatostatin analogs, such as octreotide and lanreotide, are mainly used in the treatment of NENs that are somatostatin receptor-positive, slow-growth as well as Ki-67 ≤ 10% and are usually combined with molecularly targeted drugs to control the symptom of functional NETs. Chemotherapy is typically the preferred treatment option for G3 NET and NEC. The ORR of cisplatin or carboplatin combined with etoposide in the treatment of advanced NECs ranged from 30.8%-63.2%, and the median overall survival (mOS) was between 8.9-12.5 mo[18,19]. Temozolomide combined with capecitabine has more efficacy in pancreatic NET (pNET) than in GI NET, and the mPFS and mOS in high-grade NET were longer than those in NEC (15.3 mo *vs* 3.3 mo; 22 mo *vs* 4.6 mo)[20].

Although most NENs have not demonstrated the greatest effectiveness, ICIs can still be used as the primary treatment for well-differentiated grade 3 NETs, extrapulmonary poorly differentiated NECs, and MiNENs. Patients with advanced tumor mutational burden-high [tumor mutational burden (TMB)-H], microsatellite instability-high (MSI-H), or mismatch repair deficiency (dMMR) tumors, as identified by an FDA-approved test performed after prior therapy, may be candidates for the PD-1 inhibitor pembrolizumab if no other appropriate options for therapy are available. For biologically favorable or unfavorable locally advanced or metastatic G3 NETs (unresectable with clinically considerable tumor burden or indication of disease progression), pembrolizumab is the primary treatment[21,22]. In the event of extrapulmonary, locoregional, unresectable, or metastatic NECs/MiNENs, pembrolizumab can also be considered for systemic therapy[21,22,23]. Nivolumab combined with ipilimumab (category 2B), which is known as a type of dual ICI therapy, is a recommended option for locally progressed or metastatic G3 NETs with unfavorable biologies[24]. Similarly, if the illness advances after chemotherapy, ipilimumab paired with nivolumab (category 2B) might also be taken into consideration for extrapulmonary poorly differentiated (LCNEC/SCNEC) or unknown primary tumors.

However, the Guidelines of the Chinese Society of Clinical Oncology for Neuroendocrine Neoplasms (version 2022) only suggest the use of ICIs as a treatment option for metastatic NECs. Specifically, pembrolizumab is recommended as a first-line treatment (category 3) or as a level-2 recommendation for the second-line treatment of metastatic NEC in patients with performance status (PS) scores of 0-2 and the presence of dMMR, MSI-H, or TMB-H (category 1A)[25]. In addition, ICIs such as ipilimumab, combined with nivolumab[24] or other ICIs[26-28], may be considered for patients with metastatic NECs who have previously received systemic therapy and continue to experience disease progression and who lack standard treatment options. For these patients, ICIs are recommended as a level-3 recommendation for second-line treatment (category 3A).

ICI monotherapy

ICI monotherapy has shown remarkably low RRs in NENs, especially in poorly differentiated ones. The Keynote-028 trial demonstrated the actual clinical outcomes of pembrolizumab monotherapy in patients who had carcinoid tumors and pNET with PD-L1 expression[29]. In the pNET cohort, 16 PD-L1-positive patients out of 106 pNET patients received pembrolizumab monotherapy with ORRs of 6.3% [95% confidence interval (CI): 0.2%-30.2%], only one patient confirmed partial response (PR), 31% developed stable disease (SD) lasting more than 6 mo, and 12-mo progression-free survival (PFS) and overall survival (OS) rates of 27% and 87%, respectively. However, studies comparing the efficiency of pembrolizumab in patients with or without PD-L1 expression reported no significant differences in the disease control rate (DCR), PFS, or OS between the two groups[30]. Among 29 patients who had experienced prior treatments, 48% and 34% had GI and pancreatic NENs, respectively. Only one patient (95%CI: 0.1-17.8%) with an esophageal LCNEC had an objective PR that persisted for 13 mo before he discontinued his participation in the study. Six patients (95%CI: 7.9-39.7%) had SDs, and DCR was 24.1%[30]. In an open-label phase II trial, pembrolizumab single-agent therapy in 107 well-differentiated NETs of the lung, appendix, small intestine, colon, rectum, or pancreas with previously failed standard treatments resulted in an ORR of only 3.7% (95%CI: 1.0-9.3). The median PFS (mPFS) was 4.1 mo (95%CI: 3.5-5.4), the estimated PFS rate at 6 mo was 39.3%, and the mOS was 24.2 mo. Among 40 patients with pancreatic NETs, 25 patients with small intestine NETs, and 18 patients with other GI NETs, only 4 patients had a PR as assessed by Response Evaluation Criteria in Advanced Solid Tumors version 1.1, including cases in the pancreas (3) and rectum (1); all of them were PD-L1 negative. It is noteworthy that the response rate in the pancreatic NETs subgroup was 7.5%[31]. In another

Table 1 Clinical trials mentioned in the review

Intervention	Study phase	Actual enrollment	NEN type of the digestive system	ORR (%)	mPFS (mo)	mOS (mo)	Ref.
Pembrolizumab	I	16	pNET	6.3	4.5	21.0	[29]
	II	29 (14 GI, 10 pancreas)	GI-NEN, pNEN	3.4	2.0	4.7	[30]
	II	107 (83 GEP)	WD NETs	3.7	4.1	24.2	[31]
Toripalimab	Ib	40 (23 GI, 9 pancreas)	GI-NEN	13.0	2.5	7.8	[32]
			pNEN	22.0			
Nivolumab	II	185 (93 GEP)	GEP-NEC	7.0	1.8	7.2	[33]
Spartalizumab	II	95 NETs (32 GI, 33 pancreas); 21 GEP-NECs	GI NET	3.1	3.8	Not estimable	[34]
			pNET	3.0			
			GEP-NEC	4.8	1.8	6.8	
Avelumab	II	27 (21 GEP)	GEP-NET	--	3.3	14.2	[35]
Nivolumab + Ipilimumab	--	34 (21 from digestive organs)	NENs	14.7	1.0	5.0 (from treatment initial); 14.0 (from diagnosis)	[36]
	II	32 (15 GI)	Non-pNETs	25.0	4.0	11.0	[37]
	II	19 (9 from digestive organs)	High-grade NENs	26.0	2.0	8.7	[38]
	II	185 (93 GEP)	GEP-NEC	14.9	1.9	5.8	[33]
	--	11	Metastatic EP-NEC (mainly of GEP origin)	--	8.5	Not reached	[39]
Durvalumab + Tremelimumab	II	123 (31 GI, 32 pancreas, 33 GEP)	G1/G2 GI-NETs	0	5.8	29.5	[40,41]
			G1/G2 pNETs	6.3	5.5	23.8	
			G3 GEP-NENs	9.1	2.4	5.9	
Atezolizumab + Bevacizumab	II	40 (20 pNET, 20 non-pNET)	pNET	20.0	19.6	30.1	[44,45]
			Non-pNET	15.0	14.9	Not reached	
Pembrolizumab + Lenvatinib	II	20 (10 GI)	GI-NEN	10.0	10.0	--	[46]
Pembrolizumab + Irinoteca/Paclitaxel	II	22 (16 GI)	GI-NEC	9.0	2.0	4.0	[47]
Nivolumab + Tezolomide	II	15 (12 evaluable and 7 GEP)	GEP-NET	25.0	--	--	[48]
Nivolumab + Cisplatin/Carboplatin	II	38 (31 GEP)	G3 NENs	54.1	5.7	13.9	[49,50]

WD: Well-differentiated; NET: Neuroendocrine tumor; NEN: Neuroendocrine neoplasm; NEC: Neuroendocrine carcinoma; GEP: Gastroenteropancreatic; SCLC: Small cell lung cancer; MCC: Merkel cell carcinoma; pNET: Pancreas NET; ORR: Objective response rate; mOS: Median overall survival; mPFS: Median progression-free survival; EP-NEC: Extrapulmonary neuroendocrine carcinoma.

multicenter phase Ib clinical trial investigating toripalimab for metastatic or recrudescent NENs where standard therapies had failed, 40 patients were enrolled. Of these, for ex-pancreatic GI-derived, pancreatic, and nondigestive NENs, the ORRs were 13.0% (3/23), 22.2% (2/9), and 37.5% (3/8), respectively[32].

The effectiveness of ICI monotherapy in treating NECs has also been proven in a number of clinical trials. In a phase II trial involving 185 patients with NECs (93 were GEP) and randomly assigned (1:1) to receive nivolumab monotherapy or nivolumab combined with ipilimumab. In the monotherapy group, the ORR at 8 wk, mPFS, and mOS were 7.2% (95%CI: 2.7-15.1), 1.8 mo (95%CI: 1.7-2.0), and 7.2 mo (95%CI: 3.7-14.1), respectively. However, these results indicated that the therapeutic effect was not ideal[33]. Spartalizumab, another anti-PD-1 agent, was evaluated in a clinical trial involving 21 patients with poorly differentiated GEP-NECs and 95 patients with metastatic G1 or G2 NETs (32 GI and 33 pancreatic), all of whom had received prior treatments for their advanced diseases. The ORR in the GI NET, pNET, and GEP-NEC groups was 3.1% (95%CI: 0.1-16.2), 3.0% (95%CI: 0.1-15.8), and 4.8% (95%CI: 0.1-23.8), respectively. In the NET cohort, the mPFS, 12-mo PFS, and OS rates were 3.8 mo, 19.5% (95%CI: 11.6-28.9), and 73.5% (95%CI: 63.0-81.4) respectively. For the GEP-NEC cohort, the respective values were 1.8 mo, 0%, and 19.1% (95%CI: 4.8-40.6)[34]. Although the efficacy of spartal-

izumab for digestive NEN treatment is limited and not worthy of further investigation, its AEs are mild and manageable. Fatigue (29.5%) and nausea (10.5%) were the most frequently reported spartalizumab-related AEs that emerged during the trial of the NET cohort; they were mainly distributed in the grade 1/2, while elevated aspartate/alanine aminotransferase levels (14.3% each) were common in the GEP NEC group[34]. Other trials, however, reported contrary conclusions regarding the use of ICI monotherapy. Two trials of avelumab monotherapy, which enrolled 27 patients in total, had 21 GEP-NET, with none achieving OR but only 33% obtaining SD. AEs related to avelumab were observed in 58% of patients, including grade 3-4 AEs in 3 cases, leading directly to trial termination[35].

The aforementioned ICI monotherapy regimens have indicated mild anti-tumor activity with neither NET nor NEN of the digestive system. Nonetheless, the AEs were manageable, which made them relatively safe and applicable under most conditions. It is speculated that the severity of adverse reactions may be correlated with the efficacy. In pembrolizumab treatment, for instance, only 21.5% of treatment-related adverse reactions occurred at grade ≥ 3, while the frequent adverse reactions were malaise (22.4%) and diarrhea (13.1%)[31]. Therefore, combination therapies to improve the efficacy of ICIs against NENs in the digestive system have emerged as a major research direction.

COMBINED IMMUNOTHERAPY FOR NENS OF THE DIGESTIVE SYSTEM

Dual ICI therapy

Cytotoxic T lymphocyte-associated antigen-4 (CTLA-4) antibody, another type of ICI, have mechanisms of action complementary to those of PD-1 and PD-L1 antibodies. The binding of CTLA-4 and CTLA-4 antibodies to the surface of activated T cells indirectly promotes the activation and proliferation of T cell development by relieving the inhibitory effect of antigen-presenting cells on T cells. One preliminary retrospective evaluation for the treatment with ipilimumab plus nivolumab reported ORR, DCR, and mPFS of 15%, 41.2%, and one month (95%CI: 0.54-1.46 mo), respectively, in 34 patients with G3 NENs (79% NEC and 21 from digestive organs) who had previously undergone at least one cytotoxic chemotherapy regimen and, on average, two prior lines of treatment[36]. These findings suggest that dual ICI therapy has therapeutic effects on aggressive NECs that progress after chemotherapy, as well as in heavily pre-treated NENs. The S1609DART trial established the combination of ipilimumab and nivolumab as an option for extrapulmonary poorly differentiated (LCNEC/SCNEC) or unknown primary tumors. Results of the trial revealed that the ORR of 32 cases was 25% (95%CI: 13%-64%), and the median overall survival (mOS) was 11 mo. The ORR was 44% for non-pancreatic (non-p) high-grade NECs (8/18, CR = 1, PR = 7), including lung primaries[37]. Furthermore, in the following research on high-grade NENs, 19 patients were involved, of which 11% (each) were from the pancreas, gastroesophageal junction, and rectum. The ORR of this cohort was 26% (95%CI: 11-45%), the DCR was 32% (95%CI: 13%-57%), and the 6-month PFS was 32% (95%CI: 16%-61%); however, durable control was observed in patients with long-term diseases[38]. Based on the existing outcomes, Mohamed *et al*[39] conducted a retrospective study of 70 metastatic EP-NEC cases, mostly derived from GEP, of which 11 received Nivolumab in combination with Ipilimumab. The PFS (56.5 d, 47 d, and 258 d) and OS (not reached, 18.7 mo and 10.5 mo) were compared among patients treated with ICI monotherapy (8 patients), cytotoxic agents (23 patients) and dual ICI therapy. Thus, dual ICI therapy did show some improvement in high-grade NENs, in line with previous findings.

However, not all dual ICI therapies elicit a significant response or treatment effect. The final results from a prospective Phase II study of durvalumab plus tremelimumab in 123 patients with NENs who experienced disease progression and failure to respond to standard therapy administration were presented at the ENETS Annual Conference 2022. The cases were divided into four cohorts based on grading and primary sites: 27 patients with typical/atypical lung carcinoids for Cohort 1 (C1), 31 patients with G1/G2 GI-NETs for C2, 32 patients with G1/G2 pNETs for C3, and 33 patients with G3 GEP-NENs (91% NECs) for C4. The ORRs for the last three cohorts were 0%, 6.3%, and 9.1%, respectively, and the mPFSs were 5.8, 5.5, and 2.4 mo, in the same order. The median OSs were 29.5 mo, 23.8 mo, and 5.9 mo, respectively[40]. The 9-month DCRs for these cases were 22.8% (95%CI: 16.0-30.8), and 35.5% (95%CI: 20.5-53.0), 25% (95%CI: 12.6-41.7), and 6.1% (95%CI: 1.3-18.1) for C2 to C4, respectively[41]. Therefore, this study showed that the therapeutic effectiveness of dual ICI therapy in well-differentiated NENs was limited after the failure of standard treatment and had a relatively lower ORR. Only G3 GEP-NEN or NEC cases showed a modest survival benefit. In the NIPI-NEC phase II trial, 185 patients with platinum-refractory disease, including 93 patients with GEP-NEC, were enrolled. They were randomly assigned to receive nivolumab monotherapy or nivolumab plus ipilimumab, with ORR at eight weeks as the primary outcome measure. The cohort of nivolumab combined with ipilimumab in the trial demonstrated a prominent ORR of 14.9% (95%CI: 8.2-24.2) when compared to the nivolumab single-agent cohort of 7.2% (95%CI: 2.7-15.1); however, PFS was 1.9 mo (95%CI: 1.6-2.1) *vs* 1.8 mo (95%CI: 1.7-2.0), OS was 5.8 (95%CI: 3.3-7.6) *vs* 7.2 mo (95%CI: 3.7-14.1)[33]. Thus, most patients with NECs are not eligible for ICIs monotherapy, and the anti-tumor activity of dual ICIs therapy for both NETs and NECs needs further validation.

ICI combined with targeted anti-angiogenesis

Patients with refractory tumors or those who are chemo-intolerant have a high-quality option to de-chemotherapy in the form of ICIs combined with anti-angiogenic medications. Basic research has demonstrated a synergistic impact between ICIs and anti-angiogenic medications, encouraging angiogenesis in healthy tissues and boosting anti-tumor immunity [42]. Besides, anti-angiogenic targeted medications not only prevent angiogenesis in tumor tissue but also support the efficacy of ICIs by relieving the negative regulatory process of vascular endothelial growth factor (VEGF) in the immune microenvironment. They also influence lymphocyte and macrophage infiltration into tumor tissue, thereby alleviating the suppression of the tumor immune system[43].

Daniel and colleagues examined atezolizumab with bevacizumab combination therapy in G1/G2 pNET and non-pNET patients who had progressed under any previous therapy. Preliminary results showed that ORR, mPFS, and 1-year PFS of the two cohorts with 20 patients each were 20% (95%CI: 6%-44%) and 15% (95%CI: 3%-38%), and 19.6 mo (95%CI: 10.6-NR), and 14.9 mo (95%CI: 6.1-NR), 75% and 52%, respectively. These findings manifested that pNET patients might benefit more from this drug application regimen than non-pNET patients[44]. More recently, the MD Anderson Cancer Center released the final trial results showing that the ORR of the two groups remained consistent with the previous data; however, the PFS of the pNET and the non-pNET group descended to 14.9 mo (95%CI: 4.4-32.0) and 14.2 mo (95%CI: 10.2-19.6), respectively[45].

Al-Toubah *et al*[46] tested an alternative regimen, involving pembrolizumab plus lenvatinib, with efficacy in 20 patients with well-differentiated GI or thoracic NETs (including 9 of the small intestine, and 1 of cecal), and the response rate of the treatment was unsatisfactory. Among them, only one NET presented with PR, and the mPFS was 10 mo (95%CI: 5.9-14.1) in the small intestine, and the adverse effect rate was also high. Potentially related or related grade 3 AEs, were experienced by 12 patients, 14 patients required dose reduction or discontinuation of one of the drugs. Consequently, further research into this regimen was not deserved since it did not demonstrate substantial effectiveness for GI-NET. Therefore, it may be more worthwhile to delve into the safety and beneficial effects of ICIs paired with anti-angiogenesis in NECs from the digestive organs.

ICI combined with chemotherapy

Immunotherapy paired with chemotherapy has been successfully applied in the treatment of non-small cell lung cancer, gastric cancer, and esophageal cancer due to their synergistic mechanisms. Moreover, to expand the scope of application, some clinical study outcomes on the application of this sort of regimen in the NEN of the digestive system have been published.

The result of a phase II trial reported by Chan *et al*[47] revealed an unsatisfactory treatment response rate. The trial included twenty-two patients with extrapulmonary poorly differentiated NECs who had experienced disease progression after prior first-line therapy. These patients participated in a clinical trial investigating the combination of pembrolizumab and chemotherapy combination (16 of these patients had a primary GI site), 17 (77%) were treated with irinotecan, and 5 (23%) were treated with paclitaxel. The ORR was 9% among the patients, PR was achieved only in 2 cases, SD in 14% of cases, and PD in 60%. As inferred from the results, after biomarker selection, combination therapy with pembrolizumab and chemotherapy may improve treatment efficacy in cases of poorly differentiated GI-NEC.

In another phaseIIclinical study, twelve of the fifteen patients with advanced NET who were enrolled in and treated with nivolumab and temozolomide could be assessed for their response to this treatment, with the major locations being six small bowels, one pancreas, and five bronchial tubes[48]. According to the interim efficacy results, 25% of patients (3/12) had the best response of PR, 67% of patients (8/12) had SD, and one patient (8%) had PD.

The NICE-NEC study, which included 38 patients with advanced or irresectable gastroenteritis or G3 NENs of unknown origin, was the first to assess the efficacy of first-line chemotherapy plus ICIs in G3 NENs. Of these patients, 81.6% were GEP-NENs, and 68% were NECs, that received nivolumab combined with cisplatin or carboplatin[49]. The latest results, presented at the ESMO Congress 2022, confirmed the combinations had relatively promising therapeutic action, with an ORR and mPFS of survivors of 54.1% and 5.7 mo (95%CI: 5.1-9 mo), respectively[50]. Preliminary findings suggest that adding nivolumab to chemotherapy for G3 NENs has conceivable effectiveness without noticeably raising the toxicity profile of preferred standard chemotherapy.

Naturally, in certain rare circumstances, the combined effects of immunotherapy and chemotherapy may be therapeutically productive for some patients with terminal NECs, or those who have failed to respond to initial therapies. Chorath *et al*[51] reported a female case with metastatic high-grade NEC of the gallbladder who received immunochemotherapy treatment. A substantial decrease in liver metastases was observed following six cycles of comprehensive treatment with etoposide, carboplatin, nivolumab, and ipilimumab with a sustained response. However, further investigation is needed to comprehend the specific mechanisms and biomarkers that predict treatment efficacy. This survival benefit occurred in the absence of known predictive biomarkers to immunotherapy (PD-L1 status, mismatch repair status, and TMB).

Contrary to conventional perception, chemotherapy drugs can induce immunogenic tumor cells to undergo apoptosis, which mobilizes antigen-presenting cells and primes tumor-specific immune responses[52]. This fundamental principle underlies the previously described synergistic impact and the advantages of chemotherapy paired with ICIs in the application of NEN from the digestive system.

Table 2 provides an overview of ongoing clinical trials, which can be tracked to obtain the latest research progress of immunotherapies in NENs of the digestive systems.

BIOMARKERS FOR PREDICTING IMMUNOTHERAPY RESPONSE

MSI/dMMR, TMB, and PD-L1 expression are key biomarkers used to judge the potential benefit of ICIs for patients. Among these, MSI-H/dMMR, and TMB-H are independent adverse prognostic indicators[53]. However, the incidence of MSI-H/dMMR in NENs is relatively low, reported to be present in only 8 out of 152 GEP-NECs (5.3%) and only 1 in 29 G3 NETs (3.4%)[54]. TMB is the ratio of non-synonymous mutations in somatic cells per megabase pair of a certain genomic region. Although TMB is linked to the prognostic status of patients after ICIs therapy for the majority of malignancies, the selection of detecting genes will directly impact the TMB calculation's outcomes[55]. It is unlikely that there is an exact universal value that defines TMB-H in a way that can predict the benefit of ICI in all types of cancer[56]. In a number of published trials, PD-L1 positive patients treated with ICIs had a higher ORR than PD-L1 negative patients,

Table 2 Ongoing clinical trials related to immune checkpoint inhibitors in neuroendocrine neoplasms of the digestive system

Indentifier of Clinical Trails	Intervention	Study phase	Primary outcome measures	Estimated or actual enrollment	Trial status	Estimated study completion date	Condition related to NENs of the digestive system
NCT04079712	Nivolumab + Ipilimumab + Cabozantinib	II	overall response rate	30	Active, not recruiting	October 2023	NECs: Excluding SCLC and MCC
NCT03980925	Nivolumab + Platinum-doublet chemotherapy	II	OS at 12 mo	38	Active, not recruiting	December 2023	G3 NENs: GEP or unknown primary site
NCT04197310	Cabozantinib + Nivolumab	II	ORR	35	Active, not recruiting	December 2023	WD-NET: Non-pancreatic (*i.e.*, carcinoid) origin
NCT03290079	Pembrolizumab + Lenvatinib	II	ORR	28	Active, not recruiting	January 2024	NETs: WD small bowel or colon origin, including unknown primary, excluding pNENs
NCT04400474	Cabozantinib + Atezolizumab	II	ORR	93	Active, not recruiting	March 2024	WD G1/2 NET: Digestive system; G3 NEN: Excluding SCLC
NCT04579757	Surufatinib + Tislelizumab	Ib/II	DLT, ORR	135	Active, not recruiting	June 2024	G1/2 NETs: Thoracic or GEP origins
NCT04525638	Nivolumab + 177Lu-DOTATATE	II	overall response rate	30	Recruiting	September 2024	G3 NET or NEC of GEP, lung, and unknown primary site
NCT05058651	Atezolizumab + Platinum drug (cisplatin or carboplatin) + Etoposide	II/III	OS	189	Recruiting	October 2024	NEC: Extrapulmonary
NCT05113355	Chidamide + Sintilimab	II	ORR	23	Recruiting	November 2024	High-grade NEN, advanced and metastatic
NCT04969887	Nivolumab + Ipilimumab	II	CBR, 6 mo PFS	240	Recruiting	December 2024	NECs and G3 NETs: Independent of primary site, excluding SCLC
NCT04701307	Dostarlimab + Niraparib	II	6 mo PFS, 3 mo ORR	48	Active, not recruiting	May 2025	NECs: Excluding prostate origin
NCT03475953	Avelumab + Regorafenib	I/II	Phase I: Recommended dose of regorafenib; Phase II (cohort G): CR or PR	747 (only cohort G consists of GEP-NETs)	Recruiting	December 2025	G2/3 GEP-NETs
NCT05746208	Lenvatinib + Pembrolizumab	II	ORR	29	Not yet recruiting	July 2027	WD G3 NET: GIsite and pancreas primary
NCT05289856	Avelumab + Cabozantinib	II	DCR, CR, PR, SD	30	Recruiting	December 2025	G3 NET: Excluding MCC and SCLC
NCT05627427	Surufatinib + Sintilimab	II	PFS	60	Recruiting	December 2024	G3 NET and NEC: Metastatic and advanced
NCT05262556	NP-101 (TQ Formula) + Nivolumab + Ipilimumab	I	CR, PR, SD	10	Recruiting	December 2024	GEP-NET, GEP-NEC: Poorly differentiated

CR: Complete response; CBR: Clinical benefit rate; DCR: Disease control rate; DLT: Dose-limiting toxicity; ORR: Objective response rate; OS: Overall survival; PFS: Progression-free survival; PR: Partial response; WD: Well differentiated; NET: Neuroendocrine tumor; NEN: Neuroendocrine neoplasm; NEC: Neuroendocrine carcinoma; GEP: Gastroenteropancreatic; SCLC: Small cell lung cancer; MCC: Merkel cell carcinoma; pNET: Pancreas NET; GI: gastrointestinal; G1, 2, 3: Grade 1, 2, 3.

which indicated that PD-L1 expression may be relevant to the efficacy of immunotherapy[45]. However, PD-L1 expression appears quite heterogeneous across different studies[57], even though some studies revealed no relevance between the effectiveness of ICIs and PD-L1 expression[30,31,40]. Reasons for these results may be subject to limitations due to factors such as different methods of analysis, defined cutoffs, and the freshness of biopsy tissue obtained[58]. Therefore, based on identifying the expression of PD-L1, investigate the content of other predictive biomarkers to provide patients with the best immunotherapy prediction possible.

In recent years, somatic mutation analysis of NETs has emerged as a novel approach for identification and prediction. Unlike conventional monoanalytic biomarker testing, mRNA-based liquid biopsy is a non-invasive genetic testing method. The NET transcriptome signature (NETest), a pre-spotted PCR plate that targets 51 genes, measures the amount of tumor-derived mRNA extracted from a patient's blood using PCR[59]. Compared to CGA, the diagnostic accuracy of GEP-NENs with NETest is significantly better (99% *vs* 21%-36%), and it also has good sensitivity and specificity for evaluating the course and prognosis of NENs[60]. However, despite these advancements, the gold standard for NETest has not been established in clinical practice preventing its use as a routine test for NEN and limiting its ability to completely replace biopsy procedures.

Future research should prioritize the integration of data on the circulating tumor DNA, T-cell regulatory factors, and other characteristics of NEN patients who will receive immunotherapy. By employing multidimensional and dynamic combinations of biomarkers, researchers can enhance the predictive effect and fully elucidate the potential causes of patients' poor responses to ICIs.

DISCUSSION

It is necessary for the body to trigger an appropriate anti-tumor immune response through the infiltration of immune cells into the tumor immune microenvironment (TIME). The strength of individual anti-tumor immunity depends significantly on the quantity and variety of T cells[61]. As a result, there is now broad acceptance that effector T cell plays an irreplaceable role in the anti-tumor response[62].

Malignancies that exhibit significant tumor-infiltrating lymphocyte (TIL) infiltration, high PD-L1 expression, potential genetic susceptibility, and the existence of an active anti-tumor immune response, often known as the hallmarks of "hot tumors," are more receptive to immunotherapy[63]. Although recent outcomes of clinical trials suggest that the efficacy of ICIs for NEN of the digestive system fell short of expectations, considerable TIL infiltration has been observed in various NECs, including pNECs[64]. Moreover, the likelihood that NEN will match the TIME of hot tumors increases with NEN grade. In a study of 244 patients with GEP-NEN, the G3 NEN cohort contained considerably more patients with high TILs infiltration than the G1/G2 NEN group (50% *vs* 17.1%)[65]. PD-L1-expressing GEP-NEC more frequently exhibited T cell exhaustion and an abundance of regulatory T cells than did G3-NET[66], indicating that poorly differentiated NECs are more prone to benefit from immunotherapies, particularly ICIs. Additionally, there was heterogeneity in the TIME of the primary sites of NENs. For instance, in comparison to NETs from the jejunum and ileum, the duodenum NETs had a more positive detection rate of PD-1 and immune infiltration[67]; and compared to NETs of extra-pancreatic origin, pNETs had higher expression levels of PD-1 and PD-L1, as well as more TILs[65]. At the same primary site, PD-L1 expression varies across multiple NET subtypes as well, with prior research demonstrating that the metastasis-like primary (MLP)-1 subtype expresses PD-L1 at the highest levels in pNET[68]. This illustrates the need for further research into the variations in the immune microenvironments of distinct differentiated primary sites and subtypes of NEN, which may guide the therapeutic application of ICIs and assist in selecting the best immunotherapy regimens for patients during clinical trials.In addition, probing into the processes which transform NEN with modest levels of TIL infiltration and PD-L1 expression into immunologically "hot" tumors could potentially serve as a research avenue to enhance the therapeutic effectiveness of ICIs. So far, several mechanisms have been implicated in altering the low immune state of "cold" tumors, for example, stimulating T cell priming (*e.g.*, injection of Neoepitope Cancer Vaccine), accelerating T cell expansion (*e.g.*, application of interleukin (IL)-15), and inducing T cell recruitment (*e.g.*, through the use of epigenetic modulators and chemokines), *etc*[69]. Further research is needed to evaluate the feasibility of the above treatments for NEN of the digestive system.

CONCLUSION

Due to the complexity of NENs in the digestive system, the prognosis following the failure of first-line treatment is frequently poor, and the options for subsequent treatment are constrained. ICI monotherapy for the NEN is less effective, has a shorter duration of disease control, and may only be effective in selected patients. Combination therapy may improve the efficacy of ICI treatment in certain cases. Dual immunotherapy has some effect on highly malignant NECs and may be considered after the failure of standard treatment; however, more relevant clinical studies are needed in this field. The combination of ICI and anti-angiogenic drugs has exhibited certain advantages and promising applications for advanced NETs. The combination of ICI and chemotherapy has shown some efficacy for advanced NENs and NECs; however, further studies are required to determine whether it ultimately improves patient outcomes, and how to select the best combination regimen. Additionally, several preclinical studies and clinical trials have investigated the combination of ICIs with other clinical oncology treatment modalities, including pericyte therapy (CAR-T cell therapy), cytokine therapy, oncolytic virus therapy, and cancer vaccines, but experimental data in NEN are lacking. Other strategies to modify the TME of NEN, such as enhancing T-cell homing, preventing T-cell depletion, and preserving

CD8+ T-cell immune response, are also worth investigating in conjunction with ICIs for targeted therapy[70]. TMB-H, PD-L1, and MSI-H/dMMR have been identified as biomarkers for screening patients who may benefit from immunotherapy; however, their overall predictive efficiency is limited. Further research on the immune microenvironment and the search for more predictive immunotherapy markers with higher sensitivity and specificity to guide clinical treatment are urgently needed.

Owing to the rarity of NENs of the digestive organs, most previous and ongoing clinical trials have predominantly used small samples and on small scales approaches, resulting in limited trial results on the subject. Currently, the evidence supporting the use of ICI for NENs of the digestive systems is primarily based on a small number of phase I or II studies and a few case reports. To address this limitation, it is crucial to conduct multi-center, prospective, large-sample clinical trials. Such trials can further validate the conclusions drawn from studies like those discussed here. Additionally, these trials can guide the application of ICI for the treatment of NENs from the digestive system, and provide promising ideas for future research in the field of immunotherapy.

FOOTNOTES

Author contributions: Pan WX and Zhang XM contributed equally to this work; Pan WX, Zhang XM, Hao SL, and Han W contributed to writing-review & editing; Pan WX contributed to writing-original draft, Visualization; Zhang XM and Han W contributed to supervision Zhang XM contributed to conceptualization, investigation; Han W contributed to project administration.

Supported by Capital Health Development Research Program, No. 2022-2-7081; Science and Technology Program of Tongzhou, Beijing, No. KJ2022CX016; Beijing Natural Science Foundation, No. 7234377.

Conflict-of-interest statement: The authors declare no conflicts of interest for this article.

Open-Access: This article is an open-access article that was selected by an in-house editor and fully peer-reviewed by external reviewers. It is distributed in accordance with the Creative Commons Attribution NonCommercial (CC BY-NC 4.0) license, which permits others to distribute, remix, adapt, build upon this work non-commercially, and license their derivative works on different terms, provided the original work is properly cited and the use is non-commercial. See: https://creativecommons.org/Licenses/by-nc/4.0/

Country/Territory of origin: China

ORCID number: Xin-Mu Zhang 0000-0003-2979-1144; Wei Han 0000-0003-0652-6794.

S-Editor: Liu JH
L-Editor: A
P-Editor: Liu JH

REFERENCES

1 **de Mestier L**, Cros J, Neuzillet C, Hentic O, Egal A, Muller N, Bouché O, Cadiot G, Ruszniewski P, Couvelard A, Hammel P. Digestive System Mixed Neuroendocrine-Non-Neuroendocrine Neoplasms. *Neuroendocrinology* 2017; **105**: 412-425 [PMID: 28803232 DOI: 10.1159/000475527]

2 **Anlauf M**, Garbrecht N, Bauersfeld J, Schmitt A, Henopp T, Komminoth P, Heitz PU, Perren A, Klöppel G. Hereditary neuroendocrine tumors of the gastroenteropancreatic system. *Virchows Arch* 2007; **451** Suppl 1: S29-S38 [PMID: 17684762 DOI: 10.1007/s00428-007-0450-3]

3 **Marx SJ**. Recent Topics Around Multiple Endocrine Neoplasia Type 1. *J Clin Endocrinol Metab* 2018; **103**: 1296-1301 [PMID: 29897580 DOI: 10.1210/jc.2017-02340]

4 **Anlauf M**, Perren A, Klöppel G. Endocrine precursor lesions and microadenomas of the duodenum and pancreas with and without MEN1: criteria, molecular concepts and clinical significance. *Pathobiology* 2007; **74**: 279-284 [PMID: 17890894 DOI: 10.1159/000105810]

5 **Speisky D**, Duces A, Bièche I, Rebours V, Hammel P, Sauvanet A, Richard S, Bedossa P, Vidaud M, Murat A, Niccoli P, Scoazec JY, Ruszniewski P, Couvelard A; GTE Group, Groupe d'Etude des Tumeurs Endocrines. Molecular profiling of pancreatic neuroendocrine tumors in sporadic and Von Hippel-Lindau patients. *Clin Cancer Res* 2012; **18**: 2838-2849 [PMID: 22461457 DOI: 10.1158/1078-0432.CCR-11-2759]

6 **Nagtegaal ID**, Odze RD, Klimstra D, Paradis V, Rugge M, Schirmacher P, Washington KM, Carneiro F, Cree IA; WHO Classification of Tumours Editorial Board. The 2019 WHO classification of tumours of the digestive system. *Histopathology* 2020; **76**: 182-188 [PMID: 31433515 DOI: 10.1111/his.13975]

7 **Dasari A**, Shen C, Halperin D, Zhao B, Zhou S, Xu Y, Shih T, Yao JC. Trends in the Incidence, Prevalence, and Survival Outcomes in Patients With Neuroendocrine Tumors in the United States. *JAMA Oncol* 2017; **3**: 1335-1342 [PMID: 28448665 DOI: 10.1001/jamaoncol.2017.0589]

8 **White BE**, Rous B, Chandrakumaran K, Wong K, Bouvier C, Van Hemelrijck M, George G, Russell B, Srirajaskanthan R, Ramage JK. Incidence and survival of neuroendocrine neoplasia in England 1995-2018: A retrospective, population-based study. *Lancet Reg Health Eur* 2022; **23**: 100510 [PMID: 36176500 DOI: 10.1016/j.lanepe.2022.100510]

9 **Chang JS**, Chen LT, Shan YS, Chu PY, Tsai CR, Tsai HJ. An updated analysis of the epidemiologic trends of neuroendocrine tumors in Taiwan. *Sci Rep* 2021; **11**: 7881 [PMID: 33846396 DOI: 10.1038/s41598-021-86839-2]

10 **Genus TSE**, Bouvier C, Wong KF, Srirajaskanthan R, Rous BA, Talbot DC, Valle JW, Khan M, Pearce N, Elshafie M, Reed NS, Morgan E, Deas A, White C, Huws D, Ramage J. Impact of neuroendocrine morphology on cancer outcomes and stage at diagnosis: a UK nationwide cohort study 2013-2015. *Br J Cancer* 2019; **121**: 966-972 [PMID: 31649320 DOI: 10.1038/s41416-019-0606-3]

11 **Fan JH**, Zhang YQ, Shi SS, Chen YJ, Yuan XH, Jiang LM, Wang SM, Ma L, He YT, Feng CY, Sun XB, Liu Q, Deloso K, Chi Y, Qiao YL. A nation-wide retrospective epidemiological study of gastroenteropancreatic neuroendocrine neoplasms in china. *Oncotarget* 2017; **8**: 71699-71708 [PMID: 29069739 DOI: 10.18632/oncotarget.17599]

12 **Niu C**, Wang S, Guan Q, Ren X, Ji B, Liu Y. Neuroendocrine tumors of the gallbladder. *Oncol Lett* 2020; **19**: 3381-3388 [PMID: 32269610 DOI: 10.3892/ol.2020.11461]

13 **Huang K**, Lan Z, Chen W, Zhang J, Wang J, Zhu H, Xu B, Zhang L, Lu T, Guo Y, Wen Z. Hepatectomy and pneumectomy combined with targeted therapy for primary hepatic neuroendocrine carcinoma: Case report and review of the literature. *Front Surg* 2022; **9**: 920276 [PMID: 35910478 DOI: 10.3389/fsurg.2022.920276]

14 **Frizziero M**, Chakrabarty B, Nagy B, Lamarca A, Hubner RA, Valle JW, McNamara MG. Mixed Neuroendocrine Non-Neuroendocrine Neoplasms: A Systematic Review of a Controversial and Underestimated Diagnosis. *J Clin Med* 2020; **9** [PMID: 31963850 DOI: 10.3390/jcm9010273]

15 **Cheng AL**, Hsu C, Chan SL, Choo SP, Kudo M. Challenges of combination therapy with immune checkpoint inhibitors for hepatocellular carcinoma. *J Hepatol* 2020; **72**: 307-319 [PMID: 31954494 DOI: 10.1016/j.jhep.2019.09.025]

16 **Yi M**, Zheng X, Niu M, Zhu S, Ge H, Wu K. Combination strategies with PD-1/PD-L1 blockade: current advances and future directions. *Mol Cancer* 2022; **21**: 28 [PMID: 35062949 DOI: 10.1186/s12943-021-01489-2]

17 **Yao JC**, Fazio N, Singh S, Buzzoni R, Carnaghi C, Wolin E, Tomasek J, Raderer M, Lahner H, Voi M, Pacaud LB, Rouyrre N, Sachs C, Valle JW, Fave GD, Van Cutsem E, Tesselaar M, Shimada Y, Oh DY, Strosberg J, Kulke MH, Pavel ME; RAD001 in Advanced Neuroendocrine Tumours, Fourth Trial (RADIANT-4) Study Group. Everolimus for the treatment of advanced, non-functional neuroendocrine tumours of the lung or gastrointestinal tract (RADIANT-4): a randomised, placebo-controlled, phase 3 study. *Lancet* 2016; **387**: 968-977 [PMID: 26703889 DOI: 10.1016/S0140-6736(15)00817-X]

18 **Zhang P**, Li J, Zhang X, Zhou J, Wang X, Peng Z, Shen L, Lu M. Etoposide and cisplatin *vs* irinotecan and cisplatin as the first-line therapy for patients with advanced, poorly differentiated gastroenteropancreatic neuroendocrine carcinoma: A randomized phase 2 study. *Cancer* 2020; **126** Suppl 9: 2086-2092 [PMID: 32293725 DOI: 10.1002/cncr.32750]

19 **Frizziero M**, Spada F, Lamarca A, Kordatou Z, Barriuso J, Nuttall C, McNamara MG, Hubner RA, Mansoor W, Manoharan P, Fazio N, Valle JW. Carboplatin in Combination with Oral or Intravenous Etoposide for Extra-Pulmonary, Poorly-Differentiated Neuroendocrine Carcinomas. *Neuroendocrinology* 2019; **109**: 100-112 [PMID: 30703770 DOI: 10.1159/000497336]

20 **Rogowski W**, Wachuła E, Gorzelak A, Lebiedzińska A, Sulżyc-Bielicka V, Iżycka-Świeszewska E, Żołnierek J, Kos-Kudła B. Capecitabine and temozolomide combination for treatment of high-grade, well-differentiated neuroendocrine tumour and poorly-differentiated neuroendocrine carcinoma - retrospective analysis. *Endokrynol Pol* 2019; **70**: 313-317 [PMID: 30843182 DOI: 10.5603/EP.a2019.0010]

21 **Marabelle A**, Fakih M, Lopez J, Shah M, Shapira-Frommer R, Nakagawa K, Chung HC, Kindler HL, Lopez-Martin JA, Miller WH Jr, Italiano A, Kao S, Piha-Paul SA, Delord JP, McWilliams RR, Fabrizio DA, Aurora-Garg D, Xu L, Jin F, Norwood K, Bang YJ. Association of tumour mutational burden with outcomes in patients with advanced solid tumours treated with pembrolizumab: prospective biomarker analysis of the multicohort, open-label, phase 2 KEYNOTE-158 study. *Lancet Oncol* 2020; **21**: 1353-1365 [PMID: 32919526 DOI: 10.1016/S1470-2045(20)30445-9]

22 **Merino DM**, McShane LM, Fabrizio D, Funari V, Chen SJ, White JR, Wenz P, Baden J, Barrett JC, Chaudhary R, Chen L, Chen WS, Cheng JH, Cyanam D, Dickey JS, Gupta V, Hellmann M, Helman E, Li Y, Maas J, Papin A, Patidar R, Quinn KJ, Rizvi N, Tae H, Ward C, Xie M, Zehir A, Zhao C, Dietel M, Stenzinger A, Stewart M, Allen J; TMB Harmonization Consortium. Establishing guidelines to harmonize tumor mutational burden (TMB): in silico assessment of variation in TMB quantification across diagnostic platforms: phase I of the Friends of Cancer Research TMB Harmonization Project. *J Immunother Cancer* 2020; **8** [PMID: 32217756 DOI: 10.1136/jitc-2019-000147]

23 **Marabelle A**, Le DT, Ascierto PA, Di Giacomo AM, De Jesus-Acosta A, Delord JP, Geva R, Gottfried M, Penel N, Hansen AR, Piha-Paul SA, Doi T, Gao B, Chung HC, Lopez-Martin J, Bang YJ, Frommer RS, Shah M, Ghori R, Joe AK, Pruitt SK, Diaz LA Jr. Efficacy of Pembrolizumab in Patients With Noncolorectal High Microsatellite Instability/Mismatch Repair-Deficient Cancer: Results From the Phase II KEYNOTE-158 Study. *J Clin Oncol* 2020; **38**: 1-10 [PMID: 31682550 DOI: 10.1200/JCO.19.02105]

24 **Klein O**, Kee D, Markman B, Michael M, Underhill C, Carlino MS, Jackett L, Lum C, Scott C, Nagrial A, Behren A, So JY, Palmer J, Cebon J. Immunotherapy of Ipilimumab and Nivolumab in Patients with Advanced Neuroendocrine Tumors: A Subgroup Analysis of the CA209-538 Clinical Trial for Rare Cancers. *Clin Cancer Res* 2020; **26**: 4454-4459 [PMID: 32532787 DOI: 10.1158/1078-0432.CCR-20-0621]

25 **Le DT**, Durham JN, Smith KN, Wang H, Bartlett BR, Aulakh LK, Lu S, Kemberling H, Wilt C, Luber BS, Wong F, Azad NS, Rucki AA, Laheru D, Donehower R, Zaheer A, Fisher GA, Crocenzi TS, Lee JJ, Greten TF, Duffy AG, Ciombor KK, Eyring AD, Lam BH, Joe A, Kang SP, Holdhoff M, Danilova L, Cope L, Meyer C, Zhou S, Goldberg RM, Armstrong DK, Bever KM, Fader AN, Taube J, Housseau F, Spetzler D, Xiao N, Pardoll DM, Papadopoulos N, Kinzler KW, Eshleman JR, Vogelstein B, Anders RA, Diaz LA Jr. Mismatch repair deficiency predicts response of solid tumors to PD-1 blockade. *Science* 2017; **357**: 409-413 [PMID: 28596308 DOI: 10.1126/science.aan6733]

26 **Mulvey C**, Raj NP, Chan JA, Aggarwal RR, Cinar P, Hope TA, Kolli K, Zhang L, Calabrese S, Grabowsky JA, Modarresi L, Kelly V, Stonely D, Munster PN, Reidy DL, Fong L, Bergsland EK. Phase II study of pembrolizumab-based therapy in previously treated extrapulmonary poorly differentiated neuroendocrine carcinomas: Results of Part A (pembrolizumab alone). *JCO* 2019; **37**: 363-363 [DOI: 10.1200/JCO.2019.37.4_suppl.363]

27 **Fottner C**, Apostolidis L, Ferrata M, Krug S, Michl P, Schad A, Roth W, Jaeger D, Galle PR, Weber MM. A phase II, open label, multicenter trial of avelumab in patients with advanced, metastatic high-grade neuroendocrine carcinomas NEC G3 (WHO 2010) progressive after first-line chemotherapy (AVENEC). *J Clin Oncol* 2019; **37**: 4103-4103 [DOI: 10.1200/JCO.2019.37.15_suppl.4103]

28 **Yao JC**, Strosberg J, Fazio N, Pavel ME, Ruszniewski P, Bergsland E, Li D, Tafuto S, Raj N, Campana D, Hijioka S, Raderer M, Guimbaud R, Gajate P, Pusceddu S, Reising A, Degtyarev E, Mookerjee B, Aimone P, Singh S. Activity & safety of spartalizumab (PDR001) in patients (pts) with advanced neuroendocrine tumors (NET) of pancreatic (Pan), gastrointestinal (GI), or thoracic (T) origin, & gastroenteropancreatic neuroendocrine carcinoma (GEP NEC) who have progressed on prior treatment (Tx). *Ann Oncol* 2018; **29**: viii467-viii468 [DOI: 10.1093/annonc/mdy293.001]

29 **Mehnert JM**, Bergsland E, O'Neil BH, Santoro A, Schellens JHM, Cohen RB, Doi T, Ott PA, Pishvaian MJ, Puzanov I, Aung KL, Hsu C, Le Tourneau C, Hollebecque A, Élez E, Tamura K, Gould M, Yang P, Stein K, Piha-Paul SA. Pembrolizumab for the treatment of programmed death-ligand 1-positive advanced carcinoid or pancreatic neuroendocrine tumors: Results from the KEYNOTE-028 study. *Cancer* 2020; **126**: 3021-3030 [PMID: 32320048 DOI: 10.1002/cncr.32883]

30 **Vijayvergia N**, Dasari A, Deng M, Litwin S, Al-Toubah T, Alpaugh RK, Dotan E, Hall MJ, Ross NM, Runyen MM, Denlinger CS, Halperin DM, Cohen SJ, Engstrom PF, Strosberg JR. Pembrolizumab monotherapy in patients with previously treated metastatic high-grade

neuroendocrine neoplasms: joint analysis of two prospective, non-randomised trials. *Br J Cancer* 2020; **122**: 1309-1314 [PMID: 32152503 DOI: 10.1038/s41416-020-0775-0]

31 **Strosberg J**, Mizuno N, Doi T, Grande E, Delord JP, Shapira-Frommer R, Bergsland E, Shah M, Fakih M, Takahashi S, Piha-Paul SA, O'Neil B, Thomas S, Lolkema MP, Chen M, Ibrahim N, Norwood K, Hadoux J. Efficacy and Safety of Pembrolizumab in Previously Treated Advanced Neuroendocrine Tumors: Results From the Phase II KEYNOTE-158 Study. *Clin Cancer Res* 2020; **26**: 2124-2130 [PMID: 31980466 DOI: 10.1158/1078-0432.CCR-19-3014]

32 **Lu M**, Zhang P, Zhang Y, Li Z, Gong J, Li J, Li Y, Zhang X, Lu Z, Wang X, Zhou J, Peng Z, Wang W, Feng H, Wu H, Yao S, Shen L. Efficacy, Safety, and Biomarkers of Toripalimab in Patients with Recurrent or Metastatic Neuroendocrine Neoplasms: A Multiple-Center Phase Ib Trial. *Clin Cancer Res* 2020; **26**: 2337-2345 [PMID: 32086343 DOI: 10.1158/1078-0432.CCR-19-4000]

33 **Girard N**, Mazieres J, Otto J, Lena H, Lepage C, Egenod T, Smith D, Madelaine J, Gérinière L, Hajbi FE, Ferru A, Clément-Duchêne C, Madroszyk A, Desrame J, Morin F, Langlais A, Michel P, Louvet C, Westeel V, Walter T. LBA41 Nivolumab (nivo) ± ipilimumab (ipi) in pre-treated patients with advanced, refractory pulmonary or gastroenteropancreatic poorly differentiated neuroendocrine tumors (NECs) (GCO-001 NIPINEC). *Ann Oncol* 2021; **32**: S1318 [DOI: 10.1016/j.annonc.2021.08.2119]

34 **Yao JC**, Strosberg J, Fazio N, Pavel ME, Bergsland E, Ruszniewski P, Halperin DM, Li D, Tafuto S, Raj N, Campana D, Hijioka S, Raderer M, Guimbaud R, Gajate P, Pusceddu S, Reising A, Degtyarev E, Shilkrut M, Eddy S, Singh S. Spartalizumab in metastatic, well/poorly-differentiated neuroendocrine neoplasms. *Endocr Relat Cancer* 2021 [PMID: 33480358 DOI: 10.1530/ERC-20-0382]

35 **Chan DL**, Rodriguez-Freixinos V, Doherty M, Wasson K, Iscoe N, Raskin W, Hallet J, Myrehaug S, Law C, Thawer A, Nguyen K, Singh S. Avelumab in unresectable/metastatic, progressive, grade 2-3 neuroendocrine neoplasms (NENs): Combined results from NET-001 and NET-002 trials. *Eur J Cancer* 2022; **169**: 74-81 [PMID: 35504244 DOI: 10.1016/j.ejca.2022.03.029]

36 **Al-Toubah T**, Halfdanarson T, Gile J, Morse B, Sommerer K, Strosberg J. Efficacy of ipilimumab and nivolumab in patients with high-grade neuroendocrine neoplasms. *ESMO Open* 2022; **7**: 100364 [PMID: 34973511 DOI: 10.1016/j.esmoop.2021.100364]

37 **Patel SP**, Othus M, Chae YK, Giles FJ, Hansel DE, Singh PP, Fontaine A, Shah MH, Kasi A, Baghdadi TA, Matrana M, Gatalica Z, Korn WM, Hayward J, McLeod C, Chen HX, Sharon E, Mayerson E, Ryan CW, Plets M, Blanke CD, Kurzrock R. A Phase II Basket Trial of Dual Anti-CTLA-4 and Anti-PD-1 Blockade in Rare Tumors (DART SWOG 1609) in Patients with Nonpancreatic Neuroendocrine Tumors. *Clin Cancer Res* 2020; **26**: 2290-2296 [PMID: 31969335 DOI: 10.1158/1078-0432.CCR-19-3356]

38 **Patel SP**, Mayerson E, Chae YK, Strosberg J, Wang J, Konda B, Hayward J, McLeod CM, Chen HX, Sharon E, Othus M, Ryan CW, Plets M, Blanke CD, Kurzrock R. A phase II basket trial of Dual Anti-CTLA-4 and Anti-PD-1 Blockade in Rare Tumors (DART) SWOG S1609: High-grade neuroendocrine neoplasm cohort. *Cancer* 2021; **127**: 3194-3201 [PMID: 33882143 DOI: 10.1002/cncr.33591]

39 **Mohamed A**, Vijayvergia N, Kurian M, Liu L, Fu P, Das S. Exploring Real World Outcomes with Nivolumab Plus Ipilimumab in Patients with Metastatic Extra-Pulmonary Neuroendocrine Carcinoma (EP-NEC). *Cancers (Basel)* 2022; **14** [PMID: 35681675 DOI: 10.3390/cancers14112695]

40 **Capdevila J**, Teule A, López C, García-Carbonero R, Benavent M, Custodio A, Cubillo A, Alonso V, Gordoa TA, Carmona-Bayonas A, Crespo G, Blanco-Codesido M, Jimenez-Fonseca P, Viúdez A, Muñoa ALC, Sevilla I, Llanos M, Segura A, Hernando-Cubero J, Manzano JL. 1157O A multi-cohort phase II study of durvalumab plus tremelimumab for the treatment of patients (pts) with advanced neuroendocrine neoplasms (NENs) of gastroenteropancreatic or lung origin: The DUNE trial (GETNE 1601). *Ann Oncol* 2020; **31**: S770-S771 [DOI: 10.1016/j.annonc.2020.08.1370]

41 **Capdevila J**, Hernando J, Teule A, Lopez C, Garcia-Carbonero R, Benavent M, Custodio A, Garcia-Alvarez A, Cubillo A, Alonso V, Carmona-Bayonas A, Alonso-Gordoa T, Crespo G, Jimenez-Fonseca P, Blanco M, Viudez A, Casta AL, Sevilla I, Segura A, Llanos M, Landolfi S, Nuciforo P, Manzano JL. Durvalumab plus tremelimumab for the treatment of advanced neuroendocrine neoplasms of gastroenteropancreatic and lung origin: the phase II DUNE trial (GETNE 1601). In Review [DOI: 10.21203/rs.3.rs-2174016/v1]

42 **Shigeta K**, Datta M, Hato T, Kitahara S, Chen IX, Matsui A, Kikuchi H, Mamessier E, Aoki S, Ramjiawan RR, Ochiai H, Bardeesy N, Huang P, Cobbold M, Zhu AX, Jain RK, Duda DG. Dual Programmed Death Receptor-1 and Vascular Endothelial Growth Factor Receptor-2 Blockade Promotes Vascular Normalization and Enhances Antitumor Immune Responses in Hepatocellular Carcinoma. *Hepatology* 2020; **71**: 1247-1261 [PMID: 31378984 DOI: 10.1002/hep.30889]

43 **Yang J**, Yan J, Liu B. Targeting VEGF/VEGFR to Modulate Antitumor Immunity. *Front Immunol* 2018; **9**: 978 [PMID: 29774034 DOI: 10.3389/fimmu.2018.00978]

44 **Halperin DM**, Liu S, Dasari A, Fogelman DR, Bhosale P, Mahvash A, Dervin S, Estrella J, Cortazar P, Maru DM, Mckenna EF, Wistuba II, Schulze K, Futreal PA, Darbonne WC, Yun C, Hwu P, Yao JC. A phase II trial of atezolizumab and bevacizumab in patients with advanced, progressive neuroendocrine tumors (NETs). *JCO* 2020; **38**: 619-619 [DOI: 10.1200/JCO.2020.38.4_suppl.619]

45 **Halperin DM**, Liu S, Dasari A, Fogelman D, Bhosale P, Mahvash A, Estrella JS, Rubin L, Morani AC, Knafl M, Overeem TA, Fu S-C, Solis LM, Parra Cuentas E, Verma A, Chen H-L, Gite S, Subashchandrabose P, Dervin S, Schulze K, Darbonne WC, Yun C, Wistuba II, Futreal PA, Woodman SE, Yao JC. Assessment of Clinical Response Following Atezolizumab and Bevacizumab Treatment in Patients With Neuroendocrine Tumors: A Nonrandomized Clinical Trial. *JAMA Oncology* 2022; **8**: 904-909 [DOI: 10.1001/jamaoncol.2022.0212]

46 **Al-Toubah T**, Morse B, Haider M, Valone T, Strosberg J. Phase II Study of Pembrolizumab and Lenvatinib in Advanced Well-Differentiated Neuroendocrine Tumors. *Endocrine Abstracts* 2023; **89** [DOI: 10.1530/endoabs.89.C8]

47 **Chan JA**, Raj NP, Aggarwal RR, Calabrese S, DeMore A, Dhawan MS, Fattah D, Fong L, Grabowsky J, Hope TA, Kolli KP, Munster PN, Perez K, Reidy DL, Von Fedak S, Zhang L, Bergsland EK. Phase II study of pembrolizumab-based therapy in previously treated extrapulmonary poorly differentiated neuroendocrine carcinomas: Results of Part B (pembrolizumab + chemotherapy). *JCO* 2021; **39**: 4148-4148 [DOI: 10.1200/JCO.2021.39.15_suppl.4148]

48 **Owen DH**, Wei L, Goyal A, Zhou Y, Suffren S-A, Jacob R, Pilcher C, Otterson GA, Verschraegen CF, Shah MH, Konda B. CLO20-054: A Phase 2 Trial of Nivolumab and Temozolomide in Advanced Neuroendocrine Tumors (NETs): Interim Efficacy Analysis. *J Natl Compr Canc Netw* 2020; **18**: CLO20-054 [DOI: 10.6004/jnccn.2019.7460]

49 **Riesco-Martinez MC**, Capdevila J, Alonso V, Jimenez-Fonseca P, Teule A, Grande E, Sevilla I, Viñuales MB, Alonso-Gordoa T, Custodio A, Hernando J, Polo E, Trujillo OAC, Garcia-Carbonero R. 1098O Nivolumab plus platinum-doublet chemotherapy as first-line therapy in unresectable, locally advanced or metastatic G3 neuroendocrine Neoplasms (NENs) of the gastroenteropancreatic (GEP) tract or unknown (UK) origin: Preliminary results from the phase II NICE-NEC trial (GETNE T1913). *Ann Oncol* 2021; **32**: S908-S909 [DOI: 10.1016/j.annonc.2021.08.180]

50 **Riesco Martinez MC**, Capdevila Castillon J, Alonso V, Jimenez-Fonseca P, Teule A, Grande E, Sevilla I, Benavent M, Alonso-Gordoa T, Custodio A, Antón Pascual B, Hernando J, Polo E, Castillo Trujillo OA, Garcia-Carbonero R. 496MO Final overall survival results from the

NICE-NEC trial (GETNE-T1913): A phase II study of nivolumab and platinum-doublet chemotherapy (CT) in untreated advanced G3 neuroendocrine neoplasms (NENs) of gastroenteropancreatic (GEP) or unknown (UK) origin. *Ann Oncol* 2022; **33**: S769 [DOI: 10.1016/j.annonc.2022.07.624]

51 **Chorath J**, Placencio-Hickok VR, Guan M, Nissen N, Kamrava M, Klempner SJ, Nassir Y, Hendifar A, Gong J. Durable Response to Carboplatin, Etoposide, Nivolumab, and Ipilimumab in Metastatic High-Grade Neuroendocrine Carcinoma of the Gallbladder. *Pancreas* 2020; **49**: e19-e20 [PMID: 32049953 DOI: 10.1097/MPA.0000000000001480]

52 **Galluzzi L**, Humeau J, Buqué A, Zitvogel L, Kroemer G. Immunostimulation with chemotherapy in the era of immune checkpoint inhibitors. *Nat Rev Clin Oncol* 2020; **17**: 725-741 [PMID: 32760014 DOI: 10.1038/s41571-020-0413-z]

53 **La Salvia A**, Barroso G, Espinosa Olarte P, Anton Pascual B, Modrego Sanchez A, Riesco-Martinez M, Garcia-Carbonero R. High TMB and MSI-high as independent predictors of survival in NENs. In: Journal of Neuroendocrinology. WILEY 111 RIVER ST, HOBOKEN 07030-5774, NJ USA, 2021: 108-108

54 **Venizelos A**, Elvebakken H, Perren A, Nikolaienko O, Deng W, Lothe IMB, Couvelard A, Hjortland GO, Sundlöv A, Svensson J, Garresori H, Kersten C, Hofsli E, Detlefsen S, Krogh M, Sorbye H, Knappskog S. The molecular characteristics of high-grade gastroenteropancreatic neuroendocrine neoplasms. *Endocr Relat Cancer* 2021; **29**: 1-14 [PMID: 34647903 DOI: 10.1530/ERC-21-0152]

55 **Chalmers ZR**, Connelly CF, Fabrizio D, Gay L, Ali SM, Ennis R, Schrock A, Campbell B, Shlien A, Chmielecki J, Huang F, He Y, Sun J, Tabori U, Kennedy M, Lieber DS, Roels S, White J, Otto GA, Ross JS, Garraway L, Miller VA, Stephens PJ, Frampton GM. Analysis of 100,000 human cancer genomes reveals the landscape of tumor mutational burden. *Genome Med* 2017; **9**: 34 [PMID: 28420421 DOI: 10.1186/s13073-017-0424-2]

56 **Samstein RM**, Lee CH, Shoushtari AN, Hellmann MD, Shen R, Janjigian YY, Barron DA, Zehir A, Jordan EJ, Omuro A, Kaley TJ, Kendall SM, Motzer RJ, Hakimi AA, Voss MH, Russo P, Rosenberg J, Iyer G, Bochner BH, Bajorin DF, Al-Ahmadie HA, Chaft JE, Rudin CM, Riely GJ, Baxi S, Ho AL, Wong RJ, Pfister DG, Wolchok JD, Barker CA, Gutin PH, Brennan CW, Tabar V, Mellinghoff IK, DeAngelis LM, Ariyan CE, Lee N, Tap WD, Gounder MM, D'Angelo SP, Saltz L, Stadler ZK, Scher HI, Baselga J, Razavi P, Klebanoff CA, Yaeger R, Segal NH, Ku GY, DeMatteo RP, Ladanyi M, Rizvi NA, Berger MF, Riaz N, Solit DB, Chan TA, Morris LGT. Tumor mutational load predicts survival after immunotherapy across multiple cancer types. *Nat Genet* 2019; **51**: 202-206 [PMID: 30643254 DOI: 10.1038/s41588-018-0312-8]

57 **Cives M**, Pelle' E, Strosberg J. Emerging Treatment Options for Gastroenteropancreatic Neuroendocrine Tumors. *J Clin Med* 2020; **9** [PMID: 33202931 DOI: 10.3390/jcm9113655]

58 **Robinson MD**, Livesey D, Hubner RA, Valle JW, McNamara MG. Future therapeutic strategies in the treatment of extrapulmonary neuroendocrine carcinoma: a review. *Ther Adv Med Oncol* 2023; **15**: 17588359231156870 [PMID: 36872945 DOI: 10.1177/17588359231156870]

59 **Oberg K**, Modlin IM, De Herder W, Pavel M, Klimstra D, Frilling A, Metz DC, Heaney A, Kwekkeboom D, Strosberg J, Meyer T, Moss SF, Washington K, Wolin E, Liu E, Goldenring J. Consensus on biomarkers for neuroendocrine tumour disease. *Lancet Oncol* 2015; **16**: e435-e446 [PMID: 26370353 DOI: 10.1016/S1470-2045(15)00186-2]

60 **Malczewska A**, Oberg K, Kos-Kudla B. NETest is superior to chromogranin A in neuroendocrine neoplasia: a prospective ENETS CoE analysis. *Endocr Connect* 2021; **10**: 110-123 [PMID: 33289691 DOI: 10.1530/EC-20-0417]

61 **Woolaver RA**, Wang X, Krinsky AL, Waschke BC, Chen SMY, Popolizio V, Nicklawsky AG, Gao D, Chen Z, Jimeno A, Wang XJ, Wang JH. Differences in TCR repertoire and T cell activation underlie the divergent outcomes of antitumor immune responses in tumor-eradicating *vs* tumor-progressing hosts. *J Immunother Cancer* 2021; **9** [PMID: 33414263 DOI: 10.1136/jitc-2020-001615]

62 **Galon J**, Bruni D. Approaches to treat immune hot, altered and cold tumours with combination immunotherapies. *Nat Rev Drug Discov* 2019; **18**: 197-218 [PMID: 30610226 DOI: 10.1038/s41573-018-0007-y]

63 **Hegde PS**, Karanikas V, Evers S. The Where, the When, and the How of Immune Monitoring for Cancer Immunotherapies in the Era of Checkpoint Inhibition. *Clin Cancer Res* 2016; **22**: 1865-1874 [PMID: 27084740 DOI: 10.1158/1078-0432.CCR-15-1507]

64 **Takahashi D**, Kojima M, Suzuki T, Sugimoto M, Kobayashi S, Takahashi S, Konishi M, Gotohda N, Ikeda M, Nakatsura T, Ochiai A, Nagino M. Profiling the Tumour Immune Microenvironment in Pancreatic Neuroendocrine Neoplasms with Multispectral Imaging Indicates Distinct Subpopulation Characteristics Concordant with WHO 2017 Classification. *Sci Rep* 2018; **8**: 13166 [PMID: 30177687 DOI: 10.1038/s41598-018-31383-9]

65 **Bösch F**, Brüwer K, Altendorf-Hofmann A, Auernhammer CJ, Spitzweg C, Westphalen CB, Boeck S, Schubert-Fritschle G, Werner J, Heinemann V, Kirchner T, Angele M, Knösel T. Immune checkpoint markers in gastroenteropancreatic neuroendocrine neoplasia. *Endocr Relat Cancer* 2019; **26**: 293-301 [PMID: 30608901 DOI: 10.1530/ERC-18-0494]

66 **Pinato DJ**, Vallipuram A, Evans JS, Wong C, Zhang H, Brown M, Dina RE, Trivedi P, Akarca AU, Marafioti T, Mauri FA, Sharma R. Programmed Cell Death Ligand Expression Drives Immune Tolerogenesis across the Diverse Subtypes of Neuroendocrine Tumours. *Neuroendocrinology* 2021; **111**: 465-474 [PMID: 32097935 DOI: 10.1159/000506745]

67 **Cives M**, Strosberg J, Al Diffalha S, Coppola D. Analysis of the immune landscape of small bowel neuroendocrine tumors. *Endocr Relat Cancer* 2019; **26**: 119-130 [PMID: 30400003 DOI: 10.1530/ERC-18-0189]

68 **Young K**, Lawlor RT, Ragulan C, Patil Y, Mafficini A, Bersani S, Antonello D, Mansfield D, Cingarlini S, Landoni L, Pea A, Luchini C, Piredda L, Kannan N, Nyamundanda G, Morganstein D, Chau I, Wiedenmann B, Milella M, Melcher A, Cunningham D, Starling N, Scarpa A, Sadanandam A. Immune landscape, evolution, hypoxia-mediated viral mimicry pathways and therapeutic potential in molecular subtypes of pancreatic neuroendocrine tumours. *Gut* 2021; **70**: 1904-1913 [PMID: 32883872 DOI: 10.1136/gutjnl-2020-321016]

69 **Gubbi S**, Vijayvergia N, Yu JQ, Klubo-Gwiezdzinska J, Koch CA. Immune Checkpoint Inhibitor Therapy in Neuroendocrine Tumors. *Horm Metab Res* 2022; **54**: 795-812 [PMID: 35878617 DOI: 10.1055/a-1908-7790]

70 **Kubli SP**, Berger T, Araujo DV, Siu LL, Mak TW. Beyond immune checkpoint blockade: emerging immunological strategies. *Nat Rev Drug Discov* 2021; **20**: 899-919 [PMID: 33686237 DOI: 10.1038/s41573-021-00155-y]

World Journal of Gastroenterology

Submit a Manuscript: https://www.f6publishing.com

World J Gastroenterol 2023 July 14; 29(26): 4186-4199

DOI: 10.3748/wjg.v29.i26.4186

ISSN 1007-9327 (print) ISSN 2219-2840 (online)

ORIGINAL ARTICLE

Retrospective Study

Radiomics model based on contrast-enhanced computed tomography to predict early recurrence in patients with hepatocellular carcinoma after radical resection

Shu-Qun Li, Li-Li Su, Ting-Feng Xu, Li-Ying Ren, Dong-Bo Chen, Wan-Ying Qin, Xuan-Zhi Yan, Jia-Xing Fan, Hong-Song Chen, Wei-Jia Liao

Specialty type: Gastroenterology and hepatology

Provenance and peer review: Unsolicited article; Externally peer reviewed.

Peer-review model: Single blind

Peer-review report's scientific quality classification

Grade A (Excellent): A
Grade B (Very good): 0
Grade C (Good): C, C
Grade D (Fair): 0
Grade E (Poor): 0

P-Reviewer: Ampollini L, Italy; He D, China

Received: February 11, 2023
Peer-review started: February 11, 2023
First decision: March 20, 2023
Revised: March 25, 2023
Accepted: June 6, 2023
Article in press: June 6, 2023
Published online: July 14, 2023

Shu-Qun Li, Ting-Feng Xu, Li-Ying Ren, Wan-Ying Qin, Xuan-Zhi Yan, Jia-Xing Fan, Wei-Jia Liao, Laboratory of Hepatobiliary and Pancreatic Surgery, The Affiliated Hospital of Guilin Medical University, Guilin 541001, Guangxi Zhuang Autonomous Region, China

Li-Li Su, Department of Clinical Laboratory, Nanxishan Hospital of Guangxi Zhuang Autonomous Region, Guilin 541002, Guangxi Zhuang Autonomous Region, China

Dong-Bo Chen, Hong-Song Chen, Peking University People's Hospital, Peking University Hepatology Institute, Beijing Key Laboratory of Hepatitis C and Immunotherapy for Liver Disease, Beijing 100091, China

Corresponding author: Wei-Jia Liao, BM BCh, Professor, Laboratory of Hepatobiliary and Pancreatic Surgery, The Affiliated Hospital of Guilin Medical University, No. 15 Lequn Road, Xiufeng District, Guilin 541001, Guangxi Zhuang Autonomous Region, China.
liaoweijia288@163.com

Abstract

BACKGROUND

Radical resection remains an effective strategy for patients with hepatocellular carcinoma (HCC). Unfortunately, the postoperative early recurrence (recurrence within 2 years) rate is still high.

AIM

To develop a radiomics model based on preoperative contrast-enhanced computed tomography (CECT) to evaluate early recurrence in HCC patients with a single tumour.

METHODS

We enrolled a total of 402 HCC patients from two centres who were diagnosed with a single tumour and underwent radical resection. First, the features from the portal venous and arterial phases of CECT were extracted based on the region of interest, and the early recurrence-related radiomics features were selected *via* the least absolute shrinkage and selection operator proportional hazards model (LASSO Cox) to determine radiomics scores for each patient. Then, the clinico-pathologic data were combined to develop a model to predict early recurrence by

Cox regression. Finally, we evaluated the prediction performance of this model by multiple methods.

RESULTS

A total of 1915 radiomics features were extracted from CECT images, and 31 of them were used to determine the radiomics scores, which showed a significant difference between the early recurrence and nonearly recurrence groups. Univariate and multivariate Cox regression analyses showed that radiomics scores and serum alpha-fetoprotein were independent indicators, and they were used to develop a combined model to predict early recurrence. The area under the receiver operating characteristic curve values for the training and validation cohorts were 0.77 and 0.74, respectively, while the C-indices were 0.712 and 0.674, respectively. The calibration curves and decision curve analysis showed satisfactory accuracy and clinical utilities. Kaplan-Meier curves based on recurrence-free survival and overall survival showed significant differences.

CONCLUSION

The preoperative radiomics model was shown to be effective for predicting early recurrence among HCC patients with a single tumour.

Key Words: Hepatocellular carcinoma; Contrast-enhanced computed tomography; Radiomics; Early recurrence

©The Author(s) 2023. Published by Baishideng Publishing Group Inc. All rights reserved.

Core Tip: Hepatocellular carcinoma (HCC) is a growing health issue worldwide, ranking sixth in incidence and third in mortality among all cancers. Moreover, due to the high malignancy and suppressive immune microenvironment of HCC, there remain high recurrence and metastasis rates. Therefore, we developed a radiomics model based on preoperative contrast-enhanced computed tomography to evaluate early recurrence in HCC patients with a single tumour.

Citation: Li SQ, Su LL, Xu TF, Ren LY, Chen DB, Qin WY, Yan XZ, Fan JX, Chen HS, Liao WJ. Radiomics model based on contrast-enhanced computed tomography to predict early recurrence in patients with hepatocellular carcinoma after radical resection. *World J Gastroenterol* 2023; 29(26): 4186-4199

URL: https://www.wjgnet.com/1007-9327/full/v29/i26/4186.htm

DOI: https://dx.doi.org/10.3748/wjg.v29.i26.4186

INTRODUCTION

Hepatocellular carcinoma (HCC) is a growing health issue worldwide, ranking sixth in incidence and third in mortality among all cancers[1]. For early-stage HCC patients, liver resection and liver transplantation are considered the main strategies to prolong overall survival (OS)[2,3]. However, the majority of HCC patients are diagnosed at later disease stages, and thus, surgical care is no longer a treatment option for these individuals[4]. Moreover, due to the high malignancy and suppressive immune microenvironment of HCC[5], there remain high recurrence and metastasis rates even for patients who undergo resection. Therefore, it is of vital importance to conduct systematic surveillance of HCC recurrence, and there is an urgent need to precisely predict recurrence in patients with HCC.

Currently, the recurrence rate for postoperative HCC patients is over 50% within 5 years[6], and studies have shown that patients with early recurrence – *i.e.*, recurrence occurring within 2 years – have worse outcomes and poorer prognosis than those with recurrence over 2 years[7]. Typically, the identification of primary and recurrent tumour depends on the detection of genotype, in other words, on the molecular scale[8,9]. However, its complexities have limited the widespread adoption of this method. To evaluate the prognosis of HCC patients, many staging systems have been introduced to clinical use, such as the Barcelona Clinic Liver Cancer (BCLC) staging system and albumin-bilirubin (ALBI) grading[4, 10]. Given that the staging systems above are more suitable for use in evaluating liver function or guiding treatment, there is a lack of an efficient and accurate approach to evaluate recurrence.

Radiomics is an emerging discipline based on medical imaging. Medical imaging, which includes ultrasound (US), computed tomography (CT), and magnetic resonance imaging (MRI), has played a crucial role in the screening and diagnosis of HCC[11]. However, the conventional imaging process relies on the experience and judgement of radiologists and might miss or be hard to quantify some crucial details. Many studies have shown that radiomics features may contain pathophysiological characteristics, which reflect tumour heterogeneity and are associated with patient prognosis [10]. Based on artificial intelligence technology, radiomics has shown certain potential in HCC related gene analysis, microvascular invasion, postoperative survival and recurrence prediction, *etc*[12-16]. However, there are few externally validated reports that studied on the use of radiomics to assess the risk of early recurrence in HCC patients after surgery.

In this study, we aimed to establish a radiomics model to predict early recurrence for patients who underwent radical resection based on contrast-enhanced CT (CECT) and clinical variables, evaluate this model's performance, and verify its feasibility in clinical application.

MATERIALS AND METHODS

Patients

We retrospectively enrolled 537 HCC patients from two institutions (Affiliated Hospital of Guilin Medical University; Peking University People's Hospital) who underwent radical resection. According to the exclusion criteria in Figure 1, 277 patients enrolled from October 2009 to May 2017 at the Affiliated Hospital of Guilin Medical University were set as the training cohort, while 125 patients enrolled from June 2010 to December 2017 at Peking University People's Hospital were set as the validation cohort. Along with the CECT images, information regarding demographic characteristics, clinicopathological data, and laboratory data were also retrospectively collected. Patient demographic characteristics included sex and age, while clinicopathological data were collected from electronic case records, containing tumour size and vascular invasion. Furthermore, laboratory data were collected before surgery, including routine blood test, liver function, and alpha-fetoprotein (AFP) level.

Diagnostic criteria and exclusion criteria

All enrolled patients were diagnosed with HCC by postoperative pathological examination; solitary HCC was confirmed by preoperative CECT and intraoperative palpation or US. In addition to CECT, at least US and MRI supported an HCC diagnosis. Radical resection was defined as complete removal of the tumour with no residual tumour or new lesion observed in two observations at an interval of no less than 4 wk. Two independent pathologists histopathologically examined resected tumour specimens. The main exclusion criteria were as follows: (1) CECT image unavailable; (2) CECT scan over 1 mo before operation; (3) previous treatment including hepatectomy, ablation, or transarterial chemoembolization; and (4) incomplete clinical or follow-up data.

Follow-up surveillance

Postoperative surveillance at each institution was conducted according to the protocol. Patients were followed every 2 mo within the first 2 years and every 3-6 mo after 2 years postoperatively (abdominal ultrasonography, serum AFP, and other serological tests were performed). CECT or MRI examination was performed if recurrence was suspected. OS was determined as the interval between the operation date and the date of death or last follow-up. Recurrence-free survival (RFS) was determined from the operation date of radical surgery to the date of the first recurrence at any site, death, or the last follow-up. Recurrence within 2 years after operation was considered as early recurrence.

CT image acquisition

The CECT images were obtained from each institution according to routine procedures, and the usage of contrast medium is described in the Supplementary material.

Region of interest segmentation and radiomics feature extraction

Regions of interest (ROIs) were defined as the tumour areas in both arterial and portal venous phases, which were delineated *via* 3D Slicer (v4.11, https://www.slicer.org) by two experienced radiologists (Reader 1: H.Y. with 10 years of working experience; reader 2: Z.Z. with 20 years of working experience). If they could not reach a consensus, the third radiologist intervened in the evaluation.

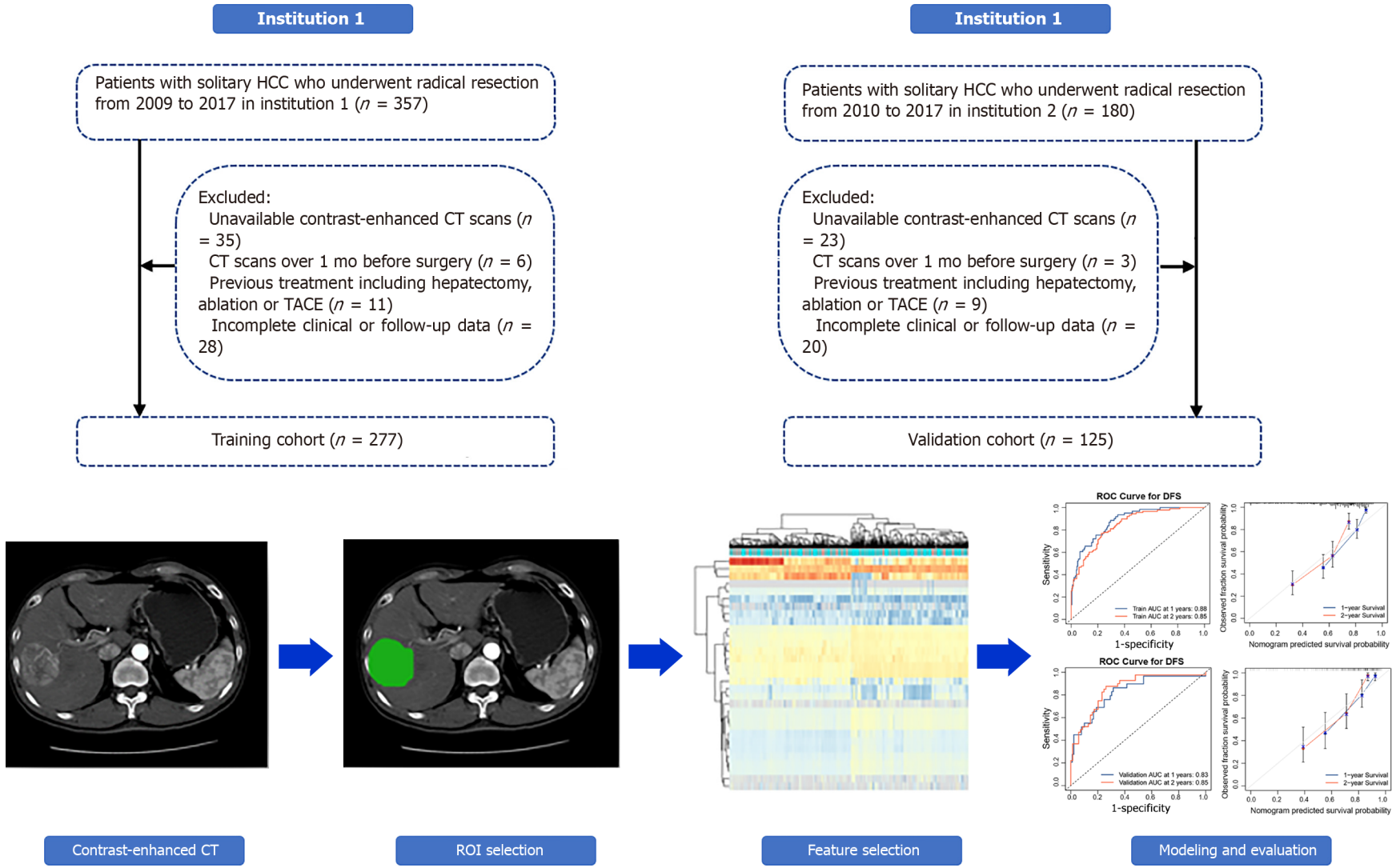
To minimize the variability and normalize the CT images, all the images were resampled to a voxel size of 1 mm × 1 mm × 1 mm. Then, the radiomics features were extracted from the ROI segments based on the Pyradiomics package (version 3.0.1). The categories of radiomics features were as follows: First-order statistics, shape-based features (2D and 3D), grey level cooccurrence matrix (GLCM), grey level run length matrix (GLRLM), grey level size zone matrix (GLZM), neighbouring grey tone difference matrix (NGTDM), and grey level dependence matrix (GLDM). LASSO Cox regression was performed to filter and obtain the early recurrence-related radiomics features according to the minimum criteria with 10-fold cross-validation. The radiomics score was determined according to the coefficients.

Modelling and validation

A radiomics and clinical combined model was developed *via* univariate and multivariate analyses, in which the optimal cut-off value of the radiomics score was determined *via* X-tile (Version 3.6.1). The candidate clinical indicators were hepatitis B surface antigen (HBsAg) (positive *vs* negative), cirrhosis (present *vs* absent), microvascular invasion (MVI) (present *vs* absent), serum AFP (> 200 *vs* ≤ 200 ng/mL), tumour size (cm), platelets (× 10^9/L), gamma-glutamyl transpeptidase (GGT) (U/L), and ALBI. The combined model was presented as a nomogram and validated in an independent cohort.

Statistical analysis

Continuous variables that follow a normal distribution are shown as the mean ± SD and were compared by using the Student's *t* test. Otherwise, the Mann-Whitney *U* test was performed. Categorical variables were compared by chi-squared tests. RFS and OS analyses were conducted by using the Kaplan-Meier method and compared by log-rank test among different groups. Time-dependent receiver operating characteristic (ROC) curves were plotted based on the timeROC package. The concordance index (C-index) was determined to evaluate the predictive ability of the combined model. The calibration curves were plotted with the rms package, while decision curve analysis (DCA) was based on the rmda package. SPSS18.0 (SPSS Inc., Chicago, IL, United States) and R (version 4.0.3, https://www.rproject.org/) were used for statistical analyses. $P < 0.05$ was considered statistically significant.



DOI: 10.3748/wjg.v29.i26.4186 **Copyright** ©The Author(s) 2023.

Figure 1 Flowchart of the study cohorts. HCC: Hepatocellular carcinoma; CT: Computed tomography; TACE: Transarterial chemoembolization; ROI: Region of interest.

RESULTS

Patient characteristics

A total of 402 patients who underwent preoperative CECT were enrolled according to the exclusion criteria from two institutions, and the baseline characteristics are illustrated in Table 1. There were no significant differences in the variables evaluated between the two cohorts except aspartate aminotransferase (AST); most patients were male (both 85.60%), with liver cirrhosis (92.06% and 93.60%) and HBV-related HCC (83.75% and 82.40%, respectively). In institution 1, the median follow-up time was 54.2 mo, the median OS time was 40.0 mo, and the early recurrence rate was 36.82% (102 recurred among 277). In institution 2, the median follow-up time was 50.7 mo, the OS time was 37.0 mo, and the early recurrence rate was 32.80% (41 recurred among 125).

Determination of the radiomics score for early recurrence

A total of 1915 CECT-based radiomics features were extracted from images acquired at both the arterial and portal venous phases among 277 patients in institution 1 as the training cohort. To filter early recurrence-related features, LASSO Cox regression was performed, and 31 features were obtained (Supplementary Figure 1). Figure 2 displays the distribution and correlations among these features. Then, a radiomics score was determined according to the coefficients in Supplementary Table 1 for each patient, and the optimal cut-off value was identified as 15.93, based on which the low and high radiomics risk groups were divided accordingly. As shown in Figure 3A, the radiomics scores were significantly different between the early and nonearly recurrence groups, while the area under curve (AUC) value was 0.73 for both institutions (Figure 3B), thus demonstrating the predictive value of the radiomics score for early recurrence HCC.

Development and assessment of the radiomics and clinical combined model

To further improve the predictive performance of the model, univariate and multivariate Cox regression analyses were conducted among the radiomics model and clinicopathologic indicators. The results from univariate analysis (Table 2) illustrated that the radiomics score, MVI, serum AFP, tumour size, and GGT were statistically significant and were included in the multivariate analysis. Multivariate analysis showed that radiomics score [hazard ratio (HR), 3.86; 95%CI: 2.41-6.16; $P < 0.001$] and serum AFP (HR, 1.52; 95%CI: 1.00-2.30; $P = 0.048$) were identified as independent predictive indicators for early HCC recurrence.

Next, a predictive and visible nomogram was developed based on the radiomics and clinical combined model (Figure 4), and the AUC values of the combined model were 0.79 (95%CI: 0.73-0.84) and 0.77 (95%CI: 0.70-0.83) for 1-year and 2-year recurrence prediction in the training cohort (Figure 5A), respectively. The AUC values of the validation cohort were 0.65 (95%CI: 0.58-0.73) and 0.74 (95%CI: 0.63-0.77) for 1-year and 2-year recurrence, respectively (Figure 5B). The C-index was 0.712 and 0.674 in the training and validation cohorts, respectively. Moreover, the calibration curves illustrated good agreement between predictive and observed outcomes (Figure 5C and D), while the DCA showed that the combined model had a relative high net benefit (Figure 5E and F).

Predictive significance and subgroup analysis of the combined model

To verify the discrimination ability of the combined model, survival curves for RFS and OS were plotted based on the median risk points in the training and validation cohorts. For early recurrence, the high-risk group was more likely to present recurrence than the low-risk group in both the training and validation cohorts (log-rank, $P < 0.0001$ for both) (Figure 6A and C). Furthermore, OS was significantly different (log-rank, $P < 0.0001$ for the training cohort and $P = 0.0446$ for the validation cohort) (Figure 6B and D).

Next, we performed subgroup analysis in AFP-negative (< 20 ng/mL) and AFP-positive (≥ 20 ng/mL) groups. Regardless of the AFP level (Figure 6E-H), the model calculated points were closely related to early recurrence and OS (log-rank, $P < 0.0001$ for all). The results above illustrated the discrimination ability of the combined model.

Representative case reports

Two representative case reports were displayed to demonstrate the distinguishing ability for similar cases (Figure 7). Both of them were male with BCLC A stage HCC and similar ages, and the ROI, also known as the tumour area, was similar in tumour size and position. MVI was present in AFP-negative case 1, while MVI was absent in AFP-positive case 2. However, their outcomes were different. Case 1 was both low risk at the radiomics score and model prediction point and without recurrence until the last follow-up. Case 2 was high risk with worse outcomes, and recurrence was present at 14 mo after the operation. Thus, we concluded that the radiomics combined model could support to distinguish similar cases using CECT in clinical practice.

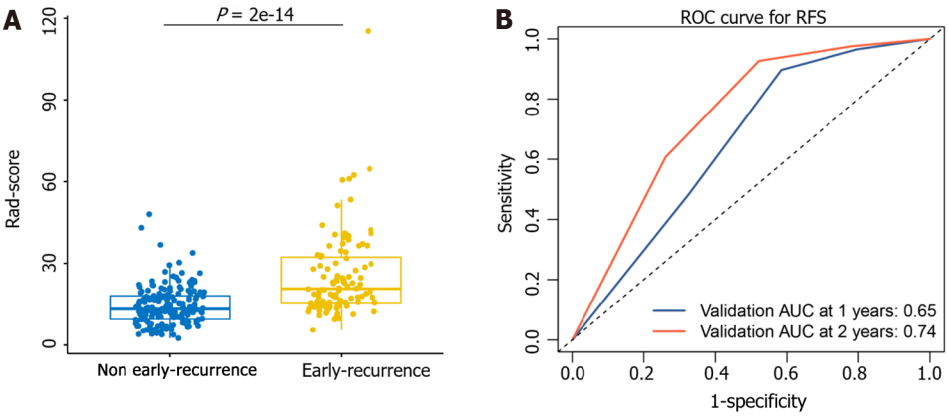
DISCUSSION

Due to the lack of indicators to predict early recurrence for patients who underwent radical resection, we determined a radiomics score based on preoperative CECT for patients from two independent centres, which was shown to be closely related to the occurrence of early recurrence. Next, serum AFP was included to establish a radiomics and clinical combined model, which elevated the accuracy of the model. The AUC values for the two cohorts were 0.77 and 0.74, respectively, and our findings supported that radiomics is able to be adopted to evaluate the RFS of HCC patients and might support preoperative risk stratification and postoperative surveillance management. Previous studies have

Table 1 Clinicopathologic characteristics of patients in the training and validation cohorts

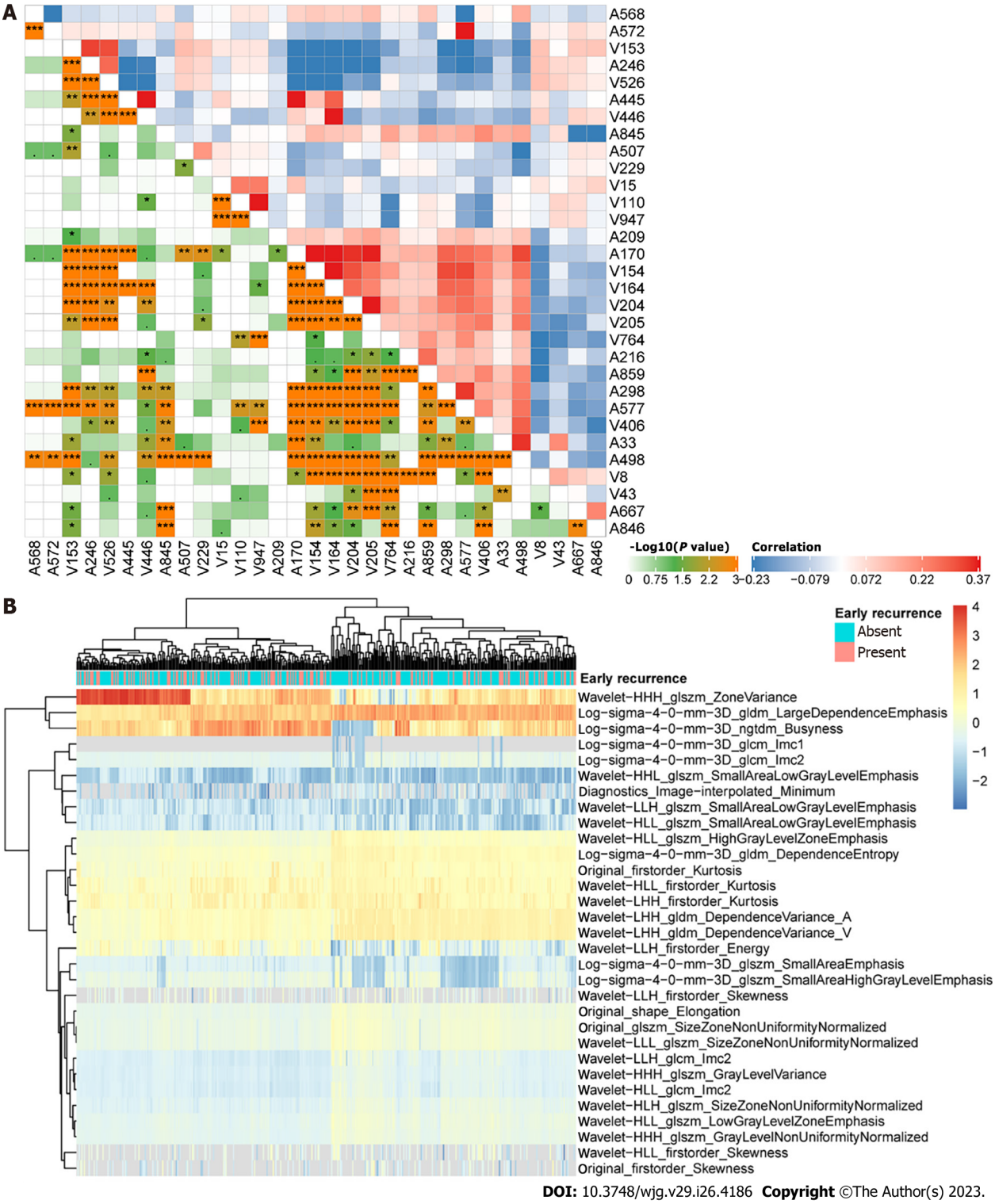
Parameter		Training cohort, *n* = 277	Validation cohort, *n* = 125	*P* value
Gender	Female	40 (14.44)	18 (14.40)	0.991
	Male	237 (85.56)	107 (85.60)	
Age (yr)		50.60 ± 11.27	51.92 ± 10.50	0.265
HBsAg	Negative	45 (16.25)	22 (17.60)	0.736
	Positive	232 (83.75)	103 (82.40)	
Child-Pugh stage	A	252 (90.97)	116 (92.80)	0.543
	B	25 (9.03)	9 (7.20)	
BCLC stage	0 + A	173 (62.45)	83 (66.40)	0.447
	B + C	104 (37.55)	42 (33.60)	
Cirrhosis	Absent	22 (7.94)	8 (6.40)	0.586
	Present	255 (92.06)	117 (93.60)	
MVI	Absent	162 (58.48)	75 (60.00)	0.775
	Present	115 (41.52)	50 (40.00)	
AFP (ng/mL)	≤ 200	130 (46.93)	67 (53.60)	0.204
	> 200	147 (53.07)	58 (46.40)	
Tumor size (cm)		7.42 ± 4.51	7.07 ± 4.03	0.464
Platelets (× 10^9/L)		198.26 ± 94.67	201.52 ± 86.77	0.743
GGT (U/L, median, IQR)		73.90 (41.74, 130.23)	80.35 (46.92, 151.00)	0.198
ALT (U/L, median, IQR)		32.80 (21.11, 51.70)	29.51 (20.50, 48.82)	0.176
AST (U/L, median, IQR)		36.47 (26.75, 53.80)	35.04 (25.90, 51.60)	0.449
TB (mg/dL)		17.41 ± 26.52	17.40 ± 23.84	0.995
DB (mg/dL)		7.99 ± 17.54	8.92 ± 23.26	0.658
ALBI		-2.50 ± 0.47	-2.53 ± 0.42	0.493

HBsAg: Hepatitis B surface antigen; BCLC: Barcelona Clinic Liver Cancer stage; MVI: Microvascular invasion; AFP: Alpha-fetoprotein; GGT: Gamma-glutamyl transpeptidase; IQR: Interquartile range; ALT: Alanine transaminase; AST: Aspartate transaminase; TB: Total bilirubin; DB: Direct bilirubin; ALBI: Albumin-bilirubin.



DOI: 10.3748/wjg.v29.i26.4186 **Copyright** ©The Author(s) 2023.

Figure 2 Correlation and distribution of early recurrence-related radiomics features. A: Correlation of the radiomics features. The red mark represents a positive correlation, while the blue mark represents a negative correlation; B: Heatmap and clustering analysis of the radiomics features. ROC: Receiver operating characteristic; RFS: Recurrence-free survival; AUC: Area under curve.



DOI: 10.3748/wjg.v29.i26.4186 **Copyright** ©The Author(s) 2023.

Figure 3 Capacity of the radiomics score to distinguish early recurrence. A: Correlation of the rad-score between the nonearly recurrence and early recurrence groups; B: Receiver operating characteristic curves of the radiomics score to predict recurrence-free survival in the training and validation cohorts.

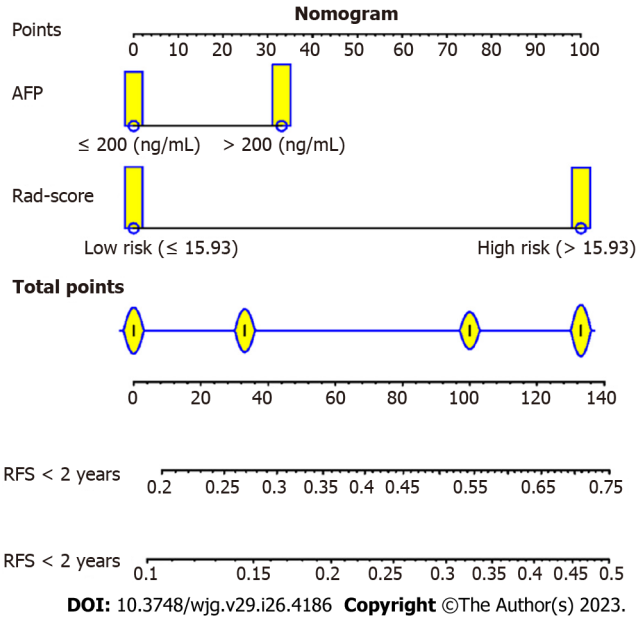
illustrated the usage of radiomics in predicting recurrence of HCC[15,16], but few studies focused on early recurrence and conducted external validation, in which early recurrence was defined as recurrence occurring within 2 years. Furthermore, the model divided the HCC patients into two risk subgroups with a favourable distinction of recurrence and a significant difference in OS. AFP-negative subgroup analysis was also performed to evaluate the reliability of the model.

The heterogeneity in primary and recurrent HCC is quite different. Typically, the gene profile and microenvironments are supposed to be able to distinguish them[8,9]. Villanueva *et al*[17] developed a composite prognostic model for HCC recurrence based on gene expression in tumour tissues. However, the majority of recurrent HCC cases occur within 2 years after surgery, which is regarded as real recurrence. Many studies have indicated that patients with early recurrence have worse outcomes than those with late recurrence[18]. Hence, it is of vital significance to monitor early recurrence in

Table 2 Univariate and multivariate Cox regression analyses of clinicopathologic characteristics for recurrence-free survival in training cohort with hepatocellular carcinoma

Variable	Univariate analysis			Multivariate analysis		
	HR	95%CI	*P* value	HR	95%CI	*P* value
Rad-score (high *vs* low) (*n*)	4.08	2.64-6.24	< 0.001	3.86	2.41-6.16	< 0.001
HBsAg (present *vs* absent) (*n*)	1.81	0.97-3.39	0.063			
Cirrhosis (present *vs* absent) (*n*)	1.84	0.75-4.52	0.183			
MVI (present *vs* absent) (*n*)	1.83	1.24-2.71	0.002	1.20	0.77-1.85	0.418
AFP (> 200 *vs* ≤ 200) (ng/mL)	1.73	1.16-2.58	0.007	1.52	1.00-2.30	0.048
Tumor size (cm)	1.05	1.01-1.09	0.005	1.00	0.94-1.04	0.621
Platelets ($\times 10^9$/L)	1.00	1.00-1.00	0.160			
GGT (U/L)	1.02	1.04-1.02	0.034	1.01	1.01-1.00	0.333
DB (mg/dL)	1.00	1.00-1.01	0.928			
ALBI	0.96	0.64-1.44	0.838			

HR: Hazard ratio; CI: Confidence interval; HBsAg: Hepatitis B surface antigen; MVI: Microvascular invasion; AFP: Alpha fetoprotein; GGT: Gamma-glutamyl transpeptidase; DB: Direct bilirubin; ALBI: Albumin-bilirubin.

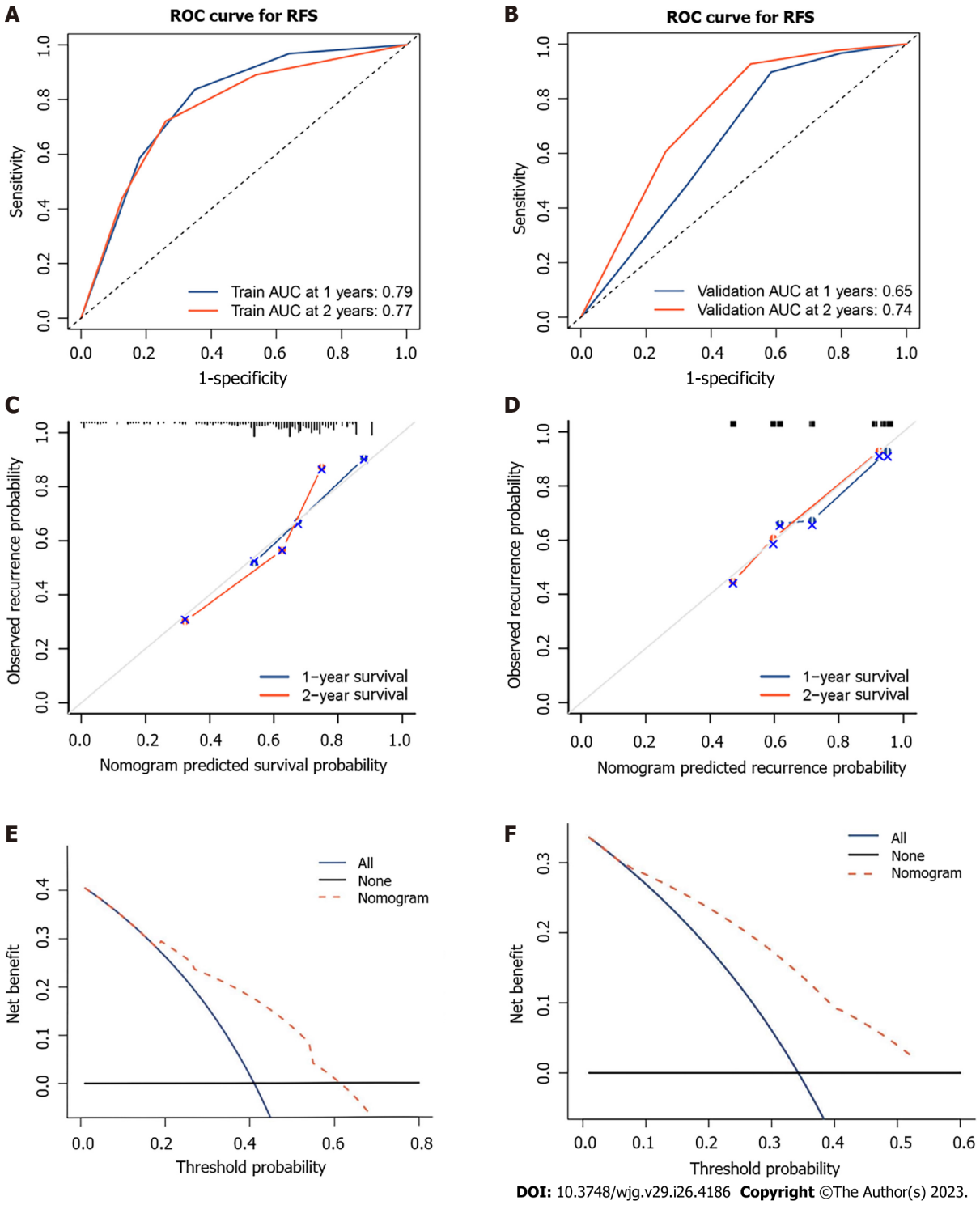


DOI: 10.3748/wjg.v29.i26.4186 **Copyright** ©The Author(s) 2023.

Figure 4 A radiomics and clinical combined model is built based on the radiomics score and preoperative alpha-fetoprotein. According to the total score of each indicator, the recurrence rate corresponding to the total score is the nomogram-predicted rate. AFP: Alpha-fetoprotein; RFS: Recurrence-free survival.

clinical practice. Increasing evidence has illustrated that the immune microenvironment plays a crucial role in the early recurrence of HCC. Sun *et al*[19] revealed the unique characteristics of early relapse HCC at single-cell resolution. Additionally, metabolic microenvironments, such as lipogenesis and glycolysis, might promote oncogenic transformation [20-23]. The mechanism above reveals the complexity of recurrent HCC. Many staging systems have been applied in the diagnosis and treatment of HCC, including the AJCC TNM staging system and the BCLC and Child-Pugh staging systems. Nevertheless, none of them are capable of predicting recurrence. Serum AFP level has long been used as an indicator to predict recurrence in both hepatectomy and liver transplantation[24,25], which showed effect in our model, as well.

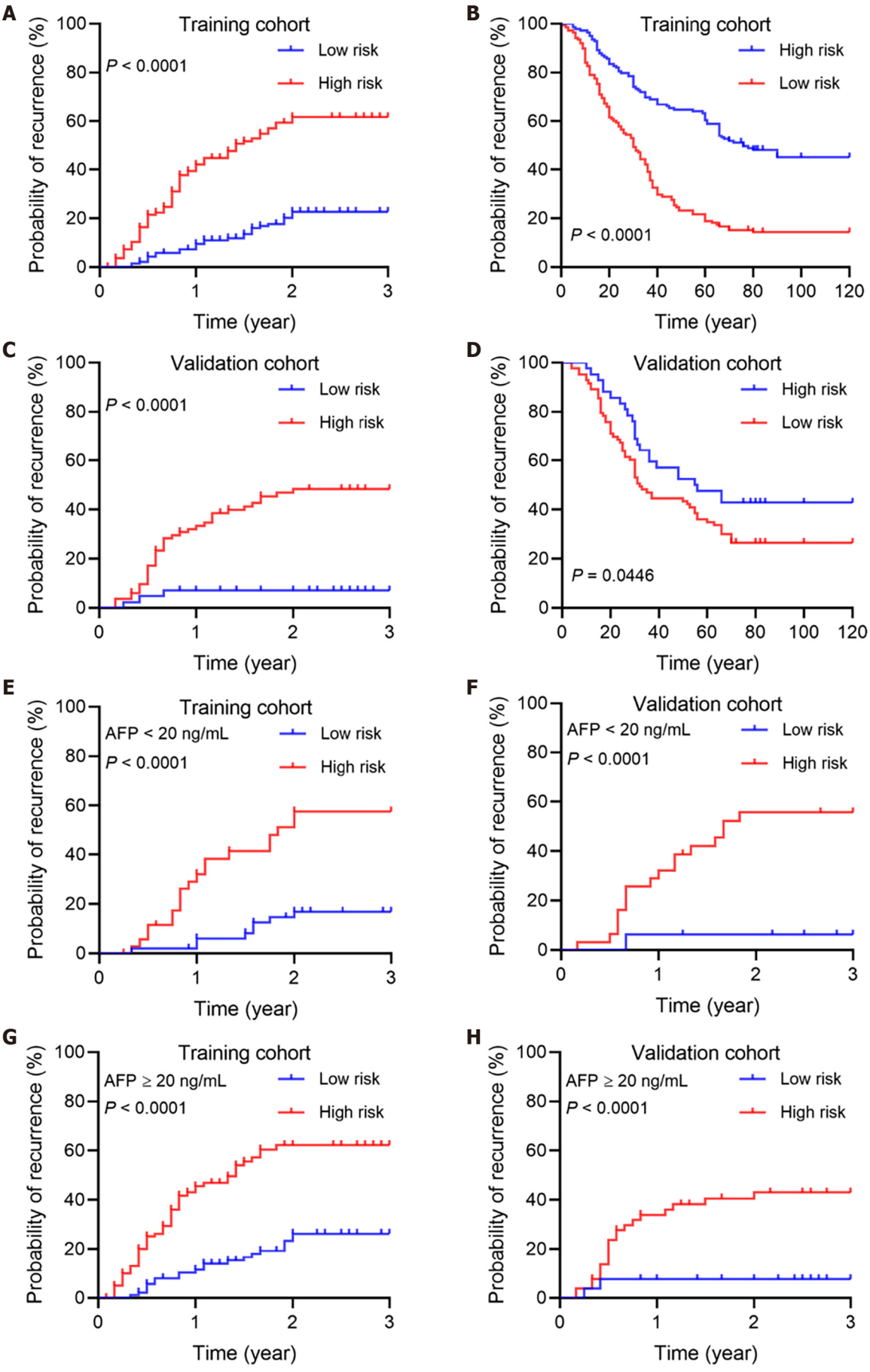
Preoperative imaging plays a very important role in the effective diagnosis and treatment of HCC, and CECT is part of this process. For BCLC stages A and B patients, liver resection is considered the main treatment strategy. However, the postoperative recurrence rate is extremely high. Hence, we employed radiomics to explore more details from CECT images. In this study, radiomics scores were determined based on the 31 features. There were 16 features extracted from images in the arterial phase and 15 features from images in the portal venous phase, which was consistent with the



DOI: 10.3748/wjg.v29.i26.4186 **Copyright** ©The Author(s) 2023.

Figure 5 Evaluation of the radiomics model to predict early recurrence. A: Receiver operating characteristic (ROC) curves to predict 1- and 2-year recurrence-free survival (RFS) in the training cohort; B: ROC curves to predict 1- and 2-year RFS in the validation cohort; C: Calibration curves of the 1- and 2-year RFS in the training cohort; D: Calibration curves of the 1- and 2-year RFS in the validation cohort; E: Decision curve analysis of the combined model in the training cohort; F: Decision curve analysis of the combined model in the validation cohort. ROC: Receiver operating characteristic; RFS: Recurrence-free survival; AUC: Area under curve.

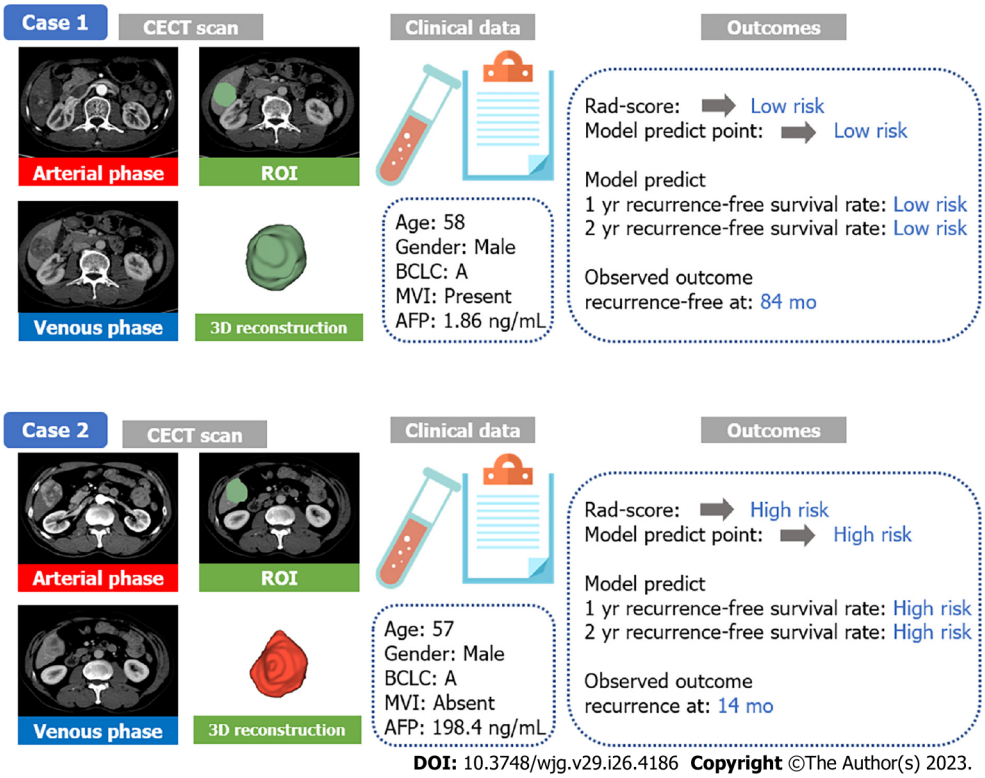
diagnosis of HCC depending on the dynamic changes in vascular findings from the arterial phase to portal venous phase [26-29]. Consistently, among these features, most of them were based on wavelet filtered features that accounted for the greatest weight, which coincided with the previous studies[15], and might represent tumour heterogeneity of HCC and peritumoral tissues that were hard to explain and easy to be ignored by the radiologist. The potential use of radiomics has been widely reported. Hence, we combined radiomics and serum indicators to evaluate the risk of early recurrence, which was validated in an independent cohort. Our findings showed favourable value in predicting early recurrence for patients with HCC *via* non-invasive indicators and might guide clinical decisions.



DOI: 10.3748/wjg.v29.i26.4186 **Copyright** ©The Author(s) 2023.

Figure 6 Cumulative rates of early recurrence and survival rates of hepatocellular carcinoma. A: Risk accumulation curve of recurrence-free

survival (RFS) in the training cohort; B: Survival curve of overall survival (OS) in the training cohort; C: Risk accumulation curve of RFS in the validation cohort; D: Survival curve of OS in the validation cohort; E and F: Risk accumulation curve of RFS in the alpha-fetoprotein (AFP)-negative group in the training and validation cohorts; G and H: Risk accumulation curve of RFS in the AFP-positive group in the training and validation cohorts. AFP: Alpha fetoprotein.



DOI: 10.3748/wjg.v29.i26.4186 **Copyright** ©The Author(s) 2023.

Figure 7 Representative case reports. AFP: Alpha-fetoprotein; BCLC: Barcelona Clinic Liver Cancer; CECT: Contrast-enhanced computed tomography; MVI: Microvascular invasion; ROI: Regions of interest.

There were several limitations in our study. First, because this was a retrospective analysis, inherent biases were inevitable. Second, even though the radiomics features were extracted *via* a standard process, the features might differ and be critically dependent across CT machines and centres. Third, with the development of multimodality radiomics, Gd-EOB-DTPA-enhanced MR or 18F-FDG PET/CT has been widely used and have more favourable discrimination in adipose tissue and tumour capsules[30,31]. Therefore, we should conduct prospective trials with multimodality radiomics to confirm our results.

CONCLUSION

In summary, the radiomics scores calculated herein revealed significant differences between early and nonearly recurrence HCC patients. Then, we integrated the scores with serum AFP to develop a radiomics and clinical combined model that showed advantages and might serve as a powerful tool to predict early recurrence of HCC. We will perform further validation and translate the results into clinical application.

ARTICLE HIGHLIGHTS

Research background

Hepatocellular carcinoma (HCC) seriously endangers human life and health, but there is still a lack of satisfactory treatment options. Even if it is diagnosed at early stage, the recurrence rate is still very high. The clinical monitoring strategy for HCC recurrence is limited, so there is a need to find a new and effective recurrence prediction model for HCC. And we developed a radiomics model based on preoperative contrast-enhanced computed tomography (CECT) to evaluate early recurrence in patients with a single tumour.

Research motivation

Due to the high malignancy and suppressive immune microenvironment of HCC, there are still high recurrence and metastasis rates even in HCC patients who have undergone radical resection. Therefore, it is of vital importance to conduct systematic surveillance of HCC recurrence, and there is an urgent need to precisely predict recurrence in patients with HCC. If tumour recurrence can be detected earlier, the survival and quality of life of HCC patients might be greatly improved.

Research objectives

Despite the rapid development in the treatment of HCC in recent decades, patients' outcomes remain unsatisfactory. One of the reasons is that the early diagnosis system of HCC recurrence is not yet well developed, so our research team established a recurrence prediction model for HCC based on medical imaging such as computed tomography (CT) to predict HCC recurrence earlier, so that timely treatment measures can be taken.

Research methods

We collected CT images from 537 clinical patients in two institutions and extracted valuable CT image features with 3D Slicer (v4.11, https://www.slicer.org). SPSS18.0 (SPSS Inc., Chicago, IL, United States) and R (version 4.0.3, https://www.rproject.org/) were used for statistical analyses and the prediction model of HCC recurrence was established jointly with AFP.

Research results

The radiomics scores calculated herein revealed significant differences between early and nonearly recurrence HCC patients. We combined radiomics and serum indicators to evaluate the risk of early recurrence, which was validated in an independent cohort. Our findings showed the value of predicting early recurrence in HCC patients by noninvasive indicators and might guide clinical decisions making. However, this is a retrospective analysis, and inherent biases are inevitable. We would conduct prospective trials with multimodality radiomics to confirm our results in future.

Research conclusions

The preoperative radiomics model was shown to be effective for predicting early recurrence among patients with single HCC. Compared with pathological biopsy or other tests, this model is noninvasive and more convenient for HCC patients.

Research perspectives

For HCC diagnosis, treatment, or prognosis assessment, more non-invasive methods are of great significance and needed.

FOOTNOTES

Author contributions: Li SQ, Su LL, Xu TF, and Ren LY contributed equally to this work; Liao WJ and Li SQ designed the study; Ren LY, Chen DB, Xu TF, and Su LL analyzed the data and wrote the manuscript; Yan XZ and Fan JX collected the data; Qin WY and Chen HS analyzed the images data; all authors have read and approved the final manuscript.

Supported by National Natural Science Foundation of China, No. 81773148; Natural Science Foundation of Guangxi, No. 2018GXNSFDA138001; Program of Guangxi Zhuang Autonomous Region Health and Family Planning Commission, No. Z20210706; Guangxi Medical and Healthcare Appropriate Technology Development and Promotion and Application Projects, No. S2022132; Guangxi Natural Science Foundation, No. 2022JJA140009; and Guangxi Zhuang Autonomous Region Health and Family Planning Commission Self-funded of Scientific Research Project, No. Z20170812.

Institutional review board statement: The study was reviewed and approved by the Medical Ethics Committee of the Affiliated Hospital of Guilin Medical University (Approval No. 2021WJWZC14).

Informed consent statement: Patients were not required to give informed consent to the study because the analysis used anonymous clinical data that were obtained after each patient agreed to treatment by written consent.

Conflict-of-interest statement: Liao WJ has received fees for serving as a speaker, a professor for the Affiliated Hospital of Guilin Medical University; Liao WJ has received research funding from the National Natural Science Foundation of China.

Data sharing statement: Technical appendix, statistical code, and dataset available from the corresponding author at liaoweijia288@163.com. Participants gave informed consent for data sharing.

Open-Access: This article is an open-access article that was selected by an in-house editor and fully peer-reviewed by external reviewers. It is distributed in accordance with the Creative Commons Attribution NonCommercial (CC BY-NC 4.0) license, which permits others to distribute, remix, adapt, build upon this work non-commercially, and license their derivative works on different terms, provided the original work is properly cited and the use is non-commercial. See: https://creativecommons.org/Licenses/by-nc/4.0/

Country/Territory of origin: China

ORCID number: Shu-Qun Li 0000-0002-6930-6855; Li-Li Su 0000-0002-4126-4366; Ting-Feng Xu 0000-0003-0303-5471; Li-Ying Ren 0000-0003-3624-5483; Dong-Bo Chen 0000-0001-5173-6999; Wan-Ying Qin 0000-0001-6040-9340; Xuan-Zhi Yan 0000-0002-0095-7190; Jia-Xing Fan 0000-0002-0926-3451; Hong-Song Chen 0000-0001-6858-8398; Wei-Jia Liao 0000-0002-8906-8612.

S-Editor: Yan JP
L-Editor: Wang TQ
P-Editor: Yu HG

REFERENCES

1 **Sung H**, Ferlay J, Siegel RL, Laversanne M, Soerjomataram I, Jemal A, Bray F. Global Cancer Statistics 2020: GLOBOCAN Estimates of Incidence and Mortality Worldwide for 36 Cancers in 185 Countries. *CA Cancer J Clin* 2021; **71**: 209-249 [PMID: 33538338 DOI: 10.3322/caac.21660]
2 **European Association for the Study of the Liver**. EASL Clinical Practice Guidelines: Management of hepatocellular carcinoma. *J Hepatol* 2018; **69**: 182-236 [PMID: 29628281 DOI: 10.1016/j.jhep.2018.03.019]
3 **Wang JH**, Wang CC, Hung CH, Chen CL, Lu SN. Survival comparison between surgical resection and radiofrequency ablation for patients in BCLC very early/early stage hepatocellular carcinoma. *J Hepatol* 2012; **56**: 412-418 [PMID: 21756858 DOI: 10.1016/j.jhep.2011.05.020]
4 **Villanueva A**. Hepatocellular Carcinoma. *N Engl J Med* 2019; **380**: 1450-1462 [PMID: 30970190 DOI: 10.1056/NEJMra1713263]
5 **Lu C**, Rong D, Zhang B, Zheng W, Wang X, Chen Z, Tang W. Current perspectives on the immunosuppressive tumor microenvironment in hepatocellular carcinoma: challenges and opportunities. *Mol Cancer* 2019; **18**: 130 [PMID: 31464625 DOI: 10.1186/s12943-019-1047-6]
6 **Cha C**, Fong Y, Jarnagin WR, Blumgart LH, DeMatteo RP. Predictors and patterns of recurrence after resection of hepatocellular carcinoma. *J Am Coll Surg* 2003; **197**: 753-758 [PMID: 14585409 DOI: 10.1016/j.jamcollsurg.2003.07.003]
7 **Tabrizian P**, Jibara G, Shrager B, Schwartz M, Roayaie S. Recurrence of hepatocellular cancer after resection: patterns, treatments, and prognosis. *Ann Surg* 2015; **261**: 947-955 [PMID: 25010665 DOI: 10.1097/SLA.0000000000000710]
8 **Chen PJ**, Chen DS, Lai MY, Chang MH, Huang GT, Yang PM, Sheu JC, Lee SC, Hsu HC, Sung JL. Clonal origin of recurrent hepatocellular carcinomas. *Gastroenterology* 1989; **96**: 527-529 [PMID: 2535996 DOI: 10.1016/0016-5085(89)91581-3]
9 **Ng IO**, Guan XY, Poon RT, Fan ST, Lee JM. Determination of the molecular relationship between multiple tumour nodules in hepatocellular carcinoma differentiates multicentric origin from intrahepatic metastasis. *J Pathol* 2003; **199**: 345-353 [PMID: 12579536 DOI: 10.1002/path.1287]
10 **Johnson PJ**, Berhane S, Kagebayashi C, Satomura S, Teng M, Reeves HL, O'Beirne J, Fox R, Skowronska A, Palmer D, Yeo W, Mo F, Lai P, Iñarrairaegui M, Chan SL, Sangro B, Miksad R, Tada T, Kumada T, Toyoda H. Assessment of liver function in patients with hepatocellular carcinoma: a new evidence-based approach-the ALBI grade. *J Clin Oncol* 2015; **33**: 550-558 [PMID: 25512453 DOI: 10.1200/JCO.2014.57.9151]
11 **Lambin P**, Leijenaar RTH, Deist TM, Peerlings J, de Jong EEC, van Timmeren J, Sanduleanu S, Larue RTHM, Even AJG, Jochems A, van Wijk Y, Woodruff H, van Soest J, Lustberg T, Roelofs E, van Elmpt W, Dekker A, Mottaghy FM, Wildberger JE, Walsh S. Radiomics: the bridge between medical imaging and personalized medicine. *Nat Rev Clin Oncol* 2017; **14**: 749-762 [PMID: 28975929 DOI: 10.1038/nrclinonc.2017.141]
12 **Kitao A**, Matsui O, Zhang Y, Ogi T, Nakada S, Sato Y, Harada K, Yoneda N, Kozaka K, Inoue D, Yoshida K, Koda W, Yamashita T, Kaneko S, Kobayashi S, Gabata T. Dynamic CT and Gadoxetic Acid-enhanced MRI Characteristics of P53-mutated Hepatocellular Carcinoma. *Radiology* 2023; **306**: e220531 [PMID: 36219111 DOI: 10.1148/radiol.220531]
13 **Xu X**, Zhang HL, Liu QP, Sun SW, Zhang J, Zhu FP, Yang G, Yan X, Zhang YD, Liu XS. Radiomic analysis of contrast-enhanced CT predicts microvascular invasion and outcome in hepatocellular carcinoma. *J Hepatol* 2019; **70**: 1133-1144 [PMID: 30876945 DOI: 10.1016/j.jhep.2019.02.023]
14 **Liu Q**, Li J, Liu F, Yang W, Ding J, Chen W, Wei Y, Li B, Zheng L. A radiomics nomogram for the prediction of overall survival in patients with hepatocellular carcinoma after hepatectomy. *Cancer Imaging* 2020; **20**: 82 [PMID: 33198809 DOI: 10.1186/s40644-020-00360-9]
15 **Ji GW**, Zhu FP, Xu Q, Wang K, Wu MY, Tang WW, Li XC, Wang XH. Radiomic Features at Contrast-enhanced CT Predict Recurrence in Early Stage Hepatocellular Carcinoma: A Multi-Institutional Study. *Radiology* 2020; **294**: 568-579 [PMID: 31934830 DOI: 10.1148/radiol.2020191470]
16 **Zhang X**, Wang C, Zheng D, Liao Y, Wang X, Huang Z, Zhong Q. Radiomics nomogram based on multi-parametric magnetic resonance imaging for predicting early recurrence in small hepatocellular carcinoma after radiofrequency ablation. *Front Oncol* 2022; **12**: 1013770 [PMID: 36439458 DOI: 10.3389/fonc.2022.1013770]
17 **Villanueva A**, Hoshida Y, Battiston C, Tovar V, Sia D, Alsinet C, Cornella H, Liberzon A, Kobayashi M, Kumada H, Thung SN, Bruix J, Newell P, April C, Fan JB, Roayaie S, Mazzaferro V, Schwartz ME, Llovet JM. Combining clinical, pathology, and gene expression data to predict recurrence of hepatocellular carcinoma. *Gastroenterology* 2011; **140**: 1501-12.e2 [PMID: 21320499 DOI: 10.1053/j.gastro.2011.02.006]
18 **Yamamoto Y**, Ikoma H, Morimura R, Konishi H, Murayama Y, Komatsu S, Shiozaki A, Kuriu Y, Kubota T, Nakanishi M, Ichikawa D, Fujiwara H, Okamoto K, Sakakura C, Ochiai T, Otsuji E. Optimal duration of the early and late recurrence of hepatocellular carcinoma after hepatectomy. *World J Gastroenterol* 2015; **21**: 1207-1215 [PMID: 25632194 DOI: 10.3748/wjg.v21.i4.1207]
19 **Sun Y**, Wu L, Zhong Y, Zhou K, Hou Y, Wang Z, Zhang Z, Xie J, Wang C, Chen D, Huang Y, Wei X, Shi Y, Zhao Z, Li Y, Guo Z, Yu Q, Xu L, Volpe G, Qiu S, Zhou J, Ward C, Sun H, Yin Y, Xu X, Wang X, Esteban MA, Yang H, Wang J, Dean M, Zhang Y, Liu S, Yang X, Fan J. Single-cell landscape of the ecosystem in early-relapse hepatocellular carcinoma. *Cell* 2021; **184**: 404-421.e16 [PMID: 33357445 DOI: 10.1016/j.cell.2020.11.041]
20 **Zuo X**, Chen Z, Gao W, Zhang Y, Wang J, Cao M, Cai J, Wu J, Wang X. M6A-mediated upregulation of LINC00958 increases lipogenesis and acts as a nanotherapeutic target in hepatocellular carcinoma. *J Hematol Oncol* 2020; **13**: 5 [PMID: 31915027 DOI: 10.1186/s13045-019-0839-x]
21 **Calvisi DF**, Wang C, Ho C, Ladu S, Lee SA, Mattu S, Destefanis G, Delogu S, Zimmermann A, Ericsson J, Brozzetti S, Staniscia T, Chen X,

Dombrowski F, Evert M. Increased lipogenesis, induced by AKT-mTORC1-RPS6 signaling, promotes development of human hepatocellular carcinoma. *Gastroenterology* 2011; **140**: 1071-1083 [PMID: 21147110 DOI: 10.1053/j.gastro.2010.12.006]

22 **Gao Q**, Zhu H, Dong L, Shi W, Chen R, Song Z, Huang C, Li J, Dong X, Zhou Y, Liu Q, Ma L, Wang X, Zhou J, Liu Y, Boja E, Robles AI, Ma W, Wang P, Li Y, Ding L, Wen B, Zhang B, Rodriguez H, Gao D, Zhou H, Fan J. Integrated Proteogenomic Characterization of HBV-Related Hepatocellular Carcinoma. *Cell* 2019; **179**: 561-577.e22 [PMID: 31585088 DOI: 10.1016/j.cell.2019.08.052]

23 **Li Q**, Pan X, Zhu D, Deng Z, Jiang R, Wang X. Circular RNA MAT2B Promotes Glycolysis and Malignancy of Hepatocellular Carcinoma Through the miR-338-3p/PKM2 Axis Under Hypoxic Stress. *Hepatology* 2019; **70**: 1298-1316 [PMID: 31004447 DOI: 10.1002/hep.30671]

24 **Ijichi M**, Takayama T, Matsumura M, Shiratori Y, Omata M, Makuuchi M. alpha-Fetoprotein mRNA in the circulation as a predictor of postsurgical recurrence of hepatocellular carcinoma: a prospective study. *Hepatology* 2002; **35**: 853-860 [PMID: 11915031 DOI: 10.1053/jhep.2002.32100]

25 **Notarpaolo A**, Layese R, Magistri P, Gambato M, Colledan M, Magini G, Miglioresi L, Vitale A, Vennarecci G, Ambrosio CD, Burra P, Di Benedetto F, Fagiuoli S, Colasanti M, Maria Ettorre G, Andreoli A, Cillo U, Laurent A, Katsahian S, Audureau E, Roudot-Thoraval F, Duvoux C. Validation of the AFP model as a predictor of HCC recurrence in patients with viral hepatitis-related cirrhosis who had received a liver transplant for HCC. *J Hepatol* 2017; **66**: 552-559 [PMID: 27899297 DOI: 10.1016/j.jhep.2016.10.038]

26 **Sun YF**, Xu Y, Yang XR, Guo W, Zhang X, Qiu SJ, Shi RY, Hu B, Zhou J, Fan J. Circulating stem cell-like epithelial cell adhesion molecule-positive tumor cells indicate poor prognosis of hepatocellular carcinoma after curative resection. *Hepatology* 2013; **57**: 1458-1468 [PMID: 23175471 DOI: 10.1002/hep.26151]

27 **Xu RH**, Wei W, Krawczyk M, Wang W, Luo H, Flagg K, Yi S, Shi W, Quan Q, Li K, Zheng L, Zhang H, Caughey BA, Zhao Q, Hou J, Zhang R, Xu Y, Cai H, Li G, Hou R, Zhong Z, Lin D, Fu X, Zhu J, Duan Y, Yu M, Ying B, Zhang W, Wang J, Zhang E, Zhang C, Li O, Guo R, Carter H, Zhu JK, Hao X, Zhang K. Circulating tumour DNA methylation markers for diagnosis and prognosis of hepatocellular carcinoma. *Nat Mater* 2017; **16**: 1155-1161 [PMID: 29035356 DOI: 10.1038/nmat4997]

28 **Bruix J**, Sherman M; Practice Guidelines Committee, American Association for the Study of Liver Diseases. Management of hepatocellular carcinoma. *Hepatology* 2005; **42**: 1208-1236 [PMID: 16250051 DOI: 10.1002/hep.20933]

29 **Clavien PA**, Lesurtel M, Bossuyt PM, Gores GJ, Langer B, Perrier A; OLT for HCC Consensus Group. Recommendations for liver transplantation for hepatocellular carcinoma: an international consensus conference report. *Lancet Oncol* 2012; **13**: e11-e22 [PMID: 22047762 DOI: 10.1016/S1470-2045(11)70175-9]

30 **Vreugdenburg TD**, Ma N, Duncan JK, Riitano D, Cameron AL, Maddern GJ. Comparative diagnostic accuracy of hepatocyte-specific gadoxetic acid (Gd-EOB-DTPA) enhanced MR imaging and contrast enhanced CT for the detection of liver metastases: a systematic review and meta-analysis. *Int J Colorectal Dis* 2016; **31**: 1739-1749 [PMID: 27682648 DOI: 10.1007/s00384-016-2664-9]

31 **Tanimoto A**, Lee JM, Murakami T, Huppertz A, Kudo M, Grazioli L. Consensus report of the 2nd International Forum for Liver MRI. *Eur Radiol* 2009; **19** Suppl 5: S975-S989 [PMID: 19851766 DOI: 10.1007/s00330-009-1624-y]

World Journal of Gastroenterology

Submit a Manuscript: https://www.f6publishing.com

World J Gastroenterol 2023 July 14; 29(26): 4200-4213

DOI: 10.3748/wjg.v29.i26.4200

ISSN 1007-9327 (print) ISSN 2219-2840 (online)

ORIGINAL ARTICLE

Clinical Trials Study

Raf kinase inhibitor protein combined with phosphorylated extracellular signal-regulated kinase offers valuable prognosis in gastrointestinal stromal tumor

Wen-Zhi Qu, Luan Wang, Juan-Juan Chen, Yang Wang

Specialty type: Gastroenterology and hepatology

Provenance and peer review: Unsolicited article; Externally peer reviewed.

Peer-review model: Single blind

Peer-review report's scientific quality classification

Grade A (Excellent): 0
Grade B (Very good): B, B
Grade C (Good): 0
Grade D (Fair): 0
Grade E (Poor): 0

P-Reviewer: Chmura SJ, United States; Kwon T, United States

Received: April 24, 2023
Peer-review started: April 24, 2023
First decision: May 16, 2023
Revised: May 20, 2023
Accepted: June 2, 2023
Article in press: June 2, 2023
Published online: July 14, 2023

Wen-Zhi Qu, Yang Wang, Department of General Surgery, The 4th Affiliated Hospital of China Medical University, Shenyang 110032, Liaoning Province, China

Luan Wang, Department of Emergency, Shengjing Hospital of China Medical University, Shenyang 110004, Liaoning Province, China

Juan-Juan Chen, Department of Medical Service, Shengjing Hospital of China Medical University, Shenyang 110004, Liaoning Province, China

Corresponding author: Yang Wang, MD, PhD, Associate Professor, Doctor, Department of General Surgery, The 4th Affiliated Hospital of China Medical University, No. 4 Chongshan Road, Huanggu District, Shenyang 110032, Liaoning Province, China. wwyy840731@126.com

Abstract

BACKGROUND

Gastrointestinal stromal tumors (GISTs) are the most common mesenchymal tumors of the gastrointestinal tract. Tyrosine kinase inhibitors, such as imatinib, have been used as first-line therapy for the treatment of GISTs. Although these drugs have achieved considerable efficacy in some patients, reports of resistance and recurrence have emerged. Extracellular signal-regulated kinase 1/2 (ERK1/2) protein, as a member of the mitogen-activated protein kinase (MAPK) family, is a core molecule of this signaling pathway. Nowadays, research reports on the important clinical and prognostic value of phosphorylated-ERK (P-ERK) and phosphorylated-MAPK/ERK kinase (P-MEK) proteins closely related to raf kinase inhibitor protein (RKIP) have gradually emerged in digestive tract tumors such as gastric cancer, colon cancer, and pancreatic cancer. However, literature on the expression of these downstream proteins combined with RKIP in GIST is scarce. This study will focus on this aspect and search for answers to the problem.

AIM

To detect the expression of RKIP, P-ERK, and P-MEK protein in GIST and to analyze their relationship with clinicopathological characteristics and prognosis of this disease. Try to establish a new prognosis evaluation model using RKIP and P-ERK in combination with analysis and its prognosis evaluation efficacy.

METHODS

The research object of our experiment was 66 pathologically diagnosed GIST patients with complete clinical and follow-up information. These patients received surgical treatment at China Medical University Affiliated Hospital from January 2015 to January 2020. Immunohistochemical method was used to detect the expression of RKIP, P-ERK, and P-MEK proteins in GIST tissue samples from these patients. Kaplan-Meier method was used to calculate the survival rate of 63 patients with complete follow-up data. A Nomogram was used to represent the new prognostic evaluation model. The Cox multivariate regression analysis was conducted separately for each set of risk evaluation factors, based on two risk classification systems [the new risk grade model *vs* the modified National Institutes of Health (NIH) 2008 risk classification system]. Receiver operating characteristic (ROC) curves were used for evaluating the accuracy and efficiency of the two prognostic evaluation systems.

RESULTS

In GIST tissues, RKIP protein showed positive expression in the cytoplasm and cell membrane, appearing as brownish-yellow or brown granules. The expression of RKIP was related to GIST tumor size, NIH grade, and mucosal invasion. P-ERK protein exhibited heterogeneous distribution in GIST cells, mainly in the cytoplasm, with occasional presence in the nucleus, and appeared as brownish-yellow granules, and the expression of P-ERK protein was associated with GIST tumor size, mitotic count, mucosal invasion, and NIH grade. Meanwhile, RKIP protein expression was negatively correlated with P-ERK expression. The results in COX multivariate regression analysis showed that RKIP protein expression was not an independent risk factor for tumor prognosis. However, RKIP combined with P-ERK protein expression were identified as independent risk factors for prognosis with statistical significance. Furthermore, we establish a new prognosis evaluation model using RKIP and P-ERK in combination and obtained the nomogram of the new prognosis evaluation model. ROC curve analysis also showed that the new evaluation model had better prognostic performance than the modified NIH 2008 risk classification system.

CONCLUSION

Our experimental results showed that the expression of RKIP and P-ERK proteins in GIST was associated with tumor size, NIH 2008 staging, and tumor invasion, and P-ERK expression was also related to mitotic count. The expression of the two proteins had a certain negative correlation. The combined expression of RKIP and P-ERK proteins can serve as an independent risk factor for predicting the prognosis of GIST patients. The new risk assessment model incorporating RKIP and P-ERK has superior evaluation efficacy and is worth further practical application to validate.

Key Words: Raf kinase inhibitory protein; Phosphorylated extracellular-signal-regulated kinase; Gastrointestinal stromal tumors; Immunohistochemistry; Survival analysis; Risk grade model

©The Author(s) 2023. Published by Baishideng Publishing Group Inc. All rights reserved.

Core Tip: Nowadays, research reports on the expression of downstream proteins of the extracellular signal-regulated kinase (ERK)/mitogen-activated protein kinase pathway combined with raf kinase inhibitor protein (RKIP) in gastrointestinal stromal tumor (GIST) is scarce. This study will focus on this aspect and use immunohistochemistry methods, large sample survival analysis data, and the latest bioinformatics analysis techniques to answer the problem. Our experimental results showed that the expression of the two proteins had a certain negative correlation. The combined expression of RKIP and phosphorylated-ERK proteins can serve as an independent risk factor for predicting the prognosis of GIST patients. Furthermore, the new risk assessment model incorporating RKIP and phosphorylated-ERK has superior evaluation efficacy.

Citation: Qu WZ, Wang L, Chen JJ, Wang Y. Raf kinase inhibitor protein combined with phosphorylated extracellular signal-regulated kinase offers valuable prognosis in gastrointestinal stromal tumor. *World J Gastroenterol* 2023; 29(26): 4200-4213
URL: https://www.wjgnet.com/1007-9327/full/v29/i26/4200.htm
DOI: https://dx.doi.org/10.3748/wjg.v29.i26.4200

INTRODUCTION

Gastrointestinal stromal tumors (GISTs) are the most common mesenchymal tumors of the gastrointestinal tract. It is believed that GISTs originate from Cajal cells, and mutations in the kit and platelet-derived growth factor receptor-alpha (PDGFR-α) genes are considered to be the cause of most cases of GISTs. Based on this discovery, specific tyrosine kinase inhibitors, such as imatinib, have been used as first-line therapy for the treatment of GISTs. Although these drugs have achieved considerable efficacy in some patients, reports of resistance and recurrence have emerged[1]. Even second-line target therapy drugs such as sunitinib, protein kinase C (PKC) 412, or BMS-354825 are not effective for all patients[2].

To overcome tumor resistance, research on GISTs has focused on the search and validation of new targeted therapy sites and regulatory genes. The Raf-MEK-ERK pathway, which is closely related to GIST, is one of the well-studied pathways. Extracellular signal-regulated kinase 1/2 (ERK1/2) protein, as a member of the mitogen-activated protein kinase (MAPK) family, is a core molecule of this signaling pathway. It works with upstream activating molecules and downstream effector molecules to form an efficient and accurate signal transduction system. The MAPK/ERK Kinase 1/2 (MEK 1/2) protein is a MAPKK (MAPK kinase) that can activate the Thr and Tyr sites on the ERK1/2 protein, thereby phosphorylating and activating it to produce the activated form of P-ERK1/2. Raf-1 protein is an upstream MAPKKK (MAPKK Kinase) that can activate the entire pathway by phosphorylating MEK1/2 to obtain P-MEK1/2. The pathway is regulated by the cell cycle and extracellular stimuli, thus regulating downstream protein kinases, phospholipases, and transcription factors to play important biological functions[3-5].

The RKIP protein is a structurally complex protein with a "multidirectional switch" regulatory role in multiple signaling pathways. First, it can regulate multiple signaling pathways and has an inhibitory effect on the Raf-MEK-ERK pathway, affecting cell invasion and proliferation[6]. Additionally, the RKIP protein is also a phosphorylation target, such as its binding to G protein-coupled receptor kinase 2 (GRK2) in the G protein-coupled pathway[7]. Recently, the study of RKIP protein's tumor regulatory function has gradually become a hot spot, and previous studies have reported that RKIP protein is related to the size of GIST tumors, National Institutes of Health (NIH) staging, and whether the tumor invades the mucosa, but RKIP cannot be used as an independent factor for GIST prognosis evaluation[8].

Nowadays, research reports on the important clinical and prognostic value of phosphorylated (P)-ERK and P-MEK proteins closely related to RKIP have gradually emerged in digestive tract tumors such as gastric cancer, colon cancer, and pancreatic cancer. However, literature on the expression of downstream proteins of the ERK/MAPK pathway combined with RKIP in GIST is scarce. This study will focus on this aspect and use immunohistochemistry methods, large sample survival analysis data, and the latest bioinformatics analysis techniques to search for answers to the problem. We aim to find new tumor treatment targets for GIST and develop more reliable and efficient diagnostic and prognostic evaluation methods.

MATERIALS AND METHODS

Patients

The research object of the immunohistochemical experiment was 66 paraffin-embedded specimens that were surgically resected and pathologically diagnosed at China Medical University Affiliated Hospital from January 2015 to January 2020, with complete clinical and follow-up information. There were 36 male cases and 30 female cases, with an age range of 21-83 years and a mean age of 56.2 years. The tumor occurrence sites were: Stomach in 37 cases (56.1%), duodenum in 12 cases (18.2%), jejunum in 15 cases (22.7%), and colon in 2 cases (3.0%) (Table 1).

The diagnostic criteria for GISTs were histopathological features consistent with GISTs and immunohistochemical positivity for CD117, immunohistochemical negativity for CD117 but positivity for CD34, or immunohistochemical negativity for CD117 and CD34 as well as smooth muscle actin, desmin, and S-100 (to exclude smooth muscle tumors and neurogenic tumors). Among them, 59 cases (90.8%) were CD117-positive, and 50 cases (76.9%) were CD34-positive.

The risk grade criteria for GIST used the modified NIH 2008 risk classification system, which combines three assessment factors: Tumor location (gastric *vs* non-gastric: Small intestine and colon, *etc*.), tumor diameter (< 2 cm, 2-5 cm, 5-10 cm, > 10 cm), and mitotic count [< 5/50 high-power fields (HPFs), 5-10/50 HPFs, > 10/50 HPFs]. GISTs were classified as very low risk (I), low risk (II), moderate risk (III), and high risk (IV).

Among the 66 cases of GIST in this study, except for 2 cases who died due to other reasons and 1 case who was lost to follow-up, the follow-up information of the remaining 63 cases was complete. The follow-up time ranged from 5 to 61 mo, with a mean of 48 mo.

Immunohistochemical staining

The GIST specimens were fixed with formalin, embedded in paraffin, and sectioned into 4 μm-thick slices. The sections underwent routine dewaxing in water, followed by H_2O_2 treatment at room temperature to inactivate endogenous enzymes. Subsequently, they were washed three times with distilled water. Antigen retrieval was performed, followed by incubation with a blocking solution containing 5% BSA at room temperature for 20 min. Primary antibodies (RKIP/P-ERK/P-MEK antibodies, rabbit IgG) were then added at an appropriate dilution and incubated at room temperature for 12 h. Next, the sections were treated with a secondary antibody (goat anti-rabbit IgG) and incubated at 25 °C for 20 min. SABC-AP reagent was applied to the sections, followed by incubation at 25 °C for 20 min. For color development, the BCIP/NBT substrate was prepared by diluting it in TBS, thoroughly mixed, and added to the slides. The sections were incubated at 25 °C for 20 min, with the reaction time monitored under a microscope. After washing with distilled water, the sections were lightly counterstained with nuclear red, rinsed, dried, and mounted with a water-soluble mounting medium for microscopic observation.

Evaluation of immunohistochemical staining

The positive staining of RKIP, P-ERK, and P-MEK proteins was mainly located in the cytoplasm and cell membrane, while P-ERK and P-MEK were occasionally observed in the nucleus. The semi-quantitative dual scoring method was used to evaluate the protein expression of proteins. Under high-power microscopy, scoring was performed based on the staining intensity and the proportion of positive cells. Ten random high-power fields were selected on each slide, and the number of positive cells was counted among 100 cells in each field. The average value was calculated and expressed as a

Table 1 Relationship between proteins expression and clinical and pathological characteristics of gastrointestinal stromal tumors

Characteristic	*n*	RKIP			P-ERK			P-MEK		
		Negative	Positive	*P* value[a]	Negative	Positive	*P* value[a]	Negative	Positive	*P* value[a]
Sex										
Male	36	16	20	0.652	16	20	0.716	22	14	0.365
Female	30	15	15		12	18		15	15	
Age in yr										
> 56	33	17	16	0.459	13	20	0.618	15	18	0.083
≤ 56	33	14	19		15	18		22	11	
Tumor location										
Stomach	37	20	17	0.585	16	21	0.902	21	16	0.224
Duodenum	12	4	8		4	8		4	8	
Jejunoileum	15	6	9		7	8		11	4	
Colon	2	1	1		1	1		1	1	
Tumor size in cm										
< 2	12	1	11	< 0.001	8	4	0.009	7	5	0.353
2-5	20	5	15		12	8		14	6	
6-10	19	14	5		6	13		10	9	
> 10	15	11	4		2	13		6	9	
NIH risk grade										
Very low	10	2	8	< 0.001	7	3	0.004	7	3	0.319
Low	20	3	17		13	7		11	9	
Moderate	11	8	3		3	8		8	3	
High	25	18	7		5	20		11	14	
Mitotic figures as /50 HPFs										
0	11	3	8	0.074	5	6	0.015	5	6	0.604
1-4	37	15	22		21	16		22	15	
5-10	7	5	2		1	6		5	2	
> 10	11	8	3		1	10		5	6	
Mucosal invasion										
Yes	34	21	13	0.013	10	24	0.027	18	16	0.599
No	32	10	22		18	14		19	13	

[a]Raf kinase inhibitory protein (RKIP)-positive percentage were compared using the χ^2 test, $P < 0.05$ were considered statistically significant.
HPFs: High-power fields; NIH: National Institutes of Health; P-ERK: Phosphorylated extracellular-signal regulated kinase; P-MEK: Phosphorylated mitogen-activated protein kinase\ERK kinase.

percentage, representing the positivity index of proteins. The detailed scoring criteria were as follows:

(1) Staining intensity scoring criteria: no staining, 0 points; yellow, 1 point; light brown, 2 points; dark brown, 3 points;

(2) Scoring criteria for the proportion of positive cells: < 25% positive cells, 0 points; 25%-50%, 1 point; 51%-75%, 2 points; > 75%, 3 points;

And (3) The overall score was the product of the staining intensity and the proportion of positive cells, and graded as negative (0-2), mildly positive (+, 3), moderately positive (++, 4-6), or strongly positive (+++, 9). RKIP/P-ERK/P-MEK expression was judged to be either negative (0-2) or positive (3-9).

Follow-up

Telephone follow-up was the primary method, with outpatient review and correspondence as secondary measures.

Survival time was calculated as the time from the date of surgery to the date of the last follow-up for surviving patients, the date of death for deceased patients, and the date of the last follow-up for lost patients. Among them, 63 cases had complete follow-up data, 2 cases were excluded due to death from other diseases or accidents, and 1 case was excluded due to loss to follow-up. The follow-up period was from January 2020 to December 2022.

Statistical analysis

SPSS 22.0 software (IBM Corp., Armonk, NY, United States) was used for statistical analysis. Chi-square test was used for comparing percentages. Spearman analysis was used for correlation analysis of two groups of ordinal data. Kaplan-Meier method was used to calculate survival rate, and log-rank test was used. Cox univariate analysis was used for single-factor prognosis analysis, and Cox multivariate regression was used for multi-factor prognosis analysis. A Nomogram was used to represent the new prognostic evaluation model. The Cox multivariate regression analysis was conducted separately for each set of risk evaluation factors, based on two risk classification systems (the new risk grade model *vs* the modified NIH 2008 risk classification system). Receiver operating characteristic (ROC) curves were used for evaluating the accuracy and efficiency of the two prognostic evaluation systems, and statistical significance was set at $P < 0.05$.

RESULTS

Immunohistochemical results of RKIP, P-ERK, and P-MEK proteins and their correlation with clinical pathology

In GIST tissues, RKIP protein showed positive expression in the cytoplasm and cell membrane, appearing as brownish-yellow or brown granules. The immunohistochemical staining result is shown in Figure 1A and B under light microscopy. Among the 66 specimens tested, RKIP protein was expressed positively in 35 cases (53%) and negatively in 31 cases (47%). Statistical analysis revealed that the expression of RKIP was related to GIST tumor size, NIH grade, and mucosal invasion ($P < 0.05$) (Table 1).

P-ERK protein exhibited heterogeneous distribution in GIST cells, mainly in the cytoplasm, with occasional presence in the nucleus, and appeared as brownish-yellow granules, as shown in Figure 1C and D. Positive expression of P-ERK protein was detected in 38 cases (57.6%), while negative expression was detected in 28 cases (42.4%). Clinical pathology analysis indicated that the expression of P-ERK protein was associated with GIST tumor size, mitotic count, mucosal invasion, and NIH grade ($P < 0.05$) (Table 1).

P-MEK protein expression in GIST cells was observed as brownish-yellow granules, mainly distributed in the cytoplasm, with some in the nucleus, and showed a relatively uniform distribution, as shown in Figure 1E and F. Among the 66 cases, positive expression of P-MEK protein was found in 29 cases (43.9%), while negative expression was detected in 37 cases (56.1%). However, no significant correlation was observed between P-MEK protein expression and any independent clinical-pathological factors of GIST (Table 1).

RKIP, P-ERK, and P-MEK protein co-expression analysis

Spearman's correlation test was used to analyze the correlation between RKIP protein expression and P-ERK/P-MEK expression. The results showed that in GIST cases, RKIP protein expression was negatively correlated with P-ERK expression (correlation coefficient = -0.575, $P < 0.001$); RKIP protein expression also had a certain negative correlation with P-MEK protein expression (correlation coefficient = -0.323, $P < 0.001$) (Table 2).

Univariate and multivariate regression analysis

Univariate regression analysis was performed on complete follow-up data from 63 cases, which indicated that tumor location, tumor size, mitotic count, RKIP protein expression, P-ERK protein expression, RKIP combined with P-ERK protein co-expression, and NIH grading were all correlated with patient prognosis ($P < 0.05$).

These univariate factors were further included in COX multivariate regression analysis. The results showed that RKIP protein expression was not an independent risk factor for tumor prognosis ($P = 0.061$). However, tumor size ($P = 0.037$), NIH grading ($P = 0.014$), P-ERK protein expression ($P = 0.041$), and RKIP combined with P-ERK protein expression ($P = 0.044$) were identified as independent risk factors for prognosis with statistical significance. Among them, the impact of RKIP combined with P-ERK protein expression on survival time was the highest with a weight factor of Exp (B) at 11.320, followed by NIH grading, P-ERK expression, and tumor size (Table 3).

Survival analysis curve of RKIP combined with P-ERK in GIST

Based on the expression of RKIP and P-ERK proteins in GIST specimens, we divided the cases into two groups: 1. RKIP (-) and P-ERK (+) group, and 2. The control group with RKIP (+) or P-ERK (-). We drew survival curves for both groups to better represent the significance of the combination of these two proteins in predicting GIST prognosis. The results showed that the survival rate and survival time of Group 1 were significantly lower than those of Group 2 ($P = 0.0312$) (Figure 2).

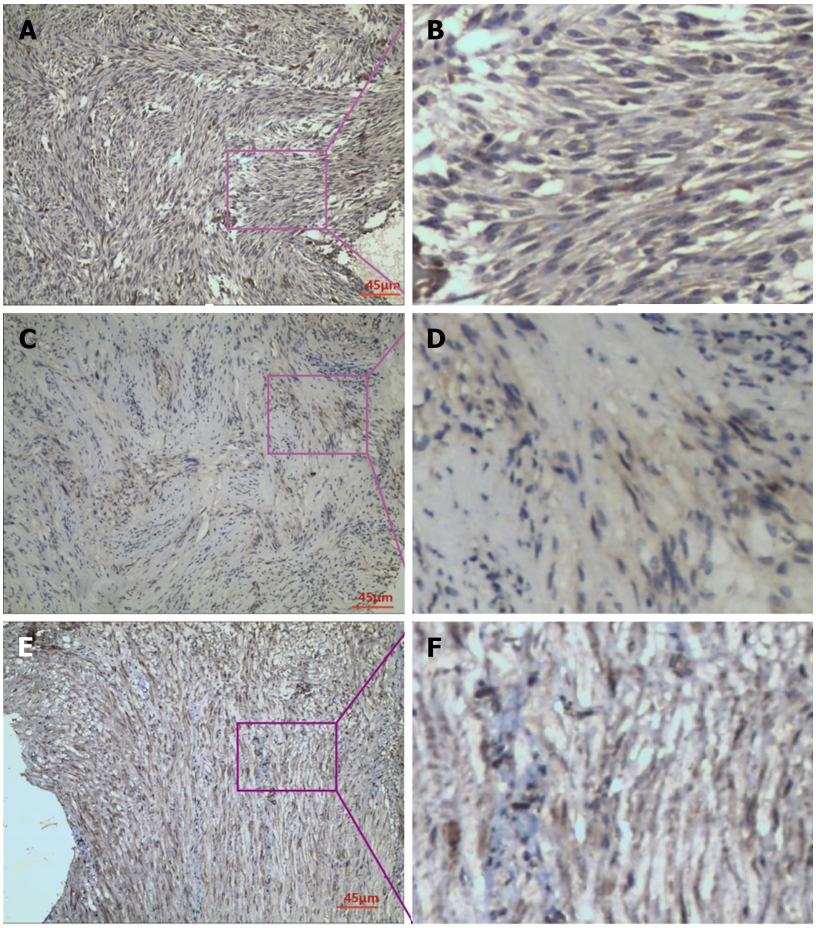
Establishment of a new prognosis evaluation model using RKIP and P-ERK in combination and its prognosis evaluation efficacy analysis

We included "RKIP expression, P-ERK protein expression, tumor size, tumor location, and mitotic count" as five risk assessment factors (Table 4: Multivariate 2) and used multivariate Cox regression analysis to draw a new nomogram for this new evaluation model. We also conducted ROC analysis to evaluate its prognostic performance. As a control, we

Table 2 Correlations among proteins expression

Protein expressions	Negative	P-ERK positive	Correlation and *P* value	Negative	P-MEK positive	Correlation and *P* value
RKIP						
Negative	3	26	C[a] = -0.575	11	18	C = -0.323
Positive	25	12	*P* < 0.001	26	11	*P* = 0.008

[a]C: Correlation coefficient value is calculated using Spearman's rho test, $P < 0.05$ were considered statistically significant.
P-ERK: Phosphorylated-extracellular-signal regulated kinase; P-MEK: Phosphorylated-mitogen-activated protein kinase\ERK kinase; RKIP: Raf kinase inhibitory protein.



DOI: 10.3748/wjg.v29.i26.4200 **Copyright** ©The Author(s) 2023.

Figure 1 Immunohistochemical staining. A: Immunohistochemical staining for raf kinase inhibitor protein (RKIP) in gastrointestinal stromal tumor (GIST) tissues; B: RKIP protein showed positive expression in the cytoplasm and cell membrane, appearing as brownish-yellow or brown granules; C: Immunohistochemical staining for phosphorylated-extracellular signal-regulated kinase (P-ERK) in GIST tissues; D: P-ERK protein exhibited heterogeneous distribution in GIST cells, mainly in the cytoplasm, with occasional presence in the nucleus, and appeared as brownish-yellow granules; E: Immunohistochemical staining for phosphorylated-mitogen-activated protein kinase/ERK Kinase (P-MEK) in GIST tissues; F: P-MEK protein expression in GIST cells was observed as brownish-yellow granules, mainly distributed in the cytoplasm, with some in the nucleus, and showed a relatively uniform distribution. A, C and E were taken under 200 × magnification.

used the three conventional risk factors (tumor location, tumor size, and mitotic count) in the modified NIH 2008 risk classification system as evaluation factors (Table 4: Multivariate 1) and performed the same statistical analysis.

After analyzing the results of the above analysis (Table 4), we obtained the nomogram of the new prognosis evaluation model (Figure 3). ROC curve analysis also showed that the new evaluation model (red curve, AUC = 0.860) had better prognostic performance than the modified NIH 2008 risk classification system (blue curve, AUC = 0.796) ($P = 0.0312$) (Figure 4).

Table 3 Analysis of factors affecting prognosis of gastrointestinal stromal tumors in Cox proportional-hazards regression models for overall survival, *n* = 63

Characteristic	*n*	Univariate[a]			Multivariate[1]		
		HR	95%CI	*P* value	B	Exp (B)	*P* value
Sex							
Male	34	0.87	0.32-2.34	0.783	0.004	1.004	0.994
Female	29						
Age in yr							
> 56	30	0.99	0.96-1.03	0.751	-0.011	0.989	0.609
≤ 56	33						
Tumor location							
Stomach	36	3.86	1.23-12.18	0.021	0.669	1.953	0.057
Duodenum	12						
Jejunoileum	15						
Tumor size in cm							
< 2	11	2.32	1.32-4.07	0.003	0.734	2.083	0.037
2-5	19						
6-10	18						
> 10	14						
NIH risk grade							
Very low	10	2.32	1.32-4.07	0.002	1.393	4.025	0.014
Low	19						
Moderate	10						
High	24						
Mitotic figures as /50 HPFs							
0	11	1.7	1.06-2.70	0.026	0.179	1.196	0.505
1-4	36						
5-10	5						
> 10	11						
RKIP expression							
Positive	35	0.14	0.04-0.50	0.002	-2.064	0.127	0.061
Negative	28						
P-ERK expression							
Positive	36	3.63	1.03-12.73	0.044	1.761	5.821	0.041
Negative	27						
P-MEK expression							
Positive	28	1.78	0.66-4.79	0.252			
Negative	35						
RKIP and P-ERK co-expression[2]							
Positive	25	0.34	012-0.94	0.037	2.427	11.32	0.044
Negative	38						

[1]Analysed factors were sex, age, tumor location, tumor size, National Institutes of Health (NIH) risk grades, mitotic figures, raf kinase inhibitory protein

(RKIP), phosphorylated-extracellular-signal regulated kinase (P-ERK) expressions, RKIP and P-ERK co-expressions.
[2]Based on the expression of RKIP and P-ERK proteins in gastrointestinal stromal tumors specimens, we defined the cases with RKIP (-) and P-ERK (+) as negative, while the cases with RKIP (+) or P-ERK (-) as positive.
[a]Log-rank test; $P < 0.05$ were considered statistically significant.
HPFs: High-power fields; HR: Hazard ratio; MAPK: Mitogen-activated protein kinase; P-MEK: Phosphorylated-MAPK\ERK kinase.

Table 4 Multivariate analysis of prognostic factors for overall survival of gastrointestinal stromal tumors with two different sets of risk factors, *n* = 63

Characteristic	*n*	Multivariate[1]			Multivariate[2]		
		HR	95%CI	*P* value[a]	HR	95%CI	*P* value[a]
Tumor location							
Stomach	36	2.59	0.69-9.69	0.156	4.13	1.07-15.98	0.04
Duodenum	12						
Jejunoileum	15						
Tumor size in cm							
< 2	11	1.92	0.93-3.96	0.079	1.17	0.52-2.62	0.71
2-5	19						
6-10	18						
> 10	14						
Mitotic figures as /50 HPFs							
0	11	1.22	0.71-2.10	0.472	1.28	0.75-2.18	0.361
1-4	36						
5-10	5						
> 10	11						
RKIP expression							
Positive	35				0.13	0.03-0.66	0.014
Negative	28						
P-ERK expression							
Positive	36				0.91	0.19-4.32	0.909
Negative	27						

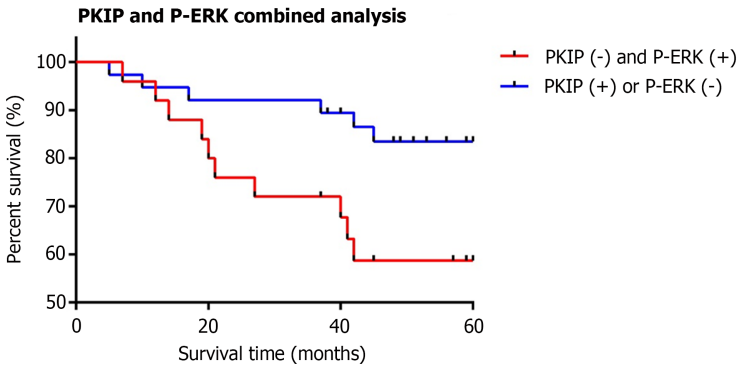
[1]Analysed factors were tumor location, tumor size, mitotic figures; above are all the risk factors included in NIH 2008 Risk Grade System.
[2]Analysed factors were tumor location, tumor size, mitotic figures, raf kinase inhibitory protein (RKIP) expressions and phosphorylated-extracellular-signal regulated kinase (P-ERK) expressions.
[a]$P < 0.05$ were considered statistically significant.
HPFs: High-power fields; HR: Hazard ratio; MAPK: Mitogen-activated protein kinase; P-MEK: Phosphorylated MAPK\ERK kinase.

DISCUSSION

GIST is the most common mesenchymal tumor in the gastrointestinal tract, accounting for approximately 60%-70% of all cases. Currently, effective treatment for GIST involves surgery combined with appropriate targeted therapy[9]. However, resistance to targeted therapy often occurs, and prognosis assessment is still being explored and modified. Therefore, there is an urgent need to find better therapeutic targets and a more efficient risk grading system.

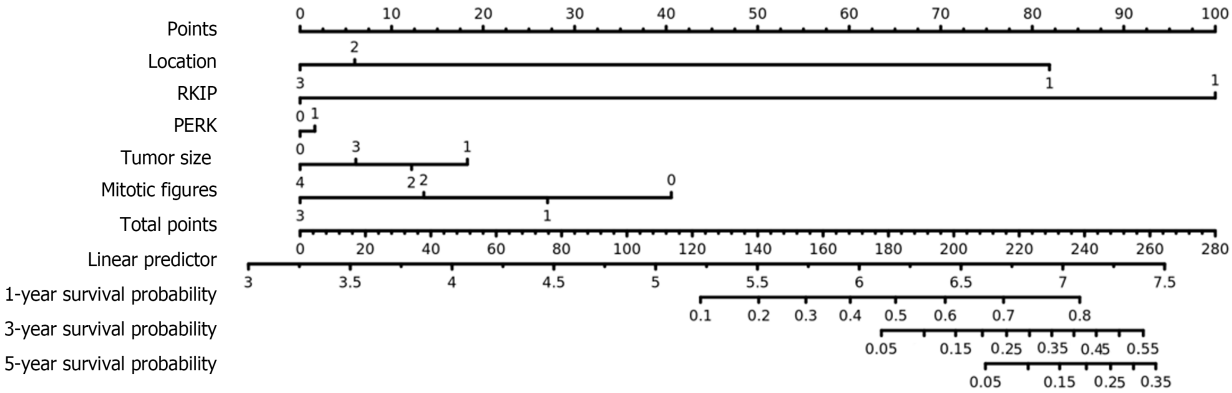
ERK and MEK proteins are two core proteins in the Raf1-MEK-ERK pathway, which are downstream targets activated by abnormal C-kit and PDGFR-α *genes* closely related to GIST. ERK protein is associated with various diseases[10] such as tumors, heart failure, developmental disorders, and autoimmune diseases[11-13]. RKIP protein is a natural inhibitor of Raf-1 protein and is widely present in living organisms. It has an inhibitory effect on the metastasis and proliferation of various tumors.

In our preliminary experiments, we found that high expression of RKIP protein was related to GIST tumor size, invasion of the mucosa, and NIH grading. However, the single expression of RKIP protein alone is not sufficient as a single risk factor for evaluating GIST prognosis. Recent reports have suggested that RKIP protein regulates the expression



DOI: 10.3748/wjg.v29.i26.4200 **Copyright** ©The Author(s) 2023.

Figure 2 Relationship between raf kinase inhibitor protein and phosphorylated-extracellular-signal regulated kinase co-expression and prognosis in gastrointestinal stromal tumors. Comparison with the raf kinase inhibitor protein (RKIP)-negative and phosphorylated-extracellular signal-regulated kinase (P-ERK)-positive groups; RKIP high expression group is correlated with a better survival rate and the difference was significant. Log-rank analysis, *P* = 0.0312.



DOI: 10.3748/wjg.v29.i26.4200 **Copyright** ©The Author(s) 2023.

Figure 3 Nomogram for the new risk grade model with consideration of raf kinase inhibitory protein and phosphorylated-extracellular-signal regulated kinase to predict the probabilities of 5-yr survival with gastrointestinal stromal tumors. Raf kinase inhibitory protein (RKIP) expression, phosphorylated-extracellular-signal regulated kinase (P-ERK) expression, tumor size, tumor location and mitotic count are involved as assessment factors.

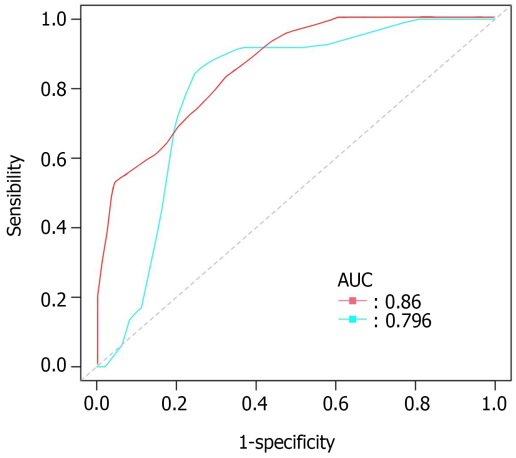
of the MEK/ERK pathway in pancreatic cancer[14,15], thereby affecting tumor resistance and invasion. Additionally, it has been found that the combination of RKIP and P-ERK proteins in gastric cancer has a predictive significance for tumor prognosis[16]. These findings inspired us to focus on the combined detection of RKIP, P-ERK, and P-MEK proteins in GIST, in hopes of gaining further insights.

Clinical and pathological correlations

In this experiment, we analyzed the expression of RKIP, P-ERK, and P-MEK proteins in GIST and found that RKIP expression is related to GIST tumor size and NIH staging. This result is consistent with the research findings of Yuan *et al* [17], who found that knocking down the RKIP gene promotes cell growth in nasopharyngeal carcinoma cell lines[17].

In addition to its correlation with tumor size and NIH staging, P-ERK protein is also related to the mitotic count in GIST cells. Zhang *et al*[18] found that high expression of RKIP protein leads to low expression of P-ERK protein in the human choriocarcinoma cell line JEG-3. Furthermore, transfection with low P-ERK level tumor cells significantly reduced their growth activity compared to the control group, indicating that P-ERK protein is related to tumor cell proliferation [18].

The mechanism may be that low RKIP expression in GIST tumor cells leads to more phosphorylation of downstream ERK1/2 protein, forming P-ERK protein, which can control important structures in cell division such as centrosomes, spindle fibers, and centromeres[19,20], accelerating the tumor cell cycle and mitosis[21]. In addition, low RKIP expression causes dysregulation of its ligand Raf-1 protein, which upregulates the cell mitotic cycle[22,23], accelerating tumor growth. Moreover, ERK protein can be rapidly transported into the nucleus, further phosphorylating and activating proliferation-related transcription factors such as AP-1, ELK-1, and Serum Response Factor Accessory Protein (SAP), promoting cell proliferation and causing abnormal nuclear division[24]. Thus, low RKIP expression in GIST upregulates P-ERK, leading to tumor enlargement and increased nuclear division.



DOI: 10.3748/wjg.v29.i26.4200 **Copyright** ©The Author(s) 2023.

Figure 4 Receiver operating characteristic curves for two risk grade system in predicting overall survival of gastrointestinal stromal tumors. The red curve represents for the new risk grade model and the blue one represents for National Institutes of Health (NIH) 2008 Risk Grade System. The area under the curve was 0.860 for the new risk grade model, while 0.796 for NIH 2008 Risk Grade System. Compared with the traditional NIH 2008 system, the new model which is with consideration of raf kinase inhibitory protein and phosphorylated-extracellular-signal regulated kinase is correlated with a better prediction efficiency for overall survival of gastrointestinal stromal tumors, the difference was significant. Log-rank analysis, $P = 0.0312$. AUC: Area under curve.

The NIH 2008 risk classification system is a recognized postoperative prognostic assessment system for GIST, which is based on three independent risk factors: Tumor location, tumor size, and mitotic index. RKIP and P-ERK proteins are associated with two of these factors, and it is easy to understand that protein expression is also related to NIH 2008 risk classification results. Schoppmann *et al*'s report suggests that loss of RKIP expression tends to increase the risk level of GIST cases in Fletcher's risk classification and a similar conclusion is drawn in Miettinen's risk classification[25]. Wang *et al*[26] also found that RKIP protein expression is related to TNM staging in non-small cell lung cancer[26].

We also found that both RKIP protein and P-ERK protein are related to the mucosal invasion status of GIST tumors. Martinho *et al*[27] found in experiments that low expression of RKIP protein often indicates a tendency of GIST tumors to invade and metastasize[27]. A similar correlation is found in gastric cancer between RKIP protein expression and tumor invasion depth, lymph node metastasis, and distant metastasis. The mechanism may be related to the interaction between RKIP protein and Snail protein, which regulates tumor Epithelial-Mesenchymal Transition (EMT)[28]: Snail protein can bind and downregulate E-cadherin protein, thereby regulating EMT; at the same time, it binds to the RKIP protein promoter E-box region to downregulate RKIP protein transcription. Thus, when Snail upregulates EMT, RKIP is often reduced[29].

In the analysis of clinical and pathological factors, no statistically significant results were found for P-MEK protein expression. However, there is a certain negative correlation between RKIP and P-MEK expression, which is statistically significant. This may indicate that RKIP has a certain regulatory effect on P-MEK. Schoppmann *et al*[25] found in their immunohistochemical study of GIST specimens that P-MEK1/2 expression is related to whether the tumor can be completely resected, but has no significant relationship with other factors. The conclusions of this study are mutually corroborated.

Analysis of co-expression of RKIP and P-ERK proteins

In this experiment, it was found that the expression of RKIP and P-ERK in GIST was negatively correlated ($P < 0.05$). Yang *et al*[14] found that inhibiting ERK phosphorylation would upregulate RKIP expression in pancreatic cancer cell lines; while Yuan *et al*[17] reported that high expression of RKIP in nasopharyngeal carcinoma cells can also inhibit ERK protein activation. Therefore, RKIP protein and P-ERK protein have mutual regulatory functions. Recently, the novel and revolutionary "Phospho-Theft" hypothesis about RKIP provides a perfect explanation for its possible mechanism[30]. RKIP protein has two completely different functions: When not phosphorylated, RKIP protein inhibits the activation and signal transmission of Raf-1 protein, which can reduce the activation of downstream MEK/ERK; after RKIP is phosphorylated by PKC protein at S153, P-RKIP substrate transfers to GRK2[31], which can enhance the activation of the β-AR pathway and activate downstream substrate ERK[32]. In addition, RKIP is regulated by feedback of KRAS-ERK pathway. At the same time, P-ERK can undergo self-phosphorylation, thereby activating downstream substrates such as Elk1, mitogen-and stress-activated protein Kinase, c-myc, *etc*[33].

Univariate and multivariate survival analysis and survival curve

Combining univariate and multivariate COX regression analysis, it was found that RKIP protein expression could not serve as an independent risk factor for predicting tumor prognosis ($P = 0.061$). Tumor size ($P = 0.037$), NIH grading ($P = 0.014$), P-ERK protein expression ($P = 0.041$), and RKIP combined with P-ERK protein expression ($P = 0.044$) could serve as independent prognostic factors with statistical significance. Among them, the combined expression of RKIP and P-ERK had the highest impact on survival, with a weight factor of Exp (B) at 11.320, followed by NIH grading, P-ERK expression, and tumor size. Furthermore, we plotted survival curves for GIST cases based on their combined RKIP and P-

ERK expression, revealing a significant difference in survival rates between groups. Therefore, the combined expression of RKIP and P-ERK has significant prognostic value for evaluating the prognosis of GIST patients and carries greater weight. This is consistent with findings in a study on nasopharyngeal carcinoma where RKIP was found to be an independent risk factor for predicting prognosis. In gastric cancer, the combined expression of P-ERK and RKIP was found to be associated with a 5-year relapse-free survival after surgery.

Establishment of a GIST prognostic model based on RKIP and P-ERK protein expression

Standardized treatment for GIST includes timely surgery and rational targeted therapy. The indication for targeted therapy is currently based on the NIH 2008 risk classification system applied to postoperative pathology results, with Imatinib (a representative TKI drug) for the intermediate and high-risk population[34]. Meanwhile, the Armed Forces Institute of Pathology and World Health Organization 2013 risk classifications are also used[35]. However, there are differences in the results among various risk classification systems, and there are difficulties in using and interpreting them for the public. As mentioned in this article, we found that the combination of RKIP and P-ERK protein expression is of great significance for the prognostic evaluation of GIST patients. Therefore, we incorporated RKIP and P-ERK protein expression, as well as tumor size, tumor location, and mitotic count, into a new GIST risk assessment model and plotted a survival curve. We analyzed its evaluation efficiency using the ROC curve, and the results showed that it is superior to the NIH 2008 risk classification system (Area Under Curve 0.860 *vs* 0.796).

Perspectives and limitations

In recent years, GIST-related research has been devoted to identifying new biomarkers and finding new therapeutic targets[36]. As one of the hotspots, our study found that the combination of RKIP and P-ERK proteins can effectively indicate the prognosis of GIST and can be used to guide GIST targeted therapy. More researchers have focused on the application and exploration of RKIP and P-ERK proteins in tumor diagnosis and treatment, such as the recent successful case of using urine RKIP monitoring to evaluate the prognosis of clear cell renal cell carcinoma (ccRCC)[37]. Serum RKIP levels have also been used to monitor the efficacy of treatment for multiple sclerosis[38]. In terms of treatment, ERK inhibitors combined with chloroquine can improve the adjuvant therapy for pancreatic cancer with K-Ras mutations[39], and imatinib combined with chloroquine (to inhibit autophagy) has also been attempted in GIST drug-resistant experimental studies[40].

Our experiment fills the gap in the research on the relevance of RKIP and P-ERK in GIST, further confirming the significance of these proteins in tumor physiology and clinical treatment. However, the experiment still has some limitations. Firstly, due to the lower incidence of GIST comparing to other gastrointestinal tumors, the sample size was limited. We will continue to recruit more samples and track their follow-up, using more abundant data for further validation and research. Secondly, this experiment used immunohistochemical methods for protein level research. In the future, we will supplement molecular level experiments to further elucidate the mechanism of action of relevant sites on the RKIP and ERK/MAPK pathways, and better guide targeted therapy. The above is also the focus of our project and ongoing work. We are confident in making improvements and will strive to promote a new chapter in the RKIP-related diagnosis and treatment of GIST.

CONCLUSION

Our experimental results showed that the expression of RKIP and p-ERK proteins in GIST was associated with tumor size, NIH 2008 staging, tumor invasion, and p-ERK expression was also related to mitotic count. The expression of the two proteins had a certain negative correlation. The combined expression of RKIP and p-ERK proteins can serve as an independent risk factor for predicting the prognosis of GIST patients. The new risk assessment model incorporating RKIP and p-ERK has superior evaluation efficacy and is worth further practical application to help validate results.

ARTICLE HIGHLIGHTS

Research background

Nowadays, research reports on the important clinical and prognostic value of phosphorylated-extracellular signal-regulated kinase (P-ERK) and phosphorylated-mitogen-activated protein kinase (MAPK/ERK) kinase (P-MEK) proteins closely related to raf kinase inhibitor protein (RKIP) have gradually emerged in digestive tract tumors.

Research motivation

The expression of downstream proteins of the ERK/MAPK pathway combined with RKIP in gastrointestinal stromal tumor (GIST) is scarce.

Research objectives

To detect the expression of RKIP, P-ERK, and P-MEK proteins in GIST and to analyze their relationship with clinicopathological characteristics and prognosis of this disease. Try to establish a new prognosis evaluation model using RKIP and P-ERK in combination and analyze its prognosis evaluation efficacy.

Research methods

This study will focus on this aspect and use immunohistochemistry methods, large sample survival analysis data, and the latest bioinformatics analysis techniques to search for answers to the problem.

Research results

Our experimental results showed that the expression of RKIP and P-ERK proteins in GIST was associated with tumor size, NIH 2008 staging, tumor invasion, and P-ERK expression was also related to mitotic count. The expression of the two proteins had a certain negative correlation.

Research conclusions

The combined expression of RKIP and P-ERK proteins can serve as an independent risk factor for predicting the prognosis of GIST patients. The new risk assessment model incorporating RKIP and P-ERK has superior evaluation efficacy and is worth further practical application to validate.

Research perspectives

As one of the hotspots, our study found that the combination of RKIP and P-ERK proteins can effectively indicate the prognosis of GIST and can be used to guide GIST targeted therapy. More researches are needed to focus on the application and exploration of RKIP and P-ERK proteins in tumor diagnosis and treatment.

FOOTNOTES

Author contributions: Wang Y designed research; Wang Y, Wang L and Qu WZ performed research; Wang Y and Qu WZ analyzed data; Wang Y, Chen JJ and Wang L wrote the paper; Wang Y edited the paper and provided primary revised opinion; All authors have read and approve the final manuscript.

Supported by Natural Science Foundation of Liaoning Province, No.2020-MS-148.

Institutional review board statement: The study was reviewed and approved by the 4th Affiliated Hospital of China Medical University's Institutional Review Board, No. EC-2020-KS-015.

Informed consent statement: Consent was not obtained but the presented data are anonymized, and risk of identification is low. With the approval of the ethics committee, informed consent was waived.

Conflict-of-interest statement: The authors report grants from Natural Science Foundation of Liaoning Province, China, during the conduct of the study. We declare that we do not have any commercial or associative interest that represents a conflict of interest in connection with the work submitted and entitled 'Raf kinase inhibitor protein combined with phosphorylated extracellular signal-regulated kinase offers valuable prognosis in gastrointestinal stromal tumor'.

Data sharing statement: Technical appendix, statistical code, and dataset available from the corresponding author at wwyy840731@126.com. Consent was not obtained but the presented data are anonymized, and risk of identification is low. No additional data are available.

CONSORT 2010 statement: The authors have read the CONSORT 2010 statement, and the manuscript was prepared and revised according to the CONSORT 2010 statement.

Open-Access: This article is an open-access article that was selected by an in-house editor and fully peer-reviewed by external reviewers. It is distributed in accordance with the Creative Commons Attribution NonCommercial (CC BY-NC 4.0) license, which permits others to distribute, remix, adapt, build upon this work non-commercially, and license their derivative works on different terms, provided the original work is properly cited and the use is non-commercial. See: https://creativecommons.org/Licenses/by-nc/4.0/

Country/Territory of origin: China

ORCID number: Wen-Zhi Qu 0009-0006-2007-7963; Luan Wang 0009-0002-2386-2407; Juan-Juan Chen 0000-0002-4874-4864; Yang Wang 0000-0002-1819-4937.

Corresponding Author's Membership in Professional Societies: Chinese Society of Clinical Oncology, 202240816.

S-Editor: Li L
L-Editor: Filipodia
P-Editor: Cai YX

REFERENCES

1 **Heinrich MC**, Corless CL, Blanke CD, Demetri GD, Joensuu H, Roberts PJ, Eisenberg BL, von Mehren M, Fletcher CD, Sandau K, McDougall K, Ou WB, Chen CJ, Fletcher JA. Molecular correlates of imatinib resistance in gastrointestinal stromal tumors. *J Clin Oncol* 2006; **24**: 4764-4774 [PMID: 16954519 DOI: 10.1200/JCO.2006.06.2265]

2 **Demetri GD**, van Oosterom AT, Garrett CR, Blackstein ME, Shah MH, Verweij J, McArthur G, Judson IR, Heinrich MC, Morgan JA, Desai J, Fletcher CD, George S, Bello CL, Huang X, Baum CM, Casali PG. Efficacy and safety of sunitinib in patients with advanced gastrointestinal stromal tumour after failure of imatinib: a randomised controlled trial. *Lancet* 2006; **368**: 1329-1338 [PMID: 17046465 DOI: 10.1016/S0140-6736(06)69446-4]

3 **Riller Q**, Rieux-Laucat F. RASopathies: From germline mutations to somatic and multigenic diseases. *Biomed J* 2021; **44**: 422-432 [PMID: 34175492 DOI: 10.1016/j.bj.2021.06.004]

4 **Yan ZP**, Li JT, Zeng N, Ni GX. Role of extracellular signal-regulated kinase 1/2 signaling underlying cardiac hypertrophy. *Cardiol J* 2021; **28**: 473-482 [PMID: 32329039 DOI: 10.5603/CJ.a2020.0061]

5 **Fan HY**, Tong C, Sun QY. [Mitogen-activated protein kinase (MAPK) Signaling Pathways: State-of-the-art]. *Donwuxue Zazhi* 2002; **37**: 98-102 [DOI: 10.3969/j.issn.0250-3263.2002.05.026]

6 **Yeung K**, Janosch P, McFerran B, Rose DW, Mischak H, Sedivy JM, Kolch W. Mechanism of suppression of the Raf/MEK/extracellular signal-regulated kinase pathway by the raf kinase inhibitor protein. *Mol Cell Biol* 2000; **20**: 3079-3085 [PMID: 10757792 DOI: 10.1128/MCB.20.9.3079-3085.2000]

7 **Granovsky AE**, Clark MC, McElheny D, Heil G, Hong J, Liu X, Kim Y, Joachimiak G, Joachimiak A, Koide S, Rosner MR. Raf kinase inhibitory protein function is regulated *via* a flexible pocket and novel phosphorylation-dependent mechanism. *Mol Cell Biol* 2009; **29**: 1306-1320 [PMID: 19103740 DOI: 10.1128/MCB.01271-08]

8 **Wang Y**, Chen JJ, Wang XF, Wang Q. Clinical and prognostic significance of Raf kinase inhibitory protein expression in gastrointestinal stromal tumors. *World J Gastroenterol* 2018; **24**: 2508-2517 [PMID: 29930472 DOI: 10.3748/wjg.v24.i23.2508]

9 **Sun K**, Lv H, Chen B, Nie C, Zhao J, Wang S, Wang J, Xu W, Chen X. Dawning precision treatment for gastric cancer: The latest biomarkers. *J Transl Int Med* 2021; **9**: 228-230 [PMID: 35136720 DOI: 10.2478/jtim-2021-0023]

10 **Lorenz K**, Rosner MR. Harnessing RKIP to Combat Heart Disease and Cancer. *Cancers (Basel)* 2022; **14** [PMID: 35205615 DOI: 10.3390/cancers14040867]

11 **Sugiura R**, Satoh R, Takasaki T. ERK: A Double-Edged Sword in Cancer. ERK-Dependent Apoptosis as a Potential Therapeutic Strategy for Cancer. *Cells* 2021; **10** [PMID: 34685488 DOI: 10.3390/cells10102509]

12 **Gilbert CJ**, Longenecker JZ, Accornero F. ERK1/2: An Integrator of Signals That Alters Cardiac Homeostasis and Growth. *Biology (Basel)* 2021; **10** [PMID: 33923899 DOI: 10.3390/biology10040346]

13 **Gallo S**, Vitacolonna A, Bonzano A, Comoglio P, Crepaldi T. ERK: A Key Player in the Pathophysiology of Cardiac Hypertrophy. *Int J Mol Sci* 2019; **20** [PMID: 31052420 DOI: 10.3390/ijms20092164]

14 **Yang K**, Li Y, Lian G, Lin H, Shang C, Zeng L, Chen S, Li J, Huang C, Huang K, Chen Y. KRAS promotes tumor metastasis and chemoresistance by repressing RKIP *via* the MAPK-ERK pathway in pancreatic cancer. *Int J Cancer* 2018; **142**: 2323-2334 [PMID: 29315556 DOI: 10.1002/ijc.31248]

15 **Bian Y**, Jiang H, Zheng J, Shao C, Lu J. Basic Pancreatic Lesions: Radiologic-pathologic Correlation. *J Transl Int Med* 2022; **10**: 18-27 [PMID: 35702187 DOI: 10.2478/jtim-2022-0003]

16 **Fujimori Y**, Inokuchi M, Takagi Y, Kato K, Kojima K, Sugihara K. Prognostic value of RKIP and p-ERK in gastric cancer. *J Exp Clin Cancer Res* 2012; **31**: 30 [PMID: 22463874 DOI: 10.1186/1756-9966-31-30]

17 **Yuan L**, Yi HM, Yi H, Qu JQ, Zhu JF, Li LN, Xiao T, Zheng Z, Lu SS, Xiao ZQ. Reduced RKIP enhances nasopharyngeal carcinoma radioresistance by increasing ERK and AKT activity. *Oncotarget* 2016; **7**: 11463-11477 [PMID: 26862850 DOI: 10.18632/oncotarget.7201]

18 **Zhang M**, Zhang D, Fan Q. RKIP suppresses the proliferation and invasion ofchoriocarcinoma cells through inhibiting the MAPK signaling pathway. *Int J Clin Exp Med* 2015; **8**: 22183-22190 [PMID: 26885193]

19 **Shapiro PS**, Vaisberg E, Hunt AJ, Tolwinski NS, Whalen AM, McIntosh JR, Ahn NG. Activation of the MKK/ERK pathway during somatic cell mitosis: direct interactions of active ERK with kinetochores and regulation of the mitotic 3F3/2 phosphoantigen. *J Cell Biol* 1998; **142**: 1533-1545 [PMID: 9744882 DOI: 10.1083/jcb.142.6.1533]

20 **Zecevic M**, Catling AD, Eblen ST, Renzi L, Hittle JC, Yen TJ, Gorbsky GJ, Weber MJ. Active MAP kinase in mitosis: localization at kinetochores and association with the motor protein CENP-E. *J Cell Biol* 1998; **142**: 1547-1558 [PMID: 9744883 DOI: 10.1083/jcb.142.6.1547]

21 **Yesilkanal AE**, Rosner MR. Raf kinase inhibitory protein (RKIP) as a metastasis suppressor: regulation of signaling networks in cancer. *Crit Rev Oncog* 2014; **19**: 447-454 [PMID: 25597354 DOI: 10.1615/CritRevOncog.2014012000]

22 **Ziogas A**, Lorenz IC, Moelling K, Radziwill G. Mitotic Raf-1 is stimulated independently of Ras and is active in the cytoplasm. *J Biol Chem* 1998; **273**: 24108-24114 [PMID: 9727031 DOI: 10.1074/jbc.273.37.24108]

23 **Hayne C**, Tzivion G, Luo Z. Raf-1/MEK/MAPK pathway is necessary for the G2/M transition induced by nocodazole. *J Biol Chem* 2000; **275**: 31876-31882 [PMID: 10884385 DOI: 10.1074/jbc.M002766200]

24 **Boilly B**, Vercoutter-Edouart AS, Hondermarck H, Nurcombe V, Le Bourhis X. FGF signals for cell proliferation and migration through different pathways. *Cytokine Growth Factor Rev* 2000; **11**: 295-302 [PMID: 10959077 DOI: 10.1016/S1359-6101(00)00014-9]

25 **Schoppmann SF**, Beer A, Nirtl N, Ba-Ssalamah A, Brodowicz T, Streubel B, Birner P. Downregulation of phosphatidylethanolamine binding protein 1 associates with clinical risk factors in gastrointestinal stromal tumors, but not with activation of the RAF-1-MEK-ETV1 pathway. *Cancer Lett* 2013; **335**: 26-30 [PMID: 23376254 DOI: 10.1016/j.canlet.2013.01.044]

26 **Wang A**, Duan G, Zhao C, Gao Y, Liu X, Wang Z, Li W, Wang K, Wang W. Reduced RKIP expression levels are associated with frequent non-small cell lung cancer metastasis and STAT3 phosphorylation and activation. *Oncol Lett* 2017; **13**: 3039-3045 [PMID: 28521411 DOI: 10.3892/ol.2017.5846]

27 **Martinho O**, Gouveia A, Silva P, Pimenta A, Reis RM, Lopes JM. Loss of RKIP expression is associated with poor survival in GISTs. *Virchows Arch* 2009; **455**: 277-284 [PMID: 19705153 DOI: 10.1007/s00428-009-0821-z]

28 **Cessna H**, Baritaki S, Zaravinos A, Bonavida B. The Role of RKIP in the Regulation of EMT in the Tumor Microenvironment. *Cancers (Basel)* 2022; **14** [PMID: 36230521 DOI: 10.3390/cancers14194596]

29 **Beach S**, Tang H, Park S, Dhillon AS, Keller ET, Kolch W, Yeung KC. Snail is a repressor of RKIP transcription in metastatic prostate cancer cells. *Oncogene* 2008; **27**: 2243-2248 [PMID: 17952120 DOI: 10.1038/sj.onc.1210860]

30 **Skinner JJ**, Wang S, Lee J, Ong C, Sommese R, Sivaramakrishnan S, Koelmel W, Hirschbeck M, Schindelin H, Kisker C, Lorenz K, Sosnick TR, Rosner MR. Conserved salt-bridge competition triggered by phosphorylation regulates the protein interactome. *Proc Natl Acad Sci U S A* 2017; **114**: 13453-13458 [PMID: 29208709 DOI: 10.1073/pnas.1711543114]

31 **Lorenz K**, Lohse MJ, Quitterer U. Protein kinase C switches the Raf kinase inhibitor from Raf-1 to GRK-2. *Nature* 2003; **426**: 574-579 [PMID: 14654844 DOI: 10.1038/nature02158]

32 **Maimari T**, Krasel C, Bünemann M, Lorenz K. The N-termini of GRK2 and GRK3 simulate the stimulating effects of RKIP on β-adrenoceptors. *Biochem Biophys Res Commun* 2019; **520**: 327-332 [PMID: 31604529 DOI: 10.1016/j.bbrc.2019.09.135]

33 **Robinson EL**, Drawnel FM, Mehdi S, Archer CR, Liu W, Okkenhaug H, Alkass K, Aronsen JM, Nagaraju CK, Sjaastad I, Sipido KR, Bergmann O, Arthur JSC, Wang X, Roderick HL. MSK-Mediated Phosphorylation of Histone H3 Ser28 Couples MAPK Signalling with Early Gene Induction and Cardiac Hypertrophy. *Cells* 2022; **11** [PMID: 35203255 DOI: 10.3390/cells11040604]

34 **Blay JY**, Hindi N, Bollard J, Aguiar S Jr, Angel M, Araya B, Badilla R, Bernabeu D, Campos F, Caro-Sánchez CHS, Carvajal B, Carvajal Montoya A, Casavilca-Zambrano S, Castro-Oliden V, Chacón M, Clara M, Collini P, Correa Genoroso R, Costa FD, Cuellar M, Dei Tos AP, Dominguez Malagon HR, Donati D, Dufresne A, Eriksson M, Farias-Loza M, Fernandez P, Frezza AM, Frisoni T, Garcia-Ortega DY, Gelderblom H, Gouin F, Gómez-Mateo MC, Gronchi A, Haro J, Huanca L, Jimenez N, Karanian M, Kasper B, Lopes David BB, Lopez-Pousa A, Lutter G, Martinez-Said H, Martinez-Tlahuel J, Mello CA, Morales Pérez JM, Moura David S, Nascimento AG, Ortiz-Cruz EJ, Palmerini E, Patel S, Pfluger Y, Provenzano S, Righi A, Rodriguez A, Salas R, Santos TTG, Scotlandi K, Soule T, Stacchiotti S, Valverde C, Waisberg F, Zamora Estrada E, Martin-Broto J. SELNET clinical practice guidelines for soft tissue sarcoma and GIST. *Cancer Treat Rev* 2022; **102**: 102312 [PMID: 34798363 DOI: 10.1016/j.ctrv.2021.102312]

35 **Chen T**, Xu L, Ye L, Qiu H, Hu Y, Liu H, Zhou Z, Li G, Yu J. A new nomogram for recurrence-free survival prediction of gastrointestinal stromal tumors: Comparison with current risk classification methods. *Eur J Surg Oncol* 2019; **45**: 1109-1114 [PMID: 30594406 DOI: 10.1016/j.ejso.2018.12.014]

36 **Dz Chen J**, Zhu Y, Wang Y. Emerging Noninvasive Neuromodulation Methods for Functional Gastrointestinal Diseases. *J Transl Int Med* 2022; **10**: 281-285 [PMID: 36860625 DOI: 10.2478/jtim-2022-0060]

37 **Papale M**, Vocino G, Lucarelli G, Rutigliano M, Gigante M, Rocchetti MT, Pesce F, Sanguedolce F, Bufo P, Battaglia M, Stallone G, Grandaliano G, Carrieri G, Gesualdo L, Ranieri E. Urinary RKIP/p-RKIP is a potential diagnostic and prognostic marker of clear cell renal cell carcinoma. *Oncotarget* 2017; **8**: 40412-40424 [PMID: 28418894 DOI: 10.18632/oncotarget.16341]

38 **Bedri SK**, Nilsson OB, Fink K, Månberg A, Hamsten C, Ayoglu B, Manouchehrinia A, Nilsson P, Olsson T, Hillert J, Grönlund H, Glaser A. Plasma protein profiling reveals candidate biomarkers for multiple sclerosis treatment. *PLoS One* 2019; **14**: e0217208 [PMID: 31141529 DOI: 10.1371/journal.pone.0217208]

39 **Bryant KL**, Stalnecker CA, Zeitouni D, Klomp JE, Peng S, Tikunov AP, Gunda V, Pierobon M, Waters AM, George SD, Tomar G, Papke B, Hobbs GA, Yan L, Hayes TK, Diehl JN, Goode GD, Chaika NV, Wang Y, Zhang GF, Witkiewicz AK, Knudsen ES, Petricoin EF 3rd, Singh PK, Macdonald JM, Tran NL, Lyssiotis CA, Ying H, Kimmelman AC, Cox AD, Der CJ. Combination of ERK and autophagy inhibition as a treatment approach for pancreatic cancer. *Nat Med* 2019; **25**: 628-640 [PMID: 30833752 DOI: 10.1038/s41591-019-0368-8]

40 **Zheng S**, Shu Y, Lu Y, Sun Y. Chloroquine Combined with Imatinib Overcomes Imatinib Resistance in Gastrointestinal Stromal Tumors by Inhibiting Autophagy *via* the MAPK/ERK Pathway. *Onco Targets Ther* 2020; **13**: 6433-6441 [PMID: 32753885 DOI: 10.2147/OTT.S256935]

World Journal of Gastroenterology

Submit a Manuscript: https://www.f6publishing.com

World J Gastroenterol 2023 July 14; 29(26): 4214-4221

DOI: 10.3748/wjg.v29.i26.4214

ISSN 1007-9327 (print) ISSN 2219-2840 (online)

CASE REPORT

Value of contrast-enhanced ultrasound in deep angiomyxoma using a biplane transrectal probe: A case report

Qiong Zhang, Hua-Lin Yan, Qiang Lu, Yan Luo

Specialty type: Gastroenterology and hepatology

Provenance and peer review: Unsolicited article; Externally peer reviewed.

Peer-review model: Single blind

Peer-review report's scientific quality classification

Grade A (Excellent): 0
Grade B (Very good): B
Grade C (Good): C
Grade D (Fair): 0
Grade E (Poor): 0

P-Reviewer: Martino A, Italy; Naganuma H, Japan

Received: March 2, 2023
Peer-review started: March 2, 2023
First decision: May 16, 2023
Revised: May 23, 2023
Accepted: June 13, 2023
Article in press: June 13, 2023
Published online: July 14, 2023

Qiong Zhang, Hua-Lin Yan, Qiang Lu, Yan Luo, Department of Medical Ultrasound, West China Hospital, Sichuan University, Chengdu 610041, Sichuan Province, China

Corresponding author: Yan Luo, Doctor, Professor, Department of Medical Ultrasound, West China Hospital, Sichuan University, No. 37 Guo Xue Xiang, Chengdu 610041, Sichuan Province, China. yanluo@scu.edu.cn

Abstract

BACKGROUND

Deep angiomyxoma (DAM) is a very rare tumor type. Magnetic resonance imaging (MRI) is considered the best imaging modality for diagnosing DAM. Computed tomography (CT) is used mainly to assess the invasion range of DAM. The value of ultrasonography in the diagnosis of DAM is still controversial. Through a literature review, we summarized the current state of ultrasonic examination for DAM and reported for the first time the contrast-enhanced ultrasound (CEUS) features of DAM seen using a biplane transrectal probe.

CASE SUMMARY

A 37-year-old woman presented with a sacrococcygeal mass that had gradually increased in size over the previous 6 mo. MRI and CT examinations failed to allow a definite diagnosis to be made. Transperineal core needle biopsy (CNB) guided by transrectal ultrasound and CEUS was suggested after a multidisciplinary discussion. Grayscale ultrasound of the lesion showed a layered appearance with alternating hyperechoic and hypoechoic patterns. Transrectal CEUS showed a laminated distribution of the contrast agent that was consistent with the layered appearance of the tumor on grayscale ultrasound. We performed transperineal CNB of the enhanced area inside the tumor under transrectal CEUS guidance and finally made a definitive diagnosis of DAM through histopathology. The patient underwent laparoscopic-assisted transabdominal surgery combined with transperineal surgery for large pelvic tumor resection and pelvic floor peritoneal reconstruction. No recurrence or metastasis was found at the nine-month follow-up.

CONCLUSION

Transrectal CEUS can show the layered perfusion characteristics of the contrast agent, guiding subsequent transperineal CNB of the enhanced area within the DAM.

Key Words: Contrast-enhanced ultrasound; Transrectal ultrasound; Transperineal core needle biopsy; Deep angiomyxoma; Pelvic tumor; Case report

©The Author(s) 2023. Published by Baishideng Publishing Group Inc. All rights reserved.

Core Tip: Deep angiomyxoma (DAM) is a very rare tumor. Imaging examinations play an important role in the diagnosis of DAM. Magnetic resonance imaging is considered the best imaging modality for diagnosing DAM. Computed tomography is used mainly to assess the invasion range of DAM. The value of ultrasonography in the diagnosis of DAM is still controversial. We reported for the first time the contrast-enhanced ultrasound (CEUS) features of DAM seen using a biplane transrectal probe. Transrectal CEUS can provide more abundant diagnostic information in terms of the blood perfusion characteristics of DAM, guiding subsequent transperineal puncture of the enhanced area within the tumor.

Citation: Zhang Q, Yan HL, Lu Q, Luo Y. Value of contrast-enhanced ultrasound in deep angiomyxoma using a biplane transrectal probe: A case report. *World J Gastroenterol* 2023; 29(26): 4214-4221
URL: https://www.wjgnet.com/1007-9327/full/v29/i26/4214.htm
DOI: https://dx.doi.org/10.3748/wjg.v29.i26.4214

INTRODUCTION

Deep angiomyxoma (DAM) is a very rare tumor that mainly occurs in the pelvis and perineum of women of reproductive age[1]. DAM is classified as a "tumor of uncertain differentiation" in the World Health Organization classification. Since it was first described in 1983, DAM has been described in multiple single case reports and some case series reports[1-3]. Imaging examinations play an important role in the diagnosis of DAM and in evaluating the scope of lesion invasion. Magnetic resonance imaging (MRI) is considered the best imaging modality for the diagnosis of DAM; computed tomography (CT) is mainly used to evaluate the invasion range of DAM, and the value of ultrasound in the diagnosis of DAM is still controversial. This article reports for the first time the contrast-enhanced ultrasound (CEUS) features of DAM seen using a biplane transrectal probe and reviews the imaging features of DAM in the literature.

CASE PRESENTATION

Chief complaints

A 37-year-old woman presented with a sacrococcygeal mass that had been increasing in size over the previous 6 mo.

History of present illness

The patient inadvertently found a sacrococcygeal mass 6 mo prior, which was approximately the size of a pigeon egg at first, without pain or other discomfort. The mass gradually increased in size, accompanied by lumbosacral distension. No definite diagnosis was made after an examination at the local hospital; thus, the patient was transferred to our hospital for further diagnosis and treatment.

History of past illness

The patient had no previous medical history.

Personal and family history

The patient and family histories were negative.

Physical examination

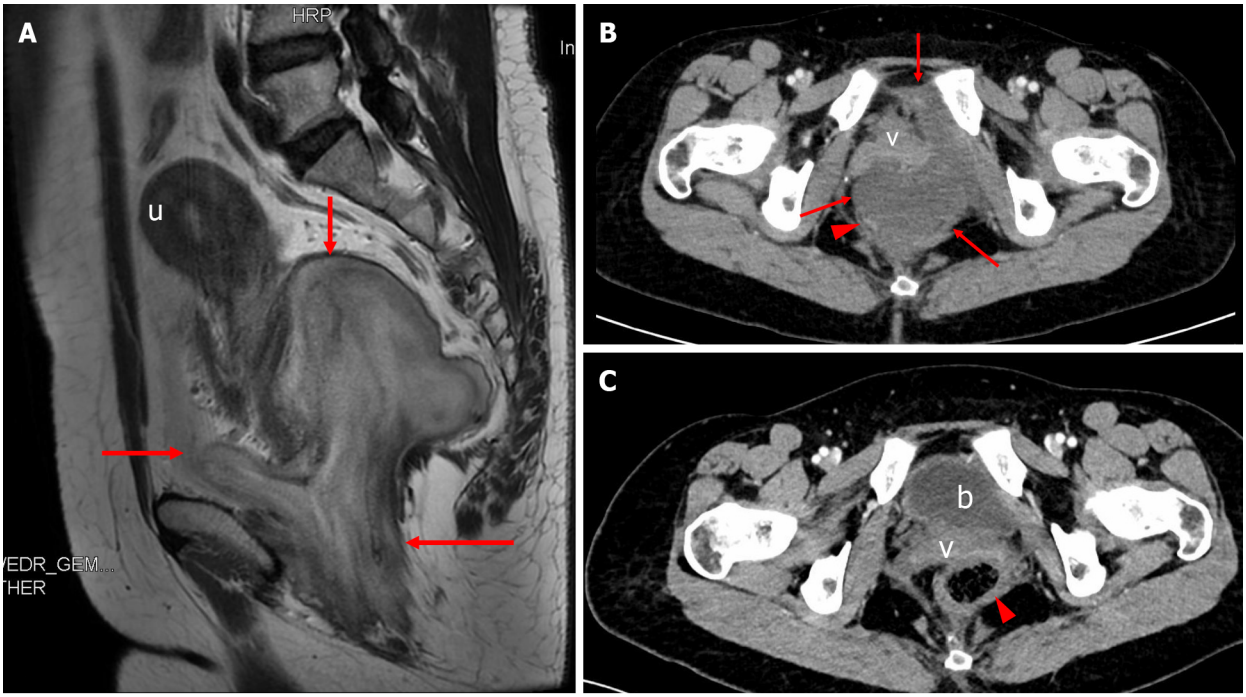
A digital rectal examination revealed a large solid mass in the anterior rectal wall, with a hard texture and fixed position. The mass boundary could not be palpated.

Laboratory examinations

The results of laboratory examinations were normal, including routine blood analysis, carcinoembryonic antigen (CEA), alpha-fetoprotein (AFP), carbohydrate antigen (CA) 19-9, and CA125 results.

Imaging examinations

Preoperative MRI showed a paracervical mass in the pelvis, measuring approximately 9.5 cm × 8.1 cm in size (Figure 1A). T2-weighted imaging (T2WI) presented stratification changes with alternating high and low signals that were clearly demarcated from the surrounding tissue, and the uterus was pushed and displaced cephalad. Preoperative contrast-



DOI: 10.3748/wjg.v29.i26.4214 **Copyright** ©The Author(s) 2023.

Figure 1 Magnetic resonance imaging and contrast-enhanced computed tomography images in our case. A: Preoperative sagittal T2-weighted imaging. The mass (arrows) was 9.5 cm × 8.1 cm in size, showing a layered appearance with alternating high and low signals and a clearly demarcated boundary with respect to surrounding tissue, and the uterus was pushed and displaced cephalad; B: Preoperative transverse contrast-enhanced computed tomography (CECT) showed that the anterior vagina and the right posterior rectum (arrowhead) were pushed by the mass (arrows); C: Six months after surgery, transverse CECT showed that the filled bladder, vagina, and rectum (arrowhead) were in normal positions, with no evidence of tumor recurrence. u: Uterus; v: Vagina; b: Bladder.

enhanced CT (CECT) demonstrated a pelvic mass between the cervix and rectum with nonenhanced areas (Figure 1B). The mass pushed against and displaced the anterior vagina and the right posterior rectum.

Preoperative transrectal ultrasound (TRUS) was performed with the MyLab Twice ultrasound system (Esaote, Genoa, Italy) equipped with a biplane endoscopic probe (TRT33, linear frequency of 4-13 MHz, convex frequency of 3-9 MHz). Grayscale ultrasound showed that the left pelvic mass had an irregular shape (Figure 2A). The internal echo of the mass presented a layered appearance with alternating hyperechoic and hypoechoic patterns, and the boundary between the mass and rectum wall was clear. Color Doppler flow imaging (CDFI) showed some blood vessels scattered in the tumor (Figure 2B), and the dispersed intratumoral blood vessels were consistent with the layered appearance of the tumor on grayscale ultrasound. Then, transrectal CEUS was performed with a bolus injection of 2.4 mL of SonoVue (Bracco, Milan, Italy) through the elbow vein (Figure 2C). A laminated distribution of the contrast agent was observed within the mass, which was also consistent with the layered appearance of the tumor on grayscale ultrasound.

Further diagnostic work-up

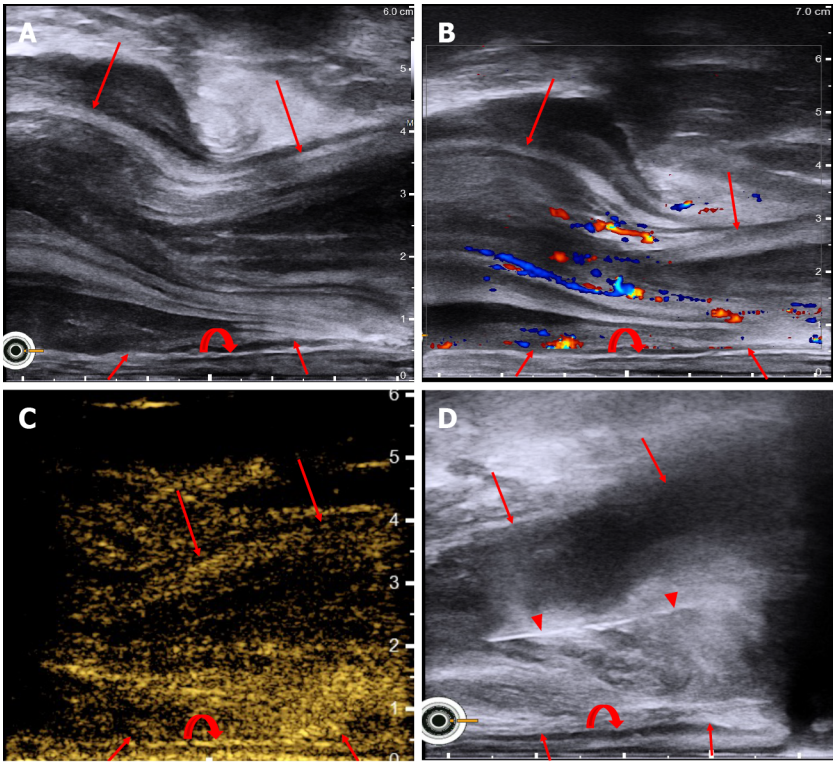
Transperineal core needle (16G) biopsy (CNB) was performed under the guidance of TRUS (Figure 2D). The probe was switched to linear mode, and puncture sampling was performed under real-time monitoring by TRUS, avoiding the nonenhanced areas of the tumor. No complications occurred during the biopsy.

FINAL DIAGNOSIS

Postoperative immunohistochemical staining showed the following results: CD34 (vascular +), CK (pan) (-), ER (+), PR (+), Desmin (+), S-100 (-), SMA (+), CDK4 (-), and MDM2 (±). FISH revealed an unbalanced translocation of the HMGA2 gene. The final diagnosis was a DAM in the deep pelvis (Figure 3).

TREATMENT

A preoperative examination was completed. The patient underwent laparoscopic-assisted transabdominal surgery combined with transperineal surgery for large pelvic tumor resection and pelvic floor peritoneal reconstruction on February 10, 2022.



DOI: 10.3748/wjg.v29.i26.4214 **Copyright** ©The Author(s) 2023.

Figure 2 Scanning with a TRT33 biplane transrectal probe linear array. A: Grayscale ultrasound showed that the mass (arrows) was irregular in shape, with a layered appearance of alternating hyperechoic and hypoechoic areas inside and a clearly demarcated boundary with respect to the rectal wall (curved arrow); B: Color Doppler flow imaging showed that the dispersed intratumoral blood vessels were consistent with the layered appearance of the mass (arrows) on grayscale ultrasound; C: Transrectal contrast-enhanced ultrasound showed a laminated distribution of the contrast agent in the mass (arrows), also consistent with the layered appearance of the tumor on grayscale ultrasound; D: Transperineal core needle (arrowheads) biopsy was performed under the guidance of transrectal ultrasound.

During surgery, the tumor was found to be located below the pelvic peritoneal reflex plane, behind the cervix, and in front of the left side of the rectum. It was irregular in shape, with a smooth capsule, and contained both cystic and solid components. The postoperative pathological report was consistent with DAM.

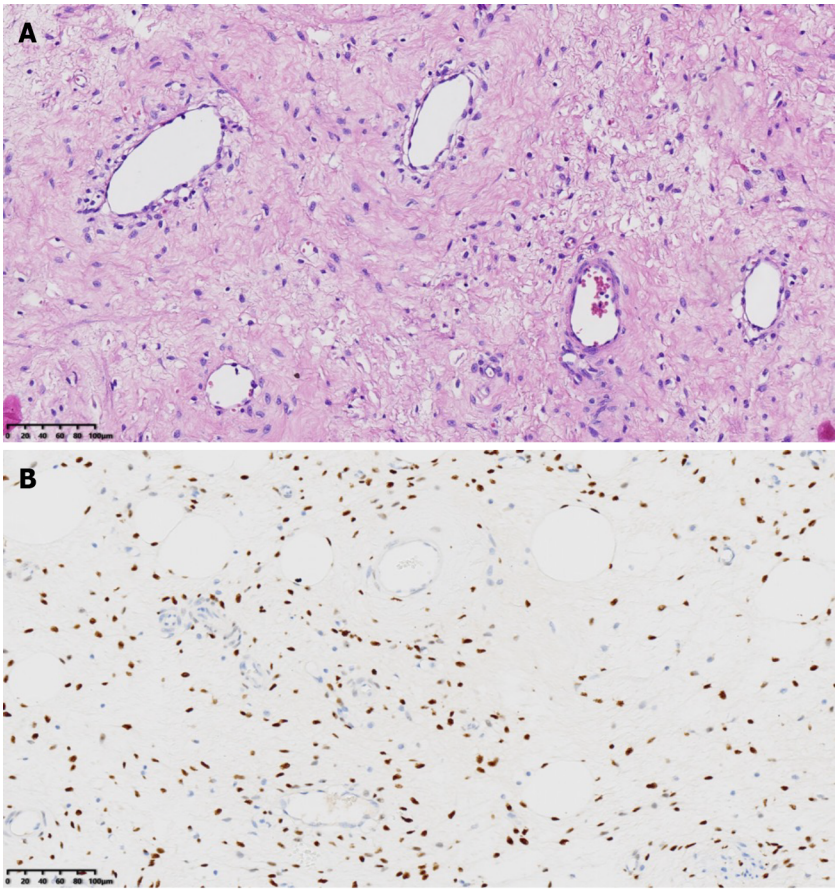
OUTCOME AND FOLLOW-UP

The patient recovered well after surgery and underwent regular outpatient follow-up examinations. CECT of the pelvic cavity was performed on August 12, 2022 (Figure 1C), six months after resection, and indicated no obvious signs of tumor recurrence. No recurrence or metastasis was found by the last follow-up on November 9, 2022.

DISCUSSION

DAM is a very rare type of tumor that most commonly occurs in the pelvis and perineum of women of reproductive age [1]. Histologically, the typical morphology of DAM is an infiltrating, uniformly hypocellular tumor, consisting of small-sized spindled or stellate cells scattered randomly in the myxoid stroma and containing many small to medium/Large blood vessels, without nuclear atypia[1] (Figure 3). Clinically, DAM presents as a slowly growing painless mass. DAM is characterized by locally aggressive growth, with recurrence and metastasis occurring in some cases[2,3]. Accurate preoperative diagnosis and complete resection of the lesion are key to the treatment and prevention of recurrence[4]. Imaging examinations play an important role in the diagnosis of DAM and in assessing the extent of lesion invasion[5]. Commonly used imaging examinations include MRI, CT, and ultrasound[6].

CT is mainly used to evaluate the invasion range of DAM and perform follow-up observations, but its value in displaying typical signs such as a laminated or swirled appearance of the DAM tissue is limited[5-7]. MRI is considered the best imaging modality for the diagnosis of DAM[6,8-10]. T2WI can reveal the swirled or layered appearance of the mass, which has been reported in at least 83% of cases[6]. MRI is also critical to determining the range of tumor extension into the surrounding space and the mode of tumor invasion into surrounding organs[6,9]. Retrospective analysis of the T2WI MRI data in our case showed a typical laminated and swirled appearance consistent with the reports in the literature[8-10] (Figure 1A). However, we failed to make a definitive diagnosis, mainly because DAM is rare; we had insufficient experience in diagnosing this tumor. Some experts believe that it is difficult to accurately diagnose DAM



DOI: 10.3748/wjg.v29.i26.4214 **Copyright** ©The Author(s) 2023.

Figure 3 Pathological results of the deep angiomyxoma puncture sample. A: Small-sized spindled or stellate cells scattered in the myxoid stroma containing many blood vessels of varying caliber, without cellular atypia or mitotic activity (HE × 200); B: Immunohistochemistry showed positive expression of estrogen receptors in the tumor cells (× 200).

before surgery, and these tumors are often misdiagnosed as other soft tissue tumors[11-13], such as Bartholin cyst, lipoma, and cellular angiofibroma. The misdiagnosis rate is as high as 82%[11].

Although MRI has many advantages in the diagnosis of DAM, the cost of MRI is relatively high, and patients with metal in the body cannot be examined by MRI. Similar to MRI, ultrasound can also be applied to avoid radiation exposure. Because of its low cost, convenient operation, and noninvasiveness, ultrasound can be used for multiple examinations in cases of DAM and follow-up examinations after surgery. In addition, ultrasound is not limited by the presence of metal objects such as heart stents and is also the preferred choice for patients with claustrophobia.

However, the literature related to ultrasound for DAM is scarce[14], and the value and role of ultrasound have not been systematically summarized. Through a literature review, we found that the previous ultrasonography methods related to DAM mainly consisted of examinations with transabdominal convex array probes[10,15], intracavity convex array probes[9,14,16,17], and transperineal linear array probes[18,19]. Among the 53 reports related to DAM, only 2[9,15] reported a typical laminated or swirled appearance on grayscale ultrasound. In all reports, CDFI did not show swirled or layered blood vessel distribution characteristics corresponding to the grayscale ultrasound findings, and CEUS examination was not performed in any of the previous reports, as shown in Table 1.

We report for the first time the CEUS features of DAM in the pelvic cavity seen using a biplane transrectal probe. In this case, transrectal grayscale ultrasound showed a laminated appearance with alternating hyperechoic and hypoechoic patterns inside the mass (Figure 2A), demonstrating the same details as MRI and excellent resolution, which confirms the high sensitivity of transrectal high-frequency ultrasound in detecting the characteristic histological structure of DAM. We also observed that the distribution of scattered blood vessels within the tumor on CDFI was consistent with the layered appearance of the tumor on grayscale ultrasound (Figure 2B). This layered distribution of vascular features has not been previously reported in the literature[9-11,15,18,19], which may be related to the fact that more anatomical details of the tumor can be displayed by high-frequency ultrasound with a biplane transrectal probe[9,20,21]; however, this is yet to be verified by subsequent cases. Reportedly, CEUS may be of great value in the diagnosis of DAM[15], as this modality can better show the characteristics of DAM and help to determine the role of ultrasound in tumor treatment. However, to our knowledge, the diagnosis of DAM by CEUS has not been reported. In our case, the mass was examined by transrectal CEUS (Figure 2C). The characteristic laminated perfusion of the contrast agent was observed within the mass, which was also consistent with the layered appearance of the tumor on grayscale ultrasound.

Table 1 Summary of sonographic features of deep angiomyxoma from the literature

No.	Ultrasonographic approach and probe	No. of tumors	Sex	Age (yr)	Location	Maximal diameter (cm)	Internal echogenicity	No. of cystic component	Laminated/swirled pattern in 2D
1	Transabdominal convex array probe	4	F	18-50	Pelvis	3-38.8 (mean: 16.2 ± 9.4)	Hypoechoic or isoechoic internal components	3	No
2	Transabdominal convex array probe	8	7F; 1M	35-64 (median 39)	Vulva, pelvis, perineal region, spermatic cord, and scrotum	7-21	Heterogeneous, isoechoic internal components	2	Yes
3	Transvaginal end-fire probe	1	F	40	Pelvis extending to the perineum	11.8	Mixed echogenicity	0	Yes
4	Transvaginal end-fire probe	1	F	54	Behind the uterus	18	Heterogeneous hypoechoic internal components	1	No
5	Transvaginal end-fire probe	1	F	44	Left pelvis	12	Hypoechoic to isoechoic internal components	0	No
6	Transrectal radial probe	1	F	61	Left perirectal mass	10.7	Hypoechoic to isoechoic internal components	NA	No
7	Transperineal linear probe	36	M	1-81 (mean 48.3 ± 20.6)	Epididymis, testes, spermatic cord, scrotum	1.6-25 (mean: 8.36)	Heterogeneous hypoechoic internal components	NA	No
8	Transperineal linear probe	1	F	28	Vulva	4.8	Heterogeneous hypoechoic internal components	0	No

F: Female; M: Male; NA: Not available.

We believe that the advantages of ultrasound with a biplane transrectal probe and CEUS in the diagnosis of DAM in the deep pelvic cavity are as follows:

First, the biplane transrectal high-frequency probe can enter the pelvic cavity along the anal canal and rectum and clearly display the laminated or swirled appearance of DAM, as well as the boundary of the mass and its relationships with adjacent structures, allowing this modality to be comparable to MRI. Typically, transperineal ultrasound and transabdominal ultrasound cannot simultaneously meet the requirements of satisfactory detection depth and high resolution of images when examining deep pelvic lesions. Additionally, the biplane transrectal probe effectively overcomes the obvious limitation of the observation angle of the convex end-fire probe.

Second, the laminated perfusion characteristics inside the mass can be displayed in real time by CEUS, which is helpful for the diagnosis and differential diagnosis of DAM.

Third, the gold standard for the diagnosis of DAM depends on histopathology and immunohistochemistry[18]. However, the proportion of cystic components in DAM is as high as 75%[10], and these components appeared as unenhanced areas on transrectal CEUS, which were easy to distinguish from enhanced areas of the mass, guiding subsequent precise and effective puncture of the enhanced area (Figure 2D). After transrectal CEUS, our patient immediately underwent transperineal CNB[22,23] guided by TRUS at the examination bed, and a clear pathological diagnosis was obtained, which provided a basis for formulating the surgical plan and reducing the patient's waiting time before surgery.

Fourth, compared with MRI and CT, TRUS is convenient, rapid, radiation-free, and economical. TRUS can dynamically display the internal and adjacent structures of the lesion in real time and can be used for repeated monitoring of the lesion before surgery.

Fifth, for patients with cardiac pacemakers, internal metal stents, or claustrophobia, ultrasound with a biplane transrectal probe and CEUS can be used instead of MRI.

Sixth, long-term follow-up is necessary due to the high recurrence rate of DAM[24]. Due to the above advantages, ultrasound with a biplane transrectal probe and CEUS are ideal tools for the postoperative follow-up of pelvic DAM patients. In summary, ultrasound with a biplane transrectal probe and CEUS can be one of the first choices for the diagnosis and follow-up of DAM patients.

CONCLUSION

In conclusion, pelvic DAM is a rare tumor. In our case, the typical laminated appearance of DAM could be observed by ultrasound with a biplane transrectal probe and CEUS. Moreover, CNB of the enhanced area inside the tumor could be accurately guided by transrectal CEUS, enabling the pathological gold standard for the diagnosis of DAM; thus, this modality is expected to be one of the preferred methods for the diagnosis of DAM in the pelvic cavity.

ACKNOWLEDGEMENTS

The authors thank Dr. Wang WY (Department of Pathology, West China Hospital, Sichuan University) for providing the pathological data.

FOOTNOTES

Author contributions: Zhang Q and Luo Y contributed to the study conceptualization; Luo Y and Lu Q supervised the study; Zhang Q and Yan HL contributed to data collection and manuscript drafting; Yan HL and Lu Q contributed to manuscript revision; and all authors have approved the final manuscript.

Informed consent statement: Informed written consent was obtained from the patient for publication of this report and any accompanying images.

Conflict-of-interest statement: All the authors report no relevant conflicts of interest for this article.

CARE Checklist (2016) statement: The authors have read the CARE Checklist (2016), and the manuscript was prepared and revised according to the CARE Checklist (2016).

Open-Access: This article is an open-access article that was selected by an in-house editor and fully peer-reviewed by external reviewers. It is distributed in accordance with the Creative Commons Attribution NonCommercial (CC BY-NC 4.0) license, which permits others to distribute, remix, adapt, build upon this work non-commercially, and license their derivative works on different terms, provided the original work is properly cited and the use is non-commercial. See: https://creativecommons.org/Licenses/by-nc/4.0/

Country/Territory of origin: China

ORCID number: Qiong Zhang 0000-0002-9330-5051; Hua-Lin Yan 0000-0003-1338-1124; Qiang Lu 0000-0002-4057-1997; Yan Luo 0000-0003-2985-1768.

S-Editor: Yan JP
L-Editor: A
P-Editor: Yan JP

REFERENCES

1 **Steeper TA**, Rosai J. Aggressive angiomyxoma of the female pelvis and perineum. Report of nine cases of a distinctive type of gynecologic soft-tissue neoplasm. *Am J Surg Pathol* 1983; **7**: 463-475 [PMID: 6684403 DOI: 10.1097/00000478-198307000-00009]
2 **Gay F**, Champigneulle J, Tortuyaux JM, Cuny T, Régent D, Laurent-Croisé V. Aggressive angiomyxoma. *Diagn Interv Imaging* 2013; **94**: 657-661 [PMID: 23453353 DOI: 10.1016/j.diii.2013.01.009]
3 **Giraudmaillet T**, Mokrane FZ, Delchier-Bellec MC, Motton S, Cron C, Rousseau H. Aggressive angiomyxoma of the pelvis with inferior vena cava involvement: MR imaging features. *Diagn Interv Imaging* 2015; **96**: 111-114 [PMID: 25533499 DOI: 10.1016/j.diii.2014.03.006]
4 **Song M**, Glasgow M, Murugan P, Rivard C. Aggressive Angiomyxoma of the Vulva and Bladder. *Obstet Gynecol* 2017; **130**: 885-888 [PMID: 28885430 DOI: 10.1097/AOG.0000000000002254]
5 **Outwater EK**, Marchetto BE, Wagner BJ, Siegelman ES. Aggressive angiomyxoma: findings on CT and MR imaging. *AJR Am J Roentgenol* 1999; **172**: 435-438 [PMID: 9930798 DOI: 10.2214/ajr.172.2.9930798]
6 **Surabhi VR**, Garg N, Frumovitz M, Bhosale P, Prasad SR, Meis JM. Aggressive angiomyxomas: a comprehensive imaging review with clinical and histopathologic correlation. *AJR Am J Roentgenol* 2014; **202**: 1171-1178 [PMID: 24848813 DOI: 10.2214/AJR.13.11668]
7 **Jeyadevan NN**, Sohaib SA, Thomas JM, Jeyarajah A, Shepherd JH, Fisher C. Imaging features of aggressive angiomyxoma. *Clin Radiol* 2003; **58**: 157-162 [PMID: 12623047 DOI: 10.1053/crad.2002.1127]
8 **Srinivasan S**, Krishnan V, Ali SZ, Chidambaranathan N. "Swirl sign" of aggressive angiomyxoma-a lesser known diagnostic sign. *Clin Imaging* 2014; **38**: 751-754 [PMID: 24852676 DOI: 10.1016/j.clinimag.2014.04.001]
9 **Tariq R**, Hasnain S, Siddiqui MT, Ahmed R. Aggressive angiomyxoma: swirled configuration on ultrasound and MR imaging. *J Pak Med Assoc* 2014; **64**: 345-348 [PMID: 24864615]
10 **Kumar N**, Goyal A, Manchanda S, Sharma R, Kumar A, Bansal VK. Aggressive pelvic angiomyxoma and its mimics: can imaging be the guiding light? *Br J Radiol* 2020; **93**: 20200255 [PMID: 32401545 DOI: 10.1259/bjr.20200255]

11 **Bai HM**, Yang JX, Huang HF, Cao DY, Chen J, Yang N, Lang JH, Shen K. Individualized managing strategies of aggressive angiomyxoma of female genital tract and pelvis. *Eur J Surg Oncol* 2013; **39**: 1101-1108 [PMID: 23899874 DOI: 10.1016/j.ejso.2013.06.013]

12 **Smith HO**, Worrell RV, Smith AY, Dorin MH, Rosenberg RD, Bartow SA. Aggressive angiomyxoma of the female pelvis and perineum: review of the literature. *Gynecol Oncol* 1991; **42**: 79-85 [PMID: 1916515 DOI: 10.1016/0090-8258(91)90235-w]

13 **Zou R**, Xu H, Shi Y, Wang J, Wang S, Zhu L. Retrospective analysis of clinicopathological features and prognosis for aggressive angiomyxoma of 27 cases in a tertiary center: a 14-year survey and related literature review. *Arch Gynecol Obstet* 2020; **302**: 219-229 [PMID: 32430760 DOI: 10.1007/s00404-020-05592-5]

14 **Yang X**, Zhang L, Zhao W, Zhang Y, Yu J. Invasive angiomyxoma diagnosed by transvaginal ultrasound: a case report. *Ann Palliat Med* 2021; **10**: 5870-5874 [PMID: 33040540 DOI: 10.21037/apm-20-321]

15 **Zhao CY**, Su N, Jiang YX, Yang M. Application of ultrasound in aggressive angiomyxoma: Eight case reports and review of literature. *World J Clin Cases* 2018; **6**: 811-819 [PMID: 30510948 DOI: 10.12998/wjcc.v6.i14.811]

16 **Hajjar R**, Alharthi M, Richard C, Gougeon F, Loungnarath R. Pelvic Aggressive Angiomyxoma: Major Challenges in Diagnosis and Treatment. *Cureus* 2019; **11**: e4419 [PMID: 31245206 DOI: 10.7759/cureus.4419]

17 **Huang CC**, Sheu CY, Chen TY, Yang YC. Aggressive angiomyxoma: a small palpable vulvar lesion with a huge mass in the pelvis. *J Low Genit Tract Dis* 2013; **17**: 75-78 [PMID: 23222052 DOI: 10.1097/LGT.0b013e3182507df8]

18 **Sun J**, Lian PH, Ye ZX, Dong X, Ji ZG, Wen J, Li HZ. Aggressive Angiomyxoma in the Scrotum: A Case Series and Literature Review. *Front Surg* 2022; **9**: 762212 [PMID: 35310439 DOI: 10.3389/fsurg.2022.762212]

19 **Ota H**, Otsuki K, Ichihara M, Ishikawa T, Okai T. A case of aggressive angiomyxoma of the vulva. *J Med Ultrason (2001)* 2013; **40**: 283-287 [PMID: 27277251 DOI: 10.1007/s10396-012-0427-y]

20 **Wenig BM**, Vinh TN, Smirniotopoulos JG, Fowler CB, Houston GD, Heffner DK. Aggressive psammomatoid ossifying fibromas of the sinonasal region: a clinicopathologic study of a distinct group of fibro-osseous lesions. *Cancer* 1995; **76**: 1155-1165 [PMID: 8630892 DOI: 10.1002/1097-0142(19951001)76:7<1155::aid-cncr2820760710>3.0.co;2-p]

21 **Granter SR**, Nucci MR, Fletcher CD. Aggressive angiomyxoma: reappraisal of its relationship to angiomyofibroblastoma in a series of 16 cases. *Histopathology* 1997; **30**: 3-10 [PMID: 9023551 DOI: 10.1046/j.1365-2559.1997.d01-556.x]

22 **Zhang Q**, Zhao JY, Zhuang H, Lu CY, Yao J, Luo Y, Yu YY. Transperineal core-needle biopsy of a rectal subepithelial lesion guided by endorectal ultrasound after contrast-enhanced ultrasound: A case report. *World J Gastroenterol* 2021; **27**: 1354-1361 [PMID: 33833488 DOI: 10.3748/wjg.v27.i13.1354]

23 **Nuernberg D**, Saftoiu A, Barreiros AP, Burmester E, Ivan ET, Clevert DA, Dietrich CF, Gilja OH, Lorentzen T, Maconi G, Mihmanli I, Nolsoe CP, Pfeffer F, Rafaelsen SR, Sparchez Z, Vilmann P, Waage JER. EFSUMB Recommendations for Gastrointestinal Ultrasound Part 3: Endorectal, Endoanal and Perineal Ultrasound. *Ultrasound Int Open* 2019; **5**: E34-E51 [PMID: 30729231 DOI: 10.1055/a-0825-6708]

24 **Draeger DL**, Protzel C, Hakenberg OW. Aggressive Angiomyxoma as a Rare Differential Diagnosis of Enlargement of the Scrotum. *Clin Genitourin Cancer* 2016; **14**: e237-e239 [PMID: 26774350 DOI: 10.1016/j.clgc.2015.12.022]



Published by **Baishideng Publishing Group Inc**
7041 Koll Center Parkway, Suite 160, Pleasanton, CA 94566, USA
Telephone: +1-925-3991568
E-mail: bpgoffice@wjgnet.com
Help Desk: https://www.f6publishing.com/helpdesk
https://www.wjgnet.com

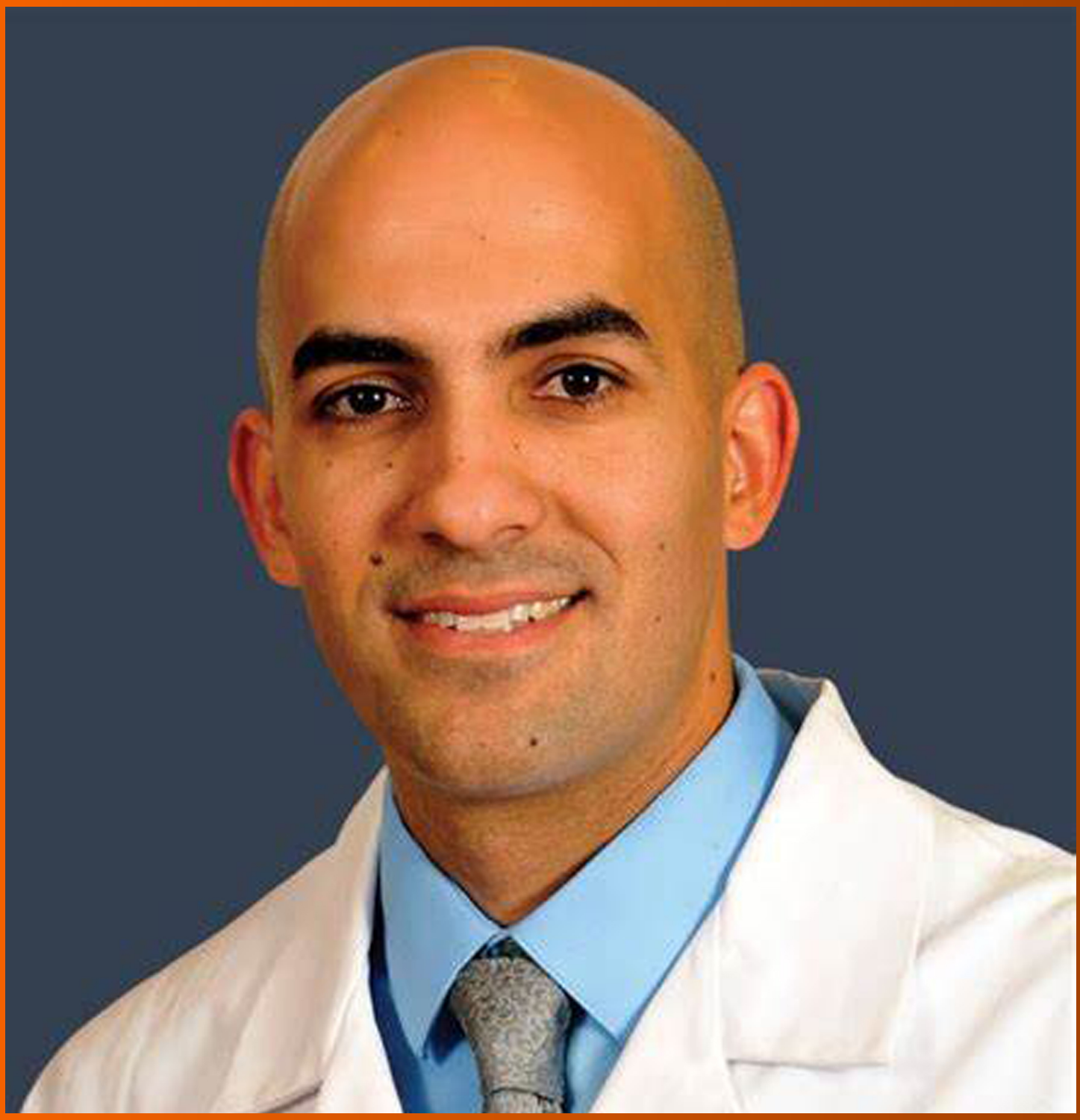


© 2023 Baishideng Publishing Group Inc. All rights reserved.

ISSN 1007-9327 (print)
ISSN 2219-2840 (online)

World Journal of *Gastroenterology*

World J Gastroenterol 2023 July 21; 29(27): 4222-4367



Published by Baishideng Publishing Group Inc

World Journal of Gastroenterology

Contents

Weekly Volume 29 Number 27 July 21, 2023

REVIEW

4222 Rare causes of acute non-variceal upper gastrointestinal bleeding: A comprehensive review

Martino A, Di Serafino M, Orsini L, Giurazza F, Fiorentino R, Crolla E, Campione S, Molino C, Romano L, Lombardi G

4236 Sarcopenia in cirrhosis: Prospects for therapy targeted to gut microbiota

Maslennikov R, Alieva A, Poluektova E, Zharikov Y, Suslov A, Letyagina Y, Vasileva E, Levshina A, Kozlov E, Ivashkin V

4252 Bile acids and their receptors: Potential therapeutic targets in inflammatory bowel disease

Long XQ, Liu MZ, Liu ZH, Xia LZ, Lu SP, Xu XP, Wu MH

4271 Serum resistin and the risk for hepatocellular carcinoma in diabetic patients

Abdalla MMI

ORIGINAL ARTICLE

Basic Study

4289 Stomach perforation-induced general occlusion/occlusion-like syndrome and stable gastric pentadecapeptide BPC 157 therapy effect

Kalogjera L, Krezic I, Smoday IM, Vranes H, Zizek H, Yago H, Oroz K, Vukovic V, Kavelj I, Novosel L, Zubcic S, Barisic I, Beketic Oreskovic L, Strbe S, Sever M, Sjekavica I, Skrtic A, Boban Blagaic A, Seiwerth S, Sikiric P

4317 18β-glycyrrhetinic acid promotes gastric cancer cell autophagy and inhibits proliferation by regulating miR-328-3p/signal transducer and activator of transcription 3

Yang Y, Nan Y, Du YH, Huang SC, Lu DD, Zhang JF, Li X, Chen Y, Zhang L, Yuan L

Observational Study

4334 Azathioprine monotherapy withdrawal in inflammatory bowel diseases: A retrospective mono-centric study

Crepaldi M, Maniero D, Massano A, Pavanato M, Barberio B, Savarino EV, Zingone F

4344 Predicting portal venous anomalies by left-sided gallbladder or right-sided ligamentum teres hepatis: A large scale, propensity score-matched study

Lin HY, Lee RC, Chai JW, Hsu CY, Chou Y, Hwang HE, Liu CA, Chiu NC, Yen HH

SCIENTOMETRICS

4356 Research landscape on COVID-19 and liver dysfunction: A bibliometric analysis

Zyoud SH

World Journal of Gastroenterology

Weekly Volume 29 Number 27 July 21, 2023

Contents

ABOUT COVER

Editorial Board Member of *World Journal of Gastroenterology*, Mark C Mattar, AGAF, FACG, MD, Professor of Medicine, Department of Gastroenterology, MedStar Georgetown University Hospital, Washington, DC 20007, United States. mark.c.mattar@medstar.net

AIMS AND SCOPE

The primary aim of *World Journal of Gastroenterology* (*WJG*, *World J Gastroenterol*) is to provide scholars and readers from various fields of gastroenterology and hepatology with a platform to publish high-quality basic and clinical research articles and communicate their research findings online. *WJG* mainly publishes articles reporting research results and findings obtained in the field of gastroenterology and hepatology and covering a wide range of topics including gastroenterology, hepatology, gastrointestinal endoscopy, gastrointestinal surgery, gastrointestinal oncology, and pediatric gastroenterology.

INDEXING/ABSTRACTING

The *WJG* is now abstracted and indexed in Science Citation Index Expanded (SCIE), MEDLINE, PubMed, PubMed Central, Scopus, Reference Citation Analysis, China Science and Technology Journal Database, and Superstar Journals Database. The 2023 edition of Journal Citation Reports® cites the 2022 impact factor (IF) for *WJG* as 4.3; Quartile category: Q2. The *WJG*'s CiteScore for 2021 is 8.3.

RESPONSIBLE EDITORS FOR THIS ISSUE

Production Editor: *Yi-Xuan Cai*; **Production Department Director:** *Xiang Li*; **Editorial Office Director:** *Jia-Ru Fan*.

NAME OF JOURNAL
World Journal of Gastroenterology

ISSN
ISSN 1007-9327 (print) ISSN 2219-2840 (online)

LAUNCH DATE
October 1, 1995

FREQUENCY
Weekly

EDITORS-IN-CHIEF
Andrzej S Tarnawski

EXECUTIVE ASSOCIATE EDITORS-IN-CHIEF
Xian-Jun Yu (Pancreatic Oncology), Jian-Gao Fan (Chronic Liver Disease), Hou-Bao Liu (Biliary Tract Disease)

EDITORIAL BOARD MEMBERS
http://www.wjgnet.com/1007-9327/editorialboard.htm

PUBLICATION DATE
July 21, 2023

COPYRIGHT
© 2023 Baishideng Publishing Group Inc

PUBLISHING PARTNER
Shanghai Pancreatic Cancer Institute and Pancreatic Cancer Institute, Fudan University
Biliary Tract Disease Institute, Fudan University

INSTRUCTIONS TO AUTHORS
https://www.wjgnet.com/bpg/gerinfo/204

GUIDELINES FOR ETHICS DOCUMENTS
https://www.wjgnet.com/bpg/GerInfo/287

GUIDELINES FOR NON-NATIVE SPEAKERS OF ENGLISH
https://www.wjgnet.com/bpg/gerinfo/240

PUBLICATION ETHICS
https://www.wjgnet.com/bpg/GerInfo/288

PUBLICATION MISCONDUCT
https://www.wjgnet.com/bpg/gerinfo/208

POLICY OF CO-AUTHORS
https://www.wjgnet.com/bpg/GerInfo/310

ARTICLE PROCESSING CHARGE
https://www.wjgnet.com/bpg/gerinfo/242

STEPS FOR SUBMITTING MANUSCRIPTS
https://www.wjgnet.com/bpg/GerInfo/239

ONLINE SUBMISSION
https://www.f6publishing.com

PUBLISHING PARTNER's OFFICIAL WEBSITE
https://www.shca.org.cn
https://www.zs-hospital.sh.cn

© 2023 Baishideng Publishing Group Inc. All rights reserved. 7041 Koll Center Parkway, Suite 160, Pleasanton, CA 94566, USA
E-mail: bpgoffice@wjgnet.com https://www.wjgnet.com

World Journal of Gastroenterology

Submit a Manuscript: https://www.f6publishing.com

World J Gastroenterol 2023 July 21; 29(27): 4222-4235

DOI: 10.3748/wjg.v29.i27.4222

ISSN 1007-9327 (print) ISSN 2219-2840 (online)

REVIEW

Rare causes of acute non-variceal upper gastrointestinal bleeding: A comprehensive review

Alberto Martino, Marco Di Serafino, Luigi Orsini, Francesco Giurazza, Roberto Fiorentino, Enrico Crolla, Severo Campione, Carlo Molino, Luigia Romano, Giovanni Lombardi

Specialty type: Gastroenterology and hepatology

Provenance and peer review: Invited article; Externally peer reviewed.

Peer-review model: Single blind

Peer-review report's scientific quality classification
Grade A (Excellent): 0
Grade B (Very good): B, B
Grade C (Good): 0
Grade D (Fair): 0
Grade E (Poor): 0

P-Reviewer: Mori H, Belgium; Zhang JW, United Kingdom

Received: February 4, 2023
Peer-review started: February 4, 2023
First decision: April 3, 2023
Revised: April 11, 2023
Accepted: May 8, 2023
Article in press: May 8, 2023
Published online: July 21, 2023

Alberto Martino, Luigi Orsini, Giovanni Lombardi, Department of Gastroenterology and Digestive Endoscopy, AORN "Antonio Cardarelli", Naples 80131, Italy

Marco Di Serafino, Luigia Romano, Department of General and Emergency Radiology, AORN "Antonio Cardarelli", Naples 80131, Italy

Francesco Giurazza, Department of Interventional Radiology, AORN "Antonio Cardarelli", Naples 80131, Italy

Roberto Fiorentino, Department of Oncology, AORN "Antonio Cardarelli", Naples 80131, Italy

Enrico Crolla, Carlo Molino, Department of Oncological Surgery, AORN "Antonio Cardarelli", Naples 80131, Italy

Severo Campione, Department of Pathology, AORN "Antonio Cardarelli", Naples 80131, Italy

Corresponding author: Alberto Martino, MD, Staff Physician, Department of Gastroenterology and Digestive Endoscopy, AORN "Antonio Cardarelli", Via Antonio Cardarelli, 9, Naples 80131, Italy. albertomartinomd@gmail.com

Abstract

Non-variceal upper gastrointestinal bleeding (NVUGIB) is a common gastroenterological emergency associated with significant morbidity and mortality. Gastroenterologists and other involved clinicians are generally assisted by international guidelines in its management. However, NVUGIB due to peptic ulcer disease only is mainly addressed by current guidelines, with upper gastrointestinal endoscopy being recommended as the gold standard modality for both diagnosis and treatment. Conversely, the management of rare and extraordinary rare causes of NVUGIB is not covered by current guidelines. Given they are frequently life-threatening conditions, all the involved clinicians, that is emergency physicians, diagnostic and interventional radiologists, surgeons, in addition obviously to gastroenterologists, should be aware of and familiar with their management. Indeed, they typically require a prompt diagnosis and treatment, engaging a dedicated, patient-tailored, multidisciplinary team approach. The aim of our review was to extensively summarize the current evidence with regard to the management of rare and extraordinary rare causes of NVUGIB.

Key Words: Gastrointestinal bleeding; Upper gastrointestinal bleeding; Non-variceal upper gastrointestinal bleeding; Rare causes; Vascular causes; Upper endoscopy

©The Author(s) 2023. Published by Baishideng Publishing Group Inc. All rights reserved.

Core Tip: Rare and extraordinary rare causes of non-variceal upper gastrointestinal bleeding (NVUGIB) are commonly life-threatening conditions. Thus, a prompt diagnosis and a subsequent equally early treatment are required, typically involving a patient-tailored, multidisciplinary team approach. However, given the rare occurrence, their management is not covered by NVUGIB current guidelines. Our study aimed to review the current evidence with regard to the management of rare and extraordinary rare causes of NVUGIB.

Citation: Martino A, Di Serafino M, Orsini L, Giurazza F, Fiorentino R, Crolla E, Campione S, Molino C, Romano L, Lombardi G. Rare causes of acute non-variceal upper gastrointestinal bleeding: A comprehensive review. *World J Gastroenterol* 2023; 29(27): 4222-4235

URL: https://www.wjgnet.com/1007-9327/full/v29/i27/4222.htm

DOI: https://dx.doi.org/10.3748/wjg.v29.i27.4222

INTRODUCTION

Acute upper gastrointestinal bleeding (UGIB) is a common medical emergency with an annual incidence of approximately 50/100000-150/100000 adults[1-3]. It is defined as hemorrhage originating above the ligament of Treitz, in the esophagus, stomach, or duodenum. According to its etiology and reflecting differences in its management, UGIB tends to be subclassified to variceal and non-variceal UGIB (NVUGIB). Peptic ulcer disease (PUD) is the most common cause for UGIB and accounts for approximately 35%-50% of cases, followed by erosive disease, esophagitis and Mallory-Weiss tear. Varices are another common source of UGIB, representing approximately 10% of all UGIB hospitalizations. Less common causes of UGIB include neoplasm, angiodysplasia, gastric antral vascular ectasia and portal hypertensive gastropathy. Finally, up to 5% of all UGIB cases are caused by rare and extraordinary rare sources[1-5].

Despite marked advances in its diagnosis and treatment, UGIB is still associated with high morbidity and mortality. Indeed, the overall mortality rate is approximately 8%-10% in *de novo* UGIB hospitalizations[5,6], increasing up to 40% in high-risk patients[7]. In accordance to current international guidelines, esophagogastroduodenoscopy (EGD) is recommended as the procedure of choice for both diagnosis and treatment of NVUGIB, with transcatheter angiographic embolization (TAE) or surgery only in case of refractory bleeding[8-12]. However, merely NVUGIB due to PUD is largely addressed by current guidelines. Conversely, rare and extraordinary rare NVUGIB causes very often require a dedicated, multidisciplinary approach, in order to provide prompt diagnosis and effective treatment[13-16]. The aim of our review was to summarize and discuss the current evidence with regard to most relevant rare and extraordinary rare causes of NVUGIB, in order to enrich the gastroenterologists and all involved physicians' knowledge of the etiology of NVUGB and to broaden their judgment in its management.

RARE CAUSES OF NVUGIB

Aorto-enteric fistula

First described by Cooper[17], aorto-enteric fistulas (AEF) are rare though life-threatening pathological communications between the aorta and the wall of an adjacent segment of the gastrointestinal (GI) tract. Pathogenesis is still not fully understood, most likely encompassing a combination of infection, aortic and GI wall degeneration, and chronic mechanical pulsatile trauma, finally resulting in erosion and fistula creation[18]. AEF are traditionally classified as either primary (PAEF) or secondary (SAEF). PAEF arise from the native aorta, in the setting most commonly of aortic aneurysm or less frequently of infection, malignancy, foreign bodies, radiation, trauma or inflammation[19]. Conversely, SAEF generally develop as late complication of either surgical or endovascular aortic reconstruction[20]. SAEF are much more common than PAEF, with a reported incidence of 0.3%-1.6% in patients after aortic reconstruction[21] and 0.02%-0.07% among general population[22], respectively. Reported mortality is still extremely high, even with prompt diagnosis and treatment[20].

The most frequent involved site is the duodenum (62%), followed by the jejunum and ileum (12%), and the colon (5%). Aorto-esophageal and aorto-gastric fistula are only rarely encountered[18,20]. The classic triad of NVUGIB, abdominal pain, and pulsatile abdominal mass was initially described by Cooper[17]. However, it is currently believed that the combination of all 3 facets of the triad tends to occur infrequently[19]. The most common clinical presentation of AEF is NVUGIB, with or without sepsis[18]. AEF patients often present with a ''sentinel or herald bleed'', in which self-limited episodes of bleeding are followed by the recurrence of massive exsanguinous hemorrhage hours or even to days later[23].

Multidetector computed tomography angiography (MDCTA) is the diagnostic modality of choice for AEF[18,24,25]. It has a relatively high sensitivity and specificity for the diagnosis of AEF, approximately of 94% and 85% respectively[25]. Although pathognomonic of AEF, active contrast medium extravasation from the aorta into the GI lumen is an exceptional MDCTA feature usually seen with ongoing exsanguination. MDCTA findings of AEF include para-aortic or intra-aortic foci of gas, loss of the fat plane between the aorta and the GI wall, and disruption of aortic wall or pseudoaneurysm. Moreover, MDCTA signs of SAEF encounter perigraft gas persisting more than 4 wk following repair of ruptured abdominal aortic aneurysm (AAA) and perigraft fluid and edema persisting more than 3 mo after elective AAA repair[24-26]. Although EGD is the first line diagnostic modality in acute NVUGIB, its usefulness in the setting of AEF is limited. AEF may occasionally be suspected by means of EGD, with endoscopic findings suggestive of AEF including visible graft, bleeding, adherent clot, GI wall defect, ulcer/erosion or pulsatile mass[27-29]. However, the experience of the GI endoscopist, a high index of suspicion and the careful exploration of the distal duodenum, are key factors to properly endoscopically identify AEF. Furthermore, given EGD may disturb the clot which had been preventing exsanguinous bleeding from the AEF, it should be performed in the operating theater and its adoption limited to hemodynamically stable patients, with other imaging suggestive of an occult AEF[18]. Among patients admitted with massive NVUGIB and with an history and a clinical presentation suggestive for AEF, emergent MDCTA should be performed as the first-line diagnostic modality.

Treatment of AEF includes either an open surgical or an endovascular approach[30]. Surgery aims to maintain perfusion while extirpating the infection and restoring GI patency. Strategies to maintain perfusion are grouped into *in situ* aortic reconstruction and extra-anatomic bypass with aortic ligation[18]. Conversely, the most commonly used endovascular technique is stent-graft repair[18,25]. Being associated with lower perioperative mortality rate as compared with open surgery, it is frequently adopted as the first-line treatment modality for AEF[20]. Moreover, endovascular balloon occlusion may be used to gain rapid control of the aortic bleeding source in hemodynamically unstable patients. Similarly, coil and plug embolization might be used as a temporizing measure to stop bleeding[18,25]. Of note, surgical and endovascular management of AEF could be integrated in a complementary approach, by the adoption of endovascular treatment as a bridge to open repair[31].

Finally, endoscopic treatment mainly as a part of multidisciplinary approach or as a bridge to definitive therapy has been anecdotally reported. The adopted endoscopic techniques mostly included clips, fully covered self-expanding metal stents, plastic stents and injection therapy[32-35]. However, evidence regarding the role of endoscopic treatment is scarce and it may not be currently recommended. Worth pointing out, especially in the absence of active bleeding (*i.e.*, adherent blood clot), the authors discourage any attempt of endoscopic hemostasis for AEF. Given the recent advent of endoscopic devices capable to realize full-thickness GI defect closure, such as endoscopic suturing systems and over-the-scope clips (OTSC), in the next future endoscopy might probably play a crucial role for the mini-invasive closure of the GI defect after endovascular aortic repair[36]. A case of AEF is shown in Figure 1.

Ruptured visceral artery aneurysms

First reported in 1809 by Wilson[37], ruptured visceral artery aneurysms (VAA) are a rare but potentially lethal cause of acute NVUGIB. Histopathologically, VAA are broadly divided into true aneurysms (TVAA) and pseudoaneurysms (VAPA). TVAA are defined as focal arterial dilatations greater than 1.5 times the diameter of the original vessel involving all 3 layers of the arterial wall, whereas VAPA, also termed false aneurysms, result from a tear in the vessel wall with extravasated blood contained by only 1 or 2 arterial wall layers[38,39]. The main cause of TVAA is atherosclerosis, followed by fibromuscular dysplasia, connective tissue diseases, inflammatory conditions, and other rare inherited illnesses. Conversely, VAPA may be secondary to trauma, inflammatory conditions such as pancreatitis, cholecystitis, and ulcer, infection, or iatrogenic injury, including surgical, endoscopic and interventional radiological procedures. To be noted, the leading cause of VAPA is chronic pancreatitis (CP). Indeed, more than half of VAPA are secondary to pancreatitis and pseudocyst formation, with up to 17% of CP patients developing VAPA[38,39].

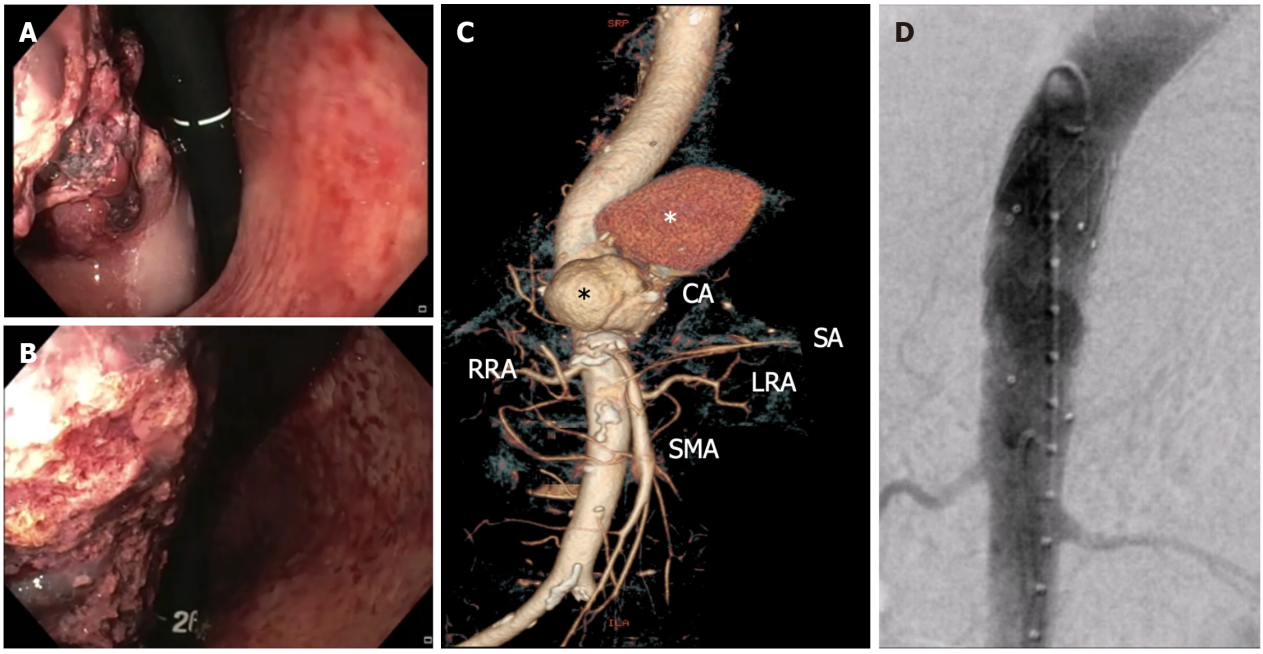
Their reported incidence is approximately 0.1%-2%[38-40]. However, because of the widespread use of advanced imaging techniques and increased aging population, VAA are being incidentally diagnosed with increased frequency [41]. Depending on size, location, and associated clinical conditions (*i.e.*, pregnancy), VAA rupture may be associated with a 20%-80% mortality rate[42].

The splenic artery (SA) is the most common site of VAA, followed by the hepatic artery (HA), accounting for nearly 60% and 20% of cases, respectively. Less common sites include in decreasing order of frequency superior mesenteric (SMA) and coeliac arteries (CA). The gastric or gastroepiploic, jejunal-ileal-colic, pancreaticoduodenal (PDA), gastroduodenal (GDA), and inferior mesenteric arteries are rarely involved[39,43].

The natural history of VAA and their potential for rupture or other complications are relatively poorly defined because of their overall scarcity. However, depending on location, size, etiology, subtype, and associated clinical conditions (*i.e.*, pregnancy), the reported risk of rupture ranges widely from 2% up to 80%[42]. Furthermore, pseudoaneurysms, CA, SMA, gastric and gastroepiploic, GDA, PDA and colic aneurysms are associated with a significantly higher risk of rupture regardless of size, requiring prompt treatment upon diagnosis[41,44].

Rupture of VAA occurs more frequently within the GI tract, manifesting with life-threatening NVUGIB, or into the peritoneal cavity. Rupture may less commonly occur into the retroperitoneal space. Finally, rupture within the hepatobiliary tract or the pancreatic duct may be rarely observed, causing hemobilia or hemosuccus pacreaticus (HP), respectively[39,43].

MDCTA is currently regarded as the diagnostic tool of choice, providing accurate vascular anatomy characterization and interventional planning. Indeed, it is frequently regarded as the "new" gold-standard, alongside with angiography [39]. Rupture is seen as an extravasation of contrast medium which is not contained within a round structure and often flows away from the point of injury. On delayed images, there will be washout of the aneurysm, whereas extravasation



DOI: 10.3748/wjg.v29.i27.4222 **Copyright** ©The Author(s) 2023.

Figure 1 Non-variceal upper gastrointestinal bleeding due to primary aorto-gastric fistula. A and B: Retroflexed endoscopic view showing gastric bulging mass partially covered by blood clots, originating from the fundus and extending to the posterior wall of the proximal body; C: Three-dimensional computed tomography angiography showing ruptured thoracoabdominal aortic aneurysm (black asterisk), retained by a periaortic hematoma (white asterisk); D: Endovascular stent graft aortic repair. CA: Celiac artery; RRA: Right renal artery; SA: Splenic artery; LRA: Left renal artery; SMA: Superior mesenteric artery.

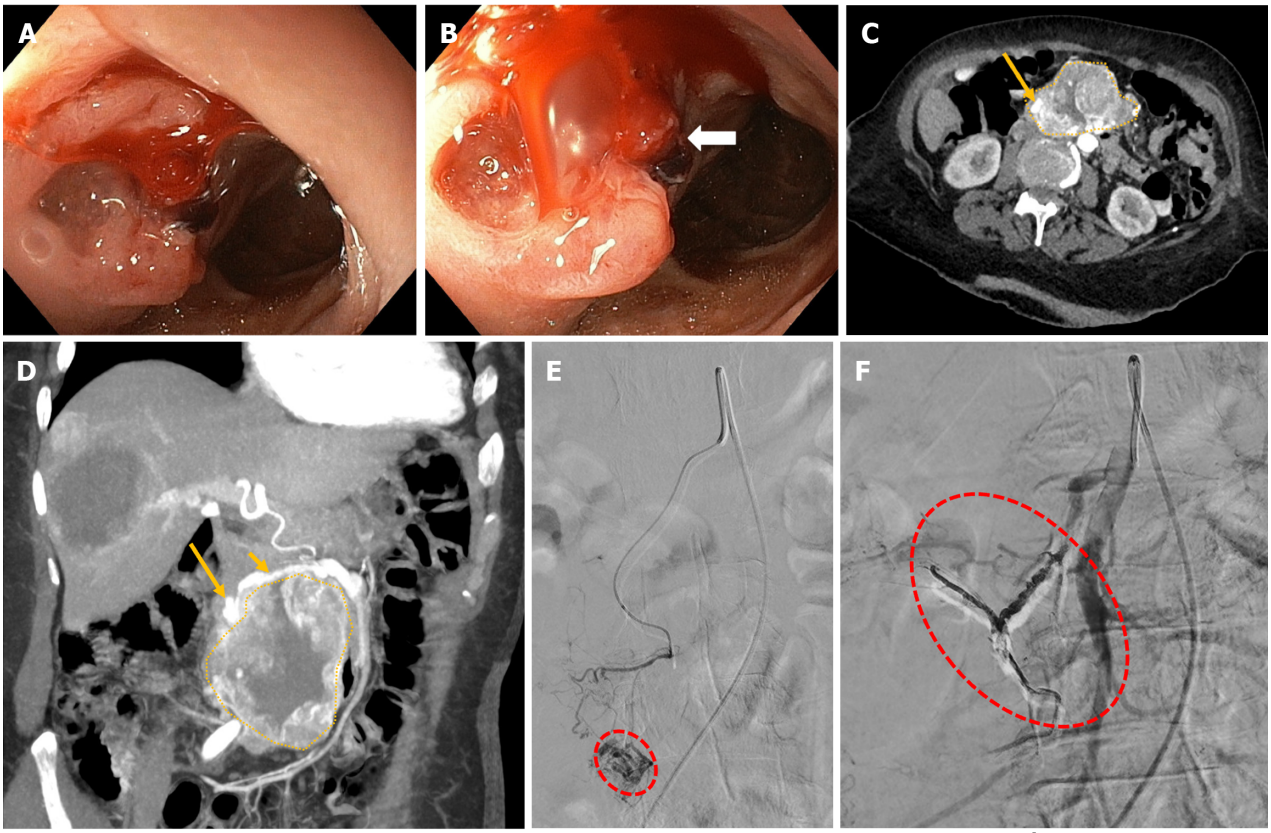
will persist[39]. Given the common presentation with NVUGIB, patients with ruptured VAA may undergo EGD if hemodynamically stable. However, the role of EGD in this setting is limited, mainly directed to exclude more common sources of NVUGIB. GI rupture of VAA may occasionally be suspected by means of EGD, with unspecific reported endoscopic findings mainly encountering gastric or duodenal ulcer/erosion with or without adherent clot, submucosal bulging mass and visible vessel[45,46]. However, a highly experienced GI endoscopist along with a high index of suspicion are necessary to suspect GI rupture of VAA. Furthermore, a detailed medical history focusing on well known risk factors for VAA development and rupture, including pancreatitis and its local complications, atherosclerosis, and recent traumatic or iatrogenic injury, such as percutaneous or endoscopic ultrasound (EUS)-guided procedures, is crucial in the diagnostic process of ruptured VAA within the GI tract.

Being associated with lower perioperative morbidity and mortality than open surgery, emergent endovascular treatment, most commonly by means of coil embolization, is currently recommended as the first-line interventional modality for ruptured VAA. Conversely, open surgery is nowadays generally reserved in case of anatomically unfeasible or failed EVT[41,44]. To date, endoscopy plays no role in the treatment of ruptured VAA. Endoscopic cyanoacrilate or epinephrine injection has been anecdotally reported[45,46]. However, we do not recommend endoscopic hemostasis attempt when GI VAA rupture is suspected or diagnosed, especially in the absence of active bleeding during endoscopic examination. Finally, EUS-guided embolization by the use of thrombin or glue injection, alone or in combination with coil deployment, has been successfully reported for the treatment of VAPA[47-49]. Although evidence is currently lacking, with growing experience, EUS-guided obliteration could represent a minimally-invasive and fashionable alternative to an endovascular approach for the treatment of selected ruptured VAPA among referral centers[50]. A case of rupture of VAA into the GI tract is shown in Figure 2.

Gastric submucosal arterial collaterals

First reported by Spriggs[51] in 1984, bleeding gastric submucosal arterial collaterals (GSAC) are an extraordinary rare cause of severe NVUGIB, with only few cases reported up to date, including a fatal one[52]. They result from either occlusion or congenital absence of the SA, being not related to portal hypertension. SA occlusion may be congenital, idiopathic, or secondary to various conditions, including surgery, endovascular intervention, trauma and extrinsic compression. In the case of SA occlusion, in order to provide splenic blood supply, extensive collaterals may arise from adjacent proximal patent arteries, such as the pancreatic, left gastric, gastroepiploic, and short gastric arteries, and pass through the gastric wall[53]. GSAC may be clinically asymptomatic or may less frequently present with severe NVUGIB from erosion of GSAC.

Since GSAC appear endoscopically as varicose shaped and tortuous submucosal vessels located at the gastric fundus [52], the differential diagnosis mainly includes type 1 isolated gastric varices (IGV)[54]. Indeed, GSAC have a very similar endoscopic appearance to IGV, being frequently misinterpreted on EGD[52]. However, they are, as opposed to GSAC, secondary to cirrhotic portal hypertension or left-sided portal hypertension[54]. Therefore, given their different management, an accurate differential diagnosis between these two entities is crucial. Indeed, endoscopic cyanoacrylate



DOI: 10.3748/wjg.v29.i27.4222 **Copyright** ©The Author(s) 2023.

Figure 2 Non-variceal upper gastrointestinal bleeding due rupture of a superior mesenteric artery pseudoaneurysm into the duodenum. A and B: Upper endoscopy showing a bulging, focally ulcerated, lesion in the second-third part of the duodenum, with a suspected small fistulous orifice on its surface (arrow); C and D: Contrast-enhanced computed tomography axial scan in the arterial phase (C) and its maximum intensity projection oblique-coronal reconstruction (D) showing a large lesion (dotted area, C and D) arising from the second-third part of the duodenum, with peripheral vascularity and a pseudoaneurysm (long arrow, C and D) arising from branches of the superior mesenteric artery (short arrow, B); E: Superselective superior mesenteric artery angiography showing a pseudoaneurysm (red dotted circle) fed by the inferior pancreaticoduodenal artery; F: Successful endovascular embolization by the use of cohesive glue (Onyx-18®, Medtronic, Dublin, Ireland) with disappearance of the pseudoaneurysm and visibility of the Onyx-18® cast (red dotted circle).

glue injection (ECGI), currently recommended as the first-line therapeutic option for bleeding IGV[55], may be complicated by systemic embolization and life-threatening adverse events when applicated to an arterial source[56,57]. Conversely, being potentially associated with severe adverse events, endoscopic mechanical hemostasis is currently not recommended for the treatment of IGV[55].

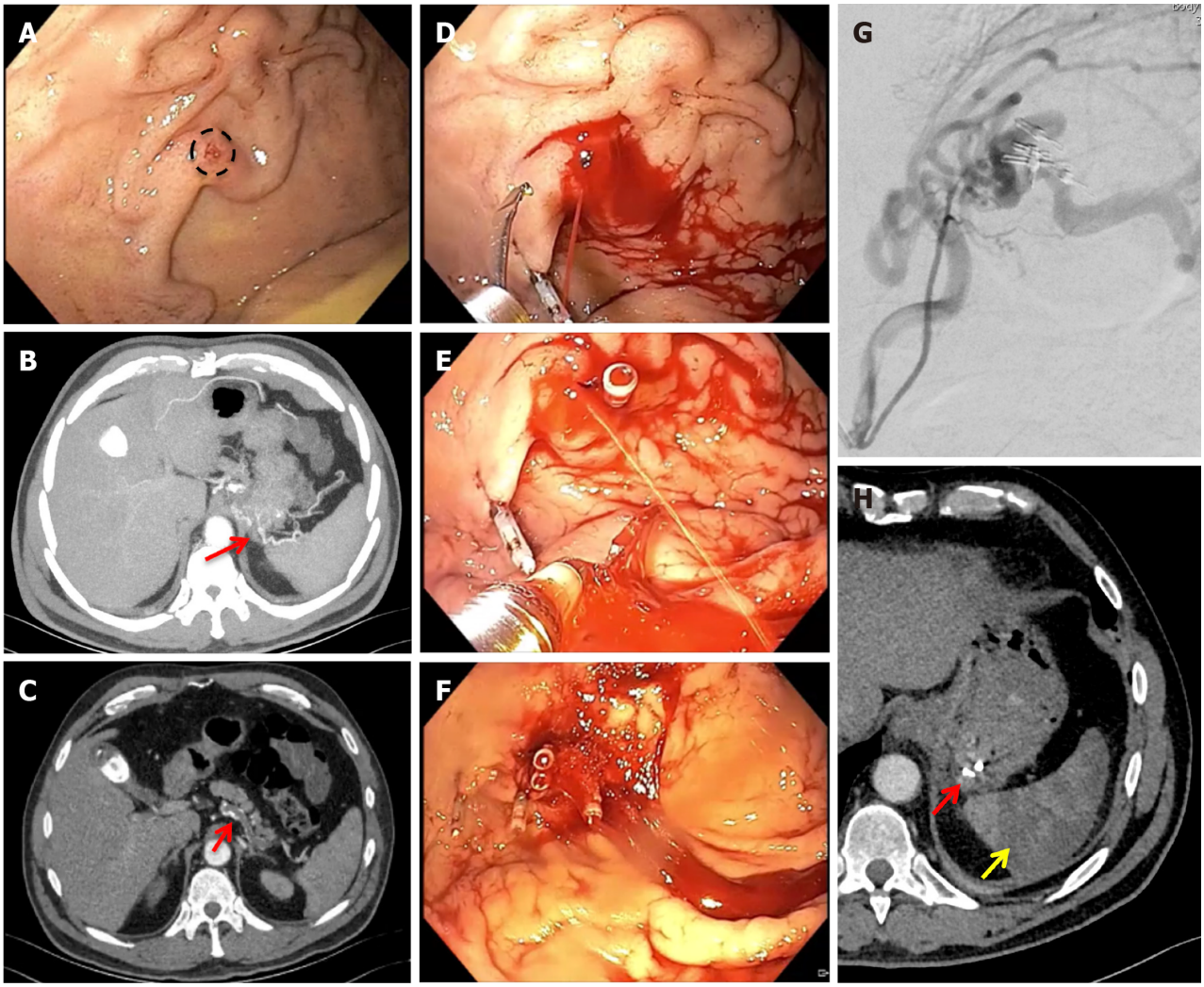
Proper diagnosis is only made by MDCTA and/or digital subtraction angiography (DSA)[52]. Thus, in case of endoscopic evidence of fundal varicose shaped submucosal vessels among UGIB patients without portal hypertension history or clinico-laboratory signs, emergent MDCTA should be performed prior to any endoscopic treatment attempt, if feasible (*i.e.*, absence of active bleeding at the time of EGD).

Definitive treatment is mainly represented by surgical splenectomy and arterial ligation with or without gastrectomy. However, effective treatment by means of endovascular embolization has also been reported. As mentioned before, endoscopic mechanical hemostasis rather than ECGI may be used for the bleeding control among experienced centers, if needed, mainly in a step-up approach[52]. A case of bleeding GSAC is shown in Figure 3.

Dieulafoy's lesions

Dieulafoy's lesion (DL) is a rare cause of acute NVUGIB, accounting for approximately 1.5% of cases, with a tendency to cause severe, life-threatening, recurrent GI bleeding[58,59]. It was originally reported by Gallard[60] in 1884 and subsequently referred to as "exulceratio simplex" in 1898 by the French surgeon Dieulafoy[61], who believed it was the first stage of a gastric ulcer. DL is a vascular abnormality, consisting of a pathologically dilated submucosal caliber-persistent artery, that typically protrudes through a small 2-5 mm mucosal defect and erodes into the GI lumen, in the absence of any abnormality such as ulcers, erosions or aneurysms[58,59]. Similarly to primary AEF, DL bleeding is thought to occur as a result of the mucosal surface disruption due to the persistent mechanical pressure perpetrated by the underlying submucosal ectatic artery[58,59].

The mortality has markedly declined from up to 80% during the pre-endoscopy era to 9%-13% currently with advances in endoscopic hemostasis[58,59]. The most common DL site is by far the stomach, typically the proximal lesser curvature within 6 cm from the gastroesophageal junction[58]. This predilection may be related to the local blood supply. Indeed, the gastric lesser curve is not irrorated by a submucosal plexus, receiving its arterial blood supply directly from the branches of the left and right gastric arteries[62]. Other less common locations include in decreasing order of frequency



DOI: 10.3748/wjg.v29.i27.4222 **Copyright** ©The Author(s) 2023.

Figure 3 Non-variceal upper gastrointestinal bleeding due to gastric submucosal arterial collaterals secondary to splenic artery thrombosis. A: Retroflexed endoscopic view of the gastric fundus showing varicose-shaped submucosal vessels with a small erosion (circle), in the absence of active bleeding; B and C: Pre-operative axial computed tomography arterial phase showing an arterial cluster at the gastric fundus (B: arrow) arising from splenic artery collateral vessels due to splenic artery complete thrombosis (C: arrow); D-F: Successful endoscopic mechanical hemostasis attempt, with intraprocedural spurting active bleeding following first endoclip application (D and E); G: Operative angiography with selective arterial embolization using microspheres; H: Post-operative axial computed tomography arterial phase showing gastric vascular lesion exclusion (red arrow) and splenic infarction (yellow arrow).

the duodenum, the colon, surgical anastomoses, the small bowel, and the esophagus[58].

Given the arterial nature of the bleeding, typical clinical presentation of DL include severe painless NVUGIB, most commonly manifesting with both hematemesis and melena and frequently associated with signs of hemodynamic instability[59]. In the absence of prompt treatment, recurrent bleeding within 72 h after the initial bleed is frequently observed, being commonly more severe. If unidentified and left untreated, DL mortality is extremely high[63].

Endoscopy is the first-line diagnostic modality and is regarded as the gold standard method for the diagnosis of DL[58, 59]. The reported endoscopic criteria for the diagnosis of DL include: (1) Active arterial spurting bleeding from a small (< 3 mm) mucosal defect or through normal mucosa; (2) Protruding vessel, with or without active bleeding, within a small mucosal defect or normal mucosa; or (3) Fresh adherent clot to a minute mucosal defect or to normal-appearing mucosa [64]. However, the reported diagnostic yield of initial EGD is only 70%, and repeat endoscopic examinations may thus be required. Main reasons for diagnostic failure of EGD encounter small lesion size, intermittently active bleeding, DL site between folds or underneath an adherent clot, or presence of a large amount of fresh blood within the gastric cavity[65]. Thus, especially in the setting of non-actively bleeding DL, endoscopic diagnosis may be challenging and a high index of clinical suspicion is required. A meticulous examination especially of the gastric cardia should be performed during EGD. In addition to adequate insufflation, in case of negative EGD, the execution of a provocative endoscopy by the use of water-jet irrigation to target wash as much of the gastric cardia as possible, particularly along the lesser curvature, has been suggested in order to disrupt a fibrin plug and provoke active bleeding from an underlying DL[15]. Of interest, in the setting of non-active bleeding, EUS may be useful to confirm the diagnosis of DL, being capable to clearly depict the pathological submucosal vessel penetrating the muscularis propria[66].

Further diagnostic modalities include MDCTA and DSA. MDCTA findings encounter abnormally enlarged submucosal vessel, which may appear tortuous, linear or as a non-specific "blush" of contrast medium at the mucosal/submucosal level[14]. However, diagnosis of DL by the use of MDCTA is usually challenging, and requires highly experienced radiologists. Conversely, angiographically, DL appears as a non-tapering, tortuous vessels in the arterial phase with no early venous return, with or without contrast medium extravasation within the GI tract[67].

Treatment is recommended for virtually all identified DL, even in the absence of recent bleeding stigmata. Dual combination endoscopic therapy with epinephrine injection followed by mechanical or thermal contact hemostasis is recommended as the first-line treatment modality for DL, being effective in more than 90% of cases. Although requiring higher endoscopic skill and experience, especially if performed in a gastric retroflexion position as frequently needed, mechanical therapy by means of band ligation or endoclip placement is currently favored over thermal hemostasis[59]. Moreover, given the risk of perforation, especially in GI tracts with thin walls such as the gastric fundus, and the risk of bands drop off with rebleeding, endoscopic band ligation may be less desirable than endoscopic clipping, especially in inexperienced hands[59,68]. Finally, mechanical hemostasis by means of OTSC has been successfully reported with good outcomes, not only for refractory cases[69,70].

If feasible (*i.e.*, absence of active bleeding), the so called acoustic Doppler mapping technique, by the use of a through-the-scope endoscopic Doppler ultrasound (DopUS) probe to delineate the subsurface route and path of the pathologically large-caliber artery, may be performed prior to endoscopic treatment, in order to treat the entire length of the superficially located artery, thus maximizing its efficacy. Furthermore, following endoscopic hemostasis achievement, the DopUS may be used to show the blood flow cessation, thus proving the successful eradication of the lesion[71].

Worth mentioning, endoscopic tattooing of the DL site should also be performed, in order to facilitate endoscopic or surgical localization in case of rebleeding occurrence[58,59]. Intriguingly, various EUS-guided treatments have been reported with good outcomes among case reports and small case series, mainly in the setting of DL refractory to standard endoscopic hemostasis. As previously mentioned, despite standard endoscopic treatment, complete ablation of a DL may be accurately evaluated at the end of treatment by Doppler EUS showing the absence of blood flow in the targeted vessel. However, up to date, evidence is still anecdotal and their adoption should be limited to referral centers in a research context[72]. TAE represents a useful second-line treatment modality, whereas surgical wedge resection has currently become the last resort for uncontrolled or unidentified DL bleeding[58,59]. A case of DL is shown in Figure 4.

Cameron lesions

Initially reported by Truesdale[73] in 1924 and subsequently extensively illustrated by Cameron[74] in 1976, Cameron lesions (CL) refer to linear gastric erosions or ulcerations located on the mucosal folds at the distal neck of a hiatal hernia (HH), in close proximity to the diaphragmatic impression. CL are thought to occur as a result of mechanical trauma and local ischemia, secondary to repetitive movement of the hernia sac against the diaphragm during respiratory excursions, and acid injury[75]. Their estimated prevalence is between 3% and 5% in the presence of a HH, reaching up to 10%-20% among patients with large HH (> 5 cm)[76-78]. Moreover, they have been reported to be the source of overt UGIB in 0.2% of cases[79].

Although commonly incidentally diagnosed during EGD, CL may clinically present with either acute or chronic NVUGIB[75,80]. EGD is considered the gold standard for the diagnosis of CL. However, they may often be missed at the index EGD[81,82]. Meticulous endoscopic evaluation of the HH neck and sac, especially in a retroflexed view, is thus required.

Although technically demanding, due to CL anatomical location requiring a retroflexed position and the movement of the HH sac with respiration, endoscopic hemostasis is indicated in case of active bleeding, visible vessel or adherent clot, similarly to peptic ulcers. Injection of epinephrine, thermal contact therapy, clipping and band ligation may be adopted [14,83,13]. However, because of the thin wall and the lack of fibrous support tissue in the gastroesophageal junction, caution is needed when attempting endoscopic therapy, given the potential risk of deep ulcer or perforation[15,75]. Finally, a surgical approach with laparoscopic or open fundoplication should be considered in patients with refractory or recurrent CL bleeding[75,80]. A case of CL is shown in Figure 5.

HP

First described in 1931 by Lower and Farrell[84], HP is an exceptionally rare cause of potentially fatal NVUGIB, with a reported incidence of about one in 1500 cases[85]. Also referred to as pseudohemobilia or wirsungorrhagia, the term HP was coined in 1970 by Sandblom[86]. It is defined as bleeding within the pancreatic duct exteriorizing through the major duodenal papilla. Of note, hemorrhage can also occur *via* the minor duodenal papilla, also known as santorinirrhage, in case of pancreas divisum. The reported mortality rate of HP is high, reaching up to approximately 10%[85]. If untreated, the mortality rate may increase up to 90%[87].

HP is commonly observed among patients with an history of pancreatic diseases, mainly including acute or CP and less frequently pancreatic neoplasms[87]. The most common cause of HP is ruptured VAPA[87]. Indeed, VAPA formation and rupture in the setting of pancreatitis, are thought to be secondary to local leakage of proteolytic enzymes with destruction of the arterial wall. Alternatively, they may also result from erosion of nearby pseudocysts or walled-off necrosis into adjacent arteries[88]. Given its close anatomical relationship with the pancreas, SA is the most common involved site of pseudoaneurysm, followed by the GDA, the PDA, and the HA[87]. Less common causes of HP include pancreatic neoplasms, pseudocysts, pancreas divisum, vascular malformations, TVAA, and traumatic or iatrogenic injuries, including endoscopic retrograde cholangiopancreatography (ERCP) and EUS interventional procedures[87,88].

The classical Sandblom's triad of clinical presentation associated with HP consists of abdominal pain radiating to the back, intermittent UGIB manifesting as melena, hematemesis, and rarely, hematochezia, and hyperamylasemia[86]. Pain is secondary to transient increase in intraductal pancreatic pressure due pancreatic duct obstruction from blood clot. It is



DOI: 10.3748/wjg.v29.i27.4222 **Copyright** ©The Author(s) 2023.

Figure 4 Non-variceal upper gastrointestinal bleeding due to Dieulafoy's lesion. A: Retroflexed endoscopic view of the gastric fundus showing a minute mucosal defect, surrounded by normal-appearing mucosa, without active bleeding; B: Active bleeding following provocative water-jet endoscopic irrigation; C: Successful endoscopic mechanical hemostasis.



DOI: 10.3748/wjg.v29.i27.4222 **Copyright** ©The Author(s) 2023.

Figure 5 Non-variceal upper gastrointestinal bleeding due to Cameron lesion. Retroflexed endoscopic view of the gastric fundus showing a fibrin covered linear erosion (arrow) at the end of a large hiatal ernia.

alleviated following bleeding episodes, due to clots clearance. Icterus from retrograde biliary obstruction may also occur [88].

Diagnosis of HP is challenging, requiring a multidisciplinary and integrative approach. Given the hidden and intermittent nature of the bleeding and its anatomical location, EGD was reported to be able to direct visualize active bleeding *via* the major duodenal papilla in only about 30%-75% of cases[87,88]. Suspicion for HP should be increased by indirect signs of bleeding, including clots within the duodenum in the absence of an alternative explanation. Furthermore, when HP is suspected, repeated endoscopy and the adjunct of a duodenoscope to properly visualize the major papilla are often necessary to establish the diagnosis[87,88].

ERCP may highlight filling defects within the pancreatic ducts, favoring the diagnosis. However, being associated with potential bleeding worsening and pancreatic duct disruption, and having a limited therapeutic role especially in the setting of ruptured VAPA, ERCP is generally not recommended for the diagnosis and treatment of HP[15,89].

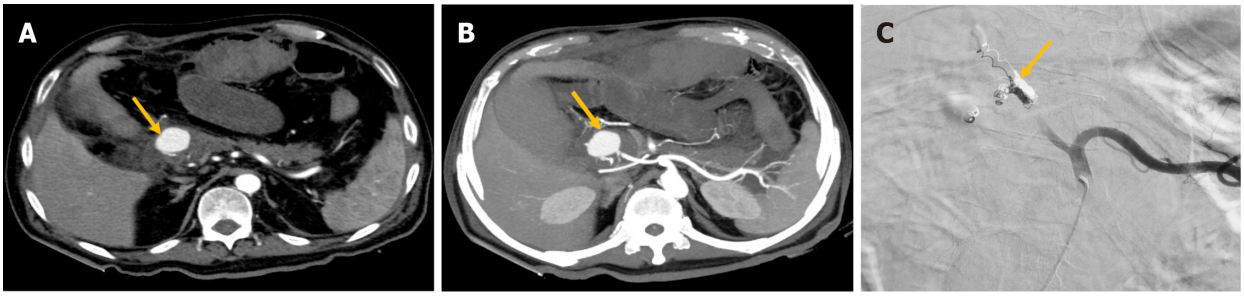
Intriguingly, EUS has been shown to be a promising tool in the diagnosis of HP, being capable to clearly depict bleeding within the pancreatic duct and its underlying cause[90,91]. Among experienced centers, EUS could be performed immediately after EGD in suspected cases, in order to provide prompt diagnosis and treatment.

MDCTA represents a very useful diagnostic tool for HP, providing characterization of the local anatomy, detection of bleeding within the pancreatic duct and its underlying etiology, thus effectively guiding further management in most of cases[15,87,88]. On pre-contrast MDCTA, the characteristic feature of clotted blood within the pancreatic duct, known as the sentinel clot sign, may also be observed. However, the diagnostic gold standard for HP is currently represented by DSA[87,88].

Percutaneous endovascular treatment, mainly by means of TAE, is currently recommended as the first choice of treatment for HP, with surgery being reserved for patients with persistent hemodynamic instability and unsuccessful embolization[89]. Although therapeutic ECRP with pancreatic multistenting has been successfully reported for the tamponade of a iatrogenic post-ERCP case of HP, its adoption may not be recommended, especially in the setting of ruptured VAPA[92]. Finally, the promising role of EUS-guided embolization in the treatment of VAPA has been previously discussed. A case of HP is shown in Figure 6.

Hemobilia

First described in 1654 by Glisson[93] on autopsy, hemobilia is defined as bleeding into the intra- or extra-hepatic biliary system exteriorizing *via* the major duodenal papilla. It occurs as a result of a fistula formation between a splanchnic blood



DOI: 10.3748/wjg.v29.i27.4222 **Copyright** ©The Author(s) 2023.

Figure 6 Non-variceal upper gastrointestinal bleeding due to hemosuccus pancreaticus. A and B: Contrast-enhanced computed tomography axial scan in the arterial phase (A) and its maximum intensity projection axial reconstruction (B) showing a large pancreaticoduodenal artery pseudoaneurysm (arrow, A and B); C: Successful endovascular coil embolization (arrow).

vessel and the biliary system. Arterial vessels are more commonly involved, due to their higher intravascular pressure. However, biliary venous fistulas have also been reported, especially in the setting of portal hypertension[94].

Due to their increased adoption, the most common reported etiology of hemobilia is currently represented by iatrogenic causes involving hepatopancreatobiliary (HPB) manipulation, including percutaneous radiological interventions, ERCP, interventional EUS, and HPB surgery. In these situations, hemobilia may be secondary to traumatic arteriobiliary fistula formation or less frequently to rupture of a HA, or rarely cistyc artery, pseudoaneurysm. Less common etiologies include traumatogenic causes, HPB malignancies, portal biliopathy, chronic ductal obstruction, inflammatory conditions, such as cholecystitis, gallstone disease, ruptured HA true aneurysms, and intraductal infection[94].

The classic clinical presentation of hemobilia is Quincke's triad, consisting of right upper quadrant pain, jaundice and UGIB[95], but all three findings are simultaneously observed in only 22%-35% of cases[94,96]. The diagnosis of hemobilia may be challenging and a high index of suspicion, mainly based on a patient's clinical presentation and suggestive medical history, is crucial. Furthermore, as with HP, bleeding can be intermittent and difficult to visualize endoscopically, even with the use of a side-viewing endoscope or a forward-viewing endoscope with distal attachment cap[94,96]. ERCP can improve diagnosis by detecting findings suggestive of hemobilia, such as amorphous, tubular, or cast-like filling defects with unexplained dilation of the common or perihilar bile duct[97]. However, it is rarely performed with a solely diagnostic intent. Of note, the use of per oral cholangioscopy has been suggested in the management of unexplained hemobilia[98]. Finally, a promising role of EUS in the diagnosis of hemobilia has been reported. Indeed, EUS was shown to be able to detect aneurysm or pseudoaneurysm in the hepatic vasculature, presence of blood within the gallbladder and common bile duct, presenting as mobile hyperechoic material, and bleeding from intra- and para-choledochal varices in portal biliopathy[99-102].

In hemodynamically stable patients with suspected major hemobilia, MDCTA should be performed in order to rule out vascular complications, such as HA aneurysms, pseudoaneurysms and cholangiovenous or arterio-ductal fistulas, and thus guiding further management[94,96].

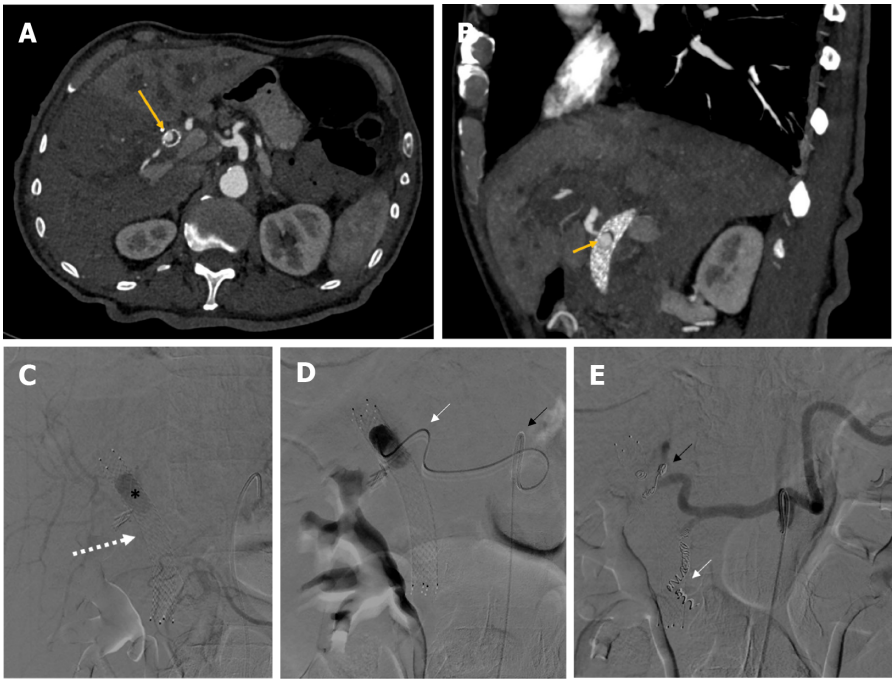
The aim of treatment consists of both hemorrhage control and maintenance of biliary patency. In the absence of vascular complications detected by MDCTA, ERCP is commonly the initial therapeutic procedure of choice, being able to provide simultaneous management of both bleeding and biliary obstruction[94,96]. Several endoscopic hemostatic techniques have been reported, varying according to etiology, location, and source of hemobilia. In case of post-sphincterotomy hemobilia, which typically is a result of injury to the posterior branch of the superior PDA, or distal hemobilia, hemostasis may be achieved by epinephrine spraying or injection, monopolar or bipolar coagulation, fibrin sealant injection, clipping, balloon tamponade, and stenting. Conversely, biliary stenting is the preferred option for proximal hemobilia[94,96]. In selected cases, biliary stents are capable to achieve immediate hemostasis, by creating a tamponade effect on the biliary wall, while maintaining luminal patency and thus bile flow. Of note, as compared with plastic stents, fully covered self-expanding metallic stents appear to have superior tamponade effect and greater patency, and should be favored in this setting[103-105]. Finally, ERCP may provide bile flow restoration, by directly extracting intraductal blood clots and/or by biliary stenting, thus preventing complications related to biliary obstruction[94,96].

In case of vascular complications, refractory hemodynamic instability, or endoscopic treatment failure, interventional radiology is recommended[94,96]. TAE is the most widely adopted technique. However, it is contraindicated in liver transplant recipients, portal vein thrombosis, and cirrhosis with concomitant shock, due to compromised collateral blood flow from the portal vein and the consequent risk of severe hepatic ischemia. In this setting, arterial stenting should be preferred[106].

Intriguingly, EUS-guided obliteration has been recently successfully reported also in the setting of hemobilia due to cystic artery pseudoaneurysm[107]. Surgery is typically reserved as a last resort, due to its high morbidity and mortality rate[94,96]. A case of hemobilia is shown in Figure 7.

CONCLUSION

Upper GI endoscopy is currently recommended as the gold standard modality for both diagnosis and treatment of



DOI: 10.3748/wjg.v29.i27.4222 **Copyright** ©The Author(s) 2023.

Figure 7 Non-variceal upper gastrointestinal bleeding due to hemobilia. A and B: Contrast-enhanced computed tomography axial scan in the arterial phase (A) and its maximum intensity projection oblique-sagittal reconstruction (B) showing a pseudoaneurysm in the lumen of the metallic biliary stent (long arrow, A), arising from the hepatic artery (short arrow, B); C: Delayed phase celiac angiography showing a pseudoaneurysm (black asterisk) into the lumen of a metallic biliary stent (white arrow); D: The pseudoaneurysm of the proper hepatic artery was reached with a 2.7 Fr microcatheter (white arrow) coaxially through a 5 Fr catheter (black arrow) positioned into the celiac trunk; E: Successful coil embolization of both the proper hepatic artery (black arrow) and the gastroduodenal artery (white arrow), in order to avoid recanalization.

NVUGIB. However, NVUGIB due to PUD only is mainly addressed by current international guidelines, whereas rare causes of NVUGIB are not covered due to their scarcity. In these instances, EGD may often not represent the gold standard for the diagnosis and may not have any role in their treatment. Conversely, a multidisciplinary approach involving not only the GI endoscopists, but also the diagnostic and the interventional radiologists, and the general and the vascular surgeons, is in most cases needed for both diagnosis and treatment. Nevertheless, EGD is inevitably the most frequently first diagnostic modality performed or requested even in NVUGIB due to rare causes. Thus, the GI endoscopists are commonly the main actors in driving further diagnostic and therapeutic process, rising the suspect of rare NVUGIB causes when appropriated. In this setting, the diagnostic role of EGD is commonly limited, mainly directed to exclude common causes of NVUGIB, whereas the diagnostic gold standard is frequently represented by MDCTA and/or DSA.

Worth mentioning, NVUGIB due to rare causes are generally associated with morbidity and mortality significantly higher as compared with those secondary to common sources. Moreover, given any delay in proper diagnosis and/or treatment is inevitably associated with increased mortality, a prompt and effective management is crucial. Thus, not only the gastroenterologists, frequently the first actors involved in the management of NVUGIB due to both common and uncommon causes, should be aware and very confident with rare NVUGIB causes, but also the diagnostic and the interventional radiologists, and the general and the vascular surgeons.

Finally, a multidisciplinary, patient-tailored, and minimally-invasive, when feasible, approach should be pursued for the management of most of the rare NVUGIB causes. Given their complexity, often requiring a strict cooperation between different specialists, rare and extraordinary rare causes of NVUGIB should be desirably managed among highly-experienced referral centers.

ACKNOWLEDGEMENTS

We are grateful to Velia De Magistris for English editing.

FOOTNOTES

Author contributions: Martino A, Di Serafino M, and Orsini L designed research and wrote, edited and finalized the text; Martino A, Di Serafino M, Orsini L, Giurazza F, Fiorentino R, Crolla E, and Campione S performed literature search and analyzed the data; Molino C, Romano L, and Lombardi G reviewed the paper for important intellectual content.

Conflict-of-interest statement: All the authors report no relevant conflicts of interest for this article.

Open-Access: This article is an open-access article that was selected by an in-house editor and fully peer-reviewed by external reviewers. It is distributed in accordance with the Creative Commons Attribution NonCommercial (CC BY-NC 4.0) license, which permits others to distribute, remix, adapt, build upon this work non-commercially, and license their derivative works on different terms, provided the original work is properly cited and the use is non-commercial. See: https://creativecommons.org/Licenses/by-nc/4.0/

Country/Territory of origin: Italy

ORCID number: Alberto Martino 0000-0002-8759-6518; Marco Di Serafino 0000-0001-6972-1859; Luigi Orsini 0000-0001-7029-3994; Francesco Giurazza 0000-0002-9080-8833; Enrico Crolla 0000-0001-7997-2715; Luigia Romano 0000-0002-5201-547X; Giovanni Lombardi 0000-0002-5957-3132.

S-Editor: Wang JJ
L-Editor: A
P-Editor: Zhang XD

REFERENCES

1 **Enestvedt BK**, Gralnek IM, Mattek N, Lieberman DA, Eisen G. An evaluation of endoscopic indications and findings related to nonvariceal upper-GI hemorrhage in a large multicenter consortium. *Gastrointest Endosc* 2008; **67**: 422-429 [PMID: 18206878 DOI: 10.1016/j.gie.2007.09.024]
2 **Tielleman T**, Bujanda D, Cryer B. Epidemiology and Risk Factors for Upper Gastrointestinal Bleeding. *Gastrointest Endosc Clin N Am* 2015; **25**: 415-428 [PMID: 26142028 DOI: 10.1016/j.giec.2015.02.010]
3 **Wuerth BA**, Rockey DC. Changing Epidemiology of Upper Gastrointestinal Hemorrhage in the Last Decade: A Nationwide Analysis. *Dig Dis Sci* 2018; **63**: 1286-1293 [PMID: 29282637 DOI: 10.1007/s10620-017-4882-6]
4 **British Society of Gastroenterology Endoscopy Committee**. Non-variceal upper gastrointestinal haemorrhage: guidelines. *Gut* 2002; **51** Suppl 4: iv1-iv6 [PMID: 12208839 DOI: 10.1136/gut.51.suppl_4.iv1]
5 **Oakland K**. Changing epidemiology and etiology of upper and lower gastrointestinal bleeding. *Best Pract Res Clin Gastroenterol* 2019; **42-43**: 101610 [PMID: 31785737 DOI: 10.1016/j.bpg.2019.04.003]
6 **Hearnshaw SA**, Logan RF, Lowe D, Travis SP, Murphy MF, Palmer KR. Acute upper gastrointestinal bleeding in the UK: patient characteristics, diagnoses and outcomes in the 2007 UK audit. *Gut* 2011; **60**: 1327-1335 [PMID: 21490373 DOI: 10.1136/gut.2010.228437]
7 **Walker TG**. Acute gastrointestinal hemorrhage. *Tech Vasc Interv Radiol* 2009; **12**: 80-91 [PMID: 19853226 DOI: 10.1053/j.tvir.2009.08.002]
8 **Laine L**, Barkun AN, Saltzman JR, Martel M, Leontiadis GI. ACG Clinical Guideline: Upper Gastrointestinal and Ulcer Bleeding. *Am J Gastroenterol* 2021; **116**: 899-917 [PMID: 33929377 DOI: 10.14309/ajg.0000000000001245]
9 **Gralnek IM**, Stanley AJ, Morris AJ, Camus M, Lau J, Lanas A, Laursen SB, Radaelli F, Papanikolaou IS, Cúrdia Gonçalves T, Dinis-Ribeiro M, Awadie H, Braun G, de Groot N, Udd M, Sanchez-Yague A, Neeman Z, van Hooft JE. Endoscopic diagnosis and management of nonvariceal upper gastrointestinal hemorrhage (NVUGIH): European Society of Gastrointestinal Endoscopy (ESGE) Guideline - Update 2021. *Endoscopy* 2021; **53**: 300-332 [PMID: 33567467 DOI: 10.1055/a-1369-5274]
10 **Sung JJ**, Chiu PW, Chan FKL, Lau JY, Goh KL, Ho LH, Jung HY, Sollano JD, Gotoda T, Reddy N, Singh R, Sugano K, Wu KC, Wu CY, Bjorkman DJ, Jensen DM, Kuipers EJ, Lanas A. Asia-Pacific working group consensus on non-variceal upper gastrointestinal bleeding: an update 2018. *Gut* 2018; **67**: 1757-1768 [PMID: 29691276 DOI: 10.1136/gutjnl-2018-316276]
11 **Mullady DK**, Wang AY, Waschke KA. AGA Clinical Practice Update on Endoscopic Therapies for Non-Variceal Upper Gastrointestinal Bleeding: Expert Review. *Gastroenterology* 2020; **159**: 1120-1128 [PMID: 32574620 DOI: 10.1053/j.gastro.2020.05.095]
12 **Barkun AN**, Almadi M, Kuipers EJ, Laine L, Sung J, Tse F, Leontiadis GI, Abraham NS, Calvet X, Chan FKL, Douketis J, Enns R, Gralnek IM, Jairath V, Jensen D, Lau J, Lip GYH, Loffroy R, Maluf-Filho F, Meltzer AC, Reddy N, Saltzman JR, Marshall JK, Bardou M. Management of Nonvariceal Upper Gastrointestinal Bleeding: Guideline Recommendations From the International Consensus Group. *Ann Intern Med* 2019; **171**: 805-822 [PMID: 31634917 DOI: 10.7326/M19-1795]
13 **Chang MA**, Savides TJ. Endoscopic Management of Nonvariceal, Nonulcer Upper Gastrointestinal Bleeding. *Gastrointest Endosc Clin N Am* 2018; **28**: 291-306 [PMID: 29933776 DOI: 10.1016/j.giec.2018.02.003]
14 **Di Serafino M**, Iacobellis F, Schillirò ML, Dell'Aversano Orabona G, Martino A, Bennato R, Borzelli A, Oliva G, D'Errico C, Pezzullo F, Barbuto L, Ronza R, Ponticiello G, Corvino F, Giurazza F, Lombardi G, Niola R, Romano L. The Role of CT-Angiography in the Acute Gastrointestinal Bleeding: A Pictorial Essay of Active and Obscure Findings. *Tomography* 2022; **8**: 2369-2402 [PMID: 36287797 DOI: 10.3390/tomography8050198]
15 **Parikh K**, Ali MA, Wong RC. Unusual Causes of Upper Gastrointestinal Bleeding. *Gastrointest Endosc Clin N Am* 2015; **25**: 583-605 [PMID: 26142040 DOI: 10.1016/j.giec.2015.02.009]
16 **Munteanu L**, Iancu I, Breazu C, Cioltean C, Brânzilă S, Odainii A, Furda P, Bocşe H, Herdean A, Bartoş D, Bartoş A. Rare Causes of Gastrointestinal Bleeding: Focus on Pancreatic Pathology and Visceral Artery Aneurysms. *Chirurgia (Bucur)* 2021; **116**: S5-S15 [PMID: 35274607]
17 **Cooper A**. Lectures on principles and practice of surgery with additional notes and cases by tyrrell. 5th edition. Philadelphia: Haswell, 1839
18 **Chung J**. Management of Aortoenteric Fistula. *Adv Surg* 2018; **52**: 155-177 [PMID: 30098611 DOI: 10.1016/j.yasu.2018.03.007]
19 **Saers SJ**, Scheltinga MR. Primary aortoenteric fistula. *Br J Surg* 2005; **92**: 143-152 [PMID: 15685700 DOI: 10.1002/bjs.4928]
20 **Kakkos SK**, Bicknell CD, Tsolakis IA, Bergqvist D; Hellenic Co-operative Group on Aortic Surgery. Editor's Choice - Management of Secondary Aorto-enteric and Other Abdominal Arterio-enteric Fistulas: A Review and Pooled Data Analysis. *Eur J Vasc Endovasc Surg* 2016; **52**: 770-786 [PMID: 27838156 DOI: 10.1016/j.ejvs.2016.09.014]

21 **Burks JA Jr**, Faries PL, Gravereaux EC, Hollier LH, Marin ML. Endovascular repair of bleeding aortoenteric fistulas: a 5-year experience. *J Vasc Surg* 2001; **34**: 1055-1059 [PMID: 11743560 DOI: 10.1067/mva.2001.119752]

22 **Voorhoeve R**, Moll FL, de Letter JA, Bast TJ, Wester JP, Slee PH. Primary aortoenteric fistula: report of eight new cases and review of the literature. *Ann Vasc Surg* 1996; **10**: 40-48 [PMID: 8688296 DOI: 10.1007/BF02002340]

23 **Chopra A**, Cieciura L, Modrall JG, Valentine RJ, Chung J. Twenty-Year Experience with Aorto-Enteric Fistula Repair: Gastrointestinal Complications Predict Mortality. *J Am Coll Surg* 2017; **225**: 9-18 [PMID: 28161484 DOI: 10.1016/j.jamcollsurg.2017.01.050]

24 **Sipe A**, McWilliams SR, Saling L, Raptis C, Mellnick V, Bhalla S. The red connection: a review of aortic and arterial fistulae with an emphasis on CT findings. *Emerg Radiol* 2017; **24**: 73-80 [PMID: 27553778 DOI: 10.1007/s10140-016-1433-y]

25 **Partovi S**, Trischman T, Sheth RA, Huynh TTT, Davidson JC, Prabhakar AM, Ganguli S. Imaging work-up and endovascular treatment options for aorto-enteric fistula. *Cardiovasc Diagn Ther* 2018; **8**: S200-S207 [PMID: 29850432 DOI: 10.21037/cdt.2017.10.05]

26 **Vu QD**, Menias CO, Bhalla S, Peterson C, Wang LL, Balfe DM. Aortoenteric fistulas: CT features and potential mimics. *Radiographics* 2009; **29**: 197-209 [PMID: 19168845 DOI: 10.1148/rg.291075185]

27 **Busuttil SJ**, Goldstone J. Diagnosis and management of aortoenteric fistulas. *Semin Vasc Surg* 2001; **14**: 302-311 [PMID: 11740838 DOI: 10.1053/svas.2001.27888]

28 **Martino A**, Bennato R, Oliva G, Pontarelli A, Picascia D, Romano L, Lombardi G. Primary aortogastric fistula: an extraordinary rare endoscopic finding in the setting of upper gastrointestinal bleeding. *Endoscopy* 2021; **53**: E60-E61 [PMID: 32559781 DOI: 10.1055/a-1180-7701]

29 **Yang DY**, Wiebe E, Peerani F. Aortoenteric fistula: A rare cause of upper gastrointestinal bleed captured on endoscopy with exceptional clarity. *Dig Liver Dis* 2018; **50**: 1367 [PMID: 30049639 DOI: 10.1016/j.dld.2018.06.023]

30 **Chakfé N**, Diener H, Lejay A, Assadian O, Berard X, Caillon J, Fourneau I, Glaudemans AWJM, Koncar I, Lindholt J, Melissano G, Saleem BR, Senneville E, Slart RHJA, Szeberin Z, Venermo M, Vermassen F, Wyss TR; Esvs Guidelines Committee, de Borst GJ, Bastos Gonçalves F, Kakkos SK, Kolh P, Tulamo R, Vega de Ceniga M, Document Reviewers, von Allmen RS, van den Berg JC, Debus ES, Koelemay MJW, Linares-Palomino JP, Moneta GL, Ricco JB, Wanhainen A. Editor's Choice - European Society for Vascular Surgery (ESVS) 2020 Clinical Practice Guidelines on the Management of Vascular Graft and Endograft Infections. *Eur J Vasc Endovasc Surg* 2020; **59**: 339-384 [PMID: 32035742 DOI: 10.1016/j.ejvs.2019.10.016]

31 **Kakkos SK**, Antoniadis PN, Klonaris CN, Papazoglou KO, Giannoukas AD, Matsagkas MI, Kotsis T, Dervisis K, Gerasimidis T, Tsolakis IA, Liapis CD. Open or endovascular repair of aortoenteric fistulas? A multicentre comparative study. *Eur J Vasc Endovasc Surg* 2011; **41**: 625-634 [PMID: 21324718 DOI: 10.1016/j.ejvs.2010.12.026]

32 **Berner-Hansen V**, Olsen AA, Brandstrup B. Endoscopic treatment of primary aorto-enteric fistulas: A case report and review of literature. *World J Gastrointest Endosc* 2021; **13**: 189-197 [PMID: 34163566 DOI: 10.4253/wjge.v13.i6.189]

33 **Donato F**, Boskoski I, Vincenzoni C, Montanari F, Tinelli G, Donati T, Tshomba Y. A New Mini-Invasive Approach for a Catastrophic Disease: Staged Endovascular and Endoscopic Treatment of Aorto-Esophageal Fistulas. *J Pers Med* 2022; **12** [PMID: 36294876 DOI: 10.3390/jpm12101735]

34 **Tsai SM**, Chen YY, Chin-Yuan Y, Lai WL. Closure of an aortoesophageal fistula with an esophageal stent and hemoclip. *Endoscopy* 2011; **43** Suppl 2: E302-E303 [PMID: 21915838 DOI: 10.1055/s-0030-1256525]

35 **Tseng KC**, Lin CW, Tan JW. Successful management of aortoesophageal fistula by combining endoscopic cyanoacrylate injection and endovascular stent grafting. *Endoscopy* 2011; **43** Suppl 2: E135-E136 [PMID: 21425013 DOI: 10.1055/s-0030-1256167]

36 **Celada-Sendino M**, Martín-Carro C, Turienzo-Santos EO, Fernández-Cadenas F, Fraile-López M. Acute upper gastrointestinal bleeding secondary to aortoesophageal fistula. Endoscopic treatment using the over-the-scope clip (OTSC®) system. *Rev Esp Enferm Dig* 2022; **114**: 682-683 [PMID: 35510315 DOI: 10.17235/reed.2022.8881/2022]

37 **Kibbler CC**, Cohen DL, Cruicshank JK, Kushwaha SS, Morgan MY, Dick RD. Use of CAT scanning in the diagnosis and management of hepatic artery aneurysm. *Gut* 1985; **26**: 752-756 [PMID: 4018639 DOI: 10.1136/gut.26.7.752]

38 **Stanley JC**, Thompson NW, Fry WJ. Splanchnic artery aneurysms. *Arch Surg* 1970; **101**: 689-697 [PMID: 5489293 DOI: 10.1001/archsurg.1970.01340300045009]

39 **Sousa J**, Costa D, Mansilha A. Visceral artery aneurysms: review on indications and current treatment strategies. *Int Angiol* 2019; **38**: 381-394 [PMID: 31284707 DOI: 10.23736/S0392-9590.19.04194-4]

40 **Pulli R**, Dorigo W, Troisi N, Pratesi G, Innocenti AA, Pratesi C. Surgical treatment of visceral artery aneurysms: A 25-year experience. *J Vasc Surg* 2008; **48**: 334-342 [PMID: 18644480 DOI: 10.1016/j.jvs.2008.03.043]

41 **Chaer RA**, Abularrage CJ, Coleman DM, Eslami MH, Kashyap VS, Rockman C, Murad MH. The Society for Vascular Surgery clinical practice guidelines on the management of visceral aneurysms. *J Vasc Surg* 2020; **72**: 3S-39S [PMID: 32201007 DOI: 10.1016/j.jvs.2020.01.039]

42 **Cordova AC**, Sumpio BE. Visceral Artery Aneurysms and Pseudoaneurysms—Should They All be Managed by Endovascular Techniques? *Ann Vasc Dis* 2013; **6**: 687-693 [PMID: 24386016 DOI: 10.3400/avd.ra.13-00045]

43 **Shanley CJ**, Shah NL, Messina LM. Common splanchnic artery aneurysms: splenic, hepatic, and celiac. *Ann Vasc Surg* 1996; **10**: 315-322 [PMID: 8793003 DOI: 10.1007/BF02001900]

44 **Björck M**, Koelemay M, Acosta S, Bastos Goncalves F, Kölbel T, Kolkman JJ, Lees T, Lefevre JH, Menyhei G, Oderich G; Esvs Guidelines Committee, Kolh P, de Borst GJ, Chakfe N, Debus S, Hinchliffe R, Kakkos S, Koncar I, Sanddal Lindholt J, Vega de Ceniga M, Vermassen F, Verzini F, Document Reviewers, Geelkerken B, Gloviczki P, Huber T, Naylor R. Editor's Choice - Management of the Diseases of Mesenteric Arteries and Veins: Clinical Practice Guidelines of the European Society of Vascular Surgery (ESVS). *Eur J Vasc Endovasc Surg* 2017; **53**: 460-510 [PMID: 28359440 DOI: 10.1016/j.ejvs.2017.01.010]

45 **Panzera F**, Inchingolo R, Rizzi M, Biscaglia A, Schievenin MG, Tallarico E, Pacifico G, Di Venere B. Giant splenic artery aneurysm presenting with massive upper gastrointestinal bleeding: A case report and review of literature. *World J Gastroenterol* 2020; **26**: 3110-3117 [PMID: 32587452 DOI: 10.3748/wjg.v26.i22.3110]

46 **Binetti M**, Lauro A, Golfieri R, Vaccari S, D'Andrea V, Marino IR, Cervellera M, Renzulli M, Tonini V. False in Name Only-Gastroduodenal Artery Pseudoaneurysm in a Recurrently Bleeding Patient: Case Report and Literature Review. *Dig Dis Sci* 2019; **64**: 3086-3091 [PMID: 31559552 DOI: 10.1007/s10620-019-05853-7]

47 **Roberts KJ**, Jones RG, Forde C, Marudanayagam R. Endoscopic ultrasound-guided treatment of visceral artery pseudoaneurysm. *HPB (Oxford)* 2012; **14**: 489-490 [PMID: 22672553 DOI: 10.1111/j.1477-2574.2012.00470.x]

48 **Gamanagatti S**, Thingujam U, Garg P, Nongthombam S, Dash NR. Endoscopic ultrasound guided thrombin injection of angiographically

occult pancreatitis associated visceral artery pseudoaneurysms: Case series. *World J Gastrointest Endosc* 2015; **7**: 1107-1113 [PMID: 26421108 DOI: 10.4253/wjge.v7.i13.1107]

49 **Maharshi S**, Sharma SS, Sharma D, Sapra B, Nijhawan S. Endoscopic ultrasound-guided thrombin injection, a management approach for visceral artery pseudoaneurysms. *Endosc Int Open* 2020; **8**: E407-E412 [PMID: 32118114 DOI: 10.1055/a-1070-9168]

50 **Anderloni A**, Auriemma F, Samarasena J. Visceral artery pseudoaneurysm: Is EUS-guided treatment ready for prime time? *Endosc Int Open* 2020; **8**: E413-E414 [PMID: 32140558 DOI: 10.1055/a-1096-0617]

51 **Spriggs DW**. Congenital absence of the splenic artery. *Cardiovasc Intervent Radiol* 1984; **7**: 303-305 [PMID: 6335674 DOI: 10.1007/BF02625116]

52 **Martino A**, Di Serafino M, Zito FP, Maglione F, Bennato R, Orsini L, Iacobelli A, Niola R, Romano L, Lombardi G. Massive bleeding from gastric submucosal arterial collaterals secondary to splenic artery thrombosis: A case report. *World J Gastroenterol* 2022; **28**: 5506-5514 [PMID: 36312836 DOI: 10.3748/wjg.v28.i37.5506]

53 **Stolze T**, Wienbeck M. [The collateral circulation in the chronic occlusion of the splenic artery]. *Rofo* 1976; **124**: 386-387 [PMID: 131773 DOI: 10.1055/s-0029-1230356]

54 **Sarin SK**, Lahoti D, Saxena SP, Murthy NS, Makwana UK. Prevalence, classification and natural history of gastric varices: a long-term follow-up study in 568 portal hypertension patients. *Hepatology* 1992; **16**: 1343-1349 [PMID: 1446890 DOI: 10.1002/hep.1840160607]

55 **Gralnek IM**, Camus Duboc M, Garcia-Pagan JC, Fuccio L, Karstensen JG, Hucl T, Jovanovic I, Awadie H, Hernandez-Gea V, Tantau M, Ebigbo A, Ibrahim M, Vlachogiannakos J, Burgmans MC, Rosasco R, Triantafyllou K. Endoscopic diagnosis and management of esophagogastric variceal hemorrhage: European Society of Gastrointestinal Endoscopy (ESGE) Guideline. *Endoscopy* 2022; **54**: 1094-1120 [PMID: 36174643 DOI: 10.1055/a-1939-4887]

56 **Lee GH**, Kim JH, Lee KJ, Yoo BM, Hahm KB, Cho SW, Park YS, Moon YS. Life-threatening intraabdominal arterial embolization after histoacryl injection for bleeding gastric ulcer. *Endoscopy* 2000; **32**: 422-424 [PMID: 10817185 DOI: 10.1055/s-2000-9002]

57 **Lee KJ**, Kim JH, Hahm KB, Cho SW, Park YS. Randomized trial of N-butyl-2-cyanoacrylate compared with injection of hypertonic saline-epinephrine in the endoscopic treatment of bleeding peptic ulcers. *Endoscopy* 2000; **32**: 505-511 [PMID: 10917181 DOI: 10.1055/s-2000-3816]

58 **Lee YT**, Walmsley RS, Leong RW, Sung JJ. Dieulafoy's lesion. *Gastrointest Endosc* 2003; **58**: 236-243 [PMID: 12872092 DOI: 10.1067/mge.2003.328]

59 **Nojkov B**, Cappell MS. Gastrointestinal bleeding from Dieulafoy's lesion: Clinical presentation, endoscopic findings, and endoscopic therapy. *World J Gastrointest Endosc* 2015; **7**: 295-307 [PMID: 25901208 DOI: 10.4253/wjge.v7.i4.295]

60 **Gallard MT**. Aneurysme miliaires de l'estomach, donnant lieu a des hematemese mortelles. *Bull Soc Med Hop Paris* 1884; **1**: 84-91

61 **Dieulafoy G**. Exulceratio simplex: Leçons 1-3. In: Dieulafoy G. Clinique medicale de l'Hotel Dieu de Paris. Paris: Masson et Cie, 1898: 1-38

62 **Barlow TE**, Bentley FH, Walder DN. Arteries, veins, and arteriovenous anastomoses in the human stomach. *Surg Gynecol Obstet* 1951; **93**: 657-671 [PMID: 14893072]

63 **Chaer RA**, Helton WS. Dieulafoy's disease. *J Am Coll Surg* 2003; **196**: 290-296 [PMID: 12595057 DOI: 10.1016/S1072-7515(02)01801-X]

64 **Dy NM**, Gostout CJ, Balm RK. Bleeding from the endoscopically-identified Dieulafoy lesion of the proximal small intestine and colon. *Am J Gastroenterol* 1995; **90**: 108-111 [PMID: 7801908]

65 **Chung YF**, Wong WK, Soo KC. Diagnostic failures in endoscopy for acute upper gastrointestinal haemorrhage. *Br J Surg* 2000; **87**: 614-617 [PMID: 10792319 DOI: 10.1046/j.1365-2168.2000.01386.x]

66 **Fockens P**, Meenan J, van Dullemen HM, Bolwerk CJ, Tytgat GN. Dieulafoy's disease: endosonographic detection and endosonography-guided treatment. *Gastrointest Endosc* 1996; **44**: 437-442 [PMID: 8905365 DOI: 10.1016/s0016-5107(96)70096-2]

67 **Durham JD**, Kumpe DA, Rothbarth LJ, Van Stiegmann G. Dieulafoy disease: arteriographic findings and treatment. *Radiology* 1990; **174**: 937-941 [PMID: 2305095 DOI: 10.1148/radiology.174.3.174-3-937]

68 **Chen YY**, Su WW, Soon MS, Yen HH. Delayed fatal hemorrhage after endoscopic band ligation for gastric Dieulafoy's lesion. *Gastrointest Endosc* 2005; **62**: 630-632 [PMID: 16185987 DOI: 10.1016/s0016-5107(05)01583-x]

69 **Skinner M**, Gutierrez JP, Neumann H, Wilcox CM, Burski C, Mönkemüller K. Over-the-scope clip placement is effective rescue therapy for severe acute upper gastrointestinal bleeding. *Endosc Int Open* 2014; **2**: E37-E40 [PMID: 26134611 DOI: 10.1055/s-0034-1365282]

70 **Manno M**, Mangiafico S, Caruso A, Barbera C, Bertani H, Mirante VG, Pigò F, Amardeep K, Conigliaro R. First-line endoscopic treatment with OTSC in patients with high-risk non-variceal upper gastrointestinal bleeding: preliminary experience in 40 cases. *Surg Endosc* 2016; **30**: 2026-2029 [PMID: 26201415 DOI: 10.1007/s00464-015-4436-y]

71 **Wong RC**. New diagnostic imaging technologies in nonvariceal upper gastrointestinal bleeding. *Gastrointest Endosc Clin N Am* 2011; **21**: 707-720 [PMID: 21944420 DOI: 10.1016/j.giec.2011.07.013]

72 **Han C**, Ling X, Liu J, Lin R, Ding Z. Management of non-variceal upper gastrointestinal bleeding: role of endoscopic ultrasound-guided treatments. *Therap Adv Gastroenterol* 2022; **15**: 17562848211056148 [PMID: 35126666 DOI: 10.1177/17562848211056148]

73 **Truesdale PE**. RECURRING HERNIA OF THE DIAPHRAGM. *Ann Surg* 1924; **79**: 751-757 [PMID: 17865033 DOI: 10.1097/00000658-192405000-00010]

74 **Cameron AJ**. Incidence of iron deficiency anemia in patients with large diaphragmatic hernia. A controlled study. *Mayo Clin Proc* 1976; **51**: 767-769 [PMID: 1086935]

75 **Kapadia S**, Jagroop S, Kumar A. Cameron ulcers: an atypical source for a massive upper gastrointestinal bleed. *World J Gastroenterol* 2012; **18**: 4959-4961 [PMID: 23002369 DOI: 10.3748/wjg.v18.i35.4959]

76 **Gray DM**, Kushnir V, Kalra G, Rosenstock A, Alsakka MA, Patel A, Sayuk G, Gyawali CP. Cameron lesions in patients with hiatal hernias: prevalence, presentation, and treatment outcome. *Dis Esophagus* 2015; **28**: 448-452 [PMID: 24758713 DOI: 10.1111/dote.12223]

77 **Weston AP**. Hiatal hernia with cameron ulcers and erosions. *Gastrointest Endosc Clin N Am* 1996; **6**: 671-679 [PMID: 8899401]

78 **Nguyen N**, Tam W, Kimber R, Roberts-Thomson IC. Gastrointestinal: Cameron's erosions. *J Gastroenterol Hepatol* 2002; **17**: 343 [PMID: 11982707 DOI: 10.1046/j.1440-1746.2002.02760.x]

79 **Camus M**, Jensen DM, Ohning GV, Kovacs TO, Ghassemi KA, Jutabha R, Machicado GA, Dulai GS, Hines OJ. Severe upper gastrointestinal hemorrhage from linear gastric ulcers in large hiatal hernias: a large prospective case series of Cameron ulcers. *Endoscopy* 2013; **45**: 397-400 [PMID: 23616128 DOI: 10.1055/s-0032-1326294]

80 **Maganty K**, Smith RL. Cameron lesions: unusual cause of gastrointestinal bleeding and anemia. *Digestion* 2008; **77**: 214-217 [PMID: 18622137 DOI: 10.1159/000144281]

81 **Zaman A**, Katon RM. Push enteroscopy for obscure gastrointestinal bleeding yields a high incidence of proximal lesions within reach of a standard endoscope. *Gastrointest Endosc* 1998; **47**: 372-376 [PMID: 9609429 DOI: 10.1016/s0016-5107(98)70221-4]

82 **Appleyard MN**, Swain CP. Endoscopic difficulties in the diagnosis of upper gastrointestinal bleeding. *World J Gastroenterol* 2001; **7**: 308-312 [PMID: 11819781 DOI: 10.3748/wjg.v7.i3.308]

83 **Lin CC**, Chen TH, Ho WC, Chen TY. Endoscopic treatment of a Cameron lesion presenting as life-threatening gastrointestinal hemorrhage. *J Clin Gastroenterol* 2001; **33**: 423-424 [PMID: 11606864 DOI: 10.1097/00004836-200111000-00018]

84 **Lower WE**, Farrell JI. Aneurysm of the splenic artery: report of a case and review of the literature. *Arch Surg* 1931; **23**: 182-190 [DOI: 10.1001/archsurg.1931.01160080010002]

85 **Rammohan A**, Palaniappan R, Ramaswami S, Perumal SK, Lakshmanan A, Srinivasan UP, Ramasamy R, Sathyanesan J. Hemosuccus Pancreaticus: 15-Year Experience from a Tertiary Care GI Bleed Centre. *ISRN Radiol* 2013; **2013**: 191794 [PMID: 24959558 DOI: 10.5402/2013/191794]

86 **Sandblom P**. Gastrointestinal hemorrhage through the pancreatic duct. *Ann Surg* 1970; **171**: 61-66 [PMID: 5308032 DOI: 10.1097/00000658-197001000-00009]

87 **Ru N**, Zou WB, Qian YY, Tang XY, Zhu JH, Hu LH, Li ZS, Liao Z. A Systematic Review of the Etiology, Diagnosis, and Treatment of Hemosuccus Pancreaticus. *Pancreas* 2019; **48**: e47-e49 [PMID: 31090670 DOI: 10.1097/MPA.0000000000001278]

88 **Abdelgabar A**, d'Archambeau O, Maes J, Van den Brande F, Cools P, Rutsaert RR. Visceral artery pseudoaneurysms: two case reports and a review of the literature. *J Med Case Rep* 2017; **11**: 126 [PMID: 28472975 DOI: 10.1186/s13256-017-1291-6]

89 **Kitano M**, Gress TM, Garg PK, Itoi T, Irisawa A, Isayama H, Kanno A, Takase K, Levy M, Yasuda I, Lévy P, Isaji S, Fernandez-Del Castillo C, Drewes AM, Sheel ARG, Neoptolemos JP, Shimosegawa T, Boermeester M, Wilcox CM, Whitcomb DC. International consensus guidelines on interventional endoscopy in chronic pancreatitis. Recommendations from the working group for the international consensus guidelines for chronic pancreatitis in collaboration with the International Association of Pancreatology, the American Pancreatic Association, the Japan Pancreas Society, and European Pancreatic Club. *Pancreatology* 2020; **20**: 1045-1055 [PMID: 32792253 DOI: 10.1016/j.pan.2020.05.022]

90 **Pham KD**, Pedersen G, Halvorsen H, Jøssang D, Flesland RH, Gjorgji GD. Usefulness of endoscopic ultrasound for the diagnosis of hemosuccus pancreaticus. *Endoscopy* 2014; **46** Suppl 1: E528 [PMID: 25409053 DOI: 10.1055/s-0034-1377641]

91 **Tarantino I**, Rizzo GEM, Ligresti D, Jukna A, Maruzzelli L, Gruttadauria S, Traina M. Hemosuccus pancreaticus: an in-motion endoscopic ultrasound view. *Endoscopy* 2022; **54**: E1038-E1040 [PMID: 36007913 DOI: 10.1055/a-1904-7312]

92 **Gutkin E**, Kim SH. A novel endoscopic treatment of hemosuccus pancreaticus: a stent tree tamponade. *JOP* 2012; **13**: 312-313 [PMID: 22572140]

93 **Glisson F**. Anatomia Hepatis. London: O. Pullein, 1654

94 **Zhornitskiy A**, Berry R, Han JY, Tabibian JH. Hemobilia: Historical overview, clinical update, and current practices. *Liver Int* 2019; **39**: 1378-1388 [PMID: 30932305 DOI: 10.1111/liv.14111]

95 **Quincke H**. Ein fall von aneurysma der leberarterie [A Case of Hepatic Artery Aneurysm]. *Berl Klin Wochenschr* 1871; **30**: 349-352

96 **Berry R**, Han J, Girotra M, Tabibian JH. Hemobilia: Perspective and Role of the Advanced Endoscopist. *Gastroenterol Res Pract* 2018; **2018**: 3670739 [PMID: 30116262 DOI: 10.1155/2018/3670739]

97 **Murugesan SD**, Sathyanesan J, Lakshmanan A, Ramaswami S, Perumal S, Perumal SU, Ramasamy R, Palaniappan R. Massive hemobilia: a diagnostic and therapeutic challenge. *World J Surg* 2014; **38**: 1755-1762 [PMID: 24381048 DOI: 10.1007/s00268-013-2435-5]

98 **Ramchandani M**, Reddy DN, Lakhtakia S, Tandan M, Maydeo A, Chandrashekhar TS, Kumar A, Sud R, Rerknimitr R, Makmun D, Khor C. Per oral cholangiopancreatoscopy in pancreatico biliary diseases--expert consensus statements. *World J Gastroenterol* 2015; **21**: 4722-4734 [PMID: 25914484 DOI: 10.3748/wjg.v21.i15.4722]

99 **Konerman MA**, Zhang Z, Piraka C. Endoscopic Ultrasound as a Diagnostic Tool in a Case of Obscure Hemobilia. *ACG Case Rep J* 2016; **3**: e170 [PMID: 28008403 DOI: 10.14309/crj.2016.143]

100 **Trakarnsanga A**, Sriprayoon T, Akaraviputh T, Tongdee T. Massive hemobilia from a ruptured hepatic artery aneurysm detected by endoscopic ultrasound (EUS) and successfully treated. *Endoscopy* 2010; **42** Suppl 2: E340-E341 [PMID: 21170839 DOI: 10.1055/s-0030-1255940]

101 **Sharma M**, Rameshbabu CS. Portal cavernoma cholangiopathy: an endoscopic ultrasound based imaging approach. *J Clin Exp Hepatol* 2014; **4**: S53-S61 [PMID: 25755596 DOI: 10.1016/j.jceh.2013.08.015]

102 **Seicean A**. Endoscopic ultrasound in the diagnosis and treatment of upper digestive bleeding: a useful tool. *J Gastrointestin Liver Dis* 2013; **22**: 465-469 [PMID: 24369332]

103 **Barresi L**, Tarantino I, Ligresti D, Curcio G, Granata A, Traina M. Fully covered self-expandable metal stent treatment of spurting bleeding into the biliary tract after endoscopic ultrasound-guided fine-needle aspiration of a solid lesion of the pancreatic head. *Endoscopy* 2015; **47** Suppl 1: E87-E88 [PMID: 25926229 DOI: 10.1055/s-0034-1391239]

104 **Song JY**, Moon JH, Choi HJ, Kim DC, Choi MH, Lee TH, Cha SW, Cho YD, Park SH. Massive hemobilia following transpapillary bile duct biopsy treated by using a covered self-expandable metal stent. *Endoscopy* 2014; **46** Suppl 1: E161-E162 [PMID: 24756274 DOI: 10.1055/s-0034-1365115]

105 **Goenka MK**, Harwani Y, Rai V, Goenka U. Fully covered self-expandable metal biliary stent for hemobilia caused by portal biliopathy. *Gastrointest Endosc* 2014; **80**: 1175 [PMID: 24818548 DOI: 10.1016/j.gie.2014.03.029]

106 **Cathcart S**, Birk JW, Tadros M, Schuster M. Hemobilia: An Uncommon But Notable Cause of Upper Gastrointestinal Bleeding. *J Clin Gastroenterol* 2017; **51**: 796-804 [PMID: 28644311 DOI: 10.1097/MCG.0000000000000876]

107 **Sharma M**, Somani P, Talele R, Kohli V, Sunkara T. EUS-guided thrombin injection of cystic artery pseudoaneurysm leading to Mirizzi's syndrome and hemobilia. *VideoGIE* 2019; **4**: 163-165 [PMID: 31032465 DOI: 10.1016/j.vgie.2018.12.004]

World Journal of Gastroenterology

Submit a Manuscript: https://www.f6publishing.com

World J Gastroenterol 2023 July 21; 29(27): 4236-4251

DOI: 10.3748/wjg.v29.i27.4236

ISSN 1007-9327 (print) ISSN 2219-2840 (online)

REVIEW

Sarcopenia in cirrhosis: Prospects for therapy targeted to gut microbiota

Roman Maslennikov, Aliya Alieva, Elena Poluektova, Yury Zharikov, Andrey Suslov, Yana Letyagina, Ekaterina Vasileva, Anna Levshina, Evgenii Kozlov, Vladimir Ivashkin

Specialty type: Gastroenterology and hepatology

Provenance and peer review: Invited article; Externally peer reviewed.

Peer-review model: Single blind

Peer-review report's scientific quality classification

Grade A (Excellent): 0
Grade B (Very good): 0
Grade C (Good): C, C, C
Grade D (Fair): D
Grade E (Poor): 0

P-Reviewer: Dai K, China; Li C, China; Zhang Y, China

Received: March 24, 2023
Peer-review started: March 24, 2023
First decision: May 13, 2023
Revised: May 25, 2023
Accepted: June 21, 2023
Article in press: June 21, 2023
Published online: July 21, 2023

Roman Maslennikov, Aliya Alieva, Elena Poluektova, Ekaterina Vasileva, Anna Levshina, Vladimir Ivashkin, Department of Internal Medicine, Gastroenterology and Hepatology, Sechenov University, Moscow 119435, Russia

Roman Maslennikov, Elena Poluektova, Vladimir Ivashkin, The Scientific Community for Human Microbiome Research, Moscow 119435, Russia

Yury Zharikov, Andrey Suslov, Yana Letyagina, Department of Human Anatomy and Histology, Sechenov University, Moscow 119435, Russia

Anna Levshina, Evgenii Kozlov, Laboratory of Immunopathology, Department of Clinical Immunology and Allergy, Sechenov University, Moscow 119991, Russia

Corresponding author: Roman Maslennikov, MD, PhD, Academic Editor, Assistant Professor, Doctor, Professor, Department of Internal Medicine, Gastroenterology and Hepatology, Sechenov University, Pogodinskaya str., 1, bld. 1, Moscow 119435, Russia.
mmmm00@yandex.ru

Abstract

Decreased muscle mass and function, also known as sarcopenia, is common in patients with cirrhosis and is associated with a poor prognosis. Although the pathogenesis of this disorder has not been fully elucidated, a disordered gut-muscle axis probably plays an important role. Decreased barrier function of the gut and liver, gut dysbiosis, and small intestinal bacterial overgrowth (SIBO) can lead to increased blood levels of ammonia, lipopolysaccharides, pro-inflammatory mediators, and myostatin. These factors have complex negative effects on muscle mass and function. Drug interventions that target the gut microbiota (long-term use of rifaximin, lactulose, lactitol, or probiotics) positively affect most links of the compromised gut-muscle axis in patients with cirrhosis by decreasing the levels of hyperammonemia, bacterial translocation, and systemic inflammation and correcting gut dysbiosis and SIBO. However, although these drugs are promising, they have not yet been investigated in randomized controlled trials specifically for the treatment and prevention of sarcopenia in patients with cirrhosis. No data exist on the effects of fecal transplantation on most links of gut-muscle axis in cirrhosis; however, the results of animal experimental studies are promising.

Key Words: Cirrhosis; Muscle; Fragility; Liver; Microbiota; Microbiome

©The Author(s) 2023. Published by Baishideng Publishing Group Inc. All rights reserved.

Core Tip: Sarcopenia is common in patients with cirrhosis and is associated with a poor prognosis. Although the pathogenesis of this disorder has not been fully elucidated, a disordered gut-muscle axis probably plays an important role. Drugs that target the gut microbiota positively affect most links of the compromised gut-muscle axis in patients with cirrhosis. However, they have not yet been investigated in randomized controlled trials specifically for the treatment and prevention of sarcopenia in patients with cirrhosis.

Citation: Maslennikov R, Alieva A, Poluektova E, Zharikov Y, Suslov A, Letyagina Y, Vasileva E, Levshina A, Kozlov E, Ivashkin V. Sarcopenia in cirrhosis: Prospects for therapy targeted to gut microbiota. *World J Gastroenterol* 2023; 29(27): 4236-4251
URL: https://www.wjgnet.com/1007-9327/full/v29/i27/4236.htm
DOI: https://dx.doi.org/10.3748/wjg.v29.i27.4236

INTRODUCTION

Sarcopenia is defined as the loss of muscle mass, strength, and physical function[1]. Sarcopenia has been detected in 14%-55% of patients with cirrhosis[2-6] and attracts the attention of researchers increasingly[7-10]. Sarcopenia was found in 68.5% of patients with cirrhosis who were admitted to the intensive care unit[11]. Recent studies have shown that sarcopenia in patients with cirrhosis is associated with poor short- and long-term prognoses[3,6,11,12]. The decrease in muscle mass in patients with cirrhosis over a year also has an unfavorable prognostic value[13]. A recent meta-analysis of 22 studies confirmed that sarcopenia is an independent predictor of increased mortality in patients with cirrhosis[14].

Sarcopenia in patients with cirrhosis is associated with a decrease in the quality of life[15], increased hepatic venous pressure gradient[12], portal hypertension-related complications (ascites and upper gastrointestinal varices), infections (urinary tract infection and spontaneous peritonitis), hepatic encephalopathy, increased risk of hepatocellular carcinoma, longer hospital stay, higher 30-d readmission rate, lower body mass index and serum albumin levels, longer prothrombin time, higher total bilirubin concentrations, and higher Child-Pugh score[16-20]. In addition, patients with cirrhosis have an increased amount of fat in the muscles (myosteatosis), which is also an unfavorable prognostic factor[21].

The exact mechanisms underlying the development of sarcopenia in patients with cirrhosis have not yet been established. Among the factors contributing to the development of sarcopenia in cirrhosis, are disorders of the metabolic function of the liver, decreased appetite[22], increased muscle autophagy[2], increased serum myostatin (a protein that blocks muscle growth)[6], catabolic effects of systemic inflammation induced by bacterial translocation from the gut[23-24], and low testosterone levels[25] were found.

GUT-MUSCLE AXIS IN CIRRHOSIS

Gut dysbiosis in patients with cirrhosis

Cirrhosis is associated with a disturbed composition of the gut microbiota, or dysbiosis[26-29]. Despite some inconsistencies, most studies have shown that in patients with cirrhosis, there was an abundance of harmful bacteria of taxa Bacilli, Streptococcaceae, Enterococcaceae, Proteobacteria, and Enterobacteriaceae, and there was a decrease in beneficial gram-positive bacteria of families Ruminococcaceae and Lachnospiraceae[30-42]. The harmful bacteria are facultative anaerobes; therefore, they can survive in oxygenated tissues, penetrate them, and spread throughout the body. This process was termed bacterial translocation and is believed to be an important contributor to the progression of cirrhosis, including the development of a systemic inflammatory response[26-29]. In addition, harmful Enterobacteriaceae of the phylum Proteobacteria, which are abundant in the gut microbiota of patients with cirrhosis, have an active endotoxin [lipopolysaccharide (LPS)]. Since cirrhosis increases the permeability of the intestinal barrier[43-46], LPS can penetrate the body (molecular bacterial translocation), leading to a systemic inflammatory response. The production of short-chain fatty acids (SCFA) by beneficial bacteria also decreases in patients with cirrhosis[30]. These SCFAs are used as a source of energy by intestinal epithelial cells, strengthen the intestinal barrier, and act on specific receptors to regulate human body functions[47]. The metabolism of bile acids, which also affect many human metabolic pathways through their special receptors[48], depends on the gut bacteria and disturbs in cirrhosis[42].

The values of the MELD scale that used to assess the risk of death in patients with cirrhosis are directly correlated with the abundance of harmful gut bacteria from the families Staphylococcaceae, Enterococcaceae, and Enterobacteriaceae, and inversely correlated with the abundance of beneficial bacteria from the families Lachnospiraceae and Ruminococcaceae [36]. Patients with acute-on-chronic liver failure have a lower abundance of beneficial gram-positive bacteria[36]. The Child–Turcotte–Pugh score, used to assess cirrhosis severity, correlates positively with the abundance of Streptococcaceae and negatively with the abundance of Lachnospiraceae[41]. Severe dysbiosis is associated with higher C-reactive protein (CRP) levels, lower serum albumin and cholinesterase levels, and poorer long-term prognosis[40]. The abundance of Lachnospiraceae is negatively correlated with the risk of hospitalization of cirrhosis patients in the intensive care unit

[49]. Abundant Enterobacteriaceae, Enterococcaceae, and Streptococcaceae are associated with hepatic encephalopathy, circulatory failure, and respiratory failure within 30 d of hospitalization of these patients, respectively[49].

Serum LPS levels are positively correlated with the abundance of Enterobacteriaceae and negatively correlated with the abundance of Lachnospiraceae and Ruminococcaceae[36]. Most of the bacterial genetic material found in the blood and ascitic fluid of patients with cirrhosis is from harmful Proteobacteria and Bacilli instead of the beneficial Lachnospiraceae and Ruminococcaceae that are dominant in the gut[50,51]. The serum level of pro-inflammatory cytokine tumor necrosis factor-alpha (TNF-α) is positively correlated with the serum LPS level and the risk of cirrhosis decompensation, spontaneous bacterial peritonitis, and acute-on-chronic liver failure[52].

Therefore, gut dysbiosis in patients with cirrhosis is associated with bacterial translocation, systemic inflammation, decompensation of liver function, and poor short- and long-term prognoses.

Small intestinal bacterial overgrowth in cirrhosis

Small intestinal bacterial overgrowth (SIBO) is an increase in the content of bacteria in the small intestine[53] and has been detected in almost half of patients with cirrhosis[54]. The prevalence of SIBO increases with increasing severity of cirrhosis[54]. Patients with cirrhosis and SIBO have ascites, minimal and overt hepatic encephalopathy, and spontaneous bacterial peritonitis more often than those without SIBO[54-55]. No relationship has been found between SIBO on the one hand and hypocoagulation, alanine aminotransferase, glutamyl transpeptidase activity, white blood cell, platelet counts, hemoglobin, ascitic fluid albumin levels, and esophageal varices on the other hand in cirrhosis[54]. In patients with cirrhosis, SIBO is associated with the presence of bacterial DNA in peripheral blood[56], higher serum LPS[57] and CRP [58] levels, splanchnic vasodilation, and hyperdynamic circulation[58]. Gut microbiota changes in patients with both cirrhosis and SIBO do not correspond to cirrhosis-associated gut dysbiosis. Therefore, gut dysbiosis and SIBO are most likely separate disorders[59] and SIBO is an independent factor associated with bacterial translocation, systemic inflammation, and the development of several complications in cirrhosis.

Gut-muscle axis in cirrhosis

The pathology of the gut microbiota (gut dysbiosis and SIBO) influences the development of sarcopenia (gut-muscle axis) in patients with cirrhosis.

Bacterial translocation-induced systemic inflammation causes protein catabolism and decreases muscle mass. This is evidenced by the association of sarcopenia with biomarkers of bacterial translocation (LPS) and systemic inflammation (TNF-α) in cirrhosis[23-24]. TNF-α reduced the formation of proteins in muscles[60]. The injection of LPS into the bodies of experimental animals had a similar effect[61].

The second mechanism of harmful effect of the gut microbiota disorders on the muscle tissue in cirrhosis is based on the fact that an excess amount of bacteria in SIBO competes with the human body for nutrients that enter the intestine with food. In support of this mechanism, an association was found between SIBO and malnutrition in cirrhosis[62].

A third mechanism linking the pathology of the gut microbiota with sarcopenia in cirrhosis is associated with an increase in the formation of myostatin, a protein that enhances protein catabolism in muscles, and inhibits their growth [63-65]. Serum myostatin levels are elevated in patients with cirrhosis and are correlated with the severity of sarcopenia [6]. Increased myostatin formation in patients with cirrhosis is likely associated with hyperammonemia that led to an increase in the myostatin level as well as a decrease in muscle mass and strength by an NF-κB-mediated mechanism in experimental animals[66]. However, such effects were not observed in mice with knockout of the myostatin gene[66]. The muscles are normally one of the main sources of ammonia in the body. Therefore, through negative feedback, hyperammonemia may reduce muscle mass to reduce the formation of ammonia by muscles. However, in patients with cirrhosis, the main source of ammonia for systemic circulation is the gut microbiota, which catabolize dietary and mucous proteins. Normally, gut microbiota-derived ammonia is neutralized by the liver; however, in patients with cirrhosis, the detoxifying function of the liver is reduced and portocaval shunts work around it, which leads to a dysfunction of this mechanism for regulating the volume of muscle mass[67-70]. In addition, hyperammonemia may lead to the development of sarcopenia in other ways[69], including increased autophagy[71] and inhibition of muscle protein anabolism[72].

The increased serum TNF-α levels are associated with the increased myostatin gene expression and the decreased muscle mass in experimental cirrhosis, suggesting that systemic inflammation can lead to sarcopenia increasing myostatin production among other mechanisms[24].

Several recent studies have reported changes in the composition of the gut microbiota associated with sarcopenia[73-76]. The abundances of Bacteroidaceae, *Eggerthella*, *Escherichia coli*, *Fusobacterium*, Micrococcaceae, *Rothia*, *Veillonella*, *Weissella*, and other bacteria are associated with a decrease in muscle mass, while the abundances of *Acidaminococcus*, *Akkermansia*, *Anaerotruncus*, *Anaerostipes*, *Barnesiellaceae*, *Bifidobacterium catenulatum*, *Catenibacterium*, *Collinsella*, *Coprococcus*, *Coriobacteriaceae*, *Desulfovibrio*, *Dialister*, *Dorea*, *Erysipelatoclostridiaceae*, *Granulicella*, *Intestinimonas*, *Lachnospiraceae*, *Megasphaera*, *Methanobrevibacter*, *Oscillospira*, *Prevotella*, *Ruminococcus flavefaciens*, *Senegalimassilia,* and other bacteria showed an association with normal muscle mass in patients with cirrhosis. The pronounced heterogeneity of these results were obtained that may be caused by different methods used to assess the muscle mass of patients. Patients with sarcopenia had higher serum levels of CRP, TNF-α, interleukin 1-beta, 2 and 6, granulocyte-macrophage-colony-stimulating factor, fibroblast growth factor, and C-X-C motif chemokine ligand 10 than patients without it[73]. Although serum LPS and myostatin levels in this study were higher in patients with sarcopenia than in those without, this increase did not reach the limit of significance[73]. There was no significant difference in zonilin and other cytokines levels and reported manifestations of cirrhosis between patients with and without sarcopenia[73]. Patients with sarcopenia were more likely to have ascites, higher Child-Pugh scores[76], and lower albumin levels[75] than patients with normal muscle mass. No other significant associations were reported in these studies on associations between gut microbiota and muscle mass in cirrhosis.

Disorders of the gut-muscle axis in cirrhosis are shown simplified in Figure 1.

Therefore, it is assumed that the condition of the gut microbiota plays an important role in the development of sarcopenia in patients with cirrhosis and therapy aimed at the gut microbiota (antibiotics, prebiotics, probiotics, and fecal transplantation) may be useful in the treatment and prevention of sarcopenia.

PROSPECTS FOR GUT-MUSCLE AXIS THERAPY IN CIRRHOSIS

Treating gut microbiota in patients with cirrhosis: rifaximin

Rifaximin is a poorly-absorbed antibiotic used against harmful intestinal bacteria. Recent meta-analyses have shown that rifaximin effectively eliminates SIBO[77,78] in patients with irritable bowel syndrome[79-82], cystic fibrosis[83], Crohn's disease[84], diabetes[85], celiac disease[86], acromegaly[87], uncomplicated diverticular disease[88,89], systemic sclerosis [90], rosacea[91], and ulcerative colitis[92]. However, rifaximin was ineffective against SIBO in patients after gastrectomy [93]. The meta-analyses also noted that rifaximin is generally well-tolerated and has a low incidence of side effects[77,78]. Other antibiotics, such as chlortetracycline[94], neomycin, doxycycline, amoxicillin/clavulanate, ciprofloxacin[95], and metronidazole[96] were less effective than rifaximin in eradicating SIBO.

Rifaximin also improved intestinal barrier function (reduced blood levels of diamine oxidase and D-lactic acid), mitigated systemic inflammation (decreased serum CRP level and erythrocyte sedimentation rate)[92], and accelerated orocecal transit[85].

Rifaximin increases the abundance of beneficial bacteria (*Akkermansia*, *Bifidobacterium*, *Faecalibacterium prausnitzii*, and Ruminococcaceae) and decreases the number of harmful ones (Alphaproteobacteria, *Eggerthella, Enterococcus*, and Streptococcaceae) in several studies (Table 1)[79,97-106].

Meta-analyses have shown that rifaximin is effective in the primary and secondary prevention of spontaneous bacterial peritonitis, a clinical manifestation of bacterial translocation in patients with cirrhosis; rifaximin was superior to norfloxacin and other antibiotics in this respect[107-110]. Rifaximin also reduces the risk of mortality and need for liver transplantation in patients with cirrhosis[111]. In addition, it is effective in the management of hepatic encephalopathy, which is associated with hyperammonemic conditions such as sarcopenia, and significantly reduces blood ammonium levels in patients with cirrhosis[111-113]. One study reported that rifaximin eradicated SIBO in 76% of patients with cirrhosis-associated minimal hepatic encephalopathy, and this was associated with a more prominent decrease in blood ammonium levels than in patients with cirrhosis without SIBO that were also treated with rifaximin[114].

Rifaximin decreased the blood LPS levels in cirrhosis[115-121], and this was associated with a decrease in serum ammonia levels[118]. Rifaximin also reduces circulating neutrophil expression of TLR-4, which is the main endotoxin receptor[122]. However, the effects of rifaximin on various biomarkers of systemic inflammation in cirrhosis have been inconsistent across studies.

Importantly, rifaximin does not alter the overall resistome[123]; *i.e.,* their intake does not lead to the development of antibacterial resistance. Rifaximin also reduces the rate of all bacterial infections[124] and variceal bleeding in patients with cirrhosis[125-126], prevents the development of hepatorenal syndrome[127-128] and refractory ascites[129-130]. The use of rifaximin in patients with cirrhosis led to a decrease in the abundance of harmful *Streptococcus*, *Eggerthella*, and *Veillonella* (Table 2)[42,117-120,122,130,131].

Overall, the literature suggests that rifaximin does positive affect the main pathogenetic links of the disordered gut-muscle axis in cirrhosis, in particular SIBO, hyperammonemia, and bacterial translocation. Rifaximin also modulates the composition of the gut microbiota reducing the number of bacterial taxa has been associated with muscle loss in patients with cirrhosis. This drug has shown excellent safety and tolerability for long-term use in patients with cirrhosis[127,132, 133]. It is very important, since the prevention and treatment of sarcopenia require long-term therapy. This suggests that rifaximin may be effective and safe for these purposes in cirrhosis.

Although other antibiotics have also had positive effects on the prevention of spontaneous bacterial peritonitis, hepatic encephalopathy, and the reduction of bacterial translocation and hyperammonemia in patients with cirrhosis[111,134-136], most of them have poorer safety profiles and fewer number of studies. Thereby, recommendations to investigate their long-term effects on the prevention and treatment of sarcopenia in patients with cirrhosis seem premature. However, this does not exclude their potential use when new data on the efficacy and safety of their long-term use become available.

Rifaximin prevents skeletal muscle atrophy and weakness by decreasing intramuscular myostatin and pro-inflammatory cytokine levels in experimental cirrhosis[24,137]. An uncontrolled study showed that the long-term use of rifaximin in patients with cirrhosis improved nutritional status and allowed patients to maintain a constant amount of muscle mass[138]. Randomized placebo-controlled studies on the effects of long-term rifaximin use on muscle mass, serum myostatin, and other biomarkers of gut-muscle axis disorders in cirrhosis are required to verify this data.

Treating gut microbiota in patients with cirrhosis: prebiotic disaccharides lactulose and lactitol

Lactulose and lactitol are artificial disaccharides that are not broken down by human digestive enzymes and are utilized by the intestinal microbiota. These drugs are primarily used as osmotic laxatives for conditions that involve constipation (including irritable bowel syndrome)[139-141]. They also used for the prevention and treatment of hepatic encephalopathy[142,143], because the abundance of these carbohydrates switches the metabolism of gut bacteria from proteolytic to saccharolytic. This leads to a decrease in the formation of ammonium and other neurotropic metabolites of amino acids[144], and their laxative effects accelerate the removal of these harmful products from the intestine.

Table 1 The effect of rifaximin on the composition of the gut microbiota in various diseases

Disease	Taxa that increase in the abundance after rifaximin	Taxa that decrease in the abundance after rifaximin
Alzheimer's disease [97]	Anaerostipes, Blautia, Erysipelotrichaceae, Erysipelatoclostridium, Faecalitalea, Lactobacillus, and *Ruminiclostridum*	
Irritable bowel syndrome[79,98-100]	Acidimicrobiales, *Acidobacteria, Alteromonas, Arthrobacter, Bacillus*, Bacteroidaceae, *Butyricimonas, Chloroflexi, Cytophagia, Coprobacillus, Bifidobacterium, Deinococcales, Devosia, Dyella, Faecalibacterium prausnitzii, Frankiales, Gordonibacter, Holdemania, Kocuria*, Methylophilales, Micrococcales, Micromonosporales, Nitriliruptorales, Parabacteroides, Prevotellaceae, Propionibacteriales, Rhizobiales, Rhodobacterales, Sphingomonadales, and Streptomycetales	Alphaproteobacteria, *Anaerotruncus, Blautia luti, Butyricimonas, Cronobacter, Escherichia, Eubacterium ventriosum, Rhodospirillales, Romboutsia, Roseburia inulinivorans*, Streptococcaceae, and *Tyzzerella*
Symptomatic uncomplicated diverticular disease [101-102]	Akkermansia, Bacteroidaceae, *Citrobacter, Coprococcus, Dialister* Ruminococcaceae, and Veillonellaceae	Anaerotruncus, Anaerostipes, Blautia, Christensenellaceae, Dehalobacteriaceae, *Eggerthella lenta, Haemophilus parainfluenzae*, Mogibacteriaceae, and Pasteurellaceae
Chronic Kidney Disease[103]	-	Anaerotruncus, *Clostridium*, and *Turicibacter*
Gut diseases[104]	Faecalibacterium	Ruminococcus and *Roseburia*
Ulcerative colitis [105]	Bacteroides and *Bifidobacterium*	Enterococcus and *Lactobacillus*
Crohn's disease[106]	Bifidobacterium, Atopobium, and *Faecalibacterium prausnitzii*	

Table 2 The effect of rifaximin on the composition of the gut microbiota in patients with cirrhosis

Ref.	Taxa that increase in the abundance after rifaximin	Taxa that decrease in the abundance after rifaximin
Bajaj *et al*[120]	Eubacteriaceae	Veillonellaceae
Kaji *et al*[117]		Streptococcus, Veillonella
Kaji *et al*[118]		Streptococcus, Veillonella
Kakiyama *et al*[42]		Veillonellaceae
Kawaguchi *et al* [131]		Lactobacillus, Streptococcus, Veillonella
Lv *et al*[130]	Bacteroidetes vulgatus	Bacteroides uniformis, Eggerthella lenta, Haemophilus, Prevotella, Roseburia
Patel *et al*[122]		Akkermansia, Hungatella, Streptococcus, Veillonella
Zeng *et al*[119]	Bacteroidaceae	Veillonellaceae

Meta-analyses have shown that lactulose and lactitol are effective against hepatic encephalopathy and that they reduce blood ammonia levels. They also decrease the risk of other serious liver-related adverse events, such as liver failure, variceal bleeding, hepatorenal syndrome, spontaneous bacterial peritonitis and other serious infections. These drugs also have excellent safety profiles and have been shown to reduce mortality[111,145-148].

Lactulose and lactitol can be safely taken for six months or more[149-151]. However, they may cause steatorrhea, which can worsen the nutritional status of patients[152].

We were unable to find any data on the effects of these disaccharides on SIBO. Two factors should be considered in this case. First, since these drugs are growth factors for bacteria, they can provoke the development of SIBO. However, SIBO can be eliminated by accelerating intestinal motility caused by these drugs. Further research is required to determine which effect outweighs the other.

The intake of lactitol was accompanied by an increase in the abundance of *Bifidobacterium, Lactobacillus, Veillonella, Enterobacter, Sutterella, Haemophilus*, and *Aggregatibacter*, and a decrease in the abundance of *Bacteroides, Clostridium, Eubacterium*, *Klebsiella*, *Pseudoflavonifractor*, and coliform bacteria (Table 3)[153-157]. In addition, there was a decrease in the LPS concentration in the blood of patients with chronic viral hepatitis[158].

The use of lactulose is associated with an increase in the levels of *Bifidobacterium* and *Lactobacillus* and a decrease in the abundance of *Clostridium*, *Eubacterium*, *Enterococcus*, and Enterobacteriaceae in patients with cirrhosis (Table 3)[153,154,159,160]. However, other studies have not shown an effect of lactulose on the composition of gut microbiota[161,162]. Several studies demonstrated that the use of lactulose in patients with minimal hepatic encephalopathy led to a decrease in the blood levels of LPS, bacterial DNA, and pro-inflammatory cytokines (TNF-α, IL-6 and IL-18)[160,163,164].

Table 3 The effect of lactitol and lactulose on the composition of the gut microbiota

Ref.	Disease	Taxa that increase in the abundance after disaccharide	Taxa that decrease in the abundance after disaccharide
Lactitol			
Riggio *et al* [153]	Cirrhosis	Lactobacilli	Enterobacteria and Enterocicci
Ballongue *et al*[154]	Healthy persons	Bifidobacterium, *Lactobacillus* and *Streptococcus*	Bacteroides, Clostridium, coliforms, and *Eubacterium*
Li *et al*[155]	Chronic constipation	Actinobacteria, Bifidobacteriales, Bifidobacteriaceae, *Anaerostipes*, and *Bifidobacterium*	-
Tarao *et al* [156]	Cirrhosis	Bifidobacterium and *Lactobacillus*	Bacteroides and *Clostridium*
Lu *et al*[157]	Cirrhosis	Bifidobacterium, Veillonella, Enterobacter, Sutterella, Haemophilus, *Aggregatibacter,* Lactobacillus salivarius, L. fermentium, and L. oris	Klebsiella *Pseudoflavonifractor*, and others
Chen *et al* [158]	Chronic viral hepatitis	Bifidobacterium and *Lactobacillus*	Clostridium perfringens
Lactulose			
Riggio *et al* [153]	Cirrhosis	Lactobacilli	-
Ballongue *et al*[154]	Healthy persons	Bifidobacterium, *Lactobacillus* and *Streptococcus*	Bacteroides, *Clostridium*, coliforms and *Eubacterium*
Ziada *et al* [159]	Minimal hepatic encephalopathy	Bifidobacterium, Lactobacillus, and Bacteroidaceae	Enterobacteriaceae and *Enterococcus*

The use of lactulose and lactitol has also been associated with a decrease in the amount of bacterial proteolysis products such as cresol, skatol, phenol, and indole in the feces, as well as an increase in the amount of lactate in the feces. Lactate can acidify the feces[154] and convert neutral ammonia to ammonium ions which, unlike ammonia, do not pass through the intestinal barrier because of the presence of an electric charge. Thus, these drugs not only decrease the bacterial catabolism of amino acids with the formation of ammonia, but also decrease ammonia absorption from the intestine. These drugs significantly reduce hyperammonemia after an amino acid load[143].

Thereby, these prebiotic disaccharides reduce the severity of the following adverse factors of the disordered gut-muscle axis in cirrhosis: hyperammonemia, bacterial translocation, and systemic inflammation. Most studies have shown positive effects of these drugs on the composition of the gut microbiota. However, their impact on SIBO is yet to be explored. These drugs are considered safe for long-term use. However, their effects on myostatin levels and muscle mass in patients with cirrhosis and other diseases have not been studied.

Treating gut microbiota in patients with cirrhosis: probiotics

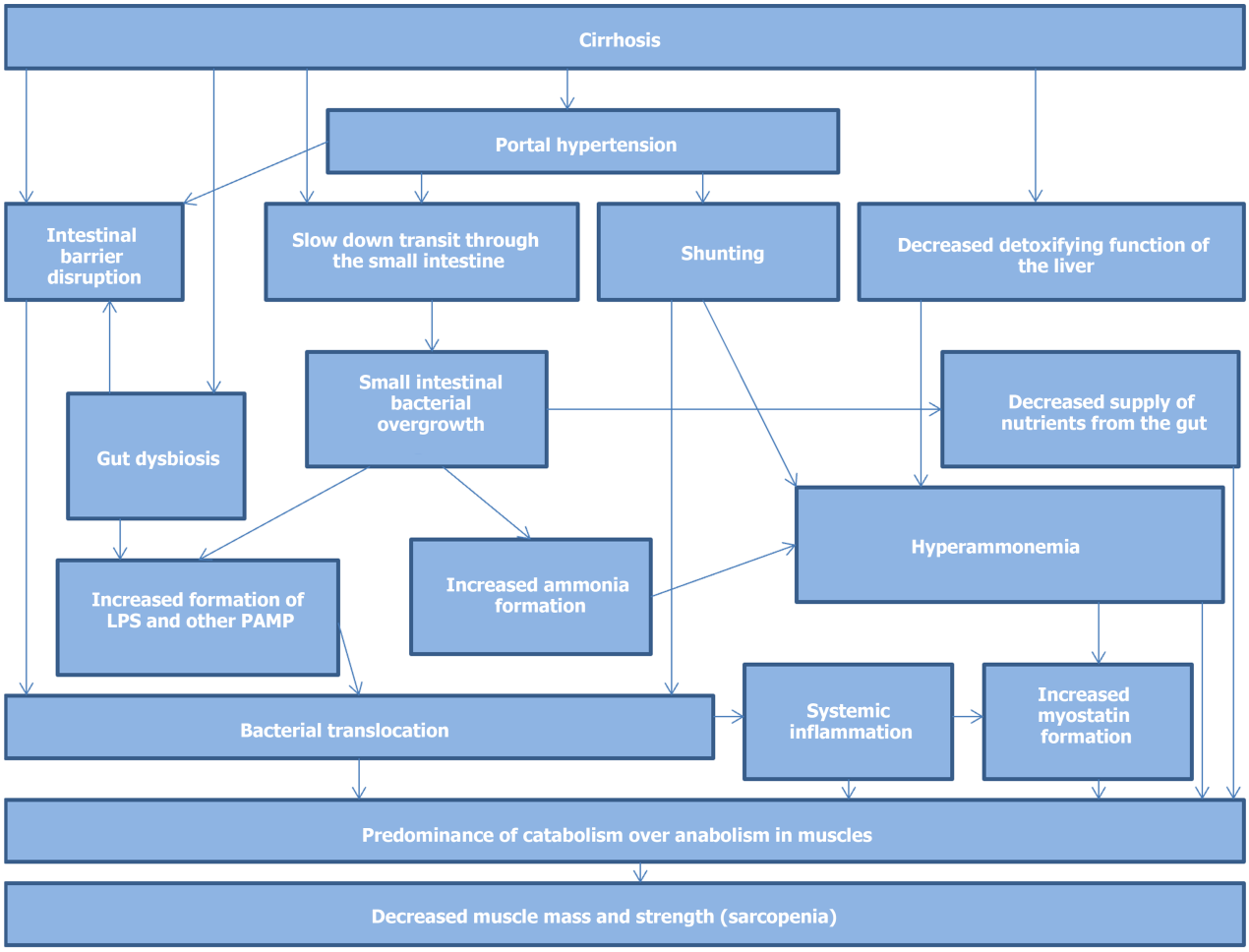
Probiotics are live microorganisms that confer health benefits to the host when administered in adequate amounts[165]. They can be used to treat liver diseases[165-166].

Meta-analyses have shown that probiotics are effective in the prevention and treatment of hepatic encephalopathy and that they decrease the blood levels of LPS and ammonia. However, they do not have a significant effect on mortality or the incidence of spontaneous bacterial peritonitis in patients with cirrhosis[111,167-170]. A meta-analysis did not show that probiotics have a significant effect on the serum level of pro-inflammatory cytokines (TNA-alpha and IL-6)[169]. Another meta-analysis revealed that prebiotics do not significantly affect CRP levels, but they lead to a decrease in TNF-α levels[171]. Among the studies not included in these meta-analyses, the following described the effect of probiotics on inflammatory biomarkers in cirrhosis. The probiotic fungus *Saccharomyces boulardii* decreases serum CRP levels and ameliorates hyperdynamic circulation in patients with decompensated cirrhosis[172]. *Escherichia coli* Nissle 1917 reduced the serum levels of IL-6, IL-8, and interferon-γ in patients with hepatic encephalopathy[160]. The probiotics that included *Clostridium butyricum* and *Bifidobacterium infantis* strengthen the intestinal barrier[173].

Probiotics have been shown to be safe when used for six months in patients with cirrhosis[174].

The use of probiotics in cirrhosis leads to an increase in the numbers of *Bifidobacterium*, *Lactobacillus*, Lachnospiraceae, Bacteroidaceae, Clostridiales incertae sedis XIV, *Faecalibacterium prausnitzii*, *Syntrophococcus sucromutans*, *Bacteroidetes vulgatus*, *Prevotella*, *Alistipes shahii*, *Clostridium* cluster I, *Clostridium coccoides*, and *Eubacterium cylindroides* and a decrease in the numbers of Enterobacteriaceae, *Enterococcus*, *Proteus hauseri*, *Citrobacter* sp., and *Morganella* (Table 4)[159,160,175-178].

Meta-analyses have also shown that probiotics effectively eliminate SIBO[179-180]. This has been observed in patients with cirrhosis[181], chronic liver disease[182], secondary lactase deficiency[183], diarrhea-predominant irritable bowel syndrome[184-186], gastric and colorectal cancer[187], systemic sclerosis[188], and bariatric surgery[189].



DOI: 10.3748/wjg.v29.i27.4236 **Copyright** ©The Author(s) 2023.

Figure 1 Simplified diagram of gut-muscle axis disorders in patients with cirrhosis. LPS: Lipopolysaccharide; PAMP: Pathogen-associated molecular patterns.

The meta-analysis showed that probiotics enhance both muscle mass and muscle strength in patients with sarcopenia that was not associated with cirrhosis[190]. The probiotic that included *Akkermansia muciniphila* and *Faecalibacterium prausnitzii* decreased myostatin levels in a mouse model of muscular atrophy[191].

Although probiotics have been shown to be effective against several pathological links of the disturbed gut-muscle axis in patients with cirrhosis (SIBO, gut dysbiosis, hyperammonemia, and bacterial translocation), improve muscle function, and increase muscle mass in sarcopenia of another origin, no study has evaluated the effect of probiotics on muscle mass and function in cirrhosis.

Treating gut microbiota in cirrhosis: fecal transplantation

Fecal transplantation involves the transfer of intestinal microbiota from the donor to the intestine of a recipient. This procedure is effective in hepatic encephalopathy[192-194] and leads to an increase in the abundance of Ruminococcaceae and Bifidobacteriaceae and a decrease in the abundance of Streptococcaceae and Veillonellaceae in patients with cirrhosis [193].

No data exist on the effects of this procedure on the severity of hyperammonemia, bacterial transplantation, systemic inflammation, myostatin levels, muscle mass and strength, or SIBO in patients with cirrhosis. No human studies have been conducted on the effect of fecal transplantation on muscle mass and strength in patients with sarcopenia of any origin; however, the results of animal experimental studies are promising[195].

CONCLUSION

Drug interventions targeting the gut microbiota positively affect most links of the compromised gut-muscle axis in cirrhosis (Table 5, Figure 2). Therefore, they are promising for the treatment and prevention of sarcopenia in cirrhosis, but have not yet been investigated in randomized controlled trials for these purposes. There are no data on the effect of fecal transplantation on most links of the gut-muscle axis and sarcopenia in cirrhosis, but the results of animal experimental studies are promising.

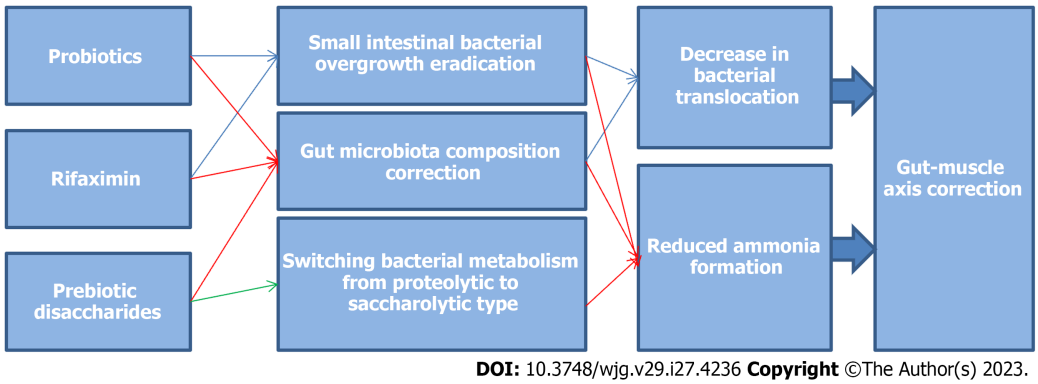
Table 4 The effect of probiotics on the composition of the gut microbiota in cirrhosis

Probiotic	Taxa that increase in the abundance after the probiotic	Taxa that decrease in the abundance after the probiotic
Lactobacillus acidophilus[159]	Bifidobacterium, Lactobacillus, and Bacteroidaceae	Enterobacteriaceae and *Enterococcus*
Escherichia coli Nissle 1917[160]	Bifidobacterium and *Lactobacillus*	Pathogenic enterobacteria
Escherichia coli Nissle 1917[175]	Bifidobacterium and *Lactobacillus*	Proteus hauseri, Citrobacter, and *Morganella*
Yakult 400[176]	Clostridium coccoides and *Eubacterium cylindroides*	Enterobacteriaceae
Lactobacillus GG[177]	Clostridiales Incertae Sedis XIV and Lachnospiracea	Enterobacteriaceae
Bifidobacterium bifidum W23, Bifidobacterium lactis W51, Bifidobacterium lactis W52, Lactobacillus acidophilus W37, Lactobacillus brevis W63, Lactobacillus casei W56, Lactobacillus salivarius W24, Lactococcus lactis W19 and Lactococcus lactis W58[178]	Faecalibacterium prausnitzii, Syntrophococcus sucromutans, Bacteroides vulgatus, Alistipes shahii, and *Prevotella*	

Table 5 Effects of interventions targeting the gut microbiota on pathogenic factors in the gut-muscle axis in cirrhosis

Intervention	SIBO	Gut dysbiosis	Hyperammonemia	Bacterial translocation	Systemic inflammation
Rifaximin	+	+	+	+	CR
Prebiotic disaccharides	ND	+	+	+	+
Probiotics	+	+	+	+	CR
Fecal transplantation	ND	+	ND	ND	ND

+: A positive effect of this drug on this disorder has been reported; SIBO: Small intestinal bacterial overgrowth; CR: Conflicting results, ND: No data.



DOI: 10.3748/wjg.v29.i27.4236 **Copyright** ©The Author(s) 2023.

Figure 2 Proposed mechanisms of action of drugs targeting the gut-muscle axis in cirrhosis.

FOOTNOTES

Author contributions: Ivashkin V suggested the idea of the review; All authors contributed to the draft editing; Maslennikov R is the guarantor.

Conflict-of-interest statement: All the authors report no relevant conflicts of interest for this article.

Open-Access: This article is an open-access article that was selected by an in-house editor and fully peer-reviewed by external reviewers. It is distributed in accordance with the Creative Commons Attribution NonCommercial (CC BY-NC 4.0) license, which permits others to distribute, remix, adapt, build upon this work non-commercially, and license their derivative works on different terms, provided the original work is properly cited and the use is non-commercial. See: https://creativecommons.org/Licenses/by-nc/4.0/

Country/Territory of origin: Russia

ORCID number: Roman Maslennikov 0000-0001-7513-1636; Aliya Alieva 0000-0002-7606-2246; Elena Poluektova 0000-0002-9038-3732; Yury Zharikov 0000-0001-9636-3807; Andrey Suslov 0000-0003-0613-8556; Yana Letyagina 0009-0003-0491-5179; Evgenii Kozlov 0000-0001-6244-1088; Vladimir Ivashkin 0000-0002-6815-6015.

S-Editor: Li L
L-Editor: A
P-Editor: Cai YX

REFERENCES

1 **Hari A**. Muscular abnormalities in liver cirrhosis. *World J Gastroenterol* 2021; **27**: 4862-4878 [PMID: 34447231 DOI: 10.3748/wjg.v27.i29.4862]
2 **Anand A**, Nambirajan A, Kumar V, Agarwal S, Sharma S, Mohta S, Gopi S, Kaushal K, Gunjan D, Singh N, Madhusudhan KS, Chauhan SS, Sharma MC, Bansal VK, Saraya A. Alterations in Autophagy and Mammalian Target of Rapamycin (mTOR) Pathways Mediate Sarcopenia in Patients with Cirrhosis. *J Clin Exp Hepatol* 2022; **12**: 510-518 [PMID: 35535114 DOI: 10.1016/j.jceh.2021.05.004]
3 **Guo G**, Li C, Hui Y, Mao L, Sun M, Li Y, Yang W, Wang X, Yu Z, Fan X, Jiang K, Sun C. Sarcopenia and frailty combined increases the risk of mortality in patients with decompensated cirrhosis. *Ther Adv Chronic Dis* 2022; **13**: 20406223221109651 [PMID: 35875834 DOI: 10.1177/20406223221109651]
4 **Hernández-Conde M**, Llop E, Gómez-Pimpollo L, Blanco S, Rodríguez L, Fernández Carrillo C, Perelló C, López-Gómez M, Martínez-Porras JL, Fernández-Puga N, Van Den Brule E, Royuela A, Calleja JL. A nomogram as an indirect method to identify sarcopenia in patients with liver cirrhosis. *Ann Hepatol* 2022; **27**: 100723 [PMID: 35580823 DOI: 10.1016/j.aohep.2022.100723]
5 **De A**, Kumari S, Kaur A, Singh A, Kalra N, Singh V. Hand-grip strength as a screening tool for sarcopenia in males with decompensated cirrhosis. *Indian J Gastroenterol* 2022; **41**: 284-291 [PMID: 35852763 DOI: 10.1007/s12664-022-01255-2]
6 **Boga S**, Yildirim AE, Ucbilek E, Koksal AR, Sisman ST, Durak I, Sen I, Dogu B, Serin E, Ucbilek AB, Yildirim MO, Erturk SM, Alkim H, Alkim C. The effect of sarcopenia and serum myokines on prognosis and survival in cirrhotic patients: a multicenter cross-sectional study. *Eur J Gastroenterol Hepatol* 2022; **34**: 1261-1268 [PMID: 36281901 DOI: 10.1097/MEG.0000000000002461]
7 **Warner Ii ER**, Satapathy SK. Sarcopenia in the Cirrhotic Patient: Current Knowledge and Future Directions. *J Clin Exp Hepatol* 2023; **13**: 162-177 [PMID: 36647414 DOI: 10.1016/j.jceh.2022.06.005]
8 **Kuchay MS**, Martínez-Montoro JI, Llamoza-Torres CJ, Fernández-García JC, Ramos-Molina B. Liver cirrhosis and sarcopenia: a dreadful combination. *Hepatobiliary Surg Nutr* 2022; **11**: 729-731 [PMID: 36268240 DOI: 10.21037/hbsn-22-355]
9 **Kumar R**, Prakash SS, Priyadarshi RN, Anand U. Sarcopenia in Chronic Liver Disease: A Metabolic Perspective. *J Clin Transl Hepatol* 2022; **10**: 1213-1222 [PMID: 36381104 DOI: 10.14218/JCTH.2022.00239]
10 **Fox R**, Stenning K, Slee A, Macnaughtan J, Davies N. Sarcopenia in liver cirrhosis: Prevalence, pathophysiology and therapeutic strategies. *Anal Biochem* 2022; **647**: 114581 [PMID: 35134388 DOI: 10.1016/j.ab.2022.114581]
11 **Khan S**, Benjamin J, Maiwall R, Tripathi H, Kapoor PB, Shasthry V, Saluja V, Agrawal P, Thapar S, Kumar G. Sarcopenia is the independent predictor of mortality in critically ill patients with cirrhosis. *J Clin Transl Res* 2022; **8**: 200-208 [PMID: 35813898]
12 **Matsui T**, Nagai H, Watanabe G, Mouri K, Yoshimine N, Amanuma M, Kobayashi K, Ogino Y, Mukozu T, Matsukiyo Y, Daidou Y, Wakui N, Nakano S, Momiyama K, Matsuda T, Igarashi Y. Measurement of skeletal muscle volume is useful for predicting prognosis in patients with liver cirrhosis. *Eur J Gastroenterol Hepatol* 2022; **34**: 1151-1157 [PMID: 36170684 DOI: 10.1097/MEG.0000000000002435]
13 **Kim TH**, Jung YK, Yim HJ, Baik JW, Yim SY, Lee YS, Seo YS, Kim JH, Yeon JE, Byun KS. Impacts of muscle mass dynamics on prognosis of outpatients with cirrhosis. *Clin Mol Hepatol* 2022; **28**: 876-889 [PMID: 36117443 DOI: 10.3350/cmh.2022.0231]
14 **Tantai X**, Liu Y, Yeo YH, Praktiknjo M, Mauro E, Hamaguchi Y, Engelmann C, Zhang P, Jeong JY, van Vugt JLA, Xiao H, Deng H, Gao X, Ye Q, Zhang J, Yang L, Cai Y, Liu N, Li Z, Han T, Kaido T, Sohn JH, Strassburg C, Berg T, Trebicka J, Hsu YC, IJzermans JNM, Wang J, Su GL, Ji F, Nguyen MH. Effect of sarcopenia on survival in patients with cirrhosis: A meta-analysis. *J Hepatol* 2022; **76**: 588-599 [PMID: 34785325 DOI: 10.1016/j.jhep.2021.11.006]
15 **Shanavas N**, Devadas K, Nahaz N, Varghese J, Cyriac R, Mathew D. Association of Sarcopenia with Health Related Quality of Life in Cirrhotics. *J Assoc Physicians India* 2021; **69**: 11-12 [PMID: 34781614]
16 **Topan MM**, Sporea I, Dănilă M, Popescu A, Ghiuchici AM, Lupușoru R, Şirli R. Impact of Sarcopenia on Survival and Clinical Outcomes in Patients With Liver Cirrhosis. *Front Nutr* 2021; **8**: 766451 [PMID: 34746216 DOI: 10.3389/fnut.2021.766451]
17 **Zeng X**, Shi ZW, Yu JJ, Wang LF, Luo YY, Jin SM, Zhang LY, Tan W, Shi PM, Yu H, Zhang CQ, Xie WF. Sarcopenia as a prognostic predictor of liver cirrhosis: a multicentre study in China. *J Cachexia Sarcopenia Muscle* 2021; **12**: 1948-1958 [PMID: 34520115 DOI: 10.1002/jcsm.12797]
18 **Nardelli S**, Riggio O, Gioia S, Merli M, Spagnoli A, di Martino M, Pelle G, Ridola L. Risk factors for hepatic encephalopathy and mortality in cirrhosis: The role of cognitive impairment, muscle alterations and shunts. *Dig Liver Dis* 2022; **54**: 1060-1065 [PMID: 35058135 DOI: 10.1016/j.dld.2021.12.015]
19 **Miwa T**, Hanai T, Nishimura K, Maeda T, Ogiso Y, Imai K, Suetsugu A, Takai K, Shiraki M, Shimizu M. Handgrip strength stratifies the risk of covert and overt hepatic encephalopathy in patients with cirrhosis. *JPEN J Parenter Enteral Nutr* 2022; **46**: 858-866 [PMID: 34287991 DOI: 10.1002/jpen.2222]
20 **Dajti E**, Renzulli M, Ravaioli F, Marasco G, Vara G, Brandi N, Rossini B, Colecchia L, Alemanni LV, Ferrarese A, Vestito A, Tamè M, Azzaroli F, Festi D, Golfieri R, Colecchia A. The interplay between sarcopenia and portal hypertension predicts ascites and mortality in cirrhosis. *Dig Liver Dis* 2023; **55**: 637-643 [PMID: 36470723 DOI: 10.1016/j.dld.2022.11.011]
21 **Ebadi M**, Tsien C, Bhanji RA, Dunichand-Hoedl AR, Rider E, Motamedrad M, Mazurak VC, Baracos V, Montano-Loza AJ. Skeletal Muscle Pathological Fat Infiltration (Myosteatosis) Is Associated with Higher Mortality in Patients with Cirrhosis. *Cells* 2022; **11** [PMID: 35456024 DOI: 10.3390/cells11081345]
22 **Ishizu Y**, Ishigami M, Honda T, Imai N, Ito T, Yamamoto K, Yokoyama S, Ishikawa T, Kawashima H. Decreased appetite is associated with the presence of sarcopenia in patients with cirrhosis. *Nutrition* 2022; **103-104**: 111807 [PMID: 36029694 DOI: 10.1016/j.nut.2022.111807]

23 **Sato S**, Namisaki T, Murata K, Fujimoto Y, Takeda S, Enomoto M, Shibamoto A, Ishida K, Ogawa H, Takagi H, Tsuji Y, Kaya D, Fujinaga Y, Furukawa M, Inoue T, Sawada Y, Nishimura N, Kitagawa K, Ozutsumi T, Takaya H, Kaji K, Shimozato N, Kawaratani H, Moriya K, Akahane T, Mitoro A, Yoshiji H. The association between sarcopenia and endotoxin in patients with alcoholic cirrhosis. *Medicine (Baltimore)* 2021; **100**: e27212 [PMID: 34516526 DOI: 10.1097/MD.0000000000027212]

24 **Han JW**, Kim DI, Nam HC, Chang UI, Yang JM, Song DS. Association between serum tumor necrosis factor-α and sarcopenia in liver cirrhosis. *Clin Mol Hepatol* 2022; **28**: 219-231 [PMID: 34281295 DOI: 10.3350/cmh.2021.0082]

25 **Sinclair M**, Grossmann M, Angus PW, Hoermann R, Hey P, Scodellaro T, Gow PJ. Low testosterone as a better predictor of mortality than sarcopenia in men with advanced liver disease. *J Gastroenterol Hepatol* 2016; **31**: 661-667 [PMID: 26414812 DOI: 10.1111/jgh.13182]

26 **Maslennikov R**, Ivashkin V, Efremova I, Poluektova E, Shirokova E. Gut-liver axis in cirrhosis: Are hemodynamic changes a missing link? *World J Clin Cases* 2021; **9**: 9320-9332 [PMID: 34877269 DOI: 10.12998/wjcc.v9.i31.9320]

27 **Giannelli V**, Di Gregorio V, Iebba V, Giusto M, Schippa S, Merli M, Thalheimer U. Microbiota and the gut-liver axis: bacterial translocation, inflammation and infection in cirrhosis. *World J Gastroenterol* 2014; **20**: 16795-16810 [PMID: 25492994 DOI: 10.3748/wjg.v20.i45.16795]

28 **Arab JP**, Martin-Mateos RM, Shah VH. Gut-liver axis, cirrhosis and portal hypertension: the chicken and the egg. *Hepatol Int* 2018; **12**: 24-33 [PMID: 28550391 DOI: 10.1007/s12072-017-9798-x]

29 **Gómez-Hurtado I**, Such J, Sanz Y, Francés R. Gut microbiota-related complications in cirrhosis. *World J Gastroenterol* 2014; **20**: 15624-15631 [PMID: 25400446 DOI: 10.3748/wjg.v20.i42.15624]

30 **Jin M**, Kalainy S, Baskota N, Chiang D, Deehan EC, McDougall C, Tandon P, Martínez I, Cervera C, Walter J, Abraldes JG. Faecal microbiota from patients with cirrhosis has a low capacity to ferment non-digestible carbohydrates into short-chain fatty acids. *Liver Int* 2019; **39**: 1437-1447 [PMID: 30919578 DOI: 10.1111/liv.14106]

31 **Zeng Y**, Chen S, Fu Y, Wu W, Chen T, Chen J, Yang B, Ou Q. Gut microbiota dysbiosis in patients with hepatitis B virus-induced chronic liver disease covering chronic hepatitis, liver cirrhosis and hepatocellular carcinoma. *J Viral Hepat* 2020; **27**: 143-155 [PMID: 31600845 DOI: 10.1111/jvh.13216]

32 **Kajihara M**, Koido S, Kanai T, Ito Z, Matsumoto Y, Takakura K, Saruta M, Kato K, Odamaki T, Xiao JZ, Sato N, Ohkusa T. Characterisation of blood microbiota in patients with liver cirrhosis. *Eur J Gastroenterol Hepatol* 2019; **31**: 1577-1583 [PMID: 31441799 DOI: 10.1097/MEG.0000000000001494]

33 **Chen Z**, Xie Y, Zhou F, Zhang B, Wu J, Yang L, Xu S, Stedtfeld R, Chen Q, Liu J, Zhang X, Xu H, Ren J. Featured Gut Microbiomes Associated With the Progression of Chronic Hepatitis B Disease. *Front Microbiol* 2020; **11**: 383 [PMID: 32265857 DOI: 10.3389/fmicb.2020.00383]

34 **Zheng R**, Wang G, Pang Z, Ran N, Gu Y, Guan X, Yuan Y, Zuo X, Pan H, Zheng J, Wang F. Liver cirrhosis contributes to the disorder of gut microbiota in patients with hepatocellular carcinoma. *Cancer Med* 2020; **9**: 4232-4250 [PMID: 32281295 DOI: 10.1002/cam4.3045]

35 **Lapidot Y**, Amir A, Nosenko R, Uzan-Yulzari A, Veitsman E, Cohen-Ezra O, Davidov Y, Weiss P, Bradichevski T, Segev S, Koren O, Safran M, Ben-Ari Z. Alterations in the Gut Microbiome in the Progression of Cirrhosis to Hepatocellular Carcinoma. *mSystems* 2020; **5** [PMID: 32546668 DOI: 10.1128/mSystems.00153-20]

36 **Bajaj JS**, Heuman DM, Hylemon PB, Sanyal AJ, White MB, Monteith P, Noble NA, Unser AB, Daita K, Fisher AR, Sikaroodi M, Gillevet PM. Altered profile of human gut microbiome is associated with cirrhosis and its complications. *J Hepatol* 2014; **60**: 940-947 [PMID: 24374295 DOI: 10.1016/j.jhep.2013.12.019]

37 **Ahluwalia V**, Betrapally NS, Hylemon PB, White MB, Gillevet PM, Unser AB, Fagan A, Daita K, Heuman DM, Zhou H, Sikaroodi M, Bajaj JS. Impaired Gut-Liver-Brain Axis in Patients with Cirrhosis. *Sci Rep* 2016; **6**: 26800 [PMID: 27225869 DOI: 10.1038/srep26800]

38 **Liu Y**, Jin Y, Li J, Zhao L, Li Z, Xu J, Zhao F, Feng J, Chen H, Fang C, Shilpakar R, Wei Y. Small Bowel Transit and Altered Gut Microbiota in Patients With Liver Cirrhosis. *Front Physiol* 2018; **9**: 470 [PMID: 29780327 DOI: 10.3389/fphys.2018.00470]

39 **Inoue T**, Nakayama J, Moriya K, Kawaratani H, Momoda R, Ito K, Iio E, Nojiri S, Fujiwara K, Yoneda M, Yoshiji H, Tanaka Y. Gut Dysbiosis Associated With Hepatitis C Virus Infection. *Clin Infect Dis* 2018; **67**: 869-877 [PMID: 29718124 DOI: 10.1093/cid/ciy205]

40 **Maslennikov R**, Ivashkin V, Efremova I, Alieva A, Kashuh E, Tsvetaeva E, Poluektova E, Shirokova E, Ivashkin K. Gut dysbiosis is associated with poorer long-term prognosis in cirrhosis. *World J Hepatol* 2021; **13**: 557-570 [PMID: 34131470 DOI: 10.4254/wjh.v13.i5.557]

41 **Chen Y**, Yang F, Lu H, Wang B, Chen Y, Lei D, Wang Y, Zhu B, Li L. Characterization of fecal microbial communities in patients with liver cirrhosis. *Hepatology* 2011; **54**: 562-572 [PMID: 21574172 DOI: 10.1002/hep.24423]

42 **Kakiyama G**, Pandak WM, Gillevet PM, Hylemon PB, Heuman DM, Daita K, Takei H, Muto A, Nittono H, Ridlon JM, White MB, Noble NA, Monteith P, Fuchs M, Thacker LR, Sikaroodi M, Bajaj JS. Modulation of the fecal bile acid profile by gut microbiota in cirrhosis. *J Hepatol* 2013; **58**: 949-955 [PMID: 23333527 DOI: 10.1016/j.jhep.2013.01.003]

43 **Nicoletti A**, Ponziani FR, Biolato M, Valenza V, Marrone G, Sganga G, Gasbarrini A, Miele L, Grieco A. Intestinal permeability in the pathogenesis of liver damage: From non-alcoholic fatty liver disease to liver transplantation. *World J Gastroenterol* 2019; **25**: 4814-4834 [PMID: 31543676 DOI: 10.3748/wjg.v25.i33.4814]

44 **Lian XX**, Sun YP, Guo XX. [Correlation between intestinal mucosal permeability and prognosis in patients with liver cirrhosis]. *Zhonghua Gan Zang Bing Za Zhi* 2020; **28**: 58-63 [PMID: 32023701 DOI: 10.3760/cma.j.issn.1007-3418.2020.01.014]

45 **Choi Y**, Jeon WK, Hwang SJ, Kim BI, Sohn CI, Park DI, Cho YK, Kim HJ, Park JH. The role of the gut barrier function in the pathophysiology of viral liver cirrhosis. *Hepatogastroenterology* 2011; **58**: 1244-1247 [PMID: 21937387 DOI: 10.5754/hge10338]

46 **Assimakopoulos SF**, Tsamandas AC, Tsiaoussis GI, Karatza E, Triantos C, Vagianos CE, Spiliopoulou I, Kaltezioti V, Charonis A, Nikolopoulou VN, Scopa CD, Thomopoulos KC. Altered intestinal tight junctions' expression in patients with liver cirrhosis: a pathogenetic mechanism of intestinal hyperpermeability. *Eur J Clin Invest* 2012; **42**: 439-446 [PMID: 22023490 DOI: 10.1111/j.1365-2362.2011.02609.x]

47 **Bach Knudsen KE**, Lærke HN, Hedemann MS, Nielsen TS, Ingerslev AK, Gundelund Nielsen DS, Theil PK, Purup S, Hald S, Schioldan AG, Marco ML, Gregersen S, Hermansen K. Impact of Diet-Modulated Butyrate Production on Intestinal Barrier Function and Inflammation. *Nutrients* 2018; **10** [PMID: 30322146 DOI: 10.3390/nu10101499]

48 **Shulpekova Y**, Zharkova M, Tkachenko P, Tikhonov I, Stepanov A, Synitsyna A, Izotov A, Butkova T, Shulpekova N, Lapina N, Nechaev V, Kardasheva S, Okhlobystin A, Ivashkin V. The Role of Bile Acids in the Human Body and in the Development of Diseases. *Molecules* 2022; **27** [PMID: 35684337 DOI: 10.3390/molecules27113401]

49 **Bajaj JS**, Vargas HE, Reddy KR, Lai JC, O'Leary JG, Tandon P, Wong F, Mitrani R, White MB, Kelly M, Fagan A, Patil R, Sait S, Sikaroodi M, Thacker LR, Gillevet PM. Association Between Intestinal Microbiota Collected at Hospital Admission and Outcomes of Patients With Cirrhosis. *Clin Gastroenterol Hepatol* 2019; **17**: 756-765.e3 [PMID: 30036646 DOI: 10.1016/j.cgh.2018.07.022]

50 **Bruns T**, Reuken PA, Stengel S, Gerber L, Appenrodt B, Schade JH, Lammert F, Zeuzem S, Stallmach A. The prognostic significance of bacterial DNA in patients with decompensated cirrhosis and suspected infection. *Liver Int* 2016; **36**: 1133-1142 [PMID: 26901072 DOI: 10.1111/liv.13095]

51 **Alvarez-Silva C**, Schierwagen R, Pohlmann A, Magdaleno F, Uschner FE, Ryan P, Vehreschild MJGT, Claria J, Latz E, Lelouvier B, Arumugam M, Trebicka J. Compartmentalization of Immune Response and Microbial Translocation in Decompensated Cirrhosis. *Front Immunol* 2019; **10**: 69 [PMID: 30800122 DOI: 10.3389/fimmu.2019.00069]

52 **Wang Z**, Wang A, Gong Z, Biviano I, Liu H, Hu J. Plasma claudin-3 is associated with tumor necrosis factor-alpha-induced intestinal endotoxemia in liver disease. *Clin Res Hepatol Gastroenterol* 2019; **43**: 410-416 [PMID: 31053499 DOI: 10.1016/j.clinre.2018.11.014]

53 **Ivashkin VT**, Maev IV, Abdulganieva DI, Alekseeva OP, Alekseenko SA, Zolnikova OYu, Korochanskaya NV, Medvedev OS, Poluektova EA, Simanenkov VI, Trukhmanov AS, Khlynov IB, Tsukanov VV, Shifrin OS, Ivashkin KV, Lapina TL, Maslennikov RV, Fadeeva MV, Ulyanin AI. Practical Recommendation of the Scientific Community for Human Microbiome Research (CHMR) and the Russian Gastroenterological Association (RGA) on Small Intestinal Bacterial Overgrowth in Adults. *Russian Journal of Gastroenterology, Hepatology, Coloproctology* 2022; **32**: 68-85 [DOI: 10.22416/1382-4376-2022-32-3-68-85]

54 **Maslennikov R**, Pavlov C, Ivashkin V. Small intestinal bacterial overgrowth in cirrhosis: systematic review and meta-analysis. *Hepatol Int* 2018; **12**: 567-576 [PMID: 30284684 DOI: 10.1007/s12072-018-9898-2]

55 **Feng X**, Li X, Zhang X, Chen W, Tian Y, Yang Q, Yang Y, Pan H, Jiang Z. Hepatic Encephalopathy in Cirrhotic Patients and Risk of Small Intestinal Bacterial Overgrowth: A Systematic Review and Meta-Analysis. *Biomed Res Int* 2022; **2022**: 2469513 [PMID: 36303585 DOI: 10.1155/2022/2469513]

56 **Jun DW**, Kim KT, Lee OY, Chae JD, Son BK, Kim SH, Jo YJ, Park YS. Association between small intestinal bacterial overgrowth and peripheral bacterial DNA in cirrhotic patients. *Dig Dis Sci* 2010; **55**: 1465-1471 [PMID: 19517230 DOI: 10.1007/s10620-009-0870-9]

57 **Wang J**, Chen M, Sun G, Et Al. Small bowel bacterial overgrowth and endotoxemia in cirrhosis. *Zhonghua Nei Ke Za Zhi* 2002; **41**: 459-461 [PMID: 12189115]

58 **Maslennikov R**, Pavlov C, Ivashkin V. Is small intestinal bacterial overgrowth a cause of hyperdynamic circulation in cirrhosis? *Turk J Gastroenterol* 2019; **30**: 964-975 [PMID: 31767551 DOI: 10.5152/tjg.2019.18551]

59 **Maslennikov R**, Ivashkin V, Efremova I, Poluektova E, Kudryavtseva A, Krasnov G. Gut dysbiosis and small intestinal bacterial overgrowth as independent forms of gut microbiota disorders in cirrhosis. *World J Gastroenterol* 2022; **28**: 1067-1077 [PMID: 35431497 DOI: 10.3748/wjg.v28.i10.1067]

60 **Lang CH**, Frost RA, Nairn AC, MacLean DA, Vary TC. TNF-α impairs heart and skeletal muscle protein synthesis by altering translation initiation. *Am J Physiol Endocrinol Metab* 2002; **282**: E336-E347 [PMID: 11788365 DOI: 10.1152/ajpendo.00366.2001]

61 **Lang CH**, Frost RA, Jefferson LS, Kimball SR, Vary TC. Endotoxin-induced decrease in muscle protein synthesis is associated with changes in eIF2B, eIF4E, and IGF-I. *Am J Physiol Endocrinol Metab* 2000; **278**: E1133-E1143 [PMID: 10827017 DOI: 10.1152/ajpendo.2000.278.6.E1133]

62 **Yao J**, Chang L, Yuan L, Duan Z. Nutrition status and small intestinal bacterial overgrowth in patients with virus-related cirrhosis. *Asia Pac J Clin Nutr* 2016; **25**: 283-291 [PMID: 27222411 DOI: 10.6133/apjcn.2016.25.2.06]

63 **Esposito P**, Picciotto D, Battaglia Y, Costigliolo F, Viazzi F, Verzola D. Myostatin: Basic biology to clinical application. *Adv Clin Chem* 2022; **106**: 181-234 [PMID: 35152972 DOI: 10.1016/bs.acc.2021.09.006]

64 **Sharma M**, McFarlane C, Kambadur R, Kukreti H, Bonala S, Srinivasan S. Myostatin: expanding horizons. *IUBMB Life* 2015; **67**: 589-600 [PMID: 26305594 DOI: 10.1002/iub.1392]

65 **Dschietzig TB**. Myostatin - From the Mighty Mouse to cardiovascular disease and cachexia. *Clin Chim Acta* 2014; **433**: 216-224 [PMID: 24680839 DOI: 10.1016/j.cca.2014.03.021]

66 **Qiu J**, Thapaliya S, Runkana A, Yang Y, Tsien C, Mohan ML, Narayanan A, Eghtesad B, Mozdziak PE, McDonald C, Stark GR, Welle S, Naga Prasad SV, Dasarathy S. Hyperammonemia in cirrhosis induces transcriptional regulation of myostatin by an NF-κB-mediated mechanism. *Proc Natl Acad Sci U S A* 2013; **110**: 18162-18167 [PMID: 24145431 DOI: 10.1073/pnas.1317049110]

67 **Richardson AJ**, McKain N, Wallace RJ. Ammonia production by human faecal bacteria, and the enumeration, isolation and characterization of bacteria capable of growth on peptides and amino acids. *BMC Microbiol* 2013; **13**: 6 [PMID: 23312016 DOI: 10.1186/1471-2180-13-6]

68 **Walker V**. Ammonia metabolism and hyperammonemic disorders. *Adv Clin Chem* 2014; **67**: 73-150 [PMID: 25735860 DOI: 10.1016/bs.acc.2014.09.002]

69 **Jindal A**, Jagdish RK. Sarcopenia: Ammonia metabolism and hepatic encephalopathy. *Clin Mol Hepatol* 2019; **25**: 270-279 [PMID: 31006226 DOI: 10.3350/cmh.2019.0015]

70 **Wright G**, Noiret L, Olde Damink SW, Jalan R. Interorgan ammonia metabolism in liver failure: the basis of current and future therapies. *Liver Int* 2011; **31**: 163-175 [PMID: 20673233 DOI: 10.1111/j.1478-3231.2010.02302.x]

71 **Qiu J**, Tsien C, Thapalaya S, Narayanan A, Weihl CC, Ching JK, Eghtesad B, Singh K, Fu X, Dubyak G, McDonald C, Almasan A, Hazen SL, Naga Prasad SV, Dasarathy S. Hyperammonemia-mediated autophagy in skeletal muscle contributes to sarcopenia of cirrhosis. *Am J Physiol Endocrinol Metab* 2012; **303**: E983-E993 [PMID: 22895779 DOI: 10.1152/ajpendo.00183.2012]

72 **Davuluri G**, Krokowski D, Guan BJ, Kumar A, Thapaliya S, Singh D, Hatzoglou M, Dasarathy S. Metabolic adaptation of skeletal muscle to hyperammonemia drives the beneficial effects of l-leucine in cirrhosis. *J Hepatol* 2016; **65**: 929-937 [PMID: 27318325 DOI: 10.1016/j.jhep.2016.06.004]

73 **Ponziani FR**, Picca A, Marzetti E, Calvani R, Conta G, Del Chierico F, Capuani G, Faccia M, Fianchi F, Funaro B, Josè Coelho-Junior H, Petito V, Rinninella E, Paroni Sterbini F, Reddel S, Vernocchi P, Cristina Mele M, Miccheli A, Putignani L, Sanguinetti M, Pompili M, Gasbarrini A; GuLiver study group. Characterization of the gut-liver-muscle axis in cirrhotic patients with sarcopenia. *Liver Int* 2021; **41**: 1320-1334 [PMID: 33713524 DOI: 10.1111/liv.14876]

74 **Ren X**, Hao S, Yang C, Yuan L, Zhou X, Zhao H, Yao J. Alterations of intestinal microbiota in liver cirrhosis with muscle wasting. *Nutrition* 2021; **83**: 111081 [PMID: 33348106 DOI: 10.1016/j.nut.2020.111081]

75 **Maslennikov R**, Ivashkin V, Alieva A, Poluektova E, Kudryavtseva A, Krasnov G, Zharkova M, Zharikov Y. Gut dysbiosis and body composition in cirrhosis. *World J Hepatol* 2022; **14**: 1210-1225 [PMID: 35978666 DOI: 10.4254/wjh.v14.i6.1210]

76 **Lee PC**, Lee KC, Yang TC, Lu HS, Cheng TY, Chen YJ, Chiou JJ, Huang CW, Yang UC, Chia-Hui Tan E, Chou SH, Kuo YL, Schnabl B, Huang YH, Hou MC. Sarcopenia-related gut microbial changes are associated with the risk of complications in people with cirrhosis. *JHEP Rep* 2023; **5**: 100619 [PMID: 36536957 DOI: 10.1016/j.jhepr.2022.100619]

77 **Wang J**, Zhang L, Hou X. Efficacy of rifaximin in treating with small intestine bacterial overgrowth: a systematic review and meta-analysis.

Expert Rev Gastroenterol Hepatol 2021; **15**: 1385-1399 [PMID: 34767484 DOI: 10.1080/17474124.2021.2005579]

78 **Gatta L**, Scarpignato C. Systematic review with meta-analysis: rifaximin is effective and safe for the treatment of small intestine bacterial overgrowth. *Aliment Pharmacol Ther* 2017; **45**: 604-616 [PMID: 28078798 DOI: 10.1111/apt.13928]

79 **Zhuang X**, Tian Z, Li L, Zeng Z, Chen M, Xiong L. Fecal Microbiota Alterations Associated With Diarrhea-Predominant Irritable Bowel Syndrome. *Front Microbiol* 2018; **9**: 1600 [PMID: 30090090 DOI: 10.3389/fmicb.2018.01600]

80 **Liu ZJ**, Wei H, Duan LP, Zhu SW, Zhang L, Wang K. [Clinical features of irritable bowel syndrome with small intestinal bacterial overgrowth and a preliminary study of effectiveness of Rifaximin]. *Zhonghua Yi Xue Za Zhi* 2016; **96**: 1896-1902 [PMID: 27373356 DOI: 10.3760/cma.j.issn.0376-2491.2016.24.005]

81 **Bae S**, Lee KJ, Kim YS, Kim KN. Determination of rifaximin treatment period according to lactulose breath test values in nonconstipated irritable bowel syndrome subjects. *J Korean Med Sci* 2015; **30**: 757-762 [PMID: 26028929 DOI: 10.3346/jkms.2015.30.6.757]

82 **Peralta S**, Cottone C, Doveri T, Almasio PL, Craxi A. Small intestine bacterial overgrowth and irritable bowel syndrome-related symptoms: experience with Rifaximin. *World J Gastroenterol* 2009; **15**: 2628-2631 [PMID: 19496193 DOI: 10.3748/wjg.15.2628]

83 **Furnari M**, De Alessandri A, Cresta F, Haupt M, Bassi M, Calvi A, Haupt R, Bodini G, Ahmed I, Bagnasco F, Giannini EG, Casciaro R. The role of small intestinal bacterial overgrowth in cystic fibrosis: a randomized case-controlled clinical trial with rifaximin. *J Gastroenterol* 2019; **54**: 261-270 [PMID: 30232597 DOI: 10.1007/s00535-018-1509-4]

84 **Biancone L**, Vernia P, Agostini D, Ferrieri A, Pallone F. Effect of rifaximin on intestinal bacterial overgrowth in Crohn's disease as assessed by the H2-Glucose Breath Test. *Curr Med Res Opin* 2000; **16**: 14-20 [PMID: 16422030 DOI: 10.1185/0300799009117003]

85 **Cuoco L**, Montalto M, Jorizzo RA, Santarelli L, Arancio F, Cammarota G, Gasbarrini G. Eradication of small intestinal bacterial overgrowth and oro-cecal transit in diabetics. *Hepatogastroenterology* 2002; **49**: 1582-1586 [PMID: 12397741]

86 **Tursi A**, Brandimarte G, Giorgetti G. High prevalence of small intestinal bacterial overgrowth in celiac patients with persistence of gastrointestinal symptoms after gluten withdrawal. *Am J Gastroenterol* 2003; **98**: 839-843 [PMID: 12738465 DOI: 10.1111/j.1572-0241.2003.07379.x]

87 **Resmini E**, Parodi A, Savarino V, Greco A, Rebora A, Minuto F, Ferone D. Evidence of prolonged orocecal transit time and small intestinal bacterial overgrowth in acromegalic patients. *J Clin Endocrinol Metab* 2007; **92**: 2119-2124 [PMID: 17405840 DOI: 10.1210/jc.2006-2509]

88 **Tursi A**, Brandimarte G, Giorgetti GM, Elisei W. Assessment of small intestinal bacterial overgrowth in uncomplicated acute diverticulitis of the colon. *World J Gastroenterol* 2005; **11**: 2773-2776 [PMID: 15884120 DOI: 10.3748/wjg.v11.i18.2773]

89 **D'Incà R**, Pomerri F, Vettorato MG, Dal Pont E, Di Leo V, Ferronato A, Medici V, Sturniolo GC. Interaction between rifaximin and dietary fibre in patients with diverticular disease. *Aliment Pharmacol Ther* 2007; **25**: 771-779 [PMID: 17373915 DOI: 10.1111/j.1365-2036.2007.03266.x]

90 **Parodi A**, Sessarego M, Greco A, Bazzica M, Filaci G, Setti M, Savarino E, Indiveri F, Savarino V, Ghio M. Small intestinal bacterial overgrowth in patients suffering from scleroderma: clinical effectiveness of its eradication. *Am J Gastroenterol* 2008; **103**: 1257-1262 [PMID: 18422815 DOI: 10.1111/j.1572-0241.2007.01758.x]

91 **Parodi A**, Paolino S, Greco A, Drago F, Mansi C, Rebora A, Parodi A, Savarino V. Small intestinal bacterial overgrowth in rosacea: clinical effectiveness of its eradication. *Clin Gastroenterol Hepatol* 2008; **6**: 759-764 [PMID: 18456568 DOI: 10.1016/j.cgh.2008.02.054]

92 **Yang C**, Zhang X, Wang S, Huo X, Wang J. Small intestinal bacterial overgrowth and evaluation of intestinal barrier function in patients with ulcerative colitis. *Am J Transl Res* 2021; **13**: 6605-6610 [PMID: 34306403]

93 **Pérez Aisa A**, García Gavilán MC, Alcaide García J, Méndez Sánchez IM, Rivera Irigoin R, Fernández Cano F, Pereda Salguero T, Rivas Ruiz F. Small intestinal bacterial overgrowth is common after gastrectomy but with little impact on nutritional status. *Gastroenterol Hepatol* 2019; **42**: 1-10 [PMID: 30197248 DOI: 10.1016/j.gastrohep.2018.07.001]

94 **Di Stefano M**, Malservisi S, Veneto G, Ferrieri A, Corazza GR. Rifaximin versus chlortetracycline in the short-term treatment of small intestinal bacterial overgrowth. *Aliment Pharmacol Ther* 2000; **14**: 551-556 [PMID: 10792117 DOI: 10.1046/j.1365-2036.2000.00751.x]

95 **Yang J**, Lee HR, Low K, Chatterjee S, Pimentel M. Rifaximin versus other antibiotics in the primary treatment and retreatment of bacterial overgrowth in IBS. *Dig Dis Sci* 2008; **53**: 169-174 [PMID: 17520365 DOI: 10.1007/s10620-007-9839-8]

96 **Lauritano EC**, Gabrielli M, Scarpellini E, Ojetti V, Roccarina D, Villita A, Fiore E, Flore R, Santoliquido A, Tondi P, Gasbarrini G, Ghirlanda G, Gasbarrini A. Antibiotic therapy in small intestinal bacterial overgrowth: rifaximin versus metronidazole. *Eur Rev Med Pharmacol Sci* 2009; **13**: 111-116 [PMID: 19499846]

97 **Suhocki PV**, Ronald JS, Diehl AME, Murdoch DM, Doraiswamy PM. Probing gut-brain links in Alzheimer's disease with rifaximin. *Alzheimers Dement (NY)* 2022; **8**: e12225 [PMID: 35128026 DOI: 10.1002/trc2.12225]

98 **Liu Z**, Zhu S, He M, Li M, Wei H, Zhang L, Sun Q, Jia Q, Hu N, Fang Y, Song L, Zhou C, Tao H, Kao JY, Zhu H, Owyang C, Duan L. Patients with breath test positive are necessary to be identified from irritable bowel syndrome: a clinical trial based on microbiomics and rifaximin sensitivity. *Chin Med J (Engl)* 2022; **135**: 1716-1727 [PMID: 36070467 DOI: 10.1097/CM9.0000000000002294]

99 **Li Y**, Hong G, Yang M, Li G, Jin Y, Xiong H, Qian W, Hou X. Fecal bacteria can predict the efficacy of rifaximin in patients with diarrhea-predominant irritable bowel syndrome. *Pharmacol Res* 2020; **159**: 104936 [PMID: 32470562 DOI: 10.1016/j.phrs.2020.104936]

100 **Soldi S**, Vasileiadis S, Uggeri F, Campanale M, Morelli L, Fogli MV, Calanni F, Grimaldi M, Gasbarrini A. Modulation of the gut microbiota composition by rifaximin in non-constipated irritable bowel syndrome patients: a molecular approach. *Clin Exp Gastroenterol* 2015; **8**: 309-325 [PMID: 26673000 DOI: 10.2147/CEG.S89999]

101 **De Vincentis A**, Santonico M, Del Chierico F, Altomare A, Marigliano B, Laudisio A, Reddel S, Grasso S, Zompanti A, Pennazza G, Putignani L, Guarino MPL, Cicala M, Antonelli Incalzi R. Gut Microbiota and Related Electronic Multisensorial System Changes in Subjects With Symptomatic Uncomplicated Diverticular Disease Undergoing Rifaximin Therapy. *Front Med (Lausanne)* 2021; **8**: 655474 [PMID: 34350192 DOI: 10.3389/fmed.2021.655474]

102 **Ivashkin V**, Shifrin O, Maslennikov R, Poluektova E, Korolev A, Kudryavtseva A, Krasnov G, Benuni N, Barbara G. Eubiotic effect of rifaximin is associated with decreasing abdominal pain in symptomatic uncomplicated diverticular disease: results from an observational cohort study. *BMC Gastroenterol* 2023; **23**: 82 [PMID: 36959568 DOI: 10.1186/s12876-023-02690-x]

103 **Kimber C**, Zhang S, Johnson C, West RE 3rd, Prokopienko AJ, Mahnken JD, Yu AS, Hoofnagle AN, Ir D, Robertson CE, Miyazaki M, Chonchol M, Jovanovich A, Kestenbaum B, Frank DN, Nolin TD, Stubbs JR. Randomized, Placebo-Controlled Trial of Rifaximin Therapy for Lowering Gut-Derived Cardiovascular Toxins and Inflammation in CKD. *Kidney360* 2020; **1**: 1206-1216 [PMID: 34322673 DOI: 10.34067/kid.0003942020]

104 **Ponziani FR**, Scaldaferri F, De Siena M, Mangiola F, Matteo MV, Pecere S, Petito V, Sterbini FP, Lopetuso LR, Masucci L, Cammarota G,

Sanguinetti M, Gasbarrini A. Increased Faecalibacterium abundance is associated with clinical improvement in patients receiving rifaximin treatment. *Benef Microbes* 2020; **11**: 519-525 [PMID: 32885687 DOI: 10.3920/BM2019.0171]

105 **Brigidi P**, Swennen E, Rizzello F, Bozzolasco M, Matteuzzi D. Effects of rifaximin administration on the intestinal microbiota in patients with ulcerative colitis. *J Chemother* 2002; **14**: 290-295 [PMID: 12120885 DOI: 10.1179/joc.2002.14.3.290]

106 **Maccaferri S**, Vitali B, Klinder A, Kolida S, Ndagijimana M, Laghi L, Calanni F, Brigidi P, Gibson GR, Costabile A. Rifaximin modulates the colonic microbiota of patients with Crohn's disease: an in vitro approach using a continuous culture colonic model system. *J Antimicrob Chemother* 2010; **65**: 2556-2565 [PMID: 20852272 DOI: 10.1093/jac/dkq345]

107 **Pimentel R**, Gregório C, Figueiredo P. Antibiotic prophylaxis for prevention of spontaneous bacterial peritonitis in liver cirrhosis: systematic review. *Acta Gastroenterol Belg* 2021; **84**: 333-342 [PMID: 34217185 DOI: 10.51821/84.2.333]

108 **Faust N**, Yamada A, Haider H, Komaki Y, Komaki F, Micic D, Sakuraba A. Systemic review and network meta-analysis: Prophylactic antibiotic therapy for spontaneous bacterial peritonitis. *World J Hepatol* 2020; **12**: 239-252 [PMID: 32547691 DOI: 10.4254/wjh.v12.i5.239]

109 **Soni H**, Kumar-M P, Sharma V, Bellam BL, Mishra S, Mahendru D, Mandavdhare HS, Medhi B, Dutta U, Singh V. Antibiotics for prophylaxis of spontaneous bacterial peritonitis: systematic review & Bayesian network meta-analysis. *Hepatol Int* 2020; **14**: 399-413 [PMID: 32266675 DOI: 10.1007/s12072-020-10025-1]

110 **Kamal F**, Khan MA, Khan Z, Cholankeril G, Hammad TA, Lee WM, Ahmed A, Waters B, Howden CW, Nair S, Satapathy SK. Rifaximin for the prevention of spontaneous bacterial peritonitis and hepatorenal syndrome in cirrhosis: a systematic review and meta-analysis. *Eur J Gastroenterol Hepatol* 2017; **29**: 1109-1117 [PMID: 28763340 DOI: 10.1097/MEG.0000000000000940]

111 **Dhiman RK**, Thumburu KK, Verma N, Chopra M, Rathi S, Dutta U, Singal AK, Taneja S, Duseja A, Singh M. Comparative Efficacy of Treatment Options for Minimal Hepatic Encephalopathy: A Systematic Review and Network Meta-Analysis. *Clin Gastroenterol Hepatol* 2020; **18**: 800-812.e25 [PMID: 31476436 DOI: 10.1016/j.cgh.2019.08.047]

112 **Eltawil KM**, Laryea M, Peltekian K, Molinari M. Rifaximin vs. conventional oral therapy for hepatic encephalopathy: a meta-analysis. *World J Gastroenterol* 2012; **18**: 767-777 [PMID: 22371636 DOI: 10.3748/wjg.v18.i8.767]

113 **Zhu GQ**, Shi KQ, Huang S, Wang LR, Lin YQ, Huang GQ, Chen YP, Braddock M, Zheng MH. Systematic review with network meta-analysis: the comparative effectiveness and safety of interventions in patients with overt hepatic encephalopathy. *Aliment Pharmacol Ther* 2015; **41**: 624-635 [PMID: 25684317 DOI: 10.1111/apt.13122]

114 **Zhang Y**, Feng Y, Cao B, Tian Q. Effects of SIBO and rifaximin therapy on MHE caused by hepatic cirrhosis. *Int J Clin Exp Med* 2015; **8**: 2954-2957 [PMID: 25932262]

115 **Vlachogiannakos J**, Saveriadis AS, Viazis N, Theodoropoulos I, Foudoulis K, Manolakopoulos S, Raptis S, Karamanolis DG. Intestinal decontamination improves liver haemodynamics in patients with alcohol-related decompensated cirrhosis. *Aliment Pharmacol Ther* 2009; **29**: 992-999 [PMID: 19210289 DOI: 10.1111/j.1365-2036.2009.03958.x]

116 **Takaya H**, Namisaki T, Sato S, Kaji K, Tsuji Y, Kaya D, Fujinaga Y, Sawada Y, Shimozato N, Kawaratani H, Moriya K, Akahane T, Mitoro A, Yoshiji H. Increased Endotoxin Activity Is Associated with the Risk of Developing Acute-on-Chronic Liver Failure. *J Clin Med* 2020; **9** [PMID: 32422875 DOI: 10.3390/jcm9051467]

117 **Kaji K**, Saikawa S, Takaya H, Fujinaga Y, Furukawa M, Kitagawa K, Ozutsumi T, Kaya D, Tsuji Y, Sawada Y, Kawaratani H, Moriya K, Namisaki T, Akahane T, Mitoro A, Yoshiji H. Rifaximin Alleviates Endotoxemia with Decreased Serum Levels of Soluble CD163 and Mannose Receptor and Partial Modification of Gut Microbiota in Cirrhotic Patients. *Antibiotics (Basel)* 2020; **9** [PMID: 32235367 DOI: 10.3390/antibiotics9040145]

118 **Kaji K**, Takaya H, Saikawa S, Furukawa M, Sato S, Kawaratani H, Kitade M, Moriya K, Namisaki T, Akahane T, Mitoro A, Yoshiji H. Rifaximin ameliorates hepatic encephalopathy and endotoxemia without affecting the gut microbiome diversity. *World J Gastroenterol* 2017; **23**: 8355-8366 [PMID: 29307995 DOI: 10.3748/wjg.v23.i47.8355]

119 **Zeng X**, Tang XJ, Sheng X, Ni W, Xin HG, Chen WZ, Jiang CF, Lin Y, Shi J, Shi B, Chen YX, Yuan ZL, Xie WF. Does low-dose rifaximin ameliorate endotoxemia in patients with liver cirrhosis: a prospective study. *J Dig Dis* 2015; **16**: 665-674 [PMID: 26474237 DOI: 10.1111/1751-2980.12294]

120 **Bajaj JS**, Heuman DM, Sanyal AJ, Hylemon PB, Sterling RK, Stravitz RT, Fuchs M, Ridlon JM, Daita K, Monteith P, Noble NA, White MB, Fisher A, Sikaroodi M, Rangwala H, Gillevet PM. Modulation of the metabiome by rifaximin in patients with cirrhosis and minimal hepatic encephalopathy. *PLoS One* 2013; **8**: e60042 [PMID: 23565181 DOI: 10.1371/journal.pone.0060042]

121 **Kalambokis GN**, Mouzaki A, Rodi M, Tsianos EV. Rifaximin improves thrombocytopenia in patients with alcoholic cirrhosis in association with reduction of endotoxaemia. *Liver Int* 2012; **32**: 467-475 [PMID: 22098272 DOI: 10.1111/j.1478-3231.2011.02650.x]

122 **Patel VC**, Lee S, McPhail MJW, Da Silva K, Guilly S, Zamalloa A, Witherden E, Støy S, Manakkat Vijay GK, Pons N, Galleron N, Huang X, Gencer S, Coen M, Tranah TH, Wendon JA, Bruce KD, Le Chatelier E, Ehrlich SD, Edwards LA, Shoaie S, Shawcross DL. Rifaximin-α reduces gut-derived inflammation and mucin degradation in cirrhosis and encephalopathy: RIFSYS randomised controlled trial. *J Hepatol* 2022; **76**: 332-342 [PMID: 34571050 DOI: 10.1016/j.jhep.2021.09.010]

123 **Yu X**, Jin Y, Zhou W, Xiao T, Wu Z, Su J, Gao H, Shen P, Zheng B, Luo Q, Li L, Xiao Y. Rifaximin Modulates the Gut Microbiota to Prevent Hepatic Encephalopathy in Liver Cirrhosis Without Impacting the Resistome. *Front Cell Infect Microbiol* 2021; **11**: 761192 [PMID: 35118004 DOI: 10.3389/fcimb.2021.761192]

124 **Mariani M**, Zuccaro V, Patruno SF, Scudeller L, Sacchi P, Lombardi A, Vecchia M, Columpsi P, Marone P, Filice G, Bruno R. The impact of rifaximin in the prevention of bacterial infections in cirrhosis. *Eur Rev Med Pharmacol Sci* 2017; **21**: 1151-1158 [PMID: 28338174]

125 **Zeng X**, Sheng X, Wang PQ, Xin HG, Guo YB, Lin Y, Zhong JW, He CZ, Yin J, Liu TT, Ma WJ, Xiao X, Shi PM, Yuan ZL, Yang L, Ma X, Xu JM, Shen XZ, Yang CQ, Zhu X, Lv NH, Xie WF. Low-dose rifaximin prevents complications and improves survival in patients with decompensated liver cirrhosis. *Hepatol Int* 2021; **15**: 155-165 [PMID: 33385299 DOI: 10.1007/s12072-020-10117-y]

126 **Flamm SL**, Mullen KD, Heimanson Z, Sanyal AJ. Rifaximin has the potential to prevent complications of cirrhosis. *Therap Adv Gastroenterol* 2018; **11**: 1756284818800307 [PMID: 30283499 DOI: 10.1177/1756284818800307]

127 **Ibrahim ES**, Alsebaey A, Zaghla H, Moawad Abdelmageed S, Gameel K, Abdelsameea E. Long-term rifaximin therapy as a primary prevention of hepatorenal syndrome. *Eur J Gastroenterol Hepatol* 2017; **29**: 1247-1250 [PMID: 28902040 DOI: 10.1097/MEG.0000000000000967]

128 **Dong T**, Aronsohn A, Gautham Reddy K, Te HS. Rifaximin Decreases the Incidence and Severity of Acute Kidney Injury and Hepatorenal Syndrome in Cirrhosis. *Dig Dis Sci* 2016; **61**: 3621-3626 [PMID: 27655104 DOI: 10.1007/s10620-016-4313-0]

129 **Wang Z**, Hou W, Zhang W, Wu HX, Zheng SJ, Hu ZJ. [Rifaximin improves clinical symptoms and short-term survival in cirrhotic patients

with refractory type ascites]. *Zhonghua Gan Zang Bing Za Zhi* 2022; **30**: 1170-1174 [PMID: 36891693 DOI: 10.3760/cma.j.cn501113-20210918-00475]

130 **Lv XY**, Ding HG, Zheng JF, Fan CL, Li L. Rifaximin improves survival in cirrhotic patients with refractory ascites: A real-world study. *World J Gastroenterol* 2020; **26**: 199-218 [PMID: 31988585 DOI: 10.3748/wjg.v26.i2.199]

131 **Kawaguchi T**, Suzuki F, Imamura M, Murashima N, Yanase M, Mine T, Fujisawa M, Sato I, Yoshiji H, Okita K, Suzuki K. Rifaximin-altered gut microbiota components associated with liver/neuropsychological functions in patients with hepatic encephalopathy: An exploratory data analysis of phase II/III clinical trials. *Hepatol Res* 2019; **49**: 404-418 [PMID: 30589492 DOI: 10.1111/hepr.13300]

132 **Yokoyama K**, Fukuda H, Yamauchi R, Higashi M, Miyayama T, Higashi T, Uchida Y, Shibata K, Tsuchiya N, Fukunaga A, Umeda K, Takata K, Tanaka T, Shakado S, Sakisaka S, Hirai F. Long-Term Effects of Rifaximin on Patients with Hepatic Encephalopathy: Its Possible Effects on the Improvement in the Blood Ammonia Concentration Levels, Hepatic Spare Ability and Refractory Ascites. *Medicina (Kaunas)* 2022; **58** [PMID: 36143954 DOI: 10.3390/medicina58091276]

133 **Kawaratani H**, Kondo Y, Tatsumi R, Kawabe N, Tanabe N, Sakamaki A, Okumoto K, Uchida Y, Endo K, Kawaguchi T, Oikawa T, Ishizu Y, Hige S, Takami T, Terai S, Ueno Y, Mochida S, Takikawa Y, Torimura T, Matsuura T, Ishigami M, Koike K, Yoshiji H. Long-Term Efficacy and Safety of Rifaximin in Japanese Patients with Hepatic Encephalopathy: A Multicenter Retrospective Study. *J Clin Med* 2022; **11** [PMID: 35329897 DOI: 10.3390/jcm11061571]

134 **Glal KAM**, Abd-Elsalam SM, Mostafa TM. Nitazoxanide versus rifaximin in preventing the recurrence of hepatic encephalopathy: A randomized double-blind controlled trial. *J Hepatobiliary Pancreat Sci* 2021; **28**: 812-824 [PMID: 33768619 DOI: 10.1002/jhbp.947]

135 **Gómez-Hurtado I**, Gimenez P, García I, Zapater P, Francés R, González-Navajas JM, Manichanh C, Ramos JM, Bellot P, Guarner F, Such J. Norfloxacin is more effective than Rifaximin in avoiding bacterial translocation in an animal model of cirrhosis. *Liver Int* 2018; **38**: 295-302 [PMID: 28834270 DOI: 10.1111/liv.13551]

136 **Pedretti G**, Calzetti C, Missale G, Fiaccadori F. Rifaximin versus neomycin on hyperammoniemia in chronic portal systemic encephalopathy of cirrhotics. A double-blind, randomized trial. *Ital J Gastroenterol* 1991; **23**: 175-178 [PMID: 1751811]

137 **Murata K**, Kaji K, Nishimura N, Enomoto M, Fujimoto Y, Takeda S, Tsuji Y, Fujinaga Y, Takaya H, Kawaratani H, Namisaki T, Akahane T, Yoshiji H. Rifaximin enhances the Lcarnitinemediated preventive effects on skeletal muscle atrophy in cirrhotic rats by modulating the gutlivermuscle axis. *Int J Mol Med* 2022; **50** [PMID: 35686541 DOI: 10.3892/ijmm.2022.5157]

138 **Ishikawa T**, Endo S, Imai M, Azumi M, Nozawa Y, Sano T, Iwanaga A, Honma T, Yoshida T. Changes in the Body Composition and Nutritional Status after Long-term Rifaximin Therapy for Hyperammonemia in Japanese Patients with Hepatic Encephalopathy. *Intern Med* 2020; **59**: 2465-2469 [PMID: 33055469 DOI: 10.2169/internalmedicine.5094-20]

139 **Miller LE**, Tennilä J, Ouwehand AC. Efficacy and tolerance of lactitol supplementation for adult constipation: a systematic review and meta-analysis. *Clin Exp Gastroenterol* 2014; **7**: 241-248 [PMID: 25050074 DOI: 10.2147/CEG.S58952]

140 **Maev IV**, Kazyulin AN, Kucheryavy YuA, Cheryomushkin SV, Goncharenko AYu, Gilyuk AV. Diagnosis of Functional Gastrointestinal Disorders and Choice of Treatment Regimen in Constipation Patients. *Russian Journal of Gastroenterology, Hepatology, Coloproctology* 2021; **31**: 7-16 [DOI: 10.22416/1382-4376-2021-31-3-7-16]

141 **Ivashkin VT**, Maev IV, Shelygin YuA, Baranskaya EK, Belous SS, Belousova EA, Beniashvili AG, Vasilyev SV, Veselov AV, Grigoryev EG, Kostenko NV, Kashnikov VN, Kulikovskiy VF, Loranskaya ID, Lyashenko OS, Poluektova EA, Rumyantsev VG, Timerbulatov VM, Fomenko OYu, Khubezov DA, Chashkova EYu, Chibisov GI, Shapina MV, Sheptulin AA, Shifrin OS, Trukhmanov AS, Alekseeva OP, Alekseenko SA, Baranovsky AYu, Zolnikova OYu, Korochanskaya NV, Mammayev SN, Khlynov IB, Tsukanov VV. Diagnosis and Treatment of Irritable Bowel Syndrome: Clinical Recommendations of the Russian Gastroenterological Association and Association of Coloproctologists of Russia. *Russian Journal of Gastroenterology, Hepatology, Coloproctology* 2021; **31**: 74-95 [DOI: 10.22416/1382-4376-2021-31-5-74-95]

142 **Morgan MY**. Current state of knowledge of hepatic encephalopathy (part III): non-absorbable disaccharides. *Metab Brain Dis* 2016; **31**: 1361-1364 [PMID: 27638474 DOI: 10.1007/s11011-016-9910-2]

143 **Sharma P**, Sharma BC. Disaccharides in the treatment of hepatic encephalopathy. *Metab Brain Dis* 2013; **28**: 313-320 [PMID: 23456517 DOI: 10.1007/s11011-013-9392-4]

144 **Masini A**, Efrati C, Merli M, Attili AF, Amodio P, Ceccanti M, Riggio O. Effect of lactitol on blood ammonia response to oral glutamine challenge in cirrhotic patients: evidence for an effect of nonabsorbable disaccharides on small intestine ammonia generation. *Am J Gastroenterol* 1999; **94**: 3323-3327 [PMID: 10566738 DOI: 10.1111/j.1572-0241.1999.01546.x]

145 **Blanc P**, Daures JP, Rouillon JM, Peray P, Pierrugues R, Larrey D, Gremy F, Michel H. Lactitol or lactulose in the treatment of chronic hepatic encephalopathy: results of a meta-analysis. *Hepatology* 1992; **15**: 222-228 [PMID: 1531204 DOI: 10.1002/hep.1840150209]

146 **Gluud LL**, Vilstrup H, Morgan MY. Nonabsorbable disaccharides for hepatic encephalopathy: A systematic review and meta-analysis. *Hepatology* 2016; **64**: 908-922 [PMID: 27081787 DOI: 10.1002/hep.28598]

147 **Gluud LL**, Vilstrup H, Morgan MY. Non-absorbable disaccharides versus placebo/no intervention and lactulose versus lactitol for the prevention and treatment of hepatic encephalopathy in people with cirrhosis. *Cochrane Database Syst Rev* 2016; **2016**: CD003044 [PMID: 27153247 DOI: 10.1002/14651858.CD003044.pub4]

148 **Sharma P**, Sharma BC, Agrawal A, Sarin SK. Primary prophylaxis of overt hepatic encephalopathy in patients with cirrhosis: an open labeled randomized controlled trial of lactulose versus no lactulose. *J Gastroenterol Hepatol* 2012; **27**: 1329-1335 [PMID: 22606978 DOI: 10.1111/j.1440-1746.2012.07186.x]

149 **Agrawal A**, Sharma BC, Sharma P, Sarin SK. Secondary prophylaxis of hepatic encephalopathy in cirrhosis: an open-label, randomized controlled trial of lactulose, probiotics, and no therapy. *Am J Gastroenterol* 2012; **107**: 1043-1050 [PMID: 22710579 DOI: 10.1038/ajg.2012.113]

150 **Riggio O**, Balducci G, Ariosto F, Merli M, Tremiterra S, Ziparo V, Capocaccia L. Lactitol in the treatment of chronic hepatic encephalopathy--a randomized cross-over comparison with lactulose. *Hepatogastroenterology* 1990; **37**: 524-527 [PMID: 2253931]

151 **Riggio O**, Balducci G, Ariosto F, Merli M, Pieche U, Pinto G, Tremiterra S, Ziparo V, Capocaccia L. Lactitol in prevention of recurrent episodes of hepatic encephalopathy in cirrhotic patients with portal-systemic shunt. *Dig Dis Sci* 1989; **34**: 823-829 [PMID: 2656134 DOI: 10.1007/BF01540265]

152 **Merli M**, Caschera M, Piat C, Pinto G, Diofebi M, Riggio O. The effect of lactulose and lactitol administration on fecal fat excretion in patients with liver cirrhosis. *J Clin Gastroenterol* 1992; **15**: 125-127 [PMID: 1401823 DOI: 10.1097/00004836-199209000-00009]

153 **Riggio O**, Varriale M, Testore GP, Di Rosa R, Di Rosa E, Merli M, Romiti A, Candiani C, Capocaccia L. Effect of lactitol and lactulose administration on the fecal flora in cirrhotic patients. *J Clin Gastroenterol* 1990; **12**: 433-436 [PMID: 2398251 DOI:

10.1097/00004836-199008000-00016]
154 **Ballongue J**, Schumann C, Quignon P. Effects of lactulose and lactitol on colonic microflora and enzymatic activity. *Scand J Gastroenterol Suppl* 1997; **222**: 41-44 [PMID: 9145445 DOI: 10.1080/00365521.1997.11720716]
155 **Li XQ**, Zhang XM, Wu X, Lan Y, Xu L, Meng XC, Li JN. Beneficial effects of lactitol on the composition of gut microbiota in constipated patients. *J Dig Dis* 2020; **21**: 445-453 [PMID: 32483935 DOI: 10.1111/1751-2980.12912]
156 **Tarao K**, Tamai S, Ito Y, Okawa S, Hayashi M. [Effects of lactitol on fecal bacterial flora in patients with liver cirrhosis and hepatic encephalopathy]. *Nihon Shokakibyo Gakkai Zasshi* 1995; **92**: 1037-1050 [PMID: 7643458]
157 **Lu H**, Chen L, Pan X, Yao Y, Zhang H, Zhu X, Lou X, Zhu C, Wang J, Li L, Wu Z. Lactitol Supplementation Modulates Intestinal Microbiome in Liver Cirrhotic Patients. *Front Med (Lausanne)* 2021; **8**: 762930 [PMID: 34722597 DOI: 10.3389/fmed.2021.762930]
158 **Chen C**, Li L, Wu Z, Chen H, Fu S. Effects of lactitol on intestinal microflora and plasma endotoxin in patients with chronic viral hepatitis. *J Infect* 2007; **54**: 98-102 [PMID: 17049992 DOI: 10.1016/j.jinf.2005.11.013]
159 **Ziada DH**, Soliman HH, El Yamany SA, Hamisa MF, Hasan AM. Can Lactobacillus acidophilus improve minimal hepatic encephalopathy? A neurometabolite study using magnetic resonance spectroscopy. *Arab J Gastroenterol* 2013; **14**: 116-122 [PMID: 24206740 DOI: 10.1016/j.ajg.2013.08.002]
160 **Manzhalii E**, Moyseyenko V, Kondratiuk V, Molochek N, Falalyeyeva T, Kobyliak N. Effect of a specific Escherichia coli Nissle 1917 strain on minimal/mild hepatic encephalopathy treatment. *World J Hepatol* 2022; **14**: 634-646 [PMID: 35582294 DOI: 10.4254/wjh.v14.i3.634]
161 **Sarangi AN**, Goel A, Singh A, Sasi A, Aggarwal R. Faecal bacterial microbiota in patients with cirrhosis and the effect of lactulose administration. *BMC Gastroenterol* 2017; **17**: 125 [PMID: 29179682 DOI: 10.1186/s12876-017-0683-9]
162 **Wang JY**, Bajaj JS, Wang JB, Shang J, Zhou XM, Guo XL, Zhu X, Meng LN, Jiang HX, Mi YQ, Xu JM, Yang JH, Wang BS, Zhang NP. Lactulose improves cognition, quality of life, and gut microbiota in minimal hepatic encephalopathy: A multicenter, randomized controlled trial. *J Dig Dis* 2019; **20**: 547-556 [PMID: 31448533 DOI: 10.1111/1751-2980.12816]
163 **Jain L**, Sharma BC, Srivastava S, Puri SK, Sharma P, Sarin S. Serum endotoxin, inflammatory mediators, and magnetic resonance spectroscopy before and after treatment in patients with minimal hepatic encephalopathy. *J Gastroenterol Hepatol* 2013; **28**: 1187-1193 [PMID: 23425082 DOI: 10.1111/jgh.12160]
164 **Moratalla A**, Ampuero J, Bellot P, Gallego-Durán R, Zapater P, Roger M, Figueruela B, Martínez-Moreno B, González-Navajas JM, Such J, Romero-Gómez M, Francés R. Lactulose reduces bacterial DNA translocation, which worsens neurocognitive shape in cirrhotic patients with minimal hepatic encephalopathy. *Liver Int* 2017; **37**: 212-223 [PMID: 27388776 DOI: 10.1111/liv.13200]
165 **Ivashkin VT**, Maev IV, Abdulganieva DI, Alekseenko SA, Gorelov AV, Zakharova IN, Zolnikova OYu, Ivashkina NYu, Korochanskaya NV, Mammayev SN, Poluektova EA, Trukhmanov AS, Usenko DV, Uspensky YuP, Tsukanov VV, Shifrin OS, Berezhnaya IV, Ivashkin KV, Lapina TL, Maslennikov RV, Nikolaeva SV, Sugyan NG, Ulyanin AI. Practical Recommendations of Scientific Society for the Study of Human Microbiome and the Russian Gastroenterological Association on Use of Probiotics, Prebiotics, Synbiotics and Functional Foods in Treatment and Prevention of Gastroenterological Diseases in Children and Adults. *Russian Journal of Gastroenterology, Hepatology, Coloproctology* 2021; **31**: 65-91 [DOI: 10.22416/1382-4376-2021-31-2-65-91]
166 **Maslennikov R**, Ivashkin V, Efremova I, Poluektova E, Shirokova E. Probiotics in hepatology: An update. *World J Hepatol* 2021; **13**: 1154-1166 [PMID: 34630882 DOI: 10.4254/wjh.v13.i9.1154]
167 **Cao Q**, Yu CB, Yang SG, Cao HC, Chen P, Deng M, Li LJ. Effect of probiotic treatment on cirrhotic patients with minimal hepatic encephalopathy: A meta-analysis. *Hepatobiliary Pancreat Dis Int* 2018; **17**: 9-16 [PMID: 29428113 DOI: 10.1016/j.hbpd.2018.01.005]
168 **Viramontes Hörner D**, Avery A, Stow R. The Effects of Probiotics and Symbiotics on Risk Factors for Hepatic Encephalopathy: A Systematic Review. *J Clin Gastroenterol* 2017; **51**: 312-323 [PMID: 28059938 DOI: 10.1097/MCG.0000000000000789]
169 **Huang L**, Yu Q, Peng H, Zhen Z. Alterations of gut microbiome and effects of probiotic therapy in patients with liver cirrhosis: A systematic review and meta-analysis. *Medicine (Baltimore)* 2022; **101**: e32335 [PMID: 36595801 DOI: 10.1097/MD.0000000000032335]
170 **Dalal R**, McGee RG, Riordan SM, Webster AC. Probiotics for people with hepatic encephalopathy. *Cochrane Database Syst Rev* 2017; **2**: CD008716 [PMID: 28230908 DOI: 10.1002/14651858.CD008716.pub3]
171 **Kazemi A**, Soltani S, Ghorabi S, Keshtkar A, Daneshzad E, Nasri F, Mazloomi SM. Effect of probiotic and synbiotic supplementation on inflammatory markers in health and disease status: A systematic review and meta-analysis of clinical trials. *Clin Nutr* 2020; **39**: 789-819 [PMID: 31060892 DOI: 10.1016/j.clnu.2019.04.004]
172 **Maslennikov R**, Efremova I, Ivashkin V, Zharkova M, Poluektova E, Shirokova E, Ivashkin K. Effect of probiotics on hemodynamic changes and complications associated with cirrhosis: A pilot randomized controlled trial. *World J Hepatol* 2022; **14**: 1667-1677 [PMID: 36157871 DOI: 10.4254/wjh.v14.i8.1667]
173 **Xia X**, Chen J, Xia J, Wang B, Liu H, Yang L, Wang Y, Ling Z. Role of probiotics in the treatment of minimal hepatic encephalopathy in patients with HBV-induced liver cirrhosis. *J Int Med Res* 2018; **46**: 3596-3604 [PMID: 29806520 DOI: 10.1177/0300060518776064]
174 **Dhiman RK**, Rana B, Agrawal S, Garg A, Chopra M, Thumburu KK, Khattri A, Malhotra S, Duseja A, Chawla YK. Probiotic VSL#3 reduces liver disease severity and hospitalization in patients with cirrhosis: a randomized, controlled trial. *Gastroenterology* 2014; **147**: 1327-37.e3 [PMID: 25450083 DOI: 10.1053/j.gastro.2014.08.031]
175 **Lata J**, Novotný I, Príbramská V, Juránková J, Fric P, Kroupa R, Stibůrek O. The effect of probiotics on gut flora, level of endotoxin and Child-Pugh score in cirrhotic patients: results of a double-blind randomized study. *Eur J Gastroenterol Hepatol* 2007; **19**: 1111-1113 [PMID: 17998837 DOI: 10.1097/MEG.0b013e3282efa40e]
176 **Koga H**, Tamiya Y, Mitsuyama K, Ishibashi M, Matsumoto S, Imaoka A, Hara T, Nakano M, Ooeda K, Umezaki Y, Sata M. Probiotics promote rapid-turnover protein production by restoring gut flora in patients with alcoholic liver cirrhosis. *Hepatol Int* 2013; **7**: 767-774 [PMID: 26201812 DOI: 10.1007/s12072-012-9408-x]
177 **Bajaj JS**, Heuman DM, Hylemon PB, Sanyal AJ, Puri P, Sterling RK, Luketic V, Stravitz RT, Siddiqui MS, Fuchs M, Thacker LR, Wade JB, Daita K, Sistrun S, White MB, Noble NA, Thorpe C, Kakiyama G, Pandak WM, Sikaroodi M, Gillevet PM. Randomised clinical trial: Lactobacillus GG modulates gut microbiome, metabolome and endotoxemia in patients with cirrhosis. *Aliment Pharmacol Ther* 2014; **39**: 1113-1125 [PMID: 24628464 DOI: 10.1111/apt.12695]
178 **Horvath A**, Durdevic M, Leber B, di Vora K, Rainer F, Krones E, Douschan P, Spindelboeck W, Durchschein F, Zollner G, Stauber RE, Fickert P, Stiegler P, Stadlbauer V. Changes in the Intestinal Microbiome during a Multispecies Probiotic Intervention in Compensated Cirrhosis. *Nutrients* 2020; **12** [PMID: 32585997 DOI: 10.3390/nu12061874]
179 **Zhong C**, Qu C, Wang B, Liang S, Zeng B. Probiotics for Preventing and Treating Small Intestinal Bacterial Overgrowth: A Meta-Analysis

and Systematic Review of Current Evidence. *J Clin Gastroenterol* 2017; **51**: 300-311 [PMID: 28267052 DOI: 10.1097/MCG.0000000000000814]

180 **Nickles MA**, Hasan A, Shakhbazova A, Wright S, Chambers CJ, Sivamani RK. Alternative Treatment Approaches to Small Intestinal Bacterial Overgrowth: A Systematic Review. *J Altern Complement Med* 2021; **27**: 108-119 [PMID: 33074705 DOI: 10.1089/acm.2020.0275]

181 **Lunia MK**, Sharma BC, Sharma P, Sachdeva S, Srivastava S. Probiotics prevent hepatic encephalopathy in patients with cirrhosis: a randomized controlled trial. *Clin Gastroenterol Hepatol* 2014; **12**: 1003-8.e1 [PMID: 24246768 DOI: 10.1016/j.cgh.2013.11.006]

182 **Kwak DS**, Jun DW, Seo JG, Chung WS, Park SE, Lee KN, Khalid-Saeed W, Lee HL, Lee OY, Yoon BC, Choi HS. Short-term probiotic therapy alleviates small intestinal bacterial overgrowth, but does not improve intestinal permeability in chronic liver disease. *Eur J Gastroenterol Hepatol* 2014; **26**: 1353-1359 [PMID: 25244414 DOI: 10.1097/MEG.0000000000000214]

183 **Ruchkina IN**, Fadeeva NA. [The role of a combined probiotic in the treatment of lactase deficiency]. *Ter Arkh* 2021; **93**: 431-434 [PMID: 36286777 DOI: 10.26442/00403660.2021.04.200808]

184 **Luo M**, Liu Q, Xiao L, Xiong LS. Golden bifid might improve diarrhea-predominant irritable bowel syndrome *via* microbiota modulation. *J Health Popul Nutr* 2022; **41**: 21 [PMID: 35578355 DOI: 10.1186/s41043-022-00302-0]

185 **Bustos Fernández LM**, Man F, Lasa JS. "Impact of Saccharomyces boulardii CNCM I-745 on bacterial overgrowth and composition of intestinal microbiota in IBS-D patients: results of a randomized pilot study". *Dig Dis* 2023 [PMID: 36630947 DOI: 10.1159/000528954]

186 **Lee SH**, Joo NS, Kim KM, Kim KN. The Therapeutic Effect of a Multistrain Probiotic on Diarrhea-Predominant Irritable Bowel Syndrome: A Pilot Study. *Gastroenterol Res Pract* 2018; **2018**: 8791916 [PMID: 30622561 DOI: 10.1155/2018/8791916]

187 **Liang S**, Xu L, Zhang D, Wu Z. Effect of probiotics on small intestinal bacterial overgrowth in patients with gastric and colorectal cancer. *Turk J Gastroenterol* 2016; **27**: 227-232 [PMID: 27210778 DOI: 10.5152/tjg.2016.15375]

188 **García-Collinot G**, Madrigal-Santillán EO, Martínez-Bencomo MA, Carranza-Muleiro RA, Jara LJ, Vera-Lastra O, Montes-Cortes DH, Medina G, Cruz-Domínguez MP. Effectiveness of Saccharomyces boulardii and Metronidazole for Small Intestinal Bacterial Overgrowth in Systemic Sclerosis. *Dig Dis Sci* 2020; **65**: 1134-1143 [PMID: 31549334 DOI: 10.1007/s10620-019-05830-0]

189 **Woodard GA**, Encarnacion B, Downey JR, Peraza J, Chong K, Hernandez-Boussard T, Morton JM. Probiotics improve outcomes after Roux-en-Y gastric bypass surgery: a prospective randomized trial. *J Gastrointest Surg* 2009; **13**: 1198-1204 [PMID: 19381735 DOI: 10.1007/s11605-009-0891-x]

190 **Prokopidis K**, Giannos P, Kirwan R, Ispoglou T, Galli F, Witard OC, Triantafyllidis KK, Kechagias KS, Morwani-Mangnani J, Ticinesi A, Isanejad M. Impact of probiotics on muscle mass, muscle strength and lean mass: a systematic review and meta-analysis of randomized controlled trials. *J Cachexia Sarcopenia Muscle* 2023; **14**: 30-44 [PMID: 36414567 DOI: 10.1002/jcsm.13132]

191 **Byeon HR**, Jang SY, Lee Y, Kim D, Hong MG, Lee D, Shin JH, Seo JG. New Strains of Akkermansia muciniphila and Faecalibacterium prausnitzii are Effective for Improving the Muscle Strength of Mice with Immobilization-Induced Muscular Atrophy. *J Med Food* 2022; **25**: 565-575 [PMID: 35708632 DOI: 10.1089/jmf.2021.K.0148]

192 **Hong AS**, Tun KM, Hong JM, Batra K, Ohning G. Fecal Microbiota Transplantation in Decompensated Cirrhosis: A Systematic Review on Safety and Efficacy. *Antibiotics (Basel)* 2022; **11** [PMID: 35884093 DOI: 10.3390/antibiotics11070838]

193 **Bajaj JS**, Salzman NH, Acharya C, Sterling RK, White MB, Gavis EA, Fagan A, Hayward M, Holtz ML, Matherly S, Lee H, Osman M, Siddiqui MS, Fuchs M, Puri P, Sikaroodi M, Gillevet PM. Fecal Microbial Transplant Capsules Are Safe in Hepatic Encephalopathy: A Phase 1, Randomized, Placebo-Controlled Trial. *Hepatology* 2019; **70**: 1690-1703 [PMID: 31038755 DOI: 10.1002/hep.30690]

194 **Tun KM**, Hong AS, Batra K, Naga Y, Ohning G. A Systematic Review of the Efficacy and Safety of Fecal Microbiota Transplantation in the Treatment of Hepatic Encephalopathy and Clostridioides difficile Infection in Patients With Cirrhosis. *Cureus* 2022; **14**: e25537 [PMID: 35800791 DOI: 10.7759/cureus.25537]

195 **Chen H**, Xu C, Zhang F, Liu Y, Guo Y, Yao Q. The gut microbiota attenuates muscle wasting by regulating energy metabolism in chemotherapy-induced malnutrition rats. *Cancer Chemother Pharmacol* 2020; **85**: 1049-1062 [PMID: 32415349 DOI: 10.1007/s00280-020-04060-w]

World Journal of Gastroenterology

Submit a Manuscript: https://www.f6publishing.com

World J Gastroenterol 2023 July 21; 29(27): 4252-4270

DOI: 10.3748/wjg.v29.i27.4252

ISSN 1007-9327 (print) ISSN 2219-2840 (online)

REVIEW

Bile acids and their receptors: Potential therapeutic targets in inflammatory bowel disease

Xiong-Quan Long, Ming-Zhu Liu, Zi-Hao Liu, Lv-Zhou Xia, Shi-Peng Lu, Xiao-Ping Xu, Ming-Hao Wu

Specialty type: Gastroenterology and hepatology

Provenance and peer review: Unsolicited article; Externally peer reviewed.

Peer-review model: Single blind

Peer-review report's scientific quality classification

Grade A (Excellent): 0
Grade B (Very good): B, B
Grade C (Good): 0
Grade D (Fair): 0
Grade E (Poor): 0

P-Reviewer: Makishima M, Japan; Rodriguez JC, Spain

Received: April 8, 2023
Peer-review started: April 8, 2023
First decision: May 12, 2023
Revised: May 19, 2023
Accepted: June 21, 2023
Article in press: June 21, 2023
Published online: July 21, 2023

Xiong-Quan Long, Ming-Zhu Liu, Zi-Hao Liu, Lv-Zhou Xia, Shi-Peng Lu, Xiao-Ping Xu, Ming-Hao Wu, Department of Gastroenterology, The First Affiliated Hospital of Hunan Normal University (Hunan Provincial People's Hospital), Changsha 410005, Hunan Province, China

Corresponding author: Ming-Hao Wu, MM, Chief Doctor, Professor, Department of Gastroenterology, The First Affiliated Hospital of Hunan Normal University (Hunan Provincial People's Hospital), No. 61 Jiefang West Road, Furong District, Changsha 410005, Hunan Province, China. wuminghao1976@sina.com

Abstract

Chronic and recurrent inflammatory disorders of the gastrointestinal tract caused by a complex interplay between genetics and intestinal dysbiosis are called inflammatory bowel disease. As a result of the interaction between the liver and the gut microbiota, bile acids are an atypical class of steroids produced in mammals and traditionally known for their function in food absorption. With the development of genomics and metabolomics, more and more data suggest that the pathophysiological mechanisms of inflammatory bowel disease are regulated by bile acids and their receptors. Bile acids operate as signalling molecules by activating a variety of bile acid receptors that impact intestinal flora, epithelial barrier function, and intestinal immunology. Inflammatory bowel disease can be treated in new ways by using these potential molecules. This paper mainly discusses the increasing function of bile acids and their receptors in inflammatory bowel disease and their prospective therapeutic applications. In addition, we explore bile acid metabolism and the interaction of bile acids and the gut microbiota.

Key Words: Bile acids; Inflammatory bowel disease; Intestinal immunology; Bile acid receptors; Bile acid metabolism; Gut microbiota

©The Author(s) 2023. Published by Baishideng Publishing Group Inc. All rights reserved.

Core Tip: Chronic and recurrent inflammatory disorders of the gastrointestinal tract caused by a complex interplay between genetics and intestinal dysbiosis are called inflammatory bowel disease. With the development of genomics and metabolomics, more and more data suggest that bile acids operate as signalling molecules by activating a variety of bile acid receptors that regulate pathophysiological mechanisms of inflammatory bowel disease. Inflammatory bowel disease can be treated in new ways by using these potential molecules.

Citation: Long XQ, Liu MZ, Liu ZH, Xia LZ, Lu SP, Xu XP, Wu MH. Bile acids and their receptors: Potential therapeutic targets in inflammatory bowel disease. *World J Gastroenterol* 2023; 29(27): 4252-4270
URL: https://www.wjgnet.com/1007-9327/full/v29/i27/4252.htm
DOI: https://dx.doi.org/10.3748/wjg.v29.i27.4252

INTRODUCTION

Inflammatory bowel disease (IBD) is a group of chronic and recurrent inflammatory diseases of the gastrointestinal tract, including two main subtypes: Ulcerative colitis (UC) and Crohn's disease (CD). Globally, the prevalence of IBD is increasing, especially in newly industrialized countries, with a prevalence of 0.5% in 2010, 0.75% in 2020, and a projected 1% in 2030, increasing the burden on health care systems around the world[1,2]. The etiology and pathogenesis of IBD are not well understood. However, it is generally accepted that IBD is a persistent and excessive immune inflammatory response in people with genetic susceptibility when exposed to environmental factors[3]. Immune homeostasis in the intestine involves the coordinated action of epithelial cells and innate and adaptive immune cells. As a result of impaired intestinal epithelial barrier function in IBD, commensal microorganisms translocate into the intestinal wall. The innate immune cells then take up the microbes and their mediators and respond, which activates immune cells and produces cytokines and chemokines. This process, in turn, upsets the homeostasis of the intestine, recruiting more immune cells to the intestinal wall and activating adaptive immunity[4,5]. IBD usually presents with chronic recurrent abdominal pain, diarrhea, mucus, and bloody stools and can also present with serious complications such as anal fistula, intestinal obstruction, and intestinal perforation[6]. Additionally, IBD patients frequently experience symptoms outside of the digestive system, such as joint, eye, or skin inflammation[7]. With the introduction of new biological and small molecule therapies, such as anti-TNF-α biologic agents, anti-interleukin (IL)-12/23 biologic agents, and anti-integrin biologic agents, significant progress has been made in the pharmacological treatment of IBD, but at a high financial and physical cost to patients. Moreover, these therapies can potentially produce life-threatening side effects and cannot cure IBD, and a significant proportion of patients still require surgical treatment. This underscores the need for new treatment strategies for IBD[8,9].

As a result of the interaction between the liver and gut bacteria, bile acids are a class of atypical steroids produced in mammals. Bile acid receptors are a type of cell membrane and nuclear receptor that is found in several digestive and immune system cells. Bile acids exert the majority of their biological effects by serving as ligands for specific bile acid receptors. In the past, bile acids were widely assumed to aid in intestinal nutrition absorption and biliary transport of lipids, toxic metabolites, and foreign substances. However, it is now well established that bile acids can act as multidirectional signaling metabolites, modulating physiopathological processes associated with a variety of digestive diseases *via* dynamic interactions with germline-encoded host receptors and microbiota[10-12]. In particular, in IBD, bile acids can modulate IBD pathophysiological pathways by acting on several bile acid receptors, including farnesol X receptor (FXR), retinoid-related orphan receptor γt (RORγt), G protein-coupled bile acid receptor 1 (GPABR1), vitamin D receptor (VDR), pregnane X receptor (PXR), constitutive androstane receptor (CAR), and sphingosine-1-phosphate receptor 2 (S1PR2)[13] (Table 1). This review primarily outlines the growing function of bile acids and their receptors in IBD, as well as their prospective therapeutic applications. Furthermore, we explore bile acid metabolism and the interaction of bile acids and microbiota to present fresh perspectives and molecular targets for diagnosing and treating IBD.

BILE ACID METABOLISM

Bile acids are the end product of cholesterol metabolism. Bile acids are composed mainly of cholesterol, and unlike other steroid hormones, bile acids are amphiphilic molecules with a hydrophobic (beta side) and a hydrophilic (alpha side) surface. They have detergent properties due to their amphiphilic nature, which helps to solubilize lipids in micelles, facilitating emulsification and absorption of dietary fatty acids and cholesterol[14,15]. Mammals have two main types of bile acids: Primary bile acids (PBAs) and secondary bile acids (SBAs). PBAs are formed by cholesterol catabolism in hepatocytes, whereas SBAs are derivatives of PBAs and are generated by the gut microbiome. The bile acid pool is maintained in balance by their hepatic synthesis, enterohepatic circulation, and microbial metabolism[16] (Figure 1).

Bile acid metabolism in the liver

In the liver, cholesterol is generated in the central hepatocyte in several steps to produce PBAs of 24 carbons. In humans, cholic acid (CA) and chenodeoxycholic acid (CDCA) are the most prevalent PBAs, while rats create the 6-hydroxylated

Table 1 Nuclear and membrane receptors of bile acids

Bile acid receptor	Abbreviation	Type	Bile acid agonists	Main tissue distribution
Farnesol X receptor	FXR	Nuclear hormone receptor	CDCA > DCA > LCA > CA	Intestinal epithelial cells, hepatocytes
Retinoid-related orphan receptor γt	RORγt	Nuclear hormone receptor	3oxo-LCA, isoLCA	Th17 cells, ILC3 and γδT cells
G protein-coupled bile acid receptor 1	GPBAR1 or TGR5	Membrane-bound receptor	LCA > DCA > CDCA > UDCA > CA	Epithelial cells, immune cells, and intestinal nerves in the gut and biliary tract
Vitamin D receptor	VDR	Nuclear hormone receptor	LCA, 3-oxoLCA, and isoalloLCA	Intestinal epithelial cells
Pregnane X receptor	PXR	Nuclear hormone receptor	CDCA, LCA	Intestinal epithelial cells, hepatocytes
Costitutive androstane receptor	CAR	Nuclear hormone receptor	CDCA, LCA	Hepatocytes
Sphingosine-1-phosphate receptor 2	S1PR2	Membrane-bound receptor	GCA, TCA, GCDCA and TCDCA	Intestinal epithelial cells, hepatocytes

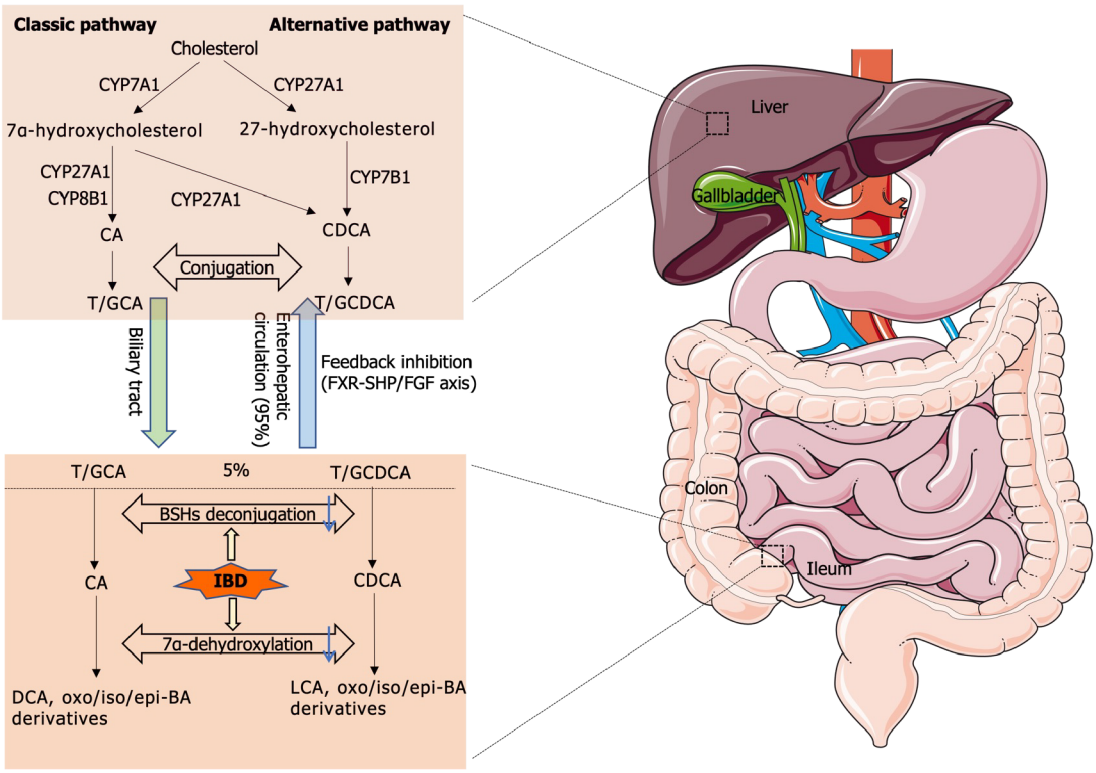
DCA: Deoxycholic acid; LCA: Lithocholic acid; CA: Cholic acid; CDCA: Chenodeoxycholic acid; isoLCA: Isolithocholic acid; isoalloLCA: Isoallolithocholic acid; 3-oxoLCA: 3-oxolithocholic acid; FXR: Farnesoid X receptor; GPABR1: G protein-coupled bile acid receptor 1; PXR: Pregnane X receptor; VDR: Vitamin D receptor; RORγt: Retinoid-related orphan receptor γt; CAR: Costitutive androstane receptor; S1PR2: Sphingosine-1-phosphate receptor 2; GCA: Glycocholic acid; TCA: Taurocholic acid; GCDCA: Glycochenodeoxycholic acid; TCDCA: Taurochenodeoxycholic acid.

versions of CA and CDCA, named muricholic acid (MCA)[17]. The conventional or alternative/acidic pathways are both possible for this process to take place in the human liver. The first limiting step in the conventional route is the 7-hydroxylation of cholesterol catalysed by cholesterol-7-hydroxylase (CYP7A1), which irreversibly transforms cholesterol to 7-hydroxycholesterol. This intermediate is then converted to 7α-hydroxy-4-cholesten-3-one by 3β-hydroxy-Δ5-C27-steroid oxidoreductase, which can be used for generating both CA and CDCA in the classic pathway. In contrast, the alternative/acidic pathway begins with the conversion of cholesterol by sterol 27-hydroxylase (CYP27A1) to 27-hydroxy-cholesterol, followed by B-ring hydroxylation and metabolic side chain modification by oxysterol 7-hydroxylase (CYP7B) to create CDCA. The alternate pathway generates solely CDCA, which accounts for 10% of the liver's total bile acids[18-20]. Subsequently, PBAs are converted to tauro-CA (TCA) and tauro-CDCA (TCDCA) and glyco-CA (GCA) and glyco-CDCA (GCDCA), respectively, by the actions of BA-CoA synthase and BA-CoA amino acid N-acetyltransferase. Conjugation turns bile acids into stronger acids and increases their aqueous solubility at acidic pH and the retention of their amphiphilic structure. This limits their passive reabsorption and is essential for their lipid emulsification activity in the acidic environment of the duodenum[21,22]. Notably, conjugation with glycine is common in the human liver, accounting for 90% of the bile acid pool. However, approximately 95% of PBAs in mice are taurine-conjugated[23]. Conjugated bile acids will be stored in the gallbladder, forming bile with phospholipids, cholesterol, and other components. Finally, the gallbladder releases bile acids into the duodenum after each meal[24].

Bile acid metabolism in the intestine

Upon release into the small intestine, bile acids form micelles with cholesterol and dietary fats to facilitate their dissolution and absorption[25,26]. However, conjugated bile acids are not absorbed and are instead retained in the small intestine. At the end of the ileum, approximately 95% of the conjugated bile acids are reabsorbed *via* the apical sodium-dependent bile acid transporter (ASBT) and enter the liver *via* the portal vein[27]. It is estimated that humans complete the enterohepatic circulation of bile acids between six and eight times a day, depending on their dietary habits. The bile acid pool in healthy persons remains between 4 and 6 g. In contrast, changes in the intestinal epithelium of individuals with IBD decrease the reabsorption of bile acids by ASBT and increase the number of bile acids discharged in the feces [28]. It is important to note that the bile acid pool that is returned from the ileum to the liver directly suppresses the production of new bile acids in hepatocytes through FXR, FXR-dependent transactivation of the small isomeric partner (SHP), and SHP-mediated suppression of CYP7A1 and CYP8B1 expression[17,29,30]. In addition, bile acid-activated FXR drives fibroblast growth factor (FGF-15/19; FGF-15 in mice and FGF-19 in humans) expression in intestinal epithelial cells (IECs). Subsequently, FGF-15/19 is secreted into the portal circulation, translocated to the liver, binds to heterodimeric receptors on hepatocytes, and reduces hepatic bile acid synthesis by inhibiting CYP7A1 expression[26,31].

The intestinal microbiota can be directly involved in the biotransformation of bile acids through microbial enzymes. The five known mechanisms of bile acid metabolism by the intestinal microbiota are dehydroxylation, dehydration, exo-embedding of the cholesterol backbone, depolymerization of amino acids (glycine or taurine), and amide conjugation of the bile acid backbone with the amino acids phenylalanine, tyrosine, and leucine. Many potential mechanisms still exist to be discovered and explored[32]. Approximately 5% of bile acids are retained in the intestinal lumen for further metabolism by the intestinal microbiota to generate SBAs *via* the aforementioned processes[33]. In particular, the depolymerization reaction of bile acid metabolism is first carried out by the gut bacteria (enzymatic hydrolysis of the C-24N-



DOI: 10.3748/wjg.v29.i27.4252 **Copyright** ©The Author(s) 2023.

Figure 1 Synthesis, recirculation, and microbial modification of bile acids in the gut. Bile acids are synthesized from cholesterol in the liver. In the classical pathway, cholesterol-7α-hydroxylase converts cholesterol to 7α-hydroxycholesterol, which is then metabolized to cholic acid *via* mitochondrial sterol-27-hydroxylase (CYP27A1) or CYP8A1, or to chenodeoxycholic acid (CDCA) *via* CYP27A1. In the alternative pathway, CYP27A1 begins the conversion of cholesterol to 27-hydroxycholesterol, which is then metabolized to CDCA by oxysterol 7α-hydroxylase. These primary bile acids are then conjugated with taurine or glycine and then released into the bile for secretion into the duodenum. At the end of the ileum, 95% of the conjugated bile acids (BAs) are reabsorbed through the enterohepatic circulation, while the remaining 5% depolymerizes and enters the colon, where BAs undergo a series of chemical modifications by intestinal bacteria, including catabolism, desulfurization, dehydrogenation, dehydroxylation, and exo-embedding reactions to form secondary bile acids (mainly lithocholic acid and deoxycholic acid) and their oxidative, isomeric, and exo-derivatives. IBD: Inflammatory bowel disease; CA: Cholic acid; CDCA: Chenodeoxycholic acid; GCA: Glycocholic acid; TCA: Taurocholic acid; GCDCA: Glycochenodeoxycholic acid; TCDCA: Taurochenodeoxycholic acid; DCA: Deoxycholic acid; LCA: Lithocholic acid; BA: Bile acid; CYP7A1: Cholesterol-7α-hydroxylase; CYP27A1: Mitochondrial sterol-27-hydroxylase; CYP8B1: Sterol-12α-hydroxylase; CYP7B1: Oxysterol 7α-hydroxylase; BSHs: Bile salt hydrolases; FXR: Farnesol X receptor; FGF: Fibroblast growth factor; SHP: Small isomeric partner.

acylamide bond). Bile salt hydrolases (BSHs), which are extensively found in both Gram-positive and Gram-negative bacteria in the gut, including *Clostridium*, *Bifidobacterium*, *Lactobacillus*, *Bacteroides*, and *Enterococcus*, mediate this process [34]. It eliminates the glycine or taurine conjugates and stops the small intestine's active reabsorption. The depolymerized PBAs are then converted to SBAs in the colon by dehydroxylation at the carbon-7 position. Bacteria that express 7-dehydroxylases, such as *Clostridiu*m and *Eubacterium*, play a major role in mediating this process. The two SBAs that are most frequently produced by these reactions are lithocholic acid (LCA from CDCA) and deoxycholic acid (DCA from CA). Additionally, a variety of oxo-, iso-, and epi-derivatives of bile acids can also arise in the colon as a result of different intestinal microbiota dehydrogenation and exo-embedding processes[35]. For example, in *Escherichia*, *Clostridium*, *Bacteroides*, and *Eubacerium*, C7β exochimerization of CDCA can occur to produce the 7β exochimer, 3α-,7β-dihydroxy-5β-cholic acid, also known as ursodeoxycholic acid (UDCA)[36]. The complete metabolic pathway for the conversion of PBAs (CA and CDCA) to the two major SBAs (DCA and LCA) has been identified[37]. It is still unclear how the gut microbiota converts PBAs into other bile acid derivatives. Moreover, it is not clear which exact bacterial species or strains are required for these processes. Furthermore, it is noteworthy that the gut microbiota can also regulate the hepatic enzymes CYP7A1 and CYP27A1, thus affecting the synthesis of bile acids in the liver[38].

The intestines of IBD patients have been found to have dysbiosis of the intestinal bacterial flora and a considerable loss in microbial diversity. Most importantly, the abundance of bacteria containing BSH and bile acid-inducible enzymes (BAIs), such as *Firmicutes, Ruminococcaceae, Lachnospiraceae*, and *Eubacterium*, was decreased. This alteration reduces depolymerization and 7α-dehydroxylation, strongly decreasing the conversion capacity of the microbiota, resulting in a decrease in SBAs (DCA and LCA) and an elevation in primary and conjugated bile acids (CA, CDCA, TCA, and GCA)[39-41]. Multiple risk factors (genetics, psychological factors, Western food, and antibiotics) may lead to intestinal flora dysbiosis and bile acid abnormalities, which are linked to the pathophysiology of IBD[42]. Notably, it has been reported that disturbances in bile acid metabolism will, in turn, exacerbate IBD damage, affect intestinal stem cell differentiation and renewal, and impair intestinal mucosal barrier function[30].

Notably, the composition of the microbiota is directly or indirectly affected by bile acids in several studies. It has been shown that bile acids inhibit bacteria by increasing cell membrane permeability and causing cell damage, as well as causing oxidative DNA damage in bacteria. Alternatively, bile acids can indirectly influence bacterial growth through FXR and VDR[40]. The overall number of bacteria in rats' feces decreased with increased CA concentration in their meal, as determined by DAPI staining, sequencing of 16S rRNA gene clone libraries, and FISH analysis. The proportion of *Bacteroidetes* and *Actinobacteria* decreased dramatically in the CA-fed group, whereas the proportion of Firmicutes increased significantly[43]. Considered together, bile acids and the gut microbiota have a bidirectional effect on each other, and this balance is critical for human health and disease.

IMPACT OF BILE ACIDS AND THEIR RECEPTORS IN IBD

FXR

FXR is a nuclear receptor belonging to a subclass of metabolic receptors, first described by Forman *et al*[44] in 1995. FXR is predominantly found in intestinal epithelial cells, hepatocytes, and some immune cells (such as macrophages and dendritic cells) of the colon and liver[45]. Its main endogenous ligand is bile acids, in the order of FXR activation potency: CDCA > DCA > LCA > CA. Numerous studies demonstrate that through modulating bile acid metabolism, FXR can improve the pathogenesis of IBD. The enzyme CYP8B1, which synthesises CA, was increased in the liver of mice with colitis. Chen *et al*[30] found that mucosal barrier repair was impaired in CYP8B1 overexpressing mice, which resulted in more severe colitis. The specific mechanism was shown that CA leads to impaired fatty acid oxidation (FAO) and LGR5+ intestinal stem cell (ISC) renewal through inhibition of peroxisome proliferator-activated receptor alpha (PPARα). Surprisingly, they found that activation of FXR inhibited hepatic CYP8B1 expression and ameliorated colitis in mice. FGF19-M52, an analog of FGF19, has been reported to inhibit bile acid synthesis, modulate bile acid pool composition, and inhibit intestinal inflammation in mice. The particular mechanisms underlying these processes are associated with maintaining intestinal epithelial barrier integrity, suppressing inflammatory immune responses, and controlling microbial composition. However, the FGF19-M52-induced anti-inflammatory effect was completely abolished in FXR-deficient animals[46]. In addition, in UC mouse models, dextran sodium sulfate (DSS)-induced colitis activates the intestinal PPARα-UDP-glucuronosyltransferases (UGTs) axis, which inhibits downstream FXR-FGF15 signaling, resulting in up-regulation of hepatic CYP7A1 and promotion of hepatic bile acids synthesis. Both inhibition of PPARα and stimulation of the FXR-FGF15 axis greatly decreased colitis induced by DSS[47]. As a result, intestinal FXR-FGF15 signaling may play a key role in controlling bile acid homeostasis and colitis development.

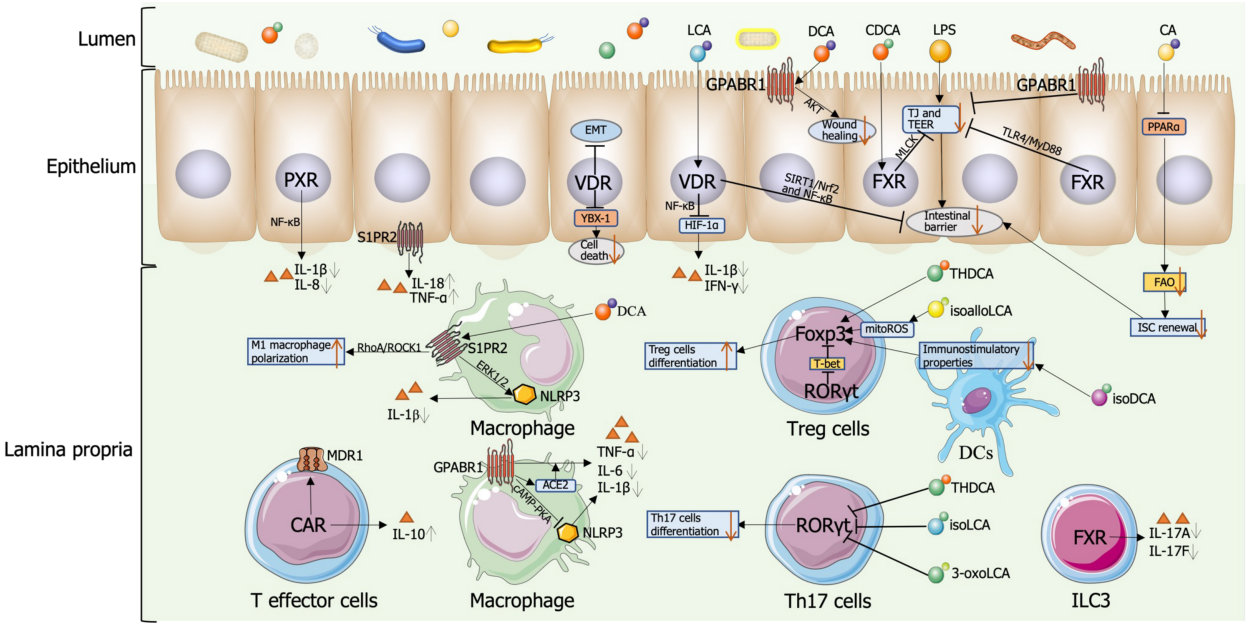
Mammalian innate lymphocyte type 3 (ILC3) is important in IBD, especially in innate intestinal immunity and mucosal barrier function[48]. Activation of FXR has been reported to block the production of IL-17A and IL-17F in ILC3, thereby eliminating ILC3-dependent intestinal inflammation and attenuating IBD injury. Interestingly, they also found that activation of FXR reduced characteristic transcription factors (including Batf3 and Tcf7)[49]. Transforming growth factor-beta (TGF-β) belongs to a family of multifunctional polypeptides produced by non-lymphoid cells and various lymphocytes. Previous studies have shown that TGF-β is essential for regulating immune cells and that TGF-β production is also associated with the pathogenesis of colitis. This implies that the pathological changes in UC may be caused by disorders of the TGF-β pathway[50]. A recent study revealed that a high-fat diet accelerated the course of DSS-induced UC and led to the down-regulation of FXR target genes (*FXR*, *Shp*, and *Ibabp*). The addition of the FXR agonist FexD repaired the high-fat diet-induced phenotype, whereas the TGF-β inhibitor SB431542 prevented FexD's restorative activity in DSS-induced UC mice[51]. This study showed that FXR alleviates inflammation in UC through a TGF-β-dependent pathway. In conclusion, these findings suggest that FXR can improve IBD by modulating intestinal immunity.

Western diets have high levels of fecal DCA, a substance that can cause inflammation in the intestines. The researchers discovered that mice fed a DCA-supplemented diet showed localised ileal and colonic inflammation, as well as changes in gut microbiota composition and faecal bile acid buildup. Dysregulation of gut microbiota homeostasis induced by DCA reduced bile acid depolymerization. This regulation was associated with the repressed expression of target genes in the FXR-FGF15 axis, leading to increased hepatic *de novo* bile acid synthesis. These results suggest that DCA-induced intestinal dysbiosis may be a key etiology of intestinal inflammation associated with disturbed bile acid metabolism and down-regulation of the FXR-FGF15 axis[52]. Subsequently, Xu *et al*[53] used the FXR agonist fexaramine to restore intestinal FXR activity. Activating FXR increased the abundance of bacteria producing short-chain fatty acids and normalized bile acid metabolism. DCA-induced intestinal inflammation can be reduced by targeting the FXR-gut microbiota signaling pathway.

In addition, FXR may ameliorate IBD through modifying the function of the intestinal mucosal barrier. By blocking lipopolysaccharide (LPS)-induced activation of the myosin light chain kinase (MLCK) pathway in an FXR-dependent manner, Song *et al*[54] showed that CDCA reversed LPS-induced decreases in intestinal permeability and tight junction protein expression and mitigated LPS-induced intestinal barrier breakdown. In another study, using the FXR agonist GW4064 to restore FXR activity, Liu *et al*[55] discovered that activation of FXR attenuates intestinal tight junction damage by inhibiting the LPS-induced TLR4/MyD88 signaling pathway. In summary, these recent findings suggest that FXR can influence the pathophysiological processes of IBD by regulating bile acid metabolism, intestinal immunity, intestinal flora, and intestinal mucosal barrier function (Figure 2). Activation of FXR may be considered a new therapeutic strategy for IBD.

RORγt

RORγ is one of three retinoid-related orphan nuclear receptors with two main isoforms: RORγ1 and RORγt (or RORγ2),



DOI: 10.3748/wjg.v29.i27.4252 **Copyright** ©The Author(s) 2023.

Figure 2 Emerging role of bile acids and their receptors. DCA: Deoxycholic acid; LCA: Lithocholic acid; CA: Cholic acid; CDCA: Chenodeoxycholic acid; isoLCA: Isolithocholic acid; isoalloLCA: Isoallolithocholic acid; 3-oxoLCA: 3-oxolithocholic acid; isoDCA: 3β-hydroxydeoxycholic acid; THDCA: Taurohyodeoxycholic acid; LPS: Lipopolysaccharide; FXR: Farnesoid X receptor; GPABR1: G protein-coupled bile acid receptor 1; PXR: Pregnane X receptor; VDR: Vitamin D receptor; RORγt: Retinoid-related orphan receptor γt; CAR: Costitutive androstane receptor; S1PR2: Sphingosine-1-phosphate receptor 2; Th17 cells: T helper 17 cells; Treg cells: Regulatory T cells; ILC3: Innate lymphocyte type 3; DCs: Dendritic cells; ISC: Intestinal stem cell; YBX-1: Y box binding protein 1; ACE2: Angiotensin-converting enzyme 2; NLRP3: The NACHT, LRR, and PYD domains-containing protein 3; mitoROS: Mitochondrial reactive oxygen species; EMT: Epithelial-mesenchymal transition; FAO: Fatty acid oxidation; PPARα: Peroxisome proliferator-activated receptor alpha; TLR4: Toll-like receptor 4; TJ: Tight junction; TEER: Trans-epithelial electrical resistance; TLR4: Toll-like receptor 4.

encoded by the *RORC* gene. RORγ1 is normally involved in the regulation of transcription of metabolic genes and some circadian rhythms in the liver and adipose tissue. However, the expression of RORγt is restricted to specific subpopulations of lymphoid spectrum immune cells, namely T helper 17 (Th17) cells, ILC3, and γδ T cells[19,56]. Recently, increasing attention has turned to RORγt, as it acts as a key transcription factor for Th17 cell and regulatory T(Treg) cell differentiation in IBD (Figure 2). Moreover, ROR-γt can depend on ILC3 to provide protective immunity[23,48]. Hang *et al* [57] discovered that 3-oxolithocholic acid (3-oxoLCA) decreased Th17 cell differentiation by directly interacting with the important transcription factor RORγt by giving mice 3-oxoLCA and isoallolithocholic acid (isoalloLCA). In contrast, isoalloLCA decreases intestinal inflammation by increasing Treg cell differentiation by generating mitochondrial reactive oxygen species (mitoROS), which enhances the expression of Forkhead box P3 (Foxp3). Interestingly, similar to 3-oxoLCA, isolithocholic acid (isoLCA) can also de-suppress Th17 cell differentiation by inhibiting RORγt[58]. In *in vivo* models, another study demonstrated that the secondary bile acid 3β-hydroxydeoxycholic acid (isoDCA) promotes Treg cell differentiation by increasing the induction of Foxp3 through its action on dendritic cells (DCs). Surprisingly, the researchers found that disruption of FXR in DCs enhanced Treg cell generation[59]. In addition, taurohyodeoxycholic acid (THDCA) was reported to not only inhibit RORγt-mediated Th17 cell differentiation, but also trigger Foxp3 expression and promote Treg cell differentiation[60]. These recent findings demonstrate the potential of bile acid derivatives to improve IBD prognosis by acting on RORγt. Kathania *et al*[61] identified a serine/threonine kinase, Pak2, directly associated with RORγt. Pak2 recognizes the conserved KRLS motif within RORγt and phosphorylates S-316 within this motif. Genetic deletion of Pak2 in Th17 cells decreases RORγt phosphorylation, increases IL-17 expression, and induces severe colitis after adoptive transfer to Rag1-/- mice. This suggests that other biological molecules *in vivo* can also regulate the developmental process of IBD by acting on RORγt and are potential targets for the treatment of IBD to be explored further.

RORγt+ immune cells are generally thought to coordinate immunity, inflammation, or tolerance in the gut. In IBD, the function of RORγt+ immune cells can be significantly altered[62-64]. According to a recent study, ILC3 in intestinal draining lymph nodes expressed numerous significant class II histocompatibility complexes (MHCIIs). To increase microbiota-specific RORγt+ Treg cells and prevent them from proliferating into inflammatory Th17 cells, ILC3 is both essential and sufficient. AlphaV integrin, competing IL-2, and ILC3-mediated antigen presentation all contributes to this impact. Single cell analysis indicated that in IBD, the interaction between ILC3 and RORγt+ Treg cells was impaired[65]. It is interesting to note that Akagbosu *et al*[66] described a class of RORγt+ antigen-presenting cells dubbed Thetis cells. These cells had dendritic cell and medullary thymic epithelial cell (mTEC) transcriptional signatures. Colitis results from the loss of MHCII or ITGB8 by Thetis cells, which severely impairs peripheral Treg (pTreg) cell differentiation in the intestine. MHCII expression by RORγt+ ILC3 and classic dendritic cells, in contrast, is neither sufficient nor essential for pTreg cell formation. In a colitis model, Liu *et al*[67] demonstrated that *Akkermansia muciniphila* improves colitis by up-

regulating the RORγt+ Treg cell-mediated immune response, and this process is regulated by Toll-like receptor 4 (TLR4). RORγt is a main transcription factor for Th17 cells. However, in the intestine, RORγt is co-expressed in peripherally induced pTreg cells together with Foxp3. Surprisingly, Bhaumik *et al*[68] observed that RORγt-mediated T-bet inhibition is essential for regulating the immunosuppressive function of pTreg cells in inflammatory states, restoring Foxp3 expression, and preventing the onset of severe colitis. Despite these advancements, the full-spectrum cellular heterogeneity of RORγt+ immune cells, the potential for functional interactions between subpopulations, and the specific mechanisms influencing the pathophysiological processes of IBD in the context of complex microbiota remain unknown and require further investigation.

GPABR1

Kawamata *et al*[69] first described GPABR1 (TGR5 or M-BAR) in 2003 as a receptor for bile acids in the membrane. GPABR1 is mainly found in epithelial cells, immune cells, and intestinal nerves in the gut and biliary tract and belongs to the superfamily of G protein-coupled receptors. Bile acids agonistically affect GPABR1 in different ways: LCA > DCA > CDCA > UDCA > CA[20]. The adaptor apoptosis-associated speck-like protein containing a caspase recruitment domain, sensor NLRP3, and procaspase-1 form the cytosolic polyprotein complex NLRP3 inflammasome. The pathogenesis of IBD is closely linked to the NLRP3 inflammasome[70,71]. An *in vivo* experimental study showed that bile acids could inhibit NLRP3 inflammasome-dependent inflammation *via* the GPABR1-cAMP-PKA axis, suggesting GPABR1 as a potential target for alleviating intestinal inflammation in IBD[72]. Biagioli *et al*[73] found that activation of GPBAR1 can lower macrophage inflammatory gene expression (mRNA for TNF-α, IL-1, IL-6, and CCL2), hence reducing inflammation in animal models of IBD. Deletion of the anti-inflammatory gene angiotensin-converting enzyme 2 (*ACE2*) from mice with colitis resulted in worse inflammation[74]. Biagioli *et al*[75] further discovered that activation of GPBAR1 could regulate ACE2 colonic expression through a glucagon-promoting factor glucagon-like peptide (GLP)-1-dependent mechanism. Furthermore, the regulation of *ACE2* mRNA in the colitis setting may contribute to the anti-inflammatory effects of GPBAR1. A recent study showed that supplementation with LCA and DCA reduced intestinal inflammation in three mouse models of colitis. This anti-inflammatory effect partially depends on GPABR1[76].

AKT, a serine/threonine kinase, is crucial for the differentiation, proliferation, survival, and metabolism of cells. In a mouse model of DSS-induced colitis and the colonic epithelium of UC patients, Azuma *et al*[77] showed that DCA could slow wound healing in the colonic epithelial cell environment by acting as a ligand for GPABR1 to activate the AKT signaling pathway. Interestingly, another recent study showed that in a Caco-2 cell model, GPABR1 activation ameliorated LPS-induced reduction in trans-epithelial electrical resistance (TEER) and up-regulated tight junction protein expression, thereby enhancing mucosal barrier function to alleviate the progression of IBD[78]. However, inhibition of GPABR1 expression in the porcine jejunal epithelial cell line IPEC-J2 did not affect the function of the intestinal barrier [54]. This may be due to the different expression levels of GPABR1 in different intestinal slices. In conclusion, these findings suggest that GPABR1 plays different roles in the gastrointestinal tract of IBD (Figure 2). Moreover, the functions of GPABR1 may also differ due to differences in species and cell types. Therefore, the role of GPABR1 on the pathophysiological mechanisms of IBD deserves further investigation.

VDR

A nuclear receptor activated by 1,25-dihydroxyvitamin D is the VDR. The human metabolism, immunity, and cancer are all regulated by this receptor, which is widely expressed in a range of tissues. Additionally, the secondary bile acid LCA and its metabolites (3-oxoLCA and isoalloLCA) can activate VDR[79,80]. LCA was reported to ameliorate the TNF-α-induced decrease in the expression and distribution of tight junction proteins (ZO-1, occludin, and claudin-1) through activation of VDR. Furthermore, it significantly blocked TNF-α-mediated down-regulation of the oxidative stress-related genes silent information regulator 1 (*SIRT1*), nuclear factor erythroid 2-related factor 2 (*Nrf2*), and heme oxygenase-1. In addition, the TNF-α-induced increase in NF-κB p-p65 and p-IκB-α was significantly suppressed by LCA[81]. This study reveals that LCA strongly protects against TNF-α-induced intestinal barrier degradation *via* VDR. Activation of hypoxia-inducible factor 1α (HIF-1α) as a heterodimeric transcription factor has been shown in previous research to accelerate the course of DSS-induced colitis in mice[82,83]. However, the association of VDR signaling and HIF-1α in the development of IBD has been enigmatic. A recent study showed that in an animal model of colitis, VDR signaling suppressed the overexpression of HIF-1α in colonic epithelial cells by regulating the NF-κB pathway, thereby inhibiting the overproduction of interferon-gamma (IFN-γ) and IL-1β in these cells and attenuating the development of colitis in the animal model[84]. Another study showed that VDR could physically bind to Y box binding protein 1 (YBX-1), blocking its nuclear translocation, thus ameliorating the death of colonic epithelial cells in the presence of inflammation[85]. Furthermore, Fernández-Barral *et al*[86] demonstrated for the first time that activation of VDR can regulate stemness-related genes, including *LGR5, SMOC2, LRIG1, MSI1, PTK7*, and *MEXA*, and decrease cell proliferation in LGR5+ human colonic stem cells. This function is essential for maintaining colonic epithelial homeostasis in IBD.

Paneth cells, which are positioned at the base of small intestinal crypts, release α-defensins and play a crucial role in regulating intestinal flora and preserving intestinal homeostasis[87]. Paneth cells showed a significant decrease in lysozyme activity, a diminished inhibition of pathogenic bacterial growth, and a reduced autophagic response in a Paneth cell-specific VDR knockout mouse model, resulting in an increased inflammatory response. These findings suggest the importance of VDR on Paneth cells in IBD in preventing intestinal inflammation[88]. Claudin-2 is a linker protein that mediates water transport between epithelial cells, and elevated claudin-2 has been reported to be associated with active human IBD[89]. Another study showed that in a Salmonella colitis model and a DSS-induced colitis model, VDR deficiency may lead to claudin-2 hyperfunction and increased permeability in an inflammatory state, resulting in more severe intestinal leakage and intestinal inflammation in mice[90]. This study highlights the importance of VDR in intestinal mucosal barrier function. In addition, intestinal fibrosis is a common complication of CD. The epithelial-

mesenchymal transition (EMT) describes the process by which epithelial cells change from epithelial to mesenchymal cells, a crucial component of fibrogenesis. In addition to inhibiting fibroblast activation and epithelial mitochondria-mediated EMT, Yu *et al*[91] revealed that VDR activation attenuates intestinal fibrosis.

Several recent studies have shown that colonic mucosal VDR expression is reduced in patients with IBD and that VDR transcript expression negatively correlates with IBD inflammation[92,93]. Yang *et al*[94] found that dysbiosis of the gut microbiota and altered fecal bile acids could regulate the immune response in UC patients. VDR may alleviate intestinal inflammation by down-regulating NF-κB signaling and activating autophagy. These findings suggest that restoring intestinal VDR expression in IBD may be a viable therapeutic strategy. In conclusion, these findings contribute to a better understanding of the role of VDR in the etiology of IBD and serve as a significant reference for future research aimed at developing more effective therapeutic options (Figure 2).

PXR and CAR

PXR and CAR are members 2 and 3 of nuclear receptor subfamily 1, group I, NR1I2, and NR1I3, respectively. PXR was first described as a major regulator of CYP family 3 subfamily A (CYP3A) transcription by Kliewer *et al*[95] and Lehmann *et al*[96] in 1998. In contrast, CAR was first reported by Baes *et al*[97] in 1994 and was later found to be a transcriptional regulator of CYP2B6. PXR and CAR have the typical modular nuclear receptor structure, which consists of a hinge, a DNA-binding domain, a ligand-binding domain, activation function 1, and activation function 2. In addition to many endogenous and exogenous complex ligands, several subsequent studies have shown that PXR and CAR are hybrid receptors that can also accommodate LCA and CDCA and function as sensors for LCA and CDCA[98]. PXR and CAR are key transcription factors that regulate intestinal homeostasis. Uehara *et al*[99] demonstrated that PXR might reduce apoptosis in a mouse model of DSS-induced colitis by lowering the mRNA expression of pro-inflammatory cytokines (TNF-α and IL-1β). CAR inhibits apoptosis by inducing Gadd45b. Both of them protected mice from DSS-induced colitis. Interestingly, they also observed that the protective effect of FXR activation on CAR knockout mice and the protective effect of CAR activation on PXR knockout mice were reduced. CAR and PXR can synergistically ameliorate DSS-induced colitis. Another study showed that PXR and CAR deficiency synergistically increased the pro-inflammatory bacteria *Helicobacteraceae* and *Helicobacter* and the relative abundance of *Lactobacillus*. *Lactobacillus* has BSHs activity, corresponding to a decrease in primary taurine-bound bile acids in feces. This may lead to an increased internal burden of taurine and unbound bile acids, which are associated with inflammation, oxidative stress, and cytotoxicity[100].

The metabolism of tryptophan produces indole-3-propionic acid (IPA) in the intestine *via Clostridium perfringens*. Previous studies have shown that it can affect mucosal barrier function and inflammation through interaction with PXR [101]. Flannigan *et al*[102] found that PXR-deficient myofibroblasts overreact to stimuli and produce higher inflammatory mediators. In addition, biopsies from CD and UC patients revealed a correlation between decreased PXR expression and increased expression of fibrosis and innate immune genes. Intriguingly, they discovered that IPA decreased intestinal inflammation and fibrosis in mice with DSS-induced colitis *via* activating PXR, whereas microbiota removal increased intestinal inflammation and fibrosis[102]. These findings suggest that the interaction of the microbiota metabolite IPA with PXR may be an important determinant of the progression of fibrotic complications in IBD. In addition, Deuring *et al* [103] found a strict negative association between colonic epithelial PXR levels and NF-B target gene expression in CD patient colon biopsy tissue. During IBD, their findings show that PXR is a substantial and clinically relevant antagonist of NF-B activity in the intestinal epithelium[103].

MDR1 is a membrane-associated, ATP-dependent efflux pump preferentially expressed in intestinal and circulating human CD4+ effector T cells[104]. Chen *et al*[105] discovered CAR as a regulator of MDR1 expression in T cells that prevents bile acid toxicity and inflammation in the mouse small intestine. Activation of CAR induces not only the expression of detoxifying enzymes and transporters in CD4+ T effector cells in the lamina propria of the small intestine, but also the expression of the key anti-inflammatory cytokine IL-10. The activation of these programs provides an unexpected strategy for treating IBD and defines the subspecialization of lymphocytes in the small intestine.

S1PR2

S1PR2 is highly expressed in the ileum and colon, and it can be activated by the conjugated main bile acids GCA and TCA as well as GCDCA and TCA[23]. Vascular and immune dysfunction is thought to be involved in the pathogenesis of IBD, but the exact mechanisms of mucosal vascular endothelial barrier dysfunction and macrophage phenotypic transformation are not fully clarified. Wang *et al*[106] discovered that S1PR2 expression was considerably enhanced in intestinal mucosal vascular endothelial cells and macrophages from IBD patients and animals with DSS-induced colitis, as well as in vascular endothelial cells and macrophages treated with LPS *in vitro*. Knockdown or inhibition of S1PR2 expression significantly reduced the expression of RhoA and ROCK1 in vascular endothelial cells and macrophages. Furthermore, they discovered that inhibiting S1PR2 and ROCK1 reversed impaired vascular barrier function and M1 macrophage polarisation *in vivo* and *in vitro*, while decreasing endoplasmic reticulum stress and macrophage glycolysis in vascular endothelial cells, and reversing LPS-induced impairment of M1 macrophage polarisation and vascular endothelial cell barrier dysfunction. The results imply that the S1PR2/RhoA/ROCK1 signalling pathway, which regulates vascular endothelial cell barrier function and M1 macrophage polarisation, may have a role in the aetiology of IBD[106]. Chen *et al*[107] previously demonstrated that S1PR2 is abundantly expressed in intestinal epithelial cells and stimulates IEC proliferation and migration. However, the precise role of S1PR2 in UC is unknown. They recently discovered that S1PR2 may play a significant role in intestinal epithelial cell proliferation and barrier maintenance by influencing the expression levels of SphK2, HDAC1, HDAC2, and ERK1/2 signaling pathways. Surprisingly, they discovered that inhibiting S1PR2 in the UC mouse model might also reduce the severity of colonic pathological injury in mice, which was followed by a drop in TNF-α and IL-18 Levels in their serum[107]. These findings reveal that S1PR2, despite its beneficial effects on intestinal epithelial cell proliferation and barrier maintenance, may be a key pathogenic

factor in UC. In addition, researchers discovered that DCA dose-dependently increased S1PR2 expression in a mouse model of colitis. Meanwhile, at least in part, DCA-induced NLRP3 inflammasome activation was achieved by stimulating the ERK1/2 signaling pathway downstream of S1PR2 to promote cathepsin B release. S1PR2/ERK1/2/cathepsin B signaling is key in triggering DCA activation of inflammatory vesicles[108]. The results of this study suggest that S1PR2 should be investigated further as a possible treatment for IBD.

POTENTIAL THERAPEUTIC TARGETS OF BILE ACIDS AND THEIR RECEPTORS IN IBD

Bile acid receptor agonists or inhibitors

Based on growing knowledge and understanding of the mechanism of action of bile acid receptors, the development of medications targeting the bile acid receptor activity that changes considerably during the progression of IBD may give a more specific therapeutic effect. The development of bile acid receptor agonists or antagonists is widely recognized as a promising therapeutic avenue for treating IBD and is a hot area of research (Table 2). Recently, Miyazaki *et al*[109] showed that administration of the novel FXR agonist nelumal A induced the expression of FXR target genes and tight junction proteins in the intestine while decreasing the expression of hepatic bile acid synthesis genes, effectively reducing colitis and inhibiting colitis-related carcinogenesis. Another study found that the FXR agonist nigakinone alleviated DSS-induced experimental colitis *via* regulating bile acid profile and the FXR/NLRP3 signaling pathway. It inhibited inflammatory cytokine production by activating the FXR/NLRP3 signaling pathway and regulated bile acid metabolism by controlling cholesterol hydroxylase and FXR-mediated transporter proteins, reducing bile acid accumulation in the colon and thereby reducing colitis[110]. Although FXR agonists exhibit very positive effects, they are also commonly associated with many side effects. Its most common side effects are dose-dependent pruritus and an increased LDL:HDL ratio, which may increase the risk of atherosclerosis. Its long-term efficacy remains to be determined[111]. Qi *et al*[112] used structure-based virtual screening to identify 2',4'-dihydroxy-2,3-dimethoxychalcone (DDC). This is a chalcone derivative enriched in plants and food, located in the binding pocket of RORγt, which can target and inhibit RORγt activity, thereby indirectly stabilizing Foxp 3 expression, achieving regulation of Th17/Treg homeostasis, and improving Th17-mediated inflammation. In another study, Chen *et al*[113] proposed a dual-targeting approach for treating IBD using RORγt and dihydroorotic dehydrogenase (DHODH). Dual RORγt/DHODH inhibitors are expected to reduce RORγt-driven Th17 cell differentiation and attenuate T cell expansion and activation, which may enhance anti-inflammatory effects. They found that the 2-aminotetrahydrobenzothiazole compound 14d could act as a potent dual RORγt/DHODH inhibitor, exhibiting significant *in vivo* anti-inflammatory activity and dose-dependently reducing the severity of DSS-induced acute colitis in mice. Furthermore, by screening a large combinatorial library of 1,5-disubstituted acylated 2-amino-4,5-dihydroimidazoles and using a positional scanning library strategy to rapidly identify a novel class of RORγ inhibitors, Ortiz *et al*[113] found that compound 1295-273 had the highest activity against RORγ in this series, with almost twofold selectivity for this receptor isoenzyme. However, they did not further validate it *via in vivo* or *in vitro* experiments.

Genistein, a key isoflavone, stimulates GPABR1 receptors in a DSS-induced mouse colitis model, dramatically lowering inflammatory cell infiltration and generation of pro-inflammatory mediators in the blood and colon and reducing weight loss and increasing colon length in mice[114,115]. In another study, Nakhi *et al*[116] observed that the acid group of CDCA can be replaced by a wide range of chemical groups that can simultaneously maintain or significantly increase its agonistic potency against GPABR1. In particular, pyrrolidinamide 9 and 1,3,4-oxadiazole analog 23 were 10- and 70-fold more potent than CDCA. There is a slight loss of potency when the hydroxyl group at position 3 of the bile acid scaffold is methylated. Surprisingly, however, a more than 100-fold increase in potency was observed upon methylation of the 7-hydroxyl group of pyrrolidinamide 9. Based on these observations, they synthesized the 7-methylated oxadiazole analogue 17, which proved to be a highly potent agonist at the GPABR1 receptor. However, the specific efficacy has to be further de-validated in IBD models[116]. However, most of the GPABR1 agonists studied are unrestricted GPABR1 agonists, and the pharmacological application would be limited by the systemic targeting effect, with associated side effects such as gallbladder overfilling and gallbladder emptying block. Recently, researchers are exploring a series of intestinal-restricted GPABR1 agonists in an attempt to avoid these side effects. Dipeptidyl peptidase IV (DPP4) is a serine exopeptidase, and DPP4 inhibitors have been reported to reduce colitis *via* the GLP pathway after colonic administration in mice[117]. Recently, Han *et al*[118] identified a series of highly potent intestine-restricted GPABR1-DPP4 bifunctional molecules for the first time by integrating GPABR1 agonistic and DPP4 inhibitory efficacy into a single molecule. The effects of GPABR1 and DPP4 on UC were exploited and made to act locally in the gut to avoid unwanted systemic effects. In particular, racemic compound 15, a highly potent GPABR1-DPP4 bifunctional molecule, showed good intestinal distribution, efficacy, and gallbladder safety in a mouse model of colitis[118]. Chen *et al*[119] also described the discovery and optimization of a series of intestinal-restricted selective thiazolidine-type GPABR1 agonists that elicit a potent response with minimal effects on the gallbladder. In this series of drugs, they mainly explored compound No. 12, with minimal systemic availability, which stimulates prolonged and potent GLP-1 (7-36) amide (tGLP-1) secretion and may have significant therapeutic value in IBD[119].

Dvořák *et al*[120] proposed microbial metabolite mimicry as a new strategy for drug discovery based on the effect of microbial metabolites on PXR and reported the functionalized indole derivative lead compound Felix Kopp Kortagere 6 (FKK6) as the first class of non-cytotoxic PXR agonists as a proof of concept for microbial metabolite mimicry. In cells, human organs, and animals, FKK6 can directly bind PXR and stimulate PXR-specific target gene expression. In mice expressing human *PXR* genes, FKK6 dramatically suppressed the production of pro-inflammatory cytokines and prevented inflammation[120]. The development of FKK6 provided the first evidence that microbial metabolite mimicry is a viable drug discovery strategy and opened the door to an underutilized chemical space for IBD drug development.

Table 2 Potential applications of bile acids and their receptors in inflammatory bowel disease

Types	Ref.	Subjects	Treatment	Major findings
Bile acid receptor agonists or inhibitors	Miyazaki *et al*[109], 2021	Mice with AOM/DSS-induced colitis	Fed nelumal A for 15 wk	Nelumal A induced the expression of FXR target genes and tight junction proteins in the intestine; Nelumal A decreased the expression of hepatic bile acid synthesis genes
	Liu *et al* [110], 2023	Mice with DSS-induced colitis	Fed nigakinone for 9 d	Nigakinone inhibited inflammatory cytokine production by activating the FXR/NLRP3 signaling pathway; Nigakinone regulated bile acid metabolism by controlling cholesterol hydroxylase and FXR-mediated transporter proteins
	Qi *et al* [112], 2022	Mice with DSS-induced colitis	DDC gavage treatment for a week	DDC targeted and inhibited RORγt activity, thereby indirectly stabilizing Foxp 3 expression and achieving regulation of Th17/Treg homeostasis
	Chen *et al* [113], 2022	Mice with DSS-induced colitis	Fed compound 14d for 9 d	Compound 14d reduced RORγt-driven Th17 cell differentiation; Compound 14d attenuated T cell expansion and activation
	Chen *et al* [115], 2019	Mice with DSS-induced colitis	Fed genistein 14d for 9 d	Genistein lowered inflammatory cell infiltration and generation of pro-inflammatory mediators in the blood and colon; Genistein reduced weight loss and increased colon length in mice
	Han *et al* [118], 2022	Mice with DSS-induced colitis	Fed racemic compound 15 for 9 d	Racemic compound 15 showed good intestinal distribution and efficacy; Racemic compound 15 avoided unwanted systemic effects and showed better gallbladder safety
	Chen *et al* [119], 2018	Diet-induced obese mice	Fed compound 12 for 4, 8, 12, or 16 h	Compound 12 elicited a potent response with minimal effects on the gallbladder; Compound 12 stimulated prolonged and potent tGLP-1 secretion
	Dvořák *et al* [120], 2020	Mice with DSS-induced colitis	FKK6 oral gavage plus FKK6 intrarectal bolus for 10 d	FKK6 dramatically suppressed the production of pro-inflammatory cytokines and prevented inflammation; FKK6 provided the first evidence that microbial metabolite mimicry is a viable drug discovery strategy
Traditional Chinese medicine	Hua *et al* [122], 2021	Mice with DSS-induced colitis	Administrated with BTWT for 7 d	BTWT normalized the levels of some bile acids, especially CA and MCA; BTWT increased the expression of FXR and TGR5 in the liver; Relative species abundance and gut microbiota diversity were significantly higher in the BTWT-exposed group; BTWT significantly ameliorated colonic inflammation and clinical signs
	Su *et al* [123], 2022	Caco-2 cells treated with bile acids	Pre-incubated with GXD at subtoxic concentration for 24 h before treatment with BAs	GXD improved intestinal barrier dysfunction caused by abnormal bile acid metabolism in IBD by regulating tight junction protein expression levels, inhibiting oxidative stress, and reducing apoptosis
	Li *et al* [125], 2022	Mice with DSS-induced colitis	Fed SFE for 11 d	SFE regulated the transcriptional levels of RORγt and Foxp 3 in the colon and down-regulating the expression of the pro-inflammatory factor IL-17 A in colon tissue
	Shi *et al* [126], 2022	Mice with DSS-induced colitis	Fed LWE for a week	LWE inhibited the transcriptional activation of RORγT and IL-17A, thereby suppressing the differentiation of Th17 lymphocytes; LWE reduced inflammation and increased the protective action of the intestinal mucosal barrier *via* the TLR4/MyD88/NF-κB signal transduction pathway
	Xia *et al* [127], 2022	Mice with DSS-induced colitis	QCWZD gavage for a week	QCWZD inhibited the phosphorylation of JAK2-STAT3 pathway, reducing the transcriptional activation of RORγT and IL-17A
	Xiong *et al* [128], 2022	Mice with DSS-induced colitis	Fed HGT for 10 d	HGT inhibited DSS-induced necrotizing lesions in the colon through up-regulation VDR levels
	Zhang *et al* [129], 2020	Mice with DSS-induced colitis	PA administered intragastrically for 10 d	PA activated PXR signaling and inhibited NF-κB signaling, thereby ameliorating inflammation
	Yu *et al* [130], 2020	Mice with DSS-induced colitis	Fed Alpinetin for 9 d	Alpinetin activated PXR/NF-kB, thereby ameliorating inflammation

IBD: Inflammatory bowel disease; FXR: Farnesoid X receptor; PXR: Pregnane X receptor; VDR: Vitamin D receptor; RORγt: Retinoid-related orphan receptor γt; DSS: Dextran sodium sulfate; HGT: Huanglian Ganjiang Tang; QCWZD: Chingchang Wenzhong Decoction; LWE: Licorice water extraction; SFE: *Sophora flavescens* Aiton total flavonoids extracts; BTWT: Baitouweng Tang; GXD: Gualou Xiebai Decoctio; MCA: Muricholic acid.

In conclusion, the research and development of bile acid receptors and their agonist or inhibitor medicines is a viable treatment method for IBD. However, there are still numerous issues, such as the increased adverse effects of non-selective agonists and activators. Increasing the intestinal restriction of agonists by identifying modifications that block the active transport of ASBT while reducing passive absorption by increasing the compounds' size and polar surface area is a feasible solution to their side effects. However, the synthesis of existing intestinal restricted activators or inhibitors is very complex and expensive, and further research is needed to explore this.

Traditional Chinese medicine

Chinese medicine is garnering more attention as the global pharmaceutical industry develops, and herbal medicine has distinct advantages in treating IBD due to allopathic treatment[121]. Many academics have recently conducted basic research on traditional Chinese medicine for the treatment of IBD from various angles, and they discovered that traditional Chinese medicine may benefit the treatment of IBD by affecting bile acids and their receptors, which support intestinal mucosal barrier function, regulate intestinal immunity, and influence bile acid metabolism (Table 2). In China, Baitouweng Tang (BTWT) is a commonly prescribed drug for the treatment of UC. In a DSS-induced mouse model of UC, mice were given BTWT for 7 d. Surprisingly, the researchers found that BTWT treatment reduced the increased UDCA, HDCA, MCA, CA, and GLCA in UC and normalized the levels of some bile acids, especially CA and MCA. Moreover, BTWT increased the expression of FXR and GPBAR1 in the liver. In addition, they found that the relative species abundance and diversity of the gut microbiota were significantly higher in the BTWT-exposed group. BTWT significantly ameliorated colonic inflammation and clinical signs, such as histological damage and colonic shortening, in mice. This result may be achieved by affecting the intestinal microbiota and bile acid metabolism[122]. Gualou Xiebai Decoction (GXD) is a classic formula used in China for thousands of years to treat inflammatory diseases. A recent study showed that GXD significantly improved intestinal barrier dysfunction caused by abnormal bile acid metabolism in IBD by regulating tight junction protein expression levels, inhibiting oxidative stress, and reducing apoptosis[123].

"Kushen", the dried root of the *Sophora flavescens* Aiton, is a classical drug widely used in China to treat UC in ancient and modern times, with alkaloids and flavonoids as the main components. Previous studies have shown that *Sophora flavescens* Aiton total flavonoids extract (SFE) exhibits anti-UC effects by restoring the balance of the "host-microbe" co-metabolic network and modulating the intestinal microbial structure in UC mice[124]. A recent study further found that SFE, especially the flavonoid component represented by kurarinone, had a significant protective effect against UC by regulating the transcriptional levels of RORγt and Foxp 3 in the colon and down-regulating the expression of the pro-inflammatory factor IL-17A in colon tissue[125]. In addition, Chingchang Wenzhong Decoction (QCWZD) and licorice water extraction (LWE) also inhibited the transcriptional activation of RORγT and IL-17A, thereby suppressing the differentiation of Th17 Lymphocytes and reducing colonic inflammation[126,127]. Huanglian Ganjiang Tang (HGT) is the classic formula in Danxi Xinfa, used to relieve diarrhea, abdominal pain, and blood in the stool; it is currently used clinically for the treatment of UC with remarkable efficacy, but its mechanism of action needs to be further elucidated. Xiong *et al*[128] recently showed that HGT could reduce DSS-induced colitis in mice by inhibiting DSS-induced necrotizing lesions in the colon through up-regulation of VDR levels. Furthermore, in animal models of IBD, researchers found that patchouli alcohol (PA) and alpinetin from ginger plants could activate PXR signaling and inhibit NF-κB signaling, thereby ameliorating inflammation[129,130]. In conclusion, the results of these herbal studies provide new options for treating IBD and provide a theoretical basis for pharmacological studies of herbal medicines, which are beneficial for their application.

UDCA

UDCA is a secondary bile acid generated from CDCA, which is found in low concentrations in humans and was initially licensed by the FDA to treat cholestatic liver disease. However, several studies have shown that UDCA may play an important role in IBD by acting on bile acid receptors. For example, a previous study showed that DCA could inhibit the expression of CFTR Cl^- channels by activating FXR, thereby delaying the repair of the intestinal mucosal barrier. Interestingly, UDCA inhibits this process and promotes epithelial cell migration and recovery[131]. In a recent study, UDCA was shown to reduce inflammatory cytokine production by activating FXR while inhibiting NF-κB activation in macrophages in a piglet model of intestinal inflammation[132]. These findings suggest a protective role for UDCA in IBD and support its use as a novel approach to treat IBD. In addition, UDCA can improve IBD injury through a few other potential mechanisms. MAdCAM-1 binds to integrin α4β7 on circulating T cells and recruits intestinal homing lymphocytes to intestinal damage sites during inflammation[133]. A recent study showed that by inhibiting NF-κB signaling, UDCA could directly attenuate the endothelial expression of MAdCAM-1 and other adhesion molecules, leading to a decrease in the accumulation of α4β7+ lymphocytes in the colon, thereby reducing the severity of colitis[134]. Another study showed that in a DSS-induced mouse model, UDCA and LCA prevented intestinal inflammation *in vivo*, at least in part by inhibiting epithelial cell apoptosis and promoting barrier function. Interestingly, LCA was more effective than UDCA in inhibiting epithelial cytokine release and preventing DSS-induced mucosal inflammation[135,136]. Mesalazine is the main drug used clinically for the treatment of UC and has been shown to induce remission of IBD and prevent IBD recurrence[137]. UDCA + mesalazine has been reported to have a better therapeutic effect than mesalazine alone, which may be related to the significant reduction of IL-23 and IL-17 and the altered distribution ratio of intestinal flora[138]. Tauroursodeoxycholic acid, a taurine conjugated UDCA, has been shown to reduce the accumulation of MPO activity, decrease colonic tissue levels of IL-1β, IFN-γ, and TNF-α, and also down-regulate nuclear receptor and bile acid transporter protein levels[139,140]. Hyodeoxycholic acid, glycine ursodeoxycholic acid, and taurocholate have similarly reduced colitis severity in in a mouse model of IBD[141-143]. However, it has also been shown that long-term use of high-dose UDCA increases the risk of colorectal neoplasia in patients with IBD, suggesting that we need to control the course and dose of the drug rationally[144]. In conclusion, secondary bile acids such as UDCA may be promising therapeutic agents for reducing ecological dysregulation and improving inflammation in human IBD and are attractive candidates for treating IBD.

Probiotics and fecal microbiota transplantation

Probiotic therapy introduces specific bacteria that have a recognized advantage in competitively suppressing pathogens and normalizing intestinal microbiota composition. Probiotics are classified by the World Health Organization as live

microorganisms that, when consumed in sufficient quantities, can help the host's health. The probiotics *Bifidobacterium, Lactobacillus*, and *Lactococcus* are the most frequently utilized. As an adjuvant therapy for addressing the functional symptoms of IBD, probiotics have shown promise in numerous human and animal studies[145-147]. Wong *et al*[148] recently demonstrated that *Lactobacillus casei* strain Shirota (LcS) not only increased beneficial bacterial species but also modified the circulating bile acid profile in a mouse model of DSS-induced acute colitis. Furthermore, LcS treatment increased mucin-2 and occludin expression in the colon while improving intestinal integrity. It was also shown that LcS therapy decreased the expression of pro-inflammatory mediators IFN-γ and NO and raised the expression of anti-inflammatory mediators in colonic tissue, possibly due to an altered bile acid profile[148]. Another study showed that probiotic mixtures containing *Lactobacillus rhamnosus* and *Lactococcus lactis* reduced the expression levels of IFN-γ, IL-17F, IL-1α, and IL-25, as well as the levels of the main NLRP3 inflammasome components (NLRP3, ASC, caspase-1, and IL-1β) and NOD2 in IBD mice. Probiotics have also increased FXR, GPABR1, vitamin D, and CAR expression in IBD mice[149]. Furthermore, the probiotic *Lactobacillus* has anti-inflammatory activity and induces cellular autophagy, and these effects are achieved by increasing VDR expression[150]. Recently, Zhou *et al*[151] designed a bile acid consortium (BAC) composed of three species of *Bacteroides ovatus*, *Clostridium* AP sp000509125, and *Eubacterium limosum*. They observed that BAC restored secondary bile acid metabolism in DSS-treated mice, thereby increasing the levels of UDCA and LCA, which induced activation of GPABR1 to improve the integrity of the intestinal barrier and reduce inflammation[151]. In addition, the probiotic strain *Bifidobacterium longum* CECT 7894 could improve the efficacy of infliximab against DSS-induced colitis by modulating intestinal flora composition and bile acid metabolism[152]. Probiotics may increase the risk of bacteremia, adverse effects, and the spread of antibiotic resistance in IBD patients because of their bioactivity and other characteristics. In addition, probiotics used for adjuvant therapy may be unsuccessful in some patients due to strain specificity or individual differences, in which case they should be discontinued. Therefore, the duration of probiotics should be dependent on various therapeutic benefits, objectives, and practical circumstances. Future clinical and animal investigations are required to study the direct effects and specific mechanisms of probiotics on bile acids and their receptors in IBD patients.

Fecal microbiota transplantation (FMT) is a novel and appropriate route to modify the microbial ecosystem in the host gastrointestinal tract. In recent decades, FMT has improved diseases such as *Clostridioides difficile* infections, IBD, and irritable bowel syndrome. However, the exact mechanisms still need to be better understood[153,154]. Several recent studies have found that FMT may improve IBD by acting on bile acids and their receptors. Lima *et al*[155] showed that FMT induced the production of RORγt+ regulatory T cells, IL-10, and short-chain fatty acids by macrogenomic analysis and strain tracing in 60 donor and recipient samples of active UC treated by FMT, thus protecting patients from colitis [155]. Another study showed that the long-term *Faecalibaterium* colonization following FMT could reduce intestinal inflammation by regulating the expression of RORγt and Foxp3 in UC, thereby ameliorating the imbalance in Th 17/Treg levels[156]. In addition, a mouse model of colitis was shown to be significantly inhibited by the intestinal fungus *C. metapsilosis* M2006 B, which was isolated from human feces. Moreover, the researchers identified two acyclic sesquiterpenoids (F4 and F5) as the main active metabolites of M2006 B. Surprisingly, in an animal model, these metabolites were able to effectively ameliorate colitis by selectively activating FXR. These findings suggest that M2006 B in human feces may be a beneficial intestinal fungus for treating and preventing IBD[157]. Interestingly, another recent study found that administering antibiotic pretreatment to IBD patients contributed to microbial implantation and possible clinical effectiveness[158]. In conclusion, these findings support the use of FMT in treating IBD, but the safety and efficacy of FMT remain to be investigated.

Bile acid sequestrants

A bile acid sequestrant is a positively charged indigestible resin that binds to bile acids in the intestine and forms insoluble compounds in the feces. They are mainly used in treating primary hypercholesterolemia and hypercholesterolemia with mild hypertriglyceridemia[159,160]. Currently, there are three major medications available for purchase: Cholestyramine, colestipol, and, more recently, colesevelam. Bile acid malabsorption (BAM), also known as bile acid diarrhea (BAD), is a prevalent, underappreciated, and frequently missed indicator of IBD. Clinically relevant BAM is most commonly seen in patients with IBD, especially in ileal resected CD patients.

In most cases, BAM in IBD is caused by impaired reabsorption of conjugated bile acids[161]. CD patients with BAM treated with bile acid sequestrants achieved a good response in 72.2% of cases. Researchers also analyzed the relationship between the degree of BAM (moderate or severe), intestinal surgery, and response to bile acid chelation therapy, but unfortunately, this was not statistically significant[162]. Another study showed a significant improvement in the quality of life of CD patients after terminal ileal resection when molecular treatment was given to them[163]. Although some research progress has been made, the specific mechanisms of bile acid chelators in treating BAM caused by IBD need to be further explained.

CONCLUSION

The data suggest that bile acid metabolism and receptor signaling play a key role in regulating dysregulated gut homeostasis in IBD. Changing bile acid metabolism and bile acid receptor signalling has been found to influence the pathogenesis of IBD *via* modulation of immunology, intestinal epithelial barrier function, and the gut microbiome. It is an attractive and highly promising therapeutic target for IBD. Many therapeutic strategies have shown positive effects, such as bile acid receptor agonists or inhibitors, traditional Chinese medicine, UDCA, probiotics, FMT, and bile acid sequestrants. However, due to the differences between species and cell types (IBD is exclusively a human disease),

valuable preclinical mechanistic studies must be performed to elucidate the function of bile acids and their receptors in human intestinal models. In this regard, human organoid technologies and bioinformatics approaches may be good tools to address this issue. In addition, the current therapeutic strategies described above have yet to be widely validated in clinical trials in patients with IBD, despite the promising results documented in cellular and animal studies. Future research efforts should focus on clinical trial data collection in IBD patients.

FOOTNOTES

Author contributions: Long XQ performed the majority of the writing; Liu MZ, Liu ZH, Xia LZ, and Lu SP designed the outline and coordinated the writing of the paper; Wu MH and Xu XP edited and checked the manuscript; all of the authors have read and approved the final manuscript.

Supported by National Natural Science Foundation of China, No. 81900466; and Hunan Provincial Natural Science Foundation of China, No. 2020JJ5307.

Conflict-of-interest statement: All the authors report no relevant conflicts of interest for this article.

Open-Access: This article is an open-access article that was selected by an in-house editor and fully peer-reviewed by external reviewers. It is distributed in accordance with the Creative Commons Attribution NonCommercial (CC BY-NC 4.0) license, which permits others to distribute, remix, adapt, build upon this work non-commercially, and license their derivative works on different terms, provided the original work is properly cited and the use is non-commercial. See: https://creativecommons.org/Licenses/by-nc/4.0/

Country/Territory of origin: China

ORCID number: Xiong-Quan Long 0009-0001-7046-9475; Ming-Hao Wu 0000-0001-7432-1788.

S-Editor: Yan JP
L-Editor: Wang TQ
P-Editor: Yan JP

REFERENCES

1 **Buie MJ**, Quan J, Windsor JW, Coward S, Hansen TM, King JA, Kotze PG, Gearry RB, Ng SC, Mak JWY, Abreu MT, Rubin DT, Bernstein CN, Banerjee R, Yamamoto-Furusho JK, Panaccione R, Seow CH, Ma C, Underwood FE, Ahuja V, Panaccione N, Shaheen AA, Holroyd-Leduc J, Kaplan GG; Global IBD Visualization of Epidemiology Studies in the 21st Century (GIVES-21) Research Group, Balderramo D, Chong VH, Juliao-Baños F, Dutta U, Simadibrata M, Kaibullayeva J, Sun Y, Hilmi I, Raja Ali RA, Paudel MS, Altuwaijri M, Hartono JL, Wei SC, Limsrivilai J, El Ouali S, Vergara BI, Dao VH, Kelly P, Hodges P, Miao Y, Li M. Global Hospitalization Trends for Crohn's Disease and Ulcerative Colitis in the 21st Century: A Systematic Review With Temporal Analyses. *Clin Gastroenterol Hepatol* 2022 [PMID: 35863682 DOI: 10.1016/j.cgh.2022.06.030]

2 **Kaplan GG**, Windsor JW. The four epidemiological stages in the global evolution of inflammatory bowel disease. *Nat Rev Gastroenterol Hepatol* 2021; **18**: 56-66 [PMID: 33033392 DOI: 10.1038/s41575-020-00360-x]

3 **Krela-Kaźmierczak I**, Zakerska-Banaszak O, Skrzypczak-Zielińska M, Łykowska-Szuber L, Szymczak-Tomczak A, Zawada A, Rychter AM, Ratajczak AE, Skoracka K, Skrzypczak D, Marcinkowska E, Słomski R, Dobrowolska A. Where Do We Stand in the Behavioral Pathogenesis of Inflammatory Bowel Disease? The Western Dietary Pattern and Microbiota-A Narrative Review. *Nutrients* 2022; **14** [PMID: 35745251 DOI: 10.3390/nu14122520]

4 **Neurath MF**. Targeting immune cell circuits and trafficking in inflammatory bowel disease. *Nat Immunol* 2019; **20**: 970-979 [PMID: 31235952 DOI: 10.1038/s41590-019-0415-0]

5 **Khor B**, Gardet A, Xavier RJ. Genetics and pathogenesis of inflammatory bowel disease. *Nature* 2011; **474**: 307-317 [PMID: 21677747 DOI: 10.1038/nature10209]

6 **Flynn S**, Eisenstein S. Inflammatory Bowel Disease Presentation and Diagnosis. *Surg Clin North Am* 2019; **99**: 1051-1062 [PMID: 31676047 DOI: 10.1016/j.suc.2019.08.001]

7 **Rogler G**, Singh A, Kavanaugh A, Rubin DT. Extraintestinal Manifestations of Inflammatory Bowel Disease: Current Concepts, Treatment, and Implications for Disease Management. *Gastroenterology* 2021; **161**: 1118-1132 [PMID: 34358489 DOI: 10.1053/j.gastro.2021.07.042]

8 **Lowe SC**, Sauk JS, Limketkai BN, Kwaan MR. Declining Rates of Surgery for Inflammatory Bowel Disease in the Era of Biologic Therapy. *J Gastrointest Surg* 2021; **25**: 211-219 [PMID: 33140318 DOI: 10.1007/s11605-020-04832-y]

9 **Baumgart DC**, Le Berre C. Newer Biologic and Small-Molecule Therapies for Inflammatory Bowel Disease. *N Engl J Med* 2021; **385**: 1302-1315 [PMID: 34587387 DOI: 10.1056/NEJMra1907607]

10 **Brandl K**, Hartmann P, Jih LJ, Pizzo DP, Argemi J, Ventura-Cots M, Coulter S, Liddle C, Ling L, Rossi SJ, DePaoli AM, Loomba R, Mehal WZ, Fouts DE, Lucey MR, Bosques-Padilla F, Mathurin P, Louvet A, Garcia-Tsao G, Verna EC, Abraldes JG, Brown RS Jr, Vargas V, Altamirano J, Caballería J, Shawcross D, Stärkel P, Ho SB, Bataller R, Schnabl B. Dysregulation of serum bile acids and FGF19 in alcoholic hepatitis. *J Hepatol* 2018; **69**: 396-405 [PMID: 29654817 DOI: 10.1016/j.jhep.2018.03.031]

11 **Hu Y**, Chau T, Liu HX, Liao D, Keane R, Nie Y, Yang H, Wan YJ. Bile acids regulate nuclear receptor (Nur77) expression and intracellular location to control proliferation and apoptosis. *Mol Cancer Res* 2015; **13**: 281-292 [PMID: 25232032 DOI: 10.1158/1541-7786.MCR-14-0230]

12 **Bertolini A**, Fiorotto R, Strazzabosco M. Bile acids and their receptors: modulators and therapeutic targets in liver inflammation. *Semin Immunopathol* 2022; **44**: 547-564 [PMID: 35415765 DOI: 10.1007/s00281-022-00935-7]

13 **Fuchs CD**, Trauner M. Role of bile acids and their receptors in gastrointestinal and hepatic pathophysiology. *Nat Rev Gastroenterol Hepatol* 2022; **19**: 432-450 [PMID: 35165436 DOI: 10.1038/s41575-021-00566-7]

14 **Hofmann AF**. Bile Acids: The Good, the Bad, and the Ugly. *News Physiol Sci* 1999; **14**: 24-29 [PMID: 11390813 DOI: 10.1152/physiologyonline.1999.14.1.24]

15 **Westergaard H**, Dietschy JM. The mechanism whereby bile acid micelles increase the rate of fatty acid and cholesterol uptake into the intestinal mucosal cell. *J Clin Invest* 1976; **58**: 97-108 [PMID: 932213 DOI: 10.1172/jci108465]

16 **Tiratterra E**, Franco P, Porru E, Katsanos KH, Christodoulou DK, Roda G. Role of bile acids in inflammatory bowel disease. *Ann Gastroenterol* 2018; **31**: 266-272 [PMID: 29720851 DOI: 10.20524/aog.2018.0239]

17 **Chiang JY**. Bile acids: regulation of synthesis. *J Lipid Res* 2009; **50**: 1955-1966 [PMID: 19346330 DOI: 10.1194/jlr.R900010-JLR200]

18 **Goodwin B**, Jones SA, Price RR, Watson MA, McKee DD, Moore LB, Galardi C, Wilson JG, Lewis MC, Roth ME, Maloney PR, Willson TM, Kliewer SA. A regulatory cascade of the nuclear receptors FXR, SHP-1, and LRH-1 represses bile acid biosynthesis. *Mol Cell* 2000; **6**: 517-526 [PMID: 11030332 DOI: 10.1016/s1097-2765(00)00051-4]

19 **Biagioli M**, Marchianò S, Carino A, Di Giorgio C, Santucci L, Distrutti E, Fiorucci S. Bile Acids Activated Receptors in Inflammatory Bowel Disease. *Cells* 2021; **10** [PMID: 34064187 DOI: 10.3390/cells10061281]

20 **Fiorucci S**, Distrutti E. The Pharmacology of Bile Acids and Their Receptors. *Handb Exp Pharmacol* 2019; **256**: 3-18 [PMID: 31201555 DOI: 10.1007/164_2019_238]

21 **Bromke MA**, Krzystek-Korpacka M. Bile Acid Signaling in Inflammatory Bowel Disease. *Int J Mol Sci* 2021; **22** [PMID: 34445800 DOI: 10.3390/ijms22169096]

22 **Monte MJ**, Marin JJ, Antelo A, Vazquez-Tato J. Bile acids: chemistry, physiology, and pathophysiology. *World J Gastroenterol* 2009; **15**: 804-816 [PMID: 19230041 DOI: 10.3748/wjg.15.804]

23 **Fiorucci S**, Carino A, Baldoni M, Santucci L, Costanzi E, Graziosi L, Distrutti E, Biagioli M. Bile Acid Signaling in Inflammatory Bowel Diseases. *Dig Dis Sci* 2021; **66**: 674-693 [PMID: 33289902 DOI: 10.1007/s10620-020-06715-3]

24 **de Aguiar Vallim TQ**, Tarling EJ, Edwards PA. Pleiotropic roles of bile acids in metabolism. *Cell Metab* 2013; **17**: 657-669 [PMID: 23602448 DOI: 10.1016/j.cmet.2013.03.013]

25 **Chandra R**, Liddle RA. Cholecystokinin. *Curr Opin Endocrinol Diabetes Obes* 2007; **14**: 63-67 [PMID: 17940422 DOI: 10.1097/MED.0b013e3280122850]

26 **Thomas JP**, Modos D, Rushbrook SM, Powell N, Korcsmaros T. The Emerging Role of Bile Acids in the Pathogenesis of Inflammatory Bowel Disease. *Front Immunol* 2022; **13**: 829525 [PMID: 35185922 DOI: 10.3389/fimmu.2022.829525]

27 **Wang C**, Zhu C, Shao L, Ye J, Shen Y, Ren Y. Role of Bile Acids in Dysbiosis and Treatment of Nonalcoholic Fatty Liver Disease. *Mediators Inflamm* 2019; **2019**: 7659509 [PMID: 31341422 DOI: 10.1155/2019/7659509]

28 **Jahnel J**, Fickert P, Hauer AC, Högenauer C, Avian A, Trauner M. Inflammatory bowel disease alters intestinal bile acid transporter expression. *Drug Metab Dispos* 2014; **42**: 1423-1431 [PMID: 24965812 DOI: 10.1124/dmd.114.058065]

29 **Lu TT**, Makishima M, Repa JJ, Schoonjans K, Kerr TA, Auwerx J, Mangelsdorf DJ. Molecular basis for feedback regulation of bile acid synthesis by nuclear receptors. *Mol Cell* 2000; **6**: 507-515 [PMID: 11030331 DOI: 10.1016/s1097-2765(00)00050-2]

30 **Chen L**, Jiao T, Liu W, Luo Y, Wang J, Guo X, Tong X, Lin Z, Sun C, Wang K, He Y, Zhang Y, Xu H, Zuo J, Ding Q, He S, Gonzalez FJ, Xie C. Hepatic cytochrome P450 8B1 and cholic acid potentiate intestinal epithelial injury in colitis by suppressing intestinal stem cell renewal. *Cell Stem Cell* 2022; **29**: 1366-1381.e9 [PMID: 36055192 DOI: 10.1016/j.stem.2022.08.008]

31 **Chen ML**, Takeda K, Sundrud MS. Emerging roles of bile acids in mucosal immunity and inflammation. *Mucosal Immunol* 2019; **12**: 851-861 [PMID: 30952999 DOI: 10.1038/s41385-019-0162-4]

32 **Quinn RA**, Melnik AV, Vrbanac A, Fu T, Patras KA, Christy MP, Bodai Z, Belda-Ferre P, Tripathi A, Chung LK, Downes M, Welch RD, Quinn M, Humphrey G, Panitchpakdi M, Weldon KC, Aksenov A, da Silva R, Avila-Pacheco J, Clish C, Bae S, Mallick H, Franzosa EA, Lloyd-Price J, Bussell R, Thron T, Nelson AT, Wang M, Leszczynski E, Vargas F, Gauglitz JM, Meehan MJ, Gentry E, Arthur TD, Komor AC, Poulsen O, Boland BS, Chang JT, Sandborn WJ, Lim M, Garg N, Lumeng JC, Xavier RJ, Kazmierczak BI, Jain R, Egan M, Rhee KE, Ferguson D, Raffatellu M, Vlamakis H, Haddad GG, Siegel D, Huttenhower C, Mazmanian SK, Evans RM, Nizet V, Knight R, Dorrestein PC. Global chemical effects of the microbiome include new bile-acid conjugations. *Nature* 2020; **579**: 123-129 [PMID: 32103176 DOI: 10.1038/s41586-020-2047-9]

33 **Pavlidis P**, Powell N, Vincent RP, Ehrlich D, Bjarnason I, Hayee B. Systematic review: bile acids and intestinal inflammation-luminal aggressors or regulators of mucosal defence? *Aliment Pharmacol Ther* 2015; **42**: 802-817 [PMID: 26223936 DOI: 10.1111/apt.13333]

34 **Ridlon JM**, Harris SC, Bhowmik S, Kang DJ, Hylemon PB. Consequences of bile salt biotransformations by intestinal bacteria. *Gut Microbes* 2016; **7**: 22-39 [PMID: 26939849 DOI: 10.1080/19490976.2015.1127483]

35 **Guzior DV**, Quinn RA. Review: microbial transformations of human bile acids. *Microbiome* 2021; **9**: 140 [PMID: 34127070 DOI: 10.1186/s40168-021-01101-1]

36 **Kriaa A**, Mariaule V, Jablaoui A, Rhimi S, Mkaouar H, Hernandez J, Korkmaz B, Lesner A, Maguin E, Aghdassi A, Rhimi M. Bile Acids: Key Players in Inflammatory Bowel Diseases? *Cells* 2022; **11** [PMID: 35269523 DOI: 10.3390/cells11050901]

37 **Funabashi M**, Grove TL, Wang M, Varma Y, McFadden ME, Brown LC, Guo C, Higginbottom S, Almo SC, Fischbach MA. A metabolic pathway for bile acid dehydroxylation by the gut microbiome. *Nature* 2020; **582**: 566-570 [PMID: 32555455 DOI: 10.1038/s41586-020-2396-4]

38 **Sayin SI**, Wahlström A, Felin J, Jäntti S, Marschall HU, Bamberg K, Angelin B, Hyötyläinen T, Orešič M, Bäckhed F. Gut microbiota regulates bile acid metabolism by reducing the levels of tauro-beta-muricholic acid, a naturally occurring FXR antagonist. *Cell Metab* 2013; **17**: 225-235 [PMID: 23395169 DOI: 10.1016/j.cmet.2013.01.003]

39 **Lavelle A**, Nancey S, Reimund JM, Laharie D, Marteau P, Treton X, Allez M, Roblin X, Malamut G, Oeuvray C, Rolhion N, Dray X, Rainteau D, Lamaziere A, Gauliard E, Kirchgesner J, Beaugerie L, Seksik P, Peyrin-Biroulet L, Sokol H. Fecal microbiota and bile acids in IBD patients undergoing screening for colorectal cancer. *Gut Microbes* 2022; **14**: 2078620 [PMID: 35638103 DOI: 10.1080/19490976.2022.2078620]

40 **Yang M**, Gu Y, Li L, Liu T, Song X, Sun Y, Cao X, Wang B, Jiang K, Cao H. Bile Acid-Gut Microbiota Axis in Inflammatory Bowel Disease: From Bench to Bedside. *Nutrients* 2021; **13** [PMID: 34579027 DOI: 10.3390/nu13093143]

41 **Duboc H**, Rajca S, Rainteau D, Benarous D, Maubert MA, Quervain E, Thomas G, Barbu V, Humbert L, Despras G, Bridonneau C, Dumetz F, Grill JP, Masliah J, Beaugerie L, Cosnes J, Chazouillères O, Poupon R, Wolf C, Mallet JM, Langella P, Trugnan G, Sokol H, Seksik P. Connecting dysbiosis, bile-acid dysmetabolism and gut inflammation in inflammatory bowel diseases. *Gut* 2013; **62**: 531-539 [PMID: 22993202 DOI: 10.1136/gutjnl-2012-302578]

42 **Feng L**, Zhou N, Li Z, Fu D, Guo Y, Gao X, Liu X. Co-occurrence of gut microbiota dysbiosis and bile acid metabolism alteration is associated with psychological disorders in Crohn's disease. *FASEB J* 2022; **36**: e22100 [PMID: 34939244 DOI: 10.1096/fj.202101088RRR]

43 **Islam KB**, Fukiya S, Hagio M, Fujii N, Ishizuka S, Ooka T, Ogura Y, Hayashi T, Yokota A. Bile acid is a host factor that regulates the composition of the cecal microbiota in rats. *Gastroenterology* 2011; **141**: 1773-1781 [PMID: 21839040 DOI: 10.1053/j.gastro.2011.07.046]

44 **Forman BM**, Goode E, Chen J, Oro AE, Bradley DJ, Perlmann T, Noonan DJ, Burka LT, McMorris T, Lamph WW, Evans RM, Weinberger C. Identification of a nuclear receptor that is activated by farnesol metabolites. *Cell* 1995; **81**: 687-693 [PMID: 7774010 DOI: 10.1016/0092-8674(95)90530-8]

45 **Fiorucci S**, Biagioli M, Zampella A, Distrutti E. Bile Acids Activated Receptors Regulate Innate Immunity. *Front Immunol* 2018; **9**: 1853 [PMID: 30150987 DOI: 10.3389/fimmu.2018.01853]

46 **Gadaleta RM**, Garcia-Irigoyen O, Cariello M, Scialpi N, Peres C, Vetrano S, Fiorino G, Danese S, Ko B, Luo J, Porru E, Roda A, Sabbà C, Moschetta A. Fibroblast Growth Factor 19 modulates intestinal microbiota and inflammation in presence of Farnesoid X Receptor. *EBioMedicine* 2020; **54**: 102719 [PMID: 32259714 DOI: 10.1016/j.ebiom.2020.102719]

47 **Zhou X**, Cao L, Jiang C, Xie Y, Cheng X, Krausz KW, Qi Y, Sun L, Shah YM, Gonzalez FJ, Wang G, Hao H. PPARα-UGT axis activation represses intestinal FXR-FGF15 feedback signalling and exacerbates experimental colitis. *Nat Commun* 2014; **5**: 4573 [PMID: 25183423 DOI: 10.1038/ncomms5573]

48 **Schroeder JH**, Howard JK, Lord GM. Transcription factor-driven regulation of ILC1 and ILC3. *Trends Immunol* 2022; **43**: 564-579 [PMID: 35618586 DOI: 10.1016/j.it.2022.04.009]

49 **Fu T**, Li Y, Oh TG, Cayabyab F, He N, Tang Q, Coulter S, Truitt M, Medina P, He M, Yu RT, Atkins A, Zheng Y, Liddle C, Downes M, Evans RM. FXR mediates ILC-intrinsic responses to intestinal inflammation. *Proc Natl Acad Sci U S A* 2022; **119**: e2213041119 [PMID: 36508655 DOI: 10.1073/pnas.2213041119]

50 **Del Zotto B**, Mumolo G, Pronio AM, Montesani C, Tersigni R, Boirivant M. TGF-beta1 production in inflammatory bowel disease: differing production patterns in Crohn's disease and ulcerative colitis. *Clin Exp Immunol* 2003; **134**: 120-126 [PMID: 12974764 DOI: 10.1046/j.1365-2249.2003.02250.x]

51 **Zhao D**, Cai C, Chen Q, Jin S, Yang B, Li N. High-Fat Diet Promotes DSS-Induced Ulcerative Colitis by Downregulated FXR Expression through the TGFB Pathway. *Biomed Res Int* 2020; **2020**: 3516128 [PMID: 33029504 DOI: 10.1155/2020/3516128]

52 **Xu M**, Cen M, Shen Y, Zhu Y, Cheng F, Tang L, Hu W, Dai N. Deoxycholic Acid-Induced Gut Dysbiosis Disrupts Bile Acid Enterohepatic Circulation and Promotes Intestinal Inflammation. *Dig Dis Sci* 2021; **66**: 568-576 [PMID: 32198567 DOI: 10.1007/s10620-020-06208-3]

53 **Xu M**, Shen Y, Cen M, Zhu Y, Cheng F, Tang L, Zheng X, Kim JJ, Dai N, Hu W. Modulation of the Gut Microbiota-farnesoid X Receptor Axis Improves Deoxycholic Acid-induced Intestinal Inflammation in Mice. *J Crohns Colitis* 2021; **15**: 1197-1210 [PMID: 33417675 DOI: 10.1093/ecco-jcc/jjab003]

54 **Song M**, Ye J, Zhang F, Su H, Yang X, He H, Liu F, Zhu X, Wang L, Gao P, Shu G, Jiang Q, Wang S. Chenodeoxycholic Acid (CDCA) Protects against the Lipopolysaccharide-Induced Impairment of the Intestinal Epithelial Barrier Function *via* the FXR-MLCK Pathway. *J Agric Food Chem* 2019; **67**: 8868-8874 [PMID: 31319027 DOI: 10.1021/acs.jafc.9b03173]

55 **Liu HM**, Liao JF, Lee TY. Farnesoid X receptor agonist GW4064 ameliorates lipopolysaccharide-induced ileocolitis through TLR4/MyD88 pathway related mitochondrial dysfunction in mice. *Biochem Biophys Res Commun* 2017; **490**: 841-848 [PMID: 28647362 DOI: 10.1016/j.bbrc.2017.06.129]

56 **Mickael ME**, Bhaumik S, Basu R. Retinoid-Related Orphan Receptor RORγt in CD4(+) T-Cell-Mediated Intestinal Homeostasis and Inflammation. *Am J Pathol* 2020; **190**: 1984-1999 [PMID: 32735890 DOI: 10.1016/j.ajpath.2020.07.010]

57 **Hang S**, Paik D, Yao L, Kim E, Trinath J, Lu J, Ha S, Nelson BN, Kelly SP, Wu L, Zheng Y, Longman RS, Rastinejad F, Devlin AS, Krout MR, Fischbach MA, Littman DR, Huh JR. Bile acid metabolites control T(H)17 and T(reg) cell differentiation. *Nature* 2019; **576**: 143-148 [PMID: 31776512 DOI: 10.1038/s41586-019-1785-z]

58 **Paik D**, Yao L, Zhang Y, Bae S, D'Agostino GD, Zhang M, Kim E, Franzosa EA, Avila-Pacheco J, Bisanz JE, Rakowski CK, Vlamakis H, Xavier RJ, Turnbaugh PJ, Longman RS, Krout MR, Clish CB, Rastinejad F, Huttenhower C, Huh JR, Devlin AS. Human gut bacteria produce T(H)17-modulating bile acid metabolites. *Nature* 2022; **603**: 907-912 [PMID: 35296854 DOI: 10.1038/s41586-022-04480-z]

59 **Campbell C**, McKenney PT, Konstantinovsky D, Isaeva OI, Schizas M, Verter J, Mai C, Jin WB, Guo CJ, Violante S, Ramos RJ, Cross JR, Kadaveru K, Hambor J, Rudensky AY. Bacterial metabolism of bile acids promotes generation of peripheral regulatory T cells. *Nature* 2020; **581**: 475-479 [PMID: 32461639 DOI: 10.1038/s41586-020-2193-0]

60 **Lv L**, Chen Z, Bai W, Hao J, Heng Z, Meng C, Wang L, Luo X, Wang X, Cao Y, He J. Taurohyodeoxycholic acid alleviates trinitrobenzene sulfonic acid induced ulcerative colitis *via* regulating Th1/Th2 and Th17/Treg cells balance. *Life Sci* 2023; **318**: 121501 [PMID: 36801213 DOI: 10.1016/j.lfs.2023.121501]

61 **Kathania M**, Kumar R, Lenou ET, Basrur V, Theiss AL, Chernoff J, Venuprasad K. Pak2-mediated phosphorylation promotes RORγt ubiquitination and inhibits colonic inflammation. *Cell Rep* 2022; **40**: 111345 [PMID: 36103814 DOI: 10.1016/j.celrep.2022.111345]

62 **Ohnmacht C**, Park JH, Cording S, Wing JB, Atarashi K, Obata Y, Gaboriau-Routhiau V, Marques R, Dulauroy S, Fedoseeva M, Busslinger M, Cerf-Bensussan N, Boneca IG, Voehringer D, Hase K, Honda K, Sakaguchi S, Eberl G. MUCOSAL IMMUNOLOGY. The microbiota regulates type 2 immunity through RORγt$^+$ T cells. *Science* 2015; **349**: 989-993 [PMID: 26160380 DOI: 10.1126/science.aac4263]

63 **Sefik E**, Geva-Zatorsky N, Oh S, Konnikova L, Zemmour D, McGuire AM, Burzyn D, Ortiz-Lopez A, Lobera M, Yang J, Ghosh S, Earl A, Snapper SB, Jupp R, Kasper D, Mathis D, Benoist C. MUCOSAL IMMUNOLOGY. Individual intestinal symbionts induce a distinct population of RORγ$^+$ regulatory T cells. *Science* 2015; **349**: 993-997 [PMID: 26272906 DOI: 10.1126/science.aaa9420]

64 **Maloy KJ**, Powrie F. Intestinal homeostasis and its breakdown in inflammatory bowel disease. *Nature* 2011; **474**: 298-306 [PMID: 21677746 DOI: 10.1038/nature10208]

65 **Lyu M**, Suzuki H, Kang L, Gaspal F, Zhou W, Goc J, Zhou L, Zhou J, Zhang W; JRI Live Cell Bank, Shen Z, Fox JG, Sockolow RE, Laufer TM, Fan Y, Eberl G, Withers DR, Sonnenberg GF. ILC3s select microbiota-specific regulatory T cells to establish tolerance in the gut. *Nature* 2022; **610**: 744-751 [PMID: 36071169 DOI: 10.1038/s41586-022-05141-x]

66 **Akagbosu B**, Tayyebi Z, Shibu G, Paucar Iza YA, Deep D, Parisotto YF, Fisher L, Pasolli HA, Thevin V, Elmentaite R, Knott M, Hemmers S, Jahn L, Friedrich C, Verter J, Wang ZM, van den Brink M, Gasteiger G, Grünewald TGP, Marie JC, Leslie C, Rudensky AY, Brown CC. Novel antigen-presenting cell imparts T(reg)-dependent tolerance to gut microbiota. *Nature* 2022; **610**: 752-760 [PMID: 36070798 DOI: 10.1038/s41586-022-05309-5]

67 **Liu Y**, Yang M, Tang L, Wang F, Huang S, Liu S, Lei Y, Wang S, Xie Z, Wang W, Zhao X, Tang B, Yang S. TLR4 regulates RORγt(+) regulatory T-cell responses and susceptibility to colon inflammation through interaction with Akkermansia muciniphila. *Microbiome* 2022; **10**:

98 [PMID: 35761415 DOI: 10.1186/s40168-022-01296-x]
68 **Bhaumik S**, Mickael ME, Moran M, Spell M, Basu R. RORγt Promotes Foxp3 Expression by Antagonizing the Effector Program in Colonic Regulatory T Cells. *J Immunol* 2021; **207**: 2027-2038 [PMID: 34518282 DOI: 10.4049/jimmunol.2100175]
69 **Kawamata Y**, Fujii R, Hosoya M, Harada M, Yoshida H, Miwa M, Fukusumi S, Habata Y, Itoh T, Shintani Y, Hinuma S, Fujisawa Y, Fujino M. A G protein-coupled receptor responsive to bile acids. *J Biol Chem* 2003; **278**: 9435-9440 [PMID: 12524422 DOI: 10.1074/jbc.M209706200]
70 **Schroder K**, Tschopp J. The inflammasomes. *Cell* 2010; **140**: 821-832 [PMID: 20303873 DOI: 10.1016/j.cell.2010.01.040]
71 **Zhen Y**, Zhang H. NLRP3 Inflammasome and Inflammatory Bowel Disease. *Front Immunol* 2019; **10**: 276 [PMID: 30873162 DOI: 10.3389/fimmu.2019.00276]
72 **Guo C**, Xie S, Chi Z, Zhang J, Liu Y, Zhang L, Zheng M, Zhang X, Xia D, Ke Y, Lu L, Wang D. Bile Acids Control Inflammation and Metabolic Disorder through Inhibition of NLRP3 Inflammasome. *Immunity* 2016; **45**: 802-816 [PMID: 27692610 DOI: 10.1016/j.immuni.2016.09.008]
73 **Biagioli M**, Carino A, Cipriani S, Francisci D, Marchianò S, Scarpelli P, Sorcini D, Zampella A, Fiorucci S. The Bile Acid Receptor GPBAR1 Regulates the M1/M2 Phenotype of Intestinal Macrophages and Activation of GPBAR1 Rescues Mice from Murine Colitis. *J Immunol* 2017; **199**: 718-733 [PMID: 28607110 DOI: 10.4049/jimmunol.1700183]
74 **Khajah MA**, Fateel MM, Ananthalakshmi KV, Luqmani YA. Anti-Inflammatory Action of Angiotensin 1-7 in Experimental Colitis. *PLoS One* 2016; **11**: e0150861 [PMID: 26963721 DOI: 10.1371/journal.pone.0150861]
75 **Biagioli M**, Marchianò S, Roselli R, Di Giorgio C, Bellini R, Bordoni M, Distrutti E, Catalanotti B, Zampella A, Graziosi L, Donini A, Fiorucci S. GLP-1 Mediates Regulation of Colonic ACE2 Expression by the Bile Acid Receptor GPBAR1 in Inflammation. *Cells* 2022; **11** [PMID: 35406751 DOI: 10.3390/cells11071187]
76 **Sinha SR**, Haileselassie Y, Nguyen LP, Tropini C, Wang M, Becker LS, Sim D, Jarr K, Spear ET, Singh G, Namkoong H, Bittinger K, Fischbach MA, Sonnenburg JL, Habtezion A. Dysbiosis-Induced Secondary Bile Acid Deficiency Promotes Intestinal Inflammation. *Cell Host Microbe* 2020; **27**: 659-670.e5 [PMID: 32101703 DOI: 10.1016/j.chom.2020.01.021]
77 **Azuma Y**, Uchiyama K, Sugaya T, Yasuda T, Hashimoto H, Kajiwara-Kubota M, Sugino S, Kitae H, Torii T, Mizushima K, Doi T, Inoue K, Dohi O, Yoshida N, Kamada K, Ishikawa T, Takagi T, Konishi H, Naito Y, Itoh Y. Deoxycholic acid delays the wound healing of colonic epithelial cells *via* transmembrane G-protein-coupled receptor 5. *J Gastroenterol Hepatol* 2022; **37**: 134-143 [PMID: 34477242 DOI: 10.1111/jgh.15676]
78 **Zhai Z**, Niu KM, Liu Y, Lin C, Wu X. The Gut Microbiota-Bile Acids-TGR5 Axis Mediates Eucommia ulmoides Leaf Extract Alleviation of Injury to Colonic Epithelium Integrity. *Front Microbiol* 2021; **12**: 727681 [PMID: 34489916 DOI: 10.3389/fmicb.2021.727681]
79 **Kellermann L**, Jensen KB, Bergenheim F, Gubatan J, Chou ND, Moss A, Nielsen OH. Mucosal vitamin D signaling in inflammatory bowel disease. *Autoimmun Rev* 2020; **19**: 102672 [PMID: 32942038 DOI: 10.1016/j.autrev.2020.102672]
80 **Makishima M**, Lu TT, Xie W, Whitfield GK, Domoto H, Evans RM, Haussler MR, Mangelsdorf DJ. Vitamin D receptor as an intestinal bile acid sensor. *Science* 2002; **296**: 1313-1316 [PMID: 12016314 DOI: 10.1126/science.1070477]
81 **Yao B**, He J, Yin X, Shi Y, Wan J, Tian Z. The protective effect of lithocholic acid on the intestinal epithelial barrier is mediated by the vitamin D receptor *via* a SIRT1/Nrf2 and NF-κB dependent mechanism in Caco-2 cells. *Toxicol Lett* 2019; **316**: 109-118 [PMID: 31472180 DOI: 10.1016/j.toxlet.2019.08.024]
82 **Bäcker V**, Cheung FY, Siveke JT, Fandrey J, Winning S. Knockdown of myeloid cell hypoxia-inducible factor-1α ameliorates the acute pathology in DSS-induced colitis. *PLoS One* 2017; **12**: e0190074 [PMID: 29261815 DOI: 10.1371/journal.pone.0190074]
83 **Kim YE**, Lee M, Gu H, Kim J, Jeong S, Yeo S, Lee YJ, Im SH, Sung YC, Kim HJ, Weissman IL, Ahn GO. HIF-1α activation in myeloid cells accelerates dextran sodium sulfate-induced colitis progression in mice. *Dis Model Mech* 2018; **11** [PMID: 29967068 DOI: 10.1242/dmm.033241]
84 **Xue G**, Gao R, Liu Z, Xu N, Cao Y, Zhao B, Du J. Vitamin D/VDR signaling inhibits colitis by suppressing HIF-1α activation in colonic epithelial cells. *Am J Physiol Gastrointest Liver Physiol* 2021; **320**: G837-G846 [PMID: 33759562 DOI: 10.1152/ajpgi.00061.2021]
85 **Wang X**, Ge X, Liao W, Cao Y, Li R, Zhang F, Zhao B, Du J. ZFP36 promotes VDR mRNA degradation to facilitate cell death in oral and colonic epithelial cells. *Cell Commun Signal* 2021; **19**: 85 [PMID: 34380509 DOI: 10.1186/s12964-021-00765-4]
86 **Fernández-Barral A**, Costales-Carrera A, Buira SP, Jung P, Ferrer-Mayorga G, Larriba MJ, Bustamante-Madrid P, Domínguez O, Real FX, Guerra-Pastrián L, Lafarga M, García-Olmo D, Cantero R, Del Peso L, Batlle E, Rojo F, Muñoz A, Barbáchano A. Vitamin D differentially regulates colon stem cells in patient-derived normal and tumor organoids. *FEBS J* 2020; **287**: 53-72 [PMID: 31306552 DOI: 10.1111/febs.14998]
87 **Yang E**, Shen J. The roles and functions of Paneth cells in Crohn's disease: A critical review. *Cell Prolif* 2021; **54**: e12958 [PMID: 33174662 DOI: 10.1111/cpr.12958]
88 **Lu R**, Zhang YG, Xia Y, Zhang J, Kaser A, Blumberg R, Sun J. Paneth Cell Alertness to Pathogens Maintained by Vitamin D Receptors. *Gastroenterology* 2021; **160**: 1269-1283 [PMID: 33217447 DOI: 10.1053/j.gastro.2020.11.015]
89 **Luettig J**, Rosenthal R, Barmeyer C, Schulzke JD. Claudin-2 as a mediator of leaky gut barrier during intestinal inflammation. *Tissue Barriers* 2015; **3**: e977176 [PMID: 25838982 DOI: 10.4161/21688370.2014.977176]
90 **Zhang YG**, Lu R, Xia Y, Zhou D, Petrof E, Claud EC, Sun J. Lack of Vitamin D Receptor Leads to Hyperfunction of Claudin-2 in Intestinal Inflammatory Responses. *Inflamm Bowel Dis* 2019; **25**: 97-110 [PMID: 30289450 DOI: 10.1093/ibd/izy292]
91 **Yu M**, Wu H, Wang J, Chen X, Pan J, Liu P, Zhang J, Chen Y, Zhu W, Tang C, Jin Q, Li C, Lu C, Zeng H, Yu C, Sun J. Vitamin D receptor inhibits EMT *via* regulation of the epithelial mitochondrial function in intestinal fibrosis. *J Biol Chem* 2021; **296**: 100531 [PMID: 33713706 DOI: 10.1016/j.jbc.2021.100531]
92 **Garg M**, Royce SG, Tikellis C, Shallue C, Sluka P, Wardan H, Hosking P, Monagle S, Thomas M, Lubel JS, Gibson PR. The intestinal vitamin D receptor in inflammatory bowel disease: inverse correlation with inflammation but no relationship with circulating vitamin D status. *Therap Adv Gastroenterol* 2019; **12**: 1756284818822566 [PMID: 30719077 DOI: 10.1177/1756284818822566]
93 **Huang J**, Chen T, Liu Y, Lyu L, Li X, Yue W. How would serum 25(OH)D level change in patients with inflammatory bowel disease depending on intestinal mucosa vitamin D receptor (VDR) and vitamin D1-α hydroxylase (CYP27B1)? *Turk J Gastroenterol* 2019; **30**: 132-138 [PMID: 30429108 DOI: 10.5152/tjg.2018.17828]
94 **Yang ZH**, Liu F, Zhu XR, Suo FY, Jia ZJ, Yao SK. Altered profiles of fecal bile acids correlate with gut microbiota and inflammatory responses in patients with ulcerative colitis. *World J Gastroenterol* 2021; **27**: 3609-3629 [PMID: 34239273 DOI: 10.3748/wjg.v27.i24.3609]
95 **Kliewer SA**, Moore JT, Wade L, Staudinger JL, Watson MA, Jones SA, McKee DD, Oliver BB, Willson TM, Zetterström RH, Perlmann T,

Lehmann JM. An orphan nuclear receptor activated by pregnanes defines a novel steroid signaling pathway. *Cell* 1998; **92**: 73-82 [PMID: 9489701 DOI: 10.1016/s0092-8674(00)80900-9]

96 **Lehmann JM**, McKee DD, Watson MA, Willson TM, Moore JT, Kliewer SA. The human orphan nuclear receptor PXR is activated by compounds that regulate CYP3A4 gene expression and cause drug interactions. *J Clin Invest* 1998; **102**: 1016-1023 [PMID: 9727070 DOI: 10.1172/jci3703]

97 **Baes M**, Gulick T, Choi HS, Martinoli MG, Simha D, Moore DD. A new orphan member of the nuclear hormone receptor superfamily that interacts with a subset of retinoic acid response elements. *Mol Cell Biol* 1994; **14**: 1544-1552 [PMID: 8114692 DOI: 10.1128/mcb.14.3.1544-1552.1994]

98 **Poudel S**, Huber AD, Chen T. Regulation of Nuclear Receptors PXR and CAR by Small Molecules and Signal Crosstalk: Roles in Drug Metabolism and Beyond. *Drug Metab Dispos* 2023; **51**: 228-236 [PMID: 36116789 DOI: 10.1124/dmd.122.000858]

99 **Uehara D**, Tojima H, Kakizaki S, Yamazaki Y, Horiguchi N, Takizawa D, Sato K, Yamada M, Uraoka T. Constitutive androstane receptor and pregnane X receptor cooperatively ameliorate DSS-induced colitis. *Dig Liver Dis* 2019; **51**: 226-235 [PMID: 30442521 DOI: 10.1016/j.dld.2018.10.008]

100 **Little M**, Dutta M, Li H, Matson A, Shi X, Mascarinas G, Molla B, Weigel K, Gu H, Mani S, Cui JY. Understanding the physiological functions of the host xenobiotic-sensing nuclear receptors PXR and CAR on the gut microbiome using genetically modified mice. *Acta Pharm Sin B* 2022; **12**: 801-820 [PMID: 35256948 DOI: 10.1016/j.apsb.2021.07.022]

101 **Venkatesh M**, Mukherjee S, Wang H, Li H, Sun K, Benechet AP, Qiu Z, Maher L, Redinbo MR, Phillips RS, Fleet JC, Kortagere S, Mukherjee P, Fasano A, Le Ven J, Nicholson JK, Dumas ME, Khanna KM, Mani S. Symbiotic bacterial metabolites regulate gastrointestinal barrier function *via* the xenobiotic sensor PXR and Toll-like receptor 4. *Immunity* 2014; **41**: 296-310 [PMID: 25065623 DOI: 10.1016/j.immuni.2014.06.014]

102 **Flannigan KL**, Nieves KM, Szczepanski HE, Serra A, Lee JW, Alston LA, Ramay H, Mani S, Hirota SA. The Pregnane X Receptor and Indole-3-Propionic Acid Shape the Intestinal Mesenchyme to Restrain Inflammation and Fibrosis. *Cell Mol Gastroenterol Hepatol* 2023; **15**: 765-795 [PMID: 36309199 DOI: 10.1016/j.jcmgh.2022.10.014]

103 **Deuring JJ**, Li M, Cao W, Chen S, Wang W, de Haar C, van der Woude CJ, Peppelenbosch M. Pregnane X receptor activation constrains mucosal NF-κB activity in active inflammatory bowel disease. *PLoS One* 2019; **14**: e0221924 [PMID: 31581194 DOI: 10.1371/journal.pone.0221924]

104 **Ramesh R**, Kozhaya L, McKevitt K, Djuretic IM, Carlson TJ, Quintero MA, McCauley JL, Abreu MT, Unutmaz D, Sundrud MS. Pro-inflammatory human Th17 cells selectively express P-glycoprotein and are refractory to glucocorticoids. *J Exp Med* 2014; **211**: 89-104 [PMID: 24395888 DOI: 10.1084/jem.20130301]

105 **Chen ML**, Huang X, Wang H, Hegner C, Liu Y, Shang J, Eliason A, Diao H, Park H, Frey B, Wang G, Mosure SA, Solt LA, Kojetin DJ, Rodriguez-Palacios A, Schady DA, Weaver CT, Pipkin ME, Moore DD, Sundrud MS. CAR directs T cell adaptation to bile acids in the small intestine. *Nature* 2021; **593**: 147-151 [PMID: 33828301 DOI: 10.1038/s41586-021-03421-6]

106 **Wang X**, Chen S, Xiang H, Wang X, Xiao J, Zhao S, Shu Z, Ouyang J, Liang Z, Deng M, Chen X, Zhang J, Liu H, Quan Q, Gao P, Fan J, Chen AF, Lu H. S1PR2/RhoA/ROCK1 pathway promotes inflammatory bowel disease by inducing intestinal vascular endothelial barrier damage and M1 macrophage polarization. *Biochem Pharmacol* 2022; **201**: 115077 [PMID: 35537530 DOI: 10.1016/j.bcp.2022.115077]

107 **Chen T**, Gu K, Lin R, Liu Y, Shan Y. The function of Sphingosine-1-phosphate receptor 2 (S1PR2) in maintaining intestinal barrier and inducing ulcerative colitis. *Bioengineered* 2022; **13**: 13703-13717 [PMID: 35707833 DOI: 10.1080/21655979.2022.2076500]

108 **Zhao S**, Gong Z, Du X, Tian C, Wang L, Zhou J, Xu C, Chen Y, Cai W, Wu J. Deoxycholic Acid-Mediated Sphingosine-1-Phosphate Receptor 2 Signaling Exacerbates DSS-Induced Colitis through Promoting Cathepsin B Release. *J Immunol Res* 2018; **2018**: 2481418 [PMID: 29854830 DOI: 10.1155/2018/2481418]

109 **Miyazaki T**, Shirakami Y, Mizutani T, Maruta A, Ideta T, Kubota M, Sakai H, Ibuka T, Genovese S, Fiorito S, Taddeo VA, Epifano F, Tanaka T, Shimizu M. Novel FXR agonist nelumal A suppresses colitis and inflammation-related colorectal carcinogenesis. *Sci Rep* 2021; **11**: 492 [PMID: 33436792 DOI: 10.1038/s41598-020-79916-5]

110 **Liu F**, Yao Y, Wang Q, Zhang F, Wang M, Zhu C, Lin C. Nigakinone alleviates DSS-induced experimental colitis *via* regulating bile acid profile and FXR/NLRP3 signaling pathways. *Phytother Res* 2023; **37**: 15-34 [PMID: 36054406 DOI: 10.1002/ptr.7588]

111 **Zhou M**, Wang D, Li X, Cao Y, Yi C, Wiredu Ocansey DK, Zhou Y, Mao F. Farnesoid-X receptor as a therapeutic target for inflammatory bowel disease and colorectal cancer. *Front Pharmacol* 2022; **13**: 1016836 [PMID: 36278234 DOI: 10.3389/fphar.2022.1016836]

112 **Qi WH**, Zhang YY, Xing K, Hao DX, Zhang F, Wang RN, Bao MY, Tian MY, Yang YN, Li X, Zhang Y. 2', 4'-Dihydroxy-2,3-dimethoxychalcone: A pharmacological inverse agonist of RORγt ameliorating Th17-driven inflammatory diseases by regulating Th17/Treg. *Int Immunopharmacol* 2022; **108**: 108769 [PMID: 35453073 DOI: 10.1016/j.intimp.2022.108769]

113 **Chen JA**, Ma H, Liu Z, Tian J, Lu S, Fang W, Ze S, Lu W, Xie Q, Huang J, Wang Y. Discovery of Orally Available Retinoic Acid Receptor-Related Orphan Receptor γ-t/Dihydroorotate Dehydrogenase Dual Inhibitors for the Treatment of Refractory Inflammatory Bowel Disease. *J Med Chem* 2022; **65**: 592-615 [PMID: 34957834 DOI: 10.1021/acs.jmedchem.1c01746]

114 **Ortiz MA**, Piedrafita FJ, Nefzi A. 1,5-Disubstituted Acylated 2-Amino-4,5-dihydroimidazoles as a New Class of Retinoic Acid Receptor-Related Orphan Receptor (ROR) Inhibitors. *Int J Mol Sci* 2022; **23** [PMID: 35457251 DOI: 10.3390/ijms23084433]

115 **Chen Y**, Le TH, Du Q, Zhao Z, Liu Y, Zou J, Hua W, Liu C, Zhu Y. Genistein protects against DSS-induced colitis by inhibiting NLRP3 inflammasome *via* TGR5-cAMP signaling. *Int Immunopharmacol* 2019; **71**: 144-154 [PMID: 30901677 DOI: 10.1016/j.intimp.2019.01.021]

116 **Nakhi A**, McDermott CM, Stoltz KL, John K, Hawkinson JE, Ambrose EA, Khoruts A, Sadowsky MJ, Dosa PI. 7-Methylation of Chenodeoxycholic Acid Derivatives Yields a Substantial Increase in TGR5 Receptor Potency. *J Med Chem* 2019; **62**: 6824-6830 [PMID: 31268316 DOI: 10.1021/acs.jmedchem.9b00770]

117 **Salaga M**, Binienda A, Draczkowski P, Kosson P, Kordek R, Jozwiak K, Fichna J. Novel peptide inhibitor of dipeptidyl peptidase IV (Tyr-Pro-D-Ala-NH(2)) with anti-inflammatory activity in the mouse models of colitis. *Peptides* 2018; **108**: 34-45 [PMID: 30179653 DOI: 10.1016/j.peptides.2018.08.011]

118 **Han F**, Ning M, Wang K, Gu Y, Qu H, Leng Y, Shen J. Design and exploration of gut-restricted bifunctional molecule with TGR5 agonistic and DPP4 inhibitory effects for treating ulcerative colitis. *Eur J Med Chem* 2022; **242**: 114697 [PMID: 36029562 DOI: 10.1016/j.ejmech.2022.114697]

119 **Chen T**, Reich NW, Bell N, Finn PD, Rodriguez D, Kohler J, Kozuka K, He L, Spencer AG, Charmot D, Navre M, Carreras CW, Koo-McCoy S, Tabora J, Caldwell JS, Jacobs JW, Lewis JG. Design of Gut-Restricted Thiazolidine Agonists of G Protein-Coupled Bile Acid Receptor 1 (GPBAR1, TGR5). *J Med Chem* 2018; **61**: 7589-7613 [PMID: 30141927 DOI: 10.1021/acs.jmedchem.8b00308]

120 **Dvořák Z**, Kopp F, Costello CM, Kemp JS, Li H, Vrzalová A, Štěpánková M, Bartoňková I, Jiskrová E, Poulíková K, Vyhlídalová B, Nordstroem LU, Karunaratne CV, Ranhotra HS, Mun KS, Naren AP, Murray IA, Perdew GH, Brtko J, Toporova L, Schön A, Wallace BD, Walton WG, Redinbo MR, Sun K, Beck A, Kortagere S, Neary MC, Chandran A, Vishveshwara S, Cavalluzzi MM, Lentini G, Cui JY, Gu H, March JC, Chatterjee S, Matson A, Wright D, Flannigan KL, Hirota SA, Sartor RB, Mani S. Targeting the pregnane X receptor using microbial metabolite mimicry. *EMBO Mol Med* 2020; **12**: e11621 [PMID: 32153125 DOI: 10.15252/emmm.201911621]

121 **Yuan S**, Wang Q, Li J, Xue JC, Li Y, Meng H, Hou XT, Nan JX, Zhang QG. Inflammatory bowel disease: an overview of Chinese herbal medicine formula-based treatment. *Chin Med* 2022; **17**: 74 [PMID: 35717380 DOI: 10.1186/s13020-022-00633-4]

122 **Hua YL**, Jia YQ, Zhang XS, Yuan ZW, Ji P, Hu JJ, Wei YM. Baitouweng Tang ameliorates DSS-induced ulcerative colitis through the regulation of the gut microbiota and bile acids *via* pathways involving FXR and TGR5. *Biomed Pharmacother* 2021; **137**: 111320 [PMID: 33578232 DOI: 10.1016/j.biopha.2021.111320]

123 **Su J**, He Z, Yu Y, Lu M, Wu Z, Zhang D. Gualou Xiebai Decoction ameliorates increased Caco-2 monolayer permeability induced by bile acids *via* tight junction regulation, oxidative stress suppression and apoptosis reduction. *J Bioenerg Biomembr* 2022; **54**: 45-57 [PMID: 34718922 DOI: 10.1007/s10863-021-09927-y]

124 **Chen L**, Shao J, Luo Y, Zhao L, Zhao K, Gao Y, Wang S, Liu Y. An integrated metabolism in vivo analysis and network pharmacology in UC rats reveal anti-ulcerative colitis effects from Sophora flavescens EtOAc extract. *J Pharm Biomed Anal* 2020; **186**: 113306 [PMID: 32371325 DOI: 10.1016/j.jpba.2020.113306]

125 **Li Z**, Lin M, Li Y, Shao J, Huang R, Qiu Y, Liu Y, Chen L. Total flavonoids of Sophora flavescens and kurarinone ameliorated ulcerative colitis by regulating Th17/Treg cell homeostasis. *J Ethnopharmacol* 2022; **297**: 115500 [PMID: 35863614 DOI: 10.1016/j.jep.2022.115500]

126 **Shi G**, Kong J, Wang Y, Xuan Z, Xu F. Glycyrrhiza uralensis Fisch. alleviates dextran sulfate sodium-induced colitis in mice through inhibiting of NF-κB signaling pathways and modulating intestinal microbiota. *J Ethnopharmacol* 2022; **298**: 115640 [PMID: 36030029 DOI: 10.1016/j.jep.2022.115640]

127 **Xia S**, Chen L, Li Z, Li Y, Zhou Y, Sun S, Su Y, Xu X, Shao J, Zhang Z, Kong D, Zhang F, Zheng S. Qingchang Wenzhong Decoction reduce ulcerative colitis in mice by inhibiting Th17 lymphocyte differentiation. *Phytomedicine* 2022; **107**: 154460 [PMID: 36182798 DOI: 10.1016/j.phymed.2022.154460]

128 **Xiong X**, Cheng Z, Zhou Y, Wu F, Xie L, Lawless L, Dong R, Zhao Y, Yu L, Chen G. HuanglianGanjiang Tang alleviates DSS-induced colitis in mice by inhibiting necroptosis through vitamin D receptor. *J Ethnopharmacol* 2022; **298**: 115655 [PMID: 35988837 DOI: 10.1016/j.jep.2022.115655]

129 **Zhang G**, Liu M, Song M, Wang J, Cai J, Lin C, Li Y, Jin X, Shen C, Chen Z, Cai D, Gao Y, Zhu C, Liu C. Patchouli alcohol activates PXR and suppresses the NF-κB-mediated intestinal inflammatory. *J Ethnopharmacol* 2020; **248**: 112302 [PMID: 31614203 DOI: 10.1016/j.jep.2019.112302]

130 **Yu Z**, Yue B, Ding L, Luo X, Ren Y, Zhang J, Mani S, Wang Z, Dou W. Activation of PXR by Alpinetin Contributes to Abrogate Chemically Induced Inflammatory Bowel Disease. *Front Pharmacol* 2020; **11**: 474 [PMID: 32372959 DOI: 10.3389/fphar.2020.00474]

131 **Mroz MS**, Lajczak NK, Goggins BJ, Keely S, Keely SJ. The bile acids, deoxycholic acid and ursodeoxycholic acid, regulate colonic epithelial wound healing. *Am J Physiol Gastrointest Liver Physiol* 2018; **314**: G378-G387 [PMID: 29351391 DOI: 10.1152/ajpgi.00435.2016]

132 **Pi Y**, Wu Y, Zhang X, Lu D, Han D, Zhao J, Zheng X, Zhang S, Ye H, Lian S, Bai Y, Wang Z, Tao S, Ni D, Zou X, Jia W, Zhang G, Li D, Wang J. Gut microbiota-derived ursodeoxycholic acid alleviates low birth weight-induced colonic inflammation by enhancing M2 macrophage polarization. *Microbiome* 2023; **11**: 19 [PMID: 36721210 DOI: 10.1186/s40168-022-01458-x]

133 **Streeter PR**, Berg EL, Rouse BT, Bargatze RF, Butcher EC. A tissue-specific endothelial cell molecule involved in lymphocyte homing. *Nature* 1988; **331**: 41-46 [PMID: 3340147 DOI: 10.1038/331041a0]

134 **Gao RY**, Shearn CT, Orlicky DJ, Battista KD, Alexeev EE, Cartwright IM, Lanis JM, Kostelecky RE, Ju C, Colgan SP, Fennimore BP. Bile acids modulate colonic MAdCAM-1 expression in a murine model of combined cholestasis and colitis. *Mucosal Immunol* 2021; **14**: 479-490 [PMID: 33004979 DOI: 10.1038/s41385-020-00347-6]

135 **Lajczak-McGinley NK**, Porru E, Fallon CM, Smyth J, Curley C, McCarron PA, Tambuwala MM, Roda A, Keely SJ. The secondary bile acids, ursodeoxycholic acid and lithocholic acid, protect against intestinal inflammation by inhibition of epithelial apoptosis. *Physiol Rep* 2020; **8**: e14456 [PMID: 32562381 DOI: 10.14814/phy2.14456]

136 **Ward JBJ**, Lajczak NK, Kelly OB, O'Dwyer AM, Giddam AK, Ní Gabhann J, Franco P, Tambuwala MM, Jefferies CA, Keely S, Roda A, Keely SJ. Ursodeoxycholic acid and lithocholic acid exert anti-inflammatory actions in the colon. *Am J Physiol Gastrointest Liver Physiol* 2017; **312**: G550-G558 [PMID: 28360029 DOI: 10.1152/ajpgi.00256.2016]

137 **Barberio B**, Segal JP, Quraishi MN, Black CJ, Savarino EV, Ford AC. Efficacy of Oral, Topical, or Combined Oral and Topical 5-Aminosalicylates, in Ulcerative Colitis: Systematic Review and Network Meta-analysis. *J Crohns Colitis* 2021; **15**: 1184-1196 [PMID: 33433562 DOI: 10.1093/ecco-jcc/jjab010]

138 **Wang Z**, Chen J, Chen Z, Xie L, Wang W. Clinical effects of ursodeoxycholic acid on patients with ulcerative colitis may improve *via* the regulation of IL-23-IL-17 axis and the changes of the proportion of intestinal microflora. *Saudi J Gastroenterol* 2021; **27**: 149-157 [PMID: 33835051 DOI: 10.4103/sjg.SJG_462_20]

139 **Van den Bossche L**, Borsboom D, Devriese S, Van Welden S, Holvoet T, Devisscher L, Hindryckx P, De Vos M, Laukens D. Tauroursodeoxycholic acid protects bile acid homeostasis under inflammatory conditions and dampens Crohn's disease-like ileitis. *Lab Invest* 2017; **97**: 519-529 [PMID: 28165466 DOI: 10.1038/labinvest.2017.6]

140 **Yang Y**, He J, Suo Y, Zheng Z, Wang J, Lv L, Huo C, Wang Z, Li J, Sun W, Zhang Y. Tauroursodeoxycholate improves 2,4,6-trinitrobenzenesulfonic acid-induced experimental acute ulcerative colitis in mice. *Int Immunopharmacol* 2016; **36**: 271-276 [PMID: 27179450 DOI: 10.1016/j.intimp.2016.04.037]

141 **Van den Bossche L**, Hindryckx P, Devisscher L, Devriese S, Van Welden S, Holvoet T, Vilchez-Vargas R, Vital M, Pieper DH, Vanden Bussche J, Vanhaecke L, Van de Wiele T, De Vos M, Laukens D. Ursodeoxycholic Acid and Its Taurine- or Glycine-Conjugated Species Reduce Colitogenic Dysbiosis and Equally Suppress Experimental Colitis in Mice. *Appl Environ Microbiol* 2017; **83** [PMID: 28115375 DOI: 10.1128/AEM.02766-16]

142 **Yang Y**, He J, Suo Y, Lv L, Wang J, Huo C, Zheng Z, Wang Z, Li J, Sun W, Zhang Y. Anti-inflammatory effect of taurocholate on TNBS-induced ulcerative colitis in mice. *Biomed Pharmacother* 2016; **81**: 424-430 [PMID: 27261622 DOI: 10.1016/j.biopha.2016.04.037]

143 **Watanabe S**, Chen Z, Fujita K, Nishikawa M, Ueda H, Iguchi Y, Une M, Nishida T, Imura J. Hyodeoxycholic Acid (HDCA) Prevents Development of Dextran Sulfate Sodium (DSS)-Induced Colitis in Mice: Possible Role of Synergism between DSS and HDCA in Increasing Fecal Bile Acid Levels. *Biol Pharm Bull* 2022; **45**: 1503-1509 [PMID: 36184509 DOI: 10.1248/bpb.b22-00373]

144 **Eaton JE**, Silveira MG, Pardi DS, Sinakos E, Kowdley KV, Luketic VA, Harrison ME, McCashland T, Befeler AS, Harnois D, Jorgensen R, Petz J, Lindor KD. High-dose ursodeoxycholic acid is associated with the development of colorectal neoplasia in patients with ulcerative colitis and primary sclerosing cholangitis. *Am J Gastroenterol* 2011; **106**: 1638-1645 [PMID: 21556038 DOI: 10.1038/ajg.2011.156]

145 **Li L**, Liu T, Gu Y, Wang X, Xie R, Sun Y, Wang B, Cao H. Regulation of gut microbiota-bile acids axis by probiotics in inflammatory bowel disease. *Front Immunol* 2022; **13**: 974305 [PMID: 36211363 DOI: 10.3389/fimmu.2022.974305]

146 **Jakubczyk D**, Leszczyńska K, Górska S. The Effectiveness of Probiotics in the Treatment of Inflammatory Bowel Disease (IBD)-A Critical Review. *Nutrients* 2020; **12** [PMID: 32630805 DOI: 10.3390/nu12071973]

147 **Binda S**, Hill C, Johansen E, Obis D, Pot B, Sanders ME, Tremblay A, Ouwehand AC. Criteria to Qualify Microorganisms as "Probiotic" in Foods and Dietary Supplements. *Front Microbiol* 2020; **11**: 1662 [PMID: 32793153 DOI: 10.3389/fmicb.2020.01662]

148 **Wong WY**, Chan BD, Sham TT, Lee MM, Chan CO, Chau CT, Mok DK, Kwan YW, Tai WC. Lactobacillus casei Strain Shirota Ameliorates Dextran Sulfate Sodium-Induced Colitis in Mice by Increasing Taurine-Conjugated Bile Acids and Inhibiting NF-κB Signaling *via* Stabilization of IκBα. *Front Nutr* 2022; **9**: 816836 [PMID: 35529468 DOI: 10.3389/fnut.2022.816836]

149 **Liu Z**, Wang H. Probiotics alleviate inflammatory bowel disease in mice by regulating intestinal microorganisms-bile acid-NLRP3 inflammasome pathway. *Acta Biochim Pol* 2021; **68**: 687-693 [PMID: 34648252 DOI: 10.18388/abp.2020_5597]

150 **Lu R**, Shang M, Zhang YG, Jiao Y, Xia Y, Garrett S, Bakke D, Bäuerl C, Martinez GP, Kim CH, Kang SM, Sun J. Lactic Acid Bacteria Isolated From Korean Kimchi Activate the Vitamin D Receptor-autophagy Signaling Pathways. *Inflamm Bowel Dis* 2020; **26**: 1199-1211 [PMID: 32170938 DOI: 10.1093/ibd/izaa049]

151 **Zhou C**, Wang Y, Li C, Xie Z, Dai L. Amelioration of Colitis by a Gut Bacterial Consortium Producing Anti-Inflammatory Secondary Bile Acids. *Microbiol Spectr* 2023; **11**: e0333022 [PMID: 36943054 DOI: 10.1128/spectrum.03330-22]

152 **Xiao F**, Dong F, Li X, Li Y, Yu G, Liu Z, Wang Y, Zhang T. Bifidobacterium longum CECT 7894 Improves the Efficacy of Infliximab for DSS-Induced Colitis *via* Regulating the Gut Microbiota and Bile Acid Metabolism. *Front Pharmacol* 2022; **13**: 902337 [PMID: 35979230 DOI: 10.3389/fphar.2022.902337]

153 **Costello SP**, Hughes PA, Waters O, Bryant RV, Vincent AD, Blatchford P, Katsikeros R, Makanyanga J, Campaniello MA, Mavrangelos C, Rosewarne CP, Bickley C, Peters C, Schoeman MN, Conlon MA, Roberts-Thomson IC, Andrews JM. Effect of Fecal Microbiota Transplantation on 8-Week Remission in Patients With Ulcerative Colitis: A Randomized Clinical Trial. *JAMA* 2019; **321**: 156-164 [PMID: 30644982 DOI: 10.1001/jama.2018.20046]

154 **Kelly CR**, Yen EF, Grinspan AM, Kahn SA, Atreja A, Lewis JD, Moore TA, Rubin DT, Kim AM, Serra S, Nersesova Y, Fredell L, Hunsicker D, McDonald D, Knight R, Allegretti JR, Pekow J, Absah I, Hsu R, Vincent J, Khanna S, Tangen L, Crawford CV, Mattar MC, Chen LA, Fischer M, Arsenescu RI, Feuerstadt P, Goldstein J, Kerman D, Ehrlich AC, Wu GD, Laine L. Fecal Microbiota Transplantation Is Highly Effective in Real-World Practice: Initial Results From the FMT National Registry. *Gastroenterology* 2021; **160**: 183-192.e3 [PMID: 33011173 DOI: 10.1053/j.gastro.2020.09.038]

155 **Lima SF**, Gogokhia L, Viladomiu M, Chou L, Putzel G, Jin WB, Pires S, Guo CJ, Gerardin Y, Crawford CV, Jacob V, Scherl E, Brown SE, Hambor J, Longman RS. Transferable Immunoglobulin A-Coated Odoribacter splanchnicus in Responders to Fecal Microbiota Transplantation for Ulcerative Colitis Limits Colonic Inflammation. *Gastroenterology* 2022; **162**: 166-178 [PMID: 34606847 DOI: 10.1053/j.gastro.2021.09.061]

156 **Huang C**, Mei Q, Lou L, Huang Z, Fu Y, Fan J, Wang J, Yin N, Zheng Y, Lu Y, Zeng Y. Ulcerative Colitis in Response to Fecal Microbiota Transplantation *via* Modulation of Gut Microbiota and Th17/Treg Cell Balance. *Cells* 2022; **11** [PMID: 35681546 DOI: 10.3390/cells11111851]

157 **Huo X**, Li D, Wu F, Li S, Qiao Y, Wang C, Wang Y, Zhou C, Sun L, Luan Z, Yan Q, Wang J, Zhang Y, Zhao T, An Y, Zhang B, Tian X, Yu Z, Ma X. Cultivated human intestinal fungus Candida metapsilosis M2006B attenuates colitis by secreting acyclic sesquiterpenoids as FXR agonists. *Gut* 2022; **71**: 2205-2217 [PMID: 35173042 DOI: 10.1136/gutjnl-2021-325413]

158 **Smith BJ**, Piceno Y, Zydek M, Zhang B, Syriani LA, Terdiman JP, Kassam Z, Ma A, Lynch SV, Pollard KS, El-Nachef N. Strain-resolved analysis in a randomized trial of antibiotic pretreatment and maintenance dose delivery mode with fecal microbiota transplant for ulcerative colitis. *Sci Rep* 2022; **12**: 5517 [PMID: 35365713 DOI: 10.1038/s41598-022-09307-5]

159 **Staels B**, Kuipers F. Bile acid sequestrants and the treatment of type 2 diabetes mellitus. *Drugs* 2007; **67**: 1383-1392 [PMID: 17600387 DOI: 10.2165/00003495-200767100-00001]

160 **Islam MS**, Sharif A, Kwan N, Tam KC. Bile Acid Sequestrants for Hypercholesterolemia Treatment Using Sustainable Biopolymers: Recent Advances and Future Perspectives. *Mol Pharm* 2022; **19**: 1248-1272 [PMID: 35333534 DOI: 10.1021/acs.molpharmaceut.2c00007]

161 **Vítek L**. Bile acid malabsorption in inflammatory bowel disease. *Inflamm Bowel Dis* 2015; **21**: 476-483 [PMID: 25248001 DOI: 10.1097/MIB.0000000000000193]

162 **Mena Bares LM[a]**, Benítez Cantero JM, Iglesias Flores E, Gros Alcalde B, Moreno Ortega E, Maza Muret FR, Carmona Asenjo E, García Sánchez MªV, Vallejo Casas JA. Bile acid malabsorption in patients with chronic diarrhea and Crohn's disease. *Rev Esp Enferm Dig* 2019; **111**: 40-45 [PMID: 30284903 DOI: 10.17235/reed.2018.5376/2017]

163 **Kumar A**, Galbraith N, Al-Hassi HO, Jain M, Phipps O, Butterworth J, Steed H, McLaughlin J, Brookes MJ. The impact of treatment with bile acid sequestrants on quality of life in patients with bile acid diarrhoea. *BMC Gastroenterol* 2022; **22**: 325 [PMID: 35778677 DOI: 10.1186/s12876-022-02404-9]

World Journal of Gastroenterology

Submit a Manuscript: https://www.f6publishing.com

World J Gastroenterol 2023 July 21; 29(27): 4271-4288

DOI: 10.3748/wjg.v29.i27.4271

ISSN 1007-9327 (print) ISSN 2219-2840 (online)

REVIEW

Serum resistin and the risk for hepatocellular carcinoma in diabetic patients

Mona Mohamed Ibrahim Abdalla

Specialty type: Gastroenterology and hepatology

Provenance and peer review: Invited article; Externally peer reviewed.

Peer-review model: Single blind

Peer-review report's scientific quality classification

Grade A (Excellent): 0
Grade B (Very good): B
Grade C (Good): C, C
Grade D (Fair): 0
Grade E (Poor): 0

P-Reviewer: Arumugam VA, India; Balbaa ME, Egypt; Yang L, China

Received: April 26, 2023
Peer-review started: April 26, 2023
First decision: May 27, 2023
Revised: June 11, 2023
Accepted: June 27, 2023
Article in press: June 27, 2023
Published online: July 21, 2023

Mona Mohamed Ibrahim Abdalla, Department of Human Biology, School of Medicine, International Medical University, Bukit Jalil 57000, Kuala Lumpur, Malaysia

Corresponding author: Mona Mohamed Ibrahim Abdalla, MSc, PhD, Senior Lecturer, Department of Human Biology, School of Medicine, International Medical University, No. 126, Jln Jalil Perkasa 19, Bukit Jalil 57000, Kuala Lumpur, Malaysia. monamohamed@imu.edu.my

Abstract

Hepatocellular carcinoma (HCC), the predominant type of liver cancer, is a major contributor to cancer-related fatalities across the globe. Diabetes has been identified as a significant risk factor for HCC, with recent research indicating that the hormone resistin could be involved in the onset and advancement of HCC in diabetic individuals. Resistin is a hormone that is known to be involved in inflammation and insulin resistance. Patients with HCC have been observed to exhibit increased resistin levels, which could be correlated with more severe disease stages and unfavourable prognoses. Nevertheless, the exact processes through which resistin influences the development and progression of HCC in diabetic patients remain unclear. This article aims to examine the existing literature on the possible use of resistin levels as a biomarker for HCC development and monitoring. Furthermore, it reviews the possible pathways of HCC initiation due to elevated resistin and offers new perspectives on comprehending the fundamen-tal mechanisms of HCC in diabetic patients. Gaining a better understanding of these processes may yield valuable insights into HCC's development and progression, as well as identify possible avenues for prevention and therapy.

Key Words: Hepatocellular carcinoma; Resistin; Insulin resistance; Obesity; Diabetes; Liver cancer

©The Author(s) 2023. Published by Baishideng Publishing Group Inc. All rights reserved.

Core Tip: Resistin, a hormone linked to the onset of insulin resistance and diabetes, could be involved in the development and advancement of hepatocellular carcinoma (HCC) in individuals with diabetes. Increased resistin levels have been observed in HCC patients and might be connected to a more severe disease stage and unfavourable prognosis. This review aims to assess the existing literature concerning the possible application of resistin as a biomarker for HCC development and monitoring while investigating the potential processes through which resistin influences HCC's development and progression in diabetic patients. Gaining a better understanding of these processes may offer valuable insights for the prevention and therapy of this condition.

Citation: Abdalla MMI. Serum resistin and the risk for hepatocellular carcinoma in diabetic patients. *World J Gastroenterol* 2023; 29(27): 4271-4288
URL: https://www.wjgnet.com/1007-9327/full/v29/i27/4271.htm
DOI: https://dx.doi.org/10.3748/wjg.v29.i27.4271

INTRODUCTION

Liver cancer, particularly hepatocellular carcinoma (HCC), poses a significant global health challenge. As the sixth most prevalent cancer and the third leading cause of cancer-related deaths worldwide, it accounts for roughly one million fatalities each year[1-3]. HCC also ranks as the second primary factor contributing to premature cancer-related deaths[4], with projections indicating that annual liver cancer diagnoses will exceed one million by 2025[5]. Moreover, between 2020 and 2040, the number of liver cancer diagnoses is predicted to rise by 55.0%[6]. Although liver cancer prevalence and mortality have decreased in some East Asian countries, they have escalated in other parts of the world[7]. HCC represents the most frequent liver cancer variety, comprising 90% of cases[8]. It is commonly associated with chronic liver diseases (CLD), including viral hepatitis[9-12], alcoholic liver disease, liver cirrhosis[13-15] and "non-alcoholic fatty liver disease (NAFLD)"[16-18]. Because of the increased prevalence of obesity and type 2 diabetes mellitus (T2DM), the incidence of NAFLD and associated consequences, such as "non-alcoholic steatohepatitis (NASH)", is rapidly increasing. NAFLD is currently the major cause of liver cirrhosis, which in turn, raises the probability of developing HCC[19]. The development of HCC is influenced by various factors, including oxidative stress[20], inflammation[21,22], and insulin resistance (IR)[22-25].

Diabetes is a chronic metabolic condition characterized by high blood sugar and IR, which is associated with an increased risk of several health complications, including cardiovascular disease, kidney disease, and fatty liver[26]. The most common form of diabetes, T2DM, is caused primarily by IR. The relationship between diabetes and HCC is complex and multifaceted. On the one hand, diabetes is a risk factor for the development of liver diseases, including liver fibrosis and HCC[27]. On the other hand, HCC can lead to diabetes due to IR, impaired glucose tolerance, and liver dysfunction[28,29].

Resistin, a hormone secreted by both adipocytes and macrophages, and linked to obesity and T2DM, has been connected to HCC development and progression[30-33]. High levels of resistin have been associated with IR, inflammation, and oxidative stress. All these factors are known risk factors for the development of HCC[32-34]. Studies have found that high resistin levels are correlated with a greater risk of getting HCC[30,32,35]. Nevertheless, the mechanisms by which resistin contributes to the initiation and progression of HCC in diabetic patients are not fully understood. Therefore, the purpose of this review is to assess the current literature on the potential use of resistin levels as a biomarker for the development and monitoring of HCC in diabetic patients. Additionally, this review aims to explore resistin's role in HCC pathogenesis among this patient group and provide novel insights into the involved underlying mechanisms. These findings could help identify new targets for preventing and treating HCC in diabetic patients.

PREVALENCE OF HCC IN DIABETIC PATIENTS

HCC is more prevalent in diabetic individuals than in those without diabetes. A thorough meta-analysis of 42 studies, including 17 case-control and 32 cohort studies, demonstrated that diabetic patients have a 2.31 times higher chance of developing HCC compared to non-diabetics. Furthermore, diabetic individuals experience a 2.43 times higher HCC mortality risk than their non-diabetic counterparts[36,37]. HCC patients also exhibit a higher prevalence of diabetes, with reported rates between 20% and 70%[38]. Additionally, a systematic review and meta-analysis of ten studies reported a 70% prevalence of liver cancer among those with elevated fasting blood glucose levels[39].

Numerous investigations have corroborated the heightened incidence of HCC in diabetic individuals. For instance, a population-based study in Taiwan discovered that diabetic patients had a 2-3 times greater risk of developing HCC than those without diabetes[40]. Similarly, a prospective cohort study of Chinese men and women in Singapore found a heightened HCC risk in diabetics[41]. Furthermore, an Italian hospital-based case-control study involving 224 HCC patients and 389 control subjects determined that the risk of HCC was significantly higher among patients with T2DM, especially those with longer disease durations[42]. Additionally, a Korean prospective cohort study using the "National Health Insurance Service-Health Screening Cohort" found a hazard ratio of 1.82, indicating an elevated HCC risk in diabetic patients[43].

Recent research has established that metabolic factors, such as diabetes mellitus, obesity, dyslipidemia, and metabolic syndromes, are substantial risk factors for HCC development[44,45]. In populations with low viral hepatitis prevalence, the overall influence of metabolic factors on HCC may be more substantial than that of viral hepatitis. A recent multicenter study in China found that 9.3% of hepatitis B virus (HBV)-infected patients undergoing curative resection for HCC had concomitant metabolic syndrome. During a median follow-up of 50.4 months, patients with metabolic syndrome had worse 5-year overall survival and recurrence-free survival rates, with increased overall recurrence rates, particularly after two years of surgery. Multivariate analyses revealed that metabolic syndrome was an independent risk factor for reduced overall survival and recurrence-free survival following curative resection for HCC. As a result, proper management of metabolic syndrome is essential for preventing post-hepatectomy recurrence. This information further emphasizes the importance of implementing a more rigorous surveillance program for recurrence in HBV-infected patients with concurrent metabolic syndrome, in addition to routine antiviral therapy[46].

POTENTIAL MECHANISMS AND RISK FACTORS FOR HCC IN DIABETIC PATIENTS

The elevated incidence of HCC in diabetic patients is attributable to a multitude of factors, such as IR, chronic inflammation, the administration of antidiabetic medications, and the progression of NAFLD and NASH[47-50]. IR and diminished glucose tolerance in diabetic individuals can result in hepatic fat accumulation, thereby promoting the onset of NAFLD[51,52]. NAFLD has been linked to a heightened risk of liver fibrosis and HCC[18,53,54]. Furthermore, the prevalence of diabetes has been recognized as a risk factor for the emergence of NASH and its subsequent progression to cirrhosis and HCC[50].

NAFLD is a multifaceted condition that can advance to severe fibrosis, cirrhosis, liver failure, and HCC[55]. In the United States, NAFLD contributes to roughly 20% of HCC cases and is associated with an increased risk of HCC development, especially in patients with metabolic syndrome, specific ethnic groups, and hepatic siderosis. The incidence of HCC in NASH-related cirrhosis varies considerably, ranging from 2.4% over seven years to 12.8% over three years, with some patients developing HCC *de novo* as a result of NASH[55]. Patients with T2DM have a higher risk of developing severe manifestations of NAFLD, such as cirrhosis and HCC[56-58].

The coexistence of diabetes and NASH may contribute to the elevated prevalence of HCC in diabetic individuals. A recent study found that the global burden of NASH-related liver cancer, attributable to increased fasting plasma glucose levels, has significantly risen over the past three decades, particularly in "low- and middle-income countries". Consequently, effective prevention and management of high fasting plasma glucose levels are vital for reducing the worldwide burden of NASH-related liver cancer[59].

Besides NAFLD and NASH, other diabetes-associated complications may also contribute to the heightened HCC risk in diabetic patients. Such patients are more prone to chronic kidney disease, leading to the accumulation of uremic toxins and oxidative stress-both implicated in HCC development[60,61]. Diabetic patients are also more prone to hypertension [62], which has been linked to a higher HCC risk in some studies[44,63,64].

The consumption of antidiabetic medications, for instance, insulin and metformin, may also influence the HCC risk in diabetic patients[49]. Some studies suggest that IR and hyperinsulinemia could promote HCC development, potentially increasing the risk of HCC with insulin therapy[64-67]. Conversely, metformin has shown protective effects against HCC development in some studies, possibly due to its antineoplastic, anti-inflammatory, and antifibrotic properties[42,64,68-70].

Hyperglycemia and hyperinsulinemia are believed to promote HCC development and progression[71,72]. These conditions can activate various signaling pathways, such as the insulin-like growth factor-1 (IGF-1) pathway, phosphatidylinositol 3-kinase (PI3K)/protein kinase B (AKT), mitogen-activated protein kinase (MAPK), and mTOR pathway, all involved in HCC development and progression[73-77].

Hyperinsulinemia can increase hepatic growth hormone receptor expression, leading to IGF-1 release and the activation of growth factor-like activity on hepatocytes. Insulin and IGF-1 inhibit cell proliferation and apoptosis, increasing the risk of HCC[78]. High glucose levels can also contribute to HCC development by generating advanced glycosylation end products, which activate inflammatory signaling pathways and produce reactive oxygen species that promote HCC development. IR might directly hasten the development of HCC by promoting the formation of new blood vessels in the liver[79,80].

Moreover, dyslipidemia, which is common in diabetic patients, may have a role in HCC initiation and progression[81,82]. Dyslipidemia can cause lipid accumulation in the liver, leading to liver damage and inflammation that promote HCC development[83]. Research has demonstrated a strong correlation between reduced total cholesterol levels and a heightened likelihood of HCC development[84-87]. Additionally, diabetic patients who exhibit high triglyceride levels and low high-density lipoprotein cholesterol levels, a pattern often seen in dyslipidemia, have been identified as being at a greater risk for HCC. However, the correlation between the levels of high-density lipoprotein cholesterol with HCC remains uncertain[85,88].

Furthermore, diabetic patients may experience weakened immune systems[89,90], which could increase the risk of developing chronic HBV or hepatitis C virus (HCV) infections, both of which are significant risk factors for HCC[91-95]. Although the connection between DM and HCC risk appears to be stronger in HCV than HBV, a United States study involving 52671 HCV-liver cirrhosis patients (including 7605 HCC cases) did not find a significant association between DM and HCC risk[96]. Moreover, immunosuppressive medications prescribed to manage diabetes-related complications, such as kidney and pancreas transplants, might also contribute to an elevated risk of HCC development[97-99].

Overall, the increased prevalence of HCC in diabetic patients is due to a combination of factors outlined in Figure 1. Further research is necessary to comprehensively understand the mechanisms linking diabetes and HCC and to devise effective strategies for preventing and treating HCC in diabetic patients.

DIAGNOSIS AND MANAGEMENT OF HCC IN DIABETIC PATIENTS

Early detection of HCC is crucial for successful treatment. Although HCC can be diagnosed early in 30%-60% of cases, recurrences can still affect up to 80% of patients within five years, even after receiving curative treatments[100].

Screening for HCC in diabetic patients is challenging due to the high prevalence of coexisting liver illnesses such as NAFLD and NASH, and there is currently a lack of effective methods to monitor NAFLD-related HCC[101]. Although guidelines recommend regular HCC surveillance for high-risk individuals, which involves at least once every six months of liver ultrasonography and serum alpha-fetoprotein monitoring[102-106], the insidious onset of HCC often leads to late detection. Consequently, it is crucial to establish effective monitoring strategies and ensure early diagnosis and treatment to enhance patient outcomes.

The lack of official guidelines for NAFLD-related HCC diagnosis criteria results in clinical symptoms being the primary diagnostic tool, which can lead to late detection of the disease. Patients with NAFLD-related cirrhosis are considered high-risk subgroups for HCC, and ultrasonography is the primary surveillance test[107-109]. Imaging modalities such as ultrasound, computed tomography, and magnetic resonance imaging are commonly used for HCC screening in diabetic patients, and diagnostic accuracy can be improved by combining different imaging techniques[108-110].

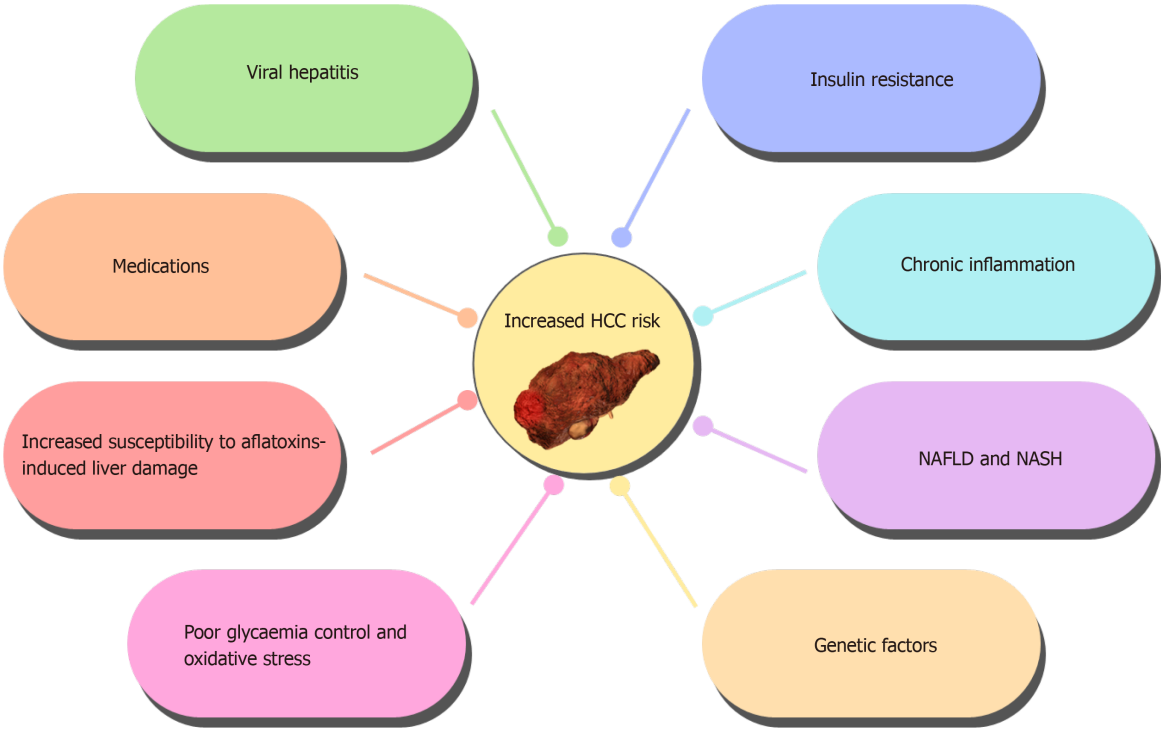
The management of HCC in diabetic patients requires a multidisciplinary approach that considers the potential interactions between diabetes medications and cancer treatments, as well as their impact on glycaemic control[49,111-113]. Although surgical removal of the tumour and liver transplant are curative treatments for HCC, they may not be suitable for all diabetic patients due to the higher risk of surgical complications in this population. Furthermore, diabetic individuals with HCC are more likely to have advanced illnesses at the time of diagnosis, which may limit the effectiveness of these treatments[107-109].

Until recently, Sorafenib was the only medication approved by the United States Food and Drug Administration (FDA) for advanced HCC. Multi-kinase inhibitors like cabozantinib and ramucirumab have been approved as second-line treatments since 2017[114-116]. Nivolumab[117] and pembrolizumab[118], the checkpoint inhibitors have either received FDA approval or are currently being investigated. However, systemic therapies may pose significant challenges in managing side effects in patients with cirrhosis[119]. Moreover, the high cost of approved medications makes their usage difficult in low-income countries[120]. Thus, HCC prevention in high-risk individuals could be a viable alternative to HCC treatment since identifying high-risk individuals is possible, and the survival rates after diagnosis are low. Local therapies such as radiofrequency ablation, percutaneous ethanol injections, and transarterial chemoembolization (TACE) are available options for early-stage HCC[121-125]. Among these options, TACE is commonly used as a treatment approach. TACE involves the direct delivery of chemotherapy drugs into the blood vessels that supply the tumour, followed by the injection of embolic agents to obstruct the tumour's blood flow. This targeted approach allows for the direct impact on the tumour while minimizing the systemic effects of chemotherapy. TACE is often recommended for patients with early-stage HCC who are not suitable candidates for surgery or liver transplantation. Additionally, it can serve as a bridge therapy prior to other definitive treatments or as a palliative measure to reduce tumor size and alleviate symptoms[124,125]. Systemic therapy with chemotherapy, targeted therapy, or immunotherapy may be used for advanced-stage HCC, but the choice of treatment should consider the potential interactions with diabetes medications and their impact on glycaemic control[126-128].

PREVENTION STRATEGIES FOR HCC IN DIABETIC PATIENTS

Preventing HCC development in diabetic patients is a crucial objective of diabetes management. Lifestyle adjustments, such as weight loss, exercise, and dietary changes, can enhance glycaemic control, diminish the risk of developing NAFLD and NASH, which are vital risk factors for HCC[101,109,111], and also minimize the risk of HCC[102,109,129]. Regular HCC screening for diabetic patients can facilitate early detection of the disease when curative therapies are more likely to succeed. The American Association for the Study of Liver Diseases recommends that diabetic patients with cirrhosis and advanced fibrosis undergo ultrasound screening every six months for HCC[107].

In addition, antidiabetic drugs may also aid in preventing HCC development in diabetic patients. Metformin, in particular, has demonstrated a protective effect against HCC development in some studies, potentially because of its anti-neoplastic, anti-inflammatory, and anti-fibrotic effects[49,64,68-70]. However, the use of other antidiabetic medications like insulin may raise the risk of HCC, though further investigation is necessary to completely comprehend the association between diabetes medications and HCC risk[67].



DOI: 10.3748/wjg.v29.i27.4271 **Copyright** ©The Author(s) 2023.

Figure 1 Factors contributing to increased risk of hepatocellular carcinoma in diabetic patients. NAFLD: Non-alcoholic fatty liver disease; NASH: Non-alcoholic steatohepatitis; HCC: Hepatocellular carcinoma.

RESISTIN AS A POTENTIAL BIOMARKER FOR HCC: INSIGHTS INTO ITS ROLE IN HCC DEVELOPMENT AND DIAGNOSIS

The timely diagnosis and detection of HCC is crucial for improving patient outcomes, which has led to an increased interest in identifying biomarkers for early detection. Resistin has emerged as a promising candidate in this regard. First identified in 2001, resistin is a hormone that is implicated in IR and is characterized by its pro-inflammatory properties. Resistin is predominantly synthesized by adipocytes in rodents. In contrast, in humans, while adipocytes have the capacity to synthesize resistin, the hormone is primarily produced by immune cells called macrophages, which are integral to immune responses and inflammation. The presence of resistin in human serum typically ranges within a physiological concentration of 7-22 ng/mL[130]. The *RETN* gene encodes resistin protein, which is also known as "adipocyte-specific secretory factor, Fizz3, RSTN, or cysteine-rich protein 1"[131-134].

Resistin contributes to IR by inducing persistent low-grade inflammation associated with obesity-induced macrophage infiltration in adipose tissues. Furthermore, resistin promotes p38 MAPK signaling, altering insulin signaling, modulating the cellular oxidative stress response, and enhancing cells proliferation by increasing the production of various inflammatory molecules such as interleukin (IL)-1β, IL-6, IL-8, IL-12, and tumor necrosis factor-alpha (TNF-α)[34,135-137]. Elevated resistin expression has been associated with inflammation, autoimmune illnesses, metabolic diseases, and malignant conditions, suggesting that it could be a reliable biomarker for HCC diagnosis, early detection, and prognosis [131,132,138,139].

Several clinical studies have investigated the potential of resistin as a diagnostic and prognostic biomarker for HCC[33,140-142]. Studies have shown that resistin is expressed in HCC tissue and is involved in the progression of HCC through its effects on cell proliferation, apoptosis, invasion, and angiogenesis[138,143-145]. Serum resistin levels have been found to be positively correlated with tumour size, TNM stage, and vascular invasion, highlighting that resistin might be a helpful HCC predictive biomarker[32]. Moreover, resistin has been assessed as a diagnostic biomarker for HCC in combination with other biomarkers, such as alpha-fetoprotein and des-gamma-carboxy prothrombin. The combination has been reported to exhibit higher diagnostic accuracy compared to any of the biomarkers alone[32,146,147].

Yagmur *et al*[139] investigated the clinical significance of resistin in CLD by measuring serum resistin levels in 82 CLD patients and 76 age and gender-matched healthy controls, and monitoring the patients for six years. The study found that resistin levels were significantly higher in liver cirrhosis patients compared to the healthy controls, with levels increasing as cirrhosis advanced. Resistin levels also showed a positive correlation with insulin secretion, a negative correlation with insulin sensitivity, and associations with inflammatory markers and clinical complications. The study concluded that patients with higher resistin levels had increased mortality within six years, suggesting that resistin could be a useful clinical biomarker for evaluating liver cirrhosis and its potential link to IR in patients with severe liver disease[140].

Da Silva *et al*[141] conducted a prospective cohort study to investigate potential factors associated with adiponectin and resistin levels in cirrhosis patients and their clinical significance. The study involved 122 cirrhosis patients from an

outpatient clinic and a control group of 30 healthy subjects. The study found that patients with cirrhosis had higher adiponectin and resistin levels compared to the control group. Adiponectin levels, but not resistin well established levels, were significantly associated with the severity of liver dysfunction and a worse prognosis in patients with alcoholic liver disease, suggesting a potential role as a prognostic biomarker[142].

A recently published systematic review and meta-analysis investigated the correlation between serum resistin levels and NAFLD in adults. The review comprised 28 studies that included 4088 participants, which were analyzed using meta-analysis techniques. The study findings indicated that patients with NAFLD had considerably higher serum resistin levels when compared to healthy individuals. In contrast, patients with NASH had lower serum resistin levels than healthy controls. No significant difference was observed in serum resistin levels between patients with NAFLD and healthy controls or between patients with NAFLD and NASH. The study also suggested that serum resistin may be a potential biomarker for predicting the risk of developing NAFLD, a known risk factor for HCC, and could also differentiate between NAFLD and NASH. However, further research is necessary to support these findings and to comprehend the underlying mechanisms of this association[148].

EVALUATION OF RESISTIN AS A DIAGNOSTIC AND PROGNOSTIC BIOMARKER FOR HCC: INSIGHTS FROM CLINICAL STUDIES

A thorough search was executed on PubMed and Google Scholar databases, employing a set of keywords including "resistin and HCC", "resistin and hepatocellular carcinoma", "resistin and liver cancer", "resistin as a biomarker for hepatocellular carcinoma", and "resistin and hepatic cancer" with the objective of identifying research that investigates the role of resistin as a biomarker specifically for HCC. The search yielded four studies that delved into the clinical utility of resistin in the diagnosis and prognosis of HCC. The ensuing compilation of studies is presented in a chronological fashion, commencing with the pioneering study conducted in 2014 and culminating with the latest research from 2022.

Elbedewy *et al*[30] conducted a study to investigate whether serum resistin and IR could be considered as risk factors for HCC in HCV-cirrhotic patients with T2DM. The study involved 50 adult patients with HCV infection who were categorized into three groups based on their HCC status, and were subjected to routine tests for DM, HCV, liver cirrhosis, and HCC. The results revealed that patients with HCC and diabetes (group I) had significantly higher levels of homeostasis model assessment-IR (HOMA-IR) and resistin than diabetic patients with cirrhosis (group II) and control subjects (group III). The study concluded that HOMA-IR and serum resistin could potentially serve as novel biomarkers to identify HCV-cirrhotic patients with T2DM who are at a greater risk of developing HCC[30].

Furthermore, a prospective case-control study was conducted by Elsayed *et al*[33] to investigate the implications of IR and serum resistin as possible risk factors for HCC among individuals with HCV-related liver cirrhosis. The study involved 200 patients with HCV-related liver cirrhosis (100 with HCC and 100 without HCC) as well as 50 healthy controls. The study found that patients with HCC had significantly higher levels of resistin and HOMA-IR than cirrhotic patients and healthy controls. Patients with resistin levels more than or equal to 12 ng/mL and HOMA-IR values higher than or equal to 4 were 1.6 times more likely to experience HCC. These data imply that HOMA as well as serum resistin, may be useful in identifying HCV-cirrhotic individuals at high risk of developing HCC[33].

Mohamed *et al*[32] conducted a study to evaluate the potential of serum resistin levels as a biomarker for assessing response to therapy in individuals with hepatic cirrhosis and HCC. The study included 50 patients with HCV-related cirrhosis, 30 of whom had HCC and the remaining 20 did not. Patients with HCC had higher levels of serum resistin, which showed strong positive correlations with hepatic focal lesions, portal vein invasion, total bilirubin, international normalized ratio, and model of end-stage liver disease score. After one month of HCC intervention, serum resistin levels were significantly lower than before the intervention. These findings suggest that serum resistin could be used as a reliable biomarker for evaluating treatment response in HCC patients[32].

More recently, Ashour *et al*[31] conducted a case-control study to investigate the relationship between serum resistin levels and HCC in patients with liver cirrhosis. The study included 80 cirrhotic patients (40 with HCC and 40 without HCC). The results showed that serum resistin levels were significantly higher in the HCC group compared to the control group, with a strong positive correlation between resistin and total cholesterol and low-density lipoprotein. Additionally, the study found that resistin levels could be used as a diagnostic marker for HCC, with a sensitivity of 90% and specificity of 95% at a cutoff value of > 13.7 ng/mL. These findings support the use of serum resistin levels as a diagnostic biomarker for HCC in patients with liver cirrhosis[31]. Table 1 provides a summary of the above-mentioned studies.

POTENTIAL MECHANISMS OF HCC INDUCTION BY ELEVATED RESISTIN LEVELS

Resistin has been implicated in cancer development through various signaling pathways. Among these, the toll-like receptor 4 (TLR4), PI3K, and nuclear factor kappa-light-chain-enhancer of activated B cells (NFκβ) pathways are particularly noteworthy. These signaling cascades are instrumental in modulating various cellular processes that are crucial for cancer development and progression. In the context of different cancer types, these signaling pathways have been demonstrated to play an imperative role in fostering cellular proliferation. Notably, specific pathways are often selectively associated with distinct types of cancer. For instance, the AKT pathway, a downstream effector of PI3K, has been predominantly associated with prostate cancer, serving as a key regulator in promoting cell survival and growth [149]. Conversely, lung cancer demonstrates a more complex network of signaling pathways. Among these, PI3K, NFκβ,

Table 1 Summary of the clinical studies assessing serum resistin as a potential biomarker for hepatocellular carcinoma

Study ID	Ref.	Study design	Number of participants (HCC/cirrhosis/control)	Age range or mean ± SD	Sex distribution	Resistin levels (ng/mL) (HCC)	Resistin levels (ng/mL) (cirrhosis)	Resistin levels (ng/mL) (control)	Main findings	Resistin as HCC biomarker
1	Elbedewy *et al*[30], 2014, Egypt	Prospective case-control study	25 (HCC), 25 (cirrhosis), 25 (control)	HCC: Mean 53.92 ± 5.9 yr; range 43-65 yr. Cirrhosis: Mean 52.92 ± 7.371 yr; range 40-66 yr. Control: Mean 51.4 ± 6.028 yr; range 38-63 yr	HCC: 19 males/6 females. Cirrhosis: 17 males/8 females. Control: 20 males/5 females	6.11 ± 1.654[1]	3.11 ± 1.533[1]	1.31 ± 0.3198[1]	Patients with HCC have significantly higher mean value of resistin than cirrhotic patients and control subjects	Promising biomarker for HCC
2	Elsayed *et al* [33], 2015, Egypt	Prospective case-control	100 (HCC)/ 100 (cirrhosis)/ 50 (control)	52.3 (HCC), 52.2 (cirrhosis), 51 (control)	85% male (HCC), 66% male (cirrhosis)	23.8 ± 7.8[1]	9.9 ± 2.7[1]	7.1 ± 1.8[1]	HCC patients had higher HOMA-IR and resistin levels; resistin and HOMA considered independent risk factors for HCC	Yes
3	Mohamed *et al*[32], 2018, Egypt	Prospective case-control	50 (HCC)/-/25 (control)	59.8 ± 9.6 (HCC), 57.6 ± 10.1 (control)	37 males/13 females (HCC), 18 males/7 females (control)	5.5 ± 1.7[1] (pre-treatment)	-	3.3 ± 1.1[1]	Higher resistin levels in HCC patients compared to controls, and significant reduction in resistin levels after treatment	Yes
4	Ashour *et al* [31], 2022, Egypt	Case-control study	80 (40 HCC/40 cirrhosis/0 control)	HCC: Median 62 yr (range 18-75). Cirrhosis: Median 59 yr (range 48-72)	HCC: 23 males/17 females. Cirrhosis: 25 males/15 females	19.4[2]	3.4[2]	N/A	Higher serum resistin levels in HCC patients compared to cirrhotic patients; resistin > 13.7 ng/mL able to diagnose HCC with 90% sensitivity and 95% specificity	Promising biomarker for HCC

[1]Data presented as mean ± SD.

[2]Data presented as median. Resistin was measured using ELISA in all studies listed in the table.

HCC: Hepatocellular carcinoma; HOMA-IR: Homeostasis model assessment-insulin resistance; N/A: Not applicable.

epidermal growth factor receptor, and TLR4 have been implicated[150]. These pathways collaboratively contribute to the progression of lung cancer through mechanisms such as cell proliferation, angiogenesis, and resistance to apoptosis.

Additionally, melanoma, a malignancy of melanocytes, has been found to be under the influence of distinct signaling axes, such as the phosphorylated AKT and Caveolin-1, which are critical in dictating the course of the disease[151].

Resistin's influence extends beyond these pathways; it has been implicated in the activation of the IL-6 dependent signal transducer and activator of transcription 3 (STAT3) signaling pathway[152,153]. This pathway is especially noteworthy in breast cancer progression. Moreover, resistin has been linked to the progression of ovarian cancer through the modulation of microRNAs, such as "miR let-7a, miR-200c, and miR-186"[154].

Diving deeper into the IL-6/STAT3 axis, this signaling pathway has been linked with various aspects of cancer biology, including tumor progression, metastasis, and therapy resistance in diverse cancer types such as breast, colorectal, and HCC. The crux of this axis lies in the overexpression of IL-6 and the consequent hyperactivation of STAT3, a combination frequently associated with a grim prognosis. Resistin further exacerbates this by promoting the secretion of pro-inflammatory cytokines like IL-6, which activates STAT3. This sets into motion an autocrine loop intensifying STAT3 signaling, leading to aggressive tumor behavior[153,155,156].

Intriguingly, Resistin dons yet another hat - that of a potential tumor suppressor. It has been shown to induce cell cycle arrest in colon cancer cells through the upregulation of suppressor of cytokine signaling 3 (SOCS3)[157]. SOCS3, part of the SOCS protein family, is integral in curbing cytokine signaling. This implies that resistin may play a role in keeping the proliferation of colon cancer cells in check, revealing its context-dependent pleiotropic nature. In summary, resistin orchestrates a plethora of pathways, including the activation of pro-inflammatory cytokines, fostering angiogenesis, modulating insulin signaling, and influencing cell proliferation and survival[155,156,158]. Its context-dependent roles in both promoting and potentially suppressing tumors accentuate the complexity of resistin's function in cancer. This warrants a nuanced understanding and approach in considering resistin as a potential target for therapeutic interventions.

Resistin's role in proinflammatory cytokine activation

The role of resistin in activating proinflammatory cytokines has been well-established in various studies. These cytokines, including TNF-α, IL-6, and monocyte chemoattractant protein-1 are crucial in inflammation, cell proliferation, and apoptosis, all of which contribute to HCC development and progression[159-163].

Resistin has been demonstrated to directly stimulate TNF-α and IL-6 production in macrophages by binding to TLR4 and initiating downstream signaling pathways, such NFκβ[164,165]. The activation of the NFκB pathway results in the transcription of proinflammatory cytokines, perpetuating chronic inflammation associated with an increased risk of HCC [166].

In addition to direct stimulation, resistin activates other inflammatory pathways, notably the c-Jun N-terminal kinase and STAT3 pathways[167-170]. These pathways contribute to the production of proinflammatory cytokines and are implicated in the pathogenesis of HCC[168,169,171]. Moreover, resistin-induced cytokines have been linked to hepatic stellate cell activation, subsequently leading to liver fibrosis and cirrhosis, both of which are significant precursors to HCC[172-174]. In this regard, resistin's activation of proinflammatory cytokines serves as a vital connection between resistin and the development of HCC in diabetic patients.

Resistin and the modulation of immune responses

In addition to resistin's proinflammatory effect, resistin has been implicated in macrophage activation and polarization of tumor-associated macrophages towards the M2 phenotype[175]. M2 macrophages are characterized by their pro-tumorigenic properties, such as promoting angiogenesis, immunosuppression, and tissue remodeling, which further advance HCC progression[176].

Additionally, resistin has been implicated in the modulation of the immune response through increased expression of the macrophage inflammatory protein-alpha (MIP-α), a chemokine also known as CC chemokine ligand 3[177]. It is a small signaling protein secreted by various immune cells, including macrophages, T cells, and dendritic cells. MIP-α plays a crucial role in immune response modulation by attracting and activating leukocytes, particularly monocytes and neutrophils, to the site of inflammation or infection. This chemokine is involved in various biological processes, including inflammation, immune cell activation, and the regulation of cell migration during an immune response. MIP-α has also been implicated in the progression of certain diseases, such as autoimmune disorders, chronic inflammatory conditions, and even cancer, due to its ability to modulate immune responses[178]. Furthermore, resistin has been reported to modulate the function of other immune cell populations, including natural killer cells and T lymphocytes, impairing their antitumor activities and allowing HCC tumor evasion[179,180]. Taken together, these findings highlight the multifaceted role of resistin in HCC pathogenesis through the modulation of the immune responses and tumour microenvironment.

Resistin and promotion of angiogenesis

Angiogenesis, the formation of new blood vessels from existing ones, is a pivotal process in tumor growth, invasion, and metastasis. Resistin promotes angiogenesis through various mechanisms, including the upregulation of vascular endothelial growth factor (VEGF), activation of the hypoxia-inducible factor-1α (HIF-1α) pathway, and modulation of other signaling pathways[181-184].

VEGF, which spurs endothelial cell proliferation, migration, and survival, is crucial for angiogenesis[185]. Studies have demonstrated that resistin boosts VEGF expression in different cell types, including cancer cells[186,187]. In a study by Tsai *et al*[178], resistin was found to upregulate VEGF expression in osteosarcoma *via* the activation of NFκβ signaling [181]. Furthermore, Chen *et al*[179] demonstrated that resistin enhanced VEGF formation in human chondrosarcoma cells through a PI3K/AKT-dependent mechanism[182]. Elevated VEGF expression in HCC tissue has been associated with a worse prognosis[188,189].

Resistin can also contribute to angiogenesis by stimulating the HIF-1α pathway[190]. Under hypoxic conditions, HIF-1α is stabilized and translocated to the nucleus, where it binds to hypoxia-response elements and promotes the transcription of various genes, including VEGF[191]. It has been demonstrated that resistin increased HIF-1α expression in human adipocytes under hypoxia, leading to enhanced VEGF expression[182].

Resistin's impact on insulin signaling

Insulin signaling is critical for maintaining glucose homeostasis and is often disrupted in diabetes, obesity, and cancer. Resistin has been implicated in modulating insulin signaling, contributing to IR and affecting HCC development in diabetic patients[158].

Resistin has been demonstrated to disrupt insulin-driven glucose uptake in peripheral tissues like adipose tissue and skeletal muscle by interfering with insulin signaling[192,193]. Fu *et al*[191] found that resistin inhibited insulin-induced glucose uptake in 3T3-L1 adipocytes by reducing the activity of glucose transporters[194]. Similar results were observed

in skeletal muscle cells, where resistin impaired insulin-stimulated glucose uptake by decreasing IRS-1-associated PI3K activity[195].

Resistin has been shown to affect liver glucose metabolism by enhancing hepatic gluconeogenesis[196]. In a study by Rajala *et al*[193], resistin administration in mice led to elevated liver glucose production and hyperglycemia. The researchers suggested that this effect occurs *via* activating the cAMP-protein kinase A pathway.

In L6 rat myotubes, resistin overexpression was shown to hinder insulin-mediated glucose uptake without altering glucose transporter type 4 (GLUT4) translocation, GLUT1 expression, or IRS signaling[197]. Moreover, resistin or RELMβ infusion in adult male Sprague Dawley rats led to hepatic IR, characterized by increased hepatic glucose production *via* AMP-activated protein kinase[198]. Lastly, resistin treatment in rat hepatocytes and mice with liver-specific resistin expression resulted in impaired hepatic insulin action by reducing phosphorylation of GSK3β at serine 9. This observation was made in a study conducted on C57BL/6 J mice[199].

The modulation of insulin signaling by resistin may indirectly contribute to HCC development by exacerbating hyperinsulinemia and IR in diabetic patients. Hyperinsulinemia has been associated with an increased risk of HCC, as insulin can promote cell proliferation and survival through the activation of mitogenic signaling pathways, such as the PI3K/Akt and Ras/MAPK pathways[200,201]. Furthermore, IR may lead to chronic inflammation and liver damage, which can promote HCC development[202,203]. Hence, resistin modulates insulin signaling by impairing insulin-stimulated glucose uptake and promoting hepatic gluconeogenesis. These effects may indirectly contribute to HCC development in diabetic patients by exacerbating hyperinsulinemia, IR, and inflammation.

Resistin's induction of matrix metalloproteinases

Matrix metalloproteinases (MMPs) are enzymes responsible for the breakdown of extracellular matrix components, thereby aiding tumour invasion and metastasis[204]. Resistin has been found to increase MMP expression in various cell types, including endothelial cells and cancer cells[136,205]. In a study by Di Simone *et al*[203], resistin was shown to stimulate MMP-2 production in human endothelial cells, potentially contributing to angiogenesis and tumour invasion [206]. Similarly, Huang *et al*[207] demonstrated that resistin increased MMP-2 and MMP-9 expression in human colorectal cancer cells. Furthermore, a study by Tsai *et al*[178] revealed that resistin enhanced MMP-2 expression *via* the activation of the AMPK/p38 signaling pathway and downregulation of miR-519d, contributing to chondrosarcoma metastasis[208].

Moreover, resistin has been implicated in the promotion of HCC metastasis through the upregulation of vascular cell adhesion molecule-1 and intercellular adhesion molecule-1, both of which are critical mediators of cancer cell adhesion and migration. Evidence suggests that resistin stimulates the expression of these adhesion molecules in endothelial cells [206], thereby facilitating the adhesion and transendothelial migration of HCC cells. Taken together, the available evidence suggests that resistin contributes to HCC progression and metastasis through multiple mechanisms, including the promotion of angiogenesis, upregulation of VEGF, activation of the HIF-1α pathway, induction of MMP expression, and increased expression of cell adhesion molecules.

Promotion of cell proliferation and survival by resistin

Resistin has been associated with the enhancement of cell proliferation as well as survival in various cell types, including cancer cells, which can contribute to HCC development and progression in diabetic patients. This is achieved through the activation of mitogenic signaling pathways like PI3K/AKT and MAPK/ERK[135,140,183,207,208]. These pathways have been found to mediate cell proliferation and HCC progression[207,208]. Additionally, resistin promotes cell survival by upregulating anti-apoptotic proteins like Bcl-2 and Bcl-xL[145]. For instance, a study by Pang *et al*[144] demonstrated that resistin increased Bcl-2 expression in human myeloma cell lines, contributing to improved cell survival and resistance to chemotherapy, potentially through the activation of the NFκβ signaling pathway.

Moreover, resistin impacts cell cycle regulation. Research revealed that resistin increased the expression of cyclin D1 in colon cancer patients[157]. Cyclin D1 is integral for cell cycle progression, particularly for the transition from the G1 to S phase. This upregulation of cyclin D1 was suggested to be a result of SOCS 3 upregulation, mediated by the activation of the ERK signaling pathway[157].

Overall, resistin contributes to cell proliferation and survival through various mechanisms, including the activation of mitogenic signaling pathways, induction of anti-apoptotic proteins, and modulation of cell cycle regulation. Figure 2 provides a schematic representation of the mechanisms through which resistin influences the development and metastasis of HCC.

CONCLUSION

Resistin, an adipokine implicated in obesity and IR, plays a crucial role in promoting HCC development and progression in diabetic patients. There is evidence supporting the potential use of resistin as a biomarker for HCC in diabetic patients. The potential mechanisms through which resistin promotes HCC include the activation of proinflammatory cytokines, promotion of angiogenesis, modulation of insulin signaling, and enhancement of cell proliferation and survival. These diverse effects highlight the need for further research to better understand the complex interplay between resistin and HCC development in diabetic patients.

Limitations

This review, while offering a comprehensive overview of resistin's role in HCC development among diabetic patients, possesses several limitations. First, the scope is bound to the literature available at the time, which may not encompass

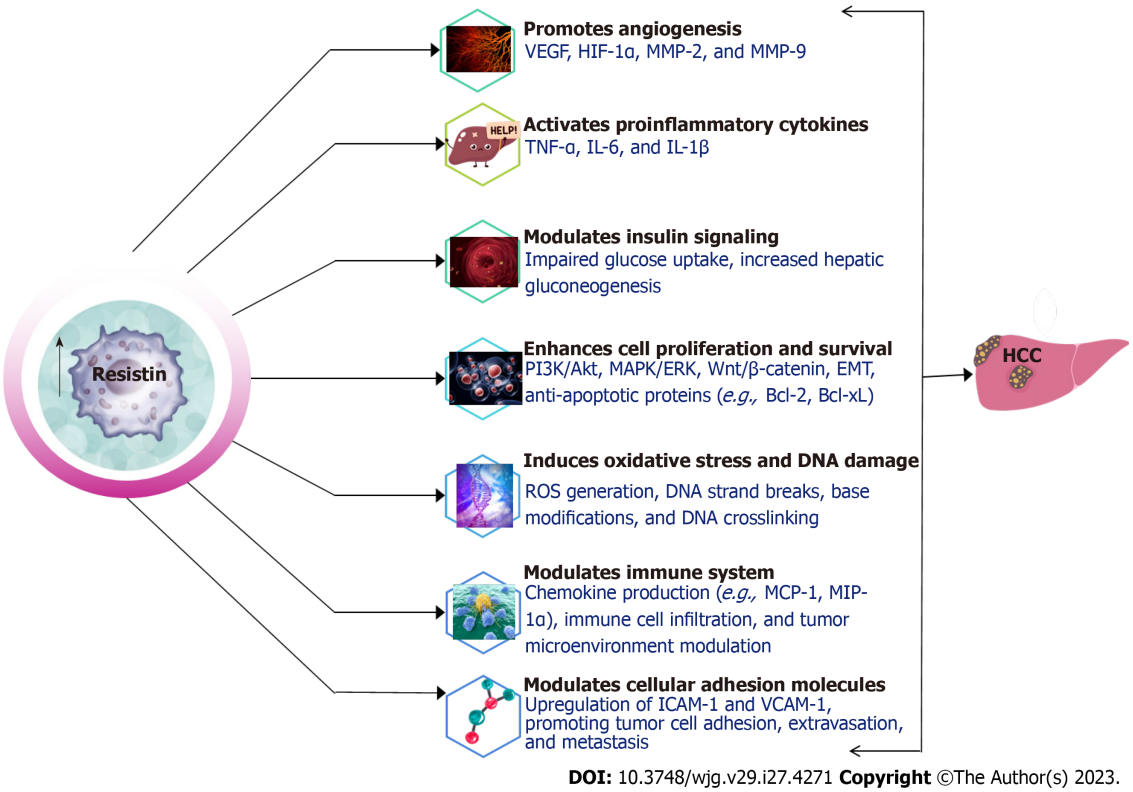


Figure 2 Mechanisms of resistin-induced hepatocellular carcinoma. VEGF: Vascular endothelial growth factor; HIF-1α: Hypoxia-inducible factor-1α; MMP-2: Matrix metalloproteinases-2; MMP-9: Matrix metalloproteinases -9; TNF-α: Tumour necrosis factor-α; IL-6: Interleukin -6; IL-1β: Interleukin--1β; ROS: Reactive-oxygen species; MCP-1: Monocyte chemoattractant protein-1; MIP-α: Macrophage inflammatory protein-alpha; ICAM-1: Intercellular adhesion molecule-1; VCAM-1: Vascular cell adhesion molecule-1; HCC: Hepatocellular carcinoma.

recent developments. Additionally, the multifaceted molecular mechanisms discussed are highly complex, and there may be aspects not extensively covered here. It is also imperative to differentiate between correlation and causation, as the review addresses associations but does not confirm causal relationships. Furthermore, the generalizability of the conclusion is uncertain, as genetic diversity, lifestyle factors, and additional health conditions could affect the interplay between resistin and HCC in different populations. Lastly, the reliance on studies that might contain biases or have their own limitations could inadvertently influence the conclusion drawn in this review. Recognizing these limitations is vital for a well-rounded understanding and highlights the importance of further studies.

Future studies

Future studies should focus on identifying novel molecular targets for therapeutic intervention and developing strategies to counteract the deleterious effects of resistin on HCC development and progression. Understanding the molecular mechanisms underlying resistin's role in HCC could lead to the development of novel diagnostic and therapeutic strategies for the management of HCC in diabetic patients. Additionally, the development of effective therapies targeting resistin and its associated signaling pathways may help mitigate the risk of HCC in diabetic patients, especially those with obesity and IR. Further research is required to assess the effectiveness and safety of such therapeutic strategies in preclinical and clinical settings.

Moreover, given the complexity of the molecular mechanisms underlying resistin's role in HCC, a multidisciplinary approach involving collaboration between experts in endocrinology, oncology, and molecular biology is essential for advancing our understanding of this complex relationship. This collaborative effort may help identify potential biomarkers for early detection and prognosis of HCC in diabetic patients and facilitate the development of personalized medicine approaches.

FOOTNOTES

Author contributions: Abdalla MMI collected the data and wrote the paper.

Conflict-of-interest statement: The author declares no conflict of interest for this article.

Open-Access: This article is an open-access article that was selected by an in-house editor and fully peer-reviewed by external reviewers. It is distributed in accordance with the Creative Commons Attribution NonCommercial (CC BY-NC 4.0) license, which permits others to

distribute, remix, adapt, build upon this work non-commercially, and license their derivative works on different terms, provided the original work is properly cited and the use is non-commercial. See: https://creativecommons.org/Licenses/by-nc/4.0/

Country/Territory of origin: Malaysia

ORCID number: Mona Mohamed Ibrahim Abdalla 0000-0002-4987-9517.

S-Editor: Wang JJ
L-Editor: A
P-Editor: Wang JJ

REFERENCES

1 **Sung H**, Ferlay J, Siegel RL, Laversanne M, Soerjomataram I, Jemal A, Bray F. Global Cancer Statistics 2020: GLOBOCAN Estimates of Incidence and Mortality Worldwide for 36 Cancers in 185 Countries. *CA Cancer J Clin* 2021; **71**: 209-249 [PMID: 33538338 DOI: 10.3322/caac.21660]
2 **Chon YE**, Park SY, Hong HP, Son D, Lee J, Yoon E, Kim SS, Ahn SB, Jeong SW, Jun DW. Hepatocellular carcinoma incidence is decreasing in Korea but increasing in the very elderly. *Clin Mol Hepatol* 2023; **29**: 120-134 [PMID: 35957547 DOI: 10.3350/cmh.2021.0395]
3 **Oh JH**, Jun DW. The latest global burden of liver cancer: A past and present threat. *Clin Mol Hepatol* 2023; **29**: 355-357 [PMID: 36891606 DOI: 10.3350/cmh.2023.0070]
4 **Ferlay J**, Colombet M, Soerjomataram I, Parkin DM, Piñeros M, Znaor A, Bray F. Cancer statistics for the year 2020: An overview. *Int J Cancer* 2021 [PMID: 33818764 DOI: 10.1002/ijc.33588]
5 **World Health Organization**. International agency for research on cancer. [cited 15 February 2023]. Available from: https://www.iarc.who.int/
6 **Rumgay H**, Arnold M, Ferlay J, Lesi O, Cabasag CJ, Vignat J, Laversanne M, McGlynn KA, Soerjomataram I. Global burden of primary liver cancer in 2020 and predictions to 2040. *J Hepatol* 2022; **77**: 1598-1606 [PMID: 36208844 DOI: 10.1016/j.jhep.2022.08.021]
7 **Arnold M**, Abnet CC, Neale RE, Vignat J, Giovannucci EL, McGlynn KA, Bray F. Global Burden of 5 Major Types of Gastrointestinal Cancer. *Gastroenterology* 2020; **159**: 335-349.e15 [PMID: 32247694 DOI: 10.1053/j.gastro.2020.02.068]
8 **Grandhi MS**, Kim AK, Ronnekleiv-Kelly SM, Kamel IR, Ghasebeh MA, Pawlik TM. Hepatocellular carcinoma: From diagnosis to treatment. *Surg Oncol* 2016; **25**: 74-85 [PMID: 27312032 DOI: 10.1016/j.suronc.2016.03.002]
9 **Askoura M**, Abbas HA, Al Sadoun H, Abdulaal WH, Abu Lila AS, Almansour K, Alshammari F, Khafagy ES, Ibrahim TS, Hegazy WAH. Elevated Levels of IL-33, IL-17 and IL-25 Indicate the Progression from Chronicity to Hepatocellular Carcinoma in Hepatitis C Virus Patients. *Pathogens* 2022; **11** [PMID: 35056005 DOI: 10.3390/pathogens11010057]
10 **Péneau C**, Imbeaud S, La Bella T, Hirsch TZ, Caruso S, Calderaro J, Paradis V, Blanc JF, Letouzé E, Nault JC, Amaddeo G, Zucman-Rossi J. Hepatitis B virus integrations promote local and distant oncogenic driver alterations in hepatocellular carcinoma. *Gut* 2022; **71**: 616-626 [PMID: 33563643 DOI: 10.1136/gutjnl-2020-323153]
11 **Luna-Cuadros MA**, Chen HW, Hanif H, Ali MJ, Khan MM, Lau DT. Risk of hepatocellular carcinoma after hepatitis C virus cure. *World J Gastroenterol* 2022; **28**: 96-107 [PMID: 35125821 DOI: 10.3748/wjg.v28.i1.96]
12 **Kudo M**. Prioritized Requirements for First-Line Systemic Therapy for Hepatocellular Carcinoma: Broad Benefit with Less Toxicity. *Liver Cancer* 2023; **12**: 1-6 [PMID: 36909143 DOI: 10.1159/000528979]
13 **Tsukuma H**, Hiyama T, Tanaka S, Nakao M, Yabuuchi T, Kitamura T, Nakanishi K, Fujimoto I, Inoue A, Yamazaki H. Risk factors for hepatocellular carcinoma among patients with chronic liver disease. *N Engl J Med* 1993; **328**: 1797-1801 [PMID: 7684822 DOI: 10.1056/NEJM199306243282501]
14 **Nakashima T**, Kojiro M, Nakashima T. Hepatocellular carcinoma and liver cirrhosis. In: Hepatocellular Carcinoma: An Atlas of Its Pathology. Janpan: Springer Tokyo, 1987: 185-204
15 **Tillman HL**, Choi SS. Risk for hepatocellular carcinoma in patients with alcoholic cirrhosis. *Ann Intern Med* 2012; **157**: 677-8; author reply 678 [PMID: 23128872 DOI: 10.7326/0003-4819-157-9-201211060-00022]
16 **Ioannou GN**, Green P, Kerr KF, Berry K. Models estimating risk of hepatocellular carcinoma in patients with alcohol or NAFLD-related cirrhosis for risk stratification. *J Hepatol* 2019; **71**: 523-533 [PMID: 31145929 DOI: 10.1016/j.jhep.2019.05.008]
17 **Thomas CE**, Diergaarde B, Kuipers AL, Adibi JJ, Luu HN, Chang X, Dorajoo R, Heng CK, Khor CC, Wang R, Jin A, Koh WP, Yuan JM. NAFLD polygenic risk score and risk of hepatocellular carcinoma in an East Asian population. *Hepatol Commun* 2022; **6**: 2310-2321 [PMID: 35503778 DOI: 10.1002/hep4.1976]
18 **Shah PA**, Patil R, Harrison SA. NAFLD-related hepatocellular carcinoma: The growing challenge. *Hepatology* 2023; **77**: 323-338 [PMID: 35478412 DOI: 10.1002/hep.32542]
19 **Estes C**, Razavi H, Loomba R, Younossi Z, Sanyal AJ. Modeling the epidemic of nonalcoholic fatty liver disease demonstrates an exponential increase in burden of disease. *Hepatology* 2018; **67**: 123-133 [PMID: 28802062 DOI: 10.1002/hep.29466]
20 **Brahma MK**, Gilglioni EH, Zhou L, Trépo E, Chen P, Gurzov EN. Oxidative stress in obesity-associated hepatocellular carcinoma: sources, signaling and therapeutic challenges. *Oncogene* 2021; **40**: 5155-5167 [PMID: 34290399 DOI: 10.1038/s41388-021-01950-y]
21 **Yu LX**, Ling Y, Wang HY. Role of nonresolving inflammation in hepatocellular carcinoma development and progression. *NPJ Precis Oncol* 2018; **2**: 6 [PMID: 29872724 DOI: 10.1038/s41698-018-0048-z]
22 **Mohamed J**, Nazratun Nafizah AH, Zariyantey AH, Budin SB. Mechanisms of Diabetes-Induced Liver Damage: The role of oxidative stress and inflammation. *Sultan Qaboos Univ Med J* 2016; **16**: e132-e141 [PMID: 27226903 DOI: 10.18295/squmj.2016.16.02.002]
23 **Sakuma T**, Nakamura M, Chiba T, Iwanaga T, Kan M, Kojima R, Ao J, Ma Y, Unozawa H, Fujita N, Kanayama K, Kanzaki H, Koroki K, Kobayashi K, Nakagawa R, Kanogawa N, Kiyono S, Kondo T, Saito T, Ogasawara S, Nakamoto S, Muroyama R, Kato J, Kishimoto T, Kato N. A diet-induced murine model for non-alcoholic fatty liver disease with obesity and insulin resistance that rapidly develops steatohepatitis

and fibrosis. *Lab Invest* 2022; **102**: 1150-1157 [PMID: 35643859 DOI: 10.1038/s41374-022-00807-6]
24 **Guerra S**, Mocciaro G, Gastaldelli A. Adipose tissue insulin resistance and lipidome alterations as the characterizing factors of non-alcoholic steatohepatitis. *Eur J Clin Invest* 2022; **52**: e13695 [PMID: 34695228 DOI: 10.1111/eci.13695]
25 **Tian Y**, Wong VW, Wong GL, Yang W, Sun H, Shen J, Tong JH, Go MY, Cheung YS, Lai PB, Zhou M, Xu G, Huang TH, Yu J, To KF, Cheng AS, Chan HL. Histone Deacetylase HDAC8 Promotes Insulin Resistance and β-Catenin Activation in NAFLD-Associated Hepatocellular Carcinoma. *Cancer Res* 2015; **75**: 4803-4816 [PMID: 26383163 DOI: 10.1158/0008-5472.CAN-14-3786]
26 **Matoori S**. Diabetes and its Complications. *ACS Pharmacol Transl Sci* 2022; **5**: 513-515 [PMID: 35983272 DOI: 10.1021/acsptsci.2c00122]
27 **Davila JA**, Morgan RO, Shaib Y, McGlynn KA, El-Serag HB. Diabetes increases the risk of hepatocellular carcinoma in the United States: a population based case control study. *Gut* 2005; **54**: 533-539 [PMID: 15753540 DOI: 10.1136/gut.2004.052167]
28 **Nakatsuka T**, Tateishi R. Development and prognosis of hepatocellular carcinoma in patients with diabetes. *Clin Mol Hepatol* 2023; **29**: 51-64 [PMID: 35903020 DOI: 10.3350/cmh.2022.0095]
29 **Mossenta M**, Busato D, Dal Bo M, Toffoli G. Glucose Metabolism and Oxidative Stress in Hepatocellular Carcinoma: Role and Possible Implications in Novel Therapeutic Strategies. *Cancers (Basel)* 2020; **12** [PMID: 32585931 DOI: 10.3390/cancers12061668]
30 **Elbedewy MM**, Ghazy MA, Elbedewy TA, Suliman GA. Serum Resistin and Insulin Resistance as Risk Factors for Hepatocellular Carcinoma in Cirrhotic Patients with Type 2 Diabetes Mellitus. *Life Sci J* 2014; **11**: 941-949 [DOI: 10.7537/marslsj111114.167]
31 **Ashour M**, Maher F, Hussein M, Mohamed AE, Elnagar A. Assessment Of Serum Resistin Relation To Hepatocellular Carcinoma In Patient With Liver Cirrhosis. *Neuroquantology* 2022 [DOI: 10.14704/nq.2022.20.11.NQ66340]
32 **Mohamed IEK**, Rasmy HS, Aly WAE. Evaluation of serum resistin levels in patients with hepatocellular carcinoma before and after treatment. *Egyptian Liver J* 2018; **8**: 61-67 [DOI: 10.1097/01.ELX.0000546516.15821.c2]
33 **Elsayed EY**, Mosalam NA, Mohamed NR. Resistin and Insulin Resistance: A Link Between Inflammation and Hepatocarcinogenesis. *Asian Pac J Cancer Prev* 2015; **16**: 7139-7142 [PMID: 26514502 DOI: 10.7314/apjcp.2015.16.16.7139]
34 **Chen C**, Jiang J, Lü JM, Chai H, Wang X, Lin PH, Yao Q. Resistin decreases expression of endothelial nitric oxide synthase through oxidative stress in human coronary artery endothelial cells. *Am J Physiol Heart Circ Physiol* 2010; **299**: H193-H201 [PMID: 20435848 DOI: 10.1152/ajpheart.00431.2009]
35 **Duan XF**, Tang P, Li Q, Yu ZT. Obesity, adipokines and hepatocellular carcinoma. *Int J Cancer* 2013; **133**: 1776-1783 [PMID: 23404222 DOI: 10.1002/ijc.28105]
36 **El-Serag HB**, Tran T, Everhart JE. Diabetes increases the risk of chronic liver disease and hepatocellular carcinoma. *Gastroenterology* 2004; **126**: 460-468 [PMID: 14762783 DOI: 10.1053/j.gastro.2003.10.065]
37 **Wang P**, Kang D, Cao W, Wang Y, Liu Z. Diabetes mellitus and risk of hepatocellular carcinoma: a systematic review and meta-analysis. *Diabetes Metab Res Rev* 2012; **28**: 109-122 [PMID: 21898753 DOI: 10.1002/dmrr.1291]
38 **Seyda Seydel G**, Kucukoglu O, Altinbasv A, Demir OO, Yilmaz S, Akkiz H, Otan E, Sowa JP, Canbay A. Economic growth leads to increase of obesity and associated hepatocellular carcinoma in developing countries. *Ann Hepatol* 2016; **15**: 662-672 [PMID: 27493104 DOI: 10.5604/16652681.1212316]
39 **Han H**, Zhang T, Jin Z, Guo H, Wei X, Liu Y, Chen Q, He J. Blood glucose concentration and risk of liver cancer: systematic review and meta-analysis of prospective studies. *Oncotarget* 2017; **8**: 50164-50173 [PMID: 28432278 DOI: 10.18632/oncotarget.16816]
40 **Chen CL**, Yang HI, Yang WS, Liu CJ, Chen PJ, You SL, Wang LY, Sun CA, Lu SN, Chen DS, Chen CJ. Metabolic factors and risk of hepatocellular carcinoma by chronic hepatitis B/C infection: a follow-up study in Taiwan. *Gastroenterology* 2008; **135**: 111-121 [PMID: 18505690 DOI: 10.1053/j.gastro.2008.03.073]
41 **Koh WP**, Wang R, Jin A, Yu MC, Yuan JM. Diabetes mellitus and risk of hepatocellular carcinoma: findings from the Singapore Chinese Health Study. *Br J Cancer* 2013; **108**: 1182-1188 [PMID: 23370206 DOI: 10.1038/bjc.2013.25]
42 **Miele L**, Bosetti C, Turati F, Rapaccini G, Gasbarrini A, La Vecchia C, Boccia S, Grieco A. Diabetes and Insulin Therapy, but Not Metformin, Are Related to Hepatocellular Cancer Risk. *Gastroenterol Res Pract* 2015; **2015**: 570356 [PMID: 26074956 DOI: 10.1155/2015/570356]
43 **Yi SW**, Choi JS, Yi JJ, Lee YH, Han KJ. Risk factors for hepatocellular carcinoma by age, sex, and liver disorder status: A prospective cohort study in Korea. *Cancer* 2018; **124**: 2748-2757 [PMID: 29669170 DOI: 10.1002/cncr.31406]
44 **Simon TG**, King LY, Chong DQ, Nguyen LH, Ma Y, VoPham T, Giovannucci EL, Fuchs CS, Meyerhardt JA, Corey KE, Khalili H, Chung RT, Zhang X, Chan AT. Diabetes, metabolic comorbidities, and risk of hepatocellular carcinoma: Results from two prospective cohort studies. *Hepatology* 2018; **67**: 1797-1806 [PMID: 29152763 DOI: 10.1002/hep.29660]
45 **Jinjuvadia R**, Patel S, Liangpunsakul S. The association between metabolic syndrome and hepatocellular carcinoma: systemic review and meta-analysis. *J Clin Gastroenterol* 2014; **48**: 172-177 [PMID: 24402120 DOI: 10.1097/MCG.0b013e3182a030c4]
46 **Wang MD**, Shen F, Zeng YY, Yang T. ASO Author Reflections: Effect of Preoperative Metabolic Syndrome for Patients with Hepatocellular Carcinoma. *Ann Surg Oncol* 2023; **30**: 359-360 [PMID: 36121580 DOI: 10.1245/s10434-022-12557-2]
47 **Shi T**, Kobara H, Oura K, Masaki T. Mechanisms Underlying Hepatocellular Carcinoma Progression in Patients with Type 2 Diabetes. *J Hepatocell Carcinoma* 2021; **8**: 45-55 [PMID: 33604315 DOI: 10.2147/JHC.S274933]
48 **Ali Kamkar MM**, Ahmad R, Alsmadi O, Behbehani K. Insight into the impact of diabetes mellitus on the increased risk of hepatocellular carcinoma: mini-review. *J Diabetes Metab Disord* 2014; **13**: 57 [PMID: 24918094 DOI: 10.1186/2251-6581-13-57]
49 **Plaz Torres MC**, Jaffe A, Perry R, Marabotto E, Strazzabosco M, Giannini EG. Diabetes medications and risk of HCC. *Hepatology* 2022; **76**: 1880-1897 [PMID: 35239194 DOI: 10.1002/hep.32439]
50 **Mantovani A**, Targher G. Type 2 diabetes mellitus and risk of hepatocellular carcinoma: spotlight on nonalcoholic fatty liver disease. *Ann Transl Med* 2017; **5**: 270 [PMID: 28758096 DOI: 10.21037/atm.2017.04.41]
51 **Cai X**, Gao J, Hu J, Wen W, Zhu Q, Wang M, Liu S, Hong J, Wu T, Yang S, Tuerxun G, Li N. Dose-Response Associations of Metabolic Score for Insulin Resistance Index with Nonalcoholic Fatty Liver Disease among a Nonobese Chinese Population: Retrospective Evidence from a Population-Based Cohort Study. *Dis Markers* 2022; **2022**: 4930355 [PMID: 35251371 DOI: 10.1155/2022/4930355]
52 **Saponaro C**, Sabatini S, Gaggini M, Carli F, Rosso C, Positano V, Armandi A, Caviglia GP, Faletti R, Bugianesi E, Gastaldelli A. Adipose tissue dysfunction and visceral fat are associated with hepatic insulin resistance and severity of NASH even in lean individuals. *Liver Int* 2022; **42**: 2418-2427 [PMID: 35900229 DOI: 10.1111/liv.15377]
53 **Tan DJH**, Ng CH, Lin SY, Pan XH, Tay P, Lim WH, Teng M, Syn N, Lim G, Yong JN, Quek J, Xiao J, Dan YY, Siddiqui MS, Sanyal AJ, Muthiah MD, Loomba R, Huang DQ. Clinical characteristics, surveillance, treatment allocation, and outcomes of non-alcoholic fatty liver disease-related hepatocellular carcinoma: a systematic review and meta-analysis. *Lancet Oncol* 2022; **23**: 521-530 [PMID: 35255263 DOI:

10.1016/S1470-2045(22)00078-X]
54 **Yip TC**, Lee HW, Chan WK, Wong GL, Wong VW. Asian perspective on NAFLD-associated HCC. *J Hepatol* 2022; **76**: 726-734 [PMID: 34619251 DOI: 10.1016/j.jhep.2021.09.024]
55 **Kumar R**, Priyadarshi RN, Anand U. Non-alcoholic Fatty Liver Disease: Growing Burden, Adverse Outcomes and Associations. *J Clin Transl Hepatol* 2020; **8**: 76-86 [PMID: 32274348 DOI: 10.14218/JCTH.2019.00051]
56 **Zarghamravanbakhsh P**, Frenkel M, Poretsky L. Metabolic causes and consequences of nonalcoholic fatty liver disease (NAFLD). *Metabol Open* 2021; **12**: 100149 [PMID: 34870138 DOI: 10.1016/j.metop.2021.100149]
57 **Björkström K**, Franzén S, Eliasson B, Miftaraj M, Gudbjörnsdottir S, Trolle-Lagerros Y, Svensson AM, Hagström H. Risk Factors for Severe Liver Disease in Patients With Type 2 Diabetes. *Clin Gastroenterol Hepatol* 2019; **17**: 2769-2775.e4 [PMID: 31009793 DOI: 10.1016/j.cgh.2019.04.038]
58 **Li Z**, Yang N, He L, Wang J, Ping F, Li W, Xu L, Zhang H, Li Y. Estimates and trends of the global burden of NASH-related liver cancer attributable to high fasting plasma glucose in 1990-2019: analysis of data from the 2019 Global Burden of Disease Study. *Diabetol Metab Syndr* 2023; **15**: 6 [PMID: 36647090 DOI: 10.1186/s13098-022-00976-w]
59 **Fabrizi F**, Cerutti R, Alfieri CM, Ridruejo E. An Update on Hepatocellular Carcinoma in Chronic Kidney Disease. *Cancers (Basel)* 2021; **13** [PMID: 34298832 DOI: 10.3390/cancers13143617]
60 **Lee CH**, Hsieh SY, Lin JL, Liu MS, Yen TH. Hepatocellular carcinoma in patients with chronic kidney disease. *World J Gastroenterol* 2013; **19**: 2466-2472 [PMID: 23674847 DOI: 10.3748/wjg.v19.i16.2466]
61 **Ramanathan RS**. Correlation of duration, hypertension and glycemic control with microvascular complications of diabetes mellitus at a tertiary care hospital. *J Integr Mol Med* 2017; **4**: 1-4 [DOI: 10.15761/IMM.1000272]
62 **Kasmari AJ**, Welch A, Liu G, Leslie D, McGarrity T, Riley T. Independent of Cirrhosis, Hepatocellular Carcinoma Risk Is Increased with Diabetes and Metabolic Syndrome. *Am J Med* 2017; **130**: 746.e1-746.e7 [PMID: 28109969 DOI: 10.1016/j.amjmed.2016.12.029]
63 **Cunha V**, Cotrim HP, Rocha R, Carvalho K, Lins-Kusterer L. Metformin in the prevention of hepatocellular carcinoma in diabetic patients: A systematic review. *Ann Hepatol* 2020; **19**: 232-237 [PMID: 31836424 DOI: 10.1016/j.aohep.2019.10.005]
64 **Siddique A**, Kowdley KV. Insulin resistance and other metabolic risk factors in the pathogenesis of hepatocellular carcinoma. *Clin Liver Dis* 2011; **15**: 281-296, vii [PMID: 21689613 DOI: 10.1016/j.cld.2011.03.007]
65 **De Minicis S**, Agostinelli L, Rychlicki C, Sorice GP, Saccomanno S, Candelaresi C, Giaccari A, Trozzi L, Pierantonelli I, Mingarelli E, Marzioni M, Muscogiuri G, Gaggini M, Benedetti A, Gastaldelli A, Guido M, Svegliati-Baroni G. HCC development is associated to peripheral insulin resistance in a mouse model of NASH. *PLoS One* 2014; **9**: e97136 [PMID: 24853141 DOI: 10.1371/journal.pone.0097136]
66 **Kawaguchi T**, Taniguchi E, Morita Y, Shirachi M, Tateishi I, Nagata E, Sata M. Association of exogenous insulin or sulphonylurea treatment with an increased incidence of hepatoma in patients with hepatitis C virus infection. *Liver Int* 2010; **30**: 479-486 [PMID: 20040053 DOI: 10.1111/j.1478-3231.2009.02191.x]
67 **Donadon V**, Balbi M, Mas MD, Casarin P, Zanette G. Metformin and reduced risk of hepatocellular carcinoma in diabetic patients with chronic liver disease. *Liver Int* 2010; **30**: 750-758 [PMID: 20331505 DOI: 10.1111/j.1478-3231.2010.02223.x]
68 **Tseng CH**. Metformin and risk of hepatocellular carcinoma in patients with type 2 diabetes. *Liver Int* 2018; **38**: 2018-2027 [PMID: 29956875 DOI: 10.1111/liv.13872]
69 **Casadei Gardini A**, Faloppi L, De Matteis S, Foschi FG, Silvestris N, Tovoli F, Palmieri V, Marisi G, Brunetti O, Vespasiani-Gentilucci U, Perrone G, Valgiusti M, Granato AM, Ercolani G, Negrini G, Tamburini E, Aprile G, Passardi A, Santini D, Cascinu S, Frassineti GL, Scartozzi M. Metformin and insulin impact on clinical outcome in patients with advanced hepatocellular carcinoma receiving sorafenib: Validation study and biological rationale. *Eur J Cancer* 2017; **86**: 106-114 [PMID: 28985579 DOI: 10.1016/j.ejca.2017.09.003]
70 **Chettouh H**, Lequoy M, Fartoux L, Vigouroux C, Desbois-Mouthon C. Hyperinsulinaemia and insulin signalling in the pathogenesis and the clinical course of hepatocellular carcinoma. *Liver Int* 2015; **35**: 2203-2217 [PMID: 26123841 DOI: 10.1111/liv.12903]
71 **Maradagi T**, Kumar R, Ponesakki G. Hyperglycaemia-induced human hepatocellular carcinoma (HepG2) cell proliferation through ROS-mediated P38 activation is effectively inhibited by a xanthophyll carotenoid, lutein. *Diabet Med* 2022; **39**: e14713 [PMID: 34614244 DOI: 10.1111/dme.14713]
72 **Liu F**, Sun Y, Liu B, Lu J, Li H, Zhu H, Gao H, Zhou X, Chang H. Insulin-like growth factor-1 induces epithelial-mesenchymal transition in hepatocellular carcinoma by activating survivin. *Oncol Rep* 2018; **40**: 952-958 [PMID: 29989646 DOI: 10.3892/or.2018.6516]
73 **Zheng Y**, Wu C, Yang J, Zhao Y, Jia H, Xue M, Xu D, Yang F, Fu D, Wang C, Hu B, Zhang Z, Li T, Yan S, Wang X, Nelson PJ, Bruns C, Qin L, Dong Q. Insulin-like growth factor 1-induced enolase 2 deacetylation by HDAC3 promotes metastasis of pancreatic cancer. *Signal Transduct Target Ther* 2020; **5**: 53 [PMID: 32398667 DOI: 10.1038/s41392-020-0146-6]
74 **Shi X**, Teng F. Down-regulated miR-28-5p in human hepatocellular carcinoma correlated with tumor proliferation and migration by targeting insulin-like growth factor-1 (IGF-1). *Mol Cell Biochem* 2015; **408**: 283-293 [PMID: 26160280 DOI: 10.1007/s11010-015-2506-z]
75 **Li TT**, Zhu D, Mou T, Guo Z, Pu JL, Chen QS, Wei XF, Wu ZJ. IL-37 induces autophagy in hepatocellular carcinoma cells by inhibiting the PI3K/AKT/mTOR pathway. *Mol Immunol* 2017; **87**: 132-140 [PMID: 28433890 DOI: 10.1016/j.molimm.2017.04.010]
76 **Wu J**, Zhu AX. Targeting insulin-like growth factor axis in hepatocellular carcinoma. *J Hematol Oncol* 2011; **4**: 30 [PMID: 21729319 DOI: 10.1186/1756-8722-4-30]
77 **Leung KC**, Doyle N, Ballesteros M, Waters MJ, Ho KK. Insulin regulation of human hepatic growth hormone receptors: divergent effects on biosynthesis and surface translocation. *J Clin Endocrinol Metab* 2000; **85**: 4712-4720 [PMID: 11134133 DOI: 10.1210/jcem.85.12.7017]
78 **Jabir NR**, Ahmad S, Tabrez S. An insight on the association of glycation with hepatocellular carcinoma. *Semin Cancer Biol* 2018; **49**: 56-63 [PMID: 28634055 DOI: 10.1016/j.semcancer.2017.06.005]
79 **Kaji K**, Yoshiji H, Kitade M, Ikenaka Y, Noguchi R, Yoshii J, Yanase K, Namisaki T, Yamazaki M, Moriya K, Tsujimoto T, Kawaratani H, Akahane T, Uemura M, Fukui H. Impact of insulin resistance on the progression of chronic liver diseases. *Int J Mol Med* 2008; **22**: 801-808 [PMID: 19020779]
80 **Filippatos T**, Tsimihodimos V, Pappa E, Elisaf M. Pathophysiology of Diabetic Dyslipidaemia. *Curr Vasc Pharmacol* 2017; **15**: 566-575 [PMID: 28155609 DOI: 10.2174/1570161115666170201105425]
81 **Shin HS**, Jun BG, Yi SW. Impact of diabetes, obesity, and dyslipidemia on the risk of hepatocellular carcinoma in patients with chronic liver diseases. *Clin Mol Hepatol* 2022; **28**: 773-789 [PMID: 35934813 DOI: 10.3350/cmh.2021.0383]
82 **Phan J**, Ng V, Sheinbaum A, French S, Choi G, El Kabany M, Durazo F, Saab S, Tong M, Busuttil R, Han SH. Hyperlipidemia and Nonalcoholic Steatohepatitis Predispose to Hepatocellular Carcinoma Development Without Cirrhosis. *J Clin Gastroenterol* 2019; **53**: 309-313

[PMID: 29912756 DOI: 10.1097/MCG.0000000000001062]
83 **Osaki Y**, Taniguchi S, Tahara A, Okamoto M, Kishimoto T. Metabolic syndrome and incidence of liver and breast cancers in Japan. *Cancer Epidemiol* 2012; **36**: 141-147 [PMID: 21890443 DOI: 10.1016/j.canep.2011.03.007]
84 **Cho Y**, Cho EJ, Yoo JJ, Chang Y, Chung GE, Jeong SM, Park SH, Han K, Shin DW, Yu SJ. Association between Lipid Profiles and the Incidence of Hepatocellular Carcinoma: A Nationwide Population-Based Study. *Cancers (Basel)* 2021; **13** [PMID: 33808412 DOI: 10.3390/cancers13071599]
85 **Yi SW**, Kim SH, Han KJ, Yi JJ, Ohrr H. Higher cholesterol levels, not statin use, are associated with a lower risk of hepatocellular carcinoma. *Br J Cancer* 2020; **122**: 630-633 [PMID: 31857717 DOI: 10.1038/s41416-019-0691-3]
86 **Sinn DH**, Kang D, Cho SJ, Paik SW, Guallar E, Cho J, Gwak GY. Risk of hepatocellular carcinoma in individuals without traditional risk factors: development and validation of a novel risk score. *Int J Epidemiol* 2020; **49**: 1562-1571 [PMID: 32725117 DOI: 10.1093/ije/dyaa089]
87 **Chiang CH**, Lee LT, Hung SH, Lin WY, Hung HF, Yang WS, Sung PK, Huang KC. Opposite association between diabetes, dyslipidemia, and hepatocellular carcinoma mortality in the middle-aged and elderly. *Hepatology* 2014; **59**: 2207-2215 [PMID: 24425422 DOI: 10.1002/hep.27014]
88 **Moutschen MP**, Scheen AJ, Lefebvre PJ. Impaired immune responses in diabetes mellitus: analysis of the factors and mechanisms involved. Relevance to the increased susceptibility of diabetic patients to specific infections. *Diabete Metab* 1992; **18**: 187-201 [PMID: 1397473]
89 **Eibl N**, Spatz M, Fischer GF, Mayr WR, Samstag A, Wolf HM, Schernthaner G, Eibl MM. Impaired primary immune response in type-1 diabetes: results from a controlled vaccination study. *Clin Immunol* 2002; **103**: 249-259 [PMID: 12173299 DOI: 10.1006/clim.2002.5220]
90 **Demir M**, Serin E, Göktürk S, Ozturk NA, Kulaksizoglu S, Ylmaz U. The prevalence of occult hepatitis B virus infection in type 2 diabetes mellitus patients. *Eur J Gastroenterol Hepatol* 2008; **20**: 668-673 [PMID: 18679070 DOI: 10.1097/MEG.0b013e3282f55e1e]
91 **Zhang X**, Zhu X, Ji Y, Li H, Hou F, Xiao C, Yuan P. Increased risk of hepatitis B virus infection amongst individuals with diabetes mellitus. *Biosci Rep* 2019; **39** [PMID: 30858308 DOI: 10.1042/BSR20181715]
92 **Fu SC**, Huang YW, Wang TC, Hu JT, Chen DS, Yang SS. Increased risk of hepatocellular carcinoma in chronic hepatitis B patients with new onset diabetes: a nationwide cohort study. *Aliment Pharmacol Ther* 2015; **41**: 1200-1209 [PMID: 25846548 DOI: 10.1111/apt.13191]
93 **Tan Y**, Wei S, Zhang W, Yang J, Yan L. Type 2 diabetes mellitus increases the risk of hepatocellular carcinoma in subjects with chronic hepatitis B virus infection: a meta-analysis and systematic review. *Cancer Manag Res* 2019; **11**: 705-713 [PMID: 30679924 DOI: 10.2147/CMAR.S188238]
94 **Villar LM**, Geloneze B, Vasques ACJ, Pires MLE, Miguel JC, da Silva EF, Marques VA, Scalioni LP, Lampe E. Prevalence of hepatitis B and hepatitis C among diabetes mellitus type 2 individuals. *PLoS One* 2019; **14**: e0211193 [PMID: 30817756 DOI: 10.1371/journal.pone.0211193]
95 **Ioannou GN**, Green P, Lowy E, Mun EJ, Berry K. Differences in hepatocellular carcinoma risk, predictors and trends over time according to etiology of cirrhosis. *PLoS One* 2018; **13**: e0204412 [PMID: 30260995 DOI: 10.1371/journal.pone.0204412]
96 **Bhat M**, Usmani SE, Azhie A, Woo M. Metabolic Consequences of Solid Organ Transplantation. *Endocr Rev* 2021; **42**: 171-197 [PMID: 33247713 DOI: 10.1210/endrev/bnaa030]
97 **Wei Q**, Gao F, Zhuang R, Ling Q, Ke Q, Wu J, Shen T, Zhang M, Xu X, Zheng S. A national report from China Liver Transplant Registry: steroid avoidance after liver transplantation for hepatocellular carcinoma. *Chin J Cancer Res* 2017; **29**: 426-437 [PMID: 29142462 DOI: 10.21147/j.issn.1000-9604.2017.05.07]
98 **Bhat M**, Mara K, Dierkhising R, Watt KDS. Immunosuppression, Race, and Donor-Related Risk Factors Affect De novo Cancer Incidence Across Solid Organ Transplant Recipients. *Mayo Clin Proc* 2018; **93**: 1236-1246 [PMID: 30064826 DOI: 10.1016/j.mayocp.2018.04.025]
99 **Lopez PM**, Villanueva A, Llovet JM. Systematic review: evidence-based management of hepatocellular carcinoma--an updated analysis of randomized controlled trials. *Aliment Pharmacol Ther* 2006; **23**: 1535-1547 [PMID: 16696801 DOI: 10.1111/j.1365-2036.2006.02932.x]
100 **Kanwal F**, Kramer JR, Mapakshi S, Natarajan Y, Chayanupatkul M, Richardson PA, Li L, Desiderio R, Thrift AP, Asch SM, Chu J, El-Serag HB. Risk of Hepatocellular Cancer in Patients With Non-Alcoholic Fatty Liver Disease. *Gastroenterology* 2018; **155**: 1828-1837.e2 [PMID: 30144434 DOI: 10.1053/j.gastro.2018.08.024]
101 **European Association for the Study of the Liver**. EASL Clinical Practice Guidelines: Management of hepatocellular carcinoma. *J Hepatol* 2018; **69**: 182-236 [PMID: 29628281 DOI: 10.1016/j.jhep.2018.03.019]
102 **Marrero JA**, Kulik LM, Sirlin CB, Zhu AX, Finn RS, Abecassis MM, Roberts LR, Heimbach JK. Diagnosis, Staging, and Management of Hepatocellular Carcinoma: 2018 Practice Guidance by the American Association for the Study of Liver Diseases. *Hepatology* 2018; **68**: 723-750 [PMID: 29624699 DOI: 10.1002/hep.29913]
103 **Zhou J**, Sun H, Wang Z, Cong W, Wang J, Zeng M, Zhou W, Bie P, Liu L, Wen T, Han G, Wang M, Liu R, Lu L, Ren Z, Chen M, Zeng Z, Liang P, Liang C, Yan F, Wang W, Ji Y, Yun J, Cai D, Chen Y, Cheng W, Cheng S, Dai C, Guo W, Hua B, Huang X, Jia W, Li Y, Liang J, Liu T, Lv G, Mao Y, Peng T, Ren W, Shi H, Shi G, Tao K, Wang X, Xiang B, Xing B, Xu J, Yang J, Yang Y, Ye S, Yin Z, Zhang B, Zhang L, Zhang S, Zhang T, Zhao Y, Zheng H, Zhu J, Zhu K, Shi Y, Xiao Y, Dai Z, Teng G, Cai J, Cai X, Li Q, Shen F, Qin S, Dong J, Fan J. Guidelines for the Diagnosis and Treatment of Hepatocellular Carcinoma (2019 Edition). *Liver Cancer* 2020; **9**: 682-720 [PMID: 33442540 DOI: 10.1159/000509424]
104 **Korean Liver Cancer Association (KLCA)**; National Cancer Center (NCC), Goyang, Korea. 2018 Korean Liver Cancer Association-National Cancer Center Korea Practice Guidelines for the Management of Hepatocellular Carcinoma. *Korean J Radiol* 2019; **20**: 1042-1113 [PMID: 31270974 DOI: 10.3348/kjr.2019.0140]
105 **Reig M**, Forner A, Rimola J, Ferrer-Fàbrega J, Burrel M, Garcia-Criado Á, Kelley RK, Galle PR, Mazzaferro V, Salem R, Sangro B, Singal AG, Vogel A, Fuster J, Ayuso C, Bruix J. BCLC strategy for prognosis prediction and treatment recommendation: The 2022 update. *J Hepatol* 2022; **76**: 681-693 [PMID: 34801630 DOI: 10.1016/j.jhep.2021.11.018]
106 **Chalasani N**, Younossi Z, Lavine JE, Charlton M, Cusi K, Rinella M, Harrison SA, Brunt EM, Sanyal AJ. The diagnosis and management of nonalcoholic fatty liver disease: Practice guidance from the American Association for the Study of Liver Diseases. *Hepatology* 2018; **67**: 328-357 [PMID: 28714183 DOI: 10.1002/hep.29367]
107 **Loomba R**, Lim JK, Patton H, El-Serag HB. AGA Clinical Practice Update on Screening and Surveillance for Hepatocellular Carcinoma in Patients With Nonalcoholic Fatty Liver Disease: Expert Review. *Gastroenterology* 2020; **158**: 1822-1830 [PMID: 32006545 DOI: 10.1053/j.gastro.2019.12.053]
108 **Kang SH**, Lee HW, Yoo JJ, Cho Y, Kim SU, Lee TH, Jang BK, Kim SG, Ahn SB, Kim H, Jun DW, Choi JI, Song DS, Kim W, Jeong SW, Kim MY, Koh H, Jeong S, Lee JW, Cho YK; Korean Association for the Study of the Liver (KASL). KASL clinical practice guidelines: Management of nonalcoholic fatty liver disease. *Clin Mol Hepatol* 2021; **27**: 363-401 [PMID: 34154309 DOI: 10.3350/cmh.2021.0178]
109 **Park HJ**, Jang HY, Kim SY, Lee SJ, Won HJ, Byun JH, Choi SH, Lee SS, An J, Lim YS. Non-enhanced magnetic resonance imaging as a

surveillance tool for hepatocellular carcinoma: Comparison with ultrasound. *J Hepatol* 2020; **72**: 718-724 [PMID: 31836549 DOI: 10.1016/j.jhep.2019.12.001]

110 **Singh MK**, Das BK, Choudhary S, Gupta D, Patil UK. Diabetes and hepatocellular carcinoma: A pathophysiological link and pharmacological management. *Biomed Pharmacother* 2018; **106**: 991-1002 [PMID: 30119271 DOI: 10.1016/j.biopha.2018.06.095]

111 **Kramer JR**, Natarajan Y, Dai J, Yu X, Li L, El-Serag HB, Kanwal F. Effect of diabetes medications and glycemic control on risk of hepatocellular cancer in patients with nonalcoholic fatty liver disease. *Hepatology* 2022; **75**: 1420-1428 [PMID: 34779535 DOI: 10.1002/hep.32244]

112 **Arvanitakis K**, Koufakis T, Kotsa K, Germanidis G. How Far beyond Diabetes Can the Benefits of Glucagon-like Peptide-1 Receptor Agonists Go? A Review of the Evidence on Their Effects on Hepatocellular Carcinoma. *Cancers (Basel)* 2022; **14** [PMID: 36230573 DOI: 10.3390/cancers14194651]

113 **Llovet JM**, Ricci S, Mazzaferro V, Hilgard P, Gane E, Blanc JF, de Oliveira AC, Santoro A, Raoul JL, Forner A, Schwartz M, Porta C, Zeuzem S, Bolondi L, Greten TF, Galle PR, Seitz JF, Borbath I, Häussinger D, Giannaris T, Shan M, Moscovici M, Voliotis D, Bruix J; SHARP Investigators Study Group. Sorafenib in advanced hepatocellular carcinoma. *N Engl J Med* 2008; **359**: 378-390 [PMID: 18650514 DOI: 10.1056/NEJMoa0708857]

114 **Abou-Alfa GK**, Meyer T, Cheng AL, El-Khoueiry AB, Rimassa L, Ryoo BY, Cicin I, Merle P, Chen Y, Park JW, Blanc JF, Bolondi L, Klümpen HJ, Chan SL, Zagonel V, Pressiani T, Ryu MH, Venook AP, Hessel C, Borgman-Hagey AE, Schwab G, Kelley RK. Cabozantinib in Patients with Advanced and Progressing Hepatocellular Carcinoma. *N Engl J Med* 2018; **379**: 54-63 [PMID: 29972759 DOI: 10.1056/NEJMoa1717002]

115 **Zhu AX**, Galle PR, Kudo M, Finn RS, Qin S, Xu Y, Abada P, Llovet J. A study of ramucirumab (LY3009806) vs placebo in patients with hepatocellular carcinoma and elevated baseline alpha-fetoprotein (REACH-2). *J Clin Oncol* 2018 [DOI: 10.1200/JCO.2018.36.4_suppl.TPS538]

116 **El-Khoueiry AB**, Sangro B, Yau T, Crocenzi TS, Kudo M, Hsu C, Kim TY, Choo SP, Trojan J, Welling TH Rd, Meyer T, Kang YK, Yeo W, Chopra A, Anderson J, Dela Cruz C, Lang L, Neely J, Tang H, Dastani HB, Melero I. Nivolumab in patients with advanced hepatocellular carcinoma (CheckMate 040): an open-label, non-comparative, phase 1/2 dose escalation and expansion trial. *Lancet* 2017; **389**: 2492-2502 [PMID: 28434648 DOI: 10.1016/S0140-6736(17)31046-2]

117 **Finn RS**, Ryoo BY, Merle P, Kudo M, Bouattour M, Lim HY, Breder VV, Edeline J, Chao Y, Ogasawara S, Yau T, Garrido M, Chan SL, Knox JJ, Daniele B, Ebbinghaus S, Chen E, Siegel AB, Zhu AX, Cheng AL. Results of KEYNOTE-240: phase 3 study of pembrolizumab (Pembro) vs best supportive care (BSC) for second line therapy in advanced hepatocellular carcinoma (HCC). *J Clin Oncol* 2019 [DOI: 10.1200/JCO.2019.37.15_suppl.4004]

118 **Pinter M**, Jain RK, Duda DG. The Current Landscape of Immune Checkpoint Blockade in Hepatocellular Carcinoma: A Review. *JAMA Oncol* 2021; **7**: 113-123 [PMID: 33090190 DOI: 10.1001/jamaoncol.2020.3381]

119 **Zhang P**, Yang Y, Wen F, He X, Tang R, Du Z, Zhou J, Zhang J, Li Q. Cost-effectiveness of sorafenib as a first-line treatment for advanced hepatocellular carcinoma. *Eur J Gastroenterol Hepatol* 2015; **27**: 853-859 [PMID: 25919775 DOI: 10.1097/MEG.0000000000000373]

120 **Lau WY**, Lai EC. The current role of radiofrequency ablation in the management of hepatocellular carcinoma: a systematic review. *Ann Surg* 2009; **249**: 20-25 [PMID: 19106671 DOI: 10.1097/SLA.0b013e31818eec29]

121 **Rhim H**, Lim HK. Radiofrequency ablation of hepatocellular carcinoma: pros and cons. *Gut Liver* 2010; **4** Suppl 1: S113-S118 [PMID: 21103289 DOI: 10.5009/gnl.2010.4.S1.S113]

122 **Chen L**, Sun J, Yang X. Radiofrequency ablation-combined multimodel therapies for hepatocellular carcinoma: Current status. *Cancer Lett* 2016; **370**: 78-84 [PMID: 26472630 DOI: 10.1016/j.canlet.2015.09.020]

123 **Zhong BY**, Jin ZC, Chen JJ, Zhu HD, Zhu XL. Role of Transarterial Chemoembolization in the Treatment of Hepatocellular Carcinoma. *J Clin Transl Hepatol* 2023; **11**: 480-489 [PMID: 36643046 DOI: 10.14218/JCTH.2022.00293]

124 **Zhu HD**, Li HL, Huang MS, Yang WZ, Yin GW, Zhong BY, Sun JH, Jin ZC, Chen JJ, Ge NJ, Ding WB, Li WH, Huang JH, Mu W, Gu SZ, Li JP, Zhao H, Wen SW, Lei YM, Song YS, Yuan CW, Wang WD, Huang M, Zhao W, Wu JB, Wang S, Zhu X, Han JJ, Ren WX, Lu ZM, Xing WG, Fan Y, Lin HL, Zhang ZS, Xu GH, Hu WH, Tu Q, Su HY, Zheng CS, Chen Y, Zhao XY, Fang ZT, Wang Q, Zhao JW, Xu AB, Xu J, Wu QH, Niu HZ, Wang J, Dai F, Feng DP, Li QD, Shi RS, Li JR, Yang G, Shi HB, Ji JS, Liu YE, Cai Z, Yang P, Zhao Y, Zhu XL, Lu LG, Teng GJ; CHANCE001 Investigators. Transarterial chemoembolization with PD-(L)1 inhibitors plus molecular targeted therapies for hepatocellular carcinoma (CHANCE001). *Signal Transduct Target Ther* 2023; **8**: 58 [PMID: 36750721 DOI: 10.1038/s41392-022-01235-0]

125 **Koulouris A**, Tsagkaris C, Spyrou V, Pappa E, Troullinou A, Nikolaou M. Hepatocellular Carcinoma: An Overview of the Changing Landscape of Treatment Options. *J Hepatocell Carcinoma* 2021; **8**: 387-401 [PMID: 34012929 DOI: 10.2147/JHC.S300182]

126 **Bruix J**, da Fonseca LG, Reig M. Insights into the success and failure of systemic therapy for hepatocellular carcinoma. *Nat Rev Gastroenterol Hepatol* 2019; **16**: 617-630 [PMID: 31371809 DOI: 10.1038/s41575-019-0179-x]

127 **Wu TC**, Shen YC, Cheng AL. Evolution of systemic treatment for advanced hepatocellular carcinoma. *Kaohsiung J Med Sci* 2021; **37**: 643-653 [PMID: 34213069 DOI: 10.1002/kjm2.12401]

128 **Islam MM**, Poly TN, Walther BA, Yang HC, Jack Li YC. Statin Use and the Risk of Hepatocellular Carcinoma: A Meta-Analysis of Observational Studies. *Cancers (Basel)* 2020; **12** [PMID: 32183029 DOI: 10.3390/cancers12030671]

129 **Patel L**, Buckels AC, Kinghorn IJ, Murdock PR, Holbrook JD, Plumpton C, Macphee CH, Smith SA. Resistin is expressed in human macrophages and directly regulated by PPAR gamma activators. *Biochem Biophys Res Commun* 2003; **300**: 472-476 [PMID: 12504108 DOI: 10.1016/s0006-291x(02)02841-3]

130 **Steppan CM**, Bailey ST, Bhat S, Brown EJ, Banerjee RR, Wright CM, Patel HR, Ahima RS, Lazar MA. The hormone resistin links obesity to diabetes. *Nature* 2001; **409**: 307-312 [PMID: 11201732 DOI: 10.1038/35053000]

131 **Al Hannan F**, Culligan KG. Human resistin and the RELM of Inflammation in diabesity. *Diabetol Metab Syndr* 2015; **7**: 54 [PMID: 26097512 DOI: 10.1186/s13098-015-0050-3]

132 **Kim KH**, Lee K, Moon YS, Sul HS. A cysteine-rich adipose tissue-specific secretory factor inhibits adipocyte differentiation. *J Biol Chem* 2001; **276**: 11252-11256 [PMID: 11278254 DOI: 10.1074/jbc.C100028200]

133 **Cao H**, Hegele RA. Single nucleotide polymorphisms of the resistin (RSTN) gene. *J Hum Genet* 2001; **46**: 553-555 [PMID: 11558907 DOI: 10.1007/s100380170040]

134 **Shen YH**, Zhang L, Gan Y, Wang X, Wang J, LeMaire SA, Coselli JS, Wang XL. Up-regulation of PTEN (phosphatase and tensin homolog deleted on chromosome ten) mediates p38 MAPK stress signal-induced inhibition of insulin signaling. A cross-talk between stress signaling and insulin signaling in resistin-treated human endothelial cells. *J Biol Chem* 2006; **281**: 7727-7736 [PMID: 16418168 DOI:

10.1074/jbc.M511105200]
135 **Mu H**, Ohashi R, Yan S, Chai H, Yang H, Lin P, Yao Q, Chen C. Adipokine resistin promotes in vitro angiogenesis of human endothelial cells. *Cardiovasc Res* 2006; **70**: 146-157 [PMID: 16515776 DOI: 10.1016/j.cardiores.2006.01.015]
136 **Codoñer-Franch P**, Alonso-Iglesias E. Resistin: insulin resistance to malignancy. *Clin Chim Acta* 2015; **438**: 46-54 [PMID: 25128719 DOI: 10.1016/j.cca.2014.07.043]
137 **Sudan SK**, Deshmukh SK, Poosarla T, Holliday NP, Dyess DL, Singh AP, Singh S. Resistin: An inflammatory cytokine with multi-faceted roles in cancer. *Biochim Biophys Acta Rev Cancer* 2020; **1874**: 188419 [PMID: 32822824 DOI: 10.1016/j.bbcan.2020.188419]
138 **Shi Y**, Zhu N, Qiu Y, Tan J, Wang F, Qin L, Dai A. Resistin-like molecules: a marker, mediator and therapeutic target for multiple diseases. *Cell Commun Signal* 2023; **21**: 18 [PMID: 36691020 DOI: 10.1186/s12964-022-01032-w]
139 **Yagmur E**, Trautwein C, Gressner AM, Tacke F. Resistin serum levels are associated with insulin resistance, disease severity, clinical complications, and prognosis in patients with chronic liver diseases. *Am J Gastroenterol* 2006; **101**: 1244-1252 [PMID: 16771945 DOI: 10.1111/j.1572-0241.2006.00543.x]
140 **Elnagar MA**. Assessment Of Serum Resistin Relation To Hepatocellular Carcinoma In Patient With Liver Cirrhosis. *Neuroquantology* 2022; **20**: 3295-3305
141 **da Silva TE**, Costa-Silva M, Correa CG, Denardin G, Alencar MLA, Coelho MSPH, Muraro-Wildner L, Luiza-Bazzo M, González-Chica DA, Dantas-Correa EB, Narciso-Schiavon JL, Schiavon LL. Clinical Significance of Serum Adiponectin and Resistin Levels in Liver Cirrhosis. *Ann Hepatol* 2018; **17**: 286-299 [PMID: 29469045 DOI: 10.5604/01.3001.0010.8659]
142 **Gong WJ**, Liu JY, Yin JY, Cui JJ, Xiao D, Zhuo W, Luo C, Liu RJ, Li X, Zhang W, Zhou HH, Liu ZQ. Resistin facilitates metastasis of lung adenocarcinoma through the TLR4/Src/EGFR/PI3K/NF-κB pathway. *Cancer Sci* 2018; **109**: 2391-2400 [PMID: 29927028 DOI: 10.1111/cas.13704]
143 **Lee JO**, Kim N, Lee HJ, Lee YW, Kim SJ, Park SH, Kim HS. Resistin, a fat-derived secretory factor, promotes metastasis of MDA-MB-231 human breast cancer cells through ERM activation. *Sci Rep* 2016; **6**: 18923 [PMID: 26729407 DOI: 10.1038/srep18923]
144 **Pang J**, Shi Q, Liu Z, He J, Liu H, Lin P, Cui J, Yang J. Resistin induces multidrug resistance in myeloma by inhibiting cell death and upregulating ABC transporter expression. *Haematologica* 2017; **102**: 1273-1280 [PMID: 28360146 DOI: 10.3324/haematol.2016.154062]
145 **Sun H**, Chua MS, Yang D, Tsalenko A, Peter BJ, So S. Antibody Arrays Identify Potential Diagnostic Markers of Hepatocellular Carcinoma. *Biomark Insights* 2008; **3**: 1-18 [PMID: 19578489 DOI: 10.4137/bmi.s595]
146 **Toniutto P**, Fornasiere E, Fumolo E, Bitetto D. Risk factors for hepatocellular carcinoma recurrence after liver transplantation. *Hepatoma Res* 2020; **6**: 50 [DOI: 10.20517/2394-5079.2020.40]
147 **Han D**, Chen J, Liu S, Zhang Z, Zhao Z, Jin W, Xin Y. Serum Resistin Levels in Adult Patients with Nonalcoholic Fatty Liver Disease: A Systematic Review and Meta-analysis. *J Clin Transl Hepatol* 2021; **9**: 484-493 [PMID: 34447677 DOI: 10.14218/JCTH.2021.00018]
148 **Kim HJ**, Lee YS, Won EH, Chang IH, Kim TH, Park ES, Kim MK, Kim W, Myung SC. Expression of resistin in the prostate and its stimulatory effect on prostate cancer cell proliferation. *BJU Int* 2011; **108**: E77-E83 [PMID: 21050358 DOI: 10.1111/j.1464-410X.2010.09813.x]
149 **Malvi P**, Chaube B, Singh SV, Mohammad N, Vijayakumar MV, Singh S, Chouhan S, Bhat MK. Elevated circulatory levels of leptin and resistin impair therapeutic efficacy of dacarbazine in melanoma under obese state. *Cancer Metab* 2018; **6**: 2 [PMID: 29568521 DOI: 10.1186/s40170-018-0176-5]
150 **Wang CH**, Wang PJ, Hsieh YC, Lo S, Lee YC, Chen YC, Tsai CH, Chiu WC, Chu-Sung Hu S, Lu CW, Yang YF, Chiu CC, Ou-Yang F, Wang YM, Hou MF, Yuan SS. Resistin facilitates breast cancer progression *via* TLR4-mediated induction of mesenchymal phenotypes and stemness properties. *Oncogene* 2018; **37**: 589-600 [PMID: 28991224 DOI: 10.1038/onc.2017.357]
151 **Deshmukh SK**, Srivastava SK, Bhardwaj A, Singh AP, Tyagi N, Marimuthu S, Dyess DL, Dal Zotto V, Carter JE, Singh S. Resistin and interleukin-6 exhibit racially-disparate expression in breast cancer patients, display molecular association and promote growth and aggressiveness of tumor cells through STAT3 activation. *Oncotarget* 2015; **6**: 11231-11241 [PMID: 25868978 DOI: 10.18632/oncotarget.3591]
152 **Qiu L**, Zhang GF, Yu L, Wang HY, Jia XJ, Wang TJ. Novel oncogenic and chemoresistance-inducing functions of resistin in ovarian cancer cells require miRNAs-mediated induction of epithelial-to-mesenchymal transition. *Sci Rep* 2018; **8**: 12522 [PMID: 30131543 DOI: 10.1038/s41598-018-30978-6]
153 **Deb A**, Deshmukh B, Ramteke P, Bhati FK, Bhat MK. Resistin: A journey from metabolism to cancer. *Transl Oncol* 2021; **14**: 101178 [PMID: 34293684 DOI: 10.1016/j.tranon.2021.101178]
154 **Singh S**, Chouhan S, Mohammad N, Bhat MK. Resistin causes G1 arrest in colon cancer cells through upregulation of SOCS3. *FEBS Lett* 2017; **591**: 1371-1382 [PMID: 28417458 DOI: 10.1002/1873-3468.12655]
155 **Ashour MA**, Wadea FM, Hussein NMM, Elnagar A-EMA. Insulin Resistance, Resistin Hormone and Hepatocellular Carcinoma Interplay: A Review Article. *Egyptian J Hospital Med* 2023; **90**: 2041-2044 [DOI: 10.21608/EJHM.2023.285028]
156 **Kelley RK**, Greten TF. Hepatocellular Carcinoma - Origins and Outcomes. *N Engl J Med* 2021; **385**: 280-282 [PMID: 34260842 DOI: 10.1056/NEJMcibr2106594]
157 **Tan W**, Luo X, Li W, Zhong J, Cao J, Zhu S, Chen X, Zhou R, Shang C, Chen Y. TNF-α is a potential therapeutic target to overcome sorafenib resistance in hepatocellular carcinoma. *EBioMedicine* 2019; **40**: 446-456 [PMID: 30594557 DOI: 10.1016/j.ebiom.2018.12.047]
158 **Malhi H**, Gores GJ. Cellular and molecular mechanisms of liver injury. *Gastroenterology* 2008; **134**: 1641-1654 [PMID: 18471544 DOI: 10.1053/j.gastro.2008.03.002]
159 **Shakiba E**, Ramezani M, Sadeghi M. Evaluation of serum interleukin-6 levels in hepatocellular carcinoma patients: a systematic review and meta-analysis. *Clin Exp Hepatol* 2018; **4**: 182-190 [PMID: 30324143 DOI: 10.5114/ceh.2018.78122]
160 **Pirvulescu MM**, Gan AM, Stan D, Simion V, Calin M, Butoi E, Manduteanu I. Subendothelial resistin enhances monocyte transmigration in a co-culture of human endothelial and smooth muscle cells by mechanisms involving fractalkine, MCP-1 and activation of TLR4 and Gi/o proteins signaling. *Int J Biochem Cell Biol* 2014; **50**: 29-37 [PMID: 24508784 DOI: 10.1016/j.biocel.2014.01.022]
161 **Silswal N**, Singh AK, Aruna B, Mukhopadhyay S, Ghosh S, Ehtesham NZ. Human resistin stimulates the pro-inflammatory cytokines TNF-alpha and IL-12 in macrophages by NF-kappaB-dependent pathway. *Biochem Biophys Res Commun* 2005; **334**: 1092-1101 [PMID: 16039994 DOI: 10.1016/j.bbrc.2005.06.202]
162 **Tarkowski A**, Bjersing J, Shestakov A, Bokarewa MI. Resistin competes with lipopolysaccharide for binding to toll-like receptor 4. *J Cell Mol Med* 2010; **14**: 1419-1431 [PMID: 19754671 DOI: 10.1111/j.1582-4934.2009.00899.x]
163 **Pikarsky E**, Porat RM, Stein I, Abramovitch R, Amit S, Kasem S, Gutkovich-Pyest E, Urieli-Shoval S, Galun E, Ben-Neriah Y. NF-kappaB

functions as a tumour promoter in inflammation-associated cancer. *Nature* 2004; **431**: 461-466 [PMID: 15329734 DOI: 10.1038/nature02924]
164 **Yung JHM**, Giacca A. Role of c-Jun N-terminal Kinase (JNK) in Obesity and Type 2 Diabetes. *Cells* 2020; **9** [PMID: 32183037 DOI: 10.3390/cells9030706]
165 **He G**, Karin M. NF-κB and STAT3 - key players in liver inflammation and cancer. *Cell Res* 2011; **21**: 159-168 [PMID: 21187858 DOI: 10.1038/cr.2010.183]
166 **Lee C**, Cheung ST. STAT3: An Emerging Therapeutic Target for Hepatocellular Carcinoma. *Cancers (Basel)* 2019; **11** [PMID: 31731457 DOI: 10.3390/cancers11111646]
167 **Pirvulescu M**, Manduteanu I, Gan AM, Stan D, Simion V, Butoi E, Calin M, Simionescu M. A novel pro-inflammatory mechanism of action of resistin in human endothelial cells: up-regulation of SOCS3 expression through STAT3 activation. *Biochem Biophys Res Commun* 2012; **422**: 321-326 [PMID: 22575502 DOI: 10.1016/j.bbrc.2012.04.159]
168 **Sakamoto T**, Kuboki S, Furukawa K, Takayashiki T, Takano S, Yoshizumi A, Ohtsuka M. TRIM27-USP7 complex promotes tumour progression *via* STAT3 activation in human hepatocellular carcinoma. *Liver Int* 2023; **43**: 194-207 [PMID: 35753056 DOI: 10.1111/liv.15346]
169 **Bertolani C**, Sancho-Bru P, Failli P, Bataller R, Aleffi S, DeFranco R, Mazzinghi B, Romagnani P, Milani S, Ginés P, Colmenero J, Parola M, Gelmini S, Tarquini R, Laffi G, Pinzani M, Marra F. Resistin as an intrahepatic cytokine: overexpression during chronic injury and induction of proinflammatory actions in hepatic stellate cells. *Am J Pathol* 2006; **169**: 2042-2053 [PMID: 17148667 DOI: 10.2353/ajpath.2006.060081]
170 **Meroni M**, Longo M, Erconi V, Valenti L, Gatti S, Fracanzani AL, Dongiovanni P. mir-101-3p Downregulation Promotes Fibrogenesis by Facilitating Hepatic Stellate Cell Transdifferentiation During Insulin Resistance. *Nutrients* 2019; **11** [PMID: 31671785 DOI: 10.3390/nu11112597]
171 **Barry AE**, Baldeosingh R, Lamm R, Patel K, Zhang K, Dominguez DA, Kirton KJ, Shah AP, Dang H. Hepatic Stellate Cells and Hepatocarcinogenesis. *Front Cell Dev Biol* 2020; **8**: 709 [PMID: 32850829 DOI: 10.3389/fcell.2020.00709]
172 **Hamaidia M**, Jamakhani M, Jacques JR, Fontaine A, Scherpereel A, Wasielewski E, Renaud L, Heinen V, Duysinx B, Willems L. Resistin mediates the immunoediting activity exerted by primary human macrophages towards mesothelioma cells. *Cancer Res* 2023; **83**: 663 [DOI: 10.1158/1538-7445.AM2023-663]
173 **Boutilier AJ**, Elsawa SF. Macrophage Polarization States in the Tumor Microenvironment. *Int J Mol Sci* 2021; **22** [PMID: 34209703 DOI: 10.3390/ijms22136995]
174 **Zhao CW**, Song WX, Liu B, Gao YH, Ding L, Huang YF, Qi X. Resistin induces chemokine and matrix metalloproteinase production *via* CAP1 receptor and activation of p38-MAPK and NF-κB signalling pathways in human chondrocytes. *Clin Exp Rheumatol* 2022; **40**: 501-513 [PMID: 33886462 DOI: 10.55563/clinexprheumatol/avcj31]
175 **De la Fuente López M**, Landskron G, Parada D, Dubois-Camacho K, Simian D, Martinez M, Romero D, Roa JC, Chahuán I, Gutiérrez R, Lopez-K F, Alvarez K, Kronberg U, López S, Sanguinetti A, Moreno N, Abedrapo M, González MJ, Quera R, Hermoso-R MA. The relationship between chemokines CCL2, CCL3, and CCL4 with the tumor microenvironment and tumor-associated macrophage markers in colorectal cancer. *Tumour Biol* 2018; **40**: 1010428318810059 [PMID: 30419802 DOI: 10.1177/1010428318810059]
176 **Bähr I**, Jahn J, Zipprich A, Pahlow I, Spielmann J, Kielstein H. Impaired natural killer cell subset phenotypes in human obesity. *Immunol Res* 2018; **66**: 234-244 [PMID: 29560551 DOI: 10.1007/s12026-018-8989-4]
177 **Jahn J**, Spielau M, Brandsch C, Stangl GI, Delank KS, Bähr I, Berreis T, Wrann CD, Kielstein H. Decreased NK cell functions in obesity can be reactivated by fat mass reduction. *Obesity (Silver Spring)* 2015; **23**: 2233-2241 [PMID: 26390898 DOI: 10.1002/oby.21229]
178 **Tsai HC**, Cheng SP, Han CK, Huang YL, Wang SW, Lee JJ, Lai CT, Fong YC, Tang CH. Resistin enhances angiogenesis in osteosarcoma *via* the MAPK signaling pathway. *Aging (Albany NY)* 2019; **11**: 9767-9777 [PMID: 31719210 DOI: 10.18632/aging.102423]
179 **Chen SS**, Tang CH, Chie MJ, Tsai CH, Fong YC, Lu YC, Chen WC, Lai CT, Wei CY, Tai HC, Chou WY, Wang SW. Resistin facilitates VEGF-A-dependent angiogenesis by inhibiting miR-16-5p in human chondrosarcoma cells. *Cell Death Dis* 2019; **10**: 31 [PMID: 30631040 DOI: 10.1038/s41419-018-1241-2]
180 **Bougatef F**, Quemener C, Kellouche S, Naïmi B, Podgorniak MP, Millot G, Gabison EE, Calvo F, Dosquet C, Lebbé C, Menashi S, Mourah S. EMMPRIN promotes angiogenesis through hypoxia-inducible factor-2alpha-mediated regulation of soluble VEGF isoforms and their receptor VEGFR-2. *Blood* 2009; **114**: 5547-5556 [PMID: 19837976 DOI: 10.1182/blood-2009-04-217380]
181 **Su CM**, Hsu CJ, Tsai CH, Huang CY, Wang SW, Tang CH. Resistin Promotes Angiogenesis in Endothelial Progenitor Cells Through Inhibition of MicroRNA206: Potential Implications for Rheumatoid Arthritis. *Stem Cells* 2015; **33**: 2243-2255 [PMID: 25828083 DOI: 10.1002/stem.2024]
182 **Carmeliet P**. Angiogenesis in health and disease. *Nat Med* 2003; **9**: 653-660 [PMID: 12778163 DOI: 10.1038/nm0603-653]
183 **Pang L**, Zhang Y, Yu Y, Zhang S. Resistin promotes the expression of vascular endothelial growth factor in ovary carcinoma cells. *Int J Mol Sci* 2013; **14**: 9751-9766 [PMID: 23652833 DOI: 10.3390/ijms14059751]
184 **Su CM**, Tang CH, Chi MJ, Lin CY, Fong YC, Liu YC, Chen WC, Wang SW. Resistin facilitates VEGF-C-associated lymphangiogenesis by inhibiting miR-186 in human chondrosarcoma cells. *Biochem Pharmacol* 2018; **154**: 234-242 [PMID: 29730230 DOI: 10.1016/j.bcp.2018.05.001]
185 **Huang GW**, Tao YM, Ding X. Endocan expression correlated with poor survival in human hepatocellular carcinoma. *Dig Dis Sci* 2009; **54**: 389-394 [PMID: 18592377 DOI: 10.1007/s10620-008-0346-3]
186 **Choi SB**, Han HJ, Kim WB, Song TJ, Choi SY. VEGF Overexpression Predicts Poor Survival in Hepatocellular Carcinoma. *Open Med (Wars)* 2017; **12**: 430-439 [PMID: 29318189 DOI: 10.1515/med-2017-0061]
187 **Theodoropoulos VE**, Lazaris ACh, Sofras F, Gerzelis I, Tsoukala V, Ghikonti I, Manikas K, Kastriotis I. Hypoxia-inducible factor 1 alpha expression correlates with angiogenesis and unfavorable prognosis in bladder cancer. *Eur Urol* 2004; **46**: 200-208 [PMID: 15245814 DOI: 10.1016/j.eururo.2004.04.008]
188 **Xu J**, Wang B, Xu Y, Sun L, Tian W, Shukla D, Barod R, Grillari J, Grillari-Voglauer R, Maxwell PH, Esteban MA. Epigenetic regulation of HIF-1α in renal cancer cells involves HIF-1α/2α binding to a reverse hypoxia-response element. *Oncogene* 2012; **31**: 1065-1072 [PMID: 21841824 DOI: 10.1038/onc.2011.305]
189 **Fan HQ**, Gu N, Liu F, Fei L, Pan XQ, Guo M, Chen RH, Guo XR. Prolonged exposure to resistin inhibits glucose uptake in rat skeletal muscles. *Acta Pharmacol Sin* 2007; **28**: 410-416 [PMID: 17303005 DOI: 10.1111/j.1745-7254.2007.00523.x]
190 **Beltowski J**. Adiponectin and resistin--new hormones of white adipose tissue. *Med Sci Monit* 2003; **9**: RA55-RA61 [PMID: 12601307]
191 **Fu Y**, Luo L, Luo N, Garvey WT. Proinflammatory cytokine production and insulin sensitivity regulated by overexpression of resistin in 3T3-L1 adipocytes. *Nutr Metab (Lond)* 2006; **3**: 28 [PMID: 16854242 DOI: 10.1186/1743-7075-3-28]
192 **Palanivel R**, Maida A, Liu Y, Sweeney G. Regulation of insulin signalling, glucose uptake and metabolism in rat skeletal muscle cells upon

prolonged exposure to resistin. *Diabetologia* 2006; **49**: 183-190 [PMID: 16341686 DOI: 10.1007/s00125-005-0060-z]

193 **Rajala MW**, Qi Y, Patel HR, Takahashi N, Banerjee R, Pajvani UB, Sinha MK, Gingerich RL, Scherer PE, Ahima RS. Regulation of resistin expression and circulating levels in obesity, diabetes, and fasting. *Diabetes* 2004; **53**: 1671-1679 [PMID: 15220189 DOI: 10.2337/diabetes.53.7.1671]

194 **Moon B**, Kwan JJ, Duddy N, Sweeney G, Begum N. Resistin inhibits glucose uptake in L6 cells independently of changes in insulin signaling and GLUT4 translocation. *Am J Physiol Endocrinol Metab* 2003; **285**: E106-E115 [PMID: 12618360 DOI: 10.1152/ajpendo.00457.2002]

195 **Wang YQ**, Dong Y, Yao MH. Chromium picolinate inhibits resistin secretion in insulin-resistant 3T3-L1 adipocytes *via* activation of amp-activated protein kinase. *Clin Exp Pharmacol Physiol* 2009; **36**: 843-849 [PMID: 19298540 DOI: 10.1111/j.1440-1681.2009.05164.x]

196 **Song R**, Wang X, Mao Y, Li H, Li Z, Xu W, Wang R, Guo T, Jin L, Zhang X, Zhang Y, Zhou N, Hu R, Jia J, Lei Z, Irwin DM, Niu G, Tan H. Resistin disrupts glycogen synthesis under high insulin and high glucose levels by down-regulating the hepatic levels of GSK3β. *Gene* 2013; **529**: 50-56 [PMID: 23860320 DOI: 10.1016/j.gene.2013.06.085]

197 **Gallagher EJ**, LeRoith D. Hyperinsulinaemia in cancer. *Nat Rev Cancer* 2020; **20**: 629-644 [PMID: 32908223 DOI: 10.1038/s41568-020-0295-5]

198 **Olatunde A**, Nigam M, Singh RK, Panwar AS, Lasisi A, Alhumaydhi FA, Jyoti Kumar V, Mishra AP, Sharifi-Rad J. Cancer and diabetes: the interlinking metabolic pathways and repurposing actions of antidiabetic drugs. *Cancer Cell Int* 2021; **21**: 499 [PMID: 34535145 DOI: 10.1186/s12935-021-02202-5]

199 **Dongiovanni P**, Rametta R, Meroni M, Valenti L. The role of insulin resistance in nonalcoholic steatohepatitis and liver disease development--a potential therapeutic target? *Expert Rev Gastroenterol Hepatol* 2016; **10**: 229-242 [PMID: 26641143 DOI: 10.1586/17474124.2016.1110018]

200 **Song C**, Long X, He J, Huang Y. Recent evaluation about inflammatory mechanisms in nonalcoholic fatty liver disease. *Front Pharmacol* 2023; **14**: 1081334 [PMID: 37007030 DOI: 10.3389/fphar.2023.1081334]

201 **Itoh Y**, Nagase H. Matrix metalloproteinases in cancer. *Essays Biochem* 2002; **38**: 21-36 [PMID: 12463159 DOI: 10.1042/bse0380021]

202 **Parafiniuk K**, Skiba W, Pawłowska A, Suszczyk D, Maciejczyk A, Wertel I. The Role of the Adipokine Resistin in the Pathogenesis and Progression of Epithelial Ovarian Cancer. *Biomedicines* 2022; **10** [PMID: 35453670 DOI: 10.3390/biomedicines10040920]

203 **Di Simone N**, Di Nicuolo F, Sanguinetti M, Castellani R, D'Asta M, Caforio L, Caruso A. Resistin regulates human choriocarcinoma cell invasive behaviour and endothelial cell angiogenic processes. *J Endocrinol* 2006; **189**: 691-699 [PMID: 16731799 DOI: 10.1677/joe.1.06610]

204 **Wågsater D**, Mumtaz M, Lofgren S, Hugander A, Dimberg J. Resistin in human colorectal cancer: increased expression independently of resistin promoter -420C > G genotype. *Cancer Invest* 2008; **26**: 1008-1014 [PMID: 18798067 DOI: 10.1080/07357900802087267]

205 **Tsai CH**, Tsai HC, Huang HN, Hung CH, Hsu CJ, Fong YC, Hsu HC, Huang YL, Tang CH. Resistin promotes tumor metastasis by down-regulation of miR-519d through the AMPK/p38 signaling pathway in human chondrosarcoma cells. *Oncotarget* 2015; **6**: 258-270 [PMID: 25404641 DOI: 10.18632/oncotarget.2724]

206 **Hsu WY**, Chao YW, Tsai YL, Lien CC, Chang CF, Deng MC, Ho LT, Kwok CF, Juan CC. Resistin induces monocyte-endothelial cell adhesion by increasing ICAM-1 and VCAM-1 expression in endothelial cells *via* p38MAPK-dependent pathway. *J Cell Physiol* 2011; **226**: 2181-2188 [PMID: 21520070 DOI: 10.1002/jcp.22555]

207 **Huang T**, Chen QF, Chang BY, Shen LJ, Li W, Wu PH, Fan WJ. TFAP4 Promotes Hepatocellular Carcinoma Invasion and Metastasis *via* Activating the PI3K/AKT Signaling Pathway. *Dis Markers* 2019; **2019**: 7129214 [PMID: 31281549 DOI: 10.1155/2019/7129214]

208 **Zhou Y**, Qiu J, Liu S, Wang P, Ma D, Zhang G, Cao Y, Hu L, Wang Z, Wu J, Jiang C. CFDP1 promotes hepatocellular carcinoma progression through activating NEDD4/PTEN/PI3K/AKT signaling pathway. *Cancer Med* 2023; **12**: 425-444 [PMID: 35861040 DOI: 10.1002/cam4.4919]

World Journal of Gastroenterology

Submit a Manuscript: https://www.f6publishing.com

World J Gastroenterol 2023 July 21; 29(27): 4289-4316

DOI: 10.3748/wjg.v29.i27.4289

ISSN 1007-9327 (print) ISSN 2219-2840 (online)

ORIGINAL ARTICLE

Basic Study

Stomach perforation-induced general occlusion/occlusion-like syndrome and stable gastric pentadecapeptide BPC 157 therapy effect

Luka Kalogjera, Ivan Krezic, Ivan Maria Smoday, Hrvoje Vranes, Helena Zizek, Haidi Yago, Katarina Oroz, Vlasta Vukovic, Ivana Kavelj, Luka Novosel, Slavica Zubcic, Ivan Barisic, Lidija Beketic Oreskovic, Sanja Strbe, Marko Sever, Ivica Sjekavica, Anita Skrtic, Alenka Boban Blagaic, Sven Seiwerth, Predrag Sikiric

Specialty type: Gastroenterology and hepatology

Provenance and peer review: Invited article; Externally peer reviewed.

Peer-review model: Single blind

Peer-review report's scientific quality classification

Grade A (Excellent): A
Grade B (Very good): B
Grade C (Good): 0
Grade D (Fair): 0
Grade E (Poor): 0

P-Reviewer: Luo W, China; Stambolija V, Croatia

Received: February 19, 2023
Peer-review started: February 19, 2023
First decision: May 23, 2023
Revised: June 1, 2023
Accepted: June 19, 2023
Article in press: June 19, 2023
Published online: July 21, 2023

Luka Kalogjera, Ivan Krezic, Ivan Maria Smoday, Hrvoje Vranes, Helena Zizek, Haidi Yago, Katarina Oroz, Vlasta Vukovic, Ivana Kavelj, Luka Novosel, Slavica Zubcic, Ivan Barisic, Sanja Strbe, Marko Sever, Ivica Sjekavica, Alenka Boban Blagaic, Predrag Sikiric, Department of Pharmacology, School of Medicine, Zagreb 10000, Croatia

Lidija Beketic Oreskovic, Division of Oncology and Radiotherapy, University Hospital for Tumors, Sestre milosrdnice University Hospital Centre, Zagreb 10000, Croatia

Anita Skrtic, Sven Seiwerth, Department of Pathology, School of Medicine, Zagreb 10000, Croatia

Corresponding author: Predrag Sikiric, MD, PhD, Full Professor, Department of Pharmacology, School of Medicine, 11 Salata, Zagreb 10000, Croatia. sikiric@mef.hr

Abstract

BACKGROUND

Using rat stomach perforation as a prototypic direct lesion applied in cytoprotection research, we focused on the first demonstration of the severe occlusion/occlusion-like syndrome induced by stomach perforation. The revealed stomach-induced occlusion/occlusion-like syndrome corresponds to the previously described occlusion/occlusion-like syndromes in rats suffering multicausal pathology and shared severe vascular and multiorgan failure. This general point was particularly reviewed. As in all the described occlusion/occlusion-like syndromes with permanent occlusion of major vessels, peripheral and central, and other similar noxious procedures that severely affect endothelium function, the stable gastric pentadecapeptide BPC 157 was resolving therapy.

AIM

To reveal the stomach perforation-induced general occlusion/occlusion-like syndrome and BPC 157 therapy effect.

METHODS

The procedure included deeply anesthetized rats, complete calvariectomy,

laparotomy at 15 min thereafter, and stomach perforation to rapidly induce vascular and multiorgan failure occlusion/occlusion-like syndrome. At 5 min post-perforation time, rats received therapy [BPC 157 (10 μg or 10 ng/kg) or saline (5 mL/kg, 1 mL/rat) (controls)] into the perforated defect in the stomach). Sacrifice was at 15 min or 60 min post-perforation time. Assessment (gross and microscopy; volume) included: Brain swelling, peripheral vessels (azygos vein, superior mesenteric vein, portal vein, inferior caval vein) and heart, other organs lesions (*i.e.*, stomach, defect closing or widening); superior sagittal sinus, and peripherally the portal vein, inferior caval vein, and abdominal aorta blood pressures and clots; electrocardiograms; and bleeding time from the perforation(s).

RESULTS

BPC 157 beneficial effects accord with those noted before in the healing of the perforated defect (raised vessel presentation; less bleeding, defect contraction) and occlusion/occlusion-like syndromes counteraction. BPC 157 therapy (into the perforated defect), induced immediate shrinking and contraction of the whole stomach (unlike considerable enlargement by saline application). Accordingly, BPC 157 therapy induced direct blood delivery *via* the azygos vein, and attenuated/eliminated the intracranial (superior sagittal sinus), portal and caval hypertension, and aortal hypotension. Thrombosis, peripherally (inferior caval vein, portal vein, abdominal aorta) and centrally (superior sagittal sinus) BPC 157 therapy markedly reduced/annihilated. Severe lesions in the brain (swelling, hemorrhage), heart (congestion and arrhythmias), lung (hemorrhage and congestion), and marked congestion in the liver, kidney, and gastrointestinal tract were markedly reduced.

CONCLUSION

We revealed stomach perforation as a severe occlusion/occlusion-like syndrome, peripherally and centrally, and rapid counteraction by BPC 157 therapy. Thereby, further BPC 157 therapy may be warranted.

Key Words: Stomach perforation; General occlusion/occlusion-like syndrome; Stable gastric pentadecapeptide BPC 157; Cytoprotection; Therapy; Rats

©The Author(s) 2023. Published by Baishideng Publishing Group Inc. All rights reserved.

Core Tip: Rats with perforated stomachs exhibited the rapidly emerging severe occlusion/occlusion-like syndrome, an innate general vascular and multiorgan failure, peripherally and centrally. The pentadecapeptide BPC 157 application into stomach defects was efficacious therapy. With an activated azygos vein-rescuing pathway, there was cause-consequence counteraction of lesions in the brain (swelling, hemorrhage), heart (congestion), lung (hemorrhage), and congestion in the liver, kidney, and gastrointestinal tract. Whole occlusion/occlusion-like syndrome, arrhythmias, blood pressure disturbances (intracranial (superior sagittal sinus), portal and caval hypertension, and aortal hypotension), major vessel failure, and widespread thrombosis, Virchow triad circumstances peripherally and centrally were all attenuated/eliminated by BPC 157 therapy.

Citation: Kalogjera L, Krezic I, Smoday IM, Vranes H, Zizek H, Yago H, Oroz K, Vukovic V, Kavelj I, Novosel L, Zubcic S, Barisic I, Beketic Oreskovic L, Strbe S, Sever M, Sjekavica I, Skrtic A, Boban Blagaic A, Seiwerth S, Sikiric P. Stomach perforation-induced general occlusion/occlusion-like syndrome and stable gastric pentadecapeptide BPC 157 therapy effect. *World J Gastroenterol* 2023; 29(27): 4289-4316

URL: https://www.wjgnet.com/1007-9327/full/v29/i27/4289.htm

DOI: https://dx.doi.org/10.3748/wjg.v29.i27.4289

INTRODUCTION

As a novel approach with the beneficial effect of the stable gastric pentadecapeptide BPC 157[1-6] to the stomach perforation therapy, we intend to better implement in practice Robert's and Szabo's cytoprotection concept[7-9]. Conceptually, this might improve the original acceptance of basic cytoprotection maxim, the direct epithelium (Robert)[7,8], endothelium (Szabo)[9] protection/maintenance in the stomach *vs* direct agent's noxious effect (*i.e.*, intragastric alcohol [7]; stomach perforation[10]). To resolve this issue, along with the recently reported stomach perforation in the rats[10], this report describes the rats with a perforated stomach rapidly emerging severe general syndrome occlusion/occlusion-like syndrome recently reviewed[1-4,11-24] as an innate general vascular and multiorgan failure and its therapy with the stable pentadecapeptide BPC 157 application (activation of the collateral pathways)[1,2,11-24].

In the rats with perforated stomachs, noxious course progression, and general detrimental syndrome peripherally and centrally, the BPC 157 therapy outcome might be similar to the beneficial effect that occurs peripherally and centrally during major vessel occlusion[11-19] and other similar noxious procedure application[20-24]. To specifically link the occlusion/occlusion-like syndrome and cytoprotection issue we should mention BPC 157 as a novel cytoprotection mediator maintaining gastrointestinal mucosa integrity, used in ulcerative colitis trials, lethal dose (LD1) not achieved in

toxicology studies, native to and stable in human gastric juice, and thereby, easy applicable cytoprotective capabilities and also permitting per-oral application[1-6]. Further, this occlusion/occlusion-like syndrome[11-24] includes, in particular, the absolute alcohol intragastric instillation as a challenge, the prototype commonly used in cytoprotection studies[7,8,24]. Given the previous therapy effects in the occlusion/occlusion-like syndrome[11-24] and in the cytoprotective studies (for review see[25-31]), including perforated defects[10,32], the stable gastric pentadecapeptide BPC 157, might be the resolving therapy (for additional review see[1-6]) equally acting peripherally and centrally. These might be the novel particular shared pathology and shared therapy indication. This might be due to the BPC 157 therapy advantages, its particular capabilities, cytoprotection[1] as a particular vascular effect[2], wound healing[5], and neuroprotection[6,33]. These implemented its particular additional cytoprotective capabilities[1], and thereby, in the severe vessel and multiorgan failure occlusion/occlusion-like syndrome[2], the prompt particular activation of the collateral pathways (*i.e.,* azygos vein direct blood flow delivery) rapidly occurred as resolving key, and recovery of the muscle disturbances, striated, smooth, and heart failure recovery as whole[3,4].

As mentioned, very recently, in the surgically perforated stomach, the stable gastric pentadecapeptide BPC 157 therapy, which locally immediately restored vessels, counteracted bleeding and contracted perforated defect, and eventually, leads to complete healing (day 7), and fewer adhesions, unlike the failed effect of the standard anti-ulcer agents[10]. Now, given the complexity of the stomach perforation lesions, given the general syndrome simultaneously progressing peripherally and centrally, some additional particular parallel effects of its therapy might be further demonstrated[1-6]. Considering the stomach perforation as the part or cause of the occlusion/occlusion-like syndrome of the vascular and multiorgan failure[11-24] might better define the whole emergency made by perforation injury. Previously, in the occlusion/occlusion-like syndrome studies[11-24], with consistently evidenced BPC 157 therapy resolving effect[11-24] due to particular activation of collateral pathways, reported were the counteractions of the severe lesions in the brain and intracerebral and intraventricular hemorrhage, heart (congestion, infarction, and arrhythmias), hemorrhage and congestion in the lung, liver, kidney and gastrointestinal tract. BPC 157 therapy effect included the attenuation/elimination of the blood pressure disturbances, (intracranial superior sagittal sinus), portal and caval hypertension, and aortal hypotension). Arterial and venous thrombosis peripherally and centrally were almost annihilated; congested inferior caval and superior mesenteric vein, collapsed azygos vein as failed major vessels were recovered to rescuing pathways organization[11-24]. Together, on the one hand, these were summarized as rapidly acting Virchow triad circumstances, and on the other hand, as rapidly acting, "key bypassing" therapy with BPC 157 application [11-24], and likely, they might occur rapidly also in the rats after stomach perforation[10]. As particular damaging points appeared the variety of the major vessel occlusion (inferior caval vein, infrarenal and suprahepatic[11,12], portal vein and hepatic artery[13], superior mesenteric vein[14,15] and artery[15,16], superior sagittal sinus[17], both carotid arteries[18], and cauterized episcleral veins[19]). A variety of other similar severe procedures appeared as additional particular points, *i.e.,* myocardial infarction and re-infarction induced by isoprenaline[21], bile duct occlusion acute pancreatitis[23], severe intra-abdominal hypertension mechanically maintained[20], and the intoxication with endothelium damaging agents, alcohol[24] or lithium[22] prototype agent in bipolar disorders, in particular, all as occlusion/occlusion-like syndrome[20-24].

As an important conceptual point to combine all these lesions and to resolve the shared therapy, the prototype ulcerogenic procedure in cytoprotection studies, the absolute alcohol intragastric instillation[24], was one of the innate injury models readily combined with full occlusion/occlusion-like syndrome[11-24]. Thereby, the resolution of the prime lesion and the resolution of the whole syndrome might be evidence of the full cytoprotective effect of the BPC 157 therapy. As the perforated defect is direct damage analogous to the intragastric alcohol-induced direct damage[10,24] (Robert's lesion by direct contact[7]), it represents an analogous prototype lesion and an essential hallmark in cytoprotection studies[10]. Thereby, the therapy for the perforated stomach defect mandated the resolution of the full occlusion/occlusion-like syndrome to be achieved as in the previous studies[11-24]. Thus, in cytoprotection terms, in the perforated stomach defect[10], the advantageous effect of the BPC 157 therapy, to the same wide extent, might likely occur. Nevertheless, the resolving intragastric alcohol stomach lesions and full occlusion/occlusion-like syndrome might be the successful therapy effects[10] (*i.e.,* activated azygos vein to provide direct blood delivery and inferior caval vein-superior caval vein rescuing pathway[2]) suited for generalization[11-24] of the activated collateral pathways occurring as resolving key.

Conceptually, within the standard view and standard cytoprotection agents, the recovery of the perforated stomach defect[10] may be still outside of the cytoprotection concept although born in the stomach[2]. Cytoprotection has essential theoretical and practical points (*i.e.,* holding direct epithelial cell protection[7,8], beneficial effect on other organs[7] (cytoprotection→organoprotection)[34]; direct endothelium cell protection[9], and endothelial maintenance→epithelial maintenance[7-9]). However, these could be hardly assumed to recover a perforated stomach[10] within the standard cytoprotective agents[1,2] as limited more to the prophylaxis, not therapy effect[7-9]. On the other hand, BPC 157 therapy, based on the noted effects[1-6], thereby, may be proof of the corresponding significance (*i.e.,* the counteraction of the leaky gut syndrome[35], and free radical scavenging activity in the various tissues[35-37]). It may be that the rapid upgrading of the minor vessel to take over and compensate for the function of the failed major vessels, and the specific activation of the collateral pathways, are highlights of the innate cytoprotection function[1-6] as an effective cytoprotection mediator. As native and stable in human gastric juice, it may take the continuous maintenance of the stomach and gastrointestinal mucosa integrity, thereby, the pleiotropic beneficial effect occurred[1-6] (including the recovery of the muscle disturbances, striated, smooth, and heart failure recovery as a whole[3,4]). As such, it might be easily applicable as therapy and might override limitations known for the standard cytoprotective agents[1-9] and contribute to the recovery of stomach perforation as both local and general (occlusion/occlusion-like syndrome) disturbance. These might be particular effects in the vascular studies[11,13-16,21,22,26,35-37], given its special interaction with nitric oxide (NO)-system[29,38-40], thrombocytes[40-42] and many molecular pathways[43-52] (*i.e.,* the counteraction of tumor-induced

muscle cachexia and the signaling process implicated in cancer cachexia)[49].

On the other hand, whatever the cause, there were all organ lesions, progressing venous/arterial thrombosis/stasis, peripherally and centrally, all counteracted by BPC 157 therapy application. As additional proof of the concept, the ECG disturbances, intracranial (superior sagittal sinus) hypertension, portal and caval hypertension, and aortal hypotension were eliminated/attenuated[11-24]. Accordingly, given the considerable blood volume that might be trapped with(in) failed vessels[11-24], there might be also a comparable syndrome that might be also induced rapidly with the stomach perforation as the initial injury[10]. Likewise, in the rats with stomach perforation, along with the therapy effect realized locally in the perforated stomach[10], BPC 157 therapy's particular beneficial effect might be realized with the rapid upgrading of the minor vessel to take over and compensate the function of the failed major vessels, making possible the specific activation of the collateral pathways, as before[11-24]. Thus, the activated azygos vein (and thereby, direct blood flow delivery from the inferior to the superior caval vein) might serve as a "bypassing vascular key" taking general significance (for review see[11-24]) to recover otherwise imminent occlusion/occlusion-like syndrome also in rats with the perforated stomachs.

For this purpose, given its cytoprotective stomach capability to counteract the whole imminent occlusion/occlusion-like syndrome, and brain lesions, in particular[11-24], we used the calvariectomized rats, for direct monitoring, and the BPC 157 therapy was given directly into the perforated stomach defect. We focused on the subsequent presentation of the stomach and the presentation of the brain swelling and all organ lesions. Then, progressing venous/arterial thrombosis/stasis, peripherally and centrally, were all counteracted by BPC 157 therapy application. These were along with attenuation/elimination of the arrhythmias, intracranial (superior sagittal sinus) hypertension, portal and caval hypertension, and aortal hypotension. Thus, full therapy effects were determined during the essential early period.

MATERIALS AND METHODS

Animals

Male Albino Wistar rats, 200 g bw, kept under standard laboratory conditions, were randomly assigned at 6 rats/group/interval for all experiments, approved by the Local Ethic Committee, carried out under a blind protocol, and the effects evaluated by the examiners who were unaware of the applied protocol.

Drugs

Stable gastric pentadecapeptide BPC 157 (GEPPPGKPADDAGLV, molecular weight 1419; Diagen, Slovenia), was used in dose and application regimens described previously (*i.e.,* without the use of a carrier or peptidase inhibitor) (for review see[1-6]).

Experimental protocol

In deep anesthesia [40 mg/kg thiopental (Rotexmedica, Germany) and 10 mg/kg diazepam (Apaurin; Krka, Slovenia) intraperitoneally] rats underwent complete calvariectomy[17], and laparotomy at 15 min thereafter, and to induce rapid vascular failure and concomitant general and peripheral occlusion/occlusion-like syndrome, stomach perforation was performed as described before[10,17]. Sacrifice was at 15 min or 60 min post-perforation time.

At 5 min post-perforation time, rats received therapy [BPC 157 (10 μg or 10 ng/kg) or saline (5 mL/kg, 1 mL/rat) (controls)] into the perforated defect in the stomach.

Before the procedure, after perforation, after therapy application, and before sacrifice, recordings [camera attached to a VMS-004 Discovery Deluxe USB microscope (Veho, United States)] of brain swelling, corresponding presentation of the peripheral vessels (azygos vein, superior mesenteric vein, portal vein, and inferior caval vein), and organ lesions, were as in our vascular studies[11-24], and assessed as before[11-24]. At all the indicated time points until the end of the 15-min period stomach defect closing or widening (both as % of the presentation immediately before therapy) was assessed as described[10].

In a separate group of animals, the stomach perforation-induced bleeding as bleeding time from the perforation(s) was assessed throughout the 15 min, given the quite short time after perforation available as described[10]. Immediately after perforation induction, rats received BPC 157 (10 μg or 10 ng/kg) or saline (5 mL/kg, 1 mL/rat) (controls) as therapy applied to the perforated defect in the stomach.

Superior sagittal sinus, portal, caval vein, and abdominal aorta pressure recording

The recording procedure in rats was described in detail in our previous vascular studies[11-24]. At 15 min and 60 min post-perforation time, under deep anesthesia, a cannula (BD Neoflon™ Cannula) connected to a pressure transducer (78534C MONITOR/ TERMINAL; Hewlett Packard, United States), inserted into the portal vein, inferior caval vein and superior sagittal sinus, as well as the abdominal aorta at the level of the bifurcation.

Accordingly[11-24], -24 mmHg to -27 mmHg values of superior sagittal sinus pressure were in healthy rats. The 3-5 mmHg values were considered normal in portal pressure in healthy rats. Similar to that were in the inferior vena cava, though with values at least 1 mmHg higher in the portal vein. Abdominal aorta blood pressure values of 100-120 mmHg at the bifurcation level were considered normal in healthy rats.

ECG recording

In rats under deep anesthesia, before the procedure, and in post-perforation time (*i.e.,* after stomach perforation, after

therapy application, and before sacrifice), precise recordings, measurements, and analysis of ECG parameters (PQ intervals, QTc, heart frequency) as specifically described[11-24] were with ECGs recorded continuously for all three main leads, by positioning stainless steel electrodes on all four limbs using an ECG monitor with a 2090 programmer (Medtronic, United States) connected to a Waverunner LT342 digital oscilloscope (LeCroy, United States)[11-24].

Thrombus assessment

After rats' sacrifice, the clots were weighed when the superior sagittal sinus, and peripherally the portal vein, inferior caval vein, and abdominal aorta were removed[11-24].

Brain volume, heart, and vessel volume presentation

We applied the procedure used in our previous vascular studies[11-24]. Brain volume and vessel volume and heart volume or stomach volume were proportional to the change in the brain or vessel or heart or stomach surface area. The presentation of the brain and peripheral vessels (superior mesenteric vein, inferior caval vein, and azygos vein) was recorded in deeply anesthetized rats, with a camera attached to a VMS-004 Discovery Deluxe USB microscope (Veho, United States). The border of the brain (or vessels, or heart or stomach) in the image was marked using ImageJ software and then the surface area of the brain (or veins, or heart or stomach) was measured. This was done with brain (or veins or stomach) images for healthy rats, and then/or for both the control (saline) group and treated (BPC 157) group of rats at the same intervals after the application and at the time of sacrifice. The arithmetic mean of the surface areas was calculated for both groups. Then, the ratio of these two areas was calculated as (A_{con}/A_{bpc}), where A_{con} is the arithmetic mean brain (or veins) area of the control group and A_{bpc} is the arithmetic mean brain (or veins or heart or stomach) area of the treated group. Starting from the square-cube law equations[1,2], an equation for the change in brain (or veins, or heart, or stomach) volume proportional to the change in brain surface area (or veins, or heart, or stomach)[6] was derived. In expressions[1-5], "*l*" is defined as any arbitrary one-dimensional length of the brain (for example rostro-caudal length of the brain) (or veins or heart or stomach), used only for defining the one-dimensional proportion (l_2/l_1) between two observed brains (or veins or heart or stomach) and as an inter-factor (and because of that not measured[6]) for deriving final expression[6].

The procedure was as follows: (1) $A_2 = A_1 \times (l_2/l_1)^2$ (square-cube law); (2) $V_2 = V_1 \times (l_2/l_1)^3$ (square-cube law); (3) $A_2/A_1 = (l_2/l_1)^2$ [from (1), after dividing both sides by A_1]; (4) $l_2/l_1 = (A_2/A_1)^{1/2}$ [from (3), after taking the square root of both sides]; (5) $V_2/V_1 = (l_2/l_1)^3$ [from (2), after dividing both sides by V_1]; and (6) $V_2/V_1 = [(A_2/A_1)^{1/2}]^3$ [after incorporating expression (4) into equation (5)].

Gross assessment of gastrointestinal lesions

In rats laparatomized under anesthesia, gross lesions in the gastrointestinal tract and in the stomach (sum of the longest diameters, mm) assessment was with the camera attached to a VMS-004 Discovery Deluxe USB microscope (Veho, United States) before sacrifice as described before[11-24].

Microscopy

As described in the previous studies[11-24], evaluation was done by light microscopy using an Olympus 71 digital camera and an Olympus BX51 microscope (OLYMPUS Europa SE & CO. KG). Digital images were saved as uncompressed 24-bit RGB TIFF files using the software program AnalySIS (Olympus Soft Imaging System GmbH, Munster, Germany). The field size was measured and marked with a manufacturer's default scale bar in the software program AnalySIS (Olympus Soft Imaging System GmbH, Munster, Germany). Representative tissue specimens (*i.e.*, the brain, liver, kidney, stomach, small and large intestine, lungs, and heart taken at the end of the experiment, fixed in 10% neutral buffered formalin (pH 7.4) at room temperature for 24 h) were embedded in paraffin, sectioned at 4 μm, stained with hemalaun and eosin.

Brain histology: As described in the previous studies[11-24], the brain was dissected according to NTP-7, at levels 3 and 6 with neuroanatomic subsites presented in certain brain sections using coronal sections with three mandatory sections. We used a semiquantitative neuropathological scoring system, and the sum of analyzed affected areas (0-4) (i) and karyopyknotic cells in the brain areas (0-4) (ii) making (i)+(ii) a combined score (0-8), as follows: (1) Specifically affected brain areas [cerebral (NTP-7, level 3), cerebellar cortex (NTP-7, level 6), hippocampus, thalamus, and hypothalamus (NTP-7, level 3)] were scored (0-4), (score 0 indicates no histopathologic change), as follows. Small, patchy, complete, or incomplete infarcts (≤ 10% of the area affected) represented score 1. Partly confluent or incomplete infarcts (20%-30% of the area affected) represented score 2. Large confluent complete infarcts (40%-60% of the area affected) represented score 3. In the cortex total disintegration of the tissue, in the hypothalamus, thalamus, and hippocampus large complete infarcts (> 75% of the area affected) represented score 4; and (2) Analyzed were karyopyknotic cells in the affected brain areas (0-4) (score 0 indicates no change), cerebral (NTP-7, level 3), cerebellar cortex (NTP-7, level 6), hippocampus, thalamus, and hypothalamus (NTP-7, level 3) as follows: A few karyopyknotic of neuronal cells (≤ 20%, score 1); patchy areas of karyopyknotic cells (50%, score 2); more extensive karyopyknotic areas (75%, score 3); complete infarction (100%, score 4). Brain tissue hemorrhage was obtained estimating a percentage of affected areas. Intraventricular hemorrhage was noted as present or absent.

We also assessed the neuronal pathological changes in acquired digital images saved as uncompressed 24-bit RGB TIFF files in the software program AnalySIS (Olympus Soft Imaging System GmbH, Munster, Germany) performing quantitative analysis of neuronal damage in the karyopyknotic areas. The neurons of the cortical cerebral, cerebellar region, hippocampus, and hypothalamus were counted in 10 different high-powered fields (HPF, 400 ×) and 3 to 5 serial

sections of each sample were used to do the count as described[53]. The field size was 0.24 μm².

We used four criteria for the estimation of the edema: Pale myelin, the sieve-like appearance of myelinated areas, dilation of perivascular and pericellular spaces, and vacuolar appearance of the neuropil of gray matter. Edema was graded as heavy, moderate, slight, or no edema (score 0-3)[54].

Lung histology: The same scoring system as in the previous studies[11-24] was used to grade the degree of lung injury in lung tissue analysis. Each of the features (*i.e.*, focal thickening of the alveolar membranes, congestion, pulmonary edema, intra-alveolar hemorrhage, interstitial neutrophil infiltration, and intra-alveolar neutrophil infiltration) was scored (0-3) as absent (0) or present a mild (1), moderate (2), or severe (3) degree and a final histology score were determined.

Renal, liver, and heart histology: The same scoring system as in the previous studies[11-24] was used to grade renal (*i.e.*, the degeneration of Bowman's space and glomeruli, degeneration of the proximal and distal tubules, vascular congestion, and interstitial edema), liver (*i.e.*, vacuolization of hepatocytes and pyknotic hepatocyte nuclei, activation of Kupffer cells, and enlargement of sinusoids) and heart (*i.e.*, dilatation and congestion of blood vessels within the myocardium and coronary arteries) histology. Each specimen was scored using a scale ranging from 0-3 (0: none, 1: mild, 2: moderate, and 3: severe) for each criterion, and a final histology score was determined (0: none, 1: mild, 2: moderate, and 3: severe).

Gastrointestinal histology: As in previous studies[11-24], we used a histologic scoring scale adapted from Chui and coworkers[55] for the stomach tissue damage scoring 0-5 (normal to severe) in three categories (mucosal injury, inflammation, hyperemia/hemorrhage) for a total score of 0 to 15, as described by Lane and coworkers[56]. Illustratively, the assessment included morphologic features of mucosal injury (*i.e.*, different grades of epithelial lifting, villi denudation, and necrosis), inflammation (*i.e.*, focal to diffuse according to lamina propria infiltration or subendothelial infiltration), and hyperemia/hemorrhage (*i.e.*, focal to diffuse according to lamina propria or subendothelial localization).

Statistical analysis

Statistical analysis was performed by parametric one-way analysis of variance (ANOVA), with the Newman-Keuls post-hoc test or the non-parametric Kruskal-Wallis test and subsequently the Mann-Whitney *U* test to compare groups. Values are presented as the mean ± SD and as the minimum/median/maximum. To compare the frequency difference between groups, the chi-squared test or Fischer's exact test was used. $P < 0.05$ was considered statistically significant.

RESULTS

Along with the recently described stomach perforation course notated in the injured stomach, particular vascular failure (vessels "disappear"/empty), prolonged bleeding, debilitated defect large widening[10], stomach perforation consistently induced the vascular and multiorgan failure, progressing thrombosis, intracranial (superior sagittal sinus), portal and caval hypertension, and aortal hypotension. These were fully compatible with the general occlusion/ occlusion-like syndrome occurring peripherally and centrally. There were also cause-consequence lesions in the brain (swelling, hemorrhage), heart (congestion), lung (hemorrhage), congestion in the liver, kidney, and gastrointestinal tract, arrhythmias, and vessel failure, peripherally and centrally. Noteworthy, the vascular failure studies confirmed similar occlusion/occlusion-like syndromes induced by major vessel occlusion or other similar noxious procedures such as alcohol or lithium intoxication, myocardial infarction, acute pancreatitis, intra-abdominal hypertension that all severely affect endothelium function[11-24].

With counteraction by BPC 157 therapy, beneficial effects were along with those noted before in the healing of the perforated defect (raised vessel presentation; less bleeding, defect contraction) comparable to the previous BPC 157 therapy of the mentioned occlusion/occlusion-like syndromes. A common key finding to recovering rats with perforated stomachs that might break instantly the injurious circle might be the prompt and sustained activation of the azygos vein direct blood flow delivery as the particular effect of the stable gastric pentadecapeptide BPC 157 therapy application. Consistently attenuated/counteracted intracranial (superior sagittal sinus) hypertension and aortal hypotension, major arrhythmias, progressing arterial and vein thrombosis, lesions in the brain, heart, lungs, liver, kidneys, and gastrointestinal tract)[11-24] all prove counteraction of whole occlusion/occlusion-like syndrome.

A perilous syndrome occurred peripherally and centrally

Blood pressure disturbances: In the rats with perforated stomachs, the rapidly presented, portal and caval hypertension, and even more the intracranial (superior sagittal sinus) hypertension (gross brain swelling) as well as the aortal hypotension were markedly attenuated by BPC 157 application. This might be a cause-consequence relation relevant to the effectiveness of the therapy application as BPC 157 reduced consistently blood pressure disturbances that were otherwise induced rapidly by similar occlusion/occlusion-like syndromes. This includes a peripheral presentation (portal and caval hypertension, aortal hypotension) as well an even more central presentation (superior sagittal sinus hypertension, Table 1).

Thrombosis

After perforation of the stomach, as a shared effect with other occlusion/occlusion-like syndromes, in the rats with perforated stomachs, thrombosis was rapidly presented, progressing peripherally in veins (*i.e.*, portal and inferior caval vein) as well as in arteries (*i.e.*, abdominal aorta) and centrally (*i.e.*, superior sagittal sinus). Contrary, with BPC 157 therapy thrombosis was promptly reduced both peripherally and centrally (Table 1) as the effective cause-consequence

Table 1 Blood pressures and thrombosis in rats at 15 min and 60 min following stomach perforation

Application of the 1 mL/rat through the perforated defect in the injured stomach at 5 min following perforation	Blood pressures and thrombosis in rats at 15 min and 60 min following stomach perforation	
	15 min	60 min
Superior sagittal sinus pressure, mmHg, mean ± SD		
Control	9 ± 1	8 ± 1
BPC 157 10 μg/kg	-3 ± 1[a]	-1 ± 1[a]
BPC 157 10 ng/kg	-1 ± 1[a]	-2 ± 1[a]
Portal pressure, mmHg, mean ± SD		
Control	16 ± 2	17 ± 1
BPC 157 10 μg/kg	9 ± 1[a]	9 ± 1[a]
BPC 157 10 ng/kg	9 ± 1[a]	8 ± 1[a]
Caval pressure, mmHg, mean ± SD		
Control	15 ± 1	15 ± 1
BPC 157 10 μg/kg	8 ± 1	9 ± 1[a]
BPC 157 10 ng/kg	7 ± 1	9 ± 1[a]
Aortal pressure, mmHg, mean ± SD		
Control	42 ± 5	45 ± 7
BPC 157 10 μg/kg	75 ± 4[a]	72 ± 5[a]
BPC 157 10 ng/kg	80 ± 5[a]	78 ± 7[a]
Superior sagittal sinus, thrombus mass, g, mean ± SD		
Control	0.0012 ± 0.0005	0.0022 ± 0.0009
BPC 157 10 μg/kg	0 ± 0[a]	0 ± 0[a]
BPC 157 10 ng/kg	0 ± 0[a]	0 ± 0[a]
Portal vein, thrombus mass, g, mean ± SD		
Control	0.0034 ± 0.0006	0.0056 ± 0.0008
BPC 157 10 μg/kg	0.0010 ± 0.0005[a]	0.0020 ± 0.0005[a]
BPC 157 10 ng/kg	0.0010 ± 0.0007[a]	0.0018 ± 0.0006[a]
Inferior caval vein, thrombus mass, g, mean ± SD		
Control	0.0039 ± 0.0007	0.0061 ± 0.0008
BPC 157 10 μg/kg	0.0002 ± 0.0001[a]	0.0003 ± 0.0001[a]
BPC 157 10 ng/kg	0.0008 ± 0.0001[a]	0.0005 ± 0.0002[a]
Abdominal aorta, thrombus mass, g, mean ± SD		
Control	0.0044 ± 0.0007	0.0063 ± 0.0009
BPC 157 10 μg/kg	0 ± 0[a]	0 ± 0[a]
BPC 157 10 ng/kg	0 ± 0[a]	0 ± 0[a]

[a]$P < 0.05$, at least *vs* control.

Blood pressures (intracranial (superior sagittal sinus), portal and caval hypertension and aortal hypotension, mmHg), and thrombosis (thrombus mass, g) in rats at 15 min and 60 min following perforation of the stomach. Saline (5 mL/kg) (control) or BPC 157 (10 μg/kg and 10 ng/kg) were given at 5 min thereafter.

course of the therapy both peripherally and centrally.

Stomach presentation

As before with the application of the BPC 157 as a bath in the abdominal cavity, which might beneath the damaged stomach[10], the application of the BPC 157 directly into the injured stomach through the perforated defect, might rapidly

Table 2 Relative volume of the stomach of the heart, azygos vein, in rats at 5 min and 15 min following stomach perforation

0 min	5 min	5 min	15 min
Relative volume (healthy/perforation, %) of the stomach in rats immediately after perforation	Application of the 1 mL/rat through the perforated defect in the injured stomach at 5 min following perforation	Relative volume (healthy/perforation, healthy/perforation + therapy, %) of the stomach, in rats at 5 min and 15 min following stomach perforation	
Relative volume (healthy/perforation, %) of the stomach, mean ± SD	Medication	Relative volume (healthy/perforation + therapy, %) of the stomach, mean ± SD	
100 ± 3	Saline 5 mL/kg (control)	114 ± 2[a,b]	118 ± 2[a,b]
100 ± 2	BPC 157 10 μg/kg	87 ± 5[a,b,c]	76 ± 8[a,b,c]
101 ± 2	BPC 157 10 ng/kg	81 ± 7[a,b,c]	79 ± 9[a,b,c]

[a]$P < 0.05$, at least *vs* healthy.
[b]$P < 0.05$, at least *vs* immediately after perforation.
[c]$P < 0.05$, at least *vs* corresponding control at the time of the assessment.
Relative volume (healthy/perforation, healthy/perforation + therapy, %) of the stomach of the heart, azygos vein, in rats at 5 min and 15 min following stomach perforation. Saline (5 mL/kg, control) or BPC 157 (10 μg/kg and 10 ng/kg) were given at 5 min after perforation.

reduce the defect size. Illustratively, given the perforation defect size ratio (%) after therapy/before therapy, considerable widening of the perforated defect occurred in the controls (235 ± 56 and 255 ± 66, at 15 min and 60 min after perforation, respectively). Contrarily, there was a marked shrinking of the defect after BPC 157 therapy (75 ± 8, 65 ± 8, BPC 157 10 μg at 15 min and 60 min perforation-time; 80 ± 8, 75 ± 8, BPC 157 10 ng at 15 min and 60 min perforation-time, $P < 0.05$, at least *vs* control). Likewise, accordingly with previous findings[10], the bleeding time (sec) was also reduced in BPC 157 treated rats (*i.e.*, 100 ± 8 in controls *vs* 50 ± 8 BPC 157 10 μg and 55 ± 7 BPC 157 10 ng, $P < 0.05$, at least *vs* control). In addition, with BPC 157 therapy into the perforated defect, upon volume application instead of volume-induced dilatation as regular finding in the rats with the perforated stomach, the whole stomach reacted with marked shrinking (Table 2, Figure 1).

Collateral pathways, blood vessels, and brain gross presentation: All rats with perforated stomachs without therapy converge to the similar failed effects consistently noted with other occlusion/occlusion-like syndromes. Indicatively for a not functioning common clue (lack of activation of collateral pathways) might be the failed azygos vein, superior mesenteric vein, inferior caval vein, and abdominal aorta. We used their disturbed presentation as indicative illustrations (Figure 2) to envisage the failed collateral pathways presentation.

On the other hand, the attenuation of blood pressure disturbances, peripherally and centrally, we perceived as an effect of BPC 157 along with progressing thrombosis fully counteracted in all vessels investigated, veins and arteries, peripherally and centrally (Table 1). Thus, the major vessel failure and blood stasis, the particular vessels recruitment might compensate. Peripherally, note the rescued presentation of the superior mesenteric vein and inferior caval vein as well as the activated azygos vein, and thereby the heart as well (Figure 2), and centrally, note brain swelling rapidly disappeared (Figure 3). Thus, with BPC 157 therapy, advanced collateral pathways presentation occurred as a key therapy effect.

The relative volume of the brain, heart, azygos vein, superior mesenteric vein, and inferior caval vein might summarize the harmful event of the stomach perforation and subsequent deleterious worsening (swollen brain, congested superior mesenteric vein and inferior caval vein for the congested lung, liver, kidney and gastrointestinal tract and heart failure) (Table 3, Figures 2 and 3). On the other hand, vice versa, relative volume change might clearly indicate the strong therapy effect of the BPC 157 application, and reversal toward the normal vessels (presentation close to normal of the superior mesenteric vein and inferior caval vein that had been over-congested), likely due to the activation of the azygos vein (direct blood delivery) that had been failed. Heart dilatation was reversed. Likewise, the brain swelling was rapidly reversed. Note, upon sacrifice, ex vivo, the control/treated brain volume ratio (%) reached for BPC 157 10 μg or 10 ng/kg ($P < 0.05$, at least *vs* control) 120 ± 4 and 122 ± 4 at 15 min and 123 ± 4 and 121 ± 4 at 60 min after perforation.

Heart and ECG disturbances: Commonly, in the procedure with the stomach perforation, BPC 157 therapy counteracted the whole noxious chain of events (*i.e.*, continuous tachycardia along with prolonged PQ prolonged and QTc intervals) (Table 4). Tachycardia, QTc intervals or PQ intervals disturbances were regularly attenuated or absent in all BPC 157-treated rats.

A perilous syndrome occurred peripherally

Gastrointestinal, lung, liver, kidney, and heart lesions: In the untreated rats, all of the post-perforation intervals consistently expressed the particular lesion severity evidenced in the affected organs (Figures 4-7, Table 5). Also, the evidenced intracranial (superior sagittal sinus), portal, and caval hypertension, aortal hypotension, progressed thrombosis, peripherally and centrally, failed collateral recruitment, and ECG disturbances may together indicate a common clue that might be failed. Thereby, there is the immediate impact of the activated collateral pathway that the reduced severity of lesions by BPC 157 therapy evidently occurred along with the reduced intracranial (superior sagittal sinus), portal, and caval hypertension, and reduced aortal hypotension, counteracted ECG disturbances. Thus, BPC 157

Table 3 Relative volume of the brain, inferior caval vein, and superior mesenteric vein, and relative volume of the heart, azygos vein, in rats at 15 min and 60 min following stomach perforation

0 min	5 min	15 min	60 min
Relative volume (healthy/perforation, %) of the brain, heart, azygos vein, inferior caval vein, superior mesenteric vein, and abdominal aorta in rats immediately after perforation	Application of the 1 mL/rat through the perforated defect in the injured stomach at 5 min following perforation	Relative volume (healthy/perforation, healthy/perforation + therapy, %) of the brain, inferior caval vein, and superior mesenteric vein, and relative volume (control/treated, %) of the heart, azygos vein, in rats at 15 min and 60 min following stomach perforation	
Relative volume (healthy/perforation) (%) of the brain, mean ± SD	Medication	Relative volume (healthy/perforation + therapy, %) of the brain, mean ± SD	
116 ± 3[a]	Saline 5 mL/kg (control)	124 ± 2[a,b]	124 ± 2[a,b]
120 ± 2[a]	BPC 157 10 µg/kg	100 ± 1[b,c]	99 ± 2[b,c]
121 ± 2[a]	BPC 157 10 ng/kg	101 ± 3[b,c]	100 ± 1[b,c]
-	Relative volume (control/treated, %) of the heart, mean ± SD		
	BPC 157 10 µg/kg	137 ± 4[c]	141 ± 5[c]
	BPC 157 10 ng/kg	136 ± 3[c]	138 ± 4[c]
	Relative volume (control/treated, %) of the azygos vein, mean ± SD		
	BPC 157 10 µg/kg	66 ± 6[c]	58 ± 7[c]
	BPC 157 10 ng/kg	64 ± 4[c]	54 ± 8[c]
	Relative volume (healthy/perforation + therapy, %) of the inferior caval vein, mean ± SD		
130 ± 3[a]	Saline 5 mL/kg (control)	164 ± 8[a,b]	174 ± 9[a,b]
128 ± 4[a]	BPC 157 10 µg/kg	98 ± 2[b,c]	100 ± 2[b,c]
126 ± 4[a]	BPC 157 10 ng/kg	100 ± 3[b,c]	99 ± 1[b,c]
	Relative volume (healthy/perforation + therapy, %) of the superior mesenteric vein, mean ± SD		
180 ± 5[a]	Saline 5 mL/kg (control)	204 ± 8[a,b]	212 ± 9[a,b]
188 ± 9[a]	BPC 157 10 µg/kg	96 ± 6[b,c]	99 ± 7[b,c]
186 ± 8[a]	BPC 157 10 ng/kg	98 ± 6[b,c]	101 ± 1[b,c]

[a]$P < 0.05$, at least *vs* healthy.
[b]$P < 0.05$, at least *vs* immediately after perforation.
[c]$P < 0.05$, at least *vs* corresponding control at the time of the assessment.
Relative volume (healthy/perforation, healthy/perforation + therapy, %) of the brain, inferior caval vein, and superior mesenteric vein, and relative volume (control/treated, %) of the heart, azygos vein, in rats at 15 min and 60 min following stomach perforation. Saline (5 mL/kg) (control) or BPC 157 (10 µg/kg and 10 ng/kg) were given at 5 min after perforation.

therapy appeared as part of the cause-consequence therapeutic course.

Gastrointestinal lesion: Transmural hyperemia of the stomach wall in the control group with marked mucosal congestion at perforation's margins (Figure 4, Table 5). No congestion of the stomach wall in the BPC 157 group, and only mild mucosal congestion was at the stomach perforation's margins (Figure 5, Table 5).

Heart: Severe myocardial congestion was commonly noted in all the control rats. Contrarily, in rats treated with BPC 157, these lesions were completely annihilated (Figures 6 and 7, Table 5). These findings were along with counteracted heart dilatation and counteracted ECG disturbances (Tables 3 and 4, Figure 2).

Lung: Without therapy, focal thickening of the alveolar membranes occurred, lung congestion, pulmonary edema, and severe intra-alveolar hemorrhage. Contrarily, BPC 157 rats exhibited only mild congestion in lung parenchyma (Figures 6 and 7, Table 5).

Liver: Severe enlargement of sinusoids with liver congestion occurred in all control rats, while BPC 157 exhibited no changes in liver parenchyma (Figures 6 and 7, Table 5).

Kidney: Severe vascular congestion and mild interstitial edema occurred in all control rats. Contrarily, no changes were found in renal parenchyma in BPC 157 treated rats (Figures 6 and 7, Table 5).

Table 4 ECG changes, PQ interval, QTc interval, msec, heart frequency, beats/min, in rats at 15 min and 60 min following stomach perforation

Application of the 1 mL/rat through the perforated defect in the injured stomach at 5 min following perforation	ECG changes in rats at 15 min and 60 min following stomach perforation	
	15 min	60 min
	PQ interval, msec mean ± SD	
Control	64 ± 5	67 ± 6
BPC 157 10 µg/kg	50 ± 5[a]	50 ± 5[a]
BPC 157 10 ng/kg	50 ± 5[a]	50 ± 5[a]
	QTc interval, msec, mean ± SD	
Control	312 ± 10	347 ± 10
BPC 157 10 µg/kg	180 ± 10[a]	188 ± 10[a]
BPC 157 10 ng/kg	185 ± 10[a]	183 ± 10[a]
	Heart frequency, beats/min, mean ± SD	
Control	530 ± 30	550 ± 30
BPC 157 10 µg/kg	375 ± 10 [a]	360 ± 10[a]
BPC 157 10 ng/kg	385 ± 10 [a]	365 ± 10[a]

[a]$P < 0.05$, at least *vs* control.

ECG changes, PQ interval, QTc interval, msec, heart frequency, beats/min, in rats at 15 min and 60 min following stomach perforation. Saline (5 mL/kg, control) or BPC 157 (10 µg/kg and 10 ng/kg) were given at 5 min thereafter.

Table 5 Lesions scored microscopically (heart, lung, liver, kidney, stomach), or macroscopically (stomach, in rats at 15 min and 60 min following stomach perforation

Application of the 1 mL/rat through the perforated defect in the injured stomach at 5 min following perforation	Lesions scored microscopically (heart, lung, liver, kidney, stomach, small and large intestine), or macroscopically (stomach), in rats at 15 min and 60 min following stomach perforation	
	15 min	60 min
	Heart (scored 0-3, min/med/max)	
Control	3/3/3	3/3/3
BPC 157 10 µg/kg	0/0/0[a]	0/0/0[a]
BPC 157 10 ng/kg	0/0/0[a]	0/0/0[a]
	Lung (scored 0-3, min/med/max)	
Control	3/3/3	3/3/3
BPC 157 10 µg/kg	1/1/1[a]	1/1/1[a]
BPC 157 10 ng/kg	1/1/1[a]	1/1/1[a]
	Liver (scored 0-3, min/med/max)	
Control	3/3/3	3/3/3
BPC 157 10 µg/kg	0/0/0[a]	0/0/0[a]
BPC 157 10 ng/kg	0/0/0[a]	0/0/0[a]
	Kidney (scored 0-3, min/med/max)	
Control	3/3/3	3/3/3
BPC 157 10 µg/kg	0/0/0[a]	0/0/0[a]
BPC 157 10 ng/kg	0/0/0[a]	0/0/0[a]

	Stomach (scored 0-15, min/med/max)	
Control	5/5/5	4/5/5
BPC 157 10 μg/kg	1/1/1[a]	1/1/1[a]
BPC 157 10 ng/kg	1/1/1[a]	1/1/1[a]

[a]$P < 0.05$, at least *vs* control.

Lesions scored microscopically (heart, lung, liver, kidney, and stomach), or macroscopically (stomach, in rats at 15 min and 60 min following stomach perforation. Saline (5 mL/kg, control) or BPC 157 (10 μg/kg and 10 ng/kg) were given at 5 min thereafter.

A perilous syndrome occurred centrally

Brain lesions, cerebral and cerebellar cortex, hypothalamus/thalamus, and hippocampus: All of the control rats with perforated stomachs converge to a similar brain lesion (Figures 7 and 8, Table 6) indicating a common clue that might be failed. Namely, these occurred along with intracranial (superior sagittal sinus), portal, and caval hypertension, aortal hypotension, progressed thrombosis, peripherally and centrally, failed collateral recruitment, disturbed ECG presentation, and peripheral organs lesion. The brain swell (Figure 3) occurred with the increased intracranial (superior sagittal sinus) hypertension in the immediate and prolonged post-application-period. These rats with perforated stomachs exhibited marked edema and congestion in neocortical brain tissue with an increased number of karyopycnotic nuclei of cortical neurons, marked edema, and an increased number of karyopycnotic nuclei of cerebellar Purkinje cells. Marked edema and congestion in the hypothalamic area appeared with an increased number of karyopycnotic cells. Marked edema and an increased number of karyopycnotic nuclei occurred also in the hippocampal area.

Contrarily, with BPC 157 therapy, there was a marked reduction of intracranial (superior sagittal sinus) hypertension (and elimination of portal and caval hypertension). These went along with the counteracted brain swelling (Figure 3). BPC 157-treated rats had only mild edema in the neocortex, no change in cerebellar Purkinje cells, only a few karyopycnotic cells in the hypothalamic area, and no change in the hippocampal area (Figures 8 and 9, Table 6).

In summary, in rats with stomach perforation after BPC 157 therapy, in either of the regimens (μg, ng, and intragastrically), there was an immediate effect on the perforated stomach (*i.e.*, decreased bleeding, shrinking of the defect and whole stomach). At the same time, rats rapidly exhibited markedly attenuated portal and caval hypertension, and superior sagittal sinus hypertension, ameliorated aortal hypotension, and had no ECG disturbance, almost annihilated venous and arterial thrombosis, both peripherally and centrally. They had reduced or eliminated central and peripheral organ lesions, in the brain, heart, lung, liver, kidney, and gastrointestinal tract. Gross assessment (*i.e.*, rapid counteraction of the brain swelling, counteraction of the heart dilatation), and microscopic assessment (*i.e.*, myocardial congestion completely annihilated) support each other. Thus, BPC 157 therapy suggests that the consistent antagonization exerted probably takes place as a network of interrelated beneficial effects. The reversal of the failed vessel presentation (*i.e.*, inferior caval and superior mesenteric vein severely congested; azygos vein collapsed) might be the key finding of an activated particular collateral pathway responsible for the noted beneficial effects. The rescued and activated azygos vein may combine in rats the inferior caval vein and the left superior caval vein, and may effectively reorganize blood flow.

DISCUSSION

In the rats with surgically perforated stomachs, Robert's direct injury[10] and occlusion/occlusion-like syndrome[11-24] occur as a particular model for cytoprotection studies[1,2]. Thus, the success of the BPC 157 therapy given directly into the perforated defect might likely resolve several cytoprotection issues.

As expected, we evidenced complete correspondence between the perforated stomach-induced occlusion/occlusion-like syndrome and the intragastric alcohol-induced stomach injuries and whole occlusion/occlusion-like syndrome equally presented in rats[24]. Thereby, the correspondence between the BPC 157 therapy resolving the immediate course after alcohol intragastric application and BPC 157 therapy resolving the immediate course after stomach perforation in the rats, might support each other effect. These findings (*i.e.*, effectively applied directly into the perforated defect) are consistent with BPC 157 as a novel cytoprotection mediator native to and stable in human gastric juice rapidly acting to maintain gastrointestinal mucosa integrity, capable to induce a general beneficial effect as well[1-6]. In the rats with perforated stomachs, there was the counteraction of the immediate triad, particular vascular failure (vessels "disappear"/empty), prolonged bleeding, and a large widening of the debilitated defect[10]. Without therapy, these might fairly extend an unresolved local cytoprotection stomach issue to the rapidly emerging severe widespread syndrome occlusion/occlusion-like syndrome as the general cytoprotection failure[10-24]. As a follow-up, the therapy essentially represents the resolution of the perforated stomach defect as the innate vascular and multiorgan failure like that which might occur during the major vessel occlusion and other alike noxious procedure application, occlusion/occlusion like-syndrome[11-24]. Consequently, this implies a wide range of the therapy effect as with the other occlusion/occlusion-like syndromes[11-24], as the perforation of the stomach in the occlusion/occlusion-like syndrome course might be rapidly complicated with the severe lesions. These lesions could be widespread in the brain with intracerebral and intraventricular hemorrhage, heart (congestion, arrhythmias), hemorrhage and congestion in the lung, liver, kidney and gastrointestinal tract. As proof of the therapy concept might be the attenuated/eliminated blood pressure disturbances [10-24]. Otherwise, the blood pressure disturbances occurred instantly (intracranial (superior sagittal sinus) hypertension

Table 6 Lesions were assessed microscopically (cerebrum, cerebellum, hypothalamus, hippocampus), in rats at 15 min and 60 min following stomach perforation

Application of the 1 ml/rat through the perforated defect in the injured stomach at 5 min following perforation	Lesions scored microscopically cerebrum, cerebellum, hypothalamus, and hippocampus in rats at 15 min and 60 min following stomach perforation	
	15 min	60 min
	Cerebrum (scored 0-8, min/med/max); percentage of karyopycnotic cells (%), mean ± SD	
Control	2/2/2; 30 ± 5	2/2/2, 35 ± 5
BPC 157 10 µg/kg	0/1/1[a], 5 ± 5[a]	0/1/1[a], 5 ± 5[a]
BPC 157 10 ng/kg	0/1/1[a], 5 ± 5[a]	0/1/1[a], 5 ± 5[a]
	Neuronal damage in the karyopyknotic areas, %, mean ± SD (10 HPF, 400 ×)	
Control	39 ± 5	42 ± 4
BPC 157 10 µg/kg	2 ± 2[a]	3 ± 2[a]
BPC 157 10 ng/kg	2 ± 2[a]	2 ± 2[a]
	Hemorrhage (% of total area), mean ± SD	
Control	30 ± 2	25 ± 2
BPC 157 10 µg/kg	5 ± 2[a]	5 ± 2[a]
BPC 157 10 ng/kg		
	Edema (scored 0-3, min/med/max)	
Control	37683	37683
BPC 157 10 µg/kg	1/1/1[a]	1/1/1[a]
BPC 157 10 ng/kg	1/1/1[a]	1/1/1[a]
	Cerebellum (scored 0-8, min/med/max); percentage of karyopycnotic cells (%), mean ± SD	
Control	1/2/2, 13 ± 5	1/1/1, 15 ± 5
BPC 157 10 µg/kg	0/0/1[a], 5 ± 5[a]	0/0/1[a], 5 ± 5[a]
BPC 157 10 ng/kg	0/0/1[a], 5 ± 5[a]	0/0/1[a], 5 ± 5[a]
	Neuronal damage in the karyopyknotic areas (%), mean ± SD (10 HPF, 400 ×)	
Control	27 ± 4	23 ± 5
BPC 157 10 µg/kg	0 ± 0[a]	0 ± 0[a]
BPC 157 10 ng/kg	0 ± 0[a]	0 ± 0[a]
	Hemorrhage (% of total area), mean ± SD	
Control	0 ± 0	0 ± 0
BPC 157 10 µg/kg	0 ± 0	0 ± 0
BPC 157 10 ng/kg	0 ± 0	0 ± 0
	Edema (scored 0-3, min/med/max)	
Control	37683	37318
BPC 157 10 µg/kg	0/0/1[a]	0/0/1[a]
BPC 157 10 ng/kg	0/0/1[a]	0/0/1[a]
	Hippocampus (scored 0-8, min/med/max); percentage of karyopycnotic cells (%), mean ± SD	
Control	37289	36924
	25 ± 3	28 ± 2
BPC 157 10 µg/kg	0/0/0[a], 0 ± 0[a]	0/0/0[a], 0 ± 0[a]

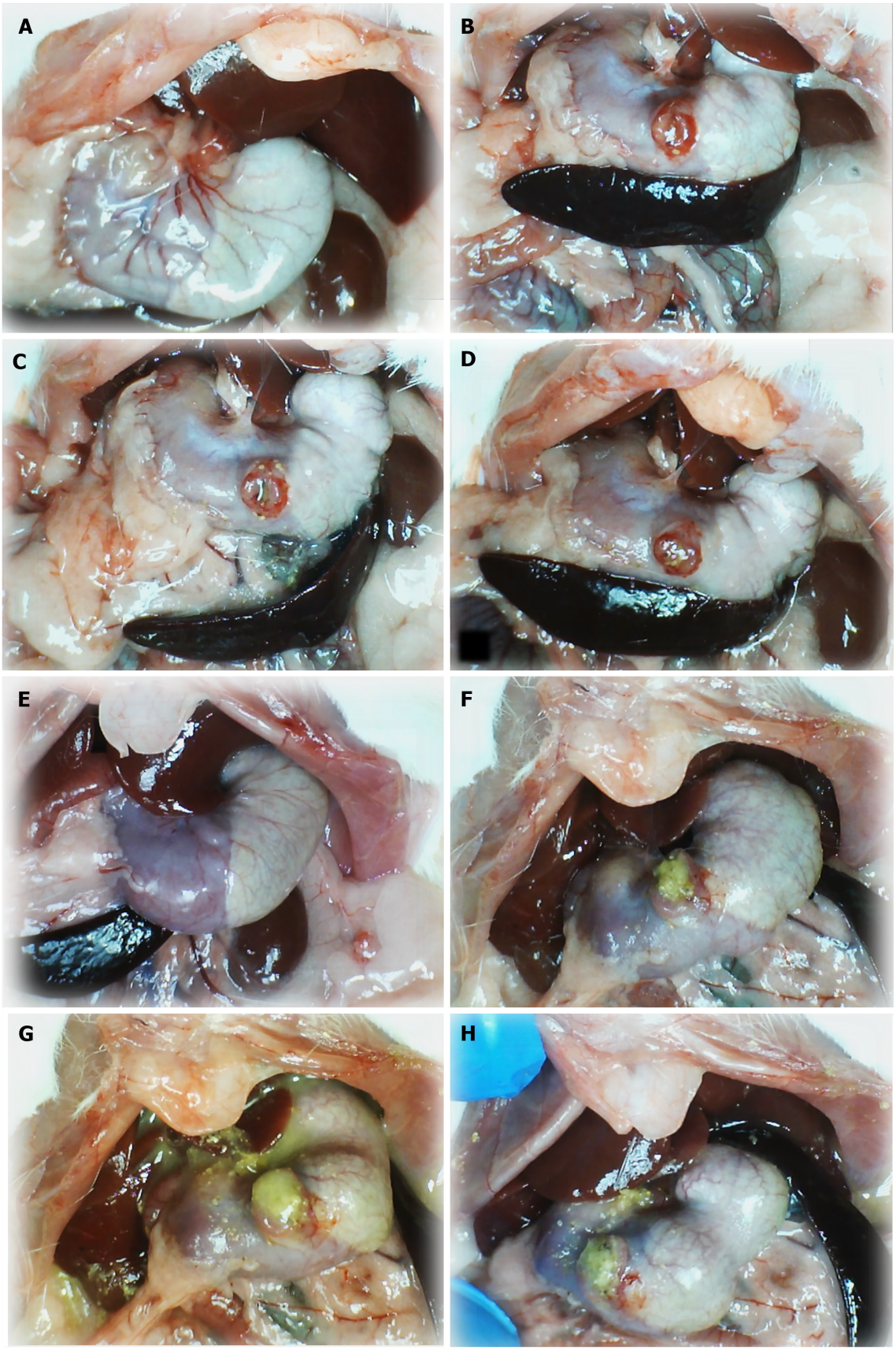
BPC 157 10 ng/kg	0/0/0[a], 0 ± 0[a]	0/0/0[a], 0 ± 0[a]
	Neuronal damage in the karyopyknotic areas (%), mean ± SD (10 HPF, 400 ×)	
Control	23 ± 2	24 ± 3
BPC 157 10 μg/kg	0 ± 0[a]	0 ± 0[a]
BPC 157 10 ng/kg	0 ± 0[a]	0 ± 0[a]
	Hemorrhage (% of total area), mean ± SD	
Control	0 ± 0	0 ± 0
BPC 157 10 μg/kg	0 ± 0	0 ± 0
BPC 157 10 ng/kg	0 ± 0	0 ± 0
	Edema (scored 0-3, min/med/max)	
Control	37683	37318
BPC 157 10 μg/kg	0/0/0[a]	0/0/0[a]
BPC 157 10 ng/kg	0/0/0[a]	0/0/0[a]
	Hypothalamus (scored 0-8, min/med/max); percentage of karyopycnotic cells (%), mean ± SD	
Control	2/2/2, 31 ± 3	1/1/1, 29 ± 4
BPC 157 10 μg/kg	0/0/1[a], 5 ± 5[a]	0/0/1[a], 5 ± 5[a]
BPC 157 10 ng/kg	0/0/1[a], 5 ± 5[a]	0/0/1[a], 5 ± 5[a]
	Neuronal damage in the karyopyknotic areas (%), mean ± SD (10 HPF, 400 ×)	
Control	24 ± 3	28 ± 5
BPC 157 10 μg/kg	5 ± 2[a]	6 ± 3[a]
BPC 157 10 ng/kg	5 ± 2[a]	6 ± 3[a]
	Hemorrhage (% of total area), mean ± SD	
Control	0 ± 0	0 ± 0
BPC 157 10 μg/kg	0 ± 0	0 ± 0
BPC 157 10 ng/kg	0 ± 0	0 ± 0
	Edema (scored 0-3, min/med/max)	
Control	37683	37318
BPC 157 10 μg/kg	0/1/1[a]	0/1/1[a]
BPC 157 10 ng/kg	0/1/1[a]	0/1/1[a]

[a]$P < 0.05$, at least *vs* control.

Lesions were assessed microscopically (cerebrum, cerebellum, hypothalamus, and hippocampus), in rats at 15 min and 60 min following stomach perforation. Saline (5 mL/kg, control) or BPC 157 (10 μg/kg and 10 ng/kg) were given at 5 min thereafter.

(grossly, immediate brain swelling), portal and caval hypertension, and aortal hypotension). These might mean the perpetuating noxious circle, initiated peripherally/centrally hampered healing, but successfully reversed by the therapy effects. This might be illustrative, as the stomach perforation combines the arterial and venous thrombosis, peripherally and centrally, failed major vessels (*i.e.*, congested inferior caval and superior mesenteric vein, collapsed azygos vein). Consequently, as in other occlusion/occlusion-like studies[11-24], the almost annihilated thrombosis, vessels presentation close to normal (inferior caval vein, superior mesenteric vein), and activated azygos vein (direct blood flow delivery) (thus stasis eliminated) might verify that Virchow triad circumstances are resolved (and thereby, attenuated/eliminated bleeding/attenuated/eliminated thrombosis). Thus, such therapy might provide an adequate resolution at both local and general levels as the perforation regularly goes with the failed spontaneous cytoprotection maxim endothelial maintenance→epithelial maintenance[7-9], failed upgrading of the minor vessels as a whole, and the widespread rapidly acting Virchow triad circumstances[10-24].

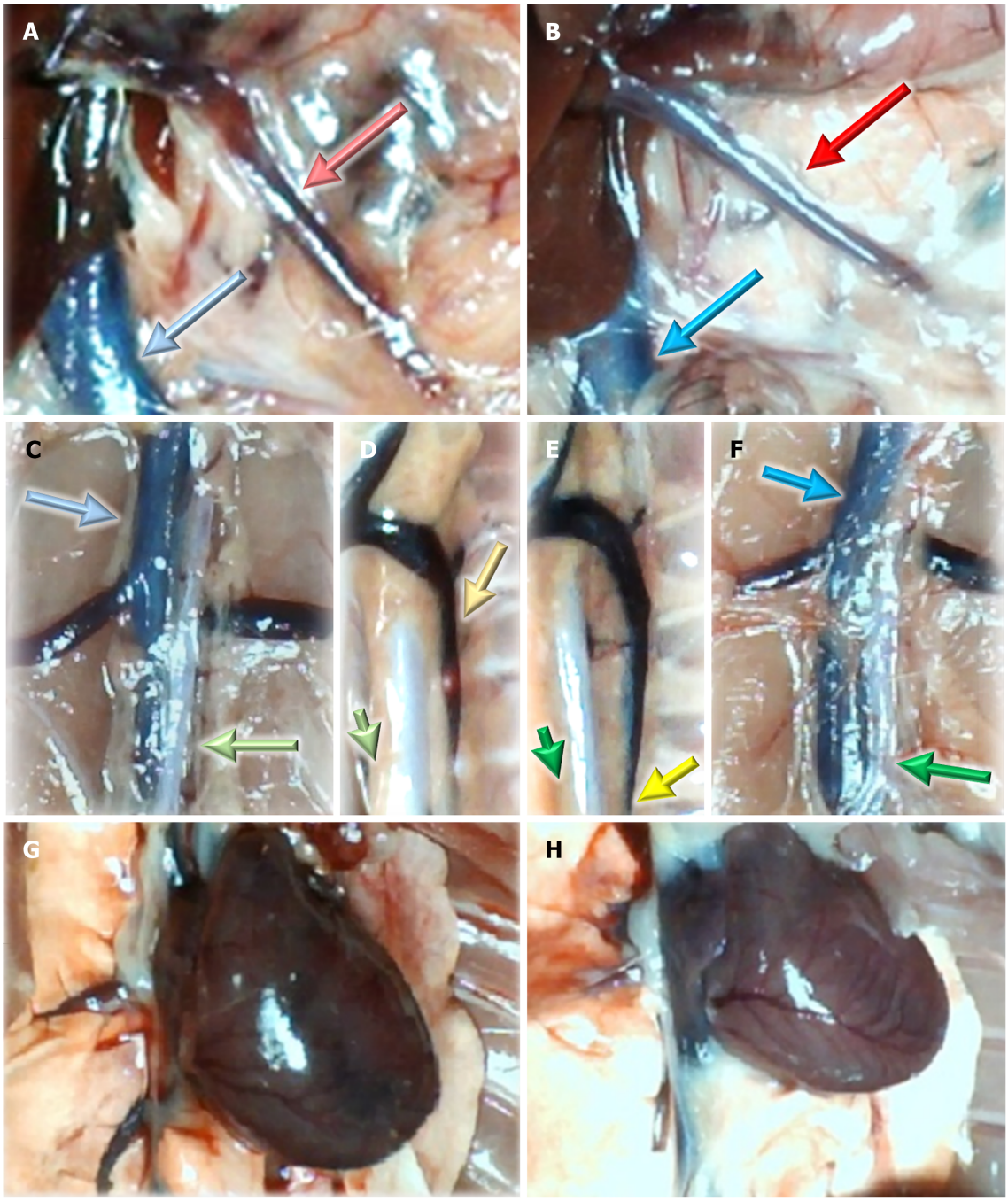
Previously, in the surgically perforated stomach, BPC 157 therapy might have particular effects[10]. Illustrating these particular effects, BPC 157 reversed to the normal healthy values in the stomach tissue surrounding the defect the otherwise increased malondialdehyde- and decreased NO-values. Likewise, already in very early post-perforation-time, BPC 157 may act beneficially in the perforated stomach lesion throughout NO- and prostaglandinds-system[10], two of



DOI: 10.3748/wjg.v29.i27.4289 **Copyright** ©The Author(s) 2023.

Figure 1 Stomach illustrative presentation. A and E: Before procedure; B and F: After perforation before therapy; C and D: Course after given therapy into the perforated defect, saline; G and H: BPC 157. Control rats: (1) Before procedure (normal rats, A); (2) after perforation before therapy application (B); (3) after saline application (1 mL/rat into the perforated defect in the stomach) (C and D), immediately thereafter (C); and (4) later (at 5 min following medication, D). BPC 157 rats: (1) Stomach before perforation (normal rats, E); (2) after perforation, but before BPC 157 therapy application (F), and (3) specifically after BPC 157 application

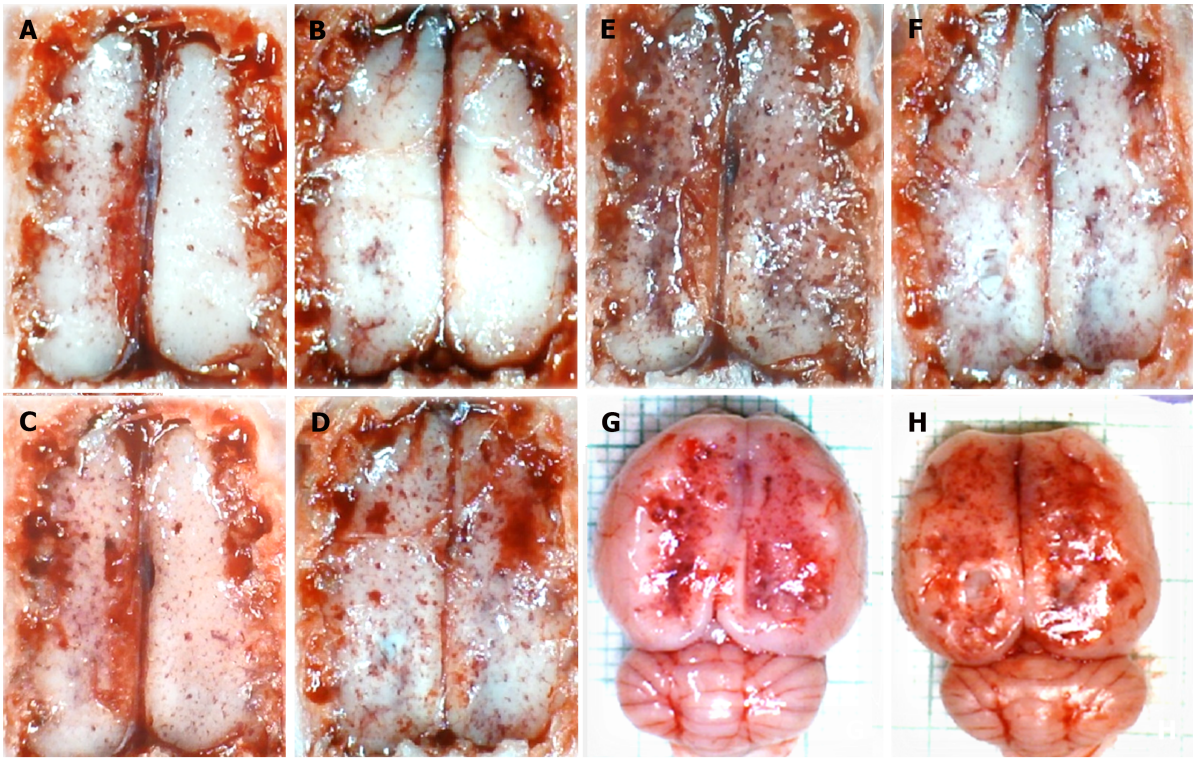
(10 μg or 10 ng/kg, 1 mL/rat into the perforated defect in the stomach, G and H), immediately thereafter (G), and later (at 5 min following medication, H).



DOI: 10.3748/wjg.v29.i27.4289 **Copyright** ©The Author(s) 2023.

Figure 2 Vessels and heart illustrative presentation. A, C, D, G: In the control rats (light color arrows); B, E, F, H: In the BPC 157 rats (dark color arrows); superior mesenteric vein (red arrows), inferior caval vein (blue arrows), aorta (green arrows), azygos vein (yellow arrows), and heart (G and H).

the essential cytoprotection systems[1-6], as shown in the findings of the mRNA expression studies (*Cox2*, *VEGFa*, *Nos1*, *Nos 2*, *Nos3*, *Nkap* (NF-kappa-B activating protein gene)), done at that very early post-perforation-time. These might be the maintenance of the proper function of the entirety of the NO-system. There was the release of the NO by its own[29,38-40,47,48], counteraction of the adverse effects of L-NAME (*i.e.*, L-NAME-hypertension[38] and pro-thrombotic[40] effect), counteraction of the adverse effects of L-arginine (*i.e.*, L-arginine-hypotension[39] and anti-thrombotic[40] effect). These suggested a modulatory effect (thereby, counteraction of NOS-blockade and counteraction of NOS-over-stimulation)[29,38-40,47,48] controlling vasomotor tone and the activation of the Src-Caveolin-1-eNOS pathway[47,48]. Thrombocyte function was maintained (*i.e.*, without interfering with coagulation pathways)[40-42]. Counteraction of all adverse effects of NSAIDs[30] includes acting as membrane stabilizers and counteracted leaky gut [26] and acting as free radical scavengers, particularly in vascular studies[11,13-16,21,22,26,35-37]. The therapy effect on NSAIDs is widespread,

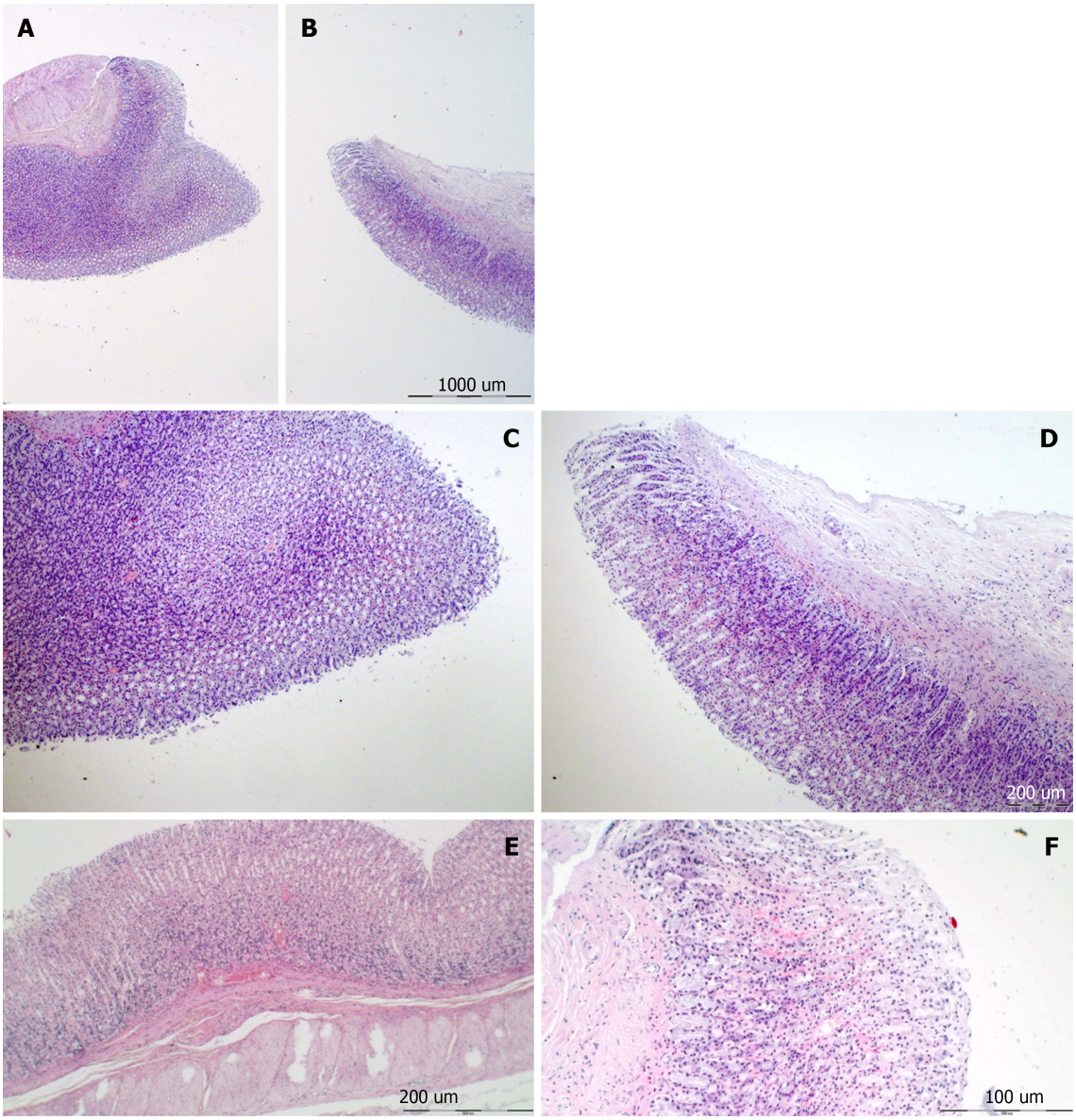


DOI: 10.3748/wjg.v29.i27.4289 **Copyright** ©The Author(s) 2023.

Figure 3 Brain illustrative presentation in the rats with perforated stomach. A, C, E, G: Control rats before perforation (A); after perforation (C, E, G), before saline medication (C), specifically after saline application (5 mL/kg, 1 mL/rat into the perforated defect in the stomach; E and G), immediately thereafter (E), and later after sacrifice (G); B, D, F, H: BPC 157 rats before perforation (B); after perforation (D, F, H), before BPC 157 medication (D), specifically after BPC 157 application (10 μg or 10 ng/kg, 1 mL/rat into the perforated defect in the stomach, capitals; F, H), immediately thereafter (F), and later after sacrifice (H).

including both nonspecific NSAIDs[26,41,42,57-61] and specific NSAID[62]. In particular, there BPC 157 may cure stomach lesions that regularly were perforated or about to perforate[58-60]. Furthermore, the healing of the fistula may be an important analogy for the perforated lesions healing, as "two sides" wounds[63], and BPC 157 may cure both external [64-66], and internal[67-69] fistulas in rats.

Summarizing, the findings presented in the rats with perforated stomachs and occlusion/occlusion-like syndrome might demonstrate how the initial cytoprotective effect (stomach epithelium maintenance) is translated to the systemic or generalized cytoprotection to many other organs (organoprotection) where the vascular endothelium might be the possible target, as it had been long-ago envisaged[34]. The local effect of the BPC 157 therapy in the stomach (*i.e.*, immediately restored stomach vessels (vessels filled/reappeared, "run" toward the defect), counteracted bleeding and contracted perforated defect, and later, complete healing (day 7), and fewer adhesions[10]), might be, at the same time, consistently translated into the rapid beneficial effect on the whole syndrome. There, BPC 157 therapy application counteracted all organs lesions, progressive venous/arterial thrombosis/stasis, peripherally and centrally, along with the ECG disturbances, intracranial (superior sagittal sinus) hypertension, portal and caval hypertension, and aortal hypotension eliminated/attenuated[10-24]. Thus, the particularly activated azygos vein (direct blood flow delivery), and minor vessel upgrading might provide a consistent basis for the demonstrated pleiotropic beneficial effect as cytoprotection endothelial maintenance→epithelial maintenance maxim as general cytoprotective (organoprotective) effect. This may implement and reorganize blood flow and instantly attenuate the consequences of maintained perforation occlusion/occlusion-like syndrome-induced vascular and multiorgan failure[10-24]. Along with the activated azygos vein, the congested inferior caval vein and superior mesenteric vein were quickly reversed to the normal vessel presentation. These highlight the inferior caval vein-superior caval vein *via* azygos vein as rescuing pathway, portal and caval hypertension eliminated, aortal hypotension attenuated, thrombosis almost annihilated, as congestion in the lung, liver, kidney, and gastrointestinal tract markedly attenuated or even eliminated[10-24]. Note, BPC 157 might specifically maintain the function of thrombocytes[42], without affecting coagulation pathways, as shown by aggregometry and thromboelastometry studies. There, BPC 157, given with aspirin, clopidogrel, or cilostazol in rats, counteracted their inhibitory effects on aggregation activated by arachidonic acid, ADP, collagen, and arachidonic acid/PGE1[42]. These findings might be responsible for the attenuation of the bleeding from the perforated defect, and lack of hemorrhage in other organs (*i.e.*, brain and lung) and thrombosis, peripherally and centrally, attenuated/eliminated[10-24]. These particular points might be along with the beforementioned particular modulatory effect on NO-system function (either NO-reduction or NO-overload can be harmful), opposing mentioned both NO-reduction (L-NAME-adverse effects) and NO-overload (L-arginine-adverse effects)[29,38-40]. Besides, BPC 157 therapy has particular wound healing capabilities (thereby, a distinctive effect on all four major events in clot formation and dissolution) as a cytoprotective agent's essential effect that realized the healing process for ruptured blood vessels as a whole[5]. Thus, BPC 157 therapy might

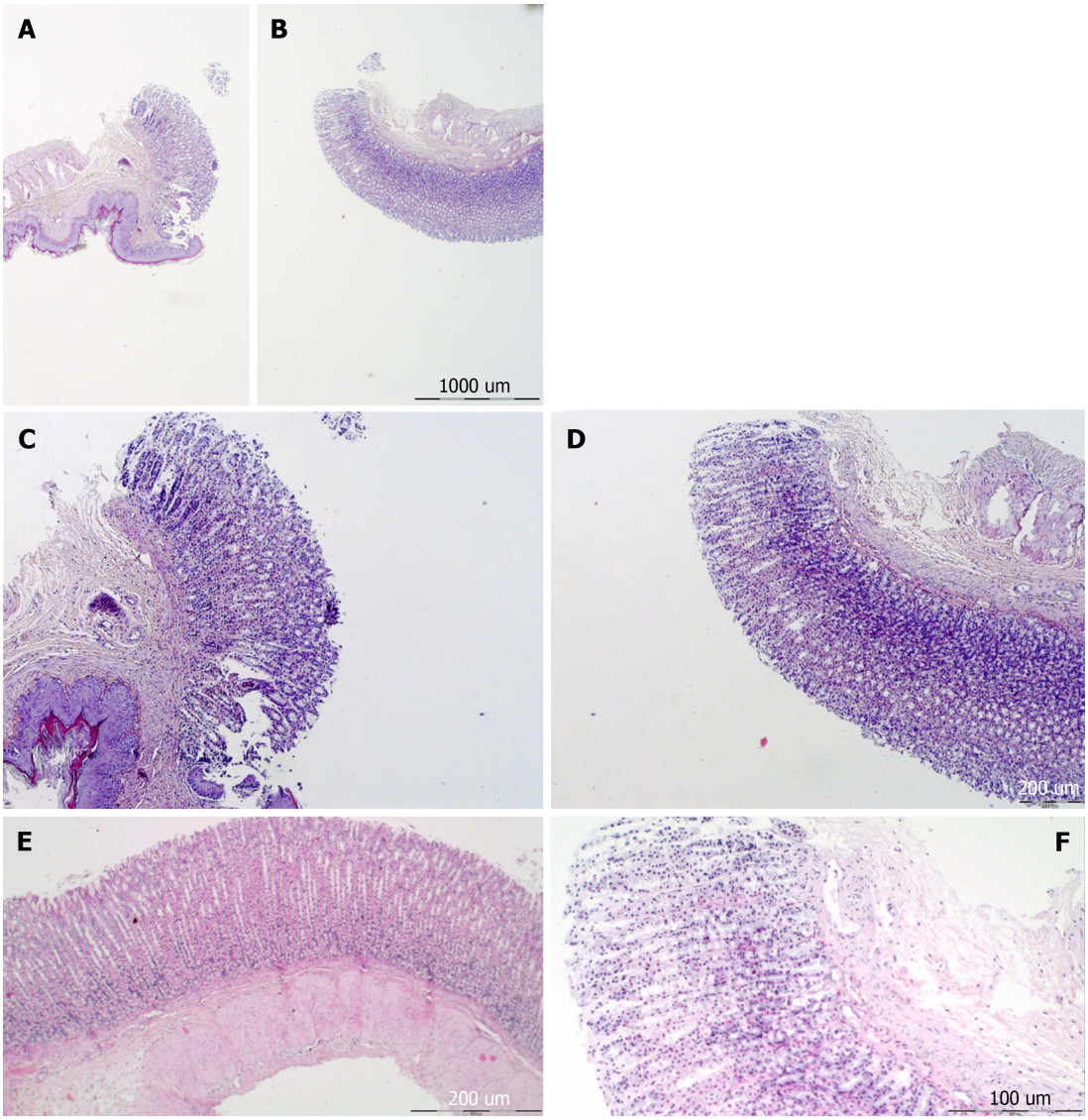


DOI: 10.3748/wjg.v29.i27.4289 **Copyright** ©The Author(s) 2023.

Figure 4 Stomach histology and control. A-F: Margins of the stomach perforation showed mucosal congestion. Transmural hyperemia of the stomach wall at the margins of the stomach perforation and in the rest of the stomach wall (A, E). HE staining: Magnification 20 × (A, B), magnification 100 × (C-E), magnification 200 × (F).

have this innate distinctive effect on all four major events in clot formation and dissolution and the therapy effects might be used in distinctive ways depending on the given injury and time of agent application[5,41]. As mentioned, these combined effects (attenuated/eliminated bleeding/attenuated/eliminated thrombosis) occurred as consistent findings commonly seen in the BPC 157 therapy of the counteraction of the occlusion/occlusion-like syndromes (intracerebral and intraventricular, and internal organs hemorrhage/progressive thrombosis, peripherally and centrally)[10-24]. This might accord with the evidence that BPC 157 therapy might reverse heart failure as a whole, including arrhythmias and thrombosis[3,4] which was also noted in the rats with stomach perforation.

Thereby, the BPC 157 therapy given into the perforated defect initiates a consistent chain of events verified by immediate counteraction of the gross brain swelling, and attenuated intracranial (superior sagittal sinus) hypertension as the upgraded venous system, adequately resolving the anatomical imbalance in venous drainage, which would thereby not occur[10-24]. Centrally, evidencing rapid counteraction of such venous and intracranial hypertension[14-17,20-24] reveals successful resolution, ability to drain venous blood adequately for a given cerebral blood inflow without rising venous pressures, and harmful inability resolved. As specifically shown in the maintained intra-abdominal hypertension studies[20], the three interconnected body cavities[14-17,20-24] require the venous system upgraded so that these might act peripherally (*i.e.*, perforated defect), centrally (*i.e.*, huge intraventricular hemorrhage), and then peripherally and centrally, and centrally and peripherally. Otherwise, if the venous system is not adequately upgraded, the disturbances may be rapidly transmitted through the venous system from the periphery to centrally, and from centrally to the periphery. Consequently, given the upgraded venous system, rats with BPC 157 therapy may smoothly sustain without major harm even the conditions of severe grade III and grade IV intra-abdominal hypertension[20]. Likely, the BPC 157



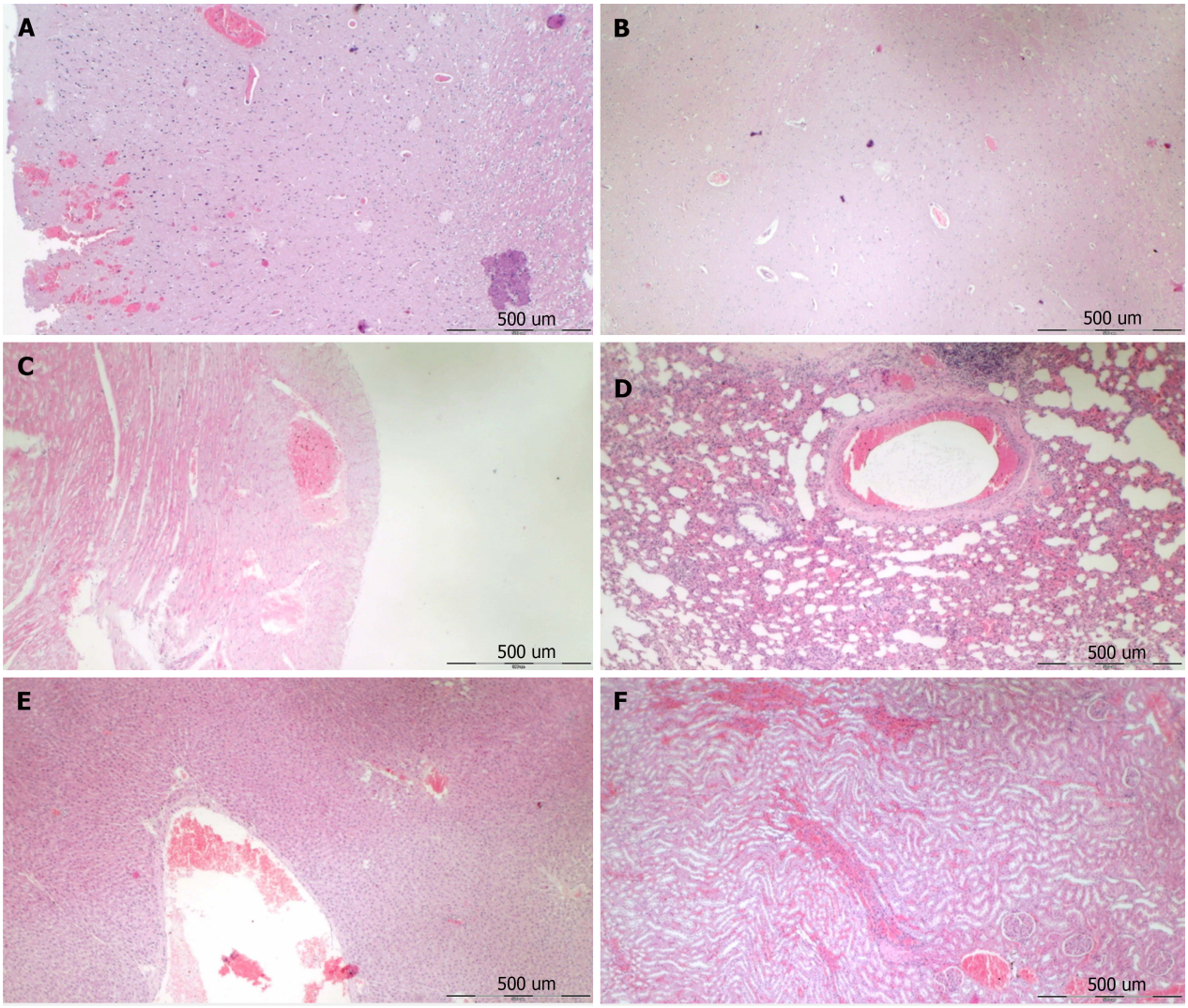
DOI: 10.3748/wjg.v29.i27.4289 **Copyright** ©The Author(s) 2023.

Figure 5 Stomach histology, BPC 157. A-F: Margins of the stomach perforation showed only mild mucosal congestion. No congestion was found in the rest of the stomach wall (A and E). HE staining: Magnification 20 × (A and B), magnification 40 × (C-E), and magnification 100 × (F).

therapy's effect in the rats with perforated stomachs might also effectively operate and might accommodate the particular central/peripheral and peripheral/central equation[10-24] to counteract perforated defect[10]. Note, with BPC 157 therapy into the perforated defect, upon volume application instead of volume-induced dilatation as regular finding in the rats with the perforated stomach, the whole stomach reacted with marked shrinking. This finding might be a sign of the rapid smooth muscle stomach function recovery and might occur along with noted smooth muscle function recovery (*i.e.*, various sphincters to counteract esophagitis development[36,57,70-74], urinary incontinence[35,67,75], pupil dysfunction, miosis[76] and mydriasis[76] (in particular in glaucoma therapy[19]). Likewise, the rapid smooth muscle stomach function might be along with the recovery as rapid adaptation following injury (*i.e.*, short bowel rats)[77]. Thus, as proof of the concept, peripherally and centrally, BPC 157 therapy might rapidly overwhelm Virchow triad circumstances, which are otherwise commonly presented in the rats with perforated stomach occlusion/occlusion-like syndrome as in the rats with occlusion/occlusion like syndromes induced with major vessel(s) occlusion or application of other similar noxious procedures[10-24].

By doing so, the pleiotropic lesions counteraction in the studies of the perforated stomach and other vascular occlusion/occlusion-like syndromes[10-24], was particular cytoprotection/organoprotection background of the cytoprotective agents' innate activity. This cytoprotection/organoprotection background of the cytoprotective agent might be also in the previous non-vascular studies since there was a particular counteraction of the lesions in the brain[57-62,78,79], lung[80-83], liver[57-62,79,84-86], kidney[87-89] and gastrointestinal tract[26,57-62,73], and in particular, the counteraction of the heart arrhythmias and infarction[83,90-95]. Together, these findings might suggest a particular regulatory role.

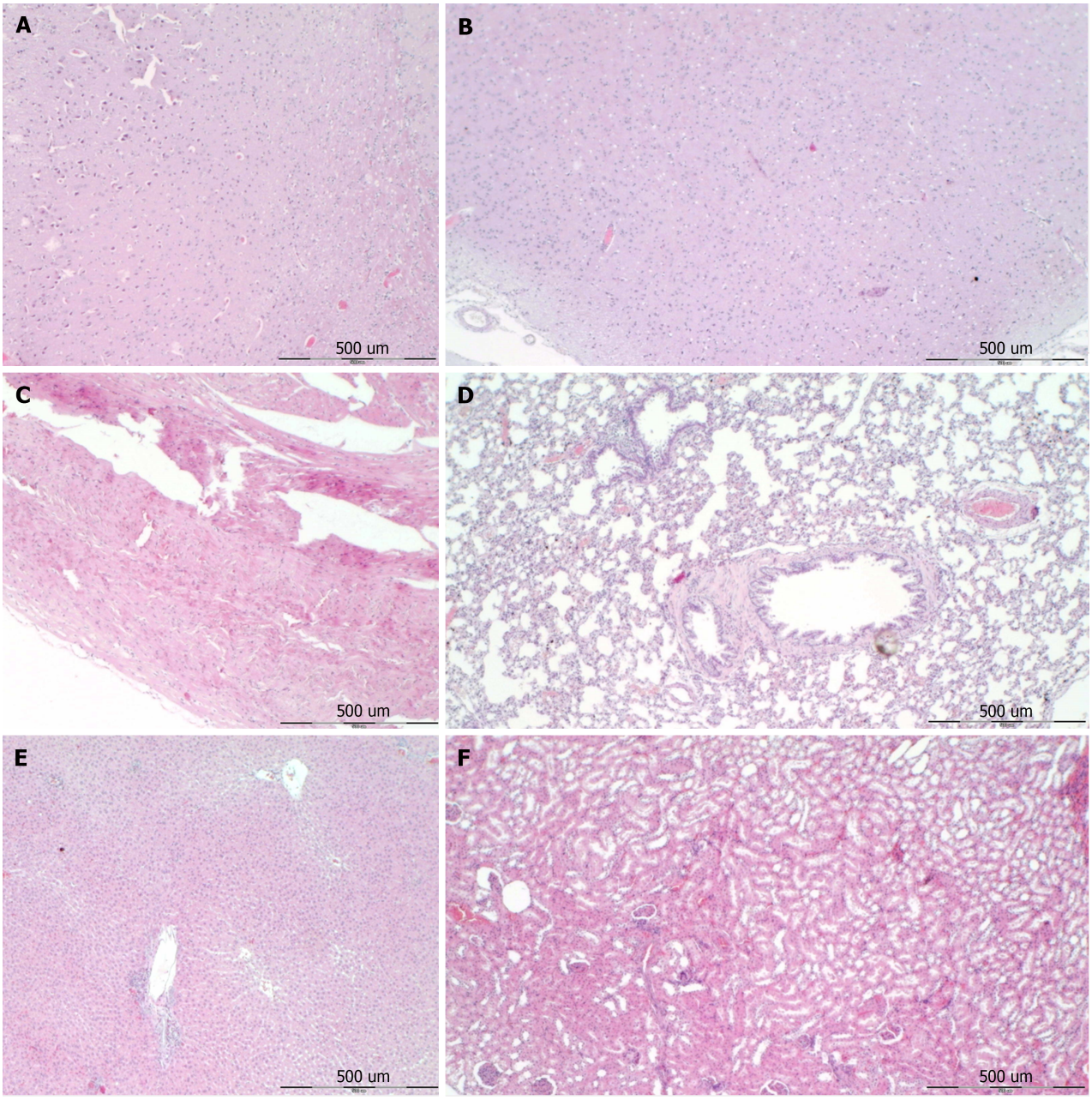
Finally, we envisaged the perforated defect as direct damage, and prototype lesion that as such should be the core hallmark in cytoprotection studies[10]. This might be further indicative for additional implementation of the cytopro-



DOI: 10.3748/wjg.v29.i27.4289 **Copyright** ©The Author(s) 2023.

Figure 6 Following stomach perforation, illustrative microscopy presentation of the organ lesion in saline-treated rats (control). A and B: Cerebral cortex, increased edema and congestion in the cerebral cortex. Severe cerebral hemorrhage of the neocortex; C: Heart, severe congestion within the myocardium; D: Lung, focal thickening of the alveolar membrane, lung congestion, pulmonary edema, and severe intra-alveolar hemorrhage; E: Liver, marked congestion of liver parenchyma with dilatation of blood vessels in portal tracts, central veins, and sinusoids; F: Kidney, a renal parenchyma showed severe vascular congestion and mild interstitial edema. HE staining: Magnification 40 ×.

tection concept into the whole occlusion/occlusion-like syndrome[10-24], and demonstration of the therapeutic potential of the stable gastric pentadecapeptide BPC 157, in particular, and cytoprotective agents in general. In conclusion, it might be the cytoprotection phenomenon with application in distinctive injuries, analogous to, if not identical with, that which might occur during major vessel occlusion and application of other alike noxious procedures[10-24]. Furthermore, it might be that in both cases, the same agent - pentadecapeptide BPC 157, also suggested being the novel cytoprotection mediator as native and stable in human gastric juice, easily applicable[1-6]-might be responsible for the effect. The investigated and counteracted lesions all attenuated/eliminated might provide full support[10-24]. The attenuated/eliminated lesions, brain swelling, and lesions, heart dysfunction, lung lesions, liver and kidney failure, gastrointestinal lesions, widespread arterial and venous thrombosis, and vessel failure, each as the ultimate outcome of the tightly interconnected network, suggests that stomach perforation-induced occlusion/occlusion syndrome was resolved in all cause-consequence terms. The additional support might provide the counteraction of the severe intracranial (superior sagittal sinus), portal and caval hypertension, and aortal hypotension, and ECG disturbances fully counteracted as well. Finally, BPC 157 was found in human fetuses and adult in various tissues (*i.e.*, gastrointestinal mucosa, lung bronchial epithelium, the epidermal layer of the skin, and kidney glomeruli) (*in situ* hybridization and immunostaining)[5,96]. Consequently, as evidenced by the resolution of the complex occlusion/occlusion-like syndrome[10-24], BPC 157 may have a regulatory physiologic role in bodily functions. Similar importance was suggested also for other species (*i.e.*, birds [72] and insects[97,98])based on the alike beneficial effects. A very safe BPC 157 profile supports a LD1 not achieved in toxicological studies and clinical trials (ulcerative colitis, phase II) without adverse effects (for review see[1-6,29,30,96]). This favorable point was recently confirmed in a large study conducted by Xu and collaborators[99]. Finally, very recently, the essential point, rapid functional improvement of minor vessels to take over the function of disabled major vessels, reorganize blood flow, and compensate failed vessel function when confronted with major vessel occlusion and



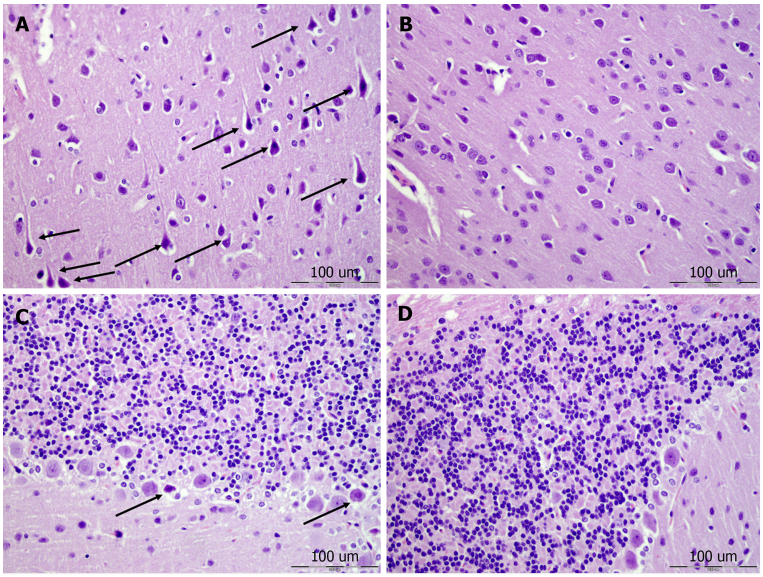
DOI: 10.3748/wjg.v29.i27.4289 **Copyright** ©The Author(s) 2023.

Figure 7 Following stomach perforation, illustrative microscopy presentation of the organs lesion in BPC 157 treated rats. A and B: Cerebral cortex, no edema and congestion in the cerebral cortex. Small cerebral hemorrhage of the neocortex; C: Heart, no changes; D: Lung, only mild congestion in the lung parenchyma; E: Liver, no changes; F: Kidney, no changes. HE staining: Magnification 40 ×.

vascular failure was supplemented with Fourier transform infrared spectroscopy evidence[100]. Illustratively, there was an increased capability of the rat thoracic aorta to function even in the worst circumstances due to the rapid change in the lipid contents and protein secondary structure conformation produced instantly by BPC 157 therapy[100].

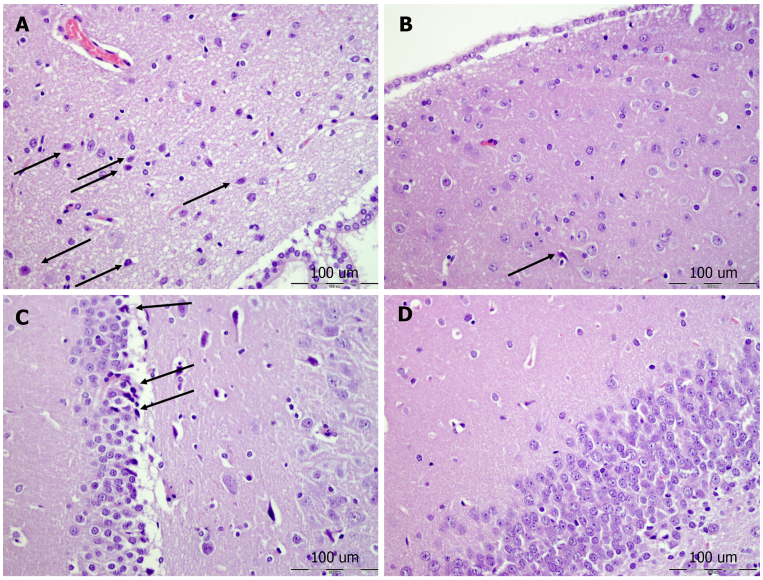
CONCLUSION

Together, these findings, providing firm evidence of the suited models (*i.e.*, perforated stomach-occlusion/occlusion-like syndrome)[1-6,29,30,96] may be suggestive for further BPC 157 therapy application. Besides, such an experimental design strongly emphasizes the need for patients to receive timely treatment, providing that in general with full medical care life-threatening situations rarely occur.



DOI: 10.3748/wjg.v29.i27.4289 **Copyright** ©The Author(s) 2023.

Figure 8 Neocortex, cerebellum, and neuropathological changes. A: In the control group marked edema and congestion in the neocortical brain tissue of the control animal with an increased number of karyopycnotic nuclei of cortical neurons; B: Only mild edema was found in the neocortex in BPC 157 treated animals; C: Edema and an increased number of karyopycnotic nuclei of the cerebellar Purkinje cells in the control animals; D: No changes were found in BPC 157 treated animals. HE staining: Magnification 400 ×.



DOI: 10.3748/wjg.v29.i27.4289 **Copyright** ©The Author(s) 2023.

Figure 9 Hypothalamus, hippocampus, neuropathological changes. A: In the control group marked edema and congestion in the hypothalamic area of control animals with brain tissue of control animal with an increased number of karyopycnotic cells; B: Only a few karyopycnotic cells in BPC 157 treated animals; C: Edema and increased number of karyopycnotic nuclei of the hippocampal area were noted in the control animals; D: While no changes were found in BPC 157 treated animals. HE staining, magnification 400 ×.

ARTICLE HIGHLIGHTS

Research background

Taking stomach perforation as a prime direct injury regularly used in cytoprotection studies, as a new insight in resolving the full extent of the cytoprotection issue, there is the rapid progression of severe occlusion/occlusion-like syndrome considerably complicating the course following stomach perforation in rats. Otherwise, such occlusion/occlusion-like syndrome may suffer rats with permanent occlusion of the major vessel(s), veins and/or arteries, peripherally and centrally, and rats who underwent similar noxious procedures that all severely affect endothelium function. There were cause-consequence lesions in the brain (intracerebral and intraventricular hemorrhage), heart (congestion), lung (hemorrhage), congestion in the liver, kidney, and gastrointestinal tract, arrhythmias, vessel failure (congested inferior

caval and superior mesenteric vein, collapsed azygos vein), and blood pressure disturbances (intracranial (superior sagittal sinus), portal and caval hypertension, and aortal hypotension), and widespread thrombosis, peripherally and centrally.

Research motivation

In occlusion/occlusion-like syndromes, stable gastric pentadecapeptide BPC 157 was recognized as counteracting therapy, and has already presented in recent reviews (*Curr Med Chem* 2023; 30: 1568-1573; *World J Gastroenterol* 2022; 28: 23-46). In the rats with perforated stomachs, and subsequent occlusion/occlusion-like syndrome, we emphasized the cytoprotection potential of the stable gastric BPC 157 as native and stable in gastric juice, thought to play the role of cytoprotection mediator maintaining stomach mucosa integrity. As a particular clue recognized also in the counteraction of stomach perforation-induced occlusion/occlusion-like syndromes, there was activation of collateral pathways depending on the injury, locally (raised vessel presentation; less bleeding, defect contraction) and systemically. Accordingly, BPC 157 therapy induced direct blood delivery from the inferior caval vein to the superior caval vein *via* the azygos vein. Application of the BPC 157 therapy (10 μg/kg and 10 ng/kg) into the perforated defect, induced immediate shrinking and contraction of the whole stomach. Simultaneously, there were attenuated/eliminated intracranial (superior sagittal sinus), portal and caval hypertension, and aortal hypotension. Thrombosis, peripherally (inferior caval vein, portal vein, abdominal aorta) and centrally (superior sagittal sinus) BPC 157 therapy markedly reduced/annihilated, and the severe lesions in the brain, heart (congestion and arrhythmias), lung (hemorrhage and congestion) and marked congestion in the liver, kidney and gastrointestinal tract markedly reduced. In conclusion, with stomach perforation severe occlusion/occlusion-like syndrome, and rapid progression peripherally and centrally, the rapid counteraction should be by BPC 157 therapy.

Research objectives

The first objective was stomach perforation presentation in rats as severe occlusion/occlusion-like syndrome, peripherally and centrally. The second objective was rapid counteraction by BPC 157 therapy.

Research methods

In deeply anesthetized rats underwent calvariectomy, stomach perforation was performed and rats received BPC 157 therapy or saline into the defect in the stomach. Then, in addition to assessing shrinking and contraction/enlargement of the whole stomach, the assessment (gross and microscopy, volume) was as in the occlusion/occlusion-like studies and included all points regularly analyzed. Assessed were swollen brain, failed peripheral vessels (azygos vein, superior mesenteric vein, portal vein, inferior caval vein) and heart, other organs lesions (*i.e.*, stomach, defect closing or widening); intracranial (superior sagittal sinus), portal and caval hypertension, aortal hypotension; clots peripherally and centrally; ECGs; and bleeding time from the perforation(s).

Research results

BPC 157 effects accord with the beneficial effect noted before in the healing of the perforated defect (raised vessel presentation; less bleeding, defect contraction) and in the occlusion/occlusion-like syndromes. In rats with perforated stomachs, BPC 157 therapy (10 μg/kg and 10 ng/kg) given into the perforated defect, induced immediate shrinking and contraction of the whole stomach (unlike saline-induced immediate stomach considerable enlargement). There were cause-consequence lesions all eliminated/attenuated by BPC 157 therapy (*i.e.*, direct blood flow delivery *via* azygos vein). There were eliminated/attenuated lesions in the brain (*i.e.*, swelling, hemorrhage), heart (congestion), lung (hemorrhage), congestion in the liver, kidney, and gastrointestinal tract, arrhythmias, and blood pressure disturbances (intracranial (superior sagittal sinus), portal and caval hypertension, and aortal hypotension). Counteracted was major vessel failure (*i.e.*, reversal of congested inferior caval vein and superior mesenteric vein, collapsed azygos vein), and eliminated widespread thrombosis, peripherally and centrally.

Research conclusions

Stomach perforation occurred as severe occlusion/occlusion-like syndrome, peripherally and centrally. Rapid counteraction was by BPC 157 therapy. Thereby, further BPC 157 therapy may be warranted.

Research perspectives

Stomach perforation as severe occlusion/occlusion-like syndrome needs immediate additional medical attention. There, BPC 157, as a prototype cytoprotective agent, should be also considered as further therapy.

FOOTNOTES

Author contributions: Kalogjera L and Smoday IM contributed to conceptualization; Zizek H, Vukovic V, and Strbe S contributed to methodology; Sikiric P, Skrtic A, and Seiwerth S contributed to writing-original draft preparation, review, and editing; Boban Blagaic A and Beketic Oreskovic L contributed to visualization; Oroz K, Yago H, and Zubcic S contributed to investigation; Krezic I, Vranes H, and Barisic I contributed to formal analysis; Sjekavica I contributed to resources; Kavelj I, Novosel L, and Sever M contributed to validation.

Institutional animal care and use committee statement: This research was reviewed and approved by the Local Ethic Committee (Approval No. 380-59-10106-17-100/290).

Conflict-of-interest statement: Authors declare no conflict of interest.

Data sharing statement: The data that support the findings of this study are available from the corresponding author, upon reasonable request.

ARRIVE guidelines statement: The authors have read the ARRIVE guidelines, and the manuscript was prepared and revised according to the ARRIVE guidelines.

Open-Access: This article is an open-access article that was selected by an in-house editor and fully peer-reviewed by external reviewers. It is distributed in accordance with the Creative Commons Attribution NonCommercial (CC BY-NC 4.0) license, which permits others to distribute, remix, adapt, build upon this work non-commercially, and license their derivative works on different terms, provided the original work is properly cited and the use is non-commercial. See: https://creativecommons.org/Licenses/by-nc/4.0/

Country/Territory of origin: Croatia

ORCID number: Ivan Krezic 0000-0001-7994-5645; Helena Zizek 0000-0001-9863-4164; Ivan Barisic 0000-0001-7397-7582; Sanja Strbe 0000-0001-7199-4530; Marko Sever 0000-0002-2599-6014; Anita Skrtic 0000-0002-9275-7283; Alenka Boban Blagaic 0000-0003-1266-3402; Sven Seiwerth 0000-0002-5894-419X; Predrag Sikiric 0000-0002-7952-2252.

S-Editor: Chen YL
L-Editor: A
P-Editor: Cai YX

REFERENCES

1 **Sikiric P**, Skrtic A, Gojkovic S, Krezic I, Zizek H, Lovric E, Sikiric S, Knezevic M, Strbe S, Milavic M, Kokot A, Blagaic AB, Seiwerth S. Cytoprotective gastric pentadecapeptide BPC 157 resolves major vessel occlusion disturbances, ischemia-reperfusion injury following Pringle maneuver, and Budd-Chiari syndrome. *World J Gastroenterol* 2022; **28**: 23-46 [PMID: 35125818 DOI: 10.3748/wjg.v28.i1.23]

2 **Sikiric P**, Gojkovic S, Knezevic M, Tepes M, Strbe S, Vukojevic J, Duzel A, Kralj T, Krezic I, Zizek H, Oroz K, Vranes H, Smoday IM, Kalogjera L, Vlainic J, Kokot A, Jurjevic I, Blagaic AB, Skrtic A, Seiwerth S. Stable Gastric Pentadecapeptide BPC 157: Prompt Particular Activation of Collateral Pathways. *Curr Med Chem* 2023; **30**: 1568-1573 [PMID: 36200148 DOI: 10.2174/0929867329666221005111553]

3 **Sikiric P**, Udovicic M, Barisic I, Balenovic D, Zivanovic Posilovic G, Strinic D, Uzun S, Sikiric S, Krezic I, Zizek H, Yago H, Gojkovic S, Smoday IM, Kalogjera L, Vranes H, Sola M, Strbe S, Koprivanac A, Premuzic Mestrovic I, Mestrovic T, Pavic P, Skrtic A, Blagaic AB, Lovric Bencic M, Seiwerth S. Stable Gastric Pentadecapeptide BPC 157 as Useful Cytoprotective Peptide Therapy in the Heart Disturbances, Myocardial Infarction, Heart Failure, Pulmonary Hypertension, Arrhythmias, and Thrombosis Presentation. *Biomedicines* 2022; **10** [PMID: 36359218 DOI: 10.3390/biomedicines10112696]

4 **Staresinic M**, Japjec M, Vranes H, Prtoric A, Zizek H, Krezic I, Gojkovic S, Smoday IM, Oroz K, Staresinic E, Dretar V, Yago H, Milavic M, Sikiric S, Lovric E, Batelja Vuletic L, Simeon P, Dobric I, Strbe S, Kokot A, Vlainic J, Blagaic AB, Skrtic A, Seiwerth S, Sikiric P. Stable Gastric Pentadecapeptide BPC 157 and Striated, Smooth, and Heart Muscle. *Biomedicines* 2022; **10** [PMID: 36551977 DOI: 10.3390/biomedicines10123221]

5 **Seiwerth S**, Milavic M, Vukojevic J, Gojkovic S, Krezic I, Vuletic LB, Pavlov KH, Petrovic A, Sikiric S, Vranes H, Prtoric A, Zizek H, Durasin T, Dobric I, Staresinic M, Strbe S, Knezevic M, Sola M, Kokot A, Sever M, Lovric E, Skrtic A, Blagaic AB, Sikiric P. Stable Gastric Pentadecapeptide BPC 157 and Wound Healing. *Front Pharmacol* 2021; **12**: 627533 [PMID: 34267654 DOI: 10.3389/fphar.2021.627533]

6 **Vukojevic J**, Milavić M, Perović D, Ilić S, Čilić AZ, Đuran N, Štrbe S, Zoričić Z, Filipčić I, Brečić P, Seiverth S, Sikirić P. Pentadecapeptide BPC 157 and the central nervous system. *Neural Regen Res* 2022; **17**: 482-487 [PMID: 34380875 DOI: 10.4103/1673-5374.320969]

7 **Robert A**. Cytoprotection by prostaglandins. *Gastroenterology* 1979; **77**: 761-767 [PMID: 38173]

8 **Robert A**, Nezamis JE, Lancaster C, Hanchar AJ. Cytoprotection by prostaglandins in rats. Prevention of gastric necrosis produced by alcohol, HCl, NaOH, hypertonic NaCl, and thermal injury. *Gastroenterology* 1979; **77**: 433-443 [PMID: 456839]

9 **Szabo S**, Trier JS, Brown A, Schnoor J. Early vascular injury and increased vascular permeability in gastric mucosal injury caused by ethanol in the rat. *Gastroenterology* 1985; **88**: 228-236 [PMID: 3871087 DOI: 10.1016/s0016-5085(85)80176-1]

10 **Bilic Z**, Gojkovic S, Kalogjera L, Krezic I, Malekinusic D, Knezevic M, Sever M, Lojo N, Kokot A, Kasnik K, Kralj T, Vukojevic J, Siroglavic M, Peklic M, Drmic D, Milavic M, Sikiric S, Skorak I, Brizic I, Hriberski K, Kubat M, Vladic J, Boban Blagaic A, Tvrdeic A, Skrtic A, Seiwerth S, Sikiric P. Novel insight into Robert's cytoprotection: complex therapeutic effect of cytoprotective pentadecapeptide pentadecapeptide BPC 157 in rats with perforated stomach throughout modulation of nitric oxide-system. Comparison with L-arginine, ranitidine and pantoprazole therapy and L-N(G)-nitro-L-arginine methyl ester worsening. *J Physiol Pharmacol* 2021; **72** [PMID: 35485358 DOI: 10.26402/jpp.2021.6.11]

11 **Vukojević J**, Siroglavić M, Kašnik K, Kralj T, Stanćić D, Kokot A, Kolarić D, Drmić D, Sever AZ, Barišić I, Šuran J, Bojić D, Patrlj MH, Sjekavica I, Pavlov KH, Vidović T, Vlainić J, Stupnišek M, Seiwerth S, Sikirić P. Rat inferior caval vein (ICV) ligature and particular new insights with the stable gastric pentadecapeptide BPC 157. *Vascul Pharmacol* 2018; **106**: 54-66 [PMID: 29510201 DOI: 10.1016/j.vph.2018.02.010]

12 **Gojkovic S**, Krezic I, Vrdoljak B, Malekinusic D, Barisic I, Petrovic A, Horvat Pavlov K, Kolovrat M, Duzel A, Knezevic M, Kasnik Kovac K, Drmic D, Batelja Vuletic L, Kokot A, Boban Blagaic A, Seiwerth S, Sikiric P. Pentadecapeptide BPC 157 resolves suprahepatic occlusion of the inferior caval vein, Budd-Chiari syndrome model in rats. *World J Gastrointest Pathophysiol* 2020; **11**: 1-19 [PMID: 32226643 DOI: 10.4291/wjgp.v11.i1.1]

13 **Kolovrat M**, Gojkovic S, Krezic I, Malekinusic D, Vrdoljak B, Kasnik Kovac K, Kralj T, Drmic D, Barisic I, Horvat Pavlov K, Petrovic A, Duzel A, Knezevic M, Mirkovic I, Kokot A, Boban Blagaic A, Seiwerth S, Sikiric P. Pentadecapeptide BPC 157 resolves Pringle maneuver in

rats, both ischemia and reperfusion. *World J Hepatol* 2020; **12**: 184-206 [PMID: 32547687 DOI: 10.4254/wjh.v12.i5.184]

14 **Knezevic M**, Gojkovic S, Krezic I, Zizek H, Vranes H, Malekinusic D, Vrdoljak B, Knezevic T, Horvat Pavlov K, Drmic D, Staroveski M, Djuzel A, Rajkovic Z, Kolak T, Lovric E, Milavic M, Sikiric S, Barisic I, Tepes M, Tvrdeic A, Patrlj L, Strbe S, Sola M, Situm A, Kokot A, Boban Blagaic A, Skrtic A, Seiwerth S, Sikiric P. Complex Syndrome of the Complete Occlusion of the End of the Superior Mesenteric Vein, Opposed with the Stable Gastric Pentadecapeptide BPC 157 in Rats. *Biomedicines* 2021; **9** [PMID: 34440233 DOI: 10.3390/biomedicines9081029]

15 **Knezevic M**, Gojkovic S, Krezic I, Zizek H, Malekinusic D, Vrdoljak B, Knezevic T, Vranes H, Drmic D, Staroveski M, Djuzel A, Rajkovic Z, Kolak T, Lovric E, Milavic M, Sikiric S, Tvrdeic A, Patrlj L, Strbe S, Sola M, Situm A, Kokot A, Boban Blagaic A, Skrtic A, Seiwerth S, Sikiric P. Occluded Superior Mesenteric Artery and Vein. Therapy with the Stable Gastric Pentadecapeptide BPC 157. *Biomedicines* 2021; **9** [PMID: 34356860 DOI: 10.3390/biomedicines9070792]

16 **Knezevic M**, Gojkovic S, Krezic I, Zizek H, Malekinusic D, Vrdoljak B, Vranes H, Knezevic T, Barisic I, Horvat Pavlov K, Drmic D, Staroveski M, Djuzel A, Rajkovic Z, Kolak T, Kocman I, Lovric E, Milavic M, Sikiric S, Tvrdeic A, Patrlj L, Strbe S, Kokot A, Boban Blagaic A, Skrtic A, Seiwerth S, Sikiric P. Occlusion of the Superior Mesenteric Artery in Rats Reversed by Collateral Pathways Activation: Gastric Pentadecapeptide BPC 157 Therapy Counteracts Multiple Organ Dysfunction Syndrome; Intracranial, Portal, and Caval Hypertension; and Aortal Hypotension. *Biomedicines* 2021; **9** [PMID: 34073625 DOI: 10.3390/biomedicines9060609]

17 **Gojkovic S**, Krezic I, Vranes H, Zizek H, Drmic D, Horvat Pavlov K, Petrovic A, Batelja Vuletic L, Milavic M, Sikiric S, Stilinovic I, Samara M, Knezevic M, Barisic I, Sjekavica I, Lovric E, Skrtic A, Seiwerth S, Sikiric P. BPC 157 Therapy and the Permanent Occlusion of the Superior Sagittal Sinus in Rat: Vascular Recruitment. *Biomedicines* 2021; **9** [PMID: 34203464 DOI: 10.3390/biomedicines9070744]

18 **Vukojević J**, Vrdoljak B, Malekinušić D, Siroglavić M, Milavić M, Kolenc D, Boban Blagaić A, Batelja L, Drmić D, Seiverth S, Sikirić P. The effect of pentadecapeptide BPC 157 on hippocampal ischemia/reperfusion injuries in rats. *Brain Behav* 2020; **10**: e01726 [PMID: 32558293 DOI: 10.1002/brb3.1726]

19 **Kralj T**, Kokot A, Zlatar M, Masnec S, Kasnik Kovac K, Milkovic Perisa M, Batelja Vuletic L, Giljanovic A, Strbe S, Sikiric S, Balog S, Sontacchi B, Sontacchi D, Buljan M, Lovric E, Boban Blagaic A, Skrtic A, Seiwerth S, Sikiric P. Stable Gastric Pentadecapeptide BPC 157 Therapy of Rat Glaucoma. *Biomedicines* 2021; **10** [PMID: 35052769 DOI: 10.3390/biomedicines10010089]

20 **Tepes M**, Gojkovic S, Krezic I, Zizek H, Vranes H, Madzar Z, Santak G, Batelja L, Milavic M, Sikiric S, Kocman I, Simonji K, Samara M, Knezevic M, Barisic I, Lovric E, Strbe S, Kokot A, Sjekavica I, Kolak T, Skrtic A, Seiwerth S, Boban Blagaic A, Sikiric P. Stable Gastric Pentadecapeptide BPC 157 Therapy for Primary Abdominal Compartment Syndrome in Rats. *Front Pharmacol* 2021; **12**: 718147 [PMID: 34966273 DOI: 10.3389/fphar.2021.718147]

21 **Barisic I**, Balenovic D, Udovicic M, Bardak D, Strinic D, Vlainić J, Vranes H, Smoday IM, Krezic I, Milavic M, Sikiric S, Uzun S, Zivanovic Posilovic G, Strbe S, Vukoja I, Lovric E, Lozic M, Sever M, Lovric Bencic M, Boban Blagaic A, Skrtic A, Seiwerth S, Sikiric P. Stable Gastric Pentadecapeptide BPC 157 May Counteract Myocardial Infarction Induced by Isoprenaline in Rats. *Biomedicines* 2022; **10** [PMID: 35203478 DOI: 10.3390/biomedicines10020265]

22 **Strbe S**, Gojkovic S, Krezic I, Zizek H, Vranes H, Barisic I, Strinic D, Orct T, Vukojevic J, Ilic S, Lovric E, Muzinic D, Kolenc D, Filipčić I, Zoricic Z, Marcinko D, Boban Blagaic A, Skrtic A, Seiwerth S, Sikiric P. Over-Dose Lithium Toxicity as an Occlusive-like Syndrome in Rats and Gastric Pentadecapeptide BPC 157. *Biomedicines* 2021; **9** [PMID: 34829735 DOI: 10.3390/biomedicines9111506]

23 **Smoday IM**, Petrovic I, Kalogjera L, Vranes H, Zizek H, Krezic I, Gojkovic S, Skorak I, Hriberski K, Brizic I, Kubat M, Strbe S, Barisic I, Sola M, Lovric E, Lozic M, Boban Blagaic A, Skrtic A, Seiwerth S, Sikiric P. Therapy Effect of the Stable Gastric Pentadecapeptide BPC 157 on Acute Pancreatitis as Vascular Failure-Induced Severe Peripheral and Central Syndrome in Rats. *Biomedicines* 2022; **10** [PMID: 35740321 DOI: 10.3390/biomedicines10061299]

24 **Gojkovic S**, Krezic I, Vranes H, Zizek H, Drmic D, Batelja Vuletic L, Milavic M, Sikiric S, Stilinovic I, Simeon P, Knezevic M, Kolak T, Tepes M, Simonji K, Strbe S, Nikolac Gabaj N, Barisic I, Oreskovic EG, Lovric E, Kokot A, Skrtic A, Boban Blagaic A, Seiwerth S, Sikiric P. Robert's Intragastric Alcohol-Induced Gastric Lesion Model as an Escalated General Peripheral and Central Syndrome, Counteracted by the Stable Gastric Pentadecapeptide BPC 157. *Biomedicines* 2021; **9** [PMID: 34680419 DOI: 10.3390/biomedicines9101300]

25 **Sikiric P**, Hahm KB, Blagaic AB, Tvrdeic A, Pavlov KH, Petrovic A, Kokot A, Gojkovic S, Krezic I, Drmic D, Rucman R, Seiwerth S. Stable Gastric Pentadecapeptide BPC 157, Robert's Stomach Cytoprotection/Adaptive Cytoprotection/Organoprotection, and Selye's Stress Coping Response: Progress, Achievements, and the Future. *Gut Liver* 2020; **14**: 153-167 [PMID: 31158953 DOI: 10.5009/gnl18490]

26 **Park JM**, Lee HJ, Sikiric P, Hahm KB. BPC 157 Rescued NSAID-cytotoxicity Via Stabilizing Intestinal Permeability and Enhancing Cytoprotection. *Curr Pharm Des* 2020; **26**: 2971-2981 [PMID: 32445447 DOI: 10.2174/1381612826666200523180301]

27 **Sikiric P**, Rucman R, Turkovic B, Sever M, Klicek R, Radic B, Drmic D, Stupnisek M, Misic M, Vuletic LB, Pavlov KH, Barisic I, Kokot A, Peklic M, Strbe S, Blagaic AB, Tvrdeic A, Rokotov DS, Vrcic H, Staresinic M, Seiwerth S. Novel Cytoprotective Mediator, Stable Gastric Pentadecapeptide BPC 157. Vascular Recruitment and Gastrointestinal Tract Healing. *Curr Pharm Des* 2018; **24**: 1990-2001 [PMID: 29879879 DOI: 10.2174/1381612824666180608101119]

28 **Sikiric P**, Seiwerth S, Rucman R, Drmic D, Stupnisek M, Kokot A, Sever M, Zoricic I, Zoricic Z, Batelja L, Ziger T, Luetic K, Vlainic J, Rasic Z, Bencic ML. Stress in Gastrointestinal Tract and Stable Gastric Pentadecapeptide BPC 157. Finally, do we have a Solution? *Curr Pharm Des* 2017; **23**: 4012-4028 [PMID: 28228068 DOI: 10.2174/1381612823666170220163219]

29 **Sikiric P**, Seiwerth S, Rucman R, Turkovic B, Rokotov DS, Brcic L, Sever M, Klicek R, Radic B, Drmic D, Ilic S, Kolenc D, Aralica G, Stupnisek M, Suran J, Barisic I, Dzidic S, Vrcic H, Sebecic B. Stable gastric pentadecapeptide BPC 157-NO-system relation. *Curr Pharm Des* 2014; **20**: 1126-1135 [PMID: 23755725 DOI: 10.2174/13816128113190990411]

30 **Sikiric P**, Seiwerth S, Rucman R, Turkovic B, Rokotov DS, Brcic L, Sever M, Klicek R, Radic B, Drmic D, Ilic S, Kolenc D, Aralica G, Safic H, Suran J, Rak D, Dzidic S, Vrcic H, Sebecic B. Toxicity by NSAIDs. Counteraction by stable gastric pentadecapeptide BPC 157. *Curr Pharm Des* 2013; **19**: 76-83 [PMID: 22950504 DOI: 10.2174/13816128130111]

31 **Sikiric P**, Seiwerth S, Brcic L, Sever M, Klicek R, Radic B, Drmic D, Ilic S, Kolenc D. Revised Robert's cytoprotection and adaptive cytoprotection and stable gastric pentadecapeptide BPC 157. Possible significance and implications for novel mediator. *Curr Pharm Des* 2010; **16**: 1224-1234 [PMID: 20166993 DOI: 10.2174/138161210790945977]

32 **Drmic D**, Samara M, Vidovic T, Malekinusic D, Antunovic M, Vrdoljak B, Ruzman J, Milkovic Perisa M, Horvat Pavlov K, Jeyakumar J, Seiwerth S, Sikiric P. Counteraction of perforated cecum lesions in rats: Effects of pentadecapeptide BPC 157, L-NAME and L-arginine. *World J Gastroenterol* 2018; **24**: 5462-5476 [PMID: 30622376 DOI: 10.3748/wjg.v24.i48.5462]

33 **Sikiric P**, Seiwerth S, Rucman R, Kolenc D, Vuletic LB, Drmic D, Grgic T, Strbe S, Zukanovic G, Crvenkovic D, Madzarac G, Rukavina I, Sucic M, Baric M, Starcevic N, Krstonijevic Z, Bencic ML, Filipcic I, Rokotov DS, Vlainic J. Brain-gut Axis and Pentadecapeptide BPC 157:

Theoretical and Practical Implications. *Curr Neuropharmacol* 2016; **14**: 857-865 [PMID: 27138887 DOI: 10.2174/1570159x13666160502153022]

34 **Szabo S**, Usadel KH. Cytoprotection - organoprotection by somatostatin: gastric and hepatic lesions. *Experientia* 1982; **38**: 254-256 [PMID: 6120852 DOI: 10.1007/BF01945097]

35 **Sucic M**, Luetic K, Jandric I, Drmic D, Sever AZ, Vuletic LB, Halle ZB, Strinic D, Kokot A, Seiwerth RS, Zoricic I, Blagaic AB, Seiwerth S, Sikiric P. Therapy of the rat hemorrhagic cystitis induced by cyclophosphamide. Stable gastric pentadecapeptide BPC 157, L-arginine, L-NAME. *Eur J Pharmacol* 2019; **861**: 172593 [PMID: 31401154 DOI: 10.1016/j.ejphar.2019.172593]

36 **Belosic Halle Z**, Vlainic J, Drmic D, Strinic D, Luetic K, Sucic M, Medvidovic-Grubisic M, Pavelic Turudic T, Petrovic I, Seiwerth S, Sikiric P. Class side effects: decreased pressure in the lower oesophageal and the pyloric sphincters after the administration of dopamine antagonists, neuroleptics, anti-emetics, L-NAME, pentadecapeptide BPC 157 and L-arginine. *Inflammopharmacology* 2017 [PMID: 28516373 DOI: 10.1007/s10787-017-0358-8]

37 **Luetic K**, Sucic M, Vlainic J, Halle ZB, Strinic D, Vidovic T, Luetic F, Marusic M, Gulic S, Pavelic TT, Kokot A, Seiwerth RS, Drmic D, Batelja L, Seiwerth S, Sikiric P. Cyclophosphamide induced stomach and duodenal lesions as a NO-system disturbance in rats: L-NAME, L-arginine, stable gastric pentadecapeptide BPC 157. *Inflammopharmacology* 2017; **25**: 255-264 [PMID: 28255738 DOI: 10.1007/s10787-017-0330-7]

38 **Sikirić P**, Seiwerth S, Grabarević Z, Rucman R, Petek M, Jagić V, Turković B, Rotkvić I, Mise S, Zoricić I, Konjevoda P, Perović D, Jurina L, Separović J, Hanzevacki M, Artuković B, Bratulić M, Tisljar M, Gjurasin M, Miklić P, Stancić-Rokotov D, Slobodnjak Z, Jelovac N, Marović A. The influence of a novel pentadecapeptide, BPC 157, on N(G)-nitro-L-arginine methylester and L-arginine effects on stomach mucosa integrity and blood pressure. *Eur J Pharmacol* 1997; **332**: 23-33 [PMID: 9298922 DOI: 10.1016/s0014-2999(97)01033-9]

39 **Turkovic B**, Sikiric P, Seiwerth S, Mise S, Anic T, Petek M. Stable gastric pentadecapeptide BPC 157 studied for inflammatory bowel disease (PLD-116, PL14736, Pliva) induces nitric oxide synthesis. *Gastroenterology* 2004; **126**: 287

40 **Stupnisek M**, Kokot A, Drmic D, Hrelec Patrlj M, Zenko Sever A, Kolenc D, Radic B, Suran J, Bojic D, Vcev A, Seiwerth S, Sikiric P. Pentadecapeptide BPC 157 Reduces Bleeding and Thrombocytopenia after Amputation in Rats Treated with Heparin, Warfarin, L-NAME and L-Arginine. *PLoS One* 2015; **10**: e0123454 [PMID: 25897838 DOI: 10.1371/journal.pone.0123454]

41 **Stupnisek M**, Franjic S, Drmic D, Hrelec M, Kolenc D, Radic B, Bojic D, Vcev A, Seiwerth S, Sikiric P. Pentadecapeptide BPC 157 reduces bleeding time and thrombocytopenia after amputation in rats treated with heparin, warfarin or aspirin. *Thromb Res* 2012; **129**: 652-659 [PMID: 21840572 DOI: 10.1016/j.thromres.2011.07.035]

42 **Konosic S**, Petricevic M, Ivancan V, Konosic L, Goluza E, Krtalic B, Drmic D, Stupnisek M, Seiwerth S, Sikiric P. Intragastric Application of Aspirin, Clopidogrel, Cilostazol, and BPC 157 in Rats: Platelet Aggregation and Blood Clot. *Oxid Med Cell Longev* 2019; **2019**: 9084643 [PMID: 31976029 DOI: 10.1155/2019/9084643]

43 **Tkalcević VI**, Cuzić S, Brajsa K, Mildner B, Bokulić A, Situm K, Perović D, Glojnarić I, Parnham MJ. Enhancement by PL 14736 of granulation and collagen organization in healing wounds and the potential role of egr-1 expression. *Eur J Pharmacol* 2007; **570**: 212-221 [PMID: 17628536 DOI: 10.1016/j.ejphar.2007.05.072]

44 **Chang CH**, Tsai WC, Hsu YH, Pang JH. Pentadecapeptide BPC 157 enhances the growth hormone receptor expression in tendon fibroblasts. *Molecules* 2014; **19**: 19066-19077 [PMID: 25415472 DOI: 10.3390/molecules191119066]

45 **Chang CH**, Tsai WC, Lin MS, Hsu YH, Pang JH. The promoting effect of pentadecapeptide BPC 157 on tendon healing involves tendon outgrowth, cell survival, and cell migration. *J Appl Physiol (1985)* 2011; **110**: 774-780 [PMID: 21030672 DOI: 10.1152/japplphysiol.00945.2010]

46 **Huang T**, Zhang K, Sun L, Xue X, Zhang C, Shu Z, Mu N, Gu J, Zhang W, Wang Y, Zhang Y. Body protective compound-157 enhances alkali-burn wound healing in vivo and promotes proliferation, migration, and angiogenesis in vitro. *Drug Des Devel Ther* 2015; **9**: 2485-2499 [PMID: 25995620 DOI: 10.2147/DDDT.S82030]

47 **Hsieh MJ**, Lee CH, Chueh HY, Chang GJ, Huang HY, Lin Y, Pang JS. Modulatory effects of BPC 157 on vasomotor tone and the activation of Src-Caveolin-1-endothelial nitric oxide synthase pathway. *Sci Rep* 2020; **10**: 17078 [PMID: 33051481 DOI: 10.1038/s41598-020-74022-y]

48 **Hsieh MJ**, Liu HT, Wang CN, Huang HY, Lin Y, Ko YS, Wang JS, Chang VH, Pang JS. Therapeutic potential of pro-angiogenic BPC157 is associated with VEGFR2 activation and up-regulation. *J Mol Med (Berl)* 2017; **95**: 323-333 [PMID: 27847966 DOI: 10.1007/s00109-016-1488-y]

49 **Kang EA**, Han YM, An JM, Park YJ, Sikiric P, Kim DH, Kwon KA, Kim YJ, Yang D, Tchah H, Hahm KB. BPC157 as Potential Agent Rescuing from Cancer Cachexia. *Curr Pharm Des* 2018; **24**: 1947-1956 [PMID: 29898649 DOI: 10.2174/1381612824666180614082950]

50 **Huang BS**, Huang SC, Chen FH, Chang Y, Mei HF, Huang HY, Chen WY, Pang JS. Pentadecapeptide BPC 157 efficiently reduces radiation-induced liver injury and lipid accumulation through Kruppel-like factor 4 upregulation both in vivo and in vitro. *Life Sci* 2022; **310**: 121072 [PMID: 36228773 DOI: 10.1016/j.lfs.2022.121072]

51 **Wu H**, Wei M, Li N, Lu Q, Shrestha SM, Tan J, Zhang Z, Wu G, Shi R. Clopidogrel-Induced Gastric Injury in Rats is Attenuated by Stable Gastric Pentadecapeptide BPC 157. *Drug Des Devel Ther* 2020; **14**: 5599-5610 [PMID: 33376304 DOI: 10.2147/DDDT.S284163]

52 **Wang XY**, Qu M, Duan R, Shi D, Jin L, Gao J, Wood JD, Li J, Wang GD. Cytoprotective Mechanism of the Novel Gastric Peptide BPC157 in Gastrointestinal Tract and Cultured Enteric Neurons and Glial Cells. *Neurosci Bull* 2019; **35**: 167-170 [PMID: 30116973 DOI: 10.1007/s12264-018-0269-8]

53 **Huang JL**, Jing X, Tian X, Qin MC, Xu ZH, Wu DP, Zhong ZG. Neuroprotective Properties of Panax notoginseng Saponins *via* Preventing Oxidative Stress Injury in SAMP8 Mice. *Evid Based Complement Alternat Med* 2017; **2017**: 8713561 [PMID: 28250796 DOI: 10.1155/2017/8713561]

54 **Bauer M**, Deigendesch N, Wittig H, Scheurer E, Lenz C. Tissue sample analysis for post mortem determination of brain edema. *Forensic Sci Int* 2021; **323**: 110808 [PMID: 33971505 DOI: 10.1016/j.forsciint.2021.110808]

55 **Chiu CJ**, McArdle AH, Brown R, Scott HJ, Gurd FN. Intestinal mucosal lesion in low-flow states. I. A morphological, hemodynamic, and metabolic reappraisal. *Arch Surg* 1970; **101**: 478-483 [PMID: 5457245 DOI: 10.1001/archsurg.1970.01340280030009]

56 **Lane JS**, Todd KE, Lewis MP, Gloor B, Ashley SW, Reber HA, McFadden DW, Chandler CF. Interleukin-10 reduces the systemic inflammatory response in a murine model of intestinal ischemia/reperfusion. *Surgery* 1997; **122**: 288-294 [PMID: 9288134 DOI: 10.1016/s0039-6060(97)90020-9]

57 **Vitaic S**, Stupnisek M, Drmic D, Bauk L, Kokot A, Klicek R, Vcev A, Luetic K, Seiwerth S, Sikiric P. Nonsteroidal anti-inflammatory drugs-induced failure of lower esophageal and pyloric sphincter and counteraction of sphincters failure with stable gatric pentadecapeptide BPC 157 in rats. *J Physiol Pharmacol* 2017; **68**: 265-272 [PMID: 28614776]

58 **Lojo N**, Rasic Z, Zenko Sever A, Kolenc D, Vukusic D, Drmic D, Zoricic I, Sever M, Seiwerth S, Sikiric P. Effects of Diclofenac, L-NAME, L-Arginine, and Pentadecapeptide BPC 157 on Gastrointestinal, Liver, and Brain Lesions, Failed Anastomosis, and Intestinal Adaptation Deterioration in 24 Hour-Short-Bowel Rats. *PLoS One* 2016; **11**: e0162590 [PMID: 27627764 DOI: 10.1371/journal.pone.0162590]

59 **Ilic S**, Drmic D, Zarkovic K, Kolenc D, Brcic L, Radic B, Djuzel V, Blagaic AB, Romic Z, Dzidic S, Kalogjera L, Seiwerth S, Sikiric P. Ibuprofen hepatic encephalopathy, hepatomegaly, gastric lesion and gastric pentadecapeptide BPC 157 in rats. *Eur J Pharmacol* 2011; **667**: 322-329 [PMID: 21645505 DOI: 10.1016/j.ejphar.2011.05.038]

60 **Ilic S**, Drmic D, Franjic S, Kolenc D, Coric M, Brcic L, Klicek R, Radic B, Sever M, Djuzel V, Filipovic M, Djakovic Z, Stambolija V, Blagaic AB, Zoricic I, Gjurasin M, Stupnisek M, Romic Z, Zarkovic K, Dzidic S, Seiwerth S, Sikiric P. Pentadecapeptide BPC 157 and its effects on a NSAID toxicity model: diclofenac-induced gastrointestinal, liver, and encephalopathy lesions. *Life Sci* 2011; **88**: 535-542 [PMID: 21295044 DOI: 10.1016/j.lfs.2011.01.015]

61 **Ilic S**, Drmic D, Zarkovic K, Kolenc D, Coric M, Brcic L, Klicek R, Radic B, Sever M, Djuzel V, Ivica M, Boban Blagaic A, Zoricic Z, Anic T, Zoricic I, Djidic S, Romic Z, Seiwerth S, Sikiric P. High hepatotoxic dose of paracetamol produces generalized convulsions and brain damage in rats. A counteraction with the stable gastric pentadecapeptide BPC 157 (PL 14736). *J Physiol Pharmacol* 2010; **61**: 241-250 [PMID: 20436226]

62 **Drmic D**, Kolenc D, Ilic S, Bauk L, Sever M, Zenko Sever A, Luetic K, Suran J, Seiwerth S, Sikiric P. Celecoxib-induced gastrointestinal, liver and brain lesions in rats, counteraction by BPC 157 or L-arginine, aggravation by L-NAME. *World J Gastroenterol* 2017; **23**: 5304-5312 [PMID: 28839430 DOI: 10.3748/wjg.v23.i29.5304]

63 **Sikiric P**, Drmic D, Sever M, Klicek R, Blagaic AB, Tvrdeic A, Kralj T, Kovac KK, Vukojevic J, Siroglavic M, Gojkovic S, Krezic I, Pavlov KH, Rasic D, Mirkovic I, Kokot A, Skrtic A, Seiwerth S. Fistulas Healing. Stable Gastric Pentadecapeptide BPC 157 Therapy. *Curr Pharm Des* 2020; **26**: 2991-3000 [PMID: 32329684 DOI: 10.2174/1381612826666200424180139]

64 **Cesarec V**, Becejac T, Misic M, Djakovic Z, Olujic D, Drmic D, Brcic L, Rokotov DS, Seiwerth S, Sikiric P. Pentadecapeptide BPC 157 and the esophagocutaneous fistula healing therapy. *Eur J Pharmacol* 2013; **701**: 203-212 [PMID: 23220707 DOI: 10.1016/j.ejphar.2012.11.055]

65 **Skorjanec S**, Kokot A, Drmic D, Radic B, Sever M, Klicek R, Kolenc D, Zenko A, Lovric Bencic M, Belosic Halle Z, Situm A, Zivanovic Posilovic G, Masnec S, Suran J, Aralica G, Seiwerth S, Sikiric P. Duodenocutaneous fistula in rats as a model for "wound healing-therapy" in ulcer healing: the effect of pentadecapeptide BPC 157, L-nitro-arginine methyl ester and L-arginine. *J Physiol Pharmacol* 2015; **66**: 581-590 [PMID: 26348082]

66 **Skorjanec S**, Dolovski Z, Kocman I, Brcic L, Blagaic Boban A, Batelja L, Coric M, Sever M, Klicek R, Berkopic L, Radic B, Drmic D, Kolenc D, Ilic S, Cesarec V, Tonkic A, Zoricic I, Mise S, Staresinic M, Ivica M, Lovric Bencic M, Anic T, Seiwerth S, Sikiric P. Therapy for unhealed gastrocutaneous fistulas in rats as a model for analogous healing of persistent skin wounds and persistent gastric ulcers: stable gastric pentadecapeptide BPC 157, atropine, ranitidine, and omeprazole. *Dig Dis Sci* 2009; **54**: 46-56 [PMID: 18649140 DOI: 10.1007/s10620-008-0332-9]

67 **Rasic D**, Zenko Sever A, Rasic F, Strbe S, Rasic Z, Djuzel A, Duplancic B, Boban Blagaic A, Skrtic A, Seiwerth S, Sikiric P, Sever M. Stable Gastric Pentadecapeptide BPC 157 Heals Established Vesicovaginal Fistula and Counteracts Stone Formation in Rats. *Biomedicines* 2021; **9** [PMID: 34572392 DOI: 10.3390/biomedicines9091206]

68 **Grgic T**, Grgic D, Drmic D, Sever AZ, Petrovic I, Sucic M, Kokot A, Klicek R, Sever M, Seiwerth S, Sikiric P. Stable gastric pentadecapeptide BPC 157 heals rat colovesical fistula. *Eur J Pharmacol* 2016; **780**: 1-7 [PMID: 26875638 DOI: 10.1016/j.ejphar.2016.02.038]

69 **Baric M**, Sever AZ, Vuletic LB, Rasic Z, Sever M, Drmic D, Pavelic-Turudic T, Sucic M, Vrcic H, Seiwerth S, Sikiric P. Stable gastric pentadecapeptide BPC 157 heals rectovaginal fistula in rats. *Life Sci* 2016; **148**: 63-70 [PMID: 26872976 DOI: 10.1016/j.lfs.2016.02.029]

70 **Petrovic I**, Dobric I, Drmic D, Sever M, Klicek R, Radic B, Brcic L, Kolenc D, Zlatar M, Kunjko K, Jurcic D, Martinac M, Rasic Z, Boban Blagaic A, Romic Z, Seiwerth S, Sikiric P. BPC 157 therapy to detriment sphincters failure-esophagitis-pancreatitis in rat and acute pancreatitis patients low sphincters pressure. *J Physiol Pharmacol* 2011; **62**: 527-534 [PMID: 22204800]

71 **Dobric I**, Drvis P, Petrovic I, Shejbal D, Brcic L, Blagaic AB, Batelja L, Sever M, Kokic N, Tonkic A, Zoricic I, Mise S, Staresinic M, Radic B, Jakir A, Babel J, Ilic S, Vuksic T, Jelic I, Anic T, Seiwerth S, Sikiric P. Prolonged esophagitis after primary dysfunction of the pyloric sphincter in the rat and therapeutic potential of the gastric pentadecapeptide BPC 157. *J Pharmacol Sci* 2007; **104**: 7-18 [PMID: 17452811 DOI: 10.1254/jphs.fp0061322]

72 **Petrovic I**, Dobric I, Drvis P, Shejbal D, Brcic L, Blagaic AB, Batelja L, Kokic N, Tonkic A, Mise S, Baotic T, Staresinic M, Radic B, Jakir A, Vuksic T, Anic T, Seiwerth S, Sikiric P. An experimental model of prolonged esophagitis with sphincter failure in the rat and the therapeutic potential of gastric pentadecapeptide BPC 157. *J Pharmacol Sci* 2006; **102**: 269-277 [PMID: 17116974 DOI: 10.1254/jphs.fp0060070]

73 **Becejac T**, Cesarec V, Drmic D, Hirsl D, Madzarac G, Djakovic Z, Bunjevac I, A Zenko Sever A, Sepac A, Batelja Vuletic L, Stancic Rokotov D, Seiwerth S, Sikiric P. An endogeous defensive concept, renewed cytoprotection/adaptive cytoprotection: intra(per)-oral/intragastric strong alcohol in rat. Involvement of pentadecapeptide BPC 157 and nitric oxide system. *J Physiol Pharmacol* 2018; **69** [PMID: 30279308 DOI: 10.26402/jpp.2018.3.11]

74 **Djakovic Z**, Djakovic I, Cesarec V, Madzarac G, Becejac T, Zukanovic G, Drmic D, Batelja L, Zenko Sever A, Kolenc D, Pajtak A, Knez N, Japjec M, Luetic K, Stancic-Rokotov D, Seiwerth S, Sikiric P. Esophagogastric anastomosis in rats: Improved healing by BPC 157 and L-arginine, aggravated by L-NAME. *World J Gastroenterol* 2016; **22**: 9127-9140 [PMID: 27895400 DOI: 10.3748/wjg.v22.i41.9127]

75 **Jandric I**, Vrcic H, Jandric Balen M, Kolenc D, Brcic L, Radic B, Drmic D, Seiwerth S, Sikiric P. Salutary effect of gastric pentadecapeptide BPC 157 in two different stress urinary incontinence models in female rats. *Med Sci Monit Basic Res* 2013; **19**: 93-102 [PMID: 23478678 DOI: 10.12659/MSMBR.883828]

76 **Kokot A**, Zlatar M, Stupnisek M, Drmic D, Radic R, Vcev A, Seiwerth S, Sikiric P. NO system dependence of atropine-induced mydriasis and L-NAME- and L-arginine-induced miosis: Reversal by the pentadecapeptide BPC 157 in rats and guinea pigs. *Eur J Pharmacol* 2016; **771**: 211-219 [PMID: 26698393 DOI: 10.1016/j.ejphar.2015.12.016]

77 **Sever M**, Klicek R, Radic B, Brcic L, Zoricic I, Drmic D, Ivica M, Barisic I, Ilic S, Berkopic L, Blagaic AB, Coric M, Kolenc D, Vrcic H, Anic T, Seiwerth S, Sikiric P. Gastric pentadecapeptide BPC 157 and short bowel syndrome in rats. *Dig Dis Sci* 2009; **54**: 2070-2083 [PMID: 19093208 DOI: 10.1007/s10620-008-0598-y]

78 **Klicek R**, Kolenc D, Suran J, Drmic D, Brcic L, Aralica G, Sever M, Holjevac J, Radic B, Turudic T, Kokot A, Patrlj L, Rucman R, Seiwerth S, Sikiric P. Stable gastric pentadecapeptide BPC 157 heals cysteamine-colitis and colon-colon-anastomosis and counteracts cuprizone brain injuries and motor disability. *J Physiol Pharmacol* 2013; **64**: 597-612 [PMID: 24304574]

79 **Ilic S**, Brcic I, Mester M, Filipovic M, Sever M, Klicek R, Barisic I, Radic B, Zoricic Z, Bilic V, Berkopic L, Brcic L, Kolenc D, Romic Z,

Pazanin L, Seiwerth S, Sikiric P. Over-dose insulin and stable gastric pentadecapeptide BPC 157. Attenuated gastric ulcers, seizures, brain lesions, hepatomegaly, fatty liver, breakdown of liver glycogen, profound hypoglycemia and calcification in rats. *J Physiol Pharmacol* 2009; **60** Suppl 7: 107-114 [PMID: 20388953]

80 **Grabarevic Z**, Tisljar M, Artukovic B, Bratulic M, Dzaja P, Seiwerth S, Sikiric P, Peric J, Geres D, Kos J. The influence of BPC 157 on nitric oxide agonist and antagonist induced lesions in broiler chicks. *J Physiol Paris* 1997; **91**: 139-149 [PMID: 9403788 DOI: 10.1016/s0928-4257(97)89478-8]

81 **Stancic-Rokotov D**, Slobodnjak Z, Aralica J, Aralica G, Perovic D, Staresinic M, Gjurasin M, Anic T, Zoricic I, Buljat G, Prkacin I, Sikiric P, Seiwerth S, Rucman R, Petek M, Turkovic B, Kokic N, Jagic V, Boban-Blagaic A. Lung lesions and anti-ulcer agents beneficial effect: anti-ulcer agents pentadecapeptide BPC 157, ranitidine, omeprazole and atropine ameliorate lung lesion in rats. *J Physiol Paris* 2001; **95**: 303-308 [PMID: 11595454 DOI: 10.1016/s0928-4257(01)00042-0]

82 **Stancic-Rokotov D**, Sikiric P, Seiwerth S, Slobodnjak Z, Aralica J, Aralica G, Perovic D, Anic T, Zoricic I, Buljat G, Prkacin I, Gjurasin M, Rucman R, Petek M, Turkovic B, Ivasovic Z, Jagic V, Staresinic M, Boban-Blagaic A. Ethanol gastric lesion aggravated by lung injury in rat. Therapy effect of antiulcer agents. *J Physiol Paris* 2001; **95**: 289-293 [PMID: 11595452 DOI: 10.1016/s0928-4257(01)00040-7]

83 **Udovicic M**, Sever M, Kavur L, Loncaric K, Barisic I, Balenovic D, Zivanovic Posilovic G, Strinic D, Uzun S, Batelja Vuletic L, Sikiric S, Skrtic A, Drmic D, Boban Blagaic A, Lovric Bencic M, Seiwerth S, Sikiric P. Stable Gastric Pentadecapeptide BPC 157 Therapy for Monocrotaline-Induced Pulmonary Hypertension in Rats Leads to Prevention and Reversal. *Biomedicines* 2021; **9** [PMID: 34356886 DOI: 10.3390/biomedicines9070822]

84 **Sever AZ**, Sever M, Vidovic T, Lojo N, Kolenc D, Vuletic LB, Drmic D, Kokot A, Zoricic I, Coric M, Vlainic J, Poljak L, Seiwerth S, Sikiric P. Stable gastric pentadecapeptide BPC 157 in the therapy of the rats with bile duct ligation. *Eur J Pharmacol* 2019; **847**: 130-142 [PMID: 30690000 DOI: 10.1016/j.ejphar.2019.01.030]

85 **Sikiric P**, Seiwerth S, Grabarevic Z, Rucman R, Petek M, Rotkvic I, Turkovic B, Jagic V, Mildner B, Duvnjak M. Hepatoprotective effect of BPC 157, a 15-amino acid peptide, on liver lesions induced by either restraint stress or bile duct and hepatic artery ligation or CCl4 administration. A comparative study with dopamine agonists and somatostatin. *Life Sci* 1993; **53**: PL291-PL296 [PMID: 7901724 DOI: 10.1016/0024-3205(93)90589-u]

86 **Prkacin I**, Separovic J, Aralicia G, Perovic D, Gjurasin M, Lovric-Bencic M, Stancic-Rokotov D, Staresinic M, Anic T, Mikus D, Sikiric P, Seiwerth S, Mise S, Rotkvic I, Jagic V, Rucman R, Petek M, Turkovic B, Marovic A, Sebecic B, Boban-Blagaic A, Kokic N. Portal hypertension and liver lesions in chronically alcohol drinking rats prevented and reversed by stable gastric pentadecapeptide BPC 157 (PL-10, PLD-116), and propranolol, but not ranitidine. *J Physiol Paris* 2001; **95**: 315-324 [PMID: 11595456 DOI: 10.1016/s0928-4257(01)00044-4]

87 **Vranes H**, Krezic I, Gojkovic S, Zizek H, Durasin T, Petrovic A, Horvat Pavlov K, Batelja L, Blagaic Boban A, Seiwerth S, Sikriic P. In hydornephrosis-rats, BPC 157 exerts a strong anti-ulcer effect in both stomach and duodenum along with marked kidney recovery. *FASEB J* 2020; **34**: 1 [DOI: 10.1096/fasebj.2020.34.s1.03972]

88 **Drmic D**, Sucic M, Zenko Sever A, Kolenc D, Suran J, Seiwerth S, Sikiric P. BPC 157 counteracts gastric lesions after bilateral nephrectomy and attenuates deleterious course in rats. *FASEB J* 2015; **29**: 628.10 [DOI: 10.1096/fasebj.29.1_supplement.628.10]

89 **Drmic D**, Sucic M, Zenko Sever A, Kolenc D, Andrijasevic V, Suran J, Seiweth S, Sikriic P. Attenuation of the deleterious course and gastric lesions after bilateral nephrectomy in rats, NO-system relation. BPC 157, L-arginine, L-NAME. *FASEB J* 2016; **30**: 720.2 [DOI: 10.1096/fasebj.30.1_supplement.720.2]

90 **Lozic M**, Stambolija V, Krezic I, Dugandzic A, Zivanovic-Posilovic G, Gojkovic S, Kovacevic J, Vrdoljak L, Mirkovic I, Kokot A, Petrovic A, Pavlov KH, Drmic D, Suran J, Blagaic AB, Seiwerth S, Sikiric P. In relation to NO-System, Stable Pentadecapeptide BPC 157 Counteracts Lidocaine-Induced Adverse Effects in Rats and Depolarisation In Vitro. *Emerg Med Int* 2020; **2020**: 6805354 [PMID: 32566305 DOI: 10.1155/2020/6805354]

91 **Strinic D**, Belosic Halle Z, Luetic K, Nedic A, Petrovic I, Sucic M, Zivanovic Posilovic G, Balenovic D, Strbe S, Udovicic M, Drmic D, Stupnisek M, Lovric Bencic M, Seiwerth S, Sikiric P. BPC 157 counteracts QTc prolongation induced by haloperidol, fluphenazine, clozapine, olanzapine, quetiapine, sulpiride, and metoclopramide in rats. *Life Sci* 2017; **186**: 66-79 [PMID: 28797793 DOI: 10.1016/j.lfs.2017.08.006]

92 **Zivanovic-Posilovic G**, Balenovic D, Barisic I, Strinic D, Stambolija V, Udovicic M, Uzun S, Drmic D, Vlainic J, Bencic ML, Sindic A, Seiwerth S, Sikiric P. Stable gastric pentadecapeptide BPC 157 and bupivacaine. *Eur J Pharmacol* 2016; **793**: 56-65 [PMID: 27815173 DOI: 10.1016/j.ejphar.2016.10.035]

93 **Barisic I**, Balenovic D, Klicek R, Radic B, Nikitovic B, Drmic D, Udovicic M, Strinic D, Bardak D, Berkopic L, Djuzel V, Sever M, Cvjetko I, Romic Z, Sindic A, Bencic ML, Seiwerth S, Sikiric P. Mortal hyperkalemia disturbances in rats are NO-system related. The life saving effect of pentadecapeptide BPC 157. *Regul Pept* 2013; **181**: 50-66 [PMID: 23327997 DOI: 10.1016/j.regpep.2012.12.007]

94 **Balenovic D**, Bencic ML, Udovicic M, Simonji K, Hanzevacki JS, Barisic I, Kranjcevic S, Prkacin I, Coric V, Brcic L, Coric M, Brcic I, Borovic S, Radic B, Drmic D, Vrcic H, Seiwerth S, Sikiric P. Inhibition of methyldigoxin-induced arrhythmias by pentadecapeptide BPC 157: a relation with NO-system. *Regul Pept* 2009; **156**: 83-89 [PMID: 19465062 DOI: 10.1016/j.regpep.2009.05.008]

95 **Lovric-Bencic M**, Sikiric P, Hanzevacki JS, Seiwerth S, Rogic D, Kusec V, Aralica G, Konjevoda P, Batelja L, Blagaic AB. Doxorubicine-congestive heart failure-increased big endothelin-1 plasma concentration: reversal by amlodipine, losartan, and gastric pentadecapeptide BPC157 in rat and mouse. *J Pharmacol Sci* 2004; **95**: 19-26 [PMID: 15153646 DOI: 10.1254/jphs.95.19]

96 **Seiwerth S**, Rucman R, Turkovic B, Sever M, Klicek R, Radic B, Drmic D, Stupnisek M, Misic M, Vuletic LB, Pavlov KH, Barisic I, Kokot A, Japjec M, Blagaic AB, Tvrdeic A, Rokotov DS, Vrcic H, Staresinic M, Sebecic B, Sikiric P. BPC 157 and Standard Angiogenic Growth Factors. Gastrointestinal Tract Healing, Lessons from Tendon, Ligament, Muscle and Bone Healing. *Curr Pharm Des* 2018; **24**: 1972-1989 [PMID: 29998800 DOI: 10.2174/1381612824666180712110447]

97 **Tlak Gajger I**, Smodiš Škerl MI, Šoštarić P, Šuran J, Sikirić P, Vlainić J. Physiological and Immunological Status of Adult Honeybees (Apis mellifera) Fed Sugar Syrup Supplemented with Pentadecapeptide BPC 157. *Biology (Basel)* 2021; **10** [PMID: 34571768 DOI: 10.3390/biology10090891]

98 **Tlak Gajger I**, Ribarić J, Smodiš Škerl M, Vlainić J, Sikirić P. Stable gastric pentadecapeptide BPC 157 in honeybee (Apis mellifera) therapy, to control Nosema ceranae invasions in apiary conditions. *J Vet Pharmacol Ther* 2018; **41**: 614-621 [PMID: 29682749 DOI: 10.1111/jvp.12509]

99 **Xu C**, Sun L, Ren F, Huang P, Tian Z, Cui J, Zhang W, Wang S, Zhang K, He L, Zhang C, Hao Q, Zhang Y, Li M, Li W. Preclinical safety evaluation of body protective compound-157, a potential drug for treating various wounds. *Regul Toxicol Pharmacol* 2020; **114**: 104665 [PMID: 32334036 DOI: 10.1016/j.yrtph.2020.104665]

100 **Gamulin O**, Oroz K, Coric L, Krajacic M, Skrabic M, Dretar V, Strbe S, Talapko J, Juzbasic M, Krezic I, Lozic M, Stambolija V, Zizek H,

Jurca I, Jurjevic I, Blagaic AB, Skrtic A, Seiwerth S, Sikiric P. Fourier Transform Infrared Spectroscopy Reveals Molecular Changes in Blood Vessels of Rats Treated with Pentadecapeptide BPC 157. *Biomedicines* 2022; **10** [PMID: 36551886 DOI: 10.3390/biomedicines10123130]

World Journal of Gastroenterology

Submit a Manuscript: https://www.f6publishing.com

World J Gastroenterol 2023 July 21; 29(27): 4317-4333

DOI: 10.3748/wjg.v29.i27.4317

ISSN 1007-9327 (print) ISSN 2219-2840 (online)

ORIGINAL ARTICLE

Basic Study

18β-glycyrrhetinic acid promotes gastric cancer cell autophagy and inhibits proliferation by regulating miR-328-3p/signal transducer and activator of transcription 3

Yi Yang, Yi Nan, Yu-Hua Du, Shi-Cong Huang, Dou-Dou Lu, Jun-Fei Zhang, Xia Li, Yan Chen, Lei Zhang, Ling Yuan

Specialty type: Gastroenterology and hepatology

Provenance and peer review: Unsolicited article; Externally peer reviewed.

Peer-review model: Single blind

Peer-review report's scientific quality classification

Grade A (Excellent): 0
Grade B (Very good): B
Grade C (Good): C
Grade D (Fair): 0
Grade E (Poor): 0

P-Reviewer: Senchukova M, Russia; Shah OJ, India

Received: March 28, 2023
Peer-review started: March 28, 2023
First decision: April 27, 2023
Revised: May 10, 2023
Accepted: June 2, 2023
Article in press: June 2, 2023
Published online: July 21, 2023

Yi Yang, Yu-Hua Du, Shi-Cong Huang, Dou-Dou Lu, Xia Li, Ling Yuan, Ningxia Medical University, Yinchuan 750004, Ningxia Hui Autonomous Region, China

Yi Nan, Jun-Fei Zhang, Yan Chen, Lei Zhang, Key Laboratory of Ningxia Minority Medicine Modernization Ministry of Education, Ningxia Medical University, Yinchuan 750004, Ningxia Hui Autonomous Region, China

Corresponding author: Ling Yuan, MD, PhD, Professor, Ningxia Medical University, No. 1160 Shengli Street, Yinchuan 750004, Ningxia Hui Autonomous Region, China. nxykdx@qq.com

Abstract

BACKGROUND

Gastric cancer (GC) is one of the most common cancer types worldwide, and its prevention and treatment methods have garnered much attention. As the active ingredient of licorice, 18β-glycyrrhetinic acid (18β-GRA) has a variety of pharmacological effects. The aim of this study was to explore the effective target of 18β-GRA in the treatment of GC, in order to provide effective ideas for the clinical prevention and treatment of GC.

AIM

To investigate the mechanism of 18β-GRA in inhibiting cell proliferation and promoting autophagy flux in GC cells.

METHODS

Whole transcriptomic analyses were used to analyze and screen differentially expressed microRNAs (miRNAs) in GC cells after 18β-GRA intervention. Lentivirus-transfected GC cells and the Cell Counting Kit-8 were used to detect cell proliferation ability, cell colony formation ability was detected by the clone formation assay, and flow cytometry was used to detect the cell cycle and apoptosis. A nude mouse transplantation tumor model of GC cells was constructed to verify the effect of miR-328-3p overexpression on the tumorigenicity of GC cells. Tumor tissue morphology was observed by hematoxylin and eosin staining, and microtubule-associated protein light chain 3 (LC3) expression was detected by immunohistochemistry. TransmiR, STRING, and miRWalk

databases were used to predict the relationship between miR-328-3p and signal transducer and activator of transcription 3 (STAT3)-related information. Expression of *STAT3* mRNA and *miR-328-3p* was detected by quantitative polymerase chain reaction (qPCR) and the expression levels of STAT3, phosphorylated STAT3 (p-STAT3), and LC3 were detected by western blot analysis. The targeted relationship between *miR-328-3p* and *STAT3* was detected using the dual-luciferase reporter gene system. AGS cells were infected with monomeric red fluorescent protein-green fluorescent protein-LC3 adenovirus double label. LC3 was labeled and autophagy flow was observed under a confocal laser microscope.

RESULTS

The expression of miR-328-3p was significantly upregulated after 18β-GRA intervention in AGS cells (P = 4.51E-06). Overexpression of miR-328-3p inhibited GC cell proliferation and colony formation ability, arrested the cell cycle in the G0/G1 phase, promoted cell apoptosis, and inhibited the growth of subcutaneous tumors in BALB/c nude mice (P < 0.01). No obvious necrosis was observed in the tumor tissue in the negative control group (no drug intervention or lentivirus transfection) and vector group (the blank vector for lentivirus transfection), and more cells were loose and necrotic in the miR-328-3p group. Bioinformatics tools predicted that miR-328-3p has a targeting relationship with STAT3, and STAT3 was closely related to autophagy markers such as p62. After overexpressing miR-328-3p, the expression level of *STAT3* mRNA was significantly decreased (P < 0.01) and p-STAT3 was downregulated (P < 0.05). The dual-luciferase reporter gene assay showed that the luciferase activity of *miR-328-3p* and *STAT3* 3′ untranslated regions of the wild-type reporter vector group was significantly decreased (P < 0.001). Overexpressed miR-328-3p combined with bafilomycin A_1 (Baf A_1) was used to detect the expression of LC3 II. Compared with the vector group, the expression level of LC3 II in the overexpressed miR-328-3p group was downregulated (P < 0.05), and compared with the Baf A_1 group, the expression level of LC3 II in the overexpressed miR-328-3p + Baf A_1 group was upregulated (P < 0.01). The expression of LC3 II was detected after intervention of 18β-GRA in GC cells, and the results were consistent with the results of miR-328-3p overexpression (P < 0.05). Additional studies showed that 18β-GRA promoted autophagy flow by promoting autophagosome synthesis (P < 0.001). qPCR showed that the expression of *STAT3* mRNA was downregulated after drug intervention (P < 0.05). Western blot analysis showed that the expression levels of STAT3 and p-STAT3 were significantly downregulated after drug intervention (P < 0.05).

CONCLUSION

18β-GRA promotes the synthesis of autophagosomes and inhibits GC cell proliferation by regulating the miR-328-3p/STAT3 signaling pathway.

Key Words: 18β-glycyrrhetinic acid; miR-328-3p; Signal transducer and activator of transcription 3; Cell proliferation; Autophagy flow

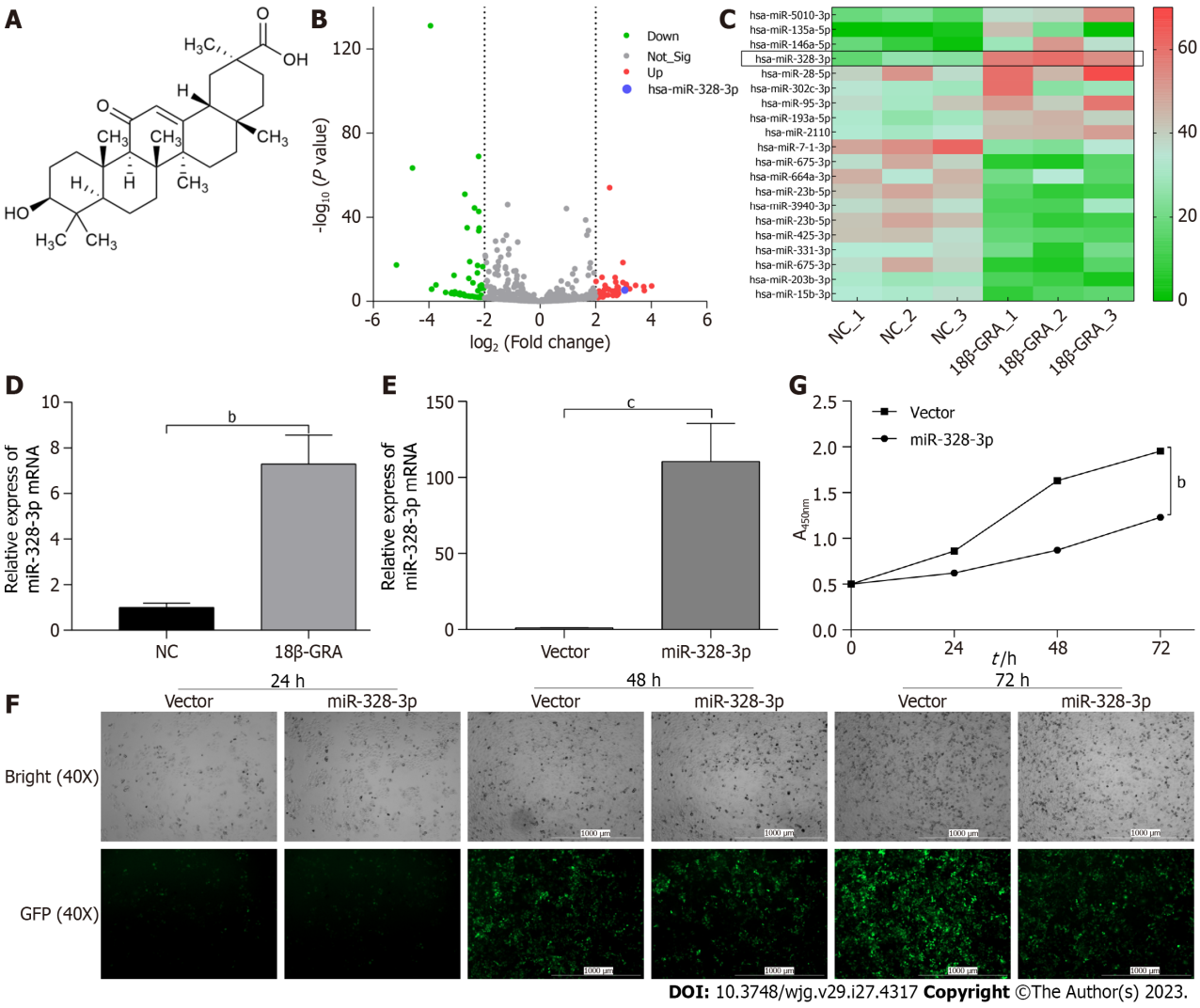
©The Author(s) 2023. Published by Baishideng Publishing Group Inc. All rights reserved.

Core Tip: 18β-glycyrrhetinic acid (18β-GRA) is an important bioactive component of glycyrrhiza liquorice. Our results showed that 18β-GRA upregulated the expression of miR-328-3p in gastric cancer (GC) cells. Overexpression of miR-328-3p inhibited GC cell proliferation and colony formation, arrested the cell cycle, promoted apoptosis, inhibited subcutaneous tumor formation, and inhibited signal transducer and activator of transcription 3 (STAT3) expression. Dual-luciferase reporter assay showed that *miR-328-3p* targeted the regulation of *STAT3*. Confocal microscopy and western blotting indicated that 18β-GRA promotes autophagy flow by promoting autophagosome synthesis. Thus, 18β-GRA appears to promote cell autophagy and inhibit GC cell proliferation by regulating miR-328-3p/STAT3.

Citation: Yang Y, Nan Y, Du YH, Huang SC, Lu DD, Zhang JF, Li X, Chen Y, Zhang L, Yuan L. 18β-glycyrrhetinic acid promotes gastric cancer cell autophagy and inhibits proliferation by regulating miR-328-3p/signal transducer and activator of transcription 3. *World J Gastroenterol* 2023; 29(27): 4317-4333
URL: https://www.wjgnet.com/1007-9327/full/v29/i27/4317.htm
DOI: https://dx.doi.org/10.3748/wjg.v29.i27.4317

INTRODUCTION

Gastric cancer (GC) is the fifth most common type of cancer and the fourth leading cause of cancer-related death worldwide[1]. GC is a local disease whose leading causes include diet, environmental and genetic factors, and *Helicobacter pylori* infection[2]. The current standard treatment for GC is surgical excision of operable tumor tissue combined with local radiotherapy, chemotherapy and conventional anticancer drugs. However, many GC cells appear to have significant invasion and metastasis after surgery. Although chemotherapy is an important management approach for preventing



DOI: 10.3748/wjg.v29.i27.4317 **Copyright** ©The Author(s) 2023.

Figure 1 Drug target miR-328-3p of 18β-glycyrrhetinic acid and its relationship with cell proliferation. A: Chemical structure of 18β-glycyrrhetinic acid (18β-GRA); B: Volcanic map; C: Heat map; D: Effect of 18β-GRA on expression of *miR-328-3p* in gastric cancer cells; E: Expression of *miR-328-3p* in gastric cancer cells transfected with lentivirus; F: Lentivirus transfected gastric cancer cells, cell status and transfection efficiency; G: Effect of overexpression of miR-328-3p on survival rate of AGS cells. All analyses were repeated three times. The data is represented as the mean ± SD. $^{b}P < 0.01$; $^{c}P < 0.001$. NC: Negative control; Vector: The blank vector for lentivirus transfection; GFP: Green fluorescent protein.

invasion and metastasis, it tends to substantially decrease the patients' quality of life due to severe toxic and side effects (*e.g.*, hair loss, bone marrow transplantation, gastrointestinal reactions) and drug resistance[3,4]. Therefore, there is an urgent need to find natural, effective, and less toxic anti-GC drugs.

Glycyrrhiza uralensis Fisch. is a traditional Chinese medicine, and 18β-glycyrrhetinic acid (18β-GRA; Figure 1A), an important bioactive component of licorice, with many pharmacological effects including anti-inflammatory, liver protection, antiviral, anti-allergic, antitumor, antioxidant, and immunomodulatory effects[5-8]. In recent years, it has been found that 18β-GRA has excellent antitumor activity against human malignant tumors such as breast cancer, glioma, lung cancer, and prostate cancer[8-12]. In GC, 18β-GRA regulates the migration of SGC-7901 cells by regulating the reactive oxygen species (ROS)/protein kinase C alpha/extracellular signal-regulated kinase signaling pathway. It also inhibits the activities of matrix metalloproteinase 2 (MMP2) and MMP9 in a dose-dependent manner[13]. Expression of the antioncogene potassium-transporting ATPase alpha chain 1 (ATP4a) is downregulated in GC, and 18-GRA can activate ATP4a, thus inhibiting the occurrence of GC[14]. In transgenic mice, 18β-GRA was found to improve the severity of gastritis and inhibit the occurrence of GC. Also, studies have shown that 18β-GRA can improve the tumor inflammatory microenvironment by downregulating the expression of cyclooxygenase-2 and inhibiting the expression of the direct target Wnt-1 by upregulating the antioncogene miR-149-3p and thus inhibiting the occurrence and development of GC[15]. Cao *et al*[16] reported that 18β-GRA regulates toll-like receptor 2 (TLR2) expression through methylation and inhibits the proliferation, energy metabolism, and carcinogenesis of TLR2-activated GC cells. Our previous study found that 18β-GRA could inhibit GC cell proliferation by regulating the mitochondrial ribosome protein L35[17]. These results suggest that 18β-GRA may be an effective drug for preventing and treating GC.

MicroRNAs (miRNAs) is a novel endogenous, highly conserved non-coding RNA molecule with a length of 18-25 nucleotides[18]. miRNAs have an important role in cancer, and to date, many human miRNA sequences have been identified to participate in cancer pathogenesis and regulate protein expression levels in a complementary manner to

their target mRNAs. miRNAs regulate and participate in the regulation of tumorigenesis, cellular processes, and pathways such as proliferation, differentiation, and apoptosis[19]. Expression profiles of miRNAs differ between cancerous and noncancerous tissues, different types and subtypes of cancer, and early and advanced cancers, depending on the aggressiveness of the disease[20-22]. Current studies have found that some miRNAs not only exist as oncogenes but also inhibit the occurrence of tumors. For example, miR-381 is upregulated in glioma, osteosarcoma and other cancers, while overexpression of miR-381 in GC and colon cancer can inhibit cell migration and invasion and promote cell apoptosis[23-26]. miRNAs also have a dual role in inducing or inhibiting tumorigenesis in GC. Previous studies have shown that the expression level of miR-148a in the plasma of GC patients is lower than that of healthy individuals, and miR-148a overexpression can inhibit proliferation, migration, cell invasion, and the epithelial-mesenchymal transition (EMT)[27]. Li *et al*[28] reported that low expression of miRNA-149 and overexpression of forkhead box C1 (FOXC1) were found in GC tissues and cells. Overexpression of miRNA-149 inhibits GC cell proliferation and migration, arrests the cell cycle, and promotes cell apoptosis. FOXC1 silencing can inhibit the biological functions of AGS and MKN28 cells in GC [28]. Overexpression of miR-140-3p can inhibit the migration and invasion ability of GC cells and directly downregulate the expression of B-cell lymphoma 2 (BCL2), thus inhibiting cell apoptosis. Downregulation of BCL2 further activates autophagy induced by Beclin 1, an autophagy marker, and inhibits the EMT[29]. An increasing number of GC-associated miRNAs have been found to participate in the formation and development of GC.

Autophagy is essential in many physiological and pathological processes, such as development, metabolism, inflammation, and cancer[30]. According to the mode of transport to lysosomes, autophagy can be divided into microautophagy, macroautophagy, and chaperone-mediated autophagy. Autophagy is closely related to the diagnosis, treatment, and prognosis of GC. In their study, Wang *et al*[31] found that there were 10 autophagy-related (*ATG*) genes with significant differences in expression between GC and paracancerous tissue. It was also found that genes such as *ATG14* were significantly associated with the tumor-node-metastasis stage, and the expression of these genes was significantly lower in early T, indicating that autophagy may participate in early GC progression[31]. The expression of miR-183 is significantly decreased in GC tissues compared with paracancerous tissues, whereas the mammalian target of rapamycin (mTOR) is significantly increased. By targeting the expression of mTOR, miR-183 inhibits cell proliferation and promotes cell apoptosis and autophagy[32]. Sec62 homolog, preprotein translocation factor (Sec62), is an endoplasmic reticulum membrane protein highly expressed in GC. Overexpression of Sec62 can increase the expression of eukaryotic translation initiation factor 2 alpha kinase 3/cyclic AMP-dependent transcription factor ATF-4, bind to light chain 3 II (LC3 II), and activate the focal adhesion kinase family interacting protein of 200 kD/Beclin 1/ATG5 pathway to activate autophagy. Therefore, dual inhibition of Sec62 and autophagy may be an effective therapeutic strategy for GC metastasis[33]. It can also be concluded that autophagy is a "double-edged sword" that promotes and inhibits cell survival[34].

Based on previous studies, this study further analyzed the differential expression of miRNAs after the intervention of 18β-GRA. Cell function and animal experiments were used to detect the cell phenotype and subcutaneous tumor formation in nude mice. We detected the targeting relationship between miRNA and signal transducer and activator of transcription 3 (STAT3) and the changes in autophagy flow rate. An important finding was that 18β-GRA could affect autophagy flow and inhibit GC cell proliferation by regulating the miR-328-3p/STAT3 signaling pathway, which may contribute to the clinical development of effective therapies.

MATERIALS AND METHODS

Cell culture

Human AGS cell lines were purchased from GeneChem (Cat. No. GCC-ST0003RT; Shanghai, China). They were cultured in Dulbecco's Modified Eagle Medium (DMEM)/F12 medium (Cat. No. SH30023.01; Hyclone, Logan, UT, United States) containing 100 mL/L fetal bovine serum (Cat. No. 35-081-CV; Corning, Corning, NY, United States), and 10 mL/L penicillin and streptomycin (Cat. No. P1400; Solarbio, Beijing, China). The culture flasks were placed in an incubator at a constant temperature of 37 °C, with 50 mL/L carbon dioxide and saturated humidity.

Whole transcriptomic analyses

Human gastric adenocarcinoma AGS cells were cultured and treated with 18β-GRA (purity > 97%, Cat. No. G10105-10G; Sigma, St. Louis, MO, United States) for 24 h. Cells in the negative control (NC) group and the 18β-GRA group were collected, and total RNA was extracted. Agarose gel electrophoresis was used to analyze the degradation degree of RNA and whether there was contamination. The NanoDrop 2000 spectrophotometer and Qubit 2.0 (Thermo Fisher Scientific, Waltham, MA, United States) were used to determine the purity and concentration of total RNA, and the Agilent 2100 Bioanalyzer (Agilent, Savage, MD, United States) was used to accurately detect the RNA integrity. After the samples were tested as qualified, a library was constructed with a Small RNA Sample Prep Kit. Using the 3'-end hydroxyl structure of the small RNA and the complete 5'-end phosphoric acid group, total RNA was taken as the starting sample, the two ends of the small RNA were added, and reverse transcription was performed to synthesize the cDNA. After polymerase chain reaction (PCR) amplification, polyacrylamide gel electrophoresis was used to isolate the target DNA fragment, after which the cDNA library was recovered.

After the library was successfully constructed, Qubit2.0 was used for preliminary quantification and Agilent 2100 was used to determine the library insert size. Once the insert size reached the expected value, quantitative PCR (qPCR) was used to accurately quantify the effective library concentration and ensure library quality (effective library concentration > 2 nmol/L). After the library was approved, different libraries were pooled into the Illumina SE50 sequencer (Illumina,

San Diego, CA, United States) as needed.

Bioinformatics analyses

TransmiR v2.0 database (http://www.cuilab.cn/transmir) was used to predict miR-328-3p-related proteins, and the STRING database (https://cn.string-db.org/) was used to predict the relationship between miR-328-3p- and autophagy-related proteins. Finally, the binding sites of miRNA-related proteins were searched on the miRWalk website (http://129.206.7.150/).

qPCR

Trizol reagent was used for total RNA extraction (Cat. No. DP424; TIANGEN Biochemical Technology, Beijing, China). cDNA reverse transcription was conducted with the PrimeScript™ RT Reagent Kit with gDNA Eraser (Cat. No. RR04B; TaKaRa Bio Inc., Shiga, Japan) and the BlazeTaq SYBR Green qPCR Mix 2.0 (Cat. No. P031-S; GeneCopoeia, Rockville, MD, United States). The primer sequences were: *miR-328-3p*: forward: ATATCTGGCCCTCTCTGCCCTTC, reverse: AGTGCAGGGTCCGAGGTATT; *U6*: forward: CTCGCTTCGGCAGCACA, reverse: AACGCTTCACGAATTTGCGT; *STAT3*: forward: ACCAGCAGTATAGCCGCTTC, reverse: GCCACAATCCGGGCAATCT; *GAPDH*: forward: CACCCACTCCTCCACCTTTGA, reverse: TCTCTCTTCCTCTTGTGCTCTTGC. All experimental groups were studied in triplicate.

Lentivirus transfection

AGS cells were cultured in a T25 cell breathable culture flask. After 24 h, GC cells were transfected with a green fluorescent protein (GFP)-labeled overexpressed miR-328-3p lentivirus (GeneChem, Shanghai, China). The virus volume = (multiplicity of infection [MOI] × number of cells)/virus titer. At 8 h after transfection, a complete fresh medium was replaced and observed under a fluorescence microscope. The lentivirus transfection efficiency was determined according to the cells with GFP fluorescence in bright and GFP fields. Follow-up experiments were performed when the transfection efficiency reached about 90%.

Cell Counting Kit-8 assay

Lentivirus-transfected AGS cells and normal AGS cells were inoculated into 96-well plates and cultured for 24 h, 48 h and 72 h. Next, the Cell Counting Kit-8 (CCK-8) reagent (Cat. No. CK04; DOJINDO Laboratories, Kumamoto, Japan) was added to each well, and absorbance (optical density [OD]) was measured at 450 nm with an enzyme marker. Cell viability = $(OD_{experiment} - OD_{blank})/(OD_{control} - OD_{blank}) \times 100\%$.

Clone formation

The AGS cells were inoculated in a 6-well plate with 600 cells per well (three wells in each group were prepared for further culture), and the cells were observed under a microscope. When the number of clones of most single cells was > 50, and the diameter was 0.3-1.0 mm, the experiment was terminated. Cells were fixed in 4 mL/L paraformaldehyde (Cat. No. D16013; Saint-Bio, Shanghai, China) for 15 min, followed by incubation in crystal indigo water solution for 4-5 min. Next, they were washed with normal saline, left to dry, photographed and visually counted.

Flow cytometry

The AGS cells transfected with lentivirus were inoculated in 6-well plates for 24 h, digested, centrifuged at 3000 r/min for 5 min, and washed once with phosphate-buffered saline (PBS). The cell concentration was adjusted to 1×10^6/mL, and 0.5 mL cold ethanol was added to fix overnight. After 16 h, the cells were washed once with PBS, and then 500 μL was added to the staining solution prepared according to Rnase A: propidium iodide = 1:9 (Cat. No. KGA511; Keygen, Changchun, China) and incubated for 30 min. Flow cytometry was used to measure the cell cycle.

The AGS cells were collected, the concentration was adjusted to 4×10^5/mL, 1 mL cell suspension was centrifuged, 500 mL of Binding Buffer was added, and 5 μL Annexin V-APC was added. The mixing process was not too forceful. Next, 5 μL 7-aminoactinomycin D staining solution (Cat. No. KGA1023; Keygen) was added, mixed, and incubated for 20 min. Apoptosis was detected with a machine.

Tumor formation experiment

The BALB/c nude mice were kept in polypropylene cages with a humidity of 50% ± 5% and temperature of 22 ± 1 °C for 1 d at a 12 h/12 h light/dark cycle, with *ad libitum* access to food and water. After 2 wk of adaptive feeding, the mice were randomly grouped. The AGS cells and lentivirus-transfected GC cells were collected, and the cell concentration of each group was adjusted to 4×10^6/200 μL. The 200 μL cell suspension was absorbed by microinjection and slowly injected into the subcutaneous area of the right back of nude mice. The subcutaneous tumor-bearing conditions of nude mice were observed daily. The long diameter (L) and short diameter (W) of the tumor were measured with an electronic vernier caliper. The formula for calculating the tumor volume (V) was as follows: $V = (W^2 \times L)/2$. When the tumor volume of nude mice grew to a certain size, all animals were euthanized with 1000 mL/L carbon dioxide, and the tumor was removed and photographed. The animal protocols were approved by the Institutional Animal Care and Use Committee of Ningxia Medical University (IACUC-NYLAC-2022-108; Yinchuan, China).

Hematoxylin and eosin staining

Tissue samples fixed in 4 mL/L paraformaldehyde were dehydrated in 75 mL/L, 85 mL/L, 90 mL/L ethanol, and

anhydrous ethanol and then embedded in paraffin. Paraffin sections 3-5 μm thick were taken from the microtome, baked at 65 °C for 1 h, and quickly sliced into xylene and ethanol for dewaxing treatment. The water was double steamed for 3 min, stained with hematoxylin dye (Cat. No. BA-4041; BaSO Diagnostics Inc., Zhuhai, China) for 5 min, double steamed with water for 3 min, incubated with acid alcohol fast differentiation solution (Cat. No. C0163M; Beyotime, Beijing, China) for 5 s, incubated with eosin dye solution (Cat. No. BA-4024; BaSO Diagnostics Inc.) for 5 min, and washed for 5 min. Next, the slices were dehydrated in 85 mL/L, 95 mL/L ethanol, and anhydrous ethanol. The dehydrated paraffin sections were placed in xylene transparent for 10 min and sealed with neutral gum (Cat. No. Zli-9555; ZSGB-Bio, Beijing, China). The cell structure and morphology were observed by optical microscope (BX43; Olympus, Tokyo, Japan).

Immunohistochemical staining

Paraffin sections were routinely dewaxed, and the sections were repaired with citric acid repair solution (pH = 6.8) under high pressure for 10 min and washed with distilled water for 5 min. The sections were incubated with 3 mL/L hydrogen peroxide for 20 min, washed with water for 5 min, and soaked in PBS for 1 min. Sections were incubated with primary antibody (LC3, 1:50, Cat. No. 12741T from Cell Signaling Technology [CST], Danvers, MA, United States; STAT3, 1:90, Cat. No. AF6294 from Affinity Biosciences, Melbourne, Australia; p-STAT3, 1:100, Cat. No. AF3293 from Affinity Biosciences) at 4 °C overnight and washed with PBS three times, 5 min each time. Next, sections were incubated with secondary antibody at 37 °C for 20 min, followed by washing with PBS, DAB (Cat. No. ZLI-9018; ZSGB-Bio) color development, and washing with tap water. Hematoxylin was used for staining, gradient alcohol was used for dehydration, and neutral gum was used for sealing. The images were observed and acquired with the Olympus Imaging System (UC90).

Western blotting

The protein lysis buffer included 10 μL phosphatase inhibitor, 1 μL protease inhibitor, and 5 μL 100 mmol/L protease inhibitor (Cat. No. KGP2100; Keygen). The cells were collected, and the protein lysate was added to extract the whole protein. The protein content was determined with the bicinchoninic acid assay (Cat. No. KGPBCA; Keygen). Appropriate protein loading buffer (Cat. No. DL101; TransGen Biotech Co., Ltd., Beijing, China) was added and boiled at 100 °C for 10 min. According to the experimental design, the sample was added to prefabricated glue (Cat. No. M00659; GenScript, Nanjing, China), and constant pressure electrophoresis was carried out at 120 V until the marker strip with the lowest molecular weight appeared. After electrophoresis, the proteins were electrotransferred to a PVDF membrane (Cat. No. ISEQ00010; Millipore, Burlington, MA, United States) and incubated overnight at 4 °C with primary antibody, followed by washing and then incubation with secondary antibody for 1 h. The luminescent solution (Cat. No. KF005; Affinity Biosciences) was prepared according to the manufacturer's instructions, and the PVDF membrane was soaked in it for 2-3 min and then placed in the intelligent chemiluminescence imaging system (iBright 1500; Invitrogen, Waltham, MA, United States) to obtain protein bands. Protein bands were analyzed using image J.

Dual-luciferase reporter assay system

Retrieval of hsa-miR-328-3p sequence from NCBI Nucleotide website: UGGCCCUCUCUGCCCUUCCGU, the binding sites of miR-328-3p and STAT3 were retrieved from the miRWalk website, and the binding sites with high binding energy were screened based on the scores.

AGS cells were cultured in 24-well plates with 2 × 10^4 cells per well, and the degree of cell confluence reached about 40%. The experimental group included: Luc-STAT3-3′ untranslated region (3′UTR) Mutant (Mut)-NC + miR-328-3p-NC, Luc-STAT3-3′UTR Mut-NC + miR-328-3p, Luc-STAT3-3′UTR Wild Type (WT) + miR-328-3p-NC, Luc-STAT3-3′UTR WT + miR-328-3p, Luc-STAT3-3′UTR Mut + miR-328-3p-NC, and Luc-STAT3-3′UTR Mut + miR-328-3p. The plasmid and transfection reagent (Cat. No. IV1216075; Invigentech, Irvine, CA, United States) were mixed 1:1 to prepare the complex, after which the complex was added and mixed, and the culture was continued for 24 h. Next, the liquid was changed and the culture was continued.

After 48 h of co-transfection with plasmids, the 24-well plates were removed and balanced to room temperature. Extraction 250 μL medium was removed from each well, and Passive lysis buffer 100 μL was added to each well and shaken for 15 min for lysis. The lysate was added into 1.5 mL EP tubes and then into black 96-well plates with 20 μL per well and 3 multiple Wells per group. Next, Luciferase Assay Reagent II 100 μL was added. Fluorescence values were detected at 560 nm with multifunctional reagent II. Then 100 μL of Stop & Glo® reagent (Cat. No. E1910; Promega, Madison, WI, United States) was added to each well, and the fluorescence value was detected at 465 nm. Luciferase activity = $OD_{\text{firefly luciferase}}/OD_{\text{renilla luciferase}}$.

Transfection with adenovirus

AGS cells with a concentration of 4 × 10^4 cells/mL were inoculated in a 15 mm confocal dish (Biosharp Biotechnology Inc., Hefei, Anhui, China) and cultured in the incubator. When the cells were fused to 40%, the fresh medium volume was changed to 1 mL. Monomeric Red Fluorescent Protein (mRFP)-GFP-LC3 tandem fluorescent protein adenovirus (Cat. No. P21071905; HanBio Therapeutics, Shanghai, China) was added, and the volume of virus = MOI × cell number/virus titer × 10^3, and then 1 mL culture medium was added and placed in the incubator for 4 h. After 16 h of infection, the culture medium was changed into a fresh medium for further culture. At 24 h and 48 h, the cell state and infection situation were observed under fluorescence microscope. The infection efficiency was determined by observing the fluorescence expression level of GFP.

Laser confocal

The AGS cells infected with adenovirus were synchronously treated for 6 h, after which the corresponding drug treatment was given (the NC group was replaced with fresh medium). Next, they were placed in an incubator for 24 h, fixed with 4 mL/L paraformaldehyde for 20 min, and observed with a laser confocal microscope. Cells infected with adenovirus using mRFP-GFP-LC3 tandem fluorescent protein were identified by observing the fluorescence of mRFP and GFP after microscopic imaging.

RESULTS

18β-GRA promotes the expression of miR-328-3p in AGS cells

Whole transcriptomics was used to analyze and screen the differentially expressed miRNAs in AGS cells after the 18β-GRA intervention. Through the selection criteria of log2 |fold change| > 1, $P < 0.05$, 283 differentially expressed miRNAs were obtained, of which 120 were upregulated and 163 were downregulated. Notably, the expression of miR-328-3p was upregulated after drug treatment, log2(fold change) = 3.04871, the P value was 4.51E-06 (Figure 1B and C).

qRT-PCR was used to verify whether the intervention process of 18β-GRA on AGS cells was related to *miR-328-3p*. Our results showed that the expression of *miR-328-3p* in AGS cells treated with 18β-GRA was significantly upregulated compared with the NC group ($P < 0.01$) (Figure 1D).

Overexpression of miR-328-3p inhibited the survival rate of AGS cells

The expression level of *miR-328-3p* after transfection was detected by qRT-PCR. *miR-328-3p* in the overexpression group was significantly higher than in the vector group (Figure 1E). Cell status and transfection efficiency were observed under the Cytation 5 microscope (Figure 1F), and cell survival rate was detected. The results showed that, compared with the vector group, the survival rate of cells in the overexpressed miR-328-3p group decreased significantly ($P < 0.01$) (Figure 1G).

Effect of overexpression of miR-328-3p on cloning formation of AGS cells

The results of the cloning formation experiment showed that compared with the vector group, the crystal violet staining positive of the overexpressing miR-328-3p group was significantly decreased (Figure 2A), and the cloning formation rate of AGS cells was significantly reduced ($P < 0.01$) (Figure 2B). These results indicated that overexpression of miR-328-3p could inhibit the colony formation of GC cells.

Overexpression of miR-328-3p arrested the cell cycle and promoted apoptosis

The cell cycle results showed that the average percentage of G0/G1 phase, S phase, and G2/M phase cells in the vector group was 49.23%, 29.41%, and 21.37%, respectively. The average percentage of G0/G1 phase, S phase, and G2/M phase cells in the overexpressed miR-328-3p group was 63.73%, 20.19%, and 16.08%, respectively. Compared with the vector group, the percentage of G0/G1 phase cells in the overexpressing miR-328-3p group was significantly higher ($P < 0.001$) (Figure 2C and D).

The results of the cell apoptosis experiment showed that the cell fragments in the vector group were increased, indicating that lentivirus transfection had a certain damage effect on AGS cells. Also, the early apoptosis rate of cells overexpressing miR-328-3p was significantly higher than that of the vector group ($P < 0.001$) (Figure 2E and F).

Overexpression of miR-328-3p inhibited subcutaneous tumor in nude mice

The results of the subcutaneous tumor experiment with nude mice showed that the subcutaneous tumor volume in the back of nude mice overexpressed with miR-328-3p was significantly smaller than that in the NC and vector groups ($n = 6$, Figure 3A and B). The tumor growth curve also showed that the tumor growth rate of the overexpressed miR-328-3p group was significantly lower compared to the vector group and the NC group ($P < 0.01$) (Figure 3C). There was no significant difference in body weight among the groups during the whole duration of the experiment(Figure 3D).

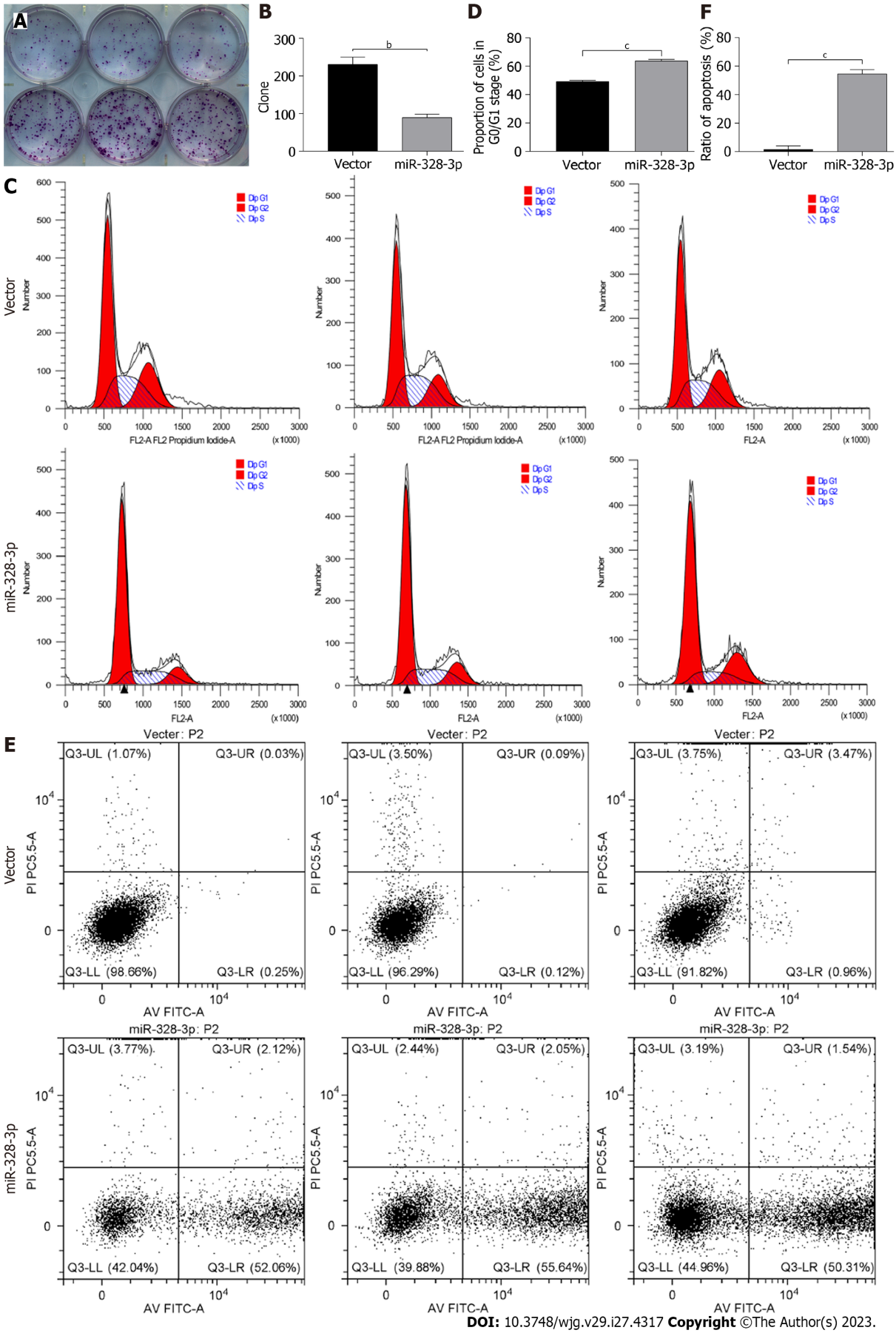
Histopathological observation of transplanted tumor and the expression of STAT3, p-STAT3, and LC3 proteins

Hematoxylin and eosin staining showed that tumor cells in the NC and vector groups grew strongly, with different sizes, certain atypia, and larger nuclei. Also, there was no obvious necrosis in the tumor tissue. In the overexpress group, the cell arrangement was loose, the tissue structure was irregular, and there were more necrotic cells (Figure 3E).

Immunohistochemical staining results showed that compared with the vector and NC groups, the expression of p-STAT3 and LC3 in the miR-328-3p group was significantly decreased ($P < 0.05$), and there was no significant difference in the positive rate of STAT3 expression in transplanted tumor tissues among all groups (Figure 3E and F).

miR-328-3p targeted STAT3 mRNA and was closely related to autophagy-related proteins

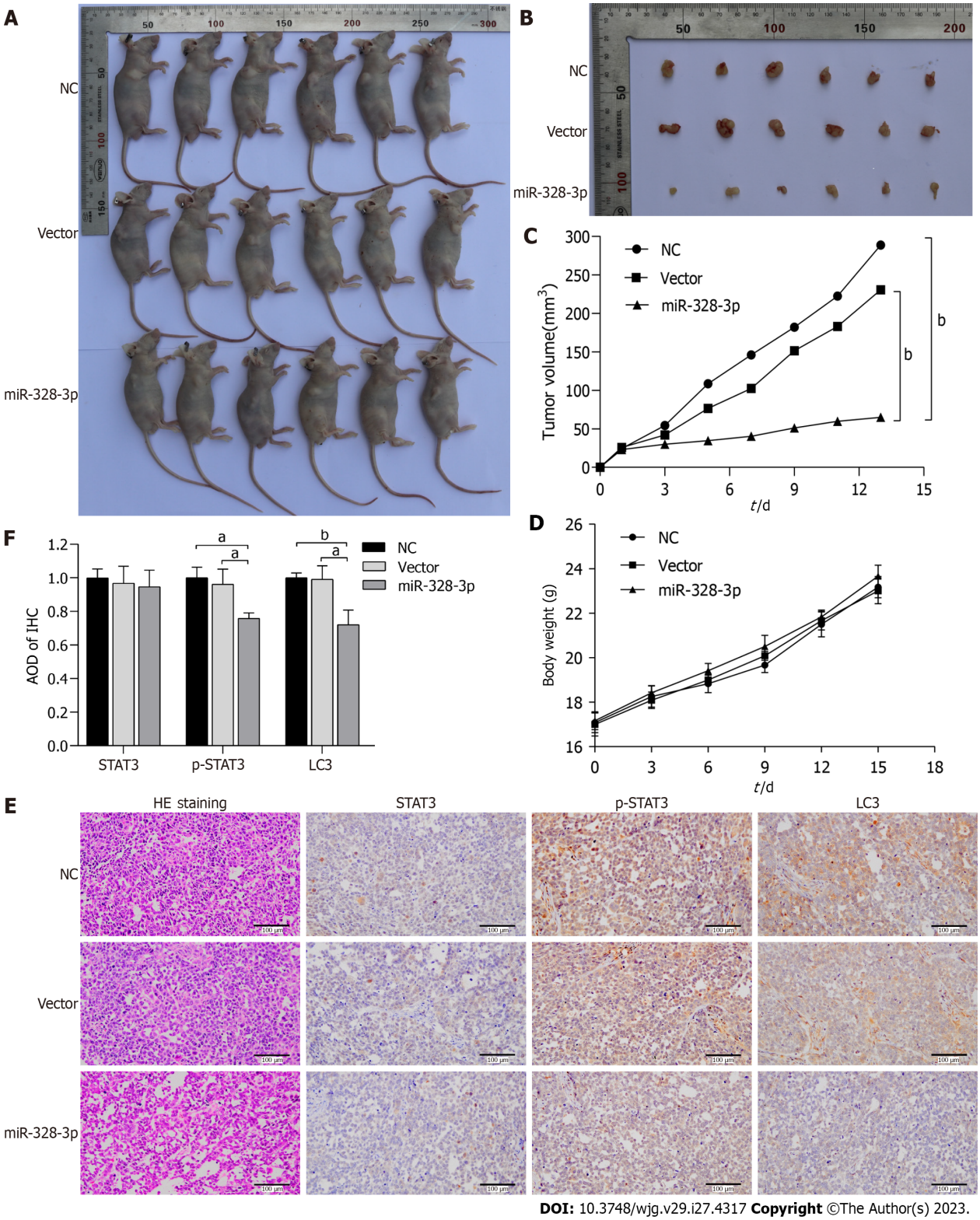
TransmiR v2.0 database predicted miR-328-3p related proteins and found that miR-328 was associated with STAT3 (Figure 4A). The relationship between STAT3 and autophagy-related proteins LC3, p62, BECN1, and ATG13 was subsequently predicted in the STRING database (Figure 4B). The above prediction results suggest that *STAT3* is a target gene of *miR-328-3p*.



DOI: 10.3748/wjg.v29.i27.4317 **Copyright** ©The Author(s) 2023.

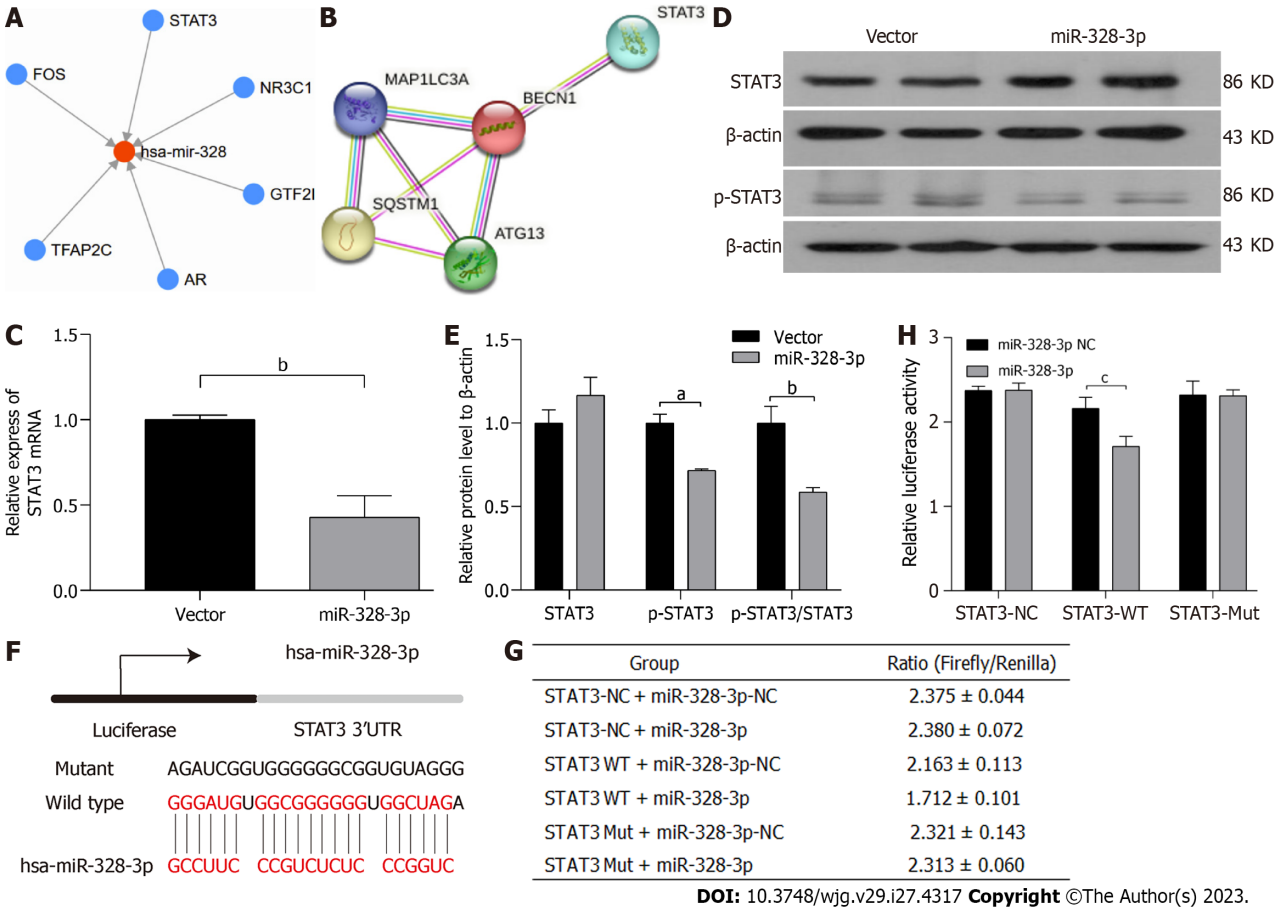
Figure 2 Effects of overexpression of miR-328-3p on clone formation ability, cell cycle and apoptosis of gastric cancer cells. A and B: Effect of miR-328-3p on colony formation ability of AGS cells; C and D: Effect of miR-328-3p on cell cycle of AGS cells; E and F: Effect of miR-328-3p on apoptosis of AGS

cells. All analyses were repeated three times. The data is represented as the mean ± SD. $^{b}P < 0.01$; $^{c}P < 0.001$. Vector: The blank vector for lentivirus transfection.



DOI: 10.3748/wjg.v29.i27.4317 **Copyright** ©The Author(s) 2023.

Figure 3 Effect of miR-328-3p on subcutaneous tumor size in nude mice. A: Comparison of xenotransplantation models of gastric cancer in nude mice; B: Subcutaneous tumor transplantation in nude mice; C: Tumor growth curves of the transplanted tumor model; D: The influence of subcutaneous tumor formation on body weight of nude mice; E: Hematoxylin and eosin (HE) staining and immunohistochemical (IHC) staining of transplanted tumor tissue; F: Statistical graph of IHC staining results. All analyses were repeated three times. The data is represented as the mean ± SD. $^{a}P < 0.05$; $^{b}P < 0.01$. NC: Negative control; Vector: The blank vector for lentivirus transfection.



DOI: 10.3748/wjg.v29.i27.4317 **Copyright** ©The Author(s) 2023.

Figure 4 ***Signal transducer and activator of transcription 3* is targeted by *miR-328-3p*.** A: TransmiR v2.0 database predicted miR-328-3p related proteins; B: STRING database predicted the relationship between Signal transducer and activator of transcription 3(STAT3) and autophagy-related proteins; C: Effect of *miR-328-3p* on the expression of *STAT3* mRNA; D and E: Effect of miR-328-3p on the expression levels of STAT3 and phosphorylated STAT3; F: Schematic diagram of binding site between *miR-328-3p* and *STAT3* 3' untranslated regions; G and H: *STAT3* is the target gene of *miR-328-3p*. All analyses were repeated three times. The data is represented as the mean ± SD. $^{a}P < 0.05$; $^{b}P < 0.01$; $^{c}P < 0.001$. NC: Negative control; Vector: The blank vector for lentivirus transfection; WT: Wild type; Mut: Mutant.

STAT3 is targeted by miR-328-3p

qRT-PCR was used to detect the expression level of *STAT3* mRNA in transfected lentivirus in AGS cells. Our results showed that the expression level of *STAT3* mRNA in the overexpressed miR-328-3p group was significantly lower than that in the vector group ($P < 0.01$) (Figure 4C).

We also detected STAT3 and p-STAT3 in AGS cells overexpressed with miR-328-3p by western blot (Figure 4D). The experimental results showed that the expression level of STAT3 in the miR-328-3p group did not significantly change, and the expression of p-STAT3 was downregulated ($P < 0.05$). After the ratio of p-STAT3 to STAT3, the p-STAT3/STAT3 ratio in the overexpressed miR-328-3p group was significantly down-regulated ($P < 0.01$) (Figure 4E).

Dual-luciferase reporter system verified the targeting relationship between miR-328-3p and STAT3

The miRWalk online tool was used to find the binding site of *miR-328-3p* and *STAT3*, suggesting that there is a targeting relationship between *miR-328-3p* and *STAT3* (Figure 4F). Dual-luciferase reporter assay was used to detect the relationship between *miR-328-3p* and *STAT3* in AGS cells (Figure 4G). Our results showed that the luciferase activity of the STAT3 WT + miR-328-3p NC group was lower than that of the STAT3 WT + miR-328-3p group, and the difference was statistically significant ($P < 0.001$) (Figure 4H). We found that *miR-328-3p* could bind specifically to the 3'UTR of *STAT3*.

miR-328-3p could regulate STAT3 and promote autophagy flow in AGS cells

In order to further investigate the effect of *miR-328-3p* targeted regulation of *STAT3* on the autophagy flow of AGS cells, western blot was used in combination with 0.5 μmoL/L Baf A_1 to detect the expression of LC3 II in AGS cells after overexpression of miR-328-3p (Figure 5A). Our experimental results showed that the expression level of LC3 II in the overexpressing miR-328-3p group was significantly downregulated compared with the vector group ($P < 0.05$). Compared with the Baf A_1 group, the expression level of LC3 II in miR-328-3p combined with the Baf A_1 group was significantly upregulated ($P < 0.01$) (Figure 5B).

18β-GRA promoted autophagosome synthesis in AGS cells

To further investigate the effect of 18β-GRA on autophagic flow in AGS cells, we treated AGS cells with different drugs. The results showed that compared with the NC group, LC3 II expression level in the 18β-GRA group was significantly downregulated ($P < 0.05$). Compared with the Baf A_1 group, LC3 II in 18β-GRA + Baf A_1 group was significantly upregulated ($P < 0.05$) (Figure 5C and D).

mRFP-GFP-LC3 tandem fluorescent protein adenovirus was also used to infect AGS cells and locally tag LC3 to detect autophagy flow. First, we explored the MOI of mRFP-GFP-LC3 tandem fluorescent protein adenovirus-infected AGS cells. The NC, MOI = 30, MOI = 50, and MOI = 80 groups were set up separately. Corresponding virus volumes were given for transfection, and photographs were taken under the fluorescence microscope at 24 h and 48 h. The results showed that, compared with MOI = 50, the virus transfection efficiency was lower when MOI = 30, while the cell state was poorer when MOI = 80. When MIO = 50 and the transfection time was 48 h, both transfection efficiency and cell state were good. Therefore, an MOI of 50 was determined as the MOI for subsequent experimental infection (Figure 5E and F). We used mRFP-GFP-LC3 tandem fluorescent protein adenovirus (MOI = 50) was used to infect AGS cells for 48 h and gave corresponding drug treatment. The experimental results showed that the number of yellow spots (GFP/mRFP) in the 18β-GRA group increased significantly compared with the NC group ($P < 0.001$). Separate red signals were also significantly increased ($P < 0.01$) (Figure 5G), suggesting that 18β-GRA could increase the number of early autophagosomes and late autolysosomes. Compared with the Baf A_1 group, the number of yellow spots in the 18β-GRA + Baf A_1 group increased significantly ($P < 0.001$), and the single red signal showed no significant change, indicating that the late autophagy inhibitor caused the blocking of late autophagic lysosome degradation. 18β-GRA promoted autophagosome synthesis, increasing the number of yellow spots (Figure 5H).

18β-GRA promoted autophagy flow and inhibited the proliferation of AGS cells by regulating the miR-328-3p/STAT3 signaling pathway

To investigate whether 18β-GRA promotes autophagy flow through the miR-328-3p/STAT3 signaling pathway, we first used qRT-PCR to collect 18β-GRA intervention AGS cells to detect the expression level of *STAT3* mRNA. Our results showed that *STAT3* mRNA expression was significantly downregulated in AGS cells after 18β-GRA intervention compared with the NC group ($P < 0.05$) (Figure 5I). Then, western blot results showed that the expression levels of STAT3 and p-STAT3 in AGS cells after 18β-GRA intervention were downregulated, and the p-STAT3/STAT3 ratio was also significantly downregulated ($P < 0.05$) (Figure 5J and K).

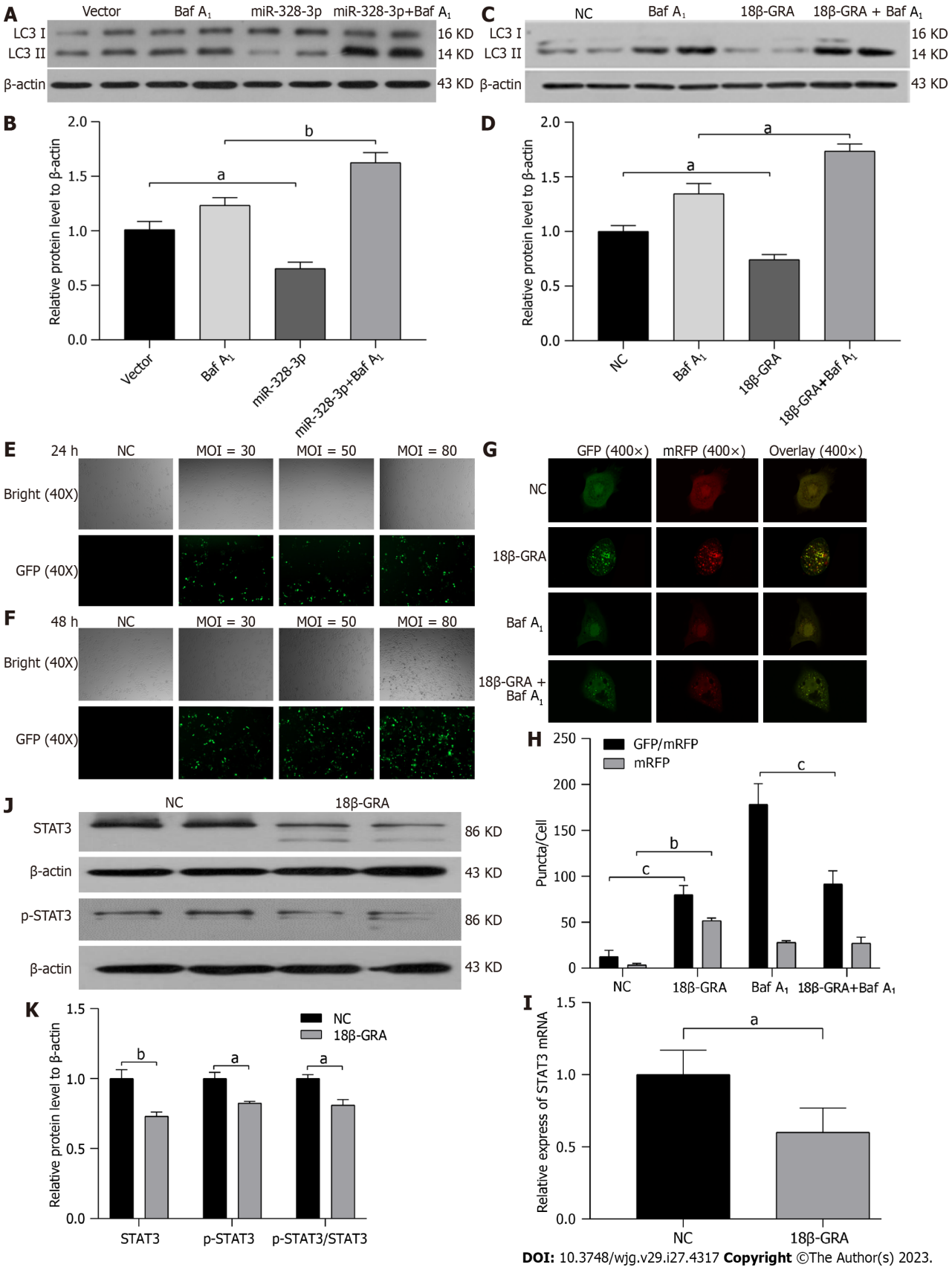
DISCUSSION

The present study found that 18β-GRA could regulate the expression of miR-328-3p, inhibit the proliferation of GC cells, arrest the cell cycle, and promote cell apoptosis. The dual-luciferase reporter gene experiment confirmed that *miR-328-3p* targeted the regulation of *STAT3* and participated in promoting autophagy. Our results suggest that 18β-GRA promoted the synthesis of autophagosomes and inhibited cell proliferation by regulating the miR-328-3p/STAT3 signaling pathway.

miR-328-3p expression was found to be significantly inhibited by palmitate-induced endoplasmic reticulum stress in liver cell lines[35]. In tumors, overexpression of miR-328-3p can inhibit the proliferation and invasion of hepatocellular carcinoma cells, promote cell apoptosis, and have an excellent targeting relationship with endoplasmic reticulum metalloproteinases[36]. Overexpression of miR-328-3p inhibited proliferation, migration, and invasion of colorectal cancer cells and inactivated the phosphatidylinositol 3 kinase/protein kinase B (Akt) signaling pathway[37]. Xu *et al*[38] analyzed the miRNA expression profiles of 389 GC patients, using forward and reverse variable selection and multiple Cox regression analysis models, finding that miR-328-3p exists in GC patients as a protective miRNA. However, Xiao *et al*[39] defined miR-328-3p as an oncogene for the first time and found that miR-328-3p promotes the progression of GC by targeting the kelch-like ECH-associated protein 1/nuclear factor erythroid 2-related factor 2 axis. Although there is some controversy about the effect of the miR-328-3p expression on GC progression, it also suggests that miR-328-3p may be a target for GC drug therapy.

Autophagy ("self-eating") usually refers to the process in which cells wrap their own pathological organelles into double-layer vesicles to form autophagosomes when they resist stress such as hunger and then deliver them to lysosomes and combine with them to form autolysosome to degrade the contents and produce energy for recycling and utilization to maintain cell survival[40]. During autophagy, the autophagy containing misfolded proteins and damaged organelles is degraded in the lysosome, which has a limiting membrane to prevent the leakage of its degrading enzymes. The autophagy process is fast and frequent and involves relatively complex membrane dynamics[41]. It is generally believed that the conversion of LC3 I to LC3 II detected in Western blot, or the increased expression level of LC3 II represents the activation of autophagy flow, and after the autophagy flow is blocked, the expression level of LC3 II is decreased (the conversion of LC3I to LC3 II was blocked) or LC3 II is excessively degraded by autolysosome[42]. In this study, autophagy marker protein LC3 was detected by combining with autophagy inhibitor Baf A_1 to explore the effects of drugs and miR-328-3p on the autophagy of GC cells, revealing that both drugs and miR-328-3p could promote the occurrence of autophagy flow.

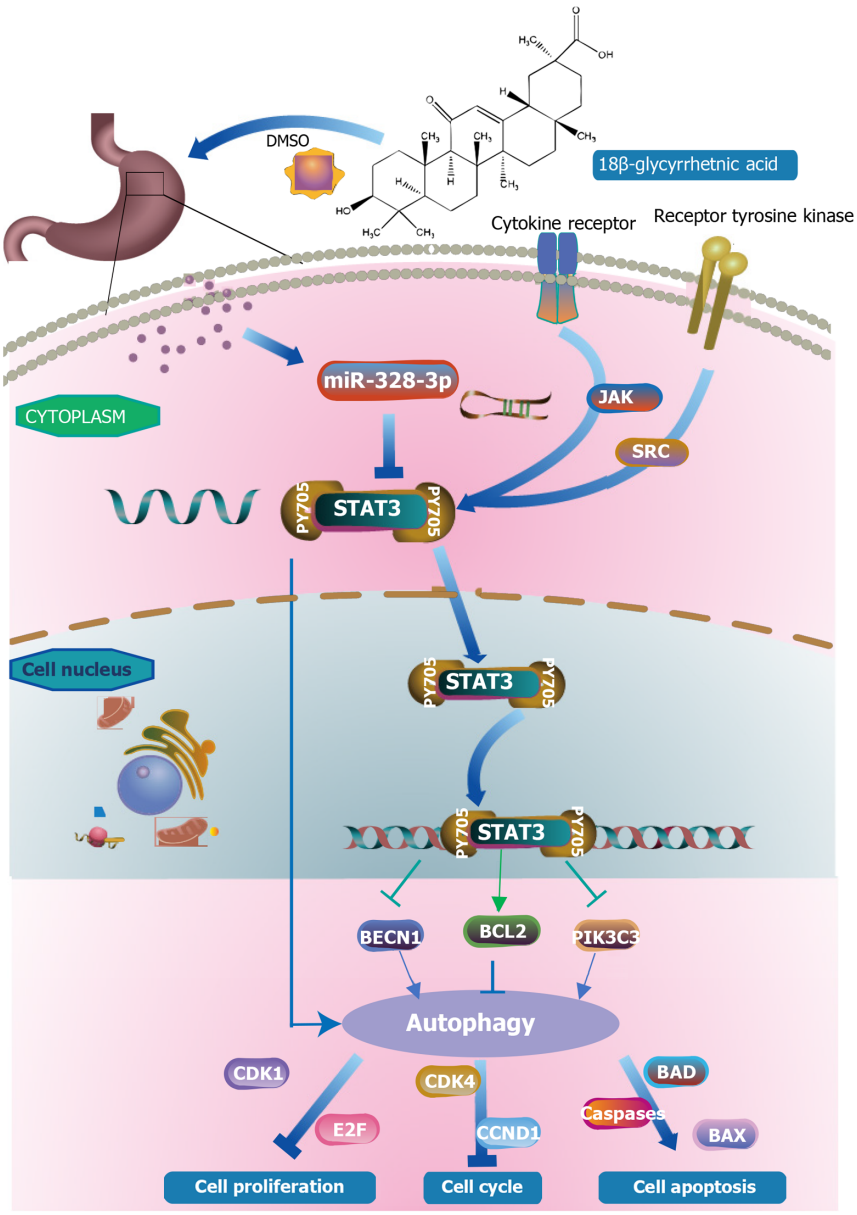
To further explore whether drugs promote the synthesis of autophagosomes or inhibit the degradation of autophagosomes, we infected GC cells with mRFP-GFP-LC3 autophagic double-labeled adenovirus, and the mRFP and GFP were used to label LC3. Because GFP fluorescent protein is sensitive to acidic environments, green fluorescence is quenched after the fusion of autophagosome and lysosome, and only mRFP fluorescence can be detected. The yellow signal



DOI: 10.3748/wjg.v29.i27.4317 **Copyright** ©The Author(s) 2023.

Figure 5 18β-glycyrrhetinic acid regulates miR-328-3p/signal transducer and activator of transcription 3 signaling pathway and promotes the synthesis of autophagosomes in gastric cancer cells. A and B: Effect of miR-328-3p on the expression level of light chain 3 II (LC3 II) in AGS cells; C and D: Effects of 18β-glycyrrhetinic acid (18β-GRA) on LC3 II expression in AGS cells; E and F: Monomeric red fluorescent protein-green fluorescent protein-LC3 tandem fluorescent protein adenovirus-infected AGS cells, and effects of different multiplicity of infection on cell status and infection efficiency; G and H: Effects of laser confocal imaging of 18β-GRA combined with bafilomycin A_1 (Baf A_1) on autophagy flow; I: Effect of 18β-GRA on the expression of signal transducer and

activator of transcription 3 (*STAT3*) in AGS cells; J and K: Effects of 18β-GRA on the expression of STAT3 and phosphorylated STAT3 in AGS cells. All analyses were repeated three times. The data are represented as the mean ± standard deviation. [a]*P* < 0.05; [b]*P* < 0.01; [c]*P* < 0.001. NC: Negative control; Vector: The blank vector for lentivirus transfection.



DOI: 10.3748/wjg.v29.i27.4317 **Copyright** ©The Author(s) 2023.

Figure 6 Graphic abstract. STAT3: Signal transducer and activator of transcription 3.

composed of GFP and mRFP fluorescence signals co-located in the cell represents the early autophagosome, while the mRFP fluorescence signal alone represents the late autophagosome. The increased yellow and red signals indicate an increased autophagic flow level[43]. Using a dual verification approach, we found that drugs promoted autophagy flow by promoting autophagy synthesis at the causal level.

Several studies have found a close relationship between STAT3 and autophagy[44]. This study validated the targeting relationship between *miR-328-3p* and *STAT3* by dual-luciferase reporter gene experiments. In conclusion, regulating the miR-328-3p/STAT3 signaling pathway promotes the synthesis of autophagosomes, and 18β-GRA inhibits the proliferation of GC cells. Typically, STAT3 monomers in the cytoplasm are phosphorylated to form STAT3 dimers, which are then shuttled into the nucleus and bind to specific DNA elements to transcriptionally activate or inhibit the expression of target genes, thereby inhibiting cell proliferation, arresting the cell cycle, and promoting autophagy[45]. At the same time, STAT3 in the unphosphorylated cytoplasm activates some autophagy-related genes, such as serine/threonine-protein kinase ULK2 and ATG12, *via* FOXO1 and FOXO3 transcription[46]. STAT3 monomer can also be transferred to mitochondria and interact with complex I/II of mitochondria to inhibit the production of reactive oxygen ROS[47] (Figure 6).

The present study showed that 18-GRA could inhibit GC cell proliferation, arrest cell cycle in G0/G1, promote apoptosis, and promote autophagosome synthesis of GC cells by regulating the miR-328-3p/STAT3 signaling pathway. Our future research program will be divided into three following phases: (1) Electrophoretic mobility shift assay was used to detect the binding ability of the STAT3 promoter regulatory region and miR-328-3p, to explore whether the transcriptional regulation of miR-328-3p on STAT3 is directly binding or indirectly binding; (2) the interaction mechanism between miR-328-3p and STAT3 proteins will be verified, and chromatin immuno-precipitation technology will be considered to further verify the binding regulation of the promoter region of the transcription factor STAT3 and miR-328-3p; (3) using Cre mice, adeno-associated virus was used for genome editing *in vivo*, and conditional gene targeting of miR-328-3p was performed in gastric mucosal epithelial cells to explore the overall phenotype and physiological status of Cre mice. This study mainly provided the scientific basis for the clinical treatment of GC and also sought effective drug targets for the prevention and treatment of GC.

CONCLUSION

18β-GRA can promote the synthesis of autophagosomes in GC cells, inhibit cell proliferation, arrest cell cycle and promote cell apoptosis by regulating miR-328-3p/STAT3 signaling pathway.

ARTICLE HIGHLIGHTS

Research background

Gastric cancer(GC) is among the most severe gastrointestinal malignancies, with high morbidity and mortality. In recent years, increasing evidence has shown that natural products can prevent and inhibit the development of GC by regulating miRNA and other genes, showing great therapeutic potential.

Research motivation

Targeting miRNA and other genes in GC with natural drugs is a promising strategy, which provides a valid reference to further elucidate the molecular mechanism of natural products in the treatment of GC.

Research objectives

The purpose of this study was to investigate the molecular mechanism of 18β-glycyrrhetinic acid (18β-GRA) regulating the miR-328-3p/ signal transducer and activator of transcription 3 (STAT3) signaling pathway, promoting the autophagy flow of GC cells and inhibiting cell proliferation.

Research methods

The differentially expressed miRNAs were screened by full transcriptomic analysis. The cells were transfected with lentivirus, and the functional indices of the cells were determined by Cell Counting Kit-8, clone forming method, and flow cytometry. The effect of overexpression of miR-328-3p on the tumorigenicity of GC cells was detected in the transplanted tumor model of nude mice. Hematoxylin-eosin staining and immunohistochemistry were used to observe tumor tissue morphology and detect protein expression, respectively. Bioinformatics analysis was performed using TransmiR, STRING, and miRWalk databases. Real-time quantitative polymerase chain reaction and western blot were used to detect mRNA and protein expression levels. Dual luciferase reporter system was used to verify the targeting relationship between genes. The autophagy flow of monomeric red fluorescent protein- green fluorescent protein - light chain 3 adenovirus double-labeled infected cells was observed under confocal laser microscopy.

Research results

18β-GRA could upregulate the expression of miR-328-3p in AGS cells. Overexpression of miR-328-3p inhibited the cell proliferation and colony formation ability, arrested the cell cycle, promoted apoptosis, inhibited the growth of subcutaneous tumors, and led to GC tissue cell necrosis increase. *miR-328-3p* can target and regulate *STAT3*. 18β-GRA intervention in GC cells and overexpression of miR-328-3p could downregulate the expression level of *STAT3* mRNA. Compared with the vector group, the expression level of LC3 II was downregulated in the overexpressed miR-328-3p + bafilomycin A_1 (Baf A_1) group and upregulated in the overexpressed miR-328-3p + Baf A_1 group. The number of yellow spots and separate red signals in the 18β-GRA group were significantly increased compared with the negative control group, and the number of yellow spots in the 18β-GRA + Baf A_1 group was significantly increased compared with the Baf A_1 group.

Research conclusions

18β-GRA promotes GC cells' autophagosome synthesis and inhibits cell proliferation by regulating the miR-328-3p/ STAT3 signaling pathway.

Research perspectives

MiR-328-3p/STAT3 can be regulated by 18β-GRA and can be used as an effective drug target for the prevention and

treatment of GC, thus providing a scientific basis for the clinical treatment of GC.

ACKNOWLEDGEMENTS

The authors would like to acknowledge Li-Qun Wang for statistical analysis assistance, as well as Joanna Japhet Tibenda for polishing the language.

FOOTNOTES

Author contributions: Yang Y carried out most of the studies, analyzed the data and wrote the manuscript; Nan Y designed the study and revised the manuscript; Nan Y, Du YH and Huang SC wrote the manuscript and carried out the chart-making work; Lu DD and Li X were responsible for the total transcriptomic and bioinformatics analyses; Zhang JF performed parts of the *in vivo* and *in vitro* experiments and conducted statistical analyses of the data; Yuan L supervised the process of research and provided clinical guidance; Yuan L, Zhang L and Chen Y provided the conceptual and technical guidance as well as revised the manuscript critically for important intellectual content; All authors have read and approved the manuscript.

Supported by Ningxia Medical University Project, No. XZ2021005; Ningxia Natural Science Foundation, Nos. 2022AAC03144 and 2022AAC02039; and National Natural Science Foundation of China, No. 82260879.

Institutional review board statement: The study was reviewed and approved by the Institutional Review Board of Ningxia Medical University (No. 2021-X003, No. 2021-N0063, Nos. 2021-N001 and 2022-G089).

Institutional animal care and use committee statement: All procedures involving animals were reviewed and approved by the Institutional Animal Care and Use Committee of the Ningxia Medical University (IACUC-NYLAC-2022-108).

Conflict-of-interest statement: All the authors report having no relevant conflicts of interest for this article.

Data sharing statement: All data generated or analyzed during this study are included in this paper, and further inquiries can be directed to the corresponding author 20080017@nxmu.edu.cn.

ARRIVE guidelines statement: The authors have read the ARRIVE guidelines, and the manuscript was prepared and revised according to the ARRIVE guidelines.

Open-Access: This article is an open-access article that was selected by an in-house editor and fully peer-reviewed by external reviewers. It is distributed in accordance with the Creative Commons Attribution NonCommercial (CC BY-NC 4.0) license, which permits others to distribute, remix, adapt, build upon this work non-commercially, and license their derivative works on different terms, provided the original work is properly cited and the use is non-commercial. See: https://creativecommons.org/Licenses/by-nc/4.0/

Country/Territory of origin: China

ORCID number: Yi Yang 0000-0002-8466-5717; Yi Nan 0000-0002-5511-9266; Yu-Hua Du 0000-0002-9669-8065; Shi-Cong Huang 0009-0002-5996-0797; Dou-Dou Lu 0009-0009-4644-9181; Jun-Fei Zhang 0000-0003-0575-4955; Xia Li 0000-0002-4981-9768; Yan Chen 0000-0002-8673-398X; Lei Zhang 0000-0002-3553-2547; Ling Yuan 0000-0003-2838-0976.

S-Editor: Wang JJ
L-Editor: Filipodia
P-Editor: Zhao S

REFERENCES

1 **Sung H**, Ferlay J, Siegel RL, Laversanne M, Soerjomataram I, Jemal A, Bray F. Global Cancer Statistics 2020: GLOBOCAN Estimates of Incidence and Mortality Worldwide for 36 Cancers in 185 Countries. *CA Cancer J Clin* 2021; **71**: 209-249 [PMID: 33538338 DOI: 10.3322/caac.21660]

2 **Lyons K**, Le LC, Pham YT, Borron C, Park JY, Tran CTD, Tran TV, Tran HT, Vu KT, Do CD, Pelucchi C, La Vecchia C, Zgibor J, Boffetta P, Luu HN. Gastric cancer: epidemiology, biology, and prevention: a mini review. *Eur J Cancer Prev* 2019; **28**: 397-412 [PMID: 31386635 DOI: 10.1097/CEJ.0000000000000480]

3 **Smyth EC**, Nilsson M, Grabsch HI, van Grieken NC, Lordick F. Gastric cancer. *Lancet* 2020; **396**: 635-648 [PMID: 32861308 DOI: 10.1016/S0140-6736(20)31288-5]

4 **Jácome AA**, Coutinho AK, Lima EM, Andrade AC, Dos Santos JS. Personalized medicine in gastric cancer: Where are we and where are we going? *World J Gastroenterol* 2016; **22**: 1160-1171 [PMID: 26811654 DOI: 10.3748/wjg.v22.i3.1160]

5 **Wang CY**, Kao TC, Lo WH, Yen GC. Glycyrrhizic acid and 18β-glycyrrhetinic acid modulate lipopolysaccharide-induced inflammatory response by suppression of NF-κB through PI3K p110δ and p110γ inhibitions. *J Agric Food Chem* 2011; **59**: 7726-7733 [PMID: 21644799 DOI: 10.1021/jf2013265]

6 **Feng Y**, Mei L, Wang M, Huang Q, Huang R. Anti-inflammatory and Pro-apoptotic Effects of 18beta-Glycyrrhetinic Acid In Vitro and In Vivo Models of Rheumatoid Arthritis. *Front Pharmacol* 2021; **12**: 681525 [PMID: 34381358 DOI: 10.3389/fphar.2021.681525]

7 **Huo X**, Meng X, Zhang J, Zhao Y. Hepatoprotective effect of different combinations of 18α-and 18β-Glycyrrhizic acid against CCl(4)-induced liver injury in rats. *Biomed Pharmacother* 2020; **122**: 109354 [PMID: 31918260 DOI: 10.1016/j.biopha.2019.109354]

8 **Luo YH**, Wang C, Xu WT, Zhang Y, Zhang T, Xue H, Li YN, Fu ZR, Wang Y, Jin CH. 18β-Glycyrrhetinic Acid Has Anti-Cancer Effects *via* Inducing Apoptosis and G2/M Cell Cycle Arrest, and Inhibiting Migration of A549 Lung Cancer Cells. *Onco Targets Ther* 2021; **14**: 5131-5144 [PMID: 34712051 DOI: 10.2147/OTT.S322852]

9 **Ye L**, Xu Y, Wang L, Zhang C, Hu P, Tong S, Liu Z, Tian D. Downregulation of CYP2E1 is associated with poor prognosis and tumor progression of gliomas. *Cancer Med* 2021; **10**: 8100-8113 [PMID: 34612013 DOI: 10.1002/cam4.4320]

10 **Wang X**, Tan Y, Zhang Y, Xu Z, Xu B, Lei H, Ding C, Cheng S, Wang X, Wei P, Wang Z, Mao Q, Ai C, Hua Q. The novel glycyrrhetinic acid-tetramethylpyrazine conjugate TOGA induces anti-hepatocarcinogenesis by inhibiting the effects of tumor-associated macrophages on tumor cells. *Pharmacol Res* 2020; **161**: 105233 [PMID: 33031908 DOI: 10.1016/j.phrs.2020.105233]

11 **Sun Y**, Jiang M, Park PH, Song K. Transcriptional suppression of androgen receptor by 18β-glycyrrhetinic acid in LNCaP human prostate cancer cells. *Arch Pharm Res* 2020; **43**: 433-448 [PMID: 32219716 DOI: 10.1007/s12272-020-01228-z]

12 **Shukla A**, Tyagi R, Meena S, Datta D, Srivastava SK, Khan F. 2D- and 3D-QSAR modelling, molecular docking and in vitro evaluation studies on 18β-glycyrrhetinic acid derivatives against triple-negative breast cancer cell line. *J Biomol Struct Dyn* 2020; **38**: 168-185 [PMID: 30686140 DOI: 10.1080/07391102.2019.1570868]

13 **Cai H**, Chen X, Zhang J, Wang J. 18β-glycyrrhetinic acid inhibits migration and invasion of human gastric cancer cells *via* the ROS/PKC-α/ERK pathway. *J Nat Med* 2018; **72**: 252-259 [PMID: 29098529 DOI: 10.1007/s11418-017-1145-y]

14 **Cao D**, Zhao D, Jia Z, Su T, Zhang Y, Wu Y, Wu M, Tsukamoto T, Oshima M, Jiang J, Cao X. Reactivation of Atp4a concomitant with intragenic DNA demethylation for cancer inhibition in a gastric cancer model. *Life Sci* 2020; **242**: 117214 [PMID: 31884095 DOI: 10.1016/j.lfs.2019.117214]

15 **Cao D**, Jia Z, You L, Wu Y, Hou Z, Suo Y, Zhang H, Wen S, Tsukamoto T, Oshima M, Jiang J, Cao X. 18β-glycyrrhetinic acid suppresses gastric cancer by activation of miR-149-3p-Wnt-1 signaling. *Oncotarget* 2016; **7**: 71960-71973 [PMID: 27713126 DOI: 10.18632/oncotarget.12443]

16 **Cao D**, Wu Y, Jia Z, Zhao D, Zhang Y, Zhou T, Wu M, Zhang H, Tsukamoto T, Oshima M, Jiang J, Cao X. 18β-glycyrrhetinic acid inhibited mitochondrial energy metabolism and gastric carcinogenesis through methylation-regulated TLR2 signaling pathway. *Carcinogenesis* 2019; **40**: 234-245 [PMID: 30364936 DOI: 10.1093/carcin/bgy150]

17 **Yuan L**, Yang Y, Li X, Zhou X, Du YH, Liu WJ, Zhang L, Yu L, Ma TT, Li JX, Chen Y, Nan Y. 18β-glycyrrhetinic acid regulates mitochondrial ribosomal protein L35-associated apoptosis signaling pathways to inhibit proliferation of gastric carcinoma cells. *World J Gastroenterol* 2022; **28**: 2437-2456 [PMID: 35979263 DOI: 10.3748/wjg.v28.i22.2437]

18 **Fabian MR**, Sonenberg N, Filipowicz W. Regulation of mRNA translation and stability by microRNAs. *Annu Rev Biochem* 2010; **79**: 351-379 [PMID: 20533884 DOI: 10.1146/annurev-biochem-060308-103103]

19 **Coradduzza D**, Cruciani S, Arru C, Garroni G, Pashchenko A, Jedea M, Zappavigna S, Caraglia M, Amler E, Carru C, Maioli M. Role of miRNA-145, 148, and 185 and Stem Cells in Prostate Cancer. *Int J Mol Sci* 2022; **23** [PMID: 35163550 DOI: 10.3390/ijms23031626]

20 **Brase JC**, Johannes M, Schlomm T, Fälth M, Haese A, Steuber T, Beissbarth T, Kuner R, Sültmann H. Circulating miRNAs are correlated with tumor progression in prostate cancer. *Int J Cancer* 2011; **128**: 608-616 [PMID: 20473869 DOI: 10.1002/ijc.25376]

21 **Di Leva G**, Croce CM. miRNA profiling of cancer. *Curr Opin Genet Dev* 2013; **23**: 3-11 [PMID: 23465882 DOI: 10.1016/j.gde.2013.01.004]

22 **Naeini MM**, Ardekani AM. Noncoding RNAs and Cancer. *Avicen J Med Biotechnol* 2009; **1**: 55-70

23 **Yin Y**, Li X, Guo Z, Zhou F. MicroRNA381 regulates the growth of gastric cancer cell by targeting TWIST1. *Mol Med Rep* 2019; **20**: 4376-4382 [PMID: 31545430 DOI: 10.3892/mmr.2019.10651]

24 **He X**, Wei Y, Wang Y, Liu L, Wang W, Li N. MiR-381 functions as a tumor suppressor in colorectal cancer by targeting Twist1. *Onco Targets Ther* 2016; **9**: 1231-1239 [PMID: 27094913 DOI: 10.2147/OTT.S99228]

25 **Wang Z**, Yang J, Xu G, Wang W, Liu C, Yang H, Yu Z, Lei Q, Xiao L, Xiong J, Zeng L, Xiang J, Ma J, Li G, Wu M. Targeting miR-381-NEFL axis sensitizes glioblastoma cells to temozolomide by regulating stemness factors and multidrug resistance factors. *Oncotarget* 2015; **6**: 3147-3164 [PMID: 25605243 DOI: 10.18632/oncotarget.3061]

26 **Li Y**, Zhao C, Yu Z, Chen J, She X, Li P, Liu C, Zhang Y, Feng J, Fu H, Wang B, Kuang L, Li L, Lv G, Wu M. Low expression of miR-381 is a favorite prognosis factor and enhances the chemosensitivity of osteosarcoma. *Oncotarget* 2016; **7**: 68585-68596 [PMID: 27612424 DOI: 10.18632/oncotarget.11861]

27 **Komatsu S**, Imamura T, Kiuchi J, Takashima Y, Kamiya H, Ohashi T, Konishi H, Shiozaki A, Kubota T, Okamoto K, Otsuji E. Depletion of tumor suppressor miRNA-148a in plasma relates to tumor progression and poor outcomes in gastric cancer. *Am J Cancer Res* 2021; **11**: 6133-6146 [PMID: 35018247]

28 **Li D**, Zhang Y, Li Y, Wang X, Wang F, Du J, Zhang H, Shi H, Wang Y, Gao Y, Feng Y, Yan J, Xue Y, Yang Y, Zhang J. miR-149 Suppresses the Proliferation and Metastasis of Human Gastric Cancer Cells by Targeting FOXC1. *Biomed Res Int* 2021; **2021**: 1503403 [PMID: 34957298 DOI: 10.1155/2021/1503403]

29 **Chen J**, Cai S, Gu T, Song F, Xue Y, Sun D. MiR-140-3p Impedes Gastric Cancer Progression and Metastasis by Regulating BCL2/BECN1-Mediated Autophagy. *Onco Targets Ther* 2021; **14**: 2879-2892 [PMID: 33953572 DOI: 10.2147/OTT.S299234]

30 **Wen X**, Klionsky DJ. At a glance: A history of autophagy and cancer. *Semin Cancer Biol* 2020; **66**: 3-11 [PMID: 31707087 DOI: 10.1016/j.semcancer.2019.11.005]

31 **Wang M**, Jing J, Li H, Liu J, Yuan Y, Sun L. The expression characteristics and prognostic roles of autophagy-related genes in gastric cancer. *PeerJ* 2021; **9**: e10814 [PMID: 33604190 DOI: 10.7717/peerj.10814]

32 **Wei Y**, Hong D, Zang A, Wang Z, Yang H, Zhang P, Wang Y. miR-183 Enhances Autophagy of GC Cells by Targeted Inhibition of mTOR. *Ann Clin Lab Sci* 2021; **51**: 837-843 [PMID: 34921037]

33 **Su S**, Shi YT, Chu Y, Jiang MZ, Wu N, Xu B, Zhou H, Lin JC, Jin YR, Li XF, Liang J. Sec62 promotes gastric cancer metastasis through mediating UPR-induced autophagy activation. *Cell Mol Life Sci* 2022; **79**: 133 [PMID: 35165763 DOI: 10.1007/s00018-022-04143-2]

34 **Xie Z**, Klionsky DJ. Autophagosome formation: core machinery and adaptations. *Nat Cell Biol* 2007; **9**: 1102-1109 [PMID: 17909521 DOI: 10.1038/ncb1007-1102]

35 **Miyamoto Y**, Mauer AS, Kumar S, Mott JL, Malhi H. Mmu-miR-615-3p regulates lipoapoptosis by inhibiting C/EBP homologous protein.

PLoS One 2014; **9**: e109637 [PMID: 25314137 DOI: 10.1371/journal.pone.0109637]

36 **Lu H**, Hu J, Li J, Lu W, Deng X, Wang X. miR-328-3p overexpression attenuates the malignant proliferation and invasion of liver cancer *via* targeting Endoplasmic Reticulum Metallo Protease 1 to inhibit AKT phosphorylation. *Ann Transl Med* 2020; **8**: 754 [PMID: 32647679 DOI: 10.21037/atm-20-3749]

37 **Pan S**, Ren F, Li L, Liu D, Li Y, Wang A, Li W, Dong Y, Guo W. MiR-328-3p inhibits cell proliferation and metastasis in colorectal cancer by targeting Girdin and inhibiting the PI3K/Akt signaling pathway. *Exp Cell Res* 2020; **390**: 111939 [PMID: 32142853 DOI: 10.1016/j.yexcr.2020.111939]

38 **Xu J**, Wen J, Li S, Shen X, You T, Huang Y, Xu C, Zhao Y. Immune-Related Nine-MicroRNA Signature for Predicting the Prognosis of Gastric Cancer. *Front Genet* 2021; **12**: 690598 [PMID: 34290743 DOI: 10.3389/fgene.2021.690598]

39 **Xiao Z**, Zheng YB, Dao WX, Luo JF, Deng WH, Yan RC, Liu JS. MicroRNA-328-3p facilitates the progression of gastric cancer *via* KEAP1/NRF2 axis. *Free Radic Res* 2021; **55**: 720-730 [PMID: 34160338 DOI: 10.1080/10715762.2021.1923705]

40 **Itakura E**, Mizushima N. Characterization of autophagosome formation site by a hierarchical analysis of mammalian Atg proteins. *Autophagy* 2010; **6**: 764-776 [PMID: 20639694 DOI: 10.4161/auto.6.6.12709]

41 **Mizushima N**, Levine B. Autophagy in Human Diseases. *N Engl J Med* 2020; **383**: 1564-1576 [PMID: 33053285 DOI: 10.1056/NEJMra2022774]

42 **LV X**, Hu Z. [Methods for detecting autophagy flow]. *Acta Pharmaceutica Sinica* 2016; **51**: 45-51

43 **Funakoshi T**, Aki T, Unuma K, Uemura K. Lysosome vacuolation disrupts the completion of autophagy during norephedrine exposure in SH-SY5Y human neuroblastoma cells. *Brain Res* 2013; **1490**: 9-22 [PMID: 23123211 DOI: 10.1016/j.brainres.2012.10.056]

44 **Pietrocola F**, Izzo V, Niso-Santano M, Vacchelli E, Galluzzi L, Maiuri MC, Kroemer G. Regulation of autophagy by stress-responsive transcription factors. *Semin Cancer Biol* 2013; **23**: 310-322 [PMID: 23726895 DOI: 10.1016/j.semcancer.2013.05.008]

45 **You L**, Wang Z, Li H, Shou J, Jing Z, Xie J, Sui X, Pan H, Han W. The role of STAT3 in autophagy. *Autophagy* 2015; **11**: 729-739 [PMID: 25951043 DOI: 10.1080/15548627.2015.1017192]

46 **Xu S**, Huang P, Yang J, Du H, Wan H, He Y. Calycosin alleviates cerebral ischemia/reperfusion injury by repressing autophagy *via* STAT3/FOXO3a signaling pathway. *Phytomedicine* 2023; **115**: 154845 [PMID: 37148714 DOI: 10.1016/j.phymed.2023.154845]

47 **Gilardini Montani MS**, Santarelli R, Granato M, Gonnella R, Torrisi MR, Faggioni A, Cirone M. EBV reduces autophagy, intracellular ROS and mitochondria to impair monocyte survival and differentiation. *Autophagy* 2019; **15**: 652-667 [PMID: 30324853 DOI: 10.1080/15548627.2018.1536530]

World Journal of Gastroenterology

Submit a Manuscript: https://www.f6publishing.com

World J Gastroenterol 2023 July 21; 29(27): 4334-4343

DOI: 10.3748/wjg.v29.i27.4334

ISSN 1007-9327 (print) ISSN 2219-2840 (online)

ORIGINAL ARTICLE

Observational Study

Azathioprine monotherapy withdrawal in inflammatory bowel diseases: A retrospective mono-centric study

Martina Crepaldi, Daria Maniero, Alessandro Massano, Margherita Pavanato, Brigida Barberio, Edoardo Vincenzo Savarino, Fabiana Zingone

Specialty type: Gastroenterology and hepatology

Provenance and peer review: Unsolicited article; Externally peer reviewed.

Peer-review model: Single blind

Peer-review report's scientific quality classification

Grade A (Excellent): 0
Grade B (Very good): 0
Grade C (Good): C, C
Grade D (Fair): D
Grade E (Poor): 0

P-Reviewer: Alex G, Australia; Moon W, South Korea; Yu CH, China

Received: March 27, 2023
Peer-review started: March 27, 2023
First decision: May 18, 2023
Revised: June 4, 2023
Accepted: July 3, 2023
Article in press: July 3, 2023
Published online: July 21, 2023

Martina Crepaldi, Daria Maniero, Alessandro Massano, Margherita Pavanato, Brigida Barberio, Edoardo Vincenzo Savarino, Fabiana Zingone, Department of Surgery, Oncology, and Gastroenterology, University of Padua, Padua 35128, Italy

Corresponding author: Fabiana Zingone, MD, PhD, Assistant Professor, Doctor, Department of Surgery, Oncology, and Gastroenterology, University of Padua, Via Giustiniani 2, Padua 35128, Italy. fabiana.zingone@unipd.it

Abstract

BACKGROUND

There is no consensus on the recommended duration of and optimal time to stop azathioprine (AZA) therapy in inflammatory bowel disease (IBD). Determining the optimal duration and cessation time can help to balance the risks of long-term intake with the possibility of relapse after cessation.

AIM

To describe the events following AZA cessation.

METHODS

Retrospective analysis was performed to examine data from adult patients affected by IBD who were followed at the University of Padua and had started but then discontinued AZA between 1995 and 2022. Data on therapy duration, reasons for cessation, and type of relapse after cessation were collected. Cox regression models were used to estimate the risk of relapse in different sub-groups.

RESULTS

A total of 133 ulcerative colitis patients and 141 Crohn's disease patients were included. Therapy with AZA was stopped in the 1st year in approximately 34% of patients but was continued for more than 10 years in approximately 10% of cases. AZA discontinuation was due to primary failure or disease relapse in 30% of patients and due to disease remission in 25.2% of patients. Most of the remaining cases stopped AZA therapy due to side effects (primarily clinical intolerance, cytopenia, and pancreatic disease). Patients who stopped AZA for clinical remission had an 83% lower risk of relapse during the observation time than other groups, with a relapse-free rate of 89% after 1 year and 79% after 2 years.

CONCLUSION
AZA administration is effective and safe, but it requires careful monitoring for potential minor and major side effects. Only 10% of patients who achieved remission with AZA needed a new treatment within 1 year of drug interruption.

Key Words: Azathioprine; Inflammatory bowel diseases; Ulcerative Colitis; Crohn's Disease; Relapse; Side effects

©The Author(s) 2023. Published by Baishideng Publishing Group Inc. All rights reserved.

Core Tip: Prolonged use of azathioprine (AZA) remains controversial, and the time of interruption is uncertain. This retrospective study analyzed our single-center data of patients affected by inflammatory bowel disease who had started and then discontinued AZA between 1995 and 2022. AZA administration was effective and safe, and only 10% of patients who achieved remission with AZA needed a new treatment within 1 year of drug interruption.

Citation: Crepaldi M, Maniero D, Massano A, Pavanato M, Barberio B, Savarino EV, Zingone F. Azathioprine monotherapy withdrawal in inflammatory bowel diseases: A retrospective mono-centric study. *World J Gastroenterol* 2023; 29(27): 4334-4343
URL: https://www.wjgnet.com/1007-9327/full/v29/i27/4334.htm
DOI: https://dx.doi.org/10.3748/wjg.v29.i27.4334

INTRODUCTION

The immunosuppressant drug azathioprine (AZA) has been used in the treatment of inflammatory bowel diseases (IBDs) since the 1950s, and it represented one of the main treatments for these disorders until the introduction of biological drugs[1]. AZA is primarily effective as a steroid-sparing therapy for obtaining steroid-free long-term remission in Crohn's disease (CD) and ulcerative colitis (UC), but its delayed onset of action precludes its use in the induction phase[2-6]. AZA indications are well defined, but controversy exists regarding the risk-benefit ratio associated with AZA suspension[5,6]. The risk of relapse after withdrawal of AZA in patients with CD and UC who reached sustained remission was lower than 50% at 5 years[7]. Other studies found that sustained remission with AZA was associated with a 1-year moderate-to-severe relapse rate of approximately 23% to 41%[8-10]. Hawthorne and co-workers showed that patients who achieved disease remission with AZA experienced a doubling of the relapse rate after AZA withdrawal[11]. Mantzaris[1] suggested that drug withdrawal should be better considered after at least 4 years of "depth" of remission (clinical, serological, endoscopic and histological for UC), and close monitoring using biological markers of inflammation after AZA withdrawal was essential[1]. In contrast, Vilien *et al*[10] observed that patients with CD who were in remission after more than 2 years of continuous AZA treatment benefit from further continued treatment[10].

The occurrence of adverse effects plays a crucial role in the decision to discontinue AZA treatment. These effects are classified as "dose-dependent" (*e.g.*, myelotoxicity, hepatitis, opportunistic infections and cancer) and "dose-independent", which includes allergic reactions, such as rash or fever. There are also idiosyncratic reactions, such as pancreatitis, that are frequently associated with AZA use[12]. The prevalence of these adverse effects among patients ranges from 6% to 30% [13]. The most critical and potentially life-threatening adverse event of AZA is myelosuppression, which occurs more frequently during the 1st months and commonly manifests as leukopenia. The overall incidence rate of myelotoxicity in IBD patients receiving AZA is approximately 3% per patient and year of treatment, while severe myelotoxicity occurs in fewer than 1% of patients, and the risk of mortality during the year of treatment is lower than 0.1%[14]. The side effects of hepatotoxicity are related to the TPMT genotype, which was reported in approximately 5% of patients with AZA/mercaptopurine therapy[15]. Discontinuation of AZA is considered when severe cholestatic jaundice develops but also with a persistent increase in liver function values despite a 50% reduction in drug dose[16]. Pancreatitis is a much less frequent adverse effect of AZA than hepatotoxicity, and it occurs within the 1st month of AZA treatment. Acute pancreatitis (AP) is diagnosed when two of three findings appear, including abdominal pain suggestive of pancreatitis, serum amylase and/or lipase levels at least three times the average level, and characteristic findings on imaging[15]. AZA treatment is associated with an increased risk of developing several types of cancer, including non-melanoma skin cancers, urinary tract cancers, and hematological malignancies, such as non-Hodgkin's lymphoma, hepatosplenic T-cell lymphoma or gastrointestinal lymphomas. The risk of hematological neoplasia correlates with the duration of AZA treatment, and it is higher in patients with leukopenia that lasts longer than 20 d[17]. Therefore, the duration of AZA therapy should balance the risks associated with long-term intake with the risks of relapse upon withdrawal/suspension.

The primary aim of our study was to examine the events following AZA suspension. Moreover, we also described reasons for cessation and side effects of AZA treatment.

MATERIALS AND METHODS

We performed a longitudinal observational retrospective study on IBD patients included in the registry "The Paduan Gastrointestinal Disease Natural History Registry": A longitudinal, retrospective and prospective study" (CESC code: 5370/AO/22), which was approved by the Ethical Committees of the Padova University Hospital. The registry collected data on the diagnosis and follow-up of IBD patients followed at our center. We selected IBD patients aged ≥ 18 years who started and then discontinued AZA monotherapy between January 1995 and January 2022. The exclusion criteria were a combination therapy of AZA and biological drugs in naïve patients, the continuation of AZA therapy, the presence of a pouch after colectomy for CU, indeterminate IBD and refusal to sign the informed consent for inclusion in the registry.

Data collection

All data were retrieved manually from the registry and collected in a specific database. The following information was considered: Type of disease, date of diagnosis, location and phenotype of diseases, familiarity with IBD, and comorbidities. The following data on AZA therapy were included: The reason for initiation of AZA therapy, duration (in months) of AZA therapy, dose of the drug and any changes during its administration, concomitant therapies with systemic or topical corticosteroids and/or oral or topical mesalazine, reason for discontinuation of AZA and any disease relapse events after AZA discontinuation. Disease relapse was considered when one of the following events after AZA suspension occurred: Disease-related hospitalizations and/or surgeries, initiation of biological drugs or resumption of AZA therapy.

Patient follow-up

All patients were assessed every 6 mo in our outpatients' clinic or earlier when needed using clinical and laboratory parameters.

Clinical activity was evaluated using the Harvey Bradshaw index for CD patients and the partial Mayo score for UC patients[18,19]. C-reactive protein (CRP) levels (positive when > 0.5 mg/dL) and fecal calprotectin values were also evaluated at each follow-up examination. Endoscopy was performed according to current guidelines[5,6]. The endoscopic activity was evaluated using the Simple Endoscopic Score or Rutgeers score for CD patients and the Mayo endoscopic score for UC patients[20-22].

Statistical analysis

The results are summarized as frequencies and percentages (categorical variables) and means with SD (continuous variables). Categorical variables were compared using the χ^2 test, and continuous variables were compared using Student's *t* test. The time of observation after AZA interruption was calculated using the date of AZA discontinuation as the start date. In contrast, the study end date was considered the earliest date of surgery, date of hospitalization, date of initiation of a new therapy (biologic therapy or AZA), or date of the last follow-up (January 31, 2022).

We calculated overall rates of disease relapse per 10 person-years. We used a Cox regression model to estimate the hazard ratios (HRs) of disease relapse in patients according to AZA suspicion. All HRs were adjusted for sex, age, and type of disease. A *P* value < 0.05 was considered statistically significant for all statistical tests. Data were analyzed using STATA11 software (Stata Corp., College Station, TX, United States).

RESULTS

Study population/ patient characteristics

The initial data collection identified 2006 IBD patients included in our registry. A total of 366 of these patients had started AZA as monotherapy during the study period, and 274 (133 UC and 141 CD) patients were ultimately included based on our inclusion and exclusion criteria. Of the included patients, 57% were male. The average age at diagnosis for CD patients was 33.2 ± 14.2 years and 28.8 ± 14.4 years for UC patients, with a statistically significant difference between the two diseases ($P = 0.01$). Table 1 summarizes the main demographic and clinical characteristics of our patients at the time of enrollment. The main reason for AZA prescription was the maintenance of remission in steroid-dependent patients (> 90% in both diseases). No patient had a history of neoplasia before AZA administration.

AZA therapy: From introduction to suspension

We evaluated the temporal trend of starting AZA in UC and CD patients as monotherapy during the study period. Figure 1 shows a peak in use in 2011-2015. AZA was started in 45.9% (61/133) of UC patients and 41.8% (59/141) of CD patients included in the study (Figure 1). Considering the time between the IBD diagnosis and the introduction of AZA therapy, 26.9% of CD patients started treatment with AZA within the 1st year of diagnosis, 29.8% within the 5th year, and 43.3% after the 5th year. In contrast, 12.8% of UC patients took AZA within the 1st year, 46.6% within 5 years, and 40.6% after the 5th year ($P = 0.002$).

We found a different age distribution for the introduction of AZA ($P = 0.001$). A higher percentage of CD (20.6%) patients started taking AZA before age 18 compared to UC (4.5%) patients. Conversely, a higher percentage of UC patients (44.4%) started AZA in the age group 19-40 years compared to CD patients (32.6%) (Figure 2).

At the introduction of AZA therapy, 13 of the patients with UC (9.6%) and 17 with CD (11.6%) had never received corticosteroid therapy, and 98.5% of patients with UC and 100% of patients with CD were naïve to biologic drugs.

Table 1 Demographic and clinical characteristics of the studied population stratified according to disease type

Characteristic	Crohn's disease	Ulcerative colitis	*P* value
Included patients	141	133	
Sex, % males	54.6%	59.4%	0.42
Mean age at IBD diagnosis in yr	33.2 ± 14.2	28.8 ± 14.4	0.01
Disease location			
Upper GI-L4	5.7%		
Small bowel-L1	17.8%		
Ileum + colon-L3	61%		
Pancolitis-L2	15.6%	61%	
Left-sided colitis		37.5%	
Proctosigmoiditis		1.5%	
Perianal	7.8%		
Phenotype			
Inflammatory	56.7%		
Stenosing	24.8%		
Fistulizing	7.8%		
Fistulizing + Stenosing	5.7%		
Inflammatory + Fistulizing	2.2%		
Inflammatory + Stenosing	2.8%		
Reasons for AZA introduction			0.23
Steroid-dependent	95.8%	90.2%	
Steroid-refractory	2.1%	5.3%	
Steroid intolerance	0.7%	3%	
Other reasons	1.4%	1.5%	
Comorbidities			
PSC	0%	2.3%	0.07
Autoimmune rheumatic diseases	7.8%	3.0%	0.08
Cardiac involvement	4.3%	7.5%	0.25

AZA: Azathioprine; IBD: Inflammatory bowel disease; PSC: Primary sclerosing cholangitis.

The duration of AZA therapy was less than 1 mo for 2 patients with UC (1.5%) and 7 patients with CD (5%) due to intolerance, and it was discontinued within 1 year in 43 patients with UC (32.3%) and 47 patients with CD (33.3%). AZA treatment was continued for 1 year to 5 years in 28.6% of UC patients and 31.9% of CD patients and continued for 5-10 years in 35 patients with UC (26.3%) and 27 patients with CD (19.1%). Therapy was administered for longer than 10 years in 15 patients with UC (11.3%) and 15 patients with CD (10.7%) (P = 0.266). Of the 274 patients undergoing treatment with AZA, 96.4% received combined therapy with oral 5-ASA. None of these patients received chronic steroid therapy.

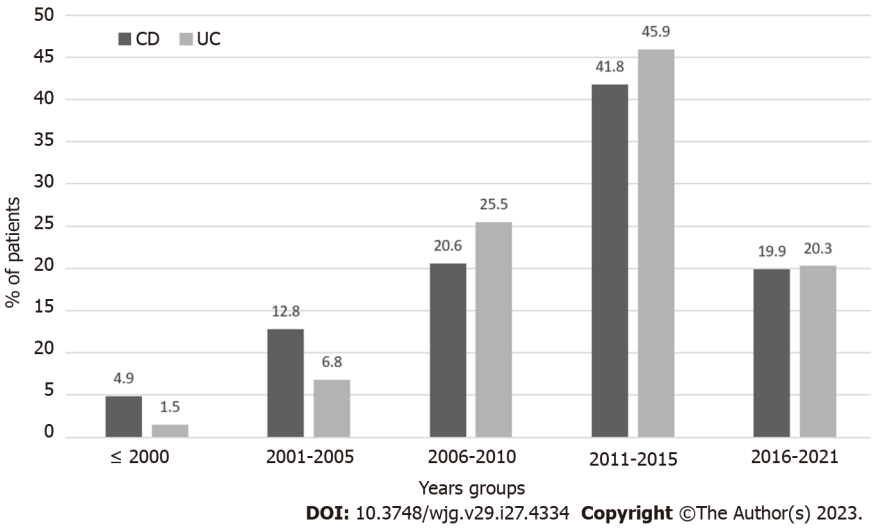
Side effects and reasons for discontinuation of AZA treatment

Overall, the onset of recurrent infections was observed in 13 patients: 6 patients experienced cytomegalovirus infections; 2 patients experienced varicella-zoster virus; 1 patient contracted herpes simplex; 1 patient had candida; and 1 patient had Staphylococcus. For 2 patients, the infections had an unknown etiology. Eleven of these 13 infections (84.6%) occurred in the 1st 5 years of treatment. Two AZA-treated patients developed cancers and discontinued the treatment within 12 mo. The first cessation was due to the onset of melanoma, and the second discontinuation was due to anal squamous cell carcinoma. Another patient developed basal cell carcinoma after 108 mo of AZA therapy, which was then discontinued. The reasons for the cessation of AZA therapy are summarized in Table 2. Forty-four patients (16.1%) discontinued therapy due to inefficacy, thirty-seven patients (13.5%) discontinued therapy due to disease relapse, sixty-nine patients (25.2%) discontinued therapy due to disease remission [average time of sustained remission: 5 years and 4 mo (SD: 3.2)], and 41% discontinued therapy due to side effects.

Table 2 Reasons for discontinuation of azathioprine treatment

Reason for discontinuation	Patients, *n*	% of 274 total
Inefficacy	44	16.1
Relapse	37	13.5
Remission	69	25.2
Pancreatitis or isolated raised in amylase/lipase or ALT > 2×ULN	48	17.5
Leukopenia	23	8.4
Infections	13	4.5
Unspecified intolerance	9	3.3
Nausea/vomiting	15	5.5
Neoplasia	3	1.1
Asthenia	2	0.7
Pregnancy desire	4	1.4
Surgery not associated with IBD	2	0.7
Unspecific patient voluntary	5	2.1

IBD: Inflammatory bowel disease.



DOI: 10.3748/wjg.v29.i27.4334 **Copyright** ©The Author(s) 2023.

Figure 1 Temporal trend of ulcerative colitis and Crohn's disease patients who started azathioprine therapy. CD: Crohn's disease; UC: Ulcerative colitis.

Side effects and reasons for discontinuation of AZA treatmentThe incidence rate of disease relapse after AZA suspension

The median follow-up duration after cessation of AZA treatment was 3.5 ± 4 years. The incidence rate of disease relapse was 1.43 per 10 person-years, with no differences between sex or type of disease (Supplementary Table 1). Patients older than 35 years had a lower rate of disease relapse after AZA discontinuation than younger patients (Table 3). The highest rate of disease relapse occurred in patients who were active at the time of AZA suspension (due to inefficacy or relapse), with a rate of 7 per 10 person-years. Otherwise, patients who stopped AZA for clinical remission had an 83% lower risk of relapse during the observation time than active patients (HR: 0.17, confidence interval: 0.01-0.03). This lower risk was also confirmed after adjustment for age. Figure 3 shows a survival of 89% after 1 year and 79% at 2 years in remission patients.

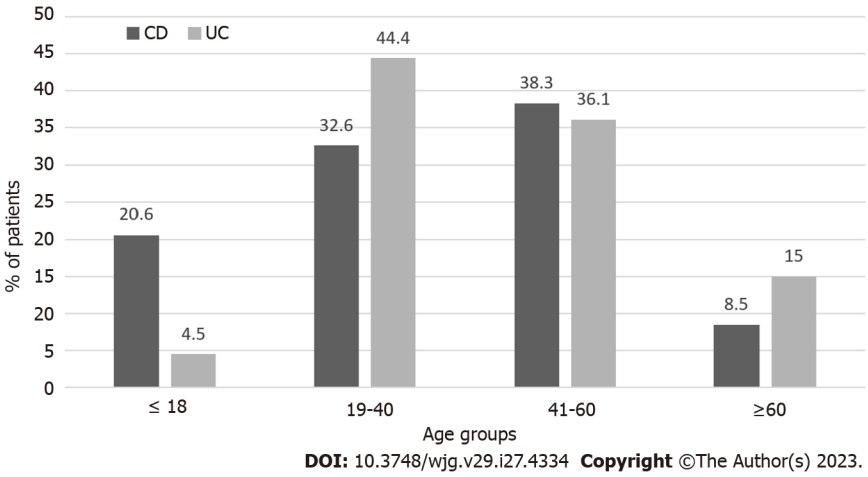
DISCUSSION

IBD is an inflammatory disease of the gastrointestinal tract with a chronic intermittent course. Although biologic and

Table 3 Incidence rates and unadjusted and adjusted hazard ratios of disease relapse in the overall population and different subgroups

Group or subgroup	Events	Rate per 10 person-yr (95%CI)	HR (95%CI)	Adjusted HR (95%CI)
Entire population	141	1.4 (1.2-1.7)		
UC	64	1.4 (1.1-1.7)	1	
CD	77	1.5 (1.2-1.8)	1.16 (0.8-1.6)	
Males	85	1.7 (1.4-2.1)	1	
Females	56	1.2 (0.9-1.5)	0.76 (0.5-1.1)	
Age ≤ 35 yr	62	1.9 (1.4-2.4)	1	
Age > 35 yr	79	1.2 (0.9-1.5)	0.69 (0.5-0.9)	
Active patients	66	7.0 (5.5-8.9)	1	1
Patients in remission	21	0.7 (0.4-1.0)	0.17 (0.1-0.3)	0.17 (0.1-0.3)
Other groups	54	0.9 (0.7-1.2)	0.25 (0.2-0.4)	0.26 (0.1-0.4)

CD: Crohn's disease; CI: Confidence interval; HR: Hazard ratios; UC: Ulcerative colitis.



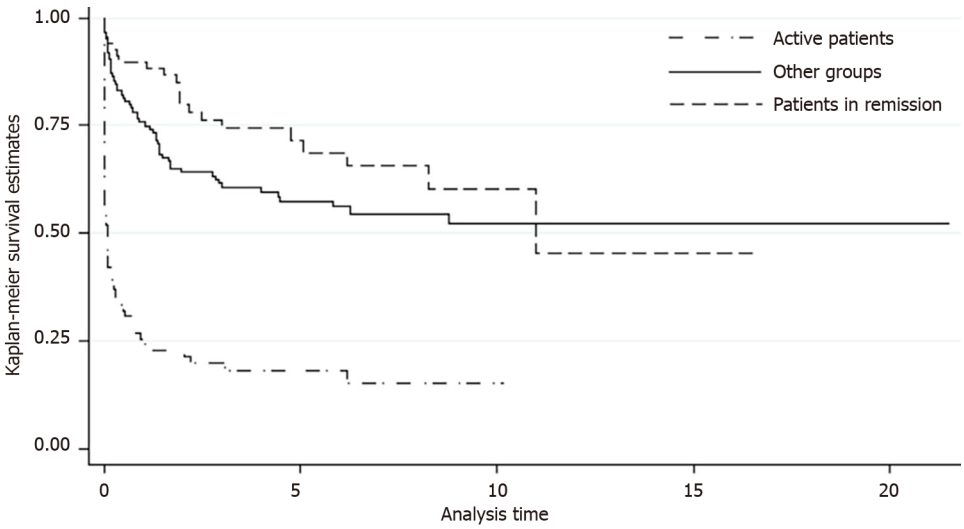
DOI: 10.3748/wjg.v29.i27.4334 **Copyright** ©The Author(s) 2023.

Figure 2 Age distribution at the introduction of azathioprine therapy. CD: Crohn's disease; UC: Ulcerative colitis.

small molecule therapies have become treatment mainstays, AZA remains an immunomodulating agent that is used to sustain corticosteroid-free remission or in cases of corticosteroid dependence/resistance. There is no consensus on the recommended duration, optimal dose, or cessation of AZA therapy[23]. The present study investigated events following AZA cessation.

The disease characteristics of our patients, including location and disease behavior, are consistent with published data regarding the efficacy and safety of AZA therapy in IBD[24-26]. However, we found a higher percentage of CD patients who started AZA before 18 years of age than UC patients. This significant difference may be explained by the earlier onset of CD and the different therapeutic management of pediatric UC and CD based on ECCO/ESPGHAN guidelines [25,27,28]. The frequency of initiating AZA therapy within 1 year after diagnosis was significantly higher in CD patients, which confirmed the different modes of treatment approach in the two diseases[5,6,29]. AZA was prescribed primarily between 2011 and 2015 (Figure 1). After this period, AZA prescriptions decreased with the parallel introduction of new biologics on the market, which suggests that the role of AZA in the management of IBD patients was progressively replaced by new, more potent and safer drugs, such as anti-tumor necrosis factor-α, vedolizumab or ustekinumab[5,9].

Regarding the optimal time for drug interruption, Holtmann *et al*[30] assessed the flare incidences and steroid doses before, during treatment and after discontinuation of AZA. They concluded that AZA continuation beyond 4 years seemed beneficial, but its discontinuation may be considered after 3-4 years in CD patients in complete remission without steroid requirement[30]. Our study showed the safety of drug continuation in half of our patients. A total of 28.6% of UC patients and 31.9% of CD patients continued AZA treatment beyond the 5th year, and 26.3% of UC patients and 19.1% of CD patients continued AZA treatment beyond the 10th year, with no difference between the two diseases. We reported 2 patients who developed cancer (melanoma and anal squamous cell carcinoma) and discontinued the treatment within 12 mo, and we reported 1 patient with basal cell carcinoma after 108 mo of AZA therapy. However, 85% of the infections required drug suspicion in the 1st 5 years of treatment.



DOI: 10.3748/wjg.v29.i27.4334 **Copyright** ©The Author(s) 2023.

Figure 3 Cox regression analysis assessing the risk of relapse in patients who discontinued azathioprine according to the reasons for suspicion.

The most common adverse events that led to AZA suspension were pancreatic and hepatic disorders, including AP, isolated raised in serum lipase and amylase or in liver enzymes, which were detected in 17.5% of patients[31]. This percentage is higher than large retrospective and prospective treatment trials, such as the SONIC trial[32]. However, only AP was considered in this study. We reported leukopenia as the second most frequent adverse effect (8.4%), which is consistent with the literature. Myelosuppression most commonly manifests as leukopenia, and the frequency in the literature varies from 2.2% to 15% of patients. The risk of recurrent infections (4.5%) was lower than the literature (7.4%-14.1%)[15]. Connell *et al*[33] did not observe an increased risk of cancer over the expected risk in a population of 755 patients treated with AZA for 30 years[33]. However, different studies showed the carcinogenic potential of AZA, particularly for the development of lymphoma, urinary tract cancer and skin cancer[34,35]. We did not report any case of tuberculosis, but AZA has recently been shown to be associated with this disease[36].

A recent Italian multicenter observational retrospective study investigated the relapse risk after withdrawal of AZA in UC and found that it occurred in one-third of patients beyond the 1st year after AZA withdrawal and in half of patients after 2 years of withdrawal. A higher risk of relapse disease was identified in patients with extensive colitis, those with a lack of sustained remission during AZA, and those with discontinuation due to toxicity[37]. A multicenter retrospective cohort study on 237 patients with sustained clinical remission (≥ 3 years) described moderate/severe relapse in 23% of CD patients and 12% of UC patients at 12 mo and 39% of CD patients and 26% of UC patients at 24 mo. Elevated CRP at withdrawal was associated with higher relapse rates at 12 mo for CD patients, and an elevated white cell count was predictive at 12 mo for UC patients[8]. A 2018 systematic review[38] described four randomized controlled trials with a total of 215 participants providing data on the rate of clinical relapse following the discontinuation of AZA monotherapy in CD patients[9,10,39,40]. The follow-up period was 12 mo for two studies[9,10], 18 mo for one study[39] and 24 mo for one study[40]. A total of 32.4% (36/111) of participants assigned to AZA withdrawal experienced clinical relapse compared to 13.5% (14/104) of patients assigned to therapeutic continuation. Our study revealed a lower rate of disease relapse than these previous studies and reported a risk of 10% at 1-year follow-up among the 69 patients who had interrupted AZA due to remission. In this subgroup, the suspicion occurred after an average time of 5 years and 4 mo (SD: 3.2) of sustained remission, and there were no differences between sex or type of diseases. In line with the recommendations provided by Holtmann *et al*[30], we suggest discontinuation of AZA after 5 years of complete remission[30].

The main strengths of our study were the inclusion of a homogeneous population followed at the same tertiary center and the very low relapse rate in the cohort. The main limitation was the small size. Moreover, our data were collected retrospectively, which is associated with the risks of missing data and recall bias. Future prospective research could examine outcomes after the withdrawal of AZA and after the long-term remission of IBD.

CONCLUSION

Our study confirmed the decreasing use of AZA in recent years due to the introduction of biological drugs and the risk of related adverse events. The present study found that the highest rate of disease relapse was observed among patients who were active at the time of AZA cessation (due to inefficacy or relapse) and patients younger than 35 years of age. Only 10% of patients who achieved a sustained remission with AZA needed a new treatment within 1 year of drug interruption.

ARTICLE HIGHLIGHTS

Research background

Before the advent of biological drugs, azathioprine (AZA) was used worldwide to treat inflammatory bowel disease (IBD) patients and is still used. It is recognized that this immunomodulating agent could induce and sustain steroid-free long-term remission. However, clinicians cannot ignore the possible adverse effects of long-term AZA treatment and the risk of relapses after its discontinuation. In this retrospective study, we want to share the experience of our tertiary center with IBD patients treated with AZA.

Research motivation

Determining the optimal duration and cessation time helps balance the risks of long-term intake with the possibility of relapse after cessation.

Research objectives

In this study, we analyzed IBD patients who started and discontinued AZA. We have focused on patients' demographic and clinical characteristics, reasons for cessation, side effects, and disease incidence rate after AZA withdrawal.

Research methods

We conducted a retrospective study, including IBD patients older than 18 who had started AZA between 1995 and 2022 and then discontinued for any reason and were followed at our IBD clinic. For categorical variables, we have used the χ^2 test and Student's t-test for continuous variables. We have estimated disease relapse hazard ratios using the Cox regression model.

Research results

AZA discontinuation was due to primary failure or disease relapse in 30% of patients and due to disease remission in 25.2% of patients. We found that patients who discontinued AZA after a sustained remission of an average time of 5 years and 4 mo had a low risk of relapse (10%) in 1 year.

Research conclusions

This study addresses an unanswered question: "When is it possible to discontinue AZA? How long should we wait before AZA cessation?". Our study proves that AZA could be safely discontinued after 5 years of sustained remission because we have observed a lower relapse rate at 1-year follow-up. The main limitation of the study was the small size of patients.

Research perspectives

For advanced evidence, future prospective research should be conducted to evaluate the long-term natural history of IBD after withdrawal of AZA.

FOOTNOTES

Author contributions: Zingone F conceived and designed the study and analyzed the findings; Crepaldi M and Maniero D collected data and wrote the manuscript; Massano A, Pavanato M, Barberio B, and Savarino EV collected data; All authors revised and approved the final version.

Institutional review board statement: The Ethical Committees of the Padova University Hospital reviewed and approved this study.

Informed consent statement: All study participants, or their legal guardian, provided informed written consent prior to study enrollment.

Conflict-of-interest statement: All the authors report no relevant conflicts of interest for this article.

Data sharing statement: Data, analytical methods, and study materials are available to other researchers upon specific request.

STROBE statement: The authors have read the STROBE Statement—checklist of items, and the manuscript was prepared and revised according to the STROBE Statement—checklist of items.

Open-Access: This article is an open-access article that was selected by an in-house editor and fully peer-reviewed by external reviewers. It is distributed in accordance with the Creative Commons Attribution NonCommercial (CC BY-NC 4.0) license, which permits others to distribute, remix, adapt, build upon this work non-commercially, and license their derivative works on different terms, provided the original work is properly cited and the use is non-commercial. See: https://creativecommons.org/Licenses/by-nc/4.0/

Country/Territory of origin: Italy

ORCID number: Martina Crepaldi 0009-0008-8388-9699; Daria Maniero 0000-0003-2468-7292; Alessandro Massano 0000-0002-9064-3434;

Margherita Pavanato 0009-0009-9450-6582; Brigida Barberio 0000-0002-3164-8243; Edoardo Vincenzo Savarino 0000-0002-3187-2894; Fabiana Zingone 0000-0003-1133-1502.

S-Editor: Fan JR
L-Editor: Filipodia
P-Editor: Yu HG

REFERENCES

1 **Mantzaris GJ**. Thiopurines and Methotrexate Use in IBD Patients in a Biologic Era. *Curr Treat Options Gastroenterol* 2017; **15**: 84-104 [PMID: 28160250 DOI: 10.1007/s11938-017-0128-0]
2 **Sandborn W**, Sutherland L, Pearson D, May G, Modigliani R, Prantera C. Azathioprine or 6-mercaptopurine for inducing remission of Crohn's disease. *Cochrane Database Syst Rev* 2000; CD000545 [PMID: 10796557 DOI: 10.1002/14651858.CD000545]
3 **Pearson DC**, May GR, Fick G, Sutherland LR. Azathioprine for maintaining remission of Crohn's disease. *Cochrane Database Syst Rev* 2000; CD000067 [PMID: 10796482 DOI: 10.1002/14651858.CD000067]
4 **Timmer A**, Patton PH, Chande N, McDonald JW, MacDonald JK. Azathioprine and 6-mercaptopurine for maintenance of remission in ulcerative colitis. *Cochrane Database Syst Rev* 2016; **2016**: CD000478 [PMID: 27192092 DOI: 10.1002/14651858.CD000478.pub4]
5 **Torres J**, Bonovas S, Doherty G, Kucharzik T, Gisbert JP, Raine T, Adamina M, Armuzzi A, Bachmann O, Bager P, Biancone L, Bokemeyer B, Bossuyt P, Burisch J, Collins P, El-Hussuna A, Ellul P, Frei-Lanter C, Furfaro F, Gingert C, Gionchetti P, Gomollon F, González-Lorenzo M, Gordon H, Hlavaty T, Juillerat P, Katsanos K, Kopylov U, Krustins E, Lytras T, Maaser C, Magro F, Marshall JK, Myrelid P, Pellino G, Rosa I, Sabino J, Savarino E, Spinelli A, Stassen L, Uzzan M, Vavricka S, Verstockt B, Warusavitarne J, Zmora O, Fiorino G. ECCO Guidelines on Therapeutics in Crohn's Disease: Medical Treatment. *J Crohns Colitis* 2020; **14**: 4-22 [PMID: 31711158 DOI: 10.1093/ecco-jcc/jjz180]
6 **Raine T**, Bonovas S, Burisch J, Kucharzik T, Adamina M, Annese V, Bachmann O, Bettenworth D, Chaparro M, Czuber-Dochan W, Eder P, Ellul P, Fidalgo C, Fiorino G, Gionchetti P, Gisbert JP, Gordon H, Hedin C, Holubar S, Iacucci M, Karmiris K, Katsanos K, Kopylov U, Lakatos PL, Lytras T, Lyutakov I, Noor N, Pellino G, Piovani D, Savarino E, Selvaggi F, Verstockt B, Spinelli A, Panis Y, Doherty G. ECCO Guidelines on Therapeutics in Ulcerative Colitis: Medical Treatment. *J Crohns Colitis* 2022; **16**: 2-17 [PMID: 34635919 DOI: 10.1093/ecco-jcc/jjab178]
7 **Iborra M**, Herreras J, Boscá-Watts MM, Cortés X, Trejo G, Cerrillo E, Hervás D, Mínguez M, Beltrán B, Nos P. Withdrawal of Azathioprine in Inflammatory Bowel Disease Patients Who Sustain Remission: New Risk Factors for Relapse. *Dig Dis Sci* 2019; **64**: 1612-1621 [PMID: 30604371 DOI: 10.1007/s10620-018-5429-1]
8 **Kennedy NA**, Kalla R, Warner B, Gambles CJ, Musy R, Reynolds S, Dattani R, Nayee H, Felwick R, Harris R, Marriott S, Senanayake SM, Lamb CA, Al-Hilou H, Gaya DR, Irving PM, Mansfield J, Parkes M, Ahmad T, Cummings JR, Arnott ID, Satsangi J, Lobo AJ, Smith M, Lindsay JO, Lees CW. Thiopurine withdrawal during sustained clinical remission in inflammatory bowel disease: relapse and recapture rates, with predictive factors in 237 patients. *Aliment Pharmacol Ther* 2014; **40**: 1313-1323 [PMID: 25284134 DOI: 10.1111/apt.12980]
9 **O'Donoghue DP**, Dawson AM, Powell-Tuck J, Bown RL, Lennard-Jones JE. Double-blind withdrawal trial of azathioprine as maintenance treatment for Crohn's disease. *Lancet* 1978; **2**: 955-957 [PMID: 81986 DOI: 10.1016/s0140-6736(78)92524-2]
10 **Vilien M**, Dahlerup JF, Munck LK, Nørregaard P, Grønbaek K, Fallingborg J. Randomized controlled azathioprine withdrawal after more than two years treatment in Crohn's disease: increased relapse rate the following year. *Aliment Pharmacol Ther* 2004; **19**: 1147-1152 [PMID: 15153167 DOI: 10.1111/j.1365-2036.2004.01944.x]
11 **Hawthorne AB**, Logan RF, Hawkey CJ, Foster PN, Axon AT, Swarbrick ET, Scott BB, Lennard-Jones JE. Randomised controlled trial of azathioprine withdrawal in ulcerative colitis. *BMJ* 1992; **305**: 20-22 [PMID: 1638191 DOI: 10.1136/bmj.305.6844.20]
12 **Triantafillidis JK**, Merikas E, Georgopoulos F. Current and emerging drugs for the treatment of inflammatory bowel disease. *Drug Des Devel Ther* 2011; **5**: 185-210 [PMID: 21552489 DOI: 10.2147/DDDT.S11290]
13 **Avallone EV**, Pica R, Cassieri C, Zippi M, Paoluzi P, Vernia P. Azathioprine treatment in inflammatory bowel disease patients: type and time of onset of side effects. *Eur Rev Med Pharmacol Sci* 2014; **18**: 165-170 [PMID: 24488903]
14 **Gisbert JP**, Gomollón F. Thiopurine-induced myelotoxicity in patients with inflammatory bowel disease: a review. *Am J Gastroenterol* 2008; **103**: 1783-1800 [PMID: 18557712 DOI: 10.1111/j.1572-0241.2008.01848.x]
15 **Teml A**, Schaeffeler E, Herrlinger KR, Klotz U, Schwab M. Thiopurine treatment in inflammatory bowel disease: clinical pharmacology and implication of pharmacogenetically guided dosing. *Clin Pharmacokinet* 2007; **46**: 187-208 [PMID: 17328579 DOI: 10.2165/00003088-200746030-00001]
16 **Khokhar OS**, Lewis JH. Hepatotoxicity of agents used in the management of inflammatory bowel disease. *Dig Dis* 2010; **28**: 508-518 [PMID: 20926880 DOI: 10.1159/000320410]
17 **Long MD**, Herfarth HH, Pipkin CA, Porter CQ, Sandler RS, Kappelman MD. Increased risk for non-melanoma skin cancer in patients with inflammatory bowel disease. *Clin Gastroenterol Hepatol* 2010; **8**: 268-274 [PMID: 20005977 DOI: 10.1016/j.cgh.2009.11.024]
18 **Gajendran M**, Loganathan P, Catinella AP, Hashash JG. A comprehensive review and update on Crohn's disease. *Dis Mon* 2018; **64**: 20-57 [PMID: 28826742 DOI: 10.1016/j.disamonth.2017.07.001]
19 **Lewis JD**, Chuai S, Nessel L, Lichtenstein GR, Aberra FN, Ellenberg JH. Use of the noninvasive components of the Mayo score to assess clinical response in ulcerative colitis. *Inflamm Bowel Dis* 2008; **14**: 1660-1666 [PMID: 18623174 DOI: 10.1002/ibd.20520]
20 **Narula N**, Pray C, Wong ECL, Colombel JF, Marshall JK, Daperno M, Reinisch W, Dulai PS. Categorising Endoscopic Severity of Crohn's Disease Using the Modified Multiplier SES-CD [MM-SES-CD]. *J Crohns Colitis* 2022; **16**: 1011-1019 [PMID: 35134140 DOI: 10.1093/ecco-jcc/jjac018]
21 **Sharara AI**, Malaeb M, Lenfant M, Ferrante M. Assessment of Endoscopic Disease Activity in Ulcerative Colitis: Is Simplicity the Ultimate Sophistication? *Inflamm Intest Dis* 2022; **7**: 7-12 [PMID: 35224012 DOI: 10.1159/000518131]
22 **Rivière P**, Vermeire S, Irles-Depe M, Van Assche G, Rutgeerts P, Denost Q, Wolthuis A, D'Hoore A, Laharie D, Ferrante M. Rates of Postoperative Recurrence of Crohn's Disease and Effects of Immunosuppressive and Biologic Therapies. *Clin Gastroenterol Hepatol* 2021; **19**:

713-720.e1 [PMID: 32272248 DOI: 10.1016/j.cgh.2020.03.064]
23 **Dart RJ**, Irving PM. Optimising use of thiopurines in inflammatory bowel disease. *Expert Rev Clin Immunol* 2017; **13**: 877-888 [PMID: 28678626 DOI: 10.1080/1744666X.2017.1351298]
24 **Baumgart DC**, Sandborn WJ. Crohn's disease. *Lancet* 2012; **380**: 1590-1605 [PMID: 22914295 DOI: 10.1016/S0140-6736(12)60026-9]
25 **Loftus EV Jr**. Clinical epidemiology of inflammatory bowel disease: Incidence, prevalence, and environmental influences. *Gastroenterology* 2004; **126**: 1504-1517 [PMID: 15168363 DOI: 10.1053/j.gastro.2004.01.063]
26 **Yu YR**, Rodriguez JR. Clinical presentation of Crohn's, ulcerative colitis, and indeterminate colitis: Symptoms, extraintestinal manifestations, and disease phenotypes. *Semin Pediatr Surg* 2017; **26**: 349-355 [PMID: 29126502 DOI: 10.1053/j.sempedsurg.2017.10.003]
27 **Ruemmele FM**, Veres G, Kolho KL, Griffiths A, Levine A, Escher JC, Amil Dias J, Barabino A, Braegger CP, Bronsky J, Buderus S, Martín-de-Carpi J, De Ridder L, Fagerberg UL, Hugot JP, Kierkus J, Kolacek S, Koletzko S, Lionetti P, Miele E, Navas López VM, Paerregaard A, Russell RK, Serban DE, Shaoul R, Van Rheenen P, Veereman G, Weiss B, Wilson D, Dignass A, Eliakim A, Winter H, Turner D; European Crohn's and Colitis Organisation; European Society of Pediatric Gastroenterology, Hepatology and Nutrition. Consensus guidelines of ECCO/ESPGHAN on the medical management of pediatric Crohn's disease. *J Crohns Colitis* 2014; **8**: 1179-1207 [PMID: 24909831 DOI: 10.1016/j.crohns.2014.04.005]
28 **Turner D**, Ruemmele FM, Orlanski-Meyer E, Griffiths AM, de Carpi JM, Bronsky J, Veres G, Aloi M, Strisciuglio C, Braegger CP, Assa A, Romano C, Hussey S, Stanton M, Pakarinen M, de Ridder L, Katsanos K, Croft N, Navas-López V, Wilson DC, Lawrence S, Russell RK. Management of Paediatric Ulcerative Colitis, Part 1: Ambulatory Care-An Evidence-based Guideline From European Crohn's and Colitis Organization and European Society of Paediatric Gastroenterology, Hepatology and Nutrition. *J Pediatr Gastroenterol Nutr* 2018; **67**: 257-291 [PMID: 30044357 DOI: 10.1097/MPG.0000000000002035]
29 **Dubinsky MC**. Azathioprine, 6-mercaptopurine in inflammatory bowel disease: pharmacology, efficacy, and safety. *Clin Gastroenterol Hepatol* 2004; **2**: 731-743 [PMID: 15354273 DOI: 10.1016/s1542-3565(04)00344-1]
30 **Holtmann MH**, Krummenauer F, Claas C, Kremeyer K, Lorenz D, Rainer O, Vogel I, Böcker U, Böhm S, Büning C, Duchmann R, Gerken G, Herfarth H, Lügering N, Kruis W, Reinshagen M, Schmidt J, Stallmach A, Stein J, Sturm A, Galle PR, Hommes DW, D'Haens G, Rutgeerts P, Neurath MF. Long-term effectiveness of azathioprine in IBD beyond 4 years: a European multicenter study in 1176 patients. *Dig Dis Sci* 2006; **51**: 1516-1524 [PMID: 16927148 DOI: 10.1007/s10620-005-9037-5]
31 **Gordon M**, Grafton-Clarke C, Akobeng A, Macdonald J, Chande N, Hanauer S, Arnott I. Pancreatitis associated with azathioprine and 6-mercaptopurine use in Crohn's disease: a systematic review. *Frontline Gastroenterol* 2021; **12**: 423-436 [PMID: 35401955 DOI: 10.1136/flgastro-2020-101405]
32 **Colombel JF**, Sandborn WJ, Reinisch W, Mantzaris GJ, Kornbluth A, Rachmilewitz D, Lichtiger S, D'Haens G, Diamond RH, Broussard DL, Tang KL, van der Woude CJ, Rutgeerts P; SONIC Study Group. Infliximab, azathioprine, or combination therapy for Crohn's disease. *N Engl J Med* 2010; **362**: 1383-1395 [PMID: 20393175 DOI: 10.1056/NEJMoa0904492]
33 **Connell WR**, Kamm MA, Dickson M, Balkwill AM, Ritchie JK, Lennard-Jones JE. Long-term neoplasia risk after azathioprine treatment in inflammatory bowel disease. *Lancet* 1994; **343**: 1249-1252 [PMID: 7910274 DOI: 10.1016/s0140-6736(94)92150-4]
34 **Armstrong RG**, West J, Card TR. Risk of cancer in inflammatory bowel disease treated with azathioprine: a UK population-based case-control study. *Am J Gastroenterol* 2010; **105**: 1604-1609 [PMID: 20104215 DOI: 10.1038/ajg.2009.745]
35 **Pasternak B**, Svanström H, Schmiegelow K, Jess T, Hviid A. Use of azathioprine and the risk of cancer in inflammatory bowel disease. *Am J Epidemiol* 2013; **177**: 1296-1305 [PMID: 23514635 DOI: 10.1093/aje/kws375]
36 **Fortes FML**, Rocha R, Santana GO. Thiopurines are an independent risk factor for active tuberculosis in inflammatory bowel disease patients. *World J Gastroenterol* 2023; **29**: 1536-1538 [PMID: 36998430 DOI: 10.3748/wjg.v29.i9.1536]
37 **Cassinotti A**, Actis GC, Duca P, Massari A, Colombo E, Gai E, Annese V, D'Albasio G, Manes G, Travis S, Porro GB, Ardizzone S. Maintenance treatment with azathioprine in ulcerative colitis: outcome and predictive factors after drug withdrawal. *Am J Gastroenterol* 2009; **104**: 2760-2767 [PMID: 19623172 DOI: 10.1038/ajg.2009.410]
38 **Boyapati RK**, Torres J, Palmela C, Parker CE, Silverberg OM, Upadhyaya SD, Nguyen TM, Colombel JF. Withdrawal of immunosuppressant or biologic therapy for patients with quiescent Crohn's disease. *Cochrane Database Syst Rev* 2018; **5**: CD012540 [PMID: 29756637 DOI: 10.1002/14651858.CD012540.pub2]
39 **Lémann M**, Mary JY, Colombel JF, Duclos B, Soule JC, Lerebours E, Modigliani R, Bouhnik Y; Groupe D'Etude Thérapeutique des Affections Inflammatoires du Tube Digestif. A randomized, double-blind, controlled withdrawal trial in Crohn's disease patients in long-term remission on azathioprine. *Gastroenterology* 2005; **128**: 1812-1818 [PMID: 15940616 DOI: 10.1053/j.gastro.2005.03.031]
40 **Wenzl HH**, Primas C, Novacek G, Teml A, Öfferlbauer-Ernst A, Högenauer C, Vogelsang H, Petritsch W, Reinisch W. Withdrawal of long-term maintenance treatment with azathioprine tends to increase relapse risk in patients with Crohn's disease. *Dig Dis Sci* 2015; **60**: 1414-1423 [PMID: 25381202 DOI: 10.1007/s10620-014-3419-5]

World Journal of Gastroenterology

Submit a Manuscript: https://www.f6publishing.com

World J Gastroenterol 2023 July 21; 29(27): 4344-4355

DOI: 10.3748/wjg.v29.i27.4344

ISSN 1007-9327 (print) ISSN 2219-2840 (online)

ORIGINAL ARTICLE

Observational Study

Predicting portal venous anomalies by left-sided gallbladder or right-sided ligamentum teres hepatis: A large scale, propensity score-matched study

Hsuan-Yin Lin, Rheun-Chuan Lee, Jyh-Wen Chai, Chiann-Yi Hsu, Yen Chou, Hsuen-En Hwang, Chien An Liu, Nai-Chi Chiu, Ho-Hsian Yen

Specialty type: Gastroenterology and hepatology

Provenance and peer review: Unsolicited article; Externally peer reviewed.

Peer-review model: Single blind

Peer-review report's scientific quality classification

Grade A (Excellent): 0
Grade B (Very good): B, B
Grade C (Good): C, C, C
Grade D (Fair): 0
Grade E (Poor): 0

P-Reviewer: Aseni P, Italy; Gad EH, Egypt; Wu SZ, China

Received: March 29, 2023
Peer-review started: March 29, 2023
First decision: May 23, 2023
Revised: June 6, 2023
Accepted: July 6, 2023
Article in press: July 6, 2023
Published online: July 21, 2023

Hsuan-Yin Lin, Jyh-Wen Chai, Department of Radiology, Taichung Veterans General Hospital, Taichung 407219, Taiwan

Rheun-Chuan Lee, Hsuen-En Hwang, Chien An Liu, Nai-Chi Chiu, Department of Radiology, Taipei Veterans General Hospital, Taipei 11267, Taiwan

Rheun-Chuan Lee, Hsuen-En Hwang, Chien An Liu, Nai-Chi Chiu, School of Medicine, National Yang Ming Chiao Tung University, Taipei 112, Taiwan

Chiann-Yi Hsu, Department of Medical Research, Taichung Veterans General Hospital, Taichung 40705, Taiwan

Yen Chou, Department of Radiology, Fu Jen Catholic University Hospital, Taipei 24352, Taiwan

Ho-Hsian Yen, Department of Radiology, Far Eastern Memorial Hospital, New Taipei City 220, Taiwan

Corresponding author: Hsuan-Yin Lin, MD, Attending Doctor, Department of Radiology, Taichung Veterans General Hospital, No. 1650 Taiwan Boulevard Section 4, Taichung 407219, Taiwan. b101096132@tmu.edu.tw

Abstract

BACKGROUND

Right-sided ligamentum teres (RSLT) is often associated with portal venous anomalies (PVA) and is regarded as a concerning feature for hepatobiliary intervention. Most studies consider RSLT to be one of the causes of left-sided gallbladder (LGB), leading to the hypothesis that LGB must always be present with RSLT. However, some cases have shown that right-sided gallbladder (RGB) can also be present in livers with RSLT.

AIM

To highlight the rare variation that RSLT may not come with LGB and to determine whether ligamentum teres (LT) or gallbladder location is reliable to predict PVA.

METHODS
This study retrospectively assessed 8552 contrast-enhanced abdominal computed tomography examinations from 2018 to 2021 [4483 men, 4069 women; mean age, 59.5 ± 16.2 (SD) years]. We defined the surrogate outcome as major PVAs. The cases were divided into 4 subgroups according to gallbladder and LT locations. On one hand, we analyzed PVA prevalence by LT locations using gallbladder location as a controlled variable (n = 36). On the other hand, we controlled LT location and computed PVA prevalence by gallbladder locations (n = 34). Finally, we investigated LT location as an independent factor of PVA by using propensity score matching (PSM) and inverse probability of treatment weighting (IPTW).

RESULTS
We found 9 cases of RSLT present with RGB. Among the LGB cases, RSLT is associated with significantly higher PVA prevalence than typical LT [80.0% *vs* 18.2%, P = 0.001; OR = 18, 95% confidence interval (CI): 2.92-110.96]. When RSLT is present, we found no statistically significant difference in PVA prevalence for RGB and LGB cases (88.9 % *vs* 80.0%, P > 0.99). Both PSM and IPTW yielded balanced cohorts in demographics and gallbladder locations. The RSLT group had a significantly higher PVA prevalence after adjusted by PSM (77.3% *vs* 4.5%, P < 0.001; OR = 16.27, 95%CI: 2.25-117.53) and IPTW (82.5% *vs* 4.7%, P < 0.001).

CONCLUSION
RSLT doesn't consistently coexist with LGB. RSLT can predict PVA independently while the gallbladder location does not serve as a sufficient predictor.

Key Words: Right-sided ligamentum teres; Left-sided gallbladder; Portal venous anomalies; Inverse probability of treatment weighting; Average treatment effect in the treated

©The Author(s) 2023. Published by Baishideng Publishing Group Inc. All rights reserved.

Core Tip: Right-sided ligamentum teres (RSLT) is often associated with intrahepatic anomalies. Most studies hypothesis that left-sided gallbladder (LGB) must exist with RSLT. However, our exploration reveals that RSLT doesn't consistently coexist with LGB. Our analysis further suggests that RSLT can predict poral venous anomalies (PVAs) independently while the gallbladder location does not serve as a sufficient predictor. Therefore, operators, interventional radiologists or interventional gastroenterologists should not use the gallbladder location as an alternative of ligamentum teres location for PVAs prediction.

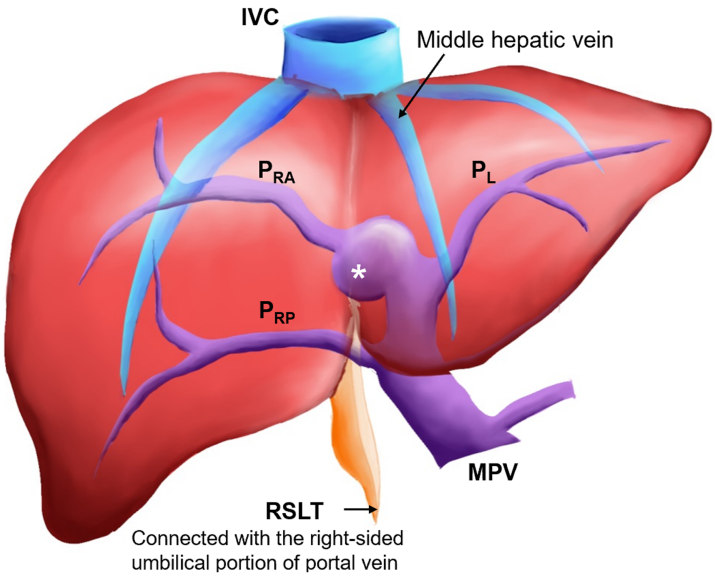
Citation: Lin HY, Lee RC, Chai JW, Hsu CY, Chou Y, Hwang HE, Liu CA, Chiu NC, Yen HH. Predicting portal venous anomalies by left-sided gallbladder or right-sided ligamentum teres hepatis: A large scale, propensity score-matched study. *World J Gastroenterol* 2023; 29(27): 4344-4355
URL: https://www.wjgnet.com/1007-9327/full/v29/i27/4344.htm
DOI: https://dx.doi.org/10.3748/wjg.v29.i27.4344

INTRODUCTION

Right-sided ligamentum teres (RSLT) is a congenital anomaly caused by misconnection of the fetal umbilical vein to the right paramedian trunk of the portal vein (Figure 1). This anomaly was first reported by Matsumoto[1] in 1986. RSLT is associated with several intrahepatic vascular anomalies and anomalous biliary confluences[2-5]. Therefore, unawareness of RSLT before an intervention may result in serious morbidities[6-8]. Specifically, RSLT strongly correlates with portal venous anomalies (PVAs), a high interventional risk morbidity feature.

PVAs result in difficulties in liver surgery and lead to surgical complications[8,9], such as active bleeding, segmental devascularization, and hepatic failure due to misinterpretation and erroneous ligation of the portal venous branch. Therefore, accurately evaluating PVAs is crucial before any major hepatobiliary intervention. In this paper, we share a case of bleeding following an ultrasound-guided liver biopsy and unsuccessful first embolization as a result of PVAs not being identified before the intervention (Supplementary Figure 1). The bleeding was finally stopped through embolization once the PVAs had been recognized.

While RSLT is the key to PVA evaluation, the presence of a left-sided gallbladder (LGB) is a more commonly used anatomical anomaly in PVA screening. This is because: (1) Nagai *et al*[10] suggested that the variant gallbladder location is an outcome of RSLT, which has been accepted in many studies[2,5,11]; and (2) LGB is relatively easy to identify. However, Yamashita *et al*[3] and Lin *et al*[4] reported some cases in which RSLT could present with a GB in the typical right-side location, which conflicted with Nagai *et al*'s hypothesis[10]. Hence, the relationship between the location of the GB and ligamentum teres (LT) remains controversial and warrants further investigation.



DOI: 10.3748/wjg.v29.i27.4344 **Copyright** ©The Author(s) 2023.

Figure 1 Coronal schematic of the most common anatomical variation in a liver with right-sided ligamentum teres. The white asterisk indicates the umbilical portion of the portal vein. IVC: Inferior vena cava; MHV: Middle hepatic vein; P_{RA}: Right anterior portal vein; P_L: Left portal vein; P_{RP}: Right posterior portal vein; RSLT: Right-sided ligamentum teres; MPV: Main portal vein.

In this paper, we present additional cases of RSLT together with a normal GB location, identified from a large data set. Then, to determine the key predictors of major PVA, we further investigate the association between GB location, LT location and PVA *via* a series of statistical analyses.

MATERIALS AND METHODS

Patients

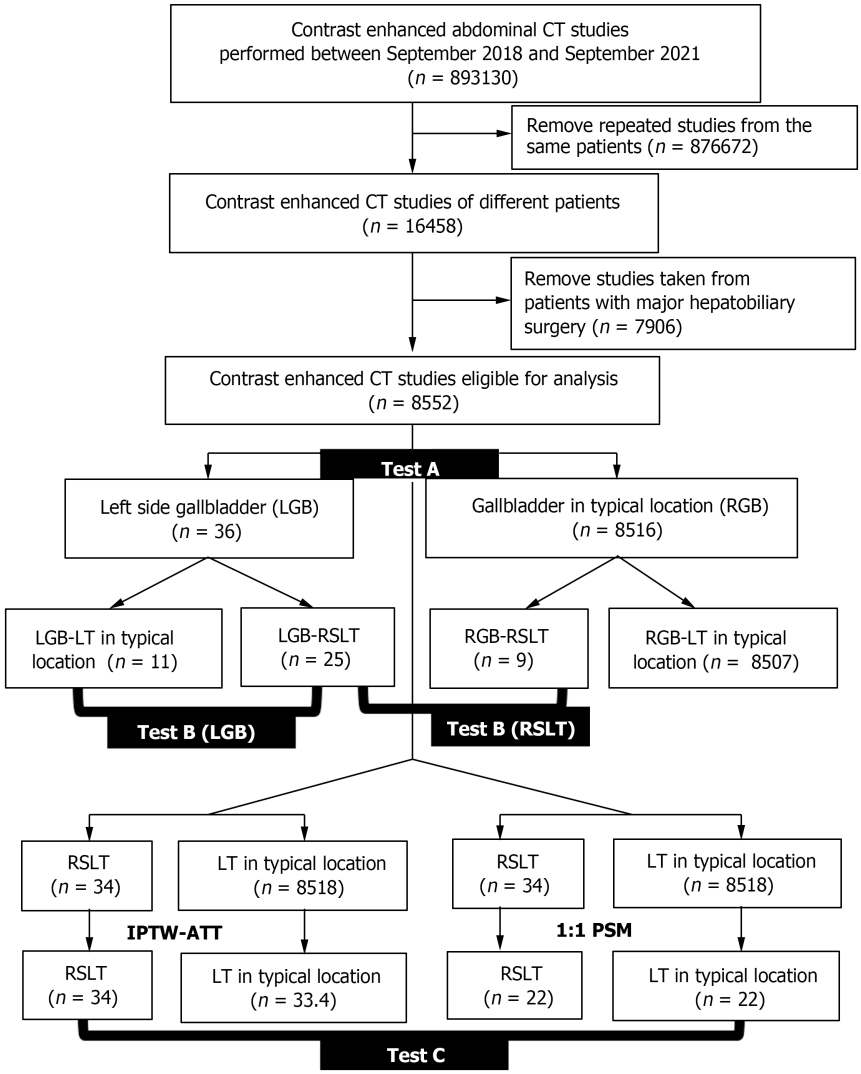
The institutional review board approved this retrospective study and waived the requirement for informed consent. We retrospectively reviewed 71822 contrast-enhanced multidetector computed tomography (MDCT) examinations conducted at the Radiology departments of Taipei Veterans General Hospital and Taichung Veterans General Hospital between September 2018 and September 2021. We excluded both repeat cases and patients who had undergone major hepatobiliary surgery. A total of 8552 cases were eligible for analysis (Figure 2). Although three of these cases have been previously reported[4], the report only highlights the existence of the rare variation. In this manuscript, we conducted a series of statistical analyses on a large number of patients. We also defined the surrogate outcome as the prevalence of major PVAs, which is the dominant risk factor for morbidity and mortality after hepatobiliary intervention.

Computed tomography examination protocol

Contrast-enhanced abdomen computed tomography (CT) studies were conducted using a Philips Brilliance iCT256, United States, or a Siemens Somatom Sensation 16 Slice CT, Germany. The examination parameters included a detector coverage of 128 × 0.625 (Philips Brilliance iCT256) or 16 × 0.75 (Siemens Somatom Sensation 16 Slice CT), a pitch of 0.91 (Philips Brilliance iCT256) or 1 (Siemens Somatom Sensation 16 Slice CT), a rotation time of 0.5 s, a section thickness of 5 mm, and a reconstruction interval of 5 mm for all images. Additional reconstructions were performed at a section thickness of 1 mm and a reconstruction interval of 0.7 mm for detailed interpretation. A total of 120 mL of nonionic iodinated contrast material with an iodine concentration of 350 mg/mL was injected. Scans were acquired in the portal venous phase by using a SmartPrep protocol, with the enhancement threshold set at 120 HU.

Image interpretation

Coronal reconstructions were performed on all raw imaging data acquired from MDCT. The commercially available GE ADW 4.6 CT Workstation was used to process oblique axial multiplanar reformation (MPR), oblique coronal MPR, and maximum-intensity projection (MIP) images. These reconstructed images were then used for the discrimination of difficult portal vein ramifications and all cases involving PVAs. The images were independently analyzed by the following six radiologists: Lin HY, a radiologist with 2 years of experience; Hwang HE and Yen HH, radiologists with 4 years of experience; Chiu NC and Liu CA, radiologists with 15-20 years of experience; and Lee RC, a radiologist with more than 30 years of experience in interpreting CT and magnetic resonance imaging scans. Identification of RSLT was based on recognition of the round ligament (or LT) notch directly connected to the umbilical portion of the portal vein, which originates from the right portal branches (Figures 3 and 4). This technique followed the three-step method proposed by Yamashita *et al*[3] (Figure 3). In all cases, RSLT was positioned to the right of the middle hepatic vein



DOI: 10.3748/wjg.v29.i27.4344 **Copyright** ©The Author(s) 2023.

Figure 2 Flowchart of study cohort retrieval, stratification, and comparison. RSLT: Right-sided ligamentum teres; CT: Computed tomography; LT: Ligamentum teres; PSM: Propensity score matching; LGB: Left-sided gallbladder; IPTW: Inverse probability of treatment weighting; ATT: Average treatment effect in the treated; RGB: Right-sided gallbladder.

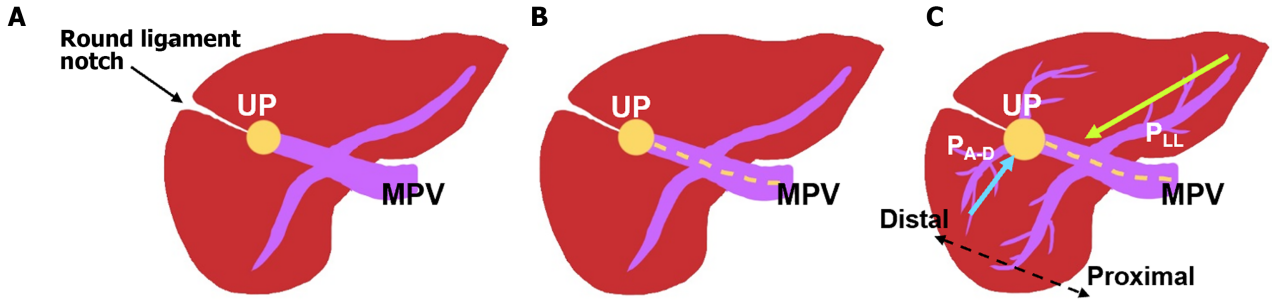


Figure 3 Three-step method for identifying right-sided ligamentum teres, proposed by Yamashita *et al*[3], in axial or oblique transverse images. A: Identify the connection of the round ligament notch to the umbilical portion of the portal vein (UP, yellow circle); B: Set an axis (dotted line) from main portal vein to the UP; C: Identify the diverging points of the dorsal branch of the right anterior portal segment (P_{A-D}, blue arrow) and left lateral portal segment (P_{LL}, green arrow). The diverging point of P_{A-D} is distal to that of P_{LL} in liver with right-sided ligamentum teres and proximal in normal liver. P_{A-D}: Right anterior portal segment; P_{LL}: Left lateral portal segment; UP: Umbilical portion of the portal vein; MPV: Main portal vein. Citation: Lin HY, Lee RC. Is right-sided ligamentum teres hepatis always accompanied by left-sided gallbladder? Case reports and literature review. *Insights Imaging* 2018; 9: 955-960. Copyright ©The Author(s) 2018. Published by Springer Nature[4]. The authors have obtained the permission for figure using (Supplementary material).

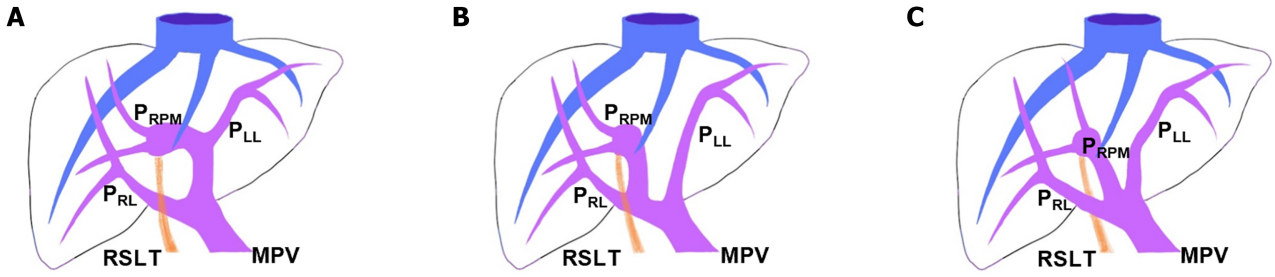


Figure 4 Intrahepatic anomalies of the portal venous system as classified by Shindoh *et al*[2]. A: Independent right lateral: The right lateral portal pedicle (P_{RL}) independently originates from the main portal vein (MPV), and the right paramedian portal pedicle (P_{RPM}) shares a trunk with the left lateral portal vein (P_{LL}); B: Bifurcation: The MPV bifurcates into left and right portal trunks, and the P_{RL} originates from the right portal trunk as the P_{RPM}; C: Trifurcation: The MPV directly divides into three branches: P_{RL}, P_{RPM}, and P_{LL}. P_{RL}: Right lateral portal pedicle; P_{RPM}: Right paramedian portal pedicle; P_{LL}: Left lateral portal vein; RSLT: Right-sided ligamentum teres; MPV: Main portal vein. Citation: Lin HY, Lee RC. Is right-sided ligamentum teres hepatis always accompanied by left-sided gallbladder? Case reports and literature review. *Insights Imaging* 2018; 9: 955-960. Copyright ©The Author(s) 2018. Published by Springer Nature[4]. The authors have obtained the permission for figure using (Supplementary material).

(MHV), consistent with the definition of Shindoh *et al*[2] (Figures 5 and 6). Major PVA cases were predominantly identified as one of three types as defined by Shindoh *et al*[2] (Figure 4). However, cases other than these types were classified following the approach of Gallego *et al*[12] and Atri *et al*[13]. Single or subsegmental PVAs—such as separate segment VI branches from the right portal vein, as reported by Covey *et al*[14]—were not defined as major PVAs. GB location was defined by its long axis position relative to the umbilical fissure (LT notch) and MHV of the liver (Figures 5 and 6).

Statistical analysis

The surrogate outcome was defined as major PVAs on which three radiologists reached a consensus. To examine the relationship between GB location, LT location, and PVAs, three-step statistical tests were conducted, namely Test A, Test B, and Test C (Figure 2). First, we compared the prevalence of PVAs based on GB locations and referred to it as Test A. According to a previous study[11], GB location and PVAs are strongly correlated. However, Test A didn't eliminate the confounding factor of LT location. To explore the effect of LT location, we divided our data into 4 subgroups based on not only GB location but also LT location and calculated PVAs prevalence for each subgroup, which was referred as Test B. Finally, we measured the PVAs prevalence per LT location as depicted in Test C. In Test C, we performed two analytical approaches: Propensity score matching (PSM) and inverse probability of treatment weighting (IPTW) with average treatment effect in the treated (ATT), to cope with data imbalance and to minimize the confounding effects of GB location, sex, and age. Hence, the PVAs analyzed in Test C were solely conditioned on LT location.

A 1:1 PSM method was used to construct matched pairs between RSLT and LT at a typical location through the nearest neighbor approach. IPTW with ATT was then used to avoid missing rare variation data from PSM. Each patient was assigned an inverse weighting of the RSLT or LT at a typical location through calculated propensity scores and the following ATT weight equation:

$$W_i = \begin{cases} 1, & RSLT_i = 1 \text{ (cases with RSLT)} \\ PS_i/(1-PS_i), & RSLT_i = 0 \text{ (cases with LT in typical location)} \end{cases}$$

Therefore, the weighting applied on these two groups improved their comparability despite the imbalance in case numbers (Figure 2).

Continuous variables were expressed in the mean ± SD. Categorical variables were expressed in number and percentage. We used the Student's *t* test to determine the differences between continuous variables and exploited the Chi-square or Fisher exact test for categorical variables. Logistic regression was performed to determine the odds ratio (OR) of the PVA prevalence. Standardized mean differences (SMDs) were calculated to diagnose the balance of matched data. Comparison of groups in matched data were performed by the paired t test for continuous variables and the McNemar's test for categorical variables. A two-sided *P* value < 0.05 indicates statistical significance. All analyses were conducted using IBM SPSS Statistics version 25.0 (IBM, Armonk, NY, United States) and R software version 3.0.2 (R Foundation for Statistical Computing, Vienna, Austria).

RESULTS

The prevalence of LGB and RSLT were 0.42% (36 out of 8552 cases) and 0.40% (34 out of 8552 cases), respectively. Overall, trifurcation-type PVA was the most common anomaly. However, when LGB or RSLT was detected, "independent right lateral type" PVA was the dominant anomaly. Patient demographics for each subgroup were demonstrated in Table 1.

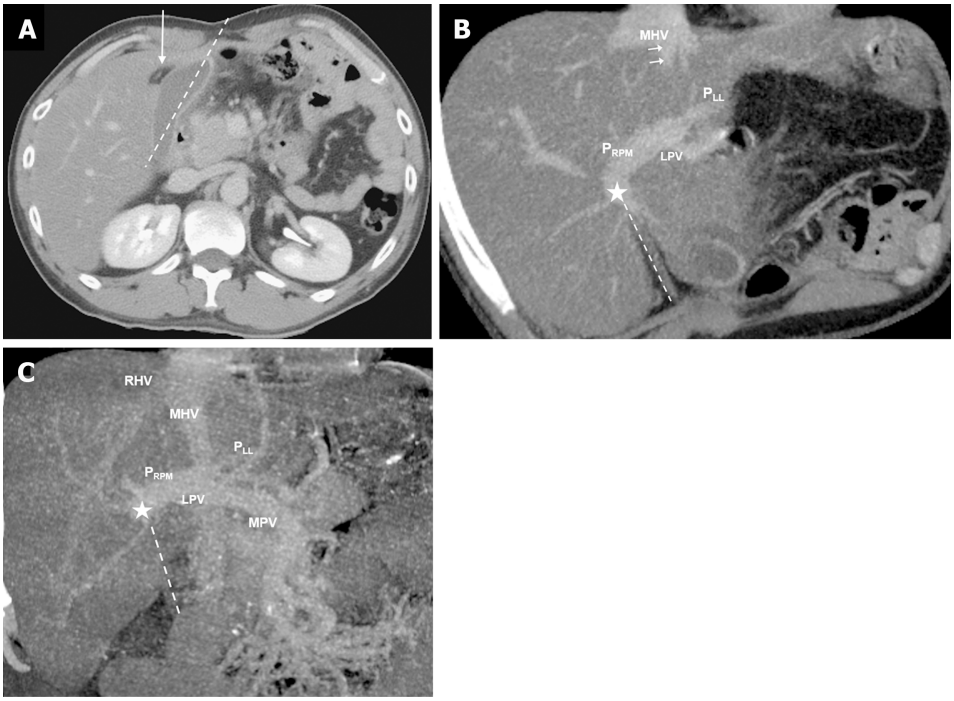
Test A

Test A investigated the population of PVA for each gallbladder location. The prevalence of major PVAs in the LGB group

Table 1 Patient demographics in the four subgroups

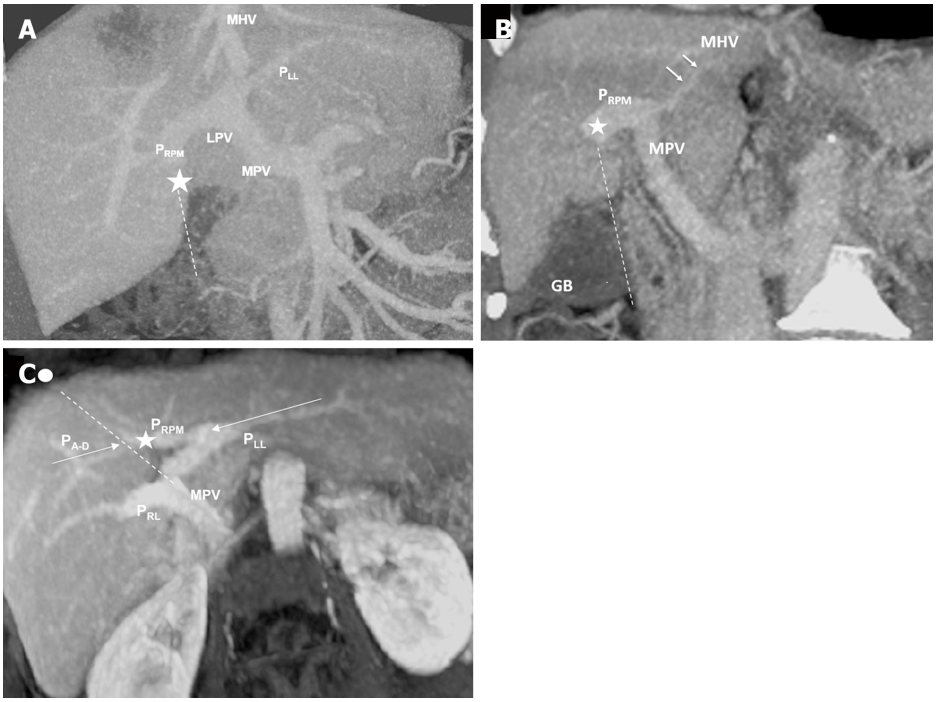
Variables		RGB (*n* = 8516)	LGB (*n* = 36)	RSLT (*n* = 34)	typical LT (*n* = 8518)
Age (yr)[1]		70.8 ± 15.9	59.6 ± 18.9	62.9 ± 17.7	79.5 ± 19.1
Sex, *n* (%)	No. of men	4460 (52.4)	23 (63.9)	21 (61.8)	4462 (52.4)
	No. of women	4056 (47.6)	13 (36.1)	13 (38.2)	4056 (47.6)
Chronic liver disease, *n* (%)	Hepatitis B virus	962 (11.3)	6 (16.7)	6 (17.6)	962 (11.3)
	Hepatitis C virus	281 (3.3)	1 (2.8)	0 (0.0)	282 (3.3)
	Other diseases	2520 (29.6)	8 (22.2)	8 (23.5)	2520 (29.6)
	None	4753 (55.8)	21 (58.3)	20 (58.8)	4754 (55.8)
Comorbidity, *n* (%)	Hepatocellular carcinoma	911 (10.7)	4 (11.1)	2 (5.9)	913 (10.7)
	Non-HCC cancer	4243 (49.8)	18 (50.0)	18 (52.9)	4243 (49.8)
	Cardiovascular disease	2127 (25.0)	10 (27.8)	8 (23.5)	2129 (25.0)
	Chronic kidney disease	845 (9.9)	4 (11.1)	5 (14.7)	844 (9.9)
	Diabetes mellitus	1899 (22.3)	6 (16.7)	9 (26.5)	1896 (22.3)
	Cholelithiasis	732 (8.6)	3 (8.3)	3 (8.8)	732 (8.6)

[1]Data are means ± SD.
RGB: Right-sided gallbladder; LGB: Left-sided gallbladder; RSLT: Right-sided ligamentum teres; LT: Ligamentum teres.



DOI: 10.3748/wjg.v29.i27.4344 **Copyright** ©The Author(s) 2023.

Figure 5 Contrast-enhanced computed tomography images of a 39-year-old man with right-sided ligamentum teres and left-sided gallbladder: Axial, maximum-intensity projection with oblique coronal multiplanar reformation. A: The cholecystic axis of the gallbladder (dotted line) is located left to the umbilical fissure and right-sided ligamentum teres (RSLT, arrow); B: Right paramedian portal pedicle (P_{RPM}) forms the right umbilical portion of the portal vein (asterisk) and joins the RSLT (dotted line). The RSLT is located right to the middle hepatic vein (MHV); C: Portal vein ramification of the Shindoh's independent right lateral type[2]. P_{RPM} shares a trunk with left lateral portal vein and forms the right umbilical portion of the portal vein (asterisk) before joining the RSLT (dotted line), which is located right to the MHV. P_{RPM}: Right paramedian portal pedicle; P_{LL}: Left lateral portal vein; MHV: Middle hepatic vein; MPV: Main portal vein; RHV: Right hepatic vein; LPV: Left portal vein.



DOI: 10.3748/wjg.v29.i27.4344 **Copyright** ©The Author(s) 2023.

Figure 6 Contrast-enhanced computed tomography images of a 72-year-old woman with right-sided ligamentum teres and right-sided gallbladder: Maximum-intensity projection with oblique coronal multiplanar reformation, coronal maximum-intensity projection, and maximum-intensity projection with oblique axial multiplanar reformation. A: Portal vein ramification of the Shindoh's independent right lateral type[2]. Right paramedian portal pedicle forms the right umbilical portion of the portal vein (asterisk) and joins the right-sided ligamentum teres (RSLT, dotted line). The RSLT is located right to the middle hepatic vein (MHV); B: The cholecystic axis of the gallbladder (dotted line) is located right to the RSLT and the round ligament notch, that is, right to the MHV; C: On the axis (dotted line) along the main portal vein to the umbilical portion of the portal vein (asterisk) and the umbilical notch (circle), the diverging point of right anterior portal segment is distal to that of left lateral portal vein in this RSLT liver, consistent with the findings described by Yamashita *et al*[3]. P_{RPM}: Right paramedian portal pedicle; P_{LL}: Left lateral portal vein; P_{RL}: Right lateral portal pedicle; P_{A-D}: Right anterior portal segment; MHV: Middle hepatic vein; MPV: Main portal vein; GB: Gallbladder; LPV: Left portal vein.

(n = 648, 61.1%) was higher than that in the right-sided GB (RGB) group (n = 22, 7.32%). A total of 670 PVA cases were identified, giving a prevalence of 7.83%, which is within the range reported in previous studies[15-19] (*i.e.*, 6% to 16.5%) without considering single or subsegmental PVAs. However, the results of Test A did not exclude possible influencing factors, particularly LT location.

Test B

Test B investigated whether an LGB is sufficient for PVA prediction.

Test B (LGB): In this analysis, we categorized LGB cases by different LT locations. Among 36 patients with LGB, 25 had RSLT (69.4%), and 11 had typical LT (30.6%) as shown in Table 2. The prevalence of PVAs was 80.0% (20 out of 25 cases) for RSLT and 18.2% (2 out of 11 cases) for typical LT, which was significantly different based on Fisher's exact test (P = 0.001). These differing results between LGB cases with different LT locations indicated that LGB alone was unreliable for predicting PVAs. To quantitatively measure the difference, we further performed logistic regression and obtained an OR of 18.00 [95% confidence interval (CI): 2.92-110.96] for RSLT over typical LT. No significant differences were observed in sex, age, and all the possible comorbidities.

Test B (RSLT): On the other hand, we performed an analysis with the RSLT cases divided by GB location. This resulted in 9 RGB cases (26.5%) and 25 LGB cases (73.5%) from a total of 34 RSLT patients, as shown in Table 3. We detected PVAs in 8 of the 9 RGB cases (88.9%) and in 20 of the 25 LGB cases (80.0%); the difference was nonsignificant according to Fisher's exact test (P > 0.99). These results indicated that GB location had no influence on the prevalence of PVAs given the existence of RSLT. The analysis showed no significant differences in demographics or confounding factors between the two subgroups.

According to the analysis results of Test B, we could conclude that GB location was not sufficient for PVA prediction. Furthermore, given the presence of RSLT, different GB locations even contributed to identical PVA prevalence.

Test C

Test C investigated the correlation between LT location and PVAs. We used PSM to handle unbalanced data and remove possible confounding factors, specifically GB location. As shown in Table 4, 22 patients of RSLT and typical LT were matched based on propensity score. Basic demographics and GB location were well balanced between the two groups,

Table 2 Demographics and clinical characteristics of the 36 patients with left-sided gallbladder stratified by location of ligamentum teres

Variables		RSLT (*n* = 25)	Typical LT (*n* = 11)	*P* value
Sex (men), *n* (%)	-	17 (68.0)	6 (54.5)	0.439
Age (yr)	-	61.4 ± 18.2	55.5 ± 20.8	0.401
Comorbidity, *n* (%)	Hepatitis B virus carrier	5 (20.0)	1 (9.1)	0.643
	Hepatitis C virus carrier	0 (0.0)	1 (9.1)	0.306
	Hepatocellular carcinoma (HCC)	2 (8.0)	2 (18.2)	0.570
	Non-HCC malignancy	13 (52.0)	5 (45.5)	0.717
	Cardiovascular disease	7 (28.0)	3 (27.3)	1.000
	Chronic kidney disease	4 (16.0)	0 (0.0)	0.290
	Diabetes mellitus	6 (24.0)	0 (0.0)	0.148
Outcomes				
Major portal vein anomalies[1], *n* (%)	Overall	20 (80.0)	2 (18.2)	0.001[2]
	Independent right lateral type	13 (52.0)	1 (9.1)	0.025
	Trifurcation	6 (24.0)	1 (9.1)	0.400
	Absence of R't PV	1 (4.0)	0 (0.0)	> 0.99

[1]Positive predictive value of left-sided gallbladder in portal vein anomalies = 61.1%.
[2]Logistic regression: Odds ratio= 18; 95% confidence interval: 2.92-110.96; *P* = 0.002.
LGB: Left-sided gallbladder; HCC: Hepatocellular carcinoma; RSLT: Right-sided ligamentum teres; LT: Ligamentum teres.

Table 3 Demographic and clinical characteristics of the 34 patients with right-sided ligamentum teres stratified by gallbladder location

Variables		RGB (*n* =9)	LGB (*n* = 25)	*P* value
Sex (men), *n* (%)	-	4 (44.4)	17 (68.0)	0.254
Age (yr)	-	66.9 ± 16.6	61.4 ± 18.2	0.434
Comorbidity, *n* (%)	Hepatitis B virus carrier	1 (11.1)	5 (20.0)	0.293
	Hepatitis C virus carrier	0 (0.0)	0 (0.0)	NA
	Hepatocellular carcinoma (HCC)	0 (0.0)	2 (8.0)	> 0.99
	Non-HCC malignancy	5 (55.6)	13 (52.0)	0.855
	Cardiovascular disease	1 (11.1)	7 (28.0)	0.403
	Chronic kidney disease	1 (16.7)	4 (16.0)	1.000
	Diabetes mellitus	3 (33.3)	6 (24.0)	0.670
Outcomes				
Major PVA, *n* (%)	Overall	8 (88.9)	20 (80.0)	> 0.99
	Independent right lateral	7 (87.5)	13 (52.0)	0.250
	Trifurcation	1 (12.5)	6 (24.0)	0.670
	Absence of R't PV	0 (0.0)	1 (4.0)	> 0.99

RSLT: Right-sided ligamentum teres; RGB: Right-sided gallbladder; LGB: Left-sided gallbladder; PVA: Portal venous anomalies; NA: Not available.

with SMDs less than 0.2. Also, both McNemar's test and the paired-*t* test revealed that the confounding factors and demographics between matched cohorts were statistically similar. The prevalence of PVAs was 77.3% (17 out of 22) for the matched RSLT group and 4.5% (1 out of 5) for the matched typical LT group; the difference between these two groups was significant according to McNemar's test ($P < 0.001$). Conditional logistic regression revealed an OR of 16.27 (95%CI: 2.25-117.53) for RSLT over typical LT. However, 12 rare variation data points in which RSLT coexisted with RGB were lost

Table 4 Characteristics of study patients before and after propensity score analysis

		Before propensity score matching				After propensity score matching			
Factors		**RSLT (*n* = 34)**	**Typical LT (*n* = 8518)**	***P* value**	**SMD[1]**	**RSLT (*n* = 22)**	**Typical LT (*n* = 22)**	***P* value**	**SMD[1]**
Age		62.9 ± 17.7	59.5 ± 16.2	0.228[2]	0.197	62.7 ± 17.1	59.9 ± 17.2	0.411[3]	0.156
Sex, *n* (%)	Men	21 (61.8)	4462 (52.4)	0.305[4]	0.193	11 (50)	11 (50)	1.000[2]	0
	Women	13 (38.2)	4056 (47.6)			11 (50)	11 (50)		
GB, *n* (%)	LGB	25 (7.35)	28 (0.3)	< 0.001[4]	2.327	13 (59.1)	13 (59.1)	1.000[2]	0
	RGB	9 (26.5)	8490 (99.7)			9 (40.9)	9 (40.9)		
Outcomes									
Major PVA, *n* (%)						17 (77.3)	1 (4.5)	< 0.001[5]	

[1]Standardized mean difference (SMD). SMD indicate very small differences for values less than 0.10; 0.1-0.3. Small differences; 0.3-0.5, moderate differences; and values higher than 0.5, large differences.
[2]Student's *t* test.
[3]Paired-*t* test.
[4]Chi-square test.
[5]Conditional logistic regression: Odds ratio = 16.27; 95% confidence interval: 2.25-117.53; *P* = 0.006.
RSLT: Right-sided ligamentum teres; LT: Ligamentum teres; RGB: Right-sided gallbladder; LGB: Left-sided gallbladder; PVA: Portal venous anomalies; SMD: Standardized mean difference; GB: Gallbladder.

during the PSM process. Therefore, we implemented IPTW with ATT to prevent data exclusion from PSM and minimize the covariate imbalance between the groups with RSLT and typical LT. Following IPTW, the SMDs between the two cohorts were smaller than 0.1, indicating they are balanced for their demographics and GB locations. Compared with the typical LT cohort, the RSLT cohort had a significantly higher prevalence of PVAs after IPTW (4.7% *vs* 82.4%, $P < 0.001$; Table 5). As possible confounding effects were removed, the result suggests that LT location per se was effective for determining PVAs.

DISCUSSION

According to our statistical analysis results, RSLT is not consistently accompanied by LGB, and the key feature of predicting major PVAs is not LGB but rather RSLT. First, nine additional cases of RSLT without LGB were identified (Figure 2 and Table 3), indicating that the four cases reported by Yamashita *et al*[3] and Lin *et al*[4] were true existing variations and that RSLT does not consistently coexist with LGB. Second, the results of Test B indicated that the prevalence of PVAs is invariant regardless of the location of GB given RSLT was detected, which suggests that GB location is not sufficient for PVA prediction. Finally, the results of Test C concludes that the LT location is an independent risk factor of PVAs after possible confounding factors are eliminated in large propensity score–matched data sets.

Because GB location is an unreliable feature of PVAs, operators should not underestimate the risk of major vascular anomalies in livers with a normal GB location. As shown in Supplementary Figure 1, hepatobiliary interventions may be technically challenging and lead to complications if the PVAs are not recognized. Our results also suggest that LT location is strongly correlates with PVAs. Therefore, operators must be aware of the high surgical risk once RSLT has been detected. In addition to PVAs, RSLT also introduces nondeterministic anomalous arterial ramifications and biliary confluences, as reported by Nishitai *et al*[5] , hence, arterial and biliary patterns must be examined in preoperative imaging studies at the presence of RSLT.

Neglecting the aforementioned anomalies before an intervention may have life-threatening consequences, such as ischemic hepatic failure or bile leak[6-8]. Specifically, because independent ramification of the right lateral portal pedicle is the most common type of PVA in livers with RSLT, ligation of the left trunk of the portal vein during hepatobiliary surgery will disrupt portal flow in two-thirds of the entire liver if the common trunk of the left portal vein and the right paramedian pedicle are misinterpreted as the left portal vein. Multiple biliary complications during major hepatobiliary interventions in patients with RSLT have also been documented[6].

With the increasing popularity of three-dimensional magnetic resonance cholangiopancreatography (a low-risk examination that does not require the injection of contrast medium), biliary confluences in livers with RSLT should be comprehensively investigated during pre-interventional assessments, especially within the context of living donor liver transplantation.

This study has several limitations. First, a normal GB location in a liver with RSLT is a substantially rare variation that results in a remarkable loss of unmatched data when performing multivariate logistic regression. However, in the present study, this problem was addressed by preprocessing data with PSM and IPTW with ATT, yielding well-balanced cohorts and minimizing imbalances. Second, the diagnoses of all the variations were made by CT images without surgical or

Table 5 Characteristics of study patients before and after inverse probability of treatment weighting

		Before IPTW				After IPTW			
Factors		**RSLT (*n* = 34)**	**Typical LT (*n* = 8518)**	***P* value**	**SMD[1]**	**RSLT (*n* = 34)**	**Typical LT (*n* = 34)**	***P* value**	**SMD[1]**
Age		62.9 ± 17.7	59.5 ± 16.2	0.228[2]	0.197	62.9 ± 17.7	62.3 ± 14.6	0.879	0.034
Sex, *n* (%)	Men	21 (61.8)	4462 (52.4)	0.305[4]	0.193	21 (61.8)	19.4 (58.1)	0.953[3]	0.076
	Women	13 (38.2)	4056 (47.6)			13 (38.2)	14 (41.9)		
GB, *n* (%)	LGB	25 (7.35)	28 (0.3)	< 0.001[4]	2.327	25 (73.5)	24.4 (73.1)	1.0003	0.011
	RGB	9 (26.5)	8490 (99.7)			9 (26.5)	9 (26.9)		
Outcomes									
Major PVA, *n* (%)						28 (82.4)	1.6 (4.7)	< 0.001[4]	2.514

[1]Standardized mean difference (SMD). SMD indicate very small differences for values less than 0.10; 0.1-0.3. Small differences; 0.3-0.5, moderate differences; and values higher than 0.5, large differences.
[2]Student's *t* test.
[3]McNemar test.
[4]Chi-square test.
IPTW: Inverse probability of treatment weighting; RSLT: Right-sided ligamentum teres; LT: Ligamentum teres; RGB: Right-sided gallbladder; LGB: Left-sided gallbladder; PVA: Portal venous anomalies; SMD: Standardized mean difference; GB: Gallbladder.

cadaveric anatomical proof. To compensate for this limitation and establish accurate image-based diagnoses, we explored several image-processing techniques, such as axial and coronal oblique MPR and MIP. We also followed the three-step method proposed by Yamashita *et al*[3] for diagnosing RSLT. In addition, the images were independently analyzed by six radiologists with 2-30 years of experience. To the best of our knowledge, this is the largest retrospective cohort study focusing on RSLTs. This is also the first article to highlight rare cases in which an RGB coexists with RSLT and further discuss the individual effects of LGB and RSLT on PVAs.

CONCLUSION

Understanding portal vein ramifications is crucial during preoperative planning of hepatobiliary interventions. We first observed that LGB is not consistently accompanied by RSLT and then performed a series of statistical analyses to evaluate the correlation between LGB, RSLT and PVAs. Our analysis results indicated that RSLT is an independent risk factor for PVAs, whereas GB location has no influence on PVAs if RSLT exists. Therefore, operators should avoid considering GB location, which is easily identified, as a surrogate feature of LT location.

ARTICLE HIGHLIGHTS

Research background

The presence of right-sided ligamentum teres (RSLT) is often accompanied by portal venous anomalies (PVAs) and is considered a worrisome characteristic in hepatobiliary interventions. Most studies hypothesis that left-sided gallbladder (LGB) must exist with RSLT. However, in a reported study, right-sided gallbladder (RGB) was observed in livers with RSLT. Therefore, the relationship between the ligamentum teres hepatis (LT), gallbladder (GB), and PVAs is controversial and requires further investigation, despite the rarity of the anatomical variation of LT and GB, which can complicate statistical analysis.

Research motivation

To verify whether the RSLT coexists with a typical RGB, represent genuine existing variations or were merely misinterpreted and to determine the key predictors of major PVA, we conducted a comprehensive investigation. Additionally, to the best of our knowledge, all previous articles focusing on the RSLT had small sample sizes, not exceeding 1000.

Research objectives

First, to draw attention to the uncommon occurrence of the RSLT without the presence of the gallbladder (LGB), and secondly, to assess the reliability of both the LT and gallbladder location in predicting PVAs.

Research methods

This retrospective study examined a total of 8552 contrast-enhanced abdominal computed tomography examinations conducted between 2018 and 2021, involving 4483 men and 4069 women, with a mean age of 59.5 ± 16.2 (SD) years. The primary focus was to assess major PVAs as a surrogate outcome. The cases were categorized into four subgroups based on the locations of the gallbladder and LT. On one hand, we analyzed the prevalence of PVAs based on LT locations while controlling for gallbladder location (n = 36). On the other hand, we controlled for LT location and determined the prevalence of PVAs based on gallbladder locations (n = 34). Lastly, we investigated the independent influence of LT location on PVA using propensity score matching (PSM) and inverse probability of treatment weighting (IPTW).

Research results

We identified a total of 9 cases where the RSLT coexisted with a typical RGB location. Among the cases with a LGB, the presence of RSLT was associated with a significantly higher prevalence of PVAs compared to those with a typical LT [80.0% *vs* 18.2%, P = 0.001; odds ratio (OR) = 18, 95% confidence interval (CI): 2.92-110.96]. However, when RSLT was present, there was no statistically significant difference in PVA prevalence between RGB and LGB cases (88.9% *vs* 80.0%, P > 0.99). We employed PSM and IPTW to ensure balanced cohorts in terms of demographics and gallbladder locations. After adjusting for these factors using PSM, the RSLT group still exhibited a significantly higher PVAs prevalence compared to the LT group (77.3% *vs* 4.5%, P < 0.001; OR = 16.27, 95%CI: 2.25-117.53). Similar results were observed when utilizing IPTW (82.5% *vs* 4.7%, P < 0.001).

Research conclusions

RSLT doesn't always coexist with LGB. RSLT can predict PVA independently while the gallbladder location does not serve as a sufficient predictor.

Research perspectives

Further investigation is needed to determine whether the existence of RSLT can predict the most predominant type of biliary or arterial anatomical variation.

ACKNOWLEDGEMENTS

We would like to express our special thanks to Chai JW, the head of the Department of Radiology at Taichung Veterans General Hospital in Taiwan, and to Lee RC, the head of the Division of Abdominal Radiology at Taipei Veterans General Hospital, for their invaluable assistance with technical support and assurance for the entire study. We would also like to thank Hsu CY from the Biostatistics Task Force and Department of Medical Research at Taichung Veterans General Hospital for kindly providing statistical advice for this manuscript.

FOOTNOTES

Author contributions: Lin HY and Lee RC contributed to the conception and design; all authors contributed to the administrative support; Lin HY, Lee RC and Chai JW contributed to the provision of study materials or patients; all authors contributed to the collection and assembly of data; Lin HY and Hsu CY contributed to the data analysis and interpretation; Lin HY contributed to the manuscript writing and final approval of manuscript.

Institutional review board statement: The study was reviewed and approved by the Institutional Review Board I&II of Taichung Veterans General Hospital (Approval No. TCVGH-IRB No. CE22408B).

Informed consent statement: Patients were not required to give informed consent to the study because the analysis used anonymous clinical data that were obtained after each patient agreed to treatment by written consent.

Conflict-of-interest statement: The authors of this manuscript declare no relationships with any companies, whose products or services may be related to the subject matter of the article.

Data sharing statement: No additional data are available.

STROBE statement: The authors have read the STROBE Statement—checklist of items, and the manuscript was prepared and revised according to the STROBE Statement—checklist of items.

Open-Access: This article is an open-access article that was selected by an in-house editor and fully peer-reviewed by external reviewers. It is distributed in accordance with the Creative Commons Attribution NonCommercial (CC BY-NC 4.0) license, which permits others to distribute, remix, adapt, build upon this work non-commercially, and license their derivative works on different terms, provided the original work is properly cited and the use is non-commercial. See: https://creativecommons.org/Licenses/by-nc/4.0/

Country/Territory of origin: Taiwan

ORCID number: Hsuan-Yin Lin 0000-0003-2309-054X; Chien An Liu 0000-0002-8838-0380.

S-Editor: Yan JP
L-Editor: A
P-Editor: Cai YX

REFERENCES

1 **Matsumoto H**. A newer concept of the segments of the liver. *Jpn J Med Ultrasonics* 1986; **13**: 551-552
2 **Shindoh J**, Akahane M, Satou S, Aoki T, Beck Y, Hasegawa K, Sugawara Y, Ohtomo K, Kokudo N. Vascular architecture in anomalous right-sided ligamentum teres: three-dimensional analyses in 35 patients. *HPB (Oxford)* 2012; **14**: 32-41 [PMID: 22151449 DOI: 10.1111/j.1477-2574.2011.00398.x]
3 **Yamashita R**, Yamaoka T, Nishitai R, Isoda H, Taura K, Arizono S, Furuta A, Ohno T, Ono A, Togashi K. Portal vein branching order helps in the recognition of anomalous right-sided round ligament: common features and variations in portal vein anatomy. *Abdom Radiol (NY)* 2017; **42**: 1832-1838 [PMID: 28389788 DOI: 10.1007/s00261-017-1128-1]
4 **Lin HY**, Lee RC. Is right-sided ligamentum teres hepatis always accompanied by left-sided gallbladder? Case reports and literature review. *Insights Imaging* 2018; **9**: 955-960 [PMID: 30456452 DOI: 10.1007/s13244-018-0671-9]
5 **Nishitai R**, Shindoh J, Yamaoka T, Akahane M, Kokudo N, Manaka D. Biliary architecture of livers exhibiting right-sided ligamentum teres: an indication for preoperative cholangiography prior to major hepatectomy. *HPB (Oxford)* 2016; **18**: 929-935 [PMID: 27594117 DOI: 10.1016/j.hpb.2016.08.002]
6 **Hai S**, Hatano E, Hirano T, Asano Y, Suzumura K, Sueoka H, Fujimoto J. Hepatectomy for Hilar Cholangiocarcinoma with Right-Sided Ligamentum Teres Using a Hepatectomy Simulation System. *Case Rep Gastroenterol* 2017; **11**: 576-583 [PMID: 29118686 DOI: 10.1159/000480375]
7 **Kaneoka Y**, Yamaguchi A, Isogai M, Harada T. Hepatectomy for cholangiocarcinoma complicated with right umbilical portion: anomalous configuration of the intrahepatic biliary tree. *J Hepatobiliary Pancreat Surg* 2000; **7**: 321-326 [PMID: 10982634 DOI: 10.1007/s005340070056]
8 **Koh MK**, Ahmad H, Watanapa P, Jalleh RP, Habib NA. Beware the anomalous portal vein. *HPB Surg* 1994; **7**: 237-9; discussion 239 [PMID: 8155591 DOI: 10.1155/1994/16017]
9 **Sureka B**, Patidar Y, Bansal K, Rajesh S, Agrawal N, Arora A. Portal vein variations in 1000 patients: surgical and radiological importance. *Br J Radiol* 2015; **88**: 20150326 [PMID: 26283261 DOI: 10.1259/bjr.20150326]
10 **Nagai M**, Kubota K, Kawasaki S, Takayama T, BandaiY, Makuuchi M. Are left-sided gallbladders really located on the left side? *Ann Surg* 1997; **225**: 274-280 [PMID: 9060583 DOI: 10.1097/00000658-199703000-00006]
11 **Hsu SL**, Chen TY, Huang TL, Sun CK, Concejero AM, Tsang LL, Cheng YF. Left-sided gallbladder: its clinical significance and imaging presentations. *World J Gastroenterol* 2007; **13**: 6404-6409 [PMID: 18081230 DOI: 10.3748/wjg.v13.i47.6404]
12 **Gallego C**, Velasco M, Marcuello P, Tejedor D, De Campo L, Friera A. Congenital and acquired anomalies of the portal venous system. *Radiographics* 2002; **22**: 141-159 [PMID: 11796904 DOI: 10.1148/radiographics.22.1.g02ja08141]
13 **Atri M**, Bret PM, Fraser-Hill MA. Intrahepatic portal venous variations: prevalence with US. *Radiology* 1992; **184**: 157-158 [PMID: 1609075 DOI: 10.1148/radiology.184.1.1609075]
14 **Covey AM**, Brody LA, Getrajdman GI, Sofocleous CT, Brown KT. Incidence, patterns, and clinical relevance of variant portal vein anatomy. *AJR Am J Roentgenol* 2004; **183**: 1055-1064 [PMID: 15385304 DOI: 10.2214/ajr.183.4.1831055]
15 **Hochstetter F**. Anomalien der Pfortader und der Nabelvene in Verbindung mit Defekt oder Linkslage der Gallenblase. *Arch Anat Entwick* **1886**: 369-384
16 **Idu M**, Jakimowicz J, Iuppa A, Cuschieri A. Hepatobiliary anatomy in patients with transposition of the gallbladder: implications for safe laparoscopic cholecystectomy. *Br J Surg* 1996; **83**: 1442-1443 [PMID: 8944467 DOI: 10.1002/bjs.1800831037]
17 **Maetani Y**, Itoh K, Kojima N, Tabuchi T, Shibata T, Asonuma K, Tanaka K, Konishi J. Portal vein anomaly associated with deviation of the ligamentum teres to the right and malposition of the gallbladder. *Radiology* 1998; **207**: 723-728 [PMID: 9609896 DOI: 10.1148/radiology.207.3.9609896]
18 **Fraser-Hill MA**, Atri M, Bret PM, Aldis AE, Illescas FF, Herschorn SD. Intrahepatic portal venous system: variations demonstrated with duplex and color Doppler US. *Radiology* 1990; **177**: 523-526 [PMID: 2217795 DOI: 10.1148/radiology.177.2.2217795]
19 **Soyer P**, Bluemke DA, Choti MA, Fishman EK. Variations in the intrahepatic portions of the hepatic and portal veins: findings on helical CT scans during arterial portography. *AJR Am J Roentgenol* 1995; **164**: 103-108 [PMID: 7998521 DOI: 10.2214/ajr.164.1.7998521]

World Journal of Gastroenterology

Submit a Manuscript: https://www.f6publishing.com

World J Gastroenterol 2023 July 21; 29(27): 4356-4367

DOI: 10.3748/wjg.v29.i27.4356

ISSN 1007-9327 (print) ISSN 2219-2840 (online)

SCIENTOMETRICS

Research landscape on COVID-19 and liver dysfunction: A bibliometric analysis

Sa'ed H Zyoud

Specialty type: Gastroenterology and hepatology

Provenance and peer review: Invited article; Externally peer reviewed.

Peer-review model: Single blind

Peer-review report's scientific quality classification
Grade A (Excellent): 0
Grade B (Very good): B
Grade C (Good): C
Grade D (Fair): D
Grade E (Poor): 0

P-Reviewer: Teles RHG, Brazil; Xie C, China

Received: February 24, 2023
Peer-review started: February 24, 2023
First decision: May 23, 2023
Revised: June 16, 2023
Accepted: June 27, 2023
Article in press: June 27, 2023
Published online: July 21, 2023

Sa'ed H Zyoud, Department of Clinical and Community Pharmacy, College of Medicine and Health Sciences, An-Najah National University, Nablus 44839, Palestine

Sa'ed H Zyoud, Poison Control and Drug Information Center (PCDIC), College of Medicine and Health Sciences, An-Najah National University, Nablus 44839, Palestine

Sa'ed H Zyoud, Clinical Research Centre, An-Najah National University Hospital, Nablus 44839, Palestine

Corresponding author: Sa'ed H Zyoud, PhD, Full Professor, Department of Clinical and Community Pharmacy, College of Medicine and Health Sciences, An-Najah National University, Academic Street, Nablus 44839, Palestine. saedzyoud@yahoo.com

Abstract

BACKGROUND

The global spread of severe acute respiratory syndrome coronavirus 2, responsible for coronavirus disease 2019 (COVID-19), poses a significant risk to public health. Beyond the respiratory issues initially associated with the condition, severe cases of COVID-19 can also lead to complications in other organs, including the liver. Patients with severe COVID-19 may exhibit various clinical signs of liver dysfunction, ranging from minor elevations in liver enzymes without symptoms to more serious cases of impaired liver function. Liver damage is more commonly observed in patients with severe or critical forms of the disease.

AIM

To present the research landscape on COVID-19 and liver dysfunction while also offering valuable insights into the prominent areas of interest within this particular domain.

METHODS

On 18 February 2023, Scopus was utilised to conduct a comprehensive exploration of the relationship between COVID-19 and the liver dysfunction. The investigation encompassed the period from 1 January 2020 to 31 December 2022. Primary sources were meticulously examined and organised in a Microsoft Excel 2013 spreadsheet, categorised by journal, institution, funding agency, country and citation type. VOSviewer version 1.6.18 was employed to explore the prominent topics and knowledge network related to the subject.

RESULTS

There were 2336 publications on COVID-19 and liver dysfunction analysed in this study, of which 558 were published in 2020, 891 in 2021 and 887 in 2022. Researchers from 111 different countries participated in the retrieved documents. The United States contributed the most studies, with 497 documents, representing 21.28% of the total, followed by China with 393 documents (16.82%) and Italy with 255 documents (10.92%). In the context of research related to COVID-19 and the liver, co-occurrence analysis identified three distinct clusters of topics: (1) 'COVID-19 vaccines in liver transplant recipients'; (2) 'liver function tests as a predictor of the severity and clinical outcomes in hospitalised patients'; and (3) 'care of patients with liver disease during the COVID-19 pandemic'.

CONCLUSION

This bibliometric study provides a comprehensive overview of liver-related publications in COVID-19 research over the past 3 years. This study highlights the significant contributions of high-income nations, particularly the United States, China, and Italy, to the production of liver-related scholarly literature in this field. Most of the articles focused on liver dysfunction in patients with COVID-19 and the implications of the virus for gastroenterologists and hepatologists.

Key Words: COVID-19; Bibliometric; Scopus; Vosviewer; Liver

©The Author(s) 2023. Published by Baishideng Publishing Group Inc. All rights reserved.

Core Tip: Severe cases of coronavirus disease 2019 (COVID-19) can lead to liver dysfunction, and this study provides a comprehensive overview of liver-related publications in COVID-19 research. The findings highlight the significant contributions of high-income countries, such as the United States, China, and Italy, to the production of liver-related scholarly literature in this field. The research clusters identified in the study focus on COVID-19 vaccines in liver transplant recipients, liver function tests as predictors of severity and clinical outcomes in hospitalized patients, and the care of patients with liver disease during the COVID-19 pandemic.

Citation: Zyoud SH. Research landscape on COVID-19 and liver dysfunction: A bibliometric analysis. *World J Gastroenterol* 2023; 29(27): 4356-4367

URL: https://www.wjgnet.com/1007-9327/full/v29/i27/4356.htm

DOI: https://dx.doi.org/10.3748/wjg.v29.i27.4356

INTRODUCTION

The novel coronavirus disease 2019 (COVID-19) has had a marked global impact. As of 3 May 2023, there have been over 765 million confirmed cases and nearly 6.92 million fatalities[1]. COVID-19 symptoms range from modest respiratory difficulties to severe respiratory distress syndrome, which can lead to organ failure and death. Older people with preexisting health issues are especially vulnerable. It is crucial to mention that in addition to its effects on the lungs, COVID-19 can cause liver damage[2-6]. COVID-19-related liver injury is defined as any liver damage that occurs in people who have COVID-19, regardless of whether they have a preexisting liver ailment[7-11]. Severe COVID-19 infections can cause liver damage through a variety of mechanisms, including immune-mediated damage, ischemic hepatitis caused by a systemic inflammatory response, drug-induced liver injury, reactivation of preexisting chronic liver disease, and direct cytopathic effects from the virus replicating in hepatocytes[12-15].

COVID-19-induced liver dysfunction has a variable prognosis and symptoms[16-20]. Because there is no cure for COVID-19-induced liver damage, treatment is only supportive. Preexisting liver diseases and nutritional support can help identify and treat liver disorders[21]. Research on COVID-19 and liver dysfunction is evolving, but there are not enough quantitative and visual studies based on bibliometrics. This chasm has stifled research in this field. Hence, this bibliometric analysis provides a view of the available COVID-19 and liver dysfunction research that is indexed in the Scopus database. This analysis has identified research hotspots for COVID-19 and liver dysfunction, as well as historical trends and future directions.

MATERIALS AND METHODS

Study design

This cross-sectional study was conducted on 18 February 2023 using a bibliometric methodology.

Bibliographic database

The Scopus database was chosen as the source of data for this study for various reasons. First, Scopus stands out as the largest scientific database compared with alternatives such as Web of Science. Second, it offers convenient options for exporting and analysing data, and it is compatible with Microsoft Excel and visualisation tools such as VOSviewer. Third, Scopus is a comprehensive database that encompasses citations from diverse fields, including social and health disciplines. Consequently, Scopus emerged as the most appropriate choice for conducting the present study[22-24].

Search strategies

The search was limited to publications between 1 January 2020 and 31 December 2022. The search strategy involved three steps.

In the first step, terms related to COVID-19 were selected from the Medical Subject Headings (MeSH) of PubMed and previous studies related to COVID-19[25-29]. Next, the retrieved terms were entered into the Scopus search engine as 'Article Title/Abstract' to retrieve publications related to COVID-19.

In the second step, the publications obtained in the first step were filtered to include only those with "liver and related words" in their title. Keywords relevant to the liver were selected from the previous liver and COVID-19 meta-analyses [30-34] and were entered into the Scopus engine to retrieve publications related to the liver.

In the third step, publications that were published as an erratum were excluded.

The final search query used for data extraction from Scopus looked like this: (TITLE-ABS ("COVID 19") OR TITLE-ABS ("2019 novel coronavirus") OR TITLE-ABS ("novel coronavirus") OR TITLE-ABS ("coronavirus 2019") OR TITLE-ABS ("* novel CoV") OR TITLE-ABS ("coronavirus disease 2019") OR TITLE-ABS ("2019-novel CoV") OR TITLE-ABS ("Wuhan coronavirus") OR TITLE-ABS ("2019 ncov") OR TITLE-ABS ("Wuhan pneumonia") OR TITLE-ABS ("COVID 2019") OR TITLE-ABS (COVID19) OR TITLE-ABS (*COVID*) OR TITLE-ABS (nCoV) OR TITLE-ABS ("corona virus 2019") OR TITLE-ABS ("nCoV-2019") OR TITLE-ABS (nCoV2019) OR TITLE-ABS ("nCoV 2019") OR TITLE-ABS (2019-ncov) OR TITLE-ABS (COVID-19) OR TITLE-ABS ("Severe acute respiratory syndrome coronavirus 2") OR TITLE-ABS ("SARS Coronavirus 2") OR TITLE-ABS ("SARS-CoV-2") OR TITLE-ABS ("SARS-CoV 2")) AND (TITLE (liver) OR TITLE (Hepati*) OR TITLE (aminotransferase) OR TITLE (bilirubin) OR TITLE (prothrombin) OR TITLE (ALT) OR TITLE (AST) OR TITLE (Hepato*) OR TITLE (Cirrhosis)) AND (LIMIT-TO (PUBYEAR,2022) OR LIMIT-TO (PUBYEAR,2021) OR LIMIT-TO (PUBYEAR,2020)) AND (EXCLUDE (DOCTYPE,"er"))

During every stage of the search process, quotation marks were employed to accurately retrieve the specific phrase. Moreover, the use of asterisk truncation acted as a flexible wildcard, enabling the retrieval of any possible term.

Validation of the search strategy

Limiting the search to the publication titles in the Scopus database can improve the accuracy of retrieved data by reducing the number of false positive results. By focusing the search on the title, the search algorithm will only retrieve articles with 'liver' in their titles, meaning that irrelevant articles that may mention 'liver' in their abstracts or full texts will not be retrieved. As mentioned, this approach may slightly reduce the level of sensitivity, meaning that some relevant articles that do not have a 'liver' in their titles may be missed[35,36]. This study employed a validated research approach to ensure dependable and precise findings. To minimise the risk of false positive results, every 15th document (15, 30, 45, 60, *etc.*) up to the end of the retrieved document list was carefully assessed by evaluating its title and abstract. The research strategy underwent continuous refinement until an entirely accurate collection of randomly selected outcomes was obtained. To confirm the absence of false-negative results or missed findings, the research productivity of 20 active authors in the field was analysed. A Spearman correlation test was utilised to compare the results derived from the research strategy with those from the authors. The study revealed a strong significant correlation ($r = 0.953$, $P < 0.001$) between the two sets of findings, underscoring the research strategy's high level of validity. Importantly, Sweileh WM[37, 38], and Zyoud SH[39] had previously employed this validation approach.

Bibliometric analysis

The data collected included the following bibliometric parameters: the types of documents (*e.g.* articles, books, or conference proceedings), the year of publication, the number of publications, the citation count (which indicates how many times other works have cited the publication), the country where the publication originated, the institution or organization that produced the publication, and the journals where the publications appeared. The *Impact Index Per Article* displayed represents the top 10 most-cited papers; it is derived from the *Reference Citation Analysis* (RCA, https://www.referencecitationanalysis.com/) database. RCA is an open citation analysis database covering various fields and is owned by Baishideng Publishing Group Inc., situated in Pleasanton, CA 94566, United States[40-42].

Visualize analysis

VOSviewer (version 1.6.18, Leiden University, Leiden, the Netherlands) was used for bibliometric visualisation[43]. In scientific research, the use of VOSviewer software for bibliometric visualisation and term co-occurrence analysis is widespread. By identifying patterns of international collaboration and analysing the co-occurrence of terms in the titles and abstracts of publications, researchers can gain insight into the hotspots in a particular field and track scientific progress[43]. Using VOSviewer software, a network of terms illustrates the relationship between terms according to the number of publications in which they appear together. This enables researchers to identify clusters of related terms that represent particular research areas or trending topics. As a result, researchers can better understand the current state of research in a particular field and identify areas for future study by identifying hotspots[44,45]. These data can be used to guide funding decisions, to identify possible collaborators and to inform policy decisions.

RESULTS

General characteristics of the retrieved articles

A total of 2336 publications on COVID-19 and liver dysfunction were analysed in this study. Among them, 558 were published in 2020, 891 in 2021, and 887 in 2022. Regarding the types of publications, 1438 (61.56%) were articles, 417 (17.85%) were letters, 357 (15.28%) were reviews, and 124 (5.31%) fell under other categories, such as editorials and notes.

Top 10 active countries

Researchers from 111 different countries participated in the retrieved documents. The United States contributed the most studies, with 497 documents, representing 21.28% of the total. China followed closely behind with 393 documents, representing 16.82% of the total, and Italy came in third with 255 documents, representing 10.92% of the total publications on research related to COVID-19 and liver dysfunction. Table 1 lists the top 10 active countries, which together represented 84.63% of all articles published. Figure 1 is a network visualisation map showing the collaboration between countries regarding co-authorship. The minimum inclusion threshold was set at 30 documents per country; a total of 22 countries met this threshold. In the visualisation, each country is represented by a circle, and the size of the circle indicates the level of contribution the country has made in terms of co-authorship. Lines represent the links between countries, and the thickness of the line indicates the strength of collaboration between the two countries. According to the centrality measures used in the map, the United States appears to be the most central country in terms of collaborations, followed by China and Italy.

Analysis of institutions

Eight thousand six hundred forty institutions participated in research in this field, of which the top 10 institutions represented 15.97% of all published articles. *INSERM* contributed the most articles (n = 26, 5.49%), followed by *Imperial College London* (n = 23, 4.85%) and *Sorbonne Université* (n = 21, 4.43%) (Table 2).

Journal analysis

The top 10 most productive journals in research related to COVID-19 and the liver are shown in Table 3. Approximately 19.91% of the articles were published on this list. The *Journal of Hepatology* published the most articles (n = 85, 3.64%), followed by *Liver International* (n = 64, 2.74%) and the *World Journal of Gastroenterology* (n = 62, 2.65%).

Analysis of citations

The retrieved documents had a total of 30,766 citations, a mean of 13.17, and an h-index of 75. A total of 638 (27.3%) documents had no citations, while 55 had 100 or more citations. The top 10 articles, ranked by the number of citations, collectively received 4,758 citations. The citations for these publications varied from 283 to 1,126 in total (Table 4) [13,46-54]. Among the top 10 most-cited articles, the *Impact Index Per Article* ranged from 88.7 to 394.7.

Term co-occurrence cluster analysis of research hotspots

In the context of COVID-19 and liver research, co-occurrence analysis was used to identify the most commonly used terms in the titles and abstracts of the relevant articles. In this case, VOSviewer was used to create a bubble map, which represents each term as a bubble, and the bubble size indicates the frequency of occurrence of that term. The analysis identified 172 terms that occurred at least 50 times in the titles and abstracts of the included publications (Figure 2). The bubbles are grouped into clusters based on the similarity of their co-occurrence patterns. There are three different groups: (1) The blue cluster, which is named 'COVID-19 vaccines in liver transplant recipients'; (2) the red group, which is titled 'liver function tests as a predictor of COVID-19 severity and clinical outcomes of COVID-19 in hospitalised patients'; and (3) the green group, which is titled 'care of patients with liver disease during the COVID-19 pandemic'.

DISCUSSION

The correlation between liver injury and COVID-19 is associated with the severity and mortality of the disease. These findings strongly indicate a relationship between liver injury and COVID-19. Despite the observation that severe and fatal cases of the disease primarily affect older adults with liver injury, the specific underlying mechanisms remain unclear[55].

The findings indicate that the United States, China and Italy have been actively involved in COVID-19 and liver dysfunction research and have produced many publications on the subject. Numerous studies on the productivity of COVID-19 research in various fields[56-60], as measured by publications, have found that the United States, China and Italy have been the leading producers of COVID-19 publications. The United States and China have dominated research output in numerous fields, including the health sciences[61,62]. According to a report released by Japan's Science and Technology Ministry, China has emerged as the global frontrunner in scientific research output, surpassing the United States in both overall volume and the number of impactful studies. The report, published by Japan's National Institute of Science and Technology Policy, revealed that China now leads the world in annual scientific research paper publications, followed by the United States and Germany[63]. There are several factors that contribute to both the United States and China being leaders in scientific research. These factors include the size of their economies, the significant amount of money invested in research and development, and the large number of researchers working across various fields[64,65]. Notably, both countries have allocated significant funds to healthcare and biotechnology[61,65-67], ensuring that

Table 1 The top 10 countries contributing to research related to coronavirus disease 2019 and liver

Ranking	Country	No. of documents	%
1st	United States	497	21.28
2nd	China	393	16.82
3rd	Italy	255	10.92
4th	India	185	7.92
5th	United Kingdom	170	7.28
6th	Spain	125	5.35
7th	Germany	107	4.58
8th	Iran	97	4.15
9th	France	74	3.17
9th	Turkey	74	3.17

Table 2 The top 10 institutions contributing to research related to coronavirus disease 2019 and liver

Ranking	Institute	Country	No. of documents	%
1st	*Huazhong University of Science and Technology*	China	55	2.35
2nd	*Tongji Medical College*	China	53	2.27
3rd	*Centro de Investigación Biomédica en Red de Enfermedades Hepáticas y Digestivas*	Spain	48	2.05
4th	*INSERM*	France	36	1.54
4th	*University of Pennsylvania*	United States	36	1.54
6th	*Yale School of Medicine*	United States	31	1.33
7th	*Hospital Clinic Barcelona*	Spain	30	1.28
8th	*AP-HP Assistance Publique - Hopitaux de Paris*	France	29	1.24
8th	*Zhejiang University School of Medicine*	China	29	1.24
10th	*Universitat de Barcelona*	Spain	26	1.11

Table 3 Top 10 active journals publishing research related to coronavirus disease 2019 and liver

Ranking	Journal/source title	No. of documents	%	IF[1]
1st	*Journal of Hepatology*	85	3.64	30.083
2nd	*Liver International*	64	2.74	8.754
3rd	*World Journal of Gastroenterology*	62	2.65	5.374
4th	*Hepatology*	50	2.14	17.298
5th	*Hepatology Communications*	37	1.58	5.701
6th	*Clinical Gastroenterology and Hepatology*	36	1.54	13.576
7th	*Liver Transplantation*	34	1.46	6.112
7th	*World Journal of Hepatology*	34	1.46	NA
9th	*World Journal of Clinical Cases*	32	1.37	1.534
10th	*Journal of Clinical and Experimental Hepatology*	31	1.33	NA

[1]Impact factors were retrieved from the 2021 Journal Citation Reports (Clarivate Analytics).

Table 4 Top 10 articles on total citations for research related to coronavirus disease 2019 and liver from 2020 to 2022

Ranking	Ref.	Title	Year	Source title	Cited by	Impact index per article[1]
1st	Zhang *et al* [13]	Liver injury in COVID-19: Management and challenges	2020	*The Lancet Gastroenterology and Hepatology*	1126	394.7
2nd	Mao *et al* [51]	Manifestations and prognosis of gastrointestinal and liver involvement in patients with COVID-19: A systematic review and meta-analysis	2020	*The Lancet Gastroenterology and Hepatology*	549	181
3rd	Cai *et al*[48]	COVID-19: Abnormal liver function tests	2020	*Journal of Hepatology*	542	177
4th	Xu *et al*[53]	Liver injury during highly pathogenic human coronavirus infections	2020	*Liver International*	522	186
5th	Fan *et al*[49]	Clinical Features of COVID-19-Related Liver Functional Abnormality	2020	*Clinical Gastroenterology and Hepatology*	460	156.7
6th	Wang *et al* [52]	SARS-CoV-2 infection of the liver directly contributes to hepatic impairment in patients with COVID-19	2020	*Journal of Hepatology*	347	117.7
7th	Boettler *et al*[47]	Care of patients with liver disease during the COVID-19 pandemic: EASL-ESCMID position paper	2020	*JHEP Reports*	326	88.7
8th	Ji *et al*[50]	Nonalcoholic fatty liver diseases in patients with COVID-19: A retrospective study	2020	*Journal of Hepatology*	314	112
9th	Zhang *et al* [54]	Liver impairment in COVID-19 patients: A retrospective analysis of 115 cases from a single center in Wuhan city, China	2020	*Liver International*	289	97.7
10th	Bangash *et al*[46]	COVID-19 and the liver: Little cause for concern	2020	*The Lancet Gastroenterology and Hepatology*	283	90.7

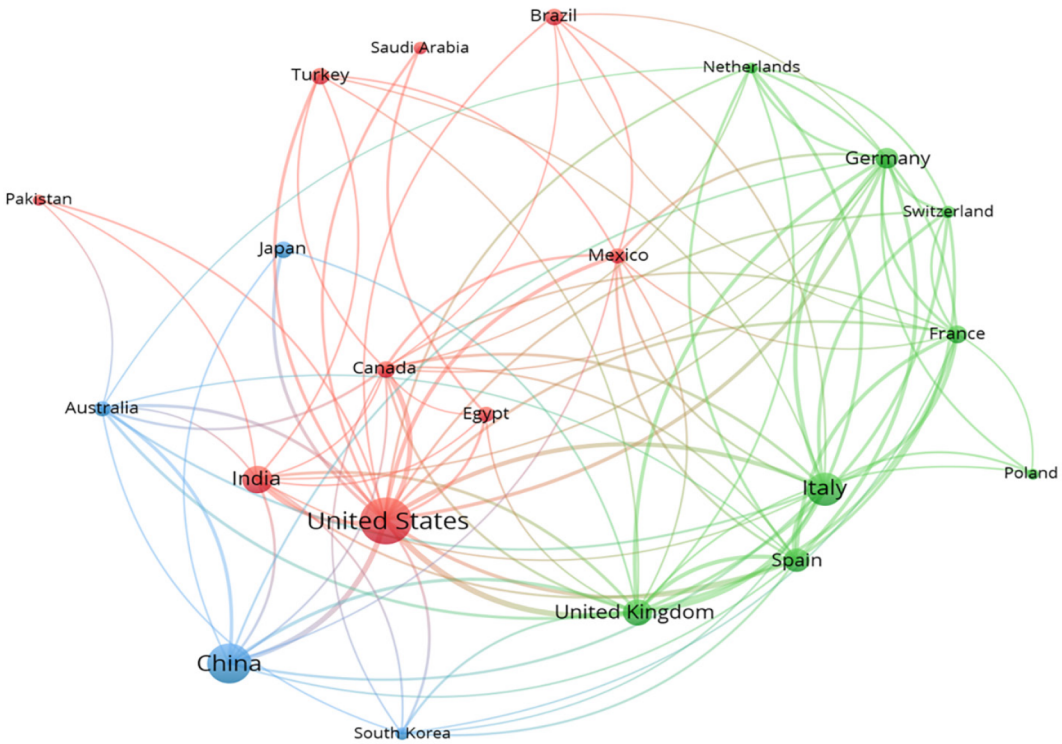
[1]The Impact Index Per Article is presented based on Reference Citation Analysis (Source: Baishideng Publishing Group Inc. Pleasanton, CA 94566, United States). COVID-19: Coronavirus disease 2019.

researchers have the resources they need to conduct thorough studies that yield reliable results. Furthermore, both countries have large and diverse scientific communities that encourage interdisciplinary research and expert collaboration. Funding also plays a pivotal role in driving research output, as researchers studying COVID-19 and liver dysfunction in both countries can seek substantial grants. These grants provide the necessary resources to pursue ambitious research projects, and thus attract top talent, and address critical health issues. Notable organizations such as the National Natural Science Foundation of China[68-70], the National Institutes of Health[71,72], and Gilead Sciences[47,73] offer sizable grants for researchers studying COVID-19 and liver dysfunction in the United States and China.

One of the key hotspots in the current study is 'COVID-19 vaccines in liver transplant recipients'. Solid organ transplant recipients face a significant risk of death from COVID-19, with mortality rates ranging from 13% to 39%[74,75]. As a result, many countries have given priority to vaccinating this vulnerable group using messenger RNA (mRNA) vaccines. Nonetheless, there is limited information available regarding their response to vaccination and its effectiveness [76]. It is critical that liver transplant recipients receive the COVID-19 vaccine to avoid hospitalisation and serious illness. COVID-19 vaccines are safe and effective in people who have had liver transplants. It should be noted, however, that these vaccines may not elicit as strong an immune response as in healthy individuals[77]. As a result, liver transplant recipients should consult their health care providers about the best time to get vaccinated, considering their specific immunosuppression regimens and recent transplant surgeries[78]. Patients who have had a liver transplant should talk to their doctors about whether they need more vaccine doses or a different vaccine to maximise their immune response[79].

'Liver function tests as a predictor of COVID-19 severity and clinical outcomes in hospitalised patients' is another study topic. Liver function tests (LFTs) are regularly conducted in hospitalised patients with COVID-19 to assess disease severity and the likelihood of poor clinical outcomes[80]. COVID-19 causes liver inflammation and abnormal LFT results [81]. In 2022, the *World Journal of Gastroenterology* reported that abnormal levels of aspartate aminotransferase (AST) and total bilirubin (T-Bil) are associated with higher mortality rates than other liver damage indicators during hospitalisation. Vasopressor medications and mechanical ventilation are linked to abnormal AST, T-Bil, and alkaline phosphatase (ALP) levels. Thus, patients with COVID-19 often have abnormal LFT results upon hospital admission, which can predict their severity and prognosis. Health care practitioners can assess risk and predict the need for advanced treatment for these individuals by measuring alanine transaminase (ALT), AST, ALP and T-Bil[82]. Patients with COVID-19 and abnormal LFT results may also have prior liver disease, medication toxicity or bacterial or viral coinfection. Thus, LFT results should be included with other clinical and laboratory data when predicting severity and clinical outcomes[83,84].

The treatment of liver disease has become increasingly important during the COVID-19 pandemic. Individuals with liver disease are more vulnerable to COVID-19-related severe illness and mortality due to factors such as a compromised immune system, advanced age and underlying health conditions[85]. Given this scenario, patients must carefully prioritise pandemic preparedness measures. Any deviation from their treatment plan – missed appointments or delayed therapy – can aggravate their liver disease and increase their COVID-19 risks[86]. Therefore, individuals with liver



DOI: 10.3748/wjg.v29.i27.4356 **Copyright** ©The Author(s) 2023.

Figure 1 Network visualization map of country collaboration. A minimum of 30 documents per country was set as a threshold, and 22 countries met the threshold. Countries can be represented as nodes in a network visualization made with VOSviewer, and lines can be created between the nodes to show correlations between co-occurrences. The strength of the co-occurrence link between the countries can be determined by the line's thickness or weight. Thicker lines are frequently used to depict stronger links.

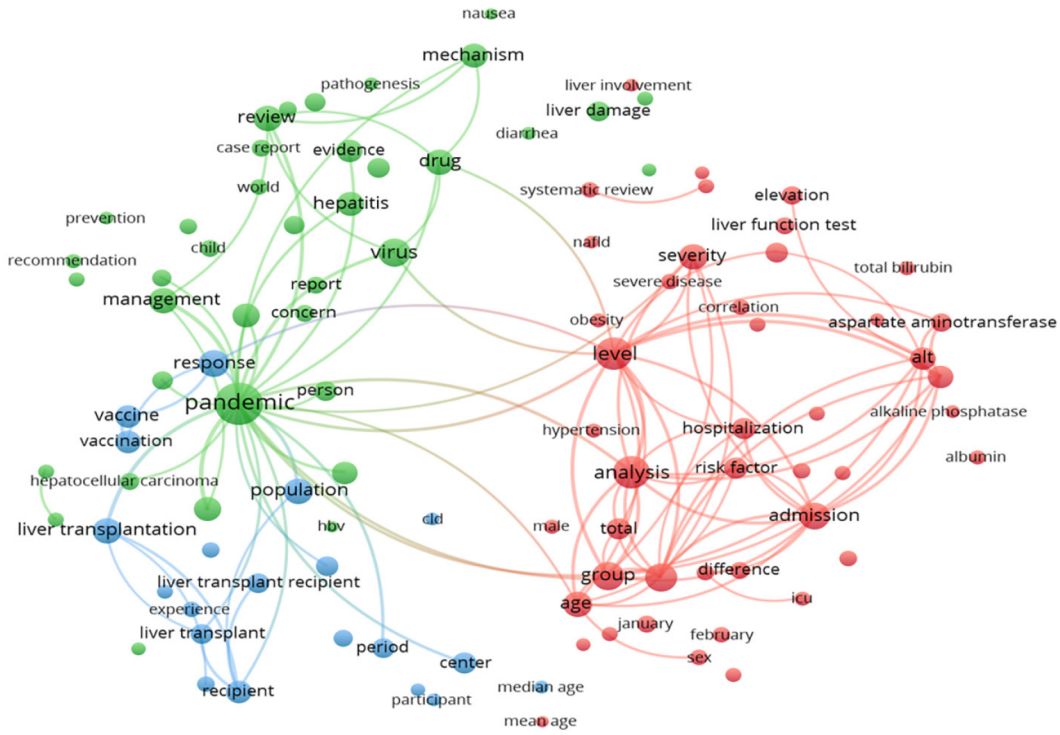
disease should take COVID-19 precautions such as frequent and thorough handwashing, avoid large crowds and wear face masks[87]. Adopting a healthy lifestyle is also important for strengthening their immune systems and preventing COVID-19 complications. This includes regular exercise, a balanced diet, abstaining from alcohol and smoking, and getting enough sleep[88,89].

Strengths and limitations

Although this is the first bibliometric analysis to assess the worldwide research output in the field of COVID-19 and liver dysfunction, according to previous similar studies, this study had several limitations, and it is essential to acknowledge them to ensure transparency and to promote further research in the field. First, Scopus is a widely used database for bibliometric analyses, and its coverage of peer-reviewed literature is generally comprehensive. However, the bibliometric analysis may not capture all the relevant COVID-19 and liver research publications because not all journals are indexed in Scopus, and some of the relevant publications may have been published in non-indexed or non-English-language journals. Second, searching for publications based on MeSH terms in the title is a common practice in bibliometric analysis to ensure the accuracy and relevance of the search results. However, including some publications that use related terms in other parts of the document may be a mistake. Therefore, it is recommended to use a combination of search terms, including title, abstract and keywords, to increase the sensitivity of the search. If false-negative results had occurred in the current study, they would have had little effect on the overall results. Third, the analysis may not account for the quality of the publications, as it only counts the number of publications without assessing their impact, significance or credibility. Furthermore, the ranking of publications based on total citations rather than annual citation averages could have excluded some recently published high-quality studies. However, this does not undermine the importance or contribution of these publications to the field. It is essential to note that the limitations identified in this bibliometric analysis could affect the precision and completeness of the obtained results. However, these limitations do not significantly compromise the study's validity.

CONCLUSION

This bibliometric study provides a comprehensive overview of liver-related publications in COVID-19 research over the past 3 years. It highlights the significant contributions of high-income nations, particularly the United States, China and Italy, to the scholarly liver-related literature in this field. Most of the articles focus on liver dysfunction in patients with COVID-19 and the implications of the virus for gastroenterologists and hepatologists. Although the study acknowledges the importance of abnormal LFTs in COVID-19, it also identifies knowledge gaps regarding their pathophysiological and



DOI: 10.3748/wjg.v29.i27.4356 **Copyright** ©The Author(s) 2023.

Figure 2 Research topics clustered by mapping the co-occurrences of terms in the title/abstract of publications on research related to coronavirus disease 2019 and liver. Of the 26722 terms, 172 terms occurred at least 50 times. The largest set of connected terms was stratified into three clusters. VOSviewer may produce a network visualization in which terms are represented as nodes and co-occurrence connections are depicted by lines connecting the nodes. The strength of the association between the terms' co-occurrence can be determined by the line's thickness or weight. Thicker lines are frequently used to depict stronger links.

prognostic value. This study indicates that well-designed prospective studies with specific research questions can be used to fill in these gaps and further investigate the topic. This bibliometric analysis provides a solid foundation for future research on liver injury and treatment for COVID-19. The findings of this study can be used by decision-makers or researchers to prioritise research areas and allocate resources to enhance our understanding of the impact of COVID-19 on liver function.

ARTICLE HIGHLIGHTS

Research background

Abnormal liver chemistry findings are commonly observed in individuals with coronavirus disease 2019 (COVID-19). As a result, there is a significant body of literature comprising published clinical studies that specifically examine the implications of hepatic involvement in COVID-19.

Research motivation

Understanding the current state of research and hotspots in the field of COVID-19 and liver dysfunction is crucial for identifying knowledge gaps and informing future research directions.

Research objectives

The purpose of this study is to present a comprehensive overview of the existing research on COVID-19 and liver dysfunction through the utilization of bibliometric analysis.

Research methods

A thorough and validated search query was conducted using the SciVerse Scopus database to identify relevant publications on the topic of COVID-19 and liver dysfunction. Subsequently, the research hotspots in related fields were examined using VOSviewer software.

Research results

Three distinct clusters of topics were identified: COVID-19 vaccines in liver transplant recipients, liver function tests as predictors of severity and clinical outcomes in hospitalized patients, and the care of patients with liver disease during the

COVID-19 pandemic.

Research conclusions

The first bibliometric analysis is presented here, which is represented by the study and offers valuable insights into the research landscape on COVID-19 and liver dysfunction. Valuable reference can be derived from the findings in this field by scholars, as a comprehensive summary is provided and the frontiers of research related to COVID-19 and liver dysfunction are identified.

Research perspectives

The goal of this study is to have current areas of focus within the field of COVID-19 and liver dysfunction identified, which can help future research be guided and clinical practice be informed. By using bibliometric analysis, a comprehensive overview of the literature on this topic is provided by the study, and the latest developments in the field can be kept up-to-date by researchers and clinicians.

FOOTNOTES

Author contributions: Zyoud S developed the concept for the manuscript, reviewed the literature, formulated research questions, collected the data, conducted analyses and interpreted the data, and wrote the manuscript; Zyoud S read and approved the final manuscript.

Conflict-of-interest statement: All the authors report no relevant conflicts of interest for this article.

PRISMA 2009 Checklist statement: The authors have read the PRISMA 2009 Checklist, and the manuscript was prepared and revised according to the PRISMA 2009 Checklist.

Open-Access: This article is an open-access article that was selected by an in-house editor and fully peer-reviewed by external reviewers. It is distributed in accordance with the Creative Commons Attribution NonCommercial (CC BY-NC 4.0) license, which permits others to distribute, remix, adapt, build upon this work non-commercially, and license their derivative works on different terms, provided the original work is properly cited and the use is non-commercial. See: https://creativecommons.org/Licenses/by-nc/4.0/

Country/Territory of origin: Palestine

ORCID number: Sa'ed H Zyoud 0000-0002-7369-2058.

S-Editor: Li L
L-Editor: A
P-Editor: Yu HG

REFERENCES

1 **World Health Organization**. WHO Coronavirus (COVID-19) Dashboard. 2023. [cited 3 May 2023]. Available from: https://covid19.who.int/

2 **Guan WJ**, Ni ZY, Hu Y, Liang WH, Ou CQ, He JX, Liu L, Shan H, Lei CL, Hui DSC, Du B, Li LJ, Zeng G, Yuen KY, Chen RC, Tang CL, Wang T, Chen PY, Xiang J, Li SY, Wang JL, Liang ZJ, Peng YX, Wei L, Liu Y, Hu YH, Peng P, Wang JM, Liu JY, Chen Z, Li G, Zheng ZJ, Qiu SQ, Luo J, Ye CJ, Zhu SY, Zhong NS; China Medical Treatment Expert Group for Covid-19. Clinical Characteristics of Coronavirus Disease 2019 in China. *N Engl J Med* 2020; **382**: 1708-1720 [PMID: 32109013 DOI: 10.1056/NEJMoa2002032]

3 **Chen G**, Wu D, Guo W, Cao Y, Huang D, Wang H, Wang T, Zhang X, Chen H, Yu H, Zhang M, Wu S, Song J, Chen T, Han M, Li S, Luo X, Zhao J, Ning Q. Clinical and immunological features of severe and moderate coronavirus disease 2019. *J Clin Invest* 2020; **130**: 2620-2629 [PMID: 32217835 DOI: 10.1172/JCI137244]

4 **Lai CC**, Shih TP, Ko WC, Tang HJ, Hsueh PR. Severe acute respiratory syndrome coronavirus 2 (SARS-CoV-2) and coronavirus disease-2019 (COVID-19): The epidemic and the challenges. *Int J Antimicrob Agents* 2020; **55**: 105924 [PMID: 32081636 DOI: 10.1016/j.ijantimicag.2020.105924]

5 **Verity R**, Okell LC, Dorigatti I, Winskill P, Whittaker C, Imai N, Cuomo-Dannenburg G, Thompson H, Walker PGT, Fu H, Dighe A, Griffin JT, Baguelin M, Bhatia S, Boonyasiri A, Cori A, Cucunubá Z, FitzJohn R, Gaythorpe K, Green W, Hamlet A, Hinsley W, Laydon D, Nedjati-Gilani G, Riley S, van Elsland S, Volz E, Wang H, Wang Y, Xi X, Donnelly CA, Ghani AC, Ferguson NM. Estimates of the severity of coronavirus disease 2019: a model-based analysis. *Lancet Infect Dis* 2020; **20**: 669-677 [PMID: 32240634 DOI: 10.1016/S1473-3099(20)30243-7]

6 **Wang C**, Pan R, Wan X, Tan Y, Xu L, Ho CS, Ho RC. Immediate Psychological Responses and Associated Factors during the Initial Stage of the 2019 Coronavirus Disease (COVID-19) Epidemic among the General Population in China. *Int J Environ Res Public Health* 2020; **17** [PMID: 32155789 DOI: 10.3390/ijerph17051729]

7 **Fu Y**, Zhu R, Bai T, Han P, He Q, Jing M, Xiong X, Zhao X, Quan R, Chen C, Zhang Y, Tao M, Yi J, Tian D, Yan W. Clinical Features of Patients Infected With Coronavirus Disease 2019 With Elevated Liver Biochemistries: A Multicenter, Retrospective Study. *Hepatology* 2021; **73**: 1509-1520 [PMID: 32602604 DOI: 10.1002/hep.31446]

8 **Hao SR**, Zhang SY, Lian JS, Jin X, Ye CY, Cai H, Zhang XL, Hu JH, Zheng L, Zhang YM, Jia HY, Yu GD, Wang XY, Gu JQ, Lu YF, Yu

XP, Yu L, Xiang DR, Jin CL, Qiu YQ, Li LJ, Sheng JF, Liang TB, Yang YD. Liver Enzyme Elevation in Coronavirus Disease 2019: A Multicenter, Retrospective, Cross-Sectional Study. *Am J Gastroenterol* 2020; **115**: 1075-1083 [PMID: 32618658 DOI: 10.14309/ajg.0000000000000717]

9 **Lippi G**, de Oliveira MHS, Henry BM. Chronic liver disease is not associated with severity or mortality in Coronavirus disease 2019 (COVID-19): a pooled analysis. *Eur J Gastroenterol Hepatol* 2021; **33**: 114-115 [PMID: 32282549 DOI: 10.1097/MEG.0000000000001742]

10 **Musa S**. Hepatic and gastrointestinal involvement in coronavirus disease 2019 (COVID-19): What do we know till now? *Arab J Gastroenterol* 2020; **21**: 3-8 [PMID: 32253172 DOI: 10.1016/j.ajg.2020.03.002]

11 **Parohan M**, Yaghoubi S, Seraji A. Liver injury is associated with severe coronavirus disease 2019 (COVID-19) infection: A systematic review and meta-analysis of retrospective studies. *Hepatol Res* 2020; **50**: 924-935 [PMID: 32386449 DOI: 10.1111/hepr.13510]

12 **Wong YJ**, Tan M, Zheng Q, Li JW, Kumar R, Fock KM, Teo EK, Ang TL. A systematic review and meta-analysis of the COVID-19 associated liver injury. *Ann Hepatol* 2020; **19**: 627-634 [PMID: 32882393 DOI: 10.1016/j.aohep.2020.08.064]

13 **Zhang C**, Shi L, Wang FS. Liver injury in COVID-19: management and challenges. *Lancet Gastroenterol Hepatol* 2020; **5**: 428-430 [PMID: 32145190 DOI: 10.1016/S2468-1253(20)30057-1]

14 **Saha L**, Vij S, Rawat K. Liver injury induced by COVID 19 treatment - what do we know? *World J Gastroenterol* 2022; **28**: 6314-6327 [PMID: 36533104 DOI: 10.3748/wjg.v28.i45.6314]

15 **Naeem M**, Bano N, Manzoor S, Ahmad A, Munawar N, Razak SIA, Lee TY, Devaraj S, Hazafa A. Pathogenetic Mechanisms of Liver-Associated Injuries, Management, and Current Challenges in COVID-19 Patients. *Biomolecules* 2023; **13** [PMID: 36671484 DOI: 10.3390/biom13010099]

16 **Bzeizi K**, Abdulla M, Mohammed N, Alqamish J, Jamshidi N, Broering D. Effect of COVID-19 on liver abnormalities: a systematic review and meta-analysis. *Sci Rep* 2021; **11**: 10599 [PMID: 34012016 DOI: 10.1038/s41598-021-89513-9]

17 **Del Zompo F**, De Siena M, Ianiro G, Gasbarrini A, Pompili M, Ponziani FR. Prevalence of liver injury and correlation with clinical outcomes in patients with COVID-19: systematic review with meta-analysis. *Eur Rev Med Pharmacol Sci* 2020; **24**: 13072-13088 [PMID: 33378061 DOI: 10.26355/eurrev_202012_24215]

18 **Abdulla S**, Hussain A, Azim D, Abduallah EH, Elawamy H, Nasim S, Kumar S, Naveed H. COVID-19-Induced Hepatic Injury: A Systematic Review and Meta-Analysis. *Cureus* 2020; **12**: e10923 [PMID: 33194489 DOI: 10.7759/cureus.10923]

19 **Puli S**, Baig M, Walayat S. Gastrointestinal Symptoms and Elevation in Liver Enzymes in COVID-19 Infection: A Systematic Review and Meta-Analysis. *Cureus* 2020; **12**: e9999 [PMID: 32983698 DOI: 10.7759/cureus.9999]

20 **Shokri Afra H**, Amiri-Dashatan N, Ghorbani F, Maleki I, Rezaei-Tavirani M. Positive association between severity of COVID-19 infection and liver damage: a systematic review and meta-analysis. *Gastroenterol Hepatol Bed Bench* 2020; **13**: 292-304 [PMID: 33244371]

21 **Vargas-Mendoza N**, García-Machorro J, Angeles-Valencia M, Martínez-Archundia M, Madrigal-Santillán EO, Morales-González Á, Anguiano-Robledo L, Morales-González JA. Liver disorders in COVID-19, nutritional approaches and the use of phytochemicals. *World J Gastroenterol* 2021; **27**: 5630-5665 [PMID: 34629792 DOI: 10.3748/wjg.v27.i34.5630]

22 **Kulkarni AV**, Aziz B, Shams I, Busse JW. Comparisons of citations in Web of Science, Scopus, and Google Scholar for articles published in general medical journals. *JAMA* 2009; **302**: 1092-1096 [PMID: 19738094 DOI: 10.1001/jama.2009.1307]

23 **De Groote SL**, Raszewski R. Coverage of Google Scholar, Scopus, and Web of Science: a case study of the h-index in nursing. *Nurs Outlook* 2012; **60**: 391-400 [PMID: 22748758 DOI: 10.1016/j.outlook.2012.04.007]

24 **Powell KR**, Peterson SR. Coverage and quality: A comparison of Web of Science and Scopus databases for reporting faculty nursing publication metrics. *Nurs Outlook* 2017; **65**: 572-578 [PMID: 28377037 DOI: 10.1016/j.outlook.2017.03.004]

25 **Zyoud SH**, Al-Jabi SW, Shahwan MJ, Jairoun AA. Global research production pertaining to gastrointestinal involvement in COVID-19: A bibliometric and visualised study. *World J Gastrointest Surg* 2022; **14**: 494-505 [PMID: 35734615 DOI: 10.4240/wjgs.v14.i5.494]

26 **Zyoud SH**, Shakhshir M, Abushanab AS, Koni A, Shahwan M, Jairoun AA, Al-Jabi SW. Mapping the output of the global literature on the links between gut microbiota and COVID-19. *J Health Popul Nutr* 2023; **42**: 3 [PMID: 36653831 DOI: 10.1186/s41043-023-00346-w]

27 **Xavier-Santos D**, Padilha M, Fabiano GA, Vinderola G, Gomes Cruz A, Sivieri K, Costa Antunes AE. Evidences and perspectives of the use of probiotics, prebiotics, synbiotics, and postbiotics as adjuvants for prevention and treatment of COVID-19: A bibliometric analysis and systematic review. *Trends Food Sci Technol* 2022; **120**: 174-192 [PMID: 35002079 DOI: 10.1016/j.tifs.2021.12.033]

28 **Al-Jabi SW**. Current global research landscape on COVID-19 and depressive disorders: Bibliometric and visualization analysis. *World J Psychiatry* 2021; **11**: 253-264 [PMID: 34168972 DOI: 10.5498/wjp.v11.i6.253]

29 **Tantengco OAG**. Investigating the evolution of COVID-19 research trends and collaborations in Southeast Asia: A bibliometric analysis. *Diabetes Metab Syndr* 2021; **15**: 102325 [PMID: 34739909 DOI: 10.1016/j.dsx.2021.102325]

30 **Cheung KS**, Mok CH, Mao X, Zhang R, Hung IF, Seto WK, Yuen MF. COVID-19 vaccine immunogenicity among chronic liver disease patients and liver transplant recipients: A meta-analysis. *Clin Mol Hepatol* 2022; **28**: 890-911 [PMID: 36263669 DOI: 10.3350/cmh.2022.0087]

31 **Dong X**, Zeng DY, Xing QQ, Hong MZ, Pan JS. Liver chemistries in severe or non-severe cases of COVID-19: A systematic review and meta-analysis. *World J Hepatol* 2022; **14**: 2012-2024 [PMID: 36618330 DOI: 10.4254/wjh.v14.i12.2012]

32 **Nagarajan R**, Krishnamoorthy Y, Rajaa S, Hariharan VS. COVID-19 Severity and Mortality Among Chronic Liver Disease Patients: A Systematic Review and Meta-Analysis. *Prev Chronic Dis* 2022; **19**: E53 [PMID: 36007255 DOI: 10.5888/pcd19.210228]

33 **Yang R**, Feng J, Wan H, Zeng X, Ji P, Zhang J. Liver injury associated with the severity of COVID-19: A meta-analysis. *Front Public Health* 2023; **11**: 1003352 [PMID: 36817905 DOI: 10.3389/fpubh.2023.1003352]

34 **Yoo JJ**, Yon DK, Lee SW, Shin JI, Kim BK. Humoral Immunogenicity to SARS-CoV-2 Vaccination in Liver Transplant Recipients: A Systematic Review and Meta-Analysis. *Int J Biol Sci* 2022; **18**: 5849-5857 [PMID: 36263175 DOI: 10.7150/ijbs.77030]

35 **Sweileh WM**. A bibliometric analysis of global research output on health and human rights (1900-2017). *Glob Health Res Policy* 2018; **3**: 30 [PMID: 30377667 DOI: 10.1186/s41256-018-0085-8]

36 **Sweileh WM**, Al-Jabi SW, Zyoud SH, Shraim NY, Anayah FMA, Sawalha AF, AbuTaha AS. Bibliometric analysis of global publications in medication adherence (1900-2017). *Int J Pharm Pract* 2019; **27**: 112-120 [PMID: 30044514 DOI: 10.1111/ijpp.12471]

37 **Sweileh WM**. Substandard and falsified medical products: bibliometric analysis and mapping of scientific research. *Global Health* 2021; **17**: 114 [PMID: 34556126 DOI: 10.1186/s12992-021-00766-5]

38 **Sweileh WM**. Global research activity on mathematical modeling of transmission and control of 23 selected infectious disease outbreak. *Global Health* 2022; **18**: 4 [PMID: 35062966 DOI: 10.1186/s12992-022-00803-x]

39 **Zyoud SH**. The state of current research on COVID-19 and antibiotic use: global implications for antimicrobial resistance. *J Health Popul Nutr* 2023; **42**: 42 [PMID: 37173756 DOI: 10.1186/s41043-023-00386-2]

40 **Wang JL**, Ma YJ, Ma L, Ma N, Guo DM, Ma LS. Baishideng's Reference Citation Analysis database announces the first Article Influence Index of multidisciplinary scholars. *World J Clin Cases* 2022; **10**: 10391-10398 [PMID: 36312463 DOI: 10.12998/wjcc.v10.i29.10391]

41 **Wang JL**, Ma YJ, Ma L, Ma N, Guo DM, Ma LS. Baishideng's Reference Citation Analysis database announces the first Journal Article Influence Index of 101 core journals and a list of high-quality academic journals in gastroenterology and hepatology. *World J Gastroenterol* 2022; **28**: 5383-5394 [PMID: 36312837 DOI: 10.3748/wjg.v28.i37.5383]

42 **Wang JL**, Ma YJ, Ma L, Ma N, Guo DM, Ma LS. Baishideng's Reference Citation Analysis database announces the first Journal Article Influence Index of 104 core journals and a list of high-quality academic journals in orthopedics. *World J Orthop* 2022; **13**: 891-902 [PMID: 36312521 DOI: 10.5312/wjo.v13.i10.891]

43 **van Eck NJ**, Waltman L. Software survey: VOSviewer, a computer program for bibliometric mapping. *Scientometrics* 2010; **84**: 523-538 [PMID: 20585380 DOI: 10.1007/s11192-009-0146-3]

44 **Flis I**, van Eck NJ. Framing psychology as a discipline (1950-1999): A large-scale term co-occurrence analysis of scientific literature in psychology. *Hist Psychol* 2018; **21**: 334-362 [PMID: 28726441 DOI: 10.1037/hop0000067]

45 **van Eck NJ**, Waltman L. Citation-based clustering of publications using CitNetExplorer and VOSviewer. *Scientometrics* 2017; **111**: 1053-1070 [PMID: 28490825 DOI: 10.1007/s11192-017-2300-7]

46 **Bangash MN**, Patel J, Parekh D. COVID-19 and the liver: little cause for concern. *Lancet Gastroenterol Hepatol* 2020; **5**: 529-530 [PMID: 32203680 DOI: 10.1016/S2468-1253(20)30084-4]

47 **Boettler T**, Newsome PN, Mondelli MU, Maticic M, Cordero E, Cornberg M, Berg T. Care of patients with liver disease during the COVID-19 pandemic: EASL-ESCMID position paper. *JHEP Rep* 2020; **2**: 100113 [PMID: 32289115 DOI: 10.1016/j.jhepr.2020.100113]

48 **Cai Q**, Huang D, Yu H, Zhu Z, Xia Z, Su Y, Li Z, Zhou G, Gou J, Qu J, Sun Y, Liu Y, He Q, Chen J, Liu L, Xu L. COVID-19: Abnormal liver function tests. *J Hepatol* 2020; **73**: 566-574 [PMID: 32298767 DOI: 10.1016/j.jhep.2020.04.006]

49 **Fan Z**, Chen L, Li J, Cheng X, Yang J, Tian C, Zhang Y, Huang S, Liu Z, Cheng J. Clinical Features of COVID-19-Related Liver Functional Abnormality. *Clin Gastroenterol Hepatol* 2020; **18**: 1561-1566 [PMID: 32283325 DOI: 10.1016/j.cgh.2020.04.002]

50 **Ji D**, Qin E, Xu J, Zhang D, Cheng G, Wang Y, Lau G. Non-alcoholic fatty liver diseases in patients with COVID-19: A retrospective study. *J Hepatol* 2020; **73**: 451-453 [PMID: 32278005 DOI: 10.1016/j.jhep.2020.03.044]

51 **Mao R**, Qiu Y, He JS, Tan JY, Li XH, Liang J, Shen J, Zhu LR, Chen Y, Iacucci M, Ng SC, Ghosh S, Chen MH. Manifestations and prognosis of gastrointestinal and liver involvement in patients with COVID-19: a systematic review and meta-analysis. *Lancet Gastroenterol Hepatol* 2020; **5**: 667-678 [PMID: 32405603 DOI: 10.1016/S2468-1253(20)30126-6]

52 **Wang Y**, Liu S, Liu H, Li W, Lin F, Jiang L, Li X, Xu P, Zhang L, Zhao L, Cao Y, Kang J, Yang J, Li L, Liu X, Li Y, Nie R, Mu J, Lu F, Zhao S, Lu J, Zhao J. SARS-CoV-2 infection of the liver directly contributes to hepatic impairment in patients with COVID-19. *J Hepatol* 2020; **73**: 807-816 [PMID: 32437830 DOI: 10.1016/j.jhep.2020.05.002]

53 **Xu L**, Liu J, Lu M, Yang D, Zheng X. Liver injury during highly pathogenic human coronavirus infections. *Liver Int* 2020; **40**: 998-1004 [PMID: 32170806 DOI: 10.1111/liv.14435]

54 **Zhang Y**, Zheng L, Liu L, Zhao M, Xiao J, Zhao Q. Liver impairment in COVID-19 patients: A retrospective analysis of 115 cases from a single centre in Wuhan city, China. *Liver Int* 2020; **40**: 2095-2103 [PMID: 32239796 DOI: 10.1111/liv.14455]

55 **Wu ZH**, Yang DL. A meta-analysis of the impact of COVID-19 on liver dysfunction. *Eur J Med Res* 2020; **25**: 54 [PMID: 33148326 DOI: 10.1186/s40001-020-00454-x]

56 **Zyoud SH**, Shakhshir M, Koni A, Shahwan M, Jairoun AA, Al-Jabi SW. Olfactory and Gustatory Dysfunction in COVID-19: A Global Bibliometric and Visualized Analysis. *Ann Otol Rhinol Laryngol* 2023; **132**: 164-172 [PMID: 35240864 DOI: 10.1177/00034894221082735]

57 **Doskaliuk B**, Yatsyshyn R, Klishch I, Zimba O. COVID-19 from a rheumatology perspective: bibliometric and altmetric analysis. *Rheumatol Int* 2021; **41**: 2091-2103 [PMID: 34596719 DOI: 10.1007/s00296-021-04987-0]

58 **Wei N**, Xu Y, Wang H, Jia Q, Shou X, Zhang X, Zhang N, Li Y, Zhai H, Hu Y. Bibliometric and visual analysis of cardiovascular diseases and COVID-19 research. *Front Public Health* 2022; **10**: 1022810 [PMID: 36568760 DOI: 10.3389/fpubh.2022.1022810]

59 **Xu SC**, Zhao XY, Xing HP, Wu W, Zhang SY. Cardiac Involvement in COVID-19: A Global Bibliometric and Visualized Analysis. *Front Cardiovasc Med* 2022; **9**: 955237 [PMID: 35966543 DOI: 10.3389/fcvm.2022.955237]

60 **Zhao J**, Zhu J, Huang C, Zhu X, Zhu Z, Wu Q, Yuan R. Uncovering the information immunology journals transmitted for COVID-19: A bibliometric and visualization analysis. *Front Immunol* 2022; **13**: 1035151 [PMID: 36405695 DOI: 10.3389/fimmu.2022.1035151]

61 **Xie Y**, Zhang C, Lai Q. China's rise as a major contributor to science and technology. *Proc Natl Acad Sci U S A* 2014; **111**: 9437-9442 [PMID: 24979796 DOI: 10.1073/pnas.1407709111]

62 **Li M**, Liu X, Zhang L. Health sciences journals: an overview of outputs by Chinese authors. *Health Info Libr J* 2015; **32**: 255-264 [PMID: 26123736 DOI: 10.1111/hir.12112]

63 **The Guardian**. China overtakes the US in scientific research output. 2022. [Cited 10 June 2023] Available from: https://www.theguardian.com/world/2022/aug/11/china-overtakes-the-us-in-scientific-research-output

64 Optimizing the Nation's Investment in Academic Research: A New Regulatory Framework for the 21st Century. Washington (DC): National Academies Press (US); 2016-Jul-27 [PMID: 27386613]

65 **Momtazmanesh S**, Saghazadeh A, Becerra JCA, Aramesh K, Barba FJ, Bella F, Blakney A, Capaccioli M, Castagna R, Crisanti U, Davtyan T, Dorigo T, Ealy J, Farokhnia M, Grancini G, Gupta M, Harbi A, Krysztofiak W, Kulasinghe A, Lam CM, Leemans A, Lighthill B, Limongelli V, Lopreiato P, Luongo L, Maboloc CR, Malekzadeh R, Gomes OC, Milosevic M, Nouwen J, Ortega-Sánchez D, Pawelek J, Pramanik S, Ramakrishna S, Renn O, Sanseviero S, Sauter D, Schreiber M, Sellke FW, Shahbazi MA, Shelkovaya N, Slater WH, Snoeck D, Sztajer S, Uddin LQ, Veramendi-Espinoza L, Vinuesa R, Willett WC, Wu D, Żyniewicz K, Rezaei N. International Scientific Collaboration Is Needed to Bridge Science to Society: USERN2020 Consensus Statement. *SN Compr Clin Med* 2021; **3**: 1699-1703 [PMID: 33997623 DOI: 10.1007/s42399-021-00896-2]

66 **Xie Q**, Freeman RB. Bigger Than You Thought: China's Contribution to Scientific Publications and Its Impact on the Global Economy. *China & World Economy* 2019; **27**: 1-27 [DOI: 10.1111/cwe.12265]

67 **Kwiek M**. Internationalists and locals: international research collaboration in a resource-poor system. *Scientometrics* 2020; **124**: 57-105 [DOI: 10.1007/s11192-020-03460-2]

68 **Feng G**, Zheng KI, Yan QQ, Rios RS, Targher G, Byrne CD, Poucke SV, Liu WY, Zheng MH. COVID-19 and Liver Dysfunction: Current

Insights and Emergent Therapeutic Strategies. *J Clin Transl Hepatol* 2020; **8**: 18-24 [PMID: 32274342 DOI: 10.14218/JCTH.2020.00018]

69 **Li J**, Fan JG. Characteristics and Mechanism of Liver Injury in 2019 Coronavirus Disease. *J Clin Transl Hepatol* 2020; **8**: 13-17 [PMID: 32274341 DOI: 10.14218/JCTH.2020.00019]

70 **Targher G**, Mantovani A, Byrne CD, Wang XB, Yan HD, Sun QF, Pan KH, Zheng KI, Chen YP, Eslam M, George J, Zheng MH. Risk of severe illness from COVID-19 in patients with metabolic dysfunction-associated fatty liver disease and increased fibrosis scores. *Gut* 2020; **69**: 1545-1547 [PMID: 32414813 DOI: 10.1136/gutjnl-2020-321611]

71 **Webb GJ**, Marjot T, Cook JA, Aloman C, Armstrong MJ, Brenner EJ, Catana MA, Cargill T, Dhanasekaran R, García-Juárez I, Hagström H, Kennedy JM, Marshall A, Masson S, Mercer CJ, Perumalswami PV, Ruiz I, Thaker S, Ufere NN, Barnes E, Barritt AS 4th, Moon AM. Outcomes following SARS-CoV-2 infection in liver transplant recipients: an international registry study. *Lancet Gastroenterol Hepatol* 2020; **5**: 1008-1016 [PMID: 32866433 DOI: 10.1016/S2468-1253(20)30271-5]

72 **Marjot T**, Moon AM, Cook JA, Abd-Elsalam S, Aloman C, Armstrong MJ, Pose E, Brenner EJ, Cargill T, Catana MA, Dhanasekaran R, Eshraghian A, García-Juárez I, Gill US, Jones PD, Kennedy J, Marshall A, Matthews C, Mells G, Mercer C, Perumalswami PV, Avitabile E, Qi X, Su F, Ufere NN, Wong YJ, Zheng MH, Barnes E, Barritt AS 4th, Webb GJ. Outcomes following SARS-CoV-2 infection in patients with chronic liver disease: An international registry study. *J Hepatol* 2021; **74**: 567-577 [PMID: 33035628 DOI: 10.1016/j.jhep.2020.09.024]

73 **Zampino R**, Mele F, Florio LL, Bertolino L, Andini R, Galdo M, De Rosa R, Corcione A, Durante-Mangoni E. Liver injury in remdesivir-treated COVID-19 patients. *Hepatol Int* 2020; **14**: 881-883 [PMID: 32725454 DOI: 10.1007/s12072-020-10077-3]

74 **Azzi Y**, Bartash R, Scalea J, Loarte-Campos P, Akalin E. COVID-19 and Solid Organ Transplantation: A Review Article. *Transplantation* 2021; **105**: 37-55 [PMID: 33148977 DOI: 10.1097/TP.0000000000003523]

75 **Dumortier J**, Duvoux C, Roux O, Altieri M, Barraud H, Besch C, Caillard S, Coilly A, Conti F, Dharancy S, Durand F, Francoz C, Garaix F, Houssel-Debry P, Kounis I, Lassailly G, Laverdure N, Leroy V, Mallet M, Mazzola A, Meunier L, Radenne S, Richardet JP, Vanlemmens C, Hazzan M, Saliba F; French Solid Organ Transplant COVID Registry; Groupe de Recherche Français en Greffe de Foie (GReF²). Covid-19 in liver transplant recipients: the French SOT COVID registry. *Clin Res Hepatol Gastroenterol* 2021; **45**: 101639 [PMID: 33636654 DOI: 10.1016/j.clinre.2021.101639]

76 **Tu ZH**, Jin PB, Chen DY, Chen ZY, Li ZW, Wu J, Lou B, Zhang BS, Zhang L, Zhang W, Liang TB. Evaluating the Response and Safety of Inactivated COVID-19 Vaccines in Liver Transplant Recipients. *Infect Drug Resist* 2022; **15**: 2469-2474 [PMID: 35592105 DOI: 10.2147/IDR.S359919]

77 **Ozaka S**, Kobayashi T, Mizukami K, Murakami K. COVID-19 vaccination and liver disease. *World J Gastroenterol* 2022; **28**: 6791-6810 [PMID: 36632314 DOI: 10.3748/wjg.v28.i48.6791]

78 **Alqahtani SA**, Barry M, Memish Z, Hashim A, Alfares MA, Alghamdi SA, Al-Hamoudi WK, Al-Judaibi B, Alhazzani W, Al-Tawfiq JA, Abaalkhail F. Use of COVID-19 vaccines in patients with liver disease and post-liver transplantation: Position statement of the Saudi association for the study of liver diseases and transplantation. *Saudi J Gastroenterol* 2021; **27**: 201-207 [PMID: 34100388 DOI: 10.4103/sjg.sjg_223_21]

79 **Luxenburger H**, Reeg DB, Lang-Meli J, Reinscheid M, Eisner M, Bettinger D, Oberhardt V, Salimi Alizei E, Wild K, Graeser A, Karl V, Sagar, Emmerich F, Klein F, Panning M, Huzly D, Bengsch B, Boettler T, Elling R, Thimme R, Hofmann M, Neumann-Haefelin C. Boosting compromised SARS-CoV-2-specific immunity with mRNA vaccination in liver transplant recipients. *J Hepatol* 2023; **78**: 1017-1027 [PMID: 36804404 DOI: 10.1016/j.jhep.2023.02.007]

80 **Abdelrahman MM**, Abdel-Baset AA, Younis MA, Mahmoud MG, Shafik NS. Liver function test abnormalities in COVID-19 patients and factors affecting them - a retrospective study. *Clin Exp Hepatol* 2021; **7**: 297-304 [PMID: 34712832 DOI: 10.5114/ceh.2021.109225]

81 **Przekop D**, Gruszewska E, Chrostek L. Liver function in COVID-19 infection. *World J Hepatol* 2021; **13**: 1909-1918 [PMID: 35069997 DOI: 10.4254/wjh.v13.i12.1909]

82 **Krishnan A**, Prichett L, Tao X, Alqahtani SA, Hamilton JP, Mezey E, Strauss AT, Kim A, Potter JJ, Chen PH, Woreta TA. Abnormal liver chemistries as a predictor of COVID-19 severity and clinical outcomes in hospitalized patients. *World J Gastroenterol* 2022; **28**: 570-587 [PMID: 35316959 DOI: 10.3748/wjg.v28.i5.570]

83 **Sivandzadeh GR**, Askari H, Safarpour AR, Ejtehadi F, Raeis-Abdollahi E, Vaez Lari A, Abazari MF, Tarkesh F, Bagheri Lankarani K. COVID-19 infection and liver injury: Clinical features, biomarkers, potential mechanisms, treatment, and management challenges. *World J Clin Cases* 2021; **9**: 6178-6200 [PMID: 34434987 DOI: 10.12998/wjcc.v9.i22.6178]

84 **Kayaaslan B**, Guner R. COVID-19 and the liver: A brief and core review. *World J Hepatol* 2021; **13**: 2013-2023 [PMID: 35070005 DOI: 10.4254/wjh.v13.i12.2013]

85 **Kariyawasam JC**, Jayarajah U, Abeysuriya V, Riza R, Seneviratne SL. Involvement of the Liver in COVID-19: A Systematic Review. *Am J Trop Med Hyg* 2022; **106**: 1026-1041 [PMID: 35203056 DOI: 10.4269/ajtmh.21-1240]

86 **Hu X**, Sun L, Guo Z, Wu C, Yu X, Li J. Management of COVID-19 patients with chronic liver diseases and liver transplants. *Ann Hepatol* 2022; **27**: 100653 [PMID: 34929350 DOI: 10.1016/j.aohep.2021.100653]

87 **Güner R**, Hasanoğlu I, Aktaş F. COVID-19: Prevention and control measures in community. *Turk J Med Sci* 2020; **50**: 571-577 [PMID: 32293835 DOI: 10.3906/sag-2004-146]

88 **Monye I**, Adelowo AB. Strengthening immunity through healthy lifestyle practices: Recommendations for lifestyle interventions in the management of COVID-19. Lifestyle Medicine 2020; 1 [DOI: 10.1002/Lim2.7]

89 **Veljković M**, Pavlović DR, Stojanović NM, Džopalić T, Popović Dragonjić L. Behavioral and Dietary Habits That Could Influence Both COVID-19 and Non-Communicable Civilization Disease Prevention-What Have We Learned Up to Now? *Medicina (Kaunas)* 2022; **58** [PMID: 36422225 DOI: 10.3390/medicina58111686]



Published by **Baishideng Publishing Group Inc**
7041 Koll Center Parkway, Suite 160, Pleasanton, CA 94566, USA
Telephone: +1-925-3991568
E-mail: bpgoffice@wjgnet.com
Help Desk: https://www.f6publishing.com/helpdesk
https://www.wjgnet.com

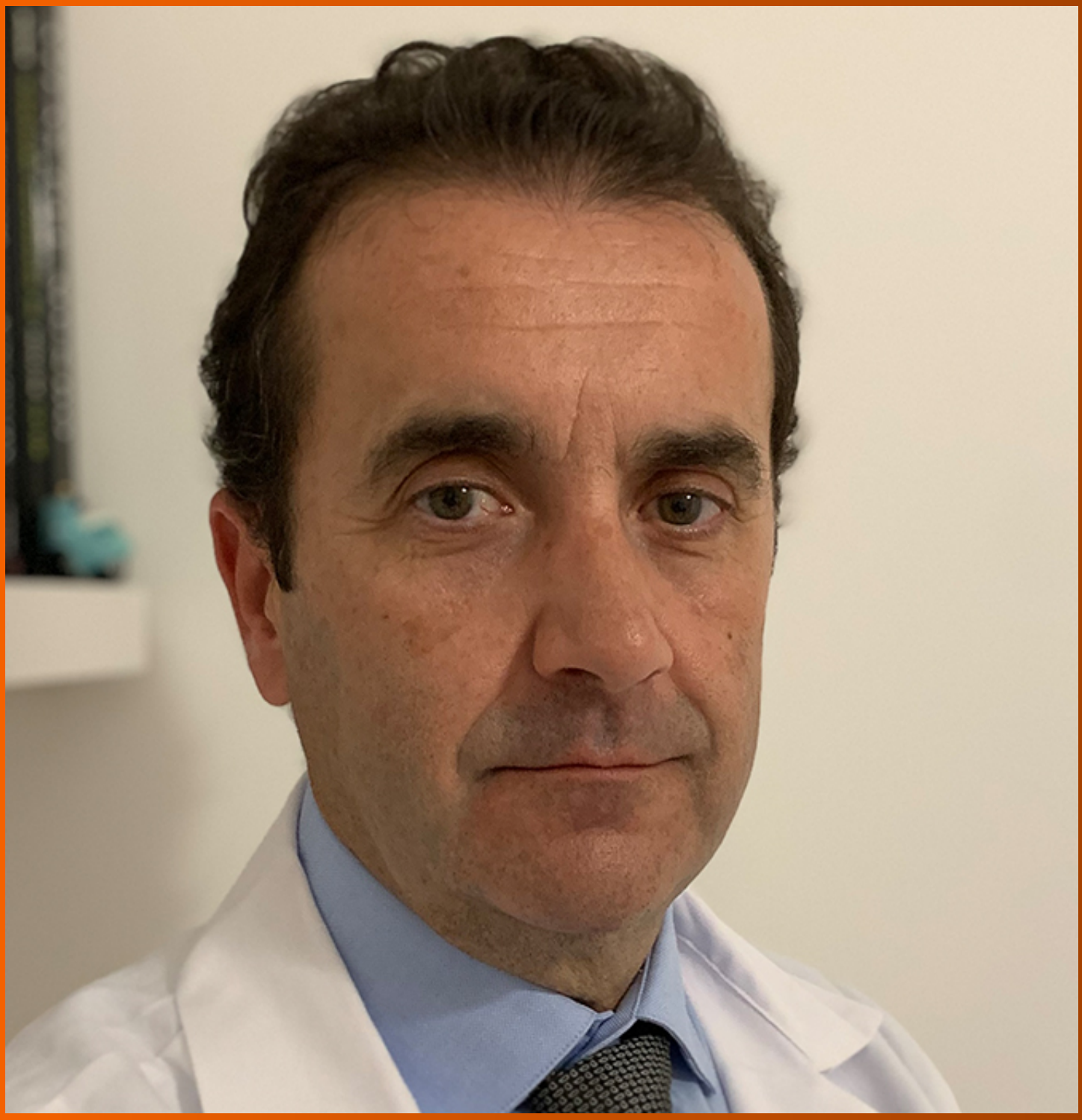


© 2023 Baishideng Publishing Group Inc. All rights reserved.

ISSN 1007-9327 (print)
ISSN 2219-2840 (online)

World Journal of *Gastroenterology*

World J Gastroenterol 2023 July 28; 29(28): 4368-4480



Published by Baishideng Publishing Group Inc

World Journal of Gastroenterology

Contents

Weekly Volume 29 Number 28 July 28, 2023

REVIEW

4368 Microbiota revolution: How gut microbes regulate our lives

Colella M, Charitos IA, Ballini A, Cafiero C, Topi S, Palmirotta R, Santacroce L

4384 Advances in application of novel magnetic resonance imaging technologies in liver disease diagnosis

Qi YM, Xiao EH

MINIREVIEWS

4397 Application of single-cell omics in inflammatory bowel disease

Zheng HB

4405 Post-acute pancreatitis diabetes: A complication waiting for more recognition and understanding

García-Compeán D, Jiménez-Rodríguez AR, Muñoz-Ayala JM, González-González JA, Maldonado-Garza HJ, Villarreal-Pérez JZ

ORIGINAL ARTICLE

Basic Study

4416 γ-aminobutyric acid B2 receptor: A potential therapeutic target for cholangiocarcinoma in patients with diabetes mellitus

Saengboonmee C, Sorin S, Sangkhamanon S, Chomphoo S, Indramanee S, Seubwai W, Thithuan K, Chiu CF, Okada S, Gingras MC, Wongkham S

4433 F-box only protein 2 exacerbates non-alcoholic fatty liver disease by targeting the hydroxyl CoA dehydrogenase alpha subunit

Liu Z, Chen NY, Zhang Z, Zhou S, Hu SY

Clinical Trials Study

4451 Efficacy and dose response of *Lactiplantibacillus plantarum* in diarrhea-predominant irritable bowel syndrome

Martoni CJ, Srivastava S, Damholt A, Leyer GJ

META-ANALYSIS

4466 One in four patients with gastrointestinal bleeding develops shock or hemodynamic instability: A systematic review and meta-analysis

Obeidat M, Teutsch B, Rancz A, Tari E, Márta K, Veres DS, Hosszúfalusi N, Mihály E, Hegyi P, Erőss B

ABOUT COVER

Editorial Board Member of *World Journal of Gastroenterology*, Miguel Jiménez Pérez, MD, PhD, Assistant Professor, Chief Doctor, Doctor, UGC de Aparato Digestivo, Unidad de Hepatología-Trasplante Hepático, Hospital Regional Universitario de Málaga, Málaga 29010, Spain. mjimenezp@commalaga.com

AIMS AND SCOPE

The primary aim of *World Journal of Gastroenterology* (*WJG*, *World J Gastroenterol*) is to provide scholars and readers from various fields of gastroenterology and hepatology with a platform to publish high-quality basic and clinical research articles and communicate their research findings online. *WJG* mainly publishes articles reporting research results and findings obtained in the field of gastroenterology and hepatology and covering a wide range of topics including gastroenterology, hepatology, gastrointestinal endoscopy, gastrointestinal surgery, gastrointestinal oncology, and pediatric gastroenterology.

INDEXING/ABSTRACTING

The *WJG* is now abstracted and indexed in Science Citation Index Expanded (SCIE, also known as SciSearch®), Current Contents/Clinical Medicine, Journal Citation Reports, Index Medicus, MEDLINE, PubMed, PubMed Central, Scopus, Reference Citation Analysis, China National Knowledge Infrastructure, China Science and Technology Journal Database, and Superstar Journals Database. The 2023 edition of Journal Citation Reports® cites the 2022 impact factor (IF) for *WJG* as 4.3; IF without journal self cites: 4.1; 5-year IF: 5.3; Journal Citation Indicator: 0.82; Ranking: 33 among 93 journals in gastroenterology and hepatology; and Quartile category: Q2. The *WJG*'s CiteScore for 2021 is 8.3 and Scopus CiteScore rank 2022: Gastroenterology is 22/149.

RESPONSIBLE EDITORS FOR THIS ISSUE

Production Editor: *Yu-Xi Chen*; **Production Department Director:** *Xu Guo*; **Editorial Office Director:** *Jia-Ru Fan*.

NAME OF JOURNAL
World Journal of Gastroenterology

ISSN
ISSN 1007-9327 (print) ISSN 2219-2840 (online)

LAUNCH DATE
October 1, 1995

FREQUENCY
Weekly

EDITORS-IN-CHIEF
Andrzej S Tarnawski

EDITORIAL BOARD MEMBERS
http://www.wjgnet.com/1007-9327/editorialboard.htm

PUBLICATION DATE
July 28, 2023

COPYRIGHT
© 2023 Baishideng Publishing Group Inc

INSTRUCTIONS TO AUTHORS
https://www.wjgnet.com/bpg/gerinfo/204

GUIDELINES FOR ETHICS DOCUMENTS
https://www.wjgnet.com/bpg/GerInfo/287

GUIDELINES FOR NON-NATIVE SPEAKERS OF ENGLISH
https://www.wjgnet.com/bpg/gerinfo/240

PUBLICATION ETHICS
https://www.wjgnet.com/bpg/GerInfo/288

PUBLICATION MISCONDUCT
https://www.wjgnet.com/bpg/gerinfo/208

ARTICLE PROCESSING CHARGE
https://www.wjgnet.com/bpg/gerinfo/242

STEPS FOR SUBMITTING MANUSCRIPTS
https://www.wjgnet.com/bpg/GerInfo/239

ONLINE SUBMISSION
https://www.f6publishing.com

© 2023 Baishideng Publishing Group Inc. All rights reserved. 7041 Koll Center Parkway, Suite 160, Pleasanton, CA 94566, USA
E-mail: bpgoffice@wjgnet.com https://www.wjgnet.com

World Journal of Gastroenterology

Submit a Manuscript: https://www.f6publishing.com

World J Gastroenterol 2023 July 28; 29(28): 4368-4383

DOI: 10.3748/wjg.v29.i28.4368

ISSN 1007-9327 (print) ISSN 2219-2840 (online)

REVIEW

Microbiota revolution: How gut microbes regulate our lives

Marica Colella, Ioannis Alexandros Charitos, Andrea Ballini, Concetta Cafiero, Skender Topi, Raffaele Palmirotta, Luigi Santacroce

Specialty type: Gastroenterology and hepatology

Provenance and peer review: Invited article; Externally peer reviewed.

Peer-review model: Single blind

Peer-review report's scientific quality classification

Grade A (Excellent): A, A
Grade B (Very good): B
Grade C (Good): 0
Grade D (Fair): 0
Grade E (Poor): 0

P-Reviewer: Ogino S, United States; Qin Y, China

Received: March 28, 2023
Peer-review started: March 28, 2023
First decision: April 26, 2023
Revised: May 16, 2023
Accepted: July 10, 2023
Article in press: July 10, 2023
Published online: July 28, 2023

Marica Colella, Raffaele Palmirotta, Luigi Santacroce, Interdisciplinary Department of Medicine, Section of Microbiology and Virology, University of Bari "Aldo Moro", Bari 70124, Italy

Ioannis Alexandros Charitos, Maugeri Clinical Scientific Research Institutes (IRCCS) of Pavia - Division of Pneumology and Respiratory Rehabilitation, Scientific Institute of Bari, Bari 70124, Italy

Andrea Ballini, Department of Clinical and Experimental Medicine, University of Foggia, Foggia 71122, Italy

Andrea Ballini, Department of Precision Medicine, University of Campania "Luigi Vanvitelli", Naples 80138, Italy

Concetta Cafiero, Area of Molecular Pathology, Anatomic Pathology Unit, Fabrizio Spaziani Hospital, Frosinone 03100, Italy

Skender Topi, Department of Clinical Disciplines, School of Technical Medical Sciences, University of Elbasan "A. Xhuvani", Elbasan 3001, Albania

Corresponding author: Luigi Santacroce, MD, Professor, Interdisciplinary Department of Medicine, Section of Microbiology and Virology, University of Bari "Aldo Moro", Pzza Giulio Cesare, 11, Bari 70124, Italy. luigi.santacroce@uniba.it

Abstract

The human intestine is a natural environment ecosystem of a complex of diversified and dynamic microorganisms, determined through a process of competition and natural selection during life. Those intestinal microorganisms called microbiota and are involved in a variety of mechanisms of the organism, they interact with the host and therefore are in contact with the organs of the various systems. However, they play a crucial role in maintaining host homeostasis, also influencing its behaviour. Thus, microorganisms perform a series of biological functions important for human well-being. The host provides the microorganisms with the environment and nutrients, simultaneously drawing many benefits such as their contribution to metabolic, trophic, immunological, and other functions. For these reasons it has been reported that its quantitative and qualitative composition can play a protective or harmful role on the host health. Therefore, a dysbiosis can lead to an association of unfavourable factors which lead to a dysregulation of the physiological processes of homeostasis. Thus, it has previously noted that the gut microbiota can participate in the pathogenesis of autoimmune diseases, chronic intestinal inflammation, diabetes mellitus, obesity

and atherosclerosis, neurological disorders (*e.g.*, neurological diseases, autism, *etc.*) colorectal cancer, and more.

Key Words: Microbiology; Human microbiota; Intestinal microbiota; Immune system; Metabolites; Dysbiosis; Probiotics; Diseases; Cancer

©The Author(s) 2023. Published by Baishideng Publishing Group Inc. All rights reserved.

Core Tip: The microbial populations that colonize the human body constitute a complex ecosystem; several cells much higher than the total number of cells in the human body. It is generally accepted that the human gut microbiota is a focus of research interest due to its complexity, involvement with health, and involvement in various pathological conditions. The need to extensively elucidate and document hitherto unknown aspects of the gastrointestinal microbiota, its associations with health fuels the need for further study. Furthermore, on the subject in question it has constituted a trigger for carrying out the present review of the research sources received so far.

Citation: Colella M, Charitos IA, Ballini A, Cafiero C, Topi S, Palmirotta R, Santacroce L. Microbiota revolution: How gut microbes regulate our lives. *World J Gastroenterol* 2023; 29(28): 4368-4383
URL: https://www.wjgnet.com/1007-9327/full/v29/i28/4368.htm
DOI: https://dx.doi.org/10.3748/wjg.v29.i28.4368

INTRODUCTION

The human organism is colonized by trillions of microbes. The microbiome refers to all the genes of microbes found in various locations in an individual's body. Instead for microbiota we mean the total of microorganisms quantitatively and qualitatively present. The human host and the microbiota have co-evolved for the benefit of both parties especially the intestinal one[1,2]. In fact, on the one hand, the host provides space, suitable conditions, and food for the growth of the intestinal microbiota and this in turn generally participates in obtaining useful substances and induces resistance to various infections. The relationship between the human gut microbiota and the host is symbiotic, in which both the host and the microorganisms are mutually beneficial. For its part, the host offers a place of growth and nourishment to the symbiotic intestinal bacteria, which in turn favors the function of the host on the one hand by inducing resistance to infections and on the other hand by facilitating the absorption of digested food[3]. It appears, therefore, that eukaryotic hosts and symbiotic bacteria have "co-evolved" with mutual interactions based on nutritional benefits enjoyed by both parties. When this balance is disturbed (dysbiosis) for various reasons, such as repeated and inappropriate use of antibiotics or alcohol abuse, pathological conditions may arise, such as mild chronic intestinal inflammation or metabolic disorders[4]. The interactions of (symbiotic) microbes with each other is of particular interest. A negative correlation has been observed between members of the phylum *Bacteroidota*, (such as that of the *Prevotellaceae* spp.) in the intestine, which may reflect alternative "metabolic specializations"[2,5]. Thus, the gut microbiota is of particular importance for the maintenance of human health. In fact, various biological mechanisms are microbiota-dependent because they cannot be performed autonomously and are useful for health homeostasis. In general, the concept of a "superorganism" refers to the bidirectional and therefore beneficial activity between the host organism and the gut microbiota. The microbiota, in addition, has both a protective and trophic role influencing, as we have mentioned, several homeostatic processes of the host organism, *e.g.*, tissue trophism, immune balance, metabolic activity, neuro-endocrine function, *etc.*[6,7]. Intestinal microbiota represents the most populous community of the entire organism. In fact, the stomach has about 10^3-10^4 bacteria, the duodenum 10^5-10^6 and the terminal ileum 10^8-10^9 bacteria (per gram of tissue). However, the most populated is the large intestinal one representing around 10^{12-14} bacteria per gram of tissue[2,6]. The colon is the part of the gastro-intestinal tract where a complex set of microorganisms develops from the moment of birth. The microbiota of the large intestine is denser and more diverse than the human microbiota of the small intestine. Intestine are enriched in the phyla of *Bacillota* and *Actinomycetota*, while *Bacteroidota* and *Lachnospiracae* are more abundant in colonic samples[8]. It is estimated that about 400-500 different genera of microorganisms constitute the intestinal microbiota, while the 90% of them species are predominantly anaerobic. Most of them belong to two genera, *Bacteroidota* and *Bacillota*. The remaining bacterial populations belong to *Pseudomonadota*, *Actinomycetota*, *Fusobacteria* and *Verrucomicrobia*[9]. An estimated 70% of these microbial communities are bacteria that cannot be cultured with conventional microbiological techniques. It has been observed that the microbial populations of the intestinal mucosa differ from those found in the intestinal lumen. The large intestine hosts the most numerous microbial cells which vary in species from individual to individual and are organized in localized microbial communities along its path. These microorganisms appear not to follow stable topological patterns along the intestine as they are influenced by the local oxygen concentration. Thus, facultative aerobic communities reside near the intestinal walls, which are sites of high oxygen concentration, and anaerobes prefer the intestinal lumen, where oxygen concentration is lower[10]. Although there is great diversity in the microbes that colonize the gut, it has been found that the gut microbiota of most individuals can be classified into three main microbial groups or "enterotypes" depending on the predominance of genera: *Bacteroides* (enterotype 1); *Prevotella* (enterotype 2) or *Ruminococcus* (enterotype 3). More recent data, however, show that the division into three enterotypes is a simplification

and that there are many intermediate states in the gut. The prevalence of each enterotype is mainly determined by dietary factors[2]. However, it appears that everyone has a fixed bacterial strain, even though the composition may vary. One of the main functions of the intestinal microbiota is to protect the intestine from pathogenic microorganisms, it also contributes to the development of a healthy immune system, regulates intestinal motility and participates in metabolism. More specifically, the gut microbiota promotes the regulation of the immune system through: (1) Stimulation of the immune response against potential pathogens; and (2) Suppression of the immune response against food and symbiotic antigens[11]. It is estimated that 80% of antibody production occurs locally in the gut, mainly supplying immunoglobulin A. In addition, they participate in host metabolism, drugs metabolism, maintenance of mucosal structural integrity, bile salts metabolism, plant fibers, mucus, and fatty acid catabolism[12]. In addition to bacteria that have already been studied quite a lot, recently it has been hypothesized that yeasts are involved in starch metabolism. Understanding the relationship between yeasts and the immune system is characterized as difficult and there are few data on their action. In some special cases, they can also act therapeutically[13]. Thus, there is an amphidromic relationship between microbes and hosts (Figure 1).

Finally, the probiotics bacteria are the "good" bacteria that are found in gut microbiota but also are added in specific dietary or ferment foods. Probiotics aid the organism by strengthening our immunity and help with gastrointestinal health, especially in conditions such as the irritable bowel syndrome (IBS)[14]. In the 1989, Fuller listed some beneficial effects and therapeutic applications of probiotic bacteria. We find probiotics in dairy products, such as yogurt and aged cheeses, but also in other foods such as pickled vegetables, *etc.* The consumption of probiotics promotes the growth of desirable microorganisms, overcoming potentially harmful bacteria and strengthening the body's defences. Several scientific articles commenting on these results, refer to studies using cultures such as of *Lactobacillus acidophilus* and *Bifidobacterium*, *Streptococcus thermophilus* and *Lactobacillus delbrueckii* subsp. *bulgaricus*[14,15]. Consuming probiotic products can cause a plethora of positives effects on the human body. Probiotics, thanks to their antimicrobial properties action can fight intestinal and other diseases, aid in various infections (such as those from coronavirus disease 2019 and other), reduce levels serum cholesterol, stimulate the immune system, reduce allergy symptoms, aid with lactose intolerance, can prevent hypercholesterolemia and osteoporosis and other[15].

MAIN FACTORS AFFECTING THE INTESTINAL MICROBIOTA

Inheritance

The mechanisms of host-bacteria interactions have not been fully described. Little is known about the relationship between the host genotype and its gut bacteria. However, there is strong evidence that it affects intestinal populations. Simple genetic mutations can lead to changes in the composition of microorganisms in the gut[16]. Further investigations are needed to delineate the mechanisms by which this occurs. There are few studies comparing the gut microbiota between family members. It has been observed that monozygotic and dizygotic twins had a greater similarity in gut microbiota between monozygotic than dizygotic siblings, indicating the importance of genetic background. Furthermore, it was observed in an animal model that the similarities in the gut microbiota of the same mouse strain were greater than in mice of a different species even with a common environmental effect. The role of parental genetic influence on the colonization of microorganisms in the intestine has not been elucidated.

Geographical location

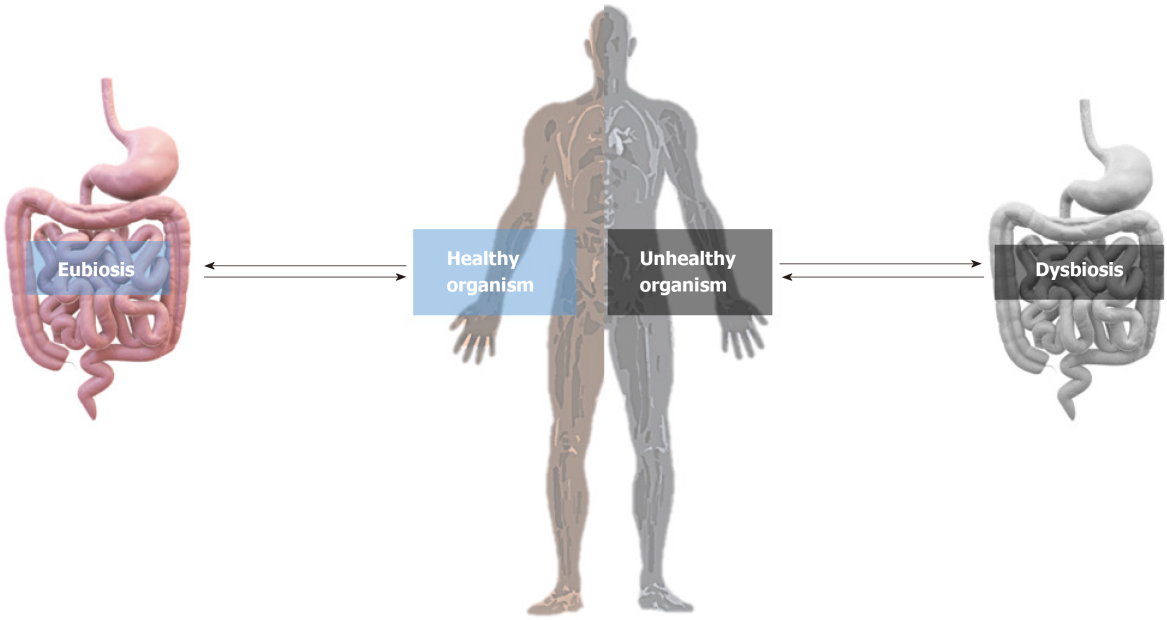
The diversity of the gut microbiota in children living in rural areas is greater than that of children in developed countries. It was noted in a study among Caucasians and Asians (Chinese) in the United States and Hong Kong that there were qualitative differences and quantitative in the intestinal microbiota[17-19]. It was found that children from a country in West Africa (Burkina Faso) that had a high presence of *Bacteroidota* with a greater presence of the genus *Xylanibacter* and *Prevotella* (which allow the hydrolysis of xylan and cellulose) with a reduced presence of *Bacillota*. Indeed, the higher presence of short-chain fatty acids (SCFAs) was noted. Therefore, the intestinal microbiota can help the host to optimize its energy intake from dietary fibers according to nutrition and needs, thus also protecting against infective and inflammatory processes[20].

Intrauterine period and delivery

There is a growing body of data suggesting that the human gut microbiota begins before infant birth. Meconium (the baby's first stool) contains bacteria, where *Bacillota* phyla predominate, the bacteria through the placenta and circulatory system enter the intestinal lumen of the foetal intestine. After human birth, the gut is colonized by many microbial strains, and everyone has their own gut microbiota which changes further throughout their life[2,6]. How the baby is born is very important as it affects the variety of microorganisms which will be installed. During normal delivery the new-born receives microorganisms from the mother's vagina or intestinal tract, whereas in caesarean section the new-born is exposed to those from the hospital environment. The gut microbiota in these newborns can be disturbed for months to years. Newborns born with normal delivery develop a microbiota that reflects the vaginal microbiota, while those born with caesarean section develop a skin microbiota resulting in delayed microbial colonization by *Bacteroides, and Bifidobacterium* spp.[16,21].

Diet

Many are observed in the first months of a person's life changes in the gut microbiota, while the stability and diversity of



DOI: 10.3748/wjg.v29.i28.4368 **Copyright** ©The Author(s) 2023.

Figure 1 The cross-talking axis host/gut microbiota: The gastrointestinal microbiota plays an important role in host physiology, metabolism, and nutrition. An organism with a regular maintenance of the physiological homeostasis leads to eubiosis of the gut microbiota and vice versa. Conversely, an altered physiological homeostasis leads to gut microbiota dysbiosis and vice versa. An alteration in the gut microbial community is linked to several disturbances gut conditions, including cancer, obesity, and a variety of gut disorders. The contribution of beneficial components of the gut microbiota to host physiology, metabolism, and immune function has become the focus of scientific research and will undoubtedly lead to new therapeutic approaches.

microbiota genes increase after the first three years of life[21]. Breastfeeding or consuming breastmilk substitutes in infancy has significant effects on intestinal microbiota of the new-born and in the development of the immune system [22]. In animal models, the two different ways of feeding babies develop different populations of microorganisms in the gut which lead to differences in the immune system. Immunity is affected up to the first five years of life[23]. In humans there are few studies on the different administration of milk to newborns. Undoubtedly, however, the intestinal microbiota of the child influences the development of the immune system and its metabolism, just as in adult life[24]. Breastfed infants are exposed to the gut microbiota offered by milk, which contains more than 700 species of bacteria. Breast milk contains many protective factors that breast milk does not contain. In addition, changes in the infant's gut microbiota appear to predispose to diseases and his later life[2,16]. Subsequently adult dietary habits are one of these most important environmental factors shaping the growth of microorganisms in the human gut. Short or long-term consumption of animal or vegetable products changes the structure of the intestinal microbiota. The short-term diet based on animal foods increases the microorganisms of genera such as *Bacteroides*, *Alistipes*, *Bilophila* and decreases the levels of *Roseburia*, *Eubacterium rectale*, *Ruminococusbromii* belonging to the *Bacillota* phyla (populations that mainly metabolize polysaccharides of plant origin)[25]. Instead, it has been noted that long-term consumption of fruit and vegetables by the elderly is associated with an increase in populations of the genus *Prevotella*. It was noticed that a change of nutrition style (*i.e.*, sugar-rich foods, a shift from a low-fat vegetable polysaccharide to a high-fat vegetable polysaccharide, and so) modifies the microbiota, qualitatively and quantitatively, through a change of the microhabitat in 24 h and so on changes in metabolic pathways also occur. Although the gut microbiota responds to short-term changes in diet, long-term nutrient changes appear to determine the type of qualitative and quantitative microorganism population also for other such as the oral ones[26,27]. There are differences in the presence of gut bacteria in the two diets, reflecting differences in metabolism. of carbohydrates and proteins. In both cases, the colonization of fungi, viruses and yeasts is observed[25]. It has been observed that the consumption of foods of plant origin is also associated with a beneficial set in the intestinal microbiota. A high correlation has been noted between a plant-based diet and increased levels of SCFAs and some dietary fibres that degrade *Bacillota* phyla. Indeed, the characteristics of the Mediterranean-type diet, *i.e.*, increased intake of cereals, fruit, vegetables, and legumes offer many benefits for the human intestine[28]. An observational study found that dietary fiber from beans, fruits, and vegetables was associated with an abundance of and *Actinomycetota* phyla and *Clostridium* spp. But also, the consumption of sour milk, many dairy products, or the consumption of fermented foods (such as Greek yogurt, kefir, and others) affect the intestinal microbiota and change its structure. The use of substances of abuse (such as alcohol, cocaine and other) or chemical xenobiotics can cause in human health is associated with quantitative and qualitative changes in the intestinal microbiota (dysbiosis)[29,30].

Lifestyle

Modern lifestyles can influence the intestinal microbiota, sedentary life contributes to obesity and combined with a positive energy balance and the consumption of foods of animal origin rich in saturated fat leads to the rearrangement of populations at the intestinal level. Although studies show conflicting results, an increase in *Bacillota* and a decrease

in *Bacteroidota* have been observed in individuals consuming foods of animal origin[6]. Frequent and moderate exercise influences the intestinal defence as well as on the genes of intestinal microorganisms. In a study on the effect of exercise on the intestinal microbiota of 22 athletes, the beneficial influence of exercise on the diversity of intestinal microorganisms is underlined and the combination with diet is claimed to affect the gut microbiota structure[31,32]. Smoking also affects the composition of the gut microbiota, increasing populations of the *Bacteroides-Prevotella* genera. Stress affects gut motility, which can change the structure of microbial populations, which has even been blamed for the development of inflammatory bowel disease (IBD)[33].

Use of antibiotics

Antibiotics target pathogenic microorganisms, but they also have a negative effect on intestinal symbionts. Unfortunately, they affect the intestinal microbiota especially if they are broad-spectrum antibiotics that are used for all diseases[34]. Gut microbiota diversity is reduced, many strains are lost, and their re-emergence is gradual and long-term, which is a major concern of experts in the field of intestinal health. It was observed that most of the bacteria affecting antibiotics response mainly belong to the *Bacillota* and *Pseudomonadota* phyla[35,36].

THE ROLE OF THE HOST/INTESTINAL MICROBIOTA CROSS-TALKING AXIS

Nutritional and gut-influenced energy conservation by metabolic processes (metabolome)

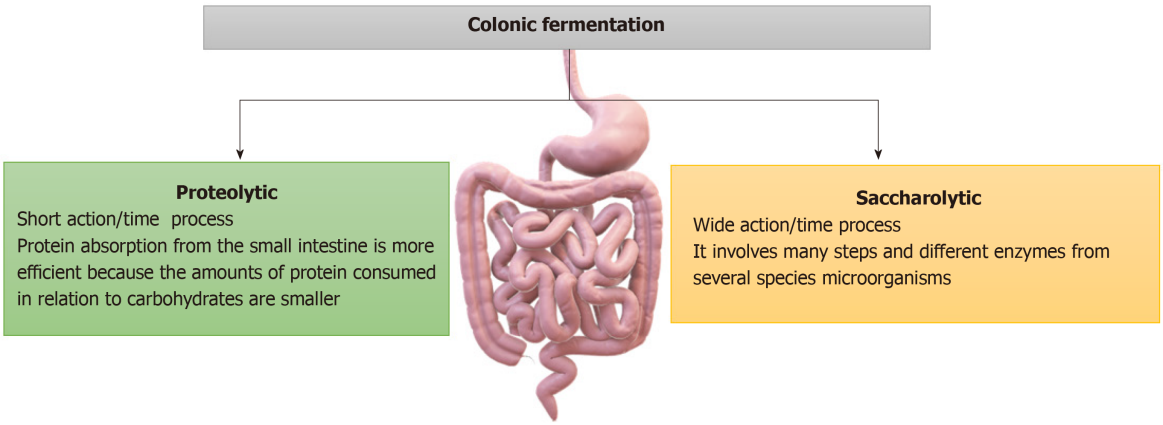
Several studies have shown that the intestinal mucosa needs to be colonized by microorganisms to take on its integral structure. For example, mice raised in a sterile environment developed fewer blood vessels in their intestinal villi. Sterile growth also showed that there is defective growth in gut-associated lymphoid tissue and antibody production. Also, in the context of the sterile environment, fewer Peyer's patches develop, there are fewer cells in the dermis, and fewer plasma cells in the germinal centres of the mesenteric lymph nodes than in the development data in a nonsterile environment[37]. The intestinal microbiota could be considered a "metabolic organ" performing multiple functions needed for maintaining the health status of the host organism orchestrating an amphidromous communication with it. The catabolism of a number of both endogenous and exogenous indigestible molecules (*i.e.*, cholesterol, fibers, bile acids, excreted mucus, *etc.*), is one of the most important activities of the intestinal microbiota accounting for 10% of the host's energy requirement every day[38,39]. So, the gut microorganisms (especially bacteria and commensal fungi) produce SCFAs to gain energy but also give trophic substances and energy to the host organism. Finally, certain bacterial species can synthesize vitamins such as B12, folic acid, thiamin, biotin, vitamin K, amino acids and more[40]. As proof, *Bacteroides thetaiotaomicron* can metabolize polysaccharides that reach the large intestine as is in Figure 2. Indeed, it has many enzymes such as glycoside hydrolases and polysaccharide lyases that break down pectins, arabinose, *etc.*

Archaea, such as *Methanobrevibacter smithii*, establish beneficial relationships with other bacteria to eliminate the H_2 by-products, thus facilitating the yield of ATP[41,42]. The gut microbiota benefits the host in many ways contributing to the conservation of energy from several common non-digestible polysaccharides through enzymes such as glycoside hydrolases and other non-encoded enzymes in the human genome[43]. Studies of mice with a germ-free gut microbiota revealed that the gut microbiota improves the regulation of fat accumulation and obesity mainly due to an increase in energy production from food. These (germ-free) mice are protected against obesity and metabolic syndrome[44]. It was noted that restoring an eubiotic intestinal microbiota in these animals leads to an increase in insulin resistance and fasting blood glucose, but also of the level of liver triglycerides and body fat amount.

The intestinal microbiota improves the absorption of monosaccharides, which in turn leads to an increased lipogenesis with consequent accumulation of triglycerides both in the liver and in the fat tissue. With food utilization, obese mice have been reported to conserve energy from food more efficiently than lean-wild-type mice[45]. Distal gut microbiota's composition of obese mice revealed that the relative increase of *Bacteroidota* and *Bacillota* resulted in a modified metabolic potential of the gut microbiota, giving it a greater ability to use energy from the diet. Interestingly, this obesity trait of his was transmissible through faecal transplants from obese mice as opposed to lean germ-free mice. Obese mice also possess multiple methanogenic archaea which can increase the efficiency of bacterial fermentation through H_2 removal[46]. It was observed that, after gut co-colonization, both *Bacteroides thetaiotaomicron* and *Methanobrevibacter smithii* boost up the efficiency and specificity of bacterial fermentation by removing bacterial polysaccharides, increasing adiposity compared to mice colonized with only one of the two organisms[47,48]. Further studies have highlighted further correlations regarding the possibility of increased energy saving through induced microbiota nutrition or genetically induced obesity microbiota[49]. For that, age and diet are important factors not only for the composition of the gut microbiota, but also for energy saving possibilities. In addition, the link between gut microbiota and liver diseases has been studied mainly in obesity and non-alcoholic steatohepatitis/nonalcoholic fatty liver disease patients, and in liver failure conditions (*e.g.*, cirrhosis, hepatic encephalopathy, infections, hepatocellular carcinoma), total parenteral nutrition-associated liver disease, cholangitis primary sclerosing, primary biliary cirrhosis[50]. It has been noted that dysbiosis of the intestinal microbiota leads to intestinal motility disorders (stasis, with bacterial proliferation). These conditions lead to increased intestinal permeability, impaired immune response with an excessive increase in tolerance in bacterial translocation by the intestinal microbiota with subsequent liver injury[50,51].

Immunological actions and resistance to colonization by pathogens

The host's organism meets both the pathogenic microbes of the environment and the microbes of the intestinal microbiota. Previous studies of the immune system have focused on the mechanisms by which this system can defend itself against pathogenic microbes. In addition, the microorganisms of the intestinal microbiota produce antimicrobial



DOI: 10.3748/wjg.v29.i28.4368 **Copyright** ©The Author(s) 2023.

Figure 2 The metabolic activity by the colonic microbiota. The intestinal microbiota finds an environment rich in polysaccharides which are not digested by stomach enzymes. Fermentation of polysaccharides by intestinal bacteria leads to the production of acetate, butyrate, and propionate, which are used as a carbon source by intestinal mucosal cells. The initial fermentation of the carbohydrate that escaped digestion in the small intestine is followed by the utilization and cross-distribution of metabolites by various members of the microbiota, and then the synthesis of short-chain fatty acids (butyrate, propionate, acetate). Proteolytic fermentation differs from saccharolytic fermentation because it releases many potentially toxic nitrogen and sulfur metabolites, such as ammonia, amines, nitrates, nitrites, and hydrogen sulfide[32,40].

substances such as bacteriocins and hydrogen peroxide which inhibit the growth of others with pathogenic behaviour [51]. The immune system has evolved in such a way that it can accommodate symbiotic bacterial communities of increasing complexity while retaining the ability to fight pathogenic bacteria. The microbiota regulates the development and function of the innate and acquired immune systems[11]. Even in healthy conditions of the host, there is a continuous stimulation of the immune system by the intestinal microbiota. This condition leads to a basal state of "low physiological inflammation" representing an effective first line of defence against pathogenic microbes. Furthermore, both resident and pathogenic microbes compete for available sites and nutrients, so the microbiota exerts a protective role metabolizing those nutrients that are necessary for the pathogens survival and producing molecules that inhibit their growth[2,52]. In fact, it has been shown that the introduction of certain molecules produced by *Bacteroides thetaiotamicron* and *Eubacterium rectale* can induce the production of specific mucosal glycans. These can be metabolized by these 2 bacterial species only but not by pathogens, thus preventing their proliferation. Hence, diet appears to have a pivotal role in microbial composition modifications[53]. The immune system works by learning, *i.e.*, at the beginning of life it has the necessary components (cells, internal cellular mediators, *etc.*) but does not have data available from the environment, which it acquires in the first years of life through contact with other people and the natural environment. If these early childhood data are inappropriate, the regulatory mechanisms of the immune system could fail. As a result, the immune system attacks not only pathogenic microorganisms but also harmless targets such as pollen, house dust and food antigens, leading to the onset of allergic diseases[54]. The microorganisms together with digestive enzymes, the mucus layer, intestinal peristalsis, and the epithelial barrier with "tight" connections (tight junctions) constitutes the non-immune component of the body's immune response. The functions of the intestinal microbiota in terms of defence of the organism are on the one hand to influence in a decisive way the arise of the gut immunity (for which reference was made to the trophic role) and on the other to prevent possible invasion of pathogens through a direct effect on them and/or through the "activation" of the host's immune mechanism[55,56]. As far as natural immunity is concerned, it has the ability, by recognizing characteristic pattern molecules [pathogen associated molecular patterns (PAMPs)] on microorganisms, to separate potentially pathogenic microbes from "unwanted" antigens. More specifically, the cells of the natural immunity using proline rich proteins (PRPs) receptors (pattern recognition receptors) detect PAMPs[57]. PRPs also participate in the release of cytokines and the activation of acquired immunity. However, there are many types of PRP, and of the most important are the Toll-like receptors (TLRs) found in dendritic cells, neutrophils, macrophages, and intestinal mucosal epithelial cells. The most known PAMPs recognized by PRP receptors are bacterial carbohydrates (*e.g.*, mannose, glucides of lipopolysaccharide), bacterial peptides (*e.g.*, flagellin), peptidoglycans and lipoteichoic acid of Gram+, fungal lipoproteins, glycans, viral genomes. Since these molecules are also found in symbiotic microorganisms, they are called microbe-associated molecular patterns (MAMPs)[58]. Thus, MAMPs seem to be able to modify the expression of TLRs in natural immunity cells. Thus, the recognition of MAMPs triggers the activation of the nuclear factor kappa-light-chain-enhancer of activated B cells (NF-κB) pathway, which results in the production of cytokines, the activation of other auxiliary and necessary molecules on the antigen-presenting cells, which ultimately results in the activation of T-cells, *i.e.*, acquired immunity[59]. However, microorganisms can modulate the natural immunity changing the quality and the amount of mucus from the intestinal mucoid cells. Mucus forms a natural barrier to stop an infection directly adhering to them, collects the bacterial by-products, and protect epithelial cells from secretions thanks to its low pH rich and richness in lytic enzymes. These events activate body's defences[60]. As far as the acquired immunity in the gastrointestinal system is concerned, it is "based" in the gut associated lymphoid tissue which is made up of the Peyer's Patches and the mesenteric lymph nodes. The spleens of germ-free mice were found to contain increasingly smaller germinal centres in the lymph nodes and reduced numbers of memory CD T4 cells in the intestinal epithelium, that the production of

cytokines belongs to a Th2-type of immune response, and that these animals have a reduced ability to secrete germicidal agents[61]. Recolonization of these muscles with muscle-specific bacteria can reverse some of these perturbations, as experimentally demonstrated by the restoration of systemic T-cell deficiency and Th1/Th2 imbalance of sterile muscle microbes after single colonization of the muscle gut with the bacterium *Bacteroides fragilis*. Such studies collectively highlight the importance of the gut microbiota for the normal development of the peripheral immune system in immunocompetent hosts[62].

Influence of the host's health condition

According to clinical studies that have been done in recent years, they show a correlation of the change in the composition of the gut microbiota with several serious pathological conditions such as: autoimmune diseases, type 2 diabetes (T2D), weight gain and obesity, IBD, asthma and chronic sinusitis, mental health disorders, dermatological problems, Alzheimer's disease, poor immune system health, gastroesophageal reflux disease, constipation or diarrhea, cancerous conditions and other[63].

INTESTINAL MICROBIOTA ROLE IN DISEASES

IBS and IBD

Functional bowel disorders such as IBS are defined solely by symptom-based diagnostic criteria. IBS is characterized by abdominal pain or discomfort and changes in bowel habits. Although the aetiology is multifactorial, recent studies to understand the pathophysiology of IBS have revealed that changes in the normal gut microbiota may play a role in IBS-associated low-grade intestinal inflammation[2,40]. Indeed, intestinal microbial dysbiosis is involved in the pathogenesis of IBS by facilitating the adhesion of the pathogenic microorganism to the intestinal wall and several studies revealed that. Indeed, there is a clear separation between the gastrointestinal microbiota of patients with IBS and that of healthy controls[64]. That is, IBS is characterized by an increase in the genera *Dorea*, *Clostridium* (as *Bacillota* phylum) and *Ruminococcus* with an important loss in the population of the genera *Bifidobacterium* and *Faecalibacterium*. According to a trial on IBS in young patients who were divided into subgroups with different bacterial fingerprints, an increase of *Bacillota* phylum compared to *Bacteroidota* phylum exists, differing from healthy patients[65,66]. Finally, another study on a paediatric population with IBS showed a variation of *Bacillota* and *Pseudomonadota* phyla amount, with many of the genera *Dorea* and *Ruminococcus*, and *Haemophilus parainfluenzae* species. The *Bacteroides* genus was found to be smaller in paediatric patients with IBS than in healthy controls. Typically, these studies could ultimately lead to the design of targeted therapies[67].

Idiopathic IBDs are immune-driven chronic diseases and represented by ulcerative colitis and Crohn's disease. Today they are an adverse immune response to endogenous symbiotic gut microorganisms with or without the involvement of the autoimmunity process. Studies have shown a change in the composition of the gut microbiota in IBD[68]. Furthermore, there is a qualitative reduction in it, *i.e.*, on the bio-diversity of the population with a typical reduction of *Bacillota* phylum strains (such as *Bifidobacteria*, spp., *Faecalibacterium prausnitzii*, and *Lactobacillaceae* families) while an increase in the microorganisms that are attached to the mucus is observed. *Bacillota* strains are the main producers of SCFAs, such as butyric acid, which has immunomodulatory properties[69]. However, it has not been clarified whether the disturbance in the microbiota is the cause of the disease or is the result of it. The normal, non-inflamed gut contains many immune cells which are in such a state of activation that there is no complete immune response to the microbes of the normal microbiota and food antigens. This is due to the activation of potent mechanisms of immune regulation, such as the stimulation of regulatory T cells expressing the transcription factor FoxP3 to suppress inflammation[66]. But, under environmental stimuli (*e.g.*, certain infections) the activation of the intestinal immune system starts on a large scale but is subsequently suppressed. In IBD patients this suppression of this immune response may not be adequately regulated. The eubiosis of the intestinal microbiota is under the control of the host through immune and epithelial responses, diet, drugs use (especially antibiotics), genetics, and more[2]. In turn, the microbiota, has significant effects on host epithelial and immune function thanks to its structural components and metabolism, that can become permanent by epigenetic effects. From childbirth, when the human microbiota is established, these host effects may influence the risk of developing IBD later in life[63]. It is worth noting here that in most studies the incidence of IBD increases particularly in the second to fourth decades of life, while some studies even report a second peak in the sixth and seventh decades. Specifically, therefore, components of the microbes can promote or protect against disease. The community microbes in patients with ulcerative colitis and Crohn's disease have been shown to be different from unaffected individuals, a state of dysbiosis: The presence of disease-causing microorganisms (such as those form *Pseudomonadota* phyla and adherent *Escherichia coli*) and to which directed immune response and/or loss of microorganisms that inhibit inflammation (*e.g.*, such as *Faecalibacterium prausnitzii*). But many changes and inflammation results in changes in the microbial community. Also, antibiotics (such as nitroimidazoles, quinolones) and certain diets change the gut microbiota and may improve Crohn's disease symptoms. In fact, the use of antibiotics really has a place in the treatment of Crohn's disease[2,16,70].

Immune dysregulation (allergies and autoimmunity)

Effectively stimulated immunity of both local and systemic mucosa is required for a mature gut microbiota. If this does not happen, a dysregulation can occur which can lead to allergic manifestations or an asthmatic phenotype from early life. It has been noted that developing countries have a lower incidence of allergic diseases such as asthma than countries developed. Thus the "hygiene hypothesis" was developed, which according to this lack of exposure to pathogenic bacteria or products of non-pathogenic bacteria can cause this condition by a negative effect on the development of the

immune system[71]. Subsequently, the "microbiota hypothesis" was formulated, in which it is proposed that changes in diet, as well as increased use of antibiotics in developed societies, lead to a less diverse gut microbiota in its microbial components. This "immature" gut microbiota, as it has been defined, alters the development of the immune system interrupting the proper evolution of events that allow the development of immune tolerance and thus increasing the risk of developing allergic hypersensitivity[72]. More specifically, levels of *Bifidobacterium* and *Enterococci* appeared to be related to allergic symptoms in the first months of life. An increased *Bacteroidota*/*Bifidobacterium* ratio was reported during the second year of life in children who developed symptoms of atopy children who eventually developed allergies were less frequently colonized with *Lactobacillaceae* phyla, *Bifidobacterium* and *Clostridiodies difficile* strains during the 2nd mo of life[73]. Autoimmune diseases (such as rheumatoid arthritis and other) can be sharing a common pathogenesis, an immune-mediated attack on the body's own organs. Autoimmune diseases usually show a variety of characteristics and symptoms. Concerning these characteristics, the most common may include, for example, an increase in epithelial (such as intestinal) and vessel permeability, mitochondrial dysfunction, progressive inflammation and chronic infections, imbalance of the hypothalamic-pituitary-adrenal (HPA) axis, and microbiota dysbiosis. Symptoms, on the other hand, can manifest as chronic fatigue, allergic phenomena, poor cognitive function, mood and mental disorders and pain, skin rashes, gastrointestinal disorders, and so[74,75]. An example of the genetically predisposed autoimmune diseases of the small intestine is celiac disease, an age-independent condition. The symptoms occur after the ingestion of the toxic epitopes of gluten (*i.e.*, the proteins present in wheat, rye, barley and, less so, in oats). In celiac disease there is an increase in intraepithelial lymphocytes and an atrophy of the intestinal villi. The autoimmune mechanism is due to the presence of various autoantigens, where the most important is tissue transglutaminase that is also an important diagnostic marker. Furthermore, it is often associated with other autoimmune diseases, such as insulin dependent diabetes mellitus (IDDM), or type 1 diabetes (T1D), thyroiditis, *etc.* This suggests that these diseases share common pathogenetic pathways[76-79]. Finally, the intestinal microbiota seems to play a fundamental role in the development and course of celiac disease. There is an unfavourable qualitative and quantitative composition of the intestinal microbiota characterized by a greater presence of the genus *Bacteroides* and *Escherichia coli* and a minor presence of *Bifidobacterium* spp. (*e.g.*, *B. longum* compared to healthy controls). Furthermore, this condition does not seem to change even after a gluten-free diet[80,81]. Finally, it has been noted that children born by caesarean section have a higher risk to develop the disease[82,83].

Diabetes mellitus

The exact role of the gut microbiota in the pathogenesis of T1D remains unknown. Data from experimental models support the idea that some bacterial families may act protectively against divalent metal transporter 1 (DMT1). Studies have shown that the use of antibiotics in experimental animals can prevent the occurrence of type 1[84]. But also, the administration of probiotics with bacterial strains in experimental animals prevented the onset or delayed the progression of the disease[85]. In another study, it was found that accidentally infecting mice with a spore forming bacterium resulted in a reduction in the incidence of DMT1[86]. Similarly, incubation of mycobacterium and streptococci in laboratory animals protected them from developing diabetes. Studies of the gut microbiota in mice that developed DMT1 and mice that did not develop diabetes reported that, at the onset of the disease, the two groups differed in the concentrations and type of microbes[87]. Stool samples from animals (mice) that developed diabetes contained higher concentrations of so-called probiotic bacteria, such as from *Lactobacillaceae* phyla and *Bifidobacterium* spp., in contrast to mice that did not develop diabetes which showed higher concentrations of *Bacteroides*, *Eubacterium* and *Ruminococcus*. It is worth mentioning that the *Lactobacillus johnsonii* strain prevents the development of diabetes when administered to mice[88,89]. Because of the possible relationship between the microbiota and IBD, most of the research around the gut microbiota has been done in patients with IBD, whereas studies in patients with type 1 diabetes mellitus (T1DM) are limited. In addition to increased intestinal permeability, patients with T1DM show an increase in inflammatory cells in the gut and decreased numbers of CD4, CD25, and T-cells, which are the master regulator of the immune system. Another study showed that individuals who developed T1DM had higher concentrations of *Bacteroidota* and lower concentrations of *Bacillota* compared to healthy controls. In addition, individuals who developed DMT1 were colonized with a lower number of bacteria compared to healthy controls[90,91].

The manifestation of T2DM is due to the combination of reduced insulin secretion from the β-cells of the pancreas and increased insulin resistance, as well as the disruption of incretin secretion from the gastrointestinal system. Several studies associated the microbiota with the development of T2DM, which is particularly characterized by a decrease in the concentrations of the phylum *Bacillota* (such as the genus *Roseburia* from the *Lachnospiraceae* family and the *Enterococcus faecalis* from genus *Enterococcus*, and other). Changes in the number of *Bifidobacteria*, *Lactobacillaceae* phylum, *Clostridioides* genus, as well as the *Bacillota*/*Bacteroidota* ratio have also been observed in the intestinal microbiota of children with T1D [91-93]. Obesity and T2D share the presence of low-grade inflammation that occurs in tissues involved in the regulation of metabolism, such as the liver, adipose tissue, and muscle. Inflammation is characterized by an increase in cytokines, interleukin (IL)-6, IL-1 and tumor necrosis factor-alpha with the result being insulin resistance. There are several studies in which the gut microbiota has been associated with the presence of obesity, insulin resistance and T2D, such as, and that probiotic treatment affects the metabolic control of patients with T2D. The gut microbiota contributes to the development of T2D[94]. Both studies showed that people with T2D had reduced concentrations of *Clostridiales* bacteria (*Roseburia* spp. and *Enterococcus faecalis*)[95]. T2D, independent of obesity, may also affect the structural composition of the microbiota. T2D may have a high presence of Gram-negative intestinal bacteria, such as *Bacteroidota*. In fact, in diabetic mice a reduction in *Bacteroides/Prevotella* spp. has been linked to an improvement in metabolic endotoxemia and lowering of laboratory tests of inflammation[96]. Changes in the number of *Bifidobacterium*, *Lactobacillaceae* phylum, *Clostridium* as well as the ratio *Bacillota*/*Bacteroidota* have also been observed in the intestinal microbiota of children with T1D[97]. Similar changes in the composition of the intestinal microbiota have been reported in patients with T2D. A lot of different theories have been proposed about the biomechanisms to explain the effect of the intestinal microbiota on insulin

resistance and T2D, the main ones being metabolic inflammation, modification of incretin secretion and the production of hydroxybutyric acid. Lipopolysaccharides are endotoxins that are usually found in the outer membrane of Gram-negative bacteria and cause so-called metabolic inflammation, which is characterized by the release of pro-inflammatory factors [98]. The role of lipopolysaccharides in the pathogenesis of metabolic diseases was demonstrated by a study in mice fed a normal diet, in which the infusion of lipopolysaccharides caused insulin resistance in the liver, glucose intolerance, as well as an increase in adipose tissue. In addition, lipopolysaccharides may can lead to the expression of NF-κB and stimulate the activity of mitogen-activated protein kinase metabolic pathways in adipocytes. A study in fed leptin-deficient mice physiologically showed that increased intestinal permeability to lipopolysaccharide resulted in a change in the proportion of Gram-negative bacteria in the intestinal lumen, which was associated with the presence of insulin resistance. The modification of the intestinal microbiota by administering probiotic treatment to obese mice acted favourably on the intestinal barrier, reducing lipopolysaccharide-induced metabolic inflammation[99]. It has been found that increasing concentrations of *Bifidobacterium* modifies the inflammatory response in obese mice by increasing the production of glucagon like peptides (GLPs), while reducing intestinal permeability. The increase in *Bifidobacterium* concentrations induced by probiotic treatment is probably associated with an increase in the levels of gut-secreted peptides GLP-1 and YY, which exert a favourable effect, reducing insulin resistance and improving β-cell function. In addition, probiotic treatment caused an increase in GLP-2 levels in the colon, improved intestinal barrier function, and ultimately reduced plasma lipopolysaccharide levels[100]. It was found that people with T2D had an increase in the number of various opportunistic gut pathogens and a decrease in the concentrations of hydroxybutyric acid-producing bacteria. Hydroxybutyric acid is the main source of energy for maintaining the function of the cells of the digestive system. In the large intestine, hydroxybutyric acid is mainly produced by the bacteria *Clostridium coccoides* and *Eubacterium rectale*. However, changes in gut bacteria were found in colon cancer patients and in elderly subjects, suggesting that hydroxybutyric acid-producing bacteria could potentially have a protective role in the functioning of the gut microbiota[101,102].

Obesity and atherosclerosis

In obese individuals the accumulation and thus the increase of energy is related to the transfer of hydrogen between certain bacterial taxa. In fact, this effect has been noted both from the hydrogen-producing *Prevotellaceae* and from the methanogenic archaea that use hydrogen[103]. In obese individuals this increase and accumulation of energy due to the relative abundance of *Gammaproteobacteria* and the less presence of *Clostridium* genus. Additionally, obese individuals harbour clusters of H_2-producing bacteria, primarily members of the family *Prevotellaceae* and some groups of *Bacillota*. These H_2-producing bacteria coexist in the gastrointestinal tracts of obese individuals with relatively large numbers of H_2-oxidizing methanogens belonging to archaea. Methanogens account up to 10% of all anaerobes in the colon[104,105]. Plant polysaccharides and dietary fibers are fermented by intestinal bacteria to produce SCFAs. An increase in methanogenic oxidation of H_2 facilitates fermentation, which produces more SCFAs[106]. It can also be utilized directly by hydrotrophic methanogenic agents, while propionate, butyrate and lactate can be fermented with acetate and H_2, where the latter is utilized by hydrotrophic methanogenic bacteria. As a consequence, the increase in methane oxidation should increase the conversion of plant polysaccharides into SCFAs, especially the acetate. SCFAs produced by fermentative bacteria are absorbed through the human intestinal epithelium, whereas H_2 is an energy exchange factor within bacterial communities[107].

Atherosclerotic vascular disease is caused by environmental and genetic factors such as food and associated microorganisms. We currently know three circulating phospholipid-related molecules considered promoters of atherosclerosis: Trimethylamine N-oxide (TMAO), choline and betaine that could be used as biomarkers to predict cardiovascular disease risk[108]. These three phospholipid-related molecules were identified by analysis of plasma metabolites from 50 patients with atherosclerotic disease using liquid chromatography/mass spectrometry compared to 50 healthy samples. It has been noted that used apoE-deficient mice as a model of atherosclerosis and showed that plasma TMAO levels in apoE-deficient mice correlated positively with the area of aortic damage. The activity level of hepatic flavin monooxygenases, which convert trimethylamine (TMA) to TMAO, correlated positively with plasma TMAO levels in both mice and humans[109,110]. In the apoE-deficient mice an antibiotic treatment modify plasma TMAO level and atherosclerosis size, suggesting that gut microbiota significantly influence the development of atherosclerosis in apoE-deficient mice reducing it. This was demonstrated by adding 1% choline to the diets of apoE-deficient mice, as it increased the formation of foam cells as well as the expression of the scavenger receptors CD36 and SRA1 on macrophages, which is normally prevented by the administration of broad-spectrum antibiotics. A new pathway linking dietary lipid intake, gut microbiota and atherosclerosis has been found. Dietary L-carnitine is metabolized to TMA by gut microbiota and further converted to TMAO in the liver, which accelerates atherosclerosis in mice[111]. 16S rRNA sequencing of cecum bacteria in mice fed a diet supplemented with L-carnitine showed that the family *Prevotellaceae* were increased and positively correlated with plasma TMA level[112]. Furthermore, circulating TMAO in individuals with non-selective diet seems to be much higher than in those with a vegetables-based diet. Faecal microbiota analysis and plasma TMAO levels have been correlated in individuals with *Prevotella* enterotype in respect of those with *Bacteroides* enterotype, showing that these are higher in the first. L-carnitine use in individuals with different diet habits showed that a varied diet led to the production of more TMAO than in vegans or vegetarians. This confirm that both diet and lifestyle can change both the gut microbiota composition and its ability to metabolize TMA and TMAO from dietary L-carnitine[113]. Based on metagenomics, the genus *Collinsella* in faecal microbiota seems to be increased in patients with symptomatic atherosclerosis, while the genera *Eubacterium* and *Roseburia* is abundant in healthy subjects. Furthermore, in patients with atherosclerosis, metabolomics of faecal microbiota suggests an increase of the expression of genes coding for peptidoglycan synthesis, and a fall of hydrogenase levels. In addition, serum carotenoids, especially β-carotene, were decreased suggesting that symptomatic patients with atherosclerosis could have changes in the gut microbiota and a basic inflammatory state[113,114].

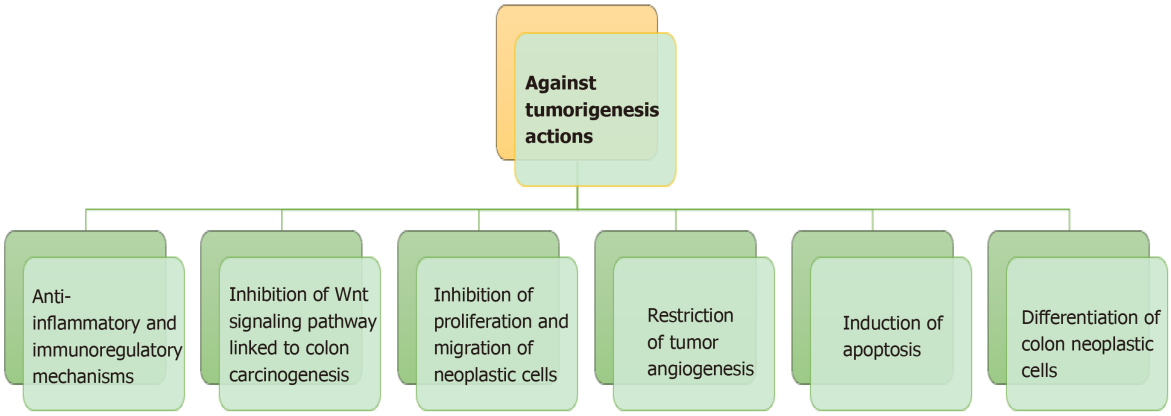
Neurological and psychiatric disturbance

As for the brain, everyone knows that it sends messages throughout the body. The intestine seems to respond. One of the most interesting effects of probiotics on the body focuses on the presence of the gut-brain axis (GBA). The GBA is the connection and the two-way communication between the gut [enteric nervous system (ENS)] and the central nervous system (CNS). This axis is a complex two-way pathway essential for metabolism homeostasis, the influence it has on emotions, mood and in general higher cognitive functions. It is a complex system in which it participates the CNS, the autonomic nervous system, the brain, the spinal cord, and the HPA axis[2,115]. The GBA axis indicates the bidirectional relationship and interdependence between CNS and ENS. It is important to understand this interaction and how a healthy intestinal microbiota can affect the body's nervous system and vice versa. Through a multitude of mechanisms, hundreds of substances and neurotransmitters, the relationship between the two complex systems is in constant change which can have both positive and negative effects. Stress is a quite common factor that can affect mood, psychology and, apparently, the body's intestinal microbiota[116,117]. When the organism exposed to a stressful social situation even for a period of only two hours, the microbiota undergoes significant changes, a significant change in its profile and change in the ratio of the main races of bacteria. Additionally, the brain, under the right conditions, can influence composition and functionality of the intestinal microbiota. It may alter intestinal permeability thereby allowing bacterial antigens to enter the epithelium and stimulate a mucosal immune response. Acute stress can increase colonic permeability, leading to overproduction of interferon-γ[116]. Finally, dysbiosis, *i.e.*, alterations caused in the gut due to stress, facilitate the expression of infectious bacteria. An example is the secretion of norepinephrine during surgery which causes expression of *Pseudomonas aeruginosa*, which can lead to intestinal sepsis. In addition, norepinephrine can stimulate the proliferation of enteric pathogens and increase the infectious properties of *Campylobacter jejuni*[117-119]. Finally, it can favour the overgrowth of non-pathogenic *Escherichia coli* isolates, as well as pathogenic *Escherichia coli* type 0157:H7[3,116]. In continuation of the above, it seems that probiotics have the mechanisms to deal with the complications of stress. Cortisol is a substance produced when the organism is in a state of stress and experiences situations related to anxiety and depression. It was found that probiotics led to a decrease in its release of this substance. In addition, the metabolic products of probiotics, SCFAs, offer beneficial actions. The ENS becomes a recipient of bacterial metabolites. SCFAs such as butyric, acetic, and propionic acids are the main metabolic products of bacterial metabolism[120]. In addition to their essential presence for the multitude of beneficial actions they offer, they can stimulate the sympathetic nervous system, release serotonin in the mucosa and positively affect memory and the learning process[116]. The above-mentioned negative effects of unpleasant psychological states indicate this strong dependence and relationship between CNS and ENS. It is worth focusing on the reverse course, that is, how the health of the body's microbiota can, through probiotic bacteria, give the appropriate signals to the brain to influence possible diseases. Studies show that balance in the microbiota is related to our emotions, as well as how our brains process information from our senses, such as sights, sounds, tastes. Scientists suspect that gut microbiota disorders may play a role in autism spectrum disorders, depression, anxiety, and chronic pain[121]. The GBA is a communication system between the gut and the brain *via* neural, hormonal, and immune circuits, offering the gut microbiota and its metabolites a potential pathway to access the brain. This communication system is bidirectional and allows the brain to regulate gastrointestinal functions such as peristaltic movements and mucus production as well as immune functions[122]. Considerable progress has been made in the past decade in understanding the ways in which the gut microbiota is linked to the brain. Stress conditions affects the gut microbiota composition and that two-way communication between gut microbiota and the CNS influences the host's response to stress. Stress has been shown to affect the integrity of the intestinal epithelium and alter peristalsis, secretions, and mucus production, thereby altering the gut microbiota environment and causing changes in microbial composition and/or metabolism[2,123]. Finally, regarding autism, it has been found that children with autism typically have a higher abundance of *Pseudomonadota*, *Bacteroidota* and a lower abundance of *Bacillota* and *Bifidobacteria* than healthy children. In fact, many classes of bacteria that make up *Bacillota* and *Clostridia* spp., have been found to appear in higher percentages in autistic children with a history of gastrointestinal problems, while at the same time and despite the overall higher abundance of *Bacteroidota*, and lower *Prevotella* were observed. Therefore, in addition to quantifying the relative increase or decrease of the populations of some phyla, it has been deemed necessary to determine the populations of specific intestinal symbiotic organisms to understand the significance of some physiological changes in the gut and/or brain[124].

Colorectal cancer

Colonic metabolism may be protective against carcinogenesis under eubiotic conditions[125] (Figure 3). Several environmental and individual factors associated with the development of colorectal cancer, and the interactions between them. It is estimated that 20% of human cancers are related to conditions of chronic inflammation and/or persistent infections. As for example *Helicobacter pylori* infection is often associated with ulcer and gastric cancer, hepatitis B virus and hepatitis C virus can facilitate hepatocellular carcinoma, IBDs can develop colorectal cancer[126]. The composition of the gut microbiota according to studies may contribute to the mechanism of carcinogenesis either through diet or through its anti-inflammatory effect on the gut mucosa. A number of research has showed a link between *Fusobacterium* genus and the development of colorectal cancer. Most recently an association between *Fusobacterium nucleatum* and colorectal cancer was established by a molecular cytogenetic technique[127,128].

The gut microbiota in patients with colorectal cancer is characterized by increased diversity in *Clostridiaceae* family (such as those from *Clostridium* genus), and an increase in *Bacteroides* and *Bifidobacterium* spp. In contrast, the gut microbiota of individuals with a reduced risk of developing cancer has a high population of lactate-producing bacteria, such as *Eubacterium aerofaciens* and *Lactobacillaceae* phyla[129]. Studies on animals led to propose a model of carcinogenesis based on the consideration that certain mutations in the intestinal epithelial cells lead to a loosening of the intercellular junctions and a reduced production of mucus, compromising the integrity of the intestinal mucosa. So, there



DOI: 10.3748/wjg.v29.i28.4368 **Copyright** ©The Author(s) 2023.

Figure 3 The inhibitory properties of butyrate on tumorigenesis through various mechanisms by the colonic microbiota. Many of the metabolites of protein fermentation can be taken up by other microorganisms and synthesized into active carcinogens. For example, amines and nitrates can be used by facultatively anaerobic and anaerobic colonic bacteria and catalysed the formation of N-nitrosamines, which are among the strongest procarcinogens. Reduced levels of butyrate in the body are not only an indication of the possibility of cancer, but also indicate the severity of the cancer and its course in the body.

is a translocation of bacteria from the lumen to the epithelium where microbial products bind to tumor-associated macrophage receptors inducing the release of inflammatory factors (such as IL-1, IL-6, IL-23) which in turn leads to the production of IL-17 stimulating T-helper lymphocytes. IL-17 activates the transcription factor signal transducer and activator of transcription 3 in epithelial cells which will lead to increased survival and proliferation of epithelial cells resulting in further mutations facilitating carcinogenesis[130,131]. These changes in the epithelium burden the already compromised epithelial integrity, exacerbating bacterial allostasis and contributing to the vicious cycle: Bacterial allostasis - inflammation - cancer. The IL-23/IL-17 axis in tumour-induced inflammation is caused by barrier loss. Thus, otherwise "good" bacteria in the gut microbiota can be transformed into a carcinogen due to the altered host defence mechanism, indicating the uniqueness of the mucosal environment in preventing the development of cancer and may can lead to a cancer progression in other sites such as make the gut/breast microbiota's axis[132-135].

CONCLUSION

A large population of microorganisms of various composition gradually colonizes the human organism, externally and internally, and forms the so-called microbiota. The most important and then populous is the intestinal one. The organism represents a stable and nutrient-rich habitat for the gut microbiota to thrive, and therefore the health of the host is of primary importance to them. In turn, the host benefits because they not only prevent colonization by pathogens, but also provide a continuous and dynamic effect on their host's homeostasis. Thus, this symbiosis creates the host/gut microbiota axis that influences its health throughout an individual's life. In fact, a gut microbiota disorder has been related to many diseases (such as asthma, diabetes, obesity, neurological disorders, *etc.*) but also psychic and mental disorders. However, not all correlation mechanisms are yet understood, which is why more research is needed into the composition of the microbiota that is the cause or result of a disease. The aim of this study is on the human microbiota and its composition for the correlation of conditions during the life course that can be physiological or pathological. In fact, the scientific community is still trying to understand and relate its development and change to various pathological conditions that occur in humans.

FOOTNOTES

Author contributions: Colella M contributed to the conceptualization and data collection; Charitos IA involved in the original manuscript writing and drafting, and resources; Ballini A take part in the manuscript revision and formal analysis; Cafiero C and Palmirotta R contributed to the investigation; Palmirotta R and Santacroce L involved in the validation of this manuscript; Santacroce L contributed to the conceptualization, project administration, and funding of this manuscript; and all the authors have read, discussed, and approved the original manuscript and the final version of it.

Conflict-of-interest statement: All the authors report no relevant conflicts of interest for this article.

Open-Access: This article is an open-access article that was selected by an in-house editor and fully peer-reviewed by external reviewers. It is distributed in accordance with the Creative Commons Attribution NonCommercial (CC BY-NC 4.0) license, which permits others to distribute, remix, adapt, build upon this work non-commercially, and license their derivative works on different terms, provided the original work is properly cited and the use is non-commercial. See: https://creativecommons.org/Licenses/by-nc/4.0/

Country/Territory of origin: Italy

ORCID number: Marica Colella 0000-0003-0806-4327; Ioannis Alexandros Charitos 0000-0003-3527-7483; Andrea Ballini 0000-0001-8758-1415; Concetta Cafiero 0000-0003-3859-2040; Skender Topi 0000-0002-6661-8116; Raffaele Palmirotta 0000-0002-9401-7377; Luigi Santacroce 0000-0001-5671-8124.

S-Editor: Wang JJ
L-Editor: A
P-Editor: Wang JJ

REFERENCES

1 **Cresci GA**, Bawden E. Gut Microbiome: What We Do and Don't Know. *Nutr Clin Pract* 2015; **30**: 734-746 [PMID: 26449893 DOI: 10.1177/0884533615609899]
2 **Santacroce L**, Man A, Charitos IA, Haxhirexha K, Topi S. Current knowledge about the connection between health status and gut microbiota from birth to elderly. A narrative review. *Front Biosci (Landmark Ed)* 2021; **26**: 135-148 [PMID: 34162042 DOI: 10.52586/4930]
3 **Duncan SH**, Lobley GE, Holtrop G, Ince J, Johnstone AM, Louis P, Flint HJ. Human colonic microbiota associated with diet, obesity and weight loss. *Int J Obes (Lond)* 2008; **32**: 1720-1724 [PMID: 18779823 DOI: 10.1038/ijo.2008.155]
4 **Conlon MA**, Bird AR. The impact of diet and lifestyle on gut microbiota and human health. *Nutrients* 2014; **7**: 17-44 [PMID: 25545101 DOI: 10.3390/nu7010017]
5 **Ferraris RP**, Vinnakota RR. Intestinal nutrient transport in genetically obese mice. *Am J Clin Nutr* 1995; **62**: 540-546 [PMID: 7661115 DOI: 10.1093/ajcn/62.3.540]
6 **Di Domenico M**, Ballini A, Boccellino M, Scacco S, Lovero R, Charitos IA, Santacroce L. The Intestinal Microbiota May Be a Potential Theranostic Tool for Personalized Medicine. *J Pers Med* 2022; **12** [PMID: 35455639 DOI: 10.3390/jpm12040523]
7 **Lazar V**, Ditu LM, Pircalabioru GG, Picu A, Petcu L, Cucu N, Chifiriuc MC. Gut Microbiota, Host Organism, and Diet Trialogue in Diabetes and Obesity. *Front Nutr* 2019; **6**: 21 [PMID: 30931309 DOI: 10.3389/fnut.2019.00021]
8 **Thursby E**, Juge N. Introduction to the human gut microbiota. *Biochem J* 2017; **474**: 1823-1836 [PMID: 28512250 DOI: 10.1042/BCJ20160510]
9 **Jeffery IB**, O'Toole PW. Diet-microbiota interactions and their implications for healthy living. *Nutrients* 2013; **5**: 234-252 [PMID: 23344252 DOI: 10.3390/nu5010234]
10 **Ravcheev DA**, Thiele I. Systematic genomic analysis reveals the complementary aerobic and anaerobic respiration capacities of the human gut microbiota. *Front Microbiol* 2014; **5**: 674 [PMID: 25538694 DOI: 10.3389/fmicb.2014.00674]
11 **Yang T**, Owen JL, Lightfoot YL, Kladde MP, Mohamadzadeh M. Microbiota impact on the epigenetic regulation of colorectal cancer. *Trends Mol Med* 2013; **19**: 714-725 [PMID: 24051204 DOI: 10.1016/j.molmed.2013.08.005]
12 **Robles Alonso V**, Guarner F. Linking the gut microbiota to human health. *Br J Nutr* 2013; **109** Suppl 2: S21-S26 [PMID: 23360877 DOI: 10.1017/S0007114512005235]
13 **Ianiro G**, Bruno G, Lopetuso L, Beghella FB, Laterza L, D'Aversa F, Gigante G, Cammarota G, Gasbarrini A. Role of yeasts in healthy and impaired gut microbiota: the gut mycome. *Curr Pharm Des* 2014; **20**: 4565-4569 [PMID: 24180411 DOI: 10.2174/1381612813196660723]
14 **Inchingolo F**, Santacroce L, Cantore S, Ballini A, Del Prete R, Topi S, Saini R, Dipalma G, Arrigoni R. Probiotics and EpiCor® in human health. *J Biol Regul Homeost Agents* 2019; **33**: 1973-1979 [PMID: 31858774 DOI: 10.23812/19-543-L]
15 **Isacco CG**, Ballini A, De Vito D, Nguyen KCD, Cantore S, Bottalico L, Quagliuolo L, Boccellino M, Di Domenico M, Santacroce L, Arrigoni R, Dipalma G, Inchingolo F. Rebalancing the Oral Microbiota as an Efficient Tool in Endocrine, Metabolic and Immune Disorders. *Endocr Metab Immune Disord Drug Targets* 2021; **21**: 777-784 [PMID: 32727337 DOI: 10.2174/1871530320666200729142504]
16 **Rodríguez JM**, Murphy K, Stanton C, Ross RP, Kober OI, Juge N, Avershina E, Rudi K, Narbad A, Jenmalm MC, Marchesi JR, Collado MC. The composition of the gut microbiota throughout life, with an emphasis on early life. *Microb Ecol Health Dis* 2015; **26**: 26050 [PMID: 25651996 DOI: 10.3402/mehd.v26.26050]
17 **Vaahtovuo J**, Toivanen P, Eerola E. Study of murine faecal microflora by cellular fatty acid analysis; effect of age and mouse strain. *Antonie Van Leeuwenhoek* 2001; **80**: 35-42 [PMID: 11761365 DOI: 10.1023/a:1012058107731]
18 **Clarke SF**, Murphy EF, O'Sullivan O, Lucey AJ, Humphreys M, Hogan A, Hayes P, O'Reilly M, Jeffery IB, Wood-Martin R, Kerins DM, Quigley E, Ross RP, O'Toole PW, Molloy MG, Falvey E, Shanahan F, Cotter PD. Exercise and associated dietary extremes impact on gut microbial diversity. *Gut* 2014; **63**: 1913-1920 [PMID: 25021423 DOI: 10.1136/gutjnl-2013-306541]
19 **Avershina E**, Storrø O, Øien T, Johnsen R, Pope P, Rudi K. Major faecal microbiota shifts in composition and diversity with age in a geographically restricted cohort of mothers and their children. *FEMS Microbiol Ecol* 2014; **87**: 280-290 [PMID: 24112053 DOI: 10.1111/1574-6941.12223]
20 **De Filippo C**, Di Paola M, Ramazzotti M, Albanese D, Pieraccini G, Banci E, Miglietta F, Cavalieri D, Lionetti P. Diet, Environments, and Gut Microbiota. A Preliminary Investigation in Children Living in Rural and Urban Burkina Faso and Italy. *Front Microbiol* 2017; **8**: 1979 [PMID: 29081768 DOI: 10.3389/fmicb.2017.01979]
21 **Santacroce L**, Charitos IA, Ballini A, Inchingolo F, Luperto P, De Nitto E, Topi S. The Human Respiratory System and its Microbiome at a Glimpse. *Biology (Basel)* 2020; **9** [PMID: 33019595 DOI: 10.3390/biology9100318]
22 **Jandhyala SM**, Talukdar R, Subramanyam C, Vuyyuru H, Sasikala M, Nageshwar Reddy D. Role of the normal gut microbiota. *World J Gastroenterol* 2015; **21**: 8787-8803 [PMID: 26269668 DOI: 10.3748/wjg.v21.i29.8787]
23 **David LA**, Maurice CF, Carmody RN, Gootenberg DB, Button JE, Wolfe BE, Ling AV, Devlin AS, Varma Y, Fischbach MA, Biddinger SB, Dutton RJ, Turnbaugh PJ. Diet rapidly and reproducibly alters the human gut microbiome. *Nature* 2014; **505**: 559-563 [PMID: 24336217 DOI: 10.1038/nature12820]
24 **Santacroce L**, Imbimbo C, Ballini A, Crocetto F, Scacco S, Cantore S, Di Zazzo E, Colella M, Jirillo E. Testicular Immunity and Its Connection with the Microbiota. Physiological and Clinical Implications in the Light of Personalized Medicine. *J Pers Med* 2022; **12** [PMID:

36013286 DOI: 10.3390/jpm12081335]
25 **De Filippis F**, Pellegrini N, Vannini L, Jeffery IB, La Storia A, Laghi L, Serrazanetti DI, Di Cagno R, Ferrocino I, Lazzi C, Turroni S, Cocolin L, Brigidi P, Neviani E, Gobbetti M, O'Toole PW, Ercolini D. High-level adherence to a Mediterranean diet beneficially impacts the gut microbiota and associated metabolome. *Gut* 2016; **65**: 1812-1821 [PMID: 26416813 DOI: 10.1136/gutjnl-2015-309957]
26 **Lovreglio P**, Bukvic N, Fustinoni S, Ballini A, Drago I, Foà V, Guanti G, Soleo L. Lack of genotoxic effect in workers exposed to very low doses of 1,3-butadiene. *Arch Toxicol* 2006; **80**: 378-381 [PMID: 16307232 DOI: 10.1007/s00204-005-0046-0]
27 **Santacroce L**, Muzio EL, Bottalico L, Spirito F, Charitos IA, Passarelli PC, Jirillo E. Subversion of the Oral Microbiota and Induction of Immune-Mediated Systemic Inflammation with Special Reference to Periodontitis: Current Knowledge and Perspectives. *Endocr Metab Immune Disord Drug Targets* 2023; **23**: 470-484 [PMID: 35770408 DOI: 10.2174/1871530322666220629101357]
28 **Dominianni C**, Sinha R, Goedert JJ, Pei Z, Yang L, Hayes RB, Ahn J. Sex, body mass index, and dietary fiber intake influence the human gut microbiome. *PLoS One* 2015; **10**: e0124599 [PMID: 25874569 DOI: 10.1371/journal.pone.0124599]
29 **Baranowski RW**, Skelly LE, Josse AR, Fajardo VA. Exploring the Effects of Greek Yogurt Supplementation and Exercise Training on Serum Lithium and Its Relationship With Musculoskeletal Outcomes in Men. *Front Nutr* 2021; **8**: 798036 [PMID: 35004824 DOI: 10.3389/fnut.2021.798036]
30 **Contuzzi N**, Casalino G, Boccaccio A, Ballini A, Charitos IA, Bottalico L, Santacroce L. Metals Biotribology and Oral Microbiota Biocorrosion Mechanisms. *J Funct Biomater* 2022; **14** [PMID: 36662061 DOI: 10.3390/jfb14010014]
31 **Arslan N**. Obesity, fatty liver disease and intestinal microbiota. *World J Gastroenterol* 2014; **20**: 16452-16463 [PMID: 25469013 DOI: 10.3748/wjg.v20.i44.16452]
32 **Wegierska AE**, Charitos IA, Topi S, Potenza MA, Montagnani M, Santacroce L. The Connection Between Physical Exercise and Gut Microbiota: Implications for Competitive Sports Athletes. *Sports Med* 2022; **52**: 2355-2369 [PMID: 35596883 DOI: 10.1007/s40279-022-01696-x]
33 **Savin Z**, Kivity S, Yonath H, Yehuda S. Smoking and the intestinal microbiome. *Arch Microbiol* 2018; **200**: 677-684 [PMID: 29626219 DOI: 10.1007/s00203-018-1506-2]
34 **Santacroce L**, Di Domenico M, Montagnani M, Jirillo E. Antibiotic Resistance and Microbiota Response. *Curr Pharm Des* 2023; **29**: 356-364 [PMID: 36537602 DOI: 10.2174/1381612829666221219093450]
35 **Ramirez J**, Guarner F, Bustos Fernandez L, Maruy A, Sdepanian VL, Cohen H. Antibiotics as Major Disruptors of Gut Microbiota. *Front Cell Infect Microbiol* 2020; **10**: 572912 [PMID: 33330122 DOI: 10.3389/fcimb.2020.572912]
36 **Bottalico L**, Charitos IA, Potenza MA, Montagnani M, Santacroce L. The war against bacteria, from the past to present and beyond. *Expert Rev Anti Infect Ther* 2022; **20**: 681-706 [PMID: 34874223 DOI: 10.1080/14787210.2022.2013809]
37 **Xu Z**, Knight R. Dietary effects on human gut microbiome diversity. *Br J Nutr* 2015; **113** Suppl: S1-S5 [PMID: 25498959 DOI: 10.1017/S0007114514004127]
38 **Vernocchi P**, Del Chierico F, Putignani L. Gut Microbiota Metabolism and Interaction with Food Components. *Int J Mol Sci* 2020; **21** [PMID: 32456257 DOI: 10.3390/ijms21103688]
39 **Rowland I**, Gibson G, Heinken A, Scott K, Swann J, Thiele I, Tuohy K. Gut microbiota functions: metabolism of nutrients and other food components. *Eur J Nutr* 2018; **57**: 1-24 [PMID: 28393285 DOI: 10.1007/s00394-017-1445-8]
40 **Bottalico L**, Castellaneta F, Charitos IA. From hydrotherapy to the discovery of the gut microbiota: the historical gastrointestinal health concept. *Pharmacophore* 2020; **11**: 82-90
41 **Ndeh D**, Munoz Munoz J, Cartmell A, Bulmer D, Wills C, Henrissat B, Gray J. The human gut microbe Bacteroides thetaiotaomicron encodes the founding member of a novel glycosaminoglycan-degrading polysaccharide lyase family PL29. *J Biol Chem* 2018; **293**: 17906-17916 [PMID: 30262663 DOI: 10.1074/jbc.RA118.004510]
42 **Turnbaugh PJ**, Ley RE, Mahowald MA, Magrini V, Mardis ER, Gordon JI. An obesity-associated gut microbiome with increased capacity for energy harvest. *Nature* 2006; **444**: 1027-1031 [PMID: 17183312 DOI: 10.1038/nature05414]
43 **Murphy EF**, Cotter PD, Healy S, Marques TM, O'Sullivan O, Fouhy F, Clarke SF, O'Toole PW, Quigley EM, Stanton C, Ross PR, O'Doherty RM, Shanahan F. Composition and energy harvesting capacity of the gut microbiota: relationship to diet, obesity and time in mouse models. *Gut* 2010; **59**: 1635-1642 [PMID: 20926643 DOI: 10.1136/gut.2010.215665]
44 **Arrigoni R**, Cammarota F, Porro R, Cantore S, Dioguardi M, Cazzolla AP, De Leonardis F, Polimeno L, Zerman N, Di Cosola M, Mastrangelo F, Santacroce L, Ballini A. Natural Bioactive Compounds against Oxidative Stress: Dietary Polyphenols Strike Back. *Endocr Metab Immune Disord Drug Targets* 2023; **23**: 764-776 [PMID: 36345247 DOI: 10.2174/1871530323666221107092553]
45 **Dao MC**, Everard A, Aron-Wisnewsky J, Sokolovska N, Prifti E, Verger EO, Kayser BD, Levenez F, Chilloux J, Hoyles L; MICRO-Obes Consortium, Dumas ME, Rizkalla SW, Doré J, Cani PD, Clément K. Akkermansia muciniphila and improved metabolic health during a dietary intervention in obesity: relationship with gut microbiome richness and ecology. *Gut* 2016; **65**: 426-436 [PMID: 26100928 DOI: 10.1136/gutjnl-2014-308778]
46 **Samuel BS**, Hansen EE, Manchester JK, Coutinho PM, Henrissat B, Fulton R, Latreille P, Kim K, Wilson RK, Gordon JI. Genomic and metabolic adaptations of Methanobrevibacter smithii to the human gut. *Proc Natl Acad Sci U S A* 2007; **104**: 10643-10648 [PMID: 17563350 DOI: 10.1073/pnas.0704189104]
47 **Schneeberger M**, Everard A, Gómez-Valadés AG, Matamoros S, Ramírez S, Delzenne NM, Gomis R, Claret M, Cani PD. Akkermansia muciniphila inversely correlates with the onset of inflammation, altered adipose tissue metabolism and metabolic disorders during obesity in mice. *Sci Rep* 2015; **5**: 16643 [PMID: 26563823 DOI: 10.1038/srep16643]
48 **Goodrich JK**, Waters JL, Poole AC, Sutter JL, Koren O, Blekhman R, Beaumont M, Van Treuren W, Knight R, Bell JT, Spector TD, Clark AG, Ley RE. Human genetics shape the gut microbiome. *Cell* 2014; **159**: 789-799 [PMID: 25417156 DOI: 10.1016/j.cell.2014.09.053]
49 **Hrncir T**, Hrncirova L, Kverka M, Hromadka R, Machova V, Trckova E, Kostovcikova K, Kralickova P, Krejsek J, Tlaskalova-Hogenova H. Gut Microbiota and NAFLD: Pathogenetic Mechanisms, Microbiota Signatures, and Therapeutic Interventions. *Microorganisms* 2021; **9** [PMID: 33946843 DOI: 10.3390/microorganisms9050957]
50 **Santacroce L**, Sardaro N, Topi S, Pettini F, Bottalico L, Cantore S, Cascella G, Del Prete R, Dipalma G, Inchingolo F. The pivotal role of oral microbiota in health and disease. *J Biol Regul Homeost Agents* 2020; **34**: 733-737 [PMID: 32492992 DOI: 10.23812/20-127-L-45]
51 **Belkaid Y**, Hand TW. Role of the microbiota in immunity and inflammation. *Cell* 2014; **157**: 121-141 [PMID: 24679531 DOI: 10.1016/j.cell.2014.03.011]
52 **Mahowald MA**, Rey FE, Seedorf H, Turnbaugh PJ, Fulton RS, Wollam A, Shah N, Wang C, Magrini V, Wilson RK, Cantarel BL, Coutinho PM, Henrissat B, Crock LW, Russell A, Verberkmoes NC, Hettich RL, Gordon JI. Characterizing a model human gut microbiota composed of

members of its two dominant bacterial phyla. *Proc Natl Acad Sci U S A* 2009; **106**: 5859-5864 [PMID: 19321416 DOI: 10.1073/pnas.0901529106]

53 **Rook GA**. Regulation of the immune system by biodiversity from the natural environment: an ecosystem service essential to health. *Proc Natl Acad Sci U S A* 2013; **110**: 18360-18367 [PMID: 24154724 DOI: 10.1073/pnas.1313731110]

54 **Gieryńska M**, Szulc-Dąbrowska L, Struzik J, Mielcarska MB, Gregorczyk-Zboroch KP. Integrity of the Intestinal Barrier: The Involvement of Epithelial Cells and Microbiota-A Mutual Relationship. *Animals (Basel)* 2022; **12** [PMID: 35049768 DOI: 10.3390/ani12020145]

55 **Ma J**, Piao X, Mahfuz S, Long S, Wang J. The interaction among gut microbes, the intestinal barrier and short chain fatty acids. *Anim Nutr* 2022; **9**: 159-174 [PMID: 35573092 DOI: 10.1016/j.aninu.2021.09.012]

56 **Amarante-Mendes GP**, Adjemian S, Branco LM, Zanetti LC, Weinlich R, Bortoluci KR. Pattern Recognition Receptors and the Host Cell Death Molecular Machinery. *Front Immunol* 2018; **9**: 2379 [PMID: 30459758 DOI: 10.3389/fimmu.2018.02379]

57 **Cochet F**, Peri F. The Role of Carbohydrates in the Lipopolysaccharide (LPS)/Toll-Like Receptor 4 (TLR4) Signalling. *Int J Mol Sci* 2017; **18** [PMID: 29099761 DOI: 10.3390/ijms18112318]

58 **Liu T**, Zhang L, Joo D, Sun SC. NF-κB signaling in inflammation. *Signal Transduct Target Ther* 2017; **2**: 17023-17023 [PMID: 29158945 DOI: 10.1038/sigtrans.2017.23]

59 **Paone P**, Cani PD. Mucus barrier, mucins and gut microbiota: the expected slimy partners? *Gut* 2020; **69**: 2232-2243 [PMID: 32917747 DOI: 10.1136/gutjnl-2020-322260]

60 **Kennedy EA**, King KY, Baldridge MT. Mouse Microbiota Models: Comparing Germ-Free Mice and Antibiotics Treatment as Tools for Modifying Gut Bacteria. *Front Physiol* 2018; **9**: 1534 [PMID: 30429801 DOI: 10.3389/fphys.2018.01534]

61 **Qi R**, Sun J, Qiu X, Zhang Y, Wang J, Wang Q, Huang J, Ge L, Liu Z. The intestinal microbiota contributes to the growth and physiological state of muscle tissue in piglets. *Sci Rep* 2021; **11**: 11237 [PMID: 34045661 DOI: 10.1038/s41598-021-90881-5]

62 **Hou K**, Wu ZX, Chen XY, Wang JQ, Zhang D, Xiao C, Zhu D, Koya JB, Wei L, Li J, Chen ZS. Microbiota in health and diseases. *Signal Transduct Target Ther* 2022; **7**: 135 [PMID: 35461318 DOI: 10.1038/s41392-022-00974-4]

63 **Tavakoli P**, Vollmer-Conna U, Hadzi-Pavlovic D, Grimm MC. A Review of Inflammatory Bowel Disease: A Model of Microbial, Immune and Neuropsychological Integration. *Public Health Rev* 2021; **42**: 1603990 [PMID: 34692176 DOI: 10.3389/phrs.2021.1603990]

64 **Ghoshal UC**, Shukla R, Ghoshal U, Gwee KA, Ng SC, Quigley EM. The gut microbiota and irritable bowel syndrome: friend or foe? *Int J Inflam* 2012; **2012**: 151085 [PMID: 22577594 DOI: 10.1155/2012/151085]

65 **Rajilić-Stojanović M**, Biagi E, Heilig HG, Kajander K, Kekkonen RA, Tims S, de Vos WM. Global and deep molecular analysis of microbiota signatures in fecal samples from patients with irritable bowel syndrome. *Gastroenterology* 2011; **141**: 1792-1801 [PMID: 21820992 DOI: 10.1053/j.gastro.2011.07.043]

66 **Jeffery IB**, O'Toole PW, Öhman L, Claesson MJ, Deane J, Quigley EM, Simrén M. An irritable bowel syndrome subtype defined by species-specific alterations in faecal microbiota. *Gut* 2012; **61**: 997-1006 [PMID: 22180058 DOI: 10.1136/gutjnl-2011-301501]

67 **Saulnier DM**, Riehle K, Mistretta TA, Diaz MA, Mandal D, Raza S, Weidler EM, Qin X, Coarfa C, Milosavljevic A, Petrosino JF, Highlander S, Gibbs R, Lynch SV, Shulman RJ, Versalovic J. Gastrointestinal microbiome signatures of pediatric patients with irritable bowel syndrome. *Gastroenterology* 2011; **141**: 1782-1791 [PMID: 21741921 DOI: 10.1053/j.gastro.2011.06.072]

68 **Vijay A**, Valdes AM. Role of the gut microbiome in chronic diseases: a narrative review. *Eur J Clin Nutr* 2022; **76**: 489-501 [PMID: 34584224 DOI: 10.1038/s41430-021-00991-6]

69 **Khan I**, Ullah N, Zha L, Bai Y, Khan A, Zhao T, Che T, Zhang C. Alteration of Gut Microbiota in Inflammatory Bowel Disease (IBD): Cause or Consequence? IBD Treatment Targeting the Gut Microbiome. *Pathogens* 2019; **8** [PMID: 31412603 DOI: 10.3390/pathogens8030126]

70 **Caparrós E**, Wiest R, Scharl M, Rogler G, Gutiérrez Casbas A, Yilmaz B, Wawrzyniak M, Francés R. Dysbiotic microbiota interactions in Crohn's disease. *Gut Microbes* 2021; **13**: 1949096 [PMID: 34313550 DOI: 10.1080/19490976.2021.1949096]

71 **Ferreira C**, Veldhoen M. Host and microbes date exclusively. *Cell* 2012; **149**: 1428-1430 [PMID: 22726431 DOI: 10.1016/j.cell.2012.06.005]

72 **Russell SL**, Gold MJ, Hartmann M, Willing BP, Thorson L, Wlodarska M, Gill N, Blanchet MR, Mohn WW, McNagny KM, Finlay BB. Early life antibiotic-driven changes in microbiota enhance susceptibility to allergic asthma. *EMBO Rep* 2012; **13**: 440-447 [PMID: 22422004 DOI: 10.1038/embor.2012.32]

73 **Sjögren YM**, Jenmalm MC, Böttcher MF, Björkstén B, Sverremark-Ekström E. Altered early infant gut microbiota in children developing allergy up to 5 years of age. *Clin Exp Allergy* 2009; **39**: 518-526 [PMID: 19220322 DOI: 10.1111/j.1365-2222.2008.03156.x]

74 **Rose NR**. Prediction and Prevention of Autoimmune Disease in the 21st Century: A Review and Preview. *Am J Epidemiol* 2016; **183**: 403-406 [PMID: 26888748 DOI: 10.1093/aje/kwv292]

75 **Topi S**, Bottalico L, Charitos IA, Colella M, Di Domenico M, Palmirotta R, Santacroce L. Biomolecular Mechanisms of Autoimmune Diseases and Their Relationship with the Resident Microbiota: Friend or Foe? *Pathophysiology* 2022; **29**: 507-536 [PMID: 36136068 DOI: 10.3390/pathophysiology29030041]

76 **Kucera P**, Nováková D, Behanová M, Novak J, Tlaskalová-Hogenová H, Andel M. Gliadin, endomysial and thyroid antibodies in patients with latent autoimmune diabetes of adults (LADA). *Clin Exp Immunol* 2003; **133**: 139-143 [PMID: 12823288 DOI: 10.1046/j.1365-2249.2003.02205.x]

77 **Tlaskalová-Hogenová H**, Stěpánková R, Kozáková H, Hudcovic T, Vannucci L, Tučková L, Rossmann P, Hrnčíř T, Kverka M, Zákostelská Z, Klimešová K, Přibylová J, Bártová J, Sanchez D, Fundová P, Borovská D, Srůtková D, Zídek Z, Schwarzer M, Drastich P, Funda DP. The role of gut microbiota (commensal bacteria) and the mucosal barrier in the pathogenesis of inflammatory and autoimmune diseases and cancer: contribution of germ-free and gnotobiotic animal models of human diseases. *Cell Mol Immunol* 2011; **8**: 110-120 [PMID: 21278760 DOI: 10.1038/cmi.2010.67]

78 **Tannock GW**, Savage DC. Influences of dietary and environmental stress on microbial populations in the murine gastrointestinal tract. *Infect Immun* 1974; **9**: 591-598 [PMID: 4593471 DOI: 10.1128/iai.9.3.591-598.1974]

79 **Nadal I**, Donant E, Ribes-Koninckx C, Calabuig M, Sanz Y. Imbalance in the composition of the duodenal microbiota of children with coeliac disease. *J Med Microbiol* 2007; **56**: 1669-1674 [PMID: 18033837 DOI: 10.1099/jmm.0.47410-0]

80 **Collado MC**, Donat E, Ribes-Koninckx C, Calabuig M, Sanz Y. Imbalances in faecal and duodenal Bifidobacterium species composition in active and non-active coeliac disease. *BMC Microbiol* 2008; **8**: 232 [PMID: 19102766 DOI: 10.1186/1471-2180-8-232]

81 **Mårild K**, Stephansson O, Montgomery S, Murray JA, Ludvigsson JF. Pregnancy outcome and risk of celiac disease in offspring: a nationwide case-control study. *Gastroenterology* 2012; **142**: 39-45.e3 [PMID: 21995948 DOI: 10.1053/j.gastro.2011.09.047]

82 **Decker E**, Engelmann G, Findeisen A, Gerner P, Laass M, Ney D, Posovszky C, Hoy L, Hornef MW. Cesarean delivery is associated with

celiac disease but not inflammatory bowel disease in children. *Pediatrics* 2010; **125**: e1433-e1440 [PMID: 20478942 DOI: 10.1542/peds.2009-2260]

83 **Durazzo M**, Ferro A, Gruden G. Gastrointestinal Microbiota and Type 1 Diabetes Mellitus: The State of Art. *J Clin Med* 2019; **8** [PMID: 31684011 DOI: 10.3390/jcm8111843]

84 **Yadav H**, Jain S, Sinha PR. Antidiabetic effect of probiotic dahi containing Lactobacillus acidophilus and Lactobacillus casei in high fructose fed rats. *Nutrition* 2007; **23**: 62-68 [PMID: 17084593 DOI: 10.1016/j.nut.2006.09.002]

85 **Elding Larsson H**, Vehik K, Gesualdo P, Akolkar B, Hagopian W, Krischer J, Lernmark Å, Rewers M, Simell O, She JX, Ziegler A, Haller MJ; TEDDY Study Group. Children followed in the TEDDY study are diagnosed with type 1 diabetes at an early stage of disease. *Pediatr Diabetes* 2014; **15**: 118-126 [PMID: 24034790 DOI: 10.1111/pedi.12066]

86 **Membrez M**, Blancher F, Jaquet M, Bibiloni R, Cani PD, Burcelin RG, Corthesy I, Macé K, Chou CJ. Gut microbiota modulation with norfloxacin and ampicillin enhances glucose tolerance in mice. *FASEB J* 2008; **22**: 2416-2426 [PMID: 18326786 DOI: 10.1096/fj.07-102723]

87 **Rebello CJ**, Burton J, Heiman M, Greenway FL. Gastrointestinal microbiome modulator improves glucose tolerance in overweight and obese subjects: A randomized controlled pilot trial. *J Diabetes Complications* 2015; **29**: 1272-1276 [PMID: 26424589 DOI: 10.1016/j.jdiacomp.2015.08.023]

88 **Cani PD**, Bibiloni R, Knauf C, Waget A, Neyrinck AM, Delzenne NM, Burcelin R. Changes in gut microbiota control metabolic endotoxemia-induced inflammation in high-fat diet-induced obesity and diabetes in mice. *Diabetes* 2008; **57**: 1470-1481 [PMID: 18305141 DOI: 10.2337/db07-1403]

89 **Mokhtari P**, Metos J, Anandh Babu PV. Impact of type 1 diabetes on the composition and functional potential of gut microbiome in children and adolescents: possible mechanisms, current knowledge, and challenges. *Gut Microbes* 2021; **13**: 1-18 [PMID: 34101547 DOI: 10.1080/19490976.2021.1926841]

90 **Whang A**, Nagpal R, Yadav H. Bi-directional drug-microbiome interactions of anti-diabetics. *EBioMedicine* 2019; **39**: 591-602 [PMID: 30553752 DOI: 10.1016/j.ebiom.2018.11.046]

91 **Moreno-Indias I**, Cardona F, Tinahones FJ, Queipo-Ortuño MI. Impact of the gut microbiota on the development of obesity and type 2 diabetes mellitus. *Front Microbiol* 2014; **5**: 190 [PMID: 24808896 DOI: 10.3389/fmicb.2014.00190]

92 **Ballini A**, Scacco S, Boccellino M, Santacroce L, Arrigoni R. Microbiota and Obesity: Where Are We Now? *Biology (Basel)* 2020; **9** [PMID: 33255588 DOI: 10.3390/biology9120415]

93 **Iatcu CO**, Steen A, Covasa M. Gut Microbiota and Complications of Type-2 Diabetes. *Nutrients* 2021; **14** [PMID: 35011044 DOI: 10.3390/nu14010166]

94 **Zhang L**, Chu J, Hao W, Zhang J, Li H, Yang C, Yang J, Chen X, Wang H. Gut Microbiota and Type 2 Diabetes Mellitus: Association, Mechanism, and Translational Applications. *Mediators Inflamm* 2021; **2021**: 5110276 [PMID: 34447287 DOI: 10.1155/2021/5110276]

95 **Craciun CI**, Neag MA, Catinean A, Mitre AO, Rusu A, Bala C, Roman G, Buzoianu AD, Muntean DM, Craciun AE. The Relationships between Gut Microbiota and Diabetes Mellitus, and Treatments for Diabetes Mellitus. *Biomedicines* 2022; **10** [PMID: 35203519 DOI: 10.3390/biomedicines10020308]

96 **Murri M**, Leiva I, Gomez-Zumaquero JM, Tinahones FJ, Cardona F, Soriguer F, Queipo-Ortuño MI. Gut microbiota in children with type 1 diabetes differs from that in healthy children: a case-control study. *BMC Med* 2013; **11**: 46 [PMID: 23433344 DOI: 10.1186/1741-7015-11-46]

97 **Sikalidis AK**, Maykish A. The Gut Microbiome and Type 2 Diabetes Mellitus: Discussing a Complex Relationship. *Biomedicines* 2020; **8** [PMID: 31936158 DOI: 10.3390/biomedicines8010008]

98 **Caesar R**, Reigstad CS, Bäckhed HK, Reinhardt C, Ketonen M, Lundén GÖ, Cani PD, Bäckhed F. Gut-derived lipopolysaccharide augments adipose macrophage accumulation but is not essential for impaired glucose or insulin tolerance in mice. *Gut* 2012; **61**: 1701-1707 [PMID: 22535377 DOI: 10.1136/gutjnl-2011-301689]

99 **Cani PD**, Possemiers S, Van de Wiele T, Guiot Y, Everard A, Rottier O, Geurts L, Naslain D, Neyrinck A, Lambert DM, Muccioli GG, Delzenne NM. Changes in gut microbiota control inflammation in obese mice through a mechanism involving GLP-2-driven improvement of gut permeability. *Gut* 2009; **58**: 1091-1103 [PMID: 19240062 DOI: 10.1136/gut.2008.165886]

100 **Dioguardi M**, Cantore S, Quarta C, Sovereto D, Zerman N, Pettini F, Muzio LL, Cosola MD, Santacroce L, Ballini A. Correlation between Diabetes Mellitus and Peri-implantitis: A Systematic Review. *Endocr Metab Immune Disord Drug Targets* 2023; **23**: 596-608 [PMID: 36281861 DOI: 10.2174/1871530323666221021100427]

101 **Markowiak-Kopeć P**, Śliżewska K. The Effect of Probiotics on the Production of Short-Chain Fatty Acids by Human Intestinal Microbiome. *Nutrients* 2020; **12** [PMID: 32316181 DOI: 10.3390/nu12041107]

102 **Zhang C**, Yin A, Li H, Wang R, Wu G, Shen J, Zhang M, Wang L, Hou Y, Ouyang H, Zhang Y, Zheng Y, Wang J, Lv X, Wang Y, Zhang F, Zeng B, Li W, Yan F, Zhao Y, Pang X, Zhang X, Fu H, Chen F, Zhao N, Hamaker BR, Bridgewater LC, Weinkove D, Clement K, Dore J, Holmes E, Xiao H, Zhao G, Yang S, Bork P, Nicholson JK, Wei H, Tang H, Zhao L. Dietary Modulation of Gut Microbiota Contributes to Alleviation of Both Genetic and Simple Obesity in Children. *EBioMedicine* 2015; **2**: 968-984 [PMID: 26425705 DOI: 10.1016/j.ebiom.2015.07.007]

103 **Marzullo P**, Di Renzo L, Pugliese G, De Siena M, Barrea L, Muscogiuri G, Colao A, Savastano S; Obesity Programs of nutrition, Education, Research and Assessment (OPERA) Group. From obesity through gut microbiota to cardiovascular diseases: a dangerous journey. *Int J Obes Suppl* 2020; **10**: 35-49 [PMID: 32714511 DOI: 10.1038/s41367-020-0017-1]

104 **Sarmiento F**, Leigh JA, Whitman WB. Genetic systems for hydrogenotrophic methanogens. *Methods Enzymol* 2011; **494**: 43-73 [PMID: 21402209 DOI: 10.1016/B978-0-12-385112-3.00003-2]

105 **Ballini A**, Cantore S, Fatone L, Montenegro V, De Vito D, Pettini F, Crincoli V, Antelmi A, Romita P, Rapone B, Miniello G, Perillo L, Grassi FR, Foti C. Transmission of nonviral sexually transmitted infections and oral sex. *J Sex Med* 2012; **9**: 372-384 [PMID: 22023797 DOI: 10.1111/j.1743-6109.2011.02515.x]

106 **Ungerfeld EM**. Corrigendum: Shifts in metabolic hydrogen sinks in the methanogenesis-inhibited ruminal fermentation: a meta-analysis. *Front Microbiol* 2015; **6**: 538 [PMID: 26082760 DOI: 10.3389/fmicb.2015.00538]

107 **Ilyas A**, Wijayasinghe YS, Khan I, El Samaloty NM, Adnan M, Dar TA, Poddar NK, Singh LR, Sharma H, Khan S. Implications of trimethylamine N-oxide (TMAO) and Betaine in Human Health: Beyond Being Osmoprotective Compounds. *Front Mol Biosci* 2022; **9**: 964624 [PMID: 36310589 DOI: 10.3389/fmolb.2022.964624]

108 **Xia X**, Li X, Xie F, Yuan G, Cheng D, Peng C. Non-targeted metabonomic analysis of plasma in patients with atherosclerosis by liquid chromatography-mass spectrometry. *Ann Transl Med* 2022; **10**: 133 [PMID: 35284547 DOI: 10.21037/atm-22-118]

109 **Wang X**, Ishimori N, Korstanje R, Rollins J, Paigen B. Identifying novel genes for atherosclerosis through mouse-human comparative

genetics. *Am J Hum Genet* 2005; **77**: 1-15 [PMID: 15931593 DOI: 10.1086/431656]

110 **Getz GS**, Reardon CA. Diet, Microbes, and Murine Atherosclerosis. *Arterioscler Thromb Vasc Biol* 2018; **38**: 2269-2271 [PMID: 30354225 DOI: 10.1161/ATVBAHA.118.311513]

111 **Koeth RA**, Wang Z, Levison BS, Buffa JA, Org E, Sheehy BT, Britt EB, Fu X, Wu Y, Li L, Smith JD, DiDonato JA, Chen J, Li H, Wu GD, Lewis JD, Warrier M, Brown JM, Krauss RM, Tang WH, Bushman FD, Lusis AJ, Hazen SL. Intestinal microbiota metabolism of L-carnitine, a nutrient in red meat, promotes atherosclerosis. *Nat Med* 2013; **19**: 576-585 [PMID: 23563705 DOI: 10.1038/nm.3145]

112 **Karlsson FH**, Fåk F, Nookaew I, Tremaroli V, Fagerberg B, Petranovic D, Bäckhed F, Nielsen J. Symptomatic atherosclerosis is associated with an altered gut metagenome. *Nat Commun* 2012; **3**: 1245 [PMID: 23212374 DOI: 10.1038/ncomms2266]

113 **Ballini A**, Charitos IA, Cantore S, Topi S, Bottalico L, Santacroce L. About Functional Foods: The Probiotics and Prebiotics State of Art. *Antibiotics (Basel)* 2023; **12** [PMID: 37106999 DOI: 10.3390/antibiotics12040635]

114 **Carabotti M**, Scirocco A, Maselli MA, Severi C. The gut-brain axis: interactions between enteric microbiota, central and enteric nervous systems. *Ann Gastroenterol* 2015; **28**: 203-209 [PMID: 25830558]

115 **Bashir Y**, Khan AU. The interplay between the gut-brain axis and the microbiome: A perspective on psychiatric and neurodegenerative disorders. *Front Neurosci* 2022; **16**: 1030694 [PMID: 36389228 DOI: 10.3389/fnins.2022.1030694]

116 **Jacobson A**, Yang D, Vella M, Chiu IM. The intestinal neuro-immune axis: crosstalk between neurons, immune cells, and microbes. *Mucosal Immunol* 2021; **14**: 555-565 [PMID: 33542493 DOI: 10.1038/s41385-020-00368-1]

117 **Charitos IA**, Topi S, Gagliano-Candela R, De Nitto E, Polimeno L, Montagnani M, Santacroce L. The Toxic Effects of Endocrine Disrupting Chemicals (EDCs) on Gut Microbiota: Bisphenol A (BPA) A Review. *Endocr Metab Immune Disord Drug Targets* 2022; **22**: 716-727 [PMID: 35339192 DOI: 10.2174/1871530322666220325114045]

118 **Gao F**, Guo R, Ma Q, Li Y, Wang W, Fan Y, Ju Y, Zhao B, Gao Y, Qian L, Yang Z, He X, Jin X, Liu Y, Peng Y, Chen C, Chen Y, Gao C, Zhu F, Ma X. Stressful events induce long-term gut microbiota dysbiosis and associated post-traumatic stress symptoms in healthcare workers fighting against COVID-19. *J Affect Disord* 2022; **303**: 187-195 [PMID: 35157946 DOI: 10.1016/j.jad.2022.02.024]

119 **Montagnani M**, Bottalico L, Potenza MA, Charitos IA, Topi S, Colella M, Santacroce L. The Crosstalk between Gut Microbiota and Nervous System: A Bidirectional Interaction between Microorganisms and Metabolome. *Int J Mol Sci* 2023; **24** [PMID: 37373470 DOI: 10.3390/ijms241210322]

120 **Ganci M**, Suleyman E, Butt H, Ball M. The role of the brain-gut-microbiota axis in psychology: The importance of considering gut microbiota in the development, perpetuation, and treatment of psychological disorders. *Brain Behav* 2019; **9**: e01408 [PMID: 31568686 DOI: 10.1002/brb3.1408]

121 **O'Mahony SM**, Clarke G, Borre YE, Dinan TG, Cryan JF. Serotonin, tryptophan metabolism and the brain-gut-microbiome axis. *Behav Brain Res* 2015; **277**: 32-48 [PMID: 25078296 DOI: 10.1016/j.bbr.2014.07.027]

122 **Foster JA**, McVey Neufeld KA. Gut-brain axis: how the microbiome influences anxiety and depression. *Trends Neurosci* 2013; **36**: 305-312 [PMID: 23384445 DOI: 10.1016/j.tins.2013.01.005]

123 **Ghaisas S**, Maher J, Kanthasamy A. Gut microbiome in health and disease: Linking the microbiome-gut-brain axis and environmental factors in the pathogenesis of systemic and neurodegenerative diseases. *Pharmacol Ther* 2016; **158**: 52-62 [PMID: 26627987 DOI: 10.1016/j.pharmthera.2015.11.012]

124 **O'Keefe SJ**. Diet, microorganisms and their metabolites, and colon cancer. *Nat Rev Gastroenterol Hepatol* 2016; **13**: 691-706 [PMID: 27848961 DOI: 10.1038/nrgastro.2016.165]

125 **Hibino S**, Kawazoe T, Kasahara H, Itoh S, Ishimoto T, Sakata-Yanagimoto M, Taniguchi K. Inflammation-Induced Tumorigenesis and Metastasis. *Int J Mol Sci* 2021; **22** [PMID: 34063828 DOI: 10.3390/ijms22115421]

126 **McCoy AN**, Araújo-Pérez F, Azcárate-Peril A, Yeh JJ, Sandler RS, Keku TO. Fusobacterium is associated with colorectal adenomas. *PLoS One* 2013; **8**: e53653 [PMID: 23335968 DOI: 10.1371/journal.pone.0053653]

127 **Inamura K**, Hamada T, Bullman S, Ugai T, Yachida S, Ogino S. Cancer as microenvironmental, systemic and environmental diseases: opportunity for transdisciplinary microbiomics science. *Gut* 2022 [PMID: 35820782 DOI: 10.1136/gutjnl-2022-327209]

128 **Rebersek M**. Gut microbiome and its role in colorectal cancer. *BMC Cancer* 2021; **21**: 1325 [PMID: 34895176 DOI: 10.1186/s12885-021-09054-2]

129 **Zhang X**, Yu D, Wu D, Gao X, Shao F, Zhao M, Wang J, Ma J, Wang W, Qin X, Chen Y, Xia P, Wang S. Tissue-resident Lachnospiraceae family bacteria protect against colorectal carcinogenesis by promoting tumor immune surveillance. *Cell Host Microbe* 2013; **31**: 418-432.e8 [PMID: 36893736 DOI: 10.1016/j.chom.2023.01.013]

130 **Polimeno L**, Barone M, Mosca A, Viggiani MT, Joukar F, Mansour-Ghanaei F, Mavaddati S, Daniele A, Debellis L, Bilancia M, Santacroce L, Di Leo A. Soy Metabolism by Gut Microbiota from Patients with Precancerous Intestinal Lesions. *Microorganisms* 2020; **8** [PMID: 32218321 DOI: 10.3390/microorganisms8040469]

131 **Murata M**. Inflammation and cancer. *Environ Health Prev Med* 2018; **23**: 50 [PMID: 30340457 DOI: 10.1186/s12199-018-0740-1]

132 **Polimeno L**, Barone M, Mosca A, Viggiani MT, Di Leo A, Debellis L, Troisi M, Daniele A, Santacroce L. Gut Microbiota Imbalance is Related to Sporadic Colorectal Neoplasms. A Pilot Study. *Appl Sci* 2019; **9**: 5491 [DOI: 10.3390/app9245491]

133 **Niekamp P**, Kim CH. Microbial Metabolite Dysbiosis and Colorectal Cancer. *Gut Liver* 2023; **17**: 190-203 [PMID: 36632785 DOI: 10.5009/gnl220260]

134 **Marino MM**, Nastri BM, D'Agostino M, Risolo R, De Angelis A, Settembre G, Rienzo M, D'Esposito V, Abbondanza C, Formisano P, Ballini A, Santacroce L, Boccellino M, Di Domenico M. Does Gut-breast Microbiota Axis Orchestrates Cancer Progression? *Endocr Metab Immune Disord Drug Targets* 2022; **22**: 1111-1122 [PMID: 35362389 DOI: 10.2174/1871530322666220331145816]

135 **Charles A**, Thomas RM. The Influence of the microbiome on the innate immune microenvironment of solid tumors. *Neoplasia* 2023; **37**: 100878 [PMID: 36696837 DOI: 10.1016/j.neo.2023.100878]

World Journal of Gastroenterology

Submit a Manuscript: https://www.f6publishing.com

World J Gastroenterol 2023 July 28; 29(28): 4384-4396

DOI: 10.3748/wjg.v29.i28.4384

ISSN 1007-9327 (print) ISSN 2219-2840 (online)

REVIEW

Advances in application of novel magnetic resonance imaging technologies in liver disease diagnosis

Yi-Ming Qi, En-Hua Xiao

Specialty type: Gastroenterology and hepatology

Provenance and peer review: Unsolicited article; Externally peer reviewed.

Peer-review model: Single blind

Peer-review report's scientific quality classification

Grade A (Excellent): 0
Grade B (Very good): B
Grade C (Good): C
Grade D (Fair): 0
Grade E (Poor): 0

P-Reviewer: Gaspar R, Portugal; Tanaka N, Japan

Received: June 1, 2023
Peer-review started: June 1, 2023
First decision: June 20, 2023
Revised: July 3, 2023
Accepted: July 7, 2023
Article in press: July 7, 2023
Published online: July 28, 2023

Yi-Ming Qi, En-Hua Xiao, Department of Radiology, The Second Xiangya Hospital of Central South University, Changsha 410000, Hunan Province, China

Corresponding author: En-Hua Xiao, PhD, Professor, Teacher, Department of Radiology, The Second Xiangya Hospital of Central South University, No. 139 Renmin Middle Road, Furong District, Changsha 410000, Hunan Province, China. xiaoenhua64@csu.edu.cn

Abstract

Liver disease is a major health concern globally, with high morbidity and mortality rates. Precise diagnosis and assessment are vital for guiding treatment approaches, predicting outcomes, and improving patient prognosis. Magnetic resonance imaging (MRI) is a non-invasive diagnostic technique that has been widely used for detecting liver disease. Recent advancements in MRI technology, such as diffusion weighted imaging, intravoxel incoherent motion, magnetic resonance elastography, chemical exchange saturation transfer, magnetic resonance spectroscopy, hyperpolarized MR, contrast-enhanced MRI, and radiomics, have significantly improved the accuracy and effectiveness of liver disease diagnosis. This review aims to discuss the progress in new MRI technologies for liver diagnosis. By summarizing current research findings, we aim to provide a comprehensive reference for researchers and clinicians to optimize the use of MRI in liver disease diagnosis and improve patient prognosis.

Key Words: Diagnostic imaging; Liver diseases; Fatty liver; Liver fibrosis; Hepatocellular carcinoma; Magnetic resonance imaging

©The Author(s) 2023. Published by Baishideng Publishing Group Inc. All rights reserved.

Core Tip: Accurate evaluation of liver disease is essential for effective treatment strategies and better patient prognosis. Magnetic resonance imaging (MRI), a non-invasive diagnostic tool, has become a necessary technique for detecting liver diseases. The advancements in various magnetic resonance techniques have significantly enriched the diagnostic methods for liver diseases, each with a different focus and expertise in examining the liver. This article reviews the principles, advantages, limitations, and clinical applications of these new technologies in the diagnosis of liver disease, providing necessary references for researchers and clinical physicians to enhance the application of MRI in liver disease diagnosis and improve patient prognosis.

Citation: Qi YM, Xiao EH. Advances in application of novel magnetic resonance imaging technologies in liver disease diagnosis. *World J Gastroenterol* 2023; 29(28): 4384-4396
URL: https://www.wjgnet.com/1007-9327/full/v29/i28/4384.htm
DOI: https://dx.doi.org/10.3748/wjg.v29.i28.4384

INTRODUCTION

Liver disease is a major global health concern with high rates of morbidity and mortality[1]. Chronic liver diseases often lead to liver fibrosis and cirrhosis, which are the primary risk factors for hepatocellular carcinoma (HCC)[2]. The accumulation of large molecules such as collagen protein and glycosaminoglycans in the extracellular matrix is the basic pathological feature of liver fibrosis[3]. Reports suggest that 80%-90% of new HCC cases occur in individuals with cirrhosis[4]. Liver cancer is the sixth most common malignancy in humans and the fourth leading cause of cancer-related deaths worldwide. HCC accounts for 90% of all liver cancer cases[5]. Surgery is the preferred method for treating early-stage HCC[6]. However, due to the absence of apparent symptoms in the early stages, most patients are diagnosed late or with distant metastasis[7]. In major Western centers, the incidence of HCC recurrence within 5 years after curative liver resection is estimated to be 60%-70%[8]. Therefore, early diagnosis and recurrence monitoring are crucial for these patients.

Imaging examinations are vital in diagnosing chronic liver disease and liver cancer. HCC can be diagnosed non-invasively without requiring pathological confirmation, unlike most solid tumors[9]. MRI is a commonly used imaging technique that provides detailed information on the pathological and physiological aspects of liver cancer. It reflects changes in the tissue structure, metabolic status, tumor microenvironment, and other relevant factors.

Recent advancements in magnetic resonance imaging (MRI) technology, such as diffusion weighted imaging (DWI), intravoxel incoherent motion (IVIM), magnetic resonance elastography (MRE), chemical exchange saturation transfer (CEST), magnetic resonance spectroscopy (MRS), hyperpolarized MR (HP MR), contrast-enhanced MRI (CE-MRI), and radiomics, have significantly improved the accuracy and effectiveness of liver disease diagnosis. These new technologies are expected to provide further important information on tumor biological behavior.

This review aims to discuss the progress in new MRI technologies for liver disease diagnosis. By summarizing current research findings, we aim to provide a comprehensive reference for researchers and clinicians to optimize the use of MRI in liver disease diagnosis and improve patient prognosis.

NEW MRI TECHNOLOGIES FOR LIVER DISEASE DIAGNOSIS

DWI and IVIM

DWI is a non-invasive imaging technique that provides information on liver tumors, diffuse liver lesions, and liver function status without the need for contrast agents[10]. DWI has become a popular tool in tumor chemotherapy response assessment and follow-up after treatment due to its ability to detect recurrent lesions earlier than traditional imaging techniques[11].

IVIM, an extension of DWI, has shown great potential in liver function assessment[12], diagnosis of diffuse liver lesions [13] and liver tumors, and liver lesion characterization[14]. It is commonly used to estimate blood flow and microvascular perfusion[15]. The IVIM analysis includes the *D* value (representing pure diffusion factors), the *D** value (representing transport and perfusion factors), and the *f* value (representing microvascular perfusion factors). Research has demonstrated that IVIM has a higher diagnostic efficacy for displaying different liver lesions than DWI. Additionally, the diagnostic efficacy of the *D* value derived from IVIM is significantly higher than that of the apparent diffusion coefficient (ADC) value[16]. IVIM can also be used to predict histological grade, as the *D* value exhibits good diagnostic performance in distinguishing high-grade from low-grade liver cancer[17].

The perfusion-diffusion ratio (PDR) is a recent concept proposed to enhance the effectiveness of DWI. PDR is the ratio of the decreased signal rate caused by IVIM to the decreased signal rate caused by diffusion. A study was conducted to compare the effectiveness of IVIM parameters, ADC value, and PDR in distinguishing solid benign and malignant liver diseases in patient imaging data. The results indicate that PDR had better accuracy compared to IVIM parameters and the ADC value, with an accuracy rate of 79%, while also exhibiting high sensitivity and specificity[18].

The technologies of DWI and IVIM show great promise in aiding the diagnosis and treatment of liver cancer. Furthermore, the introduction of PDR has provided new insights for DWI, allowing for a more precise evaluation of liver cancer. However, DWI does have some limitations, such as the low repeatability of the ADC value, which prevents it from being a dependable imaging biomarker[19]. In addition, DWI is prone to several artifacts such as blurring, ghosting, and distortion which pose a challenge in achieving the repeatability of IVIM parameters and the ADC value[20]. To address this issue, Simchick *et al*[21] proposed a two-dimensional (2D) *b*-M1-optimized data acquisition technique that offers better stability and repeatability in measuring IVIM parameters. This technique can be instrumental in establishing IVIM quantitative biomarkers for liver disease.

MRE

Liver biopsy is widely accepted as the most reliable method for diagnosing and staging liver fibrosis[22]. However, its invasiveness, cost, and potential for complications limit its use. Furthermore, the diagnostic reliability of liver biopsy is questionable due to its sampling variability and subjectivity[23]. Ultrasound elastography is a low-cost and easy-to-use alternative, but it is highly influenced by obesity[24]. For example, vibration-controlled transient elastography (VCTE) is one of the most widely used ultrasound-based methods for diagnosing liver fibrosis. Its rapid, safe, and reproducible nature has made it widely used for bedside diagnosis. However, its reliability is lower than that of MRE as 15% of its conclusions are inaccurate, which is mainly due to the impact of obesity and insufficient experience of doctors[25,26]. According to a large sample meta-analysis, the summary area under the curve (AUC) values of VCTE for diagnosing significant fibrosis, advanced fibrosis, and cirrhosis were lower than those of MRE, with values of only 0.83, 0.85, and 0.89, respectively, while MRE had AUC values as high as 0.91, 0.92, and 0.90, respectively[27]. Serum biomarkers have also been explored for liver fibrosis evaluation, but their lack of specificity poses a challenge as they may also be released during inflammation in other tissues[28].

MRE proves to be a better method for diagnosing and staging liver fibrosis as it is not influenced by factors such as obesity, ascites, inflammation, or etiology[29]. The accuracy and reliability of MRE in diagnosing all stages of liver fibrosis, especially late-stage fibrosis and cirrhosis, have been confirmed by multiple meta-analyses[27,30]. However, the clinical application of MRE is still restricted due to its long examination time and high cost.

Encouragingly, recent studies suggest that combining serum biomarkers and MRE could have unexpected benefits. For instance, fibrosis-4 (FIB-4) index, an indicator used to assess liver injury and fibrosis, includes aspartate aminotransferase, alanine aminotransferase, age, and platelet count[31]. Tamaki *et al*[32] conducted a study where they used a two-step strategy combining FIB-4 index and MRE to detect late-stage fibrosis. They found that the accuracy of the two-step strategy was equivalent to that of using MRE alone, which could lead to cost reduction by reducing excess MRE. Therefore, the two-step strategy can serve as a screening method for large populations. Another study also demonstrated that the combined use of MRE and FIB-4 index has excellent negative predictive value in liver decompensation, which has significant clinical implications[33]. In addition, MRE has acceptable specificity and sensitivity in evaluating splenic stiffness and portal hypertension[34], which is crucial for assessing the overall health status of patients with cirrhosis.

Currently, liver fibrosis assessment can be carried out using 2D MRE, but a more advanced option now available is three-dimensional (3D) MRE. Unlike 2D MRE, 3D MRE images allow analysis of the entire volume of the liver in a 3D manner, providing better accuracy by collecting and processing information in all directions. In a study by Li *et al*[35], the diagnostic performance of 2D MRE and 3D MRE was compared, and both were found to have strong performance in detecting and staging liver fibrosis. However, 3D MRE provided significantly better image quality than the 2D MRE method and had higher inter-observer consistency in measuring liver stiffness (LS). Furthermore, in their study, Catania *et al*[36] found that 3D MRE is more repeatable due to its lower sensitivity to artifacts and provides a more comprehensive liver evaluation by including a larger area of liver parenchyma.

MRE has been found to be useful in predicting the occurrence and recurrence of HCC. Reports suggest that the risk of developing HCC increases with LS as measured by MRE[37]. Late-stage HCC recurrence is predicted by LS ($P < 0.001$), which has a high specificity (90.0%)[38]. MRE has also shown potential in diagnosing microvascular invasion (MVI) in HCC. A study by Zhang *et al*[39] found that tumor stiffness (TS) increased with MVI severity, with TS/LS > 1.47 ($P = 0.001$), TS > 4.33 kPa ($P < 0.001$), and irregular tumor margins ($P = 0.006$) being important independent predictors of MVI positivity.

In summary, MRE is a valuable tool for the thorough evaluation of liver fibrosis, cirrhosis, HCC, and portal hypertension in individuals with liver disease. Although MRE has demonstrated high accuracy in identifying advanced fibrosis or cirrhosis, there are discrepancies in the diagnostic threshold for fibrosis staging based on retrospective data meta-analyses[40], which require further validation.

CEST MRI

The CEST technique, first introduced by Ward *et al*[41] in 2000, utilizes off-resonance saturation pulses to saturate a specific substance, which in turn affects the signal intensity of free water through chemical exchange, providing relevant information about the substance. There are several types of CEST, including Glu CEST, Cr CEST, LATEST, and Gluco CEST, which can, respectively, map glutamate, creatine, lactate, and glucose, all of which are important substances involved in tumor metabolism. CEST can be divided into two categories: Exogenous CEST and endogenous CEST, depending on whether exogenous CEST agents are used. In liver imaging, CEST MRI can be used to evaluate tumor metabolism and tumor microenvironment, and monitor tumor treatment response.

Tumors are known to exhibit increased glucose uptake and glycolysis. To monitor tumor glucose metabolism and treatment response, ^{18}F-fluorodeoxyglucose positron emission tomography (^{18}F-FDG PET) is commonly used. However, the high cost and radioactivity of this method limit its application. CEST MRI has emerged as a potential alternative. A study by Chan *et al*[42] showed that using D-glucose, a simple carbohydrate, to detect tumor metabolism was possible.

The Gluco CEST image showed a significant enhancement in the tumor region, consistent with PET results. However, the CEST signal decreases rapidly due to the rapid metabolism of D-glucose after entering the cells[43]. In recent years, 3-O-methyl-D-glucose (3OMG) has emerged as a promising option for monitoring tumor progression and treatment efficacy. Unlike D-glucose, 3OMG is not metabolized after being taken up by cells, and accumulates in tumor cells, giving it a different kinetic profile[44]. Its similar CEST contrast efficiency to D-glucose makes it a suitable reporter for tumor cell glucose transporters. The Gluco CEST technique, which utilizes 3OMG, offers a low-risk option for patients with renal diseases to display tumor metabolism without using radioactive tracers.

In addition, CEST MRI provides a non-invasive method for evaluating tumor pH, which is important due to the Warburg effect. This effect leads to increased lactate production within cancer cells and results in an acidic extracellular pH in the tumor microenvironment. This acidic environment can enhance tumor invasiveness, metastasis, angiogenesis, and resistance to radiotherapy and chemotherapy[45]. The CEST measurement of pH is not limited by observation depth and can be used for whole-body imaging. While amide proton transfer (APT) CEST MRI is capable of measuring pH[46], it is limited in its ability to calculate the absolute value of pH. To address this limitation, exogenous agents have been utilized to measure extracellular pH in the tumor microenvironment. The use of iodinated agents in CEST MRI has emerged as a promising non-invasive technique for pH assessment[47], as these clinically approved agents are not affected by concentration and offer advantages over APT MRI.

CEST has found another novel application in image-guided nanoparticle (NP) drug delivery. This technique can monitor the transformation and distribution of NP drugs in the body, thereby assisting in adjusting treatment plans. CEST-guided NP drug delivery systems can be divided into labeled and unlabeled systems, depending on the labeling strategy used to achieve the CEST signal[48]. For example, Law *et al*[49] successfully used CEST MRI to detect the specific distribution of iohexol-labeled liposome drugs in the brain of an animal model. In a separate study, Liu *et al*[50] introduced a new labeling-free strategy that uses CEST MRI imaging technology to detect the delivery efficiency of anti-cancer drug lentinan-functionalized SeNPs and achieve image-guided drug delivery. The ability of CEST MRI to visualize NP drug delivery provides a unique opportunity for the integration of tumor diagnosis and treatment. However, this technology is still in its infancy, and nearly all related research is currently being conducted in preclinical animal models. Therefore, extensive validation is necessary to ensure its accuracy and acceptability for clinical translation.

CE-MRI

CE-MRI is a technique used to enhance liver lesion imaging by injecting a contrast agent intravenously. The contrast agent distribution patterns in the liver can be classified into four categories[51]: (1) Extracellular fluid agents, such as Gd-DTPA and Gd-DOTA, rapidly enter the hepatic capillary network and diffuse into the tissue space after injection, eventually being excreted by the kidneys; (2) Hepatobiliary agents, such as Gd-EOB-DTPA and Gd-BOTPA, can be absorbed and metabolized by normal liver cells. During the hepatobiliary phase, regions with premalignant liver lesions or malignant tumors display low signal due to decreased contrast agent uptake[52]; (3) Superparamagnetic iron oxide (SPIO) particles can be taken up by Kupffer cells in normal liver tissue, resulting in a 'black liver' effect. Tumor tissue displays high signal because it almost does not take up SPIO particles; and (4) Molecular targeted MRI contrast agents can be modified with specific antibodies or ligands, allowing them to bind specifically to tumor tissue and highlight the tumor.

The development of MRI contrast agents with tumor targeting, safety, and efficacy has been extensively researched. The use of molecular targeted MRI contrast agents with specific antibodies or ligands has shown promising results in actively targeting tumor tissue, enabling early detection of tumors. Various specific targets can be utilized to produce specific contrast agents. This review will introduce glypican-3 (GPC3) and alpha-fetoprotein (AFP) as examples.

GPC3 is a cancer embryonic polysaccharide present on the cell membrane. Studies have shown that GPC3 is highly expressed in over 70% of HCCs, but not in hepatitis, cirrhosis, benign liver lesions, or healthy adult tissue. GPC3 promotes the progression of liver cancer by binding to molecules such as Wnt signaling proteins and growth factors[53]. In terms of diagnosis, GPC3 has a diagnostic specificity similar to AFP but with higher sensitivity[54]. Additionally, GPC3 can be used to distinguish AFP-negative HCC[55], making it a more reliable diagnostic marker for HCC. Overall, GPC3 shows promise as a potential diagnostic tool for HCC. Zhao *et al*[56] have developed a novel liver cancer-targeting probe by combining USPIO with GPC3-specific ligands. The probe demonstrated preferential binding to GPC3 in both *in vitro* and *in vivo* experiments. Furthermore, it exhibited good stability and biocompatibility, making it a promising candidate for a targeted MRI contrast agent.

AFP is not typically expressed in adults, but in liver cancer patients. AFP levels may be very high, making it a potential target for detecting liver cancer[57]. AFP antibodies can be used to create targeted probes, but as previously mentioned, AFP is not highly expressed in all liver cancer patients. To address this issue, Ma *et al*[58] conjugated AFP antibodies and GPC3 antibodies to ultra-small SPIO NPs (USPIO), resulting in the development of a dual-antibody-conjugated MRI probe that can detect heterogeneity and small HCC with higher sensitivity than single-target probes. The experiment demonstrated that using dual-antibody-conjugated USPIO probes for targeting cancer cells was more efficient and sensitive compared to using single-labeled probes that targeted AFP-USPIO and GPC3-USPIO, as well as non-targeted USPIO. This finding highlights the potential of using multi-target probes to overcome tumor heterogeneity and improve sensitivity to HCC.

Gadolinium-based contrast agents (GBCAs) are commonly used in MRI, but they carry the risk of allergic reactions and nephrogenic systemic fibrosis[59]. Furthermore, even patients with normal kidney function can experience gadolinium accumulation in all tissues with GBCA exposure[60]. Therefore, the development of effective Gd-free MRI contrast agents is becoming increasingly important. Manganese (Mn) has emerged as a promising alternative to GBCAs[61], with researchers discovering that Mn oxide nanoparticles have negligible toxicity and produce good T1-weighted contrast effects[62]. Mn^{2+} has also demonstrated potential as an anti-cancer drug or adjuvant, making it a fascinating area of

research[63]. In a recent study, researchers found that administering Mn^{2+} to a mouse model induced a strong systemic anti-cancer response. This was achieved through promoting natural killer cell function, macrophage and dendritic cell maturation and activation, CD8+ T cell differentiation and activation, and memory T cell survival in tumors. As a result, tumor growth and metastasis were greatly inhibited. Another group of researchers developed an intelligent therapeutic probe called MnTBs, which decomposes quickly in acidic and reducing cellular environments, releasing Mn^{2+} and triggering chemodynamic therapy. This probe was found to be effective in inhibiting tumor growth and metastasis, as well as detecting millimeter-sized liver metastases with a high contrast of 316%[64]. These findings suggest that Mn-based contrast agents have potential in targeted tumor therapy.

MRS

MRS is a non-invasive method that monitors organ metabolites, making it particularly suitable for the liver due to its high concentration of multiple metabolites such as ATP, glutamine, and glycogen. The liver MRS analysis primarily uses ^{1}H, ^{31}P, and ^{13}C. Its major applications include the diagnosis and grading of fatty liver and liver fibrosis, as well as the diagnosis of liver tumors.

The incidence of non-alcoholic fatty liver disease (NAFLD) is increasing, and some patients with NAFLD may develop non-alcoholic steatohepatitis, which can progress to liver cirrhosis and HCC[65]. Therefore, early diagnosis is crucial for preventing and treating NAFLD. ^{1}H-MRS is a non-invasive method that can accurately measure the content of triglycerides in the liver[66]. However, it has some limitations, such as long processing time, motion artifacts, and sampling errors.

The use of MRI proton density fat fraction (MRI-PDFF) has become a popular method for measuring liver fat content in recent years[67]. MRI-PDFF has a strong correlation with MRS ($r = 0.983$, $P < 0.001$) and can quantitatively measure the lipid content of the entire liver[68], overcoming the limitations of MRS and liver tissue biopsy. This makes MRI-PDFF a widely used reference standard for image-based fat quantification with broader application prospects than MRS[69]. In addition, the recent use of the multi-echo Dixon sequence has shown promising results in detecting NAFLD[70].

In the diagnosis and staging of liver fibrosis, ^{1}H-MRS and ^{31}P-MRS have distinct values. Ding *et al*[71] discovered that choline (Cho) levels measured by ^{1}H-MRS increased in proportion to the severity of liver fibrosis. They also found that the Cho/lipid ratio was the most significant diagnostic indicator of liver fibrosis based on the receiver operating characteristic curve. The diagnostic thresholds for liver fibrosis and early cirrhosis were ≥ 0.028 and ≥ 0.131, respectively. In comparison to ^{1}H-MRS, ^{31}P-MRS is advantageous in diagnosing cirrhosis as it can distinguish between different causes of liver disease. Through quantitative analysis of metabolite concentrations such as phosphate monoester (PME), phosphate diester (PDE), Pi, and ATP, ^{31}P-MRS has the potential to differentiate between alcoholic liver disease, viral liver disease, NAFLD, and cirrhosis[72]. However, larger-scale multi-center studies are needed to confirm the clinical relevance and usefulness of this finding.

Liver cancer patients can benefit from the use of ^{1}H-MRS and ^{31}P-MRS as well. In ^{1}H-MRS, the Cho peak is a significant indicator of focal liver lesions, and its elevation could suggest the proliferation of tumor tissue due to increased synthesis of cell membrane phospholipids. Furthermore, the information provided by the Cho peak can be further developed. Liao *et al*[73] conducted a study to compare the diagnostic performance of Cho peak area, Cho peak amplitude, and combined methods for early detection of rabbit liver cancer. The results showed that the combined method had higher accuracy in the early diagnosis of liver cancer, and the correlation between Cho peak amplitude and tumor volume was the best. In ^{31}P-MRS, the contents of PME and PDE can reflect cell membrane synthesis and breakdown, and their increase means cell proliferation. Liver tumors can be associated with an increase in PME/PDE and PME/Pi, and changes in PME/PDE after treatment are significant. However, further multi-center studies are needed to confirm their accuracy due to high heterogeneity[74]. ^{31}P-MRS is also reliable for measuring ATP consumption and identifying the degree of acute liver ischemia-reperfusion injury (IRI)[75], which is particularly meaningful for patients who require hepatectomy and liver transplantation. Diagnosis and treatment of IRI during surgery have always been a challenging task.

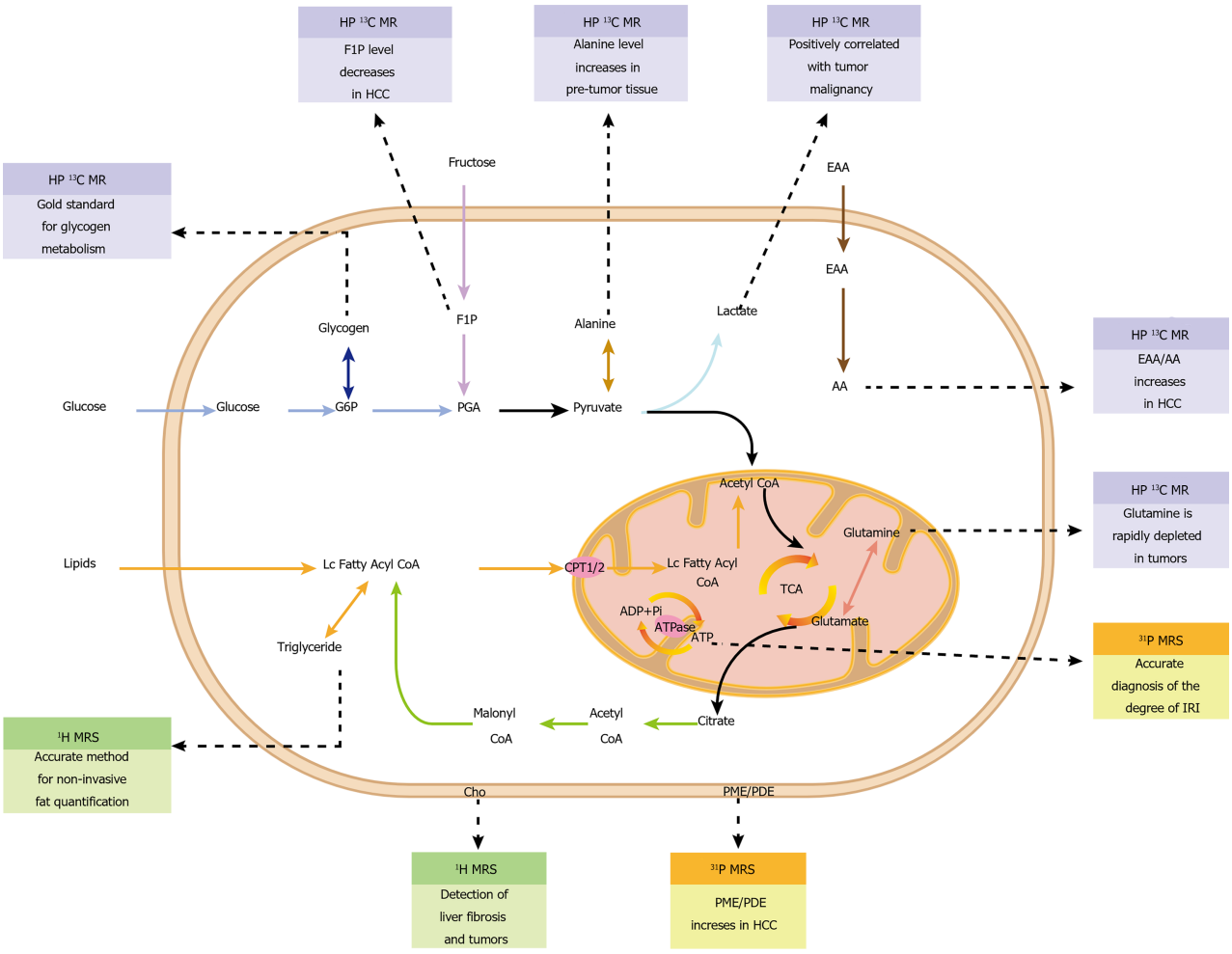
^{13}C MRS is considered the gold standard for imaging human liver glycogen metabolism after oral ingestion of ^{13}C-labeled glucose[76]. However, the low natural abundance and sensitivity of ^{13}C nuclei can limit their application. To overcome this challenge, researchers have developed hyperpolarization techniques, which will be discussed below. For readers' convenience, the targets of MRS and HP MR in liver metabolism evaluation are summarized in Figure 1.

However, motion still has an impact on the accuracy of MRS. Additionally, liver tissue has significant heterogeneity, so excluding extraneous tissue when setting the observation area is crucial. As technology continues to advance, MRS is expected to become an increasingly important tool for diagnosing and grading liver tumors, potentially replacing the need for invasive biopsies.

HP MR

The development of HP MR can be attributed to the dynamic nuclear polarization (DNP) technique, which was initially proposed by Ardenkjaer-Larsen *et al*[77]. This technique can increase MR signal by more than 10000 times. Currently, the leading HP biomarkers primarily consist of ^{13}C, with [1-^{13}C] pyruvate being the most commonly used due to its central role in cellular metabolism. When absorbed by liver cells, [1-^{13}C] pyruvate can produce three observable metabolic intermediates: Lactate, alanine, and CO_2, thus allowing visualization of liver metabolism.

Cancer cells often have higher levels of the enzyme lactate dehydrogenase[78], which convert pyruvate to lactate. Measuring the metabolic transformation from pyruvate to lactate is important for analyzing tumor invasiveness, grade, and prognosis[79]. In a study, HCC was induced in rats, and tumor cells were extracted and re-implanted into another group of nude mice. The study found that tumors re-implanted from cells with higher lactate/pyruvate ratios showed higher lactate signals. Therefore, using HP MR to evaluate glucose metabolism differences in liver cancer tissue could potentially reveal tumor phenotypes[80].



DOI: 10.3748/wjg.v29.i28.4384 **Copyright** ©The Author(s) 2023.

Figure 1 The targets of magnetic resonance spectroscopy and hyperpolarized magnetic resonance in liver metabolism evaluation. AA: Acetoacetate; CPT: Carnitine palmitoyl transferase; Cho: Choline; EAA: Ethyl acetoacetate; F1P: Fructose-1-phosphate; G6P: Glucose-6-phosphate; IRI: Ischemia-reperfusion injury; HCC: Hepatocellular carcinoma; PDE: Phosphate diester; PGA: Phosphoglyceric acid; PME: Phosphate monoester; TCA: Tricarboxylic acid; MRS: Magnetic resonance spectroscopy.

Alanine is another potential biomarker for liver cancer diagnosis. It was found that an increase in alanine generation was the earliest metabolic change detected in liver cancer models, even before the formation of primary tumors. In pre-tumor tissues, the conversion rate of pyruvate to alanine significantly increased, and the area with the most abundant alanine signal in pre-tumor tissues was often the region where tumor nodules form[81]. Thus, [1-^{13}C] pyruvate HP MR can be used for early diagnosis of liver cancer by monitoring alanine generation.

Recent studies have shown an increased interest in the use of other hyperpolarization probes, including HP [1,3-$^{13}C_2$]-ethyl acetoacetate, HP [2-^{13}C]-fructose, and HP [5-^{13}C, 4,4-$^{2}H_2$,5-^{15}N]-L-glutamine. Ethyl acetoacetate (EAA) is converted to acetoacetate (AA) at a reduced rate in HCC cells due to lower concentrations and activity of carboxylesterases. In a rat liver transplant tumor model, HP [1,3-$^{13}C_2$]-ethyl acetoacetate MR revealed that the EAA/AA ratio in tumor tissue was approximately four times higher than that in healthy tissue (P = 0.009)[82]. Similarly, HP [2-^{13}C]-fructose can be used to explain HCC cell metabolism. HCC cells have reduced generation of fructose-1-phosphate (F1P) due to lower expression of ketohexokinase[83]. HP MR has successfully detected F1P and its loss in an HCC model. Finally, evaluation of glutamine metabolism is also beneficial for liver cancer diagnosis because it is rapidly consumed by proliferating cells in tumor tissue. The newly developed HP [5-^{13}C, 4,4-$^{2}H_2$,5-^{15}N]-L-glutamine proved to be the best choice for determining *in vivo* glutamine metabolism[84].

Importantly, HP MR provides a unique advantage in obtaining information on tumor metabolism and perfusion, which is not easily obtainable through other methods. The latest technology utilizes the dual-probe imaging method, which involves the use of [1-^{13}C]-pyruvate and [^{13}C, $^{15}N_2$]-urea for simultaneous tumor perfusion and metabolic imaging [85]. The metabolic conversion rate of pyruvate indicates enzyme activity and transporter expression, whereas HP ^{13}C urea is a non-metabolically active extracellular probe that reflects tissue perfusion and distribution. The combination of these two probes can effectively explain changes in metabolism and perfusion during disease progression and treatment response.

PET is currently the preferred imaging method in clinical practice as it provides metabolic information through non-invasive analysis of cancer metabolism *in vivo*. This is achieved through the injection of ^{18}F-FDG[86]. Although PET is

useful for assessing glucose metabolism, it has limited ability to evaluate downstream metabolism, which can be important in many cases. However, HP ^{13}C-pyruvate MR can provide information about downstream metabolism. To obtain a complete picture of glucose metabolism, a combination of ^{18}F-FDG and [1-^{13}C] pyruvate methods can be used. Hansen *et al*[87] have demonstrated the feasibility of this approach through a technique called hyperPET, which shows the consistency between tumor ^{18}F-FDG uptake and [1-^{13}C] lactate production. Clemmensen *et al*[88] have also shown that combining [^{68}Ga]Ga-NODAGA-E[(cRGDyK)]$_2$ PET and HP [1-^{13}C]-pyruvate MR can enhance the ability of hyperPET to detect tumor angiogenesis. HyperPET is a promising tool for evaluating glucose metabolism direction in order to predict tumor occurrence and evaluate the malignancy degree of the tumor. It achieves this by describing the transformation of pyruvate into alanine, lactate, or entering oxidative phosphorylation in the body. While the complexity and high cost of hyperPET may seem impractical for routine use, advancements in MRI and PET-related technologies may make it a valuable tool for diagnosing liver cancer.

Recent advancements in HP MR have led to improvements in both efficiency and accuracy. The slow production of hyperpolarized pyruvate using DNP has been addressed with the MINERVA protocol, which has greatly facilitated the clinical translation of HP MR[89]. Additionally, quantification bias resulting from the use of surface transmit/receive coils has been addressed by Lee *et al*[90] through the development of a dedicated HP ^{13}C EPSI post-processing pipeline. This method has significantly improved the accuracy of measuring the pyruvate to lactate conversion rate in tumors and adjacent regions, with the average signal-to-noise ratio of pyruvate, lactate, and alanine increased by 37.4, 34.0, and 20.1 times, respectively.

MRI radiomics

The concept of radiomics was introduced by Lambin *et al*[91] in 2012. This method involves extracting features from conventional imaging at the tumor's overall level, providing a non-invasive, comprehensive, and quantitative observation of the tumor's temporal and spatial heterogeneity. Presently, MRI-based radiomics research in the liver primarily focuses on classification of liver fibrosis and hepatitis, liver cancer diagnosis, differentiation degree and immunohistochemistry prediction, and MVI evaluation.

MRI-based radiomics has shown promise in diagnosing and predicting hepatitis and liver fibrosis. While conventional MRI images can detect severe cases by observing changes in water content and distribution caused by inflammation, subtle tissue changes can prove challenging to diagnose. Radiomics technology can capture these tiny changes, allowing for more accurate diagnosis. Wei *et al*[92] proposed a grading system that simultaneously stages fibrosis and inflammation activity, with an AUC of 0.932 and 0.910 for diagnosing early-stage hepatitis and fibrosis, respectively. This study demonstrates the potential for radiomics to improve diagnosis and prediction of liver diseases. A novel technique, known as the dynamic image radiomics model, has been developed using deep learning technology to evaluate liver fibrosis. This method combines imaging features from multi-phase dynamic contrast-enhanced images with temporal features. It utilizes time-varying curves of contrast enhancement and imaging features during enhancement and eliminates manual selection bias by using an automated region of interest extraction method. Overall, compared with traditional radiomics methods and clinical serum parameters, the dynamic radiomics model has stronger predictive performance for various stages of liver fibrosis. The proposed liver fibrosis classification model is highly automated, saving time and effort. This model is significant in predicting new cases and training additional datasets[93].

Research has shown that MRI-based radiomics models are highly effective in distinguishing between HCC and non-HCC, with better discrimination efficiency than visual assessment by novice radiologists ($P < 0.05$)[94]. These models also have significant value in identifying high- and low-grade HCC. In a study by Ameli *et al*[95], radiomics features demonstrated strong differentiation ability in a multi-classification model, with an AUC of 0.83. This outperformed classification based solely on ADC or arterial-phase enhancement value, which had an AUC of only 0.75.

Moreover, research has shown that MRI radiomics features have good predictive efficacy for immunohistochemistry and molecular expression in HCC. For example, CK19+ HCC has higher invasiveness, higher lymph node metastasis rates, higher resistance to radiotherapy and chemotherapy, and poorer prognosis. Researchers have successfully constructed and validated a multi-sequence radiomics model for accurately identifying the CK19 status of HCC patients using multi-center MRI imaging data[96]. GPC3 is also associated with poor prognosis in HCC patients. Gu *et al*[97] developed a useful method for predicting GPC3 positive HCC patients without invasive procedures by combining AFP and radiomics features in a column chart. The tool showed significant predictive performance in both training and validation cohorts, with AUC values of 0.926 and 0.914, respectively. Additionally, radiomics features were found to be correlated with the protein level of the immunotherapy target programmed cell death ligand 1 (r = 0.41-0.47, $P < 0.029$) and the mRNA expression levels of programmed cell death 1 and cytotoxic T-lymphocyte-associated protein 4 (r = -0.48 to 0.47, $P < 0.037$)[98]. The findings of these studies indicate that utilizing a combination of multi-sequence MRI radiomics features can lead to precise classification of immunohistochemistry and molecular expression in liver cancer. This non-invasive approach can facilitate personalized management strategies for patients.

The use of MRI radiomics analysis can also provide a distinct advantage in preoperative diagnosis of MVI in liver cancer, as current diagnosis of MVI can only be made through postoperative histological examination. Feng *et al*[99] developed an MRI radiomics model for predicting preoperative MVI by extracting radiomics features from Gd-EOB-DTPA-enhanced MRI. The model's AUC, sensitivity, and specificity were 0.83, 90%, and 75%, respectively, which outperformed radiologists in predicting MVI. According to Liang *et al*[100]'s meta-analysis of 15 studies and 981 patients, MRI radiomics has a high accuracy in diagnosing MVI with an AUC of 0.87, sensitivity of 79%, and specificity of 81%. Based on our analysis, it can be concluded that the use of MRI radiomics for predicting MVI has a high level of accuracy. This non-invasive method can be considered as an alternative approach for evaluating MVI.

Table 1 Advanced magnetic resonance imaging techniques for liver diagnosis: Comparison of clinical applications, advantages, limitations, and developments

Technique(s)	Applications	Advantages	Limitations	Developments
DWI and IVIM	Assessment of liver tumors, diffuse liver lesions, and liver function. Assessment of liver or tumor blood perfusion	Evaluate liver or tumor blood perfusion without the use of contrast agents	Poor reproducibility of IVIM and DWI	2D *b*-M1 acquisition improves reproducibility. The new parameter PDR improves DWI performance
MRE	Diagnosis and staging of liver fibrosis and cirrhosis. Prediction of the recurrence of HCC	Diagnosis of liver fibrosis is not affected by obesity, ascites, inflammation, and etiology	The diagnostic threshold for fibrosis is variable and conflicting	The two-step strategy can screen for liver fibrosis. LS and TS can predict HCC recurrence
CEST	Assessment of tumor metabolism and microenvironment. Monitoring of tumor treatment response	An FDG substitute that does not involve ionizing radiation	Easily affected by other factors. Long scan time	The new reagent 3OMG has unique advantages. Realization of image-guided drug delivery and integration of tumor diagnosis and treatment
CE-MRI	Diagnosis and staging of liver tumors. Detection of liver metastases and diffuse liver lesions	Provides more information about lesions compared to plain MRI. Specific probes enable visualization at the molecular level	Gd chelates can cause allergic reactions and nephrotoxicity	Multi-target probes have the potential to overcome tumor heterogeneity. Potential applications of Mn-based contrast agents in targeted tumor therapy
MRS	Diagnosis and grading of fatty liver and liver fibrosis. Metabolic evaluation of liver and intrahepatic tumors	Provides quantitative data on liver metabolism non-invasively without the use of contrast agents	Low sensitivity of ^{13}C. Accuracy is affected by liver tissue heterogeneity and motion	Cho peak can provide more information. ^{31}P-MRS can differentiate liver cirrhosis etiology and evaluate IRI
HP MR	Providing metabolic, perfusion, and enzymatic information on HCC	DNP improves MR signal by 10000 times. [1-^{13}C] pyruvate has particular value in evaluating tumor metabolism	Current measurement methods still produce inevitable quantitative deviations	HyperPET is expected to elucidate complete glucose metabolism. More hyperpolarized probes are being used. Double-probe HP MR can simultaneously obtain metabolic and perfusion information
MRI radiomics	Diagnosis and prediction of immunohistochemistry features, MVI, liver fibrosis, and hepatitis.	Comprehensive, non-invasive, and quantitative observation of the spatiotemporal heterogeneity of tumors	Poor reproducibility of MRI features. MVI features are variable and conflicting in different studies	Good application value in the differential diagnosis, immunohistochemical feature prediction, and MVI prediction of HCC

CEST: Chemical exchange saturation transfer; CE-MRI: Contrast-enhanced magnetic resonance imaging; Cho: Choline; DNP: Dynamic nuclear polarization; DWI: Diffusion weighted imaging; HCC: Hepatocellular carcinoma; HP: Hyperpolarized; IRI: Ischemia-reperfusion injury; IVIM: Intravoxel incoherent motion; LS: Liver stiffness; MRE: Magnetic resonance elastography; MRI: Magnetic resonance imaging; MRS: Magnetic resonance spectroscopy; MVI: Microvascular invasion; PDR: Perfusion-diffusion ratio; TS: Tumor stiffness; PET: Positron emission tomography; FDG: Fluorodeoxyglucose; 2D: Two-dimensional.

The current limitation of MRI radiomics is the lack of reproducibility in extracting radiomics features. While previous studies have shown good interobserver reproducibility of HCC radiomics features from specific MRI systems, caution is needed when interpreting data in multi-platform radiomics studies as reproducibility can vary greatly between different platforms[101].

Additionally, there is variability and inconsistency in using MRI features to predict MVI in different studies. To combat this, Hong *et al*[102] conducted a meta-analysis of data from 36 studies involving 4410 participants. They identified seven MRI features, namely, large tumor volume, arterial edge enhancement, arterial tumor surrounding enhancement, hypointensity around the tumor in the hepatobiliary phase, irregular margins, multifocality, and low T1 signal, as important predictors of MVI in HCC. These MRI radiomics features are valuable references for future research and of great significance for developing more reliable MVI prediction strategies. Table 1 summarizes various novel MRI technologies' clinical applications, advantages, limitations, and latest developments discussed in this review for the diagnosis of liver diseases. Table 2 lists the diagnostic performance of some MR techniques for the diagnosis of liver diseases.

CONCLUSION

MRI is a promising technology for diagnosing liver diseases due to its non-invasive and radiation-free nature. The development of new technologies such as DWI, IVIM, MRE, CEST, MRS, HP MR, CE-MRI, and radiomics has expanded the capabilities of MRI, allowing for more comprehensive and accurate diagnostic results. Although these technologies have limitations, their role in liver disease diagnosis will continue to improve as they are updated and enhanced. It is important for researchers and clinical doctors to thoroughly study the application value of these new technologies in clinical practice to better guide the diagnosis, treatment, and rehabilitation of liver diseases and ultimately improve patient prognosis.

Table 2 Comparison of performance indicators of new magnetic resonance techniques in diagnosis of liver disease

Technique	Disease	Subjects	Sensitivity (%)	Specificity (%)	NPV (%)	PPV (%)	Ref.
DWI	HCC	34	54.8	90.9	34.5	95.8	[103]
DWI	LF	40	85	82	85	83	[104]
PDR	MT	83	81	77	NA	NA	[18]
MRE	LF	59	69.0	88.2	53.6	93.5	[105]
MRS	Liver steatosis	4715	72.7-88.5	92.0-95.7	NA	NA	[106]
Gd-EOB-DTPA MRI	HCC	77	88.2	96.7	90.6	95.7	[107]
SPIO MRI	HCC	30	66.0	98.0	91.4	90.0	[108]
MRI-PDFF	NAFLD	60	96	100	92.6	89.5	[70]
Radiomics	MVI	50	90	75	NA	NA	[99]
Radiomics	MVI	981	79	81	NA	NA	[100]

DWI: Diffusion weighted imaging; HCC: Hepatocellular carcinoma; LF: Liver fibrosis; MRE: Magnetic resonance elastography; MRI: Magnetic resonance imaging; MRI-PDFF: Magnetic resonance imaging proton density fat fraction; MRS: Magnetic resonance spectroscopy; MT: Malignant tumor; MVI: Microvascular invasion; NA: Not available; NAFLD: Non-alcoholic fatty liver disease; NPV: Negative predictive value; PDR: Perfusion-diffusion ratio; PPV: Positive predictive value; SPIO: Superparamagnetic iron oxide.

FOOTNOTES

Author contributions: Xiao EH was responsible for the review concept and design; Qi YM drafted the manuscript; Xiao EH provided critical revision of the manuscript for important intellectual content; and all authors critically reviewed the content and approved the final version for publication.

Supported by the National Natural Science Foundation of China, No. 81571784; the Provincial Natural Science Foundation of Hunan, No. 2022JJ70142; and the Clinical Research Center for Medical Imaging in Hunan Province, 2020SK4001.

Conflict-of-interest statement: All the authors report no relevant conflicts of interest for this article.

Open-Access: This article is an open-access article that was selected by an in-house editor and fully peer-reviewed by external reviewers. It is distributed in accordance with the Creative Commons Attribution NonCommercial (CC BY-NC 4.0) license, which permits others to distribute, remix, adapt, build upon this work non-commercially, and license their derivative works on different terms, provided the original work is properly cited and the use is non-commercial. See: https://creativecommons.org/Licenses/by-nc/4.0/

Country/Territory of origin: China

ORCID number: Yi-Ming Qi 0009-0008-4675-3717; En-Hua Xiao 0000-0002-3281-6384.

S-Editor: Wang JJ
L-Editor: Wang TQ
P-Editor: Chen YX

REFERENCES

1 **Moon AM**, Singal AG, Tapper EB. Contemporary Epidemiology of Chronic Liver Disease and Cirrhosis. *Clin Gastroenterol Hepatol* 2020; **18**: 2650-2666 [PMID: 31401364 DOI: 10.1016/j.cgh.2019.07.060]
2 **Dhar D**, Baglieri J, Kisseleva T, Brenner DA. Mechanisms of liver fibrosis and its role in liver cancer. *Exp Biol Med (Maywood)* 2020; **245**: 96-108 [PMID: 31924111 DOI: 10.1177/1535370219898141]
3 **Roehlen N**, Crouchet E, Baumert TF. Liver Fibrosis: Mechanistic Concepts and Therapeutic Perspectives. *Cells* 2020; **9** [PMID: 32260126 DOI: 10.3390/cells9040875]
4 **Harris PS**, Hansen RM, Gray ME, Massoud OI, McGuire BM, Shoreibah MG. Hepatocellular carcinoma surveillance: An evidence-based approach. *World J Gastroenterol* 2019; **25**: 1550-1559 [PMID: 30983815 DOI: 10.3748/wjg.v25.i13.1550]
5 **Donne R**, Lujambio A. The liver cancer immune microenvironment: Therapeutic implications for hepatocellular carcinoma. *Hepatology* 2023; **77**: 1773-1796 [PMID: 35989535 DOI: 10.1002/hep.32740]
6 **Zhou H**, Song T. Conversion therapy and maintenance therapy for primary hepatocellular carcinoma. *Biosci Trends* 2021; **15**: 155-160 [PMID: 34039818 DOI: 10.5582/bst.2021.01091]
7 **Fan Z**, Zhou P, Jin B, Li G, Feng L, Zhuang C, Wang S. Recent therapeutics in hepatocellular carcinoma. *Am J Cancer Res* 2023; **13**: 261-275 [PMID: 36777510]

8 **Tsuge M**, Kawaoka T, Oka S. Factors for the recurrence of hepatocellular carcinoma after hepatic resection. *J Gastroenterol* 2023; **58**: 292-293 [PMID: 36723691 DOI: 10.1007/s00535-023-01962-3]

9 **Ronot M**, Purcell Y, Vilgrain V. Hepatocellular Carcinoma: Current Imaging Modalities for Diagnosis and Prognosis. *Dig Dis Sci* 2019; **64**: 934-950 [PMID: 30825108 DOI: 10.1007/s10620-019-05547-0]

10 **Caroli A**. Diffusion-Weighted Magnetic Resonance Imaging: Clinical Potential and Applications. *J Clin Med* 2022; **11** [PMID: 35743409 DOI: 10.3390/jcm11123339]

11 **Lee S**, Kim SH, Hwang JA, Lee JE, Ha SY. Pre-operative ADC predicts early recurrence of HCC after curative resection. *Eur Radiol* 2019; **29**: 1003-1012 [PMID: 30027408 DOI: 10.1007/s00330-018-5642-5]

12 **Wáng YXJ**. Gender-specific liver aging and magnetic resonance imaging. *Quant Imaging Med Surg* 2021; **11**: 2893-2904 [PMID: 34249621 DOI: 10.21037/qims-21-227]

13 **Li T**, Che-Nordin N, Wáng YXJ, Rong PF, Qiu SW, Zhang SW, Zhang P, Jiang YF, Chevallier O, Zhao F, Xiao XY, Wang W. Intravoxel incoherent motion derived liver perfusion/diffusion readouts can be reliable biomarker for the detection of viral hepatitis B induced liver fibrosis. *Quant Imaging Med Surg* 2019; **9**: 371-385 [PMID: 31032185 DOI: 10.21037/qims.2019.02.11]

14 **Wu B**, Jia F, Li X, Li L, Wang K, Han D. Comparative Study of Amide Proton Transfer Imaging and Intravoxel Incoherent Motion Imaging for Predicting Histologic Grade of Hepatocellular Carcinoma. *Front Oncol* 2020; **10**: 562049 [PMID: 33194630 DOI: 10.3389/fonc.2020.562049]

15 **Tao YY**, Zhou Y, Wang R, Gong XQ, Zheng J, Yang C, Yang L, Zhang XM. Progress of intravoxel incoherent motion diffusion-weighted imaging in liver diseases. *World J Clin Cases* 2020; **8**: 3164-3176 [PMID: 32874971 DOI: 10.12998/wjcc.v8.i15.3164]

16 **Wang J**, Yang Z, Luo M, Xu C, Du M, Liu Y. Value of Intravoxel Incoherent Motion (IVIM) Imaging for Differentiation between Intrahepatic Cholangiocarcinoma and Hepatocellular Carcinoma. *Contrast Media Mol Imaging* 2022; **2022**: 1504463 [PMID: 35615729 DOI: 10.1155/2022/1504463]

17 **Zhu SC**, Liu YH, Wei Y, Li LL, Dou SW, Sun TY, Shi DP. Intravoxel incoherent motion diffusion-weighted magnetic resonance imaging for predicting histological grade of hepatocellular carcinoma: Comparison with conventional diffusion-weighted imaging. *World J Gastroenterol* 2018; **24**: 929-940 [PMID: 29491686 DOI: 10.3748/wjg.v24.i8.929]

18 **Podgórska J**, Pasicz K, Skrzyński W, Gołębiewski B, Kuś P, Jasieniak J, Kiliszczyk A, Rogowska A, Benkert T, Pałucki J, Grabska I, Fabiszewska E, Jagielska B, Kukołowicz P, Cieszanowski A. Perfusion-Diffusion Ratio: A New IVIM Approach in Differentiating Solid Benign and Malignant Primary Lesions of the Liver. *Biomed Res Int* 2022; **2022**: 2957759 [PMID: 35075424 DOI: 10.1155/2022/2957759]

19 **Schmeel FC**. Variability in quantitative diffusion-weighted MR imaging (DWI) across different scanners and imaging sites: is there a potential consensus that can help reducing the limits of expected bias? *Eur Radiol* 2019; **29**: 2243-2245 [PMID: 30488105 DOI: 10.1007/s00330-018-5866-4]

20 **Wáng YXJ**, Wang X, Wu P, Wang Y, Chen W, Chen H, Li J. Topics on quantitative liver magnetic resonance imaging. *Quant Imaging Med Surg* 2019; **9**: 1840-1890 [PMID: 31867237 DOI: 10.21037/qims.2019.09.18]

21 **Simchick G**, Geng R, Zhang Y, Hernando D. b value and first-order motion moment optimized data acquisition for repeatable quantitative intravoxel incoherent motion DWI. *Magn Reson Med* 2022; **87**: 2724-2740 [PMID: 35092092 DOI: 10.1002/mrm.29165]

22 **Li C**, Li R, Zhang W. Progress in non-invasive detection of liver fibrosis. *Cancer Biol Med* 2018; **15**: 124-136 [PMID: 29951337 DOI: 10.20892/j.issn.2095-3941.2018.0018]

23 **Ajmera V**, Loomba R. Imaging biomarkers of NAFLD, NASH, and fibrosis. *Mol Metab* 2021; **50**: 101167 [PMID: 33460786 DOI: 10.1016/j.molmet.2021.101167]

24 **Loomba R**, Adams LA. Advances in non-invasive assessment of hepatic fibrosis. *Gut* 2020; **69**: 1343-1352 [PMID: 32066623 DOI: 10.1136/gutjnl-2018-317593]

25 **Mózes FE**, Lee JA, Selvaraj EA, Jayaswal ANA, Trauner M, Boursier J, Fournier C, Staufer K, Stauber RE, Bugianesi E, Younes R, Gaia S, Lupşor-Platon M, Petta S, Shima T, Okanoue T, Mahadeva S, Chan WK, Eddowes PJ, Hirschfield GM, Newsome PN, Wong VW, de Ledinghen V, Fan J, Shen F, Cobbold JF, Sumida Y, Okajima A, Schattenberg JM, Labenz C, Kim W, Lee MS, Wiegand J, Karlas T, Yılmaz Y, Aithal GP, Palaniyappan N, Cassinotto C, Aggarwal S, Garg H, Ooi GJ, Nakajima A, Yoneda M, Ziol M, Barget N, Geier A, Tuthill T, Brosnan MJ, Anstee QM, Neubauer S, Harrison SA, Bossuyt PM, Pavlides M; LITMUS Investigators. Diagnostic accuracy of non-invasive tests for advanced fibrosis in patients with NAFLD: an individual patient data meta-analysis. *Gut* 2022; **71**: 1006-1019 [PMID: 34001645 DOI: 10.1136/gutjnl-2021-324243]

26 **Patel K**, Sebastiani G. Limitations of non-invasive tests for assessment of liver fibrosis. *JHEP Rep* 2020; **2**: 100067 [PMID: 32118201 DOI: 10.1016/j.jhepr.2020.100067]

27 **Selvaraj EA**, Mózes FE, Jayaswal ANA, Zafarmand MH, Vali Y, Lee JA, Levick CK, Young LAJ, Palaniyappan N, Liu CH, Aithal GP, Romero-Gómez M, Brosnan MJ, Tuthill TA, Anstee QM, Neubauer S, Harrison SA, Bossuyt PM, Pavlides M; LITMUS Investigators. Diagnostic accuracy of elastography and magnetic resonance imaging in patients with NAFLD: A systematic review and meta-analysis. *J Hepatol* 2021; **75**: 770-785 [PMID: 33991635 DOI: 10.1016/j.jhep.2021.04.044]

28 **Agbim U**, Asrani SK. Non-invasive assessment of liver fibrosis and prognosis: an update on serum and elastography markers. *Expert Rev Gastroenterol Hepatol* 2019; **13**: 361-374 [PMID: 30791772 DOI: 10.1080/17474124.2019.1579641]

29 **Gheorghe G**, Bungău S, Ceobanu G, Ilie M, Bacalbaşa N, Bratu OG, Vesa CM, Găman MA, Diaconu CC. The non-invasive assessment of hepatic fibrosis. *J Formos Med Assoc* 2021; **120**: 794-803 [PMID: 32861550 DOI: 10.1016/j.jfma.2020.08.019]

30 **Hsu C**, Caussy C, Imajo K, Chen J, Singh S, Kaulback K, Le MD, Hooker J, Tu X, Bettencourt R, Yin M, Sirlin CB, Ehman RL, Nakajima A, Loomba R. Magnetic Resonance vs Transient Elastography Analysis of Patients With Nonalcoholic Fatty Liver Disease: A Systematic Review and Pooled Analysis of Individual Participants. *Clin Gastroenterol Hepatol* 2019; **17**: 630-637.e8 [PMID: 29908362 DOI: 10.1016/j.cgh.2018.05.059]

31 **Ito H**, Kimura T, Takuro S, Higashitani M, Yamamoto K, Kobayashi D. Liver injury indicators and subsequent cancer development among non-fatty liver population. *Cancer Med* 2023; **12**: 12173-12186 [PMID: 37014815 DOI: 10.1002/cam4.5910]

32 **Tamaki N**, Imajo K, Sharpton SR, Jung J, Sutter N, Kawamura N, Yoneda M, Valasek MA, Behling C, Sirlin CB, Kurosaki M, Izumi N, Nakajima A, Loomba R. Two-Step Strategy, FIB-4 Followed by Magnetic Resonance Elastography, for Detecting Advanced Fibrosis in NAFLD. *Clin Gastroenterol Hepatol* 2023; **21**: 380-387.e3 [PMID: 35123096 DOI: 10.1016/j.cgh.2022.01.023]

33 **Ajmera V**, Kim BK, Yang K, Majzoub AM, Nayfeh T, Tamaki N, Izumi N, Nakajima A, Idilman R, Gumussoy M, Oz DK, Erden A, Quach NE, Tu X, Zhang X, Noureddin M, Allen AM, Loomba R. Liver Stiffness on Magnetic Resonance Elastography and the MEFIB Index and Liver-Related Outcomes in Nonalcoholic Fatty Liver Disease: A Systematic Review and Meta-Analysis of Individual Participants.

Gastroenterology 2022; **163**: 1079-1089.e5 [PMID: 35788349 DOI: 10.1053/j.gastro.2022.06.073]

34 **Yiyi M**, Xiaoqin Q, Lei Z. Spleen Stiffness on Magnetic Resonance Elastography for the Detection of Portal Hypertension: A Systematic Review and Meta-Analysis. *Iran J Public Health* 2022; **51**: 1925-1935 [PMID: 36743372 DOI: 10.18502/ijph.v51i9.10548]

35 **Li M**, Yang H, Liu Y, Zhang L, Chen J, Deng Y, Xiao Y, Zhu J, Yi Z, Hu B, Kuang S, He B, Glaser KJ, Yin M, Venkatesh SK, Ehman RL, Wang J. Comparison of the diagnostic performance of 2D and 3D MR elastography in staging liver fibrosis. *Eur Radiol* 2021; **31**: 9468-9478 [PMID: 34023968 DOI: 10.1007/s00330-021-08053-y]

36 **Catania R**, Lopes Vendrami C, Bolster BD, Niemzcura R, Borhani AA, Miller FH. Intra-patient comparison of 3D and 2D magnetic resonance elastography techniques for assessment of liver stiffness. *Abdom Radiol (NY)* 2022; **47**: 998-1008 [PMID: 34982182 DOI: 10.1007/s00261-021-03355-7]

37 **Higuchi M**, Tamaki N, Kurosaki M, Inada K, Kirino S, Yamashita K, Hayakawa Y, Osawa L, Takaura K, Maeyashiki C, Kaneko S, Yasui Y, Takahashi Y, Tsuchiya K, Nakanishi H, Itakura J, Loomba R, Enomoto N, Izumi N. Longitudinal association of magnetic resonance elastography-associated liver stiffness with complications and mortality. *Aliment Pharmacol Ther* 2022; **55**: 292-301 [PMID: 34927277 DOI: 10.1111/apt.16745]

38 **Zhang L**, Chen J, Jiang H, Rong D, Guo N, Yang H, Zhu J, Hu B, He B, Yin M, Venkatesh SK, Ehman RL, Wang J. MR elastography as a biomarker for prediction of early and late recurrence in HBV-related hepatocellular carcinoma patients before hepatectomy. *Eur J Radiol* 2022; **152**: 110340 [PMID: 35580445 DOI: 10.1016/j.ejrad.2022.110340]

39 **Zhang L**, Li M, Zhu J, Zhang Y, Xiao Y, Dong M, Zhang L, Wang J. The value of quantitative MR elastography-based stiffness for assessing the microvascular invasion grade in hepatocellular carcinoma. *Eur Radiol* 2023; **33**: 4103-4114 [PMID: 36435877 DOI: 10.1007/s00330-022-09290-5]

40 **Singh S**, Venkatesh SK, Wang Z, Miller FH, Motosugi U, Low RN, Hassanein T, Asbach P, Godfrey EM, Yin M, Chen J, Keaveny AP, Bridges M, Bohte A, Murad MH, Lomas DJ, Talwalkar JA, Ehman RL. Diagnostic performance of magnetic resonance elastography in staging liver fibrosis: a systematic review and meta-analysis of individual participant data. *Clin Gastroenterol Hepatol* 2015; **13**: 440-451.e6 [PMID: 25305349 DOI: 10.1016/j.cgh.2014.09.046]

41 **Ward KM**, Aletras AH, Balaban RS. A new class of contrast agents for MRI based on proton chemical exchange dependent saturation transfer (CEST). *J Magn Reson* 2000; **143**: 79-87 [PMID: 10698648 DOI: 10.1006/jmre.1999.1956]

42 **Chan KW**, McMahon MT, Kato Y, Liu G, Bulte JW, Bhujwalla ZM, Artemov D, van Zijl PC. Natural D-glucose as a biodegradable MRI contrast agent for detecting cancer. *Magn Reson Med* 2012; **68**: 1764-1773 [PMID: 23074027 DOI: 10.1002/mrm.24520]

43 **Rivlin M**, Navon G. Molecular imaging of tumors by chemical exchange saturation transfer MRI of glucose analogs. *Quant Imaging Med Surg* 2019; **9**: 1731-1746 [PMID: 31728315 DOI: 10.21037/qims.2019.09.12]

44 **Anemone A**, Capozza M, Arena F, Zullino S, Bardini P, Terreno E, Longo DL, Aime S. In vitro and in vivo comparison of MRI chemical exchange saturation transfer (CEST) properties between native glucose and 3-O-Methyl-D-glucose in a murine tumor model. *NMR Biomed* 2021; **34**: e4602 [PMID: 34423470 DOI: 10.1002/nbm.4602]

45 **Irrera P**, Roberto M, Consolino L, Anemone A, Villano D, Navarro-Tableros V, Carella A, Dastrù W, Aime S, Longo DL. Effect of Esomeprazole Treatment on Extracellular Tumor pH in a Preclinical Model of Prostate Cancer by MRI-CEST Tumor pH Imaging. *Metabolites* 2022; **13** [PMID: 36676972 DOI: 10.3390/metabo13010048]

46 **Schüre JR**, Shrestha M, Breuer S, Deichmann R, Hattingen E, Wagner M, Pilatus U. The pH sensitivity of APT-CEST using phosphorus spectroscopy as a reference method. *NMR Biomed* 2019; **32**: e4125 [PMID: 31322308 DOI: 10.1002/nbm.4125]

47 **Tao Q**, Yi P, Cai Z, Chen Z, Deng Z, Liu R, Feng Y. Ratiometric chemical exchange saturation transfer pH mapping using two iodinated agents with nonequivalent amide protons and a single low saturation power. *Quant Imaging Med Surg* 2022; **12**: 3889-3902 [PMID: 35782235 DOI: 10.21037/qims-21-1229]

48 **Han Z**, Liu G. CEST MRI trackable nanoparticle drug delivery systems. *Biomed Mater* 2021; **16**: 024103 [PMID: 33470986 DOI: 10.1088/1748-605X/abdd70]

49 **Law LH**, Huang J, Xiao P, Liu Y, Chen Z, Lai JHC, Han X, Cheng GWY, Tse KH, Chan KWY. Multiple CEST contrast imaging of nose-to-brain drug delivery using iohexol liposomes at 3T MRI. *J Control Release* 2023; **354**: 208-220 [PMID: 36623695 DOI: 10.1016/j.jconrel.2023.01.011]

50 **Liu G**, Ling J, He L, Xu Y, Chen T, Shi C, Luo L. Theranostic Cancer Treatment Using Lentinan-Coated Selenium Nanoparticles and Label-Free CEST MRI. *Pharmaceutics* 2022; **15** [PMID: 36678748 DOI: 10.3390/pharmaceutics15010120]

51 **Zhou IY**, Catalano OA, Caravan P. Advances in functional and molecular MRI technologies in chronic liver diseases. *J Hepatol* 2020; **73**: 1241-1254 [PMID: 32585160 DOI: 10.1016/j.jhep.2020.06.020]

52 **Zech CJ**, Herrmann KA, Reiser MF, Schoenberg SO. MR imaging in patients with suspected liver metastases: value of liver-specific contrast agent Gd-EOB-DTPA. *Magn Reson Med Sci* 2007; **6**: 43-52 [PMID: 17510541 DOI: 10.2463/mrms.6.43]

53 **Zhou F**, Shang W, Yu X, Tian J. Glypican-3: A promising biomarker for hepatocellular carcinoma diagnosis and treatment. *Med Res Rev* 2018; **38**: 741-767 [PMID: 28621802 DOI: 10.1002/med.21455]

54 **Tahon AM**, El-Ghanam MZ, Zaky S, Emran TM, Bersy AM, El-Raey F, A Z E, El Kharsawy AM, Johar D. Significance of Glypican-3 in Early Detection of Hepatocellular Carcinoma in Cirrhotic Patients. *J Gastrointest Cancer* 2019; **50**: 434-441 [PMID: 29623600 DOI: 10.1007/s12029-018-0095-2]

55 **Liu S**, Wang M, Zheng C, Zhong Q, Shi Y, Han X. Diagnostic value of serum glypican-3 alone and in combination with AFP as an aid in the diagnosis of liver cancer. *Clin Biochem* 2020; **79**: 54-60 [PMID: 32087138 DOI: 10.1016/j.clinbiochem.2020.02.009]

56 **Zhao M**, Liu Z, Dong L, Zhou H, Yang S, Wu W, Lin J. A GPC3-specific aptamer-mediated magnetic resonance probe for hepatocellular carcinoma. *Int J Nanomedicine* 2018; **13**: 4433-4443 [PMID: 30122918 DOI: 10.2147/IJN.S168268]

57 **Luo P**, Wu S, Yu Y, Ming X, Li S, Zuo X, Tu J. Current Status and Perspective Biomarkers in AFP Negative HCC: Towards Screening for and Diagnosing Hepatocellular Carcinoma at an Earlier Stage. *Pathol Oncol Res* 2020; **26**: 599-603 [PMID: 30661224 DOI: 10.1007/s12253-019-00585-5]

58 **Ma XH**, Wang S, Liu SY, Chen K, Wu ZY, Li DF, Mi YT, Hu LB, Chen ZW, Zhao XM. Development and in vitro study of a bi-specific magnetic resonance imaging molecular probe for hepatocellular carcinoma. *World J Gastroenterol* 2019; **25**: 3030-3043 [PMID: 31293339 DOI: 10.3748/wjg.v25.i24.3030]

59 **Davies J**, Siebenhandl-Wolff P, Tranquart F, Jones P, Evans P. Gadolinium: pharmacokinetics and toxicity in humans and laboratory animals following contrast agent administration. *Arch Toxicol* 2022; **96**: 403-429 [PMID: 34997254 DOI: 10.1007/s00204-021-03189-8]

60 **McDonald JS**, McDonald RJ. MR Imaging Safety Considerations of Gadolinium-Based Contrast Agents: Gadolinium Retention and

Nephrogenic Systemic Fibrosis. *Magn Reson Imaging Clin N Am* 2020; **28**: 497-507 [PMID: 33040991 DOI: 10.1016/j.mric.2020.06.001]

61 **Ndiaye D**, Cieslik P, Wadepohl H, Pallier A, Même S, Comba P, Tóth É. Mn(2+) Bispidine Complex Combining Exceptional Stability, Inertness, and MRI Efficiency. *J Am Chem Soc* 2022; **144**: 22212-22220 [PMID: 36445192 DOI: 10.1021/jacs.2c10108]

62 **Cai X**, Zhu Q, Zeng Y, Zeng Q, Chen X, Zhan Y. Manganese Oxide Nanoparticles As MRI Contrast Agents In Tumor Multimodal Imaging And Therapy. *Int J Nanomedicine* 2019; **14**: 8321-8344 [PMID: 31695370 DOI: 10.2147/IJN.S218085]

63 **Lv M**, Chen M, Zhang R, Zhang W, Wang C, Zhang Y, Wei X, Guan Y, Liu J, Feng K, Jing M, Wang X, Liu YC, Mei Q, Han W, Jiang Z. Manganese is critical for antitumor immune responses *via* cGAS-STING and improves the efficacy of clinical immunotherapy. *Cell Res* 2020; **30**: 966-979 [PMID: 32839553 DOI: 10.1038/s41422-020-00395-4]

64 **Zhu X**, Xiong H, Yang P, Wang S, Zhou Q, Zhang P, Zhao Z, Shi S. A pH/GSH dual responsive nanoparticle with relaxivity amplification for magnetic resonance imaging and suppression of tumors and metastases. *Nanoscale* 2023; **15**: 1583-1594 [PMID: 36594591 DOI: 10.1039/d2nr05449c]

65 **Raza S**, Rajak S, Upadhyay A, Tewari A, Anthony Sinha R. Current treatment paradigms and emerging therapies for NAFLD/NASH. *Front Biosci (Landmark Ed)* 2021; **26**: 206-237 [PMID: 33049668 DOI: 10.2741/4892]

66 **Zhang QH**, Zhao Y, Tian SF, Xie LH, Chen LH, Chen AL, Wang N, Song QW, Zhang HN, Xie LZ, Shen ZW, Liu AL. Hepatic fat quantification of magnetic resonance imaging whole-liver segmentation for assessing the severity of nonalcoholic fatty liver disease: comparison with a region of interest sampling method. *Quant Imaging Med Surg* 2021; **11**: 2933-2942 [PMID: 34249624 DOI: 10.21037/qims-20-989]

67 **Caussy C**, Alquiraish MH, Nguyen P, Hernandez C, Cepin S, Fortney LE, Ajmera V, Bettencourt R, Collier S, Hooker J, Sy E, Rizo E, Richards L, Sirlin CB, Loomba R. Optimal threshold of controlled attenuation parameter with MRI-PDFF as the gold standard for the detection of hepatic steatosis. *Hepatology* 2018; **67**: 1348-1359 [PMID: 29108123 DOI: 10.1002/hep.29639]

68 **Kim JW**, Lee CH, Yang Z, Kim BH, Lee YS, Kim KA. The spectrum of magnetic resonance imaging proton density fat fraction (MRI-PDFF), magnetic resonance spectroscopy (MRS), and two different histopathologic methods (artificial intelligence vs. pathologist) in quantifying hepatic steatosis. *Quant Imaging Med Surg* 2022; **12**: 5251-5262 [PMID: 36330193 DOI: 10.21037/qims-22-393]

69 **Yoshizawa E**, Yamada A. MRI-derived proton density fat fraction. *J Med Ultrason (2001)* 2021; **48**: 497-506 [PMID: 34669068 DOI: 10.1007/s10396-021-01135-w]

70 **Yurdaisik I**, Nurili F. Accuracy of Multi-echo Dixon Sequence in Quantification of Hepatic Steatosis. *Cureus* 2020; **12**: e7103 [PMID: 32231898 DOI: 10.7759/cureus.7103]

71 **Ding K**, Liu MR, Huang RS, Lu SJ, Wei X, Wei XX. [A comparative study of 3.0T (1)H-MRS for varying degrees of liver fibrosis in cynomolgus monkeys]. *Zhonghua Gan Zang Bing Za Zhi* 2020; **28**: 766-772 [PMID: 33053977 DOI: 10.3760/cma.j.cn501113-20190212-00044]

72 **Purvis LAB**, Valkovič L, Robson MD, Rodgers CT. Feasibility of absolute quantification for (31) P MRS at 7 T. *Magn Reson Med* 2019; **82**: 49-61 [PMID: 30892732 DOI: 10.1002/mrm.27729]

73 **Liao R**, Tang Z, Li X, Lv L, Yang C, Xiong H, Zhou B, Yu J, Zhang D. Proton Magnetic Resonance Spectroscopy at 3.0T in Rabbit With VX2 Liver Cancer: Diagnostic Efficacy and Correlations With Tumor Size. *Front Oncol* 2022; **12**: 846308 [PMID: 35433458 DOI: 10.3389/fonc.2022.846308]

74 **Seelen LWF**, van den Wildenberg L, van der Kemp WJM, Mohamed Hoesein FAA, Mohammad NH, Molenaar IQ, van Santvoort HC, Prompers JJ, Klomp DWJ. Prospective of (31) P MR Spectroscopy in Hepatopancreatobiliary Cancer: A Systematic Review of the Literature. *J Magn Reson Imaging* 2023; **57**: 1144-1155 [PMID: 35916278 DOI: 10.1002/jmri.28372]

75 **Ko SF**, Chen YL, Sung PH, Chiang JY, Chu YC, Huang CC, Huang CR, Yip HK. Hepatic (31) P-magnetic resonance spectroscopy identified the impact of melatonin-pretreated mitochondria in acute liver ischaemia-reperfusion injury. *J Cell Mol Med* 2020; **24**: 10088-10099 [PMID: 32691975 DOI: 10.1111/jcmm.15617]

76 **Stender S**, Zaha VG, Malloy CR, Sudderth J, DeBerardinis RJ, Park JM. Assessment of Rapid Hepatic Glycogen Synthesis in Humans Using Dynamic (13)C Magnetic Resonance Spectroscopy. *Hepatol Commun* 2020; **4**: 425-433 [PMID: 32140658 DOI: 10.1002/hep4.1458]

77 **Ardenkjaer-Larsen JH**, Fridlund B, Gram A, Hansson G, Hansson L, Lerche MH, Servin R, Thaning M, Golman K. Increase in signal-to-noise ratio of > 10,000 times in liquid-state NMR. *Proc Natl Acad Sci U S A* 2003; **100**: 10158-10163 [PMID: 12930897 DOI: 10.1073/pnas.1733835100]

78 **Ye Y**, Chen M, Chen X, Xiao J, Liao L, Lin F. Clinical Significance and Prognostic Value of Lactate Dehydrogenase Expression in Cervical Cancer. *Genet Test Mol Biomarkers* 2022; **26**: 107-117 [PMID: 35349377 DOI: 10.1089/gtmb.2021.0006]

79 **Granlund KL**, Tee SS, Vargas HA, Lyashchenko SK, Reznik E, Fine S, Laudone V, Eastham JA, Touijer KA, Reuter VE, Gonen M, Sosa RE, Nicholson D, Guo YW, Chen AP, Tropp J, Robb F, Hricak H, Keshari KR. Hyperpolarized MRI of Human Prostate Cancer Reveals Increased Lactate with Tumor Grade Driven by Monocarboxylate Transporter 1. *Cell Metab* 2020; **31**: 105-114.e3 [PMID: 31564440 DOI: 10.1016/j.cmet.2019.08.024]

80 **Bliemsrieder E**, Kaissis G, Grashei M, Topping G, Altomonte J, Hundshammer C, Lohöfer F, Heid I, Keim D, Gebrekidan S, Trajkovic-Arsic M, Winkelkotte AM, Steiger K, Nawroth R, Siveke J, Schwaiger M, Makowski M, Schilling F, Braren R. Hyperpolarized (13)C pyruvate magnetic resonance spectroscopy for in vivo metabolic phenotyping of rat HCC. *Sci Rep* 2021; **11**: 1191 [PMID: 33441943 DOI: 10.1038/s41598-020-80952-4]

81 **Hu S**, Balakrishnan A, Bok RA, Anderton B, Larson PE, Nelson SJ, Kurhanewicz J, Vigneron DB, Goga A. 13C-pyruvate imaging reveals alterations in glycolysis that precede c-Myc-induced tumor formation and regression. *Cell Metab* 2011; **14**: 131-142 [PMID: 21723511 DOI: 10.1016/j.cmet.2011.04.012]

82 **Jensen PR**, Serra SC, Miragoli L, Karlsson M, Cabella C, Poggi L, Venturi L, Tedoldi F, Lerche MH. Hyperpolarized [1,3-13C2]ethyl acetoacetate is a novel diagnostic metabolic marker of liver cancer. *Int J Cancer* 2015; **136**: E117-E126 [PMID: 25156718 DOI: 10.1002/ijc.29162]

83 **Tee SS**, Kim N, Cullen Q, Eskandari R, Mamakhanyan A, Srouji RM, Chirayil R, Jeong S, Shakiba M, Kastenhuber ER, Chen S, Sigel C, Lowe SW, Jarnagin WR, Thompson CB, Schietinger A, Keshari KR. Ketohexokinase-mediated fructose metabolism is lost in hepatocellular carcinoma and can be leveraged for metabolic imaging. *Sci Adv* 2022; **8**: eabm7985 [PMID: 35385296 DOI: 10.1126/sciadv.abm7985]

84 **Eskandari R**, Kim N, Mamakhanyan A, Saoi M, Zhang G, Berisaj M, Granlund KL, Poot AJ, Cross J, Thompson CB, Keshari KR. Hyperpolarized [5-(13)C,4,4-(2)H(2),5-(15)N]-L-glutamine provides a means of annotating in vivo metabolic utilization of glutamine. *Proc Natl Acad Sci U S A* 2022; **119**: e2120595119 [PMID: 35512101 DOI: 10.1073/pnas.2120595119]

85 **Qin H**, Tang S, Riselli AM, Bok RA, Delos Santos R, van Criekinge M, Gordon JW, Aggarwal R, Chen R, Goddard G, Zhang CT, Chen A,

Reed G, Ruscitto DM, Slater J, Sriram R, Larson PEZ, Vigneron DB, Kurhanewicz J. Clinical translation of hyperpolarized (13) C pyruvate and urea MRI for simultaneous metabolic and perfusion imaging. *Magn Reson Med* 2022; **87**: 138-149 [PMID: 34374471 DOI: 10.1002/mrm.28965]

86 **Witney TH**, Lewis DY. Imaging Cancer Metabolism with Positron Emission Tomography (PET). *Methods Mol Biol* 2019; **1928**: 29-44 [PMID: 30725448 DOI: 10.1007/978-1-4939-9027-6_2]

87 **Hansen AE**, Gutte H, Holst P, Johannesen HH, Rahbek S, Clemmensen AE, Larsen MME, Schøier C, Ardenkjaer-Larsen J, Klausen TL, Kristensen AT, Kjaer A. Combined hyperpolarized (13)C-pyruvate MRS and (18)F-FDG PET (hyperPET) estimates of glycolysis in canine cancer patients. *Eur J Radiol* 2018; **103**: 6-12 [PMID: 29803387 DOI: 10.1016/j.ejrad.2018.02.028]

88 **Clemmensen A**, Hansen AE, Holst P, Schøier C, Bisgaard S, Johannesen HH, Ardenkjær-Larsen JH, Kristensen AT, Kjaer A. [(68)Ga]Ga-NODAGA-E[(cRGDyK)](2) PET and hyperpolarized [1-(13)C] pyruvate MRSI (hyperPET) in canine cancer patients: simultaneous imaging of angiogenesis and the Warburg effect. *Eur J Nucl Med Mol Imaging* 2021; **48**: 395-405 [PMID: 32621132 DOI: 10.1007/s00259-020-04881-0]

89 **Hune T**, Mamone S, Schroeder H, Jagtap AP, Sternkopf S, Stevanato G, Korchak S, Fokken C, Müller CA, Schmidt AB, Becker D, Glöggler S. Metabolic Tumor Imaging with Rapidly Signal-Enhanced 1-(13) C-Pyruvate-d(3). *Chemphyschem* 2023; **24**: e202200615 [PMID: 36106366 DOI: 10.1002/cphc.202200615]

90 **Lee PM**, Chen HY, Gordon JW, Zhu Z, Larson PEZ, Dwork N, Van Criekinge M, Carvajal L, Ohliger MA, Wang ZJ, Xu D, Kurhanewicz J, Bok RA, Aggarwal R, Munster PN, Vigneron DB. Specialized computational methods for denoising, B(1) correction, and kinetic modeling in hyperpolarized (13) C MR EPSI studies of liver tumors. *Magn Reson Med* 2021; **86**: 2402-2411 [PMID: 34216051 DOI: 10.1002/mrm.28901]

91 **Lambin P**, Rios-Velazquez E, Leijenaar R, Carvalho S, van Stiphout RG, Granton P, Zegers CM, Gillies R, Boellard R, Dekker A, Aerts HJ. Radiomics: extracting more information from medical images using advanced feature analysis. *Eur J Cancer* 2012; **48**: 441-446 [PMID: 22257792 DOI: 10.1016/j.ejca.2011.11.036]

92 **Wei H**, Shao Z, Fu F, Yu X, Wu Y, Bai Y, Wei W, Meng N, Liu K, Han H, Wang M. Value of multimodal MRI radiomics and machine learning in predicting staging liver fibrosis and grading inflammatory activity. *Br J Radiol* 2023; **96**: 20220512 [PMID: 36341687 DOI: 10.1259/bjr.20220512]

93 **Zheng R**, Shi C, Wang C, Shi N, Qiu T, Chen W, Shi Y, Wang H. Imaging-Based Staging of Hepatic Fibrosis in Patients with Hepatitis B: A Dynamic Radiomics Model Based on Gd-EOB-DTPA-Enhanced MRI. *Biomolecules* 2021; **11** [PMID: 33670596 DOI: 10.3390/biom11020307]

94 **Zhang H**, Guo D, Liu H, He X, Qiao X, Liu X, Liu Y, Zhou J, Zhou Z, Fang Z. MRI-Based Radiomics Models to Discriminate Hepatocellular Carcinoma and Non-Hepatocellular Carcinoma in LR-M According to LI-RADS Version 2018. *Diagnostics (Basel)* 2022; **12** [PMID: 35626199 DOI: 10.3390/diagnostics12051043]

95 **Ameli S**, Venkatesh BA, Shaghaghi M, Ghadimi M, Hazhirkarzar B, Rezvani Habibabadi R, Aliyari Ghasabeh M, Khoshpouri P, Pandey A, Pandey P, Pan L, Grimm R, Kamel IR. Role of MRI-Derived Radiomics Features in Determining Degree of Tumor Differentiation of Hepatocellular Carcinoma. *Diagnostics (Basel)* 2022; **12** [PMID: 36292074 DOI: 10.3390/diagnostics12102386]

96 **Yang F**, Wan Y, Xu L, Wu Y, Shen X, Wang J, Lu D, Shao C, Zheng S, Niu T, Xu X. MRI-Radiomics Prediction for Cytokeratin 19-Positive Hepatocellular Carcinoma: A Multicenter Study. *Front Oncol* 2021; **11**: 672126 [PMID: 34476208 DOI: 10.3389/fonc.2021.672126]

97 **Gu D**, Xie Y, Wei J, Li W, Ye Z, Zhu Z, Tian J, Li X. MRI-Based Radiomics Signature: A Potential Biomarker for Identifying Glypican 3-Positive Hepatocellular Carcinoma. *J Magn Reson Imaging* 2020; **52**: 1679-1687 [PMID: 32491239 DOI: 10.1002/jmri.27199]

98 **Hectors SJ**, Lewis S, Besa C, King MJ, Said D, Putra J, Ward S, Higashi T, Thung S, Yao S, Laface I, Schwartz M, Gnjatic S, Merad M, Hoshida Y, Taouli B. MRI radiomics features predict immuno-oncological characteristics of hepatocellular carcinoma. *Eur Radiol* 2020; **30**: 3759-3769 [PMID: 32086577 DOI: 10.1007/s00330-020-06675-2]

99 **Feng ST**, Jia Y, Liao B, Huang B, Zhou Q, Li X, Wei K, Chen L, Li B, Wang W, Chen S, He X, Wang H, Peng S, Chen ZB, Tang M, Chen Z, Hou Y, Peng Z, Kuang M. Preoperative prediction of microvascular invasion in hepatocellular cancer: a radiomics model using Gd-EOB-DTPA-enhanced MRI. *Eur Radiol* 2019; **29**: 4648-4659 [PMID: 30689032 DOI: 10.1007/s00330-018-5935-8]

100 **Liang G**, Yu W, Liu S, Zhang M, Xie M, Liu M, Liu W. The diagnostic performance of radiomics-based MRI in predicting microvascular invasion in hepatocellular carcinoma: A meta-analysis. *Front Oncol* 2022; **12**: 960944 [PMID: 36798691 DOI: 10.3389/fonc.2022.960944]

101 **Carbonell G**, Kennedy P, Bane O, Kirmani A, El Homsi M, Stocker D, Said D, Mukherjee P, Gevaert O, Lewis S, Hectors S, Taouli B. Precision of MRI radiomics features in the liver and hepatocellular carcinoma. *Eur Radiol* 2022; **32**: 2030-2040 [PMID: 34564745 DOI: 10.1007/s00330-021-08282-1]

102 **Hong SB**, Choi SH, Kim SY, Shim JH, Lee SS, Byun JH, Park SH, Kim KW, Kim S, Lee NK. MRI Features for Predicting Microvascular Invasion of Hepatocellular Carcinoma: A Systematic Review and Meta-Analysis. *Liver Cancer* 2021; **10**: 94-106 [PMID: 33981625 DOI: 10.1159/000513704]

103 **Rimola J**, Forner A, Sapena V, Llarch N, Darnell A, Díaz A, García-Criado A, Bianchi L, Vilana R, Díaz-González Á, Ayuso C, Bruix J, Reig M. Performance of gadoxetic acid MRI and diffusion-weighted imaging for the diagnosis of early recurrence of hepatocellular carcinoma. *Eur Radiol* 2020; **30**: 186-194 [PMID: 31372783 DOI: 10.1007/s00330-019-06351-0]

104 **Razek AA**, Abdalla A, Omran E, Fathy A, Zalata K. Diagnosis and quantification of hepatic fibrosis in children with diffusion weighted MR imaging. *Eur J Radiol* 2011; **78**: 129-134 [PMID: 19926420 DOI: 10.1016/j.ejrad.2009.10.012]

105 **Furlan A**, Tublin ME, Yu L, Chopra KB, Lippello A, Behari J. Comparison of 2D Shear Wave Elastography, Transient Elastography, and MR Elastography for the Diagnosis of Fibrosis in Patients With Nonalcoholic Fatty Liver Disease. *AJR Am J Roentgenol* 2020; **214**: W20-W26 [PMID: 31714842 DOI: 10.2214/AJR.19.21267]

106 **Bohte AE**, van Werven JR, Bipat S, Stoker J. The diagnostic accuracy of US, CT, MRI and 1H-MRS for the evaluation of hepatic steatosis compared with liver biopsy: a meta-analysis. *Eur Radiol* 2011; **21**: 87-97 [PMID: 20680289 DOI: 10.1007/s00330-010-1905-5]

107 **Golfieri R**, Grazioli L, Orlando E, Dormi A, Lucidi V, Corcioni B, Dettori E, Romanini L, Renzulli M. Which is the best MRI marker of malignancy for atypical cirrhotic nodules: hypointensity in hepatobiliary phase alone or combined with other features? Classification after Gd-EOB-DTPA administration. *J Magn Reson Imaging* 2012; **36**: 648-657 [PMID: 22592930 DOI: 10.1002/jmri.23685]

108 **Nishie A**, Tajima T, Ishigami K, Ushijima Y, Okamoto D, Hirakawa M, Nishihara Y, Taketomi A, Hatakenaka M, Irie H, Yoshimitsu K, Honda H. Detection of hepatocellular carcinoma (HCC) using super paramagnetic iron oxide (SPIO)-enhanced MRI: Added value of diffusion-weighted imaging (DWI). *J Magn Reson Imaging* 2010; **31**: 373-382 [PMID: 20099351 DOI: 10.1002/jmri.22059]

World Journal of Gastroenterology

Submit a Manuscript: https://www.f6publishing.com

World J Gastroenterol 2023 July 28; 29(28): 4397-4404

DOI: 10.3748/wjg.v29.i28.4397

ISSN 1007-9327 (print) ISSN 2219-2840 (online)

MINIREVIEWS

Application of single-cell omics in inflammatory bowel disease

Hengqi Betty Zheng

Specialty type: Gastroenterology and hepatology

Provenance and peer review: Invited article; Externally peer reviewed.

Peer-review model: Single blind

Peer-review report's scientific quality classification

Grade A (Excellent): A
Grade B (Very good): B, B
Grade C (Good): 0
Grade D (Fair): D
Grade E (Poor): 0

P-Reviewer: Miyoshi E, Japan; Xiao Y, China; Yang JS, China

Received: May 25, 2023
Peer-review started: May 25, 2023
First decision: June 14, 2023
Revised: June 27, 2023
Accepted: July 7, 2023
Article in press: July 7, 2023
Published online: July 28, 2023

Hengqi Betty Zheng, Department of Pediatrics, Seattle Children's Hospital, University of Washington, Seattle, WA 98105, United States

Corresponding author: Hengqi Betty Zheng, MD, Assistant Professor, Department of Pediatrics, Seattle Children's Hospital, University of Washington, 4800 Sandpoint Way NE, Seattle, WA 98105, United States. betty.zheng@gmail.com

Abstract

Over the past decade, the advent of single cell RNA-sequencing has revolutionized the approach in cellular transcriptomics research. The current technology offers an unbiased platform to understand how genotype correlates to phenotype. Single-cell omics applications in gastrointestinal (GI) research namely inflammatory bowel disease (IBD) has become popular in the last few years with multiple publications as single-cell omics techniques can be applied directly to the target organ, the GI tract at the tissue level. Through examination of mucosal tissue and peripheral blood in IBD, the recent boom in single cell research has identified a myriad of key immune players from enterocytes to tissue resident memory T cells, and explored functional heterogeneity within cellular subsets previously unreported. As we begin to unravel the complex mucosal immune system in states of health and disease like IBD, the power of exploration through single-cell omics can change our approach to translational research. As novel techniques evolve through multiplexing single-cell omics and spatial transcriptomics come to the forefront, we can begin to fully comprehend the disease IBD and better design targets of treatment. In addition, hopefully these techniques can ultimately begin to identify biomarkers of therapeutic response and answer clinically relevant questions in how to tailor individual therapy to patients through personalized medicine.

Key Words: Single-cell omics; Inflammatory bowel disease; Crohn's disease; Ulcerative colitis; Single cell RNA-sequencing; Precision medicine

©The Author(s) 2023. Published by Baishideng Publishing Group Inc. All rights reserved.

Core Tip: Single-cell techniques and omics have taken off in the last few years and the ability to detect individual cellular transcript details has revolutionized the world of research. In the field of gastroenterology in just the last five years, several single-cell techniques have been applied to inflammatory bowel disease research with the identification of novel cellular immune players in the pathogenesis of both ulcerative colitis and Crohn's disease.

Citation: Zheng HB. Application of single-cell omics in inflammatory bowel disease. *World J Gastroenterol* 2023; 29(28): 4397-4404
URL: https://www.wjgnet.com/1007-9327/full/v29/i28/4397.htm
DOI: https://dx.doi.org/10.3748/wjg.v29.i28.4397

INTRODUCTION

The gastrointestinal (GI) tract houses a complex network of immune cells, cellular signaling, and intestinal flora. By balancing host tolerance and microbial defense response, the mucosal immune system of the GI tract performs constant surveillance and sampling of antigens and microbes to induce either tolerance or mounts a vigorous immune response to pathogens[1]. Intestinal inflammation and disease occur when this delicate balance breaks down leading to over activation of mucosal immunity and aberrant response to host antigen and commensal organisms[2]. Microscopic disruption of the epithelial barrier, over activation of proinflammatory cells, and the lack of regulatory mechanisms are some pathways that present in clinical chronic GI disorders and distinguishes mucosal immunity from systemic immunity.

The ability to detect pathogenic pathophysiology is rooted in the organ, the GI tract, and may be missed through studying the systemic immune system. In order to understand the target organ and mucosal immune system, technical advances have been made in the last few years giving us the ability to interrogate down to the microscopic single cell level, thus revolutionizing GI research. Since its inception in 2009, single cell RNA-sequencing (scRNA-seq) has enhanced our ability to comprehensively map and resolve cell types, cellular subsets, and cells states present in both healthy GI tissue and diseased states[3]. The novelty of single-cell technologies *vs* previous technologies such as bulk-sequencing is the ability to detect rare subsets of cells that may be the aberrant drivers of disease[4]. The homogeneity of bulk-sequencing lacks the capacity to decipher cellular heterogeneity and loses dimmer signals in rare subsets that may be important in disease pathogenesis[4,5]. The inherent advantage of single-cell techniques has led to its continued popularity in research. Here, we aim to review the single-cell technologies that have emerged over the last decade and its published applications to GI disease, namely in inflammatory bowel disease (IBD).

IBD which includes both ulcerative colitis (UC) and Crohn's disease (CD) is a chronic complex autoimmune condition characterized by inflammation of the GI tract. The pathogenesis of IBD is thought to develop from an inappropriate immune response towards self-antigens and commensal microbiota in a genetically susceptible host. The advent of scRNA-seq has led to a boom in the number of publications with the application of single cell techniques in IBD research [6,7]. As a disclaimer, this is by no means a comprehensive review of all single-cell studies or single-cell techniques available as the technology has massively expanded in the last few years and will continue to grow in popularity in years to come.

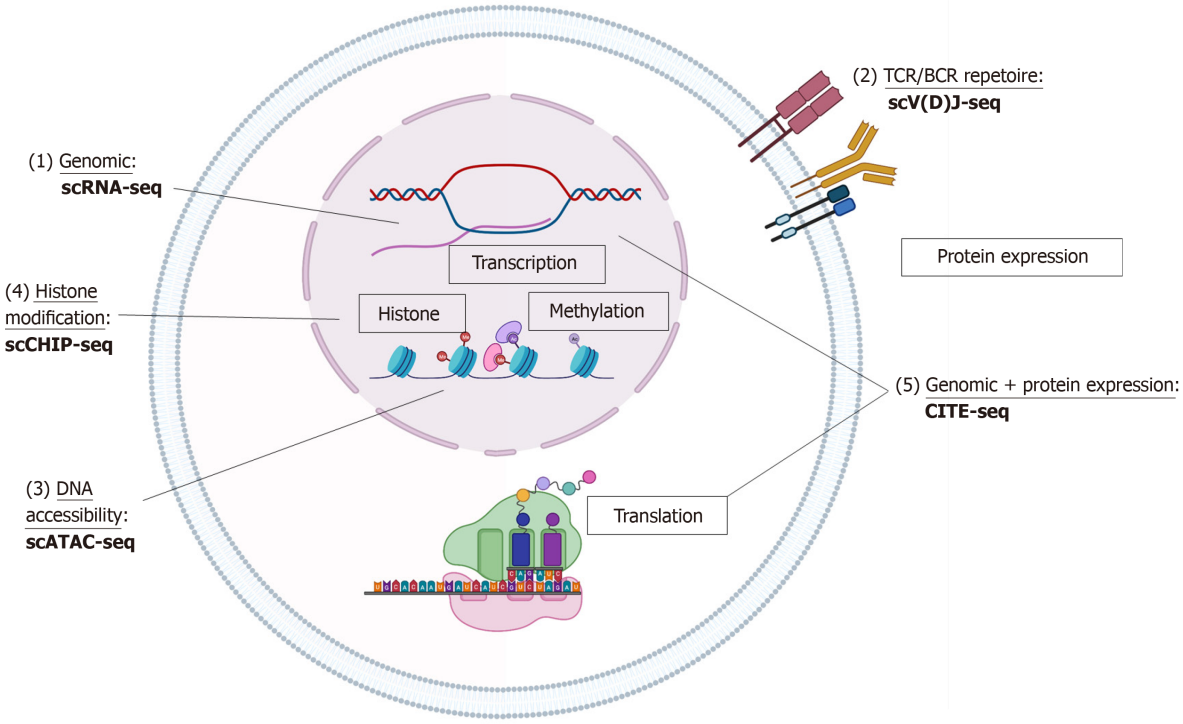
OVERVIEW OF AVAILABLE SINGLE-CELL TECHNOLOGY

scRNA-seq

With the commercialization of products and increasing user compatibility, scRNA-seq can be done using a variety of platforms and through multiple approaches (10 × Genomics, Fluidigm, BD Rhapsody, SmartSeq, *etc.*) whether with multiple well plates, microfluidics, or drop-seq[8,9]. Single-cell data sets can also be created from the 3′ end or 5′ end of mRNA. The basis behind the technology is partitioning individual cells with one uniquely barcoded mRNA-capture medium which has unique molecular code tag for each cell and its contained transcripts. The cell is then lysed and the mRNA is captured by these coded tags and each cell's mRNA is reverse transcribed into uniquely barcoded cDNA. cDNA libraries are amplified, indexed and sequenced using next-generation sequencing platforms (NextGen). Using the unique molecular code tags, the cDNA can be linked to the cell of origin and abundance of transcripts can be deciphered using the number of copies of the certain cDNA (Figure 1).

With large sets of data, bioinformatics analysis can be challenging. To perform this analysis, FASTQ files are generated from binary base call output from sequencing using software programs that then align the reads from the FASTQ files to a human reference genome/transcriptome using STAR[10]. Gene-cell matrices with principle component analysis can then be used to quantify transcripts of interest using standard workflows to give traditional visualization of single-cell datasets in the form of uniform manifold approximation and projection algorithms or T-distributed stochastic neighbor embedding plots (Figure 1).

In some cases, studies are interested not only in the current state of the cell but what the possible future of how the cell may develop ("pseudotime"). Software programs including Monocle[11] and Census[12] offer toolkits of computational bioinformatic programs specifically designed for the analysis of scRNA-Seq data to look at the temporal resolution of



DOI: 10.3748/wjg.v29.i28.4397 **Copyright** ©The Author(s) 2023.

Figure 1 Single-cell technologies. scRNA-seq: Single cell RNA-sequencing; TCR: T cell receptor; BCR: B cell receptor; scCHIP: Single-cell chromatin immunoprecipitation; scATAC: Single-cell assay for transposase-accessible chromatin; CITE: Cellular indexing of transcriptomes and epitopes. Created in biorender.com.

transcriptome dynamics using unsupervised algorithms on scRNA-Seq data collected at multiple time points. Thes programs can be used to recover single-cell gene expression kinetics from a wide array of cellular processes, including differentiation, proliferation and oncogenic transformation to identify branching patterns in the cells. The algorithm finds the longest path through the minimum spanning tree, one that corresponds to the longest sequence of transcriptionally similar cells and produces a 'trajectory' of an individual cell's progress through differentiation that is expressed in units of pseudotime (Figure 1).

T cell receptor/B cell receptor: scV(D)J- seq

T cell receptor (TCR) and B cell receptor (BCR) drive a range of antigen specific adaptive immune responses to pathogens with large highly diverse repertoires to allow for recognition of antigens[9]. The advent of 5′ single-cell sequencing allows researchers to better understand lymphocyte diversity and antigen specificity or essentially the clonality of T and B cells present in disease states. The technique of TCR/BCR is similar to scRNA-seq but utilizes a specialized switch oligo nucleotides and poly dT tail primers[9]. Untemplated C (cytosine) nucleotides to the 3′ end will pair with the end of switch oligo and reverse transcription occurs to capture the TCR/BCR sequences[9]. cDNA libraries of TCR/BCR are created and sequenced per usual protocol (Figure 1).

Single-cell assay for transposase-accessible chromatin

The modification in gene expression through epigenetics can also be studied down to a single-cell level. Through epigenetics, although the DNA sequence is unaltered, expression patterns can be affected by DNA methylation or chromatin structure. DNA chromatic accessibility is maintained by regulatory elements such as transcription factors, DNA methylation, and histone modification where DNA is wound around into nucleosomes. Single-cell assay for transposase-accessible chromatin-seq (scATAC-seq) takes advantage of the Tn5 transposase which is a bacterial enzyme primed to find and cut open DNA positions[13]. Through scATAC-seq, cells are lysed and nuclei are harvested and then undergo transposition where open DNA fragments are "cut and tagged" with adaptors[13]. Single nuclei run through a similar process as the scRNA-seq mechanism to create barcoded cDNA and sequenced and mapped to reference genome and accessible chromatic regions. These peak calling reads can then be linked to areas such as promoters and enhancers. The distribution of reads across the whole genome, functional analysis the genes associated with the peaks, and peak distribution on functional gene elements can also be done with further analysis[13] (Figure 1).

Single-cell chromatin immunoprecipitation-seq

Single-cell epigenetics in the measurement of transcription factor binding and histone modification can also be studied through single-cell chromatin immunoprecipitation-seq. Generally, cells are encapsulated and lysed within the droplets and chromatin is fragmented. DNA barcodes and chromatin fragments are merged *via* the microfluidics device[14]. DNA

barcodes are ligated to chromatin fragments and droplets are then immunoprecipitated with antibody with a carrier chromatin and library construction[14] (Figure 1).

Single-cell cellular indexing of transcriptomes and epitopes

Cell cellular indexing of transcriptomes and epitopes-seq (CITE)-seq combines traditional protein marker detection (such as flow cytometry) with scRNA-seq to provide phenotypic information such as cell-surface protein expression with transcript information[15]. Antibodies are conjugated to oligonucleotides with antibody specific barcodes using streptavidin-biotin interaction and cells are processed per scRNAseq technique[15]. The cells are then lysed and the Oligo-dT primers capture the oligonucleotides and mRNA to create cDNA[15]. cDNA is then processed into libraries and sequenced (Figure 1).

SINGLE-CELL STUDIES IN IBD

UC

Kinchen *et al*[16] published a study describing the activation of intestinal mesenchymal cells subpopulations in adult human UC and dextran-sodium sulfate colitis murine models. Through scRNA-seq, the authors identified SOX6, CD142, and WNT expressing colonic crypt mesenchymal cells consisting of fibroblasts subsets that when dysregulated can lead to impaired epithelial function and inflammation driving the UC state[16]. The human colonic epithelial layer in the UC state is again studied by Parikh *et al*[17] with further identification of various progenitor cells, colonocytes, and goblets cell also implicated in states of inflammation. The authors go on to describe a new subset of absorptive BEST4+ colonocytes cells expressing proton channel OTOP2 and uroguanylin implicated in sensing intraluminal pH and dysregulated in UC. Goblet cell expression of antiprotease molecule WFDC2 was found to be vital in bacterial defense and tight junction barrier function[17]. The study utilized inflamed human UC tissue, adjacent human UC noninflamed tissue, and healthy colonic tissue, and interestingly, the transcripts upregulated in inflamed tissue was also found to be upregulated to a lesser degree in noninflamed UC tissue implying that scRNA-seq is able to detect disease activity prior to tissue level damage[17]. Similarly, Smillie *et al*[18] described the changing landscape of inflammation in human adult UC with inflamed and noninflamed tissues. In addition, the authors describe the potential cellular players in anti-tumor necrosis factor (TNF) resistance in oncostatin M expressing monocytes and fibroblasts, and expanded on an intracellular circuitry of diseased state involving inflammatory fibroblasts, inflammatory monocytes, microfold-like cells, and CD8/interleukin (IL)17 T cells[18]. Uzzan *et al*[19] provided the first expanded adaptive immunity studies of the application of scRNA-seq in mucosal and circulating B cell and plasma cell subsets in human UC. The authors found that B cell response was dysregulated in UC through peripheral gut-homing plasmablasts that correlated with disease activity and expansion of naïve B cells and immunoglobulin (Ig)G+ plasma cells along with auto-reactive plasma cell from inflamed UC tissue[19].

Boland *et al*[20] integrated scRNA-seq with scTCR-seq and scBCR-seq to describe cellular states and clonal relationships of mucosal and peripheral adaptive immune cells in human adult UC. The authors describe an increase in IgG 1+ plasma cells and increased colonic ZEB2 transcription factor regulatory T cells in colonic tissue and gamma delta T cell subset enrichment in the peripheral blood. Of note, the authors also saw a skew in heterogeneity of CD8+ tissue-resident memory T cells in inflamed UC tissue indicating potential pathogenic role of these tissue-resident memory T cells[20]. In the same year 2020, Corridoni *et al*[21] utilized scRNA-seq, scTCR-seq, and CITE-seq to examine the repertoire and cellular subsets of tissue-resident memory CD8+ T cells in human adult UC. The study describes the heterogeneity of CD8+ T cells as both destructive expanded effector type that leads to a disease state with TNF-alpha production and post-effector type that seem to act in a more regulatory fashion through IL-26 production[21]. These studies exemplify the power and unbiased nature of single-cell technologies to understand pathogenic signatures and signify the complexity of human disease states.

CD

Martin *et al*[22] published one of the first CD scRNA-seq data sets linking anti-TNF therapy resistance with a cellular module they entitled GIMATS which stands for IgG plasma cells, inflammatory mononuclear phagocytes, activated T cells, and stromal cells. Through utilizing resected inflamed terminal ileum from adult human CD patients who did not respond to anti-TNF therapy along with uninflamed samples, the authors identified this unique cellular signature to potentially eventually develop biomarkers in prediction of therapy response[22]. Jaeger *et al*[23] further looked at the T cell composition of the terminal ileum from adult human patients with CD and resected terminal ileums, distinguishing between lamina propria and epithelial layers. Within the epithelial layer, intraepithelial lymphocytes from inflamed tissue included specific NKp30+ gamma delta T cells that expressed ROR gamma which produced IL-26 with an increased in active T helper 17 (Th17) cells[23]. The lamina propria layer also found a Th17 signature with increased CD8+ cells implicating the Th17 pathway in CD[23]. Yokoi *et al*[24] further classified T cell subsets in CD to identify CD4+ tissue-resident memory T cells that were increased in CD that expressed CD161, CCR5, and CD103 using scRNA-seq and CyTOF. Rosati *et al*[25] used both bulk TCR repertoire and scRNA-seq on peripheral blood in CD samples to identify a subpopulation of unconventional Crohn-associated invariant T (CAIT) cells with a distinctly unique TCR. These peripheral CAIT cells seem to show a gene expression similar to cells of the innate immune system and mucosal associated invariant T cells and NKT cells and seem to be present in peripheral blood in CD rather than UC[25]. Maddipatla *et al*[26] describes a pediatric CD scRNA-seq data set from treatment naïve pediatric patients, established CD patients in remission, and refractory patients. Patients in remission showed elevated apoliprotein and globlet cell trefoil factor though not in refractory Crohn's[26]. Cellular subsets of enterocyte, goblet cells and BEST4+ enterocytes, microfold and

tuft cells see, to undergo changes from treatment naïve to established CD[26].

Both UC and CD

Huang *et al*[27] describes a pediatric cohort of patients with UC, Crohn's colitis, and undefined pediatric IBD using scRNA-seq, scTCR-seq, and scBCR-seq. The authors describe a common pathway of impaired cyclic AMP-response signaling in all three pediatric cohorts along with infiltration of PDE4B-expresing and TNF-expressing macrophages within the mucosal samples. The authors also describe a decreased abundance of CD39 expressing intraepithelial T cells along with platelet aggregation and release of 5-hydroxytryptamine at the mucosal level[27]. Futhermore, they demonstrated the ability to improve clinical symptoms of some of the pediatric patients with colitis and IBD by using a drug (phosphodiesterase inhibitor dipyridamole) that targeted the pathways identified in a pilot study[27].

Mitsialis *et al*[28] also reports a study with scRNA-seq to confirm their mass cytometry (CyTOF) findings in patients with UC and CD. Within both the CD and UC cohorts, the authors found an expansion of HLA-DR+CD38+ T cells, CXCR+ plasmablasts, and IL1B+ macrophages and monocytes[28]. Expansion of IL17A+CD161+ effector memory T cells and IL17A+ T regulatory cells along with HLA-DR+CD56+ granulocytes was found within the UC cohort. Within CD, IL1B+HLA-DR+CD38+ T cells, ILB+TNF+IFNG+ naïve B cells, and IL1B+ dendritic cells, and IL1B+ plasmacytoid dendritic cells were expanded in the mucosal samples. Expanded IL1B+ T regulatory cells, IL-B+ dendritic cells, IL1B+ plasmacytoid dendritic cells, and IL1B+ monocytes were found in the peripheral blood of patients with CD but not UC [28].

FUTURE DIRECTIONS FOR SINGLE-CELL RESEARCH IN IBD

The future of single-cell technologies within gastroenterology research is already here in the ability to perform single-cell multi-omics and spatial transcriptomic on the target organ (GI tract) and peripheral blood. The ability to multiplex single-cell technologies is in development and the ability to use them on clinical samples will lead to even further growth in the field of IBD. The ability to combine transcriptomics (scRNA-seq), epitopes, (protein expression), and chromatin accessibility (scATAC-seq) from single cells was described by Swanson *et al*[29] on peripheral blood using transcriptomics, epitopes, accessibility-seq. These multimodal single-cell assays may provide a novel way to uncover and link gene expression, gene regulation, and phenotypic gene expression within a single cell and begin to fully cover genotype with phenotype in specific diseases such as IBD.

Another exciting technique that is more readily available now is spatial transcriptomics where architectural information is preserved with intact tissue[30,31]. The position of cellular location and interaction continues to be present and cell to cell interactions can be further interrogated[30,31]. Cell and tissue function can be probed to understand potential pathogenic cells and culprits of inflammation rather than bystander immune cells may be a detailed way to understand IBD. At the same time, as the GI tract is an immune active organ, spatial transcriptomics may be a way to detect the invasive pathogenic variants without losing more delicate cells in the tissue dissociation process.

SINGLE-CELL OMICS IN OTHER GI DISEASES

Given the limited scope of this minireview, we have described these technologies only in the field of IBD and did not elaborate into its use in other GI disorders such as GI cancers and other GI diseases such as allergies of the GI tract. Spatial transcriptomics and various single-cell techniques have been successfully applied to colorectal cancers using the GI cancer tissue and resections allowing researchers to better understand the tumor microenvironment to derive better chemotherapeutic targets[32-36]. Allergic disease of the GI tract such as eosinophilic esophagitis is also under interrogation using single-cell technologies[37]. The ability to study tissue level molecular changes across multiple disease is unparallel using single-cell technologies.

LIMITATIONS

The limitation to single-cell technologies is most importantly cost of reagents and cost of sequencing[38]. The ability to integrate multiple single-cell data across multiple platforms and techniques is also a challenge as there are many commercial products out in the market[38].

CONCLUSION

Single-cell techniques and omics have taken off in the last few years and the ability to detect individual cellular transcript details has revolutionized the world of research. In the field of gastroenterology in just the last five years, several single-cell techniques have been applied to IBD research with the identification of novel cellular immune players in the pathogenesis of both UC and CD. As we continue to develop further immunological techniques, we may begin to detect signals of treatment response in IBD and tailor therapies to immune signatures present in disease state.

FOOTNOTES

Author contributions: Zheng HB has written, revised, and approve the original and final versions of the manuscript.

Conflict-of-interest statement: The author reports no relevant conflicts of interest for this article.

Open-Access: This article is an open-access article that was selected by an in-house editor and fully peer-reviewed by external reviewers. It is distributed in accordance with the Creative Commons Attribution NonCommercial (CC BY-NC 4.0) license, which permits others to distribute, remix, adapt, build upon this work non-commercially, and license their derivative works on different terms, provided the original work is properly cited and the use is non-commercial. See: https://creativecommons.org/Licenses/by-nc/4.0/

Country/Territory of origin: United States

ORCID number: Hengqi Betty Zheng 0000-0003-0575-6475.

S-Editor: Wang JJ
L-Editor: A
P-Editor: Wang JJ

REFERENCES

1 **Hooper LV**, Littman DR, Macpherson AJ. Interactions between the microbiota and the immune system. *Science* 2012; **336**: 1268-1273 [PMID: 22674334 DOI: 10.1126/science.1223490]
2 **Jostins L**, Ripke S, Weersma RK, Duerr RH, McGovern DP, Hui KY, Lee JC, Schumm LP, Sharma Y, Anderson CA, Essers J, Mitrovic M, Ning K, Cleynen I, Theatre E, Spain SL, Raychaudhuri S, Goyette P, Wei Z, Abraham C, Achkar JP, Ahmad T, Amininejad L, Ananthakrishnan AN, Andersen V, Andrews JM, Baidoo L, Balschun T, Bampton PA, Bitton A, Boucher G, Brand S, Büning C, Cohain A, Cichon S, D'Amato M, De Jong D, Devaney KL, Dubinsky M, Edwards C, Ellinghaus D, Ferguson LR, Franchimont D, Fransen K, Gearry R, Georges M, Gieger C, Glas J, Haritunians T, Hart A, Hawkey C, Hedl M, Hu X, Karlsen TH, Kupcinskas L, Kugathasan S, Latiano A, Laukens D, Lawrance IC, Lees CW, Louis E, Mahy G, Mansfield J, Morgan AR, Mowat C, Newman W, Palmieri O, Ponsioen CY, Potocnik U, Prescott NJ, Regueiro M, Rotter JI, Russell RK, Sanderson JD, Sans M, Satsangi J, Schreiber S, Simms LA, Sventoraityte J, Targan SR, Taylor KD, Tremelling M, Verspaget HW, De Vos M, Wijmenga C, Wilson DC, Winkelmann J, Xavier RJ, Zeissig S, Zhang B, Zhang CK, Zhao H; International IBD Genetics Consortium (IIBDGC), Silverberg MS, Annese V, Hakonarson H, Brant SR, Radford-Smith G, Mathew CG, Rioux JD, Schadt EE, Daly MJ, Franke A, Parkes M, Vermeire S, Barrett JC, Cho JH. Host-microbe interactions have shaped the genetic architecture of inflammatory bowel disease. *Nature* 2012; **491**: 119-124 [PMID: 23128233 DOI: 10.1038/nature11582]
3 **Tang F**, Barbacioru C, Wang Y, Nordman E, Lee C, Xu N, Wang X, Bodeau J, Tuch BB, Siddiqui A, Lao K, Surani MA. mRNA-Seq whole-transcriptome analysis of a single cell. *Nat Methods* 2009; **6**: 377-382 [PMID: 19349980 DOI: 10.1038/nmeth.1315]
4 **Yu X**, Abbas-Aghababazadeh F, Chen YA, Fridley BL. Statistical and Bioinformatics Analysis of Data from Bulk and Single-Cell RNA Sequencing Experiments. *Methods Mol Biol* 2021; **2194**: 143-175 [PMID: 32926366 DOI: 10.1007/978-1-0716-0849-4_9]
5 **Nath A**, Bild AH. Leveraging Single-Cell Approaches in Cancer Precision Medicine. *Trends Cancer* 2021; **7**: 359-372 [PMID: 33563578 DOI: 10.1016/j.trecan.2021.01.007]
6 **Corridoni D**, Chapman T, Antanaviciute A, Satsangi J, Simmons A. Inflammatory Bowel Disease Through the Lens of Single-cell RNA-seq Technologies. *Inflamm Bowel Dis* 2020; **26**: 1658-1668 [PMID: 32386055 DOI: 10.1093/ibd/izaa089]
7 **Corridoni D**, Pizarro TT. Single-cell Transcriptomics Reveal the Importance of Distinct Epithelial Cell Populations in Ileal-specific, Treatment-naïve, and Treated Crohn's Disease Patients. *Inflamm Bowel Dis* 2023; **29**: 334-336 [PMID: 36610699 DOI: 10.1093/ibd/izac264]
8 **Valihrach L**, Androvic P, Kubista M. Platforms for Single-Cell Collection and Analysis. *Int J Mol Sci* 2018; **19** [PMID: 29534489 DOI: 10.3390/ijms19030807]
9 **Pai JA**, Satpathy AT. High-throughput and single-cell T cell receptor sequencing technologies. *Nat Methods* 2021; **18**: 881-892 [PMID: 34282327 DOI: 10.1038/s41592-021-01201-8]
10 **Dobin A**, Davis CA, Schlesinger F, Drenkow J, Zaleski C, Jha S, Batut P, Chaisson M, Gingeras TR. STAR: ultrafast universal RNA-seq aligner. *Bioinformatics* 2013; **29**: 15-21 [PMID: 23104886 DOI: 10.1093/bioinformatics/bts635]
11 **Trapnell C**, Cacchiarelli D, Grimsby J, Pokharel P, Li S, Morse M, Lennon NJ, Livak KJ, Mikkelsen TS, Rinn JL. The dynamics and regulators of cell fate decisions are revealed by pseudotemporal ordering of single cells. *Nat Biotechnol* 2014; **32**: 381-386 [PMID: 24658644 DOI: 10.1038/nbt.2859]
12 **Qiu X**, Hill A, Packer J, Lin D, Ma YA, Trapnell C. Single-cell mRNA quantification and differential analysis with Census. *Nat Methods* 2017; **14**: 309-315 [PMID: 28114287 DOI: 10.1038/nmeth.4150]
13 **Satpathy AT**, Granja JM, Yost KE, Qi Y, Meschi F, McDermott GP, Olsen BN, Mumbach MR, Pierce SE, Corces MR, Shah P, Bell JC, Jhutty D, Nemec CM, Wang J, Wang L, Yin Y, Giresi PG, Chang ALS, Zheng GXY, Greenleaf WJ, Chang HY. Massively parallel single-cell chromatin landscapes of human immune cell development and intratumoral T cell exhaustion. *Nat Biotechnol* 2019; **37**: 925-936 [PMID: 31375813 DOI: 10.1038/s41587-019-0206-z]
14 **Rotem A**, Ram O, Shoresh N, Sperling RA, Goren A, Weitz DA, Bernstein BE. Single-cell ChIP-seq reveals cell subpopulations defined by chromatin state. *Nat Biotechnol* 2015; **33**: 1165-1172 [PMID: 26458175 DOI: 10.1038/nbt.3383]
15 **Stoeckius M**, Hafemeister C, Stephenson W, Houck-Loomis B, Chattopadhyay PK, Swerdlow H, Satija R, Smibert P. Simultaneous epitope and transcriptome measurement in single cells. *Nat Methods* 2017; **14**: 865-868 [PMID: 28759029 DOI: 10.1038/nmeth.4380]
16 **Kinchen J**, Chen HH, Parikh K, Antanaviciute A, Jagielowicz M, Fawkner-Corbett D, Ashley N, Cubitt L, Mellado-Gomez E, Attar M, Sharma E, Wills Q, Bowden R, Richter FC, Ahern D, Puri KD, Henault J, Gervais F, Koohy H, Simmons A. Structural Remodeling of the Human Colonic Mesenchyme in Inflammatory Bowel Disease. *Cell* 2018; **175**: 372-386.e17 [PMID: 30270042 DOI: 10.1016/j.cell.2018.08.067]

17 **Parikh K**, Antanaviciute A, Fawkner-Corbett D, Jagielowicz M, Aulicino A, Lagerholm C, Davis S, Kinchen J, Chen HH, Alham NK, Ashley N, Johnson E, Hublitz P, Bao L, Lukomska J, Andev RS, Björklund E, Kessler BM, Fischer R, Goldin R, Koohy H, Simmons A. Colonic epithelial cell diversity in health and inflammatory bowel disease. *Nature* 2019; **567**: 49-55 [PMID: 30814735 DOI: 10.1038/s41586-019-0992-y]

18 **Smillie CS**, Biton M, Ordovas-Montanes J, Sullivan KM, Burgin G, Graham DB, Herbst RH, Rogel N, Slyper M, Waldman J, Sud M, Andrews E, Velonias G, Haber AL, Jagadeesh K, Vickovic S, Yao J, Stevens C, Dionne D, Nguyen LT, Villani AC, Hofree M, Creasey EA, Huang H, Rozenblatt-Rosen O, Garber JJ, Khalili H, Desch AN, Daly MJ, Ananthakrishnan AN, Shalek AK, Xavier RJ, Regev A. Intra- and Inter-cellular Rewiring of the Human Colon during Ulcerative Colitis. *Cell* 2019; **178**: 714-730.e22 [PMID: 31348891 DOI: 10.1016/j.cell.2019.06.029]

19 **Uzzan M**, Martin JC, Mesin L, Livanos AE, Castro-Dopico T, Huang R, Petralia F, Magri G, Kumar S, Zhao Q, Rosenstein AK, Tokuyama M, Sharma K, Ungaro R, Kosoy R, Jha D, Fischer J, Singh H, Keir ME, Ramamoorthi N, O'Gorman WE, Cohen BL, Rahman A, Cossarini F, Seki A, Leyre L, Vaquero ST, Gurunathan S, Grasset EK, Losic B, Dubinsky M, Greenstein AJ, Gottlieb Z, Legnani P, George J, Irizar H, Stojmirovic A, Brodmerkel C, Kasarkis A, Sands BE, Furtado G, Lira SA, Tuong ZK, Ko HM, Cerutti A, Elson CO, Clatworthy MR, Merad M, Suárez-Fariñas M, Argmann C, Hackney JA, Victora GD, Randolph GJ, Kenigsberg E, Colombel JF, Mehandru S. Ulcerative colitis is characterized by a plasmablast-skewed humoral response associated with disease activity. *Nat Med* 2022; **28**: 766-779 [PMID: 35190725 DOI: 10.1038/s41591-022-01680-y]

20 **Boland BS**, He Z, Tsai MS, Olvera JG, Omilusik KD, Duong HG, Kim ES, Limary AE, Jin W, Milner JJ, Yu B, Patel SA, Louis TL, Tysl T, Kurd NS, Bortnick A, Quezada LK, Kanbar JN, Miralles A, Huylebroeck D, Valasek MA, Dulai PS, Singh S, Lu LF, Bui JD, Murre C, Sandborn WJ, Goldrath AW, Yeo GW, Chang JT. Heterogeneity and clonal relationships of adaptive immune cells in ulcerative colitis revealed by single-cell analyses. *Sci Immunol* 2020; **5** [PMID: 32826341 DOI: 10.1126/sciimmunol.abb4432]

21 **Corridoni D**, Antanaviciute A, Gupta T, Fawkner-Corbett D, Aulicino A, Jagielowicz M, Parikh K, Repapi E, Taylor S, Ishikawa D, Hatano R, Yamada T, Xin W, Slawinski H, Bowden R, Napolitani G, Brain O, Morimoto C, Koohy H, Simmons A. Single-cell atlas of colonic CD8(+) T cells in ulcerative colitis. *Nat Med* 2020; **26**: 1480-1490 [PMID: 32747828 DOI: 10.1038/s41591-020-1003-4]

22 **Martin JC**, Chang C, Boschetti G, Ungaro R, Giri M, Grout JA, Gettler K, Chuang LS, Nayar S, Greenstein AJ, Dubinsky M, Walker L, Leader A, Fine JS, Whitehurst CE, Mbow ML, Kugathasan S, Denson LA, Hyams JS, Friedman JR, Desai PT, Ko HM, Laface I, Akturk G, Schadt EE, Salmon H, Gnjatic S, Rahman AH, Merad M, Cho JH, Kenigsberg E. Single-Cell Analysis of Crohn's Disease Lesions Identifies a Pathogenic Cellular Module Associated with Resistance to Anti-TNF Therapy. *Cell* 2019; **178**: 1493-1508.e20 [PMID: 31474370 DOI: 10.1016/j.cell.2019.08.008]

23 **Jaeger N**, Gamini R, Cella M, Schettini JL, Bugatti M, Zhao S, Rosadini CV, Esaulova E, Di Luccia B, Kinnett B, Vermi W, Artyomov MN, Wynn TA, Xavier RJ, Jelinsky SA, Colonna M. Single-cell analyses of Crohn's disease tissues reveal intestinal intraepithelial T cells heterogeneity and altered subset distributions. *Nat Commun* 2021; **12**: 1921 [PMID: 33771991 DOI: 10.1038/s41467-021-22164-6]

24 **Yokoi T**, Murakami M, Kihara T, Seno S, Arase M, Wing JB, Søndergaard JN, Kuwahara R, Minagawa T, Oguro-Igashira E, Motooka D, Okuzaki D, Mori R, Ikeda A, Sekido Y, Amano T, Iijima H, Ozono K, Mizushima T, Hirota S, Ikeuchi H, Takeda K. Identification of a unique subset of tissue-resident memory CD4(+) T cells in Crohn's disease. *Proc Natl Acad Sci U S A* 2023; **120**: e2204269120 [PMID: 36574662 DOI: 10.1073/pnas.2204269120]

25 **Rosati E**, Rios Martini G, Pogorelyy MV, Minervina AA, Degenhardt F, Wendorff M, Sari S, Mayr G, Fazio A, Dowds CM, Hauser C, Tran F, von Schönfels W, Pochhammer J, Salnikova MA, Jaeckel C, Gigla JB, Sabet SS, Hübenthal M, Schiminsky E, Schreiber S, Rosenstiel PC, Scheffold A, Thomas PG, Lieb W, Bokemeyer B, Witte M, Aden K, Hendricks A, Schafmayer C, Egberts JH, Mamedov IZ, Bacher P, Franke A. A novel unconventional T cell population enriched in Crohn's disease. *Gut* 2022; **71**: 2194-2204 [PMID: 35264446 DOI: 10.1136/gutjnl-2021-325373]

26 **Maddipatla SC**, Kolachala VL, Venkateswaran S, Dodd AF, Pelia RS, Geem D, Yin H, Sun Y, Xu C, Mo A, Kosters A, Yang J, Matthews JD, Ghosn E, Kugathasan S, Qiu P. Assessing Cellular and Transcriptional Diversity of Ileal Mucosa Among Treatment-Naïve and Treated Crohn's Disease. *Inflamm Bowel Dis* 2023; **29**: 274-285 [PMID: 36206201 DOI: 10.1093/ibd/izac201]

27 **Huang B**, Chen Z, Geng L, Wang J, Liang H, Cao Y, Chen H, Huang W, Su M, Wang H, Xu Y, Liu Y, Lu B, Xian H, Li H, Ren L, Xie J, Ye L, Zhao J, Chen P, Zhang L, Zhao S, Zhang T, Xu B, Che D, Si W, Gu X, Zeng L, Wang Y, Li D, Zhan Y, Delfouneso D, Lew AM, Cui J, Tang WH, Zhang Y, Gong S, Bai F, Yang M. Mucosal Profiling of Pediatric-Onset Colitis and IBD Reveals Common Pathogenics and Therapeutic Pathways. *Cell* 2019; **179**: 1160-1176.e24 [PMID: 31730855 DOI: 10.1016/j.cell.2019.10.027]

28 **Mitsialis V**, Wall S, Liu P, Ordovas-Montanes J, Parmet T, Vukovic M, Spencer D, Field M, McCourt C, Toothaker J, Bousvaros A; Boston Children's Hospital Inflammatory Bowel Disease Center; Brigham and Women's Hospital Crohn's and Colitis Center, Shalek AK, Kean L, Horwitz B, Goldsmith J, Tseng G, Snapper SB, Konnikova L. Single-Cell Analyses of Colon and Blood Reveal Distinct Immune Cell Signatures of Ulcerative Colitis and Crohn's Disease. *Gastroenterology* 2020; **159**: 591-608.e10 [PMID: 32428507 DOI: 10.1053/j.gastro.2020.04.074]

29 **Swanson E**, Lord C, Reading J, Heubeck AT, Genge PC, Thomson Z, Weiss MD, Li XJ, Savage AK, Green RR, Torgerson TR, Bumol TF, Graybuck LT, Skene PJ. Simultaneous trimodal single-cell measurement of transcripts, epitopes, and chromatin accessibility using TEA-seq. *Elife* 2021; **10** [PMID: 33835024 DOI: 10.7554/eLife.63632]

30 **Williams CG**, Lee HJ, Asatsuma T, Vento-Tormo R, Haque A. An introduction to spatial transcriptomics for biomedical research. *Genome Med* 2022; **14**: 68 [PMID: 35761361 DOI: 10.1186/s13073-022-01075-1]

31 **Marx V**. Method of the Year: spatially resolved transcriptomics. *Nat Methods* 2021; **18**: 9-14 [PMID: 33408395 DOI: 10.1038/s41592-020-01033-y]

32 **Guo W**, Zhang C, Wang X, Dou D, Chen D, Li J. Resolving the difference between left-sided and right-sided colorectal cancer by single-cell sequencing. *JCI Insight* 2022; **7** [PMID: 34793335 DOI: 10.1172/jci.insight.152616]

33 **Mei Y**, Xiao W, Hu H, Lu G, Chen L, Sun Z, Lü M, Ma W, Jiang T, Gao Y, Li L, Chen G, Wang Z, Li H, Wu D, Zhou P, Leng Q, Jia G. Single-cell analyses reveal suppressive tumor microenvironment of human colorectal cancer. *Clin Transl Med* 2021; **11**: e422 [PMID: 34185431 DOI: 10.1002/ctm2.422]

34 **Qi J**, Sun H, Zhang Y, Wang Z, Xun Z, Li Z, Ding X, Bao R, Hong L, Jia W, Fang F, Liu H, Chen L, Zhong J, Zou D, Liu L, Han L, Ginhoux F, Liu Y, Ye Y, Su B. Single-cell and spatial analysis reveal interaction of FAP(+) fibroblasts and SPP1(+) macrophages in colorectal cancer. *Nat Commun* 2022; **13**: 1742 [PMID: 35365629 DOI: 10.1038/s41467-022-29366-6]

35 **Roerink SF**, Sasaki N, Lee-Six H, Young MD, Alexandrov LB, Behjati S, Mitchell TJ, Grossmann S, Lightfoot H, Egan DA, Pronk A, Smakman N, van Gorp J, Anderson E, Gamble SJ, Alder C, van de Wetering M, Campbell PJ, Stratton MR, Clevers H. Intra-tumour

diversification in colorectal cancer at the single-cell level. *Nature* 2018; **556**: 457-462 [PMID: 29643510 DOI: 10.1038/s41586-018-0024-3]

36 **Wu Y**, Yang S, Ma J, Chen Z, Song G, Rao D, Cheng Y, Huang S, Liu Y, Jiang S, Liu J, Huang X, Wang X, Qiu S, Xu J, Xi R, Bai F, Zhou J, Fan J, Zhang X, Gao Q. Spatiotemporal Immune Landscape of Colorectal Cancer Liver Metastasis at Single-Cell Level. *Cancer Discov* 2022; **12**: 134-153 [PMID: 34417225 DOI: 10.1158/2159-8290.CD-21-0316]

37 **Ben-Baruch Morgenstern N**, Ballaban AY, Wen T, Shoda T, Caldwell JM, Kliewer K, Felton JM, Abonia JP, Mukkada VA, Putnam PE, Bolton SM, Dwyer DF, Barrett NA, Rothenberg ME. Single-cell RNA sequencing of mast cells in eosinophilic esophagitis reveals heterogeneity, local proliferation, and activation that persists in remission. *J Allergy Clin Immunol* 2022; **149**: 2062-2077 [PMID: 35304158 DOI: 10.1016/j.jaci.2022.02.025]

38 **Ziegenhain C**, Vieth B, Parekh S, Reinius B, Guillaumet-Adkins A, Smets M, Leonhardt H, Heyn H, Hellmann I, Enard W. Comparative Analysis of Single-Cell RNA Sequencing Methods. *Mol Cell* 2017; **65**: 631-643.e4 [PMID: 28212749 DOI: 10.1016/j.molcel.2017.01.023]

World Journal of Gastroenterology

Submit a Manuscript: https://www.f6publishing.com

World J Gastroenterol 2023 July 28; 29(28): 4405-4415

DOI: 10.3748/wjg.v29.i28.4405

ISSN 1007-9327 (print) ISSN 2219-2840 (online)

MINIREVIEWS

Post-acute pancreatitis diabetes: A complication waiting for more recognition and understanding

Diego García-Compeán, Alan R Jiménez-Rodríguez, Juan M Muñoz-Ayala, José A González-González, Héctor J Maldonado-Garza, Jesús Z Villarreal-Pérez

Specialty type: Gastroenterology and hepatology

Provenance and peer review: Unsolicited article; Externally peer reviewed.

Peer-review model: Single blind

Peer-review report's scientific quality classification

Grade A (Excellent): A
Grade B (Very good): 0
Grade C (Good): C
Grade D (Fair): 0
Grade E (Poor): 0

P-Reviewer: Kitamura K, Japan; Liu C, China

Received: June 1, 2023
Peer-review started: June 1, 2023
First decision: June 16, 2023
Revised: June 22, 2023
Accepted: July 11, 2023
Article in press: July 11, 2023
Published online: July 28, 2023

Diego García-Compeán, Alan R Jiménez-Rodríguez, Juan M Muñoz-Ayala, José A González-González, Héctor J Maldonado-Garza, Department of Gastroenterology, Autonomous University of Nuevo León, Monterrey 64700, Nuevo León, Mexico

Jesús Z Villarreal-Pérez, Department of Endocrinology, Autonomous University of Nuevo León, Monterrey 64700, Nuevo León, Mexico

Corresponding author: Diego García-Compeán, MD, MSc, Adjunct Professor, Department of Gastroenterology, Autonomous University of Nuevo León, Madero y Gonzalitos s/n Col Mitras Centro, Monterrey 64700, Nuevo León, Mexico. digarciacompean@prodigy.net.mx

Abstract

Post-acute pancreatitis diabetes (PAPD) is the second most common type of diabetes below type 2 diabetes mellitus. Due to the boom in research on this entity carried out during the last decade, its recognition has increased. However, much of the medical community still does not recognize it as a medium and long-term complication of acute pancreatitis (AP). Recent prospective cohort studies show that its incidence is about 23% globally and 34.5% in patients with severe AP. With the overall increase in the incidence of AP this complication will be certainly seen more frequently. Due to its high morbidity, mortality and difficult control, early detection and treatment are essential. However, its risk factors and pathophysiological mechanisms are not clearly defined. Its diagnosis should be made excluding pre-existing diabetes and applying the criteria of the American Diabetes Association after 90 d of resolution of one or more AP episodes. This review will show the evidence published so far on the incidence and prevalence, risk factors, possible pathophysiological mechanisms, clinical outcomes, clinical characteristics and preventive and corrective management of PAPD. Some important gaps needing to be clarified in forthcoming studies will also be discussed.

Key Words: Acute pancreatitis; Diabetes mellitus; Chronic pancreatitis; Post-pancreatitis diabetes; Pancreatogenic diabetes

©The Author(s) 2023. Published by Baishideng Publishing Group Inc. All rights reserved.

Core Tip: Post-acute pancreatitis diabetes (PAPD) is the second most common type of diabetes below type II diabetes mellitus. Its incidence is about 23% globally and 34.5% in severe acute pancreatitis (AP). With the overall increase in the incidence of AP this complication will also increase. Due to its high mortality, early detection and treatment are essential. Diagnosis should be made excluding pre-existing diabetes and applying the criteria of the American Diabetes Association after 90 d of resolution of AP episodes. This review will show published evidence on the incidence, risk factors, pathophysiology, clinical outcomes, clinical characteristics and preventive and corrective management of PAPD.

Citation: García-Compeán D, Jiménez-Rodríguez AR, Muñoz-Ayala JM, González-González JA, Maldonado-Garza HJ, Villarreal-Pérez JZ. Post-acute pancreatitis diabetes: A complication waiting for more recognition and understanding. *World J Gastroenterol* 2023; 29(28): 4405-4415
URL: https://www.wjgnet.com/1007-9327/full/v29/i28/4405.htm
DOI: https://dx.doi.org/10.3748/wjg.v29.i28.4405

INTRODUCTION

Diabetes of the exocrine pancreas (DEP) derives from the dysfunction of the exocrine component of the pancreas. It is the second most common type of diabetes after type 2 diabetes mellitus (T2DM)[1]. Its incidence has tripled in the last decade, reaching annual incidence increase of 2.8%[2]. It is associated with higher mortality compared to T2DM[3].

Despite the fact that the relationship between diabetes and diseases of the exocrine pancreas has been known for long time, there have been few advances in the knowledge of the epidemiology and pathophysiological mechanisms of the DEP, which has made it difficult to establish a clear classification of this entity[4].

Terms such as pancreatic, pancreatoprive, pancreatogenic, postpancreatectomy diabetes, and others have been used for this condition. The term "type 3c diabetes" has been attributed to the American Diabetes Association (ADA). The truth is that this nomenclature was not assigned as such to the DEP, but adopted this name because it appeared within the group "other specific types of diabetes" in subsection c of group 3 in the 1998 publication of the ADA on the classification of diabetes. In addition, the use of the term "type 3c diabetes" was not promoted in 2019 guidelines of the ADA[5]. In order to avoid more confusion, the term "diabetes of the exocrine pancreas" has been used more frequently since 2017[6-8]. There is evidence that an increase in the accumulation of intrapancreatic fat around the pancreatic islets of Langerhans may have pathophysiological role in three of the most frequent types of DEP: Post-pancreatitis diabetes (PPD), pancreatic cancer-related diabetes, and cystic fibrosis-related diabetes, but not on T2DM and T1DM[9,10]. However, each of this type of diabetes has different pathophysiology, so it is appropriate to address them separately.

On the other side, the pancreatitis giving rise to diabetes can be acute or chronic, so it is reasonable to make distinction between both: Post-acute pancreatitis diabetes (PAPD) and post-chronic pancreatitis diabetes. A simplified core classification of DEP is shown in Table 1.

Acute pancreatitis (AP) is one of the most common gastrointestinal causes of hospital admissions worldwide, accounting for more than 275000 cases per year. The global incidence rate of AP is increasing[11]. Because AP is the most common disease of the exocrine pancreas nowadays, it is probably the most common cause of DEP. However, this complication has been ignored by most physicians who care for patients recovering from AP[1]. In the last decade, epidemiological, clinical, and translational research on PAPD has boomed, and some important aspects of this pathology are now more clearly known[12,13].

In this review, the evidences published so far on the incidence, risk factors, possible pathophysiology, clinical outcomes, clinical characteristics, and management of PAPD will be discussed. However, the knowledge of a large part of these aspects is still incomplete, so some important gaps will be pointed out which will have to be clarified in future research studies.

EPIDEMIOLOGY

AP is an inflammatory disease of the exocrine pancreas whose global incidence is 34/100000 inhabitants per year, with some geographical differences[14]. This condition has mortality rate from 1 to 2/100000 person-years[15]. Biliary lithiasis, alcohol abuse, endoscopic retrograde cholangiopancreatography, hypertriglyceridemia, and some drugs are the most common causes. On the other hand, 80% of patients have mild pancreatitis associated with few complications and short hospital stay. However, up to 20% of patients may have severe or necrotizing pancreatitis, giving rise to local and systemic complications, increased mortality and long hospital stay[16].

Studies in general population have shown that an episode of AP confers at least twice the risk of subsequent diabetes compared with controls[1]. Two meta-analyses published in 2014 and 2019[17,18], (with 31 studies and 13894 adult patients with no history of DM or prediabetes), evaluated the prevalence of diabetes after one or more episodes of AP. Only 3 were case-control and 28 were non-comparative prospective cohort studies. The cumulative pooled incidence for diabetes was 23% (95%CI: 16%-31%). The diabetes incidence was higher in the populations that had severe AP than in those with mild AP (39% *vs* 14%). The case-control studies and 12 cohort studies had significant methodological shortcomings (few patients, short follow-up or deficient methods for defining diabetes). In the 16 remaining best-quality

Table 1 Classification of diabetes of exocrine pancreas

Type of diabetes	Definition
Post pancreatitis diabetes	Diabetes identified in a patient with pancreatitis without previous detection of diabetes
Post-acute pancreatitis diabetes	Diabetes identified after one or more episodes of acute pancreatitis
Post-chronic pancreatitis diabetes	Diabetes identified in a patient with diagnosis of chronic pancreatitis
Pancreatic cancer related diabetes	Diabetes associated to pancreatic cancer in a patient without history of diabetes
Cystic fibrosis related diabetes	Diabetes associated to cystic fibrosis in a patient without history of diabetes

studies, an overall incidence of PAPD of 27.8% (range 8% to 54%), and of 38.4% (range 16%-54%), only in the severe forms, was found. The cumulative incidence of diabetes reached up to 41% in studies with at least 5 years of follow-up [19-34] (Table 2). The wide range in diabetes incidence of these studies may be due to differences in methodological design, patient selection, and diabetes diagnostic methods.

The time at which diabetes appears after AP is unknown[35]. A recent prospective study, which assessed the course of glycemia over months, reported that the proportion of patients who developed diabetes after an AP episode was 3% at 6 mo, 7% at 12 mo, 9% at 18 mo, and 11% at 24 mo[36] (Figure 1).

RISK FACTORS AND PREDICTORS

Some authors have not found association between the severity of AP and the incidence of PAPD[37-39], while others have found strong relationship[28,40-43]. A higher prevalence of PAPD was found in patients with severe AP than with mild AP in the most recent meta-analysis[18]. In another study, intensive care stay during the AP episode was associated with higher risk of developing diabetes in the 2 years after discharge[44]. The differences in the prevalence of PAPD in the severe forms shown in these studies could be explained, by the different definitions of severity and the diversity of scales used for assessing severity, such as Ranson, APACHE II, BISAP, or the Atlanta classification[45]. It seems that the strongest risk factors in the development of PAPD are pancreatic necrosis and recurrent episodes of AP[40,46]. For recurrent AP, one study evaluated computed tomography evidence of pancreatic volume loss in patients with a single episode of AP compared with recurrent pancreatitis. The investigators found that total pancreatic volume was significantly reduced in those with recurrent AP and these patients also had a strong association with endocrine and exocrine insufficiency[46]. Diabetes in patients with severe and recurrent AP may be due to structural damage of the β cells of the pancreatic islets. Nevertheless, it is important to highlight that the increased risk of diabetes also in patients with mild AP (without necrosis) suggests that there could be other mechanisms involved in its pathophysiology.

Other studies have shown that advanced age and male gender are significant risk factors[47]. Additionally, the alcoholic etiology of pancreatitis seems to increase this incidence[18]. On the other hand, some parameters of metabolic dysfunction, such as obesity and dyslipidemia, could be important risk factors, including genetic factors, particularly in patients with family history of DM.

In total, PAPD risk factors have been poorly or incompletely studied, mostly in retrospective studies with unclear defining parameters. However, the definition of risk factors is important to predict the incidence of diabetes in order to adopt an effective screening strategy of diabetes in patients who recover from AP, particularly in the mild form which is the most frequently seen. Specially designed prospective studies are required in order to clear this issue.

In the other side, some biological markers with the aim of predicting the development of PAPD have been investigated. One study found that elevated plasma levels of interleukin (IL)-1β and interferon γ in individuals with AP and normal glycemia may predict the onset of de novo diabetes during follow-up[48]. Another study found that elevated basal insulin and glucagon plasma levels were associated with de novo diabetes post AP (OR: 1.99 and 3.44 respectively)[49]. Another prospective, longitudinal cohort study found that the variability of glucose plasma levels in the early stages of AP may predict the development of diabetes at 2-year follow-up[50]. Although the results of these studies may appear promising, the research on this field is still very limited and these findings need to be validated before being used in clinical practice.

PATHOPHYSIOLOGY

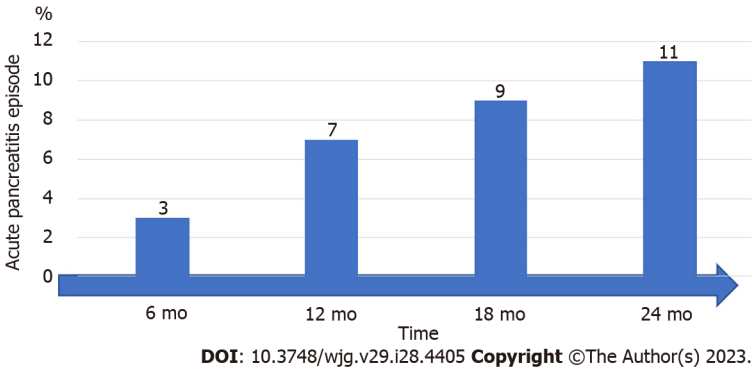
The pathophysiologic relationship between AP and diabetes seems to be bidirectional[51]. On the one hand, patients with T1DM and T2DM have higher risk of developing AP, as demonstrated in a meta-analysis with 5.7 million participants and 14124 cases. Patients with diabetes had higher risk of AP than individuals without diabetes (HR: 1.74)[52]. Likewise, other studies have reported that patients with diabetes develop more severe AP[42].

Despite it is accepted that AP can give rise to diabetes, the pathophysiological mechanisms are still unknown. In necrotizing AP, diabetes may be attributed to structural damage of pancreatic parenchyma. However, in the mild AP the involved mechanisms are less clear. Overall, it has been hypothesized that the pathophysiology of PAPD may be multifactorial, involving diverse mechanisms that could have effect at different levels of the glucose metabolism

Table 2 Prospective cohort studies with more than 12 mo of follow-up that determine the incidence of post-acute pancreatitis diabetes

Ref.	N	Follow-up, mo	AP grade, %	Definition of diabetes	Prediabetes, %	Diabetes, %
Johansen and Ornsholt[20], 1972	22	24	NS	OGTT	0	18
Olszewski *et al*[19], 1978	25	12	NS	OGTT, serum insulin	ND	28
Eriksson *et al*[21], 1992	36	74	S:56; M:44	OGTT	11	53
Angelini *et al*[22], 1993	118	53	S:70; M:30	OGTT	ND	8
Malecka *et al*[23], 2002	82	56	S:34; M:66	OGTT, serum insulin	2	16
Kaya *et al*[24], 2007	112	12	S:32; M:68	OGTT, fasting glucose, c-pep	24	21
Andersson *et al*[25], 2010	39	45	S:35; M:65	Serum insulin, OGTT	33	23
Garip *et al*[26], 2013	96	32	S:36; M:64	Fasting glucose, OGTT	ND	34
Vujasinovic *et al*[27], 2014	100	32	NS	Fasting glucose, OGTT	ND	14
Winter Gasparoto *et al*[28], 2015	16	38.4	NS	OGTT, HOMA	ND	31.2
Severe AP						
Doepel *et al*[29], 1993	37	74	S:100	Fasting glucose, C- pep, A1cHb, OGTT	ND	54
Yasuda *et al*[30], 2008	41	56	S:100	Fasting glucose	ND	39
Gupta *et al*[31], 2009	30	31	S:100	Fasting and postprandial glucose, OGTT, C-pep	20	20
Uomo *et al*[32], 2010	38	179	S:100	OGTT	ND	16
Chandrasekaran *et al*[33], 2015	35	26.2	S:100	OGTT	ND	48.5
Tu *et al*[34], 2017	113	42.9	S:90; M:10	OGTT A1cHb	ND	30

AP: Acute pancreatitis; NS: Not significant; ND: Non-determined; S: Severe; M: Mild and moderate; OGTT: Oral glucose tolerance test; C-pep: C-peptide; A1cHb: Glycosylated hemoglobin.



DOI: 10.3748/wjg.v29.i28.4405 **Copyright** ©The Author(s) 2023.

Figure 1 Trajectory of glycemia after at least one episode of acute pancreatitis.

regulation pathways. It may be possible that one or more of these mechanisms may predominate in the different diabetes phenotypes. According to some evidence collected so far, some of the possible mechanisms are discussed in the following sections (Figure 2).

Pancreatic necrosis

This complication of AP has already been discussed previously in the above sections[28,40-42,53,54]. In a recent meta-analysis, patients who displayed pancreatic necrosis during the AP attack(s) had a higher frequency of diabetes than those without necrosis (37% *vs* 11%)[18]. In other series, the incidence exceeds 50% of the cases[29]. Notwithstanding, the relation between diabetes incidence and the extension and site of necrosis has not been completely defined. In a recent study with 109 patients with AP the incidence of de novo diabetes in patients with pancreatic necrosis demonstrated by contrasted computed tomography scan was higher (66.6%) than in those without necrosis (27.8%). However, no relationship was found between diabetes incidence and necrosis rate or site of necrosis (head, body or tail of pancreas)

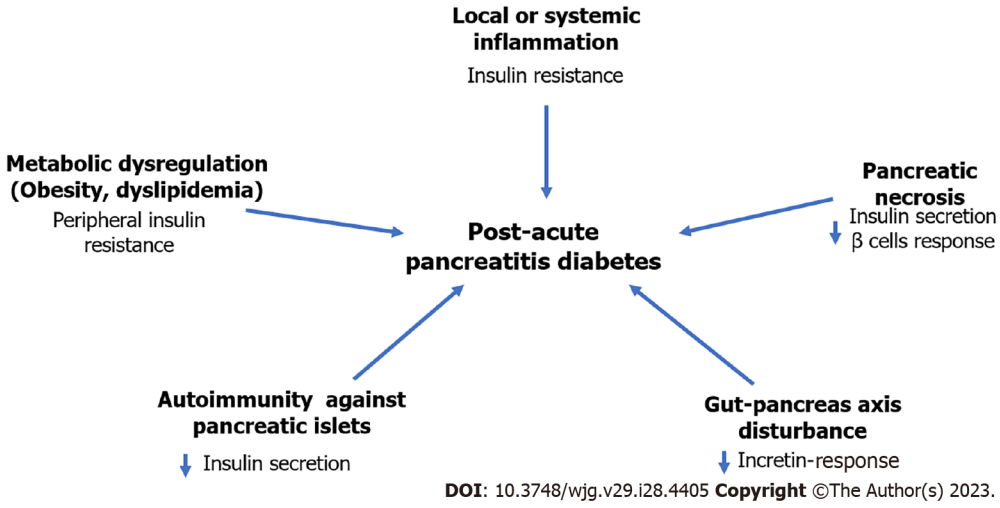


Figure 2 Possible mechanism involved in the pathophysiology of post-acute pancreatitis diabetes.

[26]. This may be explained because diabetes may be due, in addition to destruction of β cells of the pancreas, to insulin resistance. And also, because β cells are located homogeneously in the different segments of the pancreas.

Pancreatic necrosis may also induce exocrine pancreas insufficiency (EPI). From 15 to 30% of patients who have an episode of AP may have chronic pancreatitis after 3 years of follow-up[47].

Autoimmunity against β cells and other components of Langerhans islets

It has been speculated that the local and systemic inflammatory response occurring in AP patients may result in post-translational modifications of endogenous islet cell proteins, such as insulin, nucleic acids, and other proteins. Such modified neoepitopes may act as autoantigens, inducing an autoimmune response against components of the Langerhans islet[55]. To date, the frequency of autoimmunity during and after an AP episode has not been evaluated, particularly in patients who develop de novo diabetes.

Metabolic dysregulation

Obesity and hypertriglyceridemia are risk factors for the development of both T2DM and AP[56,57]. Their presence prior to AP may result in greater risk of developing diabetes and may accelerate the onset of this condition. Both factors are independently associated with increased risk of clinical severity of AP, which could explain the risk of diabetes[58,59]. In fact, hypertriglyceridemia is one of the most frequent causes of AP, only below biliary and alcoholic etiology. The impact that visceral obesity may have is unknown. However, there is evidence that increased accumulation of intrapancreatic fat around the islets of Langerhans may have pathophysiological role in acute and chronic PPD[9,10]. Insulin resistance may be the mechanism in these patients[60].

Local and systemic inflammatory response

During the course of AP, serum IL-6 levels increase as a consequence of the local and systemic inflammatory response. It has been hypothesized that this and other cytokines could favor the development of chronic hyperglycemia[61]. Multiple studies have found that the role of IL-6 on impaired glucose metabolism is primarily through insulin resistance[62,63].

Disturbance of the gut-pancreas axis

It has been suggested that of some of the pancreatic and intestine functional interconnections involved in the digestion, absorption, and utilization of nutrients which regulate glucose homeostasis may be disturbed in PAPD[53]. This assertion is based on the fact that 15% to 30% of patients who have AP show chronic pancreatitis 3 years after the acute episode[47,64]. The most common endocrine dysfunction results from decreased levels of insulin, glucagon, and pancreatic polypeptide[65]. Impaired secretion of enteral glucoregulatory hormones (incretins secreted by intestinal epithelium cells), such as glucose-dependent insulinotropic polypeptide (GIP) and glucagon-like peptide 1 (GLP-1) may also be observed. These peptides are associated with increased insulin secretion, glucagon secretion modulation and reduction of hepatic and peripheral insulin resistance[66]. It is important to underline that the reduction of glucagon secretion is the cause of severe hypoglycemia due to the loss of its counter-regulatory effect[67]. Therefore, the combined hormonal abnormalities that occur in PAPD result in a severely disrupted endocrine environment that is different from the pattern of abnormalities seen in T1DM or T2DM. Hence the need to understand and recognize these entities separately.

In summary, it is essential to determine the relative contribution of each of these pathophysiological mechanisms involved in PAPD, as well as their interrelationship with the possible genetic predispositions. In order to clarify this important issue, both clinical and basic studies in experimental models of PAPD are needed due to the difficulty in obtaining tissue samples from human beings.

DIAGNOSIS

For stablishing the diagnosis of PAPD it is important to rule out preexisting diabetes (mainly T2DM) which sometimes is difficult. The diagnostic criteria for PAPD proposed some years ago that included the demonstration of EPI as well as the absence of autoantibodies directed against β cells of the pancreas are not currently valid[68,69] because only 30% of patients show evidence of EPI 3 years after AP[64,70]. In addition, patients who develop EPI have increased risk of diabetes[71], so it should be considered as a risk factor and not as its defining characteristic. On the other hand, early and intermediate stages of EPI are difficult to demonstrate as functional tests and sophisticated imaging techniques are often not available in real life practice and are costly. In total, the term PAPD should be reserved specifically to de novo diabetes in individuals after AP with or without morphological or functional evidence of chronic pancreatitis and without the need to demonstrate the absence of anti-β cell antibodies.

The diagnosis of diabetes should be established based on the criteria recommended by the ADA: Glycosylated hemoglobin (HbA1c) ≥ 48 mm/moL or 6.5% and/or fasting glucose > 7 mmmol/L or 126 mg/dL[72], which must be performed more than 90 d after AP resolution. This is important because HbA1c levels reflect the mean plasma glucose concentration in the previous 8-12 wk and also due to the stress hyperglycemia that can occur before this period. It has been shown that the oral glucose tolerance test is better for detecting early-stage diabetes as it is not affected by stress and does not require 90 d to give reliable results.

Some clinical characteristics and biochemical markers can help to differentiate PAPD from T2DM. PAPD has greater glycemic variability and more difficult control, showing frequent hypoglycemic episodes and more insulin requirements [73]. From the biochemical point of view, PAPD patients have lower baseline and stimulated levels of insulin, glucagon and C-peptide[1]. Besides, pre and postprandial serum levels of oxyntomodulin (an intestinal peptide derived from proglucagon that participates in the regulation of the pancreatic exocrine function), have been found to be significantly higher in patients with PAPD compared to T2DM and healthy controls. This opens the possibility of being used as a specific biomarker[74]. For some, the presence of diagnostic autoimmune markers for T1DM (*i.e.*, islet cell antibodies or antibodies against glutamic acid decarboxylase, insulin, tyrosine phosphatase-like proteins, or zinc transporter)[75], rules out the diagnosis of PAPD. However, as already mentioned, an autoimmune component triggered by neoepitopes induced by the systemic inflammatory response of AP at the level of the β cells has not been ruled out as patho-physiological mechanism of PAPD in some patients[55]. Finally, it is also important to identify overlapping causes of DEP such as pancreatic surgery, cystic fibrosis, toxic pancreatic medications, hemochromatosis, and pancreatic cancer.

In summary, the diagnosis of PAPD should be based on the exclusion of any type of preexisting diabetes before AP and on identification of diabetes ninety days after AP based on the ADA criteria. For now, screening for PAPD should be performed in all patients who have had at least one episode of AP. The knowledge of the risk factors will contribute to selecting patients for screening in the future. Although there is no consensus on the frequency of screening, it is recommended to be carried out every 6 mo the first year and every year thereafter. Figure 3 shows a simplified PAPD diagnostic algorithm.

COMPLICATIONS

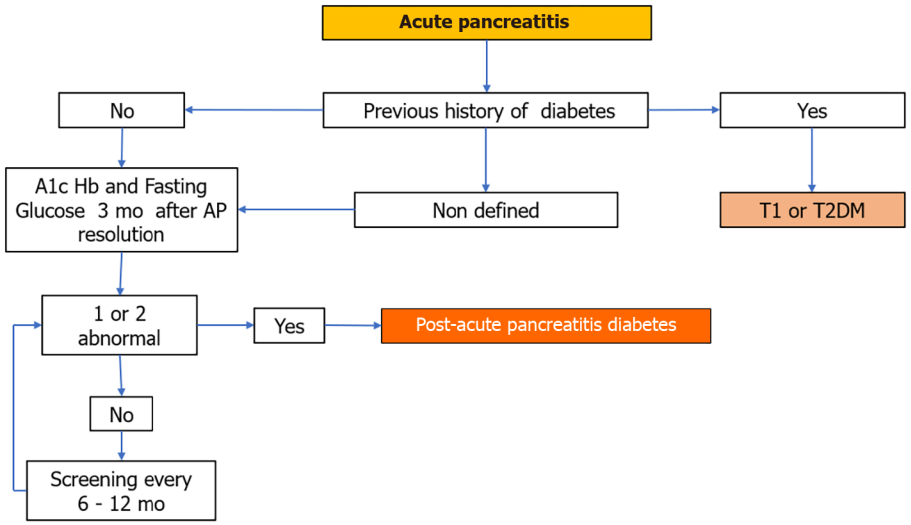
It has been demonstrated that PAPD has higher short- and long-term morbidity and mortality than T2DM[3]. A recent population-based study of 139843 individuals showed that those with PAPD had significantly higher risk of pancreatic cancer than those with T2DM or those with no history of pancreatitis (adjusted RR: 6.94; $P < 0.05$)[76]. It is important to underline that in patients recovering from AP, diabetes may be the clinical manifestation of pancreatic cancer, so early detection strategies for these neoplasms should be applied. Another recent study with 10549 individuals showed that patients with PAPD, compared to T2DM, had higher all-cause mortality (RR: 1.13), cancer (RR: 1.14), infections (RR: 2.52), and gastrointestinal disease (RR: 2.56). Likewise, the risk of rehospitalizations was significantly higher, which represented greater economic burden[77].

MANAGEMENT

The data so far available regarding the treatment of PAPD are very scarce, however, some rationale may be useful to guide treatment decisions with the understanding that refinement will be required based on the results of well-conducted future therapeutic studies. The management of PAPD should ideally be preventive and corrective.

Preventive management aims to reduce the incidence of diabetes which would be achieved if the risk factors and predictive clinical and biochemical markers were clearly known. It seems that pancreatic necrosis and recurrent episodes of AP are the most solid risk factors. Possibly in patients with these complications a more aggressive and earlier management of AP, the performance of early cholecystectomy in biliary AP and stopping alcohol consumption could have some beneficial impact. In this context, well-conducted studies are required in order to demonstrate this issue.

For corrective management it is suggested to apply the ADA recommendations for the treatment of T2DM and T1DM with some nuances[78]. It is important to be aware of the fragile stability of glycemia of these patients. This leads that a large part of patients be treated with insulin. In a large population-based study, higher proportion of patients with PAPD were already on insulin therapy within 5 years compared to T2DM (20.9% *vs* 4.1% respectively), and had poorer glycemic control (defined as HBA1c ≥ 7%)[1].



DOI: 10.3748/wjg.v29.i28.4405 **Copyright** ©The Author(s) 2023.

Figure 3 Simplified algorithm for the diagnosis of post-acute pancreatitis diabetes. AP: Acute pancreatitis; T2DM: Type 2 diabetes mellitus.

It is important to remember that about 30% of patients with AP develop EPI[70]. At this point, one study reported increased postprandial responses of GLP-1 and GIP in patients with chronic pancreatitis and EPI following pancreatic enzyme substitution (PES). Concurrently, both plasma insulin, plasma C-peptide, and total insulin secretion increased after PES. These results suggest that secretion of GLP-1 and GIP is under influence of the digestion and absorption of nutrients in the small intestine and that PES increased insulin secretion[66]. Concomitant improvement of glycemic control was not assessed in diabetic patients from this study. As a result of these findings, the assessment of therapeutic effects of PES from the early stages of diabetes development may be warranted.

Finally, the management of PAPD is complex and requires a common approach, preferably by a medical team that includes gastroenterologists, endocrinologists, primary care physicians, nutritionists, and behavioral health specialists.

CONCLUSION

PAPD is currently the second most common type of diabetes. It is increasingly known as a result of the recently published research around this entity. However, much of the medical community still ignores its existence. With the increasing global incidence of AP, the frequency of this type of diabetes will certainly increase.

Due to its high morbidity, mortality and difficult treatment, its recognition as a complication of AP is of paramount importance. Pancreatic necrosis and recurrence seem to be the strongest risk factors. Its pathophysiological mechanisms and other risk factors are not yet clearly known. The diagnosis should be based on the exclusion of any type of preexisting diabetes and on identification of diabetes ninety days after AP based on the ADA criteria. Screening for diabetes should be performed in all patients who have had at least one episode of AP. Management is not yet standardized.

It was recently announced the launch of a multicenter clinical study designed to understand the frequency and phenotypes of this type of diabetes. This study has been called Diabetes RElated to Acute Pancreatitis and its Mechanisms and is supported by The National Institute of Diabetes and Digestive and Kidney Diseases[79]. In this research project, it is planned to study risk factors and some of the mechanisms possibly involved in the pathophysiology of PAPD[80-82].

Certainly, the results of this and other similar forthcoming studies will contribute to the clarification of some important gaps that still persist in the knowledge of PAPD making possible a more effective screening and better preventive and corrective management.

FOOTNOTES

Author contributions: García-Compeán D, Jiménez-Rodríguez AR, and Muñoz-Ayala JM made a bibliographic research and wrote sections of the manuscript; Villarreal-Pérez JZ, González-González JA, and Maldonado-Garza HJ critically reviewed the manuscript; García-Compeán D conceived and coordinated the whole project.

Conflict-of-interest statement: The authors declare no conflict of interest in the preparation of this manuscript.

Open-Access: This article is an open-access article that was selected by an in-house editor and fully peer-reviewed by external reviewers. It is distributed in accordance with the Creative Commons Attribution NonCommercial (CC BY-NC 4.0) license, which permits others to distribute, remix, adapt, build upon this work non-commercially, and license their derivative works on different terms, provided the

original work is properly cited and the use is non-commercial. See: https://creativecommons.org/Licenses/by-nc/4.0/

Country/Territory of origin: Mexico

ORCID number: Diego García-Compeán 0000-0002-9642-8567; Alan R Jiménez-Rodríguez 0000-0001-8113-3144; Juan Manuel Muñoz-Ayala 0000-0001-8747-4177; José A González-González 0000-0003-4858-5717; Héctor Jesús Maldonado-Garza 0000-0001-9217-7169; Jesús Zacarías Villarreal-Pérez 0000-0002-6814-062X.

S-Editor: Fan JR
L-Editor: A
P-Editor: Yu HG

REFERENCES

1 **Woodmansey C**, McGovern AP, McCullough KA, Whyte MB, Munro NM, Correa AC, Gatenby PAC, Jones SA, de Lusignan S. Incidence, Demographics, and Clinical Characteristics of Diabetes of the Exocrine Pancreas (Type 3c): A Retrospective Cohort Study. *Diabetes Care* 2017; **40**: 1486-1493 [PMID: 28860126 DOI: 10.2337/dc17-0542]

2 **Pendharkar SA**, Mathew J, Petrov MS. Age- and sex-specific prevalence of diabetes associated with diseases of the exocrine pancreas: A population-based study. *Dig Liver Dis* 2017; **49**: 540-544 [PMID: 28110921 DOI: 10.1016/j.dld.2016.12.010]

3 **Shivaprasad C**, Aiswarya Y, Kejal S, Sridevi A, Anupam B, Ramdas B, Gautham K, Aarudhra P. Comparison of CGM-Derived Measures of Glycemic Variability Between Pancreatogenic Diabetes and Type 2 Diabetes Mellitus. *J Diabetes Sci Technol* 2021; **15**: 134-140 [PMID: 31282179 DOI: 10.1177/1932296819860133]

4 **Löhr JM**, Dominguez-Munoz E, Rosendahl J, Besselink M, Mayerle J, Lerch MM, Haas S, Akisik F, Kartalis N, Iglesias-Garcia J, Keller J, Boermeester M, Werner J, Dumonceau JM, Fockens P, Drewes A, Ceyhan G, Lindkvist B, Drenth J, Ewald N, Hardt P, de Madaria E, Witt H, Schneider A, Manfredi R, Brøndum FJ, Rudolf S, Bollen T, Bruno M; HaPanEU/UEG Working Group. United European Gastroenterology evidence-based guidelines for the diagnosis and therapy of chronic pancreatitis (HaPanEU). *United European Gastroenterol J* 2017; **5**: 153-199 [PMID: 28344786 DOI: 10.1177/2050640616684695]

5 **Expert Committee on the Diagnosis and Classification of Diabetes Mellitus**. Report of the expert committee on the diagnosis and classification of diabetes mellitus. *Diabetes Care* 2003; **26** Suppl 1: S5-20 [PMID: 12502614 DOI: 10.2337/diacare.26.2007.s5]

6 **Wynne K**, Devereaux B, Dornhorst A. Diabetes of the exocrine pancreas. *J Gastroenterol Hepatol* 2019; **34**: 346-354 [PMID: 30151918 DOI: 10.1111/jgh.14451]

7 **Duggan SN**, O'Connor DB, Antanaitis A, Campion JR, Lawal O, Ahmed M, Tisdall AR, Sherlock M, Boran G, le Roux C, Gibney J, Conlon KC. Metabolic dysfunction and diabetes mellitus during long-term follow-up of severe acute pancreatitis: A case-matched study. *Pancreatology* 2020; **20**: 813-821 [PMID: 32522508 DOI: 10.1016/j.pan.2020.03.016]

8 **Ramalho GX**, Dytz MG. Diabetes of the Exocrine Pancreas Related to Hereditary Pancreatitis, an Update. *Curr Diab Rep* 2020; **20**: 16 [PMID: 32221727 DOI: 10.1007/s11892-020-01299-8]

9 **Singh RG**, Cervantes A, Kim JU, Nguyen NN, DeSouza SV, Dokpuang D, Lu J, Petrov MS. Intrapancreatic fat deposition and visceral fat volume are associated with the presence of diabetes after acute pancreatitis. *Am J Physiol Gastrointest Liver Physiol* 2019; **316**: G806-G815 [PMID: 30920289 DOI: 10.1152/ajpgi.00385.2018]

10 **Singh RG**, Nguyen NN, DeSouza SV, Pendharkar SA, Petrov MS. Comprehensive analysis of body composition and insulin traits associated with intra-pancreatic fat deposition in healthy individuals and people with new-onset prediabetes/diabetes after acute pancreatitis. *Diabetes Obes Metab* 2019; **21**: 417-423 [PMID: 30187644 DOI: 10.1111/dom.13523]

11 **Yu B**, Li N, Li J, Wan J, He W, Zhu Y, Lu N. The Clinical Characteristics of Acute Pancreatitis in Gerontal Patients: A Retrospective Study. *Clin Interv Aging* 2020; **15**: 1541-1553 [PMID: 32982192 DOI: 10.2147/CIA.S259920]

12 **Petrov MS**. Diagnosis of endocrine disease: Post-pancreatitis diabetes mellitus: prime time for secondary disease. *Eur J Endocrinol* 2021; **184**: R137-R149 [PMID: 33460393 DOI: 10.1530/EJE-20-0468]

13 **Bendor CD**, Bardugo A, Zucker I, Cukierman-Yaffe T, Lutski M, Derazne E, Shohat T, Mosenzon O, Tzur D, Sapir A, Pinhas-Hamiel O, Kibbey RG, Raz I, Afek A, Gerstein HC, Tirosh A, Twig G. Childhood Pancreatitis and Risk for Incident Diabetes in Adulthood. *Diabetes Care* 2020; **43**: 145-151 [PMID: 31694859 DOI: 10.2337/dc19-1562]

14 **Baeza-Zapata AA**, García-Compeán D, Jaquez-Quintana JO; Collaborators. Acute Pancreatitis in Elderly Patients. *Gastroenterology* 2021; **161**: 1736-1740 [PMID: 34384746 DOI: 10.1053/j.gastro.2021.06.081]

15 **Xiao AY**, Tan ML, Wu LM, Asrani VM, Windsor JA, Yadav D, Petrov MS. Global incidence and mortality of pancreatic diseases: a systematic review, meta-analysis, and meta-regression of population-based cohort studies. *Lancet Gastroenterol Hepatol* 2016; **1**: 45-55 [PMID: 28404111 DOI: 10.1016/S2468-1253(16)30004-8]

16 **González-González JA**, Castañeda-Sepúlveda R, Martínez-Vázquez MA, García-Compean D, Flores-Rendón AR, Maldonado-Garza HJ, Bosques-Padilla F, Garza-Galindo AA. [Clinical characteristics of acute pancreatitis in Mexico]. *Rev Gastroenterol Mex* 2012; **77**: 167-173 [PMID: 23177790 DOI: 10.1016/j.rgmx.2012.08.002]

17 **Das SL**, Singh PP, Phillips AR, Murphy R, Windsor JA, Petrov MS. Newly diagnosed diabetes mellitus after acute pancreatitis: a systematic review and meta-analysis. *Gut* 2014; **63**: 818-831 [PMID: 23929695 DOI: 10.1136/gutjnl-2013-305062]

18 **Zhi M**, Zhu X, Lugea A, Waldron RT, Pandol SJ, Li L. Incidence of New Onset Diabetes Mellitus Secondary to Acute Pancreatitis: A Systematic Review and Meta-Analysis. *Front Physiol* 2019; **10**: 637 [PMID: 31231233 DOI: 10.3389/fphys.2019.00637]

19 **Olszewski S**, Kinalska I, Długosz J, Stasiewicz J, Gabryelewicz A. The glucose tolerance, insulin response and pancreatic exocrine function in patients after acute pancreatitis. *Endokrinologie* 1978; **71**: 183-191 [PMID: 668642]

20 **Johansen K**, Ornsholt J. Frequency of diabetes after acute pancreatitis. *Metabolism* 1972; **21**: 291-296 [PMID: 5061050 DOI: 10.1016/0026-0495(72)90072-8]

21 **Eriksson J**, Doepel M, Widén E, Halme L, Ekstrand A, Groop L, Höckerstedt K. Pancreatic surgery, not pancreatitis, is the primary cause of

diabetes after acute fulminant pancreatitis. *Gut* 1992; **33**: 843-847 [PMID: 1624170 DOI: 10.1136/gut.33.6.843]

22 **Angelini G**, Cavallini G, Pederzoli P, Bovo P, Bassi C, Di Francesco V, Frulloni L, Sgarbi D, Talamini G, Castagnini A. Long-term outcome of acute pancreatitis: a prospective study with 118 patients. *Digestion* 1993; **54**: 143-147 [PMID: 8359555 DOI: 10.1159/000201028]

23 **Malecka-Panas E**, Gasiorowska A, Kropiwnicka A, Zlobinska A, Drzewoski J. Endocrine pancreatic function in patients after acute pancreatitis. *Hepatogastroenterology* 2002; **49**: 1707-1712 [PMID: 12397772]

24 **Kaya E**, Dervisoglu A, Polat C. Evaluation of diagnostic findings and scoring systems in outcome prediction in acute pancreatitis. *World J Gastroenterol* 2007; **13**: 3090-3094 [PMID: 17589925 DOI: 10.3748/wjg.v13.i22.3090]

25 **Andersson B**, Pendse ML, Andersson R. Pancreatic function, quality of life and costs at long-term follow-up after acute pancreatitis. *World J Gastroenterol* 2010; **16**: 4944-4951 [PMID: 20954281 DOI: 10.3748/wjg.v16.i39.4944]

26 **Garip G**, Sarandöl E, Kaya E. Effects of disease severity and necrosis on pancreatic dysfunction after acute pancreatitis. *World J Gastroenterol* 2013; **19**: 8065-8070 [PMID: 24307801 DOI: 10.3748/wjg.v19.i44.8065]

27 **Vujasinovic M**, Tepes B, Makuc J, Rudolf S, Zaletel J, Vidmar T, Seruga M, Birsa B. Pancreatic exocrine insufficiency, diabetes mellitus and serum nutritional markers after acute pancreatitis. *World J Gastroenterol* 2014; **20**: 18432-18438 [PMID: 25561813 DOI: 10.3748/wjg.v20.i48.18432]

28 **Winter Gasparoto RC**, Racy Mde C, De Campos T. Long-term outcomes after acute necrotizing pancreatitis: what happens to the pancreas and to the patient? *JOP* 2015; **16**: 159-166 [PMID: 25791549 DOI: 10.6092/1590-8577/2958]

29 **Doepel M**, Eriksson J, Halme L, Kumpulainen T, Höckerstedt K. Good long-term results in patients surviving severe acute pancreatitis. *Br J Surg* 1993; **80**: 1583-1586 [PMID: 8298931 DOI: 10.1002/bjs.1800801229]

30 **Yasuda T**, Ueda T, Takeyama Y, Shinzeki M, Sawa H, Nakajima T, Kuroda Y. Long-term outcome of severe acute pancreatitis. *J Hepatobiliary Pancreat Surg* 2008; **15**: 397-402 [PMID: 18670841 DOI: 10.1007/s00534-007-1266-x]

31 **Gupta R**, Wig JD, Bhasin DK, Singh P, Suri S, Kang M, Rana SS, Rana S. Severe acute pancreatitis: the life after. *J Gastrointest Surg* 2009; **13**: 1328-1336 [PMID: 19415400 DOI: 10.1007/s11605-009-0901-z]

32 **Uomo G**, Gallucci F, Madrid E, Miraglia S, Manes G, Rabitti PG. Pancreatic functional impairment following acute necrotizing pancreatitis: long-term outcome of a non-surgically treated series. *Dig Liver Dis* 2010; **42**: 149-152 [PMID: 19836318 DOI: 10.1016/j.dld.2009.08.007]

33 **Chandrasekaran P**, Gupta R, Shenvi S, Kang M, Rana SS, Singh R, Bhasin DK. Prospective comparison of long term outcomes in patients with severe acute pancreatitis managed by operative and non operative measures. *Pancreatology* 2015; **15**: 478-484 [PMID: 26364168 DOI: 10.1016/j.pan.2015.08.006]

34 **Tu J**, Zhang J, Ke L, Yang Y, Yang Q, Lu G, Li B, Tong Z, Li W, Li J. Endocrine and exocrine pancreatic insufficiency after acute pancreatitis: long-term follow-up study. *BMC Gastroenterol* 2017; **17**: 114 [PMID: 29078749 DOI: 10.1186/s12876-017-0663-0]

35 **Shen HN**, Yang CC, Chang YH, Lu CL, Li CY. Risk of Diabetes Mellitus after First-Attack Acute Pancreatitis: A National Population-Based Study. *Am J Gastroenterol* 2015; **110**: 1698-1706 [PMID: 26526084 DOI: 10.1038/ajg.2015.356]

36 **Bharmal SH**, Cho J, Alarcon Ramos GC, Ko J, Stuart CE, Modesto AE, Singh RG, Petrov MS. Trajectories of glycaemia following acute pancreatitis: a prospective longitudinal cohort study with 24 months follow-up. *J Gastroenterol* 2020; **55**: 775-788 [PMID: 32494905 DOI: 10.1007/s00535-020-01682-y]

37 **Ho TW**, Wu JM, Kuo TC, Yang CY, Lai HS, Hsieh SH, Lai F, Tien YW. Change of Both Endocrine and Exocrine Insufficiencies After Acute Pancreatitis in Non-Diabetic Patients: A Nationwide Population-Based Study. *Medicine (Baltimore)* 2015; **94**: e1123 [PMID: 26166112 DOI: 10.1097/MD.0000000000001123]

38 **Nikkola J**, Laukkarinen J, Lahtela J, Seppänen H, Järvinen S, Nordback I, Sand J. The Long-term Prospective Follow-up of Pancreatic Function After the First Episode of Acute Alcoholic Pancreatitis: Recurrence Predisposes One to Pancreatic Dysfunction and Pancreatogenic Diabetes. *J Clin Gastroenterol* 2017; **51**: 183-190 [PMID: 28060789 DOI: 10.1097/MCG.0000000000000564]

39 **Ibars EP**, Sánchez de Rojas EA, Quereda LA, Ramis RF, Sanjuan VM, Peris RT. Pancreatic function after acute biliary pancreatitis: does it change? *World J Surg* 2002; **26**: 479-486 [PMID: 11910484 DOI: 10.1007/s00268-001-0253-7]

40 **Umapathy C**, Raina A, Saligram S, Tang G, Papachristou GI, Rabinovitz M, Chennat J, Zeh H, Zureikat AH, Hogg ME, Lee KK, Saul MI, Whitcomb DC, Slivka A, Yadav D. Natural History After Acute Necrotizing Pancreatitis: a Large US Tertiary Care Experience. *J Gastrointest Surg* 2016; **20**: 1844-1853 [PMID: 27619808 DOI: 10.1007/s11605-016-3264-2]

41 **Tu J**, Yang Y, Zhang J, Yang Q, Lu G, Li B, Tong Z, Ke L, Li W, Li J. Effect of the disease severity on the risk of developing new-onset diabetes after acute pancreatitis. *Medicine (Baltimore)* 2018; **97**: e10713 [PMID: 29851776 DOI: 10.1097/MD.0000000000010713]

42 **Xiao B**, Xu HB, Jiang ZQ, Hu JX, Yang GD. Acute Pancreatitis in Patients With a Medical History of Type 2 Diabetes Mellitus: Clinical Findings and Magnetic Resonance Imaging Characteristics. *Pancreas* 2020; **49**: 591-597 [PMID: 32282775 DOI: 10.1097/MPA.0000000000001530]

43 **Vipperla K**, Papachristou GI, Slivka A, Whitcomb DC, Yadav D. Risk of New-Onset Diabetes Is Determined by Severity of Acute Pancreatitis. *Pancreas* 2016; **45**: e14-e15 [PMID: 26658044 DOI: 10.1097/MPA.0000000000000536]

44 **Walker A**, O'Kelly J, Graham C, Nowell S, Kidd D, Mole DJ. Increased risk of type 3c diabetes mellitus after acute pancreatitis warrants a personalized approach including diabetes screening. *BJS Open* 2022; **6** [PMID: 36515672 DOI: 10.1093/bjsopen/zrac148]

45 **Richardson A**, Park WG. Acute pancreatitis and diabetes mellitus: a review. *Korean J Intern Med* 2021; **36**: 15-24 [PMID: 33147904 DOI: 10.3904/kjim.2020.505]

46 **Avanesov M**, Löser A, Smagarynska A, Keller S, Guerreiro H, Tahir E, Karul M, Adam G, Yamamura J. Clinico-radiological comparison and short-term prognosis of single acute pancreatitis and recurrent acute pancreatitis including pancreatic volumetry. *PLoS One* 2018; **13**: e0206062 [PMID: 30359398 DOI: 10.1371/journal.pone.0206062]

47 **Patra PS**, Das K. Longer-term outcome of acute pancreatitis: 5 years follow-up. *JGH Open* 2021; **5**: 1323-1327 [PMID: 34950774 DOI: 10.1002/jgh3.12679]

48 **Bharmal SH**, Kimita W, Ko J, Petrov MS. Cytokine signature for predicting new-onset prediabetes after acute pancreatitis: A prospective longitudinal cohort study. *Cytokine* 2022; **150**: 155768 [PMID: 34823207 DOI: 10.1016/j.cyto.2021.155768]

49 **Bharmal SH**, Kimita W, Ko J, Petrov MS. Pancreatic and gut hormones as predictors of new-onset prediabetes after non-necrotising acute pancreatitis: a prospective longitudinal cohort study. *Endocr Connect* 2021; **10**: 715-724 [PMID: 34097643 DOI: 10.1530/EC-21-0229]

50 **Bharmal SH**, Cho J, Ko J, Petrov MS. Glucose variability during the early course of acute pancreatitis predicts two-year probability of new-onset diabetes: A prospective longitudinal cohort study. *United European Gastroenterol J* 2022; **10**: 179-189 [PMID: 35188346 DOI: 10.1002/ueg2.12190]

51 **Lee YK**, Huang MY, Hsu CY, Su YC. Bidirectional Relationship Between Diabetes and Acute Pancreatitis: A Population-Based Cohort Study

in Taiwan. *Medicine (Baltimore)* 2016; **95**: e2448 [PMID: 26765434 DOI: 10.1097/MD.0000000000002448]
52 **Aune D**, Mahamat-Saleh Y, Norat T, Riboli E. Diabetes mellitus and the risk of pancreatitis: A systematic review and meta-analysis of cohort studies. *Pancreatology* 2020; **20**: 602-607 [PMID: 32409279 DOI: 10.1016/j.pan.2020.03.019]
53 **Hart PA**, Bradley D, Conwell DL, Dungan K, Krishna SG, Wyne K, Bellin MD, Yadav D, Andersen DK, Serrano J, Papachristou GI. Diabetes following acute pancreatitis. *Lancet Gastroenterol Hepatol* 2021; **6**: 668-675 [PMID: 34089654 DOI: 10.1016/S2468-1253(21)00019-4]
54 **Burkhart RA**, Gerber SM, Tholey RM, Lamb KM, Somasundaram A, McIntyre CA, Fradkin EC, Ashok AP, Felte RF, Mehta JM, Rosato EL, Lavu H, Jabbour SA, Yeo CJ, Winter JM. Incidence and severity of pancreatogenic diabetes after pancreatic resection. *J Gastrointest Surg* 2015; **19**: 217-225 [PMID: 25316483 DOI: 10.1007/s11605-014-2669-z]
55 **Kahara T**, Takamura T, Otoda T, Ishikura K, Matsushita E. Transient anti-GAD antibody positivity and acute pancreatitis with pancreas tail swelling in a patient with susceptible haplotype for type 1 diabetes mellitus. *Intern Med* 2009; **48**: 1897-1899 [PMID: 19881242 DOI: 10.2169/internalmedicine.48.2393]
56 **Ma JH**, Yuan YJ, Lin SH, Pan JY. Nomogram for predicting diabetes mellitus after the first attack of acute pancreatitis. *Eur J Gastroenterol Hepatol* 2019; **31**: 323-328 [PMID: 30433890 DOI: 10.1097/MEG.0000000000001307]
57 **Wu D**, Xu Y, Zeng Y, Wang X. Endocrine pancreatic function changes after acute pancreatitis. *Pancreas* 2011; **40**: 1006-1011 [PMID: 21705952 DOI: 10.1097/MPA.0b013e31821fde3f]
58 **Smeets XJNM**, Knoester I, Grooteman KV, Singh VK, Banks PA, Papachristou GI, Duarte-Rojo A, Robles-Diaz G, Kievit W, Besselink MGH, Verdonk RC, Van Santvoort HC, Drenth JPH, Belias M, Van Geenen EJM; Dutch Pancreatitis Study Group. The association between obesity and outcomes in acute pancreatitis: an individual patient data meta-analysis. *Eur J Gastroenterol Hepatol* 2019; **31**: 316-322 [PMID: 30399003 DOI: 10.1097/MEG.0000000000001300]
59 **Yang AL**, McNabb-Baltar J. Hypertriglyceridemia and acute pancreatitis. *Pancreatology* 2020; **20**: 795-800 [PMID: 32571534 DOI: 10.1016/j.pan.2020.06.005]
60 **Pendharkar SA**, Singh RG, Bharmal SH, Drury M, Petrov MS. Pancreatic Hormone Responses to Mixed Meal Test in New-onset Prediabetes/Diabetes After Non-necrotizing Acute Pancreatitis. *J Clin Gastroenterol* 2020; **54**: e11-e20 [PMID: 30480566 DOI: 10.1097/MCG.0000000000001145]
61 **Petrov MS**. Panorama of mediators in postpancreatitis diabetes mellitus. *Curr Opin Gastroenterol* 2020; **36**: 443-451 [PMID: 32618612 DOI: 10.1097/MOG.0000000000000654]
62 **Gillies N**, Pendharkar SA, Asrani VM, Mathew J, Windsor JA, Petrov MS. Interleukin-6 is associated with chronic hyperglycemia and insulin resistance in patients after acute pancreatitis. *Pancreatology* 2016; **16**: 748-755 [PMID: 27401909 DOI: 10.1016/j.pan.2016.06.661]
63 **Xu E**, Pereira MMA, Karakasilioti I, Theurich S, Al-Maarri M, Rappl G, Waisman A, Wunderlich FT, Brüning JC. Temporal and tissue-specific requirements for T-lymphocyte IL-6 signalling in obesity-associated inflammation and insulin resistance. *Nat Commun* 2017; **8**: 14803 [PMID: 28466852 DOI: 10.1038/ncomms14803]
64 **Hollemans RA**, Hallensleben NDL, Mager DJ, Kelder JC, Besselink MG, Bruno MJ, Verdonk RC, van Santvoort HC; Dutch Pancreatitis Study Group. Pancreatic exocrine insufficiency following acute pancreatitis: Systematic review and study level meta-analysis. *Pancreatology* 2018; **18**: 253-262 [PMID: 29482892 DOI: 10.1016/j.pan.2018.02.009]
65 **Dite P**, Bojkova M, Belobradkova J, Zak P, Kianicka B. Chronic Pancreatitis and Diabetes of Exocrine Pancreas / Type 3c Diabetes Mellitus / Post-pancreatitis Diabetes Mellitus. *J Gastrointestin Liver Dis* 2022; **31**: 371-374 [PMID: 36535041 DOI: 10.15403/jgld-4744]
66 **Knop FK**, Vilsbøll T, Larsen S, Højberg PV, Vølund A, Madsbad S, Holst JJ, Krarup T. Increased postprandial responses of GLP-1 and GIP in patients with chronic pancreatitis and steatorrhea following pancreatic enzyme substitution. *Am J Physiol Endocrinol Metab* 2007; **292**: E324-E330 [PMID: 16954337 DOI: 10.1152/ajpendo.00059.2006]
67 **Donowitz M**, Hendler R, Spiro HM, Binder HJ, Felig P. Glucagon secretion in acute and chronic pancreatitis. *Ann Intern Med* 1975; **83**: 778-781 [PMID: 1200523 DOI: 10.7326/0003-4819-83-6-778]
68 **Ewald N**, Hardt PD. Diagnosis and treatment of diabetes mellitus in chronic pancreatitis. *World J Gastroenterol* 2013; **19**: 7276-7281 [PMID: 24259958 DOI: 10.3748/wjg.v19.i42.7276]
69 **Ewald N**, Bretzel RG. Diabetes mellitus secondary to pancreatic diseases (Type 3c)--are we neglecting an important disease? *Eur J Intern Med* 2013; **24**: 203-206 [PMID: 23375619 DOI: 10.1016/j.ejim.2012.12.017]
70 **Huang W**, de la Iglesia-García D, Baston-Rey I, Calviño-Suarez C, Lariño-Noia J, Iglesias-Garcia J, Shi N, Zhang X, Cai W, Deng L, Moore D, Singh VK, Xia Q, Windsor JA, Domínguez-Muñoz JE, Sutton R. Exocrine Pancreatic Insufficiency Following Acute Pancreatitis: Systematic Review and Meta-Analysis. *Dig Dis Sci* 2019; **64**: 1985-2005 [PMID: 31161524 DOI: 10.1007/s10620-019-05568-9]
71 **Cho J**, Scragg R, Pandol SJ, Petrov MS. Exocrine Pancreatic Dysfunction Increases the Risk of New-Onset Diabetes Mellitus: Results of a Nationwide Cohort Study. *Clin Transl Sci* 2021; **14**: 170-178 [PMID: 32692901 DOI: 10.1111/cts.12837]
72 **American Diabetes Association**. Standards of medical care in diabetes--2010. *Diabetes Care* 2010; **33** Suppl 1: S11-S61 [PMID: 20042772 DOI: 10.2337/dc10-S011]
73 **Singh A**, Aggarwal M, Garg R, Stevens T, Chahal P. Post-pancreatitis diabetes mellitus: insight on optimal management with nutrition and lifestyle approaches. *Ann Med* 2022; **54**: 1776-1786 [PMID: 35786076 DOI: 10.1080/07853890.2022.2090601]
74 **Bharmal SH**, Cho J, Stuart CE, Alarcon Ramos GC, Ko J, Petrov MS. Oxyntomodulin May Distinguish New-Onset Diabetes After Acute Pancreatitis From Type 2 Diabetes. *Clin Transl Gastroenterol* 2020; **11**: e00132 [PMID: 32463621 DOI: 10.14309/ctg.0000000000000132]
75 **Petrov MS**, Basina M. DIAGNOSIS OF ENDOCRINE DISEASE: Diagnosing and classifying diabetes in diseases of the exocrine pancreas. *Eur J Endocrinol* 2021; **184**: R151-R163 [PMID: 33460395 DOI: 10.1530/EJE-20-0974]
76 **Cho J**, Scragg R, Petrov MS. Postpancreatitis Diabetes Confers Higher Risk for Pancreatic Cancer Than Type 2 Diabetes: Results From a Nationwide Cancer Registry. *Diabetes Care* 2020; **43**: 2106-2112 [PMID: 32616613 DOI: 10.2337/dc20-0207]
77 **Cho J**, Scragg R, Petrov MS. Risk of Mortality and Hospitalization After Post-Pancreatitis Diabetes Mellitus vs Type 2 Diabetes Mellitus: A Population-Based Matched Cohort Study. *Am J Gastroenterol* 2019; **114**: 804-812 [PMID: 31021833 DOI: 10.14309/ajg.0000000000000225]
78 **ElSayed NA**, Aleppo G, Aroda VR, Bannuru RR, Brown FM, Bruemmer D, Collins BS, Cusi K, Das SR, Gibbons CH, Giurini JM, Hilliard ME, Isaacs D, Johnson EL, Kahan S, Khunti K, Kosiborod M, Leon J, Lyons SK, Murdock L, Perry ML, Prahalad P, Pratley RE, Seley JJ, Stanton RC, Sun JK, Woodward CC, Young-Hyman D, Gabbay RA; on behalf of the American Diabetes Association. Introduction and Methodology: Standards of Care in Diabetes-2023. *Diabetes Care* 2023; **46**: S1-S4 [PMID: 36507647 DOI: 10.2337/dc23-Sint]
79 **Serrano J**, Laughlin MR, Bellin MD, Yadav D, Chinchilli VM, Andersen DK; Type 1 Diabetes in Acute Pancreatitis Consortium (T1DAPC). Type 1 Diabetes in Acute Pancreatitis Consortium: From Concept to Reality. *Pancreas* 2022; **51**: 563-567 [PMID: 36206459 DOI: 10.1097/MPA.0000000000002073]

80 **Casu A**, Grippo PJ, Wasserfall C, Sun Z, Linsley PS, Hamerman JA, Fife BT, Lacy-Hulbert A, Toledo FGS, Hart PA, Papachristou GI, Bellin MD, Yadav D, Laughlin MR, Goodarzi MO, Speake C; Type 1 Diabetes in Acute Pancreatitis Consortium (T1DAPC). Evaluating the Immunopathogenesis of Diabetes After Acute Pancreatitis in the Diabetes RElated to Acute Pancreatitis and Its Mechanisms Study: From the Type 1 Diabetes in Acute Pancreatitis Consortium. *Pancreas* 2022; **51**: 580-585 [PMID: 36206462 DOI: 10.1097/MPA.0000000000002076]

81 **Dungan KM**, Hart PA, Andersen DK, Basina M, Chinchilli VM, Danielson KK, Evans-Molina C, Goodarzi MO, Greenbaum CJ, Kalyani RR, Laughlin MR, Pichardo-Lowden A, Pratley RE, Serrano J, Sims EK, Speake C, Yadav D, Bellin MD, Toledo FGS; Type 1 Diabetes in Acute Pancreatitis Consortium (T1DAPC). Assessing the Pathophysiology of Hyperglycemia in the Diabetes RElated to Acute Pancreatitis and Its Mechanisms Study: From the Type 1 Diabetes in Acute Pancreatitis Consortium. *Pancreas* 2022; **51**: 575-579 [PMID: 36206461 DOI: 10.1097/MPA.0000000000002074]

82 **Tirkes T**, Chinchilli VM, Bagci U, Parker JG, Zhao X, Dasyam AK, Feranec N, Grajo JR, Shah ZK, Poullos PD, Spilseth B, Zaheer A, Xie KL, Wachsman AM, Campbell-Thompson M, Conwell DL, Fogel EL, Forsmark CE, Hart PA, Pandol SJ, Park WG, Pratley RE, Yazici C, Laughlin MR, Andersen DK, Serrano J, Bellin MD, Yadav D; Type 1 Diabetes in Acute Pancreatitis Consortium (T1DAPC). Design and Rationale for the Use of Magnetic Resonance Imaging Biomarkers to Predict Diabetes After Acute Pancreatitis in the Diabetes RElated to Acute Pancreatitis and Its Mechanisms Study: From the Type 1 Diabetes in Acute Pancreatitis Consortium. *Pancreas* 2022; **51**: 586-592 [PMID: 36206463 DOI: 10.1097/MPA.0000000000002080]

World Journal of Gastroenterology

Submit a Manuscript: https://www.f6publishing.com

World J Gastroenterol 2023 July 28; 29(28): 4416-4432

DOI: 10.3748/wjg.v29.i28.4416

ISSN 1007-9327 (print) ISSN 2219-2840 (online)

ORIGINAL ARTICLE

Basic Study

γ-aminobutyric acid B2 receptor: A potential therapeutic target for cholangiocarcinoma in patients with diabetes mellitus

Charupong Saengboonmee, Supannika Sorin, Sakkarn Sangkhamanon, Surang Chomphoo, Somsiri Indramanee, Wunchana Seubwai, Kanyarat Thithuan, Ching-Feng Chiu, Seiji Okada, Marie-Claude Gingras, Sopit Wongkham

Specialty type: Gastroenterology and hepatology

Provenance and peer review: Invited article; Externally peer reviewed.

Peer-review model: Single blind

Peer-review report's scientific quality classification

Grade A (Excellent): A
Grade B (Very good): 0
Grade C (Good): C, C
Grade D (Fair): D
Grade E (Poor): 0

P-Reviewer: Liao Z, Singapore; Rizzo A, Italy; Zhao W, China

Received: February 23, 2023
Peer-review started: February 23, 2023
First decision: May 16, 2023
Revised: June 5, 2023
Accepted: July 5, 2023
Article in press: July 5, 2023
Published online: July 28, 2023

Charupong Saengboonmee, Supannika Sorin, Somsiri Indramanee, Kanyarat Thithuan, Sopit Wongkham, Department of Biochemistry, Faculty of Medicine, Khon Kaen University, Khon Kaen 40002, Thailand

Charupong Saengboonmee, Supannika Sorin, Sakkarn Sangkhamanon, Somsiri Indramanee, Wunchana Seubwai, Sopit Wongkham, Center for Translational Medicine, Faculty of Medicine, Khon Kaen University, Khon Kaen 40002, Thailand

Charupong Saengboonmee, Supannika Sorin, Sakkarn Sangkhamanon, Somsiri Indramanee, Wunchana Seubwai, Sopit Wongkham, Cholangiocarcinoma Research Institute, Khon Kaen University, Khon Kaen 40002, Thailand

Sakkarn Sangkhamanon, Department of Pathology, Faculty of Medicine, Khon Kaen University, Khon Kaen 40002, Thailand

Surang Chomphoo, Department of Anatomy, Faculty of Medicine, Khon Kaen University, Khon Kaen 40002, Thailand

Wunchana Seubwai, Department of Forensic Medicine, Faculty of Medicine, Khon Kaen University, Khon Kaen 40002, Thailand

Ching-Feng Chiu, Graduate Institute of Metabolism and Obesity Sciences, Taipei Medical University, Taipei 11031, Taiwan

Seiji Okada, Division of Hematopoiesis, Joint Research Center for Human Retrovirus Infection, Kumamoto University, Kumamoto 860-0811, Japan

Marie-Claude Gingras, Human Genome Sequencing Center, Department of Human and Molecular Genetics, Baylor College of Medicine, Houston, TX 77030, United States

Marie-Claude Gingras, Michael E. DeBakey Department of Surgery, Baylor College of Medicine, Houston, TX 77030, United States

Corresponding author: Charupong Saengboonmee, MD, PhD, Doctor, Lecturer, Department of Biochemistry, Faculty of Medicine, Khon Kaen University, 123 Mitraphap Highway, Khon Kaen 40002, Thailand. charusa@kku.ac.th

Abstract

BACKGROUND

The association between diabetes mellitus (DM) and the increased risk and progression of cholangiocarcinoma (CCA) has been reported with unclear underlying mechanisms. Previous studies showed that γ-aminobutyric acid (GABA) B2 receptor (GABBR2) was upregulated in CCA cells cultured in high glucose (HG) conditions. Roles of GABA receptors in CCA progression have also been studied, but their association with DM and hyperglycemia in CCA remains unclarified.

AIM

To investigate the effects of hyperglycemia on GABBR2 expression and the potential use of GABBR2 as a CCA therapeutic target.

METHODS

CCA cells, KKU-055 and KKU-213A, were cultured in Dulbecco Modified Eagle's Medium supplemented with 5.6 mmol/L (normal glucose, NG) or 25 mmol/L (HG) glucose and assigned as NG and HG cells, respectively. GABBR2 expression in NG and HG cells was investigated using real-time quantitative polymerase chain reaction and western blot. Expression and localization of GABBR2 in CCA cells were determined using immunocytofluorescence. GABBR2 expression in tumor tissues from CCA patients with and without DM was studied using immunohistochemistry, and the correlations of GABBR2 with the clinicopathological characteristics of patients were analyzed using univariate analysis. Effects of baclofen, a GABA-B receptor agonist, on CCA cell proliferation and clonogenicity were tested using the MTT and clonogenic assays. Phospho-kinases arrays were used to screen the affected signaling pathways after baclofen treatment, and the candidate signaling molecules were validated using the public transcriptomic data and western blot.

RESULTS

GABBR2 expression in CCA cells was induced by HG in a dose- and time-dependent manner. CCA tissues from patients with DM and hyperglycemia also showed a significantly higher GABBR2 expression compared with tumor tissues from those with euglycemia ($P < 0.01$). High GABBR2 expression was significantly associated with a poorer non-papillary histological subtype but with smaller sizes of CCA tumors ($P < 0.05$). HG cells of both tested CCA cell lines were more sensitive to baclofen treatment. Baclofen significantly suppressed the proliferation and clonogenicity of CCA cells in both NG and HG conditions ($P < 0.05$). Phospho-kinase arrays suggested glycogen synthase kinase 3 (GSK3), β-catenin, and the signal transducer and activator of transcription 3 (STAT3) as candidate signaling molecules under the regulation of GABBR2, which were verified in NG and HG cells of the individual CCA cell lines. Cyclin D1 and c-Myc, the common downstream targets of GSK3/β-catenin and STAT3 involving cell proliferation, were accordingly downregulated after baclofen treatment.

CONCLUSION

GABBR2 is upregulated by HG and holds a promising role as a therapeutic target for CCA regardless of the glucose condition.

Key Words: Baclofen; Cholangiocarcinoma; Diabetes mellitus; Drug repurposing; Hyperglycemia; Gamma-aminobutyric acid

©The Author(s) 2023. Published by Baishideng Publishing Group Inc. All rights reserved.

Core Tip: Diabetes mellitus is associated with an increased risk and progression of cholangiocarcinoma (CCA). The γ-aminobutyric acid (GABA) B2 receptor (GABBR2) was upregulated in CCA cells cultured in high glucose and in CCA tissues from patients with hyperglycemia. High GABBR2 expressions were significantly correlated with a non-papillary histotype and smaller sizes of CCA tumors. The treatment of baclofen, a GABA-B receptor agonist, significantly suppressed CCA cell proliferation and clonogenicity, suggesting that GABBR2 is a potential target for CCA treatment. Baclofen inhibited multiple kinases and signal transducers in CCA, resulting in downregulated downstream target proteins involving cell proliferation and suppression of CCA cell growth.

Citation: Saengboonmee C, Sorin S, Sangkhamanon S, Chomphoo S, Indramanee S, Seubwai W, Thithuan K, Chiu CF, Okada S, Gingras MC, Wongkham S. γ-aminobutyric acid B2 receptor: A potential therapeutic target for cholangiocarcinoma in patients with diabetes mellitus. *World J Gastroenterol* 2023; 29(28): 4416-4432
URL: https://www.wjgnet.com/1007-9327/full/v29/i28/4416.htm
DOI: https://dx.doi.org/10.3748/wjg.v29.i28.4416

INTRODUCTION

Diabetes mellitus (DM) is a global public health problem, and its incidence is increasing every year[1]. The associations between DM and cancers have been recognized for decades from epidemiological observations[2,3]; however, the molecular mechanisms underlying the linkage are not fully elucidated. Liver cancers, including hepatocellular carcinoma and cholangiocarcinoma (CCA), are among the high-risk malignancies developing in patients with DM[4-6]. DM is not only associated with an increased risk of CCA but also associated with a poor survival of patients who have a poorly controlled blood glucose level[7]. Individuals with DM infected with *Opisthorchis viverrine* (*O. viverrini*), a carcinogenic liver fluke, are at a greater risk of developing CCA compared to those either with liver fluke infection or having DM alone[8]. The hamster CCA carcinogenesis model also showed that hamsters with DM and *O. viverrini* infection had more hepatic morbidities compared with those infected with *O. viverrini* or having DM alone[9]. CCA once developed, itself, has a poor prognosis, and the 5-year survival rate of all types is approximately 10%[10]. The attempts to investigate novel medications, *e.g.*, targeted therapy[11] or immunotherapy[12-14], reported limited efficacy or benefit for a particular population. Other underlying factors of patients have been reported to influence the progression of CCA. In line with this, the study in patients with CCA who have DM also reported that DM is associated with a shorter overall survival and is an independent prognostic factor for patients with CCA[7].

Previous studies by the current authors found that diabetogenic glucose concentration is a promoting factor for CCA aggressiveness[15,16]. High glucose (HG) promotes CCA proliferation and metastatic potential by regulating several signaling pathways, such as the signal transducer and activator of transcription 3 (STAT3)[15,17] and the nuclear factor-kappa B pathways[18]. HG also promotes cell cycle progression by enhancing cell cycle machinery proteins, namely, cyclin D1, cyclin E, cyclin A, and cyclin-dependent kinase 2, suggesting potential targets for CCA treatment in patients with DM[19]. Transcriptomic analysis of CCA cells cultured in HG *vs* normal glucose (NG) also showed several potential targets for CCA under diabetogenic glucose conditions. Among the top 5 upregulated genes, γ-aminobutyric acid (GABA) B2 receptor (GABBR2) is one of the promising therapeutic targets that are striking[18]. Given that GABBR2 is upregulated in CCA cells cultured in HG, and both agonist and antagonist of this receptor are clinically available, GABBR2 is thus a great potential target for drug repurposing for CCA treatment.

GABBR2 is a G-protein coupled receptor for GABA, an inhibitory neurotransmitter abundantly found in the central nervous system[20-22]. GABBR2 is also expressed in the gastrointestinal tract and is speculated to be important for the differentiation of several gastrointestinal epithelial cells[23,24], including cholangiocytes[25]. The roles of GABBR2 outside the central nervous system, however, are not fully understood. As a G-protein coupled receptor, GABBR2 can interact with various adaptor proteins and then signal the different downstream pathways[23]. Previous studies in CCA tissues showed that only the GABA-B receptor was differentially expressed between CCA cells and adjacent normal cholangiocytes among all subtypes of receptors (GABA-A, GABA-B, and GABA-C receptors)[26], suggesting its potential as a therapeutic target. Treatment of CCA cells with GABA showed the suppression of growth and invasive ability[26-28]. Which GABA-B receptor subtypes are responsible for the suppression of CCA aggressiveness, however, remains unclear. In contrast, in some cancers, GABA exerted pro-tumor effects on cancer cells[29], and activating the GABA-B receptor can promote the migration of cancer cells[30]. These controversial findings and the finding that HG enhanced the expression of GABBR2 in CCA cells have led to the investigation of the roles of GABBR2 in CCA under diabetic conditions. Discovering the significance of GABBR2 in CCA, especially in patients with DM, might suggest the opportunities to improve the therapeutic outcome of CCA by repurposing GABA-B receptor agonists available in clinical practice.

MATERIALS AND METHODS

CCA tissues and clinicopathological data

CCA tissues were obtained from patients who underwent surgical resection at Srinagarind Hospital, Faculty of Medicine, and archived at the Cholangiocarcinoma Research Institute, Khon Kaen University. Clinical and pathological data, including preoperative fasting blood glucose (FBG) and diabetes status, were retrieved from the medical records of Srinagarind Hospital. Patients with DM and preoperative FBG ≥ 126 mg/dL were defined as having DM, while those who had FBG < 126 mg/dL were defined as having no DM[31]. Written informed consent was obtained from all participants. The protocol of the study has been reviewed and approved by the Khon Kaen University Ethics Committee for Human Research (approval No. HE641441), based on the Declaration of Helsinki and the ICH-Good Clinical Practice Guidelines.

CCA cell lines and cell culture

CCA cell lines, KKU-055 and KKU-213A, were established from Thai CCA patients[32] and obtained from the Japanese Collection of Research Bioresources Cell Bank (Osaka, Japan). Cells were cultured in Dulbecco Modified Eagle's Medium (DMEM, Gibco, Carlsbad, CA), supplemented with 10% fetal bovine serum (Gibco) and 1% antibiotic-antimycotic (Gibco). Cells were cultured in DMEM containing 5.6 mmol/L glucose (NG) and 25 mmol/L (HG) for at least 5 passages and assigned as NG and HG cells, respectively[15,18]. Cells were subcultured when the confluence reached 80%. HG-induced GABBR2 expression was done by sequentially culturing NG cells in DMEM with 5.6, 15, and 25 mmol/L glucose for at least 5 passages, and cell lysates were collected timely for the experiments.

Reverse transcription-quantitative polymerase chain reaction

Reverse transcription-quantitative polymerase chain reaction (RT-qPCR) was used to determine GABBR2 mRNA expression in CCA cells. Confluent CCA cells were lysed using TRIzol (ThermoFisher Scientific, Waltham, MA), and RNA extraction was performed according to the manufacturer recommendations. Total RNA was reverse-transcribed using the MultiScribe Reverse Transcriptase Kit (ThermoFisher Scientific) and qPCR was performed using LightCycler® 480 System (Roche Diagnostics, Rotkreuz, Switzerland). Primers for GABBR2 are: Forward, 5′-TGGAGGCGTCT-GTCCATCCGT-3′ and reverse, 5′-GTCTTGCGTCAGCGTGCCCA-3′. β2-microglobulin was used as the internal control, and the primer sequences are: Forward, 5′-AAGATGAGTATGCCTGCCG-3′ and reverse, 5′-CGGCATCTTCAAACCTCC-3′.

Sodium dodecyl sulfate-polyacrylamide gel electrophoresis and western blot analysis

Primary antibodies used to detect the proteins by western blot were: GABBR2 (1:500, Proteintech, Rosemont, IL), pSTAT3 (Y705) (1:500, Cell Signaling Technology, Danvers, MA), pSTAT3 (S727) (1:500, Cell Signaling Technology), STAT3 (1:1000, Cell Signaling Technology), p-glycogen synthase kinase 3 (GSK3)α/β (1:1000, Cell Signaling Technology), GSK3α /β (1:1000, Cell Signaling Technology), β-catenin (1:1000, Cell Signaling Technology), cyclin D1 (1:1000, Cell Signaling Technology), c-Myc (1:500, Santa Cruz Biotechnology, Dallas, TX), and glyceraldehyde-3-phosphate dehydrogenase (GAPDH) (1:10000, Millipore Sigma, Burlington, MA).

Cell lysates were collected in radioimmunoprecipitation assay (RIPA) lysis buffer containing protease inhibitor (Sigma Aldrich, St. Louis, MO) and phosphatase inhibitor (Sigma Aldrich, St. Louis, MO). NG and HG cells of both cell lines were lysed after culture in their respective media at 72 h after incubation for determination of GABBR2 expression. Cells treated with baclofen (Sigma) were collected in the lysates at 24, 48, and 72 h after incubation with the drug. Total proteins (20 μg/well) were electrophoresed on a 10% sodium dodecyl sulfate-polyacrylamide gel electrophoresis and transferred to Amersham-Hybond® polyvinylidene fluoride membrane (GE Healthcare, Buckinghamshire, United Kingdom). After blocking with 5% skim milk in Tris-buffered saline with 0.1% Tween-20 for 1 h at room temperature, the membranes were then incubated with the primary antibodies at 4 °C overnight, followed by incubation with horseradish peroxidase-conjugated secondary antibodies for 1 h at room temperature. Enhanced Chemiluminescence kit (Millipore Sigma, Burlington, MA) was applied to develop the signals, which were detected using ImageQuant® LAS 400 (GE Healthcare, Uppsala, Sweden). Band intensities of proteins were quantified using Image J (National Institute of Health, Bethesda, MD), in which the intensities of GAPDH were used as the loading controls.

Immunocytofluorescence

CCA (NG and HG) cells were seeded into 48 well plates at a density of 5000 cells/well and incubated for 72 h. After removing media and washing with phosphate-buffered saline, cells were fixed using 4% paraformaldehyde for 30 min at room temperature, and non-specific antigens were blocked using 5% skim milk. Anti-GABBR2 antibody (1:200) was then incubated at 4 °C overnight, and Alexa-Fluo-488 conjugated secondary antibody (Invitrogen, Waltham, MA) was applied and incubated at room temperature for 1 h. Fluorescent signals were detected using a fluorescent microscope (Nikon Ti-U Inverted Fluorescence Microscope, 20X) using NIS-Elements imaging software. Mean fluorescent intensities were calculated using Image J (National Institute of Health).

Immunohistochemistry

Immunohistochemical staining for GABBR2 was performed according to the standard immunohistochemistry protocol. Briefly, paraffin-embedded formalin-fixed CCA tissues (6 μm thickness) were rehydrated using serial-graded ethanol. Antigens were retrieved by heating the sample in 0.1 M citrate buffer (pH = 6.0) in a pressure cooker for 5 min. Endogenous peroxidase was blocked using 3% H_2O_2 in methanol, and non-specific antigens were blocked using 1% fetal bovine serum (Gibco). CCA tissues were then incubated with anti-GABBR2 antibody (1:100, Abcam, Cambridge, MA) at room temperature overnight in a moisture chamber. In the DAKO EnVision™ + System, horseradish peroxidase-conjugated secondary antibody (Dako, Carpinteria, Denmark) was then applied and further incubated at room temperature for 1 h. The signals were developed using 3,3′-diaminobenzidine (DAB, Sigma, St. Louise, MO) and graded as the IHC index (intensity × frequency; where intensity: No staining = 0, mild = 1, moderate = 2, strong =3; and frequency: 0% = 0, 0%-25% = 1+, 25%-50% = 2+, > 50% = 3+), by two researchers (CS and SaS). Microscopic photographs were obtained using Nikon NIS-Elements software (Nikon, Tokyo, Japan). High and low expression of GABBR2 in CCA tissues was classified by using a median score of IHC index as a cut-off point.

Baclofen treatment and proliferation assay

CCA (NG and HG) cells (1 x 10^3 cells/well) were seeded into 96 well plates and incubated overnight, and then cells were incubated with complete media containing varied concentrations of baclofen (Sigma), a GABA-B receptor agonist, for 72 h. Then, 3-(4,5-dimethylthiazol-2-yl)-2,5-diphenyltetrazolium bromide (MTT, Invitrogen, Carlsbad, CA) was added at a final concentration of 0.5 mg/mL and further incubated for 4 h in a 37 °C incubator. Formazan crystals were dissolved in dimethyl sulfoxide, and OD540 was measured using a microplate reader (Tecan, Männedorf, Switzerland).

To determine the possible time-dependent effect of the GABA-B receptor agonist, NG and HG cells of KKU-055 were incubated with 1000 μM baclofen, and KKU-213A cells were incubated with 800 μM baclofen for 24, 48, and 72 h. MTT assay was then performed at each time point to determine the effect of baclofen on CCA cell growth in different glucose conditions.

Clonogenic assay

NG and HG cells of KKU-055 and KKU-213A in control media or media containing 800 μM baclofen were seeded into a 24-well plate at a density of 200 cells/well. Cells were allowed to grow and form the colonies for 7 d before being fixed with 4% paraformaldehyde. The colonies were stained with 0.5% crystal violet and counted under a light microscope. Only a cluster with > 50 cells was counted as a colony.

Phospho-kinase arrays

The Proteome Profiler Human Phospho-Kinase Array Kit (#ARY003B, R&D system, Minneapolis, MN) was used to screen the signaling pathways affected by baclofen. HG cells (5×10^5 cells) of KKU-213A were seeded into 6-cm dishes and allowed to adhere overnight. Then, cells were incubated with 800 μM baclofen for 24 h. Cell lysates (control and treatment) were collected using RIPA buffer containing protease and phosphatase inhibitors. Then, 200 μg of total proteins for each group were incubated with the membrane arrays overnight following the recommendation of the manufacturer. The membranes were then incubated with a cocktail-detection antibody and streptavidin-horseradish peroxidase. The signals were detected with Chemireagent provided in the same kit and quantified using an ImageQuant® LAS 400 (GE Healthcare). The candidate pathways were then selected and verified in individual cell lines cultured in different glucose conditions by western blot.

Transcriptomic analysis

The GEO datasets were retrieved using GEO2R[33]. The GSE89749 (n = 120)[34] dataset of Thai CCA cases was used for the analysis of the correlation between the expression levels of GABBR2, STAT3, GSK3B, CTNNB1, MYC, and CCND1 using Pearson's correlation coefficient.

Statistical analysis

All quantitative data, presented as the mean ± SD, were analyzed using student's t-test, one-way ANOVA, or two-way ANOVA with Tukey's multiple comparisons using IBM SPSS Statistics for Windows, version 28.0 (IBM, Armonk, NY). Univariate analysis was performed using the Chi-square test or Fisher's Exact test regarding the assumption of each model. Data visualization was done using GraphPad Prism 9 (Dotmatics, San Diego, CA). Statistical significance was considered at $P < 0.05$.

RESULTS

HG induces expression of GABBR2 in CCA cell lines

From the previous comparative transcriptomic analysis, GABBR2 is one of the top 5 upregulated genes in KKU-213A cells cultured in HG compared to those cultured in NG conditions[18]. To verify the results from the transcriptomics, determination of GABBR2 expression in different CCA cell lines was performed. GABBR2 expression was dose-dependently upregulated by various glucose concentrations ranging from 5.6 mmol/L to 25 mmol/L at both mRNA (Figure 1A) and protein levels (Figures 1B and C) in both KKU-055 and KKU-213A cells. As the expression of GABBR2 in both CCA cell lines was significantly different between those cultured in 5.6 mmol/L and 25 mmol/L ($P < 0.05$), these two glucose conditions were included in a further study and assigned as NG and HG cells, respectively.

Immunocytofluorescent staining for GABBR2 in both cell lines showed that GABBR2 was localized at membranous and cytoplasmic compartments of CCA cells (Figure 1D). Mean fluorescent intensities of GABBR2 in HG cells of both cell lines were significantly higher than those in NG cells ($P < 0.05$) (Figure 1E) and were concordant with the expression levels determined by RT-qPCR and western blot.

Hyperglycemia induces upregulation of GABBR2 in tumor tissues from CCA patients

To affirm that HG-induced GABBR2 expression in CCA cell lines is translatable to patients with CCA, the tumor tissues from patients with pre-operative hyperglycemia (FBG ≥ 126 mg/dL) and euglycemia (FBG < 126 mg/dL) were studied. Immunohistochemistry of CCA tissues revealed that GABBR2 was significantly upregulated in tumor tissues from patients with DM who had hyperglycemia compared to those without DM ($P < 0.01$) (Figures 1F-G). Cytoplasmic localization of GABBR2 was observed similarly to that found in CCA cell lines.

High GABBR2 expression is associated with a poor histological type but smaller sizes of CCA tumors

To investigate the clinical significance of GABBR2 expression, the associations between GABBR2 expression in CCA tissues and the clinicopathological characteristics of patients were analyzed by univariate analysis. High GABBR2 expression was significantly associated with a non-papillary histological type of CCA ($P < 0.05$). In contrast, high GABBR2 expression was significantly associated with CCA tumor sizes smaller than 7 cm in the longest diameter ($P < 0.05$) (Table 1), suggesting that GABBR2 is a potential target for CCA treatment.

HG cells of CCA are more sensitive to a GABA-B receptor agonist than NG cells

As GABBR2 was upregulated in HG cells and CCA tissues from patients with hyperglycemia, the therapeutic potential of using GABBR2 as a target was investigated. Baclofen, a GABA-B receptor agonist, was applied in NG and HG cells of both CCA cell lines with various concentrations and time points. The treatment of baclofen did not alter the expression levels of GABBR2 in both NG and HG cells (data not shown). The proliferation of both NG and HG cells of KKU-055 and

Table 1 Univariate analysis of γ-aminobutyric acid B2 receptor expression and clinicopathological characteristics of cholangiocarcinoma patients

Clinicopathological data	GABBR2 expression		*P* value
	High (IHC index ≥ 8)	Low (IHC index < 8)	
Diabetic status			
DM	13	2	0.109
Non-DM	8	7	
Sex			
Male	10	6	0.580
Female	8	3	
Survival			
≥ 5 mo	14	6	1.000
< 5 mo	7	3	
Histological type			
Papillary	4	6	0.030[a]
Non-papillary	17	3	
Histological grading			
Well differentiated	13	7	0.672
Moderately differentiated	5	1	
Poorly differentiated	3	1	
Tumor size (longest diameter)			
> 7 cm	6	7	0.020[a]
≤ 7 cm	15	2	
Regional lymph node involvement			
Yes	10	8	0.543
No	8	4	
Distant metastasis			
Metastasis	14	4	0.418
Non-metastasis	7	5	

[a]$P < 0.05$.
GABBR2: γ-aminobutyric acid B2 receptor.

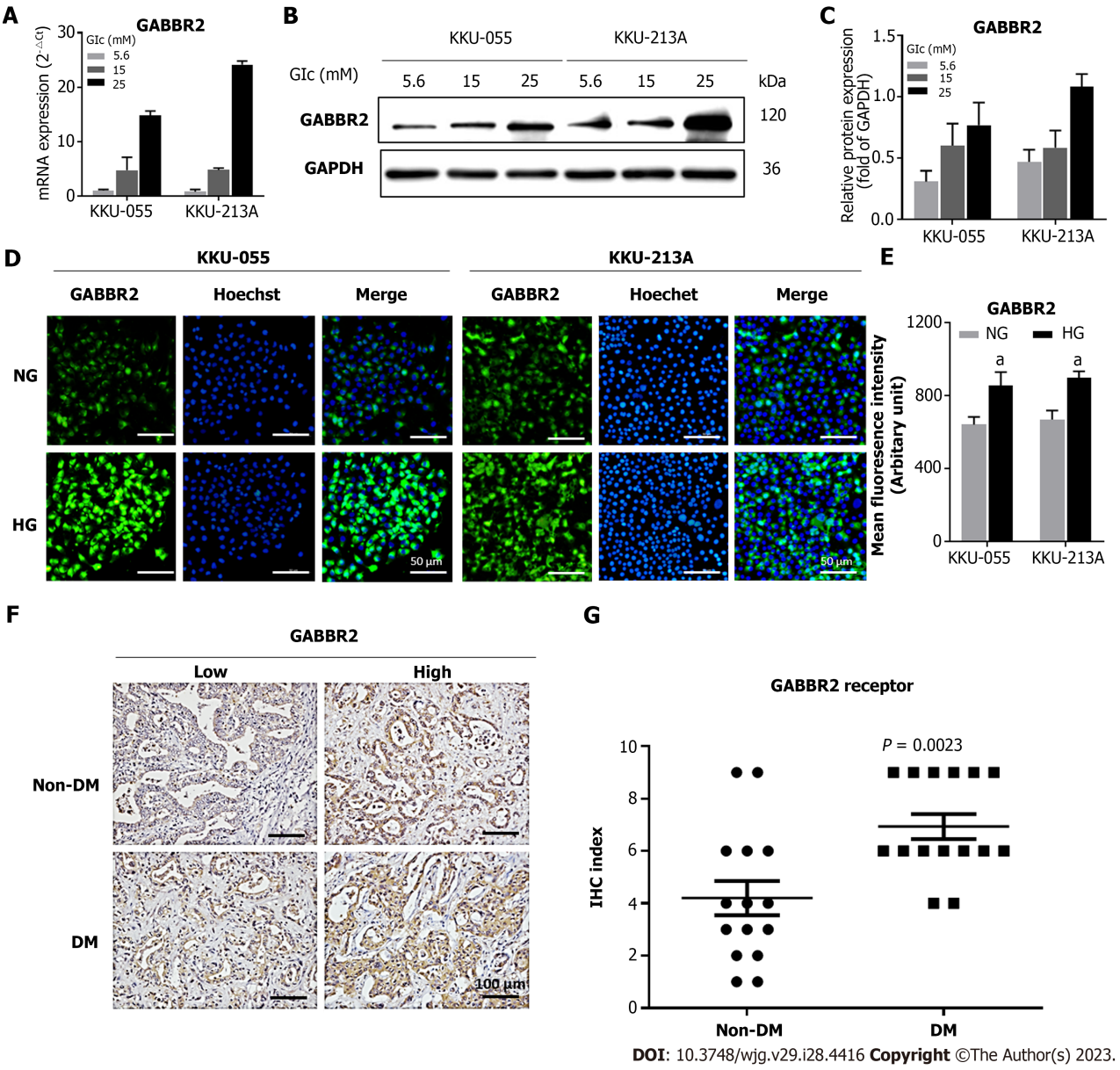
KKU-213A was significantly suppressed in a dose- and time-dependent manner, compared with the control group (Figures 2A and B). HG cells of both cell lines showed a significantly higher sensitivity to baclofen treatment at every dosage of baclofen and at 48 and 72 h of the incubation (Figures 2A and B).

Baclofen suppresses the colony formation of CCA cells

Baclofen treatment not only suppressed the proliferation of CCA cells, but the ability to form colonies was also inhibited. Clonogenicity of both NG and HG cells of KKU-055 and KKU-213A was significantly inhibited by baclofen treatment compared with the control group (Figures 2C and D).

Baclofen inhibits multiple kinases and signal transducers in CCA cells

To unveil the underlying mechanisms in which baclofen inhibits the proliferation of CCA cells, the phospho-kinase arrays were used to screen HG cells of KKU-213A with and without baclofen treatment. Phosphorylation of several kinases and signal transducers was suppressed in KKU-213A-HG after being treated with baclofen (Figures 3A and B). The kinases and signal transducers belonging to the same pathways and reported for their roles in CCA progression were prioritized and included for further verification in downstream experiments. By these criteria, GSK3α/β, β-catenin, and STAT3 were then included for validation in the individual CCA cell lines in different glucose conditions.



DOI: 10.3748/wjg.v29.i28.4416 Copyright ©The Author(s) 2023.

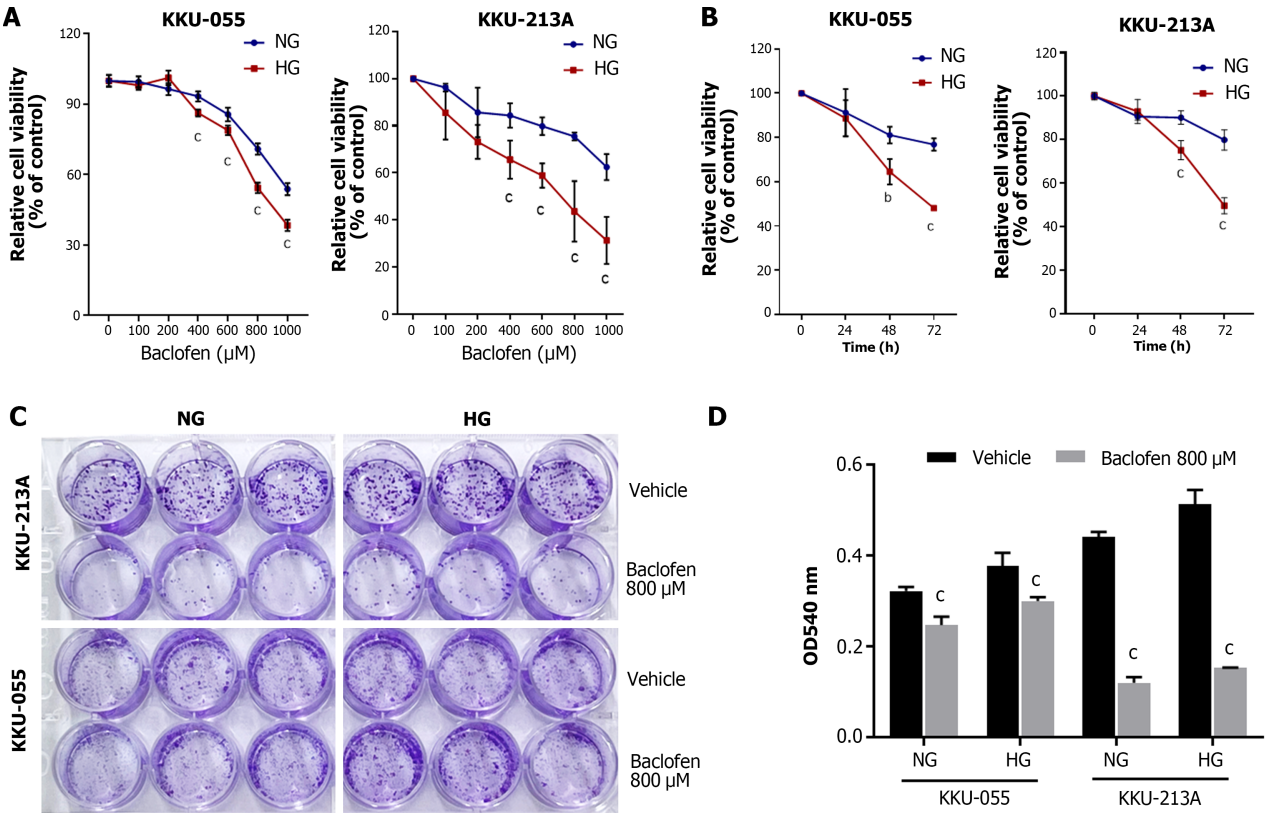
Figure 1 High glucose induces upregulation of γ-aminobutyric acid B2 receptor in cholangiocarcinoma. A-C: The expression of γ-aminobutyric acid B2 receptor (GABBR2) in cholangiocarcinoma (CCA) cell lines, KKU-055 and KKU-213A, is dose-dependently upregulated by glucose at both RNA (A) and protein (B-C) levels; D and E: Immunocytofluorescence shows the membranous and cytoplasmic localizations of GABBR2 in CCA cells, and those cultured in high glucose show significantly higher mean fluorescent intensities; F-G: GABBR2 in tumor tissues from CCA patients with hyperglycemia is also upregulated compared with those from patients without diabetes mellitus. Presented data are the average of three biological replications with triplicated experiments. NG: Normal glucose; HG: High glucose; Glc: Glucose; DM: Diabetes mellitus; GABBR2: γ-aminobutyric acid B2 receptor; GAPDH: Glyceraldehyde-3-phosphate dehydrogenase.

Expression of GABBR2 significantly correlates with STAT3 expression

The associations between GABBR2 and its signal transducers suggested by the phospho-kinase arrays were first verified for their mRNA expression using public transcriptomic databases. The expression of *GABBR2* at the RNA level was significantly correlated with the expression of *STAT3* in a transcriptomic analysis of clinical CCA samples from Thai patients ($P < 0.05$) (Figure 3C).

Baclofen suppresses STAT3 and GSK3/β-catenin signaling pathways

The effects of baclofen on the STAT3 and GSK3α/β/β-catenin signaling pathways were then validated in the individual CCA cell lines, both in NG and HG cells. Baclofen suppressed STAT3 phosphorylation at both Y705 and S272 positions and NG cells were affected the most in both cell lines. Phosphorylation of GSK3α/β was also decreased time-dependently in HG cells, and the levels of β-catenin were then accordingly decreased in both cell lines. The GSK3α/β/β-catenin signaling pathway was also inhibited in NG cells of both cell lines as shown by the decreased phosphorylation levels of GSK3α/β. Total β-catenin proteins, the GSK3α/β downstream target, were also decreased starting 24 h after treatment (Figures 4A and B).



DOI: 10.3748/wjg.v29.i28.4416 **Copyright** ©The Author(s) 2023.

Figure 2 Antiproliferative and anti-clonogenic effects of γ-aminobutyric acid-B receptor agonist. A and B: Baclofen, a γ-aminobutyric acid-B receptor agonist, exerts significant antiproliferative effects on cholangiocarcinoma (CCA) cells in a dose-dependent (A) and time-dependent (B) manner; C and D: CCA cells cultured in high glucose condition (HG) are more sensitive to baclofen than those cultured in normal glucose (NG). Baclofen also shows anti-clonogenic effects on both NG and HG cells of CCA. Presented data are representatives of three biological replications of each triplicated experiment with the same trends of results. $^{b}P < 0.01$, $^{c}P < 0.001$. NG: Normal glucose; HG: High glucose.

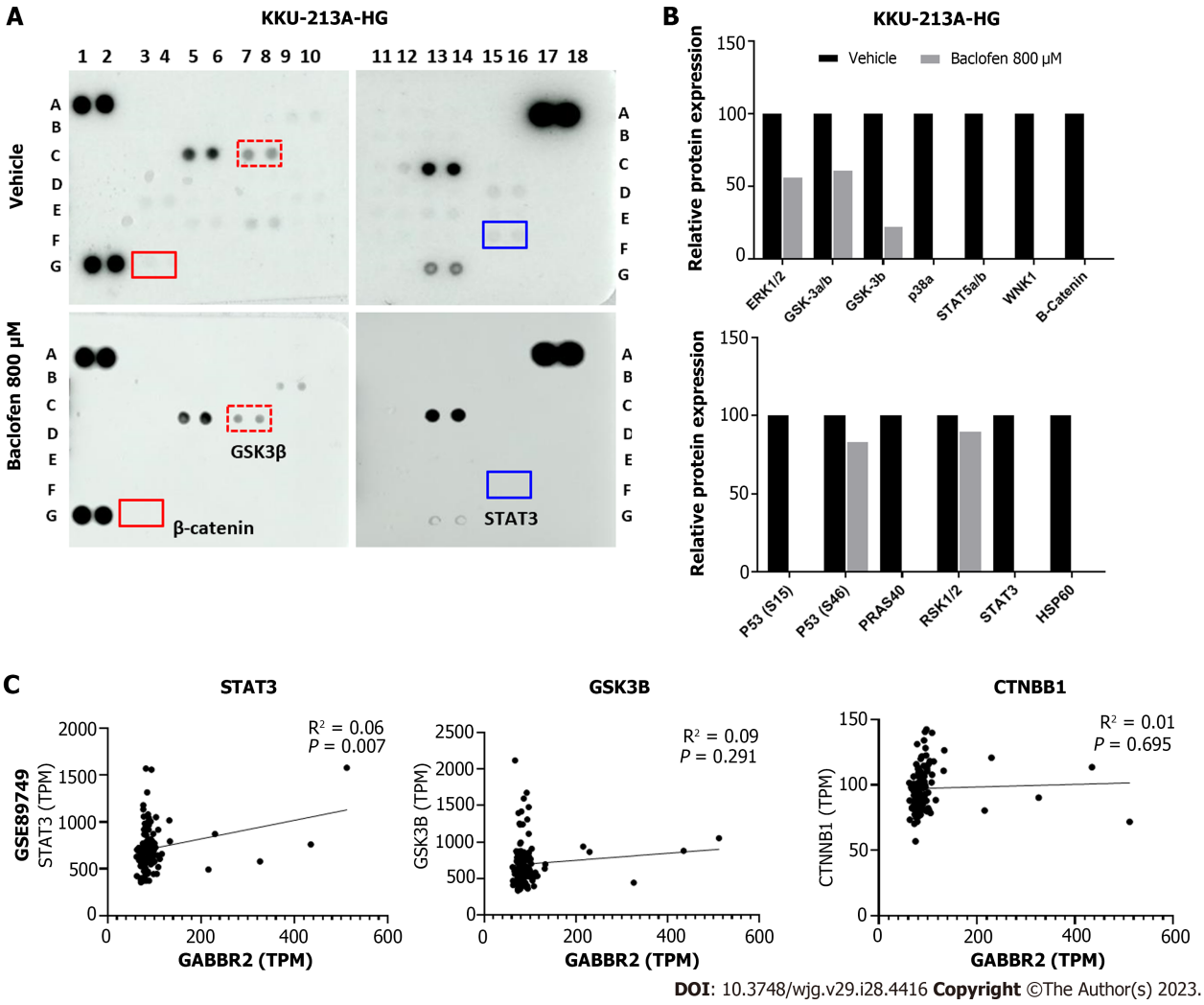
Baclofen suppresses c-Myc and cyclin D1 expression

According to the antiproliferative effects of baclofen *via* the suppression of GSK3α/β/β-catenin and STAT3 pathways, the common downstream targets of both pathways functioning in cell proliferation were then explored. Expression of c-Myc, a transcription factor involved in cell proliferation, and cyclin D1, a cell cycle regulatory protein, was examined for their correlation with GABBR2 at the mRNA and protein levels after baclofen treatment. Analyzing a public transcriptomic dataset, mRNA expression levels of *MYC* (encoding for c-Myc) and *CCND1* (encoding for cyclin D1) were not correlated with mRNA level of *GABBR2* (Supplementary Figure 1). However, both c-Myc and cyclin D1 expression at the protein level were suppressed at every time point after baclofen treatment in NG and HG cells of both CCA cell lines. Suppression of c-Myc was greater affected at the early time point in which cyclin D1 was gradually affected time-dependently in HG cells. The time-dependent suppression of c-Myc in NG cells after baclofen treatment was also observed (Figures 5A and B).

DISCUSSION

HG and hyperglycemia-induced aggressiveness of CCA cells has been reported with partially understood mechanisms [15,16,18,19]. The present study not only revealed the mechanisms by which HG activates the STAT3 and GSK3/β-catenin pathways, but also identified GABBR2 as the upstream receptor that is promising for CCA treatment, especially in patients with DM. Roles of GABA and its receptor have been studied in several types of cancer, including non-liver fluke-associated CCA[26-28,35]. The known mechanisms of actions of GABA and its receptor on CCA are by regulating several signaling pathways, *e.g.*, STAT3 and protein kinase A. This study, however, determined for the first time the association between hyperglycemia and the expression of GABBR2, and also identified GSK3/β-catenin signaling, an uncovered downstream pathway, that is modulated by GABBR2 in CCA. Roles of GABBR2 in the progression of CCA in both *in vitro* models and in the tumor tissues of CCA patients were also reported.

These current investigations first identified that GABBR2, a subtype of GABA-B receptor, was upregulated in CCA cells cultured in HG. This is of particular importance since approximately 60% of patients with CCA in Thailand had their blood glucose levels in a range of pre-DM and DM[36,37]. Targeting GABBR2 would then be beneficial to a substantial group of CCA patients. Univariate analysis revealed that high expression of GABBR2 in tumor tissues was associated

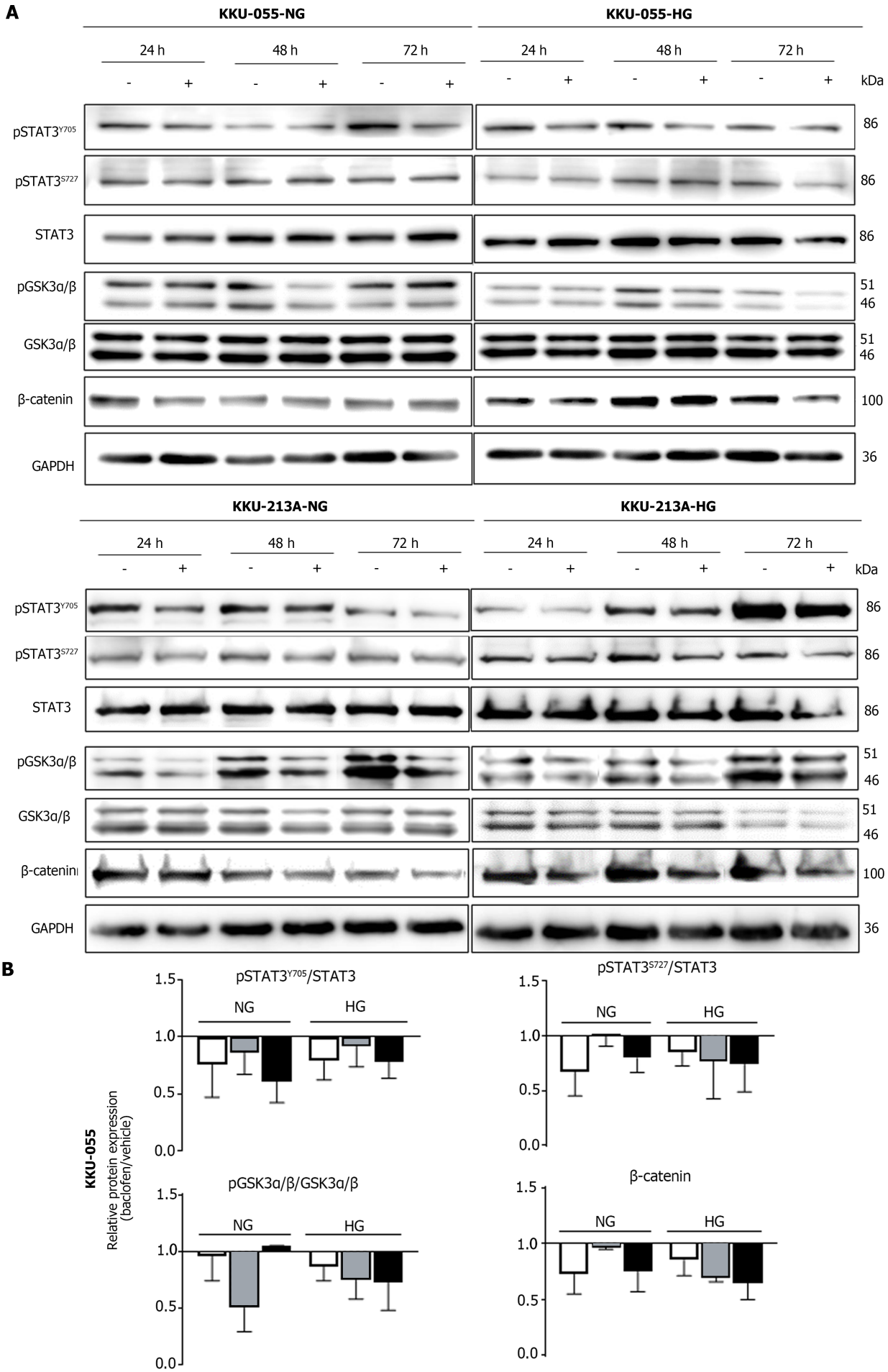


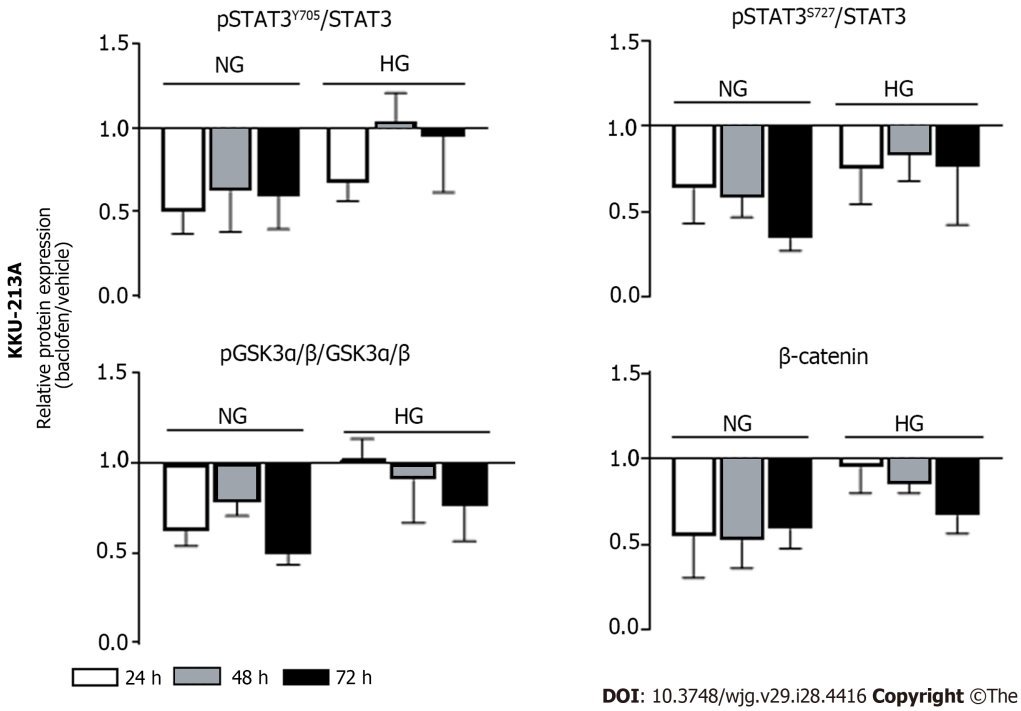
DOI: 10.3748/wjg.v29.i28.4416 **Copyright** ©The Author(s) 2023.

Figure 3 Baclofen inhibits the glycogen synthase kinase 3/β-catenin and signal transducer and activator of transcription 3 pathways. A and B: Phospho-kinase arrays reveal the inhibition of phosphorylation in multiple kinases and signal transducers; C: Glycogen synthase kinase 3 (GSK3)/β-catenin and signal transducer and activator of transcription 3 (STAT3) are included for further analysis as they are key pathways in cholangiocarcinoma (CCA) progression in which β-catenin and STAT3 are common targets of GSK3. RNA expression of γ-aminobutyric acid B2 receptor and that of STAT3 are significantly correlated in clinical CCA samples from Thai patients. HG: High glucose; GABBR2: γ-aminobutyric acid B2 receptor; GSK3: Glycogen synthase kinase 3; STAT3: Signal transducer and activator of transcription 3.

with a poorer histological subtype of CCA. High GABBR2 expression was associated with smaller tumor sizes compared with the group with low GABBR2 expression. These findings are in agreement with previous reports demonstrating that both high GABA-A or GABA-B receptors are associated with better prognostic outcomes for CCA patients[26,38]. The upregulated GABBR2 in CCA tissues of patients thus suggested a therapeutic strategy by using a natural GABA or even GABA receptor agonists. Patients with DM who have upregulated GABBR2 would, therefore, potentially benefit from targeting GABBR2 with available GABA or GABA analogs. The present study also found that HG cells of CCA with upregulated GABBR2 were more sensitive to baclofen, a GABA-B receptor agonist. This affirms the advantage of using GABA-B agonist as an add-on therapy for CCA treatment in patients with DM. As shown by western blot, the investigated signaling molecules were markedly suppressed in both NG and HG cells. This might be the result of the screening and recruitment of candidate pathways that were only from the HG cells whereas the signaling molecules in NG cells affected by baclofen were not screened and compared. Regardless of the glucose condition of the cell cultures, these results still verified that baclofen is effective for CCA treatment and is probably useful for CCA treatment in both patients with and without DM. As the available standard and developing treatment for CCA is of limited efficacy and needs more investigation[10-13], the findings in the present work may add value for alternative treatment of CCA. Especially, baclofen is a known drug in clinical practice in which its toxicity and therapeutic windows are known[39]. This medication is, therefore, highly promising for a repurposing aim. Of note, this study showed for the first time that a GABA receptor agonist is an alternative strategy to natural GABA treatment for CCA.

Suppression of GSK3/β-catenin, a new intracellular signaling mode under the regulation of GABBR2 in CCA, is shown in addition to the known affected STAT3 pathway[26]. Both GSK3/β-catenin and STAT3 are reported as crucial signaling pathways for CCA carcinogenesis and progression[40,41]. GSK3 is a kinase phosphorylating β-catenin for proteasomal degradation. The functions of GSK3 are inhibited by phosphorylation by its kinase regulators[42], hence decreased


A
KKU-055-NG
KKU-055-HG
24 h
48 h
72 h
kDa
pSTAT3Y705
pSTAT3S727
STAT3
pGSK3α/β
GSK3α/β
β-catenin
GAPDH
86
51
46
100
36
KKU-213A-NG
KKU-213A-HG
B
KKU-055
Relative protein expression (baclofen/vehicle)
pSTAT3Y705/STAT3
pSTAT3S727/STAT3
pGSK3α/β/GSK3α/β
β-catenin
NG
HG
1.5
1.0
0.5
0.0



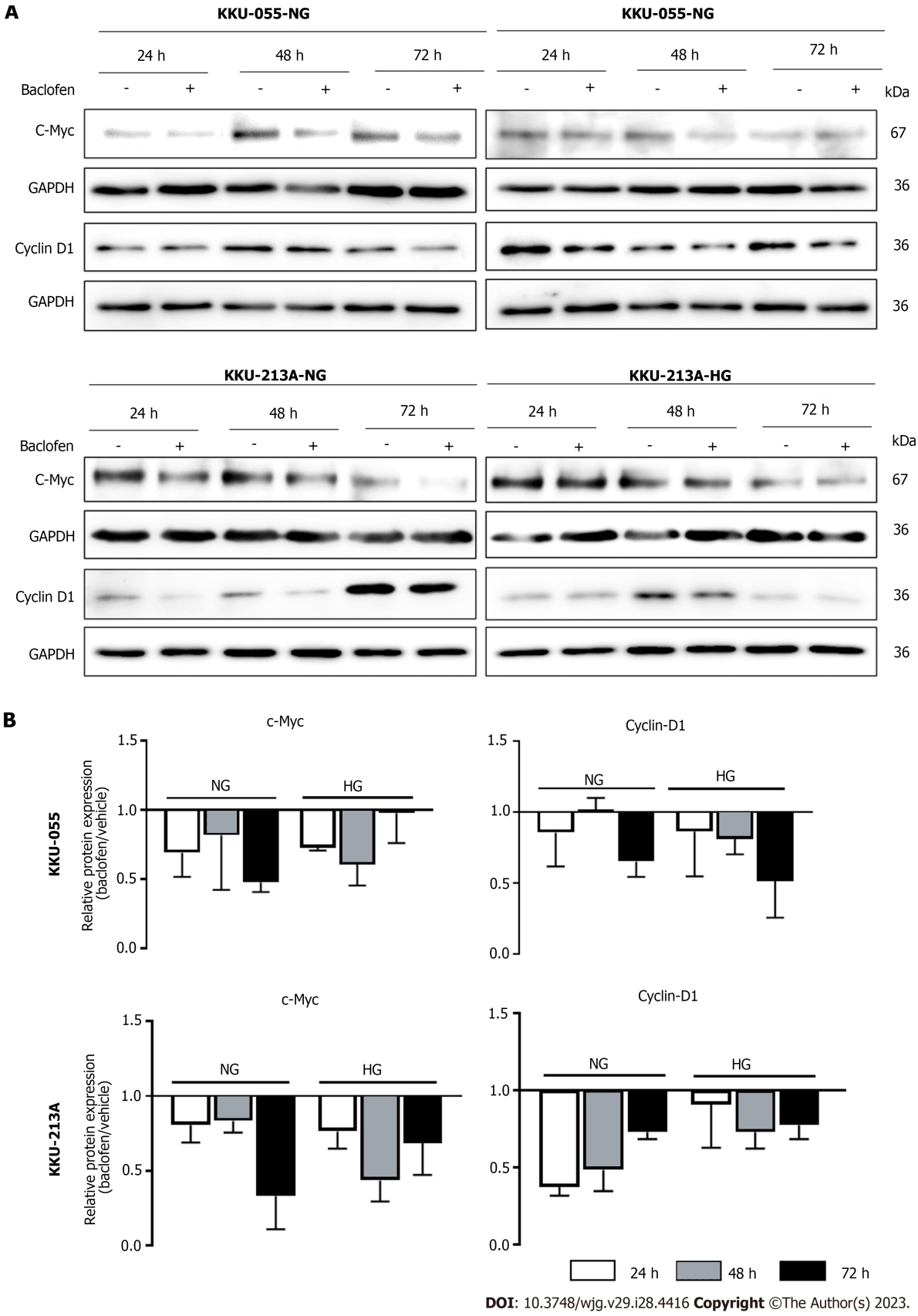
DOI: 10.3748/wjg.v29.i28.4416 **Copyright** ©The Author(s) 2023.

Figure 4 Baclofen suppresses the glycogen synthase kinase 3/β-catenin and signal transducer and activators of transcription 3 pathways. A and B: Phosphorylation of glycogen synthase kinase 3 (GSK3) and signal transducer and activators of transcription 3 is decreased after baclofen treatment in both cholangiocarcinoma cell lines, both cultured in normal glucose and high glucose conditions. Total β-catenin protein is also decreased consistently with the decreased phosphorylated GSK3α/β. Western blots show the representative of three biological replications with the same trends of results. Band intensities are the average of three biological replications which are normalized using the intensities of glyceraldehyde-3-phosphate dehydrogenase for each experiment. The levels of phosphorylated forms are normalized with the total forms of their corresponding proteins. NG: Normal glucose; HG: High glucose; GAPDH: Glyceraldehyde-3-phosphate dehydrogenase; GSK3: Glycogen synthase kinase 3; STAT3: Signal transducer and activator of transcription 3.

phosphorylated GSK3α/β in CCA cells after the baclofen treatment indicated the active state of GSK3. This is also evidenced by the decreased β-catenin, a GSK3 downstream target which is a known transcription factor for cell proliferation. Moreover, STAT3 phosphorylation was also inhibited after baclofen treatment, which is consistent with the previous findings in CCA cells treated with GABA. STAT3 has also been reported as an alternative downstream target of GSK3 phosphorylation[43]. The decreased levels of β-catenin and STAT3 phosphorylation in the present report might thus be a consequence of GSK3 inhibition by a GABBR2 agonist. As β-catenin and STAT3 control cell proliferation *via* the expression of c-Myc and cyclin D[44,45], these two common effector-proteins were also down-regulated after baclofen treatment. These suggested that the activation of GABBR2 protein by its natural or synthetic ligands might be a crucial step for the regulation of downstream signaling, although there is no correlation among *GABBR2*, *MYC*, and *CCND1* at the mRNA level. These findings not only add to the understanding of the molecular linkages among DM, hyperglycemia, and CCA progression but also imply the therapeutic strategies of the combined targeting multiple signaling pathways to improve CCA treatment outcomes. The schematic summary of the findings from the current study is depicted in Figure 6.

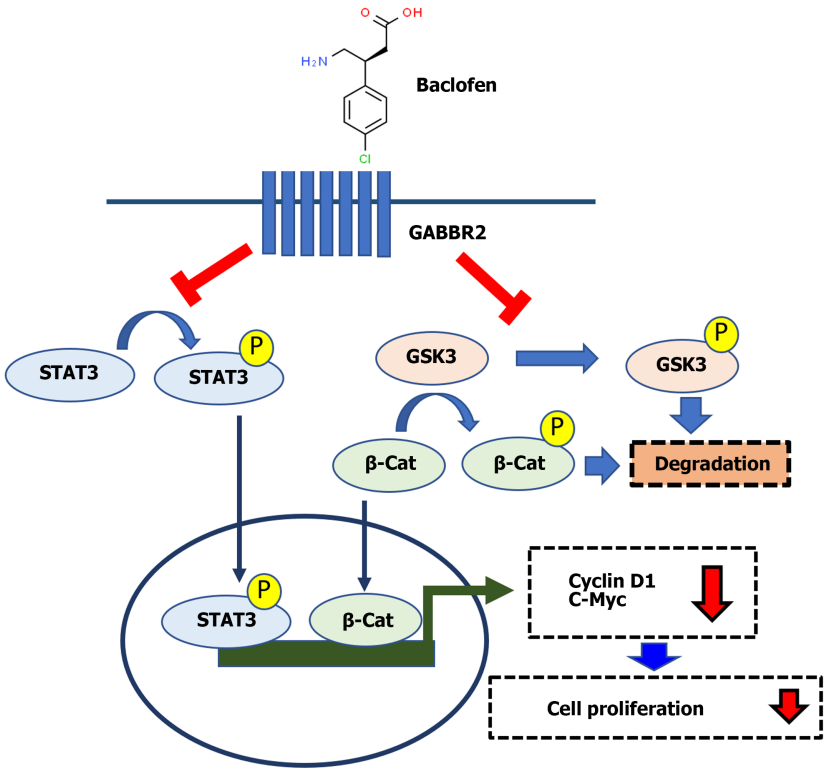
GABA is an inhibitory neurotransmitter mostly found in the central nervous system. It is a derivative of the non-essential amino acid glutamate and can be synthesized by converting glutamine as a precursor[29]. GABA functions by binding to its receptors which have three subtypes (GABA-A, GABA-B, and GABA-C receptors). Different GABA receptors are responsible for various physiological functions both within and outside the nervous system. While the GABA-A receptors are found to be important for hepatocytes[46], GABA-B receptors are also needed for the differentiation of biliary epithelial cells[25]. In addition to physiological roles, GABA and its receptors are also reported for both pro-tumor[29,30] and anti-tumor effects[28,47], depending on the cancer type. The previous study showed that all subtypes of GABA receptors were expressed in CCA cells[28]. Still, only GABA-B receptor was differentially expressed between CCA cells and normal adjacent cholangiocytes in tumor tissues from patients[26]. The GABA-B receptor then holds a high potential for targeting in CCA treatment. Treatment of GABA in CCA cells exerted antiproliferative[28] and anti-invasive effects[35] on CCA cells by inhibiting multiple pathways, *i.e.*, cyclic AMP–dependent regulation of the protein kinase A/extracellular signal-regulated kinase (PKA/ERK)[27,28] and STAT3[26,38] pathways. Low GABA-A and GABAB-B receptor expression was also associated with a poor prognosis in CCA patients[38]. The roles of GABA receptors under hyperglycemia in CCA patients with DM are for the first time reported in the present study. The study of a GABA-B receptor agonist, instead of using natural GABA, is also reiterated and suggested for a potential translation to a clinical study.

This study, nevertheless, has some limitations. First, all CCA tissues and CCA cell lines used in the study were derived from *O. viverrini*-associated CCA patients. As different molecular backgrounds of CCA in different areas have been noted [48,49], the current findings may be needed to verify in CCA from the non-endemic areas of liver fluke. Noteworthy, the



DOI: 10.3748/wjg.v29.i28.4416 **Copyright** ©The Author(s) 2023.

Figure 5 Baclofen suppresses c-Myc and cyclin D1expression in cholangiocarcinoma cells. A and B: The expression of c-Myc and cyclin D1, key proteins for cell proliferation, is suppressed in both cholangiocarcinoma cell lines after baclofen treatment. Western blots show the representatives of three biological replications with the same trends of results. Band intensities are the average of three biological replications which are normalized using the intensities of glyceraldehyde-3-phosphate dehydrogenase for each experiment. NG: Normal glucose; HG: High glucose; GAPDH: Glyceraldehyde-3-phosphate dehydrogenase.



DOI: 10.3748/wjg.v29.i28.4416 **Copyright** ©The Author(s) 2023.

Figure 6 Schematic summary of the effects of high glucose on γ-aminobutyric acid B2 receptor expression and the effects of baclofen on cholangiocarcinoma cells. High glucose induces the expression of γ-aminobutyric acid B2 receptor (GABBR2) in cholangiocarcinoma (CCA) cells. The treatment of baclofen, a GABBR2 agonist, to CCA cells inhibits phosphorylation of glycogen synthase kinase 3, resulting in the activation of the kinase activity which further phosphorylates β-catenin. Phosphorylated β-catenin is subjected to degradation preventing its function on promoting cell proliferation *via* c-Myc and cyclin D1 expression. On the other hand, activated GABBR2 by baclofen also inhibits phosphorylation of signal transducer and activator of transcription 3 (STAT3). The inhibition of STAT3 phosphorylation also suppresses its functions as a transcription factor for c-Myc and cyclin D1 expression. Activating GABBR2 by baclofen, thus, suppresses the proliferation of CCA cells. GABBR2: γ-aminobutyric acid B2 receptor; GSK3: Glycogen synthase kinase 3; STAT3: Signal transducer and activator of transcription 3.

correlations between GABBR2 and STAT3, GSK3B, and CTNNB1, were not observed in the analysis using a dataset from The Cancer Genome Atlas which included non-liver fluke-associated CCA[50].

Second, although the *in vivo* effect of natural GABA on CCA growth has been reported in several studies, the treatment of GABA receptor agonists in the animal model remains limited. A further *in vivo* study of GABA-B receptor agonists at an optimal therapeutic dosage in animal models should be certified. Third, the association of GABBR2 expression and nuclear localization of its downstream transcription factor, namely, β-catenin, needs further proof in clinical samples using appropriate techniques. Lastly, a combination of several modalities as the therapeutic regimen for CCA is recommended. The study of combining GABA-B receptor agonists with another standard or alternative modality will help translate these findings to clinical practice, especially in the treatment of CCA patients with DM who are likely suffering from a poor prognosis.

CONCLUSION

GABBR2 is upregulated by HG in both CCA cell lines and tumor tissues from patients. Targeting GABBR2 with GABA-B receptor agonists shows the potential of using GABBR2 as a therapeutic target and repurposing GABA-B receptor agonists for CCA treatment, especially for those patients with DM and hyperglycemia.

ARTICLE HIGHLIGHTS

Research background

The association between diabetes mellitus (DM) and cholangiocarcinoma (CCA) progression has been established with unclear mechanisms. Our previous study showed that γ-aminobutyric acid B2 receptor (GABBR2) is among the top 5 upregulated genes in CCA cells cultured in high glucose (HG). Thus, GABBR2 is highly potential for a repurposing aim in CCA treatment.

Research motivation

Approximately 60% of Thai patients with CCA had fasting blood glucose in a range of pre-diabetes or DM. Targeting the molecules underlying hyperglycemia-induced aggressiveness of CCA cells might improve the prognosis of CCA patients with DM.

Research objectives

This study aimed to investigate the effects of hyperglycemia on GABBR2 expression and the potential use of GABBR2 as a CCA therapeutic target.

Research methods

CCA cells cultured in normal glucose or HG conditions were used as models of *in vitro* euglycemia and hyperglycemia, respectively. Baclofen, a GABBR2 agonist, was used to study the functional roles of CCA cells. Western blot, immunocytofluorescence, and immunohistochemistry were used to study molecular mechanisms.

Research results

HG induced GABBR2 expression in both cell lines and in patients' CCA tissues. Baclofen treatment significantly suppressed CCA cell growth, while cells cultured in HG showed a significantly higher sensitivity. The effects of baclofen on CCA cell growth were achieved by the suppression of the signal transducer and activator of transcription 3 and glycogen synthase kinase 3/β-catenin pathways.

Research conclusions

The expression of GABBR2 in CCA is induced in hyperglycemic conditions. Baclofen significantly suppresses the growth of CCA cells and thus holds a high promise as a repurposing drug for CCA treatment.

Research perspectives

Investigating baclofen's effects at an optimal therapeutic dosage in *in vivo* models would verify the present work and facilitate the translation for clinical study in CCA cases.

ACKNOWLEDGEMENTS

We would like to thank Mr. Chitsakul Phuyao, Cholangiocarcinoma Research Institute, Khon Kaen University, for his technical help in histological sections. This manuscript has been edited for English presentation by Prof. James A. Will, University of Wisconsin, USA, *via* KKU Publication Clinic, Khon Kaen University.

FOOTNOTES

Author contributions: Saengboonmee C, Seubwai W, Gingras MC, and Wongkham S conceptualized the research; Saengboonmee C, Sorin S, Sangkhamanon S, Indramanee S, Chomphoo S, and Thithuan K designed and performed the experiments; Saengboonmee C, Sorin S, Sangkhamanon S, Chomphoo S, Seubwai W, Chiu CF, Okada S, Gingras MC, and Wongkham S analyzed the data; Okada S and Gingras MC contributed research resources and analysis tools; Saengbonmee C and Sorin S wrote the manuscript draft; Saengboonmee C, Chiu CF, Okada S, Gingras MC, and Wongkham S reviewed and edited the manuscript; and all authors read and approved the final version of the manuscript.

Supported by the Research Grant for Young Talented Scholars, National Research Council of Thailand, No. N41A640108.

Institutional review board statement: The protocol of this study has been reviewed and approved by the Khon Kaen University Ethics Committee for Human Research (approval No. HE641441), based on the Declaration of Helsinki and the ICH-Good Clinical Practice Guidelines.

Informed consent statement: Written informed consent was obtained from all participants.

Conflict-of-interest statement: All the authors report no relevant conflicts of interest for this article.

Data sharing statement: No additional data are available.

Open-Access: This article is an open-access article that was selected by an in-house editor and fully peer-reviewed by external reviewers. It is distributed in accordance with the Creative Commons Attribution NonCommercial (CC BY-NC 4.0) license, which permits others to distribute, remix, adapt, build upon this work non-commercially, and license their derivative works on different terms, provided the original work is properly cited and the use is non-commercial. See: https://creativecommons.org/Licenses/by-nc/4.0/

Country/Territory of origin: Thailand

ORCID number: Charupong Saengboonmee 0000-0003-1476-1129; Supannika Sorin 0000-0002-5075-0139; Sakkarn Sangkhamanon 0000-0002-520

3-8700; Surang Chomphoo 0000-0003-2879-5127; Somsiri Indramanee 0000-0003-2152-9088; Wunchana Seubwai 0000-0002-9265-5113; Kanyarat Thithuan 0000-0003-2267-210X; Ching-Feng Chiu 0000-0001-5591-0288; Seiji Okada 0000-0003-3124-5206; Marie-Claude Gingras 0000-0003-2570-6360; Sopit Wongkham 0000-0001-9578-3041.

S-Editor: Wang JJ
L-Editor: Wang TQ
P-Editor: Cai YX

REFERENCES

1 **Khan MAB**, Hashim MJ, King JK, Govender RD, Mustafa H, Al Kaabi J. Epidemiology of Type 2 Diabetes - Global Burden of Disease and Forecasted Trends. *J Epidemiol Glob Health* 2020; **10**: 107-111 [PMID: 32175717 DOI: 10.2991/jegh.k.191028.001]
2 **Zhu B**, Qu S. The Relationship Between Diabetes Mellitus and Cancers and Its Underlying Mechanisms. *Front Endocrinol (Lausanne)* 2022; **13**: 800995 [PMID: 35222270 DOI: 10.3389/fendo.2022.800995]
3 **Giovannucci E**, Harlan DM, Archer MC, Bergenstal RM, Gapstur SM, Habel LA, Pollak M, Regensteiner JG, Yee D. Diabetes and cancer: a consensus report. *Diabetes Care* 2010; **33**: 1674-1685 [PMID: 20587728 DOI: 10.2337/dc10-0666]
4 **Clements O**, Eliahoo J, Kim JU, Taylor-Robinson SD, Khan SA. Risk factors for intrahepatic and extrahepatic cholangiocarcinoma: A systematic review and meta-analysis. *J Hepatol* 2020; **72**: 95-103 [PMID: 31536748 DOI: 10.1016/j.jhep.2019.09.007]
5 **Mantovani A**, Targher G. Type 2 diabetes mellitus and risk of hepatocellular carcinoma: spotlight on nonalcoholic fatty liver disease. *Ann Transl Med* 2017; **5**: 270 [PMID: 28758096 DOI: 10.21037/atm.2017.04.41]
6 **Saengboonmee C**, Seubwai W, Lert-Itthiporn W, Sanlung T, Wongkham S. Association of Diabetes Mellitus and Cholangiocarcinoma: Update of Evidence and the Effects of Antidiabetic Medication. *Can J Diabetes* 2021; **45**: 282-290 [PMID: 33218924 DOI: 10.1016/j.jcjd.2020.09.008]
7 **Fu K**, Yang X, Wu H, Gong J, Li X. Diabetes and PKM2 affect prognosis in patients with intrahepatic cholangiocarcinoma. *Oncol Lett* 2020; **20**: 265 [PMID: 32989399 DOI: 10.3892/ol.2020.12128]
8 **Thinkhamrop K**, Khuntikeo N, Laohasiriwong W, Chupanit P, Kelly M, Suwannatrai AT. Association of comorbidity between Opisthorchis viverrini infection and diabetes mellitus in the development of cholangiocarcinoma among a high-risk population, northeastern Thailand. *PLoS Negl Trop Dis* 2021; **15**: e0009741 [PMID: 34543283 DOI: 10.1371/journal.pntd.0009741]
9 **Chaidee A**, Onsurathum S, Intuyod K, Pannangpetch P, Pongchaiyakul C, Pinlaor P, Pairojkul C, Ittiprasert W, Cochran CJ, Mann VH, Brindley PJ, Pinlaor S. Co-occurrence of opisthorchiasis and diabetes exacerbates morbidity of the hepatobiliary tract disease. *PLoS Negl Trop Dis* 2018; **12**: e0006611 [PMID: 29953446 DOI: 10.1371/journal.pntd.0006611]
10 **Rizzo A**, Brandi G. First-line Chemotherapy in Advanced Biliary Tract Cancer Ten Years After the ABC-02 Trial: "And Yet It Moves!". *Cancer Treat Res Commun* 2021; **27**: 100335 [PMID: 33592561 DOI: 10.1016/j.ctarc.2021.100335]
11 **Goyal L**, Kongpetch S, Crolley VE, Bridgewater J. Targeting FGFR inhibition in cholangiocarcinoma. *Cancer Treat Rev* 2021; **95**: 102170 [PMID: 33735689 DOI: 10.1016/j.ctrv.2021.102170]
12 **Rizzo A**, Ricci AD, Brandi G. Durvalumab: an investigational anti-PD-L1 antibody for the treatment of biliary tract cancer. *Expert Opin Investig Drugs* 2021; **30**: 343-350 [PMID: 33645367 DOI: 10.1080/13543784.2021.1897102]
13 **Ricci AD**, Rizzo A, Brandi G. Immunotherapy in Biliary Tract Cancer: Worthy of a Second Look. *Cancer Control* 2020; **27**: 1073274820948047 [PMID: 32806956 DOI: 10.1177/1073274820948047]
14 **Viscardi G**, Tralongo AC, Massari F, Lambertini M, Mollica V, Rizzo A, Comito F, Di Liello R, Alfieri S, Imbimbo M, Della Corte CM, Morgillo F, Simeon V, Lo Russo G, Proto C, Prelaj A, De Toma A, Galli G, Signorelli D, Ciardiello F, Remon J, Chaput N, Besse B, de Braud F, Garassino MC, Torri V, Cinquini M, Ferrara R. Comparative assessment of early mortality risk upon immune checkpoint inhibitors alone or in combination with other agents across solid malignancies: a systematic review and meta-analysis. *Eur J Cancer* 2022; **177**: 175-185 [PMID: 36368251 DOI: 10.1016/j.ejca.2022.09.031]
15 **Saengboonmee C**, Seubwai W, Pairojkul C, Wongkham S. High glucose enhances progression of cholangiocarcinoma cells *via* STAT3 activation. *Sci Rep* 2016; **6**: 18995 [PMID: 26743134 DOI: 10.1038/srep18995]
16 **Phoomak C**, Vaeteewoottacharn K, Silsirivanit A, Saengboonmee C, Seubwai W, Sawanyawisuth K, Wongkham C, Wongkham S. High glucose levels boost the aggressiveness of highly metastatic cholangiocarcinoma cells *via* O-GlcNAcylation. *Sci Rep* 2017; **7**: 43842 [PMID: 28262738 DOI: 10.1038/srep43842]
17 **Detarya M**, Thaenkaew S, Seubwai W, Indramanee S, Phoomak C, Saengboonmee C, Wongkham S, Wongkham C. High glucose upregulates FOXM1 expression *via* EGFR/STAT3 dependent activation to promote progression of cholangiocarcinoma. *Life Sci* 2021; **271**: 119114 [PMID: 33513399 DOI: 10.1016/j.lfs.2021.119114]
18 **Saengboonmee C**, Phoomak C, Supabphol S, Covington KR, Hampton O, Wongkham C, Gibbs RA, Umezawa K, Seubwai W, Gingras MC, Wongkham S. NF-κB and STAT3 co-operation enhances high glucose induced aggressiveness of cholangiocarcinoma cells. *Life Sci* 2020; **262**: 118548 [PMID: 33038372 DOI: 10.1016/j.lfs.2020.118548]
19 **Saengboonmee C**, Detarya M, Sangkhamanon S, Sawanyawisuth K, Seubwai W, Wongkham S. High Glucose Induced Upregulation of Cyclin a Associating with a Short Survival of Patients with Cholangiocarcinoma: A Potential Target for Treatment of Patients with Diabetes Mellitus. *Nutr Cancer* 2022; **74**: 1734-1744 [PMID: 34353198 DOI: 10.1080/01635581.2021.1961830]
20 **Smart TG**, Stephenson FA. A half century of γ-aminobutyric acid. *Brain Neurosci Adv* 2019; **3**: 2398212819858249 [PMID: 32166183 DOI: 10.1177/2398212819858249]
21 **Shaye H**, Stauch B, Gati C, Cherezov V. Molecular mechanisms of metabotropic GABA(B) receptor function. *Sci Adv* 2021; **7** [PMID: 34049877 DOI: 10.1126/sciadv.abg3362]
22 **Evenseth LSM**, Gabrielsen M, Sylte I. The GABA(B) Receptor-Structure, Ligand Binding and Drug Development. *Molecules* 2020; **25** [PMID: 32646032 DOI: 10.3390/molecules25133093]
23 **Auteri M**, Zizzo MG, Serio R. GABA and GABA receptors in the gastrointestinal tract: from motility to inflammation. *Pharmacol Res* 2015; **93**: 11-21 [PMID: 25526825 DOI: 10.1016/j.phrs.2014.12.001]

24 **Hyland NP**, Cryan JF. A Gut Feeling about GABA: Focus on GABA(B) Receptors. *Front Pharmacol* 2010; **1**: 124 [PMID: 21833169 DOI: 10.3389/fphar.2010.00124]

25 **Mancinelli R**, Franchitto A, Glaser S, Meng F, Onori P, Demorrow S, Francis H, Venter J, Carpino G, Baker K, Han Y, Ueno Y, Gaudio E, Alpini G. GABA induces the differentiation of small into large cholangiocytes by activation of Ca(2+) /CaMK I-dependent adenylyl cyclase 8. *Hepatology* 2013; **58**: 251-263 [PMID: 23389926 DOI: 10.1002/hep.26308]

26 **Huang Q**, Zhu CL, Liu CH, Xie F, Zhu K, Hu SY. Gamma-aminobutyric acid binds to GABAb receptor to inhibit cholangiocarcinoma cells growth *via* the JAK/STAT3 pathway. *Dig Dis Sci* 2013; **58**: 734-743 [PMID: 23007731 DOI: 10.1007/s10620-012-2382-2]

27 **Wang C**, Zhu CL, Huang Z, Wang G, Huang Q, Liu CH, Xie F, Wang W. γ-aminobutyric acid inhibits the growth of cholangiocarcinoma *via* cAMP / PKA signal pathway. *Int J Clin Exp Med* 2016; **9**: 9992-9998

28 **Fava G**, Marucci L, Glaser S, Francis H, De Morrow S, Benedetti A, Alvaro D, Venter J, Meininger C, Patel T, Taffetani S, Marzioni M, Summers R, Reichenbach R, Alpini G. gamma-Aminobutyric acid inhibits cholangiocarcinoma growth by cyclic AMP-dependent regulation of the protein kinase A/extracellular signal-regulated kinase 1/2 pathway. *Cancer Res* 2005; **65**: 11437-11446 [PMID: 16357152 DOI: 10.1158/0008-5472.Can-05-1470]

29 **Huang D**, Wang Y, Thompson JW, Yin T, Alexander PB, Qin D, Mudgal P, Wu H, Liang Y, Tan L, Pan C, Yuan L, Wan Y, Li QJ, Wang XF. Cancer-cell-derived GABA promotes β-catenin-mediated tumour growth and immunosuppression. *Nat Cell Biol* 2022; **24**: 230-241 [PMID: 35145222 DOI: 10.1038/s41556-021-00820-9]

30 **Xia S**, He C, Zhu Y, Wang S, Li H, Zhang Z, Jiang X, Liu J. GABA(B)R-Induced EGFR Transactivation Promotes Migration of Human Prostate Cancer Cells. *Mol Pharmacol* 2017; **92**: 265-277 [PMID: 28424220 DOI: 10.1124/mol.116.107854]

31 **ElSayed NA**, Aleppo G, Aroda VR, Bannuru RR, Brown FM, Bruemmer D, Collins BS, Hilliard ME, Isaacs D, Johnson EL, Kahan S, Khunti K, Leon J, Lyons SK, Perry ML, Prahalad P, Pratley RE, Seley JJ, Stanton RC, Gabbay RA; on behalf of the American Diabetes Association. 2. Classification and Diagnosis of Diabetes: Standards of Care in Diabetes-2023. *Diabetes Care* 2023; **46**: S19-S40 [PMID: 36507649 DOI: 10.2337/dc23-S002]

32 **Sripa B**, Seubwai W, Vaeteewoottacharn K, Sawanyawisuth K, Silsirivanit A, Kaewkong W, Muisuk K, Dana P, Phoomak C, Lert-Itthiporn W, Luvira V, Pairojkul C, Teh BT, Wongkham S, Okada S, Chamgramol Y. Functional and genetic characterization of three cell lines derived from a single tumor of an Opisthorchis viverrini-associated cholangiocarcinoma patient. *Hum Cell* 2020; **33**: 695-708 [PMID: 32207095 DOI: 10.1007/s13577-020-00334-w]

33 **Barrett T**, Wilhite SE, Ledoux P, Evangelista C, Kim IF, Tomashevsky M, Marshall KA, Phillippy KH, Sherman PM, Holko M, Yefanov A, Lee H, Zhang N, Robertson CL, Serova N, Davis S, Soboleva A. NCBI GEO: archive for functional genomics data sets--update. *Nucleic Acids Res* 2013; **41**: D991-D995 [PMID: 23193258 DOI: 10.1093/nar/gks1193]

34 **Jusakul A**, Cutcutache I, Yong CH, Lim JQ, Huang MN, Padmanabhan N, Nellore V, Kongpetch S, Ng AWT, Ng LM, Choo SP, Myint SS, Thanan R, Nagarajan S, Lim WK, Ng CCY, Boot A, Liu M, Ong CK, Rajasegaran V, Lie S, Lim AST, Lim TH, Tan J, Loh JL, McPherson JR, Khuntikeo N, Bhudhisawasdi V, Yongvanit P, Wongkham S, Totoki Y, Nakamura H, Arai Y, Yamasaki S, Chow PK, Chung AYF, Ooi LLPJ, Lim KH, Dima S, Duda DG, Popescu I, Broet P, Hsieh SY, Yu MC, Scarpa A, Lai J, Luo DX, Carvalho AL, Vettore AL, Rhee H, Park YN, Alexandrov LB, Gordân R, Rozen SG, Shibata T, Pairojkul C, Teh BT, Tan P. Whole-Genome and Epigenomic Landscapes of Etiologically Distinct Subtypes of Cholangiocarcinoma. *Cancer Discov* 2017; **7**: 1116-1135 [PMID: 28667006 DOI: 10.1158/2159-8290.CD-17-0368]

35 **Huang Q**, Liu C, Wang C, Hu Y, Qiu L, Xu P. Neurotransmitter γ-aminobutyric acid-mediated inhibition of the invasive ability of cholangiocarcinoma cells. *Oncol Lett* 2011; **2**: 519-523 [PMID: 22866114 DOI: 10.3892/ol.2011.263]

36 **Saengboonmee C**, Seubwai W, Wongkham C, Wongkham S. Diabetes mellitus: Possible risk and promoting factors of cholangiocarcinoma: Association of diabetes mellitus and cholangiocarcinoma. *Cancer Epidemiol* 2015; **39**: 274-278 [PMID: 25910864 DOI: 10.1016/j.canep.2015.04.002]

37 **Thonsri U**, Wongkham S, Wongkham C, Hino S, Nakao M, Roytrakul S, Koga T, Seubwai W. High glucose-ROS conditions enhance the progression in cholangiocarcinoma *via* upregulation of MAN2A2 and CHD8. *Cancer Sci* 2021; **112**: 254-264 [PMID: 33141432 DOI: 10.1111/cas.14719]

38 **Kawasaki K**, Kuboki S, Nojima H, Yoshitomi H, Furukawa K, Takayashiki T, Miyazaki M, Ohtsuka M. GABA signaling inhibits tumor progression by suppressing STAT3-mediated EMT in human intrahepatic cholangiocarcinoma. *HPB* 2018; **20**: S694 [DOI: 10.1016/j.hpb.2018.06.1374]

39 **Romito JW**, Turner ER, Rosener JA, Coldiron L, Udipi A, Nohrn L, Tausiani J, Romito BT. Baclofen therapeutics, toxicity, and withdrawal: A narrative review. *SAGE Open Med* 2021; **9**: 20503121211022197 [PMID: 34158937 DOI: 10.1177/20503121211022197]

40 **You L**, Lin J, Yu Z, Qian Y, Bi Y, Wang F, Zhang L, Zheng C, Zhang J, Li W, Cai Y, Gao Y, Kong X, Sun X. Nobiletin suppresses cholangiocarcinoma proliferation *via* inhibiting GSK3β. *Int J Biol Sci* 2022; **18**: 5698-5712 [PMID: 36263164 DOI: 10.7150/ijbs.78345]

41 **Dokduang H**, Techasen A, Namwat N, Khuntikeo N, Pairojkul C, Murakami Y, Loilome W, Yongvanit P. STATs profiling reveals predominantly-activated STAT3 in cholangiocarcinoma genesis and progression. *J Hepatobiliary Pancreat Sci* 2014; **21**: 767-776 [PMID: 25044480 DOI: 10.1002/jhbp.131]

42 **Glibo M**, Serman A, Karin-Kujundzic V, Bekavac Vlatkovic I, Miskovic B, Vranic S, Serman L. The role of glycogen synthase kinase 3 (GSK3) in cancer with emphasis on ovarian cancer development and progression: A comprehensive review. *Bosn J Basic Med Sci* 2021; **21**: 5-18 [PMID: 32767962 DOI: 10.17305/bjbms.2020.5036]

43 **Beurel E**, Jope RS. Differential regulation of STAT family members by glycogen synthase kinase-3. *J Biol Chem* 2008; **283**: 21934-21944 [PMID: 18550525 DOI: 10.1074/jbc.M802481200]

44 **Lecarpentier Y**, Schussler O, Hébert JL, Vallée A. Multiple Targets of the Canonical WNT/β-Catenin Signaling in Cancers. *Front Oncol* 2019; **9**: 1248 [PMID: 31803621 DOI: 10.3389/fonc.2019.01248]

45 **Carpenter RL**, Lo HW. STAT3 Target Genes Relevant to Human Cancers. *Cancers (Basel)* 2014; **6**: 897-925 [PMID: 24743777 DOI: 10.3390/cancers6020897]

46 **Erlitzki R**, Gong Y, Zhang M, Minuk G. Identification of gamma-aminobutyric acid receptor subunit types in human and rat liver. *Am J Physiol Gastrointest Liver Physiol* 2000; **279**: G733-G739 [PMID: 11005760 DOI: 10.1152/ajpgi.2000.279.4.G733]

47 **Chen ZA**, Bao MY, Xu YF, Zha RP, Shi HB, Chen TY, He XH. Suppression of Human Liver Cancer Cell Migration and Invasion *via* the GABAA Receptor. *Cancer Biol Med* 2012; **9**: 90-98 [PMID: 23691461 DOI: 10.3969/j.issn.2095-3941.2012.02.002]

48 **Chan-On W**, Nairismägi ML, Ong CK, Lim WK, Dima S, Pairojkul C, Lim KH, McPherson JR, Cutcutache I, Heng HL, Ooi L, Chung A, Chow P, Cheow PC, Lee SY, Choo SP, Tan IB, Duda D, Nastase A, Myint SS, Wong BH, Gan A, Rajasegaran V, Ng CC, Nagarajan S, Jusakul A, Zhang S, Vohra P, Yu W, Huang D, Sithithaworn P, Yongvanit P, Wongkham S, Khuntikeo N, Bhudhisawasdi V, Popescu I, Rozen

SG, Tan P, Teh BT. Exome sequencing identifies distinct mutational patterns in liver fluke-related and non-infection-related bile duct cancers. *Nat Genet* 2013; **45**: 1474-1478 [PMID: 24185513 DOI: 10.1038/ng.2806]

49 **Jinawath N**, Chamgramol Y, Furukawa Y, Obama K, Tsunoda T, Sripa B, Pairojkul C, Nakamura Y. Comparison of gene expression profiles between Opisthorchis viverrini and non-Opisthorchis viverrini associated human intrahepatic cholangiocarcinoma. *Hepatology* 2006; **44**: 1025-1038 [PMID: 17006947 DOI: 10.1002/hep.21330]

50 **Tang Z**, Li C, Kang B, Gao G, Zhang Z. GEPIA: a web server for cancer and normal gene expression profiling and interactive analyses. *Nucleic Acids Res* 2017; **45**: W98-W102 [PMID: 2WJG-29-441645 DOI: 10.1093/nar/gkx247]

World Journal of Gastroenterology

Submit a Manuscript: https://www.f6publishing.com

World J Gastroenterol 2023 July 28; 29(28): 4433-4450

DOI: 10.3748/wjg.v29.i28.4433

ISSN 1007-9327 (print) ISSN 2219-2840 (online)

ORIGINAL ARTICLE

Basic Study

F-box only protein 2 exacerbates non-alcoholic fatty liver disease by targeting the hydroxyl CoA dehydrogenase alpha subunit

Zhi Liu, Ning-Yuan Chen, Zhao Zhang, Sai Zhou, San-Yuan Hu

Specialty type: Gastroenterology and hepatology

Provenance and peer review: Unsolicited article; Externally peer reviewed.

Peer-review model: Single blind

Peer-review report's scientific quality classification

Grade A (Excellent): 0
Grade B (Very good): B, B
Grade C (Good): 0
Grade D (Fair): 0
Grade E (Poor): 0

P-Reviewer: Gasperetti A, Italy; Strong VE, United States

Received: May 24, 2023
Peer-review started: May 24, 2023
First decision: June 14, 2023
Revised: June 19, 2023
Accepted: July 11, 2023
Article in press: July 11, 2023
Published online: July 28, 2023

Zhi Liu, San-Yuan Hu, Department of General Surgery, Qilu Hospital of Shandong University, Jinan 250012, Shandong Province, China

Ning-Yuan Chen, Zhao Zhang, Department of General Surgery, Shandong Provincial Qian Foshan Hospital, Shandong University, Jinan 250014, Shandong Province, China

Sai Zhou, Department of General Surgery, Shandong First Medical University & Shandong Academy of Medical Sciences, Jinan 250117, Shandong Province, China

Corresponding author: San-Yuan Hu, Doctor, MD, Chief Doctor, Chief Physician, Doctor, Full Professor, Professor, Surgeon, Department of General Surgery, Qilu Hospital of Shandong University, No. 107 West Wenhua Road, Jinan 250012, Shandong Province, China.
husanyuan1962@hotmail.com

Abstract

BACKGROUND

Non-alcoholic fatty liver disease (NAFLD) is a major health burden with an increasing global incidence. Unfortunately, the unavailability of knowledge underlying NAFLD pathogenesis inhibits effective preventive and therapeutic measures.

AIM

To explore the molecular mechanism of NAFLD.

METHODS

Whole genome sequencing (WGS) analysis was performed on liver tissues from patients with NAFLD (n = 6) and patients with normal metabolic conditions (n = 6) to identify the target genes. A NAFLD C57BL6/J mouse model induced by 16 wk of high-fat diet feeding and a hepatocyte-specific F-box only protein 2 (FBXO2) overexpression mouse model were used for *in vivo* studies. Plasmid transfection, co-immunoprecipitation-based mass spectrometry assays, and ubiquitination in HepG2 cells and HEK293T cells were used for *in vitro* studies.

RESULTS

A total of 30982 genes were detected in WGS analysis, with 649 up-regulated and 178 down-regulated. Expression of FBXO2, an E3 ligase, was upregulated in the liver tissues of patients with NAFLD. Hepatocyte-specific FBXO2 overexpression facilitated NAFLD-associated phenotypes in mice. Overexpression of FBXO2

aggravated odium oleate (OA)-induced lipid accumulation in HepG2 cells, resulting in an abnormal expression of genes related to lipid metabolism, such as fatty acid synthase, peroxisome proliferator-activated receptor alpha, and so on. In contrast, knocking down FBXO2 in HepG2 cells significantly alleviated the OA-induced lipid accumulation and aberrant expression of lipid metabolism genes. The hydroxyl CoA dehydrogenase alpha subunit (HADHA), a protein involved in oxidative stress, was a target of FBXO2-mediated ubiquitination. FBXO2 directly bound to HADHA and facilitated its proteasomal degradation in HepG2 and HEK293T cells. Supplementation with HADHA alleviated lipid accumulation caused by FBXO2 overexpression in HepG2 cells.

CONCLUSION

FBXO2 exacerbates lipid accumulation by targeting HADHA and is a potential therapeutic target for NAFLD.

Key Words: F-box only protein 2; Nonalcoholic fatty liver disease; The hydroxyl CoA dehydrogenase alpha subunit; Liver steatosis; Ubiquitination; Lipid accumulation

©The Author(s) 2023. Published by Baishideng Publishing Group Inc. All rights reserved.

Core Tip: This study involves an assessment of the role of F-box only protein 2 (FBXO2) in non-alcoholic fatty liver disease (NAFLD). First, based on the whole genome sequencing analysis results of liver tissues from normal controls and patients with NAFLD, the expression of FBXO2 was found to be increased during NAFLD. Hepatocyte-specific FBXO2 overexpression facilitated NAFLD-associated phenotypes in mice. In contrast, the knockdown of FBXO2 expression of HepG2 cells significantly alleviated oleate-induced lipid accumulation. Mechanistically, the hydroxyl CoA dehydrogenase alpha subunit, a protein with known role in oxidative stress reaction, is one of the protein substrates of FBXO2-mediated ubiquitination.

Citation: Liu Z, Chen NY, Zhang Z, Zhou S, Hu SY. F-box only protein 2 exacerbates non-alcoholic fatty liver disease by targeting the hydroxyl CoA dehydrogenase alpha subunit. *World J Gastroenterol* 2023; 29(28): 4433-4450
URL: https://www.wjgnet.com/1007-9327/full/v29/i28/4433.htm
DOI: https://dx.doi.org/10.3748/wjg.v29.i28.4433

INTRODUCTION

Non-alcoholic fatty liver disease (NAFLD), a clinicopathologic syndrome, is characterised by an excessive deposition of fat in hepatocytes [triglyceride (TG) content exceeding 5% of the liver weight] excluding alcohol and other liver-damaging factors[1-3]. With an increase in the incidence of obesity and its associated metabolic syndrome, more than one-third of adults are affected by NAFLD globally[4-6]. NAFLD includes simple fatty liver, non-alcoholic steatohepatitis, and related cirrhosis, which can eventually develop into decompensated cirrhosis and hepatocellular carcinoma[7,8]. The key issues affecting the treatment of patients with NAFLD are atherosclerotic cardio-cerebrovascular diseases, cirrhosis, and malignant tumours associated with the metabolic syndrome[9-11]. Since the pathogenesis of NAFLD remains unclear [12], a clinically effective drug to treat NAFLD is unavailable. A healthy diet and moderate exercise remain the main measures to treat NAFLD clinically[13].

The hydroxyl CoA dehydrogenase alpha subunit (HADHA), a fatty acid β-oxidation enzyme, has been identified as a key pathogenic regulator of metabolism-related diseases, such as NAFLD, obesity, and diabetes[14-16]. Previous studies have confirmed that the expression of HADHA is decreased in L02 cells treated with free fatty acids (FFA) and in mice fed with a high-fat diet (HFD). Knocking out HADHA aggravated liver steatosis, inflammation, and oxidative stress in FFA-treated L02 cells. In addition, oxidative stress and liver damage in NAFLD mice are alleviated by the up-regulation of HADHA[17]. Meanwhile, HADHA can be affected by the ubiquitin-proteasome system (UPS), which mediates important regulatory modifications. Ubiquitination and the degradation of HADHA were reported to be mediated by ubiquitin-conjugating enzyme E2 O, thereby modulating lipid metabolism[18]. However, it remains unclear if there is another regulatory factor that could control and mediate the ubiquitination of HADHA, thus affecting the pathogenesis of HADHA-mediated NAFLD. Therefore, confirming the regulatory signaling pathway in NAFLD that inhibits or activates HADHA is necessary.

The UPS comprises an evolutionarily conserved protein degradation mechanism, including ubiquitin activation (E1), ubiquitin coupling (E2), and ubiquitin ligase (E3) enzymes[19,20]. F-box only protein 2 (FBXO2), a well-known E3 ligase, plays an indispensable role in the UPS[21] and has unique functions in various pathological processes. For example, FBXO2 regulates signal transducer and activator of transcription 3 signaling responsible for modulating the proliferation and tumorigenicity of osteosarcoma cells[22], targets glycosylated SAD1/UNC84 domain protein-2 for ubiquitination and degradation to promote the development of ovarian cancer[21] and mediates the clearance of damaged lysosomes and alters the neurodegeneration phenotype of the brain in Niemann-Pick C disease[23]. In addition, the abnormal expression of FBXO2 in obese mice disrupts glucose homeostasis through ubiquitin-mediated insulin receptor degradation[24]. However, the role of FBXO2 in NAFLD pathology remains unclear.

In this study, we found that expression of FBXO2 was upregulated in the liver tissues of patients with NAFLD when compared with those in liver tissues of normal controls *via* the whole genome sequencing (WGS) analysis. These findings urged us to explore whether FBXO2 can promote the progression of NAFLD and its mechanism. Our findings can clarify whether FBXO2 is a feasible therapeutic target for NAFLD and related metabolism disorders.

MATERIALS AND METHODS

Human liver tissue samples

Liver tissue samples were collected from 10 patients with NAFLD, who underwent sleeve gastrectomy with liver biopsy at the Qilu Hospital of Shandong University, Shandong, China. Control liver tissue samples were obtained from 10 patients with normal metabolic conditions who underwent hepatic hemangioma resection at the same hospital.

The inclusion criteria were: Physical examination, laboratory investigation, ultrasound echography, and a liver biopsy consistent with the diagnosis of NAFLD, according to the Brunt criteria. Exclusion criteria were: Excess alcohol consumption (≥ 20 g/d for women and ≥ 30 g/d for men), the presence of hepatitis B virus surface antigen or hepatitis C virus antibodies in the absence of a history of vaccination, use of drugs linked to NAFLD, evidence of other specific liver diseases, such as autoimmune liver disease, and hemochromatosis[25].

A liver biopsy during surgery was performed to provide foundation to non-alcoholic steatohepatitis (NASH) score. Clinical data of the normal controls and patients with NAFLD are shown in Table 1. Written informed consent was obtained from the patients and their families. All procedures involving human liver samples were approved by the Ethics Committee of the Qilu Hospital and adhered to the principles of the Declaration of Helsinki (approval No. KYLL-2017-073).

WGS and result analysis

RNA extraction and whole genome library sequencing were performed in 12 liver tissues (NAFLD, $n = 6$; normal, $n = 6$) by LC-BIO TECHNOLOGIES (Hangzhou, China) CO. Kyoto Encyclopedia of Genes and Genomes (KEGG) and Gene Ontology (GO) enrichment analyses of the mRNA sequencing part were performed using the DAVID programme (https://david.ncifcrf.gov/). Bar, scatter, and Gene Set Enrichment Analysis result plots were drawn using the LC-BIO Technologies platform (https://www.omicstudio.cn/).

Animals

Eight-week-old pathogen-free C57BL/6J male mice (RRID:IMSR_JAX:000664) were purchased from SPF Biotechnology Co. (Beijing, China). Five mice were placed in each cage at a temperature of 23-26 °C with a 12 h light/dark cycle. Animals had free access to food and water. Rodent food was purchased from Xiao Shu You Tai Biotechnology (Beijing, China). The mice used in this investigation were divided randomly.

To induce NAFLD, 10 mice were fed an HFD (#D12492; Research Diets, New Brunswick, NJ, United States) for 16 wk. Control mice were fed with a standard normal chow diet (ND). After 16 wk of feeding an HFD, the weight of the mice in the HFD group exceeded that of mice in the ND group by 20%, and obvious lipid accumulation was observed in the liver. Serum intracellular TG and total cholesterol (T-Cho) levels also increased significantly in the HFD group ($P < 0.001$, Supplementary Table 1). Finally, eight mice met the experimental criteria. One underweight mouse and one mouse with no significant lipid deposition in the liver were excluded from any analysis.

To establish a liver-specific FBXO2 overexpression model, six mice were injected with adeno-associated virus serotype 8 (AAV8)-His-FBXO2 through the tail vein (100 μL of virus containing 5×10^{11} vg of vectors) after 6 wk of HFD feeding. An empty vector (AAV-His-vector) was injected into the corresponding control mice ($n = 6$). The virus-infected mice were fed with HFD for an another 16 wk. The AAV used in this study was purchased from WZ Biosciences Inc. (Shandong, China). The study was approved by the Institutional Animal Care and Use Committee of Shandong Provincial Qian Foshan Hospital (approval No. S453) in accordance with internationally accepted principles for the use of laboratory animals.

Cell lines and cell culture

Human hepatoma cells (HepG2, ATCC; HB-8065 BCRC, #CL-0103) and human embryonic kidney 293 cells (HEK293T, ATCC; CRL-3216 DSMZ, #CL-0005) were cultured in Dulbecco's Modified Eagle Medium, containing 10% foetal bovine serum and 1% penicillin-streptomycin, in a humidified chamber at 37 °C with 5% CO_2. HepG2 cells were exposed to odium oleate (OA) dissolved in 0.5% fatty acid-free bovine serum albumin (BSA) at a final concentration of 0.3 mmol/L for 24 h to establish an *in vitro* cell lipid deposition model. All cells were purchased from Procell Life Science & Technology Co., Ltd. (Wuhan, China). All cell lines were authenticated *via* STR identification.

Plasmid construction and transfection

FBXO2 or HADHA overexpression was achieved by transfecting cells with His-FBXO2 plasmid (#NM_012168CH895916, WZ Bioscience Inc., Shandong, China) or Myc-HADHA plasmids (#BC009235HG15019-NM, Sino Biological, Beijing, China), respectively, as per the respective manufacturer's instructions. His-vector (#66005-1-Ig, Proteintech) and Myc-vector plasmids (#16286-1-AP, Proteintech) were used as controls. FBXO2 knockdown was achieved by transfecting cells with Sh-FBXO2 plasmid (WZ Bioscience Inc). Sh-NC plasmids were used as a control. The DNA sequences of the plasmids used are shown in Supplementary material.

Table 1 Clinical information of normal controls and patients with non-alcoholic fatty liver disease

	Normal (*n* = 10)	NAFLD (*n* = 10)	*t* value	*P* value
Gender			-	-
Male, %	4 (40)	4 (40)		
Female, %	6 (60)	6 (60)		
Age, yr	33.30 ± 2.83	32.40 ± 7.09	0.373	0.714
Height, cm	169.10 ± 7.84	169.80 ± 10.38	0.170	0.867
Body weight, kg	70.95 ± 16.48	118.04 ± 28.87	4.480	< 0.001
Body mass index, kg/m^2	24.51 ± 4.02	40.41 ± 5.41	7.454	< 0.001
Waist circumference, cm	90.80 ± 11.33	128.5 ± 3.98	9.928	< 0.001
Systolic BP, mmHg	126.40 ± 6.33	134.80 ± 10.23	2.208	0.04
ALT, U/L	12.00 ± 6.77	69.00 ± 63.20	2.836	0.011
AST, U/L	15.40 ± 3.17	46.70 ± 29.74	3.309	0.004
GLDH, U/L	1.94 ± 1.22	7.74 ± 4.98	3.580	0.002
T-Cho, mmol/L	3.97 ± 0.52	4.47 ± 0.77	1.700	0.106
HDL, mmol/L	1.31 ± 0.20	0.97 ± 0.14	4.486	< 0.001
LDL, mmol/L	2.19 ± 0.37	2.83 ± 0.62	2.824	0.011
sdLDL, mmol/L	0.34 ± 0.14	1.11 ± 0.51	4.580	< 0.001
TG, mmol/L	0.62 ± 0.20	2.05 ± 0.67	6.483	< 0.001
NEFA, μmol/L	44.41 ± 29.72	55.20 ± 15.05	1.024	0.319
FPG, mmol/L	4.82 ± 0.33	4.81 ± 1.09	0.014	0.989
NASH score	0	5.10 ± 1.30	-	-

Data are presented as the mean ± SD. $P < 0.05$ was considered statistically significant. ALT: Alanine aminotransferase; AST: Aspartate aminotransferase; BP: Blood pressure; FPG: Fasting plasma glucose; HDL: High-density lipoprotein; LDL: Low-density lipoprotein; NEFA: Nonesterified fatty acid; NAFLD: Non-alcoholic fatty liver disease; NASH: Non-alcoholic steatohepatitis; sdLDL: Small and dense low-density lipoproteins; TG: Triglycerides; T-Cho: Total cholesterol.

Western blotting, co-immunoprecipitation, and mass spectrometry assays

Briefly, liver tissues and HepG2 cells were lysed with RIPA lysis buffer containing protease inhibitors. Western blotting was performed using standard procedures[26,27]. The primary antibodies used are listed in Supplementary Table 2. Image J (RRID:SCR_003070) and GraphPad Prism software (RRID:SCR_002798) were used to analyze the western blotting results.

For the co-immunoprecipitation (co-IP) assay, HepG2 cell protein lysate was prepared. The cracking solution was then washed with 1 mL of cracking buffer (containing 100 μL of protein A/G agarose beads) and the lysate was incubated overnight with the appropriate antibodies. Next, the beads were washed thrice with cracking buffer and then re-suspended in 2 × sodium dodecyl sulfate (SDS) loading buffer. The beads were incubated at 95 °C for 5 min to elute immunoprecipitated proteins. Finally, the proteins were separated using SDS-PAGE and immunoblotted for detection. Mass spectrometry (MS)-based proteomic analysis was performed by the Jinjie Bio company (Hangzhou, China).

Quantitative reverse transcription polymerase chain reaction

Total RNA was extracted from the liver tissues and HepG2 cells using TRIzol reagent (Invitrogen, #12183555). Complementary DNA (cDNA) was synthesised from the isolated RNA using a cDNA synthesis kit (Takara, #RR047A). Subsequently, SYBR Green Master Mix (Vazyme, Q111-02) and a quantitative reverse transcription polymerase chain reaction (qRT-PCR) system (LightCycle 480 II, Roche, Japan) were used to perform qRT-PCR and analyse the results. The primer sequences used in the study are listed in Supplementary Table 3.

Homeostasis model assessment of insulin resistance (HOMA-IR), oral glucose tolerance test (OGTT) and insulin tolerance test (ITT). Blood glucose levels were measured using a Glucometer Elite monitor (ACCU-CHEK, Roche, Germany) and serum insulin was measured using an insulin ELISA kit (D721159-0048, Sangon Biotech). The HOMA-IR index was calculated based on the fasting serum glucose and insulin levels. OGTT was performed *via* the administration of glucose (2 mg/g) after an overnight fast. ITTs were performed following the *i.p.* injection of 1 U/kg insulin after 4 h of fasting. OGTT and ITT were performed at 16 wk post adenovirus injection.

Mouse serum and cell cytosol lipid analysis

Blood was collected from the tail vein of mice. Serum was obtained after the blood was centrifuged at 8000 × g for 20 min at 4 °C. HepG2 cells were lysed using an ultrasonic crusher (SCINTZ-650E; Ningbo Scientz Biotechnology Co., Ningbo, China). Serum TG and T-Cho levels were measured using commercially available assay kits (Nanjing Jiancheng Bioengineering Institute, Nanjing, China).

Histological analysis

Hematoxylin and eosin (H&E) staining was done to demonstrate the pattern of lipid accumulation. Oil Red-O staining was done to show the accumulation of fat droplets in the liver.

Immunohistochemical staining and immunofluorescence

For immunohistochemistry, paraffin sections of paired human or mouse livers were deparaffinized and rehydrated. Antigens were retrieved using sodium citrate buffer. After blocking with 1% BSA for 1 h at 25 °C, the sections were sequentially incubated with anti-FBXO2 (Proteintech Cat# 14590-1-AP, RRID:AB_2104394) and the corresponding secondary antibodies. The antibodies used in the study are listed in Supplementary Table 2.

For immunofluorescence staining, cells were fixed with 4% paraformaldehyde for 25 min at 25 °C. Cells were then washed thrice with phosphate-buffered saline (PBS) and lysed with 0.1% Triton X-100 in PBS for 20 min. After washing the cells with PBS three times, the cells were incubated in 1% BSA at 37 °C for 1.5 h followed by overnight incubation at 4 °C with rabbit anti-FBXO2 and anti-HADHA antibodies (Proteintech Cat#10758-1-AP, RRID:AB_2115593). After washing thrice with PBS, the cells were incubated with the appropriate secondary antibodies for 1 h at 37 °C. Finally, the cells were stained with 4′,6-diamidino-2-phenylindole. Images were captured using a confocal microscope (IX-73, Olympus, Japan).

Ubiquitination assay

The HADHA ubiquitination assay was performed by transfecting HEK293T cells with FBXO2, HADHA, HA-ubiquitin, or empty vectors using Lipofectamine 2000 (#11668, Invitrogen, United States). After 24 h, the cells were washed twice with PBS and lysed in RIPA lysis buffer. The lysates were then centrifuged to obtain cytoplasmic proteins. The obtained proteins were incubated overnight with anti-HADHA antibody followed by incubation with protein A/G agarose beads at 4 °C for an additional 4 h. After washing the beads three times with lysis buffer, the beads were boiled in 2 × SDS loading buffer, separated *via* the SDS-PAGE, and immunoblotted. All experiments were repeated three times independently.

Statistical analyses

The *t*-test was performed for comparisons between two groups. Statistical significance was set at $P < 0.05$.

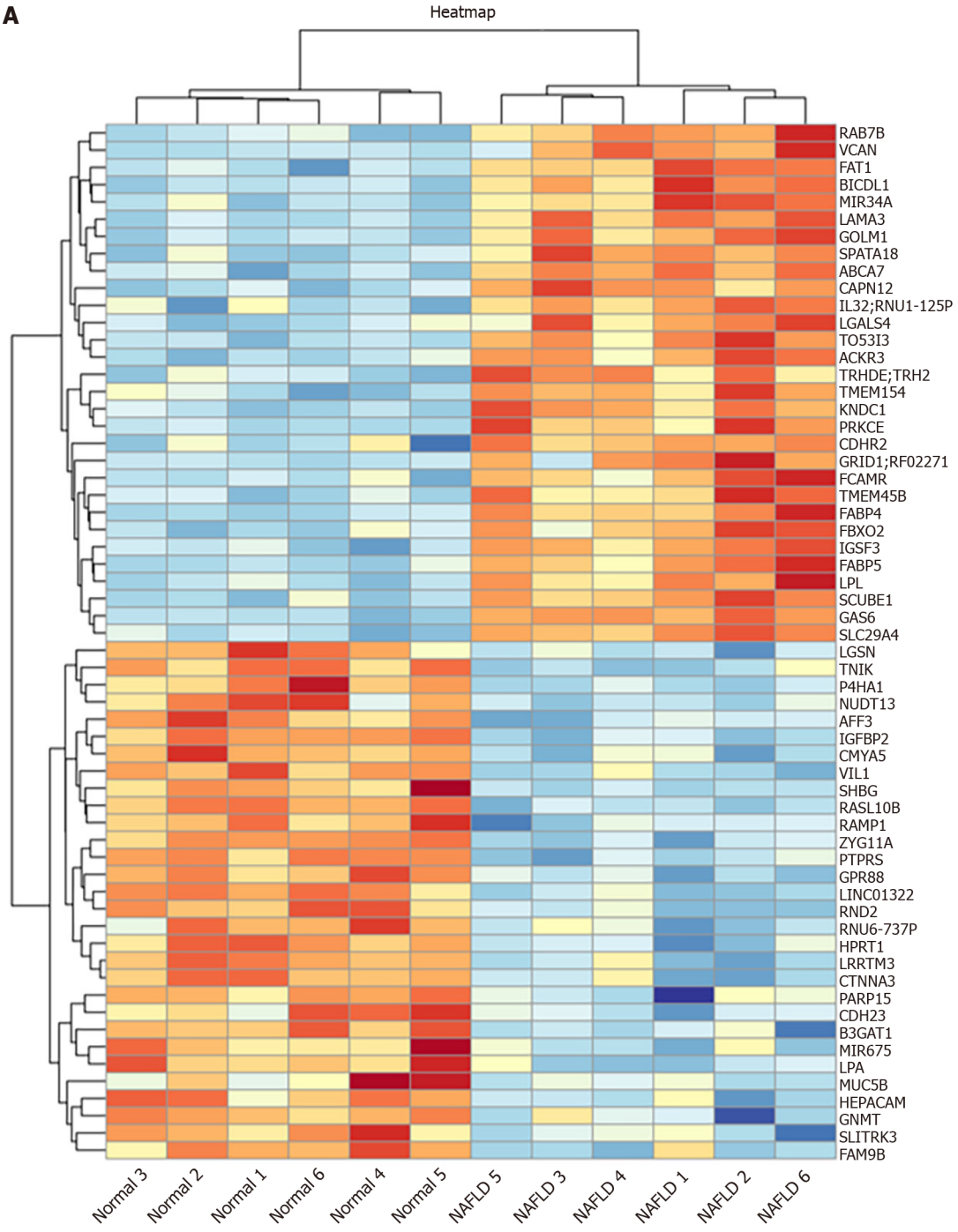
RESULTS

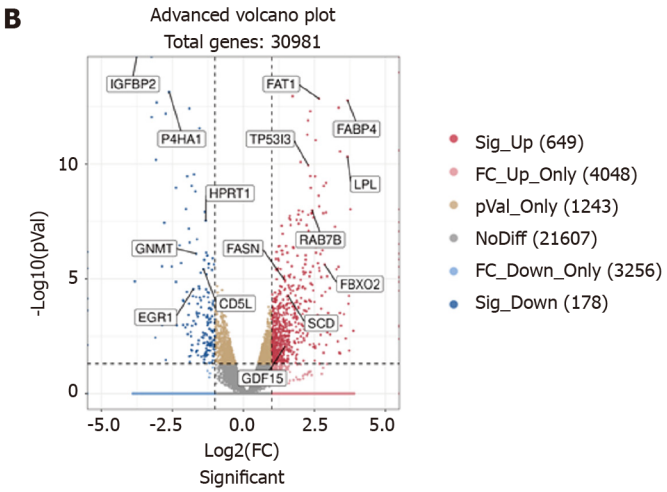
FBXO2 expression is upregulated in livers with hepatic steatosis

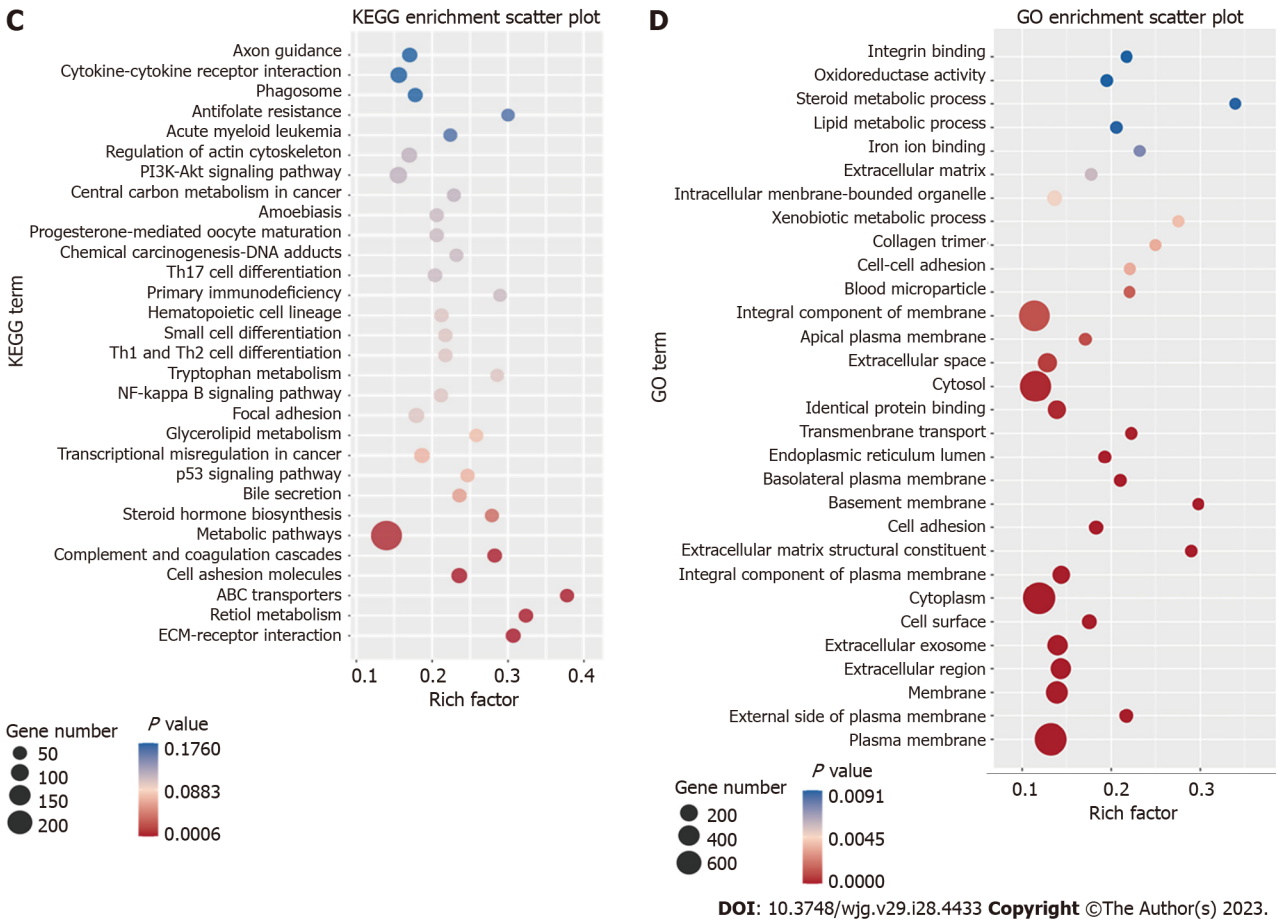
WGS was performed on the liver tissues of six patients with NAFLD and six normal controls. A total of 30982 genes were detected in the WGS analysis, of which 649 were up-regulated and 178 were down-regulated. The heat map in Figure 1A shows the 60 most significantly up- or down-regulated genes. The volcano plot in Figure 1B depicted an overview of the gene sequencing results [log2 (fold change) > 1; $P < 0.05$]. Some genes marked in our sequencing analysis were closely related to NAFLD[26,28-30], such as fatty acid synthase (FASN), growth differentiation factor 15 and insulin-like growth factor binding protein 2 (Figure 1B). GO and KEGG analyses were also performed (Figures 1C and D, Supplementary Figures 1A and B). GO-biological process analysis indicated that the differential genes were mainly involved in 'signal transduction', 'lipid metabolic process', and 'positive regulation of GTPase activity'. GO-cellular component analysis indicated that the differential genes were mainly associated with the cytoplasm, cytosol, and integral component of the membrane. GO-molecular function analysis indicated that the differential genes were mainly associated with protein binding, identical protein binding, and ATP binding processes. KEGG enrichment results revealed that the differential genes are largely enriched in 'metabolic pathways'.

Among the upregulated genes, the mRNA level of FBXO2 was significantly upregulated among patients with NAFLD. According to previous studies, the abnormal expression of FBXO2 in obese mice disrupts glucose homeostasis through ubiquitin-mediated insulin receptor degradation. We also found that sleeve gastrectomy could downregulate FBXO2 and activate in the phosphatidylinositol 3-kinase-protein kinase B (PI3K-AKT) pathway[31]. In our GO and KEGG analysis, some differential genes were enriched in the PI3K-AKT pathway. Hence, we speculated that FBXO2 may play a role in regulating lipid metabolism in NAFLD.

To investigate whether FBXO2 is involved in the occurrence and development of NAFLD, we analyzed its expression in liver tissues isolated from patients with NAFLD (Table 1, Figures 2A and B). We found that the mRNA and protein levels of FBXO2 were significantly higher in liver tissues of patients with NAFLD compared to that in control liver tissues *via* qRT-PCR analysis (Figure 2D, $P < 0.0001$), western blot analysis (Figure 2C, $P < 0.0001$), and immunohistochemical staining (Figure 2E). Moreover, we established a NAFLD mouse model by feeding C57BL6/J mice an HFD for 16 wk (Figures 2F and G, Supplementary Table 1). Similarly, we also found significantly higher FBXO2 mRNA and protein levels in liver samples obtained from HFD mice compared to ND mice *via* qRT-PCR (Figure 2I, $P < 0.0001$), western blot (Figure 2H, $P < 0.01$), and immunohistochemical staining (Figure 2J) analyses. Based on these results, we confirmed that


A
Heatmap
RAB7B
VCAN
FAT1
BICDL1
MIR34A
LAMA3
GOLM1
SPATA18
ABCA7
CAPN12
IL32;RNU1-125P
LGALS4
TO53I3
ACKR3
TRHDE;TRH2
TMEM154
KNDC1
PRKCE
CDHR2
GRID1;RF02271
FCAMR
TMEM45B
FABP4
FBXO2
IGSF3
FABP5
LPL
SCUBE1
GAS6
SLC29A4
LGSN
TNIK
P4HA1
NUDT13
AFF3
IGFBP2
CMYA5
VIL1
SHBG
RASL10B
RAMP1
ZYG11A
PTPRS
GPR88
LINC01322
RND2
RNU6-737P
HPRT1
LRRTM3
CTNNA3
PARP15
CDH23
B3GAT1
MIR675
LPA
MUC5B
HEPACAM
GNMT
SLITRK3
FAM9B
Normal 3
Normal 2
Normal 1
Normal 6
Normal 4
Normal 5
NAFLD 5
NAFLD 3
NAFLD 4
NAFLD 1
NAFLD 2
NAFLD 6


B
Advanced volcano plot
Total genes: 30981
IGFBP2
FAT1
P4HA1
TP53I3
FABP4
LPL
HPRT1
GNMT
FASN
RAB7B
FBXO2
EGR1
CD5L
SCD
GDF15
10
5
0
-Log10(pVal)
-5.0
-2.5
0.0
2.5
5.0
Log2(FC)
Significant
Sig_Up (649)
FC_Up_Only (4048)
pVal_Only (1243)
NoDiff (21607)
FC_Down_Only (3256)
Sig_Down (178)



DOI: 10.3748/wjg.v29.i28.4433 **Copyright** ©The Author(s) 2023.

Figure 1 Whole genome sequencing analysis of liver tissue from patients with non-alcoholic fatty liver disease and healthy controls. A and B: Heat map (A) and volcano plot (B) of the mRNA sequencing results; C: Scatter plot of the Kyoto Encyclopedia of Genes and Genomes enrichment analysis results; D: Scatter plot of the Gene Ontology enrich analysis results. FBXO2: F-box only protein 2; NAFLD: Non-alcoholic fatty liver disease; FC: Fold change; KEGG: Kyoto Encyclopedia of Genes and Genomes; GO: Gene Ontology.

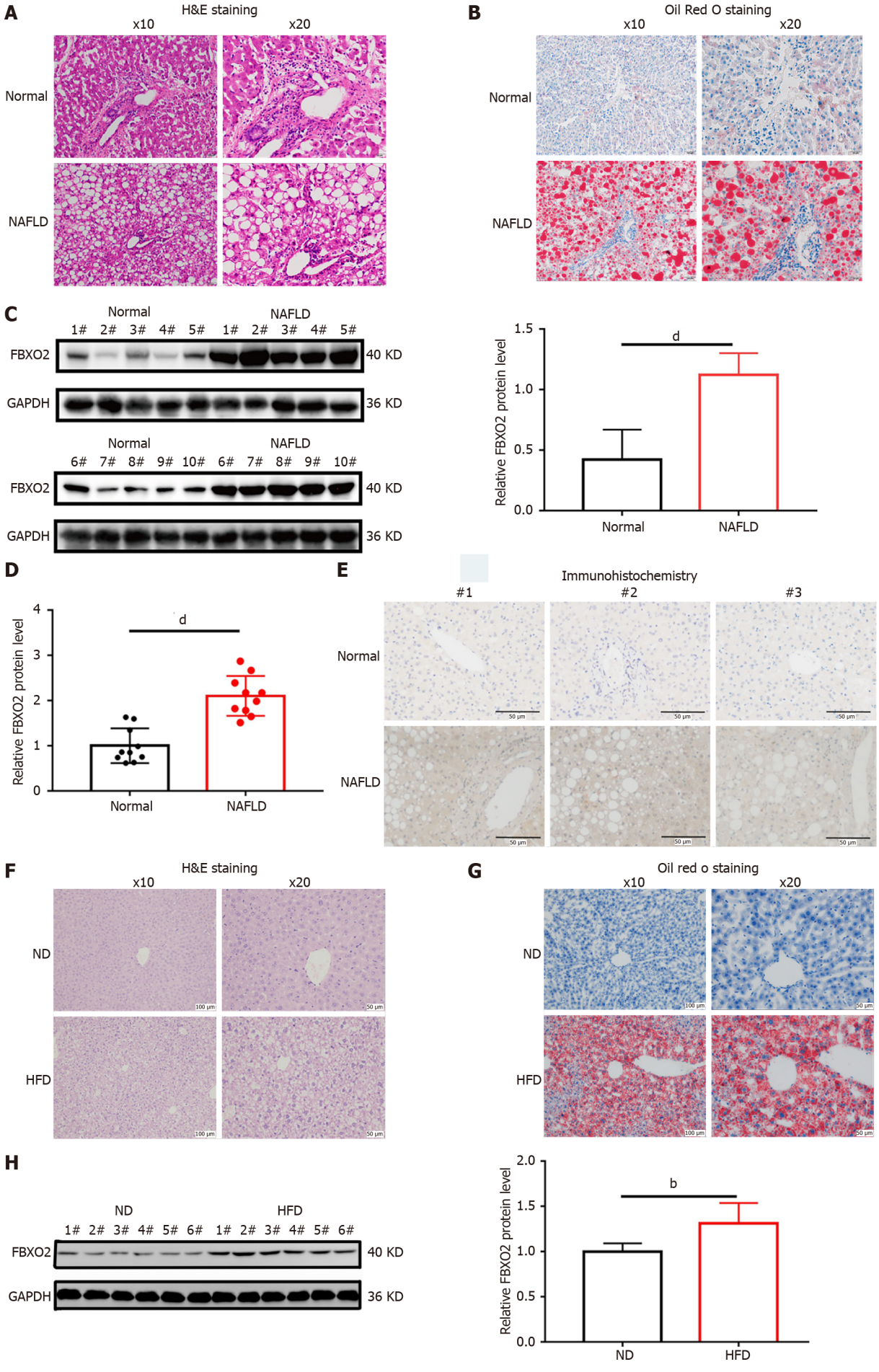
FBXO2 levels in the liver of patients with NAFLD and the HFD-fed mouse model were significantly increased compared to those in non-steatosis samples.

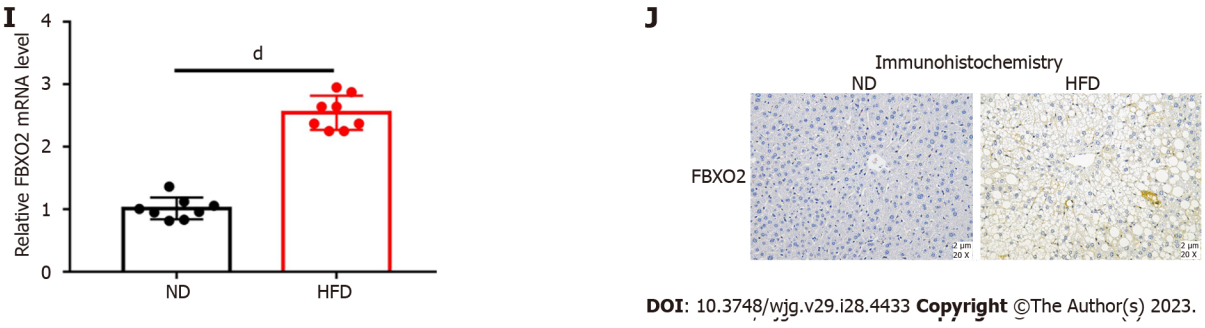
FBXO2 overexpression aggravates hepatic steatosis

Given the close correlation between FBXO2 expression and a fatty liver, we constructed a hepatocyte-specific FBXO2-overexpressing mouse model (Supplementary Figures 2A and B) to investigate the role of FBXO2 in exacerbating the HFD-induced liver steatosis, insulin resistance, and abnormal glucose metabolism. As expected, AAV-His-FBXO2-treated mice exhibited a significant increase in body weight (Supplementary Figure 2C), liver weight (Figure 3D), and the ratio of liver weight to body weight (Figure 3E) compared to AAV-His-vector-treated mice. The deposition of lipids in the liver was noticeably enhanced in AAV-His-FBXO2 mice, as determined by liver observations (Figure 3A), H&E staining (Figure 3B), Oil Red O staining (Figure 3C), and TG and T-Cho levels (Figures 3F and G). The overexpression of FBXO2 in the livers of AAV-His-FBXO2-treated mice significantly promoted the expression of lipogenesis genes [FASN and peroxisome proliferator-activated receptor gamma (PPARγ)] and fatty acid uptake genes [cluster of differentiation 36 (CD36) and fatty acid binding protein-1 (FABP1)] and suppressed the expression of fatty acid β-oxidation-related genes [acyl-CoA oxidase 1 (ACOX1), enoyl coenzyme A hydratase 1 (ECH1), medium-chain acyl-coenzyme A dehydrogenase (MCAD), and PPARα] (Figure 3H).

NAFLD is often accompanied by glucose metabolic disorders and insulin resistance. Unsurprisingly, FBXO2 overexpression significantly increased fasting blood glucose and insulin levels (Figures 3I and J). The HOMA-IR index was also increased accordingly (Figure 3K). Notably, there was no significant difference in food intake between AAV-His-FBXO2 mice and AAV-His-vector mice (Supplementary Figure 2D). In addition, the AAV-His-FBXO2 mice exhibited significantly higher blood glucose levels than AAV-His-vector mice, as determined from the OGTT and ITT data (Figures 3L-N).

We also investigated the effects of FBXO2 overexpression on lipid metabolic disorders *in vitro*. HepG2 cells were treated with OA to simulate the NAFLD phenotype. An increase in the mRNA and protein levels of FBXO2 was observed after 24 h of OA administration (Figures 4D and E). Oil Red O staining revealed that the intracellular lipid deposition (Figure 4A) and TG and T-Cho levels in HepG2 cells (Figures 4B and C) increased after OA treatment. Next, the His-FBXO2 plasmid was transfected into HepG2 cells. qRT-PCR and western blotting revealed increased FBXO2 expression (Supplementary Figures 3A and B). The effect of FBXO2 overexpression on lipid deposition was also observed in OA-


A
H&E staining
x10
x20
Normal
NAFLD
B
Oil Red O staining
x10
x20
Normal
NAFLD
C
Normal
NAFLD
1# 2# 3# 4# 5# 1# 2# 3# 4# 5#
FBXO2
40 KD
GAPDH
36 KD
Normal
NAFLD
6# 7# 8# 9# 10# 6# 7# 8# 9# 10#
FBXO2
40 KD
GAPDH
36 KD
Relative FBXO2 protein level
1.5
1.0
0.5
0.0
d
Normal
NAFLD
D
Relative FBXO2 protein level
4
3
2
1
0
d
Normal
NAFLD
E
Immunohistochemistry
#1
#2
#3
Normal
NAFLD
F
H&E staining
x10
x20
ND
HFD
G
Oil red o staining
x10
x20
ND
HFD
H
ND
HFD
1# 2# 3# 4# 5# 6# 1# 2# 3# 4# 5# 6#
FBXO2
40 KD
GAPDH
36 KD
Relative FBXO2 protein level
2.0
1.5
1.0
0.5
0.0
b
ND
HFD



DOI: 10.3748/wjg.v29.i28.4433 Copyright ©The Author(s) 2023.

Figure 2 F-box only protein 2 expression was up-regulated in livers of non-alcoholic fatty liver disease patients and high-fat diet mice models. A and B: Representative images of hematoxylin and eosin (H&E) and Oil Red O staining of liver tissues obtained from healthy controls and patients with non-alcoholic fatty liver disease (NAFLD). Scale bars, 50 μm and 100 μm; C: Western blot of F-box only protein 2 (FBXO2) expression in the liver tissues of healthy controls and patients with NAFLD (n = 10 liver samples per group); D: Expression of FBXO2 in liver tissue obtained from healthy controls and patients with NAFLD (n = 10 liver samples per group); E: Representative images of immunohistochemical staining of FBXO2 in liver tissue obtained from healthy controls and patients with NAFLD. Scale bars, 50 μm; F and G: Representative images of H&E and Oil Red O staining of liver tissue isolated from C57BL/6J mice treated with a normal chow diet (ND) or high-fat diet (HFD) for 16 wk. Scale bars, 50 μm and 100 μm; H: Representative images of FBXO2 western blots from liver tissue of C57BL/6J mice treated with an ND or HFD for 16 wk; I: Expression of FBXO2 in liver tissue obtained from C57BL/6J mice treated with an ND or HFD for 16 wk as detected using quantitative reverse transcription polymerase chain reaction (n = 8 liver samples per group); J: Representative images of immunohistochemical staining of FBXO2 in liver tissue obtained from C57BL/6J mice treated with an ND or HFD for 16 wk. Scale bars, 50 μm. $^{b}P < 0.01$, $^{d}P < 0.0001$. FBXO2: F-box only protein 2; NAFLD: Non-alcoholic fatty liver disease; HFD: High-fat diet; H&E: Hematoxylin and eosin; ND: Normal chow diet.

treated HepG2 cells. Specifically, FBXO2 overexpression after transfecting His-FBXO2 plasmids into HepG2 cells, greatly increased OA-induced lipid deposition (Figure 4F). FBXO2 overexpression also increased OA-induced cellular TG and T-Cho levels (Figures 4G and H). The overexpression of FBXO2 in OA-treated HepG2 cells also promoted the expression of FASN, PPARG, CD36, and FABP1 and suppressed the expression of ACOX1, ECH1, MCAD, and PPARα (Figure 4I). These data suggest that the up-regulation of FBXO2 expression in the liver exacerbated liver steatosis, HFD-triggered insulin resistance, and abnormal glucose metabolism.

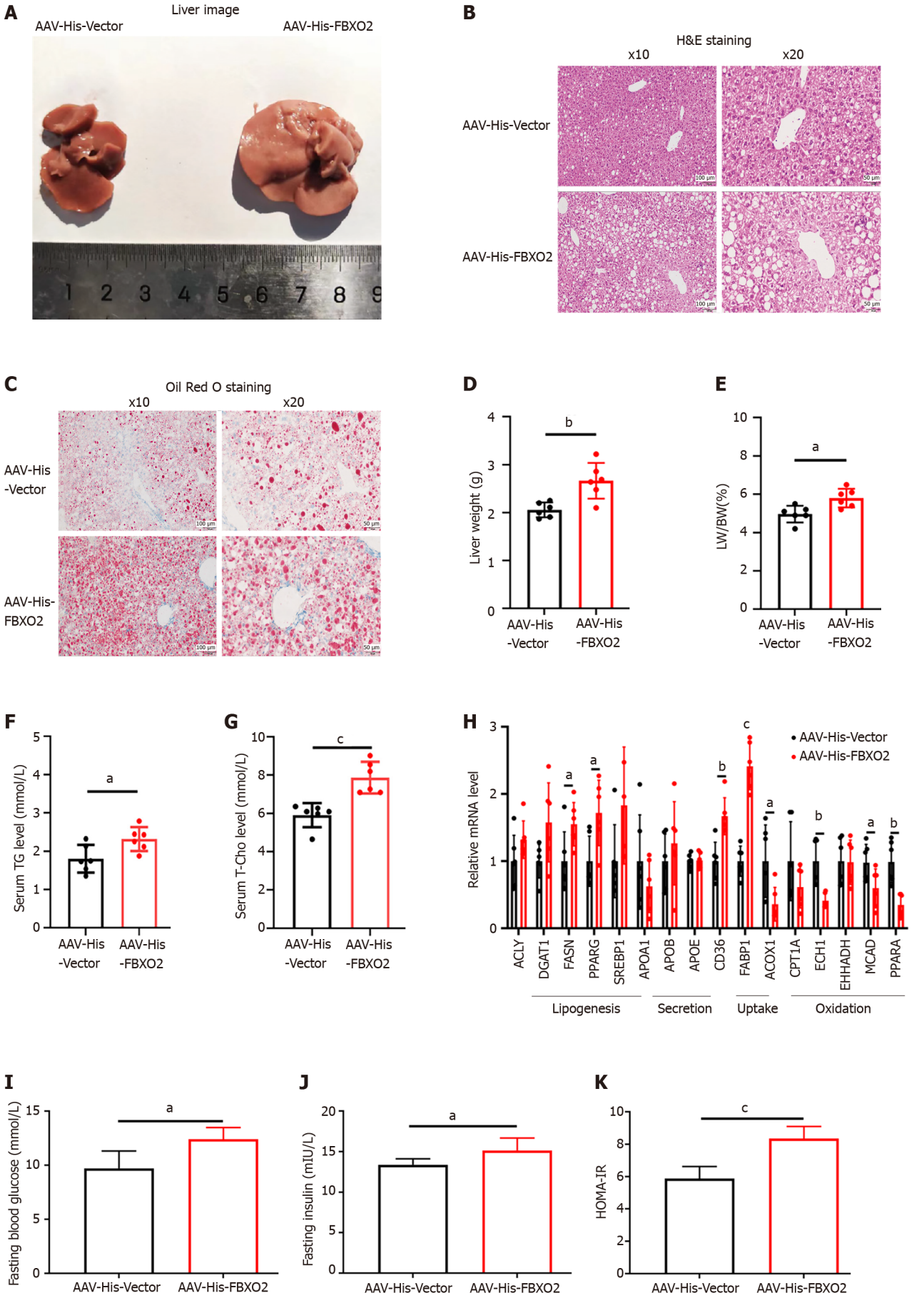
FBXO2 knockdown ameliorates lipid accumulation in hepatocytes

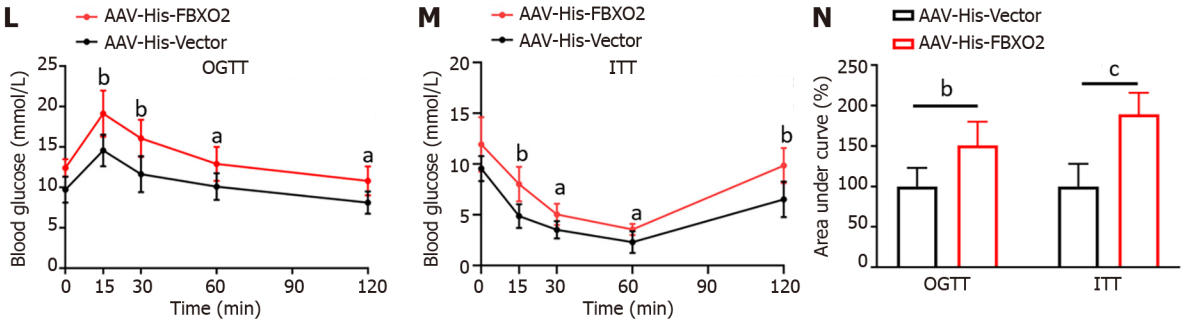
After confirming that the overexpression of FBXO2 exacerbated liver steatosis, we examined the effect of FBXO2 knockdown on lipid metabolic disorder in hepatocytes. To achieve this, the Sh-FBXO2 plasmid was transfected into HepG2 cells. Both qRT-PCR and western blot results indicated that FBXO2 expression levels decreased after transfection, confirming successful FBXO2 knockdown (Supplementary Figures 3C and D). FBXO2 knockdown decreased the OA-induced lipid deposition (Figure 4J) and regulated OA-induced TG and T-Cho secretion (Figures 4K and L). The knockdown of FBXO2 in OA-treated HepG2 cells inhibited the expression of lipogenesis genes (FASN and PPARγ) and fatty acid uptake genes (CD36 and FABP1) and promoted the expression of fatty acid β-oxidation related genes (ACOX1, ECH1, MCAD, and PPARα) (Figure 4M). Consistent with these data, *in vitro* gene therapy using Sh-FBXO2 plasmids further demonstrated that the knockdown of FBXO2 could significantly alleviate OA-induced lipid accumulation in hepatocytes (hepatic steatosis).

The up-regulation of FBXO2 expression promotes HADHA ubiquitination and degradation in HepG2 cells

We used a co-IP-based MS method to identify which proteins interact with endogenous FBXO2 in HepG2 cells. Based on peptide spectra matching protein score, HADHA was identified as a potential binding protein for FBXO2 in HepG2 cells (Figure 5A). *In vitro* interaction studies suggested that both exogenous and endogenous FBXO2 could bind directly to HADHA and vice versa. Additionally, the interaction between FBXO2 and HADHA was determined *via* a co-IP assay in HEK293T (Figures 5C and D) and HepG2 cells (Figures 5E and F). *In vitro* interaction tests suggested that both exogenous and endogenous FBXO2 could directly bind to HADHA and vice versa. Immunofluorescence staining also revealed the co-localization of FBXO2 and HADHA after the HEK293T cells were transfected with His-FBXO2 and Myc-HADHA plasmids (Figure 5B).

Next, we tested whether FBXO2 could activate the ubiquitination of HADHA. The expression of FBXO2 and HA-Ub together significantly enhanced the ubiquitination of HADHA in HEK293T cells, compared to control cells transfected with vectors expressing FBXO2 and HA-Ub alone (Figure 6A). Consistent with the results of the ubiquitination assays, gene expression analysis supported the reduction of HADHA protein levels in HepG2 cells and HFD-fed mouse models overexpressing FBXO2 (Figures 6B and D). Further, HADHA degradation was reduced after co-treatment with the proteasome inhibitor MG132 (SML1135; Sigma, United States) in HepG2 cells (Figure 6E). Moreover, FBXO2 knockdown increased the level protein of HADHA in HepG2 cells (Figure 6C). Notably, the mRNA levels of HADHA were not affected by FBXO2 overexpression or knockdown (Supplementary Figures 4A-C). Additionally, we analysed whether FBXO2 decreased the half-life of the HADHA protein. We transfected HepG2 cells with His-Vector or His-FBXO2 plasmids and treated them with the protein synthesis inhibitor cycloheximide (CHX) at different time points. The half-life of the HADHA protein was drastically reduced in FBXO2-overexpressing cells compared to the control cells (Figure 6F). These findings indicated that FBXO2 facilitates the degradation of HADHA *via* the ubiquitination machinery.


A
Liver image
AAV-His-Vector
AAV-His-FBXO2
B
H&E staining
x10
x20
AAV-His-Vector
AAV-His-FBXO2
C
Oil Red O staining
x10
x20
AAV-His -Vector
AAV-His-FBXO2
D
Liver weight (g)
b
AAV-His -Vector
AAV-His -FBXO2
E
LW/BW(%)
a
AAV-His -Vector
AAV-His -FBXO2
F
Serum TG level (mmol/L)
a
AAV-His -Vector
AAV-His -FBXO2
G
Serum T-Cho level (mmol/L)
c
AAV-His -Vector
AAV-His -FBXO2
H
Relative mRNA level
AAV-His-Vector
AAV-His-FBXO2
ACLY
DGAT1
FASN
PPARG
SREBP1
APOA1
APOB
APOE
CD36
FABP1
ACOX1
CPT1A
ECH1
EHHADH
MCAD
PPARA
Lipogenesis
Secretion
Uptake
Oxidation
I
Fasting blood glucose (mmol/L)
a
AAV-His-Vector
AAV-His-FBXO2
J
Fasting insulin (mIU/L)
a
AAV-His-Vector
AAV-His-FBXO2
K
HOMA-IR
c
AAV-His-Vector
AAV-His-FBXO2



DOI: 10.3748/wjg.v29.i28.4433 **Copyright** ©The Author(s) 2023.

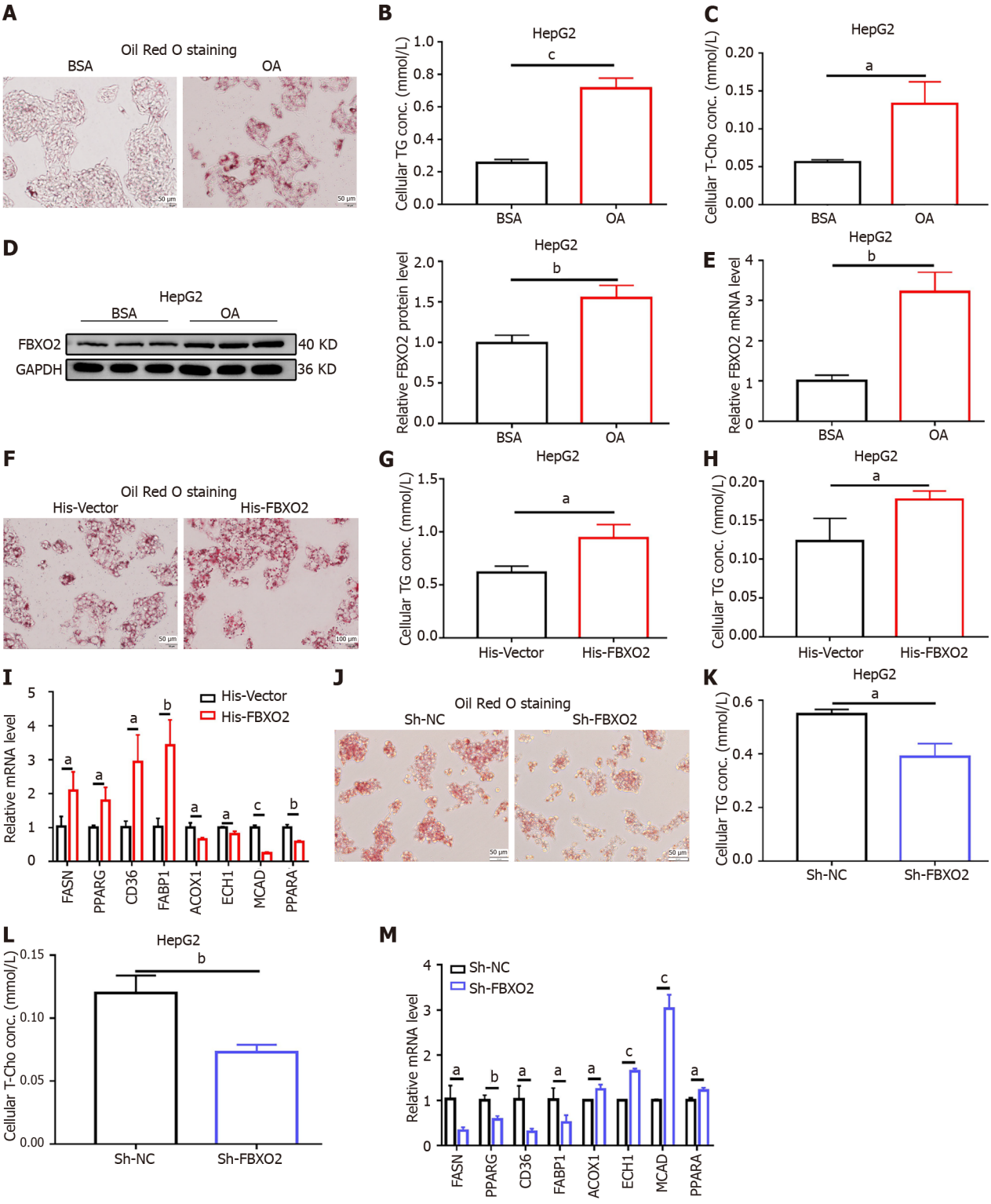
Figure 3 Overexpression of F-box only protein 2 exacerbated high-fat diet-induced liver steatosis, insulin-resistance, and abnormal glucose metabolism. A: Representative images indicating histological changes in the livers of adeno-associated virus (AAV)-His-vector and AAV-His-F-box only protein 2 (FBXO2) mice after 16 wk of administering an high-fat diet (HFD); B and C: Representative images of hematoxylin and eosin and Oil Red O staining of liver tissue obtained from AAV-His-vector and AAV-His-FBXO2 mice after 16 wk of HFD. Scale bars, 50 μm and 100 μm; D-G: The liver weight, ratio of liver weight/body weight, serum triglyceride and total cholesterol levels in AAV-His-vector and AAV-His-FBXO2 mice after 16 wk of administering an HFD (n = 6 per group); H: quantitative reverse transcription polymerase chain reaction analysis of the expression of genes associated with lipogenesis, fatty acid secretion and uptake, and oxidation in AAV-His-vector and AAV-His-FBXO2 mice after 16 wk of administering an HFD (n = 6 per group); I: Fasting blood glucose levels; J: Fasting serum insulin levels; K: The homeostatic model assessment of insulin resistance; L: Oral glucose tolerance test (OGTT) scores; M: Insulin tolerance test (ITT); N: Calculated area under curve of OGTT and ITT in the AAV-His-vector mice and AAV-His-FBXO2 mice after 16 wk of HFD (n = 6 per group). $^{a}P < 0.05$, $^{b}P < 0.01$, $^{c}P < 0.001$. AAV: Adeno-associated virus; FBXO2: F-box only protein 2; H&E: Hematoxylin and eosin; ITT: Insulin tolerance test; OGTT: Oral glucose tolerance test; LW: Liver weight; BW: Body weight; TG: Triglyceride; T-Cho: Total cholesterol; HOMA-IR: Homeostatic model assessment of insulin resistance; FASN: Fatty acid synthase; PPAR: Peroxisome proliferator-activated receptor; CD36: Cluster of differentiation 36; ACOX1: Acyl-CoA oxidase 1; ECH1: Enoyl coenzyme A hydratase 1; MCAD: Medium-chain acyl-coenzyme A dehydrogenase.

The above finding led us to determine whether HADHA alterations mediate the effect of FBXO2 on lipid accumulation in hepatocytes. First, FBXO2 overexpression increased OA-induced lipid deposition and TG and T-Cho secretion. Moreover, the overexpression of FBXO2 in OA- treated HepG2 cells enhanced the expression of FASN, PPARγ, CD36, and FABP1 and inhibited the expression of ACOX1, ECH1, MCAD, and PPARα. However, these effects were reversed after HepG2 cells were transfected with the Myc-HADHA plasmid to overexpress HADHA as indicated by the changes in lipid deposition (Figure 6G), TG and T-Cho secretion (Figures 6H and I), and mRNA expression of lipid metabolism-related genes (Figure 6J). FBXO2 and HADHA overexpression efficiency was also confirmed *via* western blot (Supplementary Figure 3E). Collectively, these indicated that the up-regulation of FBXO2 exacerbated OA-induced lipid accumulation by promoting the ubiquitination and degradation of HADHA in HepG2 cells.

DISCUSSION

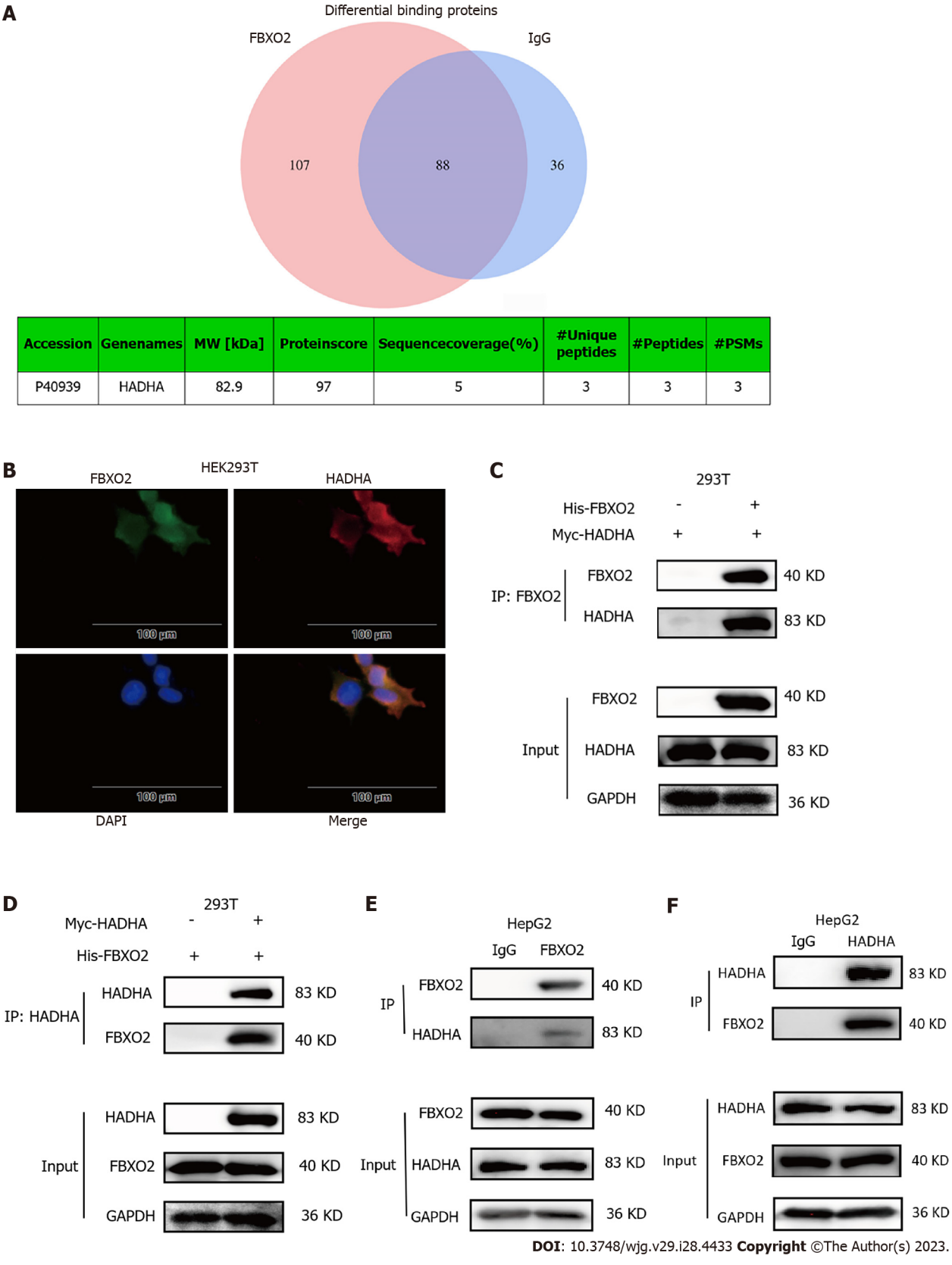
FBXO2 is an E3 ligase that can regulate protein stability through ubiquitin-mediated protein-protein interaction and plays an indispensable role in the cell cycle regulation of the UPS[21]. It regulates cell proliferation, transcription, and apoptosis through the ubiquitination and degradation of target proteins, thereby affecting the occurrence and development of various diseases, such as malignant tumours, neuronal diseases, and inflammation[22,24,32,33]. However, the status of FBXO2 expression in NAFLD and its relationship with clinicopathological parameters has not been clarified. In the present study, we found that FBXO2 levels were significantly up-regulated in NAFLD liver tissues. Subsequently, we simulated NAFLD in HFD mice and OA-treated HepG2 cells, and the results were consistent with those obtained in human liver tissue. Our sequencing results of NAFLD liver tissue samples revealed changes in multiple metabolic pathways, for example the PI3K-AKT pathway. Recent studies conducted by our team found that the expression level of FBXO2 in NAFLD mouse models was downregulated after sleeve gastrectomy. Upregulation of FBXO2 could activate the PI3K-AKT pathway[31]. Based on the above results, we speculate that FBXO2 upregulation is related to NAFLD occurrence and development.

Next, we constructed a hepatocyte-specific FBXO2-overexpressing mouse model to further explore the relationship between FBXO2 and NAFLD. Lipid accumulation in the liver is a clinical feature of NAFLD and is caused by an imbalance between lipid input and output[34]. This imbalance is regulated by four pathways: Lipid lipogenesis, lipid uptake, lipid secretion, and fatty acid oxidation[27,35]. In the present study, we found that the deposition of liver lipids was visibly enhanced in hepatocyte-specific FBXO2-overexpressing mice models. FBXO2 overexpression in the liver significantly promoted the expression of lipogenesis genes (FASN and PPARγ) and fatty acid uptake genes (CD36 and FABP1) and inhibited the expression of fatty acid β-oxidation-related genes (ACOX1, ECH1, MCAD and PPARα) in AAV-His-FBXO2 mice. In contrast, FBXO2 knockdown in OA-treated HepG2 cells had the opposite effect on the expression of lipid accumulation and the expression of lipid metabolism-related genes. The alleviative effect of FBXO2 knockdown on lipid metabolism suggests its effect in treating NAFLD. In addition, combined with the effect of the overexpression and knockdown of FBXO2 on lipid metabolism, it is worth considering that FBXO2 may promote the ubiquitination of one or more proteins that can mediate lipid metabolism. In other words, the overexpression of FBXO2 can accelerate protein



DOI: 10.3748/wjg.v29.i28.4433 **Copyright** ©The Author(s) 2023.

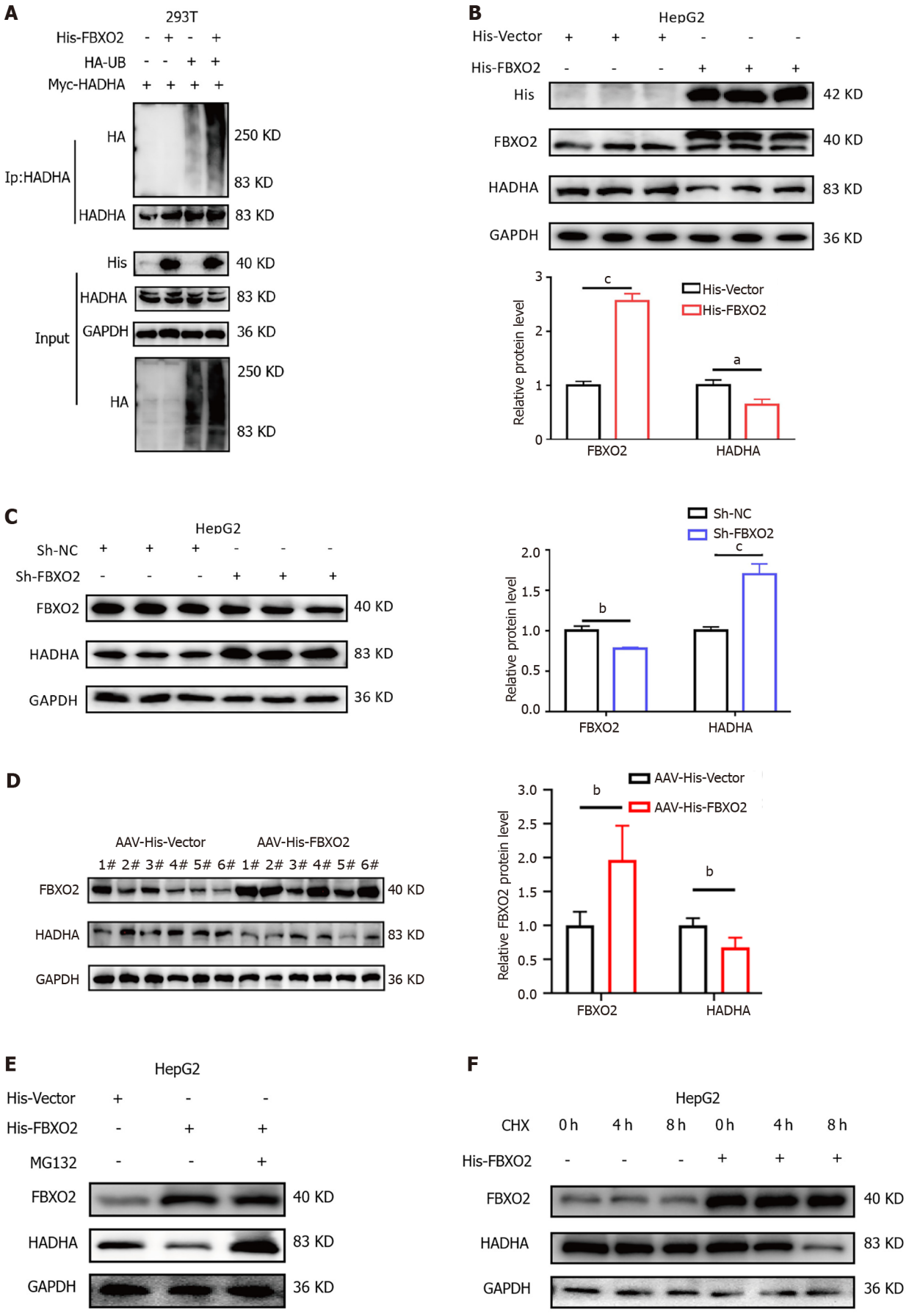
Figure 4 Effect of F-box only protein 2 overexpression or knockdown on lipid accumulation in hepatocytes. A: Representative images of Oil Red O staining of HepG2 cells treated with oleate (OA) for 24 h. Scale bar, 50 μm; B and C: Triglyceride (TG) and total cholesterol (T-Cho) levels in HepG2 cells treated with OA for 24 h; D and E: Western blot and quantitative reverse transcription polymerase chain reaction (qRT-PCR) analysis of F-box only protein 2 (FBXO2) expression in HepG2 cells treated with OA for 24 h; F-I: HepG2 cells transfected with His-FBXO2 plasmids to overexpress FBXO2, followed by OA treatment for 24 h; representative images of Oil Red O staining (F), TG (G) and T-Cho (H) levels; expression analysis of genes associated with lipogenesis, fatty acid uptake, and oxidation as detected using qRT-PCR (I); J-M: HepG2 cells were transfected with Sh-FBXO2 plasmids to knockdown FBXO2 expression, followed by OA treatment for 24 h; representative images of Oil Red O staining (J), TG (K) and T-Cho (L) levels; expression analysis of genes associated with lipogenesis, fatty acid uptake, and oxidation as detected using qRT-PCR (M). $^{a}P < 0.05$, $^{b}P < 0.01$, $^{c}P < 0.001$. FBXO2: F-box only protein 2; BSA: Bovine serum albumin; OA: Oleate; TG: Triglyceride; T-Cho: Total cholesterol; FASN: Fatty acid synthase; PPAR: Peroxisome proliferator-activated receptor; CD36: Cluster of differentiation 36; ACOX1: Acyl-CoA oxidase 1; ECH1: Enoyl coenzyme A hydratase 1; MCAD: Medium-chain acyl-coenzyme A dehydrogenase; NC: Normal control.

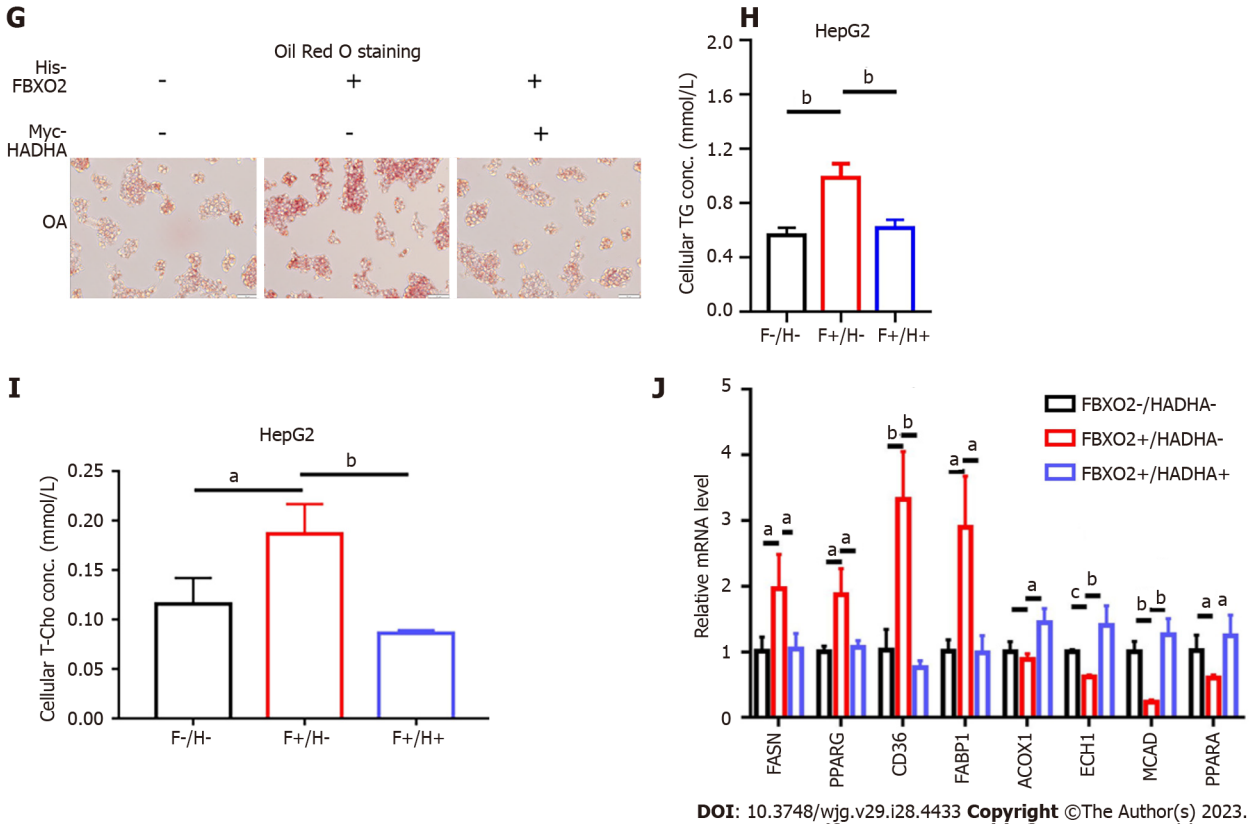


Accession	Genenames	MW [kDa]	Proteinscore	Sequencecoverage(%)	#Unique peptides	#Peptides	#PSMs
P40939	HADHA	82.9	97	5	3	3	3

DOI: 10.3748/wjg.v29.i28.4433 **Copyright** ©The Author(s) 2023.

Figure 5 F-box only protein 2 directly binds to the hydroxyl CoA dehydrogenase alpha subunit and vice versa. A: Proteins interacting with endogenous F-box only protein 2 (FBXO2) in HepG2 cells as revealed using a co-immunoprecipitation (co-IP)-based mass spectrometry method; B: Immunofluorescence staining of HEK293T cells transfected with His-FBXO2 and Myc-the hydroxyl CoA dehydrogenase alpha subunit plasmids; C-F: Co-IP assays in HEK293T and HepG2 cells. FBXO2: F-box only protein 2; HADHA: Hydroxyl CoA dehydrogenase alpha subunit; IgG: Immunoglobulin G; DAPI: 4'-6-diamidino-2-phenylindole.


A
293T
His-FBXO2 - + - +
HA-UB - - + +
Myc-HADHA + + + +
Ip:HADHA
HA
250 KD
83 KD
HADHA
83 KD
Input
His
40 KD
HADHA
83 KD
GAPDH
36 KD
HA
250 KD
83 KD
B
HepG2
His-Vector + + + - - -
His-FBXO2 - - - + + +
His
42 KD
FBXO2
40 KD
HADHA
83 KD
GAPDH
36 KD
Relative protein level
His-Vector
His-FBXO2
c
a
FBXO2
HADHA
C
HepG2
Sh-NC + + + - - -
Sh-FBXO2 - - - + + +
FBXO2
40 KD
HADHA
83 KD
GAPDH
36 KD
Sh-NC
Sh-FBXO2
Relative protein level
b
c
FBXO2
HADHA
D
AAV-His-Vector
AAV-His-FBXO2
1# 2# 3# 4# 5# 6# 1# 2# 3# 4# 5# 6#
FBXO2
40 KD
HADHA
83 KD
GAPDH
36 KD
AAV-His-Vector
AAV-His-FBXO2
Relative FBXO2 protein level
b
b
FBXO2
HADHA
E
HepG2
His-Vector + - -
His-FBXO2 - + +
MG132 - - +
FBXO2
40 KD
HADHA
83 KD
GAPDH
36 KD
F
HepG2
CHX 0 h 4 h 8 h 0 h 4 h 8 h
His-FBXO2 - - - + + +
FBXO2
40 KD
HADHA
83 KD
GAPDH
36 KD



DOI: 10.3748/wjg.v29.i28.4433 **Copyright** ©The Author(s) 2023.

Figure 6 F-box only protein 2 ubiquitinated and degraded the hydroxyl CoA dehydrogenase alpha subunit. A: The hydroxyl CoA dehydrogenase alpha subunit (HADHA) ubiquitination in HEK293T cells; B-D: Western blot of F-box only protein 2 (FBXO2) and HADHA expression in the His-Vector group *vs* His-FBXO2 group (B), Sh-NC group *vs* Sh-FBXO2 group (C), and adeno-associated virus (AAV)-His-vector mice *vs* AAV-His-FBXO2 mice (D); E: Western blot of FBXO2 and HADHA expression in HepG2 cells. HepG2 cells were transfected with His-FBXO2 plasmids for 24 h, followed by incubation with or without MG132 for 24 h; F: Western blot of FBXO2 and HADHA expression in HepG2 cells. HepG2 cells were transfected with FBXO2 adenovirus for 48 h, followed by incubation with cycloheximide (CHX) for 0, 4, or 8 h before sample collection; G-J: HepG2 cells were transfected with His-FBXO2 plasmids and Myc-HADHA plasmids to overexpress FBXO2 and HADHA, respectively, followed by treatment with oleate for 24 h; representative images of Oil Red O staining (G), triglyceride (H) and total cholesterol (I) levels; expression analysis of genes associated with lipogenesis, fatty acid uptake, and oxidation as detected using quantitative reverse transcription polymerase chain reaction (J). FBXO2: F-box only protein 2; HADHA: Hydroxyl CoA dehydrogenase alpha subunit; $^{a}P < 0.05$, $^{b}P < 0.01$, $^{c}P < 0.001$. AAV: Adeno-associated virus; OA: Oleate; TG: Triglyceride; T-Cho: Total cholesterol; FASN: Fatty acid synthase; PPAR: Peroxisome proliferator-activated receptor; CD36: Cluster of differentiation 36; ACOX1: Acyl-CoA oxidase 1; ECH1: Enoyl coenzyme A hydratase 1; MCAD: Medium-chain acyl-coenzyme A dehydrogenase; NC: Normal control.

degradation, thus aggravating NAFLD. On the contrary, the knockdown of FBXO2 protects lipid metabolising enzymes from degradation, thus maintaining normal lipid metabolism.

To further explore the mechanism through which FBXO2 affects NAFLD, we screened the proteins that could interact with endogenous FBXO2 in HepG2 cells using a co-IP-based MS method. The mitochondrial trifunctional enzyme subunit-alpha (HADHA) was identified as a potential binding protein for FBXO2. HADHA, a mitochondrial β-oxidation-associated enzyme, encodes the α-subunit of the mitochondrial trifunctional protein (hydroxyacyl-CoA dehydrogenase/3-ketoacyl-CoA thiolase/enoyl-CoA hydratase). This enzyme complex catalyses the three steps of the β-oxidation of fatty acids in the mitochondria[14]. HADHA deficiency in mice has been reported to aggravate NAFLD[36-38]. Further, HADHA knockout can lead to hyperglycemia and consequently induce liver lipid deposition[18,39]. *In vitro* interaction tests in the present study suggested that both exogenous and endogenous FBXO2 could directly bind to HADHA and vice versa. In addition, the results of our ubiquitination assays showed that FBXO2 facilitates the degradation of HADHA *via* the ubiquitination machinery. We further confirmed the interaction between FBXO2 and HADHA in hepatocytes using MG132 and CHX. We also found that FBXO2 overexpression during OA-induced liver steatosis was reversed after Myc-HADHA plasmids were transfected into HepG2 cells to overexpress HADHA.

Another interesting observation is that in addition to the exacerbation of steatosis, the targeted upregulation of FBXO2 expression in HFD-fed mouse livers led to a significant exacerbation of hyperglycemia and insulin resistance, which could be caused by various reasons. Previous studies have shown that FBXO2 targets insulin receptors to achieve ubiquitin-dependent degradation, thus regulating insulin signaling integrity[24]. The overexpression of FBXO2 can stimulate severe insulin resistance in the liver and inhibit its normal function, promoting adipogenesis. Therefore, increased insulin resistance leads to excessive lipid accumulation in the liver[34]. Recent studies have shown that HADHA knockdown augments the glucagon response[14]. This study speculates that a decrease in HADHA levels might induce an increase in blood glucose levels after the overexpression of FBXO2. In addition, the increased expression of lipogenesis- and fatty acid uptake-associated genes and decreased expression of fatty acid β-oxidation-related genes might also contribute to the observed effects on glycemic control[40-44].

CONCLUSION

Liver FBXO2 expression is upregulated in NAFLD and FBXO2 is correlated with metabolic disorders. Moreover, upregulation of FBXO2 exacerbates liver steatosis by promoting the degradation of HADHA. Finally, our findings suggest that FBXO2 can be used as a feasible therapeutic target for NAFLD.

ARTICLE HIGHLIGHTS

Research background

Non-alcoholic fatty liver disease (NAFLD) is a major health burden with an increasing global incidence. Unfortunately, the unavailability of knowledge underlying NAFLD pathogenesis inhibits effective preventive and therapeutic measures. The key issues affecting the treatment of patients with NAFLD are atherosclerotic cardio-cerebrovascular diseases, cirrhosis, and malignant tumors associated with the metabolic syndrome. The abnormal expression of F-box only protein 2 (FBXO2), an E3 ligase, in obese mice disrupts glucose homeostasis through ubiquitin-mediated insulin receptor degradation, however, the role of FBXO2 in NAFLD pathology remains unclear.

Research motivation

Recent studies conducted by our team found that the expression level of FBXO2 in NAFLD mouse models was downregulated after sleeve gastrectomy.

Research objectives

This study aimed to explore the molecular mechanism of NAFLD.

Research methods

Whole genome sequencing (WGS) analysis was performed on liver tissues from patients with NAFLD (n = 6) and patients with normal metabolic conditions (n = 6) to identify the target genes. A NAFLD C57BL6/J mouse model induced by 16 wk of high-fat diet (HFD) feeding and a hepatocyte-specific FBXO2 overexpression mouse model were used for *in vivo* studies. Plasmid transfection, co-immunoprecipitation-based mass spectrometry assays, and ubiquitination in HepG2 cells and HEK293T cells were used for *in vitro* studies.

Research results

A total of 30982 genes were detected in WGS analysis, with 649 up-regulated and 178 down-regulated. Expression of FBXO2 was upregulated in the liver tissues of patients with NAFLD. Hepatocyte-specific FBXO2 overexpression facilitated NAFLD-associated phenotypes in mice. Overexpression of FBXO2 aggravated odium oleate (OA)-induced lipid accumulation in HepG2 cells, resulting in an abnormal expression of genes related to lipid metabolism, such as fatty acid synthase, peroxisome proliferator-activated receptor alpha, and so on. In contrast, knocking down FBXO2 in HepG2 cells significantly alleviated the oleate-induced lipid accumulation and aberrant expression of lipid metabolism genes. The hydroxyl CoA dehydrogenase alpha subunit (HADHA), a protein involved in oxidative stress, was a target of FBXO2-mediated ubiquitination. FBXO2 directly bound to HADHA and facilitated its proteasomal degradation in HepG2 and HEK293T cells. Supplementation with HADHA alleviated lipid accumulation caused by FBXO2 overexpression in HepG2 cells.

Research conclusions

FBXO2 exacerbates lipid accumulation by targeting HADHA.

Research perspectives

Our results shed light on the role of FBXO2 not only in NAFLD but also in other metabolic diseases involving lipid accumulation, supporting further investigation of the therapeutic potential of this molecule in further studies.

FOOTNOTES

Author contributions: Hu SY and Liu Z contributed equally to this work; Hu SY and Liu Z designed the research study; Liu Z, Chen NY, Zhang Z, and Zhou S performed the research; Liu Z and Chen NY contributed new reagents and analytic tools; Liu Z and Chen NY analyzed the data and wrote the manuscript; and all authors have read and approve the final manuscript.

Supported by the National Natural Science Foundation of China, No. 82070869 and 82270914.

Institutional review board statement: The study was reviewed and approved by the Institutional Review Board of Qilu Hospital of Shandong University.

Institutional animal care and use committee statement: All animal experiments conformed to the internationally accepted principles for the care and use of laboratory animals (license No. S453, Institutional Animal Care and Use Committee of Shandong Provincial Qian

Foshan Hospital).

Informed consent statement: Written informed consent was obtained from the patients and their families.

Conflict-of-interest statement: All the authors report no relevant conflicts of interest for this article.

Data sharing statement: No additional data are available.

ARRIVE guidelines statement: The authors have read the ARRIVE guidelines, and the manuscript was prepared and revised according to the ARRIVE guidelines.

Open-Access: This article is an open-access article that was selected by an in-house editor and fully peer-reviewed by external reviewers. It is distributed in accordance with the Creative Commons Attribution NonCommercial (CC BY-NC 4.0) license, which permits others to distribute, remix, adapt, build upon this work non-commercially, and license their derivative works on different terms, provided the original work is properly cited and the use is non-commercial. See: https://creativecommons.org/Licenses/by-nc/4.0/

Country/Territory of origin: China

ORCID number: Zhi Liu 0000-0002-1888-1550; Ning-Yuan Chen 0000-0003-3249-1935; Zhao Zhang 0000-0003-2206-8682; Sai Zhou 0009-0001-8962-9942; San-Yuan Hu 0000-0002-0546-9778.

S-Editor: Wang JJ
L-Editor: A
P-Editor: Yu HG

REFERENCES

1 **Drescher HK**, Weiskirchen S, Weiskirchen R. Current Status in Testing for Nonalcoholic Fatty Liver Disease (NAFLD) and Nonalcoholic Steatohepatitis (NASH). *Cells* 2019; **8** [PMID: 31394730 DOI: 10.3390/cells8080845]
2 **Hirode G**, Vittinghoff E, Wong RJ. Increasing Clinical and Economic Burden of Nonalcoholic Fatty Liver Disease Among Hospitalized Adults in the United States. *J Clin Gastroenterol* 2019; **53**: 765-771 [PMID: 31135632 DOI: 10.1097/MCG.0000000000001229]
3 **Conway BN**, Han X, Munro HM, Gross AL, Shu XO, Hargreaves MK, Zheng W, Powers AC, Blot WJ. The obesity epidemic and rising diabetes incidence in a low-income racially diverse southern US cohort. *PLoS One* 2018; **13**: e0190993 [PMID: 29324894 DOI: 10.1371/journal.pone.0190993]
4 **Younossi Z**, Anstee QM, Marietti M, Hardy T, Henry L, Eslam M, George J, Bugianesi E. Global burden of NAFLD and NASH: trends, predictions, risk factors and prevention. *Nat Rev Gastroenterol Hepatol* 2018; **15**: 11-20 [PMID: 28930295 DOI: 10.1038/nrgastro.2017.109]
5 **Huby T**, Gautier EL. Immune cell-mediated features of non-alcoholic steatohepatitis. *Nat Rev Immunol* 2022; **22**: 429-443 [PMID: 34741169 DOI: 10.1038/s41577-021-00639-3]
6 **Friedman SL**, Neuschwander-Tetri BA, Rinella M, Sanyal AJ. Mechanisms of NAFLD development and therapeutic strategies. *Nat Med* 2018; **24**: 908-922 [PMID: 29967350 DOI: 10.1038/s41591-018-0104-9]
7 **Byrne CD**, Targher G. NAFLD: a multisystem disease. *J Hepatol* 2015; **62**: S47-S64 [PMID: 25920090 DOI: 10.1016/j.jhep.2014.12.012]
8 **Rinella ME**, Sanyal AJ. Management of NAFLD: a stage-based approach. *Nat Rev Gastroenterol Hepatol* 2016; **13**: 196-205 [PMID: 26907882 DOI: 10.1038/nrgastro.2016.3]
9 **Li K**, Zhang K, Wang H, Wu Y, Chen N, Chen J, Qiu C, Cai P, Li M, Liang X, Su D. Hrd1-mediated ACLY ubiquitination alleviate NAFLD in db/db mice. *Metabolism* 2021; **114**: 154349 [PMID: 32888949 DOI: 10.1016/j.metabol.2020.154349]
10 **Donne R**, Saroul-Ainama M, Cordier P, Hammoutene A, Kabore C, Stadler M, Nemazanyy I, Galy-Fauroux I, Herrag M, Riedl T, Chansel-Da Cruz M, Caruso S, Bonnafous S, Öllinger R, Rad R, Unger K, Tran A, Couty JP, Gual P, Paradis V, Celton-Morizur S, Heikenwalder M, Revy P, Desdouets C. Replication stress triggered by nucleotide pool imbalance drives DNA damage and cGAS-STING pathway activation in NAFLD. *Dev Cell* 2022; **57**: 1728-1741.e6 [PMID: 35768000 DOI: 10.1016/j.devcel.2022.06.003]
11 **Fang J**, Ji YX, Zhang P, Cheng L, Chen Y, Chen J, Su Y, Cheng X, Zhang Y, Li T, Zhu X, Zhang XJ, Wei X. Hepatic IRF2BP2 Mitigates Nonalcoholic Fatty Liver Disease by Directly Repressing the Transcription of ATF3. *Hepatology* 2020; **71**: 1592-1608 [PMID: 31529495 DOI: 10.1002/hep.30950]
12 **Chen Z**, Yu Y, Cai J, Li H. Emerging Molecular Targets for Treatment of Nonalcoholic Fatty Liver Disease. *Trends Endocrinol Metab* 2019; **30**: 903-914 [PMID: 31597607 DOI: 10.1016/j.tem.2019.08.006]
13 **Lonardo A**, Mantovani A, Petta S, Carraro A, Byrne CD, Targher G. Metabolic mechanisms for and treatment of NAFLD or NASH occurring after liver transplantation. *Nat Rev Endocrinol* 2022; **18**: 638-650 [PMID: 35840803 DOI: 10.1038/s41574-022-00711-5]
14 **Pan A**, Sun XM, Huang FQ, Liu JF, Cai YY, Wu X, Alolga RN, Li P, Liu BL, Liu Q, Qi LW. The mitochondrial β-oxidation enzyme HADHA restrains hepatic glucagon response by promoting β-hydroxybutyrate production. *Nat Commun* 2022; **13**: 386 [PMID: 35046401 DOI: 10.1038/s41467-022-28044-x]
15 **Le-Tian Z**, Cheng-Zhang H, Xuan Z, Zhang Q, Zhen-Gui Y, Qing-Qing W, Sheng-Xuan W, Zhong-Jin X, Ran-Ran L, Ting-Jun L, Zhong-Qu S, Zhong-Hua W, Ke-Rong S. Protein acetylation in mitochondria plays critical functions in the pathogenesis of fatty liver disease. *BMC Genomics* 2020; **21**: 435 [PMID: 32586350 DOI: 10.1186/s12864-020-06837-y]
16 **Nakamura MT**, Yudell BE, Loor JJ. Regulation of energy metabolism by long-chain fatty acids. *Prog Lipid Res* 2014; **53**: 124-144 [PMID: 24362249 DOI: 10.1016/j.plipres.2013.12.001]
17 **Ding J**, Wu L, Zhu G, Zhu J, Luo P, Li Y. HADHA alleviates hepatic steatosis and oxidative stress in NAFLD *via* inactivation of the MKK3/MAPK pathway. *Mol Biol Rep* 2023; **50**: 961-970 [PMID: 36376538 DOI: 10.1007/s11033-022-07965-2]

18 **Ma M**, Zhang C, Cao R, Tang D, Sang X, Zou S, Wang X, Xu H, Liu G, Dai L, Tian Y, Gao X, Fu X. UBE2O promotes lipid metabolic reprogramming and liver cancer progression by mediating HADHA ubiquitination. *Oncogene* 2022; **41**: 5199-5213 [PMID: 36273042 DOI: 10.1038/s41388-022-02509-1]

19 **Kodroń A**, Mussulini BH, Pilecka I, Chacińska A. The ubiquitin-proteasome system and its crosstalk with mitochondria as therapeutic targets in medicine. *Pharmacol Res* 2021; **163**: 105248 [PMID: 33065283 DOI: 10.1016/j.phrs.2020.105248]

20 **Kwon YT**, Ciechanover A. The Ubiquitin Code in the Ubiquitin-Proteasome System and Autophagy. *Trends Biochem Sci* 2017; **42**: 873-886 [PMID: 28947091 DOI: 10.1016/j.tibs.2017.09.002]

21 **Ji J**, Shen J, Xu Y, Xie M, Qian Q, Qiu T, Shi W, Ren D, Ma J, Liu W, Liu B. FBXO2 targets glycosylated SUN2 for ubiquitination and degradation to promote ovarian cancer development. *Cell Death Dis* 2022; **13**: 442 [PMID: 35525855 DOI: 10.1038/s41419-022-04892-9]

22 **Zhao X**, Guo W, Zou L, Hu B. FBXO2 modulates STAT3 signaling to regulate proliferation and tumorigenicity of osteosarcoma cells. *Cancer Cell Int* 2020; **20**: 245 [PMID: 32549792 DOI: 10.1186/s12935-020-01326-4]

23 **Liu EA**, Schultz ML, Mochida C, Chung C, Paulson HL, Lieberman AP. Fbxo2 mediates clearance of damaged lysosomes and modifies neurodegeneration in the Niemann-Pick C brain. *JCI Insight* 2020; **5** [PMID: 32931479 DOI: 10.1172/jci.insight.136676]

24 **Liu B**, Lu H, Li D, Xiong X, Gao L, Wu Z, Lu Y. Aberrant Expression of FBXO2 Disrupts Glucose Homeostasis Through Ubiquitin-Mediated Degradation of Insulin Receptor in Obese Mice. *Diabetes* 2017; **66**: 689-698 [PMID: 27932386 DOI: 10.2337/db16-1104]

25 **Weber M**, Mera P, Casas J, Salvador J, Rodríguez A, Alonso S, Sebastián D, Soler-Vázquez MC, Montironi C, Recalde S, Fucho R, Calderón-Domínguez M, Mir JF, Bartrons R, Escola-Gil JC, Sánchez-Infantes D, Zorzano A, Llorente-Cortes V, Casals N, Valentí V, Frühbeck G, Herrero L, Serra D. Liver CPT1A gene therapy reduces diet-induced hepatic steatosis in mice and highlights potential lipid biomarkers for human NAFLD. *FASEB J* 2020; **34**: 11816-11837 [PMID: 32666604 DOI: 10.1096/fj.202000678R]

26 **Yang H**, Deng Q, Ni T, Liu Y, Lu L, Dai H, Wang H, Yang W. Targeted Inhibition of LPL/FABP4/CPT1 fatty acid metabolic axis can effectively prevent the progression of nonalcoholic steatohepatitis to liver cancer. *Int J Biol Sci* 2021; **17**: 4207-4222 [PMID: 34803493 DOI: 10.7150/ijbs.64714]

27 **Ma N**, Wang YK, Xu S, Ni QZ, Zheng QW, Zhu B, Cao HJ, Jiang H, Zhang FK, Yuan YM, Zhang EB, Chen TW, Xia J, Ding XF, Chen ZH, Zhang XP, Wang K, Cheng SQ, Qiu L, Li ZG, Yu YC, Wang XF, Zhou B, Li JJ, Xie D. PPDPF alleviates hepatic steatosis through inhibition of mTOR signaling. *Nat Commun* 2021; **12**: 3059 [PMID: 34031390 DOI: 10.1038/s41467-021-23285-8]

28 **Wang D**, Day EA, Townsend LK, Djordjevic D, Jørgensen SB, Steinberg GR. GDF15: emerging biology and therapeutic applications for obesity and cardiometabolic disease. *Nat Rev Endocrinol* 2021; **17**: 592-607 [PMID: 34381196 DOI: 10.1038/s41574-021-00529-7]

29 **Hu Y**, He W, Huang Y, Xiang H, Guo J, Che Y, Cheng X, Hu F, Hu M, Ma T, Yu J, Tian H, Tian S, Ji YX, Zhang P, She ZG, Zhang XJ, Huang Z, Yang J, Li H. Fatty Acid Synthase-Suppressor Screening Identifies Sorting Nexin 8 as a Therapeutic Target for NAFLD. *Hepatology* 2021; **74**: 2508-2525 [PMID: 34231239 DOI: 10.1002/hep.32045]

30 **Park HS**, Song JW, Park JH, Lim BK, Moon OS, Son HY, Lee JH, Gao B, Won YS, Kwon HJ. TXNIP/VDUP1 attenuates steatohepatitis *via* autophagy and fatty acid oxidation. *Autophagy* 2021; **17**: 2549-2564 [PMID: 33190588 DOI: 10.1080/15548627.2020.1834711]

31 **Chen N**, Cao R, Zhang Z, Zhou S, Hu S. Sleeve Gastrectomy Improves Hepatic Glucose Metabolism by Downregulating FBXO2 and Activating the PI3K-AKT Pathway. *Int J Mol Sci* 2023; **24** [PMID: 36982617 DOI: 10.3390/ijms24065544]

32 **Yamada A**, Hikichi M, Nozawa T, Nakagawa I. FBXO2/SCF ubiquitin ligase complex directs xenophagy through recognizing bacterial surface glycan. *EMBO Rep* 2021; **22**: e52584 [PMID: 34515398 DOI: 10.15252/embr.202152584]

33 **Che X**, Jian F, Wang Y, Zhang J, Shen J, Cheng Q, Wang X, Jia N, Feng W. FBXO2 Promotes Proliferation of Endometrial Cancer by Ubiquitin-Mediated Degradation of FBN1 in the Regulation of the Cell Cycle and the Autophagy Pathway. *Front Cell Dev Biol* 2020; **8**: 843 [PMID: 32984335 DOI: 10.3389/fcell.2020.00843]

34 **Xu M**, Tan J, Dong W, Zou B, Teng X, Zhu L, Ge C, Dai X, Kuang Q, Zhong S, Lai L, Yi C, Tang T, Zhao J, Wang L, Liu J, Wei H, Sun Y, Yang Q, Li Q, Lou D, Hu L, Liu X, Kuang G, Luo J, Xiong M, Feng J, Zhang C, Wang B. The E3 ubiquitin-protein ligase Trim^{3}1 alleviates non-alcoholic fatty liver disease by targeting Rhbdf2 in mouse hepatocytes. *Nat Commun* 2022; **13**: 1052 [PMID: 35217669 DOI: 10.1038/s41467-022-28641-w]

35 **Yu M**, Alimujiang M, Hu L, Liu F, Bao Y, Yin J. Berberine alleviates lipid metabolism disorders *via* inhibition of mitochondrial complex I in gut and liver. *Int J Biol Sci* 2021; **17**: 1693-1707 [PMID: 33994854 DOI: 10.7150/ijbs.54604]

36 **Nassir F**, Arndt JJ, Johnson SA, Ibdah JA. Regulation of mitochondrial trifunctional protein modulates nonalcoholic fatty liver disease in mice. *J Lipid Res* 2018; **59**: 967-973 [PMID: 29581157 DOI: 10.1194/jlr.M080952]

37 **Malloy VL**, Perrone CE, Mattocks DA, Ables GP, Caliendo NS, Orentreich DS, Orentreich N. Methionine restriction prevents the progression of hepatic steatosis in leptin-deficient obese mice. *Metabolism* 2013; **62**: 1651-1661 [PMID: 23928105 DOI: 10.1016/j.metabol.2013.06.012]

38 **Dang Y**, Xu J, Zhu M, Zhou W, Zhang L, Ji G. Gan-Jiang-Ling-Zhu decoction alleviates hepatic steatosis in rats by the miR-138-5p/CPT1B axis. *Biomed Pharmacother* 2020; **127**: 110127 [PMID: 32325349 DOI: 10.1016/j.biopha.2020.110127]

39 **Bhatia H**, Pattnaik BR, Datta M. Inhibition of mitochondrial β-oxidation by miR-107 promotes hepatic lipid accumulation and impairs glucose tolerance in vivo. *Int J Obes (Lond)* 2016; **40**: 861-869 [PMID: 26499439 DOI: 10.1038/ijo.2015.225]

40 **Karagiannis F**, Masouleh SK, Wunderling K, Surendar J, Schmitt V, Kazakov A, Michla M, Hölzel M, Thiele C, Wilhelm C. Lipid-Droplet Formation Drives Pathogenic Group 2 Innate Lymphoid Cells in Airway Inflammation. *Immunity* 2020; **52**: 620-634.e6 [PMID: 32268121 DOI: 10.1016/j.immuni.2020.03.003]

41 **Cifarelli V**, Appak-Baskoy S, Peche VS, Kluzak A, Shew T, Narendran R, Pietka KM, Cella M, Walls CW, Czepielewski R, Ivanov S, Randolph GJ, Augustin HG, Abumrad NA. Visceral obesity and insulin resistance associate with CD36 deletion in lymphatic endothelial cells. *Nat Commun* 2021; **12**: 3350 [PMID: 34099721 DOI: 10.1038/s41467-021-23808-3]

42 **Manickam R**, Tur J, Badole SL, Chapalamadugu KC, Sinha P, Wang Z, Russ DW, Brotto M, Tipparaju SM. Nampt activator P7C3 ameliorates diabetes and improves skeletal muscle function modulating cell metabolism and lipid mediators. *J Cachexia Sarcopenia Muscle* 2022; **13**: 1177-1196 [PMID: 35060352 DOI: 10.1002/jcsm.12887]

43 **Castaño C**, Kalko S, Novials A, Párrizas M. Obesity-associated exosomal miRNAs modulate glucose and lipid metabolism in mice. *Proc Natl Acad Sci U S A* 2018; **115**: 12158-12163 [PMID: 30429322 DOI: 10.1073/pnas.1808855115]

44 **Tu J**, Zhu S, Li B, Xu G, Luo X, Jiang L, Yan X, Zhang R, Chen C. Gegen Qinlian Decoction Coordinately Regulates PPARγ and PPARα to Improve Glucose and Lipid Homeostasis in Diabetic Rats and Insulin Resistance 3T3-L1 Adipocytes. *Front Pharmacol* 2020; **11**: 811 [PMID: 32595495 DOI: 10.3389/fphar.2020.00811]

World Journal of Gastroenterology

Submit a Manuscript: https://www.f6publishing.com

World J Gastroenterol 2023 July 28; 29(28): 4451-4465

DOI: 10.3748/wjg.v29.i28.4451

ISSN 1007-9327 (print) ISSN 2219-2840 (online)

ORIGINAL ARTICLE

Clinical Trials Study

Efficacy and dose response of *Lactiplantibacillus plantarum* in diarrhea-predominant irritable bowel syndrome

Christopher J Martoni, Shalini Srivastava, Anders Damholt, Gregory J Leyer

Specialty type: Gastroenterology and hepatology

Provenance and peer review: Unsolicited article; Externally peer reviewed.

Peer-review model: Single blind

Peer-review report's scientific quality classification

Grade A (Excellent): A
Grade B (Very good): 0
Grade C (Good): 0
Grade D (Fair): D
Grade E (Poor): 0

P-Reviewer: McFarland LV, United States; Wen XL, China

Received: June 9, 2023
Peer-review started: June 9, 2023
First decision: June 14, 2023
Revised: June 27, 2023
Accepted: July 11, 2023
Article in press: July 11, 2023
Published online: July 28, 2023

Christopher J Martoni, Anders Damholt, Clinical Development, Human Health, Chr. Hansen A/S, Hoersholm 2970, Denmark

Shalini Srivastava, Clinical Development, Vedic Lifesciences, Mumbai 400053, India

Gregory J Leyer, Scientific Affairs,Human Health, Chr. Hansen A/S, Hoersholm 2970, Denmark

Corresponding author: Christopher J Martoni, PhD, Senior Scientist, Clinical Development, Human Health, Chr. Hansen A/S, 10-12 Boege Alle, Hoersholm 2970, Denmark. cachma@chr-hansen.com

Abstract

BACKGROUND

Probiotics have shown promise in alleviating symptoms of diarrhea-predominant irritable bowel syndrome (IBS-D); however, the certainty of evidence is low. Well-powered randomized controlled dose-ranging trials are warranted on promising single-strain candidates.

AIM

To investigate the clinical efficacy of *Lactiplantibacillus plantarum* (*L. plantarum*) Lpla33 (DSM34428) in adults with IBS-D.

METHODS

This is a randomized, double-blind, placebo-controlled, multi-center, and dose-ranging study. Three hundred and seven adults, 18-70 years of age, with IBS-D, according to Rome IV criteria, were allocated (1:1:1) to receive placebo or *L. plantarum* Lpla33 at 1×10^9 (1B) or 1×10^{10} (10B) colony-forming units/d over an 8-wk intervention period. The primary outcome was the change in IBS severity scoring system (IBS-SSS) total score after 8 wk, while secondary and exploratory outcomes included abdominal pain severity, IBS related quality of life, stool and microbial profile, and perceived stress.

RESULTS

IBS-SSS was significantly reduced, after 8 wk, in participants receiving *L. plantarum* 1B (-128.45 ± 83.30; $P < 0.001$) and *L. plantarum* 10B (-156.77 ± 99.06; $P < 0.001$), compared to placebo (-58.82 ± 74.75). Further, a dose-ranging effect was observed, with a greater absolute reduction in the *L. plantarum* 10B group ($P <$

0.05). A reduction in sub-scores related to abdominal pain, abdominal distension, bowel habits, and quality of life was observed in both *L. plantarum* groups compared to placebo ($P < 0.001$). Further, 62.5% and 88.4% of participants administered *L. plantarum* 1B and 10B, respectively, were classified as stool consistency responders based on a reduction in diarrheal stool form, as compared to 26.3% in the placebo group ($P < 0.001$). In contrast, no significant shifts were observed in microbial diversity.

CONCLUSION

L. plantarum Lpla33 (DSM34428) is well tolerated and improves IBS symptom severity with a dose-ranging effect and a corresponding normalization of bowel habits in adults with IBS-D.

Key Words: Randomized clinical trial; Diarrhea-predominant irritable bowel syndrome; Microbiome; Probiotic; *Lactiplantibacillus plantarum*

©The Author(s) 2023. Published by Baishideng Publishing Group Inc. All rights reserved.

Core Tip: The current study is unique in its dose-ranging assessment of a *Lactiplantibacillus plantarum* (*L. plantarum*) probiotic strain in a well-powered multi-center randomized controlled trial in adults with diarrhea-predominant irritable bowel syndrome (IBS-D). *L. plantarum* Lpla33 (DSM34428) was well tolerated and significantly improved global IBS symptom scores as compared to placebo, both at an absolute level and in the number of clinically relevant responders. Further, a dose-ranging effect was observed in global IBS symptom scores, abdominal pain severity, quality of life, and normalization of diarrheal stool type.

Citation: Martoni CJ, Srivastava S, Damholt A, Leyer GJ. Efficacy and dose response of *Lactiplantibacillus plantarum* in diarrhea-predominant irritable bowel syndrome. *World J Gastroenterol* 2023; 29(28): 4451-4465
URL: https://www.wjgnet.com/1007-9327/full/v29/i28/4451.htm
DOI: https://dx.doi.org/10.3748/wjg.v29.i28.4451

INTRODUCTION

Irritable bowel syndrome (IBS) is a chronic disorder of gut-brain interaction, characterized by abdominal pain in association with altered bowel habits[1]. Current estimates report a global prevalence of 4% to 9%, based on Rome IV or Rome III diagnostic criteria, respectively[2]. IBS is further classified according to the predominant stool pattern, with diarrhea predominant subtype (IBS-D) reported to be the most common, affecting approximately 40% of adults with IBS [3]. Pathophysiology is multi-factorial and may include altered gastrointestinal (GI) microbiota, motility or barrier function, immune activation, neurotransmitter imbalance, or visceral hypersensitivity[4,5]. In addition to GI symptoms, IBS significantly impacts quality of life (QoL) and is associated with work absenteeism and avoidance of daily activities [6].

IBS-D treatment options include United States Food and Drug Administration approved pharmacologic therapies such as rifaximin, eluxadoline, and alosetron[4]. However, clinical management is challenging due to chronic daily administration, safety concerns, and the heterogeneity of symptoms to address. Increasing evidence supports a link between psychological processes and IBS symptomology *via* altered gut-brain interaction, and there is a growing application of psychological interventions for IBS[7]. Within the gut, dysbiosis, including reduced abundance of lactobacilli and *Bifidobacterium*[8,9], has been reported and is linked to features of IBS-D such as intestinal permeability and low-grade inflammation[6,10]. There are conflicting reports regarding the efficacy of fecal microbiota transplantation in IBS, with enriched lactobacilli, *Streptococcus, Dorea*, and *Ruminococcaceae* reported as favorable bacterial profiles for donors[11].

Probiotics are defined as live microorganisms that, when administered in adequate amounts, confer a health benefit to the host[12]. Select strains are hypothesized to alleviate symptoms of IBS by promoting intestinal barrier function, modulating markers of inflammation, regulating immune cell balance, preventing pathogen adherence, or producing bioactive molecules such as short chain fatty acids (SCFAs), neurotransmitters, or their precursors[5]. A recent meta-analysis of probiotics for adults with IBS-D assessed ten randomized controlled trials evaluating 943 participants[13]. Probiotics were deemed safe and superior to placebo regarding global IBS-D symptoms, abdominal pain, and abdominal distension, but had no beneficial effect on QoL, stool frequency, or flatulence[13]. Additionally, the certainty of evidence was very low to low, due to heterogeneity between studies, and differences in study population, strain selection, dose, dosage form, and duration of intervention[13]. Another recent systematic review and meta-analysis accounted for probiotic strain-specific efficacy in IBS and included 42 randomized controlled trials evaluating 3856 participants[14]. The meta-analysis highlighted single-strains and combinations showing efficacy in at least one IBS outcome measure; however, most studies did not assess outcomes by IBS subtype[14]. As a result, there is a need for well-powered randomized controlled trials on promising single strain candidates with an IBS-D focus.

The present study investigated a *Lactiplantibacillus plantarum* (*L. plantarum*) strain with several relevant attributes, including GI persistence, maintenance of intestinal barrier function, and anti-pathogenic, anti-inflammatory, and bile salt hydrolase activity (Chr. Hansen internal data). The objective was to assess the efficacy and tolerability of *L. plantarum* Lpla33 (DSM34428), with respect to IBS symptomology in a randomized, double-blind, placebo-controlled, multi-center, dose-ranging study in adults with IBS-D.

MATERIALS AND METHODS

Study population and setting

Females and males, ages 18 to 70 years, meeting Rome IV diagnostic criteria for IBS-D were recruited from 12 gastroenterology specialized centers across India. As per Rome IV, included participants had recurrent abdominal pain, at least once a week for the last 3 mo, with onset of symptoms for at least 6 mo, and with at least two of the following criteria: Pain related to defecation or associated with change in stool frequency or stool form. Participants also had a history of abnormal bowel movements wherein diarrhea (type 6 or 7) was the predominant (> 25%) stool pattern on the Bristol stool scale (BSS). Further, an electronic diary was used during a 14-d placebo run-in period, wherein it was re-confirmed that predominant stool type was type 6 or 7 on the BSS. Additionally, participants had an abdominal pain severity-numeric rating score (APS-NRS) of ≥ 4 (on an 11-point scale) and an IBS severity scoring system (IBS-SSS) total score of > 175 (on a 500-point scale) prior to and after a 14-d placebo run-in period. Dietary preferences of all participants included non-vegetarian options.

The exclusion criteria included a history of organic gastrointestinal disease, including inflammatory bowel disease or ischemic colitis, a history of surgical resection of the GI tract, acute gastroenteritis or complications from infectious enteritis, a recent diagnosis of *Helicobacter pylori* infection, a history of gluten or lactose intolerance, a history of malignant tumors, or a history of neurological or psychiatric conditions. A current or recent history (*i.e.*, past 2 years) of smoking as well as heavy drinking, defined as more than 14 or 7 units per week, for males and females, respectively, was also an exclusion criterion. Additionally, individuals with type I or II diabetes, or uncontrolled hypertension were excluded, as well as individuals with abnormal thyroid-stimulating hormone (< 0.35 mIU/L or > 4.94 mIU/L) or hemoglobin (< 6.21 mmol/L) at screening. The use of probiotic/prebiotic supplements or herbal medicines for gut health, was not permitted within 4 wk prior to screening or during the study. Prohibited medications during the study period included antibiotics, antidiarrheals, or other medications affecting gastric motility and anti-depressants, among others. Lastly, participants who were pregnant or intended to get pregnant or breastfeeding were excluded. All participants provided their voluntary, written, informed consent prior to their inclusion.

Study design and procedures

The study was conducted in accordance with the ethical principles that have their origins in the current version of the Declaration of Helsinki, the International Council on Harmonization E6 Good Clinical Practice, and all applicable local regulatory requirements. The study was approved and monitored by an independent ethics committee (Approval No: VED/P-20/22/JUL/2021; Address: ACEAS, Ahmedabad, Gujarat, India). The trial was prospectively registered on clinicaltrials.gov under study number NCT04950296.

This is a prospective, randomized, double-blind, placebo-controlled, multi-center, and parallel-arm study, including two doses of the probiotic product and one placebo arm. The study population was recruited from physician databases of individuals with IBS symptoms within the gastroenterology specialized centers. Participants visited the clinical sites for screening at least 14 d prior to planned randomization. At screening, the study was explained to participants in their local language, following which written informed consent was obtained. Participants were assessed for inclusion-exclusion criteria; a clinical examination was performed, and medical history, concomitant medication, demographic details, and vitals were recorded. Participants meeting the screening criteria underwent a 2-wk placebo run-in period to observe pre-study symptomology and to identify placebo responders, defined as a decrease of more than 25% in APS-NRS. Participants not meeting the placebo responder criteria were eligible for randomization (day 0) and subsequent visits at day 28 ± 2 and day 56 ± 2 over an 8-wk intervention period.

Participants were randomized (1:1:1), without stratification, to receive either placebo, *L. plantarum* (1B), or *L. plantarum* (10B). Block randomization (block size of six) was performed using Stats Direct software (Version 3.1.17), generating distinct alphanumeric codes, with every block containing two of each arm in random sequence. The study sites were allocated randomization codes in series, and the sites dispensed blinded product and corresponding randomization code, in sequential order of participant qualification. The randomization codes were concealed from site investigators, as well as site and study teams involved in study conduct and evaluation, with blinding codes secured in tamper-evident sealed envelopes.

Study products

Placebo and *L. plantarum* capsules were prepared in compliance with standard operating and quality control procedures at Chr. Hansen Inc. (Wausau, WI, United States). Microbiological analyses were confirmed following production. *L. plantarum* 1B and 10B capsules were formulated with the lyophilized strain and microcrystalline cellulose and contained a potency of not less than (NLT) 1×10^9 colony-forming units (CFU)/capsule or 1×10^{10} CFU/capsule, respectively. Placebo capsules were formulated with microcrystalline cellulose. All capsules were size 1 hypromellose, contained minimal but identical quantities of magnesium stearate and silica as flow aids, were identical in mass, appearance, and taste, and were bottled in identical sealed 112 mL CSP bottles (Aptar CSP Technologies Inc., Auburn, AL, United States) containing 35

capsules per bottle. Participants took the allotted study product orally, one capsule daily before lunch, with a glass of water. Compliance was assessed *via* participants' investigational product diary and confirmed by examining unused study product at each visit.

Outcome measures

On days 0, 28, and 56 visits, study outcomes were assessed, a clinical examination was conducted, study product was dispensed or collected, and concomitant medication usage was recorded. Metronidazole (400 mg/d) was provided as a rescue medication in the case of severe pain and/or frequent loose stool, as it has been shown to provide symptom relief in IBS without affecting rectosigmoid motility[15]. Study product compliance was assessed *via* participants' investigational product diary and confirmed by examining unused study product at each visit. A dietary diary was completed by participants over the 14 d prior to each study visit, recording dietary intake for two weekdays and one weekend day. Dietary information was processed *via* HealthifyMe software[16] for average daily intake of calories and macronutrients over the study period.

The pre-specified ranking of primary and secondary outcomes is listed in Supplementary Table 1. The primary outcome was the change in IBS symptom severity, assessed *via* the IBS-SSS total score[17] from baseline to day 56. Scores on the IBS-SSS range from 0 to 500, with five domains related to abdominal pain severity and frequency, abdominal distention, dissatisfaction with bowel habits, and interference with QoL. A decrease of 95 points has been associated with clinically meaningful improvement[18], and was used for classification of IBS-SSS responders.

Among secondary outcomes, abdominal pain severity was assessed *via* an 11-point numeric rating scale (APS-NRS) [18], with 10 representing most severe pain and 0 representing no pain. Post-screening APS-NRS scores were submitted using a digital diary on a weekly basis. An average of the prior weeks' score was considered as the score for the corresponding visit.

Stool consistency was assessed *via* the BSS, a validated ordinal scale of stool types[19] ranging from 1 through 7, with types 6-7 being indicative of diarrhea. Stool consistency responders were defined as a decrease of 50% or more *vs* baseline in the number of days per week with at least one types 6-7 bowel movement[20].

IBS related QoL was assessed *via* the IBS-QoL, a 34-item questionnaire wherein the individual responses are summed and transformed to a 0-100 scale, with increasing scores indicating improved IBS specific QoL[21]. Lastly, mental stress was assessed using the perceived stress scale (PSS), consisting of 10 items and a total score ranging from 0-40, with higher scores indicating higher perceived stress[22].

Microbial profiling

Participants collected fecal samples, as close as possible but prior to the day 0 and day 56 visits, inside a biome collector device and ultimately a barcoded stool collection tube with preservation buffer. Stool collection tubes were stored at the individual sites, with regular shipments to a central laboratory, wherein they were shipped approximately every 8 wk to CosmosID (Germantown, MD, United States) for analysis. Cold chain (2-8 °C) was maintained during the entire process with data loggers used to confirm temperature variations during shipment.

Sample DNA isolation and quantification, library preparation, and shotgun sequencing of fecal samples were performed by CosmosID. DNA from samples was isolated using the QIAGEN DNeasy PowerSoil Pro Kit, according to the manufacturer's protocol. DNA samples were quantified using the GloMax Plate Reader System (Promega) using the QuantiFluor® dsDNA System (Promega) chemistry. DNA libraries were prepared using the Nextera XT DNA Library Preparation Kit (Illumina) and IDT Unique Dual Indexes with total DNA input of 1 ng. Genomic DNA was fragmented using a proportional amount of Illumina Nextera XT fragmentation enzyme. Unique dual indexes were added to each sample followed by 12 cycles of PCR to construct libraries. DNA libraries were purified using AMpure magnetic beads (Beckman Coulter) and eluted in QIAGEN EB buffer. DNA libraries were quantified using Qubit 4 fluorometer and Qubit dsDNA HS Assay Kit. Libraries were then sequenced on an Illumina NextSeq 2000 platform (2 × 150 bp).

Statistical analysis

The sample size calculation was based on the primary outcome. A reduction in IBS-SSS score of at least 15% in the *L. plantarum* 1B group as compared to placebo, was considered a relevant treatment effect[23]. The standard deviation of the primary outcome was estimated at 30%. A placebo effect was estimated at 20%-25%. Assuming a 90% study power and a two-sided statistical significance level of 5%, the sample size was estimated to be approximately 86 participants per group. With an estimated 15% drop-out rate, 100 participants per group were planned to be randomized.

The primary and secondary outcomes (Supplementary Table 1) were assessed on the intention-to-treat (ITT) population. Descriptive statistics are presented as the mean (SD) for continuous variables or as a percentage for qualitative variables. Data normality was assessed using the Shapiro-Wilk test. Differences between groups for demographic and clinical characteristics at baseline were analyzed using one-way ANOVA for continuous variables or Pearson chi-square test for categorical variables. An analysis of covariance (ANCOVA) was assessed for continuous outcomes on the absolute change from baseline to subsequent visit. Dunnett's test for multiple comparisons was applied to assess statistical significance for each *L. plantarum* dose group as compared to placebo. A two-sample *t*-test was used to compare the difference between the two *L. plantarum* dose groups. Categorical outcomes were assessed *via* a Pearson chi-square test. The associations between efficacy parameters were assessed *via* Pearson correlation coefficients. Descriptive and inferential statistics were performed using Statistical Package for the Social Sciences (SPSS, IBM®) Python 3.0 (Armonk, NY, United States).

Microbial profile stacked bar figures were generated using the R package ggpubr. Linear Discriminant Analysis Effect Size (LEfSe) was calculated with a Kruskal-Wallis alpha value of 0.05, a Wilcoxon alpha value of 0.05, and a logarithmic

LDA score threshold of 2.0.

RESULTS

Study parameters

A total of 333 screened participants were assessed for eligibility and 314 participants were randomized in the study (Figure 1). Enrolment and intervention occurred continuously from September 2021 through May 2022. Seven participants were incorrectly enrolled, without meeting entry criteria, and were excluded. Three hundred and seven participants were randomized as part of the ITT population, with 104, 104, and 99 allocated to the placebo, *L. plantarum* 1B, and *L. plantarum* 10B groups, respectively. A total of 298 participants completed the first follow-up visit, while nine participants were lost to follow-up with no post-baseline efficacy data. Study attrition rates over the intervention period were 5 (4.8%), 2 (1.9%), and 4 (4.0%) for the placebo, *L. plantarum* 1B, and *L. plantarum* 10B groups, respectively. A total of 294 participants completed the study per protocol.

Baseline characteristics

The screening and baseline characteristics of the ITT population are presented in Table 1. The three groups had similar demographic and clinical characteristics with no differences between groups ($P > 0.05$). The mean ages of participants were 39.5, 38.7, and 40.5 years across the three groups with a nearly even distribution of females and males. Participants met Rome IV criteria for IBS-D and demonstrated similar baseline mean IBS-SSS scores of 308.7, 315.2, and 302.9 for the placebo, *L. plantarum* 1B, and *L. plantarum* 10B groups, respectively ($P > 0.05$). At baseline, 43.4%, 41.4%, and 47.4% of participants in the placebo, *L. plantarum* 1B, and *L. plantarum* 10B groups, respectively, had moderate (175-300) IBS-SSS profiles, while 56.6%, 58.7%, and 52.6% of participants in the placebo, *L. plantarum* 1B, and *L. plantarum* 10B groups, respectively, had severe (> 300) IBS-SSS profiles.

IBS symptom severity

A significant between-group difference was observed in the primary outcome, change in IBS-SSS total score after 56 d, for both *L. plantarum* groups when compared to placebo (Table 2). On day 56, a greater reduction in IBS-SSS total score was observed in the *L. plantarum* 1B (-128.45 ± 83.30) and *L. plantarum* 10B (-156.77 ± 99.06) groups, as compared to placebo (-58.82 ± 74.75) ($P < 0.001$). Similarly, a greater reduction in IBS-SSS total score was observed on day 28 in the *L. plantarum* 1B (-66.37 ± 72.27) and *L. plantarum* 10B (-85.80 ± 89.53) groups, as compared to placebo (-35.68 ± 60.81) ($P < 0.01$). Comparing the two dose groups, the *L. plantarum* 10B group demonstrated a significantly greater reduction in IBS-SSS total score at day 56 ($P < 0.05$). End-of-study IBS-SSS profiles were considered either in remission or mild (< 175) in 48.1% and 72.6% of participants in the *L. plantarum* 1B and *L. plantarum* 10B groups, respectively. as compared to 11.1% in the placebo group ($P < 0.001$).

Participants receiving *L. plantarum* 1B capsules reported significant reductions in the scores of IBS-SSS individual domains over the intervention period, as compared to placebo, including abdominal pain severity (-28.91 ± 20.36), abdominal pain duration (-15.29 ± 13.72), abdominal distension (-29.33 ± 21.64), bowel habits (-27.73 ± 19.54) and QoL (-27.19 ± 19.19) ($P < 0.001$). Similarly, participants receiving *L. plantarum* 10B capsules reported significant reductions in IBS-SSS domain specific scores, as compared to placebo, including abdominal pain severity (-36.52 ± 24.39), abdominal pain duration (-19.68 ± 14.91), abdominal distension (-35.45 ± 24.00), bowel habits (-32.31 ± 25.12), and QoL (-32.81 ± 23.66) ($P < 0.001$). Comparing the two dose groups, the *L. plantarum* 10B group demonstrated a greater reduction in abdominal pain severity and duration scores over the intervention period ($P < 0.05$).

After 56 d, 59.6% and 72.6% of participants met 95-point reduction thresholds[18] in the *L. plantarum* 1B and *L. plantarum* 10B groups, respectively, as compared to 26.3% in the placebo group ($P < 0.001$) (Figure 2A). A post-hoc assessment showed 83.7% and 87.4% of participants met 50-point IBS-SSS reduction thresholds[17] in the *L. plantarum* 1B and *L. plantarum* 10B groups, respectively, as compared to 46.5% in the placebo group ($P < 0.001$). Additionally, 2.9% and 2.1% of participants demonstrated an increase in IBS-SSS score in the *L. plantarum* 1B and *L. plantarum* 10B groups, respectively, as compared to 18.2% in the placebo group ($P < 0.001$).

Abdominal pain severity, quality of life, and perceived stress

Baseline APS-NRS scores were 7.14 ± 0.69, 7.14 ± 0.77, and 7.17 ± 0.86 for the placebo, *L. plantarum* 1B, and *L. plantarum* 10B groups, respectively ($P > 0.05$). On day 56, a greater reduction in APS-NRS score (Table 3) was observed in the *L. plantarum* 1B (-1.83 ± 1.38) and *L. plantarum* 10B (-2.39 ± 1.47) groups, as compared to placebo (-0.94 ± 1.36) ($P < 0.001$). The mean reduction in the *L. plantarum* 10B group exceeded a clinically meaningful threshold of 30%[20] over the intervention period.

On day 56, a significant increase in IBS-Qol score (Table 3) was observed in the *L. plantarum* 1B (17.47 ± 19.54) and *L. plantarum* 10B (28.78 ± 23.64) groups, as compared to placebo (4.90 ± 14.29) ($P < 0.001$). Similarly, a greater improvement in total IBS-QoL score was demonstrated on day 28 in the *L. plantarum* 1B (8.82 ± 17.38) and *L. plantarum* 10B (17.65 ± 19.47) groups, as compared to placebo (4.20 ± 14.19) ($P < 0.01$). Comparing the two dose groups, the *L. plantarum* 10B group demonstrated a greater improvement in IBS-QoL at both timepoints ($P < 0.001$).

Perceived stress, assessed *via* the PSS, was similarly improved in the *L. plantarum* 1B and *L. plantarum* 10B groups, as compared to placebo on both day 28 and day 56 (Table 3). On day 56, a significant reduction in PSS score was observed in the *L. plantarum* 1B (-4.33 ± 6.51) and *L. plantarum* 10B (-5.59 ± 6.43) groups, as compared to placebo (-0.46 ± 4.14) ($P <$

Table 1 Baseline demographics and clinical characteristics of the intention-to-treat population, *n* (%)

	Placebo 1B (*n* = 104)	*L. plantarum* 1B (*n* = 104)	*L. plantarum* 10B (*n* = 99)	*P* value
	mean (SD) or *n* (%)	mean (SD) or *n* (%)	mean (SD) or *n* (%)	
Age (yr)	39.50 (13.26)	38.66 (11.25)	40.46 (11.15)	0.5619[1]
Female allocation	46 (44.23)	50 (48.08)	44 (44.44)	0.8232[2]
Height (m)	1.60 (0.07)	1.59 (0.08)	1.61 (0.07)	0.1775[1]
Weight (kg)	63.57 (9.10)	63.09 (9.01)	63.25 (8.50)	0.9256[1]
BMI (kg/m^2)	24.83 (3.15)	25.01 (3.31)	24.46 (2.92)	0.4506[1]
Systolic BP (mmHG)	119.68 (8.27)	119.76 (8.68)	118.88 (8.79)	0.7223[1]
Diastolic BP (mmHG)	79.29 (5.06)	79.21 (6.30)	78.75 (4.62)	0.7429[1]
Fasting glucose (mmol/L)	5.16 (0.66)	5.01 (0.65)	5.13 (0.62)	0.1961[1]
IBS-SSS aggregate score	308.70 (70.91)	315.20 (62.79)	302.85 (61.06)	0.4090[1]
APS-NRS score	7.14 (0.69)	7.14 (0.77)	7.17 (0.86)	0.9648[1]
IBS-QoL aggregate score	36.19 (17.97)	37.83 (17.25)	37.54 (17.02)	0.7787[1]
PSS score	22.06 (4.29)	22.42 (4.12)	21.93 (4.31)	0.6912[1]

[1]Between group comparison; one-way ANOVA.
[2]Between group comparison; Pearson chi-square test.
BMI: Body mass index; BP: Blood pressure; IBS-SSS: Irritable bowel syndrome-severity scoring system; APS-NRS: Abdominal pain severity-numeric rating scale; IBS-QoL: Irritable bowel syndrome-quality of life; PSS: Perceived stress scale; *L. plantarum*: *Lactiplantibacillus plantarum*.

0.001). No significant differences were observed between the dose groups in PSS. Further, a post-hoc analysis showed PSS response to be moderately but significantly correlated to IBS-SSS (r = 0.326, P < 0.001) and APS-NRS scores (r = 0.355, P < 0.001) over the intervention period.

Stool consistency

Figure 2B shows the percent of participants considered IBS-D stool consistency responders, based on a decrease of 50% or more in the number of days per week with at least one types 6-7 bowel movement, as compared to baseline[20]. On day 56, 62.5% and 88.4% of study participants met the criteria of IBS-D stool consistency responders in the *L. plantarum* 1B and *L. plantarum* 10B groups, respectively, as compared to 26.3% in the placebo group. Additionally, a greater number of responders were observed in the *L. plantarum* 10B group as compared to the *L. plantarum* 1B group (P < 0.001). A significant number of responders were also observed in the *L. plantarum* 1B (30.8%; P < 0.05 *vs* placebo) and *L. plantarum* 10B (48.4%; P < 0.001 *vs* placebo) groups after day 28.

Microbial profiling

There were no significant differences in alpha (Shannon) diversity or beta diversity between groups over the study period, suggesting no major shifts in microbiome composition. Figure 3 shows the proportional family (A) and genus (B) level abundance in participants receiving placebo, *L. plantarum* 1B, and *L. plantarum* 10B, respectively. The most abundant taxa at the phylum level, Firmicutes, Bacteroidetes, and Actinobacteria, did not differ significantly over time in the three groups. Similarly, the most abundant taxa at the family level, *Lachnospiraceae*, *Prevotellaceae*, *Ruminococcaceae*, and *Bifidobacteriaceae* were stable within group over the intervention period, with the exception of a significant reduction in *Ruminococcaceae* and *Bifidobacteriaceae* within the placebo group (LEfSe logarithmic LDA score < -3.0) that was not observed in the *L. plantarum* groups. Similarly, the placebo group demonstrated a significant reduction in *Bifidobacterium*, *Faecalibacterium,* and *F. prausnitzii* (LEfSe logarithmic LDA score < -3.0) over the study period that was not observed in the *L. plantarum* groups. LEfSe identified more taxa enriched in the higher dose *L. plantarum* group at the end of study visit as compared to placebo, including both *Lactiplantibacillus* and *L. plantarum* abundance (LEfSe logarithmic LDA score > 2.0).

Safety, compliance, and dietary profile

A total of 37 adverse events (AEs) were reported during the study, with seven reported during the run-in phase and 30 reported during the intervention phase. Of the 30 AEs reported post-randomization, 12, 13, and 5 were in the placebo, *L. plantarum* 1B, and *L. plantarum* 10B groups, respectively. A total of four AEs were suspected to be related to the study product with one AE (nausea and vomiting) in the *L. plantarum* 1B group and three AEs (heartburn and hyperacidity) in the placebo group. All AEs reported in the study were considered mild and resolved without complications. Vital signs, including systolic and diastolic blood pressure and pulse rate, were within clinically acceptable ranges over the intervention period with no significant differences between groups (Supplementary Table 2). Overall mean compliance over the study period was 98.7%, 98.4%, and 98.5% for the placebo, *L. plantarum* 1B, and *L. plantarum* 10B groups,

Table 2 Irritable bowel syndrome symptom severity total and domain-specific scores over the intervention period

	Placebo (*n* = 104)	*L. plantarum* 1B (*n* = 104)		*L. plantarum* 10B (*n* = 99)		
	mean (SD)	mean (SD)	*P vs* Placebo[1]	mean (SD)	*P vs* Placebo[1]	*P vs* 1B dose[2]
IBS-SSS total score						
Day 0	308.70 (70.91)	315.95 (62.07)		302.85 (61.06)		
AbsΔ (Day 28)	-35.68 (60.81)	-66.37 (72.27)	0.0098	-85.80 (89.53)	< 0.0001	0.0956
AbsΔ (Day 56)	-58.82 (74.75)	-128.45 (83.30)	< 0.0001	-156.77 (99.06)	< 0.0001	0.0298
Abdominal pain severity						
Day 0	67.05 (17.11)	68.80 (13.40)		67.07 (13.77)		
AbsΔ (Day 28)	-9.24 (19.67)	-15.45 (18.36)	0.0830	-20.76 (22.76)	< 0.0001	0.0736
AbsΔ (Day 56)	-14.38 (21.18)	-28.91 (20.36)	< 0.0001	-36.52 (24.39)	< 0.0001	0.0176
Abdominal pain duration						
Day 0	41.11 (14.13)	42.60 (14.55)		39.37 (13.75)		
AbsΔ (Day 28)	-5.35 (13.50)	-8.46 (12.05)	0.1975	-7.89 (12.62)	0.0484	0.7463
AbsΔ (Day 56)	-8.38 (13.75)	-15.29 (13.72)	0.0006	-19.68 (14.91)	< 0.0001	0.0315
Abdominal distension						
Day 0	65.08 (18.11)	66.31 (15.11)		63.07 (14.34)		
AbsΔ (Day 28)	-8.66 (18.19)	-14.69 (17.68)	0.0600	-18.55 (22.62)	< 0.0001	0.1849
AbsΔ (Day 56)	-14.00 (20.76)	-29.33 (21.64)	< 0.0001	-35.45 (24.00)	< 0.0001	0.0598
Bowel habits						
Day 0	68.32 (15.64)	69.35 (13.70)		66.72 (14.55)		
AbsΔ (Day 28)	-6.45 (12.02)	-14.36 (18.66)	0.0020	-19.52 (21.48)	< 0.0001	0.0714
AbsΔ (Day 56)	-11.19 (16.63)	-27.73 (19.54)	< 0.0001	-32.31 (25.12)	< 0.0001	0.1561
Effect on quality of life						
Day 0	67.13 (15.85)	68.90 (14.47)		66.62 (12.85)		
AbsΔ (Day 28)	-5.97 (12.03)	-13.40 (17.48)	0.0060	-19.08 (21.13)	< 0.0001	0.0395
AbsΔ (Day 56)	-10.86 (15.74)	-27.19 (19.19)	< 0.0001	-32.81 (23.66)	< 0.0001	0.0690

[1]ANCOVA using Dunnett's test adjustment with treatment as factor and baseline as covariate *vs* placebo.
[2]Two-sample *t*-test comparing dose groups.
IBS-SSS: Irritable bowel syndrome-severity scoring system; AbsΔ: Absolute change; *L. plantarum*: *Lactiplantibacillus plantarum*.

respectively, with no differences between groups ($P > 0.05$). Additionally, total caloric and macronutrient intake, including protein, carbohydrates, fat, and fiber, were stable over the intervention period with no significant differences between groups ($P > 0.05$) (Supplementary Table 3).

DISCUSSION

The present study was a randomized, double-blind, placebo-controlled trial to assess the efficacy of *L. plantarum* Lpla33 (DSM34428) in adults with IBS-D. The study is unique in its dose-ranging design in a well-powered study across 12 clinical sites. Enrolled participants were primarily 30 to 50 years of age, with a body mass index ranging from normal to borderline overweight and an IBS symptom score of at least moderate severity.

The study had a roughly equal allocation of females and males, which is in line with prevalence rates for the IBS-D subtype globally[24,25], as well as prior IBS studies in Asia[26-28], and in contrast with a significantly greater female prevalence among constipation-predominant (IBS-C) cohorts[2]. Within South Asia, chronic gut infections, gut microbial dysbiosis, altered intestinal permeability, and inflammation are suggested as contributing factors to IBS and IBS-D[26]. Dietary practices may also play a role, with a generally high consumption of short chain carbohydrates[29].

In the present study, *L. plantarum* Lpla33, at daily doses of 1×10^9 or 1×10^{10} CFU, reduced IBS-SSS by more than twice the magnitude of the placebo group after 56 d, thus achieving the primary outcome while surpassing a clinically

Table 3 Abdominal pain severity, quality of life, and perceived stress scores over the intervention period

	Placebo (*n* = 104)	*L. plantarum* 1B (*n* = 104)		*L. plantarum* 10B (*n* = 99)		
	mean (SD)	mean (SD)	*P vs* Placebo[1]	mean (SD)	*P vs* Placebo[1]	*P vs* 1B dose[2]
APS-NRS score						
Day 0	7.14 (0.69)	7.14 (0.77)		7.17 (0.86)		
AbsΔ (Day 28)	-0.61 (1.12)	-0.87 (1.06)	0.1356	-0.92 (0.90)	0.0733	0.7089
AbsΔ (Day 56)	-0.94 (1.36)	-1.83 (1.38)	< 0.0001	-2.39 (1.47)	< 0.0001	0.0057
IBS-QoL total score						
Day 0	36.19 (17.97)	37.83 (17.25)		37.54 (17.02)		
AbsΔ (Day 28)	4.20 (14.19)	8.82 (17.38)	0.0208	17.65 (19.47)	< 0.0001	0.0009
AbsΔ (Day 56)	4.90 (14.29)	17.47 (19.54)	< 0.0001	28.78 (23.64)	< 0.0001	0.0003
PSS score						
Day 0	22.06 (4.29)	22.42 (4.12)		21.93 (4.31)		
AbsΔ (Day 28)	-0.12 (3.92)	-2.38 (4.54)	< 0.0001	-2.76 (4.69)	< 0.0001	0.5690
AbsΔ (Day 56)	-0.46 (4.14)	-4.33 (6.51)	< 0.0001	-5.59 (6.43)	< 0.0001	0.1708

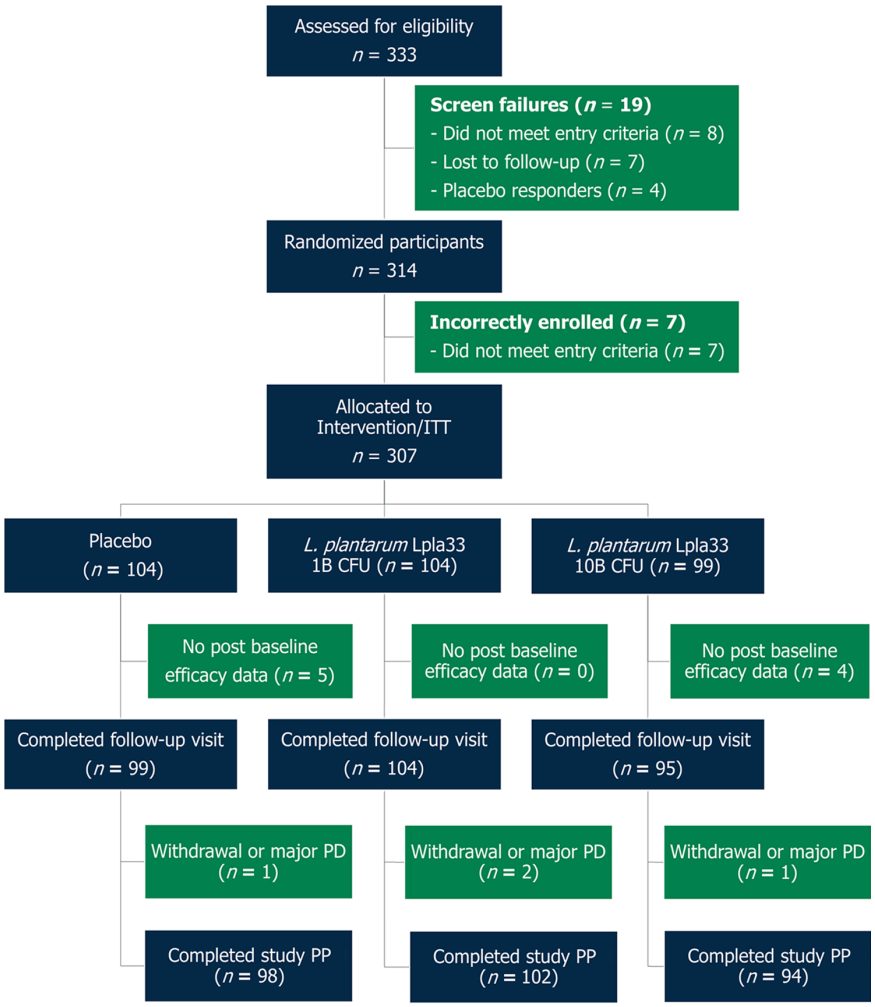
[1]ANCOVA using Dunnett's test adjustment with treatment as factor and baseline as covariate *vs* placebo.
[2]Two-sample *t*-test comparing dose groups.
APS-NRS: Abdominal pain severity-numeric rating scale; IBS-QoL: Irritable bowel syndrome-quality of life; PSS: Perceived stress scale; AbsΔ: Absolute change; *L. plantarum*: *Lactiplantibacillus plantarum*.

meaningful response[18]. Further, the higher dose *L. plantarum* group demonstrated a greater effect size than the lower dose *L. plantarum* group. Previously, an *L. acidophilus* strain, administered at daily doses of 1×10^9 and 1×10^{10} CFU for 12 wk, exhibited a treatment effect in a post-hoc analysis of IBS participants with elevated abdominal pain levels[30]. However, no dose-response was observed. Similarly, a meta-analysis reported a similar improvement in IBS symptoms when comparing probiotic regimens greater than or less than 1×10^{10} CFU daily[30]. In contrast, a *L. gasseri* strain resulted in a reduction in abdominal pain severity *vs* placebo at a daily dose of 1×10^{10} CFU, but had no effect in groups receiving 2×10^8 or 2×10^9 CFU daily[31]. Another meta-analysis looked at 14 different probiotic products over a total of 45 intervention arms, of which 36%, 51%, and 11% used a daily dose of 10^6-10^9, 10^{10}, and 10^{11} CFU, respectively[14]. Of these, a dose response was noted for a 4-strain probiotic combination at 10^{10} CFU daily[32,33], as well as a *B. infantis* strain, which demonstrated efficacy at a dose of 10^8 CFU daily but not at doses of 10^6 or 10^{10} CFU daily[34].

Both *L. plantarum* dose groups displayed a significant number of IBS-SSS responders using either 95-point[18] or 50-point[17] reduction thresholds, which have independently been correlated with clinically relevant responses. Further, the high responder rates across participants with heterogeneous baseline symptoms[35] may also be applicable to the general healthy population experiencing GI discomfort with less frequency or severity[36].

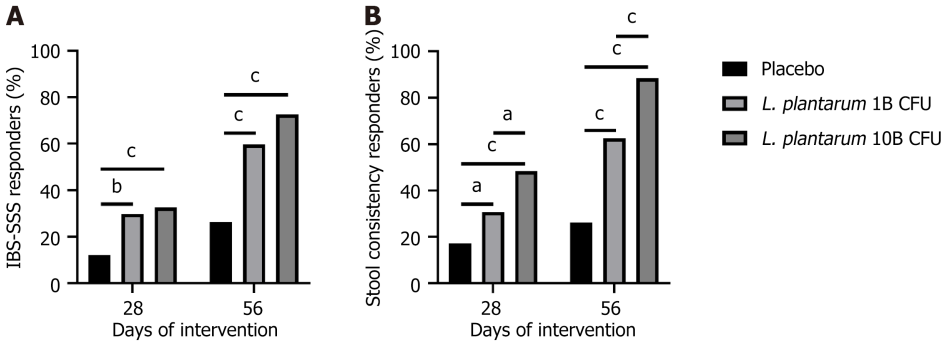
Abdominal pain severity, assessed *via* the APS-NRS, was also significantly reduced with *L. plantarum* supplementation, with the higher dose group achieving a clinically relevant reduction of over 30%[20]. It should be noted that the placebo response of approximately 20% in the current study was less than those in prior IBS-D studies, which ranged from 32% to 44%[37-39]. This may have been due, in part, to the placebo run-in period as well as geographic, cultural, or dietary differences. Additionally, the higher-dose *L. plantarum* group exhibited a mean increase in IBS related QoL of 28.8 points, above the clinically meaningful threshold of 10 points[40]. This is of note given the lower reported QoL in IBS-D as compared to IBS-C[41], in part due to unpredictable defecation habits that limit daily activity. In addition, perceived stress in the *L. plantarum* groups was reduced compared to placebo. Of note, moderate but significant correlations were observed between reduced IBS symptomology, abdominal pain, and stress levels, with effects possibly linked to a more normalized gut-brain signaling or barrier function.

Rome Foundation reports have supported the concept that the intestinal microbiota is perturbed in IBS[42,43], and both incidence and symptom severity have been inversely associated with microbiome diversity[44,45]. Further, reports have linked IBS pathogenesis to dysbiosis of the microbiota[9,46], which may in turn impact pathogen binding and mucosal barrier integrity. However, there remain no uniform characteristics of an IBS-related gut microbiota[47]. The current study demonstrated a significant reduction in type 6 or 7 stool form *via* stool consistency responder analysis[20], including a dose effect among the *L. plantarum* groups. In contrast, no significant shifts in fecal microbial diversity were observed, in line with systematic reviews of probiotic studies showing no effects on alpha diversity, richness, or evenness, as well as composition[48]. *Lactiplantibacillus* and *L. plantarum* abundances were enriched at the end of study visit in the higher dose group as compared to placebo. Further, *Ruminococcaceae, Bifidobacterium,* and *F. prausnitzii* significantly decreased over the study period in the placebo group. Multi-omics studies have implicated *F. prausnitzii*, *Ruminococcus* spp., and *Bifidobacterium* in IBS treatment response[47], but it is unclear if this played a role here. Overall, the most abundant taxa did not significantly change over time. However, the site of action of *L. plantarum* Lpla33 is postulated to



DOI: 10.3748/wjg.v29.i28.4451 **Copyright** ©The Author(s) 2023.

Figure 1 Participant flow chart. ITT: Intention-to-treat; PD: Protocol deviation; PP: Per protocol; *L. plantarum*: *Lactiplantibacillus plantarum*.

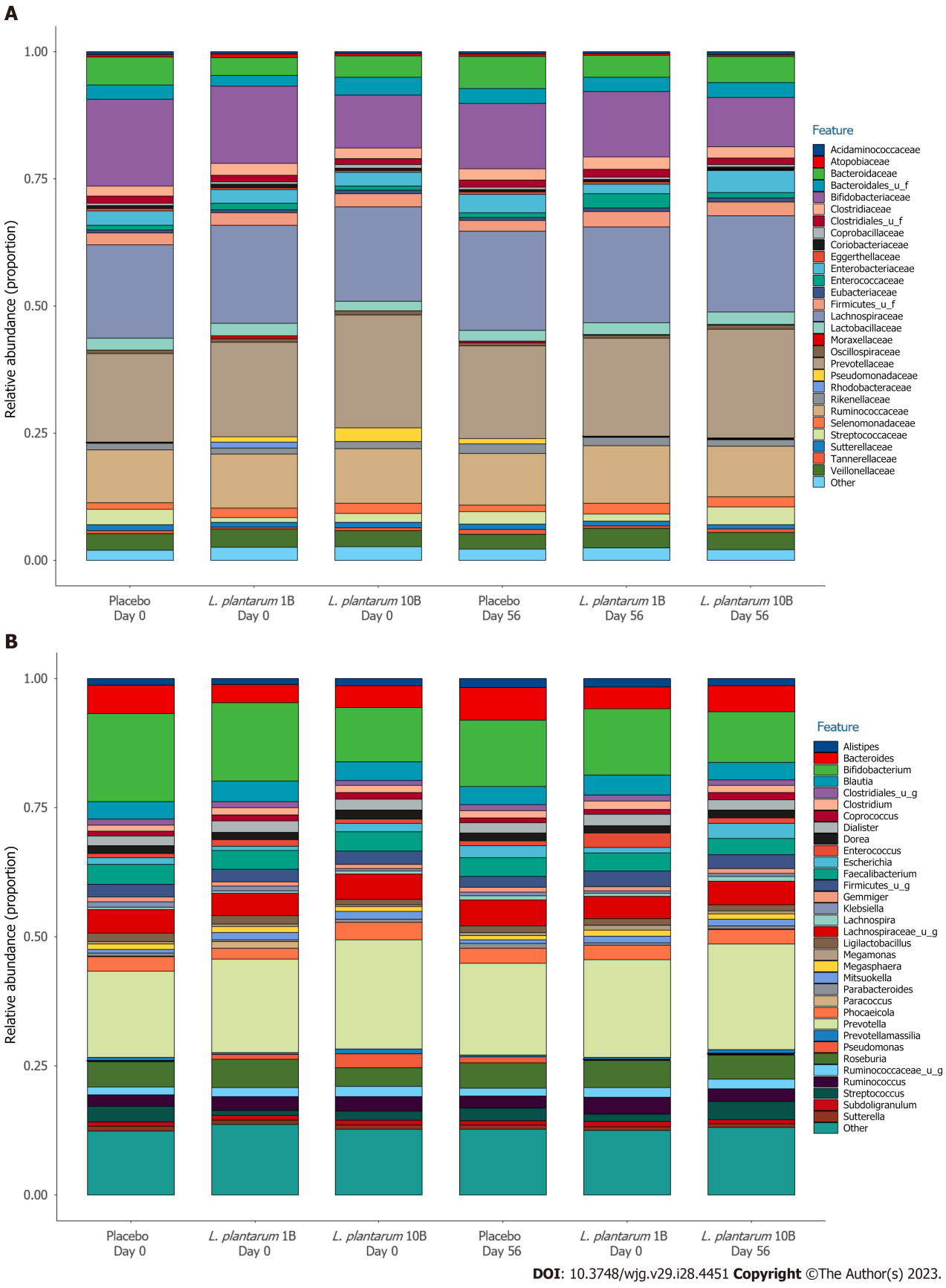


DOI: 10.3748/wjg.v29.i28.4451 **Copyright** ©The Author(s) 2023.

Figure 2 Responder profile over the intervention period. A: Percentage of irritable bowel syndrome-severity scoring system (IBS-SSS) responders, as defined by a decrease of 95 points or more in the IBS-SSS total score from baseline, in participants receiving placebo or *Lactiplantibacillus plantarum* (*L. plantarum*) (1B or 10B CFU) capsules; B: Percentage of stool consistency responders, as defined by a decrease of at least 50% in the number of days per week with at least one stool that has a consistency of type 6 or 7 compared with baseline, in participants receiving placebo or *L. plantarum* (1B or 10B CFU) capsules. Between group comparison *via* Pearson chi-square test. $^{a}P < 0.05$; $^{b}P < 0.01$; $^{c}P < 0.001$. *L. plantarum*: *Lactiplantibacillus plantarum*.

be proximal to the colon, and fecal samples may not accurately reflect the small intestinal profile or corresponding changes in mucosal inflammation or epithelial function[6].

L. plantarum is a well-documented species, with several prior studies demonstrating efficacy in managing IBS symptomology, albeit with strain specific differences[49-53]. Recent studies with *L. plantarum* strains have also reported improved QoL and defecation frequency in IBS-D[50,52]. In rodent models, *L. plantarum* strains have been shown to



DOI: 10.3748/wjg.v29.i28.4451 **Copyright** ©The Author(s) 2023.

Figure 3 Fecal microbial profile over the intervention period. A: Proportional family level abundance in participants receiving placebo or *Lactiplantibacillus plantarum* (*L. plantarum*) (1B or 10B CFU) capsules; B: Proportional genus level abundance in participants receiving placebo or *L. plantarum* (1B or 10B CFU) capsules.

relieve diarrhea through inflammation modulation and increased SCFAs[54], as well as upregulate the expression of brain-derived neurotrophic factor, serotonin transporter, and intestinal serotonin levels[55]. SCFAs play a critical role in gut homeostasis *via* mucus production, protection from inflammation, and immunomodulation[56]. Further, SCFA-producing microorganisms can also affect neurotransmitter levels and therefore gut-brain signaling, as well as activate and directly act on intestinal vagal terminals[57]. Additionally, SCFAs, particularly butyrate, may help promote intestinal barrier function[58], a feature of several *L. plantarum* strains[59]. Bile acid (BA) metabolism may also be implicated, as *L. plantarum* Lpla33 possesses significant bile salt hydrolase activity. Of note, diarrhea and visceral hypersensitivity have been associated with decreased 7α-dehydroxylation of primary BAs to secondary BAs[60]. Additionally, the ability of *L. plantarum* Lpla33 to modulate intestinal barrier function, inhibit key pathogens, and moderate inflammatory markers may have played a role in the observed effects.

Limitations of the study include the absence of biomarkers assessing immunity, inflammation, and intestinal barrier function, in part due to the large enrollment across several sites. Additionally, the study assessed fecal samples but not proximal sites of interest or corresponding changes in mucosal profile, inflammation, or epithelial function. Further, the study did not incorporate metabolite profiles in serum, feces, or urine to assess changes in immune or inflammation-related pathways[47]. Additionally, while macronutrient intake was shown to be stable over the study period, the association of diet with the microbial community or metabolite profiles would have been of interest to explore in more detail. Going forward, multi-omics studies should play an important role in further understanding therapeutic mechanisms of probiotic and diet-based interventions in IBS-D. Nevertheless, the study was well-powered to evaluate its primary outcome, incorporated 12 clinical sites and multiple doses, and integrated IBS trial design considerations[61].

CONCLUSION

The present randomized controlled trial demonstrates that *L. plantarum* Lpla33 (DSM34428) at a dose of 1×10^9 and 1×10^{10} CFU/day was well tolerated and met the primary outcome (reduction in IBS-SSS total score at day 56) in both dose groups compared to placebo. The study also met the first secondary outcome (reduction in IBS-SSS score at day 28) as well as outcomes related to abdominal pain severity, stool normalization, QoL, and perceived stress, when compared to placebo over the intervention period. Lastly, a *L. plantarum* Lpla33 dose response was observed in several key outcomes in females and males with IBS-D.

ARTICLE HIGHLIGHTS

Research background

Irritable bowel syndrome (IBS) is a disorder of gut-brain interaction characterized by abdominal pain in association with altered bowel habits and further classified by the predominant stool pattern. Global prevalence is high, with diarrhea predominant subtype (IBS-D) considered the most common. IBS-D has a significant impact on quality of life, and clinical management remains challenging due to the variety of symptoms to address.

Research motivation

A recent meta-analysis showed probiotics to be safe and superior to placebo for alleviating global IBS-D symptoms. However, the certainty of evidence is low, due in part to significant heterogeneity between studies. There is therefore a need for well-powered randomized controlled trials on promising probiotic candidates for IBS-D.

Research objectives

To assess the efficacy of a probiotic candidate strain, *Lactiplantibacillus plantarum* (*L. plantarum*) Lpla33 (DSM34428), in adults with IBS-D. The primary outcome was the change in the IBS severity scoring system (IBS-SSS) total score after 8 wk. Additional outcomes included the change in abdominal pain severity, IBS-related quality of life, stool and microbial profile, and perceived stress.

Research methods

Adults meeting Rome IV diagnostic criteria for IBS-D were recruited from 12 gastroenterology specialized centers across India. In this randomized, double-blind, placebo-controlled, multi-center, parallel-arm, and dose-ranging study, a total of 307 adults meeting the inclusion criteria were allocated (1:1:1) to receive placebo or *L. plantarum* Lpla33 at one of two doses [1×10^9 colony-forming units (CFU)/d (1B) or 1×10^{10} CFU/d (10B)] over 8 wk.

Research results

The primary outcome, IBS-SSS total score, was significantly reduced after 8 wk in participants receiving *L. plantarum* compared to placebo ($P < 0.001$), with a dose-ranging effect when comparing the two *L. plantarum* groups ($P < 0.05$). In total, 59.6% and 72.6% of participants in the *L. plantarum* 1B and *L. plantarum* 10B groups, respectively, were considered significant responders based on a 95-point reduction threshold, as compared to 26.3% in the placebo group ($P < 0.001$). Additionally, 62.5% and 88.4% of participants administered *L. plantarum* 1B and 10B, respectively, demonstrated a significant reduction in diarrheal stool form as compared to 26.3% in the placebo group ($P < 0.001$).

Research conclusions

L. plantarum Lpla33 is well tolerated and demonstrates dose-ranging efficacy in alleviating IBS symptom severity with a corresponding normalization of bowel habits in adults with IBS-D.

Research perspectives

Future research should incorporate multi-omics analyses and associated biomarkers to better understand the mechanisms of action involved.

ACKNOWLEDGEMENTS

The authors thank the site investigators (Dr. R. Dargad, Dr. S. Deshpande, Dr. J. Patel, Dr. S. Narang, Dr. P. Rahate, Dr. S. Kulkarni, Dr. A. Khanna, Dr. S. Khanna, Dr. A. Jangid, Dr. A. Pandit, Dr. R. Kushwaha, and Dr. N. Jillawar) for enabling the study, and monitors for overseeing the conduct of the study. We thank the Vedic Lifesciences team, including project, quality assurance, and data managers, as well as the consulting statistician, for professional management of the study. We thank the CosmosID team for their microbial profiling analysis and expertise. Lastly, we are thankful to J. Jensen and team for overseeing the production and quality control of the study products.

FOOTNOTES

Author contributions: Martoni CJ, Damholt A, and Leyer GL conceived, designed, and planned the study; Srivastava S directed the study, data analysis, and reporting; Martoni CJ prepared the original manuscript; Srivastava S, Damholt A, and Leyer GL reviewed and edited the manuscript; and all authors have read and approved the final version.

Institutional review board statement: This study was approved and monitored by an independent ethics committee (Approval No: VED/P-20/22/JUL/2021).

Clinical trial registration statement: This study was prospectively registered on clinicaltrials.gov under study number NCT04950296. The registry URL is as follows: https://clinicaltrials.gov/ct2/show/NCT04950296.

Informed consent statement: All study participants provided their voluntary written informed consent prior to their inclusion.

Conflict-of-interest statement: The study was funded by Chr. Hansen A/S. Christopher J Martoni, Anders Damholt and Gregory J Leyer are employees of Chr. Hansen A/S but were not involved in the study conduct, data management, or statistical analysis.

Data sharing statement: The anonymized data presented in this study are available on request from the corresponding author.

CONSORT 2010 statement: The authors have read the CONSORT 2010 Statement, and the manuscript was prepared and revised according to the CONSORT 2010 Statement.

Open-Access: This article is an open-access article that was selected by an in-house editor and fully peer-reviewed by external reviewers. It is distributed in accordance with the Creative Commons Attribution NonCommercial (CC BY-NC 4.0) license, which permits others to distribute, remix, adapt, build upon this work non-commercially, and license their derivative works on different terms, provided the original work is properly cited and the use is non-commercial. See: https://creativecommons.org/Licenses/by-nc/4.0/

Country/Territory of origin: Denmark

ORCID number: Christopher J Martoni 0000-0003-0295-8231; Shalini Srivastava 0000-0002-7635-1232; Anders Damholt 0009-0007-1657-1659; Gregory J Leyer 0000-0003-1745-4343.

S-Editor: Chen YL
L-Editor: Wang TQ
P-Editor: Chen YX

REFERENCES

1 **Holtmann GJ**, Ford AC, Talley NJ. Pathophysiology of irritable bowel syndrome. *Lancet Gastroenterol Hepatol* 2016; **1**: 133-146 [PMID: 28404070 DOI: 10.1016/S2468-1253(16)30023-1]

2 **Oka P**, Parr H, Barberio B, Black CJ, Savarino EV, Ford AC. Global prevalence of irritable bowel syndrome according to Rome III or IV criteria: a systematic review and meta-analysis. *Lancet Gastroenterol Hepatol* 2020; **5**: 908-917 [PMID: 32702295 DOI: 10.1016/S2468-1253(20)30217-X]

3 **Lovell RM**, Ford AC. Global prevalence of and risk factors for irritable bowel syndrome: a meta-analysis. *Clin Gastroenterol Hepatol* 2012; **10**: 712-721.e4 [PMID: 22426087 DOI: 10.1016/j.cgh.2012.02.029]

4 **Moshiree B**, Heidelbaugh JJ, Sayuk GS. A Narrative Review of Irritable Bowel Syndrome with Diarrhea: A Primer for Primary Care Providers. *Adv Ther* 2022; **39**: 4003-4020 [PMID: 35869354 DOI: 10.1007/s12325-022-02224-z]

5 **Dale HF**, Rasmussen SH, Asiller ÖÖ, Lied GA. Probiotics in Irritable Bowel Syndrome: An Up-to-Date Systematic Review. *Nutrients* 2019; **11** [PMID: 31480656 DOI: 10.3390/nu11092048]

6 **Altomare A**, Di Rosa C, Imperia E, Emerenziani S, Cicala M, Guarino MPL. Diarrhea Predominant-Irritable Bowel Syndrome (IBS-D): Effects of Different Nutritional Patterns on Intestinal Dysbiosis and Symptoms. *Nutrients* 2021; **13** [PMID: 33946961 DOI: 10.3390/nu13051506]

7 **Thakur ER**, Shapiro J, Chan J, Lumley MA, Cully JA, Bradford A, El-Serag HB. A Systematic Review of the Effectiveness of Psychological Treatments for IBS in Gastroenterology Settings: Promising but in Need of Further Study. *Dig Dis Sci* 2018; **63**: 2189-2201 [PMID: 29744772 DOI: 10.1007/s10620-018-5095-3]

8 **Bellini M**, Gambaccini D, Stasi C, Urbano MT, Marchi S, Usai-Satta P. Irritable bowel syndrome: a disease still searching for pathogenesis, diagnosis and therapy. *World J Gastroenterol* 2014; **20**: 8807-8820 [PMID: 25083055 DOI: 10.3748/wjg.v20.i27.8807]

9 **Chong PP**, Chin VK, Looi CY, Wong WF, Madhavan P, Yong VC. The Microbiome and Irritable Bowel Syndrome-A Review on the Pathophysiology, Current Research and Future Therapy. *Front Microbiol* 2019; **10**: 1136 [PMID: 31244784 DOI: 10.3389/fmicb.2019.01136]

10 **Burns GL**, Talley NJ, Keely S. Immune responses in the irritable bowel syndromes: time to consider the small intestine. *BMC Med* 2022; **20**: 115 [PMID: 35354471 DOI: 10.1186/s12916-022-02301-8]

11 **El-Salhy M**, Hatlebakk JG, Gilja OH, Bråthen Kristoffersen A, Hausken T. Efficacy of faecal microbiota transplantation for patients with irritable bowel syndrome in a randomised, double-blind, placebo-controlled study. *Gut* 2020; **69**: 859-867 [PMID: 31852769 DOI: 10.1136/gutjnl-2019-319630]

12 **Hill C**, Guarner F, Reid G, Gibson GR, Merenstein DJ, Pot B, Morelli L, Canani RB, Flint HJ, Salminen S, Calder PC, Sanders ME. Expert consensus document. The International Scientific Association for Probiotics and Prebiotics consensus statement on the scope and appropriate use of the term probiotic. *Nat Rev Gastroenterol Hepatol* 2014; **11**: 506-514 [PMID: 24912386 DOI: 10.1038/nrgastro.2014.66]

13 **Wang Y**, Chen N, Niu F, Li Y, Guo K, Shang X, E F, Yang C, Yang K, Li X. Probiotics therapy for adults with diarrhea-predominant irritable bowel syndrome: a systematic review and meta-analysis of 10 RCTs. *Int J Colorectal Dis* 2022; **37**: 2263-2276 [PMID: 36251040 DOI: 10.1007/s00384-022-04261-0]

14 **McFarland LV**, Karakan T, Karatas A. Strain-specific and outcome-specific efficacy of probiotics for the treatment of irritable bowel syndrome: A systematic review and meta-analysis. *EClinicalMedicine* 2021; **41**: 101154 [PMID: 34712929 DOI: 10.1016/j.eclinm.2021.101154]

15 **Nayak AK**, Karnad DR, Abraham P, Mistry FP. Metronidazole relieves symptoms in irritable bowel syndrome: the confusion with so-called 'chronic amebiasis'. *Indian J Gastroenterol* 1997; **16**: 137-139 [PMID: 9357184]

16 **Vashisht T**, Shenoy S, Cherian M. HealthifyMe App. [cited 12 June 2023]. Available from: https://www.healthifyme.com/in/

17 **Francis CY**, Morris J, Whorwell PJ. The irritable bowel severity scoring system: a simple method of monitoring irritable bowel syndrome and its progress. *Aliment Pharmacol Ther* 1997; **11**: 395-402 [PMID: 9146781 DOI: 10.1046/j.1365-2036.1997.142318000.x]

18 **Spiegel B**, Bolus R, Harris LA, Lucak S, Naliboff B, Esrailian E, Chey WD, Lembo A, Karsan H, Tillisch K, Talley J, Mayer E, Chang L. Measuring irritable bowel syndrome patient-reported outcomes with an abdominal pain numeric rating scale. *Aliment Pharmacol Ther* 2009; **30**: 1159-1170 [PMID: 19751360 DOI: 10.1111/j.1365-2036.2009.04144.x]

19 **Blake MR**, Raker JM, Whelan K. Validity and reliability of the Bristol Stool Form Scale in healthy adults and patients with diarrhoea-predominant irritable bowel syndrome. *Aliment Pharmacol Ther* 2016; **44**: 693-703 [PMID: 27492648 DOI: 10.1111/apt.13746]

20 **Food and Drug Administration**. Guidance for Industry: Irritable Bowel Syndrome-Clinical Evaluation of Drugs for Treatment. [cited 12 June 2023]. Available from: https://www.fda.gov/media/78622/download

21 **Patrick DL**, Drossman DA, Frederick IO, DiCesare J, Puder KL. Quality of life in persons with irritable bowel syndrome: development and validation of a new measure. *Dig Dis Sci* 1998; **43**: 400-411 [PMID: 9512138 DOI: 10.1023/a:1018831127942]

22 **Cohen S**. Perceived stress in a probability sample of the United States. The social psychology of health. Sage Publications, Inc. 1988. [cited 12 June 2023]. Available from: https://psycnet.apa.org/record/1988-98838-002

23 **Ford AC**, Harris LA, Lacy BE, Quigley EMM, Moayyedi P. Systematic review with meta-analysis: the efficacy of prebiotics, probiotics, synbiotics and antibiotics in irritable bowel syndrome. *Aliment Pharmacol Ther* 2018; **48**: 1044-1060 [PMID: 30294792 DOI: 10.1111/apt.15001]

24 **Lovell RM**, Ford AC. Effect of gender on prevalence of irritable bowel syndrome in the community: systematic review and meta-analysis. *Am J Gastroenterol* 2012; **107**: 991-1000 [PMID: 22613905 DOI: 10.1038/ajg.2012.131]

25 **Adeyemo MA**, Spiegel BM, Chang L. Meta-analysis: do irritable bowel syndrome symptoms vary between men and women? *Aliment Pharmacol Ther* 2010; **32**: 738-755 [PMID: 20662786 DOI: 10.1111/j.1365-2036.2010.04409.x]

26 **Rahman MM**, Mahadeva S, Ghoshal UC. Epidemiological and clinical perspectives on irritable bowel syndrome in India, Bangladesh and Malaysia: A review. *World J Gastroenterol* 2017; **23**: 6788-6801 [PMID: 29085223 DOI: 10.3748/wjg.v23.i37.6788]

27 **Barbara G**, Feinle-Bisset C, Ghoshal UC, Quigley EM, Santos J, Vanner S, Vergnolle N, Zoetendal EG. The Intestinal Microenvironment and Functional Gastrointestinal Disorders. *Gastroenterology* 2016 [PMID: 27144620 DOI: 10.1053/j.gastro.2016.02.028]

28 **Martoni CJ**, Srivastava S, Leyer GJ. Lactobacillus acidophilus DDS-1 and Bifidobacterium lactis UABla-12 Improve Abdominal Pain Severity and Symptomology in Irritable Bowel Syndrome: Randomized Controlled Trial. *Nutrients* 2020; **12** [PMID: 32019158 DOI: 10.3390/nu12020363]

29 **Hewawasam SP**, Iacovou M, Muir JG, Gibson PR. Dietary practices and FODMAPs in South Asia: Applicability of the low FODMAP diet to patients with irritable bowel syndrome. *J Gastroenterol Hepatol* 2018; **33**: 365-374 [PMID: 28700090 DOI: 10.1111/jgh.13885]

30 **Lyra A**, Hillilä M, Huttunen T, Männikkö S, Taalikka M, Tennilä J, Tarpila A, Lahtinen S, Ouwehand AC, Veijola L. Irritable bowel syndrome symptom severity improves equally with probiotic and placebo. *World J Gastroenterol* 2016; **22**: 10631-10642 [PMID: 28082816 DOI: 10.3748/wjg.v22.i48.10631]

31 **Kim JY**, Park YJ, Lee HJ, Park MY, Kwon O. Effect of Lactobacillus gasseri BNR17 on irritable bowel syndrome: a randomized, double-blind, placebo-controlled, dose-finding trial. *Food Sci Biotechnol* 2018; **27**: 853-857 [PMID: 30263811 DOI: 10.1007/s10068-017-0296-7]

32 **Kajander K**, Hatakka K, Poussa T, Färkkilä M, Korpela R. A probiotic mixture alleviates symptoms in irritable bowel syndrome patients: a controlled 6-month intervention. *Aliment Pharmacol Ther* 2005; **22**: 387-394 [PMID: 16128676 DOI: 10.1111/j.1365-2036.2005.02579.x]

33 **Kajander K**, Myllyluoma E, Rajilić-Stojanović M, Kyrönpalo S, Rasmussen M, Järvenpää S, Zoetendal EG, de Vos WM, Vapaatalo H,

Korpela R. Clinical trial: multispecies probiotic supplementation alleviates the symptoms of irritable bowel syndrome and stabilizes intestinal microbiota. *Aliment Pharmacol Ther* 2008; **27**: 48-57 [PMID: 17919270 DOI: 10.1111/j.1365-2036.2007.03542.x]

34 **Whorwell PJ**, Altringer L, Morel J, Bond Y, Charbonneau D, O'Mahony L, Kiely B, Shanahan F, Quigley EM. Efficacy of an encapsulated probiotic Bifidobacterium infantis 35624 in women with irritable bowel syndrome. *Am J Gastroenterol* 2006; **101**: 1581-1590 [PMID: 16863564 DOI: 10.1111/j.1572-0241.2006.00734.x]

35 **Wang P**, Peskoe S, Byrd R, Smith P, Breslin R, Chow SC. Statistical Evaluation of Absolute Change versus Responder Analysis in Clinical Trials. *Acta Mater Med* 2022; **1**: 320-332 [PMID: 37274016 DOI: 10.15212/amm-2022-0020]

36 **EFSA Panel on Nutrition**; Novel Foods and Food Allergens (EFSA NDA Panel), Turck D, Castenmiller J, De Henauw S, Hirsch-Ernst KI, Kearney J, Knutsen HK, Maciuk A, Mangelsdorf I, McArdle HJ, Naska A, Pelaez C, Pentieva K, Thies F, Tsabouri S, Vinceti M, Bresson JL, Burlingame B, Dean T, Fairweather-Tait S, Heinonen M, Neuhäuser-Berthold M, Nowicka G, Sanz Y, Sjödin A, Stern M, Tomé D, Van Loveren H, Willatts P, Martin A, Strain JJ, Heng L, Valtueña Martínez S, Siani A. Guidance on the scientific requirements for health claims related to muscle function and physical performance: (Revision 1). *EFSA J* 2018; **16**: e05434 [PMID: 32625715 DOI: 10.2903/j.efsa.2018.5434]

37 **Ishaque SM**, Khosruzzaman SM, Ahmed DS, Sah MP. A randomized placebo-controlled clinical trial of a multi-strain probiotic formulation (Bio-Kult®) in the management of diarrhea-predominant irritable bowel syndrome. *BMC Gastroenterol* 2018; **18**: 71 [PMID: 29801486 DOI: 10.1186/s12876-018-0788-9]

38 **Skrzydło-Radomańska B**, Prozorow-Król B, Cichoż-Lach H, Majsiak E, Bierła JB, Kosikowski W, Szczerbiński M, Gantzel J, Cukrowska B. The Effectiveness of Synbiotic Preparation Containing Lactobacillus and Bifidobacterium Probiotic Strains and Short Chain Fructooligosaccharides in Patients with Diarrhea Predominant Irritable Bowel Syndrome-A Randomized Double-Blind, Placebo-Controlled Study. *Nutrients* 2020; **12** [PMID: 32635661 DOI: 10.3390/nu12071999]

39 **Skrzydło-Radomańska B**, Prozorow-Król B, Cichoż-Lach H, Majsiak E, Bierła JB, Kanarek E, Sowińska A, Cukrowska B. The Effectiveness and Safety of Multi-Strain Probiotic Preparation in Patients with Diarrhea-Predominant Irritable Bowel Syndrome: A Randomized Controlled Study. *Nutrients* 2021; **13** [PMID: 33652763 DOI: 10.3390/nu13030756]

40 **Passos MC**, Lembo AJ, Conboy LA, Kaptchuk TJ, Kelly JM, Quilty MT, Kerr CE, Jacobson EE, Hu R, Friedlander E, Drossman DA. Adequate relief in a treatment trial with IBS patients: a prospective assessment. *Am J Gastroenterol* 2009; **104**: 912-919 [PMID: 19293784 DOI: 10.1038/ajg.2009.13]

41 **Singh P**, Staller K, Barshop K, Dai E, Newman J, Yoon S, Castel S, Kuo B. Patients with irritable bowel syndrome-diarrhea have lower disease-specific quality of life than irritable bowel syndrome-constipation. *World J Gastroenterol* 2015; **21**: 8103-8109 [PMID: 26185382 DOI: 10.3748/wjg.v21.i26.8103]

42 **Simrén M**, Barbara G, Flint HJ, Spiegel BM, Spiller RC, Vanner S, Verdu EF, Whorwell PJ, Zoetendal EG; Rome Foundation Committee. Intestinal microbiota in functional bowel disorders: a Rome foundation report. *Gut* 2013; **62**: 159-176 [PMID: 22730468 DOI: 10.1136/gutjnl-2012-302167]

43 **Barbara G**, Grover M, Bercik P, Corsetti M, Ghoshal UC, Ohman L, Rajilić-Stojanović M. Rome Foundation Working Team Report on Post-Infection Irritable Bowel Syndrome. *Gastroenterology* 2019; **156**: 46-58.e7 [PMID: 30009817 DOI: 10.1053/j.gastro.2018.07.011]

44 **Bhattarai Y**, Muniz Pedrogo DA, Kashyap PC. Irritable bowel syndrome: a gut microbiota-related disorder? *Am J Physiol Gastrointest Liver Physiol* 2017; **312**: G52-G62 [PMID: 27881403 DOI: 10.1152/ajpgi.00338.2016]

45 **Shrestha B**, Patel D, Shah H, Hanna KS, Kaur H, Alazzeh MS, Thandavaram A, Channar A, Purohit A, Venugopal S. The Role of Gut-Microbiota in the Pathophysiology and Therapy of Irritable Bowel Syndrome: A Systematic Review. *Cureus* 2022; **14**: e28064 [PMID: 36127988 DOI: 10.7759/cureus.28064]

46 **Distrutti E**, Monaldi L, Ricci P, Fiorucci S. Gut microbiota role in irritable bowel syndrome: New therapeutic strategies. *World J Gastroenterol* 2016; **22**: 2219-2241 [PMID: 26900286 DOI: 10.3748/wjg.v22.i7.2219]

47 **Ng QX**, Yau CE, Yaow CYL, Chong RIH, Chong NZ, Teoh SE, Lim YL, Soh AYS, Ng WK, Thumboo J. What Has Longitudinal 'Omics' Studies Taught Us about Irritable Bowel Syndrome? A Systematic Review. *Metabolites* 2023; **13** [PMID: 37110143 DOI: 10.3390/metabo13040484]

48 **Kristensen NB**, Bryrup T, Allin KH, Nielsen T, Hansen TH, Pedersen O. Alterations in fecal microbiota composition by probiotic supplementation in healthy adults: a systematic review of randomized controlled trials. *Genome Med* 2016; **8**: 52 [PMID: 27159972 DOI: 10.1186/s13073-016-0300-5]

49 **Niedzielin K**, Kordecki H, Birkenfeld B. A controlled, double-blind, randomized study on the efficacy of Lactobacillus plantarum 299V in patients with irritable bowel syndrome. *Eur J Gastroenterol Hepatol* 2001; **13**: 1143-1147 [PMID: 11711768 DOI: 10.1097/00042737-200110000-00004]

50 **Jung K**, Kim A, Lee JH, Cho D, Seo J, Jung ES, Kang HJ, Roh J, Kim W. Effect of Oral Intake of *Lactiplantibacillus plantarum* APsulloc 331261 (GTB1(TM)) on Diarrhea-Predominant Irritable Bowel Syndrome: A Randomized, Double-Blind, Placebo-Controlled Study. *Nutrients* 2022; **14** [PMID: 35631156 DOI: 10.3390/nu14102015]

51 **Ligaarden SC**, Axelsson L, Naterstad K, Lydersen S, Farup PG. A candidate probiotic with unfavourable effects in subjects with irritable bowel syndrome: a randomised controlled trial. *BMC Gastroenterol* 2010; **10**: 16 [PMID: 20144246 DOI: 10.1186/1471-230X-10-16]

52 **Liu Y**, Yu X, Yu L, Tian F, Zhao J, Zhang H, Qian L, Wang Q, Xue Z, Zhai Q, Chen W. Lactobacillus plantarum CCFM8610 Alleviates Irritable Bowel Syndrome and Prevents Gut Microbiota Dysbiosis: A Randomized, Double-Blind, Placebo-Controlled, Pilot Clinical Trial. *Engineering* 2021; **7**: 376-385 [DOI: 10.1016/j.eng.2020.06.026]

53 **Ducrotté P**, Sawant P, Jayanthi V. Clinical trial: Lactobacillus plantarum 299v (DSM 9843) improves symptoms of irritable bowel syndrome. *World J Gastroenterol* 2012; **18**: 4012-4018 [PMID: 22912552 DOI: 10.3748/wjg.v18.i30.4012]

54 **Yue Y**, He Z, Zhou Y, Ross RP, Stanton C, Zhao J, Zhang H, Yang B, Chen W. Lactobacillus plantarum relieves diarrhea caused by enterotoxin-producing Escherichia coli through inflammation modulation and gut microbiota regulation. *Food Funct* 2020; **11**: 10362-10374 [PMID: 33220669 DOI: 10.1039/d0fo02670k]

55 **Ranuh R**, Athiyyah AF, Darma A, Risky VP, Riawan W, Surono IS, Sudarmo SM. Effect of the probiotic Lactobacillus plantarum IS-10506 on BDNF and 5HT stimulation: role of intestinal microbiota on the gut-brain axis. *Iran J Microbiol* 2019; **11**: 145-150 [PMID: 31341569]

56 **Parada Venegas D**, De la Fuente MK, Landskron G, González MJ, Quera R, Dijkstra G, Harmsen HJM, Faber KN, Hermoso MA. Short Chain Fatty Acids (SCFAs)-Mediated Gut Epithelial and Immune Regulation and Its Relevance for Inflammatory Bowel Diseases. *Front Immunol* 2019; **10**: 277 [PMID: 30915065 DOI: 10.3389/fimmu.2019.00277]

57 **Hamamah S**, Aghazarian A, Nazaryan A, Hajnal A, Covasa M. Role of Microbiota-Gut-Brain Axis in Regulating Dopaminergic Signaling.

Biomedicines 2022; **10** [PMID: 35203645 DOI: 10.3390/biomedicines10020436]

58 **Wang RX**, Lee JS, Campbell EL, Colgan SP. Microbiota-derived butyrate dynamically regulates intestinal homeostasis through regulation of actin-associated protein synaptopodin. *Proc Natl Acad Sci U S A* 2020; **117**: 11648-11657 [PMID: 32398370 DOI: 10.1073/pnas.1917597117]

59 **Mujagic Z**, de Vos P, Boekschoten MV, Govers C, Pieters HH, de Wit NJ, Bron PA, Masclee AA, Troost FJ. The effects of Lactobacillus plantarum on small intestinal barrier function and mucosal gene transcription; a randomized double-blind placebo controlled trial. *Sci Rep* 2017; **7**: 40128 [PMID: 28045137 DOI: 10.1038/srep40128]

60 **Wei W**, Wang HF, Zhang Y, Zhang YL, Niu BY, Yao SK. Altered metabolism of bile acids correlates with clinical parameters and the gut microbiota in patients with diarrhea-predominant irritable bowel syndrome. *World J Gastroenterol* 2020; **26**: 7153-7172 [PMID: 33362374 DOI: 10.3748/wjg.v26.i45.7153]

61 **Miller LE**. Study design considerations for irritable bowel syndrome clinical trials. *Ann Gastroenterol* 2014; **27**: 338-345 [PMID: 25330749]

World Journal of Gastroenterology

Submit a Manuscript: https://www.f6publishing.com

World J Gastroenterol 2023 July 28; 29(28): 4466-4480

DOI: 10.3748/wjg.v29.i28.4466

ISSN 1007-9327 (print) ISSN 2219-2840 (online)

META-ANALYSIS

One in four patients with gastrointestinal bleeding develops shock or hemodynamic instability: A systematic review and meta-analysis

Mahmoud Obeidat, Brigitta Teutsch, Anett Rancz, Edina Tari, Katalin Márta, Dániel Sándor Veres, Nóra Hosszúfalusi, Emese Mihály, Péter Hegyi, Bálint Erőss

Specialty type: Gastroenterology and hepatology

Provenance and peer review: Unsolicited article; Externally peer reviewed.

Peer-review model: Single blind

Peer-review report's scientific quality classification

Grade A (Excellent): 0
Grade B (Very good): B
Grade C (Good): C
Grade D (Fair): 0
Grade E (Poor): 0

P-Reviewer: Kotlyarov S, Russia; Sánchez JIA, Colombia

Received: February 10, 2023
Peer-review started: February 10, 2023
First decision: May 16, 2023
Revised: May 30, 2023
Accepted: June 14, 2023
Article in press: June 14, 2023
Published online: July 28, 2023

Mahmoud Obeidat, Brigitta Teutsch, Anett Rancz, Edina Tari, Katalin Márta, Dániel Sándor Veres, Nóra Hosszúfalusi, Emese Mihály, Péter Hegyi, Bálint Erőss, Centre for Translational Medicine, Semmelweis University, Budapest 1085, Hungary

Mahmoud Obeidat, Brigitta Teutsch, Péter Hegyi, Bálint Erőss, Institute for Translational Medicine, Medical School, University of Pécs, Pécs 7623, Hungary

Anett Rancz, Nóra Hosszúfalusi, Emese Mihály, Department of Internal Medicine and Hematology, Semmelweis University, Faculty of Medicine, Budapest 1085, Hungary

Edina Tari, Katalin Márta, Péter Hegyi, Bálint Erőss, Institute of Pancreatic Diseases, Semmelweis University, Budapest 1083, Hungary

Dániel Sándor Veres, Department of Biophysics and Radiation Biology, Semmelweis University, Budapest 1085, Hungary

Corresponding author: Bálint Erőss, MD, PhD, Assistant Professor, Doctor, Centre for Translational Medicine, Semmelweis University, Üllői street 26, Budapest 1085, Hungary. dr.eross.balint@gmail.com

Abstract

BACKGROUND

Hemodynamic instability and shock are associated with untoward outcomes in gastrointestinal bleeding. However, there are no studies in the existing literature on the proportion of patients who developed these outcomes after gastrointestinal bleeding.

AIM

To determine the pooled event rates in the available literature and specify them based on the bleeding source.

METHODS

The protocol was registered on PROSPERO in advance (CRD42021283258). A systematic search was performed in three databases (PubMed, EMBASE, and CENTRAL) on 14th October 2021. Pooled proportions with 95%CI were calculated with a random-effects model. A subgroup analysis was carried out based on the time of assessment (on admission or during hospital stay). Heterogeneity was assessed by Higgins and Thompson's I^2 statistics. The Joanna Briggs Institute

Prevalence Critical Appraisal Tool was used for the risk of bias assessment. The Reference Citation Analysis (https://www.referencecitationanalysis.com/) tool was applied to obtain the latest highlight articles.

RESULTS

We identified 11589 records, of which 220 studies were eligible for data extraction. The overall proportion of shock and hemodynamic instability in general gastrointestinal bleeding patients was 0.25 (95%CI: 0.17-0.36, I^2 = 100%). In non-variceal bleeding, the proportion was 0.22 (95%CI: 0.14-0.31, I^2 = 100%), whereas it was 0.25 (95%CI: 0.19-0.32, I^2 = 100%) in variceal bleeding. The proportion of patients with colonic diverticular bleeding who developed shock or hemodynamic instability was 0.12 (95%CI: 0.06-0.22, I^2 = 90%). The risk of bias was low, and heterogeneity was high in all analyses.

CONCLUSION

One in five, one in four, and one in eight patients develops shock or hemodynamic instability on admission or during hospitalization in the case of non-variceal, variceal, and colonic diverticular bleeding, respectively.

Key Words: Gastrointestinal bleeding; Hemodynamic instability; Shock; Meta-analysis; Statistics; Review

©The Author(s) 2023. Published by Baishideng Publishing Group Inc. All rights reserved.

Core Tip: Gastrointestinal bleeding is one of the most common gastrointestinal emergencies with estimated mortality up to 10%. It is associated with significant morbidity, additional burden, and health care costs. It is documented that hemodynamic instability and shock are highly associated with untoward outcomes; they lead to a higher mortality rate, rebleeding risk, prehospital transfusion, and sedation complications. Our study provides clear evidence that hemodynamic instability and shock are common presentations and complications in gastrointestinal bleeding and gives insight into some possible predictor factors.

Citation: Obeidat M, Teutsch B, Rancz A, Tari E, Márta K, Veres DS, Hosszúfalusi N, Mihály E, Hegyi P, Erőss B. One in four patients with gastrointestinal bleeding develops shock or hemodynamic instability: A systematic review and meta-analysis. *World J Gastroenterol* 2023; 29(28): 4466-4480

URL: https://www.wjgnet.com/1007-9327/full/v29/i28/4466.htm

DOI: https://dx.doi.org/10.3748/wjg.v29.i28.4466

INTRODUCTION

The annual incidence of gastrointestinal bleeding (GIB) is 100 per 100000 population, and it is one of the most common gastroenterological emergencies with an estimated mortality rate in the range of 2%-10%, primarily due to complications related to the admission state and individual patient factors[1-3]. It is associated with significant morbidity, additional burden, and health care costs[4,5]. The mortality rate of upper GIB has not considerably decreased over the past decades, despite the improvement in the diagnosis and endoscopic treatment[6]. We contemplate that pre-endoscopic assessment and post-endoscopic care may contribute effectively to better outcomes.

Several studies showed that hemodynamic instability (HI) and shock in GIB are highly associated with untoward outcomes; they can lead to higher mortality rates, prehospital transfusion, rebleeding risk, and endoscopic sedation might be complicated with unfavorable hemodynamics if the patient presents with massive bleeding[7-9]. Furthermore, the hospital mortality rate of bleeding with shock can be 10 times higher than without shock[10].

Early intensive resuscitation of HI decreases complications in patients with upper GIB[11]. However, there are not enough details in the guidelines regarding the management of hemodynamically unstable patients; there are still some uncertainties about the optimal fluid rate and the ideal type of fluid to be used in treating those patients[12-15].

At the time of our systematic search, there were no published systematic reviews assessing the proportion of hemodynamically unstable and shocked patients in GIB. There are large variations in the proportions of these outcomes. Some studies in variceal and non-variceal bleeding resulted in proportions of 10% or lower[16-19], whereas others exceeded 60%[20-22]. Therefore, we aimed to highlight the importance of recognizing those patients by quantifying the pooled event rates based on the bleeding source. Additionally, we did a subgroup analysis based on the assessment time of these outcomes (on admission or during hospital stay).

MATERIALS AND METHODS

Our systematic review and meta-analysis was conducted following the recommendation of the Preferred Reporting Items for Systematic Reviews and Meta-Analyses (PRISMA) 2020 guideline[23]. The recommendations of the Cochrane

Handbook were also followed[24]. The study protocol was registered on PROSPERO (CRD42021283258), and we fully adhered to it[25]. In addition, we applied the Reference Citation Analysis (RCA) tool, which is based on artificial intelligence technology. This tool allowed us to access a comprehensive database of citations across multiple disciplines, aiding us in identifying the most recent and significant articles for our research.

Eligibility criteria

We applied the CoCoPop (condition, context, and population) framework to establish the eligibility criteria[26]; the condition was hemodynamic instability and/or shock, gastrointestinal bleeding as a context, and our population was adult patients. All definitions of hemodynamic instability and shock were accepted.

Randomized Controlled Trials (RCTs), cohorts, and case-control studies were included. Cross-sectional studies were included only if the hemodynamic parameters were assessed on admission. We included studies only if the primary cause of hospital admission was gastrointestinal bleeding and excluded articles that assessed our investigated outcomes after specific interventions. Articles that could not be found were sought for retrieval by contacting the journals and the authors. In the case of studies with overlapping populations, we kept the ones with larger sample sizes.

Information sources

Our systematic search was conducted in three main databases: MEDLINE (*via* PubMed), EMBASE, and Cochrane Central Register of Controlled Trials (CENTRAL) from the inception to 14th October 2021. No language or other restrictions were applied.

Search strategy

Our search key contained two main concepts: All types of bleeding sources and hemodynamic instability or shock. For the detailed search strategy, see Supplementary Table 1.

Screening and selection

Following the systematic search, the yielded articles were imported into a reference management program (EndNote 20.1). Duplicate articles were eliminated automatically and manually with overlapping publication years, authors, and titles. The screening and selection were performed by two independent reviewers (Obeidat M and Tari E) first by title and abstract, and then by full text (considering the eligibility criteria). Cohen's kappa coefficient (κ) was calculated at both levels of selection to measure the inter-reviewer reliability. In case of any disagreement, a consensus was reached after a discussion with the corresponding author (Erőss B).

Data extraction

The relevant data from the eligible studies were extracted independently by two authors (Obeidat M and Rancz A). Disagreements were resolved by involving the corresponding author (Erőss B). All data were manually collected and introduced into an Excel spreadsheet (Office 365, Microsoft, Redmond, WA, United States) for analysis. The following data were extracted: First author, the year of publication, Digital Object Identifier, geographical location, study period and design, number of centers, basic demographics, source of bleeding, the total number of GIB patients and those who developed HI or shock, definitions of the investigated outcomes, and the time of detection (on admission or during hospital stay).

Risk of bias assessment and quality of evidence

Two independent authors (Obeidat M and Tari E) performed the risk of bias assessment using the 'Joanna Briggs Institute Prevalence Critical Appraisal Tool'[26]. A third reviewer resolved potential disagreements (Rancz A). The tool contains nine items regarding the target population and study settings. Each item was rated as 'yes', 'no', 'unclear', or 'not applicable' according to information provided in each study, with a maximum score of nine points. The higher the score, the lower the risk of bias.

We followed the Grading of Recommendations Assessment, Development and Evaluation (GRADE) approach[27] to evaluate the quality of evidence of our results, and the GRADEpro tool (software) was used. Study design, risk of bias, inconsistency, indirectness, and imprecision were the determinant factors.

Statistical synthesis

The statistical analysis of the data was conducted by the R programming language using the meta package. We used forest plots to summarize the findings of the studies and show the pooled result. Pooled event rates were calculated with 95%CIs. The random-effect model was anticipated as applied in all analyses as considerable between-study heterogeneity. The random intercept logistic regression model method was used for pooling method as recommended by Schwarzer *et al*[28]. To estimate the heterogeneity variance measure τ^2, the maximum likelihood method was used. For the outcomes where the study number was at least five, a Hartung-Knapp adjustment was used[29,30]. Below five studies, we applied the adjustment if it was more conservative than without the adjustment. Statistical heterogeneity was assessed by Higgins and Thompson's I^2[31].

Egger's test with the Peter's modification and funnel plots were applied to report and visualize publication bias if at least 10 studies were involved in the analysis[32]; $P < 0.1$ indicates potential publication bias. We also performed an influential sensitivity analysis with leave-one-out method to evaluate whether a single study could have a marked influence on the overall proportional rate or heterogeneity.

A subgroup analysis was carried out based on the time of assessment (on admission or during hospitalization) of HI or shock. Studies where there were no data about the time when the patients were assessed, were considered (during hospitalization). We used a fixed-effects "plural" model. We assumed that subgroups had different τ^2 values as we anticipated differences in the between-study heterogeneity in the subgroups, although a common τ^2 assumption was used for practical reasons if the subgroup size was maximum five. To assess the difference between the subgroups, a Cochrane Q test was used between subgroups[33]. We did not calculate the overall effect and heterogeneity for subgroups where less than three studies were included. We calculated the prediction intervals for our outcomes to assess the probability that future studies would have the same result in a similar setting[34]. The statistical methods of this study were reviewed by Veres DS who is a verified biostatistician from the Centre for Translational Medicine, Semmelweis University.

RESULTS

Search and selection

Altogether, 11589 studies were identified by our search key through three main databases, 8129 in EMBASE, 3134 in Medline (*via* PubMed), and 326 in CENTRAL. Of them, 9192 records remained for title and abstract selection after duplicate removal. A total of 601 studies were sought for full-text selection, out of which 164 records were not found. We managed to retrieve 29, but 135 records were still inaccessible. In total, 466 studies were assessed for full-text eligibility, of which 246 were excluded (Supplementary Table 2). Eleven studies were removed for overlapping populations (Supplementary Table 3). Details of search and selection are illustrated in the PRISMA 2020 flow chart (Figure 1).

Basic characteristics of included studies

Most of the included studies were cohort studies. We also included 28 RCTs, 6 case-control, and 4 cross-sectional studies. Eighty records were from Asia, 66 from Europe, 25 from North America, and 13 from Africa. In total, more than six million patients were included in the analysis. However, the study with the largest sample size included 6411838 patients with different bleeding sources from a 12-year national analysis in the United States[10]. The main characteristics of the enrolled studies are detailed in Supplementary Table 4.

Hemodynamic instability and shock in general gastrointestinal bleeding sources

We included all studies with unspecified bleeding sources[8,10,35-50]. HI was assessed on admission and during hospital stay with pooled event rates of 0.29 (95%CI: 0.12-0.56, I^2 = 87%) and 0.34 (95%CI: 0.11-0.68, I^2 = 93%), respectively. Shock on admission was 0.27 (95%CI: 0.08-0.60, I^2 = 92%), whereas during hospital stay it was 0.15 (95%CI: 0.05-0.36, I^2 = 99%). One in four patients with GIB developed HI or shock; 0.25 (95%CI: 0.17-0.36, I^2 = 100%) (Figure 2).

Hemodynamic instability and shock in non-variceal upper GIB

In the case of non-variceal bleeding, more than three million patients were included in the analysis from 25 studies[10,17,20,21,51-71]. The proportion of hemodynamically unstable patients on admission was 0.21 (95%CI: 0.12-0.36, I^2 = 97%). Two studies assessed HI during hospitalization, Hwang *et al*[58] and Kwon *et al*[60] where the event rate was 0.10 (95%CI: 0.08-0.11) and 0.57 (95%CI: 0.42-0.70), respectively. Moreover, shock on admission was the highest at 0.36 (95%CI: 0.21-0.53, I^2 = 98%), with a noticeable difference from those who developed shock during hospitalization with a rate of 0.07 (95%CI: 0.02-0.18, I^2 = 100%). Altogether, 0.22 (95%CI: 0.14-0.31, I^2 = 100%) of non-variceal bleeders developed shock or HI on admission or during the hospital stay (Figure 3).

Hemodynamic instability and shock in variceal upper GIB

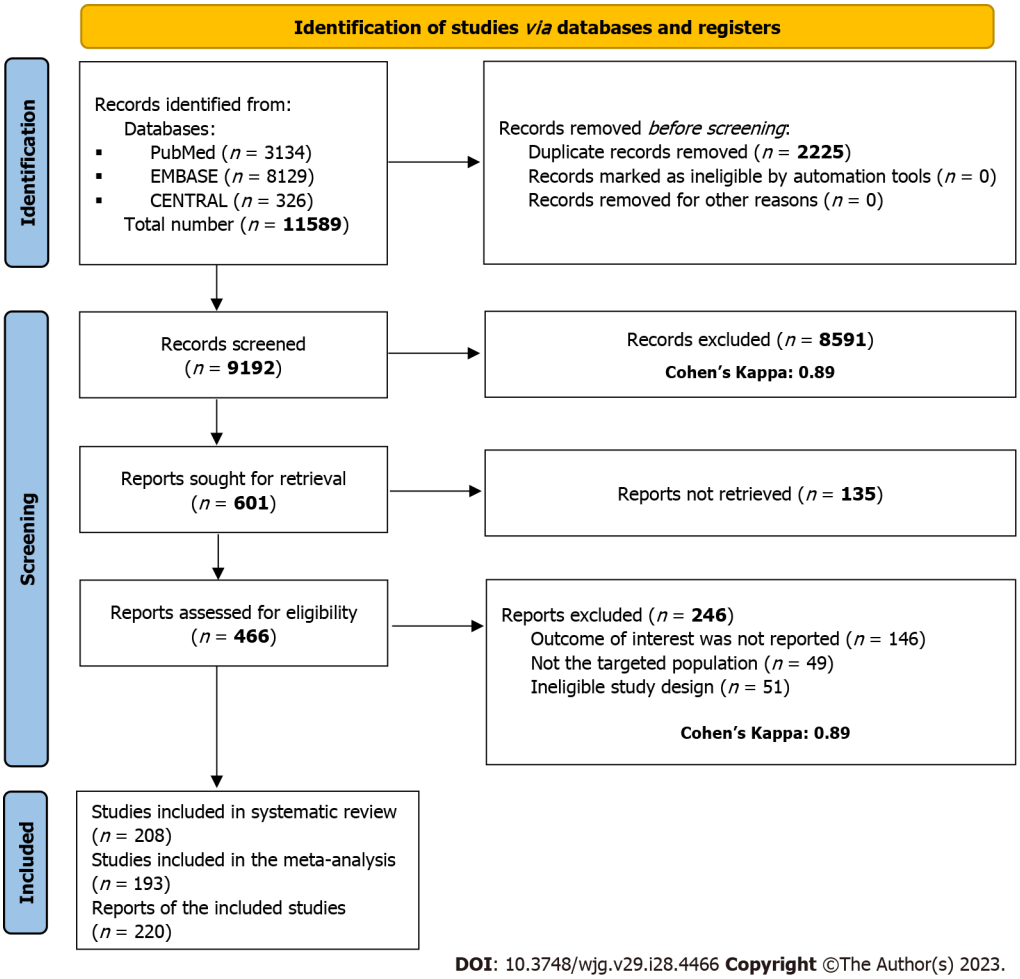
In total, 34 studies were included in this analysis[10,16,20,21,61,65,70,72-98]. The rate of patients with variceal bleeding who presented with HI on admission was 0.38 (95%CI: 0.12-0.73, I^2 = 98%). Two studies assessed HI during hospitalization, Farooqi and Farooqi[96] and Choi *et al*[75] where the event rate was 0.21 (95%CI: 0.14-0.29) and 0.52 (95%CI: 0.40-0.63), respectively. The shock rate on admission was 0.26 (95%CI: 0.18-0.36, I^2 = 100%), whereas it was 0.18 (95%CI: 0.10-0.30, I^2 = 99%) during the hospital stay. In total, one in four patients with variceal bleeding developed shock or HI at presentation or during hospital stay 0.25 (95%CI: 0.19-0.32, I^2 = 100%) (Figure 4).

Hemodynamic instability and shock in peptic ulcer bleeding

Peptic ulcer bleeding (PUB) was the most reported source of bleeding among the included studies. Sixty-seven studies were involved in the subgroups. On admission, 0.22 (95%CI: 0.09-0.44, I^2 = 96%) of the patients were hemodynamically unstable, whereas during the hospital stay, it was 0.41 (95%CI: 0.12-0.78, I^2 = 89%). The rate of shock on admission was 0.25 (95%CI: 0.19-0.32, I^2 = 98%), whereas 0.24 (95%CI: 0.17-0.33, I^2 = 97%) developed shock during hospitalization. As an overall effect, one in four PUB patients was affected by HI or shock on admission or during hospital stay; 0.25 (95%CI: 0.21-0.30, I^2 = 98%) (Supplementary Figure 1).

Hemodynamic instability and shock in upper GIB

The studies included in this plot contain various upper GIB sources. All the studies that reported HI were assessed on admission, with a rate of 0.33 (95%CI: 0.21-0.48, I^2 = 97%). Seventeen studies were included in the shock on admission subgroup with a rate of 0.15 (95%CI: 0.09-0.25, I^2 = 99%), whereas 18 studies evaluated shock during hospitalization with a rate of 0.20 (95%CI: 0.12-0.32, I^2 = 100%). In total, one in five patients with upper GIB developed shock or HI; 0.20



DOI: 10.3748/wjg.v29.i28.4466 **Copyright** ©The Author(s) 2023.

Figure 1 PRISMA 2020 flow chart of the screening and selection process of the studies.

(95%CI: 0.15-0.27, I^2 = 100%) (Supplementary Figure 2).

Hemodynamic instability and shock in lower GIB

In total, 17 studies were included in this analysis[10,48,99-113]. Thirteen studies evaluated HI in lower GIB population: Three studies on admission with a rate of 0.14 (95%CI: 0.01-0.81, I^2 = 83%), and 10 studies during hospitalization with a rate of 0.49 (95%CI: 0.27-0.71, I^2 = 94%). Two studies assessed shock on admission, Oakland *et al*[109] and Li *et al*[105] where the pooled event rates were 0.02 (95%CI: 0.02-0.03) and 0.03 (95%CI: 0.03-0.03), respectively. Another two studies assessed shock during hospital stay. In the study by Siddiqui *et al*[10] the shock rate was 0.02 (95%CI: 0.02-0.02). The study by Lv and Gu[106], which involved patients with life-threatening bleeding, resulted in the highest pooled event rate of shock with a rate of 0.68 (95%CI: 0.50-0.82). In total, of the general lower GIB population, 0.27 (95%CI: 0.13-0-49, I^2 = 100%) developed shock or HI (Figure 5).

Hemodynamic instability and shock in colonic diverticular bleeding

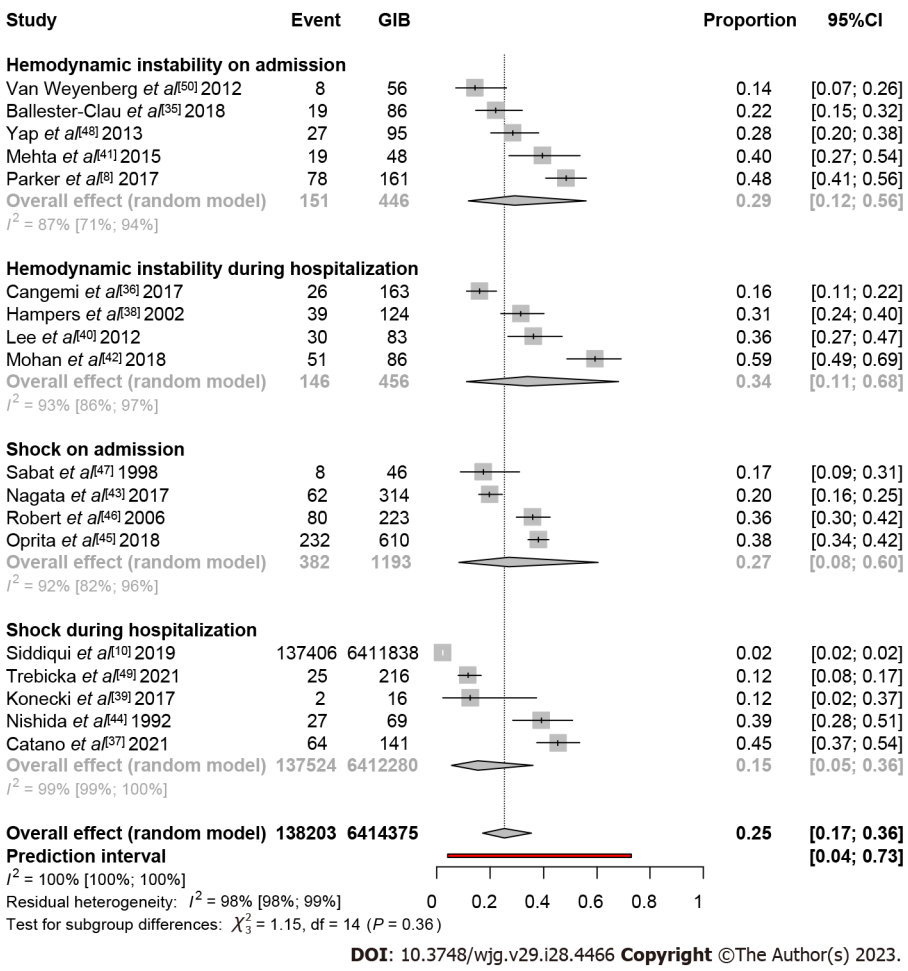
All studies assessed the investigated outcomes on admission only. Six studies evaluated shock in colonic diverticular bleeding (CDB) with a rate of 0.12 (95%CI: 0.05-0.26, I^2 = 91%). Only two studies reported HI, that of Gilshtein *et al*[114] reported a rate of 0.05 (95%CI: 0.02-0.11), and Ichiba *et al*[115] a rate of 0.21 (95%CI: 0.17-0.26). As an overall effect, the proportion of shock and HI in CDB was 0.12 (95%CI: 0.06-0.22, I^2 = 90%) (Supplementary Figure 3).

Risk of bias assessment

Most of the studies received a score of 6 or higher, indicating a moderate to low risk of bias. Only 10 studies were rated with a score less than six. The sample size was not adequate in 33 studies. The results of the risk of bias assessment are presented in Supplementary Table 5.

Heterogeneity and publication bias

Serious heterogeneity (with more than 80%) was observed in all our analyses. The large number of included studies with heterogeneous populations regarding age and sex could explain this. The definitions of HI and shock in the studies were not the same resulting in considerable heterogeneity, too.



DOI: 10.3748/wjg.v29.i28.4466 **Copyright** ©The Author(s) 2023.

Figure 2 Forest plot demonstrating the proportion rates for hemodynamic instability and shock in general gastrointestinal bleeding sources. GIB: Gastrointestinal bleeding.

All of our meta-analytical calculations that included 10 or more studies were investigated for publication bias. CDB was an exception where only eight studies were included. We found potential publication bias in all of our analyses except for non-variceal bleeding based on Egger's test. This result could be explained by the very large heterogeneity of the study estimates. Additionally, a highly influential large study by Siddiqui *et al*[10] led to a false positive result for Egger's test.

Leave-one-out sensitivity analysis showed some variability for some potential outliers. The proportion of our outcomes changed from 0.25 (95%CI: 017-0.36, I^2 = 100%) to 0.29 (95%CI: 0.22-0.37, I^2 = 90%) if Siddiqui *et al*[10] study was eliminated from the GIB analysis. This study did not only include a large sample size compared to other studies but also used the National Inpatient Sample database using International Classification of Diseases (ICD-9) codes to analyze patient data, which might have failed to identify some affected patients. Results of Egger's test, funnel plots, and leave-one-out analysis are found in Supplementary Figures 4-16.

Certainty of evidence

Based on the results and the careful evaluation of the evidence level, the certainty levels were low or very low for each outcome. The very high heterogeneity in almost all analyses was the main reason for that. In addition, all the included studies were considered observational studies, which contributes to the low level of evidence. (Supplementary Tables 6-12).

DISCUSSION

Our study found that HI and shock are common complications of GIB. Either shock or HI affects one in every four patients; even the lowest proportion, one in eight colonic diverticular bleeders, is still a significant portion of patients.

Variceal bleeding resulted in the highest HI on admission, with a rate of (38%) among various bleeding sources. In contrast, the highest HI rates during hospitalization were observed in PUB (41%) and LGIB (49%). The rate of shock on admission was generally the highest among different non-variceal bleeding sources (36%), whereas PUB specifically led to the highest rate of shock during hospitalization (24%).

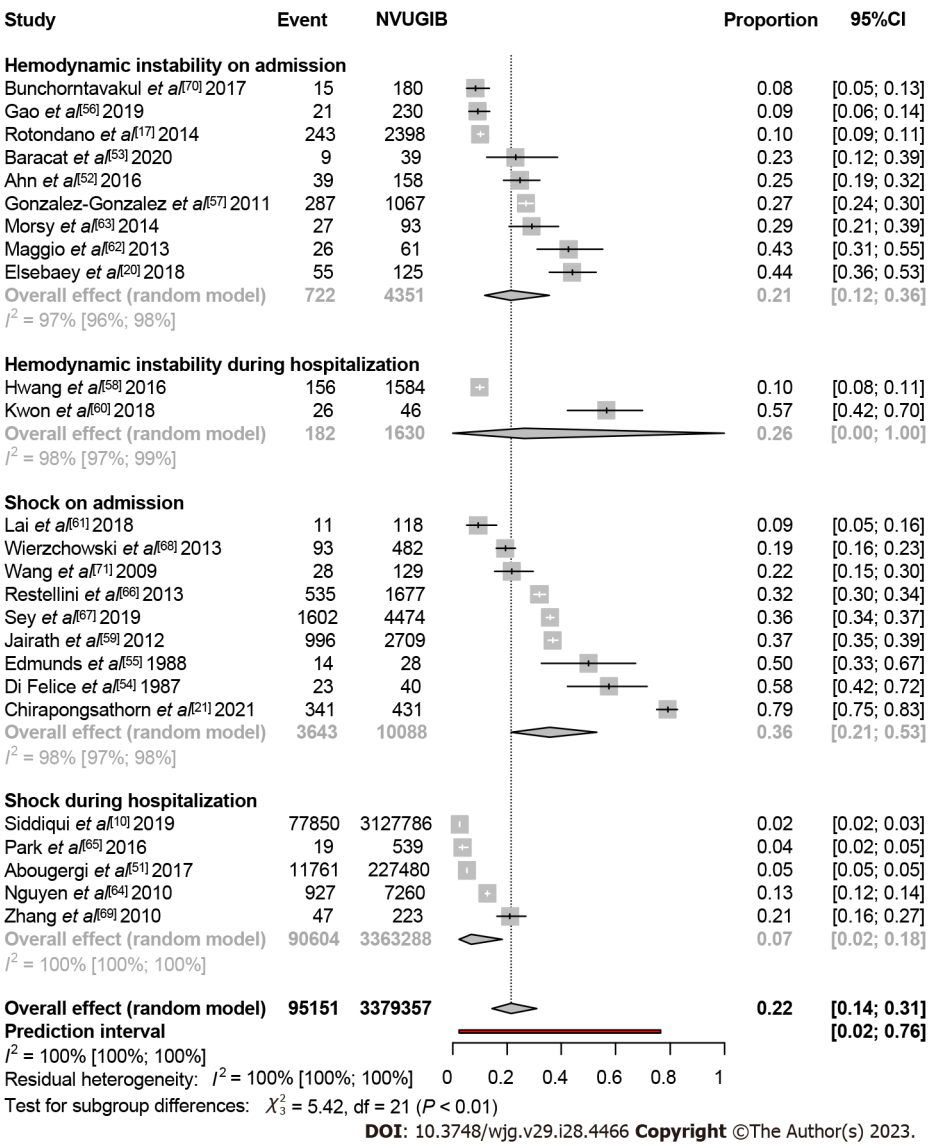


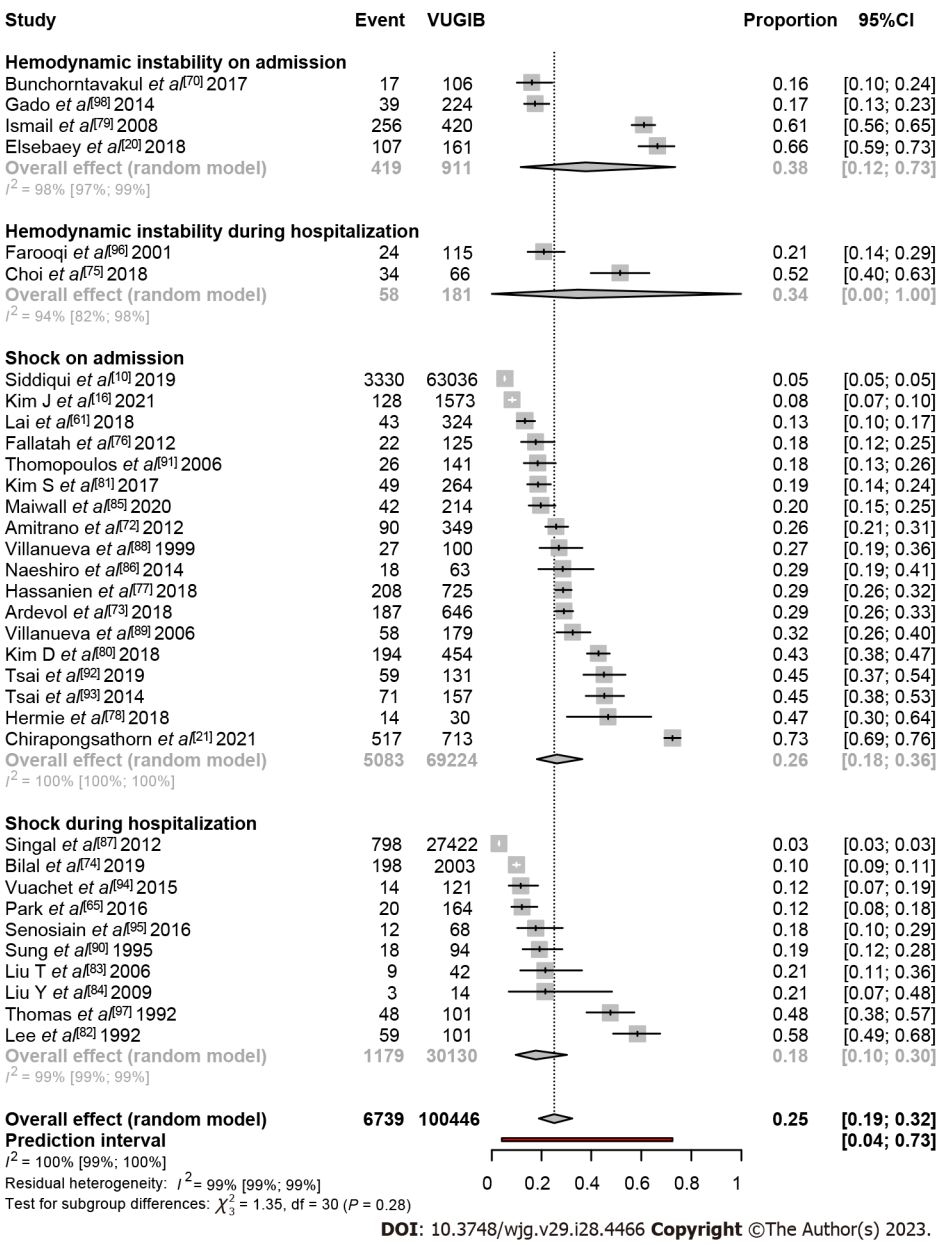
Figure 3 Forest plot demonstrating the proportion rates for hemodynamic instability and shock in non-variceal bleeding. NVUGIB: Non-variceal upper gastrointestinal bleeding.

Our results about unspecified GIB sources, non-variceal, and PUB showed higher rates of HI during hospitalization than on admission and higher rates of shock on admission than during hospitalization. In contrast, variceal bleeding showed higher rates of HI and shock on admission than during hospitalization. Lower GIB, on the other hand, showed higher rates of these outcomes during hospitalization than on admission.

Blood loss leads to HI characterized by a decrease in systolic blood pressure (BP) and an increase in heart rate (HR). Eventually, it can lead to a more severe state of shock, which is caused by a rapid reduction of intravascular blood volume resulting in decreasing hemoglobin levels, thereby decreasing the oxygen delivery capacity of the heart. HI is not just a sign; it is the starting point of a chain of events leading to hypoxemia and hypoperfusion. If it is not appropriately treated as soon as possible, it will lead to multiple organ failures. Therefore, health care providers must emphasize continuous monitoring and efficient stabilization for those patients[11].

Serious heterogeneity was observed in all our analyses. The reason for this lies in the large number of included articles. The population had different geographical locations, ethnicities, several comorbidities, age ranges, and access to different qualities of health care systems. Thus, there was even a variation in the definitions; most of the included studies defined HI as a decrease of systolic BP < 100 mmHg and/or an increase in HR > 100 bpm[6]. However, some definitions included syncope, orthostatic changes[115], or signs of organ hypoperfusion[52]. All these factors contributed noticeably, resulting in a very serious heterogeneity. All definitions of HI and shock can be found in Supplementary Tables 13 and 14, respectively.

Possible predictors were observed that resulted in higher rates of our investigated outcomes. We observed some outliers in different sources of bleeding; in variceal bleeding, intensive care unit admission[79,82,97], elderly population [20], and severe uncontrolled bleeding[75] were possible predictors for higher rates of shock and HI. In non-variceal bleeding, elderly patients > 60 years[20] and those who underwent embolization[60] accounted for the highest rate of HI on admission and during hospitalization, respectively. As for upper GIB in general, the study by Chirapongsathorn *et al*



DOI: 10.3748/wjg.v29.i28.4466 **Copyright** ©The Author(s) 2023.

Figure 4 Forest plot demonstrating the proportion rates for hemodynamic instability and shock in variceal bleeding. VUGIB: Variceal upper gastrointestinal bleeding.

[21] included variceal and non-variceal bleeders, where they defined shock as mean arterial pressure lower than 50 mmHg, which results in a very high rate of shock (75%).

Lower GIB is three times less common than upper GIB and has not been the focus of much attention yet. Mortality rises to 20%-40% in the case of massive lower GIB complicated by unstable hemodynamics[116]. Super-selective patients who underwent arterial embolization[104], angiography[112], or were diagnosed with acute severe bleeding[103] showed higher rates of the investigated outcomes.

Strengths and Limitations

This is the first comprehensive overview to assess the proportion of patients affected by HI and shock in GIB and specify it according to the bleeding source. Our study included many studies with an extensive sample size. Additionally, subgroup analysis, which was based on the time of assessment, whether on admission or during hospital stay, provided a more precise overview. This study also gives an insight into some of the possible predictors that result in higher rates of our investigated outcomes.

Considering the limitations of this work, the definitions of HI and shock were different among the included studies or even missing. Different characteristics of the included population led to high heterogeneity in almost all analyses. The presence of low certainty of evidence in some domains is another limitation.

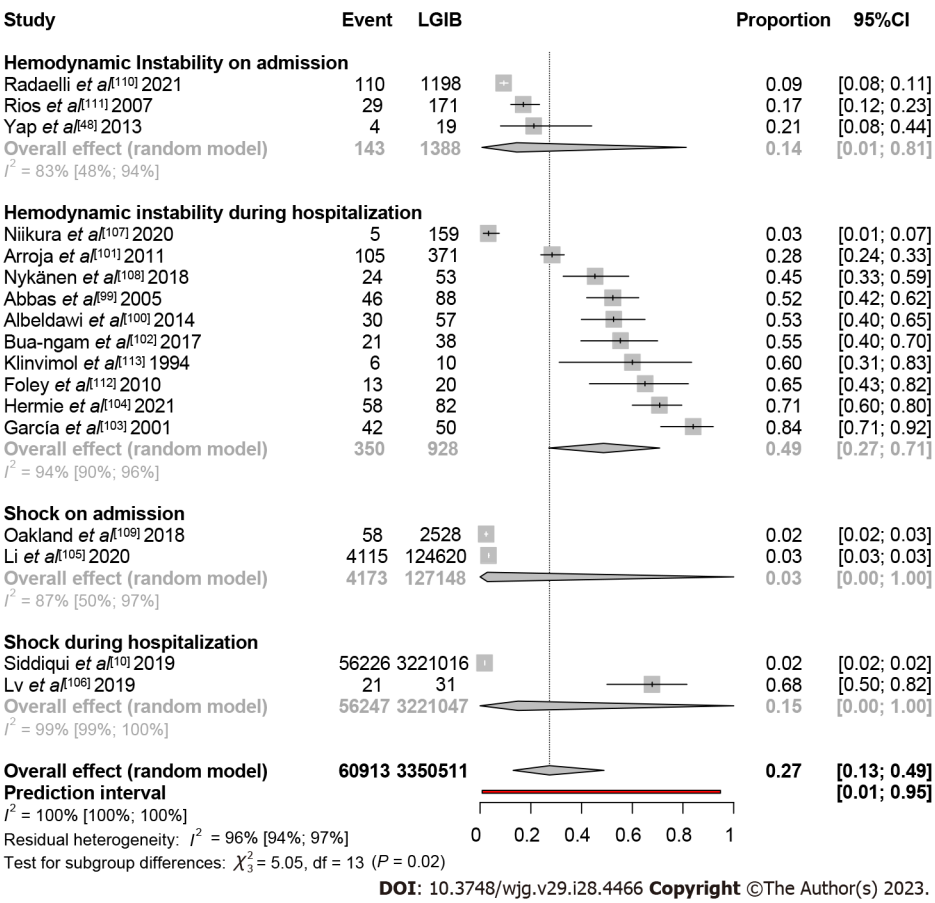


Figure 5 Forest plot demonstrating the proportion rates for hemodynamic instability and shock in lower gastrointestinal bleeding sources. LGIB: Lower gastrointestinal bleeding.

Implications for practice and research

Based on our results, we suggest standardizing the definition of HI and shock, and establishing a protocol to proactively screen and monitor the affected patients in routine management. Physicians involved in the treatment of the affected patients should focus more on early and rapid correction of hemodynamics because it significantly decreases mortality [11]. Therefore, a careful pre-endoscopic assessment and strong adherence to risk stratification scores need to be highlighted. Furthermore, cautious care and continuous monitoring of the affected patients should be emphasized, especially for high-risk patients.

CONCLUSION

Our study has provided clear evidence that hemodynamic instability and shock are common presentations and complications of GIB. On the basis of our findings, a high majority of patients are affected; one in five, one in four and one in eight patients develops shock or hemodynamic instability on admission or during the hospital stay in the case of non-variceal, variceal, and colonic diverticular bleeding, respectively. Patients need a more proactive treatment strategy and require continuous monitoring to prevent untoward outcomes.

ARTICLE HIGHLIGHTS

Research background

Hemodynamic instability (HI) and shock are associated with unfavorable outcomes in gastrointestinal bleeding (GIB). Understanding the proportion of these outcomes is essential for several reasons. Firstly, it provides valuable insight into the severity and potential risks associated with the condition. Knowing the proportion of patients who develop shock or HI helps healthcare providers anticipate the need for immediate interventions and allocate appropriate resources accordingly.

Research motivation

At the time of our systematic search, there was no data in the current literature describing these proportions in GIB based on the bleeding source. Additionally, monitoring changes in these patients over time can serve as an indicator of the effectiveness of medical interventions and guide future treatment strategies to improve patient outcomes.

Research objectives

Our aim is to quantify the pooled event rates of HI and shock in GIB. This will help in risk stratification and determining the overall severity of the condition. By understanding how frequently these outcomes occur, healthcare providers can identify high-risk patients who require immediate and intensive management.

Research methods

We conducted a systematic review with meta-analysis to determine the proportions of HI and shock in different GIB sources. The R programming language, using the meta package, was employed to perform statistical analysis on the data. Forest plots were utilized to summarize the study findings and present the results. Pooled event rates with 95%CIs, were computed to provide a measure of the overall outcomes.

Research results

The overall proportion of HI and shock was found to be 25% across all sources of GIB, 22% in non-variceal bleeding, 25% in variceal bleeding, and 12% in colonic diverticular bleeding. However, our findings also revealed a high degree of heterogeneity, highlighting the significance of our study. This heterogeneity suggests a lack of consensus in the guidelines in this field, as evidenced by the varied definitions of our included outcomes.

Research conclusions

Our study provides compelling evidence that HI and shock are frequently observed complications and presentations in GIB. One in four patients with GIB develops shock or HI on admission or during the hospital stay.

Research perspectives

Given our findings, we recommend the establishment of a standardized definition for HI and shock in GIB. Additionally, implementing a protocol for proactive screening and continuous monitoring of affected patients should be considered as part of routine management. Emphasizing a thorough pre-endoscopic assessment and strict adherence to risk stratification scores is crucial. Furthermore, rigorous care and attentive monitoring should be emphasized, particularly for high-risk patients.

FOOTNOTES

Author contributions: Obeidat M contributed to conceptualization, investigation, project administration, visualization, validation, writing – original draft; Teutsch B contributed to conceptualization, methodology, project administration, validation, writing – review & editing; Rancz A contributed to conceptualization, investigation, writing – review & editing; Tari E: conceptualization, investigation, writing – review & editing; Márta K contributed to conceptualization, writing – review & editing; Veres DS contributed to conceptualization, formal analysis, software, writing – review & editing; Hosszúfalusi N contributed to conceptualization, writing – review & editing; Mihály E contributed to conceptualization, writing – review & editing; Hegyi P contributed to conceptualization, writing – review & editing; Erőss B contributed to conceptualization, supervision, validation, writing – review & editing; All authors certify that they have participated sufficiently in the work to take public responsibility for the content, including participation in the concept, design, analysis, writing, or revision of the manuscript.

Supported by The Ministry of Innovation and Technology of Hungary from the National Research, Development, and Innovation Fund (ITM-NRDIF), No. TKP2021-EGA-23.

Conflict-of-interest statement: All the authors report no relevant conflicts of interest for this article.

PRISMA 2009 Checklist statement: All authors have read the PRISMA 2020 checklist, and the manuscript was prepared and revised according to the PRISMA 2020 checklist.

Open-Access: This article is an open-access article that was selected by an in-house editor and fully peer-reviewed by external reviewers. It is distributed in accordance with the Creative Commons Attribution NonCommercial (CC BY-NC 4.0) license, which permits others to distribute, remix, adapt, build upon this work non-commercially, and license their derivative works on different terms, provided the original work is properly cited and the use is non-commercial. See: https://creativecommons.org/Licenses/by-nc/4.0/

Country/Territory of origin: Hungary

ORCID number: Mahmoud Obeidat 0000-0002-2861-2573; Brigitta Teutsch 0000-0002-9530-7886; Anett Rancz 0000-0002-9960-6816; Edina Tari 0000-0002-8540-0614; Katalin Márta 0000-0002-2213-4865; Dániel Sándor Veres 0000-0002-9687-3556; Nóra Hosszúfalusi 0000-0002-9469-372X; Emese Mihály 0000-0003-3046-7341; Péter Hegyi 0000-0003-0399-7259; Bálint Erőss 0000-0003-3658-8427.

Corresponding Author's Membership in Professional Societies: Hungarian Society of Gastroenterology.

S-Editor: Li L
L-Editor: A
P-Editor: Yuan YY

REFERENCES

1 **Oakland K**. Changing epidemiology and etiology of upper and lower gastrointestinal bleeding. *Best Pract Res Clin Gastroenterol* 2019; **42-43**: 101610 [PMID: 31785737 DOI: 10.1016/j.bpg.2019.04.003]
2 **Marmo R**, Koch M, Cipolletta L, Capurso L, Pera A, Bianco MA, Rocca R, Dezi A, Fasoli R, Brunati S, Lorenzini I, Germani U, Di Matteo G, Giorgio P, Imperiali G, Minoli G, Barberani F, Boschetto S, Martorano M, Gatto G, Amuso M, Pastorelli A, Torre ES, Triossi O, Buzzi A, Cestari R, Della Casa D, Proietti M, Tanzilli A, Aragona G, Giangregorio F, Allegretta L, Tronci S, Michetti P, Romagnoli P, Nucci A, Rogai F, Piubello W, Tebaldi M, Bonfante F, Casadei A, Cortini C, Chiozzini G, Girardi L, Leoci C, Bagnalasta G, Segato S, Chianese G, Salvagnini M, Rotondano G. Predictive factors of mortality from nonvariceal upper gastrointestinal hemorrhage: a multicenter study. *Am J Gastroenterol* 2008; **103**: 1639-47; quiz 1648 [PMID: 18564127 DOI: 10.1111/j.1572-0241.2008.01865.x]
3 **Zheng NS**, Tsay C, Laine L, Shung DL. Trends in characteristics, management, and outcomes of patients presenting with gastrointestinal bleeding to emergency departments in the United States from 2006 to 2019. *Aliment Pharmacol Ther* 2022; **56**: 1543-1555 [PMID: 36173090 DOI: 10.1111/apt.17238]
4 **Abougergi MS**, Travis AC, Saltzman JR. The in-hospital mortality rate for upper GI hemorrhage has decreased over 2 decades in the United States: a nationwide analysis. *Gastrointest Endosc* 2015; **81**: 882-8.e1 [PMID: 25484324 DOI: 10.1016/j.gie.2014.09.027]
5 **Peery AF**, Crockett SD, Murphy CC, Lund JL, Dellon ES, Williams JL, Jensen ET, Shaheen NJ, Barritt AS, Lieber SR, Kochar B, Barnes EL, Fan YC, Pate V, Galanko J, Baron TH, Sandler RS. Burden and Cost of Gastrointestinal, Liver, and Pancreatic Diseases in the United States: Update 2018. *Gastroenterology* 2019; **156**: 254-272.e11 [PMID: 30315778 DOI: 10.1053/j.gastro.2018.08.063]
6 **Moledina SM**, Komba E. Risk factors for mortality among patients admitted with upper gastrointestinal bleeding at a tertiary hospital: a prospective cohort study. *BMC Gastroenterol* 2017; **17**: 165 [PMID: 29262794 DOI: 10.1186/s12876-017-0712-8]
7 **Laursen SB**, Leontiadis GI, Stanley AJ, Møller MH, Hansen JM, Schaffalitzky de Muckadell OB. Relationship between timing of endoscopy and mortality in patients with peptic ulcer bleeding: a nationwide cohort study. *Gastrointest Endosc* 2017; **85**: 936-944.e3 [PMID: 27623102 DOI: 10.1016/j.gie.2016.08.049]
8 **Parker ME**, Khasawneh MA, Thiels CA, Berns KS, Stubbs JR, Jenkins DH, Zietlow SP, Zielinski MD. Prehospital Transfusion for Gastrointestinal Bleeding. *Air Med J* 2017; **36**: 315-319 [PMID: 29122112 DOI: 10.1016/j.amj.2017.06.002]
9 **Edelson JC**, Edelson CV, Rockey DC, Chung KK, Robles MJ, Subramanian SR, Aden JK, Gancayco JG. Improving haemodynamics in acute gastrointestinal bleeding: Ketamine for endoscopic sedation in active gastrointestinal bleeding in critically Ill patients. *Gastro Hep* 2020; **2**: 288-294 [DOI: 10.1002/ygh2.424]
10 **Siddiqui NS**, Paul S, Khan Z, Javaid T, Hasan SS, Saleh J, Federman DJ, Khuder S, Nawras A. Rising Events and Improved Outcomes of Gastrointestinal Bleed With Shock in USA: A 12-year National Analysis. *J Clin Gastroenterol* 2019; **53**: e194-e201 [PMID: 29369239 DOI: 10.1097/MCG.0000000000000995]
11 **Baradarian R**, Ramdhaney S, Chapalamadugu R, Skoczylas L, Wang K, Rivilis S, Remus K, Mayer I, Iswara K, Tenner S. Early intensive resuscitation of patients with upper gastrointestinal bleeding decreases mortality. *Am J Gastroenterol* 2004; **99**: 619-622 [PMID: 15089891 DOI: 10.1111/j.1572-0241.2004.04073.x]
12 **Gralnek IM**, Stanley AJ, Morris AJ, Camus M, Lau J, Lanas A, Laursen SB, Radaelli F, Papanikolaou IS, Cúrdia Gonçalves T, Dinis-Ribeiro M, Awadie H, Braun G, de Groot N, Udd M, Sanchez-Yague A, Neeman Z, van Hooft JE. Endoscopic diagnosis and management of nonvariceal upper gastrointestinal hemorrhage (NVUGIH): European Society of Gastrointestinal Endoscopy (ESGE) Guideline - Update 2021. *Endoscopy* 2021; **53**: 300-332 [PMID: 33567467 DOI: 10.1055/a-1369-5274]
13 **Gralnek IM**, Camus Duboc M, Garcia-Pagan JC, Fuccio L, Karstensen JG, Hucl T, Jovanovic I, Awadie H, Hernandez-Gea V, Tantau M, Ebigbo A, Ibrahim M, Vlachogiannakos J, Burgmans MC, Rosasco R, Triantafyllou K. Endoscopic diagnosis and management of esophagogastric variceal hemorrhage: European Society of Gastrointestinal Endoscopy (ESGE) Guideline. *Endoscopy* 2022; **54**: 1094-1120 [PMID: 36174643 DOI: 10.1055/a-1939-4887]
14 **Laine L**, Barkun AN, Saltzman JR, Martel M, Leontiadis GI. ACG Clinical Guideline: Upper Gastrointestinal and Ulcer Bleeding. *Am J Gastroenterol* 2021; **116**: 899-917 [PMID: 33929377 DOI: 10.14309/ajg.0000000000001245]
15 **Sengupta N**, Feuerstein JD, Jairath V, Shergill AK, Strate LL, Wong RJ, Wan D. Management of Patients With Acute Lower Gastrointestinal Bleeding: An Updated ACG Guideline. *Am J Gastroenterol* 2023; **118**: 208-231 [PMID: 36735555 DOI: 10.14309/ajg.0000000000002130]
16 **Kim JH**, Park SW, Jung JH, Park DH, Bang CS, Park CH, Park JW, Park JG. Bedside risk-scoring model for predicting 6-week mortality in cirrhotic patients undergoing endoscopic band ligation for acute variceal bleeding. *J Gastroenterol Hepatol* 2021; **36**: 1935-1943 [PMID: 33538357 DOI: 10.1111/jgh.15426]
17 **Rotondano G**, Cipolletta L, Koch M, Bianco MA, Grossi E, Marmo R; PNED (Progetto Nazionale Emorragie Digestive) Investigators. Predictors of favourable outcome in non-variceal upper gastrointestinal bleeding: implications for early discharge? *Dig Liver Dis* 2014; **46**: 231-236 [PMID: 24361122 DOI: 10.1016/j.dld.2013.10.017]
18 **Lanas A**, Polo-Tomas M, García-Rodríguez LA, García S, Arroyo-Villarino MT, Ponce J, Bujanda L, Calleja JL, Calvet X, Feu F, Perez-Aisa A, Sung JJ. Effect of proton pump inhibitors on the outcomes of peptic ulcer bleeding: comparison of event rates in routine clinical practice and a clinical trial. *Scand J Gastroenterol* 2013; **48**: 285-294 [PMID: 23298283 DOI: 10.3109/00365521.2012.758764]
19 **Tsoi KK**, Chiu PW, Chan FK, Ching JY, Lau JY, Sung JJ. The risk of peptic ulcer bleeding mortality in relation to hospital admission on holidays: a cohort study on 8,222 cases of peptic ulcer bleeding. *Am J Gastroenterol* 2012; **107**: 405-410 [PMID: 22108453 DOI: 10.1038/ajg.2011.409]
20 **Elsebaey MA**, Elashry H, Elbedewy TA, Elhadidy AA, Esheba NE, Ezat S, Negm MS, Abo-Amer YE, Abgeegy ME, Elsergany HF, Mansour L, Abd-Elsalam S. Predictors of in-hospital mortality in a cohort of elderly Egyptian patients with acute upper gastrointestinal bleeding. *Medicine (Baltimore)* 2018; **97**: e0403 [PMID: 29668596 DOI: 10.1097/MD.0000000000010403]

21 **Chirapongsathorn S**, Akkarachinores K, Chaiprasert A. Development and validation of prognostic model to predict mortality among cirrhotic patients with acute variceal bleeding: A retrospective study. *JGH Open* 2021; **5**: 658-663 [PMID: 34124382 DOI: 10.1002/jgh3.12550]

22 **Garrido A**, Giráldez A, Trigo C, Leo E, Guil A, Márquez JL. Intravenous proton-pump inhibitor for acute peptic ulcer bleeding--is profound acid suppression beneficial to reduce the risk of rebleeding? *Rev Esp Enferm Dig* 2008; **100**: 466-469 [PMID: 18942898 DOI: 10.4321/s1130-01082008000800004]

23 **Page MJ**, McKenzie JE, Bossuyt PM, Boutron I, Hoffmann TC, Mulrow CD, Shamseer L, Tetzlaff JM, Akl EA, Brennan SE, Chou R, Glanville J, Grimshaw JM, Hróbjartsson A, Lalu MM, Li T, Loder EW, Mayo-Wilson E, McDonald S, McGuinness LA, Stewart LA, Thomas J, Tricco AC, Welch VA, Whiting P, Moher D. The PRISMA 2020 statement: an updated guideline for reporting systematic reviews. *BMJ* 2021; **372**: n71 [PMID: 33782057 DOI: 10.1136/bmj.n71]

24 **Chandler J**, Hopewell S. Cochrane methods--twenty years experience in developing systematic review methods. *Syst Rev* 2013; **2**: 76 [PMID: 24050381 DOI: 10.1186/2046-4053-2-76]

25 **Booth A**, Clarke M, Dooley G, Ghersi D, Moher D, Petticrew M, Stewart L. PROSPERO at one year: an evaluation of its utility. *Syst Rev* 2013; **2**: 4 [PMID: 23320413 DOI: 10.1186/2046-4053-2-4]

26 **Munn Z**, Moola S, Lisy K, Riitano D, Tufanaru C. Methodological guidance for systematic reviews of observational epidemiological studies reporting prevalence and cumulative incidence data. *Int J Evid Based Healthc* 2015; **13**: 147-153 [PMID: 26317388 DOI: 10.1097/XEB.0000000000000054]

27 **Guyatt G**, Oxman AD, Akl EA, Kunz R, Vist G, Brozek J, Norris S, Falck-Ytter Y, Glasziou P, DeBeer H, Jaeschke R, Rind D, Meerpohl J, Dahm P, Schünemann HJ. GRADE guidelines: 1. Introduction-GRADE evidence profiles and summary of findings tables. *J Clin Epidemiol* 2011; **64**: 383-394 [PMID: 21195583 DOI: 10.1016/j.jclinepi.2010.04.026]

28 **Schwarzer G**, Chemaitelly H, Abu-Raddad LJ, Rücker G. Seriously misleading results using inverse of Freeman-Tukey double arcsine transformation in meta-analysis of single proportions. *Res Synth Methods* 2019; **10**: 476-483 [PMID: 30945438 DOI: 10.1002/jrsm.1348]

29 **IntHout J**, Ioannidis JP, Borm GF. The Hartung-Knapp-Sidik-Jonkman method for random effects meta-analysis is straightforward and considerably outperforms the standard DerSimonian-Laird method. *BMC Med Res Methodol* 2014; **14**: 25 [PMID: 24548571 DOI: 10.1186/1471-2288-14-25]

30 **Knapp G**, Hartung J. Improved tests for a random effects meta-regression with a single covariate. *Stat Med* 2003; **22**: 2693-2710 [PMID: 12939780 DOI: 10.1002/sim.1482]

31 **Higgins JP**, Thompson SG. Quantifying heterogeneity in a meta-analysis. *Stat Med* 2002; **21**: 1539-1558 [PMID: 12111919 DOI: 10.1002/sim.1186]

32 **Sterne JA**, Sutton AJ, Ioannidis JP, Terrin N, Jones DR, Lau J, Carpenter J, Rücker G, Harbord RM, Schmid CH, Tetzlaff J, Deeks JJ, Peters J, Macaskill P, Schwarzer G, Duval S, Altman DG, Moher D, Higgins JP. Recommendations for examining and interpreting funnel plot asymmetry in meta-analyses of randomised controlled trials. *BMJ* 2011; **343**: d4002 [PMID: 21784880 DOI: 10.1136/bmj.d4002]

33 **Harrer M**, Cuijpers P, Furukawa T, Ebert D. Doing Meta-Analysis With R: A Hands-On Guide. 1st ed. New York: Chapman and Hall/CRC Press, 2021 [DOI: 10.1201/9781003107347]

34 **IntHout J**, Ioannidis JP, Rovers MM, Goeman JJ. Plea for routinely presenting prediction intervals in meta-analysis. *BMJ Open* 2016; **6**: e010247 [PMID: 27406637 DOI: 10.1136/bmjopen-2015-010247]

35 **Ballester-Clau R**, Torres Vicente G, Voltà-Pardo T, López-Barroso L, Cucala-Ramos M, Reñé-Espinet JM, Planella de Rubinat M. Clinical experience with ferric carboxymaltose in the management of anemia in acute gastrointestinal bleeding. *Eur J Gastroenterol Hepatol* 2019; **31**: 116-122 [PMID: 30335628 DOI: 10.1097/MEG.0000000000001282]

36 **Cangemi DJ**, Krill T, Weideman R, Cipher DJ, Spechler SJ, Feagins LA. A Comparison of the Rate of Gastrointestinal Bleeding in Patients Taking Non-Vitamin K Antagonist Oral Anticoagulants or Warfarin. *Am J Gastroenterol* 2017; **112**: 734-739 [PMID: 28244496 DOI: 10.1038/ajg.2017.39]

37 **Catano J**, Sacleux SC, Gornet JM, Camus M, Bigé N, Saliba F, Azoulay E, Dumas G, Zafrani L. Gastrointestinal bleeding in critically ill immunocompromised patients. *Ann Intensive Care* 2021; **11**: 130 [PMID: 34420114 DOI: 10.1186/s13613-021-00913-6]

38 **Hampers MJ**, Surgenor SD, Spanjian K, Clerico T, Corwin HL. ICU care for patients with gastrointestinal bleeding: Impact on cost and outcome. *Clin Intensive Care* 2002; **13**: 109-113 [DOI: 10.3109/tcic.13.2-3.109.113]

39 **Konecki D**, Grabowska-Derlatka L, Pacho R, Rowiński O. Correlation Between Findings of Multislice Helical Computed Tomography (CT), Endoscopic Examinations, Endovascular Procedures, and Surgery in Patients with Symptoms of Acute Gastrointestinal Bleeding. *Pol J Radiol* 2017; **82**: 676-684 [PMID: 29662594 DOI: 10.12659/PJR.902331]

40 **Lee L**, Iqbal S, Najmeh S, Fata P, Razek T, Khwaja K. Mesenteric angiography for acute gastrointestinal bleed: predictors of active extravasation and outcomes. *Can J Surg* 2012; **55**: 382-388 [PMID: 22992399 DOI: 10.1503/cjs.005611]

41 **Mehta A**, Kim S, Ahmed O, Zangan S, Ha TV, Navuluri R, Funaki B. Outcomes of Patients with Left Ventricular Assist Devices Undergoing Mesenteric Angiography for Gastrointestinal Bleeding. *J Vasc Interv Radiol* 2015; **26**: 1710-1717 [PMID: 26342883 DOI: 10.1016/j.jvir.2015.07.026]

42 **Mohan P**, Manov J, Diaz-Bode A, Venkat S, Langston M, Naidu A, Howse R, Narayanan G. Clinical predictors of arterial extravasation, rebleeding and mortality following angiographic interventions in gastrointestinal bleeding. *J Gastrointestin Liver Dis* 2018; **27**: 221-226 [PMID: 30240464 DOI: 10.15403/jgld.2014.1121.273.daz]

43 **Nagata N**, Sakurai T, Moriyasu S, Shimbo T, Okubo H, Watanabe K, Yokoi C, Yanase M, Akiyama J, Uemura N. Impact of INR monitoring, reversal agent use, heparin bridging, and anticoagulant interruption on rebleeding and thromboembolism in acute gastrointestinal bleeding. *PLoS One* 2017; **12**: e0183423 [PMID: 28863196 DOI: 10.1371/journal.pone.0183423]

44 **Nishida K**, Nojiri I, Kato M, Higashijima M, Takagi K, Akashi R. Upper gastrointestinal bleeding in the elderly. *Nihon Ronen Igakkai Zasshi* 1992; **29**: 829-835 [PMID: 1491478 DOI: 10.3143/geriatrics.29.829]

45 **Oprita R**, Ilie M, Sandru V, Berceanu D, Constantinescu G. Gastrointestinal bleeding in patients admitted to the intensive care unit. *Arch Balk Med Union* 2018; **53**: 544-550 [DOI: 10.31688/ABMU.2018.53.4.09]

46 **Robert R**, Gissot V, Pierrot M, Laksiri L, Mercier E, Prat G, Villers D, Vincent JF, Hira M, Vignon P, Charlot P, Burucoa C. Helicobacter pylori infection is not associated with an increased hemorrhagic risk in patients in the intensive care unit. *Crit Care* 2006; **10**: R77 [PMID: 16704741 DOI: 10.1186/cc4920]

47 **Sàbat M**, Kolle L, Soriano G, Ortiz J, Pamplona J, Novella MT, Villanueva C, Sainz S, Torras J, Balanzó J, Guarner C. Parenteral antibiotic prophylaxis of bacterial infections does not improve cost-efficacy of oral norfloxacin in cirrhotic patients with gastrointestinal bleeding. *Am J Gastroenterol* 1998; **93**: 2457-2462 [PMID: 9860409 DOI: 10.1111/j.1572-0241.1998.00704.x]

48 **Yap FY**, Omene BO, Patel MN, Yohannan T, Minocha J, Knuttinen MG, Owens CA, Bui JT, Gaba RC. Transcatheter embolotherapy for gastrointestinal bleeding: a single center review of safety, efficacy, and clinical outcomes. *Dig Dis Sci* 2013; **58**: 1976-1984 [PMID: 23361570 DOI: 10.1007/s10620-012-2547-z]

49 **Trebicka J**, Fernandez J, Papp M, Caraceni P, Laleman W, Gambino C, Giovo I, Uschner FE, Jansen C, Jimenez C, Mookerjee R, Gustot T, Albillos A, Bañares R, Jarcuska P, Steib C, Reiberger T, Acevedo J, Gatti P, Shawcross DL, Zeuzem S, Zipprich A, Piano S, Berg T, Bruns T, Danielsen KV, Coenraad M, Merli M, Stauber R, Zoller H, Ramos JP, Solé C, Soriano G, de Gottardi A, Gronbaek H, Saliba F, Trautwein C, Kani HT, Francque S, Ryder S, Nahon P, Romero-Gomez M, Van Vlierberghe H, Francoz C, Manns M, Garcia-Lopez E, Tufoni M, Amoros A, Pavesi M, Sanchez C, Praktiknjo M, Curto A, Pitarch C, Putignano A, Moreno E, Bernal W, Aguilar F, Clària J, Ponzo P, Vitalis Z, Zaccherini G, Balogh B, Gerbes A, Vargas V, Alessandria C, Bernardi M, Ginès P, Moreau R, Angeli P, Jalan R, Arroyo V; PREDICT STUDY group of the EASL-CLIF CONSORTIUM. PREDICT identifies precipitating events associated with the clinical course of acutely decompensated cirrhosis. *J Hepatol* 2021; **74**: 1097-1108 [PMID: 33227350 DOI: 10.1016/j.jhep.2020.11.019]

50 **Van Weyenberg SJ**, Van Turenhout ST, Jacobs MA, Bouma G, Mulder CJ. Video capsule endoscopy for previous overt obscure gastrointestinal bleeding in patients using anti-thrombotic drugs. *Dig Endosc* 2012; **24**: 247-254 [PMID: 22725110 DOI: 10.1111/j.1443-1661.2011.01228.x]

51 **Abougergi MS**, Peluso H, Mrad C, Saltzman JR. The Impact of Obesity on Mortality and Other Outcomes in Patients With Nonvariceal Upper Gastrointestinal Hemorrhage in the United States. *J Clin Gastroenterol* 2019; **53**: 114-119 [PMID: 29035976 DOI: 10.1097/MCG.0000000000000942]

52 **Ahn DW**, Park YS, Lee SH, Shin CM, Hwang JH, Kim JW, Jeong SH, Kim N, Lee DH. Clinical outcome of acute nonvariceal upper gastrointestinal bleeding after hours: the role of urgent endoscopy. *Korean J Intern Med* 2016; **31**: 470-478 [PMID: 27048253 DOI: 10.3904/kjim.2014.099]

53 **Baracat FI**, de Moura DTH, Brunaldi VO, Tranquillini CV, Baracat R, Sakai P, de Moura EGH. Randomized controlled trial of hemostatic powder versus endoscopic clipping for non-variceal upper gastrointestinal bleeding. *Surg Endosc* 2020; **34**: 317-324 [PMID: 30927124 DOI: 10.1007/s00464-019-06769-z]

54 **Di Felice G**. Endoscopic injection treatment in patients with shock and gastrointestinal bleeding or stigmata of recent hemorrhage. *Endoscopy* 1987; **19**: 185-189 [PMID: 3500038 DOI: 10.1055/s-2007-1018278]

55 **Edmunds SEJ**, Laurence BH. Endoscopic ethanol sclerotherapy in non-variceal gastrointestinal bleeding. *J Gastroen Hepatol* 1988; **3**: 355-360 [DOI: 10.1111/j.1440-1746.1988.tb00260.x]

56 **Gao F**, Chen X, Zhang J. Treatment of Acute Nonvariceal Upper Gastrointestinal Bleeding in Chinese Patients on Antithrombotic Therapy. *Gastroenterol Res Pract* 2019; **2019**: 9190367 [PMID: 31933633 DOI: 10.1155/2019/9190367]

57 **González-González JA**, Vázquez-Elizondo G, García-Compeán D, Gaytán-Torres JO, Flores-Rendón ÁR, Jáquez-Quintana JO, Garza-Galindo AA, Cárdenas-Sandoval MG, Maldonado-Garza HJ. Predictors of in-hospital mortality in patients with non-variceal upper gastrointestinal bleeding. *Rev Esp Enferm Dig* 2011; **103**: 196-203 [PMID: 21526873 DOI: 10.4321/S1130-01082011000400005]

58 **Hwang S**, Jeon SW, Kwon JG, Lee DW, Ha CY, Cho KB, Jang B, Park JB, Park YS; Daegu-Gyengbuk Gastrointestinal Study Group (DGSG). The Novel Scoring System for 30-Day Mortality in Patients with Non-variceal Upper Gastrointestinal Bleeding. *Dig Dis Sci* 2016; **61**: 2002-2010 [PMID: 26921080 DOI: 10.1007/s10620-016-4087-4]

59 **Jairath V**, Kahan BC, Stanworth SJ, Logan RF, Hearnshaw SA, Travis SP, Palmer KR, Murphy MF. Prevalence, management, and outcomes of patients with coagulopathy after acute nonvariceal upper gastrointestinal bleeding in the United Kingdom. *Transfusion* 2013; **53**: 1069-1076 [PMID: 22897615 DOI: 10.1111/j.1537-2995.2012.03849.x]

60 **Kwon JH**, Han YH. Efficacy and safety of superselective trans-catheter arterial embolization of upper and lower gastrointestinal bleeding using N-butyl-2-cyanoacrylate. *Emerg Radiol* 2018; **25**: 111-120 [PMID: 28971259 DOI: 10.1007/s10140-017-1552-0]

61 **Lai YC**, Hung MS, Chen YH, Chen YC. Comparing AIMS65 Score With MEWS, qSOFA Score, Glasgow-Blatchford Score, and Rockall Score for Predicting Clinical Outcomes in Cirrhotic Patients With Upper Gastrointestinal Bleeding. *J Acute Med* 2018; **8**: 154-167 [PMID: 32995218 DOI: 10.6705/j.jacme.201812_8(4).0003]

62 **Maggio D**, Barkun AN, Martel M, Elouali S, Gralnek IM; Reason Investigators. Predictors of early rebleeding after endoscopic therapy in patients with nonvariceal upper gastrointestinal bleeding secondary to high-risk lesions. *Can J Gastroenterol* 2013; **27**: 454-458 [PMID: 23936874 DOI: 10.1155/2013/128760]

63 **Morsy KH**, Ghaliony MA, Mohammed HS. Outcomes and predictors of in-hospital mortality among cirrhotic patients with non-variceal upper gastrointestinal bleeding in upper Egypt. *Turk J Gastroenterol* 2014; **25**: 707-713 [PMID: 25599786 DOI: 10.5152/tjg.2014.6710]

64 **Nguyen GC**, Dinani AM, Pivovarov K. Endoscopic management and outcomes of pregnant women hospitalized for nonvariceal upper GI bleeding: a nationwide analysis. *Gastrointest Endosc* 2010; **72**: 954-959 [PMID: 20875639 DOI: 10.1016/j.gie.2010.07.018]

65 **Park CH**, Han DS, Jeong JY, Eun CS, Yoo KS, Jeon YC, Sohn JH. Outcomes of Propofol Sedation During Emergency Endoscopy Performed for Upper Gastrointestinal Bleeding. *Dig Dis Sci* 2016; **61**: 825-834 [PMID: 26541992 DOI: 10.1007/s10620-015-3942-z]

66 **Restellini S**, Kherad O, Jairath V, Martel M, Barkun AN. Red blood cell transfusion is associated with increased rebleeding in patients with nonvariceal upper gastrointestinal bleeding. *Aliment Pharmacol Ther* 2013; **37**: 316-322 [PMID: 23205554 DOI: 10.1111/apt.12170]

67 **Sey MSL**, Mohammed SB, Brahmania M, Singh S, Kahan BC, Jairath V. Comparative outcomes in patients with ulcer- vs non-ulcer-related acute upper gastrointestinal bleeding in the United Kingdom: a nationwide cohort of 4474 patients. *Aliment Pharmacol Ther* 2019; **49**: 537-545 [PMID: 30628112 DOI: 10.1111/apt.15092]

68 **Wierzchowski P**, Dabrowiecki S, Szczesny W, Szmytkowski J. Nonvariceal upper gastrointestinal tract bleeding - risk factors and the value of emergency endoscopy. *Arch Med Sci* 2013; **9**: 843-848 [PMID: 24273567 DOI: 10.5114/aoms.2013.36911]

69 **Zhang JY**, Wang Y, Zhang J, Ding SG, Zhou LY, Lin SR. Risk factors associated with failure from endoscopic therapy in acute non-variceal upper gastrointestinal bleeding. *Beijing Daxue Xuebao Yixueban* 2010; **42**: 703-707 [PMID: 21170103]

70 **Bunchorntavakul C**, Yodket Y, Singhasena N. Clinical Characteristics, Treatment Outcomes and Risk Assessment of Patients with Acute Upper Gastrointestinal Bleeding in Rajavithi Hospital, Thailand. *J Med Assoc Thai* 2017; **100** Suppl 1: S104-S115 [PMID: 29927224]

71 **Wang HM**, Hsu PI, Lo GH, Chen TA, Cheng LC, Chen WC, Lin CK, Yu HC, Chan HH, Tsai WL, Wang EM, Lai KH. Comparison of hemostatic efficacy for argon plasma coagulation and distilled water injection in treating high-risk bleeding ulcers. *J Clin Gastroenterol* 2009; **43**: 941-945 [PMID: 19448567 DOI: 10.1097/MCG.0b013e31819c3885]

72 **Amitrano L**, Guardascione MA, Martino R, Manguso F, Menchise A, Balzano A. Hypoxic hepatitis occurring in cirrhosis after variceal bleeding: still a lethal disease. *J Clin Gastroenterol* 2012; **46**: 608-612 [PMID: 22772740 DOI: 10.1097/MCG.0b013e318254e9d4]

73 **Ardevol A**, Ibañez-Sanz G, Profitos J, Aracil C, Castellvi JM, Alvarado E, Cachero A, Horta D, Miñana J, Gomez-Pastrana B, Pavel O,

Dueñas E, Casas M, Planella M, Castellote J, Villanueva C. Survival of patients with cirrhosis and acute peptic ulcer bleeding compared with variceal bleeding using current first-line therapies. *Hepatology* 2018; **67**: 1458-1471 [PMID: 28714072 DOI: 10.1002/hep.29370]

74 **Bilal M**, Abougergi MS, Tayyem O, Parupudi S, Rockey DC. Thirty-Day Readmission After Esophageal Variceal Hemorrhage and its Impact on Outcomes in the United States. *J Clin Gastroenterol* 2020; **54**: 477-483 [PMID: 31373937 DOI: 10.1097/MCG.0000000000001249]

75 **Choi JY**, Jo YW, Lee SS, Kim WS, Oh HW, Kim CY, Yun EY, Kim JJ, Lee JM, Kim HJ, Kim TH, Jung WT, Lee OJ, Kim RB. Outcomes of patients treated with Sengstaken-Blakemore tube for uncontrolled variceal hemorrhage. *Korean J Intern Med* 2018; **33**: 696-704 [PMID: 29117668 DOI: 10.3904/kjim.2016.339]

76 **Fallatah HI**, Al Nahdi H, Al Khatabi M, Akbar HO, Qari YA, Sibiani AR, Bazaraa S. Variceal hemorrhage: Saudi tertiary center experience of clinical presentations, complications and mortality. *World J Hepatol* 2012; **4**: 268-273 [PMID: 23060972 DOI: 10.4254/wjh.v4.i9.268]

77 **Hassanien M**, El-Ghannam M, El-Talkawy MD, Abdelrahman Y, Attar GE, Taleb HA. Risk scoring systems to predict in-hospital mortality in patients with acute variceal bleeding due to HCV-induced liver cirrhosis. *Gastroenterology Insights* 2018; **9** [DOI: 10.4081/gi.2018.7629]

78 **Hermie L**, Dhondt E, Vanlangenhove P, Hoste E, Geerts A, Defreyne L. Model for end-stage liver disease score and hemodynamic instability as a predictor of poor outcome in early transjugular intrahepatic portosystemic shunt treatment for acute variceal hemorrhage. *Eur J Gastroenterol Hepatol* 2018; **30**: 1441-1446 [PMID: 30048333 DOI: 10.1097/MEG.0000000000001222]

79 **Ismail FW**, Shah HA, Hamid S, Abbas Z, Abid S, Mumtaz K, Jafri W. Noninvasive predictors of large varices in patients hospitalized with gastroesophageal variceal hemorrhage. *Hepatol Int* 2008; **2**: 124-128 [PMID: 19669288 DOI: 10.1007/s12072-007-9034-1]

80 **Kim DH**, Cho E, Jun CH, Son DJ, Lee MJ, Park CH, Cho SB, Park SY, Kim HS, Choi SK, Rew JS. Risk Factors and On-site Rescue Treatments for Endoscopic Variceal Ligation Failure. *Korean J Gastroenterol* 2018; **72**: 188-196 [PMID: 30419643 DOI: 10.4166/kjg.2018.72.4.188]

81 **Kim SE**, Jung DM, Park JW, Ju Y, Lee B, Kim HS, Suk KT, Jang MK, Park SH, Kang JG, Soh JS, Lim H, Kang HS, Moon SH, Kim C, Lee S, Kim JH, Lee MS, Kim DJ, Ihm SH, Park C. Baseline Renal Function Predicts Hyponatremia in Liver Cirrhosis Patients Treated with Terlipressin for Variceal Bleeding. *Gastroenterol Res Pract* 2017; **2017**: 7610374 [PMID: 29075291 DOI: 10.1155/2017/7610374]

82 **Lee H**, Hawker FH, Selby W, McWilliam DB, Herkes RG. Intensive care treatment of patients with bleeding esophageal varices: results, predictors of mortality, and predictors of the adult respiratory distress syndrome. *Crit Care Med* 1992; **20**: 1555-1563 [PMID: 1424699 DOI: 10.1097/00003246-199211000-00013]

83 **Liu TT**, Wong WJ, Hou MC, Lin HC, Chang FY, Lee SD. Hemorheology in patients with liver cirrhosis: special emphasis on its relation to severity of esophageal variceal bleeding. *J Gastroenterol Hepatol* 2006; **21**: 908-913 [PMID: 16704544 DOI: 10.1111/j.1440-1746.2006.04266.x]

84 **Liu Y**, Yang J, Wang J, Chai G, Sun G, Wang Z, Yang Y. Clinical characteristics and endoscopic treatment with cyanoacrylate injection in patients with duodenal varices. *Scand J Gastroenterol* 2009; **44**: 1012-1016 [PMID: 19513934 DOI: 10.1080/00365520903030787]

85 **Maiwall R**, Kumar A, Bhadoria AS, Jindal A, Kumar G, Bhardwaj A, Maras JS, Sharma MK, Sharma BC, Sarin SK. Utility of N-acetylcysteine in ischemic hepatitis in cirrhotics with acute variceal bleed: a randomized controlled trial. *Hepatol Int* 2020; **14**: 577-586 [PMID: 32048131 DOI: 10.1007/s12072-020-10013-5]

86 **Naeshiro N**, Aikata H, Kakizawa H, Hyogo H, Kan H, Fujino H, Kobayashi T, Fukuhara T, Honda Y, Ohno A, Miyaki D, Kawaoka T, Tsuge M, Hiraga N, Hiramatsu A, Imamura M, Kawakami Y, Takahashi S, Awai K, Chayama K. Long-term outcome of patients with gastric varices treated by balloon-occluded retrograde transvenous obliteration. *J Gastroenterol Hepatol* 2014; **29**: 1035-1042 [PMID: 24372807 DOI: 10.1111/jgh.12508]

87 **Singal AK**, Jampana SC, Singal V, Kuo YF. Hepatocellular carcinoma predicts in-hospital mortality from acute variceal hemorrhage among patients with cirrhosis. *J Clin Gastroenterol* 2012; **46**: 613-619 [PMID: 22772741 DOI: 10.1097/MCG.0b013e318256b670]

88 **Villanueva C**, Ortiz J, Sàbat M, Gallego A, Torras X, Soriano G, Sáinz S, Boadas J, Cussó X, Guarner C, Balanzó J. Somatostatin alone or combined with emergency sclerotherapy in the treatment of acute esophageal variceal bleeding: a prospective randomized trial. *Hepatology* 1999; **30**: 384-389 [PMID: 10421644 DOI: 10.1002/hep.510300222]

89 **Villanueva C**, Piqueras M, Aracil C, Gómez C, López-Balaguer JM, Gonzalez B, Gallego A, Torras X, Soriano G, Sáinz S, Benito S, Balanzó J. A randomized controlled trial comparing ligation and sclerotherapy as emergency endoscopic treatment added to somatostatin in acute variceal bleeding. *J Hepatol* 2006; **45**: 560-567 [PMID: 16904224 DOI: 10.1016/j.jhep.2006.05.016]

90 **Sung JJ**, Chung SC, Yung MY, Lai CW, Lau JY, Lee YT, Leung VK, Li MK, Li AK. Prospective randomised study of effect of octreotide on rebleeding from oesophageal varices after endoscopic ligation. *Lancet* 1995; **346**: 1666-1669 [PMID: 8551824 DOI: 10.1016/S0140-6736(95)92840-5]

91 **Thomopoulos K**, Theocharis G, Mimidis K, Lampropoulou-Karatza Ch, Alexandridis E, Nikolopoulou V. Improved survival of patients presenting with acute variceal bleeding. Prognostic indicators of short- and long-term mortality. *Dig Liver Dis* 2006; **38**: 899-904 [PMID: 17005458 DOI: 10.1016/j.dld.2006.08.002]

92 **Tsai MH**, Huang HC, Peng YS, Chen YC, Tian YC, Yang CW, Lien JM, Fang JT, Hou MC, Shen CH, Huang CC, Wu CS, Lee FY. Nutrition Risk Assessment Using the Modified NUTRIC Score in Cirrhotic Patients with Acute Gastroesophageal Variceal Bleeding: Prevalence of High Nutrition Risk and its Independent Prognostic Value. *Nutrients* 2019; **11** [PMID: 31505759 DOI: 10.3390/nu11092152]

93 **Tsai MH**, Huang HC, Peng YS, Chen YC, Tian YC, Yang CW, Lien JM, Fang JT, Wu CS, Lee FY. Critical illness-related corticosteroid insufficiency in cirrhotic patients with acute gastroesophageal variceal bleeding: risk factors and association with outcome*. *Crit Care Med* 2014; **42**: 2546-2555 [PMID: 25083978 DOI: 10.1097/CCM.0000000000000544]

94 **Vuachet D**, Cervoni JP, Vuitton L, Weil D, Dritsas S, Dussaucy A, Koch S, Di Martino V, Thevenot T. Improved survival of cirrhotic patients with variceal bleeding over the decade 2000-2010. *Clin Res Hepatol Gastroenterol* 2015; **39**: 59-67 [PMID: 25154000 DOI: 10.1016/j.clinre.2014.06.018]

95 **Senosiain Lalastra C**, Arribas Anta J, Moreira Vicente V, Martínez González J, Maroto Castellanos M, García Sánchez MC, Zaera de la Fuente C, López Durán S, Cañete Ruiz Á, Albillos Martínez A. Acute liver ischaemia after gastro-oesophageal variceal bleeding. *Gastroenterol Hepatol* 2016; **39**: 590-596 [PMID: 27112800 DOI: 10.1016/j.gastrohep.2016.03.007]

96 **Farooqi JI**, Farooqi RJ. Predictors of the outcome after the first episode of acute variceal bleeding in liver cirrhosis patients. *J Coll Physicians Surg Pak* 2001; **11**: 379-382

97 **Thomas GA**, Sugawa C, Joseph AL, Nakamura R, Saihara T, Inoue Y. Upper GI bleeding in an emergency hospital: Etiology, prognosis and improved survival by endoscopic hemostasis. *Dig Endosc* 1992; **4**: 199-208 [DOI: 10.1111/j.1443-1661.1992.tb00080.x]

98 **Gado A**, Ebeid B, Abdelmohsen A, Axon A. Predictors of mortality in patients with acute upper gastrointestinal hemorrhage who underwent endoscopy and confirmed to have variceal hemorrhage. *Alexandria journal of medicine* 2015; **51**: 295-304 [DOI: 10.1016/j.ajme.2014.08.002]

99 **Abbas SM**, Bissett IP, Holden A, Woodfield JC, Parry BR, Duncan D. Clinical variables associated with positive angiographic localization of lower gastrointestinal bleeding. *ANZ J Surg* 2005; **75**: 953-957 [PMID: 16336385 DOI: 10.1111/j.1445-2197.2005.03582.x]

100 **Albeldawi M**, Ha D, Mehta P, Lopez R, Jang S, Sanaka MR, Vargo JJ. Utility of urgent colonoscopy in acute lower gastro-intestinal bleeding: a single-center experience. *Gastroenterol Rep (Oxf)* 2014; **2**: 300-305 [PMID: 24958253 DOI: 10.1093/gastro/gou030]

101 **Arroja B**, Cremers I, Ramos R, Cardoso C, Rego AC, Caldeira A, Eliseu L, Silva JD, Glória L, Rosa I, Pedrosa J. Acute lower gastrointestinal bleeding management in Portugal: a multicentric prospective 1-year survey. *Eur J Gastroenterol Hepatol* 2011; **23**: 317-322 [PMID: 21394032 DOI: 10.1097/MEG.0b013e328344ccb5]

102 **Bua-Ngam C**, Norasetsingh J, Treesit T, Wedsart B, Chansanti O, Tapaneeyakorn J, Panpikoon T, Vallibhakara SA. Efficacy of emergency transarterial embolization in acute lower gastrointestinal bleeding: A single-center experience. *Diagn Interv Imaging* 2017; **98**: 499-505 [PMID: 28341118 DOI: 10.1016/j.diii.2017.02.005]

103 **García Sánchez M**, González Galilea A, López Vallejos P, Gálvez Calderón C, Naranjo Rodríguez A, de Dios Vega J, Miño Fugarolas G. Role of early colonoscopy in severe acute lower gastrointestinal bleeding. *Gastroenterol Hepatol* 2001; **24**: 327-332 [PMID: 11481066 DOI: 10.1016/S0210-5705(01)70187-2]

104 **Hermie L**, Dhondt E, Vanlangenhove P, De Waele J, Degroote H, Defreyne L. Empiric cone-beam CT-guided embolization in acute lower gastrointestinal bleeding. *Eur Radiol* 2021; **31**: 2161-2172 [PMID: 32964336 DOI: 10.1007/s00330-020-07232-7]

105 **Li B**, Stein DJ, Schwartz J, Lipscey M, Feuerstein JD. Outcomes in lower GI bleeding comparing weekend with weekday admission. *Gastrointest Endosc* 2020; **92**: 675-680.e6 [PMID: 32330505 DOI: 10.1016/j.gie.2020.04.031]

106 **Lv LS**, Gu JT. Super-selective arterial embolization in the control of acute lower gastrointestinal hemorrhage. *World J Clin Cases* 2019; **7**: 3728-3733 [PMID: 31799297 DOI: 10.12998/wjcc.v7.i22.3728]

107 **Niikura R**, Nagata N, Yamada A, Honda T, Hasatani K, Ishii N, Shiratori Y, Doyama H, Nishida T, Sumiyoshi T, Fujita T, Kiyotoki S, Yada T, Yamamoto K, Shinozaki T, Takata M, Mikami T, Mabe K, Hara K, Fujishiro M, Koike K. Efficacy and Safety of Early vs Elective Colonoscopy for Acute Lower Gastrointestinal Bleeding. *Gastroenterology* 2020; **158**: 168-175.e6 [PMID: 31563627 DOI: 10.1053/j.gastro.2019.09.010]

108 **Nykänen T**, Peltola E, Kylänpää L, Udd M. Transcatheter Arterial Embolization in Lower Gastrointestinal Bleeding: Ischemia Remains a Concern Even with a Superselective Approach. *J Gastrointest Surg* 2018; **22**: 1394-1403 [PMID: 29549618 DOI: 10.1007/s11605-018-3728-7]

109 **Oakland K**, Guy R, Uberoi R, Hogg R, Mortensen N, Murphy MF, Jairath V; UK Lower GI Bleeding Collaborative. Acute lower GI bleeding in the UK: patient characteristics, interventions and outcomes in the first nationwide audit. *Gut* 2018; **67**: 654-662 [PMID: 28148540 DOI: 10.1136/gutjnl-2016-313428]

110 **Radaelli F**, Frazzoni L, Repici A, Rondonotti E, Mussetto A, Feletti V, Spada C, Manes G, Segato S, Grassi E, Musso A, Di Giulio E, Coluccio C, Manno M, De Nucci G, Festa V, Di Leo A, Marini M, Ferraris L, Feliziani M, Amato A, Soriani P, Del Bono C, Paggi S, Hassan C, Fuccio L. Clinical management and patient outcomes of acute lower gastrointestinal bleeding. A multicenter, prospective, cohort study. *Dig Liver Dis* 2021; **53**: 1141-1147 [PMID: 33509737 DOI: 10.1016/j.dld.2021.01.002]

111 **Ríos A**, Montoya MJ, Rodríguez JM, Serrano A, Molina J, Ramírez P, Parrilla P. Severe acute lower gastrointestinal bleeding: risk factors for morbidity and mortality. *Langenbecks Arch Surg* 2007; **392**: 165-171 [PMID: 17131153 DOI: 10.1007/s00423-006-0117-6]

112 **Foley PT**, Ganeshan A, Anthony S, Uberoi R. Multi-detector CT angiography for lower gastrointestinal bleeding: Can it select patients for endovascular intervention? *J Med Imaging Radiat Oncol* 2010; **54**: 9-16 [PMID: 20377709 DOI: 10.1111/j.1754-9485.2010.02131.x]

113 **Klinvimol T**, Ho YH, Parry BR, Goh HS. Small bowel causes of per rectum haemorrhage. *Ann Acad Med Singap* 1994; **23**: 866-868 [PMID: 7741501]

114 **Gilshtein H**, Kluger Y, Khoury A, Issa N, Khoury W. Massive and recurrent diverticular hemorrhage, risk factors and treatment. *Int J Surg* 2016; **33** Pt A: 136-139 [PMID: 27500962 DOI: 10.1016/j.ijsu.2016.07.076]

115 **Ichiba T**, Hara M, Miyahara K, Urashima M, Shintani A, Naitou H, Higashi R. Impact of Computed Tomography Evaluation Before Colonoscopy for the Management of Colonic Diverticular Hemorrhage. *J Clin Gastroenterol* 2019; **53**: e75-e83 [PMID: 29356785 DOI: 10.1097/MCG.0000000000000988]

116 **Miyakuni Y**, Nakajima M, Ohbe H, Sasabuchi Y, Kaszynski RH, Ishimaru M, Matsui H, Fushimi K, Yamaguchi Y, Yasunaga H. Angiography versus colonoscopy in patients with severe lower gastrointestinal bleeding: a nation-wide observational study. *Acute Med Surg* 2020; **7**: e533 [PMID: 32617165 DOI: 10.1002/ams2.533]



Published by **Baishideng Publishing Group Inc**
7041 Koll Center Parkway, Suite 160, Pleasanton, CA 94566, USA
Telephone: +1-925-3991568
E-mail: bpgoffice@wjgnet.com
Help Desk: https://www.f6publishing.com/helpdesk
https://www.wjgnet.com



© 2023 Baishideng Publishing Group Inc. All rights reserved.

ISSN 1007-9327 (print)
ISSN 2219-2840 (online)

World Journal of *Gastroenterology*

World J Gastroenterol 2023 August 7; 29(29): 4481-4603



Published by Baishideng Publishing Group Inc

World Journal of Gastroenterology

Contents

Weekly Volume 29 Number 29 August 7, 2023

REVIEW

4481 Predictors and optimal management of tumor necrosis factor antagonist nonresponse in inflammatory bowel disease: A literature review

Wang LF, Chen PR, He SK, Duan SH, Zhang Y

4499 Bioenergetic alteration in gastrointestinal cancers: The good, the bad and the ugly

Chu YD, Chen CW, Lai MW, Lim SN, Lin WR

ORIGINAL ARTICLE

Basic Study

4528 Antagonizing adipose tissue-derived exosome miR-103-hepatocyte phosphatase and tensin homolog pathway alleviates autophagy in non-alcoholic steatohepatitis: A trans-cellular crosstalk

Lu MM, Ren Y, Zhou YW, Xu LL, Zhang MM, Ding LP, Cheng WX, Jin X

4542 MiR-204-3p overexpression inhibits gastric carcinoma cell proliferation by inhibiting the MAPK pathway and RIP1/MLK1 necroptosis pathway to promote apoptosis

Li X, Tibenda JJ, Nan Y, Huang SC, Ning N, Chen GQ, Du YH, Yang YT, Meng FD, Yuan L

4557 Effect of exogenous hydrogen sulfide in the nucleus tractus solitarius on gastric motility in rats

Sun HZ, Li CY, Shi Y, Li JJ, Wang YY, Han LN, Zhu LJ, Zhang YF

Case Control Study

4571 Comparison of modified gunsight suture technique and traditional interrupted suture in enterostomy closure

Chen C, Zhang X, Cheng ZQ, Zhang BB, Li X, Wang KX, Dai Y, Wang YL

Retrospective Study

4580 Prevalence and risk factors of osteoporosis detected by dual-energy X-ray absorptiometry among Chinese patients with primary biliary cholangitis

Chen JL, Liu Y, Bi YF, Wang XB

Observational Study

4593 New objective scoring system to clinically assess fecal incontinence

Garg P, Sudol-Szopinska I, Kolodziejczak M, Bhattacharya K, Kaur G

ABOUT COVER

Editorial Board Member of *World Journal of Gastroenterology*, Wan-Long Chuang, MD, PhD, Hepatobiliary Division, Department of Internal Medicine, Kaohsiung Medical University Hospital, Kaohsiung 807, Taiwan. waloch@kmu.edu.tw

AIMS AND SCOPE

The primary aim of *World Journal of Gastroenterology* (*WJG*, *World J Gastroenterol*) is to provide scholars and readers from various fields of gastroenterology and hepatology with a platform to publish high-quality basic and clinical research articles and communicate their research findings online. *WJG* mainly publishes articles reporting research results and findings obtained in the field of gastroenterology and hepatology and covering a wide range of topics including gastroenterology, hepatology, gastrointestinal endoscopy, gastrointestinal surgery, gastrointestinal oncology, and pediatric gastroenterology.

INDEXING/ABSTRACTING

The *WJG* is now abstracted and indexed in Science Citation Index Expanded (SCIE, also known as SciSearch®), Current Contents/Clinical Medicine, Journal Citation Reports, Index Medicus, MEDLINE, PubMed, PubMed Central, Scopus, Reference Citation Analysis, China National Knowledge Infrastructure, China Science and Technology Journal Database, and Superstar Journals Database. The 2023 edition of Journal Citation Reports® cites the 2022 impact factor (IF) for *WJG* as 4.3; IF without journal self cites: 4.1; 5-year IF: 5.3; Journal Citation Indicator: 0.82; Ranking: 33 among 93 journals in gastroenterology and hepatology; and Quartile category: Q2. The *WJG*'s CiteScore for 2021 is 8.3 and Scopus CiteScore rank 2022: Gastroenterology is 22/149.

RESPONSIBLE EDITORS FOR THIS ISSUE

Production Editor: *Hua-Ge Yu*; **Production Department Director:** *Xiang Li*; **Editorial Office Director:** *Jia-Ru Fan.*

NAME OF JOURNAL
World Journal of Gastroenterology

ISSN
ISSN 1007-9327 (print) ISSN 2219-2840 (online)

LAUNCH DATE
October 1, 1995

FREQUENCY
Weekly

EDITORS-IN-CHIEF
Andrzej S Tarnawski

EDITORIAL BOARD MEMBERS
http://www.wjgnet.com/1007-9327/editorialboard.htm

PUBLICATION DATE
August 7, 2023

COPYRIGHT
© 2023 Baishideng Publishing Group Inc

INSTRUCTIONS TO AUTHORS
https://www.wjgnet.com/bpg/gerinfo/204

GUIDELINES FOR ETHICS DOCUMENTS
https://www.wjgnet.com/bpg/GerInfo/287

GUIDELINES FOR NON-NATIVE SPEAKERS OF ENGLISH
https://www.wjgnet.com/bpg/gerinfo/240

PUBLICATION ETHICS
https://www.wjgnet.com/bpg/GerInfo/288

PUBLICATION MISCONDUCT
https://www.wjgnet.com/bpg/gerinfo/208

ARTICLE PROCESSING CHARGE
https://www.wjgnet.com/bpg/gerinfo/242

STEPS FOR SUBMITTING MANUSCRIPTS
https://www.wjgnet.com/bpg/GerInfo/239

ONLINE SUBMISSION
https://www.f6publishing.com

© 2023 Baishideng Publishing Group Inc. All rights reserved. 7041 Koll Center Parkway, Suite 160, Pleasanton, CA 94566, USA
E-mail: bpgoffice@wjgnet.com https://www.wjgnet.com

World Journal of Gastroenterology

Submit a Manuscript: https://www.f6publishing.com

World J Gastroenterol 2023 August 7; 29(29): 4481-4498

DOI: 10.3748/wjg.v29.i29.4481

ISSN 1007-9327 (print) ISSN 2219-2840 (online)

REVIEW

Predictors and optimal management of tumor necrosis factor antagonist nonresponse in inflammatory bowel disease: A literature review

Liang-Fang Wang, Ping-Run Chen, Si-Ke He, Shi-Hao Duan, Yan Zhang

Specialty type: Gastroenterology and hepatology

Provenance and peer review: Invited article; Externally peer reviewed.

Peer-review model: Single blind

Peer-review report's scientific quality classification

Grade A (Excellent): 0
Grade B (Very good): B, B
Grade C (Good): C
Grade D (Fair): 0
Grade E (Poor): 0

P-Reviewer: Liakina V, Lithuania; Rodrigues AT, Brazil; Tantau AI, Romania

Received: March 23, 2023
Peer-review started: March 23, 2023
First decision: June 17, 2023
Revised: June 28, 2023
Accepted: July 17, 2023
Article in press: July 17, 2023
Published online: August 7, 2023

Liang-Fang Wang, Ping-Run Chen, Shi-Hao Duan, Yan Zhang, Department of Gastroenterology and Hepatology, West China Hospital, Sichuan University, Chengdu 610041, Sichuan Province, China

Liang-Fang Wang, Ping-Run Chen, Si-Ke He, Shi-Hao Duan, Yan Zhang, West China School of Medicine, Sichuan University, Chengdu 610041, Sichuan Province, China

Corresponding author: Yan Zhang, MD, PhD, Chief Physician, Doctor, Professor, Department of Gastroenterology and Hepatology, West China Hospital, Sichuan University, No. 37 Guoxue Street, Chengdu 610041, Sichuan Province, China. hxzyan@163.com

Abstract

Tumor necrosis factor-α (TNF-α) antagonists, the first biologics approved for treating patients with inflammatory bowel disease (IBD), are effective for the induction and maintenance of remission and significantly improving prognosis. However, up to one-third of treated patients show primary nonresponse (PNR) to anti-TNF-α therapies, and 23%-50% of IBD patients experience loss of response (LOR) to these biologics during subsequent treatment. There is still no recognized predictor for evaluating the efficacy of anti-TNF drugs. This review summarizes the existing predictors of PNR and LOR to anti-TNF in IBD patients. Most predictors remain controversial, and only previous surgical history, disease manifestations, drug concentrations, antidrug antibodies, serum albumin, some biologic markers, and some genetic markers may be potentially predictive. In addition, we also discuss the next steps of treatment for patients with PNR or LOR to TNF antagonists. Therapeutic drug monitoring plays an important role in treatment selection. Dose escalation, combination therapy, switching to a different anti-TNF drug, or switching to a biologic with a different mechanism of action can be selected based on the concentration of the drug and/or antidrug antibodies.

Key Words: Predictor; Management; Tumor necrosis factor antagonist; Primary nonresponse; Secondary nonresponse; Inflammatory bowel disease

©The Author(s) 2023. Published by Baishideng Publishing Group Inc. All rights reserved.

Core Tip: Tumor necrosis factor-α (TNF-α) antagonists play an essential role in the management of inflammatory bowel disease (IBD). However, a significant number of patients experience primary or secondary nonresponse to these drugs. Here, we summarize relevant predictors of anti-TNF nonresponse in IBD and discuss the next steps for treating patients with primary or secondary nonresponse to anti-TNF agents.

Citation: Wang LF, Chen PR, He SK, Duan SH, Zhang Y. Predictors and optimal management of tumor necrosis factor antagonist nonresponse in inflammatory bowel disease: A literature review. *World J Gastroenterol* 2023; 29(29): 4481-4498
URL: https://www.wjgnet.com/1007-9327/full/v29/i29/4481.htm
DOI: https://dx.doi.org/10.3748/wjg.v29.i29.4481

INTRODUCTION

Inflammatory bowel disease (IBD), an immune-mediated inflammation of the gastrointestinal tract characterized by repeated remission and relapse, comprises Crohn's disease (CD) and ulcerative colitis (UC). Traditionally, IBD has been considered a disease of the Western world, but the newly industrialized countries of Asia, Africa, and South America are experiencing a rapid increase in incidence[1-3]; therefore, IBD has become a global disease[4,5].

IBD is a lifelong disease and is incurable. Currently, medical therapy for IBD mainly includes traditional therapeutics such as 5-aminosalicylates, thiopurines, and steroids, biologics such as antitumor necrosis factor (anti-TNF) therapy, vedolizumab and ustekinumab, and novel small-molecule drugs such as Janus kinase (JAK) inhibitors.

Anti-TNF therapies, the first biologics approved for the treatment of patients with IBD, are effective for the induction and maintenance of remission and significantly improve prognosis[6-8]. The development of anti-TNF therapies revolutionized the treatment of IBD and was a landmark event. Anti-TNF drugs are still the most commonly used biological agents in IBD at present[6]. Four TNF antagonists have been used in the treatment of IBD: infliximab, adalimumab, certolizumab, and golimumab[9]. However, up to one-third of treated patients show no primary response to anti-TNF-α therapies[10], and 23%-50% of IBD patients experience loss of response (LOR) to these biologics during subsequent treatment[11,12]. These patients not only fail to benefit from anti-TNF therapies but also suffer from the side effects of anti-TNF drugs, including increased susceptibility to infection, autoimmune diseases, and malignant tumors[13,14]. In addition, they face a serious financial burden. A retrospective study reported that direct healthcare expenditures increased significantly after the initiation of anti-TNF therapy and remained higher than preinitiation costs for up to 5 years[15].

Hence, it is important to assess the therapeutic response to anti-TNF agents in IBD before initiating treatment. In this review, we conducted a comprehensive search of studies to summarize relevant predictors of anti-TNF nonresponse in IBD and discuss the next steps of treatment for patients with primary or secondary nonresponse (SNR) to anti-TNF agents.

LITERATURE SEARCH STRATEGY

We conducted a search on PubMed and Web of Science. Keywords used include “inflammatory bowel disease”, “Crohn's disease”, “Ulcerative colitis”, “Tumor necrosis factor antagonists”, “anti-TNF”, “infliximab”, “adalimumab”, “certolizumab”, “golimumab”, “primary nonresponse”, “secondary nonresponse”, and “loss of response”. This review included articles, reviews and guidelines that investigated predictors of failure of TNF antagonists in IBD or optimized treatment (Supplementary Figure 1).

DEFINITION

Primary nonresponse

There is no consensus on the definition of primary nonresponse (PNR) in IBD patients as definitions vary across studies. Papamichael *et al*[11] defined PNR as a lack of objectively assessed improvement in baseline inflammatory signs after induction treatment in the presence of adequate concentrations of the drug and in the absence of antidrug antibodies (ADAs). In a cohort study, PNR was classified as treatment failure or use of corticosteroids (new prescription or previous dose not discontinued) or failure to reduce C-reactive protein (CRP) to 3 mg/L or less or to decrease by 50% or more from baseline and failure to decrease Harvey-Bradshaw Index score to 4 or less or by 3 or more from baseline before week 14 [16]. In general, PNR refers to the absence of improvement in clinical symptoms or objective measures during the induction phase[17-19]. The incidence of PNR has been reported to range from 13%-40%[7,20,21].

Secondary nonresponse

SNR, also named LOR, describes the clinical phenomenon of patients who have an initial response to biologics but then subsequently lose this response[22]. Notably, the two features of the SNR are that the patient's symptoms improved

during the initial treatment and that the recurrence of symptoms can only be due to the inflammatory response of IBD and not due to concurrent infection, fibrous stenosis, *etc*.[23]. SNR eventually occurs in 20%-50% of patients[12,24,25]. A recent meta-analysis found that the mean percentages of patients with SNR to infliximab, adalimumab, and certolizumab were 37.8%, 35.4%, and 43.3%, respectively[26].

PREDICTORS OF PNR

Clinical features

Age: Real-world data suggest that elderly individuals with CD benefit less from infliximab and adalimumab at 12 wk [27]. In the precision-3 study, CD patients treated with certolizumab had a reduced probability of achieving a primary response as they aged[28]. However, several other studies have reported no correlation between age and PNR to anti-TNF in CD[21,29]. In UC patients, Arias *et al*[30] found that the benefit was greater when the baseline age was less than 40 years, whereas other studies did not show the impact of age on the efficacy[31,32]. Differences between the results may have originated from variations in designs and how outcomes were defined.

Gender: A single-center study in Britain involving CD patients reported that men were significantly less likely to PNR to infliximab[21]. Another Korean study showed that among CD patients, men benefited from clinical remission at week 14 more than women[29]. However, many researchers have not found an association between sex and PNR to anti-TNF therapy in CD[33-35]. Similarly, the influence of gender on anti-TNF therapy cannot be clearly defined in UC patients. Sandborn *et al*[36] reported that women responded better when assessing the efficacy of golimumab at week 6. Other studies did not report that sex could predict TNF antagonists response in UC[30,37].

Smoking: Smoking is an environmental risk factor for CD[38] and appears to be associated with nonresponse to anti-TNF therapy in CD patients. Analysis from the precision-3 study suggested that nonsmokers are more likely to achieve early clinical remission than smokers[28]. Zorzi *et al*[39] identified a positive association between smoking and anti-TNF nonresponse in CD patients by Cox proportional hazards regression. In addition, a meta-analysis published in 2021 revealed that when smoking status was defined smoking was significantly associated with a reduction in response to infliximab or adalimumab in patients with CD[40]. However, the negative effect of smoking on response was not found in another earlier meta-analysis[41]. Studies of UC have also reported inconsistent results. One Italian study found a significantly lower response to infliximab in ex-smokers[42], while others did not reach this conclusion[37,43]. The conflicting findings may be due to different definitions of smoking among the studies. In summary, smoking cessation is recommended for current smokers diagnosed with IBD[44].

Previous surgery: Although treatment strategies for IBD have changed, 17.4%-25% of patients with CD still require surgery[45-47]. Macaluso *et al*[27] used a logistic regression model to identify a history of previous surgery as an independent risk factor for PNR in CD patients. Another group reported similar results, showing that CD patients without previous surgery had a greater chance of achieving initial remission than patients with previous surgery, with a hazard ratio of 1.387[28]. CD patients with previous surgery had a lower response rate[48]. A study involving 201 CD patients also demonstrated that previous surgery was an independent predictor of PNR[34].

Disease duration: The analysis of pooled data from CD studies indicates that CD with a shorter disease duration is associated with a superior early response[49]. In the MODIFY study, patients who received early adalimumab achieved a higher clinical response and remission rate at week 26 than those who received delayed treatment[50]. This correlation has also been confirmed by a recent meta-analysis[51]. Studies have reported that among UC patients, a shorter disease duration is associated with a better response to anti-TNF drugs[32,52]. However, in general, authors did not find a positive association between long disease duration and anti-TNF nonresponse[31,48,53]. Although the current studies available cannot explain the underlying reasons for poorer response to anti-TNF in IBD with a longer disease duration, it is intuitive that a longer disease duration may contribute to the development of fibrosis, making earlier treatment attractive to patients[54].

Phenotype: The disease phenotype seems to be related to anti-TNF treatment response. In CD patients, isolated ileitis was inversely associated with the anti-TNF response, whereas the opposite was true for isolated colitis[29,48].

Pharmacokinetic

The pharmacokinetic (PK) of anti-TNF consists of four processes: absorption, distribution, metabolism, and elimination [55]. PK failures are characterized by undetectable or subtherapeutic drug concentrations associated with rapid nonimmune clearance or immunogenicity as well as the development of ADAs[56].

Drug concentration and antidrug antibodies: Several studies have demonstrated that subtherapeutic drug concentration is a predictor of PNR, with drug concentrations lower in IBD patients who failed to respond to anti-TNF therapy than in responders[16,57]. Post hoc analysis of data from the MUSIC trial data showed that CD patients with higher levels of certolizumab were more likely to achieve endoscopic response and remission at week 10[58]. Ding *et al*[17] suggested that low anti-TNF levels and the formation of ADAs could predict PNR in CD patients. The same results were reported in another study involving patients with UC[59].

Weight: Weight is a predictor of anti-TNF nonresponse. In a multicenter cohort study, high body mass index (BMI) at baseline in CD patients was associated with an increased risk of PNR[16]. Similar results were reported in another study [60]. In UC patients, Kurnool *et al*[61] reported that an increase in BMI had a negative impact on the response to anti-TNF drug therapy. The reason may be that, on the one hand, obesity induces a proinflammatory state[62], and on the other hand, the proteolytic clearance of immunoglobulins is usually related to weight, that is, the higher the weight is, the faster the clearance[63,64].

Serum albumin: Serum albumin levels predict the PK of anti-TNF therapy. A recent prospective study noted that low albumin levels at baseline in IBD patients predicted low infliximab concentrations at week 14[16]. Several other studies have reached similar conclusions[57,63]. One study of patients with UC found significantly higher serum albumin in responders than in primary nonresponders[65]. This effect occurs because albumin is the main transporter of drugs in blood, and serum albumin binds anti-TNF drugs to protect against degradation[66].

Fcγ receptor type IIIA: Single nucleotide substitutions within the Fcγ receptor type IIIA (FCGR3A) gene result in allelic variations, one valine (V) or one phenylalanine (F) at amino acid position 158. Functional polymorphisms in FCGR3A are significantly associated with response to anti-TNF therapy in CD patients[67]. Bek *et al*[67] used mono-compartmental population modeling to describe the PK of infliximab and found that the FCGR3A-158V/V genotype was associated with increased elimination of infliximab[67]. Further studies identified the FCGR3A VV phenotype as an independent predictor of ADAs generation and associated with a reduced clinical response in IBD patients at the end of induction[68].

Pharmacodynamic

Pharmacodynamic (PD) failure is associated with underlying non-TNF-driven inflammation characterized by no improvement in symptoms even at sufficient concentrations and without ADAs[56].

Pharmacokinetic/pharmacodynamic modeling: Kimura *et al*[69] developed Pharmacokinetic/pharmacodynamic (PK/PD) modeling to predict IBD response to infliximab during induction therapy. Another team of researchers in Japan developed a PK/PD model to calculate the $K^{anti\text{-}TNF\alpha}{}_0/K^{else}$ ratio to predict the PNR to TNF in IBD patients at the second administration[70]. The validity of this model remains to be tested in larger populations.

Biologic markers

C-reactive protein: Several studies have investigated the relationship between CRP levels and anti-TNF responses. A multicenter retrospective study in Korea demonstrated that UC patients with CRP ≥ 3 mg/dL were more likely to achieve clinical remission at week 8[71]. This was also observed in CD treated with certolizumab[72]. However, opposite results were reported in another retrospective study of CD patients[73]. Presumably, high baseline CRP will exclude some patients with noninflammatory functional symptoms and predict a higher response, but it may also reflect a higher inflammatory load with increased drug loss[74].

Antineutrophil cytoplasmic antibody and anti-*Saccharomyces cerevisiae* antibody: In a cohort study involving 90 UC patients, a greater proportion of antineutrophil cytoplasmic antibody (ANCA)-negative patients achieved clinical response during infliximab induction than ANCA-positive patients[75]. Another study in CD patients found that positive perinuclear ANCN (pANCA) is a predictor of anti-TNF nonresponse[76]. In a meta-analysis, pooled results showed that pANCA-negative patients with IBD had a nearly twofold higher response to anti-TNF therapy than pANCA -positive patients[77]. A single-center study evaluating pANCA and anti-*Saccharomyces cerevisiae* antibody (ASCA) simultaneously found that pANCA+/ASCA- serotypes significantly reduced early clinical response to infliximab in CD patients[78].

Fecal calprotectin: Fecal calprotectin (FC) is an indicator of gut inflammation and disease burden in IBD. Beltrán *et al*[79] noted that FC was higher in PNR patients with CD than in responders at weeks 0, 6, and 14, with a statistically significant difference only at week 0. Another study in UC patients also showed that early high FC was predictive of infliximab nonresponse[52]. Pavlidis *et al*[80] suggested that a decrease in FC of less than 70% after induction with anti-TNF drugs could predict PNR in patients with CD. However, some authors have not shown a relationship between FC and anti-TNF PNR in UC patients[81,82].

Fecal lactoferrin: Fecal lactoferrin (FL) can be used to monitor intestinal inflammation in IBD[83]. A retrospective study involving IBD demonstrated that dynamic monitoring of FL could distinguish responders from primary nonresponders, with two sustained drops in FL observed in responders during induction therapy[84].

Genetic markers

TNF and TNF-receptor superfamily genes: Genetic polymorphisms associated with TNF and TNF receptors have been widely studied for their ability to predict the response to anti-TNF therapy. In a clinical trial studying CD, patients homozygous for the TNF/Lymphotoxin alpha (LTA) polymorphism, the LTA NcoI-TNFc-aa13L-aa26 haplotype 1-1-1-1, showed early nonresponse to infliximab[76]. Another study demonstrated that TNF-308 (rs1800629) was associated with response to anti-TNF therapy, and the presence of the minor allele (A) was associated with increased odds of nonresponse to anti-TNF therapy in IBD[85]. For TNF-receptor superfamilies (TNFRSF), Steenholdt *et al*[86] found that CD patients carrying the TNFRSF1B minor allele rs1061622 had a better response to infliximab induction therapy. In a Japanese study, TNFRSF1A (rs767455_G) and TNFRSF1B (rs1061624_A-rs3397_T) were associated with poor response in CD patients[87] and these results were replicated in another Spanish study[88]. Additionally, a meta-analysis indicated

that TNFRSF1A (rs4149570) significantly improved anti-TNF responses in IBD[67].

Autophagy-related 16 like 1: Autophagy-related 16 like 1 (ATG16L1) is a risk factor for CD[89]. Koder *et al*[90] found a strong association between ATG16L1 (rs10210302) and response to adalimumab treatment in the CD population, with the TT genotype showing a better response after 12 wk of adalimumab treatment. Future studies on the relationship between ATG16L1 and the anti-TNF response are necessary to clarify these effects.

Apoptosis genes: Infliximab and adalimumab induce apoptosis by binding to membrane-bound TNF-α, which is the main mechanism of their efficacy[54]. An earlier study observed the strongest association between the Fas ligand -843 TT genotype and nonresponse to infliximab in CD patients[91]. Furthermore, Hlavaty *et al*[92] developed a novel apoptotic pharmacogenetic index based on three single nucleotide polymorphisms (Fas ligand-843 C/T, Fas-670 G/A, and Caspase9 93 C/T), with a higher score indicating a better response to anti-TNF therapy.

Nucleotide-binding oligomerization domain 2: Nucleotide-binding oligomerization domain 2 (NOD2) mutations predict an increased risk of complications related to CD[93]. Further studies showed that NOD2 mutations were less responsive to anti-TNF therapy than wild-type NOD2 in CD patients[94]. Another study demonstrated that CD patients with either NOD2 variants alone or in combination with ATG16L1 variants were more likely to receive intensive biologic therapy, which may indicate that NOD2 variants have a negative impact on response to biologic therapy[95]. However, this effect was not observed in another trial[96].

Cytokines

Interleukin: One study conducted in CD patients found that primary nonresponders had significantly higher interleukin-8 (IL-8) concentrations at baseline[97]. In addition, the level of IL-6 in responders was significantly lower than that in primary nonresponders at week 2 and week 6[97]. Another study of CD noted that IL17A and IL1B expression was significantly upregulated in anti-TNF refractory patients during anti-TNF therapy[98]. Oncostatin M (OSM), a member of the IL-6 cytokine family, has been shown to disrupt epithelial barrier function and drive intestinal inflammation[99]. An analysis of more than 200 IBD patients treated with anti-TNF therapy found higher baseline levels of OSM expression in those who failed anti-TNF therapy[100]. A cross-sectional study suggested that higher levels of OSM in the colon were associated with PNR to anti-TNF in patients with IBD[101].

Triggering receptor expressed on myeloid cells 1: Triggering receptor expressed on myeloid cells 1 (TREM1) expression has been proposed as a potential marker for predicting response to anti-TNF therapy in IBD patients. Gaujoux *et al*[102] demonstrated that TREM1 can be an ex-ante predictor of the anti-TNF response and that TREM1 Levels were downregulated in nonresponders, with a prediction accuracy of 94%. This phenomenon is also found in the inflamed mucosa.

Gut microbes

Several studies have shown that gut microbes predict nonresponse to anti-TNF treatment in IBD. Magnusson *et al*[103] found that responders had lower dysbiosis indexes, a higher abundance of *Faecalibacterium prausnitzii* (*F. prausnitzii*) at baseline, and an increase in the abundance of *F. prausnitzii* during induction therapy compared with nonresponders. Another study found that high abundances of the genera *Blautia*, *Faecalibacterium*, *Roseburia*, and *Negativibacillus* at baseline were inversely associated with responsiveness to infliximab in CD[104]. In the same study, a high abundance of *Sutterella*, *Roseburia*, and *Intenstinibacter* appeared to predict response to infliximab in UC patients[104]. Alatawi *et al*[105] detected a reduction in the abundance of short-chain fatty acid-producing bacteria, including *Anaerostipes*, *Coprococcus*, *Lachnospira*, *Roseburia*, and *Ruminococcus,* in IBD patients unresponsive to anti-TNF therapy[105]. Nevertheless, a European multicenter study found no differences in the microbiota of anti-TNF therapy responders *vs* nonresponders in IBD[106]. Indicators that predict PNR to anti-TNF agents in patients with IBD are listed in Table 1.

PREDICTORS OF SECONDARY NONRESPONSE

Clinical features

Gender: A retrospective study identified that women were more likely to develop SNR to anti-TNF[107]. Another multicenter retrospective study found a similar result in the CD subgroup[108]. An earlier systematic review noted the male sex was a predictor of LOR in CD[109]. A single-center study demonstrated a significantly higher likelihood of SNR in men with UC[110]. However, no association has been reported between gender and SNR in most studies[21,30,31,37].

Smoking: Sandborn *et al*[28] found that current smoking was associated with LOR in individuals diagnosed with CD. This result was also validated in another single-center study[39]. Chaparro *et al*[111] reported that smoking was associated with the occurrence of LOR in CD.

Previous surgery: A Sicilian study of CD reported that previous surgery was associated with a low rate of clinical remission at 1 year[27]. However, many studies have not demonstrated a relationship between previous surgical history and SNR to anti-TNF therapy in CD[16,112].

Disease duration: Panaccione *et al*[49] showed that patients with CD whose duration was less than 1 year benefited more in maintaining remission. A retrospective cohort study reported that CD patients with a disease duration of more than 2 years had a significantly higher rate of SNR[113]. A subgroup analysis of the placebo-controlled CHARM trial also

Table 1 Predictors of primary nonresponse in Crohn's disease and ulcerative colitis

Predictor	Crohn's disease	Ulcerative colitis
Clinical features		
Age	Yes: Older[27,28]; No[21,29]	Yes: Older[30]; No[31,32]
Gender	Yes: Male[21], female[29]; No[33-35]	Yes: Male[36]; No[30,37]
Smoking	Yes: Smoker[28,39,40]; No[41]	Yes: Ex-smoker[42]; No[37,43]
Previous surgery	Yes[27,28,34,48]	
Disease duration	Yes: Longer[49-51]; No[48]	Yes: Longer[32,52]; No[30,53]
Phenotype	Yes: Isolated ileitis[29,48]	
Pharmacokinetic		
Drug concentration	Yes: Low[16,17,57,58]	Yes: Low[57,59]
Antidrug antibodies	Yes[17]	Yes[59]
Weight	Yes: High[16,60]	Yes: High[61]
Serum albumin	Yes: Low[57]	Yes: Low[57,65]
FCGR3A	Yes: FCGR3A-158V/V[67,68]	Yes: FCGR3A-158V/V[68]
Pharmacodynamic		
PK/PD model	Yes[69,70]	Yes[69,70]
Biologic markers		
CRP	Yes: Low[72], High[73]	Yes: Low[71]
ANCA and ASCA	Yes: pANCA+[76,77]	Yes: ANCA+[75], pANCA+[77], pANCA+/ASCA-[78]
Fecal calprotectin	Yes: High[79]	Yes: High[52]; No[81,82]
Fecal lactoferrin	Yes: High[84]	Yes: High[84]
Genetic markers		
TNF genes	Yes: Lymphotoxin alpha NcoI-TNFc-aa13L-aa26 haplotype 1-1-1-1[76], TNF-308A[85]	Yes: TNF-308A[85]
TNFRSF	Yes: TNFRSF1A (rs767455_G)[87], TNFRSF1B (rs1061624_A-rs3397_T)[87]	
ATG16L1	Yes: ATG16L1 (rs10210302_CC)[90]	
Apoptosis genes	Yes: Fas ligand-843 TT genotype[91]	
NOD2	Yes: NOD2 mutation[94,95]	
Cytokines		
Interleukin	Yes: IL-8 (high)[97], IL-6 (low)[97], IL17A (high)[98], IL1B (high)[98], OSM (high)[100,101]	Yes: OSM (high)[100,101]
TREM1	Yes: Low[102]	Yes: Low[102]
Gut microbes	Yes: Abundance of short-chain fatty acid-producing bacteria (decreased)[105]	Yes: Dysbiosis indexes (high)[103]; Abundance of short-chain fatty acid-producing bacteria(decreased)[105]

FCGR3A: Fcγ receptor type IIIA; PK/PD model: Pharmacokinetic/pharmacodynamic modeling; CRP: C-reactive protein; ANCA: Antineutrophil cytoplasmic antibody; ASCA: Anti-*Saccharomyces cerevisiae* antibody; pANCA: Perinuclear anti-neutrophil cytoplasmic antibody; TNF: Tumor necrosis factor; TNFRSF: TNF-receptor superfamily; ATG16L1: Autophagy-related 16 like 1; NOD2: Nucleotide-binding oligomerization domain 2; OSM: Oncostatin M; TREM1: Triggering receptor expressed on myeloid cells 1.

obtained a similar conclusion[114].

Phenotype: A recent study reported that accumulation of the upper digestive tract and the presence of fistulas at baseline were associated with SNR to adalimumab and infliximab in CD patients[27]. Another study involving 93 individuals verified that nonstructuring nonpenetrating CD was associated with sustained remission[39]. CD with concurrent fistula or stenosis had a lower clinical remission rate[115].

Pharmacokinetic

Drug concentration and antidrug antibodies: A multicenter cohort study confirmed that concentrations of infliximab < 7 mg/L and adalimumab < 12 mg/L were independently associated with SNR in CD patients[16]. A prospective study indicated that the trough level (TL) of infliximab < 5.5 μg/mL in patients with IBD was the best threshold to predict LOR [116]. Alternatively, the generation of ADAs, which in combination with circulating drugs also leads to a reduction in drug concentration, is associated with anti-TNF LOR in IBD[117].

Weight: Kennedy *et al*[16] found that obesity at baseline was associated with adalimumab treatment failure at week 54 in patients with CD. Another study also reported that IBD patients with a high BMI displayed a high rate of LOR[118]. In IBD patients treated with adalimumab, SNR was increased in those with BMI ≥ 30 kg/m^2 compared with those with BMI < 30 kg/m^2[119].

Serum albumin: In CD patients treated with certolizumab, low albumin predicted SNR[28]. Higher albumin levels were associated with lower LOR in IBD patients treated with infliximab[119]. A prospective study found that IBD patients with low albumin serum concentrations at baseline had a significantly increased risk for SNR to anti-TNF and that normalization of albumin levels during treatment did not reduce this risk[120].

Serum γ-globulin: A German study from IBD found a positive association between elevated serum γ-globulin concentrations and the risk of SNR to anti-TNF therapy[120]. Higher γ-globulin concentrations imply increased B-cell activity, resulting in increased ADAs production[120].

Matrix metalloproteinase 3: Matrix metalloproteinase 3 (MMP3) expression is significantly upregulated in inflamed colonic segments of IBD patients, suggesting the possible involvement of this enzyme in the inflammatory process[121, 122]. A retrospective study from Italy showed that in IBD patients, MMP3 levels were significantly lower in responders (11.48 ng/mL) than in nonresponders (25.96 ng/mL) at week 52[123]. In the same study, MMP3 levels tended to be higher in patients without ADAs than in those with ADAs[123]. According to a previous report, MMP3 cleaved infliximab and adalimumab which may result in reduced drug efficacy[124].

Fcγ receptor type IIIA: A Spanish team found higher serum concentration levels of both infliximab and adalimumab in FCGR3A FF carriers than in FCGR3A VV carriers during maintenance therapy in IBD and found that the proportion of VV patients who developed ADAs was significantly higher than that of FF patients diagnosed with IBD[125].

Human leukocyte antigen: The value of human leukocyte antigen-DQA1*05 (HLA-DQA1*05) in predicting anti-TNF-ADAs production has been reported in several studies. A genome-wide analysis of 1240 subjects in the PANTS cohort revealed that approximately 40% of Europeans carried HLA-DQA1*05 and significantly increased rates of ADAs production[126]. Wilson *et al*[127], using genotypic analysis, showed that HLADQA1*05 was independently associated with LOR to infliximab and increased ADAs in IBD.

Biologic markers

C-reactive protein: Post hoc analysis of ACCENT I, indicated that high levels of CRP before treatment predicted an increased likelihood of maintaining remission[128]. A study of IBD found that CRP > 5 mg/L was an independent predictor of SNR[116]. However, a Hungarian study reported that low levels of CRP at week 12 were associated with clinical remission at week 52 in CD patients on adalimumab[129]. Additionally, Angelison *et al*[82] did not find an association between CRP and SNR to anti-TNF agents in UC.

Antinuclear antibody: Among patients with IBD, those with positive antinuclear antibody (ANA) at baseline had higher odds of LOR to anti-TNF[130]. More studies are needed to investigate the relationship between ANA and response to anti-TNF therapy in the future.

Fecal calprotectin: Analyses from the 7-year PRECiSE 3 study revealed that an increase in FC implies an increased risk of LOR to anti-TNF[28]. However, Deshpande *et al*[131] reported that FC levels at week 14 could not predict the recurrence of CD one year later. Differences in the timing of FC measurement and sample size may have contributed to this discrepancy.

Fecal lactoferrin: Sorrentino *et al*[132] found that FL levels before and after anti-TNF treatment could be used to distinguish responders, partial responders, and nonresponders in IBD patients with suspected LOR[132]. In the same study, they proposed that responders had normal FL both before and after administration, partial responders had elevated FL before administration, partial FL decreased after administration but remained well above the normal threshold, and FL increased after LOR administration[132].

Genetic markers

TNF and TNF-receptor superfamily genes: Currently, only a retrospective cohort study of CD has demonstrated that carrying the TNFRSF1B minor allele rs976881 was associated with LOR to infliximab[86]. More studies are urgently needed to explore the relationship between TNF and TNFRSF genes and SNR to anti-TNF therapy.

Cytokines

Interleukin: Higher baseline OSM in IBD patients with SNR to infliximab was found in a UK study[100]. Bertani *et al*[133]

demonstrated that in CD patients treated with infliximab, those with low OSM levels at baseline and week 14 were more likely to achieve clinical remission at week 54[133]. Moreover, the level of OSM in patients with mucosal healing was significantly lower than that in patients without mucosal healing at week 54[133]. We summarize the predictors of SNR in Table 2.

OPTIMAL MANAGEMENT OF ANTI-TNF NONRESPONSE

Assessment

PNR or SNR to anti-TNF therapy was determined according to clinical symptoms, laboratory tests, endoscopy, imaging examinations, *etc.* It is worth noting that conditions such as poor adherence[134], improper drug storage medication storage[135], and co-infection[23] need to be excluded during assessment.

Therapeutic drug monitoring

The British Society of Gastroenterology consensus defines therapeutic drug monitoring (TDM) as, the measurement of the drug (± ADAs) levels to assess compliance, drug metabolism, and immunogenicity with a view to guide dose adjustments or switch off therapy[136]. TDM can be used reactively or proactively. The American Gastroenterological Association recommends reactive TDM for adults who fail to respond to anti-TNF therapy[9]. A target TL of at least 5 μg/mL, 7.5 μg/mL, and 20.0 μg/mL for infliximab, adalimumab, and certolizumab, respectively, is suggested[9]. Papamichael *et al*[137] recommend a minimum drug concentration of at least 2.5 μg/mL at week 6 and a trough concentration of at least 1 μg/mL of golimumab during maintenance therapy. Several recent reviews showed that TDM was more beneficial than empirical strategies in terms of cost-effectiveness[138-140]. TDM plays an important role in optimizing anti-TNF therapy.

Management of PNR

There is no consensus on the optimal management of PNR to TNF antagonists. A review proposed that the management of IBD patients with PNR to anti-TNF therapy consists of three major steps: prediction, prevention, and therapeutic intervention[11]. Clinical features, pharmacokinetics, genetic phenotypes, *etc*., can predict the development of PNR. Preventive measures to avoid PNR to anti-TNF include counseling patients to quit smoking, weight intervention, *etc*.[11, 17]. For IBD patients with PNR, empirical intervention can be performed, switching to another TNF antagonist, or switching to a biological agent of a different mechanism, is desirable[141]. Ding *et al*[17] suggested that a second TNF antagonist be administered when the patient is PNR to the first TNF antagonist. If the treatment fails again, switching out of class should be considered.

Some scholars have also proposed that the medication of primary nonresponders can be adjusted according to TDM. With the help of TDM, rational and optimal treatment can be provided[136]. If patients have low TLs and no or low titer ADAs formation, dose optimization or the addition of an immunomodulator is recommended. When TLs are low and high-titer ADAs are detected, switching to another TNF antagonist or biologic agent with a different mechanism may be considered. For patients with therapeutic concentrations, switching out of class is suggested (Figure 1).

Management of secondary nonresponse

The detection of TNF antagonist and ADAs concentration is helpful to guide the next treatment of SNR (Figure 2).

Dose escalation: Dose intensification can reverse nonresponse to anti-TNF in IBD patients with subtherapeutic concentrations and no or low concentrations of ADAs. A meta-analysis reported a 34% need for anti-TNF dose escalation in CD at a median follow-up of 1 year, with pooled rates of 38%, 32%, and 2% for infliximab, adalimumab, and certolizumab, respectively[26]. A multicenter cohort study in Belgium found that 34% of CD patients treated with adalimumab required an increased dose to maintain clinical response, and clinical response was induced again in 67% of these patients[142]. Billioud *et al*[109] concluded that among CD patients who experienced LOR to adalimumab, 71.4% regained response and 39.9% achieved remission after dose optimization. Interestingly, a post hoc analysis of the TAXIT trial showed a significantly higher rate of clinical response with dose intensification, regardless of the presence of ADAs[143]. Meanwhile, Bodini *et al*[144] have suggested that, based on clinical need, anti-TNF doses can be increased, even in older patients of patients receiving combination therapy, with little risk of adverse reactions occurring.

Addition of an immunomodulator: The addition of an immunomodulator is a good option for IBD patients receiving anti-TNF therapy in whom subtherapeutic and no or low concentrations of ADAs are detected. For example, van Schaik *et al*[145] observed a significant increase in mean trough concentrations and a significant decrease in the incidence of ADAs in the infliximab combined with azathioprine group compared with infliximab alone in patients with IBD, whereas no differences were observed in the adalimumab combination *vs* monotherapy groups[145]. Another study involving patients with CD reported that, for both infliximab and adalimumab, combined immunomodulators reduced the risk of ADAs formation[16]. In the SONIC trial, the response rate in corticosteroid-free clinical remission at week 50 was significantly higher with infliximab adding immunomodulator than with monotherapy (55.6% *vs* 39.6%)[146]. In the UC-SUCCESS trial, infliximab plus an immunomodulator was also superior in achieving corticosteroid-free clinical remission [147]. In a 2-year cohort study of 46 patients with IBD, the addition of a low-dose immunomodulator, either azathioprine, methotrexate, or mycophenolate mofetil, reversed clinical response in approximately 50% of IBD patients who had failed to respond to anti-TNF monotherapy[148]. With regard to when to discontinue immunomodulators, Drobne *et al*[149]

Table 2 Predictors of secondary nonresponse in Crohn's disease and ulcerative colitis

Predictor	Crohn's disease	Ulcerative colitis
Clinical features		
Gender	Yes: Female[107,108], male[109]; No[21]	Yes: Female[107], male[110]; No[31,37]
Smoking	Yes: Smoker[28,39,111]; No[41]	
Previous surgery	Yes[27]; No[16,112]	
Disease duration	Yes: Longer[49,113,114]	
Phenotype	Yes: Upper digestive tract[27], fistula[27,115], stenosis[115]	
Pharmacokinetic		
Drug concentration	Yes: Low[16,116]	Yes: Low[116]
Antidrug antibodies	Yes[117]	Yes[117]
Weight	Yes: High[16,118,119]	Yes: High[118,119]
Serum albumin	Yes: Low[28,119,120]	Yes: Low[119,120]
Serum γ-globulin	Yes: High[120]	Yes: High[120]
MMP3	Yes: High[123]	Yes: High[123]
FCGR3A	Yes: FCGR3A VV[125]	Yes: FCGR3A VV[125]
HLA	Yes: HLADQA1*05[127]	Yes: HLADQA1*05[127]
Biologic markers		
CRP	Yes: Low[128], high[129]	No[82]
ANA	Yes: ANA+ [130]	Yes: ANA[130]
Fecal calprotectin	Yes: High[28]; No[131]	
Fecal lactoferrin	Yes: High[132]	Yes: High[132]
Genetic markers		
TNFRSF	Yes: TNFRSF1B (rs976881)[86]	
Cytokines		
Interleukin	Yes: OSM (high)[100,133]	Yes: OSM (high)[100]

MMP3: Matrix metalloproteinase 3; FCGR3A: Fcγ receptor type IIIA; HLA: Human leukocyte antigen; CRP: C-reactive protein; ANA: Antinuclear antibody; TNFRSF: Tumor necrosis factor receptor superfamily; OSM: Oncostatin M.

suggest that at least 6 mo of combination therapy is required. Mahmoud *et al*[150] compared different durations of combination therapy in relation to LOR and found no significant difference between durations of combination therapy (< 0.5 years, 0.5-1 year, 1-2 years, and > 2 years); however, durations of combination therapy longer than 2 years were associated with a lower risk of ADAs formation.

Switch within class: In the case of subtherapeutic concentrations with high titers of ADAs, switching within class to another anti-TNF agent should be considered. A retrospective study of IBD showed that when ADA titers of infliximab and adalimumab were > 9 μg/mL and 4 μg/mL, respectively, switching within class achieved a longer duration of response compared with dose intensification[151]. In another study of IBD, switching patients positive for ADAs to another anti-TNF agent achieved a response rate of 92%, whereas dose optimization achieved a response rate of 17%[152]. In cases where the first anti-TNF drug failed, switching to another drug achieved remission in approximately 50% of patients, an effect that has been reported in several other studies[153,154]. Moreover, a systematic review reported that switching to a second anti-TNF agent led to successful induction of remission in 46% of patients with IBD who had failed the first anti-TNF agent[155]. Of note, the previous generation of anti-TNF antibodies increases the risk of the generation of a second anti-TNF antibody in IBD[156]. Therefore, when switching to another anti-TNF agent, a combination of immunosuppressive agents is appropriate[136,157].

Switch out of class: If TL is sufficient with high ADAs, it is recommended that the patient switches to a drug that exerts its effects through another mechanism of action, considering that TNF-α is not the primary pathogenesis. Alternatively, for low TLs with high titers of ADAs, switching out of class is also effective. Subgroup analyses of trials investigating vedolizumab[158], ustekinumab[159,160], and tofacitinib[161] all showed that patients who had failed anti-TNF therapy

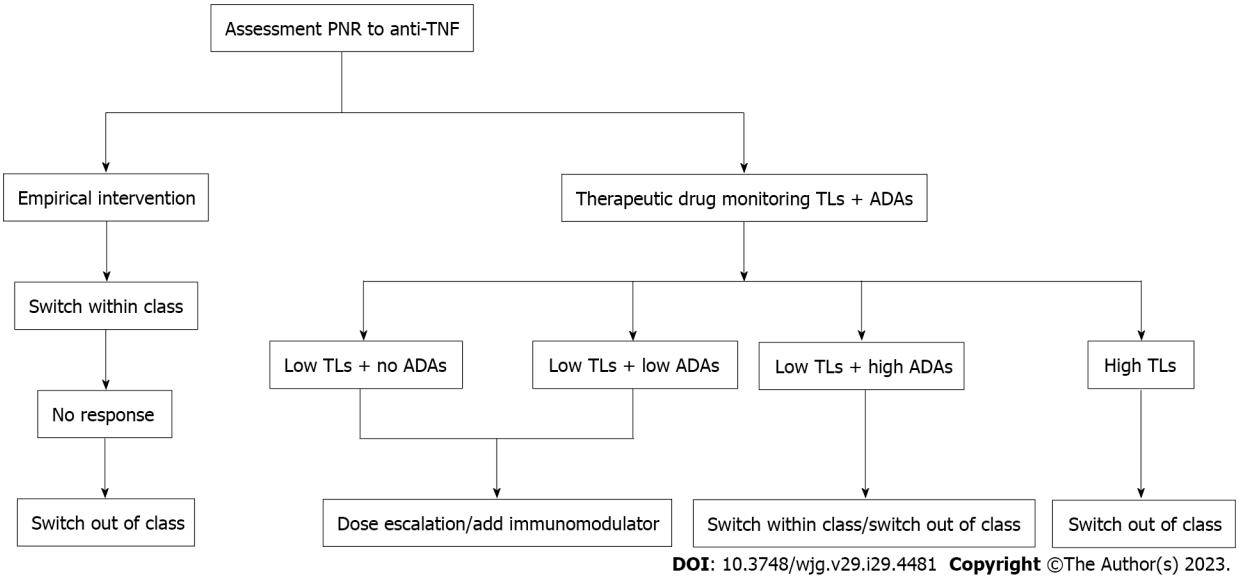


Figure 1 Flow diagram for management of primary nonresponse to tumor necrosis factor antagonists. PNR: Primary nonresponse; TNF: Tumor necrosis factor; TL: Trough level; ADA: Antidrug antibody.

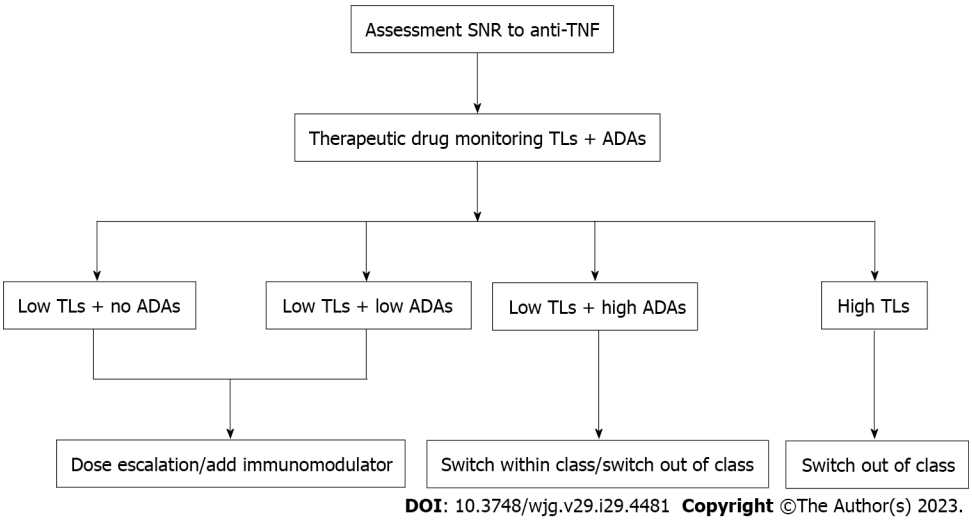


Figure 2 Flow diagram for management of secondary nonresponse to tumor necrosis factor antagonists. SNR: Secondary nonresponse; TNF: Tumor necrosis factor; TL: Trough level; ADA: Antidrug antibody.

benefited from treatment with a novel agent. One study involving 128 CD patients who had failed previous anti-TNF therapy reported that the corticosteroid-free clinical response rates of vedolizumab and ustekinumab treatment at weeks 12, 24, and 52 were 22.7%, 29.7%, 26.8% and 27.1%, 42.4%, 45.9% respectively[162]. Furthermore, propensity score matching concluded that patients who failed anti-TNF therapy benefited more from ustekinumab than vedolizumab[162].

CONCLUSION

IBD is incurable, and anti-TNF therapy plays an important role in IBD. Although existing studies have found that previous surgical history, disease manifestations, drug concentrations, ADAs, serum albumin, ANCA, p-ANCA, ANA, *etc.* have potential predictive effects, to date, there are no practically available indicators that can predict response to TNF antagonists in patients with IBD. Further research is needed to verify the accuracy of existing predictors or discover new biomarkers to achieve personalized treatment for patients with IBD.

TDM forms the core of an optimal strategy for treating IBD. It is recommended to optimize the dose or add immunomodulators when patients with low TLs and no or low titer ADAs. For nonresponders with low TLs and high titer ADAs, switching to another TNF antagonist or biologic agent with a different mechanism can be suggested. When TLs are sufficient, patients can consider switching to another biological agent. In the future, more large randomized

controlled trials are needed to investigate the efficacy of different next-step therapies for IBD patients who do not respond to anti-TNF.

FOOTNOTES

Author contributions: Wang LF and Zhang Y contributed to the study conception and design; Wang LF and Chen PR reviewed the literature and wrote the manuscript; He SK and Duan SH critically reviewed the manuscript; and all authors approved the final version of the manuscript.

Conflict-of-interest statement: Authors declare no conflict of interests for this article.

Open-Access: This article is an open-access article that was selected by an in-house editor and fully peer-reviewed by external reviewers. It is distributed in accordance with the Creative Commons Attribution NonCommercial (CC BY-NC 4.0) license, which permits others to distribute, remix, adapt, build upon this work non-commercially, and license their derivative works on different terms, provided the original work is properly cited and the use is non-commercial. See: https://creativecommons.org/Licenses/by-nc/4.0/

Country/Territory of origin: China

ORCID number: Liang-Fang Wang 0000-0003-1239-6818; Ping-Run Chen 0000-0002-5915-2530; Si-Ke He 0000-0003-3737-7568; Shi-Hao Duan 0009-0004-6197-5896; Yan Zhang 0000-0003-4854-1423.

S-Editor: Yan JP
L-Editor: A
P-Editor: Yan JP

REFERENCES

1 **Ng SC**, Kaplan GG, Tang W, Banerjee R, Adigopula B, Underwood FE, Tanyingoh D, Wei SC, Lin WC, Lin HH, Li J, Bell S, Niewiadomski O, Kamm MA, Zeng Z, Chen M, Hu P, Ong D, Ooi CJ, Ling KL, Miao Y, Miao J, Janaka de Silva H, Niriella M, Aniwan S, Limsrivilai J, Pisespongsa P, Wu K, Yang H, Ng KK, Yu HH, Wang Y, Ouyang Q, Abdullah M, Simadibrata M, Gunawan J, Hilmi I, Lee Goh K, Cao Q, Sheng H, Ong-Go A, Chong VH, Ching JYL, Wu JCY, Chan FKL, Sung JJY. Population Density and Risk of Inflammatory Bowel Disease: A Prospective Population-Based Study in 13 Countries or Regions in Asia-Pacific. *Am J Gastroenterol* 2019; **114**: 107-115 [PMID: 30177785 DOI: 10.1038/s41395-018-0233-2]

2 **Park J**, Cheon JH. Incidence and Prevalence of Inflammatory Bowel Disease across Asia. *Yonsei Med J* 2021; **62**: 99-108 [PMID: 33527789 DOI: 10.3349/ymj.2021.62.2.99]

3 **Mak WY**, Zhao M, Ng SC, Burisch J. The epidemiology of inflammatory bowel disease: East meets west. *J Gastroenterol Hepatol* 2020; **35**: 380-389 [PMID: 31596960 DOI: 10.1111/jgh.14872]

4 **Molodecky NA**, Soon IS, Rabi DM, Ghali WA, Ferris M, Chernoff G, Benchimol EI, Panaccione R, Ghosh S, Barkema HW, Kaplan GG. Increasing incidence and prevalence of the inflammatory bowel diseases with time, based on systematic review. *Gastroenterology* 2012; **142**: 46-54.e42; quiz e30 [PMID: 22001864 DOI: 10.1053/j.gastro.2011.10.001]

5 **Ng SC**, Shi HY, Hamidi N, Underwood FE, Tang W, Benchimol EI, Panaccione R, Ghosh S, Wu JCY, Chan FKL, Sung JJY, Kaplan GG. Worldwide incidence and prevalence of inflammatory bowel disease in the 21st century: a systematic review of population-based studies. *Lancet* 2017; **390**: 2769-2778 [PMID: 29050646 DOI: 10.1016/S0140-6736(17)32448-0]

6 **D'Haens GR**, van Deventer S. 25 years of anti-TNF treatment for inflammatory bowel disease: lessons from the past and a look to the future. *Gut* 2021; **70**: 1396-1405 [PMID: 33431575 DOI: 10.1136/gutjnl-2019-320022]

7 **Rutgeerts P**, Sandborn WJ, Feagan BG, Reinisch W, Olson A, Johanns J, Travers S, Rachmilewitz D, Hanauer SB, Lichtenstein GR, de Villiers WJ, Present D, Sands BE, Colombel JF. Infliximab for induction and maintenance therapy for ulcerative colitis. *N Engl J Med* 2005; **353**: 2462-2476 [PMID: 16339095 DOI: 10.1056/NEJMoa050516]

8 **Nielsen OH**, Ainsworth MA. Tumor necrosis factor inhibitors for inflammatory bowel disease. *N Engl J Med* 2013; **369**: 754-762 [PMID: 23964937 DOI: 10.1056/NEJMct1209614]

9 **Feuerstein JD**, Nguyen GC, Kupfer SS, Falck-Ytter Y, Singh S; American Gastroenterological Association Institute Clinical Guidelines Committee. American Gastroenterological Association Institute Guideline on Therapeutic Drug Monitoring in Inflammatory Bowel Disease. *Gastroenterology* 2017; **153**: 827-834 [PMID: 28780013 DOI: 10.1053/j.gastro.2017.07.032]

10 **Ben-Horin S**, Kopylov U, Chowers Y. Optimizing anti-TNF treatments in inflammatory bowel disease. *Autoimmun Rev* 2014; **13**: 24-30 [PMID: 23792214 DOI: 10.1016/j.autrev.2013.06.002]

11 **Papamichael K**, Gils A, Rutgeerts P, Levesque BG, Vermeire S, Sandborn WJ, Vande Casteele N. Role for therapeutic drug monitoring during induction therapy with TNF antagonists in IBD: evolution in the definition and management of primary nonresponse. *Inflamm Bowel Dis* 2015; **21**: 182-197 [PMID: 25222660 DOI: 10.1097/MIB.0000000000000202]

12 **Hanauer SB**, Feagan BG, Lichtenstein GR, Mayer LF, Schreiber S, Colombel JF, Rachmilewitz D, Wolf DC, Olson A, Bao W, Rutgeerts P; ACCENT I Study Group. Maintenance infliximab for Crohn's disease: the ACCENT I randomised trial. *Lancet* 2002; **359**: 1541-1549 [PMID: 12047962 DOI: 10.1016/s0140-6736(02)08512-4]

13 **Beaugerie L**, Rahier JF, Kirchgesner J. Predicting, Preventing, and Managing Treatment-Related Complications in Patients With Inflammatory Bowel Diseases. *Clin Gastroenterol Hepatol* 2020; **18**: 1324-1335.e2 [PMID: 32059920 DOI: 10.1016/j.cgh.2020.02.009]

14 **Cheon JH**. Understanding the complications of anti-tumor necrosis factor therapy in East Asian patients with inflammatory bowel disease. *J Gastroenterol Hepatol* 2017; **32**: 769-777 [PMID: 27723166 DOI: 10.1111/jgh.13612]

15 **Targownik LE**, Benchimol EI, Witt J, Bernstein CN, Singh H, Lix L, Tennakoon A, Zubieta AA, Coward S, Jones J, Kuenzig E, Murthy SK, Nguyen GC, Peña-Sánchez JN, Kaplan G. The Effect of Initiation of Anti-TNF Therapy on the Subsequent Direct Health Care Costs of Inflammatory Bowel Disease. *Inflamm Bowel Dis* 2019; **25**: 1718-1728 [PMID: 31211836 DOI: 10.1093/ibd/izz063]

16 **Kennedy NA**, Heap GA, Green HD, Hamilton B, Bewshea C, Walker GJ, Thomas A, Nice R, Perry MH, Bouri S, Chanchlani N, Heerasing NM, Hendy P, Lin S, Gaya DR, Cummings JRF, Selinger CP, Lees CW, Hart AL, Parkes M, Sebastian S, Mansfield JC, Irving PM, Lindsay J, Russell RK, McDonald TJ, McGovern D, Goodhand JR, Ahmad T; UK Inflammatory Bowel Disease Pharmacogenetics Study Group. Predictors of anti-TNF treatment failure in anti-TNF-naive patients with active luminal Crohn's disease: a prospective, multicentre, cohort study. *Lancet Gastroenterol Hepatol* 2019; **4**: 341-353 [PMID: 30824404 DOI: 10.1016/S2468-1253(19)30012-3]

17 **Ding NS**, Hart A, De Cruz P. Systematic review: predicting and optimising response to anti-TNF therapy in Crohn's disease - algorithm for practical management. *Aliment Pharmacol Ther* 2016; **43**: 30-51 [PMID: 26515897 DOI: 10.1111/apt.13445]

18 **Wong U**, Cross RK. Primary and secondary nonresponse to infliximab: mechanisms and countermeasures. *Expert Opin Drug Metab Toxicol* 2017; **13**: 1039-1046 [PMID: 28876147 DOI: 10.1080/17425255.2017.1377180]

19 **Yanai H**, Hanauer SB. Assessing response and loss of response to biological therapies in IBD. *Am J Gastroenterol* 2011; **106**: 685-698 [PMID: 21427713 DOI: 10.1038/ajg.2011.103]

20 **Ford AC**, Sandborn WJ, Khan KJ, Hanauer SB, Talley NJ, Moayyedi P. Efficacy of biological therapies in inflammatory bowel disease: systematic review and meta-analysis. *Am J Gastroenterol* 2011; **106**: 644-659, quiz 660 [PMID: 21407183 DOI: 10.1038/ajg.2011.73]

21 **Sprakes MB**, Ford AC, Warren L, Greer D, Hamlin J. Efficacy, tolerability, and predictors of response to infliximab therapy for Crohn's disease: a large single centre experience. *J Crohns Colitis* 2012; **6**: 143-153 [PMID: 22325168 DOI: 10.1016/j.crohns.2011.07.011]

22 **Marsal J**, Barreiro-de Acosta M, Blumenstein I, Cappello M, Bazin T, Sebastian S. Management of Non-response and Loss of Response to Anti-tumor Necrosis Factor Therapy in Inflammatory Bowel Disease. *Front Med (Lausanne)* 2022; **9**: 897936 [PMID: 35783628 DOI: 10.3389/fmed.2022.897936]

23 **Allez M**, Karmiris K, Louis E, Van Assche G, Ben-Horin S, Klein A, Van der Woude J, Baert F, Eliakim R, Katsanos K, Brynskov J, Steinwurz F, Danese S, Vermeire S, Teillaud JL, Lémann M, Chowers Y. Report of the ECCO pathogenesis workshop on anti-TNF therapy failures in inflammatory bowel diseases: definitions, frequency and pharmacological aspects. *J Crohns Colitis* 2010; **4**: 355-366 [PMID: 21122530 DOI: 10.1016/j.crohns.2010.04.004]

24 **Schnitzler F**, Fidder H, Ferrante M, Noman M, Arijs I, Van Assche G, Hoffman I, Van Steen K, Vermeire S, Rutgeerts P. Long-term outcome of treatment with infliximab in 614 patients with Crohn's disease: results from a single-centre cohort. *Gut* 2009; **58**: 492-500 [PMID: 18832518 DOI: 10.1136/gut.2008.155812]

25 **Zhang QW**, Shen J, Zheng Q, Ran ZH. Loss of response to scheduled infliximab therapy for Crohn's disease in adults: A systematic review and meta-analysis. *J Dig Dis* 2019; **20**: 65-72 [PMID: 30582302 DOI: 10.1111/1751-2980.12698]

26 **Qiu Y**, Chen BL, Mao R, Zhang SH, He Y, Zeng ZR, Ben-Horin S, Chen MH. Systematic review with meta-analysis: loss of response and requirement of anti-TNFα dose intensification in Crohn's disease. *J Gastroenterol* 2017; **52**: 535-554 [PMID: 28275925 DOI: 10.1007/s00535-017-1324-3]

27 **Macaluso FS**, Fries W, Privitera AC, Cappello M, Siringo S, Inserra G, Magnano A, Di Mitri R, Mocciaro F, Belluardo N, Scarpulla G, Magrì G, Trovatello A, Carroccio A, Genova S, Bertolami C, Vassallo R, Romano C, Citrano M, Accomando S, Ventimiglia M, Renna S, Orlando R, Rizzuto G, Porcari S, Ferracane C, Cottone M, Orlando A; Sicilian Network for Inflammatory Bowel Diseases [SN-IBD]. A Propensity Score-matched Comparison of Infliximab and Adalimumab in Tumour Necrosis Factor-α Inhibitor-naïve and Non-naïve Patients With Crohn's Disease: Real-Life Data From the Sicilian Network for Inflammatory Bowel Disease. *J Crohns Colitis* 2019; **13**: 209-217 [PMID: 30295785 DOI: 10.1093/ecco-jcc/jjy156]

28 **Sandborn WJ**, Melmed GY, McGovern DP, Loftus EV Jr, Choi JM, Cho JH, Abraham B, Gutierrez A, Lichtenstein G, Lee SD, Randall CW, Schwartz DA, Regueiro M, Siegel CA, Spearman M, Kosutic G, Pierre-Louis B, Coarse J, Schreiber S. Clinical and demographic characteristics predictive of treatment outcomes for certolizumab pegol in moderate to severe Crohn's disease: analyses from the 7-year PRECiSE 3 study. *Aliment Pharmacol Ther* 2015; **42**: 330-342 [PMID: 26031921 DOI: 10.1111/apt.13251]

29 **Choi CH**, Song ID, Kim YH, Koo JS, Kim YS, Kim JS, Kim N, Kim ES, Kim JH, Kim JW, Kim TO, Kim HS, Kim HJ, Park YS, Park DI, Park SJ, Song HJ, Shin SJ, Yang SK, Ye BD, Lee KM, Lee BI, Lee SY, Lee CK, Im JP, Jang BI, Jeon TJ, Cho YK, Chang SK, Jeon SR, Jung SA, Jeen YT, Cha JM, Han DS, Kim WH; IBD Study Group of the Korean Association for the Study of the Intestinal Diseases. Efficacy and Safety of Infliximab Therapy and Predictors of Response in Korean Patients with Crohn's Disease: A Nationwide, Multicenter Study. *Yonsei Med J* 2016; **57**: 1376-1385 [PMID: 27593865 DOI: 10.3349/ymj.2016.57.6.1376]

30 **Arias MT**, Vande Casteele N, Vermeire S, de Buck van Overstraeten A, Billiet T, Baert F, Wolthuis A, Van Assche G, Noman M, Hoffman I, D'Hoore A, Gils A, Rutgeerts P, Ferrante M. A panel to predict long-term outcome of infliximab therapy for patients with ulcerative colitis. *Clin Gastroenterol Hepatol* 2015; **13**: 531-538 [PMID: 25117777 DOI: 10.1016/j.cgh.2014.07.055]

31 **Taxonera C**, Rodríguez C, Bertoletti F, Menchén L, Arribas J, Sierra M, Arias L, Martínez-Montiel P, Juan A, Iglesias E, Algaba A, Manceñido N, Rivero M, Barreiro-de Acosta M, López-Serrano P, Argüelles-Arias F, Gutierrez A, Busquets D, Gisbert JP, Olivares D, Calvo M, Alba C; Collaborators. Clinical Outcomes of Golimumab as First, Second or Third Anti-TNF Agent in Patients with Moderate-to-Severe Ulcerative Colitis. *Inflamm Bowel Dis* 2017; **23**: 1394-1402 [PMID: 28671873 DOI: 10.1097/MIB.0000000000001144]

32 **Bosca-Watts MM**, Cortes X, Iborra M, Huguet JM, Sempere L, Garcia G, Gil R, Garcia M, Muñoz M, Almela P, Maroto N, Paredes JM. Short-term effectiveness of golimumab for ulcerative colitis: Observational multicenter study. *World J Gastroenterol* 2016; **22**: 10432-10439 [PMID: 28058024 DOI: 10.3748/wjg.v22.i47.10432]

33 **Narula N**, Kainz S, Petritsch W, Haas T, Feichtenschlager T, Novacek G, Eser A, Vogelsang H, Reinisch W, Papay P. The efficacy and safety of either infliximab or adalimumab in 362 patients with anti-TNF-α naïve Crohn's disease. *Aliment Pharmacol Ther* 2016; **44**: 170-180 [PMID: 27226407 DOI: 10.1111/apt.13671]

34 **Billiet T**, Papamichael K, de Bruyn M, Verstockt B, Cleynen I, Princen F, Singh S, Ferrante M, Van Assche G, Vermeire S. A Matrix-based Model Predicts Primary Response to Infliximab in Crohn's Disease. *J Crohns Colitis* 2015; **9**: 1120-1126 [PMID: 26351386 DOI: 10.1093/ecco-jcc/jjv156]

35 **Stein AC**, Rubin DT, Hanauer SB, Cohen RD. Incidence and predictors of clinical response, re-induction dose, and maintenance dose escalation with certolizumab pegol in Crohn's disease. *Inflamm Bowel Dis* 2014; **20**: 1722-1728 [PMID: 25171509 DOI: 10.1097/MIB.0000000000000146]

36 **Sandborn WJ**, Feagan BG, Marano C, Zhang H, Strauss R, Johanns J, Adedokun OJ, Guzzo C, Colombel JF, Reinisch W, Gibson PR, Collins J, Järnerot G, Hibi T, Rutgeerts P; PURSUIT-SC Study Group. Subcutaneous golimumab induces clinical response and remission in patients

with moderate-to-severe ulcerative colitis. *Gastroenterology* 2014; **146**: 85-95; quiz e14 [PMID: 23735746 DOI: 10.1053/j.gastro.2013.05.048]

37 **Gonzalez-Lama Y**, Fernandez-Blanco I, Lopez-SanRoman A, Taxonera C, Casis B, Tabernero S, Bermejo F, Martinez-Silva F, Mendoza JL, Martinez-Montiel P, Carneros JA, Sanchez F, Maté J, Gisbert JP; Group for the Study of Inflammatory Bowel Diseases from Madrid. Open-label infliximab therapy in ulcerative colitis: a multicenter survey of results and predictors of response. *Hepatogastroenterology* 2008; **55**: 1609-1614 [PMID: 19102352]

38 **Piovani D**, Danese S, Peyrin-Biroulet L, Nikolopoulos GK, Lytras T, Bonovas S. Environmental Risk Factors for Inflammatory Bowel Diseases: An Umbrella Review of Meta-analyses. *Gastroenterology* 2019; **157**: 647-659.e4 [PMID: 31014995 DOI: 10.1053/j.gastro.2019.04.016]

39 **Zorzi F**, Zuzzi S, Onali S, Calabrese E, Condino G, Petruzziello C, Ascolani M, Pallone F, Biancone L. Efficacy and safety of infliximab and adalimumab in Crohn's disease: a single centre study. *Aliment Pharmacol Ther* 2012; **35**: 1397-1407 [PMID: 22519466 DOI: 10.1111/j.1365-2036.2012.05100.x]

40 **Lee S**, Kuenzig ME, Ricciuto A, Zhang Z, Shim HH, Panaccione R, Kaplan GG, Seow CH. Smoking May Reduce the Effectiveness of Anti-TNF Therapies to Induce Clinical Response and Remission in Crohn's Disease: A Systematic Review and Meta-analysis. *J Crohns Colitis* 2021; **15**: 74-87 [PMID: 32621742 DOI: 10.1093/ecco-jcc/jjaa139]

41 **Inamdar S**, Volfson A, Rosen L, Sunday S, Katz S, Sultan K. Smoking and early infliximab response in Crohn's disease: a meta-analysis. *J Crohns Colitis* 2015; **9**: 140-146 [PMID: 25518060 DOI: 10.1093/ecco-jcc/jju018]

42 **Ribaldone DG**, Dileo I, Pellicano R, Resegotti A, Fagoonee S, Vernero M, Saracco G, Astegiano M. Severe ulcerative colitis: predictors of response and algorithm proposal for rescue therapy. *Ir J Med Sci* 2018; **187**: 385-392 [PMID: 28756540 DOI: 10.1007/s11845-017-1666-0]

43 **Ferrante M**, Vermeire S, Fidder H, Schnitzler F, Noman M, Van Assche G, De Hertogh G, Hoffman I, D'Hoore A, Van Steen K, Geboes K, Penninckx F, Rutgeerts P. Long-term outcome after infliximab for refractory ulcerative colitis. *J Crohns Colitis* 2008; **2**: 219-225 [PMID: 21172214 DOI: 10.1016/j.crohns.2008.03.004]

44 **Ananthakrishnan AN**, Kaplan GG, Bernstein CN, Burke KE, Lochhead PJ, Sasson AN, Agrawal M, Tiong JHT, Steinberg J, Kruis W, Steinwurz F, Ahuja V, Ng SC, Rubin DT, Colombel JF, Gearry R; International Organization for Study of Inflammatory Bowel Diseases. Lifestyle, behaviour, and environmental modification for the management of patients with inflammatory bowel diseases: an International Organization for Study of Inflammatory Bowel Diseases consensus. *Lancet Gastroenterol Hepatol* 2022; **7**: 666-678 [PMID: 35487235 DOI: 10.1016/S2468-1253(22)00021-8]

45 **Jeuring SF**, van den Heuvel TR, Liu LY, Zeegers MP, Hameeteman WH, Romberg-Camps MJ, Oostenbrug LE, Masclee AA, Jonkers DM, Pierik MJ. Improvements in the Long-Term Outcome of Crohn's Disease Over the Past Two Decades and the Relation to Changes in Medical Management: Results from the Population-Based IBDSL Cohort. *Am J Gastroenterol* 2017; **112**: 325-336 [PMID: 27922024 DOI: 10.1038/ajg.2016.524]

46 **Rungoe C**, Langholz E, Andersson M, Basit S, Nielsen NM, Wohlfahrt J, Jess T. Changes in medical treatment and surgery rates in inflammatory bowel disease: a nationwide cohort study 1979-2011. *Gut* 2014; **63**: 1607-1616 [PMID: 24056767 DOI: 10.1136/gutjnl-2013-305607]

47 **Ramadas AV**, Gunesh S, Thomas GA, Williams GT, Hawthorne AB. Natural history of Crohn's disease in a population-based cohort from Cardiff (1986-2003): a study of changes in medical treatment and surgical resection rates. *Gut* 2010; **59**: 1200-1206 [PMID: 20650924 DOI: 10.1136/gut.2009.202101]

48 **Vermeire S**, Louis E, Carbonez A, Van Assche G, Noman M, Belaiche J, De Vos M, Van Gossum A, Pescatore P, Fiasse R, Pelckmans P, Reynaert H, D'Haens G, Rutgeerts P; Belgian Group of Infliximab Expanded Access Program in Crohn's Disease. Demographic and clinical parameters influencing the short-term outcome of anti-tumor necrosis factor (infliximab) treatment in Crohn's disease. *Am J Gastroenterol* 2002; **97**: 2357-2363 [PMID: 12358256 DOI: 10.1111/j.1572-0241.2002.05991.x]

49 **Panaccione R**, Löfberg R, Rutgeerts P, Sandborn WJ, Schreiber S, Berg S, Maa JF, Petersson J, Robinson AM, Colombel JF. Efficacy and Safety of Adalimumab by Disease Duration: Analysis of Pooled Data From Crohn's Disease Studies. *J Crohns Colitis* 2019; **13**: 725-734 [PMID: 30753371 DOI: 10.1093/ecco-jcc/jjy223]

50 **Mantzaris GJ**, Zeglinas C, Theodoropoulou A, Koutroubakis I, Orfanoudaki E, Katsanos K, Christodoulou D, Michalopoulos G, Tzouvala M, Moschovis D, Michopoulos S, Zampeli E, Soufleris K, Ilias A, Chatzievangelinou C, Kyriakakis A, Antachopoulou K, Karmiris K. The Effect of Early *vs* Delayed Initiation of Adalimumab on Remission Rates in Patients With Crohn's Disease With Poor Prognostic Factors: The MODIFY Study. *Crohns Colitis 360* 2021; **3**: otab064 [PMID: 36777275 DOI: 10.1093/crocol/otab064]

51 **Hamdeh S**, Aziz M, Altayar O, Olyaee M, Murad MH, Hanauer SB. Early *vs* Late Use of Anti-TNFa Therapy in Adult Patients With Crohn Disease: A Systematic Review and Meta-Analysis. *Inflamm Bowel Dis* 2020; **26**: 1808-1818 [PMID: 32064534 DOI: 10.1093/ibd/izaa031]

52 **Beswick L**, Rosella O, Rosella G, Headon B, Sparrow MP, Gibson PR, van Langenberg DR. Exploration of Predictive Biomarkers of Early Infliximab Response in Acute Severe Colitis: A Prospective Pilot Study. *J Crohns Colitis* 2018; **12**: 289-297 [PMID: 29121178 DOI: 10.1093/ecco-jcc/jjx146]

53 **Iborra M**, Pérez-Gisbert J, Bosca-Watts MM, López-García A, García-Sánchez V, López-Sanromán A, Hinojosa E, Márquez L, García-López S, Chaparro M, Aceituno M, Calafat M, Guardiola J, Belloc B, Ber Y, Bujanda L, Beltrán B, Rodríguez-Gutiérrez C, Barrio J, Cabriada JL, Rivero M, Camargo R, van Domselaar M, Villoria A, Schuterman HS, Hervás D, Nos P; Spanish Working Group on Crohn's Disease and Ulcerative Colitis (GETECCU). Effectiveness of adalimumab for the treatment of ulcerative colitis in clinical practice: comparison between anti-tumour necrosis factor-naïve and non-naïve patients. *J Gastroenterol* 2017; **52**: 788-799 [PMID: 27722996 DOI: 10.1007/s00535-016-1274-1]

54 **Gisbert JP**, Chaparro M. Predictors of Primary Response to Biologic Treatment [Anti-TNF, Vedolizumab, and Ustekinumab] in Patients With Inflammatory Bowel Disease: From Basic Science to Clinical Practice. *J Crohns Colitis* 2020; **14**: 694-709 [PMID: 31777929 DOI: 10.1093/ecco-jcc/jjz195]

55 **Vande Casteele N**, Gils A. Pharmacokinetics of anti-TNF monoclonal antibodies in inflammatory bowel disease: Adding value to current practice. *J Clin Pharmacol* 2015; **55** Suppl 3: S39-S50 [PMID: 25707962 DOI: 10.1002/jcph.374]

56 **Fine S**, Papamichael K, Cheifetz AS. Etiology and Management of Lack or Loss of Response to Anti-Tumor Necrosis Factor Therapy in Patients With Inflammatory Bowel Disease. *Gastroenterol Hepatol (N Y)* 2019; **15**: 656-665 [PMID: 31892912]

57 **Buhl S**, Dorn-Rasmussen M, Brynskov J, Ainsworth MA, Bendtzen K, Klausen PH, Bolstad N, Warren DJ, Steenholdt C. Therapeutic thresholds and mechanisms for primary non-response to infliximab in inflammatory bowel disease. *Scand J Gastroenterol* 2020; **55**: 884-890 [PMID: 32631131 DOI: 10.1080/00365521.2020.1786852]

58 **Colombel JF**, Sandborn WJ, Allez M, Dupas JL, Dewit O, D'Haens G, Bouhnik Y, Parker G, Pierre-Louis B, Hébuterne X. Association

between plasma concentrations of certolizumab pegol and endoscopic outcomes of patients with Crohn's disease. *Clin Gastroenterol Hepatol* 2014; **12**: 423-31.e1 [PMID: 24184736 DOI: 10.1016/j.cgh.2013.10.025]

59 **Brandse JF**, Mathôt RA, van der Kleij D, Rispens T, Ashruf Y, Jansen JM, Rietdijk S, Löwenberg M, Ponsioen CY, Singh S, van den Brink GR, D'Haens GR. Pharmacokinetic Features and Presence of Antidrug Antibodies Associate With Response to Infliximab Induction Therapy in Patients With Moderate to Severe Ulcerative Colitis. *Clin Gastroenterol Hepatol* 2016; **14**: 251-8.e1 [PMID: 26545802 DOI: 10.1016/j.cgh.2015.10.029]

60 **Assa A**, Hartman C, Weiss B, Broide E, Rosenbach Y, Zevit N, Bujanover Y, Shamir R. Long-term outcome of tumor necrosis factor alpha antagonist's treatment in pediatric Crohn's disease. *J Crohns Colitis* 2013; **7**: 369-376 [PMID: 22483567 DOI: 10.1016/j.crohns.2012.03.006]

61 **Kurnool S**, Nguyen NH, Proudfoot J, Dulai PS, Boland BS, Vande Casteele N, Evans E, Grunvald EL, Zarrinpar A, Sandborn WJ, Singh S. High body mass index is associated with increased risk of treatment failure and surgery in biologic-treated patients with ulcerative colitis. *Aliment Pharmacol Ther* 2018; **47**: 1472-1479 [PMID: 29665045 DOI: 10.1111/apt.14665]

62 **Karagiannides I**, Pothoulakis C. Obesity, innate immunity and gut inflammation. *Curr Opin Gastroenterol* 2007; **23**: 661-666 [PMID: 17906444 DOI: 10.1097/MOG.0b013e3282c8c8d3]

63 **Dotan I**, Ron Y, Yanai H, Becker S, Fishman S, Yahav L, Ben Yehoyada M, Mould DR. Patient factors that increase infliximab clearance and shorten half-life in inflammatory bowel disease: a population pharmacokinetic study. *Inflamm Bowel Dis* 2014; **20**: 2247-2259 [PMID: 25358062 DOI: 10.1097/MIB.0000000000000212]

64 **Fasanmade AA**, Adedokun OJ, Blank M, Zhou H, Davis HM. Pharmacokinetic properties of infliximab in children and adults with Crohn's disease: a retrospective analysis of data from 2 phase III clinical trials. *Clin Ther* 2011; **33**: 946-964 [PMID: 21741088 DOI: 10.1016/j.clinthera.2011.06.002]

65 **Morita Y**, Bamba S, Takahashi K, Imaeda H, Nishida A, Inatomi O, Sasaki M, Tsujikawa T, Sugimoto M, Andoh A. Prediction of clinical and endoscopic responses to anti-tumor necrosis factor-α antibodies in ulcerative colitis. *Scand J Gastroenterol* 2016; **51**: 934-941 [PMID: 26888161 DOI: 10.3109/00365521.2016.1144781]

66 **Fasanmade AA**, Adedokun OJ, Olson A, Strauss R, Davis HM. Serum albumin concentration: a predictive factor of infliximab pharmacokinetics and clinical response in patients with ulcerative colitis. *Int J Clin Pharmacol Ther* 2010; **48**: 297-308 [PMID: 20420786 DOI: 10.5414/cpp48297]

67 **Bek S**, Nielsen JV, Bojesen AB, Franke A, Bank S, Vogel U, Andersen V. Systematic review: genetic biomarkers associated with anti-TNF treatment response in inflammatory bowel diseases. *Aliment Pharmacol Ther* 2016; **44**: 554-567 [PMID: 27417569 DOI: 10.1111/apt.13736]

68 **Curci D**, Lucafò M, Cifù A, Fabris M, Bramuzzo M, Martelossi S, Franca R, Decorti G, Stocco G. Pharmacogenetic variants of infliximab response in young patients with inflammatory bowel disease. *Clin Transl Sci* 2021; **14**: 2184-2192 [PMID: 34145770 DOI: 10.1111/cts.13075]

69 **Kimura K**, Yoshida A, Katagiri F, Takayanagi R, Yamada Y. Prediction of treatment failure during infliximab induction therapy in inflammatory bowel disease patients based on pharmacokinetic and pharmacodynamic modeling. *Eur J Pharm Sci* 2020; **150**: 105317 [PMID: 32205229 DOI: 10.1016/j.ejps.2020.105317]

70 **Yoshida A**, Kimura K, Morizane T, Ueno F. Predictor of primary response to antitumor necrosis factor-α therapy for inflammatory bowel disease: a single-center observational study. *Eur J Gastroenterol Hepatol* 2022; **34**: 640-645 [PMID: 35352693 DOI: 10.1097/MEG.0000000000002372]

71 **Lee KM**, Jeen YT, Cho JY, Lee CK, Koo JS, Park DI, Im JP, Park SJ, Kim YS, Kim TO, Lee SH, Jang BI, Kim JW, Park YS, Kim ES, Choi CH, Kim HJ; IBD study Group of Korean Association for the Study of Intestinal Diseases. Efficacy, safety, and predictors of response to infliximab therapy for ulcerative colitis: a Korean multicenter retrospective study. *J Gastroenterol Hepatol* 2013; **28**: 1829-1833 [PMID: 23829336 DOI: 10.1111/jgh.12324]

72 **Schreiber S**, Rutgeerts P, Fedorak RN, Khaliq-Kareemi M, Kamm MA, Boivin M, Bernstein CN, Staun M, Thomsen OØ, Innes A; CDP870 Crohn's Disease Study Group. A randomized, placebo-controlled trial of certolizumab pegol (CDP870) for treatment of Crohn's disease. *Gastroenterology* 2005; **129**: 807-818 [PMID: 16143120 DOI: 10.1053/j.gastro.2005.06.064]

73 **Magro F**, Rodrigues-Pinto E, Santos-Antunes J, Vilas-Boas F, Lopes S, Nunes A, Camila-Dias C, Macedo G. High C-reactive protein in Crohn's disease patients predicts nonresponse to infliximab treatment. *J Crohns Colitis* 2014; **8**: 129-136 [PMID: 23932786 DOI: 10.1016/j.crohns.2013.07.005]

74 **Kopylov U**, Seidman E. Predicting durable response or resistance to antitumor necrosis factor therapy in inflammatory bowel disease. *Therap Adv Gastroenterol* 2016; **9**: 513-526 [PMID: 27366220 DOI: 10.1177/1756283X16638833]

75 **Jürgens M**, Laubender RP, Hartl F, Weidinger M, Seiderer J, Wagner J, Wetzke M, Beigel F, Pfennig S, Stallhofer J, Schnitzler F, Tillack C, Lohse P, Göke B, Glas J, Ochsenkühn T, Brand S. Disease activity, ANCA, and IL23R genotype status determine early response to infliximab in patients with ulcerative colitis. *Am J Gastroenterol* 2010; **105**: 1811-1819 [PMID: 20197757 DOI: 10.1038/ajg.2010.95]

76 **Taylor KD**, Plevy SE, Yang H, Landers CJ, Barry MJ, Rotter JI, Targan SR. ANCA pattern and LTA haplotype relationship to clinical responses to anti-TNF antibody treatment in Crohn's disease. *Gastroenterology* 2001; **120**: 1347-1355 [PMID: 11313304 DOI: 10.1053/gast.2001.23966]

77 **Nguyen DL**, Nguyen ET, Bechtold ML. pANCA positivity predicts lower clinical response to infliximab therapy among patients with IBD. *South Med J* 2015; **108**: 139-143 [PMID: 25772045 DOI: 10.14423/SMJ.0000000000000253]

78 **Ferrante M**, Vermeire S, Katsanos KH, Noman M, Van Assche G, Schnitzler F, Arijs I, De Hertogh G, Hoffman I, Geboes JK, Rutgeerts P. Predictors of early response to infliximab in patients with ulcerative colitis. *Inflamm Bowel Dis* 2007; **13**: 123-128 [PMID: 17206703 DOI: 10.1002/ibd.20054]

79 **Beltrán B**, Iborra M, Sáez-González E, Marqués-Miñana MR, Moret I, Cerrillo E, Tortosa L, Bastida G, Hinojosa J, Poveda-Andrés JL, Nos P. Fecal Calprotectin Pretreatment and Induction Infliximab Levels for Prediction of Primary Nonresponse to Infliximab Therapy in Crohn's Disease. *Dig Dis* 2019; **37**: 108-115 [PMID: 30149385 DOI: 10.1159/000492626]

80 **Pavlidis P**, Gulati S, Dubois P, Chung-Faye G, Sherwood R, Bjarnason I, Hayee B. Early change in faecal calprotectin predicts primary non-response to anti-TNFα therapy in Crohn's disease. *Scand J Gastroenterol* 2016; **51**: 1447-1452 [PMID: 27400728 DOI: 10.1080/00365521.2016.1205128]

81 **Dahlén R**, Magnusson MK, Bajor A, Lasson A, Ung KA, Strid H, Öhman L. Global mucosal and serum cytokine profile in patients with ulcerative colitis undergoing anti-TNF therapy. *Scand J Gastroenterol* 2015; **50**: 1118-1126 [PMID: 25877762 DOI: 10.3109/00365521.2015.1031167]

82 **Angelison L**, Almer S, Eriksson A, Karling P, Fagerberg U, Halfvarson J, Thörn M, Björk J, Hindorf U, Löfberg R, Bajor A, Hjortswang H, Hammarlund P, Grip O, Torp J, Marsal J, Hertervig E; Swedish Organization for the Study of Inflammatory Bowel diseases (SOIBD). Long-

term outcome of infliximab treatment in chronic active ulcerative colitis: a Swedish multicentre study of 250 patients. *Aliment Pharmacol Ther* 2017; **45**: 519-532 [PMID: 28025840 DOI: 10.1111/apt.13893]

83 **Rubio MG**, Amo-Mensah K, Gray JM, Nguyen VQ, Nakat S, Grider D, Love K, Boone JH, Sorrentino D. Fecal lactoferrin accurately reflects mucosal inflammation in inflammatory bowel disease. *World J Gastrointest Pathophysiol* 2019; **10**: 54-63 [PMID: 31911845 DOI: 10.4291/wjgp.v10.i5.54]

84 **Sorrentino D**, Nguyen VQ, Love K. Fecal Lactoferrin Predicts Primary Nonresponse to Biologic Agents in Inflammatory Bowel Disease. *Dig Dis* 2021; **39**: 626-633 [PMID: 33631768 DOI: 10.1159/000515432]

85 **López-Hernández R**, Valdés M, Campillo JA, Martínez-Garcia P, Salama H, Salgado G, Boix F, Moya-Quiles MR, Minguela A, Sánchez-Torres A, Miras M, Garcia A, Carballo F, Álvarez-López MR, Muro M. Genetic polymorphisms of tumour necrosis factor alpha (TNF-α) promoter gene and response to TNF-α inhibitors in Spanish patients with inflammatory bowel disease. *Int J Immunogenet* 2014; **41**: 63-68 [PMID: 23590430 DOI: 10.1111/iji.12059]

86 **Steenholdt C**, Enevold C, Ainsworth MA, Brynskov J, Thomsen OØ, Bendtzen K. Genetic polymorphisms of tumour necrosis factor receptor superfamily 1b and fas ligand are associated with clinical efficacy and/or acute severe infusion reactions to infliximab in Crohn's disease. *Aliment Pharmacol Ther* 2012; **36**: 650-659 [PMID: 22860894 DOI: 10.1111/apt.12010]

87 **Matsukura H**, Ikeda S, Yoshimura N, Takazoe M, Muramatsu M. Genetic polymorphisms of tumour necrosis factor receptor superfamily 1A and 1B affect responses to infliximab in Japanese patients with Crohn's disease. *Aliment Pharmacol Ther* 2008; **27**: 765-770 [PMID: 18248655 DOI: 10.1111/j.1365-2036.2008.03630.x]

88 **Medrano LM**, Taxonera C, Márquez A, Barreiro-de Acosta M, Gómez-García M, González-Artacho C, Pérez-Calle JL, Bermejo F, Lopez-Sanromán A, Martín Arranz MD, Gisbert JP, Mendoza JL, Martín J, Urcelay E, Núñez C. Role of TNFRSF1B polymorphisms in the response of Crohn's disease patients to infliximab. *Hum Immunol* 2014; **75**: 71-75 [PMID: 24121042 DOI: 10.1016/j.humimm.2013.09.017]

89 **Franke A**, McGovern DP, Barrett JC, Wang K, Radford-Smith GL, Ahmad T, Lees CW, Balschun T, Lee J, Roberts R, Anderson CA, Bis JC, Bumpstead S, Ellinghaus D, Festen EM, Georges M, Green T, Haritunians T, Jostins L, Latiano A, Mathew CG, Montgomery GW, Prescott NJ, Raychaudhuri S, Rotter JI, Schumm P, Sharma Y, Simms LA, Taylor KD, Whiteman D, Wijmenga C, Baldassano RN, Barclay M, Bayless TM, Brand S, Büning C, Cohen A, Colombel JF, Cottone M, Stronati L, Denson T, De Vos M, D'Inca R, Dubinsky M, Edwards C, Florin T, Franchimont D, Gearry R, Glas J, Van Gossum A, Guthery SL, Halfvarson J, Verspaget HW, Hugot JP, Karban A, Laukens D, Lawrance I, Lemann M, Levine A, Libioulle C, Louis E, Mowat C, Newman W, Panés J, Phillips A, Proctor DD, Regueiro M, Russell R, Rutgeerts P, Sanderson J, Sans M, Seibold F, Steinhart AH, Stokkers PC, Torkvist L, Kullak-Ublick G, Wilson D, Walters T, Targan SR, Brant SR, Rioux JD, D'Amato M, Weersma RK, Kugathasan S, Griffiths AM, Mansfield JC, Vermeire S, Duerr RH, Silverberg MS, Satsangi J, Schreiber S, Cho JH, Annese V, Hakonarson H, Daly MJ, Parkes M. Genome-wide meta-analysis increases to 71 the number of confirmed Crohn's disease susceptibility loci. *Nat Genet* 2010; **42**: 1118-1125 [PMID: 21102463 DOI: 10.1038/ng.717]

90 **Koder S**, Repnik K, Ferkolj I, Pernat C, Skok P, Weersma RK, Potočnik U. Genetic polymorphism in ATG16L1 gene influences the response to adalimumab in Crohn's disease patients. *Pharmacogenomics* 2015; **16**: 191-204 [PMID: 25712183 DOI: 10.2217/pgs.14.172]

91 **Hlavaty T**, Pierik M, Henckaerts L, Ferrante M, Joossens S, van Schuerbeek N, Noman M, Rutgeerts P, Vermeire S. Polymorphisms in apoptosis genes predict response to infliximab therapy in luminal and fistulizing Crohn's disease. *Aliment Pharmacol Ther* 2005; **22**: 613-626 [PMID: 16181301 DOI: 10.1111/j.1365-2036.2005.02635.x]

92 **Hlavaty T**, Ferrante M, Henckaerts L, Pierik M, Rutgeerts P, Vermeire S. Predictive model for the outcome of infliximab therapy in Crohn's disease based on apoptotic pharmacogenetic index and clinical predictors. *Inflamm Bowel Dis* 2007; **13**: 372-379 [PMID: 17206723 DOI: 10.1002/ibd.20024]

93 **Adler J**, Rangwalla SC, Dwamena BA, Higgins PD. The prognostic power of the NOD2 genotype for complicated Crohn's disease: a meta-analysis. *Am J Gastroenterol* 2011; **106**: 699-712 [PMID: 21343918 DOI: 10.1038/ajg.2011.19]

94 **Niess JH**, Klaus J, Stephani J, Pflüger C, Degenkolb N, Spaniol U, Mayer B, Lahr G, von Boyen GB. NOD2 polymorphism predicts response to treatment in Crohn's disease--first steps to a personalized therapy. *Dig Dis Sci* 2012; **57**: 879-886 [PMID: 22147245 DOI: 10.1007/s10620-011-1977-3]

95 **Gutiérrez A**, Scharl M, Sempere L, Holler E, Zapater P, Almenta I, González-Navajas JM, Such J, Wiest R, Rogler G, Francés R. Genetic susceptibility to increased bacterial translocation influences the response to biological therapy in patients with Crohn's disease. *Gut* 2014; **63**: 272-280 [PMID: 23376290 DOI: 10.1136/gutjnl-2012-303557]

96 **Vermeire S**, Louis E, Rutgeerts P, De Vos M, Van Gossum A, Belaiche J, Pescatore P, Fiasse R, Pelckmans P, Vlietinck R, Merlin F, Zouali H, Thomas G, Colombel JF, Hugot JP; Belgian Group of Infliximab Expanded Access Program and Fondation Jean Dausset CEPH, Paris, France. NOD2/CARD15 does not influence response to infliximab in Crohn's disease. *Gastroenterology* 2002; **123**: 106-111 [PMID: 12105838 DOI: 10.1053/gast.2002.34172]

97 **Billiet T**, Cleynen I, Ballet V, Claes K, Princen F, Singh S, Ferrante M, Van Assche G, Gils A, Vermeire S. Evolution of cytokines and inflammatory biomarkers during infliximab induction therapy and the impact of inflammatory burden on primary response in patients with Crohn's disease. *Scand J Gastroenterol* 2017; **52**: 1086-1092 [PMID: 28622097 DOI: 10.1080/00365521.2017.1339825]

98 **Leal RF**, Planell N, Kajekar R, Lozano JJ, Ordás I, Dotti I, Esteller M, Masamunt MC, Parmar H, Ricart E, Panés J, Salas A. Identification of inflammatory mediators in patients with Crohn's disease unresponsive to anti-TNFα therapy. *Gut* 2015; **64**: 233-242 [PMID: 24700437 DOI: 10.1136/gutjnl-2013-306518]

99 **Verstockt S**, Verstockt B, Vermeire S. Oncostatin M as a new diagnostic, prognostic and therapeutic target in inflammatory bowel disease (IBD). *Expert Opin Ther Targets* 2019; **23**: 943-954 [PMID: 31587593 DOI: 10.1080/14728222.2019.1677608]

100 **West NR**, Hegazy AN, Owens BMJ, Bullers SJ, Linggi B, Buonocore S, Coccia M, Görtz D, This S, Stockenhuber K, Pott J, Friedrich M, Ryzhakov G, Baribaud F, Brodmerkel C, Cieluch C, Rahman N, Müller-Newen G, Owens RJ, Kühl AA, Maloy KJ, Plevy SE; Oxford IBD Cohort Investigators, Keshav S, Travis SPL, Powrie F. Oncostatin M drives intestinal inflammation and predicts response to tumor necrosis factor-neutralizing therapy in patients with inflammatory bowel disease. *Nat Med* 2017; **23**: 579-589 [PMID: 28368383 DOI: 10.1038/nm.4307]

101 **Verstockt S**, Verstockt B, Machiels K, Vancamelbeke M, Ferrante M, Cleynen I, De Hertogh G, Vermeire S. Oncostatin M Is a Biomarker of Diagnosis, Worse Disease Prognosis, and Therapeutic Nonresponse in Inflammatory Bowel Disease. *Inflamm Bowel Dis* 2021; **27**: 1564-1575 [PMID: 33624092 DOI: 10.1093/ibd/izab032]

102 **Gaujoux R**, Starosvetsky E, Maimon N, Vallania F, Bar-Yoseph H, Pressman S, Weisshof R, Goren I, Rabinowitz K, Waterman M, Yanai H, Dotan I, Sabo E, Chowers Y, Khatri P, Shen-Orr SS; Israeli IBD research Network (IIRN). Cell-centred meta-analysis reveals baseline predictors of anti-TNFα non-response in biopsy and blood of patients with IBD. *Gut* 2019; **68**: 604-614 [PMID: 29618496 DOI:

10.1136/gutjnl-2017-315494]

103 **Magnusson MK**, Strid H, Sapnara M, Lasson A, Bajor A, Ung KA, Öhman L. Anti-TNF Therapy Response in Patients with Ulcerative Colitis Is Associated with Colonic Antimicrobial Peptide Expression and Microbiota Composition. *J Crohns Colitis* 2016; **10**: 943-952 [PMID: 26896085 DOI: 10.1093/ecco-jcc/jjw051]

104 **Dovrolis N**, Michalopoulos G, Theodoropoulos GE, Arvanitidis K, Kolios G, Sechi LA, Eliopoulos AG, Gazouli M. The Interplay between Mucosal Microbiota Composition and Host Gene-Expression is Linked with Infliximab Response in Inflammatory Bowel Diseases. *Microorganisms* 2020; **8** [PMID: 32244928 DOI: 10.3390/microorganisms8030438]

105 **Alatawi H**, Mosli M, Saadah OI, Annese V, Al-Hindi R, Alatawy M, Al-Amrah H, Alshehri D, Bahieldin A, Edris S. Attributes of intestinal microbiota composition and their correlation with clinical primary non-response to anti-TNF-α agents in inflammatory bowel disease patients. *Bosn J Basic Med Sci* 2022; **22**: 412-426 [PMID: 34761733 DOI: 10.17305/bjbms.2021.6436]

106 **Vatn S**, Carstens A, Kristoffersen AB, Bergemalm D, Casén C, Moen AEF, Tannaes TM, Lindstrøm J, Detlie TE, Olbjørn C, Lindquist CM, Söderholm JD, Gomollón F, Kalla R, Satsangi J, Vatn MH, Jahnsen J, Halfvarson J, Ricanek P; IBD-Character Consortium. Faecal microbiota signatures of IBD and their relation to diagnosis, disease phenotype, inflammation, treatment escalation and anti-TNF response in a European Multicentre Study (IBD-Character). *Scand J Gastroenterol* 2020; **55**: 1146-1156 [PMID: 32780604 DOI: 10.1080/00365521.2020.1803396]

107 **Hong SW**, Park J, Yoon H, Yang HR, Shin CM, Park YS, Kim N, Lee DH, Kim JS. Comparison of loss of response between anti-tumor necrosis factor alone and combined use with immunomodulators in patients with inflammatory bowel disease. *Korean J Intern Med* 2021; **36**: S9-S17 [PMID: 32580540 DOI: 10.3904/kjim.2019.279]

108 **Schultheiss JPD**, Mahmoud R, Louwers JM, van der Kaaij MT, van Hellemondt BP, van Boeckel PG, Mahmmod N, Jharap B, Fidder HH, Oldenburg B. Loss of response to anti-TNFα agents depends on treatment duration in patients with inflammatory bowel disease. *Aliment Pharmacol Ther* 2021; **54**: 1298-1308 [PMID: 34559428 DOI: 10.1111/apt.16605]

109 **Billioud V**, Sandborn WJ, Peyrin-Biroulet L. Loss of response and need for adalimumab dose intensification in Crohn's disease: a systematic review. *Am J Gastroenterol* 2011; **106**: 674-684 [PMID: 21407178 DOI: 10.1038/ajg.2011.60]

110 **Nasuno M**, Miyakawa M, Tanaka H, Motoya S. Short- and Long-Term Outcomes of Infliximab Treatment for Steroid-Refractory Ulcerative Colitis and Related Prognostic Factors: A Single-Center Retrospective Study. *Digestion* 2017; **95**: 67-71 [PMID: 28052276 DOI: 10.1159/000452459]

111 **Chaparro M**, Panes J, García V, Mañosa M, Esteve M, Merino O, Andreu M, Gutierrez A, Gomollón F, Cabriada JL, Montoro MA, Mendoza JL, Nos P, Gisbert JP. Long-term durability of infliximab treatment in Crohn's disease and efficacy of dose "escalation" in patients losing response. *J Clin Gastroenterol* 2011; **45**: 113-118 [PMID: 21242747 DOI: 10.1097/MCG.0b013e3181ebaef9]

112 **Miyoshi J**, Hisamatsu T, Matsuoka K, Naganuma M, Maruyama Y, Yoneno K, Mori K, Kiyohara H, Nanki K, Okamoto S, Yajima T, Iwao Y, Ogata H, Hibi T, Kanai T. Early intervention with adalimumab may contribute to favorable clinical efficacy in patients with Crohn's disease. *Digestion* 2014; **90**: 130-136 [PMID: 25323803 DOI: 10.1159/000365783]

113 **Ma C**, Beilman CL, Huang VW, Fedorak DK, Kroeker KI, Dieleman LA, Halloran BP, Fedorak RN. Anti-TNF Therapy Within 2 Years of Crohn's Disease Diagnosis Improves Patient Outcomes: A Retrospective Cohort Study. *Inflamm Bowel Dis* 2016; **22**: 870-879 [PMID: 26818419 DOI: 10.1097/MIB.0000000000000679]

114 **Schreiber S**, Reinisch W, Colombel JF, Sandborn WJ, Hommes DW, Robinson AM, Huang B, Lomax KG, Pollack PF. Subgroup analysis of the placebo-controlled CHARM trial: increased remission rates through 3 years for adalimumab-treated patients with early Crohn's disease. *J Crohns Colitis* 2013; **7**: 213-221 [PMID: 22704916 DOI: 10.1016/j.crohns.2012.05.015]

115 **Campos C**, Perrey A, Lambert C, Pereira B, Goutte M, Dubois A, Goutorbe F, Dapoigny M, Bommelaer G, Hordonneau C, Buisson A. Medical Therapies for Stricturing Crohn's Disease: Efficacy and Cross-Sectional Imaging Predictors of Therapeutic Failure. *Dig Dis Sci* 2017; **62**: 1628-1636 [PMID: 28401425 DOI: 10.1007/s10620-017-4572-4]

116 **Roblin X**, Marotte H, Leclerc M, Del Tedesco E, Phelip JM, Peyrin-Biroulet L, Paul S. Combination of C-reactive protein, infliximab trough levels, and stable but not transient antibodies to infliximab are associated with loss of response to infliximab in inflammatory bowel disease. *J Crohns Colitis* 2015; **9**: 525-531 [PMID: 25895875 DOI: 10.1093/ecco-jcc/jjv061]

117 **Ungar B**, Chowers Y, Yavzori M, Picard O, Fudim E, Har-Noy O, Kopylov U, Eliakim R, Ben-Horin S; ABIRISK consortium. The temporal evolution of antidrug antibodies in patients with inflammatory bowel disease treated with infliximab. *Gut* 2014; **63**: 1258-1264 [PMID: 24041539 DOI: 10.1136/gutjnl-2013-305259]

118 **Scaldaferri F**, D'Ambrosio D, Holleran G, Poscia A, Petito V, Lopetuso L, Graziani C, Laterza L, Pistone MT, Pecere S, Currò D, Gaetani E, Armuzzi A, Papa A, Cammarota G, Gasbarrini A. Body mass index influences infliximab post-infusion levels and correlates with prospective loss of response to the drug in a cohort of inflammatory bowel disease patients under maintenance therapy with Infliximab. *PLoS One* 2017; **12**: e0186575 [PMID: 29073159 DOI: 10.1371/journal.pone.0186575]

119 **Chuck W**, Shadbolt BF, Nordin F, Subramaniam K. BMI is important in predicting the loss of response in inflammatory bowel disease patients on tumour necrosis factor-α inhibitors. *Eur J Gastroenterol Hepatol* 2022; **34**: 622-629 [PMID: 35352694 DOI: 10.1097/MEG.0000000000002371]

120 **Schoenefuss F**, Hoffmann P. Serum γ-globulin and albumin concentrations predict secondary loss of response to anti-TNFα in inflammatory bowel disease patients. *Eur J Gastroenterol Hepatol* 2019; **31**: 1563-1568 [PMID: 31567711 DOI: 10.1097/MEG.0000000000001493]

121 **Lakatos G**, Hritz I, Varga MZ, Juhász M, Miheller P, Cierny G, Tulassay Z, Herszényi L. The impact of matrix metalloproteinases and their tissue inhibitors in inflammatory bowel diseases. *Dig Dis* 2012; **30**: 289-295 [PMID: 22722554 DOI: 10.1159/000336995]

122 **Meijer MJ**, Mieremet-Ooms MA, van der Zon AM, van Duijn W, van Hogezand RA, Sier CF, Hommes DW, Lamers CB, Verspaget HW. Increased mucosal matrix metalloproteinase-1, -2, -3 and -9 activity in patients with inflammatory bowel disease and the relation with Crohn's disease phenotype. *Dig Liver Dis* 2007; **39**: 733-739 [PMID: 17602907 DOI: 10.1016/j.dld.2007.05.010]

123 **Barberio B**, D'Incà R, Facchin S, Dalla Gasperina M, Fohom Tagne CA, Cardin R, Ghisa M, Lorenzon G, Marinelli C, Savarino EV, Zingone F. Matrix Metalloproteinase 3 Predicts Therapeutic Response in Inflammatory Bowel Disease Patients Treated With Infliximab. *Inflamm Bowel Dis* 2020; **26**: 756-763 [PMID: 31504536 DOI: 10.1093/ibd/izz195]

124 **Biancheri P**, Brezski RJ, Di Sabatino A, Greenplate AR, Soring KL, Corazza GR, Kok KB, Rovedatti L, Vossenkämper A, Ahmad N, Snoek SA, Vermeire S, Rutgeerts P, Jordan RE, MacDonald TT. Proteolytic cleavage and loss of function of biologic agents that neutralize tumor necrosis factor in the mucosa of patients with inflammatory bowel disease. *Gastroenterology* 2015; **149**: 1564-1574.e3 [PMID: 26170138 DOI: 10.1053/j.gastro.2015.07.002]

125 **Romero-Cara P**, Torres-Moreno D, Pedregosa J, Vílchez JA, García-Simón MS, Ruiz-Merino G, Morán-Sanchez S, Conesa-Zamora P. A FCGR3A Polymorphism Predicts Anti-drug Antibodies in Chronic Inflammatory Bowel Disease Patients Treated With Anti-TNF. *Int J Med*

Sci 2018; **15**: 10-15 [PMID: 29333082 DOI: 10.7150/ijms.22812]

126 **Sazonovs A**, Kennedy NA, Moutsianas L, Heap GA, Rice DL, Reppell M, Bewshea CM, Chanchlani N, Walker GJ, Perry MH, McDonald TJ, Lees CW, Cummings JRF, Parkes M, Mansfield JC, Irving PM, Barrett JC, McGovern D, Goodhand JR, Anderson CA, Ahmad T; PANTS Consortium. HLA-DQA1*05 Carriage Associated With Development of Anti-Drug Antibodies to Infliximab and Adalimumab in Patients With Crohn's Disease. *Gastroenterology* 2020; **158**: 189-199 [PMID: 31600487 DOI: 10.1053/j.gastro.2019.09.041]

127 **Wilson A**, Peel C, Wang Q, Pananos AD, Kim RB. HLADQA1*05 genotype predicts anti-drug antibody formation and loss of response during infliximab therapy for inflammatory bowel disease. *Aliment Pharmacol Ther* 2020; **51**: 356-363 [PMID: 31650614 DOI: 10.1111/apt.15563]

128 **Reinisch W**, Wang Y, Oddens BJ, Link R. C-reactive protein, an indicator for maintained response or remission to infliximab in patients with Crohn's disease: a post-hoc analysis from ACCENT I. *Aliment Pharmacol Ther* 2012; **35**: 568-576 [PMID: 22251435 DOI: 10.1111/j.1365-2036.2011.04987.x]

129 **Kiss LS**, Szamosi T, Molnar T, Miheller P, Lakatos L, Vincze A, Palatka K, Barta Z, Gasztonyi B, Salamon A, Horvath G, Tóth GT, Farkas K, Banai J, Tulassay Z, Nagy F, Szenes M, Veres G, Lovasz BD, Vegh Z, Golovics PA, Szathmari M, Papp M, Lakatos PL; Hungarian IBD Study Group. Early clinical remission and normalisation of CRP are the strongest predictors of efficacy, mucosal healing and dose escalation during the first year of adalimumab therapy in Crohn's disease. *Aliment Pharmacol Ther* 2011; **34**: 911-922 [PMID: 21883326 DOI: 10.1111/j.1365-2036.2011.04827.x]

130 **Santos-Antunes J**, Nunes AC, Lopes S, Macedo G. The Relevance of Vitamin D and Antinuclear Antibodies in Patients with Inflammatory Bowel Disease Under Anti-TNF Treatment: A Prospective Study. *Inflamm Bowel Dis* 2016; **22**: 1101-1106 [PMID: 26818421 DOI: 10.1097/MIB.0000000000000697]

131 **Deshpande AR**, Strobel S. Prediction of Crohn's disease relapse with faecal calprotectin in infliximab responders: a prospective study. *Aliment Pharmacol Ther* 2011; **34**: 586 [PMID: 21806647 DOI: 10.1111/j.1365-2036.2011.04778.x]

132 **Sorrentino D**, Gray JM. Timely Monitoring of Inflammation by Fecal Lactoferrin Rapidly Predicts Therapeutic Response in Inflammatory Bowel Disease. *Inflamm Bowel Dis* 2021; **27**: 1237-1247 [PMID: 33501943 DOI: 10.1093/ibd/izaa348]

133 **Bertani L**, Fornai M, Fornili M, Antonioli L, Benvenuti L, Tapete G, Baiano Svizzero G, Ceccarelli L, Mumolo MG, Baglietto L, de Bortoli N, Bellini M, Marchi S, Costa F, Blandizzi C. Serum oncostatin M at baseline predicts mucosal healing in Crohn's disease patients treated with infliximab. *Aliment Pharmacol Ther* 2020; **52**: 284-291 [PMID: 32506635 DOI: 10.1111/apt.15870]

134 **van der Have M**, Oldenburg B, Kaptein AA, Jansen JM, Scheffer RC, van Tuyl BA, van der Meulen-de Jong AE, Pierik M, Siersema PD, van Oijen MG, Fidder HH. Non-adherence to Anti-TNF Therapy is Associated with Illness Perceptions and Clinical Outcomes in Outpatients with Inflammatory Bowel Disease: Results from a Prospective Multicentre Study. *J Crohns Colitis* 2016; **10**: 549-555 [PMID: 26738757 DOI: 10.1093/ecco-jcc/jjw002]

135 **Rentsch C**, Headon B, Ward MG, Gibson PR. Inadequate storage of subcutaneous biological agents by patients with inflammatory bowel disease: Another factor driving loss of response? *J Gastroenterol Hepatol* 2018; **33**: 10-11 [PMID: 29284080 DOI: 10.1111/jgh.14001]

136 **Lamb CA**, Kennedy NA, Raine T, Hendy PA, Smith PJ, Limdi JK, Hayee B, Lomer MCE, Parkes GC, Selinger C, Barrett KJ, Davies RJ, Bennett C, Gittens S, Dunlop MG, Faiz O, Fraser A, Garrick V, Johnston PD, Parkes M, Sanderson J, Terry H; IBD guidelines eDelphi consensus group, Gaya DR, Iqbal TH, Taylor SA, Smith M, Brookes M, Hansen R, Hawthorne AB. British Society of Gastroenterology consensus guidelines on the management of inflammatory bowel disease in adults. *Gut* 2019; **68**: s1-s106 [PMID: 31562236 DOI: 10.1136/gutjnl-2019-318484]

137 **Papamichael K**, Cheifetz AS, Melmed GY, Irving PM, Vande Casteele N, Kozuch PL, Raffals LE, Baidoo L, Bressler B, Devlin SM, Jones J, Kaplan GG, Sparrow MP, Velayos FS, Ullman T, Siegel CA. Appropriate Therapeutic Drug Monitoring of Biologic Agents for Patients With Inflammatory Bowel Diseases. *Clin Gastroenterol Hepatol* 2019; **17**: 1655-1668.e3 [PMID: 30928454 DOI: 10.1016/j.cgh.2019.03.037]

138 **Marquez-Megias S**, Nalda-Molina R, Sanz-Valero J, Más-Serrano P, Diaz-Gonzalez M, Candela-Boix MR, Ramon-Lopez A. Cost-Effectiveness of Therapeutic Drug Monitoring of Anti-TNF Therapy in Inflammatory Bowel Disease: A Systematic Review. *Pharmaceutics* 2022; **14** [PMID: 35631594 DOI: 10.3390/pharmaceutics14051009]

139 **Yao J**, Jiang X, You JHS. A Systematic Review on Cost-effectiveness Analyses of Therapeutic Drug Monitoring for Patients with Inflammatory Bowel Disease: From Immunosuppressive to Anti-TNF Therapy. *Inflamm Bowel Dis* 2021; **27**: 275-282 [PMID: 32311018 DOI: 10.1093/ibd/izaa073]

140 **Ricciuto A**, Dhaliwal J, Walters TD, Griffiths AM, Church PC. Clinical Outcomes With Therapeutic Drug Monitoring in Inflammatory Bowel Disease: A Systematic Review With Meta-Analysis. *J Crohns Colitis* 2018; **12**: 1302-1315 [PMID: 30107416 DOI: 10.1093/ecco-jcc/jjy109]

141 **Gisbert JP**, Chaparro M. Primary Failure to an Anti-TNF Agent in Inflammatory Bowel Disease: Switch (to a Second Anti-TNF Agent) or Swap (for Another Mechanism of Action)? *J Clin Med* 2021; **10** [PMID: 34830595 DOI: 10.3390/jcm10225318]

142 **Baert F**, Glorieus E, Reenaers C, D'Haens G, Peeters H, Franchimont D, Dewit O, Caenepeel P, Louis E, Van Assche G; BIRD (Belgian IBD Research and Development). Adalimumab dose escalation and dose de-escalation success rate and predictors in a large national cohort of Crohn's patients. *J Crohns Colitis* 2013; **7**: 154-160 [PMID: 22537637 DOI: 10.1016/j.crohns.2012.03.018]

143 **Van Stappen T**, Vande Casteele N, Van Assche G, Ferrante M, Vermeire S, Gils A. Clinical relevance of detecting anti-infliximab antibodies with a drug-tolerant assay: post hoc analysis of the TAXIT trial. *Gut* 2018; **67**: 818-826 [PMID: 28450388 DOI: 10.1136/gutjnl-2016-313071]

144 **Bodini G**, Demarzo MG, Saracco M, Coppo C, De Maria C, Baldissarro I, Savarino E, Savarino V, Giannini EG. High anti-TNF alfa drugs trough levels are not associated with the occurrence of adverse events in patients with inflammatory bowel disease. *Scand J Gastroenterol* 2019; **54**: 1220-1225 [PMID: 31553630 DOI: 10.1080/00365521.2019.1666914]

145 **van Schaik T**, Maljaars JP, Roopram RK, Verwey MH, Ipenburg N, Hardwick JC, Veenendaal RA, van der Meulen-de Jong AE. Influence of combination therapy with immune modulators on anti-TNF trough levels and antibodies in patients with IBD. *Inflamm Bowel Dis* 2014; **20**: 2292-2298 [PMID: 25230167 DOI: 10.1097/MIB.0000000000000208]

146 **Colombel JF**, Sandborn WJ, Reinisch W, Mantzaris GJ, Kornbluth A, Rachmilewitz D, Lichtiger S, D'Haens G, Diamond RH, Broussard DL, Tang KL, van der Woude CJ, Rutgeerts P; SONIC Study Group. Infliximab, azathioprine, or combination therapy for Crohn's disease. *N Engl J Med* 2010; **362**: 1383-1395 [PMID: 20393175 DOI: 10.1056/NEJMoa0904492]

147 **Panaccione R**, Ghosh S, Middleton S, Márquez JR, Scott BB, Flint L, van Hoogstraten HJ, Chen AC, Zheng H, Danese S, Rutgeerts P. Combination therapy with infliximab and azathioprine is superior to monotherapy with either agent in ulcerative colitis. *Gastroenterology* 2014; **146**: 392-400.e3 [PMID: 24512909 DOI: 10.1053/j.gastro.2013.10.052]

148 **Macaluso FS**, Sapienza C, Ventimiglia M, Renna S, Rizzuto G, Orlando R, Di Pisa M, Affronti M, Orlando E, Cottone M, Orlando A. The Addition of an Immunosuppressant After Loss of Response to Anti-TNFα Monotherapy in Inflammatory Bowel Disease: A 2-Year Study. *Inflamm Bowel Dis* 2018; **24**: 394-401 [PMID: 29361087 DOI: 10.1093/ibd/izx010]

149 **Drobne D**, Bossuyt P, Breynaert C, Cattaert T, Vande Casteele N, Compernolle G, Jürgens M, Ferrante M, Ballet V, Wollants WJ, Cleynen I, Van Steen K, Gils A, Rutgeerts P, Vermeire S, Van Assche G. Withdrawal of immunomodulators after co-treatment does not reduce trough level of infliximab in patients with Crohn's disease. *Clin Gastroenterol Hepatol* 2015; **13**: 514-521.e4 [PMID: 25066841 DOI: 10.1016/j.cgh.2014.07.027]

150 **Mahmoud R**, Schultheiss HP, Louwers J, van der Kaaij M, van Hellemondt B, Mahmmod N, van Boeckel P, Jharap B, Fidder H, Oldenburg B. Immunomodulator Withdrawal From Anti-TNF Therapy Is Not Associated With Loss of Response in Inflammatory Bowel Disease. *Clin Gastroenterol Hepatol* 2022; **20**: 2577-2587.e6 [PMID: 35101632 DOI: 10.1016/j.cgh.2022.01.019]

151 **Yanai H**, Lichtenstein L, Assa A, Mazor Y, Weiss B, Levine A, Ron Y, Kopylov U, Bujanover Y, Rosenbach Y, Ungar B, Eliakim R, Chowers Y, Shamir R, Fraser G, Dotan I, Ben-Horin S. Levels of drug and antidrug antibodies are associated with outcome of interventions after loss of response to infliximab or adalimumab. *Clin Gastroenterol Hepatol* 2015; **13**: 522-530.e2 [PMID: 25066837 DOI: 10.1016/j.cgh.2014.07.029]

152 **Afif W**, Loftus EV Jr, Faubion WA, Kane SV, Bruining DH, Hanson KA, Sandborn WJ. Clinical utility of measuring infliximab and human anti-chimeric antibody concentrations in patients with inflammatory bowel disease. *Am J Gastroenterol* 2010; **105**: 1133-1139 [PMID: 20145610 DOI: 10.1038/ajg.2010.9]

153 **R-Grau Mdel C**, Chaparro M, Mesonero F, Barreiro-de Acosta M, Castro L, Castro M, Domènech E, Mancenido N, Pérez-Calle JL, Taxonera C, Barrio J, De Francisco R, Fernández-Salgado E, Luzón L, Merino O, Oltra L, Saro C, Bermejo F, García-Sánchez V, Ginard D, Gutiérrez A, Vera I, Antón R, Ber Y, Calvet X, Gisbert JP. Effectiveness of anti-TNFα drugs in patients with Crohn's disease who do not achieve remission with their first anti-TNFα agent. *Dig Liver Dis* 2016; **48**: 613-619 [PMID: 26992847 DOI: 10.1016/j.dld.2016.02.012]

154 **Casanova MJ**, Chaparro M, Mínguez M, Ricart E, Taxonera C, García-López S, Guardiola J, López-San Román A, Iglesias E, Beltrán B, Sicilia B, Vera MI, Hinojosa J, Riestra S, Domènech E, Calvet X, Pérez-Calle JL, Martín-Arranz MD, Aldeguer X, Rivero M, Monfort D, Barrio J, Esteve M, Márquez L, Lorente R, García-Planella E, de Castro L, Bermejo F, Merino O, Rodríguez-Pérez A, Martínez-Montiel P, Van Domselaar M, Alcaín G, Domínguez-Cajal M, Muñoz C, Gomollón F, Fernández-Salazar L, García-Sepulcre MF, Rodríguez-Lago I, Gutiérrez A, Argüelles-Arias F, Rodriguez C, Rodríguez GE, Bujanda L, Llaó J, Varela P, Ramos L, Huguet JM, Almela P, Romero P, Navarro-Llavat M, Abad Á, Ramírez-de la Piscina P, Lucendo AJ, Sesé E, Madrigal RE, Charro M, García-Herola A, Pajares R, Khorrami S, Gisbert JP. Effectiveness and Safety of the Sequential Use of a Second and Third Anti-TNF Agent in Patients With Inflammatory Bowel Disease: Results From the Eneida Registry. *Inflamm Bowel Dis* 2020; **26**: 606-616 [PMID: 31504569 DOI: 10.1093/ibd/izz192]

155 **Gisbert JP**, Marín AC, McNicholl AG, Chaparro M. Systematic review with meta-analysis: the efficacy of a second anti-TNF in patients with inflammatory bowel disease whose previous anti-TNF treatment has failed. *Aliment Pharmacol Ther* 2015; **41**: 613-623 [PMID: 25652884 DOI: 10.1111/apt.13083]

156 **Chanchlani N**, Lin S, Auth MK, Lee CL, Robbins H, Looi S, Murugesan SV, Riley T, Preston C, Stephenson S, Cardozo W, Sonwalkar SA, Allah-Ditta M, Mansfield L, Durai D, Baker M, London I, London E, Gupta S, Di Mambro A, Murphy A, Gaynor E, Jones KDJ, Claridge A, Sebastian S, Ramachandran S, Selinger CP, Borg-Bartolo SP, Knight P, Sprakes MB, Burton J, Kane P, Lupton S, Fletcher A, Gaya DR, Colbert R, Seenan JP, MacDonald J, Lynch L, McLachlan I, Shields S, Hansen R, Gervais L, Jere M, Akhtar M, Black K, Henderson P, Russell RK, Lees CW, Derikx LAAP, Lockett M, Betteridge F, De Silva A, Hussenbux A, Beckly J, Bendall O, Hart JW, Thomas A, Hamilton B, Gordon C, Chee D, McDonald TJ, Nice R, Parkinson M, Gardner-Thorpe H, Butterworth JR, Javed A, Al-Shakhshir S, Yadagiri R, Maher S, Pollok RCG, Ng T, Appiahene P, Donovan F, Lok J, Chandy R, Jagdish R, Baig D, Mahmood Z, Marsh L, Moss A, Abdulgader A, Kitchin A, Walker GJ, George B, Lim YH, Gulliver J, Bloom S, Theaker H, Carlson S, Cummings JRF, Livingstone R, Beale A, Carter JO, Bell A, Coulter A, Snook J, Stone H, Kennedy NA, Goodhand JR, Ahmad T; IMSAT study investigators. Implications for sequencing of biologic therapy and choice of second anti-TNF in patients with inflammatory bowel disease: results from the IMmunogenicity to Second Anti-TNF therapy (IMSAT) therapeutic drug monitoring study. *Aliment Pharmacol Ther* 2022; **56**: 1250-1263 [PMID: 36039036 DOI: 10.1111/apt.17170]

157 **Roblin X**, Williet N, Boschetti G, Phelip JM, Del Tedesco E, Berger AE, Vedrines P, Duru G, Peyrin-Biroulet L, Nancey S, Flourie B, Paul S. Addition of azathioprine to the switch of anti-TNF in patients with IBD in clinical relapse with undetectable anti-TNF trough levels and antidrug antibodies: a prospective randomised trial. *Gut* 2020; **69**: 1206-1212 [PMID: 31980448 DOI: 10.1136/gutjnl-2019-319758]

158 **Feagan BG**, Rutgeerts P, Sands BE, Hanauer S, Colombel JF, Sandborn WJ, Van Assche G, Axler J, Kim HJ, Danese S, Fox I, Milch C, Sankoh S, Wyant T, Xu J, Parikh A; GEMINI 1 Study Group. Vedolizumab as induction and maintenance therapy for ulcerative colitis. *N Engl J Med* 2013; **369**: 699-710 [PMID: 23964932 DOI: 10.1056/NEJMoa1215734]

159 **Sandborn WJ**, Gasink C, Gao LL, Blank MA, Johanns J, Guzzo C, Sands BE, Hanauer SB, Targan S, Rutgeerts P, Ghosh S, de Villiers WJ, Panaccione R, Greenberg G, Schreiber S, Lichtiger S, Feagan BG; CERTIFI Study Group. Ustekinumab induction and maintenance therapy in refractory Crohn's disease. *N Engl J Med* 2012; **367**: 1519-1528 [PMID: 23075178 DOI: 10.1056/NEJMoa1203572]

160 **Feagan BG**, Sandborn WJ, Gasink C, Jacobstein D, Lang Y, Friedman JR, Blank MA, Johanns J, Gao LL, Miao Y, Adedokun OJ, Sands BE, Hanauer SB, Vermeire S, Targan S, Ghosh S, de Villiers WJ, Colombel JF, Tulassay Z, Seidler U, Salzberg BA, Desreumaux P, Lee SD, Loftus EV Jr, Dieleman LA, Katz S, Rutgeerts P; UNITI–IM-UNITI Study Group. Ustekinumab as Induction and Maintenance Therapy for Crohn's Disease. *N Engl J Med* 2016; **375**: 1946-1960 [PMID: 27959607 DOI: 10.1056/NEJMoa1602773]

161 **Sandborn WJ**, Ghosh S, Panes J, Vranic I, Su C, Rousell S, Niezychowski W; Study A3921063 Investigators. Tofacitinib, an oral Janus kinase inhibitor, in active ulcerative colitis. *N Engl J Med* 2012; **367**: 616-624 [PMID: 22894574 DOI: 10.1056/NEJMoa1112168]

162 **Biemans VBC**, van der Woude CJ, Dijkstra G, van der Meulen-de Jong AE, Löwenberg M, de Boer NK, Oldenburg B, Srivastava N, Jansen JM, Bodelier AGL, West RL, de Vries AC, Haans JJL, de Jong D, Hoentjen F, Pierik MJ; Dutch Initiative on Crohn and Colitis (ICC). Ustekinumab is associated with superior effectiveness outcomes compared to vedolizumab in Crohn's disease patients with prior failure to anti-TNF treatment. *Aliment Pharmacol Ther* 2020; **52**: 123-134 [PMID: 32441396 DOI: 10.1111/apt.15745]

World Journal of Gastroenterology

Submit a Manuscript: https://www.f6publishing.com

World J Gastroenterol 2023 August 7; 29(29): 4499-4527

DOI: 10.3748/wjg.v29.i29.4499

ISSN 1007-9327 (print) ISSN 2219-2840 (online)

REVIEW

Bioenergetic alteration in gastrointestinal cancers: The good, the bad and the ugly

Yu-De Chu, Chun-Wei Chen, Ming-Wei Lai, Siew-Na Lim, Wey-Ran Lin

Specialty type: Gastroenterology and hepatology

Provenance and peer review: Invited article; Externally peer reviewed.

Peer-review model: Single blind

Peer-review report's scientific quality classification

Grade A (Excellent): 0
Grade B (Very good): B
Grade C (Good): C
Grade D (Fair): 0
Grade E (Poor): 0

P-Reviewer: Masaru T, Hungary; Sun G, China

Received: March 28, 2023
Peer-review started: March 28, 2023
First decision: May 12, 2023
Revised: May 23, 2023
Accepted: July 3, 2023
Article in press: July 3, 2023
Published online: August 7, 2023

Yu-De Chu, Liver Research Center, Linkou Chang Gung Memorial Hospital, Taoyuan 333, Taiwan

Chun-Wei Chen, Wey-Ran Lin, Department of Gastroenterology and Hepatology, Linkou Chang Gung Memorial Hospital, Taoyuan 333, Taiwan

Ming-Wei Lai, Department of Pediatrics, Linkou Chang Gung Memorial Hospital, Taoyuan 333, Taiwan

Siew-Na Lim, Department of Neurology, Linkou Chang Gung Memorial Hospital, Taoyuan 333, Taiwan

Wey-Ran Lin, Department of Medicine, Chang Gung University, Taoyuan 333, Taiwan

Corresponding author: Wey-Ran Lin, AGAF, MD, PhD, Professor, Department of Gastroenterology and Hepatology, Linkou Chang Gung Memorial Hospital, No. 5 Fu-Shin Street, Taoyuan 333, Taiwan. t12360@adm.cgmh.org.tw

Abstract

Cancer cells exhibit metabolic reprogramming and bioenergetic alteration, utilizing glucose fermentation for energy production, known as the Warburg effect. However, there are a lack of comprehensive reviews summarizing the metabolic reprogramming, bioenergetic alteration, and their oncogenetic links in gastrointestinal (GI) cancers. Furthermore, the efficacy and treatment potential of emerging anticancer drugs targeting these alterations in GI cancers require further evaluation. This review highlights the interplay between aerobic glycolysis, the tricarboxylic acid (TCA) cycle, and oxidative phosphorylation (OXPHOS) in cancer cells, as well as hypotheses on the molecular mechanisms that trigger this alteration. The role of hypoxia-inducible transcription factors, tumor suppressors, and the oncogenetic link between hypoxia-related enzymes, bioenergetic changes, and GI cancer are also discussed. This review emphasizes the potential of targeting bioenergetic regulators for anti-cancer therapy, particularly for GI cancers. Emphasizing the potential of targeting bioenergetic regulators for GI cancer therapy, the review categorizes these regulators into aerobic glycolysis/ lactate biosynthesis/transportation and TCA cycle/coupled OXPHOS. We also detail various anti-cancer drugs and strategies that have produced pre-clinical and/or clinical evidence in treating GI cancers, as well as the challenges posed by these drugs. Here we highlight that understanding dysregulated cancer cell bioenergetics is critical for effective treatments, although the diverse metabolic patterns

present challenges for targeted therapies. Further research is needed to comprehend the specific mechanisms of inhibiting bioenergetic enzymes, address side effects, and leverage high-throughput multi-omics and spatial omics to gain insights into cancer cell heterogeneity for targeted bioenergetic therapies.

Key Words: Energy metabolism; Mitochondria; Hypoxia; Oxidative phosphorylation; Glycolysis; Gastrointestinal neoplasms

©The Author(s) 2023. Published by Baishideng Publishing Group Inc. All rights reserved.

Core Tip: This review discusses the bioenergetic alteration and metabolic reprogramming in gastrointestinal (GI) cancers, including the interplay between aerobic glycolysis, tricarboxylic acid cycle, and oxidative phosphorylation. The review also highlights potential strategies for targeting bioenergetic regulators for anti-cancer therapy in GI cancers, summarizing the efficacy and challenges of several drugs.

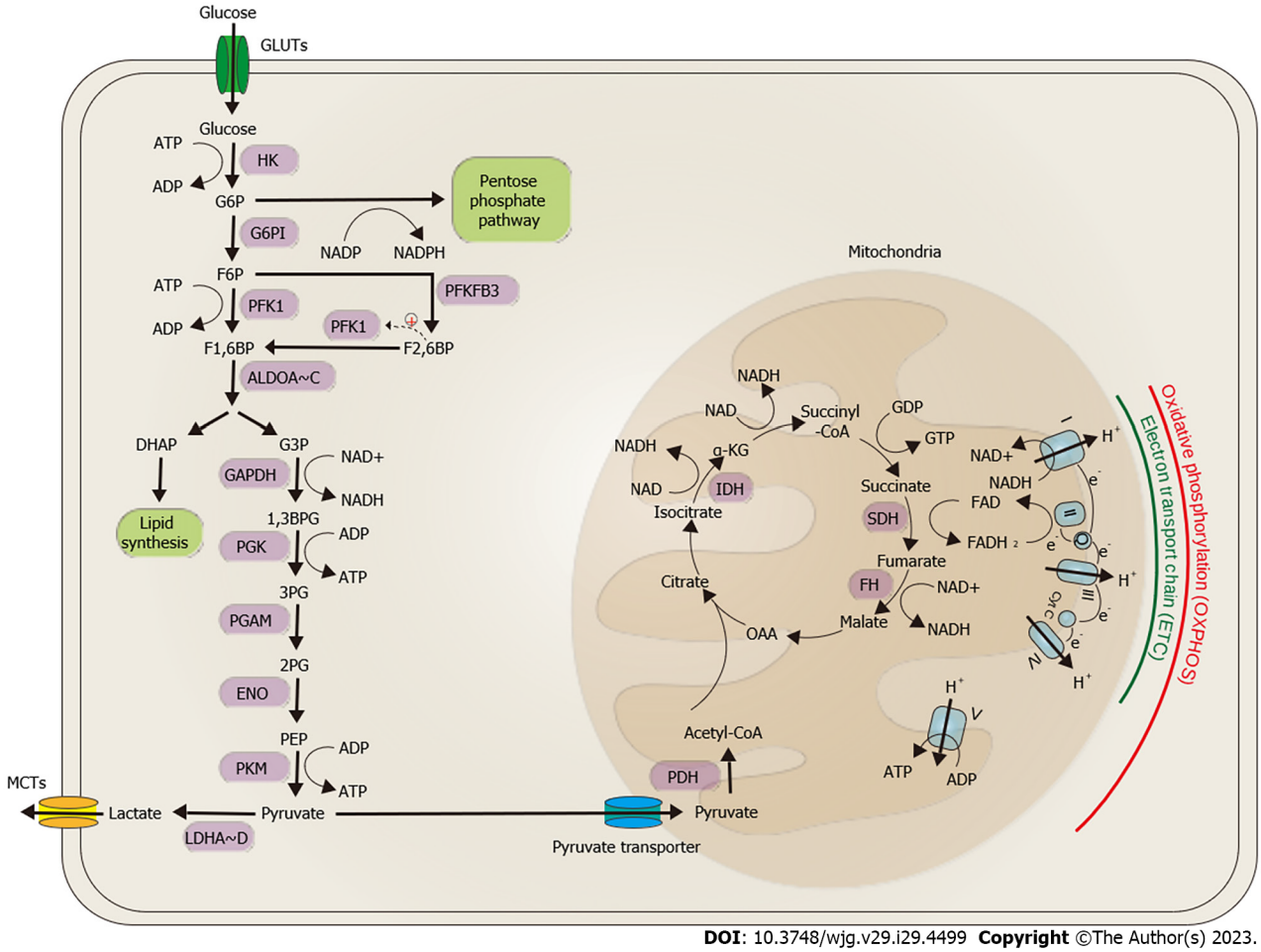
Citation: Chu YD, Chen CW, Lai MW, Lim SN, Lin WR. Bioenergetic alteration in gastrointestinal cancers: The good, the bad and the ugly. *World J Gastroenterol* 2023; 29(29): 4499-4527
URL: https://www.wjgnet.com/1007-9327/full/v29/i29/4499.htm
DOI: https://dx.doi.org/10.3748/wjg.v29.i29.4499

INTRODUCTION

Cells require energy to carry out their functions, and the most common form of cellular energy is adenosine triphosphate (ATP). This energy is typically produced by oxidative phosphorylation (OXPHOS) in the mitochondria of normal cells[1]. However, in cancer cells, there is a shift in the way energy is generated. Instead of using OXPHOS, cancer cells use glycolysis, a process that results in increased uptake of glucose and secretion of lactate[2]. This phenomenon is known as the Warburg effect and is observed in many types of cancer[3,4]. By understanding the altered energy metabolism in cancer cells, researchers can gain new insights into cancer cell biology and identify potential targets for cancer therapy.

Glycolysis is the process by which glucose is broken down to produce ATP, and it does not require oxygen (Figure 1). Glucose enters cells through glucose transporters and is converted to glucose-6-phosphate (G6P) by hexokinase (HK). Glucose-6-phosphate isomerase (G6PI) converts G6P to fructose-6-phosphate (F6P), which is used in both the glycolytic pathway to generate pyruvate or lactate and the pentose phosphate pathway (PPP) to produce nucleotides and nicotinamide adenine dinucleotide phosphate (NADPH). Phosphofructokinase-1 (PFK1) converts F6P and fructose-2,6-bisphosphate (F2,6BP), a metabolite from a branch driven by fructose-2,6-biphosphatase 3 (PFKBP3), to fructose-1,6-bisphosphate (F1,6BP), which is further processed by aldolase to generate glyceraldehyde-3-phosphate (G3P) and dihydroxyacetone phosphate (DHAP). G3P is converted by glyceraldehyde 3-phosphate dehydrogenase (GAPDH) to 1,3-bisphosphoglycerate (1,3BPG), which is further converted to 3-phosphoglycerate (3PG) by phosphoglycerate kinase (PGK1). The 3PG is subsequently converted by phosphoglycerate mutase (PGAM) to 2-phosphoglycerate (2PG). The 2PG then serves as a substrate for enolase (ENO) to convert to phosphoenolpyruvate (PEP). Pyruvate kinase isozyme M1/M2 (PKM1/2) catalyzes the conversion of PEP to pyruvate, which can be converted to acetyl-CoA or lactate. This process generates NAD+ from NADH, which is important for the continuation of the glycolysis process. Although glycolysis itself does not require oxygen, the fate of the pyruvate produced by glycolysis depends on the availability of oxygen, and the overall efficiency of ATP production is much higher when oxygen is present[5].

Pyruvate, a product of glycolysis, enters the mitochondria where it is converted to acetyl-CoA. The resulting acetyl-CoA can then enter the tricarboxylic acid (TCA) cycle, also known as the Krebs cycle, which plays a pivotal role in generating ATP through the electron transport chain (ETC). The TCA cycle completes the breakdown of glucose by breaking down acetyl-CoA into carbon dioxide (CO_2) and water, releasing energy in the form of NADH and flavin adenine dinucleotide (FADH2). NADH and FADH2 donate their electrons to the ETC at Complex I and II, respectively. The ETC, specifically Complexes I-IV, transfers electrons from NADH and FADH2 to generate a proton gradient across the inner mitochondrial membrane. This gradient is then used by ATP synthase to produce ATP. Complex I, also known as NADH dehydrogenase or NADH ubiquinone oxidoreductase, is the largest of the five mitochondrial complexes and marks the initiation of the ETC[6]. Electrons are transferred from Complex I to coenzyme Q (CoQ) across the inner mitochondrial membrane and then from CoQ to Complex III, although an alternative pathway exists *via* Complex II, succinate dehydrogenase (SDH)[7,8]. Following reduction of succinate by Complex II, electrons are transported to CoQ and then transferred to Complex III. Complex III and cytochrome c transfer electrons to Complex IV, cytochrome c oxidase (COX). The ETC complexes act as proton pumps, creating an electrochemical gradient across the inner mitochondrial membrane, and this energy is harnessed by Complex V, ATP synthase, which generates ATP by using the energy from the movement of protons down their electrochemical gradient. This whole process is known as OXPHOS and is a time-consuming process compared to glycolysis, but is the most efficient way to generate ATP in the cell, producing up to 36-38 ATP molecules per glucose molecule. Complexes I-IV are known as the ETC, while Complex V (ATP synthase) does not (Figure 1). Except for Complex II, all OXPHOS-related complexes are partially encoded by mitochondrial DNA (mtDNA)[9]. Unfortunately, OXPHOS also produces reactive oxygen species (ROS) as a byproduct,



DOI: 10.3748/wjg.v29.i29.4499 **Copyright** ©The Author(s) 2023.

Figure 1 Illustration of the pathway of glucose metabolism. Glucose is taken up by cells and undergoes a series of reactions to convert it to pyruvate *via* the process of glycolysis. Pyruvate can then enter the tricarboxylic acid cycle in the mitochondria to produce energy, or it can be converted to lactate in the cytosol under anaerobic conditions. The key enzymes involved in these reactions are highlighted in pale-purple, and linked pathways are depicted in pale-green. The mitochondrial complexes that are critical for oxidative phosphorylation and adenosine triphosphate production are shown in pale-blue. GLUT: Glucose transporter; HK: Hexokinase; G6P: Glucose-6-phosphate; G6PI: Glucose-6-phosphate isomerase; F6P: Fructose-6-phosphate; NADPH: Nicotinamide adenine dinucleotide phosphate; PFK1: Phosphofructokinase-1; F2,6BP: Fructose-2,6-bisphosphate; PFKBP3: Fructose-2,6-biphosphatase 3; F1,6BP: Fructose-1,6-bisphosphate; G3P: Glyceraldehyde-3-phosphate; DHAP: Dihydroxyacetone phosphate; GAPDH: Glyceraldehyde 3-phosphate dehydrogenase; 1,3BPG: 1,3-bisphosphoglycerate; 3PG: 3-phosphoglycerate; PGK: Phosphoglycerate kinase; PGAM: Phosphoglycerate mutase; 2PG: 2-phosphoglycerate; ENO: Enolase; PEP: Phosphoenolpyruvate; PKM1/2: Pyruvate kinase isozyme M1/M2; LDH: Lactate dehydrogenase; MCT: Monocarboxylate transporter family; PDH: Pyruvate dehydrogenase; IDH: Isocitrate dehydrogenase; α-KG: α-ketoglutarate; OAA: Oxaloacetate; SDH: Succinate dehydrogenase; FH: Fumarate hydratase; I: Mitochondrial complex I; II: Mitochondrial complex II; III: Mitochondrial complex III; IV: Mitochondrial complex IV; V: Mitochondrial complex V; Q: Co-enzyme Q; cyto C: Cytochrome *c*; ATP: Adenosine triphosphate; ADP: Adenosine diphosphate; FADH2: Flavin adenine dinucleotide; e⁻: Electrons.

which can cause damage to mitochondrial or nuclear DNA and activate oncogenic signaling pathways, potentially leading to diseases and carcinogenesis[10-12]. Mutations in mtDNA are also implicated in cancer[13]. Overall, the process of OXPHOS is vital for cellular energy production, but careful regulation is necessary to prevent the damaging effects of ROS production.

In cancer cells, certain enzymes and molecules involved in the conversion of glucose to energy are upregulated, which provides an attractive target for anti-cancer therapies[14]. Disrupting this process could prevent cancer cells from producing energy and lead to their death. In addition to the upregulation of these enzymes, alterations in certain mitochondrial enzymes and oncometabolites have been identified in cancer cells. Oncometabolites are small molecules that are produced in cancer cells and contribute to their growth and proliferation[15]. These alterations can be caused by genetic and epigenetic changes in the genes involved in energy production[13,16]. Recent research has focused on understanding these bioenergetic alterations in gastrointestinal (GI) cancers, such as esophageal cancer (ESCA), gastric cancer (GC), hepatocellular carcinoma (HCC), cholangiocarcinoma (CCA), pancreatic cancer (PAC), and colorectal cancer (CRC). Understanding these specific metabolic changes in cancer cells can provide insight into developing more effective targeted therapies for GI cancers. In addition to the potential for targeted therapy, these metabolic changes could also serve as biomarkers for cancer diagnosis and prognosis. By identifying alterations in the genes and molecules involved in energy production, clinicians may be able to more accurately diagnose and predict the course of the disease. Overall, understanding the bioenergetic alterations in cancer cells is a promising avenue for developing new therapies and improving cancer diagnosis and treatment. In this review, we summarize the latest findings on bioenergetic alterations in

various GI cancers, and discuss the potential therapeutic strategies that target these alterations. Such strategies may include inhibitors of specific enzymes or molecules involved in energy production, as well as interventions aimed at modulating the metabolic environment of cancer cells. Further research in this area could lead to new and more effective treatments for GI cancers.

BIOENERGETIC ALTERATION AND THE WARBURG EFFECT

The process of bioenergetic alteration in cancer involves changes in the way cancer cells generate energy. One well-known component of bioenergetic alteration is the Warburg effect. This phenomenon describes how cancer cells prefer to use glucose fermentation to produce energy even in the presence of oxygen[2]. This process, called aerobic glycolysis, is less efficient than mitochondrial OXPHOS in terms of ATP production[17,18]. However, it has been noted that respiration alone can maintain tumor viability, suggesting that glucose and oxygen must be eliminated to kill cancer cells by depriving them of energy[2]. The underlying mechanisms of the Warburg effect have been investigated for decades. Otto Warburg originally proposed that mitochondrial dysfunction could be responsible for aerobic glycolysis[19]. This theory was later confirmed and explored by another group that demonstrated the Warburg effect could be caused by an imbalance of intracellular pH and mitochondrial ATPase dysfunction[20]. Moreover, it was observed that aerobic glycolysis could be controlled by cascade signaling mediated by growth factors and oncogenes, questioning whether the Warburg effect was a mere bystander in the pathogenesis of cancer[21-24]. It was not until later that the Warburg effect was discovered to be crucial for tumor growth in genetic and pharmacological studies[25,26].

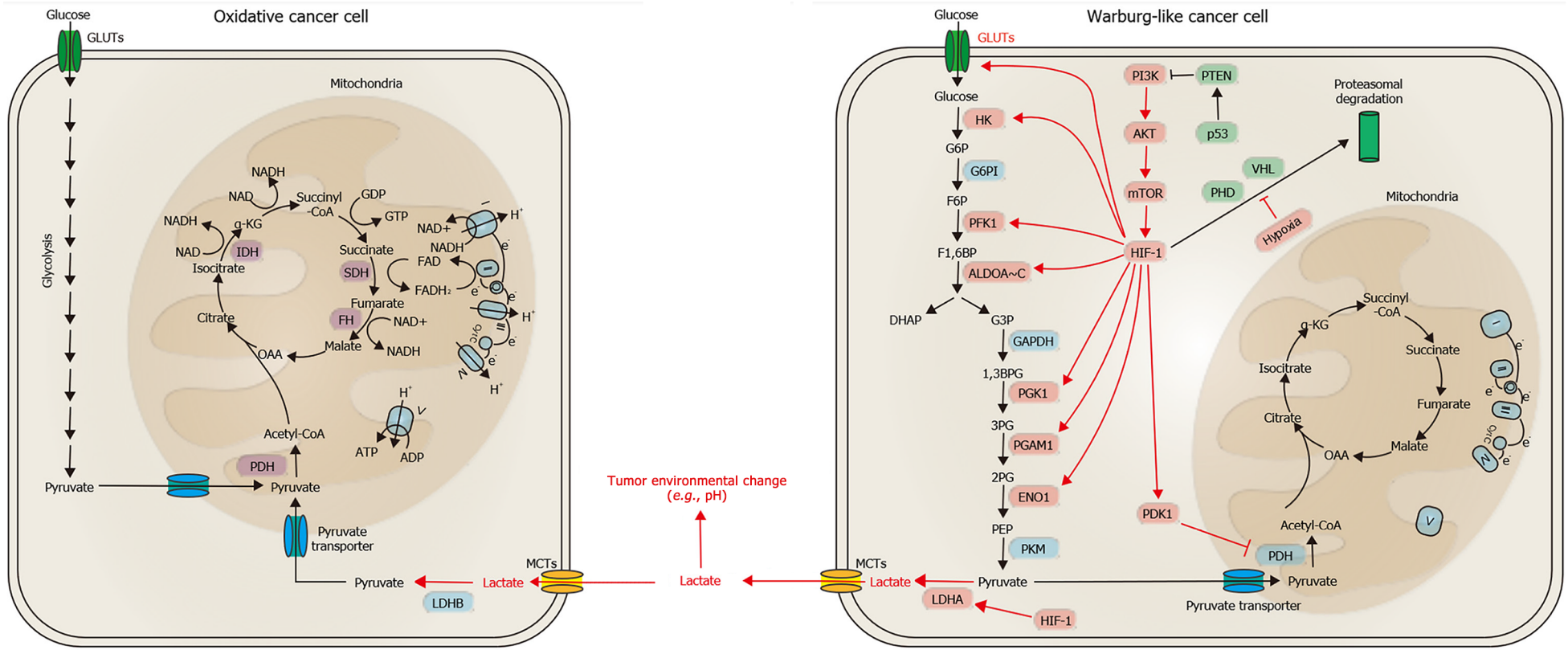
Scientists have been trying to understand why cancer cells prefer aerobic glycolysis to mitochondrial OXPHOS for decades, given that the ATP generated by aerobic glycolysis is much lower than that produced by mitochondrial OXPHOS[27-29]. Recent studies have shed light on this phenomenon. For example, when changes in the cellular environment increase ATP demand through alteration of ATP-dependent membrane activity, aerobic glycolysis increases rapidly and OXPHOS remains unchanged[30]. Another study showed high aerobic glycolysis as a metabolic strategy which cancer cells use to optimally respond to fluctuating energy availability[31]. Together, this literature suggests that the Warburg effect is a metabolic strategy that allows flexibility among cancer cells under an unpredictable tumor microenvironment.

THE DYNAMIC INTERPLAY BETWEEN OXPHOS AND AEROBIC GLYCOLYSIS

Not all pyruvate produced during glycolysis is converted to lactate. Indeed, a significant amount of pyruvate can enter the TCA cycle for oxidation and further metabolism. The intermediates generated during the TCA cycle, such as NAD+/NADH and NADP+/NADPH, can continue to enter the OXPHOS pathway, which can further generate bioenergy[32,33]. Although the role of the Warburg effect in cancers remains controversial, interfering with tumor metabolism and targeting both aerobic glycolysis and mitochondrial OXPHOS pathways have been shown to be necessary[34-37]. It is evident from current literature that there exists crosstalk between aerobic glycolysis, the TCA cycle, and coupled OXPHOS, suggesting cooperative and competitive roles in cancer. Interestingly, some studies suggest that targeting mitochondrial metabolism alone may not be sufficient to inhibit tumor growth, as cancer cells can redirect their metabolism to rely on other energy sources. In such cases, blocking both the glycolytic and mitochondrial pathways may be necessary to prevent cancer cell growth[34-37]. Therefore, a better understanding of the metabolic pathways in cancer cells and their interactions is required to develop effective cancer therapies.

Although the exact molecular mechanism that triggers the Warburg effect in cancer remains unclear, multiple hypotheses have been proposed, including the involvement of tumor suppressors (*e.g.*, p53) and oncogenes (*e.g.*, PI3K, AKT, mTOR), all of which appear to converge on the role of hypoxia-inducible transcription factors (HIFs), particularly HIF-1. HIF-1 is a transcription factor that regulates cellular responses to oxygen deprivation, and it was initially identified as a protein that is present only under hypoxic conditions[38-41]. However, it was later discovered that HIF-1 can also be stabilized under normoxia in a microenvironment with high lactate concentration[42,43]. Under normal conditions, HIF-1 α, a subunit of HIF-1, is targeted for degradation by prolyl hydroxylases (PHDs), which utilize molecular oxygen to hydroxylate HIF-1α, leading to its recognition by the von Hippel-Lindau tumor suppressor (VHL), and degradation *via* proteasome-mediated pathways[44-47].

HIF-1 regulates the expression of several key glycolytic enzymes, such as glucose transporter-1 (GLUT1), GLUT3, HK, aldolase A (ALDOA), PGK1, PKM1/2, ENO1, pyruvate dehydrogenase kinase (PDKs), and lactate dehydrogenase subunit A (LDHA), by directly promoting their expression[48-54]. This leads to an increased level of pyruvate, the final product of glycolysis. However, it is important to note that cancer cells with high glycolytic activity are not guaranteed to catabolize all pyruvate to lactate, as significant amounts of pyruvate can enter the TCA cycle for oxidation and metabolism. In cancer cells, it is suggested that the HIF-1 induced increased expression of PDKs can inhibit the function of pyruvate dehydrogenase (PDH), which blocks pyruvate entry into the TCA cycle and promotes lactate production. Since HIF-1 also promotes the expression of LDHA, an important subunit of LDH necessary for lactate biosynthesis from pyruvate, it is thought to be crucial in cancers affecting terminal lactate levels[55] (Figure 2). Therefore, HIF-1 plays a significant role in the Warburg effect, which may have implications for cancer diagnosis and treatment. While the precise molecular mechanism behind the Warburg effect remains to be elucidated, the involvement of HIF-1 is clear. Understanding the interplay between HIF-1, glycolysis, and OXPHOS in cancer cells may lead to the development of novel cancer therapies that target both pathways.



DOI: 10.3748/wjg.v29.i29.4499 **Copyright** ©The Author(s) 2023.

Figure 2 The complex interplay between glycolysis and oxidative phosphorylation in cancer cells. This figure highlights the signaling networks and metabolic regulation in both Warburg-like and oxidative cancer cells. p53 induces PTEN and represses PI3K activity, which inhibits glycolysis and opposes the Warburg effect. Hypoxia and the subsequent activation of hypoxia-inducible factor 1 (HIF-1) play a crucial role in modulating various aspects of cancer cell metabolism, including glycolysis, lactate production, and the tricarboxylic acid (TCA) cycle. Hypoxia counteracts the degradation of HIF-1 by prolyl hydroxylases and von Hippel-Lindau, which stabilizes and activates HIF-1. HIF-1 then transcriptionally activates genes such as hexokinase, phosphofructokinase-1, aldolase A, PGK1, PGAM1, ENO1, and LDHA, as indicated by the red arrows. During glycolysis, excessive lactate can be exported to the extracellular environment, leading to microenvironmental changes such as a lower pH. Intracellular lactate can also be transferred to adjacent cells and re-converted to pyruvate, which can enter the TCA cycle and drive oxidative phosphorylation in oxidative cancer cells. GLUT: Glucose transporter; HK: Hexokinase; G6P: Glucose-6-phosphate; G6PI: Glucose-6-phosphate isomerase; F6P: Fructose-6-phosphate; NADPH: Nicotinamide adenine dinucleotide phosphate; PFK1: Phosphofructokinase-1; F2,6BP: Fructose-2,6-bisphosphate; PFKBP3: Fructose-2,6-biphosphatase 3; F1,6BP: Fructose-1,6-bisphosphate; G3P: Glyceraldehyde-3-phosphate; DHAP: Dihydroxyacetone phosphate; GAPDH: Glyceraldehyde 3-phosphate dehydrogenase; 1,3BPG: 1,3-bisphosphoglycerate; 3PG: 3-phosphoglycerate; PGK: Phosphoglycerate kinase; PGAM: Phosphoglycerate mutase; 2PG: 2-phosphoglycerate; ENO: Enolase; PEP: Phosphoenolpyruvate; PKM1/2: Pyruvate kinase isozyme M1/M2; LDH: Lactate dehydrogenase; MCT: Monocarboxylate transporter family; PDH: Pyruvate dehydrogenase; IDH: Isocitrate dehydrogenase; α-KG: α-ketoglutarate; OAA: Oxaloacetate; SDH: Succinate dehydrogenase; FH: Fumarate hydratase; I: Mitochondrial complex I; II: Mitochondrial complex II; III: Mitochondrial complex III; IV: Mitochondrial complex IV; V: Mitochondrial complex V; Q: Co-enzyme Q; cyto C: Cytochrome *c*; HIF-1: Hypoxia-inducible factor 1; PHD: Prolyl hydroxylases; VHL: Von Hippel-Lindau.

The concept of lactate as a metabolic waste product has been revised with the latest findings in lactate metabolism and transport. It is now known that lactate can serve as an alternative fuel for certain types of cells, including cancer cells[56,57]. In cancer, the excess lactate is transported between the intracellular and extracellular matrix by the monocarboxylate transporter family (MCT1-4), which depends on the gradients of the protons and monocarboxylate ions[58,59]. Imported extracellular lactate can be converted to pyruvate *via* LDH primarily composed by the LDHB subunit[60,61]. In oxidative cancer cells with a functional TCA cycle and OXPHOS, pyruvate can be further converted to acetyl-CoA through PDH, thus linking aerobic glycolysis and OXPHOS[62,63]. It has been demonstrated that HIF-1 and downstream oncometabolite lactate play causal roles in these regulatory events. Therefore, current findings provide a possible explanation for the Warburg effect and crosstalk of bioenergetic homeostatic transition between aerobic glycolysis and OXPHOS observed in cancer. The importance of lactate in cancer metabolism and its potential as a therapeutic target have been recognized by others in the field. Thus, a better understanding of the metabolic pathways and their interactions could lead to the development of new strategies for cancer treatment.

THE LINK BETWEEN HYPOXIA-RELATED ENZYMES, BIOENERGETIC CHANGES, AND GI CANCER: A GENETIC AND EPIGENETIC PERSPECTIVE

Cancer cells often undergo a metabolic shift characterized by increased glycolysis and decreased mitochondrial respiration, a phenomenon known as the Warburg effect. This metabolic reprogramming has been linked to the activity of HIF-1 under low-oxygen conditions[64,65]. Genetic and epigenetic alterations in HIF-1 regulatory genes contribute to the development of the Warburg effect in cancer. Methylation-induced epigenetic changes can drive transcriptional changes, leading to impaired expression of key enzymes involved in bioenergetic homeostasis. Additionally, mutations in nuclear and mitochondrial genomes may cause a loss of function or decreased expression of glycolytic/OXPHOS enzymes. Therefore, mutations, transcriptional changes, or epigenetic alterations that enhance HIF-1 stability or activity can lead to increased aerobic glycolysis, resembling the Warburg effect (Table 1).

Studies have found that alterations in PHD enzymes, which target HIF-1 for degradation, contribute to cancer development and progression. Reduced expression or loss-of-function due to PHD2 mutations lead to constitutive activation of HIF-1 and have been found to stimulate HCC and CC development and progression in mouse models[66,67]. In contrast, decreased PHD1-3 expression correlates with increased HIF-1 and vascular endothelial growth factor (VEGF) levels, invasive tumor behavior, and poor prognosis in certain GI cancers such as HCC[68], GC[69-71], and CRC[72]. Interestingly, the opposite effect has been observed in patients with PAC[73]. Another protein involved in HIF-1 stabilization, VHL, also plays a role in GI cancers. Mutations or promoter methylation within the *VHL* gene lead to increased cytoplasmic HIF-1 levels and an unfavorable prognosis in patients with PAC and CRC[74,75]. However, the general status of VHL protein expression in GI cancers remains unclear, with the exception of HCC, whose levels have been shown to decrease, and low levels correlate with poor prognosis[76]. Further investigation is needed to determine the impact of mutations, genetic, or epigenetic alterations in these hypoxia-associated enzymes on bioenergetic alterations in GI cancers, since understanding the mechanisms behind the Warburg effect and the role of HIF-1 regulatory genes could potentially provide new therapeutic targets for treating GI cancers.

THE LINK BETWEEN MITOCHONDRIAL AND NUCLEAR GENE EXPRESSION, BIOENERGETIC HOMEOSTASIS, AND THE PROGRESSION OF GI CANCERS

Cancer development and progression are often accompanied by changes in cellular metabolism that contribute to tumor growth and survival. In addition to genetic and epigenetic alterations in hypoxia-associated regulatory enzymes that promote aerobic glycolysis, emerging evidence suggests that changes in nuclear-encoded genes for enzymes and subunits involved in OXPHOS and the TCA cycle may also play a role in driving the switch to glycolysis and altering bioenergetic homeostasis in cancer. Studies have shown that changes in the expression of key enzymes involved in OXPHOS, such as cytochrome *c* oxidase (COX) and ATP synthase, as well as the TCA cycle enzymes isocitrate dehydrogenase (IDH), fumarate hydratase (FH), and succinate dehydrogenase (SDH), may contribute to glycolysis transition and cancer progression[77-80]. Furthermore, mutations and copy number alterations in mtDNA have also been identified as important factors in the development and progression of GI cancer by altering bioenergetic homeostasis[81]. These emerging factors and their potential contribution to the complex mechanisms underlying the progression of GI cancer are discussed in more detail in the following sections.

ROLE OF MITOCHONDRIAL-NUCLEAR ENCODED COX SUBUNITS IN BIOENERGETIC CHANGES AND PROGRESSION OF GI CANCERS

The COX complex, also known as respiratory chain complex IV, is a multi-subunit enzyme complex, consisting of 14 subunits, and a vital component of the final step in the mitochondrial ETC responsible for catalyzing the transfer of electrons from cytochrome c to oxygen, a crucial step in the process of OXPHOS[82]. Recent studies have shown that alterations in the expression of both mtDNA-encoded and nuclear-encoded COX subunits are associated with tumori-

Table 1 Genetic and epigenetic alterations in hypoxia-related enzymes correlated with the development and progression of gastrointestinal cancers

Cancer type	Gene	Type of change	Consequence	Model	Ref.
HCC and CCA	PHD2	Haplo-deficiency	Stabilized HIF-1 and promoted carcinogenesis and progression of HCC/CCA	Mice	[66, 67]
HCC	PHD3	Reduced tumor level	Correlated with elevated levels of HIF-1, aggressive tumor behavior, and a poor prognosis in HCC patients	HCC patient	[68]
GC	PHD3	Reduced tumor level	Correlated negatively with tumor size and stage, as well as HIF-1 and VEGF expression	GC patient	[69, 70]
GC	PHD2	Reduced tumor level	Correlated with shortened overall survival	GC patient	[71]
CRC	PHD1-3	Reduced tumor level	Although not correlated with HIF-1 expression, PHD2 was the only factor found to be associated with unfavorable overall survival	CRC patient	[72]
PAC	PHD1-3	Increased tumor level	PHD1-3 expression was elevated, and specifically PHD3 expression was found to be associated with unfavorable overall disease-specific survival	PAC patient	[73]
PAC	VHL	Promoter methylation or deletion of VHL	Correlated with decreased VHL expression and poor prognosis	PAC patient	[74]
CRC	VHL	*VHL* mutation	Elevated cytoplasmic expression of HIF-1 in tumors	CRC patient	[75]
HCC	VHL	Reduced tumor level	Negative VHL expression was correlated with an unfavorable prognosis	HCC patient	[76]

ESCA: Esophageal cancer; GC: Gastric cancer; HCC: Hepatocellular carcinoma; CCA: Cholangiocarcinoma; PAC: Pancreatic cancer; CRC: Colorectal cancer; PHD: Prolyl hydroxylase; VHL: Von Hippel-Lindau tumor suppressor.

genesis, cancer progression, and bioenergetic homeostasis in cancer. In GI cancers, alterations in the expression of the mitochondrial-nuclear encoded subunits of the COX complex have been implicated in driving disease progression. Studies have shown that the overall levels of the COX complex are increased in GI cancers, and higher levels have been associated with poor clinical outcomes[83,84]. Of the three mtDNA-encoded core subunits essential for the basic functions of the COX complex, including MTCO1, MTCO2, and MTCO3[85], MTCO1 is the most frequently investigated in GI cancers (Table 2). In ESCA, MTCO1 expression was found to be elevated but did not correlate with clinicopathological variables or survival[86]. On the other hand, elevated levels of MTCO1 were associated with diffuse GC types, suggesting a link between MTCO1 expression and GC carcinogenesis, de-differentiation, and distant metastasis[87,88]. In contrast, defective MTCO1 expression was observed in patients with HCC and CCA, while MTCO1 levels have been shown to predict postoperative survival in patients with HCC[89,90]. Elevated MTCO3 levels have been observed only in HCC, especially among patients with hepatitis B virus (HBV)-related HCC. This is likely due to the ability of the HBV X protein (HBx) to interact and increase MTCO3 expression[91,92]. Additionally, genetic variants identified within MTCO1 and MTCO3 are associated with increased carcinogenic risk in CRC[93,94], GC[95], and HCC[96], possibly due to reduced COX activity leading to intrinsic proton leak and a reduction in overall bioenergetic production efficiency[93,94]. However, studies on the expression or genetic variation of MTCO2 in GI cancers are relatively few and need further investigation.

While the three core mtDNA-encoded COX subunits have been extensively studied, 11 nuclear-encoded protein subunits are also required for the full functionality of the COX complex[97]. Of these 11 subunits, six can be replaced by isoforms, leading to heterogeneity in the composition and activity of this large complex[98]. In GI cancers, altered expression of nuclear-encoded COX subunits has been shown to play a crucial role in the switch to glycolysis and the promotion of tumor growth and progression (Table 2). For example, in ESCA, the silencing of COX4I1 and COX5B has been shown to promote bioenergetic changes and increased aggressiveness of ESCA cells *in vitro*[99]. In HCC and CRC, COX5B levels were found to correlate with prognosis, and changes in COX5B expression were associated with alterations in bioenergetics, cell proliferation, tumor growth, migration, and chemosensitivity. HCC and CRC, however, showed different COX5B expression patterns[100-102]. Similarly in CRC, increased COX4I2 has been shown to promote cell proliferation, migration, tumorigenesis, and angiogenesis[103]. COX6C and COX6B2 were also found to be increased in PAC, with changes in expression levels of COX6C affecting COX activity and cell growth *in vitro*. Meanwhile, COX6B2 levels were associated with prognosis, metastatic potential in PAC cells, and altered bioenergetic homeostasis[104,105].

The roles of remaining subunits in GI cancer are currently unknown, and studies focusing on the level of nuclear-encoded COX subunit in GI cancer largely suggest that altered expression leads to decreased OXPHOS activity in a Warburg effect-like phenotype. Increased GI cancer growth and/or progression is also suggested. Together, these findings highlight the crucial role COX subunits play in GI cancer progression and underscore the need for continued research. The identification of altered COX subunit expression and function may lead to the development of novel therapeutic targets for the treatment of GI cancers. Therefore, further research on the COX complex and its subunits is

Table 2 Defects in cytochrome c oxidase subunits correlated with bioenergetic alterations and the growth or progression of gastrointestinal cancers

Type	Gene	Type of defect	Consequence	Model	Ref.
GC	Full COX complex	Increased expression	Correlated with poor prognosis	GC patient	[83]
CRC	Full COX complex	Increased expression	May be involved in the initiation of carcinogenesis, but not in cancer progression	CRC patient	[84]
ESCA	MTCO1	Increased expression	There is no correlation with clinical variables or survival	ESCA patient	[86]
GC	MTCO1	Increased expression	Correlated with gastric tumorigenesis, dedifferentiation, and distant metastasis, but showed no significant correlation with prognosis	GC patient	[87,88]
HCC	MTCO1	Reduced expression	Correlated with postoperative prognosis	HCC patient	[89]
CCA	MTCO1	Reduced expression	Reduced MTCO1 correlates with increased VDAC1 expression but not with other clinicopathological factors	CCA patient	[90]
HCC	MTCO3	Increased expression	HBx interacted with MTCO3, leading to an increase in MTCO3 expression levels and an enhancement in OXPHOS activity	Cell line	[91,92]
CRC	MTCO1	Genetic variation	The Gly125Asp substitution in MTCO1 correlated with an increased risk of CRC and caused proton leak in COX	CRC patient	[93,94]
GC	MTCO3	Genetic variation	Polymorphisms at mtDNA positions 9540 and 9548 correlated with an increased risk of GC	GC patient	[95]
HCC	MTCO3	Genetic variation	Polymorphisms at mtDNA position 9545 correlated with an increased risk of HCC	HCC patient	[96]
ESCA	COX4I1	Expression silenced	Promotes alterations in cellular bioenergetics and increases cancer cell aggressiveness	ESCA Cell line	[99]
ESCA	COX5B	Expression silenced	Promotes alterations in cellular bioenergetics and increases cancer cell aggressiveness	ESCA Cell line	[99]
HCC	COX5B	Increased in tumor	Correlated with prognosis, regulated bioenergetic alterations, and influenced cell proliferation, tumor growth, and migration	HCC patient, cell line, mouse model	[100]
CRC	COX5B	Reduced in tumor	Correlated with prognosis, modulated COX activity, and controlled cell proliferation, apoptosis, and response to chemotherapy	CRC patient and cell line	[101,102]
CRC	COX4I2	Increased in tumor	Promoted cell proliferation, migration, tumorigenesis, and angiogenesis	CRC patient and cell line	[103]
PAC	COX6C	Increased expression	Modulated COX activity and cell proliferation	PAC cell line	[104]
PAC	COX6B2	Increased in tumor	Correlated with prognosis, and modulated cancer cell metastatic potential, and altered bioenergetic homeostasis	PCA patient and cell line	[105]

COX: Cytochrome *c* oxidase; GI: Gastrointestinal; ESCA: Esophageal cancer; GC: Gastric cancer; HCC: Hepatocellular carcinoma; CCA: Cholangiocarcinoma; PAC: Pancreatic cancer; CRC: Colorectal cancer; MTCO1: Mitochondrially encoded cytochrome *c* oxidase I; MTCO2: Mitochondrially encoded cytochrome *c* oxidase II; MTCO3: Mitochondrially encoded cytochrome *c* oxidase III; COX4I1: Cytochrome *c* oxidase subunit 4I1; COX4I2: Cytochrome *c* oxidase subunit 4I2; COX5B: Cytochrome *c* oxidase subunit 5B; COX6C: Cytochrome *c* oxidase subunit 6C; COX6B2: Cytochrome *c* oxidase subunit 6B2.

needed to fully elucidate their role in GI cancer.

THE ROLE OF ATP SYNTHASE SUBUNITS IN DRIVING BIOENERGETIC CHANGES AND GI CANCER PROGRESSION

ATP synthase, also known as Complex V, is a crucial mitochondrial protein complex that plays a vital role in cellular ATP synthesis. The F1 beta-catalytic subunit (ATP5F1B) is a critical component that has been extensively studied to find a significant reduction in various cancer types, including GI cancers[106] (Table 3). However, the expression patterns of ATP5F1B in patients with GC remain controversial. While one study reported increased ATP5F1B expression in tumors,

Table 3 Implications of defects in adenosine triphosphate synthase subunits on bioenergetic alterations and the development or progression of gastrointestinal cancer

Type	Gene	Type of defect	Consequence	Model	Ref.
GC	ATP5F1B	Increased in tumor	Higher ATP5B expression correlated with poor prognosis. Over-expression of ATP5F1B increased intracellular and extracellular ATP levels, cell proliferation, migration, and invasion	GC patient, cell line, and xeno-transplantation mouse model	[107]
GC	ATP5F1B	Reduced in tumor	Reduced ATP5F1B expression correlated with elevated glycolytic enzyme levels	GC patient	[108]
HCC	ATP5F1B	Reduced in tumor	Reduced ATP5F1B expression correlated with impaired OXPHOS	HCC patient	[109, 110]
ESCA	ATP5F1B	Reduced in tumor	Reduced ATP5F1B expression correlated with elevated glycolytic enzyme levels	ESCA patient	[108]
CRC	ATP5F1B	Reduced in tumor	Reduced ATP5F1B expression correlated with poor prognosis in CRC patients	CRC patient	[109]
PAC	ATP5F1B	Reduced in tumor	Unknown	PAC patient and cell line	[111]
CRC	ATP5F1A	Increased in liver metastasized tumor	Silencing of ATP5F1A inhibited cell invasion and reduced cell proliferation in CRC cancer cells	CRC patient and cell line	[112]
CRC	ATP5F1E	Increased in tumor	Higher ATP5E levels correlated with poor prognosis. Silencing of ATP5F1E inhibited cancer cell migration and invasion *in vitro*, and distal metastasis *in vivo*	CRC patient, cell line, and tail vein injected mouse model	[113]
CRC	ATP5F1D	Increased in liver metastasized tumor	Higher ATP5F1D expression correlated with poor prognosis, and silencing of ATP5F1D inhibited cell invasion	CRC patient and cell line	[112]

ATP: Adenosine triphosphate; GI: Gastrointestinal; ESCA: Esophageal cancer; GC: Gastric cancer; HCC: Hepatocellular carcinoma; CCA: Cholangiocarcinoma; PAC: Pancreatic cancer; CRC: Colorectal cancer; ATP5F1A: ATP synthase F1 subunit alpha; ATP5F1B: ATP synthase F1 subunit beta; ATP5F1D: ATP synthase F1 subunit delta; ATP5F1E: ATP synthase F1 subunit epsilon.

correlating with poor prognosis[107], consistent findings from other GI cancer studies indicate that decreased ATP5F1B expression results in reduced ATP production efficiency from OXPHOS and a subsequent shift towards the glycolysis-dependent Warburg effect phenotype[108-111]. These findings highlight the critical role of ATP synthase in GI cancer progression, suggesting that mitochondrial defects in ATP synthesis may contribute to the bioenergetic alterations observed in these cancers.

Apart from the F1 beta-subunit, other subunits of the ATP synthase F1 region have been implicated as crucial to CRC carcinogenesis/progression. Interestingly, in contrast to the finding that ATP5F1B generally decreases in tumors, ATP5F1A, ATP5F1E, and ATP5F1D were found to be increased in patients with CRC. Moreover, higher levels correlated with poorer prognosis as well as increased risk of CRC liver metastasis[112,113]. Currently, there are no reports on the expression patterns or role of ATP synthase subunits in CCA. The mechanisms underlying opposing expression patterns in ATP synthase subunits are thus unknown pending further investigation.

To provide more insight into the development of novel therapeutic targets for the treatment of GI cancers, further research on ATP synthase expression and function is necessary. In this regard, potential avenues of research may focus on clarifying the controversial findings regarding ATP5F1B expression patterns in GC and elucidating the mechanisms underlying these opposing expression patterns seen in differing ATP synthase subunits in CRC. Such research may uncover novel therapeutic targets, leading to improved treatment outcomes.

LINKING IDH, FH, AND SDH TO BIOENERGETICS AND GI CANCER PROGRESSION

Fumarate and succinate are critical metabolites that are produced during the TCA cycle, which is an essential process for energy production in cells. While these metabolites are important for normal cellular function, they have been shown to act as oncometabolites in various types of cancer by inducing pseudohypoxia[114]. Specifically, aberrant fumarate and succinate accumulation resulting from mutations or abnormal expression in FH and SDH, respectively, can impede the production of α-ketoglutarate in the TCA cycle, which is a key substrate in tumor suppression pathways. Similarly, mutations in IDH enzymes, which are responsible for α-ketoglutarate synthesis, can directly reduce the levels of α-ketoglutarate. This reduction in α-ketoglutarate can limit the availability of substrate for the hydroxylation of HIF-1 by PHDs for subsequent degradation by the proteasome. Consequently, stabilized HIFs activate the transcription of genes involved in cancer-related processes such as angiogenesis, glucose metabolism, and cell proliferation, thereby promoting cancer development and progression[114].

In addition to their effects on HIFs, high levels of fumarate and succinate have been shown to cause abnormal methylation of DNA and histones, leading to dysregulation of gene expression and cell function. This is due to

attenuation of enzymes responsible for DNA and histone demethylation such as tet-eleven translocation methyl-cytosine dioxygenase (TET) and lysine demethylase (KDM, also known as the Jumonji C domain-containing histone demethylase, JHDM)). Dysregulation of gene expression, increased carcinogenicity, and cancer progression can result from decreased α -ketoglutarate under high fumarate and succinate levels[115,116] (Figure 3).

The FH and SDH enzymes responsible for the catabolism of fumarate and succinate have been implicated as tumor suppressors[117]. Genetic variants in FH or SDH complex subunits, including SDHA, SDHB, SDHC, and SDHD, have been associated with increased risk of certain cancers such as hereditary leiomyomatosis and renal cell cancer (HLRCC) [118,119] as well as paraganglioma and pheochromocytoma[120-123]. Although there is limited evidence involving genetic mutants of FH or SDH complex subunit genes in GI cancer, an unusual mutation of the FH gene was found to be associated with the development of gastric leiomyoma following cutaneous and uterine leiomyomatosis[124]. Except for loss-of-function mutations, some researchers have revealed FH and SDH complex subunit gene single nucleotide polymorphisms (SNP) in patients with HCC and CRC[125,126]. Interestingly, FH was found to be downregulated in HCC patients with portal vein thrombosis due to currently unknown underlying mechanisms[127]. However, the role of FH and SDH in GI cancer remains largely unknown. Further investigation is thus necessary.

Understanding the role of oncometabolites in GI cancer could provide valuable insights into the development of novel therapeutic targets for the treatment of these cancers. Further research should be conducted to investigate the potential roles of FH and SDH in the development and progression of GI cancer and explore the possible therapeutic targets associated with the regulation of these enzymes. By gaining a better understanding of oncometabolites in GI cancer, we may be able to develop more effective therapies and improve patient outcome.

EXPLORING BIOENERGETIC REGULATORS AS TARGETS FOR GI CANCER THERAPY

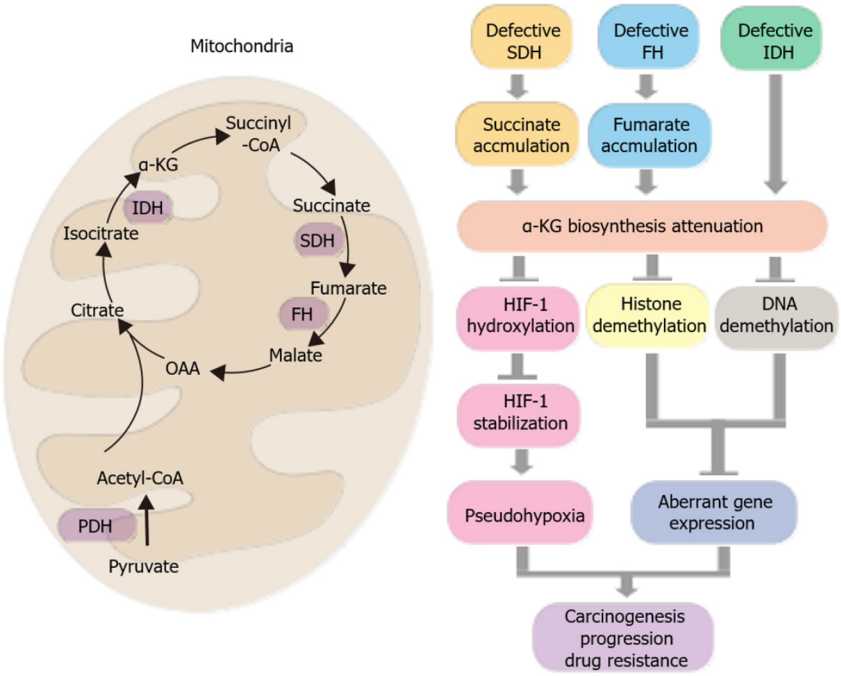
Our current understanding of metabolic reprogramming and bioenergetic alterations in cancer has led to the emergence of several potential drugs that target the bioenergetics of cancer cells, offering a promising avenue for anti-cancer therapy. These drugs can be classified into two main categories based on their mode of action: targeting aerobic glycolysis/lactate biosynthesis and transportation, or targeting the TCA cycle and coupled OXPHOS (Figure 4).

To target aerobic glycolysis, several strategies have been developed including blocking glucose import by targeting GLUT1, reducing glycolysis activity by targeting hexokinase 2 (HK2), PKMFB3, and PKM2, inhibiting lactate biosynthesis by targeting LDHA and PDK, and blocking lactate transportation through targeting MCT1/2. Targeting the TCA cycle and OXPHOS involves PDH and mitochondrial complex inhibitors. Several bioenergetic-targeted drugs have provided pre-clinical or clinical evidence in treating GI cancers. Table 4 provides a summary of these drugs. In the following sections, we will discuss the details of such strategies and the drugs used to target bioenergetic regulators during GI cancer therapy.

UNLOCKING THE POTENTIAL OF GLUCOSE METABOLISM TARGETS IN GI CANCER THERAPY

Cancer cells typically rely on increased glucose uptake, a phenomenon known as the Warburg effect, to meet energy requirements, making glucose uptake a promising target for anti-cancer therapy. As a result, GLUT1 has been identified as a potential drug target for blocking glucose uptake. Several GLUT1 inhibitors, including genistein, apigenin, fasentin, WZB117, WZB27, WZB115, STF-31, and BAY-876 have shown an ability to block glucose uptake[14]. Genistein and apigenin are natural compounds belonging to the flavonoid group, and they have been shown to inhibit hypoxia-inducible factor 1A (HIF1A) mRNA and protein expression, which leads to inactivation of downstream genes such as GLUT1 and HK2, thereby attenuating glycolysis activity[128-130]. In GI cancers, these compounds have demonstrated the ability to inhibit cancer cell proliferation, cell cycle progression, colony formation, migration, invasion, angiogenesis, stemness, spheroid formation, EMT, and to enhance cell death[131-146]. Although the majority of evidence pertaining to efficacy comes from *in vitro* cell-based assays, genistein and apigenin have entered clinical trials as a combination anti-cancer therapy for patients with CRC (NCT10985763 and NCT00609310) and PAC (NCT02336087, NCT00376948 and NCT00882765). Moreover, dietary supplementation with apigenin has been shown to significantly prevent CRC recurrence in a prospective study[147]. Fasentin, WZB117, WZB27, WZB115, STF-31, and BAY-876 are synthetic chemicals with selective activity on GLUT1 inhibition. Fasentin, WZB27, and WZB115 have shown anti-cancer potential in other pre-clinical cancer models, although there is currently little to no research on GI cancers. WZB117 has been shown to reduce glucose uptake, inhibit cell proliferation/invasion, and enhance chemosensitivity in GI cancer cell lines, as well as in xenograft models[148-151]. STF-31 has been implicated in reducing cancer stem cell stemness, cell proliferation, viability, and tumor growth in PAC and CRC cell lines, as well as in xenograft models[152,153]. BAY-876 has been found to inhibit cell proliferation, tumor growth, glucose uptake, and promote chemosensitivity in ESCA, PCA, and CRC cell lines, and in xenograft mouse models[154-156]. Although these findings are promising, WZB117, STF-31, and BAY-876 are not currently in clinical trials for GI cancer. Thus, their safety, dosage, and therapeutic response in GI cancer patients remain to be determined in future studies.

Another strategy to block glycolysis is by targeting glycolytic enzymes or attenuating glycolytic activity. A well-studied example of this strategy is the use of 2-deoxy-D-glucose (2-DG), a glucose molecule with a 2-hydroxyl group replaced by hydrogen. 2-DG is taken up by cells with high glucose uptake ability, such as cancer cells, where it serves as a competitive inhibitor of glucose[157]. Once inside the cell, 2-DG enters the glycolytic pathway and is phosphorylated by HK2 to become 2-DG-6-phosphate (2-DG-6-P), which cannot be further processed by G6P isomerase and therefore



DOI: 10.3748/wjg.v29.i29.4499 **Copyright** ©The Author(s) 2023.

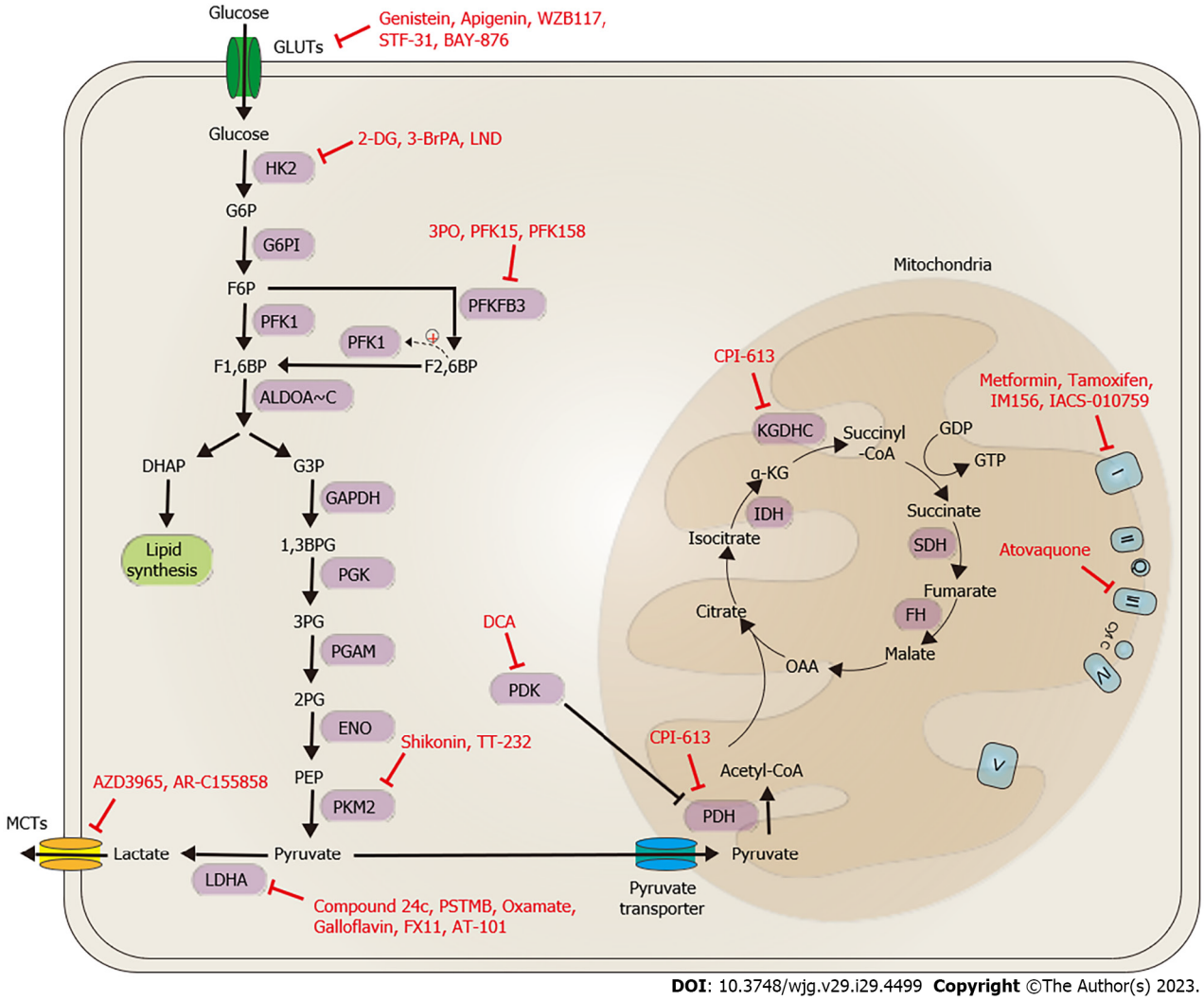
Figure 3 Tricarboxylic acid cycle dysfunction in cancer and its role in carcinogenesis, progression, and anti-cancer drug resistance. The left panel depicts the tricarboxylic acid cycle, with succinate dehydrogenase and fumarate hydratase as key regulatory enzymes responsible for the formation of oncometabolites succinate and fumarate. The isocitrate dehydrogenase enzyme synthesizes α-ketoglutarate, which serves as a substrate for tumor suppressor pathways, such as hypoxia-inducible factor 1 hydroxylation for degradation, as well as histone and DNA demethylation. These processes can lead to pseudohypoxia and aberrant gene expression, promoting carcinogenesis, progression, and anti-cancer drug resistance. The right panel provides a summary of these relationships. OAA: Oxaloacetate; SDH: Succinate dehydrogenase; FH: Fumarate hydratase; PDH: Pyruvate dehydrogenase; IDH: Isocitrate dehydrogenase; α-KG: α-ketoglutarate; HIF-1: Hypoxia-inducible factor 1.

accumulates. Accumulated 2-DG-6-P reversely negatively inhibits HK2 activity, leading to a reduction in glycolytic activity. A derivative of 2-DG, fluorodeoxyglucose (18F-FDG), has been extensively employed in positron emission tomography (PET) to visualize the location and status of certain types of cancers[158]. In pre-clinical studies using GI cancer cell lines, as well as xenograft models and rat HCC and hamster PAC models, 2-DG has been shown to inhibit cell proliferation, tumor growth, and promote chemosensitivity[159-165]. Although 2-DG has entered clinical trials for other cancer types, only a phase I trial (NCT00096707) was conducted for patients with PAC, and the safety, dose, and efficacy of 2-DG in treating patients with other GI cancers are unknown.

Several other chemical drugs have been claimed to inhibit HK2 function, but their roles in GI cancers are unclear, with the exception of 3-bromopyruvate (3-BrPA) and lonidamine (LND). 3-BrPA is an analog of both lactate and pyruvate and shows an inhibitory effect on HK2, possibly due to its ability to induce protein alkylation[166,167]. In pre-clinical studies of GI cancers, 3-BrPA has shown its ability to inhibit cellular ATP generation, cell proliferation, tumor growth, induce mitochondrial depolarization, reduce animal serum VEGF levels, and promote cell death and chemosensitivity in GC, HCC, PAC, and CRC cell lines, as well as rabbit, transgenic mice, and xenograft mouse models[167-171]. Therapeutic efficacy and safety were only evaluated in a case report study, providing a safe and tolerable dose of 3-BrPA in patients with fibrolamellar HCC[172].

LND is an indazole derivative that was previously utilized as an anti-spermatogenic agent. In drug re-purposing studies, LND was found to have anti-cancer activity by affecting bioenergetic homeostasis, including the glycolytic pathway, through targeting HK2 *via* currently unclear mechanisms[173]. LND showed promising therapeutic efficacy by inhibiting cell proliferation, migration, invasion, cell cycle progression, and increasing chemosensitivity in HCC, CCA, and CRC cell lines, as well as in a hamster CCA model[174-179]. Encouraging results were observed in a clinical trial recruiting patients with GC, showing improved overall response rate and duration of disease progression[174]. Reversely, it was reported that administration of LND was ineffective and toxic in clinical trials recruiting patients with CRC[178, 179].

Targeting PFKFB3 is another approach to block cancer glycolysis, as it is considered an oncogene in cancers due to its high expression and role in glycolysis[180]. PFKFB3 is activated by multiple cancer-associated stimuli, including cytokines, chemokines, growth factors, and hypoxia, and then participates in glycolysis through catalyzing fructose-6-P to become F2,6BP, which can further positively enhance PFK1 activity and thus accelerate glycolysis[180]. Accordingly, PFKFB3 drugs have been identified and tested in pre-clinical and clinical studies. Among the list of candidate drugs that target PFKFB3, 3-(3-pyridinyl)-1-(4-pyridinyl)-2-propen-1-one (3PO), 1-(4-pyridinyl)-3-(2-quinolinyl)-2-propen-1-one (PFK15), and 1-pyridin-4-yl-3-[7-(trifluoromethyl)-quinolin-2-yl]-prop-2-en-1-one (PFK158) have drawn more attention than others[181]. It was found that 3PO and PFK15 inhibit cell proliferation, reduce tumor growth, attenuate angiogenesis, prevent fibrogenesis, and increase cell death in pre-clinical studies using GI cancer cell lines, transgenic mice,



DOI: 10.3748/wjg.v29.i29.4499 **Copyright** ©The Author(s) 2023.

Figure 4 Potent bioenergetic-targeting drugs for gastrointestinal cancers. Promising bioenergetic drugs for gastrointestinal cancers can be classified into two main categories based on their mode of action. The first category involves targeting aerobic glycolysis and lactate biosynthesis/transportation, while the second category involves targeting the tricarboxylic acid (TCA) cycle and oxidative phosphorylation (OXPHOS). Strategies to target aerobic glycolysis include blocking glucose importation through the targeting of glucose transporter 1 with compounds such as genistein, apigenin, WZB117, STF-31, and BAY-876, reducing glycolysis activity by targeting HK2 with compounds such as 2-DG, 3-BrPA, and LND, and targeting PKMFB3 and PKM2 with compounds such as 3PO, PFK15, PFK158, shikonin, and TT-232. Lactate biosynthesis can be inhibited by targeting LDHA with compounds such as compound 24c, PSTMB, oxamate, galloflavin, FX11, and AT-101, and PDK with DCA. Lactate transportation can be blocked by targeting MCT1/2 with compounds such as AZD3965 and AR-C155858. Targeting the TCA cycle and OXPHOS involves using inhibitors of pyruvate dehydrogenase, such as CPI-613, and mitochondrial complex I with metformin, tamoxifen, IM156, IACS-010759, and complex III with atovaquone. GLUT: Glucose transporter; HK: Hexokinase; G6P: Glucose-6-phosphate; G6PI: Glucose-6-phosphate isomerase; F6P: Fructose-6-phosphate; NADPH: Nicotinamide adenine dinucleotide phosphate; PFK1: Phosphofructokinase-1; F2,6BP: Fructose-2,6-bisphosphate; PFKBP3: Fructose-2,6-biphosphatase 3; F1,6BP: Fructose-1,6-bisphosphate; G3P: Glyceraldehyde-3-phosphate; DHAP: Dihydroxyacetone phosphate; GAPDH: Glyceraldehyde 3-phosphate dehydrogenase; 1,3BPG: 1,3-bisphosphoglycerate; 3PG: 3-phosphoglycerate; PGK: Phosphoglycerate kinase; PGAM: Phosphoglycerate mutase; 2PG: 2-phosphoglycerate; ENO: Enolase; PEP: Phosphoenolpyruvate; PKM1/2: Pyruvate kinase isozyme M1/M2; LDH: Lactate dehydrogenase; MCT: Monocarboxylate transporter family; PDH: Pyruvate dehydrogenase; IDH: Isocitrate dehydrogenase; α-KG: α-ketoglutarate; OAA: Oxaloacetate; SDH: Succinate dehydrogenase; FH: Fumarate hydratase; I: Mitochondrial complex I; II: Mitochondrial complex II; III: Mitochondrial complex III; IV: Mitochondrial complex IV; V: Mitochondrial complex V; Q: Co-enzyme Q; cyto C: Cytochrome *c*; KGDHC: α-ketoglutarate dehydrogenase complex.

xenograft mouse models, and HCC rat models[182-189]. Intriguingly, it was also found that 3PO suppresses glucose uptake *via* a 14C-2-DG tracing system[184]. Although there is no pre-clinical evidence of efficacy in GI cancers, the safety, tolerated dose, and therapeutic efficacy of PKF158 have been evaluated in a Phase I clinical trial (NCT02044861) that involved patients with solid tumors[190].

One strategy proposed to inhibit glycolysis activity is to target the last enzyme in the glycolytic pathway –PKM2. PKM2 targeting is based on its glycolysis role as well as aberrant expression in cancer-associated events[191]. While many drugs have shown the ability to inhibit PKM activity, only two, TT-232 and Shikonin, have been confirmed efficacious in pre-clinical studies. Both TT-232 and Shikonin have been found to inhibit GI cancer cell proliferation, migration, invasion, cell cycle progression, and tumor growth, as well as enhance cell death[192-200]. However, the efficacy of these drugs in treating GI cancers is still unclear and requires further investigation. Both drugs have entered clinical trials for specific cancers, showing promise as cancer therapy targets.

Table 4 Promising novel bioenergetics targeting drugs for gastrointestinal cancer therapy

Inhibitor	Target	GI model	Consequence	Clinical trial	Ref.
Targeting glucose transportation					
Genistein	HIF1A, GLUT1 and HK2	GC, ESCA, HCC, CCA, PCA, and CRC cell lines	Inhibited cancer cell proliferation, cell cycle progression, migration, invasion, angiogenesis, stemness, spheroid formation, EMT, and promoted apoptosis	CRC patient, phase I/II (NCT10985763), and PAC patient, phase I/II (NCT02336087, NCT00376948 and NCT00882765)	[131-140]
Apigenin	HIF1A, GLUT1 and HK2	GC, ESCA, HCC, CCA, PCA, and CRC cell lines	Inhibited cancer cell proliferation, colony-forming, cell cycle progression, migration, invasion, angiogenesis, and induced apoptosis	CRC patient, phase II (NCT00609310)	[141-146]
WZB117	GLUT1	HCC, CCA, PAC, and CRC cell lines, and xenograft models	Reduced glucose uptake, inhibits cell proliferation, and invasion, and enhanced chemosensitivity	None in GI cancers	[148-151]
STF-31	GLUT1	PAC and CRC cell lines, and xenograft model	Reduced cancer stem cell properties, such as stemness, and inhibits cell proliferation, viability, and tumor growth	None in GI cancers	[152, 153]
BAY-876	GLUT1	ESCA, PCA, and CRC cell lines, and xenograft mouse models	Reduced cancer cell proliferation, tumor growth, and glucose uptake, while also increased chemosensitivity	None in GI cancers	[154-156]
Targeting glucose metabolism					
2-Deoxy-D-glucose (2-DG)	HK2	GC, ESCA, HCC, PAC and CRC cell lines, xenograft models, and rat HCC and hamster PAC models	Inhibited cell proliferation, tumor growth, and promoted chemosensitivity	PAC patient, phase I (NCT00096707)	[159-165]
3-Bromopyruvate (3-BrPA)	HK2	GC, HCC, PCA, and CRC cell lines, and rabbit, transgenic mouse and xenograft mouse models	Inhibited cellular ATP generation, cell proliferation, and tumor growth. Also induced mitochondrial depolarization, reduced animal serum VEGF levels, and promoted cell death and chemosensitivity	HCC patient, case report[170]	[167-170]
Lonidamine (LND)	HK2	HCC, CCA, and CRC cell lines, hamster CCA model, and GC and CRC patients	Inhibited cell proliferation, migration, invasion, and cell cycle progression. Increased chemosensitivity, patient overall response rate, and duration of disease progression in GC patients. However, was ineffective and toxic in advanced CRC patients	GC patient, phase II[172], CRC patients, phase II[176,177]	[174-179]
3-(3-pyridinyl)-1-(4-pyridinyl)-2-propen-1-one (3PO)	PFKFB3	HCC, PAC, and CRC cell lines, and transgenic and xenograft mouse models	Inhibited glucose uptake, cell proliferation, tumor growth, angiogenesis, fibrogenesis, and promoted cell death	None in GI cancers	[182-184]
1-(4-pyridinyl)-3-(2-quinolinyl)-2-propen-1-one (PFK15)	PFKFB3	GC, HCC, PAC, and CRC cell lines, xenograft models, and HCC rat model	Inhibited cell proliferation, migration, invasion, cell cycle progression, tumor growth, and enhanced cell death	None in GI cancers	[185-189]
1-pyridin-4-yl-3-[7-(trifluoromethyl)-quinolin-2-yl]-prop-2-en-1-one (PFK158)	PFKFB3	None in GI cancers	None in GI cancers	Solid tumor patients, phase I (NCT02044861)	[190]
Shikonin	PKM2	GC, ESCA, HCC, CCA, PCA, and CRC cell lines, and xenograft mouse models	Inhibited cell proliferation, migration, invasion, cell cycle progression, tumor growth, and enhanced cell death	None in GI cancers	[192-197]
TT-232	PKM2	HCC, PAC, and CRC cell lines,	Inhibited cell proliferation, tumor growth, and enhanced cell death	None in GI cancers	[198-200]

		and xenograft mouse models			
Targeting lactate biosynthesis					
Dichloroacetate (DCA)	PDK	GC, ESCA, HCC, PAC, and CRC cell lines, xenograft models, and B6C3F1 mice	Reduced lactate production, cell proliferation, migration, and increased chemosensitivity. Showed synergistic anticancer effects in HCC. However, promoted hepatocarcinogenesis in B6C3F1 mice	CRC patient, phase I (NCT00566410)	[203-207]
Compound 24c	LDHA	PAC cell lines, and xenograft model	Suppressed cell proliferation, colony formation, enhanced cell apoptosis, arrested cell at G2 phase, repressed xenograft growth, and re-programmed cancer metabolism, with minimal impact on mouse weight	None in GI cancers	[210]
1-(Phenylseleno)-4-(Trifluoromethyl) Benzene (PSTMB)	LDHA	HCC and CRC cell lines	Inhibited cell proliferation, reduced cell viability, attenuated LDHA activity, lowered lactate levels, and induced mitochondria-mediated apoptosis	None in GI cancers	[211]
Oxamate	LDHA	GC, ESCA, HCC, PCA, and CRC cell lines	Suppressed LDHA activity, lactate production, cell proliferation, migration, MMP9 expression, pro-inflammatory cytokines, EMT transition, and AKT/ERK/mTOR signaling pathways, while enhanced apoptosis, senescence, protective autophagy, and metabolic rewiring	None in GI cancers	[212-218]
Galloflavin	LDHA	HCC, PCA, and CRC cell lines	Reduced ATPase activity and expression levels of heat shock proteins, inhibited cell proliferation, lactate production, pro-inflammatory cytokines, and EMT transition, while promoting apoptosis and senescence	None in GI cancers	[215, 218-220]
FX11	LDHA	HCC, PCA, and CRC cell lines, and xenograft mouse models	FX11 reduced lactate production and ATP levels, suppressed cell proliferation, migration, invasion, and xenograft tumor growth, while enhancing apoptosis. However, in a PCA patient-derived mouse xenograft model, FX11 was only effective in attenuating tumor growth in the presence of mutant TP53	None in GI cancers	[221-225]
Gossypol (AT-101) or its derivatives	LDHA	GC, ESCA, HCC, PAC and CRC cell lines, GC and xenograft mouse models, and ESCA patient	Reduced cell viability, suppressed cell proliferation, migration, and tumor growth, down-regulated cancer stem cell markers CD133, Nanog, LC3, and YAP-1, enhanced apoptosis, protective autophagy. and complete response rate/prognosis	ESCA patient, phase I/II (NCT00561197)	[226-240]
Targeting lactate transportation					
AZD3965	MCT1/2	GC, ESCA, HCC, CRC cell lines	Inhibited cell proliferation and tumor growth, while increasing intracellular lactate concentration, TCA-related metabolites, mitochondrial metabolism, and chemosensitivity. Also decreased intracellular pH	None in GI cancers	[242-246]
AR-C155858	MCT1/2	GC, PAC, and CRC cell lines, and xenograft mouse models	Inhibited cell proliferation, spheroid forming ability, and tumor growth, while decreased glycolysis and increased intracellular lactate concentration, TCA-related metabolites, mitochondrial metabolism, and chemosensitivity	None in GI cancers	[247-249]
Targeting mitochondrial OXPHOS					
Metformin	Mitochondrial complex I	GC, ESCA, HCC, CCA, PAC, and CRC cell lines, xenograft models, and ESCA, HCC, CCA, PCA and CRC patients	Suppressed cell proliferation, migration, cell cycle progression, and tumor growth while increasing chemosensitivity and cell death. Also re-programmed the tumor immune microenvironment in ESCA patients	ESCA patient, phase II (ChiCTR-ICR-15005940), HCC patient, phase I (CTRI/2018/07/014865), CCA patient, phase Ib (NCT0249674), PCA patient, phase II (NCT01210911 and NCT01167738), and CRC patient, phase II (NCT01312467, NCT03047837, and NCT01941953)	[252-265]

Tamoxifen	Mitochondrial complex I	GC, ESCA, HCC, CCA, PAC and CRC cell lines, CRC murine model, and ESCA, HCC and PAC patients	Inhibited cell proliferation, tumor growth, metastasis, and increased chemosensitivity. However, no prolonged survival benefits have been observed in HCC patients, and in some cases, there may even be a higher risk of death	ESCA patient, phase I (NCT02513849), PAC patient, phase II[272-274], and HCC patient, phase III (NCT00003424)	[267-273, 277]
IM156	Mitochondrial complex I	GC and CRC patients	Considered tolerable in human subjects, with stable disease being the most common response. Combinatorial therapy may be necessary for improved efficacy	GC and CRC patients, phase I (NCT03272256), and PAC patient, phase Ib (NCT05497778)	[278]
IACS-010759	Mitochondrial complex I	PAC cell lines, and CCA, PAC, and CRC patients	Reduced cell viability and generally well tolerated, but may induce neurotoxicity, peripheral neuropathy, and behavioral/physiological changes in mice. Increased blood lactate levels	CCA, PAC, and CRC patient, phase I (NCT03291938)	[279, 280]
Atovaquone	Mitochondrial complex III	GC, HCC, PAC and CRC cell lines, and xenograft models	Reduced OXPHOS, oxygen consumption rate, cell viability, cell proliferation, and cell cycle progression. Inhibited tumor growth and enhanced cell death	None in GI cancers	[283-285]
Targeting TCA cycle					
CPI-613	PDH and KGDHC	GC, ESCA, PAC and CRC cell lines, xenograft mouse models, and GC mouse model	Inhibited cell proliferation, cell viability, tumor growth, and metastasis, while increased cell death and chemosensitivity. In PAC patients, also increased the overall response rate	PAC patient, phase I (NCT01835041) and III (NCT03504423), HCC and CCA patients, phase I/II (NCT01766219), and CRC patients, phase I (NCT05070104 and NCT02232152)	[287-291]

GI: Gastrointestinal; ESCA: Esophageal cancer; GC: Gastric cancer; HCC: Hepatocellular carcinoma; CCA: Cholangiocarcinoma; PAC: Pancreatic cancer; CRC: Colorectal cancer; LDHA: Lactate dehydrogenase subunit A; MCT1/2: Monocarboxylate transporter family 1/2; HIF1A: Hypoxia inducible factor 1A; GLUT1: Glucose transporter 1; HK2: Hexokinase 2; PFKFB3: Fructose-2,6-biphosphatase 3; PKM2: Pyruvate kinase isozyme M2; PDK: Pyruvate dehydrogenase kinase; PDH: Pyruvate dehydrogenase; KGDHC: Alpha-ketoglutarate dehydrogenase complex; EMT: Epithelial-mesenchymal transition; OXPHOS: Oxidative phosphorylation.

EXPLORING LACTATE BIOSYNTHESIS AND TRANSPORT AS A POTENTIAL STRATEGY FOR GI CANCER THERAPY

As mentioned above, the Warburg effect is a common phenomenon in many cancers for which glycolysis is upregulated even in the presence of oxygen. This results in the accumulation of lactate, which is the last product of glycolysis. The PDK class of enzymes play a key role in deciding whether pyruvate is converted to lactate or enters the TCA cycle. Under hypoxia, PDKs are transcriptionally upregulated by HIF1A in cancers, promoting the inactivation of PDH through PDK-mediated phosphorylation. This leads to elevated lactate biosynthesis, resulting in excessive lactate levels that can promote carcinogenesis or progression[201]. Therefore, targeting PDKs is a potential strategy to inhibit lactate synthesis. Although several candidate drugs that target PDKs have been proposed, dichloroacetate (DCA) has been the most convincing inactivator of PDKs[202]. DCA has been shown in numerous pre-clinical studies on GI cancer to reduce lactate production, cell proliferation, migration, and increase chemosensitivity[203-207]. It has also shown synergistic anti-cancer activity in HCC despite concerns that it may promote hepatic carcinogenesis in B6C3F1 mice[205,208]. Despite promising pre-clinical results, clinical studies are still necessary to determine the efficacy and safety of DCA during cancer therapy. A clinical trial recruiting patients with CRC has been conducted to evaluate DCA as a potential anti-cancer drug (NCT00566410).

In previous studies on lactic acid inhibitors for anti-cancer therapy, the focus has been on inhibiting the enzymes responsible for lactate biosynthesis, namely LDH. TLDH complex composition has been investigated as a crucial factor in determining the fate of lactate biosynthesis or catabolism, and LDHA homo-tetramer (LDH5 or A4) has been considered the most effective complex for lactate biosynthesis. Accordingly, the currently established strategy is to identify LDH inhibitors with high selectivity against LDHA[209]. Although many candidates exist, including small peptides, small interfering RNAs (siRNAs), small chemical molecules, and natural compounds, only a few have progressed towards clinical use in anti-cancer therapy. Compound 24c and 1-(Phenylseleno)-4-(Trifluoromethyl) Benzene (PSTMB) are small compounds that have recently been identified as capable of selectively inhibiting LDHA, suppressing cancer cell aggressiveness, and enhancing cell death in both PCA cells and xenograft mouse models[210] as well as HCC and CRC cells [211]. Notably, Compound 24c has little effect on mouse weight, perhaps due to its relatively strong activity to reprogram metabolic profiling[210]. In contrast, oxamate, galloflavin, and FX11 have a longer history than Compound 24c and PSTMB in targeting LDHA. Pre-clinical evidence shows promise in suppressing GI cancer cell aggressiveness by targeting LDHA and other cancer-associated signaling pathways, suggesting possible treatment of GI cancers[212-225]. Despite this evidence, there is still a lack of clinical results to support the safety and efficacy of these LDHA-targeting drugs in GI cancer patients. An early natural compound, gossypol (AT-101), derived from the cotton plant, is one exception. Gossypol

and its derivatives have proven potent inhibitors of LDHA[226]. Gossypol not only reduces the aggressiveness of GI and other cancers, but also has a strong cytotoxic effect on cancer cells[226-240]. Most importantly, gossypol has entered a phase I/II clinical trial (NCT00561197) to evaluate its safety and efficacy in treating patients with esophageal cancer, showing significant improvement in complete response and survival rates[231]. Therefore, gossypol may be the most promising clinical drug targeting LDHA to date for use in GI cancers.

Excessive intracellular accumulation of lactate is a hallmark of many cancer types, which necessitates MCTs in transporting lactate from highly glycolytic cancer cells. Secretory lactate can acidify the extracellular microenvironment, which can impact the tumor microenvironment[241]. While secretory lactate was initially considered a waste product of cancer cells, recent evidence has suggested that it serves as an alternative fuel for oxidative cancer cells, leading to enhanced aggressiveness[56]. Therefore, MCT targets have emerged as an alternative strategy for anti-cancer therapy [241]. Among the various compounds proposed to target MCTs in cancer, AZD3965 and AR-C155858 have received more attention from researchers. Both drugs have demonstrated potential in targeting MCTs, inhibiting GI cancer cell aggressiveness, and stunting tumor growth both *in vitro* and *in vivo*[242-249]. While AZD3965 has entered the clinical trial phase, further investigation is needed to determine the safety and therapeutic efficacy of these drugs in patients with GI cancer. Notably, the development of MCT inhibitors has faced several challenges, including the presence of MCT isoforms and the need for inhibitors that selectively target cancer cells without affecting normal tissues[58,250]. In this regard, approaches and strategies to develop selective MCT inhibitors are being actively pursued. While MCT inhibitors hold promise as a potential anti-cancer therapy, further research is needed to fully understand their mechanisms of action and optimize their clinical applications.

TARGETING OXPHOS AS A POTENTIAL THERAPEUTIC STRATEGY FOR GI CANCER

Excessive OXPHOS activity has been observed in certain cancers and has been associated with more aggressive phenotypes/unfavorable clinical outcomes, making it a novel target for anti-cancer therapy[251]. Attenuating OXPHOS activity has been proposed as the best strategy to target OXPHOS, leading to the identification of a large number of candidate compounds that target mitochondrial complex I. Metformin, a compound that has long been used to treat diabetes, has been reported to exhibit mitochondrial complex I inhibition activity and can impact cancer cell aggressiveness/tumor growth in both GI cancer cell lines and xenograft models[252-265]. Metformin has advanced to clinical trials in combination with other anti-cancer regimens for patients with GI cancers, such as ESCA patients in Phase II (ChiCTR-ICR-15005940), HCC patients in Phase I (CTRI/2018/07/014865), CCA patients in Phase Ib (NCT0249674), PCA patients in Phase II (NCT01210911 and NCT01167738), and CRC patients in Phase II (NCT01312467, NCT03047837, and NCT01941953). It was found that metformin combination therapy can provide benefit to patients, perhaps through reprogramming the tumor immune microenvironment[258].

Recent studies have proposed several candidates as mitochondrial complex I-targeting compounds in addition to metformin. Among them, tamoxifen, IM156, and IACS-010759 have gained attention as potential anti-cancer agents. Tamoxifen is an anti-estrogen agent that has been clinically used to treat breast cancer patients with positive estrogen-receptor (ER) expression[266]. Interestingly, tamoxifen has also been shown to inhibit cancer cell aggressiveness, tumor growth, metastasis, and increase chemosensitivity in GI cancers[267-273]. This effect is thought to be through an ER-independent anti-cancer pathway[269]. Tamoxifen has been used as a monotherapy or combined therapy in several clinical trials, including an early phase trial in ESCA patients, Phase II trials in PAC patients[274-276], and a Phase III trial in HCC patients (NCT00003424). Tamoxifen has been found to be tolerable, safe, and with manageable adverse effects, while a Phase III trial in HCC patients found that tamoxifen monotherapy either offered no effect or decreased survival in patients with unresectable HCC[277]. This result has slowed the advancement of tamoxifen in GI cancers and requires further investigation.

IM156 and IACS-010759 are two novel mitochondria-targeting drugs that specifically inhibit mitochondrial complex I. While both compounds have shown promising results in pre-clinical studies against certain cancer cell lines, their potential in treating GI cancers involves limited evidence. Interestingly, IM156 has entered Phase I clinical trials in patients with GC, CRC and PCA (NCT03272256 and Janku *et al*[278]), demonstrating tolerability and safety. However, IM156 monotherapy in patients with GC and CRC offered only disease stabilization, indicating the need for further study.

On the other hand, IACS-010759 has shown significant cell viability reduction in PCA cell lines[279], leading to the initiation of a Phase I clinical trial (NCT03291938) to evaluate clinical efficacy and safety in patients with solid tumors due to CCA, PAC, and CRC. However, a recent publication reported that although IACS-010759 was tolerable and safe, it increased blood lactate levels and neurotoxicity while offering only limited anti-cancer efficacy. A reverse translational study using mice also found IACS-010759 to induce behavioral and physiological changes indicative of peripheral neuropathy, minimizing the possibility of combined therapy with specific anti-cancer compounds (*e.g.*, histone deacetylase 6 inhibitor). The development of mitochondrial complex I inhibitors is ongoing[280].

While the mitochondrial complex I inhibitors metformin, tamoxifen, IM156, and IACS-010759 hold promise as potential treatments for GI cancer, further studies are needed to evaluate their efficacy and safety, particularly in combination with other anti-cancer compounds. The development of more selective and potent mitochondrial complex I inhibitors may help overcome side effects and improve efficacy in cancer treatment.

The targeting of mitochondrial complexes other than complex I has also been proposed as a strategy for anti-cancer therapy[281]. One such compound of note is atovaquone, which was identified as a mitochondrial complex III inhibitor during a drug re-purposing study[282]. Pre-clinical studies have evaluated the potential of atovaquone as an anti-cancer agent in GI cancer cell lines and xenograft models, and have shown its ability to reduce OXPHOS, OCR, cell viability, cell

proliferation, cell cycle progression, and tumor growth, while enhancing cell death[283-285]. Despite promising results, atovaquone is currently in clinical trials for patients with non-small cell lung cancer (NCT04648033) and acute myeloid leukemia (NCT03568994) but not for patients with GI cancer. Further studies are needed to determine drug tolerability, safety, and therapeutic efficacy in patients with GI cancer. Nonetheless, the potential benefits of targeting OXPHOS make for a promising strategy in GI cancer therapy. However, the potential toxicity of these inhibitors in normal cells must be carefully evaluated before being considered as viable anti-cancer agents. In addition, the development of resistance to mitochondrial inhibitors, similar to the resistance seen with other anti-cancer agents, highlights the need for combination therapy.

POTENTIAL OF TCA CYCLE TARGETS IN GI CANCER THERAPY

The TCA cycle is a critical metabolic pathway that fuels bioenergetic processes in cells. Targeting the TCA cycle has emerged as a potential strategy for anti-cancer therapy[286]. Various agents have been tested for their anti-cancer efficacy, including AGI-5195, AG-221, AG-881, and CPI-613[286]. Among these compounds, CPI-613 is the only PDH and alpha-ketoglutarate dehydrogenase complex (KGDHC) dual targeting agent that has shown promising anti-cancer properties in GI cancer models both *in vitro* and *in vivo*[287-291]. The tolerability and safety of CPI-613, alone or in combination with other agents, has been evaluated or is currently being studied in patients with HCC, CCA, and CRC (NCT01766219, NCT05070104 and NCT02232152). However, a recent Phase III trial (NCT03504423) evaluating the anti-cancer efficacy of CPI-613 in patients with advanced PAC failed to improve survival rate but improved overall response rate[292]. This outcome is disappointing, combining CPI-613 with other drugs such as gemcitabine or nab-paclitaxel may provide better results.

The TCA cycle is a complex pathway, and there are multiple enzymes and metabolites that could be targeted for anti-cancer therapy. For example, the isocitrate dehydrogenase 1 and 2 (IDH1/2) enzymes play a crucial role in the TCA cycle, and mutations in these enzymes have been observed in several types of cancer, including gliomas and acute myeloid leukemia (AML)[293]. Enasidenib and ivosidenib are two IDH1/2 inhibitors that have been approved for the treatment of relapsed or refractory AML[294,295]. In GI cancers, however, the efficacy of IDH1/2 inhibitors is still under investigation [296]. In addition to IDH1/2 inhibitors, other TCA cycle inhibitors are being explored for anti-cancer therapy. For example, IDH1/2 mutant tumors are sensitive to glutaminase inhibitor CB-839, which targets glutamine metabolism [297]. Another TCA cycle inhibitor, BPTES, has shown anti-cancer efficacy in pre-clinical studies by blocking the activity of the glutaminase enzyme[298]. However, our understanding of these inhibitors in GI cancer treatment is still limited.

Targeting the TCA cycle and associated bioenergetic processes is a promising approach for anti-cancer therapy. While CPI-613 has shown some success in GI cancer models, the failure in Phase III trial underscores the need for continued research and combination therapy. Other TCA cycle inhibitors, such as IDH1/2 and glutaminase inhibitors, are being evaluated for their anti-cancer efficacy in GI cancers, offering hope for future treatments.

DISCUSSION AND FUTURE PERSPECTIVE

Cancer cells undergo significant metabolic changes which involve alteration to the nuclear and mitochondrial genomes as well as cell microenvironment. Understanding the molecular mechanisms behind these alterations is critical for the development of effective cancer therapies. Next-generation technologies such as metabolic profiling, single-cell sequencing, and metabolic tracing can provide insights into the regulation of mitochondrial metabolism in different cancer types. However, developing therapies based on altered metabolism is challenging due to the diverse metabolic patterns observed across different cancer cells.

Simply targeting a single bioenergetic enzyme or pathway may not be enough to effectively inhibit cancer cell growth, as metabolic symbiosis enables cancer cells to adapt to harsh tumor environments. One potential strategy is to treat the metabolic patterns of different cellular subpopulations in the tumor microenvironment to create a homogeneous metabolic population for targeting.

Bioenergetic enzymes have been explored as a way to inhibit cancer cell growth, with some small-molecule inhibitors of glucose metabolism showing significant inhibition in various cancers. However, clinical translation of these inhibitors has been limited by side effects. Other small-molecule inhibitors and natural products that regulate key bioenergy enzymes have also shown promise, but their specific mechanisms and targets require further investigation. Developing anticancer drugs targeting bioenergetic enzymes remains a significant challenge due to the unique metabolic features of cancer cells. Targeted drugs have shown anticancer effects in various tumor models, and combining them with conventional anticancer drugs is a promising strategy.

High-throughput multi-omics and spatial omics can help elucidate the heterogeneity of cancer cells and provide opportunities for therapeutic drugs targeting the bioenergetics of malignant tumors. Unbiased CRISPR-Cas9 synthetic lethality screening of metabolic genes that favor anti-cancer responses, particularly *in vivo*, could provide an avenue towards the identification of bioenergetic targets of interest. The ultimate goal is to develop drugs that simultaneously disable cancer cells while synergizing with targeted therapies.

However, while targeting bioenergetic pathways in cancer cells shows promise, it also has the potential to affect normal cells and tissues that rely on these pathways. Therefore, careful consideration and further research are needed to ensure that therapies targeting bioenergetics in cancer cells are specific and effective while minimizing potential side effects on normal cells and tissues. Additionally, combination therapies that target multiple pathways may be necessary

to achieve optimal therapeutic effects.

CONCLUSION

The metabolic reprogramming and bioenergetic alteration of cancer cells, particularly their utilization of glucose fermentation (the Warburg effect) for energy production, are well-known phenomena. However, comprehensive summaries of these alterations and their oncogenetic links in GI cancers are lacking. This review provides a summary of the interplay between aerobic glycolysis, the TCA cycle, and OXPHOS in cancer cells, including the molecular mechanisms that trigger these alterations. It also explores the role of HIFs, tumor suppressors, and the oncogenetic link between hypoxia-related enzymes, bioenergetic changes, and GI cancer. Additionally, this review details various anti-cancer drugs and strategies for treating GI cancers, along with the challenges associated with them. Understanding dysregulated cancer cell bioenergetics is critical for effective treatments, although the diverse metabolic patterns present challenges for targeted therapies. Further research is needed to comprehensively understand the specific mechanisms of inhibiting bioenergetic enzymes, address side effects, and utilize high-throughput multi-omics and spatial omics for insights into the heterogeneity of GI cancer cells in targeted bioenergetic therapies.

FOOTNOTES

Author contributions: Chu YD and Chen CW contributed equally to this article; Chu YD and Chen CW wrote the draft of the manuscript; Lai MW and Lim SN collected the data; Lin WR reviewed and edited the manuscript.

Supported by Ministry of Science and Technology, Taiwan, No. MOST-110-2314-B-182A-095- and No. MOST-111-2314-B-182A-126- (to Lin WR); and Chang Gung Memorial Hospital, Linkou Branch, Taiwan, No. CMRPG3K2292, No. CMRPG3J0693 (to Lin WR), No. CORPG3J0531, No. CORPG3L0261, No. CORPG3J0501, and No. CMRPG3K0771 (to Chen CW).

Conflict-of-interest statement: The authors declare no conflicts of interests.

Open-Access: This article is an open-access article that was selected by an in-house editor and fully peer-reviewed by external reviewers. It is distributed in accordance with the Creative Commons Attribution NonCommercial (CC BY-NC 4.0) license, which permits others to distribute, remix, adapt, build upon this work non-commercially, and license their derivative works on different terms, provided the original work is properly cited and the use is non-commercial. See: https://creativecommons.org/Licenses/by-nc/4.0/

Country/Territory of origin: Taiwan

ORCID number: Chun-Wei Chen 0000-0001-9438-0398; Siew-Na Lim 0000-0001-6867-8449; Wey-Ran Lin 0000-0001-6078-1396.

Corresponding Author's Membership in Professional Societies: The Gastroenterological Society of Taiwan, No. 001565; American Gastroenterological Association, No. 337214; American Society for Gastrointestinal Endoscopy, No. 161580.

S-Editor: Yan JP
L-Editor: Webster JR
P-Editor: Yu HG

REFERENCES

1 **Herrera AS**, Del C A Esparza M, Md Ashraf G, Zamyatnin AA, Aliev G. Beyond mitochondria, what would be the energy source of the cell? *Cent Nerv Syst Agents Med Chem* 2015; **15**: 32-41 [PMID: 25645910 DOI: 10.2174/1871524915666150203093656]
2 **Warburg O**, Wind F, Negelein E. The metabolism of tumors in the body. *J Gen Physiol* 1927; **8**: 519-530 [PMID: 19872213 DOI: 10.1085/jgp.8.6.519]
3 **Liberti MV**, Locasale JW. The Warburg Effect: How Does it Benefit Cancer Cells? *Trends Biochem Sci* 2016; **41**: 211-218 [PMID: 26778478 DOI: 10.1016/j.tibs.2015.12.001]
4 **Hanahan D**, Weinberg RA. Hallmarks of cancer: the next generation. *Cell* 2011; **144**: 646-674 [PMID: 21376230 DOI: 10.1016/j.cell.2011.02.013]
5 **El Hassouni B**, Granchi C, Vallés-Martí A, Supadmanaba IGP, Bononi G, Tuccinardi T, Funel N, Jimenez CR, Peters GJ, Giovannetti E, Minutolo F. The dichotomous role of the glycolytic metabolism pathway in cancer metastasis: Interplay with the complex tumor microenvironment and novel therapeutic strategies. *Semin Cancer Biol* 2020; **60**: 238-248 [PMID: 31445217 DOI: 10.1016/j.semcancer.2019.08.025]
6 **Mimaki M**, Wang X, McKenzie M, Thorburn DR, Ryan MT. Understanding mitochondrial complex I assembly in health and disease. *Biochim Biophys Acta* 2012; **1817**: 851-862 [PMID: 21924235 DOI: 10.1016/j.bbabio.2011.08.010]
7 **Banerjee R**, Purhonen J, Kallijärvi J. The mitochondrial coenzyme Q junction and complex III: biochemistry and pathophysiology. *FEBS J* 2022; **289**: 6936-6958 [PMID: 34428349 DOI: 10.1111/febs.16164]
8 **Bénit P**, Goncalves J, El Khoury R, Rak M, Favier J, Gimenez-Roqueplo AP, Rustin P. Succinate Dehydrogenase, Succinate, and Superoxides: A Genetic, Epigenetic, Metabolic, Environmental Explosive Crossroad. *Biomedicines* 2022; **10** [PMID: 35892689 DOI:

10.3390/biomedicines10081788]
9 **Lin YH**, Lim SN, Chen CY, Chi HC, Yeh CT, Lin WR. Functional Role of Mitochondrial DNA in Cancer Progression. *Int J Mol Sci* 2022; **23** [PMID: 35163579 DOI: 10.3390/ijms23031659]
10 **Zhao RZ**, Jiang S, Zhang L, Yu ZB. Mitochondrial electron transport chain, ROS generation and uncoupling (Review). *Int J Mol Med* 2019; **44**: 3-15 [PMID: 31115493 DOI: 10.3892/ijmm.2019.4188]
11 **Moloney JN**, Cotter TG. ROS signalling in the biology of cancer. *Semin Cell Dev Biol* 2018; **80**: 50-64 [PMID: 28587975 DOI: 10.1016/j.semcdb.2017.05.023]
12 **Kowalczyk P**, Sulejczak D, Kleczkowska P, Bukowska-Ośko I, Kucia M, Popiel M, Wietrak E, Kramkowski K, Wrzosek K, Kaczyńska K. Mitochondrial Oxidative Stress-A Causative Factor and Therapeutic Target in Many Diseases. *Int J Mol Sci* 2021; **22** [PMID: 34948180 DOI: 10.3390/ijms222413384]
13 **Kim M**, Mahmood M, Reznik E, Gammage PA. Mitochondrial DNA is a major source of driver mutations in cancer. *Trends Cancer* 2022; **8**: 1046-1059 [PMID: 36041967 DOI: 10.1016/j.trecan.2022.08.001]
14 **Zhang Y**, Li Q, Huang Z, Li B, Nice EC, Huang C, Wei L, Zou B. Targeting Glucose Metabolism Enzymes in Cancer Treatment: Current and Emerging Strategies. *Cancers (Basel)* 2022; **14** [PMID: 36230492 DOI: 10.3390/cancers14194568]
15 **Godel M**, Ortone G, Anobile DP, Pasino M, Randazzo G, Riganti C, Kopecka J. Targeting Mitochondrial Oncometabolites: A New Approach to Overcome Drug Resistance in Cancer. *Pharmaceutics* 2021; **13** [PMID: 34065551 DOI: 10.3390/pharmaceutics13050762]
16 **Wagner A**, Kosnacova H, Chovanec M, Jurkovicova D. Mitochondrial Genetic and Epigenetic Regulations in Cancer: Therapeutic Potential. *Int J Mol Sci* 2022; **23** [PMID: 35887244 DOI: 10.3390/ijms23147897]
17 **Schiliro C**, Firestein BL. Mechanisms of Metabolic Reprogramming in Cancer Cells Supporting Enhanced Growth and Proliferation. *Cells* 2021; **10** [PMID: 33946927 DOI: 10.3390/cells10051056]
18 **Schmidt CA**, Fisher-Wellman KH, Neufer PD. From OCR and ECAR to energy: Perspectives on the design and interpretation of bioenergetics studies. *J Biol Chem* 2021; **297**: 101140 [PMID: 34461088 DOI: 10.1016/j.jbc.2021.101140]
19 **WARBURG O**. On the origin of cancer cells. *Science* 1956; **123**: 309-314 [PMID: 13298683 DOI: 10.1126/science.123.3191.309]
20 **Racker E**. Bioenergetics and the problem of tumor growth. *Am Sci* 1972; **60**: 56-63 [PMID: 4332766]
21 **Boerner P**, Resnick RJ, Racker E. Stimulation of glycolysis and amino acid uptake in NRK-49F cells by transforming growth factor beta and epidermal growth factor. *Proc Natl Acad Sci U S A* 1985; **82**: 1350-1353 [PMID: 3871948 DOI: 10.1073/pnas.82.5.1350]
22 **Flier JS**, Mueckler MM, Usher P, Lodish HF. Elevated levels of glucose transport and transporter messenger RNA are induced by ras or src oncogenes. *Science* 1987; **235**: 1492-1495 [PMID: 3103217 DOI: 10.1126/science.3103217]
23 **Birnbaum MJ**, Haspel HC, Rosen OM. Transformation of rat fibroblasts by FSV rapidly increases glucose transporter gene transcription. *Science* 1987; **235**: 1495-1498 [PMID: 3029870 DOI: 10.1126/science.3029870]
24 **Hiraki Y**, Rosen OM, Birnbaum MJ. Growth factors rapidly induce expression of the glucose transporter gene. *J Biol Chem* 1988; **263**: 13655-13662 [PMID: 3262104 DOI: 10.1016/s0021-9258(18)68291-2]
25 **Fantin VR**, St-Pierre J, Leder P. Attenuation of LDH-A expression uncovers a link between glycolysis, mitochondrial physiology, and tumor maintenance. *Cancer Cell* 2006; **9**: 425-434 [PMID: 16766262 DOI: 10.1016/j.ccr.2006.04.023]
26 **Shim H**, Chun YS, Lewis BC, Dang CV. A unique glucose-dependent apoptotic pathway induced by c-Myc. *Proc Natl Acad Sci U S A* 1998; **95**: 1511-1516 [PMID: 9465046 DOI: 10.1073/pnas.95.4.1511]
27 **Locasale JW**, Cantley LC. Metabolic flux and the regulation of mammalian cell growth. *Cell Metab* 2011; **14**: 443-451 [PMID: 21982705 DOI: 10.1016/j.cmet.2011.07.014]
28 **Lunt SY**, Vander Heiden MG. Aerobic glycolysis: meeting the metabolic requirements of cell proliferation. *Annu Rev Cell Dev Biol* 2011; **27**: 441-464 [PMID: 21985671 DOI: 10.1146/annurev-cellbio-092910-154237]
29 **Slavov N**, Budnik BA, Schwab D, Airoldi EM, van Oudenaarden A. Constant growth rate can be supported by decreasing energy flux and increasing aerobic glycolysis. *Cell Rep* 2014; **7**: 705-714 [PMID: 24767987 DOI: 10.1016/j.celrep.2014.03.057]
30 **Epstein T**, Xu L, Gillies RJ, Gatenby RA. Separation of metabolic supply and demand: aerobic glycolysis as a normal physiological response to fluctuating energetic demands in the membrane. *Cancer Metab* 2014; **2**: 7 [PMID: 24982758 DOI: 10.1186/2049-3002-2-7]
31 **Epstein T**, Gatenby RA, Brown JS. The Warburg effect as an adaptation of cancer cells to rapid fluctuations in energy demand. *PLoS One* 2017; **12**: e0185085 [PMID: 28922380 DOI: 10.1371/journal.pone.0185085]
32 **DeBerardinis RJ**, Mancuso A, Daikhin E, Nissim I, Yudkoff M, Wehrli S, Thompson CB. Beyond aerobic glycolysis: transformed cells can engage in glutamine metabolism that exceeds the requirement for protein and nucleotide synthesis. *Proc Natl Acad Sci U S A* 2007; **104**: 19345-19350 [PMID: 18032601 DOI: 10.1073/pnas.0709747104]
33 **Grashei M**, Biechl P, Schilling F, Otto AM. Conversion of Hyperpolarized [1-(13)C]Pyruvate in Breast Cancer Cells Depends on Their Malignancy, Metabolic Program and Nutrient Microenvironment. *Cancers (Basel)* 2022; **14** [PMID: 35406616 DOI: 10.3390/cancers14071845]
34 **Birsoy K**, Wang T, Chen WW, Freinkman E, Abu-Remaileh M, Sabatini DM. An Essential Role of the Mitochondrial Electron Transport Chain in Cell Proliferation Is to Enable Aspartate Synthesis. *Cell* 2015; **162**: 540-551 [PMID: 26232224 DOI: 10.1016/j.cell.2015.07.016]
35 **Flaveny CA**, Griffett K, El-Gendy Bel-D, Kazantzis M, Sengupta M, Amelio AL, Chatterjee A, Walker J, Solt LA, Kamenecka TM, Burris TP. Broad Anti-tumor Activity of a Small Molecule that Selectively Targets the Warburg Effect and Lipogenesis. *Cancer Cell* 2015; **28**: 42-56 [PMID: 26120082 DOI: 10.1016/j.ccell.2015.05.007]
36 **Sullivan LB**, Gui DY, Hosios AM, Bush LN, Freinkman E, Vander Heiden MG. Supporting Aspartate Biosynthesis Is an Essential Function of Respiration in Proliferating Cells. *Cell* 2015; **162**: 552-563 [PMID: 26232225 DOI: 10.1016/j.cell.2015.07.017]
37 **Viale A**, Pettazzoni P, Lyssiotis CA, Ying H, Sánchez N, Marchesini M, Carugo A, Green T, Seth S, Giuliani V, Kost-Alimova M, Muller F, Colla S, Nezi L, Genovese G, Deem AK, Kapoor A, Yao W, Brunetto E, Kang Y, Yuan M, Asara JM, Wang YA, Heffernan TP, Kimmelman AC, Wang H, Fleming JB, Cantley LC, DePinho RA, Draetta GF. Oncogene ablation-resistant pancreatic cancer cells depend on mitochondrial function. *Nature* 2014; **514**: 628-632 [PMID: 25119024 DOI: 10.1038/nature13611]
38 **Semenza GL**, Wang GL. A nuclear factor induced by hypoxia *via* de novo protein synthesis binds to the human erythropoietin gene enhancer at a site required for transcriptional activation. *Mol Cell Biol* 1992; **12**: 5447-5454 [PMID: 1448077 DOI: 10.1128/mcb.12.12.5447-5454.1992]
39 **Wang GL**, Semenza GL. Characterization of hypoxia-inducible factor 1 and regulation of DNA binding activity by hypoxia. *J Biol Chem* 1993; **268**: 21513-21518 [PMID: 8408001 DOI: 10.1016/s0021-9258(20)80571-7]
40 **Beck I**, Weinmann R, Caro J. Characterization of hypoxia-responsive enhancer in the human erythropoietin gene shows presence of hypoxia-

inducible 120-Kd nuclear DNA-binding protein in erythropoietin-producing and nonproducing cells. *Blood* 1993; **82**: 704-711 [PMID: 8338939 DOI: 10.1182/blood.V82.3.704.704]

41 **Soni S**, Padwad YS. HIF-1 in cancer therapy: two decade long story of a transcription factor. *Acta Oncol* 2017; **56**: 503-515 [PMID: 28358664 DOI: 10.1080/0284186X.2017.1301680]

42 **De Saedeleer CJ**, Copetti T, Porporato PE, Verrax J, Feron O, Sonveaux P. Lactate activates HIF-1 in oxidative but not in Warburg-phenotype human tumor cells. *PLoS One* 2012; **7**: e46571 [PMID: 23082126 DOI: 10.1371/journal.pone.0046571]

43 **Sonveaux P**, Copetti T, De Saedeleer CJ, Végran F, Verrax J, Kennedy KM, Moon EJ, Dhup S, Danhier P, Frérart F, Gallez B, Ribeiro A, Michiels C, Dewhirst MW, Feron O. Targeting the lactate transporter MCT1 in endothelial cells inhibits lactate-induced HIF-1 activation and tumor angiogenesis. *PLoS One* 2012; **7**: e33418 [PMID: 22428047 DOI: 10.1371/journal.pone.0033418]

44 **To KK**, Huang LE. Suppression of hypoxia-inducible factor 1alpha (HIF-1alpha) transcriptional activity by the HIF prolyl hydroxylase EGLN1. *J Biol Chem* 2005; **280**: 38102-38107 [PMID: 16157596 DOI: 10.1074/jbc.M504342200]

45 **Berra E**, Benizri E, Ginouvès A, Volmat V, Roux D, Pouysségur J. HIF prolyl-hydroxylase 2 is the key oxygen sensor setting low steady-state levels of HIF-1alpha in normoxia. *EMBO J* 2003; **22**: 4082-4090 [PMID: 12912907 DOI: 10.1093/emboj/cdg392]

46 **Maxwell PH**, Wiesener MS, Chang GW, Clifford SC, Vaux EC, Cockman ME, Wykoff CC, Pugh CW, Maher ER, Ratcliffe PJ. The tumour suppressor protein VHL targets hypoxia-inducible factors for oxygen-dependent proteolysis. *Nature* 1999; **399**: 271-275 [PMID: 10353251 DOI: 10.1038/20459]

47 **Ohh M**, Park CW, Ivan M, Hoffman MA, Kim TY, Huang LE, Pavletich N, Chau V, Kaelin WG. Ubiquitination of hypoxia-inducible factor requires direct binding to the beta-domain of the von Hippel-Lindau protein. *Nat Cell Biol* 2000; **2**: 423-427 [PMID: 10878807 DOI: 10.1038/35017054]

48 **Semenza GL**, Roth PH, Fang HM, Wang GL. Transcriptional regulation of genes encoding glycolytic enzymes by hypoxia-inducible factor 1. *J Biol Chem* 1994; **269**: 23757-23763 [PMID: 8089148 DOI: 10.1016/s0021-9258(17)31580-6]

49 **Jiang BH**, Agani F, Passaniti A, Semenza GL. V-SRC induces expression of hypoxia-inducible factor 1 (HIF-1) and transcription of genes encoding vascular endothelial growth factor and enolase 1: involvement of HIF-1 in tumor progression. *Cancer Res* 1997; **57**: 5328-5335 [PMID: 9393757]

50 **Semenza GL**, Jiang BH, Leung SW, Passantino R, Concordet JP, Maire P, Giallongo A. Hypoxia response elements in the aldolase A, enolase 1, and lactate dehydrogenase A gene promoters contain essential binding sites for hypoxia-inducible factor 1. *J Biol Chem* 1996; **271**: 32529-32537 [PMID: 8955077 DOI: 10.1074/jbc.271.51.32529]

51 **O'Rourke JF**, Pugh CW, Bartlett SM, Ratcliffe PJ. Identification of hypoxically inducible mRNAs in HeLa cells using differential-display PCR. Role of hypoxia-inducible factor-1. *Eur J Biochem* 1996; **241**: 403-410 [PMID: 8917436 DOI: 10.1111/j.1432-1033.1996.00403.x]

52 **Ebert BL**, Firth JD, Ratcliffe PJ. Hypoxia and mitochondrial inhibitors regulate expression of glucose transporter-1 *via* distinct Cis-acting sequences. *J Biol Chem* 1995; **270**: 29083-29089 [PMID: 7493931 DOI: 10.1074/jbc.270.49.29083]

53 **Riddle SR**, Ahmad A, Ahmad S, Deeb SS, Malkki M, Schneider BK, Allen CB, White CW. Hypoxia induces hexokinase II gene expression in human lung cell line A549. *Am J Physiol Lung Cell Mol Physiol* 2000; **278**: L407-L416 [PMID: 10666126 DOI: 10.1152/ajplung.2000.278.2.L407]

54 **Kim JW**, Tchernyshyov I, Semenza GL, Dang CV. HIF-1-mediated expression of pyruvate dehydrogenase kinase: a metabolic switch required for cellular adaptation to hypoxia. *Cell Metab* 2006; **3**: 177-185 [PMID: 16517405 DOI: 10.1016/j.cmet.2006.02.002]

55 **Nagao A**, Kobayashi M, Koyasu S, Chow CCT, Harada H. HIF-1-Dependent Reprogramming of Glucose Metabolic Pathway of Cancer Cells and Its Therapeutic Significance. *Int J Mol Sci* 2019; **20** [PMID: 30634433 DOI: 10.3390/ijms20020238]

56 **de la Cruz-López KG**, Castro-Muñoz LJ, Reyes-Hernández DO, García-Carrancá A, Manzo-Merino J. Lactate in the Regulation of Tumor Microenvironment and Therapeutic Approaches. *Front Oncol* 2019; **9**: 1143 [PMID: 31737570 DOI: 10.3389/fonc.2019.01143]

57 **Muñoz-Pinedo C**, El Mjiyad N, Ricci JE. Cancer metabolism: current perspectives and future directions. *Cell Death Dis* 2012; **3**: e248 [PMID: 22237205 DOI: 10.1038/cddis.2011.123]

58 **Halestrap AP**. The SLC16 gene family - structure, role and regulation in health and disease. *Mol Aspects Med* 2013; **34**: 337-349 [PMID: 23506875 DOI: 10.1016/j.mam.2012.05.003]

59 **Payen VL**, Mina E, Van Hée VF, Porporato PE, Sonveaux P. Monocarboxylate transporters in cancer. *Mol Metab* 2020; **33**: 48-66 [PMID: 31395464 DOI: 10.1016/j.molmet.2019.07.006]

60 **Urbańska K**, Orzechowski A. Unappreciated Role of LDHA and LDHB to Control Apoptosis and Autophagy in Tumor Cells. *Int J Mol Sci* 2019; **20** [PMID: 31035592 DOI: 10.3390/ijms20092085]

61 **Mishra D**, Banerjee D. Lactate Dehydrogenases as Metabolic Links between Tumor and Stroma in the Tumor Microenvironment. *Cancers (Basel)* 2019; **11** [PMID: 31146503 DOI: 10.3390/cancers11060750]

62 **Mendes C**, Serpa J. Revisiting lactate dynamics in cancer-a metabolic expertise or an alternative attempt to survive? *J Mol Med (Berl)* 2020; **98**: 1397-1414 [PMID: 32827258 DOI: 10.1007/s00109-020-01965-0]

63 **Moldogazieva NT**, Mokhosoev IM, Terentiev AA. Metabolic Heterogeneity of Cancer Cells: An Interplay between HIF-1, GLUTs, and AMPK. *Cancers (Basel)* 2020; **12** [PMID: 32252351 DOI: 10.3390/cancers12040862]

64 **Liu Y**, Chen C, Wang X, Sun Y, Zhang J, Chen J, Shi Y. An Epigenetic Role of Mitochondria in Cancer. *Cells* 2022; **11** [PMID: 36010594 DOI: 10.3390/cells11162518]

65 **Zhu X**, Xuan Z, Chen J, Li Z, Zheng S, Song P. How DNA methylation affects the Warburg effect. *Int J Biol Sci* 2020; **16**: 2029-2041 [PMID: 32549751 DOI: 10.7150/ijbs.45420]

66 **Bogaerts E**, Paridaens A, Verhelst X, Carmeliet P, Geerts A, Van Vlierberghe H, Devisscher L. Effect of prolyl hydroxylase domain 2 haplodeficiency on liver progenitor cell characteristics in early mouse hepatocarcinogenesis. *EXCLI J* 2016; **15**: 687-698 [PMID: 28337100 DOI: 10.17179/excli2016-607]

67 **Heindryckx F**, Kuchnio A, Casteleyn C, Coulon S, Olievier K, Colle I, Geerts A, Libbrecht L, Carmeliet P, Van Vlierberghe H. Effect of prolyl hydroxylase domain-2 haplodeficiency on the hepatocarcinogenesis in mice. *J Hepatol* 2012; **57**: 61-68 [PMID: 22420978 DOI: 10.1016/j.jhep.2012.02.021]

68 **Ma M**, Hua S, Li G, Wang S, Cheng X, He S, Wu P, Chen X. Prolyl hydroxylase domain protein 3 and asparaginyl hydroxylase factor inhibiting HIF-1 levels are predictive of tumoral behavior and prognosis in hepatocellular carcinoma. *Oncotarget* 2017; **8**: 12983-13002 [PMID: 28099905 DOI: 10.18632/oncotarget.14677]

69 **Cui L**, Qu J, Dang S, Mao Z, Wang X, Fan X, Sun K, Zhang J. Prolyl hydroxylase 3 inhibited the tumorigenecity of gastric cancer cells. *Mol*

Carcinog 2014; **53**: 736-743 [PMID: 23533015 DOI: 10.1002/mc.22025]
70 **Xia YJ**, Jiang XT, Jiang SB, He XJ, Luo JG, Liu ZC, Wang L, Tao HQ, Chen JZ. PHD3 affects gastric cancer progression by negatively regulating HIF1A. *Mol Med Rep* 2017; **16**: 6882-6889 [PMID: 28901473 DOI: 10.3892/mmr.2017.7455]
71 **Kamphues C**, Wittschieber D, Klauschen F, Kasajima A, Dietel M, Schmidt SC, Glanemann M, Bahra M, Neuhaus P, Weichert W, Stenzinger A. Prolyl hydroxylase domain 2 protein is a strong prognostic marker in human gastric cancer. *Pathobiology* 2012; **79**: 11-17 [PMID: 22236543 DOI: 10.1159/000330170]
72 **Xie G**, Zheng L, Ou J, Huang H, He J, Li J, Pan F, Liang H. Low expression of prolyl hydroxylase 2 is associated with tumor grade and poor prognosis in patients with colorectal cancer. *Exp Biol Med (Maywood)* 2012; **237**: 860-866 [PMID: 22802519 DOI: 10.1258/ebm.2012.011331]
73 **Gossage L**, Zaitoun A, Fareed KR, Turley H, Aloysius M, Lobo DN, Harris AL, Madhusudan S. Expression of key hypoxia sensing prolyl-hydroxylases PHD1, -2 and -3 in pancreaticobiliary cancer. *Histopathology* 2010; **56**: 908-920 [PMID: 20497244 DOI: 10.1111/j.1365-2559.2010.03566.x]
74 **Schmitt AM**, Schmid S, Rudolph T, Anlauf M, Prinz C, Klöppel G, Moch H, Heitz PU, Komminoth P, Perren A. VHL inactivation is an important pathway for the development of malignant sporadic pancreatic endocrine tumors. *Endocr Relat Cancer* 2009; **16**: 1219-1227 [PMID: 19690016 DOI: 10.1677/ERC-08-0297]
75 **Kuwai T**, Kitadai Y, Tanaka S, Hiyama T, Tanimoto K, Chayama K. Mutation of the von Hippel-Lindau (VHL) gene in human colorectal carcinoma: association with cytoplasmic accumulation of hypoxia-inducible factor (HIF)-1alpha. *Cancer Sci* 2004; **95**: 149-153 [PMID: 14965365 DOI: 10.1111/j.1349-7006.2004.tb03196.x]
76 **Li G**, Shen Y, Wang F, Hong S, Cai M. Correlation Between von Hippel-Lindau Gene Expression and Tumor SUVmax and Survival Prognosis in Hepatocellular Carcinoma. *Med Sci Monit* 2020; **26**: e920473 [PMID: 32075951 DOI: 10.12659/MSM.920473]
77 **Linehan WM**, Rouault TA. Molecular pathways: Fumarate hydratase-deficient kidney cancer--targeting the Warburg effect in cancer. *Clin Cancer Res* 2013; **19**: 3345-3352 [PMID: 23633457 DOI: 10.1158/1078-0432.CCR-13-0304]
78 **Rasheed MRHA**, Tarjan G. Succinate Dehydrogenase Complex: An Updated Review. *Arch Pathol Lab Med* 2018; **142**: 1564-1570 [PMID: 30289269 DOI: 10.5858/arpa.2017-0285-RS]
79 **Herrmann PC**, Herrmann EC. Oxygen metabolism and a potential role for cytochrome c oxidase in the Warburg effect. *J Bioenerg Biomembr* 2007; **39**: 247-250 [PMID: 17587160 DOI: 10.1007/s10863-007-9084-z]
80 **Sánchez-Aragó M**, Formentini L, Cuezva JM. Mitochondria-mediated energy adaption in cancer: the H(+)-ATP synthase-geared switch of metabolism in human tumors. *Antioxid Redox Signal* 2013; **19**: 285-298 [PMID: 22901241 DOI: 10.1089/ars.2012.4883]
81 **Lee HC**, Wei YH. Mitochondrial DNA instability and metabolic shift in human cancers. *Int J Mol Sci* 2009; **10**: 674-701 [PMID: 19333428 DOI: 10.3390/ijms10020674]
82 **Balsa E**, Marco R, Perales-Clemente E, Szklarczyk R, Calvo E, Landázuri MO, Enríquez JA. NDUFA4 is a subunit of complex IV of the mammalian electron transport chain. *Cell Metab* 2012; **16**: 378-386 [PMID: 22902835 DOI: 10.1016/j.cmet.2012.07.015]
83 **Kim SH**, Choi SI, Won KY, Lim SJ. Distinctive interrelation of p53 with SCO2, COX, and TIGAR in human gastric cancer. *Pathol Res Pract* 2016; **212**: 904-910 [PMID: 27499152 DOI: 10.1016/j.prp.2016.07.014]
84 **Zhang K**, Chen Y, Huang X, Qu P, Pan Q, Lü L, Jiang S, Ren T, Su H. Expression and clinical significance of cytochrome c oxidase subunit IV in colorectal cancer patients. *Arch Med Sci* 2016; **12**: 68-77 [PMID: 26925120 DOI: 10.5114/aoms.2016.57581]
85 **Ramzan R**, Kadenbach B, Vogt S. Multiple Mechanisms Regulate Eukaryotic Cytochrome C Oxidase. *Cells* 2021; **10** [PMID: 33671025 DOI: 10.3390/cells10030514]
86 **Huhta H**, Helminen O, Palomäki S, Kauppila JH, Saarnio J, Lehenkari PP, Karttunen TJ. Intratumoral lactate metabolism in Barrett's esophagus and adenocarcinoma. *Oncotarget* 2017; **8**: 22894-22902 [PMID: 28206968 DOI: 10.18632/oncotarget.15284]
87 **Ma JT**, Han CB, Zhou Y, Zhao JZ, Jing W, Zou HW. Altered expression of mitochondrial cytochrome c oxidase I and NADH dehydrogenase 4 transcripts associated with gastric tumorigenesis and tumor dedifferentiation. *Mol Med Rep* 2012; **5**: 1526-1530 [PMID: 22407105 DOI: 10.3892/mmr.2012.832]
88 **Eskuri M**, Kemi N, Kauppila JH. Monocarboxylate Transporters 1 and 4 and MTCO1 in Gastric Cancer. *Cancers (Basel)* 2021; **13** [PMID: 33946786 DOI: 10.3390/cancers13092142]
89 **LE PH**, Huang SC, Lim SN, Chou CH, Yeh TS, Chen TC, Yen TH, Su MY, Chiu CT, Yeh CT, Lin WR. Complex IV subunit 1 defect predicts postoperative survival in hepatocellular carcinoma. *Oncol Lett* 2014; **7**: 1430-1438 [PMID: 24765151 DOI: 10.3892/ol.2014.1966]
90 **Feichtinger RG**, Neureiter D, Kemmerling R, Mayr JA, Kiesslich T, Kofler B. Low VDAC1 Expression Is Associated with an Aggressive Phenotype and Reduced Overall Patient Survival in Cholangiocellular Carcinoma. *Cells* 2019; **8** [PMID: 31167495 DOI: 10.3390/cells8060539]
91 **Li D**, Wang XZ, Yu JP, Chen ZX, Huang YH, Tao QM. Cytochrome C oxidase III interacts with hepatitis B virus X protein in vivo by yeast two-hybrid system. *World J Gastroenterol* 2004; **10**: 2805-2808 [PMID: 15334674 DOI: 10.3748/wjg.v10.i19.2805]
92 **Zou LY**, Zheng BY, Fang XF, Li D, Huang YH, Chen ZX, Zhou LY, Wang XZ. HBx co-localizes with COXIII in HL-7702 cells to upregulate mitochondrial function and ROS generation. *Oncol Rep* 2015; **33**: 2461-2467 [PMID: 25778742 DOI: 10.3892/or.2015.3852]
93 **Greaves LC**, Preston SL, Tadrous PJ, Taylor RW, Barron MJ, Oukrif D, Leedham SJ, Deheragoda M, Sasieni P, Novelli MR, Jankowski JA, Turnbull DM, Wright NA, McDonald SA. Mitochondrial DNA mutations are established in human colonic stem cells, and mutated clones expand by crypt fission. *Proc Natl Acad Sci U S A* 2006; **103**: 714-719 [PMID: 16407113 DOI: 10.1073/pnas.0505903103]
94 **Namslauer I**, Brzezinski P. A mitochondrial DNA mutation linked to colon cancer results in proton leaks in cytochrome c oxidase. *Proc Natl Acad Sci U S A* 2009; **106**: 3402-3407 [PMID: 19218458 DOI: 10.1073/pnas.0811450106]
95 **Wang Y**, Wang H, Yin S, Zhang J, Zhang R, Guo Z. Identification of polymorphisms in mitochondrial cytochrome c oxidase genes as risk factors for gastric cancer. *Transl Cancer Res* 2020; **9**: 3854-3859 [PMID: 35117752 DOI: 10.21037/tcr-19-2227]
96 **Wang H**, Xu J, Li D, Zhang S, Guo Z. Identification of sequence polymorphisms in the mitochondrial cytochrome c oxidase genes as risk factors for hepatocellular carcinoma. *J Clin Lab Anal* 2018; **32** [PMID: 28703354 DOI: 10.1002/jcla.22299]
97 **Zong S**, Wu M, Gu J, Liu T, Guo R, Yang M. Structure of the intact 14-subunit human cytochrome c oxidase. *Cell Res* 2018; **28**: 1026-1034 [PMID: 30030519 DOI: 10.1038/s41422-018-0071-1]
98 **Kadenbach B**. Regulation of Mammalian 13-Subunit Cytochrome c Oxidase and Binding of other Proteins: Role of NDUFA4. *Trends Endocrinol Metab* 2017; **28**: 761-770 [PMID: 28988874 DOI: 10.1016/j.tem.2017.09.003]
99 **Srinivasan S**, Guha M, Dong DW, Whelan KA, Ruthel G, Uchikado Y, Natsugoe S, Nakagawa H, Avadhani NG. Disruption of cytochrome c oxidase function induces the Warburg effect and metabolic reprogramming. *Oncogene* 2016; **35**: 1585-1595 [PMID: 26148236 DOI:

10.1038/onc.2015.227]
100 **Chu YD**, Lin WR, Lin YH, Kuo WH, Tseng CJ, Lim SN, Huang YL, Huang SC, Wu TJ, Lin KH, Yeh CT. COX5B-Mediated Bioenergetic Alteration Regulates Tumor Growth and Migration by Modulating AMPK-UHMK1-ERK Cascade in Hepatoma. *Cancers (Basel)* 2020; **12** [PMID: 32580279 DOI: 10.3390/cancers12061646]
101 **Chen ZX**, Pervaiz S. Involvement of cytochrome c oxidase subunits Va and Vb in the regulation of cancer cell metabolism by Bcl-2. *Cell Death Differ* 2010; **17**: 408-420 [PMID: 19834492 DOI: 10.1038/cdd.2009.132]
102 **Chu YD**, Lim SN, Yeh CT, Lin WR. COX5B-Mediated Bioenergetic Alterations Modulate Cell Growth and Anticancer Drug Susceptibility by Orchestrating Claudin-2 Expression in Colorectal Cancers. *Biomedicines* 2021; **10** [PMID: 35052740 DOI: 10.3390/biomedicines10010060]
103 **Li JP**, Liu YJ, Zeng SH, Gao HJ, Chen YG, Zou X. Identification of COX4I2 as a hypoxia-associated gene acting through FGF1 to promote EMT and angiogenesis in CRC. *Cell Mol Biol Lett* 2022; **27**: 76 [PMID: 36064310 DOI: 10.1186/s11658-022-00380-2]
104 **Yang J**, Liu J, Zhang S, Yang Y, Gong J. The overexpression of cytochrome c oxidase subunit 6C activated by Kras mutation is related to energy metabolism in pancreatic cancer. *Transl Cancer Res* 2018; **7**: 290-300 [DOI: 10.21037/tcr.2018.03.02]
105 **Nie K**, Li J, He X, Wang Y, Zhao Q, Du M, Sun H, Wang J, Lyu J, Fang H, Jin L. COX6B2 drives metabolic reprogramming toward oxidative phosphorylation to promote metastasis in pancreatic ductal cancer cells. *Oncogenesis* 2020; **9**: 51 [PMID: 32415061 DOI: 10.1038/s41389-020-0231-2]
106 **Esparza-Moltó PB**, Cuezva JM. The Role of Mitochondrial H(+)-ATP Synthase in Cancer. *Front Oncol* 2018; **8**: 53 [PMID: 29564224 DOI: 10.3389/fonc.2018.00053]
107 **Wang X**, Chang X, He C, Fan Z, Yu Z, Yu B, Wu X, Hou J, Li J, Su L, Liu B, Zhu Z. ATP5B promotes the metastasis and growth of gastric cancer by activating the FAK/AKT/MMP2 pathway. *FASEB J* 2021; **35**: e20649 [PMID: 33715234 DOI: 10.1096/fj.202000608R]
108 **Isidoro A**, Martínez M, Fernández PL, Ortega AD, Santamaría G, Chamorro M, Reed JC, Cuezva JM. Alteration of the bioenergetic phenotype of mitochondria is a hallmark of breast, gastric, lung and oesophageal cancer. *Biochem J* 2004; **378**: 17-20 [PMID: 14683524 DOI: 10.1042/BJ20031541]
109 **Cuezva JM**, Krajewska M, de Heredia ML, Krajewski S, Santamaría G, Kim H, Zapata JM, Marusawa H, Chamorro M, Reed JC. The bioenergetic signature of cancer: a marker of tumor progression. *Cancer Res* 2002; **62**: 6674-6681 [PMID: 12438266]
110 **Capuano F**, Varone D, D'Eri N, Russo E, Tommasi S, Montemurro S, Prete F, Papa S. Oxidative phosphorylation and F(O)F(1) ATP synthase activity of human hepatocellular carcinoma. *Biochem Mol Biol Int* 1996; **38**: 1013-1022 [PMID: 9132148]
111 **Tanton H**, Voronina S, Evans A, Armstrong J, Sutton R, Criddle DN, Haynes L, Schmid MC, Campbell F, Costello E, Tepikin AV. F(1)F(0)-ATP Synthase Inhibitory Factor 1 in the Normal Pancreas and in Pancreatic Ductal Adenocarcinoma: Effects on Bioenergetics, Invasion and Proliferation. *Front Physiol* 2018; **9**: 833 [PMID: 30050450 DOI: 10.3389/fphys.2018.00833]
112 **Chang HJ**, Lee MR, Hong SH, Yoo BC, Shin YK, Jeong JY, Lim SB, Choi HS, Jeong SY, Park JG. Identification of mitochondrial FoF1-ATP synthase involved in liver metastasis of colorectal cancer. *Cancer Sci* 2007; **98**: 1184-1191 [PMID: 17559425 DOI: 10.1111/j.1349-7006.2007.00527.x]
113 **Huang YJ**, Jan YH, Chang YC, Tsai HF, Wu AT, Chen CL, Hsiao M. ATP Synthase Subunit Epsilon Overexpression Promotes Metastasis by Modulating AMPK Signaling to Induce Epithelial-to-Mesenchymal Transition and Is a Poor Prognostic Marker in Colorectal Cancer Patients. *J Clin Med* 2019; **8** [PMID: 31330880 DOI: 10.3390/jcm8071070]
114 **Martínez-Reyes I**, Chandel NS. Mitochondrial TCA cycle metabolites control physiology and disease. *Nat Commun* 2020; **11**: 102 [PMID: 31900386 DOI: 10.1038/s41467-019-13668-3]
115 **Beyoğlu D**, Idle JR. Metabolic Rewiring and the Characterization of Oncometabolites. *Cancers (Basel)* 2021; **13** [PMID: 34200553 DOI: 10.3390/cancers13122900]
116 **Missiroli S**, Perrone M, Genovese I, Pinton P, Giorgi C. Cancer metabolism and mitochondria: Finding novel mechanisms to fight tumours. *EBioMedicine* 2020; **59**: 102943 [PMID: 32818805 DOI: 10.1016/j.ebiom.2020.102943]
117 **Kaelin WG Jr**. Cancer and altered metabolism: potential importance of hypoxia-inducible factor and 2-oxoglutarate-dependent dioxygenases. *Cold Spring Harb Symp Quant Biol* 2011; **76**: 335-345 [PMID: 22089927 DOI: 10.1101/sqb.2011.76.010975]
118 **Carvajal-Carmona LG**, Alam NA, Pollard PJ, Jones AM, Barclay E, Wortham N, Pignatelli M, Freeman A, Pomplun S, Ellis I, Poulsom R, El-Bahrawy MA, Berney DM, Tomlinson IP. Adult leydig cell tumors of the testis caused by germline fumarate hydratase mutations. *J Clin Endocrinol Metab* 2006; **91**: 3071-3075 [PMID: 16757530 DOI: 10.1210/jc.2006-0183]
119 **Tomlinson IP**, Alam NA, Rowan AJ, Barclay E, Jaeger EE, Kelsell D, Leigh I, Gorman P, Lamlum H, Rahman S, Roylance RR, Olpin S, Bevan S, Barker K, Hearle N, Houlston RS, Kiuru M, Lehtonen R, Karhu A, Vilkki S, Laiho P, Eklund C, Vierimaa O, Aittomäki K, Hietala M, Sistonen P, Paetau A, Salovaara R, Herva R, Launonen V, Aaltonen LA; Multiple Leiomyoma Consortium. Germline mutations in FH predispose to dominantly inherited uterine fibroids, skin leiomyomata and papillary renal cell cancer. *Nat Genet* 2002; **30**: 406-410 [PMID: 11865300 DOI: 10.1038/ng849]
120 **Baysal BE**, Ferrell RE, Willett-Brozick JE, Lawrence EC, Myssiorek D, Bosch A, van der Mey A, Taschner PE, Rubinstein WS, Myers EN, Richard CW 3rd, Cornelisse CJ, Devilee P, Devlin B. Mutations in SDHD, a mitochondrial complex II gene, in hereditary paraganglioma. *Science* 2000; **287**: 848-851 [PMID: 10657297 DOI: 10.1126/science.287.5454.848]
121 **Niemann S**, Müller U. Mutations in SDHC cause autosomal dominant paraganglioma, type 3. *Nat Genet* 2000; **26**: 268-270 [PMID: 11062460 DOI: 10.1038/81551]
122 **Burnichon N**, Brière JJ, Libé R, Vescovo L, Rivière J, Tissier F, Jouanno E, Jeunemaitre X, Bénit P, Tzagoloff A, Rustin P, Bertherat J, Favier J, Gimenez-Roqueplo AP. SDHA is a tumor suppressor gene causing paraganglioma. *Hum Mol Genet* 2010; **19**: 3011-3020 [PMID: 20484225 DOI: 10.1093/hmg/ddq206]
123 **Astuti D**, Latif F, Dallol A, Dahia PL, Douglas F, George E, Sköldberg F, Husebye ES, Eng C, Maher ER. Gene mutations in the succinate dehydrogenase subunit SDHB cause susceptibility to familial pheochromocytoma and to familial paraganglioma. *Am J Hum Genet* 2001; **69**: 49-54 [PMID: 11404820 DOI: 10.1086/321282]
124 **Serra D**, Amaro P, Gonçalo M, Silva M, Ferrando B, Pasini B, Figueiredo A. Gastric leiomyoma and hyperplastic polyposis coli in a patient with multiple cutaneous and uterine leiomyomatosis. *J Cutan Med Surg* 2012; **16**: 208-211 [PMID: 22713448 DOI: 10.1177/120347541201600315]
125 **Du X**, Wan S, Chen Y, Qu P, Huang X, Yu X, Yang H, Zhang Y, Xing J. Genetic variants in genes of tricarboxylic acid cycle key enzymes predict postsurgical overall survival of patients with hepatocellular carcinoma. *Ann Surg Oncol* 2014; **21**: 4300-4307 [PMID: 25081338 DOI: 10.1245/s10434-014-3876-2]
126 **Dong G**, He X, Chen Y, Cao H, Wang J, Liu X, Wang S, Wan S, Xing J. Genetic variations in genes of metabolic enzymes predict

postoperational prognosis of patients with colorectal cancer. *Mol Cancer* 2015; **14**: 171 [PMID: 26377099 DOI: 10.1186/s12943-015-0442-x]

127 **Lee WC**, Chou HS, Wu TJ, Lee CF, Hsu PY, Hsu HY, Wu TH, Chan KM. Down-regulation of metabolic proteins in hepatocellular carcinoma with portal vein thrombosis. *Clin Proteomics* 2017; **14**: 29 [PMID: 28785178 DOI: 10.1186/s12014-017-9164-y]

128 **Tuli HS**, Tuorkey MJ, Thakral F, Sak K, Kumar M, Sharma AK, Sharma U, Jain A, Aggarwal V, Bishayee A. Molecular Mechanisms of Action of Genistein in Cancer: Recent Advances. *Front Pharmacol* 2019; **10**: 1336 [PMID: 31866857 DOI: 10.3389/fphar.2019.01336]

129 **Samec M**, Liskova A, Koklesova L, Mersakova S, Strnadel J, Kajo K, Pec M, Zhai K, Smejkal K, Mirzaei S, Hushmandi K, Ashrafizadeh M, Saso L, Brockmueller A, Shakibaei M, Büsselberg D, Kubatka P. Flavonoids Targeting HIF-1: Implications on Cancer Metabolism. *Cancers (Basel)* 2021; **13** [PMID: 33401572 DOI: 10.3390/cancers13010130]

130 **Ashrafizadeh M**, Bakhoda MR, Bahmanpour Z, Ilkhani K, Zarrabi A, Makvandi P, Khan H, Mazaheri S, Darvish M, Mirzaei H. Apigenin as Tumor Suppressor in Cancers: Biotherapeutic Activity, Nanodelivery, and Mechanisms With Emphasis on Pancreatic Cancer. *Front Chem* 2020; **8**: 829 [PMID: 33195038 DOI: 10.3389/fchem.2020.00829]

131 **Cao X**, Ren K, Song Z, Li D, Quan M, Zheng Y, Cao J, Zeng W, Zou H. 7-Difluoromethoxyl-5,4'-di-n-octyl genistein inhibits the stem-like characteristics of gastric cancer stem-like cells and reverses the phenotype of epithelial-mesenchymal transition in gastric cancer cells. *Oncol Rep* 2016; **36**: 1157-1165 [PMID: 27279287 DOI: 10.3892/or.2016.4848]

132 **Yanagihara K**, Ito A, Toge T, Numoto M. Antiproliferative effects of isoflavones on human cancer cell lines established from the gastrointestinal tract. *Cancer Res* 1993; **53**: 5815-5821 [PMID: 8242641]

133 **Gao J**, Xia R, Chen J, Gao J, Luo X, Ke C, Ren C, Li J, Mi Y. Inhibition of esophageal-carcinoma cell proliferation by genistein *via* suppression of JAK1/2-STAT3 and AKT/MDM2/p53 signaling pathways. *Aging (Albany NY)* 2020; **12**: 6240-6259 [PMID: 32276266 DOI: 10.18632/aging.103019]

134 **Mousavi Y**, Adlercreutz H. Genistein is an effective stimulator of sex hormone-binding globulin production in hepatocarcinoma human liver cancer cells and suppresses proliferation of these cells in culture. *Steroids* 1993; **58**: 301-304 [PMID: 8212077 DOI: 10.1016/0039-128x(93)90088-5]

135 **Dai W**, Wang F, He L, Lin C, Wu S, Chen P, Zhang Y, Shen M, Wu D, Wang C, Lu J, Zhou Y, Xu X, Xu L, Guo C. Genistein inhibits hepatocellular carcinoma cell migration by reversing the epithelial-mesenchymal transition: partial mediation by the transcription factor NFAT1. *Mol Carcinog* 2015; **54**: 301-311 [PMID: 24243709 DOI: 10.1002/mc.22100]

136 **Li S**, Li J, Dai W, Zhang Q, Feng J, Wu L, Liu T, Yu Q, Xu S, Wang W, Lu X, Chen K, Xia Y, Lu J, Zhou Y, Fan X, Mo W, Xu L, Guo C. Genistein suppresses aerobic glycolysis and induces hepatocellular carcinoma cell death. *Br J Cancer* 2017; **117**: 1518-1528 [PMID: 28926527 DOI: 10.1038/bjc.2017.323]

137 **Tanjak P**, Thiantanawat A, Watcharasit P, Satayavivad J. Genistein reduces the activation of AKT and EGFR, and the production of IL6 in cholangiocarcinoma cells involving estrogen and estrogen receptors. *Int J Oncol* 2018; **53**: 177-188 [PMID: 29693152 DOI: 10.3892/ijo.2018.4375]

138 **Mouria M**, Gukovskaya AS, Jung Y, Buechler P, Hines OJ, Reber HA, Pandol SJ. Food-derived polyphenols inhibit pancreatic cancer growth through mitochondrial cytochrome C release and apoptosis. *Int J Cancer* 2002; **98**: 761-769 [PMID: 11920648 DOI: 10.1002/ijc.10202]

139 **Büchler P**, Reber HA, Büchler MW, Friess H, Lavey RS, Hines OJ. Antiangiogenic activity of genistein in pancreatic carcinoma cells is mediated by the inhibition of hypoxia-inducible factor-1 and the down-regulation of VEGF gene expression. *Cancer* 2004; **100**: 201-210 [PMID: 14692041 DOI: 10.1002/cncr.11873]

140 **Yu Z**, Li W, Liu F. Inhibition of proliferation and induction of apoptosis by genistein in colon cancer HT-29 cells. *Cancer Lett* 2004; **215**: 159-166 [PMID: 15488634 DOI: 10.1016/j.canlet.2004.06.010]

141 **Wu K**, Yuan LH, Xia W. Inhibitory effects of apigenin on the growth of gastric carcinoma SGC-7901 cells. *World J Gastroenterol* 2005; **11**: 4461-4464 [PMID: 16052672 DOI: 10.3748/wjg.v11.i29.4461]

142 **Zhang Q**, Zhao XH, Wang ZJ. Flavones and flavonols exert cytotoxic effects on a human oesophageal adenocarcinoma cell line (OE33) by causing G2/M arrest and inducing apoptosis. *Food Chem Toxicol* 2008; **46**: 2042-2053 [PMID: 18331776 DOI: 10.1016/j.fct.2008.01.049]

143 **Chiang LC**, Ng LT, Lin IC, Kuo PL, Lin CC. Anti-proliferative effect of apigenin and its apoptotic induction in human Hep G2 cells. *Cancer Lett* 2006; **237**: 207-214 [PMID: 16023288 DOI: 10.1016/j.canlet.2005.06.002]

144 **Subhasitanont P**, Chokchaichamnankit D, Chiablaem K, Keeratichamroen S, Ngiwsara L, Paricharttanakul NM, Lirdprapamongkol K, Weeraphan C, Svasti J, Srisomsap C. Apigenin inhibits growth and induces apoptosis in human cholangiocarcinoma cells. *Oncol Lett* 2017; **14**: 4361-4371 [PMID: 28943950 DOI: 10.3892/ol.2017.6705]

145 **Ujiki MB**, Ding XZ, Salabat MR, Bentrem DJ, Golkar L, Milam B, Talamonti MS, Bell RH Jr, Iwamura T, Adrian TE. Apigenin inhibits pancreatic cancer cell proliferation through G2/M cell cycle arrest. *Mol Cancer* 2006; **5**: 76 [PMID: 17196098 DOI: 10.1186/1476-4598-5-76]

146 **Engelmann C**, Blot E, Panis Y, Bauer S, Trochon V, Nagy HJ, Lu H, Soria C. Apigenin--strong cytostatic and anti-angiogenic action in vitro contrasted by lack of efficacy in vivo. *Phytomedicine* 2002; **9**: 489-495 [PMID: 12403156 DOI: 10.1078/09447110260573100]

147 **Hoensch H**, Groh B, Edler L, Kirch W. Prospective cohort comparison of flavonoid treatment in patients with resected colorectal cancer to prevent recurrence. *World J Gastroenterol* 2008; **14**: 2187-2193 [PMID: 18407592 DOI: 10.3748/wjg.14.2187]

148 **Hung MH**, Chen YL, Chen LJ, Chu PY, Hsieh FS, Tsai MH, Shih CT, Chao TI, Huang CY, Chen KF. Canagliflozin inhibits growth of hepatocellular carcinoma *via* blocking glucose-influx-induced β-catenin activation. *Cell Death Dis* 2019; **10**: 420 [PMID: 31142735 DOI: 10.1038/s41419-019-1646-6]

149 **Tiemin P**, Peng X, Qingfu L, Yan W, Junlin X, Zhefeng H, Ming Z, Desen L, Qinghui M. Dysregulation of the miR-148a-GLUT1 axis promotes the progression and chemoresistance of human intrahepatic cholangiocarcinoma. *Oncogenesis* 2020; **9**: 19 [PMID: 32054829 DOI: 10.1038/s41389-020-0207-2]

150 **Shibuya K**, Okada M, Suzuki S, Seino M, Seino S, Takeda H, Kitanaka C. Targeting the facilitative glucose transporter GLUT1 inhibits the self-renewal and tumor-initiating capacity of cancer stem cells. *Oncotarget* 2015; **6**: 651-661 [PMID: 25528771 DOI: 10.18632/oncotarget.2892]

151 **Liu W**, Fang Y, Wang XT, Liu J, Dan X, Sun LL. Overcoming 5-Fu resistance of colon cells through inhibition of Glut1 by the specific inhibitor WZB117. *Asian Pac J Cancer Prev* 2014; **15**: 7037-7041 [PMID: 25227787 DOI: 10.7314/apjcp.2014.15.17.7037]

152 **Cao X**, Cao Y, Zhao H, Wang P, Zhu Z. Prolyl 4-hydroxylase P4HA1 Mediates the Interplay Between Glucose Metabolism and Stemness in Pancreatic Cancer Cells. *Curr Stem Cell Res Ther* 2023; **18**: 712-719 [PMID: 36043766 DOI: 10.2174/1574888X17666220827113434]

153 **Kraus D**, Reckenbeil J, Veit N, Kuerpig S, Meisenheimer M, Beier I, Stark H, Winter J, Probstmeier R. Targeting glucose transport and the NAD pathway in tumor cells with STF-31: a re-evaluation. *Cell Oncol (Dordr)* 2018; **41**: 485-494 [PMID: 29949049 DOI: 10.1007/s13402-018-0385-5]

154 **Sawayama H**, Ogata Y, Ishimoto T, Mima K, Hiyoshi Y, Iwatsuki M, Baba Y, Miyamoto Y, Yoshida N, Baba H. Glucose transporter 1 regulates the proliferation and cisplatin sensitivity of esophageal cancer. *Cancer Sci* 2019; **110**: 1705-1714 [PMID: 30861255 DOI: 10.1111/cas.13995]

155 **Gauthier-Coles G**, Bröer A, McLeod MD, George AJ, Hannan RD, Bröer S. Identification and characterization of a novel SNAT2 (SLC38A2) inhibitor reveals synergy with glucose transport inhibition in cancer cells. *Front Pharmacol* 2022; **13**: 963066 [PMID: 36210829 DOI: 10.3389/fphar.2022.963066]

156 **Guo L**, Zhang W, Xie Y, Chen X, Olmstead EE, Lian M, Zhang B, Zaytseva YY, Evers BM, Spielmann HP, Liu X, Watt DS, Liu C. Diaminobutoxy-substituted Isoflavonoid (DBI-1) Enhances the Therapeutic Efficacy of GLUT1 Inhibitor BAY-876 by Modulating Metabolic Pathways in Colon Cancer Cells. *Mol Cancer Ther* 2022; **21**: 740-750 [PMID: 35247917 DOI: 10.1158/1535-7163.MCT-21-0925]

157 **Laussel C**, Léon S. Cellular toxicity of the metabolic inhibitor 2-deoxyglucose and associated resistance mechanisms. *Biochem Pharmacol* 2020; **182**: 114213 [PMID: 32890467 DOI: 10.1016/j.bcp.2020.114213]

158 **Shen K**, Liu B, Zhou X, Ji Y, Chen L, Wang Q, Xue W. The Evolving Role of (18)F-FDG PET/CT in Diagnosis and Prognosis Prediction in Progressive Prostate Cancer. *Front Oncol* 2021; **11**: 683793 [PMID: 34395251 DOI: 10.3389/fonc.2021.683793]

159 **Xu Y**, Wang Q, Zhang L, Zheng M. 2-Deoxy-D-glucose enhances TRAIL-induced apoptosis in human gastric cancer cells through downregulating JNK-mediated cytoprotective autophagy. *Cancer Chemother Pharmacol* 2018; **81**: 555-564 [PMID: 29383484 DOI: 10.1007/s00280-018-3526-7]

160 **Mack P**, Ahrén B, Jeppsson B, Kan Z, Bengmark S. Influence of 2-deoxy-D-glucose and arterial ischaemia on glucose oxidation and growth of liver cancer in the rat. *Eur J Cancer Clin Oncol* 1988; **24**: 1433-1437 [PMID: 3181267 DOI: 10.1016/0277-5379(88)90333-1]

161 **Saydjari R**, Alexander RW, Barranco SC, Townsend CM Jr, Thompson JC. The effects of 2-deoxy-D-glucose and alpha-difluoromethylornithine on the growth of pancreatic cancer in vivo. *Pancreas* 1989; **4**: 38-43 [PMID: 2497460 DOI: 10.1097/00006676-198902000-00006]

162 **Takemura A**, Che XF, Tabuchi T, Moriya S, Miyazawa K, Tomoda A. Enhancement of cytotoxic and pro-apoptotic effects of 2-aminophenoxazine-3-one on the rat hepatocellular carcinoma cell line dRLh-84, the human hepatocellular carcinoma cell line HepG2, and the rat normal hepatocellular cell line RLN-10 in combination with 2-deoxy-D-glucose. *Oncol Rep* 2012; **27**: 347-355 [PMID: 22076586 DOI: 10.3892/or.2011.1531]

163 **Maher JC**, Savaraj N, Priebe W, Liu H, Lampidis TJ. Differential sensitivity to 2-deoxy-D-glucose between two pancreatic cell lines correlates with GLUT-1 expression. *Pancreas* 2005; **30**: e34-e39 [PMID: 15714127 DOI: 10.1097/01.mpa.0000153327.46945.26]

164 **Zhang XD**, Deslandes E, Villedieu M, Poulain L, Duval M, Gauduchon P, Schwartz L, Icard P. Effect of 2-deoxy-D-glucose on various malignant cell lines in vitro. *Anticancer Res* 2006; **26**: 3561-3566 [PMID: 17094483]

165 **Cui Y**, Yang D, Wang W, Zhang L, Liu H, Ma S, Guo W, Yao M, Zhang K, Li W, Zhang Y, Guan F. Nicotinamide N-methyltransferase decreases 5-fluorouracil sensitivity in human esophageal squamous cell carcinoma through metabolic reprogramming and promoting the Warburg effect. *Mol Carcinog* 2020; **59**: 940-954 [PMID: 32367570 DOI: 10.1002/mc.23209]

166 **Fan T**, Sun G, Sun X, Zhao L, Zhong R, Peng Y. Tumor Energy Metabolism and Potential of 3-Bromopyruvate as an Inhibitor of Aerobic Glycolysis: Implications in Tumor Treatment. *Cancers (Basel)* 2019; **11** [PMID: 30845728 DOI: 10.3390/cancers11030317]

167 **Ko YH**, Pedersen PL, Geschwind JF. Glucose catabolism in the rabbit VX2 tumor model for liver cancer: characterization and targeting hexokinase. *Cancer Lett* 2001; **173**: 83-91 [PMID: 11578813 DOI: 10.1016/s0304-3835(01)00667-x]

168 **Xian SL**, Cao W, Zhang XD, Lu YF. Inhibitory effects of 3-bromopyruvate on human gastric cancer implant tumors in nude mice. *Asian Pac J Cancer Prev* 2014; **15**: 3175-3178 [PMID: 24815466 DOI: 10.7314/apjcp.2014.15.7.3175]

169 **Cao X**, Jia G, Zhang T, Yang M, Wang B, Wassenaar PA, Cheng H, Knopp MV, Sun D. Non-invasive MRI tumor imaging and synergistic anticancer effect of HSP90 inhibitor and glycolysis inhibitor in RIP1-Tag2 transgenic pancreatic tumor model. *Cancer Chemother Pharmacol* 2008; **62**: 985-994 [PMID: 18253734 DOI: 10.1007/s00280-008-0688-8]

170 **Ihrlund LS**, Hernlund E, Khan O, Shoshan MC. 3-Bromopyruvate as inhibitor of tumour cell energy metabolism and chemopotentiator of platinum drugs. *Mol Oncol* 2008; **2**: 94-101 [PMID: 19383331 DOI: 10.1016/j.molonc.2008.01.003]

171 **Sun X**, Sun G, Huang Y, Hao Y, Tang X, Zhang N, Zhao L, Zhong R, Peng Y. 3-Bromopyruvate regulates the status of glycolysis and BCNU sensitivity in human hepatocellular carcinoma cells. *Biochem Pharmacol* 2020; **177**: 113988 [PMID: 32330495 DOI: 10.1016/j.bcp.2020.113988]

172 **Ko YH**, Verhoeven HA, Lee MJ, Corbin DJ, Vogl TJ, Pedersen PL. A translational study "case report" on the small molecule "energy blocker" 3-bromopyruvate (3BP) as a potent anticancer agent: from bench side to bedside. *J Bioenerg Biomembr* 2012; **44**: 163-170 [PMID: 22328020 DOI: 10.1007/s10863-012-9417-4]

173 **Huang Y**, Sun G, Sun X, Li F, Zhao L, Zhong R, Peng Y. The Potential of Lonidamine in Combination with Chemotherapy and Physical Therapy in Cancer Treatment. *Cancers (Basel)* 2020; **12** [PMID: 33187214 DOI: 10.3390/cancers12113332]

174 **Calabresi F**, Di Lauro L, Marolla P, Curcio CG, Paoletti G, Calabró A, Giannarelli D, Ballatore P, Foggi CM, Di Palma M. Fluorouracil, doxorubicin, and cyclophosphamide versus fluorouracil, doxorubicin, and cyclophosphamide plus lonidamine for the treatment of advanced breast cancer: a multicentric randomized clinical study. *Semin Oncol* 1991; **18**: 66-72 [PMID: 2031201]

175 **Ricotti L**, Tesei A, De Paola F, Milandri C, Amadori D, Frassineti GL, Ulivi P, Zoli W. Potentiation of antiproliferative drug activity by lonidamine in hepatocellular carcinoma cells. *J Chemother* 2003; **15**: 480-487 [PMID: 14598941 DOI: 10.1179/joc.2003.15.5.480]

176 **Thamrongwaranggoon U**, Seubwai W, Phoomak C, Sangkhamanon S, Cha'on U, Boonmars T, Wongkham S. Targeting hexokinase II as a possible therapy for cholangiocarcinoma. *Biochem Biophys Res Commun* 2017; **484**: 409-415 [PMID: 28131825 DOI: 10.1016/j.bbrc.2017.01.139]

177 **Villa R**, Zaffaroni N, Orlandi L, Bearzatto A, Costa A, Silvestrini R. In vitro effect of lonidamine on the cytotoxicity of mitomycin C and BCNU in human colon adenocarcinoma cells. *Eur J Cancer* 1994; **30A**: 1534-1540 [PMID: 7833114 DOI: 10.1016/0959-8049(94)e0162-w]

178 **Zaniboni A**, Meriggi F, Alghisi A, Mutti S, Distefano L, Rizzi A, Bettini L, Simoncini E, Marpicati P, Montini E. Mitomycin-C and lonidamine as second-line therapy for colorectal cancer: a phase II study. *Tumori* 1995; **81**: 435-437 [PMID: 8804471 DOI: 10.1177/030089169508100610]

179 **Gebbia V**, Testa A, Cannata G, Tirrito M, Longo A, Sciume C, Valdesi M, Salamone G, Gebbia N, Leo P. Second line chemotherapy for metastatic colorectal carcinoma. *Oncol Rep* 1996; **3**: 867-869 [PMID: 21594470 DOI: 10.3892/or.3.5.867]

180 **Shi L**, Pan H, Liu Z, Xie J, Han W. Roles of PFKFB3 in cancer. *Signal Transduct Target Ther* 2017; **2**: 17044 [PMID: 29263928 DOI: 10.1038/sigtrans.2017.44]

181 **Varghese E**, Samuel SM, Líšková A, Samec M, Kubatka P, Büsselberg D. Targeting Glucose Metabolism to Overcome Resistance to

Anticancer Chemotherapy in Breast Cancer. *Cancers (Basel)* 2020; **12** [PMID: 32806533 DOI: 10.3390/cancers12082252]
182 **Mejias M**, Gallego J, Naranjo-Suarez S, Ramirez M, Pell N, Manzano A, Suñer C, Bartrons R, Mendez R, Fernandez M. CPEB4 Increases Expression of PFKFB3 to Induce Glycolysis and Activate Mouse and Human Hepatic Stellate Cells, Promoting Liver Fibrosis. *Gastroenterology* 2020; **159**: 273-288 [PMID: 32169429 DOI: 10.1053/j.gastro.2020.03.008]
183 **Conradi LC**, Brajic A, Cantelmo AR, Bouché A, Kalucka J, Pircher A, Brüning U, Teuwen LA, Vinckier S, Ghesquière B, Dewerchin M, Carmeliet P. Tumor vessel disintegration by maximum tolerable PFKFB3 blockade. *Angiogenesis* 2017; **20**: 599-613 [PMID: 28875379 DOI: 10.1007/s10456-017-9573-6]
184 **Klarer AC**, O'Neal J, Imbert-Fernandez Y, Clem A, Ellis SR, Clark J, Clem B, Chesney J, Telang S. Inhibition of 6-phosphofructo-2-kinase (PFKFB3) induces autophagy as a survival mechanism. *Cancer Metab* 2014; **2**: 2 [PMID: 24451478 DOI: 10.1186/2049-3002-2-2]
185 **Zhu W**, Ye L, Zhang J, Yu P, Wang H, Ye Z, Tian J. PFK15, a Small Molecule Inhibitor of PFKFB3, Induces Cell Cycle Arrest, Apoptosis and Inhibits Invasion in Gastric Cancer. *PLoS One* 2016; **11**: e0163768 [PMID: 27669567 DOI: 10.1371/journal.pone.0163768]
186 **Shi WK**, Zhu XD, Wang CH, Zhang YY, Cai H, Li XL, Cao MQ, Zhang SZ, Li KS, Sun HC. PFKFB3 blockade inhibits hepatocellular carcinoma growth by impairing DNA repair through AKT. *Cell Death Dis* 2018; **9**: 428 [PMID: 29559632 DOI: 10.1038/s41419-018-0435-y]
187 **Dou Q**, Grant AK, Callahan C, Coutinho de Souza P, Mwin D, Booth AL, Nasser I, Moussa M, Ahmed M, Tsai LL. PFKFB3-mediated Pro-glycolytic Shift in Hepatocellular Carcinoma Proliferation. *Cell Mol Gastroenterol Hepatol* 2023; **15**: 61-75 [PMID: 36162723 DOI: 10.1016/j.jcmgh.2022.09.009]
188 **Richardson DA**, Sritangos P, James AD, Sultan A, Bruce JIE. Metabolic regulation of calcium pumps in pancreatic cancer: role of phosphofructokinase-fructose-bisphosphatase-3 (PFKFB3). *Cancer Metab* 2020; **8**: 2 [PMID: 32266066 DOI: 10.1186/s40170-020-0210-2]
189 **Horváthová J**, Moravčík R, Matúšková M, Šišovský V, Boháč A, Zeman M. Inhibition of Glycolysis Suppresses Cell Proliferation and Tumor Progression In Vivo: Perspectives for Chronotherapy. *Int J Mol Sci* 2021; **22** [PMID: 33922320 DOI: 10.3390/ijms22094390]
190 **Redman RA**, Pohlmann PR, Kurman MR, Tapolsky G, Chesney JA. A phase I, dose-escalation, multi-center study of PFK-158 in patients with advanced solid malignancies explores a first-in-man inhbibitor of glycolysis. *J Clin Oncol* 2015; **33**: tps2606 [DOI: 10.1200/jco.2015.33.15_suppl.tps2606]
191 **Chhipa AS**, Patel S. Targeting pyruvate kinase muscle isoform 2 (PKM2) in cancer: What do we know so far? *Life Sci* 2021; **280**: 119694 [PMID: 34102192 DOI: 10.1016/j.lfs.2021.119694]
192 **Kim SJ**, Kim JM, Shim SH, Chang HI. Shikonin induces cell cycle arrest in human gastric cancer (AGS) by early growth response 1 (Egr1)-mediated p21 gene expression. *J Ethnopharmacol* 2014; **151**: 1064-1071 [PMID: 24384380 DOI: 10.1016/j.jep.2013.11.055]
193 **Tang JC**, Zhao J, Long F, Chen JY, Mu B, Jiang Z, Ren Y, Yang J. Efficacy of Shikonin against Esophageal Cancer Cells and its possible mechanisms in vitro and in vivo. *J Cancer* 2018; **9**: 32-40 [PMID: 29290767 DOI: 10.7150/jca.21224]
194 **Yingkun N**, Lvsong Z, Huimin Y. Shikonin inhibits the proliferation and induces the apoptosis of human HepG2 cells. *Can J Physiol Pharmacol* 2010; **88**: 1138-1146 [PMID: 21164560 DOI: 10.1139/Y10-085]
195 **Zhou G**, Yang Z, Wang X, Tao R, Zhou Y. TRAIL Enhances Shikonin Induced Apoptosis through ROS/JNK Signaling in Cholangiocarcinoma Cells. *Cell Physiol Biochem* 2017; **42**: 1073-1086 [PMID: 28662515 DOI: 10.1159/000478758]
196 **Wang Y**, Zhou Y, Jia G, Han B, Liu J, Teng Y, Lv J, Song Z, Li Y, Ji L, Pan S, Jiang H, Sun B. Shikonin suppresses tumor growth and synergizes with gemcitabine in a pancreatic cancer xenograft model: Involvement of NF-κB signaling pathway. *Biochem Pharmacol* 2014; **88**: 322-333 [PMID: 24522113 DOI: 10.1016/j.bcp.2014.01.041]
197 **Li MY**, Mi C, Wang KS, Wang Z, Zuo HX, Piao LX, Xu GH, Li X, Ma J, Jin X. Shikonin suppresses proliferation and induces cell cycle arrest through the inhibition of hypoxia-inducible factor-1α signaling. *Chem Biol Interact* 2017; **274**: 58-67 [PMID: 28684144 DOI: 10.1016/j.cbi.2017.06.029]
198 **Diaconu CC**, Szathmári M, Kéri G, Venetianer A. Apoptosis is induced in both drug-sensitive and multidrug-resistant hepatoma cells by somatostatin analogue TT-232. *Br J Cancer* 1999; **80**: 1197-1203 [PMID: 10376972 DOI: 10.1038/sj.bjc.6690486]
199 **Lee JU**, Hosotani R, Wada M, Doi R, Koshiba T, Fujimoto K, Miyamoto Y, Tsuji S, Nakajima S, Hirohashi M, Uehara T, Arano Y, Fujii N, Imamura M. Antiproliferative activity induced by the somatostatin analogue, TT-232, in human pancreatic cancer cells. *Eur J Cancer* 2002; **38**: 1526-1534 [PMID: 12110500 DOI: 10.1016/s0959-8049(02)00101-6]
200 **Tejeda M**, Gaal D, Barna K, Csuka O, Kéri G. The antitumor activity of the somatostatin structural derivative (TT-232) on different human tumor xenografts. *Anticancer Res* 2003; **23**: 4061-4066 [PMID: 14666719]
201 **Zhao Y**, Butler EB, Tan M. Targeting cellular metabolism to improve cancer therapeutics. *Cell Death Dis* 2013; **4**: e532 [PMID: 23470539 DOI: 10.1038/cddis.2013.60]
202 **Michelakis ED**, Webster L, Mackey JR. Dichloroacetate (DCA) as a potential metabolic-targeting therapy for cancer. *Br J Cancer* 2008; **99**: 989-994 [PMID: 18766181 DOI: 10.1038/sj.bjc.6604554]
203 **Hur H**, Xuan Y, Kim YB, Lee G, Shim W, Yun J, Ham IH, Han SU. Expression of pyruvate dehydrogenase kinase-1 in gastric cancer as a potential therapeutic target. *Int J Oncol* 2013; **42**: 44-54 [PMID: 23135628 DOI: 10.3892/ijo.2012.1687]
204 **Twarock S**, Reichert C, Bach K, Reiners O, Kretschmer I, Gorski DJ, Gorges K, Grandoch M, Fischer JW. Inhibition of the hyaluronan matrix enhances metabolic anticancer therapy by dichloroacetate in vitro and in vivo. *Br J Pharmacol* 2019; **176**: 4474-4490 [PMID: 31351004 DOI: 10.1111/bph.14808]
205 **Sun L**, Jiang Y, Yan X, Dai X, Huang C, Chen L, Li T, Zhang Y, Xiao H, Yang M, Xiang L, Chen S, Li S, Chen A, He F, Lian J. Dichloroacetate enhances the anti-tumor effect of sorafenib *via* modulating the ROS-JNK-Mcl-1 pathway in liver cancer cells. *Exp Cell Res* 2021; **406**: 112755 [PMID: 34332981 DOI: 10.1016/j.yexcr.2021.112755]
206 **Tataranni T**, Agriesti F, Pacelli C, Ruggieri V, Laurenzana I, Mazzoccoli C, Sala GD, Panebianco C, Pazienza V, Capitanio N, Piccoli C. Dichloroacetate Affects Mitochondrial Function and Stemness-Associated Properties in Pancreatic Cancer Cell Lines. *Cells* 2019; **8** [PMID: 31109089 DOI: 10.3390/cells8050478]
207 **Babu E**, Ramachandran S, CoothanKandaswamy V, Elangovan S, Prasad PD, Ganapathy V, Thangaraju M. Role of SLC5A8, a plasma membrane transporter and a tumor suppressor, in the antitumor activity of dichloroacetate. *Oncogene* 2011; **30**: 4026-4037 [PMID: 21499304 DOI: 10.1038/onc.2011.113]
208 **Bull RJ**, Sanchez IM, Nelson MA, Larson JL, Lansing AJ. Liver tumor induction in B6C3F1 mice by dichloroacetate and trichloroacetate. *Toxicology* 1990; **63**: 341-359 [PMID: 2219130 DOI: 10.1016/0300-483x(90)90195-m]
209 **Claps G**, Faouzi S, Quidville V, Chehade F, Shen S, Vagner S, Robert C. The multiple roles of LDH in cancer. *Nat Rev Clin Oncol* 2022; **19**: 749-762 [PMID: 36207413 DOI: 10.1038/s41571-022-00686-2]

210 **Zhou Y**, Tao P, Wang M, Xu P, Lu W, Lei P, You Q. Development of novel human lactate dehydrogenase A inhibitors: High-throughput screening, synthesis, and biological evaluations. *Eur J Med Chem* 2019; **177**: 105-115 [PMID: 31129449 DOI: 10.1016/j.ejmech.2019.05.033]

211 **Kim EY**, Chung TW, Han CW, Park SY, Park KH, Jang SB, Ha KT. A Novel Lactate Dehydrogenase Inhibitor, 1-(Phenylseleno)-4-(Trifluoromethyl) Benzene, Suppresses Tumor Growth through Apoptotic Cell Death. *Sci Rep* 2019; **9**: 3969 [PMID: 30850682 DOI: 10.1038/s41598-019-40617-3]

212 **Liu X**, Yang Z, Chen Z, Chen R, Zhao D, Zhou Y, Qiao L. Effects of the suppression of lactate dehydrogenase A on the growth and invasion of human gastric cancer cells. *Oncol Rep* 2015; **33**: 157-162 [PMID: 25394466 DOI: 10.3892/or.2014.3600]

213 **Zhao Z**, Han F, Yang S, Wu J, Zhan W. Oxamate-mediated inhibition of lactate dehydrogenase induces protective autophagy in gastric cancer cells: involvement of the Akt-mTOR signaling pathway. *Cancer Lett* 2015; **358**: 17-26 [PMID: 25524555 DOI: 10.1016/j.canlet.2014.11.046]

214 **Forkasiewicz A**, Stach W, Wierzbicki J, Stach K, Tabola R, Hryniewicz-Jankowska A, Augoff K. Effect of LDHA Inhibition on TNF-α-Induced Cell Migration in Esophageal Cancers. *Int J Mol Sci* 2022; **23** [PMID: 36555705 DOI: 10.3390/ijms232416062]

215 **Manerba M**, Di Ianni L, Govoni M, Roberti M, Recanatini M, Di Stefano G. LDH inhibition impacts on heat shock response and induces senescence of hepatocellular carcinoma cells. *Eur J Pharm Sci* 2017; **105**: 91-98 [PMID: 28501492 DOI: 10.1016/j.ejps.2017.05.015]

216 **Lu QY**, Zhang L, Yee JK, Go VW, Lee WN. Metabolic Consequences of LDHA inhibition by Epigallocatechin Gallate and Oxamate in MIA PaCa-2 Pancreatic Cancer Cells. *Metabolomics* 2015; **11**: 71-80 [PMID: 26246802 DOI: 10.1007/s11306-014-0672-8]

217 **Miskimins WK**, Ahn HJ, Kim JY, Ryu S, Jung YS, Choi JY. Synergistic anti-cancer effect of phenformin and oxamate. *PLoS One* 2014; **9**: e85576 [PMID: 24465604 DOI: 10.1371/journal.pone.0085576]

218 **Manerba M**, Di Ianni L, Govoni M, Roberti M, Recanatini M, Di Stefano G. Lactate dehydrogenase inhibitors can reverse inflammation induced changes in colon cancer cells. *Eur J Pharm Sci* 2017; **96**: 37-44 [PMID: 27622920 DOI: 10.1016/j.ejps.2016.09.014]

219 **Wendt EHU**, Schoenrogge M, Vollmar B, Zechner D. Galloflavin Plus Metformin Treatment Impairs Pancreatic Cancer Cells. *Anticancer Res* 2020; **40**: 153-160 [PMID: 31892563 DOI: 10.21873/anticanres.13936]

220 **Moir JAG**, Long A, Haugk B, French JJ, Charnley RM, Manas DM, Wedge SR, Mann J, Robinson SM, White SA. Therapeutic Strategies Toward Lactate Dehydrogenase Within the Tumor Microenvironment of Pancreatic Cancer. *Pancreas* 2020; **49**: 1364-1371 [PMID: 33122526 DOI: 10.1097/MPA.0000000000001689]

221 **Yang J**, Wang C, Zhao F, Luo X, Qin M, Arunachalam E, Ge Z, Wang N, Deng X, Jin G, Cong W, Qin W. Loss of FBP1 facilitates aggressive features of hepatocellular carcinoma cells through the Warburg effect. *Carcinogenesis* 2017; **38**: 134-143 [PMID: 27742690 DOI: 10.1093/carcin/bgw109]

222 **Le A**, Cooper CR, Gouw AM, Dinavahi R, Maitra A, Deck LM, Royer RE, Vander Jagt DL, Semenza GL, Dang CV. Inhibition of lactate dehydrogenase A induces oxidative stress and inhibits tumor progression. *Proc Natl Acad Sci U S A* 2010; **107**: 2037-2042 [PMID: 20133848 DOI: 10.1073/pnas.0914433107]

223 **Rajeshkumar NV**, Dutta P, Yabuuchi S, de Wilde RF, Martinez GV, Le A, Kamphorst JJ, Rabinowitz JD, Jain SK, Hidalgo M, Dang CV, Gillies RJ, Maitra A. Therapeutic Targeting of the Warburg Effect in Pancreatic Cancer Relies on an Absence of p53 Function. *Cancer Res* 2015; **75**: 3355-3364 [PMID: 26113084 DOI: 10.1158/0008-5472.CAN-15-0108]

224 **Mohammad GH**, Vassileva V, Acedo P, Olde Damink SWM, Malago M, Dhar DK, Pereira SP. Targeting Pyruvate Kinase M2 and Lactate Dehydrogenase A Is an Effective Combination Strategy for the Treatment of Pancreatic Cancer. *Cancers (Basel)* 2019; **11** [PMID: 31527446 DOI: 10.3390/cancers11091372]

225 **Kim D**, Koh B, Kim KR, Kim KY, Jung WH, Kim HY, Kim S, Dal Rhee S. Anticancer effect of XAV939 is observed by inhibiting lactose dehydrogenase A in a 3-dimensional culture of colorectal cancer cells. *Oncol Lett* 2019; **18**: 4858-4864 [PMID: 31611996 DOI: 10.3892/ol.2019.10813]

226 **Yu Y**, Deck JA, Hunsaker LA, Deck LM, Royer RE, Goldberg E, Vander Jagt DL. Selective active site inhibitors of human lactate dehydrogenases A4, B4, and C4. *Biochem Pharmacol* 2001; **62**: 81-89 [PMID: 11377399 DOI: 10.1016/s0006-2952(01)00636-0]

227 **Gunassekaran GR**, Priya DK, Gayathri R, Sakthisekaran D. In vitro and in vivo studies on antitumor effects of gossypol on human stomach adenocarcinoma (AGS) cell line and MNNG induced experimental gastric cancer. *Biochem Biophys Res Commun* 2011; **411**: 661-666 [PMID: 21782799 DOI: 10.1016/j.bbrc.2011.06.167]

228 **Xin J**, Zhan YH, Xia LM, Zhu HW, Nie YZ, Liang JM, Tian J. ApoG2 as the most potent gossypol derivatives inhibits cell growth and induces apoptosis on gastric cancer cells. *Biomed Pharmacother* 2013; **67**: 88-95 [PMID: 23201009 DOI: 10.1016/j.biopha.2012.10.016]

229 **Xin J**, Zhan Y, Liu M, Hu H, Xia L, Nie Y, Wu K, Liang J, Tian J. ApoG2 induces ER stress-dependent apoptosis in gastric cancer cells in vitro and its real-time evaluation by bioluminescence imaging in vivo. *Cancer Lett* 2013; **336**: 260-269 [PMID: 23523614 DOI: 10.1016/j.canlet.2013.03.019]

230 **Wei X**, Duan W, Li Y, Zhang S, Xin X, Sun L, Gao M, Li Q, Wang D. AT101 exerts a synergetic efficacy in gastric cancer patients with 5-FU based treatment through promoting apoptosis and autophagy. *Oncotarget* 2016; **7**: 34430-34441 [PMID: 27144437 DOI: 10.18632/oncotarget.9119]

231 **Song S**, Chen Q, Li Y, Lei G, Scott A, Huo L, Li CY, Estrella JS, Correa A, Pizzi MP, Ma L, Jin J, Liu B, Wang Y, Xiao L, Hofstetter WL, Lee JH, Weston B, Bhutani M, Shanbhag N, Johnson RL, Gan B, Wei S, Ajani JA. Targeting cancer stem cells with a pan-BCL-2 inhibitor in preclinical and clinical settings in patients with gastroesophageal carcinoma. *Gut* 2021; **70**: 2238-2248 [PMID: 33487592 DOI: 10.1136/gutjnl-2020-321175]

232 **Wang Y**, Lonard DM, Yu Y, Chow DC, Palzkill TG, O'Malley BW. Small molecule inhibition of the steroid receptor coactivators, SRC-3 and SRC-1. *Mol Endocrinol* 2011; **25**: 2041-2053 [PMID: 22053001 DOI: 10.1210/me.2011-1222]

233 **Cheng P**, Ni Z, Dai X, Wang B, Ding W, Rae Smith A, Xu L, Wu D, He F, Lian J. The novel BH-3 mimetic apogossypolone induces Beclin-1- and ROS-mediated autophagy in human hepatocellular carcinoma [corrected] cells. *Cell Death Dis* 2013; **4**: e489 [PMID: 23392177 DOI: 10.1038/cddis.2013.17]

234 **Mohammad RM**, Wang S, Banerjee S, Wu X, Chen J, Sarkar FH. Nonpeptidic small-molecule inhibitor of Bcl-2 and Bcl-XL, (-)-Gossypol, enhances biological effect of genistein against BxPC-3 human pancreatic cancer cell line. *Pancreas* 2005; **31**: 317-324 [PMID: 16258364 DOI: 10.1097/01.mpa.0000179731.46210.01]

235 **Thakur A**, Lum LG, Schalk D, Azmi A, Banerjee S, Sarkar FH, Mohommad R. Pan-Bcl-2 inhibitor AT-101 enhances tumor cell killing by EGFR targeted T cells. *PLoS One* 2012; **7**: e47520 [PMID: 23185240 DOI: 10.1371/journal.pone.0047520]

236 **Yuan Y**, Tang AJ, Castoreno AB, Kuo SY, Wang Q, Kuballa P, Xavier R, Shamji AF, Schreiber SL, Wagner BK. Gossypol and an HMT G9a inhibitor act in synergy to induce cell death in pancreatic cancer cells. *Cell Death Dis* 2013; **4**: e690 [PMID: 23807219 DOI: 10.1038/cddis.2013.191]

237 **Lee S**, Hong E, Jo E, Kim ZH, Yim KJ, Woo SH, Choi YS, Jang HJ. Gossypol Induces Apoptosis of Human Pancreatic Cancer Cells *via* CHOP/Endoplasmic Reticulum Stress Signaling Pathway. *J Microbiol Biotechnol* 2022; **32**: 645-656 [PMID: 35283426 DOI: 10.4014/jmb.2110.10019]

238 **Wang X**, Wang J, Wong SC, Chow LS, Nicholls JM, Wong YC, Liu Y, Kwong DL, Sham JS, Tsa SW. Cytotoxic effect of gossypol on colon carcinoma cells. *Life Sci* 2000; **67**: 2663-2671 [PMID: 11105982 DOI: 10.1016/s0024-3205(00)00857-2]

239 **Zhang M**, Liu H, Guo R, Ling Y, Wu X, Li B, Roller PP, Wang S, Yang D. Molecular mechanism of gossypol-induced cell growth inhibition and cell death of HT-29 human colon carcinoma cells. *Biochem Pharmacol* 2003; **66**: 93-103 [PMID: 12818369 DOI: 10.1016/s0006-2952(03)00248-x]

240 **Wang X**, Zhang C, Yan X, Lan B, Wang J, Wei C, Cao X, Wang R, Yao J, Zhou T, Zhou M, Liu Q, Jiang B, Jiang P, Kesari S, Lin X, Guo F. A Novel Bioavailable BH3 Mimetic Efficiently Inhibits Colon Cancer *via* Cascade Effects of Mitochondria. *Clin Cancer Res* 2016; **22**: 1445-1458 [PMID: 26515494 DOI: 10.1158/1078-0432.CCR-15-0732]

241 **Sun X**, Wang M, Yao L, Li X, Dong H, Li M, Sun T, Liu X, Liu Y, Xu Y. Role of Proton-Coupled Monocarboxylate Transporters in Cancer: From Metabolic Crosstalk to Therapeutic Potential. *Front Cell Dev Biol* 2020; **8**: 651 [PMID: 32766253 DOI: 10.3389/fcell.2020.00651]

242 **Tao Z**, Huang C, Wang D, Wang Q, Gao Q, Zhang H, Zhao Y, Wang M, Xu J, Shen B, Zhou C, Zhu W. Lactate induced mesenchymal stem cells activation promotes gastric cancer cells migration and proliferation. *Exp Cell Res* 2023; **424**: 113492 [PMID: 36702194 DOI: 10.1016/j.yexcr.2023.113492]

243 **Wang C**, Wen Z, Xie J, Zhao Y, Zhao L, Zhang S, Liu Y, Xue Y, Shi M. MACC1 mediates chemotherapy sensitivity of 5-FU and cisplatin *via* regulating MCT1 expression in gastric cancer. *Biochem Biophys Res Commun* 2017; **485**: 665-671 [PMID: 28235486 DOI: 10.1016/j.bbrc.2017.02.096]

244 **Grasa L**, Chueca E, Arechavaleta S, García-González MA, Sáenz MÁ, Valero A, Hördnler C, Lanas Á, Piazuelo E. Antitumor effects of lactate transport inhibition on esophageal adenocarcinoma cells. *J Physiol Biochem* 2023; **79**: 147-161 [PMID: 36342616 DOI: 10.1007/s13105-022-00931-3]

245 **Behrends V**, Giskeødegård GF, Bravo-Santano N, Letek M, Keun HC. Acetaminophen cytotoxicity in HepG2 cells is associated with a decoupling of glycolysis from the TCA cycle, loss of NADPH production, and suppression of anabolism. *Arch Toxicol* 2019; **93**: 341-353 [PMID: 30552463 DOI: 10.1007/s00204-018-2371-0]

246 **Beloueche-Babari M**, Wantuch S, Casals Galobart T, Koniordou M, Parkes HG, Arunan V, Chung YL, Eykyn TR, Smith PD, Leach MO. MCT1 Inhibitor AZD3965 Increases Mitochondrial Metabolism, Facilitating Combination Therapy and Noninvasive Magnetic Resonance Spectroscopy. *Cancer Res* 2017; **77**: 5913-5924 [PMID: 28923861 DOI: 10.1158/0008-5472.CAN-16-2686]

247 **Lee JY**, Lee I, Chang WJ, Ahn SM, Lim SH, Kim HS, Yoo KH, Jung KS, Song HN, Cho JH, Kim SY, Kim KM, Lee S, Kim ST, Park SH, Lee J, Park JO, Park YS, Lim HY, Kang WK. MCT4 as a potential therapeutic target for metastatic gastric cancer with peritoneal carcinomatosis. *Oncotarget* 2016; **7**: 43492-43503 [PMID: 27224918 DOI: 10.18632/oncotarget.9523]

248 **Kong SC**, Nøhr-Nielsen A, Zeeberg K, Reshkin SJ, Hoffmann EK, Novak I, Pedersen SF. Monocarboxylate Transporters MCT1 and MCT4 Regulate Migration and Invasion of Pancreatic Ductal Adenocarcinoma Cells. *Pancreas* 2016; **45**: 1036-1047 [PMID: 26765963 DOI: 10.1097/MPA.0000000000000571]

249 **Le Floch R**, Chiche J, Marchiq I, Naiken T, Ilc K, Murray CM, Critchlow SE, Roux D, Simon MP, Pouysségur J. CD147 subunit of lactate/H+ symporters MCT1 and hypoxia-inducible MCT4 is critical for energetics and growth of glycolytic tumors. *Proc Natl Acad Sci U S A* 2011; **108**: 16663-16668 [PMID: 21930917 DOI: 10.1073/pnas.1106123108]

250 **Fisel P**, Schaeffeler E, Schwab M. Clinical and Functional Relevance of the Monocarboxylate Transporter Family in Disease Pathophysiology and Drug Therapy. *Clin Transl Sci* 2018; **11**: 352-364 [PMID: 29660777 DOI: 10.1111/cts.12551]

251 **Frattaruolo L**, Brindisi M, Curcio R, Marra F, Dolce V, Cappello AR. Targeting the Mitochondrial Metabolic Network: A Promising Strategy in Cancer Treatment. *Int J Mol Sci* 2020; **21** [PMID: 32825551 DOI: 10.3390/ijms21176014]

252 **Kato K**, Gong J, Iwama H, Kitanaka A, Tani J, Miyoshi H, Nomura K, Mimura S, Kobayashi M, Aritomo Y, Kobara H, Mori H, Himoto T, Okano K, Suzuki Y, Murao K, Masaki T. The antidiabetic drug metformin inhibits gastric cancer cell proliferation in vitro and in vivo. *Mol Cancer Ther* 2012; **11**: 549-560 [PMID: 22222629 DOI: 10.1158/1535-7163.MCT-11-0594]

253 **Feng Y**, Ke C, Tang Q, Dong H, Zheng X, Lin W, Ke J, Huang J, Yeung SC, Zhang H. Metformin promotes autophagy and apoptosis in esophageal squamous cell carcinoma by downregulating Stat3 signaling. *Cell Death Dis* 2014; **5**: e1088 [PMID: 24577086 DOI: 10.1038/cddis.2014.59]

254 **Cai X**, Hu X, Cai B, Wang Q, Li Y, Tan X, Hu H, Chen X, Huang J, Cheng J, Jing X. Metformin suppresses hepatocellular carcinoma cell growth through induction of cell cycle G1/G0 phase arrest and p21CIP and p27KIP expression and downregulation of cyclin D1 in vitro and in vivo. *Oncol Rep* 2013; **30**: 2449-2457 [PMID: 24008375 DOI: 10.3892/or.2013.2718]

255 **Fujimori T**, Kato K, Fujihara S, Iwama H, Yamashita T, Kobayashi K, Kamada H, Morishita A, Kobara H, Mori H, Okano K, Suzuki Y, Masaki T. Antitumor effect of metformin on cholangiocarcinoma: In vitro and in vivo studies. *Oncol Rep* 2015; **34**: 2987-2996 [PMID: 26398221 DOI: 10.3892/or.2015.4284]

256 **Wang LW**, Li ZS, Zou DW, Jin ZD, Gao J, Xu GM. Metformin induces apoptosis of pancreatic cancer cells. *World J Gastroenterol* 2008; **14**: 7192-7198 [PMID: 19084933 DOI: 10.3748/wjg.14.7192]

257 **Tsai CC**, Chuang TW, Chen LJ, Niu HS, Chung KM, Cheng JT, Lin KC. Increase in apoptosis by combination of metformin with silibinin in human colorectal cancer cells. *World J Gastroenterol* 2015; **21**: 4169-4177 [PMID: 25892866 DOI: 10.3748/wjg.v21.i14.4169]

258 **Wang S**, Lin Y, Xiong X, Wang L, Guo Y, Chen Y, Chen S, Wang G, Lin P, Chen H, Yeung SJ, Bremer E, Zhang H. Low-Dose Metformin Reprograms the Tumor Immune Microenvironment in Human Esophageal Cancer: Results of a Phase II Clinical Trial. *Clin Cancer Res* 2020; **26**: 4921-4932 [PMID: 32646922 DOI: 10.1158/1078-0432.CCR-20-0113]

259 **Ostwal V**, Ramaswamy A, Gota V, Bhargava PG, Srinivas S, Shriyan B, Jadhav S, Goel M, Patkar S, Mandavkar S, Naughane D, Daddi A, Nashikkar C, Shetty N, Ankathi SK, Banavali SD. Phase I Study Evaluating Dose De-escalation of Sorafenib with Metformin and Atorvastatin in Hepatocellular Carcinoma (SMASH). *Oncologist* 2022; **27**: 165-e222 [PMID: 35274724 DOI: 10.1093/oncolo/oyab008]

260 **Khurshed M**, Molenaar RJ, van Linde ME, Mathôt RA, Struys EA, van Wezel T, van Noorden CJF, Klümpen HJ, Bovée JVMG, Wilmink JW. A Phase Ib Clinical Trial of Metformin and Chloroquine in Patients with IDH1-Mutated Solid Tumors. *Cancers (Basel)* 2021; **13** [PMID: 34069550 DOI: 10.3390/cancers13102474]

261 **Kordes S**, Pollak MN, Zwinderman AH, Mathôt RA, Weterman MJ, Beeker A, Punt CJ, Richel DJ, Wilmink JW. Metformin in patients with advanced pancreatic cancer: a double-blind, randomised, placebo-controlled phase 2 trial. *Lancet Oncol* 2015; **16**: 839-847 [PMID: 26067687 DOI: 10.1016/S1470-2045(15)00027-3]

262 **Reni M**, Dugnani E, Cereda S, Belli C, Balzano G, Nicoletti R, Liberati D, Pasquale V, Scavini M, Maggiora P, Sordi V, Lampasona V, Ceraulo D, Di Terlizzi G, Doglioni C, Falconi M, Piemonti L. (Ir)relevance of Metformin Treatment in Patients with Metastatic Pancreatic Cancer: An Open-Label, Randomized Phase II Trial. *Clin Cancer Res* 2016; **22**: 1076-1085 [PMID: 26459175 DOI: 10.1158/1078-0432.CCR-15-1722]

263 **Zell JA**, McLaren CE, Morgan TR, Lawson MJ, Rezk S, Albers CG, Chen WP, Carmichael JC, Chung J, Richmond E, Rodriguez LM, Szabo E, Ford LG, Pollak MN, Meyskens FL. A Phase IIa Trial of Metformin for Colorectal Cancer Risk Reduction among Individuals with History of Colorectal Adenomas and Elevated Body Mass Index. *Cancer Prev Res (Phila)* 2020; **13**: 203-212 [PMID: 31818851 DOI: 10.1158/1940-6207.CAPR-18-0262]

264 **Petrera M**, Paleari L, Clavarezza M, Puntoni M, Caviglia S, Briata IM, Oppezzi M, Mislej EM, Stabuc B, Gnant M, Bachleitner-Hofmann T, Roth W, Scherer D, Haefeli WE, Ulrich CM, DeCensi A. The ASAMET trial: a randomized, phase II, double-blind, placebo-controlled, multicenter, 2 × 2 factorial biomarker study of tertiary prevention with low-dose aspirin and metformin in stage I-III colorectal cancer patients. *BMC Cancer* 2018; **18**: 1210 [PMID: 30514262 DOI: 10.1186/s12885-018-5126-7]

265 **Miranda VC**, Braghiroli MI, Faria LD, Bariani G, Alex A, Bezerra Neto JE, Capareli FC, Sabbaga J, Lobo Dos Santos JF, Hoff PM, Riechelmann RP. Phase 2 Trial of Metformin Combined With 5-Fluorouracil in Patients With Refractory Metastatic Colorectal Cancer. *Clin Colorectal Cancer* 2016; **15**: 321-328.e1 [PMID: 27262895 DOI: 10.1016/j.clcc.2016.04.011]

266 **Hoskins JM**, Carey LA, McLeod HL. CYP2D6 and tamoxifen: DNA matters in breast cancer. *Nat Rev Cancer* 2009; **9**: 576-586 [PMID: 19629072 DOI: 10.1038/nrc2683]

267 **Hosoya Y**, Kitoh Y, Kobayashi E, Okabe R, Fujimura A, Kanazawa K. Combination effects of tamoxifen plus 5-fluorouracil on gastric cancer cell lines in vitro. *Cancer Lett* 1999; **140**: 139-143 [PMID: 10403552 DOI: 10.1016/s0304-3835(99)00059-2]

268 **Due SL**, Watson DI, Bastian I, Ding GQ, Sukocheva OA, Astill DS, Vat L, Hussey DJ. Tamoxifen enhances the cytotoxicity of conventional chemotherapy in esophageal adenocarcinoma cells. *Surg Oncol* 2016; **25**: 269-277 [PMID: 27566033 DOI: 10.1016/j.suronc.2016.05.029]

269 **Jiang SY**, Shyu RY, Yeh MY, Jordan VC. Tamoxifen inhibits hepatoma cell growth through an estrogen receptor independent mechanism. *J Hepatol* 1995; **23**: 712-719 [PMID: 8750171 DOI: 10.1016/0168-8278(95)80038-7]

270 **Sampson LK**, Vickers SM, Ying W, Phillips JO. Tamoxifen-mediated growth inhibition of human cholangiocarcinoma. *Cancer Res* 1997; **57**: 1743-1749 [PMID: 9135018]

271 **Xie X**, Wu MY, Shou LM, Chen LP, Gong FR, Chen K, Li DM, Duan WM, Xie YF, Mao YX, Li W, Tao M. Tamoxifen enhances the anticancer effect of cantharidin and norcantharidin in pancreatic cancer cell lines through inhibition of the protein kinase C signaling pathway. *Oncol Lett* 2015; **9**: 837-844 [PMID: 25624908 DOI: 10.3892/ol.2014.2711]

272 **Lointier P**, Wildrick DM, Boman BM. Growth effects of tamoxifen on Lovo colon carcinoma cells and cultured cells from normal colonic mucosa. *Anticancer Res* 1992; **12**: 1523-1525 [PMID: 1444215]

273 **Kuruppu D**, Christophi C, Bertram JF, O'Brien PE. Tamoxifen inhibits colorectal cancer metastases in the liver: a study in a murine model. *J Gastroenterol Hepatol* 1998; **13**: 521-527 [PMID: 9641652 DOI: 10.1111/j.1440-1746.1998.tb00680.x]

274 **Tomao S**, Romiti A, Massidda B, Ionta MT, Farris A, Zullo A, Brescia A, Santuari L, Frati L. A phase II study of gemcitabine and tamoxifen in advanced pancreatic cancer. *Anticancer Res* 2002; **22**: 2361-2364 [PMID: 12174927]

275 **Eckel F**, Lersch C, Lippl F, Assmann G, Schulte-Frohlinde E. Phase II trial of cyclophosphamide, leucovorin, 5-fluorouracil 24-hour infusion and tamoxifen in pancreatic cancer. *J Exp Clin Cancer Res* 2000; **19**: 295-300 [PMID: 11144522]

276 **Lissoni P**, Paolorossi F, Tancini G, Ardizzoia A, Barni S, Brivio F, Maestroni GJ, Chilelli M. A phase II study of tamoxifen plus melatonin in metastatic solid tumour patients. *Br J Cancer* 1996; **74**: 1466-1468 [PMID: 8912546 DOI: 10.1038/bjc.1996.566]

277 **Chow PK**, Tai BC, Tan CK, Machin D, Win KM, Johnson PJ, Soo KC; Asian-Pacific Hepatocellular Carcinoma Trials Group. High-dose tamoxifen in the treatment of inoperable hepatocellular carcinoma: A multicenter randomized controlled trial. *Hepatology* 2002; **36**: 1221-1226 [PMID: 12395333 DOI: 10.1053/jhep.2002.36824]

278 **Janku F**, Beom SH, Moon YW, Kim TW, Shin YG, Yim DS, Kim GM, Kim HS, Kim SY, Cheong JH, Lee YW, Geiger B, Yoo S, Thurston A, Welsch D, Rudoltz MS, Rha SY. First-in-human study of IM156, a novel potent biguanide oxidative phosphorylation (OXPHOS) inhibitor, in patients with advanced solid tumors. *Invest New Drugs* 2022; **40**: 1001-1010 [PMID: 35802288 DOI: 10.1007/s10637-022-01277-9]

279 **Aguilar-Valdés A**, Noriega LG, Tovar AR, Ibarra-Sánchez MJ, Sosa-Hernández VA, Maravillas-Montero JL, Martínez-Aguilar J. SWATH-MS proteomics of PANC-1 and MIA PaCa-2 pancreatic cancer cells allows identification of drug targets alternative to MEK and PI3K inhibition. *Biochem Biophys Res Commun* 2021; **552**: 23-29 [PMID: 33740661 DOI: 10.1016/j.bbrc.2021.03.018]

280 **Yap TA**, Daver N, Mahendra M, Zhang J, Kamiya-Matsuoka C, Meric-Bernstam F, Kantarjian HM, Ravandi F, Collins ME, Francesco MED, Dumbrava EE, Fu S, Gao S, Gay JP, Gera S, Han J, Hong DS, Jabbour EJ, Ju Z, Karp DD, Lodi A, Molina JR, Baran N, Naing A, Ohanian M, Pant S, Pemmaraju N, Bose P, Piha-Paul SA, Rodon J, Salguero C, Sasaki K, Singh AK, Subbiah V, Tsimberidou AM, Xu QA, Yilmaz M, Zhang Q, Li Y, Bristow CA, Bhattacharjee MB, Tiziani S, Heffernan TP, Vellano CP, Jones P, Heijnen CJ, Kavelaars A, Marszalek JR, Konopleva M. Complex I inhibitor of oxidative phosphorylation in advanced solid tumors and acute myeloid leukemia: phase I trials. *Nat Med* 2023; **29**: 115-126 [PMID: 36658425 DOI: 10.1038/s41591-022-02103-8]

281 **Roth KG**, Mambetsariev I, Kulkarni P, Salgia R. The Mitochondrion as an Emerging Therapeutic Target in Cancer. *Trends Mol Med* 2020; **26**: 119-134 [PMID: 31327706 DOI: 10.1016/j.molmed.2019.06.009]

282 **Aminzadeh-Gohari S**, Weber DD, Vidali S, Catalano L, Kofler B, Feichtinger RG. From old to new - Repurposing drugs to target mitochondrial energy metabolism in cancer. *Semin Cell Dev Biol* 2020; **98**: 211-223 [PMID: 31145995 DOI: 10.1016/j.semcdb.2019.05.025]

283 **Li X**, Wang H, Li Z, Li D, Lu X, Ai S, Dong Y, Liu S, Wu J, Guan W. Oxygen tank for synergistic hypoxia relief to enhance mitochondria-targeted photodynamic therapy. *Biomater Res* 2022; **26**: 47 [PMID: 36138489 DOI: 10.1186/s40824-022-00296-0]

284 **Gao X**, Liu X, Shan W, Liu Q, Wang C, Zheng J, Yao H, Tang R. Anti-malarial atovaquone exhibits anti-tumor effects by inducing DNA damage in hepatocellular carcinoma. *Am J Cancer Res* 2018; **8**: 1697-1711 [PMID: 30323964]

285 **Cheng G**, Hardy M, You M, Kalyanaraman B. Combining PEGylated mito-atovaquone with MCT and Krebs cycle redox inhibitors as a potential strategy to abrogate tumor cell proliferation. *Sci Rep* 2022; **12**: 5143 [PMID: 35332210 DOI: 10.1038/s41598-022-08984-6]

286 **Sainero-Alcolado L**, Liaño-Pons J, Ruiz-Pérez MV, Arsenian-Henriksson M. Targeting mitochondrial metabolism for precision medicine in cancer. *Cell Death Differ* 2022; **29**: 1304-1317 [PMID: 35831624 DOI: 10.1038/s41418-022-01022-y]

287 **Rabben HL**, Andersen GT, Olsen MK, Øverby A, Ianevski A, Kainov D, Wang TC, Lundgren S, Grønbech JE, Chen D, Zhao CM. Neural signaling modulates metabolism of gastric cancer. *iScience* 2021; **24**: 102091 [PMID: 33598644 DOI: 10.1016/j.isci.2021.102091]

288 **Inoue J**, Kishikawa M, Tsuda H, Nakajima Y, Asakage T, Inazawa J. Identification of PDHX as a metabolic target for esophageal squamous

cell carcinoma. *Cancer Sci* 2021; **112**: 2792-2802 [PMID: 33964039 DOI: 10.1111/cas.14938]

289 **Zachar Z**, Marecek J, Maturo C, Gupta S, Stuart SD, Howell K, Schauble A, Lem J, Piramzadian A, Karnik S, Lee K, Rodriguez R, Shorr R, Bingham PM. Non-redox-active lipoate derivates disrupt cancer cell mitochondrial metabolism and are potent anticancer agents in vivo. *J Mol Med (Berl)* 2011; **89**: 1137-1148 [PMID: 21769686 DOI: 10.1007/s00109-011-0785-8]

290 **Alistar A**, Morris BB, Desnoyer R, Klepin HD, Hosseinzadeh K, Clark C, Cameron A, Leyendecker J, D'Agostino R Jr, Topaloglu U, Boteju LW, Boteju AR, Shorr R, Zachar Z, Bingham PM, Ahmed T, Crane S, Shah R, Migliano JJ, Pardee TS, Miller L, Hawkins G, Jin G, Zhang W, Pasche B. Safety and tolerability of the first-in-class agent CPI-613 in combination with modified FOLFIRINOX in patients with metastatic pancreatic cancer: a single-centre, open-label, dose-escalation, phase 1 trial. *Lancet Oncol* 2017; **18**: 770-778 [PMID: 28495639 DOI: 10.1016/S1470-2045(17)30314-5]

291 **Arnold C**, Demuth P, Seiwert N, Wittmann S, Boengler K, Rasenberger B, Christmann M, Huber M, Brunner T, Linnebacher M, Fahrer J. The Mitochondrial Disruptor Devimistat (CPI-613) Synergizes with Genotoxic Anticancer Drugs in Colorectal Cancer Therapy in a Bim-Dependent Manner. *Mol Cancer Ther* 2022; **21**: 100-112 [PMID: 34750196 DOI: 10.1158/1535-7163.MCT-21-0393]

292 **Philip PA**, Buyse ME, Alistar AT, Rocha Lima CM, Luther S, Pardee TS, Van Cutsem E. A Phase III open-label trial to evaluate efficacy and safety of CPI-613 plus modified FOLFIRINOX (mFFX) versus FOLFIRINOX (FFX) in patients with metastatic adenocarcinoma of the pancreas. *Future Oncol* 2019; **15**: 3189-3196 [PMID: 31512497 DOI: 10.2217/fon-2019-0209]

293 **Dang L**, Su SM. Isocitrate Dehydrogenase Mutation and (R)-2-Hydroxyglutarate: From Basic Discovery to Therapeutics Development. *Annu Rev Biochem* 2017; **86**: 305-331 [PMID: 28375741 DOI: 10.1146/annurev-biochem-061516-044732]

294 **DiNardo CD**, Stein EM, de Botton S, Roboz GJ, Altman JK, Mims AS, Swords R, Collins RH, Mannis GN, Pollyea DA, Donnellan W, Fathi AT, Pigneux A, Erba HP, Prince GT, Stein AS, Uy GL, Foran JM, Traer E, Stuart RK, Arellano ML, Slack JL, Sekeres MA, Willekens C, Choe S, Wang H, Zhang V, Yen KE, Kapsalis SM, Yang H, Dai D, Fan B, Goldwasser M, Liu H, Agresta S, Wu B, Attar EC, Tallman MS, Stone RM, Kantarjian HM. Durable Remissions with Ivosidenib in IDH1-Mutated Relapsed or Refractory AML. *N Engl J Med* 2018; **378**: 2386-2398 [PMID: 29860938 DOI: 10.1056/NEJMoa1716984]

295 **Stein EM**, DiNardo CD, Fathi AT, Pollyea DA, Stone RM, Altman JK, Roboz GJ, Patel MR, Collins R, Flinn IW, Sekeres MA, Stein AS, Kantarjian HM, Levine RL, Vyas P, MacBeth KJ, Tosolini A, VanOostendorp J, Xu Q, Gupta I, Lila T, Risueno A, Yen KE, Wu B, Attar EC, Tallman MS, de Botton S. Molecular remission and response patterns in patients with mutant-IDH2 acute myeloid leukemia treated with enasidenib. *Blood* 2019; **133**: 676-687 [PMID: 30510081 DOI: 10.1182/blood-2018-08-869008]

296 **Khurshed M**, Aarnoudse N, Hulsbos R, Hira VVV, van Laarhoven HWM, Wilmink JW, Molenaar RJ, van Noorden CJF. IDH1-mutant cancer cells are sensitive to cisplatin and an IDH1-mutant inhibitor counteracts this sensitivity. *FASEB J* 2018; **32**: fj201800547R [PMID: 29879375 DOI: 10.1096/fj.201800547R]

297 **Gross MI**, Demo SD, Dennison JB, Chen L, Chernov-Rogan T, Goyal B, Janes JR, Laidig GJ, Lewis ER, Li J, Mackinnon AL, Parlati F, Rodriguez ML, Shwonek PJ, Sjogren EB, Stanton TF, Wang T, Yang J, Zhao F, Bennett MK. Antitumor activity of the glutaminase inhibitor CB-839 in triple-negative breast cancer. *Mol Cancer Ther* 2014; **13**: 890-901 [PMID: 24523301 DOI: 10.1158/1535-7163.MCT-13-0870]

298 **Le A**, Lane AN, Hamaker M, Bose S, Gouw A, Barbi J, Tsukamoto T, Rojas CJ, Slusher BS, Zhang H, Zimmerman LJ, Liebler DC, Slebos RJ, Lorkiewicz PK, Higashi RM, Fan TW, Dang CV. Glucose-independent glutamine metabolism *via* TCA cycling for proliferation and survival in B cells. *Cell Metab* 2012; **15**: 110-121 [PMID: 22225880 DOI: 10.1016/j.cmet.2011.12.009]

World Journal of Gastroenterology

Submit a Manuscript: https://www.f6publishing.com

World J Gastroenterol 2023 August 7; 29(29): 4528-4541

DOI: 10.3748/wjg.v29.i29.4528

ISSN 1007-9327 (print) ISSN 2219-2840 (online)

ORIGINAL ARTICLE

Basic Study

Antagonizing adipose tissue-derived exosome miR-103-hepatocyte phosphatase and tensin homolog pathway alleviates autophagy in non-alcoholic steatohepatitis: A trans-cellular crosstalk

Miao-Miao Lu, Yue Ren, Yu-Wei Zhou, Ling-Ling Xu, Meng-Meng Zhang, Lin-Ping Ding, Wei-Xin Cheng, Xi Jin

Specialty type: Gastroenterology and hepatology

Provenance and peer review: Unsolicited article; Externally peer reviewed.

Peer-review model: Single blind

Peer-review report's scientific quality classification

Grade A (Excellent): 0
Grade B (Very good): B
Grade C (Good): C
Grade D (Fair): 0
Grade E (Poor): 0

P-Reviewer: Herrera B, Spain; Sukocheva OA, Australia

Received: April 5, 2023
Peer-review started: April 5, 2023
First decision: May 23, 2023
Revised: June 11, 2023
Accepted: July 4, 2023
Article in press: July 4, 2023
Published online: August 7, 2023

Miao-Miao Lu, Endoscopy Center, Children's Hospital of Zhejiang University School of Medicine, Hangzhou 310003, Zhejiang Province, China

Yue Ren, Yu-Wei Zhou, Lin-Ping Ding, Wei-Xin Cheng, Department of Medicine, Zhejiang University School of Medicine, Hangzhou 310003, Zhejiang Province, China

Ling-Ling Xu, Department of Gastroenterology, The Second People's Hospital of Yuhang District, Hangzhou 310003, Zhejiang Province, China

Meng-Meng Zhang, Department of Gastroenterology, Hangzhou Shangcheng District People's Hospital, Hangzhou 310003, Zhejiang Province, China

Xi Jin, Department of Gastroenterology, The First Affiliated Hospital of Zhejiang University School of Medicine, Hangzhou 310003, Zhejiang Province, China

Corresponding author: Xi Jin, MD, PhD, Doctor, Department of Gastroenterology, The First Affiliated Hospital of Zhejiang University School of Medicine, No. 79 Qingchun Road, Hangzhou 310003, Zhejiang Province, China. jxfl007@zju.edu.cn

Abstract

BACKGROUND

Obesity plays a vital role in the occurrence and development of non-alcoholic steatohepatitis (NASH). However, the underlining mechanism is still unclear, where adipose tissue (AT) derived exosomes may actively participate. MicroRNAs (miRNAs) are commonly secreted from exosomes for cell communication. Though the regulation of miR-103 on insulin sensitivity has been reported, the specific role of AT-derived exosomes miR-103 in NASH is still vague and further investigation may provide novel therapeutic choices.

AIM

To determine the specific role of AT-derived exosomes miR-103 in developing NASH through various methods.

METHODS

The expression levels of miR-103 in the AT-derived exosomes and livers were detected and compared between NASH mice and control. The effect of miR-103

on NASH progression was also explored by antagonizing miR-103, including steatosis and inflammation degree changes. The interaction between miR-103 and the autophagy-related gene phosphatase and tensin homolog (PTEN) was confirmed by dual-luciferase reporter assay. The role of the interaction between miR-103 and PTEN on autophagy was verified in NASH-like cells. Finally, the effects of miR-103 from adipose-derived exosomes on NASH and autophagy were analyzed through animal experiments.

RESULTS

The expression of miR-103 was increased in NASH mice, compared to the control, and inhibition of miR-103 could alleviate NASH. The results of the dual-luciferase reporter assay showed miR-103 could interact with PTEN. MiR-103-anta decreased p-AMPKa, p-mammalian target of rapamycin (mTOR), and p62 but increased the protein levels of PTEN and LC3-II/I and the number of autophagosomes in NASH mice. Similar results were also observed in NASH-like cells, and further experiments showed PTEN silencing inhibited the effect of miR-103-anta. AT derived-exosome miR-103 aggravated NASH and increased the expressions of p-AMPKa, p-mTOR, and p62 but decreased the protein levels of PTEN and LC3-II/I and the number of autophagosomes in mice.

CONCLUSION

AT derived-exosome increased the levels of miR-103 in the liver, and miR-103 aggravated NASH. Mechanically, miR-103 could interact with PTEN and inhibit autophagy.

Key Words: Non-alcoholic steatohepatitis; Nonalcoholic fatty liver disease; Exosomes; Phosphatase and tensin homolog

©The Author(s) 2023. Published by Baishideng Publishing Group Inc. All rights reserved.

Core Tip: Our study confirms the important role of miR-103-phosphatase and tensin homolog-autophagy axis in the pathogenesis of non-alcoholic steatohepatitis (NASH). More importantly, the elevation of miR-103 in the liver of NASH mice is partly due to adipose tissue exosome secretion and integration, which also partially explains the mechanism of obesity leading to NASH.

Citation: Lu MM, Ren Y, Zhou YW, Xu LL, Zhang MM, Ding LP, Cheng WX, Jin X. Antagonizing adipose tissue-derived exosome miR-103-hepatocyte phosphatase and tensin homolog pathway alleviates autophagy in non-alcoholic steatohepatitis: A trans-cellular crosstalk. *World J Gastroenterol* 2023; 29(29): 4528-4541
URL: https://www.wjgnet.com/1007-9327/full/v29/i29/4528.htm
DOI: https://dx.doi.org/10.3748/wjg.v29.i29.4528

INTRODUCTION

Non-alcoholic fatty liver disease (NAFLD) is recognized as the hepatocellular manifestation of metabolic syndrome, characterized by hepatic lipid accumulation and inflammation, and precluded with secondary causes, such as chronic viral hepatitis, significant alcohol consumption, long-term use of steatogenic medication, and other chronic liver diseases including autoimmune hepatitis, hemochromatosis, Wilson's disease[1]. NAFLD is categorized into NAFL, non-alcoholic steatohepatitis (NASH), fibrosis, and even cirrhosis according to histological changes in different disease stages. Among them, NASH is considered the watershed in NAFLD and is defined as the presence of 5% hepatic steatosis and ensuing hepatocyte injury[1]. According to a previous meta-analysis, the pooled overall global prevalence of NAFLD was estimated to be 25.24% [95% confidence interval (CI): 22.10-28.65], while the pooled overall NASH prevalence among biopsied NAFLD patients was 59.10% (95%CI: 47.55-69.73)[2]. Moreover, fibrosis, which is closely related to liver cirrhosis, liver cancer, and other end-stage liver diseases, is more likely to occur in NASH patients than NAFL patients [3]. Those findings support the importance of NASH and suggest that the burden of disease caused by NASH needs to be paid adequate attention. NASH has become one of the leading causes of cirrhosis and the second leading cause of liver transplantation in the United States[4,5].

NAFLD is commonly associated with metabolic comorbidities such as obesity, diabetes mellitus, and dyslipidemia[2,6]. The prevalence of obesity is as high as 51.34% (95%CI: 41.38-61.20) and 81.83% (95%CI: 55.16-94.28) among NAFLD and NASH patients, respectively[2]. The effect of obesity on NAFLD has been intensively explored. On the one hand, the expansion of adipose tissue (AT) in obese people leads to increased circulating free fatty acids (FFAs) and leptin and decreased adiponectin, which leads to intrahepatic fat accumulation. On the other hand, the chronic inflammatory state caused by obesity will further lead to the infiltration of inflammatory cells in the liver, resulting in the progression of NAFLD[7]. Due to the important role of obesity in the occurrence and development of NAFLD, in-depth research on the mechanism of obesity leading to NASH may provide new therapeutic targets.

Exosomes are extracellular vesicles secreted by various cells and serve as an essential means of intercellular communication by delivering microRNAs (miRNAs), bioactive lipids, and regulatory proteins from one cell to another [8]. Previous studies have shown that AT-derived exosomes are essential in regulating insulin sensitivity[9,10], a common

manifestation of metabolic syndrome in patients with NAFLD. Previous studies have also shown that AT-derived exosome miRNAs are involved in the occurrence and development of various metabolic-related diseases[11]. Among them, miR-103 attracted our attention since previous studies have shown that miR-103 is involved in regulating insulin sensitivity[12]. The specific role of AT-derived exosomes in the development of NASH also deserves further study. Therefore, in this study, we focused on the specific role of AT-derived exosomes miR-103 in developing NASH through various methods.

MATERIALS AND METHODS

Ethics statement

This study followed the guidelines for the Care and Use of Laboratory Animals of the National Institute of Health. The animal protocol was approved by the institutional review board of the Tab of Animal Experimental Ethical Inspection of the First Affiliated Hospital of Zhejiang University. The Reference Number is 2020-1407.

The successful construction of NASH animal and cell models

C57BL/6 mice were routinely fed a high-fat diet for 12 wk to establish the NASH animal model. According to different treatments, they were initially divided into the control group (12% kcal fat, 66% kcal carbohydrate, 22% kcal protein) and the model group (60% kcal fat, 20% kcal carbohydrate, 20% kcal protein)[13]. Starting from the 13th wk, 40 mg/kg miR-negative control (NC)-anta and miR-103-anta were injected into the mice from the model group (dissolved in 0.2 mL normal saline) through the tail vein every 2 d thrice to construct miR-NC-anta model group and miR-103-anta model group. The control and model groups were injected with blank normal saline thrice (n = 10 in each group). Finally, the mice were sacrificed, where liver tissue, abdominal AT, and serum were collected and stored in a cryostorage tube at -80 °C for further analysis.

NASH-like cell model was constructed by conventional oleic acid (OA)-palmitic acid (PA) mixture culture (OA:PA = 2:1)[14]. Firstly, 128.2 mg PA (molecular weight: 256.42) was sequentially retrieved on a precision balance, 1 mL 1 M OA was added, vortex dissolved, and mixed in a small whirlpool, and then completely dissolved in a water bath at 55 °C-65 °C to obtain 1.5 M FFA mixture. After that, 1.5 M FFA with DMSO was dissolved into 0.1 M working solution. In the model group, Alpha mouse liver 12 (AML-12) cells were added with 400 μM FFA and cultured for 24 h, followed by transfection with miR-103-anta and its sh-phosphatase and tensin homolog (PTEN) and their relative controls. All further *in vitro* experiments were performed on those cells.

Exosome isolation and confirmation

Exosomes were extracted from the filtrate according to the manufacturer's instructions[15]. The diluted exosomes were subjected to NanoFCM (China) for transmission electron microscopy (TEM) and size distribution analysis for further confirmation.

Quantitative real-time polymerase chain reaction, ELISA, and western blotting

Total RNA was isolated using Trizol (Invitrogen, United States) and reverse-transcribed into cDNA using the First Strand cDNA Synthesis Kit (TransGen, China) following the manufacturer's instructions. Quantitative real-time polymerase chain reaction (qRT-PCR) was routinely performed using the SYBR Premix Ex Taq qPCR kit (TaKaRa, Japan). The alanine aminotransferase (ALT), aspartate aminotransferase (AST), total triglycerides (TG), total cholesterol (CHOL), superoxide dismutase (SOD), malondialdehyde (MDA), and H_2O_2 concentrations were detected using test kits according to the manufacturer's instructions. Total protein was isolated using radioimmune precipitation assay buffer (TaKaRa, Japan) supplemented with a protease inhibitor (Roche, Switzerland). After quantification using the BCA Protein Assay Kit (Thermo, United States), the proteins were separated by sodium-dodecyl sulfate gel electrophoresis and transferred onto polyvinylidene fluoride membranes. The membranes were blocked and incubated overnight with antibodies against PTEN (9188T, CST), p-AMPK (ab32047, Abcam), p-mammalian target of rapamycin (mTOR) (CSB-PA271384, Cusabio), LC3 (12741T, CST), p62 (ab91526, Abcam), and GAPDH (ab245355, Abcam) at 4 °C. The membranes were incubated with HRP-conjugated secondary antibodies (ab205718, Abcam). Finally, the protein bands were detected using enhanced chemiluminescence (ECL) kits (Thermo, United States).

Hematoxylin and eosin staining and oil red staining

The hematoxylin and eosin (HE) staining was performed using the HE staining kit (C0105S, Beyotime) according to the manufacturer's instructions. Oil red staining was performed using an oil red staining solution (G 1262, Solarbio; C0157S, Beyotime). Briefly, 5-10 μm thick fresh frozen tissue was placed on the slide and dried at room temperature for 30-60 min. The sections were fixed with 10% paraformaldehyde for 10 min, washed thrice with distilled water, and dried for several minutes. After that, the oil red was diluted with deionized water in a 3:2 ratio, with impurities removed by filter paper, and left for 10 min at room temperature. Preheated oil red was used for tissue dye in a 6 °C temperature box for 8-10 min. After the 85% propylene glycol solution was differentiated for 2-5 min, it was washed twice with distilled water and restained with hematoxylin for 30 s. After rinsing with running water for 3 min, the tablets can be sealed with glycerine gelatin.

Luciferase reporter assay and TEM

The luciferase reporter assay was performed according to the manufacturer's instructions of Pierce™ Cypridina-Firefly Luciferase Dual Assay Kit (16184, Thermo). Briefly, AML-12 cells were co-transfected with a 10 nM miR-103 or NC control, a 2 ng pRL-CMV, and a 20 ng firefly luciferase reporter plasmid containing PTEN of the wild-type or mutant 30-untranslated region. Then, 48 h after transfection, the cell lysates were determined by luciferase to observe the interaction between miR-103 and PTEN. The liver tissues with the size of 1 mm × 1 mm × 1 mm were fixed, dehydrated, impregnated, and embedded to make ultrathin sections (50-70 nm) and then stained with uranium acetate and lead citrate successively and dried for observation under TEM.

Immunofluorescence

The frozen slices of 5-10 μm thick liver tissue were dried at room temperature for 30-60 min. They were sequentially fixed with 10% paraformaldehyde for 10 min, rinsed thrice with distilled water, and dried for several minutes. After that, the antigen was repaired by microwave at 92 °C-96 °C for 10-15 min, cooled to room temperature naturally, and sealed with 5% BSA at 37 °C for 60 min. After pouring the excess serum, LC3-II/I antibody was diluted at 1:100, added into samples, and incubated at 4 °C overnight. Rinsed with phosphate buffered saline (PBS) the next day, samples were added to the mixture of the fluorescent secondary antibody and 4',6-diamidino-2-phenylindole at a ratio of 1:200 and incubated for 60 min at room temperature. After washing with PBS, laser confocal scanning for immunofluorescence was performed.

Transwell analysis

3T3-L1 cells were first routinely induced to differentiate into adipocytes to identify the transfer of miR-103 from adipocytes to AML-12 cells. After that, Cy3-labeled miR-103 was transfected and then co-cultured with the underlying AML-12 cells through a transwell chamber. AML-12 cells were then isolated, and immunofluorescence determined the red fluorescence value.

Cell transfection

Cells for transfection were incubated into a 6-well plate. 5-10 μL miR-NC-anta and miR-103-anta were absorbed and diluted into 250 μL Opti-MEMI reduced serum medium, mixed gently, and incubated at room temperature for 5 min. Then, 3-6 μL Lipofectamine® 2000 Reagent was diluted to 250 μL of Opti-MempI reduced-serum medium, lightly mixed, and incubated at room temperature for 5 min. Diluted miR-NC-anta, miR-103-anta, and diluted Lipofectamine® 2000 Reagent were carefully mixed, gently blended, and incubated at room temperature for 20 min to form the reagent complex. After that, cells were washed with 2 mL serum-free medium, added with 2 mL of Opti-MEMI low serum medium to each well, and then added to 500 μL of miR-NC-anta and miR-103-anta-Lipofectamine® 2000 Reagent complex. These reagents were gently mixed and prepared for use.

Statistical analysis

All data are presented as mean ± SD. Differences between the two groups were analyzed using the student's *t*-test for categorical data and the chi-square method for numerical data. All statistical analyses were performed using GraphPad 9.0.2 software. Statistical significance between groups was set at $P < 0.05$.

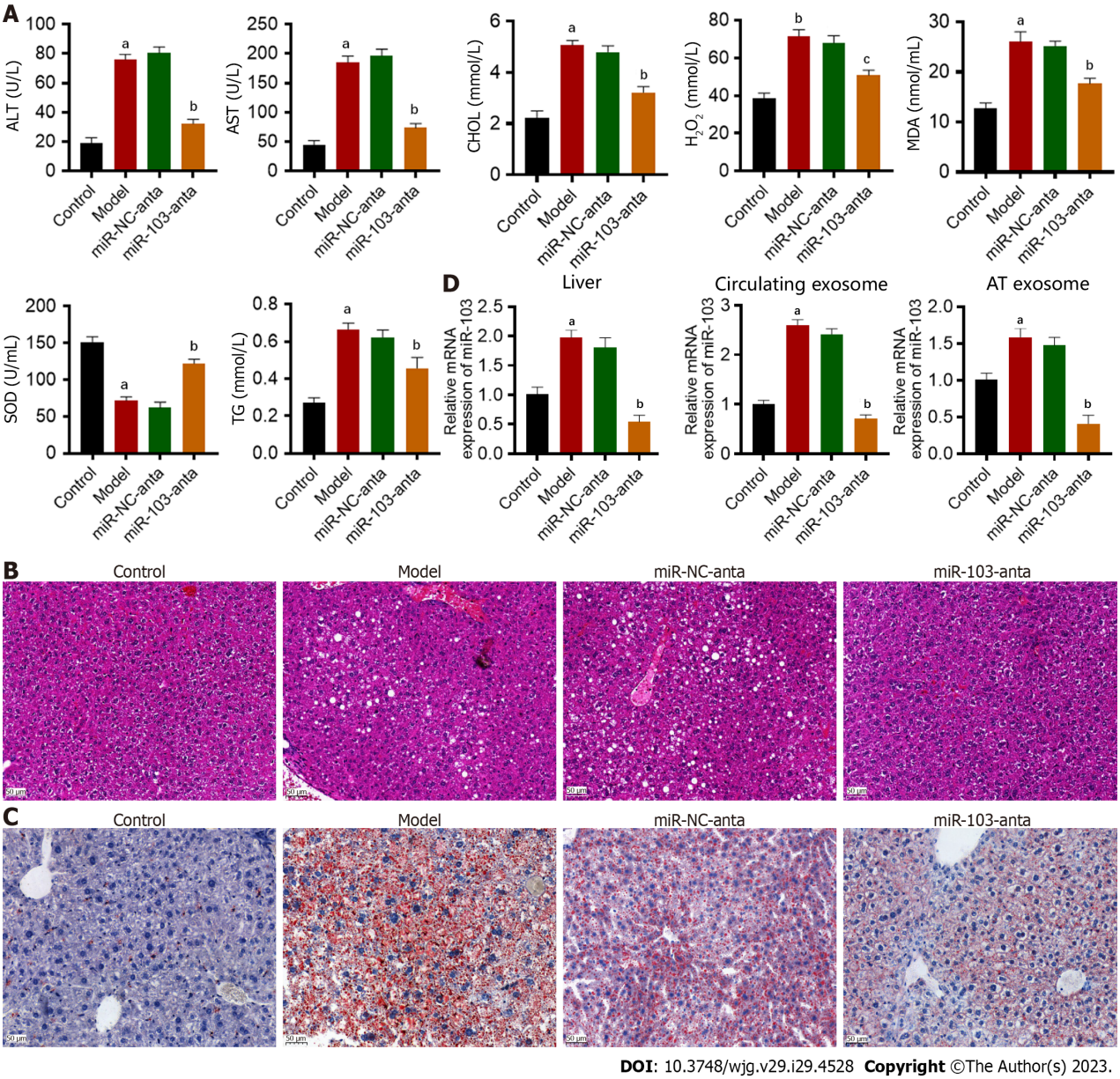
RESULTS

The expression of miR-103 was increased in NASH mice, and inhibition of miR-103 could alleviate NASH

First, we successfully constructed animal models of NASH. Compared with the control, ALT, AST, TG, and CHOL were increased in NASH mice (Figure 1A). Hepatocyte ballooning, inflammatory cell infiltration, and hepatic lipid accumulation were observed in the livers of NASH mice (Figures 1B and C). Furthermore, we successfully extracted and confirmed AT-derived and circulating exosomes (Supplementary Figure 1). Subsequently, the expression of miR-103 in the livers, AT-derived exosomes, and circulating exosomes was detected by qRT-PCR. MiR-103 expression levels in the livers, AT-derived exosomes, and circulating exosomes were significantly increased in the NASH model group compared with the control group. Antagonizing miR-103 decreased miR-103 expression in NASH mice, but miR-NC-anta had no significant effect in NASH mice (Figure 1D). In addition, compared with miR-NC-anta and the model group, miR-103-anta treatment significantly reduced serum ALT and AST, decreased serum CHOL and TG, and alleviated oxidative stress (Figure 1A). Histologically, HE and oil red staining of the liver also indicated that inhibition of miR-103 alleviated hepatocyte ballooning, inflammatory cell infiltration, and hepatic lipid accumulation. (Figures 1B and C). Our above results indicate that the miR-103 level is elevated in NASH model mice, and reducing the expression of miR-103 can alleviate NASH, suggesting the potential involvement of miR-103.

The interaction between miR-103 and PTEN is involved in the process of autophagy

To further investigate the regulatory mechanism of miR-103 on NASH, we used *TargetScan* to predict its downstream targets[16]. The predicted results showed that PTEN, a gene that plays an essential role in autophagy, might interact with miR-103. Therefore, we used a dual-luciferase reporting experiment to further confirm their interaction (Figure 2A). The wild-type PTEN could interact with miR-103, while the mutant PTEN could not. Next, the protein content of PTEN and autophagy-related proteins such as p-AMPKa, p-mTOR, LC3-II/I, and p62 were determined by western blot. The results showed that compared with the control group, the expressions of p-AMPKa, p-mTOR, and p62 were significantly



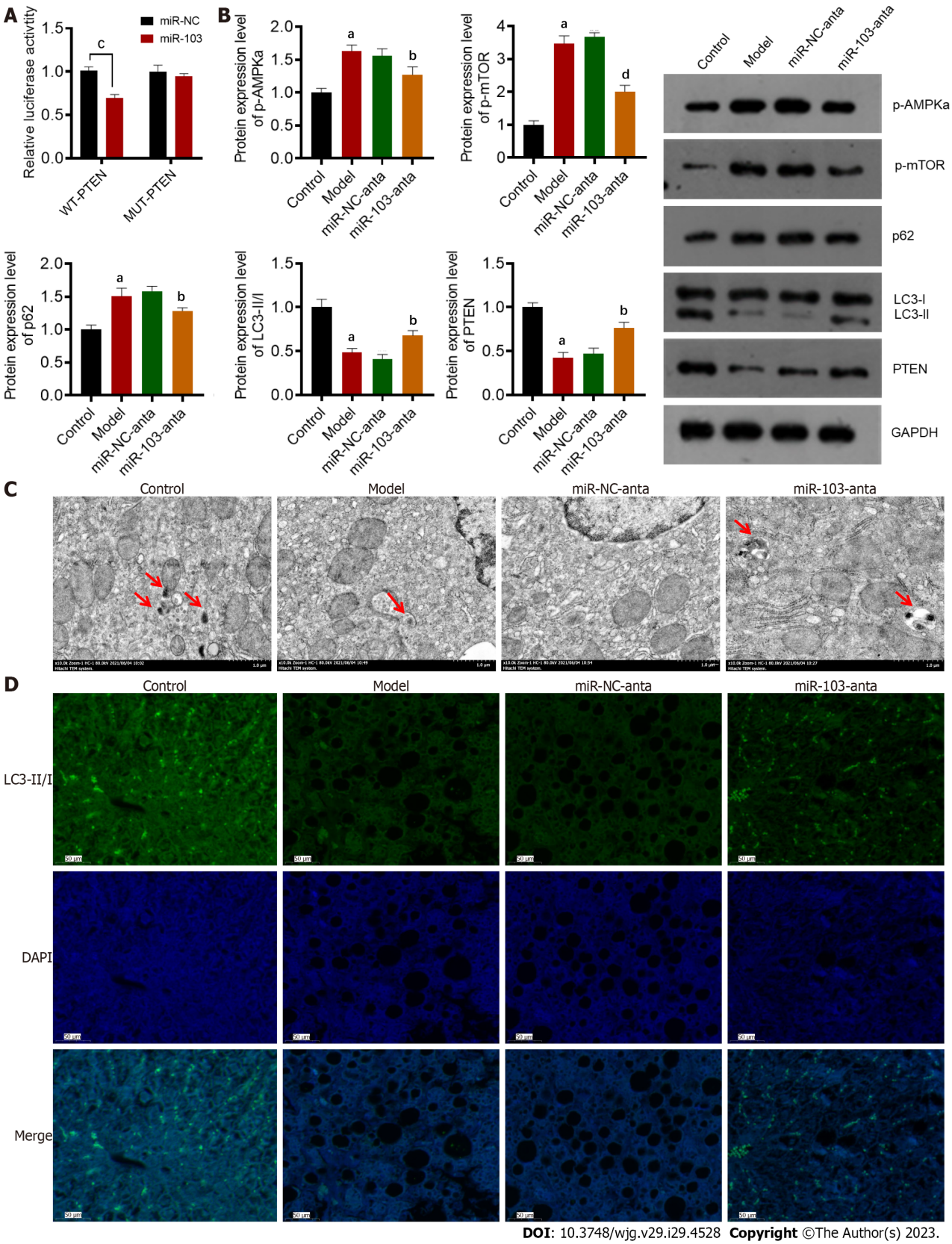
DOI: 10.3748/wjg.v29.i29.4528 **Copyright** ©The Author(s) 2023.

Figure 1 The effect of miR-103 on the development of non-alcoholic steatohepatitis in mice. A: The results of ELISA to measure serum alanine aminotransferase (ALT), aspartate aminotransferase, total triglycerides, total cholesterol, superoxide dismutase, malondialdehyde, and H_2O_2; B: Hematoxylin and eosin staining of mice liver from different groups; C: Oil-red staining of mice liver from different groups; D: The expression of miR-103 in the liver, circulating exosomes, and adipose tissue-derived exosomes. $^{a}P < 0.01$ *vs* control; $^{b}P < 0.01$ *vs* model. ALT: Alanine aminotransferase; AST: Aspartate aminotransferase; TG: Total triglycerides; CHOL: Cholesterol; SOD: Superoxide dismutase; MDA: Malondialdehyde.

increased in the model group, while the protein levels of PTEN and LC3-II/I were decreased (Figure 2B). In addition, TEM and immunofluorescence staining showed that the number of autophagosomes in the liver of NASH model mice was significantly reduced compared with control mice (Figures 2C and D). However, compared with the model and miR-NC-anta groups, p-AMPKa, p-mTOR, p62, and the number of autophagosomes were significantly decreased in the miR-103-anta group. Similarly, the protein levels of PTEN and LC3-II/I was increased (Figures 2C and D). All these results indicate that autophagy is inhibited in the development of NASH, while miR-103-anta treatment could antagonize those changes. These results indicate that miR-103 interacts with PTEN and interferes with the downstream autophagy process, suggesting that the inhibition of autophagy in NASH may be attributed to the increased expression of miR-103.

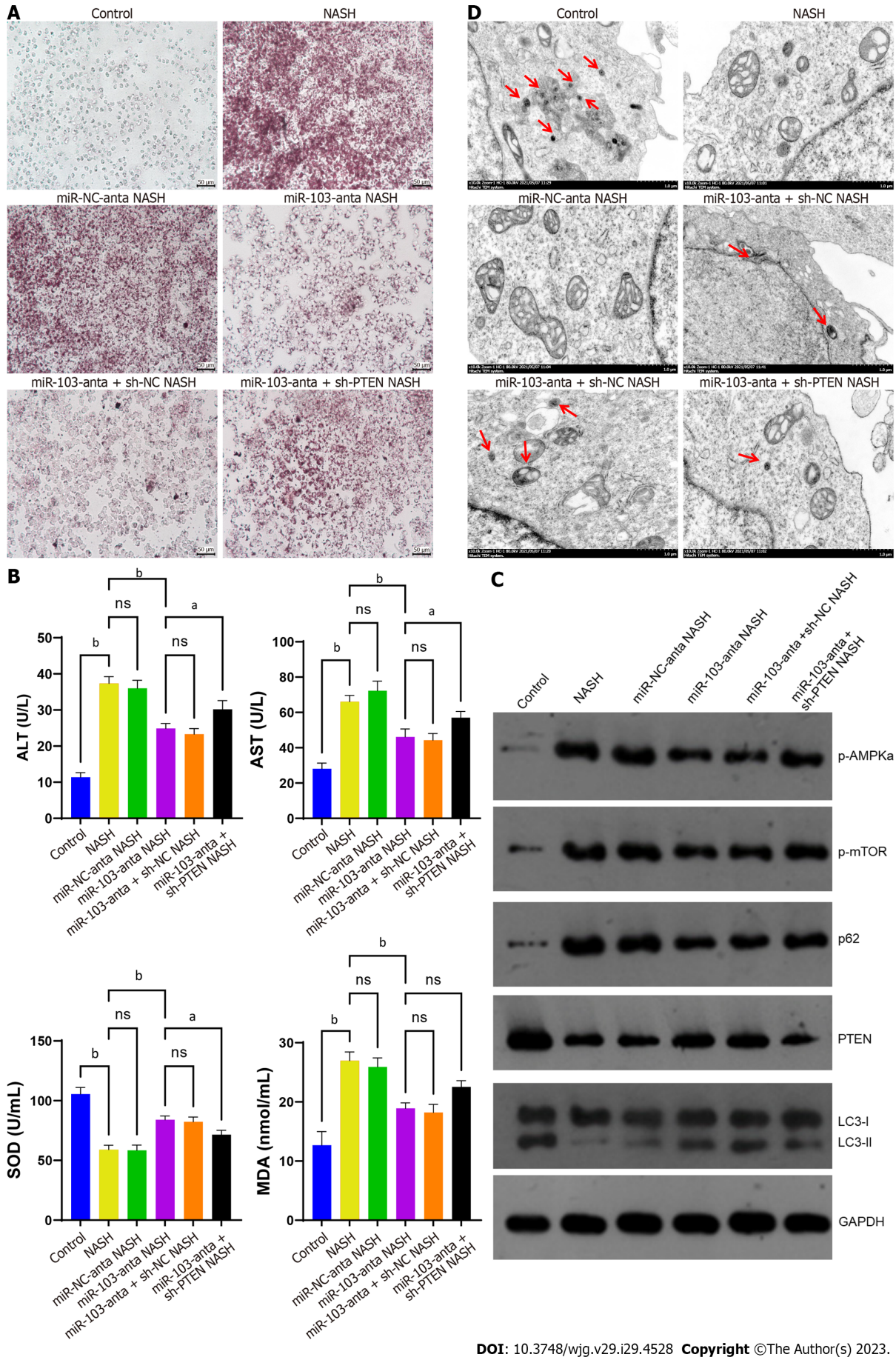
MiR-103 participates in the development of NASH by inhibiting autophagy via interacting with PTEN

We then conducted *in vitro* experiments to further confirm our hypothesis. The results showed that inhibition of miR-103 expression could reduce the accumulation of lipids in NASH model cells, decrease the release of ALT and AST, and relieve oxidative stress. However, the effect of miR-103-anta was partially eliminated by silencing PTEN (Figures 3A and B). The above results indicate that miR-103 is involved in NASH formation partially through its interaction with PTEN. In addition, we detected the expression of autophagy-related proteins. We found that the expression of p-AMPKa, p-mTOR, and p62 was increased in NASH cells, while the expression of PTEN and LC3-II/I was decreased. Treatment with miR-



DOI: 10.3748/wjg.v29.i29.4528 **Copyright** ©The Author(s) 2023.

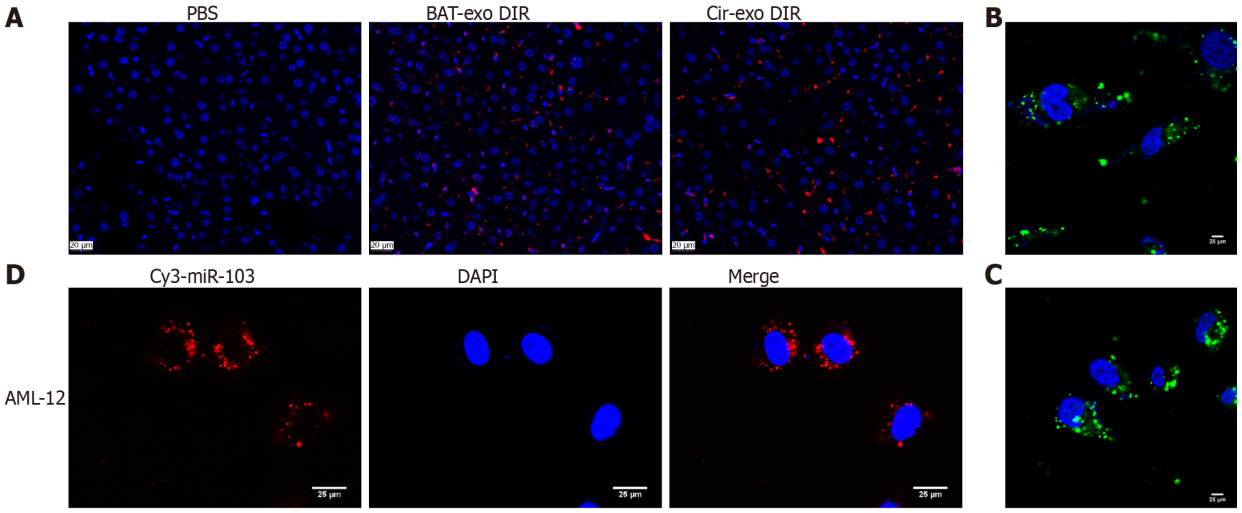
Figure 2 The capacity of miR-103 in targeting phosphatase and tensin homolog gene and affecting autophagy. A: The luciferase reporter assay results verified the interaction between miR-103 and phosphatase and tensin homolog; B: Western blotting showed the differential expression of the autophagy-related protein; C: Transmission electron microscopy images of autophagosomes (red arrowhead) in the liver; D: The results of immunofluorescence staining showed liver autophagosomes in different groups. $^{a}P < 0.01$ *vs* control; $^{b}P < 0.01$ *vs* model; $^{c}P < 0.01$ *vs* miR-103; $^{d}P < 0.05$ *vs* model. PTEN: Phosphatase and tensin homolog; WT: Wild type; MUT: Mutant; DAPI: 4',6-diamidino-2-phenylindole; mTOR: Mammalian target of rapamycin; NC: Negative control.



DOI: 10.3748/wjg.v29.i29.4528 **Copyright** ©The Author(s) 2023.

Figure 3 *In vitro* experiments confirmed the interaction between miR-103 and phosphatase and tensin homolog gene. A: Oil-red staining of

cells from different groups showed different lipid droplet accumulation and inflammatory cell infiltration; B: The results of ELISA to measure serum alanine aminotransferase, aspartate aminotransferase, superoxide dismutase and malondialdehyde; C: Western blotting detected the expression of the autophagy-related protein of cells from different groups; D: Transmission electron microscopy pictures of autophagosomes (red arrowhead) in cells from different groups. $^{a}P < 0.05$, $^{b}P < 0.01$, ns: No significance. NASH: Non-alcoholic steatohepatitis; PTEN: Phosphatase and tensin homolog; NC: Negative control; ALT: Alanine aminotransferase; AST: Aspartate aminotransferase; TG: Total triglycerides; CHOL: Cholesterol; SOD: Superoxide dismutase; MDA: Malondialdehyde.



DOI: 10.3748/wjg.v29.i29.4528 **Copyright** ©The Author(s) 2023.

Figure 4 MiR-103 transfers from adipocytes to hepatocytes. A: The fluorescence of liver tissue of mice injected with adipose tissue (AT)-exosomes or phosphate buffered saline; B: AT exosomes can be absorbed into alpha mouse liver 12 (AML-12) cells; C: Circulating exosomes can be absorbed into AML-12 cells; D: Transewell assay confirmed that miR-103 could be transferred from adipocytes to AML-12 cells. BAT: Brown adipose tissue; Exo: Exosomes; DIR: 1,1-dioctadecyl-3,3,3,3-tetramethylindotricarbocyaine iodide; Cir: Circulating; PBS: Phosphate buffered saline; DAPI: 4',6-diamidino-2-phenylindole; AML-12: Alpha mouse liver 12.

103-anta elevated the expression of PTEN and LC3-II/I and reduced the expression of p-AMPKa, p-mTOR, and p62 in NASH cells, while PTEN silencing inhibited the effect of miR-103-anta (Figure 3C). Finally, we also found that the number of autophagosomes decreased in NASH cells, and such declination was partially antagonized after the inhibition of miR-103. Similarly, PTEN silencing inhibited the effect of miR-103-anta (Figure 3D). To sum up, we confirmed the role of the miR-103-PTEN-autophagy axis in NASH through *in vitro* experiments.

Hepatocyte absorption of AT-derived exosome miR-103

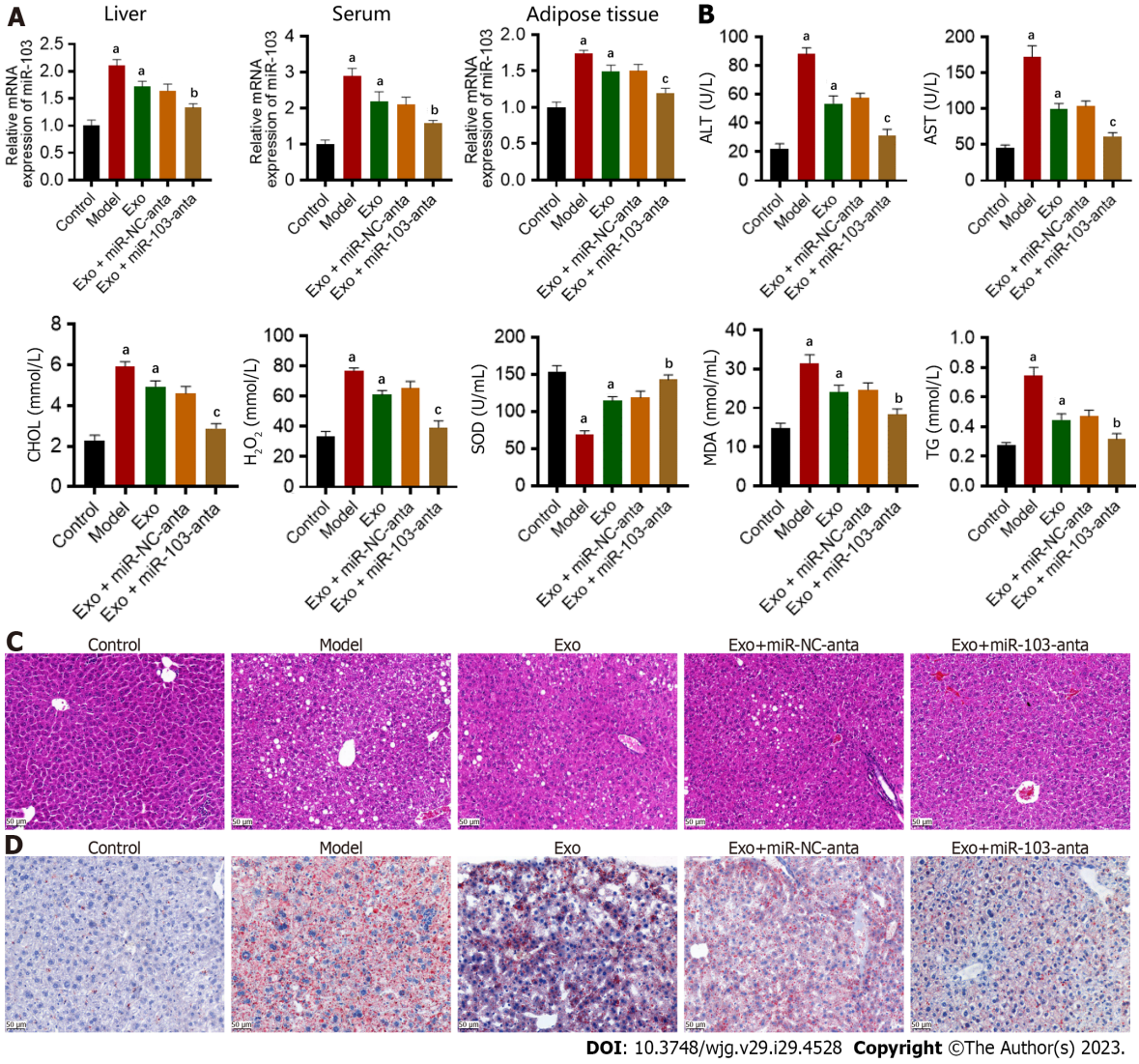
To confirm that AT-derived exosomes can encapsulate miR-103 and target the liver, we conducted *in vivo* and *in vitro* experiments. In the *in vivo* experiment, AT and circulating exosomes of mice were extracted. The exo-DIR complex collected by centrifugation was injected into the tail vein of mice, and the PBS group was used as a control. The fluorescence of liver tissue was observed after mice scarification. There was no fluorescence in the PBS group but observed in AT-exo-DIR and cir-exo-DIR groups, with similar fluorescence intensity (Figure 4A). In the part of the *in vitro* experiment, the AT exosomes and circulating exosomes were detected by the FISH probe to migrate into AML-12 cells (Figures 4B and C). Further transewell assay showed that Cy3-labeled miR-103 could be transferred from adipocytes to AML-12 cells (Figure 4D).

Role of AT-derived exosome miR-103 in NASH

To verify the role of AT-derived exosome miR-103 in NASH through *in vivo* experiments, we extracted exosomes from mouse AT. We injected the extracted exosomes without other treatments and with miR-103-anta or miR-NC-anta into mice through the tail vein. Firstly, we found that injection of AT-derived exosomes increased the level of miR-103 in the liver, serum, and AT compared with the control group (Figure 5A). In addition, compared with the control group, treating AT-derived exosomes can increase serum ALT, AST, CHOL, and TG levels and aggravate oxidative stress (Figure 5B). Histologically, HE and oil red staining of the liver showed that treating AT-derived exosomes could aggravate hepatocyte ballooning, inflammatory cell infiltration, and intrahepatic lipid accumulation (Figures 5C and D). However, miR-103-anta treatment could partially eliminate such an effect while miR-NC-anta treatment could not, suggesting that AT-derived exosome aggravates NASH, and this effect is partly dependent on its encapsulated miR-103.

AT derived-exosome miR-103 inhibits autophagy in hepatocytes

To further verify *in vivo* that miR-103 in AT-derived exosomes is involved in NASH formation by influencing autophagy, we detected the expression of autophagy-related proteins in the liver of mice in each group. We found that compared with the control group, the expression of p-AMPKa, p-mTOR, and p62 in the livers of AT exosome-treated group was increased, while the expression of PTEN and LC3-II/I was decreased. Further miR-103-anta treatment increased the



DOI: 10.3748/wjg.v29.i29.4528 **Copyright** ©The Author(s) 2023.

Figure 5 The effect of adipose tissue-derived exosomes miR-103 on the development of non-alcoholic steatohepatitis in mice. A: The expression of miR-103 in the liver, serum, and adipose tissue; B: The results of ELISA to measure serum alanine aminotransferase, aspartate aminotransferase, total triglycerides, total cholesterol, superoxide dismutase, malondialdehyde, and H_2O_2; C: Hematoxylin and eosin staining of mice liver from different groups; D: Oil-red staining of mice liver from different groups. $^{a}P < 0.01$ *vs* control; $^{b}P < 0.05$ *vs* exosomes; $^{c}P < 0.01$ *vs* exosomes. Exo: Exosomes; NC: Negative control; ALT: Alanine aminotransferase; AST: Aspartate aminotransferase; TG: Total triglycerides; CHOL: Cholesterol; SOD: Superoxide dismutase; MDA: Malondialdehyde.

expression level of PTEN and LC3-II/I and reduced the expression level of p-AMPKa, p-mTOR, and p62, while miR-NC-anta had no similar effect (Figures 6A and B). Finally, through TEM and immunofluorescence, we found that the number of autophagosomes in the livers of mice treated with AT-derived exosomes was decreased, while miR-103-anta could partially antagonize such effect (Figures 6C and D).

DISCUSSION

NASH is considered the watershed in the progress of NAFLD, which is more closely related to the occurrence of liver cirrhosis and other complications. The prevalence of NASH has been increasing in recent years, resulting in a big challenge in disease burden and patient suffering. For instance, the lifetime cost of care for patients with NASH was around US $222 billion in 2017 in the United States[17]. More intriguingly, many NASH patients are obese and tend to have higher healthcare costs than non-obese NASH patients[18], but the etiology is still vague. Therefore, it is necessary to study the role and underlying mechanisms of obesity on NASH and further provide possible therapeutic targets. In this study, we confirmed the important role of AT-derived exosomes miR-103 in NASH and preliminary revealed its regulation on hepatocyte autophagy through targeting PTEN, which might partially provide the mechanisms by which obesity affects NASH.

MiRNA belongs to the family of non-coding RNA, which generally consists of 22 nucleotides[19] and regulates the mRNA levels of target genes[20]. Previous studies have identified a variety of miRNAs involved in metabolism-related diseases[21]. For example, miR-200 and miR-29 families play an important role in maintaining the balance between the

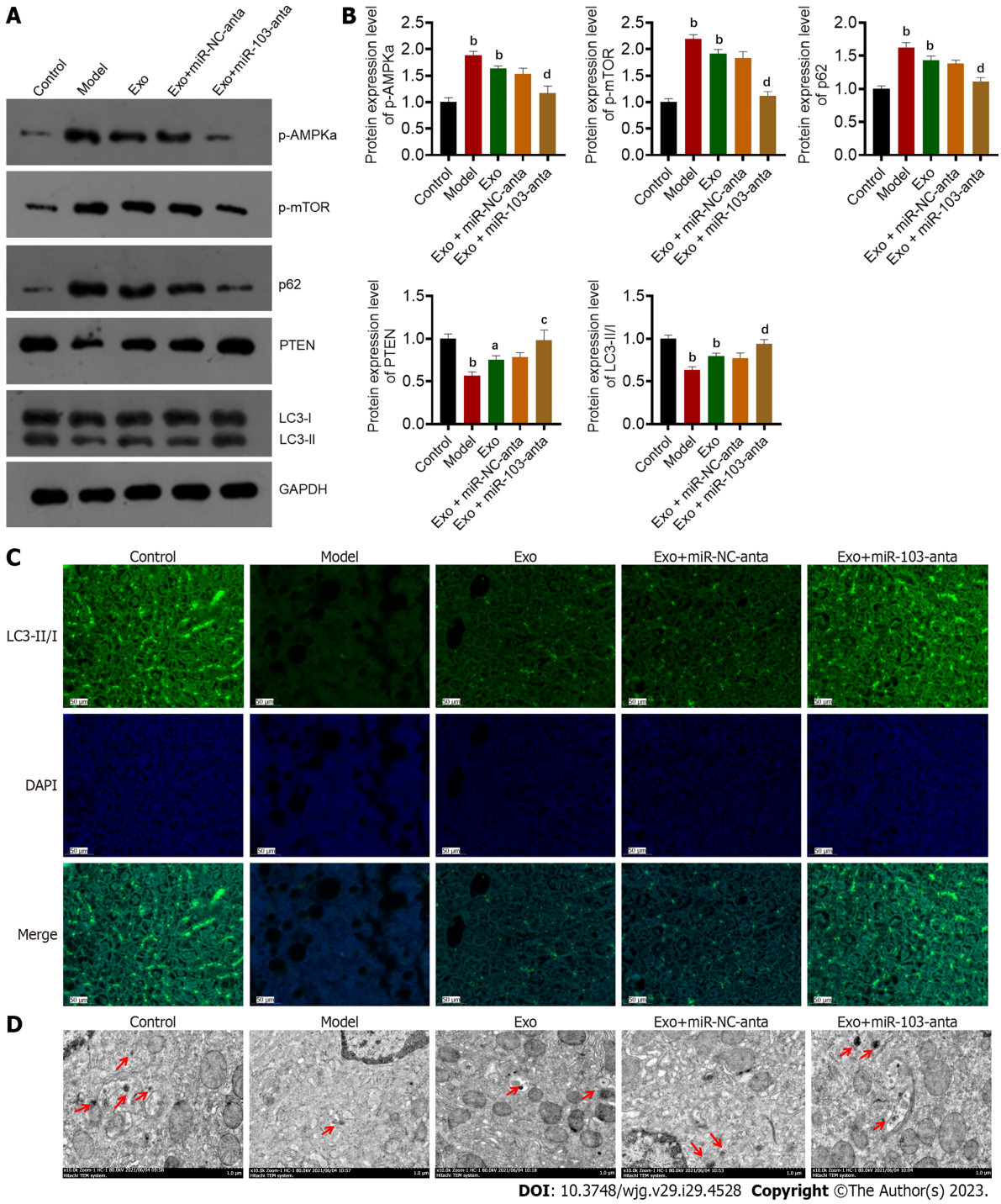
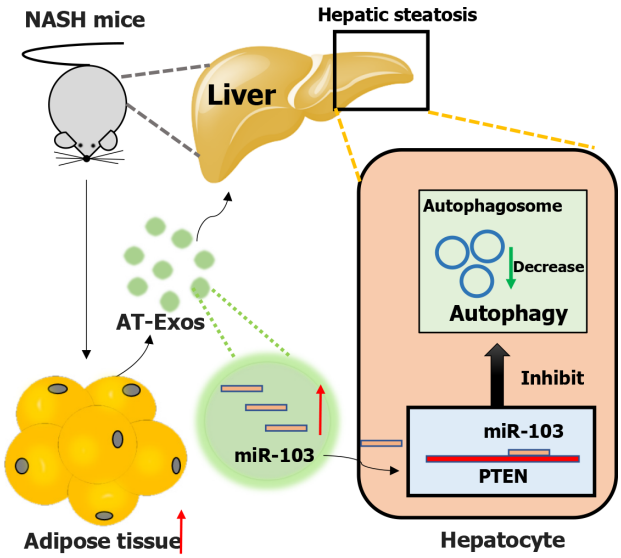


Figure 6 The effect of adipose tissue-derived exosomes miR-103 on autophagy in mice. A and B: Western blotting detected the expression of the autophagy-related protein; C: The results of immunofluorescence staining to observe autophagosomes in the liver from different groups; D: Transmission electron microscopy images of autophagosomes (red arrowhead) in the liver from different groups. $^{a}P < 0.05$ *vs* control; $^{b}P < 0.01$ *vs* control; $^{c}P < 0.05$ *vs* exosomes; $^{d}P < 0.01$ *vs* exosomes. Exo: Exosomes; PTEN: Phosphatase and tensin homolog; DAPI: 4',6-diamidino-2-phenylindole; mTOR: Mammalian target of rapamycin; NC: Negative control.

proliferation and differentiation of pancreatic β cells[22,23]. MiR-33a and miR-33b are involved in cholesterol and lipid metabolism[24,25]. Furthermore, several miRNAs are also targeting the liver to regulate metabolic processes. For instance, miR-122, one of the most abundant miRNAs in the liver, is involved in hepatic cholesterol and lipid metabolism [26,27]. Besides, miR-103, the focus of our study, has also been confirmed to be closely related to hepatic insulin sensitivity and the regulation of glucose homeostasis in previous studies[12]. Since NAFLD is the hepatic manifestation of metabolic syndrome, it is theoretically possible that miR-103 participates in NAFLD, but related research is still lacking. NASH was linked to menopause[28], and miR-103 was found to be linked to G protein-coupled estrogen receptor 1[29]. Therefore, the estrogen signaling pathway is the potential mechanism where miR-103 promotes NASH. However, in this study, for the first time, we showed that the miR-103 level in the liver of NASH mice was significantly increased while inhibiting miR-103 expression could alleviate NASH, suggesting that miR-103 is one of the potential targets for NASH



DOI: 10.3748/wjg.v29.i29.4528 **Copyright** ©The Author(s) 2023.

Figure 7 The hypothesis of obesity-induced non-alcoholic steatohepatitis. The increased adipocyte tissue will secret more adipose tissue (AT)-derived exosomes, which include various contents, and miR-103 is our focus. The increased AT-derived exosomes miR-103 could be absorbed by hepatocytes and further regulate non-alcoholic steatohepatitis progression by affecting the autophagy process by targeting phosphatase and tensin homolog gene. AT: Adipose tissue; NASH: Non-alcoholic steatohepatitis; Exo: Exosomes; PTEN: Phosphatase and tensin homolog.

treatment.

We further identified the AT-derived exosomes as the source of miR-103 upregulation in the NASH mouse model. There have been many studies on the role of AT-derived exosomes in the development of NAFLD in obese people[30]. For instance, Fuchs *et al*[31] showed that the concentration of free exosomes is significantly higher in obese with NAFLD (OB-NAFLD) patients compared with lean with normal intrahepatic triglyceride content (LEAN) and obese with normal intrahepatic triglyceride content (OB-NL) populations and that these exosomes are at least partially derived from AT. Compared with exosomes derived from the LEAN and OB-NL groups, plasma and AT-derived exosomes from the OB-NAFLD group caused insulin resistance in both myotubes and hepatocytes, demonstrated by impaired insulin signaling. However, the underlying mechanism of the above effects of AT-derived exosomes in NAFLD patients has not been further explored. Our results complement this by revealing the effect of AT-derived exosomes through the miR-103-PTEN pathway, which broadens our understanding of NASH pathogenesis from the angle of trans-cellular crosstalk.

We also confirmed that autophagy is the downstream of the action of miR-103 through *in vivo* and *in vitro* experiments. Autophagy is an evolutionarily conserved cellular degradation process that delivers some intracellular components to lysosomes for degradation[32]. Current studies suggest that autophagy includes three subtypes: Macroautophagy, microautophagy, and chaperon-mediated autophagy[33]. Autophagy plays a vital role in the liver. It involves many basic liver functions, such as glycogenolysis, gluconeogenesis, and β-oxidation[34]. Previous studies have also shown that autophagy is hampered in NAFLD patients. Our previous study also revealed that autophagy inhibition plays an important role in NASH development[35]. Furthermore, restoring autophagy through certain drugs (trehalose, rapamycin, carbamazepine, or other pharmaceutical agents) or gene targets (overexpression of Atg7 or TFEB) can also alleviate NAFLD[36]. In addition, thyroxine[37] and caffeine[38] were also identified to reduce NAFLD by regulating liver autophagy. Therefore, miR-103 is expected to be one of the therapeutic targets for its autophagy regulation capacity and needs further clinical investigation in the future.

Some limitations in this study should be acknowledged. Firstly, AT-derived exosomes contain many non-coding RNAs, and we did not detect changes in the expression of other non-coding RNAs. Moreover, inhibition of miR-103 only partially inhibited the effect of AT-derived exosomes. Therefore, the above results suggest that AT-derived exosomes promote the development of NASH in multiple ways, and miR-103 is only one of them. Further research is needed on other reasons why AT-derived exosomes promote the development of NASH. Secondly, we did not design *in vivo* experiments to verify whether inhibition of autophagy could abolish the role of miR-103 in NASH. Therefore, in future studies, we may improve this part of the experiment and further explore the mechanism of miR-103 affecting autophagy. Finally, the preliminary data on the hepatocyte absorption of AT-derived exosome miR-103 needs further verification.

CONCLUSION

To sum up, our study confirms the important role of miR-103-PTEN - autophagy axis in NASH, and the elevation of miR-103 in the liver of the NASH model is partly due to hepatocyte absorption of AT derived-exosomes, which also partially explains the underlining mechanism of obesity leading to NASH (Figure 7).

ARTICLE HIGHLIGHTS

Research background

Non-alcoholic steatohepatitis (NASH) has become one of the leading causes of cirrhosis and the second leading cause of liver transplantation. miR-103 is involved in regulating insulin sensitivity, a common manifestation of metabolic syndrome in patients with NASH.

Research motivation

The specific role of miR-103 in the development of NASH also deserves further study.

Research objectives

To explore the specific role of miR-103 in the development of NASH and provide new therapeutic targets for NASH.

Research methods

The expression levels of miR-103 were detected and compared between NASH mice and control. The effect of miR-103 on NASH progression was explored by miR-103 antagonizing, including both changes of steatosis and inflammation degree. The interaction between miR-103 and the autophagy-related gene phosphatase and tensin homolog (PTEN) was confirmed by dual-luciferase reporter assay. The role of the interaction between miR-103 and PTEN on autophagy was verified in NASH cells. Finally, the effects of miR-103 from adipose tissue (AT)-derived exosomes on NASH and autophagy were analyzed through animal experiments.

Research results

The expression of miR-103 was increased in NASH mice, compared with the control, and inhibition of miR-103 could alleviate NASH. MiR-103 could interact with PTEN. MiR-103-anta inhibited autophagy in NASH mice. Further experiments showed PTEN silencing inhibited the effect of miR-103-anta. AT-derived exosome miR-103 aggravated NASH and inhibited autophagy in mice.

Research conclusions

AT derived-exosome increased the levels of miR-103 in the liver, and miR-103 aggravated NASH. Mechanically speaking, miR-103 could interact with PTEN and inhibit autophagy.

Research perspectives

MiR-103 may be a potential target for NASH treatment in the future.

FOOTNOTES

Author contributions: Jin X designed the report; Lu MM performed experiments, wrote the paper and assisted to design the report; Ren Y and Zhou YW performed experiments and statistical analysis; Zhang MM, Ding LP, and Cheng WX assisted to perform experiments and analyzed data; and all authors had access to the study data and reviewed and approved the final manuscript.

Supported by the Natural Science Foundation of Zhejiang Province, No. LZ21H030002.

Institutional animal care and use committee statement: This study was carried out following the recommendations in the Guide for the Care and Use of Laboratory Animals of the National Institute of Health. The animal protocol was approved by the institutional review board of the Tab of Animal Experimental Ethical Inspection of the First Affiliated Hospital of Zhejiang University. The Reference Number is 2020-1407.

Conflict-of-interest statement: All the authors report no relevant conflicts of interest for this article.

Data sharing statement: All the data included in this study are available upon request by contact with the corresponding author.

ARRIVE guidelines statement: The authors have read the ARRIVE guidelines, and the manuscript was prepared and revised according to the ARRIVE guidelines.

Open-Access: This article is an open-access article that was selected by an in-house editor and fully peer-reviewed by external reviewers. It is distributed in accordance with the Creative Commons Attribution NonCommercial (CC BY-NC 4.0) license, which permits others to distribute, remix, adapt, build upon this work non-commercially, and license their derivative works on different terms, provided the original work is properly cited and the use is non-commercial. See: https://creativecommons.org/Licenses/by-nc/4.0/

Country/Territory of origin: China

ORCID number: Miao-Miao Lu 0000-0002-9328-8239; Yue Ren 0000-0001-9071-2738; Ling-Ling Xu 0000-0002-6668-3057; Wei-Xin Cheng 0000-0003-1764-0779; Xi Jin 0000-0002-2975-977X.

S-Editor: Wang JJ
L-Editor: A
P-Editor: Zhao S

REFERENCES

1 **Chalasani N**, Younossi Z, Lavine JE, Charlton M, Cusi K, Rinella M, Harrison SA, Brunt EM, Sanyal AJ. The diagnosis and management of nonalcoholic fatty liver disease: Practice guidance from the American Association for the Study of Liver Diseases. *Hepatology* 2018; **67**: 328-357 [PMID: 28714183 DOI: 10.1002/hep.29367]
2 **Younossi ZM**, Koenig AB, Abdelatif D, Fazel Y, Henry L, Wymer M. Global epidemiology of nonalcoholic fatty liver disease-Meta-analytic assessment of prevalence, incidence, and outcomes. *Hepatology* 2016; **64**: 73-84 [PMID: 26707365 DOI: 10.1002/hep.28431]
3 **Wong VW**, Wong GL, Choi PC, Chan AW, Li MK, Chan HY, Chim AM, Yu J, Sung JJ, Chan HL. Disease progression of non-alcoholic fatty liver disease: a prospective study with paired liver biopsies at 3 years. *Gut* 2010; **59**: 969-974 [PMID: 20581244 DOI: 10.1136/gut.2009.205088]
4 **Wong RJ**, Aguilar M, Cheung R, Perumpail RB, Harrison SA, Younossi ZM, Ahmed A. Nonalcoholic steatohepatitis is the second leading etiology of liver disease among adults awaiting liver transplantation in the United States. *Gastroenterology* 2015; **148**: 547-555 [PMID: 25461851 DOI: 10.1053/j.gastro.2014.11.039]
5 **Charlton MR**, Burns JM, Pedersen RA, Watt KD, Heimbach JK, Dierkhising RA. Frequency and outcomes of liver transplantation for nonalcoholic steatohepatitis in the United States. *Gastroenterology* 2011; **141**: 1249-1253 [PMID: 21726509 DOI: 10.1053/j.gastro.2011.06.061]
6 **Byrne CD**, Targher G. NAFLD: a multisystem disease. *J Hepatol* 2015; **62**: S47-S64 [PMID: 25920090 DOI: 10.1016/j.jhep.2014.12.012]
7 **Polyzos SA**, Kountouras J, Mantzoros CS. Obesity and nonalcoholic fatty liver disease: From pathophysiology to therapeutics. *Metabolism* 2019; **92**: 82-97 [PMID: 30502373 DOI: 10.1016/j.metabol.2018.11.014]
8 **Crewe C**, Scherer PE. Intercellular and interorgan crosstalk through adipocyte extracellular vesicles. *Rev Endocr Metab Disord* 2022; **23**: 61-69 [PMID: 33447986 DOI: 10.1007/s11154-020-09625-x]
9 **Ying W**, Riopel M, Bandyopadhyay G, Dong Y, Birmingham A, Seo JB, Ofrecio JM, Wollam J, Hernandez-Carretero A, Fu W, Li P, Olefsky JM. Adipose Tissue Macrophage-Derived Exosomal miRNAs Can Modulate In Vivo and In Vitro Insulin Sensitivity. *Cell* 2017; **171**: 372-384.e12 [PMID: 28942920 DOI: 10.1016/j.cell.2017.08.035]
10 **Liu T**, Sun YC, Cheng P, Shao HG. Adipose tissue macrophage-derived exosomal miR-29a regulates obesity-associated insulin resistance. *Biochem Biophys Res Commun* 2019; **515**: 352-358 [PMID: 31153636 DOI: 10.1016/j.bbrc.2019.05.113]
11 **Rottiers V**, Näär AM. MicroRNAs in metabolism and metabolic disorders. *Nat Rev Mol Cell Biol* 2012; **13**: 239-250 [PMID: 22436747 DOI: 10.1038/nrm3313]
12 **Trajkovski M**, Hausser J, Soutschek J, Bhat B, Akin A, Zavolan M, Heim MH, Stoffel M. MicroRNAs 103 and 107 regulate insulin sensitivity. *Nature* 2011; **474**: 649-653 [PMID: 21654750 DOI: 10.1038/nature10112]
13 **Recena Aydos L**, Aparecida do Amaral L, Serafim de Souza R, Jacobowski AC, Freitas Dos Santos E, Rodrigues Macedo ML. Nonalcoholic Fatty Liver Disease Induced by High-Fat Diet in C57bl/6 Models. *Nutrients* 2019; **11** [PMID: 31888190 DOI: 10.3390/nu11123067]
14 **Wang L**, Zhang X, Lin ZB, Yang PJ, Xu H, Duan JL, Ruan B, Song P, Liu JJ, Yue ZS, Fang ZQ, Hu H, Liu Z, Huang XL, Yang L, Tian S, Tao KS, Han H, Dou KF. Tripartite motif 16 ameliorates nonalcoholic steatohepatitis by promoting the degradation of phospho-TAK1. *Cell Metab* 2021; **33**: 1372-1388.e7 [PMID: 34146477 DOI: 10.1016/j.cmet.2021.05.019]
15 **Gao J**, Li X, Wang Y, Cao Y, Yao D, Sun L, Qin L, Qiu H, Zhan X. Adipocyte-derived extracellular vesicles modulate appetite and weight through mTOR signalling in the hypothalamus. *Acta Physiol (Oxf)* 2020; **228**: e13339 [PMID: 31278836 DOI: 10.1111/apha.13339]
16 **Agarwal V**, Bell GW, Nam JW, Bartel DP. Predicting effective microRNA target sites in mammalian mRNAs. *Elife* 2015; **4** [PMID: 26267216 DOI: 10.7554/eLife.05005]
17 **Younossi ZM**, Tampi R, Priyadarshini M, Nader F, Younossi IM, Racila A. Burden of Illness and Economic Model for Patients With Nonalcoholic Steatohepatitis in the United States. *Hepatology* 2019; **69**: 564-572 [PMID: 30180285 DOI: 10.1002/hep.30254]
18 **Allen AM**, Lazarus JV, Younossi ZM. Healthcare and socioeconomic costs of NAFLD: A global framework to navigate the uncertainties. *J Hepatol* 2023; **79**: 209-217 [PMID: 36740046 DOI: 10.1016/j.jhep.2023.01.026]
19 **Lagos-Quintana M**, Rauhut R, Lendeckel W, Tuschl T. Identification of novel genes coding for small expressed RNAs. *Science* 2001; **294**: 853-858 [PMID: 11679670 DOI: 10.1126/science.1064921]
20 **Voinnet O**. Origin, biogenesis, and activity of plant microRNAs. *Cell* 2009; **136**: 669-687 [PMID: 19239888 DOI: 10.1016/j.cell.2009.01.046]
21 **Vienberg S**, Geiger J, Madsen S, Dalgaard LT. MicroRNAs in metabolism. *Acta Physiol (Oxf)* 2017; **219**: 346-361 [PMID: 27009502 DOI: 10.1111/apha.12681]
22 **Pullen TJ**, da Silva Xavier G, Kelsey G, Rutter GA. miR-29a and miR-29b contribute to pancreatic beta-cell-specific silencing of monocarboxylate transporter 1 (Mct1). *Mol Cell Biol* 2011; **31**: 3182-3194 [PMID: 21646425 DOI: 10.1128/MCB.01433-10]
23 **Belgardt BF**, Ahmed K, Spranger M, Latreille M, Denzler R, Kondratiuk N, von Meyenn F, Villena FN, Herrmanns K, Bosco D, Kerr-Conte J, Pattou F, Rülicke T, Stoffel M. The microRNA-200 family regulates pancreatic beta cell survival in type 2 diabetes. *Nat Med* 2015; **21**: 619-627 [PMID: 25985365 DOI: 10.1038/nm.3862]
24 **Dávalos A**, Goedeke L, Smibert P, Ramírez CM, Warrier NP, Andreo U, Cirera-Salinas D, Rayner K, Suresh U, Pastor-Pareja JC, Esplugues E, Fisher EA, Penalva LO, Moore KJ, Suárez Y, Lai EC, Fernández-Hernando C. miR-33a/b contribute to the regulation of fatty acid metabolism and insulin signaling. *Proc Natl Acad Sci U S A* 2011; **108**: 9232-9237 [PMID: 21576456 DOI: 10.1073/pnas.1102281108]
25 **Rayner KJ**, Esau CC, Hussain FN, McDaniel AL, Marshall SM, van Gils JM, Ray TD, Sheedy FJ, Goedeke L, Liu X, Khatsenko OG, Kaimal V, Lees CJ, Fernandez-Hernando C, Fisher EA, Temel RE, Moore KJ. Inhibition of miR-33a/b in non-human primates raises plasma HDL and lowers VLDL triglycerides. *Nature* 2011; **478**: 404-407 [PMID: 22012398 DOI: 10.1038/nature10486]
26 **Krützfeldt J**, Rajewsky N, Braich R, Rajeev KG, Tuschl T, Manoharan M, Stoffel M. Silencing of microRNAs *in vivo* with 'antagomirs'. *Nature* 2005; **438**: 685-689 [PMID: 16258535 DOI: 10.1038/nature04303]

27 **Esau C**, Davis S, Murray SF, Yu XX, Pandey SK, Pear M, Watts L, Booten SL, Graham M, McKay R, Subramaniam A, Propp S, Lollo BA, Freier S, Bennett CF, Bhanot S, Monia BP. miR-122 regulation of lipid metabolism revealed by *in vivo* antisense targeting. *Cell Metab* 2006; **3**: 87-98 [PMID: 16459310 DOI: 10.1016/j.cmet.2006.01.005]

28 **DiStefano JK**. NAFLD and NASH in Postmenopausal Women: Implications for Diagnosis and Treatment. *Endocrinology* 2020; **161** [PMID: 32776116 DOI: 10.1210/endocr/bqaa134]

29 **Fang T**, Li J, Wu X. Shenmai injection improves the postoperative immune function of papillary thyroid carcinoma patients by inhibiting differentiation into Treg cells *via* miR-103/GPER1 axis. *Drug Dev Res* 2018; **79**: 324-331 [PMID: 30267584 DOI: 10.1002/ddr.21459]

30 **Thietart S**, Rautou PE. Extracellular vesicles as biomarkers in liver diseases: A clinician's point of view. *J Hepatol* 2020; **73**: 1507-1525 [PMID: 32682050 DOI: 10.1016/j.jhep.2020.07.014]

31 **Fuchs A**, Samovski D, Smith GI, Cifarelli V, Farabi SS, Yoshino J, Pietka T, Chang SW, Ghosh S, Myckatyn TM, Klein S. Associations Among Adipose Tissue Immunology, Inflammation, Exosomes and Insulin Sensitivity in People With Obesity and Nonalcoholic Fatty Liver Disease. *Gastroenterology* 2021; **161**: 968-981.e12 [PMID: 34004161 DOI: 10.1053/j.gastro.2021.05.008]

32 **Klionsky DJ**, Emr SD. Autophagy as a regulated pathway of cellular degradation. *Science* 2000; **290**: 1717-1721 [PMID: 11099404 DOI: 10.1126/science.290.5497.1717]

33 **Mizushima N**, Levine B, Cuervo AM, Klionsky DJ. Autophagy fights disease through cellular self-digestion. *Nature* 2008; **451**: 1069-1075 [PMID: 18305538 DOI: 10.1038/nature06639]

34 **Ueno T**, Komatsu M. Autophagy in the liver: functions in health and disease. *Nat Rev Gastroenterol Hepatol* 2017; **14**: 170-184 [PMID: 28053338 DOI: 10.1038/nrgastro.2016.185]

35 **Jin X**, Gao J, Zheng R, Yu M, Ren Y, Yan T, Huang Y, Li Y. Antagonizing circRNA_002581-miR-122-CPEB1 axis alleviates NASH through restoring PTEN-AMPK-mTOR pathway regulated autophagy. *Cell Death Dis* 2020; **11**: 123 [PMID: 32054840 DOI: 10.1038/s41419-020-2293-7]

36 **Qian H**, Chao X, Williams J, Fulte S, Li T, Yang L, Ding WX. Autophagy in liver diseases: A review. *Mol Aspects Med* 2021; **82**: 100973 [PMID: 34120768 DOI: 10.1016/j.mam.2021.100973]

37 **Zhou J**, Tripathi M, Ho JP, Widjaja AA, Shekeran SG, Camat MD, James A, Wu Y, Ching J, Kovalik JP, Lim KH, Cook SA, Bay BH, Singh BK, Yen PM. Thyroid Hormone Decreases Hepatic Steatosis, Inflammation, and Fibrosis in a Dietary Mouse Model of Nonalcoholic Steatohepatitis. *Thyroid* 2022; **32**: 725-738 [PMID: 35317606 DOI: 10.1089/thy.2021.0621]

38 **Sinha RA**, Farah BL, Singh BK, Siddique MM, Li Y, Wu Y, Ilkayeva OR, Gooding J, Ching J, Zhou J, Martinez L, Xie S, Bay BH, Summers SA, Newgard CB, Yen PM. Caffeine stimulates hepatic lipid metabolism by the autophagy-lysosomal pathway in mice. *Hepatology* 2014; **59**: 1366-1380 [PMID: 23929677 DOI: 10.1002/hep.26667]

World Journal of Gastroenterology

Submit a Manuscript: https://www.f6publishing.com

World J Gastroenterol 2023 August 7; 29(29): 4542-4556

DOI: 10.3748/wjg.v29.i29.4542

ISSN 1007-9327 (print) ISSN 2219-2840 (online)

ORIGINAL ARTICLE

Basic Study

MiR-204-3p overexpression inhibits gastric carcinoma cell proliferation by inhibiting the MAPK pathway and RIP1/MLK1 necroptosis pathway to promote apoptosis

Xia Li, Joanna J Tibenda, Yi Nan, Shi-Cong Huang, Na Ning, Guo-Qing Chen, Yu-Hua Du, Ya-Ting Yang, Fan-Di Meng, Ling Yuan

Specialty type: Gastroenterology and hepatology

Provenance and peer review: Unsolicited article; Externally peer reviewed.

Peer-review model: Single blind

Peer-review report's scientific quality classification

Grade A (Excellent): 0
Grade B (Very good): B
Grade C (Good): C, C
Grade D (Fair): 0
Grade E (Poor): 0

P-Reviewer: Gupta S, Brazil; Wang L, China

Received: May 6, 2023
Peer-review started: May 6, 2023
First decision: May 17, 2023
Revised: May 24, 2023
Accepted: July 5, 2023
Article in press: July 5, 2023
Published online: August 7, 2023

Xia Li, Joanna J Tibenda, Shi-Cong Huang, Na Ning, Guo-Qing Chen, Yu-Hua Du, Ling Yuan, College of Pharmacy, Ningxia Medical University, Yinchuan 750004, Ningxia Hui Autonomous Region, China

Xia Li, Ningxia Chinese Medicine Reserch Center, Yinchuan 750004, Ningxia Hui Autonomous Region, China

Yi Nan, Fan-Di Meng, Key Laboratory of Hui Ethnic Medicine Modernization of Ministry of Education, Ningxia Medical University, Yinchuan 750004, Ningxia Hui Autonomous Region, China

Yi Nan, Ya-Ting Yang, Traditional Chinese Medicine College, Ningxia Medical University, Yinchuan 750004, Ningxia Hui Autonomous Region, China

Corresponding author: Ling Yuan, PhD, Professor, College of Pharmacy, Ningxia Medical University, No. 1160 Shengli Street, Yinchuan 750004, Ningxia Hui Autonomous Region, China. 20080017@nxmu.edu.cn

Abstract

BACKGROUND

Gastric carcinoma (GC) is the third most frequent cause of cancer-related death, highlighting the pressing need for novel clinical treatment options. In this regard, microRNAs (miRNAs) have emerged as a promising therapeutic strategy. Studies have shown that miRNAs can regulate related signaling pathways, acting as tumor suppressors or tumor promoters.

AIM

To explore the effect of miR-204-3p on GC cells.

METHODS

We measured the expression levels of miR-204-3p in GC cells using quantitative real-time polymerase chain reaction, followed by the delivery of miR-204-3p overexpression and miR-204-3p knockdown vectors into GC cells. CCK-8 was used to detect the effect of miR-204-3p on the proliferation of GC cells, and the colony formation ability of GC cells was detected by the clonal formation assay.

The effects of miR-204-3p on GC cell cycle and apoptosis were detected by flow cytometry. The BABL/c nude mouse subcutaneous tumor model using MKN-45 cells was constructed to verify the effect of miR-204-3p on the tumorigenicity of GC cells. Furthermore, the study investigated the effects of miR-204-3p on various proteins related to the MAPK signaling pathway, necroptosis signaling pathway and apoptosis signaling pathway on GC cells using Western blot techniques.

RESULTS

Firstly, we found that the expression of miR-204-3p in GC was low. When treated with the lentivirus overexpression vector, miR-204-3p expression significantly increased, but the lentivirus knockout vector had no significant effect on miR-204-3p. *In vitro* experiments confirmed that miR-204-3p overexpression inhibited GC cell viability, promoted cell apoptosis, blocked the cell cycle, and inhibited colony formation ability. *In vivo* animal experiments confirmed that miR-204-3p overexpression inhibited subcutaneous tumorigenesis ability in BABL/c nude mice. Simultaneously, our results verified that miR-204-3p overexpression can inhibit GC cell proliferation by inhibiting protein expression levels of KRAS and p-ERK1/2 in the MAPK pathway, as well as inhibiting protein expression levels of p-RIP1 and p-MLK1 in the necroptosis pathway to promote the BCL-2/BAX/Caspase-3 apoptosis pathway.

CONCLUSION

MiR-204-3p overexpression inhibited GC cell proliferation by inhibiting the MAPK pathway and necroptosis pathway to promote apoptosis of GC cells. Thus, miR-204-3p may represent a new potential therapeutic target for GC.

Key Words: miR-204-3p; Gastric carcinoma; MAPK signaling pathway; Apoptosis; Necroptosis

©The Author(s) 2023. Published by Baishideng Publishing Group Inc. All rights reserved.

Core Tip: Gastric carcinoma (GC) is a global health problem that seriously endangers human life; therefore, it is important to identify effective treatment targets. In this regard, microRNAs (miRNAs) have emerged as a promising therapeutic strategy. Studies have shown that miRNAs regulated signaling pathways, acting as tumor suppressors or tumor promoters. In this study, we first verified the inhibitory effect of miR-204-3p overexpression on GC cells through *in vitro* and *in vivo* experiments. Simultaneously, miR-204-3p overexpression induced GC cell apoptosis by inhibiting the MAPK pathway and the necroptosis pathway. Thus, miR-204-3p may represent a new potential therapeutic target for GC.

Citation: Li X, Tibenda JJ, Nan Y, Huang SC, Ning N, Chen GQ, Du YH, Yang YT, Meng FD, Yuan L. MiR-204-3p overexpression inhibits gastric carcinoma cell proliferation by inhibiting the MAPK pathway and RIP1/MLK1 necroptosis pathway to promote apoptosis. *World J Gastroenterol* 2023; 29(29): 4542-4556
URL: https://www.wjgnet.com/1007-9327/full/v29/i29/4542.htm
DOI: https://dx.doi.org/10.3748/wjg.v29.i29.4542

INTRODUCTION

Gastric carcinoma (GC) is a gastrointestinal tumor and the third major cause of cancer-related death[1,2]. Early clinical symptoms are mild or asymptomatic, resulting in difficult diagnosis and a low patient survival rate[3,4]. Currently, the clinical therapy of GC primarily consists of radiotherapy, chemotherapy, and surgical excision, but the therapeutic effect is unsatisfactory[5,6]. Therefore, feasible targeted therapies are particularly important for GC patients. As research has progressed, molecular targets have been found to have a role in the occurrence and development of GC.

MicroRNAs (miRNAs) are small non-coding RNAs that regulate gene expression by binding to the 3'-untranslated region of target mRNA[7]. With further study in genetic engineering, it has been confirmed that miRNAs regulate different signaling pathways to take part in important cellular processes[8]. miRNAs can act as tumor promoters or inhibitors to target mRNA to regulate GC proliferation, metastasis, angiogenesis, and drug resistance[9-11]. Consequently, it is necessary to strengthen miRNA research for the diagnosis and clinical treatment of GC.

MiR-204-3p has demonstrated efficacy in treating various pathologies, including retinopathy, diabetes, and cancer[12-15]. Crucially, miR-204-3p is underexpressed in melanoma, thyroid carcinoma, glioma and bladder carcinoma, and is related to patient prognosis[16-19]. However, the mechanism of miR-204-3p in GC remains unclear.

Our team's previous research confirmed that the expression of miR-204-3p in GC tissue is low and is associated with poor prognosis in GC patients. In addition, we also verified that KRAS is its direct target[20]. However, the anti-GC effect of miR-204-3p still requires further research to support the possibility of miR-204-3p becoming a new target for the treatment of GC. In this study, we focused on determining the impact of miR-204-3p on GC cells phenotype and its anti-GC molecular mechanism, to provide theoretical support for the treatment of GC by miR-204-3p.

Table 1 Primer sequences

Primer	Forward sequence (5'-3')	Reverse sequence (5'-3')
KRAS	TGTGGACGAATATGATCCAACA	GCAAATACACAAAGAAAGCCCT
ERK1	ATGTCATCGGCATCCGAGAC	GGATCTGGTAGAGGAAGTAGCA
ERK2	TACACCAACCTCTCGTACATCG	ATGTCTGAAGCGCAGTAAGATT
GAPDH	CACCCACTCCTCCACCTTTGA	TCTCTCTTCCTCTTGTGCTCTCTTGC
miR-204-3p	CAAGTCGCTGGGAAGGCAA	CAGTGCAGGGTCCGAGGT
U6	CTCGCTTCGGCAGCACA	AACGCTTCACGAATTTGCGT

MATERIALS AND METHODS

Cell culture and cell transfection

A normal human gastric epithelial cell line (GES-1) and three GC cell lines (HGC-27, AGS and MKN-45) were acquired from BNCC (Beijing, China). MKN-45 and HGC-27 cells were cultured in RPIM-1640 medium, AGS cells in DMEM/F-12 medium and GES-1 cells in DMEM medium. All culture media were purchased from Gibco (United States), and were supplemented with 1% penicillin-streptomycin and 10% fetal bovine serum. Genechem (Shanghai, China) provided the green fluorescent protein-labeled miR-204-3p overexpression lentiviral vector (OE group), miR-204-3p knockdown lentiviral vector (KD group) and empty lentiviral vector (NC group), which were then transfected into HGC-27, MKN-45 and AGS cells using the tool virus user manual as a guide.

CCK-8 assay

Cell viability was evaluated using the CCK-8 assay. Specifically, lentivirus-transfected AGS and HGC-27 cells were seeded into 96-well plates (5000 cells/well) and cultured for 24 h, 48 h and 72 h, respectively. Following this step, each well was treated with 10 μL CCK-8 reagent (MedChemExpress, United States), and a microplate reader was used to measure the value at 450 nm following incubation for 2 h at 37°C.

Colony formation assay

Lentivirus-transfected AGS and HGC-27 cells were inoculated into 6-well plates (500 cells/well), and fixed with 4% paraformaldehyde for 30 min after 2 wk of continuous culture. Next, the fixing solution was washed off and the cells were stained using 0.5% crystal violet for 10 min. Finally, the cell clones were photographed and statistically analyzed based on clone sizes (diameter > 1 mm).

Flow cytometric analysis

Cell cycle was confirmed using the cell cycle kit (KeyGEN BioTECH, China). Lentivirus-transfected HGC-27 and AGS cells were collected at 1 × 10^6 cells/mL, and then fixed overnight at 37°C with 4% paraformaldehyde. On the second day, the fixing solution was washed off with PBS and 500 μL cell cycle detection working solution (Rnase A:PI = 1:9) was added. The distribution of various groups of cells in the cell cycle was detected after they had reacted for 30 min.

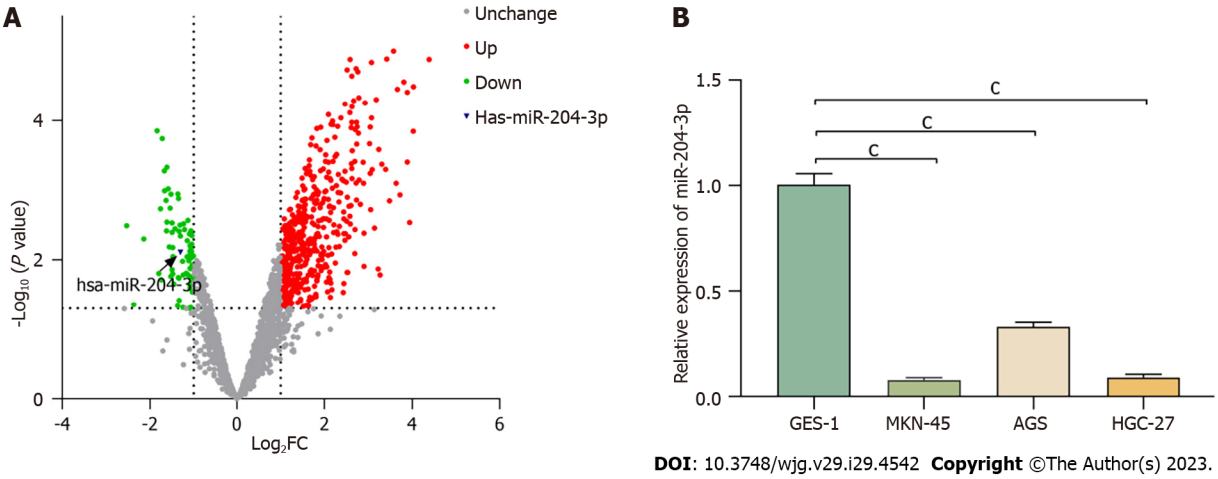
The Annexin V-APC/7-AAD double staining kit (KeyGEN BioTECH, China) was used to confirm apoptosis (early apoptosis and late apoptosis) in each group. Lentivirus-transfected AGS and HGC-27 cells were collected, and 500 μL Binding Buffer, 5 μL Annexin V-APC and 5 μL 7-AAD were added sequentially and gently mixed. Apoptosis was observed after the cells had reacted for 10 min.

Western blot

The expression of related proteins in lentivirus-transfected AGS and HGC-27 cells was detected. Firstly, total protein was extracted with RIPA (Epizyme Biotech, China) from GC cells and their content was confirmed using the BCA assay (Epizyme Biotech, China). Next, the proteins were isolated and transferred onto a polyvinylidene fluoride membrane, which was sealed with 5% skim milk powder, soaked in primary antibody and incubated overnight. On the second day, it was washed with TBST and soaked in HRP-linked secondary antibody (1:1000, 7074/7076, CST, United States) for 1 h. Finally, protein bands were visualized with ECL reagent (KeyGEN BioTECH, China), and the gray values of the protein bands were analyzed using Image J. GAPDH or β-tubulin was used as an internal control to standardize target proteins. p-ERK1/2 (1:5000, 4370), ERK1/2 (1:5000, 9102), RIP1 (1:1000, 3493), p-RIP1 (1:1000, 65746), MLK1 (1:1000, 5029) and p-MLK1 (1:1000, 91689) antibodies were purchased from CST. BAX (1:2000, ab32503), Caspase-3 (1:1000, ab13847), BCL-2 (1:5000, ab182858) and KRAS (1:1000, ab275876) antibodies were purchased from Abcam.

Quantitative real-time polymerase chain reaction

The related genes expressed in each group of GC cells were determined using quantitative real-time polymerase chain reaction (qRT-PCR). Briefly, total RNA was extracted from GC cells using TRIzol reagent (Invitrogen, United States), then cDNA was synthesized (Takara Bio, Japan) and gene expression levels were measured (Takara Bio, Japan). The primer sequences are shown in Table 1. U6 or GAPDH was used as a housekeeping gene, and target genes were calculated using



DOI: 10.3748/wjg.v29.i29.4542 **Copyright** ©The Author(s) 2023.

Figure 1 Expression of miR-204-3p in gastric carcinoma. A: The expression level of miR-204-3p in gastric carcinoma tissues and para-carcinoma tissues was analyzed by the GEO database; B: The expression level of miR-204-3p in normal gastric mucosal epithelial cells and gastric carcinoma cells, $^{c}P < 0.001$.

the $2^{-\Delta\Delta Ct}$ method.

Tumor xenograft experiment

BABL/c nude mice (male, 4 wk, SPF) were provided by the Animal Laboratory Center of Ningxia Medical University. The animal protocol (IACUC-NYLAC-2022-251) was approved by the Institutional Animal Care and Use Committee of Ningxia Medical University. Following 7 d of adaptive feeding in BALB/c nude mice, lentivirus-transfected MKN-45 cells were cultured, and the cell concentration adjusted to 5×10^7 cells/mL. A suspension containing 100 μL cells was slowly subcutaneously injected into the back of nude mice, which were then returned to their cage for feeding. Growth of the subcutaneous tumor and mouse body weight were observed daily. The tumor volume (V) was calculated by $V = (W^2 \times L)/2$ (long diameter: L; short diameter: W). When the tumor on the back grew to an appropriate size and conformed to animal ethics, the animals were killed by CO_2 and photographed.

Differential expression analysis of miRNAs

We used the GEO database (https://www.ncbi.nlm.nih.gov/geo/) to screen differentially expressed miRNAs. We searched the keywords " miRNAs" and "gastric carcinoma, and downloaded Differential expression microarrays of miRNAs (series: GES79973). Then adjusted for $P < 0.05$, $|\log_2 (\text{fold change})| > 1$, and analyzed significant miRNAs.

Statistical analysis

The statistical methods used in this study were reviewed by Li-Qun Wang from the Department of Epidemiology, Department of Medical Statistics, Institute of Public Health and Management, Ningxia Medical University. All data represent the mean ± SD of at least three independent samples. Statistical analysis was conducted using SPSS 27.0 and GraphPad Prism 8.0. One-way analysis of variance was used to analyze the differences between groups. $P < 0.05$ indicated a statistically significant difference.

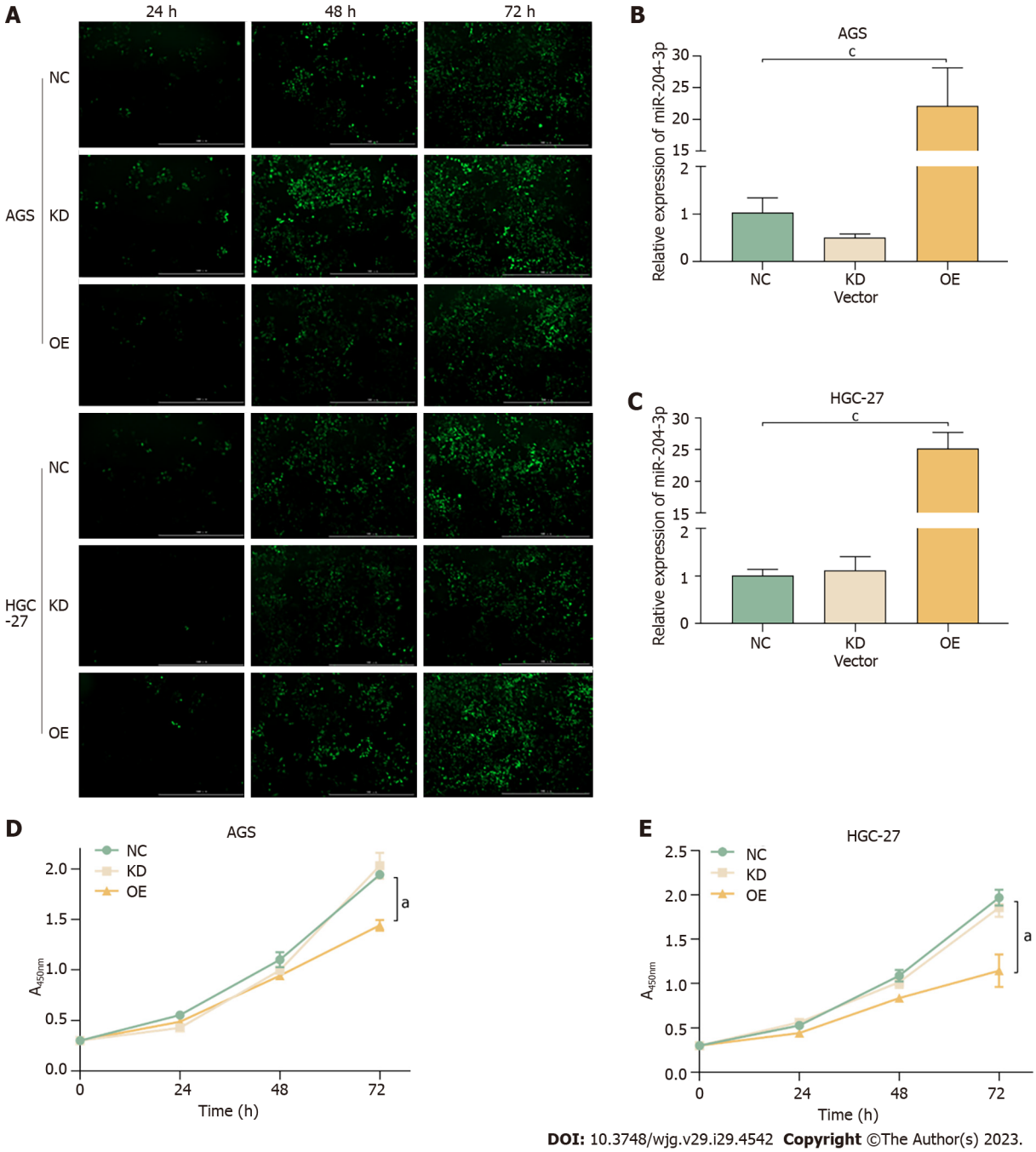
RESULTS

MiR-204-3p was underexpressed in GC

In our previous study, we analyzed 40 pairs of tissue samples and discovered that miR-204-3p expression was lower in GC tissues compared to normal tissues[20]. To further validate this finding, we utilized the GEO database to identify differentially expressed miRNAs in GC tissues and paracancerous tissues, which confirmed the downregulation of miR-204-3p in GC tissues (Figure 1A). Subsequently, we investigated miR-204-3p expression between GC cell lines (AGS, MKN-45 and HGC-27) and the normal gastric epithelial cell line GES-1. The results revealed that miR-204-3p was underexpressed in MKN-45, AGS, and HGC-27 cells compared to GES-1 cells (Figure 1B).

MiR-204-3p inhibited GC cell viability

Lentivirus transfection caused miR-204-3p overexpression and miR-204-3p knockdown in AGS and HGC-27 cells. The transfection rate was found to be approximately 90% after 72 h, indicating high transfection efficiency (Figure 2A). The qRT-PCR results demonstrated that the miR-204-3p overexpression lentivirus significantly upregulated its expression compared to the NC group in AGS and HGC-27 cells, but the miR-204-3p knockdown lentivirus did not result in downregulation of its expression (Figure 2B and C). These findings indicated that miR-204-3p overexpression in GC cells was highly satisfactory, while miR-204-3p knockdown does not yield meaningful outcomes. Subsequently, the cell viability assay showed that miR-204-3p overexpression significantly inhibited GC cell viability (Figure 2D and E).



DOI: 10.3748/wjg.v29.i29.4542 **Copyright** ©The Author(s) 2023.

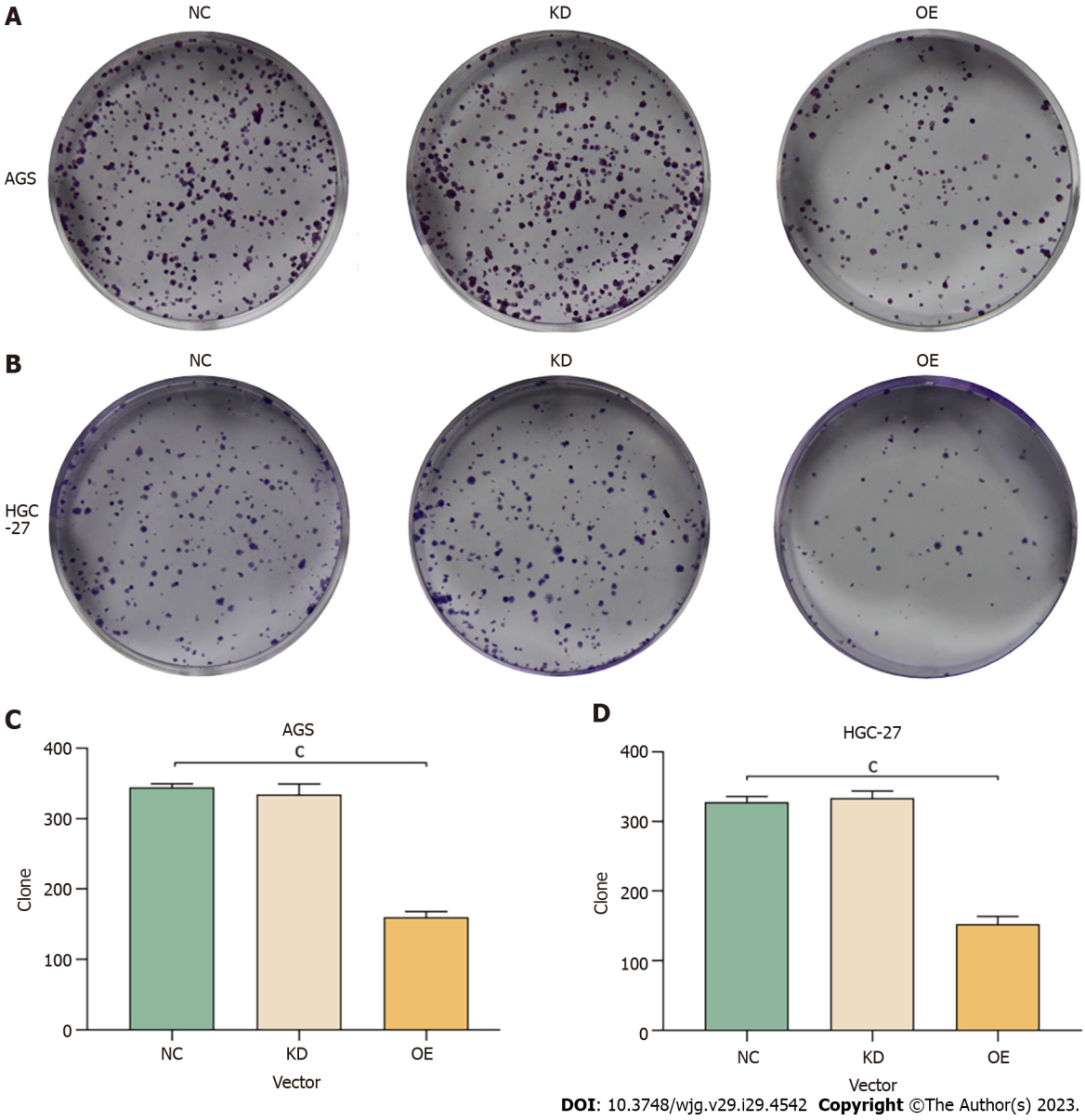
Figure 2 Effect of miR-204-3p on AGS and HGC-27 cell viability. A: Transfection efficiency of lentiviral vector. Scale bar: 1000 μm, with representative images shown, fluorescence distribution of green fluorescent protein in cells indicating transfection efficiency; B and C: The expression level of miR-204-3p in lentivirus transfected AGS and HGC-27 cells; D and E: Effect of miR-204-3p on AGS and HGC-27 cell viability. $^{a}P < 0.05$, $^{c}P < 0.001$. NC: Empty lentiviral vector; KD: miR-204-3p knockdown lentiviral vector; OE: miR-204-3p overexpression lentiviral vector.

MiR-204-3p inhibited the colony forming ability of GC cells

The impact of miR-204-3p on the colony forming ability of GC cells was evaluated. The crystal violet positive staining in the miR-204-3p overexpression group decreased (Figure 3A and B), and simultaneously, the number of clones formed in AGS and HGC-27 cells was distinctly reduced compared to the NC group (Figure 3C and D). This indicated that miR-204-3p overexpression inhibited the colony forming ability of GC cells.

MiR-204-3p promoted GC cell apoptosis

We evaluated apoptosis by collecting cells from each group (Figure 4). The apoptosis rates of AGS cells were 2.53 ± 0.12%, 3.73 ± 0.83% and 10.6 ± 0.70% in the NC, KD and OE groups, respectively (Figure 4A and C). Among HGC-27 cells, the apoptosis rates were 9.47 ± 0.58%, 7.87 ± 1.63% and 18.40 ± 1.27% in the NC, KD and OE groups, respectively (Figure 4B and D). The findings revealed that HGC-27 and AGS cells with miR-204-3p overexpression had a notably higher apoptosis rate, which indicated that miR-204-3p overexpression stimulated GC cell apoptosis.



DOI: 10.3748/wjg.v29.i29.4542 **Copyright** ©The Author(s) 2023.

Figure 3 Effect of miR-204-3p on colony forming ability in AGS and HGC-27 cells. A and B: Crystal violet staining diagram of AGS and HGC-27 cells; C and D: Statistical results of colony forming ability in AGS and HGC-27 cells. °P < 0.001. NC: Empty lentiviral vector; KD: miR-204-3p knockdown lentiviral vector; OE: miR-204-3p overexpression lentiviral vector.

MiR-204-3p retarded GC cell cycle

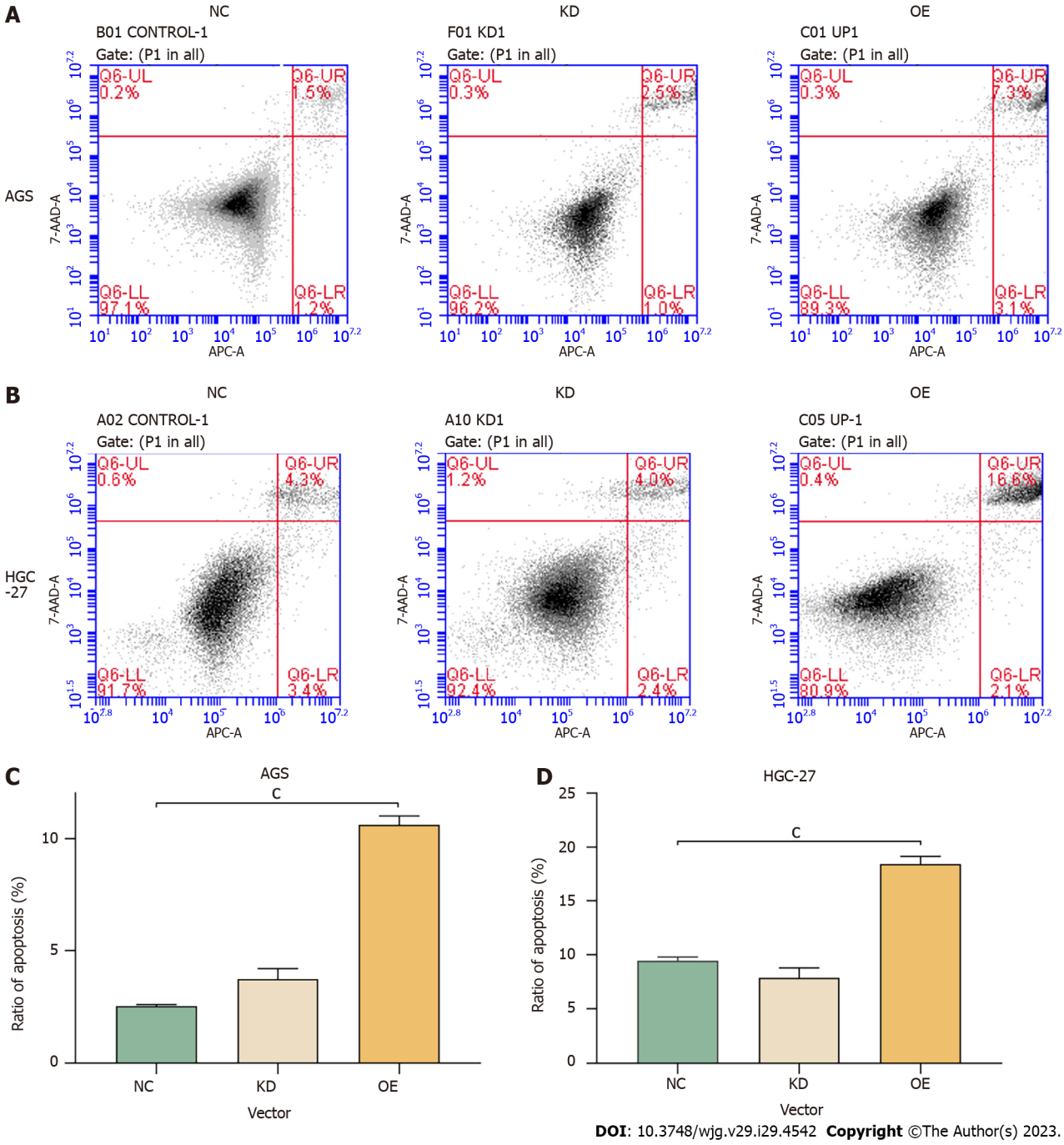
We analyzed cell cycle distribution to investigate whether miR-204-3p inhibited GC cell proliferation by mediating the cell cycle (Figure 5). Among AGS cells, the G0/G1 phase percentages were 44.91 ± 1.15%, 45.36 ± 0.70% and 49.30 ± 0.41% in the NC, KD and OE groups, respectively (Figure 5A and C). Among HGC-27 cells, the G0/G1 phase percentages were 29.36 ± 0.29%, 29.57 ± 1.11% and 41.03 ± 0.47% in the NC, KD and OE groups, respectively (Figure 5B and D). These results revealed that AGS and HGC-27 cells with miR-204-3p overexpression had a notably higher number of cells in G0/G1 phase, which indicated that miR-204-3p overexpression blocked GC cell cycle in the G0/G1 phase.

MiR-204-3p inhibited the formation of subcutaneous tumor in BABL/c nude mice

A subcutaneous tumor formation experiment was conducted in BABL/c nude mice using lentivirus-transfected MKN-45 cells to observe the changes in tumor size and body weight. The results revealed that the OE group had smaller tumors compared to the NC group (Figure 6A and B). According to tumor growth data, it was found that back tumor growth was notably slower in the OE group compared to the NC group (Figure 6C). Additionally, the weight of BABL/c nude mice in the OE group increased significantly (Figure 6D), which indicated that miR-204-3p overexpression suppressed subcutaneous tumorigenesis in BABL/c nude mice.

Effect of miR-204-3p on the MAPK signaling pathway

We investigated the effect of miR-204-3p on the MAPK signaling pathway. Firstly, the impact of miR-204-3p on the



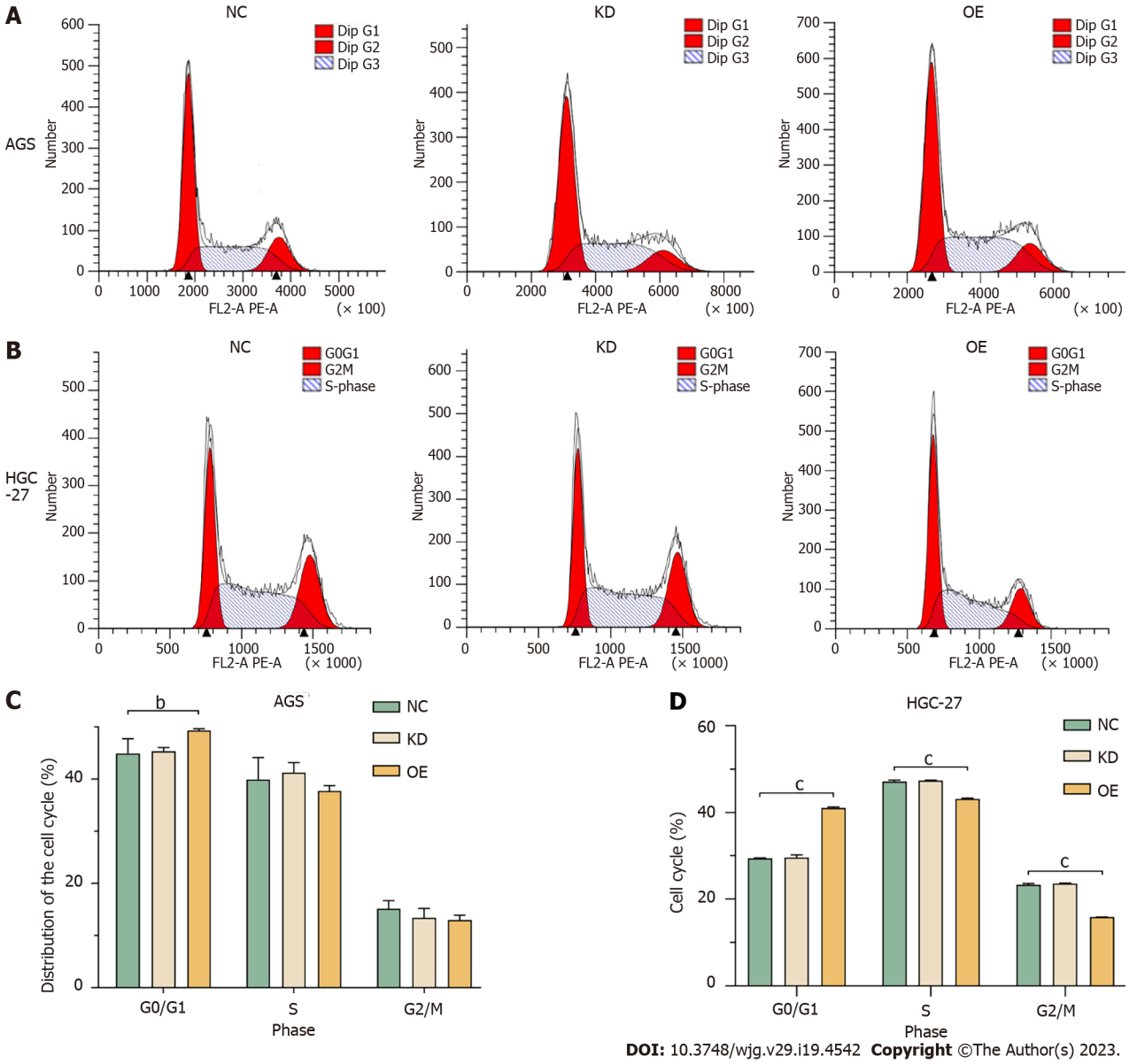
DOI: 10.3748/wjg.v29.i29.4542 **Copyright** ©The Author(s) 2023.

Figure 4 Effects of miR-204-3p on apoptosis in AGS and HGC-27 cells. A and B: Flow cytometry was used to analyze apoptosis of AGS and HGC-27 cells; C and D: Statistical results of AGS and HGC-27 cell apoptosis. °$P < 0.001$. NC: Empty lentiviral vector; KD: miR-204-3p knockdown lentiviral vector; OE: miR-204-3p overexpression lentiviral vector.

mRNA levels of *KRAS*, *ERK1* and *ERK2* was detected using qRT-PCR. The results revealed that miR-204-3p overexpression resulted in a significant decrease in *KRAS*, *ERK1* and *ERK2* in AGS and HGC-27 cells (Figure 7A and B). We further investigated the impact of miR-204-3p on the MAPK signaling pathway-related proteins, including KRAS, ERK1/2, and p-ERK1/2. The results showed that in HGC-27 and AGS cells, miR-204-3p overexpression caused noteworthy lower levels of KRAS and p-ERK1/2, but no significant difference was observed in ERK1/2 (Figure 7C-F). These findings indicated that miR-204-3p overexpression effectively inhibited GC cell proliferation, and this effect was achieved through the inhibition of KRAS, which subsequently prevented the phosphorylation of downstream effector protein ERK1/2 in the MAPK signaling pathway.

Effects of miR-204-3p on apoptosis-related proteins

The effect of miR-204-3p on apoptosis-related proteins in GC cells was investigated. The results indicated a reduction in BCL-2 and the BCL-2/BAX ratio, as well as an increase in Caspase-3 in the OE group (Figure 8A-D), which confirmed that miR-204-3p overexpression stimulated GC cell apoptosis *via* the BCL-2/BAX signaling pathway.



DOI: 10.3748/wjg.v29.i19.4542 **Copyright** ©The Author(s) 2023.

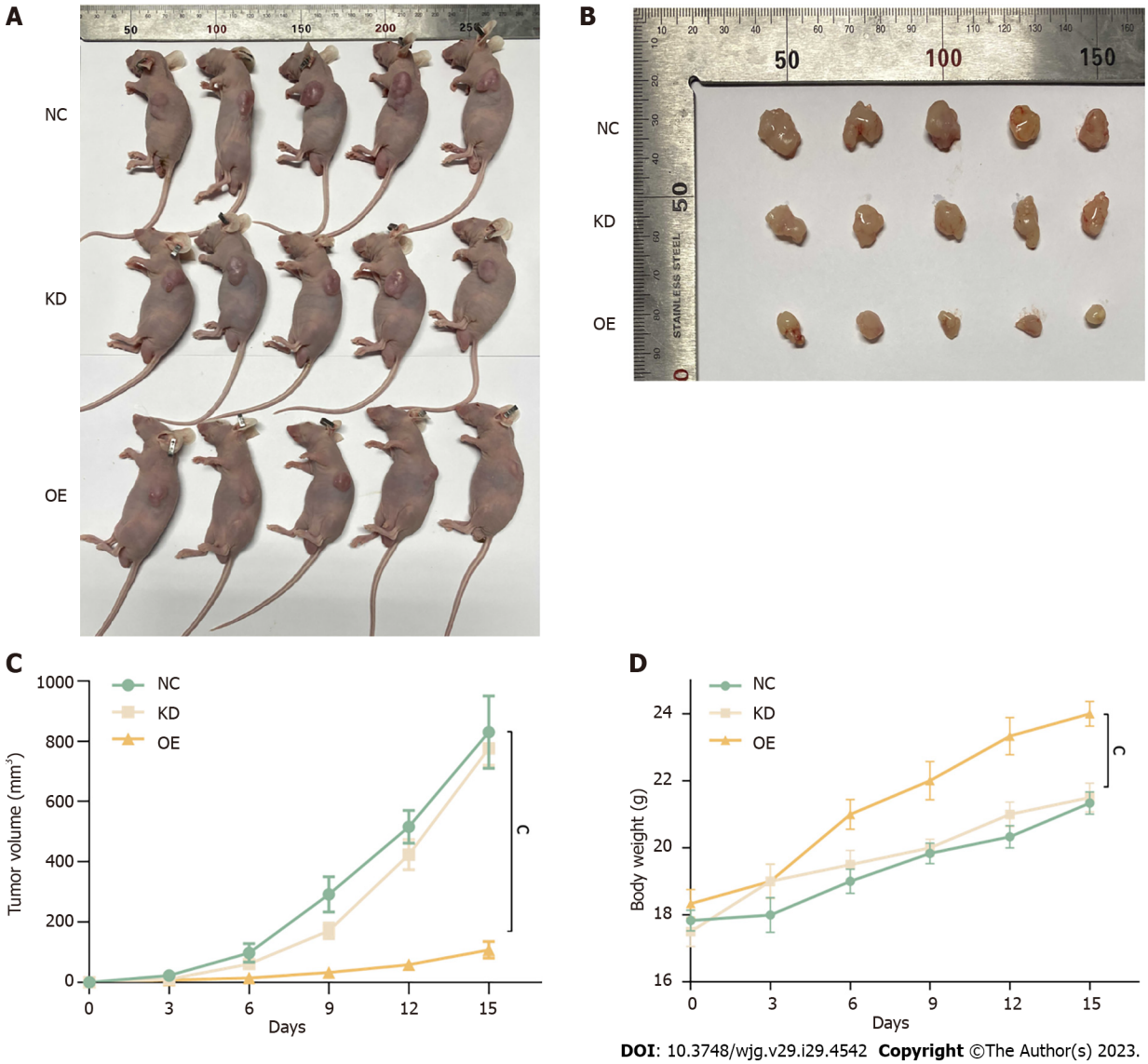
Figure 5 Effects of miR-204-3p on the cell cycle in AGS and HGC-27 cells. A and B: Cell cycle analysis in AGS and HGC-27 cells by flow cytometry; C and D: Percentage of cell cycle distribution in AGS and HGC-27 cells. $^{b}P < 0.01$, $^{c}P < 0.001$. NC: Empty lentiviral vector; KD: miR-204-3p knockdown lentiviral vector; OE: miR-204-3p overexpression lentiviral vector.

Effect of miR-204-3p on necroptosis-related proteins

We examined the protein changes in RIP1, p-RIP1, MLK1 and p-MLK1 during necroptosis and investigated the impact of miR-204-3p on GC cells necroptosis. The results revealed that miR-204-3p overexpression significantly inhibited the protein expression levels of p-RIP1 and p-MLK1 (Figure 8E-H), which confirmed that miR-204-3p overexpression inhibited GC cells necroptosis *via* the RIP1/MLK1 signaling pathway.

DISCUSSION

MiR-204-3p plays a crucial role in various diseases. Some studies have confirmed that miR-204-3p upregulation can be targeted to inhibit Nox4 to reduce memory deficits[21]. Moreover, its overexpression inhibited high glucose induced lens epithelial cells migration and epithelial-mesenchymal transition (EMT), and inhibited high glucose induced podocytes apoptosis and dysfunction[13,15]. Notably, miR-204-3p upregulation inhibited malignant melanoma migration, invasion and EMT progression by targeting inhibition of PAX2[19], its upregulation also inhibited hepatocellular carcinoma cell proliferation by targeting inhibition of FN1[22]. MiR-204-3p was found to be underexpressed in bladder cancer tissues and was related to poor prognosis, it regulated bladder cancer cell proliferation by targeting LDHA mediated glycolysis [16]. Apoptosis of glioma cells is induced by miR-204-3p targeting IGFBP2[23]. Furthermore, LINC00963 was overexpressed in osteosarcoma tissues and was related to poor prognosis, miR-204-3p reversed LINC00963 in promoted



DOI: 10.3748/wjg.v29.i29.4542 **Copyright** ©The Author(s) 2023.

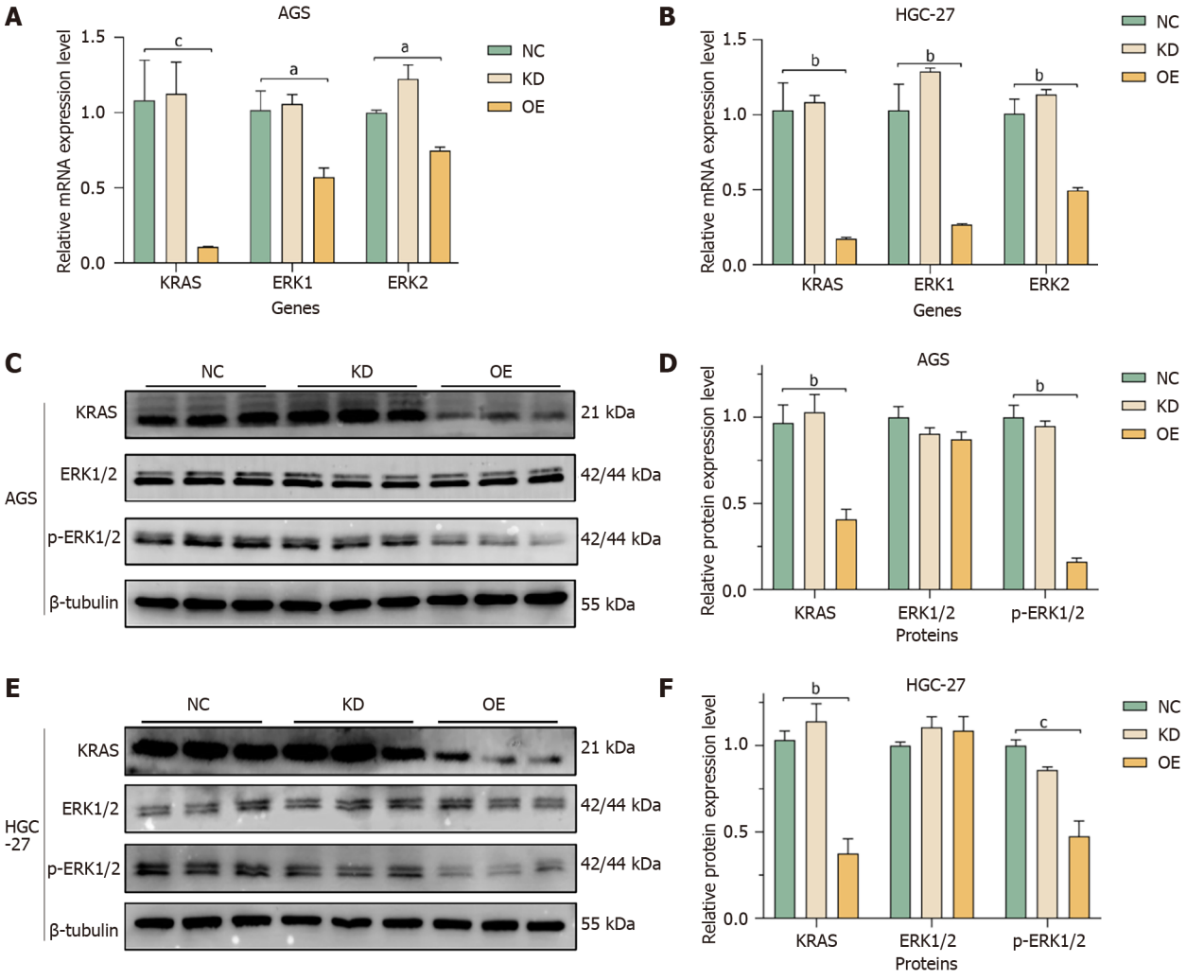
Figure 6 Effect of miR-204-3p on tumor size in BABL/c nude mice. A: Comparison of gastric carcinoma tumor xenograft models in BABL/c nude mice; B: Comparison of subcutaneous tumors on the back in BABL/c nude mice; C: Statistical graph of tumor growth curve for gastric carcinoma tumor xenograft models in BABL/c nude mice; D: Statistical graph of body weight growth curve in BABL/c nude mice. $^{c}P < 0.001$. NC: Empty lentiviral vector; KD: miR-204-3p knockdown lentiviral vector; OE: miR-204-3p overexpression lentiviral vector.

osteosarcoma cell proliferation and inhibited migration and invasion[24]. LINC00514 was upregulated in GC tissues, its overexpression stimulated GC cell growth and inhibited EMT by sponging miR-204-3p/KRAS[20]. These results suggest that miR-204-3p may be a new target for cancer therapy.

Firstly, we found that the expression of miR-204-3p was low in GC cells, and its overexpression resulted in the inhibition of cell proliferation, colony formation ability, and the cell cycle, while promoting apoptosis. *In vivo* tumor formation experiments in 4-week-old BABL/c nude mice verified that miR-204-3p overexpression inhibited subcutaneous tumor growth. Thus, both *in vitro* and *in vivo* experiments demonstrated the inhibitory influence of miR-204-3p overexpression on GC cells.

Apoptosis, a programmed cell death, is a natural barrier against tumorigenesis. However, in cancer, abnormal expression of anti-apoptotic or pro-apoptotic proteins causes inhibition of apoptotic pathways[25]. For instance, BCL-2 functions as an anti-apoptotic protein, preventing cytochrome C liberation from mitochondria, thereby inhibiting apoptosis. On the other hand, BAX is a common pro-apoptotic protein that can form homodimers or bind to BCL-2 to form heterodimers that activate Caspase-3 to promote apoptosis[26]. The BCL-2/BAX ratio is closely related to tumor progression, and a lower ratio indicates a stronger apoptosis effect. Therefore, most anti-cancer drugs rely on the BCL-2/BAX mechanism to kill cancer cells[27]. This study verified that miR-204-3p overexpression led to the upregulation of Caspase-3 in GC cells, while downregulating BCL-2 and the BCL-2/BAX ratio. These findings provide evidence that miR-204-3p overexpression can stimulate apoptosis and inhibit GC cell proliferation through the BCL-2/BAX/Caspase-3 apoptosis pathway.

In tumors, the MAPK pathway is frequently activated to control apoptosis, cell growth, and cell division[28]. Signal transmission of the MAPK signaling pathway follows a three-step enzyme-linked reaction. KRAS, as an upstream



DOI: 10.3748/wjg.v29.i29.4542 **Copyright** ©The Author(s) 2023.

Figure 7 Effect of miR-204-3p on the MAPK signaling pathway in AGS and HGC-27 cells. A and B: Effects of miR-204-3p on mRNA levels of *KRAS*, *ERK1* and *ERK2* in AGS and HGC-27 cells; C and D: Effects of miR-204-3p on protein levels of *KRAS*, *ERK1/2* and *p-ERK1/2* in AGS cells; E and F: Effects of miR-204-3p on protein levels of *KRAS*, *ERK1/2* and *p-ERK1/2* in HGC-27 cells. $^{a}P < 0.05$, $^{b}P < 0.01$, $^{c}P < 0.001$. NC: Empty lentiviral vector; KD: miR-204-3p knockdown lentiviral vector; OE: miR-204-3p overexpression lentiviral vector.

activation protein, is activated when bound to GTP. This change causes the recruitment of KRAS to RAF on the cell membrane and promotes RAF activation. Activated RAF phosphorylates and activates MEK, while MEK phosphorylates and further activates ERK, which is located at the end of the signaling pathway and can transfer into the nucleus and bind to transcription factors, thereby regulating transcription programs and mediating cell growth, migration and differentiation[29-31]. Previously, we established that miR-204-3p targeted KRAS[20]. The current study confirmed that miR-204-3p upregulation can inhibit KRAS and p-ERK1/2, which suggested that miR-204-3p overexpression could inhibit the MAPK signaling pathway.

Necroptosis is a newly discovered mechanism of programmed cell death that has the potential to regulate tumorigenesis[32]. This process is primarily regulated by three proteins: RIP1, RIP3 and MLK1. Specifically, RIP1 is activated through phosphorylation, which then recruits RIP3[33]. Once activated, phosphorylated RIP3 can oligomerize MLK1 and transfer it to the plasma membrane, ultimately resulting in necroptosis characterized by cell swelling and organelle damage[34,35]. Interestingly, necroptosis has been found to both promote and inhibit cancer growth. As a form of cell death, necroptosis inhibits the development of tumors, yet it may also incite an inflammatory reaction that encourages cancer metastasis and immunosuppression. Research has revealed that glioblastoma, pancreatic cancer, and lung cancer can be impacted by the upregulation of RIP1, RIP3, and MLK1[36-38]. It was found that downregulation of MLK1 inhibited tumor cell growth and increased sensitivity to radiotherapy in both GC and ovarian cancer[39,40]. We detected necroptosis-related proteins and discovered that miR-204-3p overexpression decreased p-RIP1 and p-MLK1. These findings suggest that miR-204-3p overexpression can inhibit necroptosis through the RIP1/MLK1 pathway, ultimately inhibiting GC cell proliferation.

To sum up, our study verified that miR-204-3p is underexpressed in GC, and that its overexpression inhibits GC cell proliferation, promotes apoptosis, arrests the cell cycle in the G0/G1 phase, inhibits cell colony formation and the formation of subcutaneous tumors. Necroptosis is typically initiated by tumor necrosis factor (TNF) stimulation[41]. RIP1 binds to FADD, which then recruits caspase-8. The activation of caspase-8 promotes the process of RIP1-dependent

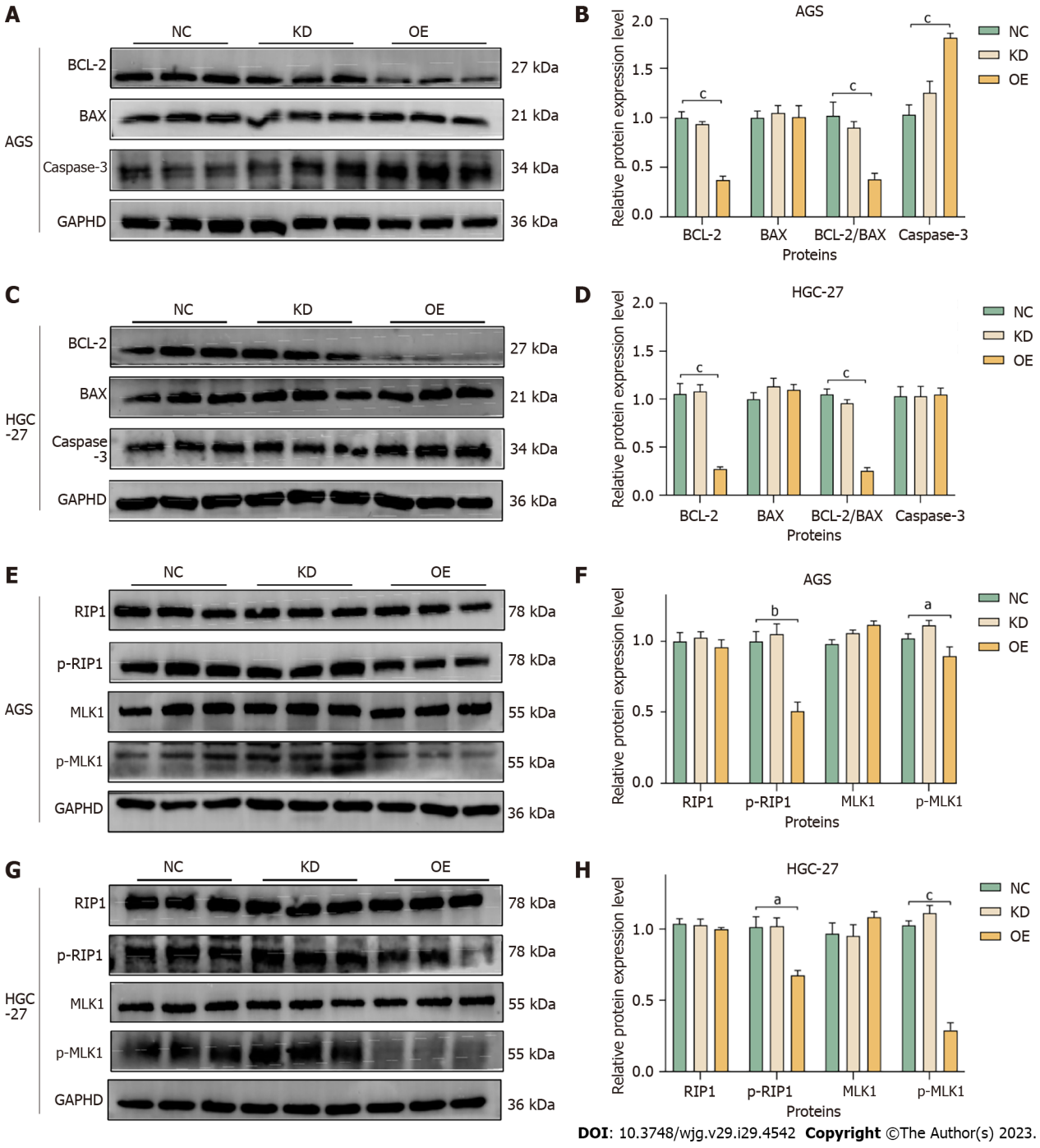
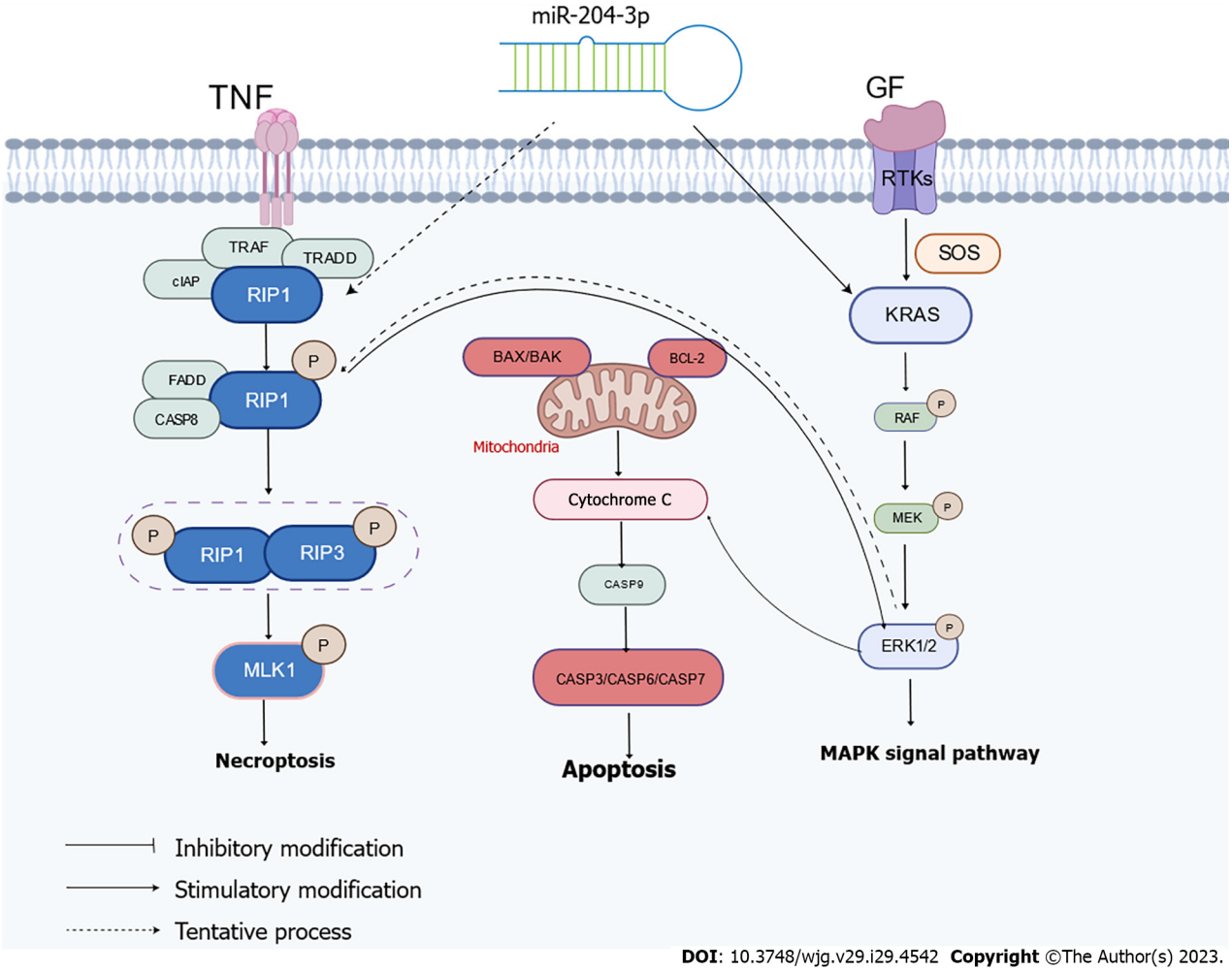


Figure 8 Effects of miR-204-3p on apoptosis-related proteins and necroptosis-related proteins in AGS and HGC-27 cells. A and B: Effect of miR-204-3p on apoptosis-related proteins BCL-2, BAX and Caspase-3 in AGS cells; C and D: Effect of miR-204-3p on apoptosis-related proteins BCL-2, BAX and Caspase-3 in HGC-27 cells; E and F: Effects of miR-204-3p on necroptosis-related proteins RIP1, p-RIP1, MLK1, and p-MLK1 in AGS cells; G and H: Effects of miR-204-3p on necroptosis-related proteins RIP1, p-RIP1, MLK1, and p-MLK1 in HGC-27 cells. $^{a}P < 0.05$, $^{b}P < 0.01$, $^{c}P < 0.001$. NC: Empty lentiviral vector; KD: miR-204-3p knockdown lentiviral vector; OE: miR-204-3p overexpression lentiviral vector.

apoptosis[32]. Additionally, RIP1 activates ERK to regulate the MAPK signaling pathway[42-44]. In the MAPK signaling pathway, phosphorylation of ERK can activate BCL-2, which in turn stimulates the apoptosis pathway and accelerates the process of apoptosis[45,46]. We verified that miR-204-3p overexpression can inhibit GC cell proliferation by inhibiting the MAPK signaling pathway and inhibiting the RIP1/MLK1 necroptosis pathway to promote the BCL-2/BAX/Caspase-3 apoptosis pathway (Figure 9).

CONCLUSION

MiR-204-3p overexpression inhibited GC cell proliferation by inhibiting the MAPK pathway and necroptosis pathway to



DOI: 10.3748/wjg.v29.i29.4542 **Copyright** ©The Author(s) 2023.

Figure 9 Mechanism of the effect of miR-204-3p on the MAPK signaling pathway, apoptosis and necroptosis. TNF: Tumor necrosis factor; GF: Germ-free.

promote GC cell apoptosis. Thus, miR-204-3p may represent a new potential therapeutic target for GC.

ARTICLE HIGHLIGHTS

Research background

Gastric carcinoma (GC) is a common gastrointestinal malignancy worldwide. Based on the cancer-related mortality, the current prevention and treatment strategies for GC still show poor clinical results. Therefore, it is important to find effective treatment targets.

Research motivation

At present, the main treatment for GC is surgery, chemotherapy and radiotherapy, but the therapeutic effect is not ideal.

Research objectives

To explore the effect of miR-204-3p on GC cells.

Research methods

We determined the expression level of miR-204-3p in GC, and then used an miR-204-3p overexpression vector and an miR-204-3p knockdown vector in GC cells. The influence of miR-204-3p on the changes in cell phenotype and tumorigenicity *in vivo* was assessed. Furthermore, the effects of miR-204-3p on various proteins related to the MAPK signaling pathway, necroptosis signaling pathway and apoptosis signaling pathway in GC cells were investigated.

Research results

It was found that miR-204-3p was underexpressed in GC, and miR-204-3p overexpression inhibited GC cell viability, promoted cell apoptosis, blocked the cell cycle, inhibited colony formation ability and inhibited tumorigenicity *in vivo*. It

was also verified that miR-204-3p overexpression can promote apoptosis by inhibiting the MAPK pathway and the necroptosis pathway, thus inhibiting GC cell proliferation.

Research conclusions

MiR-204-3p overexpression inhibited GC cell proliferation by inhibiting the MAPK pathway and the necroptosis pathway to promote GC cell apoptosis.

Research perspectives

MiR-204-3p can be used for targeted therapy of GC, and can also be used as a new biomarker for GC.

ACKNOWLEDGEMENTS

The authors would like to acknowledge Li-Qun Wang for statistical analysis assistance. Thanks to the Key Laboratory of Hui Ethnic Medicine Modernization of Ministry of Education for providing experimental equipment and space.

FOOTNOTES

Author contributions: Li X carried out most of the studies, analyzed the data, and wrote the manuscript; Nan Y designed the study and revised the manuscript; Tibenda JJ, Du YH and Huang SC wrote the manuscript, and conducted the chart-making work; Ning N and Chen GQ were responsible for the total transcriptomic; Yang YT and Meng FD performed parts of the *in vivo* and *in vitro* experiments, and conducted statistical analysis of the data; Yuan L and Nan Y provided the conceptual and technical guidance and revised the manuscript critically for important intellectual content; all authors have read and approved the manuscript.

Supported by Ningxia Natural Science Foundation, No. 2022AAC03144.

Institutional review board statement: This manuscript does not involve human experiments.

Institutional animal care and use committee statement: The animal study protocol was approved by the Institutional Animal Care and Use Committee of Ningxia Medical University, No. IACUC-NYLAC-2022-251.

Conflict-of-interest statement: All authors declare no financial or commercial conflict of interest for this article. This article was published during the period of Ling Yuan granted "Young Scholars of Western China"(Class A)_West Light Foundation of the Chinese Academy of Sciences.

Data sharing statement: All data generated or analyzed during this study are included in this paper, and further inquiries can be directed to the corresponding author (E-mail: 20080017@nxmu.edu.cn).

ARRIVE guidelines statement: The authors have read the ARRIVE guidelines, and the manuscript was prepared and revised according to the ARRIVE guidelines.

Open-Access: This article is an open-access article that was selected by an in-house editor and fully peer-reviewed by external reviewers. It is distributed in accordance with the Creative Commons Attribution NonCommercial (CC BY-NC 4.0) license, which permits others to distribute, remix, adapt, build upon this work non-commercially, and license their derivative works on different terms, provided the original work is properly cited and the use is non-commercial. See: https://creativecommons.org/Licenses/by-nc/4.0/

Country/Territory of origin: China

ORCID number: Xia Li 0000-0002-4981-9768; Yi Nan 0000-0002-5511-9266; Shi-Cong Huang 0009-0002-5996-0797; Yu-Hua Du 0000-0002-9669-8065; Ling Yuan 0000-0003-2838-0976.

S-Editor: Fan JR
L-Editor: Webster JR
P-Editor: Yu HG

REFERENCES

1 **Smyth EC**, Nilsson M, Grabsch HI, van Grieken NC, Lordick F. Gastric cancer. *Lancet* 2020; **396**: 635-648 [PMID: 32861308 DOI: 10.1016/S0140-6736(20)31288-5]

2 **Sung H**, Ferlay J, Siegel RL, Laversanne M, Soerjomataram I, Jemal A, Bray F. Global Cancer Statistics 2020: GLOBOCAN Estimates of Incidence and Mortality Worldwide for 36 Cancers in 185 Countries. *CA Cancer J Clin* 2021; **71**: 209-249 [PMID: 33538338 DOI: 10.3322/caac.21660]

3 **Banks M**, Graham D, Jansen M, Gotoda T, Coda S, di Pietro M, Uedo N, Bhandari P, Pritchard DM, Kuipers EJ, Rodriguez-Justo M, Novelli

MR, Ragunath K, Shepherd N, Dinis-Ribeiro M. British Society of Gastroenterology guidelines on the diagnosis and management of patients at risk of gastric adenocarcinoma. *Gut* 2019; **68**: 1545-1575 [PMID: 31278206 DOI: 10.1136/gutjnl-2018-318126]

4 **Sung JK**. Diagnosis and management of gastric dysplasia. *Korean J Intern Med* 2016; **31**: 201-209 [PMID: 26932397 DOI: 10.3904/kjim.2016.021]

5 **Miller KD**, Nogueira L, Mariotto AB, Rowland JH, Yabroff KR, Alfano CM, Jemal A, Kramer JL, Siegel RL. Cancer treatment and survivorship statistics, 2019. *CA Cancer J Clin* 2019; **69**: 363-385 [PMID: 31184787 DOI: 10.3322/caac.21565]

6 **Liu H**, Xu J, Yao Q, Zhang Z, Guo Q, Lin J. Rab7 Is Associated with Poor Prognosis of Gastric Cancer and Promotes Proliferation, Invasion, and Migration of Gastric Cancer Cells. *Med Sci Monit* 2020; **26**: e922217 [PMID: 32591494 DOI: 10.12659/MSM.922217]

7 **Hill M**, Tran N. miRNA interplay: mechanisms and consequences in cancer. *Dis Model Mech* 2021; **14** [PMID: 33973623 DOI: 10.1242/dmm.047662]

8 **Saliminejad K**, Khorram Khorshid HR, Soleymani FS, Ghaffari SH. An overview of mi-croRNAs: Biology, functions, therapeutics, and analysis methods. *J Cell Physiol* 2019; **234**: 5451-5465 [DOI: 10.1002/jcp.27486]

9 **Matsuo M**, Nakada C, Tsukamoto Y, Noguchi T, Uchida T, Hijiya N, Matsuura K, Moriyama M. MiR-29c is downregulated in gastric carcinomas and regulates cell proliferation by targeting RCC2. *Mol Cancer* 2013; **12**: 15 [PMID: 23442884 DOI: 10.1186/1476-4598-12-15]

10 **Shin JY**, Kim YI, Cho SJ, Lee MK, Kook MC, Lee JH, Lee SS, Ashktorab H, Smoot DT, Ryu KW, Kim YW, Choi IJ. MicroRNA 135a suppresses lymph node metastasis through down-regulation of ROCK1 in early gastric cancer. *PLoS One* 2014; **9**: e85205 [PMID: 24465504 DOI: 10.1371/journal.pone.0085205]

11 **Yang M**, Shan X, Zhou X, Qiu T, Zhu W, Ding Y, Shu Y, Liu P. miR-1271 regulates cisplatin resistance of human gastric cancer cell lines by targeting IGF1R, IRS1, mTOR, and BCL2. *Anticancer Agents Med Chem* 2014; **14**: 884-891 [PMID: 24875127 DOI: 10.2174/1871520614666140528161318]

12 **Gao L**, Zhao C, Li S, Dou Z, Wang Q, Liu J, Ren W, Zhi K. circ-PKD2 inhibits carcinogenesis *via* the miR-204-3p/APC2 axis in oral squamous cell carcinoma. *Mol Carcinog* 2019; **58**: 1783-1794 [PMID: 31206208 DOI: 10.1002/mc.23065]

13 **Han X**, Li Q, Wang C, Li Y. MicroRNA-204-3p Attenuates High Glucose-Induced MPC5 Podocytes Apoptosis by Targeting Braykinin B2 Receptor. *Exp Clin Endocrinol Diabetes* 2019; **127**: 387-395 [PMID: 29940664 DOI: 10.1055/a-0630-0173]

14 **Liu X**, Guo JW, Lin XC, Tuo YH, Peng WL, He SY, Li ZQ, Ye YC, Yu J, Zhang FR, Ma MM, Shang JY, Lv XF, Zhou AD, Ouyang Y, Wang C, Pang RP, Sun JX, Ou JS, Zhou JG, Liang SJ. Macrophage NFATc3 prevents foam cell formation and atherosclerosis: evidence and mechanisms. *Eur Heart J* 2021; **42**: 4847-4861 [PMID: 34570211 DOI: 10.1093/eurheartj/ehab660]

15 **Li X**, Sun M, Cheng A, Zheng G. LncRNA GAS5 regulates migration and epithelial-to-mesenchymal transition in lens epithelial cells *via* the miR-204-3p/TGFBR1 axis. *Lab Invest* 2022; **102**: 452-460 [PMID: 34916611 DOI: 10.1038/s41374-021-00713-3]

16 **Guo J**, Zhao P, Liu Z, Li Z, Yuan Y, Zhang X, Yu Z, Fang J, Xiao K. MiR-204-3p Inhibited the Proliferation of Bladder Cancer Cells *via* Modulating Lactate Dehydrogenase-Mediated Glycolysis. *Front Oncol* 2019; **9**: 1242 [PMID: 31850191 DOI: 10.3389/fonc.2019.01242]

17 **Guo Q**, Fan Y, Wang Q, Li B, Qiu W, Qi Y, Pan Z, Zhang S, Zhao S, Yang K, Xu H, Li M, Gao Z, Xu J, Wang H, Wang S, Tang Q, Qiu J, Guo X, Deng L, Zhang P, Zhao R, Xue H, Wang C, Li G. Glioblastoma upregulates SUMOylation of hnRNP A2/B1 to eliminate the tumor suppressor miR-204-3p, accelerating angiogenesis under hypoxia. *Cell Death Dis* 2023; **14**: 147 [PMID: 36810326 DOI: 10.1038/s41419-023-05663-w]

18 **Ma H**, Shi Q, Fang J, Wang R, Zhao J, Lin S, Dong J, Zhang Y, Shen X, Chen J, Zhong Q. Long non-coding RNA AFAP1-AS1 promotes thyroid cancer progression by sponging miR-204-3p and upregulating DUSP4. *J Biochem* 2022; **171**: 131-140 [PMID: 34652441 DOI: 10.1093/jb/mvab109]

19 **Song J**, Chen X, Zhang L, Song D, Xiong H. MicroRNA-204-3p modulates epithelial-mesenchymal transition by targeting paired box gene 2 in human melanoma A-375 cells. *Transl Cancer Res* 2019; **8**: 2032-2043 [PMID: 35116952 DOI: 10.21037/tcr.2019.09.10]

20 **Yuan L**, Li J, Yang Y, Chen Y, Bu Y, Ye M, Mao X, Ma T, Yu L, Nan Y. LINC00514 promotes gastric cancer cell growth and EMT progression *via* miR-204-3p/KRAS. *Aging (Albany NY)* 2021; **13**: 12007-12015 [PMID: 33888645 DOI: 10.18632/aging.202905]

21 **Tao W**, Yu L, Shu S, Liu Y, Zhuang Z, Xu S, Bao X, Gu Y, Cai F, Song W, Xu Y, Zhu X. miR-204-3p/Nox4 Mediates Memory Deficits in a Mouse Model of Alzheimer's Disease. *Mol Ther* 2021; **29**: 396-408 [PMID: 32950103 DOI: 10.1016/j.ymthe.2020.09.006]

22 **Cui ZH**, Shen SQ, Chen ZB, Hu C. Growth inhibition of hepatocellular carcinoma tumor endothelial cells by miR-204-3p and underlying mechanism. *World J Gastroenterol* 2014; **20**: 5493-5504 [PMID: 24833879 DOI: 10.3748/wjg.v20.i18.5493]

23 **Chen PH**, Chang CK, Shih CM, Cheng CH, Lin CW, Lee CC, Liu AJ, Ho KH, Chen KC. The miR-204-3p-targeted IGFBP2 pathway is involved in xanthohumol-induced glioma cell apoptotic death. *Neuropharmacology* 2016; **110**: 362-375 [PMID: 27487563 DOI: 10.1016/j.neuropharm.2016.07.038]

24 **Zhou Y**, Yin L, Li H, Liu LH, Xiao T. The LncRNA LINC00963 facilitates osteosarcoma proliferation and invasion by suppressing miR-204-3p/FN1 axis. *Cancer Biol Ther* 2019; **20**: 1141-1148 [PMID: 30975024 DOI: 10.1080/15384047.2019.1598766]

25 **Holdenrieder S**, Stieber P. Apoptotic markers in cancer. *Clin Biochem* 2004; **37**: 605-617 [PMID: 15234242 DOI: 10.1016/j.clinbiochem.2004.05.003]

26 **Pistritto G**, Trisciuoglio D, Ceci C, Garufi A, D'Orazi G. Apoptosis as anticancer mechanism: function and dysfunction of its modulators and targeted therapeutic strategies. *Aging (Albany NY)* 2016; **8**: 603-619 [PMID: 27019364 DOI: 10.18632/aging.100934]

27 **Pan LL**, Wang AY, Huang YQ, Luo Y, Ling M. Mangiferin induces apoptosis by regulating Bcl-2 and Bax expression in the CNE2 nasopharyngeal carcinoma cell line. *Asian Pac J Cancer Prev* 2014; **15**: 7065-7068 [PMID: 25227792 DOI: 10.7314/apjcp.2014.15.17.7065]

28 **Buchegger K**, Silva R, López J, Ili C, Araya JC, Leal P, Brebi P, Riquelme I, Roa JC. The ERK/MAPK pathway is overexpressed and activated in gallbladder cancer. *Pathol Res Pract* 2017; **213**: 476-482 [PMID: 28285962 DOI: 10.1016/j.prp.2017.01.025]

29 **Santarpia L**, Lippman SM, El-Naggar AK. Targeting the MAPK-RAS-RAF signaling pathway in cancer therapy. *Expert Opin Ther Targets* 2012; **16**: 103-119 [PMID: 22239440 DOI: 10.1517/14728222.2011.645805]

30 **Whelan JT**, Hollis SE, Cha DS, Asch AS, Lee MH. Post-transcriptional regulation of the Ras-ERK/MAPK signaling pathway. *J Cell Physiol* 2012; **227**: 1235-1241 [PMID: 21688267 DOI: 10.1002/jcp.22899]

31 **Yuan J**, Dong X, Yap J, Hu J. The MAPK and AMPK signalings: interplay and implication in targeted cancer therapy. *J Hematol Oncol* 2020; **13**: 113 [PMID: 32807225 DOI: 10.1186/s13045-020-00949-4]

32 **Gong Y**, Fan Z, Luo G, Yang C, Huang Q, Fan K, Cheng H, Jin K, Ni Q, Yu X, Liu C. The role of necroptosis in cancer biology and therapy. *Mol Cancer* 2019; **18**: 100 [PMID: 31122251 DOI: 10.1186/s12943-019-1029-8]

33 **Zhang Y**, Su SS, Zhao S, Yang Z, Zhong CQ, Chen X, Cai Q, Yang ZH, Huang D, Wu R, Han J. RIP1 autophosphorylation is promoted by mitochondrial ROS and is essential for RIP3 recruitment into necrosome. *Nat Commun* 2017; **8**: 14329 [PMID: 28176780 DOI:

10.1038/ncomms14329]
34 **Cai Z**, Jitkaew S, Zhao J, Chiang HC, Choksi S, Liu J, Ward Y, Wu LG, Liu ZG. Plasma membrane translocation of trimerized MLKL protein is required for TNF-induced necroptosis. *Nat Cell Biol* 2014; **16**: 55-65 [PMID: 24316671 DOI: 10.1038/ncb2883]
35 **Sun L**, Wang H, Wang Z, He S, Chen S, Liao D, Wang L, Yan J, Liu W, Lei X, Wang X. Mixed lineage kinase domain-like protein mediates necrosis signaling downstream of RIP3 kinase. *Cell* 2012; **148**: 213-227 [PMID: 22265413 DOI: 10.1016/j.cell.2011.11.031]
36 **Seifert L**, Werba G, Tiwari S, Giao Ly NN, Alothman S, Alqunaibit D, Avanzi A, Barilla R, Daley D, Greco SH, Torres-Hernandez A, Pergamo M, Ochi A, Zambirinis CP, Pansari M, Rendon M, Tippens D, Hundeyin M, Mani VR, Hajdu C, Engle D, Miller G. The necrosome promotes pancreatic oncogenesis *via* CXCL1 and Mincle-induced immune suppression. *Nature* 2016; **532**: 245-249 [PMID: 27049944 DOI: 10.1038/nature17403]
37 **Wang Q**, Chen W, Xu X, Li B, He W, Padilla MT, Jang JH, Nyunoya T, Amin S, Wang X, Lin Y. RIP1 potentiates BPDE-induced transformation in human bronchial epithelial cells through catalase-mediated suppression of excessive reactive oxygen species. *Carcinogenesis* 2013; **34**: 2119-2128 [PMID: 23633517 DOI: 10.1093/carcin/bgt143]
38 **Park S**, Hatanpaa KJ, Xie Y, Mickey BE, Madden CJ, Raisanen JM, Ramnarain DB, Xiao G, Saha D, Boothman DA, Zhao D, Bachoo RM, Pieper RO, Habib AA. The receptor interacting protein 1 inhibits p53 induction through NF-kappaB activation and confers a worse prognosis in glioblastoma. *Cancer Res* 2009; **69**: 2809-2816 [PMID: 19339267 DOI: 10.1158/0008-5472.CAN-08-4079]
39 **He L**, Peng K, Liu Y, Xiong J, Zhu FF. Low expression of mixed lineage kinase domain-like protein is associated with poor prognosis in ovarian cancer patients. *Onco Targets Ther* 2013; **6**: 1539-1543 [PMID: 24204164 DOI: 10.2147/OTT.S52805]
40 **Ertao Z**, Jianhui C, Kang W, Zhijun Y, Hui W, Chuangqi C, Changjiang Q, Sile C, Yulong H, Shirong C. Prognostic value of mixed lineage kinase domain-like protein expression in the survival of patients with gastric caner. *Tumour Biol* 2016; **37**: 13679-13685 [PMID: 27473085 DOI: 10.1007/s13277-016-5229-1]
41 **Vandenabeele P**, Declercq W, Van Herreweghe F, Vanden Berghe T. The role of the kinases RIP1 and RIP3 in TNF-induced necrosis. *Sci Signal* 2010; **3**: re4 [PMID: 20354226 DOI: 10.1126/scisignal.3115re4]
42 **Liu Y**, Liu T, Lei T, Zhang D, Du S, Girani L, Qi D, Lin C, Tong R, Wang Y. RIP1/RIP3-regulated necroptosis as a target for multifaceted disease therapy (Review). *Int J Mol Med* 2019; **44**: 771-786 [PMID: 31198981 DOI: 10.3892/ijmm.2019.4244]
43 **Obitsu S**, Sakata K, Teshima R, Kondo K. Eleostearic acid induces RIP1-mediated atypical apoptosis in a kinase-independent manner *via* ERK phosphorylation, ROS generation and mitochondrial dysfunction. *Cell Death Dis* 2013; **4**: e674 [PMID: 23788031 DOI: 10.1038/cddis.2013.188]
44 **Filipczak PT**, Thomas C, Chen W, Salzman A, McDonald JD, Lin Y, Belinsky SA. TSC2 Deficiency Unmasks a Novel Necrosis Pathway That Is Suppressed by the RIP1/RIP3/MLKL Signaling Cascade. *Cancer Res* 2016; **76**: 7130-7139 [PMID: 27756752 DOI: 10.1158/0008-5472.CAN-16-1052]
45 **Vitagliano O**, Addeo R, D'Angelo V, Indolfi C, Indolfi P, Casale F. The Bcl-2/Bax and Ras/Raf/MEK/ERK signaling pathways: implications in pediatric leukemia pathogenesis and new prospects for therapeutic approaches. *Expert Rev Hematol* 2013; **6**: 587-597 [PMID: 24083449 DOI: 10.1586/17474086.2013.827415]
46 **Chang F**, Steelman LS, Shelton JG, Lee JT, Navolanic PM, Blalock WL, Franklin R, McCubrey JA. Regulation of cell cycle progression and apoptosis by the Ras/Raf/MEK/ERK pathway (Review). *Int J Oncol* 2003; **22**: 469-480 [PMID: 12579299]

World Journal of Gastroenterology

Submit a Manuscript: https://www.f6publishing.com

World J Gastroenterol 2023 August 7; 29(29): 4557-4570

DOI: 10.3748/wjg.v29.i29.4557

ISSN 1007-9327 (print) ISSN 2219-2840 (online)

ORIGINAL ARTICLE

Basic Study

Effect of exogenous hydrogen sulfide in the nucleus tractus solitarius on gastric motility in rats

Hong-Zhao Sun, Chen-Yu Li, Yuan Shi, Jin-Jin Li, Yi-Ya Wang, Li-Na Han, Lu-Jie Zhu, Ya-Fei Zhang

Specialty type: Gastroenterology and hepatology

Provenance and peer review: Unsolicited article; Externally peer reviewed.

Peer-review model: Single blind

Peer-review report's scientific quality classification

Grade A (Excellent): 0
Grade B (Very good): 0
Grade C (Good): C, C
Grade D (Fair): 0
Grade E (Poor): 0

P-Reviewer: Sato T, Japan; Zayachkivska O, Ukraine

Received: May 18, 2023
Peer-review started: May 18, 2023
First decision: June 20, 2023
Revised: June 29, 2023
Accepted: July 19, 2023
Article in press: July 19, 2023
Published online: August 7, 2023

Hong-Zhao Sun, Chen-Yu Li, Yuan Shi, Jin-Jin Li, Yi-Ya Wang, Li-Na Han, Lu-Jie Zhu, Ya-Fei Zhang, College of Life Science, Qi Lu Normal University, Zhangqiu 250200, Shandong Province, China

Corresponding author: Hong-Zhao Sun, PhD, Professor, College of Life Science, Qi Lu Normal University, No. 2 Wenbo Road, Zhangqiu 250200, Shandong Province, China.
sunhongzhao18@126.com

Abstract

BACKGROUND

Hydrogen sulfide (H_2S) is a recently discovered gaseous neurotransmitter in the nervous and gastrointestinal systems. It exerts its effects through multiple signaling pathways, impacting various physiological activities. The nucleus tractus solitarius (NTS), a vital nucleus involved in visceral sensation, was investigated in this study to understand the role of H_2S in regulating gastric function in rats.

AIM

To examine whether H_2S affects the nuclear factor kappa-B (NF-κB) and transient receptor potential vanilloid 1 pathways and the neurokinin 1 (NK1) receptor in the NTS.

METHODS

Immunohistochemical and fluorescent double-labeling techniques were employed to identify cystathionine beta-synthase (CBS) and c-Fos co-expressed positive neurons in the NTS during rat stress. Gastric motility curves were recorded by inserting a pressure-sensing balloon into the pylorus through the stomach fundus. Changes in gastric motility were observed before and after injecting different doses of NaHS (4 nmol and 8 nmol), physiological saline, Capsazepine (4 nmol) + NaHS (4 nmol), pyrrolidine dithiocarbamate (PDTC, 4 nmol) + NaHS (4 nmol), and L703606 (4 nmol) + NaHS (4 nmol).

RESULTS

We identified a significant increase in the co-expression of c-Fos and CBS positive neurons in the NTS after 1 h and 3 h of restraint water-immersion stress compared to the expressions observed in the control group. Intra-NTS injection of NaHS at different doses significantly inhibited gastric motility in rats ($P < 0.01$). However, injection of saline, first injection NF-κB inhibitor PDTC or transient receptor potential vanilloid 1 (TRPV1) antagonist Capsazepine or NK1 receptor blockers

L703606 and then injection NaHS did not produce significant changes ($P > 0.05$).

CONCLUSION

NTS contains neurons co-expressing CBS and c-Fos, and the injection of NaHS into the NTS can suppress gastric motility in rats. This effect may be mediated by activating TRPV1 and NK1 receptors *via* the NF-κB channel.

Key Words: Nucleus tractus solitarius; Hydrogen sulfide; Gastric motility; Nuclear factor kappa-B; Transient receptor potential vanilloid 1

©The Author(s) 2023. Published by Baishideng Publishing Group Inc. All rights reserved.

Core Tip: This study revealed a significant inhibitory effect of exogenous hydrogen sulfide on gastric motility in rats. This effect appeared to involve the release of substance P, potentially activating the transient receptor potential vanilloid 1 pathway mediated by nuclear factor kappa-B channels.

Citation: Sun HZ, Li CY, Shi Y, Li JJ, Wang YY, Han LN, Zhu LJ, Zhang YF. Effect of exogenous hydrogen sulfide in the nucleus tractus solitarius on gastric motility in rats. *World J Gastroenterol* 2023; 29(29): 4557-4570

URL: https://www.wjgnet.com/1007-9327/full/v29/i29/4557.htm

DOI: https://dx.doi.org/10.3748/wjg.v29.i29.4557

INTRODUCTION

The number of patients with stress-induced gastric ulcers has increased dramatically[1], and stress is highly associated with several functional gastrointestinal disorders, such as functional dyspepsia and irritable bowel syndrome[2]. The nucleus tractus solitarius (NTS) is a relay nucleus for visceral primary afferent neural signaling. It receives sensory afferents from visceral organs and projects to the spinal cord to regulate respiratory and cardiovascular activity. The NTS is also closely connected with various brain nuclei[3]. Recent studies have demonstrated the role of the NTS in cardiovascular and respiratory regulation and the reflex regulation of intragastric pressure. Synapses mediate the vagal-dependent gastric reflex between vagal afferent fibers and NTS neurons, and through the vagal preganglionic parasympathetic neurons in the dorsal vagal complex[4]. Neuronal firing studies in the NTS have shown that H_2S increases NTS-evoked postsynaptic currents by enhancing presynaptic glutamate release and affects the membrane potential of NTS neurons in a concentration-dependent manner[5].

Vagal afferent transmission primarily terminates in the NTS[6], which may act as a relay activator to inhibit spinal neuronal activity. Vagal-mediated glutamate release can regulate homeostasis by activating NTS neurons and metabotropic glutamate receptors, contributing to homeostatic regulation. Injection of oxytocin in the NTS has been observed to inhibit gastric smooth muscle diastole in rats, possibly through the cAMP-PKA signaling pathway[7]. The microinjection of monosodium glutamate in the NTS and the activation of NTS opioid receptors inhibit gastric motility and significant c-Fos expression in the dorsal motor nucleus of the vagus (DMV) neurons[8].

However, hydrogen sulfide (H_2S) is a recently discovered gas transmitter endogenously produced in the human and animal brain and organ tissues. Cystathionine beta-synthase (CBS) mainly synthesizes H_2S in the central nervous system and plays a significant physiological role[9] and has a protective role in neurodegenerative diseases such as Parkinson's disease[10] and Alzheimer's disease[11]. CBS is present in neurons and glial cells of the NTS, exerting excitatory effects and modulating synaptic neuronal activity[12]. Blocking CBS attenuates synaptic transmission in NTS neurons. Applying the H_2S donor NaHS also enhances synaptic transmission in NTS neurons. H_2S in the NTS plays an equally important role as a gaseous neuromodulator in maintaining or modulating autonomicand other systems[13]. In vitro experiments have shown that H_2S relaxes gastrointestinal smooth muscles, inhibiting spontaneous movements and responses to chemical or electrical stimuli[14]. H_2S also plays a role in other types of smooth muscle relaxation *via* K^+-ATP channels[15], suggesting that endogenous H_2S has a regulatory role in the gastrointestinal tract's motor function.

The nuclear factor kappa-B (NF-κB) pathway is activated by various factors and plays a crucial role in the immune response and inflammation. A study found that NaHS administration in the rat intraperitoneal *via* sulfhydration caused NF-κB activation and lung inflammation, a significant increase in p65 protein levels, vascular congestion, and neutrophil infiltration. Also, slight neuronal degeneration was observed in the rat heart, liver, and brain, suggesting that H_2S acts on NF-κB channels for messaging[16]. H_2S also interacts with nitric oxide to cause vasodilation, down-regulates NF-kB pathway-induced inflammation, fibrosis and damage from prolonged or intense oxidative stress; protects tissues from ischemia- and reperfusion-induced injury; and reduces immune rejection by reducing oxygen free radicals produced *in vivo*[17]. Additionally, H_2S demonstrates antioxidant and anti-apoptotic effects on neurons and glial cells[18].

Transient receptor potential vanilloid type 1 (TRPV1) is a non-selective calcium channel associated with nociceptive sensations in peripheral nerves. Its activation can lead to neurokinin 1 (NK1) receptor activation, pain, local neurogenic inflammation, and systemic anti-inflammatory/analgesic effects, and enhanced transmitter release in the NTS. TRPV1 involves various physiological and pathological processes[19,20]. Electrophysiological studies have shown that the

activation of TRPV1 by capsaicin enhances glutamate release to visceral sensory neurons, affecting NTS preganglionic neurons[21]. H_2S can cause peripheral inflammation and synaptic enhancement of glutamatergic signaling in the spinal cord by activating TRPV1 channels, thus stimulating other receptors at the terminals of capsaicin-sensitive neurons[22]. TRPV1 activation also leads to the release of substance P (SP), while NK1 receptors are responsible for neurally mediated digestive secretion and contributes to brain homeostasis and sensory neuronal transmission associated with depression, stress, anxiety and vomiting[23]. H_2S causes gastric juice secretion by stimulating TRPV1 receptors on primary afferent nerve fibers and modulates cholinergic neurons by releasing SP to act on NK1, NK2, or NK3 receptors[24]. Therefore, we speculate that TRPV1 channels may be involved in the effect of H_2S donors on gastric emptying.

SP is a neuroactive peptide involved in pain and inflammation[25]. It is widely present in the mammalian organism in the central, peripheral, and gastrointestinal nervous systems[26] and other tissues, participating in various physiopathological processes, including stress, emotional anxiety, and immune regulation. NK1 receptors are the primary receptors for SP and are widely expressed in the brain, contributing to stress and emotional anxiety[27]. SP is widely expressed in the NTS, mainly in the primary sensory neurons in the peripheral nervous system, and intrinsic neurons of the gastrointestinal tract. It has been shown to have neurotransmitter effects in the central and peripheral nervous systems and is associated with immune and inflammatory diseases of the respiratory and gastrointestinal systems[28].

Herein, we investigated the regulatory effects of H_2S in the NTS on rat gastric function and explore whether these effects were mediated by SP release *via* NF-κB channel-dependent activation of the TRPV1 pathway.

MATERIALS AND METHODS

Animal

The animals used in this experiment were 240-280 g adult male Wistar rats purchased from Jinan Panyue Experimental Animal Breeding Co and housed in separate cages at a constant temperature (22 °C ± 2 °C) given appropriate food and water based on their body weight. To allow them to acclimate to their surroundings, the rats were exposed to natural rhythmic light for one week before the start of the experiment.

Before the experiment, the rats underwent a 24-h fasting period, during which they were allowed to freely drink. The other environmental conditions remained consistent throughout the experiment. The Experimental Animal Ethics Committee of Qilu Normal University approved the experiment. All experiments complied with internationally accepted ethical standards. The study also adhered to the guidelines set by the International Association for the Study of Pain[29].

Chemicals

NaHS, L703606, PDTC, Capsazepine, and protamine sky blue were purchased from Sigma-Aldrich (St. Louis, MO, United States). NaHS was dissolved in 0.9% saline, while the other chemicals were dissolved in dimethyl sulfoxide and reconstituted in saline. For the immunohistochemical fluorescence double labeling, the following reagents were purchased from Servicebio (Wuhan, China): Goat serum, anti-CBS rabbit pAb, FITC-conjugated goat anti-rabbit IgG, Cy3-conjugated goat anti-mouse IgG, and anti-c-Fos mouse pAb.

Immunohistochemical fluorescence double labeling

We used the restraint water immersion stress model to investigate acute stress-induced gastric mucosal injury in rats. This acute compound stress model causes changes in gastric function in rats under stress through enhanced parasympathetic activity in the innervated stomach[30]. Once anesthetized, the rats were swiftly removed from the bottle and secured to a wooden board using medical tape to immobilize their limbs and teeth. When awake, the rats were then immersed in cold water (21 °C ± 1 °C) with the sternal process aligned with the water level. To minimize experimental error, consistent time points were selected for each experiment.

The rats were randomly divided into three groups (n = 6) based on the duration of restraint water-immersion stress (RWIS) (0 h, 1 h, or 3 h). Cardiac perfusion was performed using 500 mL of prepared 0.01 mol/L phosphate-buffered saline (PBS) followed by 500 mL of 4% 0.1 mol/L paraformaldehyde (PFA). After administering an overdose of isoflurane to sacrifice the rat, the thoracic cavity was opened along the sternal process, and the heart was exposed. The infuser needle was inserted into the heart's left ventricle, securing the heart, while the right auricle was incised to allow blood to drain. The rat's liver was flushed with 0.01 mol/L PBS buffer until it turned white, followed by perfusion with 4% PFA solution using a "fast and then slow" principle, gradually reducing the flow rate when the rat's limbs twitched.

Upon completion of perfusion, the rat's head was severed, and the brain was extracted. The brain was placed in a small wide-mouth flask containing 4% PFA and kept at 4 °C for 24 h. Subsequently, the fixed rat brain was transferred to a 0.1 mol/L 30% sucrose solution for dehydration. The frozen target nuclei region was then sectioned into 30 μm thick coronal sections using a sectioning machine and stored in 0.01 mol/L PBS.

Next, each well of a multi-well plate was filled with 500 μL of 0.01 mol/L PBS buffer to clean the brain slices and remove impurities. A methanolic solution of 3% H_2O_2 was added to block endogenous peroxidase activity. The wells were then incubated with a goat serum closure solution for 1 h to enhance cell membrane permeability. Subsequently, 500 μL of each primary antibody working solution was added, consisting of mouse anti-c-Fos (diluted at 1:500) and rabbit anti-CBS (diluted at 1:500), and incubated overnight at 4 °C.

Finally, 500 μL of each fluorescent secondary antibody working solution was added for 1 h. Any residual fluorescent secondary antibody was washed off with PBST. Previously treated with chromium-vanadium gelatin, the brain slides were placed on glass slides and allowed to dry naturally. The slides were sealed with an anti-fluorescence quencher, ensuring the removal of air bubbles using a vacuum. Finally, the sealed fluorescent glass slide was placed under an

Olympus Fluorescence confocal microscopy to observe and compare the brain atlas to determine the position of the NTS, observe the CBS and c-Fos-positive neurons number, and take pictures. The expression of c-Fos and CBS in the NTS was counted using Image Pro-Plus 6.0 software (Number/0.01 mm^2).

Experimental grouping

We evaluated the following subgroups to investigate the regulatory effects of NaHS in the NTS on gastric function and its underlying mechanisms. The chosen doses were based on pre-experiments and relevant literature[31]: (1) The effect of microinjection of NaHS (0.1 μL, 4 nmol; n = 6) in NTS on gastric motility; (2) the effect of microinjection of NaHS (0.1 μL, 8 nmol; n = 6) in NTS on gastric motility; (3) the effect of microinjection of saline (0.1 μL; n = 6) in NTS on gastric motility as a control group; (4) the effect of microinjection of NaHS (0.1 μL, 4 nmol) + PDTC (0.1 μL; n = 6) in NTS on gastric motility; (5) microinjection of NaHS (0.1 μL, 4 nmol) + Capsazepine (0.1 μL, 4 nmol; n = 6) in NTS on gastric motility; and (6) microinjection of NaHS (0.1 μL, 4 nmol) + L703606 (0.1 μL, 4 nmol; n = 6) in NTS on gastric motility.

Microinjection

Before conducting the experiments, the rats were anesthetized with 4% chloral hydrate at (400 mg/kg body weight) by intraperitoneal injection until the eyelids and corneal reflexes disappeared, the muscles were relaxed, and the breathing was uniform. The anesthetized rat head was fixed on a brain stereotaxic apparatus (Stoelting 68002, Shenzhen Ruiwode Company, China).

Next, the animal was fixed according to the rat brain stereotaxic atlas (Paxinos and Watson, 2007) using the three points of the animal's bilateral inner ear holes and incisors. With the left and right ear rods reading the same, fontanelle and bregma were kept at the same level with an error of no more than 0.3 mm.

The head hair was removed with hair clippers to expose the scalp and disinfected with 75% alcohol. Then, the scalp was cut along the sagittal suture of the skull with ophthalmic clippers to expose the skull, the excess connective tissue around the skull was cut away, and the surface of the skull was gently wiped with saline until the fontanelle and herringbone suture were exposed. The three-dimensional coordinates of fontanelle were used as the zero point. A small hole of approximately 2 mm in diameter was drilled in the skull ipsilateral to the coordinates of the NTS center point (13.3 mm posterior to fontanelle, 0.8 mm paracentral opening, 7.9 mm subdural) in the atlas using an electric cranial drill. A glass microelectrode with a tip of approximately 30 μm was placed into the brain at the depth of the coordinates.

Recording gastric motility

The anesthetized rats were placed abdomen side up, and a small incision was made in the fundus of the stomach to clean the gastric residue. A 5 mm diameter balloon filled with warm water was inserted into the pylorus of the gastric sinus and kept at a constant baseline pressure. The balloon inserted into the rat's stomach was connected to the pressure transducer and BL-420 (Biological Function Experimental System; Chengdu Taimeng Company, China) *via* a polyethylene plastic tube. The stimulation parameters of the transducer were adjusted to 25 mm/min speed, 0.5 mV/cm sensitivity, and 10 Hz filter. Once the gastric motility curve was stabilized, the drug's microinjections and contaminate sky blue were administered. A heat lamp was used throughout the experiment to maintain a constant ambient temperature, and gastric motility was recorded.

Histological identification of the microinjection site

After gastric motility recording, 2% pontamine sky blue (0.1 μL) was injected into the NTS, the rats were executed with an excess of sodium pentobarbital, and the thorax was opened for cardiac perfusion. After perfusion, the heads of the rats were cut off, and the brain tissues were removed and placed in a 4% formaldehyde solution for fixation.

Subsequently, the brain tissues were frozen at -16 °C for 30 min and sectioned into successive coronal sections with a thickness of 16 μm. The brainstem sections were stained, allowing for the identification of injection sites. The brain slices on slides were treated with a neutral red stain and dehydrated to achieve transparency. The sections were observed and photographed using a microscope (Nikon Optiphot, Nikon, Shanghai, China) and photographed with a digital camera (Magnafire; Optronics, Goleta, CA, United States) connected to a computer. The blue dot marking the precise location of the NTS was identified for further statistical analysis.

Data analysis and statistics

The gastric motility of the rats was assessed by counting the number of contractions before and 5 min after injection were counted respectively. The total duration of contraction waves (T.D.C.W) within 5 min, the total amplitude of contraction waves (T.A.C.W) within 5 min and the gastric motility index (the product of amplitude and duration) before and after the 5-min microinjection were evaluated statistically. To calculate the inhibition rate of gastric motility, the following formula was used: Inhibition rate (%) = (pre-injection value-post-injection value) × 100%/pre-injection value. The height between the highest point of the contraction curve and the baseline is the amplitude of the contraction wave. The time duration between the starting point and the ending point of the contraction wave is the time duration of the contraction wave.

Statistical analysis was performed using SPSS v25.0 (IBM SPSS Inc., Chicago, IL, United States) using Student's t-test or one-way ANOVA, followed by a posthoc test using the Student-Newman-Keuls test. All data are presented as mean ± SE. A P value less than 0.05 was considered statistically significant.

RESULTS

Observation of c-Fos and CBS expression in NTS at different times in RWIS

In this experiment, the number of CBS and c-Fos co-expressing neurons in the NTS (Figure 1, n = 6) was revealed by immunohistochemical fluorescence double-labeling. The expression of c-Fos protein in the NTS showed varying degrees of increase at 1 h (7.00 ± 0.37) and 3 h (4.83 ± 0.31) after RWIS compared to the control group at 0 h (1.83 ± 0.30) (P < 0.01). This finding indicates that CBS neurons in the NTS of rats were activated during the RWIS procedure.

NTS injection site identification

Following neutral red staining, the brain slices were examined under a light microscope to determine the localization of the injected blue spots and drugs within the NTS. The observed data regarding the gastric motility of rats in the correct position were analyzed. Figure 2 presents the diagram for identifying the degree of tissue localization.

NaHS inhibits gastrointestinal motility within NTS

The microinjection of physiological saline (PS) (0.1 μL, n = 6) under the same conditions did not produce a significant change in gastric motility (Figure 3A). In contrast, the microinjection of NaHS at different concentrations (4 nmol and 8 nmol, 0.1 μL, n = 6) into the rat NTS resulted in significant inhibition of gastric motility (Figure 3B and C).

We compared gastric motility curves measured before and 5 min after the drug injection and after 4 nmol NaHS injection in the NTS. The T.A.C.W. decreased from 553.08 mm 5 min^{-1} ± 9.59 mm 5 min^{-1} to 421.30 mm 5 min^{-1} ± 10.58 mm 5 min^{-1} (P < 0.01). The T.D.C.W. decreased from 179.79 s 5 min^{-1} ± 13.33 s 5 min^{-1} to 132.56 s 5 min^{-1} ± 6.67 s 5 min^{-1} (P < 0.01), and the gastric motility index (G.M.I.) decreased from 5219.88 ± 182.11 to 4250.28 ± 159.03 (P < 0.01). At a NTS microinjection dose of 8 nmol NaHS, the T.A.C.W. decreased from 587.62 mm 5 min^{-1} ± 9.58 mm 5 min^{-1} to 407.44 mm 5 min^{-1} ± 10.61 mm 5 min^{-1} (P < 0.01) and the T.D.C.W. decreased from 234.11 s 5 min^{-1} ± 11.74 s 5 min^{-1} to 145.13 s 5 min^{-1} ± 3.93 s 5 min^{-1} (P < 0.01) and the G.M.I. decreased from 5906.07 ± 181.71 to 4105.60 ± 49.35. After PS injection in the NTS, the T.A.C.W. decreased from 468.72 mm 5 min^{-1} ± 6.42 mm 5 min^{-1} to 467.34 mm 5 min^{-1} ± 5.04 mm 5 min^{-1} (P > 0.05), the T.D.C.W. from 236.96 s 5 min^{-1} ± 8.51 s 5 min^{-1} to 232.38 s 5 min^{-1} ± 16.31 s 5 min^{-1} (P > 0.05), and the G.M.I. from 5797.17 ± 141.87 to 5778.08 ± 125.32 (P > 0.05) (Figure 4A-C).

The inhibition rates of the T.A.C.W. in the 4 nmol NaHS, 8 nmol NaHS, and saline groups were 23.83%, 30.69%, and 0.27%, respectively. The inhibition rates of T.D.C.W. in the 4 nmol NaHS, 8 nmol NaHS, and saline groups were 26.21%, 37.43%, and 2.06%, respectively. The inhibition rates of G.M.I. in the 4 nmol NaHS, 8 nmol NaHS, and saline groups were 18.55%, 30.17%, and 0.30%, respectively (Figure 4D). The data indicated that the inhibition rates of T.A.C.W., T.D.C.W., and G.M.I. were significantly higher in the 8 nmol NaHS group compared to the 4 nmol NaHS group. These findings suggest a dose-dependent inhibitory effect of NTS injection of NaHS on gastric motility.

PDTC eliminates the inhibitory effect of NaHS on gastric motility

Injection of PDTC followed by NaHS into the NTS eliminated the inhibitory effect of NaHS on gastric motility (Figure 5A, n = 6). The T.A.C.W. changed from 500.15 mm 5 min^{-1} ± 7.56 mm 5 min^{-1} to 491.06 mm 5 min^{-1} ± 17.19 mm 5 min^{-1} (P > 0.05), the T.D.C.W. changed from 169.84 s 5 min^{-1} ± 3.40 s 5 min^{-1} (P > 0.05), and the G.M.I. changed from 5494.78 ± 140.32 to 5490.60 ± 88.80 after PDTC followed by NaHS injection (P > 0.05) (Figure 5B-D). These data suggest that NaHS can regulate gastric motility through the NF-κB signaling pathway.

Capsazepine eliminates the inhibitory effect of NaHS on gastric motility

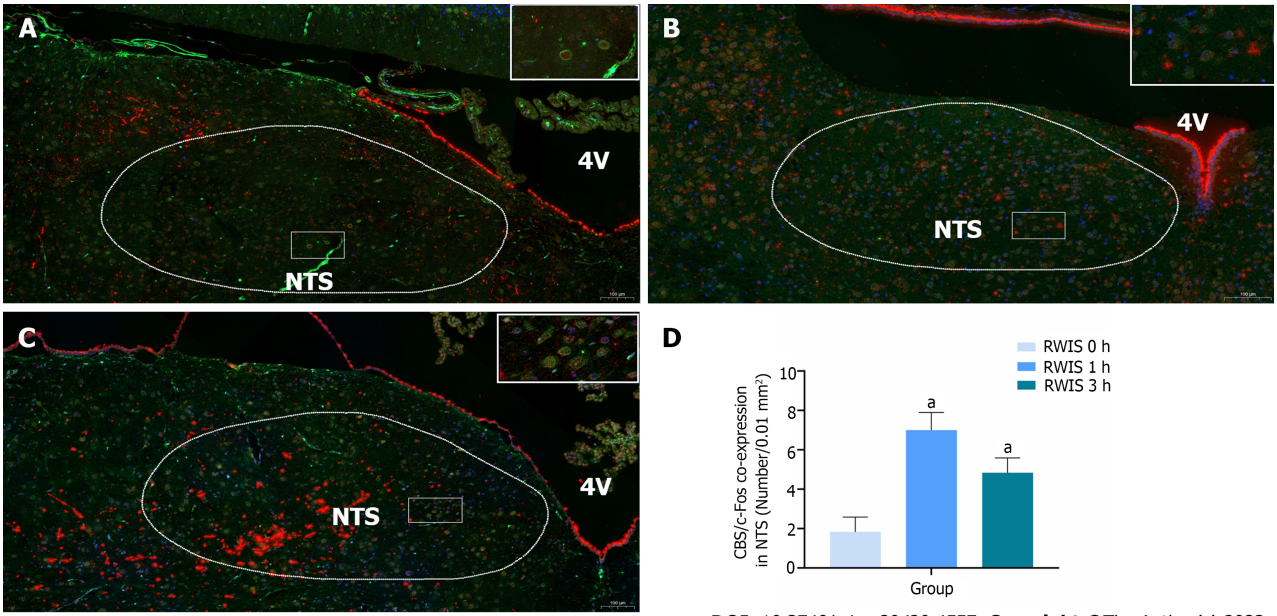
Injection of Capsazepine followed by NaHS into the NTS eliminated the inhibitory effect of NaHS on gastric motility (Figure 6A, n = 6). As a result, the T.A.C.W. changed from 514.46 mm 5 min^{-1} ± 6.56 mm 5 min^{-1} to 523.87 mm 5 min^{-1} ± 9.21 mm 5 min^{-1} (P > 0.05), the T.D.C.W. changed from 175.90 s 5 min^{-1} ± 4.22 s 5 min^{-1} to 172.13 s 5 min^{-1} ± 4.68 s 5 min^{-1} (P > 0.05), and the G.M.I. changed from 5932.97 ± 104.93 to 5946.45 ± 184.14 (P > 0.05) (Figure 6B-D). These data suggest that NaHS can regulate gastric motility through TRPV1 channels.

L703606 eliminates the inhibitory effect of NaHS on gastric motility

Injection of L703606 followed by NaHS into the NTS eliminated the inhibitory effect of NaHS on gastric motility (Figure 7A, n = 6). The T.A.C.W. changed from 494.46 mm 5 min^{-1} ± 11.86 mm 5 min^{-1} to 490.53 mm 5 min^{-1} ± 14.00 mm 5 min^{-1} (P > 0.05), the T.D.C.W. changed from 164.10 s 5 min^{-1} ± 5.53 s 5 min^{-1} to 158.39 s 5 min^{-1} ± 10.64 s 5 min^{-1} (P > 0.05), and the G.M.I. changed from 5827.59 ± 133.74 to 5762.80 ± 114.34 (P > 0.05) (Figure 7B-D). These data suggest that NaHS can act on NK1 receptors to regulate gastric motility.

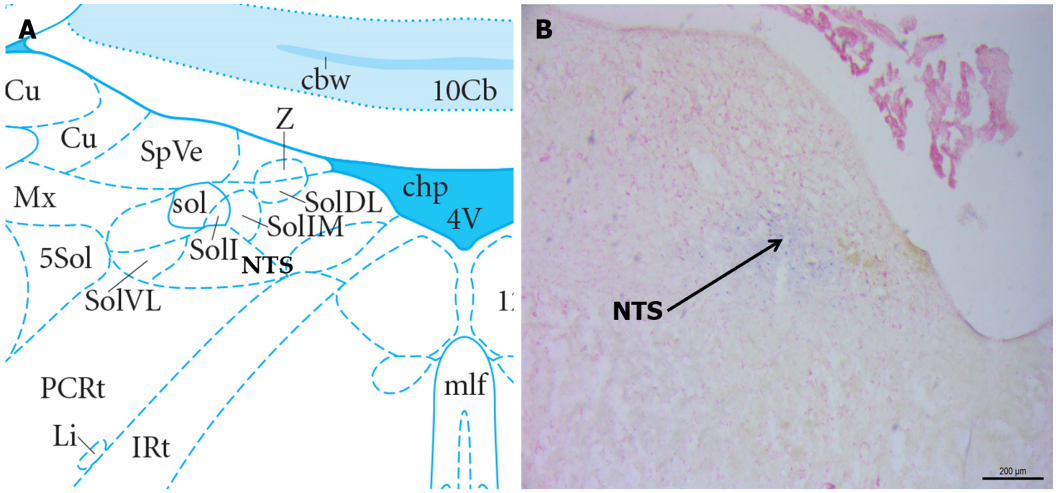
DISCUSSION

Endogenous H_2S concentrations in the brain range between 10 nM and 160 nM[32], and approximately 33% of H_2S is produced by volatilization in NaHS solutions when measurements are made in a closed environment. H_2S (10 mmol/L) in NTS neurons can maintain excitatory postsynaptic potential excitation for 10 minutes, which is equivalent to the time it takes for a microinjection NaHS to work[33]. Moreover, H_2S can cross the cell membrane by free diffusion to modulate cellular properties[34]. We selected NaHS as an exogenous H_2S rapid drug-delivery donor.



DOI: 10.3748/wjg.v29.i29.4557 **Copyright** ©The Author(s) 2023.

Figure 1 Co-expression of cystathionine beta-synthase (green) and c-Fos (red) neurons in the nucleus tractus solitarius at different times of restraint water-immersion stress. A: Expression of cystathionine beta-synthase (CBS) and c-Fos in restraint water-immersion stress (RWIS) at 0 h; B: Expressions of CBS and c-Fos in RWIS at 1 h; C: Expression of CBS and c-Fos in RWIS at 3 h; D: Quantification of neurons co-expressing CBS and c-Fos in the nucleus tractus solitarius (n = 6). $^aP < 0.01$ *vs* RWIS 0 h group. NTS: Nucleus tractus solitarius; RWIS: Restraint water-immersion stress; CBS: Cystathionine beta-synthase.

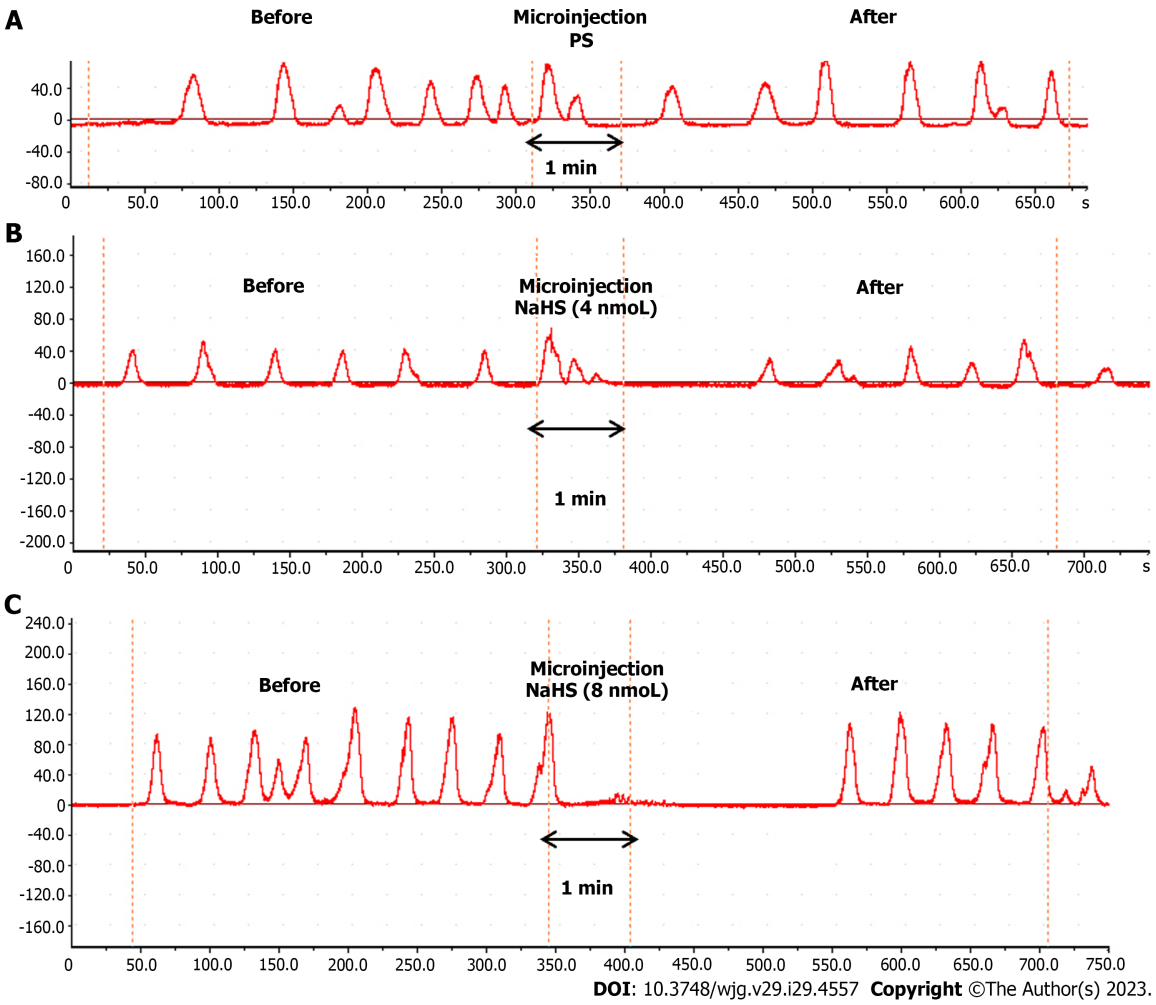


DOI: 10.3748/wjg.v29.i29.4557 **Copyright** ©The Author(s) 2023.

Figure 2 Histological identification of microinjections located at the nucleus tractus solitarius in the brain. A: Location of the nucleus tractus solitarius (NTS) in the brain atlas; B: Neutral red stained brain section with blue dot sites representing injection into the NTS. NTS: Nucleus tractus solitarius.

H_2S, an emerging gaseous signaling molecule, plays an important role in regulating digestion and the nervous system [35]. Placing coronal NTS slices into NaHS solution was found to cause rapid concentration-dependent depolarization of neurons at NTS sites, with H_2S increasing the postsynaptic currents in NTS neurons by promoting presynaptic glutamate release[36]. Herein, we observed a significant increase in the co-expression of neurons between CBS and c-Fos in rat NTS after RWIS, indicating that H_2S in the NTS is involved in gastrointestinal regulation and stress.

In this experiment, we found that the amplitude and duration of gastric motility and the index of gastric motility were significantly lower in the NTS than in the control group, in a dose-dependent manner, after the injection of different concentrations of NaHS in rats. Sensory information from the upper gastrointestinal tract is transmitted to the NTS *via* vagal afferent fibers, and c-Fos-positive neurons are significantly increased in the NTS following stressful processes. Glutamate release from vagal afferent fibers activates NTS neurons, which can regulate gastrointestinal activity by inhibiting the vagal excitatory cholinergic efferent pathway *via* the inhibitory neurotransmitter GABA or by exciting the vagal inhibitory non-adrenergic non-cholinergic (NANC) efferent pathway[37]. In addition, vagal afferent nerves from the gastrointestinal tract can activate the NANC efferent pathway leading to gastric smooth muscle relaxation. Vagal



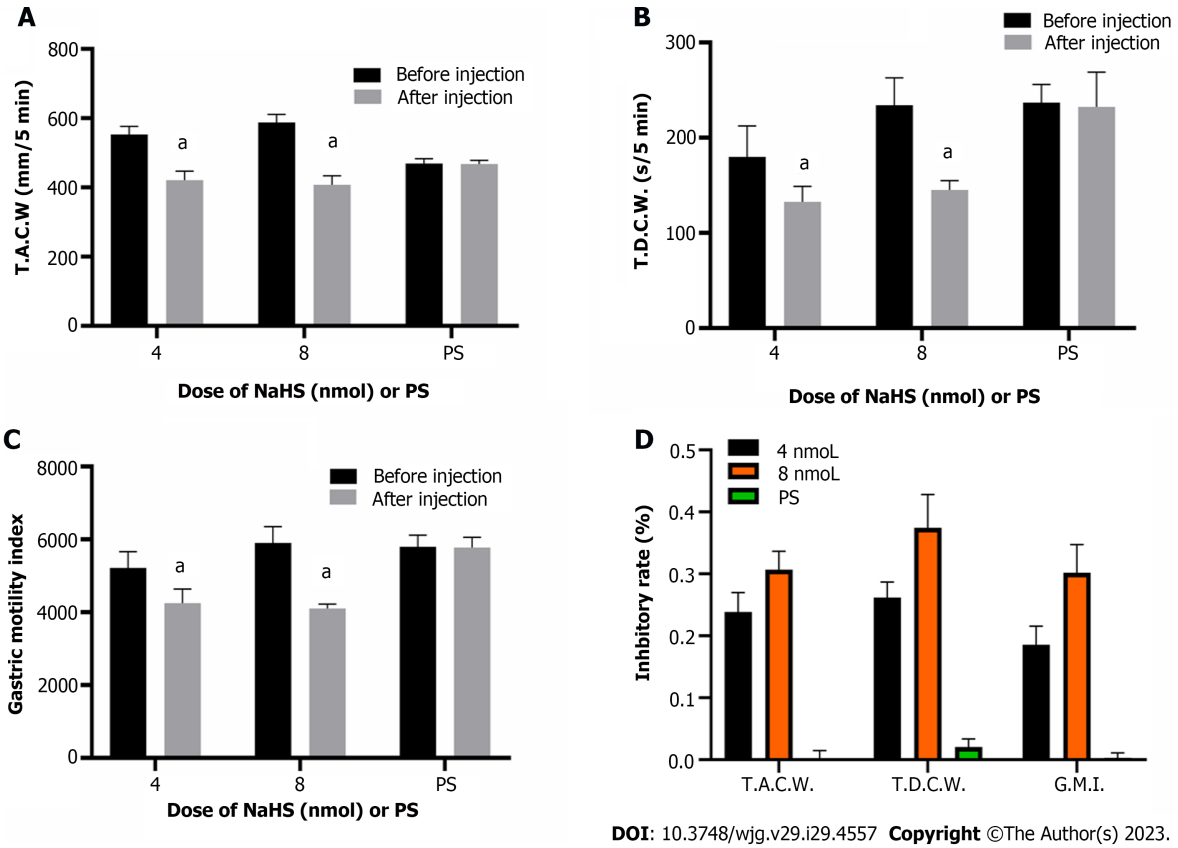
DOI: 10.3748/wjg.v29.i29.4557 **Copyright** ©The Author(s) 2023.

Figure 3 Effect of microinjection of drugs in the nucleus tractus solitarius on gastric motility in rats. A: Gastric motility curves were recorded in rats microinjected with saline at the nucleus tractus solitarius (NTS); B: Gastric motility curves were recorded in rats microinjected with 4 nmol NaHS in the NTS; C: Gastric motility curves were recorded in rats microinjected with 8 nmol NaHS in the NTS. PS: Physiological saline.

efferent fibers activate the noradrenergic neurons in the NTS, which in turn activate the NANC pathway neurons in the DMV. These NANC-DMV neurons transmit to the gastrointestinal plexus to activate postganglionic cholinergic neurons, thus causing gastric relaxation[38].

In vivo studies found that the microinjection of D-glucose into the NTS resulted in decreased gastric motility and increased intragastric pressure in rats *via* K^+-ATP channel relaxation of the smooth muscles and increased firing of GABAergic neurons[39]. Injection of cholecystokinin in the rat NTS modulates the gastrointestinal motility and secretory function in the upper gastrointestinal tract by activating postganglionic cholinergic excitatory or NANC inhibitory pathways[40]. Increased glutamate content within the NTS directly activates excitatory postsynaptic potentials in NTS neurons, which in turn stimulates local circuit GABAergic and glutamatergic neurons. GABAergic signals at the NTS determine the state of the gastric tone and contraction and mediate changes in gastric mechanical function at the onset of the vagal-vagal reflex[41,42]. The intra-NTS injection of GLP-1 reduces the gastric tone by activating NANC and delays gastric emptying in a dose-dependent manner[43]. Therefore, NaHS injection in the rat NTS may inhibit gastric motility by releasing inhibitory neurotransmitters such as GABA from preganglionic cholinergic neurons.

The activation of TRPV1 leads to the release of various pro-inflammatory cytokines, which can activate NF-kB translocation to the nucleus. Our experiments revealed that the injection of the NF-κB pathway blocker PDTC followed by NaHS eliminated the modulation of gastric function by NaHS. H_2S is mainly synthesized in the brain by the CBS enzyme, andwe found that NaHS injection in both the ambiguous and paraventricular nuclei inhibited gastric motility in rats *via* the NF-κB pathway[44,45], that the injection of NaHS to the brain blocked inflammation-associated apoptosis, and that treatment with NaHS reduced the expression of inflammatory factors in astrocytes and microglia due to Alzheimer's disease[46]. H_2S reduces the levels of phosphorylated p38 MAPK and phosphorylated p65 NF-κB *in vivo*. NaHS also reduces LPS-induced inflammation by inhibiting p38 MAPK and p65 NF-κB in rat cells[47]. SP is the main presynaptically released excitatory transmitter from injured primary afferent fibers. It binds to NK1 receptors on the postsynaptic membrane to activate NF-kB-induced inflammatory factor synthesis. NF-κB is reportedly involved in the transcriptional regulation of various response-related genes, including gastrointestinal mucosal damage, and that the downregulation of NF-κB signaling can inhibit stress-induced local inflammatory responses in the gastric mucosa and can repair local lesions in the gastric mucosa[48,49]. Therefore, physiological concentrations of H_2S can modulate the inflam-



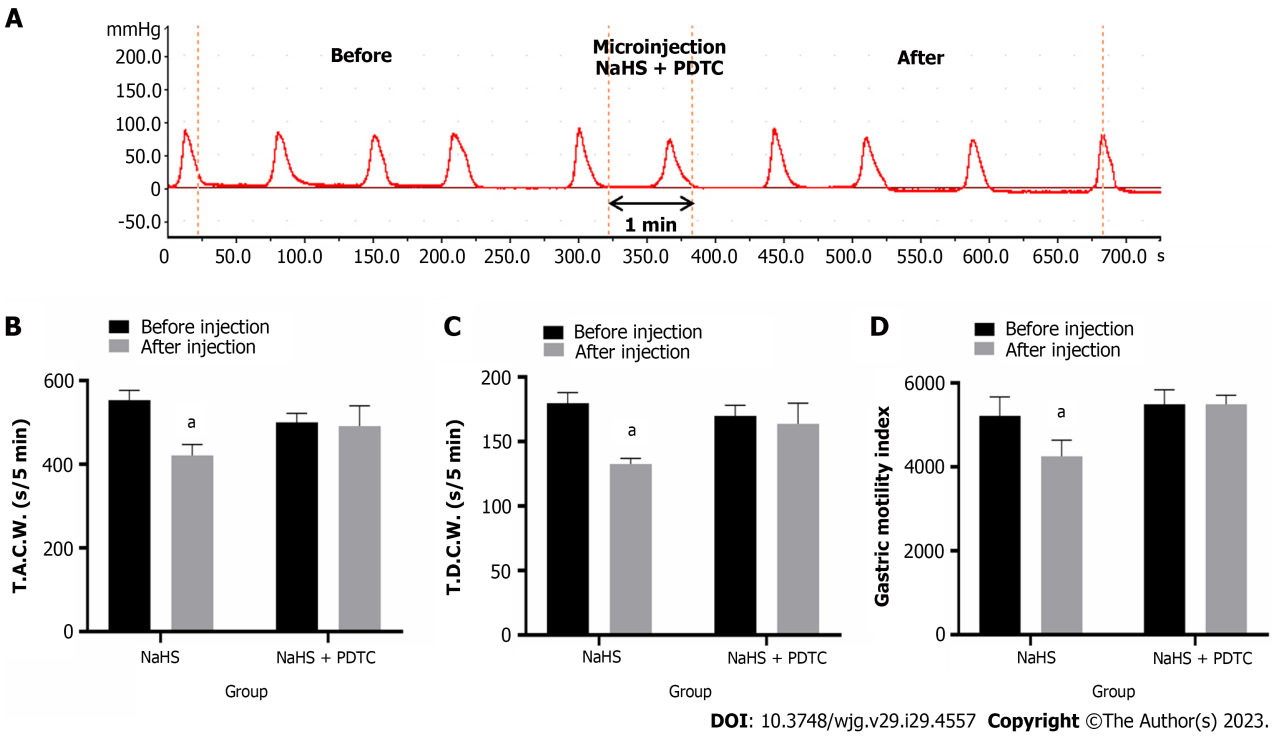
DOI: 10.3748/wjg.v29.i29.4557 **Copyright** ©The Author(s) 2023.

Figure 4 Effects of the microinjection of NaHS (4 nmol and 8 nmol) and physiological saline into the nucleus tractus solitarius before and after the gastric motility data. A: Total amplitude of the contraction wave (T.A.C.W.); B: Total duration of the contraction wave (T.D.C.W.); C: Gastric motility index (G.M.I.); D: Inhibition rates of T.A.C.W., T.D.C.W., and G.M.I. $^aP < 0.01$ *vs* before injection. PS: Physiological saline; T.A.C.W.: Total amplitude of the contraction wave; T.D.C.W.: Total duration of the contraction wave; G.M.I.: Gastric motility index.

matory process and regulate gastric dysfunction by down-regulating the inflammatory response.

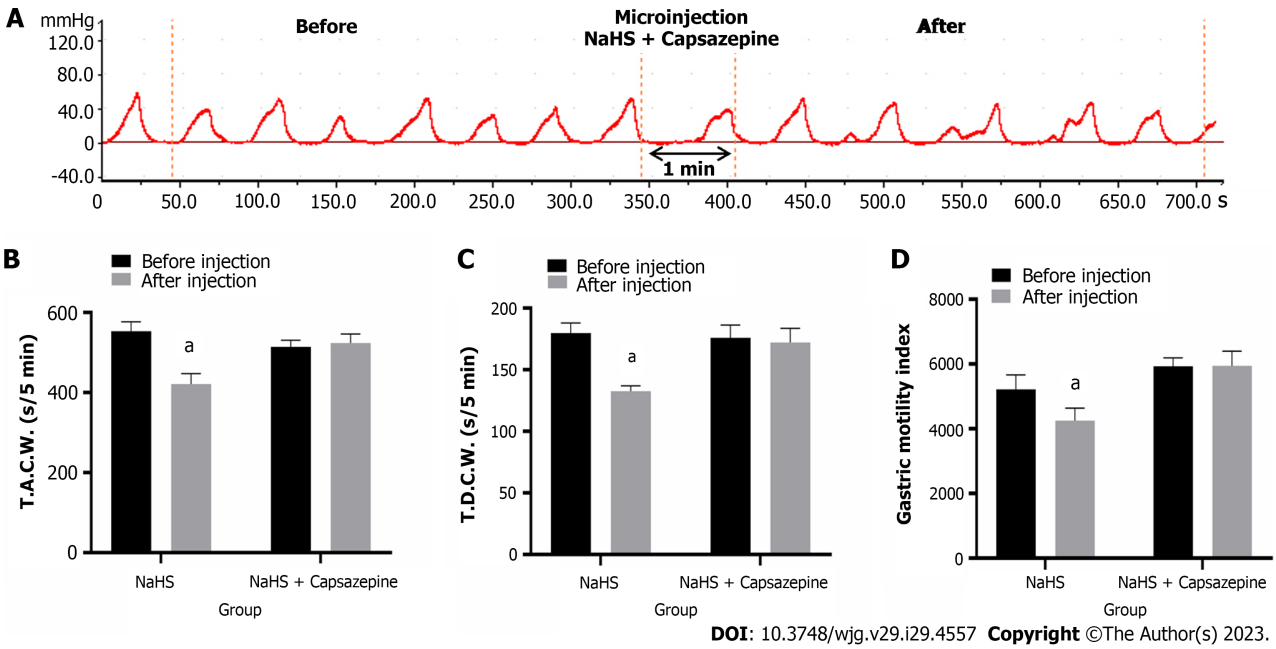
To investigate the signaling pathways involved in H_2S regulation, we focused on the TRPV1-SP-NF-kB pathway[50]. TRPV1 activation, enhanced pro-inflammatory cytokine expression, and oxidative stress *via* the NF-kB pathway led to reduced phosphorylation of the ERK signaling pathway, activation of PAG involved in the ERK-NF-kB pathway, and production of SP, which in turn regulated TRPV1-mediated neurogenic inflammation[51]. Our experiments showed that the administration of the TRPV1 blocker Capsazepine followed by NaHS eliminated the modulation of gastric function by NaHS. TRPV1 is widely expressed in spinal and vagal afferent neurons. It innervates the gastrointestinal tract, and its upregulated sensitivity may be associated with the pathophysiological functions of diseases such as visceral pain, irritable bowel syndrome, inflammatory bowel disease and pancreatitis[52]. TRPV1 presents two sides to inflammation. There are even studies showing the alternating effects of TRPV1 on inflammation[53]. Capsaicin induces inflammation in the stomach by activating TRPV1, damages the gastrointestinal mucosa, causes structural changes in the intestinal barrier and further leads to other gastrointestinal symptoms[54-56]. It also decreases the expression of anti-inflammatory cytokines in the stomach and intestine and promotes the release of gastrointestinal neuropeptide SP, which is closely associated with gastrointestinal visceral pain[57]. The findings suggest that the TRPV1 receptor antagonist caspofungin abrogates H_2S donor-induced enhancement of gastric emptying and that TRPV1-dependent pathways have been shown to produce modulation of vagally mediated muscle contractions in the gastrointestinal tract[58]. Capsaicin also activates the enterocholinergic neurons in guinea pig's small intestine and induces contractile effects and inhibition of gastric emptying, thus inducing the relaxation of smooth muscles of the fundus[59]. Capsazepine was also found to inhibit NaHS-induced pyloric smooth muscle relaxation, indicating that the effect of H_2S donors on enhancing gastric emptying and inducing pyloric sphincter relaxation is mediated by the activation of TRPV1 receptors. Although there are many mechanisms by which this effect can be manifested, our data support the theory of smooth muscle relaxation induced by afferent neuronal TRPV1 receptor activation[45,60].

TRPV1 receptors may act as molecular sensors involved in processing cardiac injury information in spinal neurons. Harmful environmental stimuli can activate TRPV1 to produce pro-inflammatory mediators in the epithelial cells, thus triggering neurogenic inflammatory responses. TRPV1 antagonists reportedly inhibited H_2S-induced neuropeptide release and bronchoconstriction in vitro, whereas H_2S induced the release of an endogenous tachykinin, SP, by stimulating sensory nerve endings, and that NaHS-induced SP release is significantly reduced when the TRPV1 blocker Capsazepine is applied[61]. Capsaicin also slows down gastric motility through TRPV1-induced excitation of gastric sensory nerve fibers[62]. A possible role of capsaicin-sensitive vagal afferent nerves in gastric mucosal injury and prevention has been demonstrated and is associated with the release of SP[31].



DOI: 10.3748/wjg.v29.i29.4557 **Copyright** ©The Author(s) 2023.

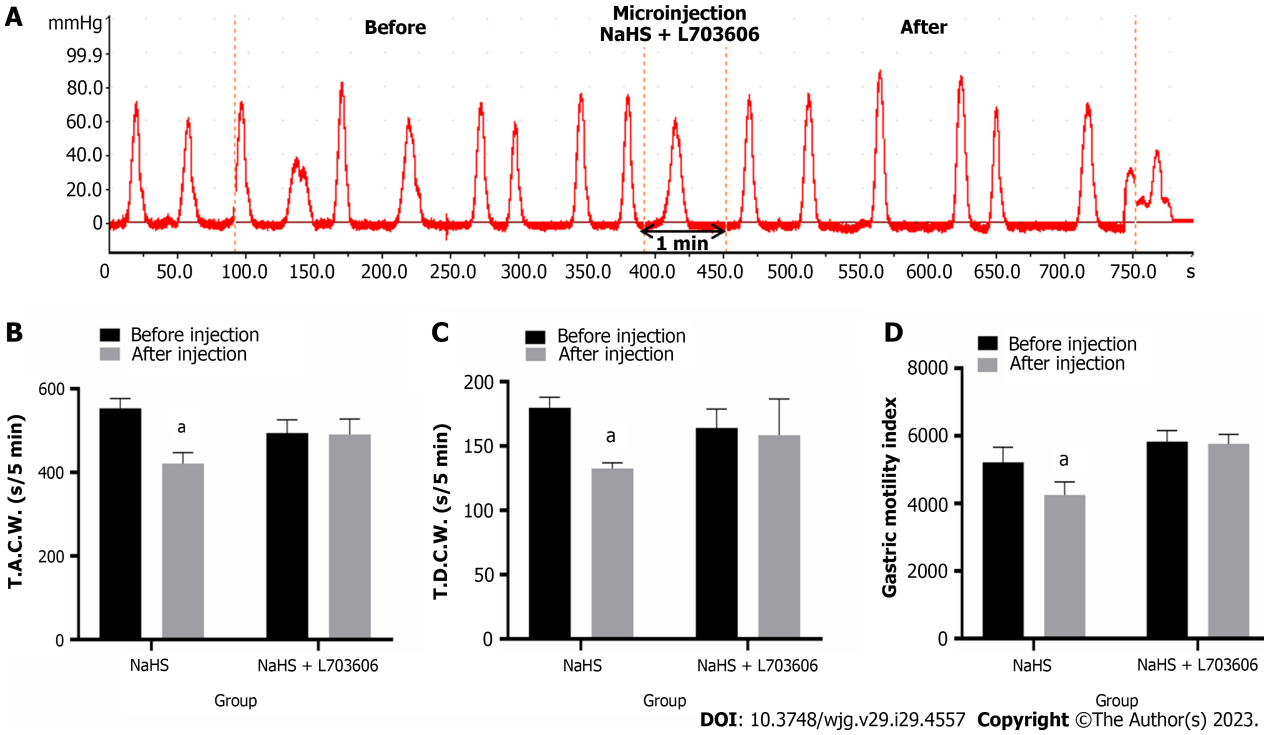
Figure 5 Effect of microinjection of 4 nmol NaHS and 4 nmol NaHS + pyrrolidine dithiocarbamate into the nucleus tractus solitarius on gastric motility in rats. A: Gastric motility curve recorded in rats with 4 nmol NaHS + pyrrolidine dithiocarbamate microinjection in nucleus tractus solitarius; B: Data of total amplitude of the contraction wave; C: Data of total duration of the contraction wave; D: Data of gastric motility index. $^aP < 0.01$ *vs* before injection. PDTC: Pyrrolidine dithiocarbamate; T.A.C.W.: Total amplitude of the contraction wave; T.D.C.W.: Total duration of the contraction wave.



DOI: 10.3748/wjg.v29.i29.4557 **Copyright** ©The Author(s) 2023.

Figure 6 Effects of microinjection of 4 nmol NaHS and 4 nmol NaHS + Capsazepine into the nucleus tractus solitarius on gastric motility in rats. A: Gastric motility curve recorded in rats with 4 nmol NaHS + Capsazepine microinjection in nucleus tractus solitarius; B: Data of total amplitude of the contraction wave; C: Data of total duration of the contraction wave; D: Data of gastric motility index. $^aP < 0.01$ *vs* before injection. T.A.C.W.: Total amplitude of the contraction wave; T.D.C.W.: Total duration of the contraction wave.

We eliminated the inhibitory effect of NaHS on gastric motility in our experiments by injecting the NK1 receptor blocker L703606 followed by NaHS. SP is a brain-gut peptide abundant in mammals that acts as a neurotransmitter for specific receptors to mediate NANC expression in the autonomic nervous system. Numerous studies have shown its role in stress and nociceptive transmission[63]. Injection of exogenous SP into the NTS resulted in the reduction of gastric motility. In contrast, injection of NK1 blockers enhanced the gastric motility. Therefore, SP in the NTS may play a



DOI: 10.3748/wjg.v29.i29.4557 **Copyright** ©The Author(s) 2023.

Figure 7 Effects of microinjection of 4 nmol NaHS and 4 nmol NaHS + L703606 into the nucleus tractus solitarius on gastric motility in rats. A: Gastric motility curve recorded in rats with 4 nmol NaHS + L703606 microinjection in nucleus tractus solitarius; B: Data of total amplitude of the contraction wave; C: Data of total duration of the contraction wave; D: Data of gastric motility index. $^aP < 0.01$ *vs* before injection. T.A.C.W.: Total amplitude of the contraction wave; T.D.C.W.: Total duration of the contraction wave.

predominantly inhibitory role in gastrointestinal regulation. Administration of NK1 receptor antagonists also prevented H_2S-induced contractile responses, indicating that SP released from sensory nerve endings is the ultimate mediator of H_2S-induced excitation of smooth muscle in rats, possibly leading to altered gastric motility and the formation of gastric ulcers[64]. Injection of glutamate and SP in the NTS modulates gastric motility and emptying, and leads to a dose-dependent decrease in tonic gastric pressure and inhibition of gastric motility[65,66]. It has been shown that glutamate, acting through N-methyl-D-aspartic acid receptors with glutamate ion channels, and tachykinin, acting through NK1 and NK2 receptors, act synergistically in the transmission of acid stimuli from the gastric mucosa to the NTS[67]. SP regulates gastric smooth muscle contraction by both inhibition and enhancement mechanisms. Studies have found that SP microinjections in the brain have inhibitory effects on gastric motility. Furthermore, microinjections of SP in the rat DMV inhibited gastric EMG fast waves and gastric motility. These effects could be abolished by SP receptor antagonists and by severing the vagus nerve, respectively[68]. SP in the brain plays a role in stress-induced physiological and behavioral activity. The effects of NK1 can be blocked using injectable drugs or knockout methods[69-71]. Moreover, c-Fos expression can be downregulated, with the nucleus involved in stress in the brain and pain, causing pain through increased SP release in the hypothalamic and spinal cord tissue. This results in a sterile inflammatory response, with persistent pain leading to increased levels of SP receptors in the posterior horn of the spinal cord[72]. SP also plays a role in transmitting injurious information, with low doses given ventrally to produce analgesia, acting in a neuroendocrine manner on various immune cells involved in immune regulation and enhancing immune function[73]. We, therefore, consider that H_2S enhances the inhibitory effect of SP on gastric motility by excitation of NTS neurons which are then transmitted to the DMV.

CONCLUSION

Our experiments revealed that CBSergic neurons affecting gastric function were present in the NTS and were activated by stress. Furthermore, exogenous H_2S in the NTS significantly inhibited gastric motility in rats, possibly by activating the TRPV1 pathway through NF-κB channels to release SP. This is the first study to report that H_2S in the NTS may regulate gastric function. It provides an important experimental basis for the clinical prevention and treatment of gastric ulcers.

ARTICLE HIGHLIGHTS

Research background

Recent studies have revealed that hydrogen sulfide is the third class of gas signaling molecules after nitric oxide (NO) and carbon monoxide (CO). The high level of endogenous hydrogen sulfide found in the brain, which is mainly produced by cystathionine beta-synthase, suggests that it may have a physiological function, and the nucleus tractus solitarius is important nucleus that regulates the function of internal organs, so we want to elucidate the role of hydrogen sulfide in the NTS in regulating gastric function in rats.

Research motivation

To investigate whether hydrogen sulfide in the nucleus tractus solitarius is involved in the regulation of gastric dysfunction by restraint water-immersion stress, this study will examine the role of hydrogen sulfide in the nucleus tractus solitarius in the regulation of gastric motility.

Research objectives

It is the first time to propose that hydrogen sulfide in the nucleus tractus solitarius has a regulatory effect on the gastric motility caused by restraint water-immersion stress, and to investigate its mechanism of action, which can not only elucidate the mechanism of regulation of gastric dysfunction by hydrogen sulfide in the nucleus tractus solitarius, and also provide an important experimental basis for the prevention and treatment of stress gastric ulcer from the central aspect in clinical practice.

Research methods

We used immunohistochemical, fluorescent double-labeling technique and restraint water-immersion stress model to confirm the involvement of hydrogen sulfide-producing cystathionine beta-synthase neurons in the nucleus tractus solitarius in the regulation of gastric function, and physiological methods to record changes in gastric motility before and after their brain injection.

Research results

After restraint water-immersion stress, cystathionine beta-synthase neurons containing c-Fos were significantly increased and gastric motility was inhibited in rats after nucleus tractus solitarius injection of NaHS, and this inhibitory effect was eliminated after pre-injection of transient receptor potential vanilloid 1 channels, NF-κB channel blockers, and NK1 receptor antagonists followed by NaHS injection.

Research conclusions

Injection NaHS into the nucleus tractus solitarius can inhibit gastric motility in rats and this effect may be mediated by TRPV1 and NK1 receptors *via* NF-κB channel-dependent activation.

Research perspectives

Our next step will be to continue our work on the effects of endogenous hydrogen sulfide in the nucleus tractus solitarius on gastric function.

FOOTNOTES

Author contributions: Sun HZ and Li CY contributed equally to this work; Sun HZ conceived and designed the experiments; Li CY, Shi Y, Li JJ, Wang YY, Han LN, Zhu LJ, and Zhang YF performed the experiments; Sun HZ and Li CY analyzed the data; Sun HZ provided reagents/materials/analysis tools; Li CY authored the paper; all authors have read and approved the final manuscript.

Supported by the Natural Science Foundation of Shandong Province, No. ZR2019MC020.

Institutional animal care and use committee statement: All animal procedures were reviewed and approved by the Institutional Animal Care and Use Committee (IACUC) of Qi Lu Normal University (Approval No. 14276).

Conflict-of-interest statement: The authors declare no conflicts of interest.

Data sharing statement: No additional data are available.

ARRIVE guidelines statement: The authors have read the ARRIVE Guidelines, and the manuscript was prepared and revised according to the ARRIVE Guidelines.

Open-Access: This article is an open-access article that was selected by an in-house editor and fully peer-reviewed by external reviewers. It is distributed in accordance with the Creative Commons Attribution NonCommercial (CC BY-NC 4.0) license, which permits others to distribute, remix, adapt, build upon this work non-commercially, and license their derivative works on different terms, provided the original work is properly cited and the use is non-commercial. See: https://creativecommons.org/Licenses/by-nc/4.0/

Country/Territory of origin: China

ORCID number: Hong-Zhao Sun 0000-0001-5094-469X; Chen-Yu Li 0000-0001-8102-1978; Jin-Jin Li 0000-0002-6125-4181.

S-Editor: Chen YL
L-Editor: A
P-Editor: Cai YX

REFERENCES

1 **Gong SN**, Zhu JP, Ma YJ, Zhao DQ. Proteomics of the mediodorsal thalamic nucleus of rats with stress-induced gastric ulcer. *World J Gastroenterol* 2019; **25**: 2911-2923 [PMID: 31249449 DOI: 10.3748/wjg.v25.i23.2911]
2 **Travagli RA**, Anselmi L. Vagal neurocircuitry and its influence on gastric motility. *Nat Rev Gastroenterol Hepatol* 2016; **13**: 389-401 [PMID: 27251213 DOI: 10.1038/nrgastro.2016.76]
3 **Hyde TM**, Miselis RR. Subnuclear organization of the human caudal nucleus of the solitary tract. *Brain Res Bull* 1992; **29**: 95-109 [PMID: 1504855 DOI: 10.1016/0361-9230(92)90013-n]
4 **Zhang X**, Fogel R, Renehan WE. Relationships between the morphology and function of gastric- and intestine-sensitive neurons in the nucleus of the solitary tract. *J Comp Neurol* 1995; **363**: 37-52 [PMID: 8682936 DOI: 10.1002/cne.903630105]
5 **Qiao W**, Yang L, Li XY, Cao N, Wang WZ, Chai C, Lu Y. The cardiovascular inhibition functions of hydrogen sulfide within the nucleus tractus solitarii are mediated by the activation of KATP channels and glutamate receptors mechanisms. *Pharmazie* 2011; **66**: 287-292 [PMID: 21612157]
6 **Cao J**, Wang X, Powley TL, Liu Z. Gastric neurons in the nucleus tractus solitarius are selective to the orientation of gastric electrical stimulation. *J Neural Eng* 2021; **18** [PMID: 34634781 DOI: 10.1088/1741-2552/ac2ec6]
7 **Holmes GM**, Browning KN, Babic T, Fortna SR, Coleman FH, Travagli RA. Vagal afferent fibres determine the oxytocin-induced modulation of gastric tone. *J Physiol* 2013; **591**: 3081-3100 [PMID: 23587885 DOI: 10.1113/jphysiol.2013.253732]
8 **Gillis RA**, Dezfuli G, Bellusci L, Vicini S, Sahibzada N. Brainstem Neuronal Circuitries Controlling Gastric Tonic and Phasic Contractions: A Review. *Cell Mol Neurobiol* 2022; **42**: 333-360 [PMID: 33813668 DOI: 10.1007/s10571-021-01084-5]
9 **Jimenez M**. Hydrogen sulfide as a signaling molecule in the enteric nervous system. *Neurogastroenterol Motil* 2010; **22**: 1149-1153 [PMID: 21069935 DOI: 10.1111/j.1365-2982.2010.01600.x]
10 **Hacioglu G**, Cirrik S, Tezcan Yavuz B, Tomruk C, Keskin A, Uzunoglu E, Takir S. The BDNF-TrkB signaling pathway is partially involved in the neuroprotective effects of hydrogen sulfide in Parkinson's disease. *Eur J Pharmacol* 2023; **944**: 175595 [PMID: 36804547 DOI: 10.1016/j.ejphar.2023.175595]
11 **Paul BD**, Pieper AA. Protective Roles of Hydrogen Sulfide in Alzheimer's Disease and Traumatic Brain Injury. *Antioxidants (Basel)* 2023; **12** [PMID: 37237961 DOI: 10.3390/antiox12051095]
12 **Wang S**, Paton JF, Kasparov S. Differential sensitivity of excitatory and inhibitory synaptic transmission to modulation by nitric oxide in rat nucleus tractus solitarii. *Exp Physiol* 2007; **92**: 371-382 [PMID: 17138620 DOI: 10.1113/expphysiol.2006.036103]
13 **Li Q**, Sun B, Wang X, Jin Z, Zhou Y, Dong L, Jiang LH, Rong W. A crucial role for hydrogen sulfide in oxygen sensing *via* modulating large conductance calcium-activated potassium channels. *Antioxid Redox Signal* 2010; **12**: 1179-1189 [PMID: 19803741 DOI: 10.1089/ars.2009.2926]
14 **Gallego D**, Clavé P, Donovan J, Rahmati R, Grundy D, Jiménez M, Beyak MJ. The gaseous mediator, hydrogen sulphide, inhibits in vitro motor patterns in the human, rat and mouse colon and jejunum. *Neurogastroenterol Motil* 2008; **20**: 1306-1316 [PMID: 19019033 DOI: 10.1111/j.1365-2982.2008.01201.x]
15 **Fernandes VS**, Ribeiro AS, Barahona MV, Orensanz LM, Martínez-Sáenz A, Recio P, Martínez AC, Bustamante S, Carballido J, García-Sacristán A, Prieto D, Hernández M. Hydrogen sulfide mediated inhibitory neurotransmission to the pig bladder neck: role of KATP channels, sensory nerves and calcium signaling. *J Urol* 2013; **190**: 746-756 [PMID: 23454157 DOI: 10.1016/j.juro.2013.02.103]
16 **Unuma K**, Aki T, Yamashita A, Yoshikawa A, Uemura K. Hydrogen sulfide donor NaHS causes bronchitis with enhanced respiratory secretion in rats. *J Toxicol Sci* 2019; **44**: 107-112 [PMID: 30726810 DOI: 10.2131/jts.44.107]
17 **Scammahorn JJ**, Nguyen ITN, Bos EM, Van Goor H, Joles JA. Fighting Oxidative Stress with Sulfur: Hydrogen Sulfide in the Renal and Cardiovascular Systems. *Antioxidants (Basel)* 2021; **10** [PMID: 33801446 DOI: 10.3390/antiox10030373]
18 **Kimura Y**, Shibuya N, Kimura H. Sulfite protects neurons from oxidative stress. *Br J Pharmacol* 2019; **176**: 571-582 [PMID: 29808913 DOI: 10.1111/bph.14373]
19 **Derbenev AV**, Monroe MJ, Glatzer NR, Smith BN. Vanilloid-mediated heterosynaptic facilitation of inhibitory synaptic input to neurons of the rat dorsal motor nucleus of the vagus. *J Neurosci* 2006; **26**: 9666-9672 [PMID: 16988037 DOI: 10.1523/JNEUROSCI.1591-06.2006]
20 **Peters JH**, McDougall SJ, Fawley JA, Smith SM, Andresen MC. Primary afferent activation of thermosensitive TRPV1 triggers asynchronous glutamate release at central neurons. *Neuron* 2010; **65**: 657-669 [PMID: 20223201 DOI: 10.1016/j.neuron.2010.02.017]
21 **Jin YH**, Bailey TW, Andresen MC. Cranial afferent glutamate heterosynaptically modulates GABA release onto second-order neurons *via* distinctly segregated metabotropic glutamate receptors. *J Neurosci* 2004; **24**: 9332-9340 [PMID: 15496669 DOI: 10.1523/JNEUROSCI.1991-04.2004]
22 **Lappin SC**, Randall AD, Gunthorpe MJ, Morisset V. TRPV1 antagonist, SB-366791, inhibits glutamatergic synaptic transmission in rat spinal dorsal horn following peripheral inflammation. *Eur J Pharmacol* 2006; **540**: 73-81 [PMID: 16737693 DOI: 10.1016/j.ejphar.2006.04.046]
23 **Garcia-Recio S**, Gascón P. Biological and Pharmacological Aspects of the NK1-Receptor. *Biomed Res Int* 2015; **2015**: 495704 [PMID: 26421291 DOI: 10.1155/2015/495704]
24 **Krueger D**, Foerster M, Mueller K, Zeller F, Slotta-Huspenina J, Donovan J, Grundy D, Schemann M. Signaling mechanisms involved in the intestinal pro-secretory actions of hydrogen sulfide. *Neurogastroenterol Motil* 2010; **22**: 1224-1231, e319 [PMID: 20659296 DOI: 10.1111/j.1365-2982.2010.01571.x]
25 **Couture R**, Harrisson M, Vianna RM, Cloutier F. Kinin receptors in pain and inflammation. *Eur J Pharmacol* 2001; **429**: 161-176 [PMID:

11698039 DOI: 10.1016/S0014-2999(01)01318-8]
26 **Severini C**, Improta G, Falconieri-Erspamer G, Salvadori S, Erspamer V. The tachykinin peptide family. *Pharmacol Rev* 2002; **54**: 285-322 [PMID: 12037144 DOI: 10.1124/pr.54.2.285]
27 **Nakaya Y**, Kaneko T, Shigemoto R, Nakanishi S, Mizuno N. Immunohistochemical localization of substance P receptor in the central nervous system of the adult rat. *J Comp Neurol* 1994; **347**: 249-274 [PMID: 7814667 DOI: 10.1002/cne.903470208]
28 **Mashaghi A**, Marmalidou A, Tehrani M, Grace PM, Pothoulakis C, Dana R. Neuropeptide substance P and the immune response. *Cell Mol Life Sci* 2016; **73**: 4249-4264 [PMID: 27314883 DOI: 10.1007/s00018-016-2293-z]
29 **Zimmermann M**. Ethical considerations in relation to pain in animal experimentation. *Acta Physiol Scand Suppl* 1986; **554**: 221-233 [PMID: 3469880]
30 **Murison R**, Overmier JB. Some psychosomatic causal factors of restraint-in-water stress ulcers. *Physiol Behav* 1993; **53**: 577-581 [PMID: 8451325 DOI: 10.1016/0031-9384(93)90155-9]
31 **Sun H**, Yang J, Shi Y, Wang Y, Li C, Zhu M. Hydrogen sulfide in the nucleus tractus solitarii regulates gastric acid secretion in rats. *J Physiol Pharmacol* 2020; **71** [PMID: 33214338 DOI: 10.26402/jpp.2020.4.05]
32 **Mancuso C**, Navarra P, Preziosi P. Roles of nitric oxide, carbon monoxide, and hydrogen sulfide in the regulation of the hypothalamic-pituitary-adrenal axis. *J Neurochem* 2010; **113**: 563-575 [PMID: 20089135 DOI: 10.1111/j.1471-4159.2010.06606.x]
33 **Levitt MD**, Abdel-Rehim MS, Furne J. Free and acid-labile hydrogen sulfide concentrations in mouse tissues: anomalously high free hydrogen sulfide in aortic tissue. *Antioxid Redox Signal* 2011; **15**: 373-378 [PMID: 20812866 DOI: 10.1089/ars.2010.3525]
34 **Ritter JM**. Human pharmacology of hydrogen sulfide, putative gaseous mediator. *Br J Clin Pharmacol* 2010; **69**: 573-575 [PMID: 20565447 DOI: 10.1111/j.1365-2125.2010.03690.x]
35 **Fiorucci S**, Antonelli E, Distrutti E, Rizzo G, Mencarelli A, Orlandi S, Zanardo R, Renga B, Di Sante M, Morelli A, Cirino G, Wallace JL. Inhibition of hydrogen sulfide generation contributes to gastric injury caused by anti-inflammatory nonsteroidal drugs. *Gastroenterology* 2005; **129**: 1210-1224 [PMID: 16230075 DOI: 10.1053/j.gastro.2005.07.060]
36 **Malik R**, Ferguson AV. Hydrogen sulfide depolarizes neurons in the nucleus of the solitary tract of the rat. *Brain Res* 2016; **1633**: 1-9 [PMID: 26721687 DOI: 10.1016/j.brainres.2015.12.029]
37 **Bellusci L**, Kim E, Garcia DuBar S, Gillis RA, Vicini S, Sahibzada N. Brainstem activation of GABA(B) receptors in the nucleus tractus solitarius increases gastric motility. *Front Neurosci* 2022; **16**: 961042 [PMID: 35983226 DOI: 10.3389/fnins.2022.961042]
38 **McDougal DH**, Viard E, Hermann GE, Rogers RC. Astrocytes in the hindbrain detect glucoprivation and regulate gastric motility. *Auton Neurosci* 2013; **175**: 61-69 [PMID: 23313342 DOI: 10.1016/j.autneu.2012.12.006]
39 **Ferreira M Jr**, Browning KN, Sahibzada N, Verbalis JG, Gillis RA, Travagli RA. Glucose effects on gastric motility and tone evoked from the rat dorsal vagal complex. *J Physiol* 2001; **536**: 141-152 [PMID: 11579164 DOI: 10.1111/j.1469-7793.2001.t01-1-00141.x]
40 **Talman WT**, Andreasen K, Calvin J, Eversmann-Johanns S. Cholecystokinin in nucleus tractus solitarii modulates tonic and phasic gastric pressure. *Am J Physiol* 1991; **261**: R217-R222 [PMID: 1858949 DOI: 10.1152/ajpregu.1991.261.1.R217]
41 **Cruz MT**, Dezfuli G, Murphy EC, Vicini S, Sahibzada N, Gillis RA. GABA(B) Receptor Signaling in the Dorsal Motor Nucleus of the Vagus Stimulates Gastric Motility *via* a Cholinergic Pathway. *Front Neurosci* 2019; **13**: 967 [PMID: 31572117 DOI: 10.3389/fnins.2019.00967]
42 **Herman MA**, Cruz MT, Sahibzada N, Verbalis J, Gillis RA. GABA signaling in the nucleus tractus solitarius sets the level of activity in dorsal motor nucleus of the vagus cholinergic neurons in the vagovagal circuit. *Am J Physiol Gastrointest Liver Physiol* 2009; **296**: G101-G111 [PMID: 19008339 DOI: 10.1152/ajpgi.90504.2008]
43 **Holmes GM**, Browning KN, Tong M, Qualls-Creekmore E, Travagli RA. Vagally mediated effects of glucagon-like peptide 1: in vitro and in vivo gastric actions. *J Physiol* 2009; **587**: 4749-4759 [PMID: 19675064 DOI: 10.1113/jphysiol.2009.175067]
44 **Li C**, Sun H, Shi Y, Yu Y, Ji X, Li E, Zhou X, Liu X, Xue X. Effects of Exogenous Hydrogen Sulfide in the Hypothalamic Paraventricular Nucleus on Gastric Function in Rats. *Front Pharmacol* 2021; **12**: 806012 [PMID: 35095514 DOI: 10.3389/fphar.2021.806012]
45 **Sun H**, Ding H, Shi Y, Li C, Jin H, Yang X, Chen Z, Tian P, Zhu J, Sun H. Exogenous Hydrogen Sulfide Within the Nucleus Ambiguus Inhibits Gastrointestinal Motility in Rats. *Front Physiol* 2020; **11**: 545184 [PMID: 33013478 DOI: 10.3389/fphys.2020.545184]
46 **Xuan A**, Long D, Li J, Ji W, Zhang M, Hong L, Liu J. Hydrogen sulfide attenuates spatial memory impairment and hippocampal neuroinflammation in β-amyloid rat model of Alzheimer's disease. *J Neuroinflammation* 2012; **9**: 202 [PMID: 22898621 DOI: 10.1186/1742-2094-9-202]
47 **Hu LF**, Wong PT, Moore PK, Bian JS. Hydrogen sulfide attenuates lipopolysaccharide-induced inflammation by inhibition of p38 mitogen-activated protein kinase in microglia. *J Neurochem* 2007; **100**: 1121-1128 [PMID: 17212697 DOI: 10.1111/j.1471-4159.2006.04283.x]
48 **Sun HZ**, Zheng S, Lu K, Hou FT, Bi JX, Liu XL, Wang SS. Hydrogen sulfide attenuates gastric mucosal injury induced by restraint water-immersion stress *via* activation of K(ATP) channel and NF-κB dependent pathway. *World J Gastroenterol* 2017; **23**: 87-92 [PMID: 28104983 DOI: 10.3748/wjg.v23.i1.87]
49 **Guo C**, Liang F, Shah Masood W, Yan X. Hydrogen sulfide protected gastric epithelial cell from ischemia/reperfusion injury by Keap1 s-sulfhydration, MAPK dependent anti-apoptosis and NF-κB dependent anti-inflammation pathway. *Eur J Pharmacol* 2014; **725**: 70-78 [PMID: 24444438 DOI: 10.1016/j.ejphar.2014.01.009]
50 **Bhatia M**. H_2S and substance P in inflammation. *Methods Enzymol* 2015; **555**: 195-205 [PMID: 25747481 DOI: 10.1016/bs.mie.2014.11.024]
51 **Ang SF**, Moochhala SM, MacAry PA, Bhatia M. Hydrogen sulfide and neurogenic inflammation in polymicrobial sepsis: involvement of substance P and ERK-NF-κB signaling. *PLoS One* 2011; **6**: e24535 [PMID: 21931742 DOI: 10.1371/journal.pone.0024535]
52 **Holzer P**. TRPV1 and the gut: from a tasty receptor for a painful vanilloid to a key player in hyperalgesia. *Eur J Pharmacol* 2004; **500**: 231-241 [PMID: 15464036 DOI: 10.1016/j.ejphar.2004.07.028]
53 **Wang Y**, Cui L, Xu H, Liu S, Zhu F, Yan F, Shen S, Zhu M. TRPV1 agonism inhibits endothelial cell inflammation *via* activation of eNOS/NO pathway. *Atherosclerosis* 2017; **260**: 13-19 [PMID: 28324760 DOI: 10.1016/j.atherosclerosis.2017.03.016]
54 **Han J**, Zhang S, Liu X, Xiao C. Fabrication of capsaicin emulsions: improving the stability of the system and relieving the irritation to the gastrointestinal tract of rats. *J Sci Food Agric* 2020; **100**: 129-138 [PMID: 31452202 DOI: 10.1002/jsfa.10002]
55 **Lu M**, Cao Y, Ho CT, Huang Q. The enhanced anti-obesity effect and reduced gastric mucosa irritation of capsaicin-loaded nanoemulsions. *Food Funct* 2017; **8**: 1803-1809 [PMID: 28443906 DOI: 10.1039/c7fo00173h]
56 **van Wanrooij SJ**, Wouters MM, Van Oudenhove L, Vanbrabant W, Mondelaers S, Kollmann P, Kreutz F, Schemann M, Boeckxstaens GE. Sensitivity testing in irritable bowel syndrome with rectal capsaicin stimulations: role of TRPV1 upregulation and sensitization in visceral hypersensitivity? *Am J Gastroenterol* 2014; **109**: 99-109 [PMID: 24189713 DOI: 10.1038/ajg.2013.371]

57 **Xiang Q**, Tang X, Cui S, Zhang Q, Liu X, Zhao J, Zhang H, Mao B, Chen W. Capsaicin, the Spicy Ingredient of Chili Peppers: Effects on Gastrointestinal Tract and Composition of Gut Microbiota at Various Dosages. *Foods* 2022; **11** [PMID: 35267319 DOI: 10.3390/foods11050686]

58 **Boudaka A**, Wörl J, Shiina T, Neuhuber WL, Kobayashi H, Shimizu Y, Takewaki T. Involvement of TRPV1-dependent and -independent components in the regulation of vagally induced contractions in the mouse esophagus. *Eur J Pharmacol* 2007; **556**: 157-165 [PMID: 17156774 DOI: 10.1016/j.ejphar.2006.11.005]

59 **Benko R**, Lazar Z, Undi S, Illenyi L, Antal A, Horvath OP, Rumbus Z, Wolf M, Maggi CA, Bartho L. Inhibition of nitric oxide synthesis blocks the inhibitory response to capsaicin in intestinal circular muscle preparations from different species. *Life Sci* 2005; **76**: 2773-2782 [PMID: 15808879 DOI: 10.1016/j.lfs.2004.07.033]

60 **Medeiros JV**, Bezerra VH, Lucetti LT, Lima-Júnior RC, Barbosa AL, Tavares BM, Magalhães PJ, Santos AA, Cunha FQ, Soares PM, Souza MH. Role of KATP channels and TRPV1 receptors in hydrogen sulfide-enhanced gastric emptying of liquid in awake mice. *Eur J Pharmacol* 2012; **693**: 57-63 [PMID: 22884438 DOI: 10.1016/j.ejphar.2012.07.004]

61 **Trevisani M**, Patacchini R, Nicoletti P, Gatti R, Gazzieri D, Lissi N, Zagli G, Creminon C, Geppetti P, Harrison S. Hydrogen sulfide causes vanilloid receptor 1-mediated neurogenic inflammation in the airways. *Br J Pharmacol* 2005; **145**: 1123-1131 [PMID: 15937520 DOI: 10.1038/sj.bjp.0706277]

62 **Holzer P**. Efferent-like roles of afferent neurons in the gut: Blood flow regulation and tissue protection. *Auton Neurosci* 2006; **125**: 70-75 [PMID: 16542883 DOI: 10.1016/j.autneu.2006.01.004]

63 **Zieglgänsberger W**. Substance P and pain chronicity. *Cell Tissue Res* 2019; **375**: 227-241 [PMID: 30284083 DOI: 10.1007/s00441-018-2922-y]

64 **Patacchini R**, Santicioli P, Giuliani S, Maggi CA. Hydrogen sulfide (H2S) stimulates capsaicin-sensitive primary afferent neurons in the rat urinary bladder. *Br J Pharmacol* 2004; **142**: 31-34 [PMID: 15051627 DOI: 10.1038/sj.bjp.0705764]

65 **Spencer SE**, Talman WT. Central modulation of gastric pressure by substance P: a comparison with glutamate and acetylcholine. *Brain Res* 1986; **385**: 371-374 [PMID: 2430670 DOI: 10.1016/0006-8993(86)91085-1]

66 **Clyburn C**, Browning KN. Glutamatergic plasticity within neurocircuits of the dorsal vagal complex and the regulation of gastric functions. *Am J Physiol Gastrointest Liver Physiol* 2021; **320**: G880-G887 [PMID: 33730858 DOI: 10.1152/ajpgi.00014.2021]

67 **Jocic M**, Schuligoi R, Schöninkle E, Pabst MA, Holzer P. Cooperation of NMDA and tachykinin NK(1) and NK(2) receptors in the medullary transmission of vagal afferent input from the acid-threatened rat stomach. *Pain* 2001; **89**: 147-157 [PMID: 11166470 DOI: 10.1016/s0304-3959(00)00357-2]

68 **Krowicki ZK**, Hornby PJ. Substance P in the dorsal motor nucleus of the vagus evokes gastric motor inhibition *via* neurokinin 1 receptor in rat. *J Pharmacol Exp Ther* 2000; **293**: 214-221 [PMID: 10734172]

69 **Hahn MK**, Bannon MJ. Stress-induced C-fos expression in the rat locus coeruleus is dependent on neurokinin 1 receptor activation. *Neuroscience* 1999; **94**: 1183-1188 [PMID: 10625057 DOI: 10.1016/s0306-4522(99)00319-x]

70 **Santarelli L**, Gobbi G, Blier P, Hen R. Behavioral and physiologic effects of genetic or pharmacologic inactivation of the substance P receptor (NK1). *J Clin Psychiatry* 2002; **63** Suppl 11: 11-17 [PMID: 12562138]

71 **Singewald N**, Chicchi GG, Thurner CC, Tsao KL, Spetea M, Schmidhammer H, Sreepathi HK, Ferraguti F, Singewald GM, Ebner K. Modulation of basal and stress-induced amygdaloid substance P release by the potent and selective NK1 receptor antagonist L-822429. *J Neurochem* 2008; **106**: 2476-2488 [PMID: 18673452 DOI: 10.1111/j.1471-4159.2008.05596.x]

72 **Abbadie C**, Brown JL, Mantyh PW, Basbaum AI. Spinal cord substance P receptor immunoreactivity increases in both inflammatory and nerve injury models of persistent pain. *Neuroscience* 1996; **70**: 201-209 [PMID: 8848125 DOI: 10.1016/0306-4522(95)00343-h]

73 **Souza-Moreira L**, Campos-Salinas J, Caro M, Gonzalez-Rey E. Neuropeptides as pleiotropic modulators of the immune response. *Neuroendocrinology* 2011; **94**: 89-100 [PMID: 21734355 DOI: 10.1159/000328636]

World Journal of Gastroenterology

Submit a Manuscript: https://www.f6publishing.com

World J Gastroenterol 2023 August 7; 29(29): 4571-4579

DOI: 10.3748/wjg.v29.i29.4571

ISSN 1007-9327 (print) ISSN 2219-2840 (online)

ORIGINAL ARTICLE

Case Control Study

Comparison of modified gunsight suture technique and traditional interrupted suture in enterostomy closure

Chang Chen, Xiang Zhang, Zhi-Qiang Cheng, Bin-Bin Zhang, Xin Li, Ke-Xin Wang, Yong Dai, Yan-Lei Wang

Specialty type: Surgery

Provenance and peer review: Unsolicited article; Externally peer reviewed.

Peer-review model: Single blind

Peer-review report's scientific quality classification

Grade A (Excellent): 0
Grade B (Very good): B, B
Grade C (Good): C
Grade D (Fair): 0
Grade E (Poor): 0

P-Reviewer: Maher CA, United States; Tie J, Australia; Zingg U, Switzerland

Received: June 19, 2023
Peer-review started: June 19, 2023
First decision: July 6, 2023
Revised: July 10, 2023
Accepted: July 17, 2023
Article in press: July 17, 2023
Published online: August 7, 2023

Chang Chen, Xiang Zhang, Zhi-Qiang Cheng, Ke-Xin Wang, Yong Dai, Yan-Lei Wang, Department of Colorectal Surgery, Qilu Hospital, Shandong University, Jinan 250012, Shandong Province, China

Bin-Bin Zhang, Department of Nursing, Qilu Hospital of Shandong University De Zhou Hospital, Dezhou 254300, Shandong Province, China

Xin Li, Department of General Surgery, Huantai Branch of Qilu Hospital of Shandong University, Zibo 255000, Shandong Province, China

Corresponding author: Yan-Lei Wang, MD, PhD, Adjunct Associate Professor, Deputy Director, Doctor, Department of Colorectal Surgery, Qilu Hospital, Shandong University, No. 107 Wenhua West Road, Lixia District, Jinan 250012, Shandong Province, China.
yanleiwang@hotmail.com

Abstract

BACKGROUND

Prophylactic enterostomy surgery is a common surgical approach used to reduce the risk of anastomotic leakage in patients who have undergone partial intestinal resection due to trauma or tumors. However, the traditional interrupted suturing technique used in enterostomy closure surgery has several issues, including longer surgical incisions and higher incision tension, which can increase the risk of postoperative complications. To address these issues, scholars have proposed the use of a "gunsight suture" technique. This technique involves using a gunsight incision instead of a traditional linear incision, leaving a gap in the center for the drainage of blood and fluid to reduce the risk of infection. Building on this technique, we propose an improved gunsight suture technique. A drainage tube is placed at the lowest point of the incision and close the gap in the center of the gunsight suture, which theoretically facilitates early postoperative mobility and reduces the burden of dressing changes, thereby reducing the risk of postoperative complications.

AIM

To compare the effectiveness of improved gunsight suture technique with traditional interrupted suture in closing intestinal stomas.

METHODS

In this study, a retrospective, single-center case analysis was conducted on 270

patients who underwent prophylactic ileostomy closure surgery at the Department of Colorectal Surgery of Qilu Hospital from April 2017 to December 2021. The patients were divided into two groups: 135 patients received sutures using the improved gunsight method, while the remaining 135 patients were sutured with the traditional interrupted suture method. We collected data on a variety of parameters, such as operation time, postoperative pain score, body temperature, length of hospital stays, laboratory indicators, incidence of incisional complications, number of wound dressing changes, and hospitalization costs. Non-parametric tests and chi-square tests were utilized for data analysis.

RESULTS

There were no statistically significant differences in general patient information between the two groups, including the interval between the first surgery and the stoma closure [132 (105, 184) d *vs* 134 (109, 181) d, $P = 0.63$], gender ratio (0.64 *vs* 0.69, $P = 0.44$), age [62 (52, 68) years *vs* 60 (52, 68) years, $P = 0.33$], preoperative body mass index (BMI) [23.83 (21.60, 25.95) kg/m² *vs* 23.12 (20.94, 25.06) kg/m², $P = 0.17$]. The incidence of incision infection in the improved gunsight suture group tended to be lower than that in the traditional interrupted suture group [($n = 2/135$, 1.4%) *vs* ($n = 10/135$, 7.4%), $P < 0.05$], and the postoperative hospital stay in the improved gunsight suture group was significantly shorter than that in the traditional interrupted suture group [5 (4, 7) d *vs* 7 (6, 8) d, $P < 0.05$]. Additionally, the surgical cost in the modified gunsight suture group was slightly lower than that in the traditional suture group [4840 (4330, 5138) yuan *vs* 4980 (4726, 5221) yuan, $P > 0.05$], but there was no significant difference in the total hospitalization cost between the two groups.

CONCLUSION

In stoma closure surgery, the improved gunsight technique can reduce the incision infection rate, shorten the postoperative hospital stay, reduce wound tension, and provide better wound cosmetic effects compared to traditional interrupted suture.

Key Words: Enterostomy; Abdominal wound closure technique; Suture techniques; Surgical wound infection; Hospital costs; Hospital stay

©The Author(s) 2023. Published by Baishideng Publishing Group Inc. All rights reserved.

Core Tip: Based on the gunsight technique, we proposed an improved gunsight closure method for enterostomy surgery in this study. This closure method can reduce the incision tension, lower the risk of incision infection, decrease the length of hospital stay, and reduce hospitalization costs. Additionally, it requires less postoperative wound care and provides a better cosmetic outcome.

Citation: Chen C, Zhang X, Cheng ZQ, Zhang BB, Li X, Wang KX, Dai Y, Wang YL. Comparison of modified gunsight suture technique and traditional interrupted suture in enterostomy closure. *World J Gastroenterol* 2023; 29(29): 4571-4579
URL: https://www.wjgnet.com/1007-9327/full/v29/i29/4571.htm
DOI: https://dx.doi.org/10.3748/wjg.v29.i29.4571

INTRODUCTION

Patients with colon cancer, inflammatory bowel disease, or intestinal trauma may require partial bowel resection. However, a simple one-stage surgery may result in complications such as anastomotic leakage, significantly affecting patient health and increasing the economic burden. To reduce this risk, a prophylactic intestinal stoma is often performed in patients at high risk for anastomotic leakage during routine surgery[1,2]. After 2-3 mo, the patient's condition was evaluated and a second-stage anastomosis was performed to restore gastrointestinal continuity[3]. Although prophylactic intestinal stoma can reduce complications such as anastomotic leakage[4], second-stage anastomotic surgery also has its own risks, including incision infection, intestinal obstruction, and incisional hernia[5-8]. Unlike Class II incisions in other gastrointestinal surgeries, the skin around the colostomy site is continuously exposed to feces, classifying it as a Class III incision. Incision infections are particularly common, with an incidence of up to 41% reported[9]. Due to factors, such as contamination of the intestinal contents, preventing incision infections may be challenging.

According to guidelines published by different countries, surgical site infection increases hospital stay and the risk of death by 2-11 times[10-13]. To address this issue, researchers have proposed improved surgical methods, such as placing drainage tubes at the incision site, selecting special suture materials, and modifying the suture technique[14-19]. Some special antimicrobial suture materials and techniques are highly regarded; however, there is currently no recognized surgical procedure to reduce the incidence of incision infections. Studies have shown that compared with traditional interrupted sutures, the purse-string suture technique can effectively drain subcutaneous fluid and significantly reduce the incidence of incision infections. However, owing to the high tension at the center of the incision[20-22], the healing

process of the abdominal incision after closure may take up to 3 wk.

In 2010, Lim *et al*[23] proposed a suture technique called "gunsight suture" that can reduce tension at the incision site and leave a smaller drainage gap at the center of the incision. This technique can effectively drain subcutaneous blood and fluid, reduce infection rate, and provide good cosmetic results with minimal scarring[20,24,25]. However, it is difficult to drain all the subcutaneous blood and fluid by placing a drainage tube or strip at an angle in the central gap. In addition, the vertical placement of the drainage tube significantly affects the postoperative activity range, and frequent dressing changes are required owing to leakage at the center of the incision, which can cause serious psychological and economic burdens on patients. Moreover, fixing the drainage tube in the central gap of the gunsight suture incision is challenging; therefore, drainage strips are often used, resulting in a shorter drainage time and a slightly inferior drainage effect.

Therefore, in our hospital, we reserve a smaller gap (approximately 0.2 cm) at the center and place a drainage tube through the entire subcutaneous gap in a small incision next to the incision. The catheter was left in place for approximately 14 d and removed after the incision healed (Figure 1). This design effectively drained the subcutaneous fluid and reduced the local tension at the incision site (Figure 1C). Theoretically, it can reduce the incidence of incision infection, shorten the postoperative hospital stay, provide better cosmetic results, and reduce hospitalization costs. To verify the significance of the improved gunsight suture method in clinical practice, data were collected from 270 patients who underwent ileostomy closure surgery between April 2017 and December 2022. Our findings are reported below.

MATERIALS AND METHODS

Study design

This retrospective case-control study was conducted between April 2017 and December 2022 to evaluate the effectiveness of a modified surgical technique for ileostomy closure and lateral ileal anastomosis. This study was approved by the Ethics Committee of Qilu Hospital, Shandong University (Approval No: KYLL-2020-120).

Participants

A total of 270 patients who underwent ileostomy closure and ileo-ileal lateral anastomosis surgery at the Department of Colorectal Surgery at Qilu Hospital were included in this study.

Inclusion criteria: Age > 18 years, patients who underwent ileostomy closure and ileo-ileal lateral anastomosis surgery, no stenosis of the intestinal lumen near the stoma on preoperative colonoscopy, and no concomitant colitis.

Exclusion criteria: Patients who required hernia repair due to concomitant incisional hernia, patients with mental dysfunction, and patients with other tumors, serious illnesses, or severe abdominal adhesions.

Preoperative preparation

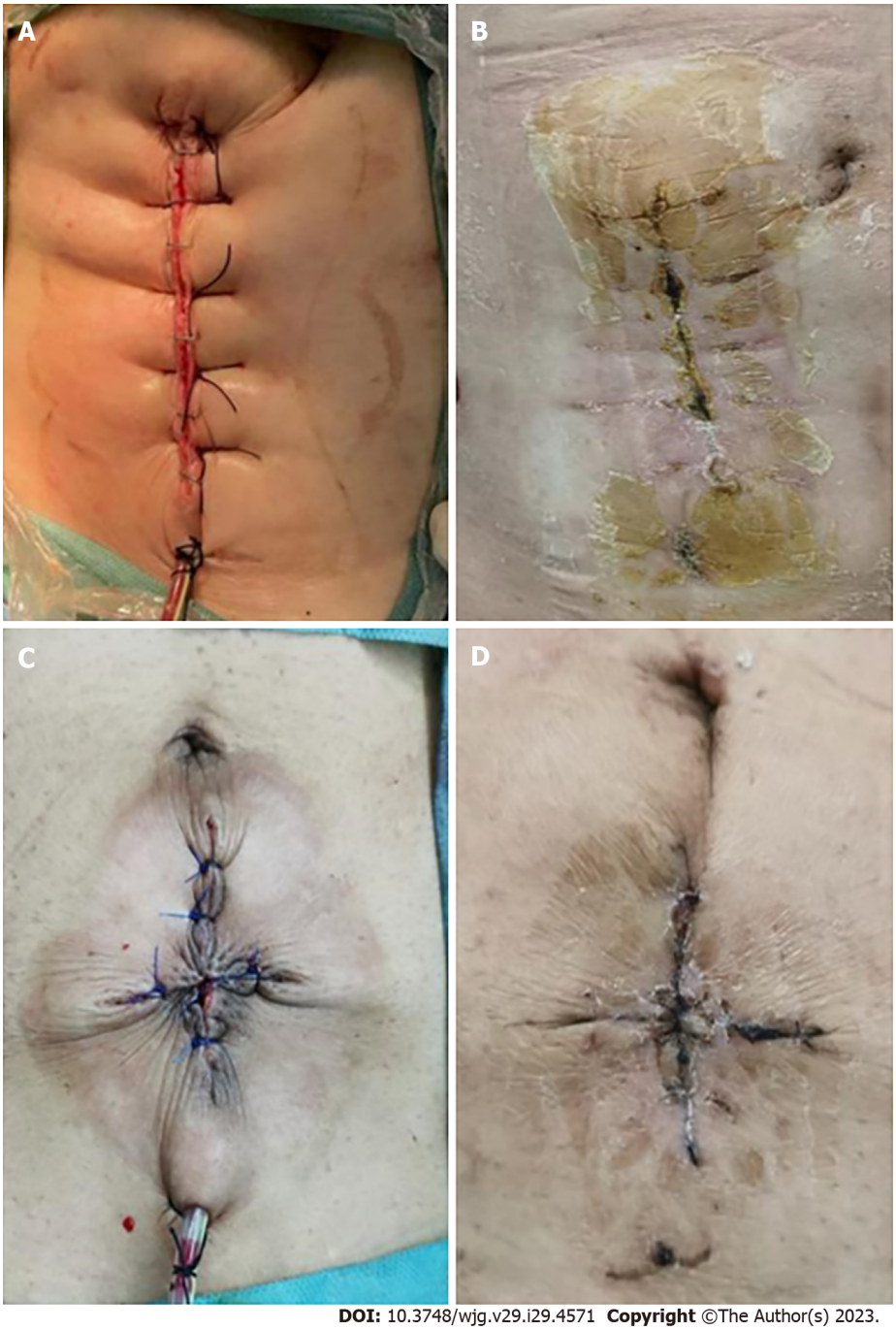
The day before surgery, the patient underwent mechanical bowel preparation with polyethylene glycol and rectal cleansing enema. This procedure improved the patient's general condition, eliminated distant obstruction, and controlled the inflammation around the stoma. Prophylactic antibiotics were administered 30 min before surgery to prevent infection.

Surgical procedure

After the patients were fully anesthetized, they were placed in the supine position. First, a 2-0 silk suture was used to close the ileostomy and prevent intestinal contents from spilling out during the reduction process. After re-disinfecting, an appropriate stoma incision was made using the suturing method. The tissues surrounding the stoma were separated layer by layer to avoid damage to the intestinal wall. The freed intestine was then separated in all directions, and the direction with less adhesion was chosen to cut open the peritoneum and enter the abdominal cavity where the adhesions were loosened. The two ends of the freed intestinal tube were pulled out of the abdominal wall by > 5 cm, and a linear cutting closure device was used to perform a side-to-side anastomosis of the proximal and distal ends of the ileum to restore intestinal continuity. The 4-0 absorbable suture (Vycrl, Ethicon) was used to intermittently suture and reinforce the ileal muscularis layers. The bowel is returned to the abdominal cavity without placement of an abdominal drainage tube. Subsequently, a continuous suture is performed using 2-0 absorbable antibacterial sutures (VCP-603) to close the peritoneum and rectal sheath, leaving a subcutaneous drainage tube in place. The appropriate skin closure method is chosen based on the group.

Simple interrupted suture group (A, B): No or only minimal trimming is required at the site of repositioning. A 2-0 suture is used for full-thickness vertical mattress suturing, with a needle margin of 1 cm, a stitch spacing of 2 cm, and avoiding residual ineffective cavities. Reinforcement sutures can be placed between every two stitches, with a needle margin of 0.5 cm. This approach can better support skin closure and reduce tension on the surgical incision. After disinfection, sterile auxiliary materials are used for compression and bandaging.

Modified gunsight suture group (C, D): The incision was marked at the 3, 6, 9, and 12 o'clock positions, and the skin tissue between the marked points was triangularly excised to form a gunsight incision. A 2-0 silk suture was used to suture the subcutaneous tissue at the four marked points, and the skin was tightened and knotted after closure. The central part of the incision was brought together as closely as possible without leaving or leaving a gap of approximately



DOI: 10.3748/wjg.v29.i29.4571 **Copyright** ©The Author(s) 2023.

Figure 1 Surgical stitching result diagram. A: Photo of incision closed with traditional interrupted suture; B: Postoperative photo of incision healing after traditional interrupted suture; C: Photo of incision closed with improved gunsight suture; D: Postoperative photo of incision healing after improved gunsight suture.

0.2 cm. Finally, a 2-0 silk suture was used to suture the midpoints of the four edges of the gunsight incision to complete the reinforcement. After disinfection, sterile auxiliary materials were applied for compression and bandaging.

Observation indicators

The patients' baseline data included age, sex, surgery time, postoperative pain score, postoperative temperature changes, hospitalization time, postoperative laboratory indicators, incision infection rate, and hospitalization costs. The temperature was recorded for 3 d after surgery. The Numeric Rating Scale (NRS) was used to assess the pain scores.

Statistical analysis

Data analysis was performed using the SPSS 26 statistical software. Normally distributed metric data were expressed as mean ± SD and intergroup comparisons were performed using independent sample *t*-tests. Non-normally distributed quantitative data were expressed as median (interquartile range) [M (IQR)], and intergroup comparisons were performed using the Mann-Whitney *U* test. Categorical variables were expressed as frequencies, and intergroup comparisons were

performed using Chi-squared test or Fisher's exact test. Statistical significance was set at $P < 0.05$.

RESULTS

The study included 270 patients who underwent stoma closure surgery at Qilu Hospital. All the patients completed the procedure without anastomotic leakage. Among them, 135 patients received modified Gunsight sutures, and 135 received traditional simple interrupted sutures. Statistical comparisons showed no significant differences in sex ratio, age, preoperative BMI, or the proportion of patients with diabetes between the two groups (Table 1).

Laboratory indicators included the systemic immune inflammation index (SII), red blood cell count, and hemoglobin levels. The SII was calculated as the platelet count multiplied by the ratio of neutrophils to lymphocytes and was used as a simple and effective evaluation index to assess the immune and inflammatory status and prognosis of patients before and after colorectal surgery. Previous studies have shown that the SII is an independent risk factor for the prognosis of colorectal cancer patients. There were no statistically significant differences in the laboratory indicators between the two groups[26-28].

According to the comparison of the main observation indicators (Table 2), the incidence of surgical site infection (SSI) in the modified gunsight suture group was lower than that in the traditional simple interrupted suture group [(n = 2/135, 1.4%) *vs* (n = 10/135, 7.4%), $P < 0.05$], and the length of hospital stay and the number of dressing changes were also significantly better than those in the traditional simple interrupted suture group. However, there were no significant differences in the postoperative body temperature, pain score, or postoperative first bowel gas passage time between the two groups ($P > 0.05$). In addition, we compared the surgical and hospitalization costs between the two groups and found that the surgical cost in the modified Gunsight suture group was slightly lower than that in the traditional suture group [4840 (4330, 5138) yuan *vs* 4980 (4726, 5221) yuan, $P > 0.05$], but there was no significant difference in the total hospitalization cost between the two groups. Furthermore, scar formation after incision healing was significantly lower in the modified Gunsight suture group than in the control group (Figure 1B and D).

DISCUSSION

During stoma closure surgery in patients who undergo preventive ostomy, there is a high incidence of incisional infections due to environmental contamination, subcutaneous fluid accumulation, and other reasons, with reported rates ranging from 3% to 41%[29]. This delay in wound healing can severely affect patients' quality of life. To reduce the risk of postoperative incisional infections, many clinicians have proposed improvements in the suture method of the incision [20], among which the modified Gunsight suture technique has shown promise.

Reid *et al*[30] conducted a randomized controlled clinical trial involving 61 patients to compare postoperative complications of the purse-string suture technique with those of the traditional simple interrupted suture technique. They found that purse-string sutures had fewer surgical site infections than conventional sutures, with two out of 30 patients experiencing infections compared to 12 out of 31 patients in the conventional suture group[30]. In a multicenter prospective study by Han *et al*[20], the effectiveness of the gunsight and purse-string suture techniques in closing skin incisions was compared. This study found that the gunsight suture technique has a lower incision infection rate, similar to that of the purse-string suture technique. Additionally, patients in the Gunsight suture group had shorter incision healing times and higher patient satisfaction[20]. In a case-review study of 233 patients, Li *et al*[31] compared the clinical characteristics between patients with traditional simple interrupted sutures and those with gunsight sutures. The incidence of surgical site infections was significantly lower in the Gunsight suture group than in the traditional simple interrupted suture group. Gunsight sutures were identified as an independent protective risk factor for surgical site infections, with a dominance ratio of 0.212 and a P value of 0.048.

This study showed that our modified Gunsight suture technique is associated with a lower incidence of surgical site infection when compared with the traditional simple interrupted suture technique. Specifically, 10 patients in the traditional simple interrupted suture group experienced postoperative incisional infections, with three of these patients requiring a second surgical intervention and wound resuturing after failed conservative treatment. In contrast, only two patients in the modified gunsight suture group developed postoperative incisional infections, which resolved after conservative treatment. These findings provide evidence supporting the effectiveness of the modified Gunsight suture technique in reducing the risk of incisional infection.

In addition to the reduced incidence of SSI, patients in the modified Gunsight suture group also experienced shorter postoperative hospitalization days than those in the simple interrupted suture group. This difference in hospitalization time may be due to an increased risk of incision infection and the need for more frequent and longer wound care, such as wet alcohol dressing, in the simple interrupted suture group.

Furthermore, the surgical costs for patients in the gunsight suture group were slightly lower than those in the traditional suture group, and there was no significant difference in total hospitalization costs between the two groups. Furthermore, there were no significant differences between the two groups in terms of postoperative pain scores, exhaust time, and related laboratory indicators. Postoperative pain scores were evaluated using the NRS, with most patients scoring between 1 and 3 indicating mild pain. This may explain the lack of significant differences between the two groups. Additionally, the postoperative exhaust time and laboratory test results were not significantly associated with wound closure.

Table 1 General information

Group	Gunsight suture	Traditional suture	Statistical quantity	*P* value
Case number	135	135	-	-
Male (%)	86 (63.7)	92 (68.1)	$\chi^2 = 0.59$	0.440
Age in yr (IQR)	62 (52, 68)	60 (52, 68)	$Z = -0.97$	0.332
BMI (IQR)	23.83 (21.60, 25.95)	23.12 (20.94, 25.06)	$Z = -1.377$	0.169
DM (%)	17 (12.6)	23 (17.0)	$\chi^2 = 1.06$	0.300
Length of time between two surgeries, d (IQR)	132 (105, 184)	134 (109, 181)	$Z = -0.489$	0.625

BMI: Body mass index [a commonly used index to assess the relationship between weight and height, usually expressed in units of kilograms per square meter (kg/m²)]; DM: Diabetes mellitus (a chronic metabolic disease characterized by prolonged high blood sugar levels); IQR: Interquartile range [a statistical measure used to describe the spread of a dataset, it represents the span of the middle 50% of the data and is calculated as the difference between the first quartile (Q1) and the third quartile (Q3)].

Table 2 Patient observation indicators

Group		Gunsight suture (IQR)	Traditional suture (IQR)	Statistical quantity	*P* value
SII (postoperative/preoperative)		3.24 (2.16, 4.78)	3.14 (2.10, 5.47)	$Z = -0.592$	0.554
Red blood cell (postoperative/preoperative)		0.90 (0.84, 0.95)	0.91 (0.87, 9.96)	$Z = -1.445$	0.148
Haemoglobin (postoperative/postoperative)		0.91 (0.85, 0.97)	0.92 (0.88, 0.96)	$Z = -1.231$	0.218
SSI (%)		2 (1.4)	10 (7.4)	$\chi^2 = -5.580$	0.018
Postoperative intestinal exhaust time (d)		3 (2, 3)	3 (2, 3)	$Z = -1.171$	0.242
Total cost of hospitalization (Yuan)		33569 (30545, 36757)	32782 (29134, 36199)	$Z = -1.199$	0.230
Cost of surgery (Yuan)		4840 (4330, 5138)	4980 (4726, 5221)	$Z = -2.745$	0.006
Number of dressing changes for surgical incision		2 (1, 3)	4 (3, 6)	$Z = -2.460$	< 0.001
Operation time		80 (70, 90)	80 (70, 85)	$Z = -1.210$	0.220
Early postoperative pain score (NRS)	DAY1	3 (3, 3)	3 (3, 3)	$Z = -1.145$	0.252
	DAY2	2 (2, 2)	2 (2, 2)	$Z = -0.044$	0.965
	DAY3	2.0 (1.5, 2.0)	1.5 (1.5, 2.0)	$Z = -0.603$	0.547
Early postoperative body temperature (°C)	DAY1	36.7 (36.4, 36.9)	36.7 (36.4, 36.9)	$Z = -0.476$	0.634
	DAY2	37.4 (37.1, 37.9)	37.6 (37.1, 38.1)	$Z = -1.769$	0.077
	DAY3	37.1 (36.9, 37.4)	37.20 (36.85, 37.50)	$Z = -1.385$	0.166
	DAY4	36.9 (36.7, 37.1)	36.9 (36.7, 37.3)	$Z = -1.315$	0.189
Postoperative hospital stay (d)		5 (4, 7)	7 (6, 8)	$Z = -5.181$	< 0.001

SII: Systemic immune inflammation index (a composite index based on peripheral blood neutrophil, lymphocyte, and platelet counts, used to reflect the systemic inflammatory response in patients with various diseases); SSI: Surgical site infection (an infection that occurs after surgery in the part of the body where the surgery took place); Postoperative Pain Score (NRS): Numeric Rating Scale (a commonly used tool to assess the intensity of postoperative pain. It consists of a scale from 0 to 10, where 0 represents no pain and 10 represents the worst possible pain).

CONCLUSION

The modified Gunsight suture technique is an effective method for reducing the risk of surgical site infection and shortening postoperative hospitalization. Although this technique may require additional surgical steps, the reduced incidence of SSI and lower surgical costs make it a viable option for wound closure. Further research is needed to investigate the potential benefits of this technique in larger patient populations and evaluate its long-term effectiveness.

ARTICLE HIGHLIGHTS

Research background

In the traditional intestinal stoma closure surgery, the interrupted suturing technique used has some issues, such as longer incisions and higher tension on the incision, which may increase the risk of postoperative complications. To address these concerns, scholars have proposed the use of the "gunsight suture" technique. This method involves using a gun-shaped incision instead of the conventional linear incision, leaving a gap in the center for drainage of blood and fluids to reduce the risk of infection. Building on this, we have proposed an improved gunsight suture technique.

Research motivation

Motivated by the need to enhance patient outcomes, this study focuses on developing an improved prophylactic stoma reversal abdominal closure suturing technique. Our goal is to reduce incision infection rates and alleviate patient burden, improving a key issue in stoma closure methods. We strive to contribute to the advancement of surgical research and help shape safer and more effective surgical practices in the future.

Research objectives

To compare the outcomes of the improved gunsight suture technique with traditional interrupted suture techniques in enterostomy closure. The objective is to minimize complications and related burdens following prophylactic ileostomy closure.

Research methods

This study analyzed 270 patients who underwent prophylactic ileostomy closure surgery at Qilu Hospital from April 2017 to December 2021. The patients were divided into two groups, one group received sutures using the improved gunsight method while the other group was sutured with the traditional interrupted suture method, and data on various parameters such as operation time, postoperative pain score, and hospitalization costs were collected. Non-parametric tests and chi-square tests were used for data analysis.

Research results

This retrospective study compared two suture methods for prophylactic ileostomy closure surgery in 270 patients. The modified gunsight suture group had better outcomes, including lower incidence of surgical site infections, shorter hospital stays, and fewer dressing changes than the traditional simple interrupted suture group. Laboratory parameters, postoperative temperature, pain scores, and time to first bowel gas passage did not differ significantly. The modified gunsight suture group had slightly lower surgical costs and significantly lower scar formation after incision healing.

Research conclusions

The modified Gunsight suture technique reduces the risk of surgical site infection and shortens postoperative hospitalization. Despite requiring additional surgical steps, the technique lowers surgical costs and is a viable option for wound closure.

Research perspectives

Despite the study's retrospective design and challenges in obtaining accurate data on bowel obstruction incidence and long-term complications like incisional hernias, it provides valuable insights. However, the single-center data source may introduce bias during data collection and analysis. Further research on larger patient populations is needed to evaluate the technique's long-term effectiveness and potential benefits.

FOOTNOTES

Author contributions: Chen C and Zhang X contributed equally to this work; Wang YL, Zhang X, Cheng ZQ, Zhang BB, Wang KX, and Dai Y designed the study; Chen C and Li X carried out relevant clinical work and data collection; Chen C and Zhang X analyzed the data and wrote the manuscript; and all authors have read and approved the final manuscript.

Supported by the Natural Science Foundation of Shandong Province, No. ZR2020MH257.

Institutional review board statement: The study was reviewed and approved by the Ethics Committee of Qilu Hospital (Approval No. KYLL-2020-120).

Informed consent statement: Patients were not required to give informed consent to the study because the analysis used anonymous clinical data that were obtained after each patient agreed to treatment by written consent.

Conflict-of-interest statement: The authors declare that they have no conflict of interest.

Data sharing statement: The dataset generated or analyzed in this study is not available to the public. Due to privacy and ethical considerations, we are unable to provide relevant data. We will ensure compliance with relevant regulations and policies to protect the

privacy and confidentiality of participants. If you have specific questions or questions about this study, please feel free to contact the corresponding author at any time.

STROBE statement: The authors have read the STROBE Statement—checklist of items, and the manuscript was prepared and revised according to the STROBE Statement—checklist of items.

Open-Access: This article is an open-access article that was selected by an in-house editor and fully peer-reviewed by external reviewers. It is distributed in accordance with the Creative Commons Attribution NonCommercial (CC BY-NC 4.0) license, which permits others to distribute, remix, adapt, build upon this work non-commercially, and license their derivative works on different terms, provided the original work is properly cited and the use is non-commercial. See: https://creativecommons.org/Licenses/by-nc/4.0/

Country/Territory of origin: China

ORCID number: Chang Chen 0000-0001-7964-1473; Yong Dai 0000-0001-6163-8022; Yan-Lei Wang 0000-0002-4227-0274.

S-Editor: Chen YL
L-Editor: A
P-Editor: Yu HG

REFERENCES

1 **Hüser N**, Michalski CW, Erkan M, Schuster T, Rosenberg R, Kleeff J, Friess H. Systematic review and meta-analysis of the role of defunctioning stoma in low rectal cancer surgery. *Ann Surg* 2008; **248**: 52-60 [PMID: 18580207 DOI: 10.1097/SLA.0b013e318176bf65]
2 **Gastinger I**, Marusch F, Steinert R, Wolff S, Koeckerling F, Lippert H; Working Group 'Colon/Rectum Carcinoma'. Protective defunctioning stoma in low anterior resection for rectal carcinoma. *Br J Surg* 2005; **92**: 1137-1142 [PMID: 15997447 DOI: 10.1002/bjs.5045]
3 **Chow A**, Tilney HS, Paraskeva P, Jeyarajah S, Zacharakis E, Purkayastha S. The morbidity surrounding reversal of defunctioning ileostomies: a systematic review of 48 studies including 6,107 cases. *Int J Colorectal Dis* 2009; **24**: 711-723 [PMID: 19221766 DOI: 10.1007/s00384-009-0660-z]
4 **Mrak K**, Uranitsch S, Pedross F, Heuberger A, Klingler A, Jagoditsch M, Weihs D, Eberl T, Tschmelitsch J. Diverting ileostomy *vs* no diversion after low anterior resection for rectal cancer: A prospective, randomized, multicenter trial. *Surgery* 2016; **159**: 1129-1139 [PMID: 26706610 DOI: 10.1016/j.surg.2015.11.006]
5 **Krebs B**, Ivanecz A, Potrc S, Horvat M. Factors affecting the morbidity and mortality of diverting stoma closure: retrospective cohort analysis of twelve-year period. *Radiol Oncol* 2019; **53**: 331-336 [PMID: 31553701 DOI: 10.2478/raon-2019-0037]
6 **Åkesson O**, Syk I, Lindmark G, Buchwald P. Morbidity related to defunctioning loop ileostomy in low anterior resection. *Int J Colorectal Dis* 2012; **27**: 1619-1623 [PMID: 22576906 DOI: 10.1007/s00384-012-1490-y]
7 **Sajid MS**, Craciunas L, Baig MK, Sains P. Systematic review and meta-analysis of published, randomized, controlled trials comparing suture anastomosis to stapled anastomosis for ileostomy closure. *Tech Coloproctol* 2013; **17**: 631-639 [PMID: 23681301 DOI: 10.1007/s10151-013-1027-6]
8 **Faunø L**, Rasmussen C, Sloth KK, Sloth AM, Tøttrup A. Low complication rate after stoma closure. Consultants attended 90% of the operations. *Colorectal Dis* 2012; **14**: e499-e505 [PMID: 22340709 DOI: 10.1111/j.1463-1318.2012.02991.x]
9 **Milanchi S**, Nasseri Y, Kidner T, Fleshner P. Wound infection after ileostomy closure can be eliminated by circumferential subcuticular wound approximation. *Dis Colon Rectum* 2009; **52**: 469-474 [PMID: 19333048 DOI: 10.1007/DCR.0b013e31819acc90]
10 **Anderson DJ**, Podgorny K, Berríos-Torres SI, Bratzler DW, Dellinger EP, Greene L, Nyquist AC, Saiman L, Yokoe DS, Maragakis LL, Kaye KS. Strategies to prevent surgical site infections in acute care hospitals: 2014 update. *Infect Control Hosp Epidemiol* 2014; **35**: 605-627 [PMID: 24799638 DOI: 10.1086/676022]
11 **Bratzler DW**, Dellinger EP, Olsen KM, Perl TM, Auwaerter PG, Bolon MK, Fish DN, Napolitano LM, Sawyer RG, Slain D, Steinberg JP, Weinstein RA; American Society of Health-System Pharmacists; Infectious Disease Society of America; Surgical Infection Society; Society for Healthcare Epidemiology of America. Clinical practice guidelines for antimicrobial prophylaxis in surgery. *Am J Health Syst Pharm* 2013; **70**: 195-283 [PMID: 23327981 DOI: 10.2146/ajhp120568]
12 **Mangram AJ**, Horan TC, Pearson ML, Silver LC, Jarvis WR. Guideline for prevention of surgical site infection, 1999. Hospital Infection Control Practices Advisory Committee. *Infect Control Hosp Epidemiol* 1999; **20**: 250-78; quiz 279 [PMID: 10219875 DOI: 10.1086/501620]
13 **Magill SS**, Edwards JR, Bamberg W, Beldavs ZG, Dumyati G, Kainer MA, Lynfield R, Maloney M, McAllister-Hollod L, Nadle J, Ray SM, Thompson DL, Wilson LE, Fridkin SK; Emerging Infections Program Healthcare-Associated Infections and Antimicrobial Use Prevalence Survey Team. Multistate point-prevalence survey of health care-associated infections. *N Engl J Med* 2014; **370**: 1198-1208 [PMID: 24670166 DOI: 10.1056/NEJMoa1306801]
14 **Banerjee A**. Pursestring skin closure after stoma reversal. *Dis Colon Rectum* 1997; **40**: 993-994 [PMID: 9269819 DOI: 10.1007/BF02051210]
15 **Pan HD**, Wang L, Peng YF, Li M, Yao YF, Zhao J, Zhan TC, Du CZ, Gu J. Subcutaneous vacuum drains reduce surgical site infection after primary closure of defunctioning ileostomy. *Int J Colorectal Dis* 2015; **30**: 977-982 [PMID: 25700809 DOI: 10.1007/s00384-015-2168-z]
16 **Cantero R**, Rubio-Perez I, Leon M, Alvarez M, Diaz B, Herrera A, Diaz-Dominguez J, Rodriguez-Montes JA. Negative-Pressure Therapy to Reduce the Risk of Wound Infection Following Diverting Loop Ileostomy Reversal: An Initial Study. *Adv Skin Wound Care* 2016; **29**: 114-118 [PMID: 26866867 DOI: 10.1097/01.ASW.0000480458.60005.34]
17 **Blinov AV**, Kachanov MD, Gvozdenko AA, Nagdalian AA, Blinova AA, Rekhman ZA, Golik AB, Vakalov DS, Maglakelidze DG, Nagapetova AG, Pokhilko AD, Burkina IV. Synthesis and Characterization of Zinc Oxide Nanoparticles Stabilized with Biopolymers for Application in Wound-Healing Mixed Gels. *Gels* 2023; **9** [PMID: 36661823 DOI: 10.3390/gels9010057]
18 **Blinov AV**, Nagdalian AA, Povetkin SN, Gvozdenko AA, Verevkina MN, Rzhepakovsky IV, Lopteva MS, Maglakelidze DG, Kataeva TS,

Blinova AA, Golik AB, Osipchuk GV, Shariati MA. Surface-Oxidized Polymer-Stabilized Silver Nanoparticles as a Covering Component of Suture Materials. *Micromachines (Basel)* 2022; **13** [PMID: 35888922 DOI: 10.3390/mi13071105]

19 **Dragovic M**, Pejovic M, Stepic J, Colic S, Dozic B, Dragovic S, Lazarevic M, Nikolic N, Milasin J, Milicic B. Comparison of four different suture materials in respect to oral wound healing, microbial colonization, tissue reaction and clinical features-randomized clinical study. *Clin Oral Investig* 2020; **24**: 1527-1541 [PMID: 31342245 DOI: 10.1007/s00784-019-03034-4]

20 **Han JG**, Yao HW, Zhou JP, Zhang H, Wang GY, Shen ZL, Gong JF, Wang ZJ; Colorectal Surgery Group of Chinese Academic Society of Young Surgeons. Gunsight Procedure Versus the Purse-String Procedure for Closing Wounds After Stoma Reversal: A Multicenter Prospective Randomized Trial. *Dis Colon Rectum* 2020; **63**: 1411-1418 [PMID: 32969884 DOI: 10.1097/DCR.0000000000001755]

21 **Amano K**, Ishida H, Kumamoto K, Okada N, Hatano S, Chika N, Tajima Y, Ohsawa T, Yokoyama M, Ishibashi K, Mochiki E. Purse-string approximation *vs* primary closure with a drain for stoma reversal surgery: results of a randomized clinical trial. *Surg Today* 2019; **49**: 231-237 [PMID: 30367238 DOI: 10.1007/s00595-018-1729-5]

22 **Hajibandeh S**, Hajibandeh S, Kennedy-Dalby A, Rehman S, Zadeh RA. Purse-string skin closure *vs* linear skin closure techniques in stoma closure: a comprehensive meta-analysis with trial sequential analysis of randomised trials. *Int J Colorectal Dis* 2018; **33**: 1319-1332 [PMID: 30074070 DOI: 10.1007/s00384-018-3139-y]

23 **Lim JT**, Shedda SM, Hayes IP. "Gunsight" skin incision and closure technique for stoma reversal. *Dis Colon Rectum* 2010; **53**: 1569-1575 [PMID: 20940608 DOI: 10.1007/DCR.0b013e3181f0535a]

24 **Lee JR**, Kim YW, Sung JJ, Song OP, Kim HC, Lim CW, Cho GS, Jung JC, Shin EJ. Conventional Linear *vs* Purse-string Skin Closure after Loop Ileostomy Reversal: Comparison of Wound Infection Rates and Operative Outcomes. *J Korean Soc Coloproctol* 2011; **27**: 58-63 [PMID: 21602963 DOI: 10.3393/jksc.2011.27.2.58]

25 **Moreton A**, Shankar S, Jones S. Randomized clinical trial of short-term outcomes following purse-string *vs* conventional closure of ileostomy wounds (Br J Surg 2010; 97: 1511-1517). *Br J Surg* 2011; **98**: 458; author reply 458 [PMID: 21254027 DOI: 10.1002/bjs.7439]

26 **Xie QK**, Chen P, Hu WM, Sun P, He WZ, Jiang C, Kong PF, Liu SS, Chen HT, Yang YZ, Wang D, Yang L, Xia LP. The systemic immune-inflammation index is an independent predictor of survival for metastatic colorectal cancer and its association with the lymphocytic response to the tumor. *J Transl Med* 2018; **16**: 273 [PMID: 30286769 DOI: 10.1186/s12967-018-1638-9]

27 **Mangalesh S**, Dudani S, Malik A. The systemic immune-inflammation index in predicting sepsis mortality. *Postgrad Med* 2023; **135**: 345-351 [PMID: 36287784 DOI: 10.1080/00325481.2022.2140535]

28 **Dong M**, Shi Y, Yang J, Zhou Q, Lian Y, Wang D, Ma T, Zhang Y, Mi Y, Gu X, Fan R. Prognostic and clinicopathological significance of systemic immune-inflammation index in colorectal cancer: a meta-analysis. *Ther Adv Med Oncol* 2020; **12**: 1758835920937425 [PMID: 32699557 DOI: 10.1177/1758835920937425]

29 **Dusch N**, Goranova D, Herrle F, Niedergethmann M, Kienle P. Randomized controlled trial: comparison of two surgical techniques for closing the wound following ileostomy closure: purse string *vs* direct suture. *Colorectal Dis* 2013; **15**: 1033-1040 [PMID: 23634717 DOI: 10.1111/codi.12211]

30 **Reid K**, Pockney P, Pollitt T, Draganic B, Smith SR. Randomized clinical trial of short-term outcomes following purse-string *versus* conventional closure of ileostomy wounds. *Br J Surg* 2010; **97**: 1511-1517 [PMID: 20575111 DOI: 10.1002/bjs.7151]

31 **Li CK**, Liang WW, Wang HM, Guo WT, Qin XS, Zhao J, Zhou WB, Li Y, Wang H, Huang RK. Gunsight sutures significantly reduce surgical-site infection after ileostomy reversal compared with linear sutures. *Gastroenterol Rep (Oxf)* 2021; **9**: 357-362 [PMID: 34567568 DOI: 10.1093/gastro/goaa075]

World Journal of Gastroenterology

Submit a Manuscript: https://www.f6publishing.com

World J Gastroenterol 2023 August 7; 29(29): 4580-4592

DOI: 10.3748/wjg.v29.i29.4580

ISSN 1007-9327 (print) ISSN 2219-2840 (online)

ORIGINAL ARTICLE

Retrospective Study

Prevalence and risk factors of osteoporosis detected by dual-energy X-ray absorptiometry among Chinese patients with primary biliary cholangitis

Jia-Liang Chen, Yao Liu, Yu-Fei Bi, Xian-Bo Wang

Specialty type: Gastroenterology and hepatology

Provenance and peer review: Unsolicited article; Externally peer reviewed.

Peer-review model: Single blind

Peer-review report's scientific quality classification

Grade A (Excellent): A
Grade B (Very good): B
Grade C (Good): C
Grade D (Fair): 0
Grade E (Poor): 0

P-Reviewer: Jennane R, France; Kuroki H, Japan; Lee MK, South Korea

Received: June 7, 2023
Peer-review started: June 7, 2023
First decision: June 16, 2023
Revised: June 21, 2023
Accepted: July 19, 2023
Article in press: July 19, 2023
Published online: August 7, 2023

Jia-Liang Chen, Yao Liu, Yu-Fei Bi, Xian-Bo Wang, Center of Integrative Medicine, Beijing Ditan Hospital, Capital Medical University, Beijing 100015, China

Corresponding author: Xian-Bo Wang, MD, PhD, Chief Physician, Professor, Center of Integrative Medicine, Beijing Ditan Hospital, Capital Medical University, No. 8 Jing Shun East Street, Beijing 100015, China. wangxb@ccmu.edu.cn

Abstract

BACKGROUND

Osteoporosis is an extrahepatic complication of primary biliary cholangitis (PBC) that increases the risk of fractures and mortality. However, Epidemiological studies of osteoporosis in patients with PBC in China and the Asia-Pacific region is lack.

AIM

To assess the prevalence and clinical characteristics of osteoporosis in Chinese patients with PBC.

METHODS

This retrospective analysis included consecutive patients with PBC from a tertiary care center in China who underwent bone mineral density (BMD) assessment using dual-energy X-ray absorptiometry between January 2013 and December 2021. We defined subjects with T-scores ≤ -2.5 in any sites (L1 to L4, femoral neck, or total hip) as having osteoporosis. Demographic, serological, clinical, and histological data were collected. Independent risk factors for osteoporosis were identified by multivariate logistic regression analysis.

RESULTS

A total of 268 patients with PBC [236 women (88.1%); mean age, 56.7 ± 10.6 years; 163 liver biopsies (60.8%)] were included. The overall prevalence of osteoporosis in patients with PBC was 45.5% (122/268), with the prevalence of osteoporosis in women and men being 47.0% and 34.4%, respectively. The prevalence of osteoporosis in postmenopausal women was significantly higher than that in premenopausal women (56.3% *vs* 21.0%, $P < 0.001$). Osteoporosis in patients with PBC is associated with age, fatigue, menopausal status, previous steroid therapy, body mass index (BMI), splenomegaly, gastroesophageal varices, ascites, Mayo

risk score, histological stage, alanine aminotransferase, albumin, bilirubin, platelet and prothrombin activity. Multivariate regression analysis identified that older age, lower BMI, previous steroid therapy, higher Mayo risk score, and advanced histological stage as the main independent risk factors for osteoporosis in PBC.

CONCLUSION

Osteoporosis is very common in Chinese patients with PBC, allowing for prior screening of BMD in those PBC patients with older age, lower BMI, previous steroid therapy and advanced liver disease.

Key Words: Primary biliary cholangitis; Osteoporosis; Bone mineral density; Dual-energy X-ray absorptiometry; Prevalence; Chinese

©The Author(s) 2023. Published by Baishideng Publishing Group Inc. All rights reserved.

Core Tip: In this paper, we reported for the first large-sample study to explore the prevalence and potential risk factors for osteoporosis in Chinese patients with primary biliary cholangitis (PBC). The prevalence of osteoporosis in Chinese patients with PBC was 45.5%. Osteoporosis in PBC is strongly associated with older age, lower body mass index, previous steroid use, the severity of liver disease, and advanced histological stage. This study provides reference information for future PBC-related guideline development and public policy formulation in China and the Asia-Pacific region.

Citation: Chen JL, Liu Y, Bi YF, Wang XB. Prevalence and risk factors of osteoporosis detected by dual-energy X-ray absorptiometry among Chinese patients with primary biliary cholangitis. *World J Gastroenterol* 2023; 29(29): 4580-4592
URL: https://www.wjgnet.com/1007-9327/full/v29/i29/4580.htm
DOI: https://dx.doi.org/10.3748/wjg.v29.i29.4580

INTRODUCTION

Primary biliary cholangitis (PBC, also known as primary biliary cirrhosis) is a chronic immune-mediated, progressive cholestatic liver disease characterized by nonsuppurative destructive intrahepatic cholangitis focused on the small bile ducts, which mainly affects middle-aged women over 40 years old, typically manifested as fatigue, pruritus and even metabolic bone disease[1,2]. Currently, ursodeoxycholic acid (UDCA) is its first-line treatment drug, and untreated PBC may eventually lead to cirrhosis and liver failure, requiring liver transplantation[3]. Moreover, PBC affects all races and ethnicities with significant regional differences[1,4]. It is estimated that at least 1 in 1000 women older than 40 years globally has PBC[5], and the prevalence and incidence of PBC in Europe and the United States are higher than that in the Asia-Pacific region[6]. However, the prevalence of PBC in China ranks second only to Japan in the Asia-Pacific region and is increasing[6].

Osteoporosis is a disease characterized by decreased bone density or bone loss, leading to an increased risk of fracture [7]. The prevalence of osteoporosis in patients with PBC is at least three times that of age- or sex-matched controls[8,9]. Thus, osteoporosis is considered an extrahepatic complication of PBC[10]. Unlike increased bone resorption in postmenopausal osteoporosis, osteoporosis in PBC is mainly caused by decreased bone formation[11]. Moreover, recently, a large cohort study indicated that the risk of fracture and post-fracture mortality of PBC patients were significantly higher than those of the control group in the general population[12]. Prevention and timely diagnosis of osteoporosis are key to reducing the associated complications for patients with PBC. With the increasing prevalence of PBC, most likely due to the improvement of diagnosis and awareness, it is likely that the incidence and prevalence of PBC-related osteoporosis will also increase[11]. According to previous studies from Europe, Africa and North America, the prevalence of osteoporosis in patients with PBC is approximately 30% (range 20%-52%) and higher in postmenopause or advanced stages of liver disease[8,9,13-18], and up to 44% of patients waiting for liver transplantation[16]. However, to our knowledge, in China and other Asia–Pacific regions, the prevalence and clinical features of osteoporosis in patients with PBC, including men and women, have not been well defined.

Therefore, this study aimed to investigate the prevalence and clinical features of osteoporosis and independent risk factors associated with osteoporosis using bone mineral density (BMD) detected by dual-energy X-ray absorptiometry (DEXA) in a large series of Chinese patients with PBC.

MATERIALS AND METHODS

Study design

We carried out a retrospective observational study of all consecutive PBC patients between January 2013 and December 2021 from Beijing Ditan Hospital, China. The baseline date was the first admission with a diagnosis of PBC and completion of a BMD examination in the hospital. The study protocol was approved by the Ethics Committee of Beijing

Ditan Hospital, Beijing, China (No. DTEC-KT2022-010-01).

The inclusion criteria were as follows: (1) Age greater than 18 years old; (2) at least two of the following: Elevated γ-glutamyl transpeptidase (GGT) or alkaline phosphatase (ALP), positive antimitochondrial antibody (AMA) or gp210, sp100, and pathological features of non-suppurative cholangitis or small bile duct destruction[19]; and (3) complete BMD examination using DEXA method at baseline. The exclusion criteria were as follows: (1) Alcoholic liver disease, non-alcoholic fatty liver disease, viral hepatitis, drug-induced liver injury, or inherited liver disease; (2) liver transplantation, liver cancer, or other malignant lesions; (3) evidence of intrahepatic or extrahepatic biliary obstruction; (4) severe cardiac or renal insufficiency; (5) previous or current hormone replacement therapy; and (6) pregnancy or breast-feeding.

Data collection

A history of UDCA or steroid treatment, prior fractures, and comorbidities were recorded. Symptoms of chronic cholestasis, such as fatigue and pruritus, and physical signs of liver disease, such as splenomegaly, hepatomegaly, edema and ascites, were collected. Blood was collected for hematological, biochemical and immunological tests after an overnight fast and tested at the Laboratory of Beijing Ditan Hospital using standard methods. These laboratory parameters include serum bilirubin, albumin, ALP, GGT, calcium, phosphorus, creatinine, 25-hydroxyvitamin D, aspartate aminotransferase, alanine aminotransferase (ALT), prothrombin activity (PTA), platelet count (PLT), immunoglobulin G, serum immunoglobulin M, and autoantibodies [AMA, antinuclear antibody (ANA), anti-centromere antibody (ACA), gp210, and sp100] were measured at the time of the first BMD examination. Age, smoking status, body mass index (BMI), menopausal status, duration of PBC, histological stage, and cirrhosis status were recorded. Esophagogastroscopy and abdominal ultrasonography were also evaluated. The Mayo risk score (MRS) was calculated using the previous algorithm[20]. The liver histological stage was determined according to Ludwig's criteria[21].

BMD measurement

Certified technicians measured BMD at the lumbar spine (L1 to L4), femoral neck, and total hip using a DEXA scanner (Lunar, GE Healthcare, United States). The diagnoses of osteopenia and osteoporosis were based on the World Health Organization thresholds: T-score is between -1.0 and -2.5 and ≤ -2.5, respectively[22]. T-score were presented as absolute values (g/cm^2) and the number of SD lower than the average peak value of young sex-matched normal individuals. Z-score are also presented as the number of SD from normal values corrected for sex and age. We defined patients with T-scores ≤ -2.5 in any sites (L1 to L4, femoral neck, or total hip) as having osteoporosis[23].

Statistical analysis

All statistical analyses were performed using SPSS 20.0 (SPSS Inc., Chicago, IL, United States). Quantitative data are expressed as mean ± SD or median and interquartile range, and categorical data are expressed as frequencies with percentages. Student *t*-test or Mann-Whitney U test was used to analyse differences in continuous variables. Chi-squared or Fisher's exact tests were used for categorical variables. The independent risk factor of significant variable associated with osteoporosis with (P value < 0.05) in univariate analyses was determined using multivariate logistic regression with the backward stepwise selection method (the criteria for entering and removing variables were P < 0.05 and > 0.10, respectively). Statistical significance was defined as a two-tailed P value < 0.05.

RESULTS

Demographic and clinical characteristics

From January 2013 to December 2021, we retrospectively enrolled 268 subjects in the final analysis who had undergone BMD examination by DEXA scanner from 1272 patients with PBC. Figure 1 summarizes the enrolment process. The demographic, clinical, serological, histological, and BMD characteristics of all patients with PBC are shown in Table 1. The mean age of the overall patients was 56.7 ± 10.6 years (range 29-94 years). The ratio of women:men was 7.38:1. Liver biopsies were performed in 60.8% of patients. Among the women, 73.7% were postmenopausal. Prior fractures had occurred in 11 patients, including six vertebral fractures and five peripheral fractures. Compared with women, men PBC patients had more smoker, UDCA-treated patients, fewer ACA positive, lower serum calcium, and higher serum creatinine as well as BMD absolute value (all P < 0.05). However, there was no difference between men and women in the T- and Z-score (P > 0.05).

Prevalence of osteoporosis

There were significant differences in the BMD value, T-score, and Z-score at any sites (L1 to L4, femoral neck, or total hip) in patients with osteoporosis compared to those without (all P < 0.001) (Supplementary Table 1). The prevalence of osteoporosis and osteopenia in the lumbar spine (L1 to L4), femoral neck and total hip were 40.3% and 35.8%, 29.1% and 45.9%, 16.8% and 47.4%, respectively (Table 1). Overall, the prevalence of osteoporosis was 45.5% (122/268) in all PBC patients, considering the lowest BMD values at the lumbar spine, femoral neck and total hip (Table 1 and Supplementary Table 2). The prevalence of osteoporosis 47.0% (111/236) was higher among women than among men 34.4% (11/32), but it was not statistically significant (P = 0.177) (Supplementary Table 2 and Figure 2). The prevalence of osteoporosis in postmenopausal women was significantly higher than that in premenopausal women (56.3% *vs* 21.0%, P < 0.001) (Supplementary Table 2 and Figure 2). The prevalence of osteoporosis was assessed according to age, cirrhosis status, histological stage and BMI. Regardless of overall patients or only women patients, the prevalence of osteoporosis

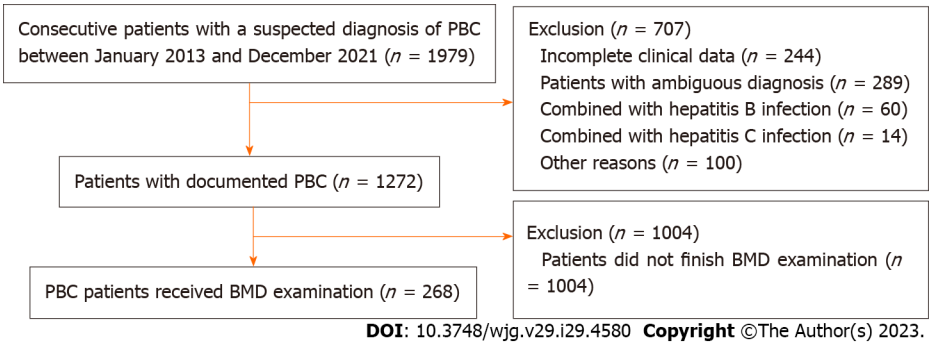
Table 1 Demographic, clinical, laboratory, and bone mineral density data in patients with primary biliary cholangitis

Characteristics	Overall (*n* = 268)	Men (*n* = 32)	Women (*n* = 236)	*P* value
Age (years) (range)	56.7 ± 10.6 (29-94)	60.0 ± 9.3 (38-79)	56.3 ± 10.7 (29-94)	0.059
Age group (years), *n* (%)				0.201
29-39	13 (4.9)	1 (3.1)	12 (5.1)	
40-49	53 (19.8)	2 (6.3)	51 (21.6)	
50-59	93 (34.7)	11 (34.4)	82 (34.7)	
60-69	77 (28.7)	12 (37.5)	65 (27.5)	
≥ 70	32 (11.9)	6 (18.8)	26 (11.0)	
Duration of PBC (years)	3.0 (1.0-6.0)	4.0 (1.6-6.8)	3.0 (1.0-6.0)	0.246
Smoking, *n* (%)	20 (7.5)	17 (53.1)	3 (1.3)	< 0.001
Postmenopausal, *n* (%)	174 (73.7)		174 (73.7)	
Pruritus, *n* (%)	45 (16.8)	4 (12.5)	41 (17.4)	0.489
Fatigue, *n* (%)	91 (34.0)	10 (31.3)	81 (34.3)	0.731
Hepatomegaly, *n* (%)	9 (3.4)	1 (3.1)	8 (3.4)	1.000
Splenomegaly, *n* (%)	187 (69.8)	20 (62.5)	167 (70.8)	0.340
Gastroesophageal varices, *n* (%)	110 (41.0)	14 (43.8)	96 (40.7)	0.740
Ascites, *n* (%)	103 (38.4)	11 (34.4)	92 (39.0)	0.615
Prior fractures, *n* (%)	11 (4.1)	0 (0.0)	11 (4.7)	0.371
BMI (kg/m^2)	22.6 ± 3.3	22.1 ± 3.0	22.7 ± 3.4	0.367
Comorbidities				
Diabetes mellitus, *n* (%)	46 (17.2)	8 (25.0)	38 (16.1)	0.210
Hypertension, *n* (%)	58 (21.6)	7 (21.9)	51 (21.6)	0.973
Hashimoto's thyroiditis, *n* (%)	66 (24.6)	7 (21.9)	59 (25.0)	0.700
Rheumatoid arthritis, *n* (%)	8 (3.0)	0 (0.0)	8 (3.4)	0.602
Sicca syndrome, *n* (%)	18 (6.7)	1 (3.1)	17 (7.2)	0.706
Previous medication, *n* (%)				
UDCA use	155 (57.8)	24 (75.0)	131 (55.5)	0.036
Steroid use	32 (11.9)	3 (9.4)	29 (12.3)	0.633
Cirrhosis status, *n* (%)				0.661
Non-cirrhosis	107 (39.9)	15 (46.9)	92 (39.0)	
Compensated	53 (19.8)	5 (15.6)	48 (20.3)	
Decompensated	108 (40.3)	12 (37.5)	96 (40.7)	
PBC-AIH overlap syndrome, *n* (%)	42 (15.7)	5 (15.6)	37 (15.7)	0.994
Mayo risk score	5.2 ± 1.4	5.4 ± 1.4	5.1 ± 1.5	0.301
Histological stage, *n* (%)[1]				0.630
I-II	65 (39.9)	6 (46.2)	59 (39.3)	
III-IV	98 (60.1)	7 (53.8)	91 (60.7)	
Laboratory data				
ALT (U/L)	36.2 (22.2-70.0)	42.8 (29.0-74.4)	35.8 (21.3-69.7)	0.236
AST (U/L)	46.4 (29.2-88.7)	39.2 (30.1-62.2)	48.1 (29.0-87.7)	0.642
Bilirubin (mg/dL)	1.1 (0.7-1.9)	0.9 (0.7-1.5)	1.1 (0.7-2.0)	0.708
Albumin (g/L)	37.2 ± 6.6	35.5 ± 6.0	37.4 ± 6.6	0.124

ALP (U/L)	157.2 (101.7-263.1)	166.3 (102.8-315.8)	156.5 (101.2-262.4)	0.747
GGT (U/L)	118.2 (48.0-276.3)	146.3 (52.3-321.2)	117.0 (47.6-276.3)	0.568
PTA (%)	93.0 ± 20.6	92.6 ± 19.9	93.0 ± 20.8	0.922
PLT (× 10^9/L)	140.2 ± 79.4	140.7 ± 80.1	136.2 ± 74.4	0.761
Calcium (mmol/L)	2.22 ± 0.14	2.17 ± 0.16	2.23 ± 0.14	0.018
Phosphorous (mmol/L)	1.14 ± 0.24	1.09 ± 0.17	1.15 ± 0.25	0.201
25-hydroxyvitamin D (ng/mL)[2]	14.3 ± 6.9	17.2 ± 6.6	13.6 ± 6.9	0.224
Creatinine (μmol/L)	56.4 (49.5-65.9)	67.1 (60.2-86.6)	55.0 (48.6-63.6)	< 0.001
IgM (g/L)	2.86 (1.60-4.40)	2.55 (1.16-4.14)	2.87 (1.64-4.49)	0.240
IgG (g/L)	15.3 (12.0-19.1)	15.0 (11.9-19.3)	15.6 (12.0-19.1)	0.674
gp210 (+), *n* (%)	99 (36.9)	10 (31.3)	89 (37.7)	0.477
Sp100 (+), *n* (%)	38 (14.2)	1 (12.5)	34 (14.4)	0.772
ACA, *n* (%)	54 (20.1)	2 (6.3)	52 (22.0)	0.037
ANA, *n* (%)	165 (61.6)	21 (65.6)	144 (61.0)	0.615
Lumbar spine BMD (L1-L4), g/cm^2	0.828 ± 0.142	0.893 ± 0.146	0.818 ± 0.139	0.005
T-score	-2.04 ± 1.27	-1.81 ± 1.31	-2.1 ± 1.27	0.267
Z-score	-0.929 ± 1.182	-1.18 ± 1.33	-0.89 ± 1.16	0.198
BMD classification, *n* (%)				0.536
Osteoporosis	108 (40.3)	10 (31.3)	98 (41.5)	
Osteopenia	96 (35.8)	13 (40.6)	83 (35.2)	
Normal	64 (23.9)	9 (28.1)	55 (23.3)	
Femoral neck BMD, g/cm^2	0.654 ± 0.128	0.714 ± 0.139	0.646 ± 0.125	0.005
T-score	-1.80 ± 1.12	-1.59 ± 1.03	-1.83 ± 1.13	0.262
Z-score	-0.73 ± 1.02	-0.63 ± 0.99	-0.74 ± 1.03	0.590
BMD classification, *n* (%)				0.374
Osteoporosis	78 (29.1)	7 (21.9)	71 (30.1)	
Osteopenia	123 (45.9)	14 (43.8)	109 (46.2)	
Normal	67 (25.0)	11 (34.4)	56 (23.7)	
Total Hip BMD, g/cm^2	0.784 ± 0.153	0.855 ± 0.148	0.774 ± 0.152	0.005
T-score	-1.42 ± 1.06	-1.19 ± 0.98	-1.45 ± 1.07	0.198
Z-score	-0.64 ± 0.98	-0.70 ± 0.96	-0.63 ± 1.00	0.714
BMD classification, *n* (%)				0.601
Osteoporosis	45 (16.8)	5 (15.6)	40 (16.9)	
Osteopenia	127 (47.4)	13 (40.6)	114 (48.3)	
Normal	96 (35.8)	14 (43.8)	82 (34.7)	
Osteoporosis lumbar or neck or hip	122 (45.5)	11 (34.4)	111 (47.0)	0.177

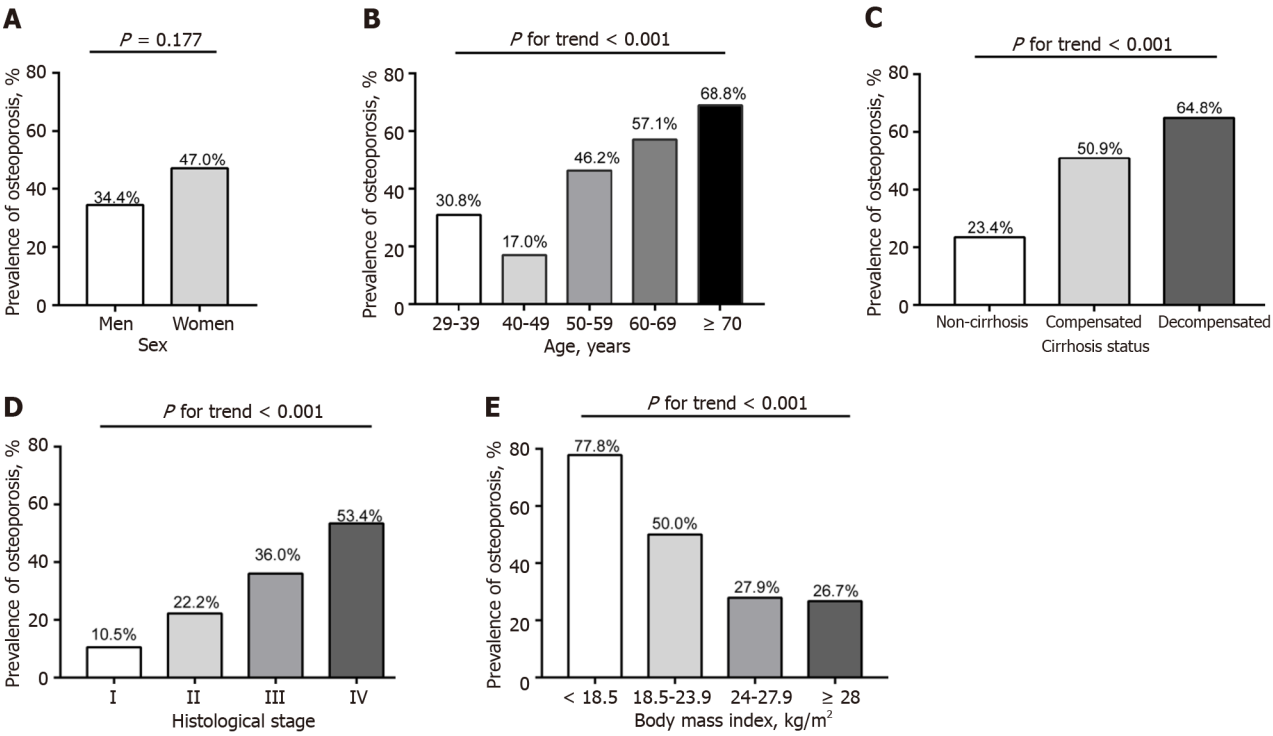
[1]Available in 163 patients.
[2]Available in 46 patients.
Data are presented as mean ± SD or median (interquartile range) or *n* (%). ACA: Anti-centromere antibody; AIH: Autoimmune hepatitis; ALP: Alkaline phosphatase; ALT: Alanine aminotransferase; ANA: Antinuclear antibody; AST: Aspartate aminotransferase; BMD: Bone mineral density; BMI: Body mass index; GGT: γ-glutamyl transpeptidase; IgG: Immunoglobulin G; IgM: Immunoglobulin M; PBC: Primary biliary cholangitis; PLT: Platelet count; PTA: Prothrombin activity; UDCA: Ursodeoxycholic acid.

increased with age, cirrhosis status, and histological stage, but decreased with BMI (all *P* for trend < 0.001) (Supplementary Table 2, Figures 2 and 3).



DOI: 10.3748/wjg.v29.i29.4580 **Copyright** ©The Author(s) 2023.

Figure 1 The flowchart of patient enrolment. PBC: Primary biliary cholangitis; BMD: Bone mineral density.



DOI: 10.3748/wjg.v29.i29.4580 **Copyright** ©The Author(s) 2023.

Figure 2 Prevalence of osteoporosis in different subgroups for overall patients with primary biliary cholangitis (*n* = 268). A: Sex; B: Age; C: Cirrhosis status; D: Histological stage; E: Body mass index.

Risk factors of osteoporosis

Table 2 shows the results of univariate analysis of the association between osteoporosis and potential risk factors in patients with PBC. In the univariate analysis, osteoporosis was correlated with older age, fatigue, postmenopausal status, previous steroids use, splenomegaly, gastroesophageal varices, ascites, advanced histological stage (III or IV), higher MRS and bilirubin levels, and lower BMI, ALT, albumin, PTA, and PLT regardless of overall or women patients (all $P < 0.05$). However, there was no association between osteoporosis and other biochemical parameters or immunological indicators such as immunoglobulin, gp210, sp100, ACA, PBC-autoimmune hepatitis (AIH) overlap syndrome, or extrahepatic autoimmune diseases.

In multivariate analysis, older age [odds ratio (OR), 1.80; 95%CI (confidence interval): 1.33-2.44, $P < 0.001$] per 10 years, gastroesophageal varices (OR, 2.11; 95%CI: 1.14-3.92, $P = 0.018$), lower BMI (OR, 0.85; 95%CI: 0.77-0.93, $P < 0.001$), previous steroid use (OR, 4.19; 95%CI: 1.66-10.56, $P = 0.002$), higher MRS (OR, 1.36; 95%CI: 1.08-1.71, $P = 0.009$) were the independent risk factors associated with the presence of osteoporosis in all patients with PBC (Table 3). In addition, when the histological stage was included in the multivariate analysis, higher bilirubin (OR, 1.20; 95%CI: 1.0-1.42, $P = 0.044$) and advanced histological stage (OR, 3.74; 95%CI: 1.60-8.77, $P = 0.002$) gained statistical significance, but the effects of gastroesophageal varices, previous steroid use, and higher MRS were removed. When menopausal status was included in the multivariate analysis (only for female patients), the splenomegaly (OR, 2.62; 95%CI: 1.18-5.80, $P = 0.018$) and postmenopausal (OR, 2.92; 95%CI: 1.02-8.38, $P = 0.046$) gained statistical significance. When both menopausal status and histological stage were included in the multivariate analysis, advanced histological stage, older age, lower BMI, previous

Table 2 Univariate analysis of risk factors for osteoporosis in overall and women patients with primary biliary cholangitis

Variables	Overall patients (*n* = 268)		*P* value	Women patients (*n* = 236)		*P* value
	Osteoporosis (*n* = 122)	No osteoporosis (*n* = 146)		Osteoporosis (*n* = 111)	No osteoporosis (*n* = 125)	
Women, *n* (%)	111 (91.0)	125 (85.6)	0.177	111 (100)	125 (100)	
Age (year)	60.5 ± 10.5	53.6 ± 9.7	< 0.001	60.4 ± 10.7	52.6 ± 9.4	< 0.001
Duration of PBC (year)	3.0 (1.0-7.0)	2.3 (1.0-5.0)	0.125	3.0 (1.0-7.0)	2.0 (1.0-5.0)	0.217
Smoking, *n* (%)	9 (7.4)	11 (7.5)	0.961	2 (1.8)	1 (1.6)	0.602
Postmenopausal, *n* (%)	98 (88.3)	76 (60.8)	< 0.001	98 (88.3)	76 (60.8)	< 0.001
Pruritus, *n* (%)	22 (18.0)	23 (15.8)	0.619	21 (18.9)	20 (16.0)	0.555
Fatigue, *n* (%)	50 (41.0)	41 (28.1)	0.026	48 (43.2)	33 (26.4)	0.007
Hepatomegaly, *n* (%)	2 (1.6)	7 (4.8)	0.188	2 (1.8)	6 (4.8)	0.204
Splenomegaly, *n* (%)	103 (84.4)	84 (57.5)	< 0.001	96 (86.5)	71 (56.8)	< 0.001
Gastroesophageal varices, *n* (%)	72 (59.0)	38 (26.0)	< 0.001	66 (59.5)	30 (24.0)	< 0.001
Ascites, *n* (%)	67 (54.9)	36 (24.7)	< 0.001	61 (55.0)	31 (24.8)	< 0.001
Prior fractures, *n* (%)	8 (5.0)	3 (2.1)	0.064	8 (7.2)	3 (2.4)	0.080
BMI (kg/m^2)	21.6 ± 3.2	23.4 ± 3.3	< 0.001	21.8 ± 3.1	23.4 ± 3.4	< 0.001
Comorbidities						
Diabetes mellitus, *n* (%)	23 (18.9)	23 (15.8)	0.503	20 (18.0)	18 (14.4)	0.450
Hypertension, *n* (%)	28 (23.0)	30 (20.5)	0.634	26 (23.4)	25 (20.0)	0.524
Hashimoto's thyroiditis, *n* (%)	27 (22.1)	39 (26.7)	0.386	26 (23.4)	33 (26.4)	0.598
Rheumatoid arthritis, *n* (%)	4 (3.3)	4 (2.7)	0.796	4 (3.6)	4 (3.2)	0.864
Sicca syndrome, *n* (%)	8 (6.6)	10 (6.8)	0.924	8 (7.2)	9 (7.2)	0.998
Previous medication						
UDCA use, *n* (%)	78 (63.9)	77 (52.7)	0.065	69 (62.2)	62 (49.6)	0.053
Steroid use, *n* (%)	23 (18.9)	9 (6.2)	0.001	21 (18.9)	8 (6.4)	0.003
PBC-AIH overlap syndrome, *n* (%)	17 (13.9)	25 (17.1)	0.475	17 (15.3)	20 (16.0)	0.885
Mayo risk score	5.7 ± 1.5	4.7 ± 1.3	< 0.001	5.7 ± 1.4	4.6 ± 1.2	< 0.001
Histological stage, *n* (%)[1]			< 0.001			< 0.001
I-II	10 (17.2)	55 (52.4)		9 (16.1)	50 (53.2)	
III-IV	48 (82.8)	50 (47.6)		47 (83.9)	44 (46.8)	
ALT (U/L)	32.0 (20.8-54.8)	43.7 (23.7-84.4)	0.007	31.2 (20.5-31.2)	46.3 (29.1-84.4)	0.013
AST (U/L)	44.0 (29.1-83.7)	49.5 (29.2-91.5)	0.782	46.3 (29.1-84.4)	50.9 (28.7-91.5)	0.899
Bilirubin (mg/dL)	1.2 (0.8-2.40	0.9 (0.7-1.7)	0.002	1.2 (0.8-2.5)	0.9 (0.7-1.6)	0.001
Albumin (g/L)	35.5 ± 6.9	38.7 ± 5.9	< 0.001	35.7 ± 6.9	39.0 ± 5.9	< 0.001
ALP (U/L)	164.2 (110.8-266.3)	149.3 (94.4-261.5)	0.180	164.3 (112.3-265.0)	144.5 (93.6-257.4)	0.175
GGT (U/L)	107.7 (47.9-237.1)	143.1 (47.7-307.3)	0.320	108.5 (45.4-242.5)	129.1 (48.6-303.3)	0.432
PTA (%)	87.9 ± 20.2	97.2 ± 20.1	< 0.001	87.6 ± 20.2	97.8 ± 20.1	< 0.001
PLT (× 10^9/L)	119.3 ± 71.4	157.7 ± 81.7	< 0.001	116.4 ± 67.4	162.4 ± 84.5	< 0.001
Calcium (mmol/L)	2.20 ± 0.15	2.24 ± 0.13	0.065	2.21 ± 0.14	2.24 ± 0.13	0.100
Phosphorous (mmol/L)	1.15 ± 0.30	1.14 ± 0.17	0.703	1.15 ± 0.31	1.15 ± 0.17	0.869

25-hydroxyvitamin D (ng/mL)[2]	14.0 ± 7.8	14.5 ± 6.2	0.823	14.1 ± 8.0	13.4 ± 5.8	0.748
Creatinine (μmol/L)	58.4 (47.2-67.5)	56.2 (50.6-65.4)	0.724	55.9 (46.9-67.5)	54.9 (49.9-60.7)	0.710
IgM (g/L)	2.80 (1.53-4.39)	2.87 (1.64-4.63)	0.497	2.87 (1.61-4.49)	2.93 (1.65-4.49)	0.776
IgG (g/L)	15.7 (12.0-19.5)	15.2 (11.9-18.9)	0.453	15.7 (12.3-19.6)	15.3 (11.8-18.6)	0.420
gp210 (+), *n* (%)	48 (39.3)	51 (34.9)	0.456	45 (40.5)	44 (35.2)	0.398
Sp100 (+), *n* (%)	19 (15.6)	19 (13.0)	0.550	18 (16.2)	16 (12.8)	0.456
ACA, *n* (%)	30 (24.6)	24 (16.4)	0.098	29 (26.1)	23 (18.4)	0.153
ANA, *n* (%)	74 (60.7)	91 (62.3)	0.779	69 (62.2)	75 (60.0)	0.734

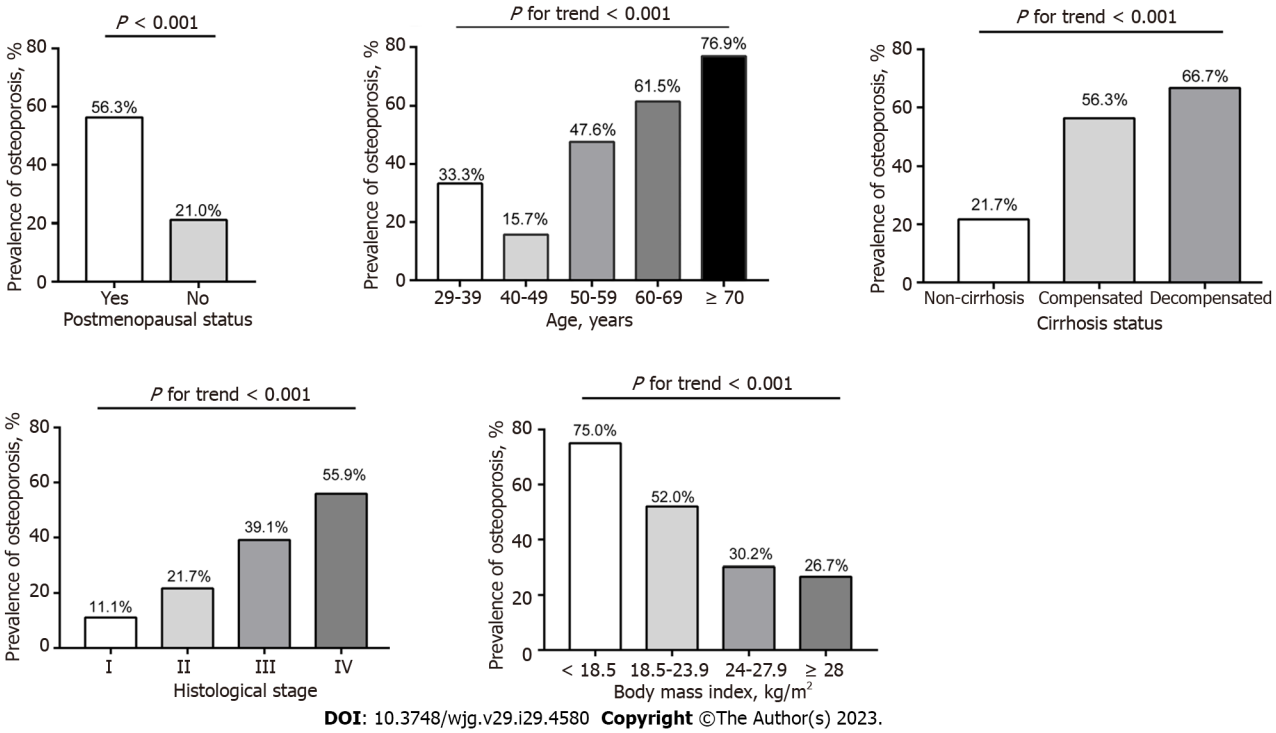
[1]Available in 163 patients.
[2]Available in 46 patients.
Data are presented as mean ± SD or median (interquartile range) or *n* (%). ACA: Anti-centromere antibody; AIH: Autoimmune hepatitis; ALP: Alkaline phosphatase; ALT: Alanine aminotransferase; ANA: Antinuclear antibody; AST: Aspartate aminotransferase; BMI: Body mass index; GGT: γ-glutamyl transpeptidase; IgG: Immunoglobulin G; IgM: Immunoglobulin M; PBC: Primary biliary cholangitis; PLT: Platelet count; PTA: Prothrombin activity; UDCA: Ursodeoxycholic acid.

Table 3 Multivariate analysis of risk factors for osteoporosis in overall and women patients with primary biliary cholangitis

Variables	Overall patients (*n* = 268)		Overall patients underwent liver biopsy (*n* = 163)		Women patients (*n* = 236)		Women patients underwent liver biopsy (*n* = 150)	
	OR (95%CI)	*P* value	OR (95%CI)	*P* value	OR (95%CI)	*P* value	OR (95%CI)	*P* value
Age, per 10 years	1.80 (1.33-2.44)	< 0.001	1.95 (1.30-2.92)	0.001	1.63 (1.04-2.57)	0.035	2.02 (1.27-3.20)	0.003
Fatigue		NS		NS		NS		NS
Splenomegaly		NS		NS	2.62 (1.18-5.80)	0.018		NS
Gastroesophageal varices	2.11 (1.14-3.92)	0.018		NS		NS		NS
Ascites		NS		NS		NS		NS
BMI	0.85 (0.77-0.93)	< 0.001	0.87 (0.77-0.98)	0.023	0.83 (0.75-0.92)	< 0.001	0.85 (0.74-0.97)	0.014
Previous steroid use	4.19 (1.66-10.56)	0.002		NS	4.01 (1.42-11.31)	0.009	3.99 (1.24-12.87)	0.020
Mayo risk score	1.36 (1.08-1.71)	0.009		NS	1.61 (1.22-2.14)	0.001	1.64 (1.12-2.41)	0.011
ALT		NS		NS		NS		NS
Bilirubin		NS	1.20 (1.01-1.42)	0.044		NS		NS
Albumin		NS		NS		NS		NS
PTA		NS		NS		NS		NS
PLT		NS		NS		NS		NS
Postmenopausal					2.92 (1.02-8.38)	0.046		NS
Histological stage III or IV			3.74 (1.60-8.77)	0.002			3.02 (1.13-8.06)	0.027

ALT: Alanine aminotransferase; BMI: Body mass index; CI: Confidence interval; NS: Not significant; OR: Odds ratio; PLT: Platelet count; PTA: Prothrombin activity.

steroid use, and higher MRS were identified as independent risk factors for osteoporosis. However, menopausal status and other variables, such as bilirubin, were not entered as independent factors of osteoporosis in the final model.



DOI: 10.3748/wjg.v29.i29.4580 **Copyright** ©The Author(s) 2023.

Figure 3 Prevalence of osteoporosis in different subgroups for women patients with primary biliary cholangitis (*n* = 236). A: Postmenopausal status; B: Age; C: Cirrhosis status; D: Histological stage; E: Body mass index.

DISCUSSION

To our knowledge, this observational study is the largest population study on BMD in PBC among currently published studies, whether in China, the Asia-Pacific region, or globally. Moreover, this is the first large-sample study to explore the prevalence and potential risk factors for osteoporosis in Asian patients with PBC. PBC patients with advanced stage (Ludwig III/IV) had more than 2-fold increased risk of osteoporosis compared to patients with early stage (Ludwig I/II). The main independent risk factors identified for osteoporosis include older age, lower BMI, previous steroid use, liver disease severity determined by the MRS, and advanced histological stage. These factors are consistent with those of previous studies in Europe and the United States[8,9].

A recent meta-analysis indicated that the risk of osteoporosis increased by 1.8 times in PBC patients compared with non-PBC participants[24]. Similar to this result, our study indicated a 2.3-time increased risk of osteoporosis in PBC patients aged 40 years or older, accounting for 95% of the total patients, compared to age-matched controls in China[23]. However, by searching the literature, we found that since 2001, the prevalence of PBC osteoporosis evaluated by DEXA has been verified in European, African, and American populations but not in Asian populations (Supplementary Table 3). As is well known, genetic factors play a crucial role in the pathogenesis of PBC[1], it is imperative to explore the prevalence of PBC osteoporosis in Asian populations. The findings of our study fill the gap in the epidemiological data on PBC-related osteoporosis in China and Asia. Notably, in our study, the prevalence of osteoporosis (45.5%) in PBC patients was higher than that of PBC patients in Europe and America (approximately 30%). The reason for this difference may be ethnic differences or a high proportion of patients with cirrhosis (60.1%) or decompensated cirrhosis (40.3%) in our study. However, the prevalence of osteoporosis in noncirrhotic PBC patients (23.4%) in our study was similar to that reported in Europe and the United States.

It has been recognized that glucocorticoid administration can significantly increase the risk of osteoporosis and bone fragility[25]. Consistently, our study found that the osteoporosis rate of PBC patients previously treated with steroid was significantly higher than that of patients without steroid treatment (71.9% *vs* 41.0%, $P = 0.001$). However, although many patients in our study were treated with UDCA (64%), it had no effect on the prevalence of osteoporosis. Previous studies have also shown that the treatment of PBC itself has not been shown to improve BMD[10]. In addition, PBC-related osteoporosis is strongly correlated with the severity of liver disease[8,9,14]. Our study results also showed that the more severe liver disease determined by MRS and histological stage in PBC, the more prone the individual is to osteoporosis. Moreover, the univariate analysis in this study demonstrated that osteoporosis in PBC was related to fatigue, higher bilirubin, lower albumin, PTA, and features of portal hypertension, including splenomegaly, gastroesophageal varices, ascites and thrombocytopenia, which are also common clinical indicators of liver disease severity. Moreover, although the pathogenesis of hepatic osteodystrophy has not been clarified, it is generally believed that chronic cholestasis itself may lead to bone loss in PBC patients[14]. Bilirubin inhibits the function of osteoblasts in vitro, which may be related to the low bone formation rate of PBC patients[26]. In our study, bilirubin levels were also statistically significant when the histological stage was considered as a variable in multivariate analysis. Similarly, Menon *et al*[9] found that higher baseline bilirubin level rather than the histological stage was the only variable independently related to bone loss rate

after 3 years of follow up[9].

In addition, lower BMI and older age are recognized risk factors for osteoporosis in postmenopausal women as well as in the general population[27]. Our study also verified the association between lower BMI and older age in PBC and osteoporosis, thus further proving that this may be associated with similar pathogenesis in the general population. However, although the menopausal status was not statistically significant when including histological stage in our multivariate analysis, it was selected as an independent indicator of osteoporosis when excluding histological stage from the model, indicating that histological stage captured the impact of menopausal status when the two variables competed in the model. Interestingly, lower ALT levels were also found to be related to a higher osteoporosis rate in the current univariate analysis, which is similar to our previous study that indicated that the biochemical response rate of PBC patients with lower ALT levels at baseline were worse than that of patients with higher ALT levels[28]. However, the ALT level was not an independent factor of osteoporosis in multivariate analysis.

In addition, one advantage of our study was that it explored the correlation between immune indicators and PBC osteoporosis, which has not been discussed in previous studies. Anti-gp210 and sp100 antibodies are two specific ANAs for PBC diagnosis[2]. Previous studies showed that gp210-positive is associated with poor prognosis in PBC patients[29]. Meanwhile, PBC is an immune-mediated cholangitis with complex pathogenesis, which often occurs concomitantly with PBC-AIH overlap syndrome and other extrahepatic autoimmune diseases such as sicca syndrome, rheumatoid arthritis, and Hashimoto's thyroiditis[2,30]. However, our study showed that osteoporosis in PBC patients was not related to these immunological features.

Up to now, the pathogenesis of PBC osteoporosis is still unclear. Most experts believed that it seems to be mainly caused by reduced bone formation, although increased bone resorption may play a role in certain situations, such as in post-menopausal women and patients with hypogonadism[10]. Osteoblast mediated bone formation and osteoclast dependent bone resorption are two opposite processes that affect bone mass: when absorption exceeds formation, bone mass will inevitably decrease, and this negative balance will lead to bone loss and osteoporosis[31]. Several studies assessing bone histomorphometry have shown that most of the osteoporosis patients with PBC had reduced tetracycline double labeling, bone formation rate, osteoblasts numbers, and reduced serum osteocalcin level, all of which indicate that osteoblast dysfunction and bone formation deficiency are the core of the pathogenesis of PBC-related osteoporosis[32-34]. In addition, other changes, increased levels of bilirubin and bile salts, and production of fibronectin may also reduce bone formation by inhibiting the proliferation and survival of osteoblasts in PBC or cholestasis[26,35]. Other conditions of PBC patients, including increased formation of osteoclast, low vitamin D levels, calcium malabsorption and sarcopenia, may be contributing factors to the panorama of PBC osteopathy[31,33,36,37].

Nevertheless, our study has several limitations. First, despite being the largest DEXA-based BMD measurement cohort of PBC to date, the sample size was relatively small, especially for men. Thus, it would be interesting and necessary to explore the same objective for larger sample size with a fairly balanced number of women and men. Second, this was a single-center, retrospective study. As a tertiary care center in China, our patients come from different regions of China and may not be representative of those at primary or secondary medical institutions. Prospective studies in Chinese populations may validate our findings. Third, a history of use of anti-osteoporosis treatments such as bisphosphonate, Vitamin D, and calcium supplementation was not included in this study for the analysis of the factors influencing osteoporosis. However, data on osteoporosis therapies related to PBC are insufficient and controversial, and the overall quality of evidence is low[11]. Therefore, we do not think that receiving anti-osteoporosis treatments in the past affected our results. In the future, it is necessary to conduct high-quality research and explore PBC specific therapies focused on improving bone formation.

CONCLUSION

In summary, we found a significantly higher prevalence of osteoporosis in Chinese patients with PBC. Osteoporosis in PBC is strongly associated with older age, lower BMI, previous steroid use, the severity of liver disease, and advanced histological stage. Thus, this study contributes to identifying PBC patients who require early screening for BMD, and potential interventions to diminish the risk of osteoporosis and fractures. This study may help to provide reference information for the development and formulation of future PBC-related guideline and public health policy in China and the Asia-Pacific region.

ARTICLE HIGHLIGHTS

Research background

Primary biliary cholangitis (PBC) is a chronic immune-mediated, progressive cholestatic liver disease. Osteoporosis is an extrahepatic complication of PBC that increases the risk of fractures and mortality.

Research motivation

Although the prevalence of osteoporosis in PBC is high in Europe and North America, relevant epidemiological studies of osteoporosis in patients with PBC in China and the Asia-Pacific region is lack.

Research objectives
To assess the prevalence and clinical characteristics of osteoporosis in Chinese patients with PBC.

Research methods
We performed a retrospective observational study to evaluation the prevalence and risk factors of osteoporosis in Chinese patients with PBC from a tertiary care center who underwent bone mineral density (BMD) assessment using dual-energy X-ray absorptiometry between January 2013 and December 2021. Demographic, serological, clinical, and histological data were collected. Independent risk factors for osteoporosis were identified by multivariate logistic regression analysis.

Research results
The prevalence of osteoporosis in Chinese patients with PBC was 45.5%. Osteoporosis in PBC is strongly associated with older age, lower body mass index (BMI), previous steroid use, the severity of liver disease, and advanced histological stage.

Research conclusions
Osteoporosis is very common in Chinese patients with PBC, allowing for prior screening of BMD in those PBC patients with older age, lower BMI, previous steroid therapy, and advanced liver disease.

Research perspectives
This study provides reference information for future PBC-related guideline development and public policy formulation in China and the Asia-Pacific region.

FOOTNOTES

Author contributions: Chen JL and Wang XB designed the research; Chen JL, Liu Y and Bi YF performed the research; Chen JL and Liu Y analyzed the data; Chen JL wrote the manuscript; Wang XB supervised the report; all authors reviewed and approved the final manuscript.

Supported by Capital's Funds for Health Improvement and Research, No. CFH2018-1-2172; and Beijing Ditan Hospital Scientific Research Fund Project, No. DTYM202102.

Institutional review board statement: The study was approved by the Institutional Ethical Review Board of Beijing Ditan Hospital, No. DTEC-KT2022-010-01.

Informed consent statement: As this study used anonymous and pre-existing data, the requirement for the informed consent from patients was waived.

Conflict-of-interest statement: We have no financial relationships to disclose.

Data sharing statement: No additional data are available.

Open-Access: This article is an open-access article that was selected by an in-house editor and fully peer-reviewed by external reviewers. It is distributed in accordance with the Creative Commons Attribution NonCommercial (CC BY-NC 4.0) license, which permits others to distribute, remix, adapt, build upon this work non-commercially, and license their derivative works on different terms, provided the original work is properly cited and the use is non-commercial. See: https://creativecommons.org/Licenses/by-nc/4.0/

Country/Territory of origin: China

ORCID number: Jia-Liang Chen 0000-0002-3007-0451; Yao Liu 0009-0001-7443-902X; Yu-Fei Bi 0009-0008-6871-8322; Xian-Bo Wang 0000-0002-3593-5741.

S-Editor: Fan JR
L-Editor: A
P-Editor: Yu HG

REFERENCES

1 **Lleo A**, Wang GQ, Gershwin ME, Hirschfield GM. Primary biliary cholangitis. *Lancet* 2020; **396**: 1915-1926 [PMID: 33308474 DOI: 10.1016/S0140-6736(20)31607-X]

2 **Lindor KD**, Bowlus CL, Boyer J, Levy C, Mayo M. Primary Biliary Cholangitis: 2018 Practice Guidance from the American Association for the Study of Liver Diseases. *Hepatology* 2019; **69**: 394-419 [PMID: 30070375 DOI: 10.1002/hep.30145]

3 **Levy C**, Manns M, Hirschfield G. New Treatment Paradigms in Primary Biliary Cholangitis. *Clin Gastroenterol Hepatol* 2023; **21**: 2076-2087 [PMID: 36809835 DOI: 10.1016/j.cgh.2023.02.005]

4 **Lv T**, Chen S, Li M, Zhang D, Kong Y, Jia J. Regional variation and temporal trend of primary biliary cholangitis epidemiology: A systematic review and meta-analysis. *J Gastroenterol Hepatol* 2021; **36**: 1423-1434 [PMID: 33141955 DOI: 10.1111/jgh.15329]

5 **Jepsen P**, Grønbæk L, Vilstrup H. Worldwide Incidence of Autoimmune Liver Disease. *Dig Dis* 2015; **33** Suppl 2: 2-12 [PMID: 26641102 DOI: 10.1159/000440705]

6 **Zeng N**, Duan W, Chen S, Wu S, Ma H, Ou X, You H, Kong Y, Jia J. Epidemiology and clinical course of primary biliary cholangitis in the Asia-Pacific region: a systematic review and meta-analysis. *Hepatol Int* 2019; **13**: 788-799 [PMID: 31552558 DOI: 10.1007/s12072-019-09984-x]

7 **Compston JE**, McClung MR, Leslie WD. Osteoporosis. *Lancet* 2019; **393**: 364-376 [PMID: 30696576 DOI: 10.1016/S0140-6736(18)32112-3]

8 **Guañabens N**, Parés A, Ros I, Caballería L, Pons F, Vidal S, Monegal A, Peris P, Rodés J. Severity of cholestasis and advanced histological stage but not menopausal status are the major risk factors for osteoporosis in primary biliary cirrhosis. *J Hepatol* 2005; **42**: 573-577 [PMID: 15763344 DOI: 10.1016/j.jhep.2004.11.035]

9 **Menon KV**, Angulo P, Weston S, Dickson ER, Lindor KD. Bone disease in primary biliary cirrhosis: independent indicators and rate of progression. *J Hepatol* 2001; **35**: 316-323 [PMID: 11592591 DOI: 10.1016/s0168-8278(01)00144-1]

10 **Danford CJ**, Trivedi HD, Papamichael K, Tapper EB, Bonder A. Osteoporosis in primary biliary cholangitis. *World J Gastroenterol* 2018; **24**: 3513-3520 [PMID: 30131657 DOI: 10.3748/wjg.v24.i31.3513]

11 **Trivedi HD**, Danford CJ, Goyes D, Bonder A. Osteoporosis in Primary Biliary Cholangitis: Prevalence, Impact and Management Challenges. *Clin Exp Gastroenterol* 2020; **13**: 17-24 [PMID: 32021374 DOI: 10.2147/CEG.S204638]

12 **Schönau J**, Wester A, Schattenberg JM, Hagström H. Risk of fractures and postfracture mortality in 3980 people with primary biliary cholangitis: A population-based cohort study. *J Intern Med* 2023; **294**: 164-177 [PMID: 36823685 DOI: 10.1111/joim.13624]

13 **Wariaghli G**, Mounach A, Achemlal L, Benbaghdadi I, Aouragh A, Bezza A, El Maghraoui A. Osteoporosis in chronic liver disease: a case-control study. *Rheumatol Int* 2010; **30**: 893-899 [PMID: 19636560 DOI: 10.1007/s00296-009-1071-8]

14 **Guañabens N**, Cerdá D, Monegal A, Pons F, Caballería L, Peris P, Parés A. Low bone mass and severity of cholestasis affect fracture risk in patients with primary biliary cirrhosis. *Gastroenterology* 2010; **138**: 2348-2356 [PMID: 20178794 DOI: 10.1053/j.gastro.2010.02.016]

15 **Floreani A**, Mega A, Camozzi V, Baldo V, Plebani M, Burra P, Luisetto G. Is osteoporosis a peculiar association with primary biliary cirrhosis? *World J Gastroenterol* 2005; **11**: 5347-5350 [PMID: 16149144 DOI: 10.3748/wjg.v11.i34.5347]

16 **Guichelaar MM**, Kendall R, Malinchoc M, Hay JE. Bone mineral density before and after OLT: long-term follow-up and predictive factors. *Liver Transpl* 2006; **12**: 1390-1402 [PMID: 16933236 DOI: 10.1002/Lt.20874]

17 **Benetti A**, Crosignani A, Varenna M, Giussani CS, Allocca M, Zuin M, Podda M, Battezzati PM. Primary biliary cirrhosis is not an additional risk factor for bone loss in women receiving regular calcium and vitamin D supplementation: a controlled longitudinal study. *J Clin Gastroenterol* 2008; **42**: 306-311 [PMID: 18223492 DOI: 10.1097/01.mcg.0000248017.31386.39]

18 **Boulton-Jones JR**, Fenn RM, West J, Logan RF, Ryder SD. Fracture risk of women with primary biliary cirrhosis: no increase compared with general population controls. *Aliment Pharmacol Ther* 2004; **20**: 551-557 [PMID: 15339326 DOI: 10.1111/j.1365-2036.2004.02089.x]

19 **You H**, Ma X, Efe C, Wang G, Jeong SH, Abe K, Duan W, Chen S, Kong Y, Zhang D, Wei L, Wang FS, Lin HC, Yang JM, Tanwandee T, Gani RA, Payawal DA, Sharma BC, Hou J, Yokosuka O, Dokmeci AK, Crawford D, Kao JH, Piratvisuth T, Suh DJ, Lesmana LA, Sollano J, Lau G, Sarin SK, Omata M, Tanaka A, Jia J. APASL clinical practice guidance: the diagnosis and management of patients with primary biliary cholangitis. *Hepatol Int* 2022; **16**: 1-23 [PMID: 35119627 DOI: 10.1007/s12072-021-10276-6]

20 **Dickson ER**, Grambsch PM, Fleming TR, Fisher LD, Langworthy A. Prognosis in primary biliary cirrhosis: model for decision making. *Hepatology* 1989; **10**: 1-7 [PMID: 2737595 DOI: 10.1002/hep.1840100102]

21 **Ludwig J**, Dickson ER, McDonald GS. Staging of chronic nonsuppurative destructive cholangitis (syndrome of primary biliary cirrhosis). *Virchows Arch A Pathol Anat Histol* 1978; **379**: 103-112 [PMID: 150690 DOI: 10.1007/bf00432479]

22 **Kanis JA**, Melton LJ 3rd, Christiansen C, Johnston CC, Khaltaev N. The diagnosis of osteoporosis. *J Bone Miner Res* 1994; **9**: 1137-1141 [PMID: 7976495 DOI: 10.1002/jbmr.5650090802]

23 **Wang L**, Yu W, Yin X, Cui L, Tang S, Jiang N, Zhao N, Lin Q, Chen L, Lin H, Jin X, Dong Z, Ren Z, Hou Z, Zhang Y, Zhong J, Cai S, Liu Y, Meng R, Deng Y, Ding X, Ma J, Xie Z, Shen L, Wu W, Zhang M, Ying Q, Zeng Y, Dong J, Cummings SR, Li Z, Xia W. Prevalence of Osteoporosis and Fracture in China: The China Osteoporosis Prevalence Study. *JAMA Netw Open* 2021; **4**: e2121106 [PMID: 34398202 DOI: 10.1001/jamanetworkopen.2021.21106]

24 **Fan J**, Wang Q, Sun L. Association between primary biliary cholangitis and osteoporosis: meta-analysis. *Clin Rheumatol* 2017; **36**: 2565-2571 [PMID: 28948408 DOI: 10.1007/s10067-017-3844-x]

25 **van Staa TP**, Leufkens HG, Cooper C. The epidemiology of corticosteroid-induced osteoporosis: a meta-analysis. *Osteoporos Int* 2002; **13**: 777-787 [PMID: 12378366 DOI: 10.1007/s001980200108]

26 **Janes CH**, Dickson ER, Okazaki R, Bonde S, McDonagh AF, Riggs BL. Role of hyperbilirubinemia in the impairment of osteoblast proliferation associated with cholestatic jaundice. *J Clin Invest* 1995; **95**: 2581-2586 [PMID: 7769100 DOI: 10.1172/jci117959]

27 **Kröger H**, Tuppurainen M, Honkanen R, Alhava E, Saarikoski S. Bone mineral density and risk factors for osteoporosis--a population-based study of 1600 perimenopausal women. *Calcif Tissue Int* 1994; **55**: 1-7 [PMID: 7922782 DOI: 10.1007/bf00310160]

28 **Chen J**, Xue D, Gao F, Tao L, Li Y, Zhang Q, Wang R, Sun L, Yang X, Liu Y, Zhu B, Niu S, Wang X. Influence factors and a predictive scoring model for measuring the biochemical response of primary biliary cholangitis to ursodeoxycholic acid treatment. *Eur J Gastroenterol Hepatol* 2018; **30**: 1352-1360 [PMID: 29889683 DOI: 10.1097/MEG.0000000000001186]

29 **Yang F**, Yang Y, Wang Q, Wang Z, Miao Q, Xiao X, Wei Y, Bian Z, Sheng L, Chen X, Qiu D, Fang J, Tang R, Gershwin ME, Ma X. The risk predictive values of UK-PBC and GLOBE scoring system in Chinese patients with primary biliary cholangitis: the additional effect of anti-gp210. *Aliment Pharmacol Ther* 2017; **45**: 733-743 [PMID: 28083929 DOI: 10.1111/apt.13927]

30 **European Association for the Study of the Liver**. EASL Clinical Practice Guidelines: The diagnosis and management of patients with primary biliary cholangitis. *J Hepatol* 2017; **67**: 145-172 [PMID: 28427765 DOI: 10.1016/j.jhep.2017.03.022]

31 **Pugliese N**, Arcari I, Aghemo A, Lania AG, Lleo A, Mazziotti G. Osteosarcopenia in autoimmune cholestatic liver diseases: Causes, management, and challenges. *World J Gastroenterol* 2022; **28**: 1430-1443 [PMID: 35582674 DOI: 10.3748/wjg.v28.i14.1430]

32 **Hodgson SF**, Dickson ER, Wahner HW, Johnson KA, Mann KG, Riggs BL. Bone loss and reduced osteoblast function in primary biliary cirrhosis. *Ann Intern Med* 1985; **103**: 855-860 [PMID: 4062087 DOI: 10.7326/0003-4819-103-6-855]

33 **Guañabens N**, Parés A, Mariñoso L, Brancós MA, Piera C, Serrano S, Rivera F, Rodés J. Factors influencing the development of metabolic

bone disease in primary biliary cirrhosis. *Am J Gastroenterol* 1990; **85**: 1356-1362 [PMID: 2220729]

34 **Guichelaar MM**, Malinchoc M, Sibonga J, Clarke BL, Hay JE. Bone metabolism in advanced cholestatic liver disease: analysis by bone histomorphometry. *Hepatology* 2002; **36**: 895-903 [PMID: 12297836 DOI: 10.1053/jhep.2002.36357]

35 **Kawelke N**, Bentmann A, Hackl N, Hager HD, Feick P, Geursen A, Singer MV, Nakchbandi IA. Isoform of fibronectin mediates bone loss in patients with primary biliary cirrhosis by suppressing bone formation. *J Bone Miner Res* 2008; **23**: 1278-1286 [PMID: 18348696 DOI: 10.1359/jbmr.080313]

36 **Olivier BJ**, Schoenmaker T, Mebius RE, Everts V, Mulder CJ, van Nieuwkerk KM, de Vries TJ, van der Merwe SW. Increased osteoclast formation and activity by peripheral blood mononuclear cells in chronic liver disease patients with osteopenia. *Hepatology* 2008; **47**: 259-267 [PMID: 18022900 DOI: 10.1002/hep.21971]

37 **Saeki C**, Oikawa T, Kanai T, Nakano M, Torisu Y, Sasaki N, Abo M, Saruta M, Tsubota A. Relationship between osteoporosis, sarcopenia, vertebral fracture, and osteosarcopenia in patients with primary biliary cholangitis. *Eur J Gastroenterol Hepatol* 2021; **33**: 731-737 [PMID: 32558699 DOI: 10.1097/MEG.0000000000001791]

World Journal of Gastroenterology

Submit a Manuscript: https://www.f6publishing.com

World J Gastroenterol 2023 August 7; 29(29): 4593-4603

DOI: 10.3748/wjg.v29.i29.4593

ISSN 1007-9327 (print) ISSN 2219-2840 (online)

ORIGINAL ARTICLE

Observational Study

New objective scoring system to clinically assess fecal incontinence

Pankaj Garg, Iwona Sudol-Szopinska, Małgorzata Kolodziejczak, Kaushik Bhattacharya, Gurleen Kaur

Specialty type: Gastroenterology and hepatology

Provenance and peer review: Invited article; Externally peer reviewed.

Peer-review model: Single blind

Peer-review report's scientific quality classification

Grade A (Excellent): 0
Grade B (Very good): B, B
Grade C (Good): 0
Grade D (Fair): 0
Grade E (Poor): 0

P-Reviewer: Ammarullah MI, Indonesia; Qi L, China

Received: April 27, 2023
Peer-review started: April 27, 2023
First decision: June 7, 2023
Revised: June 9, 2023
Accepted: July 11, 2023
Article in press: July 11, 2023
Published online: August 7, 2023

Pankaj Garg, Colorectal Surgery, Garg Fistula Research Institute (GFRI), Panchkula 134113, Haryana, India

Pankaj Garg, Colorectal Surgery, Indus International Hospital, Mohali 140507, Punjab, India

Iwona Sudol-Szopinska, Department ofRadiology, National Institute of Geriatrics, Rheumatology and Rehabilitation, Warsaw 02-637, Poland

Małgorzata Kolodziejczak, Department of Proctology, Proctologic Center, St. Elizabeth Hospital, Warsaw 02-616, Poland

Kaushik Bhattacharya, Department of Surgery, MGM Medical College and LSK Hospital, Kishanganj 855107, Bihar, India

Gurleen Kaur, Department of Pharmacology, Adesh Medical College and Hospital, Shahbad 136143, Haryana, India

Corresponding author: Pankaj Garg, MS, CEO, Chief Colorectal Surgeon, Colorectal Surgery, Garg Fistula Research Institute (GFRI), 1042, Sector-15, Panchkula 134113, Haryana, India. drgargpankaj@gmail.com

Abstract

BACKGROUND

Several scoring systems are used to assess fecal incontinence (FI), among which, the most commonly used are Wexner and Vaizey's scoring systems. However, there are significant lacunae in these scoring systems, due to which they are neither accurate nor comprehensive.

AIM

To develop a new scoring system for FI that is accurate, comprehensive, and easy to use.

METHODS

A pro forma was made in which six types of FI were included: solid, liquid, flatus, mucous, stress, and urge. The weight for each FI was determined by asking a group of patients and laypersons to give a disability score to each type of FI from 0 to 100 (0- least, 100- maximum disability). The disability was assessed on a modified EQ-5D+ (EuroQol) description system, 4D3L (4 dimensions and 3 levels) for each FI. The average score of each FI was calculated, divided by 10, and rounded off to determine the weight of each FI type. The scores for the three levels of frequency of each FI were assigned as never = 0 (No episode of FI ever),

occasional = 1 (≤ 1 episode of FI/ wk), and common = 2 (> 1 episode of FI/ wk), and was termed as frequency score. The score for each FI would be derived by multiplying the frequency score and the weight for that FI type. In the second phase of the study, a group of colorectal surgeons was asked to rank the six FI types in order of severity, and their ranking was compared with the patient and laypersons' rankings.

RESULTS

Fifty patients and 50 laypersons participated in the study. The weight was assigned to each FI (solid-8, liquid-8, urge-7, flatus-6, mucus-6, and stress-5), and an new scoring system was formulated. The maximum possible score was 80 (total incontinence), and the least 0 (no incontinence). The surgeons' ranking of FI severity did not correlate well with patients' and laypersons' rankings of FI, highlighting that surgeons and patients may perceive the severity of FI differently.

CONCLUSION

A new scoring system for FI was formulated, which was simple, logical, comprehensive, and easy to use, and eliminated previous shortcomings. Patients' and surgeons' perceptions of FI severity of FI did not correlate well.

Key Words: Feal incontinence; Scoring system; Urge; Stress; Flatus

©The Author(s) 2023. Published by Baishideng Publishing Group Inc. All rights reserved.

Core tip: There are several scoring systems to assess fecal incontinence (FI), among which, the most commonly used are Wexner's, Vaizey's, and FI Severity Index scoring systems. However, there are major lacunae and shortcomings in these scoring systems, due to which, they are neither accurate and scientific nor comprehensive. We have developed a new scoring system to assess FI, which is better and more accurate than the existing scoring systems. The new system is more comprehensive and simple and easy to use, and most shortcomings of previous scoring systems have been addressed.

Citation: Garg P, Sudol-Szopinska I, Kolodziejczak M, Bhattacharya K, Kaur G. New objective scoring system to clinically assess fecal incontinence. *World J Gastroenterol* 2023; 29(29): 4593-4603
URL: https://www.wjgnet.com/1007-9327/full/v29/i29/4593.htm
DOI: https://dx.doi.org/10.3748/wjg.v29.i29.4593

INTRODUCTION

Fecal incontinence (FI) is defined as the accidental leakage of stools, flatus, or mucus and is a common gastrointestinal disorder. It affects between 1% and 16% of the population[1-7]. FI drastically impacts the quality of life, and cause embarrassment, anxiety, fear, or reluctance to go out, often leading to social isolation and the need to carry clothes or wear incontinence pads regularly[1,3,8-13]. The sensitive nature of FI makes it a taboo subject, and many people are reluctant to discuss these with family members or even doctors[2,9,14-16].

There are three scoring systems commonly used to assess FI: Cleveland Clinic or Wexner[17] (Table 1), St. Marks Hospital or Vaizey's[18] (Table 2), and FI Severity Index (FISI)[19] (Table 3). The Wexner and Vaizey scores are the most commonly used[20]. However, there are major lacunae in these scoring systems, due to which they are not an accurate reflection of incontinence level and its correlation with the quality of life.

First, the existing scoring systems are not comprehensive. Wexner scores evaluate only three parameters: solid, liquid, and flatus (gas) FI[17], and Vaizey scores include only four parameters: solid, gas, flatus, and urge (lack of ability to defer defecation for 15 min due to sudden need to defecate)[18]. FISI scores include mucus FI (leakage) as the fifth parameter to evaluate FI but do not include urge FI[19]. None of the scoring systems includes stress FI (leakage of fecal matter or flatus on increasing intraabdominal pressure like coughing, lifting weights, *etc.*) as a parameter to evaluate FI.

Stress FI is an essential independent parameter that should be included in a scoring system. The prevention of stress FI primarily depends on the proper functioning of the external anal sphincter (EAS) and intact straining puborectalis reflex [21]. The latter is a coordinated contraction of EAS and puborectalis muscle on coughing or straining. The damage to EAS and puborectalis during surgery or by peripheral neuritis due to any condition (like diabetes, *etc.*) can cause disruption of straining puborectalis reflex and lead to stress FI[22]. Stress FI is prevalent and is independent of other FIs with distinct etiopathogenesis and treatment, and therefore should be separately evaluated in all patients of FI[22].

Second, the different types of FIs are assigned the same weights in Wexner and Vaizey scoring system[17,18]. This implies that uncontrolled passage of flatus is given equal weight to uncontrolled leakage of solid motion. It does not seem logical and scientifically sound to equate and give equal weights to different types of FI. This was perhaps done for the sake of simplicity[20]. Keeping a scoring system simple and easy to use should be a priority, but it is not justified at the cost of accuracy and sacrifice of scientific principles.

Table 1 Wexner scoring

	Never	Rarely	Sometimes	Usually	Always
Solid	0	1	2	3	4
Liquid	0	1	2	3	4
Gas	0	1	2	3	4
Wears a pad	0	1	2	3	4
Lifestyle alteration	0	1	2	3	4

Rarely: < 1/mo; sometimes: < 1/wk to ≥ 1/mo; usually: < 1/d to ≥ 1/wk; always: ≥ 1/d.

Table 2 Vaizey's scoring

	Never	Rarely	Sometimes	Weekly	Daily
Solid stool incontinence	0	1	2	3	4
Liquid stool incontinence	0	1	2	3	4
Gas incontinence	0	1	2	3	4
Alteration in lifestyle	0	1	2	3	4
	No	Yes			
Need to wear a pad or plug	0	2			
Constipating medication	0	2			
Lack of ability to defer defecation for 15 min	0	4			

Never: No episodes in last 4 wk; rarely: 1 episode in last 4 wk; sometimes: ≥ 1 in last 4 wk but < 1/wk; weekly: ≥ 1/wk to < 1/d; always: ≥ 1/d.

Table 3 Fecal incontinence Severity Index scoring

	≥ 2 times/day (patient/surgeon scores)	Once/day (patient/surgeon scores)	≥ 2 times/week (patient/surgeon scores)	Once/week (patient/surgeon)	1-3 times/month (patient/surgeon scores)
Gas	12/9	11/8	8/6	6/4	4/2
Mucous	12/11	10/9	7/7	5/7	3/5
Liquid	19/18	17/16	13/14	10/13	8/10
Solid	18/19	16/17	13/16	10/14	8/11

Third, there are parameters included in the existing scoring systems that are not a direct measure of the degree or severity of FI. This leads to error (confounding bias). The same symptom is scored multiple times due to the inclusion of parameters like "Need to wear a pad"[17,18], "Alteration in lifestyle"[17,18], and "Need to take a constipating medicine"[18] in the Wexner and Vaizey scoring systems. For example, a patient having liquid or stool FI would also wear a pad daily, would have an alteration in lifestyle, and could also be taking constipating medicines to counter the symptom. This way, the patient with liquid or solid FI would be scored four times for the same symptom. These included questions are not independent types of FI but are corrective actions taken to control the symptoms of FI. So, apart from being the indirect measures, they would cause a multiplicity of scoring as the primary direct symptom (liquid or solid FI) would anyway be getting points.

Fourth, the patient perceptions were not taken into consideration while developing these scoring systems. As any FI scoring system is being developed for the patients, the latter's perception is paramount. It would be incorrect to assume that the surgeons' perception of different FIs would be similar to that of the patients. The FISI scoring system is the only one that has compared the surgeons' and patients' perceptions and found them to be different, yet they failed to formulate a simple and clear scoring system that was patient-centric[19]. There were several other discrepancies in the FISI study[23]. The sample size was small (26 surgeons and 34 patients)[19]. The forms were filled by interview as well as through mail. The standard definitions and the disability parameters on the basis of which scoring was made were not used[19]. The lack of proper statistical methods, the scoring system becoming too complex, and no proper weights being

allotted to each FI type were important shortcomings of the FISI system (Table 3). These could be the reasons that the FISI scoring system did not become popular with gastroenterologists and surgeons[19].

Due to these major lacunae in the existing scoring systems (not comprehensive, the different types of FIs were assigned the same weights, parameters included were not a direct measure of the degree or severity of FI, the patient perceptions were not taken into consideration while developing these scoring systems, *etc.*), a need was felt to develop a new scoring system that would be comprehensive, based primarily on patients' and laypersons' perceptions, was scientifically sound, accurate (free of bias or overlapping parameters), faithfully reflected the degree of disability, and yet would be simple and easy to use. Against this background, this study was done in two phases. In the first phase, a new scoring system was developed based on patients' and laypersons' perceptions, and in the second phase, it was analyzed to determine whether patients' perception and surgeons' assessments of the disability of different FIs were similar or not.

MATERIALS AND METHODS

The study was designed in two phases. In the first phase, the assignment of weights to six types of FI and the formulation of a new scoring system based on patients' and laypersons' perceptions were performed. In the second phase, the colorectal surgeons were also interviewed, and their assessment of the severity of different FI types was compared with the rankings of patients and laypersons.

First phase of the study: development of new scoring system

Study group: The first phase of the study comprised the patients and laypersons.

Patients group: (1) Inclusion criteria: the patients were defined as those who knew about FI and could potentially develop it secondary to the treatment of the disease condition they were suffering from. Therefore, patients suffering from anal fistula were included. Since they were experiencing the fear of incontinence, their perception was relevant; and (2) Exclusion criteria: the patients already suffering from any FI were excluded as they would rate their type of incontinence worse than other types.

Laypersons group: The layperson group was included because the patients with FI were expected to be emotionally involved. Therefore, a group that was not directly involved in the disease process was also included. Inclusion criteria: the relatives of the patients suffering from a disease, the treatment of which could potentially cause FI (anal fistula), were included. These persons were aware of the details and the risk of FI in their close relatives but were not actually directly afflicted by the disease. Therefore, they would balance out any extreme response by the patients.

Parameters of FI

The six parameters directly reflecting FI were included: solid, liquid, flatus (gas), urge, stress, and mucus.

Study methodology

Measuring weight for each FI type: The six FI parameters were defined in simple language (English as well as the native language, Hindi), which a patient and layperson could easily understand (Table 4). An interviewer was assigned to interview each person. Both the interviewer and interviewee (study subject) were blinded to the goals or the purpose of the study. The interviewees were shown the proforma, and after they understood the definitions of six FI parameters, they were asked to arrange the six parameters in order of decreasing severity. After this, each parameter was to be assigned numbers (disability score) between 0 and 100. The disability score was the measure of the impact of FI on all aspects of the life of the person. The worst parameter would be assigned a disability score of 100, and all other parameters would be assigned disability scores according to that. The same weight could be assigned to different parameters if the interviewee perceived them as of equal magnitude. In order to guide the interviewee regarding the weight assignment, a modified EQ-5D+ (EuroQol) description system was utilized[24]. EQ-5D+ includes a structured approach in which each health state parameter is described in terms of dimensions and severity levels within each dimension. In the present study, a 4D3L (4 dimensions, 3 levels) description system was used (Table 5). The impact of FI type on four dimensions of daily life, usual routine activity, anxiety/depression, self-esteem, and social life, was assessed, and a maximum of 25 points were assigned to each dimension. Each dimension had three levels, and depending on the severity level of that dimension, the points out of 25 were to be assigned to that dimension (Table 5). For example, an interviewee assessing liquid FI assigns 18 points to usual routine activity (out of 25), 20 points to anxiety/depression (out of 25), 15 points to self-esteem (out of 25), and 22 points to social life dimension (out of 25), then the total disability score assigned to liquid FI would be 75 (out of 100) for that interviewee (Table 5). Similarly, every interviewee would assign disability scores to each of the six types of fecal FIs. The 4D3L system was used to make the procedure objective and also helped the interviewee to fill the proforma easily. The two dimensions, self-esteem and anxiety, are relevant to evaluate the impact of a medical condition and were not given much importance in earlier scoring systems[25,26]. The inclusion of the parameters used as independent parameters in previous scoring systems like "Need to wear a pad"[17,18], "Alteration in lifestyle"[17,18], and "Need to take a constipating medicine"[18], were included as a part of the 4D3L proforma and therefore had an influence on assigning disability score to each type of FI. As discussed above, these parameters are not a type of incontinence, and their independent inclusion in the scoring system would have led to the error.

A pilot study was done before commencing the main study to assess any shortcomings. This was helpful in removing questions that were irrelevant or difficult to comprehend, improving the proforma's content, and making the language

Table 4 Detailed description of different types of incontinence [it was also translated into the local language (Hindi)]

Incontinence	Description
Urge	Whenever there is an urge to pass motion, normally, a person can hold the motion for a few minutes. In urge IC, the person faces difficulty holding the motions whenever there is an urge of passing motions. Although the motion does not come out, the feeling and fear that it will come out force the patient to rush to the toilet
Stress	Whenever there is an increase in pressure inside the tummy like in coughing or lifting weights, a person with normal anal sphincters can tighten his sphincters and hold the motions. A person can hold the motion for a few minutes. In stress IC, on increasing the pressure inside the tummy like in coughing or lifting weights, a little bit of motion or flatus leak from the anus
Mucus	A person with normal anal sphincters has a good anal tone due to which no leakage of mucus (normally present in the rectum as there is saliva in the mouth) occurs. However, in a person with weak sphincters, some mucus may leak out into the area around the anus spontaneously
Flatus	A person with normal anal sphincters has a good anal tone due to which he/she has control over the passage of gas/flatus. The person can hold the gas/flatus for some time. However, in a person with weak sphincters, gas/flatus may leak out of the anus with the person having no control over it
Liquid	A person with normal anal sphincters has a good anal tone due to which no leakage of liquid stool occurs. However, in a person with weak sphincters, some amount of liquid stool may leak out into the area around the anus spontaneously
Solid	A person with normal anal sphincters has a good anal tone due to which no leakage of solid stool occurs. However, in a person with weak sphincters, some amount of solid stool may leak out into the area around the anus spontaneously

Table 5 Four dimensions, 3 levels [modified EQ-5D+ (EuroQol)] description system utilized in the study and assignment of disability score for each fecal incontinence

Dimension	Dimension description	Perception of severity level
Usual routine activity	Performance of usual role activities such as working at a job, housework, child care, volunteer work, *etc.* Need to wear a pad, take a constipating medicine	Minimal problems with performing usual activities (0–5)
		Some problems with performing usual activities and moderate alteration in lifestyle (6–15)
		Unable to perform usual activities and severe alteration in lifestyle (16–25)
Anxiety/depression	Negative psychological states include anxiety, depression, behavioral, emotional control, loneliness, *etc.*	Minimal anxiety or depression (0–5)
		Moderate anxiety or depression (social isolation and loss of appetite) (6–15)
		Extremely anxious or depressed (suicidal ideation) (16–25)
Self-esteem	Perception about self	Minimal loss of self-esteem (0–5)
		Some loss of self-esteem (6–15)
		Marked loss of self-esteem (16–25)
Social life	How frequently the person goes out for socializing, like going to the cinema to watch a movie, going to a party, going out of the station for vacation	Minimal impact on social life (0–5)
		Some loss of social life (6–15)
		Marked curtailment of social life (16–25)

For example, an interviewee assessing liquid fecal incontinence assigns 18 points to Usual routine activity (out of 25), 20 points to anxiety/depression (out of 25), 15 points to self-esteem (out of 25), and 22 points to social life dimension (out of 25), then the total disability score assigned to liquid FI would be 75 (out of 100).

simpler. The subjects in the pilot study were not included in the final study.

Calculating the final weight for each FI type: The data of patients and laypersons were combined. The disability scores for each FI type were tabulated, and the average disability score for each FI type was calculated. Th weight for that FI was calculated by dividing the average disability score by 10 and rounding off the number to the nearest whole number (Table 6). This was done for simplicity, as a numbers with decimals would would have been difficult to use.

Development of a scoring system: Once the weights for each FI type were determined based on patients' and laypersons' perceptions, the three frequencies of each FI type were fixed as never (No episode of FI ever), occasional (≤ 1 episode of FI/ wk) or common (> 1 episode of FI/ wk). These were assigned linear scores of 0, 1 and 2, respectively. The frequency system of never, daily, weekly, monthly or yearly was not used for a few reasons. First, the patients found it difficult to calculate the frequency when there were too many columns. Secondly, the frequency of any FI type could vary in

Table 6 Weight assignment to different types of incontinence by study group

	Solid	Liquid	Flatus	Mucous	Stress	Urge
Patients' (n = 50) average disability score	82.5 ± 19.1	84.8 ± 15.4	58.1 ± 23.6	55.3 ± 21.2	52.0 ± 23.9	68.5 ± 23.5
Laypersons' (n = 50) average disability score	83.0 ± 22.4	81.4 ± 19.2	54.6 ± 21.1	55.2 ± 19.3	48.8 ± 22.0	68.3 ± 22.8
Total average disability score	82.7 ± 20.7	83.1 ± 17.4	56.3 ± 22.3	55.2 ± 20.1	50.4 ± 22.9	68.4 ± 23.0
Division by 10	8.27	8.31	5.63	5.52	5.04	6.84
Final weight (after rounding-off)	8	8	6	6	5	7

frequency over a period of time. Third, increasing the columns would have made the scoring system more cumbersome.

Second phase of the study: comparison of ranking of six types of FI according to severity by patients, laypersons and surgeons

In this phase, the assessment of FI was done by surgeons, and FI ranking in decreasing order of severity was done by three participating groups: patients, laypersons and surgeons. As discussed above, this was not done to assign weights or for formulation of the new scoring system but to check whether there was a correlation between patients, laypersons and colorectal surgeons regarding perception of severity of different types of FI.

Surgeons: Inclusion criteria: colorectal surgeons who had performed at least 30 anal fistula procedures in their surgical career were included. The persons in each group (patients, laypersons and surgeons) were asked to rank the six FI in decreasing order of severity. The most severe FI was given a rank of 6, and the least severe FI was given a rank of 1. The other types of FI were given ranks between 2 and 5, depending on the severity. The average of each FI type in each group was calculated, and the final ranking of FI in the groups was tabulated and compared (Table 7).

Ethics

The study was approved by the Ethics Committee of Adesh Medical College and Hospital, Shahbad, India (reference number AMCH/IEC/2022/02/04).

Statistical analysis

The categorical variables were compared by performing the χ^2 or Fisher's exact test. For normally distributed data, the continuous variables were tested by Student's t test when there were two samples, and analysis of variance (ANOVA) there were three or more samples. For non-normally distributed data, the Wilcoxon signed-rank test was performed for paired samples, and Mann–Whitney U test for unpaired samples. The significant cut-off point was set at $P < 0.05$.

RESULTS

Fifty patients and 50 laypersons were included in the first phase of the study. All the proformas were filled over a period of 1 year by the same interviewer between March 2022 and March 2023. The mean age was 40.7 ± 11.7 years (41.7 ± 12.0 in patients and 39.8 ± 11.4 in laypersons), and 71 were male (44 in patients and 27 in the laypersons groups).

The mean disability scores assigned to solid, liquid, flatus, mucous, stress, and urge FI by the patients were 82.5 ± 19.1, 84.8 ± 15.4, 58.1 ± 23.6, 55.3 ± 21.2, 52.0 ± 23.9, and 68.5 ± 23.5 respectively and by the laypersons were 83.0 ± 22.4, 81.4 ± 19.2, 54.6 ± 21.1, 55.2 ± 19.3, 48.8 ± 22.0, and 68.3 ± 22.8 respectively (Table 6). The overall mean disability scores assigned to solid, liquid, flatus, mucous, stress, and urge FI were 82.7 ± 20.7, 83.1 ± 17.4, 56.3 ± 22.3, 55.2 ± 20.1, 50.4 ± 22.9, and 68.4 ± 23.0 respectively (Table 6). After dividing these by 10 and rounding them off, the final weights assigned to solid, liquid, flatus, mucous, stress, and urge FI were 8, 8, 6, 6, 5, and 7, respectively (Table 6).

The three frequencies fixed for all FIs were never, occasional and common and were assigned points of 0, 1 and 2, respectively (Table 8). Thus, a new scoring system was finalized (Table 8). The maximum possible score was 80, which implied total incontinence, and the minimum score possible was 0, which implied normal continence (no incontinence) (Table 8).

In the second phase of the study, 50 patients and 50 laypersons from the first phase of the study were included, and 33 colorectal surgeons were interviewed to rank the six different types of FI according to severity. The ranking of the surgeons, patients and laypersons was compared. The perception of the patients and the laypersons correlated well, whereas it did not correlate with the surgeons' perception (Tables 7 and 9). The patients rated liquid FI, while the surgeons perceived solid FI as the most severe (Table 7). After solid and liquid FI, the patients and laypersons ranked urge FI as the most severe, whereas the surgeons ranked stress FI at that level (Table 7). The severity perception of the patients and laypersons regarding solid and urge FI was significantly different from the surgeons ($P < 0.00001$, ANOVA) (Table 9).

Table 7 Comparison of ranking of six types of fecal incontinence as per severity perceived by patients, laypersons and surgeons

Ranking	Patients (*n* = 50)		Laypersons (*n* = 50)		Surgeons (*n* = 33)	
Most severe to least severe	Type of FI	Ranking mean ± SD	Type of FI	Ranking mean ± SD	Type of FI	Ranking mean ± SD
6	Liquid	4.73 ± 1.25	Solid	4.80 ± 1.50	Solid	6.0 ± 0.0
5	Solid	4.51 ± 1.50	Liquid	4.64 ± 1.35	Liquid	5.0 ± 0.0
4	Urge	3.65 ± 1.52	Urge	3.70 ± 1.44	Stress	2.90 ± 1.07
3	Flatus	2.87 ± 1.50	Flatus	2.72 ± 1.45	Mucous	2.81 ± 0.91
2	Mucous	2.57 ± 1.38	Mucous	2.70 ± 1.44	Flatus	2.57 ± 1.06
1	Stress	2.53 ± 1.53	Stress	2.46 ± 1.38	Urge	1.69 ± 1.07

The persons in each group (patients, laypersons and surgeons) were asked to rank the six types of fecal incontinence (FI) in decreasing order of severity. The most severe was given 6 points, and the least severe FI was given 1 point. The average of each FI type in each group was calculated, and the final ranking of FI in that group was calculated.

Table 8 New scoring system

Incontinence type	Weight	Frequency			Maximum score
		Never (points)	Occasional (points) (≤ 1 episode/ wk)	Common (points) (> 1 episode/ wk)	
Solid	8	0	1	2	16
Liquid	8	0	1	2	16
Urge	7	0	1	2	14
Flatus	6	0	1	2	12
Mucus	6	0	1	2	12
Stress	5	0	1	2	10
Total					80

Score in a cell = Weight for that incontinence type × frequency points. For example, a person with occasional liquid incontinence would have an 8 × 1 = 8 score. Maximum possible score = 80 (total incontinence), minimum score possible = 0 (no incontinence).

Table 9 Difference in mean ranking six types of fecal incontinence as per severity perceived by patients, laypersons and surgeons

Type of FI	Ranking mean ± SD			Significance
	Patients (*n* = 50)	Laypersons (*n* = 50)	Surgeons (*n* = 33)	(ANOVA)
Solid	4.51 ± 1.50	4.80 ± 1.50	6.00 ± 0.00	$P < 0.00001$
Liquid	4.73 ± 1.25	4.64 ± 1.35	5.00 ± 0.00	$P = 0.35$
Urge	3.65 ± 1.52	3.70 ± 1.44	1.69 ± 1.07	$P < 0.00001$
Flatus	2.87 ± 1.50	2.72 ± 1.45	2.57 ± 1.06	$P = 0.88$
Mucous	2.57 ± 1.38	2.70 ± 1.44	2.81 ± 0.91	$P = 0.90$
Stress	2.53 ± 1.53	2.46 ± 1.38	2.90 ± 1.07	$P = 0.29$

The persons in each group (patients, laypersons, and surgeons) were asked to rank the six fecal incontinence (FI) in decreasing order of severity. The most severe was given 6, and the least severe FI was given 1 point. The average of each FI type in each group was calculated and compared.

DISCUSSION

The objective scoring of FI is an important and necessary tool, especially for gastroenterologists, gastrointestinal and colorectal surgeons, and neurologists. Out of the few scoring systems published, the Wexner and Vaizey scoring systems

are the most popular and commonly used[17,18]. However, as discussed above, there are a few major shortcomings in these scoring systems, due to which they are not accurate, comprehensive, and bias-free. In the present system, it was attempted to remove the lacunae of existing scoring systems (Table 10).

FI missed out in previous scoring systems, such as urge in Wexner, mucous in Wexner and Vaizey, and stress FI in all previous systems, were included in the new scoring system[18]. The new system is the first in which all six types of FI were included: solid, liquid, flatus, mucus, stress, and urge. It is logical to include all these six FI in a scoring system as all of these are distinct, and the presence of any of these indicates a malfunction in the coordinated function of a portion of the sphincter mechanism.

The biggest lacuna in the Wexner and Vaizey scores is that all types of FIs are assigned the same weight (Tables 1 and 2)[17,18]. In fact, no attempt was made to assign differential weights to different types of FI[18]. It is difficult to understand how all types of FI could be assigned exactly the same scores when all six FI types are different. The present study highlighted that weights calculated for different FIs could have significant variations ranging from 5 (urge FI) to 8 (liquid and solid FI) (Tables 6 and 8). Therefore, assigning these FIs equal weight was too simplistic and a source of significant error.

In the past, patients' perceptions were not given due importance, or it was assumed that surgeons' and patients' perceptions would be similar. We were of the opinion that the patients' subjective perception should be the basis of any FI scoring system. If there is any discrepancy between surgeons' and patients' perceptions regarding FI, then the patients' perceptions should be given priority over surgeons' perceptions. Even taking an average of both would be inappropriate. This is because, ultimately, the patients are the sufferers, and before making any decision regarding a treatment/surgery, fellow patients' perceptions would be of more relevance to any patient. Therefore, we did not include surgeons' perceptions in determining the weight of the different types of FI. In the second phase of the study, we compared the severity ranking of different FI according to the patients, laypersons, and surgeons' perceptions. The patients' and layperson's ranking of different FI was similar, but both were significantly different from the surgeons' rankings (Tables 7 and 9).

In the FISI scoring system, as in the present study, the surgeons' and patients' perceptions were different as the surgeons gave more importance to solid than liquid FI (Tables 3, 7, and 9). The reason mentioned in the FISI study was that surgeons viewed solid FI as a reflection of sphincter integrity and the adequacy of surgical repairs[19]. It was further discussed that professionals tended to assign a higher value to more severe elements, whereas patients placed greater importance on more common events[19,27]. In such a scenario where discrepancy arises, the patients' perception should be given priority in formulating a scoring system, and it would be inappropriate to force surgeons' opinions on the patients.

The FISI study also had several lacunae. When compared to the present study, the sample size in the FISI study was smaller (n = 34 *vs* 100 in the present study)[19]. About one-third of patients (12/34) in the FISI study completed the questionnaire through email[19]. Also, their questionnaire was not detailed and contained a single 20-cell table that was to be filled by the patients (Table 3)[19]. Each cell had to be assigned a number between 1 and 20 according to the severity, and no number could be repeated (Table 3)[19]. This step in their methodology could lead to error as two different cells could be perceived to be of similar severity by patients and could have deserved the same number (*e.g.*, mucus leakage once weekly could be perceived as severe as gas leakage once daily by the patient). Also, the present study showed that detailed definitions (Table 4) and the EuroQol descriptive system (Table 5) helped to guide the patients to understand the parameters properly and filling the charts accordingly. In our study, the interviewer took at least 1 h in every case to accurately fill out the chart. It seemed highly improbable that such detailed charts could be filled appropriately *via* email, as was done in the FISI study[19]. The proper statistical methods were also not followed in the FISI study, such as assigning weights to each FI type, linear increase in scores on the increasing frequency of symptoms, *etc.* Therefore, the end result of FISI scoring was haphazard and not amenable to usage (Table 3). This was perhaps the main reason that the FISI scoring system did not become popular and was not widely utilized. All the existing lacunae were removed in the present study, and the latter utilized detailed and sound scientific methods and in a much larger sample than in the FISI study (Table 10).

In the present study, like in the FISI study[19], the surgeons perceived solid FI as the worst, while the patients perceived liquid FI as the worst. Another interesting aspect was that after excluding solid and liquid FI, the surgeons perceived stress FI while patients and laypersons perceived urge FI as the worst (Table 7). On detailed questioning, most surgeons opined that in stress FI, there was actual leakage of fecal matter, while in urge FI, one had to rush to the toilet, and actual leakage could be prevented in most cases. In contrast, the patients and laypersons opined that stress FI would only happen when there was stress (lifting weights, and coughing, *etc.*), and many times, such stressful situations (and hence stress FI) could be avoided (not lifting weights) or curtailed (coughing lightly) but in urge FI, the person had to rush to the toilet every time, and this would hamper the quality of life in a bigger way. It was difficult to ascertain the reason behind this difference in perception between the surgeons and patients.

The parameters included in the existing scoring systems (Wexner and Vaizey) which were not a type of FI and were not a direct measure of the degree of FI like "Need to wear a pad"[17,18], "Alteration in lifestyle"[17,18], and "Need to take a constipating medicine"[18], which led to error, were excluded as parameters in the new scoring system. Rather, these were included in the 4D3L [modified EQ-5D+ (EuroQol)] description system (Table 5), which served as the basis for assigning weights to different types of FI. As discussed above, these parameters are the outcome/side effects of FI, and adding them as separate parameters for scoring was leading to a confounding bias.

It is pertinent that there is an optimal balance between scientific soundness and simplicity of a scoring system. Steps were taken to simplify the new scoring system, such as rounding off the assigned weights to the nearest whole number and decreasing the frequency of FI episodes from 5 (earlier scoring systems) (daily, weekly, monthly, yearly and never) to 3 (common, occasional and never). During the pilot study, it was realized that dividing the symptoms (episodes) into

Table 10 Comparison of existing scoring systems with new scoring system

	Wexner	Vaizey	FISI	NSS
Comprehensive	No	No	No	Yes
FI type included: urge FI	No	Yes	No	Yes
FI type included: mucous FI	No	No	Yes	Yes
Presence of confounding parameters like "Need to wear a pad", "Need to take constipating medicine", and "Alteration of lifestyle"	Yes	Yes	No	No
Assigning weights to each FI by an objective method	No	No	No	Yes
Inclusion of patient perceptions (*n*)	0	0	34	50
Inclusion of laypersons' perceptions (*n*)	0	0	0	50
Simple and easy to use	+++++	+++++	+	+++++
Detailed structured definitions	No	No	No	Yes
In-depth disability scores based on an objective description system	No	No	No	4D3L [modified EQ-5D+ (EuroQol)] used

FI: Fecal incontinence.

daily, weekly or monthly was difficult for the patients as the frequency of FI episodes is not strictly regular or periodic. Therefore, the broad categories of FI episodes as common or occasional made the scoring task easier for the patient while also simplifying the system without significantly impacting the scientific quotient. In contrast, giving equal weight to all types of FI for the sake of simplicity would be inappropriate as that would significantly compromise accuracy.

The subjective evaluation of study subjects could lead to deviation of the results. Therefore, several steps were taken to maximize objectivity while developing the new scoring system. First, in the proforma, the six FI parameters were defined in simple as well as two languages (English and the native language, Hindi), which a patient and layperson could easily understand. Second, both the interviewer and interviewee were blinded to the goals or purpose of the study. Third, all the proformas were filled out by the same interviewer. Fourth, to increase objectivity while filling out the proforma by the study subjects, a modified EQ-5D+ (EuroQol), 4D3L descriptive system was utilized. Scoring (0–25) was also utilized in each dimension to guide study subjects and to increase objectivity.

The study had some limitations. The new scoring system was not tested for inter- and intra-observer variability and test–retest reliability. However, these are planned for the next phase of the study. The validity of the new scoring system could not be checked because there was no gold standard against which it could be validated. The system was based on assigning weights and had more types of FI, due to which it was fundamentally different from the commonly used Wexner and Vaizey scoring systems. Nonetheless, this was a single-center study, and the new scoring system should be validated in a larger sample, preferably in multiple centers.

CONCLUSION

The new scoring system to objectively assess and grade FI clinically is more accurate than the existing scoring systems. It is simple and easy to use, and addresses most of the shortcomings of previous scoring systems. However, further studies are needed to corroborate the results of the present study.

ACKNOWLEDGMENTS

We would like to thank Khushhreet Garg for providing software support and editing the tables.

ARTICLE HIGHLIGHTS

Research background

Fecal incontinence (FI) is a common problem. Its assessment is difficult, and an objective scoring system needs to be developed so that FI can be evaluated uniformly all across the globe.

Research objectives

To develop a new effective, and scientifically sound scoring system in which the shortcomings of the existing scoring

systems are removed.

Research motivation
The existing scoring systems had many lacunae, due to which they were not scientifically accurate.

Research methods
A proforma was made in simple language in which all definitions of FI were included so that the study participants (patients and laypersons) could understand them. The study participants were then assigned disability scores (ranging from 0 to 100) for each type of FI based on a modified EQ-5D+ (EuroQol) descriptive system. The average score of each type of FI was calculated, divided by 10, and rounded off to determine the weight of each type. In the second phase of the study, a group of colorectal surgeons was asked to rank the six FI types in order of severity, and their ranking was compared with that of the patients and laypersons.

Research results
One hundred participants (50 patients and 50 laypersons) were included in the study. A new scoring system was formulated in which the maximum possible score was 80 (total incontinence), and the least 0 (no incontinence). The surgeons' ranking of FI severity differed significantly from the patients' and the laypersons' rankings, highlighting that the surgeons and the patients may perceive the severity of different FIs differently.

Research conclusions
A new scoring system for FI was formulated, which was simple, logical, comprehensive, and easy to use. The perceptions of patients and surgeons regarding the severity of different FIs differed significantly.

Research perspectives
The new scoring system would be useful for clinicians worldwide to objectively assess FI in the clinical setting.

FOOTNOTES

Author contributions: Garg P conceived and designed the study, collected and analyzed the data, revised the data, and finally approved and submitted the manuscript (Guarantor of the study); Sudoł-Szopińska I collected and analyzed the data, revised the data, finally approved and submitted the manuscript; Kołodziejczak M critically analyzed the data, reviewed and edited the manuscript, finally approved and submitted the manuscript; Bhattacharya K analyzed the data, revised the data, finally approved and submitted the manuscript; Kaur G analyzed the data, revised the data, and finally approved and submitted the manuscript.

Institutional review board statement: The study was approved by the Ethics Committee of Adesh Medical College and Hospital (Approval No. AMCH/IEC/2022/02/04).

Informed consent statement: All study participants, or their legal guardian, provided informed written consent prior to study enrollment.

Conflict-of-interest statement: There are no conflicts of interest to report.

Data sharing statement: Technical appendix, statistical code, and dataset available from the corresponding author at drgargpankaj@gmail.com.

Open-Access: This article is an open-access article that was selected by an in-house editor and fully peer-reviewed by external reviewers. It is distributed in accordance with the Creative Commons Attribution NonCommercial (CC BY-NC 4.0) license, which permits others to distribute, remix, adapt, build upon this work non-commercially, and license their derivative works on different terms, provided the original work is properly cited and the use is non-commercial. See: https://creativecommons.org/Licenses/by-nc/4.0/

Country/Territory of origin: India

ORCID number: Pankaj Garg 0000-0002-0800-3578; Iwona Sudol-Szopinska 0000-0003-2671-3036; Małgorzata Kolodziejczak 0009-0002-3817-9280; Kaushik Bhattacharya 0000-0002-4825-9148; Gurleen Kaur 0000-0001-8405-2913.

S-Editor: Chen YL
L-Editor: Kerr C
P-Editor: Chen YL

REFERENCES

1 **Sun G**, Trzpis M, Ding H, Gao X, Zhang W, Broens PMA. Validation of the Chinese DeFeC questionnaire: a comprehensive screening tool for symptoms and causes of constipation and incontinence. *Ann Palliat Med* 2023; **12**: 507-515 [PMID: 37038059 DOI: 10.21037/apm-22-1009]

2 **Goodoory VC**, Ng CE, Black CJ, Ford AC. Prevalence and impact of faecal incontinence among individuals with Rome IV irritable bowel syndrome. *Aliment Pharmacol Ther* 2023; **57**: 1083-1092 [PMID: 36914979 DOI: 10.1111/apt.17465]

3 **Cuinas K**, Ferrari L, Igbedioh C, Solanki D, Williams A, Schizas A, Hainsworth A. Pelvic floor investigations for anal incontinence: Are they useful to predict outcomes from conservative treatment? *Neurourol Urodyn* 2023; **42**: 1122-1131 [PMID: 37010063 DOI: 10.1002/nau.25182]

4 **Whitehead WE**, Simren M, Busby-Whitehead J, Heymen S, van Tilburg MAL, Sperber AD, Palsson OS. Fecal Incontinence Diagnosed by the Rome IV Criteria in the United States, Canada, and the United Kingdom. *Clin Gastroenterol Hepatol* 2020; **18**: 385-391 [PMID: 31154029 DOI: 10.1016/j.cgh.2019.05.040]

5 **Menees SB**, Almario CV, Spiegel BMR, Chey WD. Prevalence of and Factors Associated With Fecal Incontinence: Results From a Population-Based Survey. *Gastroenterology* 2018; **154**: 1672-1681.e3 [PMID: 29408460 DOI: 10.1053/j.gastro.2018.01.062]

6 **Rao SS**, Bharucha AE, Chiarioni G, Felt-Bersma R, Knowles C, Malcolm A, Wald A. Functional Anorectal Disorders. *Gastroenterology* 2016 [PMID: 27144630 DOI: 10.1053/j.gastro.2016.02.009]

7 **Whitehead WE**, Borrud L, Goode PS, Meikle S, Mueller ER, Tuteja A, Weidner A, Weinstein M, Ye W; Pelvic Floor Disorders Network. Fecal incontinence in US adults: epidemiology and risk factors. *Gastroenterology* 2009; **137**: 512-517, 517.e1 [PMID: 19410574 DOI: 10.1053/j.gastro.2009.04.054]

8 **Vasant DH**, Nigam GB, Bate S, Hamdy S, Limdi JK. The prevalence and burden of Rome IV faecal incontinence in ulcerative colitis: A cross-sectional study. *Aliment Pharmacol Ther* 2023; **58**: 26-34 [PMID: 37012703 DOI: 10.1111/apt.17502]

9 **Bordeianou LG**, Thorsen AJ, Keller DS, Hawkins AT, Messick C, Oliveira L, Feingold DL, Lightner AL, Paquette IM. The American Society of Colon and Rectal Surgeons Clinical Practice Guidelines for the Management of Fecal Incontinence. *Dis Colon Rectum* 2023; **66**: 647-661 [PMID: 36799739 DOI: 10.1097/DCR.0000000000002776]

10 **Rao SSC**. Keys to the Diagnosis and Management of Patients With Fecal Incontinence. *Gastroenterol Hepatol (N Y)* 2022; **18**: 169-171 [PMID: 35506006]

11 **Futaba K**, Chen SC, Leung WW, Wong C, Mak T, Ng S, Gregersen H. Fecobionics Evaluation of Biofeedback Therapy in Patients With Fecal Incontinence. *Clin Transl Gastroenterol* 2022; **13**: e00491 [PMID: 35363631 DOI: 10.14309/ctg.0000000000000491]

12 **de Miguel Valencia MJ**, Margallo Lana A, Pérez Sola MÁ, Sánchez Iriso E, Cabasés Hita JM, Alberdi Ibáñez I, Ciga Lozano MÁ, de Miguel Velasco M. Economic burden of long-term treatment of severe fecal incontinence. *Cir Esp (Engl Ed)* 2022; **100**: 422-430 [PMID: 35537695 DOI: 10.1016/j.cireng.2022.05.006]

13 **Cerdán Santacruz C**, Cerdán Santacruz DM, Milla Collado L, Ruiz de León A, Cerdán Miguel J. Multimodal Management of Fecal Incontinence Focused on Sphincteroplasty: Long-Term Outcomes from a Single Center Case Series. *J Clin Med* 2022; **11** [PMID: 35807037 DOI: 10.3390/jcm11133755]

14 **Knol ME**, Bastiaannet E, DeRuiter MC, Snijders HS, van der Heyden JTM, Baeten CIM. Clinical characteristics of phenotypes of fecal incontinence. *Tech Coloproctol* 2023; **27**: 475-480 [PMID: 36967451 DOI: 10.1007/s10151-023-02778-2]

15 **Hovan HM**. Instructing Clinicians and Providers on Care Principles and Management of Fecal and Urinary Incontinence. *J Wound Ostomy Continence Nurs* 2023; **50**: 171-173 [PMID: 36867042 DOI: 10.1097/WON.0000000000000952]

16 **de Codes LMG**, de Jesus ACC, de Codes JJG, Ferreira RF, da Silva Beda Sacramento C, da Cruz IDM, de Castro Ribeiro Fidelis F, de Carvalho AL, Motta MP, de Oliveira Alves C, Netto EM, Santana GO. Anorectal function and clinical characteristics associated with fecal incontinence in patients with Crohn's disease. *J Crohns Colitis* 2023 [PMID: 36951290 DOI: 10.1093/ecco-jcc/jjad048]

17 **Jorge JM**, Wexner SD. Etiology and management of fecal incontinence. *Dis Colon Rectum* 1993; **36**: 77-97 [PMID: 8416784 DOI: 10.1007/BF02050307]

18 **Vaizey CJ**, Carapeti E, Cahill JA, Kamm MA. Prospective comparison of faecal incontinence grading systems. *Gut* 1999; **44**: 77-80 [PMID: 9862829 DOI: 10.1136/gut.44.1.77]

19 **Rockwood TH**, Church JM, Fleshman JW, Kane RL, Mavrantonis C, Thorson AG, Wexner SD, Bliss D, Lowry AC. Patient and surgeon ranking of the severity of symptoms associated with fecal incontinence: the fecal incontinence severity index. *Dis Colon Rectum* 1999; **42**: 1525-1532 [PMID: 10613469 DOI: 10.1007/BF02236199]

20 **Wexner SD**. Further validation of the Wexner Incontinence Score: A note of appreciation and gratitude. *Surgery* 2021; **170**: 53-54 [PMID: 33863582 DOI: 10.1016/j.surg.2021.02.039]

21 **Shafik A**. Anorectal tightening reflex: role in fecal incontinence. *Eur Surg Res* 1993; **25**: 399-405 [PMID: 8276040 DOI: 10.1159/000129308]

22 **Shafik A**, El Sibai O, Shafik IA, Shafik AA. Stress, urge, and mixed types of partial fecal incontinence: pathogenesis, clinical presentation, and treatment. *Am Surg* 2007; **73**: 6-9 [PMID: 17249447]

23 **Rockwood TH**, Church JM, Fleshman JW, Kane RL, Mavrantonis C, Thorson AG, Wexner SD, Bliss D, Lowry AC. Fecal Incontinence Quality of Life Scale: quality of life instrument for patients with fecal incontinence. *Dis Colon Rectum* 2000; **43**: 9-16; discussion 16 [PMID: 10813117 DOI: 10.1007/BF02237236]

24 **Dolan P**. Modeling valuations for EuroQol health states. *Med Care* 1997; **35**: 1095-1108 [PMID: 9366889 DOI: 10.1097/00005650-199711000-00002]

25 **Afif IY**, Manik AR, Munthe K, Maula MI, Ammarullah MI, Jamari J, Winarni TI. Physiological Effect of Deep Pressure in Reducing Anxiety of Children with ASD during Traveling: A Public Transportation Setting. *Bioengineering (Basel)* 2022; **9** [PMID: 35447717 DOI: 10.3390/bioengineering9040157]

26 **Afif IY**, Farkhan M, Kurdi O, Maula MI, Ammarullah MI, Setiyana B, Jamari J, Winarni TI. Effect of Short-Term Deep-Pressure Portable Seat on Behavioral and Biological Stress in Children with Autism Spectrum Disorders: A Pilot Study. *Bioengineering (Basel)* 2022; **9** [PMID: 35200402 DOI: 10.3390/bioengineering9020048]

27 **Kane RL**, Rockwood T, Finch M, Philp I. Consumer and professional ratings of the importance of functional status components. *Health Care Financ Rev* 1997; **19**: 11-22 [PMID: 10345400]



Published by **Baishideng Publishing Group Inc**
7041 Koll Center Parkway, Suite 160, Pleasanton, CA 94566, USA
Telephone: +1-925-3991568
E-mail: bpgoffice@wjgnet.com
Help Desk: https://www.f6publishing.com/helpdesk
https://www.wjgnet.com



© 2023 Baishideng Publishing Group Inc. All rights reserved.

ISSN 1007-9327 (print)
ISSN 2219-2840 (online)

World Journal of *Gastroenterology*

World J Gastroenterol 2023 August 14; 29(30): 4604-4705



Published by Baishideng Publishing Group Inc

World Journal of Gastroenterology

Contents

Weekly Volume 29 Number 30 August 14, 2023

REVIEW

4604 Immune response modulation in inflammatory bowel diseases by *Helicobacter pylori* infection

Feilstrecker Balani G, dos Santos Cortez M, Picasky da Silveira Freitas JE, Freire de Melo F, Zarpelon-Schutz AC, Teixeira KN

4616 *Helicobacter pylori* intragastric colonization and migration: Endoscopic manifestations and potential mechanisms

Mu T, Lu ZM, Wang WW, Feng H, Jin Y, Ding Q, Wang LF

MINIREVIEWS

4628 Systemic treatments for resectable carcinoma of the esophagus

Leowattana W, Leowattana P, Leowattana T

ORIGINAL ARTICLE

Basic Study

4642 Exploring the regulatory mechanism of tRNA-derived fragments 36 in acute pancreatitis based on small RNA sequencing and experiments

Fan XR, Huang Y, Su Y, Chen SJ, Zhang YL, Huang WK, Wang H

4657 Fecal microbiota transplantation alleviates experimental colitis through the Toll-like receptor 4 signaling pathway

Wen X, Xie R, Wang HG, Zhang MN, He L, Zhang MH, Yang XZ

Observational Study

4671 Incidence, prevalence, and comorbidities of chronic pancreatitis: A 7-year population-based study

Cai QY, Tan K, Zhang XL, Han X, Pan JP, Huang ZY, Tang CW, Li J

META-ANALYSIS

4685 Diagnostic value of conventional endoscopic ultrasound for lymph node metastasis in upper gastrointestinal neoplasia: A meta-analysis

Chen C, Song YL, Wu ZY, Chen J, Zhang Y, Chen L

LETTER TO THE EDITOR

4701 Pitfalls and promises of bile duct alternatives: There is plenty of room in the regenerative surgery

Klabukov ID, Baranovskii DS, Shegay PV, Kaprin AD

ABOUT COVER

Editorial Board Member of *World Journal of Gastroenterology*, Goran Hauser, FEBG, MD, PhD, Professor, Department of Internal Medicine, Division of Gastroenterology, Clinical Hospital Centre, Faculty of Medicine Rijeka-University of Rijeka, Rijeka 51000, Croatia. goran.hauser@medri.uniri.hr

AIMS AND SCOPE

The primary aim of *World Journal of Gastroenterology* (*WJG*, *World J Gastroenterol*) is to provide scholars and readers from various fields of gastroenterology and hepatology with a platform to publish high-quality basic and clinical research articles and communicate their research findings online. *WJG* mainly publishes articles reporting research results and findings obtained in the field of gastroenterology and hepatology and covering a wide range of topics including gastroenterology, hepatology, gastrointestinal endoscopy, gastrointestinal surgery, gastrointestinal oncology, and pediatric gastroenterology.

INDEXING/ABSTRACTING

The *WJG* is now abstracted and indexed in Science Citation Index Expanded (SCIE, also known as SciSearch®), Current Contents/Clinical Medicine, Journal Citation Reports, Index Medicus, MEDLINE, PubMed, PubMed Central, Scopus, Reference Citation Analysis, China National Knowledge Infrastructure, China Science and Technology Journal Database, and Superstar Journals Database. The 2023 edition of Journal Citation Reports® cites the 2022 impact factor (IF) for *WJG* as 4.3; IF without journal self cites: 4.1; 5-year IF: 5.3; Journal Citation Indicator: 0.82; Ranking: 33 among 93 journals in gastroenterology and hepatology; and Quartile category: Q2. The *WJG*'s CiteScore for 2021 is 8.3 and Scopus CiteScore rank 2022: Gastroenterology is 22/149.

RESPONSIBLE EDITORS FOR THIS ISSUE

Production Editor: *Ying-Yi Yuan*; **Production Department Director:** *Xu Guo*; **Editorial Office Director:** *Jia-Ru Fan*.

NAME OF JOURNAL
World Journal of Gastroenterology

ISSN
ISSN 1007-9327 (print) ISSN 2219-2840 (online)

LAUNCH DATE
October 1, 1995

FREQUENCY
Weekly

EDITORS-IN-CHIEF
Andrzej S Tarnawski

EDITORIAL BOARD MEMBERS
http://www.wjgnet.com/1007-9327/editorialboard.htm

PUBLICATION DATE
August 14, 2023

COPYRIGHT
© 2023 Baishideng Publishing Group Inc

INSTRUCTIONS TO AUTHORS
https://www.wjgnet.com/bpg/gerinfo/204

GUIDELINES FOR ETHICS DOCUMENTS
https://www.wjgnet.com/bpg/GerInfo/287

GUIDELINES FOR NON-NATIVE SPEAKERS OF ENGLISH
https://www.wjgnet.com/bpg/gerinfo/240

PUBLICATION ETHICS
https://www.wjgnet.com/bpg/GerInfo/288

PUBLICATION MISCONDUCT
https://www.wjgnet.com/bpg/gerinfo/208

ARTICLE PROCESSING CHARGE
https://www.wjgnet.com/bpg/gerinfo/242

STEPS FOR SUBMITTING MANUSCRIPTS
https://www.wjgnet.com/bpg/GerInfo/239

ONLINE SUBMISSION
https://www.f6publishing.com

© 2023 Baishideng Publishing Group Inc. All rights reserved. 7041 Koll Center Parkway, Suite 160, Pleasanton, CA 94566, USA
E-mail: bpgoffice@wjgnet.com https://www.wjgnet.com

World Journal of Gastroenterology

Submit a Manuscript: https://www.f6publishing.com

World J Gastroenterol 2023 August 14; 29(30): 4604-4615

DOI: 10.3748/wjg.v29.i30.4604

ISSN 1007-9327 (print) ISSN 2219-2840 (online)

REVIEW

Immune response modulation in inflammatory bowel diseases by *Helicobacter pylori* infection

Gabriella Feilstrecker Balani, Mariana dos Santos Cortez, Jayme Euclydes Picasky da Silveira Freitas, Fabrício Freire de Melo, Ana Carla Zarpelon-Schutz, Kádima Nayara Teixeira

Specialty type: Gastroenterology and hepatology

Provenance and peer review: Invited article; Externally peer reviewed.

Peer-review model: Single blind

Peer-review report's scientific quality classification

Grade A (Excellent): 0
Grade B (Very good): B, B
Grade C (Good): C
Grade D (Fair): 0
Grade E (Poor): 0

P-Reviewer: B Lankarani K, Iran; Bernal G, Chile; Wang D, China

Received: April 28, 2023
Peer-review started: April 28, 2023
First decision: June 17, 2023
Revised: July 1, 2023
Accepted: July 24, 2023
Article in press: July 24, 2023
Published online: August 14, 2023

Gabriella Feilstrecker Balani, Mariana dos Santos Cortez, Jayme Euclydes Picasky da Silveira Freitas, Ana Carla Zarpelon-Schutz, Kádima Nayara Teixeira, Campus Toledo, Universidade Federal do Paraná, Toledo 85.919-899, Paraná, Brazil

Fabrício Freire de Melo, Campus Anísio Teixeira, Universidade Federal da Bahia, Instituto Multidisciplinar em Saúde, Vitória da Conquista 45.029-094, Bahia, Brazil

Ana Carla Zarpelon-Schutz, Programa de Pós-graduação em Biotecnologia - Setor Palotina, Universidade Federal do Paraná, Palotina 85.950-000, Paraná, Brazil

Kádima Nayara Teixeira, Programa Multicêntrico de Pós-graduação em Bioquímica e Biologia Molecular - Setor Palotina, Universidade Federal do Paraná, Palotina 85.950-000, Paraná, Brazil

Corresponding author: Kádima Nayara Teixeira, PhD, Professor, Campus Toledo, Universidade Federal do Paraná, Max Planck 3796, Toledo 85.919-899, Paraná, Brazil.
kadimateixeira@ufpr.br

Abstract

Many studies point to an association between *Helicobacter pylori* (*H. pylori*) infection and inflammatory bowel diseases (IBD). Although controversial, this association indicates that the presence of the bacterium somehow affects the course of IBD. It appears that *H. pylori* infection influences IBD through changes in the diversity of the gut microbiota, and hence in local chemical characteristics, and alteration in the pattern of gut immune response. The gut immune response appears to be modulated by *H. pylori* infection towards a less aggressive inflammatory response and the establishment of a targeted response to tissue repair. Therefore, a T helper 2 (Th2)/macrophage M2 response is stimulated, while the Th1/macrophage M1 response is suppressed. The immunomodulation appears to be associated with intrinsic factors of the bacteria, such as virulence factors - such oncogenic protein cytotoxin-associated antigen A, proteins such *H. pylori* neutrophil-activating protein, but also with microenvironmental changes that favor permanence of *H. pylori* in the stomach. These changes include the increase of gastric mucosal pH by urease activity, and suppression of the stomach immune response promoted by evasion mechanisms of the bacterium. Furthermore, there is a causal relationship between *H. pylori* infection and components of the innate immunity such as the NLR family pyrin domain containing 3 inflammasome that

directs IBD toward a better prognosis.

Key Words: Cytotoxin-associated antigen A oncoprotein; Gut microbiota; *Helicobacter pylori*; *Helicobacter pylori* neutrophil-activating protein; Immunological modulation; Inflammatory bowel disease; NLR family pyrin domain containing 3 inflammasome

©The Author(s) 2023. Published by Baishideng Publishing Group Inc. All rights reserved.

Core Tip: *Helicobacter pylori* (*H. pylori*) infection seems to modulate the immune response triggered by inflammatory bowel disease in a way that makes it less aggressive. The virulence factors of *H. pylori*, as well as the mechanisms that allow it to remain in the stomach environment, appear to change the intestinal microenvironment and modulate the local immune response, contributing to a disease with milder symptoms and less tissue damage.

Citation: Feilstrecker Balani G, dos Santos Cortez M, Picasky da Silveira Freitas JE, Freire de Melo F, Zarpelon-Schutz AC, Teixeira KN. Immune response modulation in inflammatory bowel diseases by *Helicobacter pylori* infection. *World J Gastroenterol* 2023; 29(30): 4604-4615
URL: https://www.wjgnet.com/1007-9327/full/v29/i30/4604.htm
DOI: https://dx.doi.org/10.3748/wjg.v29.i30.4604

INTRODUCTION

Inflammatory bowel diseases (IBD) are a group of chronic conditions affecting the gastrointestinal tract, characterized by episodes of abdominal pain, diarrhea, bloody stools, and weight loss. The two main types of IBD are Crohn's disease (CD) and ulcerative colitis (UC)[1]. In CD any area of the gastrointestinal tract can be affected, but the most affected regions are the terminal ileum, the cecum, the perianal region, and the colon, while in UC the inflammation is restricted to the colon and rectum[1]. Regarding histology, in CD the intestine presents thickened submucosa, transmural inflammation, ulceration and non-caseating granulomas, while in UC the inflammation is limited to the mucosa, with crypts and abscesses[2].

The pathogenesis of IBD is complex and involves a combination of genetic, environmental, and immunological factors. The gut microbiota is critical to homeostasis in this organ and contributes to the tolerance process, to the development and differentiation of the local and systemic immune system, and may protect the host from pathogenic enteric infections. However, in IBD, luminal bacteria trigger deregulated immune responses, acting as the main environmental factor for the development of these pathologies[3,4].

The loss of tolerance to the commensal microbiota seems to be related to the genetic susceptibility of the individual and to an imbalance in the composition of the microbiota[5]. IBD patients have changes in stool composition, with less bacterial quantity and diversity[6,7].

Genome wide association studies of IBD have identified 99 non-overlapping genetic risk loci including 28 that are shared between CD and UC[8]. These genetic alterations seem to implicate several important pathways, such as intestinal barrier function, regulation of innate and adaptive immunity, reactive oxygen species formation, autophagy, and endoplasmic reticulum stress[9]; associations were identified between polymorphisms in the genes for interleukin (IL)-10, IL-10 receptor alpha, and components of this signaling pathway - signal transducer and activator of transcription 3, tyrosine kinase 2, and JAK2, with the early development of IBD[10].

Dysregulation of the immune component in IBD is marked by abnormal mucus production, failure to repair the epithelial barrier, and excessive and persistent activation of T lymphocytes, B cells, dendritic cells, macrophages, and natural killer cells[11,12].

Naive TCD4+ cells can differentiate into T helper 1 (Th1), Th2, Th9, Th17 and regulatory T (Treg) subpopulations; the main stimulus for differentiation into Th1 cells - secreting interferon (IFN)-γ, tumor necrosis factor (TNF) and IL-2, is the expression of IL-12, while IL-4 leads to differentiation into Th2 cells, whose cytokine pattern is marked by the expression of IL-4, IL-5, IL-13 and IL-25[13]. Classically, CD and UC are described as diseases with a Th1 and Th2 immune pattern, respectively[14-16], since typically CD patients have higher IFN-γ and IL-2 expression than UC patients[17,18], that express more IL-5 and IL-13[19,20]. However, some studies contradict this information, since lower levels of IL-13 were seen in UC patients compared to CD patients[21], and high levels of IFN-γ were found in carriers of both diseases[22]. In line with this, Bernardo *et al*[23] found a mixed cytokine pattern in biopsies from UC patients, associated with low IL-13 levels.

A Th17 pattern response prevails in the gut. The differentiation into Th17 cells leads to the expression of IL-17, IL- 21, IL- 22, and IL-23, which are found in large quantities in the intestine of IBD patients[24]. A study using IL-17 receptor (IL-17R) knockout mice showed that IL-17R deficiency protected the animals from developing trinitrobenzene sulfonic acid (TNBS)-induced colitis[25-27].

Although not conclusive, there is evidence to indicate that two members of this cytokine family have different effects; IL-17A appears to have a protective effect through inhibition of the Th1 response[28], furthermore, other studies indicate that deficiency of this cytokine causes exacerbation of colitis, while IL-17F contributes to and aggravates the inflammatory process[29]. Despite the prevalence of Th17 cells in the gut in the absence of IBD, this response pattern appears to be exacerbated with disease onset leading to increased production of pattern marker cytokines. Perhaps this increase occurs relatively disproportionately, prioritizing the increase in cytokines that induce an inflammatory response, such as IL-17F.

Treg cells which is characterized by constitutive expression of forkhead/winged helix transcriptional factor P3 (FoxP3), CD25 and cytotoxic T lymphocyte-associated protein 4, play a major role in the pathogenesis of IBD[30]. In these diseases, there is a significant dysfunction in the activity of these cells, either by being in low numbers or by having their function suppressed. It has been observed that effector cells from IBD patients exhibit relative resistance to Treg-mediated suppression by expressing high levels of Smad7, an inhibitor of the transforming growth factor (TGF)-β signaling pathway[31,32]. The unbalanced and uncontrolled local immune response against the bacterial microbiota in the IBD occurs when it is poorly controlled by endogenous counter regulatory mechanisms, such as the immunosuppressive cytokine TGF-β. Studies show that the inefficiency in control occurs due to a blockade of TGF-β signaling, caused by a blockade in the phosphorylation of the signaling molecule associated with the TGF-β activated receptor, Smad3. The blockade of Smad3 activity is caused by the upregulation of the Smad7[33].

Individuals with a mutation in the *FOXP3* gene often suffer from intestinal inflammation[34]. Treg cells are able to convert to Th17 cells under inflammatory conditions, and the cytokine IL-1β is key in this process[35]. The balance between the Th17 and Treg response is important, especially in places such as the gut, where there is a commensal microbiota, to prevent deregulated immune responses. IBD patients have a reduced Treg/Th17 ratio in peripheral blood compared to healthy individuals. The installation of the inflammatory process in IBD seems to be fueled by an unbalanced increase in the production of Th17 cytokines, which promote the Th1 pattern. Pro-inflammatory cytokines produced by Th1 cells, such as IL-1β, potentiate the inflammatory process by decreasing the Treg/Th17 ratio, both by proportionally increasing the Th17 response and by reducing the suppression of the inflammatory response by Treg cells. Regarding Th9 cells - capable of exacerbating inflammatory processes by increasing epithelial permeability[36], are at high levels in CD and UC[37,38].

IMMUNOMODULATION OF THE INFLAMMATORY PROCESS AND PATHOGENESIS OF IBD BY *HELICOBACTER PYLORI*

Influence of Helicobacter pylori cytotoxin-associated antigen A+ infection on IBD prognosis

Cytotoxin-associated antigen A (*CagA*) is a gene found in the final portion of the Cag pathogenicity island of the *Helicobacter pylori* (*H. pylori*) genome and encodes the oncogenic protein CagA. Its presence is more frequent in East Asian populations than in those from the West, and determines a number of interactions between the bacterium and the host [39]. Although there is a causal relationship between *H. pylori* CagA+ and the incidence of cancers of the gastrointestinal tract[39,40], when it comes to IBD, especially CD and UC, the presence of the *CagA* gene may positively influence the prognosis of patients[41].

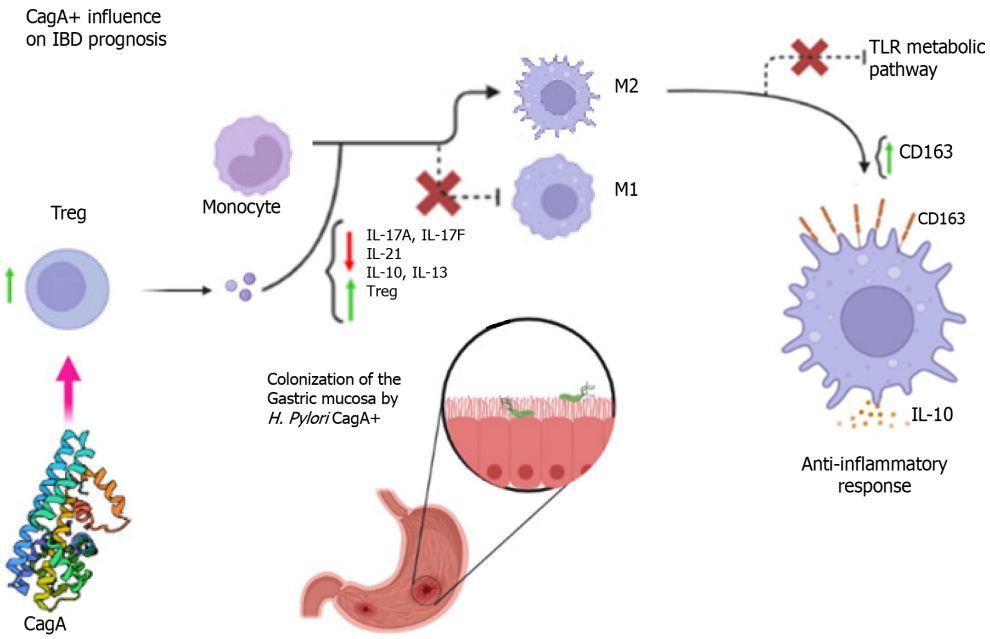
In a first analysis, age, genetic and environmental factors associated with innate and adaptive immunity are key factors in the development of IBD[42,43], thus the presence of *H. pylori* infection becomes yet another variable. Some studies point to several hypotheses for the improved prognosis of IBD in the presence of the *H. pylori CagA* gene, such as the conversion of the M1 macrophage lineage into M2 through modulation of the Th17/Treg immune response, in which there is a decrease in the levels of IL-17F and IL-21 with concomitant increase in the expression of IL-10 and Treg cells[44] due to increased plasma IL-13[45].

Also contributing to the process are increased anti-inflammatory responses through increased expression of CD163 and IL-10, suppression of toll like receptors (TLR) mediated signaling pathways[46], and control of the immune response through activation of pathways mediated by the basic leucine zipper transcription factor ATF-like 2 (BATF2)[47-49] (Figure 1).

The CD163 is a macrophage/monocyte scavenger receptor whose expression is positively regulated by IL-10. The upregulated expression of this receptor is one of the most marked changes in the M2/M1 phenotype switch; therefore, high expression of CD163 is characteristic in inflammatory processes[50,51]. According to studies, the number of CD163- M1 monocytes, as well as CD163+ and CD163+/IL-10+ M2 monocytes are significantly increased in individuals infected with *H. pylori*, in addition to having higher levels of IL-10. IL-10 production is significantly higher by M2 cells from individuals with *H. pylori* infection. In addition, individuals infected with CagA-positive *H. pylori* strains had a significantly higher number of CD163+ and CD163+/IL-10+ monocytes compared to those infected with CagA-negative strains[52].

The TLRs are expressed by cells of the intestinal epithelium, and by cells of the immune system present in the gut, such as leukocytes, dendritic cells, and various polymorphisms of these receptors have been associated with susceptibility to IBD[53,54] and they are involved in signaling pathways leading to the expression of several inflammatory genes[55,56]. BATF2 has unique functions in the regulation of cytokine gene expression by TLR signaling in macrophages[57].

H. pylori has metabolic adaptations for gastric colonization that, in the background, participate in modulating the inflammatory process of IBD. The urease enzyme that confers *H. pylori* resistance to stomach acidity, participates in immunomodulation as it alters particle opsonization, facilitates apoptosis, and by being presented by MHC II increases the expression of pro-inflammatory cytokines[58].



DOI: 10.3748/wjg.v29.i30.4604 **Copyright** ©The Author(s) 2023.

Figure 1 Mechanisms of *Helicobacter pylori* cytotoxin-associated antigen A+ on favorable prognosis of inflammatory bowel diseases. The presence of the cytotoxin-associated antigen A gene at the Cag pathogenicity island induces the modulation of T helper 17/Treg immunological response (1), which reduces levels of interleukin (IL)-17F, IL-17A, and IL-21 and increases the expression of IL-13, IL-10, and Treg (2). These two factors are synergists in the conversion process of the M1 to M2 macrophage lineage (3). Then, M2 macrophages suppress signaling mediated by toll-like receptors (4) and activate metabolic pathways mediated by basic leucine zipper transcription factor ATF-like 2, increasing CD163, a macrophage/monocyte scavenger receptor (5). Finally, the levels of IL-10 expression also increase (6), leading to anti-inflammatory effects (7) and, therefore, to a better prognosis on inflammatory bowel diseases. *H. pylori*: *Helicobacter pylori*; IL: Interleukin; TLR: Toll-like receptor; IBD: Inflammatory bowel disease; CagA: Cytotoxin-associated antigen A; Treg: Regulatory T.

The flagella of *H. pylori*, besides the fundamental importance in its motility for gastric colonization, also induces an inflammatory response. FlaA and FlaB flagellins can promote a humoral response by stimulating the production of specific antibodies[59,60]. Furthermore, studies report that bacteria with increased motility increase IL-8 release and suggest that genes which regulate flagellin production may alter adhesin expression[61-63] facilitating colonization. The chemoattractant effect of IL-8 is all too well known, however, data on the association of IL-8 with *H. pylori* infection are still scarce[64].

Superoxide dismutase from *H. pylori* has also been shown to have a potential immune suppressive effect by inhibiting the production of pro-inflammatory cytokines, through inhibition of pathways activated by the transcription factor nuclear factor kappa B (NF-κB), as well as macrophage inflammatory protein 1-α[65].

Modification of bacterial gut microbiota by H. pylori

The alteration in the pattern of gastric secretion by *H. pylori* is closely related to the modification of the microbiota of the gastrointestinal tract[66]. Hypochlorhydria enables colonization of the distal intestine by acidic pH-sensitive bacteria; this causes people infected with *H. pylori* to have a more diverse alpha intestinal microbiota compared to uninfected people [66-68]. These changes reflect higher percentages of acidophilic bacteria, proteobacteria, bacteria of the genera *Lactobacillus*, *Haemophilus*, *Streptococcus* and *Gemella*; in contrast, there is a decrease in the percentage of pathogenic anaerobic bacteria such as *Clostridium*[69-72].

In addition to the variation in intestinal pH being one of the factors that alter the diversity of the gut bacterial microbiota, it can also be influenced by the virulence factors CagA and VacA of *H. pylori*, which alter the immune response of the infected individual[73-75]. Hormonal factors, influenced by *H. pylori* infection such as an increase of gastrin secretion alter gut metabolism, in addition, leptin has been directly related to an increase of the amount of the probiotic bacteria *Bifidobacterium* and *Lactobacillus*[76].

Indeed, there is an altered composition of the local microbiota of IBD patients[77]. In these diseases an exacerbated immune response against the commensal microbiota occurs in genetically predisposed individuals and, studies suggest that the balance between pathogenic and beneficial bacterial species is altered in these ones[78]. Therefore, the dysbiosis promoted by *H. pylori* infection may help explain the inverse relationship between bacterial infection and IBD in individuals with the two conditions concomitantly, although the underlying molecular mechanisms are not fully understood[79].

CO-IMMUNOMODULATION OF IBD BY NLR FAMILY PYRIN DOMAIN CONTAINING 3 INFLAMMASOME AND *H. PYLORI* INFECTION

The NLR family pyrin domain containing 3 (NLRP3) inflammasome is a multiprotein complex that plays a crucial role in the innate immune response. The complex is formed by the NLRP3 receptor, the adaptor protein caspase-recruitment domain (ASC) and the enzyme caspase-1 and, appears to play a role in the negative association between IBD and *H. pylori* infection by the IL-1β and IL-18 activity. NLRP3 recognizes a wide variety of stimuli linked to pathogen-associated molecular patterns and damage-associated molecular patterns through pattern recognition receptors such as TLRs and nucleotide-binding oligomerization domain 2. Activation of NLRP3 includes a priming process which components are expressed in greater quantities and depends on several upstream signals such as potassium and chloride efflux, calcium mobilization, lysosomal disruption, and mitochondrial dysfunction with increased reactive oxygen species[80].

Activation of the inflammasome culminates i4n expression of NF-κB and cleavage/activation of caspase-1, responsible for processing pro-IL-1β and pro-IL-18, which are cleaved into their active forms[81,82]. Furthermore, activation of NLRP3 leads to proptosis, a form of programmed cell death mediated by gasdermin D protein. Caspase-1 cleaves gasdermin D, removing its carboxy-terminal portion, which allows its insertion and polymerization into the plasma membrane forming pores. Proptosis also appears to induce the secretion of IL-1β and IL-18[83].

Caspase-1 is highly expressed in the mucosa of the patients infected with *H. pylori*. However, it is observed that together, IL-1β and IL-18 seem to play different roles in controlling the infection and the pathogenicity of the bacterium. While IL-1β presents itself as a potent pro-inflammatory agent, IL-18 has regulatory properties and controls responses mediated by TCD4+ cells. Studies have shown that mice that failed to process IL-18 in the absence of caspase-1 had less bacterial colonization, more robust Th17 responses, and more evident immune pathogenicity compared to control animals[84]. Furthermore, mesenchymal stem cells stimulated by this cytokine promote differentiation of Treg cells into virgin TCD4+ cells, limiting the Th17 response[85], promoting a tolerogenic activity and adjusting chronic inflammation in the gastric mucosa (Figure 2).

The absence of caspase-1 results in an inefficient protective immune response, with a less pronounced Th1 and Th17 pattern[86,87]. There is strong evidence of an association between IL-18 and the prevention and control of allergic diseases such as asthma and rhinitis, through pulmonary infiltration of large amounts of Treg and tolerogenic dendritic cells. This association seems especially beneficial in relation to infection with *H. pylori* CagA+ strains, as observed in a study wherein mice infected with the bacteria in the neonatal period developed specific immunological tolerance and protection against gastric immunopathology resulting from *H. pylori* CagA+ infection[88].

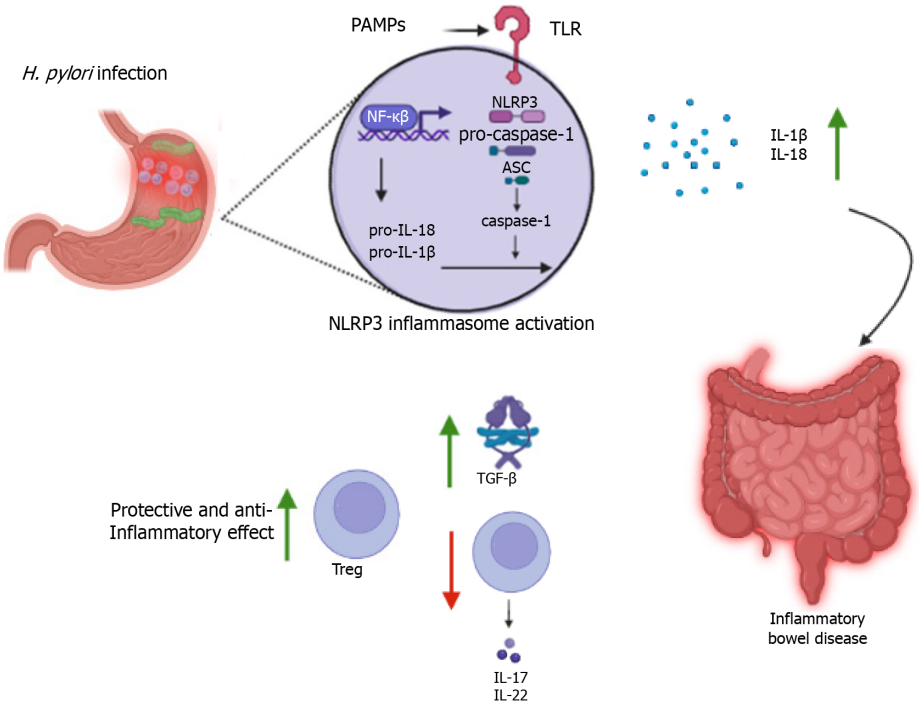
Studies with animal models have shown that NLRP3 activation induced by *H. pylori* infection appears to improve the prognosis of IBD. Engler *et al*[89] observed that mice exposed to the bacterium developed less severe forms of dextran sulfate sodium (DSS)-induced colitis, with significantly milder inflammation and epithelial changes. These positive effects were also observed in animals treated with *H. pylori* extracts. Such beneficial effects are accompanied by positive regulation of TGF-β and the transcription factor caudal-related homeobox transcription factor 2, which regulates the expression of mucins such as mucin 2, a fact that was associated with signaling by NLRP3 and IL-18 production by caspase-1.

Zaki *et al*[90] demonstrated that NLRP3 -/- or ASC -/- mice are more susceptible to DSS-induced colitis and caspase-1 -/- mice are more susceptible to weight loss, diarrhea, rectal bleeding and mortality during the chronic and acute phases of DSS- or TNBS-induced colitis. These findings are related to IL-18 production and its mucosal barrier repair function. Furthermore, IL-18 -/- and IL-18R -/- mice exhibit greater susceptibility to DSS-induced colitis, associated with higher mortality and more severe histopathological changes[91]. Previous studies have reported that the absence of the adaptor protein myeloid differentiation primary response 88 (MyD88), which is involved in the production of IL-18 and IL-1β, increases the severity of inflammatory disease, indicating the importance of MyD88-dependent signaling pathways, such as the TLR4-MyD88 pathway, in blocking the onset and progression of IBD[92-94]. MyD88 is the main signaling adaptor protein of the TLR family. Studies using MyD88-deficient mice suggest a dominant role for TLR/MyD88 signal transduction in preventing intestinal inflammation after acute epithelial injury by promoting epithelial repair[94,95].

Yao *et al*[96] conducted a study with NLRP3R258W mutant mice, a mutation homologous to NLRP3R260W in humans, which causes increased inflammasome activity. The mutant mice developed DSS-induced colitis with milder symptoms compared to wild-type animals, in addition to lower expression of inflammatory mediators, higher expression of IL-18 and IL-1β, and fewer colon tumors. These positive effects were associated with higher activity of Treg cells, positively regulated by IL-1β and fundamental in controlling inflammation. In this study no evidence was found that directly points to IL-18 as an effector molecule in the activation of the inflammasome, but it is believed that this cytokine may be indirectly affected by NLRP3 through secondary effects. However, IL-18 deficiency was shown to override the protective effect of the NLRP3R258W mutation.

IMMUNOMODULATION OF IBD BY NEUTROPHIL-ACTIVATING PROTEIN OF *H. PYLORI*

H. pylori neutrophil-activating protein (HP-NAP) is a virulence factor that plays an important role in immunomodulation. HP-NAP refers to *H. pylori* mini-ferritin, a protein with the ability to activate the production of oxygen radicals by neutrophils promoting their adhesion to the vascular endothelium[97]. Neutrophil adhesion occurs by the positive regulation of β-2-integrin (CD18) expression in a high-affinity state[98,99].



DOI: 10.3748/wjg.v29.i30.4604 **Copyright** ©The Author(s) 2023.

Figure 2 Immunomodulation of the NLR family pyrin domain containing 3 inflammasome and protection against inflammatory bowel diseases. Pathogen-associated molecular patterns from *Helicobacter pylori* are recognized by the NLR family pyrin domain containing 3 (NLRP3) inflammasome toll-like receptors leading to responses that appear to be associated with improved prognosis and an anti-inflammatory effect. Activated NLRP3 is able to increase the expression of caspase-1 which activates the cytokines interleukin (IL)-18 and IL-1β. The positive regulation of these cytokines leads to extragastric immunomodulation by suppressing the T helper 17 subpopulation and increasing regulatory T, transforming growth factor-β and mucins. *H. pylori*: *Helicobacter pylori*; IL: Interleukin; PAMPs: Pathogen-associated molecular patterns; TLR: Toll-like receptor; TGF: Transforming growth factor; NLRP3: NLR family pyrin domain containing 3; Treg: Regulatory T.

The mini-ferritins have the ability to influence host immune cells in addition to protecting bacterial DNA from oxidizing radicals[100]. HP-NAP is released by *H. pylori* near the gastric epithelial monolayer, thus activating macrophages/monocytes and mast cells, with the release of pro-inflammatory cytokines TNF-α, IL-6, IL-12 and IL-23[101,102]. Similar to the chemokine CXCL8, HP-NAP directly promotes leukocyte recruitment; after HP-NAP transcytosis by endothelial cells, part of these proteins remain bound to the luminal portion of the endothelium, increasing the expression of β-2-integrin and changing the local spatial conformation, a fact that culminates in the extravasation of immune cells[99,103].

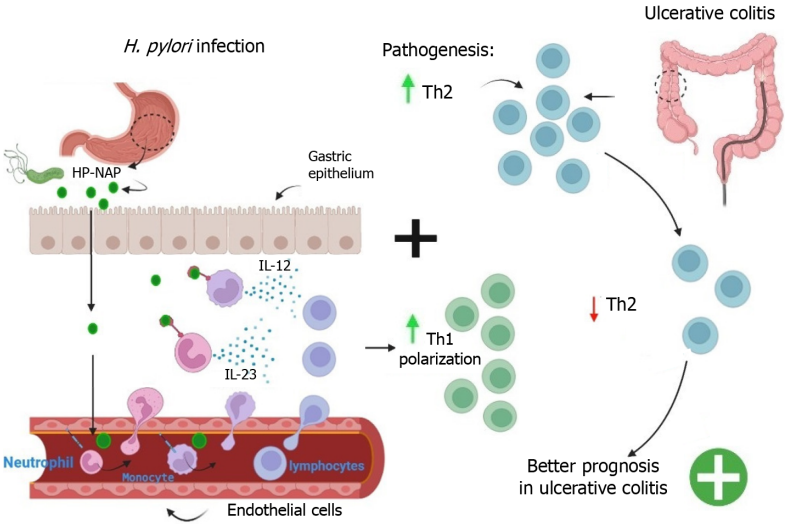
The IL-8 secretion by neutrophils present at the site of inflammation enables the recruitment of more neutrophils and other immune cells. IL-8 secretion is promoted by HP-NAP and mediated through interactions with TLR2 receptors and pertussis toxin-sensitive G proteins[104]. HP-NAP also induces mast cells and basophils to secrete TNF-α, IL-6, IL-8, IL-12 and IL-23, and stimulates mast cells to release histamine and IL-6[101,102,105]. Besides influencing innate immunity, HP-NAP modulates adaptive immunity by promoting the release of IL-12 and IL-23 by neutrophils and monocytes, thereby causing a Th1 polarization, and directing the maturation of monocytes to mature dendritic cells[102].

The mature dendritic cells are stimulated by HP-NAP to express MHCII and release Th1 pattern cytokines such as IL-12[102,106]. The increased secretion of IL-12 in the gastrointestinal microenvironment, promoted by HP-NAP, causes gastric specific T lymphocyte subpopulations to be able to produce large amounts of IFN-γ and TNF-α and, to exhibit cytotoxic activity[102]. Increased Th1 pattern and cytotoxic response, induced by *H. pylori* infection, may be beneficial in pathologies which the Th2 response is the detrimental mechanism (Figure 3). The ability of HP-NAP to reduce Th2 activity due to the polarization towards Th1 was proven in experiments using mice with atopic dermatitis[107]. Therefore, HP-NAP may have a therapeutic effect in situations which there is a predominance of Th2 response, as was observed in HP-NAP inoculation assays in mice with allergic asthma, which significantly reduced serum immunoglobulin E levels with concomitant increase in IL-2, thus decreasing eosinophil infiltration[108].

Thus, the Th1-directed polarization promoted by HP-NAP, may be a possible explanation for the improvement of IBD symptoms, whose pathogenesis may be the result of a dysregulated Th2 response, as occurs in UC, in which there is a predominance of a Th2 response and inhibition of the Th1 response, in individuals infected with *H. pylori*[109-112].

CONCLUSION

Although significant progress has been made over the last few years in defining the mechanisms that *H. pylori* use to influence on IBD evolution, there is clearly much that remains to be elucidated and many questions persist. In this review



DOI: 10.3748/wjg.v29.i30.4604 **Copyright** ©The Author(s) 2023.

Figure 3 Hypothesis on correlation between concomitant infection with *Helicobacter pylori* and the presence of ulcerative colitis (inflammatory bowel disease), which has a pathological pattern of exacerbated T helper 2 response. The schematic shows HP-NAP being secreted into the gastric mucosa by *Helicobacter pylori* (*H. pylori*). Then, HP-NAP undergoes a process of transcytosis by endothelial cells, binding to the luminal side of the blood vessel. With this, there is an alteration in the expression of β-2-integrin, with the recruitment of neutrophils and monocytes, which carry out diapedesis. The recruited leukocytes secrete cytokines [interleukin (IL)-12 and IL-23], which promote a polarization of the circulating lymphocytes to a T helper 1 (Th1) pattern. The Th1 polarization causes a reduction in the Th2 response, this could explain the improvement of ulcerative colitis symptoms in patients infected with *H. pylori*. *H. pylori*: *Helicobacter pylori*; IL: Interleukin; Th: T helper; HP-NAP: *Helicobacter pylori* neutrophil-activating protein.

we emphasize the role of *H. pylori* CagA+ and HP-NAP on favorable prognosis of IBD. The pathogenesis of IBD is complex and involves a combination of genetic, environmental, and immunological factors. Classically, CD and UC are described as diseases with a Th1 and Th2 immune pattern, but the prevalence of type response remains under study.

Regarding the cellular pattern, Th17 cells have been demonstrated at the site of inflammation, but the levels of total cytokine markers of these patterns remain variable on models' diversity. Treg cells play a major role in the pathogenesis of IBD by suppression of Smad3 and consequently overexpression Smad7, an inhibitor of the TGF-β signaling pathway. Moreover, Th9 cells - capable of exacerbating inflammatory processes by increasing epithelial permeability, are at high levels in CD and UC.

In summary, targeting NLRP3 inflammasome by *H. pylori* infection allows the exacerbation of IL-1β and IL-18 that culminates in high levels of TGF-β and low levels of IL-17 and IL-22 on IBD. The patients with *CagA* gene can induce the Treg cells which contributes to the polarization of the M1 macrophage into M2 macrophage lineage through concomitant increase of the expression of IL-10 and more Treg cells. At the same time, HP-NAP has an important role in immunomodulation by reactive oxygen species production neutrophil-induced. The ability of HP-NAP to reduce Th2 activity due to the polarization towards Th1 response may be a possible explanation for the improvement of IBD symptoms, in which there is a predominance of a Th2 response and inhibition of the Th1 response like occurs in individuals infected with *H. pylori*.

Regarding the capacity of CagA+ and HP-NAP to control inflammation and autoimmunity, and their implication in preventing IBD evolution, it seems probable that a clear understanding of how CagA+ and HP-NAP work on Treg cells, cytokines and macrophages-induced will present definitive opportunities for therapeutic intervention.

FOOTNOTES

Author contributions: Feilstrecker Balani G, Picasky da Silveira Freitas JE, dos Santos Cortez M collected the data and wrote the manuscript; Freire de Melo F performed the critical analysis of the manuscript; Zarpelon-Schutz AC and Teixeira KN performed the critical analysis, corrected the manuscript and coordinated the study; and all authors approved the final version of the manuscript.

Conflict-of-interest statement: All the authors report no relevant conflicts of interest for this article.

Open-Access: This article is an open-access article that was selected by an in-house editor and fully peer-reviewed by external reviewers. It is distributed in accordance with the Creative Commons Attribution NonCommercial (CC BY-NC 4.0) license, which permits others to distribute, remix, adapt, build upon this work non-commercially, and license their derivative works on different terms, provided the original work is properly cited and the use is non-commercial. See: https://creativecommons.org/Licenses/by-nc/4.0/

Country/Territory of origin: Brazil

ORCID number: Gabriella Feilstrecker Balani 0009-0000-6528-2166; Mariana dos Santos Cortez 0000-0001-6518-0792; Jayme Euclydes Picasky da

Silveira Freitas 0000-0002-3249-6536; Fabrício Freire de Melo 0000-0002-5680-2753; Ana Carla Zarpelon-Schutz 0000-0002-8320-3633; Kádima Nayara Teixeira 0000-0002-2928-9181.

S-Editor: Wang JJ
L-Editor: A
P-Editor: Zhao S

REFERENCES

1 **Flynn S**, Eisenstein S. Inflammatory Bowel Disease Presentation and Diagnosis. *Surg Clin North Am* 2019; **99**: 1051-1062 [PMID: 31676047 DOI: 10.1016/j.suc.2019.08.001]
2 **Baumgart DC**, Sandborn WJ. Inflammatory bowel disease: clinical aspects and established and evolving therapies. *Lancet* 2007; **369**: 1641-1657 [PMID: 17499606 DOI: 10.1016/S0140-6736(07)60751-X]
3 **Nell S**, Suerbaum S, Josenhans C. The impact of the microbiota on the pathogenesis of IBD: lessons from mouse infection models. *Nat Rev Microbiol* 2010; **8**: 564-577 [PMID: 20622892 DOI: 10.1038/nrmicro2403]
4 **Saleh M**, Elson CO. Experimental inflammatory bowel disease: insights into the host-microbiota dialog. *Immunity* 2011; **34**: 293-302 [PMID: 21435584 DOI: 10.1016/j.immuni.2011.03.008]
5 **Strober W**, Fuss I, Mannon P. The fundamental basis of inflammatory bowel disease. *J Clin Invest* 2007; **117**: 514-521 [PMID: 17332878 DOI: 10.1172/JCI30587]
6 **Frank DN**, St Amand AL, Feldman RA, Boedeker EC, Harpaz N, Pace NR. Molecular-phylogenetic characterization of microbial community imbalances in human inflammatory bowel diseases. *Proc Natl Acad Sci U S A* 2007; **104**: 13780-13785 [PMID: 17699621 DOI: 10.1073/pnas.0706625104]
7 **Ott SJ**, Musfeldt M, Wenderoth DF, Hampe J, Brant O, Fölsch UR, Timmis KN, Schreiber S. Reduction in diversity of the colonic mucosa associated bacterial microflora in patients with active inflammatory bowel disease. *Gut* 2004; **53**: 685-693 [PMID: 15082587 DOI: 10.1136/gut.2003.025403]
8 **Anderson CA**, Boucher G, Lees CW, Franke A, D'Amato M, Taylor KD, Lee JC, Goyette P, Imielinski M, Latiano A, Lagacé C, Scott R, Amininejad L, Bumpstead S, Baidoo L, Baldassano RN, Barclay M, Bayless TM, Brand S, Büning C, Colombel JF, Denson LA, De Vos M, Dubinsky M, Edwards C, Ellinghaus D, Fehrmann RS, Floyd JA, Florin T, Franchimont D, Franke L, Georges M, Glas J, Glazer NL, Guthery SL, Haritunians T, Hayward NK, Hugot JP, Jobin G, Laukens D, Lawrance I, Lémann M, Levine A, Libioulle C, Louis E, McGovern DP, Milla M, Montgomery GW, Morley KI, Mowat C, Ng A, Newman W, Ophoff RA, Papi L, Palmieri O, Peyrin-Biroulet L, Panés J, Phillips A, Prescott NJ, Proctor DD, Roberts R, Russell R, Rutgeerts P, Sanderson J, Sans M, Schumm P, Seibold F, Sharma Y, Simms LA, Seielstad M, Steinhart AH, Targan SR, van den Berg LH, Vatn M, Verspaget H, Walters T, Wijmenga C, Wilson DC, Westra HJ, Xavier RJ, Zhao ZZ, Ponsioen CY, Andersen V, Torkvist L, Gazouli M, Anagnou NP, Karlsen TH, Kupcinskas L, Sventoraityte J, Mansfield JC, Kugathasan S, Silverberg MS, Halfvarson J, Rotter JI, Mathew CG, Griffiths AM, Gearry R, Ahmad T, Brant SR, Chamaillard M, Satsangi J, Cho JH, Schreiber S, Daly MJ, Barrett JC, Parkes M, Annese V, Hakonarson H, Radford-Smith G, Duerr RH, Vermeire S, Weersma RK, Rioux JD. Meta-analysis identifies 29 additional ulcerative colitis risk loci, increasing the number of confirmed associations to 47. *Nat Genet* 2011; **43**: 246-252 [PMID: 21297633 DOI: 10.1038/ng.764]
9 **Franke A**, McGovern DP, Barrett JC, Wang K, Radford-Smith GL, Ahmad T, Lees CW, Balschun T, Lee J, Roberts R, Anderson CA, Bis JC, Bumpstead S, Ellinghaus D, Festen EM, Georges M, Green T, Haritunians T, Jostins L, Latiano A, Mathew CG, Montgomery GW, Prescott NJ, Raychaudhuri S, Rotter JI, Schumm P, Sharma Y, Simms LA, Taylor KD, Whiteman D, Wijmenga C, Baldassano RN, Barclay M, Bayless TM, Brand S, Büning C, Cohen A, Colombel JF, Cottone M, Stronati L, Denson T, De Vos M, D'Inca R, Dubinsky M, Edwards C, Florin T, Franchimont D, Gearry R, Glas J, Van Gossum A, Guthery SL, Halfvarson J, Verspaget HW, Hugot JP, Karban A, Laukens D, Lawrance I, Lemann M, Levine A, Libioulle C, Louis E, Mowat C, Newman W, Panés J, Phillips A, Proctor DD, Regueiro M, Russell R, Rutgeerts P, Sanderson J, Sans M, Seibold F, Steinhart AH, Stokkers PC, Torkvist L, Kullak-Ublick G, Wilson D, Walters T, Targan SR, Brant SR, Rioux JD, D'Amato M, Weersma RK, Kugathasan S, Griffiths AM, Mansfield JC, Vermeire S, Duerr RH, Silverberg MS, Satsangi J, Schreiber S, Cho JH, Annese V, Hakonarson H, Daly MJ, Parkes M. Genome-wide meta-analysis increases to 71 the number of confirmed Crohn's disease susceptibility loci. *Nat Genet* 2010; **42**: 1118-1125 [PMID: 21102463 DOI: 10.1038/ng.717]
10 **Glocker EO**, Kotlarz D, Boztug K, Gertz EM, Schäffer AA, Noyan F, Perro M, Diestelhorst J, Allroth A, Murugan D, Hätscher N, Pfeifer D, Sykora KW, Sauer M, Kreipe H, Lacher M, Nustede R, Woellner C, Baumann U, Salzer U, Koletzko S, Shah N, Segal AW, Sauerbrey A, Buderus S, Snapper SB, Grimbacher B, Klein C. Inflammatory bowel disease and mutations affecting the interleukin-10 receptor. *N Engl J Med* 2009; **361**: 2033-2045 [PMID: 19890111 DOI: 10.1056/NEJMoa0907206]
11 **Korzenik JR**, Podolsky DK. Evolving knowledge and therapy of inflammatory bowel disease. *Nat Rev Drug Discov* 2006; **5**: 197-209 [PMID: 16518373 DOI: 10.1038/nrd1986]
12 **Choy MC**, Visvanathan K, De Cruz P. An Overview of the Innate and Adaptive Immune System in Inflammatory Bowel Disease. *Inflamm Bowel Dis* 2017; **23**: 2-13 [PMID: 27779499 DOI: 10.1097/MIB.0000000000000955]
13 **Ahluwalia B**, Moraes L, Magnusson MK, Öhman L. Immunopathogenesis of inflammatory bowel disease and mechanisms of biological therapies. *Scand J Gastroenterol* 2018; **53**: 379-389 [PMID: 29523023 DOI: 10.1080/00365521.2018.1447597]
14 **Shih DQ**, Targan SR, McGovern D. Recent advances in IBD pathogenesis: genetics and immunobiology. *Curr Gastroenterol Rep* 2008; **10**: 568-575 [PMID: 19006613 DOI: 10.1007/s11894-008-0104-x]
15 **Di Sabatino A**, Biancheri P, Rovedatti L, MacDonald TT, Corazza GR. New pathogenic paradigms in inflammatory bowel disease. *Inflamm Bowel Dis* 2012; **18**: 368-371 [PMID: 21538717 DOI: 10.1002/ibd.21735]
16 **Strober W**, Fuss IJ. Proinflammatory cytokines in the pathogenesis of inflammatory bowel diseases. *Gastroenterology* 2011; **140**: 1756-1767 [PMID: 21530742 DOI: 10.1053/j.gastro.2011.02.016]
17 **Breese E**, Braegger CP, Corrigan CJ, Walker-Smith JA, MacDonald TT. Interleukin-2- and interferon-gamma-secreting T cells in normal and diseased human intestinal mucosa. *Immunology* 1993; **78**: 127-131 [PMID: 8436398]
18 **Noguchi M**, Hiwatashi N, Liu Z, Toyota T. Enhanced interferon-gamma production and B7-2 expression in isolated intestinal mononuclear

cells from patients with Crohn's disease. *J Gastroenterol* 1995; **30** Suppl 8: 52-55 [PMID: 8563891]
19 **Fuss IJ**, Neurath M, Boirivant M, Klein JS, de la Motte C, Strong SA, Fiocchi C, Strober W. Disparate CD4+ lamina propria (LP) lymphokine secretion profiles in inflammatory bowel disease. Crohn's disease LP cells manifest increased secretion of IFN-gamma, whereas ulcerative colitis LP cells manifest increased secretion of IL-5. *J Immunol* 1996; **157**: 1261-1270 [PMID: 8757634 DOI: 10.4049/jimmunol.157.3.1261]
20 **Heller F**, Florian P, Bojarski C, Richter J, Christ M, Hillenbrand B, Mankertz J, Gitter AH, Bürgel N, Fromm M, Zeitz M, Fuss I, Strober W, Schulzke JD. Interleukin-13 is the key effector Th2 cytokine in ulcerative colitis that affects epithelial tight junctions, apoptosis, and cell restitution. *Gastroenterology* 2005; **129**: 550-564 [PMID: 16083712 DOI: 10.1016/j.gastro.2005.05.002]
21 **Vainer B**, Nielsen OH, Hendel J, Horn T, Kirman I. Colonic expression and synthesis of interleukin 13 and interleukin 15 in inflammatory bowel disease. *Cytokine* 2000; **12**: 1531-1536 [PMID: 11023669 DOI: 10.1006/cyto.2000.0744]
22 **Rovedatti L**, Kudo T, Biancheri P, Sarra M, Knowles CH, Rampton DS, Corazza GR, Monteleone G, Di Sabatino A, Macdonald TT. Differential regulation of interleukin 17 and interferon gamma production in inflammatory bowel disease. *Gut* 2009; **58**: 1629-1636 [PMID: 19740775 DOI: 10.1136/gut.2009.182170]
23 **Bernardo D**, Vallejo-Díez S, Mann ER, Al-Hassi HO, Martínez-Abad B, Montalvillo E, Tee CT, Murugananthan AU, Núñez H, Peake ST, Hart AL, Fernández-Salazar L, Garrote JA, Arranz E, Knight SC. IL-6 promotes immune responses in human ulcerative colitis and induces a skin-homing phenotype in the dendritic cells and Tcells they stimulate. *Eur J Immunol* 2012; **42**: 1337-1353 [PMID: 22539302 DOI: 10.1002/eji.201142327]
24 **Fujino S**, Andoh A, Bamba S, Ogawa A, Hata K, Araki Y, Bamba T, Fujiyama Y. Increased expression of interleukin 17 in inflammatory bowel disease. *Gut* 2003; **52**: 65-70 [PMID: 12477762 DOI: 10.1136/gut.52.1.65]
25 **Zhang Z**, Zheng M, Bindas J, Schwarzenberger P, Kolls JK. Critical role of IL-17 receptor signaling in acute TNBS-induced colitis. *Inflamm Bowel Dis* 2006; **12**: 382-388 [PMID: 16670527 DOI: 10.1097/01.MIB.0000218764.06959.91]
26 **Gálvez J**. Role of Th17 Cells in the Pathogenesis of Human IBD. *ISRN Inflamm* 2014; **2014**: 928461 [PMID: 25101191 DOI: 10.1155/2014/928461]
27 **Pène J**, Chevalier S, Preisser L, Vénéreau E, Guilleux MH, Ghannam S, Molès JP, Danger Y, Ravon E, Lesaux S, Yssel H, Gascan H. Chronically inflamed human tissues are infiltrated by highly differentiated Th17 lymphocytes. *J Immunol* 2008; **180**: 7423-7430 [PMID: 18490742 DOI: 10.4049/jimmunol.180.11.7423]
28 **O'Connor W Jr**, Kamanaka M, Booth CJ, Town T, Nakae S, Iwakura Y, Kolls JK, Flavell RA. A protective function for interleukin 17A in T cell-mediated intestinal inflammation. *Nat Immunol* 2009; **10**: 603-609 [PMID: 19448631 DOI: 10.1038/ni.1736]
29 **Awasthi A**, Kuchroo VK. IL-17A directly inhibits TH1 cells and thereby suppresses development of intestinal inflammation. *Nat Immunol* 2009; **10**: 568-570 [PMID: 19448657 DOI: 10.1038/ni0609-568]
30 **Hardenberg G**, Steiner TS, Levings MK. Environmental influences on T regulatory cells in inflammatory bowel disease. *Semin Immunol* 2011; **23**: 130-138 [PMID: 21295492 DOI: 10.1016/j.smim.2011.01.012]
31 **Giuffrida P**, Di Sabatino A. Targeting T cells in inflammatory bowel disease. *Pharmacol Res* 2020; **159**: 105040 [PMID: 32585338 DOI: 10.1016/j.phrs.2020.105040]
32 **Fantini MC**, Rizzo A, Fina D, Caruso R, Sarra M, Stolfi C, Becker C, Macdonald TT, Pallone F, Neurath MF, Monteleone G. Smad7 controls resistance of colitogenic T cells to regulatory T cell-mediated suppression. *Gastroenterology* 2009; **136**: 1308-1316, e1 [PMID: 19192480 DOI: 10.1053/j.gastro.2008.12.053]
33 **Monteleone G**, Boirivant M, Pallone F, MacDonald TT. TGF-beta1 and Smad7 in the regulation of IBD. *Mucosal Immunol* 2008; **1** Suppl 1: S50-S53 [PMID: 19079231 DOI: 10.1038/mi.2008.55]
34 **Gambineri E**, Perroni L, Passerini L, Bianchi L, Doglioni C, Meschi F, Bonfanti R, Sznajer Y, Tommasini A, Lawitschka A, Junker A, Dunstheimer D, Heidemann PH, Cazzola G, Cipolli M, Friedrich W, Janic D, Azzi N, Richmond E, Vignola S, Barabino A, Chiumello G, Azzari C, Roncarolo MG, Bacchetta R. Clinical and molecular profile of a new series of patients with immune dysregulation, polyendocrinopathy, enteropathy, X-linked syndrome: inconsistent correlation between forkhead box protein 3 expression and disease severity. *J Allergy Clin Immunol* 2008; **122**: 1105-1112.e1 [PMID: 18951619 DOI: 10.1016/j.jaci.2008.09.027]
35 **Koenen HJ**, Smeets RL, Vink PM, van Rijssen E, Boots AM, Joosten I. Human CD25highFoxp3pos regulatory T cells differentiate into IL-17-producing cells. *Blood* 2008; **112**: 2340-2352 [PMID: 18617638 DOI: 10.1182/blood-2008-01-133967]
36 **Gerlach K**, McKenzie AN, Neurath MF, Weigmann B. IL-9 regulates intestinal barrier function in experimental T cell-mediated colitis. *Tissue Barriers* 2015; **3**: e983777 [PMID: 25838986 DOI: 10.4161/21688370.2014.983777]
37 **Gerlach K**, Hwang Y, Nikolaev A, Atreya R, Dornhoff H, Steiner S, Lehr HA, Wirtz S, Vieth M, Waisman A, Rosenbauer F, McKenzie AN, Weigmann B, Neurath MF. TH9 cells that express the transcription factor PU.1 drive T cell-mediated colitis *via* IL-9 receptor signaling in intestinal epithelial cells. *Nat Immunol* 2014; **15**: 676-686 [PMID: 24908389 DOI: 10.1038/ni.2920]
38 **Weigmann B**, Neurath MF. Th9 cells in inflammatory bowel diseases. *Semin Immunopathol* 2017; **39**: 89-95 [PMID: 27837255 DOI: 10.1007/s00281-016-0603-z]
39 **Hatakeyama M**. Structure and function of Helicobacter pylori CagA, the first-identified bacterial protein involved in human cancer. *Proc Jpn Acad Ser B Phys Biol Sci* 2017; **93**: 196-219 [PMID: 28413197 DOI: 10.2183/pjab.93.013]
40 **Wu AH**, Crabtree JE, Bernstein L, Hawtin P, Cockburn M, Tseng CC, Forman D. Role of Helicobacter pylori CagA+ strains and risk of adenocarcinoma of the stomach and esophagus. *Int J Cancer* 2003; **103**: 815-821 [PMID: 12516104 DOI: 10.1002/ijc.10887]
41 **Tepler A**, Narula N, Peek RM Jr, Patel A, Edelson C, Colombel JF, Shah SC. Systematic review with meta-analysis: association between Helicobacter pylori CagA seropositivity and odds of inflammatory bowel disease. *Aliment Pharmacol Ther* 2019; **50**: 121-131 [PMID: 31165513 DOI: 10.1111/apt.15306]
42 **Zhang YZ**, Li YY. Inflammatory bowel disease: pathogenesis. *World J Gastroenterol* 2014; **20**: 91-99 [PMID: 24415861 DOI: 10.3748/wjg.v20.i1.91]
43 **Khan I**, Ullah N, Zha L, Bai Y, Khan A, Zhao T, Che T, Zhang C. Alteration of Gut Microbiota in Inflammatory Bowel Disease (IBD): Cause or Consequence? IBD Treatment Targeting the Gut Microbiome. *Pathogens* 2019; **8** [PMID: 31412603 DOI: 10.3390/pathogens8030126]
44 **Zhang H**, Dai Y, Liu Y, Wu T, Li J, Wang X, Wang W. Helicobacter pylori Colonization Protects Against Chronic Experimental Colitis by Regulating Th17/Treg Balance. *Inflamm Bowel Dis* 2018; **24**: 1481-1492 [PMID: 29788098 DOI: 10.1093/ibd/izy107]
45 **Marotti B**, Rocco A, De Colibus P, Compare D, de Nucci G, Staibano S, Tatangelo F, Romano M, Nardone G. Interleukin-13 mucosal production in Helicobacter pylori-related gastric diseases. *Dig Liver Dis* 2008; **40**: 240-247 [PMID: 18243827 DOI: 10.1016/j.dld.2007.11.021]
46 **Michalkiewicz J**, Helmin-Basa A, Grzywa R, Czerwionka-Szaflarska M, Szaflarska-Poplawska A, Mierzwa G, Marszalek A, Bodnar M, Nowak M, Dzierzanowska-Fangrat K. Innate immunity components and cytokines in gastric mucosa in children with Helicobacter pylori

infection. *Mediators Inflamm* 2015; **2015**: 176726 [PMID: 25948881 DOI: 10.1155/2015/176726]
47 **Guler R**, Roy S, Suzuki H, Brombacher F. Targeting Batf2 for infectious diseases and cancer. *Oncotarget* 2015; **6**: 26575-26582 [PMID: 26376615 DOI: 10.18632/oncotarget.5576]
48 **Murphy TL**, Tussiwand R, Murphy KM. Specificity through cooperation: BATF-IRF interactions control immune-regulatory networks. *Nat Rev Immunol* 2013; **13**: 499-509 [PMID: 23787991 DOI: 10.1038/nri3470]
49 **Roy S**, Guler R, Parihar SP, Schmeier S, Kaczkowski B, Nishimura H, Shin JW, Negishi Y, Ozturk M, Hurdayal R, Kubosaki A, Kimura Y, de Hoon MJ, Hayashizaki Y, Brombacher F, Suzuki H. Batf2/Irf1 induces inflammatory responses in classically activated macrophages, lipopolysaccharides, and mycobacterial infection. *J Immunol* 2015; **194**: 6035-6044 [PMID: 25957166 DOI: 10.4049/jimmunol.1402521]
50 **Etzerodt A**, Moestrup SK. CD163 and inflammation: biological, diagnostic, and therapeutic aspects. *Antioxid Redox Signal* 2013; **18**: 2352-2363 [PMID: 22900885 DOI: 10.1089/ars.2012.4834]
51 **Skytthe MK**, Graversen JH, Moestrup SK. Targeting of CD163(+) Macrophages in Inflammatory and Malignant Diseases. *Int J Mol Sci* 2020; **21** [PMID: 32752088 DOI: 10.3390/ijms21155497]
52 **Hou J**, Wang X, Zhang M, Wang M, Gao P, Jiang Y. Circulating CD14(+)CD163(+)CD209(+) M2-like monocytes are associated with the severity of infection in Helicobacter pylori-positive patients. *Mol Immunol* 2019; **108**: 13-22 [PMID: 30771733 DOI: 10.1016/j.molimm.2019.01.017]
53 **Cario E**, Gerken G, Podolsky DK. Toll-like receptor 2 controls mucosal inflammation by regulating epithelial barrier function. *Gastroenterology* 2007; **132**: 1359-1374 [PMID: 17408640 DOI: 10.1053/j.gastro.2007.02.056]
54 **Himmel ME**, Hardenberg G, Piccirillo CA, Steiner TS, Levings MK. The role of T-regulatory cells and Toll-like receptors in the pathogenesis of human inflammatory bowel disease. *Immunology* 2008; **125**: 145-153 [PMID: 18798918 DOI: 10.1111/j.1365-2567.2008.02939.x]
55 **Korbecki J**, Bajdak-Rusinek K. The effect of palmitic acid on inflammatory response in macrophages: an overview of molecular mechanisms. *Inflamm Res* 2019; **68**: 915-932 [PMID: 31363792 DOI: 10.1007/s00011-019-01273-5]
56 **Rocha DM**, Caldas AP, Oliveira LL, Bressan J, Hermsdorff HH. Saturated fatty acids trigger TLR4-mediated inflammatory response. *Atherosclerosis* 2016; **244**: 211-215 [PMID: 26687466 DOI: 10.1016/j.atherosclerosis.2015.11.015]
57 **Kanemaru H**, Yamane F, Tanaka H, Maeda K, Satoh T, Akira S. BATF2 activates DUSP2 gene expression and up-regulates NF-κB activity *via* phospho-STAT3 dephosphorylation. *Int Immunol* 2018; **30**: 255-265 [PMID: 29534174 DOI: 10.1093/intimm/dxy023]
58 **Schmalstig AA**, Benoit SL, Misra SK, Sharp JS, Maier RJ. Noncatalytic Antioxidant Role for Helicobacter pylori Urease. *J Bacteriol* 2018; **200** [PMID: 29866802 DOI: 10.1128/JB.00124-18]
59 **Skene C**, Young A, Every A, Sutton P. Helicobacter pylori flagella: antigenic profile and protective immunity. *FEMS Immunol Med Microbiol* 2007; **50**: 249-256 [PMID: 17521391 DOI: 10.1111/j.1574-695X.2007.00263.x]
60 **Tang RX**, Luo DJ, Sun AH, Yan J. Diversity of Helicobacter pylori isolates in expression of antigens and induction of antibodies. *World J Gastroenterol* 2008; **14**: 4816-4822 [PMID: 18720546 DOI: 10.3748/wjg.14.4816]
61 **Lawson AJ**. Helicobacter. In: James V, Carroll KC, Guido F, Jorgensen JH, Landry ML, Warnock DW. Manual of Clinical Microbiology, 10 th ed. Washington: Wiley, 2011: 900-915
62 **Lee SK**, Stack A, Katzowitsch E, Aizawa SI, Suerbaum S, Josenhans C. Helicobacter pylori flagellins have very low intrinsic activity to stimulate human gastric epithelial cells *via* TLR5. *Microbes Infect* 2003; **5**: 1345-1356 [PMID: 14670447 DOI: 10.1016/j.micinf.2003.09.018]
63 **Clyne M**, Ocroinin T, Suerbaum S, Josenhans C, Drumm B. Adherence of isogenic flagellum-negative mutants of Helicobacter pylori and Helicobacter mustelae to human and ferret gastric epithelial cells. *Infect Immun* 2000; **68**: 4335-4339 [PMID: 10858255 DOI: 10.1128/IAI.68.7.4335-4339.2000]
64 **Dincă AL**, Meliț LE, Mărginean CO. Old and New Aspects of H. pylori-Associated Inflammation and Gastric Cancer. *Children (Basel)* 2022; **9** [PMID: 35884067 DOI: 10.3390/children9071083]
65 **Stent A**, Every AL, Chionh YT, Ng GZ, Sutton P. Superoxide dismutase from Helicobacter pylori suppresses the production of pro-inflammatory cytokines during in vivo infection. *Helicobacter* 2018; **23** [PMID: 29235197 DOI: 10.1111/hel.12459]
66 **Chen CC**, Liou JM, Lee YC, Hong TC, El-Omar EM, Wu MS. The interplay between Helicobacter pylori and gastrointestinal microbiota. *Gut Microbes* 2021; **13**: 1-22 [PMID: 33938378 DOI: 10.1080/19490976.2021.1909459]
67 **Martín-Núñez GM**, Cornejo-Pareja I, Coin-Aragüez L, Roca-Rodríguez MDM, Muñoz-Garach A, Clemente-Postigo M, Cardona F, Moreno-Indias I, Tinahones FJ. H. pylori eradication with antibiotic treatment causes changes in glucose homeostasis related to modifications in the gut microbiota. *PLoS One* 2019; **14**: e0213548 [PMID: 30870471 DOI: 10.1371/journal.pone.0213548]
68 **Heimesaat MM**, Fischer A, Plickert R, Wiedemann T, Loddenkemper C, Göbel UB, Bereswill S, Rieder G. Helicobacter pylori induced gastric immunopathology is associated with distinct microbiota changes in the large intestines of long-term infected Mongolian gerbils. *PLoS One* 2014; **9**: e100362 [PMID: 24941045 DOI: 10.1371/journal.pone.0100362]
69 **Bühling A**, Radun D, Müller WA, Malfertheiner P. Influence of anti-Helicobacter triple-therapy with metronidazole, omeprazole and clarithromycin on intestinal microflora. *Aliment Pharmacol Ther* 2001; **15**: 1445-1452 [PMID: 11552917 DOI: 10.1046/j.1365-2036.2001.01033.x]
70 **He C**, Peng C, Wang H, Ouyang Y, Zhu Z, Shu X, Zhu Y, Lu N. The eradication of Helicobacter pylori restores rather than disturbs the gastrointestinal microbiota in asymptomatic young adults. *Helicobacter* 2019; **24**: e12590 [PMID: 31124220 DOI: 10.1111/hel.12590]
71 **Iino C**, Shimoyama T, Chinda D, Sakuraba H, Fukuda S, Nakaji S. Influence of Helicobacter pylori Infection and Atrophic Gastritis on the Gut Microbiota in a Japanese Population. *Digestion* 2020; **101**: 422-432 [PMID: 31394526 DOI: 10.1159/000500634]
72 **Myllyluoma E**, Ahlroos T, Veijola L, Rautelin H, Tynkkynen S, Korpela R. Effects of anti-Helicobacter pylori treatment and probiotic supplementation on intestinal microbiota. *Int J Antimicrob Agents* 2007; **29**: 66-72 [PMID: 17141481 DOI: 10.1016/j.ijantimicag.2006.08.034]
73 **Jones TA**, Hernandez DZ, Wong ZC, Wandler AM, Guillemin K. The bacterial virulence factor CagA induces microbial dysbiosis that contributes to excessive epithelial cell proliferation in the Drosophila gut. *PLoS Pathog* 2017; **13**: e1006631 [PMID: 29049360 DOI: 10.1371/journal.ppat.1006631]
74 **Chen L**, Xu W, Lee A, He J, Huang B, Zheng W, Su T, Lai S, Long Y, Chu H, Chen Y, Wang L, Wang K, Si J, Chen S. The impact of Helicobacter pylori infection, eradication therapy and probiotic supplementation on gut microenvironment homeostasis: An open-label, randomized clinical trial. *EBioMedicine* 2018; **35**: 87-96 [PMID: 30145102 DOI: 10.1016/j.ebiom.2018.08.028]
75 **Peek RM Jr**, Fiske C, Wilson KT. Role of innate immunity in Helicobacter pylori-induced gastric malignancy. *Physiol Rev* 2010; **90**: 831-858 [PMID: 20664074 DOI: 10.1152/physrev.00039.2009]
76 **Mohammadi SO**, Yadegar A, Kargar M, Mirjalali H, Kafilzadeh F. The impact of Helicobacter pylori infection on gut microbiota-endocrine

system axis; modulation of metabolic hormone levels and energy homeostasis. *J Diabetes Metab Disord* 2020; **19**: 1855-1861 [PMID: 33553045 DOI: 10.1007/s40200-020-00608-y]

77 **Lee M**, Chang EB. Inflammatory Bowel Diseases (IBD) and the Microbiome-Searching the Crime Scene for Clues. *Gastroenterology* 2021; **160**: 524-537 [PMID: 33253681 DOI: 10.1053/j.gastro.2020.09.056]

78 **Sartor RB**. Therapeutic manipulation of the enteric microflora in inflammatory bowel diseases: antibiotics, probiotics, and prebiotics. *Gastroenterology* 2004; **126**: 1620-1633 [PMID: 15168372 DOI: 10.1053/j.gastro.2004.03.024]

79 **Bai X**, Jiang L, Ruan G, Liu T, Yang H. Helicobacter pylori may participate in the development of inflammatory bowel disease by modulating the intestinal microbiota. *Chin Med J (Engl)* 2022; **135**: 634-638 [PMID: 35234697 DOI: 10.1097/CM9.0000000000002008]

80 **Swanson KV**, Deng M, Ting JP. The NLRP3 inflammasome: molecular activation and regulation to therapeutics. *Nat Rev Immunol* 2019; **19**: 477-489 [PMID: 31036962 DOI: 10.1038/s41577-019-0165-0]

81 **von Moltke J**, Ayres JS, Kofoed EM, Chavarría-Smith J, Vance RE. Recognition of bacteria by inflammasomes. *Annu Rev Immunol* 2013; **31**: 73-106 [PMID: 23215645 DOI: 10.1146/annurev-immunol-032712-095944]

82 **Martinon F**, Burns K, Tschopp J. The inflammasome: a molecular platform triggering activation of inflammatory caspases and processing of proIL-beta. *Mol Cell* 2002; **10**: 417-426 [PMID: 12191486 DOI: 10.1016/s1097-2765(02)00599-3]

83 **Zhang X**, Li C, Chen D, He X, Zhao Y, Bao L, Wang Q, Zhou J, Xie Y. H. pylori CagA activates the NLRP3 inflammasome to promote gastric cancer cell migration and invasion. *Inflamm Res* 2022; **71**: 141-155 [PMID: 34854954 DOI: 10.1007/s00011-021-01522-6]

84 **Hitzler I**, Sayi A, Kohler E, Engler DB, Koch KN, Hardt WD, Müller A. Caspase-1 has both proinflammatory and regulatory properties in Helicobacter infections, which are differentially mediated by its substrates IL-1β and IL-18. *J Immunol* 2012; **188**: 3594-3602 [PMID: 22403439 DOI: 10.4049/jimmunol.1103212]

85 **Oertli M**, Sundquist M, Hitzler I, Engler DB, Arnold IC, Reuter S, Maxeiner J, Hansson M, Taube C, Quiding-Järbrink M, Müller A. DC-derived IL-18 drives Treg differentiation, murine Helicobacter pylori-specific immune tolerance, and asthma protection. *J Clin Invest* 2012; **122**: 1082-1096 [PMID: 22307326 DOI: 10.1172/JCI61029]

86 **El-Omar EM**, Carrington M, Chow WH, McColl KE, Bream JH, Young HA, Herrera J, Lissowska J, Yuan CC, Rothman N, Lanyon G, Martin M, Fraumeni JF Jr, Rabkin CS. Interleukin-1 polymorphisms associated with increased risk of gastric cancer. *Nature* 2000; **404**: 398-402 [PMID: 10746728 DOI: 10.1038/35006081]

87 **Tu S**, Bhagat G, Cui G, Takaishi S, Kurt-Jones EA, Rickman B, Betz KS, Penz-Oesterreicher M, Bjorkdahl O, Fox JG, Wang TC. Overexpression of interleukin-1beta induces gastric inflammation and cancer and mobilizes myeloid-derived suppressor cells in mice. *Cancer Cell* 2008; **14**: 408-419 [PMID: 18977329 DOI: 10.1016/j.ccr.2008.10.011]

88 **Arnold IC**, Dehzad N, Reuter S, Martin H, Becher B, Taube C, Müller A. Helicobacter pylori infection prevents allergic asthma in mouse models through the induction of regulatory T cells. *J Clin Invest* 2011; **121**: 3088-3093 [PMID: 21737881 DOI: 10.1172/JCI45041]

89 **Engler DB**, Leonardi I, Hartung ML, Kyburz A, Spath S, Becher B, Rogler G, Müller A. Helicobacter pylori-specific protection against inflammatory bowel disease requires the NLRP3 inflammasome and IL-18. *Inflamm Bowel Dis* 2015; **21**: 854-861 [PMID: 25742401 DOI: 10.1097/MIB.0000000000000318]

90 **Zaki MH**, Boyd KL, Vogel P, Kastan MB, Lamkanfi M, Kanneganti TD. The NLRP3 inflammasome protects against loss of epithelial integrity and mortality during experimental colitis. *Immunity* 2010; **32**: 379-391 [PMID: 20303296 DOI: 10.1016/j.immuni.2010.03.003]

91 **Takagi H**, Kanai T, Okazawa A, Kishi Y, Sato T, Takaishi H, Inoue N, Ogata H, Iwao Y, Hoshino K, Takeda K, Akira S, Watanabe M, Ishii H, Hibi T. Contrasting action of IL-12 and IL-18 in the development of dextran sodium sulphate colitis in mice. *Scand J Gastroenterol* 2003; **38**: 837-844 [PMID: 12940437 DOI: 10.1080/00365520310004047]

92 **Araki A**, Kanai T, Ishikura T, Makita S, Uraushihara K, Iiyama R, Totsuka T, Takeda K, Akira S, Watanabe M. MyD88-deficient mice develop severe intestinal inflammation in dextran sodium sulfate colitis. *J Gastroenterol* 2005; **40**: 16-23 [PMID: 15692785 DOI: 10.1007/s00535-004-1492-9]

93 **Fukata M**, Breglio K, Chen A, Vamadevan AS, Goo T, Hsu D, Conduah D, Xu R, Abreu MT. The myeloid differentiation factor 88 (MyD88) is required for CD4+ T cell effector function in a murine model of inflammatory bowel disease. *J Immunol* 2008; **180**: 1886-1894 [PMID: 18209086 DOI: 10.4049/jimmunol.180.3.1886]

94 **Rakoff-Nahoum S**, Paglino J, Eslami-Varzaneh F, Edberg S, Medzhitov R. Recognition of commensal microflora by toll-like receptors is required for intestinal homeostasis. *Cell* 2004; **118**: 229-241 [PMID: 15260992 DOI: 10.1016/j.cell.2004.07.002]

95 **Gibson DL**, Ma C, Bergstrom KS, Huang JT, Man C, Vallance BA. MyD88 signalling plays a critical role in host defence by controlling pathogen burden and promoting epithelial cell homeostasis during Citrobacter rodentium-induced colitis. *Cell Microbiol* 2008; **10**: 618-631 [PMID: 17979981 DOI: 10.1111/j.1462-5822.2007.01071.x]

96 **Yao X**, Zhang C, Xing Y, Xue G, Zhang Q, Pan F, Wu G, Hu Y, Guo Q, Lu A, Zhang X, Zhou R, Tian Z, Zeng B, Wei H, Strober W, Zhao L, Meng G. Remodelling of the gut microbiota by hyperactive NLRP3 induces regulatory T cells to maintain homeostasis. *Nat Commun* 2017; **8**: 1896 [PMID: 29196621 DOI: 10.1038/s41467-017-01917-2]

97 **Evans DJ Jr**, Evans DG, Takemura T, Nakano H, Lampert HC, Graham DY, Granger DN, Kvietys PR. Characterization of a Helicobacter pylori neutrophil-activating protein. *Infect Immun* 1995; **63**: 2213-2220 [PMID: 7768601 DOI: 10.1128/iai.63.6.2213-2220.1995]

98 **Satin B**, Del Giudice G, Della Bianca V, Dusi S, Laudanna C, Tonello F, Kelleher D, Rappuoli R, Montecucco C, Rossi F. The neutrophil-activating protein (HP-NAP) of Helicobacter pylori is a protective antigen and a major virulence factor. *J Exp Med* 2000; **191**: 1467-1476 [PMID: 10790422 DOI: 10.1084/jem.191.9.1467]

99 **Polenghi A**, Bossi F, Fischetti F, Durigutto P, Cabrelle A, Tamassia N, Cassatella MA, Montecucco C, Tedesco F, de Bernard M. The neutrophil-activating protein of Helicobacter pylori crosses endothelia to promote neutrophil adhesion in vivo. *J Immunol* 2007; **178**: 1312-1320 [PMID: 17237377 DOI: 10.4049/jimmunol.178.3.1312]

100 **Codolo G**, Coletta S, D'Elios MM, de Bernard M. HP-NAP of Helicobacter pylori: The Power of the Immunomodulation. *Front Immunol* 2022; **13**: 944139 [PMID: 35844568 DOI: 10.3389/fimmu.2022.944139]

101 **Montemurro P**, Nishioka H, Dundon WG, de Bernard M, Del Giudice G, Rappuoli R, Montecucco C. The neutrophil-activating protein (HP-NAP) of Helicobacter pylori is a potent stimulant of mast cells. *Eur J Immunol* 2002; **32**: 671-676 [PMID: 11857341 DOI: 10.1002/1521-4141(200203)32:3<671::AID-IMMU671>3.0.CO;2-5]

102 **Amedei A**, Cappon A, Codolo G, Cabrelle A, Polenghi A, Benagiano M, Tasca E, Azzurri A, D'Elios MM, Del Prete G, de Bernard M. The neutrophil-activating protein of Helicobacter pylori promotes Th1 immune responses. *J Clin Invest* 2006; **116**: 1092-1101 [PMID: 16543949 DOI: 10.1172/JCI27177]

103 **Middleton J**, Neil S, Wintle J, Clark-Lewis I, Moore H, Lam C, Auer M, Hub E, Rot A. Transcytosis and surface presentation of IL-8 by venular endothelial cells. *Cell* 1997; **91**: 385-395 [PMID: 9363947 DOI: 10.1016/s0092-8674(00)80422-5]

104 **Wen SH**, Hong ZW, Chen CC, Chang HW, Fu HW. Helicobacter pylori Neutrophil-Activating Protein Directly Interacts with and Activates Toll-like Receptor 2 to Induce the Secretion of Interleukin-8 from Neutrophils and ATRA-Induced Differentiated HL-60 Cells. *Int J Mol Sci* 2021; **22** [PMID: 34768994 DOI: 10.3390/ijms222111560]

105 **Tsai CC**, Kuo TY, Hong ZW, Yeh YC, Shih KS, Du SY, Fu HW. Helicobacter pylori neutrophil-activating protein induces release of histamine and interleukin-6 through G protein-mediated MAPKs and PI3K/Akt pathways in HMC-1 cells. *Virulence* 2015; **6**: 755-765 [PMID: 26375619 DOI: 10.1080/21505594.2015.1043505]

106 **Ramachandran M**, Jin C, Yu D, Eriksson F, Essand M. Vector-encoded Helicobacter pylori neutrophil-activating protein promotes maturation of dendritic cells with Th1 polarization and improved migration. *J Immunol* 2014; **193**: 2287-2296 [PMID: 25049358 DOI: 10.4049/jimmunol.1400339]

107 **Guo X**, Ding C, Lu J, Zhou T, Liang T, Ji Z, Xie P, Liu X, Kang Q. HP-NAP ameliorates OXA-induced atopic dermatitis symptoms in mice. *Immunopharmacol Immunotoxicol* 2020; **42**: 416-422 [PMID: 32762390 DOI: 10.1080/08923973.2020.1806869]

108 **Codolo G**, Mazzi P, Amedei A, Del Prete G, Berton G, D'Elios MM, de Bernard M. The neutrophil-activating protein of Helicobacter pylori down-modulates Th2 inflammation in ovalbumin-induced allergic asthma. *Cell Microbiol* 2008; **10**: 2355-2363 [PMID: 18671823 DOI: 10.1111/j.1462-5822.2008.01217.x]

109 **Kałużna A**, Olczyk P, Komosińska-Vassev K. The Role of Innate and Adaptive Immune Cells in the Pathogenesis and Development of the Inflammatory Response in Ulcerative Colitis. *J Clin Med* 2022; **11** [PMID: 35054093 DOI: 10.3390/jcm11020400]

110 **Kmieć Z**, Cyman M, Ślebioda TJ. Cells of the innate and adaptive immunity and their interactions in inflammatory bowel disease. *Adv Med Sci* 2017; **62**: 1-16 [PMID: 28126697 DOI: 10.1016/j.advms.2016.09.001]

111 **Bamias G**, Cominelli F. Role of type 2 immunity in intestinal inflammation. *Curr Opin Gastroenterol* 2015; **31**: 471-476 [PMID: 26376478 DOI: 10.1097/MOG.0000000000000212]

112 **Ding ZH**, Xu XP, Wang TR, Liang X, Ran ZH, Lu H. The prevalence of Helicobacter pylori infection in inflammatory bowel disease in China: A case-control study. *PLoS One* 2021; **16**: e0248427 [PMID: 33711050 DOI: 10.1371/journal.pone.0248427]

World Journal of Gastroenterology

Submit a Manuscript: https://www.f6publishing.com

World J Gastroenterol 2023 August 14; 29(30): 4616-4627

DOI: 10.3748/wjg.v29.i30.4616

ISSN 1007-9327 (print) ISSN 2219-2840 (online)

REVIEW

Helicobacter pylori intragastric colonization and migration: Endoscopic manifestations and potential mechanisms

Tong Mu, Zhi-Ming Lu, Wen-Wen Wang, Hua Feng, Yan Jin, Qian Ding, Li-Fen Wang

Specialty type: Gastroenterology and hepatology

Provenance and peer review: Unsolicited article; Externally peer reviewed.

Peer-review model: Single blind

Peer-review report's scientific quality classification

Grade A (Excellent): 0
Grade B (Very good): 0
Grade C (Good): C, C
Grade D (Fair): 0
Grade E (Poor): 0

P-Reviewer: Miklos BG, Hungary; Sano W, Japan

Received: May 9, 2023
Peer-review started: May 9, 2023
First decision: June 14, 2023
Revised: July 1, 2023
Accepted: July 25, 2023
Article in press: July 25, 2023
Published online: August 14, 2023

Tong Mu, Wen-Wen Wang, Hua Feng, Qian Ding, Li-Fen Wang, Department of Gastroenterology, Shandong Provincial Hospital Affiliated to Shandong First Medical University, Jinan 250021, Shandong Province, China

Zhi-Ming Lu, Yan Jin, Department of Clinical Laboratory Medicine, Shandong Provincial Hospital Affiliated to Shandong First Medical University, Jinan 250021, Shandong Province, China

Corresponding author: Li-Fen Wang, MD, Associate Chief Physician, Department of Gastroenterology, Shandong Provincial Hospital Affiliated to Shandong First Medical University, No. 9677 Jing Shi Road, Jinan 250021, Shandong Province, China.
inuonuobao@163.com

Abstract

After being ingested and entering the human stomach, *Helicobacter pylori* (*H. pylori*) adopts several effective strategies to adhere to and colonize the gastric mucosa and move to different regions of the stomach to obtain more nutrients and escape from the harsher environments of the stomach, leading to acute infection and chronic gastritis, which is the basis of malignant gastric tumors. The endoscopic manifestations and pathological features of *H. pylori* infection are diverse and vary with the duration of infection. In this review, we describe the endoscopic manifestations of each stage of *H. pylori* gastritis and then reveal the potential mechanisms of bacterial intragastric colonization and migration from the perspective of endoscopists to provide direction for future research on the effective therapy and management of *H. pylori* infection.

Key Words: *Helicobacter pylori*; Colonization; Endoscopy; Gastritis; Infection

©The Author(s) 2023. Published by Baishideng Publishing Group Inc. All rights reserved.

Core Tip: *Helicobacter pylori* (*H. pylori*) adopts several effective strategies to adhere to and colonize the gastric mucosa and move to different regions of the stomach, leading to acute infection and chronic gastritis that can be observed through endoscopy. Herein, we describe the endoscopic manifestations of each stage of *H. pylori* gastritis and then discuss the potential mechanisms of bacterial intragastric colonization and migration from the perspective of endoscopists to provide direction for future research on the effective therapy and management of *H. pylori* infection.

Citation: Mu T, Lu ZM, Wang WW, Feng H, Jin Y, Ding Q, Wang LF. *Helicobacter pylori* intragastric colonization and migration: Endoscopic manifestations and potential mechanisms. *World J Gastroenterol* 2023; 29(30): 4616-4627
URL: https://www.wjgnet.com/1007-9327/full/v29/i30/4616.htm
DOI: https://dx.doi.org/10.3748/wjg.v29.i30.4616

INTRODUCTION

More than half of the world's population is estimated to be infected by the gram-negative, flagellated, spiral-shaped bacterium *Helicobacter pylori* (*H. pylori*)[1]. The bacterium has received intensive attention because *H. pylori* infection is closely associated with the development of peptic ulcers, mucosa-associated lymphoid tissue lymphoma and gastric cancer (GC), resulting in at least 500000 deaths per year[2-4]. The slow carcinogenic process is known as Correa's cascade [5]: At first, gastritis occurs in all infected individuals[2], and then a series of intermediate stages (characterized by precancerous lesions), including atrophy, intestinal metaplasia (IM) and dysplasia, may slowly develop, and eventually, 1%-3% of infected patients develop gastric malignant tumors[6].

All gastric mucosal lesions that occur after *H. pylori* infection can be observed by skilled endoscopists through upper gastrointestinal endoscopy. Based on the Kyoto classification of gastritis, endoscopic features, such as nodularity, diffuse redness, spotty redness, mucosal swelling, enlarged folds, xanthoma, atrophy and IM, are helpful in diagnosing *H. pylori* gastritis[7]. Atrophy can be endoscopically identified with high confidence by applying the Kimura-Takemoto classification[8], while IM and dysplasia can be diagnosed more accurately with advanced image-enhanced endoscopy (IEE) [9].

The highly motile pathogen *H. pylori* usually infects young children[3] and initiates acute infection that lasts for only a few weeks[10,11] and chronic inflammation that can last for the lifetime of the host[12]. Its ability to swim in the gastric mucus and colonize the stomach enables it to survive in the hostile gastric environment[13] and leads to various endoscopic and histological features as gastric mucosal lesions progress[14]. Many articles and reviews have reported the underlying mechanisms, but few have linked endoscopic features to mechanisms. Therefore, in the following sections, we describe the endoscopic manifestations of each stage of *H. pylori* gastritis and summarize the process and potential mechanisms of intragastric colonization by *H. pylori* and its migration.

ACUTE INFECTION

Acute *H. pylori* infection only lasts for a few weeks[10,11] and has been rarely observed or reported in recent decades. The endoscopic manifestation of gastric erythema and a gaping pylorus[10,11] is always featureless. Although the gastric mucosa does not appear damaged at this stage, initial colonization of the mucosa is the basis of a series of lesions, such as atrophic gastritis, peptic ulcer and even gastric carcinoma.

The prevalence of *H. pylori* infection is high, but colonization by this microbe is not easy. Multiple spontaneous eradication events may occur before colonization, leading to acute infection[15]. Sophisticated strategies have been adopted by *H. pylori* that have enabled it to adapt to and survive in the hostile gastric environment.

When *H. pylori* is ingested by adults, it is almost completely destroyed in the gastric acid, while it is easier to survive in the stomach of children younger than the age of five, both in developing and developed countries[3]. Bucker *et al*[3] simulated the pH changes of the postprandial stage in babies, young children and adults and suggested that the bacteria were easiest to reach the mucus layer in young children, whose feature of postprandial gastric condition is moderate food-induced pH elevation and slow reacidification.

During the process of slow reacidification, the urease enzyme is believed to play a key role in bacterial survival and adhesion. Urea is degraded by the urease enzyme, which buffers the cytoplasm and periplasm[16]. This confers many benefits. First, *H. pylori* prefers to live in an environment with elevated pH. A recent study[17] showed that *H. pylori* does not escape from phosphate buffer solutions of pH 6.6 and 7.0. Second, intracellular urease could also increase membrane potential, thereby allowing protein synthesis at a low pH[18]. Third, mucosal viscosity highly depends on acidity[19]. At a less acidic pH, the mucus is less gel-like, which enables *H. pylori* to more easily move through the mucus layer[20]. Fourth, trefoil factor 1 (TFF1) is a member of the trefoil peptide family of proteins and is coexpressed with Mucin-5AC (MUC5AC), a gel-forming mucin that is predominantly secreted and expressed by gastric surface epithelial cells in the stomach[21]. The optimum pH for bacterial binding to TFF1, which thereby promotes colonization, was found to be 5.0-6.0[22]. In addition, urea and bicarbonate were considered to have a chemotactic effect on *H. pylori in vitro*[23], but research by Schreiber *et al*[13] shows that neither the urea/ammonium gradient nor the bicarbonate/CO_2 gradient are essential for the orientation of *H. pylori in vivo*.

However, this does not mean that a neutral or alkaline environment is suitable for *H. pylori*. Previous studies have shown that *H. pylori* is sensitive to alkaline conditions[24], and its growth is limited at neutral pH[25]. To prevent lethal alkalinization of the cytoplasm, *H. pylori* utilizes a proton-gated channel, UreI, which regulates the uptake of urea[26] and only functions in conditions of an acidic pH; thus, the transport of urea into the bacterial cell does not occur at a neutral pH[24]. Therefore, *H. pylori* prefers a weakly acidic environment.

The epithelial surface of the stomach is covered with an approximately 300 μm thick layer of secreted mucus, which mainly consists of mucins Mucin 6 (MUC6) and MUC5AC[27]. MUC6 exists in each layer of the mucus gel, while MUC5AC is mainly present on the surface and bottom. The increase in the viscosity of gastric mucus gel is due to this natural stratification of mucins[28]. While protecting gastric epithelial cells, the mucus layer also plays an important role in the colonization process. The pH is approximately neutral at the epithelium and very acidic (pH 1-2) close to the lumen [21], resulting in a mucus pH gradient that can be used by *H. pylori* for precise spatial orientation[13]. The membrane-bound chemoreceptor TlpA of *H. pylori* detects and mediates repulsion from environments with a lower pH, and the cytoplasmic chemoreceptor TlpD mediates both attraction to higher pH environments and repulsion from lower pH environments[17,29]. Under this chemotactic effect, *H. pylori* penetrates the gastric mucus quickly and reaches the narrow region within 25 μm of the gastric epithelial surface with the help of its two to six sheathed unipolar flagella and helical shape[30,31].

After approaching the lower mucus layer, the majority of *H. pylori* swim in gastric mucus, while others directly adhere to epithelial cells[13,31]. Although it is considered a noninvasive gastric pathogen to date[19], *H. pylori* can indeed bind to, invade, be internalized into and proliferate in gastric epithelial cells[27,32]. The invasiveness of *H. pylori* may partially depend on the strain. Research by Camorlinga-Ponce *et al*[33] showed that CagA-negative bacteria adhered to the surface of the apical epithelium, while CagA-positive bacteria were identified in the intercellular spaces or the immediate vicinity of epithelial cells. Sigal *et al*[34] found a subgroup of *H. pylori* associated with cells deep in the antral glands. These microbes can promote gland hyperplasia by inducing stem cell proliferation and expansion and altering gene expression of stem cells[34].

H. pylori adheres to epithelial cells mainly by outer membrane proteins (OMPs). Blood group antigen-binding adhesion (BabA) and sialic acid-binding adhesion (SabA) are important OMPs[19,27]. Lewis antigens are common in normal, infected and inflamed gastric mucosa[35,36]. BabA can identify and bind to Lewis b antigen[35], while SabA can bind to the antigens Lewis a and Lewis X[36], and its expression can quickly respond to the changes in the stomach or different areas of the stomach, enabling the bacteria to adapt to host's immune responses and varied microenvironments to maintain long-term colonization and infection[37]. In addition to BabA and SabA, other surface proteins, such as AlpA, AlpB, DupA, outer inflammatory protein A (OipA) and HopZ, are considered related to adhesion, but none of them has been shown to be essential to adhesive mechanisms[38]. After *H. pylori* adheres to epithelial cells, the Cag type IV secretion system (T4SS) promotes CagA translocation into host cells, resulting in changes in cell shape, disruption of cell□cell junctions, altered cell polarity and cell adhesion, increased cell motility and cell migration, increased cell proliferation, β-catenin activation, and epithelial-mesenchymal transition[39]. Some bacteria are internalized into the cytoplasm of gastric epithelial cells through endocytosis within 45 minutes of bacterial attachment to the cell surface[32]. *H. pylori* can replicate and proliferate in epithelial cells[40], escape the immune response, and exit cells to colonize and infect cells again when the external environment is suitable for survival[27].

In an artificial ingestion study[10], histological examination during the acute phase of *H. pylori* infection showed many polymorphonuclear neutrophil leucocytes (PMNs) in the lamina propria and on the surface of the mucosa and an absence of intracellular mucus. Spiral bacilli adhered to the surface and glandular epithelium as well as among PMNs in the mucus[10]. Zhao *et al*[41] proposed a novel staging strategy according to the depth and degree of gastric mucosal injury induced by *H. pylori* infection and the progression of lesions. Stage I means the bacteria were present in the mucus layer, stage IIA refers to the specific adhesion to and selective destruction of gastric epithelial cells, and stage IIB refers to the degeneration and shedding of surface mucus cells[41]. It seems that stages I and II are consistent with the pathological characteristics of acute *H. pylori* infection.

CHRONIC GASTRITIS

Cases of *H. pylori* gastritis that are observed by doctors usually involve chronic gastritis that has lasted for years[42]. Chronic gastritis has various endoscopic findings, among which nodularity, diffuse redness, spotty redness, xanthoma, mucosal swelling, enlarged folds, atrophy, and IM are common in *H. pylori*-infected gastric mucosa[43,44] (Figure 1). Considering the severity and progression of chronic *H. pylori* gastritis, we discuss endoscopic manifestations and potential mechanisms from the following three aspects: (1) Early stage of *H. pylori* infection; (2) corpus inflammation; and (3) atrophy and intestinal metaplasia, which are summarized in Table 1.

Early stage of H. pylori infection

Nodular gastritis is considered a feature of an early stage of *H. pylori* infection in adults and is more common in children, with an incidence of 32.9% to 85%[45,46]. It appears more frequently in the antral mucosa than in the corpus mucosa[47]. Nodularity is characterized by a miliary pattern resembling "gooseflesh" in the gastric mucosa on endoscopy[46] and follicular lymphoid hyperplasia with intraepithelial lymphocytosis on histological examination[47]. Okamura *et al*[48] further demonstrated that superficially located, enlarged hyperplastic lymphoid follicles corresponded to nodular and/or granular lesions, and the percentage of MECA-79 high endothelial venule (HEV)-like vessels was greater in areas with gooseflesh-like lesions in nodules than in normal gastric mucosa. The pathogenesis of nodular gastritis may involve a Th2

Table 1 The mechanisms of common endoscopic features

Endoscopic features	Mechanisms
Nodularity	Follicular lymphoid hyperplasia with intraepithelial lymphocytosis[47]; Superficially located, enlarged hyperplastic lymphoid follicles [48]; Increased numbers of MECA-79 HEV-like vessels[48]; Th2 immune response[49]
Diffuse redness	Infiltration of neutrophils and monocytes[44,58]
Spotty redness	Unclear
Mucosal swelling	Infiltration by neutrophils and monocytes[44]
Enlarged folds	Tumor necrosis factor-alpha gene polymorphism[64]; Genome wide hypomethylation and regional hypermethylation[65,66]; Stimulation of epithelial cell proliferation and inhibition of acid secretion induced by interleukin 1 beta and hepatocyte growth factor [61,62]; Inhibition of acid secretion caused by morphological changes in parietal cells[63]
Xanthoma	Unclear
Atrophy	Cellular injury inflicted by *Helicobacter pylori* or mediated by inflammation or apoptosis[77]; Th1 immune response[78]; C-X-C motif chemokine receptor 2-mediated cellular senescence[79]
Intestinal metaplasia	Death of parietal cells and reprograming of chief cells[82]

immune response, which is more likely to occur in children[49,50].

Early colonization usually occurs in the gastric antrum, and early inflammation is always more serious in the gastric antrum, which is consistent with endoscopic findings. Animal research suggested that the wild-type *H. pylori* strain mostly colonized the antrum and the transition zone between the antrum and corpus rather than the corpus[31,34]. Rolig *et al*[51] demonstrated that inflammation was worse in the antrum than in the corpus in mice infected with wild-type *H. pylori* strains. This may be associated with the particularity of antral glands and chemotaxis of the bacterium.

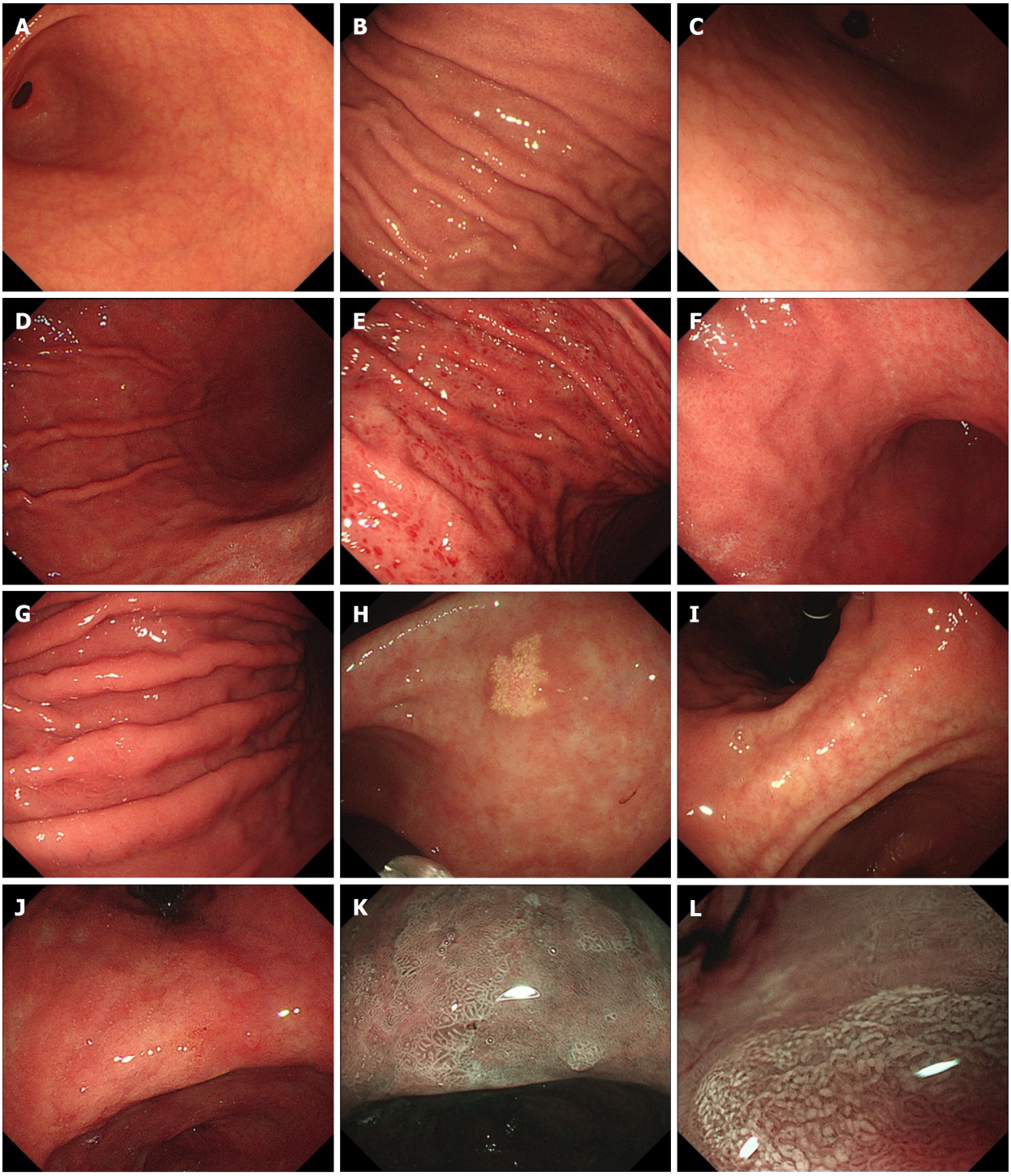
It is well known that the corpus is populated by oxyntic glands containing many acid-secreting parietal cells that promote acidic conditions in the stomach. In contrast, the antrum, which is defined by the presence of gastrin-expressing G cells, mainly comprises the pyloric or antral glands containing MUC6-expressing deep mucous cells, G cells, D cells, enterochromaffin cells and foveolar surface mucous cells[52]. Interestingly, oxyntic glands also exist in the human gastric antrum, but the proportion of parietal cells and chief parietal cells is significantly less than that in corpus glands[53]. The effects of parietal cells in the antrum on *H. pylori* colonization remains unclear. However, generally, the weaker acidic environment of the antrum provides the bacteria with more opportunities to survive and colonize.

The chemotaxis system of *H. pylori* includes three membrane-bound chemoreceptors, including TlpA, TlpB, and TlpC; one cytoplasmic chemoreceptor, TlpD[29]; three core signaling complex proteins, including CheW, CheA and CheY[54,55]; and auxiliary chemotaxis proteins containing CheV-type coupling proteins (CheV1, CheV2, and CheV3), CheZ phosphatase and ChePep[56]. The role of pH sensing in chemotaxis has been mentioned above. In addition, a study by Rolig *et al*[51] shows that chemotaxis is required for *H. pylori* to swim to and achieve normal bacterial loads in the antrum and transition zone. The number of nonchemotactic mutant (Che-) *H. pylori* strains at this site was found to increase more slowly than that of the wild-type strains. TlpD plays a major role in this process. Therefore, chemotaxis may be necessary for *H. pylori* to locate or to maintain colonization of the antrum.

Corpus inflammation

Previous clinical studies focused on the relationship between endoscopic findings and *H. pylori* infection and demonstrated that diffuse redness, spotty redness, mucosal swelling and enlarged folds under endoscopy are associated with *H. pylori* infection[14,46]. Diffuse redness, defined as uniform redness with continuous expansion involving the nonatrophic mucosa in the region of fundic gland, and mucosal swelling, defined as swollen gastric mucosa in the region of fundic gland or thick, uneven mucosa in the region of pyloric gland, correlate predominantly with the degree of neutrophilic and mononuclear cell infiltration caused by *H. pylori* infection[44,57-59]. Spotty redness comprises multiple spotted small flat erythema, commonly observed in the upper corpus and fornix[44], but its mechanism remains unclear. An enlarged fold is defined as a fold with a width of 5 mm or more in the gastric greater curvature, which is not or only partially flattened by air insufflation[60]. Stimulation of epithelial cell proliferation, inhibition of acid secretion, tumor necrosis factor-alpha gene polymorphism, genome-wide hypomethylation and regional hypermethylation may play a role in the generation of enlarged folds caused by bacterial infection[61-66]. We describe another perspective: these endoscopic features that are mainly observed in the corpus indicate the existence of corpus inflammation, the development of gastric mucosal lesions, and a later stage of *H. pylori* infection that differs from the early stage and mainly manifests as antral inflammation.

H. pylori can survive in and colonize the harsh conditions of the corpus that are promoted by oxyntic glands. This has been indicated by previous studies. *H. pylori* was identified in the corpus in 83% of patients with a previous diagnosis of intestinal metaplasia and known *H. pylori* infection[67]. Biopsies taken from the corpus are conducive to an accurate histologic diagnosis and assessment of *H. pylori* infection[68,69]. Combined antrum and corpus biopsies can lead to a significantly better success rate of *H. pylori* culture than single antrum biopsy[4].



DOI: 10.3748/wjg.v29.i30.4616 **Copyright** ©The Author(s) 2023.

Figure 1 Endoscopic features without and with *Helicobacter pylori* infection. A: Antrum without *Helicobacter pylori* infection; B: Corpus without *Helicobacter pylori* infection; C: Nodularity; D: Diffuse redness; E: Spotty redness; F: Mucosal swelling; G: Enlarged folds; H: Xanthoma; I: Atrophy; J: Intestinal metaplasia; K: Light-blue crest; L: White opaque substance.

H. pylori also reaches the corpus under the guidance of chemotaxis, but afterward, chemotaxis is not needed for *H. pylori* populations to increase[51]. It is likely that the spontaneous eradication of the bacteria is almost impossible at this stage. However, to live, proliferate and induce chronic infection, bacteria need to acquire nutrients and escape immune reactions in addition to adapting to acidic environments, as mentioned above. Due to the low permeability of the mucosal layer, essential nutrients (for example, Fe^{3+}) for ingested microorganisms are scarce in the stomach[70]. Following the successful colonization of gastric epithelial cells, *H. pylori* induces immune cells that cause cell damage to shed nutrients onto the surface of the gastric mucosa for survival[71]. However, *H. pylori* needs to take measures to protect itself from host immunity. Sophisticated mechanisms participate in the response to innate immunity; these mechanisms include: (1) The induction of mitochondrial-dependent apoptosis in macrophages; (2) the defense against NO products available in the gastric microniche through production of peroxiredoxin by the AhpC gene; and (3) the reduction of NO or O_2^- radicals

by arginase due to substrate competition; responses to adaptive immunity, which have been elaborated in a previous review, include: (1) The binding of the VacA toxin to an unknown surface ligand in T cells, which results in actin rearrangement and then inhibition of cell proliferation; (2) The promotion of vacuoles in host cells, which leads to apoptosis by an anion-selective channel formed by the VacA toxin; and (3) VacA binding to mitochondria, which activates the associated apoptotic pathway[19]. In addition, *H. pylori* can be internalized into epithelial cells through endocytosis[32]. Long-term exposure to VacA during chronic infection causes the formation of immature autophagosomes, resulting in a failure to clear the bacteria[72].

In the novel pathological staging strategy mentioned above[41], stage III, the laminar lesion stage, may be consistent with the early stage of gastric antrum and corpus inflammation. Stage III is subdivided into: (1) Stage IIIA: Infiltration of inflammatory cells and vacuolar-like degeneration; (2) stage IIIB: The development of mucous neck cell hyperplasia, glandular hyperplasia and heteroplasia, and serrated structures; (3) stage IIIC: Mucosal ulcers develop; and (4) stage IIID: Histologically diffuse lymphocyte proliferation occurs, and many lymphatic follicles of varying sizes are present.

Atrophy and intestinal metaplasia

In the absence of treatment, the inflammation and immune response caused by *H. pylori* infection may lead to atrophic gastritis[73], which is defined as the loss of gastric glands, with or without metaplasia[74]. This process takes several years in humans[75]. Early *H. pylori* eradication should be considered for preventing GC development prior to the appearance of atrophy or metaplasia because the benefits of *H. pylori* eradication diminish after the gastric IM stage is reached, which is referred to as the "point of no return"[76].

Gastric gland replacement by connective tissue or inflammatory cells is referred to as atrophy[73,74]. Previous studies have reported that atrophy may be related to the Th1 immune response and cellular injury, which is directly inflicted by the bacteria or mediated by inflammation or apoptosis[77,78]. A recent study showed a new mechanism of *H. pylori* –induced atrophy through C-X-C motif chemokine receptor 2 (CXCR2)-mediated cellular senescence[79]. However, in general, the pathogenetic mechanisms that trigger atrophy are still debated.

Color changes (yellowish pale) in the mucosa, mucosal thinning and visible vascular patterns are typical endoscopic atrophic features[80]. In 1966, Kimura and Takemoto described the appearance of an "atrophic transitional zone" in patients with gastritis for the first time, which was subsequently known as the endoscopic atrophic border[8]. The differences in mucosal color and the visibility of capillary networks are remarkable between the two sides of the endoscopic atrophic border[81]. The degree of atrophy can be divided into 6 types based on the location of the endoscopic atrophic border. Endoscopic atrophic findings that are only visible in the antrum are referred to as closed type C-1. In closed types C-2 and C-3, atrophy can be observed in the angulus and the lesser curvature of the corpus. In open type O-1, the atrophic border lies between the lesser curvature and the anterior wall; in type O-2, it lies within the anterior wall; and in type O-3, the endoscopic atrophic area is widely spread within the border between the anterior wall and the greater curvature[81].

When deep damage to the gastric mucosa occurs, acid-secreting parietal cells die, and pepsin-secreting chief cells are reprogrammed into mucin-secreting, wound-healing cells to reduce endogenous production of caustic substances; this response to injury is known as metaplasia[82]. Pathologically, metaplasia refers to gland replacement by a different type of epithelium in a tissue where it is not normally found[74,83]. The characteristics of mucus secretion were used to discriminate metaplastic lineages[83]. Pseudopyloric metaplasia is defined as the presence of MUC6- and trefoil factor 2 (TFF2)-expressing cells at the base of corpus glands with a morphology more characteristic of mucus-producing deep antral glands[84]. IM refers to the presence of Mucin2 (MUC2)/trefoil factor 3 (TFF3)-expressing intestinal-type goblet cells in the stomach[85]. IM can be divided into two types: (1) Incomplete IM, which may be found in either the superficial or foveolar epithelium and in the glands and is characterized by secretive columnar cells that secrete mucin into the apical cytoplasm and the presence of goblet cells; and (2) complete IM, which is characterized by columnar absorptive cells without mucin secretion and the presence of goblet cells[86]. Both incomplete and complete IM can be subdivided into small intestinal type and colonic type (Table 2).

An ash-colored flat nodular change has been considered a typical endoscopic finding of IM since the last century[80]. With the development of endoscopic technology, advanced IEE, including narrow band imaging (NBI) endoscopy, has been used as a more accurate IM diagnostic tool than traditional white light endoscopy[9]. Various markers are related to gastric IM[87]. Light-blue crest (LBC) (Figure 1K), a light blue line observed on the surface of gastric mucosal epithelium, is the earliest mentioned IEE finding[88]. Combining the findings of white opaque substance (WOS) (Figure 1L), white mucosal epithelium observed under IEE, and LBC improves the sensitivity of diagnosing IM[89]. Through systematic review and meta-analysis, the diagnostic sensitivity and specificity of LBC were found to be 0.79 [95% confidence interval (CI): 0.76-0.81] and 0.95 (95%CI: 0.94-0.96), respectively. The sensitivities of the groove type (GT) and marginal turbid band (MTB) were 0.49 (95%CI: 0.43-0.54) and 0.47 (95%CI: 0.40-0.53), respectively, and the specificities were 0.92 (95%CI, 0.89-0.94) and 0.92 (95%CI: 0.89-0.95)[87], respectively. In addition, researchers derived a classification for endoscopic grading of gastric IM (EGGIM) using IEE, which permits immediate grading of intestinal metaplasia without biopsies and is beneficial for GC risk stratification[90].

In addition, gastric xanthoma is a common endoscopic finding in patients with *H. pylori* infection and may serve as a warning endoscopic sign for advanced atrophic gastritis, intestinal metaplasia and GC[91-93]. It is a small yellowish or yellowish-white plaque-like or nodular lesion characterized by the accumulation of lipids, containing cholesterol, low-density oxidized lipoprotein, low-density lipoprotein and neutral fat, in histiocytic foam cells[93,94]. However, the etiopathogenesis is also unclear.

Table 2 Intestinal metaplasia with different mucin secretion

Cells	Incomplete intestinal metaplasia		Complete intestinal metaplasia	
	Small intestinal type	Colonic type	Small intestinal type	Colonic type
Columnar cells	Neutral and scanty sialomucins	Sulpho- and scanty sialomucins	No mucin secretion	No mucin secretion
Goblet cells	Sialomucins	sialomucins	Neutral and sialomucins	Sulpho- and sialomucins

INTRAGASTRIC MIGRATION

H. pylori has shared a coevolutionary history with humans for more than 60000 years[41,95]. Human migration has led to the global distribution of the bacterium from East Africa to other continents[19]. In addition to geographical migration, *H. pylori* has the ability to move between different regions of the stomach.

The motility of *H. pylori* provided by its flagella and helical shape is the basis of intragastric migration. The bacterium possesses two to six sheathed unipolar flagella[96]. The sheath, which consists of both proteins and lipopolysaccharide, protects the flagellar filaments from gastric acid[97]. Expression of the two major flagellar proteins, FlaA and FlaB, is required for full motility of the bacteria[21]. An efficient screw-like movement resulting from the characteristic helical shape of *H. pylori* also provides an advantage for penetrating the gastric mucus layer[98]. Any mutation in the genes associated with bacterial morphology, such as Ccrp89, Ccrp58, Ccrp1142 and Ccrp1143, can lead to a deficiency in bacterial shape and motility[99].

The chemotaxis system of *H. pylori* is necessary for intragastric migration. Chemotactic signals sensed by chemoreceptors are transmitted to the histidine kinase CheA through the coupling protein CheW or CheV1[100]. Repellents activate CheA autophosphorylation, and CheY is subsequently phosphorylated *via* histidine-to-aspartate phosphorelay [101]. Phosphorylated CheY interacts with the flagellar motor, causing it to rotate clockwise and the bacteria to reverse or change direction[56]. Alternatively, the bacteria swim straight because chemicals perceived as attractants squelch CheA autophosphorylation[56]. As described above, the ability of chemoreceptors to sense pH guides the bacteria to the surface of the gastric epithelium. It has been suggested that different regions of the stomach contain unique chemotactic signals [51]. The gastric antrum is usually the first colonized area because of its weaker acidic environment but not due to chemotaxis. The chemotactic signals produced by the antrum or transition zone play an important role in the increase in *H. pylori* numbers that occurs from 14 h to 1 wk after colonization[51]. Chemotaxis is also required when *H. pylori* migrates to the corpus from the antrum but is not needed for the increase in bacterial populations after the initial colonization of the corpus[27]. In addition, *H. pylori* can swim toward injured epithelia[102].

H. pylori can simultaneously survive in the antrum and the corpus in general. However, when atrophy occurs, an environment that is unfavorable to the growth of *H. pylori* develops, and the bacteria can only be found in a small percentage of endoscopic biopsy specimens[103]. Research has revealed that atrophy in the corpus manifests as a continuous sheet of pseudopyloric metaplasia and forms an advancing histologically atrophic front, the presence of which is similar to the spread of antral mucosa toward the corpus and is faster in the lesser curvature[104]. This pattern is the same as the endoscopic atrophic border described by Kimura and Takemoto[8]. This may indicate that the suitable region in which *H. pylori* survives shrinks as the atrophic front advances and is well discriminated by the endoscopic atrophic border.

In addition, *H. pylori* can migrate to the duodenum and colonize the duodenal gastric metaplasia (DGM) with a bacterial density 100-fold lower than that in the antrum[105,106]. DGM is characterized by the metaplastic replacement of normal duodenal epithelial cells with cells displaying a phenotype similar to that of mucus-secreting cells of the gastric mucosa[107]. It is frequently found in patients with duodenal ulcers with a prevalence of 72 to 90% and is associated with the chronicity and recurrence of duodenal ulcer disease[108-110]. The exact pathogenesis of DGM remains unclear. It is speculated that a high acid burden in the duodenum caused by increased gastrin secretion and the inflammatory damage to duodenal mucosa induced by bacterial cytotoxin may lead to the development of DGM in patients with *H. pylori* infection[109]. Liu and Wright[111] considered that metaplastic cells originate from Brunner's gland duct epithelium or basal buds growing out of the crypts of Lieberkühn and migrate in straight lines. However, Shaoul *et al*[112] suggested that DGM develops from goblet cells that simultaneously express gastric antigens, MUC5AC and TFF1, and intestinal antigen, MUC2 core antigen, migrate upward and transform to foveolar-like cells at the site of early metaplastic patches. Published results about the association between *H. pylori* infection and DGM are also conflicting. Some studies reported that *H. pylori* infection was one of the independent risk factors for DGM[113], the amount of *H. pylori* in the duodenal bulb might be related to the extent of gastric metaplasia in the duodenal bulb[114], and the presence of DGM significantly decreased after *H. pylori* eradication[109]. However, some researchers have suggested that DGM is associated with high acid output in the stomach rather than gastric *H. pylori* infection[115-117].

CARDIA

The endoscopic characteristics of the cardia have received little attention in previous studies. In recent years, cardiac nodularity, which involves the appearance of miliary nodules or scattered small whitish circular colorations within 2 cm of the esophagogastric junction, has been proposed by researchers[46,118].

Cardia glands lack chief cells and parietal cells, and have similar characteristics to the pyloric glands[53]. The cardiac and pyloric glands secrete mucus and bicarbonate and are involved in the defense of the gastric epithelium[46]. In addition, both of them secrete MUC6 and pepsinogen II rather than pepsinogen I[46]. Unlike the fundic glands, the similarity of the cardiac and pyloric glands may lead to the appearance of cardiac nodularity.

Nodularity can be observed more frequently in the stomach of children and improves gradually with age[119,120]. Reportedly, the eradication of *H. pylori* in patients with antral nodularity could effectively prevent diffuse-type GC[119]. A study by Nishikawa *et al*[119] suggested that compared with patients without cardiac nodularity, patients with cardiac nodularity were significantly younger and had lower IM scores. Therefore, cardiac nodularity may also be a feature of the early stage of *H. pylori* infection, but further research is needed to analyze its clinicopathological importance.

CONCLUSION

H. pylori infection has received worldwide attention for decades. In this review, we described the process of intragastric colonization by *H. pylori* and its migration and tried to identify a link between endoscopic manifestations and potential mechanisms. Upper gastrointestinal endoscopy and pathological examination of biopsy specimens are useful tools for diagnosing *H. pylori*-induced gastritis and estimating the risk of *H. pylori*-induced GC. In addition to animal models, exploring the mechanisms of *H. pylori* infection requires biopsy sampling. However, extensive study is needed to evaluate the association between endoscopic manifestations and mechanisms.

FOOTNOTES

Author contributions: Mu T drafted the article; Lu ZM and Jin Y made contributions to the design of the article; Wang WW, Feng H and Ding Q revised the article; Wang LF provides figures, revised the article and made the decision to submit for publication; all authors have read and approved the final manuscript.

Supported by Medical Health Science and Technology Development Plan Project of Shandong Province, No. 202103030765; and Natural Science Foundation of Shandong Province, No. ZR2021QH195 and No. ZR2020QH035.

Conflict-of-interest statement: All authors declare no conflict of interests for this article.

Open-Access: This article is an open-access article that was selected by an in-house editor and fully peer-reviewed by external reviewers. It is distributed in accordance with the Creative Commons Attribution NonCommercial (CC BY-NC 4.0) license, which permits others to distribute, remix, adapt, build upon this work non-commercially, and license their derivative works on different terms, provided the original work is properly cited and the use is non-commercial. See: https://creativecommons.org/Licenses/by-nc/4.0/

Country/Territory of origin: China

ORCID number: Tong Mu 0000-0001-7053-9181; Zhi-Ming Lu 0000-0003-1228-5739; Wen-Wen Wang 0000-0001-7300-2304; Hua Feng 0000-0002-5751-4163; Yan Jin 0009-0009-2288-8753; Qian Ding 0000-0002-2301-8487; Li-Fen Wang 0009-0007-5314-3055.

S-Editor: Yan JP
L-Editor: A
P-Editor: Yan JP

REFERENCES

1 **Suerbaum S**, Michetti P. Helicobacter pylori infection. *N Engl J Med* 2002; **347**: 1175-1186 [PMID: 12374879 DOI: 10.1056/NEJMra020542]
2 **Buck GE**, Gourley WK, Lee WK, Subramanyam K, Latimer JM, DiNuzzo AR. Relation of Campylobacter pyloridis to gastritis and peptic ulcer. *J Infect Dis* 1986; **153**: 664-669 [PMID: 3950448 DOI: 10.1093/infdis/153.4.664]
3 **Bücker R**, Azevedo-Vethacke M, Groll C, Garten D, Josenhans C, Suerbaum S, Schreiber S. Helicobacter pylori colonization critically depends on postprandial gastric conditions. *Sci Rep* 2012; **2**: 994 [PMID: 23251780 DOI: 10.1038/srep00994]
4 **Brennan DE**, O'Morain C, McNamara D, Smith SM. Combined antrum and corpus biopsy protocol improves Helicobacter pylori culture success. *World J Gastrointest Pathophysiol* 2022; **13**: 34-40 [PMID: 35116178 DOI: 10.4291/wjgp.v13.i1.34]
5 **Correa P**. Human gastric carcinogenesis: a multistep and multifactorial process--First American Cancer Society Award Lecture on Cancer Epidemiology and Prevention. *Cancer Res* 1992; **52**: 6735-6740 [PMID: 1458460]
6 **Cirak MY**, Akyön Y, Mégraud F. Diagnosis of Helicobacter pylori. *Helicobacter* 2007; **12** Suppl 1: 4-9 [PMID: 17727453 DOI: 10.1111/j.1523-5378.2007.00542.x]
7 **Yoshii S**, Mabe K, Watano K, Ohno M, Matsumoto M, Ono S, Kudo T, Nojima M, Kato M, Sakamoto N. Validity of endoscopic features for the diagnosis of Helicobacter pylori infection status based on the Kyoto classification of gastritis. *Dig Endosc* 2020; **32**: 74-83 [PMID: 31309632 DOI: 10.1111/den.13486]
8 **Quach DT**, Hiyama T. Assessment of Endoscopic Gastric Atrophy according to the Kimura-Takemoto Classification and Its Potential Application in Daily Practice. *Clin Endosc* 2019; **52**: 321-327 [PMID: 31327182 DOI: 10.5946/ce.2019.072]

9 **Pimentel-Nunes P**, Dinis-Ribeiro M, Soares JB, Marcos-Pinto R, Santos C, Rolanda C, Bastos RP, Areia M, Afonso L, Bergman J, Sharma P, Gotoda T, Henrique R, Moreira-Dias L. A multicenter validation of an endoscopic classification with narrow band imaging for gastric precancerous and cancerous lesions. *Endoscopy* 2012; **44**: 236-246 [PMID: 22294194 DOI: 10.1055/s-0031-1291537]

10 **Marshall BJ**, Armstrong JA, McGechie DB, Glancy RJ. Attempt to fulfil Koch's postulates for pyloric Campylobacter. *Med J Aust* 1985; **142**: 436-439 [PMID: 3982345 DOI: 10.5694/j.1326-5377.1985.tb113443.x]

11 **Sobala GM**, Crabtree JE, Dixon MF, Schorah CJ, Taylor JD, Rathbone BJ, Heatley RV, Axon AT. Acute Helicobacter pylori infection: clinical features, local and systemic immune response, gastric mucosal histology, and gastric juice ascorbic acid concentrations. *Gut* 1991; **32**: 1415-1418 [PMID: 1752479 DOI: 10.1136/gut.32.11.1415]

12 **Thorell K**, Lehours P, Vale FF. Genomics of Helicobacter pylori. *Helicobacter* 2017; **22**: Suppl 1 [PMID: 28891132 DOI: 10.1111/hel.12409]

13 **Schreiber S**, Konradt M, Groll C, Scheid P, Hanauer G, Werling HO, Josenhans C, Suerbaum S. The spatial orientation of Helicobacter pylori in the gastric mucus. *Proc Natl Acad Sci U S A* 2004; **101**: 5024-5029 [PMID: 15044704 DOI: 10.1073/pnas.0308386101]

14 **Kato T**, Yagi N, Kamada T, Shimbo T, Watanabe H, Ida K; Study Group for Establishing Endoscopic Diagnosis of Chronic Gastritis. Diagnosis of Helicobacter pylori infection in gastric mucosa by endoscopic features: a multicenter prospective study. *Dig Endosc* 2013; **25**: 508-518 [PMID: 23369058 DOI: 10.1111/den.12031]

15 **Perri F**, Pastore M, Clemente R, Festa V, Quitadamo M, Niro G, Conoscitore P, Rutgeerts P, Andriulli A. Helicobacter pylori infection may undergo spontaneous eradication in children: a 2-year follow-up study. *J Pediatr Gastroenterol Nutr* 1998; **27**: 181-183 [PMID: 9702650 DOI: 10.1097/00005176-199808000-00010]

16 **Scott DR**, Weeks D, Hong C, Postius S, Melchers K, Sachs G. The role of internal urease in acid resistance of Helicobacter pylori. *Gastroenterology* 1998; **114**: 58-70 [PMID: 9428219 DOI: 10.1016/s0016-5085(98)70633-x]

17 **Huang JY**, Goers Sweeney E, Guillemin K, Amieva MR. Multiple Acid Sensors Control Helicobacter pylori Colonization of the Stomach. *PLoS Pathog* 2017; **13**: e1006118 [PMID: 28103315 DOI: 10.1371/journal.ppat.1006118]

18 **Stingl K**, Altendorf K, Bakker EP. Acid survival of Helicobacter pylori: how does urease activity trigger cytoplasmic pH homeostasis? *Trends Microbiol* 2002; **10**: 70-74 [PMID: 11827807 DOI: 10.1016/s0966-842x(01)02287-9]

19 **Abadi ATB**. Strategies used by helicobacter pylori to establish persistent infection. *World J Gastroenterol* 2017; **23**: 2870-2882 [PMID: 28522905 DOI: 10.3748/wjg.v23.i16.2870]

20 **Celli JP**, Turner BS, Afdhal NH, Keates S, Ghiran I, Kelly CP, Ewoldt RH, McKinley GH, So P, Erramilli S, Bansil R. Helicobacter pylori moves through mucus by reducing mucin viscoelasticity. *Proc Natl Acad Sci U S A* 2009; **106**: 14321-14326 [PMID: 19706518 DOI: 10.1073/pnas.0903438106]

21 **Dunne C**, Dolan B, Clyne M. Factors that mediate colonization of the human stomach by Helicobacter pylori. *World J Gastroenterol* 2014; **20**: 5610-5624 [PMID: 24914320 DOI: 10.3748/wjg.v20.i19.5610]

22 **Reeves EP**, Ali T, Leonard P, Hearty S, O'Kennedy R, May FE, Westley BR, Josenhans C, Rust M, Suerbaum S, Smith A, Drumm B, Clyne M. Helicobacter pylori lipopolysaccharide interacts with TFF1 in a pH-dependent manner. *Gastroenterology* 2008; **135**: 2043-2054, 2054.e1 [PMID: 18848942 DOI: 10.1053/j.gastro.2008.08.049]

23 **Nakamura H**, Yoshiyama H, Takeuchi H, Mizote T, Okita K, Nakazawa T. Urease plays an important role in the chemotactic motility of Helicobacter pylori in a viscous environment. *Infect Immun* 1998; **66**: 4832-4837 [PMID: 9746586 DOI: 10.1128/IAI.66.10.4832-4837.1998]

24 **Clyne M**, Labigne A, Drumm B. Helicobacter pylori requires an acidic environment to survive in the presence of urea. *Infect Immun* 1995; **63**: 1669-1673 [PMID: 7729871 DOI: 10.1128/iai.63.5.1669-1673.1995]

25 **van Vliet AH**. Use of pan-genome analysis for the identification of lineage-specific genes of Helicobacter pylori. *FEMS Microbiol Lett* 2017; **364** [PMID: 28011701 DOI: 10.1093/femsle/fnw296]

26 **Weeks DL**, Eskandari S, Scott DR, Sachs G. A H+-gated urea channel: the link between Helicobacter pylori urease and gastric colonization. *Science* 2000; **287**: 482-485 [PMID: 10642549 DOI: 10.1126/science.287.5452.482]

27 **Huang Y**, Wang QL, Cheng DD, Xu WT, Lu NH. Adhesion and Invasion of Gastric Mucosa Epithelial Cells by Helicobacter pylori. *Front Cell Infect Microbiol* 2016; **6**: 159 [PMID: 27921009 DOI: 10.3389/fcimb.2016.00159]

28 **Ho SB**, Takamura K, Anway R, Shekels LL, Toribara NW, Ota H. The adherent gastric mucous layer is composed of alternating layers of MUC5AC and MUC6 mucin proteins. *Dig Dis Sci* 2004; **49**: 1598-1606 [PMID: 15573912 DOI: 10.1023/b:ddas.0000043371.12671.98]

29 **Lertsethtakarn P**, Ottemann KM, Hendrixson DR. Motility and chemotaxis in Campylobacter and Helicobacter. *Annu Rev Microbiol* 2011; **65**: 389-410 [PMID: 21939377 DOI: 10.1146/annurev-micro-090110-102908]

30 **Ottemann KM**, Lowenthal AC. Helicobacter pylori uses motility for initial colonization and to attain robust infection. *Infect Immun* 2002; **70**: 1984-1990 [PMID: 11895962 DOI: 10.1128/IAI.70.4.1984-1990.2002]

31 **Howitt MR**, Lee JY, Lertsethtakarn P, Vogelmann R, Joubert LM, Ottemann KM, Amieva MR. ChePep controls Helicobacter pylori Infection of the gastric glands and chemotaxis in the Epsilonproteobacteria. *mBio* 2011; **2** [PMID: 21791582 DOI: 10.1128/mBio.00098-11]

32 **Ozbek A**, Ozbek E, Dursun H, Kalkan Y, Demirci T. Can Helicobacter pylori invade human gastric mucosa?: an in vivo study using electron microscopy, immunohistochemical methods, and real-time polymerase chain reaction. *J Clin Gastroenterol* 2010; **44**: 416-422 [PMID: 19904218 DOI: 10.1097/MCG.0b013e3181c21c69]

33 **Camorlinga-Ponce M**, Romo C, González-Valencia G, Muñoz O, Torres J. Topographical localisation of cagA positive and cagA negative Helicobacter pylori strains in the gastric mucosa; an in situ hybridisation study. *J Clin Pathol* 2004; **57**: 822-828 [PMID: 15280402 DOI: 10.1136/jcp.2004.017087]

34 **Sigal M**, Rothenberg ME, Logan CY, Lee JY, Honaker RW, Cooper RL, Passarelli B, Camorlinga M, Bouley DM, Alvarez G, Nusse R, Torres J, Amieva MR. Helicobacter pylori Activates and Expands Lgr5(+) Stem Cells Through Direct Colonization of the Gastric Glands. *Gastroenterology* 2015; **148**: 1392-404.e21 [PMID: 25725293 DOI: 10.1053/j.gastro.2015.02.049]

35 **Van de Bovenkamp JH**, Mahdavi J, Korteland-Van Male AM, Büller HA, Einerhand AW, Borén T, Dekker J. The MUC5AC glycoprotein is the primary receptor for Helicobacter pylori in the human stomach. *Helicobacter* 2003; **8**: 521-532 [PMID: 14535999 DOI: 10.1046/j.1523-5378.2003.00173.x]

36 **Lindén S**, Mahdavi J, Semino-Mora C, Olsen C, Carlstedt I, Borén T, Dubois A. Role of ABO secretor status in mucosal innate immunity and H. pylori infection. *PLoS Pathog* 2008; **4**: e2 [PMID: 18179282 DOI: 10.1371/journal.ppat.0040002]

37 **Goodwin AC**, Weinberger DM, Ford CB, Nelson JC, Snider JD, Hall JD, Paules CI, Peek RM, Forsyth MH. Expression of the Helicobacter pylori adhesin SabA is controlled *via* phase variation and the ArsRS signal transduction system. *Microbiology (Reading)* 2008; **154**: 2231-2240 [PMID: 18667556 DOI: 10.1099/mic.0.2007/016055-0]

38 **Oleastro M**, Ménard A. The Role of Helicobacter pylori Outer Membrane Proteins in Adherence and Pathogenesis. *Biology (Basel)* 2013; **2**: 1110-1134 [PMID: 24833057 DOI: 10.3390/biology2031110]

39 **Cover TL**, Lacy DB, Ohi MD. The Helicobacter pylori Cag Type IV Secretion System. *Trends Microbiol* 2020; **28**: 682-695 [PMID: 32451226 DOI: 10.1016/j.tim.2020.02.004]

40 **Chu YT**, Wang YH, Wu JJ, Lei HY. Invasion and multiplication of Helicobacter pylori in gastric epithelial cells and implications for antibiotic resistance. *Infect Immun* 2010; **78**: 4157-4165 [PMID: 20696835 DOI: 10.1128/IAI.00524-10]

41 **Zhao G**, Zhang Z, Li B, Huang S, Li W, Zhu C, Jiang B, He S, Wang Y, Wang S. Follow-up analysis and histopathological study of gastric mucosa in patients with Helicobacter pylori infection. *J Int Med Res* 2021; **49**: 3000605211055397 [PMID: 34939874 DOI: 10.1177/03000605211055397]

42 **Andersen LP**. Colonization and infection by Helicobacter pylori in humans. *Helicobacter* 2007; **12** Suppl 2: 12-15 [PMID: 17991171 DOI: 10.1111/j.1523-5378.2007.00574.x]

43 **Toyoshima O**, Nishizawa T, Sakitani K, Yamakawa T, Takahashi Y, Yamamichi N, Hata K, Seto Y, Koike K, Watanabe H, Suzuki H. Serum anti-Helicobacter pylori antibody titer and its association with gastric nodularity, atrophy, and age: A cross-sectional study. *World J Gastroenterol* 2018; **24**: 4061-4068 [PMID: 30254410 DOI: 10.3748/wjg.v24.i35.4061]

44 **Nomura S**, Terao S, Adachi K, Kato T, Ida K, Watanabe H, Shimbo T; Research Group for Establishment of Endoscopic Diagnosis of Chronic Gastritis. Endoscopic diagnosis of gastric mucosal activity and inflammation. *Dig Endosc* 2013; **25**: 136-146 [PMID: 23362997 DOI: 10.1111/j.1443-1661.2012.01357.x]

45 **Miyamoto M**, Haruma K, Yoshihara M, Hiyama T, Sumioka M, Nishisaka T, Tanaka S, Chayama K. Nodular gastritis in adults is caused by Helicobacter pylori infection. *Dig Dis Sci* 2003; **48**: 968-975 [PMID: 12772798 DOI: 10.1023/a:1023016000096]

46 **Toyoshima O**, Nishizawa T, Sakitani K, Yamakawa T, Watanabe H, Yoshida S, Nakai Y, Hata K, Ebinuma H, Suzuki H, Koike K. Nodularity-like appearance in the cardia: novel endoscopic findings for Helicobacter pylori infection. *Endosc Int Open* 2020; **8**: E770-E774 [PMID: 32490162 DOI: 10.1055/a-1136-9890]

47 **Hayashi S**, Imamura J, Kimura K, Saeki S, Hishima T. Endoscopic features of lymphoid follicles in Helicobacter pylori-associated chronic gastritis. *Dig Endosc* 2015; **27**: 53-60 [PMID: 25092073 DOI: 10.1111/den.12335]

48 **Okamura T**, Sakai Y, Hoshino H, Iwaya Y, Tanaka E, Kobayashi M. Superficially located enlarged lymphoid follicles characterise nodular gastritis. *Pathology* 2015; **47**: 38-44 [PMID: 25474513 DOI: 10.1097/PAT.0000000000000195]

49 **Uchida K**, Okazaki K, Debrecceni A, Nishi T, Iwano H, Inai M, Uose S, Nakase H, Ohana M, Oshima C, Matsushima Y, Kawanami C, Hiai H, Masuda T, Chiba T. Analysis of cytokines in the early development of gastric secondary lymphoid follicles in Helicobacter pylori-infected BALB/c mice with neonatal thymectomy. *Infect Immun* 2001; **69**: 6749-6754 [PMID: 11598047 DOI: 10.1128/IAI.69.11.6749-6754.2001]

50 **Kako S**, Iwaya Y, Nagaya T, Hara D, Okamura T, Iwaya M, Kurasawa S, Kato S, Nakayama Y, Akamatsu T, Umemura T. Clinicopathological features of nodular gastritis in three classes of age. *Helicobacter* 2021; **26**: e12845 [PMID: 34396629 DOI: 10.1111/hel.12845]

51 **Rolig AS**, Shanks J, Carter JE, Ottemann KM. Helicobacter pylori requires TlpD-driven chemotaxis to proliferate in the antrum. *Infect Immun* 2012; **80**: 3713-3720 [PMID: 22802346 DOI: 10.1128/IAI.00407-12]

52 **Choi E**, Roland JT, Barlow BJ, O'Neal R, Rich AE, Nam KT, Shi C, Goldenring JR. Cell lineage distribution atlas of the human stomach reveals heterogeneous gland populations in the gastric antrum. *Gut* 2014; **63**: 1711-1720 [PMID: 24488499 DOI: 10.1136/gutjnl-2013-305964]

53 **Engevik AC**, Kaji I, Goldenring JR. The Physiology of the Gastric Parietal Cell. *Physiol Rev* 2020; **100**: 573-602 [PMID: 31670611 DOI: 10.1152/physrev.00016.2019]

54 **Foynes S**, Dorrell N, Ward SJ, Stabler RA, McColm AA, Rycroft AN, Wren BW. Helicobacter pylori possesses two CheY response regulators and a histidine kinase sensor, CheA, which are essential for chemotaxis and colonization of the gastric mucosa. *Infect Immun* 2000; **68**: 2016-2023 [PMID: 10722597 DOI: 10.1128/IAI.68.4.2016-2023.2000]

55 **Pittman MS**, Goodwin M, Kelly DJ. Chemotaxis in the human gastric pathogen Helicobacter pylori: different roles for CheW and the three CheV paralogues, and evidence for CheV2 phosphorylation. *Microbiology (Reading)* 2001; **147**: 2493-2504 [PMID: 11535789 DOI: 10.1099/00221287-147-9-2493]

56 **Johnson KS**, Ottemann KM. Colonization, localization, and inflammation: the roles of H. pylori chemotaxis in vivo. *Curr Opin Microbiol* 2018; **41**: 51-57 [PMID: 29202336 DOI: 10.1016/j.mib.2017.11.019]

57 **Toyoshima O**, Nishizawa T, Koike K. Endoscopic Kyoto classification of Helicobacter pylori infection and gastric cancer risk diagnosis. *World J Gastroenterol* 2020; **26**: 466-477 [PMID: 32089624 DOI: 10.3748/wjg.v26.i5.466]

58 **Uchiyama K**, Ida K, Okuda J, Asai Y, Ohyama Y, Kuroda M, Matsumoto N, Takami T, Ogawa T, Takaori K. Correlations of hemoglobin index (IHb) of gastric mucosa with Helicobacter pylori (H. pylori) infection and inflammation of gastric mucosa. *Scand J Gastroenterol* 2004; **39**: 1054-1060 [PMID: 15545161 DOI: 10.1080/00365520410009645]

59 **Hojo M**, Nagahara A, Kudo T, Takeda T, Ikuse T, Matsumoto K, Ueda K, Ueyama H, Asaoka D, Shimizu T. Endoscopic findings of Helicobacter pylori gastritis in children and young adults based on the Kyoto classification of gastritis and age-associated changes. *JGH Open* 2021; **5**: 1197-1202 [PMID: 34622008 DOI: 10.1002/jgh3.12652]

60 **Toyoshima O**, Yoshida S, Nishizawa T, Toyoshima A, Sakitani K, Matsuno T, Yamada T, Matsuo T, Nakagawa H, Koike K. Enlarged folds on endoscopic gastritis as a predictor for submucosal invasion of gastric cancers. *World J Gastrointest Endosc* 2021; **13**: 426-436 [PMID: 34630892 DOI: 10.4253/wjge.v13.i9.426]

61 **Yasunaga Y**, Shinomura Y, Kanayama S, Higashimoto Y, Yabu M, Miyazaki Y, Kondo S, Murayama Y, Nishibayashi H, Kitamura S, Matsuzawa Y. Increased production of interleukin 1 beta and hepatocyte growth factor may contribute to foveolar hyperplasia in enlarged fold gastritis. *Gut* 1996; **39**: 787-794 [PMID: 9038658 DOI: 10.1136/gut.39.6.787]

62 **Yasunaga Y**, Shinomura Y, Kanayama S, Higashimoto Y, Yabu M, Miyazaki Y, Murayama Y, Nishibayashi H, Kitamura S, Matsuzawa Y. Mucosal interleukin-1 beta production and acid secretion in enlarged fold gastritis. *Aliment Pharmacol Ther* 1997; **11**: 801-809 [PMID: 9305492 DOI: 10.1046/j.1365-2036.1997.00200.x]

63 **Murayama Y**, Miyagawa J, Shinomura Y, Kanayama S, Yasunaga Y, Nishibayashi H, Yamamori K, Higashimoto Y, Matsuzawa Y. Morphological and functional restoration of parietal cells in helicobacter pylori associated enlarged fold gastritis after eradication. *Gut* 1999; **45**: 653-661 [PMID: 10517899 DOI: 10.1136/gut.45.5.653]

64 **Ohyama I**, Ohmiya N, Niwa Y, Shirai K, Taguchi A, Itoh A, Hirooka Y, Wakai K, Hamajima N, Mori N, Goto H. The association between tumour necrosis factor-alpha gene polymorphism and the susceptibility to rugal hyperplastic gastritis and gastric carcinoma. *Eur J Gastroenterol Hepatol* 2004; **16**: 693-700 [PMID: 15201584 DOI: 10.1097/01.meg.0000108315.52416.bf]

65 **Yamamoto E**, Toyota M, Suzuki H, Kondo Y, Sanomura T, Murayama Y, Ohe-Toyota M, Maruyama R, Nojima M, Ashida M, Fujii K, Sasaki

Y, Hayashi N, Mori M, Imai K, Tokino T, Shinomura Y. LINE-1 hypomethylation is associated with increased CpG island methylation in Helicobacter pylori-related enlarged-fold gastritis. *Cancer Epidemiol Biomarkers Prev* 2008; **17**: 2555-2564 [PMID: 18842996 DOI: 10.1158/1055-9965.EPI-08-0112]

66 **Tahara T**, Tahara S, Horiguchi N, Kato T, Shinkai Y, Okubo M, Terada T, Yoshida D, Funasaka K, Nagasaka M, Nakagawa Y, Kurahashi H, Shibata T, Tsukamoto T, Ohmiya N. Prostate Stem Cell Antigen Gene Polymorphism Is Associated with H. pylori-related Promoter DNA Methylation in Nonneoplastic Gastric Epithelium. *Cancer Prev Res (Phila)* 2019; **12**: 579-584 [PMID: 31213476 DOI: 10.1158/1940-6207.CAPR-19-0035]

67 **el-Zimaity HM**, al-Assi MT, Genta RM, Graham DY. Confirmation of successful therapy of Helicobacter pylori infection: number and site of biopsies or a rapid urease test. *Am J Gastroenterol* 1995; **90**: 1962-1964 [PMID: 7485000]

68 **Satoh K**, Kimura K, Taniguchi Y, Kihira K, Takimoto T, Saifuku K, Kawata H, Tokumaru K, Kojima T, Seki M, Ido K, Fujioka T. Biopsy sites suitable for the diagnosis of Helicobacter pylori infection and the assessment of the extent of atrophic gastritis. *Am J Gastroenterol* 1998; **93**: 569-573 [PMID: 9576449 DOI: 10.1111/j.1572-0241.1998.166_b.x]

69 **El-Zimaity HM**, Graham DY. Evaluation of gastric mucosal biopsy site and number for identification of Helicobacter pylori or intestinal metaplasia: role of the Sydney System. *Hum Pathol* 1999; **30**: 72-77 [PMID: 9923930 DOI: 10.1016/s0046-8177(99)90303-9]

70 **Basso D**, Plebani M, Kusters JG. Pathogenesis of Helicobacter pylori infection. *Helicobacter* 2010; **15** Suppl 1: 14-20 [PMID: 21054648 DOI: 10.1111/j.1523-5378.2010.00781.x]

71 **Talebi Bezmin Abadi A**. Helicobacter pylori: Emergence of a Superbug. *Front Med (Lausanne)* 2014; **1**: 34 [PMID: 25593908 DOI: 10.3389/fmed.2014.00034]

72 **Raju D**, Hussey S, Ang M, Terebiznik MR, Sibony M, Galindo-Mata E, Gupta V, Blanke SR, Delgado A, Romero-Gallo J, Ramjeet MS, Mascarenhas H, Peek RM, Correa P, Streutker C, Hold G, Kunstmann E, Yoshimori T, Silverberg MS, Girardin SE, Philpott DJ, El Omar E, Jones NL. Vacuolating cytotoxin and variants in Atg16L1 that disrupt autophagy promote Helicobacter pylori infection in humans. *Gastroenterology* 2012; **142**: 1160-1171 [PMID: 22333951 DOI: 10.1053/j.gastro.2012.01.043]

73 **de Brito BB**, da Silva FAF, Soares AS, Pereira VA, Santos MLC, Sampaio MM, Neves PHM, de Melo FF. Pathogenesis and clinical management of Helicobacter pylori gastric infection. *World J Gastroenterol* 2019; **25**: 5578-5589 [PMID: 31602159 DOI: 10.3748/wjg.v25.i37.5578]

74 **Shah SC**, Piazuelo MB, Kuipers EJ, Li D. AGA Clinical Practice Update on the Diagnosis and Management of Atrophic Gastritis: Expert Review. *Gastroenterology* 2021; **161**: 1325-1332.e7 [PMID: 34454714 DOI: 10.1053/j.gastro.2021.06.078]

75 **Burkitt MD**, Duckworth CA, Williams JM, Pritchard DM. Helicobacter pylori-induced gastric pathology: insights from in vivo and ex vivo models. *Dis Model Mech* 2017; **10**: 89-104 [PMID: 28151409 DOI: 10.1242/dmm.027649]

76 **Watari J**, Chen N, Amenta PS, Fukui H, Oshima T, Tomita T, Miwa H, Lim KJ, Das KM. Helicobacter pylori associated chronic gastritis, clinical syndromes, precancerous lesions, and pathogenesis of gastric cancer development. *World J Gastroenterol* 2014; **20**: 5461-5473 [PMID: 24833876 DOI: 10.3748/wjg.v20.i18.5461]

77 **Genta RM**. Review article: Gastric atrophy and atrophic gastritis--nebulous concepts in search of a definition. *Aliment Pharmacol Ther* 1998; **12** Suppl 1: 17-23 [PMID: 9701001 DOI: 10.1111/j.1365-2036.1998.00003.x]

78 **Freire de Melo F**, Rocha GA, Rocha AM, Teixeira KN, Pedroso SH, Pereira Junior JB, Fonseca de Castro LP, Cabral MM, Carvalho SD, Bittencourt PF, de Oliveira CA, Queiroz DM. Th1 immune response to H. pylori infection varies according to the age of the patients and influences the gastric inflammatory patterns. *Int J Med Microbiol* 2014; **304**: 300-306 [PMID: 24373859 DOI: 10.1016/j.ijmm.2013.11.001]

79 **Cai Q**, Shi P, Yuan Y, Peng J, Ou X, Zhou W, Li J, Su T, Lin L, Cai S, He Y, Xu J. Inflammation-Associated Senescence Promotes Helicobacter pylori-Induced Atrophic Gastritis. *Cell Mol Gastroenterol Hepatol* 2021; **11**: 857-880 [PMID: 33161156 DOI: 10.1016/j.jcmgh.2020.10.015]

80 **Kaminishi M**, Yamaguchi H, Nomura S, Oohara T, Sakita T. Endoscopic classification of chronic gastritis based on a pilot study by the Research Society for Gastritis. *Digest Endosc* 2002; **14**: 138-151 [DOI: 10.1046/j.1443-1661.2002.00199.x]

81 **Kimura K**, Takemoto T. An Endoscopic Recognition of the Atrophic Border and its Significance in Chronic Gastritis. *Endoscopy* 1969; **1**: 87-97 [DOI: 10.1055/s-0028-1098086]

82 **Goldenring JR**, Mills JC. Cellular Plasticity, Reprogramming, and Regeneration: Metaplasia in the Stomach and Beyond. *Gastroenterology* 2022; **162**: 415-430 [PMID: 34728185 DOI: 10.1053/j.gastro.2021.10.036]

83 **Petersen CP**, Mills JC, Goldenring JR. Murine Models of Gastric Corpus Preneoplasia. *Cell Mol Gastroenterol Hepatol* 2017; **3**: 11-26 [PMID: 28174755 DOI: 10.1016/j.jcmgh.2016.11.001]

84 **Weis VG**, Sousa JF, LaFleur BJ, Nam KT, Weis JA, Finke PE, Ameen NA, Fox JG, Goldenring JR. Heterogeneity in mouse spasmolytic polypeptide-expressing metaplasia lineages identifies markers of metaplastic progression. *Gut* 2013; **62**: 1270-1279 [PMID: 22773549 DOI: 10.1136/gutjnl-2012-302401]

85 **Correa P**, Piazuelo MB, Wilson KT. Pathology of gastric intestinal metaplasia: clinical implications. *Am J Gastroenterol* 2010; **105**: 493-498 [PMID: 20203636 DOI: 10.1038/ajg.2009.728]

86 **Baracchini P**, Fulcheri E, Lapertosa G. Patterns of intestinal metaplasia in gastric biopsies. A comparison of different histochemical classifications. *Histochem J* 1991; **23**: 1-9 [PMID: 1938465 DOI: 10.1007/BF01886501]

87 **Wei N**, Mulmi Shrestha S, Shi RH. Markers of gastric intestinal metaplasia under digital chromoendoscopy: systematic review and meta-analysis. *Eur J Gastroenterol Hepatol* 2021; **33**: 470-478 [PMID: 32675780 DOI: 10.1097/MEG.0000000000001834]

88 **Uedo N**, Ishihara R, Iishi H, Yamamoto S, Yamada T, Imanaka K, Takeuchi Y, Higashino K, Ishiguro S, Tatsuta M. A new method of diagnosing gastric intestinal metaplasia: narrow-band imaging with magnifying endoscopy. *Endoscopy* 2006; **38**: 819-824 [PMID: 17001572 DOI: 10.1055/s-2006-944632]

89 **Kanemitsu T**, Yao K, Nagahama T, Imamura K, Fujiwara S, Ueki T, Chuman K, Tanabe H, Atsuko O, Iwashita A, Shimokawa T, Uchita K, Kanesaka T. Extending magnifying NBI diagnosis of intestinal metaplasia in the stomach: the white opaque substance marker. *Endoscopy* 2017; **49**: 529-535 [PMID: 28395383 DOI: 10.1055/s-0043-103409]

90 **Pimentel-Nunes P**, Libânio D, Lage J, Abrantes D, Coimbra M, Esposito G, Hormozdi D, Pepper M, Drasovean S, White JR, Dobru D, Buxbaum J, Ragunath K, Annibale B, Dinis-Ribeiro M. A multicenter prospective study of the real-time use of narrow-band imaging in the diagnosis of premalignant gastric conditions and lesions. *Endoscopy* 2016; **48**: 723-730 [PMID: 27280384 DOI: 10.1055/s-0042-108435]

91 **Isomoto H**, Mizuta Y, Inoue K, Matsuo T, Hayakawa T, Miyazaki M, Onita K, Takeshima F, Murase K, Shimokawa I, Kohno S. A close relationship between Helicobacter pylori infection and gastric xanthoma. *Scand J Gastroenterol* 1999; **34**: 346-352 [PMID: 10365893 DOI: 10.1080/003655299750026344]

92 **Köksal AŞ**, Suna N, Kalkan İH, Eminler AT, Sakaoğulları ŞZ, Turhan N, Saygılı F, Kuzu UB, Öztaş E, Parlak E. Is Gastric Xanthelasma an Alarming Endoscopic Marker for Advanced Atrophic Gastritis and Intestinal Metaplasia? *Dig Dis Sci* 2016; **61**: 2949-2955 [PMID: 27250981 DOI: 10.1007/s10620-016-4210-6]

93 **Sekikawa A**, Fukui H, Maruo T, Tsumura T, Kanesaka T, Okabe Y, Osaki Y. Gastric xanthelasma may be a warning sign for the presence of early gastric cancer. *J Gastroenterol Hepatol* 2014; **29**: 951-956 [PMID: 24372908 DOI: 10.1111/jgh.12512]

94 **Moumin FA**, Mohamed AA, Osman AA, Cai J. Gastric Xanthoma Associated with Gastric Cancer Development: An Updated Review. *Can J Gastroenterol Hepatol* 2020; **2020**: 3578927 [PMID: 32149048 DOI: 10.1155/2020/3578927]

95 **Moodley Y**, Brunelli A, Ghirotto S, Klyubin A, Maady AS, Tyne W, Muñoz-Ramirez ZY, Zhou Z, Manica A, Linz B, Achtman M. Helicobacter pylori's historical journey through Siberia and the Americas. *Proc Natl Acad Sci U S A* 2021; **118** [PMID: 34161258 DOI: 10.1073/pnas.2015523118]

96 **Geis G**, Leying H, Suerbaum S, Mai U, Opferkuch W. Ultrastructure and chemical analysis of Campylobacter pylori flagella. *J Clin Microbiol* 1989; **27**: 436-441 [PMID: 2715319 DOI: 10.1128/jcm.27.3.436-441.1989]

97 **Geis G**, Suerbaum S, Forsthoff B, Leying H, Opferkuch W. Ultrastructure and biochemical studies of the flagellar sheath of Helicobacter pylori. *J Med Microbiol* 1993; **38**: 371-377 [PMID: 8487294 DOI: 10.1099/00222615-38-5-371]

98 **Sycuro LK**, Wyckoff TJ, Biboy J, Born P, Pincus Z, Vollmer W, Salama NR. Multiple peptidoglycan modification networks modulate Helicobacter pylori's cell shape, motility, and colonization potential. *PLoS Pathog* 2012; **8**: e1002603 [PMID: 22457625 DOI: 10.1371/journal.ppat.1002603]

99 **Sycuro LK**, Pincus Z, Gutierrez KD, Biboy J, Stern CA, Vollmer W, Salama NR. Peptidoglycan crosslinking relaxation promotes Helicobacter pylori's helical shape and stomach colonization. *Cell* 2010; **141**: 822-833 [PMID: 20510929 DOI: 10.1016/j.cell.2010.03.046]

100 **Abedrabbo S**, Castellon J, Collins KD, Johnson KS, Ottemann KM. Cooperation of two distinct coupling proteins creates chemosensory network connections. *Proc Natl Acad Sci U S A* 2017; **114**: 2970-2975 [PMID: 28242706 DOI: 10.1073/pnas.1618227114]

101 **Jiménez-Pearson MA**, Delany I, Scarlato V, Beier D. Phosphate flow in the chemotactic response system of Helicobacter pylori. *Microbiology (Reading)* 2005; **151**: 3299-3311 [PMID: 16207913 DOI: 10.1099/mic.0.28217-0]

102 **Aihara E**, Closson C, Matthis AL, Schumacher MA, Engevik AC, Zavros Y, Ottemann KM, Montrose MH. Motility and chemotaxis mediate the preferential colonization of gastric injury sites by Helicobacter pylori. *PLoS Pathog* 2014; **10**: e1004275 [PMID: 25033386 DOI: 10.1371/journal.ppat.1004275]

103 **Perez-Perez GI**. Accurate diagnosis of Helicobacter pylori. Culture, including transport. *Gastroenterol Clin North Am* 2000; **29**: 879-884 [PMID: 11190072 DOI: 10.1016/s0889-8553(05)70155-2]

104 **El-Zimaity HM**, Ota H, Graham DY, Akamatsu T, Katsuyama T. Patterns of gastric atrophy in intestinal type gastric carcinoma. *Cancer* 2002; **94**: 1428-1436 [PMID: 11920498 DOI: 10.1002/cncr.10375]

105 **Hamlet A**, Thoreson AC, Nilsson O, Svennerholm AM, Olbe L. Duodenal Helicobacter pylori infection differs in cagA genotype between asymptomatic subjects and patients with duodenal ulcers. *Gastroenterology* 1999; **116**: 259-268 [PMID: 9922305 DOI: 10.1016/s0016-5085(99)70121-6]

106 **Cui R**, Zhou L, Yan X, Jin Z, Zhang H. Clinicopathological features of duodenal bulb biopsies and their relationship with upper gastrointestinal diseases. *Ann Diagn Pathol* 2019; **40**: 40-44 [PMID: 30921623 DOI: 10.1016/j.anndiagpath.2019.02.006]

107 **Carrick J**, Lee A, Hazell S, Ralston M, Daskalopoulos G. Campylobacter pylori, duodenal ulcer, and gastric metaplasia: possible role of functional heterotopic tissue in ulcerogenesis. *Gut* 1989; **30**: 790-797 [PMID: 2753403 DOI: 10.1136/gut.30.6.790]

108 **Kawaguchi M**, Saito T. Incidence of Gastric Metaplasia and Helicobacter pylori Infection in Duodenal Bulb - With Specific Reference to Patients With Duodenal Ulcers. *Diagn Ther Endosc* 1999; **6**: 17-23 [PMID: 18493520 DOI: 10.1155/DTE.6.17]

109 **Li XB**, Ge ZZ, Chen XY, Liu WZ. Duodenal gastric metaplasia and Helicobacter pylori infection in patients with diffuse nodular duodenitis. *Braz J Med Biol Res* 2007; **40**: 897-902 [PMID: 17653441 DOI: 10.1590/s0100-879x2006005000117]

110 **Gisbert JP**, Blanco M, Cruzado AI, Pajares JM. Helicobacter pylori infection, gastric metaplasia in the duodenum and the relationship with ulcer recurrence. *Eur J Gastroenterol Hepatol* 2000; **12**: 1295-1298 [PMID: 11192318 DOI: 10.1097/00042737-200012120-00006]

111 **Liu KC**, Wright NA. The migration pathway of epithelial cells on human duodenal villi: the origin and fate of 'gastric metaplastic' cells in duodenal mucosa. *Epithelial Cell Biol* 1992; **1**: 53-58 [PMID: 1307939]

112 **Shaoul R**, Marcon P, Okada Y, Cutz E, Forstner G. The pathogenesis of duodenal gastric metaplasia: the role of local goblet cell transformation. *Gut* 2000; **46**: 632-638 [PMID: 10764705 DOI: 10.1136/gut.46.5.632]

113 **Voutilainen M**, Juhola M, Färkkilä M, Sipponen P. Gastric metaplasia and chronic inflammation at the duodenal bulb mucosa. *Dig Liver Dis* 2003; **35**: 94-98 [PMID: 12747627 DOI: 10.1016/s1590-8658(03)00003-3]

114 **Futami H**, Takashima M, Furuta T, Hanai H, Kaneko E. Relationship between Helicobacter pylori infection and gastric metaplasia in the duodenal bulb in the pathogenesis of duodenal ulcer. *J Gastroenterol Hepatol* 1999; **14**: 114-119 [PMID: 10029290 DOI: 10.1046/j.1440-1746.1999.01824.x]

115 **Veijola L**, Sankila A, Rautelin H, Kosunen TU, Sipponen P, Hyvärinen H, Tilvis R, Sarna S, Arkkila PE, Seppälä K. Clinical significance of widespread gastric metaplasia in the duodenal bulb. *J Clin Gastroenterol* 2006; **40**: 510-514 [PMID: 16825933 DOI: 10.1097/00004836-200607000-00009]

116 **Seo JH**, Do HJ, Park CH, Woo HO, Youn HS, Ko GH, Baik SC, Lee WK, Cho MJ, Rhee KH, Lee JH. Helicobacter pylori infection and duodenal gastric metaplasia in healthy young adults. *Korean J Gastroenterol* 2013; **61**: 191-195 [PMID: 23624732 DOI: 10.4166/kjg.2013.61.4.191]

117 **Harris AW**, Gummett PA, Walker MM, Misiewicz JJ, Baron JH. Relation between gastric acid output, Helicobacter pylori, and gastric metaplasia in the duodenal bulb. *Gut* 1996; **39**: 513-520 [PMID: 8944558 DOI: 10.1136/gut.39.4.513]

118 **Nishizawa T**, Sakitani K, Suzuki H, Yoshida S, Kataoka Y, Nakai Y, Ebinuma H, Kanai T, Toyoshima O, Koike K. Clinical features of cardiac nodularity-like appearance induced by Helicobacter pylori infection. *World J Gastroenterol* 2020; **26**: 5354-5361 [PMID: 32994693 DOI: 10.3748/wjg.v26.i35.5354]

119 **Nishikawa I**, Kato J, Terasoma S, Matsutani H, Tamaki H, Tamaki T, Kuwashima F, Nakata H, Tomeki T, Matsunaka H, Ibata Y, Yamashita Y, Maekita T, Higashi K, Ichinose M. Nodular gastritis in association with gastric cancer development before and after Helicobacter pylori eradication. *JGH Open* 2018; **2**: 80-86 [PMID: 30483568 DOI: 10.1002/jgh3.12049]

120 **Shiotani A**, Kamada T, Kumamoto M, Nakae Y, Nakamura Y, Kakudo K, Haruma K. Nodular gastritis in Japanese young adults: endoscopic and histological observations. *J Gastroenterol* 2007; **42**: 610-615 [PMID: 17701123 DOI: 10.1007/s00535-007-2073-5]

World Journal of Gastroenterology

Submit a Manuscript: https://www.f6publishing.com

World J Gastroenterol 2023 August 14; 29(30): 4628-4641

DOI: 10.3748/wjg.v29.i30.4628

ISSN 1007-9327 (print) ISSN 2219-2840 (online)

MINIREVIEWS

Systemic treatments for resectable carcinoma of the esophagus

Wattana Leowattana, Pathomthep Leowattana, Tawithep Leowattana

Specialty type: Gastroenterology and hepatology

Provenance and peer review: Invited article; Externally peer reviewed.

Peer-review model: Single blind

Peer-review report's scientific quality classification

Grade A (Excellent): A
Grade B (Very good): 0
Grade C (Good): C, C
Grade D (Fair): 0
Grade E (Poor): 0

P-Reviewer: Ogino S, United States; Tan X, China; Wang LH, China

Received: May 10, 2023
Peer-review started: May 10, 2023
First decision: July 9, 2023
Revised: July 18, 2023
Accepted: July 28, 2023
Article in press: July 28, 2023
Published online: August 14, 2023

Wattana Leowattana, Pathomthep Leowattana, Department of Clinical Tropical Medicine, Faculty of Tropical Medicine, Mahidol University, Rachatawee 10400, Bangkok, Thailand

Tawithep Leowattana, Department of Medicine, Faculty of Medicine, Srinakarinwirot University, Wattana 10110, Bangkok, Thailand

Corresponding author: Wattana Leowattana, BMed, MD, MSc, PhD, Professor, Department of Clinical Tropical Medicine, Faculty of Tropical Medicine, Mahidol University, 420/6 Rajavithi road, Rachatawee 10400, Bangkok, Thailand. wattana.leo@mahidol.ac.th

Abstract

One of the most prevalent malignancies in the world is esophageal cancer (EC). The 5-year survival rate of EC remains pitiful despite treatment advancements. Neoadjuvant chemoradiotherapy in conjunction with esophagectomy is the standard of care for patients with resectable disease. The pathological complete response rate, however, is not acceptable. A distant metastasis or a locoregional recurrence will occur in about half of the patients. To increase the clinical effectiveness of therapy, it is consequently vital to investigate cutting-edge and potent therapeutic modalities. The approach to the management of resectable EC using immunotherapy has been considerably altered by immune checkpoint inhibitors. Systemic immunotherapy has recently been shown to have the potential to increase the survival of patients with resectable EC, according to growing clinical data. A combination of chemotherapy, radiation, and immunotherapy may have a synergistic antitumor impact because, according to mounting evidence, these treatments can stimulate the immune system *via* a number of different pathways. In light of this, it makes sense to consider the value of neoadjuvant immunotherapy for patients with surgically treatable EC. In this review, we clarify the rationale for neoadjuvant immunotherapy in resectable EC patients, recap the clinical outcomes of these approaches, go through the upcoming and ongoing investigations, and emphasize the difficulties and unmet research requirements.

Key Words: Systemic treatment; Resectable carcinoma of the esophagus; Personalized medicine; Biomarkers; Chemotherapy; Chemoradiotherapy; Immunotherapy; Immune checkpoint inhibitors

©The Author(s) 2023. Published by Baishideng Publishing Group Inc. All rights reserved.

Core Tip: Despite improvements in neoadjuvant and adjuvant treatment approaches in recent years, the average life expectancy of patients with resectable esophageal cancer (EC) still falls below 5 years. Immunotherapy has been effectively used as a first-line therapy for many oncological diseases at advanced stages for over ten years. Immunotherapy drugs are also making great progress in resectable situations, while it is still debatable whether this treatment should be limited to a certain patient subgroup based on biomarker selection. In order to treat resectable EC, immunotherapy, in particular immune checkpoint inhibitors, has made significant strides. This review also provides a brief overview of potential ongoing clinical studies.

Citation: Leowattana W, Leowattana P, Leowattana T. Systemic treatments for resectable carcinoma of the esophagus. *World J Gastroenterol* 2023; 29(30): 4628-4641
URL: https://www.wjgnet.com/1007-9327/full/v29/i30/4628.htm
DOI: https://dx.doi.org/10.3748/wjg.v29.i30.4628

INTRODUCTION

With over 544000 expected deaths from esophageal cancer (EC) in 2020, EC is the sixth most common cancer-related cause of death globally. In East Asia, esophageal squamous cell carcinoma (ESCC) covers up around 90% of cases of EC, in contrast to Western nations[1-3]. Surgery continues to be the therapy of choice for early-stage EC. Unfortunately, the majority of EC patients are stage 4 or advanced stage at the time of diagnosis, and only surgery has a modest impact, hence a 5-year survival rate is only 25%. Systemic treatment, as opposed to surgery alone, may increase survival for resectable locally advanced EC. As a result, preoperative systemic treatment combined with surgery has become the norm for treating EC patients. Despite this, approximately half of these patients experience local recurrence or distant metastases following surgery[4-6]. To enhance survival, it is therefore vital to investigate innovative and effective therapies. Immune checkpoint inhibitors (ICIs) have recently made substantial advancements in a range of malignancies, including EC, with several trials demonstrating longer overall survival (OS), a higher objective response rate (ORR), and a decreased frequency of grade 3-5 adverse events (AEs) as second-line therapy. According to the most recent findings, treating resectable EC patients as first-line therapy with programmed death 1 (PD-1) inhibitors combined with chemotherapy resulted in considerably longer progression-free survival (PFS) and OS than treatment with only chemotherapy. These findings imply that ICIs have a bright future in EC management. ICI systemic treatment is now being extensively researched for EC patients and has been tested in a number of malignancies[7-10]. The rationale for ICI neoadjuvant treatment in EC, the published findings, the upcoming and ongoing studies, the unanswered questions, and the suggestions for more research will all be included in this review.

ROLE OF DIET AND MICROBIOTA IN EC

Some of the traditional risk factors for EC seem to be linked to changes in the esophagus' natural microbiome. In ESCC patients, drinking alcohol has been connected to changes in the microbiota's diversity. In animal studies, high-fat diets have been related to esophageal dysplasia and changes in the microbiome. Gram-negative organisms, which are present in lesions that are precursors to EC, were shown to be more prevalent in those who consumed less fiber. Changes in the esophagus bacterial population have been linked to smoking and medications like proton pump inhibitors and antibiotics. Firmicutes, Proteobacteria, Bacteriodetes, Actinobacteria, and Fusobacteria make up the majority of the microbiota in a healthy esophagus. In comparison, reduced microbial diversity, which appears to start in the precursor stages of EC, is a characteristic of malignancy of the esophagus. The EC microbiome is distinguished at the taxonomic level by a switch from Gram-positive to Gram-negative bacteria. The genera *Fusobacterium*, *Streptococcus*, *Veilonella*, and *Prevotella* are those that are most often enriched in EC. Although particular changes in the EC microbiome can be detected, a consistent microbiota profile linked with EC has not yet been discovered. The varied technical processes, such as the sampling strategy, the types of samples examined, and the analytic approach used to profile the microbiome, as well as the relatively small number of people participated in each experiment, may be to blame for this discrepancy. Future research should take method standardization into account. To study and integrate the impacts of various exposures, including those of nutrition, with the microbiome and the changes that occur during the carcinogenesis process, multidisciplinary research efforts will be necessary. This is especially true in studies of esophageal carcinogenesis associated with the microbiome. Large, well-characterized prospective cohort studies would be beneficial for dissecting these complicated connections, and they would undoubtedly aid in the development of creative preventive and treatment plans that would lessen the incidence of EC[11].

SYSTEMIC TREATMENT OPTIONS FOR RESECTABLE EC

Squamous cell carcinoma and adenocarcinoma, the two principal histological forms of EC, have very different epidemi-

ologies. To some extent, the therapy choices for these two categories differ. The two main therapeutic options for EC are local and systemic therapies. The tumor's histological type, location, extension, and size can all contribute to guiding therapy selections. Endoscopic and surgical resection are the primary treatments for locally advanced EC. Lymphatic node metastases arise early in EC due to the extensive lymphatic drainage in the esophagus submucosa, and the cancer is frequently detected at an advanced stage[12]. For resectable EC, the main systemic treatment options include neoadjuvant chemotherapy (NCT), neoadjuvant chemoradiotherapy (NCRT), and perioperative chemotherapy (PCT). According to the most recent National Comprehensive Cancer Network guidelines for esophageal and esophagogastric junction cancers, the optimal treatment options for both localized squamous cell carcinoma (SCC) and actinic cheilitis (AC) staged as Tis-T2 (low-risk lesions: < 3 cm, well-differentiated) without lymph node metastases include esophagectomy and endoscopic treatments. Patients with unresectable EC should get definitive chemoradiation. Current clinical research focuses mostly on locally progressed EC between the preferable single surgery and the recommended final chemoradiation. The systemic therapeutic approaches listed encompass NCT, NCRT, and PCT indicating a range between the two histological groups. As an adjuvant therapy, immunotherapy is employed[13].

The most prevalent subtype of EC in the world is ESCC, which manifests in the naturally occurring esophageal epithelium. An estimated 456000 people were diagnosed with EC in 2012, of whom 398000 had ESCC. Around 80% of ESCC cases worldwide were found in Central and Southeast Asia. More than half of all cases globally originated in China alone[14]. For 366 patients with locally advanced resectable esophageal or esophagogastric junctional cancer, NCRT that included carboplatin, paclitaxel, and concurrent 41.4 Gy radiotherapy was compared to surgery alone (178 for NCRT and surgery *vs.* 188 for surgery alone). A minimum projected follow-up term of 10 years was guaranteed by the follow-up period, which ended on December 31, 2018. In the first year, patients visited the outpatient clinic once every three months. In the second year, they visited once every six months, and so on until the fifth year, when they visited once a year. After 5 years of follow-up, patients with symptoms could visit the outpatient clinic. Participants in the chemoradiotherapy-surgery group survived more than those in the surgery arm, with 10-year OS rates of 38% and 25%, respectively. The respective 10-year OS rates in the chemoradiotherapy-surgery and surgery groups for patients with SCC were 46% and 23%, respectively, and 36% and 26% for patients with AC. Participants in the chemoradiotherapy-surgical group died from EC at a lower rate than those in the surgery arm, with 10-year absolute risks of 47% and 64%, respectively. Other causes of death were comparable in the chemoradiotherapy-surgery and surgery arms, with 10-year absolute risks of 15% and 11%, respectively. They concluded that the OS advantage of preoperative NCRT for patients with locally advanced resectable esophageal or junctional carcinoma, according to the ChemoRadiotherapy for Oesophageal cancer followed by Surgery Study (CROSS) study, lasts at least ten years[15].

NEOCRTEC 5010, a phase 3 randomized, open-label, multicenter, clinical trial, supported the findings of ESCC patients from the CROSS study. The NCRT group outperformed the surgery-only group in terms of R0 resection rate (98.4% *vs.* 91.2%), median OS (100.1 mo *vs.* 66.5 mo), and disease-free survival (DFS, 100.1 mos vs. 41.7 mos). According to the long-term efficacy of the NEOCRTEC 5010 research, the OS advantage in patients with locally advanced resectable ESCC who received the NCRT regimen was maintained for at least 10 years[16]. The CROSS trial also discovered that NCRT decreased solitary distant relapse (27% *vs.* 28%) but did not lessen isolated distant relapse (8% *vs.* 18%) or synchronous locoregional and distant relapse (13% *vs.* 22%). Relapse following NCRT is thus a critical obstacle to overcome[15].

Esophageal adenocarcinoma (EAC), also known as gastroesophageal adenocarcinoma or esophagogastric junction cancer, usually develops in the lower third of the esophagus. Obesity is its main risk factor since it mostly affects people with a history of gastroesophageal reflux disease[14]. About two-thirds of the histological categories of EC in high-income nations are AC. It is currently the most common histological type in seven high-income countries, including Canada, Denmark, Norway, Australia, New Zealand, Ireland, and the United Kingdom[17]. The CROSS-study's findings similarly positioned NCRT as the therapy of choice for resectable EAC, although superior NCRT effectiveness was shown in ESCC. As a result, depending on specific circumstances, PCT and NCT are different tactics. In order to successfully treat resectable EAC, PCT is crucial. The landmark-like phase 3 Medical Research Council Adjuvant Gastric Infusion Chemotherapy Study (MAGIC) initially showed the survival advantage of PCT in AC. This study revealed that patients with non-metastatic AC who had PCT with epirubicin, cisplatin, and fluorouracil (FU) had better PFS and OS. The MAGIC trial had more treatment-related AEs (TRAEs) than the CROSS study did[15,18]. The FU plus Leucovorin, Oxaliplatin, and Docetaxel triplet FU plus Leucovorin, Oxaliplatin, and Docetaxel (FLOT) regimen was used in a later, important phase 2/3 trial, the FLOT4 trial, which demonstrated superiority in R0 resection rate (85% *vs.* 78%) and median OS (50 mo *vs.* 35 mo). In recent score-matched research, the therapeutic effects of NCRT and PCT were contrasted. The findings demonstrated no discernible differences in tumor response or survival rates between these two common regimens. After PCT, there were more TRAEs (42/97 *vs.* 30/97)[19]. Another effective therapy for resectable EAC is NCT. Preoperative FU and cisplatin (FC) showed a survival benefit over surgery alone in the Medical Research Council OEO2 study[20,21]. The survival benefit remained at a median follow-up of 6 years [hazard ratio (HR), 0.84; 95% confidence interval (CI), 0.72-0.98; $P = 0.03$], while the cisplatin group had a better OS at 2 years (HR, 0.79; 95% CI, 0.67- 0.93; $P = 0.004$). Another sizable experiment, nevertheless, was unable to show the same result[22]. Triplet chemotherapy (epirubicin, cisplatin, and capecitabine) did not improve OS in the OE05 study. Additionally, it was connected to greater toxicity than FC[23]. NCT is therefore hardly employed.

A few noteworthy clinical studies on neoadjuvant therapy for resectable EC have recently been conducted. As a preoperative treatment for locally advanced ESCC, the NExT study seeks to demonstrate that docetaxel, cisplatin plus 5-FU (DCF), and radiotherapy with cisplatin plus 5-FU are superior than FC in terms of OS. The superior OS and manageable toxicity of DCF indicate a new standard therapeutic strategy for ESCC[24]. In 2021, Wang *et al*[25] conducted a prospective, multicenter, open-label, randomized clinical study on 264 patients with locally advanced ESCC to assess the efficacy and safety of NCRT *vs.* NCT followed by minimally invasive esophagectomy (MIE). The postoperative

morbidity rates of 264 patients, 47.4% in the NCRT group and 42.6% in the NCT group, did not significantly vary between the two groups. Based on the Clavien-Dindo classification, the degree of complications was distributed similarly across the two groups. For the NCRT group and the NCT group, the 90-day perioperative mortality rate was 3.5% and 2.8%, respectively. Patients in the NCRT group, however, showed higher rates of negative lymph nodes (66.1% *vs.* 46.2%) and pathologic complete responses (35.7% *vs.* 3.8%). They came to the conclusion that NCRT followed by MIE was safer and produced better histopathologic results than NCT followed by MIE for the treatment of locally advanced ESCC. According to a recent publication by Tang *et al*[26], among patients with cT3-4aN0-1M0 ESCC, NCRT followed by MIE was not significantly related to a better OS than NCT. The findings highlight the ongoing question of the ideal neoadjuvant therapeutic plan for locally progressing bulky ESCC. In the Neo-AEGIS study, 377 European patients were assigned at random to receive PCT, or CROSS. In the 3-year OS, the first OS analysis did not reveal any statistically significant differences (HR, 1.02; 95% CI, 0.74-1.42). However, the results must be taken seriously because the majority of the evaluable perioperative patients did not get the current standard of care FLOT (epirubicin, cisplatin and FU/epirubicin, cisplatin and capecitabine/epirubicin, oxaliplatin and FU/epirubicin, oxaliplatin and capecitabine prior to 2018, FLOT option 2019-2020, only 15% of chemotherapy arm patients received FLOT)[27].

MOLECULAR MECHANISMS OF ICIS FOR EC TREATMENT

Utilizing one's own immune system to find and eliminate tumor cells is the goal of immunotherapy. Understanding the anti-tumor response and the strategies a malignancy may use to modify or inhibit the immune response has seen significant breakthroughs. This has made it possible for a new field of medicine to flourish, one that has shown considerable promise in treating conditions like EC that previously had a low survival rate. Our knowledge of the tumor microenvironment (TME) is one of the essential components for the creation of novel therapies. The TME is a complicated environment where a variety of immune and stromal cell subtypes interact to either promote or prevent tumor growth [28,29]. A crucial component of the immune response against tumors is the effector T cell. To maintain the immune system's equilibrium, negative regulators are produced on the surface of T cells during the activation process. Immune checkpoints are what they are known as. T cell activation, function, proliferation, and survival may be diminished when these immune checkpoints and their ligands are triggered during T cell receptor (TCR) signaling, which promotes tumor immune evasion. When compared to other solid tumor forms, EC is distinguished by having a significant amount of tumor-infiltrating T cells and monocytes/macrophages. The bulk of the tumor-infiltrating T cells are worn-out cluster of differentiation (CD) 8+ T cells and regulatory T cells (Tregs). Tregs, tumor-associated macrophages (TAMs), myeloid-derived suppressor cells, and cancer-associated fibroblasts all contribute to the immunosuppressive TME of EC through immune checkpoint-related mechanisms. The CD8+ T cells in the EC TME display high quantities of immunological checkpoint molecules such the lymphocyte activation gene-3 (LAG-3), cytotoxic T lymphocyte antigen-4 (CTLA-4), programmed cell death PD-1, and programmed cell death-ligand (PD-L) 1[30,31].

PD-1 and PD-L1

Activated cytotoxic T cells and their primary ligands are the best examples of how PD-1 functions. Cancer cells and antigen-presenting cells (APCs) both have PD-L1 and PD-L2 molecules on their surfaces. T cell immunological fatigue is promoted by intracellular phosphorylation events that occur as a result of PD-1 engagement with its ligands, either through processes that depend on or are independent of TCR-CD28. The phosphoinositide 3-kinase route and the mitogen-activated protein kinase pathway are the two principals downstream signaling pathways involved in the TCR-CD28-dependent process. T cell depression that is not caused by TCR-CD28 is also caused by increased expression of the B-cell activating transcriptional factor[32-34]. CD8+ T cells in EC TME consistently exhibit significant levels of PD-1 expression. The findings of several clinical studies revealed that the objective response to immunotherapy was highly correlated with the high level of PD-L1 expression in EC tumor cells[35-37]. As a result, one of the suggested biomarkers for identifying EC patients who may benefit from ICIs is the degree of PD-L1 expression. Other than tumoral or healthy epithelial cells, TAMs play a significant role in the expression of PD-1 ligands in the EC TME. M2 polarization increases PD-L2 expression in TAMs and leads to immune evasion *via* the PD-1 signaling cascade regulated by the C-C motif chemokine ligand 2-C-C motif chemokine receptor 2 axis[38]. Additionally, TAMs showed PD-1 expression, which may increase PD-L1 expression in tumor cells. Increased CD8+ T cell abundance was seen in the responders in the clinical trials of PD-1 blockade therapy for EC, suggesting that the PD-1 inhibitors were successful in saving the worn-out T cells. To increase anti-tumor activity, these T cells settle on the tumor and fill the EC TME. Additionally, the decrease in the fraction of M2-type TAMs coincided with the rise in CD8+ T cell density, demonstrating that other innate immune cells in the EC TME were highly significant to the effectiveness of PD-1 blockade therapy for EC patients. In addition to the PD-1/PD-L1 pathway, interactions between PD-L1, CD80, and PD-L2-repulsive guidance molecule family member B are necessary for ICIs that target PD-L1 to be efficacious[39,40] (Figure 1).

LAG-3

The precise signaling pathways downstream of LAG-3 are unclear, although it is known that LAG-3 has a distinct signaling route that is not shared by other immunological checkpoints. It is not unexpected that LAG-3 binds to major histocompatibility complex (MHC)-II given that their structures are comparable. However, the affinity of the interaction between LAG-3 and MHC-II is substantially stronger. LAG-3 affects CD8+ T cell activity as well, pointing to the possibility of new LAG-3 ligands. LAG-3 is one of the hallmarks of worn-out CD8+ T cells and is considerably overexpressed in ESCC. Positive LAG-3 expression strongly predicted lower recurrence-free survival and OS in ESCC patients

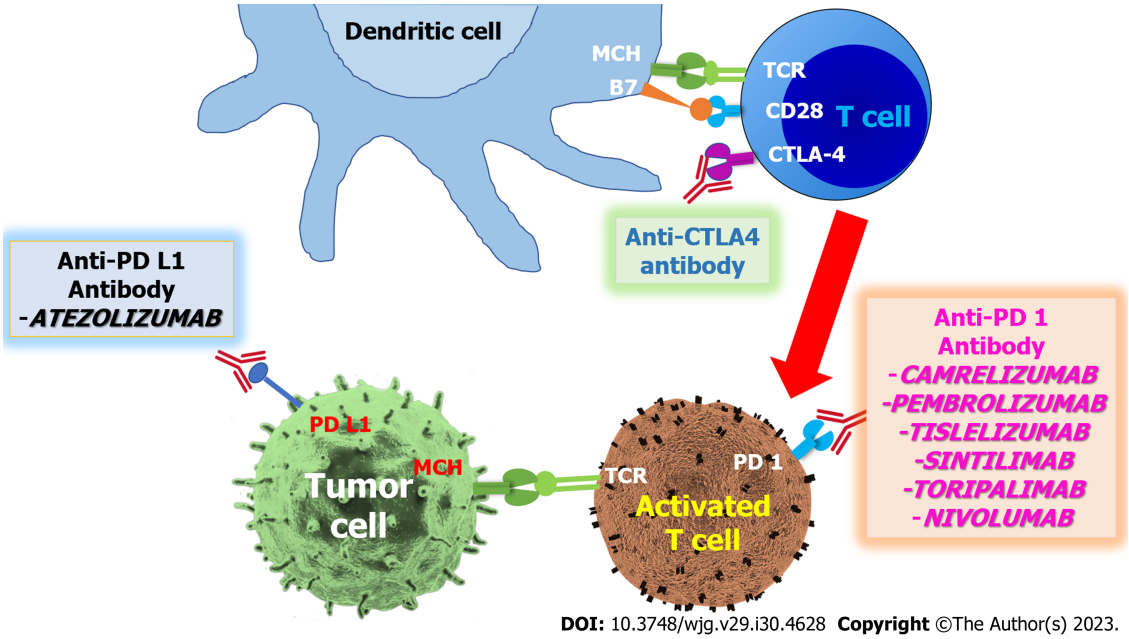


Figure 1 The mechanisms of action of immune checkpoint inhibitors in resectable esophageal cancer immunotherapy. CD28: Cluster of differentiation 28; CTLA-4: Cytotoxic T lymphocyte antigen 4; MHC: Major histocompatibility complex; PD-1: Programmed cell death protein 1; PD-L1: Programmed death-ligand 1; TCR: T cell receptor.

and was significantly correlated with CTLA-4 expression. Strong correlations were found between high levels of CD8+ tumor-infiltrating lymphocytes (TILs) in the EAC TME and high levels of LAG-3 expression. Research on individuals with unresectable EAC found connections between the LAG-3 gene and their response to the combination treatment of nivolumab and ipilimumab. Numerous LAG-3+ CD8+ T cells in the EAC TME are thought to be remnants of a robust anti-tumor immune response that was suppressed by PD-L1 and LAG-3-related mechanisms. The EAC patients who exhibit this TME trait are a good fit for ICIs. As a result, LAG-3 is a novel target for ICI's treatment of EC and is generating a lot of attention[41-44].

CTLA-4

The engagement of the TCR by peptides from the MHC and crucial positive co-stimulatory signals produced by the interaction of CD80 (B7.1) or CD86 (B7.2) on the surface of APCs and CD28 on the surface of T cells are both necessary for T cell activation. This process is damaged by CTLA-4. Intracellularly stored CTLA-4 is transferred onto the surface of T cells during the initial stages of T cell activation, competing with CD80 with a higher affinity and diminishing the signal. *Via* phosphorylation reactions, CTLA-4 attenuates signals downstream of the TCR intrinsically after interacting with CD80. The primary professional APCs whose immunological capabilities are compromised in individuals with EC, along with a reduction in CD80 and CD86 expression, are dendritic cells. The high level of CTLA-4 expression on the surface of Tregs in the EC TME significantly contributes to immunosuppression. Further weakening the anti-tumor immune response, elevated expression of CTLA-4 is found in ESCC tumor cells on both an mRNA and protein level, in addition to effector T cells and Tregs in EC patients. Previous research has shown that ESCC patients with high tumor cell CTLA-4 expression had a poor prognosis, patients with ESCC who exhibited little tumor cell CTLA-4 expression, however, had a longer OS. Additionally, it's been proven that CD80 guards against metaplasia in inflammatory esophageal carcinogenesis, which is linked to EAC. In light of these findings, scientists developed ICIs that specifically target CTLA-4 to enhance EC's anti-tumor immunity. We still don't know how CTLA-4 blocking treatment impacts EC TME and effector T cells[45-47].

ICIS FOR RESECTABLE EC TREATMENT

Neoadjuvant immunotherapy is the main subgroup of the clinical studies on ICI treatment for resectable EC. Camrelizumab, Pembrolizumab, Tremelimumab, Tislelizumab, Sintilimab, Atezolizumab, Nivolumab, Durvalumab, Relatlimab, Toripalimab, and IMC-001 were among the ICIs employed in these research. According to the CROSS-study's protocol, neoadjuvant immunotherapies are frequently used in conjunction with NCRT or NCT.

Camrelizumab

The National Medical Products Administration has authorized the PD-1 inhibitor Camrelizumab as a first-line therapy for unresectable ESCC. The neoadjuvant use of Camrelizumab for resectable locally advanced ESCC has been the focus of a significant number of clinical trials, making it one of the most popular ICIs being studied for its therapeutic efficacy. The

majority of these trials have proven the beneficial effects of combining Camrelizumab with NCT and NCRT. In research done by Wu *et al*[48], 38 patients with resectable ESCC were examined to determine the effectiveness and safety of NCT coupled with immunotherapy. Pembrolizumab (55.26%) and Camrelizumab (31.58%) were the two drugs most often taken by patients. The results of their analysis of 19 individuals revealed that 13 patients (68.42%) had a radiological partial response (PR) on computed tomography scans. 35 patients (92.11%) underwent R0 resection, and postoperative problems occurred in 10 individuals (26.32%). A substantial positive correlation between the pathological remission rate and the regression rate of the sum of lesion diameters was also found. Major pathologic response (MPR) rates were 42.11% in ESCC patients.

In a trial by Liu *et al*[49,50], the primary endpoint was used to assess the safety as well as the efficacy of Camrelizumab with NCT in 60 patients with locally advanced ESCC. Fifty-five (91.7%) of these patients successfully completed the whole two-cycle therapy. Fifty-one patients had surgery, and 50 (98.0%) of them had R0 resection. Twenty patients (39.2%) had pathological complete response (pCR) (ypT0N0), while five patients (9%; ypT0N+) had a full response to the main tumor but persistent illness in the lymph nodes alone. Leukocytopenia (86.7%) was the most prevalent of the 58 TRAEs that affected individuals (96.7%). One patient (1.7% of patients) experienced a grade 5 adverse event, while 34 patients (56.7%) experienced AEs of grade 3 or worse. They stated that chemotherapy and Camrelizumab had strong anticancer effects that had been validated and shown without any unanticipated safety effects. These results demonstrated the efficacy of Camrelizumab with chemotherapy as a neoadjuvant therapy for locally advanced ESCC. It is necessary to conduct a phase 3 randomized controlled study to further illustrate potential survival gains (Table 1).

Pembrolizumab

The United States Food and Drug Administration (FDA) has authorized the PD-1 inhibitor pembrolizumab as a first-line therapy for unresectable ESCC and EAC when combined with chemotherapy. Neoadjuvant immunotherapy has undergone clinical testing to treat both resectable ESCC and EAC. Preoperative Pembrolizumab with concurrent chemoradiotherapy for resectable locally advanced ESCC is being tested in the phase 1b, single-arm PALACE I trial, with safety as the main end measure. Of the 20 participants, 18 (90%) underwent surgery, and 19 (95%) received complete preoperative care. The patient had grade 3 lymphopenia and leukopenia, and she passed away while undergoing surgery, which is why the neoadjuvant therapy was not completed. The disease progression led to the discontinuation of surgery for one participant after full neoadjuvant therapy. All 20 patients experienced the development of TRAEs of any grade during the neoadjuvant therapy phase. The most frequent TRAEs were leukopenia (100%), lymphopenia (100%), anemia (80%), esophagitis (55%), alopecia (55%), and fatigue (55%), the majority of which were grade 1 or 2. With a pCR rate of 56% and a substantial pathological response of 89%, the R0 resection rate was 94%. All of the patients who received radical resection were free of disease recurrence at the median postoperative follow-up of 6.6 mo[51]. The PALACE II multicenter trial is still underway and has a larger sample size (143 participants), with pCR set as the major end measure[52]. Thirty-one eligible patients were included in a phase 1b/2 study to examine the effects of trimodal therapy with Pembrolizumab in the treatment of gastroesophageal junction (GEJ) adenocarcinoma. Twenty-eight individuals got R0 resection, and 29 of the 31 patients received all recommended doses of neoadjuvant Pembrolizumab. All safety criteria were satisfied. The primary efficacy goal was not attained [7/31 (22.6%)]. Individuals with high baseline expression of PD-L1 in the TME [combined positive score (CPS) > 10] had a substantially higher pCR rate than patients with low expression. Additionally, PFS and OS were longer for patients with high PD-L1 expression compared to propensity-score-matched patients. Extracellular vesicles (EV) were investigated to determine whether they may detect additional responders among trial participants with PD-L1 CPS < 10. A greater plasma level of PD-L1-expressing EVs was substantially linked with a higher pCR. They indicated that when Pembrolizumab was added to trimodal treatment, it did not achieve the intended pCR endpoint because of its satisfactory tolerability. Exploratory findings revealed that individuals who are most likely to achieve tumor response may be identified by having high levels of PD-L1 expression in the TME or on EVs[53].

Pembrolizumab in conjunction with chemotherapy and simple chemotherapy were compared for their effectiveness and safety in a trial by Huang *et al*[54], which involved 54 ESCC patients with stages II–IVa (23 in the combination group and 31 in the simple chemotherapy group). After two cycles of neoadjuvant therapy, major surgical intervention was given to all patients. They discovered that the combination group's pCR, ORR, and tumor regression 2 score were all considerably greater than those of the basic chemotherapy group (30.4% *vs.* 9.7% and 80.7% *vs.* 50.0%, respectively). Additionally, there was no statistically significant difference between the two groups' complete esophagectomy and R0/R1 resection rates. They concluded that pembrolizumab with chemotherapy demonstrated encouraging activity with a tolerable safety profile. Additionally, it might present a brand-new neoadjuvant treatment strategy for ESCC patients. In a single-arm study, Duan *et al*[55] evaluated the efficacy and safety of neoadjuvant pembrolizumab with chemotherapy in 18 patients with resectable ESCC. They found that postoperative pathology showed pCR in 6 cases (6/13, 46.2%) and MPR in 9 cases (9/13, 69.2%). Grade 3 or higher: Significant TRAEs occurred in 5 individuals (5/18, 27.8%). The amount of residual viable tumor (RVT) in pretreatment specimens was not substantially correlated with PD-L1 expression. While there was a weak association between postoperative forkhead box P3-positive+ T cells/CD4+ T cell ratios and RVT, there was a substantial correlation between changes in CD68+ macrophage counts between pre- and post-treatment specimens.

Tislelizumab

Another inhibitor of PD-1 is Tislelizumab. Following systemic therapy, ESCCs that cannot be removed, have relapsed, or have spread have been approved for consideration by the FDA. Tislelizumab was combined with NCT in the TD-NICE study, a phase 2, single-arm clinical study. The MPR served as the study's main outcome indicator. Of the 45 patients, 36 had surgery and received comprehensive neoadjuvant care. Eighty percent of R0 resections were successful, with 72% of pCR and 50% of MPR. Leukopenia (73%), anemia (51%), and thrombocytopenia (49%) were the most prevalent TRAEs.

Table 1 The immunotherapies for resectable esophageal cancer patients

Name	Ref.	Number of patients	Treatment regimens	Outcome	Conclusion
Camrelizumab	Wu *et al* [48], 2021	12	Cisplatin + paclitaxel + camrelizumab = 8; carboplatin + paclitaxel + camrelizumab = 4	MPR, 5/7 (71.43%)	Patients with ESCC had an MPR rate of 42.11%; The SLD regression rate has a certain guiding relevance for the impact of immunotherapy, and the adoption of the NACI regimen may not raise the likelihood of problems in neoadjuvant treatment and surgery
Camrelizumab	Liu *et al* [49], 2022	60	Carboplatin + paclitaxel + camrelizumab	Proceeded to surgery, 51/60 (85.00%); R0 resection, 50/51 (98.00%); pCR, 5/20 (39.20%)	Camrelizumab plus weekly chemotherapy as a promising neoadjuvant treatment for locally advanced ESCC, and further phase 3 randomized controlled trial is warranted
Camrelizumab	Liu *et al* [50], 2022	56	Cisplatin + paclitaxel + camrelizumab	Proceeded to surgery, 51/56 (77.40%); pCR, 18/56 (39.20%); MPR, 12/56 (21.43%)	Camrelizumab plus neoadjuvant chemotherapy in resectable ESCC demonstrates promising efficacy with acceptable toxicity, providing a feasible and effective option
Pembrolizumab	Li *et al* [51], 2021	20	Carboplatin + paclitaxel + pembrolizumab + radiotherapy	Proceeded to surgery, 18/20 (90.00%); pCR, 10/18 (55.60%)	PPCT was safe and did not delay surgery in resectable EC
Pembrolizumab	Zhu *et al* [53], 2022	31	Carboplatin + paclitaxel + pembrolizumab + radiotherapy	Proceeded to surgery, 28/29 (96.55%); pCR, 7/31 (22.58%)	Incorporating anti–PD-1 therapy into neoadjuvant chemoradiation and adjuvant treatment of GEJ adenocarcinoma may improve pCR and survival
Pembrolizumab	Huang *et al*[54], 2021	54	Nedaplatin + docetaxel + pembrolizumab = 23 *vs.* nedaplatin + docetaxel = 31	pCR 30.4%/9.7%; ORR 86.9%/95.7%	Pembrolizumab combined with chemotherapy showed promising activity with a manageable safety profile and it could offer a potential new neoadjuvant treatment approach for patients with ESCC
Pembrolizumab	Duan *et al*[55], 2022	18	Nedaplatin + paclitaxel + pembrolizumab = 13 or nedaplatin + docetaxel + pembrolizumab = 5	Proceeded to surgery, 13/18 (72.22%); MPR, 9/13 (69.20%); pCR, 6/13 (46.15%)	The combination of neoadjuvant immunotherapy and chemotherapy for ESCC is associated with a high pathological response and immunologic effects in the tumor microenvironment
Tislelizumab	Yan *et al* [56], 2022	45	Carboplatin + paclitaxel + tislelizumab	Proceeded to surgery, 36/45 (80.00%); MPR (69.20%); pCR (50.00%)	Tislelizumab plus chemotherapy as neoadjuvant therapy demonstrates promising antitumor activity for resectable ESCC with high rates of MPR, pCR, and R0 resection, as well as acceptable tolerability
Sintilimab	Chen *et al* [57], 2023	30	Cisplatin + S1 + paclitaxel + sintilimab	Proceeded to surgery, 30/30 (100.00%); MPR (50.00%); pCR (20.00%)	Neoadjuvant sintilimab plus platinum-based triplet chemotherapy appeared safe and feasible, did not delay surgery and induced a pCR rate of 20.0% in patients with potentially resectable ESCC
Atezolizumab	van den Ende *et al* [58], 2021	40	Carboplatin + Paclitaxel + Atezolizumab + Radiotherapy	Proceeded to surgery, 33/40 (82.50%); MPR (50.00%); pCR, 10/40 (25.00%)	The addition of atezolizumab to conventional nCRT for resectable EC was feasible without compromising surgical outcomes
Toripalimab	Xing *et al* [59], 2021	30	Cisplatin + paclitaxel + toripalimab D3 *vs.* cisplatin + paclitaxel + toripalimab D1	Proceeded to surgery, 11/15 *vs.* 13/15; pCR 4/15 *vs.* 1/15	The study showed that delaying toripalimab to day 3 in chemoimmunotherapy might achieve a higher pCR rate than that on the same day
Toripalimab	He *et al* [60], 2022	20	Carboplatin + paclitaxel + toripalimab	Proceeded to surgery, 16/20; R0 resection, 14/16; MPR, 7/16; pCR, 4/16	The combination of toripalimab plus paclitaxel and carboplatin is safe, feasible, and effective in locally advanced resectable ESCC
Toripalimab	Gao *et al* [61], 2022	20	Cisplatin + docetaxel + toripalimab	ORR, 14/20; MPR, 5/12; pCR, 2/12	Toripalimab combined with docetaxel and cisplatin as a novel neoadjuvant therapy was safe and effective in locally advanced ESCC
Toripalimab	Zhang *et al*[62], 2023	60	S1 + paclitaxel + toripalimab	R0 resection, 55/60; MPR, 27/60; pCR, 16/60	Neoadjuvant therapy with toripalimab, nab-paclitaxel and S1 was less toxic and showed promising antitumor activity in patients with resectable ESCC
Nivolumab	Kelly *et al* [63], 2021	794	Chemoradiotherapy+ nivolumab = 532 *vs.* chemoradiotherapy+ placebo = 262	DFS, 22.4/11.0 mo; distant recurrence, 29/39%; locoregional recurrence, 12/17%	Nivolumab adjuvant treatment significantly increased DFS compared to placebo in patients with resected esophagus or gastroesophageal junction cancer who had received neoadjuvant chemoradiotherapy

DFS: Disease-free survival; EC: Esophageal cancer; ESCC: Esophageal squamous cell carcinoma; GEJ: Gastroesophageal junction; MPR: Major pathological

response; NACI: Neoadjuvant chemotherapy combined with immunotherapy; nCRT: Neoadjuvant chemoradiotherapy; ORR: Objective response rate; pCR: Pathological complete response; PD-1: Programmed cell death protein 1; SLD: Sum of lesion diameter; PPCT: Preoperative pembrolizumab with concurrent chemoradiotherapy.

Nineteen (42.2%) of the 45 patients had TRAEs in grades 3 to 4. Seventy-eight percent of the 36 individuals had postoperative problems. There were no surgical delays or deaths brought on by the therapy. They discovered that Tislelizumab in combination with chemotherapy as neoadjuvant therapy shows encouraging anticancer effectiveness for resectable ESCC with high rates of MPR, pCR, and R0 resection, as well as moderate tolerability[56].

Sintilimab

Sintilimab, another PD-1 inhibitor, has been approved by the FDA for the treatment of certain subtypes of non-small cell lung cancer (NSCLC) and Hodgkin's lymphoma. The primary use of Sintilimab is as a neoadjuvant therapy for ESCC. In 30 patients with possibly resectable ESCC, Chen *et al*[57] performed a single-arm, phase 2, open-label study to evaluate the safety and surgical viability of intravenous Sintilimab preoperatively with triplet chemotherapy (cisplatin, liposomal paclitaxel, and S-1) for a total of two cycles every 3 wk. The MPR and pCR rates were discovered to be 50.0% and 20.0%, respectively. Patients were more likely to react if they had a greater TMB and more clonal mutations. Changes in the circulating tumor DNA high-releaser status and the v-erb-b2 avian erythroblastic leukemia viral oncogene homolog 2 are adversely linked with the response to neoadjuvant ICI. They discovered that neoadjuvant Sintilimab in conjunction with platinum-based triplet chemotherapy was safe and effective, did not delay surgery, and led to a 20.0% pCR rate in patients with ESCC who would be eligible for resection. A total of 36.7% (11/30) of patients experienced TRAEs of grades 3–4. Reduced neutrophil count (73.3%), anemia (76.7%), and reduced white cell count (76.7%) were the most common TRAEs. Hematological toxicities constituted all TRAEs. This confirmed that it was safe to use. To confirm the viability of the suggested approach, more investigation is needed.

Atezolizumab

A PD-L1 inhibitor called Atezolizumab has been given FDA approval for the treatment of melanoma, NSCLC, small cell lung cancer, and some types of urothelial cancer. In the phase 2 feasibility trial PD-L1 Targeting in Resectable EC (PERFECT), NCRT is coupled with Atezolizumab to treat resectable EAC. The major end measure of this trial was feasibility, which was determined as the percentage of Atezolizumab treatments that were completed. Thirty-four (85%) of the 40 patients finished the full course of atezolizumab treatment. Any missed cycles were brought on by autoimmune-related toxicity (n = 3), progression (n = 2), and death (n = 1). The R0 resection rate was 100% with 30% pCR. The PERFECT study had a median OS of 29.7 mo and a median PFS of 19.4 mo[58]. Fatigue (95%), mucositis (60%), nausea (53%), and anorexia (43%) were the most prevalent TRAEs. A grade 3–4 TRAE was encountered by 16 patients (40%). The three most prevalent symptoms were syncope (8%), nausea (8%), and anorexia (10%). The aforementioned TRAEs mostly took place during NCRT in conjunction with ICI. One patient who passed away from a pulmonary embolus had a grade 5 TRAE. Thirteen individuals (33%) had serious TRAEs that resulted in hospitalization or death.

Toripalimab

The FDA authorized Toripalimab, an anti-PD-1 monoclonal antibody, for the treatment of ESCC, nasopharyngeal carcinoma, mucosal melanoma, and sarcoma. In order to assess the efficacy of neoadjuvant chemoimmunotherapy (Toripalimab) in 30 patients with locally advanced ESCC, Xing *et al*[59] conducted an open-label, randomized phase 2 investigation. The patients were divided into two groups: The experimental group, which got chemotherapy on day 1 and Toripalimab on day 3, and the control group, which received chemotherapy and Toripalimab on day 1. The patients were then randomly allocated to either group. Paclitaxel and cisplatin were the components of the chemotherapy regimen. Four to six weeks following the second course of chemoimmunotherapy, surgery was undertaken. They reported that 13 participants in the control group and 11 participants in the experimental group had surgery. In each of these 24 cases, a R0 resection was done. Four patients (36%) in the experimental group and one patient (7%) in the control group both achieved pCR. Statistically non-significantly increased pCR rates were observed in the experimental group. One patient in the control group had a PD-L1 CPS of 10, and pCR was achieved. The other 13 patients all had PD-L1 CPSs of 1, and 11 of the 13 underwent surgery, with two of the 13 patients (in the experimental group) attaining pCR. After one round of chemoimmunotherapy, two patients experienced grade 3 adverse effects, and one patient withdrew out of the research due to immune-related enteritis that was grade 3. After surgery, a second patient passed away from a severe lung infection and elevated troponin. They concluded that postponing Toripalimab until day 3 of chemotherapy could result in a greater pCR rate than that on the same day.

In a study conducted by He *et al*[60], 20 patients with locally advanced resectable ESCC were examined to determine the effectiveness of Toripalimab with paclitaxel and carboplatin as neoadjuvant treatment and the possible prognostic biomarkers. For the 16 patients who underwent surgery without a related delay in treatment, the R0 resection rate was 87.5% (14/16). The pCR rate was 18.8% (3/16), and the MPR rate was 43.8% (7/16) among the 16 patients. Following neoadjuvant treatment, the fraction of M2-type TAMs reduced, and the number of CD8+ T cells rose in surgical tissues. Responders had greater baseline C-X-C motif chemokine 5 gene expression levels and lower baseline chemokine (C-C motif) ligand 19 and uromodulin-like 1 gene expression levels. They concluded that the treatment of locally progressed resectable ESCC with the combination of Toripalimab, paclitaxel, and carboplatin is dependable, doable, and effective, indicating its promise as a neoadjuvant therapy for ESCC. An open-label, non-randomized, single-arm, single-center

phase 2 study also looked at Toripalimab for usage as neoadjuvant treatment in conjunction with Docetaxel and Cisplatin in 20 patients with locally advanced ESCC. The ORR was reported to be 70% (14/20). McKeown's MIE was performed on twelve individuals. Sixteen percent (2/12) of initial tumors achieved pCR, while 41.7% (5/12) of primary tumors achieved MPR. The median time before surgery was 33.2 d, and no patients had surgery delayed as a result of AEs from the medication. The most typical 30-day postoperative consequence (3/12, 25%) was pneumonia. Only 1 patient experienced anastomotic leakage while they were in the hospital. No patients passed away as a result of medical care or surgery. They concluded that Toripalimab was a safe and effective new neoadjuvant treatment for locally progressed ESCC when coupled with Docetaxel and Cisplatin[61]. Toripalimab combined with nab-Paclitaxel and S-1 was evaluated in a phase 2 single-center, open-label, single-arm study in 60 ESCC patients. They discovered that 55 patients (98.21%) had successful R0 resections. In 27 patients (49.09%) with MPR, pCR was attained in 16 individuals (29.09%). There were 37 (61.67%), 21 (35.00%), and 2 (3.33%) patients with PR, stable illness, and progressing disease, respectively. Following therapy, the overall staging, Stooler dysphagia scores, and daily living ability were considerably reduced. Eleven patients (18.3%) had grade 3 AEs. Patients with PD-L1-high levels exhibited a considerably greater PR ratio than those with PD-L1-low levels. In patients who had a PR, the TMB and tumor neoantigen burden considerably decreased with treatment[62].

Nivolumab

The first immunotherapy to be recommended for resectable EC is adjuvant immunotherapy, which is appropriate for both ESCC and EAC with R0 resection following NCRT but staged as ypT-positive and/or N-positive. A PD-1 inhibitor known as Nivolumab is the ICI employed in this treatment plan. With a median follow-up of 24.4 mo, Kelly *et al*[63] conducted the worldwide, randomized, double-blind, placebo-controlled phase 3 study CheckMate 577 to assess Nivolumab as adjuvant treatment in 794 patients with esophageal or GEJ cancer. In contrast to the 262 patients who received a placebo, the authors found that the median DFS for the 532 individuals who received Nivolumab was 22.4 mo, as opposed to 11.0 mo for those who received the placebo (HR for disease recurrence or death, 0.69; 96.4% CI, 0.56 to 0.86; P = 0.001). In the Nivolumab group, 71 of 532 patients (13%), and 15 of 260 (6%) patients in the placebo group, encountered grade 3 or higher AEs. The trial regimen was discontinued in 9% of participants receiving Nivolumab and 3% of patients receiving a placebo owing to adverse drug or placebo-related events. They concluded that DFS was significantly longer in patients with resectable esophageal or GEJ cancer who had received NCRT who got Nivolumab adjuvant treatment than in those who received a placebo.

SUMMARY

Neoadjuvant ICIs are often used to treat ESCC patients, whereas perioperative ICIs are frequently used to treat EAC patients from the perspective of therapeutic models. This could be a result of NCRT having a better pathological outcome for ESCC than for EAC in earlier investigations[64]. A few clinical studies have moved into phase 3, and the majority are still in phase 2. It's important to be aware of phase 2 trial limitations, such as the limited sample size and lack of a control group. Trials investigating the use of ICIs in combination with NCRT, NCT, and PCT for resectable EC are still in their early phases in general. Credibility and generality are insufficient and need to be enhanced going forward. To get over these restrictions, multicenter or international phase 3 studies should be conducted. Very few studies have revealed the specifics of the response evaluation criteria and methodologies used in the various preoperative systemic therapy trials. The full metabolic response was the criterion used in the PALACE I investigation, which made use of the positron emission tomography-computed tomography scan. To help choose the best course of therapy, it is necessary to confirm how to more accurately gauge the reaction and specify the circumstances warranting surgery. TRAEs continue to endanger the safety of ICI therapy regimens, even if an acceptable rate of them has been recorded. All the research mentioned the above-mentioned TRAEs, and in certain situations, TRAE-related surgical delay or mortality happened. The safety of the ICIs is anticipated to drastically increase.

Immunotherapy for resectable EC patients primarily focuses on blocking the PD-1 and PD-L1 pathways, which have demonstrated impressive anti-tumor effects. But for some patients, ICIs treatment was ineffective, and in certain instances, medication resistance developed. PD-L1 expression in ESCC and microsatellite instability-high (MSI-H) or microsatellite instability-deficiency in mismatch repair are two indicators for successful ICIs treatment[65]. Unfortunately, PD-L1-positive ESCC did not significantly improve objective response to ICI treatment in a clinical investigation[66]. Furthermore, only 7% of EAC patients have MSI-H. Their predictive values are constrained. A critical issue that has to be solved is how to more effectively identify the EC patients who will benefit from PD-1 blocking treatment. A number of processes are involved in the PD-1/PD-L1 pathway's signaling process, such as chromosomal changes, mechanisms controlling molecule expression during and after transcription, and post-translational modification of molecules[67,68]. Scientists have identified various immune-related genes and chromosomal alterations unique to EC through the ongoing improvement of gene analysis techniques[69-71]. These are all possible biomarkers for EC patients who react to PD-1/PD-L1 blocking drugs. Furthermore, an immune-related long non-coding RNA signature of this pathway in ESCC was discovered, and it has the potential to be exploited as a stand-alone predictor of ESCC immunotherapy prognosis. PD-L1 expression inside the EC TME is now linked to immune infiltration frequency, which is what makes PD-1/PD-L1 blocking therapy beneficial. The frequencies of TILs, TAMs, CD8+ T cells, and Tregs are among the factors that are connected to clinical outcomes[72].

There aren't many active clinical studies of anti-CTLA-4 immunotherapy for resectable EC, in contrast to PD-1/PD-L1 blocking treatment. Severe TRAEs, the bulk of which were immune-related AEs (irAEs), limited the efficacy of CTLA-4 inhibiting therapy for a number of solid tumors. A deadly autoimmune illness is prevented by the intrinsic immune

checkpoint CTLA-4 on Tregs. Inhibiting CTLA-4 increases anti-cancer immunity but also upregulates auto-immune responses, leading to irAEs. For a safer and more effective immune checkpoint treatment, several scientists concluded that the CTLA-4 checkpoint should be preserved rather than blocked. Some people overcome this obstacle by creating anti-CTLA-4 antibodies that are specific to TMEs. There is an ongoing debate about whether CTLA-4-targeted immunotherapy should be permitted[73,74].

The immunosuppressive mechanism of LAG-3 is a recent area of study that has drawn a lot of interest. According to a recent study, MHC-II-independent fibrinogen-like protein 1 (FGL1) was a significant LAG-3 functional ligand. A poor prognosis and resistance to anti-PD-1 therapy are associated with high levels of FGL1 expression in the plasma of cancer patients, and it has been abundantly produced by human cancer cells[75,76]. The results of the clinical trial employing the Nivolumab and Relatlimab combination treatment for resectable EC may provide some insight into the riddle. Certainly, the positive results of immunotherapy for resectable EC in recent times give reason for optimism, but there are still many shortcomings to be overcome. The ICIs therapy for resectable EC will be ideal with a dependable effect and high safety in the next few days if these problems are promptly addressed.

CONCLUSION

Although systemic immunotherapy has produced encouraging preliminary findings in resectable EC in some clinical studies, and although preoperative immunotherapy may potentially be more beneficial than adjuvant therapy, more confirmation of the feasibility, safety, and effectiveness of neoadjuvant immunotherapy in sizable randomized clinical trials is still needed. Additionally, before neoadjuvant ICI techniques can be extensively used as the standard of treatment, a number of unsolved concerns must be overcome. To choose the right populations, it will be essential to identify predictive biomarkers, and the function of adjuvant treatment must be clearly understood. In order to assess any delayed toxicity and ascertain the long-term consequences, long-term follow-up is also required. Systemic immunotherapy will undoubtedly enter a new phase soon.

FOOTNOTES

Author contributions: Leowattana W wrote the paper; Leowattana T and Leowattana P collected the data.

Conflict-of-interest statement: The authors declare no conflicts of interest related to this article.

Open-Access: This article is an open-access article that was selected by an in-house editor and fully peer-reviewed by external reviewers. It is distributed in accordance with the Creative Commons Attribution NonCommercial (CC BY-NC 4.0) license, which permits others to distribute, remix, adapt, build upon this work non-commercially, and license their derivative works on different terms, provided the original work is properly cited and the use is non-commercial. See: https://creativecommons.org/Licenses/by-nc/4.0/

Country/Territory of origin: Thailand

ORCID number: Wattana Leowattana 0000-0003-4257-2480; Tawithep Leowattana 0000-0003-2316-3585.

S-Editor: Lin C
L-Editor: A
P-Editor: Cai YX

REFERENCES

1 **Sung H**, Ferlay J, Siegel RL, Laversanne M, Soerjomataram I, Jemal A, Bray F. Global Cancer Statistics 2020: GLOBOCAN Estimates of Incidence and Mortality Worldwide for 36 Cancers in 185 Countries. *CA Cancer J Clin* 2021; **71**: 209-249 [PMID: 33538338 DOI: 10.3322/caac.21660]

2 **Jiang Y**, Lin Y, Wen Y, Fu W, Wang R, He J, Zhang J, Wang Z, Ge F, Huo Z, Peng H, Wu X, Li S. Global trends in the burden of esophageal cancer, 1990-2019: results from the Global Burden of Disease Study 2019. *J Thorac Dis* 2023; **15**: 348-364 [PMID: 36910098 DOI: 10.21037/jtd-22-856]

3 **Huang J**, Koulaouzidis A, Marlicz W, Lok V, Chu C, Ngai CH, Zhang L, Chen P, Wang S, Yuan J, Lao XQ, Tse SLA, Xu W, Zheng ZJ, Xie SH, Wong MCS. Global Burden, Risk Factors, and Trends of Esophageal Cancer: An Analysis of Cancer Registries from 48 Countries. *Cancers (Basel)* 2021; **13** [PMID: 33466239 DOI: 10.3390/cancers13010141]

4 **Yang H**, Liu H, Chen Y, Zhu C, Fang W, Yu Z, Mao W, Xiang J, Han Y, Chen Z, Yang H, Wang J, Pang Q, Zheng X, Li T, Lordick F, D'Journo XB, Cerfolio RJ, Korst RJ, Novoa NM, Swanson SJ, Brunelli A, Ismail M, Fernando HC, Zhang X, Li Q, Wang G, Chen B, Mao T, Kong M, Guo X, Lin T, Liu M, Fu J; AME Thoracic Surgery Collaborative Group. Neoadjuvant Chemoradiotherapy Followed by Surgery Versus Surgery Alone for Locally Advanced Squamous Cell Carcinoma of the Esophagus (NEOCRTEC5010): A Phase III Multicenter, Randomized, Open-Label Clinical Trial. *J Clin Oncol* 2018; **36**: 2796-2803 [PMID: 30089078 DOI: 10.1200/JCO.2018.79.1483]

5 **Ajani JA**, D'Amico TA, Bentrem DJ, Chao J, Corvera C, Das P, Denlinger CS, Enzinger PC, Fanta P, Farjah F, Gerdes H, Gibson M, Glasgow RE, Hayman JA, Hochwald S, Hofstetter WL, Ilson DH, Jaroszewski D, Johung KL, Keswani RN, Kleinberg LR, Leong S, Ly QP,

Matkowskyj KA, McNamara M, Mulcahy MF, Paluri RK, Park H, Perry KA, Pimiento J, Poultsides GA, Roses R, Strong VE, Wiesner G, Willett CG, Wright CD, McMillian NR, Pluchino LA. Esophageal and Esophagogastric Junction Cancers, Version 2.2019, NCCN Clinical Practice Guidelines in Oncology. *J Natl Compr Canc Netw* 2019; **17**: 855-883 [PMID: 31319389 DOI: 10.6004/jnccn.2019.0033]

6 **Shapiro J**, van Lanschot JJB, Hulshof MCCM, van Hagen P, van Berge Henegouwen MI, Wijnhoven BPL, van Laarhoven HWM, Nieuwenhuijzen GAP, Hospers GAP, Bonenkamp JJ, Cuesta MA, Blaisse RJB, Busch ORC, Ten Kate FJW, Creemers GM, Punt CJA, Plukker JTM, Verheul HMW, Bilgen EJS, van Dekken H, van der Sangen MJC, Rozema T, Biermann K, Beukema JC, Piet AHM, van Rij CM, Reinders JG, Tilanus HW, Steyerberg EW, van der Gaast A; CROSS study group. Neoadjuvant chemoradiotherapy plus surgery versus surgery alone for oesophageal or junctional cancer (CROSS): long-term results of a randomised controlled trial. *Lancet Oncol* 2015; **16**: 1090-1098 [PMID: 26254683 DOI: 10.1016/S1470-2045(15)00040-6]

7 **Shen L**, Kato K, Kim SB, Ajani JA, Zhao K, He Z, Yu X, Shu Y, Luo Q, Wang J, Chen Z, Niu Z, Zhang L, Yi T, Sun JM, Chen J, Yu G, Lin CY, Hara H, Bi Q, Satoh T, Pazo-Cid R, Arkenau HT, Borg C, Lordick F, Li L, Ding N, Tao A, Shi J, Van Cutsem E; RATIONALE-302 Investigators. Tislelizumab Versus Chemotherapy as Second-Line Treatment for Advanced or Metastatic Esophageal Squamous Cell Carcinoma (RATIONALE-302): A Randomized Phase III Study. *J Clin Oncol* 2022; **40**: 3065-3076 [PMID: 35442766 DOI: 10.1200/JCO.21.01926]

8 **de Miguel M**, Calvo E. Clinical Challenges of Immune Checkpoint Inhibitors. *Cancer Cell* 2020; **38**: 326-333 [PMID: 32750319 DOI: 10.1016/j.ccell.2020.07.004]

9 **Kojima T**, Shah MA, Muro K, Francois E, Adenis A, Hsu CH, Doi T, Moriwaki T, Kim SB, Lee SH, Bennouna J, Kato K, Shen L, Enzinger P, Qin SK, Ferreira P, Chen J, Girotto G, de la Fouchardiere C, Senellart H, Al-Rajabi R, Lordick F, Wang R, Suryawanshi S, Bhagia P, Kang SP, Metges JP; KEYNOTE-181 Investigators. Randomized Phase III KEYNOTE-181 Study of Pembrolizumab Versus Chemotherapy in Advanced Esophageal Cancer. *J Clin Oncol* 2020; **38**: 4138-4148 [PMID: 33026938 DOI: 10.1200/JCO.20.01888]

10 **Luo H**, Lu J, Bai Y, Mao T, Wang J, Fan Q, Zhang Y, Zhao K, Chen Z, Gao S, Li J, Fu Z, Gu K, Liu Z, Wu L, Zhang X, Feng J, Niu Z, Ba Y, Zhang H, Liu Y, Zhang L, Min X, Huang J, Cheng Y, Wang D, Shen Y, Yang Q, Zou J, Xu RH; ESCORT-1st Investigators. Effect of Camrelizumab *vs* Placebo Added to Chemotherapy on Survival and Progression-Free Survival in Patients With Advanced or Metastatic Esophageal Squamous Cell Carcinoma: The ESCORT-1st Randomized Clinical Trial. *JAMA* 2021; **326**: 916-925 [PMID: 34519801 DOI: 10.1001/jama.2021.12836]

11 **Moreira C**, Figueiredo C, Ferreira RM. The Role of the Microbiota in Esophageal Cancer. *Cancers (Basel)* 2023; **15** [PMID: 37174041 DOI: 10.3390/cancers15092576]

12 **Tanaka T**, Ueno M, Iizuka T, Hoteya S, Haruta S, Udagawa H. Comparison of long-term outcomes between esophagectomy and chemoradiotherapy after endoscopic resection of submucosal esophageal squamous cell carcinoma. *Dis Esophagus* 2019; **32** [PMID: 30980070 DOI: 10.1093/dote/doz023]

13 **Ajani JA**, D'Amico TA, Bentrem DJ, Cooke D, Corvera C, Das P, Enzinger PC, Enzler T, Farjah F, Gerdes H, Gibson M, Grierson P, Hofstetter WL, Ilson DH, Jalal S, Keswani RN, Kim S, Kleinberg LR, Klempner S, Lacy J, Licciardi F, Ly QP, Matkowskyj KA, McNamara M, Miller A, Mukherjee S, Mulcahy MF, Outlaw D, Perry KA, Pimiento J, Poultsides GA, Reznik S, Roses RE, Strong VE, Su S, Wang HL, Wiesner G, Willett CG, Yakoub D, Yoon H, McMillian NR, Pluchino LA. Esophageal and Esophagogastric Junction Cancers, Version 2.2023, NCCN Clinical Practice Guidelines in Oncology. *J Natl Compr Canc Netw* 2023; **21**: 393-422 [PMID: 37015332 DOI: 10.6004/jnccn.2023.0019]

14 **Arnold M**, Soerjomataram I, Ferlay J, Forman D. Global incidence of oesophageal cancer by histological subtype in 2012. *Gut* 2015; **64**: 381-387 [PMID: 25320104 DOI: 10.1136/gutjnl-2014-308124]

15 **Eyck BM**, van Lanschot JJB, Hulshof MCCM, van der Wilk BJ, Shapiro J, van Hagen P, van Berge Henegouwen MI, Wijnhoven BPL, van Laarhoven HWM, Nieuwenhuijzen GAP, Hospers GAP, Bonenkamp JJ, Cuesta MA, Blaisse RJB, Busch OR, Creemers GM, Punt CJA, Plukker JTM, Verheul HMW, Spillenaar Bilgen EJ, van der Sangen MJC, Rozema T, Ten Kate FJW, Beukema JC, Piet AHM, van Rij CM, Reinders JG, Tilanus HW, Steyerberg EW, van der Gaast A; CROSS Study Group. Ten-Year Outcome of Neoadjuvant Chemoradiotherapy Plus Surgery for Esophageal Cancer: The Randomized Controlled CROSS Trial. *J Clin Oncol* 2021; **39**: 1995-2004 [PMID: 33891478 DOI: 10.1200/JCO.20.03614]

16 **Yang H**, Liu H, Chen Y, Zhu C, Fang W, Yu Z, Mao W, Xiang J, Han Y, Chen Z, Yang H, Wang J, Pang Q, Zheng X, Li T, Zhang X, Li Q, Wang G, Chen B, Mao T, Kong M, Guo X, Lin T, Liu M, Fu J. Long-term Efficacy of Neoadjuvant Chemoradiotherapy Plus Surgery for the Treatment of Locally Advanced Esophageal Squamous Cell Carcinoma: The NEOCRTEC5010 Randomized Clinical Trial. *JAMA Surg* 2021; **156**: 721-729 [PMID: 34160577 DOI: 10.1001/jamasurg.2021.2373]

17 **Morgan E**, Soerjomataram I, Gavin AT, Rutherford MJ, Gatenby P, Bardot A, Ferlay J, Bucher O, De P, Engholm G, Jackson C, Kozie S, Little A, Møller B, Shack L, Tervonen H, Thursfield V, Vernon S, Walsh PM, Woods RR, Finley C, Merrett N, O'Connell DL, Reynolds JV, Bray F, Arnold M. International trends in oesophageal cancer survival by histological subtype between 1995 and 2014. *Gut* 2021; **70**: 234-242 [PMID: 32554620 DOI: 10.1136/gutjnl-2020-321089]

18 **Cunningham D**, Allum WH, Stenning SP, Thompson JN, Van de Velde CJ, Nicolson M, Scarffe JH, Lofts FJ, Falk SJ, Iveson TJ, Smith DB, Langley RE, Verma M, Weeden S, Chua YJ, MAGIC Trial Participants. Perioperative chemotherapy versus surgery alone for resectable gastroesophageal cancer. *N Engl J Med* 2006; **355**: 11-20 [PMID: 16822992 DOI: 10.1056/NEJMoa055531]

19 **Al-Batran SE**, Homann N, Pauligk C, Goetze TO, Meiler J, Kasper S, Kopp HG, Mayer F, Haag GM, Luley K, Lindig U, Schmiegel W, Pohl M, Stoehlmacher J, Folprecht G, Probst S, Prasnikar N, Fischbach W, Mahlberg R, Trojan J, Koenigsmann M, Martens UM, Thuss-Patience P, Egger M, Block A, Heinemann V, Illerhaus G, Moehler M, Schenk M, Kullmann F, Behringer DM, Heike M, Pink D, Teschendorf C, Löhr C, Bernhard H, Schuch G, Rethwisch V, von Weikersthal LF, Hartmann JT, Kneba M, Daum S, Schulmann K, Weniger J, Belle S, Gaiser T, Oduncu FS, Güntner M, Hozaeel W, Reichart A, Jäger E, Kraus T, Mönig S, Bechstein WO, Schuler M, Schmalenberg H, Hofheinz RD; FLOT4-AIO Investigators. Perioperative chemotherapy with fluorouracil plus leucovorin, oxaliplatin, and docetaxel versus fluorouracil or capecitabine plus cisplatin and epirubicin for locally advanced, resectable gastric or gastro-oesophageal junction adenocarcinoma (FLOT4): a randomised, phase 2/3 trial. *Lancet* 2019; **393**: 1948-1957 [PMID: 30982686 DOI: 10.1016/S0140-6736(18)32557-1]

20 **Medical Research Council Oesophageal Cancer Working Group**. Surgical resection with or without preoperative chemotherapy in oesophageal cancer: a randomised controlled trial. *Lancet* 2002; **359**: 1727-1733 [PMID: 12049861 DOI: 10.1016/S0140-6736(02)08651-8]

21 **Allum WH**, Stenning SP, Bancewicz J, Clark PI, Langley RE. Long-term results of a randomized trial of surgery with or without preoperative chemotherapy in esophageal cancer. *J Clin Oncol* 2009; **27**: 5062-5067 [PMID: 19770374 DOI: 10.1200/JCO.2009.22.2083]

22 **Kelsen DP**, Winter KA, Gunderson LL, Mortimer J, Estes NC, Haller DG, Ajani JA, Kocha W, Minsky BD, Roth JA, Willett CG; Radiation Therapy Oncology Group; USA Intergroup. Long-term results of RTOG trial 8911 (USA Intergroup 113): a random assignment trial

comparison of chemotherapy followed by surgery compared with surgery alone for esophageal cancer. *J Clin Oncol* 2007; **25**: 3719-3725 [PMID: 17704421 DOI: 10.1200/JCO.2006.10.4760]

23 **Alderson D**, Cunningham D, Nankivell M, Blazeby JM, Griffin SM, Crellin A, Grabsch HI, Langer R, Pritchard S, Okines A, Krysztopik R, Coxon F, Thompson J, Falk S, Robb C, Stenning S, Langley RE. Neoadjuvant cisplatin and fluorouracil versus epirubicin, cisplatin, and capecitabine followed by resection in patients with oesophageal adenocarcinoma (UK MRC OE05): an open-label, randomised phase 3 trial. *Lancet Oncol* 2017; **18**: 1249-1260 [PMID: 28784312 DOI: 10.1016/S1470-2045(17)30447-3]

24 **Nakamura K**, Kato K, Igaki H, Ito Y, Mizusawa J, Ando N, Udagawa H, Tsubosa Y, Daiko H, Hironaka S, Fukuda H, Kitagawa Y; Japan Esophageal Oncology Group/Japan Clinical Oncology Group. Three-arm phase III trial comparing cisplatin plus 5-FU (CF) versus docetaxel, cisplatin plus 5-FU (DCF) versus radiotherapy with CF (CF-RT) as preoperative therapy for locally advanced esophageal cancer (JCOG1109, NExT study). *Jpn J Clin Oncol* 2013; **43**: 752-755 [PMID: 23625063 DOI: 10.1093/jjco/hyt061]

25 **Wang H**, Tang H, Fang Y, Tan L, Yin J, Shen Y, Zeng Z, Zhu J, Hou Y, Du M, Jiao J, Jiang H, Gong L, Li Z, Liu J, Xie D, Li W, Lian C, Zhao Q, Chen C, Zheng B, Liao Y, Li K, Li H, Wu H, Dai L, Chen KN. Morbidity and Mortality of Patients Who Underwent Minimally Invasive Esophagectomy After Neoadjuvant Chemoradiotherapy *vs* Neoadjuvant Chemotherapy for Locally Advanced Esophageal Squamous Cell Carcinoma: A Randomized Clinical Trial. *JAMA Surg* 2021; **156**: 444-451 [PMID: 33729467 DOI: 10.1001/jamasurg.2021.0133]

26 **Tang H**, Wang H, Fang Y, Zhu JY, Yin J, Shen YX, Zeng ZC, Jiang DX, Hou YY, Du M, Lian CH, Zhao Q, Jiang HJ, Gong L, Li ZG, Liu J, Xie DY, Li WF, Chen C, Zheng B, Chen KN, Dai L, Liao YD, Li K, Li HC, Zhao NQ, Tan LJ. Neoadjuvant chemoradiotherapy versus neoadjuvant chemotherapy followed by minimally invasive esophagectomy for locally advanced esophageal squamous cell carcinoma: a prospective multicenter randomized clinical trial. *Ann Oncol* 2023; **34**: 163-172 [PMID: 36400384 DOI: 10.1016/j.annonc.2022.10.508]

27 **Reynolds JV**, Preston SR, O'Neill B, Lowery MA, Baeksgaard L, Crosby T, Cunningham M, Cuffe S, Griffiths GO, Roy R, Falk S, Hanna G, Bartlett FR, Parker I, Alvarez-Iglesias A, Nilsson M, Piessen G, Risum S, Ravi N, McDermott RS. Neo-AEGIS (Neoadjuvant trial in Adenocarcinoma of the Esophagus and Esophago-Gastric Junction International Study): Preliminary results of phase III RCT of CROSS versus perioperative chemotherapy (Modified MAGIC or FLOT protocol). (NCT01726452). *J Clin Oncol* 2021; **39** [DOI: 10.1200/JCO.2021.39.15_suppl.4004]

28 **Murciano-Goroff YR**, Warner AB, Wolchok JD. The future of cancer immunotherapy: microenvironment-targeting combinations. *Cell Res* 2020; **30**: 507-519 [PMID: 32467593 DOI: 10.1038/s41422-020-0337-2]

29 **Davern M**, Donlon NE, Power R, Hayes C, King R, Dunne MR, Reynolds JV. The tumour immune microenvironment in oesophageal cancer. *Br J Cancer* 2021; **125**: 479-494 [PMID: 33903730 DOI: 10.1038/s41416-021-01331-y]

30 **Zheng Y**, Chen Z, Han Y, Han L, Zou X, Zhou B, Hu R, Hao J, Bai S, Xiao H, Li WV, Bueker A, Ma Y, Xie G, Yang J, Chen S, Li H, Cao J, Shen L. Immune suppressive landscape in the human esophageal squamous cell carcinoma microenvironment. *Nat Commun* 2020; **11**: 6268 [PMID: 33293583 DOI: 10.1038/s41467-020-20019-0]

31 **Cui K**, Hu S, Mei X, Cheng M. Innate Immune Cells in the Esophageal Tumor Microenvironment. *Front Immunol* 2021; **12**: 654731 [PMID: 33995371 DOI: 10.3389/fimmu.2021.654731]

32 **Dermani FK**, Samadi P, Rahmani G, Kohlan AK, Najafi R. PD-1/PD-L1 immune checkpoint: Potential target for cancer therapy. *J Cell Physiol* 2019; **234**: 1313-1325 [PMID: 30191996 DOI: 10.1002/jcp.27172]

33 **Jiang Y**, Chen M, Nie H, Yuan Y. PD-1 and PD-L1 in cancer immunotherapy: clinical implications and future considerations. *Hum Vaccin Immunother* 2019; **15**: 1111-1122 [PMID: 30888929 DOI: 10.1080/21645515.2019.1571892]

34 **Yi M**, Zheng X, Niu M, Zhu S, Ge H, Wu K. Combination strategies with PD-1/PD-L1 blockade: current advances and future directions. *Mol Cancer* 2022; **21**: 28 [PMID: 35062949 DOI: 10.1186/s12943-021-01489-2]

35 **Schneider BJ**, Chang AC. ASO Perspectives: Adjuvant Nivolumab in Resected Esophageal or Gastroesophageal Junction Cancer: Never Stop Questioning. *Ann Surg Oncol* 2022; **29**: 2735-2738 [PMID: 35182309 DOI: 10.1245/s10434-021-11276-4]

36 **Zhang W**, Yan C, Gao X, Li X, Cao F, Zhao G, Zhao J, Er P, Zhang T, Chen X, Wang Y, Jiang Y, Wang Q, Zhang B, Qian D, Wang J, Zhou D, Ren X, Yu Z, Zhao L, Yuan Z, Wang P, Pang Q. Safety and Feasibility of Radiotherapy Plus Camrelizumab for Locally Advanced Esophageal Squamous Cell Carcinoma. *Oncologist* 2021; **26**: e1110-e1124 [PMID: 33893689 DOI: 10.1002/onco.13797]

37 **Huang J**, Xu J, Chen Y, Zhuang W, Zhang Y, Chen Z, Chen J, Zhang H, Niu Z, Fan Q, Lin L, Gu K, Liu Y, Ba Y, Miao Z, Jiang X, Zeng M, Fu Z, Gan L, Wang J, Zhan X, Liu T, Li Z, Shen L, Shu Y, Zhang T, Yang Q, Zou J; ESCORT Study Group. Camrelizumab versus investigator's choice of chemotherapy as second-line therapy for advanced or metastatic oesophageal squamous cell carcinoma (ESCORT): a multicentre, randomised, open-label, phase 3 study. *Lancet Oncol* 2020; **21**: 832-842 [PMID: 32416073 DOI: 10.1016/S1470-2045(20)30110-8]

38 **Pan C**, Wang Y, Liu Q, Hu Y, Fu J, Xie X, Zhang S, Xi M, Wen J. Phenotypic profiling and prognostic significance of immune infiltrates in esophageal squamous cell carcinoma. *Oncoimmunology* 2021; **10**: 1883890 [PMID: 33628625 DOI: 10.1080/2162402X.2021.1883890]

39 **Yang H**, Zhang Q, Xu M, Wang L, Chen X, Feng Y, Li Y, Zhang X, Cui W, Jia X. CCL2-CCR2 axis recruits tumor associated macrophages to induce immune evasion through PD-1 signaling in esophageal carcinogenesis. *Mol Cancer* 2020; **19**: 41 [PMID: 32103760 DOI: 10.1186/s12943-020-01165-x]

40 **Bagchi S**, Yuan R, Engleman EG. Immune Checkpoint Inhibitors for the Treatment of Cancer: Clinical Impact and Mechanisms of Response and Resistance. *Annu Rev Pathol* 2021; **16**: 223-249 [PMID: 33197221 DOI: 10.1146/annurev-pathol-042020-042741]

41 **Andrews LP**, Marciscano AE, Drake CG, Vignali DA. LAG3 (CD223) as a cancer immunotherapy target. *Immunol Rev* 2017; **276**: 80-96 [PMID: 28258692 DOI: 10.1111/imr.12519]

42 **Chen Z**, Zhao M, Liang J, Hu Z, Huang Y, Li M, Pang Y, Lu T, Sui Q, Zhan C, Lin M, Guo W, Wang Q, Tan L. Dissecting the single-cell transcriptome network underlying esophagus non-malignant tissues and esophageal squamous cell carcinoma. *EBioMedicine* 2021; **69**: 103459 [PMID: 34192657 DOI: 10.1016/j.ebiom.2021.103459]

43 **Gebauer F**, Krämer M, Bruns C, Schlößer HA, Thelen M, Lohneis P, Schröder W, Zander T, Alakus H, Buettner R, Loeser H, Quaas A. Lymphocyte activation gene-3 (LAG3) mRNA and protein expression on tumour infiltrating lymphocytes (TILs) in oesophageal adenocarcinoma. *J Cancer Res Clin Oncol* 2020; **146**: 2319-2327 [PMID: 32592066 DOI: 10.1007/s00432-020-03295-7]

44 **Wang W**, Chen D, Zhao Y, Zhao T, Wen J, Mao Y, Chen C, Sang Y, Zhang Y, Chen Y. Characterization of LAG-3, CTLA-4, and CD8(+) TIL density and their joint influence on the prognosis of patients with esophageal squamous cell carcinoma. *Ann Transl Med* 2019; **7**: 776 [PMID: 32042792 DOI: 10.21037/atm.2019.11.38]

45 **Zhang CY**, Zhang J, Ma YF, Zhe H, Zhao R, Wang YY. Prognostic Value of Combined Analysis of CTLA-4 and PLR in Esophageal Squamous Cell Carcinoma (ESCC) Patients. *Dis Markers* 2019; **2019**: 1601072 [PMID: 31485274 DOI: 10.1155/2019/1601072]

46 **Cai Z**, Ang X, Xu Z, Li S, Zhang J, Pei C, Zhou F. A pan-cancer study of PD-1 and CTLA-4 as therapeutic targets. *Transl Cancer Res* 2021;

10: 3993-4001 [PMID: 35116697 DOI: 10.21037/tcr-21-561]

47 **Zhang XF**, Pan K, Weng DS, Chen CL, Wang QJ, Zhao JJ, Pan QZ, Liu Q, Jiang SS, Li YQ, Zhang HX, Xia JC. Cytotoxic T lymphocyte antigen-4 expression in esophageal carcinoma: implications for prognosis. *Oncotarget* 2016; **7**: 26670-26679 [PMID: 27050369 DOI: 10.18632/oncotarget.8476]

48 **Wu Z**, Zheng Q, Chen H, Xiang J, Hu H, Li H, Pan Y, Peng Y, Yao X, Liu P, Sun Y, Li B, Zhang Y. Efficacy and safety of neoadjuvant chemotherapy and immunotherapy in locally resectable advanced esophageal squamous cell carcinoma. *J Thorac Dis* 2021; **13**: 3518-3528 [PMID: 34277047 DOI: 10.21037/jtd-21-340]

49 **Liu J**, Yang Y, Liu Z, Fu X, Cai X, Li H, Zhu L, Shen Y, Zhang H, Sun Y, Chen H, Yu B, Zhang R, Shao J, Zhang M, Li Z. Multicenter, single-arm, phase II trial of camrelizumab and chemotherapy as neoadjuvant treatment for locally advanced esophageal squamous cell carcinoma. *J Immunother Cancer* 2022; **10** [PMID: 35338088 DOI: 10.1136/jitc-2021-004291]

50 **Liu J**, Li J, Lin W, Shao D, Depypere L, Zhang Z, Li Z, Cui F, Du Z, Zeng Y, Jiang S, He P, Gu X, Chen H, Zhang H, Lin X, Huang H, Lv W, Cai W, Liang W, Liang H, Jiang W, Wang W, Xu K, Wu K, Lerut T, Fu J, He J. Neoadjuvant camrelizumab plus chemotherapy for resectable, locally advanced esophageal squamous cell carcinoma (NIC-ESCC2019): A multicenter, phase 2 study. *Int J Cancer* 2022; **151**: 128-137 [PMID: 35188268 DOI: 10.1002/ijc.33976]

51 **Li C**, Zhao S, Zheng Y, Han Y, Chen X, Cheng Z, Wu Y, Feng X, Qi W, Chen K, Xiang J, Li J, Lerut T, Li H. Preoperative pembrolizumab combined with chemoradiotherapy for oesophageal squamous cell carcinoma (PALACE-1). *Eur J Cancer* 2021; **144**: 232-241 [PMID: 33373868 DOI: 10.1016/j.ejca.2020.11.039]

52 **Zheng Y**, Li C, Yu B, Zhao S, Li J, Chen X, Li H. Preoperative pembrolizumab combined with chemoradiotherapy for esophageal squamous cell carcinoma: Trial design. *JTCVS Open* 2022; **9**: 293-299 [PMID: 36003437 DOI: 10.1016/j.xjon.2021.11.003]

53 **Zhu M**, Chen C, Foster NR, Hartley C, Mounajjed T, Salomao MA, Fruth BF, Beamer SE, Kim Y, Harrington SM, Pitot HC, Sanhueza CT, Feng Y, Herrmann J, McWilliams RR, Lucien F, Huang BQ, Ma WW, Bekaii-Saab TS, Dong H, Wigle D, Ahn DH, Hallemeier CL, Blackmon S, Yoon HH. Pembrolizumab in Combination with Neoadjuvant Chemoradiotherapy for Patients with Resectable Adenocarcinoma of the Gastroesophageal Junction. *Clin Cancer Res* 2022; **28**: 3021-3031 [PMID: 35552651 DOI: 10.1158/1078-0432.CCR-22-0413]

54 **Huang B**, Shi H, Gong X, Yu J, Xiao C, Zhou B, Liang Z, Li X. Comparison of efficacy and safety between pembrolizumab combined with chemotherapy and simple chemotherapy in neoadjuvant therapy for esophageal squamous cell carcinoma. *J Gastrointest Oncol* 2021; **12**: 2013-2021 [PMID: 34790369 DOI: 10.21037/jgo-21-610]

55 **Duan H**, Shao C, Pan M, Liu H, Dong X, Zhang Y, Tong L, Feng Y, Wang Y, Wang L, Newman NB, Sarkaria IS, Reynolds JV, De Cobelli F, Ma Z, Jiang T, Yan X. Neoadjuvant Pembrolizumab and Chemotherapy in Resectable Esophageal Cancer: An Open-Label, Single-Arm Study (PEN-ICE). *Front Immunol* 2022; **13**: 849984 [PMID: 35720388 DOI: 10.3389/fimmu.2022.849984]

56 **Yan X**, Duan H, Ni Y, Zhou Y, Wang X, Qi H, Gong L, Liu H, Tian F, Lu Q, Sun J, Yang E, Zhong D, Wang T, Huang L, Wang J, Chaoyang Wang, Wang Y, Wan Z, Lei J, Zhao J, Jiang T. Tislelizumab combined with chemotherapy as neoadjuvant therapy for surgically resectable esophageal cancer: A prospective, single-arm, phase II study (TD-NICE). *Int J Surg* 2022; **103**: 106680 [PMID: 35595021 DOI: 10.1016/j.ijsu.2022.106680]

57 **Chen X**, Xu X, Wang D, Liu J, Sun J, Lu M, Wang R, Hui B, Li X, Zhou C, Wang M, Qiu T, Cui S, Sun N, Li Y, Wang F, Liu C, Shao Y, Luo J, Gu Y. Neoadjuvant sintilimab and chemotherapy in patients with potentially resectable esophageal squamous cell carcinoma (KEEP-G 03): an open-label, single-arm, phase 2 trial. *J Immunother Cancer* 2023; **11** [PMID: 36759013 DOI: 10.1136/jitc-2022-005830]

58 **van den Ende T**, de Clercq NC, van Berge Henegouwen MI, Gisbertz SS, Geijsen ED, Verhoeven RHA, Meijer SL, Schokker S, Dings MPG, Bergman JJGHM, Haj Mohammad N, Ruurda JP, van Hillegersberg R, Mook S, Nieuwdorp M, de Gruijl TD, Soeratram TTD, Ylstra B, van Grieken NCT, Bijlsma MF, Hulshof MCCM, van Laarhoven HWM. Neoadjuvant Chemoradiotherapy Combined with Atezolizumab for Resectable Esophageal Adenocarcinoma: A Single-arm Phase II Feasibility Trial (PERFECT). *Clin Cancer Res* 2021; **27**: 3351-3359 [PMID: 33504550 DOI: 10.1158/1078-0432.CCR-20-4443]

59 **Xing W**, Zhao L, Zheng Y, Liu B, Liu X, Li T, Zhang Y, Ma B, Yang Y, Shang Y, Fu X, Liang G, Yuan D, Qu J, Chai X, Zhang H, Wang Z, Lin H, Liu L, Ren X, Zhang J, Gao Q. The Sequence of Chemotherapy and Toripalimab Might Influence the Efficacy of Neoadjuvant Chemoimmunotherapy in Locally Advanced Esophageal Squamous Cell Cancer-A Phase II Study. *Front Immunol* 2021; **12**: 772450 [PMID: 34938292 DOI: 10.3389/fimmu.2021.772450]

60 **He W**, Leng X, Mao T, Luo X, Zhou L, Yan J, Peng L, Fang Q, Liu G, Wei X, Wang K, Wang C, Zhang S, Zhang X, Shen X, Huang D, Yi H, Bei T, She X, Xiao W, Han Y. Toripalimab Plus Paclitaxel and Carboplatin as Neoadjuvant Therapy in Locally Advanced Resectable Esophageal Squamous Cell Carcinoma. *Oncologist* 2022; **27**: e18-e28 [PMID: 35305102 DOI: 10.1093/oncolo/oyab011]

61 **Gao L**, Lu J, Zhang P, Hong ZN, Kang M. Toripalimab combined with docetaxel and cisplatin neoadjuvant therapy for locally advanced esophageal squamous cell carcinoma: a single-center, single-arm clinical trial (ESONICT-2). *J Gastrointest Oncol* 2022; **13**: 478-487 [PMID: 35557591 DOI: 10.21037/jgo-22-131]

62 **Zhang G**, Yuan J, Pan C, Xu Q, Cui X, Zhang J, Liu M, Song Z, Wu L, Wu D, Luo H, Hu Y, Jiao S, Yang B. Multi-omics analysis uncovers tumor ecosystem dynamics during neoadjuvant toripalimab plus nab-paclitaxel and S-1 for esophageal squamous cell carcinoma: a single-center, open-label, single-arm phase 2 trial. *EBioMedicine* 2023; **90**: 104515 [PMID: 36921563 DOI: 10.1016/j.ebiom.2023.104515]

63 **Kelly RJ**, Ajani JA, Kuzdzal J, Zander T, Van Cutsem E, Piessen G, Mendez G, Feliciano J, Motoyama S, Lièvre A, Uronis H, Elimova E, Grootscholten C, Geboes K, Zafar S, Snow S, Ko AH, Feeney K, Schenker M, Kocon P, Zhang J, Zhu L, Lei M, Singh P, Kondo K, Cleary JM, Moehler M; CheckMate 577 Investigators. Adjuvant Nivolumab in Resected Esophageal or Gastroesophageal Junction Cancer. *N Engl J Med* 2021; **384**: 1191-1203 [PMID: 33789008 DOI: 10.1056/NEJMoa2032125]

64 **van Hagen P**, Hulshof MC, van Lanschot JJ, Steyerberg EW, van Berge Henegouwen MI, Wijnhoven BP, Richel DJ, Nieuwenhuijzen GA, Hospers GA, Bonenkamp JJ, Cuesta MA, Blaisse RJ, Busch OR, ten Kate FJ, Creemers GJ, Punt CJ, Plukker JT, Verheul HM, Spillenaar Bilgen EJ, van Dekken H, van der Sangen MJ, Rozema T, Biermann K, Beukema JC, Piet AH, van Rij CM, Reinders JG, Tilanus HW, van der Gaast A; CROSS Group. Preoperative chemoradiotherapy for esophageal or junctional cancer. *N Engl J Med* 2012; **366**: 2074-2084 [PMID: 22646630 DOI: 10.1056/NEJMoa1112088]

65 **Luchini C**, Bibeau F, Ligtenberg MJL, Singh N, Nottegar A, Bosse T, Miller R, Riaz N, Douillard JY, Andre F, Scarpa A. ESMO recommendations on microsatellite instability testing for immunotherapy in cancer, and its relationship with PD-1/PD-L1 expression and tumour mutational burden: a systematic review-based approach. *Ann Oncol* 2019; **30**: 1232-1243 [PMID: 31056702 DOI: 10.1093/annonc/mdz116]

66 **Huang J**, Xu B, Mo H, Zhang W, Chen X, Wu D, Qu D, Wang X, Lan B, Yang B, Wang P, Zhang H, Yang Q, Jiao Y. Safety, Activity, and Biomarkers of SHR-1210, an Anti-PD-1 Antibody, for Patients with Advanced Esophageal Carcinoma. *Clin Cancer Res* 2018; **24**: 1296-1304

[PMID: 29358502 DOI: 10.1158/1078-0432.CCR-17-2439]

67 **Nihira NT**, Miki Y. Regulation of Intrinsic Functions of PD-L1 by Post-Translational Modification in Tumors. *Front Oncol* 2022; **12**: 825284 [PMID: 35402280 DOI: 10.3389/fonc.2022.825284]

68 **Dudley JC**, Lin MT, Le DT, Eshleman JR. Microsatellite Instability as a Biomarker for PD-1 Blockade. *Clin Cancer Res* 2016; **22**: 813-820 [PMID: 26880610 DOI: 10.1158/1078-0432.CCR-15-1678]

69 **Qiu R**, Wang W, Li J, Wang Y. Roles of PTEN inactivation and PD-1/PD-L1 activation in esophageal squamous cell carcinoma. *Mol Biol Rep* 2022; **49**: 6633-6645 [PMID: 35301651 DOI: 10.1007/s11033-022-07246-y]

70 **Li L**, Wei JR, Dong J, Lin QG, Tang H, Jia YX, Tan W, Chen QY, Zeng TT, Xing S, Qin YR, Zhu YH, Li Y, Guan XY. Laminin γ2-mediating T cell exclusion attenuates response to anti-PD-1 therapy. *Sci Adv* 2021; **7** [PMID: 33536206 DOI: 10.1126/sciadv.abc8346]

71 **Zheng S**, Liu B, Guan X. The Role of Tumor Microenvironment in Invasion and Metastasis of Esophageal Squamous Cell Carcinoma. *Front Oncol* 2022; **12**: 911285 [PMID: 35814365 DOI: 10.3389/fonc.2022.911285]

72 **Wu X**, Ke X, Ni Y, Kuang L, Zhang F, Lin Y, Lin W, Xiong X, Huang H, Lin X, Zhang H. Tumor-Infiltrating Immune Cells and PD-L1 as Prognostic Biomarkers in Primary Esophageal Small Cell Carcinoma. *J Immunol Res* 2020; **2020**: 8884683 [PMID: 33457428 DOI: 10.1155/2020/8884683]

73 **Liu Y**, Zheng P. Preserving the CTLA-4 Checkpoint for Safer and More Effective Cancer Immunotherapy. *Trends Pharmacol Sci* 2020; **41**: 4-12 [PMID: 31836191 DOI: 10.1016/j.tips.2019.11.003]

74 **Pai CS**, Simons DM, Lu X, Evans M, Wei J, Wang YH, Chen M, Huang J, Park C, Chang A, Wang J, Westmoreland S, Beam C, Banach D, Bowley D, Dong F, Seagal J, Ritacco W, Richardson PL, Mitra S, Lynch G, Bousquet P, Mankovich J, Kingsbury G, Fong L. Tumor-conditional anti-CTLA4 uncouples antitumor efficacy from immunotherapy-related toxicity. *J Clin Invest* 2019; **129**: 349-363 [PMID: 30530991 DOI: 10.1172/JCI123391]

75 **Duan J**, Xie Y, Qu L, Wang L, Zhou S, Wang Y, Fan Z, Yang S, Jiao S. A nomogram-based immunoprofile predicts overall survival for previously untreated patients with esophageal squamous cell carcinoma after esophagectomy. *J Immunother Cancer* 2018; **6**: 100 [PMID: 30285868 DOI: 10.1186/s40425-018-0418-7]

76 **Zhang Y**, Liu YD, Luo YL, Liu BL, Huang QT, Wang F, Zhong Q. Prognostic Value of Lymphocyte Activation Gene-3 (LAG-3) Expression in Esophageal Squamous Cell Carcinoma. *J Cancer* 2018; **9**: 4287-4293 [PMID: 30519331 DOI: 10.7150/jca.26949]

World Journal of Gastroenterology

Submit a Manuscript: https://www.f6publishing.com

World J Gastroenterol 2023 August 14; 29(30): 4642-4656

DOI: 10.3748/wjg.v29.i30.4642

ISSN 1007-9327 (print) ISSN 2219-2840 (online)

ORIGINAL ARTICLE

Basic Study

Exploring the regulatory mechanism of tRNA-derived fragments 36 in acute pancreatitis based on small RNA sequencing and experiments

Xi-Rui Fan, Yun Huang, Yu Su, Si-Jin Chen, Yu-Lu Zhang, Wei-Kang Huang, Hui Wang

Specialty type: Gastroenterology and hepatology

Provenance and peer review: Unsolicited article; Externally peer reviewed.

Peer-review model: Single blind

Peer-review report's scientific quality classification

Grade A (Excellent): 0
Grade B (Very good): 0
Grade C (Good): C, C
Grade D (Fair): D
Grade E (Poor): 0

P-Reviewer: Nagaya M, Japan; Tzeng IS, Taiwan

Received: February 9, 2023
Peer-review started: February 9, 2023
First decision: May 16, 2023
Revised: May 26, 2023
Accepted: July 17, 2023
Article in press: July 17, 2023
Published online: August 14, 2023

Xi-Rui Fan, Yun Huang, Yu Su, Si-Jin Chen, Yu-Lu Zhang, Wei-Kang Huang, Hui Wang, Department of Gastroenterology, The Affiliated Yan'an Hospital of Kunming Medical University, Kunming 650051, Yunnan Province, China

Xi-Rui Fan, Hui Wang, Key Laboratory of Tumor Immunological Prevention and Treatment of Yunnan Province, Yan'an Hospital of Kunming, Kunming 650051, Yunnan Province, China

Corresponding author: Hui Wang, PhD, Doctor, Department of Gastroenterology, The Affiliated Yan'an Hospital of Kunming Medical University, Renmin East Road, Panlong District, Kunming 650051, Yunnan Province, China. wanghui@kmmu.edu.cn

Abstract

BACKGROUND

Acute pancreatitis (AP) is a disease featuring acute inflammation of the pancreas and histological destruction of acinar cells. Approximately 20% of AP patients progress to moderately severe or severe pancreatitis, with a case fatality rate of up to 30%. However, a single indicator that can serve as the gold standard for prognostic prediction has not been discovered. Therefore, gaining deeper insights into the underlying mechanism of AP progression and the evolution of the disease and exploring effective biomarkers are important for early diagnosis, progression evaluation, and precise treatment of AP.

AIM

To determine the regulatory mechanisms of tRNA-derived fragments (tRFs) in AP based on small RNA sequencing and experiments.

METHODS

Small RNA sequencing and functional enrichment analyses were performed to identify key tRFs and the potential mechanisms in AP. Reverse transcription quantitative polymerase chain reaction (RT-qPCR) was conducted to determine tRF expression. AP cell and mouse models were created to investigate the role of tRF36 in AP progression. Lipase, amylase, and cytokine levels were assayed to examine AP progression. Ferritin expression, reactive oxygen species, malondialdehyde, and ferric ion levels were assayed to evaluate cellular ferroptosis. RNA pull down assays and methylated RNA immunoprecipitation were performed to explore the molecular mechanisms.

RESULTS

RT-qPCR results showed that tRF36 was significantly upregulated in the serum of AP patients, compared to healthy controls. Functional enrichment analysis indicated that target genes of tRF36 were involved in ferroptosis-related pathways, including the Hippo signaling pathway and ion transport. Moreover, the occurrence of pancreatic cell ferroptosis was detected in AP cells and mouse models. The results of interference experiments and AP cell models suggested that tRF-36 could promote AP progression through the regulation of ferroptosis. Furthermore, ferroptosis gene microarray, database prediction, and immunoprecipitation suggested that tRF-36 accelerated the progression of AP by recruiting insulin-like growth factor 2 mRNA binding protein 3 (IGF2BP3) to the p53 mRNA m6A modification site by binding to IGF2BP3, which enhanced p53 mRNA stability and promoted the ferroptosis of pancreatic follicle cells.

CONCLUSION

In conclusion, regulation of nuclear pre-mRNA domain-containing protein 1B promoted AP development by regulating the ferroptosis of pancreatic cells, thereby acting as a prospective therapeutic target for AP. In addition, this study provided a basis for understanding the regulatory mechanisms of tRFs in AP.

Key Words: Acute pancreatitis; tRNA-derived fragments; tRNA-derived fragments 36; Mouse models; Ferroptosis; Reverse transcription quantitative polymerase chain reaction

©The Author(s) 2023. Published by Baishideng Publishing Group Inc. All rights reserved.

Core Tip: Based on reverse transcription quantitative polymerase chain reaction and bioinformatic analysis of small RNA sequencing data extracted from three patients and three healthy controls, and validated by 20 acute pancreatitis (AP) patients and 20 healthy controls, we found that tRNA-derived fragments 36 (tRF36) was significantly upregulated in AP. Furthermore, the results of the cell model of the MCP-83 cell line and knockdown of tRF36 suggested that tRF36 contributed to AP progression by promoting cell death.

Citation: Fan XR, Huang Y, Su Y, Chen SJ, Zhang YL, Huang WK, Wang H. Exploring the regulatory mechanism of tRNA-derived fragments 36 in acute pancreatitis based on small RNA sequencing and experiments. *World J Gastroenterol* 2023; 29(30): 4642-4656
URL: https://www.wjgnet.com/1007-9327/full/v29/i30/4642.htm
DOI: https://dx.doi.org/10.3748/wjg.v29.i30.4642

INTRODUCTION

As a common acute and critical condition of the digestive system, acute pancreatitis (AP) refers to local inflammation of the pancreas and even organ dysfunction due to self-digestion of the pancreas and surrounding organs after abnormal activation of pancreatic enzymes. The prevalence of AP is rising annually, with a global incidence of 4.9-73.4 per 100000 person-years[1]. Most patients display mild symptoms, recover gradually with treatment and have a good prognosis, however, approximately 20% of patients progress to moderately severe or severe pancreatitis, with a case fatality rate (CFR) of up to 30%[2]. Organ failure and pancreatic infection necrosis are believed to be the common causes of mortality in AP patients, and prompt and effective early intervention can improve the prognosis[3]. Accordingly, the prognosis of AP must be predicted at onset. However, a single indicator that can serve as the gold standard for prognostic prediction has not been discovered. Therefore, gaining deeper insights into the underlying mechanism of AP progression and the evolution of the disease and exploring effective biomarkers are important for early diagnosis, progression evaluation, and precise treatment of AP.

Programmed death of pancreatic acinar cells is the major pathophysiological change in the early stages of AP, with the mode of pancreatic acinar cell death playing a vital role in determining AP advancement and prognosis[4,5]. Ferroptosis is a new type of cell death characterized by intracellular iron-dependent lipid peroxidation. In recent years, excessive cellular ferroptosis has been demonstrated to exert a vital role in the pathogenesis of aseptic inflammatory conditions, such as ischemia-reperfusion injury and nonalcoholic steatohepatitis[6]. According to recent studies using a mouse model of AP with knockout of pancreatic tissue glutathione peroxidase 4 (GPX4), the ferroptosis of pancreatic acinar cells exacerbates pancreatic tissue injury, leading to significantly elevated levels of relevant biomarkers and accelerated AP progression[7,8]. The core proteoglycan released from the cells that have undergone ferroptosis can trigger immune responses and the production of proinflammatory cytokines, thereby exacerbating pancreatic acinar cell death and leading to further exacerbation of AP[9]. As shown above, ferroptosis of pancreatic acinar cells promotes the aggravation of AP; however, the molecular mechanism regulating the ferroptosis of pancreatic acinar cells remains unclear.

Non-coding RNAs (ncRNAs) are gaining increasing interest for AP diagnosis and treatment and are expected to be potential biomarkers and therapeutic targets[10]. tRNA-derived fragments (tRFs) have recently been identified as ncRNAs produced from mature tRNAs or tRNA precursors through a specific mechanism of action[11]. tRFs are widespread in various organisms and are extremely conserved, structurally robust, and tissue specific, participating in

different physiological and pathological processes[12]. A sequencing study revealed that several tRFs were abnormally expressed in AP cell models, among which tRF3-Thr-AGT affected AP progression by regulating trypsinogen activation in pancreatic acini[13]. Subsequently, another study revealed that tRF3-Thr-AGT expression was significantly downregulated in the pancreatic tissues of an AP cell model and an AP animal model, while overexpression of tRF3-Thr-AGT inhibited NACHT, LRR, and PYD domains-containing protein 3 (NLRP3)-mediated pyroptosis and the inflammatory responses of pancreatic acinar cells and alleviated AP progression[14]. Accordingly, tRF3-Thr-AGT may be deployed as a biomarker for AP diagnosis and treatment[14].

In this study, serum RNA extraction for AP patients and healthy controls and small RNA sequencing were performed. Thereafter, candidate tRFs were identified using bioinformatics and validated using reverse transcription quantitative polymerase chain reaction (RT-qPCR). The most significantly differentially expressed tRF36 was selected for subsequent investigation. An AP cell model and an AP mouse model were constructed to probe the role and mechanism of tRF36 in regulating ferroptosis and promoting AP progression and to identify the downstream effector pathways and targets. tRF36 was found to promote AP development and progression by regulating P53 expression and ferroptosis by binding to insulin-like growth factor 2 mRNA binding protein 3 (IGF2BP3). This finding provides a theoretical foundation for gaining further insights into the pathogenesis of AP and identifying new potential therapeutic targets.

MATERIALS AND METHODS

Small RNA sequencing

Serum was collected from three patients with AP and three healthy controls. Total RNA was retrieved utilizing the TRizol method, and libraries were constructed utilizing the Multiplex Small RNA Library Prep Kit for Illumina (NEB, United States). The procedure included: (1) 3′ splice ligation; (2) Reverse primer hybridization; (3) 5′ splice ligation; (4) One-strand cDNA synthesis; (5) PCR enrichment; and (6) 8% sodium dodecyl-sulfate polyacrylamide gel electrophoresis fragment sorting (SDS-PAGE). Thereafter, 2 × 150 bp sequencing was performed on an Illumina platform (Yingbiotech, Shanghai, China). This study was approved by Medical Ethics Committee of Yan'an Hospital Affiliated To Kunming Medical University (Approval No. 2022-024-01).

Identification of the differentially expressed tRFs

The overall quality of the sequencing data was evaluated *via* Fast-QC software (http://www.bioinformatics.babraham.ac.uk/projects/fastqc/). For tRFs, sequences that did not match the miRBase (12-23 bp, 34-43 bp) and piRNAcluster (24-33 bp) were compared to rRNA. After we filtered out sequences that could be matched to rRNA, sequences that could be matched to the GtRNA database were matched to the tRFdb and tRFMINTbase databases to obtain tRF expression profiles. Finally, differential expression analysis of tRFs was performed using the DESeq2.0 algorithm (P value < 0.05 and $|\log_2$ fold change$|$ > 1).

Functional enrichment analysis

The target genes for the tRFs were mined *via* miranda (score > 150, energy < -20) and RNAhybrid (energy < -25), and the ultimate target genes were recognized by intersecting the two algorithms. For Gene Ontology (GO) analysis, the significance level of each GO was calculated depending on the GO database (http://www.geneontology.org/) and Fisher's test. The target genes were also annotated with pathways depending on the Kyoto Encyclopedia of Genes and Genomes (KEGG) database (http://www.genome.jp/kegg/) to obtain all pathways involving the genes. The significance level (P value) of each pathway was calculated using Fisher's test and pathways with P value < 0.05 were deemed significantly enriched.

RT-qPCR

We collected serum from 20 patients with AP and 20 healthy controls. Total RNA was retrieved utilizing TRizol (Invitrogen), and reverse transcribed according to the manufacturer's instructions (Thermo, K1622). qPCR was carried out using 2 × Master Mix (Roche). The following thermocycling program was employed for qPCR: 1 cycle at 95 °C for 10 min, followed by 40 cycles at 95 °C for 15 s, and 60 °C for 60 s. The relative expression level was normalized to that of the endogenous control U6 and calculated using the $2^{-\Delta\Delta Ct}$ method[15].

Establishment of the AP cell model and mouse model

Cerulein is a cholecystokinin analogue that provokes the secretion of digestive enzymes in the pancreas of humans and rodents[16]. Cerulein-induced pancreatitis is one of the best featured animal models of pancreatitis, which was first described in 1977 and is highly reproducible and economical[16-18]. Briefly, 10 nM cerulein (MCE, HY-A0190) was administered to the mouse pancreatic acinar carcinoma cell line MPC-83 (Shanghai Bei Nuo Biotechnology Co., Ltd., China) to develop an AP cell model. Male BALB/C mice (age, 6-8 wk; weight 25 ± 3 g; Beijing SiPeiFu Biotechnology Co., Ltd., China) were intraperitoneally administered cerulein 10 times at 1-h intervals to establish the AP mouse model. This study was approved by Animal Ethics and Welfare Committee of Kunming Yan'an hospital (Approval No. 2022013) in accordance with internationally accepted principles for the use of laboratory animals.

tRF interference

According to the manufacturer's protocols, Lipofectamine™ 2000 Transfection reagent (Invitrogen, United States) was

utilized to transfect the tRF-36 inhibitor into MPC-83 cells to knock down the expression of tRF-36. qRT-PCR was conducted to determine the knockdown efficiency of tRF-36.

Cell Counting Kit-8 assay

The viability of cells was determined *via* Cell Counting Kit-8 (CCK-8) assays (Beyotime, China). Then, we seeded 10^3 cells into a 96-well plate and added 10 μL of CCK-8 per well. The absorbance was measured at 450 nm by an enzyme-linked immunosorbent assay (ELISA) microplate reader (Infinite M1000, Tecan) after 1 h of incubation.

ELISA

The levels of tumor necrosis factor (TNF)-α, interleukin (IL)-6, IL-1β, mouse amylase (AMS), and mouse lipase (R&D Systems, MN, United States) were determined using ELISA kits and the absorbance was measured at 450 nm using a microplate reader (Infinite M1000, Tecan).

Detection of cell death

Cell death was assessed using the TUNEL Kit (Sangon Biotech), as described by the manufacturer. A fluorescent microscope (Nikon, Japan) was utilized to observe the specimens.

Reactive oxygen species and malondialdehyde detection

The oxidative-sensitive fluorescent probe DCFH-DA in the reactive oxygen species (ROS) Assay Kit (Beyotime, China) was utilized to assess the generation of intracellular ROS. A laser confocal microscope (Nikon, Japan) was utilized to observe the green fluorescence intensity. Malondialdehyde (MDA) is a metabolite of lipid oxidation and is widely used as an indicator of lipid oxidation. An MDA detection kit (Beyotime, S0131) was used to measure the MDA level in cells or tissues according to the manufacturer's instructions.

Ferric ion detection

A ferric ion colorimetric assay kit (Pulley's, #E1042) was used to measure ferric ion levels in mouse pancreatic tissue, according to the manufacturer's manuals.

Western blot analysis

Cells were lysed using RIPA lysis buffer, homogenized, and centrifuged. Thereafter, the supernatant was collected. Then, the protein concentration was measured using the bicinchoninic acid assay. The proteins were separated *via* SDS-PAGE and transferred to polyvinylidene fluoride membranes. After that, the membranes were incubated at 4 °C overnight with specific primary antibodies against p53 (Proteintech, 60004-1-Lg) and ferritin (Abcam, ab75973) after blocking with 5% nonfat milk. The membrane was then incubated with secondary antibody for 60 min. After the membrane was washed with TBST solution, it was analyzed using the chemiluminescence method. The relative quantification was performed using scanning software (ImageJ grayscale).

Hematoxylin and eosin staining

The mouse lung and pancreatic tissues were washed with phosphate buffered saline and fixed for 24 h in 4% paraformaldehyde fixative solution. Thereafter, conventional paraffin embedding was conducted, and tissue sections (4 μm) were prepared for hematoxylin and eosin (HE) staining. Finally, the histopathological morphology of the sections was observed under a microscope (Olympus, Tokyo, Japan).

Immunohistochemical staining

The tissue sections were dewaxed, rehydrated with xylene, and washed with an alcohol gradient. After soaking and washing with distilled water, H_2O_2 was used to destroy endogenous peroxidase activity. After incubation with anti-ferritin antibody (Abcam, ab75973), the sections were exposed to secondary antibodies. Instillation with diaminobenzidine for 5 min was then performed. Thereafter, the sections were counterstained with hematoxylin, dehydrated with ethanol, and clarified with xylene. Observation and image capture were performed using a microscope (Olympus, Tokyo, Japan).

RNA pulldown assay

The tRF36 probe labeled by biotin was generated, and a Magnetic RNA-Protein Pull-Down Kit [Sangon Biotech (Shanghai, China)] was utilized to implement the RNA pull-down assay depending on the manufacturer's instructions. First, the tRF36 probe or control probe was incubated with streptavidin magnetic beads for 30 min at room temperature. Thereafter, the cell lysates were incubated with probe-bead complexes for 1 h at 4 °C to enable binding of the proteins to RNAs. The RNA-protein complexes were washed and eluted from beads *via* incubation at 37 °C for 30 min with agitation. The eluted proteins were finally analyzed *via* silver staining. The differential protein bands of immunoglobulin G and tRF36-IP lanes were cut and sent to the mass spectrometry platform for protein profiling.

Methylated RNA immunoprecipitation-qPCR

The methylated RNA immunoprecipitation (MeRIP) experiments were completed *via* the riboMeRIPTM m6A Transcriptome Profiling Kit (Merck Millipore) to capture the RNA modified by m6A. Briefly, the total RNA of AP model cells and control cells was extracted by TRizol (Invitrogen). After fragmentation, RNA was incubated with the magnetic

bead-m6A antibody complex for immunoprecipitation. MeRIPed p53 was then analyzed using qRT-PCR.

Statistical analysis

The experimental data were compared *via* student's *t* test to determine the group difference. If not specified above, a *P* value < 0.05 was considered statistically significant.

RESULTS

Differentially expressed tRFs in AP

Based on quality control and preprocessing of the raw small RNA sequencing data for three serum samples from three AP patients and three control samples, we found that the sequencing quality met the criteria for subsequent analysis (Supplementary Figure 1). By RNA mapping based on the BWA algorithm, tRF expression data were extracted. A total of 116 upregulated tRFs and 95 downregulated tRFs in AP were screened *via* differential expression analysis (Figures 1A and B, Supplementary Table 1). According to functional enrichment analysis, many biological processes and pathways, including the Wnt signaling pathway, Hippo signaling pathway, and ion transport, were associated with the target genes of these differentially expressed tRFs (DE-tRFs) (Supplementary Figure 2).

tRF36 is upregulated in AP and contributes to AP progression

Due to the uncertainty of high-throughput sequencing, we collected serum from 20 AP patients and 20 healthy controls and verified the five most significant DE-tRFs using RT-qPCR (Figure 1C). As shown in Figure 1C, tRF36 was downregulated in the serum of AP patients, and its differential expression was the most significant ($P < 0.05$, Figure 1C). This finding implied that tRF36 played an important role in AP progression. To test our hypothesis, we generated an AP cell model using the MCP-83 cell line. Figure 2A revealed that the expression of tRF-36 was significantly reduced after the use of inhibitor. It is well known that AMS and lipase have diagnostic value for AP[19], and the inflammatory response is associated with AP-induced injury[20]. Therefore, we measured the expression of AMS and lipase as well as inflammatory factors to determine the feasibility of the model. After MCP-83 cells were treated with cerulein, the levels of AMS and lipase and the inflammatory factors TNF-α, IL-6, and IL-1β in the cell supernatant increased significantly, indicating successful establishment of the AP cell model (Figures 2B-F). After knockdown of tRF36, these markers were further assayed in the cell supernatants. Based on the results, the levels of AMS and lipase and the inflammatory factors TNF-α, IL-6, and IL-1β in the cell supernatant were significantly reduced after knockdown of tRF36 (Figures 2B-F). Cell viability and cell death were measured by CCK-8 and TUNEL assays, respectively. Knockdown of tRF36 was found to significantly increase cell viability, and significantly reduce cell death (Figures 2G and H). These results suggest that tRF36 contributes to AP progression by promoting cell death.

Presence of cell ferroptosis in AP

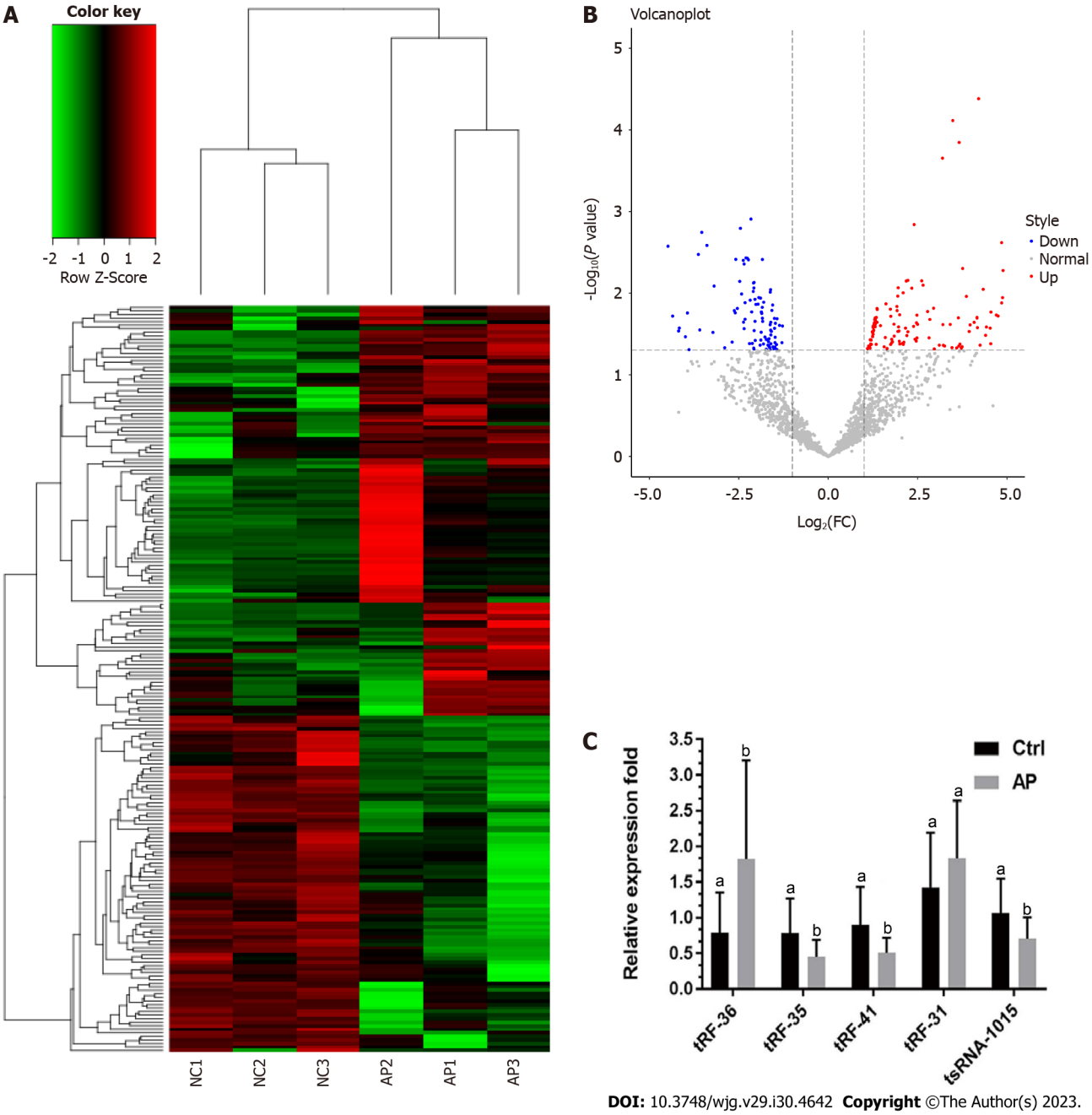
We proceeded to conduct functional enrichment analysis of the target genes of tRF36 (KEGG pathway). The target genes of tRF36 were found to be involved in ferroptosis-related pathways, namely, the P53 signaling pathway and mechanistic target of rapamycin (mTOR) signaling pathway (Figure 3A). To confirm the presence of ferroptosis in AP progression, we constructed an AP mouse model. Based on HE staining of lung and pancreatic tissues, significant changes were observed in pancreatic tissue cell morphology (Figure 3B). Furthermore, the serum levels of lipase and AMS in the AP model mice were significantly higher than those in the controls (Figures 3C and D). The serum levels of the inflammatory factors TNF-α, IL-6, and IL-1β were also significantly increased in the AP model mice (Figures 3E-G). Therefore, the AP mouse model was successfully established. Subsequently, the levels of ferritin expression, ferric ions, and the lipid oxidation metabolite MDA were examined in pancreatic tissue. The expression of ferritin in the pancreatic tissues of the AP model mice was significantly reduced (Figure 3H). Correspondingly, the levels of ferric ion concentration and MDA were significantly increased (Figures 3I and J). These results highlighted the presence of cell ferroptosis in AP.

tRF36 promotes AP progression through the regulation of ferroptosis

Based on the above results, we hypothesized that tRF36 may promote AP progression by regulating cell ferroptosis. Hence, we examined the ROS levels in AP model cells. The ROS levels of cells in the model group were found to be significantly higher than those in the control group (Figure 4A). Similar results were obtained using the AP cell model (*e.g.*, decreased ferritin expression and increased MDA levels) compared to control cells, which were similar to those of the mouse model (Figures 4B and C), suggesting the presence of cell ferroptosis in the AP model. After knockdown of tRF36 in MCP-83 cells, a significant decrease in ROS levels and MDA and a significant increase in ferritin expression levels were found in cells (Figures 4A-C). Therefore, we concluded that tRF36 could promote AP progression through the regulation of ferroptosis.

Exploring the molecular mechanisms by which tRF36 promotes AP progression

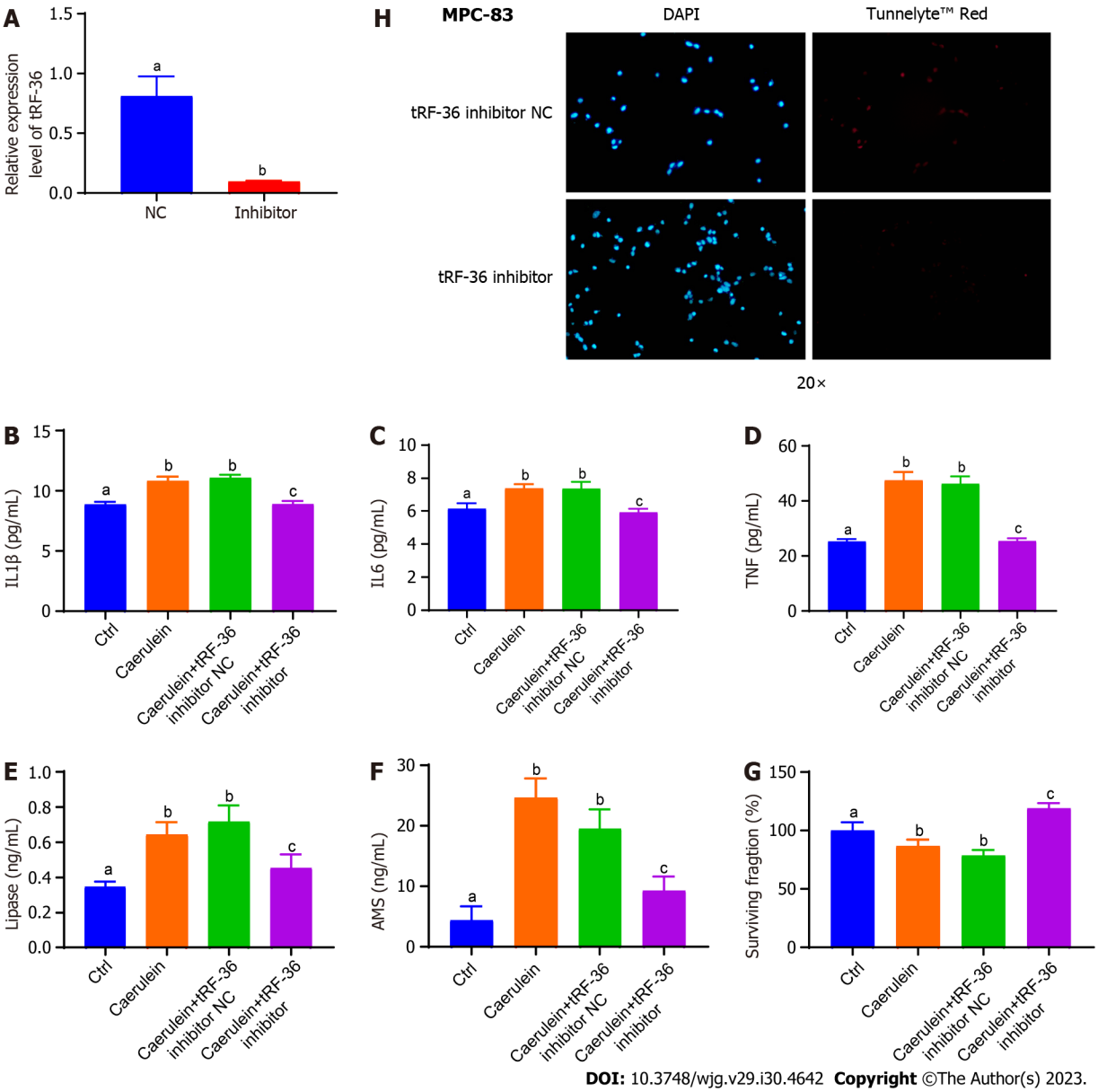
To further probe the molecular mechanisms underlying the regulation of ferroptosis by tRF36, we utilized a ferroptosis gene microarray to determine the differentially expressed ferroptosis genes after tRF36 knockdown. The gene expression of p53 was the most significantly downregulated of the genes (Figure 5A). Database analysis revealed that p53 mRNA interacts with several m6A proteins, including METTL3, ALKBH5, IGF2BP3, and others (Figure 5B). The SRAMP database (http://www.cuilab.cn/sramp) predicted that p53 mRNA has m6A modification sites with a very high



DOI: 10.3748/wjg.v29.i30.4642 **Copyright** ©The Author(s) 2023.

Figure 1 Identification of 116 upregulated tRNA-derived fragments and 95 downregulated tRNA-derived fragments in acute pancreatitis by the differential expression analysis. A: Heatmap of the differentially expressed tRNA-derived fragments (DE-tRFs); B: Volcano plot for the 116 upregulated and 95 downregulated DE-tRFs; C: Gene expression of the five most significant DE-tRFs using reverse transcription quantitative polymerase chain reaction. Error bars represent the mean ± SD, a and b represent different expression levels, the same letter represents no significant difference between groups ($P > 0.05$), different letters represent significant difference between groups ($P < 0.05$). AP: Acute pancreatitis; tRF: tRNA-derived fragment.

probability of modification (Figure 5C). Therefore, we searched for proteins interacting with tRF-36 using an RNA pull down assay and mass spectrometry, which revealed that tRF-36 interacts with the m6A methylation regulator IGF2BP3 (Figures 5D and E, Supplementary Table 2). IGF2BP3 is a unique m6A reader protein that promotes stable mRNA expression and prevents mRNA degradation[21]. MeRIP-qPCR results revealed that the level of m6A modification of p53 was elevated in the AP cell model (Figure 5F). Western blot and qPCR analyses revealed that the knockdown of tRF36 in the AP cell model resulted in a significant reduction in p53 expression (Figures 5G and H). Interestingly, p53 expression was significantly restored after the overexpression of IGF2BP3 in cells with tRF36 knockdown (Figures 5G and H). Therefore, we speculated that tRF36 accelerated the progression of AP by recruiting IGF2BP3 to the p53 mRNA m6A modification site through binding to IGF2BP3, which enhanced p53 mRNA stability and promoted the ferroptosis of pancreatic follicle cells (Figure 6). The p53 expression level after the knockdown of tRF36 was determined by western blot qPCR.



DOI: 10.3748/wjg.v29.i30.4642 **Copyright** ©The Author(s) 2023.

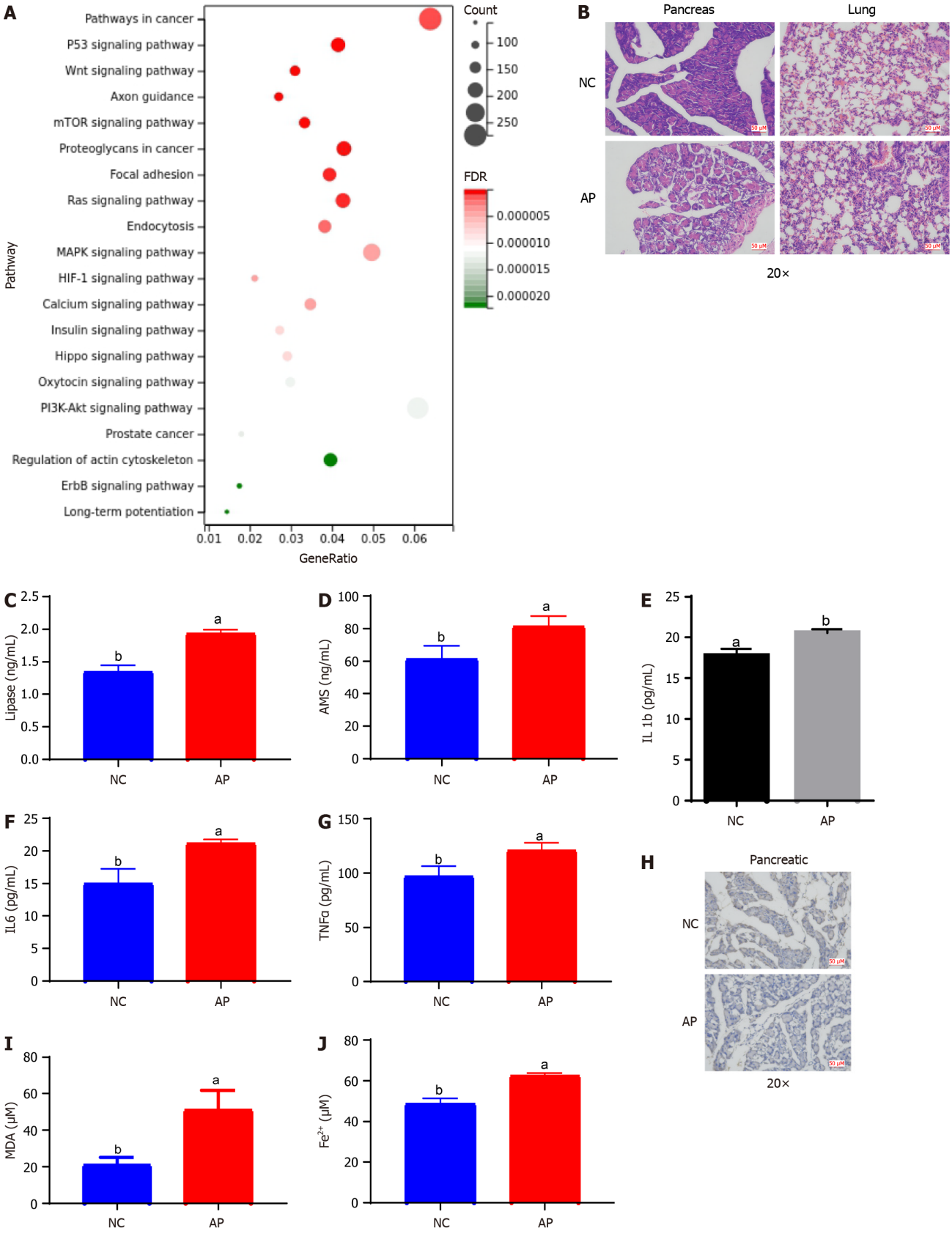
Figure 2 Effects of tRNA-derived fragments 36 on acute pancreatitis progression in MCP-83 cells. A: Gene expression of tRNA-derived fragments 36 using reverse transcription quantitative polymerase chain reaction; B-D: The expression levels of inflammatory factors in the acute pancreatitis (AP) cell model, including interleukin-1β (B), interleukin-6 (C), and tumor necrosis factor-α (D); E: The expression levels of lipase in the AP cell model; F: The expression levels of amylase in the AP cell model; G: Cell viability examination using Cell Counting Kit-8 assays; H: Cell death examination using terminal deoxynucleotidyl transferase dUTP nick-end labeling analysis. Error bars represent the mean ± SD. a, b, and c represent different expression levels, the same letter represents no significant difference between groups ($P > 0.05$), different letters represent significant difference between groups ($P < 0.05$). tRF-36: tRNA-derived fragments 36; IL: Interleukin; TNF: Tumor necrosis factor; AMS: Amylase; NC: Normal control; DAPI: 4',6-diamidino-2-phenylindole.

DISCUSSION

The incidence of AP is increasing annually, with a global incidence of 4.9-73.4 per 100000 person-years[1]. Approximately 20% of AP cases will progress to moderate or severe pancreatitis, with a CFR of up to 30%[2]. The pathogenesis of AP is complex, and no effective clinical treatment has been developed to date. Therefore, gaining deeper insights into the underlying mechanism of AP progression and exploring effective biomarkers are important for AP diagnosis and treatment[9]. In this study, tRF36 was discovered to play an important role in AP progression; thus, its regulatory mechanism was explored.

Sequencing and bioinformatics analyses were performed using the small RNAs extracted from the serum samples of AP patients and healthy controls. Validation of tRF36, the most significantly expressed molecule, was performed using qPCR. The downstream target genes of tRF36 were then predicted and analyzed to explore their potential biological functions.

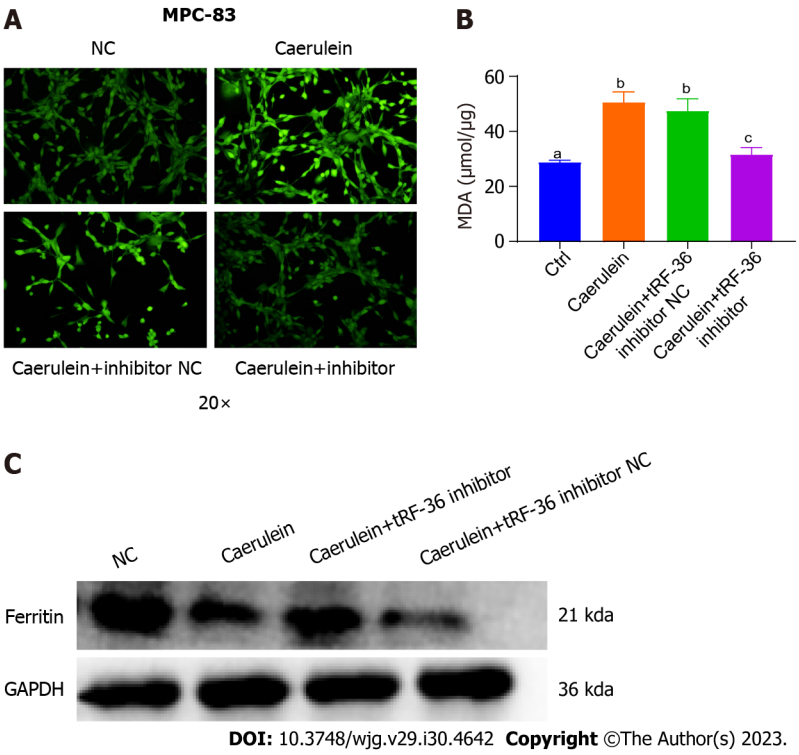
KEGG pathway enrichment analysis revealed that the target genes of tRF36 were mainly enriched in the ferroptosis-related p53 and mTOR signaling pathways. Numerous studies have confirmed that the p53 signaling pathway can regulate ferroptosis. For example, Chen *et al*[22] found that iPLA2 β-mediated lipid detoxification is vital for inhibiting



DOI: 10.3748/wjg.v29.i30.4642 **Copyright** ©The Author(s) 2023.

Figure 3 Evaluation of the target genes of tRNA-derived fragments 36 for the cell ferroptosis process in acute pancreatitis. A: Functional enrichment analysis for the target genes of tRNA-derived fragments 36; B: Hematoxylin and eosin staining results of lung and pancreatic tissues in the acute pancreatitis (AP) mouse model; C and D: The serum levels of lipase and amylase in the AP mouse model; E-G: The serum levels of the inflammatory factors interleukin-1β (E), interleukin-6 (F), and tumor necrosis factor-α (G); H: The expression of ferritin in the mouse pancreatic tissues with AP; I: The levels of malondialdehyde in mouse pancreatic tissues with AP; J: The ferric ion concentration in mouse pancreatic tissues with AP. a and b represent different expression

levels, the same letter represents no significant difference between groups ($P > 0.05$), different letters represent significant difference between groups ($P < 0.05$). tRF-36: tRNA-derived fragments 36; IL: Interleukin; TNF: Tumor necrosis factor; NC: Normal control; mTOR: Mechanistic target of rapamycin; HIF-1: Hypoxia-inducible factor 1; FDR: False discovery rate; PI3K-AKT: Phosphatidylinositol-4,5-bisphosphate 3-kinase-protein kinase B; ErbB: Erythroblastic oncogene B; AP: Acute pancreatitis; MDA: Malondialdehyde; AMS: Amylase.



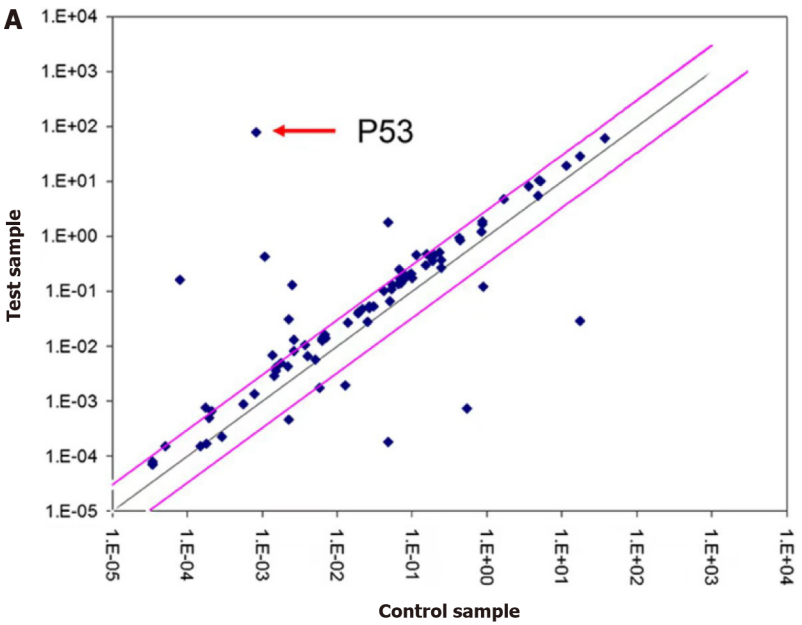
DOI: 10.3748/wjg.v29.i30.4642 **Copyright** ©The Author(s) 2023.

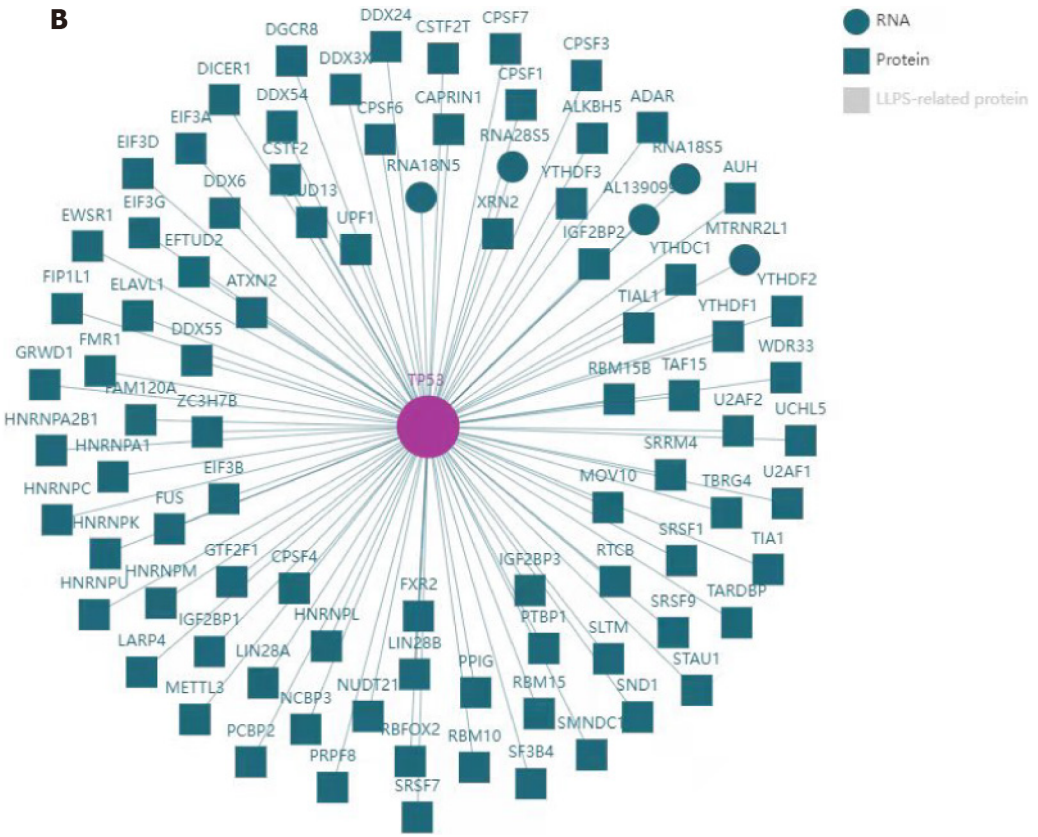
Figure 4 Effect of tRNA-derived fragments 36 on ferroptosis regulation in acute pancreatitis progression. A: The reactive oxygen species levels were detected under a laser confocal microscope; B: Exploration of the malondialdehyde levels in the acute pancreatitis cell model; C: Ferritin levels using western blot analysis. a, b, and c represent different expression levels, the same letter represents no significant difference between groups ($P > 0.05$), different letters represent significant difference between groups ($P < 0.05$). tRF-36: tRNA-derived fragments 36; NC: Normal control.

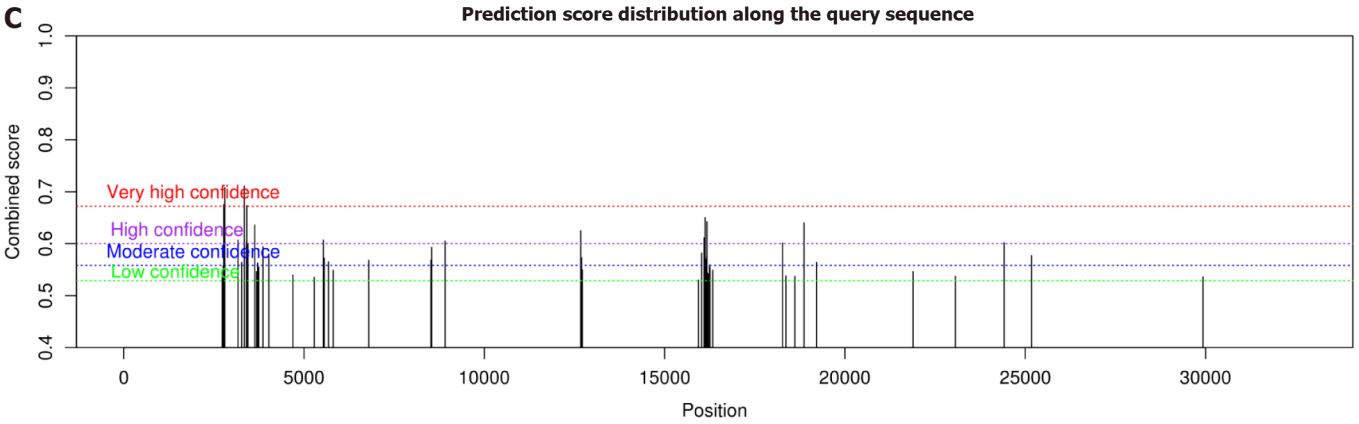
the ROS-induced ferroptosis of cancer cells. Chu *et al*[23] found an ALOX12-mediated, ACSL4-independent ferroptosis pathway that is vital for p53-dependent tumor suppression. Lei *et al*[24] found that radiotherapy (RT)-mediated p53 activation antagonizes RT-induced SLC7A11 expression and inhibits glutathione synthesis, thereby promoting RT-induced lipid peroxidation and ferroptosis. Li *et al*[25] found that ferroptosis contributes to acute lung injury induced by intestinal ischemia/reperfusion and that iASPP treatment partially inhibits ferroptosis *via* nuclear factor E2-related factor 2 (Nrf2). Jiang *et al*[26] found that p53 inhibits cystine uptake and sensitizes cells to ferroptosis by suppressing SLC7A11 expression.

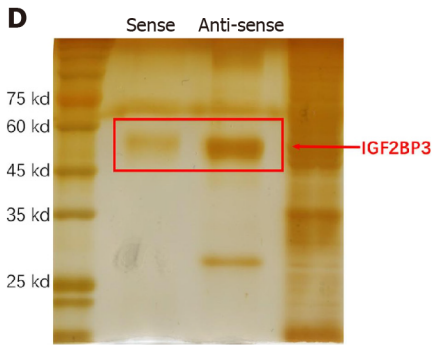
Numerous studies have shown that the mTOR signaling pathway regulates ferroptosis. For example, Conlon *et al*[27] found that acute amino acid deprivation-induced proliferative arrest correlates with protection from ferroptosis in a manner independent of mTOR inhibition and GCN2/ATF4 pathway activation. Sun *et al*[28] not only supported the concept that ferroptosis is autophagy-dependent cell death but also suggested that the combined application of ferroptosis inducers and mTOR inhibitors is a promising approach to improve bladder cancer treatment options. Hsieh *et al*[29] found that ZVI-NP selectively triggered the ferroptosis of cancer cells by inhibiting the Nrf2-mediated cytoprotective program, which was attributed to ZVI-NP-induced disruption of AMPK/mTOR signaling and activation of the GSK3βSK-TrCP-dependent degradation system.

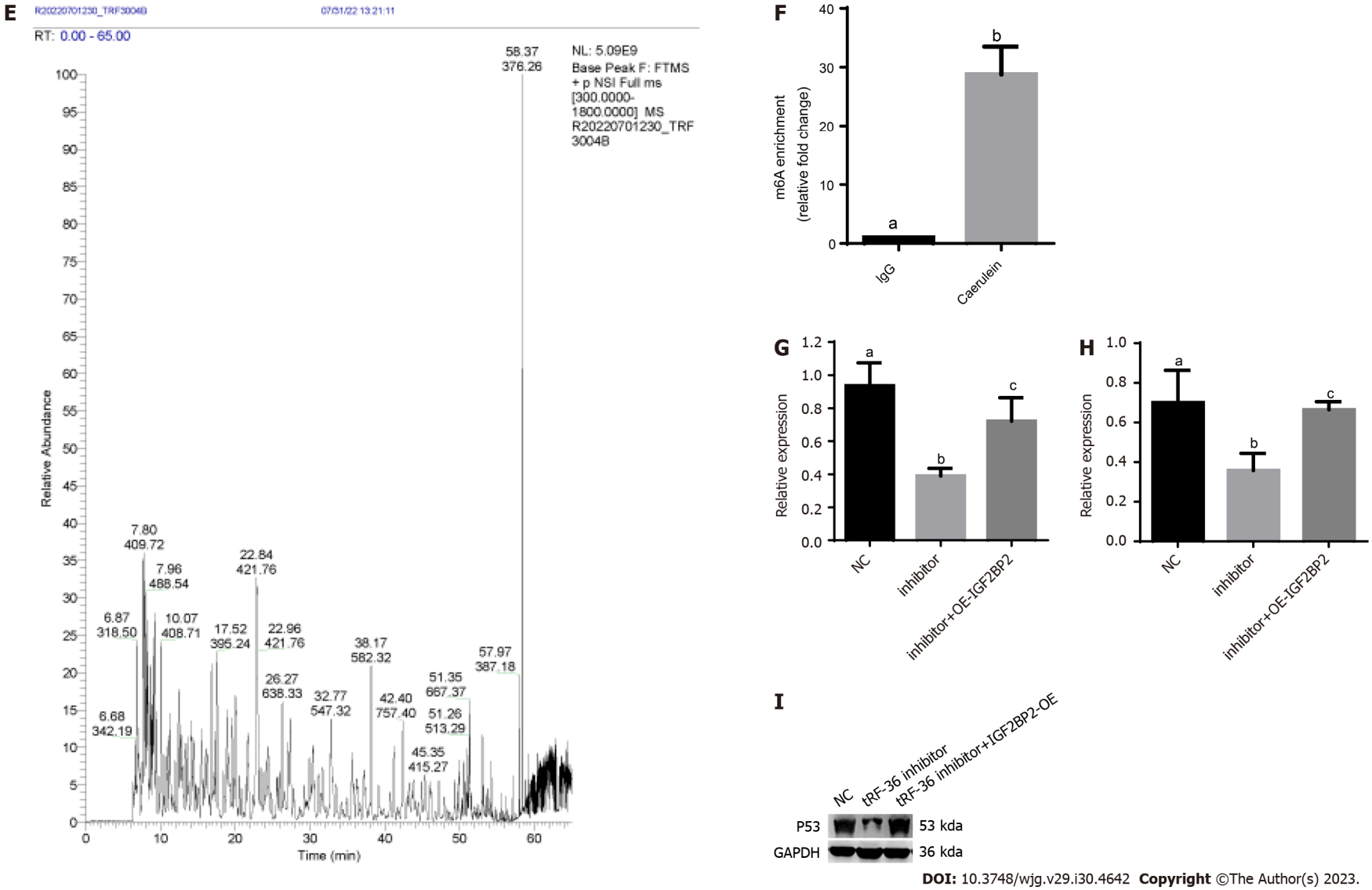
In recent years, the role of ncRNAs in AP has received increasing attention, and ncRNAs are expected to be a potential biomarker and therapeutic target. Owing to the development of sequencing technology, many AP-associated ncRNAs have been identified, such as long ncRNAs, microRNAs, and tRFs[30,31], suggesting that ncRNA dysregulation plays an important role in the development of AP. For example, Li *et al*[32] demonstrated that tRNA-derived small RNAs (tsRNAs) can be used as a potential therapeutic biomarker for bile duct cancer. The sequencing results of Yang *et al*[13] revealed that different tRFs were abnormally expressed in AP cell models, and tRF3-Thr-AGT affected AP progression by regulating trypsinogen activation in pancreatic acini. A later study further showed that tRF3-Thr-AGT expression was significantly downregulated in the pancreatic tissues of an AP cell model and an AP animal model, while overexpression of tRF3-Thr-AGT inhibited the NLRP3-mediated pyroptosis and inflammatory responses of pancreatic acinar cells, thereby alleviating AP progression[14]. However, no existing studies have reported the involvement of tRF36 in regulating the pathogenesis of AP. In the present study, tRF36 expression was upregulated in the serum of AP patients,


A
P53
Test sample
Control sample
1.E+04
1.E+03
1.E+02
1.E+01
1.E+00
1.E-01
1.E-02
1.E-03
1.E-04
1.E-05


B
RNA
Protein
LLPS-related protein
TP53
DDX24
CSTF2T
CPSF7
DGCR8
DDX3X
CPSF3
DICER1
CPSF1
DDX54
CAPRIN1
ALKBH5
ADAR
EIF3A
CPSF6
RNA28S5
EIF3D
CSTF2
RNA18S5
RNA18N5
YTHDF3
AUH
DDX6
UD13
XRN2
AL139095
EIF3G
UPF1
IGF2BP2
MTRNR2L1
EWSR1
EFTUD2
YTHDC1
FIP1L1
ELAVL1
ATXN2
YTHDF2
TIAL1
YTHDF1
DDX55
FMR1
WDR33
GRWD1
RBM15B
TAF15
FAM120A
ZC3H7B
U2AF2
UCHL5
HNRNPA2B1
SRRM4
HNRNPA1
EIF3B
MOV10
TBRG4
U2AF1
HNRNPC
FUS
SRSF1
HNRNPK
TIA1
GTF2F1
CPSF4
IGF2BP3
RTCB
HNRNPM
FXR2
SRSF9
TARDBP
HNRNPU
PTBP1
IGF2BP1
HNRNPL
SLTM
LARP4
LIN28A
LIN28B
STAU1
PPIG
METTL3
NUDT21
RBM15
SND1
NCBP3
SMNDC1
PCBP2
RBFOX2
RBM10
SF3B4
PRPF8
SRSF7


C
Prediction score distribution along the query sequence
Combined score
Position
Very high confidence
High confidence
Moderate confidence
Low confidence
0
5000
10000
15000
20000
25000
30000
0.4
0.5
0.6
0.7
0.8
0.9
1.0


D
Sense
Anti-sense
75 kd
60 kd
45 kd
35 kd
25 kd
IGF2BP3



DOI: 10.3748/wjg.v29.i30.4642 **Copyright** ©The Author(s) 2023.

Figure 5 Exploration of the molecular mechanisms of tRNA-derived fragments 36 in acute pancreatitis progression. A: p53 was the most significantly downregulated gene in ferroptosis gene microarray analysis after tRNA-derived fragments 36 (tRF-36) knockdown; B: The interaction network of p53 and m6A proteins; C: The m6A modification analysis for p53 mRNA by SRAMP; D: The RNA pull down assay for tRF-36 with insulin-like growth factor 2 mRNA binding

protein 3; E: Mass spectrometry results for tRF-36; F: The level of m6A modification of p53 by methylated RNA immunoprecipitation-quantitative polymerase chain reaction.; G: The p53 expression level after the knockdown of tRF-36 by reverse transcription quantitative polymerase chain reaction; H: The p53 expression level after the knockdown of tRF-36 by western blot; I: The changes in P53 expression. a, b, and c represent different expression levels, the same letter represents no significant difference between groups ($P > 0.05$), different letters represent significant difference between groups ($P < 0.05$). tRF-36: tRNA-derived fragments 36; NC: Normal control; IgG: Immunoglobulin G; OE: Overexpression; IGF2BP3: Insulin-like growth factor 2 mRNA binding protein 3.

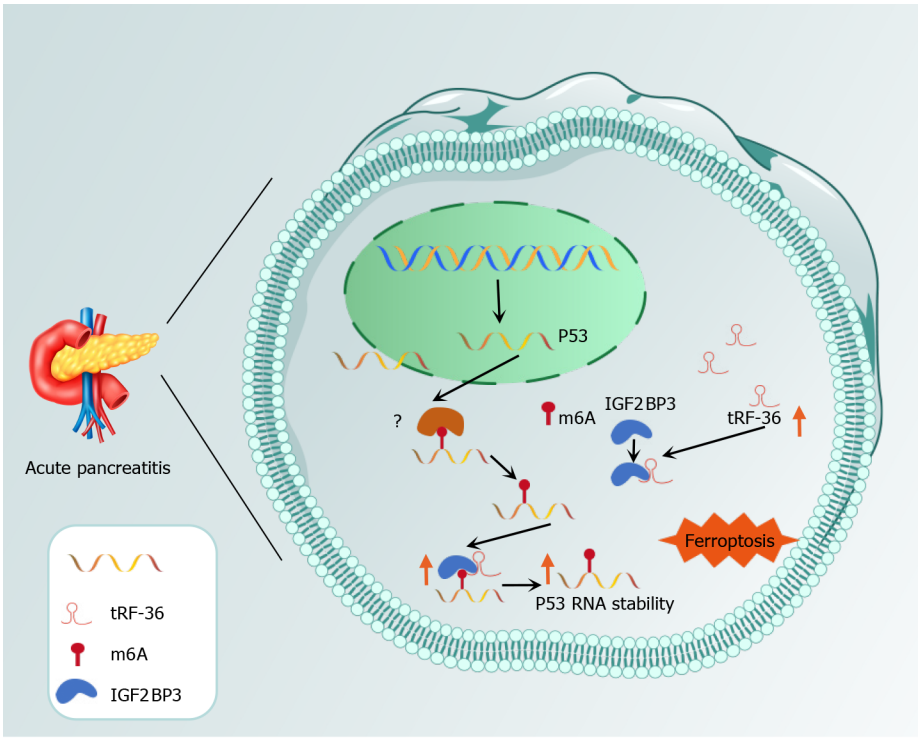
and knockdown of tRF36 resulted in a significant decrease in AMS and lipase levels in cell supernatants and a reduction in pancreatic acinar cell death. Therefore, tRF36 exacerbates AP by promoting pancreatic acinar cell death and may be a diagnostic biomarker in clinical treatment.

In AP mouse models in which GPX4 was knocked out in pancreatic tissues, the ferroptosis of pancreatic acinar cells exacerbated pancreatic tissue damage, leading to a significant increase in the levels of relevant biomarkers and accelerated progression of AP[7,8]. The core proteoglycan released from cells that have undergone ferroptosis can trigger immune responses and the production of proinflammatory cytokines, thereby exacerbating pancreatic acinar cell death and leading to further exacerbation of AP[9]. In mice and cell models of AP, the expression of ferritin decreased and MDA level increased. Hou *et al*[33] suggested that ferritin was a major intracellular iron storage protein complex, and its increased expression would limit ferroptosis. On the contrary, there was a low ferritin expression level during ferroptosis. As shown above, ferroptosis of pancreatic acinar cells promotes the aggravation of AP.

In the present study, we constructed an AP cell model in which tRF36 was knocked down in the pancreatic acinar cells. A ferroptosis gene microarray was performed to identify the key genes involved in ferroptosis, among which P53 was demonstrated to exhibit the most significant expression. Database-based prediction revealed that p53 mRNA has an m6A modification site where p53 mRNA interacts with some m6A-reader proteins. Goodarzi *et al*[34] found that tsRNA can inhibit the stability of multiple proto-oncogene transcripts in breast cancer cells by competitively binding to the RNA-binding protein YBX1. Thus, tRFs can regulate the stability of downstream gene transcripts *via* RNA-binding proteins. Accordingly, an RNA pulldown assay combined with mass spectrometry was performed in the present study, which revealed that tRF36 interacted with IGF2BP3. Finally, based on gene interference, overexpression, MeRIP-PCR, RNA pulldown assays, western blotting, and rescue assays, IGF2BP3 was confirmed to regulate the ferroptosis of pancreatic acinar cells by regulating P53 expression by enhancing P53 mRNA stability. Taken together, the above findings suggest that the acceleration of AP progression by tRF36 may involve the process of tRF36 recruiting IGF2BP3 to the m6A modification site of P53 mRNA by binding to IGF2BP3, which enhances P53 mRNA stability, ultimately promoting the ferroptosis of pancreatic acinar cells.

To our knowledge, this is the first study to identify a tRF, tRF36, that promotes AP progression by regulating the ferroptosis of pancreatic acinar cells and to elucidate the molecular mechanism whereby tRF36 is involved in AP progression (*e.g.*, tRF36 regulates the ferroptosis of pancreatic acinar cells by regulating P53 expression through binding to IGF2BP3). The findings fill the knowledge gap by revealing how tRFs are involved in AP progression *via* the regulation of ferroptosis and provide a new direction for further studies on AP development.

The present study had some limitations. The sample size of the study cohort was small. Future studies should employ a larger sample size to further verify the expression of tRF36 in AP. The expression levels of ROS and MDA were determined only by knocking down tRF36. Accordingly, their expression should also be examined by overexpressing tRF36.



DOI: 10.3748/wjg.v29.i30.4642 **Copyright** ©The Author(s) 2023.

Figure 6 A schematic of a putative mechanism of tRNA-derived fragments 36 in the progression of acute pancreatitis. In this model, tRNA-derived fragments 36 might recruit insulin-like growth factor 2 mRNA binding protein 3 (IGF2BP3) to the p53 mRNA m6A modification site by binding to IGF2BP3 to enhance p53 mRNA stability and promote the ferroptosis of pancreatic follicle cells. tRF-36: tRNA-derived fragments 36; IGF2BP3: Insulin-like growth factor 2 mRNA binding protein 3.

CONCLUSION

In this study, the most significantly differentially expressed candidate, tRF36, was identified using bioinformatics and validated using qRT-PCR based on serum RNA extraction and small RNA sequencing data from AP patients and healthy controls. The AP cell model and the AP mouse model were constructed to explore the role and mechanism of tRF36 in regulating ferroptosis and promoting AP progression, indicating that tRF36 might recruit IGF2BP3 to the p53 mRNA m6A modification site by binding to IGF2BP3 to enhance p53 mRNA stability and promote the ferroptosis of pancreatic follicle cells. This finding provides a theoretical basis for gaining further insights into the pathogenesis of AP and identifying new potential therapeutic targets.

ARTICLE HIGHLIGHTS

Research background

Acute pancreatitis (AP), also known as acute inflammation of the pancreas, is an inflammatory injury resulting from the activation of pancreatic enzymes caused by a variety of pathogenic factors, leading to self-digestion of pancreatic tissue.

Research motivation

Difficult treatment, high morbidity, many complications, high cost, and poor prognosis are the current clinical status. Therefore, it is particularly important to investigate the pathogenesis of AP.

Research objectives

Screening for tRNA-derived fragments (tRFs) contribute to AP progression and exploring the molecular mechanism of its action were the main objectives of our study.

Research methods

Firstly, key tRFs and the potential mechanisms of action were explored based on the small RNA sequencing and functional enrichment analyses in AP. The role of tRF36 was investigated by constructing the AP cell and mouse models. Subsequently, the lipase, amylase, and cytokine levels were assayed to examine AP progression. Evaluation of cellular ferroptosis was implemented by analyzing the ferritin expression, reactive oxygen species, malondialdehyde, and ferric ion levels. Finally, RNA pull down assays and methylated RNA immunoprecipitation were performed to explore the

molecular mechanisms.

Research results

In total, 211 differentially expressed tRFs including 116 upregulated and 95 downregulated were identified. According to reverse transcription quantitative polymerase chain reaction, tRF36 was significantly upregulated in the serum of AP patients, compared to healthy controls. Moreover, the occurrence of pancreatic cell ferroptosis was detected in AP cells and mouse models. Furthermore, we hypothesized that tRF36 accelerated AP progression by binding to insulin-like growth factor 2 mRNA binding protein 3, which was recruited to the p53 mRNA m6A modification site, thereby enhancing the stability of p53 mRNA and promoting ferroptosis in pancreatic follicular cells.

Research conclusions

tRF36 promoted AP development by regulating the ferroptosis of pancreatic cells, which would provide a new theoretical basis for understanding the regulatory mechanism of tRF in AP, and also provide new targets for the treatment of AP.

Research perspectives

We will further validate the results of this study and continue to monitor the role of tRF36 in the development process of AP.

FOOTNOTES

Author contributions: Fan XR and Huang Y contributed equally to this work. Wang H conceived, designed, and supervised the study; Fan XR, Huang Y, and Chen SJ performed the majority of experiments and collected the data; Su Y and Huang WK performed data analysis and drafted the manuscript; and all authors have read and agreed to the published version of the manuscript.

Supported by the National Natural Science Foundation of China, No. 81860424.

Institutional review board statement: This study was approved by the Medical Ethics Committee of Yan'an Hospital Affiliated to Kunming Medical University (Approval No. 2022-024-01).

Institutional animal care and use committee statement: This study was approved by Animal Ethics and Welfare Committee (AEWC) of Kunming Yan'an hospital (Approval No. 2022013) in accordance with internationally accepted principles for the use of laboratory animals.

Conflict-of-interest statement: All the authors report no relevant conflicts of interest for this article.

Data sharing statement: The data used during the current study are available from the corresponding author on reasonable request.

ARRIVE guidelines statement: The authors have read the ARRIVE guidelines, and the manuscript was prepared and revised according to the ARRIVE guidelines.

Open-Access: This article is an open-access article that was selected by an in-house editor and fully peer-reviewed by external reviewers. It is distributed in accordance with the Creative Commons Attribution NonCommercial (CC BY-NC 4.0) license, which permits others to distribute, remix, adapt, build upon this work non-commercially, and license their derivative works on different terms, provided the original work is properly cited and the use is non-commercial. See: https://creativecommons.org/Licenses/by-nc/4.0/

Country/Territory of origin: China

ORCID number: Xi-Rui Fan 0000-0002-9111-7823; Wei-Kang Huang 0000-0003-4825-8337; Hui Wang 0000-0003-4804-8559.

S-Editor: Wang JJ
L-Editor: A
P-Editor: Yuan YY

REFERENCES

1 **Li CL**, Jiang M, Pan CQ, Li J, Xu LG. The global, regional, and national burden of acute pancreatitis in 204 countries and territories, 1990-2019. *BMC Gastroenterol* 2021; **21**: 332 [PMID: 34433418 DOI: 10.1186/s12876-021-01906-2]

2 **Schepers NJ**, Bakker OJ, Besselink MG, Ahmed Ali U, Bollen TL, Gooszen HG, van Santvoort HC, Bruno MJ; Dutch Pancreatitis Study Group. Impact of characteristics of organ failure and infected necrosis on mortality in necrotising pancreatitis. *Gut* 2019; **68**: 1044-1051 [PMID: 29950344 DOI: 10.1136/gutjnl-2017-314657]

3 **Wolbrink DRJ**, Kolwijck E, Ten Oever J, Horvath KD, Bouwense SAW, Schouten JA. Management of infected pancreatic necrosis in the intensive care unit: a narrative review. *Clin Microbiol Infect* 2020; **26**: 18-25 [PMID: 31238118 DOI: 10.1016/j.cmi.2019.06.017]

4 **Mayerle J**, Sendler M, Hegyi E, Beyer G, Lerch MM, Sahin-Tóth M. Genetics, Cell Biology, and Pathophysiology of Pancreatitis.

Gastroenterology 2019; **156**: 1951-1968.e1 [PMID: 30660731 DOI: 10.1053/j.gastro.2018.11.081]
5 **Bai Y**, Lam HC, Lei X. Dissecting Programmed Cell Death with Small Molecules. *Acc Chem Res* 2020; **53**: 1034-1045 [PMID: 32297735 DOI: 10.1021/acs.accounts.9b00600]
6 **Tang D**, Chen X, Kang R, Kroemer G. Ferroptosis: molecular mechanisms and health implications. *Cell Res* 2021; **31**: 107-125 [PMID: 33268902 DOI: 10.1038/s41422-020-00441-1]
7 **Dai E**, Han L, Liu J, Xie Y, Zeh HJ, Kang R, Bai L, Tang D. Ferroptotic damage promotes pancreatic tumorigenesis through a TMEM173/STING-dependent DNA sensor pathway. *Nat Commun* 2020; **11**: 6339 [PMID: 33311482 DOI: 10.1038/s41467-020-20154-8]
8 **Liu K**, Liu J, Zou B, Li C, Zeh HJ, Kang R, Kroemer G, Huang J, Tang D. Trypsin-Mediated Sensitization to Ferroptosis Increases the Severity of Pancreatitis in Mice. *Cell Mol Gastroenterol Hepatol* 2022; **13**: 483-500 [PMID: 34562639 DOI: 10.1016/j.jcmgh.2021.09.008]
9 **Liu J**, Zhu S, Zeng L, Li J, Klionsky DJ, Kroemer G, Jiang J, Tang D, Kang R. DCN released from ferroptotic cells ignites AGER-dependent immune responses. *Autophagy* 2022; **18**: 2036-2049 [PMID: 34964698 DOI: 10.1080/15548627.2021.2008692]
10 **Li J**, Bu X, Chen X, Xiong P, Chen Z, Yu L. Predictive value of long non-coding RNA intersectin 1-2 for occurrence and in-hospital mortality of severe acute pancreatitis. *J Clin Lab Anal* 2020; **34**: e23170 [PMID: 31880027 DOI: 10.1002/jcla.23170]
11 **Krishna S**, Raghavan S, DasGupta R, Palakodeti D. tRNA-derived fragments (tRFs): establishing their turf in post-transcriptional gene regulation. *Cell Mol Life Sci* 2021; **78**: 2607-2619 [PMID: 33388834 DOI: 10.1007/s00018-020-03720-7]
12 **Pandey KK**, Madhry D, Ravi Kumar YS, Malvankar S, Sapra L, Srivastava RK, Bhattacharyya S, Verma B. Regulatory roles of tRNA-derived RNA fragments in human pathophysiology. *Mol Ther Nucleic Acids* 2021; **26**: 161-173 [PMID: 34513302 DOI: 10.1016/j.omtn.2021.06.023]
13 **Yang H**, Zhang H, Chen Z, Wang Y, Gao B. Effects of tRNA-derived fragments and microRNAs regulatory network on pancreatic acinar intracellular trypsinogen activation. *Bioengineered* 2022; **13**: 3207-3220 [PMID: 35045793 DOI: 10.1080/21655979.2021.2018880]
14 **Sun B**, Chen Z, Chi Q, Zhang Y, Gao B. Endogenous tRNA-derived small RNA (tRF3-Thr-AGT) inhibits ZBP1/NLRP3 pathway-mediated cell pyroptosis to attenuate acute pancreatitis (AP). *J Cell Mol Med* 2021; **25**: 10441-10453 [PMID: 34643045 DOI: 10.1111/jcmm.16972]
15 **Livak KJ**, Schmittgen TD. Analysis of relative gene expression data using real-time quantitative PCR and the 2(-Delta Delta C(T)) Method. *Methods* 2001; **25**: 402-408 [PMID: 11846609 DOI: 10.1006/meth.2001.1262]
16 **Zhang KY**, Rosenkrantz L, Sellers ZM. Chemically Induced Models of Pancreatitis. *Pancreapedia* 2022 [DOI: 10.3998/panc.2022.01]
17 **Lampel M**, Kern HF. Acute interstitial pancreatitis in the rat induced by excessive doses of a pancreatic secretagogue. *Virchows Arch A Pathol Anat Histol* 1977; **373**: 97-117 [PMID: 139754 DOI: 10.1007/BF00432156]
18 **Saluja A**, Saito I, Saluja M, Houlihan MJ, Powers RE, Meldolesi J, Steer M. In vivo rat pancreatic acinar cell function during supramaximal stimulation with caerulein. *Am J Physiol* 1985; **249**: G702-G710 [PMID: 2417493 DOI: 10.1152/ajpgi.1985.249.6.G702]
19 **Itzkowitz SH**, Sands BE, Ullman TA, Rustgi AK. Mark Warren Babyatsky, MD (June 29, 1959-August 25, 2014). *Gastroenterology* 2014; **147**: 1189-1190 [PMID: 25449021 DOI: 10.1053/j.gastro.2014.10.030]
20 **Tu HJ**, Zhao CF, Chen ZW, Lin W, Jiang YC. Fibroblast Growth Factor (FGF) Signaling Protects Against Acute Pancreatitis-Induced Damage by Modulating Inflammatory Responses. *Med Sci Monit* 2020; **26**: e920684 [PMID: 32283546 DOI: 10.12659/MSM.920684]
21 **Bi Z**, Liu Y, Zhao Y, Yao Y, Wu R, Liu Q, Wang Y, Wang X. A dynamic reversible RNA N^6-methyladenosine modification: current status and perspectives. *J Cell Physiol* 2019; **234**: 7948-7956 [DOI: 10.1002/jcp.28014]
22 **Chen D**, Chu B, Yang X, Liu Z, Jin Y, Kon N, Rabadan R, Jiang X, Stockwell BR, Gu W. iPLA2β-mediated lipid detoxification controls p53-driven ferroptosis independent of GPX4. *Nat Commun* 2021; **12**: 3644 [PMID: 34131139 DOI: 10.1038/s41467-021-23902-6]
23 **Chu B**, Kon N, Chen D, Li T, Liu T, Jiang L, Song S, Tavana O, Gu W. ALOX12 is required for p53-mediated tumour suppression through a distinct ferroptosis pathway. *Nat Cell Biol* 2019; **21**: 579-591 [PMID: 30962574 DOI: 10.1038/s41556-019-0305-6]
24 **Lei G**, Zhang Y, Hong T, Zhang X, Liu X, Mao C, Yan Y, Koppula P, Cheng W, Sood AK, Liu J, Gan B. Ferroptosis as a mechanism to mediate p53 function in tumor radiosensitivity. *Oncogene* 2021; **40**: 3533-3547 [PMID: 33927351 DOI: 10.1038/s41388-021-01790-w]
25 **Li Y**, Cao Y, Xiao J, Shang J, Tan Q, Ping F, Huang W, Wu F, Zhang H, Zhang X. Inhibitor of apoptosis-stimulating protein of p53 inhibits ferroptosis and alleviates intestinal ischemia/reperfusion-induced acute lung injury. *Cell Death Differ* 2020; **27**: 2635-2650 [PMID: 32203170 DOI: 10.1038/s41418-020-0528-x]
26 **Jiang L**, Kon N, Li T, Wang SJ, Su T, Hibshoosh H, Baer R, Gu W. Ferroptosis as a p53-mediated activity during tumour suppression. *Nature* 2015; **520**: 57-62 [PMID: 25799988 DOI: 10.1038/nature14344]
27 **Conlon M**, Poltorack CD, Forcina GC, Armenta DA, Mallais M, Perez MA, Wells A, Kahanu A, Magtanong L, Watts JL, Pratt DA, Dixon SJ. A compendium of kinetic modulatory profiles identifies ferroptosis regulators. *Nat Chem Biol* 2021; **17**: 665-674 [PMID: 33686292 DOI: 10.1038/s41589-021-00751-4]
28 **Sun Y**, Berleth N, Wu W, Schlütermann D, Deitersen J, Stuhldreier F, Berning L, Friedrich A, Akgün S, Mendiburo MJ, Wesselborg S, Conrad M, Berndt C, Stork B. Fin56-induced ferroptosis is supported by autophagy-mediated GPX4 degradation and functions synergistically with mTOR inhibition to kill bladder cancer cells. *Cell Death Dis* 2021; **12**: 1028 [PMID: 34716292 DOI: 10.1038/s41419-021-04306-2]
29 **Hsieh CH**, Hsieh HC, Shih FS, Wang PW, Yang LX, Shieh DB, Wang YC. An innovative NRF2 nano-modulator induces lung cancer ferroptosis and elicits an immunostimulatory tumor microenvironment. *Theranostics* 2021; **11**: 7072-7091 [PMID: 34093872 DOI: 10.7150/thno.57803]
30 **Natarajan SK**, Pachunka JM, Mott JL. Role of microRNAs in Alcohol-Induced Multi-Organ Injury. *Biomolecules* 2015; **5**: 3309-3338 [PMID: 26610589 DOI: 10.3390/biom5043309]
31 **Tirronen A**, Hokkanen K, Vuorio T, Ylä-Herttuala S. Recent advances in novel therapies for lipid disorders. *Hum Mol Genet* 2019; **28**: R49-R54 [PMID: 31227825 DOI: 10.1093/hmg/ddz132]
32 **Li YK**, Yan LR, Wang A, Jiang LY, Xu Q, Wang BG. RNA-sequencing reveals the expression profiles of tsRNAs and their potential carcinogenic role in cholangiocarcinoma. *J Clin Lab Anal* 2022; **36**: e24694 [PMID: 36098712 DOI: 10.1002/jcla.24694]
33 **Hou W**, Xie Y, Song X, Sun X, Lotze MT, Zeh HJ 3rd, Kang R, Tang D. Autophagy promotes ferroptosis by degradation of ferritin. *Autophagy* 2016; **12**: 1425-1428 [PMID: 27245739 DOI: 10.1080/15548627.2016.1187366]
34 **Goodarzi H**, Liu X, Nguyen HC, Zhang S, Fish L, Tavazoie SF. Endogenous tRNA-Derived Fragments Suppress Breast Cancer Progression *via* YBX1 Displacement. *Cell* 2015; **161**: 790-802 [PMID: 25957686 DOI: 10.1016/j.cell.2015.02.053]

World Journal of Gastroenterology

Submit a Manuscript: https://www.f6publishing.com

World J Gastroenterol 2023 August 14; 29(30): 4657-4670

DOI: 10.3748/wjg.v29.i30.4657

ISSN 1007-9327 (print) ISSN 2219-2840 (online)

ORIGINAL ARTICLE

Basic Study

Fecal microbiota transplantation alleviates experimental colitis through the Toll-like receptor 4 signaling pathway

Xin Wen, Rui Xie, Hong-Gang Wang, Min-Na Zhang, Le He, Meng-Hui Zhang, Xiao-Zhong Yang

Specialty type: Gastroenterology and hepatology

Provenance and peer review: Unsolicited article; Externally peer reviewed.

Peer-review model: Single blind

Peer-review report's scientific quality classification

Grade A (Excellent): 0
Grade B (Very good): B, B
Grade C (Good): 0
Grade D (Fair): 0
Grade E (Poor): 0

P-Reviewer: El-Nakeep S, Egypt; Xu QB, China

Received: May 22, 2023
Peer-review started: May 22, 2023
First decision: June 20, 2023
Revised: July 3, 2023
Accepted: July 11, 2023
Article in press: July 11, 2023
Published online: August 14, 2023

Xin Wen, Rui Xie, Hong-Gang Wang, Min-Na Zhang, Le He, Meng-Hui Zhang, Xiao-Zhong Yang, Department of Gastroenterology, The Affiliated Huaian No. 1 People's Hospital of Nanjing Medical University, Huai'an 223300, Jiangsu Province, China

Corresponding author: Xiao-Zhong Yang, MD, PhD, Chief Doctor, Doctor, Professor, Department of Gastroenterology, The Affiliated Huaian No. 1 People's Hospital of Nanjing Medical University, No. 1 Huanghe Road, Huai'an 223300, Jiangsu Province, China. hayyyxzh@njmu.edu.cn

Abstract

BACKGROUND

Fecal microbiota transplantation (FMT) has shown promising therapeutic effects on mice with experimental colitis and patients with ulcerative colitis (UC). FMT modulates the Toll-like receptor 4 (TLR4) signaling pathway to treat some other diseases. However, it remains unknown whether this modulation is also involved in the treatment of UC.

AIM

To clarify the necessity of TLR4 signaling pathway in FMT on dextran sodium sulphate (DSS)-induced mice and explain the mechanism of FMT on UC, through association analysis of gut microbiota with colon transcriptome in mice.

METHODS

A mouse colitis model was constructed with wild-type (WT) and TLR4-knockout (KO) mice. Fecal microbiota was transplanted by gavage. Colon inflammation severity was measured by disease activity index (DAI) scoring and hematoxylin and eosin staining. Gut microbiota structure was analyzed through 16S ribosomal RNA sequencing. Gene expression in the mouse colon was obtained by transcriptome sequencing.

RESULTS

The KO (DSS + Water) and KO (DSS + FMT) groups displayed indistinguishable body weight loss, colon length, DAI score, and histology score, which showed that FMT could not inhibit the disease in KO mice. In mice treated with FMT, the relative abundance of *Akkermansia* decreased, and *Lactobacillus* became dominant. In particular, compared with those in WT mice, the scores of DAI and colon histology were clearly decreased in the KO-DSS group. Microbiota structure showed a significant difference between KO and WT mice. *Akkermansia* were the

dominant genus in healthy KO mice. The ineffectiveness of FMT in KO mice was related to the decreased abundance of *Akkermansia*. Gene Ontology enrichment analysis showed that differentially expressed genes between each group were mainly involved in cytoplasmic translation and cellular response to DNA damage stimulus. The top nine genes correlating with *Akkermansia* included Aqp4, Clca4a, Dpm^3, Fau, Mcrip1, Meis3, Nupr1 L, Pank3, and Rps13 ($|R| > 0.9$, $P < 0.01$).

CONCLUSION

FMT may ameliorate DSS-induced colitis by regulating the TLR4 signaling pathway. TLR4 modulates the composition of gut microbiota and the expression of related genes to ameliorate colitis and maintain the stability of the intestinal environment. *Akkermansia* bear great therapeutic potential for colitis.

Key Words: Toll-like receptor 4; Fecal microbiota transplantation; Colitis; *Akkermansia*; *Lactobacillus*; Aquaporin 4; Transcriptome sequencing

©The Author(s) 2023. Published by Baishideng Publishing Group Inc. All rights reserved.

Core Tip: Recent studies have shown that fecal microbiota transplantation (FMT) has a therapeutic role in patients with inflammatory bowel disease. The Toll-like receptor 4 (TLR4) signaling pathway may play a critical role in intestinal injury and repair. Here, we conducted animal experiments to explore the role of TLR4 in dextran sodium sulphate-induced colitis in mice and the treatment of FMT.

Citation: Wen X, Xie R, Wang HG, Zhang MN, He L, Zhang MH, Yang XZ. Fecal microbiota transplantation alleviates experimental colitis through the Toll-like receptor 4 signaling pathway. *World J Gastroenterol* 2023; 29(30): 4657-4670
URL: https://www.wjgnet.com/1007-9327/full/v29/i30/4657.htm
DOI: https://dx.doi.org/10.3748/wjg.v29.i30.4657

INTRODUCTION

Recent studies support that inflammatory bowel disease (IBD) can be categorized as a "microbial dysbiosis disease," because of its progression synchronizing the dysbacteriosis of gut microbiota[1]. Host physiology such as barrier function, metabolism, immune responses, and homeostasis involves microbiome-induced cell signaling, proliferation, and neurotransmitter biosynthesis[2]. In IBD patients, intestinal bacterial diversity decreases and the bacterial community structure changes[3]. In dextran sodium sulphate (DSS)-induced colitis in mice, some probiotics, including *Lactbacillus* and *Bifidobacterium*, are significantly reduced[4]. New evidence indicates that IBD is not merely a consequence of chronic inflammation, but also of disruption of the gut microbiome and destruction of the intestinal epithelial barrier[5].

Gut microbiota play a role in inflammation-related activities. Fecal microbiota transplantation (FMT) has shown high efficacy and safety in treating ulcerative colitis (UC)[6,7] due to its immunomodulatory and anti-inflammatory functions [8]. Our previous study showed that FMT can counter DSS-induced colitis in mice by increasing the relative abundance of *Lactobacillus*[9]. FMT has also shown therapeutic potential for a range of other diseases, such as hepatic disorders and metabolic syndrome[10]. Recent studies have demonstrated that Toll-like receptor 4 (TLR4) is exploited by FMT in treating many diseases such as spleen deficiency diarrhea[11], Parkinson's disease[12,13], developmental arsenic neurotoxicity[14], fluorosis[15], and acute lung injury[16]. Previous studies have indicated that FMT intervention can inhibit activation of the nuclear factor kappa B (NF-κB) signaling pathway[17], which is downstream of TLR4. However, there have been limited studies investigating the role of TLR4 in FMT for UC.

As a class of transmembrane proteins that recognize invading microbes and activate immune cells, Toll-like receptors (TLRs) regulate gene transcription and the acquired intestinal immune response[18]. In the etiology of IBD, microbes in the intestinal lumen induce abnormal immune responses, along with excessive leakage of bacterial antigens into the mucosa[19]. TLR4, an important immune activator, is highly expressed in the intestinal epithelial cells and lamina propria cells of UC patients[20]. It binds to ligands to activate cytokine signaling, recruit inflammatory cells, and damage intestinal mucosal barrier, all of which aggravate intestinal inflammatory lesions. More importantly, substantial evidence supports a pro-inflammatory role of the TLR4 signaling pathway in UC. Expression levels of TLR4 are positively correlated with disease activity indices (DAIs), endoscopy scores, and histopathological scores[21]. DSS-induced colitis deteriorates in mice with TLR4 overexpression[22,23], but is stably maintained in TLR4-deficient mice[24,25]. Multiple experiments have shown that inhibiting the TLR4 signaling pathway can prevent DSS-induced colitis[26,27]. While TLR4 plays a crucial role in intestinal injury and repair, its role in shaping colonic bacterial homeostasis and microbiota-related immunity remains poorly understood.

Our previous studies confirmed the efficacy FMT on IBD, but the mechanism has not been reported[9]. Therefore, we explored the role of TLR4 in the mechanism by which FMT treats DSS-induced colitis in the mice.

MATERIALS AND METHODS

Animals

Wild-type (WT) C57BL/10J mice and TLR4-knockout (KO) mice on the C57BL/10J background (female; 6 to 8 wk of age; weighing 18-20 g; specific pathogen-free (SPF) grade) were purchased from the Model Animal Research Center of Nanjing University (Nanjing, China). All mice were reared in an SPF condition at the experimental animal center of the Affiliated Huaian No. 1 People's Hospital of Nanjing Medical University. Throughout the acclimatization and study periods, all mice were maintained in a 12 h-light/12 h-dark cycle (21 °C ± 2 °C with a relatively constant humidity of 45% ± 10%) and had access to food and water *ad libitum*. All mice were group-housed and reared in a standard cage, with TLR4 KO mice kept separately from C57BL/10J mice in different cages.

DSS-induced colitis

DSS (36-50 kDa) was purchased from MP Biomedicals LLC (Irvine, CA, United States) and dissolved in distilled water. Experimental colitis was induced as previously described with minor changes[9]. For different groups, the mice were administered 2.5% (w/v) DSS in drinking water for 7 d. Mice in the KO (DSS + FMT) group were fed fecal microbiota from healthy WT mice from day 8 (once every 2 d) until the end of the experiment, while mice in the KO (DSS + water) group were fed normal saline at the same time. The mice were evaluated daily by scoring *via* the disease activity index (DAI)[28]. The DAI score was calculated on a 0-4 scale as previously described[29].

Fecal preparation and transplantation

The process of FMT was performed as previously described[9]. Briefly, feces from donor mice (healthy WT mice) were collected and resuspended in sterile normal saline at 0.125 g/mL. Then 0.2 mL of this suspension was administered to mice once every 2 d by oral gavage. This process lasted 7 d.

Histopathology

Mice were euthanized by cervical dislocation, and their abdominal cavity was opened immediately. The colon tissue was dissected; colons were measured for colon length, and tissues were examined for gross macroscopic appearance and stool consistency. The distal colon segment was placed in 10% neutral buffered formalin for 24 h, embedded in paraffin, and cut into sections 4 μm in thickness. Then the sections were stained with hematoxylin and eosin (H&E). H&E-stained sections were examined for inflammation and tissue damage by an experienced pathologist in a blinded manner. Tissue histology was scored by summing the scores of the following parameters according to a previous study[30]: Extent of inflammation, aberrant crypt foci, lymphocyte infiltration, and aberrant colon wall.

Fecal DNA extraction and 16S ribosomal RNA sequencing

Fecal DNA extraction and 16S ribosomal RNA (rRNA) sequencing were performed as previously reported[9]. The V3-V4 hypervariable region of the bacterial 16S-rRNA gene was amplified with primers 338F (5′-ACTCCTACGGGAG-GCAGCAG-3′) and 806R (5′-GGACTACHVGGGTWTCTAA T-3′) with the ABI GeneAmp® 9700 PCR thermocycler (Applied Biosystems, Foster City, CA, United States)[9]. All PCR products were extracted from a 2% agarose gel and purified using the AxyPrep DNA Gel Extraction Kit (Axygen Biosciences, Union City, CA, United States)[31]. Purified amplicons were sequenced on the Illumina MiSeq PE300 platform (Illumina, San Diego, CA, United States). The raw 16S rRNA gene sequencing reads were demultiplexed, quality-filtered by fastp version 0.20.0, and merged by FLASH version 1.2.7. Operational taxonomic units (OTUs) with 97% similarity cutoff[32] were clustered using UPARSE version 7.1[33], and chimeric sequences were identified and removed. Bacterial alpha-diversity was determined by sampling-based OTU analysis. Analysis of species accumulation curves was performed to assess the rationality and efficiency of the sequencing depth. Principal component analysis (PCA) was implemented in R programming. Using the Wilcoxon rank-sum test, the bacterial taxonomic analysis was performed for comparison at the bacterial phylum, class, order, family, genus levels between two groups. Based on the matrix of normalized relative abundance, bacteria with significantly different abundances between assigned taxa were determined by linear discriminant analysis effect size (LEfSe) with the Kruskal-Wallis rank-sum test ($P < 0.05$). LDA was used to assess the effect size of each feature (LDA score [log10] = 3 as the cut-off value).

Transcriptome analysis

Total RNA was extracted from inflammatory colonic tissue. For sequencing, a 1 cm colon tissue was sampled from the site about 2 cm from the anus, regardless of whether there was visible inflammation. The tissue samples with minimum and maximum histological scores were removed. Then the colon samples from four randomly chosen animals in each group was used for sequencing. Methods for amplifying and sequencing followed those previously published[9,29]. Briefly, 2 μg RNA per sample was used to sequence on the Illumina Hiseq 4000 platform. Differential expression analysis was performed using the DESeq R package (1.10.1) according to the manufacturer's protocol. Then, to explore the potential function of the differentially expressed genes (DEGs), GOseq R package[34] and KOBAS software[35] were used to test the enrichment of DEGs in Gene Ontology (GO) functional annotations[36] and Kyoto Encyclopedia of Genes and Genomes (KEGG) pathways[37].

Correlation analysis for gut microbiota and transcriptome

We used Metastats software to confirm the difference in the relative abundance of microbiota among the samples ($P \leq$

0.05). We used DEG sequencing to carry out transcriptome difference analysis (the threshold was *P*adj < 0.05 & |log2FC| > 1). Finally, R psych software package was used to analyze the Spearman association between the transcriptome and intestinal microflora. Those with $|R| > 0.8$ and $P < 0.05$ (strong correlation) were screened for mapping.

Statistical analysis

Differences were analyzed using the *t*-test with Graphpad Prism 8.0 software (GraphPad Software Inc., La Jolla, CA, United States). Results are shown as the mean ± standard error of the mean. $P < 0.05$ was considered statistically significant.

RESULTS

FMT does not improve acute colitis induced by DSS in TLR4-KO mice

In our previous experiment, we found that FMT is effective to treat colitis[9]. We further explored whether this efficacy is related to the TLR4 pathway. Acute DSS-induced colitis was induced in eight animals per group using 2.5% DSS in the drinking water. After gavage with fecal microbiota from the WT mice, mice in the KO (DSS + water) and KO (DSS + FMT) groups displayed indistinguishable body weight loss, colon length, DAI score, and histology score (Figure 1A-D). Beyond our expectation, FMT had no effect on colonic inflammation in TLR4-KO mice. We compared the expression of TLR4 gene in the intestine of WT mice before and after FMT. The transcriptome sequence data indicated that DSS increased, but FMT effectively decreased the expression of TLR4 (Figure 1E).

FMT changes the intestinal flora of TLR4-KO mice

We investigated whether FMT changed the composition of gut microbiota in the KO (DSS + water) and KO (DSS + FMT) groups. We employed LEfSe to evaluate the bacterial taxa (at genus level) in the two groups (Figure 2A). The dominating taxa in KO (DSS + FMT) group were enriched in *Lactobacillus*, which indicated that we had successfully transplanted the gut microbiota of healthy WT mice. Meanwhile, the KO (DSS + FMT) group had a lower abundance of *Akkermansia*, indicating that FMT could alter the relative abundance of *Akkermansia* in KO mice (Figure 2B).

TLR4 KO alleviates DSS-induced colitis

We used TLR4-deficient mice and WT mice to determine whether TLR4 may protect mice from DSS-induced colitis. Mice in the KO-DSS ($n = 8$) and WT-DSS ($n = 7$) groups were given distilled drinking water containing 2.5% DSS for 7 d (Figure 3A). Compared with WT mice, KO mice showed lower susceptibility to DSS, as manifested by their much smaller body weight loss (Figure 3B), lower DAI (Figure 3C), and longer colons (Figure 3D). Compared to the WT-DSS group, mice in the KO-DSS group exhibited a more intact colon structure, less severe crypt damage, and reduced inflammatory infiltration (Figure 3E). In summary, KO mice showed increased tolerance to DSS-induced colitis.

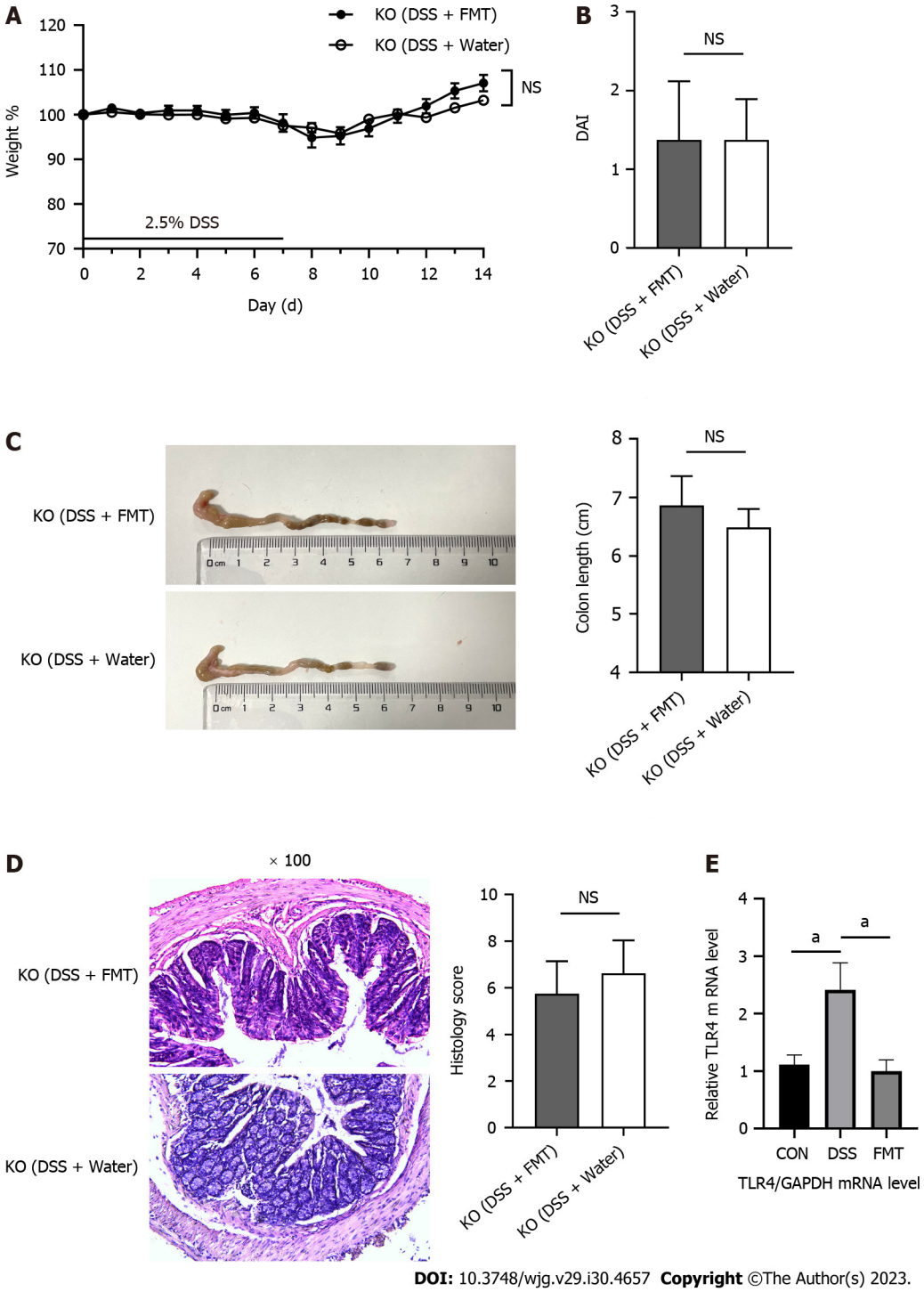
TLR4 deficiency influences the diversity and composition of gut microbiota

We further investigated whether the protection against DSS-induced colitis was due to TLR4 KO or microbiota re-composition. We detected the gut microbiota of WT and KO mice in the basal and DSS-treated states. We analyzed the beta-diversity of microbiota based on PCA. An evident clustering separation between OTUs revealed the different community structures between each two groups, suggesting that these communities are distinct in terms of their compositional structure (Figure 4A and 5A).

At the phylum level, TLR4 deficiency decreased the abundance of *Bacteroidetes* and increased the abundances of *Actinobacteria* and *Verrucomicrobia* ($P < 0.05$; Figure 4B), compared to those in WT mice. After DSS induction, a significant increase of phylum *Proteobacteria* was observed in the WT-DSS group compared to the KO-DSS group ($P < 0.05$; Figure 5B). *Verrucomicrobia* was the most abundant phylum among those with significant differences ($P < 0.05$). At the genus level, *Akkermansia* abundance was significantly higher in KO mice than in WT mice either healthy or diseased ($P < 0.05$; Figure 4C and 5C). To further investigate the potential effect of microbiota composition on DSS-induced colitis, we used the LEfSe to detect the marked differences in the dominant bacterial communities between the two groups (Figure 4D and 5D). Specifically, *Lactobacillus* and *Peptococcus* were enriched in the WT-CON group (Figure 4D), while *Escherichia Shigella* and *Anaerotruncus* were enriched in the WT-DSS group (Figure 5D). Interestingly, *Akkermansia* and *Bifidobacterium* were enriched either in healthy and diseased KO mice (Figure 4D and 5D). The collective results of our study indicated clear differences in the intestinal microbiome between WT mice and KO mice, both in healthy conditions and during illness. These findings highlight the important role of TLR4 in shaping the composition and diversity of the intestinal microbiota.

TLR4-KO-shaped microbiota affect the transcriptome in the colon of mice

To further explore whether FMT can change the gene expression related to TLR4, we investigated the DEGs between groups. Compared to those in the WT-DSS group, 1436 genes were differentially expressed in the KO-DSS group, and 309 genes in the KO (DSS + FMT) group. Furthermore, 193 DEGs were found among the KO-DSS group, WT-DSS group, and KO (DSS + FMT) group (Figure 6A). GO enrichment analysis showed that these DEGs were mainly involved in cytoplasmic translation and cellular response to DNA damage stimulus (Figure 6B). According to 16S rRNA sequencing analysis, we found that *Akkermansia* was dominant in the KO group. To characterize potential gene-microbe interactions, we computed gene-microbe correlations with Spearman correlation efficients (Figure 6C). The top nine genes correlating



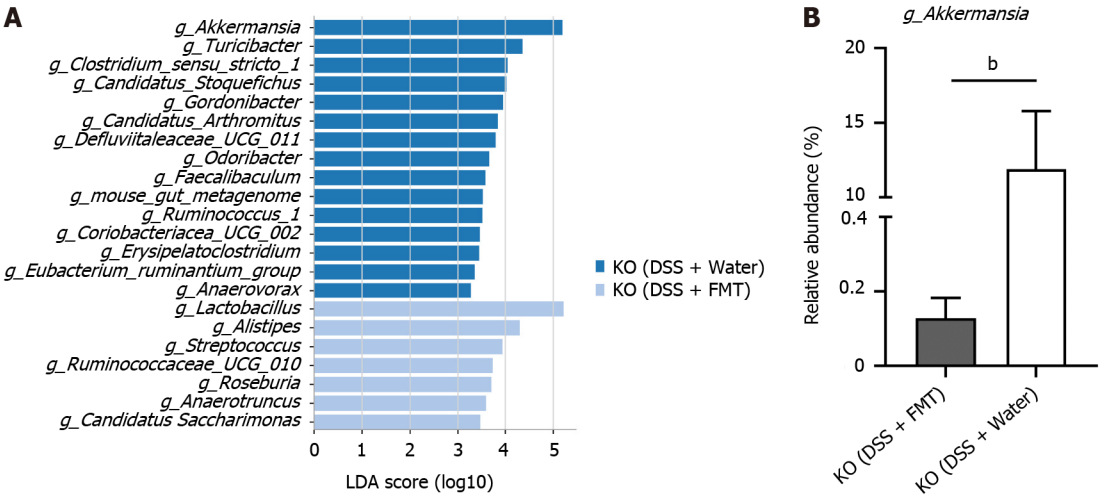
DOI: 10.3748/wjg.v29.i30.4657 **Copyright** ©The Author(s) 2023.

Figure 1 Fecal microbiota transplantation did not alleviate acute colitis induced by dextran sodium sulphate in Toll-like receptor 4 knockout mice. A: Body weight of mice during the course of colitis; B: The bar chart represents the disease activity index (DAI) score of mice on day 14; C: Representative images of colons from mice (left) and statistical analysis of colon length (right); D: Representative hematoxylin and eosin staining of colon tissues, original magnification 100 ×, and histological scores (right); E: Relative quantification of the transcription level of Toll-like receptor 4 (TLR4) among groups. $^{a}P < 0.05$. DSS: Dextran sodium sulphate; FMT: Fecal microbiota transplantation; KO: Knockout.

with *Akkermansia* included Aqp4, Clca4a, Dpm^{3}, Fau, Mcrip1, Meis3, Nupr1 L, Pank3, and Rps13 ($|R| > 0.9$, $P < 0.01$).

DISCUSSION

Researchers have found that patients with active UC can benefit from FMT[38]. Moreover, our previous study also verified that FMT can treat colitis in mice. In the present study, the expression of TLR4 was upregulated by DSS, and downregulated after FMT. It therefore stands to reason that, by inhibiting TLR4, a protective effect from intestinal inflam-



DOI: 10.3748/wjg.v29.i30.4657 **Copyright** ©The Author(s) 2023.

Figure 2 Fecal microbiota transplantation changed the gut microbiota of Toll-like receptor 4 knockout mice. A: Linear discriminant analysis (LDA) effect size (LEfSe) analysis in two groups with an LDA score > 3.0; B: The relative abundance of *Akkermansia* in Toll-like receptor 4 knockout mice. [a]*P* < 0.05, [b]*P* < 0.01. DSS: Dextran sodium sulphate; FMT: Fecal microbiota transplantation.

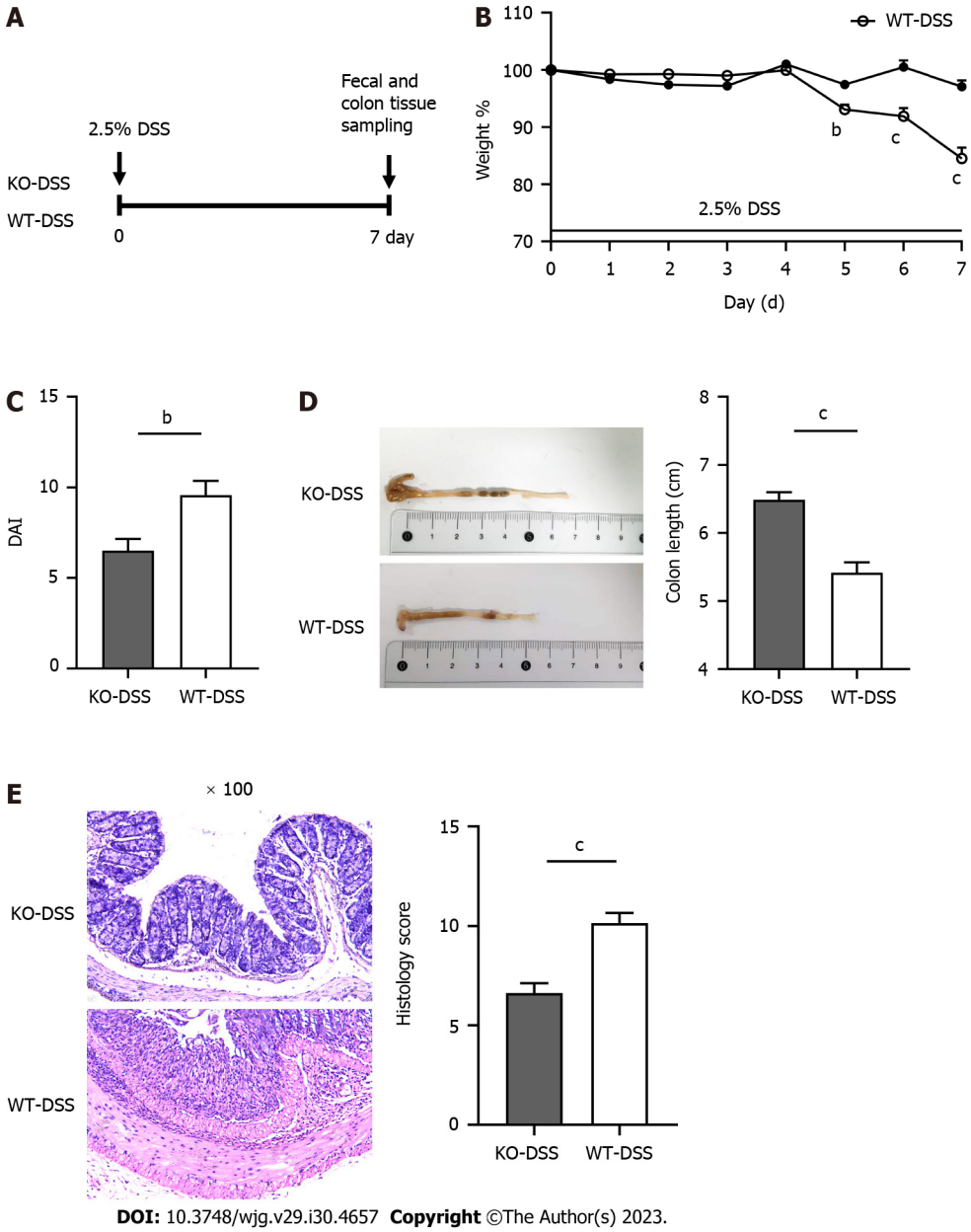
mation will be induced. Considering the ubiquitous involvement of the TLR4 signaling pathway in the activities of the mucosa, we designed this animal study to elucidate its interaction with FMT in UC. In this study, TLR4 KO significantly alleviated the clinical and histological manifestations of DSS-induced colitis. Notably, the increased relative abundance of the predominant *Akkermansia* species contributed to the heightened resistance against colon inflammation. Through further investigation, we discovered that genetic KO of TLR4 significantly impacted the structure and composition of the gut microbiota, resulting in a shift towards an anti-inflammatory configuration. This shift plays a crucial role in promoting enhanced resistance and tolerance to colitis.

At the phylum level, DSS changed the relative abundances of *Bacteroidetes*, *Actinobacteria,* and *Verrucomicrobia* in TLR4-KO mice compared to WT mice. Possibly, the high abundance of anti-inflammatory *Akkermansia* in the gut microbiota curbs the aggravation of colitis, despite the absence of TLR4 signaling. *Akkermansia* was the dominant genus in healthy KO mice, while after the treatment of FMT, their level decreased. Compared with that in the WT group, the status of colitis in the KO group was not significantly attenuated by FMT, suggesting that the therapeutic effect of FMT on colitis is closely related to the TLR4 signaling pathway and *Akkermansia*.

In the gut, the expression of TLRs changes with the composition of microbiota[39], as well as the activity of the intestinal epithelium such as inflammation[40]. In the present study, we observed the difference in microbial composition between WT-DSS and KO-DSS groups. At the phylum level, the KO-DSS group had a higher relative abundance of *Actinobacteria* and *Verrucomicrobia*, while WT-DSS had a higher relative abundance of *Proteobacteria*. In addition, *Verrucomicrobia* demonstrated the most significant difference at the phylum level. Lo Sasso *et al*[41] analyzed the composition of gut microbiota in UC patients *via* fecal microbiota whole-genome sequencing, finding increased abundance of *Proteobacteria* and decreased abundance of *Verrucomicrobia*. In addition, one study characterized the mucosal microbiome of pediatric UC patients, noting a significant decrease in the phylum *Verrucomicrobia* at the phylum level[42]. It has been reported that the abundance of *Proteobacteria* increases in UC mice[43]. Moreover, the relative abundance of *Proteobacteria* in DSS-induced mice rises remarkably, compared with that in WT mice, which can be restored to normal after Lizhong therapy[44]. Consistently, this study proves that DSS can raise the abundance of *Proteobacteria* in WT mice, rather than KO mice.

In particular, we found that the abundance of *Akkermansia* increased in the KO-DSS group, but then dropped notably after FMT, indicating its role in the effect of FMT on UC. As previously reported, the abundance of *Akkermansia* decreases in UC patients[45], but it is unclear whether this is a cause or consequence of UC. *Akkermansia* can protect intestinal barrier function and reduce the production of inflammatory cytokines[46]. On the other hand, *Akkermansia* can increase the production of short-chain fatty acids and antioxidant enzymes, indicating that *Akkermansia* may proliferate to alleviate colitis[47]. According to our experiment, the relative abundance of *Akkermansia* was negatively correlated with the severity of colitis in our animal models. *Akkermansia* bear great therapeutic potential for colitis. Studies on human and mice have revealed that the injection of beneficial bacteria such as *Lactobacillus*, *Akkermansia,* and *Bifidobacterium* can alleviate the inflammation in UC patients[48-50]. In a systematic review of three studies, the abundance of *Akkermansia* decreased in all UC patients[51]. A high abundance of *Akkermansia* can modulate host metabolism to prevent seizures [52]. Several *Akkermansia* species have demonstrated the ability to modulate immune responses and protect barrier function[53].

Despite the widely recognized beneficial properties of *Akkermansia* as a potential probiotic, it is crucial to take into account the potential occurrence of adverse effects. Patients with colorectal cancer have a higher abundance of *A. muciniphila*[3]. A prior study demonstrated that the genetic deletion of TLR4 exacerbates the severity of colon inflammation, resulting in the decreased abundance of *Akkermansia*[54]. This conflicting conclusion may be explained by various factors, such as the different mouse species and different experimental models used. When the equilibrium of the gut

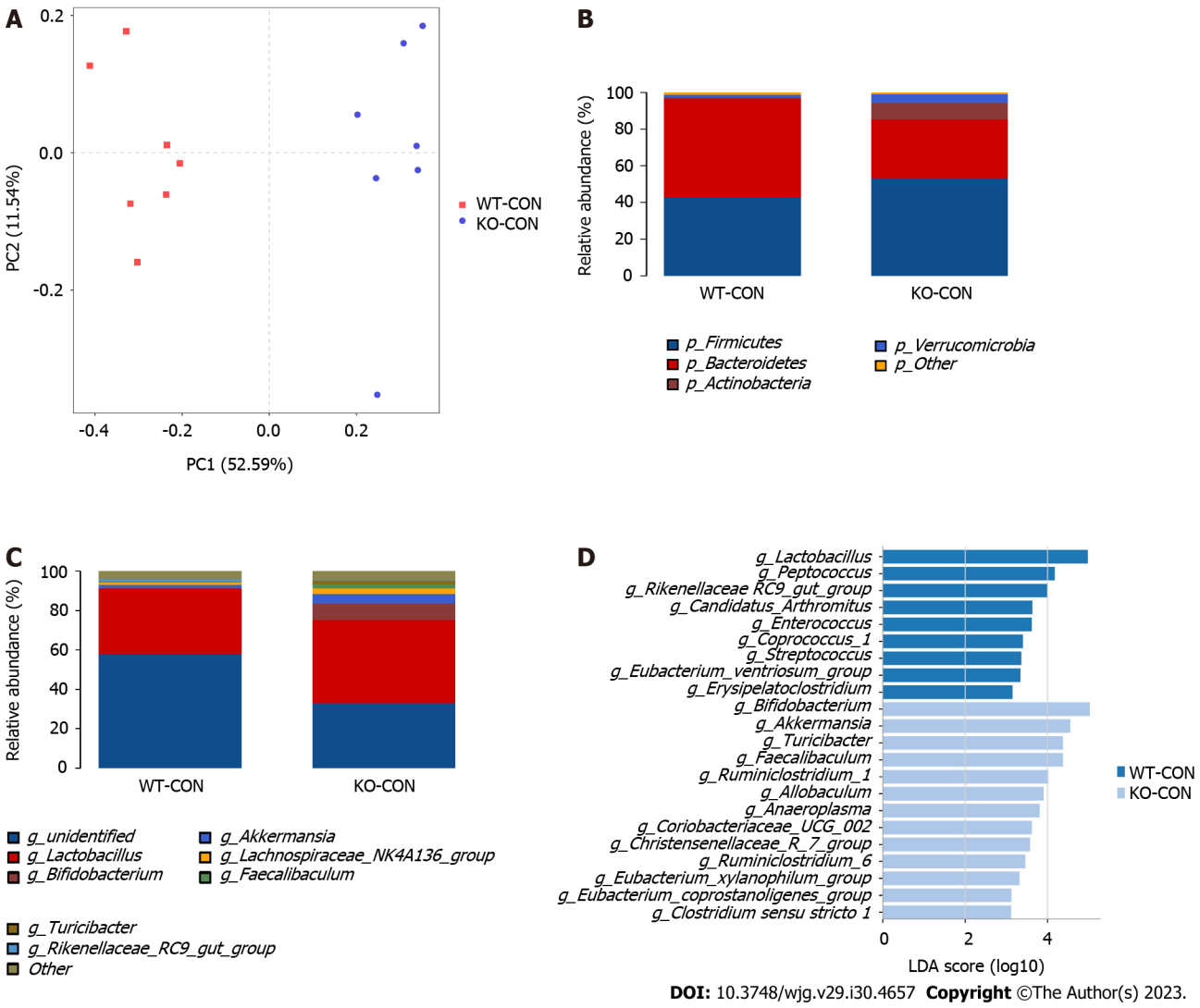


DOI: 10.3748/wjg.v29.i30.4657 **Copyright** ©The Author(s) 2023.

Figure 3 Toll-like receptor 4 knockout alleviated dextran sodium sulphate-induced inflammation in the colon. A: Scheme of the animal experimental design; B: The change in body weight of mice from days 0 to 7 during the disease course (knockout-dextran sodium sulphate [KO-DSS]: $n = 8$; wild type [WT]-DSS: $n = 7$); C: The bar chart represents the disease activity index (DAI) score on day 7; D: Representative colons (left) and statistical analysis (right) of colonic length; E: Representative hematoxylin and eosin staining of colon tissues (left), original magnification 100 ×, and histological scores (right). $^{a}P < 0.05$, $^{b}P < 0.01$, and $^{c}P < 0.001$ were considered statistically significant. FMT: Fecal microbiota transplantation.

microbiota is disturbed, beneficial microbes have the potential to shift towards virulent species, leading to adverse effects on the host. Studies have suggested a potential link between *Akkermansia* and TLR4 signaling. A study demonstrated that the administration of anthocyanins extracted from *Lycium ruthenicum* (ACs) increases the abundance of *Akkermansia*, thus inhibiting the lipopolysaccharide/NF-κB/TLR4 pathway to improve intestinal function[55]. It has also been observed that inhibition of the TLR4 signaling pathway can increase the abundance of *Akkermansia*[56]. *Akkermansia* promotes the integrity of the intestinal barrier and regulates immune homeostasis, potentially by interacting with TLR4[57,58]. In this study, the composition and structure of gut microbiota presented a significant difference between KO-DSS mice and WT-DSS mice. Based on the above results, we advocate that *Akkermansia* can increase resistance to acute colitis in TLR4-KO mice. However, more in-depth investigations are needed to determine if *Akkermansia* negatively associated with TLR4 are a potential target of FMT in treating UC.

TLR4 is differentially expressed in patients with early and advanced UC, indicating a close correlation between TLR4 and UC[59]. Inhibition of TLR4 significantly decreases the expression of cell cycle regulatory genes. Furthermore, TLR4 signaling in colonic epithelial cells promotes the recruitment of inflammatory cells through microRNA 155-mediated posttranscriptional regulation[60]. In the current study, our results showed that FMT downregulated the expression of genes related to the TLR4/myosin light chain kinase signaling pathway in WT mice, highlighting the importance of TLR4 in the effectiveness of FMT. Functional analysis revealed that most DEGs were enriched in cytoplasmic translation and

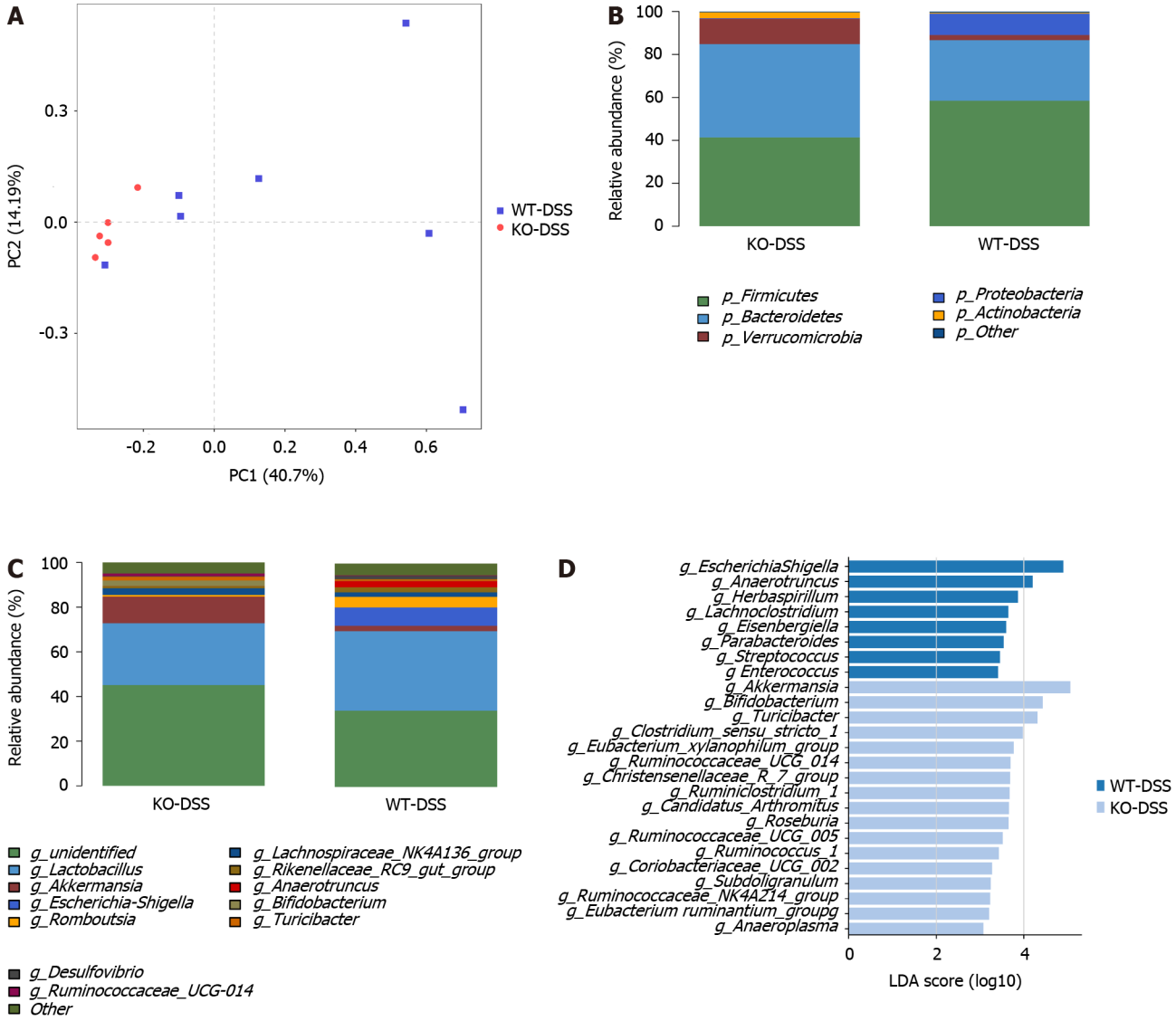


DOI: 10.3748/wjg.v29.i30.4657 **Copyright** ©The Author(s) 2023.

Figure 4 Diversities and compositions of gut microbiota in knockdown-control and wild type-control groups. A: β-diversity evaluated using the weighted UniFrac-based PCA (knockdown-control [KO-CON]: *n* = 7; wild type [WT]-CON: *n* = 7); B and C: Bar graphs showing the relative abundances of different bacteria at the phylum and genus levels; D: Linear discriminant analysis (LDA) effect size analysis in groups with an LDA score > 3.0 between two groups.

cellular response to DNA damage stimulus. The top nine DEGs strongly related to *Akkermansia* were primarily associated with cell cycle regulation, transcriptional control, apoptosis, stress responses, and inflammatory responses. Their functions aligned with the main processes identified in GO analysis, indicating their involvement in crucial biological pathways. These functions highlight its potential role in modulating various cellular activities. Aquaporin 4 (AQP4), a water channel protein that facilitates transmembrane water movement, has the strongest correlation[61]. AQPs are widely distributed in mammals' secretory and absorptive epithelial cells and are responsible for transport and trafficking processes. In colonic inflammation, AQP4 is abundantly expressed in the basolateral membrane of colonic epithelial cells in humans and mice. The permeability of cell membranes is positively correlated with AQP4 expression[62]. AQP4 overexpression facilitates the entry of water into cytes, thereby contributing to cytotoxic edema[63-65]. AQP4 deficiency alleviates experimental colitis in the mice[66]. Although we did not use the same mouse KO model in the present study, the effect of AQP4 on colonic inflammation is consistent with that of TLR4. Activating the high mobility group box 1 protein/TLR4/NF-κB pathway can increase the expression of AQP4[67,68]. Furthermore, lipopolysaccharide, a potent TLR4 agonist, significantly increases the mRNA level of AQP4 expression through TLR4 signaling in the cortex and astrocytes[62]. We speculate that TLR4 deficiency can protect against colitis by increasing the abundance of *Akkermansia* and reducing the expression of AQP4. As shown by previous results, FMT can relieve colitis in WT mice[9]. However, in this study, FMT did not exert effects on colonic inflammation in TLR4-KO mice. It was intriguing to determine that the abundance of *Akkermansia*, which was dominant in TLR4-KO mice, was significantly decreased after FMT. This may be related to the decreased relative abundance of *Akkermansia*. While the DEGs mentioned above may have roles in immune regulation, inflammation, or cellular processes that can intersect with TLR4 signaling, their specific relationships with TLR4 are not extensively characterized. Notwithstanding, further studies are needed to determine whether FMT also targets *Akkermansia* to regulate the expression of related DEGs in countering colon inflammation.

In this study, we assessed the microbial diversity and composition in DSS-induced mice. The bacteria inhabited in the mucosa may play major roles in the development of IBD. So it is necessary to explore the function of microbiota in



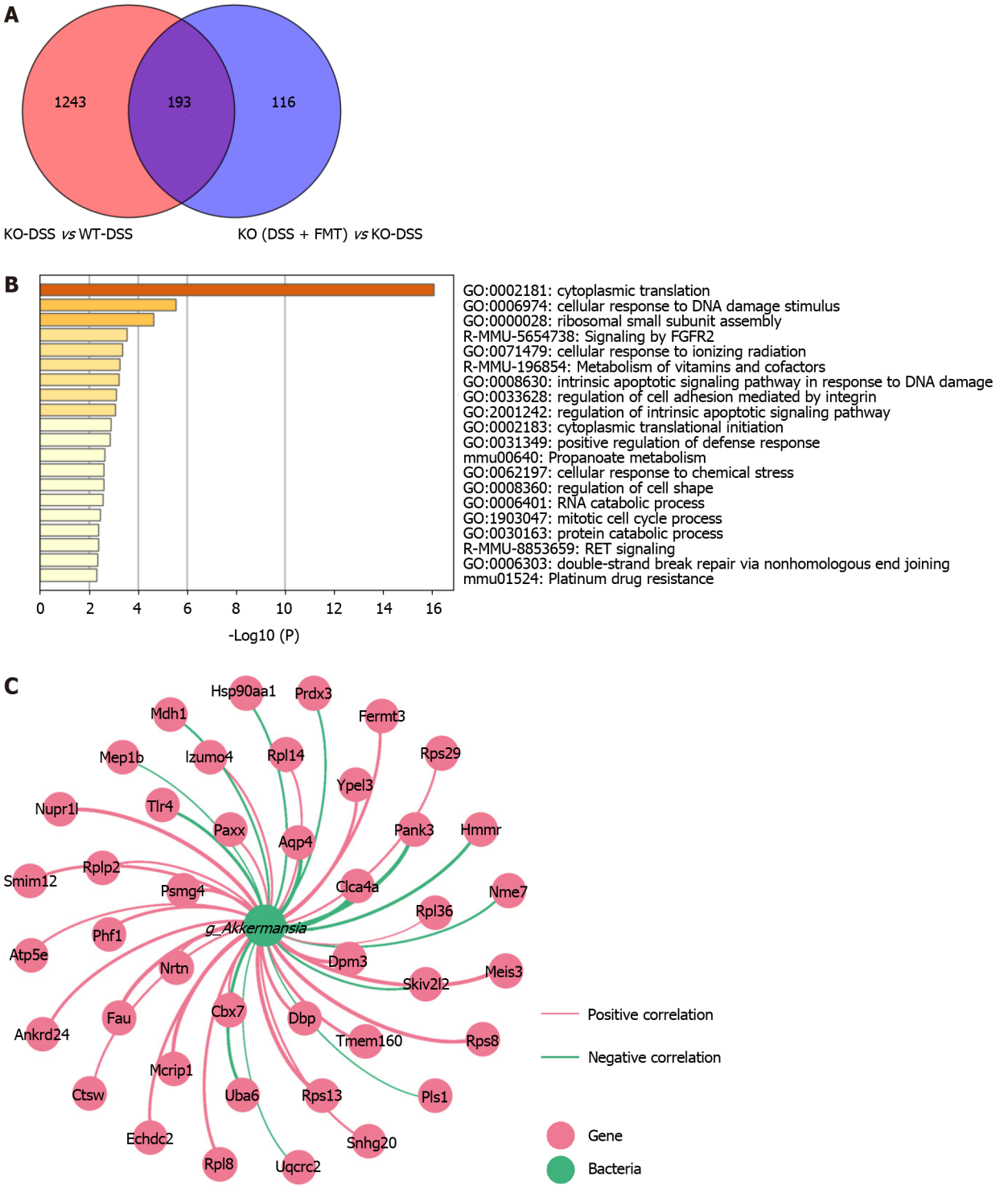
DOI: 10.3748/wjg.v29.i30.4657 **Copyright** ©The Author(s) 2023.

Figure 5 Diversities and compositions of gut microbiota in knockout-dextran sodium sulphate and wild type-dextran sodium sulphate groups. A: Multiple sample principal component analysis (knockout-dextran sodium sulphate [KO-DSS]: *n* = 5; wild type [WT]-DSS: *n* = 7); B and C: Bar graphs showing the relative abundances of different bacteria at the phylum and genus levels; D: Linear discriminant analysis (LDA) effect size (LEfSe) analysis in groups with an LDA score > 3.0.

mucosal tissues in future study. However, animal studies have certain limitations in evaluating the mechanism of TLR4. Therefore, clinical studies should be designed to unveil the interplay among TLR4, gut microbiota, and UC.

CONCLUSION

TLR4 modulates the composition of gut microbiota and regulates the expression of microbiome-related genes to ameliorate colitis and maintain the stability of the intestinal environment. For the first time, we find that FMT may ameliorate DSS-induced colitis by regulating the TLR4 signaling pathway. Our findings will make the treatment of patients more targeted and is worthy of clinical trials in the future.



DOI: 10.3748/wjg.v29.i30.4657 **Copyright** ©The Author(s) 2023.

Figure 6 Colonic transcriptome profile and gene-microbe correlation. A: Venn diagram illustrates genes regulated by fecal microbiota transplantation (FMT) and Toll-like receptor 4 knockout (KO); B: The top 20 Gene Ontology terms enriched in these 193 differentially expressed genes (DEGs); C: Network visualizing 193 DEGs associated with *Akkermansia* (|R| > 0.8, $P < 0.05$). CON: Control; DSS: Dextran Sodium Sulphate; WT: Wild type.

ARTICLE HIGHLIGHTS

Research background

It is well known that microbiota dysbiosis contributes to the occurrence of inflammatory bowel disease (IBD). Fecal microbiota transplantation (FMT) has shown promising therapeutic effects on both clinical and basic studies of ulcerative colitis (UC). Substantial evidence supports a negative pro-inflammatory role of Toll-like receptor 4 (TLR4) signaling pathway in IBD. However, it remains unknown whether this modulation is also involved in the treatment of FMT on UC.

Research motivation

FMT treats other diseases by regulating the TLR4 signaling pathway. Previous studies have shown that the expression of TLR4 is higher in the intestinal mucosa of patients with effective FMT and lower in patients with poor FMT. We speculate that the TLR4 signaling pathway may be involved in the therapeutic mechanism of FMT on IBD.

Research objectives

To clarify the necessity of TLR4 signaling pathway in FMT on regulating gut microbiota in dextran sodium sulphate (DSS)-induced colitis.

Research methods

Experimental colitis was constructed in wild-type (WT) and TLR4-knockout (KO) mice and fecal microbiota was transplanted by gavage. Colon inflammation severity in mouse model was measured by disease activity index (DAI) score and hematoxylin and eosin (H&E) staining. Gut microbiota alteration was analyzed through 16S ribosomal RNA sequencing. The difference of gene expression in mouse colon was obtained by transcriptome sequencing of colon tissue.

Research results

In KO mice treated with FMT or water, these two groups displayed indistinguishable body weight loss, colon length, DAI score, and histology score, which showed that FMT could hardly alter the disease progress in KO mice. Next, compared with WT mice, the scores of DAI and colon histology clearly decreased in the KO-DSS group. KO mice experienced enhanced resistibility to DSS-induced colitis. There was a significant difference in the microbiota structure between KO and WT mice. *Akkermansia* was the dominant genus in healthy KO mice. But unexpectedly, after treatment with FMT, the relative abundance of *Akkermansia* decreased, while the level of *Lactobacillus* in the intestine of mice was maintained. The ineffectiveness in KO mice after FMT was related to the decrease of *Akkermansia*. GO enrichment analysis showed that DEGs between each group were mainly involved in cytoplasmic translation and cellular response to DNA damage stimulus. Finally, we listed the top nine genes related to *Akkermansia*.

Research conclusions

FMT may ameliorate DSS-induced colitis by regulating the TLR4 signaling pathway.

Research perspectives

This study provides new insights into the underlying mechanisms of FMT as a treatment for UC, which greatly helps to optimize FMT treatment in the future.

FOOTNOTES

Author contributions: Wen X, Xie R, and Wang HG contributed equally to this work; Wen X, Xie R, and Wang HG conceived and designed this work, and drafted and revised the manuscript; Wen X, Zhang MN, He L, and Zhang MH performed the experiments, collected samples, and analyzed the data; Yang XZ and Wang HG worked on the concept and guidance of this study; Yang XZ and Wang HG provided the funding support and project administration; All authors have read and approved the final manuscript.

Supported by the Scientific Research Project of Jiangsu Provincial Health Commission, No. H2018082; Huai'an Natural Science Research Project Project, No. HAB201926; and Scientific Research Project of Translational Medicine Innovation Team of Huai'an First People's Hospital, No. YZHT201905.

Institutional animal care and use committee statement: The animal experimental protocol was approved by experimental animal ethics committee of the Affiliated Huaian No. 1 People's Hospital of Nanjing Medical University (Approval No. DW-P-2018-008-01).

Conflict-of-interest statement: The authors have no conflicts interest to declare.

Data sharing statement: The data presented in the study are available in article. The datasets analysed during the current study are available in the NCBI Sequence Read Archive (SRA) database, submission number: SUB11829874.

ARRIVE guidelines statement: The authors have read the ARRIVE guidelines, and the manuscript was prepared and revised according to the ARRIVE guidelines.

Open-Access: This article is an open-access article that was selected by an in-house editor and fully peer-reviewed by external reviewers. It is distributed in accordance with the Creative Commons Attribution NonCommercial (CC BY-NC 4.0) license, which permits others to distribute, remix, adapt, build upon this work non-commercially, and license their derivative works on different terms, provided the original work is properly cited and the use is non-commercial. See: https://creativecommons.org/Licenses/by-nc/4.0/

Country/Territory of origin: China

ORCID number: Xin Wen 0000-0001-8904-1340; Hong-Gang Wang 0000-0003-4761-0407; Min-Na Zhang 0000-0003-1567-3788; Meng-Hui Zhang 0000-0002-8679-386X; Xiao-Zhong Yang 0000-0003-2036-5878.

S-Editor: Chen YL
L-Editor: Filipodia
P-Editor: Yuan YY

REFERENCES

1 **Ni J**, Wu GD, Albenberg L, Tomov VT. Gut microbiota and IBD: causation or correlation? *Nat Rev Gastroenterol Hepatol* 2017; **14**: 573-584 [PMID: 28743984 DOI: 10.1038/nrgastro.2017.88]
2 **Schirmer M**, Garner A, Vlamakis H, Xavier RJ. Microbial genes and pathways in inflammatory bowel disease. *Nat Rev Microbiol* 2019; **17**: 497-511 [PMID: 31249397 DOI: 10.1038/s41579-019-0213-6]
3 **Ma Y**, Zhang Y, Xiang J, Xiang S, Zhao Y, Xiao M, Du F, Ji H, Kaboli PJ, Wu X, Li M, Wen Q, Shen J, Yang Z, Li J, Xiao Z. Metagenome Analysis of Intestinal Bacteria in Healthy People, Patients With Inflammatory Bowel Disease and Colorectal Cancer. *Front Cell Infect Microbiol* 2021; **11**: 599734 [PMID: 33738265 DOI: 10.3389/fcimb.2021.599734]
4 **Liu Y**, Luo L, Luo Y, Zhang J, Wang X, Sun K, Zeng L. Prebiotic Properties of Green and Dark Tea Contribute to Protective Effects in Chemical-Induced Colitis in Mice: A Fecal Microbiota Transplantation Study. *J Agric Food Chem* 2020; **68**: 6368-6380 [PMID: 32419454 DOI: 10.1021/acs.jafc.0c02336]
5 **Mehandru S**, Colombel JF. The intestinal barrier, an arbitrator turned provocateur in IBD. *Nat Rev Gastroenterol Hepatol* 2021; **18**: 83-84 [PMID: 33318680 DOI: 10.1038/s41575-020-00399-w]
6 **Thomas H**. IBD: FMT induces clinical remission in ulcerative colitis. *Nat Rev Gastroenterol Hepatol* 2017; **14**: 196 [PMID: 28250470 DOI: 10.1038/nrgastro.2017.27]
7 **Moayyedi P**, Surette MG, Kim PT, Libertucci J, Wolfe M, Onischi C, Armstrong D, Marshall JK, Kassam Z, Reinisch W, Lee CH. Fecal Microbiota Transplantation Induces Remission in Patients With Active Ulcerative Colitis in a Randomized Controlled Trial. *Gastroenterology* 2015; **149**: 102-109.e6 [PMID: 25857665 DOI: 10.1053/j.gastro.2015.04.001]
8 **Lima SF**, Gogokhia L, Viladomiu M, Chou L, Putzel G, Jin WB, Pires S, Guo CJ, Gerardin Y, Crawford CV, Jacob V, Scherl E, Brown SE, Hambor J, Longman RS. Transferable Immunoglobulin A-Coated Odoribacter splanchnicus in Responders to Fecal Microbiota Transplantation for Ulcerative Colitis Limits Colonic Inflammation. *Gastroenterology* 2022; **162**: 166-178 [PMID: 34606847 DOI: 10.1053/j.gastro.2021.09.061]
9 **Wen X**, Wang HG, Zhang MN, Zhang MH, Wang H, Yang XZ. Fecal microbiota transplantation ameliorates experimental colitis *via* gut microbiota and T-cell modulation. *World J Gastroenterol* 2021; **27**: 2834-2849 [PMID: 34135557 DOI: 10.3748/wjg.v27.i21.2834]
10 **Green JE**, Davis JA, Berk M, Hair C, Loughman A, Castle D, Athan E, Nierenberg AA, Cryan JF, Jacka F, Marx W. Efficacy and safety of fecal microbiota transplantation for the treatment of diseases other than Clostridium difficile infection: a systematic review and meta-analysis. *Gut Microbes* 2020; **12**: 1-25 [PMID: 33345703 DOI: 10.1080/19490976.2020.1854640]
11 **Xu J**, Liu C, Shi K, Sun X, Song C, Xu K, Liu Y. Atractyloside-A ameliorates spleen deficiency diarrhea by interfering with TLR4/MyD88/NF-κB signaling activation and regulating intestinal flora homeostasis. *Int Immunopharmacol* 2022; **107**: 108679 [PMID: 35279514 DOI: 10.1016/j.intimp.2022.108679]
12 **Zhao Z**, Ning J, Bao XQ, Shang M, Ma J, Li G, Zhang D. Fecal microbiota transplantation protects rotenone-induced Parkinson's disease mice *via* suppressing inflammation mediated by the lipopolysaccharide-TLR4 signaling pathway through the microbiota-gut-brain axis. *Microbiome* 2021; **9**: 226 [PMID: 34784980 DOI: 10.1186/s40168-021-01107-9]
13 **Zhong Z**, Chen W, Gao H, Che N, Xu M, Yang L, Zhang Y, Ye M. Fecal Microbiota Transplantation Exerts a Protective Role in MPTP-Induced Parkinson's Disease *via* the TLR4/PI3K/AKT/NF-κB Pathway Stimulated by α-Synuclein. *Neurochem Res* 2021; **46**: 3050-3058 [PMID: 34347266 DOI: 10.1007/s11064-021-03411-0]
14 **Zhao Q**, Hao Y, Yang X, Mao J, Tian F, Gao Y, Tian X, Yan X, Qiu Y. Mitigation of maternal fecal microbiota transplantation on neurobehavioral deficits of offspring rats prenatally exposed to arsenic: Role of microbiota-gut-brain axis. *J Hazard Mater* 2023; **457**: 131816 [PMID: 37307732 DOI: 10.1016/j.jhazmat.2023.131816]
15 **Zhang S**, Zhao T, Wang Y, Mi J, Liu J, Fan X, Niu R, Sun Z. Intestinal microbiota regulates colonic inflammation in fluorosis mice by TLR/NF-κB pathway through short-chain fatty acids. *Food Chem Toxicol* 2023; **178**: 113866 [PMID: 37269894 DOI: 10.1016/j.fct.2023.113866]
16 **Tang J**, Xu L, Zeng Y, Gong F. Effect of gut microbiota on LPS-induced acute lung injury by regulating the TLR4/NF-κB signaling pathway. *Int Immunopharmacol* 2021; **91**: 107272 [PMID: 33360370 DOI: 10.1016/j.intimp.2020.107272]
17 **Zhang W**, Zou G, Li B, Du X, Sun Z, Sun Y, Jiang X. Fecal Microbiota Transplantation (FMT) Alleviates Experimental Colitis in Mice by Gut Microbiota Regulation. *J Microbiol Biotechnol* 2020; **30**: 1132-1141 [PMID: 32423189 DOI: 10.4014/jmb.2002.02044]
18 **Ley RE**, Peterson DA, Gordon JI. Ecological and evolutionary forces shaping microbial diversity in the human intestine. *Cell* 2006; **124**: 837-848 [PMID: 16497592 DOI: 10.1016/j.cell.2006.02.017]
19 **Park JH**, Peyrin-Biroulet L, Eisenhut M, Shin JI. IBD immunopathogenesis: A comprehensive review of inflammatory molecules. *Autoimmun Rev* 2017; **16**: 416-426 [PMID: 28212924 DOI: 10.1016/j.autrev.2017.02.013]
20 **Ocansey DKW**, Wang L, Wang J, Yan Y, Qian H, Zhang X, Xu W, Mao F. Mesenchymal stem cell-gut microbiota interaction in the repair of inflammatory bowel disease: an enhanced therapeutic effect. *Clin Transl Med* 2019; **8**: 31 [PMID: 31872304 DOI: 10.1186/s40169-019-0251-8]
21 **Tan Y**, Zou KF, Qian W, Chen S, Hou XH. Expression and implication of toll-like receptors TLR2, TLR4 and TLR9 in colonic mucosa of patients with ulcerative colitis. *J Huazhong Univ Sci Technolog Med Sci* 2014; **34**: 785-790 [PMID: 25318894 DOI: 10.1007/s11596-014-1353-6]
22 **Shi D**, Das J, Das G. Inflammatory bowel disease requires the interplay between innate and adaptive immune signals. *Cell Res* 2006; **16**: 70-74 [PMID: 16467877 DOI: 10.1038/sj.cr.7310009]
23 **Tun X**, Yasukawa K, Yamada K. Involvement of nitric oxide with activation of Toll-like receptor 4 signaling in mice with dextran sodium sulfate-induced colitis. *Free Radic Biol Med* 2014; **74**: 108-117 [PMID: 24992835 DOI: 10.1016/j.freeradbiomed.2014.06.020]
24 **Shi YJ**, Gong HF, Zhao QQ, Liu XS, Liu C, Wang H. Critical role of toll-like receptor 4 (TLR4) in dextran sulfate sodium (DSS)-Induced intestinal injury and repair. *Toxicol Lett* 2019; **315**: 23-30 [PMID: 31442584 DOI: 10.1016/j.toxlet.2019.08.012]

25 **Tam JSY**, Coller JK, Hughes PA, Prestidge CA, Bowen JM. Toll-like receptor 4 (TLR4) antagonists as potential therapeutics for intestinal inflammation. *Indian J Gastroenterol* 2021; **40**: 5-21 [PMID: 33666891 DOI: 10.1007/s12664-020-01114-y]

26 **Ge X**, Wen H, Fei Y, Xue R, Cheng Z, Li Y, Cai K, Li L, Li M, Luo Z. Structurally dynamic self-healable hydrogel cooperatively inhibits intestinal inflammation and promotes mucosal repair for enhanced ulcerative colitis treatment. *Biomaterials* 2023; **299**: 122184 [PMID: 37276796 DOI: 10.1016/j.biomaterials.2023.122184]

27 **Elkholy SE**, Maher SA, Abd El-Hamid NR, Elsayed HA, Hassan WA, Abdelmaogood AKK, Hussein SM, Jaremko M, Alshawwa SZ, Alharbi HM, Imbaby S. The immunomodulatory effects of probiotics and azithromycin in dextran sodium sulfate-induced ulcerative colitis in rats *via* TLR4-NF-κB and p38-MAPK pathway. *Biomed Pharmacother* 2023; **165**: 115005 [PMID: 37327586 DOI: 10.1016/j.biopha.2023.115005]

28 **Wang H**, Liu N, Yang Z, Zhao K, Pang H, Shao K, Zhou Z, Li S, He N. Preventive effect of pectic oligosaccharides on acute colitis model mice: modulating epithelial barrier, gut microbiota and Treg/Th17 balance. *Food Funct* 2022; **13**: 9999-10012 [PMID: 36065954 DOI: 10.1039/d2fo01448c]

29 **Wang HG**, Zhang MN, Wen X, He L, Zhang MH, Zhang JL, Yang XZ. Cepharanthine ameliorates dextran sulphate sodium-induced colitis through modulating gut microbiota. *Microb Biotechnol* 2022; **15**: 2208-2222 [PMID: 35439340 DOI: 10.1111/1751-7915.14059]

30 **Li C**, Ai G, Wang Y, Lu Q, Luo C, Tan L, Lin G, Liu Y, Li Y, Zeng H, Chen J, Lin Z, Xian Y, Huang X, Xie J, Su Z. Oxyberberine, a novel gut microbiota-mediated metabolite of berberine, possesses superior anti-colitis effect: Impact on intestinal epithelial barrier, gut microbiota profile and TLR4-MyD88-NF-κB pathway. *Pharmacol Res* 2020; **152**: 104603 [PMID: 31863867 DOI: 10.1016/j.phrs.2019.104603]

31 **Yu J**, Zhang W, Dao Y, Yang M, Pang X. Characterization of the Fungal Community in Fritillariae Cirrhosae Bulbus through DNA Metabarcoding. *J Fungi (Basel)* 2022; **8** [PMID: 36012863 DOI: 10.3390/jof8080876]

32 **Edgar RC**. UPARSE: highly accurate OTU sequences from microbial amplicon reads. *Nat Methods* 2013; **10**: 996-998 [PMID: 23955772 DOI: 10.1038/nmeth.2604]

33 **Stackebrandt E**, Goebel BM. Taxonomic note: A place for DNA:DNA reassociation and 16s rRNA sequence analysis in the present species definition in bacteriology. *Physics* 1994; **44**: 846-849 [DOI: 10.1099/00207713-44-4-846]

34 **Yan A**, Ban Y, Gao Z, Chen X, Wang L. PathwaySplice: an R package for unbiased pathway analysis of alternative splicing in RNA-Seq data. *Bioinformatics* 2018; **34**: 3220-3222 [PMID: 29688305 DOI: 10.1093/bioinformatics/bty317]

35 **Mao X**, Cai T, Olyarchuk JG, Wei L. Automated genome annotation and pathway identification using the KEGG Orthology (KO) as a controlled vocabulary. *Bioinformatics* 2005; **21**: 3787-3793 [PMID: 15817693 DOI: 10.1093/bioinformatics/bti430]

36 **Young MD**, Wakefield MJ, Smyth GK, Oshlack A. Gene ontology analysis for RNA-seq: accounting for selection bias. *Genome Biol* 2010; **11**: R14 [PMID: 20132535 DOI: 10.1186/gb-2010-11-2-r14]

37 **Kanehisa M**, Araki M, Goto S, Hattori M, Hirakawa M, Itoh M, Katayama T, Kawashima S, Okuda S, Tokimatsu T, Yamanishi Y. KEGG for linking genomes to life and the environment. *Nucleic Acids Res* 2008; **36**: D480-D484 [PMID: 18077471 DOI: 10.1093/nar/gkm882]

38 **Zhang WH**, Jin ZY, Yang ZH, Zhang JY, Ma XH, Guan J, Sun BL, Chen X. Fecal Microbiota Transplantation Ameliorates Active Ulcerative Colitis by Downregulating Pro-inflammatory Cytokines in Mucosa and Serum. *Front Microbiol* 2022; **13**: 818111 [PMID: 35444617 DOI: 10.3389/fmicb.2022.818111]

39 **Yang H**, Wang W, Romano KA, Gu M, Sanidad KZ, Kim D, Yang J, Schmidt B, Panigrahy D, Pei R, Martin DA, Ozay EI, Wang Y, Song M, Bolling BW, Xiao H, Minter LM, Yang GY, Liu Z, Rey FE, Zhang G. A common antimicrobial additive increases colonic inflammation and colitis-associated colon tumorigenesis in mice. *Sci Transl Med* 2018; **10** [PMID: 29848663 DOI: 10.1126/scitranslmed.aan4116]

40 **Dheer R**, Santaolalla R, Davies JM, Lang JK, Phillips MC, Pastorini C, Vazquez-Pertejo MT, Abreu MT. Intestinal Epithelial Toll-Like Receptor 4 Signaling Affects Epithelial Function and Colonic Microbiota and Promotes a Risk for Transmissible Colitis. *Infect Immun* 2016; **84**: 798-810 [PMID: 26755160 DOI: 10.1128/IAI.01374-15]

41 **Lo Sasso G**, Khachatryan L, Kondylis A, Battey JND, Sierro N, Danilova NA, Grigoryeva TV, Markelova MI, Khusnutdinova DR, Laikov AV, Salafutdinov II, Romanova YD, Siniagina MN, Vasiliev IY, Boulygina EA, Solovyeva VV, Garanina EE, Kitaeva KV, Ivanov KY, Chulpanova DS, Kletenkov KS, Valeeva AR, Odintsova AK, Ardatskaya MD, Abdulkhakov RA, Ivanov NV, Peitsch MC, Hoeng J, Abdulkhakov SR. Inflammatory Bowel Disease-Associated Changes in the Gut: Focus on Kazan Patients. *Inflamm Bowel Dis* 2021; **27**: 418-433 [PMID: 32766755 DOI: 10.1093/ibd/izaa188]

42 **Shah R**, Cope JL, Nagy-Szakal D, Dowd S, Versalovic J, Hollister EB, Kellermayer R. Composition and function of the pediatric colonic mucosal microbiome in untreated patients with ulcerative colitis. *Gut Microbes* 2016; **7**: 384-396 [PMID: 27217061 DOI: 10.1080/19490976.2016.1190073]

43 **Zhang XJ**, Yuan ZW, Qu C, Yu XT, Huang T, Chen PV, Su ZR, Dou YX, Wu JZ, Zeng HF, Xie Y, Chen JN. Palmatine ameliorated murine colitis by suppressing tryptophan metabolism and regulating gut microbiota. *Pharmacol Res* 2018; **137**: 34-46 [PMID: 30243842 DOI: 10.1016/j.phrs.2018.09.010]

44 **Zou J**, Shen Y, Chen M, Zhang Z, Xiao S, Liu C, Wan Y, Yang L, Jiang S, Shang E, Qian D, Duan J. Lizhong decoction ameliorates ulcerative colitis in mice *via* modulating gut microbiota and its metabolites. *Appl Microbiol Biotechnol* 2020; **104**: 5999-6012 [PMID: 32418127 DOI: 10.1007/s00253-020-10665-1]

45 **Zhang T**, Ji X, Lu G, Zhang F. The potential of Akkermansia muciniphila in inflammatory bowel disease. *Appl Microbiol Biotechnol* 2021; **105**: 5785-5794 [PMID: 34312713 DOI: 10.1007/s00253-021-11453-1]

46 **Kong C**, Yan X, Liu Y, Huang L, Zhu Y, He J, Gao R, Kalady MF, Goel A, Qin H, Ma Y. Ketogenic diet alleviates colitis by reduction of colonic group 3 innate lymphoid cells through altering gut microbiome. *Signal Transduct Target Ther* 2021; **6**: 154 [PMID: 33888680 DOI: 10.1038/s41392-021-00549-9]

47 **Wu Z**, Huang S, Li T, Li N, Han D, Zhang B, Xu ZZ, Zhang S, Pang J, Wang S, Zhang G, Zhao J, Wang J. Gut microbiota from green tea polyphenol-dosed mice improves intestinal epithelial homeostasis and ameliorates experimental colitis. *Microbiome* 2021; **9**: 184 [PMID: 34493333 DOI: 10.1186/s40168-021-01115-9]

48 **Wang L**, Tang L, Feng Y, Zhao S, Han M, Zhang C, Yuan G, Zhu J, Cao S, Wu Q, Li L, Zhang Z. A purified membrane protein from Akkermansia muciniphila or the pasteurised bacterium blunts colitis associated tumourigenesis by modulation of CD8(+) T cells in mice. *Gut* 2020; **69**: 1988-1997 [PMID: 32169907 DOI: 10.1136/gutjnl-2019-320105]

49 **von Schillde MA**, Hörmannsperger G, Weiher M, Alpert CA, Hahne H, Bäuerl C, van Huynegem K, Steidler L, Hrncir T, Pérez-Martínez G, Kuster B, Haller D. Lactocepin secreted by Lactobacillus exerts anti-inflammatory effects by selectively degrading proinflammatory chemokines. *Cell Host Microbe* 2012; **11**: 387-396 [PMID: 22520466 DOI: 10.1016/j.chom.2012.02.006]

50 **Bian X**, Wu W, Yang L, Lv L, Wang Q, Li Y, Ye J, Fang D, Wu J, Jiang X, Shi D, Li L. Administration of Akkermansia muciniphila Ameliorates Dextran Sulfate Sodium-Induced Ulcerative Colitis in Mice. *Front Microbiol* 2019; **10**: 2259 [PMID: 31632373 DOI:

10.3389/fmicb.2019.02259]
51 **Pittayanon R**, Lau JT, Leontiadis GI, Tse F, Yuan Y, Surette M, Moayyedi P. Differences in Gut Microbiota in Patients With vs Without Inflammatory Bowel Diseases: A Systematic Review. *Gastroenterology* 2020; **158**: 930-946.e1 [PMID: 31812509 DOI: 10.1053/j.gastro.2019.11.294]
52 **Olson CA**, Vuong HE, Yano JM, Liang QY, Nusbaum DJ, Hsiao EY. The Gut Microbiota Mediates the Anti-Seizure Effects of the Ketogenic Diet. *Cell* 2018; **173**: 1728-1741.e13 [PMID: 29804833 DOI: 10.1016/j.cell.2018.04.027]
53 **Chang ZP**, Deng GF, Shao YY, Xu D, Zhao YN, Sun YF, Zhang SQ, Hou RG, Liu JJ. Shaoyao-Gancao Decoction Ameliorates the Inflammation State in Polycystic Ovary Syndrome Rats *via* Remodeling Gut Microbiota and Suppressing the TLR4/NF-κB Pathway. *Front Pharmacol* 2021; **12**: 670054 [PMID: 34054541 DOI: 10.3389/fphar.2021.670054]
54 **Liu Y**, Yang M, Tang L, Wang F, Huang S, Liu S, Lei Y, Wang S, Xie Z, Wang W, Zhao X, Tang B, Yang S. TLR4 regulates RORγt(+) regulatory T-cell responses and susceptibility to colon inflammation through interaction with Akkermansia muciniphila. *Microbiome* 2022; **10**: 98 [PMID: 35761415 DOI: 10.1186/s40168-022-01296-x]
55 **Tian B**, Zhao J, Zhang M, Chen Z, Ma Q, Liu H, Nie C, Zhang Z, An W, Li J. Lycium ruthenicum Anthocyanins Attenuate High-Fat Diet-Induced Colonic Barrier Dysfunction and Inflammation in Mice by Modulating the Gut Microbiota. *Mol Nutr Food Res* 2021; **65**: e2000745 [PMID: 33629483 DOI: 10.1002/mnfr.202000745]
56 **Liu Y**, Zhang H, Xie A, Sun J, Yang H, Li J, Li Y, Chen F, Mei Y, Liang Y. Lactobacillus rhamnosus and L. plantarum Combination Treatment Ameliorated Colitis Symptoms in a Mouse Model by Altering Intestinal Microbial Composition and Suppressing Inflammatory Response. *Mol Nutr Food Res* 2023; **67**: e2200340 [PMID: 36988616 DOI: 10.1002/mnfr.202200340]
57 **Zhou S**, Yang L, Hu L, Qin W, Cao Y, Tang Z, Li H, Hu X, Fang Z, Li S, Huang Z, Chen H. Blueberry extract alleviated lipopolysaccharide-induced inflammation responses in mice through activating the FXR/TGR5 signaling pathway and regulating gut microbiota. *J Sci Food Agric* 2023; **103**: 4638-4648 [PMID: 36935348 DOI: 10.1002/jsfa.12560]
58 **Shi J**, Wang F, Tang L, Li Z, Yu M, Bai Y, Weng Z, Sheng M, He W, Chen Y. Akkermansia muciniphila attenuates LPS-induced acute kidney injury by inhibiting TLR4/NF-κB pathway. *FEMS Microbiol Lett* 2022; **369** [PMID: 36368696 DOI: 10.1093/femsle/fnac103]
59 **Song R**, Li Y, Hao W, Wang B, Yang L, Xu F. Identification and analysis of key genes associated with ulcerative colitis based on DNA microarray data. *Medicine (Baltimore)* 2018; **97**: e10658 [PMID: 29794741 DOI: 10.1097/MD.0000000000010658]
60 **Guo J**, Liao M, Wang J. TLR4 signaling in the development of colitis-associated cancer and its possible interplay with microRNA-155. *Cell Commun Signal* 2021; **19**: 90 [PMID: 34479599 DOI: 10.1186/s12964-021-00771-6]
61 **Verkman AS**, Anderson MO, Papadopoulos MC. Aquaporins: important but elusive drug targets. *Nat Rev Drug Discov* 2014; **13**: 259-277 [PMID: 24625825 DOI: 10.1038/nrd4226]
62 **Song TT**, Bi YH, Gao YQ, Huang R, Hao K, Xu G, Tang JW, Ma ZQ, Kong FP, Coote JH, Chen XQ, Du JZ. Systemic pro-inflammatory response facilitates the development of cerebral edema during short hypoxia. *J Neuroinflammation* 2016; **13**: 63 [PMID: 26968975 DOI: 10.1186/s12974-016-0528-4]
63 **Saadoun S**, Papadopoulos MC. Aquaporin-4 in brain and spinal cord oedema. *Neuroscience* 2010; **168**: 1036-1046 [PMID: 19682555 DOI: 10.1016/j.neuroscience.2009.08.019]
64 **Hemley SJ**, Bilston LE, Cheng S, Chan JN, Stoodley MA. Aquaporin-4 expression in post-traumatic syringomyelia. *J Neurotrauma* 2013; **30**: 1457-1467 [PMID: 23441695 DOI: 10.1089/neu.2012.2614]
65 **Zu J**, Wang Y, Xu G, Zhuang J, Gong H, Yan J. Curcumin improves the recovery of motor function and reduces spinal cord edema in a rat acute spinal cord injury model by inhibiting the JAK/STAT signaling pathway. *Acta Histochem* 2014; **116**: 1331-1336 [PMID: 25201116 DOI: 10.1016/j.acthis.2014.08.004]
66 **Wang L**, Tang H, Wang C, Hu Y, Wang S, Shen L. Aquaporin 4 deficiency alleviates experimental colitis in mice. *FASEB J* 2019; **33**: 8935-8944 [PMID: 31034776 DOI: 10.1096/fj.201802769RR]
67 **Deng S**, Qiu K, Tu R, Zheng H, Lu W. Relationship Between Pregnancy and Acute Disseminated Encephalomyelitis: A Single-Case Study. *Front Immunol* 2020; **11**: 609476 [PMID: 33597947 DOI: 10.3389/fimmu.2020.609476]
68 **Sun L**, Li M, Ma X, Feng H, Song J, Lv C, He Y. Inhibition of HMGB1 reduces rat spinal cord astrocytic swelling and AQP4 expression after oxygen-glucose deprivation and reoxygenation *via* TLR4 and NF-κB signaling in an IL-6-dependent manner. *J Neuroinflammation* 2017; **14**: 231 [PMID: 29178911 DOI: 10.1186/s12974-017-1008-1]

World Journal of Gastroenterology

Submit a Manuscript: https://www.f6publishing.com

World J Gastroenterol 2023 August 14; 29(30): 4671-4684

DOI: 10.3748/wjg.v29.i30.4671

ISSN 1007-9327 (print) ISSN 2219-2840 (online)

ORIGINAL ARTICLE

Observational Study

Incidence, prevalence, and comorbidities of chronic pancreatitis: A 7-year population-based study

Qiu-Yu Cai, Kun Tan, Xue-Li Zhang, Xu Han, Jing-Ping Pan, Zhi-Yin Huang, Cheng-Wei Tang, Jing Li

Specialty type: Gastroenterology and hepatology

Provenance and peer review: Invited article; Externally peer reviewed.

Peer-review model: Single blind

Peer-review report's scientific quality classification

Grade A (Excellent): 0
Grade B (Very good): 0
Grade C (Good): C, C, C
Grade D (Fair): 0
Grade E (Poor): 0

P-Reviewer: Poddighe D, Kazakhstan; Rathnaswami A, India

Received: March 27, 2023
Peer-review started: March 27, 2023
First decision: April 26, 2023
Revised: May 20, 2023
Accepted: July 11, 2023
Article in press: July 11, 2023
Published online: August 14, 2023

Qiu-Yu Cai, Zhi-Yin Huang, Cheng-Wei Tang, Jing Li, Department of Gastroenterology, West China Hospital, Sichuan University, Chengdu 610041, Sichuan Province, China

Kun Tan, Xue-Li Zhang, Xu Han, Jing-Ping Pan, Sichuan Health Information Association, Chengdu 610041, Sichuan Province, China

Corresponding author: Jing Li, MD, PhD, Doctor, Department of Gastroenterology, West China Hospital, Sichuan University, No. 37 Guoxue Xiang, Chengdu 610041, Sichuan Province, China. melody224@163.com

Abstract

BACKGROUND

Chronic pancreatitis (CP) is a fibroinflammatory syndrome leading to reduced quality of life and shortened life expectancy. Population-based estimates of the incidence, prevalence, and comorbidities of CP in China are scarce.

AIM

To characterize the incidence, prevalence, and comorbidities of CP in Sichuan Province, China, with population-based data.

METHODS

Data on CP from 2015 to 2021 were obtained from the Health Information Center of Sichuan Province. During the study period, a total of 38090 individuals were diagnosed with CP in Sichuan Province. The yearly incidence rate and point prevalence rate (December 31, 2021) of CP were calculated. The prevalence of comorbid conditions in CP patients was estimated. The annual number of CP-related hospitalizations, hospital length of stay, and hospitalization costs for CP were evaluated. Yearly incidence rates were standardized for age by the direct method using the permanent population of Sichuan Province in the 2020 census as the standard population. An analysis of variance test for the linearity of scaled variables and the Cochran-Armitage trend test for categorical data were performed to investigate the yearly trends, and a two-sided test with $P < 0.05$ was considered statistically significant.

RESULTS

The 38090 CP patients comprised 23280 males and 14810 females. The mean age of patients at CP diagnosis was 57.83 years, with male patients (55.87 years) being younger than female patients (60.11 years) ($P < 0.001$). The mean incidence rate of

CP during the study period was 6.81 per 100000 person-years, and the incidence of CP increased each year, from 4.03 per 100000 person-years in 2015 to 8.27 per 100000 person-years in 2021 ($P < 0.001$). The point prevalence rate of CP in 2021 was 45.52 per 100000 individuals for the total population, with rates of 55.04 per 100000 individuals for men and 35.78 per 100000 individuals for women ($P < 0.001$). Individuals aged 65 years or older had the highest prevalence of CP (113.38 per 100000 individuals) ($P < 0.001$). Diabetes (26.32%) was the most common comorbidity in CP patients. The number of CP-related hospitalizations increased from 3739 in 2015 to 11009 in 2021. The total costs for CP-related hospitalizations for CP patients over the study period were 667.96 million yuan, with an average of 17538 yuan per patient.

CONCLUSION

The yearly incidence of CP is increasing, and the overall CP hospitalization cost has increased by 1.4 times during the last 7 years, indicating that CP remains a heavy health burden.

Key Words: Chronic pancreatitis; Epidemiology; Incidence; Prevalence; Comorbidities; Disease burden

©The Author(s) 2023. Published by Baishideng Publishing Group Inc. All rights reserved.

Core Tip: Chronic pancreatitis (CP) remains a heavy health burden worldwide. However, available epidemiological data on CP in China are scarce. We conducted a population-based study on the incidence, prevalence, comorbidities, and disease burden of CP in Sichuan Province, China, from 2015 to 2021. We analyzed a total of 38090 patients, which represents the largest series of CP patients ever reported in China. We observed an increasing incidence and rising costs for CP-related hospitalization. The point prevalence rate of CP was 45.52 per 100000 individuals in 2021. Metabolic-related diseases and pancreatic tumors were among the most common comorbidities among CP patients.

Citation: Cai QY, Tan K, Zhang XL, Han X, Pan JP, Huang ZY, Tang CW, Li J. Incidence, prevalence, and comorbidities of chronic pancreatitis: A 7-year population-based study. *World J Gastroenterol* 2023; 29(30): 4671-4684
URL: https://www.wjgnet.com/1007-9327/full/v29/i30/4671.htm
DOI: https://dx.doi.org/10.3748/wjg.v29.i30.4671

INTRODUCTION

Chronic pancreatitis (CP) is a fibroinflammatory syndrome characterized by chronic upper abdominal pain and exocrine and endocrine pancreatic insufficiency[1]. Although some cases of CP may begin with one or recurrent bouts of pancreatitis, approximately 50% of CP patients have no history of acute pancreatitis[2,3]. Therefore, for a considerable proportion of patients, the development of CP might be attributable to different pathogeneses. As CP progresses, diabetes mellitus, malnutrition, and pancreatic cancer may develop[3,4], leading to reduced quality of life (QoL) and shortened life expectancy. The current strategies for CP include relieving symptoms, preventing disease progression, and managing complications[5]. CP causes a heavy health burden worldwide, consuming many medical resources due to less effective curative treatments for reversing the course of the disease[1,6,7]. Nevertheless, available epidemiological studies on CP are mainly from registry-based analyses and questionnaire-based surveys in European countries and the United States. Reportedly, the prevalence of CP ranges from 13.5 to 163 cases per 100000 individuals, and the incidence of CP ranges from 5 to 31.7 new cases per 100000 person-years[8-14]. The wide CP prevalence and incidence ranges may be related to the differences in case definitions, settings, patient cohorts, and statistical methods. China is one of the most populous countries in the world. However, only two epidemiological studies on CP in the eastern part of China have been conducted[15,16]. These data were mainly based on one or several databases from hospitals with small sample sizes. Population-based epidemiological data from other regions may provide a better picture of the incidence and prevalence of CP in China[1].

In addition, comorbidities, defined as the cooccurrence of two or more chronic medical conditions in one person[17], usually alter the disease management implications. Multiple comorbidities may reduce QoL and increase the risk of death and the consumption of medical resources[18]. Therefore, comorbidities have become an important part of epidemiological studies for chronic diseases[19]. However, data on the comorbidities of CP are still insufficient[20]. This epidemiological study aimed to characterize the incidence, prevalence, and comorbidities of CP in Sichuan Province in Southwest China from 2015 to 2021 with population-based data.

MATERIALS AND METHODS

Study design and population

Data on CP from 2015 to 2021 were obtained from the Health Information Center of Sichuan Province (HIC-SC), which collects electronic hospitalization summary reports (HSRs) from the electronic medical record systems of all hospitals in Sichuan Province. These records contain encrypted patient identification numbers and data on age, sex, admission and discharge dates, International Classification of Diseases, Tenth Revision (ICD-10) codes, and relevant discharge diagnoses. The HIC-SC has provided data for many scientific studies[21-23], verifying the reliability of the database. The data of permanent residents in Sichuan Province over the study years were obtained from the Sichuan Provincial Bureau of Statistics. This study was approved by the biomedical ethics review committee of West China Hospital, Sichuan Univer -sity on February 8, 2022 (IRB approval number: 2022-296), and the requirement for informed consent was waived.

Diagnosis and classification of CP

In China, the definition of CP as a continuing inflammatory disease of the pancreas, characterized by irreversible morphological changes and pain and/or permanent loss of function, has been widely accepted[7,24]. In clinical practice, computed tomography (CT) or magnetic resonance imaging (MRI) are usually recommended as first-line tests for patients with clinical symptoms of an inflammatory disorder of the pancreas (such as a previous episode of acute pancreatitis, characteristic pain, and/or maldigestion) because they are universally available and reproducible. The major imaging characteristics of CP include pancreatic atrophy, fibrosis, duct distortion and strictures, stones in pancreatic ducts or multiple calcifications distributed throughout the entire pancreas, *etc*. Endoscopic ultrasound, because of its invasiveness, is used only if the diagnosis is in question after CT or MRI. The diagnosis of CP in some patients is established by histopathological examination after surgery due to unexplained pancreatic masses. Therefore, patients who had a discharge diagnosis of CP in their HSR provided by the HIC-SC with the following ICD-10 codes were included in this study: K86.102 for CP, K86.852 for pancreatic atrophy, K86.811 for pancreatic calcifications, K86.809 for stones in pancreatic ducts, K86.806/807 for duct distortion and strictures, K86.154 for pancreatic fibrosis, K86.201 for pancreatic cysts, K86.804 for pancreatemphraxis, and K86.901/902 for pancreatic masses. Furthermore, this study classified CP according to the following ICD-10 codes: K86.051 for alcoholic CP, K86.153 for autoimmune pancreatitis (AIP), and K86.151 for biliary pancreatitis. Patients with conflicting information, *i.e.*, different birth dates at each admission, were excluded.

Identification of comorbidities

The comorbidities of CP in this study were selected by referring to previous studies[4,13,25]. Data on comorbidities were extracted from the electronic database by identifying their corresponding ICD-10 codes (Table 1).

Epidemiological outcomes

The major outcomes were the incidence and prevalence of CP. Incident cases were defined as patients with a first-time diagnosis of CP. Patients with a diagnosis of CP before the calculated year were excluded from the incidence estimate calculation. Prevalent cases were defined as patients with a diagnosis at some timepoint before the end of 2021. Crude incidence rates were calculated for each year between 2015 and 2021 as the number of incident CP cases divided by the average permanent population in a year (per 100000 person-years). Yearly incidence rates were standardized for age by the direct method using the permanent population of Sichuan Province in the 2020 census as the standard population. The point prevalence rate (December 31, 2021) was calculated as the number of patients who were diagnosed with CP before the end of 2021 divided by the permanent population of Sichuan Province in 2021. Other outcomes were the number of hospitalizations, the hospital length of stay (LoS), and the hospitalization costs. LoS was defined as the total length of hospital stay of the patient within one year. Costs for hospitalization, including total costs and the mean costs per patient, were calculated. Costs were adjusted by the consumer price index for each year to 2021 costs.

Statistical analysis

Data management and computations were performed using Oracle version 11.2.0 (https://www.oracle.com) and R version 4.1.3 (R Foundation for Statistical Computing; https://www.R-project.org/). Continuous variables are shown as the means ± SD. Since this was a population-based study including the entire permanent population of Sichuan Province during the observation period, no confidence intervals are provided for the estimates of the incidence or prevalence rates. Statistical analysis, such as the student's *t*-test for continuous variables and the chi-squared test for categorical variables, was used for the comparison of statistics between sexes and age groups. To investigate yearly trends, we performed an analysis of variance tests for the linearity of scaled variables and the Cochran-Armitage trend test for categorical data. A two-sided test with $P < 0.05$ was considered statistically significant.

RESULTS

Data collection

There were a total of 61112 electronic records (38296 individuals) with a diagnosis of CP from 2015 to 2021. Among all the records, 3180 records were excluded due to missing encrypted patient identification numbers (1518 records) and conflicting information (1662 records from 206 individuals). The exclusion of the data resulted in the loss of 5.2% of the

Table 1 The comorbidities and the corresponding International Classification of Diseases, Tenth Revision codes

Comorbidities	ICD-10 codes
Diabetes	E10, E11, E12, E13, E14
Type I diabetes	E10
Type II diabetes	E11
Secondary diabetes	E13, E14
Hypertension	I10, I11, I12, I13, I15, O10
Dyslipidemia	E78
Cholelithiasis	K80, O99.603, K56.3
Fatty liver disease	K76.0, K70.0
Alcoholic fatty liver disease	K70.0
Coronary heart disease	I21, I22, I23, I24, I25
Cerebrovascular disease	I60, I61, I62, I63, I64, I65, I66, I67, I69, G45
Ischemic cerebrovascular disease	I63, I64, I65, I66, I67, G45
Hemorrhagic cerebrovascular disease	I60, I61, I62
Pancreatic cyst	K86.2
Pancreatic pseudocyst	K86.3
Acute pancreatitis	K85
Heart failure	I50, I11.0, I13.0, I13.2
Hyperuricemia	M10, E79
Gastrointestinal bleeding	K92.0, K92.1, K92.2
Liver cirrhosis/fibrosis	K70.3, K74
Alcoholic cirrhosis	K70.3
Pancreatic tumor	C24.102, C25, D13.6, D37.752, D37.703, D37.704
Malignant tumor of the pancreas	C25, C24.102
Malnutrition	E12, E40, E41, E42, E43, E44, E45, E46
Ulcer disease	K25, K26, K27, K28
Gastric ulcer	K25
Duodenal ulcer	K26
Osteoporosis	M80, M81
Inflammatory bowel disease	K50, K51
Crohn's disease	K50
Ulcerative enteritis	K51

ICD: International Classification of Diseases.

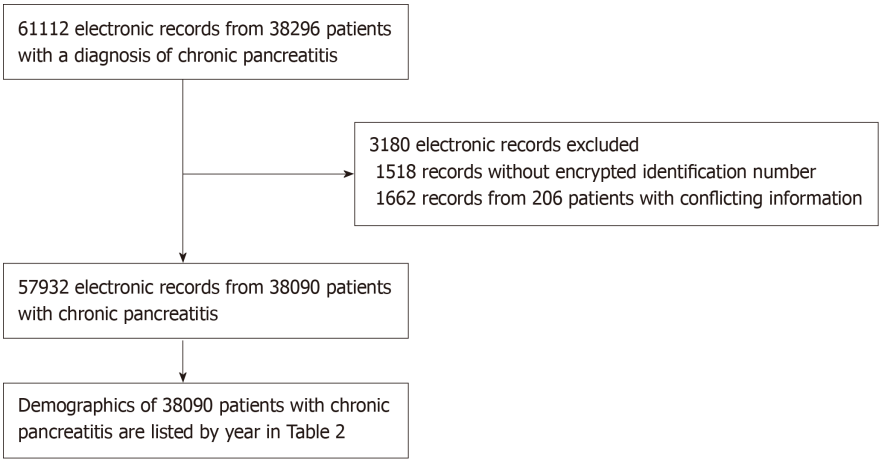
original electronic records and a loss of 0.5% from the original patient cohort. Therefore, 57932 electronic records from 38090 unique patients were ultimately analyzed in this study (Figure 1). Data for 30756 CP patients (80.7% of the cohort) were extracted by the ICD-code K86.102. A total of 3641 CP patients (9.6%) were identified by the ICD-10 code K86.809 (pancreatic calculus). The left 9.7% of the CP patients were included by other ICD-10 codes (K86). Only 397 CP patients (1%) were classified as having alcoholic CP. Sichuan Province is one of the most populous provinces in China, with approximately 83.67 million permanent residents in 2020.

Characteristics of the patients

The demographics of the CP patients with a first diagnosis are presented in Table 2 by calendar year. The number of new cases increased each year from 2015 to 2021, with a significant upward trend ($P < 0.001$). There were 1.56-fold more male patients than female patients. The mean age of the patients at CP diagnosis was 57.83 years, with males (55.87 years) being younger than females (60.11 years) ($P < 0.001$). More than 60% of the patients diagnosed each year were aged 15-64

Table 2 Demographics of chronic pancreatitis patients with a first diagnosis by calendar year

	2015	2016	2017	2018	2019	2020	2021	*P* value
Electronic records, *n*	3739	5760	7688	9488	9865	10383	11009	< 0.001
New case, *n*	3088	4334	5299	5945	5987	6475	6962	< 0.001
Mean hospitalizations per patient, *n*	1.21	1.16	1.19	1.20	1.17	1.16	1.15	0.097
Sex, %								
Male	62.01	59.23	60.52	59.73	60.23	62.63	62.90	0.282
Female	37.99	40.77	39.48	40.27	39.77	37.37	37.10	
Age, yr, mean ± SD	57.48 ± 15.78	58.01 ± 15.31	58.28 ± 15.59	58.84 ± 15.81	58.27 ± 15.77	57.52 ± 15.99	56.57 ± 16.57	0.387
Male	55.87 ± 15.35	56.58 ± 15.19	56.85 ± 15.17	57.37 ± 15.62	56.74 ± 15.38	56.10 ± 15.58	54.98 ± 16.41	0.415
Female	60.11 ± 16.12	60.09 ± 15.25	60.48 ± 15.96	61.01 ± 15.86	60.60 ± 16.06	59.88 ± 16.38	59.27 ± 16.51	0.389
Age group, %								
0-14	0.39	0.35	0.51	0.64	0.33	0.34	0.39	0.902
15-64	64.57	63.99	63.37	60.52	61.78	63.83	64.97	0.820
≥ 65	35.04	35.65	36.12	38.84	37.88	35.83	34.65	0.807
Ethnicity, %								
Han	94.36	94.78	95.32	95.31	94.27	94.18	95.17	0.722
Yi	1.33	1.80	1.91	1.55	2.04	2.12	2.08	0.515
Zang	1.69	2.03	1.83	2.27	2.24	2.30	1.74	0.923
Qiang	0.36	0.39	0.47	0.37	0.45	0.83	0.43	0.646
Other	2.27	0.99	0.47	0.50	1.00	0.57	0.57	0.007



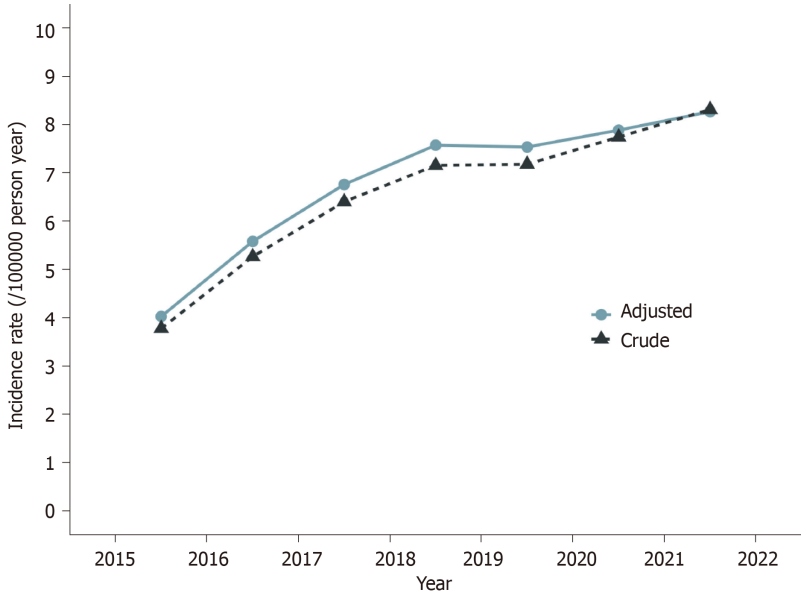
DOI: 10.3748/wjg.v29.i30.4671 **Copyright** ©The Author(s) 2023.

Figure 1 Flowchart of the inclusion and exclusion processes. A total of 61112 electronic records from 38296 patients with a diagnosis of chronic pancreatitis were retrieved from the Health Information Center of Sichuan Province. A total of 3180 records were excluded due to missing encrypted patient identification numbers (1518 records) and conflicting information (1662 records from 206 individuals). A total of 57932 electronic records from 38090 unique patients with chronic pancreatitis were ultimately included in this study.

years, and the proportion of each group remained stable over time (Table 2). Similar to the population ratio, the component ratio of the Han Chinese was the highest (94.92%) in CP patients, although Sichuan is a multiethnic province.

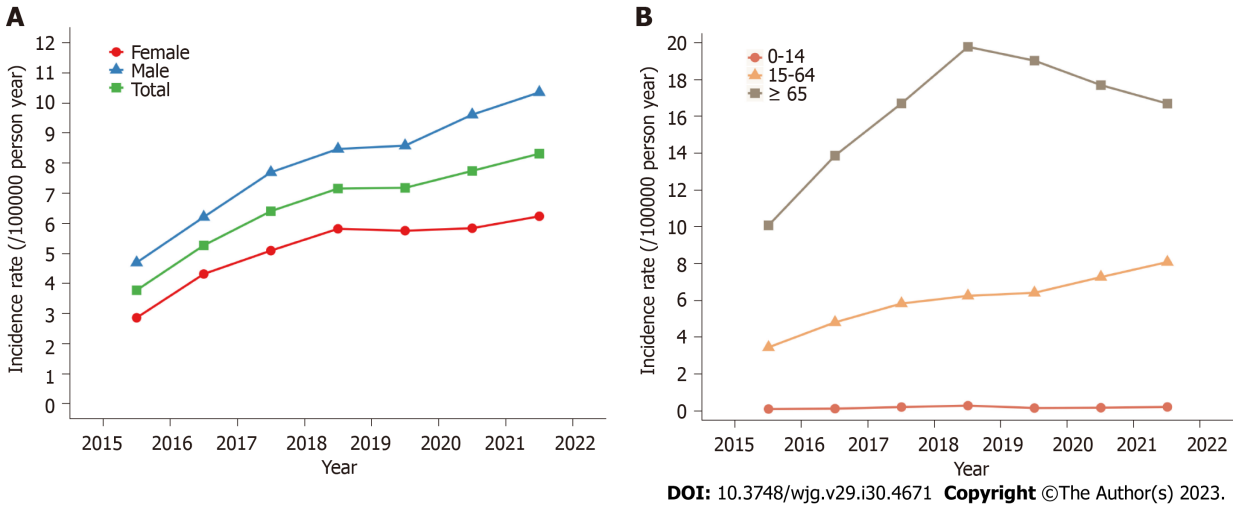
Incidence

The mean standardized incidence of CP was 6.81 per 100000 person-years, and the incidence of CP increased yearly during the study period ($P < 0.001$), from 4.03 per 100000 person-years in 2015 to 8.27 per 100000 person-years in 2021 (Figure 2). The mean incidence of CP in males was 7.95 per 100000 person-years, which was significantly higher than that in females (5.13 per 100000 person-years) ($P < 0.001$). Both sexes presented similar upward trends ($P < 0.001$) (Figure 3A).



DOI: 10.3748/wjg.v29.i30.4671 **Copyright** ©The Author(s) 2023.

Figure 2 Incidence trends of chronic pancreatitis. Crude and age-adjusted annual incidence trends of chronic pancreatitis from 2015 to 2021 in Sichuan Province, China (per 100000 person-years).



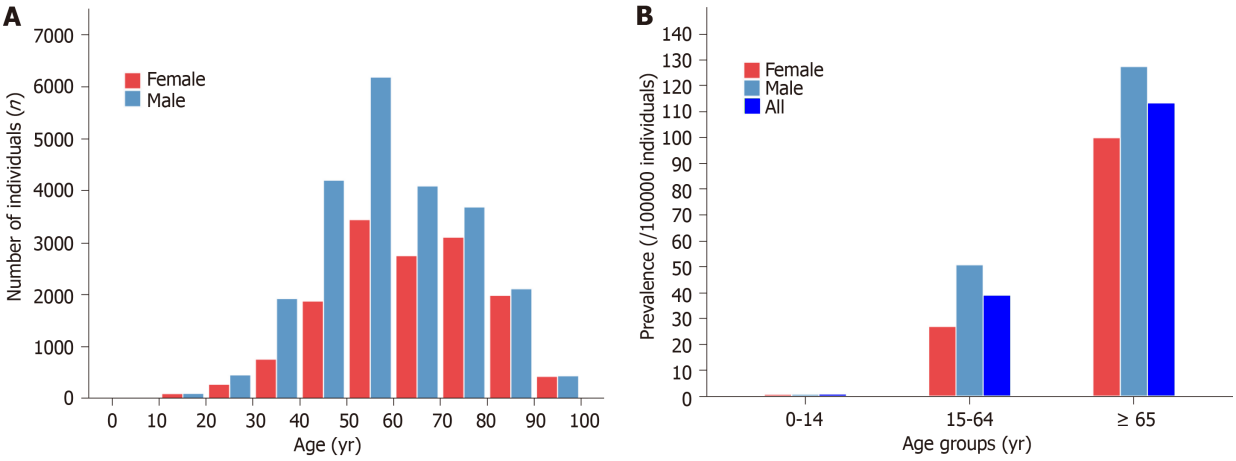
DOI: 10.3748/wjg.v29.i30.4671 **Copyright** ©The Author(s) 2023.

Figure 3 Sex- and age-grouped incidence of chronic pancreatitis. A and B: The crude incidence of chronic pancreatitis in the population grouped by sex (A) and age (B) (per 100000 person-years) from 2015 to 2021.

For males, the incidence of CP was 4.70 per 100000 person-years in 2015 and 10.36 per 100000 person-years in 2021; for females, the incidence of CP was 2.86 per 100000 person-years in 2015 and 6.24 per 100000 person-years in 2021. The highest CP incidence (16.27 per 100000 person-years) was observed in patients aged ≥ 65 years, with an upward trend from 10.08 per 100000 person-years in 2015 to 16.70 per 100000 person-years in 2021 ($P < 0.001$) (Figure 3B). Individuals aged 14 years or younger showed the lowest CP incidence (0.17 per 100000 person-years), which remained stable during the 7 years ($P = 0.830$) (Figure 3B). The seven-year mean incidence for the 15-64-year age group was 6.01 per 100000 person-years, with an increase from 3.45 per 100000 person-years in 2015 to 8.08 per 100000 person-years in 2021 ($P < 0.001$) (Figure 3B).

Prevalence

A total of 38090 individuals were diagnosed with CP in Sichuan Province during the study period. The age distribution of the CP patients up to 2021 is shown in Figure 4A. Among all the patients, 23280 (61.12%) were men, and 14810 (38.88%) were women ($P < 0.001$). The point prevalence of CP was 45.52 per 100000 individuals in 2021 for the total population, 55.04 per 100000 individuals for the male population, and 35.78 per 100000 individuals for the female population ($P < 0.001$). The prevalence of CP was 1.53 times higher [95% confidence interval (CI): 1.51-1.57; $P < 0.001$] for men than for women. Individuals aged 65 years or older had the highest prevalence of CP (113.38 per 100000 individuals), with a prevalence of 127.58 per 100000 individuals for men and 100.03 per 100000 individuals for women ($P < 0.001$) (Figure 4B).



DOI: 10.3748/wjg.v29.i30.4671 **Copyright** ©The Author(s) 2023.

Figure 4 The prevalence of chronic pancreatitis. A and B: The age distribution of chronic pancreatitis patients (A) and the prevalence of chronic pancreatitis by sex and age groups (B) in 2021.

For individuals aged between 15 and 64 years, the prevalence of CP was 39.11 per 100000 individuals, with a prevalence of 50.86 per 100000 individuals for men and 27.00 per 100000 individuals for women ($P < 0.001$) (Figure 4B). The prevalence of CP was 2.90 times higher (95%CI: 2.84-2.96; $P < 0.001$) for individuals aged 65 years or older than for individuals aged between 15 and 64 years. Individuals aged 14 years or younger had the lowest prevalence of CP (0.81 per 100000 individuals), with a prevalence of 0.82 per 100000 individuals for boys and 0.80 per 100000 individuals for girls ($P = 1$) (Figure 4B).

Prevalence of comorbid conditions

Diabetes (26.32%) was the most common comorbidity in CP patients, and patients with diabetes were similar in age to the overall cohort (Table 3). Metabolic-related diseases, including hypertension (21.51%), cholelithiasis (16.79%), dyslipidemia (16.70%), and fatty liver diseases (12.39%), were also common comorbidities among CP patients. The incidence of acute exacerbations of CP was 5.08% in all CP patients, with an incidence of 6.35% in males and 3.07% in females. A total of 2.65% of the CP patients were also diagnosed with pancreatic tumors, and 2.36% were diagnosed with malignant tumors of the pancreas.

Disease burden of CP

The number of CP-related hospitalizations increased approximately 2-fold, from 3739 in 2015 to 11009 in 2021 ($P < 0.001$) (Figure 5A). The LoS per CP patient decreased from 14.52 d in 2016 to 12.38 d in 2021 ($P = 0.008$) (Figure 5B). The total costs for CP-related hospitalizations for CP patients over the study period were 667.96 million yuan, with an average of 17538 yuan per patient. Total costs for CP-related hospitalizations increased from 50.60 million yuan in 2015 to 124.16 million in 2021 ($P < 0.001$) (Figure 5C), while the costs per patient decreased from 16387 yuan in 2015 to 13986 yuan in 2021 ($P = 0.024$) (Figure 5D).

DISCUSSION

We conducted a population-based study on the epidemiology of CP in Sichuan Province, China, from 2015 to 2021. This study showed that the mean incidence of CP was 6.81 per 100000 person-years in the last 7 years, and the point prevalence of CP was 45.52 per 100000 individuals in 2021 for the total population in Sichuan Province. The incidence and prevalence of CP increased with age and were significantly higher in males than in females over the study years. Metabolic-related diseases, including diabetes (26.32%), hypertension (21.51%), cholelithiasis (16.79%), dyslipidemia (16.70%), and fatty liver disease (12.39%), were common comorbidities in CP patients. In addition, 2.65% of the CP patients were diagnosed with pancreatic tumors. During the 7-year period, CP-related hospitalizations increased approximately 2-fold, and the overall hospitalization cost of CP increased by 1.4-fold. However, the LoS and the costs per CP patient decreased over the study years.

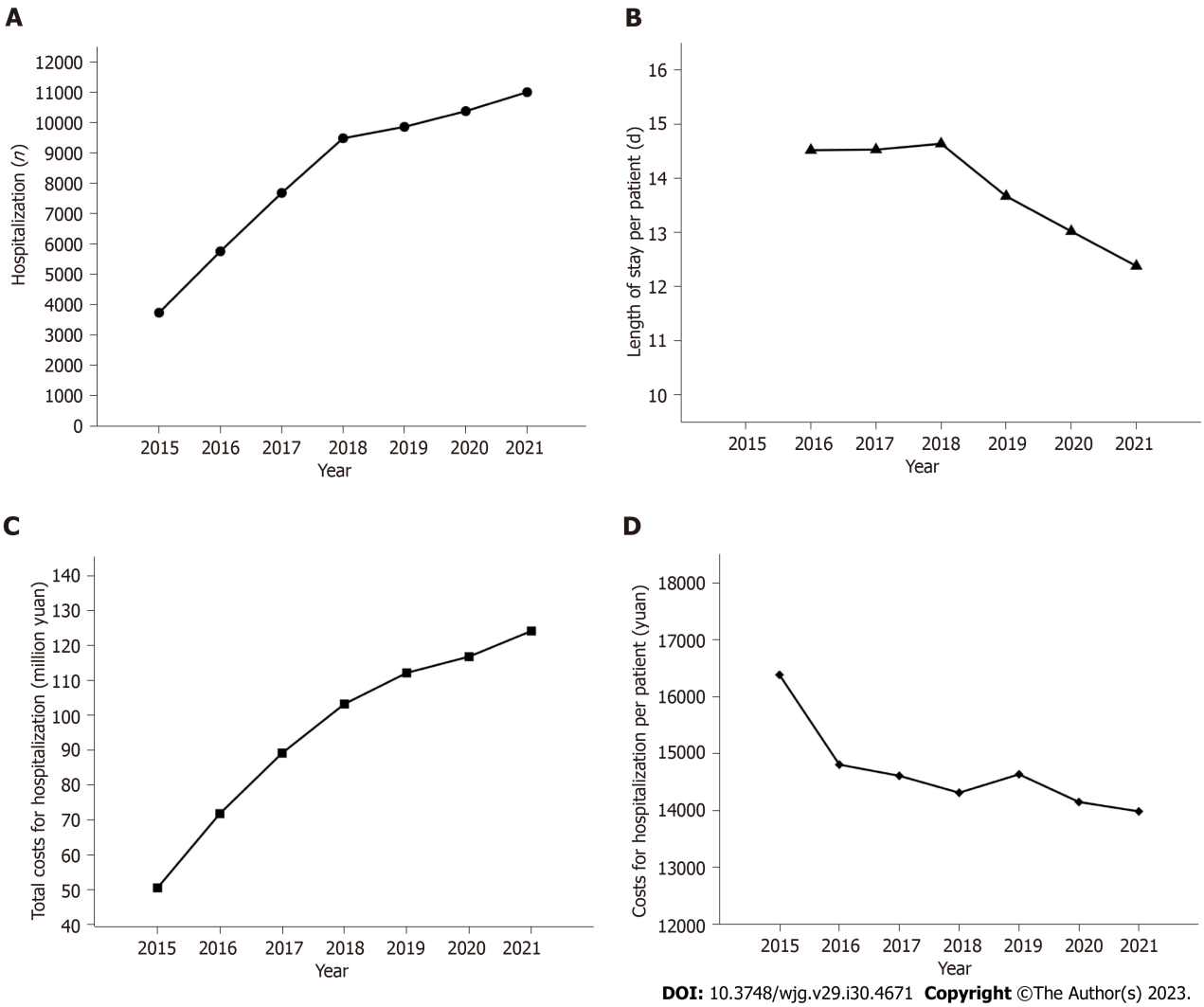
It may be valuable to improve epidemiological data of CP in the southwest area of China due to the rapid economic and societal development of the country. The first population-based epidemiological study of CP reported a mean CP incidence of 6.81 per 100000 person-years in Sichuan Province in the last 7 years. In other words, Sichuan Province has an average of 5652 new cases of CP every year. Thus, although hospitalization costs per patient decreased yearly, overall hospitalization costs still increased year by year. The overall hospitalization cost of CP increased by 1.4 times during the 7-year period. Although this study was analyzed with big data, the incidence rate may be underestimated because the data only covered inpatients with CP, and outpatients with CP were not included. A variety of databases have been used for the epidemiological analysis of CP[8,9,14,26], but it is still difficult to accurately describe the epidemic status of CP

Table 3 Prevalence of comorbidities in chronic pancreatitis patients

Diseases	Total cohort, *n* = 38090		Males, *n* = 23280		Females, *n* = 14810		*P* value
	n, %	Age, yr, mean ± SD	*n*, %	Age, yr, mean ± SD	*n*, %	Age, yr, mean ± SD	
Total	100.00	57.58 ± 15.79	100.00	56.26 ± 15.25	100.00	59.99 ± 16.44	-
Diabetes	26.32	56.57 ± 14.60	28.94	55.43 ± 14.03	22.20	59.14 ± 15.51	< 0.001
Type I diabetes	0.79	45.33 ± 15.11	0.81	47.32 ± 12.81	0.76	42.23 ± 17.70	0.591
Type II diabetes	21.84	58.04 ± 14.26	23.73	56.78 ± 13.89	18.87	60.75 ± 14.66	< 0.001
Secondary diabetes	2.05	50.04 ± 13.24	2.71	49.35 ± 12.40	1.01	53.27 ± 16.27	< 0.001
Hypertension	21.51	66.32 ± 14.41	20.23	64.27 ± 14.43	23.51	69.36 ± 13.82	< 0.001
Cholelithiasis	16.79	62.33 ± 16.14	14.95	60.23 ± 15.37	19.67	64.90 ± 16.68	< 0.001
Dyslipidemia	16.70	51.49 ± 14.28	16.76	48.57 ± 13.12	16.61	56.01 ± 14.81	0.708
Cerebrovascular disease	12.76	69.75 ± 13.34	12.19	68.52 ± 13.55	13.65	71.60 ± 12.79	< 0.001
Ischemic cerebrovascular disease	11.75	69.55 ± 13.38	11.17	68.54 ± 13.57	12.65	71.09 ± 12.92	< 0.001
Hemorrhagic cerebrovascular disease	0.34	64.05 ± 14.42	0.43	62.63 ± 14.55	0.20	69.39 ± 12.79	< 0.001
Fatty liver disease	12.39	49.53 ± 13.50	13.46	47.20 ± 12.63	10.72	54.28 ± 13.96	< 0.001
Alcoholic fatty liver disease	0.35	54.07 ± 12.45	0.53	54.32 ± 12.38	0.07	50.50 ± 13.39	< 0.001
Coronary heart disease	10.07	72.15 ± 12.77	8.37	71.13 ± 13.10	12.75	73.27 ± 12.31	< 0.001
Heart failure	5.27	74.15 ± 13.38	4.72	72.62 ± 13.98	6.14	76.06 ± 12.33	< 0.001
Acute pancreatitis	5.08	51.38 ± 15.68	6.35	52.17 ± 14.18	3.07	48.80 ± 19.57	< 0.001
Hyperuricemia	4.93	56.86 ± 17.25	6.42	55.07 ± 16.87	2.59	64.28 ± 16.85	< 0.001
Ulcer disease	4.68	60.16 ± 14.54	5.28	59.30 ± 14.06	3.73	62.22 ± 15.46	< 0.001
Gastric ulcer	2.17	60.34 ± 13.91	2.40	59.36 ± 13.34	1.80	62.60 ± 14.92	< 0.001
Duodenal ulcer	1.30	59.15 ± 14.46	1.65	58.53 ± 14.65	0.74	61.28 ± 13.62	< 0.001
Liver cirrhosis/fibrosis	3.49	58.70 ± 13.92	4.35	57.05 ± 13.12	2.13	65.09 ± 15.04	< 0.001
Alcoholic cirrhosis	0.72	53.23 ± 10.21	1.15	53.31 ± 10.19	0.05	49.60 ± 10.54	< 0.001
Pancreatic pseudocyst	3.45	52.55 ± 14.28	4.46	51.57 ± 12.92	1.85	56.38 ± 18.17	< 0.001
Malnutrition	3.36	64.04 ± 16.53	3.80	62.74 ± 15.52	2.67	66.86 ± 18.23	< 0.001
Gastrointestinal bleeding	2.93	61.76 ± 16.38	3.46	59.78 ± 15.84	2.10	67.13 ± 16.64	< 0.001
Pancreatic tumor	2.65	61.43 ± 12.13	2.97	61.27 ± 11.77	2.15	61.79 ± 12.89	< 0.001
Malignant tumor of pancreas	2.36	61.74 ± 11.99	2.64	61.50 ± 11.67	1.91	62.27 ± 12.65	< 0.001
Osteoporosis	2.03	75.28 ± 13.19	1.37	70.13 ± 13.89	3.06	78.02 ± 11.94	< 0.001
Inflammatory bowel disease	0.14	56.13 ± 15.76	0.13	56.75 ± 14.03	0.17	55.43 ± 17.76	0.388
Crohn's disease	0.03	56.40 ± 14.07	0.03	58.67 ± 10.76	0.03	53.00 ± 19.37	1
Ulcerative enteritis	0.12	56.00 ± 16.05	0.11	56.15 ± 14.56	0.14	55.83 ± 17.90	0.429

due to the limitations of various databases. There may be many CP outpatients, but if their condition is not severe enough to require hospitalization, the medical costs and the disease burden would be relatively low, and the epidemiological significance may not be very important. Reportedly, the rates of harmful drinking behaviors and smoking, which may be risk factors for CP, have increased in Chinese individuals in the last 10 years[27,28]. In contrast, the incidences of CP remained stable or even decreased yearly in recent years in the United States and Denmark, indicating that the decline in CP incidence might be due to the decrease in tobacco and alcohol consumption in both countries[8,14,29]. However, it was difficult to evaluate the factors related to the increasing incidence of CP in this study because electronic HSRs did not include risk factors associated with CP. CT and MRI have become universally available in hospitals at all levels in Sichuan Province, China. This greatly enhances the detection rate of CP and may partly contribute to the increasing CP incidence rate.

The point prevalence of CP was 45.52 per 100000 individuals in 2021 for the total population in Sichuan Province. The prevalence of CP was 39.11 and 113.38 per 100000 individuals for the population aged between 15 and 64 years and the population aged 65 years or older, respectively. The current results are consistent with those of studies in Minnesota



DOI: 10.3748/wjg.v29.i30.4671 **Copyright** ©The Author(s) 2023.

Figure 5 Disease burden of chronic pancreatitis. A: Annual number of chronic pancreatitis-associated hospitalizations; B: Mean length of stay per patient; C: Total costs for hospitalization; D: Costs for hospitalization per patient. Costs were adjusted by the consumer price index every year to 2021 costs (yuan).

(41.76/100000 individuals), Japan (52.4/100000 individuals), and Spain (49.3/100000 individuals), which were all based on questionnaire-based surveys[10,11,30]. In contrast, the prevalence of CP was considerably higher in register-based studies covering inpatients as well as outpatients[8,9,14]. Based on insurance claims databases, Machicado *et al*[9] and Sellers *et al*[14] reported similar results for the prevalence of CP in adults in America, which was 98.7/100000 individuals (2001-2013) and 91.9/100000 individuals (2007-2014), respectively. Using nationwide health care registries over a long period (1994–2018), Olesen *et al*[8] estimated the prevalence of CP at 153.9/100000 individuals in Denmark. This discrepancy may be explained by differences in study designs or by true differences in the CP prevalence across regions. Compared to the multicenter study in 2003, our current study adds to the prevalence data on CP over the past decades and verifies the upward trend in the prevalence of CP[15]. The increase in the CP prevalence could be explained by the increasing CP incidence and improved prognosis and life expectancy of CP patients[31-33].

Both the incidence and prevalence of CP in males were significantly higher than those in females over the study years. The prevalence for men was 1.53 times higher than that for women. Of all CP patients, 61.12% were men and 38.88% were women. Both the incidence and prevalence of CP were higher among men than women in all age groups, which was consistent with most previous studies[8,11,15,34,35]. This difference may be due to higher alcohol and tobacco exposure and increased genetic susceptibility to alcoholic CP among men[36,37]. The male hemizygous CLDN2 genotype and the female homozygous CLDN2 genotype are known to confer an amplified risk of pancreatitis together with alcohol use, and the frequency of the male hemizygous CLDN2 genotype (0.26) is much higher than that of the female homozygous CLDN2 genotype (0.07); thus, males have a higher genetic susceptibility to alcoholic CP than females[37]. In addition, the prevalence and incidence of CP were the highest among elderly individuals compared with young and middle-aged people in our study. These results are also similar to those of previous studies, suggesting that the incidence and prevalence of CP increases with aging[8,14]. Although the results might represent the prevalence of CP, it is undeniable that there was bias. In terms of the inpatient database, elderly people had the highest rate of hospitalization, which was accompanied by a higher detection rate of CP. In comparison, the detection rates of CP might be lower in other age groups, leading to an underestimation of the incidence and prevalence of CP.

Table 4 Available studies on comorbidities of chronic pancreatitis

Region	Study design	Study period	Total CP patients	Frequent comorbidities compared with controls	Ref.
Denmark	Nationwide retrospective cohort study	1995-2010	11972	Cerebrovascular disease, chronic pulmonary disease, ulcer disease, diabetes, chronic renal disease, and pancreatic cancer	[4]
United States and Denmark	Cross-sectional, multicenter prospective study	Not available	171	Anxiety and depression	[40]
United States	Retrospective cohort study	2015-2020	63230	Hypertension, diabetes, and myocardial Infarction	[41]
United States	Ongoing longitudinal cohort study	2017-2022	488	Depression, anxiety, sleep disturbance, and physical disability	[42]
United States	Cohort study (NAPS2 cohort)	2000-2014	1024	Gallstones, diabetes, heart disease/heart attack/stroke, liver disease, renal disease, or prior history of cancer	[25]
United Kingdom	Cohort Study (the United Kingdom BioBank cohort)	2000-2020	1027	Gallstones, hyperlipidemia, diabetes, hypertriglyceridemia, hypercalcemia, pancreatic cancer, celiac, and ulcerative colitis	[13]
Canada	Retrospective study	2007-2014	75744	Anxiety and depression	[43]
China	Population-based cohort study	2000-2011	15848	Urolithiasis	[44]
China	Population-based cohort study	2000-2011	17810	Subsequent pyogenic liver abscess	[45]
China	Population-based cohort study	2000-2011	16672	Cerebrovascular disease	[46]
China	Population-based cohort study	2000-2011	17778	Deep vein thrombosis and pulmonary embolism	[20]
China	Population-based cohort study	2000-2011	17796	Inflammatory bowel disease	[47]
China	Prospective observational study	2019-2021	720	Anxiety and depression	[48]

As comorbidity, diabetes was reported in 26.32% of CP patients in this study. The prevalence of diabetes in CP patients reported in the previous literature was 15.2%-41.5%[4,13,25]. The high comorbidity of CP with diabetes suggests the importance of the identification of post-pancreatitis diabetes mellitus, which might be greatly different from type 2 diabetes mellitus in its manifestation and treatment. In addition, hypertension (21.51%), cholelithiasis (16.79%), and fatty liver disease (12.39%) were also common comorbidities in CP patients. A cohort study of the United Kingdom Biobank reported an even higher prevalence of gallstones (32.4%), hyperlipidemia (34.7%), and pancreatic cancer (4.7%) in CP patients and a strong association between CP and essential hypertension[13]. In the same cohort (United Kingdom Biobank), a case-control study reported that CP was associated with a significantly higher risk of pancreatic cancer in patients within the first 3 years[38]. These comorbidities may be explained by shared etiologies resulting from general exposure to risk factors such as tobacco use and alcohol consumption among CP patients. However, it is also possible that some of these comorbidities are involved in the pathogenesis of CP development, and some comorbidities may be complications caused by CP. Prospective studies, including longitudinal cohort studies and randomized control trials, may provide more definitive evidence on potential associations with multimorbidity. As shown in Table 4, different comorbidities were reported to be associated with CP in European, American, and East Asian countries. This may be related to different regions, times, and types of research. In addition, the pattern of comorbidities of CP is still under exploration, and the comorbidities reported by the abovementioned studies are similar to our findings. Smaller sample sizes and more accurate and complete diagnoses of diseases in cohort studies as well as different study inclusion criteria could explain the discrepancy between cohort and register-based studies.

AIP represents < 5%-10% of pancreatitis cases and has a smaller prevalence of approximately 1-2/100000 individuals [39]. In the design of this study, AIP was classified as a type of CP. However, data on AIP were not extracted from the electronic HSRs because there is no special ICD-10 code for AIP. Moreover, only 1% of CP patients were classified as having alcoholic CP, which might be underestimated because doctors may not have paid enough attention to alcoholic CP when they filled out the electronic HSRs. This study suggests some improvements for the HIC-SC to enhance the quality of electronic HSR completion.

CONCLUSION

The yearly incidence of CP increased, along with the absolute number of CP patients and associated costs for hospitalization in Sichuan Province over the study period. The current work shows that CP remains a heavy burden on patients and the healthcare system. The implication of the high prevalence of diabetes (26.32%) in CP patients may vary with different people.

ARTICLE HIGHLIGHTS

Research background

Chronic pancreatitis (CP) is a fibroinflammatory syndrome leading to reduced quality of life and shortened life expectancy. Population-based estimates of the prevalence and incidence of CP in China are scarce.

Research motivation

Accurate epidemiological estimates of CP are vital in shaping health resource allocation and medical provider training priorities.

Research objectives

To evaluate the prevalence and time trends of the incidence of CP and describe the comorbidities and disease burden of CP in Sichuan Province, China.

Research methods

Data on CP from 2015 to 2021 were obtained from the Health Information Center of Sichuan Province. During the study period, a total of 38090 individuals were diagnosed with CP in Sichuan Province. The yearly incidence rate and point prevalence rate (December 31, 2021) of CP were calculated. The prevalence of comorbid conditions in CP patients was estimated. The annual number of CP-related hospitalizations, hospital length of stay, and costs for hospitalization for CP were evaluated. Yearly incidence rates were standardized for age by the direct method using the permanent population of Sichuan Province in the 2020 census as the standard population. An analysis of variance test for the linearity of scaled variables and the Cochran-Armitage trend test for categorical data were performed to investigate the yearly trends, and a two-sided test with $P < 0.05$ was considered statistically significant.

Research results

The 38090 CP patients comprised 23280 males and 14810 females. The mean age of patients at CP diagnosis was 57.83 years, with males (55.87 years) being younger than females (60.11 years) ($P < 0.001$). The mean incidence rate of CP during the study period was 6.81 per 100000 person-years, and the incidence of CP increased each year, from 4.03 per 100000 person-years in 2015 to 8.27 per 100000 person-years in 2021 ($P < 0.001$). The point prevalence rate of CP in 2021 was 45.52 per 100000 individuals for the total population, with rates of 55.04 per 100000 individuals for men and 35.78 per 100000 individuals for women ($P < 0.001$). Individuals aged 65 years or older had the highest prevalence of CP (113.38 per 100000 individuals) ($P < 0.001$). Diabetes (26.32%) was the most common comorbidity in CP patients. The number of CP-related hospitalizations increased from 3739 in 2015 to 11009 in 2021. The total costs for CP-related hospitalizations for CP patients over the study period were 667.96 million yuan, with an average of 17538 yuan per patient.

Research conclusions

The yearly incidence of CP increased in Sichuan Province, along with the absolute number of CP patients and associated costs for hospitalization between 2015 and 2021. The point prevalence rate of CP in 2021 was 45.52/100000 individuals for the total population. Diabetes (26.32%), other metabolic-related diseases, and pancreatic cancer are among the common comorbidities in CP patients. The current work shows that CP continues to place a heavy burden on patients and the healthcare system.

Research perspectives

Further studies are needed to identify CP and its comorbidities earlier, triggering potentially preventive mana-gement to relieve the disease burden.

ACKNOWLEDGEMENTS

The authors are grateful to the staff of the Department of Gastroenterology, West China Hospital, Sichuan University, and the Health Information Center of Sichuan Province for their valuable assistance in this work.

FOOTNOTES

Author contributions: Cai QY analyzed the data and wrote the manuscript; Tan K and Zhang XL collected the data; Han X established the database and cleaned the data; Pan JP managed the data; Huang ZY analyzed the data; Tang CW designed the study and revised the manuscript; Li J designed the study and revised the manuscript.

Supported by the Special Project on "Digital Development of Health" of the Health Information Center of Sichuan Province, China, No. 2021ZXKY06007; and the National Natural Science Fund of China, No. 82241054 and 82000613.

Institutional review board statement: This study was approved by the biomedical ethics review committee of West China Hospital,

Sichuan University.

Informed consent statement: The requirement for informed consent was waived in this study.

Conflict-of-interest statement: All the authors report no relevant conflicts of interest for this article.

Data sharing statement: No additional data are available.

STROBE statement: The authors have read the STROBE Statement checklist of items, and the manuscript was prepared and revised according to the STROBE Statement checklist of items.

Open-Access: This article is an open-access article that was selected by an in-house editor and fully peer-reviewed by external reviewers. It is distributed in accordance with the Creative Commons Attribution NonCommercial (CC BY-NC 4.0) license, which permits others to distribute, remix, adapt, build upon this work non-commercially, and license their derivative works on different terms, provided the original work is properly cited and the use is non-commercial. See: https://creativecommons.org/Licenses/by-nc/4.0/

Country/Territory of origin: China

ORCID number: Qiu-Yu Cai 0000-0002-0400-5314; Zhi-Yin Huang 0000-0002-8322-1768; Cheng-Wei Tang 0000-0002-2289-8240; Jing Li 0000-0002-6929-409X.

S-Editor: Wang JJ
L-Editor: A
P-Editor: Wang JJ

REFERENCES

1 **Beyer G**, Habtezion A, Werner J, Lerch MM, Mayerle J. Chronic pancreatitis. *Lancet* 2020; **396**: 499-512 [PMID: 32798493 DOI: 10.1016/S0140-6736(20)31318-0]
2 **Hori Y**, Vege SS, Chari ST, Gleeson FC, Levy MJ, Pearson RK, Petersen BT, Kendrick ML, Takahashi N, Truty MJ, Smoot RL, Topazian MD. Classic chronic pancreatitis is associated with prior acute pancreatitis in only 50% of patients in a large single-institution study. *Pancreatology* 2019; **19**: 224-229 [PMID: 30795927 DOI: 10.1016/j.pan.2019.02.004]
3 **Vege SS**, Chari ST. Chronic Pancreatitis. *N Engl J Med* 2022; **386**: 869-878 [PMID: 35235728 DOI: 10.1056/NEJMcp1809396]
4 **Bang UC**, Benfield T, Hyldstrup L, Bendtsen F, Beck Jensen JE. Mortality, cancer, and comorbidities associated with chronic pancreatitis: a Danish nationwide matched-cohort study. *Gastroenterology* 2014; **146**: 989-994 [PMID: 24389306 DOI: 10.1053/j.gastro.2013.12.033]
5 **Cohen SM**, Kent TS. Etiology, Diagnosis, and Modern Management of Chronic Pancreatitis: A Systematic Review. *JAMA Surg* 2023; **158**: 652-661 [PMID: 37074693 DOI: 10.1001/jamasurg.2023.0367]
6 **Masamune A**, Kikuta K, Kume K, Hamada S, Tsuji I, Takeyama Y, Shimosegawa T, Okazaki K; Japan Pancreas Society. Nationwide epidemiological survey of chronic pancreatitis in Japan: introduction and validation of the new Japanese diagnostic criteria 2019. *J Gastroenterol* 2020; **55**: 1062-1071 [PMID: 32676800 DOI: 10.1007/s00535-020-01704-9]
7 **Gardner TB**, Adler DG, Forsmark CE, Sauer BG, Taylor JR, Whitcomb DC. ACG Clinical Guideline: Chronic Pancreatitis. *Am J Gastroenterol* 2020; **115**: 322-339 [PMID: 32022720 DOI: 10.14309/ajg.0000000000000535]
8 **Olesen SS**, Mortensen LH, Zinck E, Becker U, Drewes AM, Nøjgaard C, Novovic S, Yadav D, Tolstrup JS. Time trends in incidence and prevalence of chronic pancreatitis: A 25-year population-based nationwide study. *United European Gastroenterol J* 2021; **9**: 82-90 [PMID: 33176616 DOI: 10.1177/2050640620966513]
9 **Machicado JD**, Dudekula A, Tang G, Xu H, Wu BU, Forsmark CE, Yadav D. Period prevalence of chronic pancreatitis diagnosis from 2001-2013 in the commercially insured population of the United States. *Pancreatology* 2019; **19**: 813-818 [PMID: 31350077 DOI: 10.1016/j.pan.2019.07.003]
10 **Domínguez-Muñoz JE**, Lucendo A, Carballo LF, Iglesias-García J, Tenías JM. A Spanish multicenter study to estimate the prevalence and incidence of chronic pancreatitis and its complications. *Rev Esp Enferm Dig* 2014; **106**: 239-245 [PMID: 25075654]
11 **Hirota M**, Shimosegawa T, Masamune A, Kikuta K, Kume K, Hamada S, Kanno A, Kimura K, Tsuji I, Kuriyama S; Research Committee of Intractable Pancreatic Diseases. The seventh nationwide epidemiological survey for chronic pancreatitis in Japan: clinical significance of smoking habit in Japanese patients. *Pancreatology* 2014; **14**: 490-496 [PMID: 25224249 DOI: 10.1016/j.pan.2014.08.008]
12 **Capurso G**, Archibugi L, Pasquali P, Aceti A, Balducci P, Bianchi P, Buono F, Camerucci S, Cantarini R, Centofanti S, Colantonio P, Cremaschi R, Crescenzi S, Di Mauro C, Di Renzi D, Filabozzi A, Fiorillo A, Giancaspro G, Giovannetti P, Lanna G, Medori C, Merletti E, Nunnari E, Paris F, Pavone M, Piacenti A, Rossi A, Scamuffa MC, Spinelli G, Taborchi M, Valente B, Villanova A, Chiriatti A, Delle Fave G. Prevalence of chronic pancreatitis: Results of a primary care physician-based population study. *Dig Liver Dis* 2017; **49**: 535-539 [PMID: 28089214 DOI: 10.1016/j.dld.2016.12.024]
13 **Spagnolo DM**, Greer PJ, Ohlsen CS, Mance S, Ellison M, Breze C, Busby B, Whitcomb DC, Haupt M. Acute and Chronic Pancreatitis Disease Prevalence, Classification, and Comorbidities: A Cohort Study of the UK BioBank. *Clin Transl Gastroenterol* 2022; **13**: e00455 [PMID: 35060944 DOI: 10.14309/ctg.0000000000000455]
14 **Sellers ZM**, MacIsaac D, Yu H, Dehghan M, Zhang KY, Bensen R, Wong JJ, Kin C, Park KT. Nationwide Trends in Acute and Chronic Pancreatitis Among Privately Insured Children and Non-Elderly Adults in the United States, 2007-2014. *Gastroenterology* 2018; **155**: 469-478.e1 [PMID: 29660323 DOI: 10.1053/j.gastro.2018.04.013]
15 **Wang LW**, Li ZS, Li SD, Jin ZD, Zou DW, Chen F. Prevalence and clinical features of chronic pancreatitis in China: a retrospective multicenter analysis over 10 years. *Pancreas* 2009; **38**: 248-254 [PMID: 19034057 DOI: 10.1097/MPA.0b013e31818f6ac1]

16 **Li JN**, Lai YM, Qian JM, Guo T, Lü H, Tang XY. Trends in etiologies of chronic pancreatitis within 20 years: analysis of 636 cases. *Chin Med J (Engl)* 2011; **124**: 3556-3559 [PMID: 22340177]

17 **Beard JR**, Officer A, de Carvalho IA, Sadana R, Pot AM, Michel JP, Lloyd-Sherlock P, Epping-Jordan JE, Peeters GMEEG, Mahanani WR, Thiyagarajan JA, Chatterji S. The World report on ageing and health: a policy framework for healthy ageing. *Lancet* 2016; **387**: 2145-2154 [PMID: 26520231 DOI: 10.1016/S0140-6736(15)00516-4]

18 **Emerging Risk Factors Collaboration**, Di Angelantonio E, Kaptoge S, Wormser D, Willeit P, Butterworth AS, Bansal N, O'Keeffe LM, Gao P, Wood AM, Burgess S, Freitag DF, Pennells L, Peters SA, Hart CL, Håheim LL, Gillum RF, Nordestgaard BG, Psaty BM, Yeap BB, Knuiman MW, Nietert PJ, Kauhanen J, Salonen JT, Kuller LH, Simons LA, van der Schouw YT, Barrett-Connor E, Selmer R, Crespo CJ, Rodriguez B, Verschuren WM, Salomaa V, Svärdsudd K, van der Harst P, Björkelund C, Wilhelmsen L, Wallace RB, Brenner H, Amouyel P, Barr EL, Iso H, Onat A, Trevisan M, D'Agostino RB Sr, Cooper C, Kavousi M, Welin L, Roussel R, Hu FB, Sato S, Davidson KW, Howard BV, Leening MJ, Leening M, Rosengren A, Dörr M, Deeg DJ, Kiechl S, Stehouwer CD, Nissinen A, Giampaoli S, Donfrancesco C, Kromhout D, Price JF, Peters A, Meade TW, Casiglia E, Lawlor DA, Gallacher J, Nagel D, Franco OH, Assmann G, Dagenais GR, Jukema JW, Sundström J, Woodward M, Brunner EJ, Khaw KT, Wareham NJ, Whitsel EA, Njølstad I, Hedblad B, Wassertheil-Smoller S, Engström G, Rosamond WD, Selvin E, Sattar N, Thompson SG, Danesh J. Association of Cardiometabolic Multimorbidity With Mortality. *JAMA* 2015; **314**: 52-60 [PMID: 26151266 DOI: 10.1001/jama.2015.7008]

19 **Jepsen P**. Comorbidity in cirrhosis. *World J Gastroenterol* 2014; **20**: 7223-7230 [PMID: 24966593 DOI: 10.3748/wjg.v20.i23.7223]

20 **Chung WS**, Lin CL. Comorbid risks of deep vein thrombosis and pulmonary thromboembolism in patients with chronic pancreatitis: a nationwide cohort study. *J Thromb Haemost* 2016; **14**: 98-104 [PMID: 26563680 DOI: 10.1111/jth.13195]

21 **Qiu H**, Tan K, Long F, Wang L, Yu H, Deng R, Long H, Zhang Y, Pan J. The Burden of COPD Morbidity Attributable to the Interaction between Ambient Air Pollution and Temperature in Chengdu, China. *Int J Environ Res Public Health* 2018; **15** [PMID: 29534476 DOI: 10.3390/ijerph15030492]

22 **Zhu X**, Qiu H, Wang L, Duan Z, Yu H, Deng R, Zhang Y, Zhou L. Risks of hospital admissions from a spectrum of causes associated with particulate matter pollution. *Sci Total Environ* 2019; **656**: 90-100 [PMID: 30502738 DOI: 10.1016/j.scitotenv.2018.11.240]

23 **Qiu H**, Zhu X, Wang L, Pan J, Pu X, Zeng X, Zhang L, Peng Z, Zhou L. Attributable risk of hospital admissions for overall and specific mental disorders due to particulate matter pollution: A time-series study in Chengdu, China. *Environ Res* 2019; **170**: 230-237 [PMID: 30594694 DOI: 10.1016/j.envres.2018.12.019]

24 **Zou WB**, Ru N, Wu H, Hu LH, Ren X, Jin G, Wang Z, Du YQ, Cao YN, Zhang L, Chang XY, Zhang RC, Li XB, Shen Y, Li P, Li ZS, Liao Z; Chronic Pancreatitis Group of Chinese Medical Doctor Association. Guidelines for the diagnosis and treatment of chronic pancreatitis in China (2018 edition). *Hepatobiliary Pancreat Dis Int* 2019; **18**: 103-109 [PMID: 30922816 DOI: 10.1016/j.hbpd.2019.02.004]

25 **Machicado JD**, Amann ST, Anderson MA, Abberbock J, Sherman S, Conwell DL, Cote GA, Singh VK, Lewis MD, Alkaade S, Sandhu BS, Guda NM, Muniraj T, Tang G, Baillie J, Brand RE, Gardner TB, Gelrud A, Forsmark CE, Banks PA, Slivka A, Wilcox CM, Whitcomb DC, Yadav D. Quality of Life in Chronic Pancreatitis is Determined by Constant Pain, Disability/Unemployment, Current Smoking, and Associated Co-Morbidities. *Am J Gastroenterol* 2017; **112**: 633-642 [PMID: 28244497 DOI: 10.1038/ajg.2017.42]

26 **Alkhayyat M**, Abou Saleh M, Coronado W, Abureesh M, Al-Otoom O, Qapaja T, Mansoor E, Simons-Linares CR, Stevens T, Chahal P. Increasing Prevalence of Anxiety and Depression Disorders After Diagnosis of Chronic Pancreatitis: A 5-Year Population-Based Study. *Pancreas* 2021; **50**: 153-159 [PMID: 33565791 DOI: 10.1097/MPA.0000000000001746]

27 **Im PK**, Millwood IY, Guo Y, Du H, Chen Y, Bian Z, Tan Y, Guo Z, Wu S, Hua Y, Li L, Yang L, Chen Z; China Kadoorie Biobank (CKB) collaborative group. Patterns and trends of alcohol consumption in rural and urban areas of China: findings from the China Kadoorie Biobank. *BMC Public Health* 2019; **19**: 217 [PMID: 30786877 DOI: 10.1186/s12889-019-6502-1]

28 **Wang M**, Luo X, Xu S, Liu W, Ding F, Zhang X, Wang L, Liu J, Hu J, Wang W. Trends in smoking prevalence and implication for chronic diseases in China: serial national cross-sectional surveys from 2003 to 2013. *Lancet Respir Med* 2019; **7**: 35-45 [PMID: 30482646 DOI: 10.1016/S2213-2600(18)30432-6]

29 **Pernenkil V**, Wyatt T, Akinyemiju T. Trends in smoking and obesity among US adults before, during, and after the great recession and Affordable Care Act roll-out. *Prev Med* 2017; **102**: 86-92 [PMID: 28694062 DOI: 10.1016/j.ypmed.2017.07.001]

30 **Yadav D**, Timmons L, Benson JT, Dierkhising RA, Chari ST. Incidence, prevalence, and survival of chronic pancreatitis: a population-based study. *Am J Gastroenterol* 2011; **106**: 2192-2199 [PMID: 21946280 DOI: 10.1038/ajg.2011.328]

31 **Löhr JM**, Dominguez-Munoz E, Rosendahl J, Besselink M, Mayerle J, Lerch MM, Haas S, Akisik F, Kartalis N, Iglesias-Garcia J, Keller J, Boermeester M, Werner J, Dumonceau JM, Fockens P, Drewes A, Ceyhan G, Lindkvist B, Drenth J, Ewald N, Hardt P, de Madaria E, Witt H, Schneider A, Manfredi R, Brøndum FJ, Rudolf S, Bollen T, Bruno M; HaPanEU/UEG Working Group. United European Gastroenterology evidence-based guidelines for the diagnosis and therapy of chronic pancreatitis (HaPanEU). *United European Gastroenterol J* 2017; **5**: 153-199 [PMID: 28344786 DOI: 10.1177/2050640616684695]

32 **Madzak A**, Olesen SS, Wathle GK, Haldorsen IS, Drewes AM, Frøkjær JB. Secretin-Stimulated Magnetic Resonance Imaging Assessment of the Benign Pancreatic Disorders: Systematic Review and Proposal for a Standardized Protocol. *Pancreas* 2016; **45**: 1092-1103 [PMID: 27171509 DOI: 10.1097/MPA.0000000000000606]

33 **Rosman DA**, Duszak R Jr, Wang W, Hughes DR, Rosenkrantz AB. Changing Utilization of Noninvasive Diagnostic Imaging Over 2 Decades: An Examination Family-Focused Analysis of Medicare Claims Using the Neiman Imaging Types of Service Categorization System. *AJR Am J Roentgenol* 2018; **210**: 364-368 [PMID: 29220208 DOI: 10.2214/AJr17.18214]

34 **Xiao AY**, Tan ML, Wu LM, Asrani VM, Windsor JA, Yadav D, Petrov MS. Global incidence and mortality of pancreatic diseases: a systematic review, meta-analysis, and meta-regression of population-based cohort studies. *Lancet Gastroenterol Hepatol* 2016; **1**: 45-55 [PMID: 28404111 DOI: 10.1016/S2468-1253(16)30004-8]

35 **Hirota M**, Shimosegawa T, Masamune A, Kikuta K, Kume K, Hamada S, Kihara Y, Satoh A, Kimura K, Tsuji I, Kuriyama S; Research Committee of Intractable Pancreatic Diseases. The sixth nationwide epidemiological survey of chronic pancreatitis in Japan. *Pancreatology* 2012; **12**: 79-84 [PMID: 22487515 DOI: 10.1016/j.pan.2012.02.005]

36 **Petrov MS**, Yadav D. Global epidemiology and holistic prevention of pancreatitis. *Nat Rev Gastroenterol Hepatol* 2019; **16**: 175-184 [PMID: 30482911 DOI: 10.1038/s41575-018-0087-5]

37 **Whitcomb DC**, LaRusch J, Krasinskas AM, Klei L, Smith JP, Brand RE, Neoptolemos JP, Lerch MM, Tector M, Sandhu BS, Guda NM, Orlichenko L; Alzheimer's Disease Genetics Consortium, Alkaade S, Amann ST, Anderson MA, Baillie J, Banks PA, Conwell D, Coté GA, Cotton PB, DiSario J, Farrer LA, Forsmark CE, Johnstone M, Gardner TB, Gelrud A, Greenhalf W, Haines JL, Hartman DJ, Hawes RA,

Lawrence C, Lewis M, Mayerle J, Mayeux R, Melhem NM, Money ME, Muniraj T, Papachristou GI, Pericak-Vance MA, Romagnuolo J, Schellenberg GD, Sherman S, Simon P, Singh VP, Slivka A, Stolz D, Sutton R, Weiss FU, Wilcox CM, Zarnescu NO, Wisniewski SR, O'Connell MR, Kienholz ML, Roeder K, Barmada MM, Yadav D, Devlin B. Common genetic variants in the CLDN2 and PRSS1-PRSS2 loci alter risk for alcohol-related and sporadic pancreatitis. *Nat Genet* 2012; **44**: 1349-1354 [PMID: 23143602 DOI: 10.1038/ng.2466]

38 **Ma DM**, Dong XW, Han X, Ling Z, Lu GT, Sun YY, Yin XD. Pancreatitis and Pancreatic Cancer Risk. *Technol Cancer Res Treat* 2023; **22**: 15330338231164875 [PMID: 36972517 DOI: 10.1177/15330338231164875]

39 **Poddighe D**. Autoimmune pancreatitis and pancreatic cancer: Epidemiological aspects and immunological considerations. *World J Gastroenterol* 2021; **27**: 3825-3836 [PMID: 34321847 DOI: 10.3748/wjg.v27.i25.3825]

40 **Phillips AE**, Faghih M, Drewes AM, Singh VK, Yadav D, Olesen SS; Pancreatic Quantitative Sensory Testing (P-QST) Consortium. Psychiatric Comorbidity in Patients With Chronic Pancreatitis Associates With Pain and Reduced Quality of Life. *Am J Gastroenterol* 2020; **115**: 2077-2085 [PMID: 32740078 DOI: 10.14309/ajg.0000000000000782]

41 **Khan D**, Abureesh M, Alkhayyat M, Sadiq W, Alshami M, Munir AB, Karam B, Deeb L, Lafferty J. Prevalence of Myocardial Infarction in Patients With Chronic Pancreatitis. *Pancreas* 2021; **50**: 99-103 [PMID: 33370030 DOI: 10.1097/MPA.0000000000001721]

42 **Yadav D**, Askew RL, Palermo T, Li L, Andersen DK, Chen M, Fisher WE, Fogel EL, Forsmark CE, Hart PA, Othman MO, Pandol SJ, Park WG, Topazian MD, Van Den Eeden SK, Vege SS, Yang Y, Serrano J, Conwell DL; Consortium for the Study of Chronic Pancreatitis, Diabetes; Pancreatic Cancer (CPDPC). Association of Chronic Pancreatitis Pain Features With Physical, Mental, and Social Health. *Clin Gastroenterol Hepatol* 2023; **21**: 1781-1791.e4 [PMID: 36191836 DOI: 10.1016/j.cgh.2022.09.026]

43 **Makar M**, Vodusek Z, Xia W, Greenberg P, Abdelsayed GG. Rising Prevalence of Anxiety and Depression in Chronic Pancreatitis: A Nationwide Analysis. *Pancreas* 2022; **51**: 325-329 [PMID: 35695767 DOI: 10.1097/MPA.0000000000002019]

44 **Chen CH**, Lin CL, Jeng LB. Association between chronic pancreatitis and urolithiasis: A population-based cohort study. *PLoS One* 2018; **13**: e0194019 [PMID: 29522553 DOI: 10.1371/journal.pone.0194019]

45 **Tseng CW**, Chen YT, Lin CL, Liang JA. Association between chronic pancreatitis and pyogenic liver abscess: a nationwide population study. *Curr Med Res Opin* 2017; **33**: 505-510 [PMID: 27892720 DOI: 10.1080/03007995.2016.1266312]

46 **Wong TS**, Liao KF, Lin CM, Lin CL, Chen WC, Lai SW. Chronic Pancreatitis Correlates With Increased Risk of Cerebrovascular Disease: A Retrospective Population-Based Cohort Study in Taiwan. *Medicine (Baltimore)* 2016; **95**: e3266 [PMID: 27082563 DOI: 10.1097/MD.0000000000003266]

47 **Chen YL**, Hsu CW, Cheng CC, Yiang GT, Lin CS, Lin CL, Sung FC, Liang JA. Increased subsequent risk of inflammatory bowel disease association in patients with chronic pancreatitis: a nationwide population-based cohort study. *Curr Med Res Opin* 2017; **33**: 1077-1082 [PMID: 28277863 DOI: 10.1080/03007995.2017.1300143]

48 **Chen C**, Zhou Y, Wang D, Li G, Yin K, Tao H, Wang CY, Li ZS, Wei C, Hu LH. Anxiety, depression, and coping styles among patients with chronic pancreatitis in East China. *BMC Psychiatry* 2023; **23**: 212 [PMID: 36991480 DOI: 10.1186/s12888-023-04691-2]

World Journal of Gastroenterology

Submit a Manuscript: https://www.f6publishing.com

World J Gastroenterol 2023 August 14; 29(30): 4685-4700

DOI: 10.3748/wjg.v29.i30.4685

ISSN 1007-9327 (print) ISSN 2219-2840 (online)

META-ANALYSIS

Diagnostic value of conventional endoscopic ultrasound for lymph node metastasis in upper gastrointestinal neoplasia: A meta-analysis

Cong Chen, Ya-Lan Song, Zhen-Yu Wu, Jing Chen, Yao Zhang, Lei Chen

Specialty type: Gastroenterology and hepatology

Provenance and peer review: Unsolicited article; Externally peer reviewed.

Peer-review model: Single blind

Peer-review report's scientific quality classification

Grade A (Excellent): 0
Grade B (Very good): B, B
Grade C (Good): C
Grade D (Fair): 0
Grade E (Poor): 0

P-Reviewer: Grgurevic I, Croatia; Massironi S, Italy; Redondo-Cerezo E, Spain

Received: May 5, 2023
Peer-review started: May 5, 2023
First decision: July 9, 2023
Revised: July 16, 2023
Accepted: July 27, 2023
Article in press: July 27, 2023
Published online: August 14, 2023

Cong Chen, Ya-Lan Song, Zhen-Yu Wu, Jing Chen, Lei Chen, Institute of Gastroenterology, Southwest Hospital, Army Medical University (Third Military Medical University), Chongqing 400038, China

Yao Zhang, Department of Epidemiology, College of Preventive Medicine, Army Medical University (Third Military Medical University), Chongqing 400038, China

Corresponding author: Lei Chen, MD, PhD, Professor, Institute of Gastroenterology, Southwest Hospital, Army Medical University (Third Military Medical University), No. 30 Gaotanyan Main Street, Xinqiao Street, Shapingba District, Chongqing 400038, China.
chenlei_1977603@126.com

Abstract

BACKGROUND

Upper gastrointestinal neoplasia mainly includes esophageal cancer and gastric cancer, both of which have high morbidity and mortality. Lymph node metastasis (LNM), as the most common metastasis mode of both diseases, is an important factor affecting tumor stage, treatment strategy and clinical prognosis. As a new fusion technology, endoscopic ultrasound (EUS) is becoming increasingly used in the diagnosis and treatment of digestive system diseases, but its use in detecting LNM in clinical practice remains limited.

AIM

To evaluate the diagnostic value of conventional EUS for LNM in upper gastrointestinal neoplasia.

METHODS

Using the search mode of "MeSH + Entry Terms" and according to the predetermined inclusion and exclusion criteria, we conducted a comprehensive search and screening of the PubMed, EMBASE and Cochrane Library databases from January 1, 2000 to October 1, 2022. Study data were extracted according to the predetermined data extraction form. The quality of the included studies was assessed using the Quality Assessment of Diagnostic Accuracy Studies tool, and the results of the quality assessment were presented using Review Manager 5.3.5 software. Finally, Stata14.0 software was used for a series of statistical analyses.

RESULTS

A total of 22 studies were included in our study, including 2986 patients. The pooled sensitivity, specificity, positive likelihood ratio, negative likelihood ratio, diagnostic score and diagnostic odds ratio of conventional EUS in the diagnosis of upper gastrointestinal neoplasia LNM were 0.62 [95% confidence interval (CI): 0.50-0.73], 0.80 (95%CI: 0.73-0.86), 3.15 (95%CI: 2.46-4.03), 0.47 (95%CI: 0.36-0.61), 1.90 (95%CI: 1.51-2.29) and 6.67 (95%CI: 4.52-9.84), respectively. The area under the summary receiver operating characteristic curve was 0.80 (95%CI: 0.76-0.83). Sensitivity analysis indicated that the results of the meta-analysis were stable. There was considerable heterogeneity among the included studies, and the threshold effect was an important source of heterogeneity. Univariable meta-regression and subgroup analysis showed that tumor type, sample size and EUS diagnostic criteria were significant sources of heterogeneity in specificity ($P < 0.05$). No significant publication bias was found.

CONCLUSION
Conventional EUS has certain clinical value and can assist in the detection of LNM in upper gastrointestinal neoplasia, but it cannot be used as a confirmatory or exclusionary test.

Key Words: Endosonography; Esophageal neoplasms; Stomach neoplasms; Lymphatic metastasis; Diagnosis; Meta-analysis

©The Author(s) 2023. Published by Baishideng Publishing Group Inc. All rights reserved.

Core Tip: This meta-analysis examined the diagnostic value of conventional endoscopic ultrasound (EUS) for lymph node metastasis (LNM) in upper gastrointestinal neoplasia. The pooled analyses of 2986 patients from 22 studies performed herein show that conventional EUS has certain clinical value and can assist in the detection of LNM in upper gastrointestinal neoplasia, but it cannot be used as a confirmatory or exclusionary test. More high-quality studies are needed to further verify the diagnostic value of EUS and determine the best diagnostic criteria.

Citation: Chen C, Song YL, Wu ZY, Chen J, Zhang Y, Chen L. Diagnostic value of conventional endoscopic ultrasound for lymph node metastasis in upper gastrointestinal neoplasia: A meta-analysis. *World J Gastroenterol* 2023; 29(30): 4685-4700
URL: https://www.wjgnet.com/1007-9327/full/v29/i30/4685.htm
DOI: https://dx.doi.org/10.3748/wjg.v29.i30.4685

INTRODUCTION

Upper gastrointestinal neoplasia mainly includes esophageal cancer and gastric cancer, and their morbidity and mortality have long been among the top ten of the global cancer list, bringing great pain and burden to countries all over the world, and they are major global public health problems[1-4]. The onset of esophageal cancer and gastric cancer is hidden, and the best time for treatment has often been passed by the time they are clinically diagnosed. Lymph node metastasis (LNM), as the most common metastasis mode of both diseases, is an important basis for tumor staging, which largely determines the treatment plan and clinical prognosis of patients[5-8]. For patients with early tumor stages and no LNM, we can attempt endoscopic minimally invasive treatment, but for patients with LNM or advanced tumor stages, it is often necessary to consider comprehensive treatment, including radiotherapy, chemotherapy or surgery[9-11]. One study showed that when esophageal cancer has 0, 1-2 or more than 2 malignant lymph nodes, the median patient survival time is 66 mo, 14.5 mo or 6.5 mo, respectively[12]. Therefore, it is very important to accurately predict LNM.

Endoscopic ultrasound (EUS) combines the advantages of endoscopic technology and ultrasound technology; that is, it can evaluate the mucous membrane of the digestive tract with the naked eye, and it can also be used to detect the hierarchical structure and surrounding tissues of the digestive tract wall with ultrasound wave. EUS has the advantages of close observation distance, high resolution, low price and few adverse events. Since the 1980s, EUS has been gradually used in the diagnosis and treatment of many digestive system diseases, including the staging of gastrointestinal tumors, the identification of submucosal tumors, and the study of pancreatic or biliary tract diseases[13,14]. Conventional EUS uses grayscale imaging technology for analysis, which can clearly display the status of lymph nodes near upper gastrointestinal neoplasia and identify the nature of lymph nodes according to the imaging features. When the endosonographic characteristics of lymph nodes are hypoechoic, round in shape, with a clear boundary and a size greater than 1 cm, the accuracy of conventional EUS in predicting malignant lymph nodes is more than 80%[15]. Some studies have shown that the ability of conventional EUS to detect LNM in upper gastrointestinal neoplasia is better than that of computed tomography and positron emission tomography, but some scholars believe that the diagnostic performance of conventional EUS is poor, and study results have varied widely[16-20]. The purpose of this meta-analysis was to explore the diagnostic value of conventional EUS for LNM in upper gastrointestinal neoplasia to guide clinical practice more effectively.

MATERIALS AND METHODS

This meta-analysis was conducted according to the Preferred Reporting Items for Systematic Review and Meta-Analysis statement[21,22]. The study protocol was registered in the PROSPERO database with the number CRD42022372170.

Literature search

We used the "MeSH + Entry Terms" search mode to conduct a comprehensive search of the PubMed, EMBASE and Cochrane Library databases before October 1, 2022. The specific search terms were as follows: ("esophageal neoplasms" OR "stomach neoplasms" OR "duodenal neoplasms") AND ("lymphatic metastasis" OR "lymph nodes") AND "endosonography" AND "diagnostic test search strategy". We also manually searched the references of related studies.

Study selection

We imported all the retrieved articles into EndNote software (Version X9.1; Clarivate Analytics; Philadelphia, United States). Two researchers independently conducted study selection according to the predetermined inclusion and exclusion criteria with the process of identification, screening, eligibility and inclusion. To ensure consistency, we conducted exercises and tests before the formal selection, and the data were verified for internal consistency with the Kappa test during the selection process. If there was any disagreement, the decision was made by the two researchers together through consultation.

The study inclusion criteria were as follows: (1) Patients older than 18 who had recently been diagnosed with upper gastrointestinal neoplasia such as esophageal cancer, gastric cancer, and duodenal cancer; (2) LNM detected by conventional EUS; and (3) Diagnostic testing.

The exclusion criteria were as follows: (1) Studies published before 2000; (2) Case reports, conference abstracts, reviews, comments, letters, meta-analyses and systematic reviews; (3) Animal or *in vitro* models used as the objects of the study; (4) Sample size less than ten cases; (5) Inclusion of only stage cN0 patients; (6) Patients with other malignant tumors; (7) Patients who received or may have received preoperative neoadjuvant therapy; (8) Use of assistive technologies such as fine needle aspiration (FNA); (9) LNM diagnosis not made with postoperative pathological examination as the gold standard or radical surgery not performed for all patients; (10) Per patient not used as the analysis unit; (11) Inability to extract 2 × 2 tables of true positives (TP), false positives (FP), false negatives (FN), and true negatives (TN); (12) Repeated publication of the same data; and (13) Full text of English literature not found.

Data extraction and quality assessment

Two researchers independently extracted the study data using the predetermined data extraction form, and when they faced disagreement, a third researcher was consulted. Extracted data included: (1) Study characteristics such as first author, publication year, study country, study design and participating center; (2) Diagnostic test characteristics such as EUS model, EUS scan type, EUS examination method, EUS scan frequency, EUS diagnostic criteria, type and number of image interpretation experts, blinding, interval between EUS and surgery, gold standard and analysis unit; (3) Patient/tumor characteristics such as tumor type, tumor location, tumor stage, tumor histological type, neoadjuvant therapy, location of metastatic lymph nodes, age, sex and sample size; and (4) Statistical indicators such as TP, FP, FN, and TN. If the data were not reported directly, the sensitivity, specificity, accuracy and other indicators were used for reverse calculation.

Two researchers independently assessed the quality of the included studies using the Quality Assessment of Diagnostic Accuracy Studies (QUADAS-2) tool[23]. Disagreements were resolved through consultation. The results of the quality assessment were presented using Review Manager software (Version 5.3.5; Nordic Cochrane Centre; Copenhagen, Denmark).

Statistical analysis

All data evaluation and picture generation were completed by Stata software (Version 14.0; StataCorp LP; Texas, United States) using the MIDAS module of the bivariable mixed effects model. This model not only considers factors such as heterogeneity between studies, threshold effect and study size but also enables the bivariate nature of the original data to remain unchanged throughout the analysis process, thereby generating reliable statistical indicators. The pooled sensitivity, specificity, positive likelihood ratio (PLR), negative likelihood ratio (NLR), diagnostic score (DS) and diagnostic odds ratio (DOR) were calculated by drawing forest plots. The higher the values of DS and DOR were, the better the diagnostic effect of conventional EUS. The area under the curve (AUC) was obtained by drawing a summary receiver operating characteristic (SROC) curve, and the diagnostic performance was considered low, moderate, and high for AUCs of 0.5-0.7, 0.7-0.9 and 0.9-1.0, respectively. Fagan's nomogram was used to reveal changes in the posttest probabilities. Likelihood ratio scatter diagram was used to evaluate the diagnostic performance of conventional EUS. Sensitivity analysis was used to assess the influence of individual studies on heterogeneity and observe the stability of the summary statistics. The threshold effect was determined according to whether the ROC plane showed a "shoulder-arm" point distribution. The Q statistical test was applied to assess the heterogeneity among the included studies, and heterogeneity was considered statistically significant when $P < 0.05$. The degree of heterogeneity was estimated based on the I^2 statistic, where $I^2 < 25\%$, 25%-50%, 50%-75%, and ≥ 75% were considered low, moderate, substantial, and considerable heterogeneity, respectively. If the heterogeneity was high, meta-regression and subgroup analysis were used to explore the most significant source of heterogeneity. Publication bias was assessed with Deeks' funnel plot, and $P < 0.05$ indicated statistical significance. The statistical methods of this study were reviewed by Professor Yao Zhang from the Department of Epidemiology, College of Preventive Medicine, Army Medical University of China.

RESULTS

Study selection

The study selection process is shown in Figure 1. A total of 729 articles were retrieved from three databases, and 22 articles were included in the manual search. The complete retrieval strategy of each database and manual search literature catalog can be found in Supplementary Table 1. Among them, 99 repeated articles were excluded after checking duplicates with EndNote software, 525 obviously irrelevant articles were excluded after reading the publication year, title and abstract, 8 articles were not published in English, 97 articles that did not meet the requirements were excluded after full-text reading, and 22 articles were included in the analysis according to the screening criteria[24-45]. In addition, the Kappa coefficient of the consistency test of the final selection results of the two researchers was 0.810 (P = 0.000).

Characteristics and quality of the included studies

This meta-analysis included 22 studies with 2986 patients. The basic information of the studies is shown in Table 1, and the detailed information is shown in Supplementary Table 2. Among them, the vast majority of studies were retrospective studies (21/22, 95.5%) and single center studies (20/22, 90.9%); ten studies were conducted in eastern countries, and twelve studies were conducted in western countries; the objects of twelve studies and ten studies were esophageal cancer and gastric cancer, respectively; none of the patients received neoadjuvant therapy before EUS and surgery, and the gold standard for the diagnosis of LNM in all studies was postoperative pathology. The results of the quality assessment based on the QUADAS-2 tool are shown in Figure 2, and detailed quality assessment information is shown in Supplementary Table 3.

Meta-analysis outcomes

Primary outcomes: The pooled sensitivity and specificity of conventional EUS in the diagnosis of upper gastrointestinal neoplasia LNM were 0.62 [95% confidence interval (CI): 0.50-0.73, I^2 = 91.50%] and 0.80 (95%CI: 0.73-0.86, I^2 = 86.10%), respectively, as shown in Figure 3A. According to the SROC curve, the AUC was 0.80 (95%CI: 0.76-0.83), as shown in Figure 4.

Secondary outcomes: The pooled PLR, NLR, DS, and DOR of conventional EUS in the diagnosis of upper gastrointestinal neoplasia LNM were 3.15 (95%CI: 2.46-4.03, I^2 = 61.17%), 0.47 (95%CI: 0.36-0.61, I^2 = 92.21%), 1.90 (95%CI: 1.51-2.29, I^2 = 60.94%) and 6.67 (95%CI: 4.52-9.84, I^2 = 99.99%), respectively, as shown in Figures 3B and C. The likelihood ratio scatter diagram showed that the summary PLR and NLR for the index test were in the fourth quadrant, suggesting that conventional EUS cannot be used as a confirmatory or exclusionary test, as shown in Figure 5. According to Fagan's nomogram, when the EUS results were positive, the probability of diagnosing LNM increased from 50% to 76%; when the EUS results were negative, the probability of diagnosing LNM decreased from 50% to 32%, as shown in Figure 6.

Validation of meta-analysis results

Sensitivity analysis: We conducted sensitivity analysis by eliminating studies one by one, and the results showed that the pooled sensitivity change rate was ≤ 4.84% (I^2 change rate ≤ 2.75%), and the pooled specificity change rate was ≤ 2.50% (I^2 change rate ≤ 5.04%), indicating that the results of the meta-analysis were stable. Detailed data from the sensitivity analysis are shown in Supplementary Table 4.

Heterogeneity: Based on the Q statistical test and I^2 statistic, considerable heterogeneity was observed in the analysis for diagnostic sensitivity and specificity of conventional EUS. The ROC plane showed that the sensitivity was positively correlated with (1 - specificity), resulting in a "shoulder-arm" point distribution and indicating the existence of a threshold effect, as shown in Figure 7. According to the calculations from Stata software, the proportion of heterogeneity likely due to the threshold effect was 0.54. Because of the obvious heterogeneity among studies, we included five covariates: Tumor type (esophageal cancer or gastric cancer), study area (eastern country or western country), publication year (2010-2018 or 2000-2009), sample size (≥ 100 cases or < 100 cases) and EUS diagnostic criteria (criteria 1 or criteria 2). Univariable meta-regression and subgroup analysis were performed to identify the significant sources of heterogeneity. The results showed that tumor type, sample size and EUS diagnostic criteria were significant sources of heterogeneity in specificity (P < 0.05), as shown in Figure 8. The covariable assignment instructions are shown in Supplementary Table 5. The indicators for evaluating the diagnostic value of conventional EUS in each subgroup are shown in Table 2.

Publication bias

Deeks' funnel plot showed that the distribution of all studies was relatively symmetrical; the asymmetry was not statistically significant (P = 0.654), indicating that there was no significant publication bias among the 22 studies, as shown in Figure 9.

DISCUSSION

In this meta-analysis, upper gastrointestinal neoplasia was considered as a whole, and the diagnostic value of conventional EUS for LNM was analysed. To ensure the reliability of the research results, we excluded studies that were old, had incomplete data, had small sample sizes and were published in languages other than English. The effects of incomplete surgical resection, neoadjuvant therapy, animal experiments, assistive technologies and other malignant tumors on the

Table 1 Characteristics of the included studies

Ref.	Country	Study design	Center	EUS scan type	EUS scan frequency (MHz)	EUS diagnostic criteria[1]	Gold standard	Tumor type	Age[2] (yr)	Sample size (cases)	TP	FP	FN	TN
Jeong *et al* [24], 2018	Korea	Retrospective	1	Radial	12/20	Criteria 1	Postoperative pathology	Esophageal cancer	64	435	57	31	80	267
Shi *et al* [25], 2017	China	Retrospective	1	Radial	-	Criteria 2	Postoperative pathology	Esophageal cancer	59	86	28	5	8	45
Shan *et al* [26], 2015	China	Prospective	1	Radial	7.5	Criteria 1	Postoperative pathology	Esophageal cancer	≥ 44	94	11	5	23	55
Lee *et al* [27], 2014	Korea	Retrospective	1	Radial	7.5/12/20	Criteria 2	Postoperative pathology	Esophageal cancer	69	12	2	0	3	7
Meister *et al* [28], 2013	Germany	Retrospective	5	Radial	20	Criteria 1	Postoperative pathology	Esophageal cancer	≥ 34	93	39	12	12	30
Yen *et al* [29], 2012	China	Retrospective	1	Radial	12/20	Criteria 2	Postoperative pathology	Esophageal cancer	≥ 43	27	5	12	0	10
Pech *et al* [30], 2010	Germany	Retrospective	1	Radial	7.5-10	Criteria 1	Postoperative pathology	Esophageal cancer	64	179	48	29	20	82
Machlenkin *et al*[31], 2009	Israel	Retrospective	1	Radial	7.5-12	Criteria 1	Postoperative pathology	Esophageal cancer	≥ 28	13	2	0	2	9
Mennigen *et al*[32], 2008	Germany	Retrospective	1	-	7.5/15	Criteria 1	Postoperative pathology	Esophageal cancer	65	97	49	15	10	23
Shimpi *et al* [33], 2007	United States	Retrospective	1	Radial	20	Criteria 1	Postoperative pathology	Esophageal cancer	-	37	9	1	3	24
Shinkai *et al* [34], 2000	Japan	Retrospective	1	Radial	7.5/12/ 15/20	Criteria 1	Postoperative pathology	Esophageal cancer	≥ 42	102	41	20	13	28
Richards *et al*[35], 2000	United Kingdom	Retrospective	1	Radial	7.5/12	Criteria 1	Postoperative pathology	Esophageal cancer	≥ 35	69	19	9	23	18
Li *et al*[36], 2017	China	Retrospective	1	Radial	5/7.5/ 10/12	Criteria 2	Postoperative pathology	Gastric cancer	57	81	48	4	3	26
Serrano *et al*[37], 2016	United States	Retrospective	1	Radial	7.5/10	Criteria 2	Postoperative pathology	Gastric cancer	≥ 42	46	8	6	8	24
Spolverato *et al*[38], 2015	United States	Retrospective	7	-	-	Criteria 2	Postoperative pathology	Gastric cancer	-	144	34	12	36	62
Fairweather *et al*[39], 2015	United States	Retrospective	1	Radial	5-10	Criteria 2	Postoperative pathology	Gastric cancer	67	49	2	3	25	19
Feng *et al* [40], 2013	China	Retrospective	1	-	5/7.5/12/ 15/20	Criteria 2	Postoperative pathology	Gastric cancer	57	610	307	45	118	140
Kutup *et al* [41], 2012	Germany	Retrospective	1	Radial	7.5/10/12	Criteria 2	Postoperative pathology	Gastric cancer	61	123	64	18	17	24
Zheng *et al* [42], 2011	China	Retrospective	1	Radial	7.5/12	Criteria 2	Postoperative pathology	Gastric cancer	58	162	48	20	49	45
Bohle *et al* [43], 2011	Germany	Retrospective	1	Radial	5-20	Criteria 1	Postoperative pathology	Gastric cancer	63	62	30	5	9	18
Hwang *et al* [44], 2010	Korea	Retrospective	1	Radial	5/7.5/ 12/20	Criteria 2	Postoperative pathology	Gastric cancer	≥ 49	247	16	6	67	158
Bentrem *et al*[45], 2007	United States	Retrospective	1	-	7.5-12	Criteria 2	Postoperative pathology	Gastric cancer	-	218	81	39	27	71

[1]Criteria 1 (hypoechoic, round, well-defined margin, diameter ≥ 10 mm), Criteria 2 (others).

[2]Mean age or youngest age.

EUS: Endoscopic ultrasound; TP: True positives; FP: False positives; FN: False negatives; TN: True negatives.

Table 2 Subgroup analysis of the diagnostic value of conventional endoscopic ultrasound for lymph node metastasis in upper gastrointestinal neoplasia

Subgroup		Studies	Sensitivity (95%CI)	Specificity (95%CI)	PLR (95%CI)	NLR (95%CI)	DS (95%CI)	DOR (95%CI)	AUC (95%CI)
	All studies	22	0.62 (0.50-0.73)	0.80 (0.73-0.86)	3.15 (2.46-4.03)	0.47 (0.36-0.61)	1.90 (1.51-2.29)	6.67 (4.52-9.84)	0.80 (0.76-0.83)
Tumor type	Esophageal cancer	12	0.64 (0.51-0.76)	0.81 (0.70-0.88)	3.33 (2.27-4.87)	0.44 (0.33-0.59)	2.02 (1.53-2.50)	7.52 (4.64-12.18)	0.79 (0.75-0.83)
	Gastric cancer	10	0.59 (0.38-0.76)	0.80 (0.71-0.87)	2.95 (2.09-4.17)	0.52 (0.34-0.79)	1.74 (1.09-2.40)	5.71 (2.96-10.99)	0.79 (0.75-0.82)
Study area	Eastern country	10	0.63 (0.42-0.80)	0.84 (0.72-0.91)	3.83 (2.46-5.95)	0.44 (0.28-0.71)	2.15 (1.48-2.83)	8.62 (4.38-16.94)	0.82 (0.79-0.85)
	Western country	12	0.61 (0.48-0.73)	0.76 (0.69-0.82)	2.57 (2.13-3.11)	0.51 (0.38-0.67)	1.62 (1.26-1.99)	5.07 (3.53-7.30)	0.77 (0.73-0.80)
Publication year	2010-2018	16	0.60 (0.44-0.74)	0.82 (0.75-0.88)	3.36 (2.58-4.38)	0.48 (0.35-0.68)	1.94 (1.47-2.41)	6.93 (4.34-11.08)	0.81 (0.77-0.84)
	2000-2009	6	0.70 (0.56-0.81)	0.75 (0.56-0.88)	2.79 (1.50-5.18)	0.41 (0.27-0.62)	1.93 (1.01-2.85)	6.87 (2.74-17.22)	0.78 (0.74-0.81)
Sample size	≥ 100 cases	9	0.60 (0.46-0.73)	0.78 (0.67-0.87)	2.79 (2.14-3.65)	0.51 (0.40-0.65)	1.71 (1.45-1.97)	5.52 (4.24-7.18)	0.76 (0.72-0.80)
	< 100 cases	13	0.65 (0.61-0.90)	0.83 (0.72-0.89)	3.80 (2.45-5.89)	0.42 (0.26-0.69)	2.20 (1.42-2.99)	9.04 (4.13-19.81)	0.83 (0.80-0.86)
EUS diagnostic criteria[1]	Criteria 1	10	0.62 (0.50-0.73)	0.79 (0.71-0.86)	3.04 (2.38-3.88)	0.47 (0.37-0.60)	1.86 (1.58-2.14)	6.43 (4.84-8.54)	0.78 (0.74-0.82)
	Criteria 2	12	0.61 (0.41-0.79)	0.81 (0.70-0.88)	3.17 (2.19-4.60)	0.48 (0.30-0.75)	1.89 (1.22-2.57)	6.63 (3.37-13.05)	0.80 (0.76-0.83)

[1]Criteria 1 (hypoechoic, round, well-defined margin, diameter ≥ 10mm), Criteria 2 (others).

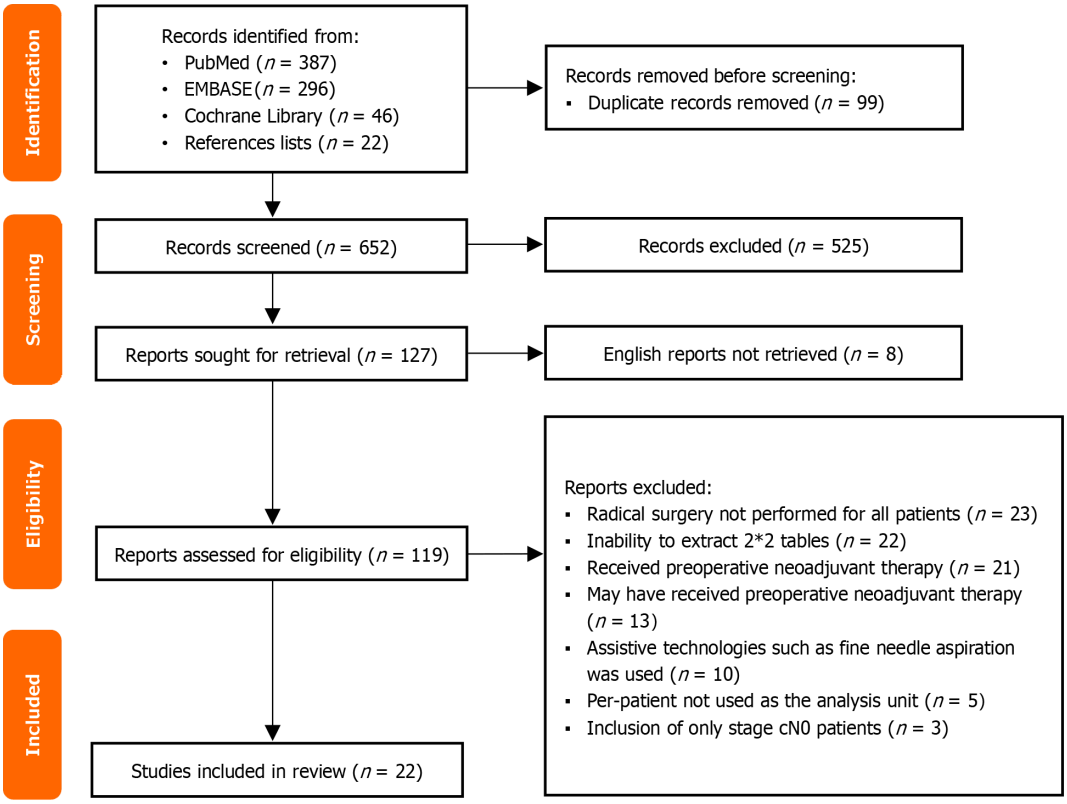
PLR: Positive likelihood ratio; NLR: Negative likelihood ratio; DS: Diagnostic score; DOR: Diagnostic odds ratio; AUC: Area under the curve.

statistical results were excluded (which is also the reason for the small number of studies included in this meta-analysis). The results of conventional EUS were compared with postoperative pathology, and the data of 2986 patients in 22 studies were analyzed in detail.

The results of the quality assessment showed that many studies had a risk of bias, mainly because the proportion of retrospective studies was too high, and selective bias may have been present in the patient inclusion process. Four studies did not clearly describe the diagnostic criteria in the use of EUS, five studies unreasonably excluded some tumor patients (two studies limited the tumor location, two studies defined the location of metastatic lymph nodes, and one study only included esophageal cancer of ≤ pT2 stage), and fifteen studies did not specify the interval between EUS and surgery. However, we believe that since both esophageal cancer and gastric cancer are malignancies, examination and surgery should be arranged as soon as possible after clinical diagnosis. Although many studies did not specify the interval, it should not have had a significant impact on the research results. Regarding concerns regarding applicability, we think that the main reasons were the difference in diagnostic criteria of EUS and bias in patient selection. Therefore, caution should be taken in interpreting the results of the meta-analysis.

Due to the significant heterogeneity among the included studies, we used the bivariate mixed effect model to calculate statistics on various diagnostic evaluation indicators. The results showed that the pooled sensitivity and specificity of conventional EUS in diagnosing LNM in upper gastrointestinal neoplasia were 0.62 and 0.80, respectively, and the AUC of the SROC curve was 0.80, which indicated that the diagnostic value of conventional EUS was moderate. When EUS indicated positive or negative results, the posttest probability could be adjusted from the previous 50% to 76% and 32%, respectively. This result is meaningful for noninvasive examinations, indicating that conventional EUS has certain clinical value. However, it is undeniable that because the PLR < 10 and NLR > 0.1 in conventional EUS diagnosis and the DS and DOR were relatively small, this examination cannot be used to confirm or exclude LNM, which is consistent with the results of previous studies[46-49]. It is not difficult to understand that, as with other imaging examinations, it is difficult for conventional EUS to reach such a high diagnostic level without obtaining lymph node tissue.

We explored the sources of heterogeneity among the included studies. First, we believe that the threshold effect could lead to heterogeneity because the 22 studies adopted a variety of EUS diagnostic criteria, and the "shoulder-arm" point distribution in the ROC plane also confirmed our view; the threshold effect might contribute 54% of the heterogeneity. Then, in view of the differences among the various studies, we included five covariables that could be easily grouped according to the collected data for meta-regression and subgroup analysis. Considering the limited number of studies, it would have been difficult to guarantee the accuracy of the statistical results of the simultaneous inclusion of five covariates, so we included individual covariates one by one for analysis. Although we were unable to identify significant

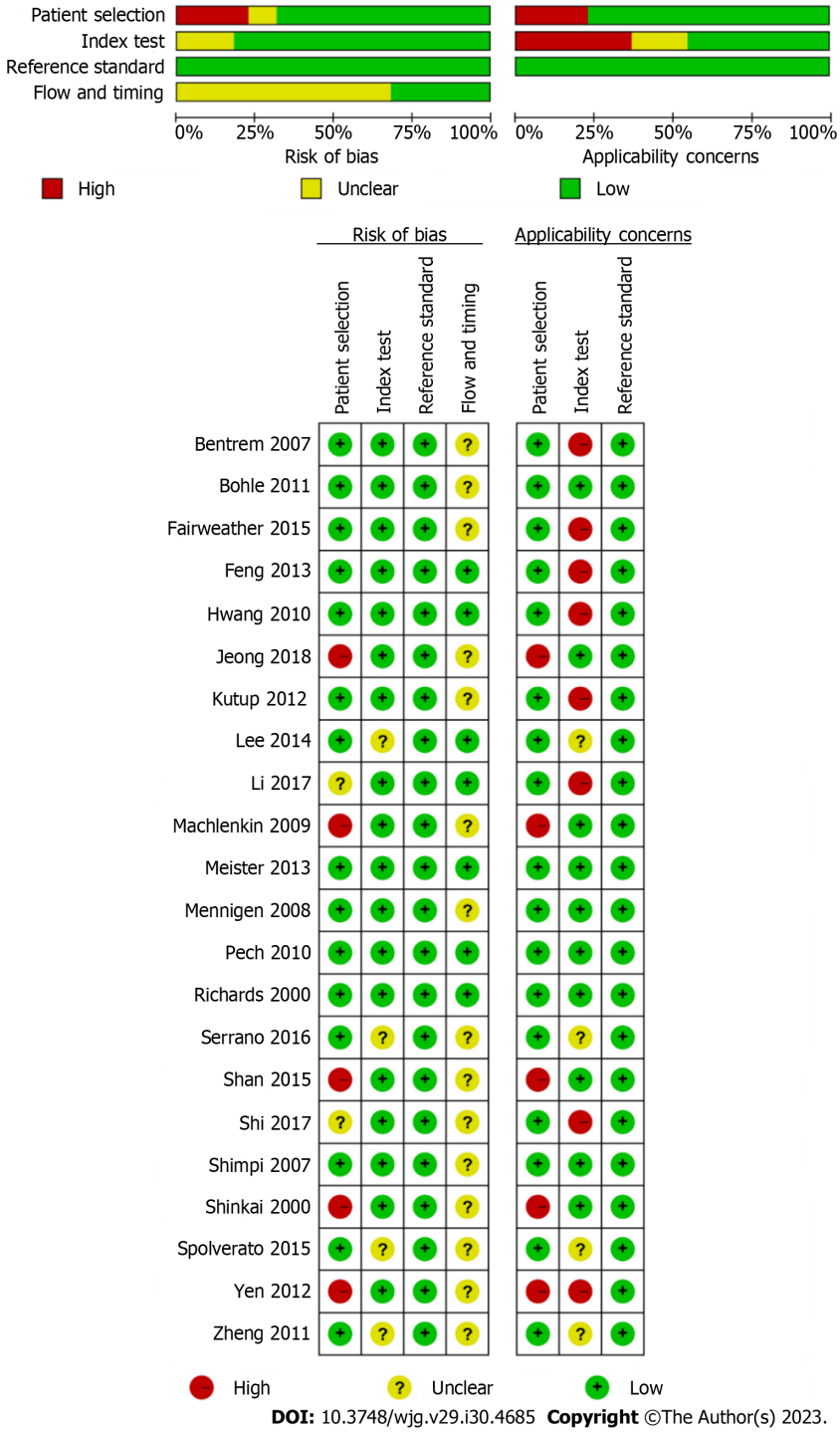


DOI: 10.3748/wjg.v29.i30.4685 **Copyright** ©The Author(s) 2023.

Figure 1 Flow chart for study selection.

sources of heterogeneity in sensitivity, we found that the significant sources of heterogeneity in specificity included tumor type, sample size, and EUS diagnostic criteria. However, after excluding the influence of the above factors, the heterogeneity within each subgroup was still obvious. Therefore, we have reason to believe that the heterogeneity was caused by a combination of factors. Many unincluded factors may also have been sources of heterogeneity; examples and the reasons they were not analyzed in detail included the study design, participating center and EUS scan type (because of the proportion imbalance within the group), the qualifications of the endoscopists, the EUS model and scan frequency (because of the complexity of the data), and the tumor stage, tumor location and location of metastatic lymph nodes (because these could not be accurately distinguished). We also found that the study area was not a significant source of heterogeneity, indicating that the diagnostic performance of conventional EUS for LNM in patients with upper gastrointestinal neoplasia in eastern and western countries is comparable. Publication year was also not a significant source of heterogeneity, indicating that the diagnostic performance of conventional EUS has not changed significantly in the past 20 years and that there may be technical barriers in conventional EUS that limit opportunities to significantly improve the ability of conventional EUS to identify malignant lymph nodes by relying solely on the diagnostic criteria of size, shape, boundary and echo.

Although the performance of conventional EUS in diagnosing LNM in upper gastrointestinal neoplasia remains nonideal, the diagnostic ability can be greatly improved with the assistance of EUS-guided FNA (EUS-FNA), EUS elastography (EUS-E) and contrast-enhanced EUS (CE-EUS)[50-52]. EUS-FNA uses a slender biopsy needle to perform puncture biopsy for suspicious lesions under the guidance of EUS, which can provide histopathological information and is an accurate method to distinguish between benign and malignant lymph nodes. The sensitivity and accuracy of EUS-FNA in the diagnosis of regional LNM of upper gastrointestinal neoplasia are higher than those of conventional EUS. Chen *et al*[53] included 26 studies with 2753 patients for meta-analysis and found that the pooled sensitivity and specificity of EUS-FNA in differentiating benign and malignant lymph nodes were 87% and 100%, respectively, and the AUC was as high as 0.9912. EUS-E uses different colors to distinguish tissue hardness and displays different color images according to the elastic difference between lymph nodes and surrounding tissues, which can more clearly identify metastatic lymph nodes, improve the diagnostic performance of conventional EUS, and reduce unnecessary biopsies. Xu *et al*[54] included seven studies with 368 patients for meta-analysis and showed that the pooled sensitivity, specificity and AUC of EUS-E in the diagnosis of LNM were 88%, 85% and 0.9456, respectively. CE-EUS obtains enhanced images by using contrast agents, which can provide more information about the lesion tissue and can be used to identify metastatic lymph nodes. Lisotti *et al*[55] included four studies with 336 patients in their meta-analysis and indicated that the pooled sensitivity and specificity of CE-EUS in diagnosing LNM were 82.1% and 90.7%, respectively. However, our study only analyzed the diagnostic value of conventional EUS for LNM of upper gastrointestinal neoplasia, without considering the role of the above assistive technologies, which may underestimate the diagnostic value of EUS and affect the choice of clinicians. Therefore, we can carry out relevant studies in the next stage to evaluate the diagnostic value of various EUS assistive technologies in detail.

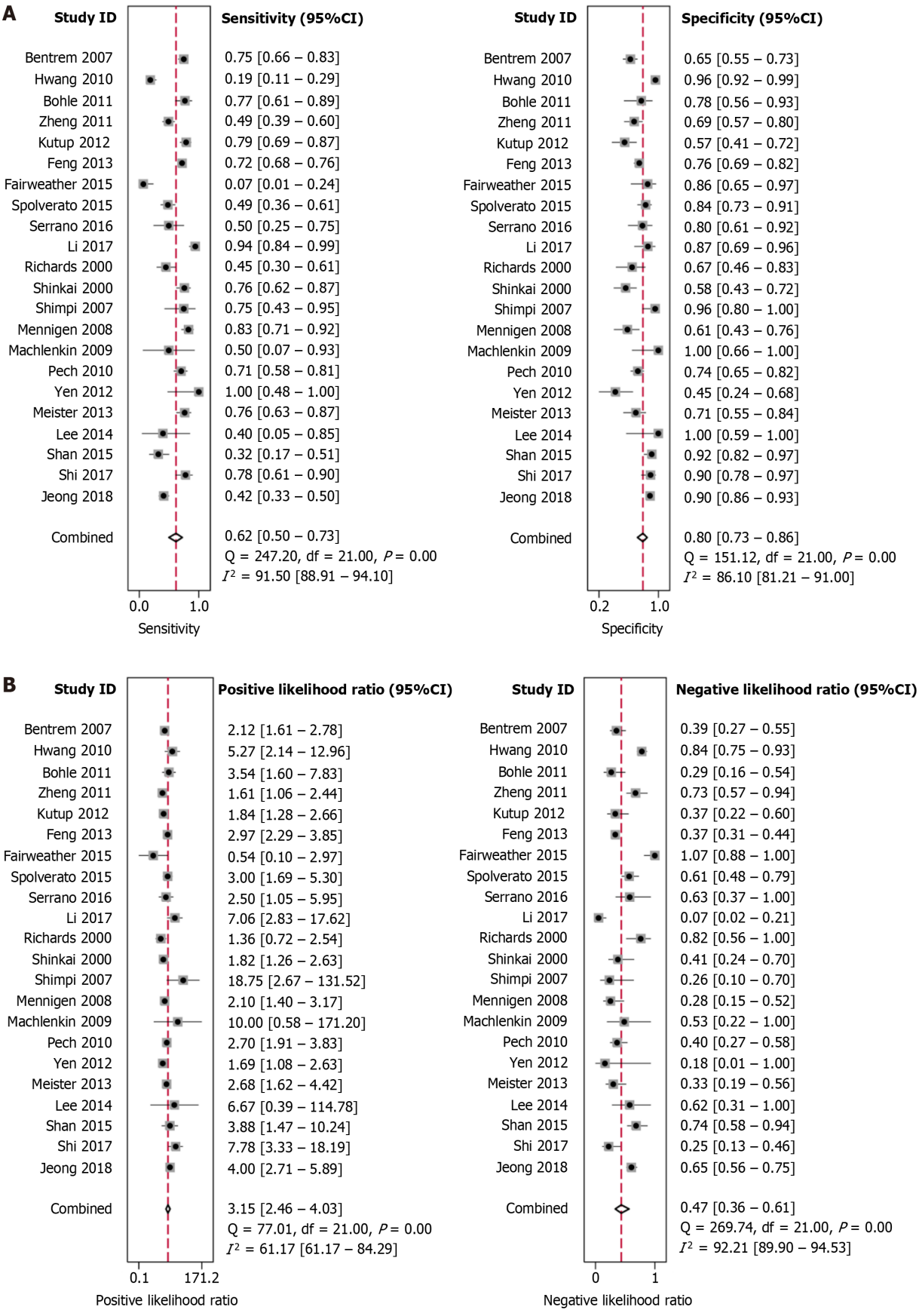


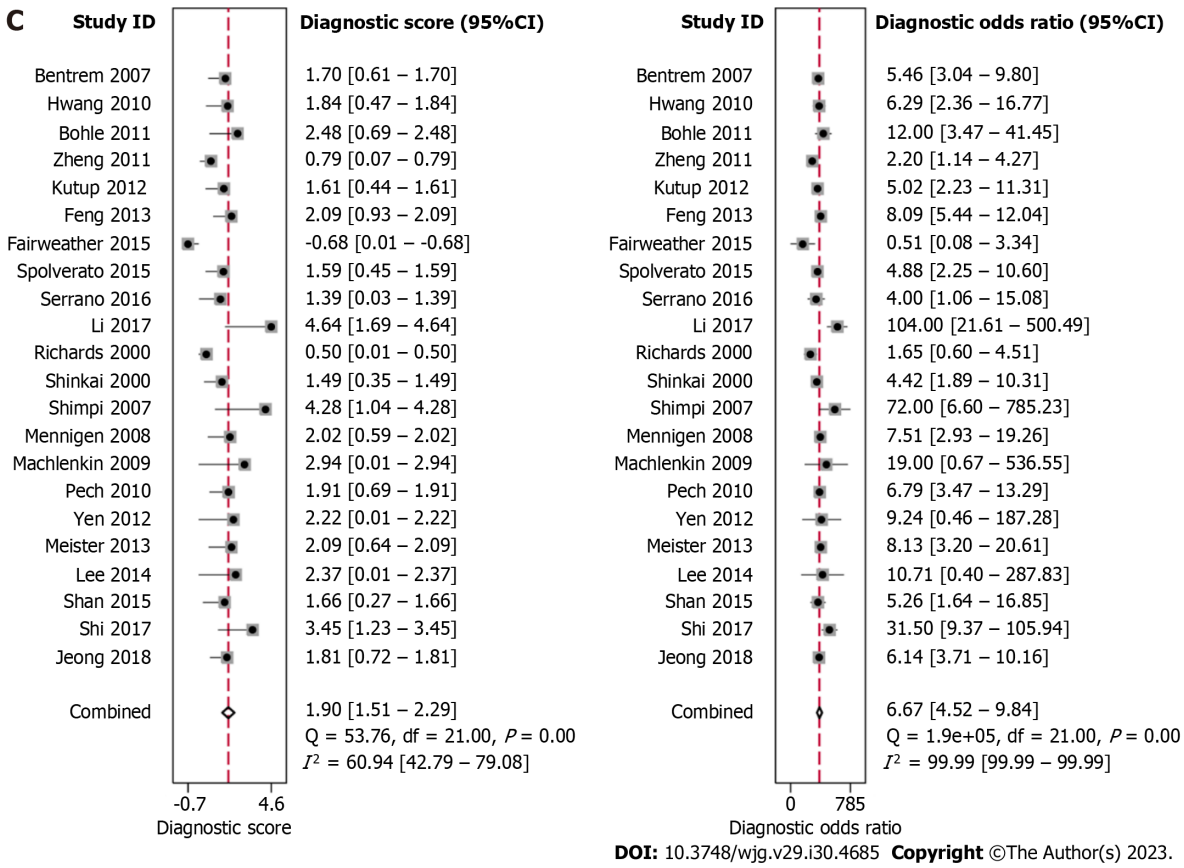
DOI: 10.3748/wjg.v29.i30.4685 **Copyright** ©The Author(s) 2023.

Figure 2 Quality assessment of included studies based on the Quality Assessment of Diagnostic Accuracy Studies tool criteria.

Our study only included patients who underwent radical surgery and did not receive preoperative neoadjuvant therapy, which inevitably led to case selection bias and excluded some patients with early tumors suitable for endoscopic treatment or patients with advanced tumors not suitable for surgical treatment. In addition, because preoperative neoadjuvant chemoradiotherapy can improve the treatment effect and prolong the survival time of some patients with upper gastrointestinal neoplasia, some patients with positive LNM may not have received the best treatment in this study. However, it is difficult to know the exact situation of LNM without obtaining complete pathological tissue, and preoperative neoadjuvant therapy will cause necrosis, fibrosis or inflammation of lymph nodes, which will affect the diagnostic effect of conventional EUS and the manifestations of postoperative histopathology. Therefore, to provide a reliable reference standard, we had to abandon the above cases in the study design stage.

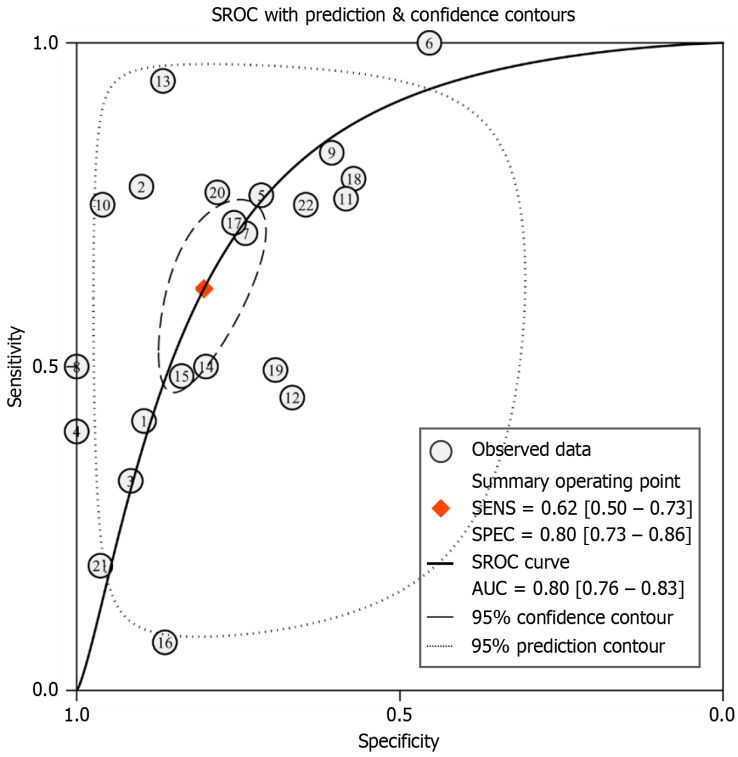
Our study also has the following limitations. First, there were many retrospective studies with a long time span and use of different technologies and tools, which may have led to selection bias. Second, only studies published in English were included, which may have led to information bias. Third, there were differences in the study designs and implementation processes, which may have led to confounding bias. In addition, the significant heterogeneity may have


A
Study ID
Sensitivity (95%CI)
Bentrem 2007 0.75 [0.66 – 0.83]
Hwang 2010 0.19 [0.11 – 0.29]
Bohle 2011 0.77 [0.61 – 0.89]
Zheng 2011 0.49 [0.39 – 0.60]
Kutup 2012 0.79 [0.69 – 0.87]
Feng 2013 0.72 [0.68 – 0.76]
Fairweather 2015 0.07 [0.01 – 0.24]
Spolverato 2015 0.49 [0.36 – 0.61]
Serrano 2016 0.50 [0.25 – 0.75]
Li 2017 0.94 [0.84 – 0.99]
Richards 2000 0.45 [0.30 – 0.61]
Shinkai 2000 0.76 [0.62 – 0.87]
Shimpi 2007 0.75 [0.43 – 0.95]
Mennigen 2008 0.83 [0.71 – 0.92]
Machlenkin 2009 0.50 [0.07 – 0.93]
Pech 2010 0.71 [0.58 – 0.81]
Yen 2012 1.00 [0.48 – 1.00]
Meister 2013 0.76 [0.63 – 0.87]
Lee 2014 0.40 [0.05 – 0.85]
Shan 2015 0.32 [0.17 – 0.51]
Shi 2017 0.78 [0.61 – 0.90]
Jeong 2018 0.42 [0.33 – 0.50]
Combined 0.62 [0.50 – 0.73]
Q = 247.20, df = 21.00, P = 0.00
I² = 91.50 [88.91 – 94.10]
0.0 1.0
Sensitivity
Study ID
Specificity (95%CI)
Bentrem 2007 0.65 [0.55 – 0.73]
Hwang 2010 0.96 [0.92 – 0.99]
Bohle 2011 0.78 [0.56 – 0.93]
Zheng 2011 0.69 [0.57 – 0.80]
Kutup 2012 0.57 [0.41 – 0.72]
Feng 2013 0.76 [0.69 – 0.82]
Fairweather 2015 0.86 [0.65 – 0.97]
Spolverato 2015 0.84 [0.73 – 0.91]
Serrano 2016 0.80 [0.61 – 0.92]
Li 2017 0.87 [0.69 – 0.96]
Richards 2000 0.67 [0.46 – 0.83]
Shinkai 2000 0.58 [0.43 – 0.72]
Shimpi 2007 0.96 [0.80 – 1.00]
Mennigen 2008 0.61 [0.43 – 0.76]
Machlenkin 2009 1.00 [0.66 – 1.00]
Pech 2010 0.74 [0.65 – 0.82]
Yen 2012 0.45 [0.24 – 0.68]
Meister 2013 0.71 [0.55 – 0.84]
Lee 2014 1.00 [0.59 – 1.00]
Shan 2015 0.92 [0.82 – 0.97]
Shi 2017 0.90 [0.78 – 0.97]
Jeong 2018 0.90 [0.86 – 0.93]
Combined 0.80 [0.73 – 0.86]
Q = 151.12, df = 21.00, P = 0.00
I² = 86.10 [81.21 – 91.00]
0.2 1.0
Specificity
B
Study ID
Positive likelihood ratio (95%CI)
Bentrem 2007 2.12 [1.61 – 2.78]
Hwang 2010 5.27 [2.14 – 12.96]
Bohle 2011 3.54 [1.60 – 7.83]
Zheng 2011 1.61 [1.06 – 2.44]
Kutup 2012 1.84 [1.28 – 2.66]
Feng 2013 2.97 [2.29 – 3.85]
Fairweather 2015 0.54 [0.10 – 2.97]
Spolverato 2015 3.00 [1.69 – 5.30]
Serrano 2016 2.50 [1.05 – 5.95]
Li 2017 7.06 [2.83 – 17.62]
Richards 2000 1.36 [0.72 – 2.54]
Shinkai 2000 1.82 [1.26 – 2.63]
Shimpi 2007 18.75 [2.67 – 131.52]
Mennigen 2008 2.10 [1.40 – 3.17]
Machlenkin 2009 10.00 [0.58 – 171.20]
Pech 2010 2.70 [1.91 – 3.83]
Yen 2012 1.69 [1.08 – 2.63]
Meister 2013 2.68 [1.62 – 4.42]
Lee 2014 6.67 [0.39 – 114.78]
Shan 2015 3.88 [1.47 – 10.24]
Shi 2017 7.78 [3.33 – 18.19]
Jeong 2018 4.00 [2.71 – 5.89]
Combined 3.15 [2.46 – 4.03]
Q = 77.01, df = 21.00, P = 0.00
I² = 61.17 [61.17 – 84.29]
0.1 171.2
Positive likelihood ratio
Study ID
Negative likelihood ratio (95%CI)
Bentrem 2007 0.39 [0.27 – 0.55]
Hwang 2010 0.84 [0.75 – 0.93]
Bohle 2011 0.29 [0.16 – 0.54]
Zheng 2011 0.73 [0.57 – 0.94]
Kutup 2012 0.37 [0.22 – 0.60]
Feng 2013 0.37 [0.31 – 0.44]
Fairweather 2015 1.07 [0.88 – 1.00]
Spolverato 2015 0.61 [0.48 – 0.79]
Serrano 2016 0.63 [0.37 – 1.00]
Li 2017 0.07 [0.02 – 0.21]
Richards 2000 0.82 [0.56 – 1.00]
Shinkai 2000 0.41 [0.24 – 0.70]
Shimpi 2007 0.26 [0.10 – 0.70]
Mennigen 2008 0.28 [0.15 – 0.52]
Machlenkin 2009 0.53 [0.22 – 1.00]
Pech 2010 0.40 [0.27 – 0.58]
Yen 2012 0.18 [0.01 – 1.00]
Meister 2013 0.33 [0.19 – 0.56]
Lee 2014 0.62 [0.31 – 1.00]
Shan 2015 0.74 [0.58 – 0.94]
Shi 2017 0.25 [0.13 – 0.46]
Jeong 2018 0.65 [0.56 – 0.75]
Combined 0.47 [0.36 – 0.61]
Q = 269.74, df = 21.00, P = 0.00
I² = 92.21 [89.90 – 94.53]
0 1
Negative likelihood ratio



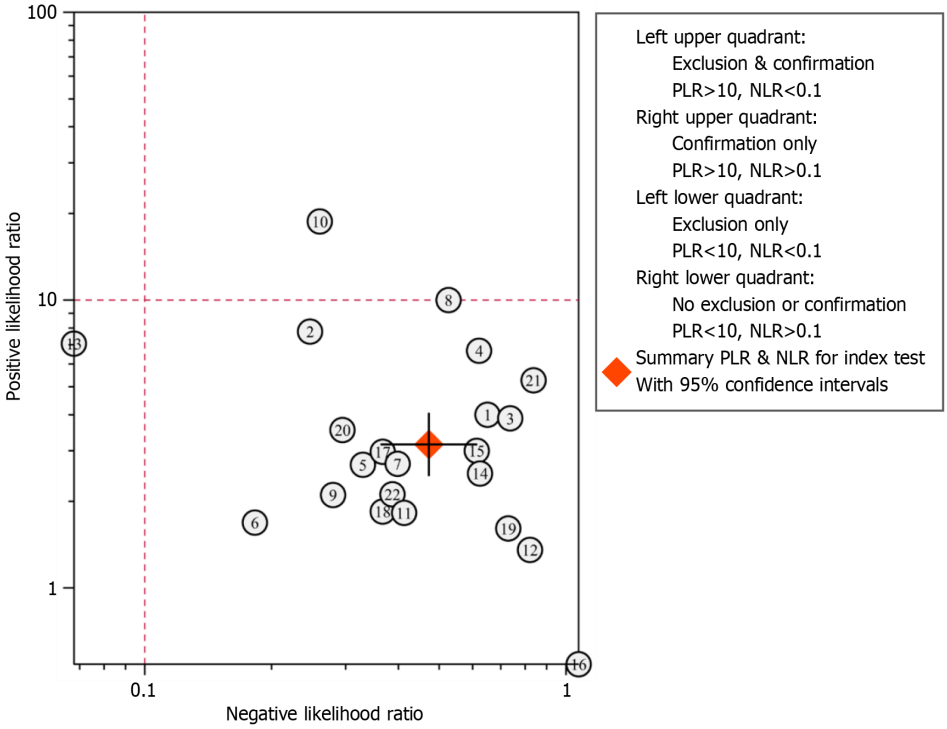
DOI: 10.3748/wjg.v29.i30.4685 **Copyright** ©The Author(s) 2023.

Figure 3 Forest plots showing the pooled evaluation indicators and heterogeneity test results. A: Pooled sensitivity and specificity; B: Pooled positive likelihood ratio and negative likelihood ratio; C: Pooled diagnostic score and diagnostic odds ratio. CI: Confidence interval.



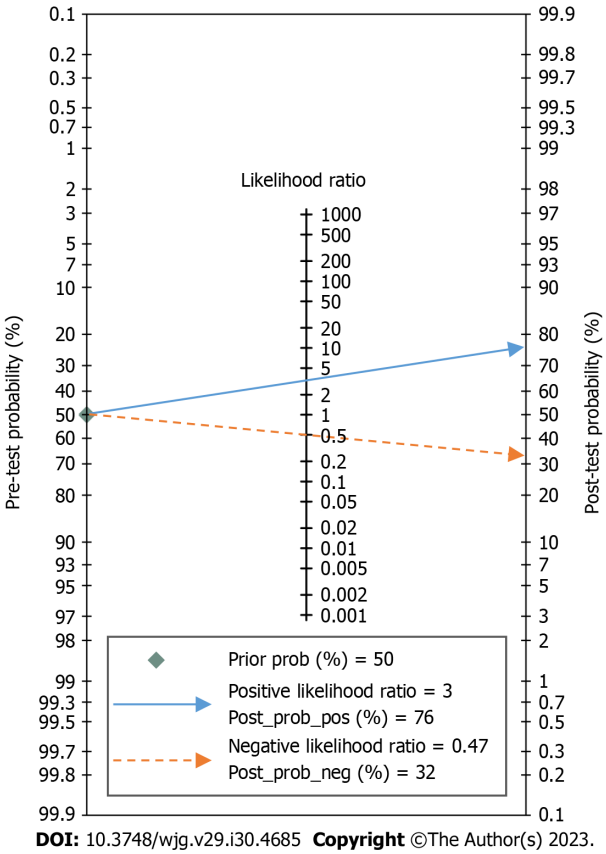
DOI: 10.3748/wjg.v29.i30.4685 **Copyright** ©The Author(s) 2023.

Figure 4 Summary receiver operating characteristic curve for evaluating the diagnostic performance of conventional endoscopic ultrasound. SROC: Summary receiver operating characteristic; SENS: Sensitivity; SPEC: Specificity; AUC: Area under the curve.



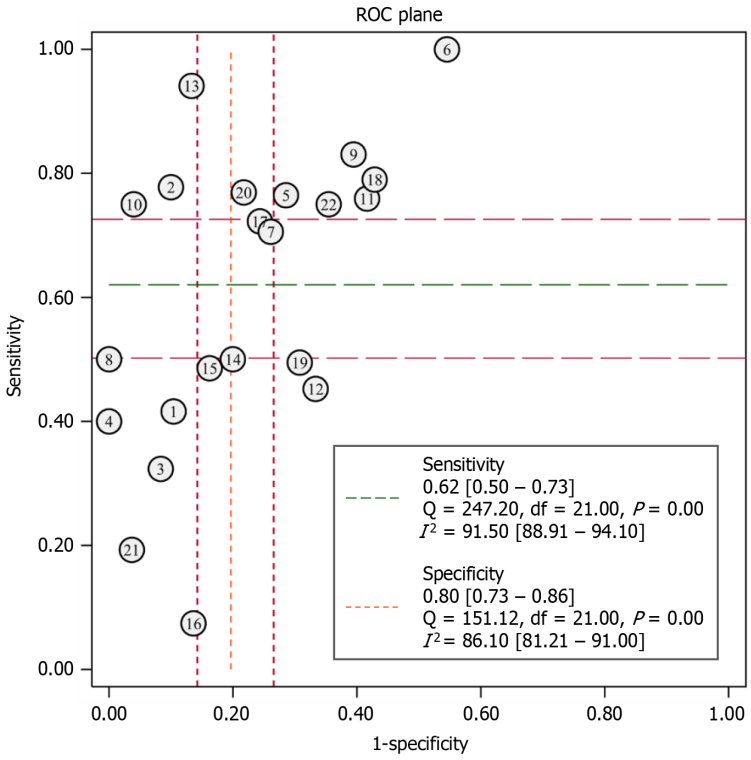
DOI: 10.3748/wjg.v29.i30.4685 **Copyright** ©The Author(s) 2023.

Figure 5 Likelihood ratio scatter diagram for evaluating the diagnostic performance of conventional endoscopic ultrasound. PLR: Positive likelihood ratio; NLR: Negative likelihood ratio.



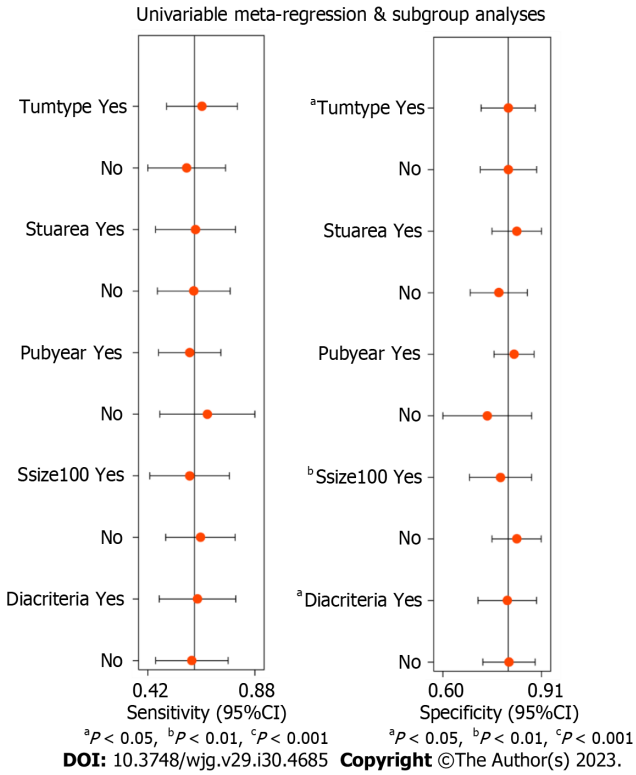
DOI: 10.3748/wjg.v29.i30.4685 **Copyright** ©The Author(s) 2023.

Figure 6 Fagan's nomogram for the diagnosis of lymph node metastasis with conventional endoscopic ultrasound.



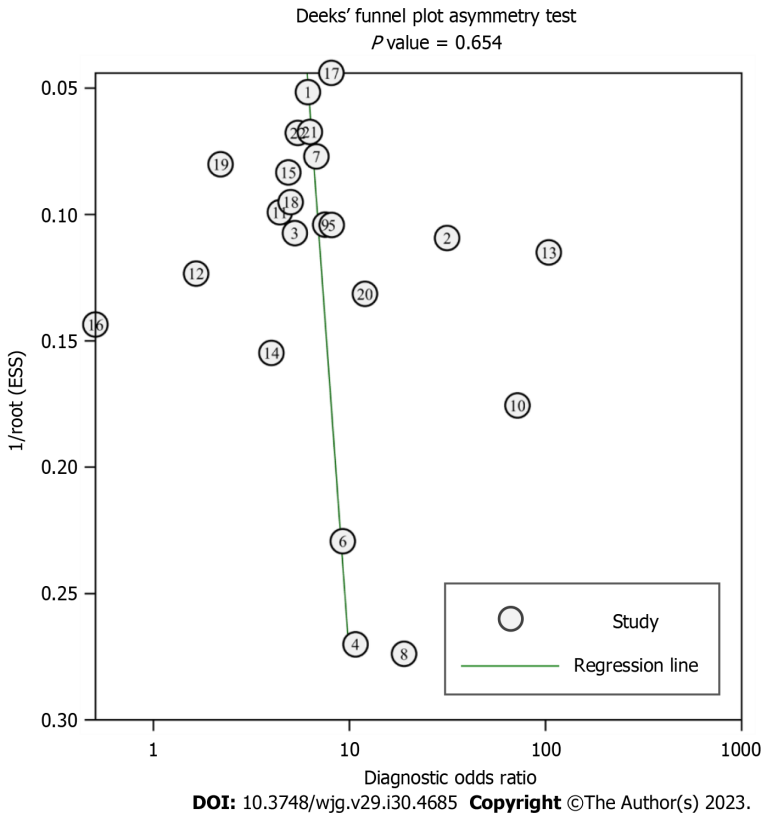
DOI: 10.3748/wjg.v29.i30.4685 **Copyright** ©The Author(s) 2023.

Figure 7 Receiver operating characteristic plane for testing the threshold effect. ROC: Receiver operating characteristic.



DOI: 10.3748/wjg.v29.i30.4685 **Copyright** ©The Author(s) 2023.

Figure 8 Univariable meta-regression and subgroup analyses for finding sources of heterogeneity. Tumtype: Tumor type (Yes: Esophageal cancer; No: Gastric cancer); Stuarea: Study area (Yes: Eastern countries; No: Western countries); Pubyear: Publication year (Yes: 2010-2018; No: 2000-2009); Ssize: Sample size (Yes: At least 100 cases; No: Less than 100 cases); Diacriteria: Diagnostic criteria (Yes: Hypoechoic, round, well-defined margin, diameter ≥ 10mm; No: Others). CI: Confidence interval.



DOI: 10.3748/wjg.v29.i30.4685 **Copyright** ©The Author(s) 2023.

Figure 9 Deeks' funnel plot for assessing publication bias of the included studies.

affected the reliability and repeatability of the analysis results.

CONCLUSION

In conclusion, conventional EUS has certain clinical value and can assist in the detection of LNM in upper gastrointestinal neoplasia, but it cannot be used as a confirmatory or exclusionary test. There was great heterogeneity among the included studies, and more high-quality studies are needed to further verify the diagnostic value of EUS and determine its best diagnostic criteria. However, with the popularization of EUS technology, the use of assistive technologies such as EUS-FNA, EUS-E or CE-EUS, and the training of high-quality endoscopists, we believe that EUS will be increasingly valuable in the diagnosis of LNM in upper gastrointestinal neoplasia.

ARTICLE HIGHLIGHTS

Research background

Upper gastrointestinal neoplasia, mainly including esophageal cancer and gastric cancer, is a common cancer with high mortality. Accurate prediction of lymph node metastasis (LNM) is of great significance for guiding clinical treatment and improving the prognosis of patients. In recent years, endoscopic ultrasound (EUS) has become increasingly used in the diagnosis and treatment of gastrointestinal diseases, but its application in the detection of LNM remains limited.

Research motivation

Although previous studies have reported the diagnostic value of conventional EUS for LNM in upper gastrointestinal neoplasia, the relevant research conclusions were controversial, and the research results have varied widely. Therefore, we intend to further carry out this research through meta-analysis.

Research objectives

This study aimed to systematically search the literature and examine the diagnostic value of conventional EUS for LNM in upper gastrointestinal neoplasia by summarizing and analyzing the data.

Research methods

We conducted a comprehensive search and screening of the PubMed, EMBASE and Cochrane Library databases from January 1, 2000 to October 1, 2022. Then, relevant study data were extracted, and the quality of the included studies was assessed based on the Quality Assessment of Diagnostic Accuracy Studies tool. Afterward, a meta-analysis was performed using the statistical software Stata 14.0.

Research results

A total of 2986 patients in 22 studies were included. The results showed that the pooled sensitivity, specificity and area under the summary receiver operating characteristic curve of conventional EUS in the diagnosis of upper gastrointestinal neoplasia LNM were acceptable, which were 0.62 [95% confidence interval (CI): 0.50-0.73], 0.80 (95%CI: 0.73-0.86) and 0.80 (95%CI: 0.76-0.83), respectively. However, the pooled positive likelihood ratio and negative likelihood ratio were relatively poor, at 3.15 (95%CI: 2.46-4.03) and 0.47 (95%CI: 0.36-0.61), respectively. The pooled diagnostic score and diagnostic odds ratio were relatively small, at 1.90 (95%CI: 1.51-2.29) and 6.67 (95%CI: 4.52-9.84), respectively.

Research conclusions

Conventional EUS has certain clinical value and can assist in the detection of LNM in upper gastrointestinal neoplasia, but it cannot be used as a confirmatory or exclusionary test. More high-quality studies are needed to further verify the diagnostic value of EUS and determine the best diagnostic criteria.

Research perspectives

In the future, further clinical studies should be carried out to evaluate the diagnostic value of various EUS assistive technologies for LNM in upper gastrointestinal neoplasia and to evaluate the influence of neoadjuvant therapy on the diagnostic value of EUS for LNM in upper gastrointestinal neoplasia.

FOOTNOTES

Author contributions: Chen C and Chen L conceived and designed the study; Chen C and Song YL contributed to the literature search, study selection and drafted the manuscript; Chen C, Wu ZY, and Chen L extracted the data; Chen C and Chen J contributed to the quality assessment; Chen C, Song YL, and Zhang Y analyzed the data; Chen C, Wu ZY, and Chen J interpreted the data; Wu ZY edited the manuscript; Chen J revised the manuscript; Chen L and Zhang Y contributed to the critical revision; and all authors have read and approved the final manuscript.

Conflict-of-interest statement: All the authors report no relevant conflicts of interest for this article.

PRISMA 2009 Checklist statement: The authors have read the PRISMA 2009 Checklist, and the manuscript was prepared and revised according to the PRISMA 2009 Checklist.

Open-Access: This article is an open-access article that was selected by an in-house editor and fully peer-reviewed by external reviewers. It is distributed in accordance with the Creative Commons Attribution NonCommercial (CC BY-NC 4.0) license, which permits others to distribute, remix, adapt, build upon this work non-commercially, and license their derivative works on different terms, provided the original work is properly cited and the use is non-commercial. See: https://creativecommons.org/Licenses/by-nc/4.0/

Country/Territory of origin: China

ORCID number: Cong Chen 0000-0002-2585-2942; Ya-Lan Song 0009-0006-3658-6068; Zhen-Yu Wu 0000-0003-4172-2213; Lei Chen 0000-0002-1400-0728.

S-Editor: Wang JJ
L-Editor: A
P-Editor: Zhao S

REFERENCES

1 **Sung H**, Ferlay J, Siegel RL, Laversanne M, Soerjomataram I, Jemal A, Bray F. Global Cancer Statistics 2020: GLOBOCAN Estimates of Incidence and Mortality Worldwide for 36 Cancers in 185 Countries. *CA Cancer J Clin* 2021; **71**: 209-249 [PMID: 33538338 DOI: 10.3322/caac.21660]

2 **Xia C**, Dong X, Li H, Cao M, Sun D, He S, Yang F, Yan X, Zhang S, Li N, Chen W. Cancer statistics in China and United States, 2022: profiles, trends, and determinants. *Chin Med J (Engl)* 2022; **135**: 584-590 [PMID: 35143424 DOI: 10.1097/CM9.0000000000002108]

3 **Qiu H**, Cao S, Xu R. Cancer incidence, mortality, and burden in China: a time-trend analysis and comparison with the United States and United Kingdom based on the global epidemiological data released in 2020. *Cancer Commun (Lond)* 2021; **41**: 1037-1048 [PMID: 34288593 DOI: 10.1002/cac2.12197]

4 **Huang J**, Koulaouzidis A, Marlicz W, Lok V, Chu C, Ngai CH, Zhang L, Chen P, Wang S, Yuan J, Lao XQ, Tse SLA, Xu W, Zheng ZJ, Xie SH, Wong MCS. Global Burden, Risk Factors, and Trends of Esophageal Cancer: An Analysis of Cancer Registries from 48 Countries.

Cancers (Basel) 2021; **13** [PMID: 33466239 DOI: 10.3390/cancers13010141]

5 **Visser E**, Markar SR, Ruurda JP, Hanna GB, van Hillegersberg R. Prognostic Value of Lymph Node Yield on Overall Survival in Esophageal Cancer Patients: A Systematic Review and Meta-analysis. *Ann Surg* 2019; **269**: 261-268 [PMID: 29794846 DOI: 10.1097/SLA.0000000000002824]

6 **Watanabe M**, Toh Y, Ishihara R, Kono K, Matsubara H, Murakami K, Muro K, Numasaki H, Oyama T, Ozawa S, Saeki H, Tanaka K, Tsushima T, Ueno M, Uno T, Yoshio T, Usune S, Takahashi A, Miyata H; Registration Committee for Esophageal Cancer of the Japan Esophageal Society. Comprehensive registry of esophageal cancer in Japan, 2014. *Esophagus* 2022; **19**: 1-26 [PMID: 34550491 DOI: 10.1007/s10388-021-00879-1]

7 **Wang FH**, Zhang XT, Li YF, Tang L, Qu XJ, Ying JE, Zhang J, Sun LY, Lin RB, Qiu H, Wang C, Qiu MZ, Cai MY, Wu Q, Liu H, Guan WL, Zhou AP, Zhang YJ, Liu TS, Bi F, Yuan XL, Rao SX, Xin Y, Sheng WQ, Xu HM, Li GX, Ji JF, Zhou ZW, Liang H, Zhang YQ, Jin J, Shen L, Li J, Xu RH. The Chinese Society of Clinical Oncology (CSCO): Clinical guidelines for the diagnosis and treatment of gastric cancer, 2021. *Cancer Commun (Lond)* 2021; **41**: 747-795 [PMID: 34197702 DOI: 10.1002/cac2.12193]

8 **Askari A**, Munster AB, Jambulingam P, Riaz A. Critical number of lymph node involvement in esophageal and gastric cancer and its impact on long-term survival-A single-center 8-year study. *J Surg Oncol* 2020; **122**: 1364-1372 [PMID: 32803769 DOI: 10.1002/jso.26145]

9 **Li H**, Fang W, Yu Z, Mao Y, Chen L, He J, Rong T, Chen C, Chen H, Chen K, Du M, Han Y, Hu J, Fu J, Hou X, Gong T, Li Y, Liu J, Liu S, Tan L, Tian H, Wang Q, Xiang J, Xu M, Ye X, You B, Zhang R, Zhao Y; Society of Esophageal Tumor, Chinese Anti-Cancer Association. Chinese expert consensus on mediastinal lymph node dissection in esophagectomy for esophageal cancer (2017 edition). *J Thorac Dis* 2018; **10**: 2481-2489 [PMID: 29850156 DOI: 10.21037/jtd.2018.03.175]

10 **Ajani JA**, D'Amico TA, Bentrem DJ, Chao J, Cooke D, Corvera C, Das P, Enzinger PC, Enzler T, Fanta P, Farjah F, Gerdes H, Gibson MK, Hochwald S, Hofstetter WL, Ilson DH, Keswani RN, Kim S, Kleinberg LR, Klempner SJ, Lacy J, Ly QP, Matkowskyj KA, McNamara M, Mulcahy MF, Outlaw D, Park H, Perry KA, Pimiento J, Poultsides GA, Reznik S, Roses RE, Strong VE, Su S, Wang HL, Wiesner G, Willett CG, Yakoub D, Yoon H, McMillian N, Pluchino LA. Gastric Cancer, Version 2.2022, NCCN Clinical Practice Guidelines in Oncology. *J Natl Compr Canc Netw* 2022; **20**: 167-192 [PMID: 35130500 DOI: 10.6004/jnccn.2022.0008]

11 **Muro K**, Lordick F, Tsushima T, Pentheroudakis G, Baba E, Lu Z, Cho BC, Nor IM, Ng M, Chen LT, Kato K, Li J, Ryu MH, Zamaniah WIW, Yong WP, Yeh KH, Nakajima TE, Shitara K, Kawakami H, Narita Y, Yoshino T, Van Cutsem E, Martinelli E, Smyth EC, Arnold D, Minami H, Tabernero J, Douillard JY. Pan-Asian adapted ESMO Clinical Practice Guidelines for the management of patients with metastatic oesophageal cancer: a JSMO-ESMO initiative endorsed by CSCO, KSMO, MOS, SSO and TOS. *Ann Oncol* 2019; **30**: 34-43 [PMID: 30475943 DOI: 10.1093/annonc/mdy498]

12 **Radlinski M**, Shami VM. Role of endoscopic ultrasound in esophageal cancer. *World J Gastrointest Endosc* 2022; **14**: 205-214 [PMID: 35634483 DOI: 10.4253/wjge.v14.i4.205]

13 **Dhar J**, Samanta J. Role of therapeutic endoscopic ultrasound in gastrointestinal malignancy- current evidence and future directions. *Clin J Gastroenterol* 2022; **15**: 11-29 [PMID: 35028906 DOI: 10.1007/s12328-021-01559-4]

14 **Serrani M**, Calvanese C, Lisotti A, Caletti G, Abenavoli L, Fusaroli P. Basics in Endoscopic Ultrasound Part 1: Diagnostic Indications and Tissue Sampling. *Rev Recent Clin Trials* 2018; **13**: 27-36 [PMID: 29032763 DOI: 10.2174/1574887112666171009170119]

15 **Krill T**, Baliss M, Roark R, Sydor M, Samuel R, Zaibaq J, Guturu P, Parupudi S. Accuracy of endoscopic ultrasound in esophageal cancer staging. *J Thorac Dis* 2019; **11**: S1602-S1609 [PMID: 31489227 DOI: 10.21037/jtd.2019.06.50]

16 **Zhou H**, Li M. The Value of Gastric Cancer Staging by Endoscopic Ultrasonography Features in the Diagnosis of Gastroenterology. *Comput Math Methods Med* 2022; **2022**: 6192190 [PMID: 35222686 DOI: 10.1155/2022/6192190]

17 **Schmidlin EJ**, Gill RR. New frontiers in esophageal radiology. *Ann Transl Med* 2021; **9**: 904 [PMID: 34164538 DOI: 10.21037/atm-20-2909]

18 **Jayaprakasam VS**, Yeh R, Ku GY, Petkovska I, Fuqua JL 3rd, Gollub M, Paroder V. Role of Imaging in Esophageal Cancer Management in 2020: Update for Radiologists. *AJR Am J Roentgenol* 2020; **215**: 1072-1084 [PMID: 32901568 DOI: 10.2214/AJR.20.22791]

19 **Peng T**, Lou Z, Wang X, Huang D, Zhang G, Gao H, Li S. Clinical Comparison of Endoscopic Ultrasonography and CT in Preoperative TN Staging of Esophagogastric Junction Cancer. *Contrast Media Mol Imaging* 2022; **2022**: 5810405 [PMID: 36128174 DOI: 10.1155/2022/5810405]

20 **Yang H**, Hu B. Recent advances in early esophageal cancer: diagnosis and treatment based on endoscopy. *Postgrad Med* 2021; **133**: 665-673 [PMID: 34030580 DOI: 10.1080/00325481.2021.1934495]

21 **Page MJ**, McKenzie JE, Bossuyt PM, Boutron I, Hoffmann TC, Mulrow CD, Shamseer L, Tetzlaff JM, Akl EA, Brennan SE, Chou R, Glanville J, Grimshaw JM, Hróbjartsson A, Lalu MM, Li T, Loder EW, Mayo-Wilson E, McDonald S, McGuinness LA, Stewart LA, Thomas J, Tricco AC, Welch VA, Whiting P, Moher D. The PRISMA 2020 statement: an updated guideline for reporting systematic reviews. *BMJ* 2021; **372**: n71 [PMID: 33782057 DOI: 10.1136/bmj.n71]

22 **Page MJ**, Moher D, Bossuyt PM, Boutron I, Hoffmann TC, Mulrow CD, Shamseer L, Tetzlaff JM, Akl EA, Brennan SE, Chou R, Glanville J, Grimshaw JM, Hróbjartsson A, Lalu MM, Li T, Loder EW, Mayo-Wilson E, McDonald S, McGuinness LA, Stewart LA, Thomas J, Tricco AC, Welch VA, Whiting P, McKenzie JE. PRISMA 2020 explanation and elaboration: updated guidance and exemplars for reporting systematic reviews. *BMJ* 2021; **372**: n160 [PMID: 33781993 DOI: 10.1136/bmj.n160]

23 **Whiting PF**, Rutjes AW, Westwood ME, Mallett S, Deeks JJ, Reitsma JB, Leeflang MM, Sterne JA, Bossuyt PM; QUADAS-2 Group. QUADAS-2: a revised tool for the quality assessment of diagnostic accuracy studies. *Ann Intern Med* 2011; **155**: 529-536 [PMID: 22007046 DOI: 10.7326/0003-4819-155-8-201110180-00009]

24 **Jeong DY**, Kim MY, Lee KS, Choi JY, Kim SJ, Chung MJ, Min YW, Kim HK, Zo JI, Shim YM, Sun JM. Surgically resected T1- and T2-stage esophageal squamous cell carcinoma: T and N staging performance of EUS and PET/CT. *Cancer Med* 2018; **7**: 3561-3570 [PMID: 29932307 DOI: 10.1002/cam4.1617]

25 **Shi H**, Ma S, Zhao P, Jiang J, Cheng Y, Zhao J, Wang J, Qiao Z, Li S, Wu J. Endoscopic ultrasonography for preoperative staging of esophageal carcinoma. *Scand J Gastroenterol* 2017; **52**: 1052-1056 [PMID: 28625089 DOI: 10.1080/00365521.2017.1339829]

26 **Shan HB**, Zhang R, Li Y, Gao XY, Lin SY, Luo GY, Li JJ, Xu GL. Application of Endobronchial Ultrasonography for the Preoperative Detecting Recurrent Laryngeal Nerve Lymph Node Metastasis of Esophageal Cancer. *PLoS One* 2015; **10**: e0137400 [PMID: 26372339 DOI: 10.1371/journal.pone.0137400]

27 **Lee G**, I H, Kim SJ, Jeong YJ, Kim IJ, Pak K, Park DY, Kim GH. Clinical implication of PET/MR imaging in preoperative esophageal cancer staging: comparison with PET/CT, endoscopic ultrasonography, and CT. *J Nucl Med* 2014; **55**: 1242-1247 [PMID: 24868109 DOI: 10.2967/jnumed.114.138974]

28 **Meister T**, Heinzow HS, Osterkamp R, Wehrmann T, Kucharzik T, Domschke W, Domagk D, Seifert H. Miniprobe endoscopic ultrasound

accurately stages esophageal cancer and guides therapeutic decisions in the era of neoadjuvant therapy: results of a multicenter cohort analysis. *Surg Endosc* 2013; **27**: 2813-2819 [PMID: 23404148 DOI: 10.1007/s00464-013-2817-7]

29 **Yen TJ**, Chung CS, Wu YW, Yen RF, Cheng MF, Lee JM, Hsu CH, Chang YL, Wang HP. Comparative study between endoscopic ultrasonography and positron emission tomography-computed tomography in staging patients with esophageal squamous cell carcinoma. *Dis Esophagus* 2012; **25**: 40-47 [PMID: 21595776 DOI: 10.1111/j.1442-2050.2011.01204.x]

30 **Pech O**, Günter E, Dusemund F, Origer J, Lorenz D, Ell C. Accuracy of endoscopic ultrasound in preoperative staging of esophageal cancer: results from a referral center for early esophageal cancer. *Endoscopy* 2010; **42**: 456-461 [PMID: 20306385 DOI: 10.1055/s-0029-1244022]

31 **Machlenkin S**, Melzer E, Idelevich E, Ziv-Sokolovsky N, Klein Y, Kashtan H. Endoscopic ultrasound: doubtful accuracy for restaging esophageal cancer after preoperative chemotherapy. *Isr Med Assoc J* 2009; **11**: 166-169 [PMID: 19544707]

32 **Mennigen R**, Tuebergen D, Koehler G, Sauerland C, Senninger N, Bruewer M. Endoscopic ultrasound with conventional probe and miniprobe in preoperative staging of esophageal cancer. *J Gastrointest Surg* 2008; **12**: 256-262 [PMID: 17823841 DOI: 10.1007/s11605-007-0300-2]

33 **Shimpi RA**, George J, Jowell P, Gress FG. Staging of esophageal cancer by EUS: staging accuracy revisited. *Gastrointest Endosc* 2007; **66**: 475-482 [PMID: 17725937 DOI: 10.1016/j.gie.2007.03.1051]

34 **Shinkai M**, Niwa Y, Arisawa T, Ohmiya N, Goto H, Hayakawa T. Evaluation of prognosis of squamous cell carcinoma of the oesophagus by endoscopic ultrasonography. *Gut* 2000; **47**: 120-125 [PMID: 10861273 DOI: 10.1136/gut.47.1.120]

35 **Richards DG**, Brown TH, Manson JM. Endoscopic ultrasound in the staging of tumours of the oesophagus and gastro-oesophageal junction. *Ann R Coll Surg Engl* 2000; **82**: 311-317 [PMID: 11041028]

36 **Li JH**, Shen WZ, Gu XQ, Hong WK, Wang ZQ. Prognostic value of EUS combined with MSCT in predicting the recurrence and metastasis of patients with gastric cancer. *Jpn J Clin Oncol* 2017; **47**: 487-493 [PMID: 28334806 DOI: 10.1093/jjco/hyx024]

37 **Serrano OK**, Huang K, Ng N, Yang J, Friedmann P, Libutti SK, Kennedy TJ. Correlation between preoperative endoscopic ultrasound and surgical pathology staging of gastric adenocarcinoma: A single institution retrospective review. *J Surg Oncol* 2016; **113**: 42-45 [PMID: 26784562 DOI: 10.1002/jso.24098]

38 **Spolverato G**, Ejaz A, Kim Y, Squires MH, Poultsides GA, Fields RC, Schmidt C, Weber SM, Votanopoulos K, Maithel SK, Pawlik TM. Use of endoscopic ultrasound in the preoperative staging of gastric cancer: a multi-institutional study of the US gastric cancer collaborative. *J Am Coll Surg* 2015; **220**: 48-56 [PMID: 25283742 DOI: 10.1016/j.jamcollsurg.2014.06.023]

39 **Fairweather M**, Jajoo K, Sainani N, Bertagnolli MM, Wang J. Accuracy of EUS and CT imaging in preoperative gastric cancer staging. *J Surg Oncol* 2015; **111**: 1016-1020 [PMID: 25872753 DOI: 10.1002/jso.23919]

40 **Feng XY**, Wang W, Luo GY, Wu J, Zhou ZW, Li W, Sun XW, Li YF, Xu DZ, Guan YX, Chen S, Zhan YQ, Zhang XS, Xu GL, Zhang R, Chen YB. Comparison of endoscopic ultrasonography and multislice spiral computed tomography for the preoperative staging of gastric cancer - results of a single institution study of 610 Chinese patients. *PLoS One* 2013; **8**: e78846 [PMID: 24223855 DOI: 10.1371/journal.pone.0078846]

41 **Kutup A**, Vashist YK, Groth S, Vettorazzi E, Yekebas EF, Soehendra N, Izbicki JR. Endoscopic ultrasound staging in gastric cancer: Does it help management decisions in the era of neoadjuvant treatment? *Endoscopy* 2012; **44**: 572-576 [PMID: 22528672 DOI: 10.1055/s-0032-1308950]

42 **Zheng Z**, Yu Y, Lu M, Sun W, Wang F, Li P, Zhang Y, Lin L, Huang P, Chen J, Zhang H, Xie Z, Dong Xda E. Double contrast-enhanced ultrasonography for the preoperative evaluation of gastric cancer: a comparison to endoscopic ultrasonography with respect to histopathology. *Am J Surg* 2011; **202**: 605-611 [PMID: 21824594 DOI: 10.1016/j.amjsurg.2010.09.033]

43 **Bohle W**, Scheidig A, Zoller WG. Endosonographic tumor staging for treatment decision in resectable gastric cancer. *J Gastrointestin Liver Dis* 2011; **20**: 135-139 [PMID: 21725509]

44 **Hwang SW**, Lee DH, Lee SH, Park YS, Hwang JH, Kim JW, Jung SH, Kim NY, Kim YH, Lee KH, Kim HH, Park DJ, Lee HS, Jung HC, Song IS. Preoperative staging of gastric cancer by endoscopic ultrasonography and multidetector-row computed tomography. *J Gastroenterol Hepatol* 2010; **25**: 512-518 [PMID: 20370729 DOI: 10.1111/j.1440-1746.2009.06106.x]

45 **Bentrem D**, Gerdes H, Tang L, Brennan M, Coit D. Clinical correlation of endoscopic ultrasonography with pathologic stage and outcome in patients undergoing curative resection for gastric cancer. *Ann Surg Oncol* 2007; **14**: 1853-1859 [PMID: 17357856 DOI: 10.1245/s10434-006-9037-5]

46 **Klamt AL**, Neyeloff JL, Santos LM, Mazzini GDS, Campos VJ, Gurski RR. Echoendoscopy in Preoperative Evaluation of Esophageal Adenocarcinoma and Gastroesophageal Junction: Systematic Review and Meta-analysis. *Ultrasound Med Biol* 2021; **47**: 1657-1669 [PMID: 33896677 DOI: 10.1016/j.ultrasmedbio.2021.03.013]

47 **Chen J**, Zhou C, He M, Zhen Z, Wang J, Hu X. A Meta-Analysis And Systematic Review Of Accuracy Of Endoscopic Ultrasound For N Staging Of Gastric Cancers. *Cancer Manag Res* 2019; **11**: 8755-8764 [PMID: 31632135 DOI: 10.2147/CMAR.S200318]

48 **Mocellin S**, Pasquali S. Diagnostic accuracy of endoscopic ultrasonography (EUS) for the preoperative locoregional staging of primary gastric cancer. *Cochrane Database Syst Rev* 2015; **2015**: CD009944 [PMID: 25914908 DOI: 10.1002/14651858.CD009944.pub2]

49 **Mocellin S**, Marchet A, Nitti D. EUS for the staging of gastric cancer: a meta-analysis. *Gastrointest Endosc* 2011; **73**: 1122-1134 [PMID: 21444080 DOI: 10.1016/j.gie.2011.01.030]

50 **Tamanini G**, Cominardi A, Brighi N, Fusaroli P, Lisotti A. Endoscopic ultrasound assessment and tissue acquisition of mediastinal and abdominal lymph nodes. *World J Gastrointest Oncol* 2021; **13**: 1475-1491 [PMID: 34721779 DOI: 10.4251/wjgo.v13.i10.1475]

51 **Dietrich CF**, Jenssen C, Arcidiacono PG, Cui XW, Giovannini M, Hocke M, Iglesias-Garcia J, Saftoiu A, Sun S, Chiorean L. Endoscopic ultrasound: Elastographic lymph node evaluation. *Endosc Ultrasound* 2015; **4**: 176-190 [PMID: 26374575 DOI: 10.4103/2303-9027.162995]

52 **Ang TL**, Kwek ABE, Wang LM. Diagnostic Endoscopic Ultrasound: Technique, Current Status and Future Directions. *Gut Liver* 2018; **12**: 483-496 [PMID: 29291601 DOI: 10.5009/gnl17348]

53 **Chen L**, Li Y, Gao X, Lin S, He L, Luo G, Li J, Huang C, Wang G, Yang Q, Shan H. High Diagnostic Accuracy and Safety of Endoscopic Ultrasound-Guided Fine-Needle Aspiration in Malignant Lymph Nodes: A Systematic Review and Meta-Analysis. *Dig Dis Sci* 2021; **66**: 2763-2775 [PMID: 32979158 DOI: 10.1007/s10620-020-06554-2]

54 **Xu W**, Shi J, Zeng X, Li X, Xie WF, Guo J, Lin Y. EUS elastography for the differentiation of benign and malignant lymph nodes: a meta-analysis. *Gastrointest Endosc* 2011; **74**: 1001-9; quiz 1115.e1 [PMID: 22032315 DOI: 10.1016/j.gie.2011.07.026]

55 **Lisotti A**, Ricci C, Serrani M, Calvanese C, Sferrazza S, Brighi N, Casadei R, Fusaroli P. Contrast-enhanced endoscopic ultrasound for the differential diagnosis between benign and malignant lymph nodes: a meta-analysis. *Endosc Int Open* 2019; **7**: E504-E513 [PMID: 31044153 DOI: 10.1055/a-0854-3785]

World Journal of Gastroenterology

Submit a Manuscript: https://www.f6publishing.com

World J Gastroenterol 2023 August 14; 29(30): 4701-4705

DOI: 10.3748/wjg.v29.i30.4701

ISSN 1007-9327 (print) ISSN 2219-2840 (online)

LETTER TO THE EDITOR

Pitfalls and promises of bile duct alternatives: There is plenty of room in the regenerative surgery

Ilya D Klabukov, Denis S Baranovskii, Peter V Shegay, Andrey D Kaprin

Specialty type: Gastroenterology and hepatology

Provenance and peer review: Unsolicited article; Externally peer reviewed.

Peer-review model: Single blind

Peer-review report's scientific quality classification

Grade A (Excellent): 0
Grade B (Very good): B
Grade C (Good): C
Grade D (Fair): 0
Grade E (Poor): 0

P-Reviewer: Midgley AC, China; Wang G, China

Received: May 31, 2023
Peer-review started: May 31, 2023
First decision: July 8, 2023
Revised: July 11, 2023
Accepted: July 25, 2023
Article in press: July 25, 2023
Published online: August 14, 2023

Ilya D Klabukov, Denis S Baranovskii, Department of Regenerative Medicine, National Medical Research Radiological Center of the Ministry of Health of the Russian Federation, Obninsk 249036, Russia

Peter V Shegay, Andrey D Kaprin, Center for Innovative Radiological and Regenerative Technologies, National Medical Research Radiological Center of the Ministry of Health of the Russian Federation, Obninsk 249036, Russia

Corresponding author: Ilya D Klabukov, MSc, PhD, Director, Department of Regenerative Medicine, National Medical Research Radiological Center of the Ministry of Health of the Russian Federation, 4 Koroleva Street, Obninsk 249036, Russia. ilya.klabukov@gmail.com

Abstract

Current abdominal surgery has several approaches for biliary reconstruction. However, the creation of functional and clinically applicable bile duct substitutes still represents an unmet need. In the paper by Miyazawa and colleagues, approaches to the creation of bile duct alternatives were summarized, and the reasons for the lack of development in this area were explained. The history of bile duct surgery since the nineteenth century was also traced, leading to the conclusion that the use of bioabsorbable materials holds promise for the creation of bile duct substitutes in the future. We suggest three ideas that may stimulate progress in the field of bile duct substitute creation. First, a systematic analysis of the causative factors leading to failure or success in the creation of bile duct substitutes may help to develop more effective approaches. Second, the regeneration of a bile duct is delicately balanced between epithelialization and subsequent submucosal maturation within limited time frames, which may be more apparent when using quantitative models to estimate outcomes. Third, the utilization of the organism's endogenous regeneration abilities may enhance the creation of bile duct substitutes. We are convinced that an interdisciplinary approach, including quantitative methods, machine learning, and deep retrospective analysis of the causes that led to success and failure in studies on the creation of bile duct substitutes, holds great value. Additionally, more attention should be directed towards the balance of epithelialization and submucosal maturation rates, as well as induced angiogenesis. These ideas deserve further investigation to pave the way for bile duct restoration with physiologically relevant outcomes.

Key Words: Bile duct alternative; Bile duct substitute; Regenerative medicine; Regene-

rative surgery; Theoretical surgery; Quantitative human physiology

©The Author(s) 2023. Published by Baishideng Publishing Group Inc. All rights reserved.

Core Tip: Progress towards the development of clinically applicable bile duct substitutes can be achieved by applying an interdisciplinary approach. This approach should include the utilization of quantitative mathematical methods, principles of cross-tissue interactions for epithelial and submucosal tissues, as well as deep retrospective data analysis of the causes of success and failure in studies on the creation of bile duct substitutes.

Citation: Klabukov ID, Baranovskii DS, Shegay PV, Kaprin AD. Pitfalls and promises of bile duct alternatives: There is plenty of room in the regenerative surgery. *World J Gastroenterol* 2023; 29(30): 4701-4705
URL: https://www.wjgnet.com/1007-9327/full/v29/i30/4701.htm
DOI: https://dx.doi.org/10.3748/wjg.v29.i30.4701

TO THE EDITOR

We read with great interest the paper by Miyazawa *et al*[1], who analyzed the drawbacks and advantages of various alternatives for bile ducts. The authors described the current approaches for substituting the bile duct and acknowledged that a suitable graft has not yet been developed due to limited understanding of the mechanisms involved in the healing and regeneration of bile duct tissue. They are convinced that the use of bioabsorbable materials may facilitate the creation of bile duct substitutes in the future.

The authors have fairly mentioned that there is a 100-year history of attempts to create satisfactory bile duct substitutes [2]. However, despite significant advancements in material and life sciences, the development of engineered bile ducts has not been successful. None of the grafts currently available are reliable enough for use in clinical practice. Additionally, due to the variant anatomy of bile ducts (Figure 1A)[3,4], it is nearly impossible to completely prevent iatrogenic injuries.

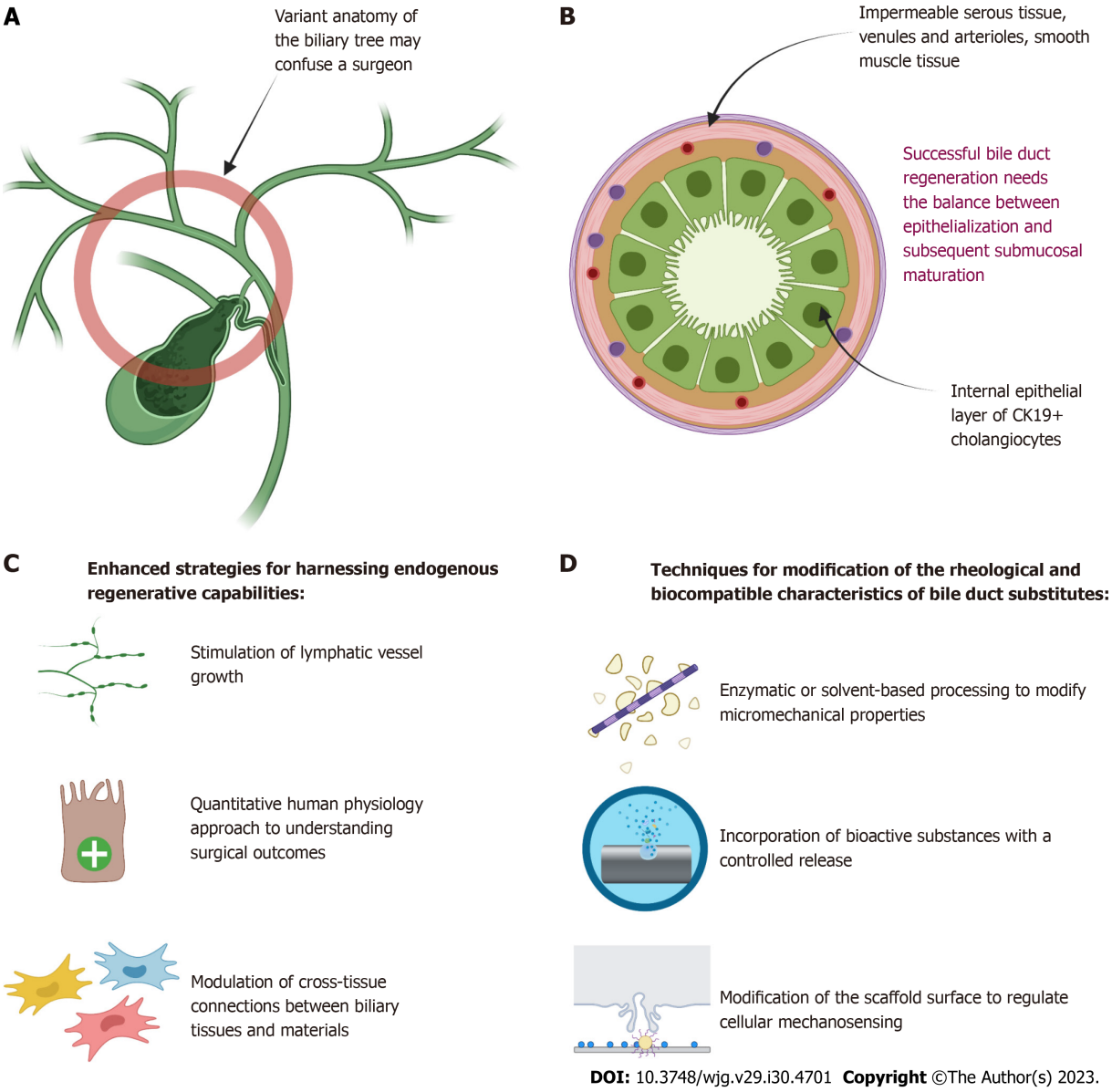
One of the most valuable features of the paper by Miyazawa *et al*[1] is the systematization and analysis of the early attempts to create bile duct alternatives, as application of a systematic approach. The authors traced the history of reconstructive hepatobiliary surgery since the 1880s and discussed many intriguing studies. However, we noticed that the causes of negative or positive results are not usually analyzed or systematized in these studies. For example, in the study by Doillon *et al*[5], it was shown that pre-exposure of a venous graft in glycerol improves surgical outcomes, but the fundamental reasons for such improvement were not investigated in this study, as well as in many other papers.

First, we want to emphasize that the analysis of the causes of negative and positive results is just as important as the results themselves. Additionally, studies that describe the unsuccessful use of rubber tubes[6], polyvinyl chloride[7], silastic[8], lyophilized and siliconized dura mater[9] in both humans and animals are valuable as they shed light on the various causes of postoperative surprises. We believe that a systematic analysis of the factors that contribute to failure or success in creating bile duct substitutes could help develop more effective approaches. It is important to note that such a systematic review has never been conducted before.

Secondly, quantitative methods of analysis can also highlight interesting patterns. Specifically, the studies reviewed by the authors revealed the limitations of bile duct epithelialization, which was found to be approximately 3 cm long and not more than 1-2 mm per week[10-12]. Additionally, the required time for submucosal maturation was estimated to be around 6-12 mo[10,13]. These findings provide support for the hypothesis that there are several deterministic mechanisms of bile duct regeneration that have yet to be discovered and completely understood. Furthermore, this suggests that the regeneration of the bile duct is delicately balanced between epithelialization and subsequent submucosal maturation within limited time frames (Figure 1B).

Thirdly, the utilization of the organism's endogenous regeneration abilities may enhance the effectiveness of bile duct substitutes. Cross-tissue interactions play a crucial role in the process of regeneration, as they determine the normal and pathological proliferation and maturation of tissues[14]. Moreover, in interconnected tissues, not only interactions but also division of labor and competition between different tissues become relevant[15]. This phenomenon has gained significant importance, particularly in relation to the biliary microbiota's role in inflammatory diseases of the biliary tract [16]. Therefore, the correct surgical approach with incompatible tissues, or the reconstruction of biliary tissues with incompatible materials, may lead to the development of chronic disorders and require additional supplementation. For example, some methods that have been underestimated include the stimulation of not only blood vessel growth but also lymphatic vessel growth in the interstitium, as well as the specific chemotaxis of mesenchymal stromal cells to the site of injury (Figure 1C).

Miyazawa *et al*[1] have demonstrated a connection between vascularization/angiogenesis and the maturation of biliary glands, as well as the stabilization of inflammation[17]. Considering the recently discovered crucial role played by vascular endothelial growth factor in biliary tree development and cell cycle regulation[18], inducing angiogenesis could be a promising avenue for future research. It is worth noting that the use of grafts may yield varying outcomes, mainly due to differences in their structure, immunogenicity, and vascular density, regardless of whether they are autologous or



DOI: 10.3748/wjg.v29.i30.4701 **Copyright** ©The Author(s) 2023.

Figure 1 Bioengineer's Bile duct wallet cards. A: Variant anatomy of the biliary tree may confuse the surgeon; B: Successful bile duct regeneration needs the balance between epithelialization and subsequent submucosal maturation; C: Advanced techniques for the use of endogenous regeneration abilities; D: Techniques for modification of the rheological and biocompatible characteristics of bile duct substitutes. Created with BioRender.com.

allogeneic. Therefore, the mechanical (rheological) and cyto compatible properties of the substitute material are important (Figure 1D).

The functional and biomimetic properties of the bile duct substitute are expected to promote the growth of resident cells and facilitate tissue regeneration[19]. However, significant advancements in regenerative medicine necessitate innovative ideas from interdisciplinary fields. The application of mathematical logic to human physiology has the potential to accelerate progress in tissue engineering[20]. For example, the phase space method, well known in physics, can provide new insights into physiological relevance in bioengineering[21]. This promising and novel concept relies on the application of mathematical logic and machine learning to forecast surgical outcomes, commonly referred to as theoretical surgery[22].

We assume that the views of the surgeon and the biophysicist on the same facts and problems differ, particularly in terms of abstract concepts. This highlights the necessity for collaborative work among specialists from various fields (Table 1). We firmly believe that the integration of quantitative methods and retrospective analysis in bioengineering will open up new avenues for developing models of inter-tissue interaction, ultimately yielding groundbreaking outcomes in bile duct engineering.

Table 1 Differences in understanding of the clinical evidences between a surgeon and a physiologist

Clinical evidences	Understanding of a surgeon	Understanding of a physiologist
There are many negative results of the use of materials for bile duct repair	Materials associated with complications are not suitable for clinical practice	The causes of failure are what we need to determine. Can we cluster these causes to understand the underlying mechanisms? If we only consider successful cases, we will commit survival bias and be unable to determine the reasons for successful outcomes
Bile duct epithelialization never exceed the following limits: About 3 cm long and growth not more than 1-2 mm per week	We must avoid implanting grafts (autografts) longer than 3 cm. This is an interesting fact. My experience supports these values, so I am aware of the potential outcomes that may be achieved after a surgical procedure	The presence of stable values indicates the conservatism of the underlying regenerative mechanisms, which are not dependent on the surgeon's skills or the quality of the materials
The normal human bile is not sterile and contains both living cholangiocytes and normal biliary microbiota	These are interesting facts, but we still lack the necessary tools to support endogenous regeneration in routine clinical practice. The application of cells remains unproven	The presence of living cells in bile may support the existence of unknown ways for the migration of bile duct cells. These methods need to be discovered and applied for bile duct regeneration

FOOTNOTES

Author contributions: Klabukov ID designed and performed research, and wrote the letter; Baranovskii DS analyzed data; Baranovskii DS, Shegay PV, and Kaprin AD revised the letter.

Conflict-of-interest statement: All the authors report no relevant conflicts of interest for this article.

Open-Access: This article is an open-access article that was selected by an in-house editor and fully peer-reviewed by external reviewers. It is distributed in accordance with the Creative Commons Attribution NonCommercial (CC BY-NC 4.0) license, which permits others to distribute, remix, adapt, build upon this work non-commercially, and license their derivative works on different terms, provided the original work is properly cited and the use is non-commercial. See: https://creativecommons.org/Licenses/by-nc/4.0/

Country/Territory of origin: Russia

ORCID number: Ilya D Klabukov 0000-0002-2888-7999; Denis S Baranovskii 0000-0002-6154-9959; Peter V Shegay 0000-0001-8901-4596; Andrey D Kaprin 0000-0001-8784-8415.

S-Editor: Wang JJ
L-Editor: A
P-Editor: Wang JJ

REFERENCES

1 **Miyazawa M**, Aikawa M, Takashima J, Kobayashi H, Ohnishi S, Ikada Y. Pitfalls and promises of bile duct alternatives: A narrative review. *World J Gastroenterol* 2022; **28**: 5707-5722 [PMID: 36338889 DOI: 10.3748/wjg.v28.i39.5707]
2 **Ahrendt SA**, Pitt HA. A history of the bilioenteric anastomosis. *Arch Surg* 1990; **125**: 1493-1500 [PMID: 2241564 DOI: 10.1001/archsurg.1990.01410230087016]
3 **Kowalczyk KA**, Majewski A. Analysis of surgical errors associated with anatomical variations clinically relevant in general surgery. Review of the literature. *Transl Res Anat* 2021; **23**: 100107 [DOI: 10.1016/j.tria.2020.100107]
4 **Żytkowski A**, Tubbs RS, Iwanaga J, Clarke E, Polguj M, Wysiadecki G. Anatomical normality and variability: historical perspective and methodological considerations. *Transl Res Anat* 2021; **23**: 100105 [DOI: 10.1016/j.tria.2020.100105]
5 **Doillon C**, Dureau G, Clendinnen G, Eloy R. Effects of glycerol pretreatment upon biliary or venous grafts in bile duct replacement. *Surg Gynecol Obstet* 1981; **152**: 613-620 [PMID: 7221844]
6 **Sullivan AG**. Reconstruction of the Bile Ducts. *JAMA* 1909; **53**: 774-777 [DOI: 10.1001/jama.1909.92550100001001f]
7 **Apalakis A**. An experimental evaluation of the types of material used for bile duct drainage tubes. *Br J Surg* 1976; **63**: 440-445 [PMID: 1276671 DOI: 10.1002/bjs.1800630608]
8 **Cantor MO**. Silicone rubber t tubes for common duct drainage. *Am J Surg* 1964; **107**: 666-668 [PMID: 14136357 DOI: 10.1016/0002-9610(64)90341-1]
9 **Gagni G**, Favaretto P, Luzzani A, Ferrini S, Marchi F, Ciprian V, Gadioli P, Mastropasqua D, Dal Cortivo G, Sovran C. Choledochal prostheses with lyophilized and siliconed dura mater. Experimental research; preliminary results. *Minerva Chir* 1979; **34**: 1209-1216 [PMID: 548824]
10 **Montalvo-Javé EE**, Mendoza Barrera GE, Valderrama Treviño AI, Piña Barba MC, Montalvo-Arenas C, Rojas Mendoza F, León Mancilla B, García Pineda MA, Jaime Limón Á, Albores Saavedra J, Tapia-Jurado J. Absorbable bioprosthesis for the treatment of bile duct injury in an experimental model. *Int J Surg* 2015; **20**: 163-169 [PMID: 26166740 DOI: 10.1016/j.ijsu.2015.06.074]
11 **Heistermann HP**, Palmes D, Stratmann U, Hohlbach G, Hierlemann H, Langer M, Spiegel HU. A new technique for reconstruction of the common bile duct by an autologous vein graft and a biodegradable endoluminal stent. *J Invest Surg* 2006; **19**: 57-60 [PMID: 16546930 DOI: 10.1080/08941930500444560]

12 **Palmes D**, Wolters H, Spiegel HU, M Ller E, Minin E, Heistermann HP. Morphological changes during creation of a neo-bile duct using a vein and a biodegradable endoluminal stent. *J Invest Surg* 2009; **22**: 435-444 [PMID: 20001814 DOI: 10.3109/08941930903410791]

13 **Lahey FH**, Pyrtek LJ. Experience with the operative management of 280 strictures of the bile ducts, with a description of a new method and a complete follow-up study of the end results in 229 of the cases. *Surg Gynecol Obstet* 1950; **91**: 25-56 [PMID: 15442823]

14 **Cote LE**, Feldman JL. Won't You be My Neighbor: How Epithelial Cells Connect Together to Build Global Tissue Polarity. *Front Cell Dev Biol* 2022; **10**: 887107 [PMID: 35800889 DOI: 10.3389/fcell.2022.887107]

15 **Adler M**, Moriel N, Goeva A, Avraham-Davidi I, Mages S, Adams TS, Kaminski N, Macosko EZ, Regev A, Medzhitov R, Nitzan M. Emergence of division of labor in tissues through cell interactions and spatial cues. *Cell Rep* 2023; **42**: 112412 [PMID: 37086403 DOI: 10.1016/j.celrep.2023.112412]

16 **Liu Y**, Sun LY, Zhu ZJ, Wei L, Qu W, Zeng ZG. Bile microbiota: new insights into biliary complications in liver transplant recipients. *Ann Transl Med* 2020; **8**: 354 [PMID: 32355798 DOI: 10.21037/atm.2020.02.60]

17 **Shang H**, Zeng JP, Wang SY, Xiao Y, Yang JH, Yu SQ, Liu XC, Jiang N, Shi XL, Jin S. Extrahepatic bile duct reconstruction in pigs with heterogenous animal-derived artificial bile ducts: A preliminary experience. *World J Gastroenterol* 2020; **26**: 7312-7324 [PMID: 33362386 DOI: 10.3748/wjg.v26.i46.7312]

18 **Mariotti V**, Fiorotto R, Cadamuro M, Fabris L, Strazzabosco M. New insights on the role of vascular endothelial growth factor in biliary pathophysiology. *JHEP Rep* 2021; **3**: 100251 [PMID: 34151244 DOI: 10.1016/j.jhepr.2021.100251]

19 **Sun Q**, Shen Z, Liang X, He Y, Kong D, Midgley AC, Wang K. Progress and Current Limitations of Materials for Artificial Bile Duct Engineering. *Materials (Basel)* 2021; **14** [PMID: 34885623 DOI: 10.3390/ma14237468]

20 **Klabukov ID**, Krasilnikova OA, Baranovskii DS. Quantitative human physiology: An introduction guide for advanced tissue engineering. *Biotechnol J* 2021; e2100481 [PMID: 34605205 DOI: 10.1002/biot.202100481]

21 **Klabukov I**, Tenchurin T, Shepelev A, Baranovskii D, Mamagulashvili V, Dyuzheva T, Krasilnikova O, Balyasin M, Lyundup A, Krasheninnikov M, Sulina Y, Gomzyak V, Krasheninnikov S, Buzin A, Zayratyants G, Yakimova A, Demchenko A, Ivanov S, Shegay P, Kaprin A, Chvalun S. Biomechanical Behaviors and Degradation Properties of Multilayered Polymer Scaffolds: The Phase Space Method for Bile Duct Design and Bioengineering. *Biomedicines* 2023; **11** [PMID: 36979723 DOI: 10.3390/biomedicines11030745]

22 **Lorenz W**, Rothmund M. Theoretical surgery: a new specialty in operative medicine. *World J Surg* 1989; **13**: 292-299 [PMID: 2662629 DOI: 10.1007/BF01659037]



Published by **Baishideng Publishing Group Inc**
7041 Koll Center Parkway, Suite 160, Pleasanton, CA 94566, USA
Telephone: +1-925-3991568
E-mail: bpgoffice@wjgnet.com
Help Desk: https://www.f6publishing.com/helpdesk
https://www.wjgnet.com



© 2023 Baishideng Publishing Group Inc. All rights reserved.

ISSN 1007-9327 (print)
ISSN 2219-2840 (online)

World Journal of *Gastroenterology*

World J Gastroenterol 2023 August 21; 29(31): 4706-4814



Published by Baishideng Publishing Group Inc

World Journal of Gastroenterology

Contents

Weekly Volume 29 Number 31 August 21, 2023

REVIEW

4706 Dysregulated microRNAs as a biomarker for diagnosis and prognosis of hepatitis B virus-associated hepatocellular carcinoma

Zhang MH, Yuan YF, Liu LJ, Wei YX, Yin WY, Zheng LZY, Tang YY, Lv Z, Zhu F

MINIREVIEWS

4736 Diabetes as a consequence of acute pancreatitis

Charley E, Dinner B, Pham K, Vyas N

ORIGINAL ARTICLE

Basic Study

4744 Huangqin decoction alleviates lipid metabolism disorders and insulin resistance in nonalcoholic fatty liver disease by triggering Sirt1/NF-κB pathway

Yan BF, Pan LF, Quan YF, Sha Q, Zhang JZ, Zhang YF, Zhou LB, Qian XL, Gu XM, Li FT, Wang T, Liu J, Zheng X

Retrospective Cohort Study

4763 Gastric cancer incidence based on endoscopic Kyoto classification of gastritis

Toyoshima O, Nishizawa T, Yoshida S, Matsuno T, Fujisawa G, Toyoshima A, Ebinuma H, Fujishiro M, Saito Y, Suzuki H

Observational Study

4774 Dental evaluation is helpful in the differentiation of functional heartburn and gastroesophageal reflux disease

Helle K, Árok AZ, Ollé G, Antal M, Rosztóczy A

Randomized Controlled Trial

4783 Poly(A)-specific ribonuclease protein promotes the proliferation, invasion and migration of esophageal cancer cells

Zhang FW, Xie XW, Chen MH, Tong J, Chen QQ, Feng J, Chen FT, Liu WQ

META-ANALYSIS

4797 Circulating copeptin level and the clinical prognosis of patients with chronic liver disease

Tan HQ, Zhao M, Huang Z, Liu Y, Li H, Ma LH, Liu JY

CASE REPORT

4809 Inherited CHEK2 p.H371Y mutation in solitary rectal ulcer syndrome among familial patients: A case report

He CC, Wang SP, Zhou PR, Li ZJ, Li N, Li MS

ABOUT COVER

Editorial Board Member of *World Journal of Gastroenterology*, De-Liang Fu, MD, PhD, Chief Doctor, Professor, Department of Pancreatic Surgery, Pancreatic Disease Institute, Huashan Hospital, Shanghai 200040, China. surgeonfu@163.com

AIMS AND SCOPE

The primary aim of *World Journal of Gastroenterology* (*WJG*, *World J Gastroenterol*) is to provide scholars and readers from various fields of gastroenterology and hepatology with a platform to publish high-quality basic and clinical research articles and communicate their research findings online. *WJG* mainly publishes articles reporting research results and findings obtained in the field of gastroenterology and hepatology and covering a wide range of topics including gastroenterology, hepatology, gastrointestinal endoscopy, gastrointestinal surgery, gastrointestinal oncology, and pediatric gastroenterology.

INDEXING/ABSTRACTING

The *WJG* is now abstracted and indexed in Science Citation Index Expanded (SCIE, also known as SciSearch®), Current Contents/Clinical Medicine, Journal Citation Reports, Index Medicus, MEDLINE, PubMed, PubMed Central, Scopus, Reference Citation Analysis, China National Knowledge Infrastructure, China Science and Technology Journal Database, and Superstar Journals Database. The 2023 edition of Journal Citation Reports® cites the 2022 impact factor (IF) for *WJG* as 4.3; IF without journal self cites: 4.1; 5-year IF: 5.3; Journal Citation Indicator: 0.82; Ranking: 33 among 93 journals in gastroenterology and hepatology; and Quartile category: Q2. The *WJG*'s CiteScore for 2021 is 8.3 and Scopus CiteScore rank 2022: Gastroenterology is 22/149.

RESPONSIBLE EDITORS FOR THIS ISSUE

Production Editor: *Yi-Xuan Cai*; **Production Department Director:** *Xiang Li*; **Editorial Office Director:** *Jia-Ru Fan.*

NAME OF JOURNAL
World Journal of Gastroenterology

ISSN
ISSN 1007-9327 (print) ISSN 2219-2840 (online)

LAUNCH DATE
October 1, 1995

FREQUENCY
Weekly

EDITORS-IN-CHIEF
Andrzej S Tarnawski

EDITORIAL BOARD MEMBERS
http://www.wjgnet.com/1007-9327/editorialboard.htm

PUBLICATION DATE
August 21, 2023

COPYRIGHT
© 2023 Baishideng Publishing Group Inc

INSTRUCTIONS TO AUTHORS
https://www.wjgnet.com/bpg/gerinfo/204

GUIDELINES FOR ETHICS DOCUMENTS
https://www.wjgnet.com/bpg/GerInfo/287

GUIDELINES FOR NON-NATIVE SPEAKERS OF ENGLISH
https://www.wjgnet.com/bpg/gerinfo/240

PUBLICATION ETHICS
https://www.wjgnet.com/bpg/GerInfo/288

PUBLICATION MISCONDUCT
https://www.wjgnet.com/bpg/gerinfo/208

ARTICLE PROCESSING CHARGE
https://www.wjgnet.com/bpg/gerinfo/242

STEPS FOR SUBMITTING MANUSCRIPTS
https://www.wjgnet.com/bpg/GerInfo/239

ONLINE SUBMISSION
https://www.f6publishing.com

© 2023 Baishideng Publishing Group Inc. All rights reserved. 7041 Koll Center Parkway, Suite 160, Pleasanton, CA 94566, USA
E-mail: bpgoffice@wjgnet.com https://www.wjgnet.com

World Journal of Gastroenterology

Submit a Manuscript: https://www.f6publishing.com

World J Gastroenterol 2023 August 21; 29(31): 4706-4735

DOI: 10.3748/wjg.v29.i31.4706

ISSN 1007-9327 (print) ISSN 2219-2840 (online)

REVIEW

Dysregulated microRNAs as a biomarker for diagnosis and prognosis of hepatitis B virus-associated hepatocellular carcinoma

Ming-He Zhang, Yu-Feng Yuan, Li-Juan Liu, Yu-Xin Wei, Wan-Yue Yin, Lan-Zhuo-Yin Zheng, Ying-Ying Tang, Zhao Lv, Fan Zhu

Specialty type: Gastroenterology and hepatology

Provenance and peer review: Invited article; Externally peer reviewed.

Peer-review model: Single blind

Peer-review report's scientific quality classification

Grade A (Excellent): A
Grade B (Very good): 0
Grade C (Good): C
Grade D (Fair): D
Grade E (Poor): 0

P-Reviewer: Korkmaz P, Turkey; Oura S, Japan; Quarleri J, Argentina

Received: March 28, 2023
Peer-review started: March 28, 2023
First decision: June 17, 2023
Revised: June 29, 2023
Accepted: August 1, 2023
Article in press: August 1, 2023
Published online: August 21, 2023

Ming-He Zhang, Yu-Feng Yuan, Department of Hepatobiliary & Pancreatic Surgery, Zhongnan Hospital of Wuhan University, Wuhan 430071, Hubei Province, China

Ming-He Zhang, Li-Juan Liu, Yu-Xin Wei, Wan-Yue Yin, Lan-Zhuo-Yin Zheng, Ying-Ying Tang, Zhao Lv, Fan Zhu, State Key Laboratory of Virology, Department of Medical Microbiology, School of Basic Medical Sciences, Wuhan University, Wuhan 430071, Hubei Province, China

Yu-Xin Wei, Department of Neurosurgery, Renmin Hospital of Wuhan University, Wuhan 430060, Hubei Province, China

Lan-Zhuo-Yin Zheng, Department of Cardiology, Zhongnan Hospital of Wuhan University, Wuhan 430071, Hubei Province, China

Ying-Ying Tang, Department of Neurology, Zhongnan Hospital of Wuhan University, Wuhan 430071, Hubei Province, China

Fan Zhu, Hubei Province Key Laboratory of Allergy & Immunology, Wuhan University, Wuhan 430071, Hubei Province, China

Corresponding author: Fan Zhu, PhD, Professor, State Key Laboratory of Virology, Department of Medical Microbiology, School of Basic Medical Sciences, Wuhan University, No. 185 Donghu Road, Wuhan 430071, Hubei Province, China. fanzhu@whu.edu.cn

Abstract

Hepatocellular carcinoma (HCC) is a malignancy with a high incidence and fatality rate worldwide. Hepatitis B virus (HBV) infection is one of the most important risk factors for its occurrence and development. Early detection of HBV-associated HCC (HBV-HCC) can improve clinical decision-making and patient outcomes. Biomarkers are extremely helpful, not only for early diagnosis, but also for the development of therapeutics. MicroRNAs (miRNAs), a subset of non-coding RNAs approximately 22 nucleotides in length, have increasingly attracted scientists' attention due to their potential utility as biomarkers for cancer detection and therapy. HBV profoundly impacts the expression of miRNAs potentially involved in the development of hepatocarcinogenesis. In this review, we summarize the current progress on the role of miRNAs in the diagnosis and treatment of HBV-HCC. From a molecular standpoint, we discuss the mechanism by which HBV regulates miRNAs and investigate the exact effect of miRNAs on the promotion of HCC. In the near future, miRNA-based diagnostic, prognostic,

and therapeutic applications will make their way into the clinical routine.

Key Words: Hepatitis B virus; Hepatocellular carcinoma; MicroRNA; Diagnosis; Prognosis; Biomarker

©The Author(s) 2023. Published by Baishideng Publishing Group Inc. All rights reserved.

Core Tip: Hepatocellular carcinoma (HCC) is one of the most common malignancies worldwide. Hepatitis B virus (HBV) infection is one of the predominant risk factors for developing HCC. Early diagnosis and prognosis prediction are pivotal for patients with HBV-associated HCC (HBV-HCC) in their clinical management. MicroRNAs (miRNAs), a subset of non-coding RNAs, play an essential role in human diseases including HBV-HCC. Here, we summarize the role of miRNAs in the diagnosis and prognosis prediction of patients with HBV-HCC. Furthermore, we discuss the underlying mechanism by which HBV dysregulates miRNAs, and the potential role of dysregulated miRNAs in promoting hepatocarcinogenesis, laying the foundation for applying potential therapeutic targets.

Citation: Zhang MH, Yuan YF, Liu LJ, Wei YX, Yin WY, Zheng LZY, Tang YY, Lv Z, Zhu F. Dysregulated microRNAs as a biomarker for diagnosis and prognosis of hepatitis B virus-associated hepatocellular carcinoma. *World J Gastroenterol* 2023; 29(31): 4706-4735
URL: https://www.wjgnet.com/1007-9327/full/v29/i31/4706.htm
DOI: https://dx.doi.org/10.3748/wjg.v29.i31.4706

INTRODUCTION

According to World Health Organization (WHO) reports, in 2020, primary liver cancer is the sixth most frequently occurring cancer worldwide, with mortality ranking third among all cancers. Hepatocellular carcinoma (HCC) accounted for about 75%-85% of cases. Chronic hepatitis B virus (HBV) infection is one of the major known risk factors[1]. Although the HBV-vaccination program has greatly reduced the incidence of HBV infection, it is estimated that nearly 292 million people are living with chronic hepatitis B (CHB) globally, and approximately 900000 people die annually because of HBV-induced liver cirrhosis and HCC, according to WHO estimates[2]. Liver surgery, including liver resection and liver transplantation, has become an established therapy for HCC and cirrhosis. Early diagnosis is a key factor for liver resection. Biomarkers are widely used for the early diagnosis of several cancers. But HCC biomarkers cannot be clinically useful for early HCC diagnosis due to their low sensitivity[3]. Similarly essential is the construction of prognosis of HBV-associated HCC (HBV-HCC), which can help make treatment decisions[3]. At present, circulating nucleic acid biomarkers, including microRNAs (miRNA), are identified as possible biomarkers for the diagnosis, prognosis, and therapeutics of liver diseases, especially HBV-HCC[4].

miRNA, a subset of non-coding RNAs, possess 19-25 nucleotides in length and play crucial biological roles in the process of gene silencing. Given that up to 60% of human protein-coding genes have conserved miRNA target sites, it is not surprising that dysregulated miRNAs can disrupt homeostasis and cause diseases including cancer[5]. miRNAs play a vital role in different stages of the HBV-HCC continuum, including early HBV infection, chronic inflammation, fibrosis/cirrhosis, and the emergence of HCC[6].

Although most miRNAs are located within cells, circulating miRNAs are present in body fluids and may reflect the pathophysiology of tissues. Several desirable characteristics of circulating miRNAs, such as their high stability in biological samples, non-invasive methods for sampling, and high sensitivity and accuracy, make them suitable as biomarker candidates for cancer diagnosis, prognosis, and therapeutic response prediction[7]. In this review, we summarize the application of miRNAs as diagnostic, prognostic, and therapeutic markers in HBV-HCC. We further discuss the mechanism by which HBV affects miRNA transcription and stability. We also try to understand the mechanisms by which miRNAs participate in the development of HCC. This will provide an in-depth understanding to identify promising biomarkers in HBV-HCC diagnosis, prognosis, and treatment.

DYSREGULATED MIRNAS IN THE DIAGNOSIS OF HBV-HCC

miRNAs are expressed with high tissue and cell selectivity. For example, some miRNAs, such as miR-122-5p, are particularly abundant in the liver, suggesting that certain miRNAs participate in HCC carcinogenesis and progression[8]. After tumor resection in HCC patients, some serum circulating miRNAs exhibit significant changes[9-13], indicating that circulating miRNAs may be specific non-invasive and diagnostic markers for HBV-HCC.

In clinical diagnostic tests, area under the receiver operating characteristic curve (AUC) is widely used to judge the diagnostic accuracy. Generally, an AUC between 0.7 and 0.8 is considered clinically useful, between 0.8 and 0.9 is deemed excellent, and greater than 0.9 is considered outstanding discrimination[14]. Numerous individual miRNAs have shown good diagnostic efficacy, with miR-93-5p[15], miR-122[16], miR-125b[17], miR-150[13], miR-487b[18,19], miR-768-3p[20],

and miR-5193[21] achieving AUC > 0.9 in discriminating HBV-HCC patients from healthy controls (HC) (Table 1), miR-122[22], miR-125b[23], and miR-192[22] in differentiating HBV-HCC from CHB patients (Table 2), and miR-101[24] and miR-125b[17,23] in discriminating HBV-HCC from HBV related liver cirrhosis (HBV-LC) patients (Table 2). Additionally, some HBV dysregulated miRNAs show different expression profiles in the serum or plasma of HBV-HCC patients compared to control populations[25-29], suggesting a potential value of these miRNAs in diagnosing HBV-HCC. In addition, one study reveals that urine miR-93-5p demonstrates diagnostic performance comparable to plasma miR-93-5p for diagnosing early HBV-HCC. Urine sample is non-invasive and simple to perform on humans. Therefore, urine miRNAs may have more clinical application potential than plasma miRNAs[15]. However, individual miRNAs may have limitations in sensitivity and specificity due to HBV-associated chronic liver disease. In addition, despite the fact that numerous miRNAs were highly effective at distinguishing HBV-HCC patients from healthy populations or all control populations, the efficacy used to differentiate HBV-HCC from CHB or HBV-LC is nonspecific. Hence, new methods are required to improve the diagnostic efficacy of miRNAs in diagnosing HBV-HCC patients, particularly in distinguishing them from CHB and LC populations.

Individual miRNAs are altered in different infectious diseases, nonspecific inflammation, and acute lesions in addition to cancer, revealing their lack of specificity. Forming a miRNA panel may help serve as diagnostic biomarkers for HBV-HCC (Table 3). Several miRNA panels, such as miR-21 + miR-122 + miR-192[22], miR-125b + miR-223 + miR-27a + miR-26a[30], and miR-23b + miR-423 + miR-375 + miR-23a + miR-342-3p[31] reach a high value in differentiating HBV-HCC from HC, CHB and HBV-LC patients. However, the good diagnostic efficiency of miRNA profiles does not necessitate the combination of as many miRNAs as feasible to improve diagnostic accuracy, due to the complexity of the method necessary to detect miRNAs and the lengthy timeframes involved. In some cases, the combination of multiple biomarkers showed no additive effect on HBV-HCC diagnosis[32]. Several studies demonstrate that panels with only two miRNAs can also reach a high AUC as panels with more miRNAs, such as miR-10a + miR-125b[31] and miR-15b + miR-130b[9]. Consequently, additional research is required to determine the optimal combination of the fewest possible number of miRNAs and to reduce the cost of diagnosis as much as possible, all while attaining a good diagnostic capacity.

It will be better to combine miRNAs with other biomarkers in HBV-HCC diagnosis (Table 4). The most prevalent combination biomarker is alpha fetoprotein (AFP), a traditional biomarker in HCC. Obviously, the combination of most miRNAs with AFP demonstrates a high AUC and diagnostic accuracy for discriminating HBV-HCC from HC or patients with CHB, HBV-CLD, and HBV-LC, such as miR-24-3p[33], miR-96[34], miR-101[24], miR-122[35], miR-126[32], miR-142-3p[32], miR-205[36] and miR-224[11]. Another study combines miR-122 with AFP and TERT gene promoter mutations in cfDNA. The results show that it reaches a 0.98 and 0.88 AUC in discriminating HBV-HCC patients from CHB and HBV-LC patients, respectively, demonstrating a high diagnostic value in HBV-HCC[35]. Similarly, the combination of miR-122 with AFP and prothrombin induced by vitamin K deficiency or antagonist- II (PIVKA-II) reaches a 0.918 AUC in separating HBV-HCC from HBV-LC patients[37]. Consequently, the combination of single miRNA with other biomarkers may improve the diagnostic accuracy for HBV-HCC from other HBV-related diseases. Moreover, some miRNAs panels show a better diagnostic value than AFP[38], and combination of these miRNA panels with AFP further increased the efficacy[22,30,32]. Therefore, the use of miRNA profiles paired with AFP may be the optimum modality for the diagnosis of HBV-HCC.

In addition, miRNAs may be of particular value in the diagnosis of HBV-HCC with low AFP levels. Despite the fact that AFP is the most often utilized biomarker for HCC worldwide, serum AFP levels stay normal in 15%-30% of advanced HCC. Meanwhile, approximately 30% of early-stage HCC cannot be diagnosed *via* AFP measurement, which delays therapy. Therefore, it is crucial to establish biomarkers capable of identifying HCC patients with negative AFP levels[39]. Different miRNAs and miRNA panels have shown good capacity for separating HBV-HCC patients with negative AFP expression from HC and CHB patients (Table 5), such as miR-125b[23], miR-15b + miR-130b[9] miR-21 + miR-122 + miR-192[22], and miR-125b + miR-223 + miR-27a + miR-26a[30]. A meta-analysis suggests that circulating miRNAs have a relatively high diagnostic accuracy in distinguishing HBV-HCC patients with low AFP levels from non-HCC controls[40]. Therefore, circulating miRNAs may be an ideal potential diagnostic biomarker for HBV-HCC patients with low AFP levels. Notably, these miRNAs or miRNAs panels only show ordinary effects when differentiating HBV-HCC with HBV-LC, and thus, more research is needed to improve the value of miRNA in differentiating HBV-LC and HBV-HCC patients with negative AFP expression.

Overall, miRNAs have great potential for use in the diagnosis of HBV-HCC. Two meta-analyses also show that miRNAs attain a level between moderate and high in terms of diagnostic evaluation criteria, and also demonstrate superior diagnostic performance than AFP[41,42]. According to both studies, miR-125b demonstrates a stronger diagnostic value for HBV-related HCC than other single miRNAs[41,42]. The subgroup analysis further concludes that downregulated miRNAs, miRNA panels, and serum-type miRNAs provide the most accurate diagnostic function for HBV-HCC[42]. Notably, the majority of patients with HCC are frequently diagnosed at an advanced stage, with a 1-year survival rate of less than 50% and a 5-year survival rate of only 10%[43]. This is due to the lack of accurate early diagnostic biomarkers. Several other studies also evaluate the ability of miRNAs to discriminate between early-stage HBV-HCC and controls. In one study, the combination of AFP and miR-125b, miR-223, miR-27a, and miR-26a has the highest diagnostic accuracy for early-stage HBV-HCC[30]. Another study finds that one miRNA panel consisting of seven miRNAs shows significant diagnostic accuracy for HBV-HCC, particularly in patients with early Barcelona Clinic Liver Cancer (BCLC) stages (0/A)[44]. Consequently, these miRNA profiles may serve as possible early diagnostic markers for HBV-HCC.

Notably, in addition to circulating miRNAs, exosome miRNAs may also have diagnostic and prognostic value in HBV-HCC. Exosome miRNAs are miRNAs contained within exosomes and released by various cells. Exosome miRNAs are frequently more stable in bodily fluids than other circulating miRNAs because the exosome membrane protects them from degradation, indicating a higher value as cancer biomarkers[45]. As HBV can impact the production of exosomes

Table 1 Efficacy of single microRNAs used in diagnosing hepatitis B virus-associated hepatocellular carcinoma patients from healthy control

miRNA	AUC	Sensitivity	Specificity	Ref.
miR-18a	0.881	0.861	0.750	[228]
miR-26a	0.711	0.876	0.600	[30]
miR-26a[1]	0.685	0.907	0.600	[30]
miR-26a-5p	0.762	0.689	0.744	[38]
miR-27a	0.859	0.933	0.733	[30]
miR-27a[1]	0.809	0.926	0.733	[30]
miR-34a	0.736	0.920	0.600	[21]
miR-93-5p	0.906	0.859	0.954	[15]
miR-93-5p	0.903	0.879	0.938	[15]
miR-93-5p	0.905	0.862	0.954	[15]
miR-101	0.788	0.761	0.700	[24]
miR-122	0.984	0.960	0.940	[16]
miR-122	0.869	0.816	0.833	[10]
miR-122-5p	0.697	0.489	0.822	[38]
miR-125b	0.835	0.798	0.867	[30]
miR-125b	0.891	0.859	0.786	[23]
miR-125b	0.940	0.830	0.960	[17]
miR-125b[1]	0.822	0.815	0.867	[30]
miR-141-3p	0.758	0.681	0.833	[38]
miR-143	0.813	0.776	0.860	[229]
miR-145	0.852	0.882	0.780	[229]
miR-150	0.931	0.825	0.837	[13]
miR-192-5p	0.695	0.719	0.756	[38]
miR-199a-5p	0.638	0.593	0.667	[38]
miR-205	0.885	0.969	0.679	[36]
miR-206	0.615	0.481	0.788	[38]
miR-212	0.886	0.696	0.950	[230]
miR-214	0.747	0.760	0.740	[21]
miR-223	0.736	0.921	0.633	[30]
miR-223[1]	0.822	0.907	0.633	[30]
miR-433-5p	0.736	0.793	0.644	[38]
miR-487b	0.946	0.888	0.909	[18]
miR-487b	0.929	0.839	0.928	[19]
miR-768-3p	0.908	0.873	0.800	[20]
miR-1228-5p	0.552	0.793	0.278	[38]
miR-5193	0.993	0.960	1.000	[21]
miR-6510	0.839	0.720	0.910	[21]

[1]Comparing early-stage hepatitis B virus-associated hepatocellular carcinoma patients to patients with other stages.
AUC: Area under the receiver operating characteristic curve; miRNAs: MicroRNAs.

Table 2 Efficacy of single microRNAs used in diagnosing hepatitis B virus-associated hepatocellular carcinoma patients from hepatitis B virus-positive patients

Comparison	miRNA	AUC	Sensitivity	Specificity	Ref.
HBV-carriers	miR-20a-5p	0.770	0.866	0.573	[231]
HBV-carriers	miR-25-3p	0.718	0.553	0.793	[231]
HBV-carriers	miR-30a-5p	0.681	0.642	0.683	[231]
HBV-carriers	miR-92a-3p	0.765	0.761	0.683	[231]
HBV-carriers	miR-132-3p	0.722	0.910	0.366	[231]
HBV-carriers	miR-185-5p	0.788	0.910	0.390	[231]
HBV-carriers	miR-320a	0.678	0.388	0.878	[231]
HBV-carriers	miR-324-3p	0.656	0.746	0.500	[231]
CHB	miR-26a	0.650	0.533	0.833	[30]
CHB	miR-26a[1]	0.411	0.582	0.500	[30]
CHB	miR-27a	0.761	0.677	0.833	[30]
CHB	miR-27a[1]	0.690	0.527	0.833	[30]
CHB	miR-34a	0.619	0.400	0.870	[21]
CHB	miR-96	0.803	0.779	0.753	[34]
CHB	miR-99a[2]	0.694	0.844	0.567	[232]
CHB	miR-101	0.777	0.881	0.620	[24]
CHB	miR-122	0.190	0.250	0.250	[16]
CHB	miR-122	0.630	0.776	0.578	[10]
CHB	miR-125b	0.675	0.522	0.867	[30]
CHB	miR-125b	0.958	0.938	0.857	[23]
CHB	miR-125b	0.792	0.906	0.567	[232]
CHB	miR-125b	0.800	0.810	0.870	[17]
CHB	miR-125b[1]	0.631	0.400	0.870	[30]
CHB	miR-126	0.670	0.630	0.580	[32]
CHB	miR-142-3p	0.550	0.320	0.910	[32]
CHB	miR-150	0.881	0.791	0.765	[13]
CHB	miR-214	0.520	0.850	0.430	[21]
CHB	miR-223	0.737	0.544	0.933	[30]
CHB	miR-223[1]	0.656	0.782	0.533	[30]
CHB	miR-224	0.846	0.865	0.745	[11]
CHB	miR-487b	0.815	0.836	0.667	[18]
CHB	miR-487b	0.856	0.759	0.897	[19]
CHB	miR-768-3p	0.819	0.850	0.727	[20]
CHB	miR-5193	0.817	0.798	0.820	[21]
CHB	miR-6510	0.531	0.810	0.390	[21]
HBV-DN	let-7b	0.633	0.825	0.467	[233]
HBV-DN	miR-122	0.648	0.667	0.567	[233]
HBV-LC	miR-26a-5p	0.744	0.607	0.909	[38]
HBV-LC	miR-99a[2]	0.696	0.967	0.563	[232]
HBV-LC	miR-101	0.976	0.955	0.902	[24]

HBV-LC	miR-122	0.675	0.610	0.760	[37]
HBV-LC	miR-122-5p	0.751	0.489	0.902	[38]
HBV-LC	miR-125b	0.958	0.891	0.881	[23]
HBV-LC	miR-125b	0.910	0.780	0.960	[17]
HBV-LC	miR-126	0.578	0.550	0.580	[32]
HBV-LC	miR-141-3p	0.663	0.607	0.727	[38]
HBV-LC	miR-142-3p	0.566	0.550	0.630	[32]
HBV-LC	miR-192-5p	0.687	0.548	0.833	[38]
HBV-LC	miR-199a-5p	0.589	0.593	0.576	[38]
HBV-LC	miR-205	0.781	0.969	0.542	[36]
HBV-LC	miR-206	0.693	0.778	0.689	[38]
HBV-LC	miR-224	0.832	0.865	0.667	[11]
HBV-LC	miR-433-5p	0.644	0.564	0.674	[38]
HBV-LC	miR-1228-5p	0.542	0.667	0.470	[38]
CHB + HBV-LC	miR-18a	0.775	0.772	0.700	[228]
CHB + HBV-LC	miR-224	0.840	0.865	0.711	[11]
CHB + HBV-LC	miR-375	0.768	0.938	0.639	[234]

[1]Comparing early-stage hepatitis B virus (HBV)-associated hepatocellular carcinoma (HCC) patients to patients with other stages.
[2]Comparing advanced HBV-HCC to patients with other stages.
CHB: Chronic hepatitis B patient, HBV-DN: Hepatitis B virus-related dysplastic nodule patient; HBV-LC: Hepatitis B virus-related liver cirrhosis patient; AUC: Area under the receiver operating characteristic curve; miRNAs: MicroRNAs.

and their cargos to promote HBV replication and diseases progression[46], exosomes derived from HBV-infected cells may be useful biomarkers for HBV-related diseases[47,48]. Several studies have validated and reviewed exosome-encapsulated miRNAs as circulating diagnostic markers for HCC[49,50], which may be beneficial for monitoring CHB progression and for detecting HBV-HCC at an early stage[51,52].

DYSREGULATED MIRNAS IN THE PROGNOSIS OF HBV-HCC

miRNAs, whose expression level is correlated with disease severity and survival rate in HCC patients, have shown good prognostic value for HCC[53]. For HBV-HCC patients, several miRNAs from HCC tissues or blood are found to be significantly correlated with overall survival, diseases-free survival (DFS) and progression-free survival (Table 6). For tissue miRNAs, higher expression of miR-122[54,55], miR-143[55], miR-145[56], miR-193b[57], miR-203a[58], miR-216b [59], miR-375[55,60], and miR-384[61] is associated with a better prognosis, and higher expression of miR-9-3[62], miR-10b [62], miR-21[56], miR-29a-5p[63], miR-31[62], miR-106b[64], miR-224[55], miR-371a-5p[27], miR-519c[62], miR-522[62,65], miR-523[65], miR-3188[28], miR-3682-3p[66], miR-3660[62], miR-4784[62], miR-5188[67], and miR-6883[62] is associated with a significantly poorer long-term prognosis. For circulating miRNAs, higher expression of miR-150[13], miR-223-3p [68], and miR-768-3p[20] is associated with a better prognosis, higher expression of miR-24-3p[33], miR-29a-3p[69], miR-96[34], miR-155[70], miR-192-5p[69], and miR-487b[18,19] is associated with a significantly poorer long-term prognosis. Therefore, tissues or circulating miRNAs can be a promising tool in predicting the prognosis of HBV-HCC patients. Specifically, due to the fact that miRNAs are abundant in serum exosomes, serum exosomal miRNAs can be used to predict the outcome of HCC patients. In addition, tissue miR-21[56], miR-203a[58], miR-375[60], and miR-5188[67], and serum miR-26a[30], miR-27a[30], miR-29a-3p[69], miR-125b[30], miR-150[13], miR-192-5p[69], miR-223[30,68], miR-487b [18,19], and miR-768-3p[20] are independent prognostic factors of HBV-HCC patients.

Researchers also develop different models to predict HBV-HCC survival. One study constructs a multivariate risk model that incorporates BCLC stage, miR-192-5p, and miR-29-3p. This risk model is significantly correlated with patient survival and has a good prognostic value. Consequently, the serum miRNA signature can offer predictive value for the BCLC stage classification. In addition, one random forests model made with miRNAs can predict HBV-HCC survival well[62].

It is worthy of note that miRNAs are also correlated with the probability of HBV-HCC recurrence. Several miRNAs may serve as a potential predictor for early tumor recurrence after HCC resection. For instance, the amount of miR-29a-5p in HCC tissues is strongly linked with early HCC recurrence following surgery, including in early-stage HCCs. Stages 0 and A of BCLC are regarded as the early stages, it implies that these HCC patients may have a better prognosis. However, in clinical practice, some patients still have a bad prognosis. Predicting the prognosis of these individuals is a

Table 3 Efficacy of microRNAs panels used in diagnosing hepatitis B virus-associated hepatocellular carcinoma

Comparison	miRNA	AUC	Sensitivity	Specificity	Ref.
HC	miR-125b + miR-223[1]	0.881	0.891	0.833	[30]
HC	miR-125b + miR-26a[1]	0.884	0.873	0.867	[30]
HC	miR-223 + miR-27a[1]	0.892	0.909	0.833	[30]
HC	miR-223 + miR-26a[1]	0.828	0.927	0.667	[30]
HC	miR-27a + miR-26a[1]	0.895	0.945	0.833	[30]
HC	miR-125b + miR-223 + miR-27a + miR-26a	0.932	0.865	0.933	[30]
HC	miR-125b + miR-223 + miR-27a + miR-26a[1]	0.910	0.852	0.933	[30]
HC	miR-375 + miR-25 + and let-7f	0.997	0.979	0.991	[31]
HC	miR-23b + miR-423 + miR-375 + miR-23a + miR-342-3p	0.999	0.969	0.994	[31]
HC	miR-122 + miR-192 + miR-21 + miR-223 + miR-26a + miR-27a + miR-801	0.941	0.832	0.939	[44]
HC	miR-27b-3p + miR-192-5p	0.823	0.685	0.952	[235]
HC	miR-206 + miR-141-3p + miR-433-5p + miR-1228-5p + miR-199a-5p + miR-122-5p + miR-192-5p + miR-26a-5p	0.893	0.828	0.833	[38]
HBV-carriers	miR-20a-5p + miR-25-3p + miR-30a-5p + miR-92a-3p + miR-132-3p + miR-185-5p + miR-320a + miR-324-3p	0.802	0.866	0.646	[231]
HBV-carriers	miR-20a-5p + miR-320a + miR-324-3p + miR-375	0.768	0.650	0.775	[231]
HBV-carriers	miR-20a-5p + miR-320a + miR-324-3p + miR-375	0.706	0.560	0.838	[231]
CHB	miR-125b + miR-223[1]	0.680	0.473	0.867	[30]
CHB	miR-125b + miR-26a[1]	0.668	0.509	0.833	[30]
CHB	miR-223 + miR-27a[1]	0.714	0.582	0.833	[30]
CHB	miR-223 + miR-26a[1]	0.708	0.509	0.900	[30]
CHB	miR-27a + miR-26a[1]	0.741	0.873	0.533	[30]
CHB	miR-125b + miR-223 + miR-27a + miR-26a	0.761	0.622	0.867	[30]
CHB	miR-125b + miR-223 + miR-27a + miR-26a[1]	0.687	0.818	0.533	[30]
CHB	miR-10a + miR-125b	0.992	0.985	0.985	[31]
CHB	miR-122 + miR-192 + miR-21 + miR-223 + miR-26a + miR-27a + miR-801	0.842	0.791	0.764	[44]
HBV-LC	miR-122 + miR-192 + miR-21 + miR-223 + miR-26a + miR-27a + miR-801	0.884	0.750	0.911	[44]
HBV-LC	miR-27b-3p + miR-192-5p	0.859	0.785	0.793	[235]
HBV-LC	miR-206 + miR-141-3p + miR-433-5p + miR-1228-5p + miR-199a-5p + miR-122-5p + miR-192-5p + miR-26a-5p	0.892	0.816	0.846	[38]

[1]Comparing early-stage hepatitis B virus-associated hepatocellular carcinoma patients to patients with other stages.
HC: Healthy control, CHB: Chronic hepatitis B patient; HBV-LC: Hepatitis B virus-related liver cirrhosis patient; AUC: Area under the receiver operating characteristic curve; miRNAs: MicroRNAs.

huge challenge for clinicians. As miR-29a-5p sensitivity and specificity may reach approximately 70% for HCC patients with BCLC 0/A stage, their miR-29a-5p expression level may provide a visual aid to distinguish them from other early-stage patients[63]. In addition, it has been discovered that the recurrence of HBV-HCC is closely associated with dysregulation of miR-21 and miR-145[56].

In addition, one study reveals that miRNAs are related with the development risk of HCC in CHB. In CHB patients who do not develop HCC, nucleos(t)ide analogue (NA) treatment restores expression of these miRNAs to near-normal levels, whereas the expression profile is not fully restored in individuals who ultimately develop HCC. Therefore, in CHB patients treated with NA, the changes in miRNAs expression may help identify HCC development risks[71].

MECHANISMS OF HBV-INDUCED DYSREGULATION OF MIRNA

In HCC, HBV and its proteins [HBV surface antigen (HBs), HBV core antigen (HBc), HBV envelope antigen (HBe), HBV x

Table 4 Efficacy of microRNAs combined with other biomarkers used in diagnosing hepatitis B virus-associated hepatocellular carcinoma

Comparison	miRNA	AUC	Sensitivity	Specificity	Ref.
HC	miR-125b + miR-27a + AFP[1]	0.937	0.909	0.933	[30]
HC	miR-125b + miR-223 + miR-27a + miR-26a + AFP	0.945	0.910	0.933	[30]
HC	miR-125b + miR-223 + miR-27a + miR-26a + AFP[2]	0.972	0.944	0.900	[30]
HC	miR-125b + miR-223 + miR-27a + miR-26a + AFP[1]	0.936	0.907	0.933	[30]
HC	miR-125b + miR-223 + miR-27a + miR-26a + AFP[1,2]	0.956	0.800	1.000	[30]
HBV-carriers	miR-20a-5p + miR-320a + miR-324-3p + miR-375 + AFP	0.789	0.700	0.775	[231]
HBV-carriers	miR-20a-5p + miR-320a + miR-324-3p + miR-375 + AFP	0.767	0.640	0.838	[231]
CHB	miR-96 + AFP	0.889	0.836	0.824	[34]
CHB	miR-126 + AFP	0.920	0.840	0.920	[32]
CHB	miR-142-3p + AFP	0.910	0.860	0.940	[32]
CHB	miR-224 + AFP	0.867	0.875	0.765	[11]
CHB	miR-125b + miR-27a + AFP[1]	0.722	0.600	0.833	[30]
CHB	miR-125b + miR-223 + miR-27a + miR-26a + AFP	0.790	0.689	0.867	[30]
CHB	miR-125b + miR-223 + miR-27a + miR-26a + AFP[2]	0.833	0.820	0.767	[30]
CHB	miR-125b + miR-223 + miR-27a + miR-26a + AFP[1]	0.728	0.582	0.867	[30]
CHB	miR-125b + miR-223 + miR-27a + miR-26a + AFP[1,2]	0.812	0.704	0.833	[30]
CHB	miR-126 + miR-142-3p + AFP	0.930	0.880	0.970	[32]
HBV-DN	let-7b + AFP	0.706	0.508	0.767	[233]
HBV-DN	miR-122 + AFP	0.714	0.792	0.533	[233]
HBV-LC	miR-99a + AFP	0.780	0.719	0.828	[232]
HBV-LC	miR-101 + AFP	0.973	0.966	0.879	[24]
HBV-LC	miR-122 + AFP + PIVKA-II	0.918	0.910	0.880	[37]
HBV-LC	miR-126 + AFP	0.897	0.800	0.790	[32]
HBV-LC	miR-142-3p + AFP	0.899	0.850	1.000	[32]
HBV-LC	miR-205 + AFP	0.893	0.750	0.860	[36]
HBV-LC	miR-224 + AFP	0.844	0.969	0.641	[11]
HBV-LC	miR-126 + miR-142-3p + AFP	0.939	0.850	0.840	[32]
CHB + HBV-LC	miR-224 + AFP	0.857	0.875	0.722	[11]

[1]Comparing early-stage hepatitis B virus-associated hepatocellular carcinoma patients to patients with other stages.
[2]Adjusting for gender and age differences.
HC: Healthy control; CHB: Chronic hepatitis B patient; HBV: Hepatitis B virus; HBV-DN: Hepatitis B virus-related dysplastic nodule patient; HBV-LC: Hepatitis B virus-related liver cirrhosis patient; AFP: Alpha fetoprotein; PIVKA-II: Prothrombin induced by vitamin K deficiency or antagonist- II; AUC: Area under the receiver operating characteristic curve; miRNAs: MicroRNAs.

protein (HBx), and HBV polymerase protein (HBp)] dysregulate miRNAs to promote hepatocarcinogenesis. In this part, we summarize the available studies deciphering the way in which HBV regulates the expression profiles of miRNAs through modulating miRNA processing genes and proteins and influencing transcriptional, posttranscriptional, and epigenetic mechanisms, as well as the factors affecting the regulation process, which may help to identify the novel

Table 5 Efficacy of microRNAs used in diagnosing hepatitis B virus-associated hepatocellular carcinoma with low alpha fetoprotein expression

AFP level in HBV-HCC patients	Comparison	miRNA	AUC	Sensitivity	Specificity	Ref.
< 15 ng/mL	HBV-DN	let-7b	0.645	0.848	0.500	[233]
< 15 ng/mL	HBV-DN	miR-122	0.629	0.712	0.577	[233]
< 15 ng/mL	HBV-DN	miR-122 + let-7b	0.646	0.848	0.500	[233]
≤ 20 ng/mL	CHB + HC	miR-26a	0.733	0.868	0.574	[30]
≤ 20 ng/mL	CHB + HC	miR-26a[1]	0.701	0.880	0.574	[30]
≤ 20 ng/mL	CHB + HC	miR-27a	0.832	0.838	0.723	[30]
≤ 20 ng/mL	CHB + HC	miR-27a[1]	0.771	0.800	0.723	[30]
≤ 20 ng/mL	CHB + HC	miR-125b	0.778	0.760	0.790	[30]
≤ 20 ng/mL	CHB + HC	miR-125b[1]	0.775	0.800	0.787	[30]
≤ 20 ng/mL	CHB + HC	miR-223	0.759	0.789	0.702	[30]
≤ 20 ng/mL	CHB + HC	miR-223[1]	0.715	0.720	0.723	[30]
< 20 ng/mL	CHB + HC	miR-15b + miR-130b	0.980	0.967	0.915	[9]
≤ 20 ng/mL	CHB + HC	miR-125b + miR-223 + miR-27a + and miR-26a	0.874	0.842	0.851	[30]
≤ 20 ng/mL	CHB + HC	miR-125b + miR-223 + miR-27a + miR-26a[1]	0.849	0.800	0.894	[30]
< 200 ng/mL	CHB	miR-125b	0.943	1.000	0.755	[23]
< 250 ng/mL	CHB	miR-126	0.765	0.610	0.690	[32]
< 250 ng/mL	HBV-LC	miR-126	0.643	0.610	0.580	[32]
< 400 ng/mL	HBV-LC	miR-205	0.815	1.000	0.560	[36]
20-400 ng/mL	CHB + HC	miR-15b + miR-130b	0.976	1.000	0.915	[9]
< 400 ng/mL	CHB + HBV-LC + HC	miR-122 + miR-192 + miR-21 + miR-223 + miR-26a + miR-27a + miR-801	0.879	0.777	0.845	[44]

[1]Comparing early-stage hepatitis B virus-associated hepatocellular carcinoma patients to patients with other stages.
HBV-DN: Hepatitis B virus-related dysplastic nodule patient; CHB: Chronic hepatitis B patient; HC: Healthy control; HBV: Hepatitis B virus; HCC: Hepatocellular carcinoma; HBV-LC: Hepatitis B virus-related liver cirrhosis patient; AFP: Alpha fetoprotein; AUC: Area under the receiver operating characteristic curve; miRNAs: MicroRNAs.

therapeutic pathways (Figure 1).

HBV modulates miRNA processing proteins to affect the biogenesis of miRNAs

It takes a complex process to form mature miRNAs. Firstly, miRNA genes, encoded by introns of noncoding or coding regions, are transcribed to pri-miRNAs by RNA polymerase II (Pol II) in the nucleus. Then, pri-miRNAs are spliced to pre-miRNAs by the Microprocessor complex (composed by the nuclear RNase III Drosha and DGCR8). Depending on the protein exportin 5 (EXP5), pre-miRNAs are exported to the cytosol, and are cleaved to a small RNA duplex by Dicer. The duplex is subsequently sorted and loaded onto Ago proteins, of which the guide strand is selected and preserved to form the RNA-induced silencing complex and silence gene expression[72].

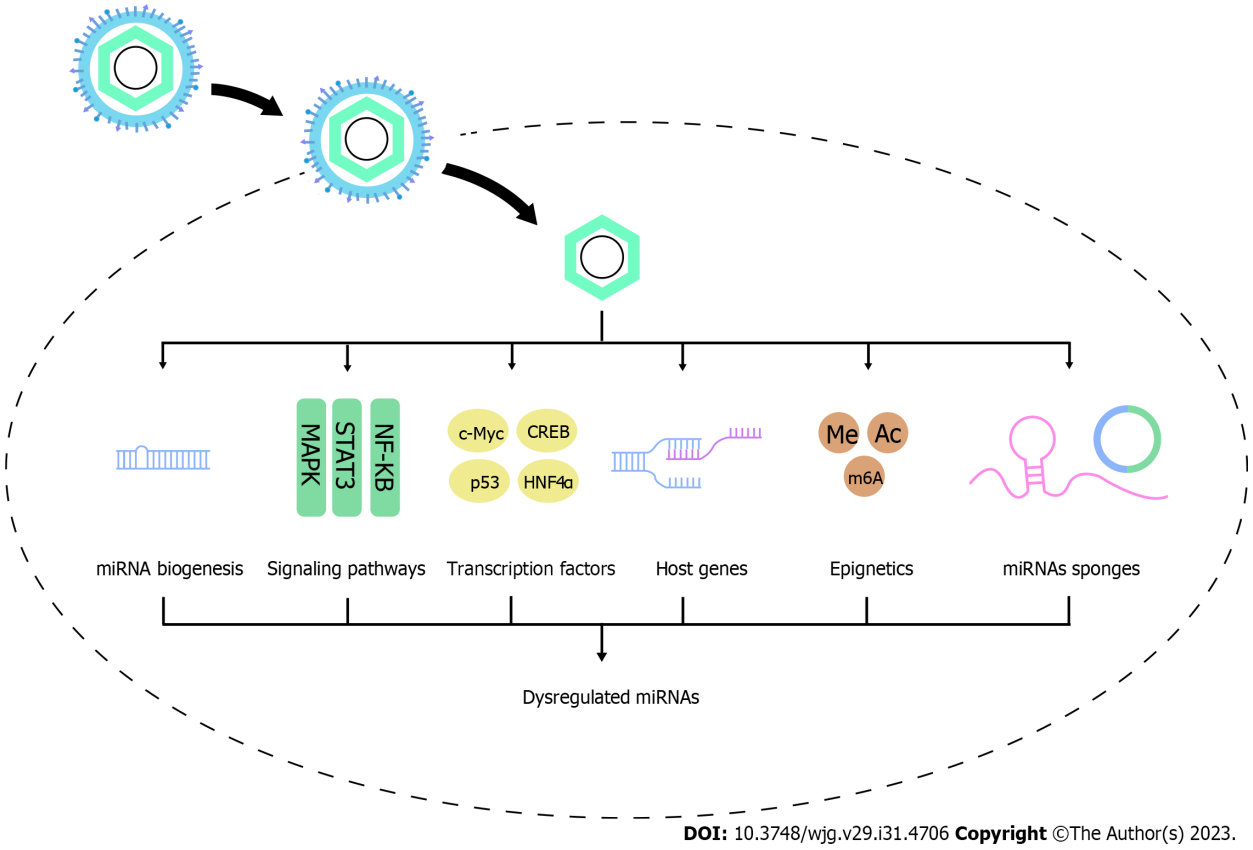
There is evidence that HBV contributes to pre-miRNA production. Rather than pri-miR-18a levels, pre-miR-18a levels are associated with miR-18a elevation in HBV-HCC cases, indicating increased processing of pri- to pre-miR-18a[73]. Another study demonstrates that ectopic expression of HBx stimulates the transcription of pri-miR-1269b and hence induces the expression of pre-miR-1269b in HCC cell lines[74]. Therefore, HBV may affect miRNA expression through modulating its synthesis process.

Studies have verified a strong correlation between HBV and miRNA processing proteins. CHB patients with high HBV loads have lower mRNA and protein levels of Drosha, Dicer and Ago2 compared with patients with low viral loads[75]. In HBV-positive HCC patients, Drosha, DGCR8, Ago1, and Ago2 are significantly overexpressed[76], whereas Dicer and Ago3 are significantly downregulated in HCC tissues than that in adjacent nontumor tissues[76,77].

Table 6 Efficacy of microRNAs used to predict the prognosis of hepatitis B virus-associated hepatocellular carcinoma

Tissues/serum	miRNA panels	Risk/protective factors	Outcome	HR	CI	Ref.
Tissues	miR-9-3[a]	Risk	OS	-	-	[62]
Tissues	miR-10b[a]	Risk	OS	-	-	[62]
Tissues	miR-21[b]	Risk	DFS	3.019	0.219-6.939	[56]
Tissues	miR-29a-5p[b]	Risk	TTR	0.5	0.3-0.8	[63]
Tissues	miR-29a-5p[b]	Risk	OS	-	-	[63]
Tissues	miR-31[a]	Risk	OS	-	-	[62]
Tissues	miR-106b[a]	Risk	OS, DFS	-	-	[64]
Tissues	miR-122[a]	Protect	OS	-	-	[54]
Tissues	miR-122[b]	Protect	OS	-	-	[55]
Tissues	miR-143[b]	Protect	OS	-	-	[55]
Tissues	miR-145[a]	Protect	DFS	1.12	0.293-2.958	[56]
Tissues	miR-193b[c]	Protect	OS	-	-	[57]
Tissues	miR-203a	Protect	OS	0.63	0.41-0.97	[58]
Tissues	miR-216b[c]	Protect	OS, DFS	-	-	[59]
Tissues	miR-224[b]	Risk	OS	-	-	[55]
Tissues	miR-371a-5p[b]	Risk	OS	-	-	[27]
Tissues	miR-375	Protect	DFS	-	-	[60]
Tissues	miR-375[b]	Protect	OS	-	-	[55]
Tissues	miR-384[a]	Protect	OS	-	-	[61]
Tissues	miR-519c[a]	Risk	OS	-	-	[62]
Tissues	miR-522[a]	Risk	OS	-	-	[62]
Tissues	miR-522[b]	Risk	OS	2.19	1.33-3.6	[65]
Tissues	miR-523[b]	Risk	OS	1.5	1-2.44	[65]
Tissues	miR-3188[c]	Risk	OS, DFS	-	-	[28]
Tissues	miR-3660[a]	Risk	OS	-	-	[62]
Tissues	miR-3682-3p[c]	Risk	OS	-	-	[66]
Tissues	miR-4784[a]	Risk	OS	-	-	[62]
Tissues	miR-5188[b]	Risk	OS	-	-	[67]
Tissues	miR-6883[a]	Risk	OS	-	-	[62]
Serum	miR-24-3p[b]	Risk	OS	2.141	1.158-3.960	[33]
Serum	miR-24-3p[b]	Risk	DFS	2.055	1.114-3.792	[33]
Serum	miR-29a-3p[b]	Risk	OS	4.0	1.2-13.9	[69]
Serum	miR-29a-3p[a]	Risk	PFS	-	-	[69]
Serum	miR-96[a]	Risk	OS	-	-	[34]
Serum	miR-150[c]	Protect	OS	0.446	0.233-0.854	[13]
Serum	miR-192-5p[b]	Risk	OS	-	-	[69]
Serum	miR-192-5p[b]	Risk	PFS	2.2	1.1-4.2	[69]
Serum	miR-487b[a]	Risk	OS	2.846	1.139-7.114	[19]
Serum	miR-487b[c]	Risk	OS	2.115	1.083-4.132	[18]
Serum	miR-768-3p[b]	Protect	OS	3.057	1.136-8.225	[20]
Plasma	miR-155	Risk	OS	-	-	[70]

[a]*P* < 0.05.
[b]*P* < 0.01.
[c]*P* < 0.001.
OS: Overall survival; DFS: Disease-free survival; TTR: Time to tumor recurrence; PFS: Progression-free survival; HR: Hazard ratio; CI: Confidence interval; miRNAs: MicroRNAs.



DOI: 10.3748/wjg.v29.i31.4706 **Copyright** ©The Author(s) 2023.

Figure 1 Mechanisms of hepatitis B virus-induced dysregulation of microRNAs. miRNAs: MicroRNAs.

For Drosha protein, researchers find that HBV inhibits Drosha promoter activity to downregulate its expression. HBx are inferred to interact with SP1 and AP-2a to downregulate Drosha expression[78]. HBV can downregulate DGCR8 expression *via* suppressing its promoter activity through upregulating transcription factor YY-1, in which HBs and HBx may play a role[79]. No study has provided direct evidence that the EXP5 protein is controlled by HBV. PIN1 decreases mature miRNA expression by catalyzing EXP5's conformational change and reducing its ability to export pre-miRNAs from the nucleus to the cytoplasm[80]. It is reported that PIN1 can bind specifically to the HBx to synergistically increase cell proliferation[81], indicating that HBx interacts with PIN1 and may affect pre-miRNAs export. Upon export to the cytoplasm, pre-miRNA is cleaved by Dicer in Drosophila. MiRNAs and siRNAs share a similar step in splicing and partitioning[82]. Considering that HBx can inhibit the Dicer-mediated processing of dsRNAs into siRNAs[75], HBV may also modulate miRNA through inhibiting Dicer and Dicer-mediated splicing of pre-miRNAs. Researchers discover that Ago2 mRNA is repressed by miR-99a in Huh7 and Hep3B cells[83], whereas miR-99a is found to be up-regulated in serum of HBV patients[84], indicating that there may be an HBV/miR-99a/Ago2 regulatory axis.

Overall, there is still no evidence directly indicating that HBV affects miRNA expression by altering miRNA processing proteins. But due to the crucial role of these proteins in miRNA biogenesis, it is reasonable to infer that this is possible. It's worth noting that in a study with non-viral-associated HCC samples, DGCR8, Dicer, Ago3 and Ago4 are also significantly downregulated, in which epigenetic regulation may be implicated[77]. Therefore, the regulatory role and mechanisms of HBV on miRNA machinery components still need further investigation (Figure 2).

HBV alters signaling pathways to modulate miRNAs

Although miRNAs share a common synthesis machinery, specific miRNA is regulated by different transcriptional and posttranscriptional mechanisms. HBV generally leads to a range of aberration of signaling pathways, Sartorius *et al*[6] summarize the miRNAs that are dysregulated by HBV and are involved in regulating these signaling pathways. However, miRNAs are also regulated by these signaling pathways induced by HBV infection (Table 7).

Table 7 Dysregulated signaling pathways mediates hepatitis B virus-induced microRNAs dysregulation

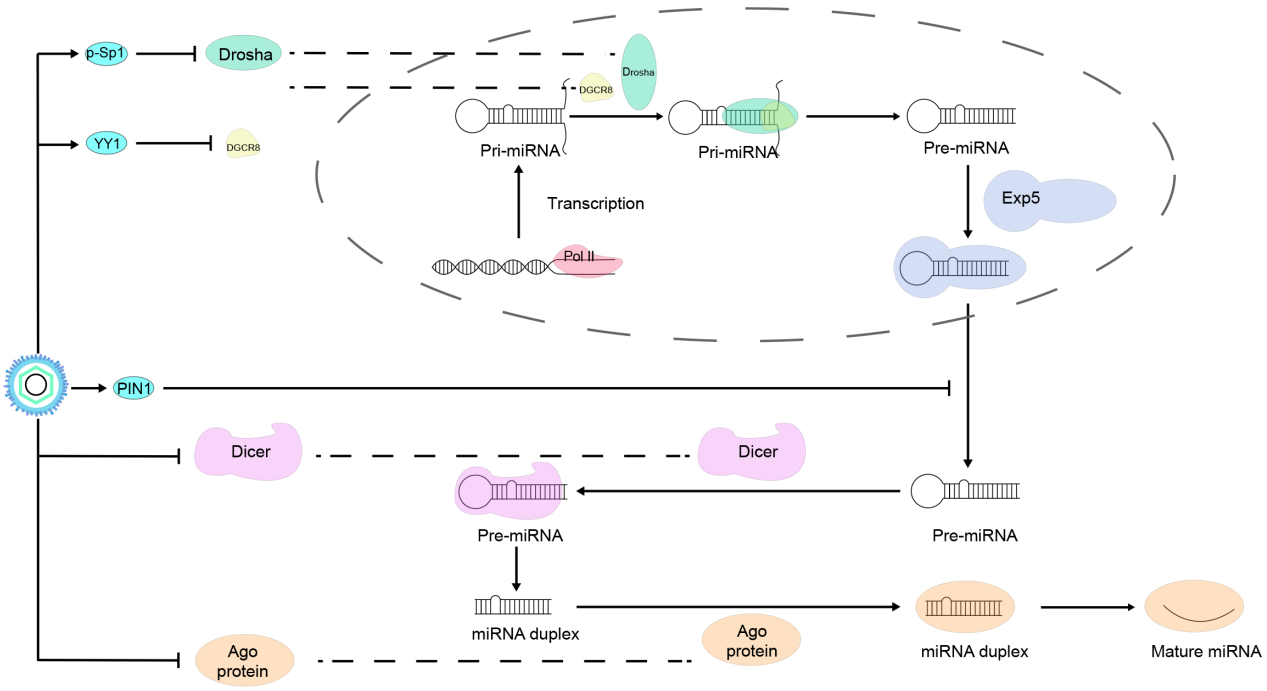
Upstream signaling pathway	miRNA	HBV protein	Expression	Ref.
ERK1/2/CREB	miR-212-3p	HBe	Up	[85]
MAPK/Ap1	miR-21	HBx	Up	[87,88]
MAPK/YY1	miR-129-2	HBV	Down	[89]
MAPK/YY1	miR-203	HBV	Down	[89]
MAPK/YY1	miR-335	HBV	Down	[89]
IL-6/STAT3	miR-21	HBx	Up	[91]
STAT3	miR-328-3p	HBV, HBx, HBc	Up	[90]
STAT3	miR-34a	HBx	Down	[95]
STAT3/SALL4	miR-200c	HBV	Down	[94]
STAT3	miR-204	HBV	Down	[93]
STAT3	miR-539	HBx	Up	[92]
NF-κB	miR-23a	HBV	Up	[103]
NF-κB	miR-143	HBx	Up	[98,99]
NF-κB	miR-146a	HBx	Up	[100]
NF-κB	miR-146a-5p	HBx, HBc	Up	[97]
NF-κB	miR-1269b	HBx	Up	[74]
PI3K, NF-κB	miR-155	HBe	Up	[101]
IKKα/NF-κB	miR-7	HBx	Up	[104]
IKKα/NF-κB	miR-21	HBx	Up	[104]
IKKα/NF-κB	miR-103	HBx	Up	[104]
IKKα/NF-κB	miR-107	HBx	Up	[104]
Androgen pathway	miR-216a	HBx	Up	[111]
TLR7/NF-κB	miR-155	HBV	Down	[106]
LEF-1	miR-371a-5p	HBV	Up	[27]
PPARγ/NF-κB/p65	miR-130a	HBV	Down	[105]

HBV: Hepatitis B virus; HBe: Hepatitis B virus envelope antigen; HBx: Hepatitis B virus x protein, HBc: Hepatitis B virus core antigen; miRNAs: MicroRNAs.

MAPK pathway plays a crucial role during the innate immune response. HBeAg is able to activate ERK, one of the MAP kinases, to induce the expression of phosphorylated CREB, which is able to bind to the promoter of miR-212-3p and subsequently enhance miR-212-3p expression[85]. In addition, several AP-1 components including Fra-1, c-Jun, and JunB are found to be recruited on a miR-21 50-flanking region, thus promoting miR-21 transcription. HBx has been previously shown to activate Ap-1, which is activated predominately by MAPK signaling cascade[86]. Therefore, there is a potential HBx/MAPK/Ap1/miR-21 regulatory pathway[87,88]. Meanwhile, HBV also induces YY1 expression through MAPK signaling, and negatively regulates the expression of miR-335, miR-129-2, and miR-203[89].

STAT3 is crucial for transducing signals and regulating the expression of a wide range of genes to promote tumor progression. Studies have found that HBV, HBc and HBx but not HBs and HBp increase STAT3 phosphorylation[90], suggesting that HBV and its viral proteins underline a role in STAT3 activation. STAT3 has been proved to directly bind to several miRNAs' promotors, increase the promotors activity, and subsequently activate miRNAs transcription. STAT3 mediates upregulation of miR-21[91], miR-328-3p[90] and miR-539[92], which are dysregulated by HBV infection. However, Huang *et al*[93] found that STAT3 mediates HBV-induced miR-204 suppression. HBV also activates STAT3 to induce SALL4 expression, while SALL4 suppresses miR-200c expression through directly binding to miR-200c promoter [94]. In addition, STAT3 may mediate the suppression of miR-34a caused by HBx[95].

NF-κB is a transcription factor with broad roles in gene induction in a variety of cellular responses, particularly throughout the immune system. HBV and its proteins have been shown to increase NF-κB content and facilitate its translocation from the cytoplasm to the nucleus[74,96]. Researches show that multiple miRNAs are dysregulated by HBV through modulating NF-κB signaling. For example, HBx and HBc upregulate miR-146a-5p through activating NF-κB signaling[97]. HBx upregulates miR-143[98,99], miR-146a[100] and miR-1269b[74] by activating NF-κB binding to the



DOI: 10.3748/wjg.v29.i31.4706 **Copyright** ©The Author(s) 2023.

Figure 2 Hepatitis B virus modulates microRNAs processing proteins to affect the biogenesis of microRNAs. miRNAs: MicroRNAs.

miRNAs promotor. Meanwhile, inhibitors of NF-κB and PI3K decrease miR-155 in HBeAg-stimulated macrophages, suggesting NF-κB and PI3K mediate HBeAg-induced miR-155 upregulation in macrophages[101]. In addition, NF-κB subunit p50 but not p65 mediates upregulation of miR-942 by LPS through binding to miR-942 promotor, and miR-942 expression is increased with progression of HBV-mediated liver fibrosis, implying a putative regulation of HBV on miR-942[102]. As a consensus p65-binding sequence (AGGGATTTCC) is located in the miR-23a promoter region, p65 dominantly represses miR-23a promoter activity, and suppresses miR-23a transcription[103]. Therefore, HBV has the potential to upregulate miR-23a by suppressing p65 expression. In addition, nuclear IKKα coordinates the transcriptional activity of NF-κB to mediate the expression of miR-7, miR-21, miR-103, and miR-107 caused by HBx[104]. Intriguingly, HBV induced PPARγ to negatively control NF-κB/p65 protein *via* ubiquitination and degradation. Repressed NF-κB/p65 then reduces the endogenous miR-130a expression[105]. The discrepancy in the NF-κB results may be due to the different HBV viral proteins.

Toll-like receptors (TLRs), the main cellular innate immune cell receptor, play crucial roles in immune responses against viral infections, including HBV. Sarkar *et al*[106] find that TLR7 expression is reduced by HBV infection, while TLR7 is able to induce miR-155 through the NF-κB pathway. Considering that HBV suppresses TLR7 and its subsequent signaling pathway including MAPK/Ap-1, NF-κB, IRF3 and IRF7[107], HBV may impact miRNAs expression through regulating TLR proteins and their signaling pathways. In addition, one study finds that HBV upregulates LEF-1, a key component of the Wnt signaling pathway, to induce miR-371a-5p expression through binding with miR-371a-5p promoter[27].

Membrane-initiated estrogen receptor (ER) and androgen receptor (AR) signaling participate significantly in physiology and disease[108]. HBx enhances AR-responsive gene expression[109], and represses ERα responsive gene transcription[110]. Therefore, HBV has the potential to regulate the miRNAs that act as AR or ERα responsive elements. HBx amplified the transcription of pri-miR-216a which is activated as a result of ligand-stimulated AR binding to the ARE site at the 5′ promoter region. However, when applied to AR-negative cells, HBx failed to stimulate an increase in pri-miR-216a[111].

HBV modulates transcription factors to regulate miRNAs

HBV protein and its RNA can modulate the expression of some transcription factors or other proteins, which in turn regulate miRNAs expression (Table 8).

HBV promotes the expression of oncogenic proteins to regulate miRNAs. c-Myc oncoprotein is a transcription factor that regulates numerous physiological processes. Chang *et al*[112] identify 13 miRNAs which are prominently repressed by c-Myc through binding to miRNA promotors. HBV can directly interact with c-Myc and stimulate its expression, thereby affecting the expression of miRNAs. For example, HBx induces c-Myc, and then c-Myc is recruited to a region of miR-192 promotor, which leads to decreased promotor activity, and subsequently downregulates miR-192-3p expression [113]. Similarly, HBx also downregulates miR-15a/16 expression[114], and suppresses let-7 family through c-Myc[115]. In addition, Jung *et al*[116] find that c-Myc mediates HBV-induced miR-17-92 overexpression. c-Myc also binds to the miR-3682-3p promoter, thus HBx may also induce miR-3682-3p expression *via* c-Myc[66]. CREB is an essential subset of phosphorylation-dependent transcription factors. HBx promotes CREB-mediated activation of miR-3188[28]. Similarly,

Table 8 Dysregulated transcription factors or upstream regulatory elements mediates hepatitis B virus-induced microRNAs dysregulation

Transcription factors or upstream regulatory elements	miRNA	HBV protein	Expression	Ref.
c-Myc	let-7	HBx	Down	[115]
c-Myc	miR-15a/16	HBx	Down	[114]
c-Myc	miR-17-92	HBV	Up	[116]
c-Myc	miR-192	HBx	Down	[113]
c-Myc	miR-3682-3p	HBx	Up	[66]
CREB1	miR-520c-3p	HBx	Up	[117]
CREB	miR-3188	HBx	Up	[28]
Survivin, Sp1	miR-520b	HBx	Up	[118]
FOXO3	miR-30b-5p	HBp	Up	[119]
URG11	miR-148a	HBx	Up	[126]
JNK/c-Jun	miR-199a-3p	HBx	Up	[120]
p53	miR-216b	HBx	Down	[59]
p53	miR-148a	HBx	Down	[122]
Hnf4α	miR-122	HBV	Down	[123]
Hnf4α	miR-548p	HBx	Down	[124]
DDX3	miR-34	HBx	Down	[127]

HBV: Hepatitis B virus; HBx: Hepatitis B virus x protein; HBp: Hepatitis B virus polymerase protein; miRNAs: MicroRNAs.

HBx promotes miR-520c transcription through CREB1[117]. Meanwhile, HBx, survivin and Sp1 form a complex in the promotor of miR-520b, and the interaction between HBx and survivin or Sp1 is indispensable for the regulation of miR-520b[118]. FOXO3 is a transcriptional factor that promotes oncogenesis, HBp can promote the expression of miR-30b-5p through its interaction with FOXO3[119]. Moreover, HBx and TGF-1 induce JNK-dependent activation of c-Jun, which is then recruited to the miR-199a-3p promoter to stimulate its transcription[120].

HBV inhibits the expression of tumor suppressor proteins to regulate miRNAs. Acting as an important tumor suppressor gene, TP53 is the most frequently mutated gene in HBV-related HCC[121]. HBx can decrease the recruitment of p53 to the miR-216b promoter, and then inhibit miR-216b transcription[59]. Another research indicates that HBx can also repress miR-148a *via* suppressing p53-mediated activation[122]. Hepatocyte nuclear factor 4α (Hnf4α), a liver-enriched transcription factor that activates miR-122 gene transcription by binding to its promotor, is found to be repressed by HBV infection in both mRNA and protein levels[123]. Similarly, Hnf4α mediates HBx induced downregulation of miR-548p, possibly through direct binding to the miR-548p promoter[124].

In addition to these transcription factors, HBV also regulates some other proteins to affect miRNAs expression. URG4/URGCP, up-regulated by HBx, can up-regulate 77 miRNAs and down-regulate 9 miRNAs in HepG2 cells[125]. Yuan *et al* [126] find that HBx-induced miR-148a is dependent on oncogenic URG11. HBx also downregulates DDX3, which upregulates miR-34 expression[127]. Meanwhile, one study also identifies 75 miRNAs by ChIP-Seq whose promotor regions are putatively targeted by HBx protein, some of which have been implicated in hepatocarcinogenesis[128].

HBV affects production of miRNAs from their host genes

As the majority of miRNA genes are encoded in the introns of either noncoding or coding regions, multiple studies have demonstrated that only one-third of intronic miRNAs are transcribed from their own promoters. The coregulation of intronic miRNAs with their host genes can be further illustrated by their tissue- or disease-specific co-expression patterns [129].

Some miRNAs are derived from lncRNA precursors, which have the potential to be affected by HBV. LncRNA H19 has been proved to harbor a miRNA containing hairpin in its exon 1, which serves as the precursor for miRNA-675[130]. HBx upregulates H19 expression, leading to a corresponding increase of miR-675[131,132]. Therefore, HBV may affect the LncRNA-derived miRNAs. However, HBx can positively regulate miR-545/374a cluster in the Ftx lncRNA, but fails to regulate miR-421/374b cluster which is also encoded in Ftx introns. Even though miR-374a and miR-545 are transcribed off the same promoter, their abundances are not always correlated[12].

In addition, intronic miRNAs may be coupled with their host genes. miR-26b gene resides in an intron of CTDSP1. They share the same transcription start sites (TSS). miR-26b is therefore transcribed as part of its host transcription unit [133,134]. HBV downregulates miR-26b expression, partly because of the suppression of CTDSP1 mRNA transcription. Notably, the extent of the decrease in miR-26b level was greater than that of CTDSP1 mRNA, implying the other putative

regulatory pathway[135]. Similarly, HBx promotes miR-106b, miR-93, and miR-25 transcription in HCC cells, whose host gene MCM7 is also co-transcribed and upregulated, suggesting that MCM7 activation may be involved in the regulation of these miRNAs by HBV[64].

Notably, despite the fact that some miRNA genes share the promoter of their host gene, the vast majority of miRNA genes have multiple TSS, and the promoters of intronic miRNAs are sometimes distinct from the promoters of their host genes.

HBV participants in epigenetic regulation of miRNAs

Epigenetic mechanisms mainly include DNA methylation, posttranslational histone modifications, chromatin remodeling, ncRNA interactions and RNA modification. Despite the significant involvement of miRNAs in epigenetic regulation, miRNAs are also regulated by epigenetic modifications and involved in diverse human diseases[136]. HBV can regulate epigenetics of miRNAs, leading to the functional disruption of miRNAs and consequently promoting HCC.

HBx has been found to increase the DNA methyltransferase (DNMT) activities and promote regional hypermethylation of specific tumor suppressor genes (TSG)[137]. It has been elucidated that HBx induces DNA hypermethylation of CpG islands in miR-18b[138], miR-30e[139], miR-132[140], and miR-205 promoter[141] to affect their expression. Shang *et al*[89] identify that miR-335, miR-129-2, and miR-203 are repressed by HBV, but are significantly activated by 5-azacytidine, the DNMT inhibitor, indicating that HBV regulates these miRNAs through DNMT-mediated methylation. Meanwhile, Tsang *et al*[142] find that knockdown of HBV-upregulated YY1[89] significantly decreases DNA methylation levels in the miR-9 Loci, leading to an increased miR-9 in HCC cells. Thus, YY1 may mediate the suppression of miRNAs caused by HBV through inducing DNA methylation. Conversely, although HBx leads to overall hypomethylation, HBx highly interferes methylation levels of -550 CpG site in the miR-125a promoter, and therefore triggers miR-125 expression[143]. Further study is needed to elaborate this phenomenon.

As for the histone modification, Guerrieri *et al*[128] verify that HBx decreases H4 acetylation level in the promoter regions of miR-138-2, miR-224, miR-302e, miR-576-3p and miR-596, which may explain their downregulation. Conversely, HBx increases H4 acetylation at the miR-26b promoter. These imply HBx ability to regulate miRNAs by modulating the histone modification of miRNAs promotors[128]. In addition, H3K27me3 is an epigenetic modification to the DNA packaging protein Histone H3[144]. The genomic regions enriched for H3K27me3 can function as silencers to repress gene expression *via* chromatin interactions[145]. Knockdown of HBV-upregulated YY1 reduced not only global H3K27me3 levels, but also EZH2 and H3K27me3 promoter occupancy, leading to the increased miR-9 in HCC cells. It is also found that HBV-upregulated YY1 Leads to EZH2 recruitment for H3K27me3-mediated silencing of tumor-suppressing miRNAs[142], supporting the idea that HBV may indirectly regulate miRNAs through impacting H3K27me3 Levels mediated by EZH2 and YY1.

PPARγ, a ligand-activated transcription factor, is able to form a heterodimer with RXRα. The complex binds to DR1 and DR2 motifs in the miR-122 gene promoter to enhance miR-122 gene transcription, which will be amplified by 5-Aza-CdR (DNA methylation inhibitor) and PBA (histone deacetylation inhibitor). However, this positive regulation is abrogated by HBx which suppresses PPARγ-mediated transactivation through binding to the PPARγ DNA binding domain[146], indicating HBx may affect miR-122 epigenetics through binding and inhibiting PPARγ.

N6methyladenosine (m6A) modification is the most widespread post-transcriptional modification in mammalian mRNAs. MiRNAs can control the expression of m6A regulator, but they are also frequently modified with m6A[147]. HBV infection enhances the expression of METTL3, promotes miR-146a-5p maturation in an m6A-dependent manner [148]. In addition, Gld2 is a cytoplasmic non-canonical poly(A) RNA polymerase that adds successive AMP monomers to the 3'-end of specific RNAs. It can directly monoadenylate specific miRNAs, including miR-122, to stabilize and prolong the activity of miRNAs[149]. HBx also downregulates Gld2 expression, decreasing miR-122 3’ monoadenylation and ultimately suppressing mature miR-122 expression[150].

A variety of endogenous RNAs are able to bind to miRNAs to reduce the number of free miRNAs. These competitive endogenous RNAs (ceRNAs) mainly include lncRNAs and circRNAs, showing an increasing significance in multiple diseases[151]. HBV has been shown to regulate miRNAs through lncRNAs or circRNAs (Table 9). HBV-induced lncRNA-Unigene56159 directly targets miR-140-5p and suppresses its expression[152]. HBV infection also elevates lncRNA PCNAP1 to target miR-154[153]. HBV also enhances LncRNA n335586 to competitively bind with miR-924[154]. Meanwhile, HBx is found to stimulate lncRNA H19 to directly target to miR-138[131] and miR-22[155] through endogenous competition. HBx upregulates TRERNA1, which functions as a ceRNA sponge for miR-22-3p[156]. Additionally, HBx upregulates lncRNA MALAT1 and downregulates miR-124 expression. Further study indicates that MALAT1 directly binds to miR-124[157]. HBx also upregulates HMMR-AS1 and downregulates miR-627-3p expression. And HMMR-AS1 directly targets miR-627-3p[158]. Conversely, HBx inhibits LINC01352, which functions as a tumor suppressor by sponging miR-135b, through binding to the site where ERα binds[159]. HBx also downregulates lncRNA F11-AS1 expression and elevates expression of miR-211-5p, while lncRNA F11-AS1 is capable of binding to miR-211-5p [160]. In HBV-positive HCC cells, LncRNA XIST[161], LINC01232[162] are markedly increased and TFAP2A-AS1[163] are significantly decreased. Further studies show that XIST targets miR-192[161], LINC01232 targets miR-708-5p[162] and TFAP2A-AS1 targets miR-933[163] in HCC, suggesting HBV may dysregulate these miRNAs through lncRNAs. Similarly, HBV may downregulate LINC00924 expression, while LINC00924 interacts with miR-6755-5p, suggesting a potential HBV/ LINC00924/ miR-6755-5p regulatory axis[164]. HBx also promotes the progression of HCC through translocation and secretion of HMGB1, as a sponge to competitively bind the miR-200 family, *via* calcium dependent cascades[165,166]. Therefore, HBx may affect miR-200 expression through HMGB1.

HBV also regulates circRNAs to affect miRNAs (Table 9). HBx upregulates METTL3 expression to increase the m6A modification of circ-ARL3, and further favors circ-ARL3 reverse splicing and biogenesis. circ-ARL3 binds to miR-1305, antagonizing the inhibitory effects of miR-1305 on target oncogenes[167]. HBV also upregulated Circ-RNF13, as a sponge

Table 9 MicroRNAs sponges dysregulated by hepatitis B virus to induce microRNAs dysregulation

	miRNAs sponges	miRNA	Expression	Ref.
LncRNA	LncRNA Unigene56159	miR-140-5p	Down	[152]
	LncRNA PCNAP1	miR-154	Down	[153]
	LncRNA n335586	miR-924	Down	[154]
	LncRNA H19	miR-138	Down	[131]
	LncRNA H19	miR-22	Down	[155]
	LncRNA TRERNA1	miR-22-3p	Down	[156]
	LncRNA MALAT1	miR-124	Down	[157]
	LncRNA HMMR-AS1	miR-627-3p	Down	[158]
	LncRNA LINC01352	miR-135b	Up	[159]
	LncRNA F11-AS1	miR-211-5p	Up	[160]
	LncRNA XIST	miR-192	Down	[161]
	LncRNA LINC01232	miR-708-5p	Down	[162]
	LncRNA TFAP2A-AS1	miR-933	Up	[163]
	LncRNA LINC00924	miR-6755-5p	Up	[164]
	LncRNA HMGB1	miR-200	Down	[165,166]
CircRNA	CircRNA ARL3	miR-1305	Down	[167]
	CircRNA RNF13	miR-424-5p	Down	[168]
	CircRNA BACH1	miR-200a-3p	Down	[169]
	CircRNA ATP5H	miR-138-5p	Down	[170]
	CircRNA 0027089	miR-136-5p	Down	[171]
HBV mRNAs	HBx mRNA	miR-15a/miR-16-1	Down	[172]
	HBV mRNAs	miR-15a/miR-16	Down	[173]
	HBV mRNAs	miR-122	Down	[174]
	HBV mRNAs	let-7a	Down	[175]
	HBs mRNA	let-7g	Down	[176]
	HBx mRNA	miR-129-5p	Down	[177]
	HBx-LINE1	miR-122	Down	[179]

HBV: Hepatitis B virus; HBx: Hepatitis B virus x protein; HBs: Hepatitis B virus surface protein; miRNAs: MicroRNAs.

for miR-424-5p[168]. HBV upregulates Circ-BACH1, which sponges miR-200a-3p to reduce its expression[169]. Meanwhile, HBV upregulates Circ-ATP5H expression, while Circ-ATP5H directly targets miR-138-5p[170]. In HBV-positive HCC cells compared to HBV-negative HCC cells, circ_0027089 is markedly increased and specifically binds to miR-136-5p[171].

HBV sponges miRNAs to inhibits miRNAs' function

In addition to the lncRNAs and circRNAs, ceRNAs also include viral RNAs and host mRNAs[151]. HBV RNA could function as sponges to directly bind with miRNAs. Studies have implicated that HBV RNA may dysregulate miRNAs by binding to the complementary binding sites of miRNAs and depletion of miRNAs (Table 9).

HBV mRNAs, including pre-C/C (pgRNA), pre-S, S 3'-UTR, and X mRNAs, act as sponges to bind and sequester miR-15a/16-1, subsequently resulting in a depletion of miR-15a/16-1[172,173]. Li *et al*[174] validate that HBV mRNAs (pre-C/C (or pgRNA), pre-S, S 3'-UTR, and X mRNAs) can sponge miR-122 to inhibit its expression and function. Deng *et al*[175] identify that there is a let-7a complementary region in the HBV genome in HBV pre-C/C, pre-S, and S mRNAs. Notably, HBV regulates downstream targets of let-7a in a sequence-dependent manner. In addition, HBV transcripts harboring the preS2 region, such as HBV large S mRNA, can almost entirely interact with let-7g and subsequently promote HCC[176]. Ochi *et al*[177] find that HBx mRNA has complementary sequences with the central region of miR-129-5p, HBx mRNA interacts with the responsive element in the 3' UTR of miR-129-5p and sequesters it from forming a complex with Ago2. It is noted that the abundances of viral RNAs may affect their regulation on miRNAs. Although HCV 5'UTR may be able to

bind miR-122, it fails to change miR-122 expression like HBV mRNAs do. This discrepancy may be due to the fact that HCV mRNAs copy numbers are much less than miR-122, while HBV mRNAs copy numbers are more than miR-122[174]. Besides, HBV RNA copies per cell are much higher than those of let-7a[175], which may be essential for HBV RNA sequestration.

Of note, HBV genome gene is frequently inserted to host genes, which may lead to the transcription of the integrated virus-human chimeric fusion. It is exemplified by the discovery of a novel chimeric HBx-LINE1 RNA, which is generated from a normally silenced region of chromosome 8p11.21 after HBV integration[178]. Functioning as a long noncoding RNA (lncRNA)-like transcript, HBx-LINE1 sequesters cellular miR-122 by directly absorbing it, which ultimately leads to the depletion of miR-122[178,179].

HBV affects miRNAs through autophagy

Autophagy is the major intracellular degradation system and plays a pivotal role in multiple physiological processes [180], some of which have been delineated to function through modulating specific miRNAs. Majority of existing works have shown that HBV is able to induce autophagy. However, Lan *et al*[181] find that HBx transgenesis leads to a lower autophagic level, and miR-224 is preferentially recruited and degraded through autophagic progression. In addition, the selective autophagy receptor NDP52 targets Dicer and Ago2 proteins for the degradation. Autophagy is required for miRNA homeostasis and activity. Moreover, autophagy participates in the posttranscriptional regulation of Dicer mRNA, and chronic autophagy deficits impair miRNA stability after pre-miRNA processing[182]. Therefore, HBV has the potential to affect autophagy to disrupt the homeostasis of miRNAs biogenesis.

C-terminal truncated HBx and HBV integration may affect the ability of HBV in inducing dysregulation of miRNA

Carboxyl-terminal truncated HBx proteins (Ct-HBx, also called HBxΔC or trHBx) are variants transcribed from the mutant HBV X gene whose 3′-end are deleted during HBV genome integration into the host cells. Ct-HBx plays a pivotal role in hepatocarcinogenesis[183,184]. Ct-HBx regulates specific miRNAs more effectively than full-length HBx (HBx-FL). For instance, HBx-D35 enhances miR-21 promoter occupancy and upregulates miR-21 expression compared to HBx-FL [91]. HBxD127 also remarkably increases miR-215 expression relative to HBx[185]. A possible explanation is that C-terminal truncation may affect the binding of HBx to cellular proteins, resulting in altered miRNA gene expression patterns in cells[184]. Notably, Ct-HBx directly binds to some miRNAs promotors, such as miR-26a and miR-29c, resulting in direct transcriptional suppression which HBx-FL is unable to induce. The reason for this discrepancy may be that HBx-FL and Ct-HBx bind to different chromatin binding regions of miRNAs[186]. However, not all miRNAs are under this regulation. miR-23a and miR-27a are concordantly regulated by both HBx-FL and Ct-HBx, and their binding regions are similar[186]. For miR-146a, Ct-HBx does not lead to the same elevation as HBx-FL does[187].

HBV pre-S2 mutant protein may also play a role in the dysregulation of miRNA. HBV pre-S2 mutant induces endoplasmic reticulum stress and the mTOR signal cascade in transgenic livers and HCC tissues[188,189]. Meanwhile, Mdm^2-dependent ubiquitinoylation of Drosha by mTOR activates miRNA synthesis and controls many cancer-related miRNAs[190]. Since PreS/S proteins initiate a cascade of events that lead to malignancy[189], it's worth to investigate whether PreS mutant dysregulates miRNAs.

Considering HBV integration severely disrupts host cellular gene expression, genomic loci containing miRNA sequences inserted by HBV may impact miRNA expression. It has been found that HBV DNA integration into fragile sites may alter the expression of a couple of miRNAs which are located in or near fragile sites, including miR-200a near FRA1A, miR-143, miR-145 and miR-224 near FRA5C, miRNA-17–92 cluster near FRA13D, miR-195 near FRA17A, miR-99b, miR-125a and let-7e near FRA19A, and miR-199a-1 near FRA19B[191-193]. These miRNAs have been documented in HCC[191], and there are still a great many miRNAs that are potentially dysregulated by HBV integration[192].

In addition, Yang *et al*[194] also find miR-602 is upregulated by HBV or HBx, and they speculate that the chromosome 9q34.3 containing miR-602 sequence is commonly integrated by HBV, which may lead to increased miR-602 expression. Similarly, Guo *et al*[195] speculate that HBV-induced chromosome instability caused by HBV integration may play a role in promoting the miRNAs-371-3 gene cluster expression. Further study is needed to support this hypothesis. Therefore, HBV DNA integration may alter miRNA expression, but the underlying mechanism requires additional study.

MECHANISMS OF HBV DYSREGULATED MIRNAS IN PROMOTING HCC

By dysregulating miRNAs, HBV exacerbates its function in the oncogenesis of HCC. Currently, multiple reviews have summarized the essential role of HBV-dysregulated miRNAs in affecting tumor cell cycle, cell proliferation, cell apoptosis, cell migration and invasion, and epithelial-mesenchymal transition (EMT)[6,196-199]. Therefore, we provided an updated supplementary list of miRNAs dysregulated by HBV and involved in these processes (Supplementary Tables 1 and 2), which will not be elaborated here. In this section, we discuss the role of HBV-dysregulated miRNAs in the tumor stemness, metabolic reprogramming, anti-tumor immunity, and tumor drug resistance of HCC, which may shed light on potential treatment approaches (Table 10 and Figure 3).

Dysregulated miRNAs promote tumor stemness

Liver cancer stem cells (CSCs) are a distinct population of HCC cells with stem cell characteristics, defining a hierarchical structure and contributing to treatment resistance and tumor recurrence. HBV is one of the most prominent players in liver CSCs. miRNAs partially mediate the stemness progression[200] (Table 11).

Table 10 Functions of hepatitis B virus-dysregulated microRNAs in promoting hepatocellular carcinoma

miRNA	HBV protein	Expression	Target genes	Abnormal function in HBV-HCC	Ref.
miR-7	HBV, HBx	Up	Mapsin	Conferring HBx-mediated anoikis resistance and doxorubicin resistance	[213]
miR-15a/16	HBV mRNA	Down	-	Inducing etoposide-induced apoptosis	[173]
miR-21	HBV, HBx	Up	Mapsin	Conferring HBx-mediated anoikis resistance and doxorubicin resistance	[213]
miR-23a	HBV	Down	CCL22	Inhibiting Tregs recruitment	[103]
miR-30b-5p	HBp	Up	MINPP1	Promoting tumor growth, enhancing cell proliferation, promoting cell migration and invasion, regulating glycolytic bypass metabolism	[119]
miR-34a	HBV	Down	CCL22	Inhibiting Tregs recruitment	[209]
miR-103	HBV, HBx	Up	Mapsin	Conferring HBx-mediated anoikis resistance and doxorubicin resistance	[213]
miR-107	HBV, HBx	Up	Mapsin	Conferring HBx-mediated anoikis resistance and doxorubicin resistance	[213]
miR-124	HBx	Down	PI3K/Akt	Suppressing CSC differentiation	[157]
miR-135a-5p	HBc	Up	VAMP2	Preventing Doxorubicin hydrochloride-induced apoptosis	[212]
miR-138	HBV	Down	PD-1	Regulating cytokine secretion of T cells and improving T-cell immune responses	[208]
miR-146a	HBV	Up	STAT1	Suppressing IFN-induced anti-HBV effect	[187]
miR-152	HBV	Down	HLA-G	Enhanced NK cytolysis against hepatoma cells	[210]
miR-193b	HBV	Down	Mcl-1	Sensitizing sorafenib-induced apoptosis	[57]
miR-200a/200b/429	HBx	Down	RICTOR	Impairing HCC stem cell properties, regulating glutamine metabolism, sensitizing the response to anti-PD-L1 immuno-therapy	[165, 166]
miR-203a	HBs	Down	BMI1	Sensitizing 5-FU-induced apoptosis, impairing HCC stem cell properties	[58]
miR-205	HBx	Down	ACSL1	May promote lipogenesis	[141] [206]
miR-325-3p	HBV	Down	DPAGT1	Sensitizing the response to Doxorubicin chemotherapy	[201, 202]
miR-329	HBV, HBx	Down	AFP	Sensitizing chemotherapy induced apoptosis	[214]
miR-384	HBV, HBx	Down	PTN/PI3K/AKT/mTORC1	Inhibiting high glucose-induced lipogenesis	[61]
miR-429	HBx	Down	Rab18	Inhibiting dysregulation of lipogenesis	[205]
miR-1236	HBV, HBx	Down	AFP	Sensitizing chemotherapy induced apoptosis	[214]
miR-3682-3p	HBx	Up	FOXO3/PI3K/AKT1/β-catenin/c-Myc	Promoting HCC stemness	[66]
miR-5188	HBx	Up	FOXO1/β-catenin	Resisting the effects of chemotherapy 5-FU, CDDP and EPI, promoting HCC stemness	[67]

HBV: Hepatitis B virus; HBx: Hepatitis B virus x protein; HBp: Hepatitis B virus polymerase protein; HBc: Hepatitis B virus core antigen; HBs: Hepatitis B virus surface antigen; HCC: Hepatocellular carcinoma; miRNAs: MicroRNAs.

In HCC cells, the expression of CD44, CD133, and EpCAM is markedly reduced by miR-124, indicating the pivotal effects of miR-124 in suppressing CSCs differentiation. HBx downregulates miR-124, and may therefore interfere CSCs differentiation[157]. In one research, HBx supports the progression of HCC *via* translocation and secretion of HMGB1, which regulates RICTOR expression in HCC by competitively binding to the miR-200 family[166]. Both HMGB1 and RICTOR mRNAs can augment HCC stemness characteristics in HCC[165]. HBsAg inhibits the expression of miR-203a in HCC cells. miR-203a decreases the proportion of CD133-positive HCC cells but not CD90, and it also significantly lowers

Table 11 Hepatitis B virus-dysregulated microRNAs that play different roles in hepatitis B virus-associated hepatocellular carcinoma

Process	HBV-dysregulated miRNAs
Tumor stemness	miR-124[157], miR-200a/200b/429[165], miR-203[58], miR-325-3p[201], miR-3682-3p[66], miR-5188[67]
Metabolic reprogramming	miR-30b-5p[119], miR-200[165], miR-205[141,206], miR-384[61], miR-429[205]
Anti-tumor immunity	miR-23a[103], miR-34a[209], miR-138[208], miR-146a[187], miR-152[210], miR-200[165,166]
Drug resistance	miR-7[213], miR-21[213], miR-103[213], miR-107[213], miR-135a-5p[212], miR-5188[67], miR-15a/16[173], miR-193b[57], miR-203a[58], miR-325-3p[201,202], miR-329[214], miR-1236[214]

HBV: Hepatitis B virus; miRNAs: MicroRNAs.

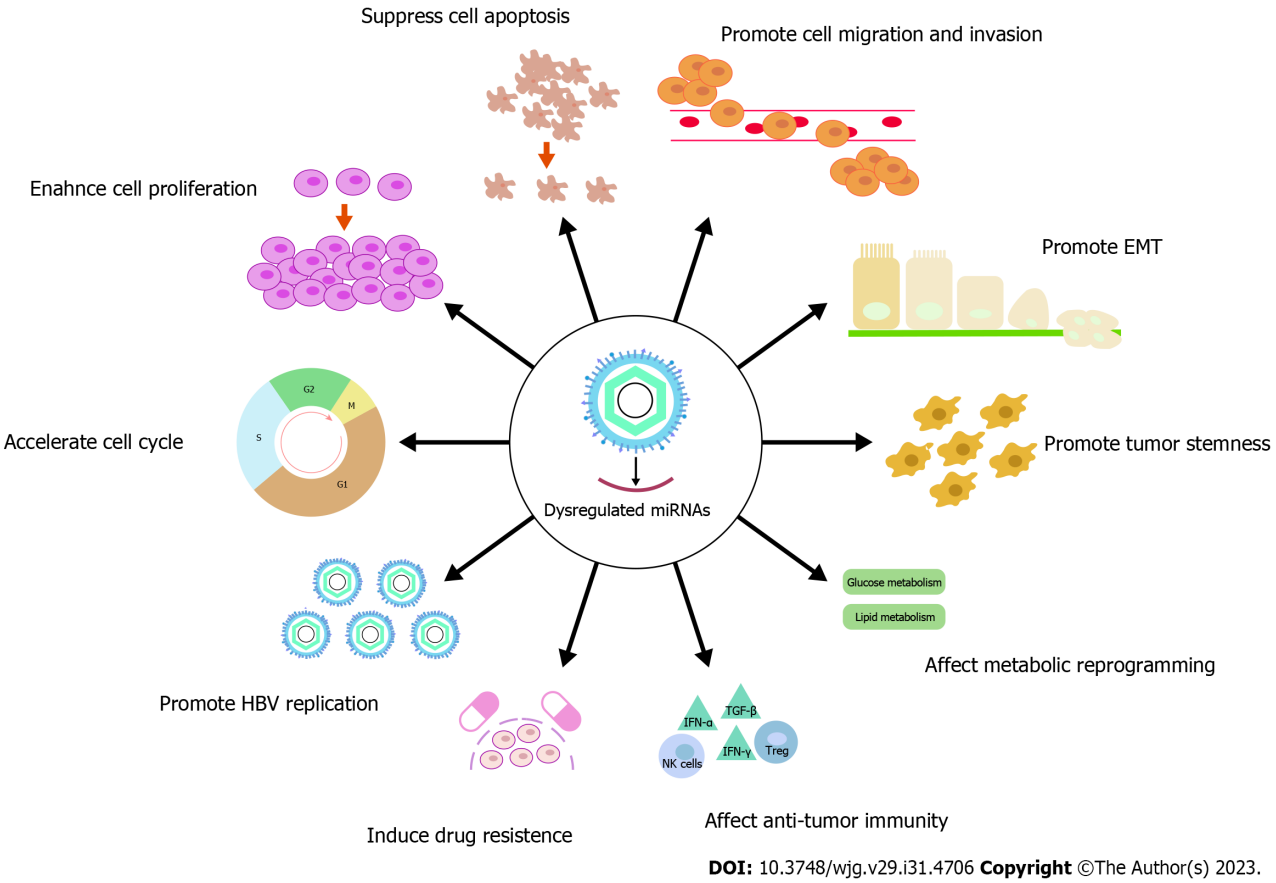


Figure 3 Mechanisms of hepatitis B virus dysregulated microRNAs in promoting hepatocellular carcinoma. miRNAs: MicroRNAs; HBV: Hepatitis B virus; EMT: Epithelial-mesenchymal transition.

the average percentage of ALDH-positive malignant stem cells. Therefore, HBV infection may promote the stemness of HCC *via* regulating miR-203a[58]. HBV also inhibits miR-325-3p[201], which suppresses the expression of critical stemness markers, including SOX-2, Nestin, Notch-1, OCT4, and Nanog. miR-325-3p/DPAGT1 may presumably have a role in HBV-induced HCC stemness[202]. In addition, miR-3682-3p mediates the oncogenic consequences of HBx-induced PI3K/AKT/c-Myc signaling. HBx increases stemness by elevating miR-3682-3p expression[66]. Meanwhile, miR-5188 directly targets FOXO1, which inhibits the nuclear translocation of β-catenin and promotes Wnt signaling activation and downstream tumor stemness. HBx modulates the miR-5188/FOXO1/β-catenin/c-Jun feedback loop to drive Wnt/β-catenin activation, subsequently promoting HCC stemness[67].

Dysregulated miRNAs affect metabolic reprogramming

Metabolic reprogramming plays a crucial role in the initiation and progression of cancer. A few studies have revealed that HBV affects the process of HCC by regulating metabolism (Table 11). Aerobic glycolysis is a distinguishing feature of HCC and is responsible for regulating proliferation, immune evasion, invasion, metastasis, and drug resistance in HCC [203]. The miR-30b-5p/MINPP1 axis is capable of accelerating the conversion of glucose to lactate and 2,3-bisphosphoglycerate (2,3-BPG), as well as regulating the glycolytic bypass to generate more 2-PG for energy supplementation. HBV

protein P (HBp) regulates the miR-30b-5p/MINPP1 axis, contributing to the development of HBV-positive HCC cells *via* glycolytic bypass[119]. RICTOR regulates glutamine metabolism *via* mTOR signaling[165]. HBx stimulates the translocation and secretion of HMGB1[166], which regulates RICTOR expression in HCC by binding competitively to the miR-200 family. Therefore, HBx may affect miR-200 to dysregulate glutamine metabolism. As for lipid metabolism, changes in fatty acid synthesis, β-oxidation, and cellular lipidic composition contribute to hepatocarcinogenesis[204]. HBx inhibits miR-384 and upregulates its target PTN expression, while PTN promotes hepatoma cell lipogenesis[61]. Knockdown of Rab18b decreases the lipogenesis. HBx activates Rab18 through downregulating miR-429. Therefore, HBx could enhance hepatocarcinogenesis by leading to the dysregulation of lipogenesis *via* the miR-429/Rab18 axis[205]. Meanwhile, HBx inhibits miR-205 expression[141], and miR-205 inhibits lipogenesis in hepatoma cells dependent on ACSL1, suggesting that HBx inhibits miR-205 to promote lipogenesis[206].

Dysregulated miRNAs affect anti-tumor immunity

It is widely acknowledged that HBV causes chronic liver damage through aberrant immunological reactions. During chronic HBV infection in humans, adaptive immunity transitions may be immune pathogenic factors for the development of HCC[207]. A number of research have revealed the function of miRNAs in HBV-induced immunological dysregulation (Table 11). HBV infection increases the expression of miR-146a, which impairs the IFN-induced anti-HBV immune response. Additionally, inhibition of miR-146a improves IFN-α-mediated anti-HBV efficacy[187]. In HBV-HCC patients, miR-138 is significantly higher than in asymptomatic carriers. By targeting the 3'-UTR region of PD-1, miR-138 alters its expression directly. miR-138 exerts its regulatory effects on T-cell cytokine production by suppressing PD-1 expression [208].

HBV also represses some miRNAs to affect anti-tumor immunity. One study finds that HBV-elevated CCL22 induction is mediated by transcriptionally repressing miR-23a. It is hypothesized that the axis of p65/miR-23a/CCL22 is present in the HCC cells and may drive tumor progression by recruiting Tregs, particularly when HBV infection was involved[103]. In HBV-expressing HepG2.215 cells, miR-34a is downregulated, while suppressed miR-34a leads to enhanced production of chemokine CCL22, which recruits Tregs to facilitate immune escape[209]. In addition, HLA-G, which inhibits different kinds of immune cells directly, such as NK, is downregulated by miR-152 in hepatoma cells. HBV inhibits miR-152 and increases the expression of its target HLA-G, which may further suppress NK against cancer cells[210]. Additionally, mRNAs of HMGB1 regulated by HBV and RICTOR regulated by HMGB1 mediated by miR-200[166] inhibit the response to anti-PD-L1 immunotherapy in HCC by elevating PD-L1+ exosomes[165].

Dysregulated miRNAs promote tumor drug resistance

Chemoresistance, resulting in cancer relapse and spread, is frequently mentioned as the largest cause of cancer therapeutic failure. In HCC, HBV commonly drives chemoresistance[211]. Accumulating evidence implicates the role of miRNAs in HBV-driven chemoresistance of HCC (Table 11).

HBc upregulates miR-135a-5p to suppress VAMP2 expression, blocking doxorubicin hydrochloride-induced apoptosis in HCC[212]. Similarly, HBV-upregulated miR-5188 Leads to an increase in resistance to the chemotherapy drugs 5-FU, cisplatin, and pharmorubicin[67]. Meanwhile, it is inferred that HBx elevates miR-7, -103, -107, and -21 expression to downregulate their target mapsin. Silencing maspin boosts HCC resistance to doxorubicin and other chemotherapeutic drugs[213]. These miRNAs may contribute to HBV-induced resistance to chemotherapy.

For some anti-tumor miRNAs, HBV suppresses their expression to promote HCC drug resistance. HBV mRNA can directly sponge miR-15a/16 and inhibit the subsequent cascade of etoposide-induced apoptosis in hepatoma cells[173]. miR-193b is downregulated in HBV-positive cells and tissues. Recent research shows that it increases the sensitivity of HCC cells to sorafenib by suppressing the expression of the anti-apoptotic protein Mcl-1[57]. miR-203a reduces HCC cell viability after 5-fluorouracil (5-FU) treatment and also increases the apoptosis rate of HCC cells in response to 5-FU[58]. HBV suppresses miR-203a expression, and subsequently renders HCC cells resistant to chemotherapy drug-induced apoptosis. HBV inhibits miR-325-3p[201], which remarkably increases chemosensitivity to doxorubicin in HCC cells[202]. Similarly, HBV negatively regulates miR-329 and miR-1236 to elevate their target AFP expression, while AFP further attenuates the proapoptotic effect of chemotherapy agents cisplatinum[214].

At present, the research on HBV-dysregulated miRNAs to enhance drug resistance in HCC is in its infancy. It has been discovered that miRNA promotes tumor treatment resistance through targeted regulation of multiple drug-related genes and DNA damage repair-related genes[215]. Therefore, more in-depth studies are needed.

Dysregulated miRNAs promote HBV replication to perpetuate its infection

The majority of HBV-infected patients have strong viral replication. By promoting self-replication, HBV maintains a high titer and promotes hepatocarcinogenesis. The complex relationship between HBV replication and miRNA has been described in a number of reviews[53,199,216]. We have enumerated the currently known miRNAs dysregulated by HBV that regulate HBV replication in the Supplementary Tables 1 and 2. Intriguingly, HBx upregulates miR-125a-5p expression[217], which interferes with expression of HBV surface antigen[218]. HBV may modulate miRNAs to restrict self-replication, therefore maintaining a long period of existence.

Others

DNA hypermethylation is responsible for suppressing TSGs in hepatocarcinogenesis. The inhibition of miR-101 by HBx leads to an increase in DNMT3A expression, while miR-101 inhibition or overexpression drastically affects the mRNA expression of different TSGs, demonstrating that miR-101 operates upstream to enhance TSG expression[219].

During the process of metastasis, cancer cells detaching from extracellular matrix (ECM) acquire the ability to persist in circulation by evading anoikis-induced cell death[220]. It is found that HBx induces miR-7, -103, -107, and -21 to suppress maspin expression, while maspin downregulation conferes HBx-mediated anoikis resistance in HCC cells[213]. Therefore, it can be speculated that these miRNAs may similarly confer HBx-mediated anoikis resistance.

In addition to directly affecting tumor cells, miRNA can indirectly accelerate the development of HCC *via* acting on other liver cells. Exosomal miR-142-3p from HBV-positive cells induces ferroptosis in HBV-infected M1-type macrophages *via* SLC3A2[221]. Similarly, exosomal miR-222 from HBV-infected hepatic cells boosts LX-2 cell activation by suppressing TFRC-induced ferroptosis, which ultimately exacerbates liver fibrosis[222]. Besides that, HBx-elevated P4HA2 enhances the collagen deposition in the liver *in vivo* and *in vitro* by inhibiting miR-30e, leading to liver fibrosis and liver cancer progression[139]. Moreover, HBx and TGF-β1 exposure induces the upregulation of miR-199a-3p, which contributes to the malignant transformation of hepatic progenitor cells (HPCs)[120]. As HPCs have the capacity to generate HCC with the cooperation of HBx and AFB1 in the liver microenvironment, this may provide new insight of HBV promoting HCC[223].

FUTURE PROSPECTS - CHALLENGES AND POTENTIAL CLINICAL USE OF MIRNAS IN DIAGNOSIS AND TREATMENT OF HBV-HCC

Due to the significant changes of miRNA in bodily fluid and tissues of HBV-HCC, its utility as a biomarker for the diagnosis of HCC incidence and prognostic risk has been extensively evaluated. However, since the PLR of miRNAs diagnosing HBV-HCC is less than 10 and the NLR is greater than 0.1[41,42], the clinical use of miRNAs for detecting HBV-HCC may still be limited. Traditional techniques for detecting miRNAs include Northern blotting, quantitative reverse transcription polymerase chain reaction (qRT-PCR), next-generation sequencing, and microarray-based hybridization[7,224]. However, quantifying miRNA in a dependable and robust manner can be challenging, and these methods may involve significant trade-offs between cost, complexity, and efficacy[7,224]. Therefore, using standardized measurements with unified standards will facilitate the collection of trustworthy miRNA data that can be compared across institutions[7]. It is crucial to minimize the influence of confounding factors, such as measurement technical characteristics, when detecting miRNA. Additionally, novel miRNA detection assays, such as miRacles which utilize conformationally responsive DNA nanoswitches, have been proved to be a simple, inexpensive, and accurate method for detecting miRNAs[224]. With the continuous development of new materials, it is anticipated that the miRNAs detection technology will increase in precision and sensitivity while decreasing in cost and operational complexity.

In addition to their use as diagnostics, miRNAs have significant promise for prognostication. Current relevant research has focused on miRNAs to predict the risk of recurrence, OS, and DFS in patients with HBV-HCC. There are few studies and insufficient data on circulating miRNAs. As circulating miRNAs offer numerous advantages, such as being convenient, safe, and noninvasive, their potential as biomarkers can be exploited further. For instance, miRNAs can be used to predict or evaluate the efficacy of neoadjuvant chemotherapy[225], radiotherapy[226], and immunotherapy[227] in cancer patients. Hence, miRNAs have the potential to anticipate therapeutic efficacy in HBV-HCC, which warrants further investigation.

Since HBV-dysregulated miRNAs play a significant role in hepatocarcinogenesis, miRNAs can be used as viable alternative therapeutic targets. Despite the fact that miRNA delivery to specific locations is hampered by many challenges, several techniques, such as conjugation, virus-associated delivery, and nanoparticles, have been researched to improve the efficacy of miRNA delivery[8]. In fact, multiple miRNA-based therapeutics have entered the clinical phase of cancer therapy. The combination of miRNAs therapy with chemotherapy, radiotherapy, and immunotherapy has shown encouraging outcomes against different malignancies[215]. Unfortunately, there is no relevant clinical research on the use of miRNAs in the treatment of HCC. Given that miRNAs play a crucial part in the occurrence and progression of HBV-HCC, the approaches of combining diverse strategies, applying complementary miRNAs together, or inventing new forms of miRNAs may bring considerable clinical benefits for HBV-HCC patients. To reach the ultimate objective of enhancing patient OS and DFS, additional research is required in this area.

CONCLUSION

HBV dysregulates miRNAs in multiple ways, thereby contributing to the occurrence and progression of HCC. Consequently, miRNAs are anticipated to become HBV-HCC biomarkers for diagnosis and prognosis. miRNAs-based therapies may also improve the efficacy of HBV-HCC. More research is required for miRNA clinical transformation.

FOOTNOTES

Author contributions: Zhang MH gathered the pertinent literature, drafted the initial manuscript, and conceptualized the tables and figures; Yuan YF, Liu LJ, Wei YX, Yin WY, Zheng LZY, Tang YY, Lv Z, and Zhu F conceptualized the text's structure and revised it for significant intellectual content; all authors have viewed and approved the final manuscript version.

Supported by the Translational Medicine and Interdisciplinary Research Joint Fund of Zhongnan Hospital of Wuhan University, No.

ZNLH201902.

Conflict-of-interest statement: Authors declare no conflict of interests for this article.

Open-Access: This article is an open-access article that was selected by an in-house editor and fully peer-reviewed by external reviewers. It is distributed in accordance with the Creative Commons Attribution NonCommercial (CC BY-NC 4.0) license, which permits others to distribute, remix, adapt, build upon this work non-commercially, and license their derivative works on different terms, provided the original work is properly cited and the use is non-commercial. See: https://creativecommons.org/Licenses/by-nc/4.0/

Country/Territory of origin: China

ORCID number: Ming-He Zhang 0009-0000-4161-2204; Yu-Feng Yuan 0000-0003-3924-3803; Li-Juan Liu 0000-0002-2549-5463; Yu-Xin Wei 0009-0005-7930-2662; Wan-Yue Yin 0009-0004-6034-8014; Lan-Zhuo-Yin Zheng 0000-0002-0616-7990; Ying-Ying Tang 0009-0005-1122-2906; Zhao Lv 0009-0008-6499-213X; Fan Zhu 0000-0001-7031-2956.

S-Editor: Yan JP
L-Editor: A
P-Editor: Zhao S

REFERENCES

1 **Sung H**, Ferlay J, Siegel RL, Laversanne M, Soerjomataram I, Jemal A, Bray F. Global Cancer Statistics 2020: GLOBOCAN Estimates of Incidence and Mortality Worldwide for 36 Cancers in 185 Countries. *CA Cancer J Clin* 2021; **71**: 209-249 [PMID: 33538338 DOI: 10.3322/caac.21660]
2 **World Health Organization**. Global hepatitis report 2017. Geneva: World Health Organization; 2017
3 **Piñero F**, Dirchwolf M, Pessôa MG. Biomarkers in Hepatocellular Carcinoma: Diagnosis, Prognosis and Treatment Response Assessment. *Cells* 2020; **9** [PMID: 32492896 DOI: 10.3390/cells9061370]
4 **Johnson P**, Zhou Q, Dao DY, Lo YMD. Circulating biomarkers in the diagnosis and management of hepatocellular carcinoma. *Nat Rev Gastroenterol Hepatol* 2022; **19**: 670-681 [PMID: 35676420 DOI: 10.1038/s41575-022-00620-y]
5 **Ha M**, Kim VN. Regulation of microRNA biogenesis. *Nat Rev Mol Cell Biol* 2014; **15**: 509-524 [PMID: 25027649 DOI: 10.1038/nrm3838]
6 **Sartorius K**, Makarova J, Sartorius B, An P, Winkler C, Chuturgoon A, Kramvis A. The Regulatory Role of MicroRNA in Hepatitis-B Virus-Associated Hepatocellular Carcinoma (HBV-HCC) Pathogenesis. *Cells* 2019; **8** [PMID: 31771261 DOI: 10.3390/cells8121504]
7 **Valihrach L**, Androvic P, Kubista M. Circulating miRNA analysis for cancer diagnostics and therapy. *Mol Aspects Med* 2020; **72**: 100825 [PMID: 31635843 DOI: 10.1016/j.mam.2019.10.002]
8 **Ho PTB**, Clark IM, Le LTT. MicroRNA-Based Diagnosis and Therapy. *Int J Mol Sci* 2022; **23** [PMID: 35806173 DOI: 10.3390/ijms23137167]
9 **Liu AM**, Yao TJ, Wang W, Wong KF, Lee NP, Fan ST, Poon RT, Gao C, Luk JM. Circulating miR-15b and miR-130b in serum as potential markers for detecting hepatocellular carcinoma: a retrospective cohort study. *BMJ Open* 2012; **2**: e000825 [PMID: 22403344 DOI: 10.1136/bmjopen-2012-000825]
10 **Qi P**, Cheng SQ, Wang H, Li N, Chen YF, Gao CF. Serum microRNAs as biomarkers for hepatocellular carcinoma in Chinese patients with chronic hepatitis B virus infection. *PLoS One* 2011; **6**: e28486 [PMID: 22174818 DOI: 10.1371/journal.pone.0028486]
11 **Lin L**, Lu B, Yu J, Liu W, Zhou A. Serum miR-224 as a biomarker for detection of hepatocellular carcinoma at early stage. *Clin Res Hepatol Gastroenterol* 2016; **40**: 397-404 [PMID: 26724963 DOI: 10.1016/j.clinre.2015.11.005]
12 **Zhao Q**, Li T, Qi J, Liu J, Qin C. The miR-545/374a cluster encoded in the Ftx lncRNA is overexpressed in HBV-related hepatocellular carcinoma and promotes tumorigenesis and tumor progression. *PLoS One* 2014; **9**: e109782 [PMID: 25299640 DOI: 10.1371/journal.pone.0109782]
13 **Yu F**, Lu Z, Chen B, Dong P, Zheng J. microRNA-150: a promising novel biomarker for hepatitis B virus-related hepatocellular carcinoma. *Diagn Pathol* 2015; **10**: 129 [PMID: 26215970 DOI: 10.1186/s13000-015-0369-y]
14 **Mandrekar JN**. Receiver operating characteristic curve in diagnostic test assessment. *J Thorac Oncol* 2010; **5**: 1315-1316 [PMID: 20736804 DOI: 10.1097/JTO.0b013e3181ec173d]
15 **Zhou G**, Zeng Y, Luo Y, Guo S, Bao L, Zhang Q. Urine miR-93-5p is a promising biomarker for early detection of HBV-related hepatocellular carcinoma. *Eur J Surg Oncol* 2022; **48**: 95-102 [PMID: 34175168 DOI: 10.1016/j.ejso.2021.06.015]
16 **Quoc NB**, Phuong NDN, Ngan TK, Linh NTM, Cuong PH, Chau NNB. Expression of Plasma hsa-miR122 in HBV-Related Hepatocellular Carcinoma (HCC) in Vietnamese Patients. *Microrna* 2018; **7**: 92-99 [PMID: 29701140 DOI: 10.2174/2211536607666180427165114]
17 **Xu L**, Wei B, Hui H, Liu Y. Association of serum microRNA-125b and HBV-related hepatocellular carcinoma in Chinese Han patients. *Int J Clin Exp Med* 2018; **11**: 3699-3703
18 **Li X**, Guo Y, Wang X, Ge A, Wang H, Fan K, Guo C. Clinical significance of serum miR-487b in HBV-related hepatocellular carcinoma and its potential mechanism. *Infect Dis (Lond)* 2021; **53**: 546-554 [PMID: 33783293 DOI: 10.1080/23744235.2021.1901981]
19 **Cao X**, Yang Q, Yu Q. Increased Expression of miR-487b Is Associated With Poor Prognosis and Tumor Progression of HBV-Related Hepatocellular Carcinoma. *Open Forum Infect Dis* 2020; **7**: ofaa498 [PMID: 33364257 DOI: 10.1093/ofid/ofaa498]
20 **Cao C**, Wang C. Clinical significance of serum miR-768-3p in HBV-related hepatocellular carcinoma and its potential mechanism. *Clin Exp Med* 2020; **20**: 569-576 [PMID: 32712720 DOI: 10.1007/s10238-020-00646-z]
21 **Moradi N**, Paryan M, Khansarinejad B, Sarmadian H, Mondanizadeh M. Plasma Level of miR-5193 As a Novel Biomarker for Diagnosis of HBV-Related Hepatocellular Carcinoma. *Hepat Mon* 2019; In Press [DOI: 10.5812/hepatmon.84455]
22 **Tat Trung N**, Duong DC, Tong HV, Hien TTT, Hoan PQ, Bang MH, Binh MT, Ky TD, Tung NL, Thinh NT, Sang VV, Thao LTP, Bock CT,

Velavan TP, Meyer CG, Song LH, Toan NL. Optimisation of quantitative miRNA panels to consolidate the diagnostic surveillance of HBV-related hepatocellular carcinoma. *PLoS One* 2018; **13**: e0196081 [PMID: 29672637 DOI: 10.1371/journal.pone.0196081]

23 **Chen S**, Chen H, Gao S, Qiu S, Zhou H, Yu M, Tu J. Differential expression of plasma microRNA-125b in hepatitis B virus-related liver diseases and diagnostic potential for hepatitis B virus-induced hepatocellular carcinoma. *Hepatol Res* 2017; **47**: 312-320 [PMID: 27152955 DOI: 10.1111/hepr.12739]

24 **Xie Y**, Yao Q, Butt AM, Guo J, Tian Z, Bao X, Li H, Meng Q, Lu J. Expression profiling of serum microRNA-101 in HBV-associated chronic hepatitis, liver cirrhosis, and hepatocellular carcinoma. *Cancer Biol Ther* 2014; **15**: 1248-1255 [PMID: 24971953 DOI: 10.4161/cbt.29688]

25 **Mjelle R**, Dima SO, Bacalbasa N, Chawla K, Sorop A, Cucu D, Herlea V, Sætrom P, Popescu I. Comprehensive transcriptomic analyses of tissue, serum, and serum exosomes from hepatocellular carcinoma patients. *BMC Cancer* 2019; **19**: 1007 [PMID: 31660891 DOI: 10.1186/s12885-019-6249-1]

26 **Xia G**, Xie Y, He Q. Hepatitis B Virus Affected Serum MicroRNA-203a Level in Hepatocellular Carcinoma. *Clin Lab* 2021; **67** [PMID: 33739050 DOI: 10.7754/Clin.Lab.2020.200748]

27 **Bai PS**, Hou P, Kong Y. Hepatitis B virus promotes proliferation and metastasis in male Chinese hepatocellular carcinoma patients through the LEF-1/miR-371a-5p/SRCIN1/pleiotrophin/Slug pathway. *Exp Cell Res* 2018; **370**: 174-188 [PMID: 29928866 DOI: 10.1016/j.yexcr.2018.06.020]

28 **Zhou SJ**, Deng YL, Liang HF, Jaoude JC, Liu FY. Hepatitis B virus X protein promotes CREB-mediated activation of miR-3188 and Notch signaling in hepatocellular carcinoma. *Cell Death Differ* 2017; **24**: 1577-1587 [PMID: 28574502 DOI: 10.1038/cdd.2017.87]

29 **Riazalhosseini B**, Mohamed R, Apalasamy YD, Langmia IM, Mohamed Z. Circulating microRNA as a marker for predicting liver disease progression in patients with chronic hepatitis B. *Rev Soc Bras Med Trop* 2017; **50**: 161-166 [PMID: 28562750 DOI: 10.1590/0037-8682-0416-2016]

30 **Zuo D**, Chen L, Liu X, Wang X, Xi Q, Luo Y, Zhang N, Guo H. Combination of miR-125b and miR-27a enhances sensitivity and specificity of AFP-based diagnosis of hepatocellular carcinoma. *Tumour Biol* 2016; **37**: 6539-6549 [PMID: 26637228 DOI: 10.1007/s13277-015-4545-1]

31 **Li LM**, Hu ZB, Zhou ZX, Chen X, Liu FY, Zhang JF, Shen HB, Zhang CY, Zen K. Serum microRNA profiles serve as novel biomarkers for HBV infection and diagnosis of HBV-positive hepatocarcinoma. *Cancer Res* 2010; **70**: 9798-9807 [PMID: 21098710 DOI: 10.1158/0008-5472.CAN-10-1001]

32 **Ghosh A**, Ghosh A, Datta S, Dasgupta D, Das S, Ray S, Gupta S, Chowdhury A, Chatterjee R, Mohapatra SK, Banerjee S. Hepatic miR-126 is a potential plasma biomarker for detection of hepatitis B virus infected hepatocellular carcinoma. *Int J Cancer* 2016; **138**: 2732-2744 [PMID: 26756996 DOI: 10.1002/ijc.29999]

33 **Meng FL**, Wang W, Jia WD. Diagnostic and prognostic significance of serum miR-24-3p in HBV-related hepatocellular carcinoma. *Med Oncol* 2014; **31**: 177 [PMID: 25129312 DOI: 10.1007/s12032-014-0177-3]

34 **Chen Y**, Dong X, Yu D, Wang X. Serum miR-96 is a promising biomarker for hepatocellular carcinoma in patients with chronic hepatitis B virus infection. *Int J Clin Exp Med* 2015; **8**: 18462-18468 [PMID: 26770453]

35 **Trung NT**, Hoan NX, Trung PQ, Binh MT, Van Tong H, Toan NL, Bang MH, Song LH. Clinical significance of combined circulating TERT promoter mutations and miR-122 expression for screening HBV-related hepatocellular carcinoma. *Sci Rep* 2020; **10**: 8181 [PMID: 32424223 DOI: 10.1038/s41598-020-65213-8]

36 **Chen SS**, Chen H, Gao SS, Zhou H, Qiu SL, Yu MX, Tu JC. Differential expression of plasma miR-205 in HBV-related liver diseases and diagnostic potential for HBV-induced hepatocellular carcinoma. *Wuhan Daxue Xuebao (Yixueban)* 2016; **37**: 445-450

37 **Caviglia GP**, Abate ML, Gaia S, Petrini E, Bosco C, Olivero A, Rosso C, Ciancio A, Pellicano R, Saracco GM, Rizzetto M, Smedile A. Risk of hepatocellular carcinoma in HBV cirrhotic patients assessed by the combination of miR-122, AFP and PIVKA-II. *Panminerva Med* 2017; **59**: 283-289 [PMID: 28650134 DOI: 10.23736/S0031-0808.17.03353-5]

38 **Tan Y**, Ge G, Pan T, Wen D, Chen L, Yu X, Zhou X, Gan J. A serum microRNA panel as potential biomarkers for hepatocellular carcinoma related with hepatitis B virus. *PLoS One* 2014; **9**: e107986 [PMID: 25238238 DOI: 10.1371/journal.pone.0107986]

39 **Luo P**, Wu S, Yu Y, Ming X, Li S, Zuo X, Tu J. Current Status and Perspective Biomarkers in AFP Negative HCC: Towards Screening for and Diagnosing Hepatocellular Carcinoma at an Earlier Stage. *Pathol Oncol Res* 2020; **26**: 599-603 [PMID: 30661224 DOI: 10.1007/s12253-019-00585-5]

40 **Peng C**, Li Z, Xie Z, Wang Z, Ye Y, Li B, Li W. The role of circulating microRNAs for the diagnosis of hepatitis B virus-associated hepatocellular carcinoma with low alpha-fetoprotein level: a systematic review and meta-analysis. *BMC Gastroenterol* 2020; **20**: 249 [PMID: 32736604 DOI: 10.1186/s12876-020-01345-5]

41 **Zhang WT**, Gil-Gómez A, Liu CH, Gao SS, Romero-Gómez M. Diagnostic accuracy of circulating microRNA in hepatitis B virus-related hepatocellular carcinoma: a meta-analysis based on Asian data. *Rev Esp Enferm Dig* 2022; **114**: 280-288 [PMID: 34423645 DOI: 10.17235/reed.2021.8139/2021]

42 **Jin X**, Cai C, Qiu Y. Diagnostic Value of Circulating microRNAs in Hepatitis B Virus-Related Hepatocellular Carcinoma: A Systematic Review and Meta-Analysis. *J Cancer* 2019; **10**: 4754-4764 [PMID: 31598147 DOI: 10.7150/jca.32833]

43 **Shi J**, Liu J, Tu X, Li B, Tong Z, Wang T, Zheng Y, Shi H, Zeng X, Chen W, Yin W, Fang W. Single-cell immune signature for detecting early-stage HCC and early assessing anti-PD-1 immunotherapy efficacy. *J Immunother Cancer* 2022; **10** [PMID: 35101942 DOI: 10.1136/jitc-2021-003133]

44 **Zhou J**, Yu L, Gao X, Hu J, Wang J, Dai Z, Wang JF, Zhang Z, Lu S, Huang X, Wang Z, Qiu S, Wang X, Yang G, Sun H, Tang Z, Wu Y, Zhu H, Fan J. Plasma microRNA panel to diagnose hepatitis B virus-related hepatocellular carcinoma. *J Clin Oncol* 2011; **29**: 4781-4788 [PMID: 22105822 DOI: 10.1200/JCO.2011.38.2697]

45 **Sanz-Rubio D**, Martin-Burriel I, Gil A, Cubero P, Forner M, Khalyfa A, Marin JM. Stability of Circulating Exosomal miRNAs in Healthy Subjects. *Sci Rep* 2018; **8**: 10306 [PMID: 29985466 DOI: 10.1038/s41598-018-28748-5]

46 **Karamichali E**, Foka P, Papadopoulou G, Loukaki-Gkountara D, Andresaki K, Koskinas I, Georgopoulou U. Hepatitis Viruses Control Host Immune Responses by Modifying the Exosomal Biogenesis Pathway and Cargo. *Int J Mol Sci* 2022; **23** [PMID: 36142773 DOI: 10.3390/ijms231810862]

47 **Liu Z**, Li Y, Wang Y, Bai X, Zhang Y. Exosomes in HBV infection. *Clin Chim Acta* 2023; **538**: 65-69 [PMID: 36375524 DOI: 10.1016/j.cca.2022.11.012]

48 **Li S**, Li S, Wu S, Chen L. Exosomes Modulate the Viral Replication and Host Immune Responses in HBV Infection. *Biomed Res Int* 2019; **2019**: 2103943 [PMID: 31275965 DOI: 10.1155/2019/2103943]

49 **Ghosh S**, Bhowmik S, Majumdar S, Goswami A, Chakraborty J, Gupta S, Aggarwal S, Ray S, Chatterjee R, Bhattacharyya S, Dutta M, Datta

S, Chowdhury A, Dhali GK, Banerjee S. The exosome encapsulated microRNAs as circulating diagnostic marker for hepatocellular carcinoma with low alpha-fetoprotein. *Int J Cancer* 2020; **147**: 2934-2947 [PMID: 32441313 DOI: 10.1002/ijc.33111]

50 **Wei XC**, Liu LJ, Zhu F. Exosomes as potential diagnosis and treatment for liver cancer. *World J Gastrointest Oncol* 2022; **14**: 334-347 [PMID: 35116120 DOI: 10.4251/wjgo.v14.i1.334]

51 **Pandyarajan V**, Govalan R, Yang JD. Risk Factors and Biomarkers for Chronic Hepatitis B Associated Hepatocellular Carcinoma. *Int J Mol Sci* 2021; **22** [PMID: 33418899 DOI: 10.3390/ijms22020479]

52 **Bandopadhyay M**, Bharadwaj M. Exosomal miRNAs in hepatitis B virus related liver disease: a new hope for biomarker. *Gut Pathog* 2020; **12**: 23 [PMID: 32346400 DOI: 10.1186/s13099-020-00353-w]

53 **Xu J**, An P, Winkler CA, Yu Y. Dysregulated microRNAs in Hepatitis B Virus-Related Hepatocellular Carcinoma: Potential as Biomarkers and Therapeutic Targets. *Front Oncol* 2020; **10**: 1271 [PMID: 32850386 DOI: 10.3389/fonc.2020.01271]

54 **Yuan LT**, Lee WJ, Yang YC, Chen BR, Yang CY, Chen MW, Chen JQ, Hsiao M, Chien MH, Hua KT. Histone Methyltransferase G9a-Promoted Progression of Hepatocellular Carcinoma Is Targeted by Liver-Specific Hsa-miR-122. *Cancers (Basel)* 2021; **13** [PMID: 34069116 DOI: 10.3390/cancers13102376]

55 **Zhang Q**, Xu HF, Song WY, Zhang PJ, Song YB. Potential microRNA panel for the diagnosis and prediction of overall survival of hepatocellular carcinoma with hepatitis B virus infection. *World J Gastrointest Oncol* 2020; **12**: 383-393 [PMID: 32368317 DOI: 10.4251/wjgo.v12.i4.383]

56 **Dundar HZ**, Aksoy F, Aksoy SA, Tasar P, Ugras N, Tunca B, Egeli U, Cecener G, Yerci O, Kaya E. Overexpression of miR-21 Is Associated With Recurrence in Patients With Hepatitis B Virus-Mediated Hepatocellular Carcinoma Undergoing Liver Transplantation. *Transplant Proc* 2019; **51**: 1157-1161 [PMID: 31101191 DOI: 10.1016/j.transproceed.2019.01.089]

57 **Mao K**, Zhang J, He C, Xu K, Liu J, Sun J, Wu G, Tan C, Zeng Y, Wang J, Xiao Z. Restoration of miR-193b sensitizes Hepatitis B virus-associated hepatocellular carcinoma to sorafenib. *Cancer Lett* 2014; **352**: 245-252 [PMID: 25034398 DOI: 10.1016/j.canlet.2014.07.004]

58 **Qin YF**, Zhou ZY, Fu HW, Lin HM, Xu LB, Wu WR, Liu C, Xu XL, Zhang R. Hepatitis B Virus Surface Antigen Promotes Stemness of Hepatocellular Carcinoma through Regulating MicroRNA-203a. *J Clin Transl Hepatol* 2023; **11**: 118-129 [PMID: 36406317 DOI: 10.14218/JCTH.2021.00373]

59 **Liu FY**, Zhou SJ, Deng YL, Zhang ZY, Zhang EL, Wu ZB, Huang ZY, Chen XP. MiR-216b is involved in pathogenesis and progression of hepatocellular carcinoma through HBx-miR-216b-IGF2BP2 signaling pathway. *Cell Death Dis* 2015; **6**: e1670 [PMID: 25741595 DOI: 10.1038/cddis.2015.46]

60 **Zhou N**, Wu J, Wang X, Sun Z, Han Q, Zhao L. Low-level expression of microRNA-375 predicts poor prognosis in hepatocellular carcinoma. *Tumour Biol* 2016; **37**: 2145-2152 [PMID: 26349912 DOI: 10.1007/s13277-015-3841-0]

61 **Bai PS**, Xia N, Sun H, Kong Y. Pleiotrophin, a target of miR-384, promotes proliferation, metastasis and lipogenesis in HBV-related hepatocellular carcinoma. *J Cell Mol Med* 2017; **21**: 3023-3043 [PMID: 28557334 DOI: 10.1111/jcmm.13213]

62 **Zhen Y**, Xinghui Z, Chao W, Yi Z, Jinwen C, Ruifang G, Chao Z, Min Z, Chunlei G, Yan F, Lingfang D, Long S, Wenzhi S, Xiaohe L, Rong X. Several microRNAs could predict survival in patients with hepatitis B-related liver cancer. *Sci Rep* 2017; **7**: 45195 [PMID: 28322348 DOI: 10.1038/srep45195]

63 **Zhu HT**, Dong QZ, Sheng YY, Wei JW, Wang G, Zhou HJ, Ren N, Jia HL, Ye QH, Qin LX. MicroRNA-29a-5p is a novel predictor for early recurrence of hepatitis B virus-related hepatocellular carcinoma after surgical resection. *PLoS One* 2012; **7**: e52393 [PMID: 23285022 DOI: 10.1371/journal.pone.0052393]

64 **Yen CS**, Su ZR, Lee YP, Liu IT, Yen CJ. miR-106b promotes cancer progression in hepatitis B virus-associated hepatocellular carcinoma. *World J Gastroenterol* 2016; **22**: 5183-5192 [PMID: 27298561 DOI: 10.3748/wjg.v22.i22.5183]

65 **Dai X**, Huang R, Hu S, Zhou Y, Sun X, Gui P, Yu Z, Zhou P. A novel miR-0308-3p revealed by miRNA-seq of HBV-positive hepatocellular carcinoma suppresses cell proliferation and promotes G1/S arrest by targeting double CDK6/Cyclin D1 genes. *Cell Biosci* 2020; **10**: 24 [PMID: 32128112 DOI: 10.1186/s13578-020-00382-7]

66 **Chen Q**, Yang SB, Zhang YW, Han SY, Jia L, Li B, Zhang Y, Zuo S. miR-3682-3p directly targets FOXO3 and stimulates tumor stemness in hepatocellular carcinoma *via* a positive feedback loop involving FOXO3/PI3K/AKT/c-Myc. *World J Stem Cells* 2022; **14**: 539-555 [PMID: 36157524 DOI: 10.4252/wjsc.v14.i7.539]

67 **Lin X**, Zuo S, Luo R, Li Y, Yu G, Zou Y, Zhou Y, Liu Z, Liu Y, Hu Y, Xie Y, Fang W. HBX-induced miR-5188 impairs FOXO1 to stimulate β-catenin nuclear translocation and promotes tumor stemness in hepatocellular carcinoma. *Theranostics* 2019; **9**: 7583-7598 [PMID: 31695788 DOI: 10.7150/thno.37717]

68 **Pratedrat P**, Chuaypen N, Nimsamer P, Payungporn S, Pinjaroen N, Sirichindakul B, Tangkijvanich P. Diagnostic and prognostic roles of circulating miRNA-223-3p in hepatitis B virus-related hepatocellular carcinoma. *PLoS One* 2020; **15**: e0232211 [PMID: 32330203 DOI: 10.1371/journal.pone.0232211]

69 **Zhu HT**, Hasan AM, Liu RB, Zhang ZC, Zhang X, Wang J, Wang HY, Wang F, Shao JY. Serum microRNA profiles as prognostic biomarkers for HBV-positive hepatocellular carcinoma. *Oncotarget* 2016; **7**: 45637-45648 [PMID: 27317768 DOI: 10.18632/oncotarget.10082]

70 **Niu LJ**, Huang T, Wang L, Sun XF, Zhang YM. HBX suppresses PTEN to promote the malignant progression of hepatocellular carcinoma through mi-R155 activation. *Ann Hepatol* 2022; **27**: 100688 [PMID: 35196550 DOI: 10.1016/j.aohep.2022.100688]

71 **Wakasugi H**, Takahashi H, Niinuma T, Kitajima H, Oikawa R, Matsumoto N, Takeba Y, Otsubo T, Takagi M, Ariizumi Y, Suzuki M, Okuse C, Iwabuchi S, Nakano M, Akutsu N, Kang JH, Matsui T, Yamada N, Sasaki H, Yamamoto E, Kai M, Sasaki Y, Sasaki S, Tanaka Y, Yotsuyanagi H, Tsutsumi T, Yamamoto H, Tokino T, Nakase H, Suzuki H, Itoh F. Dysregulation of miRNA in chronic hepatitis B is associated with hepatocellular carcinoma risk after nucleos(t)ide analogue treatment. *Cancer Lett* 2018; **434**: 91-100 [PMID: 30026054 DOI: 10.1016/j.canlet.2018.07.019]

72 **Kim VN**. MicroRNA biogenesis: coordinated cropping and dicing. *Nat Rev Mol Cell Biol* 2005; **6**: 376-385 [PMID: 15852042 DOI: 10.1038/nrm1644]

73 **Li CL**, Yeh KH, Liu WH, Chen CL, Chen DS, Chen PJ, Yeh SH. Elevated p53 promotes the processing of miR-18a to decrease estrogen receptor-α in female hepatocellular carcinoma. *Int J Cancer* 2015; **136**: 761-770 [PMID: 24975878 DOI: 10.1002/ijc.29052]

74 **Kong XX**, Lv YR, Shao LP, Nong XY, Zhang GL, Zhang Y, Fan HX, Liu M, Li X, Tang H. HBx-induced MiR-1269b in NF-κB dependent manner upregulates cell division cycle 40 homolog (CDC40) to promote proliferation and migration in hepatoma cells. *J Transl Med* 2016; **14**: 189 [PMID: 27349221 DOI: 10.1186/s12967-016-0949-y]

75 **Chinnappan M**, Singh AK, Kakumani PK, Kumar G, Rooge SB, Kumari A, Varshney A, Rastogi A, Sarin SK, Malhotra P, Mukherjee SK, Bhatnagar RK. Key elements of the RNAi pathway are regulated by hepatitis B virus replication and HBx acts as a viral suppressor of RNA

silencing. *Biochem J* 2014; **462**: 347-358 [PMID: 24902849 DOI: 10.1042/BJ20140316]

76 **Liu AM**, Zhang C, Burchard J, Fan ST, Wong KF, Dai H, Poon RT, Luk JM. Global regulation on microRNA in hepatitis B virus-associated hepatocellular carcinoma. *OMICS* 2011; **15**: 187-191 [PMID: 21319996 DOI: 10.1089/omi.2010.0098]

77 **Kitagawa N**, Ojima H, Shirakihara T, Shimizu H, Kokubu A, Urushidate T, Totoki Y, Kosuge T, Miyagawa S, Shibata T. Downregulation of the microRNA biogenesis components and its association with poor prognosis in hepatocellular carcinoma. *Cancer Sci* 2013; **104**: 543-551 [PMID: 23398123 DOI: 10.1111/cas.12126]

78 **Ren M**, Qin D, Li K, Qu J, Wang L, Wang Z, Huang A, Tang H. Correlation between hepatitis B virus protein and microRNA processor Drosha in cells expressing HBV. *Antiviral Res* 2012; **94**: 225-231 [PMID: 22554933 DOI: 10.1016/j.antiviral.2012.04.004]

79 **Shan X**, Ren M, Chen K, Huang A, Tang H. Regulation of the microRNA processor DGCR8 by hepatitis B virus proteins *via* the transcription factor YY1. *Arch Virol* 2015; **160**: 795-803 [PMID: 25427980 DOI: 10.1007/s00705-014-2286-x]

80 **Li J**, Pu W, Sun HL, Zhou JK, Fan X, Zheng Y, He J, Liu X, Xia Z, Liu L, Wei YQ, Peng Y. Pin1 impairs microRNA biogenesis by mediating conformation change of XPO5 in hepatocellular carcinoma. *Cell Death Differ* 2018; **25**: 1612-1624 [PMID: 29445125 DOI: 10.1038/s41418-018-0065-z]

81 **Pang R**, Lee TK, Poon RT, Fan ST, Wong KB, Kwong YL, Tse E. Pin1 interacts with a specific serine-proline motif of hepatitis B virus X-protein to enhance hepatocarcinogenesis. *Gastroenterology* 2007; **132**: 1088-1103 [PMID: 17383430 DOI: 10.1053/j.gastro.2006.12.030]

82 **Förstemann K**, Horwich MD, Wee L, Tomari Y, Zamore PD. Drosophila microRNAs are sorted into functionally distinct argonaute complexes after production by dicer-1. *Cell* 2007; **130**: 287-297 [PMID: 17662943 DOI: 10.1016/j.cell.2007.05.056]

83 **Zhang J**, Jin H, Liu H, Lv S, Wang B, Wang R, Ding M, Yang Y, Li L, Zhang J, Fu S, Xie D, Wu M, Zhou W, Qian Q. MiRNA-99a directly regulates AGO2 through translational repression in hepatocellular carcinoma. *Oncogenesis* 2014; **3**: e97 [PMID: 24732044 DOI: 10.1038/oncsis.2014.11]

84 **Hayes CN**, Akamatsu S, Tsuge M, Miki D, Akiyama R, Abe H, Ochi H, Hiraga N, Imamura M, Takahashi S, Aikata H, Kawaoka T, Kawakami Y, Ohishi W, Chayama K. Hepatitis B virus-specific miRNAs and Argonaute2 play a role in the viral life cycle. *PLoS One* 2012; **7**: e47490 [PMID: 23091627 DOI: 10.1371/journal.pone.0047490]

85 **Chen W**, Bian H, Xie X, Yang X, Bi B, Li C, Zhang Y, Zhu Q, Song J, Qin C, Qi J. Negative feedback loop of ERK/CREB/miR-212-3p inhibits HBeAg-induced macrophage activation. *J Cell Mol Med* 2020; **24**: 10935-10945 [PMID: 32767729 DOI: 10.1111/jcmm.15723]

86 **Atsaves V**, Leventaki V, Rassidakis GZ, Claret FX. AP-1 Transcription Factors as Regulators of Immune Responses in Cancer. *Cancers (Basel)* 2019; **11** [PMID: 31340499 DOI: 10.3390/cancers11071037]

87 **Talotta F**, Cimmino A, Matarazzo MR, Casalino L, De Vita G, D'Esposito M, Di Lauro R, Verde P. An autoregulatory loop mediated by miR-21 and PDCD4 controls the AP-1 activity in RAS transformation. *Oncogene* 2009; **28**: 73-84 [PMID: 18850008 DOI: 10.1038/onc.2008.370]

88 **Tanaka Y**, Kanai F, Ichimura T, Tateishi K, Asaoka Y, Guleng B, Jazag A, Ohta M, Imamura J, Ikenoue T, Ijichi H, Kawabe T, Isobe T, Omata M. The hepatitis B virus X protein enhances AP-1 activation through interaction with Jab1. *Oncogene* 2006; **25**: 633-642 [PMID: 16247477 DOI: 10.1038/sj.onc.1209093]

89 **Shang J**, Zheng Y, Guo X, Mo J, Xie X, Xiong Y, Liu Y, Wu K, Wu J. Hepatitis B virus replication and sex-determining region Y box 4 production are tightly controlled by a novel positive feedback mechanism. *Sci Rep* 2015; **5**: 10066 [PMID: 25970172 DOI: 10.1038/srep10066]

90 **Fu X**, Ouyang Y, Mo J, Li R, Fu L, Peng S. Upregulation of microRNA-328-3p by hepatitis B virus contributes to THLE-2 cell injury by downregulating FOXO4. *J Transl Med* 2020; **18**: 143 [PMID: 32228643 DOI: 10.1186/s12967-020-02299-8]

91 **Li CH**, Xu F, Chow S, Feng L, Yin D, Ng TB, Chen Y. Hepatitis B virus X protein promotes hepatocellular carcinoma transformation through interleukin-6 activation of microRNA-21 expression. *Eur J Cancer* 2014; **50**: 2560-2569 [PMID: 25087183 DOI: 10.1016/j.ejca.2014.07.008]

92 **Liu Y**, Feng J, Sun M, Yang G, Yuan H, Wang Y, Bu Y, Zhao M, Zhang S, Zhang X. Long non-coding RNA HULC activates HBV by modulating HBx/STAT3/miR-539/APOBEC3B signaling in HBV-related hepatocellular carcinoma. *Cancer Lett* 2019; **454**: 158-170 [PMID: 30981758 DOI: 10.1016/j.canlet.2019.04.008]

93 **Huang JY**, Chen HL, Shih C. MicroRNA miR-204 and miR-1236 inhibit hepatitis B virus replication *via* two different mechanisms. *Sci Rep* 2016; **6**: 34740 [PMID: 27734898 DOI: 10.1038/srep34740]

94 **Sun C**, Lan P, Han Q, Huang M, Zhang Z, Xu G, Song J, Wang J, Wei H, Zhang J, Sun R, Zhang C, Tian Z. Oncofetal gene SALL4 reactivation by hepatitis B virus counteracts miR-200c in PD-L1-induced T cell exhaustion. *Nat Commun* 2018; **9**: 1241 [PMID: 29593314 DOI: 10.1038/s41467-018-03584-3]

95 **Zhang Y**, Ren H, Li J, Xue R, Liu H, Zhu Z, Pan C, Lin Y, Hu A, Gou P, Cai J, Zhou J, Zhu W, Shi X. Elevated HMGB1 expression induced by hepatitis B virus X protein promotes epithelial-mesenchymal transition and angiogenesis through STAT3/miR-34a/NF-κB in primary liver cancer. *Am J Cancer Res* 2021; **11**: 479-494 [PMID: 33575082]

96 **Yi H**, Zhang Y, Yang X, Li M, Hu H, Xiong J, Wang N, Jin J, Song Y, Wang X, Chen L, Lian J. Hepatitis B Core Antigen Impairs the Polarization While Promoting the Production of Inflammatory Cytokines of M2 Macrophages *via* the TLR2 Pathway. *Front Immunol* 2020; **11**: 535 [PMID: 32292408 DOI: 10.3389/fimmu.2020.00535]

97 **Fu L**, Fu X, Mo J, Li X, Li R, Peng S. miR-146a-5p enhances hepatitis B virus replication through autophagy to promote aggravation of chronic hepatitis B. *IUBMB Life* 2019; **71**: 1336-1346 [PMID: 31018043 DOI: 10.1002/iub.2044]

98 **Zhang X**, Liu S, Hu T, He Y, Sun S. Up-regulated microRNA-143 transcribed by nuclear factor kappa B enhances hepatocarcinoma metastasis by repressing fibronectin expression. *Hepatology* 2009; **50**: 490-499 [PMID: 19472311 DOI: 10.1002/hep.23008]

99 **Yin X**, Sun S, Zhao J, Yang J, Lei X, Xu C, Li K. Rs4705342 polymorphism is involved in the tumorigenesis of HBV positive HCC by altering the binding affinity of HBV induced NF-kB with the promoter region of microRNA-143. *J Cell Biochem* 2018; **119**: 5233-5242 [PMID: 29236306 DOI: 10.1002/jcb.26581]

100 **Li JF**, Dai XP, Zhang W, Sun SH, Zeng Y, Zhao GY, Kou ZH, Guo Y, Yu H, Du LY, Jiang SB, Zhou YS. Upregulation of microRNA-146a by hepatitis B virus X protein contributes to hepatitis development by downregulating complement factor H. *mBio* 2015; **6** [PMID: 25805734 DOI: 10.1128/mBio.02459-14]

101 **Wang W**, Bian H, Li F, Li X, Zhang D, Sun S, Song S, Zhu Q, Ren W, Qin C, Qi J. HBeAg induces the expression of macrophage miR-155 to accelerate liver injury *via* promoting production of inflammatory cytokines. *Cell Mol Life Sci* 2018; **75**: 2627-2641 [PMID: 29349567 DOI: 10.1007/s00018-018-2753-8]

102 **Tao L**, Xue D, Shen D, Ma W, Zhang J, Wang X, Zhang W, Wu L, Pan K, Yang Y, Nwosu ZC, Dooley S, Seki E, Liu C. MicroRNA-942 mediates hepatic stellate cell activation by regulating BAMBI expression in human liver fibrosis. *Arch Toxicol* 2018; **92**: 2935-2946 [PMID: 30097701 DOI: 10.1007/s00204-018-2278-9]

103 **Li ZQ**, Wang HY, Zeng QL, Yan JY, Hu YS, Li H, Yu ZJ. p65/miR-23a/CCL22 axis regulated regulatory T cells recruitment in hepatitis B virus positive hepatocellular carcinoma. *Cancer Med* 2020; **9**: 711-723 [PMID: 31769216 DOI: 10.1002/cam4.2611]

104 **Chen WS**, Liu LC, Yen CJ, Chen YJ, Chen JY, Ho CY, Liu SH, Chen CC, Huang WC. Nuclear IKKα mediates microRNA-7/-103/107/21 inductions to downregulate maspin expression in response to HBx overexpression. *Oncotarget* 2016; **7**: 56309-56323 [PMID: 27409165 DOI: 10.18632/oncotarget.10462]

105 **Huang JY**, Chou SF, Lee JW, Chen HL, Chen CM, Tao MH, Shih C. MicroRNA-130a can inhibit hepatitis B virus replication *via* targeting PGC1α and PPARγ. *RNA* 2015; **21**: 385-400 [PMID: 25595716 DOI: 10.1261/rna.048744.114]

106 **Sarkar N**, Panigrahi R, Pal A, Biswas A, Singh SP, Kar SK, Bandopadhyay M, Das D, Saha D, Kanda T, Sugiyama M, Chakrabarti S, Banerjee A, Chakravarty R. Expression of microRNA-155 correlates positively with the expression of Toll-like receptor 7 and modulates hepatitis B virus *via* C/EBP-β in hepatocytes. *J Viral Hepat* 2015; **22**: 817-827 [PMID: 25720442 DOI: 10.1111/jvh.12390]

107 **Sepehri Z**, Kiani Z, Alavian SM, Arababadi MK, Kennedy D. The link between TLR7 signaling and hepatitis B virus infection. *Life Sci* 2016; **158**: 63-69 [PMID: 27373425 DOI: 10.1016/j.lfs.2016.06.026]

108 **Mauvais-Jarvis F**, Lange CA, Levin ER. Membrane-Initiated Estrogen, Androgen, and Progesterone Receptor Signaling in Health and Disease. *Endocr Rev* 2022; **43**: 720-742 [PMID: 34791092 DOI: 10.1210/endrev/bnab041]

109 **Yang WJ**, Chang CJ, Yeh SH, Lin WH, Wang SH, Tsai TF, Chen DS, Chen PJ. Hepatitis B virus X protein enhances the transcriptional activity of the androgen receptor through c-Src and glycogen synthase kinase-3beta kinase pathways. *Hepatology* 2009; **49**: 1515-1524 [PMID: 19205031 DOI: 10.1002/hep.22833]

110 **Han J**, Ding L, Yuan B, Yang X, Wang X, Li J, Lu Q, Huang C, Ye Q. Hepatitis B virus X protein and the estrogen receptor variant lacking exon 5 inhibit estrogen receptor signaling in hepatoma cells. *Nucleic Acids Res* 2006; **34**: 3095-3106 [PMID: 16757575 DOI: 10.1093/nar/gkl389]

111 **Chen PJ**, Yeh SH, Liu WH, Lin CC, Huang HC, Chen CL, Chen DS, Chen PJ. Androgen pathway stimulates microRNA-216a transcription to suppress the tumor suppressor in lung cancer-1 gene in early hepatocarcinogenesis. *Hepatology* 2012; **56**: 632-643 [PMID: 22392644 DOI: 10.1002/hep.25695]

112 **Chang TC**, Yu D, Lee YS, Wentzel EA, Arking DE, West KM, Dang CV, Thomas-Tikhonenko A, Mendell JT. Widespread microRNA repression by Myc contributes to tumorigenesis. *Nat Genet* 2008; **40**: 43-50 [PMID: 18066065 DOI: 10.1038/ng.2007.30]

113 **Wang J**, Chen J, Liu Y, Zeng X, Wei M, Wu S, Xiong Q, Song F, Yuan X, Xiao Y, Cao Y, Li C, Chen L, Guo M, Shi YB, Sun G, Guo D. Hepatitis B Virus Induces Autophagy to Promote its Replication by the Axis of miR-192-3p-XIAP Through NF kappa B Signaling. *Hepatology* 2019; **69**: 974-992 [PMID: 30180281 DOI: 10.1002/hep.30248]

114 **Wu G**, Yu F, Xiao Z, Xu K, Xu J, Tang W, Wang J, Song E. Hepatitis B virus X protein downregulates expression of the miR-16 family in malignant hepatocytes in vitro. *Br J Cancer* 2011; **105**: 146-153 [PMID: 21629246 DOI: 10.1038/bjc.2011.190]

115 **Wu G**, Huang P, Ju X, Li Z, Wang Y. Lin28B over-expression mediates the repression of let-7 by hepatitis B virus X protein in hepatoma cells. *Int J Clin Exp Med* 2015; **8**: 15108-15116 [PMID: 26628994]

116 **Jung YJ**, Kim JW, Park SJ, Min BY, Jang ES, Kim NY, Jeong SH, Shin CM, Lee SH, Park YS, Hwang JH, Kim N, Lee DH. c-Myc-mediated overexpression of miR-17-92 suppresses replication of hepatitis B virus in human hepatoma cells. *J Med Virol* 2013; **85**: 969-978 [PMID: 23532756 DOI: 10.1002/jmv.23534]

117 **Liu Y**, Wang J, Chen J, Wu S, Zeng X, Xiong Q, Guo Y, Sun J, Song F, Xu J, Yuan S, Li C, He Y, Wang M, Chen L, Shi YB, Guo M, Guo D, Sun G. Upregulation of miR-520c-3p *via* hepatitis B virus drives hepatocellular migration and invasion by the PTEN/AKT/NF-κB axis. *Mol Ther Nucleic Acids* 2022; **29**: 47-63 [PMID: 35795482 DOI: 10.1016/j.omtn.2022.05.031]

118 **Zhang W**, Lu Z, Kong G, Gao Y, Wang T, Wang Q, Cai N, Wang H, Liu F, Ye L, Zhang X. Hepatitis B virus X protein accelerates hepatocarcinogenesis with partner survivin through modulating miR-520b and HBXIP. *Mol Cancer* 2014; **13**: 128 [PMID: 24886421 DOI: 10.1186/1476-4598-13-128]

119 **Chen W**, Jiang J, Gong L, Shu Z, Xiang D, Zhang X, Bi K, Diao H. Hepatitis B virus P protein initiates glycolytic bypass in HBV-related hepatocellular carcinoma *via* a FOXO3/miRNA-30b-5p/MINPP1 axis. *J Exp Clin Cancer Res* 2021; **40**: 1 [PMID: 33390177 DOI: 10.1186/s13046-020-01803-8]

120 **Dong KS**, Chen Y, Yang G, Liao ZB, Zhang HW, Liang HF, Chen XP, Dong HH. TGF-β1 accelerates the hepatitis B virus X-induced malignant transformation of hepatic progenitor cells by upregulating miR-199a-3p. *Oncogene* 2020; **39**: 1807-1820 [PMID: 31740785 DOI: 10.1038/s41388-019-1107-9]

121 **Gao Q**, Zhu H, Dong L, Shi W, Chen R, Song Z, Huang C, Li J, Dong X, Zhou Y, Liu Q, Ma L, Wang X, Zhou J, Liu Y, Boja E, Robles AI, Ma W, Wang P, Li Y, Ding L, Wen B, Zhang B, Rodriguez H, Gao D, Zhou H, Fan J. Integrated Proteogenomic Characterization of HBV-Related Hepatocellular Carcinoma. *Cell* 2019; **179**: 561-577.e22 [PMID: 31585088 DOI: 10.1016/j.cell.2019.08.052]

122 **Xu X**, Fan Z, Kang L, Han J, Jiang C, Zheng X, Zhu Z, Jiao H, Lin J, Jiang K, Ding L, Zhang H, Cheng L, Fu H, Song Y, Jiang Y, Liu J, Wang R, Du N, Ye Q. Hepatitis B virus X protein represses miRNA-148a to enhance tumorigenesis. *J Clin Invest* 2013; **123**: 630-645 [PMID: 23321675 DOI: 10.1172/JCI64265]

123 **Wu Q**, Liu HO, Liu YD, Liu WS, Pan D, Zhang WJ, Yang L, Fu Q, Xu JJ, Gu JX. Decreased expression of hepatocyte nuclear factor 4α (Hnf4α)/microRNA-122 (miR-122) axis in hepatitis B virus-associated hepatocellular carcinoma enhances potential oncogenic GALNT10 protein activity. *J Biol Chem* 2015; **290**: 1170-1185 [PMID: 25422324 DOI: 10.1074/jbc.M114.601203]

124 **Hu XM**, Yan XH, Hu YW, Huang JL, Cao SW, Ren TY, Tang YT, Lin L, Zheng L, Wang Q. miRNA-548p suppresses hepatitis B virus X protein associated hepatocellular carcinoma by downregulating oncoprotein hepatitis B x-interacting protein. *Hepatol Res* 2016; **46**: 804-815 [PMID: 26583881 DOI: 10.1111/hepr.12618]

125 **Dodurga Y**, Yonguc GN, Avci CB, Bagci G, Gunduz C, Satiroglu-Tufan NL. Investigation of microRNA expression changes in HepG2 cell line in presence of URG4/URGCP and in absence of URG4/URGCP suppressed by RNA interference. *Mol Biol Rep* 2012; **39**: 11119-11124 [PMID: 23053999 DOI: 10.1007/s11033-012-2019-8]

126 **Yuan K**, Lian Z, Sun B, Clayton MM, Ng IO, Feitelson MA. Role of miR-148a in hepatitis B associated hepatocellular carcinoma. *PLoS One* 2012; **7**: e35331 [PMID: 22496917 DOI: 10.1371/journal.pone.0035331]

127 **Mishra AK**, Hossain MM, Umar M, Sata TN, Yadav AK, Sah AK, Ismail M, Nayak B, Shalimar, Venugopal SK. DDX3-mediated miR-34 expression inhibits autophagy and HBV replication in hepatic cells. *J Viral Hepat* 2023; **30**: 327-334 [PMID: 36597176 DOI: 10.1111/jvh.13799]

128 **Guerrieri F**, Belloni L, D'Andrea D, Pediconi N, Le Pera L, Testoni B, Scisciani C, Floriot O, Zoulim F, Tramontano A, Levrero M. Genome-wide identification of direct HBx genomic targets. *BMC Genomics* 2017; **18**: 184 [PMID: 28212627 DOI: 10.1186/s12864-017-3561-5]

129 **Kwok ZH**, Zhang B, Chew XH, Chan JJ, Teh V, Yang H, Kappei D, Tay Y. Systematic Analysis of Intronic miRNAs Reveals Cooperativity within the Multicomponent FTX Locus to Promote Colon Cancer Development. *Cancer Res* 2021; **81**: 1308-1320 [PMID: 33172934 DOI: 10.1158/0008-5472.CAN-20-1406]

130 **Keniry A**, Oxley D, Monnier P, Kyba M, Dandolo L, Smits G, Reik W. The H19 lincRNA is a developmental reservoir of miR-675 that suppresses growth and Igf1r. *Nat Cell Biol* 2012; **14**: 659-665 [PMID: 22684254 DOI: 10.1038/ncb2521]

131 **Ge L**, Zhang X, Hu S, Song Y, Kong J, Zhang B, Yang X. H19 suppresses the growth of hepatoblastoma cells by promoting their apoptosis *via* the signaling pathways of miR-675/FADD and miR-138/PTK2. *J Cell Biochem* 2019; **120**: 5218-5231 [PMID: 30367502 DOI: 10.1002/jcb.27797]

132 **Liu Y**, Xu L, Lu B, Zhao M, Li L, Sun W, Qiu Z, Zhang B. LncRNA H19/microRNA-675/PPARα axis regulates liver cell injury and energy metabolism remodelling induced by hepatitis B X protein *via* Akt/mTOR signalling. *Mol Immunol* 2019; **116**: 18-28 [PMID: 31574452 DOI: 10.1016/j.molimm.2019.09.006]

133 **Zhu Y**, Lu Y, Zhang Q, Liu JJ, Li TJ, Yang JR, Zeng C, Zhuang SM. MicroRNA-26a/b and their host genes cooperate to inhibit the G1/S transition by activating the pRb protein. *Nucleic Acids Res* 2012; **40**: 4615-4625 [PMID: 22210897 DOI: 10.1093/nar/gkr1278]

134 **Wang H**, Luo J, He Q, Yao D, Wu J, Loor JJ. miR-26b promoter analysis reveals regulatory mechanisms by lipid-related transcription factors in goat mammary epithelial cells. *J Dairy Sci* 2017; **100**: 5837-5849 [PMID: 28527797 DOI: 10.3168/jds.2016-12440]

135 **Zhao F**, Xu G, Zhou Y, Wang L, Xie J, Ren S, Liu S, Zhu Y. MicroRNA-26b inhibits hepatitis B virus transcription and replication by targeting the host factor CHORDC1 protein. *J Biol Chem* 2014; **289**: 35029-35041 [PMID: 25342750 DOI: 10.1074/jbc.M114.589978]

136 **Piletič K**, Kunej T. MicroRNA epigenetic signatures in human disease. *Arch Toxicol* 2016; **90**: 2405-2419 [PMID: 27557899 DOI: 10.1007/s00204-016-1815-7]

137 **Park IY**, Sohn BH, Yu E, Suh DJ, Chung YH, Lee JH, Surzycki SJ, Lee YI. Aberrant epigenetic modifications in hepatocarcinogenesis induced by hepatitis B virus X protein. *Gastroenterology* 2007; **132**: 1476-1494 [PMID: 17408664 DOI: 10.1053/j.gastro.2007.01.034]

138 **Yang Z**, Li J, Feng G, Wang Y, Yang G, Liu Y, Zhang S, Feng J, Zhang X. Hepatitis B virus X protein enhances hepatocarcinogenesis by depressing the targeting of NUSAP1 mRNA by miR-18b. *Cancer Biol Med* 2019; **16**: 276-287 [PMID: 31516748 DOI: 10.20892/j.issn.2095-3941.2018.0283]

139 **Feng GX**, Li J, Yang Z, Zhang SQ, Liu YX, Zhang WY, Ye LH, Zhang XD. Hepatitis B virus X protein promotes the development of liver fibrosis and hepatoma through downregulation of miR-30e targeting P4HA2 mRNA. *Oncogene* 2017; **36**: 6895-6905 [PMID: 28846110 DOI: 10.1038/onc.2017.291]

140 **Wei X**, Tan C, Tang C, Ren G, Xiang T, Qiu Z, Liu R, Wu Z. Epigenetic repression of miR-132 expression by the hepatitis B virus x protein in hepatitis B virus-related hepatocellular carcinoma. *Cell Signal* 2013; **25**: 1037-1043 [PMID: 23376496 DOI: 10.1016/j.cellsig.2013.01.019]

141 **Zhang T**, Zhang J, Cui M, Liu F, You X, Du Y, Gao Y, Zhang S, Lu Z, Ye L, Zhang X. Hepatitis B virus X protein inhibits tumor suppressor miR-205 through inducing hypermethylation of miR-205 promoter to enhance carcinogenesis. *Neoplasia* 2013; **15**: 1282-1291 [PMID: 24339740 DOI: 10.1593/neo.131362]

142 **Tsang DP**, Wu WK, Kang W, Lee YY, Wu F, Yu Z, Xiong L, Chan AW, Tong JH, Yang W, Li MS, Lau SS, Li X, Lee SD, Yang Y, Lai PB, Yu DY, Xu G, Lo KW, Chan MT, Wang H, Lee TL, Yu J, Wong N, Yip KY, To KF, Cheng AS. Yin Yang 1-mediated epigenetic silencing of tumour-suppressive microRNAs activates nuclear factor-κB in hepatocellular carcinoma. *J Pathol* 2016; **238**: 651-664 [PMID: 26800240 DOI: 10.1002/path.4688]

143 **Zhang H**, Huang C, Wang Y, Lu Z, Zhuang N, Zhao D, He J, Shi L. Hepatitis B Virus X Protein Sensitizes TRAIL-Induced Hepatocyte Apoptosis by Inhibiting the E3 Ubiquitin Ligase A20. *PLoS One* 2015; **10**: e0127329 [PMID: 25993287 DOI: 10.1371/journal.pone.0127329]

144 **Ferrari KJ**, Scelfo A, Jammula S, Cuomo A, Barozzi I, Stützer A, Fischle W, Bonaldi T, Pasini D. Polycomb-dependent H3K27me1 and H3K27me2 regulate active transcription and enhancer fidelity. *Mol Cell* 2014; **53**: 49-62 [PMID: 24289921 DOI: 10.1016/j.molcel.2013.10.030]

145 **Cai Y**, Zhang Y, Loh YP, Tng JQ, Lim MC, Cao Z, Raju A, Lieberman Aiden E, Li S, Manikandan L, Tergaonkar V, Tucker-Kellogg G, Fullwood MJ. H3K27me3-rich genomic regions can function as silencers to repress gene expression *via* chromatin interactions. *Nat Commun* 2021; **12**: 719 [PMID: 33514712 DOI: 10.1038/s41467-021-20940-y]

146 **Song K**, Han C, Zhang J, Lu D, Dash S, Feitelson M, Lim K, Wu T. Epigenetic regulation of MicroRNA-122 by peroxisome proliferator activated receptor-gamma and hepatitis b virus X protein in hepatocellular carcinoma cells. *Hepatology* 2013; **58**: 1681-1692 [PMID: 23703729 DOI: 10.1002/hep.26514]

147 **Feng H**, Yuan X, Wu S, Yuan Y, Cui L, Lin D, Peng X, Liu X, Wang F. Effects of writers, erasers and readers within miRNA-related m6A modification in cancers. *Cell Prolif* 2023; **56**: e13340 [PMID: 36162823 DOI: 10.1111/cpr.13340]

148 **Cheng D**, Wu C, Li Y, Liu Y, Mo J, Fu L, Peng S. METTL3 inhibition ameliorates liver damage in mouse with hepatitis B virus-associated acute-on-chronic liver failure by regulating miR-146a-5p maturation. *Biochim Biophys Acta Gene Regul Mech* 2022; **1865**: 194782 [PMID: 34968770 DOI: 10.1016/j.bbagrm.2021.194782]

149 **D'Ambrogio A**, Gu W, Udagawa T, Mello CC, Richter JD. Specific miRNA stabilization by Gld2-catalyzed monoadenylation. *Cell Rep* 2012; **2**: 1537-1545 [PMID: 23200856 DOI: 10.1016/j.celrep.2012.10.023]

150 **Peng F**, Xiao X, Jiang Y, Luo K, Tian Y, Peng M, Zhang M, Xu Y, Gong G. HBx down-regulated Gld2 plays a critical role in HBV-related dysregulation of miR-122. *PLoS One* 2014; **9**: e92998 [PMID: 24667324 DOI: 10.1371/journal.pone.0092998]

151 **Thomson DW**, Dinger ME. Endogenous microRNA sponges: evidence and controversy. *Nat Rev Genet* 2016; **17**: 272-283 [PMID: 27040487 DOI: 10.1038/nrg.2016.20]

152 **Lv J**, Fan HX, Zhao XP, Lv P, Fan JY, Zhang Y, Liu M, Tang H. Long non-coding RNA Unigene56159 promotes epithelial-mesenchymal transition by acting as a ceRNA of miR-140-5p in hepatocellular carcinoma cells. *Cancer Lett* 2016; **382**: 166-175 [PMID: 27597739 DOI: 10.1016/j.canlet.2016.08.029]

153 **Feng J**, Yang G, Liu Y, Gao Y, Zhao M, Bu Y, Yuan H, Yuan Y, Yun H, Sun M, Gao H, Zhang S, Liu Z, Yin M, Song X, Miao Z, Lin Z, Zhang X. LncRNA PCNAP1 modulates hepatitis B virus replication and enhances tumor growth of liver cancer. *Theranostics* 2019; **9**: 5227-5245 [PMID: 31410212 DOI: 10.7150/thno.34273]

154 **Fan H**, Lv P, Mu T, Zhao X, Liu Y, Feng Y, Lv J, Liu M, Tang H. LncRNA n335586/miR-924/CKMT1A axis contributes to cell migration and invasion in hepatocellular carcinoma cells. *Cancer Lett* 2018; **429**: 89-99 [PMID: 29753758 DOI: 10.1016/j.canlet.2018.05.010]

155 **Li L**, Han T, Liu K, Lei CG, Wang ZC, Shi GJ. LncRNA H19 promotes the development of hepatitis B related hepatocellular carcinoma through regulating microRNA-22 *via* EMT pathway. *Eur Rev Med Pharmacol Sci* 2019; **23**: 5392-5401 [PMID: 31298392 DOI: 10.26355/eurrev_201906_18208]

156 **Song W**, Zheng C, Liu M, Xu Y, Qian Y, Zhang Z, Su H, Li X, Wu H, Gong P, Li Y, Fan H. TRERNA1 upregulation mediated by HBx promotes sorafenib resistance and cell proliferation in HCC *via* targeting NRAS by sponging miR-22-3p. *Mol Ther* 2021; **29**: 2601-2616 [PMID: 33839325 DOI: 10.1016/j.ymthe.2021.04.011]

157 **He B**, Peng F, Li W, Jiang Y. Interaction of lncRNA-MALAT1 and miR-124 regulates HBx-induced cancer stem cell properties in HepG2 through PI3K/Akt signaling. *J Cell Biochem* 2019; **120**: 2908-2918 [PMID: 30500989 DOI: 10.1002/jcb.26823]

158 **Zhuang H**, Ma X, Liu X, Li C, Li X, Wu L, Wen M, Shi W, Yang X. Hyaluronan-mediated motility receptor antisense RNA 1 promotes hepatitis B virus-related hepatocellular carcinoma progression by regulating miR-627-3p/High Mobility Group AT-hook 2 axis. *Bioengineered* 2022; **13**: 8617-8630 [PMID: 35322735 DOI: 10.1080/21655979.2022.2054151]

159 **Huang P**, Xu Q, Yan Y, Lu Y, Hu Z, Ou B, Zhang H, Mao K, Zhang J, Wang J, Xiao Z. HBx/ERα complex-mediated LINC01352 downregulation promotes HBV-related hepatocellular carcinoma *via* the miR-135b-APC axis. *Oncogene* 2020; **39**: 3774-3789 [PMID: 32157216 DOI: 10.1038/s41388-020-1254-z]

160 **Deng Y**, Wei Z, Huang M, Xu G, Wei W, Peng B, Nong S, Qin H. Long non-coding RNA F11-AS1 inhibits HBV-related hepatocellular carcinoma progression by regulating NR1I3 *via* binding to microRNA-211-5p. *J Cell Mol Med* 2020; **24**: 1848-1865 [PMID: 31880390 DOI: 10.1111/jcmm.14881]

161 **Wang J**, Yin G, Bian H, Yang J, Zhou P, Yan K, Liu C, Chen P, Zhu J, Li Z, Xue T. LncRNA XIST upregulates TRIM25 *via* negatively regulating miR-192 in hepatitis B virus-related hepatocellular carcinoma. *Mol Med* 2021; **27**: 41 [PMID: 33858324 DOI: 10.1186/s10020-021-00278-3]

162 **Guo L**, Gao S, Sun W, Wang Y, Zhao J. Elevated LINC01232 is associated with poor prognosis and HBV infection in hepatocellular carcinoma patients and contributes to tumor progression in vitro. *Clin Res Hepatol Gastroenterol* 2022; **46**: 101813 [PMID: 34583064 DOI: 10.1016/j.clinre.2021.101813]

163 **Cheng Y**, Shi W, Cui X, Sun L, Nan Y, Yao H, Fan J, Zhu L, Yu L. Long Noncoding RNA TFAP2A-AS1 Suppressed Hepatitis B Virus Replication by Modulating miR-933/HDAC11. *Dis Markers* 2022; **2022**: 7733390 [PMID: 35478990 DOI: 10.1155/2022/7733390]

164 **Yu K**, Mei Y, Wang Z, Liu B, Deng M. LncRNA LINC00924 upregulates NDRG2 to inhibit epithelial-mesenchymal transition *via* sponging miR-6755-5p in hepatitis B virus-related hepatocellular carcinoma. *J Med Virol* 2022; **94**: 2702-2713 [PMID: 34997970 DOI: 10.1002/jmv.27578]

165 **Wei Y**, Tang X, Ren Y, Yang Y, Song F, Fu J, Liu S, Yu M, Chen J, Wang S, Zhang K, Tan Y, Han Z, Wei L, Zhang B, Cheng Z, Li L, Wang H. An RNA-RNA crosstalk network involving HMGB1 and RICTOR facilitates hepatocellular carcinoma tumorigenesis by promoting glutamine metabolism and impedes immunotherapy by PD-L1+ exosomes activity. *Signal Transduct Target Ther* 2021; **6**: 421 [PMID: 34916485 DOI: 10.1038/s41392-021-00801-2]

166 **Chen S**, Dong Z, Yang P, Wang X, Jin G, Yu H, Chen L, Li L, Tang L, Bai S, Yan H, Shen F, Cong W, Wen W, Wang H. Hepatitis B virus X protein stimulates high mobility group box 1 secretion and enhances hepatocellular carcinoma metastasis. *Cancer Lett* 2017; **394**: 22-32 [PMID: 28216372 DOI: 10.1016/j.canlet.2017.02.011]

167 **Rao X**, Lai L, Li X, Wang L, Li A, Yang Q. N(6) -methyladenosine modification of circular RNA circ-ARL3 facilitates Hepatitis B virus-associated hepatocellular carcinoma *via* sponging miR-1305. *IUBMB Life* 2021; **73**: 408-417 [PMID: 33372396 DOI: 10.1002/iub.2438]

168 **Chen Y**, Li S, Wei Y, Xu Z, Wu X. Circ-RNF13, as an oncogene, regulates malignant progression of HBV-associated hepatocellular carcinoma cells and HBV infection through ceRNA pathway of circ-RNF13/miR-424-5p/TGIF2. *Bosn J Basic Med Sci* 2021; **21**: 555-568 [PMID: 33714261 DOI: 10.17305/bjbms.2020.5266]

169 **Du N**, Li K, Wang Y, Song B, Zhou X, Duan S. CircRNA circBACH1 facilitates hepatitis B virus replication and hepatoma development by regulating the miR-200a-3p/MAP3K2 axis. *Histol Histopathol* 2022; **37**: 863-877 [PMID: 35352818 DOI: 10.14670/HH-18-452]

170 **Jiang W**, Wang L, Zhang Y, Li H. Circ-ATP5H Induces Hepatitis B Virus Replication and Expression by Regulating miR-138-5p/TNFAIP3 Axis. *Cancer Manag Res* 2020; **12**: 11031-11040 [PMID: 33173336 DOI: 10.2147/CMAR.S272983]

171 **He W**, Zhu X, Tang X, Xiang X, Yu J, Sun H. Circ_0027089 regulates NACC1 by targeting miR-136-5p to aggravate the development of hepatitis B virus-related hepatocellular carcinoma. *Anticancer Drugs* 2022; **33**: e336-e348 [PMID: 34419960 DOI: 10.1097/CAD.0000000000001211]

172 **Wang Y**, Jiang L, Ji X, Yang B, Zhang Y, Fu XD. Hepatitis B viral RNA directly mediates down-regulation of the tumor suppressor microRNA miR-15a/miR-16-1 in hepatocytes. *J Biol Chem* 2013; **288**: 18484-18493 [PMID: 23649629 DOI: 10.1074/jbc.M113.458158]

173 **Liu N**, Zhang J, Jiao T, Li Z, Peng J, Cui Z, Ye X. Hepatitis B virus inhibits apoptosis of hepatoma cells by sponging the MicroRNA 15a/16 cluster. *J Virol* 2013; **87**: 13370-13378 [PMID: 24089558 DOI: 10.1128/JVI.02130-13]

174 **Li C**, Wang Y, Wang S, Wu B, Hao J, Fan H, Ju Y, Ding Y, Chen L, Chu X, Liu W, Ye X, Meng S. Hepatitis B virus mRNA-mediated miR-122 inhibition upregulates PTTG1-binding protein, which promotes hepatocellular carcinoma tumor growth and cell invasion. *J Virol* 2013; **87**: 2193-2205 [PMID: 23221562 DOI: 10.1128/JVI.02831-12]

175 **Deng M**, Hou J, Hu J, Wang S, Chen M, Chen L, Ju Y, Li C, Meng S. Hepatitis B virus mRNAs functionally sequester let-7a and enhance hepatocellular carcinoma. *Cancer Lett* 2016; **383**: 62-72 [PMID: 27693636 DOI: 10.1016/j.canlet.2016.09.028]

176 **Takata A**, Otsuka M, Ohno M, Kishikawa T, Yoshikawa T, Koike K. Mutual antagonism between hepatitis B viral mRNA and host microRNA let-7. *Sci Rep* 2016; **6**: 23237 [PMID: 26979389 DOI: 10.1038/srep23237]

177 **Ochi M**, Otsuka M, Maruyama R, Koike K. HBx increases EGFR expression by inhibiting miR129-5p function. *Biochem Biophys Res Commun* 2020; **529**: 198-203 [PMID: 32703411 DOI: 10.1016/j.bbrc.2020.06.018]

178 **Lau CC**, Sun T, Ching AK, He M, Li JW, Wong AM, Co NN, Chan AW, Li PS, Lung RW, Tong JH, Lai PB, Chan HL, To KF, Chan TF, Wong N. Viral-human chimeric transcript predisposes risk to liver cancer development and progression. *Cancer Cell* 2014; **25**: 335-349 [PMID: 24582836 DOI: 10.1016/j.ccr.2014.01.030]

179 **Liang HW**, Wang N, Wang Y, Wang F, Fu Z, Yan X, Zhu H, Diao W, Ding Y, Chen X, Zhang CY, Zen K. Hepatitis B virus-human chimeric transcript HBx-LINE1 promotes hepatic injury *via* sequestering cellular microRNA-122. *J Hepatol* 2016; **64**: 278-291 [PMID: 26409216 DOI: 10.1016/j.jhep.2015.09.013]

180 **Levine B**, Kroemer G. Biological Functions of Autophagy Genes: A Disease Perspective. *Cell* 2019; **176**: 11-42 [PMID: 30633901 DOI: 10.1016/j.cell.2018.09.048]

181 **Lan SH**, Wu SY, Zuchini R, Lin XZ, Su IJ, Tsai TF, Lin YJ, Wu CT, Liu HS. Autophagy suppresses tumorigenesis of hepatitis B virus-associated hepatocellular carcinoma through degradation of microRNA-224. *Hepatology* 2014; **59**: 505-517 [PMID: 23913306 DOI: 10.1002/hep.26659]

182 **Gibbings D**, Mostowy S, Jay F, Schwab Y, Cossart P, Voinnet O. Selective autophagy degrades DICER and AGO2 and regulates miRNA

activity. *Nat Cell Biol* 2012; **14**: 1314-1321 [DOI: 10.1038/ncb2611]

183 **Ma NF**, Lau SH, Hu L, Xie D, Wu J, Yang J, Wang Y, Wu MC, Fung J, Bai X, Tzang CH, Fu L, Yang M, Su YA, Guan XY. COOH-terminal truncated HBV X protein plays key role in hepatocarcinogenesis. *Clin Cancer Res* 2008; **14**: 5061-5068 [PMID: 18698024 DOI: 10.1158/1078-0432.CCR-07-5082]

184 **Minarovits J**, Niller HH. Truncated oncoproteins of retroviruses and hepatitis B virus: A lesson in contrasts. *Infect Genet Evol* 2019; **73**: 342-357 [PMID: 31152910 DOI: 10.1016/j.meegid.2019.05.020]

185 **Liu F**, You X, Chi X, Wang T, Ye L, Niu J, Zhang X. Hepatitis B virus X protein mutant HBxΔ127 promotes proliferation of hepatoma cells through up-regulating miR-215 targeting PTPRT. *Biochem Biophys Res Commun* 2014; **444**: 128-134 [PMID: 24434140 DOI: 10.1016/j.bbrc.2014.01.004]

186 **Yip WK**, Cheng AS, Zhu R, Lung RW, Tsang DP, Lau SS, Chen Y, Sung JG, Lai PB, Ng EK, Yu J, Wong N, To KF, Wong VW, Sung JJ, Chan HL. Carboxyl-terminal truncated HBx regulates a distinct microRNA transcription program in hepatocellular carcinoma development. *PLoS One* 2011; **6**: e22888 [PMID: 21829663 DOI: 10.1371/journal.pone.0022888]

187 **Hou ZH**, Han QJ, Zhang C, Tian ZG, Zhang J. miR146a impairs the IFN-induced anti-HBV immune response by downregulating STAT1 in hepatocytes. *Liver Int* 2014; **34**: 58-68 [PMID: 23890093 DOI: 10.1111/liv.12244]

188 **Su IJ**, Wang LH, Hsieh WC, Wu HC, Teng CF, Tsai HW, Huang W. The emerging role of hepatitis B virus pre-S2 deletion mutant proteins in HBV tumorigenesis. *J Biomed Sci* 2014; **21**: 98 [PMID: 25316153 DOI: 10.1186/s12929-014-0098-7]

189 **Levrero M**, Zucman-Rossi J. Mechanisms of HBV-induced hepatocellular carcinoma. *J Hepatol* 2016; **64**: S84-S101 [PMID: 27084040 DOI: 10.1016/j.jhep.2016.02.021]

190 **Zhang Y**, Huang B, Wang HY, Chang A, Zheng XFS. Emerging Role of MicroRNAs in mTOR Signaling. *Cell Mol Life Sci* 2017; **74**: 2613-2625 [PMID: 28238105 DOI: 10.1007/s00018-017-2485-1]

191 **Murakami Y**, Yasuda T, Saigo K, Urashima T, Toyoda H, Okanoue T, Shimotohno K. Comprehensive analysis of microRNA expression patterns in hepatocellular carcinoma and non-tumorous tissues. *Oncogene* 2006; **25**: 2537-2545 [PMID: 16331254 DOI: 10.1038/sj.onc.1209283]

192 **Feitelson MA**, Lee J. Hepatitis B virus integration, fragile sites, and hepatocarcinogenesis. *Cancer Lett* 2007; **252**: 157-170 [PMID: 17188425 DOI: 10.1016/j.canlet.2006.11.010]

193 **Calin GA**, Sevignani C, Dumitru CD, Hyslop T, Noch E, Yendamuri S, Shimizu M, Rattan S, Bullrich F, Negrini M, Croce CM. Human microRNA genes are frequently located at fragile sites and genomic regions involved in cancers. *Proc Natl Acad Sci U S A* 2004; **101**: 2999-3004 [PMID: 14973191 DOI: 10.1073/pnas.0307323101]

194 **Yang L**, Ma Z, Wang D, Zhao W, Chen L, Wang G. MicroRNA-602 regulating tumor suppressive gene RASSF1A is overexpressed in hepatitis B virus-infected liver and hepatocellular carcinoma. *Cancer Biol Ther* 2010; **9**: 803-808 [PMID: 20364114 DOI: 10.4161/cbt.9.10.11440]

195 **Guo H**, Liu H, Mitchelson K, Rao H, Luo M, Xie L, Sun Y, Zhang L, Lu Y, Liu R, Ren A, Liu S, Zhou S, Zhu J, Zhou Y, Huang A, Wei L, Guo Y, Cheng J. MicroRNAs-372/373 promote the expression of hepatitis B virus through the targeting of nuclear factor I/B. *Hepatology* 2011; **54**: 808-819 [PMID: 21608007 DOI: 10.1002/hep.24441]

196 **Zhang B**, Han S, Feng B, Chu X, Chen L, Wang R. Hepatitis B virus X protein-mediated non-coding RNA aberrations in the development of human hepatocellular carcinoma. *Exp Mol Med* 2017; **49**: e293 [PMID: 28186085 DOI: 10.1038/emm.2016.177]

197 **Sartorius K**, Swadling L, An P, Makarova J, Winkler C, Chuturgoon A, Kramvis A. The Multiple Roles of Hepatitis B Virus X Protein (HBx) Dysregulated MicroRNA in Hepatitis B Virus-Associated Hepatocellular Carcinoma (HBV-HCC) and Immune Pathways. *Viruses* 2020; **12** [PMID: 32664401 DOI: 10.3390/v12070746]

198 **Sartorius K**, An P, Winkler C, Chuturgoon A, Li X, Makarova J, Kramvis A. The Epigenetic Modulation of Cancer and Immune Pathways in Hepatitis B Virus-Associated Hepatocellular Carcinoma: The Influence of HBx and miRNA Dysregulation. *Front Immunol* 2021; **12**: 661204 [PMID: 33995383 DOI: 10.3389/fimmu.2021.661204]

199 **Xie KL**, Zhang YG, Liu J, Zeng Y, Wu H. MicroRNAs associated with HBV infection and HBV-related HCC. *Theranostics* 2014; **4**: 1176-1192 [PMID: 25285167 DOI: 10.7150/thno.8715]

200 **Lee TK**, Guan XY, Ma S. Cancer stem cells in hepatocellular carcinoma - from origin to clinical implications. *Nat Rev Gastroenterol Hepatol* 2022; **19**: 26-44 [PMID: 34504325 DOI: 10.1038/s41575-021-00508-3]

201 **Zhang Z**, Han Y, Sun G, Liu X, Jia X, Yu X. MicroRNA-325-3p inhibits cell proliferation and induces apoptosis in hepatitis B virus-related hepatocellular carcinoma by down-regulation of aquaporin 5. *Cell Mol Biol Lett* 2019; **24**: 13 [PMID: 30805015 DOI: 10.1186/s11658-019-0137-1]

202 **Li R**, Xu T, Wang H, Wu N, Liu F, Jia X, Mi J, Lv J, Gao H. Dysregulation of the miR-325-3p/DPAGT1 axis supports HBV-positive HCC chemoresistance. *Biochem Biophys Res Commun* 2019; **519**: 358-365 [PMID: 31519321 DOI: 10.1016/j.bbrc.2019.08.116]

203 **Feng J**, Li J, Wu L, Yu Q, Ji J, Wu J, Dai W, Guo C. Emerging roles and the regulation of aerobic glycolysis in hepatocellular carcinoma. *J Exp Clin Cancer Res* 2020; **39**: 126 [PMID: 32631382 DOI: 10.1186/s13046-020-01629-4]

204 **Sangineto M**, Villani R, Cavallone F, Romano A, Loizzi D, Serviddio G. Lipid Metabolism in Development and Progression of Hepatocellular Carcinoma. *Cancers (Basel)* 2020; **12** [PMID: 32486341 DOI: 10.3390/cancers12061419]

205 **You X**, Liu F, Zhang T, Li Y, Ye L, Zhang X. Hepatitis B virus X protein upregulates oncogene Rab18 to result in the dysregulation of lipogenesis and proliferation of hepatoma cells. *Carcinogenesis* 2013; **34**: 1644-1652 [PMID: 23471881 DOI: 10.1093/carcin/bgt089]

206 **Cui M**, Wang Y, Sun B, Xiao Z, Ye L, Zhang X. MiR-205 modulates abnormal lipid metabolism of hepatoma cells *via* targeting acyl-CoA synthetase long-chain family member 1 (ACSL1) mRNA. *Biochem Biophys Res Commun* 2014; **444**: 270-275 [PMID: 24462768 DOI: 10.1016/j.bbrc.2014.01.051]

207 **Chen Y**, Tian Z. HBV-Induced Immune Imbalance in the Development of HCC. *Front Immunol* 2019; **10**: 2048 [PMID: 31507621 DOI: 10.3389/fimmu.2019.02048]

208 **Liu W**, Zheng X, Wang J, He Q, Li J, Zhang Z, Liu H. MicroRNA-138 Regulates T-Cell Function by Targeting PD-1 in Patients with Hepatitis B Virus-Related Liver Diseases. *Lab Med* 2021; **52**: 439-451 [PMID: 33410459 DOI: 10.1093/labmed/lmaa110]

209 **Yang P**, Li QJ, Feng Y, Zhang Y, Markowitz GJ, Ning S, Deng Y, Zhao J, Jiang S, Yuan Y, Wang HY, Cheng SQ, Xie D, Wang XF. TGF-β-miR-34a-CCL22 signaling-induced Treg cell recruitment promotes venous metastases of HBV-positive hepatocellular carcinoma. *Cancer Cell* 2012; **22**: 291-303 [PMID: 22975373 DOI: 10.1016/j.ccr.2012.07.023]

210 **Bian X**, Si Y, Zhang M, Wei R, Yang X, Ren H, Zheng G, Wang C, Zhang Y. Down-expression of miR-152 lead to impaired anti-tumor effect of NK *via* upregulation of HLA-G. *Tumour Biol* 2016; **37**: 3749-3756 [PMID: 26468017 DOI: 10.1007/s13277-015-3669-7]

211 **Sadri Nahand J**, Rabiei N, Fathazam R, Taghizadieh M, Ebrahimi MS, Mahjoubin-Tehran M, Bannazadeh Baghi H, Khatami A, Abbasi-Kolli M, Mirzaei HR, Rahimian N, Darvish M, Mirzaei H. Oncogenic viruses and chemoresistance: What do we know? *Pharmacol Res* 2021; **170**: 105730 [PMID: 34119621 DOI: 10.1016/j.phrs.2021.105730]

212 **Wei XC**, Xia YR, Zhou P, Xue X, Ding S, Liu LJ, Zhu F. Hepatitis B core antigen modulates exosomal miR-135a to target vesicle-associated membrane protein 2 promoting chemoresistance in hepatocellular carcinoma. *World J Gastroenterol* 2021; **27**: 8302-8322 [PMID: 35068871 DOI: 10.3748/wjg.v27.i48.8302]

213 **Chen WS**, Yen CJ, Chen YJ, Chen JY, Wang LY, Chiu SJ, Shih WL, Ho CY, Wei TT, Pan HL, Chien PH, Hung MC, Chen CC, Huang WC. miRNA-7/21/107 contribute to HBx-induced hepatocellular carcinoma progression through suppression of maspin. *Oncotarget* 2015; **6**: 25962-25974 [PMID: 26296971 DOI: 10.18632/oncotarget.4504]

214 **Zhang C**, Liu P, Zhang C. Hepatitis B virus X protein upregulates alpha-fetoprotein to promote hepatocellular carcinoma by targeting miR-1236 and miR-329. *J Cell Biochem* 2020; **121**: 2489-2499 [PMID: 31680299 DOI: 10.1002/jcb.29471]

215 **He B**, Zhao Z, Cai Q, Zhang Y, Zhang P, Shi S, Xie H, Peng X, Yin W, Tao Y, Wang X. miRNA-based biomarkers, therapies, and resistance in Cancer. *Int J Biol Sci* 2020; **16**: 2628-2647 [PMID: 32792861 DOI: 10.7150/ijbs.47203]

216 **Lamontagne J**, Steel LF, Bouchard MJ. Hepatitis B virus and microRNAs: Complex interactions affecting hepatitis B virus replication and hepatitis B virus-associated diseases. *World J Gastroenterol* 2015; **21**: 7375-7399 [PMID: 26139985 DOI: 10.3748/wjg.v21.i24.7375]

217 **Mosca N**, Castiello F, Coppola N, Trotta MC, Sagnelli C, Pisaturo M, Sagnelli E, Russo A, Potenza N. Functional interplay between hepatitis B virus X protein and human miR-125a in HBV infection. *Biochem Biophys Res Commun* 2014; **449**: 141-145 [PMID: 24824183 DOI: 10.1016/j.bbrc.2014.05.009]

218 **Potenza N**, Papa U, Mosca N, Zerbini F, Nobile V, Russo A. Human microRNA hsa-miR-125a-5p interferes with expression of hepatitis B virus surface antigen. *Nucleic Acids Res* 2011; **39**: 5157-5163 [PMID: 21317190 DOI: 10.1093/nar/gkr067]

219 **Wei X**, Xiang T, Ren G, Tan C, Liu R, Xu X, Wu Z. miR-101 is down-regulated by the hepatitis B virus x protein and induces aberrant DNA methylation by targeting DNA methyltransferase 3A. *Cell Signal* 2013; **25**: 439-446 [PMID: 23124077 DOI: 10.1016/j.cellsig.2012.10.013]

220 **Liu Y**, Lou G, Wu W, Zheng M, Shi Y, Zhao D, Chen Z. Involvement of the NF-κB pathway in multidrug resistance induced by HBx in a hepatoma cell line. *J Viral Hepat* 2011; **18**: e439-e446 [PMID: 21914061 DOI: 10.1111/j.1365-2893.2011.01463.x]

221 **Hu Z**, Yin Y, Jiang J, Yan C, Wang Y, Wang D, Li L. Exosomal miR-142-3p secreted by hepatitis B virus (HBV)-hepatocellular carcinoma (HCC) cells promotes ferroptosis of M1-type macrophages through SLC3A2 and the mechanism of HCC progression. *J Gastrointest Oncol* 2022; **13**: 754-767 [PMID: 35557596 DOI: 10.21037/jgo-21-916]

222 **Zhang Q**, Qu Y, Zhang Q, Li F, Li B, Li Z, Dong Y, Lu L, Cai X. Exosomes derived from hepatitis B virus-infected hepatocytes promote liver fibrosis *via* miR-222/TFRC axis. *Cell Biol Toxicol* 2023; **39**: 467-481 [PMID: 34978008 DOI: 10.1007/s10565-021-09684-z]

223 **Li CH**, Wang YJ, Dong W, Xiang S, Liang HF, Wang HY, Dong HH, Chen L, Chen XP. Hepatic oval cell lines generate hepatocellular carcinoma following transfection with HBx gene and treatment with aflatoxin B1 in vivo. *Cancer Lett* 2011; **311**: 1-10 [PMID: 21821357 DOI: 10.1016/j.canlet.2011.05.035]

224 **Chandrasekaran AR**, MacIsaac M, Dey P, Levchenko O, Zhou L, Andres M, Dey BK, Halvorsen K. Cellular microRNA detection with miRacles: microRNA- activated conditional looping of engineered switches. *Sci Adv* 2019; **5**: eaau9443 [PMID: 30891499 DOI: 10.1126/sciadv.aau9443]

225 **Guo T**, Tang XH, Gao XY, Zhou Y, Jin B, Deng ZQ, Hu Y, Xing XF, Li ZY, Ji JF. A liquid biopsy signature of circulating exosome-derived mRNAs, miRNAs and lncRNAs predict therapeutic efficacy to neoadjuvant chemotherapy in patients with advanced gastric cancer. *Mol Cancer* 2022; **21**: 216 [PMID: 36510184 DOI: 10.1186/s12943-022-01684-9]

226 **To NH**, Nguyen HQ, Thiolat A, Liu B, Cohen J, Radosevic-Robin N, Belkacemi Y; TransAtlantic Radiation Oncology Network (TRONE) & Association of Radiotherapy, and Oncology of the Mediterranean Area (AROME). Radiation therapy for triple-negative breast cancer: emerging role of microRNAs as biomarkers and radiosensitivity modifiers. A systematic review. *Breast Cancer Res Treat* 2022; **193**: 265-279 [PMID: 35397079 DOI: 10.1007/s10549-022-06533-3]

227 **Peng XX**, Yu R, Wu X, Wu SY, Pi C, Chen ZH, Zhang XC, Gao CY, Shao YW, Liu L, Wu YL, Zhou Q. Correlation of plasma exosomal microRNAs with the efficacy of immunotherapy in EGFR/ALK wild-type advanced non-small cell lung cancer. *J Immunother Cancer* 2020; **8** [PMID: 31959728 DOI: 10.1136/jitc-2019-000376]

228 **Li L**, Guo Z, Wang J, Mao Y, Gao Q. Serum miR-18a: a potential marker for hepatitis B virus-related hepatocellular carcinoma screening. *Dig Dis Sci* 2012; **57**: 2910-2916 [PMID: 22865399 DOI: 10.1007/s10620-012-2317-y]

229 **Zhao Q**, Sun X, Liu C, Li T, Cui J, Qin C. Expression of the microRNA-143/145 cluster is decreased in hepatitis B virus-associated hepatocellular carcinoma and may serve as a biomarker for tumorigenesis in patients with chronic hepatitis B. *Oncol Lett* 2018; **15**: 6115-6122 [PMID: 29616093 DOI: 10.3892/ol.2018.8117]

230 **Zhang Y**, Xi H, Nie X, Zhang P, Lan N, Lu Y, Liu J, Yuan W. Assessment of miR-212 and Other Biomarkers in the Diagnosis and Treatment of HBV-infection-related Liver Diseases. *Curr Drug Metab* 2019; **20**: 785-798 [PMID: 31608838 DOI: 10.2174/1389200220666191011120434]

231 **Wen Y**, Han J, Chen J, Dong J, Xia Y, Liu J, Jiang Y, Dai J, Lu J, Jin G, Wei Q, Shen H, Sun B, Hu Z. Plasma miRNAs as early biomarkers for detecting hepatocellular carcinoma. *Int J Cancer* 2015; **137**: 1679-1690 [PMID: 25845839 DOI: 10.1002/ijc.29544]

232 **Xiong F**, Ma H, Qu Y, Wen F, Bao X, Han D, Lu J. Profiles of serum miR-99a, let-7c and miR-125b in hepatitis B virus (HBV)-associated chronic hepatitis, liver cirrhosis and hepatocellular carcinoma. *Int J Clin Exp Pathol* 2016; **9**: 7087-7095

233 **Hung CH**, Hu TH, Lu SN, Kuo FY, Chen CH, Wang JH, Huang CM, Lee CM, Lin CY, Yen YH, Chiu YC. Circulating microRNAs as biomarkers for diagnosis of early hepatocellular carcinoma associated with hepatitis B virus. *Int J Cancer* 2016; **138**: 714-720 [PMID: 26264553 DOI: 10.1002/ijc.29802]

234 **Zhang W**, Fu T, Guo Z, Zhang Y, Zhang L, Su H, Long Y, Ji Z, Yan Y, Shao Z. Serum miR-375 Levels Are Closely Related to Disease Progression from HBV Infection to HBV-Related Hepatocellular Carcinoma. *Biomed Res Int* 2020; **2020**: 5819385 [PMID: 32382558 DOI: 10.1155/2020/5819385]

235 **Zhu HT**, Liu RB, Liang YY, Hasan AME, Wang HY, Shao Q, Zhang ZC, Wang J, He CY, Wang F, Shao JY. Serum microRNA profiles as diagnostic biomarkers for HBV-positive hepatocellular carcinoma. *Liver Int* 2017; **37**: 888-896 [PMID: 28061012 DOI: 10.1111/liv.13356]

World Journal of Gastroenterology

Submit a Manuscript: https://www.f6publishing.com

World J Gastroenterol 2023 August 21; 29(31): 4736-4743

DOI: 10.3748/wjg.v29.i31.4736

ISSN 1007-9327 (print) ISSN 2219-2840 (online)

MINIREVIEWS

Diabetes as a consequence of acute pancreatitis

Ericka Charley, Brett Dinner, Kimberly Pham, Neil Vyas

Specialty type: Gastroenterology and hepatology

Provenance and peer review: Unsolicited article; Externally peer reviewed.

Peer-review model: Single blind

Peer-review report's scientific quality classification

Grade A (Excellent): 0
Grade B (Very good): B
Grade C (Good): C
Grade D (Fair): 0
Grade E (Poor): 0

P-Reviewer: Mao EQ, China; Xiao B, China

Received: June 26, 2023
Peer-review started: June 26, 2023
First decision: July 5, 2023
Revised: July 17, 2023
Accepted: July 28, 2023
Article in press: July 28, 2023
Published online: August 21, 2023

Ericka Charley, Department of Gastroenterology, Creighton University - St. Joseph's Hospital and Medical Center Phoenix, AZ 85013, United States

Brett Dinner, Kimberly Pham, Department of Internal Medicine, Creighton University St. Joseph's Hospital and Medical Center, Phoenix, AZ 85013, United States

Neil Vyas, Department of Gastroenterology, Creighton University St. Joseph's Hospital and Medical Center, Phoenix, AZ 85013, United States

Corresponding author: Ericka Charley, MD, Gastroenterology Fellow Department of Gastroenterology, Creighton University - Phoenix, 350 W Thomas Road, Phoenix, AZ 85013, United States. erickaziggycharley@gmail.com

Abstract

Diabetes is a highly prevalent disease that was initially simplified into three major types: Type 1, type 2 and gestational diabetes. With the global rise in incidence of acute pancreatitis (AP), a lesser-known type of diabetes referred to as diabetes of the exocrine pancreas (DEP) is becoming more recognized. However, there is a poor understanding of the inherent relationship between diabetes and AP. There is established data about certain diseases affecting the exocrine function of the pancreas which can lead to diabetes. More specifically, there are well established guidelines for diagnosis and management of DEP caused be chronic pancreatitis. Conversely, the sequelae of AP leading to diabetes has limited recognition and data. The purpose of this review is to provide a comprehensive summary of the prevalence, epidemiology, pathophysiology and future research aims of AP-related diabetes. In addition, we propose a screening and diagnostic algorithm to aid clinicians in providing better care for their patients.

Key Words: Acute pancreatitis; Type 3c diabetes; Diabetes of the exocrine pancreas; Sequelae of acute pancreatitis; Screening and diagnostic algorithm

©The Author(s) 2023. Published by Baishideng Publishing Group Inc. All rights reserved.

Core Tip: Acute pancreatitis (AP)-related diabetes has limited recognition and data. The disease occurs more often than previously recognized and patients are often misdiagnosed with type 2 diabetes. The purpose of this review is to provide a comprehensive summary of the prevalence, epidemiology, pathophysiology and future research aims of AP-related diabetes. In addition, we propose a screening and diagnostic algorithm to aid clinicians in providing better care for their patients.

Citation: Charley E, Dinner B, Pham K, Vyas N. Diabetes as a consequence of acute pancreatitis. *World J Gastroenterol* 2023; 29(31): 4736-4743
URL: https://www.wjgnet.com/1007-9327/full/v29/i31/4736.htm
DOI: https://dx.doi.org/10.3748/wjg.v29.i31.4736

INTRODUCTION

Acute pancreatitis (AP) is a condition defined by rapid onset pancreatic inflammation that is short-lived and may be associated with local and systemic complications[1]. Alcohol use and gallstones are the most common etiologies, which may explain its standing as one of the leading gastrointestinal diseases requiring hospitalization in the United States[2]. The severity of AP is graded based on the presence or absence of local complications, systemic complications, and persistent organ failure. Patients with mild disease recover with supportive care alone while those with severe disease may experience prolonged hospitalization and require procedural interventions to treat various complications. The severe form of the disease occurs in 20% of all patients with AP and carries a mortality rate as high as 30%-40%[1,3]. Following a single episode of AP, all patients are susceptible to the potential sequela of the injury sustained by the pancreas regardless of the severity of the episode[4]. The complication acquiring interest of late is new-onset diabetes mellitus (DM) after AP.

Diabetes is a term used to classify a group of diseases characterized by persistent hyperglycemia that afflicts 37 million adults in the United States alone. Type I diabetes (T1D) accounts for 5%-10% of the total prevalence of diabetes and is hypothesized to be a consequence of autoimmune destruction of beta cells, resulting in inadequate insulin levels[5]. The most common form of diabetes, type II DM (T2DM), is caused by insufficient insulin secretion by pancreatic beta cells and progressive development of insulin resistance (IR). Persistent impairment in glucose control may also be promoted by diseases of the exocrine pancreas, including AP[6]. This form of diabetes has been referred to as type 3c diabetes or diabetes of the exocrine pancreas (DEP)[6,7].

Hyperglycemia during AP was previously speculated to be a transient event that resolved as the inflammatory process improved[4]. Recent meta-analyses have questioned this notion by showing evidence of a high incidence of AP-related DM[4]. Two meta-analyses found 15%-23% of patients developed new-onset diabetes following a single episode of AP and the remaining patients had greater than a two-fold risk of diabetes over five years[8,9].

The various pancreatic diseases known to potentially cause DEP are often grouped together despite this collection encompassing multiple distinct conditions that should be further investigated on an individual basis. The unique mechanisms in which these conditions cause damage to the pancreas is important to take into consideration as they may allow for specific therapeutic options, change screening recommendations, and affect the length of time to diabetes. AP in particular, the most common disease of the exocrine pancreas, warrants further discussion. The goal of this review is to summarize the prevalence and pathophysiology of DEP after episode(s) of AP, elucidate diagnostic criteria for AP-related DM and identify risk factors of those at highest risk of developing the complication. We will also suggest management and screening recommendations, including the emergence of potential new ways to diagnose AP-related DM and identify areas for further study.

PREVALENCE OF DM AFTER AP

In the United States, AP is estimated to account for approximately 275000 hospital admissions and $2.5 billion in healthcare costs annually[10]. A meta-analysis of the global incidence of AP from 1961 to 2016 found the incidence of AP has been increasing over time. Select populations were noted to have disproportionate rises in incidence especially throughout the majority of countries within the Western world, including North America, Europe, and Oceania[3]. One study aimed at determining the global incidence of AP reported the countries with the greatest incidence of AP in 2019 were India, China, and the United States. Alcohol was found to be an important cause of increased morbidity and mortality. The study also uncovered the existence of significant differences in the burden of AP across geographic regions and differences in outcomes based on socioeconomic factors. For example, patients admitted to smaller hospitals with fewer resources were noted to have a higher risk of pancreatitis-related mortality[10].

The lesser-known sequelae of AP are the development of endocrine and exocrine insufficiency, which in turn can contribute to the development of diabetes. All patients are susceptible to these effects, even those with a mild case of AP and after a first-time episode[11]. In one cohort study, exocrine pancreatic dysfunction was associated with significantly increased risk for new-onset DM, including when the analysis was limited to mild AP[12]. A systematic review and meta-analysis from May 2019 found the incidence of AP-related DM was 23% and new onset insulin dependent DM (IDDM) was 15%. The incidence of DM was higher for severe AP (SAP) compared to mild AP, pancreatic necrosis compared to without, and alcoholic compared to biliary AP. The incidence of IDDM after SAP was 21% and 18% following an episode

of alcohol-related AP. Within five years of the initial episode of AP, the rate of DM and IDDM was 20% and 14%, respectively. The rate of DM and IDDM after AP increased to 37% and 25%, respectively[9]. Another study demonstrated similar findings of the development of endocrine and exocrine insufficiency despite severity of AP, number of or time from episodes of AP, gender, and etiology. However, there was a statistically significant difference in the prevalence of DM when patients with SAP were compared with non-SAP[12].

PATHOPHYSIOLOGY

Ongoing investigations have proposed multiple mechanisms believed to contribute to the development of AP-related DM. These mechanisms presumably occur in parallel and it is unknown which mechanism has the greatest impact. Prior to further discussing the theories it is important to understand the roles of the individual cell types of the pancreas and where they reside. This will aid in demonstrating the clinical implications of their malfunction or loss.

The pancreas consists of two tissue types which give rise to the distinct actions of the pancreas, the exocrine and endocrine functions. Exocrine tissue makes up an estimated 95% of the pancreas and produces enzymes necessary for digestion. The remaining tissue is made up of special endocrine cells embedded within the exocrine pancreas that are collectively known as the islets of Langerhans[13]. This collection consists of four cell types that play exclusive roles in regulating glucose levels and pancreatic secretions: Alpha cells, beta cells, pancreatic polypeptide (PP) cells and delta cells. Alpha cells release glucagon and make up 15% of the total islet cell volume in the anterior portions of the pancreas (head, body and tail). Glucagon is important in preventing hypoglycemia through several well-known mechanisms. Insulin-releasing beta cells make up 80% of the islet volume in the anterior pancreas and 20% of the volume in the posterior head. Insulin regulates glucose by promoting uptake and storage of glucose in the liver, muscle and adipose tissue. The hormone also regulates the action of alpha cells through paracrine inhibition. PP cells make up 80% of the islet volume in the posterior head and have a small presence (< 1%) in the anterior portions of the pancreas. They produce PP, which enhances the effect of insulin on the liver. Delta cells have a small overall existence, contributing to < 1% of islet volume in the posterior head and 5% in the anterior pancreas. Nevertheless, they are essential for their release of somatostatin which has multiple functions throughout the body. In the gastrointestinal system, somatostatin is important for regulating the release of glucagon and insulin through paracrine inhibition. The hormone also slows both gastric emptying and nutrient absorption from the intestinal tract[7].

MECHANICAL DESTRUCTION OF THE PANCREAS *VS* LOSS OF ISLET MASS

Unlike T1D and T2DM, DEP is a consequence of damage to the pancreas that affects all of the highly specialized cells of the organ. Based on this observation and previous data showing a higher incidence of DEP in patients suffering from necrotizing pancreatitis compared to those without necrosis, a correlation between the extent of loss of islet cells and the risk of developing AP-related DM has been suggested[9]. This inference has been further substantiated by evidence that patients with T1D and T2DM have decreased pancreatic volume compared to non-diabetics[14]. Nevertheless, emerging evidence indicates the overall pathogenesis is likely more complicated and requires more investigation. One systematic review examining the risk of developing DM after partial pancreatectomy found the incidence of new-onset DM was significantly different between various types of resection. Those who underwent a distal pancreatectomy had the highest incidence of developing DEP followed by patients who underwent a Whipple. Patients who underwent a central pancreatectomy had the smallest incidence[15]. A study by Tu *et al*[16] reports that in comparison to necrosis in the head and body of the pancreas, necrosis in the tail was associated with a greater risk of developing diabetes. Others also report that surgical resection of up to 50% of the pancreas did not necessarily lead to diabetes[14]. These new findings may explain why the severity of AP does not necessarily positively correlate with the risk of developing AP-related DM.

DYSFUNCTION OF THE EXOCRINE PANCREAS

Damage to the exocrine pancreas may contribute to endocrine dysfunction through mechanisms still undergoing analysis. When chronic pancreatic exocrine disease occurs, findings of decreased pancreatic endocrine function including islet function and insulin secretion can be seen. For example, one of the results of chronic pancreatitis is damage to nerve bundles, specifically vagal afferents, which are necessary for PP secretion. Volume loss within the posterior head of the pancreas, in which resides the majority of PP cells, further exacerbates the reduction in insulin secretion. Significant pancreatic endocrine dysfunction can thereby lead to DEP[14].

In a recent cohort study, Cho *et al*[12] found that patients with exocrine pancreatic dysfunction requiring pancreatic enzyme replacement therapy (PERT) after their initial attack of pancreatitis were at increased risk of new-onset DM. New-onset DM was defined as diagnostic coding of DM and/or receiving a new oral hypoglycemic medication. This association remained even when the analysis was limited to mild AP. Patients with exocrine dysfunction are prone to deficiencies in fat-soluble vitamins.

In the past, vitamin D was found to play a role in glucose control. Mirhosseini *et al*[17] describe the mechanism in a meta-analysis, reporting that the active form of vitamin D regulates the expression of the insulin receptor gene and facilitates the transport of glucose into muscle cells. The authors conclude that vitamin D supplementation may

significantly reduce serum fasting plasma glucose (FPG) and hemoglobin A1c (HbA1c)[17]. However, study results regarding the association of vitamin D and glucose control have been inconsistent. One randomized placebo-controlled trial found that daily vitamin D and calcium supplementation did not have a significant effect on insulin sensitivity, insulin secretion, or β-cell function in vitamin D deficient individuals at risk of T2DM[18]. An important point to note is that the authors classified patients "at risk of T2DM" based on a diabetes risk questionnaire. In a *post hoc* analysis restricted to patients with clinically diagnosed prediabetes, they found a significant beneficial effect of vitamin D and calcium supplementation on insulin sensitivity. There were no changes in insulin secretion or beta cell function.

In a more recent study, Norbitt *et al*[19] investigated potential connections between the intake of fat- and water-soluble vitamins with markers of glucose metabolism in patients after AP. They found a significant association between three fat-soluble vitamins (α-carotene, β-carotene, and total carotene) and homeostasis model assessment of β-cell function (HOMA-β) in patients with new-onset prediabetes/diabetes after AP[19]. Despite this association, there were no significant associations with FPG or HOMA-IR index. Although more studies are needed to help uncover the role of vitamin deficiencies in oxidative stress-driven disorders, it appears that optimizing the exocrine function of the pancreas plays an important role in glucose control. This may provide a key opportunity for intervention to prevent AP-related DM.

RISK FACTORS

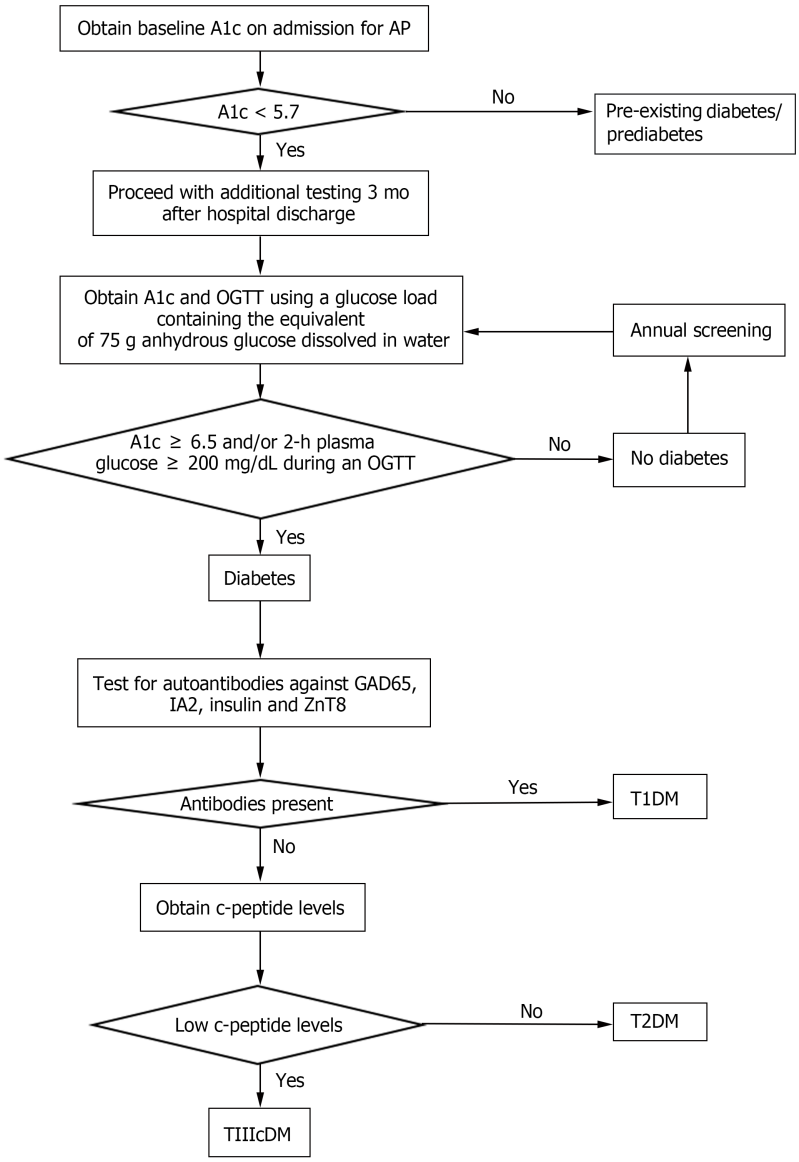
An important component of understanding the etiology of AP-related DM is identifying risk factors linked with heightened endocrine dysfunction after AP. One case-controlled study with multivariable analysis found AP-related DM occurred more often in patients with components of metabolic syndrome such as hypertension, obesity and hyperlipidemia[20]. The potential explanation is that this particular population has an underlying predisposition toward T2DM and the additional insult of AP accelerates the progression to sustained hyperglycemia[21,22]. In another study, Lv *et al* [23] found similar results but also discovered non-alcoholic fatty liver disease (NAFLD) was an additional independent risk factor. Until now, most studies have focused on the effect of the exocrine pancreas on endocrine function yet the liver also plays a critical role in regulating and maintaining glucose levels. Those with NAFLD have underlying IR due to chronic inflammation from the release of inflammatory mediators by adipose tissue. These mediators which include leucine-rich alpha-2-glycoprotein 1 and interleukin-6 have been found to inhibit insulin receptors and the action of insulin through different signaling pathways[23]. The authors suggest chronic inflammation combined with inflammation-induced lipolysis contribute to the process of IR. Investigations to further characterize risk factors for AP-related DM are needed to help identify patients who will benefit from closer follow-up and earlier interventions to control glucose levels following an episode of AP.

DIAGNOSIS

Diagnostic criteria for T1D and T2DM have been well established and have undergone very minor revision over the last decades. The diagnosis of DEP has been more challenging to standardize as it shares clinical features that overlap with T1D and T2DM. The development of standardized criteria is also complicated by the fact that DEP is the result of multiple clinically distinct diseases and/or mechanisms. These individual etiologies lead to variable levels of pancreatic dysfunction and have varying rates of progression to diabetes, making the timing of the initiation of screening difficult to determine[7,24]. Previously, Ewald and Bretzel[25] suggested the following to diagnose DEP: Major criteria (all must be fulfilled): Presence of exocrine pancreatic insufficiency (according to the monoclonal fecal elastase-1 test or direct function tests); pathological pancreatic imaging (endoscopic ultrasound, magnetic resonance imaging, computed tomography); absence of T1DM associated autoimmune markers. Minor criteria: Impaired beta cell function (*e.g.*, HOMA-B, C-peptide/glucose-ratio); no excessive IR (*e.g.*, HOMA-IR); impaired incretin secretion [*e.g.*, glucagon-like peptide 1 (GLP-1), PP]; low serum levels of lipid-soluble vitamins (A, D, E, and K).

Although cited in numerous articles over the years, the criteria were never universally accepted. As we learn more about the underlying mechanisms of each disease process and how they may lead to DEP, most of the above criteria have become invalid. For example, pancreatic insufficiency is not a specific characteristic of any of the diseases of the exocrine pancreas. Pancreatic insufficiency is a risk factor for the development of DEP and therefore should not be considered a defining characteristic. Additionally, pathological pancreatic imaging varies among the different diseases and is not a reliable marker of pancreatic function. Not all patients with imaging findings consistent with necrotizing pancreatitis develop DEP. Patients with mild pancreatitis may lack significant radiographic findings yet are still at risk of developing DEP. Furthermore, patients with pancreatic adenocarcinoma are commonly diagnosed with diabetes prior to developing cancer visible on cross-sectional imaging[26].

Here, we will focus on screening and diagnosis of AP-related diabetes (Figure 1). The first step should be to rule out undiagnosed diabetes/prediabetes by obtaining an HbA1c on admission for AP. We recommend screening for diabetes three months after hospital discharge by obtaining an HbA1c and an oral glucose tolerance test (OGTT). The timing of screening at three months post-hospitalization was selected to limit confounding by stress-related hyperglycemia and to help ensure that the HbA1c is an accurate reflection of changes in glucose levels after AP. Recommendations to use an OGTT are based on several observations. First, studies have shown poor test performance of HbA1c in diagnosing diabetes in patients with cystic fibrosis, another well-known disease affecting the exocrine pancreas. As a result, screening guidelines for cystic fibrosis-related diabetes recommend use of OGTT over HbA1c, and the committee concluded HbA1c



DOI: 10.3748/wjg.v29.i31.4736 **Copyright** ©The Author(s) 2023.

Figure 1 Diagnostic algorithm for acute pancreatitis related diabetes. OGTT: Oral glucose tolerance test; GAD65: Glutamic acid decarboxylase; IA2: Tyrosine phosphatase; ZnT8: Zinc transporter 8; T1DM: Type 1 diabetes mellitus; AP: Acute pancreatitis.

was not sufficiently sensitive for diagnosis of diabetes in this patient population[27]. Similarly, Meier and Giese[28] advocate for the use of OGTT for earlier detection of diabetes in those with pancreatic disease. They found the OGTT diagnosed diabetes when the beta cell area was reduced by 64% compared to a more sizeable beta cell area loss of 89% when diabetes was diagnosed by HbA1c. A more recent study found that fasting glucose and HbA1c underestimate the prevalence of DEP and also recommend use of OGTT[29]. In this study, the diagnosis of over half of the new cases of diabetes after SAP were only possible by using the OGTT.

Once a diagnosis of diabetes is established, the next steps involve ruling out T1D and T2DM. The exclusion of T1D is more straightforward and can be performed by demonstrating the absence of autoantibodies. Duggan *et al*[29] suggest that c-peptide levels may be used to differentiate DEP and T2DM. Levels of c-peptide are typically used to distinguish T1D from T2DM, as levels are low in T1D and high in T2DM. They found that SAP patients with diabetes demonstrated a lower insulin response to glucose ingestion and had lower c-peptide secretion. This suggests the diagnosis of AP-related DM/DEP should be made in the setting of low c-peptide levels and the absence of autoantibodies[29]. More studies are needed to confirm the correlation, but it is a reasonable place to start. As studies showed risk of developing DEP up to five years after a single attack, it would be reasonable to consider continuing annual screening with HbA1c and OGTT *vs* more frequently depending on the presence of other risk factors.

MANAGEMENT

While the overall pathophysiology of DEP is far more complex than the more common types of diabetes, the treatment

algorithms for T2DM are often applied for management of DEP. This may be problematic on several fronts. Studies have shown that patients with CP have an increased risk of developing pancreatic adenocarcinoma through a mechanism potentiated by hyperinsulinemia[2,7,30]. As a result, interventions that reduce ambient insulin levels (*i.e.*, exercise, weight loss, low-carb diet) coupled with the anti-neoplastic properties of Metformin has become the preferred first-line treatment option. If glucose levels remain elevated it is reasonable to consider the addition of oral agents from the thiazolidinedione and/or alpha-glucosidase inhibitor classes. Clinical trials evaluating the safety of sulfonylureas, GLP-1 analogs, and dipeptidyl peptidase-IV inhibitors are lacking and these medications should be avoided due to possible association with pancreatitis[7,30]. All patients should also be counseled on the importance of abstinence from alcohol and tobacco use.

Screening for malabsorption and fat-soluble vitamin deficiencies can help guide the initiation of PERT and vitamin supplementation. The response and release of incretins, such as GLP-1, to fat hydrolysis may even be impaired with subclinical fat-soluble vitamin deficiency and thereby promote post-prandial hyperglycemia. PERT may augment the post-prandial incretin response and has been demonstrated to stabilize glucose levels in patients with alcoholic pancreatitis and cystic fibrosis. Additionally, some believe that PERT may help improve pain associated with pancreatitis.

Every effort should be made to detect AP-related DM before the development of critical insulin deficiency. If insulin therapy is necessary, it is important to remember that DEP may cause enhanced peripheral sensitivity to insulin, increasing the risk of hypoglycemia[7,30]. Dosing calculations similar to those used for T1D should be used rather than those used for T2DM[7]. Additionally, patients with DEP may require more frequent dose adjustments compared to patients with T2DM.

FUTURE RESEARCH

Further investigation should focus on how to use IR and insufficient insulin production to distinguish T2DM from DEP. Although we have proposed a set of diagnostic criteria, further research is needed to confirm whether the absence of autoantibodies in conjunction with low c-peptide levels is enough to diagnose DEP. Additionally, exploration into the possible contribution of PP cell tracking and other biomarkers to characterize DEP is necessary[4].

Improved characterization of alpha cells, beta cells, PP cells and delta cells may also have implications on the diagnosis and treatment of DEP[4]. Methods to do so may include new radiological techniques as well as neural networks. Newer advanced magnetic resonance techniques, including diffusion-weighted imaging, T1 mapping, and T2 mapping, provide quantifiable imaging features to gain additional understanding of underlying irregularities in AP. This goes beyond the traditional magnetic resonance sequences' qualitative imaging features to detect morphological changes in AP[31]. Further, these newer radiological techniques may be able to improve the detection of islet volume changes involved in DEP. Advanced analytic techniques, including radiomics and artificial neural networks, may be able to uncover imaging biomarkers to enable further risk stratification of DEP secondary to AP.

Artificial intelligence (AI) offers risk stratification and prognostication information for AP, including DEP secondary to AP. Machine learning through large data sets may be able to better determine an association between AP disease severity and DEP. An ongoing clinical trial is investigating whether AI machine learning can be used to estimate the disease severity in AP according to the revised Atlanta criteria, which may have implications on DEP[32]. Similarly, while parameters used in handcrafted AP severity prediction scores, such as APACHE II and Ranson, are typically unavailable until 24 to 72 h after hospitalization, the early achievable severity index prediction score which was developed using machine learning, can identify patients at high risk for SAP within 24 h of hospital admission[33]. Early identification of patients at risk of SAP allows for early interventions to decrease mortality, which may also be critical in preventing the development of DEP.

As deficiency of fat-soluble vitamins associated with exocrine pancreatic dysfunction may be linked to new-onset DM, early administration of fat-soluble vitamins needs to be further studied as a possible preventative measure against the development of DEP[12]. Additionally, serum levels of fat-soluble vitamins (vitamin D in particular) may have the potential to be used as markers of risk of AP-related DM, as mentioned by Norbitt *et al*[19]. The connection comes from previous findings that vitamin D levels negatively correlated with AP severity indexes[19,34].

Based on the data mentioned earlier, the incidence of AP continues to rise and we should anticipate an increasing incidence of AP-related DM. This escalates the importance of needing to screen for, monitor, and treat DEP[3]. The next major step in research should also include investigating the reasons for the increased incidence of AP to prevent the disease and DEP by extension.

CONCLUSION

AP is the most common disease of the exocrine pancreas and places a significant strain on healthcare costs as the incidence continues to rise. While many studies have focused on treatment during hospitalization, the sequela of the disease are becoming more important as more patients develop AP and recover from the disease. AP-related diabetes, a type of DEP, is likely more prevalent than initially thought as it is often misclassified as T2DM and treated as such. As new studies emerge, we have learned that the diagnostic criteria for AP-related diabetes needs to be better defined in order to improve management of this unique type of diabetes. Through common knowledge of the pathophysiology of T1D and T2DM and the review of newer studies attempting to find biomarkers to help characterize DEP, we were able to propose a set of diagnostic criteria for AP-related DM. Although studies are needed to test the utility, this may at least provide a starting point. Furthermore, we have identified specific areas in need of further research in hopes that it may

help lead to the development of guidelines for the diagnosis and management of AP-related DM.

FOOTNOTES

Author contributions: Charley E contributed to the final review; Charley E and Dinner B composed the paper; Dinner B added to the literature review and created the included figure; Charley E and Pham K conducted the literature review; Pham K made critical revisions; Vyas N provided mentorship, contributed to the overall concept and made critical revisions; and all authors have read and approve the final manuscript.

Conflict-of-interest statement: All the authors report no relevant conflicts of interest for this article.

Open-Access: This article is an open-access article that was selected by an in-house editor and fully peer-reviewed by external reviewers. It is distributed in accordance with the Creative Commons Attribution NonCommercial (CC BY-NC 4.0) license, which permits others to distribute, remix, adapt, build upon this work non-commercially, and license their derivative works on different terms, provided the original work is properly cited and the use is non-commercial. See: https://creativecommons.org/Licenses/by-nc/4.0/

Country/Territory of origin: United States

ORCID number: Ericka Charley 0009-0004-3647-2971; Neil Vyas 0000-0002-0166-3928.

S-Editor: Wang JJ
L-Editor: A
P-Editor: Cai YX

REFERENCES

1 **Garg PK**, Singh VP. Organ Failure Due to Systemic Injury in Acute Pancreatitis. *Gastroenterology* 2019; **156**: 2008-2023 [PMID: 30768987 DOI: 10.1053/j.gastro.2018.12.041]
2 **Gapp J**, Tariq A, Chandra S. Acute Pancreatitis. 2023 Feb 9. In: StatPearls [Internet]. Treasure Island (FL): StatPearls Publishing; 2023 Jan- [PMID: 29494075]
3 **Iannuzzi JP**, King JA, Leong JH, Quan J, Windsor JW, Tanyingoh D, Coward S, Forbes N, Heitman SJ, Shaheen AA, Swain M, Buie M, Underwood FE, Kaplan GG. Global Incidence of Acute Pancreatitis Is Increasing Over Time: A Systematic Review and Meta-Analysis. *Gastroenterology* 2022; **162**: 122-134 [PMID: 34571026 DOI: 10.1053/j.gastro.2021.09.043]
4 **Hart PA**, Bradley D, Conwell DL, Dungan K, Krishna SG, Wyne K, Bellin MD, Yadav D, Andersen DK, Serrano J, Papachristou GI. Diabetes following acute pancreatitis. *Lancet Gastroenterol Hepatol* 2021; **6**: 668-675 [PMID: 34089654 DOI: 10.1016/S2468-1253(21)00019-4]
5 **Centers for Disease Control and Prevention**. What Is Diabetes? [cited 26 November 2022]. Available from: https://www.cdc.gov/diabetes/basics/diabetes.html
6 **Hart PA**, Bellin MD, Andersen DK, Bradley D, Cruz-Monserrate Z, Forsmark CE, Goodarzi MO, Habtezion A, Korc M, Kudva YC, Pandol SJ, Yadav D, Chari ST; Consortium for the Study of Chronic Pancreatitis, Diabetes, and Pancreatic Cancer(CPDPC). Type 3c (pancreatogenic) diabetes mellitus secondary to chronic pancreatitis and pancreatic cancer. *Lancet Gastroenterol Hepatol* 2016; **1**: 226-237 [PMID: 28404095 DOI: 10.1016/S2468-1253(16)30106-6]
7 **Wynne K**, Devereaux B, Dornhorst A. Diabetes of the exocrine pancreas. *J Gastroenterol Hepatol* 2019; **34**: 346-354 [PMID: 30151918 DOI: 10.1111/jgh.14451]
8 **Das SL**, Singh PP, Phillips AR, Murphy R, Windsor JA, Petrov MS. Newly diagnosed diabetes mellitus after acute pancreatitis: a systematic review and meta-analysis. *Gut* 2014; **63**: 818-831 [PMID: 23929695 DOI: 10.1136/gutjnl-2013-305062]
9 **Zhi M**, Zhu X, Lugea A, Waldron RT, Pandol SJ, Li L. Incidence of New Onset Diabetes Mellitus Secondary to Acute Pancreatitis: A Systematic Review and Meta-Analysis. *Front Physiol* 2019; **10**: 637 [PMID: 31231233 DOI: 10.3389/fphys.2019.00637]
10 **Li CL**, Jiang M, Pan CQ, Li J, Xu LG. The global, regional, and national burden of acute pancreatitis in 204 countries and territories, 1990-2019. *BMC Gastroenterol* 2021; **21**: 332 [PMID: 34433418 DOI: 10.1186/s12876-021-01906-2]
11 **Mederos MA**, Reber HA, Girgis MD. Acute Pancreatitis: A Review. *JAMA* 2021; **325**: 382-390 [PMID: 33496779 DOI: 10.1001/jama.2020.20317]
12 **Cho J**, Scragg R, Pandol SJ, Petrov MS. Exocrine Pancreatic Dysfunction Increases the Risk of New-Onset Diabetes Mellitus: Results of a Nationwide Cohort Study. *Clin Transl Sci* 2021; **14**: 170-178 [PMID: 32692901 DOI: 10.1111/cts.12837]
13 **Columbia Surgery**. The pancreas and its functions. [cited 15 November 2022]. Available from: https://columbiasurgery.org/pancreas/pancreas-and-its-functions
14 **Rickels MR**, Norris AW, Hull RL. A tale of two pancreases: exocrine pathology and endocrine dysfunction. *Diabetologia* 2020; **63**: 2030-2039 [PMID: 32894313 DOI: 10.1007/s00125-020-05210-8]
15 **Wu L**, Nahm CB, Jamieson NB, Samra J, Clifton-Bligh R, Mittal A, Tsang V. Risk factors for development of diabetes mellitus (Type 3c) after partial pancreatectomy: A systematic review. *Clin Endocrinol (Oxf)* 2020; **92**: 396-406 [PMID: 32017157 DOI: 10.1111/cen.14168]
16 **Tu J**, Zhang J, Ke L, Yang Y, Yang Q, Lu G, Li B, Tong Z, Li W, Li J. Endocrine and exocrine pancreatic insufficiency after acute pancreatitis: long-term follow-up study. *BMC Gastroenterol* 2017; **17**: 114 [PMID: 29078749 DOI: 10.1186/s12876-017-0663-0]
17 **Mirhosseini N**, Vatanparast H, Mazidi M, Kimball SM. The Effect of Improved Serum 25-Hydroxyvitamin D Status on Glycemic Control in Diabetic Patients: A Meta-Analysis. *J Clin Endocrinol Metab* 2017; **102**: 3097-3110 [PMID: 28957454 DOI: 10.1210/jc.2017-01024]
18 **Gagnon C**, Daly RM, Carpentier A, Lu ZX, Shore-Lorenti C, Sikaris K, Jean S, Ebeling PR. Effects of combined calcium and vitamin D supplementation on insulin secretion, insulin sensitivity and β-cell function in multi-ethnic vitamin D-deficient adults at risk for type 2

diabetes: a pilot randomized, placebo-controlled trial. *PLoS One* 2014; **9**: e109607 [PMID: 25299668 DOI: 10.1371/journal.pone.0109607]

19 **Norbitt CF**, Kimita W, Bharmal SH, Ko J, Petrov MS. Relationship between Habitual Intake of Vitamins and New-Onset Prediabetes/Diabetes after Acute Pancreatitis. *Nutrients* 2022; **14** [PMID: 35406092 DOI: 10.3390/nu14071480]

20 **Firkins SA**, Hart PA, Papachristou GI, Lara LF, Cruz-Monserrate Z, Hinton A, Conwell DL, Bradley DP, Krishna SG. Identification of a Risk Profile for New-Onset Diabetes After Acute Pancreatitis. *Pancreas* 2021; **50**: 696-703 [PMID: 34016890 DOI: 10.1097/MPA.0000000000001818]

21 **Goodarzi MO**, Petrov MS, Andersen DK, Hart PA. Diabetes in chronic pancreatitis: risk factors and natural history. *Curr Opin Gastroenterol* 2021; **37**: 526-531 [PMID: 34074860 DOI: 10.1097/MOG.0000000000000756]

22 **Woodmansey C**, McGovern AP, McCullough KA, Whyte MB, Munro NM, Correa AC, Gatenby PAC, Jones SA, de Lusignan S. Incidence, Demographics, and Clinical Characteristics of Diabetes of the Exocrine Pancreas (Type 3c): A Retrospective Cohort Study. *Diabetes Care* 2017; **40**: 1486-1493 [PMID: 28860126 DOI: 10.2337/dc17-0542]

23 **Lv Y**, Zhang J, Yang T, Sun J, Hou J, Chen Z, Yu X, Yuan X, Lu X, Xie T, Yu T, Su X, Liu G, Zhang C, Li L. Non-Alcoholic Fatty Liver Disease (NAFLD) Is an Independent Risk Factor for Developing New-Onset Diabetes After Acute Pancreatitis: A Multicenter Retrospective Cohort Study in Chinese Population. *Front Endocrinol (Lausanne)* 2022; **13**: 903731 [PMID: 35692404 DOI: 10.3389/fendo.2022.903731]

24 **Richardson A**, Park WG. Acute pancreatitis and diabetes mellitus: a review. *Korean J Intern Med* 2021; **36**: 15-24 [PMID: 33147904 DOI: 10.3904/kjim.2020.505]

25 **Ewald N**, Bretzel RG. Diabetes mellitus secondary to pancreatic diseases (Type 3c)--are we neglecting an important disease? *Eur J Intern Med* 2013; **24**: 203-206 [PMID: 23375619 DOI: 10.1016/j.ejim.2012.12.017]

26 **Petrov MS**, Basina M. DIAGNOSIS OF ENDOCRINE DISEASE: Diagnosing and classifying diabetes in diseases of the exocrine pancreas. *Eur J Endocrinol* 2021; **184**: R151-R163 [PMID: 33460395 DOI: 10.1530/EJE-20-0974]

27 **Moran A**, Brunzell C, Cohen RC, Katz M, Marshall BC, Onady G, Robinson KA, Sabadosa KA, Stecenko A, Slovis B; CFRD Guidelines Committee. Clinical care guidelines for cystic fibrosis-related diabetes: a position statement of the American Diabetes Association and a clinical practice guideline of the Cystic Fibrosis Foundation, endorsed by the Pediatric Endocrine Society. *Diabetes Care* 2010; **33**: 2697-2708 [PMID: 21115772 DOI: 10.2337/dc10-1768]

28 **Meier JJ**, Giese A. Diabetes associated with pancreatic diseases. *Curr Opin Gastroenterol* 2015; **31**: 400-406 [PMID: 26125315 DOI: 10.1097/MOG.0000000000000199]

29 **Duggan SN**, O'Connor DB, Antanaitis A, Campion JR, Lawal O, Ahmed M, Tisdall AR, Sherlock M, Boran G, le Roux C, Gibney J, Conlon KC. Metabolic dysfunction and diabetes mellitus during long-term follow-up of severe acute pancreatitis: A case-matched study. *Pancreatology* 2020; **20**: 813-821 [PMID: 32522508 DOI: 10.1016/j.pan.2020.03.016]

30 **Cui Y**, Andersen DK. Pancreatogenic diabetes: special considerations for management. *Pancreatology* 2011; **11**: 279-294 [PMID: 21757968 DOI: 10.1159/000329188]

31 **Ghandili S**, Shayesteh S, Fouladi DF, Blanco A, Chu LC. Emerging imaging techniques for acute pancreatitis. *Abdom Radiol (NY)* 2020; **45**: 1299-1307 [PMID: 31428811 DOI: 10.1007/s00261-019-02192-z]

32 **İnce AT**. Artificial Intelligence Prediction for the Severity of Acute Pancreatitis. [accessed 2023 Jan 24]. In: ClinicalTrials.gov [Internet]. Bethesda (MD): U.S. National Library of Medicine. Available from: https://clinicaltrials.gov/study/NCT04735055 ClinicalTrials.gov Identifier: NCT04735055

33 **Kui B**, Pintér J, Molontay R, Nagy M, Farkas N, Gede N, Vincze Á, Bajor J, Gódi S, Czimmer J, Szabó I, Illés A, Sarlós P, Hágendorn R, Pár G, Papp M, Vitális Z, Kovács G, Fehér E, Földi I, Izbéki F, Gajdán L, Fejes R, Németh BC, Török I, Farkas H, Mickevicius A, Sallinen V, Galeev S, Ramírez-Maldonado E, Párniczky A, Erőss B, Hegyi PJ, Márta K, Váncsa S, Sutton R, Szatmary P, Latawiec D, Halloran C, de-Madaria E, Pando E, Alberti P, Gómez-Jurado MJ, Tantau A, Szentesi A, Hegyi P; Hungarian Pancreatic Study Group. EASY-APP: An artificial intelligence model and application for early and easy prediction of severity in acute pancreatitis. *Clin Transl Med* 2022; **12**: e842 [PMID: 35653504 DOI: 10.1002/ctm2.842]

34 **Huh JH**, Kim JW, Lee KJ. Vitamin D deficiency predicts severe acute pancreatitis. *United European Gastroenterol J* 2019; **7**: 90-95 [PMID: 30788120 DOI: 10.1177/2050640618811489]

World Journal of Gastroenterology

Submit a Manuscript: https://www.f6publishing.com

World J Gastroenterol 2023 August 21; 29(31): 4744-4762

DOI: 10.3748/wjg.v29.i31.4744

ISSN 1007-9327 (print) ISSN 2219-2840 (online)

ORIGINAL ARTICLE

Basic Study

Huangqin decoction alleviates lipid metabolism disorders and insulin resistance in nonalcoholic fatty liver disease by triggering Sirt1/NF-κB pathway

Bao-Fei Yan, Lan-Fen Pan, Yi-Fang Quan, Qian Sha, Jing-Zheng Zhang, Yi-Feng Zhang, Li-Bing Zhou, Xi-Long Qian, Xiao-Mei Gu, Feng-Tao Li, Ting Wang, Jia Liu, Xian Zheng

Specialty type: Gastroenterology and hepatology

Provenance and peer review: Unsolicited article; Externally peer reviewed.

Peer-review model: Single blind

Peer-review report's scientific quality classification

Grade A (Excellent): 0
Grade B (Very good): B, B
Grade C (Good): 0
Grade D (Fair): 0
Grade E (Poor): 0

P-Reviewer: Bugaj AM, Poland; Dietrich CG, Germany

Received: April 27, 2023
Peer-review started: April 27, 2023
First decision: July 9, 2023
Revised: July 23, 2023
Accepted: July 31, 2023
Article in press: July 31, 2023
Published online: August 21, 2023

Bao-Fei Yan, Jing-Zheng Zhang, Feng-Tao Li, Jia Liu, College of Pharmacy, Jiangsu Health Vocational College, Nanjing 211800, Jiangsu Province, China

Lan-Fen Pan, Department of Pathology, Affiliated Kunshan Hospital of Jiangsu University, Kunshan 215300, Jiangsu Province, China

Yi-Fang Quan, Department of Education and Science, The First People's Hospital of Taicang, Kunshan 215400, Jiangsu Province, China

Qian Sha, Department of Pharmacy, Affiliated Hospital of Xuzhou Medical University, Xuzhou 221006, Jiangsu Province, China

Yi-Feng Zhang, School of Pharmacy, Nantong University, Nantong 226019, Jiangsu Province, China

Li-Bing Zhou, Xiao-Mei Gu, Ting Wang, Xian Zheng, Department of Pharmacy, Affiliated Kunshan Hospital of Jiangsu University, Kunshan 215300, Jiangsu Province, China

Xi-Long Qian, School of Pharmacy, Nanjing University of Chinese Medicine, Nanjing 210023, Jiangsu Province, China

Corresponding author: Xian Zheng, PhD, Pharmacist, Postdoc, Department of Pharmacy, Affiliated Kunshan Hospital of Jiangsu University, No. 566 Qianjin East Road, Development Zone, Kunshan 215300, Jiangsu Province, China. zhengxiannew@163.com

Abstract

BACKGROUND

Nonalcoholic fatty liver disease (NAFLD) is a clinicopathological entity characterized by intrahepatic ectopic steatosis. As a consequence of increased consumption of high-calorie diet and adoption of a sedentary lifestyle, the incidence of NAFLD has surpassed that of viral hepatitis, making it the most common cause of chronic liver disease globally. Huangqin decoction (HQD), a Chinese medicinal formulation that has been used clinically for thousands of years, has beneficial outcomes in patients with liver diseases, including NAFLD. However, the role and mechanism of action of HQD in lipid metabolism disorders

and insulin resistance in NAFLD remain poorly understood.

AIM
To evaluate the ameliorative effects of HQD in NAFLD, with a focus on lipid metabolism and insulin resistance, and to elucidate the underlying mechanism of action.

METHODS
High-fat diet-induced NAFLD rats and palmitic acid (PA)-stimulated HepG2 cells were used to investigate the effects of HQD and identify its potential mechanism of action. Phytochemicals in HQD were analyzed by high-performance liquid chromatography (HPLC) to identify the key components.

RESULTS
Ten primary chemical components of HQD were identified by HPLC analysis. *In vivo*, HQD effectively prevented rats from gaining body and liver weight, improved the liver index, ameliorated hepatic histological aberrations, decreased transaminase and lipid profile disorders, and reduced the levels of pro-inflammatory factors and insulin resistance. *In vitro* studies revealed that HQD effectively alleviated PA-induced lipid accumulation, inflammation, and insulin resistance in HepG2 cells. In-depth investigation revealed that HQD triggers Sirt1/NF-κB pathway-modulated lipogenesis and inflammation, contributing to its beneficial actions, which was further corroborated by the addition of the Sirt1 antagonist EX-527 that compromised the favorable effects of HQD.

CONCLUSION
In summary, our study confirmed that HQD mitigates lipid metabolism disorders and insulin resistance in NAFLD by triggering the Sirt1/NF-κB pathway.

Key Words: Nonalcoholic fatty liver disease; Huangqin decoction; Lipid metabolism disorders; Insulin resistance; Sirt1/NF-κB pathway

©The Author(s) 2023. Published by Baishideng Publishing Group Inc. All rights reserved.

Core Tip: Huangqin decoction (HQD) has substantial therapeutic effects in liver diseases. We previously showed that HQD mitigates hepatic inflammation in a rat model of High-fat diet (HFD)-induced Nonalcoholic fatty liver disease (NAFLD) by inhibiting the TLR4/NF-κB/NLRP3 pathway. Here, we investigated the effects of HQD on lipid metabolism disorders and insulin resistance in NAFLD. Our results demonstrated that HQD effectively antagonizes hepatocyte steatosis and insulin resistance in HFD-fed rats and palmitic acid-challenged HepG2 cells by triggering Sirt1/NF-κB pathway-modulated lipogenesis and inflammation. These data will significantly promote the clinical application of HQD in the treatment of NAFLD.

Citation: Yan BF, Pan LF, Quan YF, Sha Q, Zhang JZ, Zhang YF, Zhou LB, Qian XL, Gu XM, Li FT, Wang T, Liu J, Zheng X. Huangqin decoction alleviates lipid metabolism disorders and insulin resistance in nonalcoholic fatty liver disease by triggering Sirt1/NF-κB pathway. *World J Gastroenterol* 2023; 29(31): 4744-4762
URL: https://www.wjgnet.com/1007-9327/full/v29/i31/4744.htm
DOI: https://dx.doi.org/10.3748/wjg.v29.i31.4744

INTRODUCTION

As lifestyles have been increasingly shifting to "eat more, move less", overweight and obese cohorts is on a monumental rise. Consequently, the incidence of obesity-related chronic diseases, such as type 2 diabetes, cardiovascular disease, and nonalcoholic fatty liver disease (NAFLD) is on the rise. NAFLD is the most common liver disease characterized by excessive hepatocellular lipid build-up, which is caused by factors other than alcohol intake, drugs, viral infections, and autoimmunity[1]. The initial signs and symptoms of NAFLD are limited to benign steatosis[2]. However, if not managed, approximately 30% of NAFLD cases will progress to nonalcoholic steatohepatitis (NASH). Subsequently approximately 30%–40% of NASH cases will further progress to fibrosis and cirrhosis, and approximately 5%–25% of NASH patients will die from advanced liver diseases within ten years[2-5]. Additionally, epidemiological studies suggest that NAFLD patients are more prone to develop heart disease and die from heart attacks compared to healthy individuals[6]. Currently, NAFLD affects approximately 25% of the general population worldwide, and the associated morbidity in China has increased substantially from 18% to approximately 30% in recent decades[7]. It is estimated that more than 300 million cases of NAFLD will emerge in China by 2030, causing a tremendous strain on its healthcare and economy[8]. Unfortunately, no specific drug has been approved by the Food and Drug Administration for NAFLD; invasive bariatric surgery and lifestyle modifications are thought to be effective strategies[9]. Therefore, there is an urgent need to identify more efficacious agents for NAFLD treatment.

NAFLD is driven by multiple factors and its etiology remains complex and elusive. Several hypotheses have been proposed over the past few decades to explain its pathogenesis. According to the canonical "two-hit" hypothesis originally proposed by Day and James[10], obesity and insulin resistance-evoked excessive intrahepatic lipid accumulation constitutes the "first hit," and ensuing oxidative stress and inflammation constitute the "second hit". Subsequent studies found that hepatocyte regeneration and proliferation were impeded during the progression of NAFLD, which was termed as the "third-hit"[11]. Following further in-depth investigations, a more precise "multiple-hit" hypothesis was proposed that deems that hepatic steatosis increases the susceptibility of the liver to intra- and extrahepatic offenders, such as hepatic oxidative stress and inflammation, gut dysbiosis, and disturbed adipokines, and the multiple insults simultaneously and synergistically induce and advance NAFLD[12]. However, in both the hypotheses, hepatic steatosis is considered to be the paramount driver of NAFLD, and numerous studies have focused on lipid metabolism-associated targets (*e.g.*, Sirt1) in an attempt to reduce intrahepatic fat[9]. Sirt1, a nicotinamide adenine dinucleotide-dependent lysine deacetylase, is a metabolic sensor that is highly expressed in metabolically active organs (*e.g.*, the liver and skeletal muscles) and is extensively involved in glucose and lipid metabolism[9,13,14]. Clinical evidence indicates that patients with NAFLD exhibit defective Sirt1 expression in the liver[15]. Additionally, inhibition of Sirt1 exacerbated high-fat diet (HFD)-induced hepatic steatosis in mice, whereas activation of Sirt1 exerted anti-steatotic effect[16]. Importantly, it was reported that Sirt1 deacetylates lysine residues of NF-κB (RelA/p65 subunit), thereby affecting its transcriptional activity and restricting the expression of pro-inflammatory target genes[17]. Curative effects including anti-steatosis, anti-inflammation, and anti-apoptosis were noted when Sirt1/NF-κB pathway was triggered in methionine-choline-deficient diet-induced NASH mice, indicating the vital role of Sirt1/NF-κB pathway in defense against NAFLD[18]. In addition, recent studies suggest that NF-κB-stimulated pro-inflammatory factors activate hepatic insulin resistance, and thereby aggravate hepatic steatosis[17,19]. Therefore, triggering the Sirt1/NF-κB pathway represents a potential strategy for counteracting insulin resistance and hepatic steatosis in NAFLD.

Huangqin decoction (HQD) is a classical traditional Chinese medicine (TCM) formulation that was first mentioned in "Treatise on Febrile Diseases" by the medical sage Zhong-Jing Zhang. According to records, HQD harbors the efficacy of "clearing away heat and treating dysentery" and "regulating the stomach and relieving pain," and has long been utilized to treat inflammatory diseases. It has a positive reputation as "the ancestral agent for curing dysentery in all ages" and "the first decoction for febrile diseases"[20]. Notably, HQD has been used to treat liver disorders (*e.g.*, NAFLD) at the First Affiliated Hospital of Nanjing University of Chinese Medicine for decades with positive outcomes. HQD is composed of four botanical herbs, *Scutellariae Radix* (Huangqin in Chinese), *Paeoniae Radix Alba* (Baishao in Chinese), *Glycyrrhizae Radix et Rhizome* (Gancao in Chinese), and *Jujubae Fructus* (Dazao in Chinese), which are clinically combined in a 3:2:2:2 ratio. Previous studies reported that these herbs can alleviate NAFLD when used independently[21-23]. More importantly, in our recent study, the anti-hepatitis effects of HQD in HFD-induced NAFLD rats were found to be mediated *via* inhibition of the TLR4/NF-κB/NLRP3 pathway[24]. However, the regulatory mechanisms of HQD in hepatic steatosis and its ameliorative effects in insulin resistance remain undefined.

To address this gap, we used HFD-induced NAFLD rats and palmitic acid (PA)-induced HepG2 cells to investigate the ameliorative effects of HQD in lipid metabolism disorders and insulin resistance, and identify the potential molecular mechanisms by focusing on the Sirt1/NF-κB pathway.

MATERIALS AND METHODS

Plant materials and reagents

Scutellariae Radix, *Paeoniae Radix Alba*, Glycyrrhizae Radix et Rhizome, and *Jujubae Fructus* were obtained from Wansheng Herbal Decoction Pieces Co. Ltd. (Bozhou, China) and authenticated by Professor Sheng-Jin Liu of the Nanjing University of Chinese Medicine (Nanjing, China). All voucher specimens (Voucher No. 220301, 220302, 220303, and 220304) were deposited at the Central Laboratory of Jiangsu Health Vocational College (Nanjing, China). Gallic acid, paeoniflorin, scutellarin, liquiritin, baicalin, scutellarein, wogonoside, baicalein, wogonin, and chrysin (purity ≥ 98%) were purchased from Yuanye Biotechnology Co. Ltd. (Shanghai, China). Fenofibrate (Fen) was obtained from SPGC Sine Pharmaceutical Co. Ltd. (Shanghai, China). Enzyme-linked immunosorbent assay (ELISA) kits for insulin, tumor necrosis factor (TNF)-α, interleukin (IL)-6, and IL-1β were obtained from Solarbio (Beijing, China). Commercial biochemical kits for triacylglycerol (TG), total cholesterol (TC), free fatty acids (FFA), low-density lipoprotein cholesterol (LDL-c), high-density lipoprotein cholesterol (HDL-c), alanine transaminase (ALT), and aspartate transaminase (AST) were obtained from the Nanjing Jiancheng Bioengineering Institute (Nanjing, China). Hematoxylin and eosin (H&E) and Oil Red O staining kits were supplied by Beyotime (Shanghai, China). Dulbecco's modified Eagle's medium (DMEM), fetal bovine serum (FBS), bovine serum albumin (BSA), and PA were purchased from Sigma-Aldrich (St. Louis, MO, United States). Penicillin-streptomycin solution was obtained from Thermo Fisher Scientific (Waltham, MA, United States). EX-527 was purchased from Selleck Chemicals (Houston, TX, United States). A colorimetric 2-deoxydglucose (2DG) uptake assay kit and antibodies against IL-1β, sterol regulatory element-binding protein (SREBP)-1, fatty acid synthase (FAS), cluster of differentiation 36 (CD36), Sirt1, NF-κB, p-NF-κB, IRS-2, p-IRS-2, and glyceraldehyde-3-phosphate dehydrogenase (GAPDH) were purchased from Abcam (Cambridge, MA, United Kingdom). All the chemicals used were of analytical grade.

Preparation of HQD

HQD was prepared using established protocols. Briefly, 300 g *Scutellariae Radix*, 200 g *Paeoniae Radix Alba*, 200 g *Glycyrrhizae Radix et Rhizome*, and 200 g *Jujubae Fructus* were combined in 10-fold volume of double-distilled water and extracted in boiling water for 1 h. Following filtration through gauze, the herbal residue was extracted again for 1 h at 100

°C with 8-fold volume of double-distilled water. Subsequently, the two extracts were pooled, concentrated under reduced pressure, and lyophilized to yield 173.1 g of the extract powder. The extract ratio of HQD was 19.23% (w/w). The lyophilized extract powder was stored at -80 °C for subsequent experiments.

High-performance liquid chromatography analysis of HQD

An Agilent 1260 high-performance liquid chromatography (HPLC) separation system (Agilent, Santa Clara, CA, United States) equipped with a diode array detector was used to analyze the chemical composition of HQD. Briefly, the lyophilized powder (0.5 g) was dissolved in 20 mL of ultrapure water using ultrasonication. Following filtration through a 0.22 μm syringe filter, 20 μL of the supernatant was injected into the HPLC system and separated chromatographically through an Agilent ZORBAX SB-C18 column (4.6 mm × 150 mm, 5 μm). The mobile phase comprised of linear gradients of 0.1% (v/v) formic acid in water and acetonitrile. Gradient elution was performed as follows: 0–10 min, 5%–8% acetonitrile; 10–20 min, 8%–16% acetonitrile; 20–40 min, 16%–22% acetonitrile; 40–50 min, 22%–25% acetonitrile; 50–60 min, 25%–40% acetonitrile; 60–70 min, 40%–60% acetonitrile; 70–75 min, 60%–5% acetonitrile; 75–80 min, 5% acetonitrile. Programmable parameters for flow rate, injection volume, and detector wavelength were 1 mL/min, 5 μL, and 270 nm, respectively.

Animals

Male Sprague-Dawley rats (seven weeks old, weighing 180–200 g) were obtained from the Hangzhou Medical College (Hangzhou, China). The rats were housed in a conventional habitat (40%–50% humidity, 25 ± 1 °C, and 12 h light/dark) at the Laboratory Animal Center of the Jiangsu Health Vocational College. The experimental protocols strictly complied with the European Community criteria and were authorized by the Animal Ethics Committee of the Jiangsu Health Vocational College (Permission No. JHVC-IACUC-2022-B007).

Animal grouping and treatment

Following one week of acclimatization, the rats were randomly allocated to five groups (n = 8/group): Normal, HFD, HFD plus Fen (30 mg/kg), and HFD plus HQD (400 and 800 mg/kg). Rats in the normal group were fed a normal chow diet (10% calories from fat), whereas the rats in the other groups were fed a HFD (60% calories from fat) for 16 wk to establish the NAFLD model[25]. Both diets were provided by Jiangsu Xietong Pharmaceutical Bioengineering Co. Ltd. (Nanjing, China). Starting from the 8th week, the rats were orally administered Fen or HQD once daily for intervention, whereas the rats in the normal and HFD groups received an equal volume of 0.5% sodium carboxymethylcellulose (CMC-Na) orally as the control. Body weights of the animals were monitored weekly during the experimental period. At the end of the experiment, the rats were fasted overnight prior to being anesthetized with 1% pentobarbital sodium. To obtain serum, blood samples were collected from the abdominal aorta and centrifuged at 3500 rpm for 15 min. The rat livers were swiftly resected and flushed with phosphate buffered saline. Liver weights were measured and the liver indices (liver weight/body weight) were calculated. Portions of the liver were fixed in 4% paraformaldehyde for histological analysis and the remaining liver specimen was snap-frozen and stored at -80 °C for future molecular biology analyses.

Evaluation of insulin sensitivity

Two days prior to the termination of the experiment, the mice were fasted for 12 h and then orally administered 2 g/kg glucose. Blood was drawn from the tail vein before or at the indicated time points (30, 60, 90, and 120 min) after gavage. Blood glucose levels were measured using a glucometer (Yuwell, Inc., Zhenjiang, China). The oral glucose tolerance test (OGTT) curve and area under the curve (AUC) of the OGTT were drawn and calculated using GraphPad Prism 8.0. At the end of the experiment, fasting blood glucose (FBG) and serum insulin levels were determined using a glucometer and an insulin ELISA kit, respectively. The homeostasis model assessment of insulin resistance (HOMA-IR) was calculated as follows: (FBG × fasting serum insulin)/22.5.

Cell culture and treatment

HepG2 cells were purchased from the Chinese Academy of Cell Resource Center (Shanghai, China) and cultured in DMEM (supplemented with 10% FBS and 1% penicillin-streptomycin) at 37 °C in a humid environment containing 5% CO_2. PA stock solution (5 mmol/L) was dissolved in 5% BSA by incubating at 55 °C for 15 min. Subsequently, the PA-BSA solution was incorporated into the medium at a final concentration of 125 μM. HQD-mediated cytotoxicity was determined using the 3-(4,5-dimethylthiazol-2-yl)-2,5-diphenyltetrazolium bromide (MTT) assay. For the interventions, HepG2 cells (70% confluent and serum-starved for 12 h) were treated with insulin (1 IU/mL), various doses of HQD (0, 25, 75, or 125 μg/mL) or a combination of HQD (100 μg/mL) and EX-527 (10 μM) under PA (125 μM) challenge for 24 h. HepG2 cells grown in serum-free media with 5% BSA served as the blank control.

MTT assay

HepG2 cells were seeded in 96-well plates (1×10^4 cells/well) and cultured overnight, followed by exposure to different concentrations of HQD (0, 25, 50, 75, 100, 120, 150, 175, and 200 μg/mL) with or without 125 μM PA for 24 h. MTT solution (10 μL of 5 mg/mL) was added to each well and incubated at 37 °C for 4 h. Dimethyl sulfoxide (150 μL) was added to dissolve the formazan crystals with vigorously shaking for 5 min. Finally, a Multiskan MK3 microplate reader (Thermo Fisher Scientific) was used to measure the absorbance at 490 nm. Cell viability (% of control) was calculated using the following formula: [Optical density (OD) 490 (sample-blank)/OD 490 (control-blank)] × 100%.

Glucose uptake assay

HepG2 cells were cultured overnight in 96-well plates (5 × 10^3 cells/well) and then starved for 12 h. The cells were stimulated without or with 1 μM insulin for 20 min to activate the glucose transporters. A colorimetric 2DG uptake test was performed according to the manufacturer's protocol to evaluate glucose absorption by HepG2 cells in response to insulin.

ELISA and biochemical analyses

TNF-β, IL-6, and IL-1β levels in the liver and cell supernatants, as well as serum insulin levels, were measured using the corresponding ELISA kits following the manufacturer's instructions. Biochemical parameters in the serum, liver, and HepG2 cells, including TG, TC, LDL-c, HDL-c, FFA, ALT, and AST were determined using commercial kits following the manufacturer's instructions.

Histological and immunohistochemistrical/immunofluorescent analyses

Fixed liver tissues were embedded in paraffin, cut into 5 μm slices, and stained with H&E according to the standard procedure. Immunohistochemical analyses were performed as described previously[25]. Briefly, primary antibodies against IL-1β, SREBP-1, Sirt1, and p-NF-κB were diluted 200-fold and then incubated with the tissue samples overnight at 4 °C. Following that, 100 μL of secondary antibody (diluted 400-fold) was added dropwise to each section. Horseradish peroxidase (HRP)-conjugated goat anti-rabbit IgG (H + L) was used for IL-1β and SREBP-1. HRP- or Alexa Fluor594-conjugated goat anti-rabbit IgG (H + L) was used for Sirt1 and p-NF-κB. Subsequently, 4',6-diamidino-2-phenylindole (DAPI) or 3,3'-diaminobenzidine substrate solution was sequentially added to each section. Images were captured using either a DM2500 optical microscope (Leica, Wetzlar, Germany) or an LSM 700 confocal laser microscope (Zeiss, Oberkochen, Germany). Finally, the data were quantified using the Image-Pro Plus software (version 6.0; Media Cybernetics, Rockville, MD, United States). For immunofluorescence analysis, HepG2 cells were immobilized in 4% paraformaldehyde solution for 10 min, blocked with 5% BSA, and incubated overnight with primary antibodies against Sirt1 and NF-κB (both diluted 200-fold). Thereafter, the cells were probed with Alexa Fluor 488-conjugated secondary antibodies (diluted 500-fold) and counterstained with DAPI to visualize the nuclei. Fluorescence images were acquired using an LSM 700 confocal laser microscope (Zeiss).

Oil Red O staining

Paraffin-embedded liver tissues were cut into 5 μm sections, followed by staining with Oil Red O dye according to standard procedure. HepG2 cells were fixed in 4% paraformaldehyde for 15 min, rinsed with distilled water, and stained with Oil Red O dye. Images were captured using a DM2500 optical microscope (Leica).

Western blotting

Pre-chilled radio immunoprecipitation assay buffer (containing a protease inhibitor cocktail) was used to lyse liver samples. A commercial bicinchoninic acid assay kit was used to quantify total proteins. Immunoblot analysis was performed as previously described[25]. Specific primary antibodies against SREBP-1c, FAS, CD36, Sirt1, NF-κB, p-NF-κB, IRS-2, p-IRS-2, and GAPDH were used at 1000-fold dilution. The protein bands were visualized and semi-quantified using Azure Biosystems C600 (Azure Biosystems Inc., Dublin, CA, United States) and ImageJ software (NIH, Bethesda, MD, United States), respectively.

Statistical analysis

Data were analyzed using IBM SPSS software (version 21.0; Armonk, NY, United States) and expressed as mean ± SD. One-way analysis of variance followed by a least significant difference test for multiple comparisons was used to assess significant differences among groups. Statistical significance was set at $P \leq 0.05$.

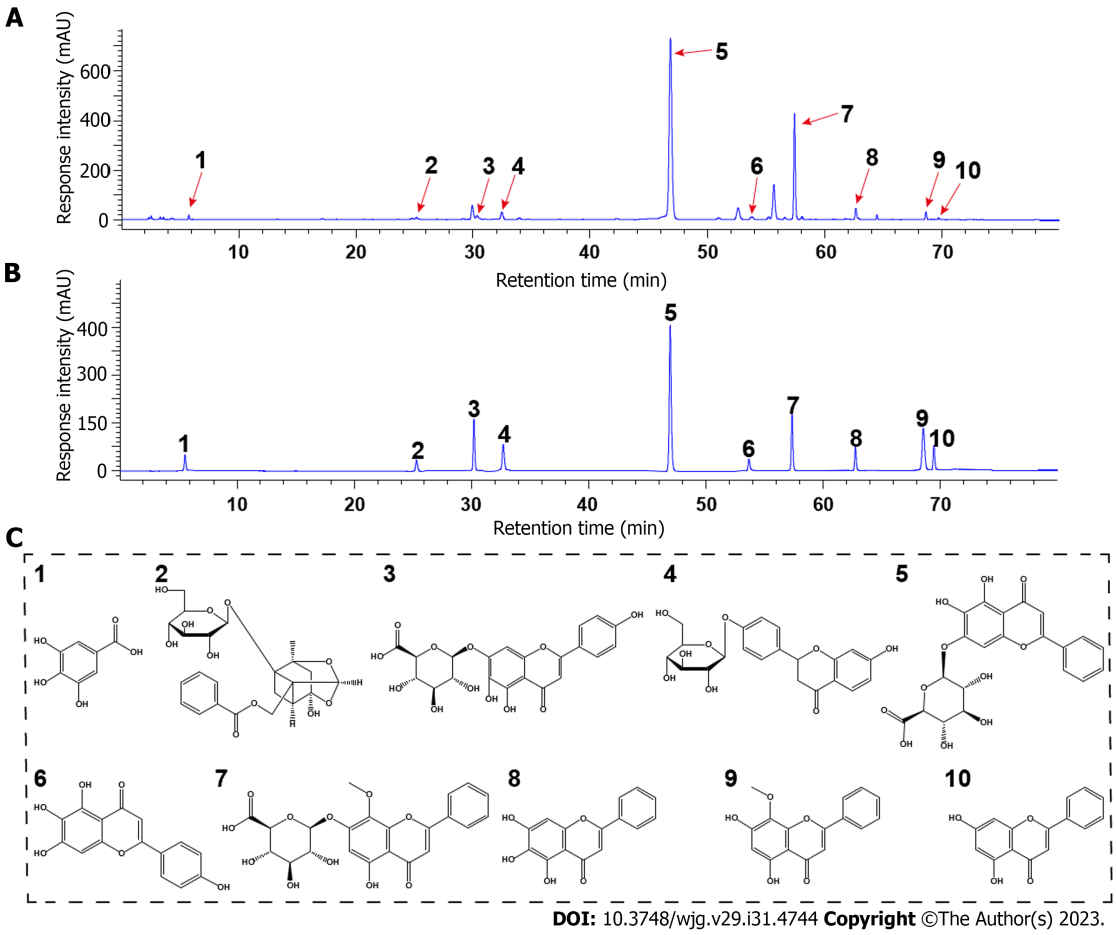
RESULTS

Phytochemical analysis of HQD

The multifaceted effectiveness of TCMs stem from their multi-component trait. First, we sought to identify the primary chemical components of HQD using HPLC analysis. As shown in Figure 1, ten major monomeric components were identified in HQD by comparing the retention times of the standards. Based on the standards, the concentrations of: (1) Gallic acid, (2) paeoniflorin, (3) scutellarin, (4) liquiritin, (5) baicalin, (6) scutellarein, (7) wogonoside, (8) baicalein, (9) wogonin, and (10) chrysin were determined to be 0.709, 2.005, 1.417, 1.626, 60.092, 0.916, 13.471, 1.905, 2.088, and 0.559 mg/g, respectively.

HQD alleviated adiposity and hepatic histological abnormalities in HFD-induced NAFLD rats

Patients with NAFLD frequently present with increased body and liver weight. Fen, a lipid-lowering medication that is clinically used for NAFLD treatment, was chosen as the positive control drug. The experimental scheme is indicated in Figure 2A. As shown in Figure 2B-E, HQD treatment (400 and 800 mg/kg) significantly attenuated HFD-induced increase in body and liver weight, as well as the liver index. As hepatic steatosis is the primary hallmark of NAFLD, we performed histological analysis to assess the effect of HQD on hepatic steatosis. H&E staining indicated that rats in the HFD group presented with severe structural disruption of the hepatic lobules, steatosis, and hepatocellular ballooning degeneration,



DOI: 10.3748/wjg.v29.i31.4744 **Copyright** ©The Author(s) 2023.

Figure 1 High-performance liquid chromatography fingerprint spectrum of Huangqin decoction and structures of the major phytochemicals in Huangqin decoction. A and B: High-performance liquid chromatography profiles of Huangqin decoction (HQD) and the standard mixture: (1) Gallic acid, (2) paeoniflorin, (3) scutellarin, (4) liquiritin, (5) baicalin, (6) scutellarein, (7) wogonoside, (8) baicalein, (9) wogonin, and (10) chrysin; C: Structures of the major phytochemicals in HQD.

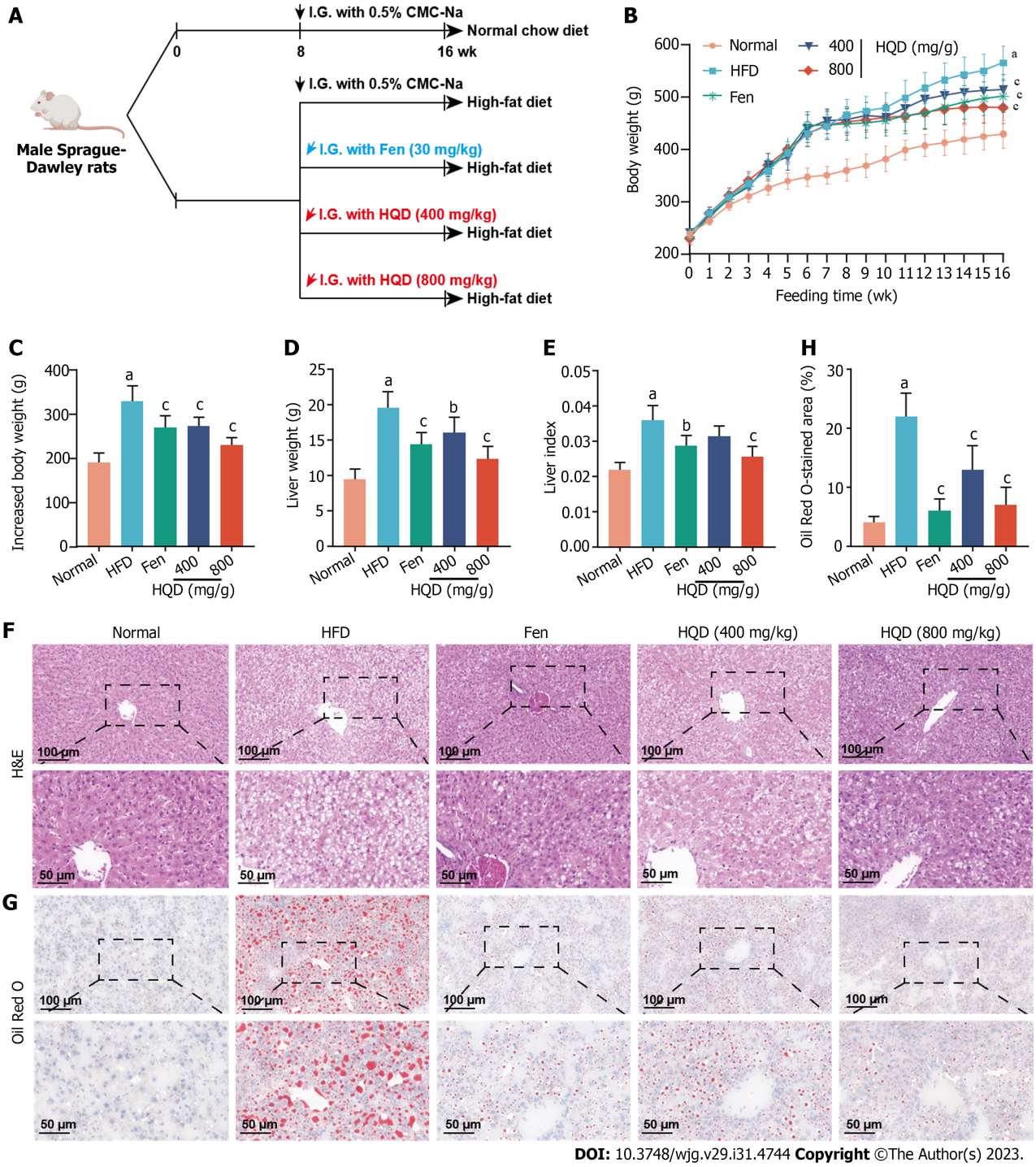
whereas oral administration of HQD mitigated these pathological alterations in a dose-dependent manner, as evidenced by relatively intact hepatic lobules and smaller fat vacuoles (Figure 2F). Additionally, Oil Red O staining showed numerous lipid droplets in the HFD group that reduced significantly following HQD treatment (Figure 2G and H). Notably, high-dose HQD exerted anti-steatosis effects comparable to those of Fen.

HQD mitigated liver damage and lipid metabolism disorders in HFD-induced NAFLD rats

Biochemical parameters of liver damage and lipid metabolism disorders, including ALT, AST, TC, TG, FFA, LDL-c, and HDL-c, are robust diagnostic markers for NAFLD. As shown in Figure 3, serum levels of ALT, AST, TC, TG, FFA, and LDL-c, as well as hepatic TC, TG, and FFA in the HFD group were noticeably higher than those in the control group. These levels were markedly reduced following HQD treatment. In contrast, the HFD-challenged group exhibited lower serum HDL-c level than the normal group, which was markedly restored following HQD treatment. In addition, the therapeutic efficacy of a high dose of HQD was equivalent to that of Fen.

HQD relieved hepatic inflammation and insulin resistance in HFD-induced NAFLD rats

Liver inflammation and insulin resistance are pivotal concomitant factors that facilitate NAFLD progression. Inflammation exacerbates insulin resistance, and both form a vicious cycle with each promoting the other and accelerating NAFLD progression[26]. As shown in Figure 4A and B, IL-1β-positive area in the liver of the HFD group was significantly higher relative to that in the control group, indicating extensive inflammatory response in the liver, which was further supported by markedly elevated levels of IL-6, IL-1β, and TNF-α in the liver (Figure 4C-E). However, all these alterations were reversed following HQD interventions. To ascertain the effect of HQD on glucose tolerance, an OGTT was performed. As shown in Figure 4F and G, higher levels of blood glucose (0–120 min) were noted in the HFD group following intragastric administration of glucose, which was robustly attenuated by HQD treatment. This was quantitatively verified by the AUC of the OGTT. Moreover, the HFD-induced elevation in serum insulin levels also decreased markedly following HQD treatment (Figure 4H). As shown in Figure 4I, the HOMA-IR value in HFD-challenged rats was significantly higher than that in normal rats, and was effectively reduced following HQD intervention. Notably, high-dose HQD showed curative efficacy similar to that of Fen.

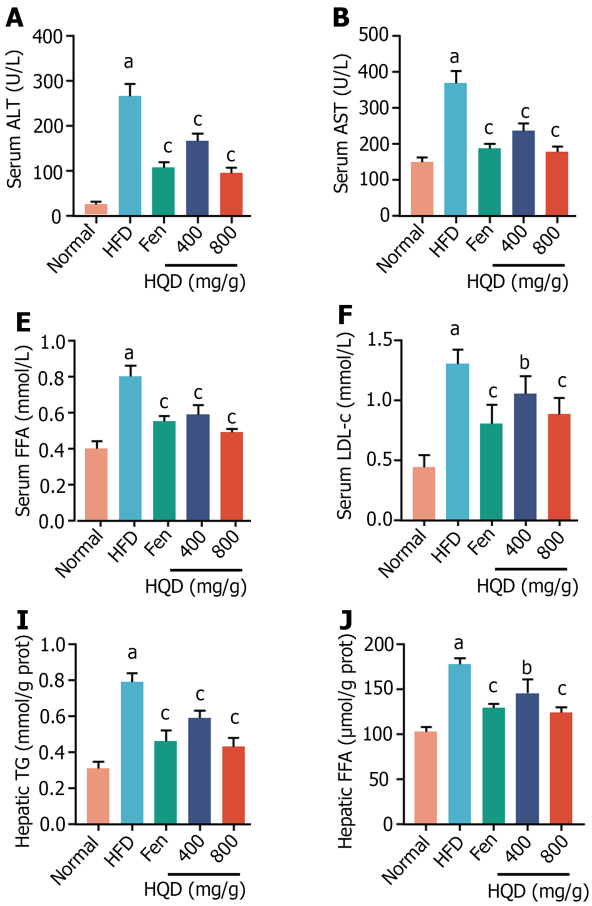


DOI: 10.3748/wjg.v29.i31.4744 **Copyright** ©The Author(s) 2023.

Figure 2 Huangqin decoction improves adiposity and hepatic histological abnormalities in high-fat diet-induced nonalcoholic fatty liver disease rats. Data are presented as mean ± SD (n = 4–8). $^{a}P < 0.01$ *vs* the normal group, $^{b}P < 0.05$ and $^{c}P < 0.01$ *vs* the high-fat diet group. A: Workflow of the experimental design; B: Dynamic curve of the body weight; C-E: Barcharts showing the effects of different treatments on body weight (C), liver weight at the termination of the experiment (D), and liver index (liver weight/body weight) (E) at the termination of the experiment; F and G: Representative micrographs of Hematoxylin and eosin and Oil Red O stained liver sections; H: Quantitative analysis of positive areas in Oil Red O staining. CMC-Na: Sodium carboxymethylcellulose; Fen: fenofibrate; HQD: Huangqin decoction; I.G.: Intragastric administration.

HQD triggered the Sirt1/NF-κB pathway in HFD-induced NAFLD rats

Sirt1/NF-κB pathway-modulated insulin resistance and hepatic steatosis play an important role in the progression of NAFLD. Therefore, protein levels of Sirt1, NF-κB, p-NF-κB, and the downstream insulin signal transduction- and lipid metabolism-related proteins (*i.e.*, IRS-2, p-IRS-2, SREBP-1, FAS, and CD36) in the liver were examined. As shown in Figure 5A-G, Sirt1 and p-IRS-2 protein levels were significantly lower in the HFD group relative to that in the normal group, whereas those of p-NF-κB, SREBP-1, FAS, and CD36 were clearly elevated in response to HFD challenge. Oral supplementation with HQD markedly reversed these changes in a dose-dependent manner. To further validate these findings, the levels of Sirt1, p-NF-κB, and SREBP-1 were evaluated immunohistochemically. Consistent with the previous



DOI: 10.3748/wjg.v29.i31.4744 **Copyright** ©The Author(s) 2023.

Figure 3 Huangqin decoction alleviates liver damage and lipid metabolism disorders in high-fat diet-induced nonalcoholic fatty liver disease rats. Data are presented as mean ± SD (n = 8). $^{a}P < 0.01$ *vs* the normal group, $^{b}P < 0.05$ and $^{c}P < 0.01$ *vs* high-fat diet group. A-J: Effects of different treatments on levels of alanine transaminase (A); aspartate transaminase (B); total cholesterol (TC) (C); triacylglycerol (TG) (D); free fatty acid (FFA) (E); low-density lipoprotein cholesterol (F); high-density lipoprotein cholesterol (G); TC (H); TG (I); FFA (J) levels in rats are shown. ALT: Alanine transaminase; AST: Aspartate transaminase; Fen: Fenofibrate; FFA: Free fatty acid; HDL-c: High-density lipoprotein cholesterol; HFD: High-fat diet; HQD: Huangqin decoction; LDL-c: Low-density lipoprotein cholesterol; TC: Total cholesterol; TG: Triacylglycerol.

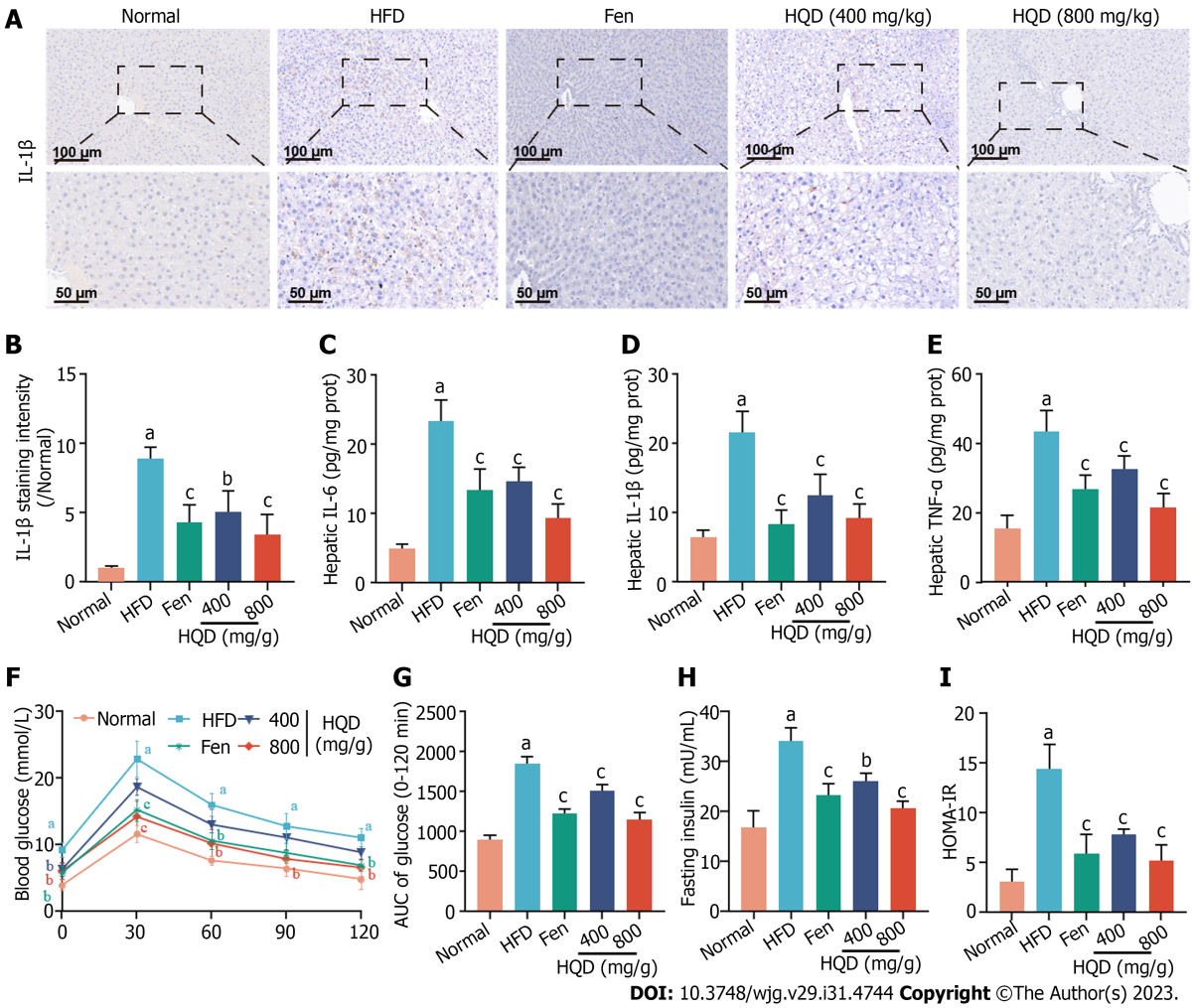
data, mild staining intensity of Sirt1 (brown/fluorescence) and strong staining intensities of p-NF-κB (brown/fluorescence) and SREBP-1 (brown) were observed in the HFD group, indicating the up-regulation of these proteins and activation of Sirt1/NF-κB pathway (Figure 5H-P). However, HQD administration substantially reduced the increased expression noted in immunohistochemical analyses. Overall, these findings suggest that the therapeutic effects of HQD on HFD-induced disorders in insulin signaling and lipid metabolism are closely associated with the Sirt1/NF-κB pathway.

HQD improved steatosis, inflammation, and insulin resistance in PA-induced HepG2 cells

The direct exposure of HepG2 cells to PA is a commonly used approach to mimic the symptoms of NAFLD *in vitro*[27, 28]. PA-induced HepG2 cells were used to investigate the therapeutic effects of HQD in NAFLD *in vitro*. Initially, MTT assay was used to examine the cytotoxicity of HQD in HepG2 cells. As shown in Figure 6A and B, HQD presented no obvious cytotoxic effect in HepG2 cells at doses ≤ 150 μg/mL, and the safe concentration of HQD when co-incubated with PA (125 μM) was determined to be ≤ 125 μg/mL. Accordingly, HQD at doses of 25, 75, and 125 μg/mL were selected for the treatment of PA-induced HepG2 cells in subsequent experiments. As shown in Figure 6C and D, the levels of neutral lipids (TC and TG) in PA-challenged HepG2 cells were noticeably increased relative to that in the control cells, but markedly reduced following HQD intervention. This was further supported by the results of Oil Red O staining, which showed reduced lipid droplets in the HQD-treated groups (Figure 6E). As inflammation is a major cause of NAFLD and is strongly associated with insulin resistance, we examined the effects of HQD on the release of inflammatory factors in PA-challenged HepG2 cells. Figure 6F-H shows that HQD attenuated the PA-induced increase in the levels of IL-6, IL-1β, and TNF-β in a dose-dependent manner. A 2DG assay was performed to assess insulin resistance. The results showed that 2DG uptake was significantly lower in PA-treated HepG2 cells, whereas it increased markedly following HQD treatment (Figure 6I), indicative of the ameliorative effect of HQD on insulin resistance.

HQD exerted hepatocyte protection by triggering Sirt1/NF-κB pathway in PA-induced HepG2 cells

Consistent with the *in vivo* results, we noted that PA-stimulated HepG2 cells showed markedly decreased expression of



DOI: 10.3748/wjg.v29.i31.4744 **Copyright** ©The Author(s) 2023.

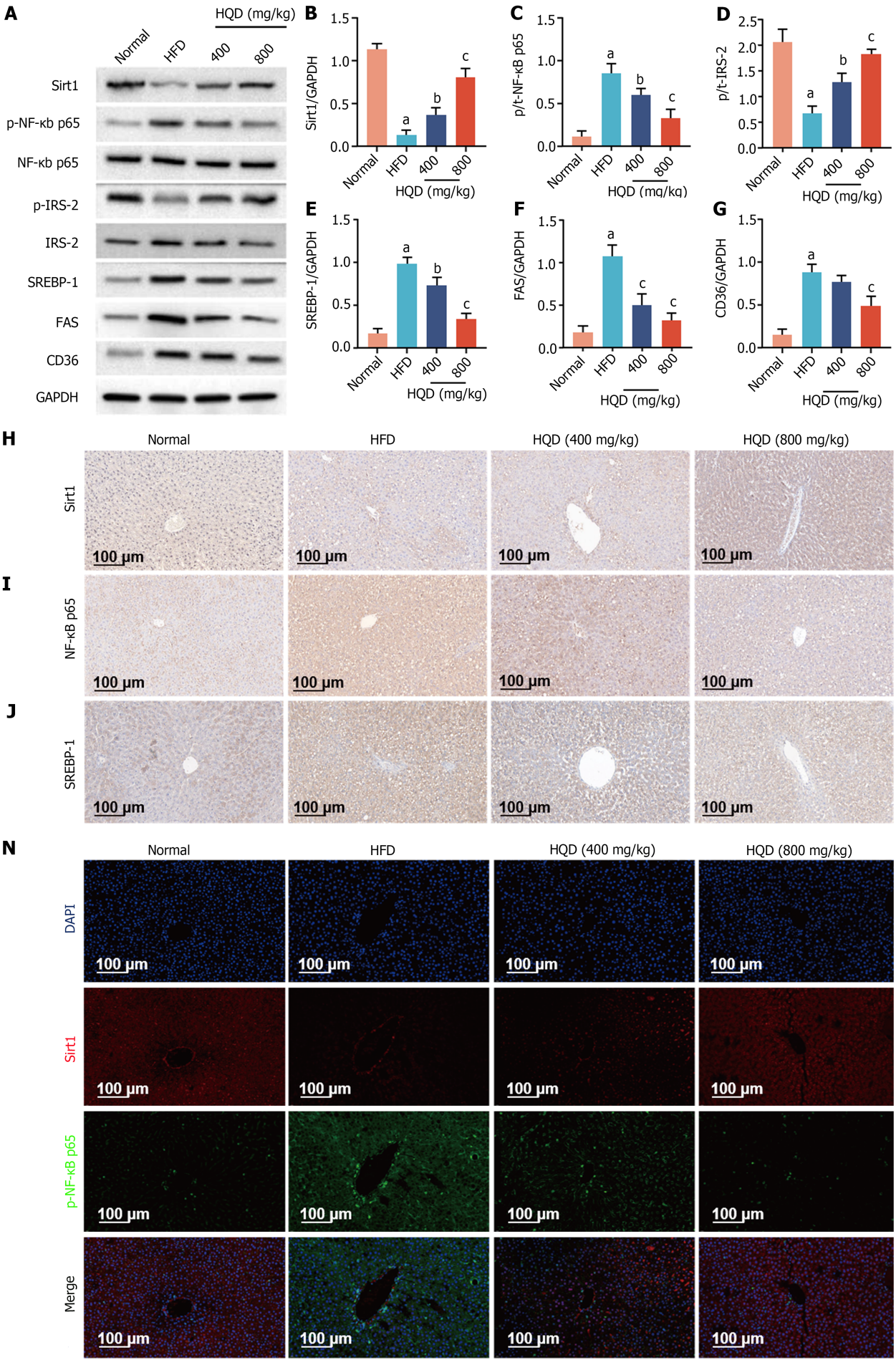
Figure 4 Huangqin decoction suppresses hepatic inflammation and insulin resistance in high-fat diet-induced nonalcoholic fatty liver disease rats. Data are presented as mean ± SD (n = 4–8). $^{a}P < 0.01$ *vs* the normal group, $^{b}P < 0.05$ and $^{c}P < 0.01$ *vs* the high-fat diet (HFD) group. A: Representative images of immunohistochemical staining of interleukin (IL)-1β in liver sections; B: Quantitative analysis of staining intensity of IL-1β; C-E: Levels of IL-6 (C), IL-1β (D), and tumor necrosis factor-α (E) in the liver of HFD-fed rats; F: Oral glucose tolerance test (OGTT); G: Area under the curve from OGTT; H: Level of fasting serum insulin; I: Values of homeostasis model assessment of insulin resistance. AUC: Area under the curve; Fen: Fenofibrate; HFD: High-fat diet; HOMA-IR: Homeostasis model assessment of insulin resistance; HQD: Huangqin decoction; IL: Interleukin; TNF: Tumor necrosis factor.

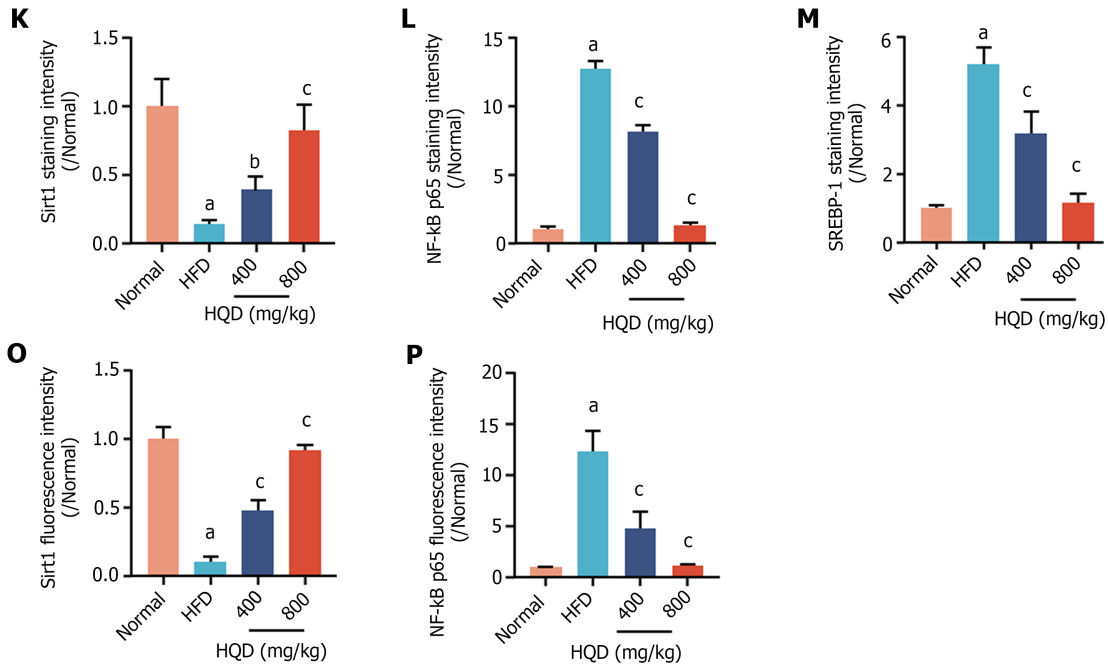
Sirt1 and p-IRS-2, and increased expression of p-NF-κB, SREBP-1, FAS, and CD36 compared with that in the control cells (Figure 7A-G), indicative of inhibition of the Sirt1/NF-B pathway. However, these changes were restored following HQD treatment. To further determine the expression and distribution of Sirt1 and NF-κB, immunofluorescence analyses were performed. Consistently, the intensity of Sirt1 staining in the PA group was clearly lower compared to that in the control group. Furthermore, significantly increased NF-κB nuclear translocation was noted in PA-induced HepG2 cells, which was conspicuously reversed following HQD treatment (Figure 7H). Collectively, these data suggest that HQD protects hepatocytes against PA-induced insults *via* the Sirt1/NF-κB pathway.

To further confirm that the HQD-mediated mitigatory effects on insulin resistance and lipid accumulation occurs *via* the Sirt1/NF-κB pathway, we used a Sirt1 inhibitor, EX-527 to block the pathway. As shown in Figure 8A-G, the ameliorative effects of HQD on lipid accumulation, inflammation, and 2DG uptake were significantly compromised following co-treatment with EX-527. More importantly, EX-527 abolished the regulatory effects of HQD on Sirt1/NF-κB pathway and its downstream-modulated insulin signal transduction- and lipid metabolism-related proteins (Figure 8H-O). In summary, our data indicate that the protective effects of HQD against hepatic lipid accumulation, inflammation, and insulin resistance are mediated through triggering of the Sirt1/NF-κB pathway.

DISCUSSION

NAFLD is the most prevalent chronic liver disease for which no specific effective drug has been approved, making its treatment a top research priority[29]. Unlike synthetic drugs, whose efficacy depends mainly on their action on one target, the efficacy of TCM depends on its holistic effects on multiple targets and pathways. Therefore, TCMs are promising complementary and auxiliary agents for metabolic diseases with multifactorial pathogeneses, such as NAFLD


A
HQD (mg/kg)
Normal
HFD
400
800
Sirt1
p-NF-κb p65
NF-κb p65
p-IRS-2
IRS-2
SREBP-1
FAS
CD36
GAPDH
B
Sirt1/GAPDH
C
p/t-NF-κB p65
D
p/t-IRS-2
E
SREBP-1/GAPDH
F
FAS/GAPDH
G
CD36/GAPDH
HQD (mg/kg)
H
Normal
HFD
HQD (400 mg/kg)
HQD (800 mg/kg)
Sirt1
I
NF-κB p65
J
SREBP-1
N
DAPI
Sirt1
p-NF-κB p65
Merge
100 μm



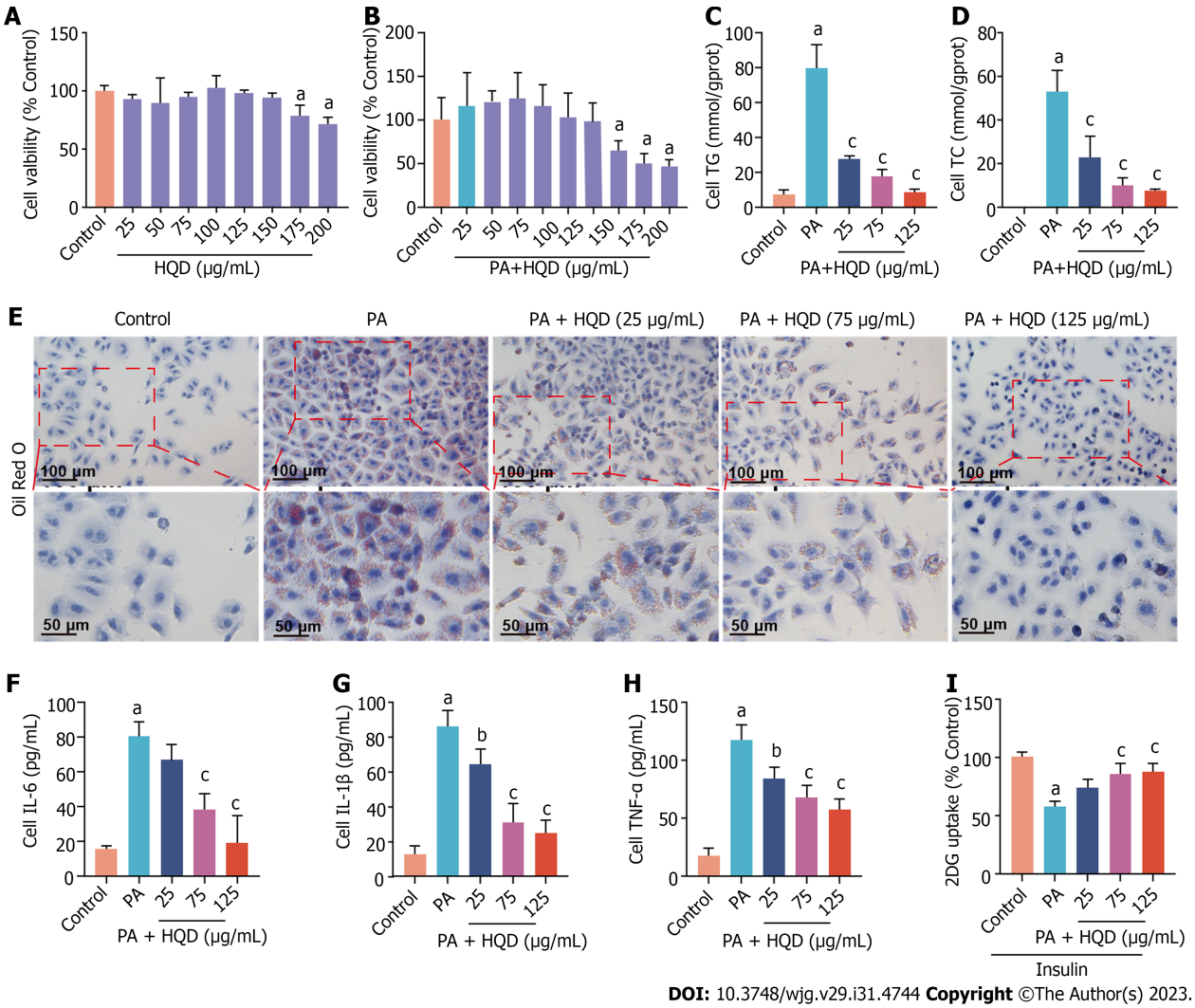
DOI: 10.3748/wjg.v29.i31.4744 **Copyright** ©The Author(s) 2023.

Figure 5 Huangqin decoction activates the Sirt1/NF-Kb pathway in high-fat diet-induced nonalcoholic fatty liver disease rats. Data are presented as mean ± SD (n = 3–4). $^{a}P < 0.01$ *vs* the normal group, $^{b}P < 0.05$ and $^{c}P < 0.01$ *vs* the high-fat diet group. A: Expression levels of Sirt1, p-NF-κB/NF-κB, p-IRS-2/IRS-2, sterol regulatory element-binding protein (SREBP)-1c, fatty acid synthase, and cluster of differentiation 36; B-G: Semi-quantitative analysis of these proteins; H-J: Representative images of immunohistochemical staining of Sirt1 (H), NF-κB (I), and SREBP-1c (J) in liver sections; K-M: Quantitative analysis of the staining intensity; N: Representative images of immunofluorescent staining of Sirt1 and NF-κB in liver sections; O and P: Quantitative analysis of the fluorescence intensity. CD36: Cluster of differentiation 36; DAPI: 4',6-diamidino-2-phenylindole; FAS: Fatty acid synthase; GAPDH: Glyceraldehyde-3-phosphate dehydrogenase; HFD: High-fat diet; HQD, Huangqin decoction; SREBP: Sterol regulatory element-binding protein.

[30-32]. HQD, a well-known TCM formula, has emerged as a potentially effective modality for the clinical treatment of liver diseases, including NAFLD. In our study, several constituents of HQD, including gallic acid, paeoniflorin, scutellarin, liquiritin, baicalin, scutellarein, wogonoside, baicalein, wogonin, and chrysin were identified by HPLC analysis. The beneficial effects of these compounds in NAFLD have been reported both *in vivo* and *in vitro*[33-36], which provide the basis for the potential application of HQD in NAFLD therapy. In the present study, using both *in vivo* and *in vitro* experiments, we demonstrated that HQD mitigates insulin resistance and hepatic steatosis by modulating the Sirt1/NF-κB pathway.

Overconsumption of HFD, which is associated with a modern lifestyle, plays a role in the progression of NAFLD[37]. Currently, NAFLD murine models are most commonly developed by long-term consumption of an HFD, resulting in symptoms similar to those observed in patients with NAFLD[37]. PA is an essential fatty acid for TG synthesis in the liver and increased concentrations of PA in hepatocytes accelerate the progression[38]. Typically, the exogenous addition of PA induces hepatocellular lipid accumulation to mimic the pathological process of NAFLD *in vitro*. We used HFD-fed rats and PA-treated HepG2 cells to study the therapeutic effects of HQD on NAFLD. Our results showed that the HFD-fed rats had higher body and liver weights. Histological analysis revealed hepatic steatosis and injuries, which were further supported by aberrant levels of TC, TG, ALT, and AST in the serum and liver. Furthermore, abnormal levels of serum FFA, LDL-c, HDL-c, OGTT, insulin, and HOMA-IR were observed in the HFD-fed rats, indicating the onset of dyslipidemia and insulin resistance. Consistent with these findings, PA-stimulated HepG2 cells exhibited a marked increase in lipid accumulation, intracellular TC and TG levels, and glucose uptake. Notably, all the above mentioned NAFLD symptoms were dose-dependently reversed following HQD treatment, indicating that HQD mitigates lipid metabolism disorders and insulin resistance in NAFLD.

Compromised lipid metabolism contributes to hepatic steatosis, thereby triggering the onset of NAFLD[39,40]. Several studies have confirmed that the activation of *de novo* lipogenesis (DNL) promotes FFA generation and esterification into TG, which are crucial driving factors contributing to lipid metabolism dysfunction[41]. A previous clinical trial revealed that individuals with NAFLD had higher nighttime plasma FFA levels and a threefold increase in DNL[42]. SREBP-1c is a key transcription factor that controls hepatic DNL and lipolysis by modulating the activities of lipogenic enzymes (FAS) and fatty acid importer proteins (CD36) as downstream targets[43-45]. The active state of SREBP-1c directly influences FLD progression in fatty liver[43]. In the present study, rats with HFD-induced NAFLD and PA-treated HepG2 cells showed elevated SREBP-1, FAS, and CD36 Levels, indicating increased DNL and fatty acid uptake. However, oral HQD supplementation effectively reversed these changes. Sirt1 plays a critical role in cellular energy metabolism and deacetylates and inhibits SREBP-1c activity in the regulation of hepatic lipid metabolism; however, it is downregulated in patients with NAFLD[15]. In the rat liver and HepG2 cells, we observed deactivation of Sirt1 following exposure to HFD or PA, whereas HQD treatment increased Sirt1 levels, resulting in NAFLD mitigation.

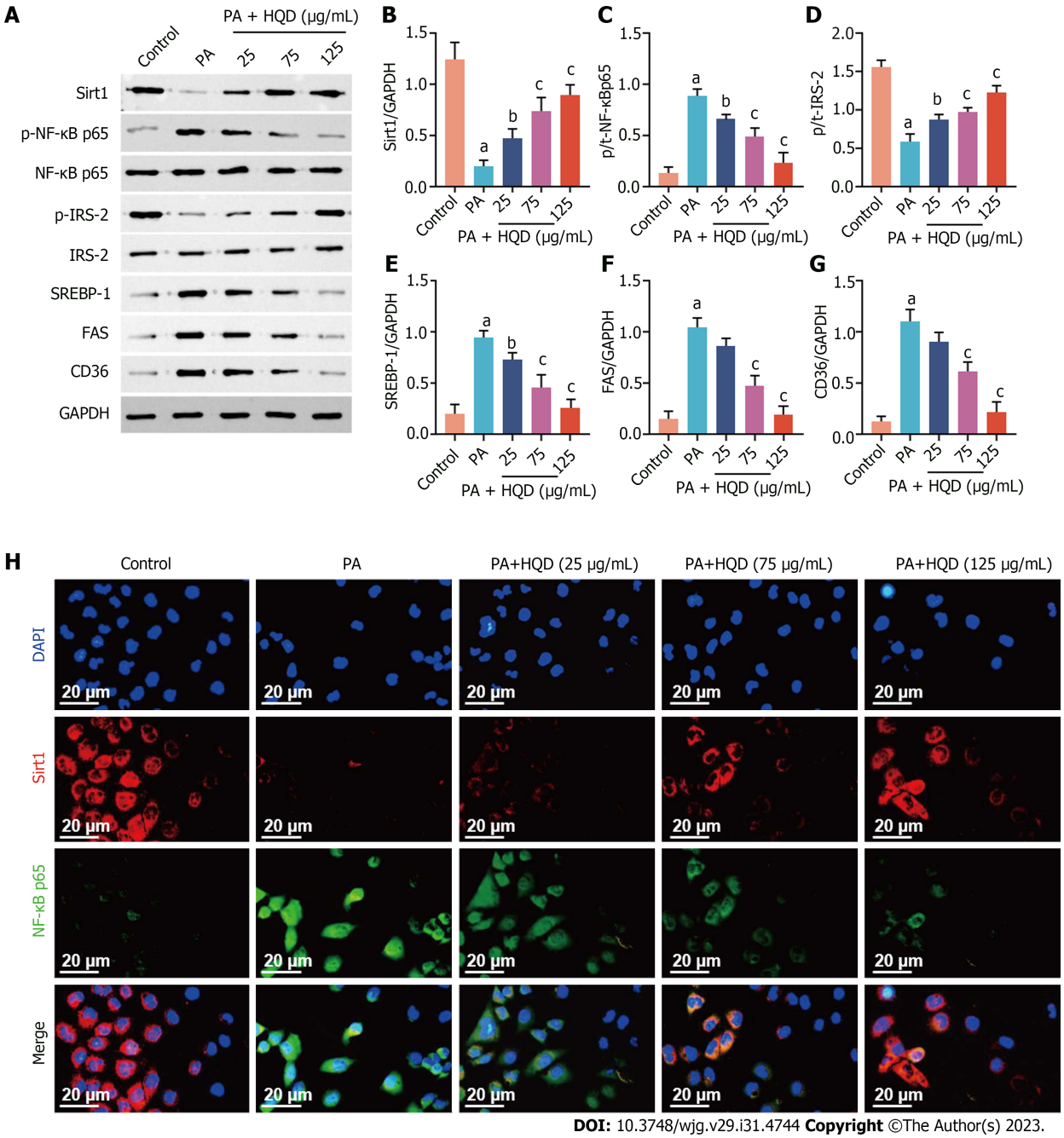


DOI: 10.3748/wjg.v29.i31.4744 **Copyright** ©The Author(s) 2023.

Figure 6 Huangqin decoction improves lipotoxicity, inflammation, and insulin resistance in palmitic acid-induced HepG2 cells. Data are presented as mean ± SD of at least three independent experiments. $^{a}P < 0.01$ *vs* the control group, $^{b}P < 0.05$ and $^{c}P < 0.01$ *vs* the palmitic acid (PA) group. A: Viability of HepG2 cells following incubation with different concentrations of Huangqin decoction (HQD); B: Viability of HepG2 cells following co-culture with PA and different concentrations of HQD; C and D: Levels of triacylglycerol and total cholesterol in HepG2 cells; E: Representative micrographs of Oil Red O staining of HepG2 cells; F–H: Levels of interleukin (IL)-6, IL-1β, and tumor necrosis factor-α in HepG2 cells; I: Level of glucose uptake in HepG2 cells. 2DG: 2-deoxydglucose; HQD, Huangqin decoction; IL: Interleukin; TC: Total cholesterol; TG: Triacylglycerol; TNF: Tumor necrosis factor; PA: Palmitic acid.

Insulin resistance is the initial driver of hepatic steatosis in NAFLD[10,11,46]. Moreover, recent studies have suggested that obesity-induced chronic low-grade inflammation exacerbates insulin resistance[26,47]. Specifically, hypertrophic adipocytes promote macrophage infiltration and secrete pro-inflammatory factors including IL-6, IL-1β, and TNF-α, which downregulate insulin signaling molecules by inhibiting the phosphorylation of IRS-2, ultimately promoting insulin resistance[48-50]. NF-κB acts as an inducible transcription factor and induces the production of pro-inflammatory factors [51]. A previous study reported that FFA-induced insulin resistance is strongly associated with the activation of the pro-inflammatory NF-κB pathway[52]. More importantly, Sirt1 can inactivate NF-κB by deacetylating lysine 310, impeding the expression of pro-inflammatory target genes, whereas patients with NAFLD are more susceptible to inactivation of the Sirt1/NF-κB pathway[17,53]. In both, *in vivo* and *in vitro* NAFLD models, phosphorylation of NF-κB was upregulated and accompanied by increased levels of pro-inflammatory factors (IL-1β, TNF-α, and IL-6), whereas phosphorylation of IRS-2 was downregulated, suggesting that Sirt1/NF-κB pathway-mediated insulin resistance occurred in NAFLD. In contrast, the HQD intervention clearly restored these changes. Furthermore, treatment with the Sirt1 inhibitor, EX-527, abolished all HQD-mediated favorable effects in PA-challenged HepG2 cells, confirming that HQD mitigated hepatic steatosis and insulin resistance *via* the Sirt1/NF-κB pathway.

Fen, a peroxisome proliferator-activated receptor α (PPARα) agonist, offers potential therapeutic efficacy against NAFLD by inducing fatty acid oxidation and inhibiting inflammatory gene expression in the liver[54,55]. Clinical studies have shown that Fen may have positive therapeutic outcomes in NAFLD/NASH[56,57]. Herein, we found that HQD achieved therapeutic effects comparable to those of Fen by activating Sirt1. Several studies have shown that Sirt1, a key regulator of PPARα signaling, can trigger PPARα-mediated fatty acid oxidation in the liver, showing favorable effects in NAFLD[9,58,59]. Although HQD and Fen act on different targets, their therapeutic effects could be interpreted from the upstream and downstream regulatory relationships between Sirt1 and PPARα make.

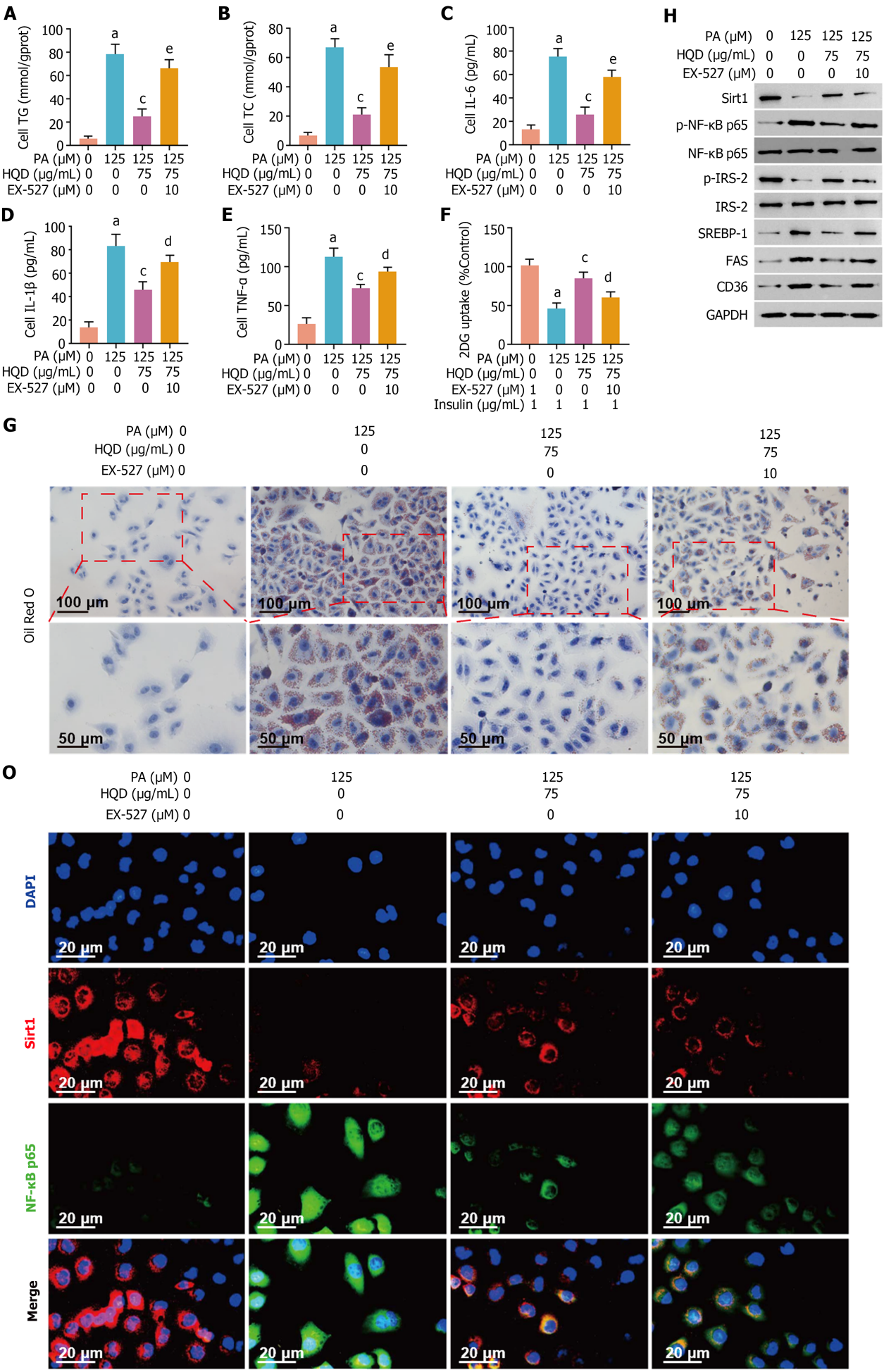


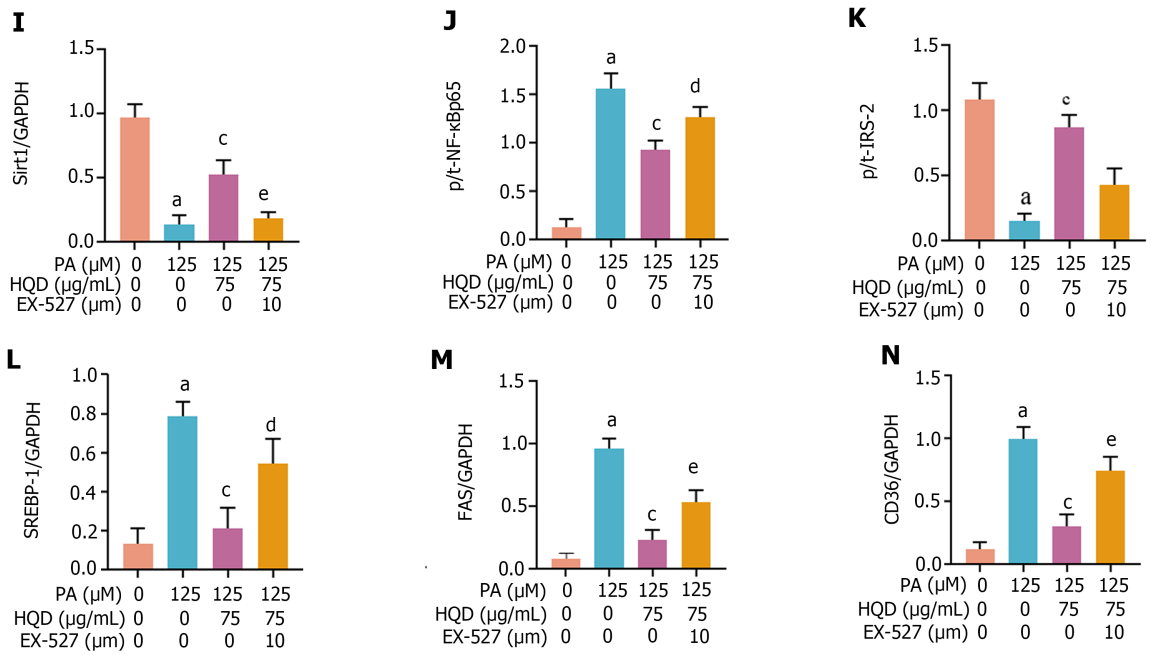
DOI: 10.3748/wjg.v29.i31.4744 **Copyright** ©The Author(s) 2023.

Figure 7 Huangqin decoction activates the Sirt1/NF-κB pathway in palmitic acid-induced HepG2 cells. Data are presented as mean ± SD of at least three independent experiments. $^{a}P < 0.01$ *vs* the control group, $^{b}P < 0.05$ and $^{c}P < 0.01$ *vs* the palmitic acid group. A: Expression levels of Sirt1, p-NF-κB/NF-κB, p-IRS-2/IRS-2, sterol regulatory element-binding protein 1, fatty acid synthase, and cluster of differentiation 36 in HepG2 cells; B–G: Semi-quantitative analysis of these proteins; H: Representative images of immunofluorescent staining of Sirt1 and NF-κB in HepG2 cells. CD36: Cluster of differentiation 36; DAPI: 4',6-diamidino-2-phenylindole; FAS: Fatty acid synthase; GAPDH: Glyceraldehyde-3-phosphate dehydrogenase; HQD, Huangqin decoction; PA: Palmitic acid; SREBP: Sterol regulatory element-binding protein.

CONCLUSION

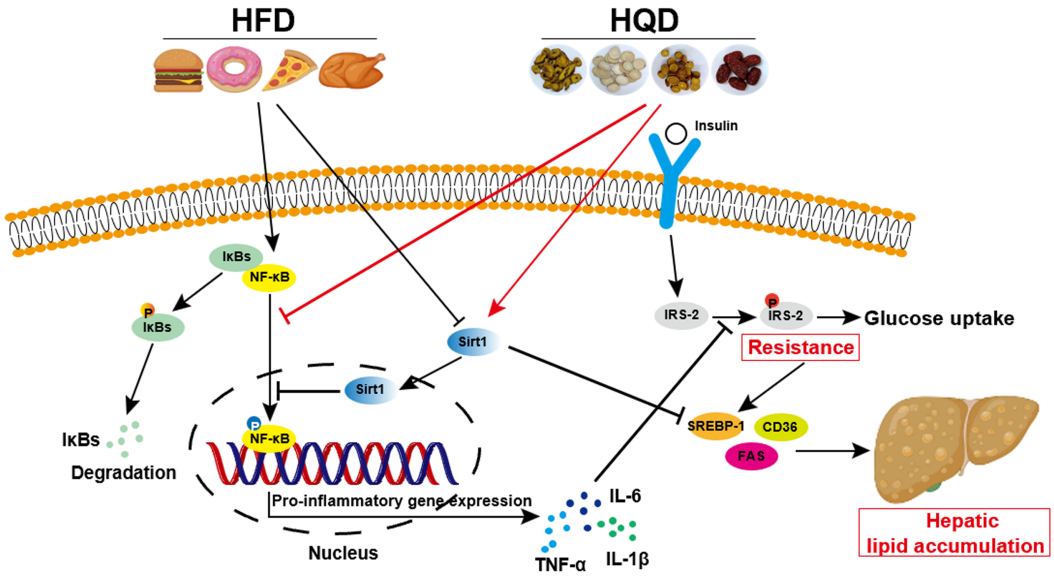
In summary, we have demonstrated the mitigating effects of HQD on lipid metabolism disorders and insulin resistance. Our investigations revealed that HQD mediates these beneficial effects by modulating lipogenesis and inflammatory responses which trigger the Sirt1/NF-κB pathway (Figure 9). Our study provides strong evidence supporting HQD as a promising agent for NAFLD treatment.


A
Cell TG (mmol/gprot)
B
Cell TC (mmol/gprot)
C
Cell IL-6 (pg/mL)
D
Cell IL-1β (pg/mL)
E
Cell TNF-α (pg/mL)
F
2DG uptake (%Control)
PA (μM) 0 125 125 125
HQD (μg/mL) 0 0 75 75
EX-527 (μM) 0 0 0 10
Insulin (μg/mL) 1 1 1 1
H
Sirt1
p-NF-κB p65
NF-κB p65
p-IRS-2
IRS-2
SREBP-1
FAS
CD36
GAPDH
G
Oil Red O
100 μm
50 μm
O
DAPI
Sirt1
NF-κB p65
Merge
20 μm



DOI: 10.3748/wjg.v29.i31.4744 **Copyright** ©The Author(s) 2023.

Figure 8 Huangqin decoction protects hepatocytes by triggering Sirt1/NF-κB pathway in palmitic acid-induced HepG2 cells. Data are presented as mean ± SD of at least three independent experiments. [a]*P* < 0.01 *vs* the control group, [b]*P* < 0.05 and [c]*P* < 0.01 *vs* the palmitic acid group, [d]*P* < 0.05 and [e]*P* < 0.01 *vs* the Huangqin decoction group. A and B: Levels of triacylglycerol (A) and total cholesterol (B) in HepG2 cells co-cultured with or without EX-527; C-E: Levels of interleukin (IL)-6, IL-1β, and tumor necrosis factor-α in HepG2 cells co-cultured with or without EX-527; F: Level of glucose uptake in HepG2 cells co-cultured with or without EX-527; G: Representative micrographs of Oil Red O staining of HepG2 cells co-cultured with or without EX-527; H: Expression levels of Sirt1, p-NF-κB/NF-κB, p-IRS-2/IRS-2, sterol regulatory element-binding protein-1c, fatty acid synthase, and cluster of differentiation 36 in HepG2 cells co-cultured with or without EX-527; I-N: Semi-quantitative analysis of these proteins; O: Representative images of immunofluorescent staining of Sirt1 and NF-κB in HepG2 cells co-cultured with or without EX-527. 2DG: 2-deoxydglucose; CD36: Cluster of differentiation 36; DAPI: 4',6-diamidino-2-phenylindole; FAS: Fatty acid synthase; GAPDH: Glyceraldehyde-3-phosphate dehydrogenase; HQD: Huangqin decoction; IL: Interleukin; PA: Palmitic acid; SREBP: Sterol regulatory element-binding protein; TC: Total cholesterol; TG: Triacylglycerol; TNF: Tumor necrosis factor.



DOI: 10.3748/wjg.v29.i31.4744 **Copyright** ©The Author(s) 2023.

Figure 9 Schematic diagram illustrating the effects of Huangqin decoction on Sirt1/NF-κB pathway-modulated hepatic steatosis and insulin resistance. CD36: Cluster of differentiation 36; FAS: Fatty acid synthase; HFD: High-fat diet; HQD: Huangqin decoction; IL: Interleukin; SREBP: Sterol regulatory element-binding protein; TNF: Tumor necrosis factor.

ARTICLE HIGHLIGHTS

Research background

Non-alcoholic fatty liver disease (NAFLD) is the most common chronic liver disease, for which no effective therapeutic drugs have been approved. Huangqin decoction (HQD), a traditional Chinese medicine, has been widely used to treat liver diseases in clinical practice. Our study confirmed that HQD effectively mitigates high-fat diet (HFD)-induced hepatic inflammation. However, whether HQD has ameliorative effects on lipid metabolism disorders and insulin resistance, as well as the underlying mechanisms, remains unclear.

Research motivation

Convincing evidence for HQD in the clinical treatment of NAFLD is required.

Research objectives

This study aimed to investigate the therapeutic efficacy of HQD on lipid metabolism disorders and insulin resistance and explore the possible molecular mechanisms by focusing on the Sirt1/NF-κB pathway.

Research methods

High-performance liquid chromatography was used to identify the key components of HQD. HFD-induced NAFLD rats and palmitic acid-induced HepG2 cells were treated with HQD to investigate the mitigating effects of HQD on lipid metabolism disorders and insulin resistance. Finally, molecular biology techniques, including western blotting, immunohistochemistry, and immunofluorescence, were applied to explore the protein expression in the Sirt1/NF-κB pathway.

Research results

Ten key components of HQD were identified. The results showed that HQD effectively prevented lipid metabolism disorders in rats and HepG2 cells, inflammatory responses, and insulin resistance. Mechanistic exploration revealed that triggering Sirt1/NF-κB pathway-modulated lipogenesis and inflammation contributed to the favorable effects of HQD, which was further validated by the addition of EX-527 (a Sirt1 antagonist).

Research conclusions

Supported by our previous findings, we strongly believe that HQD is a promising complementary or auxiliary agent for the clinical treatment of NAFLD.

Research perspectives

HQD has been used to treat liver diseases in clinical practice for decades, with positive outcomes. More in-depth and precise research on the molecular mechanisms of HQD could guide and promote the clinical treatment of NAFLD more effectively.

ACKNOWLEDGEMENTS

The authors are grateful to Yue-Tao He (Leishenhe Mechanical and Electrical Equipment Co. Ltd.) for kindly providing high-quality reagents.

FOOTNOTES

Author contributions: Yan BF, Pan LF, and Quan YF contributed equally to this work and performed the research; Liu J and Zheng X designed the research and proofread the manuscript; Sha Q, Zhang JZ, and Zhou LB analyzed the data; Zhang YF carefully revised the manuscript; Qian XL, Gu XM, Li FT, and Wang T interpreted the data; All authors approved the final version of the article.

Supported by the Scientific Research Project of Jiangsu Health Commission, No. Z2022078; the Natural Science Foundation of Jiangsu Province, No. BK20220299.

Institutional review board statement: The study was reviewed and approved by the Institutional Review Board at Jiangsu Health Vocational College.

Institutional animal care and use committee statement: The experimental protocols strictly complied with the European Community criteria and were authorized by the Animal Ethics Committee of Jiangsu Health Vocational College (Permission No. JHVC-IACUC-2022-B007).

Conflict-of-interest statement: The authors declare that they have no competing interests.

Data sharing statement: No additional data are available.

ARRIVE guidelines statement: The authors have read the ARRIVE guidelines, and the manuscript was prepared and revised according to the ARRIVE guidelines.

Open-Access: This article is an open-access article that was selected by an in-house editor and fully peer-reviewed by external reviewers. It is distributed in accordance with the Creative Commons Attribution NonCommercial (CC BY-NC 4.0) license, which permits others to distribute, remix, adapt, build upon this work non-commercially, and license their derivative works on different terms, provided the original work is properly cited and the use is non-commercial. See: https://creativecommons.org/Licenses/by-nc/4.0/

Country/Territory of origin: China

ORCID number: Xian Zheng 0000-0003-3342-7636.

S-Editor: Lin C
L-Editor: A
P-Editor: Cai YX

REFERENCES

1 **Seval GC**, Kabacam G, Yakut M, Seven G, Savas B, Elhan A, Cinar K, Idilman R. The natural course of non-alcoholic fatty liver disease. *Hepatol Forum* 2020; **1**: 20-24 [PMID: 35949661 DOI: 10.14744/hf.2020.0008]
2 **Rafiq N**, Bai C, Fang Y, Srishord M, McCullough A, Gramlich T, Younossi ZM. Long-term follow-up of patients with nonalcoholic fatty liver. *Clin Gastroenterol Hepatol* 2009; **7**: 234-238 [PMID: 19049831 DOI: 10.1016/j.cgh.2008.11.005]
3 **Dam-Larsen S**, Becker U, Franzmann MB, Larsen K, Christoffersen P, Bendtsen F. Final results of a long-term, clinical follow-up in fatty liver patients. *Scand J Gastroenterol* 2009; **44**: 1236-1243 [PMID: 19670076 DOI: 10.1080/00365520903171284]
4 **McPherson S**, Hardy T, Henderson E, Burt AD, Day CP, Anstee QM. Evidence of NAFLD progression from steatosis to fibrosing-steatohepatitis using paired biopsies: implications for prognosis and clinical management. *J Hepatol* 2015; **62**: 1148-1155 [PMID: 25477264 DOI: 10.1016/j.jhep.2014.11.034]
5 **Yan T**, Yan N, Wang P, Xia Y, Hao H, Wang G, Gonzalez FJ. Herbal drug discovery for the treatment of nonalcoholic fatty liver disease. *Acta Pharm Sin B* 2020; **10**: 3-18 [PMID: 31993304 DOI: 10.1016/j.apsb.2019.11.017]
6 **Targher G**, Day CP, Bonora E. Risk of cardiovascular disease in patients with nonalcoholic fatty liver disease. *N Engl J Med* 2010; **363**: 1341-1350 [PMID: 20879883 DOI: 10.1056/NEJMra0912063]
7 **Younossi Z**, Anstee QM, Marietti M, Hardy T, Henry L, Eslam M, George J, Bugianesi E. Global burden of NAFLD and NASH: trends, predictions, risk factors and prevention. *Nat Rev Gastroenterol Hepatol* 2018; **15**: 11-20 [PMID: 28930295 DOI: 10.1038/nrgastro.2017.109]
8 **Estes C**, Anstee QM, Arias-Loste MT, Bantel H, Bellentani S, Caballeria J, Colombo M, Craxi A, Crespo J, Day CP, Eguchi Y, Geier A, Kondili LA, Kroy DC, Lazarus JV, Loomba R, Manns MP, Marchesini G, Nakajima A, Negro F, Petta S, Ratziu V, Romero-Gomez M, Sanyal A, Schattenberg JM, Tacke F, Tanaka J, Trautwein C, Wei L, Zeuzem S, Razavi H. Modeling NAFLD disease burden in China, France, Germany, Italy, Japan, Spain, United Kingdom, and United States for the period 2016-2030. *J Hepatol* 2018; **69**: 896-904 [PMID: 29886156 DOI: 10.1016/j.jhep.2018.05.036]
9 **Zheng X**, Zhang XG, Liu Y, Zhu LP, Liang XS, Jiang H, Shi GF, Zhao YY, Zhao ZW, Teng Y, Pan K, Zhang J, Yin ZQ. Arjunolic acid from Cyclocarya paliurus ameliorates nonalcoholic fatty liver disease in mice *via* activating Sirt1/AMPK, triggering autophagy and improving gut barrier function. *J Funct Foods* 2021; **86**: 104686 [DOI: 10.1016/j.jff.2021.104686]
10 **Day CP**, James OF. Steatohepatitis: a tale of two "hits"? *Gastroenterology* 1998; **114**: 842-845 [PMID: 9547102 DOI: 10.1016/s0016-5085(98)70599-2]
11 **Mouzaki M**, Loomba R. An update on the role of the microbiome in non-alcoholic fatty liver disease pathogenesis, diagnosis, and treatment. *Curr Treat Options Gastroenterol* 2020; **18**: 270-280 [PMID: 33716495 DOI: 10.1007/s11938-020-00290-2]
12 **Buzzetti E**, Pinzani M, Tsochatzis EA. The multiple-hit pathogenesis of non-alcoholic fatty liver disease (NAFLD). *Metabolism* 2016; **65**: 1038-1048 [PMID: 26823198 DOI: 10.1016/j.metabol.2015.12.012]
13 **Cao Y**, Jiang X, Ma H, Wang Y, Xue P, Liu Y. SIRT1 and insulin resistance. *J Diabetes Complications* 2016; **30**: 178-183 [PMID: 26422395 DOI: 10.1016/j.jdiacomp.2015.08.022]
14 **Li X**. SIRT1 and energy metabolism. *Acta Biochim Biophys Sin (Shanghai)* 2013; **45**: 51-60 [PMID: 23257294 DOI: 10.1093/abbs/gms108]
15 **Wu T**, Liu YH, Fu YC, Liu XM, Zhou XH. Direct evidence of sirtuin downregulation in the liver of non-alcoholic fatty liver disease patients. *Ann Clin Lab Sci* 2014; **44**: 410-418 [PMID: 25361925]
16 **Zhang Y**, Geng C, Liu X, Li M, Gao M, Fang F, Chang Y. Celastrol ameliorates liver metabolic damage caused by a high-fat diet through Sirt1. *Mol Metab* 2017; **6**: 138-147 [PMID: 28123944 DOI: 10.1016/j.molmet.2016.11.002]
17 **de Gregorio E**, Colell A, Morales A, Marí M. Relevance of SIRT1-NF-κB Axis as Therapeutic Target to Ameliorate Inflammation in Liver Disease. *Int J Mol Sci* 2020; **21** [PMID: 32485811 DOI: 10.3390/ijms21113858]
18 **Komeili-Movahhed T**, Bassirian M, Changizi Z, Moslehi A. SIRT1/NFκB pathway mediates anti-inflammatory and anti-apoptotic effects of rosmarinic acid on in a mouse model of nonalcoholic steatohepatitis (NASH). *J Recept Signal Transduct Res* 2022; **42**: 241-250 [PMID: 33787460 DOI: 10.1080/10799893.2021.1905665]
19 **Cobbina E**, Akhlaghi F. Non-alcoholic fatty liver disease (NAFLD) - pathogenesis, classification, and effect on drug metabolizing enzymes and transporters. *Drug Metab Rev* 2017; **49**: 197-211 [PMID: 28303724 DOI: 10.1080/03602532.2017.1293683]
20 **Liu SH**, Cheng YC. Old formula, new Rx: the journey of PHY906 as cancer adjuvant therapy. *J Ethnopharmacol* 2012; **140**: 614-623 [PMID: 22326673 DOI: 10.1016/j.jep.2012.01.047]
21 **Chen Q**, Liu M, Yu H, Li J, Wang S, Zhang Y, Qiu F, Wang T. Scutellaria baicalensis regulates FFA metabolism to ameliorate NAFLD through the AMPK-mediated SREBP signaling pathway. *J Nat Med* 2018; **72**: 655-666 [PMID: 29542003 DOI: 10.1007/s11418-018-1199-5]

22 **Luo Z**, Liu Y, Han X, Yang W, Wang G, Wang J, Jiang X, Sen M, Li X, Yu G, Shi Y. Mechanism of Paeoniae Radix Alba in the Treatment of Non-alcoholic Fatty Liver Disease Based on Sequential Metabolites Identification Approach, Network Pharmacology, and Binding Affinity Measurement. *Front Nutr* 2021; **8**: 677659 [PMID: 34604271 DOI: 10.3389/fnut.2021.677659]

23 **Hajiaghamohammadi AA**, Ziaee A, Samimi R. The efficacy of licorice root extract in decreasing transaminase activities in non-alcoholic fatty liver disease: a randomized controlled clinical trial. *Phytother Res* 2012; **26**: 1381-1384 [PMID: 22308054 DOI: 10.1002/ptr.3728]

24 **Yan BF**, Wang Y, Wang WB, Ding XJ, Wei B, Liu SJ, Fu TM, Chen L, Zhang JZ, Liu J, Zheng X. Huangqin decoction mitigates hepatic inflammation in high-fat diet-challenged rats by inhibiting TLR4/NF-κB/NLRP3 pathway. *J Ethnopharmacol* 2023; **303**: 115999 [PMID: 36509260 DOI: 10.1016/j.jep.2022.115999]

25 **Yan BF**, Chen X, Chen YF, Liu SJ, Xu CX, Chen L, Wang WB, Wen TT, Zheng X, Liu J. Aqueous extract of Paeoniae Radix Alba (Paeonia lactiflora Pall.) ameliorates DSS-induced colitis in mice by tunning the intestinal physical barrier, immune responses, and microbiota. *J Ethnopharmacol* 2022; **294**: 115365 [PMID: 35597411 DOI: 10.1016/j.jep.2022.115365]

26 **Zhu Y**, Wan N, Shan X, Deng G, Xu Q, Ye H, Sun Y. Celastrol targets adenylyl cyclase-associated protein 1 to reduce macrophages-mediated inflammation and ameliorates high fat diet-induced metabolic syndrome in mice. *Acta Pharm Sin B* 2021; **11**: 1200-1212 [PMID: 34094828 DOI: 10.1016/j.apsb.2020.12.008]

27 **Wang Y**, Zhao H, Li X, Li N, Wang Q, Liu Y, Liang Q, Shao Z, Zhang N, Zhao T, Peng L, Li P. Tangshen Formula Alleviates Hepatic Steatosis by Inducing Autophagy Through the AMPK/SIRT1 Pathway. *Front Physiol* 2019; **10**: 494 [PMID: 31105592 DOI: 10.3389/fphys.2019.00494]

28 **Xiao Q**, Zhang S, Yang C, Du R, Zhao J, Li J, Xu Y, Qin Y, Gao Y, Huang W. Ginsenoside Rg1 Ameliorates Palmitic Acid-Induced Hepatic Steatosis and Inflammation in HepG2 Cells *via* the AMPK/NF-κB Pathway. *Int J Endocrinol* 2019; **2019**: 7514802 [PMID: 31467529 DOI: 10.1155/2019/7514802]

29 **Badolati N**, Masselli R, Sommella E, Sagliocchi S, Di Minno A, Salviati E, Campiglia P, Dentice M, Tenore GC, Stornaiuolo M, Novellino E. The Hepatoprotective Effect of Taurisolo, a Nutraceutical Enriched in Resveratrol and Polyphenols, Involves Activation of Mitochondrial Metabolism in Mice Liver. *Antioxidants (Basel)* 2020; **9** [PMID: 32403305 DOI: 10.3390/antiox9050410]

30 **Shi H**, Dong C, Wang M, Liu R, Wang Y, Kan Z, Wang L, Si G. Exploring the mechanism of Yizhi Tongmai decoction in the treatment of vascular dementia through network pharmacology and molecular docking. *Ann Transl Med* 2021; **9**: 164 [PMID: 33569466 DOI: 10.21037/atm-20-8165]

31 **Huo M**, Ma L, Liu G. Exploring the mechanism of Yixinyin for myocardial infarction by weighted co-expression network and molecular docking. *Sci Rep* 2021; **11**: 22567 [PMID: 34799616 DOI: 10.1038/s41598-021-01691-8]

32 **Liu W**, Shang J, Deng Y, Han X, Chen Y, Wang S, Yang R, Dong F, Shang H. Network pharmacology analysis on mechanism of Jian Pi Qing Gan Yin decoction ameliorating high fat diet-induced non-alcoholic fatty liver disease and validated in vivo. *J Ethnopharmacol* 2022; **295**: 115382 [PMID: 35577161 DOI: 10.1016/j.jep.2022.115382]

33 **Chao J**, Cheng HY, Chang ML, Huang SS, Liao JW, Cheng YC, Peng WH, Pao LH. Gallic Acid Ameliorated Impaired Lipid Homeostasis in a Mouse Model of High-Fat Diet-and Streptozotocin-Induced NAFLD and Diabetes through Improvement of β-oxidation and Ketogenesis. *Front Pharmacol* 2020; **11**: 606759 [PMID: 33643038 DOI: 10.3389/fphar.2020.606759]

34 **Li YC**, Qiao JY, Wang BY, Bai M, Shen JD, Cheng YX. Paeoniflorin Ameliorates Fructose-Induced Insulin Resistance and Hepatic Steatosis by Activating LKB1/AMPK and AKT Pathways. *Nutrients* 2018; **10** [PMID: 30081580 DOI: 10.3390/nu10081024]

35 **Zhang X**, Huo Z, Luan H, Huang Y, Shen Y, Sheng L, Liang J, Wu F. Scutellarin ameliorates hepatic lipid accumulation by enhancing autophagy and suppressing IRE1α/XBP1 pathway. *Phytother Res* 2022; **36**: 433-447 [PMID: 34859513 DOI: 10.1002/ptr.7344]

36 **Hu Q**, Zhang W, Wu Z, Tian X, Xiang J, Li L, Li Z, Peng X, Wei S, Ma X, Zhao Y. Baicalin and the liver-gut system: Pharmacological bases explaining its therapeutic effects. *Pharmacol Res* 2021; **165**: 105444 [PMID: 33493657 DOI: 10.1016/j.phrs.2021.105444]

37 **Zheng X**, Zhao MG, Jiang CH, Sheng XP, Yang HM, Liu Y, Yao XM, Zhang J, Yin ZQ. Triterpenic acids-enriched fraction from Cyclocarya paliurus attenuates insulin resistance and hepatic steatosis *via* PI3K/Akt/GSK3β pathway. *Phytomedicine* 2020; **66**: 153130 [PMID: 31790897 DOI: 10.1016/j.phymed.2019.153130]

38 **Araya J**, Rodrigo R, Videla LA, Thielemann L, Orellana M, Pettinelli P, Poniachik J. Increase in long-chain polyunsaturated fatty acid n - 6/n - 3 ratio in relation to hepatic steatosis in patients with non-alcoholic fatty liver disease. *Clin Sci (Lond)* 2004; **106**: 635-643 [PMID: 14720121 DOI: 10.1042/cs20030326]

39 **Park JC**, Jeong WJ, Seo SH, Choi KY. WDR76 mediates obesity and hepatic steatosis *via* HRas destabilization. *Sci Rep* 2019; **9**: 19676 [PMID: 31873167 DOI: 10.1038/s41598-019-56211-6]

40 **Bechmann LP**, Hannivoort RA, Gerken G, Hotamisligil GS, Trauner M, Canbay A. The interaction of hepatic lipid and glucose metabolism in liver diseases. *J Hepatol* 2012; **56**: 952-964 [PMID: 22173168 DOI: 10.1016/j.jhep.2011.08.025]

41 **Tilg H**, Moschen AR, Roden M. NAFLD and diabetes mellitus. *Nat Rev Gastroenterol Hepatol* 2017; **14**: 32-42 [PMID: 27729660 DOI: 10.1038/nrgastro.2016.147]

42 **Lambert JE**, Ramos-Roman MA, Browning JD, Parks EJ. Increased de novo lipogenesis is a distinct characteristic of individuals with nonalcoholic fatty liver disease. *Gastroenterology* 2014; **146**: 726-735 [PMID: 24316260 DOI: 10.1053/j.gastro.2013.11.049]

43 **Song Z**, Xiaoli AM, Yang F. Regulation and Metabolic Significance of De Novo Lipogenesis in Adipose Tissues. *Nutrients* 2018; **10** [PMID: 30274245 DOI: 10.3390/nu10101383]

44 **Horton JD**, Goldstein JL, Brown MS. SREBPs: activators of the complete program of cholesterol and fatty acid synthesis in the liver. *J Clin Invest* 2002; **109**: 1125-1131 [PMID: 11994399 DOI: 10.1172/jci15593]

45 **Manzoor M**, Muroi M, Ogawa N, Kobayashi H, Nishimura H, Chen D, Fasina OB, Wang J, Osada H, Yoshida M, Xiang L, Qi J. Isoquercitrin from Apocynum venetum L. produces an anti-obesity effect on obese mice by targeting C-1-tetrahydrofolate synthase, carbonyl reductase, and glutathione S-transferase P and modification of the AMPK/SREBP-1c/FAS/CD36 signaling pathway in mice in vivo. *Food Funct* 2022; **13**: 10923-10936 [PMID: 36205648 DOI: 10.1039/d2fo02438a]

46 **Tilg H**, Moschen AR. Evolution of inflammation in nonalcoholic fatty liver disease: the multiple parallel hits hypothesis. *Hepatology* 2010; **52**: 1836-1846 [PMID: 21038418 DOI: 10.1002/hep.24001]

47 **Sakurai Y**, Kubota N, Yamauchi T, Kadowaki T. Role of Insulin Resistance in MAFLD. *Int J Mol Sci* 2021; **22** [PMID: 33923817 DOI: 10.3390/ijms22084156]

48 **Zhang HH**, Halbleib M, Ahmad F, Manganiello VC, Greenberg AS. Tumor necrosis factor-alpha stimulates lipolysis in differentiated human adipocytes through activation of extracellular signal-related kinase and elevation of intracellular cAMP. *Diabetes* 2002; **51**: 2929-2935 [PMID: 12351429 DOI: 10.2337/diabetes.51.10.2929]

49 **Hotamisligil GS**, Shargill NS, Spiegelman BM. Adipose expression of tumor necrosis factor-alpha: direct role in obesity-linked insulin resistance. *Science* 1993; **259**: 87-91 [PMID: 7678183 DOI: 10.1126/science.7678183]

50 **Sabio G**, Das M, Mora A, Zhang Z, Jun JY, Ko HJ, Barrett T, Kim JK, Davis RJ. A stress signaling pathway in adipose tissue regulates hepatic insulin resistance. *Science* 2008; **322**: 1539-1543 [PMID: 19056984 DOI: 10.1126/science.1160794]

51 **Zhang JN**, Ma Y, Wei XY, Liu KY, Wang H, Han H, Cui Y, Zhang MX, Qin WD. Remifentanil Protects against Lipopolysaccharide-Induced Inflammation through PARP-1/NF-κB Signaling Pathway. *Mediators Inflamm* 2019; **2019**: 3013716 [PMID: 32082073 DOI: 10.1155/2019/3013716]

52 **Boden G**, She P, Mozzoli M, Cheung P, Gumireddy K, Reddy P, Xiang X, Luo Z, Ruderman N. Free fatty acids produce insulin resistance and activate the proinflammatory nuclear factor-kappaB pathway in rat liver. *Diabetes* 2005; **54**: 3458-3465 [PMID: 16306362 DOI: 10.2337/diabetes.54.12.3458]

53 **Yeung F**, Hoberg JE, Ramsey CS, Keller MD, Jones DR, Frye RA, Mayo MW. Modulation of NF-kappaB-dependent transcription and cell survival by the SIRT1 deacetylase. *EMBO J* 2004; **23**: 2369-2380 [PMID: 15152190 DOI: 10.1038/sj.emboj.7600244]

54 **Yoo J**, Jeong IK, Ahn KJ, Chung HY, Hwang YC. Fenofibrate, a PPARα agonist, reduces hepatic fat accumulation through the upregulation of TFEB-mediated lipophagy. *Metabolism* 2021; **120**: 154798 [PMID: 33984335 DOI: 10.1016/j.metabol.2021.154798]

55 **Mahmoudi A**, Moallem SA, Johnston TP, Sahebkar A. Liver Protective Effect of Fenofibrate in NASH/NAFLD Animal Models. *PPAR Res* 2022; **2022**: 5805398 [PMID: 35754743 DOI: 10.1155/2022/5805398]

56 **El-Haggar SM**, Mostafa TM. Comparative clinical study between the effect of fenofibrate alone and its combination with pentoxifylline on biochemical parameters and liver stiffness in patients with non-alcoholic fatty liver disease. *Hepatol Int* 2015; **9**: 471-479 [PMID: 25956613 DOI: 10.1007/s12072-015-9633-1]

57 **Oscarsson J**, Önnerhag K, Risérus U, Sundén M, Johansson L, Jansson PA, Moris L, Nilsson PM, Eriksson JW, Lind L. Effects of free omega-3 carboxylic acids and fenofibrate on liver fat content in patients with hypertriglyceridemia and non-alcoholic fatty liver disease: A double-blind, randomized, placebo-controlled study. *J Clin Lipidol* 2018; **12**: 1390-1403.e4 [PMID: 30197273 DOI: 10.1016/j.jacl.2018.08.003]

58 **Huang K**, Du M, Tan X, Yang L, Li X, Jiang Y, Wang C, Zhang F, Zhu F, Cheng M, Yang Q, Yu L, Wang L, Huang D, Huang K. PARP1-mediated PPARα poly(ADP-ribosyl)ation suppresses fatty acid oxidation in non-alcoholic fatty liver disease. *J Hepatol* 2017; **66**: 962-977 [PMID: 27979751 DOI: 10.1016/j.jhep.2016.11.020]

59 **Kim TH**, Yang YM, Han CY, Koo JH, Oh H, Kim SS, You BH, Choi YH, Park TS, Lee CH, Kurose H, Noureddin M, Seki E, Wan YY, Choi CS, Kim SG. Gα12 ablation exacerbates liver steatosis and obesity by suppressing USP22/SIRT1-regulated mitochondrial respiration. *J Clin Invest* 2018; **128**: 5587-5602 [PMID: 30300140 DOI: 10.1172/jci97831]

World Journal of Gastroenterology

Submit a Manuscript: https://www.f6publishing.com

World J Gastroenterol 2023 August 21; 29(31): 4763-4773

DOI: 10.3748/wjg.v29.i31.4763

ISSN 1007-9327 (print) ISSN 2219-2840 (online)

ORIGINAL ARTICLE

Retrospective Cohort Study

Gastric cancer incidence based on endoscopic Kyoto classification of gastritis

Osamu Toyoshima, Toshihiro Nishizawa, Shuntaro Yoshida, Tatsuya Matsuno, Gota Fujisawa, Akira Toyoshima, Hirotoshi Ebinuma, Mitsuhiro Fujishiro, Yutaka Saito, Hidekazu Suzuki

Specialty type: Gastroenterology and hepatology

Provenance and peer review: Unsolicited article; Externally peer reviewed.

Peer-review model: Single blind

Peer-review report's scientific quality classification

Grade A (Excellent): 0
Grade B (Very good): B
Grade C (Good): C
Grade D (Fair): 0
Grade E (Poor): 0

P-Reviewer: Ma L, China; Senchukova M, Russia

Received: June 3, 2023
Peer-review started: June 3, 2023
First decision: July 10, 2023
Revised: July 20, 2023
Accepted: July 28, 2023
Article in press: July 28, 2023
Published online: August 21, 2023

Osamu Toyoshima, Shuntaro Yoshida, Tatsuya Matsuno, Gota Fujisawa, Department of Gastroenterology, Toyoshima Endoscopy Clinic, Tokyo 157-0066, Japan

Toshihiro Nishizawa, Hirotoshi Ebinuma, Department of Gastroenterology and Hepatology, International University of Health and Welfare, Narita Hospital, Narita 286-8520, Japan

Akira Toyoshima, Department of Colorectal Surgery, Japanese Red Cross Medical Center, Tokyo 150-8935, Japan

Mitsuhiro Fujishiro, Department of Gastroenterology, Graduate School of Medicine, The University of Tokyo, Tokyo 113-8655, Japan

Yutaka Saito, Division of Endoscopy, National Cancer Center Hospital, Tokyo 104-0045, Japan

Hidekazu Suzuki, Division of Gastroenterology and Hepatology, Department of Internal Medicine, Tokai University School of Medicine, Isehara 259-1193, Japan

Corresponding author: Toshihiro Nishizawa, MD, PhD, Professor, Department of Gastroenterology and Hepatology, International University of Health and Welfare, Narita Hospital, Hatakeda 852, Narita, Chiba, Narita 286-8520, Japan. nisizawa@kf7.so-net.ne.jp

Abstract

BACKGROUND

Gastric cancer (GC) incidence based on the endoscopic Kyoto classification of gastritis has not been systematically investigated using time-to-event analysis.

AIM

To examine GC incidence in an endoscopic surveillance cohort.

METHODS

This study was retrospectively conducted at the Toyoshima Endoscopy Clinic. Patients who underwent two or more esophagogastroduodenoscopies were enrolled. GC incidence was based on Kyoto classification scores, such as atrophy, intestinal metaplasia (IM), enlarged folds (EFs), nodularity, diffuse redness (DR), and total Kyoto scores. Hazard ratios (HRs) adjusted for age and sex were calculated using a Cox hazard model.

RESULTS

A total of 6718 patients were enrolled (median age 54.0 years; men 44.2%). During the follow-up period (max 5.02 years; median 2.56 years), GC developed in 34 patients. The average frequency of GCs per year was 0.19%. Kyoto atrophy scores 1 [HR with score 0 as reference: 3.66, 95% confidence interval (CI): 1.06 to 12.61], 2 (11.60, 3.82-35.27), IM score 2 (9.92, 4.37-22.54), EF score 1 (4.03, 1.63-9.96), DR scores 1 (6.22, 2.65-14.56), and 2 (10.01, 3.73-26.86) were associated with GC incidence, whereas nodularity scores were not. The total Kyoto scores of 4 (HR with total Kyoto scores 0-1 as reference: 6.23, 95%CI: 1.93 to 20.13, $P = 0.002$) and 5-8 (16.45, 6.29-43.03, $P < 0.001$) were more likely to develop GC, whereas the total Kyoto scores 2-3 were not. The HR of the total Kyoto score for developing GC per 1 rank was 1.75 (95%CI: 1.46 to 2.09, $P < 0.001$).

CONCLUSION

A high total Kyoto score (≥ 4) was associated with GC incidence. The endoscopy-based diagnosis of gastritis can stratify GC risk.

Key Words: Gastric cancer; Gastritis; Endoscopy; Atrophy; Intestinal metaplasia; Kyoto classification

©The Author(s) 2023. Published by Baishideng Publishing Group Inc. All rights reserved.

Core Tip: A high total Kyoto score (≥ 4) was associated with gastric cancer (GC) incidence. Adjusted hazard ratios (HRs) for the total Kyoto scores of 4 and 5-8 were high at 6.23 and 16.45, respectively, compared to the total Kyoto scores of 0-1. The HR of the total Kyoto score for developing GC per 1 rank was 1.75.

Citation: Toyoshima O, Nishizawa T, Yoshida S, Matsuno T, Fujisawa G, Toyoshima A, Ebinuma H, Fujishiro M, Saito Y, Suzuki H. Gastric cancer incidence based on endoscopic Kyoto classification of gastritis. *World J Gastroenterol* 2023; 29(31): 4763-4773
URL: https://www.wjgnet.com/1007-9327/full/v29/i31/4763.htm
DOI: https://dx.doi.org/10.3748/wjg.v29.i31.4763

INTRODUCTION

Gastric cancer (GC) is a global health problem and the third most common cause of cancer-related deaths worldwide[1]. *Helicobacter pylori* (*H. pylori*) infection is estimated to account for 89% of GC cases, and *H. pylori*-related gastritis is a precursor of GC[2-6]. Evaluation of *H. pylori*-related gastritis is clinically important because it allows for the risk stratification of GC[2,7-9]. Endoscopy detects early GCs and precisely diagnoses gastritis. Periodic endoscopic screening can reduce deaths from GC[10]. Recent advances in endoscopic technology allow for more accurate endoscopic diagnosis of gastritis[11,12].

The endoscopy-based Kyoto classification of gastritis was advocated by the Japan Society for Gastrointestinal Endoscopy in 2013. This classification aims to ensure that the endoscopic diagnosis of gastritis is unified and matched with the histopathology[13]. Recently, the Kyoto classification has been widely used in clinical practice and vigorously studied worldwide[14,15]. To assess GC risk, the Kyoto classification individually scores five *H. pylori*-related gastritis findings, such as atrophy, intestinal metaplasia (IM), enlarged fold (EF), nodularity, and diffuse redness (DR), and defines their sum as the total Kyoto score.

Several investigations have clarified that not only individual Kyoto scores but also the total Kyoto score are associated with *H. pylori* infection and GC risks[14]. For example, the total Kyoto score was associated with *H. pylori* infection, presence of GC[16-19], and GC risk indicators, such as serum pepsinogen titer, serum *H. pylori* antibody titer, histological distribution of neutrophil infiltration in the gastric mucosa, and genotype of the single nucleotide polymorphism. Collectively, total Kyoto scores of 0, ≥ 2, and ≥ 4 indicated a normal stomach, *H. pylori*-infected gastritis, and gastritis at risk for GC, respectively[14].

To date, GC incidence based on the Kyoto classification scores has not been systematically investigated using time-to-event analysis. Therefore, we examined GC incidence according to the five individual Kyoto scores and the total Kyoto score in the endoscopic surveillance cohort and verified the GC risks of endoscopic gastritis in Japan, which is a high GC morbidity area.

MATERIALS AND METHODS

Study design and overview

This cohort study was retrospectively conducted at the Toyoshima Endoscopy Clinic. We obtained data from the Toyoshima Endoscopy Clinic Database. This study was approved by the institutional review board of the Yoyogi Mental Clinic (approval no. RKK227). Written informed consent was obtained from patients at the time of esophagogastroduodenoscopy (EGD) to use their data for research purposes. The study's protocol was published on our institute's website (

www.ichou.com) so that patients could opt out of the study. All clinical investigations were conducted in accordance with the ethical guidelines of the Declaration of Helsinki.

Patients

This study enrolled patients who underwent two or more EGDs at the Toyoshima Endoscopy Clinic, an urban area in Tokyo, Japan, between April 2017 and April 2022. We excluded patients with a previous surgical gastrectomy at baseline and those who underwent the last EGD within one month after the index EGD. The indications for the index EGD included screening, surveillance for gastritis or other upper gastrointestinal diseases, and examination for symptoms or abnormal findings on other tests. *H. pylori* status was determined using serum anti-*H. pylori* antibodies, urea breath test, histology, and/or endoscopy.

Kyoto classification score

In the Kyoto classification, the total Kyoto score was developed as a GC risk score[14]. The total Kyoto score is calculated as the sum of the following five Kyoto scores: Atrophy, IM, EF, nodularity, and DR, and ranges from 0 to 8 (Supplementary Table 1). Atrophy was classified based on the extent of mucosal atrophy using the Kimura-Takemoto classification[20]. Non-atrophy and Closed I, Closed II and III, and Open I to III were scored as atrophy scores of 0, 1, and 2, respectively. The IM commonly appears as a grayish-white, slightly elevated patch. IM scores of 0, 1, and 2 were defined as the absence of IM, IM limited to the antrum, and IM extending into the corpus, respectively. EF was defined as a width of ≥ 5 mm in the greater curvature of the corpus, which was not flattened by stomach insufflation. The absence and presence of EF were scored as 0 and 1, respectively. Nodularity was identified by a miliary pattern resembling "goose flesh", which was typically located in the antrum. The absence and presence of nodularity were scored 0 and 1, respectively. DR indicated uniform redness observed in the non-atrophic mucosa, mainly in the greater curvature of the corpus. The regular arrangement of collecting venules (RAC) in the corpus appears as numerous dots, which are starfish-like shapes in close view. DR scores of 0, 1, and 2 were defined as the absence of DR, mild DR and/or DR with partial RAC, and severe DR without RAC, respectively[14].

EGD

EGDs were performed by gastrointestinal endoscopists using the Olympus' (Tokyo, Japan) endoscopic system (EVIS X1 or LUCERA ELITE) and endoscope (GIF-XZ1200, GIF-1200N, GIF-HQ290, GIF-H290Z, or GIF-XP290N). The T-File System (STS-MEDIC Inc., Tokyo, Japan) was used to file endoscopic images and document endoscopic findings.

The Kyoto classification scores were assessed using white light imaging without magnification. The endoscopists diagnosed the Kyoto classification scores on-site during EGD, and it was retrospectively reviewed by experienced endoscopists. Endoscopists performed EGDs after learning from textbooks and journal articles on the Kyoto classification of gastritis[14,21].

GC

GC was histologically diagnosed based on biopsy or resected specimens. GC morphology and histology were classified based on the Japanese classification of gastric carcinoma[22] and Lauren's classification[23], respectively.

Outcomes

This cohort study evaluated GC incidence based on patients' age, sex, *H. pylori* status, and endoscopic Kyoto classification scores of gastritis, such as atrophy, IM, EF, nodularity, DR, and total Kyoto scores. The primary outcome was GC incidence according to the total Kyoto score. We performed a time-to-event analysis with the start time as the date of index EGD. Data were censored on the date of the last EGD. The effects of Kyoto classification scores on GC development were estimated. The total Kyoto scores were categorized into 4 (*i.e.*, 0-1, 2-3, 4, and 5-8) based on the frequency of GC increasing stepwise with the total Kyoto scores of 0-1, 2-3, and ≥ 4 in a cross-sectional study[24] and the number of patients in this study. The secondary outcomes were GC incidence according to the Kyoto atrophy, IM, EF, nodularity, and DR scores.

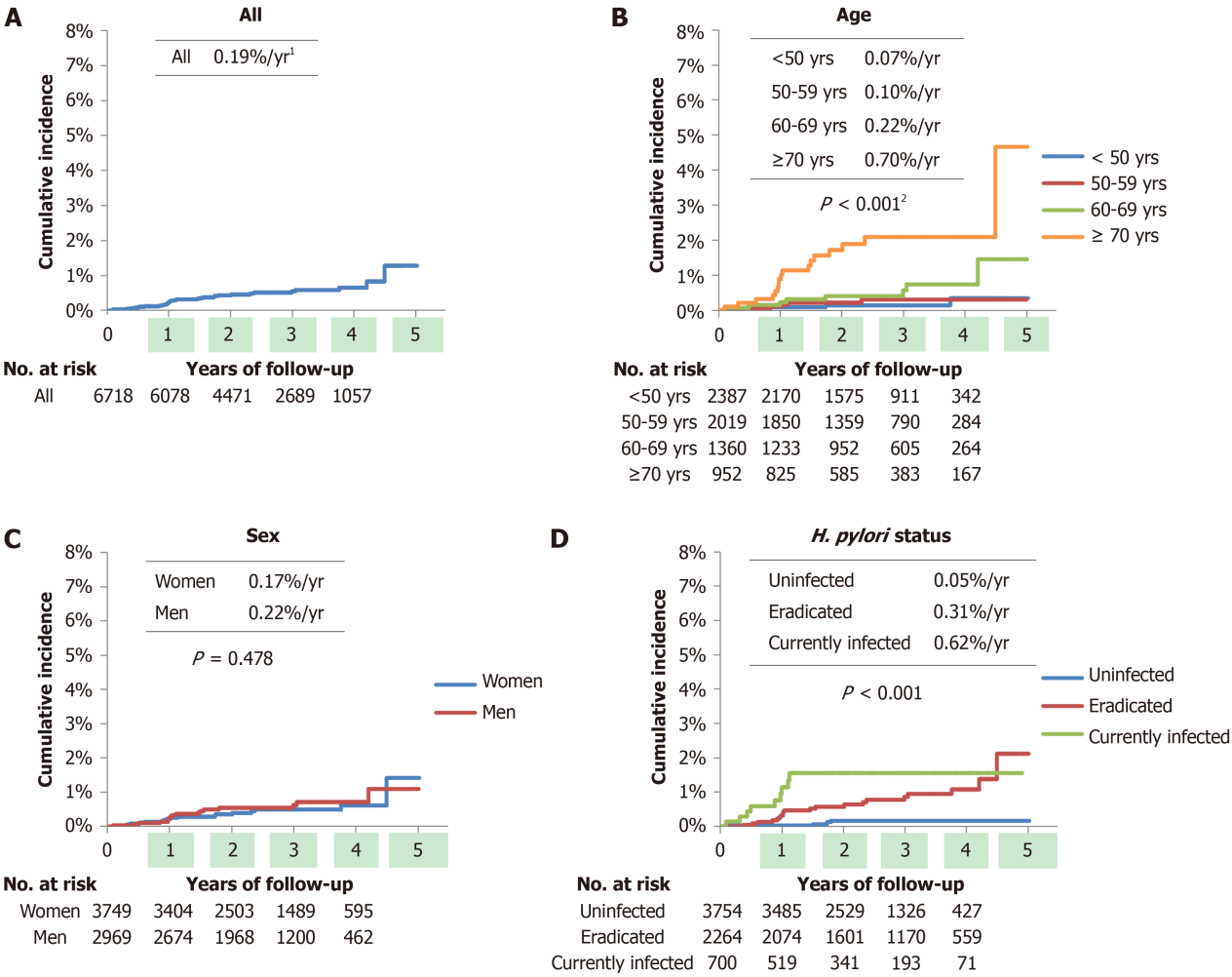
Statistical analysis

Baseline characteristics were compared between GC and non-GC groups using binomial logistic regression model. Kaplan-Meier curves were constructed according to patient age, sex, *H. pylori* status, and Kyoto classification scores (*i.e.*, atrophy, IM, EF, nodularity, DR, and the total Kyoto scores). Statistical differences were estimated using the log-rank tests. The average frequency of GCs per year was calculated by dividing the number of events by the total person-years of observation. Hazard ratios (HRs) with 95% confidence intervals (CIs) for GC development were estimated using the Cox proportional hazards regression model. In multivariate analysis, HRs were adjusted for patient age and sex. A P value < 0.05 (two-sided) was defined as statistically significant. Statistical analysis was conducted using BellCurve for Excel version 4.03 (Social Survey Research Information Co., Ltd., Tokyo, Japan).

RESULTS

Patient enrollment

A total of 30585 EGDs in 16969 patients were performed during the study period. Six thousand seven hundred forty-four



DOI: 10.3748/wjg.v29.i31.4763 **Copyright** ©The Author(s) 2023.

Figure 1 Cumulative incidence of gastric cancer according to patient demographic characteristics. A-D: Kaplan-Meier curves of gastric cancer development for all patients (A), according to age (B), sex (C), and *Helicobacter pylori* status (D). [1]The average frequency of gastric cancer per year. [2]*P* values were calculated using a log-rank test.

patients underwent two or more EGDs. Of these, 19 patients with a previous surgical gastrectomy and 7 with a follow-up period of less than 1 mo were excluded. A total of 6718 patients were enrolled.

The baseline patient characteristics are shown in Table 1. The median age of the patients was 54 years with the interquartile range (IQR) of 46-64 years. Men accounted for 44.2% of the cases. The proportion of patients with *H. pylori* status of uninfected, eradicated, and currently infected was 55.9%, 33.7%, and 10.4%, respectively. Patients were followed up for up to 5.02 years (median 2.56 years, IQR 1.74-3.64 years). The median (IQR) of Kyoto classification scores were 0 (0-1) for atrophy; 0 (0-0) for IM, EF, nodularity, and DR; and 0 (0-2) for total Kyoto. Supplementary Table 2 is shown with the mean and standard deviation. During the follow-up period, 37 GCs occurred in 34 patients. The characteristics of GCs are presented in Table 2. All GCs were superficial and within the submucosal depth. Lauren's intestinal type made up 89.1% of GCs.

GC incidence

Kaplan-Meier curves of GC development according to patient demographic characteristics are shown in Figure 1. In this study, the average frequency of GCs was 0.19%/year. Age and *H. pylori* status were associated with GC incidence (both $P < 0.001$), whereas sex was not.

Figures 2A-E show the cumulative incidence using the Kaplan-Meier method for each Kyoto classification score. Atrophy, IM, EF, and DR scores were associated with GC development (all $P < 0.001$), whereas nodularity was not. The average frequencies of GCs per year were 0.04%, 0.17%, and 0.73% for atrophy scores of 0, 1, and 2; 0.07%, 0.25%, and 1.10% for IM scores of 0, 1, and 2; 0.17% and 0.92% for EF scores of 0 and 1; and 0.06%, 0.55%, and 0.74% for DR scores of 0, 1, and 2, respectively. The total Kyoto score was associated with GC development ($P < 0.001$), as shown in Figure 2F. The average frequencies of GCs were 0.05, 0.07, 0.47, and 1.27% per year for the total Kyoto scores of 0-1, 2-3, 4, and 5-8, respectively.

Table 1 Demographic characteristics and endoscopic findings of the patient at baseline

	All	Gastric cancer	Non-gastric cancer	*P* value[1]
No.	6718	34	6684	
Age, median (IQR), yr	54 (46-64)	69.5 (57.8-73.8)	54 (46-64)	< 0.001
Male sex, No. (%)	2969 (44.2)	17 (50.0)	2952 (44.2)	0.495
H. pylori status, No. (%)				< 0.001
Uninfected	3754 (55.9)	5 (14.7)	3749 (56.1)	
Eradicated	2264 (33.7)	20 (58.8)	2244 (33.6)	
Currently infected	700 (10.4)	9 (26.5)	691 (10.3)	
Duration of follow up, median (IQR), yr	2.56 (1.74-3.64)	1.03 (0.85-1.78)	2.57 (1.76-3.64)	< 0.001
No. EGD per patient, median (IQR)	2 (2-4)	2 (2-3)	2 (2-4)	0.652
Kyoto classification score, median (IQR)				
Atrophy	0 (0-1)	2 (1-2)	0 (0-1)	< 0.001
Intestinal metaplasia	0 (0-0)	2 (0-2)	0 (0-0)	< 0.001
Enlarged folds	0 (0-0)	0 (0-0)	0 (0-0)	< 0.001
Nodularity	0 (0-0)	0 (0-0)	0 (0-0)	0.916
Diffuse redness	0 (0-0)	1 (1-1)	0 (0-0)	< 0.001
Total Kyoto	0 (0-2)	5 (4-5)	0 (0-2)	< 0.001

[1]*P* values were calculated using binomial logistic regression model.
IQR: Interquartile range; EGD: Esophagogastroduodenoscopy; *H. pylori*: *Helicobacter pylori*.

Table 2 Characteristics of gastric cancers

	n
Gastric cancer patient	34
Gastric cancer lesion	37
Morphological type[1]	
Superficial elevated (0-IIa)	7
Superficial flat (0-IIb)	5
Superficial depressed (0-IIc)	25
Depth	
Mucosa	33
Submucosa	4
Lauren's histological type	
Diffuse	4
Intestinal	33

[1]According to the Japanese classification of gastric carcinoma[22].

Multivariate analysis of GC incidence

Table 3 provides the crude and adjusted HRs for GC development according to Kyoto classification scores. Multivariate analysis showed that atrophy scores 1 (adjusted HR with score 0 as reference: 3.66, 95%CI: 1.06 to 12.61), 2 (11.60, 3.82-35.27), IM score 2 (9.92, 4.37-22.54), EF score 1 (4.03, 1.63-9.96), DR scores 1 (6.22, 2.65-14.56), and 2 (10.01, 3.73-26.86) were significantly associated with GC incidence, independent of patient age and sex, whereas nodularity score was not.

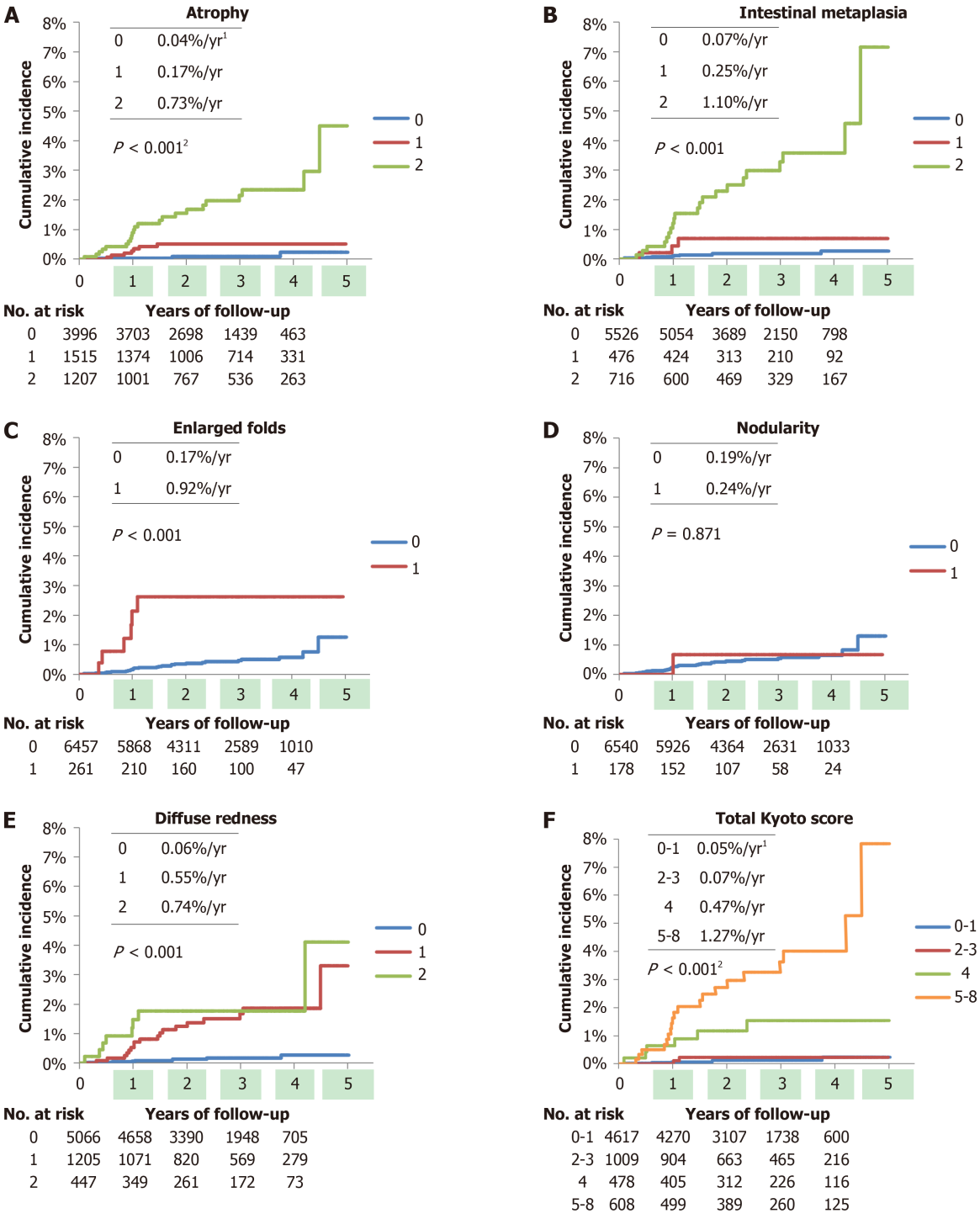
The total Kyoto scores of 4 (adjusted HR with total Kyoto scores 0-1 as reference: 6.23, 95%CI: 1.93 to 20.13, $P = 0.002$) and 5-8 (16.45, 6.29-43.03, $P < 0.001$) were more likely to develop GC, whereas the total Kyoto scores of 2-3 were not. In

Table 3 Univariate and multivariate analysis of gastric cancer development

	GC patients, No.	Non-GC patients, No.	Crude HR[1]	95%CI	*P* value	Adjusted HR[1,2]	95%CI	*P* value
Age (yr)								
< 50	4	2383	Reference					
50-59	5	2014	1.48	0.40-5.50	0.562			
60-69	8	1352	3.37	1.01-11.19	0.047			
≥ 70	17	935	10.75	3.62-31.96	< 0.001			
Sex								
Women	17	3732	Reference					
Men	17	2952	1.27	0.65-2.48	0.488			
H. pylori status								
Uninfected	5	3749	Reference			Reference		
Eradicated	20	2244	6.00	2.25-16.05	< 0.001	3.81	1.40-10.38	0.009
Currently infected	9	691	11.60	3.88-34.64	< 0.001	9.53	3.17-28.65	< 0.001
Atrophy								
0	4	3992	Reference			Reference		
1	7	1508	4.40	1.29-15.06	0.018	3.66	1.06-12.61	0.040
2	23	1184	19.02	6.56-55.12	< 0.001	11.60	3.82-35.27	< 0.001
Intestinal metaplasia								
0	10	5516	Reference			Reference		
1	3	473	3.42	0.94-12.44	0.062	2.25	0.60-8.43	0.228
2	21	695	16.01	7.52-34.05	< 0.001	9.92	4.37-22.54	< 0.001
Enlarged folds								
0	28	6429	Reference			Reference		
1	6	255	5.41	2.23-13.10	< 0.001	4.03	1.63-9.96	0.003
Nodularity								
0	33	6507	Reference			Reference		
1	1	177	1.18	0.16-8.62	0.872	2.51	0.33-18.86	0.372
Diffuse redness								
0	8	5058	Reference			Reference		
1	18	1187	9.05	3.92-20.85	< 0.001	6.22	2.65-14.56	< 0.001
2	8	439	12.26	4.60-32.68	< 0.001	10.01	3.73-26.86	< 0.001
Total Kyoto								
0-1	6	4615	Reference			Reference		
2-3	2	1008	1.48	0.30-7.34	0.631	1.12	0.22-5.63	0.887
4	6	473	9.54	3.07-29.62	< 0.001	6.23	1.93-20.13	0.002
5-8	20	588	25.58	10.25-63.84	< 0.001	16.45	6.29-43.03	< 0.001

[1]Hazard ratios were calculated using the Cox proportional hazards model.
[2]Hazard ratios were adjusted for age and sex.
GC: Gastric cancer; HR: Hazard ratio; CI: Confidence interval; *H. pylori*: *Helicobacter pylori*.

per 1 rank analysis, an adjusted HR of the total Kyoto score for developing GC was 1.75 (95%CI: 1.46 to 2.09, $P < 0.001$).



DOI: 10.3748/wjg.v29.i31.4763 **Copyright** ©The Author(s) 2023.

Figure 2 Cumulative incidence of gastric cancer according to the Kyoto classification scores. A-E: Kaplan-Meier curves of gastric cancer development according to atrophy (A), intestinal metaplasia (B), enlarged folds (C), nodularity (D), and diffuse redness (E) scores, respectively; F: Kaplan-Meier curves of gastric cancer development according to total Kyoto scores. [1]The average frequency of gastric cancer per year. [2]*P* values were calculated using a log-rank test.

DISCUSSION

We found that high total Kyoto scores, especially ≥ 4, were associated with GC incidence. The adjusted HR of the total Kyoto score for GC development was 1.75 per 1 rank analysis. Additionally, adjusted HRs for the total Kyoto scores of 4 and 5-8 were high at 6.23 and 16.45, respectively, compared to the total Kyoto scores of 0-1. The total Kyoto score was associated with the cumulative incidence of GC ($P < 0.001$). The average frequencies of GCs per year increased with the total Kyoto score (0.05%, 0.07%, 0.47%, and 1.27% for the total Kyoto scores of 0-1, 2-3, 4, and 5-8, respectively). This is the first report that shows that high total Kyoto scores represent GC risks in a time-to-event analysis. This finding is consistent with those of several previous studies. In cross-sectional studies, we and Lin *et al*[19] reported that the odds

ratios of the total Kyoto score for GC were 1.6 and 1.5 per 1 rank, respectively[18]. Liu *et al*[24] indicated an increased trend of GC frequency in patients with total Kyoto scores of 0-1, 2-3, and ≥ 4. Some investigators showed that the mean total Kyoto scores of the patients with GC, *H. pylori*-infected GC, and *H. pylori*-eradicated GC were 4.0-4.6, 4.8-5.6, and 4.2, respectively[18,25,26]. Taken together, a total Kyoto score ≥ 4 was available for determining GC risks.

This cohort study demonstrated that patients with endoscopy-based atrophy, IM, EF, and DR are more likely to develop GC. In contrast, nodularity was not associated with GC incidence. Endoscopic atrophy has been shown to be a predictor of GC development. Shichijo *et al*[27] described a significantly higher adjusted HR of severe atrophy for developing GC as 9.3, while we identified significantly higher adjusted HRs of Kyoto atrophy scores 1 and 2 as 3.7 and 11.6, respectively. Several cohort studies have shown that severe endoscopic atrophy is associated with a high incidence of GC, especially in patients who have undergone *H. pylori* eradication[9,27,28]. These studies revealed that the average frequencies of GCs per year for non-to-mild, moderate, and severe atrophy were 0.06%-0.15%, 0.12%-0.34%, and 0.31%-1.60%, respectively. Similarly, our study showed that the average frequencies of GCs per year for total Kyoto scores of 0, 1, and 2 were 0.04%, 0.17%, and 0.73%, respectively. Since more than half of the study patients were uninfected with *H. pylori*, our study may present a lower GC incidence in patients with a Kyoto atrophy score of 0. Two meta-analyses also showed that a high Kyoto atrophy score provided a high-risk ratio of 2.8-8.0[29,30]. Thus, our study results are in line with those of previous studies.

Although the risk of GC in histological IM has been well studied[2,8,27,31,32], few studies have examined GC risks associated with endoscopic IM. A high Kyoto IM score has been identified as a risk factor for GC, especially multiple GC [14,18]. This study revealed that endoscopic corpus IM was associated with GC development (adjusted HR: 9.92), which is supported by Sakitani *et al*[33], who clarified histological corpus IM as a predictor of GC. The consistency of IM between endoscopy and histology has been demonstrated[13]; we successfully verified endoscopic IM as a risk factor for GC using event history analysis.

Watanabe *et al*[34] provided an adjusted HR of EF for GC development as high as 43.3, whereas our study's adjusted HR was 4.03. These results are similar; however, the difference in HRs between them may be attributed to the inclusion of many *H. pylori*-uninfected individuals in the study population. However, whether nodularity is a risk factor for GC remains controversial. Nodularity has been reported to be a juvenile and histologically diffuse-type GC risk[35,36], whereas we have shown in a cross-sectional study that the odds ratio for GC of nodularity is low at 0.5[18]. After adjusting for age and sex, no association between nodularity and GC was observed. Although nodularity decreases with age[37], the risk of intestinal-type GC increases with age. Furthermore, intestinal-type cancers are more common than diffuse-type cancers. Therefore, age offsets the association of nodularity with GC, especially in older generations, although nodularity is associated with diffuse-type GC in the young generation[35]. As the association between nodularity and the risk of developing GC is still debated, nodularity might be listed separately. For example, the total Kyoto classification score for atrophy 1, IM 0, EF 1, nodularity 1, and DR 1 might be reported as 3 + 1 instead of 4.

Several studies have reported that DR is strongly associated with *H. pylori* infection[15,38-40], but little is known about the association between DR and GC incidence. This study identified Kyoto DR scores of 1 and 2 as indicators of GC incidence (adjusted HRs: 6.22 and 10.01, respectively). Since DR presents inflammatory cell infiltration caused by *H. pylori* [13] and *H. pylori* infection is a definite risk factor for GC[2,3], DR is expressed as a GC risk. Additionally, since the Kyoto DR score includes RAC as a negative factor and RAC is inversely associated with GC development[41], a high Kyoto DR score may be associated with high GC incidence.

This study has some limitations. First, this was a single-center, retrospective cohort study. Although the endoscopy data were well-organized, multi-center, prospective studies are warranted. Second, this study was conducted only in areas with a high GC prevalence in Asia. Therefore, studies in Western countries are warranted. Third, the total Kyoto score has shortcomings in the scoring design, which simply adds five individual Kyoto scores[14]. IM is associated with a high risk of intestinal-type GC but a low risk of diffuse-type GC[18]. In addition, EF and nodularity are high risks for diffuse-type GC but low risks for intestinal-type GC. Therefore, the evaluation of GC risk using a scoring system that individually predicts the risks of intestinal- and diffuse-type GCs is needed.

CONCLUSION

In conclusion, a high total Kyoto score of ≥ 4 was associated with GC incidence in a cohort study. The endoscopy-based diagnosis of gastritis can stratify GC risk.

ARTICLE HIGHLIGHTS

Research background

The Japan Gastroenterological Endoscopy Society advocated the Kyoto classification, a new grading system for endoscopic gastritis in 2013.

Research motivation

Although a high Kyoto score is believed to reflect an increased gastric cancer (GC) risk, it has not been systematically investigated using time-to-event analysis.

Research objectives
We examined GC incidence according to the total Kyoto score in the endoscopic surveillance cohort and verified the GC risks of endoscopic gastritis.

Research methods
Patients who underwent two or more esophagogastroduodenoscopies were enrolled. GC incidence was based on Kyoto classification scores. Hazard ratios (HRs) adjusted for age and sex were calculated using a Cox hazard model.

Research results
A total of 6718 patients were enrolled. The annual incidence rate of GC was 0.19%. The total Kyoto scores of 4 [HR with total Kyoto scores 0-1 as reference: 6.23, 95% confidence interval (CI): 1.93 to 20.13, $P = 0.002$] and 5-8 (16.45, 6.29-43.03, $P < 0.001$) were more likely to develop GC, whereas the total Kyoto scores 2-3 were not. The HR of the total Kyoto score for developing GC per 1 rank was 1.75 (95%CI: 1.46 to 2.09, $P < 0.001$).

Research conclusions
A total Kyoto score ≥ 4 could predict GC risk. The endoscopic Kyoto classification of gastritis can stratify GC risk.

Research perspectives
This was a single-center, retrospective cohort study, and multi-center, prospective studies are warranted.

ACKNOWLEDGEMENTS

We would like to thank Shido Inc. (www.Shido.co.jp) for consulting the statistical analysis. We would like to thank clinical laboratory engineer Tadahiro Yamakawa for managing the endoscopy database of the Toyoshima Endoscopy Clinic.

FOOTNOTES

Author contributions: Toyoshima O, Nishizawa T, Yoshida S, Matsuno T, Fujisawa G, and Toyoshima A contributed to the conception of article; Toyoshima O drafted the article; Toyoshima O, Nishizawa T, Yoshida S, and Matsuno T involved in the review of endoscopic images; Toyoshima O contributed to the statistical analysis; Nishizawa T edited the article; Toyoshima O, Nishizawa T, Yoshida S, Matsuno T, Fujisawa G, Toyoshima A, Ebinuma H, Fujishiro M, Saito Y, and Suzuki H contributed to the critical review; and all authors approved the final manuscript.

Institutional review board statement: This study was approved by the institutional review board of the Yoyogi Mental Clinic (approval no. RKK227).

Informed consent statement: Written informed consent was obtained from patients at the time of esophagogastroduodenoscopy to use their data for research purposes. The study's protocol was published on our institute's website (www.ichou.com) so that patients could opt out of the study.

Conflict-of-interest statement: All the authors report no relevant conflicts of interest for this article.

Data sharing statement: No additional data are available.

STROBE statement: The authors have read the STROBE Statement-checklist of items, and the manuscript was prepared and revised according to the STROBE Statement-checklist of items.

Open-Access: This article is an open-access article that was selected by an in-house editor and fully peer-reviewed by external reviewers. It is distributed in accordance with the Creative Commons Attribution NonCommercial (CC BY-NC 4.0) license, which permits others to distribute, remix, adapt, build upon this work non-commercially, and license their derivative works on different terms, provided the original work is properly cited and the use is non-commercial. See: https://creativecommons.org/Licenses/by-nc/4.0/

Country/Territory of origin: Japan

ORCID number: Osamu Toyoshima 0000-0002-6953-6079; Toshihiro Nishizawa 0000-0003-4876-3384; Shuntaro Yoshida 0000-0002-9437-9132; Tatsuya Matsuno 0000-0002-1935-3506; Gota Fujisawa 0000-0002-0218-200X; Akira Toyoshima 0000-0002-5697-6251; Hirotoshi Ebinuma 0000-0001-6604-053X; Mitsuhiro Fujishiro 0000-0002-4074-1140; Yutaka Saito 0000-0003-2296-8373; Hidekazu Suzuki 0000-0002-8994-6163.

S-Editor: Wang JJ
L-Editor: A
P-Editor: Xu ZH

REFERENCES

1 **Bray F**, Ferlay J, Soerjomataram I, Siegel RL, Torre LA, Jemal A. Global cancer statistics 2018: GLOBOCAN estimates of incidence and mortality worldwide for 36 cancers in 185 countries. *CA Cancer J Clin* 2018; **68**: 394-424 [PMID: 30207593 DOI: 10.3322/caac.21492]

2 **Uemura N**, Okamoto S, Yamamoto S, Matsumura N, Yamaguchi S, Yamakido M, Taniyama K, Sasaki N, Schlemper RJ. Helicobacter pylori infection and the development of gastric cancer. *N Engl J Med* 2001; **345**: 784-789 [PMID: 11556297 DOI: 10.1056/NEJMoa001999]

3 **Plummer M**, Franceschi S, Vignat J, Forman D, de Martel C. Global burden of gastric cancer attributable to Helicobacter pylori. *Int J Cancer* 2015; **136**: 487-490 [PMID: 24889903 DOI: 10.1002/ijc.28999]

4 **Sugano K**. Effect of Helicobacter pylori eradication on the incidence of gastric cancer: a systematic review and meta-analysis. *Gastric Cancer* 2019; **22**: 435-445 [PMID: 30206731 DOI: 10.1007/s10120-018-0876-0]

5 **Choi Y**, Kim N, Yun CY, Choi YJ, Yoon H, Shin CM, Park YS, Ahn SH, Joong Park D, Lee HS, Kim JW, Lee KW, Chang W, Park JH, Lee YJ, Lee KH, Kim YH, Lee DH, Kim HH. Effect of Helicobacter pylori eradication after subtotal gastrectomy on the survival rate of patients with gastric cancer: follow-up for up to 15 years. *Gastric Cancer* 2020; **23**: 1051-1063 [PMID: 32361784 DOI: 10.1007/s10120-020-01076-2]

6 **Takahashi Y**, Yamamichi N, Kubota D, Shimamoto T, Nagao S, Sakuma N, Sakaguchi Y, Yakabi S, Tsuji Y, Wada R, Mitsushima T, Ichinose M, Fujishiro M. Risk factors for gastric cancer in Japan in the 2010s: a large, long-term observational study. *Gastric Cancer* 2022; **25**: 481-489 [PMID: 35067826 DOI: 10.1007/s10120-021-01273-7]

7 **Song H**, Ekheden IG, Zheng Z, Ericsson J, Nyrén O, Ye W. Incidence of gastric cancer among patients with gastric precancerous lesions: observational cohort study in a low risk Western population. *BMJ* 2015; **351**: h3867 [PMID: 26215280 DOI: 10.1136/bmj.h3867]

8 **Pimentel-Nunes P**, Libânio D, Marcos-Pinto R, Areia M, Leja M, Esposito G, Garrido M, Kikuste I, Megraud F, Matysiak-Budnik T, Annibale B, Dumonceau JM, Barros R, Fléjou JF, Carneiro F, van Hooft JE, Kuipers EJ, Dinis-Ribeiro M. Management of epithelial precancerous conditions and lesions in the stomach (MAPS II): European Society of Gastrointestinal Endoscopy (ESGE), European Helicobacter and Microbiota Study Group (EHMSG), European Society of Pathology (ESP), and Sociedade Portuguesa de Endoscopia Digestiva (SPED) guideline update 2019. *Endoscopy* 2019; **51**: 365-388 [PMID: 30841008 DOI: 10.1055/a-0859-1883]

9 **Take S**, Mizuno M, Ishiki K, Kusumoto C, Imada T, Hamada F, Yoshida T, Yokota K, Mitsuhashi T, Okada H. Risk of gastric cancer in the second decade of follow-up after Helicobacter pylori eradication. *J Gastroenterol* 2020; **55**: 281-288 [PMID: 31667586 DOI: 10.1007/s00535-019-01639-w]

10 **Hamashima C**, Shabana M, Okada K, Okamoto M, Osaki Y. Mortality reduction from gastric cancer by endoscopic and radiographic screening. *Cancer Sci* 2015; **106**: 1744-1749 [PMID: 26432528 DOI: 10.1111/cas.12829]

11 **Shah SC**, Piazuelo MB, Kuipers EJ, Li D. AGA Clinical Practice Update on the Diagnosis and Management of Atrophic Gastritis: Expert Review. *Gastroenterology* 2021; **161**: 1325-1332.e7 [PMID: 34454714 DOI: 10.1053/j.gastro.2021.06.078]

12 **Takeda T**, Asaoka D, Nojiri S, Nishiyama M, Ikeda A, Yatagai N, Ishizuka K, Hiromoto T, Okubo S, Suzuki M, Nakajima A, Nakatsu Y, Komori H, Akazawa Y, Nakagawa Y, Izumi K, Matsumoto K, Ueyama H, Sasaki H, Shimada Y, Osada T, Hojo M, Kato M, Nagahara A. Linked Color Imaging and the Kyoto Classification of Gastritis: Evaluation of Visibility and Inter-Rater Reliability. *Digestion* 2020; **101**: 598-607 [PMID: 31302654 DOI: 10.1159/000501534]

13 **Toyoshima O**, Nishizawa T, Yoshida S, Matsuno T, Odawara N, Toyoshima A, Sakitani K, Watanabe H, Fujishiro M, Suzuki H. Consistency between the endoscopic Kyoto classification and pathological updated Sydney system for gastritis: A cross-sectional study. *J Gastroenterol Hepatol* 2022; **37**: 291-300 [PMID: 34569096 DOI: 10.1111/jgh.15693]

14 **Toyoshima O**, Nishizawa T. Kyoto classification of gastritis: Advances and future perspectives in endoscopic diagnosis of gastritis. *World J Gastroenterol* 2022; **28**: 6078-6089 [PMID: 36483157 DOI: 10.3748/wjg.v28.i43.6078]

15 **Wang K**, Zhao J, Jin H, Meng L, Fan Y, Zhou Y, Ye C, Li M, Ma P, Zhu L, Ye Y, Lyu B. Establishment of a modified Kyoto classification scoring model and its significance in the diagnosis of Helicobacter pylori current infection. *Gastrointest Endosc* 2023; **97**: 684-693 [PMID: 36403805 DOI: 10.1016/j.gie.2022.11.008]

16 **Shichijo S**, Hirata Y, Niikura R, Hayakawa Y, Yamada A, Koike K. Association between gastric cancer and the Kyoto classification of gastritis. *J Gastroenterol Hepatol* 2017; **32**: 1581-1586 [PMID: 28217843 DOI: 10.1111/jgh.13764]

17 **Sugimoto M**, Ban H, Ichikawa H, Sahara S, Otsuka T, Inatomi O, Bamba S, Furuta T, Andoh A. Efficacy of the Kyoto Classification of Gastritis in Identifying Patients at High Risk for Gastric Cancer. *Intern Med* 2017; **56**: 579-586 [PMID: 28321054 DOI: 10.2169/internalmedicine.56.7775]

18 **Toyoshima O**, Nishizawa T, Yoshida S, Aoki T, Nagura F, Sakitani K, Tsuji Y, Nakagawa H, Suzuki H, Koike K. Comparison of endoscopic gastritis based on Kyoto classification between diffuse and intestinal gastric cancer. *World J Gastrointest Endosc* 2021; **13**: 125-136 [PMID: 34046150 DOI: 10.4253/wjge.v13.i5.125]

19 **Lin J**, Su H, Zhou Q, Pan J, Zhou L. Predictive value of nomogram based on Kyoto classification of gastritis to diagnosis of gastric cancer. *Scand J Gastroenterol* 2022; **57**: 574-580 [PMID: 34994675 DOI: 10.1080/00365521.2021.2023626]

20 **Kimura K**, Takemoto T. An endoscopic recognition of the atrophic border and its significance in chronic gastritis. *Endoscopy* 1969; **1**: 87-97 [DOI: 10.1055/S-0028-1098086]

21 **Haruma K**, Kato M, Inoue K, Murakami K, Kamada T. Kyoto Classification of Gastritis. 1st Edition. Tokyo Japan: Nihon Medical Center, 2017

22 **Japanese Gastric Cancer Association**. Japanese classification of gastric carcinoma: 3rd English edition. *Gastric Cancer* 2011; **14**: 101-112 [PMID: 21573743 DOI: 10.1007/s10120-011-0041-5]

23 **Lauren P**. The two histological main types of gastric carcinoma: Diffuse and so-called intestinal-type carcinoma. an attempt at a histo-clinical classification. *Acta Pathol Microbiol Scand* 1965; **64**: 31-49 [PMID: 14320675 DOI: 10.1111/apm.1965.64.1.31]

24 **Liu XM**, Ma XY, Liu F, Liu ZL, Tang XY, Ji MZ, Zheng JX. Gastric Cancer Screening Methods: A Comparative Study of the Chinese New Gastric Cancer Screening Score and Kyoto Classification of Gastritis. *Gastroenterol Res Pract* 2022; **2022**: 7639968 [PMID: 35309108 DOI: 10.1155/2022/7639968]

25 **Ohno A**, Miyoshi J, Kato A, Miyamoto N, Yatagai T, Hada Y, Kusuhara M, Jimbo Y, Ida Y, Tokunaga K, Okamoto S, Hisamatsu T. Endoscopic severe mucosal atrophy indicates the presence of gastric cancer after Helicobacter pylori eradication -analysis based on the Kyoto classification. *BMC Gastroenterol* 2020; **20**: 232 [PMID: 32689949 DOI: 10.1186/s12876-020-01375-z]

26 **Sugimoto M**, Kawai Y, Morino Y, Hamada M, Iwata E, Niikura R, Nagata N, Koyama Y, Fukuzawa M, Itoi T, Kawai T. Efficacy of high-vision transnasal endoscopy using texture and colour enhancement imaging and narrow-band imaging to evaluate gastritis: a randomized

controlled trial. *Ann Med* 2022; **54**: 1004-1013 [PMID: 35441573 DOI: 10.1080/07853890.2022.2063372]

27 **Shichijo S**, Hirata Y, Niikura R, Hayakawa Y, Yamada A, Ushiku T, Fukayama M, Koike K. Histologic intestinal metaplasia and endoscopic atrophy are predictors of gastric cancer development after Helicobacter pylori eradication. *Gastrointest Endosc* 2016; **84**: 618-624 [PMID: 26995689 DOI: 10.1016/j.gie.2016.03.791]

28 **Kaji K**, Hashiba A, Uotani C, Yamaguchi Y, Ueno T, Ohno K, Takabatake I, Wakabayashi T, Doyama H, Ninomiya I, Kiriyama M, Ohyama S, Yoneshima M, Koyama N, Takeda Y, Yasuda K. Grading of Atrophic Gastritis is Useful for Risk Stratification in Endoscopic Screening for Gastric Cancer. *Am J Gastroenterol* 2019; **114**: 71-79 [PMID: 30315306 DOI: 10.1038/s41395-018-0259-5]

29 **Sui Z**, Chen J, Li P, Shao L, Ye J, Lu X, Cai J. Risk for gastric cancer in patients with gastric atrophy: a systematic review and meta-analysis. *Transl Cancer Res* 2020; **9**: 1618-1624 [PMID: 35117509 DOI: 10.21037/tcr.2020.01.54]

30 **Xiao S**, Fan Y, Yin Z, Zhou L. Endoscopic grading of gastric atrophy on risk assessment of gastric neoplasia: A systematic review and meta-analysis. *J Gastroenterol Hepatol* 2021; **36**: 55-63 [PMID: 32656803 DOI: 10.1111/jgh.15177]

31 **Yue H**, Shan L, Bin L. The significance of OLGA and OLGIM staging systems in the risk assessment of gastric cancer: a systematic review and meta-analysis. *Gastric Cancer* 2018; **21**: 579-587 [PMID: 29460004 DOI: 10.1007/s10120-018-0812-3]

32 **Na YS**, Kim SG, Cho SJ. Risk assessment of metachronous gastric cancer development using OLGA and OLGIM systems after endoscopic submucosal dissection for early gastric cancer: a long-term follow-up study. *Gastric Cancer* 2023; **26**: 298-306 [PMID: 36609936 DOI: 10.1007/s10120-022-01361-2]

33 **Sakitani K**, Hirata Y, Watabe H, Yamada A, Sugimoto T, Yamaji Y, Yoshida H, Maeda S, Omata M, Koike K. Gastric cancer risk according to the distribution of intestinal metaplasia and neutrophil infiltration. *J Gastroenterol Hepatol* 2011; **26**: 1570-1575 [PMID: 21575058 DOI: 10.1111/j.1440-1746.2011.06767.x]

34 **Watanabe M**, Kato J, Inoue I, Yoshimura N, Yoshida T, Mukoubayashi C, Deguchi H, Enomoto S, Ueda K, Maekita T, Iguchi M, Tamai H, Utsunomiya H, Yamamichi N, Fujishiro M, Iwane M, Tekeshita T, Mohara O, Ushijima T, Ichinose M. Development of gastric cancer in nonatrophic stomach with highly active inflammation identified by serum levels of pepsinogen and Helicobacter pylori antibody together with endoscopic rugal hyperplastic gastritis. *Int J Cancer* 2012; **131**: 2632-2642 [PMID: 22383377 DOI: 10.1002/ijc.27514]

35 **Kamada T**, Tanaka A, Yamanaka Y, Manabe N, Kusunoki H, Miyamoto M, Tanaka S, Hata J, Chayama K, Haruma K. Nodular gastritis with helicobacter pylori infection is strongly associated with diffuse-type gastric cancer in young patients. *Dig Endosc* 2007; **19**: 180-184 [DOI: 10.1111/j.1443-1661.2007.00750.x]

36 **Nishikawa I**, Kato J, Terasoma S, Matsutani H, Tamaki H, Tamaki T, Kuwashima F, Nakata H, Tomeki T, Matsunaka H, Ibata Y, Yamashita Y, Maekita T, Higashi K, Ichinose M. Nodular gastritis in association with gastric cancer development before and after Helicobacter pylori eradication. *JGH Open* 2018; **2**: 80-86 [PMID: 30483568 DOI: 10.1002/jgh3.12049]

37 **Nishizawa T**, Sakitani K, Suzuki H, Yoshida S, Kataoka Y, Nakai Y, Ebinuma H, Kanai T, Toyoshima O, Koike K. Clinical features of cardiac nodularity-like appearance induced by Helicobacter pylori infection. *World J Gastroenterol* 2020; **26**: 5354-5361 [PMID: 32994693 DOI: 10.3748/wjg.v26.i35.5354]

38 **Yoshii S**, Mabe K, Watano K, Ohno M, Matsumoto M, Ono S, Kudo T, Nojima M, Kato M, Sakamoto N. Validity of endoscopic features for the diagnosis of Helicobacter pylori infection status based on the Kyoto classification of gastritis. *Dig Endosc* 2020; **32**: 74-83 [PMID: 31309632 DOI: 10.1111/den.13486]

39 **Zhao J**, Xu S, Gao Y, Lei Y, Zou B, Zhou M, Chang D, Dong L, Qin B. Accuracy of Endoscopic Diagnosis of Helicobacter pylori Based on the Kyoto Classification of Gastritis: A Multicenter Study. *Front Oncol* 2020; **10**: 599218 [PMID: 33344250 DOI: 10.3389/fonc.2020.599218]

40 **Fiuza F**, Maluf-Filho F, Ide E, Furuya CK Jr, Fylyk SN, Ruas JN, Stabach L, Araujo GA, Matuguma SE, Uemura RS, Sakai CM, Yamazaki K, Ueda SS, Sakai P, Martins BC. Association between mucosal surface pattern under near focus technology and Helicobacter pylori infection. *World J Gastrointest Endosc* 2021; **13**: 518-528 [PMID: 34733412 DOI: 10.4253/wjge.v13.i10.518]

41 **Kawamura M**, Uedo N, Koike T, Kanesaka T, Hatta W, Ogata Y, Oikawa T, Iwai W, Yokosawa S, Honda J, Asonuma S, Okata H, Ohyauchi M, Ito H, Abe Y, Ara N, Kayaba S, Shinkai H, Shimokawa T. Kyoto classification risk scoring system and endoscopic grading of gastric intestinal metaplasia for gastric cancer: Multicenter observation study in Japan. *Dig Endosc* 2022; **34**: 508-516 [PMID: 34415621 DOI: 10.1111/den.14114]

World Journal of Gastroenterology

Submit a Manuscript: https://www.f6publishing.com

World J Gastroenterol 2023 August 21; 29(31): 4774-4782

DOI: 10.3748/wjg.v29.i31.4774

ISSN 1007-9327 (print) ISSN 2219-2840 (online)

ORIGINAL ARTICLE

Observational Study

Dental evaluation is helpful in the differentiation of functional heartburn and gastroesophageal reflux disease

Krisztina Helle, Anna Zsófia Árok, Georgina Ollé, Márk Antal, András Rosztóczy

Specialty type: Gastroenterology and hepatology

Provenance and peer review: Unsolicited article; Externally peer reviewed.

Peer-review model: Single blind

Peer-review report's scientific quality classification

Grade A (Excellent): 0
Grade B (Very good): B
Grade C (Good): C
Grade D (Fair): 0
Grade E (Poor): 0

P-Reviewer: Montasser IF, Egypt; Wang ZF, China

Received: June 20, 2023
Peer-review started: June 20, 2023
First decision: July 10, 2023
Revised: July 19, 2023
Accepted: July 27, 2023
Article in press: July 27, 2023
Published online: August 21, 2023

Krisztina Helle, Georgina Ollé, András Rosztóczy, Department of Internal Medicine, Division of Gastroenterology, University of Szeged, Szeged 6725, Hungary

Anna Zsófia Árok, Márk Antal, Department of Operative and Esthetic Dentistry, University of Szeged, Szeged 6725, Hungary

Corresponding author: András Rosztóczy, MD, PhD, Associate Professor, Department of Internal Medicine, Division of Gastroenterology, University of Szeged, 57 Kálvária Sugárút, Szeged 6725, Hungary. rosztoczy.andras@med.u-szeged.hu

Abstract

BACKGROUND

Heartburn is identically the key symptom of both, gastroesophageal reflux disease (GERD) and functional heartburn (FHB), making the differential diagnosis resource-intensive. Oral manifestations of GERD can be easily examined; therefore, their exploration might be a cheap, widely available, and useful tool in the differentiation of GERD and FHB.

AIM

To evaluate the prevalence of dental erosions (DE) and periodontal diseases (PD) in patients with heartburn and their association with GERD and FHB.

METHODS

A total of 116 [M/F: 51/65, mean age: 54 (17-80) years] consecutive patients with heartburn were enrolled for detailed esophageal function and orodental examinations.

RESULTS

Dental disorders were detected in 89% (103/116). Patients with PD + DE had significantly more often pathologic reflux (90.0% *vs* 27.8%; $P < 0.05$), higher esophagitis scores (1.8 *vs* 0.9; $P < 0.05$), and a significantly different mean impedance curve ($P = 0.04$) than those without any dental diseases. The opposite approach established that patients with GERD had significantly higher prevalence of DE and PD, especially if both were present (28.9% *vs* 2.0%; $P < 0.01$), more severe PD (1.5 *vs* 1.0; $P < 0.01$), and longer history of heartburn (15 years *vs* 9 years; $P < 0.01$) than those with FHB.

CONCLUSION

The dental evaluation of patients with heartburn seems to be useful in the differential diagnosis of GERD and FHB. Among the studied parameters, the co-appearance of DE and PD seems to be the best predictor of GERD, whereas the absence of dental disorders was mostly observed in FHB.

Key Words: Gastroesophageal reflux disease; Gastric acid; Heartburn; Differential diagnosis; Epidemiology; Oral manifestations; Prevalence; Risk factors; Dental erosion; Periodontal diseases

©The Author(s) 2023. Published by Baishideng Publishing Group Inc. All rights reserved.

Core Tip: Heartburn is identically the key symptom of gastroesophageal reflux disease (GERD) and functional heartburn (FHB), making the differential diagnosis resource-intensive. Oral manifestations of GERD can be easily examined to differentiate GERD and FHB. A total of 116 consecutive patients with heartburn were enrolled to evaluate the prevalence of dental erosions (DE) and periodontal diseases (PD). The dental evaluation of patients with heartburn seems to be useful in the differential diagnosis of GERD and FHB. The co-appearance of DE and PD seems to be the best predictor of GERD, while the absence of dental disorders was mostly observed in FHB.

Citation: Helle K, Árok AZ, Ollé G, Antal M, Rosztóczy A. Dental evaluation is helpful in the differentiation of functional heartburn and gastroesophageal reflux disease. *World J Gastroenterol* 2023; 29(31): 4774-4782
URL: https://www.wjgnet.com/1007-9327/full/v29/i31/4774.htm
DOI: https://dx.doi.org/10.3748/wjg.v29.i31.4774

INTRODUCTION

Heartburn is mostly considered a typical symptom of gastroesophageal reflux disease (GERD) and has a global prevalence of 11.9%. However, it cannot be diagnosed without performing detailed esophageal function tests based on the symptom of patients with functional heartburn (FHB)[1].

According to the Montreal definition, GERD may be associated with supraesophageal manifestations, including oropharyngeal symptoms[2]. Among various oropharyngeal symptoms (salivation, mouth burning, and tongue burning), dental erosion (DE) is considered to have a proven correlation with GERD. The association between DE and GERD was apparently first reported in 1933[3]. By definition, DE is a progressive loss of tough tissues of the teeth due to the action of extrinsic or intrinsic acids. Its median prevalence has been reported to be 24% in all patients with GERD and 32.5% in adult patients with GERD[4]. However, DE can be accompanied by other disorders, such as bulimia, rumination, and the consumption of acidic foods or drinks.

Much less data are available regarding other oral symptoms, especially periodontal diseases (PD), which have recently been suggested to be associated with GERD[5]. PD, which represent a group of oral inflammatory conditions caused by oral pathogens, lead to the destruction of tooth-supporting soft tissues. DE and PD may be considered as cumulative lesions, representing the long-term consequences of gastroesophageal reflux.

To the best of our knowledge, currently, no studies have been performed to assess hard and soft tissue injuries (DE and PD), and their relationship has never been investigated from dental and gastroenterological perspectives. Moreover, there are no studies about the possibility to distinguish GERD from FHB on the basis of oral manifestations.

Therefore, we aimed to obtain data on the prevalence of DE and PD in patients with heartburn and evaluate their association with GERD.

MATERIALS AND METHODS

One-hundred and sixteen consecutive patients (M/F: 51/65, mean age: 54.00 years ± 15.62 years) with heartburn were enrolled in our tertiary center for detailed esophageal function testing, including upper gastrointestinal endoscopy, high-resolution esophageal manometry [medical measurement systems (MMS) solar with a 22-channel, water-perfused catheter], and 24-h multi-channel intra-esophageal pH-impedance monitoring (MMS Ohmega®, with a pHersaflex Z61A pH probe). Any medications with any effect on gastrointestinal motility or gastric secretion were suspended one month before the esophageal testing. For gastroscopy, Olympus GIF-Q165 endoscopes were used, and the procedure was carried out under local, topical anesthesia. The presence of esophageal manifestations was recorded. Esophagitis was classified per the Los Angeles criteria[6]. On this basis, the following scoring system (no erosion = 0, LA-A = 1, LA-B = 2, LA-C = 3, LA-D = 4) was applied for quantitative comparison of the degree of esophagitis. Esophagogastric junction outflow obstruction and other major motility disorders were excluded *via* high-resolution esophageal manometry according to the Chicago classification 3.0[7]. During pH-impedance monitoring, the pH sensor was placed 5 cm above the lower esophageal sphincter as determined *via* manometry.

The significance of GERD was judged by the Lyon consensus[8]. The diagnosis of FHB was established according to the Rome IV criteria[9], including < 4% acid exposure time in the esophagus and the independence of symptoms of acidic and non-acidic reflux episodes. The occurrence of reflux hypersensitivity was also evaluated, but none of the studied patients fulfilled the accepted Rome IV criteria of this disease. Moreover, baseline impedance values were above 2000 Ω in this patient group[10]. We also calculated the mean 24-h impedance in all channels, the impedance values of the six channels during the 24-h measurement were exported to a .csv file and averaged.

Before dental examinations, general personal data, social and dental habits, and the presence, frequency, and appearance of typical and atypical reflux symptoms were assessed using standardized questionnaires that were collected by an interviewer (medical doctor and student). Among the enrolled subjects, 116 patients [M/F: 51/65, mean age: 56 (22-82) years] with heartburn were participating in further oral and dental examinations. Oral evaluations were carried out by a dentist who was blinded to the results of the esophageal function tests. The tooth wear index was evaluated and scored using the Smith and Knight's criteria, while the clinical staging of periodontitis was performed according to some study[11,12]. To quantitatively compare the severity of periodontitis, the following score system was used: No sign = 0, mild = 1, moderate = 2, severe = 3). The plaque index was calculated *via* percentage of plaque area in relation to total area.

Based on the presence of DE and/or PD, subgroups were formed.

Statistical analyses (one-way analysis of variance, chi-squared test, and unpaired *t*-test) were performed using R program; the significance level was set at $P = 0.05$. Data are expressed using the mean ± SD. This study was approved by the Regional Human Research Ethics Committee of the University of Szeged (Ethical approval No. 4564).

RESULTS

Detailed esophageal testing identified 66 patients with GERD (56.9%) and 50 patients with FHB (43.1%) among the 116 enrolled patients. Dental disorders were detected in 89% (103/116) of the enrolled patients with heartburn. The global prevalence of DE among the enrolled patients was 23.3%. In the group of subjects with GERD, the mean DeMeester score (DMS) was 29.84 ± 27.06. In contrast, in the other group, the mean DMS was 3.34 ± 2.94. Fourteen subjects were diagnosed with Barrett's esophagus. Among patients with GERD, LA-A in 12 (18.2%), LA-B in 15 (22.7%), LA-C in 20 (30.3%), and LA-D in 4 cases (6.1%) were detected, and 15 (22.7%) of them had no sign of esophagitis. In the group with FHB, there was no esophagitis on gastroscopy. Based on the results of pH-impedance monitoring, proximal reflux was found in 41 cases. Dental erosions were significantly more common among patients with GERD (66/116) than among those with FHB (21/66, 31.8% *vs* 6/50, 12.0%; $P = 0.0312$). The mean body mass index (BMI) in the GERD group was 27.8 kg/m^2 ± 4.45 kg/m^2 while that in the FHB group was 26.2 kg/m^2 ± 4.53 kg/m^2 ($P = 0.0192$). Eleven patients were toothless. Furthermore, we established significantly more severe periodontal problems in patients with GERD ($P = 0.0253$). However, instead of the fact that neither only DE nor only PD was significantly more common in any of the study groups, PD and DE together were significantly more prevalent among patients with GERD ($P = 0.00008$). DEs alone were less common among patients with GERD (3/8, 37.5%) than among those with FHB (5/8, 62.5%). Moreover, more patients were toothless in the GERD group (8/11, 72.7%). However, the most prominent difference is the presence of DE and PD together: 19/20 (95%) in the group of patients with GERD and 1/20 (5%) in the control group. The mean plaque index was 52 (0-100) in both groups. Fewer teeth were detected in the GERD group; however, the difference was not statistically significant (18 *vs* 21; $P = 0.098$). Patients with GERD had a longer history of symptoms than those with FHB (15 years *vs* 9 years, $P = 0.0041$) (Table 1).

Mean impedance values were compared between the two study groups and found to be significantly lower among patients with GERD than among those with FHB, and a characteristic tendency of GERD was detected (Figure 1).

In the entire study population, the periodontal examination was possible in only 105 patients because 11 of them were toothless. Among the examined subjects, 17/105 (16.2%) had DE alone, 24/105 (22.9%) had PD alone, 10/105 (9.5%) had both, and 54/105 (51.4%) had neither. Patients with DE alone had no more pathologic reflux than those with intact teeth (41.2% *vs* 27.8%). Among patients with both PD and DE, pathologic reflux was significantly more prevalent (27.8% and 90.0%; $P = 0.03$) than among patients without DE and PD. Furthermore, patients with PD and DE had higher esophagitis scores (1.8 *vs* 0.9; $P = 0.05$) than those without any dental diseases, and there was a tendency for more proximal reflux ($P = 0.08$). The presence of PD causing tooth loss was more common than the presence of DE or both (18 *vs* 22 and 24, $P = 0.11$) On the other hand, the mean plaque index was significantly higher among patients with PD than among patients without PD and/or DE (72 *vs* 49, $P < 0.0001$; Table 2). Other oral, atypical symptoms were not significant in the studied group, such as burning sensation of the mouth and tongue, sore throat, bad breath, sour taste, and ageusia.

Evaluating the mean impedance values, the tendency in patients with DE and PD was similar to that in patients with GERD (Figure 2).

Besides the abovementioned risk factors, no other ones were detected in the study. Furthermore, there was no difference between the four groups in terms of smoking ($P = 0.36$), alcohol consumption ($P = 0.59$), and coffee consumption ($P = 0.86$). There was also no significant difference in different habits resulting in DEs, such as drinking carbonated drinks ($P = 0.58$), teeth grinding ($P = 0.71$), and eating sour foods ($P = 0.23$).

DISCUSSION

The complete symptom similarity of GERD and FHB makes the differential diagnosis of heartburn complicated and resource-intensive. According to the Rome IV classification, it is not possible to differentiate the role of acid and

Table 1 Comparison of parameters between patients with gastroesophageal reflux disease and those with functional heartburn

		GERD (*n* = 66)	FHB (*n* = 50)	*P* value
Gender (male/female)		32 (48.5%)/34 (51.5%)	19 (38%)/31 (62%)	NS
Age, yr (min-max)		57 (22-82)	51 (25-79)	NS
BMI, kg/m^2 (min-max)		28 (16-37)	26 (17-39)	< 0.05
Mean DMS		29.84	3.34	< 0.0001
Mean impedance ± SD		2175 ± 650	2489 ± 731	< 0.05
Number of teeth (min-max)		18.3 (0-32)	20.7 (0-32)	NS
Toothless		8 (12.1%)	3 (6%)	NS
DE all		22 (33.3%)	6 (12%)	< 0.01
DE only		3 (4.5%)	5 (10%)	NS
PD all		52 (78.8%)	32 (64%)	NS
PD only		33 (50%)	31 (62%)	NS
DE and PD		19 (28.9%)	1 (2%)	< 0.01
Neither DE, nor PD		3 (4.5%)	10 (20%)	< 0.01
Periodontal scores (mean ± SD)		1.45 ± 0.85	0.97 ± 0.84	< 0.01
Drinking carbonated drinks	Nowadays	8 (12.2%)	10 (20%)	NS
	Previously	22 (33.3%)	15 (30%)	
	Never	36 (54.5%)	25 (50%)	
Eating sour foods	Nowadays	15 (22.7%)	9 (18%)	NS
	Previously	13 (19.7%)	9 (18%)	
	Never	38 (57.6%)	32 (64%)	
Bruxism/teeth grinding		9 (13.6%)	8 (16%)	NS
Total duration of heartburn, mean years (range)		15 (0-64)	9 (0-35)	< 0.01
Duration of heartburn until diagnosis, mean years (range)		5.3 (0-49)	2.9 (0-30)	NS

GERD: Gastroesophageal reflux disease; FHB: Functional heartburn; BMI: Body mass index; DMS: DeMeester score; PD: Periodontal disease; DE: Dental erosion; DE all: All the patients who had DE, and some of them have associated PD as well; DE only: Such patients have only DE and have not PD; PD all: All the patients who had PD, and some of them have associated DE as well; PD only: Such patients have only PD and have not DE; SD: Standard deviation; NS: Not significant.

hypersensitivity in the development of heartburn on the basis of the frequency and subjective severity of heartburn symptom. To confirm the diagnosis, detailed esophageal examinations are mandatory. That is why the necessity of comparative studies was also raised in the latest Rome IV criteria[13]; however, such studies had not been carried out. To the best of our knowledge, this study attempted the first differentiation between FHB and GERD based on oral manifestations. The rationale behind the use of oral evaluation is based on its low cost, wide availability, and the fact that the suggested parameters are not temporary symptoms but long-term consequences of GERD.

In the literature, there are many studies on the association between GERD and DE or PD. However, to the best of our knowledge, studies assessing the hard and soft tissue injuries, namely DE and PD, together have not been conducted yet. Furthermore, none of the previous studies examined their relations from both dental and gastroenterological perspectives.

Several studies discussed and concluded a clear but variable relationship between DE and GERD[14,15]. The proposed pathogenesis of DEs is attributed the direct contact of acid and the enamel, resulting in dissolution of the enamel crystals and destruction of the interprismatic matrix and subsequently, the dentin[16-19].

As a result of our research, 41.2% of those with DE had reflux, which did not prove to be a significant result. However, this result differed from the findings recorded in the literature. Pace *et al*[4] published a recent systematic review involving 17 eligible studies, mainly observational and case-control studies on GERD and DE, in which they reported a strong association between the two conditions. The median prevalence of DE among all patients with GERD was 24%, and the median prevalence of GERD among adults with DEs was 32.5% (21.0%-83.0%) However, in this population, there were wide percentage ranges and degrees of tooth tissue loss, and not all studies and evaluations of patients included esophageal endoscopy and/or 24 h esophageal pH-metry[4].

Table 2 Comparison of parameters between patients with or without dental erosion and periodontal disease

		DE (*n* = 17)	PD (*n* = 24)	Both (*n* = 10)	Neither (*n* = 54)	*P* value
Gender (male/female)		7 (41.2%)/10 (58.8%)	12 (50%)/12 (50%)	7 (70%)/3 (30%)	21 (38.9%)/33 (61.1%)	NS
Age, yr (min-max)		50 (24-79)	60 (41-82)	62 (40-71)	53 (22-80)	NS
BMI, kg/m^2 (min-max)		27 (17-35)	28 (16-39)	29 (26-35)	26 (18-37)	NS
Heartburn		17 (100%)	24 (100%)	10 (100%)	54 (100%)	NS
Nausea		12 (70.6%)	9 (37.5%)	7 (70%)	23 (42.6%)	NS
Vomiting		4 (23.6%)	5 (20.8%)	5 (50%)	9 (16.7%)	NS
Dysphagia		11 (64.7%)	10 (41.7%)	5 (50%)	21 (38.9%)	NS
Regurgitation		15 (88.2%)	15 (62.5%)	8 (80%)	39 (72.2%)	NS
Drinking carbonated drinks	Nowadays	2 (11.8%)	5 (20.8%)	2 (20%)	8 (14.8%)	NS
	Previously	6 (35.3%)	10 (41.7%)	1 (10%)	17 (31.5%)	
	Never	9 (52.9%)	9 (37.5%)	7 (70%)	29 (53.7%)	
Eating sour foods	Nowadays	5 (29.4%)	6 (25%)	0 (0%)	11 (20.4%)	NS
	Previously	2 (11.8%)	6 (25%)	4 (40%)	7 (13%)	
	Never	10 (58.8%)	12 (50%)	6 (60%)	36 (66.7%)	
Bruxism (teeth grinding)		4 (23.6%)	4 (16.7%)	2 (20%)	7 (13%)	NS
Number of teeth (min-max)		24 (13-31)	18 (1-30)	21 (13-28)	22 (2-32)	NS
Plaque Index (min-max)		58 (15-100)	72 (32-100)	67 (35-97)	49 (0-94)	< 0.01
Esophagitis score (mean ± SD)		1.6 ± 1.4	1.5 ± 1.4	1.8 ± 1.2	0.9 ± 1.1	0.05
Mean DMS		23.11	17.5	26.91	13.94	NS
Mean impedance ± SD		2390 ± 878	2393 ± 714	1708 ± 249	2427 ± 690	NS
Pathological reflux		7 (41.2%)	9 (37.5%)	9 (90%)	15 (27.8%)	< 0.01
Any proximal reflux		8 (47.1%)	9 (37.5%)	7 (70%)	19 (35.2%)	NS
Distal reflux		11 (64.7%)	13 (54.2%)	10 (100%)	21 (38.9%)	< 0.01

PD: Periodontal disease; DE: Dental erosion; BMI: Body mass index; DMS: DeMeester score; SD: Standard deviation; NS: Not significant.

Another systematic review was carried out and used different references since 2007. From a total of 273 articles, the mean prevalence values of DE were 48.8% in GERD patients and 20.5% in non-GERD controls. The prevalence of DE among adults with GERD was 38.9%, compared to 98.1% among children with GERD[20].

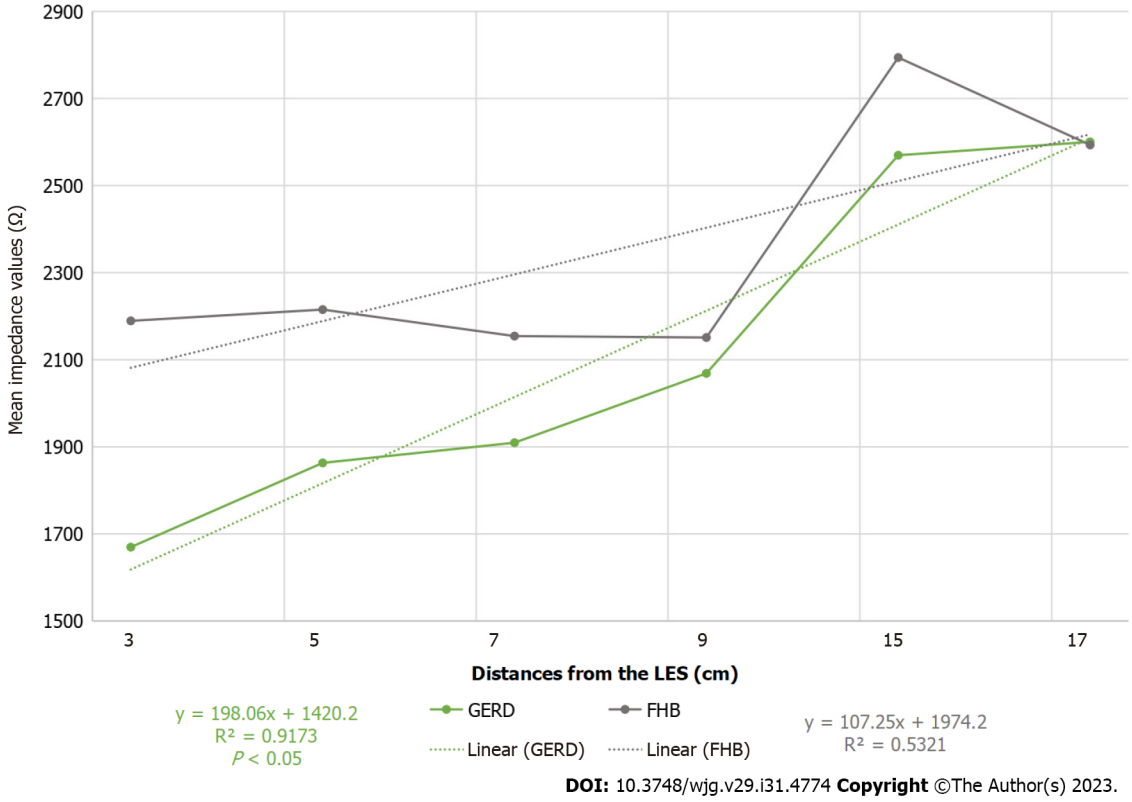
The total prevalence of DE (23.3%) in all subjects was less than the known global prevalence of DE. It can be stated that in the patient group we examined, the prevalence of DEs was found to be significantly higher among patients with GERD (33.1%) than among patients with FHB (12.0%) ($P < 0.01$). Our findings differ from those of studies conducted in different parts of the world.

A recent study conducted in China in 2016, reported a 60.8% presence of DE among patients diagnosed with GERD [21]. Another study carried out in Italy could not establish a significant co-appearance in the association between GERD and DE[22].

Previous studies have confirmed the association between DE and GERD. However, other manifestations (xerostomia, halitosis, oral burning, altered taste, bruxism, and soft tissue injuries, such as mucositis/stomatitis, aphthous-like ulcerations, gingivitis, and periodontal disease) are less likely to be investigated. The relationship between these diseases and GERD could either be direct or indirect[23].

In the literature, the presence of extrinsic factors resulting in DE was uncertain. According to a cross-sectional study, there was a clear relationship between DE and extrinsic dietary factors in patients with GERD[24]. This result was supported by a systematic review that highlighted the etiological complexity of DE (dietary habits, lifestyle, abrasion, bruxism, *etc*.), and the importance of taking a detailed medical history[25]. In contrast, based on an Indian cross-sectional study, extrinsic factors were not related to DE in GERD. In our study, there was no significant difference between the different habits resulting in DE ($P = 0.23$)[26].

In contrast to Song *et al*[27], our results could not confirm a close association between GERD and such manifestations except PD. The mechanism by which PD develops in GERD is mainly attributed to the direct action of acid on the mucosa, although hyposalivation is also suggested to play a role[28,29]. Watanabe *et al*[30] reported significant presence of soft tissue symptoms (stinging, bad breath, and burning sensation), oral cavity symptoms (sour/sour taste sensation),



DOI: 10.3748/wjg.v29.i31.4774 **Copyright** ©The Author(s) 2023.

Figure 1 Mean impedance values in patients with gastroesophageal reflux disease and those with functional heartburn. GERD: Gastroesophageal reflux disease; FHB: Functional heartburn; LES: Lower esophageal sphincter.

and the presence of GERD.

Di Fede *et al*[22] assessed the occurrence of oral pathological changes and symptoms in patients with GERD. Two hundred patients with GERD and 100 matched healthy controls were enrolled and studied. Univariate analyses revealed that xerostomia, oral burning sensation, subjective halitosis, and soft, hard palate mucosa, and uvula erythema were more common among patients with GERD than among matched controls ($P < 0.05$). The main outcome of this study was that no significant association between GERD and DEs was found, whereas some other symptoms or objective oral mucosal changes were found to be significantly associated with GERD[22]. In contrast, based on the responses of the patients we interviewed and examined, we did not find any data indicating a significant occurrence of oral complaints (such as the mouth and tongue burning, unpleasant breath, taste perception problems, inflammation of the mucous membrane, hypersensitivity, and sensations of sour taste).

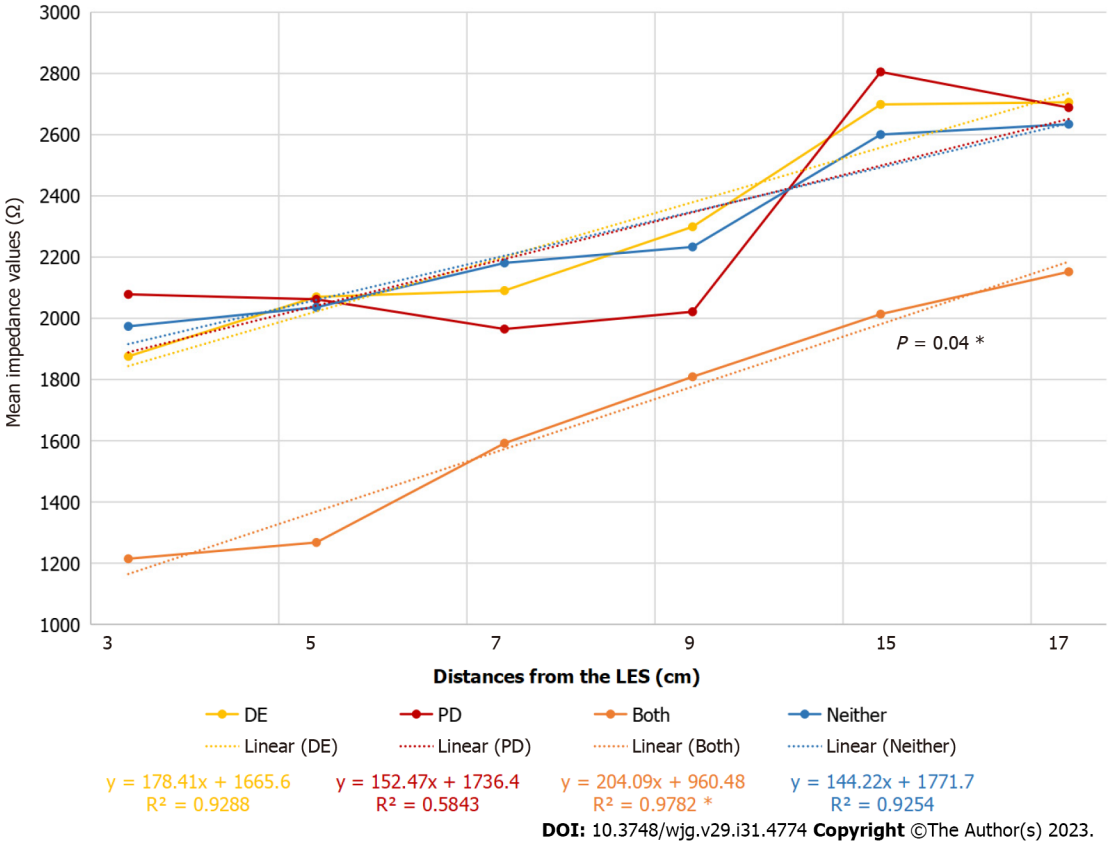
A Chinese study found that periodontal factors were significantly associated with the risk of GERD in the studied 50183 patients. Severe periodontitis (OR = 1.40, $P < 0.001$) and lower frequency of tooth brushing (OR = 2.01, $P < 0.001$) were significantly associated with GERD[31].

In our study, neither DE nor PD alone was predictive of the presence of pathological reflux. There is not significantly more reflux in these cases. However, if both are present, the simultaneous presence of pathological reflux is more likely, as evidenced by the characteristic impedance deviations following the reflux pattern.

Increased BMI is commonly mentioned as a predictor of GERD. In their population-based study, Locke *et al*[31] found a significant relationship between higher BMI and the presence of GERD compared to subjects without reflux disease. Conversely, Watanabe *et al*[30] failed to establish a significant correlation between an increase in BMI and the presence of GERD. Our results seem to support the suggested association because our patients with GERD had significantly higher BMI than those with FHB. However, the observed difference is not significant enough to allow the prediction of GERD on the basis of this parameter alone.

In our study, higher esophagitis scores were detected in patients with DE and PD together than those without any dental diseases. This result suggests that there is more severe esophagitis in case of DE and PD than in the other groups. The correlation between the degree of DE and the severity of esophagitis was barely studied. A study conducted among the Mexican population found that 3/4 of the patients with mild grade DE had normal esophageal mucosa or LA-A esophagitis, whereas patients with severe DE were associated with a higher frequency of esophagitis LA-C and -D ($P = 0.021$)[32].

There are limitations to our study: First, the study was carried out in a single tertiary referral center; therefore, the prevalence of GERD phenotypes is different from the values of the general population. Second, during the process of pH-MII, inpatients were examined under standard conditions that do not correspond to their everyday conditions at home. DEs could be considered as cumulative lesions, representing the long-term consequences of reflux. Therefore, the dental status does not necessarily correlate with the current reflux state, since the bolus exposure time is not always the same, and it may significantly vary day by day, especially in the proximal part of the esophagus.



DOI: 10.3748/wjg.v29.i31.4774 **Copyright** ©The Author(s) 2023.

Figure 2 Mean impedance values in patients with or without dental erosion and periodontal disease. The asterisk (*) the curve of "Both" group is significantly different from the others, and similar to the one in patients with gastroesophageal reflux disease. PD: Periodontal disease; DE: Dental erosion; LES: Lower esophageal sphincter.

CONCLUSION

The dental evaluation of patients with heartburn seems to be useful in the differential diagnosis of GERD and FHB. The co-appearance of dental erosions and periodontal diseases was present mostly in patients with GERD, whereas DE or PD (especially its mild forms) alone were not predictive for the disease. In contrast, the absence of dental disorders in patients with heartburn was predictive of FHB.

ARTICLE HIGHLIGHTS

Research background

Heartburn is a typical symptom of gastroesophageal reflux disease (GERD) and other functional gastrointestinal diseases. To diagnose them, detailed esophageal function tests are required. Oral manifestations are also common in patients with GERD. The dental evaluation is cheap and widely available.

Research motivation

This study raised the hypothesis that dental evaluation (dental erosions, periodontal diseases) in patients with heartburn may be useful in the differential diagnosis of GERD and functional heartburn (FHB).

Research objectives

To evaluate the prevalence of oral manifestations in patients with heartburn and their association with GERD and FHB.

Research methods

We enrolled 116 [M/F: 51/65, mean age: 54 (17-80) years] consecutive patients with heartburn for detailed esophageal function tests and dental evaluation.

Research results

The prevalence of dental diseases in patients with heartburn was about 89%. Compared with heartburn patients without any dental diseases, heartburn patients with both DE and PD had more significant pathological reflux, higher grade of

esophagitis, and significantly different mean impedance curves. Compared to FHB, GERD had a higher prevalence of DE and PD, especially when they coexisted. When evaluating the mean impedance curve, the trend of patients with both PD and DE was similar to those with GERD. The results of the study confirmed the abovementioned hypothesis experimentally.

Research conclusions

The co-existence of PD and DE is more likely to have pathological reflux, and the severity of esophagitis is higher than that of other groups. This study provides a new, inexpensive, widely available, and useful method for the differential diagnosis of GERD and FHB.

Research perspectives

On the one hand, our aim is to expand the study multicentrally in the direction of patients with heartburn presenting in primary care, and thereby reach a larger number of cases. On the other hand, this would probably also enable the inclusion of patients with reflux hypersensitivity, which is defined as a special borderline area between GERD and FHB in the Rome IV criteria system, which may help to decide whether this group of patients is more similar to patients GERD or FHB based on the oral status.

FOOTNOTES

Author contributions: Antal M and Rosztóczy A contributed tools and further data; Ollé G contributed help in the research; Rosztóczy A designed the research study; Árok AZ and Helle K performed the research; Helle K analyzed the data and wrote the manuscript; and all authors have read and approved the final manuscript.

Supported by the University of Szeged Open Access Fund, No. 6373.

Institutional review board statement: The study was reviewed and approved by the Institutional Review Board of the University of Szeged.

Informed consent statement: All study participants, or their legal guardian, provided informed written consent prior to study enrollment.

Conflict-of-interest statement: The authors have no conflict of interest to disclose.

Data sharing statement: No additional data are available.

STROBE statement: The authors have read the STROBE Statement—checklist of items, and the manuscript was prepared and revised according to the STROBE Statement—checklist of items.

Open-Access: This article is an open-access article that was selected by an in-house editor and fully peer-reviewed by external reviewers. It is distributed in accordance with the Creative Commons Attribution NonCommercial (CC BY-NC 4.0) license, which permits others to distribute, remix, adapt, build upon this work non-commercially, and license their derivative works on different terms, provided the original work is properly cited and the use is non-commercial. See: https://creativecommons.org/Licenses/by-nc/4.0/

Country/Territory of origin: Hungary

ORCID number: Krisztina Helle 0000-0002-5477-2618; Georgina Ollé 0000-0003-1726-8436; Márk Antal 0000-0002-4109-9356; András Rosztóczy 0000-0002-8597-8934.

S-Editor: Chen YL
L-Editor: A
P-Editor: Yuan YY

REFERENCES

1 **Moraes-Filho JP**, Chinzon D, Eisig JN, Hashimoto CL, Zaterka S. Prevalence of heartburn and gastroesophageal reflux disease in the urban Brazilian population. *Arq Gastroenterol* 2005; **42**: 122-127 [PMID: 16127569 DOI: 10.1590/s0004-28032005000200011]

2 **Vakil N**, van Zanten SV, Kahrilas P, Dent J, Jones R; Global Consensus Group. The Montreal definition and classification of gastroesophageal reflux disease: a global evidence-based consensus. *Am J Gastroenterol* 2006; **101**: 1900-20; quiz 1943 [PMID: 16928254 DOI: 10.1111/j.1572-0241.2006.00630.x]

3 **Bodecker CF**. Dental erosion: its possible causes and treatment. *Dental Cosmos* 1933; **75**: 1056-1062 [DOI: 10.14219/jada.archive.1938.0134]

4 **Pace F**, Pallotta S, Tonini M, Vakil N, Bianchi Porro G. Systematic review: gastro-oesophageal reflux disease and dental lesions. *Aliment Pharmacol Ther* 2008; **27**: 1179-1186 [PMID: 18373634 DOI: 10.1111/j.1365-2036.2008.03694.x]

5 **Boyapati R**, Vudathaneni VKP, Nadella SB, Bollepalli AC, Marella Y, Adurty C. Reflex Gastroesophageal Disorders and Functional Dyspepsia: Potential Confounding Variables for the Progression of Chronic Periodontitis: A Clinical Study. *Int J Prev Med* 2020; **11**: 138

[PMID: 33088466 DOI: 10.4103/ijpvm.IJPVM_141_19]

6 **Lundell LR**, Dent J, Bennett JR, Blum AL, Armstrong D, Galmiche JP, Johnson F, Hongo M, Richter JE, Spechler SJ, Tytgat GN, Wallin L. Endoscopic assessment of oesophagitis: clinical and functional correlates and further validation of the Los Angeles classification. *Gut* 1999; **45**: 172-180 [PMID: 10403727 DOI: 10.1136/gut.45.2.172]

7 **Kahrilas PJ**, Bredenoord AJ, Fox M, Gyawali CP, Roman S, Smout AJ, Pandolfino JE; International High Resolution Manometry Working Group. The Chicago Classification of esophageal motility disorders, v3.0. *Neurogastroenterol Motil* 2015; **27**: 160-174 [PMID: 25469569 DOI: 10.1111/nmo.12477]

8 **Gyawali CP**, Kahrilas PJ, Savarino E, Zerbib F, Mion F, Smout AJPM, Vaezi M, Sifrim D, Fox MR, Vela MF, Tutuian R, Tack J, Bredenoord AJ, Pandolfino J, Roman S. Modern diagnosis of GERD: the Lyon Consensus. *Gut* 2018; **67**: 1351-1362 [PMID: 29437910 DOI: 10.1136/gutjnl-2017-314722]

9 **Palsson OS**, Whitehead WE, van Tilburg MA, Chang L, Chey W, Crowell MD, Keefer L, Lembo AJ, Parkman HP, Rao SS, Sperber A, Spiegel B, Tack J, Vanner S, Walker LS, Whorwell P, Yang Y. Rome IV Diagnostic Questionnaires and Tables for Investigators and Clinicians. *Gastroenterology* 2016 [PMID: 27144634 DOI: 10.1053/j.gastro.2016.02.014]

10 **Zhong C**, Duan L, Wang K, Xu Z, Ge Y, Yang C, Han Y. Esophageal intraluminal baseline impedance is associated with severity of acid reflux and epithelial structural abnormalities in patients with gastroesophageal reflux disease. *J Gastroenterol* 2013; **48**: 601-610 [PMID: 23076541 DOI: 10.1007/s00535-012-0689-6]

11 **Smith BG**, Knight JK. An index for measuring the wear of teeth. *Br Dent J* 1984; **156**: 435-438 [PMID: 6590081 DOI: 10.1038/sj.bdj.4805394]

12 **Eke PI**, Page RC, Wei L, Thornton-Evans G, Genco RJ. Update of the case definitions for population-based surveillance of periodontitis. *J Periodontol* 2012; **83**: 1449-1454 [PMID: 22420873 DOI: 10.1902/jop.2012.110664]

13 **Aziz Q**, Fass R, Gyawali CP, Miwa H, Pandolfino JE, Zerbib F. Functional Esophageal Disorders. *Gastroenterology* 2016 [PMID: 27144625 DOI: 10.1053/j.gastro.2016.02.012]

14 **Bartlett D**. Intrinsic causes of erosion. *Monogr Oral Sci* 2006; **20**: 119-139 [PMID: 16687891 DOI: 10.1159/000093359]

15 **Ranjitkar S**, Kaidonis JA, Smales RJ. Gastroesophageal reflux disease and tooth erosion. *Int J Dent* 2012; **2012**: 479850 [PMID: 22194748 DOI: 10.1155/2012/479850]

16 **Hannig C**, Hannig M, Attin T. Enzymes in the acquired enamel pellicle. *Eur J Oral Sci* 2005; **113**: 2-13 [PMID: 15693823 DOI: 10.1111/j.1600-0722.2004.00180.x]

17 **Meurman JH**, Frank RM. Scanning electron microscopic study of the effect of salivary pellicle on enamel erosion. *Caries Res* 1991; **25**: 1-6 [PMID: 2070377 DOI: 10.1159/000261335]

18 **Lussi A**, Jäggi T, Schärer S. The influence of different factors on in vitro enamel erosion. *Caries Res* 1993; **27**: 387-393 [PMID: 8242676 DOI: 10.1159/000261569]

19 **Cairns AM**, Watson M, Creanor SL, Foye RH. The pH and titratable acidity of a range of diluting drinks and their potential effect on dental erosion. *J Dent* 2002; **30**: 313-317 [PMID: 12554112 DOI: 10.1016/s0300-5712(02)00044-1]

20 **Picos A**, Badea ME, Dumitrascu DL. Dental erosion in gastro-esophageal reflux disease. A systematic review. *Clujul Med* 2018; **91**: 387-390 [PMID: 30564013 DOI: 10.15386/cjmed-1017]

21 **Li W**, Liu J, Chen S, Wang Y, Zhang Z. Prevalence of dental erosion among people with gastroesophageal reflux disease in China. *J Prosthet Dent* 2017; **117**: 48-54 [PMID: 27616724 DOI: 10.1016/j.prosdent.2016.04.029]

22 **Di Fede O**, Di Liberto C, Occhipinti G, Vigneri S, Lo Russo L, Fedele S, Lo Muzio L, Campisi G. Oral manifestations in patients with gastro-oesophageal reflux disease: a single-center case-control study. *J Oral Pathol Med* 2008; **37**: 336-340 [PMID: 18284539 DOI: 10.1111/j.1600-0714.2008.00646.x]

23 **Mahajan R**, Kulkarni R, Stoopler ET. Gastroesophageal reflux disease and oral health: A narrative review. *Spec Care Dentist* 2022; **42**: 555-564 [PMID: 35605234 DOI: 10.1111/scd.12726]

24 **Ortiz AC**, Fideles SOM, Pomini KT, Buchaim RL. Updates in association of gastroesophageal reflux disease and dental erosion: systematic review. *Expert Rev Gastroenterol Hepatol* 2021; **15**: 1037-1046 [PMID: 33571021 DOI: 10.1080/17474124.2021.1890030]

25 **Chauhan N**, Manjunath BC, Malhotra P, Yadav V, Kumar JS, Muppalla L, Bhukal S. Dietary Practices as a Potential Predictor for Dental Erosion among Patients Having Gastroesophageal Reflux Disease: An Analytical Cross-sectional Study. *J Int Soc Prev Community Dent* 2022; **12**: 583-589 [PMID: 36777015 DOI: 10.4103/jispcd.JISPCD_95_22]

26 **Liu Z**, Gao X, Liang L, Zhou X, Han X, Yang T, Huang K, Lin Y, Deng S, Wang Z, Wang C. Prevalence, General and Periodontal Risk Factors of Gastroesophageal Reflux Disease in China. *J Inflamm Res* 2023; **16**: 235-244 [PMID: 36691403 DOI: 10.2147/JIR.S395777]

27 **Song JY**, Kim HH, Cho EJ, Kim TY. The relationship between gastroesophageal reflux disease and chronic periodontitis. *Gut Liver* 2014; **8**: 35-40 [PMID: 24516699 DOI: 10.5009/gnl.2014.8.1.35]

28 **Hauk L**. Laparoscopic Roux-en-Y gastric bypass. *AORN J* 2018; **107**: P12-P14 [PMID: 29486072 DOI: 10.1002/aorn.12107]

29 **Jajam M**, Bozzolo P, Niklander S. Oral manifestations of gastrointestinal disorders. *J Clin Exp Dent* 2017; **9**: e1242-e1248 [PMID: 29167716 DOI: 10.4317/jced.54008]

30 **Watanabe M**, Nakatani E, Yoshikawa H, Kanno T, Nariai Y, Yoshino A, Vieth M, Kinoshita Y, Sekine J. Oral soft tissue disorders are associated with gastroesophageal reflux disease: retrospective study. *BMC Gastroenterol* 2017; **17**: 92 [PMID: 28784097 DOI: 10.1186/s12876-017-0650-5]

31 **Locke GR 3rd**, Talley NJ, Fett SL, Zinsmeister AR, Melton LJ 3rd. Risk factors associated with symptoms of gastroesophageal reflux. *Am J Med* 1999; **106**: 642-649 [PMID: 10378622 DOI: 10.1016/s0002-9343(99)00121-7]

32 **Roesch-Ramos L**, Roesch-Dietlen F, Remes-Troche JM, Romero-Sierra G, Mata-Tovar Cde J, Azamar-Jácome AA, Barranca-Enríquez A. Dental erosion, an extraesophageal manifestation of gastroesophageal reflux disease. The experience of a center for digestive physiology in Southeastern Mexico. *Rev Esp Enferm Dig* 2014; **106**: 92-97 [PMID: 24852734 DOI: 10.4321/S1130-01082014000200004]

World Journal of Gastroenterology

Submit a Manuscript: https://www.f6publishing.com

World J Gastroenterol 2023 August 21; 29(31): 4783-4796

DOI: 10.3748/wjg.v29.i31.4783

ISSN 1007-9327 (print) ISSN 2219-2840 (online)

ORIGINAL ARTICLE

Randomized Controlled Trial

Poly(A)-specific ribonuclease protein promotes the proliferation, invasion and migration of esophageal cancer cells

Fu-Wei Zhang, Xiao-Wei Xie, Meng-Hua Chen, Jian Tong, Qun-Qing Chen, Jing Feng, Feng-Ti Chen, Wen-Qi Liu

Specialty type: Gastroenterology and hepatology

Provenance and peer review: Unsolicited article; Externally peer reviewed.

Peer-review model: Single blind

Peer-review report's scientific quality classification

Grade A (Excellent): 0
Grade B (Very good): B
Grade C (Good): C
Grade D (Fair): 0
Grade E (Poor): 0

P-Reviewer: Arigami T, Japan; Luyer MDP, Netherlands

Received: April 4, 2023
Peer-review started: April 4, 2023
First decision: April 12, 2023
Revised: April 29, 2023
Accepted: July 27, 2023
Article in press: July 27, 2023
Published online: August 21, 2023

Fu-Wei Zhang, Jian Tong, Qun-Qing Chen, Jing Feng, Department of Thoracic Surgery, Zhujiang Hospital, Southern Medical University, Guangzhou 510282, Guangdong Province, China

Xiao-Wei Xie, Meng-Hua Chen, Feng-Ti Chen, Wen-Qi Liu, Department of Radiation Oncology, The Second Affiliated Hospital of Guangxi Medical University, Nanning 530000, Guangxi Zhuang Autonomous Region, China

Corresponding author: Wen-Qi Liu, PhD, Chief Doctor, Doctor, Department of Radiation Oncology, The Second Affiliated Hospital of Guangxi Medical University, No. 166 East University Road, Nanning 530000, Guangxi Zhuang Autonomous Region, China.
liuwenqigx@163.com

Abstract

BACKGROUND

Bioinformatics analysis showed that the expression of the poly(A)-specific ribonuclease (PARN) gene in gastric cancer, head and neck squamous cell carcinoma, melanoma, cervical cancer and lung squamous cell carcinoma tissues was significantly higher than that in normal tissues and was associated with high stage and poor prognosis. The expression of the PARN gene in esophageal cancer (EC) tissue is also significantly higher than that in normal tissues, but the effect of PARN on the proliferation, migration and invasion of EC cells remains unclear.

AIM

To investigate the relationship between PARN and the proliferation, migration and invasion of EC cells.

METHODS

The EC tissues of 91 patients after EC surgery and 63 paired precancerous healthy tissues were collected. PARN mRNA levels were measured using a tissue microarray, and the PARN expression level was evaluated using immunohistochemistry to analyze the relationship between PARN expression and clinicopathologic features as well as the survival and prognosis of patients. In addition, the effects of PARN gene knockout on tumor cell proliferation, invasion and migration were studied by using shRNA during the *in vitro* culture of EC cell lines Eca-109 and TE-1, and the effects of the PARN gene on tumor growth *in vivo* were verified by a xenotransplantation nude mice model.

RESULTS

The expression of PARN in EC tissues was higher than that in adjacent normal tissues, and the level of PARN expression was significantly positively correlated with lymphatic metastasis. Patients with high PARN levels had poor overall survival. BIM, IGFBP-5 and p21 levels were significantly increased in the PARN knockout group, while the expression levels of the antiapoptotic proteins Survivin and sTNF-R1 were significantly decreased in the apoptotic antibody array data. In addition, the expression levels of Akt, p-Akt, PIK3CA and CCND1 in the downstream signaling pathway regulating EC progression were significantly decreased. The culture of EC cell lines confirmed that the apoptosis rate of EC cells was significantly increased, the growth and proliferation of tumor cells were significantly inhibited, and the invasion and migration ability of tumor cells were significantly decreased after PARN gene knockout. *In vivo* experiments of BALB/c nude mice transfected with Eca-109 cells expressing control shRNA (sh-NC) and PARN shRNA (sh-PARN) showed that the tumor volume and weight of nude mice treated with sh-PARN were significantly decreased compared with those of nude mice treated with sh-NC, indicating that PARN knockdown significantly inhibited tumor growth *in vivo*.

CONCLUSION

PARN has antiapoptotic effects on EC cells and promotes their proliferation, invasion and migration, which is associated with the development of EC and poor patient prognosis. PARN may become a potential target for the diagnosis, prognosis prediction and treatment of EC.

Key Words: Poly(A)-specific ribonuclease; Esophageal cancer; Apoptotic; Phosphatidylinositol 3-kinase/protein kinase B

©The Author(s) 2023. Published by Baishideng Publishing Group Inc. All rights reserved.

Core Tip: Bioinformatics analysis showed that the expression of the poly(A)-specific ribonuclease (PARN) gene in gastric cancer, head and neck squamous cell carcinoma, melanoma, cervical cancer and lung squamous cell carcinoma tissues was significantly higher than that in normal tissues and was associated with high stage and poor prognosis. The expression of the PARN gene in esophageal cancer (EC) tissue is also significantly higher than that in normal tissues, but the effect of PARN on the proliferation, migration and invasion of EC cells remains unclear. This study investigated the relationship between PARN and the proliferation, migration and invasion of EC cells.

Citation: Zhang FW, Xie XW, Chen MH, Tong J, Chen QQ, Feng J, Chen FT, Liu WQ. Poly(A)-specific ribonuclease protein promotes the proliferation, invasion and migration of esophageal cancer cells. *World J Gastroenterol* 2023; 29(31): 4783-4796
URL: https://www.wjgnet.com/1007-9327/full/v29/i31/4783.htm
DOI: https://dx.doi.org/10.3748/wjg.v29.i31.4783

INTRODUCTION

Esophageal cancer (EC) is one of the most common malignancies in the world and the sixth leading cause of cancer-related mortality worldwide[1]. The main pathological types of esophageal carcinoma include esophageal squamous cell carcinoma (ESCC) and esophageal adenocarcinoma. In contrast to Europe and America, Asia has the most ESCC cases, which account for the vast majority of EC cases[2,3]. Currently, the main treatments for EC include surgery, radiotherapy and chemotherapy[4]. Since the clinical symptoms of early EC are not obvious, more than half of patients are in the advanced stage at the time of detection, and only 20% of patients with EC can be treated with surgery. Inoperable EC patients can only use radiotherapy, chemotherapy and other comprehensive treatments. Since it is highly invasive and has a high recurrence and metastasis rate, the prognosis for ESCC patients remains poor despite the use of multidisciplinary therapies[5]. The overall 5-year survival rate for ESCC patients is only 30%-40%. Patients with advanced or metastatic EC have a worse prognosis, with a 5-year overall survival of less than 15 years[2,4,5].

Increasing evidence shows that the resistance of some ECs to radiotherapy and chemotherapy is the cause of relapse and metastasis. Obviously, it is necessary to study the molecular mechanism of EC progression through genomics and proteomics and explore effective cancer biomarkers to predict treatment efficacy and EC patient prognosis.

Bioinformatics analysis from The Cancer Genome Atlas (TCGA) database showed that the expression of the PARN gene in breast cancer, head and neck squamous cell carcinoma, skin cancer, testicular cancer, thymic carcinoma and lung cancer tissues was significantly higher than that in normal tissues and was positively correlated with high stage and poor prognosis. In addition, the expression of the PARN gene in EC tissues in the TCGA database was also significantly higher than that in adjacent tissues. However, the effect of PARN on the proliferation, migration and invasion of EC cells is not clear and is worth further discussion.

Poly(A)-specific ribonuclease (PARN) is a deadenylase enzyme that is present in mammalian cells[6,7]. As a deadenylase, PARN interacts with the cap and the poly(A) tail of mRNA to control the length of the poly(A) tail and regulate gene expression. Therefore, it plays a role in mRNA degradation in the nucleus and cytoplasm[8,9]. Interference

in RNA stability is closely related to tumorigenesis and tumor development, and factors that affect RNA stability may become new targets for the treatment of malignant tumors[10]. Recent studies have shown that RNA-degrading enzymes, called RNases, are involved in the development of malignant tumors, so the regulation of mRNA turnover is a promising mechanism[11].

However, the biological function of PARN and its basic molecular mechanism in the carcinogenesis of the esophagus are still unclear and are worthy of further investigation. In the present study, EC tissues and adjacent normal tissues were immunohistochemically stained and analyzed to detect PARN expression. Moreover, we also investigated the clinicopathological characteristics of PARN and explored the value of PARN expression in predicting prognosis. In addition, we investigated the role of PARN knockdown in the biological characteristics of EC cells *in vitro* and *in vivo*.

MATERIALS AND METHODS

Online databases used in this study

Data on PARN expression in EC cell lines were obtained from the Cancer Cell Line Encyclopedia (CCLE) (www.broadinstitute.org/ccle). Mutation data were obtained from cBioPortal (https://www.cbioportal.org/). The mRNA expression level data of EC patients were downloaded from TCGA Portal (https://tcga-data.nci.nih.gov/tcga/).

Clinical samples

Ninety-one EC tissues and 63 healthy mucosa tissues were taken from EC patients who underwent resection at the Second Affiliated Hospital of Guangxi Medical University and the Affiliated Zhujiang Hospital of Southern Medical University from 2017 to 2018. The study ethics were approved by the Research Ethics Committee of the Second Affiliated Hospital of Guangxi Medical University and Zhujiang Hospital Affiliated to Southern Medical University, and written patient consent was obtained from all patients.

Immunohistochemistry

Immunohistochemistry (IHC) was conducted as previously described[12]. Briefly, the unstained tissue sections were deparaffinized by xylene and then rehydrated with a graded alcohol series. The sections were placed in EDTA buffer (pH = 8.0) buffer at 95-100 °C for 20 min to retrieve antigens. Then, the sections were incubated with rabbit anti-human PARN primary antibodies at 4 °C (1:100; Abcam, ab188333) overnight and then incubated with secondary antibodies for 1 h at room temperature.

Tissue microarray

The mRNA transcription levels of PARN in tumor tissues and adjacent normal mucosal tissues were measured using a tissue microarray (TMA).

Construction of a protein-protein interaction network and enrichment of functions and pathways

In this research, we obtained the protein-protein interaction by using an online tool, the String Database (STRING, https://string-db.org/). Then, the protein-protein interaction (PPI) we obtained was analyzed by using the software CytoScape (https://cytoscape.org/) and its plug-ins ClueGO and CluePedia. Then, Gene Ontology and Kyoto Encyclopedia of Genes and Genomes analyses were performed. The results of the PPI network and functional and pathway enrichment analyses are shown in Figures 1A and B.

Human apoptosis antibody array

The *Homo sapiens* apoptosis antibody array kit was purchased from Abcam (ab134001). Total protein samples were prepared as described above and incubated with the array according to the kit instructions. After the addition of chemiluminescence detection reagent, a signal proportional to the protein binding amount was detected. After RNA interference with the PARN gene in Eca-109 cells, the expression levels of apoptosis signaling pathway-related genes and proteins BIM, IGFBP-5 and p21 were evaluated.

Cell culture and transfection

We purchased human EC cell lines (Eca-109 and TE-1) from the Chinese Academy of Sciences Cell Bank (Shanghai, China). We cultured all cells in RPMI 1640 (Gibco, Grand Island, NY, United States) supplemented with 10% fetal bovine serum and maintained all cells in a humidified chamber at 37 °C with 5% CO_2. Control shRNA, shPARN-1, shPARN-2, and shPARN-3 were constructed by our group (the list of shRNA sequences is shown in Table 1). Viral transduction and selection of stable transfectants were carried out as mentioned above.

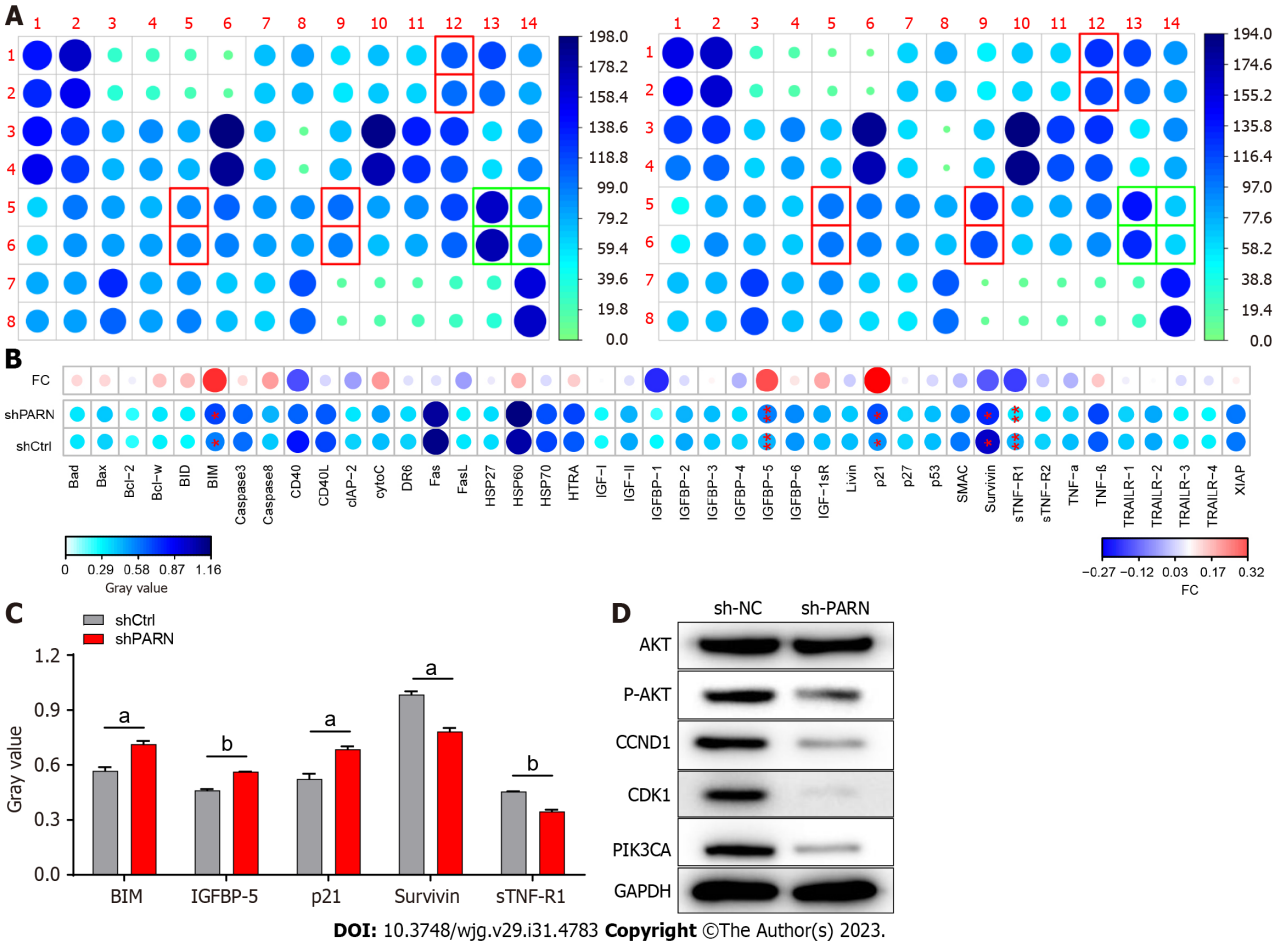
Western blot assay and antibodies

We collected cells and lysed them in RIPA lysis buffer. Aliquots of protein were then loaded and separated on SDS-PAGE gels and transferred to a polyvinylidene difluoride membrane. After blocking, the membrane was incubated with the appropriate primary antibody, followed by incubation with the corresponding secondary antibody. The primary antibodies and dilution factors were as follows: Rabbit anti-PARN (ab1883331, 1:1000 dilution; Abcam, United States), rabbit anti-CDK1 (ab133327, 1:3000 dilution, Abcam, United States), rabbit anti-PIK3CA (ab40776, 1:1000 dilution, Abcam, United States), rabbit anti-AKT [4685, 1:1000 dilution, Cell Signaling Technology (CST), United States], rabbit anti-

Table 1 Poly(A)-specific ribonuclease shRNA target sequence

Target number	Target sequence
Human-PARN-1	TATGACACAGCCTCTGAACA
Human-PARN-2	TGGATACTAAATTGATGGCCA
Human-PARN-3	CAACACATCCCTTGCGGAATT

PARN: Poly(A)-specific ribonuclease.



DOI: 10.3748/wjg.v29.i31.4783 **Copyright** ©The Author(s) 2023.

Figure 1 Exploration of the downstream molecular mechanism of poly(A)-specific ribonuclease in esophageal cancer cells. A: Human apoptosis antibody array analysis was performed in Eca-109 cells transfected with control shRNA or poly(A)-specific ribonuclease shRNA; B: Differences in the human apoptotic antibody array were visualized; C: Densitometry analysis was performed, and the gray values of differentially expressed proteins are shown; D: The expression of the target protein pathway in Eca-109 cells was observed by western blot. The data are expressed as the mean ± SD, $^{a}P < 0.05$, $^{b}P < 0.01$. sh PARN: Poly(A)-specific ribonuclease shRNA; sh-NC: Control shRNA.

CCND1 (2978, 1:1000 dilution, CST, United States), rabbit anti-P-AKT (AF887-sp, 1:500 dilution, R&D Systems, United States), and rabbit anti-GAPDH (AP0063, 1:3000 dilution, Bioworld, United States).

Quantitative real-time polymerase chain reaction

Total RNA was isolated using TRIzol (Sigma-Aldrich, T9424-100 m), and cDNA was obtained with HiScript Q RT SuperMix for quantitative real-time polymerase chain reaction qRT-PCR (+gDNA wiper) (Vazyme, R123-01). PCRs were performed on an ABI 7500 qRT-PCR machine. GAPDH was used as an endogenous control. We assessed the qualified expression by employing the $2^{-\Delta\Delta Ct}$ formula, while statistical analysis was conducted by using the fold change. All primer sequences used in this research are available in Table 2.

Cell viability assay

The cell viability of the TE-1 and Eca-109 cell lines was calculated using the Celigo cell counting assay after transfection. Logarithmic-phase transfected cells were collected, and cell suspensions were obtained by trypsin digestion. Then, we

Table 2 Primer sequences

Gene		Sequence (5'-3')	Tm (°C)
GAPDH	Forward primer	GAAAGCCTGCCGGTGACTAA	60.32
	Reverse primer	GCCCAATACGACCAAATCAGAG	59.39
PARN	Forward primer	GCCGCGGAATTCGATTTTAAG	58.63
	Reverse primer	ATCGATGGCGAAGAAGTCGG	60.25

PARN: Poly(A)-specific ribonuclease.

seeded the cell suspensions (2000 cells/well) into 96-well plates and cultured them for 5 d. The cell number was recorded, and the cell growth curve was plotted.

Apoptosis and cell cycle assay

Apoptosis and cell cycle analyses were performed by flow cytometry. As mentioned above, transfected TE-1 and Eca-109 cells were cultured in 6-well plates and then collected, washed with D-Hanks buffer and incubated with 1 × binding buffer. The cells were centrifuged and resuspended in 200 μL 1 × binding buffer, and an additional 10 μL Annexin V from the Annexin V Apoptosis Detection kit APC (cat. no. 88-8007; eBioscience; Thermo Fisher Scientific, Inc.) was added. Then, the cells were incubated in the dark for 15 min. The cell cycle distribution phases were detected based on propidium iodide (PI; Sigma, P4170) staining. The samples were analyzed on an easy Cyte HT flow cytometer (Merck Millipore).

Wound healing assay

In this study, we detected cell migratory abilities by using a wound healing assay. Cells were seeded into 96-well plates (5.0×10^4) and cultured to 90% confluence. Confluent monolayer cells were scratched gently with a 96 Wounding Replicator (VP scientific, VP408FH), and images were captured using a Cellomics ArrayScan VTI (Thermo Scientific) at 0 h, 4 h, 8 h, 24 h and 72 h. The wound area was quantified using a Cellomics ArrayScan HCS Reader (Thermo Scientific).

Migration assay

Transwell plates (Corning, 3422) were used for migration assays, which were carried out according to the manufacturer's protocol. Cells were seeded in transwell inserts (100 μL, 6.0×10^4/inserts), and RPMI 1640 medium with 30% foetal bovine serum (600 μL) was added to the bottom chamber. Following incubation for 24 h, the inserts were removed and stained with crystal violet. Photos were obtained using an inverted microscope (Olympus I × 73) and analyzed by ImageJ software.

BALB/c nude mouse xenograft model

This study was approved by the Guangxi Medical University Ethics Committee. All BALB/c nude mice (male; 4 wk old) were purchased from Charles River (Beijing, China). All BALB/c nude mice (male; 4 wk old) were maintained in a specific-pathogen-free environment. Cells were collected and suspended in D-Hanks solution (1×10^7 cells/mL) and then subcutaneously injected into the right front limb of 20 nude mice (n = 10 for each group). After injection, the size of the tumor was measured with calipers every 4 d for 23 d. On day 23 after injection, the mice were deeply anesthetized with isoflurane gas, and tumor growth and metastases were visualized and analyzed using a whole-body fluorescence imaging system (Berthold Technologies, LB983). After the live imaging experiment, mice were sacrificed by cervical dislocation under anesthesia. Additionally, the tumors were isolated, weighed and photographed. Tumor tissues were saved for further experimentation.

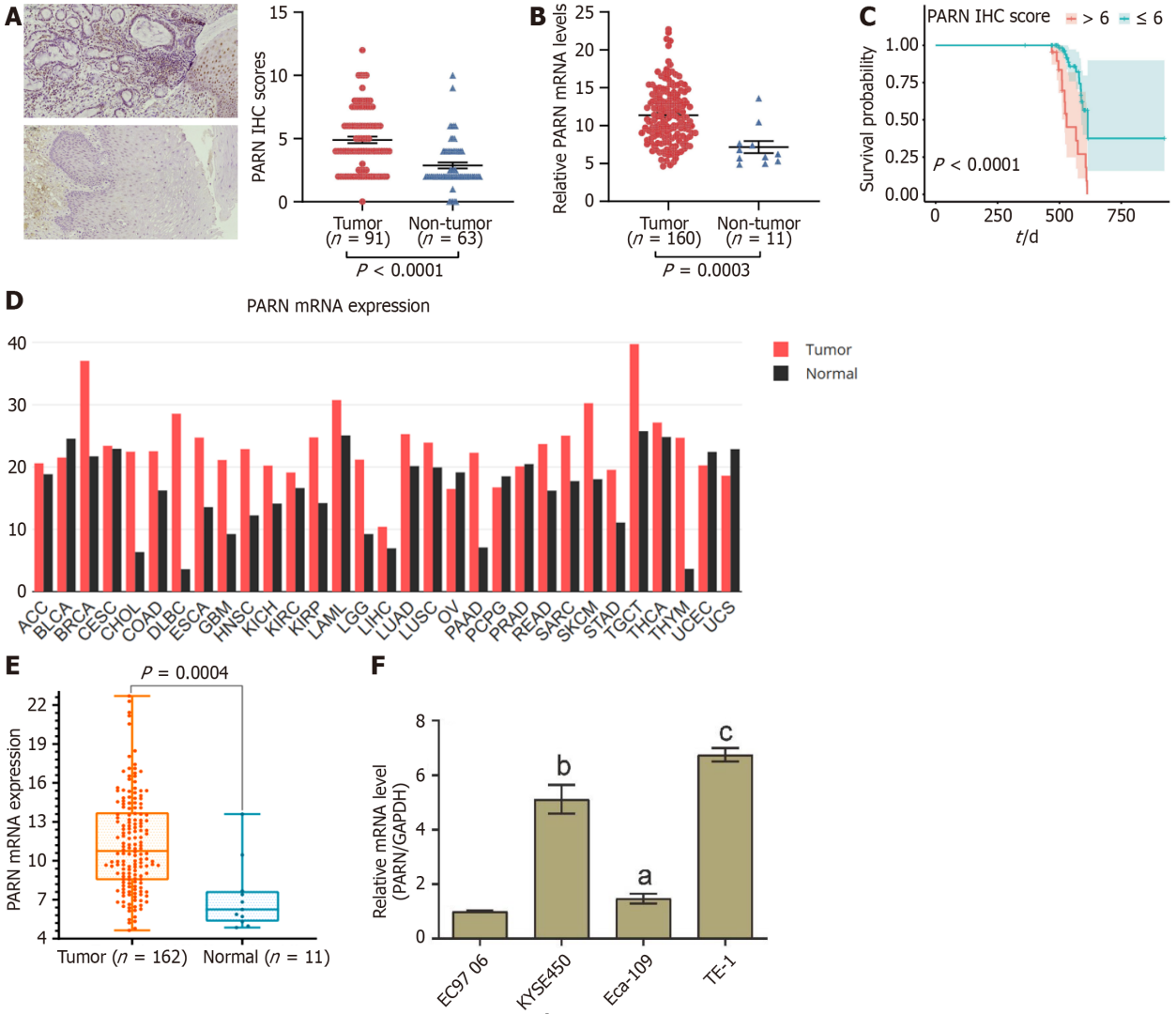
Statistical analysis

In this study, data are reported as the mean ± SD, and statistical analysis was carried out using GraphPad Prism 8.3 and SPSS 23.0. The Kaplan-Meier log rank test was used for survival curve analysis. Unpaired student's t test was used to assess statistically significant differences between two groups, and one-way ANOVA with Dunnett's posttest was used to compare the differences among three or more groups. P values < 0.05 represented a statistically significant difference.

RESULTS

Cancer data and bioinformatics analysis

Analysis of EC datasets from TCGA demonstrated that PARN mRNA levels were significantly increased in EC tissues compared with adjacent nontumor tissues (Figure 2B). Then, we extended the detailed annotation process of the preclinical human cancer model by compiling CCLE data and proved that PARN was abnormally upregulated in EC cell lines (Figures 2D and E). We found that PARN expression was upregulated in various EC cell lines, including Eca-109,



DOI: 10.3748/wjg.v29.i31.4783 **Copyright** ©The Author(s) 2023.

Figure 2 Poly(A)-specific ribonuclease protein expression was upregulated in both esophageal cancer tissue and cell lines and correlated with poor prognosis in esophageal cancer patients. A: Left panel: Representative immunohistochemistry (IHC) staining images of poly(A)-specific ribonuclease (PARN) in esophageal cancer tissue specimens (magnification × 400, bar = 50 μm). Right panel: Summary of IHC staining of PARN in esophageal cancer tissues (n = 91) and adjacent normal tissues (n = 63) in an esophageal tissue microarray; B: PARN mRNA levels were significantly increased in esophageal cancer tissue (n = 160) compared with adjacent normal tissues (n = 11). The data were obtained from The Cancer Genome Atlas; C: Kaplan-Meier survival analysis showed that high expression of PARN was correlated with poor prognosis in esophageal cancer patients (the PARN IHC score criteria: Table 5); D and E: Exploration of PARN gene expression in various malignant tumors using TCGA database, and the expression of PARN gene in EC was significantly higher than that in adjacent tissues in the TCGA database, P = 0.0004; F: PARN mRNA levels in esophageal cancer cell lines. $^{a}P < 0.05$, $^{b}P < 0.01$, $^{c}P < 0.001$, mean ± SD is shown. PARN: Poly(A)-specific ribonuclease; IHC: Immunohistochemistry.

KYSE450 and TE-1 cells (Figure 2F). In this study, we observed PARN mutations in < 2% of EC patients based on the cBioportal datasets, suggesting that gene mutation is not a major mechanism contributing to the frequent upregulation of PARN in EC patients (Supplementary Figure 1).

IHC and TMA of clinical samples

The IHC staining and the TMA assay results indicated that PARN protein expression is exceedingly upregulated in EC tissues compared with nontumor tissues (Figure 2A). Additionally, to assess the clinical significance of PARN expression in EC, we investigated the relationship between PARN expression and clinicopathologic data in 91 EC patients (Table 3). After statistical analysis, we found that PARN expression was correlated with lymphatic metastasis (P = 0.028). The expression of PARN was positively correlated with tumor lymph node metastasis (N value). With increasing tumor malignancy, the expression levels of PARN increased (Table 4). However, PARN expression was not correlated with tumor size (P = 0.110), T cell infiltration (P = 0.680) or stage (P = 0.336). To determine the relationship between PARN expression and EC patient clinical prognosis, we performed survival analysis using the survival data of 91 EC patients. The Kaplan-Meier analysis results indicated that high PARN levels were linked with poor survival (Figure 2C and Table 5). In summary, the above results demonstrated that high PARN expression may be implicated in the progression and metastasis of EC and that high PARN expression may predict a worse prognosis.

Table 3 Relationship between poly(A)-specific ribonuclease expression and tumor characteristics in patients with esophageal cancer

Features	No. of patients	PARN expression		*P* value
		Low	High	
All patients	91	48	43	
Age (yr)				0.758
< 65	45	23	22	
≥ 65	46	25	21	
Gender				0.433
Male	73	40	33	
Female	18	8	10	
Tumor size				0.110
≤ 5 cm	46	28	18	
> 5 cm	35	15	20	
T Infiltrate				0.680
T0	1	1	0	
T1	3	1	2	
T2	15	8	7	
T3	39	22	17	
T4	10	4	6	
Lymphatic metastasis (*n*)				0.028[a]
N0	31	20	11	
N1	18	10	8	
N2	11	4	7	
N3	8	2	6	
Stage				0.336
I	3	2	1	
II	30	18	12	
III	33	14	19	
IV	2	2	0	
Lymphoid positive number				0.164
< 1	43	26	17	
≥ 1	46	21	25	
Grade				0.516
I	7	4	3	
II	49	25	24	
III	26	16	10	

[a]$P < 0.05$.

The high expression group: Poly(A)-specific ribonuclease immunohistochemistry scores > 6; the low expression group: Poly(A)-specific ribonuclease immunohistochemistry scores ≤ 6. PARN: Poly(A)-specific ribonuclease.

Construction of a PPI network, enrichment analyses and human apoptosis antibody array results

Functional and pathway enrichment and differential gene analysis showed that PARN plays a role in tumor apoptosis. To further identify the potential mechanism by which PARN induces apoptosis, a Human Apoptosis Antibody Array kit (ab134001), including 43 human apoptosis-related proteins, was used to investigate the mechanisms of PARN knockdown treatment-induced apoptosis. Among all detected proteins, BIM, IGFBP-5 and p21 were found to be significantly

Table 4 Relationship between poly(A)-specific ribonuclease expression and tumor characteristics (lymphatic metastasis) in patients with esophageal cancer (Spearman's correlation coefficient for ranked data)

		PARN
Lymphatic metastasis (N)	Spearman correlation analysis	0.269
	Significance (two-tailed)	0.027[a]
	N	68

[a]$P < 0.05$.
PARN: Poly(A)-specific ribonuclease.

Table 5 Immunohistochemistry scoring criteria

Score type	Score point	Score
Positive cell score	No positive signal	0 (negative)
	0% < the proportion of positive cells < 25%	1
	25% ≤ the proportion of positive cells < 50%	2
	50% ≤ the proportion of positive cells < 75%	3
	75% ≤ the proportion of positive cells	4
Staining intensity score (the staining intensity of cytoplasm, membrane or nucleus)	No signal color	0 (negative)
	Pale yellow	1
	Brown yellow	2
	Dark brown	3

The positive cell score × staining color intensity score was used to judge the immunohistochemistry results, and the higher the score, the higher the antibody expression (score 0: Negative, score 1-4: Positive, score 5-8: Positive ++, score 9-12: Positive +++).

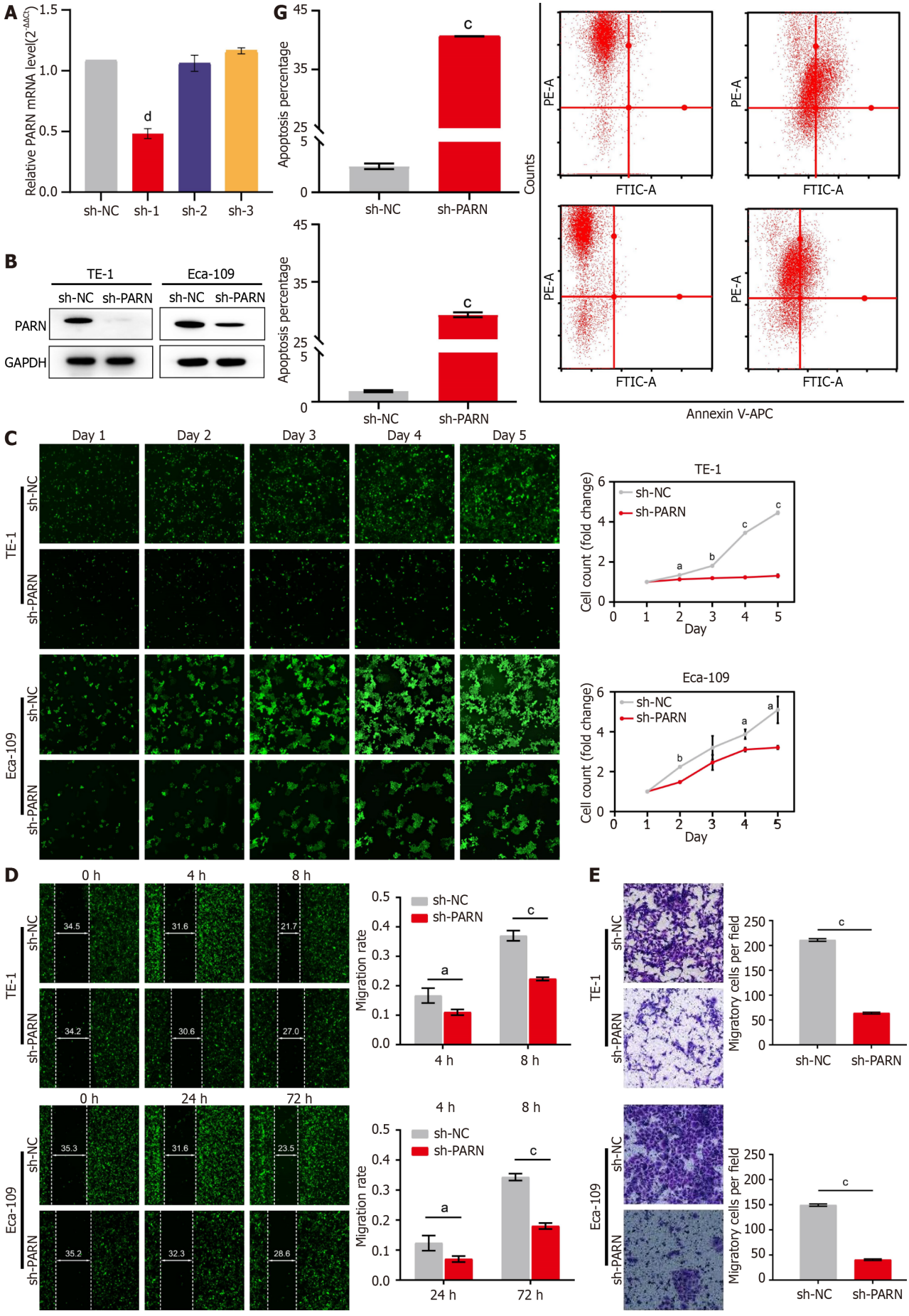
upregulated in the PARN knockdown group, while knockdown of PARN significantly downregulated the expression of the antiapoptotic proteins Surviving and sTNF-R1 (Figures 1A-C). Changes in apoptosis-associated proteins strongly demonstrated that PARN is involved in preventing apoptosis of EC cells by regulating these apoptotic proteins. The original figures of the Human Apoptosis Antibody Array in this study are provided (Supplementary Figure 2). Furthermore, the expression of Akt, p-Akt, CCND1, CDK1 and PIK3CA was downregulated in the sh-PARN group compared with the sh-NC group (Figure 1D).

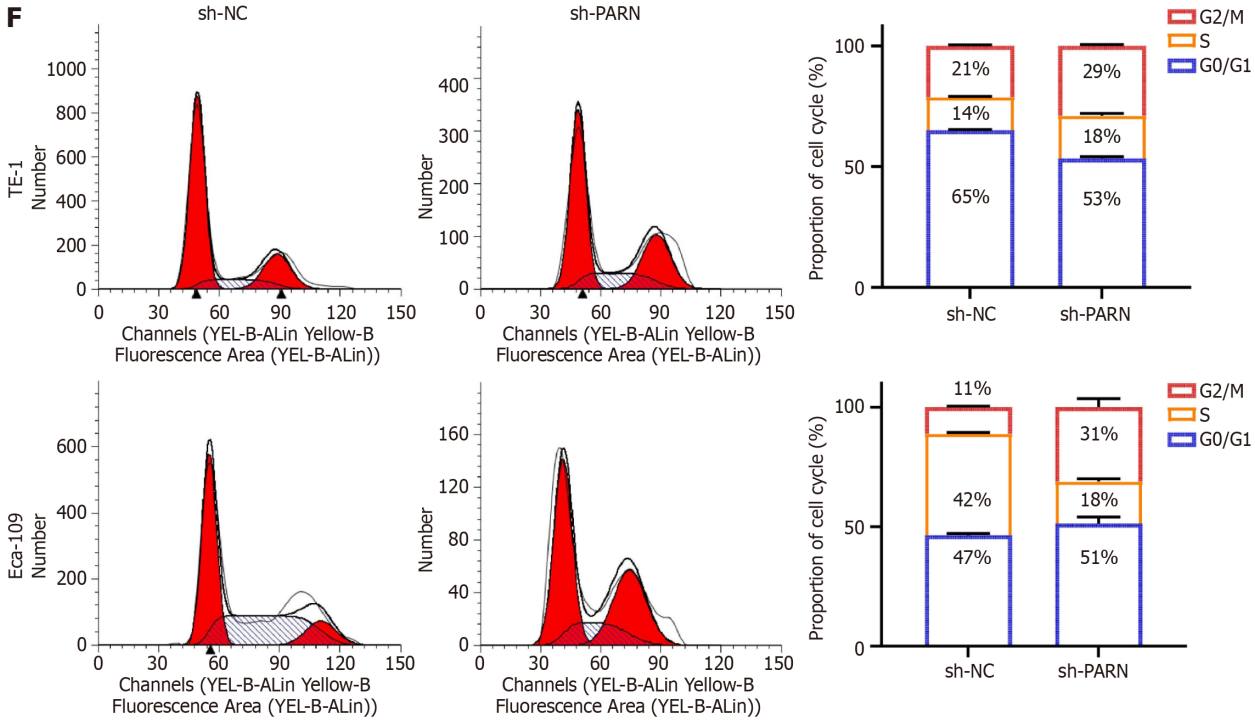
Effects of PARN on the proliferation, apoptosis and cell cycle of tumor cells in vitro

To investigate the effect of PARN on the biological characteristics of esophageal tumor cells, TE-1 and Eca-109 cells were transfected with sh-NC, shPARN-1, shPARN-2, and shPARN-3. The knockdown efficiency of PARN was validated by RT-qPCR. The results showed that shPARN-1 achieved the most efficient knockdown of PARN (Figure 3A), and thereafter, it was used to represent PARN knockdown in all follow-up experiments. The knockdown efficiency was verified at the protein level by western blotting (Figure 3B). The potential effect of PARN on the proliferation of Eca-109 and TE-1 cells was evaluated using the Celigo cell counting method. The results showed that the proliferation rate of Eca-109 and TE-1 cells infected with sh-PARN was significantly reduced compared with that of control cells (Figure 3C). It was confirmed that PARN knockout could significantly inhibit the proliferation of tumor cells. Apoptosis was analyzed by flow cytometry with Annexin V staining and showed a significantly increased percentage of apoptotic cells in sh-PARN-infected TE-1 and Eca-109 cells compared to sh-NC cells (Figure 3G). These results suggest that PARN knockout inhibits cell proliferation by inducing apoptosis. It was also found that compared with the sh-NC group, the sh-PARN group exhibited a significantly increased percentage of cells in the G2/M phase (Figure 3F), suggesting that PARN affects the proliferation of TE-1 and Eca-109 cells by regulating the cell cycle. Together, these findings confirm that PARN promotes EC cell proliferation by blocking cell cycle arrest and apoptosis.

Wound healing assay and transwell invasion assay

In the wound healing assay, the migration rates were significantly decreased in the sh-PARN group compared to the sh-NC group after lentivirus transfection. The migration abilities of Eca-109 cells in the sh-PARN group (72 h) were 47% lower than those in the sh-NC group ($P < 0.001$). In TE-1 cells, migration abilities in the sh-PARN group (8 h) were reduced by 40% ($P < 0.001$). (Figures 3D and E). Transwell invasion assays showed that after lentivirus transfection, the invasion ability of Eca-109 cells in the sh-PARN group was reduced by 73% compared with that in the sh-NC group ($P <$


A
Relative PARN mRNA level(2^-ΔΔCt)
1.5
1.0
0.5
0.0
d
sh-NC
sh-1
sh-2
sh-3
B
TE-1
Eca-109
sh-NC
sh-PARN
sh-NC
sh-PARN
PARN
GAPDH
G
Apoptosis percentage
45
35
25
5
0
c
sh-NC
sh-PARN
Apoptosis percentage
45
35
25
5
0
c
sh-NC
sh-PARN
Counts
PE-A
FTIC-A
PE-A
FTIC-A
PE-A
FTIC-A
PE-A
FTIC-A
Annexin V-APC
C
Day 1
Day 2
Day 3
Day 4
Day 5
TE-1
sh-NC
sh-PARN
Eca-109
sh-NC
sh-PARN
TE-1
sh-NC
sh-PARN
Cell count (fold change)
Day
Eca-109
sh-NC
sh-PARN
Cell count (fold change)
Day
D
0 h
4 h
8 h
TE-1
sh-NC
sh-PARN
34.5
31.6
21.7
34.2
30.6
27.0
Migration rate
sh-NC
sh-PARN
4 h
8 h
0 h
24 h
72 h
Eca-109
sh-NC
sh-PARN
35.3
31.6
23.5
35.2
32.3
28.6
Migration rate
sh-NC
sh-PARN
4 h
8 h
24 h
72 h
E
TE-1
sh-NC
sh-PARN
Migratory cells per field
sh-NC
sh-PARN
Eca-109
sh-NC
sh-PARN
Migratory cells per field
sh-NC
sh-PARN



DOI: 10.3748/wjg.v29.i31.4783 **Copyright** ©The Author(s) 2023.

Figure 3 Effect of poly(A)-specific ribonuclease on esophageal cancer cell proliferation, migration and invasion, cell cycle, and cell apoptosis *in vitro*. A and B: The interference efficiency of poly(A)-specific ribonuclease (PARN) *via* shRNA; C: Representative images of the Celigo cell count assay (magnification, × 100) and cumulative data of cell numbers in TE-1 and Eca-109 cells transfected with control shRNA or PARN shRNA; D: Representative images and statistical analysis of the wound healing assay; E: Representative images and statistical analysis of the transwell assay; F and G: Representative images and statistical analysis of flow cytometry analysis of TE-1 and Eca-109 cells after transfection. Cell cycle analysis revealed that PARN affected TE-1 and Eca-109 cell proliferation (F), and cell apoptosis analysis showed that PARN affected the apoptosis of TE-1 and Eca-109 cells (G). $^{a}P < 0.05$, $^{b}P < 0.01$, $^{a}P < 0.0001$, $^{c}P < 0.001$, means ± SDs are shown. sh PARN: Poly(A)-specific ribonuclease shRNA; sh-NC: Control shRNA.

0.001). In TE-1 cells, cell invasion was 70% lower in the sh-PARN group than in the sh-NC group ($P < 0.001$).

PARN facilitates tumor growth in vivo

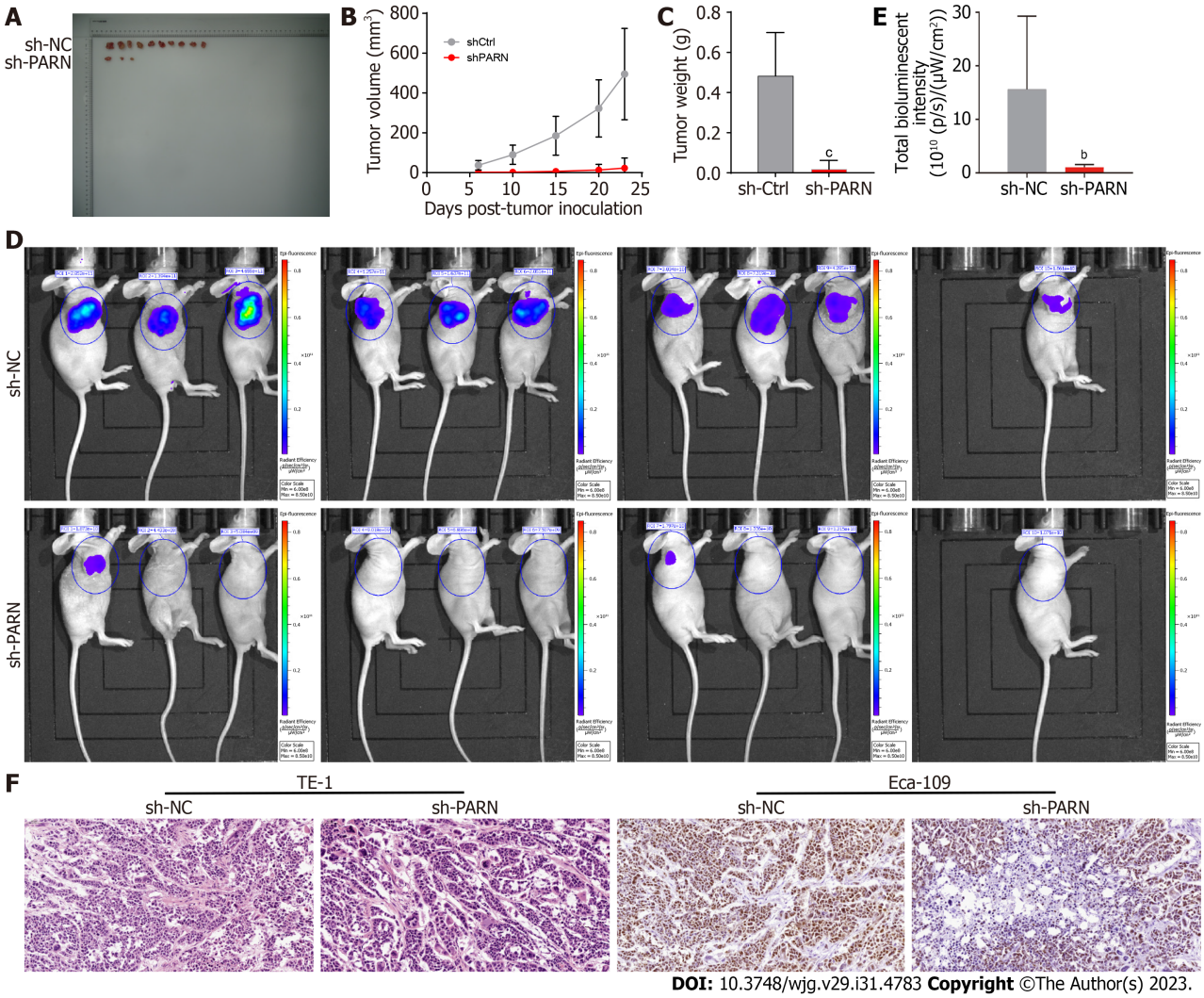
The above results showed that knockdown of PARN inhibits cell proliferation and promotes cell apoptosis *in vitro*. We next wanted to examine the tumor suppression effects of PARN *in vivo*. To establish the xenograft tumor model, Eca-109 cells that were stably transfected with sh-NC and sh-PARN were subcutaneously implanted into BALB/c nude mice. Tumor weight and volume in the shPARN group were significantly reduced compared with those in the sh-NC-treated group (Figures 4A-C). Additionally, bioluminescence imaging suggested that tumor growth in the sh-PARN group was substantially suppressed (Figures 4D and E), which was similar to the results presented above. The sh-PARN group exhibited significantly repressed tumor development *in vivo*, suggesting that the tumor-forming capacity of Eca-109 cells in nude mice was significantly accelerated by PARN downregulation. Additionally, Ki67 staining was used to examine the proliferative cells in tumors. IHC data of tumor tissue showed that the number of Ki-67-positive tumor cells in the sh-PARN group markedly declined in comparison to that in the sh-NC group (Figure 4F). These *in vivo* results confirmed the *in vitro* results and showed that PARN significantly accelerated EC formation in nude mice.

DISCUSSION

Tumor progression is a complicated process, and increasing the degradation rate of homologous mRNAs affects the expression of dominant oncogenes, dysfunctional trans-acting factors and/or destruction of specific tumor suppressor genes. Therefore, precise control of mRNA levels is important for the regulation of gene expression[13,14].

As an RNA-processing enzymes, PARN may have an important role in tumor development and progression[15-17]. Currently, there is little evidence indicating a correlation between PARN expression and EC. Our study found that PARN expression levels in EC tissues are clearly higher than those in adjacent normal tissues and are significantly correlated with lymph node metastasis and poor patient survival. Since PARN expression has potential clinical implications in EC, the investigation of its regulatory mechanisms attracted our attention.

The main function of PARN is to cut the mRNA poly(A) tail and produce AMP in the process. The shortening of the eukaryotic poly(A) mRNA tail inhibits mRNA translation and induces transcript renewal; the deregulation of this process is common in cancer. A shortened poly(A) tail destabilizes mRNA and induces degradation. Thus, PARN is considered to be one of the important posttranscriptional regulators in cells. Previous studies have reported that the poly(A) tail of



DOI: 10.3748/wjg.v29.i31.4783 **Copyright** ©The Author(s) 2023.

Figure 4 Poly(A)-specific ribonuclease promotes tumor growth *in vivo*. A: Representative image of tumors separated from nude mice; B and C: Tumor volume and weight were measured in nude mice; D and E: Representative bioluminescence imaging (BLI) images and quantification of BLI in the tumor regions of nude mice; F: Representative images of Ki-67 staining in tumors isolated from the nude mice. Scale bars are indicated in the upper left corner of the picture (Bar = 50 μm). Assays were conducted in triplicate. °$P < 0.001$, mean ± SD is shown. sh PARN: Poly(A)-specific ribonuclease shRNA; sh-NC: Control shRNA.

mRNA transcripts is removed by 3′ to 5′ exonucleases (deadenylases), and this process is referred to as the rate-limiting step of mRNA degradation[9,18-21]. After mRNA transcript degradation, the protein expression levels also change accordingly. The levels of these mRNAs are low under normal conditions due to deadenylase activity[22-24].

In our study, compared with normal tissues, EC tissues exhibited significantly increased mRNA levels of PARN, and we also observed this trend in EC cell lines. Interestingly, we found that high PARN expression predicted a poor prognosis in EC patients.

Furthermore, compared with the those of the respective control cell lines, the growth and proliferation of EC cells were significantly inhibited after PARN knockdown. In contrast, it was confirmed that high PARN levels can promote the growth and proliferation of EC cells.

In addition, it was also found that compared with the sh-NC group, the sh-PARN group exhibited a significantly increased percentage of cells in the G2/M phase, suggesting that PARN affects the proliferation of carcinoma cells by regulating the cell cycle.

Escape from apoptosis is beneficial for malignant cell survival and thus could be one of the important mechanisms in cancer pathogenesis[25,26]. Apoptosis involves many biochemical processes that are induced by multiple signaling pathways[27,28]. In our study, PARN knockdown significantly downregulated multiple apoptosis-related proteins (for example, the antiapoptotic proteins Surviving and sTNF-R1) and promoted apoptosis. Therefore, knockdown of the PARN gene promotes apoptosis by regulating apoptotic proteins. In addition, PARN knockdown not only affects the apoptosis rate but also regulates a wide range of downstream signaling factors, including Akt, p-Akt, PIK3CA and CCND1. There has been much evidence suggesting that the PI3K/Akt pathway is one of the most important signaling pathways for cell proliferation, survival, apoptosis and malignant transformation[29,30]. These results suggest that PARN may inhibit tumor cell apoptosis and promote tumor proliferation through the PI3K/Akt pathway in EC. Subsequent wound healing tests and transwell invasion tests confirmed the promoting effect of PARN on the migration and invasion of EC cells. In a BALB/c nude mouse xenograft model, the apoptosis ratio of Eca-109 and TE-1 cells was significantly

increased after PARN knockout, and the cell proliferation rate was significantly decreased, as well as the percentage of cells in G2/M phase arrest. It has been confirmed that PARN promotes tumor cell proliferation by blocking cell cycle arrest and apoptosis in EC.

CONCLUSION

Our study preliminarily concluded that PARN may inhibit in EC cell apoptosis and cell cycle arrest through the PI3K/Akt pathway, thus promoting tumor proliferation, invasion and migration and further accelerating the progression of EC. Therefore, PARN can be used as a prognostic marker and therapeutic target for the diagnosis and treatment of EC.

ARTICLE HIGHLIGHTS

Research background

Esophageal cancer (EC) is a common malignant cancer type and the sixth leading cause of cancer-related mortality worldwide. The main treatment options for esophageal squamous cell carcinoma (ESCC) include surgery, radiotherapy, and chemotherapy. Due to its high invasiveness and high recurrence and metastasis rates, the prognosis of ESCC patients remains poor despite the use of multidisciplinary treatment. The 5-year overall survival rate of ESCC patients is only 30%-40%. However, the prognosis of patients with advanced or metastatic EC is even worse, with a 5-year overall survival rate of less than 15%.

Research motivation

Poly(A)-specific ribonuclease (PARN) is a multifunctional enzyme that plays a crucial role in the occurrence and development of a variety of cancer types. The aim of this study was to explore the relationship between PARN and the proliferation, metastasis and invasion of EC cells to evaluate whether PARN could be a potential biomarker and drug target for the treatment of EC.

Research objectives

The objects of this study are as follows: (1) EC tissues and paired adjacent normal tissues were obtained from 91 patients with EC after surgery; (2) EC lines Eca-109 and TE-1; and (3) Nude mice.

Research methods

The expression of PARN mRNA was measured using a tissue microarray, and the expression of PARN was also detected using immunohistochemistry. The relationship between PARN expression and clinicopathological features and the survival prognosis of patients was analyzed. The effect of PARN on the proliferation, invasion and migration of Eca-109 and TE-1 EC cells was investigated *in vitro* by knocking down PARN using shRNA. The effect of PARN on tumor growth *in vivo* was verified by a nude mouse xenograft model.

Research results

Our study found that PARN expression in EC tissues is clearly higher than that in adjacent healthy tissues and is significantly correlated with lymph node metastasis and poor survival. It was confirmed that PARN can promote the growth and proliferation of EC cells. Compared with the control shRNA group, the PARN shRNA group exhibited a significantly increased percentage of cells in the G2/M phase, suggesting that PARN affects the proliferation of carcinoma cells by regulating their cell cycle. Knockdown of the PARN gene promoted apoptosis by regulating apoptotic proteins. Wound healing tests and transwell invasion tests confirmed the promoting effect of PARN on the migration and invasion of EC cells. In the BALB/c nude mouse xenograft model, the apoptosis ratio of Eca-109 and TE-1 cells was significantly increased after PARN knockout, and the cell proliferation rate was significantly decreased, as well as the percentage of cells in G2/M phase arrest.

Research conclusions

Our study preliminarily concluded that PARN may inhibit EC cell apoptosis and cell cycle arrest through the PI3K/Akt pathway, thus promoting tumor cell proliferation, invasion and migration and further accelerating the progression of EC.

Research perspectives

PARN can be used as a prognostic marker and therapeutic target for the diagnosis and treatment of EC.

FOOTNOTES

Author contributions: Zhang FW and Liu WQ contributed to the conceptualization of this manuscript; Tong J, Chen QQ, and Feng J collected and curated the data and contributed to the supervision of this study; Xie XW contributed to the experiments; Tong J contributed to the data analysis; Zhang FW wrote the original draft; Liu WQ contributed to the writing, review and editing of this article;

and all authors reviewed, discussed, and agreed with manuscript.

Institutional review board statement: The study was reviewed and approved by the Second Affiliated Hospital of Guangxi Medical University Ethics Committee.

Clinical trial registration statement: Our study was not a prospective, randomized, controlled clinical trial and did not give a population one or more pre-defined interventions. Our study was a retrospective study of postoperative tissue samples from patients who had completed treatment. Cell experiments and animal experiments were conducted according to the results of clinical specimens. Therefore, our study should not apply the registration policy and should not require registration for clinical studies.

Informed consent statement: Written patient consent was obtained from all patients.

Conflict-of-interest statement: All the authors report no relevant conflicts of interest for this article.

Data sharing statement: No additional data are available.

CONSORT 2010 statement: The authors have read the CONSORT 2010 statement, and the manuscript was prepared and revised according to the CONSORT 2010 statement.

Open-Access: This article is an open-access article that was selected by an in-house editor and fully peer-reviewed by external reviewers. It is distributed in accordance with the Creative Commons Attribution NonCommercial (CC BY-NC 4.0) license, which permits others to distribute, remix, adapt, build upon this work non-commercially, and license their derivative works on different terms, provided the original work is properly cited and the use is non-commercial. See: https://creativecommons.org/Licenses/by-nc/4.0/

Country/Territory of origin: China

ORCID number: Wen-Qi Liu 0000-0003-4986-1234.

S-Editor: Wang JJ
L-Editor: A
P-Editor: Zhao S

REFERENCES

1 **Kashyap MK**, Abdel-Rahman O. Expression, regulation and targeting of receptor tyrosine kinases in esophageal squamous cell carcinoma. *Mol Cancer* 2018; **17**: 54 [PMID: 29455652 DOI: 10.1186/s12943-018-0790-4]
2 **van den Ende T**, Ter Veer E, Mali RMA, van Berge Henegouwen MI, Hulshof MCCM, van Oijen MGH, van Laarhoven HWM. Prognostic and Predictive Factors for the Curative Treatment of Esophageal and Gastric Cancer in Randomized Controlled Trials: A Systematic Review and Meta-Analysis. *Cancers (Basel)* 2019; **11** [PMID: 31013858 DOI: 10.3390/cancers11040530]
3 **Tepper J**, Krasna MJ, Niedzwiecki D, Hollis D, Reed CE, Goldberg R, Kiel K, Willett C, Sugarbaker D, Mayer R. Phase III trial of trimodality therapy with cisplatin, fluorouracil, radiotherapy, and surgery compared with surgery alone for esophageal cancer: CALGB 9781. *J Clin Oncol* 2008; **26**: 1086-1092 [PMID: 18309943 DOI: 10.1200/JCO.2007.12.9593]
4 **Sjoquist KM**, Burmeister BH, Smithers BM, Zalcberg JR, Simes RJ, Barbour A, Gebski V; Australasian Gastro-Intestinal Trials Group. Survival after neoadjuvant chemotherapy or chemoradiotherapy for resectable oesophageal carcinoma: an updated meta-analysis. *Lancet Oncol* 2011; **12**: 681-692 [PMID: 21684205 DOI: 10.1016/S1470-2045(11)70142-5]
5 **van Hagen P**, Hulshof MC, van Lanschot JJ, Steyerberg EW, van Berge Henegouwen MI, Wijnhoven BP, Richel DJ, Nieuwenhuijzen GA, Hospers GA, Bonenkamp JJ, Cuesta MA, Blaisse RJ, Busch OR, ten Kate FJ, Creemers GJ, Punt CJ, Plukker JT, Verheul HM, Spillenaar Bilgen EJ, van Dekken H, van der Sangen MJ, Rozema T, Biermann K, Beukema JC, Piet AH, van Rij CM, Reinders JG, Tilanus HW, van der Gaast A; CROSS Group. Preoperative chemoradiotherapy for esophageal or junctional cancer. *N Engl J Med* 2012; **366**: 2074-2084 [PMID: 22646630 DOI: 10.1056/NEJMoa1112088]
6 **Balatsos NA**, Maragozidis P, Anastasakis D, Stathopoulos C. Modulation of poly(A)-specific ribonuclease (PARN): current knowledge and perspectives. *Curr Med Chem* 2012; **19**: 4838-4849 [PMID: 22834816 DOI: 10.2174/092986712803341539]
7 **Dejene EA**, Li Y, Showkatian Z, Ling H, Seto E. Regulation of poly(a)-specific ribonuclease activity by reversible lysine acetylation. *J Biol Chem* 2020; **295**: 10255-10270 [PMID: 32457045 DOI: 10.1074/jbc.RA120.012552]
8 **Delis C**, Krokida A, Tomatsidou A, Tsikou D, Beta RA, Tsioumpekou M, Moustaka J, Stravodimos G, Leonidas DD, Balatsos NA, Papadopoulou KK. AtHESPERIN: a novel regulator of circadian rhythms with poly(A)-degrading activity in plants. *RNA Biol* 2016; **13**: 68-82 [PMID: 26619288 DOI: 10.1080/15476286.2015.1119363]
9 **Virtanen A**, Henriksson N, Nilsson P, Nissbeck M. Poly(A)-specific ribonuclease (PARN): an allosterically regulated, processive and mRNA cap-interacting deadenylase. *Crit Rev Biochem Mol Biol* 2013; **48**: 192-209 [PMID: 23496118 DOI: 10.3109/10409238.2013.771132]
10 **Dehan E**, Ben-Dor A, Liao W, Lipson D, Frimer H, Rienstein S, Simansky D, Krupsky M, Yaron P, Friedman E, Rechavi G, Perlman M, Aviram-Goldring A, Izraeli S, Bittner M, Yakhini Z, Kaminski N. Chromosomal aberrations and gene expression profiles in non-small cell lung cancer. *Lung Cancer* 2007; **56**: 175-184 [PMID: 17258348 DOI: 10.1016/j.lungcan.2006.12.010]
11 **Valles I**, Pajares MJ, Segura V, Guruceaga E, Gomez-Roman J, Blanco D, Tamura A, Montuenga LM, Pio R. Identification of novel deregulated RNA metabolism-related genes in non-small cell lung cancer. *PLoS One* 2012; **7**: e42086 [PMID: 22876301 DOI: 10.1371/journal.pone.0042086]
12 **Yu K**, Ahrens S, Zhang X, Schiff H, Ramakrishnan C, Fenno L, Deisseroth K, Zhao F, Luo MH, Gong L, He M, Zhou P, Paninski L, Li B. The

central amygdala controls learning in the lateral amygdala. *Nat Neurosci* 2017; **20**: 1680-1685 [PMID: 29184202 DOI: 10.1038/s41593-017-0009-9]

13 **Audic Y**, Hartley RS. Post-transcriptional regulation in cancer. *Biol Cell* 2004; **96**: 479-498 [PMID: 15380615 DOI: 10.1016/j.biolcel.2004.05.002]

14 **Tang Y**, Shu G, Yuan X, Jing N, Song J. FOXA2 functions as a suppressor of tumor metastasis by inhibition of epithelial-to-mesenchymal transition in human lung cancers. *Cell Res* 2011; **21**: 316-326 [PMID: 20820189 DOI: 10.1038/cr.2010.126]

15 **Maragozidis P**, Karangeli M, Labrou M, Dimoulou G, Papaspyrou K, Salataj E, Pournaras S, Matsouka P, Gourgoulianis KI, Balatsos NA. Alterations of deadenylase expression in acute leukemias: evidence for poly(a)-specific ribonuclease as a potential biomarker. *Acta Haematol* 2012; **128**: 39-46 [PMID: 22614729 DOI: 10.1159/000337418]

16 **Maragozidis P**, Papanastasi E, Scutelnic D, Totomi A, Kokkori I, Zarogiannis SG, Kerenidi T, Gourgoulianis KI, Balatsos NA. Poly(A)-specific ribonuclease and Nocturnin in squamous cell lung cancer: prognostic value and impact on gene expression. *Mol Cancer* 2015; **14**: 187 [PMID: 26541675 DOI: 10.1186/s12943-015-0457-3]

17 **Zhang LN**, Yan YB. Depletion of poly(A)-specific ribonuclease (PARN) inhibits proliferation of human gastric cancer cells by blocking cell cycle progression. *Biochim Biophys Acta* 2015; **1853**: 522-534 [PMID: 25499764 DOI: 10.1016/j.bbamcr.2014.12.004]

18 **Funakoshi Y**, Doi Y, Hosoda N, Uchida N, Osawa M, Shimada I, Tsujimoto M, Suzuki T, Katada T, Hoshino S. Mechanism of mRNA deadenylation: evidence for a molecular interplay between translation termination factor eRF3 and mRNA deadenylases. *Genes Dev* 2007; **21**: 3135-3148 [PMID: 18056425 DOI: 10.1101/gad.1597707]

19 **Nousch M**, Techritz N, Hampel D, Millonigg S, Eckmann CR. The Ccr4-Not deadenylase complex constitutes the main poly(A) removal activity in C. elegans. *J Cell Sci* 2013; **126**: 4274-4285 [PMID: 23843623 DOI: 10.1242/jcs.132936]

20 **Wilson T**, Treisman R. Removal of poly(A) and consequent degradation of c-fos mRNA facilitated by 3' AU-rich sequences. *Nature* 1988; **336**: 396-399 [PMID: 3194021 DOI: 10.1038/336396a0]

21 **Wolf J**, Passmore LA. mRNA deadenylation by Pan2-Pan3. *Biochem Soc Trans* 2014; **42**: 184-187 [PMID: 24450649 DOI: 10.1042/BST20130211]

22 **Cevher MA**, Zhang X, Fernandez S, Kim S, Baquero J, Nilsson P, Lee S, Virtanen A, Kleiman FE. Nuclear deadenylation/polyadenylation factors regulate 3' processing in response to DNA damage. *EMBO J* 2010; **29**: 1674-1687 [PMID: 20379136 DOI: 10.1038/emboj.2010.59]

23 **Devany E**, Zhang X, Park JY, Tian B, Kleiman FE. Positive and negative feedback loops in the p53 and mRNA 3' processing pathways. *Proc Natl Acad Sci U S A* 2013; **110**: 3351-3356 [PMID: 23401530 DOI: 10.1073/pnas.1212533110]

24 **Moraes KC**, Wilusz CJ, Wilusz J. CUG-BP binds to RNA substrates and recruits PARN deadenylase. *RNA* 2006; **12**: 1084-1091 [PMID: 16601207 DOI: 10.1261/rna.59606]

25 **Chen T**, Dai X, Dai J, Ding C, Zhang Z, Lin Z, Hu J, Lu M, Wang Z, Qi Y, Zhang L, Pan R, Zhao Z, Lu L, Liao W, Lu X. AFP promotes HCC progression by suppressing the HuR-mediated Fas/FADD apoptotic pathway. *Cell Death Dis* 2020; **11**: 822 [PMID: 33009373 DOI: 10.1038/s41419-020-03030-7]

26 **Zhivotovsky B**, Kroemer G. Apoptosis and genomic instability. *Nat Rev Mol Cell Biol* 2004; **5**: 752-762 [PMID: 15340382 DOI: 10.1038/nrm1443]

27 **Fuchs Y**, Steller H. Live to die another way: modes of programmed cell death and the signals emanating from dying cells. *Nat Rev Mol Cell Biol* 2015; **16**: 329-344 [PMID: 25991373 DOI: 10.1038/nrm3999]

28 **Jeong SY**, Seol DW. The role of mitochondria in apoptosis. *BMB Rep* 2008; **41**: 11-22 [PMID: 18304445 DOI: 10.5483/bmbrep.2008.41.1.011]

29 **Downward J**. Mechanisms and consequences of activation of protein kinase B/Akt. *Curr Opin Cell Biol* 1998; **10**: 262-267 [PMID: 9561851 DOI: 10.1016/s0955-0674(98)80149-x]

30 **Duan C**, Bauchat JR, Hsieh T. Phosphatidylinositol 3-kinase is required for insulin-like growth factor-I-induced vascular smooth muscle cell proliferation and migration. *Circ Res* 2000; **86**: 15-23 [PMID: 10625300 DOI: 10.1161/01.res.86.1.15]

World Journal of Gastroenterology

Submit a Manuscript: https://www.f6publishing.com

World J Gastroenterol 2023 August 21; 29(31): 4797-4808

DOI: 10.3748/wjg.v29.i31.4797

ISSN 1007-9327 (print) ISSN 2219-2840 (online)

META-ANALYSIS

Circulating copeptin level and the clinical prognosis of patients with chronic liver disease

Hao-Qian Tan, Ming Zhao, Zan Huang, Yang Liu, Han Li, Long-Hui Ma, Jun-Ying Liu

Specialty type: Gastroenterology and hepatology

Provenance and peer review: Unsolicited article; Externally peer reviewed.

Peer-review model: Single blind

Peer-review report's scientific quality classification

Grade A (Excellent): A
Grade B (Very good): B
Grade C (Good): 0
Grade D (Fair): 0
Grade E (Poor): 0

P-Reviewer: El-Shabrawi MH, Egypt; Rodrigues AT, Brazil

Received: June 15, 2023
Peer-review started: June 15, 2023
First decision: July 14, 2023
Revised: July 21, 2023
Accepted: July 28, 2023
Article in press: July 28, 2023
Published online: August 21, 2023

Hao-Qian Tan, Department of Gastroenterology, Zhoukou Central Hospital Affiliated to Xinxiang Medical University, Zhoukou 466000, Henan Province, China

Ming Zhao, Yang Liu, Han Li, Jun-Ying Liu, Department of Gastroenterology, Zhoukou Central Hospital, Zhoukou 466000, Henan Province, China

Zan Huang, Long-Hui Ma, Department of Teaching and Research, Zhoukou Central Hospital, Zhoukou 466000, Henan Province, China

Corresponding author: Jun-Ying Liu, MD, Director, Department of Gastroenterology, Zhoukou Central Hospital, No. 26 Renmin Road East Section, Chuanhui District, Zhoukou 466000, Henan Province, China. liujunying781025@163.com

Abstract

BACKGROUND

The relationship between copeptin and the severity of circulatory dysfunction and systemic stress response in patients with chronic liver disease (CLD) has been established. Nevertheless, the potential of serum copeptin levels to predict the prognosis of CLD patients remains unclear.

AIM

To conduct a systematic review and meta-analysis to investigate the correlation between serum copeptin and transplant-free survival (TFS) in this population.

METHODS

To achieve the objective of the meta-analysis, PubMed, Embase, the Cochrane Library, and the Web of Science were searched to identify observational studies with longitudinal follow-up. The Cochrane *Q* test was utilized to assess between-study heterogeneity, and the I^2 statistic was estimated. Random-effects models were employed to combine the outcomes, taking into account the potential influence of heterogeneity.

RESULTS

Ten datasets including 3133 patients were involved. The follow-up durations were 1 to 48 mo (mean: 12.5 mo). Overall, it was shown that a high level of serum copeptin was associated with a poor TFS [risk ratio (RR): 1.82, 95% confidence interval: 1.52-2.19, $P < 0.001$; $I^2 = 0\%$]. In addition, sensitivity analysis by omitting one dataset at a time showed consistent results (RR: 1.73-2.00, $P < 0.05$). Finally, subgroup analyses according to study country, study design, patient diagnosis,

cutoff of copeptin, follow-up duration, and study quality score also showed similar results (*P* for subgroup difference all > 0.05).

CONCLUSION
Patients with CLD who have high serum copeptin concentrations may be associated with a poor clinical prognosis.

Key Words: Chronic liver disease; Liver cirrhosis; Copeptin; Prognosis; Mortality; Meta-analysis

©The Author(s) 2023. Published by Baishideng Publishing Group Inc. All rights reserved.

Core Tip: Serum copeptin has been related to the severity of circulatory dysfunction and systemic stress response in patients with chronic liver disease (CLD). However, little is known about the relationship between serum copeptin and the prognosis of patients with CLD. In this systematic review and meta-analysis, evidence from ten datasets including 3133 patients were integrated. The results showed that a high level of serum copeptin was associated with a poor transplant-free survival in these patients. These findings support the use of serum copeptin as a prognostic biomarker for patients with CLD.

Citation: Tan HQ, Zhao M, Huang Z, Liu Y, Li H, Ma LH, Liu JY. Circulating copeptin level and the clinical prognosis of patients with chronic liver disease. *World J Gastroenterol* 2023; 29(31): 4797-4808
URL: https://www.wjgnet.com/1007-9327/full/v29/i31/4797.htm
DOI: https://dx.doi.org/10.3748/wjg.v29.i31.4797

INTRODUCTION

Chronic liver disease (CLD) patients are more likely to develop complications associated with the progression of the disease, such as portal hypertension, ascites, spontaneous bacterial peritonitis, gastroesophageal varices, and hepatic encephalopathy[1,2]. For those with advanced CLD (ACLD), the clinical prognosis is generally poor, which has become a substantial cause of morbidity and mortality worldwide[3,4]. Accumulating evidence suggests that patients with ACLD may have multiple features of circulatory dysfunction, such as incremental intrahepatic vascular resistance, decrease of portal blood flow, and a reduced systemic vascular resistance[5,6], all of which could subsequently activate the neurohormonal system for counter regulation, including the upregulated systemic arginine vasopressin (AVP)[7,8]. As a biomarker of disease progression, the AVP increment in patients with CLD has been hypothesized as a predictor of poor prognosis[9]. However, as a small peptide of nine amino acids, the blood level of AVP is difficult to quantitatively analyze due to its short half-life[10]. Copeptin is a 39-amino-acid glycopeptide which contains the C-terminus of AVP precursor, making it an effective surrogate marker for AVP release[11,12]. As a result of osmotic stress and osmotic stimulation, a high level of copeptin has been demonstrated in patients with ACLD[13,14]. However, it remains unknown whether the serum level of copeptin may predict the prognosis of patients with CLD. Therefore, in this study, we conducted a systematic review and meta-analysis to investigate the potential association between serum copeptin and clinical outcomes in this patient population.

MATERIALS AND METHODS

Throughout the process of planning, conducting, and reporting the study, the Preferred Reporting Items for Systematic Reviews and Meta-Analyses statement[15,16] and Cochrane Handbook[17] were followed.

Search of databases

We searched electronic databases including PubMed, Embase, the Cochrane Library, and Web of Science, starting from inception and ending April 21st, 2023, for studies that had been published up to that date. The search was performed with terms related to our study including: (1) "Copeptin" OR "C-terminal provasopressin"; and (2) "cirrhosis" OR "cirrhotic" OR "liver" OR "hepatic" OR "hepatitis". There was no limitation on the language of the publication in the search for human studies. As part of our manual screening process, references from relevant original and review articles were screened for possible relevant studies.

Inclusion and exclusion criteria of studies

Inclusion criteria were developed in accordance with PICOS recommendations and according to the aim of the meta-analysis.

P (patients): Adult patients (18 years or older) with a confirmed diagnosis of CLD; I (exposure): Patients with a high serum concentration of copeptin at baseline. Methods for measuring serum copeptin and cutoffs for defining high serum copeptin were consistent with those of the original studies; C (control): Patients with a low serum concentration of

copeptin at baseline; O (outcomes): Incidence of transplant-free survival (TFS) compared between CLD patients with high *vs* low serum levels of copeptin at baseline. S (study design): Studies with longitudinal follow-up, including cohort and case-control studies, as well as post-hoc analyses of clinical trials.

Excluded from the meta-analysis were reviews, editorials, preclinical studies, and studies that did not involve patients with CLD, failed to measure serum copeptin, or did not report the relevant outcome. In instances where there was a patient population overlap, the study with the greatest sample size was incorporated into the meta-analysis.

Data extraction and quality evaluation

Two of the authors conducted literature searches, data collection, and assessments of study quality independently. In instances where discrepancies arose, a third author was consulted for discussion, and a consensus was reached. The analysis of studies included the collection of information pertaining to study information, design characteristics, patient diagnosis, demographic factors, measuring methods, serum copeptin cutoffs, follow-up durations, and adjusted variables for the evaluation of the association between serum copeptin levels and TFS in patients with CLD. In terms of quality, the study was scored using the Newcastle-Ottawa Scale[18] based on the criteria for participant selection, the comparability of the groups, and the validity of the outcomes. There were nine stars on the scale, with a larger number of stars representing a higher quality study.

Statistics

Risk ratios (RRs) and corresponding 95% confidence interval (CI) were used as the variables to indicate the association between serum concentration of copeptin and the survival of patients with CLD. A logarithmical transformation was performed on the RR and its corresponding standard error from each study to stabilize and normalize its variance[19]. In order to estimate between-study heterogeneity, the Cochrane Q test and the I^2 statistic[20] were used. An $I^2 > 50\%$ indicates that there is significant heterogeneity between studies. The utilization of a random-effects model was employed to amalgamate the findings, as it has been acknowledged to encompass the impact of potential heterogeneity[17]. In order to assess the impact of individual studies on the meta-analysis outcomes, sensitivity analyses were conducted by eliminating one dataset at a time[21]. To ascertain the effect of study characteristics on the outcome, subgroup analyses were executed based on the study country, design, patient diagnosis, cutoffs of copeptin, follow-up duration, and study quality scores. The subgroups were defined based on the medians of continuous variables. A funnel plot was used to estimate publication bias based on visual judgments of symmetry, along with Egger's regression asymmetry test[22]. The statistical analyses were carried out with RevMan (Version 5.1; Cochrane Collaboration, Oxford, United Kingdom) and Stata software (version 12.0; Stata Corporation, College Station, TX, United States).

RESULTS

Database search and study retrieval

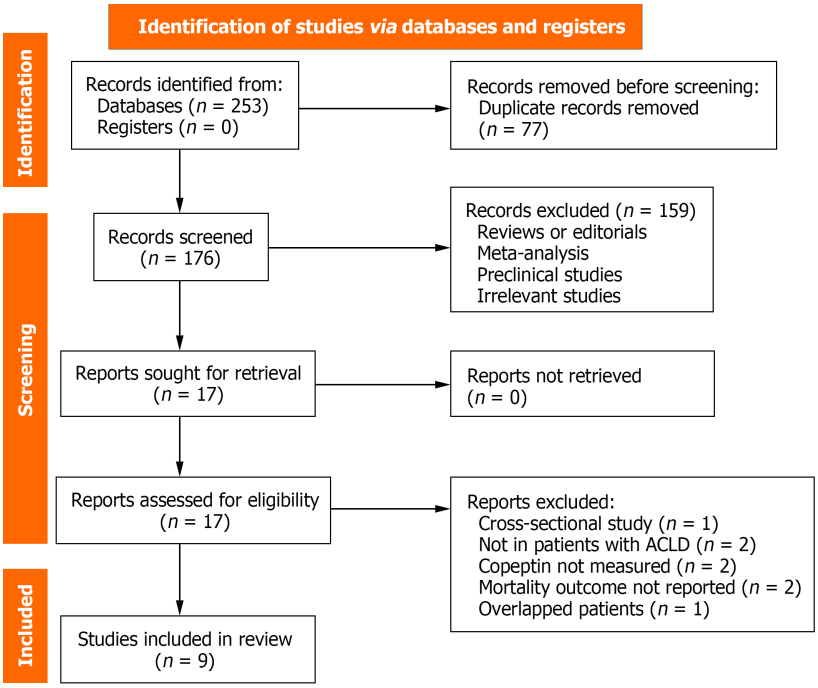
Figure 1 shows the process of the literature search and study retrieval. Initially, 253 records were obtained from the database, and 77 duplicate entries were removed. After screening the titles and abstracts, a further 159 studies were removed as they did not fit the meta-analysis' objectives. Following full-text reviews of 17 studies, eight were excluded because of the reasons listed in Figure 1. Accordingly, 9 studies were obtained for subsequent meta-analysis[23-31].

Study characteristics

One of the studies reported two datasets from two cohort studies[26], and these datasets were independently incorporated into the meta-analysis. Overall, ten datasets from nine cohort studies[23-31], which included 3133 patients with CLD, were used for the meta-analysis. The characteristics of the included studies are summarized in Table 1. These studies were published between 2013 and 2021, and performed in European and Asian countries. As for the study design, four cohorts were prospective[23,25,26,29], and six were retrospective[24,26-28,30,31]. Patients with cirrhosis were included in six cohorts of the included studies[23-27], while patients with various CLD were included in the other four cohorts[28-31]. The mean ages of the patients were 49.0 years to 67.3 years, and the proportions of men were 58.2% to 83.4%. Serum copeptin was measured with the Kryptor immunoassay in eight cohorts[23-28,30], while other methods such as enzyme-linked immunosorbent assay and the automated copeptin immunofluorescent assay were used in the other two studies[29,31]. A high serum level of copeptin was defined according to receiver operating characteristic analysis in four cohorts[24,25,27,31], medians in three cohorts[26,29], tertiles in two cohorts[23,28], and the upper limit of normal level in one cohort[30]. The follow-up durations were 1 mo to 48 mo (mean: 12.5 mo). Multivariate regression analyses were applied in all of the included studies when the association between serum copeptin and TFS of patients with CLD were estimated, and factors including age, sex, and scores for hepatic dysfunction were adjusted, such as the Child-Pugh score, the Model for End-Stage Liver Disease score, and the albumin-bilirubin score. Among the included studies, all had quality scores between seven and nine stars, indicating that they were of good quality (Table 2).

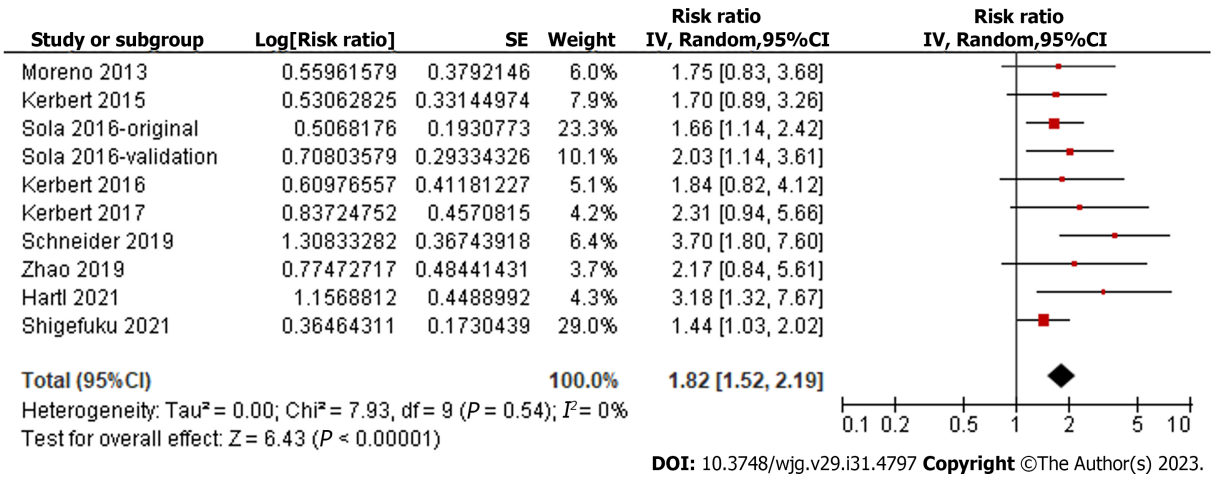
Meta-analysis results

Overall, pooled results of ten datasets from nine cohort studies showed that a high level of serum copeptin at baseline was associated with a poor TFS (RR: 1.82, 95%CI: 1.52-2.19, $P < 0.001$; Figure 2) with no evidence of significant heterogeneity (P for Cochrane Q test = 0.54, $I^2 = 0\%$). In addition, sensitivity analysis by omitting one dataset at a time showed consistent results (RR: 1.73-2.00, $P < 0.05$). Finally, subgroup analyses showed that the association between serum



DOI: 10.3748/wjg.v29.i31.4797 **Copyright** ©The Author(s) 2023.

Figure 1 Flowchart of database search and study inclusion. ACLD: Advanced chronic liver diseases.



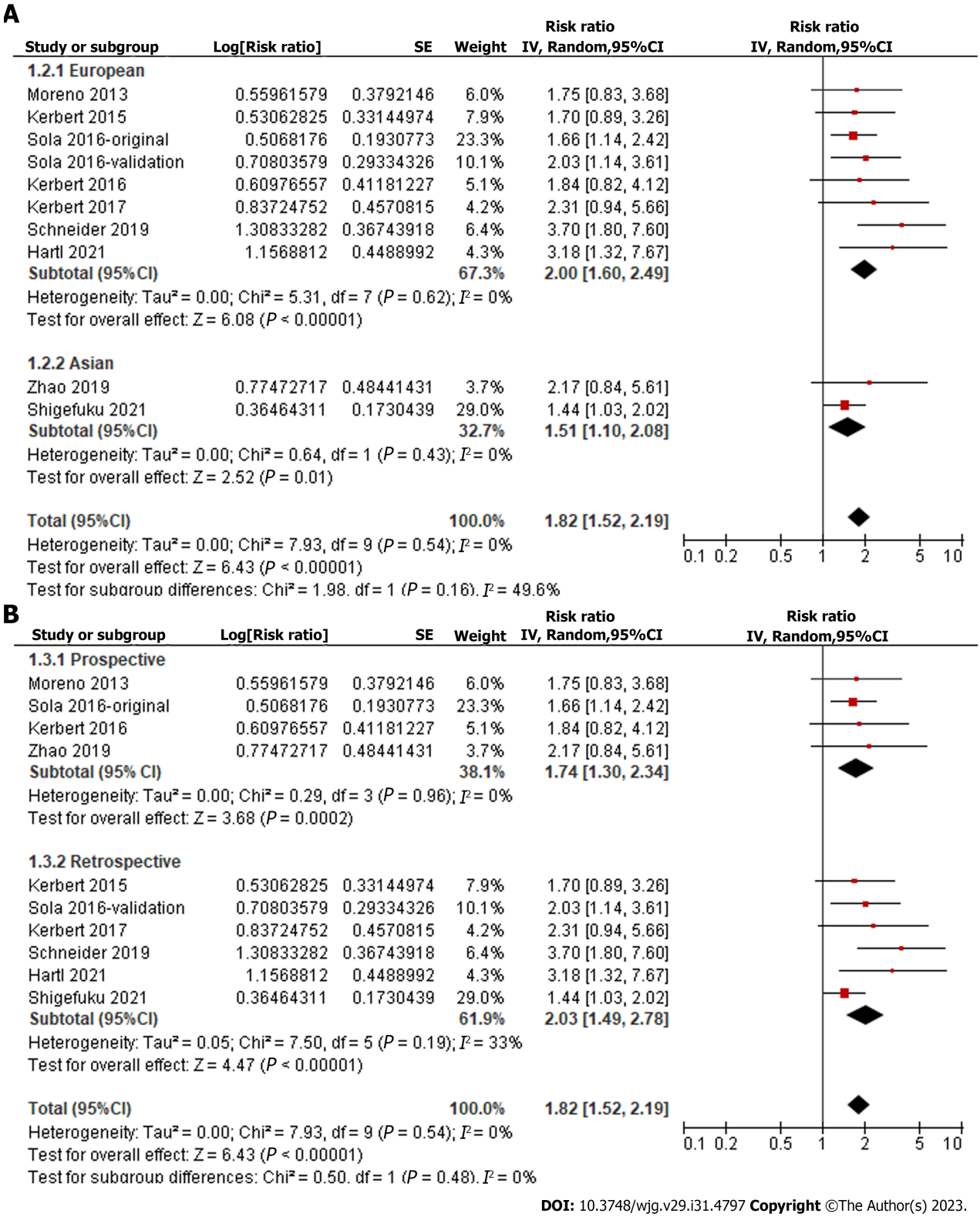
DOI: 10.3748/wjg.v29.i31.4797 **Copyright** ©The Author(s) 2023.

Figure 2 Forest plots for the overall meta-analyses regarding the association between serum copeptin and transplant-free survival of patients with chronic liver diseases. 95%CI: 95% confidence interval.

copeptin and poor TFS was consistent between European and Asian studies (*P* for subgroup difference = 0.16, Figure 3A), between prospective and retrospective cohorts (*P* for subgroup difference = 0.48, Figure 3B), between studies of patients with cirrhosis and all CLD (*P* for subgroup difference = 0.42, Figure 4A), between studies with cutoffs for copeptin < and ≥ 15 pmol/L (P for subgroup difference = 0.17, Figure 4B), between studies with mean follow-up durations < and ≥ 1 year (*P* for subgroup difference = 0.29, Figure 5A), and between studies with different quality scores (*P* for subgroup difference = 0.14, Figure 5B).

Publication bias

The funnel plots for the meta-analysis of the association between copeptin and TFS in patients with CLD are shown in Figure 6. Based on visual examination, the plots are symmetrical, suggesting that publication bias is low. Additionally, Egger's regression tests indicated a low likelihood of publication bias (*P* = 0.47).



DOI: 10.3748/wjg.v29.i31.4797 **Copyright** ©The Author(s) 2023.

Figure 3 Forest plots for the subgroup analyses regarding the association between serum copeptin and transplant-free survival of patients with chronic liver diseases. A: subgroup analysis according to study country; B: Subgroup analysis according to study design. 95%CI: 95% confidence interval.

DISCUSSION

This systematic review and meta-analysis synthesized data from ten cohort studies to investigate the association between serum copeptin concentration and poor TFS in patients with CLD. Our findings indicate that patients with a high serum copeptin level at baseline are at a greater risk of experiencing poor TFS during follow-up, compared to those with a low serum copeptin concentration. The robustness of our results was confirmed through sensitivity analyses that excluded

Table 1 Characteristics of the included studies

Ref.	Country	Design	Diagnosis	Patient number	Mean age (yr)	Male (%)	CP class C (%)	Methods for copeptin measuring	Copeptin analysis	Median follow-up duration (mo)	Variables adjusted
Moreno *et al*[23], 2013	France	PC	Cirrhosis (alcohol 84.2%)	125	58	69	33.7	Kryptor immunoassay	13 pmol/L, T3:T1-2	11	Age, sex, CP Class, and CRP
Kerbert *et al*[24], 2015	The Netherlands	RC	Cirrhosis (alcohol 34.4%, viral 18%)	61	54	75.4	31.1	Kryptor immunoassay	21.9 pmol/L, ROC analysis	12	Age, sex, and MELD score
Sola 2016-original	Spain	PC	Cirrhosis (alcohol 43%, HCV 34%)	265	60	66	NR	Kryptor immunoassay	14 pmol/L, median	3	Age, sex, MELD score, and leukocyte count
Sola 2016-validation	Multiple European countries	RC	Cirrhosis (alcohol 51%, HCV 19%)	120	57	72	NR	Kryptor immunoassay	19 pmol/L, median	3	Age, sex, and MELD score
Kerbert *et al*[25], 2016	The Netherlands and France	PC	Cirrhosis (alcohol 70.1%, viral 11.4%)	184	55.7	70.7	21.2	Kryptor immunoassay	12.3 pmol/L, ROC analysis	12	Age, sex, CP class, and CRP
Kerbert *et al*[27], 2017	Multiple European countries	RC	Acute decompensated cirrhosis (alcohol 61%, HCV 31.9%, and HBV 5.7%)	779	58	65.7	NR	Kryptor immunoassay	13.6 pmol/L, ROC analysis	3	Age, sex, WBC, sodium, and MELD score
Schneider *et al*[28], 2019	Germany	RC	End-stage liver disease (alcohol 63.4%, viral 8.5%)	615	57.2	61.9	NR	Kryptor immunoassay	16.3 pmol/L, T3:T1-2	9.3	Age, sex, and MELD-Na score
Zhao *et al* [29], 2019	China	PC	HBV related ACLF	151	49	83.4	NR	ELISA	18.7 pmol/L, median	1	Age, sex, and MELD score
Hartl *et al* [30], 2021	Austria	RC	ACLD (alcohol 36.2%, viral 35.9%)	663	56.6	68.2	16.5	Kryptor immunoassay	11.4 pmol/L, ULN	26.2	Age, sex, MELD score, HVPG, albumin, sodium, and presence of HCC
Shigefuku *et al*[36], 2021	Japan	RC	CLD (alcohol 45.9%, viral 57.0%), cirrhosis 66.5%	170	67.3	58.2	NR	Automated copeptin immuno-fluorescent assay	4.8 pmol/L, ROC analysis	48	Age, sex, eGFR, ALBI score, and presence of HCC

CP: Child-Pugh; PC: Prospective cohort; RC: Retrospective cohort; HBV: Hepatitis B virus; HCV: Hepatitis C virus; ACLF: Acute-on-chronic liver failure; ACLD: Advanced chronic liver diseases; CLD: Chronic liver diseases; NR: Not Reported; ELISA: Enzyme-linked immunosorbent assay; T: Tertile; ROC: Receiver operating characteristic; ULN: Upper limit of normal; CRP: C-reactive protein; MELD: Model for end-stage liver disease; WBC: White blood cell; HVPG: Hepatic venous pressure gradient; HCC: Hepatocellular carcinoma; ALBI: Albumin-bilirubin; eGFR: Estimated glomerular infiltrating rate.

individual datasets and subgroup analyses based on various study characteristics, including country, design, patient diagnosis, copeptin cutoffs, follow-up duration, and study quality scores. These findings demonstrate that a high serum copeptin level may be a useful index which is associated with poor prognosis for patients with CLD.

To the best of our knowledge, this is the first meta-analysis investigating the potential role of serum copeptin concentration as a prognostic factor of patients with CLD. Several advantages in meta-analysis methodologies deserve to be noticed. For example, we performed a comprehensive literature search in four commonly used databases, which could provide current evidence regarding the relationship of serum copeptin and TFS of patients with CLD. Furthermore, it is noteworthy that all of the studies incorporated in this analysis were cohort studies, implying a potential longitudinal correlation between elevated serum copeptin levels and diminished transplant-free survival among individuals with

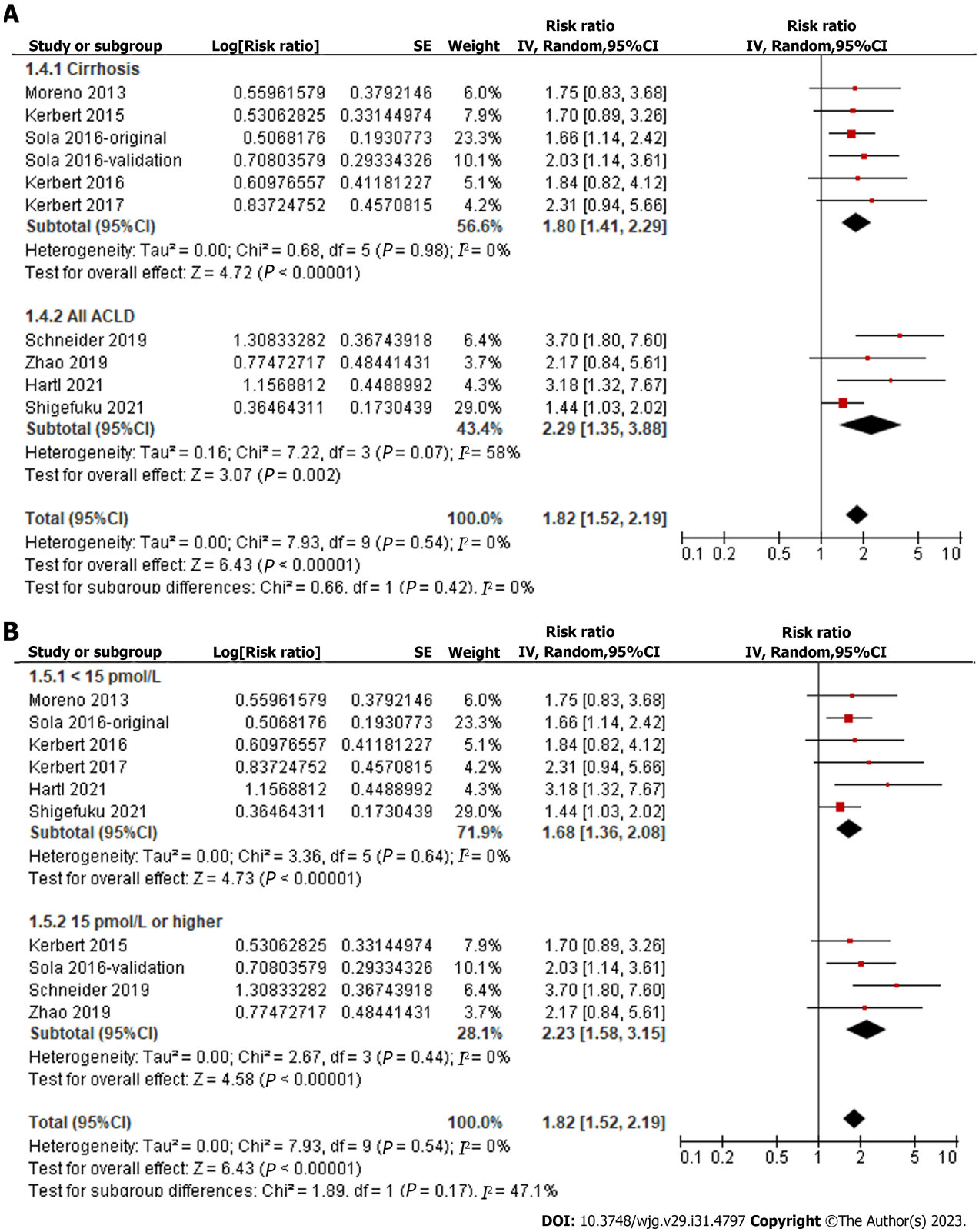
Table 2 Quality evaluation of the included studies *via* the Newcastle-Ottawa scale

Ref.	Representativeness of the exposed cohort	Selection of the non-exposed cohort	Ascertainment of exposure	Outcome not present at baseline	Control for age and sex	Control for other confounding factors	Assessment of outcome	Suitable follow-up duration	Adequacy of follow-up of cohorts	Total
Moreno *et al*[23], 2013	1	1	1	1	1	1	1	0	1	8
Kerbert *et al*[24], 2015	0	1	1	1	1	1	1	1	1	8
Sola 2016-original	1	1	1	1	1	1	1	0	1	8
Sola 2016-validation	0	1	1	1	1	1	1	0	1	7
Kerbert *et al*[25], 2016	1	1	1	1	1	1	1	1	1	9
Kerbert *et al*[27], 2017	0	1	1	1	1	1	1	0	1	7
Schneider *et al*[28], 2019	0	1	1	1	1	1	1	0	1	7
Zhao *et al* [29], 2019	1	1	1	1	1	1	1	0	1	8
Hartl *et al* [30], 2021	0	1	1	1	1	1	1	1	1	8
Shigefuku *et al*[36], 2021	1	1	1	1	1	1	1	1	1	9

CLD. Additionally, the utilization of multivariate regression analysis in all of the studies included in this review indicates that the relationship between heightened serum copeptin levels and reduced TFS in this population may be autonomous of potential confounding factors, such as age, gender, and hepatic dysfunction scores. Ultimately, multiple sensitivity and subgroup analyses were executed, and the uniform outcomes reinforced the durability and stability of the conclusions. Collectively, these conclusions substantiate that elevated serum levels of copeptin in individuals with CLD may serve as an indicator of unfavorable prognosis.

There may be multiple mechanisms underlying the relationship between a high serum copeptin level and a poor survival outcome in patients with CLD. Previous studies have shown that a high copeptin level in patients with cirrhosis was correlated to the risk of various complications that may lead to a poor prognosis of these patients, such as gastrointestinal hemorrhage due to portal hypertension, hepatorenal syndrome, hepatic encephalopathy, and larger amounts of ascites[32,33]. Pathophysiologically, as a surrogate marker of AVP, increased copeptin may reflect the enhanced systemic release of AVP in these patients[34]. A high AVP in patients with cirrhosis may deteriorate the status of vasoconstriction, water retention, and hyponatremia, which have all been recognized as key risk factors for poor survival of these patients[35]. The role of copeptin in the pathogenesis and progression of CLD should be further investigated, either as a simple biomarker or an active participant in the disease.

This study is subject to certain limitations. Firstly, the meta-analysis results were predominantly influenced by studies involving patients with ACLD, including those with decompensated cirrhosis and other end-stage liver diseases. The efficacy of copeptin as a prognostic factor in patients with early CLD requires further validation in future research. Additionally, despite the utilization of multivariate regression analyses across all the studies included, the potential for residual factors to confound the association between copeptin and TFS cannot be entirely ruled out. For example, serum copeptin may predict the response to tolvaptan in patients with decompensated cirrhosis[36]. Accordingly, use of treatments such as tolvaptan may confound the association between copeptin and TFS. Furthermore, the determination of an optimal serum copeptin cutoff for predicting the survival of patients with CLD remains elusive, necessitating further investigation. Moreover, the absence of a causal association between elevated copeptin levels and unfavorable TFS in CLD patients is attributable to the reliance on observational studies in the meta-analysis.

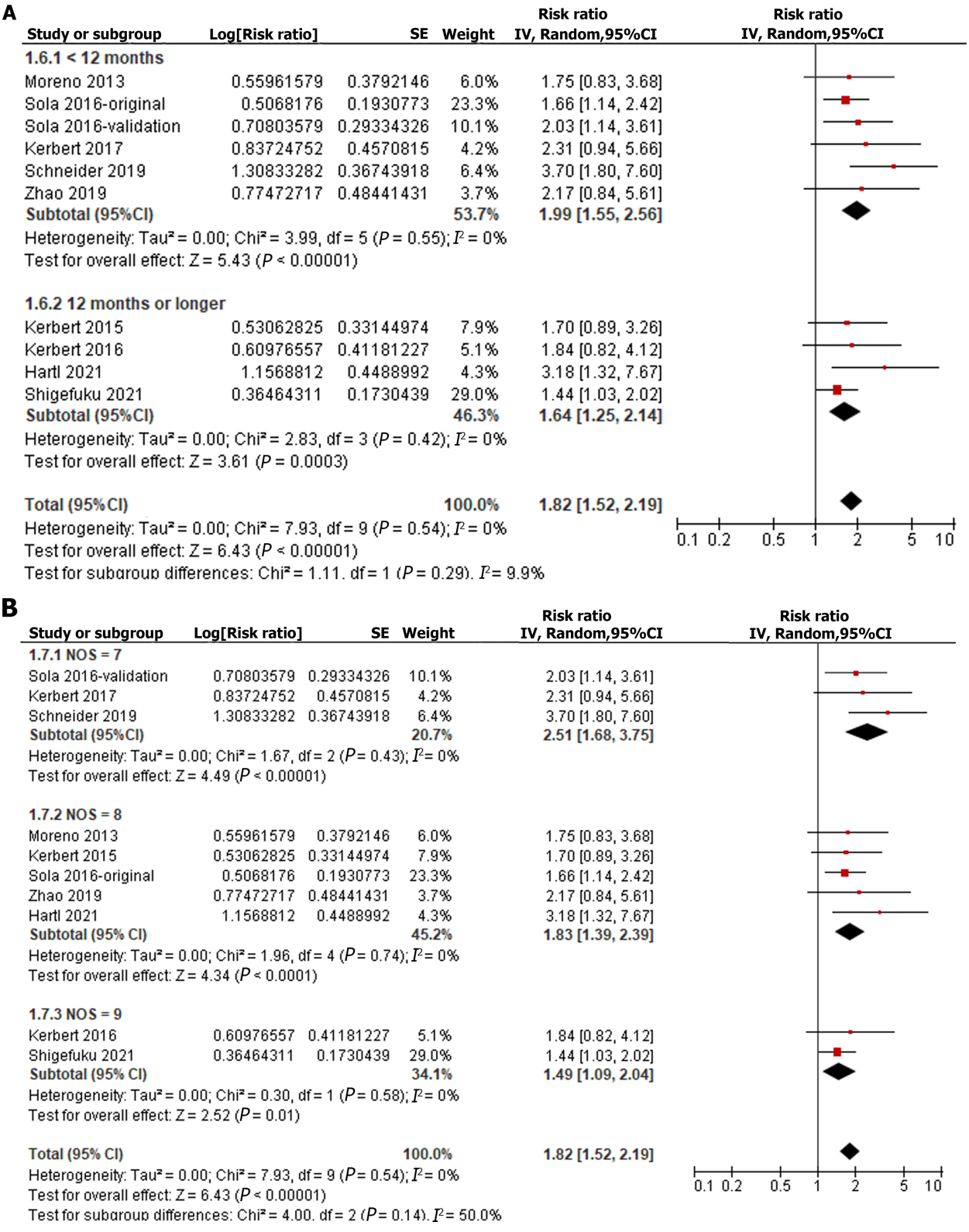


DOI: 10.3748/wjg.v29.i31.4797 **Copyright** ©The Author(s) 2023.

Figure 4 Forest plots for the subgroup analyses regarding the association between serum copeptin and transplant-free survival of patients with chronic liver diseases. A: Subgroup analysis according to the diagnosis of the patients; B: Subgroup analysis according to the cutoffs of serum copeptin. 95%CI: 95% confidence interval.

CONCLUSION

The findings of the meta-analysis indicate that an elevated serum copeptin concentration in individuals with CLD is linked to unfavorable TFS. The assessment of serum copeptin levels may hold significance in the stratification of risk among CLD patients. Furthermore, it is imperative to investigate whether the reduction of copeptin levels in these patients is correlated with a better clinical outcome, particularly in those with ACLD.



DOI: 10.3748/wjg.v29.i31.4797 **Copyright** ©The Author(s) 2023.

Figure 5 Forest plots for the subgroup analyses regarding the association between serum copeptin and transplant-free survival of patients with chronic liver diseases. A: Subgroup analysis according to the follow-up durations; B: Subgroup analysis according to the study quality scores. 95%CI: 95% confidence interval.

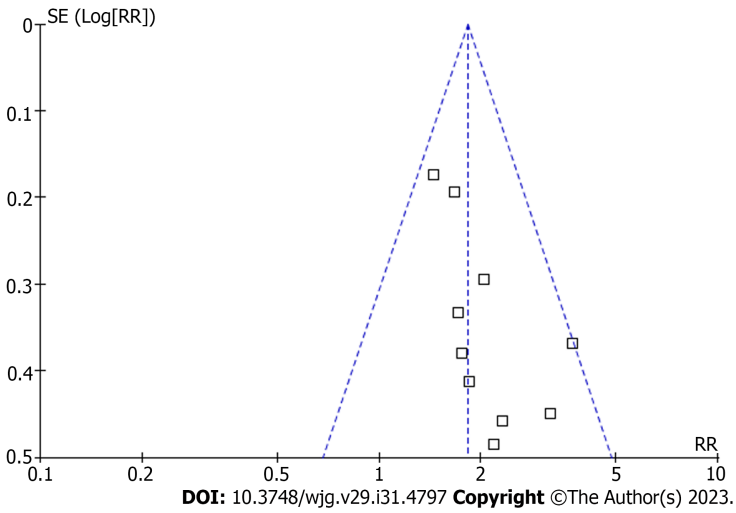


Figure 6 Funnel plots for the publication bias underlying the meta-analysis regarding the association between serum copeptin and transplant-free survival of patients with chronic liver diseases. RR: Risk ratio.

ARTICLE HIGHLIGHTS

Research background

Patients with chronic liver disease (CLD) will develop various complications with the progression of the disease. Upregulated systemic arginine vasopressin (AVP) has been observed in patients with advanced CLD. However, measuring AVP is clinically challenging due to the short half-life. Copeptin is a C-terminus of AVP precursor, which may be of importance for prognostic prediction in patients with CLD.

Research motivation

Identifying biomarkers that predict the prognosis of patients with CLD is clinically important. Although there are pilot studies aiming to correlate copeptin with survival of patients with CLD, the results are not always consistent. In this regard, a systematic review with meta-analysis is particularly useful.

Research objectives

To investigate the correlation between serum copeptin and transplant-free survival (TFS) in patients with CLD with a systematic review and meta-analysis.

Research methods

Studies were obtained by search of PubMed, Embase, the Cochrane Library, and Web of Science. Two authors independently screened the studies, assessed the study quality with Newcastle-Ottawa Scale, and extracted the data. Risk ratios and corresponding 95% confidence intervals were used as the variables to indicate the association between serum concentration of copeptin and the survival of patients with CLD. The RevMan and Stata software were used for the statistical analyses.

Research results

This meta-analysis enrolled ten datasets involving 3133 patients, who were followed for 1 to 48 mo (mean: 12.5 mo). We found that a high level of serum copeptin was associated with a poor TFS, with a risk ratio of 1.82. Additionally, sensitivity analysis retrieved similar results by omitting one dataset at a time. The robustness of the finding was further evidenced by consistent results of subgroup analyses according to study country, study design, patient diagnosis, cutoff of copeptin, follow-up duration, and study quality score.

Research conclusions

High serum concentration of copeptin may be associated with a poor clinical prognosis in patients with CLD. These findings were not significantly affected by either of the included studies and were not influenced by multiple study characteristics within the subgroup analysis.

Research perspectives

In view of the standard methods for the measuring copeptin in clinical practice, as well as the finding of the meta-analysis, evaluating serum copeptin may be considered at the initial management of patients with CLD, which may provide prognostic significance.

FOOTNOTES

Author contributions: Tan HQ and Liu JY conceived and designed the study; Tan HQ, Zhao M, Huang Z, and Liu Y performed database search, data collection, and study quality evaluation; Tan HQ, Li H, and Ma LH performed statistical analysis; Tan HQ, Zhao M, Huang Z, and Liu JY interpreted the results; Tan HQ wrote the initial draft; all authors revised the manuscript, read and approved the final version of the manuscript.

Conflict-of-interest statement: The authors have no conflicts of interest to declare.

PRISMA 2009 Checklist statement: The authors have read the PRISMA 2009 Checklist, and the manuscript was prepared and revised according to the PRISMA 2009 Checklist.

Open-Access: This article is an open-access article that was selected by an in-house editor and fully peer-reviewed by external reviewers. It is distributed in accordance with the Creative Commons Attribution NonCommercial (CC BY-NC 4.0) license, which permits others to distribute, remix, adapt, build upon this work non-commercially, and license their derivative works on different terms, provided the original work is properly cited and the use is non-commercial. See: https://creativecommons.org/Licenses/by-nc/4.0/

Country/Territory of origin: China

ORCID number: Hao-Qian Tan 0000-0001-5349-0507; Ming Zhao 0009-0005-8792-0612; Zan Huang 0009-0000-6942-212X; Yang Liu 0009-0003-8587-2800; Han Li 0009-0001-6171-8783; Long-Hui Ma 0009-0003-4569-2346; Jun-Ying Liu 0009-0002-8058-6197.

S-Editor: Chen YL
L-Editor: A
P-Editor: Cai YX

REFERENCES

1 **Br VK**, Sarin SK. Acute-on-chronic liver failure: Terminology, mechanisms and management. *Clin Mol Hepatol* 2023; **29**: 670-689 [PMID: 36938601 DOI: 10.3350/cmh.2022.0103]
2 **Huang DQ**, Terrault NA, Tacke F, Gluud LL, Arrese M, Bugianesi E, Loomba R. Global epidemiology of cirrhosis - aetiology, trends and predictions. *Nat Rev Gastroenterol Hepatol* 2023; **20**: 388-398 [PMID: 36977794 DOI: 10.1038/s41575-023-00759-2]
3 **Moon AM**, Singal AG, Tapper EB. Contemporary Epidemiology of Chronic Liver Disease and Cirrhosis. *Clin Gastroenterol Hepatol* 2020; **18**: 2650-2666 [PMID: 31401364 DOI: 10.1016/j.cgh.2019.07.060]
4 **Younossi ZM**, Wong G, Anstee QM, Henry L. The Global Burden of Liver Disease. *Clin Gastroenterol Hepatol* 2023; **21**: 1978-1991 [PMID: 37121527 DOI: 10.1016/j.cgh.2023.04.015]
5 **Engelmann C**, Clària J, Szabo G, Bosch J, Bernardi M. Pathophysiology of decompensated cirrhosis: Portal hypertension, circulatory dysfunction, inflammation, metabolism and mitochondrial dysfunction. *J Hepatol* 2021; **75** Suppl 1: S49-S66 [PMID: 34039492 DOI: 10.1016/j.jhep.2021.01.002]
6 **Møller S**, Bendtsen F. The pathophysiology of arterial vasodilatation and hyperdynamic circulation in cirrhosis. *Liver Int* 2018; **38**: 570-580 [PMID: 28921803 DOI: 10.1111/liv.13589]
7 **Tapper EB**, Parikh ND. Diagnosis and Management of Cirrhosis and Its Complications: A Review. *JAMA* 2023; **329**: 1589-1602 [PMID: 37159031 DOI: 10.1001/jama.2023.5997]
8 **Wagener G**, Bakker J. Vasopressin in cirrhosis and sepsis: physiology and clinical implications. *Minerva Anestesiol* 2015; **81**: 1377-1383 [PMID: 25384691]
9 **Rondon-Berrios H**, Velez JCQ. Hyponatremia in Cirrhosis. *Clin Liver Dis* 2022; **26**: 149-164 [PMID: 35487602 DOI: 10.1016/j.cld.2022.01.001]
10 **Leng G**, Sabatier N. Measuring Oxytocin and Vasopressin: Bioassays, Immunoassays and Random Numbers. *J Neuroendocrinol* 2016; **28** [PMID: 27467712 DOI: 10.1111/jne.12413]
11 **Bankir L**, Bichet DG, Morgenthaler NG. Vasopressin: physiology, assessment and osmosensation. *J Intern Med* 2017; **282**: 284-297 [PMID: 28649750 DOI: 10.1111/joim.12645]
12 **Szmygin H**, Szydełko J, Matyjaszek-Matuszek B. Copeptin as a novel biomarker of cardiometabolic syndrome. *Endokrynol Pol* 2021; **72**: 566-571 [PMID: 34378786 DOI: 10.5603/EP.a2021.0072]
13 **Di Martino V**, Weil D, Cervoni JP, Thevenot T. New prognostic markers in liver cirrhosis. *World J Hepatol* 2015; **7**: 1244-1250 [PMID: 26019739 DOI: 10.4254/wjh.v7.i9.1244]
14 **Mookerjee RP**. Prognosis and Biomarkers in Acute-on-Chronic Liver Failure. *Semin Liver Dis* 2016; **36**: 127-132 [PMID: 27172354 DOI: 10.1055/s-0036-1583200]
15 **Page MJ**, Moher D, Bossuyt PM, Boutron I, Hoffmann TC, Mulrow CD, Shamseer L, Tetzlaff JM, Akl EA, Brennan SE, Chou R, Glanville J, Grimshaw JM, Hróbjartsson A, Lalu MM, Li T, Loder EW, Mayo-Wilson E, McDonald S, McGuinness LA, Stewart LA, Thomas J, Tricco AC, Welch VA, Whiting P, McKenzie JE. PRISMA 2020 explanation and elaboration: updated guidance and exemplars for reporting systematic reviews. *BMJ* 2021; **372**: n160 [PMID: 33781993 DOI: 10.1136/bmj.n160]
16 **Page MJ**, McKenzie JE, Bossuyt PM, Boutron I, Hoffmann TC, Mulrow CD, Shamseer L, Tetzlaff JM, Akl EA, Brennan SE, Chou R, Glanville J, Grimshaw JM, Hróbjartsson A, Lalu MM, Li T, Loder EW, Mayo-Wilson E, McDonald S, McGuinness LA, Stewart LA, Thomas J, Tricco AC, Welch VA, Whiting P, Moher D. The PRISMA 2020 statement: an updated guideline for reporting systematic reviews. *BMJ* 2021; **372**: n71 [PMID: 33782057 DOI: 10.1136/bmj.n71]
17 **Higgins J**, Thomas J, Chandler J, Cumpston M, Li T, Page M, Welch V. Cochrane Handbook for Systematic Reviews of Interventions version 6.2. 2021. [cited 5 July 2023]. Available from: https://training.cochrane.org/handbook

18 **Wells GA**, Shea B, O'Connell D, Peterson J, Welch V, Losos M, Tugwell P. The Newcastle-Ottawa Scale (NOS) for assessing the quality of nonrandomised studies in meta-analyses. 2010. [cited 5 July 2023]. Available from: https://www.semanticscholar.org/paper/The-Newcastle-Ottawa-Scale-(NOS)-for-Assessing-the-Wells-Wells/c293fb316b6176154c3fdbb8340a107d9c8c82bf

19 **Higgins J**, Green S. Cochrane Handbook for Systematic Reviews of Interventions Version 5.1.0. 2011. [cited 5 July 2023]. Available from: http://handbook-5-1.cochrane.org/

20 **Higgins JP**, Thompson SG. Quantifying heterogeneity in a meta-analysis. *Stat Med* 2002; **21**: 1539-1558 [PMID: 12111919 DOI: 10.1002/sim.1186]

21 **Patsopoulos NA**, Evangelou E, Ioannidis JP. Sensitivity of between-study heterogeneity in meta-analysis: proposed metrics and empirical evaluation. *Int J Epidemiol* 2008; **37**: 1148-1157 [PMID: 18424475 DOI: 10.1093/ije/dyn065]

22 **Egger M**, Davey Smith G, Schneider M, Minder C. Bias in meta-analysis detected by a simple, graphical test. *BMJ* 1997; **315**: 629-634 [PMID: 9310563]

23 **Moreno JP**, Grandclement E, Monnet E, Clerc B, Agin A, Cervoni JP, Richou C, Vanlemmens C, Dritsas S, Dumoulin G, Di Martino V, Thevenot T. Plasma copeptin, a possible prognostic marker in cirrhosis. *Liver Int* 2013; **33**: 843-851 [PMID: 23560938 DOI: 10.1111/liv.12175]

24 **Kerbert AJ**, Verbeke L, Chiang FW, Laleman W, van der Reijden JJ, van Duijn W, Nevens F, Wolterbeek R, van Hoek B, Verspaget HW, Coenraad MJ. Copeptin as an Indicator of Hemodynamic Derangement and Prognosis in Liver Cirrhosis. *PLoS One* 2015; **10**: e0138264 [PMID: 26378453 DOI: 10.1371/journal.pone.0138264]

25 **Kerbert AJ**, Weil D, Verspaget HW, Moréno JP, van Hoek B, Cervoni JP, Di Martino V, Coenraad MJ, Thevenot T. Copeptin is an independent prognostic factor for transplant-free survival in cirrhosis. *Liver Int* 2016; **36**: 530-537 [PMID: 26502363 DOI: 10.1111/liv.12992]

26 **Solà E**, Kerbert AJ, Verspaget HW, Moreira R, Pose E, Ruiz P, Cela R, Morales-Ruiz M, López E, Graupera I, Solé C, Huelin P, Navarro AA, Ariza X, Jalan R, Fabrellas N, Benten D, de Prada G, Durand F, Jimenez W, van der Reijden JJ, Fernandez J, van Hoek B, Coenraad MJ, Ginès P. Plasma copeptin as biomarker of disease progression and prognosis in cirrhosis. *J Hepatol* 2016; **65**: 914-920 [PMID: 27422752 DOI: 10.1016/j.jhep.2016.07.003]

27 **Kerbert AJC**, Verspaget HW, Navarro ÀA, Jalan R, Solà E, Benten D, Durand F, Ginès P, van der Reijden JJ, van Hoek B, Coenraad MJ; CANONIC Study Investigators of the EASL-CLIF Consortium. Copeptin in acute decompensation of liver cirrhosis: relationship with acute-on-chronic liver failure and short-term survival. *Crit Care* 2017; **21**: 321 [PMID: 29268760 DOI: 10.1186/s13054-017-1894-8]

28 **Schneider C**, Remmler J, Netto J, Seehofer D, Engelmann C, Berg T, Thiery J, Kaiser T. Copeptin - a biomarker of short-term mortality risk (7 days) in patients with end-stage liver disease. *Clin Chem Lab Med* 2019; **57**: 1897-1905 [PMID: 31199758 DOI: 10.1515/cclm-2019-0023]

29 **Zhao R**, Wu W, Zhou Z, Zheng X, Sun W, Shi Y, Yu H, Wang F, Zhao H, Sun S, Jin L, Sheng J. Prognostic utility of novel biomarkers in acute-on-chronic liver failure (ACLF) associated with hepatitis B: A multicenter prospective study. *Hepatol Res* 2019; **49**: 42-50 [PMID: 30246902 DOI: 10.1111/hepr.13251]

30 **Hartl L**, Jachs M, Desbalmes C, Schaufler D, Simbrunner B, Paternostro R, Schwabl P, Bauer DJM, Semmler G, Scheiner B, Bucsics T, Eigenbauer E, Marculescu R, Szekeres T, Peck-Radosavljevic M, Kastl S, Trauner M, Mandorfer M, Reiberger T. The differential activation of cardiovascular hormones across distinct stages of portal hypertension predicts clinical outcomes. *Hepatol Int* 2021; **15**: 1160-1173 [PMID: 34021479 DOI: 10.1007/s12072-021-10203-9]

31 **Shigefuku R**, Iwasa M, Eguchi A, Tamai Y, Yoshikawa K, Sugimoto R, Takei Y. Serum copeptin level is a biomarker associated with ascites retention and the formation of a portosystemic shunt in chronic liver disease. *J Gastroenterol Hepatol* 2021; **36**: 1006-1014 [PMID: 32790956 DOI: 10.1111/jgh.15215]

32 **Tawfik AK**, Helmy A, Yousef M, Abou-Saif S, Kobtan A, Asaad E, Abd-Elsalam S. Copeptin as a novel marker predicting prognosis of liver cirrhosis and its major complications. *Hepat Med* 2018; **10**: 87-93 [PMID: 30214326 DOI: 10.2147/HMER.S174267]

33 **Abudeif A**, Hashim MS, Ahmed NM, Ahmed AO. Serum copeptin is associated with major complications of liver cirrhosis and spontaneous bacterial peritonitis. *Clin Exp Hepatol* 2023; **9**: 71-78 [PMID: 37064833 DOI: 10.5114/ceh.2023.125970]

34 **Glavaš M**, Gitlin-Domagalska A, Dębowski D, Ptaszyńska N, Łęgowska A, Rolka K. Vasopressin and Its Analogues: From Natural Hormones to Multitasking Peptides. *Int J Mol Sci* 2022; **23** [PMID: 35328489 DOI: 10.3390/ijms23063068]

35 **Alukal JJ**, John S, Thuluvath PJ. Hyponatremia in Cirrhosis: An Update. *Am J Gastroenterol* 2020; **115**: 1775-1785 [PMID: 33156095 DOI: 10.14309/ajg.0000000000000786]

36 **Shigefuku R**, Iwasa M, Eguchi A, Tempaku M, Tamai Y, Suzuki T, Takei Y. Serum Copeptin and Zinc-α2-glycoprotein Levels Are Novel Biomarkers of Tolvaptan Treatment in Decompensated Cirrhotic Patients with Ascites. *Intern Med* 2021; **60**: 3359-3368 [PMID: 34719623 DOI: 10.2169/internalmedicine.7291-21]

World Journal of Gastroenterology

Submit a Manuscript: https://www.f6publishing.com

World J Gastroenterol 2023 August 21; 29(31): 4809-4814

DOI: 10.3748/wjg.v29.i31.4809

ISSN 1007-9327 (print) ISSN 2219-2840 (online)

CASE REPORT

Inherited CHEK2 p.H371Y mutation in solitary rectal ulcer syndrome among familial patients: A case report

Cheng-Cheng He, Shan-Ping Wang, Pei-Rong Zhou, Zhi-Jun Li, Na Li, Ming-Song Li

Specialty type: Gastroenterology and hepatology

Provenance and peer review: Unsolicited article; Externally peer reviewed.

Peer-review model: Single blind

Peer-review report's scientific quality classification

Grade A (Excellent): 0
Grade B (Very good): B
Grade C (Good): C, C
Grade D (Fair): 0
Grade E (Poor): 0

P-Reviewer: Choi YS, South Korea; Zamani M, Iran

Received: June 5, 2023
Peer-review started: June 5, 2023
First decision: July 7, 2023
Revised: July 18, 2023
Accepted: July 31, 2023
Article in press: July 31, 2023
Published online: August 21, 2023

Cheng-Cheng He, Shan-Ping Wang, Pei-Rong Zhou, Zhi-Jun Li, Na Li, Ming-Song Li, Department of Gastroenterology, The Third Affiliated Hospital of Guangzhou Medical University, Guangzhou 510150, Guangdong Province, China

Corresponding author: Ming-Song Li, MD, PhD, Chief Physician, Professor, Department of Gastroenterology, The Third Affiliated Hospital of Guangzhou Medical University, No. 63 Duobao Road, Liwan District, Guangzhou 510150, Guangdong Province, China.
2020683127@gzhmu.edu.cn

Abstract

BACKGROUND

Solitary rectal ulcer syndrome (SRUS) is a rare rectal disease with unknown etiology. Data on the genetic background in SRUS is lacking.

CASE SUMMARY

Here, we report the first case of SRUS in a mother-son relationship. Gene sequencing was conducted on the whole family, which revealed an inherited CHEK2 p.H371Y mutation. The experiment preliminarily revealed that the CHEK2 mutation did not affect the expression of CHEK2 protein, but affected the function of CHEK2, resulting in the expression level changes of downstream genes such as CDC25A.

CONCLUSION

SRUS is a genetic susceptibility disease where CHEK2 p.H371Y mutation may play a crucial role in the development and prognosis of SRUS.

Key Words: Solitary rectal ulcer syndrome; CHEK2 mutation; CDC25A; Genetic background; Gene sequencing; Case report

©The Author(s) 2023. Published by Baishideng Publishing Group Inc. All rights reserved.

Core Tip: Solitary rectal ulcer syndrome (SRUS) is a rare rectal disease with unknown etiology. Data on the genetic background in SRUS is lacking. Here, we present the first case of SRUS in a mother-son relationship. Gene sequencing and experiment preliminarily indicate that SRUS may serve as a genetic susceptibility disease in which CHEK2 p.H371Y mutation may play a crucial role in the development and prognosis of SRUS. This case may offer some new insights into the virulence genes and genetic background of SRUS.

Citation: He CC, Wang SP, Zhou PR, Li ZJ, Li N, Li MS. Inherited CHEK2 p.H371Y mutation in solitary rectal ulcer syndrome among familial patients: A case report. *World J Gastroenterol* 2023; 29(31): 4809-4814
URL: https://www.wjgnet.com/1007-9327/full/v29/i31/4809.htm
DOI: https://dx.doi.org/10.3748/wjg.v29.i31.4809

INTRODUCTION

Solitary rectal ulcer syndrome (SRUS) is a chronic rectal disease characterized by difficulty in defecation, mucous hematochezia, and anal pain, and bulging. SRUS is a rare disease with unknown etiology that was proposed by Rutter in 1975[1]. We have a detailed understanding of the clinical, endoscopy, pathology and images characteristics based on recent reports about SRUS, but data about the etiology, especially the virulence genes and genetic background, are limited[2,3]. Herein, we present the first case that describes a Chinese female patient with SRUS and one of her sons diagnosed with SRUS. Her daughter and the other son demonstrated healthy gastrointestinal tracts. Next-generation sequencing of family inheritance results indicated an inherited CHEK2 p.H371Y mutation may contributes to SRUS.

CASE PRESENTATION

Chief complaints

A 63-year-old female patient was admitted to the Third Affiliated Hospital of Guangzhou Medical University for abdominal pain, anal irritation, and repeated hematochezia. Her 31-year-old son was previously diagnosed with SRUS and underwent an inpatient examination.

History of present illness

Her symptoms started 1 year before the presentation of abdominal pain, anal irritation, and repeated hematochezia. Additionally, her 31-year-old son started to present with repeated diarrhea and intermittent hematochezia at the age of 26. He suffered from chronic diarrhea of up to 30 times a day, with the worst demonstrating fecal incontinence. He was subsequently diagnosed with SRUS 3 years ago and underwent surgical removal. The surgical pathology was consistent with the pathological features of SRUS (Supplementary Figure 1). Hematochezia disappeared postoperatively, but his diarrhea remained. Chronic diarrhea causes his anxiety because his symptoms worsen as his mood changed.

History of past illness

The patients were healthy before the SRUS incidence.

Personal and family history

The patient has two sons and one daughter. Notably, one of her sons was diagnosed with SRUS before her diagnosis and underwent partial rectal resection. The other son was healthy. Additionally, she and her son with SRUS like to eat mixed and coarse grains, and they have high-fiber eating habits and a sedentary lifestyle. Moreover, they are accustomed to squatting for a long time to defecate. Furthermore, they were healthy before the SRUS incidence, but are prone to anxious behaviors in life.

Physical examination

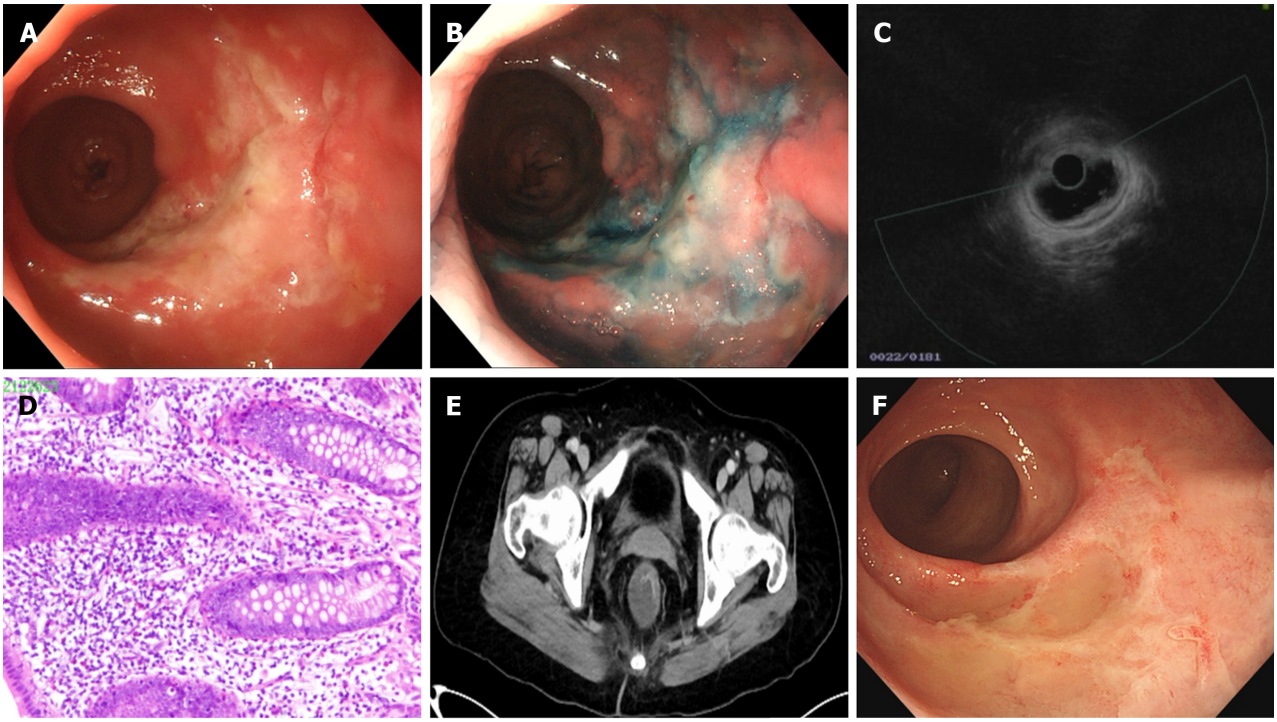
A physical examination upon admission revealed no obvious abnormality in both patients.

Laboratory examinations

Laboratory tests of the female patient revealed high triglyceride (2.11 mmol/L), while others were all within normal ranges. Further, Epstein-Barr virus, and cytomegalovirus were negative. Blood routine, coagulation function and autoimmune tests were within normal ranges. Additionally, laboratory tests of the male patient upon admission revealed no obvious abnormality.

Imaging examinations

Her total digestive tract endoscopy results revealed a rectal solitary ulcer (Figure 1A), the indicarmine dyeing demonstrated a clear boundary (Figure 1B), and pathological results indicated the fibrous tissue hyperplasia in the lamina



DOI: 10.3748/wjg.v29.i31.4809 **Copyright** ©The Author(s) 2023.

Figure 1 Clinical features of the female patient with solitary rectal ulcer syndrome. A: Colonoscopy image upon her admission; B: Chromoendoscopy result upon her admission using the Indicarmine dyeing; C: Ultrasonic endoscopy was used for solitary rectal ulcer observation; D: Pathological results of the solitary rectal ulcer; E: Imaging of the solitary rectal ulcer, using the intestine computed tomography enhancement; F: Colonoscopy image upon her reexamination after therapy.

propria layer as well as glands destruction (Figure 1D). Ultrasonic endoscopy revealed clearly demarcated mucosal layers, missing ulcerative mucosa and submucosa layers, and intact and thickened muscularis propria (Figure 1C). Moreover, the intestinal computed tomography enhancement revealed segmental rectal wall thickening (Figure 1E). The anorectal function test demonstrated a low resting pressure of the anal canal and normal contractile response and anorectal inhibition reflex but with increased anorectal sensitivity. Further, a colonoscopy of the male patient showed that the mucosa of his rectal anastomosis was smooth without any erosion or ulcer (Supplementary Figure 1).

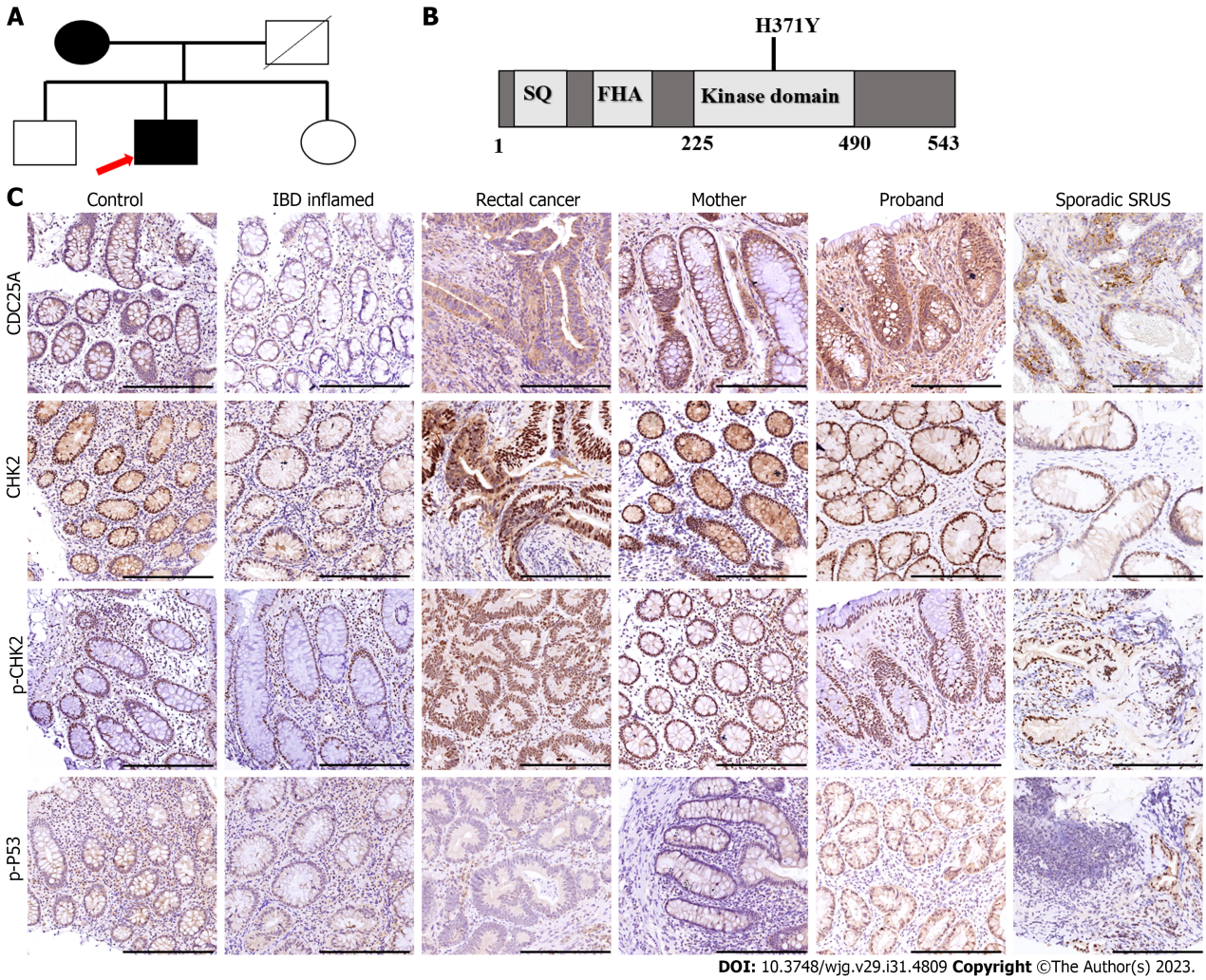
Further diagnostic work-up

Whereas their complicate family history and next-generation sequencing of heritage whole exome sequencing was then conducted with their consent. The results (Figure 2) exhibited a CHEK2 gene (c.1111C>T, p.His371Tyr) missense mutation in the patient and her son with SRUS, but not in the other son and the daughter. The CHEK2 p.H371Y mutation was reported as a kind of pathologic mutation[4]. Then we conduct the immunohistochemical staining (IHC) to analyze the expression and function of CHEK2 (Antibody: CHEK2, CST#3440, 1:1600; p-CHEK2, CST#82263, 1:500; CDC25A, CST#3652, 1:100; p-P53, CST#9287, 1:100), which revealed a normal CHEK2 protein level but an impaired downstream gene protein level. As shown in Figure 2, CHEK2 protein levels and autophosphorylation CHEK2 protein levels showed no significant difference among the healthy control, inflammatory bowel diseases, rectal cancer and SRUS groups (including familial and sporadic cases). In contrast, the downstream gene of CHEK2, such as CDC25A and p-P53 (Ser 20), exhibit differential expression among these groups. CDC25A and p-p53 protein expression levels were the highest and the lowest in the SRUS group, while the differences between the SRUS and rectal cancer groups do not reach significance.

The SRUS groups contain familial patients in our case and non-familial cases (sporadic cases). The IHC results revealed that the CHEK2 mutation did not affect the expression of CHEK2 protein whether in familial SRUS cases or sporadic SRUS cases, but it would affect CHEK2 functions to different degrees. CDC25A expression level variations are more significant in familial SRUS cases, while p-p53 expression level changes are more pronounced in sporadic SRUS cases.

FINAL DIAGNOSIS

Both patients with a mother-son relationship were diagnosed with SRUS based on the above-mentioned results.



DOI: 10.3748/wjg.v29.i31.4809 **Copyright** ©The Author(s) 2023.

Figure 2 Genetic background of the patients with solitary rectal ulcer syndrome patients in a mother-son relationship. A: Family tree of the familial patients with solitary rectal ulcer syndrome. Squares indicate male family members; circles indicate female family members; black indicate affected patients; white indicate healthy family members; slashes indicate deceased family members; arrow indicate the first diagnosed patient of the family; B: Schematic diagram of the CHEK2 protein; C: The differential expressions of CHEK2 and the downstream genes among the healthy control, and patients with inflammatory bowel diseases, rectal cancer, and solitary rectal ulcer syndrome, using the immunohistochemical staining; scale bars, 100 μm. IBD: Inflammatory bowel diseases; SRUS: Solitary rectal ulcer syndrome.

TREATMENT

SRUS treatment should be comprehensive and aimed at restoring the patient's normal bowel pattern, including behavior modification, medication, biofeedback, and surgery. Initially, we guided patient's lifestyles and eating habits and advised them to change their sedentary habits and appropriately reduce the amount of dietary fiber in their food. Simultaneously, we guided them to develop good defecation habits, avoid forceful defecation, set defecation time and body position, and artificially limit defecation frequency. Then, we provide psychological care to patients and encourage them to appropriately participate in social activities to vent their bad emotions. Concurrently, biofeedback, which can limit the change of toilet frequency in patients with frequent bowel movements, was recommended as an effective treatment. Biofeedback training can help resolve symptoms, especially in patients who remain symptomatic postoperatively. Finally, we advise patients to use thalidomide and mesalazine for rapid improvement of inflammation, considering the long medical history of the patient, especially frequent diarrhea in the male patients. Mesalazine is a commonly used drug for SRUS and thalidomide is used for anti-inflammation and its side effects of constipation and improved sleeping happen to help patients relieve diarrhea and help them sleep.

OUTCOME AND FOLLOW-UP

Changes in eating and living habits need to be maintained for a long time. Patients are advised to undergo re-examination 3 mo after drug treatment and biofeedback adjuvant therapy. A significant improvement can be maintained for a long time under the condition of monitoring drug side effects. Additionally, the medication regimen was adjusted

following the patient's symptoms during the follow-up. Patients' symptoms were significantly improved under the comprehensive treatment. The reexamination results after 3 mo indicated a significantly relieved mucosa (Figure 1F). Patients remain under regular follow-up and treatment annually.

DISCUSSION

Previous studies have reported the relevance of rectal mucosal prolapse, ischemia, or injury to SRUS pathogens. These main SRUS features include the following clinical manifestations: defecation difficulty with mucous blood stools and lower abdominal pain, normal general physical examination condition, colonoscopy revealing an isolated rectal ulcer, ultrasound colonoscopy showing proliferative mucosal lesions, pathological results demonstrating mucosal myometrium hyperplasia and fibrosis, dynamic examination indicating abnormal rectal and pelvic floor dynamics, normal blood and inflammatory markers, and negative tumor markers[5].

SRUS has no specific clinical manifestation, thus it is frequently misdiagnosed because its clinical diagnosis mainly depends on endoscopy and histopathology. Current SRUS treatment includes medical, surgical treatment, and biofeedback therapy. Drug therapy aims to inhibit inflammatory response and proliferation. Literature reports revealed a similar treatment plan to ulcerative colitis (UC), which can be used orally with mesalazine and locally with rectal administration. This disease has a long treatment period, causing a non-exact therapeutic effect, although biofeedback therapy aims to harmonize and improve pelvic floor muscle function. However, biofeedback therapy may be effective for patients with pelvic floor dysfunction[6]. Surgical treatment is an alternative option, but it is only effective for some patients and has a risk of recurrence postoperatively. Hence, surgical treatment should not be the first therapeutic choice.

To the best of our knowledge, this is the first case of two patients with SRUS in a mother-son relationship. Thus, this is the first study to indicate a possible genetic background for SRUS. The mother in our cases had a very late onset although SRUS was rarely reported in patients over 60 years old. Meanwhile, the symptoms of both patients have commonalities and differences. Her ulcer and symptom significantly improved after medication, while her young son's symptoms did not improve much even with surgery, although a follow-up colonoscopy revealed no further rectal mucosa damage and anastomosis. Concurrently, long-term diarrhea caused psychologically abnormalities, specifically anxiety, in the young male thereby aggravating diarrhea symptoms. Therefore, surgery may be not available for all patients. Most importantly, the psychological symptoms of the disease should also be considered an important treatment scheme aspect.

Genetic data on SRUS is limited. Genes, heritage data, and features need to be explored for a better understanding of the SRUS pathogen and mechanism. Our cases demonstrated that CHEK2 p.H371Y mutation may be relevant to SRUS development and prognosis. CHEK2 is a cell cycle checkpoint regulator, and it plays an essential role in DNA damage repair. Phosphorylation of p53/TP53 at "Ser-20" by CHEK2 is required for the accumulation of active TP53. When activated, the encoded CHEK2 is known to inhibit CDC25A through phosphorylation of CDC25A and cause its degradation[7]. The CHEK2 p.H371Y mutation was reported as a pathogenic mutation causing decreased kinase activity because p.H371Y is located within the activation region of the CHEK2 protein kinase domain. Here, we performed a series of clinical specimens, which revealed no changes in the CHEK2 expression level while the downstream gene expression was significantly modified, exhibiting an impaired CHEK2 protein function. Both familial and sporadic SRUS cases showed weakened function in CHEK2 protein, and familial SRUS cases are mainly characterized by changes in CDC25A of CHEK2 downstream, while sporadic SRUS cases are mainly characterized by variations in p-p53 of CHEK2 downstream. We speculate similarities and differences in the pathogenesis and prognosis between familial SRUS and non-familial SRUS.

Previous studies have revealed that CHEK2 is associated with inflammation and functions through the kinase mechanism to down-regulate the nuclear factor kappa-light-chain-enhancer of activated B cells (NF-κB) pathway in macrophages to alleviate *Staphylococcus aureus*-induced pneumonia in mice. Additionally, phospho-CHEK2 was associated with high macrophage infiltration in UC[8]. Moreover, SRUS is a manifestation of inflammation and CHEK2 mutation may contribute to the development of SRUS *via* effects on inflammatory pathways, such as the NF-κB pathway [9]. Furthermore, the CHEK2 gene is associated with rectal cancer and inflammatory bowel diseases (IBD). SRUS is closely correlated with rectal cancer and IBD, thus it is difficult to differentiate the diagnosis between SRUS from IBD, especially through UC[10]. Rectal cancer is the most important aspect of SRUS prognostic follow-up, but whether the CHEK2 gene is a pathological gene causing SRUS or a gene for assessing the SRUS prognosis or a potential cause of rectal cancer remains uncertain, as well as the exact role of CHEK2 p.H371Y mutation in familial SRUS.

Limitations related to a small-cohort study and the patient heterogeneity exist. The following possible drawbacks may occur in our study. Firstly, this is a single case report and a retrospective study, and the role of CHEK2 mutation in SRUS pathogenesis needs further investigation. Secondly, this study did not involve the detailed mechanism of CHEK2 mutation causing SRUS. Therefore, subsequent verification of large samples and more detailed experimental verification should be prepared.

CONCLUSION

In summary, this is the first study to report two patients with SRUS in a mother-son relationship with an inherited CHEK2 p.H371Y mutation, which provides insights that SRUS may serve as a genetic susceptibility disease, and CHEK2 p.H371Y mutation may play a crucial role in the development and prognosis of SRUS.

ACKNOWLEDGEMENTS

The authors thank Wei Zhang, BS, from the Department of Pathology in The Third Affiliated Hospital of Guangzhou Medical University for the histology slides and for providing helpful advice.

FOOTNOTES

Author contributions: He CC wrote the manuscript and designed the study; Wang SP performed the experiments; Li ZJ and Li N helped to collect the data; Zhou PR and Li MS supervised the study; All authors have read and approved the final manuscript.

Supported by This work was supported by the Guangdong Basic and Applied Basic Research Fund, No. 2022A1515111193; and the Guangzhou Science and technology plan project, No. 2023A04J0581.

Informed consent statement: Collection and usage of clinical specimens were approved by The Third Affiliated Hospital of Guangzhou Medical University's Ethical Committee Board (Approval number: EN-2022010). All patients were informed of sample collection and usage.

Conflict-of-interest statement: All the authors declare that they have no competing financial or other interests to disclose.

CARE Checklist (2016) statement: The authors have read the CARE Checklist (2016), and the manuscript was prepared and revised according to the CARE Checklist (2016).

Open-Access: This article is an open-access article that was selected by an in-house editor and fully peer-reviewed by external reviewers. It is distributed in accordance with the Creative Commons Attribution NonCommercial (CC BY-NC 4.0) license, which permits others to distribute, remix, adapt, build upon this work non-commercially, and license their derivative works on different terms, provided the original work is properly cited and the use is non-commercial. See: https://creativecommons.org/Licenses/by-nc/4.0/

Country/Territory of origin: China

ORCID number: Cheng-Cheng He 0000-0001-8176-8588; Shan-Ping Wang 0000-0003-1313-369X; Pei-Rong Zhou 0000-0002-6799-6792; Zhi-Jun Li 0009-0000-8528-6498; Na Li 0009-0003-7703-8285; Ming-Song Li 0000-0003-2115-5928.

S-Editor: Liu JH
L-Editor: A
P-Editor: Cai YX

REFERENCES

1 **Rutter KR**. Solitary rectal ulcer syndrome. *Proc Royal Soc Med* 1975; **68**: 22-26 [PMID: 1863712 DOI: 10.1177/003591577506800110]
2 **Gouriou C**, Siproudhis L, Chambaz M, Ropert A, Wallenhorst T, Merlini-l'Héritier A, Carlo A, Bouguen G, Brochard C. Solitary rectal ulcer syndrome in 102 patients: Do different phenotypes make sense? *Dig Liver Dis* 2021; **53**: 190-195 [PMID: 33199231 DOI: 10.1016/j.dld.2020.10.041]
3 **Felt-Bersma RJF**. Solitary rectal ulcer syndrome. *Curr Opin Gastroenterol* 2021; **37**: 59-65 [PMID: 33060396 DOI: 10.1097/MOG.0000000000000689]
4 **Bartek J**, Falck J, Lukas J. CHK2 kinase--a busy messenger. *Nat Rev Mol Cell Biol* 2001; **2**: 877-886 [PMID: 11733767 DOI: 10.1038/35103059]
5 **Abusharifah O**, Bokhary RY, Mosli MH, Saadah OI. Solitary rectal ulcer syndrome in children and adolescents: a descriptive clinicopathologic study. *Int J Clin Exp Pathol* 2021; **14**: 399-407 [PMID: 33936361]
6 **Forootan M**, Shekarchizadeh M, Farmanara H, Esfahani ARS, Esfahani MS. Biofeedback efficacy to improve clinical symptoms and endoscopic signs of solitary rectal ulcer syndrome. *Eur J Transl Myol* 2018; **28**: 7327 [PMID: 29686820 DOI: 10.4081/ejtm.2018.7327]
7 **Xu X**, Tsvetkov LM, Stern DF. Chk2 activation and phosphorylation-dependent oligomerization. *Mol Cell Biol* 2002; **22**: 4419-4432 [PMID: 12024051 DOI: 10.1128/MCB.22.12.4419-4432.2002]
8 **Xie F**, Chen R, Zhao J, Xu C, Zan C, Yue B, Tian W, Yi W. Cell cycle kinase CHEK2 in macrophages alleviates the inflammatory response to Staphylococcus aureus-induced pneumonia. *Exp Lung Res* 2022; **48**: 53-60 [PMID: 35075953 DOI: 10.1080/01902148.2022.2029625]
9 **Sohn JJ**, Schetter AJ, Yfantis HG, Ridnour LA, Horikawa I, Khan MA, Robles AI, Hussain SP, Goto A, Bowman ED, Hofseth LJ, Bartkova J, Bartek J, Wogan GN, Wink DA, Harris CC. Macrophages, nitric oxide and microRNAs are associated with DNA damage response pathway and senescence in inflammatory bowel disease. *PLoS One* 2012; **7**: e44156 [PMID: 22970173 DOI: 10.1371/journal.pone.0044156]
10 **Abid S**, Khawaja A, Bhimani SA, Ahmad Z, Hamid S, Jafri W. The clinical, endoscopic and histological spectrum of the solitary rectal ulcer syndrome: a single-center experience of 116 cases. *BMC Gastroenterol* 2012; **12**: 72 [PMID: 22697798 DOI: 10.1186/1471-230X-12-72]



Published by **Baishideng Publishing Group Inc**
7041 Koll Center Parkway, Suite 160, Pleasanton, CA 94566, USA
Telephone: +1-925-3991568
E-mail: bpgoffice@wjgnet.com
Help Desk: https://www.f6publishing.com/helpdesk
https://www.wjgnet.com



© 2023 Baishideng Publishing Group Inc. All rights reserved.

ISSN 1007-9327 (print)
ISSN 2219-2840 (online)

World Journal of *Gastroenterology*

World J Gastroenterol 2023 August 28; 29(32): 4815-4919



Published by Baishideng Publishing Group Inc

World Journal of Gastroenterology

Contents

Weekly Volume 29 Number 32 August 28, 2023

GUIDELINES

4815 International experts consensus guidelines on robotic liver resection in 2023

Liu R, Abu Hilal M, Wakabayashi G, Han HS, Palanivelu C, Boggi U, Hackert T, Kim HJ, Wang XY, Hu MG, Choi GH, Panaro F, He J, Efanov M, Yin XY, Croner RS, Fong YM, Zhu JY, Wu Z, Sun CD, Lee JH, Marino MV, Ganpati IS, Zhu P, Wang ZZ, Yang KH, Fan J, Chen XP, Lau WY

REVIEW

4831 Non-alcoholic fatty liver disease: Immunological mechanisms and current treatments

Petagine L, Zariwala MG, Patel VB

MINIREVIEWS

4851 Role of non-*Helicobacter pylori* gastric Helicobacters in *helicobacter pylori*-negative gastric mucosa-associated lymphoid tissue lymphoma

Lemos FFB, Silva Luz M, Rocha Pinheiro SL, Teixeira KN, Freire de Melo F

ORIGINAL ARTICLE

Basic Study

4860 Linolenic acid-metronidazole inhibits the growth of *Helicobacter pylori* through oxidation

Zhou WT, Dai YY, Liao LJ, Yang SX, Chen H, Huang L, Zhao JL, Huang YQ

Retrospective Cohort Study

4873 Validation of the albumin-bilirubin score for identifying decompensation risk in patients with compensated cirrhosis

Navadurong H, Thanapirom K, Wejnaruemarn S, Prasoppokakorn T, Chaiteerakij R, Komolmit P, Treeprasertsuk S

4883 Different oncological features of colorectal cancer codon-specific *KRAS* mutations: Not codon 13 but codon 12 have prognostic value

Ahn HM, Kim DW, Oh HJ, Kim HK, Lee HS, Lee TG, Shin HR, Yang IJ, Lee J, Suh JW, Oh HK, Kang SB

4900 Hepatitis B virus infection in patients with Wilson disease: A large retrospective study

Zhou HY, Yang X, Luo KZ, Jiang YF, Wang WL, Liang J, Li MM, Luo HY

CASE REPORT

4912 Drug-induced entero-colitis due to interleukin-17 inhibitor use; capsule endoscopic findings and pathological characteristics: A case report

Saito K, Yoza K, Takeda S, Shimoyama Y, Takeuchi K

ABOUT COVER

Editorial Board of *World Journal of Gastroenterology*, Haruhiko Sugimura, MD, PhD, Director, Sasaki Institute, Sasaki Foundation, Tokyo 101-0062, Japan. hsugimur@po.kyoundo.jp

AIMS AND SCOPE

The primary aim of *World Journal of Gastroenterology* (*WJG*, *World J Gastroenterol*) is to provide scholars and readers from various fields of gastroenterology and hepatology with a platform to publish high-quality basic and clinical research articles and communicate their research findings online. *WJG* mainly publishes articles reporting research results and findings obtained in the field of gastroenterology and hepatology and covering a wide range of topics including gastroenterology, hepatology, gastrointestinal endoscopy, gastrointestinal surgery, gastrointestinal oncology, and pediatric gastroenterology.

INDEXING/ABSTRACTING

The *WJG* is now abstracted and indexed in Science Citation Index Expanded (SCIE, also known as SciSearch®), Current Contents/Clinical Medicine, Journal Citation Reports, Index Medicus, MEDLINE, PubMed, PubMed Central, Scopus, Reference Citation Analysis, China National Knowledge Infrastructure, China Science and Technology Journal Database, and Superstar Journals Database. The 2023 edition of Journal Citation Reports® cites the 2022 impact factor (IF) for *WJG* as 4.3; IF without journal self cites: 4.1; 5-year IF: 5.3; Journal Citation Indicator: 0.82; Ranking: 33 among 93 journals in gastroenterology and hepatology; and Quartile category: Q2. The *WJG*'s CiteScore for 2021 is 8.3 and Scopus CiteScore rank 2022: Gastroenterology is 22/149.

RESPONSIBLE EDITORS FOR THIS ISSUE

Production Editor: *Yu-Xi Chen*; **Production Department Director:** *Xu Guo*; **Editorial Office Director:** *Jia-Ru Fan*.

NAME OF JOURNAL
World Journal of Gastroenterology

ISSN
ISSN 1007-9327 (print) ISSN 2219-2840 (online)

LAUNCH DATE
October 1, 1995

FREQUENCY
Weekly

EDITORS-IN-CHIEF
Andrzej S Tarnawski

EDITORIAL BOARD MEMBERS
http://www.wjgnet.com/1007-9327/editorialboard.htm

PUBLICATION DATE
August 28, 2023

COPYRIGHT
© 2023 Baishideng Publishing Group Inc

INSTRUCTIONS TO AUTHORS
https://www.wjgnet.com/bpg/gerinfo/204

GUIDELINES FOR ETHICS DOCUMENTS
https://www.wjgnet.com/bpg/GerInfo/287

GUIDELINES FOR NON-NATIVE SPEAKERS OF ENGLISH
https://www.wjgnet.com/bpg/gerinfo/240

PUBLICATION ETHICS
https://www.wjgnet.com/bpg/GerInfo/288

PUBLICATION MISCONDUCT
https://www.wjgnet.com/bpg/gerinfo/208

ARTICLE PROCESSING CHARGE
https://www.wjgnet.com/bpg/gerinfo/242

STEPS FOR SUBMITTING MANUSCRIPTS
https://www.wjgnet.com/bpg/GerInfo/239

ONLINE SUBMISSION
https://www.f6publishing.com

© 2023 Baishideng Publishing Group Inc. All rights reserved. 7041 Koll Center Parkway, Suite 160, Pleasanton, CA 94566, USA

E-mail: bpgoffice@wjgnet.com https://www.wjgnet.com

World Journal of Gastroenterology

Submit a Manuscript: https://www.f6publishing.com

World J Gastroenterol 2023 August 28; 29(32): 4815-4830

DOI: 10.3748/wjg.v29.i32.4815

ISSN 1007-9327 (print) ISSN 2219-2840 (online)

GUIDELINES

International experts consensus guidelines on robotic liver resection in 2023

Rong Liu, Mohammed Abu Hilal, Go Wakabayashi, Ho-Seong Han, Chinnusamy Palanivelu, Ugo Boggi, Thilo Hackert, Hong-Jin Kim, Xiao-Ying Wang, Ming-Gen Hu, Gi Hong Choi, Fabrizio Panaro, Jin He, Mikhail Efanov, Xiao-Yu Yin, Roland S Croner, Yu-Man Fong, Ji-Ye Zhu, Zheng Wu, Chuan-Dong Sun, Jae Hoon Lee, Marco V Marino, Iyer Shridhar Ganpati, Peng Zhu, Zi-Zheng Wang, Ke-Hu Yang, Jia Fan, Xiao-Ping Chen, Wan Yee Lau

Specialty type: Surgery

Provenance and peer review: Unsolicited article; Externally peer reviewed.

Peer-review model: Single blind

Peer-review report's scientific quality classification

Grade A (Excellent): A, A
Grade B (Very good): B
Grade C (Good): 0
Grade D (Fair): 0
Grade E (Poor): 0

P-Reviewer: Goja S, India; Montasser IF, Egypt; Morise Z, Japan

Received: June 5, 2023
Peer-review started: June 5, 2023
First decision: July 8, 2023
Revised: July 22, 2023
Accepted: August 9, 2023
Article in press: August 9, 2023
Published online: August 28, 2023

Rong Liu, Ming-Gen Hu, Faculty of Hepato-Pancreato-Biliary Surgery, The First Medical Center of Chinese PLA General Hospital, Beijing 100000, China

Mohammed Abu Hilal, Hepatobiliary Pancreatic, Robotic & Laparoscopic Surgery, Poliambulanza Foundation Hospital, Brescia 25100, Italy

Go Wakabayashi, Center for Advanced Treatment of HBP Diseases, Ageo Central General Hospital, Saitama 362-0075, Japan

Ho-Seong Han, Department of Surgery, Seoul National University Bundang Hospital, Seoul National University College of Medicine, Seoul 03080, South Korea

Chinnusamy Palanivelu, GEM Hospital & Research Centre, GEM Hospital & Research Centre, Coimbatore 641045, India

Ugo Boggi, Division of General and Transplant Surgery, University of Pisa, Pisa 56126, Italy

Thilo Hackert, Department of General, Visceral and Thoracic Surgery, University Hospital Hamburg-Eppendorf, Hamburg 20251, Germany

Hong-Jin Kim, Department of Surgery, Yeungnam University Hospital, Daegu 42415, South Korea

Xiao-Ying Wang, Department of Liver Surgery and Transplantation, Liver Cancer Institute, Zhongshan Hospital, Fudan University, Shanghai 200032, China

Gi Hong Choi, Division of Hepato-Biliary-Pancreatic Surgery, Department of Surgery, Severance Hospital, Yonsei University, College of Medicine, Seoul 03722, South Korea

Fabrizio Panaro, Department of Surgery/Division of Robotic and HBP Surgery, Montpellier University Hospital-School of Medicine, Montpellier 34090, France

Jin He, Department of Surgery, Johns Hopkins University School of Medicine, Baltimore, MD 21218, United States

Mikhail Efanov, Department of Hepato-Pancreato-Biliary Surgery, Moscow Clinical Scientific Center, Moscow 111123, Russia

Xiao-Yu Yin, Department of Pancreatobiliary Surgery, The First Affiliated Hospital, Sun Yat-Sen University, Guangzhou 510080, Guangdong Province, China

Roland S Croner, Department of General, Visceral, Vascular and Transplant Surgery, University Hospital Magdeburg, Magdeburg 39120, Germany

Yu-Man Fong, Department of Surgery, City of Hope Medical Center, Duarte, CA 91010, United States

Ji-Ye Zhu, Department of Hepatobiliary Surgery, Peking University People's Hospital, Beijing 100000, China

Zheng Wu, Department of Hepatobiliary Surgery, The First Affiliated Hospital of Xi'an Jiaotong University, Xi'an 710061, Shaanxi Province, China

Chuan-Dong Sun, Department of Hepatobiliary and Pancreatic Surgery, The Affiliated Hospital of Qingdao University, Qingdao 266000, Shandong Province, China

Jae Hoon Lee, Division of Hepatobiliary & Pancreatic surgery, Asan Medical Center, University of Ulsan College of Medicine, Ulsan 682, South Korea

Marco V Marino, General Surgery Department, F. Tappeiner Hospital, Merano 39012, Italy

Iyer Shridhar Ganpati, Hepatobiliary and Pancreatic Surgery, National University Hospital, Singapore 189969, Singapore

Peng Zhu, Xiao-Ping Chen, Hepatic Surgery Center, Tongji Hospital, Tongji Medical College, Huazhong University of Science and Technology, Wuhan 430000, Hubei Province, China

Zi-Zheng Wang, Department of Hepatobiliary Surgery, Senior Department of Hepatology, The Fifth Medical Center of Chinese PLA General Hospital, Beijing 100000, China

Ke-Hu Yang, Evidence-Based Medicine Center, Lanzhou University, Lanzhou 730000, Gansu Province, China

Jia Fan, Zhongshan Hospital, Fudan University, Shanghai 200000, China

Wan Yee Lau, Faculty of Medicine, The Chinese University of Hong Kong, Hong Kong 999077, China

Corresponding author: Rong Liu, MD, PhD, Chief Doctor, Professor, Faculty of Hepato-Pancreato-Biliary Surgery, The First Medical Center of Chinese PLA General Hospital, No. 28 Fuxing Road, Beijing 100000, China. liurong301@126.com

Abstract

The robotic liver resection (RLR) has been increasingly applied in recent years and its benefits shown in some aspects owing to the technical advancement of robotic surgical system, however, controversies still exist. Based on the foundation of the previous consensus statement, this new consensus document aimed to update clinical recommendations and provide guidance to improve the outcomes of RLR clinical practice. The guideline steering group and guideline expert group were formed by 29 international experts of liver surgery and evidence-based medicine (EBM). Relevant literature was reviewed and analyzed by the evidence evaluation group. According to the WHO Handbook for Guideline Development, the Guidance Principles of Development and Amendment of the Guidelines for Clinical Diagnosis and Treatment in China 2022, a total of 14 recommendations were generated. Among them were 8 recommendations formulated by the GRADE method, and the remaining 6 recommendations were formulated based on literature review and experts' opinion due to insufficient EBM results. This international experts consensus guideline offered guidance for the safe and effective clinical practice and the research direction of RLR in future.

Key Words: Robotic liver resection; Laparoscopic liver resection; Guidelines; Expert consensus

©The Author(s) 2023. Published by Baishideng Publishing Group Inc. All rights reserved.

Core Tip: The robotic liver resection (RLR) has been increasingly applied in recent years. Based on the foundation of the previous consensus statement, this new consensus guideline document aimed to update clinical recommendations and provide guidance to improve the outcomes of RLR clinical practice. The guideline steering group and guideline expert group were formed by 29 international experts of liver surgery and evidence-based medicine. Relevant literature was reviewed and analyzed by the evidence evaluation group. According to the WHO Handbook for Guideline Development, the Guidance Principles of Development and Amendment of the Guidelines for Clinical Diagnosis and Treatment in China 2022, a total of 14 recommendations were generated.

Citation: Liu R, Abu Hilal M, Wakabayashi G, Han HS, Palanivelu C, Boggi U, Hackert T, Kim HJ, Wang XY, Hu MG, Choi GH, Panaro F, He J, Efanov M, Yin XY, Croner RS, Fong YM, Zhu JY, Wu Z, Sun CD, Lee JH, Marino MV, Ganpati IS, Zhu P, Wang ZZ, Yang KH, Fan J, Chen XP, Lau WY. International experts consensus guidelines on robotic liver resection in 2023. *World J Gastroenterol* 2023; 29(32): 4815-4830

URL: https://www.wjgnet.com/1007-9327/full/v29/i32/4815.htm

DOI: https://dx.doi.org/10.3748/wjg.v29.i32.4815

INTRODUCTION

Laparoscopic liver resection (LLR) was first introduced in the 1990s for treatment of benign and malignant tumors[1,2]. Over the past few decades, laparoscopic hepatectomy has developed rapidly and gained widespread acceptance around the world. In 2008, the Louisville Statement indicated the feasibility of laparoscopic hepatectomy[3], and the second international consensus conference in Morioka recommended LLR as a standard practice in specific types of hepatectomy [4]. After that, the Southampton consensus guidelines promoted the safe expansion of LLR and improved patient care after LLR[5]. Since then, laparoscopic techniques have occupied an important place in hepatobiliary surgery. At the same time, with the approval of clinical application and technique developments of robotic surgery systems, robotic hepatectomy has gradually been used in clinical practice. Experience in robotic liver resection (RLR) has been reported in many parts of the world and its feasibility has gradually been identified by clinical studies[6-8]. The robotic system is superior in providing three-dimensional magnified field of vision and robotic arms offer flexibility and tremor filter to surgeons to overcome the shortages of conventional laparoscopic hepatectomy. However, the high cost of the mainstream models and the lack of surgical instruments and experience limit the application of RLR.

With the advent of advanced technique and with experience accumulation, the indications of RLR have been expanded. The robotic system can be used in almost all types of liver resection, including minor hepatectomy, major hepatectomy, donor hepatectomy, and complex liver resections[9-16]. In 2018, an international consensus statement on robotic hepatectomy provided recommendations for RLR based on relevant research and experts' opinions, which contribute to standardization of robotic hepatectomy[17]. However, the recommendation grades were relatively low due to the lack of high-quality evidence. Furthermore, some important issues, like cost-effectiveness of RLR, learning curve of RLR, and outcomes of RLR for difficult liver segments, remain controversial. Available data derive from case series, case-comparative studies, reviews and meta-analyses have been published in recent years, and some new theories also provide new views and perspectives on RLR[18-25].

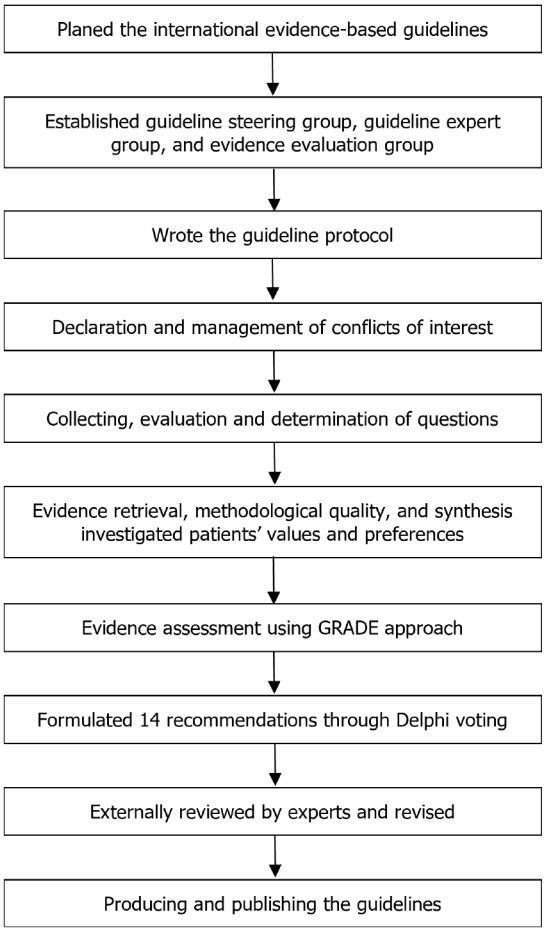
Based on the foundation of the previous statement, the 2023 international consensus statement on RLR aimed to update clinical recommendations and provide guidance to improve the outcomes of RLR clinical practice. We invited a team of robotic surgeon experts to provide their views related to RLR. Based on the related topics, we searched the online databases for RLR studies and the GRADE system was used to grade the evidence. The final consensus was reached by using a combination of clinical evidence and experts' opinions with the aim to improve the clinical outcome of RLR.

METHODS

This international evidence-based guideline is based on the WHO Handbook for Guideline Development and refers to the Guidance Principles of Development and Amendment of the Guidelines for Clinical Diagnosis and Treatment in China 2022. Reporting of the guideline follows the Appraisal of Guidelines, Research, and Evaluation (AGREE II)[26]. A flow chart describes the process and steps of the guideline development (Figure 1).

The guideline development group included the Steering Committee, Consensus Expert Group, and Evidence Evaluation Group. The Steering Committee and Consensus Expert Group consisted of 29 members from different countries or regions. Literature review, questionnaires, and expert discussions were implemented to initially identify clinical questions. All members of the Steering Committee and Consensus Expert Group were encouraged to submit suggestions and add potential questions. Each question was then evaluated and confirmed by the Steering Committee through meetings or emails. The Evidence Evaluation Group performed a literature search, literature screening, method quality evaluation, and data extraction, and thus formed the body of evidence.

PubMed, Cochrane Library, Web of Science, Embase, Scottish Intercollegiate Guidelines Network, WHO, National Guideline Clearing-house, Guidelines International Network, and National Institute for Health and Care Excellence



DOI: 10.3748/wjg.v29.i32.4815 **Copyright** ©The Author(s) 2023.

Figure 1 The flow chart illustrates the process of guideline development.

databases were systematically searched from inception to September 5, 2022, to retrieval potential eligible studies. There were no regional and language restrictions, but it was limited to human studies. The Evidence Evaluation Group evaluated titles, abstracts, and full texts to identify the eligible publications based on inclusion and exclusion criteria approved by the Steering Committee. The eligible literature included clinical guidelines, systematic reviews and meta-analyses, randomized controlled trials (RCT), non-RCT, cohort studies, case-comparative studies, and case reports or case series that were considered for inclusion when necessary. Information on the included studies was extracted according to a pre-designed extraction form. A Measure Tool to Assess Systematic Reviews (AMSTAR II) was used to evaluate the methodological quality of the included systematic reviews and meta-analyses[27]. The revised Cochrane Risk of Bias Tool and the Newcastle-Ottawa Scale were performed to assess the methodological quality of their corresponding types of clinical studies[28,29]. All the above processes were completed by two independent terms of the Evidence Evaluation Group. If there are differences, they will be resolved by discussing or consulting third parties.

According to the WHO Handbook for Guideline Development, the Evidence Evaluation Group evaluated the need for an update or rapid development of systematic review[30]. The method of GRADE was used to assess the quality of the evidence[31]. Based on the GRADE approach, clinical outcomes, patients' benefit, and economic evaluation, the Steering Committee and Consensus Expert Group used the GRADE decision form and Delphi voting to formulate the strength of recommendations. The consensus was considered to have been reached when 80% of the experts approved a proposal. Before submitting the manuscript for publication, the final draft was reviewed and approved by all members of the guideline development group. This evidence-based guideline is expected to be updated again in 2026.

RESULTS

Question 1: What are the indications of RLR?

In general, the indications of the RLR are similar to those of LLR and open liver resection (OLR). RLR can be applied for treating various liver diseases, including hepatocellular carcinoma (HCC), intrahepatic cholangiocarcinoma (ICC), colorectal liver metastases (CRLM), benign tumors of liver, and living donor hepatectomy. RLR is associated with the following advantages over OLR and LLR in the majority of the currently available studies: less intraoperative blood loss, shorter postoperative hospital stay, less overall complications, and lower pain intensity after surgery[21,22,32-45].

However, in complex hepatectomies such as large tumor size or proximity of tumor to vital vascular structures, RLR should be performed with caution and by highly experienced surgeons (clinical recommendation: Expert agreement 100%).

In a prospective study using propensity score matching, Zhu *et al*[21] compared the short-term perioperative outcomes and long-term survival outcomes of RLR, LLR, and OLR in patients with BCLC stage 0-A hepatocellular carcinoma. The results showed that there were no significant differences among the three interventions except for a shorter hospital stay in the minimally invasive group (RLR and LLR)[21]. Hu *et al*[33] evaluated the clinical efficacy of robotic, laparoscopic, and open liver resection for giant liver haemangiomas (> 10 cm in diameter). They reported robotic hemihepatectomy to be associated with less intraoperative blood loss, better postoperative recovery and lower pain score than OLR. When compared with laparoscopic hemihepatectomy, robotic hemihepatectomy was associated with significantly less intraoperative blood loss and a shorter operative time[33]. Masetti *et al*[46] analyzed the short-term outcomes of patients with CRLM comparing from a multicenter study who underwent RLR *vs* LLR. The results showed RLR and LLR to be comparable in postoperative overall complication rates, intraoperative blood loss, conversion rates, operation time, and hospital stay, but RLR showed a reduced rate of R1 resection margins compared with LLR. Masetti *et al*[46] found the effect size of RLR to be increased for posterosuperior lesions and difficult procedures, which may be due to RLR being able to offer some technical advantages over conventional laparoscopy to improve the short-term outcomes of these patients.

Question 2: Is RLR safe and effective in patients with HCC?

Recommendation: RLR is safe and feasible for HCC, as it is associated with lower overall complication rates than LLR and OLR and a shorter hospital stay than OLR, although it has a longer operative time than LLR and OLR. Other perioperative outcomes are comparable among the three interventions. Regarding oncologic outcomes, limited evidence suggested there is also no significant difference.

Level of evidence: Low level of recommendation: Weak (Grade 2C). Expert agreement: 96.55%.

Two systematic reviews[47,48] and 15 publications[21,35,37,43,49-59] were included to evaluate the perioperative and oncologic outcomes of robotic *vs* laparoscopic or open hepatectomy for treatment of HCC patients, respectively. When compared with LLR for HCC patients, the pooled results indicated that RLR had a lower overall complications rate (RR = 0.72, 95%CI: 0.57 to 0.90; P = 0.003), lower minor complication (Clavien-Dindo I-II) rate (RR = 0.72, 95%CI: 0.54 to 0.96; P = 0.030), and longer operative time (SMD = 0.66, 95%CI: 0.22 to 1.10; P = 0.003)[21,50,52-57]. When compared with OLR for HCC patients, RLR was associated with a shorter hospital stay (SMD = -0.42, 95%CI: -0.57 to -0.28; P < 0.00001), lower overall complication rate (RR = 0.61, 95%CI: 0.45 to 0.84; P = 0.002), lower minor complication rate (RR = 0.59, 95%CI: 0.42 to 0.84; P = 0.003), and longer operative time (SMD = 0.82, 95%CI: 0.18 to 1.46; P = 0.01)[21,35,37,43,49,51,58,59]. For other outcomes, RLR showed similar results when compared with LLR or OLR, including estimated blood loss, transfusion rate, severe complication (Clavien-Dindo III-IV), and 90-d mortality. Thus, RLR was comparable to OLR and LLR in feasibility and safety for patients with HCC.

Regarding oncologic outcomes, the three interventions showed comparable R0 resection rates and similar short- and long-term oncological outcomes[21,35,37,43,49,51,53-56,58,59]. Also, a recently published study with a large sample size suggested that robotics may be associated with improved overall survival[54]. The study reported that the RLR group had significantly higher 1- , 3- , and 5- year overall survival rates of 92%, 75%, and 63% compared with the LLR group of 86%, 60%, and 45%, respectively (all P < 0.01)[54]. Based on the currently available studies, the implementation of RLR is feasible and safe and is associated with similar oncologic outcomes. Prospective studies are recommended to further evaluate whether the safety and efficacy of RLR can be affected by tumor size, resection complexity, and the quality of the underlying liver parenchyma.

Question 3: Is RLR safe and effective in patients with ICC?

Recommendation: Currently, there is insufficient evidence to compare the safety and feasibility between RLR and LLR for treatment of ICC. Limited evidence suggests that RLR has less intraoperative blood loss, shorter hospital stay, and better overall survival than OLR.

Level of evidence: Very low. Level of recommendation: Weak (Grade 2D). Expert agreement: 86.21%.

Two comparative studies were reported to evaluate the safety and feasibility of robotic *vs* open hepatectomy for ICC [36,60]. The pooled results suggested that RLR had less intraoperative blood loss (SMD = -0.75, 95%CI: -1.46 to -0.05; P = 0.04) and shorter hospital stay (SMD = -0.31, 95%CI: -0.54 to -0.09; P = 0.006) than OLR[36,60]. There were no significant differences in other perioperative outcomes between the two groups. Limited evidence suggests RLR may improve the outcomes of ICC when compared to OLR, but we need to carefully interpret these findings. Shapera *et al*[60] suggested that patients after RLR or OLR had similar resection margins, and median overall survival was similar in patients with any resection margin distance. Hamad *et al*[36] compared short- and long-term outcomes between RLR and OLR for patients with ICC, and they reported that patients who underwent RLR had shorter hospital stays and similar long-term risk of death between the two groups. These results suggested RLR for ICC could shorten hospital stay without compromising oncological outcomes such as negative margins, postoperative mortality, and long-term survival[36]. As there have been few comparative studies focusing on ICC and there is no meta-analysis on the short- and long-term clinical outcomes of RLR *vs* LLR or OLR for ICC, higher levels of evidence are urgently needed to answer this question.

Question 4: Is RLR safe and effective in patients with CRLM?

Recommendation: RLR is safe and feasible for patients with CRLM, since it is associated with a lower conversion rate but

longer hospital stay than that of LLR. Limited evidence suggests no significant difference in all the perioperative outcomes between RLR and OLR in patients with CRLM. Oncologic outcomes with limited evidence suggested there was also no significant difference between RLR *vs* LLR and RLR *vs* OLR.

Level of evidence: Very low. Level of recommendation: Weak (Grade 2D). Expert agreement: 89.66%.

Studies on RLR *vs* LLR or OLR for CRLM have been extensively published in the past three years[45,46,61-63]. The evidence suggested RLR to have a lower conversion rate (RR = 0.42, 95%CI: 0.23 to 0.77; P = 0.005) and longer hospital stays (SMD = 0.19, 95%CI: 0.03 to 0.35; P = 0.020) than LLR for patients with CRLM, and there were no significant difference in operation time, estimated blood loss, intraoperative blood transfusion rates, R0 resection, postoperative morbidity, and overall survival[45,46,61,62]. In addition, limited evidence showed there were no significant differences in operation time, estimated blood loss, R0 resection, hospital stays, overall complications, minor and major complications, postoperative 30-d mortality, and survival outcomes between RLR and OLR for patients with CRLM[61,63]. With appropriate expertise and experience, robotic-assisted surgery can be considered to be an alternative minimally invasive approach to CRLM resections[64,65].

Currently, there is insufficient evidence on patients who underwent simultaneous robotic-assisted resections of CRLM and the primary tumor. A conference abstract on one RCT in comparing RLR and OLR for simultaneous resections suggested a longer operating time in the robotic arm, and patients who underwent RLR had less blood loss, less Clavien-Dindo III-IV complications, a shorter time to pass first flatus, and a shorter hospital stay when compared to open surgery [40]. A recent systematic review reported that all patients who underwent robot-assisted R0 resection had no perioperative deaths[65]. However, when patients who underwent simultaneous major hepatectomy combined with complex colorectal surgery, the operative risks were increased, leading to poorer perioperative outcomes with increased length of stay, morbidity, and mortality, and unfavorable patient recovery due to delay in the initiation of subsequent adjuvant therapy[5,65].

Question 5: Is robot approach safe and feasible for living donor hepatectomy?

Recommendation: Robotic living donor hepatectomy can be a safe and feasible alternative to open and laparoscopic approach. Robotic living donor hepatectomy has a longer operative time than that of OLR and LLR, but a shorter hospital stay compared with OLR. The other donor and recipient outcomes were reported to be comparable among the three interventions.

Level of evidence: Very low. Level of recommendation: Weak (Grade 2D). Expert agreement: 96.55%.

We systematically reviewed 4 studies that investigated the safety and feasibility of robotic and open living donor hepatectomy, with a total of 972 patients being included in the meta-analysis[41,66-68]. The pooled results suggested that RLR had lower postoperative peak serum bilirubin (SMD = -0.59, 95%CI: -0.81 to -0.37; P < 0.0001), shorter postoperative hospital stays (SMD = -0.53, 95%CI: -0.90 to -0.17; P = 0.004) and a longer operative time (SMD = 1.45, 95%CI: 0.66 to 2.25; P = 0.003) compared to the open group[41,66-68]. There were no significant differences in terms of other donor and recipient outcomes. Rho *et al*[41] evaluated the clinical and perioperative outcomes of robotic living donor right hepatectomy from carried out on 52 consecutive cases patients and compared with patients who underwent comparison with open (n = 62) and laparoscopic (n = 118) donor hepatectomy. They reported that although RLR was associated with a longer operation time, the mean estimated blood loss was significantly lower compared with LLR and OLR, and donor satisfaction (body image and cosmetic appearance scores) was higher in RLR than that of LLR[41].

Large incisions resulting in large scars are an ongoing concern for surgeons performing open living donor hepatectomy. For robotic living donor hepatectomy, there is a better body image, improved cosmetic appearance, and fewer wound-related complications[41]. Living donor hepatectomy is considered to be the pinnacle of hepatobiliary surgery, which requires assurance of donor survival, good graft status and minimization of associated complications[66]. Based on the currently available studies, RLR reduced postoperative pain, resulted in rapid donor recovery and with similar postoperative complications[41,66-68]. However, studies comparing RLR with LLR are insufficient[41]. In summary, RLR for living donor hepatectomy is feasible and safe when performed by surgeons with both excellent knowledge of liver anatomy and long experience of open living donor hepatectomy[41,66]. However, biliary complications are a problem that should never be ignored. The combination of robotic-assisted procedures and indocyanine green (ICG) fluoroscopy is recommended for precise division and fine suturing of the divided bile ducts[41,66].

Question 6: Is robotic approach safe and feasible for minor hepatectomy?

Recommendation: For minor hepatectomy, the safety and feasibility of RLR are comparable to that of LLR and OLR. Robotic minor hepatectomy was reported to have a longer operative time than LLR, but there was less overall complication. RLR resulted in a shorten hospital stay and decreased overall morbidity compared to the open approach. The other perioperative outcomes were comparable among the three interventions.

Level of evidence: Low. Level of recommendation: Weak (Grade 2C). Expert agreement: 96.55%.

Minor hepatectomy with fewer than 3 adjacent hepatic segmental resections is the most commonly carried out procedure in RLR. As a minimally invasive surgery, the benefits of the robotic approach for minor hepatectomy have been controversial[36,37,49,51,69-72]. An updated meta-analysis based on new evidence was conducted by the Evidence Evaluation Group on 13 retrospective cohort studies with 735 robotic and 1362 laparoscopic minor hepatectomies[12,22,34,53,73-81]. The results showed that the operative time was significantly longer (SMD = 0.44, 95%CI: 0.19 to 0.69; P = 0.0006) with the robotic approach, but it had less overall complication (RR = 0.76, 95%CI: 0.61 to 0.95; P = 0.01) than LLR. No statistically significant differences were observed in estimated blood loss, conversion rate, blood transfusion rate,

postoperative hospital stays, 90-d mortality, and R0 resection. Based on the currently available studies and expert opinions, RLH was associated with a longer operation time when compared with LLH because of the additional time required to dock and undock the robot, and the large extent to exchange instruments required by the robot-assisted procedures[34,69,70].

We also systematically reviewed 6 studies to investigate the safety and feasibility between RLR and OLR[9,38,71,73,82,83]. The results showed that robotic minor hepatectomy had a shorter postoperative hospital stay (SMD = -0.91, 95%CI: -1.27 to -0.55; P < 0.00001), less overall complications (RR = 0.39, 95%CI: 0.23 to 0.64; P = 0.0002), and less severe complications (RR = 0.28, 95%CI: 0.08 to 0.97; P = 0.04) when compared to open surgery. There were no significant differences in terms of operation time, estimated blood loss, intra-operative blood transfusion rate, and readmission rate, and R0 resection for malignancy between robotic and open minor hepatectomies. Liver resections for difficult-located segments (1, 4a, 7, and 8) are recommended to be defined as technical major hepatectomy.

Question 7: Is robotic approach safe and feasible for major hepatectomy?

Recommendation: For major hepatectomy, robotic hepatectomy is as safe and feasible as laparoscopic and open hepatectomy. Compared with LLR, RLR was significantly better in estimated blood loss and conversion rate. In comparison with OLR, the estimated blood loss and hospital stay of RLR are significantly better than those of OLR, but there is a longer operation time in the RLR group.

Level of evidence: Low. Level of recommendation: Weak (Grade 2C). Expert agreement: 93.10%.

Chong *et al*[32] compared the efficacy and safety of 989 individuals, including 220 who underwent robotic and 769 who underwent laparoscopic right and extended right hepatectomy (RH/ERH). They reported a lower open conversion rate and a shorter postoperative hospital stay for robotic RH/ERH. We systematically reviewed 10 studies that investigated the safety and feasibility of robotic and laparoscopic major hepatectomy[22,32,33,39,84-89]. The results showed that robotic major hepatectomy resulted in less estimated blood loss (SMD = -0.52, 95%CI: -0.88 to -0.16; P = 0.005) and a lower conversion rate (RR = 0.44, 95%CI: 0.29 to 0.67; P = 0.0001) compared to laparoscopic surgery. There were no significant differences between robotic and laparoscopic major hepatectomies in transfusion rate, R0 resection, readmission, mortality within 90 d, overall complications, mild/severe complication, bile leakage and liver failure rates.

Hamad *et al*[36] investigated 1876 patients who underwent open (n = 1804) and robotic assisted (n = 72) resection between 2004 and 2017. The results showed that the patients who underwent RLR had a shorter length of hospital stays yet there was no difference in 30-d readmission or 90-d mortality[36]. Lee *et al*[43] matched 36 patients each in the robotic and open group. They found that operative time was significantly longer but the postoperative hospital stays was significantly shorter in the robotic group[43]. An updated meta-analysis based on the latest evidence was conducted by the Evidence Evaluation Group on 8 retrospective cohort studies. The pooled results suggested the estimated blood loss and hospital stay of the robotic group to be significantly shorter than the open group, but there was a longer operation time in the robotic group[22,33,37,43,49,51,71,72].

We also focused on the safety and feasibility of RLR in technically "major" resections (segment 1, 4a, 7, and 8). Liver resection on segments 1, 4a, 7, and 8 is relatively more technically difficult owing to a large parenchymal transection plane with proximity to critical structures and major vessels[90-92]. RLR on difficult liver segments has been reported to be a safe and feasible procedure, and many experienced surgeons tend to perform robotic resections on these selected patients. In a recent international multicenter retrospective study comparing robotic *vs* laparoscopic right posterior sectionectomy, the author reported RLR to be associated with reduced blood loss and lower open conversion rates than LLR, and suggested that RLR and LLR could be performed in expert centers with good outcomes in well selected patients [93]. A study reported a patient with hepatocellular carcinoma which involved segments 4 and 8 to undergo robotic central bisectionectomy. The outcomes indicated that robotic central bisectionectomy could be performed safely using proper exposure techniques and an appropriate combination of several useful technical tips[16]. A multicenter study reported that robotic right posterior sectionectomy could be performed in expert centers with less blood loss and lower conversion rates in well-selected patients[93,94]. Another study indicated that RLR on segments 1, 4a, 7, and 8 showed similar surgical outcomes, including blood loss, hospital stay, R0 negative margin rate, and morbidity, when compared with laparoscopic liver resection[95]. The application of robotic approach has also been reported for caudate lobectomy, including Spiegelian lobectomy, isolated partial and complete caudate lobectomy[96,97]. However, most studies reported only a few cases with the potential of selection bias, thus limiting the application of the results. It is necessary to conduct high-quality clinical studies in the future to further clarify the impact of robotic hepatectomy on difficult liver segments.

Question 8: Is RLR more cost-effective than LLR and OLR?

Recommendation: As the policy on medical expense and definition of cost are different in the literature, the real cost of three interventions should be calculated and compared based on a standard method in the future. Limited evidence suggests the total cost of RLR to be higher than LLR, but there were no significant differences between RLR and OLR. The cost-effectiveness of the three interventions should be synthetically evaluated based on many factors, including direct and indirect costs, hidden benefits from favorable clinical outcomes and local social and economic situations.

Level of evidence: Very low. Level of recommendation: Weak (Grade 2D). Expert agreement: 89.66%.

The most common concern about cost-effectiveness analysis of RLR is simply on the total cost, hospitalization costs, and readmission costs. One systematic review and meta-analysis and nine additional updated original studies were included to answer this question[9,34,42,84,98-103]. The resynthesized evidence suggests that the total costs (SMD = 1.15, 95%CI: 0.24 to 2.07; P = 0.01) and hospitalization costs (SMD = 0.96, 95%CI: 0.50 to 1.41; P < 0.0001) of RLR is higher compared to LLR[34,42,75,78,104]. However, no statistically significant differences were observed regarding total costs,

hospitalization costs, and readmission costs between RLR and OLR[9,42,44,68,101]. In addition, total costs were assessed for different type of liver resection. For the included studies which investigated RLR *vs* LLR, these studies were more focused on the cost-effectiveness in minor liver resections, and the results showed that RLR had higher total costs than LLR (SMD = 1.22, 95%CI: 0.60 to 1.83; $P < 0.0001$)[34,75,78]. When various types of pathologies in patients were included in the comparison between RLR and OLR, including complex hepatolithiasis, donor right hepatectomy, minor and major resections, these confounders were introduced to become an important reason to decrease the level of evidence[9,44,68,103]. According to the currently available studies, even though the higher total costs of RLR were closely associated with more operating room supplies[34,68,73,79,80,84], the higher total costs were mainly due to longer hospital stays and more treatment of complications in the laparoscopic and open group than the robotic group[9,71,100,105,106]. The favorable perioperative outcomes in RLR should be weighed against the higher operative costs when compared with laparoscopic or open approaches[98].

Robotic surgical systems have evolved rapidly in recent years, and the trends in the total cost and operative cost are worth future investigating. Although the costs of RLR may differ among countries or regions due to differences in medical policy or insurance premium, a serious obstacle to the widespread use of robotic surgical system is the large indirect cost[34,78-80]. Furthermore, a comprehensive evaluation of the cost-effectiveness should also consider the hidden benefits from favorable clinical outcomes associated with robotic hepatectomy to include patient's psychological benefits and social benefits.

Question 9: What is the role of RLR for cirrhotic patients?

In the setting of cirrhotic patients, similar to LLR, RLR could also be performed in to selected patients. Currently, there are insufficient studies focusing on the application of RLR on cirrhotic patients (clinical recommendation: Expert agreement 100%).

The improvement of surgical techniques, perioperative management, and patient selection improved the surgical outcome of patients with cirrhosis, and the overall improvement of surgical techniques as represented by the minimally invasive approach improved the outcomes of perioperative management in patients with cirrhosis[107-109]. Minimally invasive hepatectomy for cirrhotic patients has been reported to be associated with less complications, shorter postoperative hospital stay, and similar outcomes in operative time, estimated blood loss and postoperative complications when compared with non-cirrhotic patients, and laparoscopic surgery may provide potential benefits in reducing the incidence of postoperative ascites and liver failure[5,110]. Only a few patients were included in these studies and the outcome of robotic hepatectomy in patients with cirrhosis were not evaluated separately[47]. It is necessary to conduct more research on RLR for liver cancer patients with cirrhosis to further evaluate the safety and efficacy of the robotic approach.

Question 10: What is the role of RLR for lesions located close to major vascular and biliary structures?

For lesions located close to major vascular and biliary structures, especially for deeply located lesions, parenchyma-sparing liver resection should be performed by using the robotic approach to rely on the delicate dissection offered by the stable and flexible movements of the robotic arms, as an alternative approach to major liver resection. Compared to robotic major liver resection, robotic parenchyma-sparing liver resection could potentially increase resectability of these lesions. However, as this is a technically demanding procedure, it should be performed by experienced surgeons on well-selected patients (clinical recommendation: Expert agreement 100%).

For malignant liver lesion with a small tumor size but in close proximity to important vessels such as the hepatocaval confluence, or the bifurcation of the primary or secondary Glissonean pedicles, the conventional approach is to use major resection to remove the vessel in its entirety along with the liver tissues it supplies or drains. However, in patients with a poor liver function and insufficient liver remnant volume, the safety of major resection is difficult to ensure, resulting in a reduced operative resection rate. Parenchyma-sparing liver resection addresses this dilemma to some extent. Removal of the tumor off the adjacent vascular structures or combined vascular resection and reconstruction could increase the resection rate of the tumor. In contrast to the laparoscopic approach with its intrinsic drawbacks including the fulcrum effect and rigid instruments, the robotic system could offer stable and flexible movements of the instruments, which facilitate the operative procedures to achieve a higher level of difficulty. RLR for treatment of centrally located lesions has been reported and shown to be safe and feasible in small case series[111,112]. In addition, with the help of intraoperative ultrasound, it has been shown that the robotic approach allowed optimal access to all liver segments and facilitated parenchymal-sparing surgery for lesions located in the posterosuperior segments or in contact with main liver vessels, not only for colorectal liver metastasis but also for HCC[113]. Robotic parenchyma-sparing liver resection for lesions located close to major vascular and biliary structures allows for sufficient liver remnant to be retained, thus allowing patients to start their postoperative adjuvant therapy early, which is important in improving patients' survival in today's rapidly evolving of comprehensive treatment.

Question 11: What is the role of robotic approach for associating liver partition and portal vein ligation for staged hepatectomy?

Robotic first- or second-stage associating liver partition and portal vein ligation for staged hepatectomy (ALPPS) is an optional strategy for treatment of primary and metastatic liver cancer in patients with insufficient residual liver volume. Due to the complexity of ALPPS surgery and the high morbidity rate, the benefit of robotic ALPPS is unclear on the curative effect of the initially unresectable liver cancer, as there have been rapidly evolving developments in locoregional and systemic therapies. Robotic ALPPS must be evaluated with caution before operation and should only be performed in highly selected patients (clinical recommendation: Expert agreement 100%).

ALPPS has been introduced to treat patients with advanced liver tumors and insufficient residual liver volumes for more than 10 years. However, there is still a lot of controversies on the value of this approach due to its high mortality rate[114,115]. Minimally invasive approach for ALPPS has been applied for the purpose of reducing mortality and improving recovery of patients. Most of the ALPPS procedures were used for the first-stage[116]. A systematic review of 27 patients who underwent ALPPS reported the potential benefit of using the minimally invasive ALPPS in reducing morbidity and mortality[117]. However, there was selective bias in this study and the sample size was small, which compromised the robustness of the conclusions. Previous studies with small case numbers showed that the robotic approach could be used for the first-stage ALPPS for HCC, CRLM and ICC[118-120]. Complex robotic ALPPS procedures (*e.g.*, robotic ALPPS for patients with portal vein thrombosis, robotic ALPPS with simultaneous left colectomy) have also been reported to be safe and feasible carried out by experienced surgeons[121-124]. After the long period of development of ALPPS and its modified approaches, the role of ALPPS should be revisited due to its complexity in treating patients with advanced stage of malignancy and the high morbidity rate, especially when facing the major developments in locoregional and systemic therapies[125-128]. Although the robotic ALPPS is technically feasible, the oncological and health economic benefits are still unclear. The efficacy of robotic ALPPS still needs to be evaluated through high-quality clinical researches.

Question 12: Could the robotic approach shorten the learning curve of liver resection?

The case number required to surmount the learning curve for RLR has been reported to be lower than that for LLR. The case number required to surmount the learning curve of RLR varied among different studies[12,32,129-134]. The surgeons' experience in LLR could have a significant influence on the learning curve of RLR. About 25 consecutive cases are needed for an experienced surgeon to surmount the learning curve of major RLR and 15 cases for minor RLR (clinical recommendation: Expert agreement 100%).

Because of the enhanced surgical dexterity offered by the robotic system, robotic hepatectomy may have a shorter learning curve compared to laparoscopic hepatectomy. However, the large experience in LLR surgeons had before embarking on robotic liver surgery could have an impact on the learning curve[100,135]. Chua *et al*[136] reviewed the literature reported up to July 2019 pertaining to the learning curves in minimally invasive hepatectomy (MIH) by searching PubMed and Scopus databases. Forty studies were included to explore quantitatively the learning curve for MIH. They reported the case number required to surmount the learning curve for RLR was 25 consecutive cases (range: 16-50)[136].

Liu *et al*[131], by analyzing the learning curve of 100 robotic left and right hemihepatectomy (RLH/RRH) in terms of operative time, reported that the learning process was completed in the RLH group after an initial phase of 35 cases, which was shorter than the RRH group (n = 45). Given that, mobilization and resection of the left liver are easier to perform than the right liver, RLH might be the first choice for beginners.

Question 13: Which difficulty scoring systems should be used for RLR?

Ban and Iwate reported on the difficulty scoring system for LLR which was externally validated for RLR. The two difficulty scoring systems are currently recommended. A difficulty scoring system exclusively for RLR should be established by further studies (clinical recommendation: Expert agreement 100%).

By predicting the complexity of different surgeries, the difficulty scoring system (DSS) can recommend suitable patients to surgeons at their corresponding learning stages. Current DSS scores on the basis of the weighted combination of predicted factors that affect the surgeries' complexity include tumor size, position, number of the tumor, extent of liver resection and liver function[137,138].

However, the scoring system for RLR remains to be designed. Linn *et al*[137] summarized 11 types of DSS for LLR based on previously reported studies and conducted a meta-analysis. The results showed that 5 DSS (including Ban DSS, Iwate DSS, Hasegawa DSS, IMM DSS, and Southampton DSS) could be used for predicting the difficulty of LLR surgeries [138-141]. Though no DSS has significant advantages, Ban and Iwate DSS were externally validated for RLR[137,138].

Question 14: What is the role of intraoperative navigation techniques in RLR?

Intraoperative ultrasonography (IOUS) and indocyanine green (ICG) imaging has been used for tumor locating and surgical margin delineation in RLR. Surgeons are supposed to master these techniques and choose the suitable navigation tools to increase the safety of RLR (clinical recommendation: Expert agreement 100%).

Studies have supported the importance of IOUS in liver operations[142,143]. Based on the experience of IOUS in 110 consecutive patients, Zhu *et al*[144] put forward a standardized 4-step IOUS agreement to ensure the safety of RLR operation. Moreover, when using IOUS to examine all the patients, they found 11 patients (10%) had extra lesions, and 7 of these patients (63.64%) underwent improved surgical strategies[144]. However, IOUS has the limitations to accurately show irregular hepatic segmental demarcation and anatomical structure, while ICG imaging has become a supplementary tool for IOUS due to its ability on real-time 3D recognition of tumor margins and to guide liver transection plane. Wakabayashi *et al*[145] reviewed articles related to ICG imaging in liver resection and showed that the combination of IOUS and ICG imaging can increase the safety of liver resection, but the timing and dose administration of ICG remain uncertain. Furthermore, Liu and his team reported the application of ICG using "four-zone three-phase" fluorescence imaging in robot-assisted anatomical hepatectomy in which the liver was divided into 4 anatomical zones include the "tumor zone", "peritumor zone", "ischemia zone", and "reserved liver zone"[146]. The ICG "four-zone three-phase" fluorescence imaging could accurately locate most tumors, clearly display the liver resection plane in a real-time manner and achieved the precision and standardization of anatomical hepatectomy.

The application of augmented reality (AR) technology can increase the accuracy of tumor positioning and surgical margin delineation. At present, only a few cases have been reported on the application of AR technology in RLR. Further technological advance and studies on evaluation of AR technology in clinical applications remain to be done.

CONCLUSION

This international experts consensus guideline offered guidance for the safe and effective clinical practice and the research direction of RLR in future. This evidence-based guideline is expected to be updated again in 2026 and further randomized controlled trials are needed to validate these recommendations.

ACKNOWLEDGEMENTS

We thank all the external reviewers for giving responses to the consensus; and all Members of the Evidence Evaluation Group: Shao-Ming Song and Lin Zhu (The First School of Clinical Medicine, Lanzhou University, Lanzhou 730000, China), Gui-Neng Zeng and Yue Li (School of Medicine, Nankai University, Tianjin 300300, China), Zhao-Da Deng and Zhi-Yuan Yao (Medical School of Chinese PLA, Beijing 100000, China).

FOOTNOTES

Author contributions: Members of the guideline steering group: Liu R, Abu Hilal M, Wakabayashi G, Fan J, Chen XP, and Lau WY contributed to designing guidelines, identifying problems, and providing comments; Members of the guideline expert group: Han HS, Palanivelu C, Boggi U, Hackert T, Kim HJ, Wang XY, Hu MG, Choi GH, Panaro F, He J, Efanov M, Yin XY, Croner RS, Fong YM, Zhu JY, Wu Z, Sun CD, Lee JH, Marino MV, Ganpati IS, Zhu P, Wang ZZ, and Yang KH provided expert's opinion; and all authors approved the final version of the manuscript.

Conflict-of-interest statement: The authors declare no conflict of interest in the development of consensus guidelines.

Open-Access: This article is an open-access article that was selected by an in-house editor and fully peer-reviewed by external reviewers. It is distributed in accordance with the Creative Commons Attribution NonCommercial (CC BY-NC 4.0) license, which permits others to distribute, remix, adapt, build upon this work non-commercially, and license their derivative works on different terms, provided the original work is properly cited and the use is non-commercial. See: https://creativecommons.org/Licenses/by-nc/4.0/

Country/Territory of origin: China

ORCID number: Rong Liu 0000-0001-5170-6474; Mohammed Abu Hilal 0000-0002-3162-4639; Go Wakabayashi 0000-0002-8383-9666; Ho-Seong Han 0000-0001-9659-1260; Ugo Boggi 0000-0002-7505-5896; Hong-Jin Kim 0000-0002-5965-8339; Ming-Gen Hu 0000-0003-3612-2870; Gi Hong Choi 0000-0001-7511-9581; Fabrizio Panaro 0000-0001-8200-4969; Jin He 0000-0001-9149-2247; Mikhail Efanov 0000-0003-0738-7642; Xiao-Yu Yin 0000-0002-5518-5984; Yu-Man Fong 0000-0002-8934-9959; Ji-Ye Zhu 0000-0003-0456-7584; Zheng Wu 0000-0002-7102-9543; Chuan-Dong Sun 0000-0002-6724-2747; Jae Hoon Lee 0000-0002-6170-8729; Iyer Shridhar Ganpati 0000-0002-4630-9842; Peng Zhu 0000-0001-8088-0615; Zi-Zheng Wang 0009-0000-5963-7493; Jia Fan 0000-0002-2127-4102; Xiao-Ping Chen 0000-0001-8636-0493.

S-Editor: Chen YL
L-Editor: A
P-Editor: Chen YL

REFERENCES

1 **Reich H**, McGlynn F, DeCaprio J, Budin R. Laparoscopic excision of benign liver lesions. *Obstet Gynecol* 1991; **78**: 956-958 [PMID: 1833688]

2 **Katkhouda N**, Fabiani P, Benizri E, Mouiel J. Laser resection of a liver hydatid cyst under videolaparoscopy. *Br J Surg* 1992; **79**: 560-561 [PMID: 1535261 DOI: 10.1002/bjs.1800790628]

3 **Buell JF**, Cherqui D, Geller DA, O'Rourke N, Iannitti D, Dagher I, Koffron AJ, Thomas M, Gayet B, Han HS, Wakabayashi G, Belli G, Kaneko H, Ker CG, Scatton O, Laurent A, Abdalla EK, Chaudhury P, Dutson E, Gamblin C, D'Angelica M, Nagorney D, Testa G, Labow D, Manas D, Poon RT, Nelson H, Martin R, Clary B, Pinson WC, Martinie J, Vauthey JN, Goldstein R, Roayaie S, Barlet D, Espat J, Abecassis M, Rees M, Fong Y, McMasters KM, Broelsch C, Busuttil R, Belghiti J, Strasberg S, Chari RS; World Consensus Conference on Laparoscopic Surgery. The international position on laparoscopic liver surgery: The Louisville Statement, 2008. *Ann Surg* 2009; **250**: 825-830 [PMID: 19916210 DOI: 10.1097/sla.0b013e3181b3b2d8]

4 **Wakabayashi G**, Cherqui D, Geller DA, Buell JF, Kaneko H, Han HS, Asbun H, O'Rourke N, Tanabe M, Koffron AJ, Tsung A, Soubrane O, Machado MA, Gayet B, Troisi RI, Pessaux P, Van Dam RM, Scatton O, Abu Hilal M, Belli G, Kwon CH, Edwin B, Choi GH, Aldrighetti LA, Cai X, Cleary S, Chen KH, Schön MR, Sugioka A, Tang CN, Herman P, Pekolj J, Chen XP, Dagher I, Jarnagin W, Yamamoto M, Strong R, Jagannath P, Lo CM, Clavien PA, Kokudo N, Barkun J, Strasberg SM. Recommendations for laparoscopic liver resection: a report from the

second international consensus conference held in Morioka. *Ann Surg* 2015; **261**: 619-629 [PMID: 25742461 DOI: 10.1097/SLA.0000000000001184]

5 **Abu Hilal M**, Aldrighetti L, Dagher I, Edwin B, Troisi RI, Alikhanov R, Aroori S, Belli G, Besselink M, Briceno J, Gayet B, D'Hondt M, Lesurtel M, Menon K, Lodge P, Rotellar F, Santoyo J, Scatton O, Soubrane O, Sutcliffe R, Van Dam R, White S, Halls MC, Cipriani F, Van der Poel M, Ciria R, Barkhatov L, Gomez-Luque Y, Ocana-Garcia S, Cook A, Buell J, Clavien PA, Dervenis C, Fusai G, Geller D, Lang H, Primrose J, Taylor M, Van Gulik T, Wakabayashi G, Asbun H, Cherqui D. The Southampton Consensus Guidelines for Laparoscopic Liver Surgery: From Indication to Implementation. *Ann Surg* 2018; **268**: 11-18 [PMID: 29064908 DOI: 10.1097/SLA.0000000000002524]

6 **Choi GH**, Chong JU, Han DH, Choi JS, Lee WJ. Robotic hepatectomy: the Korean experience and perspective. *Hepatobiliary Surg Nutr* 2017; **6**: 230-238 [PMID: 28848745 DOI: 10.21037/hbsn.2017.01.14]

7 **Goja S**, Singh MK, Vohra V, Soin AS. Robotic Left Hepatectomy: a Case Report (First Reported Case of Robotic Hepatectomy in India). *Indian J Surg* 2015; **77**: 338-340 [PMID: 26702246 DOI: 10.1007/s12262-015-1307-7]

8 **Kam JH**, Goh BK, Chan CY, Wong JS, Lee SY, Cheow PC, Chung AY, Ooi LL. Robotic hepatectomy: initial experience of a single institution in Singapore. *Singapore Med J* 2016; **57**: 209-214 [PMID: 26843059 DOI: 10.11622/smedj.2016024]

9 **Stewart C**, Wong P, Warner S, Raoof M, Singh G, Fong Y, Melstrom L. Robotic minor hepatectomy: optimizing outcomes and cost of care. *HPB (Oxford)* 2021; **23**: 700-706 [PMID: 32988754 DOI: 10.1016/j.hpb.2020.09.005]

10 **Sucandy I**, Jacoby H, Crespo K, Syblis C, App S, Ignatius J, Ross S, Rosemurgy A. A Single Institution's Experience With Robotic Minor and Major Hepatectomy. *Am Surg* 2023; **89**: 1387-1391 [PMID: 34798777 DOI: 10.1177/00031348211047500]

11 **Sucandy I**, Luberice K, Lippert T, Castro M, Krill E, Ross S, Rosemurgy A. Robotic Major Hepatectomy: An Institutional Experience and Clinical Outcomes. *Ann Surg Oncol* 2020; **27**: 4970-4979 [PMID: 32661848 DOI: 10.1245/s10434-020-08845-4]

12 **O'Connor VV**, Vuong B, Yang ST, DiFronzo A. Robotic Minor Hepatectomy Offers a Favorable Learning Curve and May Result in Superior Perioperative Outcomes Compared with Laparoscopic Approach. *Am Surg* 2017; **83**: 1085-1088 [PMID: 29391100 DOI: 10.1177/000313481708301014]

13 **Chen PD**, Wu CY, Hu RH, Ho CM, Lee PH, Lai HS, Lin MT, Wu YM. Robotic liver donor right hepatectomy: A pure, minimally invasive approach. *Liver Transpl* 2016; **22**: 1509-1518 [PMID: 27509325 DOI: 10.1002/lt.24522]

14 **Broering DC**, Elsheikh Y, Alnemary Y, Zidan A, Elsarawy A, Saleh Y, Alabbad S, Sturdevant M, Wu YM, Troisi RI. Robotic Versus Open Right Lobe Donor Hepatectomy for Adult Living Donor Liver Transplantation: A Propensity Score-Matched Analysis. *Liver Transpl* 2020; **26**: 1455-1464 [PMID: 32542956 DOI: 10.1002/lt.25820]

15 **Camerlo A**, Delayre T, Fara R. Robotic central hepatectomy for hepatocarcinoma by glissonean approach (with video). *Surg Oncol* 2021; **36**: 82-83 [PMID: 33316683 DOI: 10.1016/j.suronc.2020.11.011]

16 **Rojas AE**, Paterakos P, Choi SH. Robotic Central Bisectionectomy for Centrally Located Hepatic Malignant Tumor. *Ann Surg Oncol* 2022 [PMID: 35357613 DOI: 10.1245/s10434-022-11646-6]

17 **Liu R**, Wakabayashi G, Kim HJ, Choi GH, Yiengpruksawan A, Fong Y, He J, Boggi U, Troisi RI, Efanov M, Azoulay D, Panaro F, Pessaux P, Wang XY, Zhu JY, Zhang SG, Sun CD, Wu Z, Tao KS, Yang KH, Fan J, Chen XP. International consensus statement on robotic hepatectomy surgery in 2018. *World J Gastroenterol* 2019; **25**: 1432-1444 [PMID: 30948907 DOI: 10.3748/wjg.v25.i12.1432]

18 **Chong CC**, Fuks D, Lee KF, Zhao JJ, Choi GH, Sucandy I, Chiow AKH, Marino MV, Gastaca M, Wang X, Lee JH, Efanov M, Kingham TP, D'Hondt M, Troisi RI, Choi SH, Sutcliffe RP, Chan CY, Lai ECH, Park JO, Di Benedetto F, Rotellar F, Sugioka A, Coelho FF, Ferrero A, Long TCD, Lim C, Scatton O, Liu Q, Schmelzle M, Pratschke J, Cheung TT, Liu R, Han HS, Tang CN, Goh BKP; International Robotic and Laparoscopic Liver Resection study group investigators. Propensity Score-Matched Analysis Comparing Robotic and Laparoscopic Right and Extended Right Hepatectomy. *JAMA Surg* 2022; **157**: 436-444 [PMID: 35262660 DOI: 10.1001/jamasurg.2022.0161]

19 **Varghese CT**, Chandran B, Sudhindran S. Robotic Donor Hepatectomy-Safety in Novelty Is the Essence. *JAMA Surg* 2021; **156**: 1171-1172 [PMID: 34668937 DOI: 10.1001/jamasurg.2021.4428]

20 **Muaddi H**, Hafid ME, Choi WJ, Lillie E, de Mestral C, Nathens A, Stukel TA, Karanicolas PJ. Clinical Outcomes of Robotic Surgery Compared to Conventional Surgical Approaches (Laparoscopic or Open): A Systematic Overview of Reviews. *Ann Surg* 2021; **273**: 467-473 [PMID: 32398482 DOI: 10.1097/SLA.0000000000003915]

21 **Zhu P**, Liao W, Zhang WG, Chen L, Shu C, Zhang ZW, Huang ZY, Chen YF, Lau WY, Zhang BX, Chen XP. A Prospective Study Using Propensity Score Matching to Compare Long-term Survival Outcomes After Robotic-assisted, Laparoscopic, or Open Liver Resection for Patients With BCLC Stage 0-A Hepatocellular Carcinoma. *Ann Surg* 2023; **277**: e103-e111 [PMID: 35081573 DOI: 10.1097/SLA.0000000000005380]

22 **Tsung A**, Geller DA, Sukato DC, Sabbaghian S, Tohme S, Steel J, Marsh W, Reddy SK, Bartlett DL. Robotic versus laparoscopic hepatectomy: a matched comparison. *Ann Surg* 2014; **259**: 549-555 [PMID: 24045442 DOI: 10.1097/SLA.0000000000000250]

23 **Ji WB**, Wang HG, Zhao ZM, Duan WD, Lu F, Dong JH. Robotic-assisted laparoscopic anatomic hepatectomy in China: initial experience. *Ann Surg* 2011; **253**: 342-348 [PMID: 21135692 DOI: 10.1097/SLA.0b013e3181ff4601]

24 **Liu R**, Liu Q, Wang F. Prognosis control surgery: From theory to practice. *Zhongguo Kexue Jianbao* 2019; **64**: 1137-48 [DOI: 10.1360/N972019-00141]

25 **Liu R**, Wang Y, Zhang XP. Revisiting human liver anatomy: dynamic watershed theory. *Hepatobiliary Surg Nutr* 2021; **10**: 139-141 [PMID: 33575307 DOI: 10.21037/hbsn-20-666]

26 **Brouwers MC**, Kho ME, Browman GP, Burgers JS, Cluzeau F, Feder G, Fervers B, Graham ID, Grimshaw J, Hanna SE, Littlejohns P, Makarski J, Zitzelsberger L; AGREE Next Steps Consortium. AGREE II: advancing guideline development, reporting and evaluation in health care. *CMAJ* 2010; **182**: E839-E842 [PMID: 20603348 DOI: 10.1503/cmaj.090449]

27 **Shea BJ**, Reeves BC, Wells G, Thuku M, Hamel C, Moran J, Moher D, Tugwell P, Welch V, Kristjansson E, Henry DA. AMSTAR 2: a critical appraisal tool for systematic reviews that include randomised or non-randomised studies of healthcare interventions, or both. *BMJ* 2017; **358**: j4008 [PMID: 28935701 DOI: 10.1136/bmj.j4008]

28 **Sterne JAC**, Savović J, Page MJ, Elbers RG, Blencowe NS, Boutron I, Cates CJ, Cheng HY, Corbett MS, Eldridge SM, Emberson JR, Hernán MA, Hopewell S, Hróbjartsson A, Junqueira DR, Jüni P, Kirkham JJ, Lasserson T, Li T, McAleenan A, Reeves BC, Shepperd S, Shrier I, Stewart LA, Tilling K, White IR, Whiting PF, Higgins JPT. RoB 2: a revised tool for assessing risk of bias in randomised trials. *BMJ* 2019; **366**: l4898 [PMID: 31462531 DOI: 10.1136/bmj.l4898]

29 **Stang A**. Critical evaluation of the Newcastle-Ottawa scale for the assessment of the quality of nonrandomized studies in meta-analyses. *Eur J Epidemiol* 2010; **25**: 603-605 [PMID: 20652370 DOI: 10.1007/s10654-010-9491-z]

30 **Elliott JH**, Synnot A, Turner T, Simmonds M, Akl EA, McDonald S, Salanti G, Meerpohl J, MacLehose H, Hilton J, Tovey D, Shemilt I,

Thomas J; Living Systematic Review Network. Living systematic review: 1. Introduction-the why, what, when, and how. *J Clin Epidemiol* 2017; **91**: 23-30 [PMID: 28912002 DOI: 10.1016/j.jclinepi.2017.08.010]

31 **Guyatt GH**, Oxman AD, Vist GE, Kunz R, Falck-Ytter Y, Alonso-Coello P, Schünemann HJ; GRADE Working Group. GRADE: an emerging consensus on rating quality of evidence and strength of recommendations. *BMJ* 2008; **336**: 924-926 [PMID: 18436948 DOI: 10.1136/bmj.39489.470347.AD]

32 **Beard RE**, Tsung A. Minimally Invasive Approaches for Surgical Management of Primary Liver Cancers. *Cancer Control* 2017; **24**: 1073274817729234 [PMID: 28975827 DOI: 10.1177/1073274817729234]

33 **Hu M**, Chen K, Zhang X, Li C, Song D, Liu R. Robotic, laparoscopic or open hemihepatectomy for giant liver haemangiomas over 10 cm in diameter. *BMC Surg* 2020; **20**: 93 [PMID: 32375738 DOI: 10.1186/s12893-020-00760-5]

34 **Zhu L**, Liu Y, Hu M, Zhao Z, Li C, Zhang X, Tan X, Wang F, Liu R. Comparison of robotic and laparoscopic liver resection in ordinary cases of left lateral sectionectomy. *Surg Endosc* 2022; **36**: 4923-4931 [PMID: 34750706 DOI: 10.1007/s00464-021-08846-8]

35 **Zhang XP**, Xu S, Hu MG, Zhao ZM, Wang ZH, Zhao GD, Li CG, Tan XL, Liu R. Short- and long-term outcomes after robotic and open liver resection for elderly patients with hepatocellular carcinoma: a propensity score-matched study. *Surg Endosc* 2022; **36**: 8132-8143 [PMID: 35534731 DOI: 10.1007/s00464-022-09236-4]

36 **Hamad A**, Ansari A, Li Y, Shen C, Cloyd J, Pawlik TM, Ejaz A. Short- and long-term outcomes following robotic and open resection for intrahepatic cholangiocarcinoma: A national cohort study. *Surg Oncol* 2022; **43**: 101790 [PMID: 35717859 DOI: 10.1016/j.suronc.2022.101790]

37 **Chen PD**, Wu CY, Hu RH, Chou WH, Lai HS, Liang JT, Lee PH, Wu YM. Robotic Versus Open Hepatectomy for Hepatocellular Carcinoma: A Matched Comparison. *Ann Surg Oncol* 2017; **24**: 1021-1028 [PMID: 27778128 DOI: 10.1245/s10434-016-5638-9]

38 **Nota CL**, Woo Y, Raoof M, Boerner T, Molenaar IQ, Choi GH, Kingham TP, Latorre K, Borel Rinkes IHM, Hagendoorn J, Fong Y. Robotic Versus Open Minor Liver Resections of the Posterosuperior Segments: A Multinational, Propensity Score-Matched Study. *Ann Surg Oncol* 2019; **26**: 583-590 [PMID: 30334196 DOI: 10.1245/s10434-018-6928-1]

39 **Sucandy I**, Rayman S, Lai EC, Tang CN, Chong Y, Efanov M, Fuks D, Choi GH, Chong CC, Chiow AKH, Marino MV, Prieto M, Lee JH, Kingham TP, D'Hondt M, Troisi RI, Choi SH, Sutcliffe RP, Cheung TT, Rotellar F, Park JO, Scatton O, Han HS, Pratschke J, Wang X, Liu R, Goh BKP; International Robotic, Laparoscopic Liver Resection Study Group Investigators. Robotic Versus Laparoscopic Left and Extended Left Hepatectomy: An International Multicenter Study Propensity Score-Matched Analysis. *Ann Surg Oncol* 2022; **29**: 8398-8406 [PMID: 35997903 DOI: 10.1245/s10434-022-12216-6]

40 **Xu J**, Wei Y, Chang W. Robot-assisted procedure vs open surgery for simultaneous resection of colorectal cancer with liver metastases: short-term outcomes of a randomized controlled study. *Ann Oncol* 2017; **28**: x42- [DOI: 10.1093/annonc/mdx659.001]

41 **Rho SY**, Lee JG, Joo DJ, Kim MS, Kim SI, Han DH, Choi JS, Choi GH. Outcomes of Robotic Living Donor Right Hepatectomy From 52 Consecutive Cases: Comparison With Open and Laparoscopy-assisted Donor Hepatectomy. *Ann Surg* 2022; **275**: e433-e442 [PMID: 32773621 DOI: 10.1097/SLA.0000000000004067]

42 **Cortolillo N**, Patel C, Parreco J, Kaza S, Castillo A. Nationwide outcomes and costs of laparoscopic and robotic vs. open hepatectomy. *J Robot Surg* 2019; **13**: 557-565 [PMID: 30484059 DOI: 10.1007/s11701-018-0896-0]

43 **Lee KF**, Chong C, Cheung S, Wong J, Fung A, Lok HT, Lo E, Lai P. Robotic versus open hemihepatectomy: a propensity score-matched study. *Surg Endosc* 2021; **35**: 2316-2323 [PMID: 33185767 DOI: 10.1007/s00464-020-07645-x]

44 **Shu J**, Wang XJ, Li JW, Bie P, Chen J, Zheng SG. Robotic-assisted laparoscopic surgery for complex hepatolithiasis: a propensity score matching analysis. *Surg Endosc* 2019; **33**: 2539-2547 [PMID: 30350102 DOI: 10.1007/s00464-018-6547-8]

45 **Beard RE**, Khan S, Troisi RI, Montalti R, Vanlander A, Fong Y, Kingham TP, Boerner T, Berber E, Kahramangil B, Buell JF, Martinie JB, Vrochides D, Shen C, Molinari M, Geller DA, Tsung A. Long-Term and Oncologic Outcomes of Robotic Versus Laparoscopic Liver Resection for Metastatic Colorectal Cancer: A Multicenter, Propensity Score Matching Analysis. *World J Surg* 2020; **44**: 887-895 [PMID: 31748885 DOI: 10.1007/s00268-019-05270-x]

46 **Masetti M**, Fallani G, Ratti F, Ferrero A, Giuliante F, Cillo U, Guglielmi A, Ettorre GM, Torzilli G, Vincenti L, Ercolani G, Cipressi C, Lombardi R, Aldrighetti L, Jovine E. Minimally invasive treatment of colorectal liver metastases: does robotic surgery provide any technical advantages over laparoscopy? A multicenter analysis from the IGoMILS (Italian Group of Minimally Invasive Liver Surgery) registry. *Updates Surg* 2022; **74**: 535-545 [PMID: 35099776 DOI: 10.1007/s13304-022-01245-1]

47 **Murtha-Lemekhova A**, Fuchs J, Hoffmann K. Innovation for the Sake of Innovation? How Does Robotic Hepatectomy Compare to Laparoscopic or Open Resection for HCC-A Systematic Review and Meta-Analysis. *Cancers (Basel)* 2022; **14** [PMID: 35884420 DOI: 10.3390/cancers14143359]

48 **Hu Y**, Guo K, Xu J, Xia T, Wang T, Liu N, Fu Y. Robotic versus laparoscopic hepatectomy for malignancy: A systematic review and meta-analysis. *Asian J Surg* 2021; **44**: 615-628 [PMID: 33468382 DOI: 10.1016/j.asjsur.2020.12.016]

49 **Sucandy I**, Shapera E, Syblis CC, Crespo K, Przetocki VA, Ross SB, Rosemurgy AS. Propensity score matched comparison of robotic and open major hepatectomy for malignant liver tumors. *Surg Endosc* 2022; **36**: 6724-6732 [PMID: 34981238 DOI: 10.1007/s00464-021-08948-3]

50 **Wu YM**, Hu RH, Lai HS, Lee PH. Robotic-assisted minimally invasive liver resection. *Asian J Surg* 2014; **37**: 53-57 [PMID: 24642128 DOI: 10.1016/j.asjsur.2014.01.015]

51 **Yang HY**, Rho SY, Han DH, Choi JS, Choi GH. Robotic major liver resections: Surgical outcomes compared with open major liver resections. *Ann Hepatobiliary Pancreat Surg* 2021; **25**: 8-17 [PMID: 33649249 DOI: 10.14701/ahbps.2021.25.1.8]

52 **Yu S**, Yuan G, Lu S, Li J, Tang B, Zhong F, Su H, He S. Application of da Vinci robot and laparoscopy on repeat hepatocellular carcinoma. *J Minim Access Surg* 2022; **18**: 378-383 [PMID: 35708383 DOI: 10.4103/jmas.JMAS_111_21]

53 **Balzano E**, Bernardi L, Tincani G, Ghinolfi D, Melandro F, Bronzoni J, Meli S, Arenga G, Biancofiore G, Crocetti L, De Simone P. Implementing a robotic liver resection program does not always require prior laparoscopic experience. *Surg Endosc* 2022; **36**: 3317-3322 [PMID: 34606006 DOI: 10.1007/s00464-021-08645-1]

54 **Duong LM**, Cai H, Shrubsole MJ, Bailey CE, Idrees K, Shu XO. Outcomes of robotic-assisted liver surgery versus laparoscopic liver surgery for treatment of stage I hepatocellular carcinoma. *Cancer* 2022; **128**: 762-769 [PMID: 34674225 DOI: 10.1002/cncr.33979]

55 **Lai EC**, Tang CN. Long-term Survival Analysis of Robotic Versus Conventional Laparoscopic Hepatectomy for Hepatocellular Carcinoma: A Comparative Study. *Surg Laparosc Endosc Percutan Tech* 2016; **26**: 162-166 [PMID: 27031650 DOI: 10.1097/SLE.0000000000000254]

56 **Lim C**, Goumard C, Salloum C, Tudisco A, Napoli N, Boggi U, Azoulay D, Scatton O. Outcomes after 3D laparoscopic and robotic liver resection for hepatocellular carcinoma: a multicenter comparative study. *Surg Endosc* 2021; **35**: 3258-3266 [PMID: 32617657 DOI: 10.1007/s00464-020-07762-7]

57 **Magistri P**, Tarantino G, Guidetti C, Assirati G, Olivieri T, Ballarin R, Coratti A, Di Benedetto F. Laparoscopic versus robotic surgery for hepatocellular carcinoma: the first 46 consecutive cases. *J Surg Res* 2017; **217**: 92-99 [PMID: 28641762 DOI: 10.1016/j.jss.2017.05.005]

58 **Pesi B**, Bencini L, Moraldi L, Tofani F, Batignani G, Bechi P, Farsi M, Annecchiarico M, Coratti A. Robotic Versus Open Liver Resection in Hepatocarcinoma: Surgical and Oncological Outcomes. *Surg Laparosc Endosc Percutan Tech* 2021; **31**: 468-474 [PMID: 33480668 DOI: 10.1097/SLE.0000000000000904]

59 **Wang WH**, Kuo KK, Wang SN, Lee KT. Oncological and surgical result of hepatoma after robot surgery. *Surg Endosc* 2018; **32**: 3918-3924 [PMID: 29488090 DOI: 10.1007/s00464-018-6131-2]

60 **Shapera EA**, Ross S, Syblis C, Crespo K, Rosemurgy A, Sucandy I. Analysis of Oncological Outcomes After Robotic Liver Resection for Intrahepatic Cholangiocarcinoma. *Am Surg* 2023; **89**: 2399-2412 [PMID: 35512632 DOI: 10.1177/00031348221093933]

61 **Gumbs AA**, Lorenz E, Tsai TJ, Starker L, Flanagan J, Benedetti Cacciaguerra A, Yu NJ, Bajul M, Chouillard E, Croner R, Abu Hilal M. Study: International Multicentric Minimally Invasive Liver Resection for Colorectal Liver Metastases (SIMMILR-CRLM). *Cancers (Basel)* 2022; **14** [PMID: 35326532 DOI: 10.3390/cancers14061379]

62 **Rahimli M**, Perrakis A, Schellerer V, Gumbs A, Lorenz E, Franz M, Arend J, Negrini VR, Croner RS. Robotic and laparoscopic liver surgery for colorectal liver metastases: an experience from a German Academic Center. *World J Surg Oncol* 2020; **18**: 333 [PMID: 33353551 DOI: 10.1186/s12957-020-02113-1]

63 **Shapera E**, Ross S, Crespo K, Syblis C, Przetocki V, Rosemurgy A, Sucandy I. Analysis of surgical approach and tumor distance to margin after liver resection for colorectal liver metastasis. *J Robot Surg* 2022; **16**: 1427-1439 [PMID: 35199291 DOI: 10.1007/s11701-022-01387-9]

64 **Rocca A**, Scacchi A, Cappuccio M, Avella P, Bugiantella W, De Rosa M, Costa G, Polistena A, Codacci-Pisanelli M, Amato B, Carbone F, Ceccarelli G. Robotic surgery for colorectal liver metastases resection: A systematic review. *Int J Med Robot* 2021; **17**: e2330 [PMID: 34498805 DOI: 10.1002/rcs.2330]

65 **Machairas N**, Dorovinis P, Kykalos S, Stamopoulos P, Schizas D, Zoe G, Terra A, Nikiteas N. Simultaneous robotic-assisted resection of colorectal cancer and synchronous liver metastases: a systematic review. *J Robot Surg* 2021; **15**: 841-848 [PMID: 33598830 DOI: 10.1007/s11701-021-01213-8]

66 **Amma BSPT**, Mathew JS, Varghese CT, Nair K, Mallick S, Chandran B, Menon RN, Gopalakrishnan U, Balakrishnan D, George PS, Vayoth SO, Sudhindran S. Open to robotic right donor hepatectomy: A tectonic shift in surgical technique. *Clin Transplant* 2022; **36**: e14775 [PMID: 35876772 DOI: 10.1111/ctr.14775]

67 **Lincango Naranjo EP**, Garces-Delgado E, Siepmann T, Mirow L, Solis-Pazmino P, Alexander-Leon H, Restrepo-Rodas G, Mancero-Montalvo R, Ponce CJ, Cadena-Semanate R, Vargas-Cordova R, Herrera-Cevallos G, Vallejo S, Liu-Sanchez C, Prokop LJ, Ziogas IA, Vailas MG, Guerron AD, Visser BC, Ponce OJ, Barbas AS, Moris D. Robotic Living Donor Right Hepatectomy: A Systematic Review and Meta-Analysis. *J Clin Med* 2022; **11** [PMID: 35566727 DOI: 10.3390/jcm11092603]

68 **Yeow M**, Soh S, Starkey G, Perini MV, Koh YX, Tan EK, Chan CY, Raj P, Goh BKP, Kabir T. A systematic review and network meta-analysis of outcomes after open, mini-laparotomy, hybrid, totally laparoscopic, and robotic living donor right hepatectomy. *Surgery* 2022; **172**: 741-750 [PMID: 35644687 DOI: 10.1016/j.surg.2022.03.042]

69 **Nota CL**, Rinkes IHB, Molenaar IQ, van Santvoort HC, Fong Y, Hagendoorn J. Robot-assisted laparoscopic liver resection: a systematic review and pooled analysis of minor and major hepatectomies. *HPB (Oxford)* 2016; **18**: 113-120 [PMID: 26902129 DOI: 10.1016/j.hpb.2015.09.003]

70 **Wang JM**, Li JF, Yuan GD, He SQ. Robot-assisted versus laparoscopic minor hepatectomy: A systematic review and meta-analysis. *Medicine (Baltimore)* 2021; **100**: e25648 [PMID: 33907124 DOI: 10.1097/MD.0000000000025648]

71 **Daskalaki D**, Gonzalez-Heredia R, Brown M, Bianco FM, Tzvetanov I, Davis M, Kim J, Benedetti E, Giulianotti PC. Financial Impact of the Robotic Approach in Liver Surgery: A Comparative Study of Clinical Outcomes and Costs Between the Robotic and Open Technique in a Single Institution. *J Laparoendosc Adv Surg Tech A* 2017; **27**: 375-382 [PMID: 28186429 DOI: 10.1089/lap.2016.0576]

72 **Valverde A**, Abdallah S, Danoussou D, Goasguen N, Jouvin I, Oberlin O, Lupinacci RM. Transitioning From Open to Robotic Liver Resection. Results of 46 Consecutive Procedures Including a Majority of Major Hepatectomies. *Surg Innov* 2021; **28**: 309-315 [PMID: 32857664 DOI: 10.1177/1553350620954580]

73 **Croner RS**, Perrakis A, Hohenberger W, Brunner M. Robotic liver surgery for minor hepatic resections: a comparison with laparoscopic and open standard procedures. *Langenbecks Arch Surg* 2016; **401**: 707-714 [PMID: 27207697 DOI: 10.1007/s00423-016-1440-1]

74 **Kadam P**, Sutcliffe RP, Scatton O, Sucandy I, Kingham TP, Liu R, Choi GH, Syn NL, Gastaca M, Choi SH, Chiow AKH, Marino MV, Efanov M, Lee JH, Chong CC, Tang CN, Cheung TT, Pratschke J, Wang X, Campos RR, Ivanecz A, Park JO, Rotellar F, Fuks D, D'Hondt M, Han HS, Troisi RI, Goh BKP; International Robotic and Laparoscopic Liver Resection Study Group Investigators. An international multicenter propensity-score matched and coarsened-exact matched analysis comparing robotic versus laparoscopic partial liver resections of the anterolateral segments. *J Hepatobiliary Pancreat Sci* 2022; **29**: 843-854 [PMID: 35393759 DOI: 10.1002/jhbp.1149]

75 **Kim JK**, Park JS, Han DH, Choi GH, Kim KS, Choi JS, Yoon DS. Robotic versus laparoscopic left lateral sectionectomy of liver. *Surg Endosc* 2016; **30**: 4756-4764 [PMID: 26902613 DOI: 10.1007/s00464-016-4803-3]

76 **Lai EC**, Yang GP, Tang CN. Robot-assisted laparoscopic liver resection for hepatocellular carcinoma: short-term outcome. *Am J Surg* 2013; **205**: 697-702 [PMID: 23561638 DOI: 10.1016/j.amjsurg.2012.08.015]

77 **Lee KF**, Cheung YS, Chong CC, Wong J, Fong AK, Lai PB. Laparoscopic and robotic hepatectomy: experience from a single centre. *ANZ J Surg* 2016; **86**: 122-126 [PMID: 26423216 DOI: 10.1111/ans.13339]

78 **Mejia A**, Cheng SS, Vivian E, Shah J, Oduor H, Archarya P. Minimally invasive liver resection in the era of robotics: analysis of 214 cases. *Surg Endosc* 2020; **34**: 339-348 [PMID: 30937618 DOI: 10.1007/s00464-019-06773-3]

79 **Packiam V**, Bartlett DL, Tohme S, Reddy S, Marsh JW, Geller DA, Tsung A. Minimally invasive liver resection: robotic versus laparoscopic left lateral sectionectomy. *J Gastrointest Surg* 2012; **16**: 2233-2238 [PMID: 23054901 DOI: 10.1007/s11605-012-2040-1]

80 **Salloum C**, Lim C, Lahat E, Gavara CG, Levesque E, Compagnon P, Azoulay D. Robotic-Assisted Versus Laparoscopic Left Lateral Sectionectomy: Analysis of Surgical Outcomes and Costs by a Propensity Score Matched Cohort Study. *World J Surg* 2017; **41**: 516-524 [PMID: 27743071 DOI: 10.1007/s00268-016-3736-2]

81 **Tranchart H**, Ceribelli C, Ferretti S, Dagher I, Patriti A. Traditional versus robot-assisted full laparoscopic liver resection: a matched-pair comparative study. *World J Surg* 2014; **38**: 2904-2909 [PMID: 24984879 DOI: 10.1007/s00268-014-2679-8]

82 **Lee KF**, Fong AK, Chong CC, Cheung SY, Wong J, Lai PB. Robotic Liver Resection For Primary Hepatolithiasis: Is It Beneficial? *World J Surg* 2016; **40**: 2490-2496 [PMID: 27138884 DOI: 10.1007/s00268-016-3528-8]

83 **Morel P**, Jung M, Cornateanu S, Buehler L, Majno P, Toso C, Buchs NC, Rubbia-Brandt L, Hagen ME. Robotic versus open liver resections:

A case-matched comparison. *Int J Med Robot* 2017; **13** [PMID: 28058770 DOI: 10.1002/rcs.1800]

84 **Cai JP**, Chen W, Chen LH, Wan XY, Lai JM, Yin XY. Comparison between robotic-assisted and laparoscopic left hemi-hepatectomy. *Asian J Surg* 2022; **45**: 265-268 [PMID: 34120821 DOI: 10.1016/j.asjsur.2021.05.017]

85 **Fruscione M**, Pickens R, Baker EH, Cochran A, Khan A, Ocuin L, Iannitti DA, Vrochides D, Martinie JB. Robotic-assisted versus laparoscopic major liver resection: analysis of outcomes from a single center. *HPB (Oxford)* 2019; **21**: 906-911 [PMID: 30617001 DOI: 10.1016/j.hpb.2018.11.011]

86 **Lorenz E**, Arend J, Franz M, Rahimli M, Perrakis A, Negrini V, Gumbs AA, Croner RS. Robotic and laparoscopic liver resection-comparative experiences at a high-volume German academic center. *Langenbecks Arch Surg* 2021; **406**: 753-761 [PMID: 33834295 DOI: 10.1007/s00423-021-02152-6]

87 **Marino MV**, Shabat G, Guarrasi D, Gulotta G, Komorowski AL. Comparative Study of the Initial Experience in Performing Robotic and Laparoscopic Right Hepatectomy with Technical Description of the Robotic Technique. *Dig Surg* 2019; **36**: 241-250 [PMID: 29539603 DOI: 10.1159/000487686]

88 **Spampinato MG**, Coratti A, Bianco L, Caniglia F, Laurenzi A, Puleo F, Ettorre GM, Boggi U. Perioperative outcomes of laparoscopic and robot-assisted major hepatectomies: an Italian multi-institutional comparative study. *Surg Endosc* 2014; **28**: 2973-2979 [PMID: 24853851 DOI: 10.1007/s00464-014-3560-4]

89 **Wang ZZ**, Tang WB, Hu MG, Zhao ZM, Zhao GD, Li CG, Tan XL, Zhang X, Lau WY, Liu R. Robotic vs laparoscopic hemihepatectomy: A comparative study from a single center. *J Surg Oncol* 2019; **120**: 646-653 [PMID: 31313324 DOI: 10.1002/jso.25640]

90 **Chin KM**, Linn YL, Cheong CK, Koh YX, Teo JY, Chung AYF, Chan CY, Goh BKP. Minimally invasive versus open right anterior sectionectomy and central hepatectomy for central liver malignancies: a propensity-score-matched analysis. *ANZ J Surg* 2021; **91**: E174-E182 [PMID: 33719128 DOI: 10.1111/ans.16719]

91 **Cho CW**, Rhu J, Kwon CHD, Choi GS, Kim JM, Joh JW, Koh KC, Kim GS. Short-Term Outcomes of Totally Laparoscopic Central Hepatectomy and Right Anterior Sectionectomy for Centrally Located Tumors: A Case-Matched Study with Propensity Score Matching. *World J Surg* 2017; **41**: 2838-2846 [PMID: 28752429 DOI: 10.1007/s00268-017-4105-5]

92 **Jeung IH**, Choi SH, Kim S, Kwon SW. Laparoscopic Central Bisectionectomy and Right Anterior Sectionectomy Using Two Retraction Methods: Technical Aspects with Video. *World J Surg* 2019; **43**: 3120-3127 [PMID: 31493192 DOI: 10.1007/s00268-019-05154-0]

93 **Chiow AKH**, Fuks D, Choi GH, Syn N, Sucandy I, Marino MV, Prieto M, Chong CC, Lee JH, Efanov M, Kingham TP, Choi SH, Sutcliffe RP, Troisi RI, Pratschke J, Cheung TT, Wang X, Liu R, D'Hondt M, Chan CY, Tang CN, Han HS, Goh BKP; International Robotic and Laparoscopic Liver Resection Study Group collaborators. International multicentre propensity score-matched analysis comparing robotic versus laparoscopic right posterior sectionectomy. *Br J Surg* 2021; **108**: 1513-1520 [PMID: 34750608 DOI: 10.1093/bjs/znab321]

94 **Patriti A**, Cipriani F, Ratti F, Bartoli A, Ceccarelli G, Casciola L, Aldrighetti L. Robot-assisted versus open liver resection in the right posterior section. *JSLS* 2014; **18** [PMID: 25516700 DOI: 10.4293/JSLS.2014.00040]

95 **Montalti R**, Scuderi V, Patriti A, Vivarelli M, Troisi RI. Robotic versus laparoscopic resections of posterosuperior segments of the liver: a propensity score-matched comparison. *Surg Endosc* 2016; **30**: 1004-1013 [PMID: 26123328 DOI: 10.1007/s00464-015-4284-9]

96 **Zhao ZM**, Yin ZZ, Pan LC, Hu MG, Tan XL, Liu R. Robotic isolated partial and complete hepatic caudate lobectomy: A single institution experience. *Hepatobiliary Pancreat Dis Int* 2020; **19**: 435-439 [PMID: 32513586 DOI: 10.1016/j.hbpd.2020.05.003]

97 **Zhao ZM**, Yin ZZ, Pan LC, Jiang N, Tan XL, Chen X, Liu R. Robotic anatomic isolated complete caudate lobectomy: Left-side approach and techniques. *Asian J Surg* 2021; **44**: 269-274 [PMID: 32747143 DOI: 10.1016/j.asjsur.2020.07.011]

98 **Ziogas IA**, Evangeliou AP, Mylonas KS, Athanasiadis DI, Cherouveim P, Geller DA, Schulick RD, Alexopoulos SP, Tsoulfas G. Economic analysis of open versus laparoscopic versus robotic hepatectomy: a systematic review and meta-analysis. *Eur J Health Econ* 2021; **22**: 585-604 [PMID: 33740153 DOI: 10.1007/s10198-021-01277-1]

99 **Aziz H**, Hanna K, Lashkari N, Ahmad NU, Genyk Y, Sheikh MR. Hospitalization Costs and Outcomes of Open, Laparoscopic, and Robotic Liver Resections. *Am Surg* 2022; **88**: 2331-2337 [PMID: 33861658 DOI: 10.1177/00031348211011063]

100 **D'Hondt M**, Devooght A, Willems E, Wicherts D, De Meyere C, Parmentier I, Provoost A, Pottel H, Verslype C. Transition from laparoscopic to robotic liver surgery: clinical outcomes, learning curve effect, and cost-effectiveness. *J Robot Surg* 2023; **17**: 79-88 [PMID: 35322342 DOI: 10.1007/s11701-022-01405-w]

101 **Hawksworth J**, Llore N, Holzner ML, Radkani P, Meslar E, Winslow E, Satoskar R, He R, Jha R, Haddad N, Fishbein T. Robotic Hepatectomy Is a Safe and Cost-Effective Alternative to Conventional Open Hepatectomy: a Single-Center Preliminary Experience. *J Gastrointest Surg* 2021; **25**: 825-828 [PMID: 33001352 DOI: 10.1007/s11605-020-04793-2]

102 **Miller HP**, Hakim A, Kellish A, Wozniak M, Gaughan J, Sensenig R, Atabek UM, Spitz FR, Hong YK. Cost-Benefit Analysis of Robotic vs. Laparoscopic Hepatectomy: A Propensity-Matched Retrospective Cohort Study of American College of Surgeons National Surgical Quality Improvement Program Database. *Am Surg* 2022; **88**: 2886-2892 [PMID: 33861656 DOI: 10.1177/00031348211011124]

103 **Shapera E**, Sucandy I, Syblis C, Crespo K, Ja'Karri T, Ross S, Rosemurgy A. Cost analysis of robotic versus open hepatectomy: Is the robotic platform more expensive? *J Robot Surg* 2022; **16**: 1409-1417 [PMID: 35152343 DOI: 10.1007/s11701-022-01375-z]

104 **Yu YD**, Kim KH, Jung DH, Namkoong JM, Yoon SY, Jung SW, Lee SK, Lee SG. Robotic versus laparoscopic liver resection: a comparative study from a single center. *Langenbecks Arch Surg* 2014; **399**: 1039-1045 [PMID: 25366357 DOI: 10.1007/s00423-014-1238-y]

105 **Sham JG**, Richards MK, Seo YD, Pillarisetty VG, Yeung RS, Park JO. Efficacy and cost of robotic hepatectomy: is the robot cost-prohibitive? *J Robot Surg* 2016; **10**: 307-313 [PMID: 27153838 DOI: 10.1007/s11701-016-0598-4]

106 **Wu CY**, Chen PD, Chou WH, Liang JT, Huang CS, Wu YM. Is robotic hepatectomy cost-effective? In view of patient-reported outcomes. *Asian J Surg* 2019; **42**: 543-550 [PMID: 30704965 DOI: 10.1016/j.asjsur.2018.12.010]

107 **Coletta D**, De Padua C, Parrino C, De Peppo V, Oddi A, Frigieri C, Grazi GL. Laparoscopic Liver Surgery: What Are the Advantages in Patients with Cirrhosis and Portal Hypertension? Systematic Review and Meta-Analysis with Personal Experience. *J Laparoendosc Adv Surg Tech A* 2020; **30**: 1054-1065 [PMID: 32707003 DOI: 10.1089/lap.2020.0408]

108 **Dong KS**, Liang BY, Zhang ZY, Zhang EL, Yang G, Xia SL, Chen XP, Huang ZY. Histologic severity of liver cirrhosis: A key factor affecting surgical outcomes of hepatocellular carcinoma in patients with portal hypertension. *Asian J Surg* 2019; **42**: 981-989 [PMID: 30782497 DOI: 10.1016/j.asjsur.2019.01.009]

109 **Lin CH**, Ho CM, Wu CH, Liang PC, Wu YM, Hu RH, Lee PH, Ho MC. Minimally invasive surgery versus radiofrequency ablation for single subcapsular hepatocellular carcinoma ≤ 2 cm with compensated liver cirrhosis. *Surg Endosc* 2020; **34**: 5566-5573 [PMID: 31993821 DOI: 10.1007/s00464-019-07357-x]

110 **European Association for the Study of the Liver**. EASL Clinical Practice Guidelines: Management of hepatocellular carcinoma. *J Hepatol*

2018; **69**: 182-236 [PMID: 29628281 DOI: 10.1016/j.jhep.2018.03.019]
111 **Birgin E**, Hartwig V, Rasbach E, Seyfried S, Rahbari M, Reeg A, Jentschura SL, Téoule P, Reißfelder C, Rahbari NN. Minimally invasive mesohepatectomy for centrally located liver lesions-a case series. *Surg Endosc* 2022; **36**: 8935-8942 [PMID: 35668311 DOI: 10.1007/s00464-022-09342-3]
112 **Hawksworth J**, Radkani P, Filice R, Aguirre O, Nguyen B, Fishbein T, Winslow E. Robotic Central Hepatectomy and Right Anterior Sectionectomy: Minimally Invasive Parenchyma Sparing Surgery for Central Liver Tumors. *J Gastrointest Surg* 2023; **27**: 407-410 [PMID: 36600076 DOI: 10.1007/s11605-022-05554-z]
113 **Casciola L**, Patriti A, Ceccarelli G, Bartoli A, Ceribelli C, Spaziani A. Robot-assisted parenchymal-sparing liver surgery including lesions located in the posterosuperior segments. *Surg Endosc* 2011; **25**: 3815-3824 [PMID: 21656067 DOI: 10.1007/s00464-011-1796-9]
114 **Au KP**, Chan ACY. Current status of associating liver partition with portal vein ligation for staged hepatectomy: Comparison with two-stage hepatectomy and strategies for better outcomes. *World J Gastroenterol* 2019; **25**: 6373-6385 [PMID: 31798275 DOI: 10.3748/wjg.v25.i43.6373]
115 **Lang H**. ALPPS - Beneficial or detrimental? *Surg Oncol* 2020; **33**: 249-253 [PMID: 31740102 DOI: 10.1016/j.suronc.2019.10.013]
116 **Michal K**, Sau M, Tamara GMH, Long JR. A better route to ALPPS: minimally invasive vs open ALPPS. *Surg Endosc* 2020; **34**: 2379-2389 [PMID: 32274625 DOI: 10.1007/s00464-020-07437-3]
117 **Melandro F**, Giovanardi F, Hassan R, Larghi Laureiro Z, Ferri F, Rossi M, Mennini G, Pawlik TM, Lai Q. Minimally Invasive Approach in the Setting of ALPPS Procedure: a Systematic Review of the Literature. *J Gastrointest Surg* 2019; **23**: 1917-1924 [PMID: 31197682 DOI: 10.1007/s11605-018-04092-x]
118 **Vicente E**, Quijano Y, Ielpo B, Fabra I. First ALPPS procedure using a total robotic approach. *Surg Oncol* 2016; **25**: 457 [PMID: 26856770 DOI: 10.1016/j.suronc.2015.10.001]
119 **Krishnamurthy J**, Naragund AV, Mahadevappa B. First Ever Robotic Stage One ALPPS Procedure in India: for Colorectal Liver Metastases. *Indian J Surg* 2018; **80**: 269-271 [PMID: 29973758 DOI: 10.1007/s12262-017-1713-0]
120 **Machado MAC**, Surjan RC, Makdissi F. Robotic ALPPS. *Ann Surg Oncol* 2020; **27**: 1174-1179 [PMID: 31686346 DOI: 10.1245/s10434-019-08027-x]
121 **Di Benedetto F**, Assirati G, Magistri P. Full robotic ALPPS for HCC with intrahepatic portal vein thrombosis. *Int J Med Robot* 2020; **16**: e2087 [PMID: 32011081 DOI: 10.1002/rcs.2087]
122 **Masetti M**, Lombardi R, Romboli A, Jovine E. Fully Robotic ALPPS and Simultaneous Left Colectomy for Synchronous Colorectal Liver Metastases. *J Laparoendosc Adv Surg Tech A* 2020; **30**: 1106-1109 [PMID: 32762603 DOI: 10.1089/lap.2020.0589]
123 **Hu MG**, Wang J, Yin ZZ, Liu R. First two-stage robotic ALPPS in HCC patients with hepatic vein invasion: a step-by-step procedure from a clinical case. *World J Surg Oncol* 2021; **19**: 58 [PMID: 33612103 DOI: 10.1186/s12957-021-02170-0]
124 **Di Benedetto F**, Magistri P. First Case of Full Robotic ALPPS for Intrahepatic Cholangiocarcinoma. *Ann Surg Oncol* 2021; **28**: 865 [PMID: 32638168 DOI: 10.1245/s10434-020-08794-y]
125 **Schadde E**, Ardiles V, Robles-Campos R, Malago M, Machado M, Hernandez-Alejandro R, Soubrane O, Schnitzbauer AA, Raptis D, Tschuor C, Petrowsky H, De Santibanes E, Clavien PA; ALPPS Registry Group. Early survival and safety of ALPPS: first report of the International ALPPS Registry. *Ann Surg* 2014; **260**: 829-36; discussion 836 [PMID: 25379854 DOI: 10.1097/SLA.0000000000000947]
126 **Schadde E**, Raptis DA, Schnitzbauer AA, Ardiles V, Tschuor C, Lesurtel M, Abdalla EK, Hernandez-Alejandro R, Jovine E, Machado M, Malago M, Robles-Campos R, Petrowsky H, Santibanes ED, Clavien PA. Prediction of Mortality After ALPPS Stage-1: An Analysis of 320 Patients From the International ALPPS Registry. *Ann Surg* 2015; **262**: 780-5; discussion 785 [PMID: 26583666 DOI: 10.1097/SLA.0000000000001450]
127 **Rimassa L**, Finn RS, Sangro B. Combination immunotherapy for hepatocellular carcinoma. *J Hepatol* 2023; **79**: 506-515 [PMID: 36933770 DOI: 10.1016/j.jhep.2023.03.003]
128 **Sadeghi S**, Bejjani A, Finn RS. Systemic Therapy for Primary Liver Tumors: Cholangiocarcinoma and Hepatocellular Carcinoma. *Surg Oncol Clin N Am* 2019; **28**: 695-715 [PMID: 31472914 DOI: 10.1016/j.soc.2019.06.015]
129 **Zhu P**, Liao W, Ding ZY, Chen L, Zhang WG, Zhang BX, Chen XP. Learning Curve in Robot-Assisted Laparoscopic Liver Resection. *J Gastrointest Surg* 2019; **23**: 1778-1787 [PMID: 30406576 DOI: 10.1007/s11605-018-3689-x]
130 **Varghese CT**, Chandran B, Gopalakrishnan U, Nair K, Mallick S, Mathew JS, Sivasankara Pillai Thankamony Amma B, Balakrishnan D, Othiyil Vayoth S, Sudhindran S. Extended criteria donors for robotic right hepatectomy: A propensity score matched analysis. *J Hepatobiliary Pancreat Sci* 2022; **29**: 874-883 [PMID: 35411725 DOI: 10.1002/jhbp.1145]
131 **Liu Q**, Zhang T, Hu M, Zhao Z, Zhao G, Li C, Zhang X, Lau WY, Liu R. Comparison of the learning curves for robotic left and right hemihepatectomy: A prospective cohort study. *Int J Surg* 2020; **81**: 19-25 [PMID: 32739547 DOI: 10.1016/j.ijsu.2020.07.022]
132 **Gravetz A**, Sucandy I, Wilfong C, Patel N, Spence J, Ross S, Rosemurgy A. Single-Institution Early Experience and Learning Curve with Robotic Liver Resections. *Am Surg* 2019; **85**: 115-119 [PMID: 30760356 DOI: 10.1177/000313481908500143]
133 **Efanov M**, Alikhanov R, Tsvirkun V, Kazakov I, Melekhina O, Kim P, Vankovich A, Grendal K, Berelavichus S, Khatkov I. Comparative analysis of learning curve in complex robot-assisted and laparoscopic liver resection. *HPB (Oxford)* 2017; **19**: 818-824 [PMID: 28599892 DOI: 10.1016/j.hpb.2017.05.003]
134 **Chen PD**, Wu CY, Hu RH, Chen CN, Yuan RH, Liang JT, Lai HS, Wu YM. Robotic major hepatectomy: Is there a learning curve? *Surgery* 2017; **161**: 642-649 [PMID: 27884614 DOI: 10.1016/j.surg.2016.09.025]
135 Goh BKP, Teo JY, Lee SY, Kam JH, Cheow PC, Jeyaraj P, Chow PKH, Ooi L, Chung AYF, Chan CY. Critical appraisal of the impact of individual surgeon experience on the outcomes of laparoscopic liver resection in the modern era: collective experience of multiple surgeons at a single institution with 324 consecutive cases. *Surg Endosc* 2018; 32:1802-11 [PMID: 28916894 DOI: 10.1007/s00464-017-5864-7]
136 **Chua D**, Syn N, Koh YX, Goh BKP. Learning curves in minimally invasive hepatectomy: systematic review and meta-regression analysis. *Br J Surg* 2021; **108**: 351-358 [PMID: 33779690 DOI: 10.1093/bjs/znaa118]
137 **Linn YL**, Wu AG, Han HS, Liu R, Chen KH, Fuks D, Soubrane O, Cherqui D, Geller D, Cheung TT, Edwin B, Aldrighetti L, Abu Hilal M, Troisi RI, Wakabayashi G, Goh BKP; International Robotic and Laparoscopic Liver Resection Study Group Investigators. Systematic review and meta-analysis of difficulty scoring systems for laparoscopic and robotic liver resections. *J Hepatobiliary Pancreat Sci* 2023; **30**: 36-59 [PMID: 35780493 DOI: 10.1002/jhbp.1211]
138 **Wakabayashi G**. What has changed after the Morioka consensus conference 2014 on laparoscopic liver resection? *Hepatobiliary Surg Nutr* 2016; **5**: 281-289 [PMID: 27500140 DOI: 10.21037/hbsn.2016.03.03]

139 **Hasegawa Y**, Wakabayashi G, Nitta H, Takahara T, Katagiri H, Umemura A, Makabe K, Sasaki A. A novel model for prediction of pure laparoscopic liver resection surgical difficulty. *Surg Endosc* 2017; **31**: 5356-5363 [PMID: 28593408 DOI: 10.1007/s00464-017-5616-8]

140 **Kawaguchi Y**, Fuks D, Kokudo N, Gayet B. Difficulty of Laparoscopic Liver Resection: Proposal for a New Classification. *Ann Surg* 2018; **267**: 13-17 [PMID: 28187043 DOI: 10.1097/SLA.0000000000002176]

141 **Halls MC**, Berardi G, Cipriani F, Barkhatov L, Lainas P, Harris S, D'Hondt M, Rotellar F, Dagher I, Aldrighetti L, Troisi RI, Edwin B, Abu Hilal M. Development and validation of a difficulty score to predict intraoperative complications during laparoscopic liver resection. *Br J Surg* 2018; **105**: 1182-1191 [PMID: 29737513 DOI: 10.1002/bjs.10821]

142 **Castaing D**, Emond J, Kunstlinger F, Bismuth H. Utility of operative ultrasound in the surgical management of liver tumors. *Ann Surg* 1986; **204**: 600-605 [PMID: 3021072 DOI: 10.1097/00000658-198611000-00015]

143 **Ferrero A**, Lo Tesoriere R, Russolillo N, Viganò L, Forchino F, Capussotti L. Ultrasound-guided laparoscopic liver resections. *Surg Endosc* 2015; **29**: 1002-1005 [PMID: 25135446 DOI: 10.1007/s00464-014-3762-9]

144 **Zhu P**, Liao W, Ding ZY, Luo HC, Zhang BH, Zhang WG, Zhang W, Zhang ZG, Zhang BX, Chen XP. Intraoperative ultrasonography of robot-assisted laparoscopic hepatectomy: initial experiences from 110 consecutive cases. *Surg Endosc* 2018; **32**: 4071-4077 [PMID: 30151749 DOI: 10.1007/s00464-017-5854-9]

145 **Wakabayashi T**, Cacciaguerra AB, Abe Y, Bona ED, Nicolini D, Mocchegiani F, Kabeshima Y, Vivarelli M, Wakabayashi G, Kitagawa Y. Indocyanine Green Fluorescence Navigation in Liver Surgery: A Systematic Review on Dose and Timing of Administration. *Ann Surg* 2022; **275**: 1025-1034 [PMID: 35121701 DOI: 10.1097/SLA.0000000000005406]

146 **Zhang X**, Xu S, Zhao Z. Application of ICG "four-zone three-phase" fluorescence imaging in robot-assisted anatomical hepatectomy. *Chin J Hepat Surg* 2021; **10**: 191-6

World Journal of Gastroenterology

Submit a Manuscript: https://www.f6publishing.com

World J Gastroenterol 2023 August 28; 29(32): 4831-4850

DOI: 10.3748/wjg.v29.i32.4831

ISSN 1007-9327 (print) ISSN 2219-2840 (online)

REVIEW

Non-alcoholic fatty liver disease: Immunological mechanisms and current treatments

Lucy Petagine, Mohammed Gulrez Zariwala, Vinood B Patel

Specialty type: Gastroenterology and hepatology

Provenance and peer review: Invited article; Externally peer reviewed.

Peer-review model: Single blind

Peer-review report's scientific quality classification

Grade A (Excellent): 0
Grade B (Very good): B
Grade C (Good): C
Grade D (Fair): 0
Grade E (Poor): 0

P-Reviewer: Sun H, China; Zhang Y, China

Received: May 3, 2023
Peer-review started: May 3, 2023
First decision: June 14, 2023
Revised: July 14, 2023
Accepted: August 7, 2023
Article in press: August 7, 2023
Published online: August 28, 2023

Lucy Petagine, Mohammed Gulrez Zariwala, Vinood B Patel, Centre for Nutraceuticals, School of Life Sciences, University of Westminster, London W1W6UW, United Kingdom

Corresponding author: Vinood B Patel, FRSC, PhD, Professor, Centre for Nutraceuticals, School of Life Sciences, University of Westminster, No. 115 New Cavendish Street, London W1W6UW, United Kingdom. v.b.patel@westminster.ac.uk

Abstract

Non-alcoholic fatty liver disease (NAFLD) causes significant global disease burden and is a leading cause of mortality. NAFLD induces a myriad of aberrant changes in hepatocytes at both the cellular and molecular level. Although the disease spectrum of NAFLD is widely recognised, the precise triggers for disease progression are still to be fully elucidated. Furthermore, the propagation to cirrhosis is poorly understood. Whilst some progress in terms of treatment options have been explored, an incomplete understanding of the hepatic cellular and molecular alterations limits their clinical utility. We have therefore reviewed some of the key pathways responsible for the pathogenesis of NAFLD such as innate and adaptative immunity, lipotoxicity and fibrogenesis, and highlighted current trials and treatment options for NAFLD patients.

Key Words: Liver; Fat; Inflammation; Mitochondria; Immune system

©The Author(s) 2023. Published by Baishideng Publishing Group Inc. All rights reserved.

Core Tip: Non-alcoholic fatty liver disease (NAFLD) is a significant global disease burden and a leading cause of mortality causing aberrant changes in hepatocytes. Although the disease spectrum is widely recognised, precise triggers for disease progression remain poorly understood. Whilst some progress has evolved in terms of treatment, there are still no approved pharmacological therapies for NAFLD treatment due to the incomplete understanding of the hepatic cellular and molecular alterations in disease pathogenesis.

Citation: Petagine L, Zariwala MG, Patel VB. Non-alcoholic fatty liver disease: Immunological mechanisms and current treatments. *World J Gastroenterol* 2023; 29(32): 4831-4850
URL: https://www.wjgnet.com/1007-9327/full/v29/i32/4831.htm
DOI: https://dx.doi.org/10.3748/wjg.v29.i32.4831

INTRODUCTION

Non-alcoholic fatty liver disease (NAFL) (NAFLD) is the most common cause of liver disease globally which occurs due to an excessive accumulation of fat in the liver in the absence of secondary causes or other liver disease aetiologies[1]. NAFLD encompasses the spectrum of disease from simple NAFL, non-alcoholic steatohepatitis (NASH), fibrosis, cirrhosis, and in many cases hepatocellular carcinoma (HCC)[1]. Due to increasing trends of sedentary lifestyles and dietary choices the prevalence of NAFLD continues to rise[1].

NAFLD has a significant global disease burden (882 million cases in 2017)[2], with cases likely to be higher due to poor screening of high risk asymptomatic populations. Furthermore, inaccurate disease progression predication markers and a lack of available licenced therapeutics hinders the treatment of NAFLD. Management of NAFLD is largely based on lifestyle modifications, but many newer therapies are being evaluated (discussed later). Further understanding into the mechanisms of disease progression, diagnostic biomarkers and therapeutic intervention should help mitigate burden of disease. Finally, liver disease combination therapies are becoming increasingly popular. This review will highlight some of the recent developments in NAFLD and aims to define the pathological features associated with disease progression including the immunological mechanisms as well as the current therapeutic interventions used for NAFLD.

Epidemiology and prevalence

Global reports relating to the epidemiology of NAFLD have estimated a global prevalence of NAFLD between 25% and 35%[3-5], with Europe as high as 30%[6], 35% in South American countries[6,7], and 35% in North America[6]. During the period of 1991 to 2019, trend analysis shown that increasing global prevalence increased yearly by 0.7%, rising from 21.9% in 1991 to 37.3% in 2019[5].

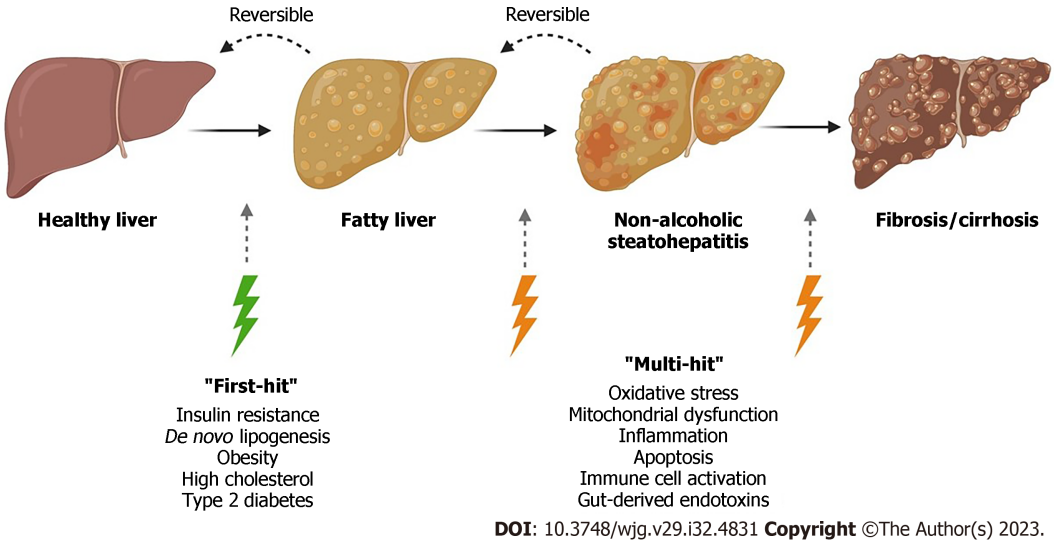
NAFLD has a global impact on health care systems due to its high rates of morbidity and mortality[8]. NASH is a particularly prevalent cause of chronic liver disease which in turn leads to cirrhosis and HCC, whereas NAFLD has been noted as the biggest cause of HCC in the United States, France, and the United Kingdom, with NAFLD-related HCC predicted to increase globally alongside the rise in obesity[3]. In the United States, by 2030, almost 49% of the total population is projected to be obese[3].

Globally, the phenotype of patients with NAFLD appears to be men of a mean age of 51.7 years old, with obesity and/or type 2 diabetes[6]. A linear increase prevalence of NAFLD, diabetes and metabolic disorders have also been documented[9,10], and especially occurs in those with central obesity, diabetes and metabolic syndrome[11,12]. Metabolic comorbidities include hypertension (37%) and metabolic syndrome (40%)[6]. NAFLD prevalence in type-2 diabetes mellitus (T2DM) is as high as 70%[13], and patients with T2DM also have a twofold increased risk of all-cause mortality [4,14]. Prevalence of NAFLD in patients with morbid obesity also rises to 90%[4]. Therefore, prevalence of NAFLD poses a significant global health burden requiring clinical attention.

Histopathology and disease spectrum

NAFLD is the most common cause of liver dysfunction with a high association for obesity and insulin resistance (IR). The spectrum of NAFLD can lead to progressive NASH, fibrosis, and lastly HCC and liver failure. NAFLD is a complex disease which results from environmental causes as well as polygenic background and risk factors (Figure 1). Although the molecular mechanisms underlying disease progression are complex, the histological spectrum of disease has been well described[15].

NAFLD is defined as a disease of the liver which is characterised by macrovesicular fat deposition and storage (> 5% of the hepatocytes) due to dysregulation in the mechanisms of fat synthesis and utilisation by the liver[7,16]. Steatosis is predominantly graded on a four-step scale, from 0 to 3. Grade 0 is defined as a normal liver containing fat in < 5% of hepatocytes[17,18]; grade 1 occurs when fat deposits occur in < 33% of hepatocytes, and grade 2 when fat occurs in 33%-66%[17,18]; grade 3 is the final stage in the spectrum of steatosis which occurs when > 66% hepatocytes contain fat[17,18]. The most important histological feature of NASH is hepatocyte ballooning and lobular inflammation as well as a steatotic liver. Hepatocyte ballooning is the second histological feature of NASH. Hepatocyte ballooning is defined by a clear, flocculent, not vacuolar cytoplasm with a ballooned shape. Inflammation occurs in a lobular pattern in NASH, containing Kupffer cells (KC), aggregates of neutrophils, and Mallory-Denk bodies[15]. NASH is defined as a chronic state of inflammation whereby hepatic stellate cells (HSCs) transform into myofibroblasts[19]. These transformed cells produce extracellular collagen matrix[19]. Normally fibrogenesis is a wound healing process. However, in NAFLD, sustained and progressive insults occurring over many years causes unregulated fibrogenesis[19]. Initially collagen deposits form in the perisinusoidal space. As collagen bundles form, architectural remodelling occurs which can lead to cirrhosis and HCC. Fibrosis stage 1 (F1) occurs when mild perisinusoidal/pericellular fibrosis is documented without septa[20]. Stage two occurs when fibrosis occurs in perisinusoidal/pericellular and portal/periportal regions with few septa (F2)[20]. Stage three (F3) is seen when numerous septa are documented, also known as bridging fibrosis[20]. Lastly, stage four is a cirrhotic liver[20]. An overview of NAFLD progression is shown in Figure 1.



DOI: 10.3748/wjg.v29.i32.4831 **Copyright** ©The Author(s) 2023.

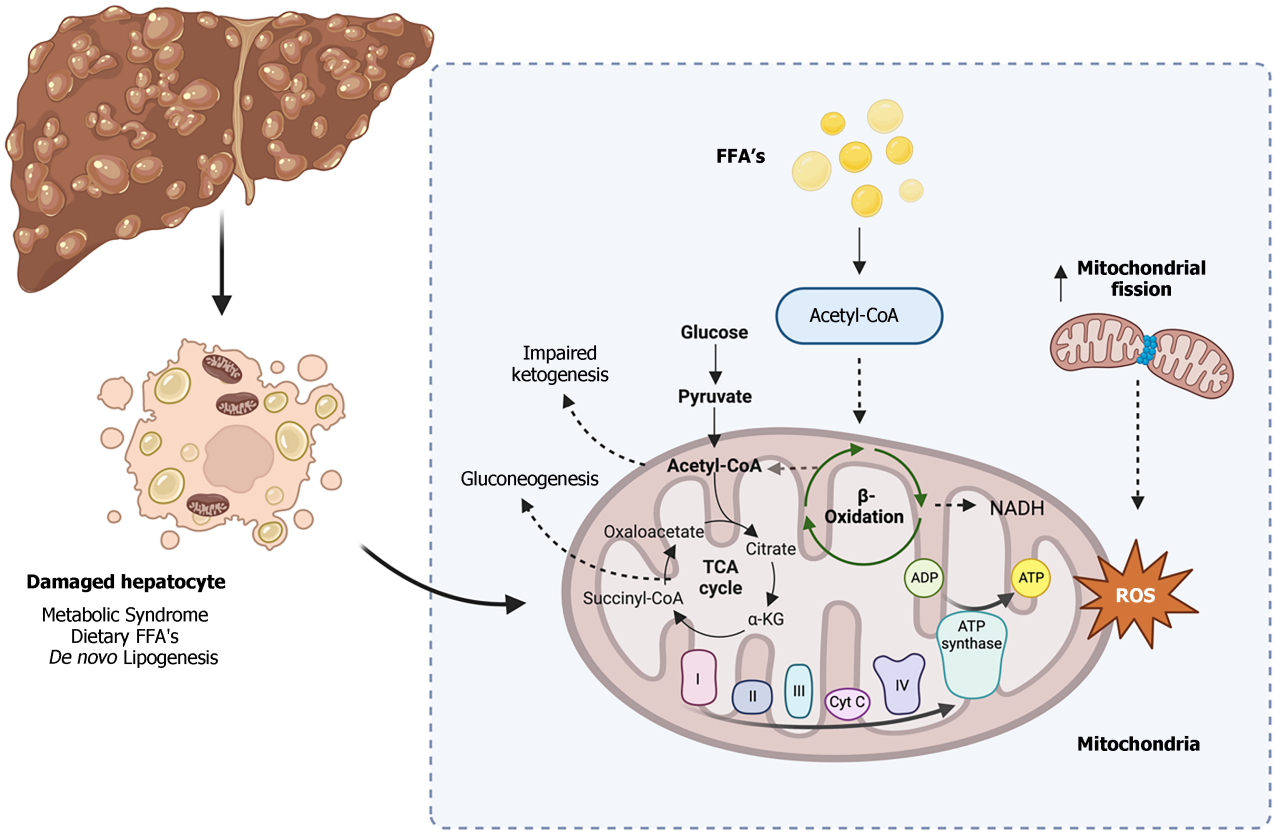
Figure 1 Overview of the current understanding of non-alcoholic fatty liver disease progression. Non-alcoholic fatty liver disease (NAFLD) encompasses a range of liver damage, from simple accumulation of fat in liver cells, named steatosis, to more severe forms of the diseases such as steatohepatitis, involving inflammation which can lead to fibrosis and cirrhosis. In the "multiple-hit" theory of progression, the first cause or "first-hit" in NAFLD is insulin resistance, obesity, type 2 diabetes, and metabolic syndrome. As the first hit occurs, free fatty acids are stored in the liver as triglycerides, resulting in simple steatosis. Disease progresses when multiple factors, or "multi-hits", such as oxidative stress, inflammatory mediators, apoptosis, and mitochondrial dysfunction cause liver damage (created with BioRender.com).

Progression of the fibrosis stage to a cirrhotic scarred liver can vary between individuals, with cirrhosis occurring up to 15 to 20 years after initial diagnosis[19,21]. The median survival rate for patients with compensated cirrhosis is approximately 9 to 12 years, however, patients with decompensated cirrhosis have a significantly lower median survival rate of approximately 2 years[22]. Patients in the compensated stage are frequently asymptomatic, and often remain undiagnosed[22]. Therefore, early detection of cirrhotic patients who are still in the compensated stage is crucial, as early diagnosis could prevent or slow down disease progression. The onset of decompensated cirrhosis occurs when symptoms such as ascites, hepatic encephalopathy, and/or gastroesophageal variceal haemorrhage are found[22]. Histologically, cirrhosis is diagnosed when a disconnection of the hepatocytes from the central vein occurs as well as capillarisation of the liver sinusoids[19]. These modifications that occur to the liver structure and integrity lead to elevated intravascular resistance within the portal system and decreased hepatic perfusion, ultimately causing a loss of liver function[19]. Hence, timely diagnosis and management of cirrhosis is required to improve patient outcomes.

IR in NAFLD

Many studies have shown that metabolic dysfunction and IR play a significant role in the development of NAFLD. Various animal and clinical studies suggest that chronic low grade inflammation may play a role in the development of IR and NAFLD as well as extrahepatic complications such as cardiovascular diseases, T2DM, and renal dysfunction[23]. IR is a complex state by which the skeletal muscle, liver, and adipose tissue become less sensitive to insulin and its metabolic effects[24]. IR is related to obesity, hypertension, hyperglycaemia and metabolic syndrome. During a carbohydrate-rich diet, excess glucose is converted into fatty acids *via* lipogenesis, using acetyl-CoA which is generated from glycolysis-driven pyruvate[25]. These fatty acids are then incorporated into very low-density lipoproteins (VLDL) for transport to white adipose tissue for storage[25]. Accumulation of lipids in adipocytes trigger downstream signalling of pathways including c-Jun N-terminal kinase (JNK) and nuclear factor-kappa B (NF-κB), leading to production of proinflammatory cytokines, such as tumour necrosis factor-alpha (TNF-α) and interleukin (IL)-6[26,27]. JNK regulates the production of proinflammatory cytokines, karyomitosis, and cellular apoptosis, and therefore, contributes to inflammation and IR. Research has proposed activation of JNK also accelerates lipid accumulation, thus, exacerbating liver injury. JNK-1 deficiency in adipose tissue shows protection from development of hepatic steatosis and promotes glucose intolerance, insulin clearance, IR, and hepatic steatosis[24]. Kluwe *et al*[28] also showed that in a mouse model, inhibition of JNK lead to modulation of fibrosis in hepatocytes. In a high fat diet (HFD) model of NAFLD, IR, liver injury and increased autophagy were documented[29]. However, JNK inhibition decreased autophagy and IR[29]. Therefore, JNK signalling plays a significant role in NAFLD progression.

The hormone adiponectin is secreted by adipocytes and is associated with improved insulin sensitivity. Adiponectin-mediated signalling is also able to stimulate fatty acid β-oxidation, glucose utilisation and uptake, as well as suppression of fatty acid synthesis[30]. Adiponectin can also inhibit the glycerol 3 phosphate (G3P) pathway; however, research has shown that during NAFLD serum levels of adiponectin are reduced[30]. Another metabolite of the G3P pathway is fatty acyl-CoA which is involved in mitochondrial β-oxidation. In patients with NAFLD, an increase in mitochondrial β-oxidation can lead to a state of oxidative stress due to increased substrate delivery to the mitochondrial electron transport chain (ETC), increasing reactive oxygen species (ROS) and damaging mitochondrial DNA[30,31]. Although β-oxidation is upregulated, ATP levels are decreased in NAFLD due to reduced activity of ETC complexes I and IV[32], and have been



DOI: 10.3748/wjg.v29.i32.4831 **Copyright** ©The Author(s) 2023.

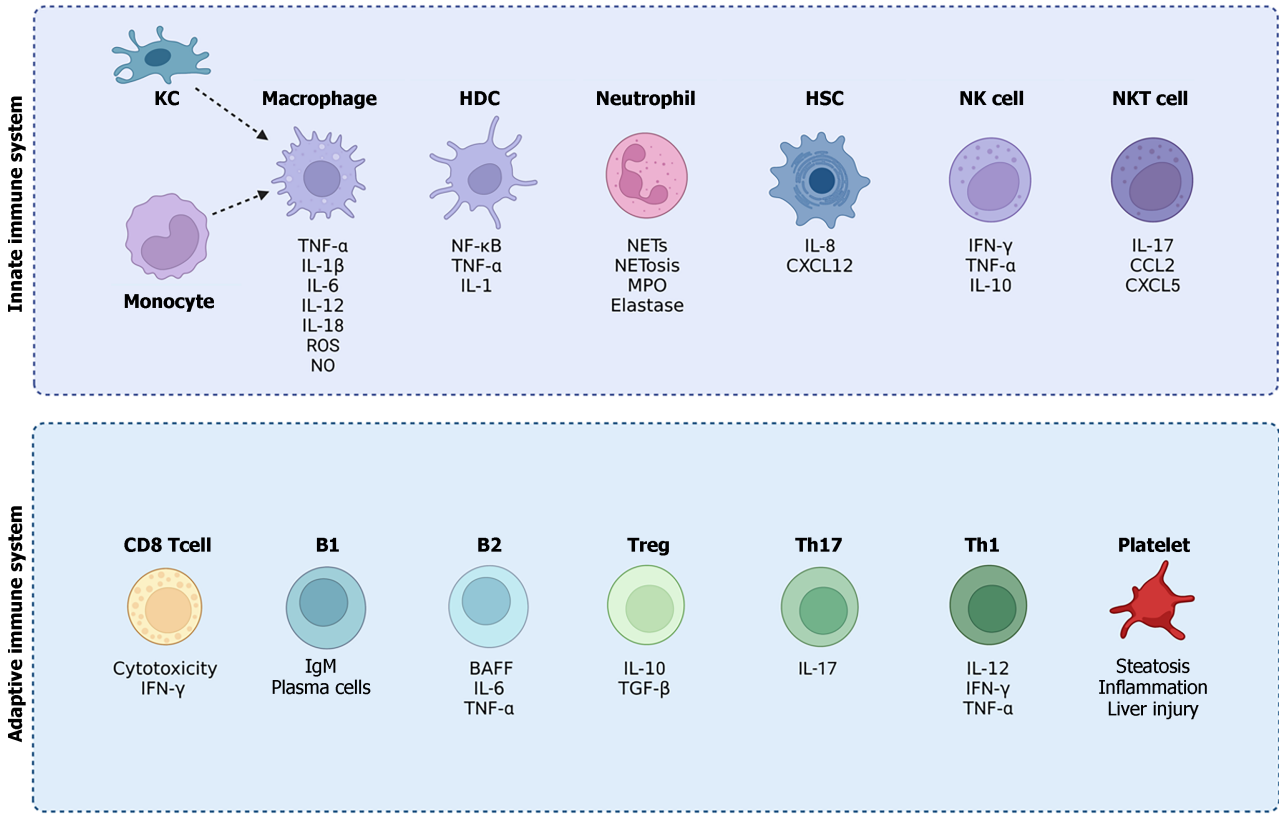
Figure 2 Overview of mitochondrial dynamics in non-alcoholic fatty liver disease. The accumulation of triglycerides and free fatty acids (FFAs) in the liver are converted to fatty acyl-CoA, which is then transported to the mitochondria for β-oxidation, generating acetyl-CoA. However, increased accumulation of FFA can cause insufficient hepatic β-oxidation, triggering inflammation and oxidative stress. Acetyl-CoA enters the mitochondrial tricarboxylic acid cycle allowing continuation of gluconeogenesis. The by-product nicotinamide adenine dinucleotide, produced though β-oxidation are transported to the electron transport chain (ETC) for oxidative phosphorylation. Disruption and dysfunction of the ETC can cause electron leakage and hepatocyte damage leading to reactive oxygen species production and oxidative stress. Accumulation of FFAs can cause mitochondrial damage, resulting in increased mitochondrial fission and degradation *via* mitophagy processes (created with BioRender.com). ROS: Reactive oxygen species; NADH: Nicotinamide adenine dinucleotide; TCA: Tricarboxylic acid; ADP: Adenosine diphosphate; ATP: Adenosine triphosphate.

correlated to levels of disease progression. Therefore, modifications to mitochondrial function can exacerbate disease progression in NAFLD. Hyperinsulinemia alongside increased levels of ROS also leads to an imbalance between mitochondrial fission and fusion proteins such as dynamin-related protein 1 (Drp1) and mitofusin-2 proteins (Mfn2)[33]. It is possible that an excessive mitochondrial fission in the liver plays an important role in NAFLD progression. Increases in the Drp1-to-Mfn2 ratio causes enhanced mitochondrial fission which in turn causes reduced endoplasmic reticulum association, decreases oxidative phosphorylation capacity, and elevated mitochondrial ROS production[33], which can exacerbate disease state. Therefore, it is plausible that a reduction in mitochondrial oxidative capacity as well as the impairment of metabolic fuels provides a plausible relationship between mitochondrial dysfunction, lipotoxicity and IR. Therefore, metabolic health and mitochondrial function are fundamental to progression of NAFLD (Figure 2).

The inflammasome pathway and macrophages are known to play a significant role in the development of IR. Production of IL-1β and IL-18 can be regulated by the inflammasome pathway, which contains complexes including nucleotide-binding oligomerization domain (NOD)-, leucine-rich repeats-and pyrin domain-containing protein 3 (NLRP3) and activation of caspase-1[34]. In NAFLD, inflammasome formation can be activated upon a variety of stress stimuli such as damage-associated molecular patterns, pathogen-associated molecular patterns, for example, lipopolysaccharide (LPS) from the gut-liver axis, mitochondrial ROS, endoplasmic reticulum stress, and ROS[34-36]. Activation of the NLPR3 inflammasome has shown to contribute to disease progression from steatosis to NASH[34,37]. MRNA levels of NLRP3 inflammasome components such as NLRP3, caspase-1, IL-1β, and IL-18 were also found to be significantly upregulated in NAFLD patients[37-39]. Therefore, targeted modulation of the inflammasome will lead to improved insulin signalling and mitochondrial function.

Immunological Mechanisms

In chronic liver disease, the activation of the immune response can both restore tissue function as well as cause tissue injury. Therefore, an amplified immune response may lead to organ dysfunction. The following section describes the involvement of various immune cell types in the pathogenesis of NAFLD (Figure 3).



DOI: 10.3748/wjg.v29.i32.4831 **Copyright** ©The Author(s) 2023.

Figure 3 Overview of innate and adaptive immune cells involved in non-alcoholic fatty liver disease (NAFLD). Activation of immune cells can promote inflammation and liver injury in NAFLD. The innate immune system cells include Kupffer cells, monocytes, and macrophages as well as hepatic dendritic cells, neutrophils and natural killer cells. Natural killer T cells provide a bridge between both the innate and adaptive immune system. The adaptive immune system includes T cells such as CD8 T cells and CD4 T cells (Th1, Th17 and regulatory T cells). The adaptive immune system also comprises of B1 and B2 cells as well as platelets. Although the contribution of immune cells to the development of NAFLD has been explored, the crosstalk between the distinctive immune cell subsets in the pathogenesis of NAFLD requires further investigation (created with BioRender.com). KC: Kupffer cells; TNF-α: Tumour necrosis factor-alpha; IFN-γ: Interferon-γ; IL: Interleukin; ROS: Reactive oxygen species; NO: Nitric oxide; NETs: Neutrophil extracellular traps; NF-κB: Nuclear factor-kappa B; HDC: Hepatic dendritic cells; MPO: Myeloperoxidase; HSC: Hepatic stellate cells ; CXCL: C-X-C motif chemokine ligand; BAFF: B cell activating factor; TGF-β: Transforming growth factor-β; NK: Natural killer; NKT: Natural killer T cells; Treg: Regulatory T cells.

Innate immune system in NAFLD: During NAFLD, the innate immune system is involved in the activation of resident KCs, with recruitment of innate immune cells such as neutrophils, monocytes, natural killer (NK) cells and natural killer T (NKT) cells[40], and inflammation is further exacerbated *via* the production of cytokines, (*e.g.* TNF-α, IL-1β, IL-6, IL-12, IL-18), chemokines, nitric oxide (NO) and ROS[40-42].

Macrophages: The main role of macrophages in the liver is predominantly for immunoregulatory and detoxifying functions, however, alterations in macrophage phenotypes and dynamics have been reported to be involved in the pathogenesis of NAFLD[43,44]. Liver resident KCs are a large population of macrophages as well as other subsets of macrophages such as monocyte-derived macrophages and liver capsular macrophages[45]. M1 macrophages have a pro-inflammatory phenotype and are induced by mediators such as LPS and interferon-γ (IFN-γ) and their activation causes secretion of pro-inflammatory cytokines such as IL-1β, IL-6 and TNF-α[46,47]. On the other hand, M2 macrophages have an anti-inflammatory phenotype and are induced by Th2 cytokines such as IL-4 and IL-13, causing secretion of anti-inflammatory factors such as IL-10 and transforming growth factor-β (TGF-β)[46,47]. M2-type macrophages have also been reported to induce M1-type KCs apoptosis decreasing disease progression[48]. Therefore, the balance between M1 and M2 macrophages is important for homeostasis in the liver.

During NAFLD, macrophages can recognise and respond to stimuli through pattern recognition receptors such as membrane-bound toll-like receptors (TLRs), such as TLR4 and TLR9, and cytoplasmic NOD-like receptors [43,45,49]. LPS translocated from the gut can activate TRL4 and TLR9, and this recognition of stimuli can then result in inflammation *via* secretion of proinflammatory cytokines such as TNF-α, IL-1β, IL-6, IL-12, and IL-18, as well as molecules such as ROS and NO. Activation of TLR9 can induce the release of IL-1β from KCs, which occurs during processes such as lipid accumulation, fibrinogenesis and cell death[50]. In NAFLD patients, TLR4 expression is often correlated with hepatic inflammation and fibrosis[51]. There are also many advantages to the activation of macrophages due to their immunosuppressive effects and secretion of anti-inflammatory cytokines, however, they also have pro-fibrinogenic effects. Activation of M2-type macrophages can release TGF-β1 and IL-13, leading to a fibrotic response of liver remodelling and tissue repair[52].

During IR, circulating free fatty acids (FFA) can also directly activate KCs causing activation of the stress-response kinases (JNK1 and JNK2) producing pro-inflammatory cytokines and extracellular vesicles (EVs), stimulating macrophage activation. EVs have been studied in their contribution to pathobiology of NAFLD, and have been found to mediate inflammation[53,54]. Hepatocytes can release EVs containing cargoes which activate signalling pathways[53,54]. Some EVs can carry mitochondrial DNA, which in mice and humans have been shown to activate macrophages *via* TLR9 [53,54]. Activation of TLR9 then causes inflammation though resultant downstream activation of NF-κB-dependent pro-inflammatory cytokines in macrophages[53,54]. Macrophage activation and inflammation may also occur *via* EV formation in response to lipid-associated toxicity[55]. Therefore, both harmful and beneficial macrophage phenotypes can co-exist during NAFLD, and the balance between these phenotypes must be considered for therapeutic strategies. Both cellular and molecular macrophage targets for therapy may provide a new perspective as well as the adoptive transfer therapies.

Neutrophils: Neutrophil infiltration during NASH has been documented in both patients and in mouse models. In the early stages of NAFLD, recruitment of neutrophils occurs *via* chemokines such as C-X-C motif chemokine ligand (CXCL) 1, IL-8, and CXCL2[56]. Research has shown that various neutrophil specific components are released in NAFLD. Neutrophil elastase is a major inflammatory protease which can be released by neutrophils. In a mouse model of NAFLD, elastase suppression has been shown to improve disease severity[57]. As well as elastase, neutrophil proteinase-3 has also been reported as elevated in NASH and both the levels of proteinase-3 and elastase were correlated with liver fibrosis [58]. Elastase has also been shown to play a role in metabolic dysfunction and IR, and therefore, targeting or improving IR and metabolic disease may improve inflammation in NAFLD. Myeloperoxidase (MPO), a neutrophil derived enzyme has been shown to become increased in NASH. It is thought that both neutrophils and MPO may cause activation of HSCs inducing liver fibrosis and inflammation in NASH[59,60]. Plasma levels of MPO have been found to be correlated with fibrosis in NAFLD patients[61]. More research is required to determine how neutrophils contribute to disease pathogenesis in NAFLD.

NKT cells: NKT cells provide a bridge between the innate and adaptive immune system and express both NK cell and T cell markers[40]. NKT cells become activated upon antigen presentation by CD1d which can be expressed by a variety of cells such as hepatocytes, macrophages, dendritic cells, and B cells[40]. Pro-inflammatory cytokines such as IL-4 and IFN-γ are secreted after NKT activation causing further tissue injury. Although there is conflicting evidence, during steatosis levels of NKT cells become reduced, whereas in NASH and fibrosis they are increased[40]. This has been shown by in vivo studies where NKT cells were elevated in the blood and liver of patients with moderate-to-severe steatosis[62]. During early-stage NAFLD such at fatty liver, the phenotype of NKT cells demonstrate a pro-inflammatory Th1 cytokines profile such as IFN-γ, whereas, in advanced end stage disease, they have a profibrotic role[40].

NK cells: NK cells have a cytotoxic role and can attack cells *via* perforin-mediated pathways or cell-cell interactions, for example Fas. NK cells can also act as regulatory cells by releasing various cytokines and chemokines, such as IFN-γ, TNF-α, and IL-10 as well as growth factors[40]. NK cell-associated cytotoxic ligands, such as TNF-related apoptosis-inducing ligand (TRAIL), NK group 2 member D, and major histocompatibility (MHC) class I chain-related protein A and B mRNAs, have been reported to be elevated in obese NASH patients[63]. NK cells therefore may possibly promote inflammation and hepatocyte apoptosis *via* TRAIL secretion[63], leading to progression of fibrosis.

Dendritic cells**:** Hepatic dendritic cells (HDCs), which highly express MHC-class II molecules and CD45 are important immune cells in the liver which have migratory capabilities as well as production of cytokines such as TNF-α, IFN-γ, IL-2, IL-4, and IL-6[64]. Three distinct subsets of HDCs have been described in experimental models of HDCs: Lymphoid, myeloid and plasmacytoid[64]. They play a crucial role in the progression of metabolic steatohepatitis bridging lipid metabolism and inflammation. HDCs can shift from a tolerant state to an active state, triggering an inflammatory process [65]. In an immune tolerant state, immature HDCs secrete IL-10, and TGF-β, as well as limit T cell expansion[64]. In a tolerant state they supress inflammasome activation, maintaining homeostasis in the liver. This regulatory role of HDC in NASH can therefore restrict inflammation as well as clear apoptotic cells and necrotic debris[65]. Additionally, they are involved in lipid storage within the liver and are important for antigen presentation and induction of inflammatory pathways[64]. Recent studies suggest that HDCs have antifibrogenic effects by activating metalloproteinases, such as matrix metallopeptidase 9 which has been found to be involved in regression of fibrosis as well as remodelling of the extracellular matrix.

On the other hand, in an active state HDCs cause inflammation and liver damage as well as contribute to fibrosis. In an active or inflammatory state, mature recruit macrophages to the liver and can activate the NF-κB pathway as well as produce pro-inflammatory cytokines such as TNF-α and IL-1, contributing to the inflammatory microenvironment[64]. In humans, a subset of HDCs (CD11C + cDC2) have been shown to play an important role in development of fibrosis and have been positively correlated with metabolic steatohepatitis[64]. HDC's in a mouse model of metabolic associated fatty liver disease (MAFLD) have shown that in a matured form they produce more inflammatory cytokines and may be responsible for proinflammatory responses[65]. HDC may therefore play dual roles in both the suppression and progression of disease state.

Adaptive immune system in NAFLD: The adaptive immune system is defined by antigenic specificity and immunological memory and includes predominantly B and T lymphocytes. Experimental research has suggested that sustained immune responses activated by oxidative stress-related antigens can affect the pathogenesis of disease *via* activation of CD4+ T-cells, which, in turn, stimulate macrophage M1 responses and liver CD8+ T- and NKT cell recruitment[66]. Experimental in vitro data as well as in vivo data supports adaptive immunity in NAFLD disease progression.

T cells: Conventional T cells have been well studied in their involvement in the pathogenesis of NAFLD. The main CD4+ T-cell are divided into Th1, Th2, and Th17 populations characterised by production of specific cytokines. Recruitment of CD4+ T-cell in the liver have been reported to be increased in individuals diagnosed with NASH[67-71],

as well as in animal models fed a high calorie diet[72]. Upon presentation to inflammatory stimuli, CD4+ T cells can differentiate into Th17 cells[73], a subset of pro-inflammatory T helper cells defined by their ability to produce IL-17. In animal models of NAFLD, in the liver it has been documented that the Th-17 phenotype was favoured, promoting inflammation[74]. Human studies in obese and overweight patients have also shown an increase in the Th17 population[74]. The IL-17 family of cytokines have been implicated in the progression of fatty liver disease through interference of the insulin signalling pathway[75]. In mouse models, deficiency of IL-17A, IL-17F or IL-17A receptor (IL-17RA) results in increased steatosis but reduced steatohepatitis[76,77]. In HFD mouse model, neutralisation or IL-17RA deficiency as well as treatment with anti-IL-17mAb therapy has shown to protect mice from diet-induced liver injury *via* improvement of lipid accumulation, suppressing KCs activation, decreased pro-inflammatory cytokines levels and inhibition downstream of NF-κB signalling[40,78]. IL-17 has also been shown to activate the signal transducer and activator of transcription 3 pathway in HSCs causing progression of fibrosis in the liver[79]. These studies indicate the involvement of IL-17 in the pathogenesis of NAFLD.

Regulatory T cells (Tregs), a subset of cells which promote immune tolerance and facilitate tissue repair and express the transcription factor forkhead box P3. Although there is limited data available, the number of hepatic Tregs have been documented to be decreased in in animal models of NAFLD[80]. In humans, the levels of Tregs in the liver and the circulation of patients with NAFLD is also reported to be decreased[80]. Also, in a NASH mouse model, induced by a HFD and endotoxin challenge, a decrease in liver Tregs was documented, however, transfer of Tregs into mice showed reduced liver injury and inflammation, through decreased expression of TNF-α[81].

B cells: Until recently, the role of B cells is the pathogenesis of NAFLD was less understood. B cells are highly specific antibody producing cells of the adaptive immune system. B cells contribute to approximately 6% of intrahepatic cells[40,82]. B cells produce the B cell activating factor (BAFF), a cytokine controlling the process of B cell survival and maturation [83,84]. Liver biopsies from patients with NASH have been shown to contain both B and T cells in the inflammatory infiltrates [73,85,86].

In mouse models, B cells have been shown to become activated in NASH, concomitantly with the onset of steatohepatitis and thus, maturing to plasma blasts and plasma cells[73,86]. Another study has also shown that BAFF signalling increased IR in an NAFLD model as well as promoting fatty liver[87]. Whereas, in mice models of NASH, B2 cell responses upregulate BAFF[73]. Levels of BAFF in patients with NASH appear to occur at a higher level than with patients with fatty liver, therefore it has been proposed BAFF levels correlate with severity of steatohepatitis fibrosis[88]. BAFF receptor-deficient mice showed an improvement in HFD-induced obesity and IR, as well as a reduction in the number of B cells and a decrease in serum immunoglobulin G level[40]. The involvement of B cells in the progression of liver disease can also be due to production of pro-inflammatory mediators and antigen-presentation[89,90]. In patients with NASH, MHC class II molecules become upregulated causing inflammatory infiltration and recruitment of CD4+ and CD8+ T cells to the liver[73], whereby Th1 CD4 + T cell activation and IFN-γ production occurs[86]. Therefore, this research suggests B cells and BAFF play an important role in NAFLD pathogenesis and can contribute to pathogenesis of NAFLD *via* autoimmune hepatitis and liver fibrogenesis [87,90,91].

Serum levels of IgA has been found to be associated with patients with NASH and levels of IgA can predict advanced liver disease progression[92]. Patients with HCC have also been documented to have higher serum IgA[93-95]. In both mouse models and human studies, liver resident IgA accumulation in hepatic cells has been associated with chronic inflammation and fibrosis[93]. Regression of HCC has also been documented when IgA is inhibited, causing reactivation of CD8+ T cell function[93,94].

B cell deficiency also has been shown to improve development of NASH. The mechanisms and signalling of B cell activation in NASH is *via* myeloid differentiation early response protein 88[40,96]. Studies have shown that elimination of myeloid differentiation early response protein 88 on B cells reduced hepatic T cell-mediated inflammation and fibrosis, but had no effects on steatosis[40,96]. Therefore, B cells show involvement in the pathogenesis of NAFLD, and manipulation on B cells may provide a therapeutic opportunity for NAFLD treatment. An overview of innate and adaptive immune cells involved in NAFLD is shown in Figure 3.

Diagnostic procedures

Most commonly a combination of clinical history, laboratory findings, biopsies and radiological testing are used in the diagnosis of NAFLD. The clinical diagnosis of NAFLD is usually considered when aminotransferases become elevated or imaging on the liver detects high hepatic fat[97]. Both the American and European guidelines agree that suspicion of fibrosis warrants a confirmatory liver biopsy[98].

Current biomarkers: Liver function tests, particularly alanine aminotransferase (ALT) and aspartate aminotransferase (AST) levels, can indicate liver damage in NAFLD/NASH[12,99]. These levels may be elevated by two to four times the normal limit. Mild elevations in aminotransferase levels may be present in lower stages of the disease, but routine tests may appear normal. Alkaline phosphatase and gamma-glutamyl transferase (GGT) levels may be up to three times the upper limit even in the absence of advanced disease[100]. A serum GGT cut-off value of 96.5 can predict advanced fibrosis with a sensitivity of 83% and specificity of 69%[101].

Several different biomarker panels have been described in their use to assess liver fat. These include the liver fat score (LFS) (sensitivity 86%, specificity 71%), hepatic steatosis index (sensitivity 92.5%, specificity 92.4%), fatty liver index (FLI) (sensitivity 87%, specificity 86%) and the steatotest (sensitivity 95.5%, positive predictive value 97.0%)[102]. LFS is calculated using a patients serum AST/ALT ratio, fasting serum AST level, fasting serum insulin level, any presence of metabolic syndrome and diagnosed diabetes mellitus. Studies have shown that a score greater than -0.640 can predict NAFLD with a sensitivity of 86% and specificity of 71%. The FLI uses waist circumference, body mass index (BMI), triglyceride, and GGT and this was initially developed to detect fatty liver in western countries.

Screening tools: The fibrosis-4 scoring system uses a patients age, platelet count, AST, and ALT to determine a liver fibrosis score and can help to predict advanced fibrosis. A score < 1.45 defines a negative predictive value or low probability of advanced liver fibrosis[103]. Scores of A score > 3.25 indicated a higher likelihood and has a positive predictive value of 65%, and specificity of 97% at predicting advanced fibrosis[103]. Recently, a new FAST™ screening tool has been used which compromises a combination of FibroScan® parameters such as liver stiffness measurement and controlled attenuation parameter as well as AST. This screening tool has been shown to have diagnostic accuracy when predicting those at risk of NASH. The FAST™ screening tool may provide a better non-invasive algorithm for diagnosis of NASH. FAST™ performed better than other non-invasive algorithms for the diagnosis of at-risk NASH[104,105]. Results have shown that the FAST score had the highest area under curve for the most high-risk NASH criteria as well as liver stiffness showing a consistently acceptable performance in predicting NASH[106].

Emerging biomarkers: Various non-invasive biomarkers for NAFLD have been developed and validated over the last 20 years, however, there is a need to develop and validate new biomarkers for NAFLD which encompass IR, inflammation and fibrogenesis[107-109].

Cell Death**:** As well as current markers such as cytokeratin 18, necroptosis is a form of cell death which is characterised by changes such as organelle swelling, plasma membrane damage, and release of cellular contents[110]. Proteins such as receptor-interacting protein kinase (RIPK) family members such as RIPK1 and RIPK3, and mixed lineage kinase domain-like (MLKL) are involved in the process[111]. During NAFLD, TLR4 ligands such as LPS cause activation of the TLR4 receptor causing activation of proteins such as RIPK3 and MLKL leading to necroptosis[112]. In patients with MAFLD, necroptosis components such as RIPK3 have been shown to be upregulated, therefore, it may be important to consider markers of necroptosis in NAFLD.

MicroRNAs (miRNAs): miRNAs are non-coding RNAs which play a role in gene expression regulation[113] and have been implicated as potential biomarkers in NAFLD. Research has shown that miRNAS such as miR-21, miR-34a, miR-122, and miR-451 have been found to be upregulated in NAFLD patients[114-117]. Various studies have also shown that profiles of miRNAs in NAFLD patients can differentiate between disease stage. In NAFLD and NASH, miR-122, miR-192, miR-19a, miR-19b, miR-125b, and miR-375 have been found to be increased greater than 2-fold, whereas continuous upregulated expression of miR-122, miR-192, and miR-375 was found in NASH patients[118,119]. Furthermore, higher expression of miR-122 and miR-21 have been reported in people with high fasting blood glucose, obesity and fatty liver infiltrations[119,120]. Therefore, these findings suggest that miRNAs may be promising biomarkers for NAFLD and metabolic disease, in particular miR-122, miR-192, and miR-34a, which have been shown to be correlated with severity of NAFLD.

EVs**:** Growing evidence suggests that EVs play a significant role pathological disease including those associated with obesity and metabolic syndrome. Obesity, IR, T2DM and NAFLD have all been linked to changes in the abundance and phenotype of circulating EVs[121] and therefore circulating EVs and their composition may be a candidate biomarker for NAFLD. EVs contain substances such as genetic material including miRNAs[122]. It has been documented that in humans, the number of AD-EVs is correlated with IR in overweight people[123], as well as visceral AD-EV number correlated with liver injury measured by ALT and AST and metabolic syndrome[124]. Circulating EVs have also been shown to become elevated during the progression of NASH and have reported to be correlated with histological findings [125]. Research has also shown that EVs from a NAFLD model in mice contained miR-122 and miR-192[125]. In cirrhotic patients, plasma hepatocyte-EVs were found to contain elevated levels of CK-18[126]. EVs from visceral adipose tissue can exacerbate disease in NAFLD by causing further inflammation, fibrosis and IR. Both pro- and anti-fibrotic EVs have been documented in the liver and therefore it is plausible to investigate the differences in the pro- and anti-fibrotic phenotypes to track disease progression and likelihood of fibrosis development. Future research should consider the use of EVs in monitoring metabolic dysfunction and IR in NAFLD, with focus on EV phenotypes, cargo and cell specific markers.

Therapeutic interventions

Despite NAFLD being an extremely prevalent liver disease, no specific pharmacological interventions are currently Food and Drug Administration approved for treatment. Some therapeutic agents used as anti-diabetics, antilipidemic and natural bile treatments have previously been evaluated in their ability to treat liver disease, although they have limitations. Predominantly, lifestyle interventions including diet and exercise are most commonly used to treat NAFLD. The current therapeutic interventions used for NAFLD are outlined below including future potential agents such as sirtuins, antioxidants and vitamins.

Lifestyle modifications: A substantial amount of research indicated that changes to lifestyle are a primary approach for the treatment of NAFLD[127]. Diet changes and weight loss can reverse liver disease. Weight loss in the range of 5%-10% can provide beneficial effects to NAFLD patients *via* a reduction in NAFLD activity score (NAS)[128,129]. A weight reduction greater than 10% has also been shown to reduce the severity of fibrosis as well as resolution of NASH[12,129,130].

European Association for the Study of the Liver (EASL), National Institute for Health and Care Excellence and American Association for the Study of Liver Diseases guidelines provide recommendations in terms of diet and physical activity for the management of NAFLD. These bodies recommend caloric restriction with a calorie deficit of 500-1000 kcal a day, as well as limiting the consumption of alcohol, fats and coffee. EASL also favours the Mediterranean diet, with studies indicating a reduction in liver fat in NAFLD patients[131]. Lifestyle modifications in terms of physical exercise can also positively effect liver fat content. Both resistance/weight training, high-intensity interval training and aerobic exercise have all equally been shown to reduce liver fat content; however, in men with NAFLD, high-intensity interval

training was the most effective in restoring hepatic fat, reducing hepatic stiffness and improving Kupffer cell function; key features of NASH[132].

Evidence has suggested that the ketogenic diet (KD) is an effective treatment for NAFLD. Ketogenesis is a metabolic process resulting in the production of ketone bodies, namely acetoacetate, beta-hydroxybutyrate (BHB), and acetone, which act as alternative energy sources[33,133]. The KD has been shown to change hepatic mitochondrial fluxes and redox state as well as significantly reducing liver fat content and hepatic IR[134]. These changes were found to be accompanied by an increase in the net hydrolysis of liver triglycerides, a decrease in endogenous glucose production, and lower serum insulin levels[134]. BHB has also been shown to interact with inflammasomes[135,136] and neutralise ROS [137], leading to a reduction in inflammatory cytokines and oxidative damage *via* its antioxidant capacity. These findings suggest a KD can contribute to the reversal of NAFLD through improvement of IR and cellular redox function.

Bariatric surgery: Bariatric surgery been shown to be an effective treatment for NAFLD improving overall liver health *via* facilitating weight loss, improving insulin sensitivity, and subsiding inflammation[138,139]. Roux-en-Y gastric bypass (RYGB) and laparoscopic sleeve gastrectomy (LSG) are the most prevalent bariatric procedures, which lead to significant weight loss and metabolic health improvements[140].

Several research studies have investigated the impact of bariatric surgery in NAFLD and have shown positive results. Studies have indicated that bariatric surgery resulted in significant improvements in liver enzymes and histology, with a decrease in liver fat and fibrosis. Results from two meta-analyses have shown that treatment of NAFLD using bariatric surgery resulted in a biopsy-confirmed resolution of steatosis (56%-66%), inflammation (45%-50%), ballooning degeneration (49%-76%), and fibrosis (25%-40%), as well as showing a decrease in NAS scoring[140-142]. Bariatric surgery has therefore proven to be effective in ameliorating NAFLD, however, it is important to clarify which type of surgery is most effective. A study by Baldwin *et al*[143] compared RYGB and LSG against its effectiveness at improving AST and ALT concentration, NAS and NAFLD fibrosis score. Overall, both procedures reduce AST and ALT levels, however, LSG showed slightly more favourable results[139]. Another study has shown NAS scoring reduced significantly in patients who underwent both surgery types 12-mo after the surgery[139]. RYGB patients had a more significantly decreased steatosis and superior improvement in plasma lipid profile[144]. Furthermore, bariatric surgery has been demonstrated to lower the risk of liver-related complications and death in individuals with NAFLD. Bariatric surgery can therefore be considered as a promising treatment option for those with NAFLD who are overweight or obese.

Insulin sensitising agents: IR is believed to play an essential role in the development and progression of NAFLD. In recent years, various insulin sensitizers such as biguanides, thiazolidinediones (TZDs), glucagon-like peptide-1 receptor agonists (GLP-1), and dipeptidyl peptidase 4 inhibitors have been investigated as potential therapeutic targets for NAFLD[145]. However, there are safety concerns associated with long-term use of these targets[145].

Biguanides*:* As the development of NAFLD is closely associated with IR, diabetes, hyperglycaemia and hyperlipidaemia, antidiabetic drugs are often utilised in the treatment of NAFLD[145]. Metformin is considered the first-line treatment for T2DM due to its ability to improve insulin sensitivity and promote weight loss without causing hypoglycaemia[145,146]. Although its mechanisms of action are not fully understood, it works by lowering hepatic glucose production[145]. Previous open-label studies have suggested that metformin may have a positive impact on hepatic steatosis and necroinflammation, although excessive weight loss may have confounded these results[30]. However, some studies have shown that metformin does not significantly improve the histological response in NAFLD [30,147], but improves liver function and BMI[148]. In a mouse model, metformin treatment showed improvements to the gut-liver axis *via* attenuation of the loss of tight junction proteins in the small intestine as well as reducing the increase of endotoxin levels in the portal circulation[149].

GLP-1: GLP-1 receptor agonists can alter IR by promoting weight loss *via* suppressing appetite and delaying gastric emptying[150]. In NAFLD patients, research has shown GLP-1 receptor agonists improve hepatic and adipose tissue IR, suppress de novo lipogenesis and oxidative stress as well as increased clearance of VLDL[30,150]. GLP-1 may also modulate the immune system *via* the reprogramming of macrophages to the M2 phenotype. In the exenatide study of cardiovascular event lowering trial, GLP-1 receptor agonists reduced cardiovascular risk[151] and visceral fat, improved glucose tolerance, body fat percentage and resting energy rate (NCT01144338). The trial semaglutide unabated sustainability in treatment of type 2 diabetes (NCT02054897) are a series of phase III clinical trials which suggest treatment with semaglutide has a higher effectiveness than other GLP-1 therapeutics in the reduction of HbA1c in patients with T2DM. In a phase 2 trial with patients diagnosed with NASH receiving semaglutide treatment of 0.1 mg (80 patients), 0.2 mg (78 patients), or 0.4 mg (82 patients), patients resulted in a significantly higher NASH resolution when compared to the placebo (NCT02970942)[152]. Although NASH resolution was significantly improved, no significant difference was shown in the fibrosis stage[152].

Fibroblast growth factor (FGF) based therapeutics: FGF analogs have been proposed to target steps of disease pathogenesis. FGF-21 treatments are currently in clinical development for the treatment of NASH[153,154] and data suggests that FGF21 is anti-fibrotic and has the potential to improve the metabolic syndrome and is effective in treating NASH. The BALANCED trial (NCT03976401) evaluated the effects of efruxifermin, a long-acting Fc-FGF21 fusion protein [155]. In this study, 80 patients were given either placebo (n = 21) or efruxifermin 28 mg (n = 19), efruxifermin 50 mg (n = 20) or efruxifermin 70 mg (n = 20) *via* weekly subcutaneous injection for 16 wk[155]. Treatment with efruxifermin was found to significantly reduced hepatic fat fraction (HFF) in patients with F1-F3 stage NASH[155]. FGF based compounds which are currently in phase II are efruxifermin (FGF-21), pegbelfirmin (FGF-21), aldafermin (FGF-19), pegozafermin (FGF-21) and BFK8588A (FGF-21), which have been shown to achieve a reduction in ALT levels[109].

Thyroid hormone receptor-β (THRβ) 1 agonists: Currently, several different THRβ specific agonists have been shown to produce positive therapeutic effects in both animal models and clinical trials for treatment of NAFLD. Treatment with

TG68, a novel THRβ agonist, has positive effects on resolution of NAFLD *via* reduction in liver weight, hepatic steatosis, serum transaminases, and circulating triglycerides in a NAFLD model[156]. Resmetirom (MGL-3196) has also been found to significantly reduce hepatic lipid content and improve liver enzyme levels and plasma lipid levels in NASH patients [157], however, glucose or insulin levels remained unchanged. Another THRβ agonist, VK2809 has been shown to reduce hepatic steatosis in a mouse model and in a phase II clinical trial reduced liver lipid content[158,159].

Currently there are many ongoing clinical trials studying the effects of THRβ agonists in NAFLD. The VOYAGE study is assessing VK2809 to determine its efficacy in the resolution of biopsy proven NASH (NCT04173065). The DUET study is also assessing the effects of orally administered TERN-501 and TERN-101 in presumed NASH (NCT05415722), whilst the LIFT study is assessing TERN-101 alone in NASH patients (NCT04328077)[160]. In a NASH mouse model, TERN-501 reduced steatosis as well as reducing serum total cholesterol, triglyceride and ALT levels[161].

Peroxisome proliferator-activated receptor-γ (PPAR-γ) agonists: PPAR-γ is a ligand-activated nuclear receptor and its activation causes insulin sensitization and enhances glucose metabolism. TZDs are a group of insulin sensitisers used to treat T2DM by action on PPAR-γ. PPAR agonists have been shown to modulate the innate immune response. PPAR-δ can promote anti-inflammatory polarization of macrophages and modulate their activation[162], whilst PPAR-γ ligands can inhibit the activation of macrophages and cytokine production (TNF-α, IL-6, and IL-1β), thus, reducing inflammation [163]. Activated PPARs can also regulate immune cells (macrophages, DCs, T cells, and B cells) as well as decrease inflammatory cytokine production[163].

Pioglitazone, a TZD, has been used for treatment of NASH with its effects improving steatohepatitis, ballooning degeneration and lobular inflammation[164]. Pioglitazone (45 mg/d) for 6 mo has been shown in patients with prediabetes or T2DM to improve the fibrosis stage (NCT00227110)[165]. Elafibranor is a dual PPAR-α/δ agonist. PPAR-δ functions to regulates peroxisomal β-oxidation of FFA as well as improve insulin sensitivity, lipid and glucose homeostasis[30]. Several clinical trials have assessed the effects of elafibronor in improving histology in NASH patients such as RESOLVE-IT (NCT02704403), and the GOLDEN trial[166]. In both trials elafibranor showed no effect.

Sodium glucose cotransporter 2 (SGLT2) Inhibitors: Another class of drugs lower serum glucose levels *via* inhibition of the SGLT2 and promote weight loss. Studies have shown that SGLT2 inhibitors reduce ALT levels correlating with changes in bodyweight and glycaemic control[30], although further studies are required to identify whether SGLT2 inhibitors can prevent progression of NAFLD/NASH.

Current clinical trials are underway to assess the efficacy and effectiveness of SGLT2 inhibitors. A randomised clinical trial aims to compare the effect of the pioglitazone and empagliflozin combination on liver fat mass (NCT04976283). Another trial is investigating dapagliflozin in NASH (NCT05254626).

Farnesoid X receptor (FXR) agonists: The FXR is a nuclear receptor which is activated by bile acids. FXR inhibits the expression sterol regulatory element binding protein-1 and carbohydrate-responsive element-binding protein. FXR also enhances the clearance of high-density lipoprotein and VLDL in the liver and well as promoting hepatic regeneration. However, little is documented regarding the immune modulation in this class of drugs.

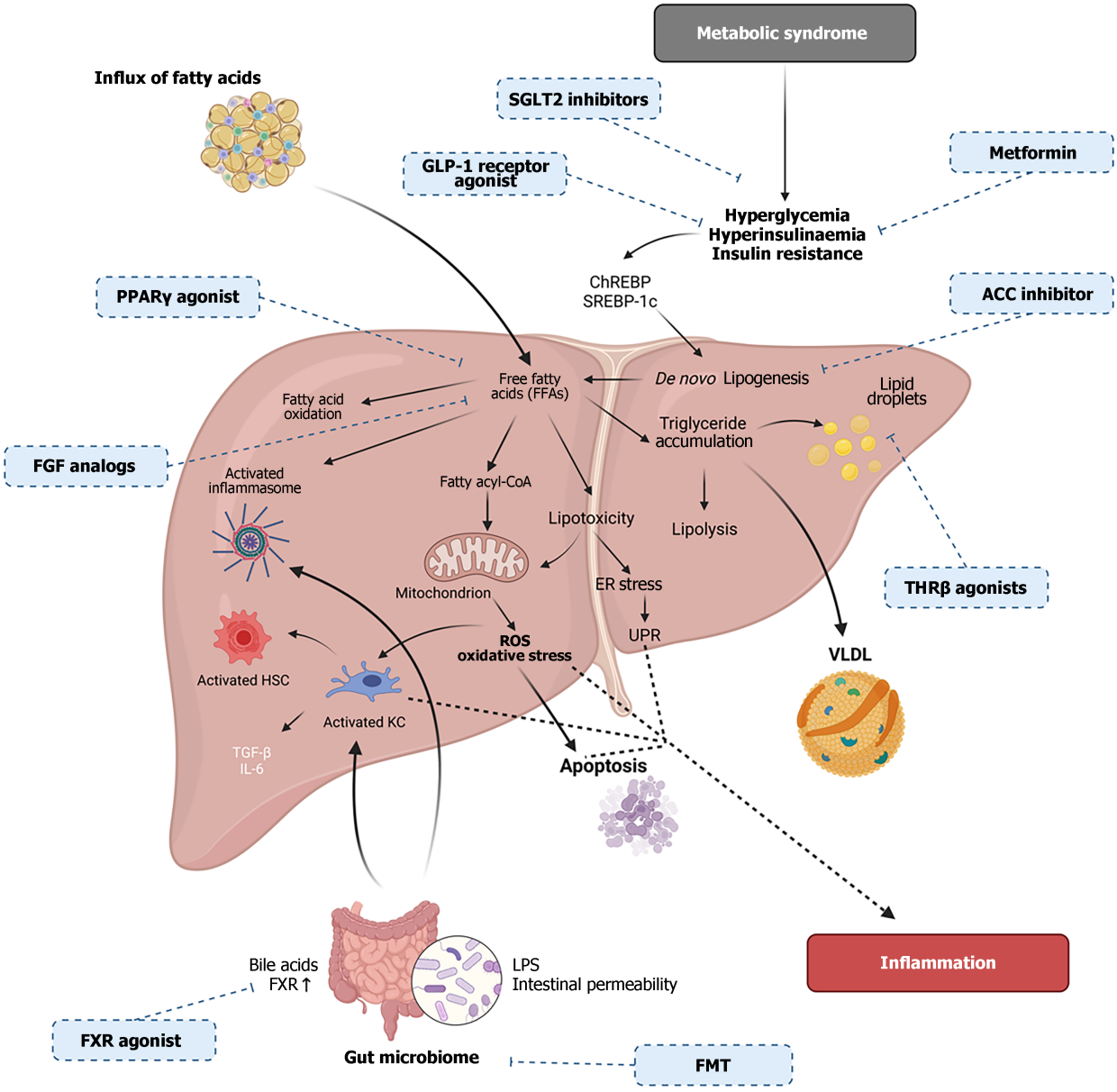
Obeticholic acid (OCA) is a synthetic bile acid which acts as a FXR agonist. The use of OCA for NASH is still under investigation, due to reported side effects. The FLINT trial (NCT01265498) was a multicentre, randomized, double-blind, placebo-controlled phase IIb study assessing the effects of 25 mg of OCA for 72 wk. Treatment with OCA was linked with a significant improvement fibrosis stage in the treated group (35% *vs*. 19%; $P = 0.004$), although there was no difference in rates of NASH resolution. A phase III trial (REGENERATE) is currently active to further assess the treatment of OCA in patients with NASH (NCT02548351).

Other FXR agonists, such as tropifexor, have been studied in the treatment of NASH in the FLIGHT-FXR study (NCT02855164). This 48-wk study using tropifexor found sustained decreases in ALT and liver fat content (measured by HFF using magnetic resonance imaging-estimated proton density fat fraction) during the therapy duration[167]. A Phase IIa (LIFT trial) studying TERN-101, a FXR agonist, showed that in a 12-wk controlled trial, significant improvements in cT1, a marker of fibro-inflammation was observed[160].

Other treatment approaches: Modulation of the gut microbiome: Gut dysbiosis is a common feature of NAFLD[168]. Whilst pre- and pro- biotics are being evaluated, faecal microbiota transplant (FMT) may provide an alternative approach. HFD-fed mice which received FMT from healthy donors showed a significant reduction in intracellular hepatic lipid and proinflammatory cytokines concentration (IFN-γ and IL-17)[169]. Small intestinal microbiota transplants from healthy lean individuals to obese individuals have reported improvements in insulin sensitivity in those patients with metabolic syndrome[170]. A phase I pilot study is currently underway to study FMT in patients with NASH (NCT02469272). FMT as a treatment for NASH patients seems to be both a safe and efficient treatment, although, more high quality studies, trials and follow-ups are required to verify its therapeutic potential[168].

Modulation of the immune system: Methods for modulating the immune system as potential therapies for NAFLD are currently under investigation. Various pleiotropic effects of platelets have recently been discovered in liver homeostasis and disease as platelets are also involved in inflammatory regulation. Anti-platelet therapy (APT) has been shown to reduce NASH pathogenesis in rats[171]. Evidence has shown that APT may have a protective effect in patients with NAFLD[172]. In the liver, platelet and neutrophils can interact leading to neutrophil extracellular trap formation[173]. APT has been shown to reduce both NASH and HCC development[174]. It has been observed that APT reduced platelet accumulation in hepatocytes as well as reducing immune cell interaction, which led to decreases in cytokine and chemokine release, thus attenuating macrovesicular steatosis and liver damage[174].

It is well documented that NASH can progress to HCC. Immunotherapy, including programmed cell death 1 (PD-1) treatment, has been approved for the treatment of HCC[175]. PD-1 can interfere with the immune response and contributes to the growth and expansion of cancer. It has been documented that in NASH there is a progressive accumulation of exhausted, unconventionally activated CD8+ PD1 + T cells[175] and data has shown that in HCC, immune



DOI: 10.3748/wjg.v29.i32.4831 **Copyright** ©The Author(s) 2023.

Figure 4 Overview of the metabolic and molecular mechanisms occurring in non-alcoholic fatty liver disease pathogenesis with therapeutic targets. Non-alcoholic fatty liver disease (NAFLD) is a multifactorial disease, including metabolic syndrome, insulin resistance (IR) and gut microbiome changes. IR and metabolic syndrome cause increased free fatty acids (FFAs) which lead to endoplasmic reticulum stress, reactive oxygen species accumulation, oxidative stress, apoptosis, immune cell activation and inflammasome activation. Changes in the gut barrier can cause changes to bile acids and intestinal permeability causing lipopolysaccharides translocation from the gut causing immune activation, thus, inducing inflammation. FFA's can also activate transcription factors such as sterol regulatory binding protein-1c and carbohydrate response element binding protein causing the storage of FFAs as triglycerides in lipid droplets. Accumulated triglycerides can be exported as very low-density lipoprotein or oxidized by mitochondrial β-oxidation. Pharmacologic treatments for NAFLD are identified with corresponding drug mechanism of action (created with BioRender.com). ROS: Reactive oxygen species; LPS: Lipopolysaccharide; UPR: Unfolded protein response; FMT: Faecal microbiota transplant; VLDL: Very low-density lipoproteins; PPAR-γ: Peroxisome proliferator-activated receptor-γ; KC: Kupffer cells; HSC: Hepatic stellate cells; FXR: Farnesoid X Receptor; SGLT2: Sodium-glucose cotransporter 2; SREBP-1c: Sterol regulatory binding protein-1c; ChREBP: Carbohydrate response element binding protein.

surveillance was impaired[175]. Several pharmaceutical agents have been developed to target PD-1 receptors. Pembrolizumab has shown significant enhancement in overall survival and progression-free survival although statistical significance was not met[176]. However, it is also thought that NASH-derived HCC may be less responsive to immune modulated therapy due to NASH-related aberrant T cell activation, causing damage to tissues[175,177,178]. A summary of current clinical trials is shown in Table 1; and an overview of the metabolic and molecular mechanisms occurring in NAFLD pathogenesis with therapeutic targets in Figure 4.

Table 1 Current active and recruiting clinical trials assessing therapeutics for non-alcoholic fatty liver disease

Drug name	Condition	Target	Clinical trial Number	Phase	Status	Primary endpoint
GH509	NASH NAFLD		NCT05784779	Phase Ib/II	Recruiting	Change in liver fat content assessed by MRI-PDFF
LUM-201	NASH NAFLD	Lipid accumulation	NCT05364684	Phase II	Recruiting	Change in intrahepatic lipid content measured by proton magnetic resonance spectroscopy
Choline	NAFLD	Choline deficiency	NCT05200156	N/A	Recruiting	Change in Thiobarbituric acid reactive substances serum level
Dasatinib and quercetin	Fibrosis	Senescence	NCT05506488	Phase I	Recruiting	Improvement of fibrosis NAFLD score based on histology after 21 wk
GSK4532990	NAFLD fibrosis	17 β-HSD	NCT05583344	Phase II	Recruiting	Improvement of fibrosis measured by clinical research network scoring
Lisinopril	NASH HCC	ACE inhibitor	NCT04550481	Phase II	Recruiting	Changes in fibrosis marker PRO-C3
Rencofilstat	NASH Fibrosis NAFLD	Cyclophilin inhibitor	NCT05402371	Phase II	Recruiting	Improvement in fibrosis score CRN or NASH resolution
Lactobacillus reuteri GMNL-263 and GMNL-89 and lactobacillus rhamnosus GMNL-74	NAFLD	Gut microbiome	NCT05402449	N/A	Recruiting	Changes in serum ALT levels
Lubiprostone	NAFLD	Type 2 chloride channel activator	NCT05768334	Phase III	Recruiting	Changes in liver fat by measured by MRI-PDFF
Bacillus coagulans TCI711	NAFLD	Gut microbiome	NCT05635474	N/A	Recruiting	Changes measured by fibroscan
TVB-2640	NAFLD	FASN inhibitor	NCT04906421	Phase III	Active, not recruiting	Improvement in NAS and CRN scoring
ASC41		THRβ agonist	NCT05462353	Phase II	Recruiting	Improvement in NAS score
Ketohexokinase inhibition	NAFLD		NCT05463575	Phase II	Recruiting	Insulin-mediated suppression of endogenous glucose production
PF-06865571/ PF-05221304	NAFLD NASH with fibrosis	DGAT2 inhibitor/ACC inhibitor	NCT04321031	Phase II	Active, not recruiting	Resolution of NASH
ZED1227		TG2 inhibitor	NCT05305599	Phase II	Recruiting	Relative change of serum PRO-C3 levels
MK-3655	NASH	FGF21 agonist	NCT04583423	Phase II	Active, not recruiting	Resolution of NASH
MXP22 (probiotic and antioxidant capsule)	NAFLD	Gut microbiome	NCT05808049	N/A	Recruiting	Changes in steatosis measure by fibroscan
TERN 501/TERN-101	NASH	THRβ agonist/ FXR agonist	NCT05415722	Phase II	Active, not recruiting	Relative change in liver fat content (MRI-PDFF)
MET642	NASH	FXR agonist	NCT04773964	Phase II	Active, not recruiting	Safety study to measure adverse events
VK2809	NASH	THRβ agonist	NCT04173065	Phase II	Recruiting	Relative change in liver fat content (MRI-PDFF)

MRI-PDFF: Magnetic resonance imaging-estimated proton density fat fraction; NASH: Non-alcoholic steatohepatitis; FXR: Farnesoid X receptor; NAFLD: Non-alcoholic fatty liver disease; THRβ: Thyroid hormone receptor-β; NAS: Non-alcoholic fatty liver disease activity score; HCC: Hepatocellular carcinoma; ALT: Alanine aminotransferase; FASN: Fatty acid synthase; HSD: High-salt diet; CRN: Clinical research network; N/A: Not applicable.

CONCLUSION

NAFLD is a prevalent and progressive disease that can lead to liver damage and is strongly associated with obesity, IR,

and metabolic syndrome. Current treatments for NAFLD include lifestyle modifications such as diet and exercise, surgery, as well as medications to sensitise insulin. However, there is a need for effective and safe interventions that can directly target the underlying mechanisms of NASH/NAFLD in relation to IR, the gut microbiome and immunological mechanisms.

There is a growing body of evidence that NAFLD and metabolic syndrome are closely linked, and it is crucial for future research to prospectively evaluate interventions and therapeutics which both target improvement to liver outcomes as well as comorbidities associated with NAFLD (including cardiovascular diseases, T2DM, renal dysfunction). It is also essential to develop more refined and early risk stratification tools and biomarkers to identify individuals at the highest risk for NAFLD, considering that this condition affects a substantial portion of the world. Understanding the implications of metabolic signatures, chronic insulin signalling, mitochondrial dysfunction and cellular redox, is important for accurate prognosis and potential therapeutics.

Significant progress in the field has been made using bioinformatics to integrate intra- and extra-hepatic signals including gut and adipose interactions as well as patient information regarding lifestyle, nutrition, and comorbidities. The interplay between this multitude of factors provides promise for advancing therapeutics targeting immune regulation and mitochondrial function during progression of NAFLD. Advancements to the field should consider multidisciplinary approaches for the prevention, diagnosis, treatment, and care of patients with NAFLD.

FOOTNOTES

Author contributions: Petagine L performed the literature search, wrote the original draft, designed the figures, and reviewed and edited the final manuscript; Patel VB reviewed and edited the final manuscript; Zariwala MG reviewed and edited the final manuscript; All authors have read and agreed to the published version of the manuscript.

Conflict-of-interest statement: Authors declare no conflict of interests for this article.

Open-Access: This article is an open-access article that was selected by an in-house editor and fully peer-reviewed by external reviewers. It is distributed in accordance with the Creative Commons Attribution NonCommercial (CC BY-NC 4.0) license, which permits others to distribute, remix, adapt, build upon this work non-commercially, and license their derivative works on different terms, provided the original work is properly cited and the use is non-commercial. See: https://creativecommons.org/Licenses/by-nc/4.0/

Country/Territory of origin: United Kingdom

ORCID number: Mohammed Gulrez Zariwala 0000-0001-9944-8451; Vinood B Patel 0000-0001-9334-2525.

S-Editor: Qu XL
L-Editor: A
P-Editor: Chen YX

REFERENCES

1 **Sayiner M**, Koenig A, Henry L, Younossi ZM. Epidemiology of Nonalcoholic Fatty Liver Disease and Nonalcoholic Steatohepatitis in the United States and the Rest of the World. *Clin Liver Dis* 2016; **20**: 205-214 [PMID: 27063264 DOI: 10.1016/j.cld.2015.10.001]
2 **Ge X**, Zheng L, Wang M, Du Y, Jiang J. Prevalence trends in non-alcoholic fatty liver disease at the global, regional and national levels, 1990-2017: a population-based observational study. *BMJ Open* 2020; **10**: e036663 [PMID: 32747349 DOI: 10.1136/bmjopen-2019-036663]
3 **Huang DQ**, El-Serag HB, Loomba R. Global epidemiology of NAFLD-related HCC: trends, predictions, risk factors and prevention. *Nat Rev Gastroenterol Hepatol* 2021; **18**: 223-238 [PMID: 33349658 DOI: 10.1038/s41575-020-00381-6]
4 **Alexander M**, Loomis AK, Fairburn-Beech J, van der Lei J, Duarte-Salles T, Prieto-Alhambra D, Ansell D, Pasqua A, Lapi F, Rijnbeek P, Mosseveld M, Avillach P, Egger P, Kendrick S, Waterworth DM, Sattar N, Alazawi W. Real-world data reveal a diagnostic gap in non-alcoholic fatty liver disease. *BMC Med* 2018; **16**: 130 [PMID: 30099968 DOI: 10.1186/s12916-018-1103-x]
5 **Teng ML**, Ng CH, Huang DQ, Chan KE, Tan DJ, Lim WH, Yang JD, Tan E, Muthiah MD. Global incidence and prevalence of nonalcoholic fatty liver disease. *Clin Mol Hepatol* 2023; **29**: S32-S42 [PMID: 36517002 DOI: 10.3350/cmh.2022.0365]
6 **Le MH**, Yeo YH, Li X, Li J, Zou B, Wu Y, Ye Q, Huang DQ, Zhao C, Zhang J, Liu C, Chang N, Xing F, Yan S, Wan ZH, Tang NSY, Mayumi M, Liu X, Rui F, Yang H, Yang Y, Jin R, Le RHX, Xu Y, Le DM, Barnett S, Stave CD, Cheung R, Zhu Q, Nguyen MH. 2019 Global NAFLD Prevalence: A Systematic Review and Meta-analysis. *Clin Gastroenterol Hepatol* 2022; **20**: 2809-2817.e28 [PMID: 34890795 DOI: 10.1016/j.cgh.2021.12.002]
7 **Mitra S**, De A, Chowdhury A. Epidemiology of non-alcoholic and alcoholic fatty liver diseases. *Transl Gastroenterol Hepatol* 2020; **5**: 16 [PMID: 32258520 DOI: 10.21037/tgh.2019.09.08]
8 **Younossi Z**, Anstee QM, Marietti M, Hardy T, Henry L, Eslam M, George J, Bugianesi E. Global burden of NAFLD and NASH: trends, predictions, risk factors and prevention. *Nat Rev Gastroenterol Hepatol* 2018; **15**: 11-20 [PMID: 28930295 DOI: 10.1038/nrgastro.2017.109]
9 **Calzadilla Bertot L**, Adams LA. The Natural Course of Non-Alcoholic Fatty Liver Disease. *Int J Mol Sci* 2016; **17** [PMID: 27213358 DOI: 10.3390/ijms17050774]
10 **Kanwar P**, Kowdley KV. The Metabolic Syndrome and Its Influence on Nonalcoholic Steatohepatitis. *Clin Liver Dis* 2016; **20**: 225-243 [PMID: 27063266 DOI: 10.1016/j.cld.2015.10.002]
11 **Browning JD**, Szczepaniak LS, Dobbins R, Nuremberg P, Horton JD, Cohen JC, Grundy SM, Hobbs HH. Prevalence of hepatic steatosis in an

urban population in the United States: impact of ethnicity. *Hepatology* 2004; **40**: 1387-1395 [PMID: 15565570 DOI: 10.1002/HEP.20466]
12 **Pouwels S**, Sakran N, Graham Y, Leal A, Pintar T, Yang W, Kassir R, Singhal R, Mahawar K, Ramnarain D. Non-alcoholic fatty liver disease (NAFLD): a review of pathophysiology, clinical management and effects of weight loss. *BMC Endocr Disord* 2022; **22**: 63 [PMID: 35287643 DOI: 10.1186/s12902-022-00980-1]
13 **Ali A**, Amin MJ, Ahmed MU, Taj A, Aasim M, Tabrez E. Frequency of non-alcoholic fatty liver disease (NAFLD) and its associated risk factors among Type-2 diabetics. *Pak J Med Sci* 2022; **38**: 28-33 [PMID: 35035396 DOI: 10.12669/pjms.38.1.4968]
14 **Allen AM**, Therneau TM, Larson JJ, Coward A, Somers VK, Kamath PS. Nonalcoholic fatty liver disease incidence and impact on metabolic burden and death: A 20 year-community study. *Hepatology* 2018; **67**: 1726-1736 [PMID: 28941364 DOI: 10.1002/hep.29546]
15 **Hardy T**, Oakley F, Anstee QM, Day CP. Nonalcoholic Fatty Liver Disease: Pathogenesis and Disease Spectrum. *Annu Rev Pathol* 2016; **11**: 451-496 [PMID: 26980160 DOI: 10.1146/annurev-pathol-012615-044224]
16 **Bedossa P**. Histological Assessment of NAFLD. *Dig Dis Sci* 2016; **61**: 1348-1355 [PMID: 26874689 DOI: 10.1007/s10620-016-4062-0]
17 **Nassir F**, Rector RS, Hammoud GM, Ibdah JA. Pathogenesis and Prevention of Hepatic Steatosis. *Gastroenterol Hepatol (N Y)* 2015; **11**: 167-175 [PMID: 27099587]
18 **Qayyum A**, Nystrom M, Noworolski SM, Chu P, Mohanty A, Merriman R. MRI steatosis grading: development and initial validation of a color mapping system. *AJR Am J Roentgenol* 2012; **198**: 582-588 [PMID: 22357996 DOI: 10.2214/AJR.11.6729]
19 **Heyens LJM**, Busschots D, Koek GH, Robaeys G, Francque S. Liver Fibrosis in Non-alcoholic Fatty Liver Disease: From Liver Biopsy to Non-invasive Biomarkers in Diagnosis and Treatment. *Front Med (Lausanne)* 2021; **8**: 615978 [PMID: 33937277 DOI: 10.3389/fmed.2021.615978]
20 **El-Kamary SS**, Mohamed MM, El-Raziky M, Shardell MD, Shaker OG, ElAkel WA, Esmat G. Liver fibrosis staging through a stepwise analysis of non-invasive markers (FibroSteps) in patients with chronic hepatitis C infection. *Liver Int* 2013; **33**: 982-990 [PMID: 23509874 DOI: 10.1111/liv.12139]
21 **Bataller R**, Brenner DA. Liver fibrosis. *J Clin Invest* 2005; **115**: 209-218 [PMID: 15690074 DOI: 10.1172/JCI24282]
22 **Shetty A**, Jun Yum J, Saab S. The Gastroenterologist's Guide to Preventive Management of Compensated Cirrhosis. *Gastroenterol Hepatol (N Y)* 2019; **15**: 423-430 [PMID: 31592079]
23 **Petrescu M**, Vlaicu SI, Ciumărnean L, Milaciu MV, Mărginean C, Florea M, Vesa ȘC, Popa M. Chronic Inflammation-A Link between Nonalcoholic Fatty Liver Disease (NAFLD) and Dysfunctional Adipose Tissue. *Medicina (Kaunas)* 2022; **58** [PMID: 35630058 DOI: 10.3390/medicina58050641]
24 **Chen L**, Chen R, Wang H, Liang F. Mechanisms Linking Inflammation to Insulin Resistance. *Int J Endocrinol* 2015; **2015**: 508409 [PMID: 26136779 DOI: 10.1155/2015/508409]
25 **Han HS**, Kang G, Kim JS, Choi BH, Koo SH. Regulation of glucose metabolism from a liver-centric perspective. *Exp Mol Med* 2016; **48**: e218 [PMID: 26964834 DOI: 10.1038/emm.2015.122]
26 **Utzschneider KM**, Kahn SE. Review: The role of insulin resistance in nonalcoholic fatty liver disease. *J Clin Endocrinol Metab* 2006; **91**: 4753-4761 [PMID: 16968800 DOI: 10.1210/JC.2006-0587]
27 **Sakurai Y**, Kubota N, Yamauchi T, Kadowaki T. Role of Insulin Resistance in MAFLD. *Int J Mol Sci* 2021; **22** [PMID: 33923817 DOI: 10.3390/ijms22084156]
28 **Kluwe J**, Pradere JP, Gwak GY, Mencin A, De Minicis S, Osterreicher CH, Colmenero J, Bataller R, Schwabe RF. Modulation of hepatic fibrosis by c-Jun-N-terminal kinase inhibition. *Gastroenterology* 2010; **138**: 347-359 [PMID: 19782079 DOI: 10.1053/j.gastro.2009.09.015]
29 **Yan H**, Gao Y, Zhang Y. Inhibition of JNK suppresses autophagy and attenuates insulin resistance in a rat model of nonalcoholic fatty liver disease. *Mol Med Rep* 2017; **15**: 180-186 [PMID: 27909723 DOI: 10.3892/mmr.2016.5966]
30 **Khan RS**, Bril F, Cusi K, Newsome PN. Modulation of Insulin Resistance in Nonalcoholic Fatty Liver Disease. *Hepatology* 2019; **70**: 711-724 [PMID: 30556145 DOI: 10.1002/hep.30429]
31 **Delli Bovi AP**, Marciano F, Mandato C, Siano MA, Savoia M, Vajro P. Oxidative Stress in Non-alcoholic Fatty Liver Disease. An Updated Mini Review. *Front Med (Lausanne)* 2021; **8**: 595371 [PMID: 33718398 DOI: 10.3389/fmed.2021.595371]
32 **Gusdon AM**, Song KX, Qu S. Nonalcoholic Fatty liver disease: pathogenesis and therapeutics from a mitochondria-centric perspective. *Oxid Med Cell Longev* 2014; **2014**: 637027 [PMID: 25371775 DOI: 10.1155/2014/637027]
33 **Cooper ID**, Brookler KH, Kyriakidou Y, Elliott BT, Crofts CAP. Metabolic Phenotypes and Step by Step Evolution of Type 2 Diabetes: A New Paradigm. *Biomedicines* 2021; **9** [PMID: 34356863 DOI: 10.3390/biomedicines9070800]
34 **Yu L**, Hong W, Lu S, Li Y, Guan Y, Weng X, Feng Z. The NLRP3 Inflammasome in Non-Alcoholic Fatty Liver Disease and Steatohepatitis: Therapeutic Targets and Treatment. *Front Pharmacol* 2022; **13**: 780496 [PMID: 35350750 DOI: 10.3389/fphar.2022.780496]
35 **Lalor P F**. The Impact of the NLRP3 Pathway in the Pathogenesis of Non-Alcoholic Fatty Liver Disease and Alcohol-Related Liver Disease**.** *Livers* 2021. [DOI: 10.3390/livers1020007]
36 **Xu GX**, Wei S, Yu C, Zhao SQ, Yang WJ, Feng YH, Pan C, Yang KX, Ma Y. Activation of Kupffer cells in NAFLD and NASH: mechanisms and therapeutic interventions. *Front Cell Dev Biol* 2023; **11**: 1199519 [PMID: 37261074 DOI: 10.3389/fcell.2023.1199519]
37 **Wan X**, Xu C, Yu C, Li Y. Role of NLRP3 Inflammasome in the Progression of NAFLD to NASH. *Can J Gastroenterol Hepatol* 2016; **2016**: 6489012 [PMID: 27446858 DOI: 10.1155/2016/6489012]
38 **Zhu X**, Lin X, Zhang P, Liu Y, Ling W, Guo H. Upregulated NLRP3 inflammasome activation is attenuated by anthocyanins in patients with nonalcoholic fatty liver disease: A case-control and an intervention study. *Clin Res Hepatol Gastroenterol* 2022; **46**: 101843 [PMID: 34922061 DOI: 10.1016/j.clinre.2021.101843]
39 **Wree A**, McGeough MD, Peña CA, Schlattjan M, Li H, Inzaugarat ME, Messer K, Canbay A, Hoffman HM, Feldstein AE. NLRP3 inflammasome activation is required for fibrosis development in NAFLD. *J Mol Med (Berl)* 2014; **92**: 1069-1082 [PMID: 24861026 DOI: 10.1007/s00109-014-1170-1]
40 **Moayedfard Z**, Sani F, Alizadeh A, Bagheri Lankarani K, Zarei M, Azarpira N. The role of the immune system in the pathogenesis of NAFLD and potential therapeutic impacts of mesenchymal stem cell-derived extracellular vesicles. *Stem Cell Res Ther* 2022; **13**: 242 [PMID: 35672797 DOI: 10.1186/s13287-022-02929-6]
41 **Tilg H**, Moschen AR. Evolution of inflammation in nonalcoholic fatty liver disease: the multiple parallel hits hypothesis. *Hepatology* 2010; **52**: 1836-1846 [PMID: 21038418 DOI: 10.1002/hep.24001]
42 **Friedman SL**, Neuschwander-Tetri BA, Rinella M, Sanyal AJ. Mechanisms of NAFLD development and therapeutic strategies. *Nat Med* 2018; **24**: 908-922 [PMID: 29967350 DOI: 10.1038/s41591-018-0104-9]

43 **Kazankov K**, Jørgensen SMD, Thomsen KL, Møller HJ, Vilstrup H, George J, Schuppan D, Grønbæk H. The role of macrophages in nonalcoholic fatty liver disease and nonalcoholic steatohepatitis. *Nat Rev Gastroenterol Hepatol* 2019; **16**: 145-159 [PMID: 30482910 DOI: 10.1038/s41575-018-0082-x]

44 **Barreby E**, Chen P, Aouadi M. Macrophage functional diversity in NAFLD - more than inflammation. *Nat Rev Endocrinol* 2022; **18**: 461-472 [PMID: 35534573 DOI: 10.1038/s41574-022-00675-6]

45 **Xu L**, Liu W, Bai F, Xu Y, Liang X, Ma C, Gao L. Hepatic Macrophage as a Key Player in Fatty Liver Disease. *Front Immunol* 2021; **12**: 708978 [PMID: 34956171 DOI: 10.3389/fimmu.2021.708978]

46 **Mantovani A**, Biswas SK, Galdiero MR, Sica A, Locati M. Macrophage plasticity and polarization in tissue repair and remodelling. *J Pathol* 2013; **229**: 176-185 [PMID: 23096265 DOI: 10.1002/path.4133]

47 **Xiao Z**, Liu M, Yang F, Liu G, Liu J, Zhao W, Ma S, Duan Z. Programmed cell death and lipid metabolism of macrophages in NAFLD. *Front Immunol* 2023; **14**: 1118449 [PMID: 36742318 DOI: 10.3389/fimmu.2023.1118449]

48 **Wan J**, Benkdane M, Teixeira-Clerc F, Bonnafous S, Louvet A, Lafdil F, Pecker F, Tran A, Gual P, Mallat A, Lotersztajn S, Pavoine C. M2 Kupffer cells promote M1 Kupffer cell apoptosis: a protective mechanism against alcoholic and nonalcoholic fatty liver disease. *Hepatology* 2014; **59**: 130-142 [PMID: 23832548 DOI: 10.1002/hep.26607]

49 **Arrese M**, Cabrera D, Kalergis AM, Feldstein AE. Innate Immunity and Inflammation in NAFLD/NASH. *Dig Dis Sci* 2016; **61**: 1294-1303 [PMID: 26841783 DOI: 10.1007/s10620-016-4049-x]

50 **Miura K**, Kodama Y, Inokuchi S, Schnabl B, Aoyama T, Ohnishi H, Olefsky JM, Brenner DA, Seki E. Toll-like receptor 9 promotes steatohepatitis by induction of interleukin-1beta in mice. *Gastroenterology* 2010; **139**: 323-34.e7 [PMID: 20347818 DOI: 10.1053/j.gastro.2010.03.052]

51 **Nati M**, Chung KJ, Chavakis T. The Role of Innate Immune Cells in Nonalcoholic Fatty Liver Disease. *J Innate Immun* 2022; **14**: 31-41 [PMID: 34515137 DOI: 10.1159/000518407]

52 **Schuppan D**, Surabattula R, Wang XY. Determinants of fibrosis progression and regression in NASH. *J Hepatol* 2018; **68**: 238-250 [PMID: 29154966 DOI: 10.1016/j.jhep.2017.11.012]

53 **Srinivas AN**, Suresh D, Santhekadur PK, Suvarna D, Kumar DP. Extracellular Vesicles as Inflammatory Drivers in NAFLD. *Front Immunol* 2020; **11**: 627424 [PMID: 33603757 DOI: 10.3389/fimmu.2020.627424]

54 **Dorairaj V**, Sulaiman SA, Abu N, Abdul Murad NA. Extracellular Vesicles in the Development of the Non-Alcoholic Fatty Liver Disease: An Update. *Biomolecules* 2020; **10** [PMID: 33143043 DOI: 10.3390/biom10111494]

55 **Schattenberg JM**, Lee MS. Extracellular Vesicles as Messengers Between Hepatocytes and Macrophages in Nonalcoholic Steatohepatitis. *Gastroenterology* 2016; **150**: 815-818 [PMID: 26924096 DOI: 10.1053/j.gastro.2016.02.064]

56 **Lalor PF**, Faint J, Aarbodem Y, Hubscher SG, Adams DH. The role of cytokines and chemokines in the development of steatohepatitis. *Semin Liver Dis* 2007; **27**: 173-193 [PMID: 17520517 DOI: 10.1055/s-2007-979470]

57 **Zang S**, Wang L, Ma X, Zhu G, Zhuang Z, Xun Y, Zhao F, Yang W, Liu J, Luo Y, Liu Y, Ye D, Shi J. Neutrophils Play a Crucial Role in the Early Stage of Nonalcoholic Steatohepatitis *via* Neutrophil Elastase in Mice. *Cell Biochem Biophys* 2015; **73**: 479-487 [PMID: 27352342 DOI: 10.1007/s12013-015-0682-9]

58 **Mirea AM**, Toonen EJM, van den Munckhof I, Munsterman ID, Tjwa ETTL, Jaeger M, Oosting M, Schraa K, Rutten JHW, van der Graaf M, Riksen NP, de Graaf J, Netea MG, Tack CJ, Chavakis T, Joosten LAB. Increased proteinase 3 and neutrophil elastase plasma concentrations are associated with non-alcoholic fatty liver disease (NAFLD) and type 2 diabetes. *Mol Med* 2019; **25**: 16 [PMID: 31046673 DOI: 10.1186/s10020-019-0084-3]

59 **Pulli B**, Ali M, Iwamoto Y, Zeller MW, Schob S, Linnoila JJ, Chen JW. Myeloperoxidase-Hepatocyte-Stellate Cell Cross Talk Promotes Hepatocyte Injury and Fibrosis in Experimental Nonalcoholic Steatohepatitis. *Antioxid Redox Signal* 2015; **23**: 1255-1269 [PMID: 26058518 DOI: 10.1089/ars.2014.6108]

60 **Rensen SS**, Slaats Y, Nijhuis J, Jans A, Bieghs V, Driessen A, Malle E, Greve JW, Buurman WA. Increased hepatic myeloperoxidase activity in obese subjects with nonalcoholic steatohepatitis. *Am J Pathol* 2009; **175**: 1473-1482 [PMID: 19729473 DOI: 10.2353/ajpath.2009.080999]

61 **Alkhouri N**, Li L, Hanouneh I, Feldstein A, Hazen S. Plasma Myeloperoxidase Levels Correlate with the Presence of Fibrosis in Patients with Nonalcoholic Fatty Liver Disease. Am J Gastroenterol 2012; 107: S181 [DOI: 10.14309/00000434-201210001-00433]

62 **Adler M**, Taylor S, Okebugwu K, Yee H, Fielding C, Fielding G, Poles M. Intrahepatic natural killer T cell populations are increased in human hepatic steatosis. *World J Gastroenterol* 2011; **17**: 1725-1731 [PMID: 21483633 DOI: 10.3748/wjg.v17.i13.1725]

63 **Kahraman A**, Fingas CD, Syn WK, Gerken G, Canbay A. Role of stress-induced NKG2D ligands in liver diseases. *Liver Int* 2012; **32**: 370-382 [PMID: 22097967 DOI: 10.1111/j.1478-3231.2011.02608.x]

64 **Méndez-Sánchez N**, Córdova-Gallardo J, Barranco-Fragoso B, Eslam M. Hepatic Dendritic Cells in the Development and Progression of Metabolic Steatohepatitis. *Front Immunol* 2021; **12**: 641240 [PMID: 33833761 DOI: 10.3389/fimmu.2021.641240]

65 **Henning JR**, Graffeo CS, Rehman A, Fallon NC, Zambirinis CP, Ochi A, Barilla R, Jamal M, Deutsch M, Greco S, Ego-Osuala M, Bin-Saeed U, Rao RS, Badar S, Quesada JP, Acehan D, Miller G. Dendritic cells limit fibroinflammatory injury in nonalcoholic steatohepatitis in mice. *Hepatology* 2013; **58**: 589-602 [PMID: 23322710 DOI: 10.1002/hep.26267]

66 **Sutti S**, Jindal A, Bruzzì S, Locatelli I, Bozzola C, Albano E. Is there a role for adaptive immunity in nonalcoholic steatohepatitis? *World J Hepatol* 2015; **7**: 1725-1729 [PMID: 26167244 DOI: 10.4254/wjh.v7.i13.1725]

67 **Li Z**, Soloski MJ, Diehl AM. Dietary factors alter hepatic innate immune system in mice with nonalcoholic fatty liver disease. *Hepatology* 2005; **42**: 880-885 [PMID: 16175608 DOI: 10.1002/HEP.20826]

68 **Weston CJ**, Shepherd EL, Claridge LC, Rantakari P, Curbishley SM, Tomlinson JW, Hubscher SG, Reynolds GM, Aalto K, Anstee QM, Jalkanen S, Salmi M, Smith DJ, Day CP, Adams DH. Vascular adhesion protein-1 promotes liver inflammation and drives hepatic fibrosis. *J Clin Invest* 2015; **125**: 501-520 [PMID: 25562318 DOI: 10.1172/JCI73722]

69 **Inzaugarat ME**, Ferreyra Solari NE, Billordo LA, Abecasis R, Gadano AC, Cherñavsky AC. Altered phenotype and functionality of circulating immune cells characterize adult patients with nonalcoholic steatohepatitis. *J Clin Immunol* 2011; **31**: 1120-1130 [PMID: 21845516 DOI: 10.1007/s10875-011-9571-1]

70 **Wolf MJ**, Adili A, Piotrowitz K, Abdullah Z, Boege Y, Stemmer K, Ringelhan M, Simonavicius N, Egger M, Wohlleber D, Lorentzen A, Einer C, Schulz S, Clavel T, Protzer U, Thiele C, Zischka H, Moch H, Tschöp M, Tumanov AV, Haller D, Unger K, Karin M, Kopf M, Knolle P, Weber A, Heikenwalder M. Metabolic activation of intrahepatic CD8+ T cells and NKT cells causes nonalcoholic steatohepatitis and liver cancer *via* cross-talk with hepatocytes. *Cancer Cell* 2014; **26**: 549-564 [PMID: 25314080 DOI: 10.1016/j.ccell.2014.09.003]

71 **Sutti S**, Jindal A, Locatelli I, Vacchiano M, Gigliotti L, Bozzola C, Albano E. Adaptive immune responses triggered by oxidative stress contribute to hepatic inflammation in NASH. *Hepatology* 2014; **59**: 886-897 [PMID: 24115128 DOI: 10.1002/hep.26749]

72 **Hirsova P**, Bamidele AO, Wang H, Povero D, Revelo XS. Emerging Roles of T Cells in the Pathogenesis of Nonalcoholic Steatohepatitis and Hepatocellular Carcinoma. *Front Endocrinol (Lausanne)* 2021; **12**: 760860 [PMID: 34777255 DOI: 10.3389/fendo.2021.760860]

73 **Sutti S**, Albano E. Adaptive immunity: an emerging player in the progression of NAFLD. *Nat Rev Gastroenterol Hepatol* 2020; **17**: 81-92 [PMID: 31605031 DOI: 10.1038/s41575-019-0210-2]

74 **Chackelevicius CM**, Gambaro SE, Tiribelli C, Rosso N. Th17 involvement in nonalcoholic fatty liver disease progression to non-alcoholic steatohepatitis. *World J Gastroenterol* 2016; **22**: 9096-9103 [PMID: 27895397 DOI: 10.3748/wjg.v22.i41.9096]

75 **Tang Y**, Bian Z, Zhao L, Liu Y, Liang S, Wang Q, Han X, Peng Y, Chen X, Shen L, Qiu D, Li Z, Ma X. Interleukin-17 exacerbates hepatic steatosis and inflammation in non-alcoholic fatty liver disease. *Clin Exp Immunol* 2011; **166**: 281-290 [PMID: 21985374 DOI: 10.1111/j.1365-2249.2011.04471.x]

76 **Giles DA**, Moreno-Fernandez ME, Stankiewicz TE, Cappelletti M, Huppert SS, Iwakura Y, Dong C, Shanmukhappa SK, Divanovic S. Regulation of Inflammation by IL-17A and IL-17F Modulates Non-Alcoholic Fatty Liver Disease Pathogenesis. *PLoS One* 2016; **11**: e0149783 [PMID: 26895034 DOI: 10.1371/journal.pone.0149783]

77 **Harley IT**, Stankiewicz TE, Giles DA, Softic S, Flick LM, Cappelletti M, Sheridan R, Xanthakos SA, Steinbrecher KA, Sartor RB, Kohli R, Karp CL, Divanovic S. IL-17 signaling accelerates the progression of nonalcoholic fatty liver disease in mice. *Hepatology* 2014; **59**: 1830-1839 [PMID: 24115079 DOI: 10.1002/hep.26746]

78 **Xu R**, Tao A, Zhang S, Zhang M. Neutralization of interleukin-17 attenuates high fat diet-induced non-alcoholic fatty liver disease in mice. *Acta Biochim Biophys Sin (Shanghai)* 2013; **45**: 726-733 [PMID: 23786840 DOI: 10.1093/abbs/gmt065]

79 **Meng F**, Wang K, Aoyama T, Grivennikov SI, Paik Y, Scholten D, Cong M, Iwaisako K, Liu X, Zhang M, Österreicher CH, Stickel F, Ley K, Brenner DA, Kisseleva T. Interleukin-17 signaling in inflammatory, Kupffer cells, and hepatic stellate cells exacerbates liver fibrosis in mice. *Gastroenterology* 2012; **143**: 765-776.e3 [PMID: 22687286 DOI: 10.1053/j.gastro.2012.05.049]

80 **Van Herck MA**, Weyler J, Kwanten WJ, Dirinck EL, De Winter BY, Francque SM, Vonghia L. The Differential Roles of T Cells in Non-alcoholic Fatty Liver Disease and Obesity. *Front Immunol* 2019; **10**: 82 [PMID: 30787925 DOI: 10.3389/fimmu.2019.00082]

81 **Rau M**, Schilling AK, Meertens J, Hering I, Weiss J, Jurowich C, Kudlich T, Hermanns HM, Bantel H, Beyersdorf N, Geier A. Progression from Nonalcoholic Fatty Liver to Nonalcoholic Steatohepatitis Is Marked by a Higher Frequency of Th17 Cells in the Liver and an Increased Th17/Resting Regulatory T Cell Ratio in Peripheral Blood and in the Liver. *J Immunol* 2016; **196**: 97-105 [PMID: 26621860 DOI: 10.4049/jimmunol.1501175]

82 **Williams CD**, Stengel J, Asike MI, Torres DM, Shaw J, Contreras M, Landt CL, Harrison SA. Prevalence of nonalcoholic fatty liver disease and nonalcoholic steatohepatitis among a largely middle-aged population utilizing ultrasound and liver biopsy: a prospective study. *Gastroenterology* 2011; **140**: 124-131 [PMID: 20858492 DOI: 10.1053/j.gastro.2010.09.038]

83 **Racanelli V**, Rehermann B. The liver as an immunological organ. *Hepatology* 2006; **43**: S54-S62 [PMID: 16447271 DOI: 10.1002/hep.21060]

84 **Tsiantoulas D**, Sage AP, Mallat Z, Binder CJ. Targeting B cells in atherosclerosis: closing the gap from bench to bedside. *Arterioscler Thromb Vasc Biol* 2015; **35**: 296-302 [PMID: 25359862 DOI: 10.1161/ATVBAHA.114.303569]

85 **Grohmann M**, Wiede F, Dodd GT, Gurzov EN, Ooi GJ, Butt T, Rasmiena AA, Kaur S, Gulati T, Goh PK, Treloar AE, Archer S, Brown WA, Muller M, Watt MJ, Ohara O, McLean CA, Tiganis T. Obesity Drives STAT-1-Dependent NASH and STAT-3-Dependent HCC. *Cell* 2018; **175**: 1289-1306.e20 [PMID: 30454647 DOI: 10.1016/j.cell.2018.09.053]

86 **Bruzzì S**, Sutti S, Giudici G, Burlone ME, Ramavath NN, Toscani A, Bozzola C, Schneider P, Morello E, Parola M, Pirisi M, Albano E. B2-Lymphocyte responses to oxidative stress-derived antigens contribute to the evolution of nonalcoholic fatty liver disease (NAFLD). *Free Radic Biol Med* 2018; **124**: 249-259 [PMID: 29920340 DOI: 10.1016/j.freeradbiomed.2018.06.015]

87 **Kawasaki K**, Abe M, Tada F, Tokumoto Y, Chen S, Miyake T, Furukawa S, Matsuura B, Hiasa Y, Onji M. Blockade of B-cell-activating factor signaling enhances hepatic steatosis induced by a high-fat diet and improves insulin sensitivity. *Lab Invest* 2013; **93**: 311-321 [PMID: 23318884 DOI: 10.1038/labinvest.2012.176]

88 **Miyake T**, Abe M, Tokumoto Y, Hirooka M, Furukawa S, Kumagi T, Hamada M, Kawasaki K, Tada F, Ueda T, Hiasa Y, Matsuura B, Onji M. B cell-activating factor is associated with the histological severity of nonalcoholic fatty liver disease. *Hepatol Int* 2013; **7**: 539-547 [PMID: 26201785 DOI: 10.1007/s12072-012-9345-8]

89 **Lund FE**. Cytokine-producing B lymphocytes-key regulators of immunity. *Curr Opin Immunol* 2008; **20**: 332-338 [PMID: 18417336 DOI: 10.1016/j.coi.2008.03.003]

90 **DiLillo DJ**, Horikawa M, Tedder TF. B-lymphocyte effector functions in health and disease. *Immunol Res* 2011; **49**: 281-292 [PMID: 21125343 DOI: 10.1007/s12026-010-8189-3]

91 **Béland K**, Marceau G, Labardy A, Bourbonnais S, Alvarez F. Depletion of B cells induces remission of autoimmune hepatitis in mice through reduced antigen presentation and help to T cells. *Hepatology* 2015; **62**: 1511-1523 [PMID: 26175263 DOI: 10.1002/hep.27991]

92 **McPherson S**, Henderson E, Burt AD, Day CP, Anstee QM. Serum immunoglobulin levels predict fibrosis in patients with non-alcoholic fatty liver disease. *J Hepatol* 2014; **60**: 1055-1062 [PMID: 24445215 DOI: 10.1016/j.jhep.2014.01.010]

93 **Shalapour S**, Lin XJ, Bastian IN, Brain J, Burt AD, Aksenov AA, Vrbanac AF, Li W, Perkins A, Matsutani T, Zhong Z, Dhar D, Navas-Molina JA, Xu J, Loomba R, Downes M, Yu RT, Evans RM, Dorrestein PC, Knight R, Benner C, Anstee QM, Karin M. Inflammation-induced IgA+ cells dismantle anti-liver cancer immunity. *Nature* 2017; **551**: 340-345 [PMID: 29144460 DOI: 10.1038/nature24302]

94 **Gregory SN**, Perati SR, Brown ZJ. Alteration in immune function in patients with fatty liver disease. Hepatoma Res 2022; 8: 31 [DOI: 10.20517/2394-5079.2022.34]

95 **Sung PS**, Park DJ, Roh PR, Mun KD, Cho SW, Lee GW, Jung ES, Lee SH, Jang JW, Bae SH, Choi JY, Choi J, Ahn J, Yoon SK. Intrahepatic inflammatory IgA(+)PD-L1(high) monocytes in hepatocellular carcinoma development and immunotherapy. *J Immunother Cancer* 2022; **10** [PMID: 35577505 DOI: 10.1136/jitc-2021-003618]

96 **Barrow F**, Khan S, Fredrickson G, Wang H, Dietsche K, Parthiban P, Robert S, Kaiser T, Winer S, Herman A, Adeyi O, Mouzaki M, Khoruts A, Hogquist KA, Staley C, Winer DA, Revelo XS. Microbiota-Driven Activation of Intrahepatic B Cells Aggravates NASH Through Innate and Adaptive Signaling. *Hepatology* 2021; **74**: 704-722 [PMID: 33609303 DOI: 10.1002/hep.31755]

97 **Nassir F**. NAFLD: Mechanisms, Treatments, and Biomarkers. *Biomolecules* 2022; **12** [PMID: 35740949 DOI: 10.3390/biom12060824]

98 **Ando Y**, Jou JH. Nonalcoholic Fatty Liver Disease and Recent Guideline Updates. *Clin Liver Dis (Hoboken)* 2021; **17**: 23-28 [PMID: 33552482 DOI: 10.1002/cld.1045]

99 **Piazzolla VA**, Mangia A. Noninvasive Diagnosis of NAFLD and NASH. *Cells* 2020; **9** [PMID: 32316690 DOI: 10.3390/cells9041005]

100 **Sanyal D**, Mukherjee P, Raychaudhuri M, Ghosh S, Mukherjee S, Chowdhury S. Profile of liver enzymes in non-alcoholic fatty liver disease in patients with impaired glucose tolerance and newly detected untreated type 2 diabetes. *Indian J Endocrinol Metab* 2015; **19**: 597-601 [PMID: 26425466 DOI: 10.4103/2230-8210.163172]

101 **Obika M**, Noguchi H. Diagnosis and evaluation of nonalcoholic fatty liver disease. *Exp Diabetes Res* 2012; **2012**: 145754 [PMID: 22110476 DOI: 10.1155/2012/145754]

102 **Zeng Y**, He H, An Z. Advance of Serum Biomarkers and Combined Diagnostic Panels in Nonalcoholic Fatty Liver Disease. *Dis Markers* 2022; **2022**: 1254014 [PMID: 35811662 DOI: 10.1155/2022/1254014]

103 **Kumar R**, Teo EK, How CH, Wong TY, Ang TL. A practical clinical approach to liver fibrosis. *Singapore Med J* 2018; **59**: 628-633 [PMID: 30631885 DOI: 10.11622/smedj.2018145]

104 **Woreta TA**, Van Natta ML, Lazo M, Krishnan A, Neuschwander-Tetri BA, Loomba R, Mae Diehl A, Abdelmalek MF, Chalasani N, Gawrieh S, Dasarathy S, Vuppalanchi R, Siddiqui MS, Kowdley KV, McCullough A, Terrault NA, Behling C, Kleiner DE, Fishbein M, Hertel P, Wilson LA, Mitchell EP, Miriel LA, Clark JM, Tonascia J, Sanyal AJ; NASH Clinical Research Network. Validation of the accuracy of the FAST™ score for detecting patients with at-risk nonalcoholic steatohepatitis (NASH) in a North American cohort and comparison to other non-invasive algorithms. *PLoS One* 2022; **17**: e0266859 [PMID: 35427375 DOI: 10.1371/journal.pone.0266859]

105 **Newsome PN**, Sasso M, Deeks JJ, Paredes A, Boursier J, Chan WK, Yilmaz Y, Czernichow S, Zheng MH, Wong VW, Allison M, Tsochatzis E, Anstee QM, Sheridan DA, Eddowes PJ, Guha IN, Cobbold JF, Paradis V, Bedossa P, Miette V, Fournier-Poizat C, Sandrin L, Harrison SA. FibroScan-AST (FAST) score for the non-invasive identification of patients with non-alcoholic steatohepatitis with significant activity and fibrosis: a prospective derivation and global validation study. *Lancet Gastroenterol Hepatol* 2020; **5**: 362-373 [PMID: 32027858 DOI: 10.1016/S2468-1253(19)30383-8]

106 **Lee JS**, Lee HW, Kim BK, Park JY, Kim DY, Ahn SH, Jang JY, Park SY, Lee CK, Kim SU. Comparison of FibroScan-Aspartate Aminotransferase (FAST) Score and Other Non-invasive Surrogates in Predicting High-Risk Non-alcoholic Steatohepatitis Criteria. *Front Med (Lausanne)* 2022; **9**: 869190 [PMID: 35492369 DOI: 10.3389/fmed.2022.869190]

107 **Reinson T**, Buchanan RM, Byrne CD. Noninvasive serum biomarkers for liver fibrosis in NAFLD: current and future. *Clin Mol Hepatol* 2023; **29**: S157-S170 [PMID: 36417894 DOI: 10.3350/cmh.2022.0348]

108 **Singh SP**, Barik RK. NonInvasive Biomarkers in Nonalcoholic Fatty Liver Disease: Are We There Yet? *J Clin Exp Hepatol* 2020; **10**: 88-98 [PMID: 32025168 DOI: 10.1016/j.jceh.2019.09.006]

109 **Dufour JF**, Anstee QM, Bugianesi E, Harrison S, Loomba R, Paradis V, Tilg H, Wong VW, Zelber-Sagi S. Current therapies and new developments in NASH. *Gut* 2022; **71**: 2123-2134 [PMID: 35710299 DOI: 10.1136/gutjnl-2021-326874]

110 **Choi ME**, Price DR, Ryter SW, Choi AMK. Necroptosis: a crucial pathogenic mediator of human disease. *JCI Insight* 2019; **4** [PMID: 31391333 DOI: 10.1172/jci.insight.128834]

111 **Zhao J**, Hu Y, Peng J. Targeting programmed cell death in metabolic dysfunction-associated fatty liver disease (MAFLD): a promising new therapy. *Cell Mol Biol Lett* 2021; **26**: 17 [PMID: 33962586 DOI: 10.1186/s11658-021-00254-z]

112 **Kaiser WJ**, Sridharan H, Huang C, Mandal P, Upton JW, Gough PJ, Sehon CA, Marquis RW, Bertin J, Mocarski ES. Toll-like receptor 3-mediated necrosis *via* TRIF, RIP3, and MLKL. *J Biol Chem* 2013; **288**: 31268-31279 [PMID: 24019532 DOI: 10.1074/jbc.M113.462341]

113 **O'Brien J**, Hayder H, Zayed Y, Peng C. Overview of MicroRNA Biogenesis, Mechanisms of Actions, and Circulation. *Front Endocrinol (Lausanne)* 2018; **9**: 402 [PMID: 30123182 DOI: 10.3389/fendo.2018.00402]

114 **Salvoza NC**, Klinzing DC, Gopez-Cervantes J, Baclig MO. Association of Circulating Serum miR-34a and miR-122 with Dyslipidemia among Patients with Non-Alcoholic Fatty Liver Disease. *PLoS One* 2016; **11**: e0153497 [PMID: 27077736 DOI: 10.1371/journal.pone.0153497]

115 **Yamada H**, Suzuki K, Ichino N, Ando Y, Sawada A, Osakabe K, Sugimoto K, Ohashi K, Teradaira R, Inoue T, Hamajima N, Hashimoto S. Associations between circulating microRNAs (miR-21, miR-34a, miR-122 and miR-451) and non-alcoholic fatty liver. *Clin Chim Acta* 2013; **424**: 99-103 [PMID: 23727030 DOI: 10.1016/j.cca.2013.05.021]

116 **Celikbilek M**, Baskol M, Taheri S, Deniz K, Dogan S, Zararsiz G, Gursoy S, Guven K, Ozbakır O, Dundar M, Yucesoy M. Circulating microRNAs in patients with non-alcoholic fatty liver disease. *World J Hepatol* 2014; **6**: 613-620 [PMID: 25232454 DOI: 10.4254/wjh.v6.i8.613]

117 **Cermelli S**, Ruggieri A, Marrero JA, Ioannou GN, Beretta L. Circulating microRNAs in patients with chronic hepatitis C and non-alcoholic fatty liver disease. *PLoS One* 2011; **6**: e23937 [PMID: 21886843 DOI: 10.1371/journal.pone.0023937]

118 **Liu XL**, Pan Q, Zhang RN, Shen F, Yan SY, Sun C, Xu ZJ, Chen YW, Fan JG. Disease-specific miR-34a as diagnostic marker of non-alcoholic steatohepatitis in a Chinese population. *World J Gastroenterol* 2016; **22**: 9844-9852 [PMID: 27956809 DOI: 10.3748/wjg.v22.i44.9844]

119 **Sun Y**, Shen Y, Liang X, Zheng H, Zhang Y. MicroRNAs as Biomarkers and Therapeutic Targets for Nonalcoholic Fatty Liver Disease: A Narrative Review. *Clin Ther* 2023; **45**: 234-247 [PMID: 36841739 DOI: 10.1016/j.clinthera.2023.02.001]

120 **Pillai SS**, Lakhani HV, Zehra M, Wang J, Dilip A, Puri N, O'Hanlon K, Sodhi K. Predicting Nonalcoholic Fatty Liver Disease through a Panel of Plasma Biomarkers and MicroRNAs in Female West Virginia Population. *Int J Mol Sci* 2020; **21** [PMID: 32933141 DOI: 10.3390/ijms21186698]

121 **Eguchi A**, Iwasa M, Nakagawa H. Extracellular vesicles in fatty liver disease and steatohepatitis: Role as biomarkers and therapeutic targets. *Liver Int* 2023; **43**: 292-298 [PMID: 36462157 DOI: 10.1111/liv.15490]

122 **Wu D**, Zhu H, Wang H. Extracellular Vesicles in Non-alcoholic Fatty Liver Disease and Alcoholic Liver Disease. *Front Physiol* 2021; **12**: 707429 [PMID: 34335310 DOI: 10.3389/fphys.2021.707429]

123 **Kranendonk ME**, Visseren FL, van Balkom BW, Nolte-'t Hoen EN, van Herwaarden JA, de Jager W, Schipper HS, Brenkman AB, Verhaar MC, Wauben MH, Kalkhoven E. Human adipocyte extracellular vesicles in reciprocal signaling between adipocytes and macrophages. *Obesity (Silver Spring)* 2014; **22**: 1296-1308 [PMID: 24339422 DOI: 10.1002/oby.20679]

124 **Kranendonk ME**, Visseren FL, van Herwaarden JA, Nolte-'t Hoen EN, de Jager W, Wauben MH, Kalkhoven E. Effect of extracellular vesicles of human adipose tissue on insulin signaling in liver and muscle cells. *Obesity (Silver Spring)* 2014; **22**: 2216-2223 [PMID: 25045057 DOI: 10.1002/oby.20847]

125 **Povero D**, Eguchi A, Li H, Johnson CD, Papouchado BG, Wree A, Messer K, Feldstein AE. Circulating extracellular vesicles with specific proteome and liver microRNAs are potential biomarkers for liver injury in experimental fatty liver disease. *PLoS One* 2014; **9**: e113651 [PMID: 25470250 DOI: 10.1371/journal.pone.0113651]

126 **Garcia-Martinez I**, Alen R, Rada P, Valverde AM. Insights Into Extracellular Vesicles as Biomarker of NAFLD Pathogenesis. *Front Med (Lausanne)* 2020; **7**: 395 [PMID: 32850903 DOI: 10.3389/fmed.2020.00395]

127 **Moore MP**, Cunningham RP, Dashek RJ, Mucinski JM, Rector RS. A Fad too Far? Dietary Strategies for the Prevention and Treatment of NAFLD. *Obesity (Silver Spring)* 2020; **28**: 1843-1852 [PMID: 32893456 DOI: 10.1002/oby.22964]

128 **Mantovani A**, Dalbeni A. Treatments for NAFLD: State of Art. *Int J Mol Sci* 2021; **22** [PMID: 33652942 DOI: 10.3390/ijms22052350]

129 **Vilar-Gomez E**, Martinez-Perez Y, Calzadilla-Bertot L, Torres-Gonzalez A, Gra-Oramas B, Gonzalez-Fabian L, Friedman SL, Diago M, Romero-Gomez M. Weight Loss Through Lifestyle Modification Significantly Reduces Features of Nonalcoholic Steatohepatitis. *Gastroenterology* 2015; **149**: 367-78.e5; quiz e14 [PMID: 25865049 DOI: 10.1053/j.gastro.2015.04.005]

130 **Wong VW**, Chan RS, Wong GL, Cheung BH, Chu WC, Yeung DK, Chim AM, Lai JW, Li LS, Sea MM, Chan FK, Sung JJ, Woo J, Chan HL. Community-based lifestyle modification programme for non-alcoholic fatty liver disease: a randomized controlled trial. *J Hepatol* 2013; **59**: 536-542 [PMID: 23623998 DOI: 10.1016/j.jhep.2013.04.013]

131 **Mascaró CM**, Bouzas C, Tur JA. Association between Non-Alcoholic Fatty Liver Disease and Mediterranean Lifestyle: A Systematic Review. *Nutrients* 2021; **14** [PMID: 35010923 DOI: 10.3390/nu14010049]

132 **Oh S**, So R, Shida T, Matsuo T, Kim B, Akiyama K, Isobe T, Okamoto Y, Tanaka K, Shoda J. High-Intensity Aerobic Exercise Improves Both Hepatic Fat Content and Stiffness in Sedentary Obese Men with Nonalcoholic Fatty Liver Disease. *Sci Rep* 2017; **7**: 43029 [PMID: 28223710 DOI: 10.1038/srep43029]

133 **Watanabe M**, Tozzi R, Risi R, Tuccinardi D, Mariani S, Basciani S, Spera G, Lubrano C, Gnessi L. Beneficial effects of the ketogenic diet on nonalcoholic fatty liver disease: A comprehensive review of the literature. *Obes Rev* 2020; **21**: e13024 [PMID: 32207237 DOI: 10.1111/obr.13024]

134 **Luukkonen PK**, Dufour S, Lyu K, Zhang XM, Hakkarainen A, Lehtimäki TE, Cline GW, Petersen KF, Shulman GI, Yki-Järvinen H. Effect of a ketogenic diet on hepatic steatosis and hepatic mitochondrial metabolism in nonalcoholic fatty liver disease. *Proc Natl Acad Sci U S A* 2020; **117**: 7347-7354 [PMID: 32179679 DOI: 10.1073/pnas.1922344117]

135 **Achanta LB**, Rae CD. β-Hydroxybutyrate in the Brain: One Molecule, Multiple Mechanisms. *Neurochem Res* 2017; **42**: 35-49 [PMID: 27826689 DOI: 10.1007/s11064-016-2099-2]

136 **Wu Y**, Teng Y, Zhang C, Pan Y, Zhang Q, Zhu X, Liu N, Su X, Lin J. The ketone body β-hydroxybutyrate alleviates CoCrMo alloy particles induced osteolysis by regulating NLRP3 inflammasome and osteoclast differentiation. *J Nanobiotechnology* 2022; **20**: 120 [PMID: 35264201 DOI: 10.1186/s12951-022-01320-0]

137 **Miller VJ**, Villamena FA, Volek JS. Nutritional Ketosis and Mitohormesis: Potential Implications for Mitochondrial Function and Human Health. *J Nutr Metab* 2018; **2018**: 5157645 [PMID: 29607218 DOI: 10.1155/2018/5157645]

138 **O'Brien PE**, Hindle A, Brennan L, Skinner S, Burton P, Smith A, Crosthwaite G, Brown W. Long-Term Outcomes After Bariatric Surgery: a Systematic Review and Meta-analysis of Weight Loss at 10 or More Years for All Bariatric Procedures and a Single-Centre Review of 20-Year Outcomes After Adjustable Gastric Banding. *Obes Surg* 2019; **29**: 3-14 [PMID: 30293134 DOI: 10.1007/s11695-018-3525-0]

139 **Głuszyńska P**, Lemancewicz D, Dzięcioł JB, Razak Hady H. Non-Alcoholic Fatty Liver Disease (NAFLD) and Bariatric/Metabolic Surgery as Its Treatment Option: A Review. *J Clin Med* 2021; **10** [PMID: 34945016 DOI: 10.3390/jcm10245721]

140 **Lee KC**, Wu PS, Lin HC. Pathogenesis and treatment of non-alcoholic steatohepatitis and its fibrosis. *Clin Mol Hepatol* 2023; **29**: 77-98 [PMID: 36226471 DOI: 10.3350/cmh.2022.0237]

141 **Lee Y**, Doumouras AG, Yu J, Brar K, Banfield L, Gmora S, Anvari M, Hong D. Complete Resolution of Nonalcoholic Fatty Liver Disease After Bariatric Surgery: A Systematic Review and Meta-analysis. *Clin Gastroenterol Hepatol* 2019; **17**: 1040-1060.e11 [PMID: 30326299 DOI: 10.1016/j.cgh.2018.10.017]

142 **Fakhry TK**, Mhaskar R, Schwitalla T, Muradova E, Gonzalvo JP, Murr MM. Bariatric surgery improves nonalcoholic fatty liver disease: a contemporary systematic review and meta-analysis. *Surg Obes Relat Dis* 2019; **15**: 502-511 [PMID: 30683512 DOI: 10.1016/j.soard.2018.12.002]

143 **Baldwin D**, Chennakesavalu M, Gangemi A. Systematic review and meta-analysis of Roux-en-Y gastric bypass against laparoscopic sleeve gastrectomy for amelioration of NAFLD using four criteria. *Surg Obes Relat Dis* 2019; **15**: 2123-2130 [PMID: 31711944 DOI: 10.1016/j.soard.2019.09.060]

144 **Pedersen JS**, Rygg MO, Serizawa RR, Kristiansen VB, Albrechtsen NJW, Gluud LL, Madsbad S, Bendtsen F. Effects of Roux-en-Y Gastric Bypass and Sleeve Gastrectomy on Non-Alcoholic Fatty Liver Disease: A 12-Month Follow-Up Study with Paired Liver Biopsies. *J Clin Med* 2021; **10** [PMID: 34501231 DOI: 10.3390/jcm10173783]

145 **Ozturk ZA**, Kadayifci A. Insulin sensitizers for the treatment of non-alcoholic fatty liver disease. *World J Hepatol* 2014; **6**: 199-206 [PMID: 24799988 DOI: 10.4254/wjh.v6.i4.199]

146 **Pinyopornpanish K**, Leerapun A, Pinyopornpanish K, Chattipakorn N. Effects of Metformin on Hepatic Steatosis in Adults with Nonalcoholic Fatty Liver Disease and Diabetes: Insights from the Cellular to Patient Levels. *Gut Liver* 2021; **15**: 827-840 [PMID: 33820884 DOI: 10.5009/gnl20367]

147 **Chalasani N**, Younossi Z, Lavine JE, Charlton M, Cusi K, Rinella M, Harrison SA, Brunt EM, Sanyal AJ. The diagnosis and management of nonalcoholic fatty liver disease: Practice guidance from the American Association for the Study of Liver Diseases. *Hepatology* 2018; **67**: 328-357 [PMID: 28714183 DOI: 10.1002/hep.29367]

148 **Li Y**, Liu L, Wang B, Wang J, Chen D. Metformin in non-alcoholic fatty liver disease: A systematic review and meta-analysis. *Biomed Rep* 2013; **1**: 57-64 [PMID: 24648894 DOI: 10.3892/br.2012.18]

149 **Brandt A**, Hernández-Arriaga A, Kehm R, Sánchez V, Jin CJ, Nier A, Baumann A, Camarinha-Silva A, Bergheim I. Metformin attenuates the onset of non-alcoholic fatty liver disease and affects intestinal microbiota and barrier in small intestine. *Sci Rep* 2019; **9**: 6668 [PMID: 31040374 DOI: 10.1038/s41598-019-43228-0]

150 **Nevola R**, Epifani R, Imbriani S, Tortorella G, Aprea C, Galiero R, Rinaldi L, Marfella R, Sasso FC. GLP-1 Receptor Agonists in Non-Alcoholic Fatty Liver Disease: Current Evidence and Future Perspectives. *Int J Mol Sci* 2023; **24** [PMID: 36675217 DOI: 10.3390/ijms24021703]

151 **Holman RR**, Bethel MA, Mentz RJ, Thompson VP, Lokhnygina Y, Buse JB, Chan JC, Choi J, Gustavson SM, Iqbal N, Maggioni AP, Marso SP, Öhman P, Pagidipati NJ, Poulter N, Ramachandran A, Zinman B, Hernandez AF; EXSCEL Study Group. Effects of Once-Weekly Exenatide on Cardiovascular Outcomes in Type 2 Diabetes. *N Engl J Med* 2017; **377**: 1228-1239 [PMID: 28910237 DOI: 10.1056/NEJMoa1612917]

152 **Newsome PN**, Buchholtz K, Cusi K, Linder M, Okanoue T, Ratziu V, Sanyal AJ, Sejling AS, Harrison SA; NN9931-4296 Investigators. A

Placebo-Controlled Trial of Subcutaneous Semaglutide in Nonalcoholic Steatohepatitis. *N Engl J Med* 2021; **384**: 1113-1124 [PMID: 33185364 DOI: 10.1056/NEJMoa2028395]

153 **Raptis DD**, Mantzoros CS, Polyzos SA. Fibroblast Growth Factor-21 as a Potential Therapeutic Target of Nonalcoholic Fatty Liver Disease. *Ther Clin Risk Manag* 2023; **19**: 77-96 [PMID: 36713291 DOI: 10.2147/TCRM.S352008]

154 **Tian H**, Zhang S, Liu Y, Wu Y, Zhang D. Fibroblast Growth Factors for Nonalcoholic Fatty Liver Disease: Opportunities and Challenges. *Int J Mol Sci* 2023; **24** [PMID: 36902015 DOI: 10.3390/ijms24054583]

155 **Harrison SA**, Ruane PJ, Freilich BL, Neff G, Patil R, Behling CA, Hu C, Fong E, de Temple B, Tillman EJ, Rolph TP, Cheng A, Yale K. Efruxifermin in non-alcoholic steatohepatitis: a randomized, double-blind, placebo-controlled, phase 2a trial. *Nat Med* 2021; **27**: 1262-1271 [PMID: 34239138 DOI: 10.1038/s41591-021-01425-3]

156 **Caddeo A**, Kowalik MA, Serra M, Runfola M, Bacci A, Rapposelli S, Columbano A, Perra A. TG68, a Novel Thyroid Hormone Receptor-β Agonist for the Treatment of NAFLD. *Int J Mol Sci* 2021; **22** [PMID: 34884910 DOI: 10.3390/ijms222313105]

157 **Harrison SA**, Bashir MR, Guy CD, Zhou R, Moylan CA, Frias JP, Alkhouri N, Bansal MB, Baum S, Neuschwander-Tetri BA, Taub R, Moussa SE. Resmetirom (MGL-3196) for the treatment of non-alcoholic steatohepatitis: a multicentre, randomised, double-blind, placebo-controlled, phase 2 trial. *Lancet* 2019; **394**: 2012-2024 [PMID: 31727409 DOI: 10.1016/S0140-6736(19)32517-6]

158 **Zhou J**, Waskowicz LR, Lim A, Liao XH, Lian B, Masamune H, Refetoff S, Tran B, Koeberl DD, Yen PM. A Liver-Specific Thyromimetic, VK2809, Decreases Hepatosteatosis in Glycogen Storage Disease Type Ia. *Thyroid* 2019; **29**: 1158-1167 [PMID: 31337282 DOI: 10.1089/thy.2019.0007]

159 **Ferguson D**, Finck BN. Emerging therapeutic approaches for the treatment of NAFLD and type 2 diabetes mellitus. *Nat Rev Endocrinol* 2021; **17**: 484-495 [PMID: 34131333 DOI: 10.1038/s41574-021-00507-z]

160 **Nelson CH**, Jones C, Klucher K, Jin F, Marmon T, Chung D et al. Liver-distributed farnesoid X receptor agonist TERN-101 demonstrates potent target engagement with a favorable exposure-response profile in non-alcoholic steatohepatitis patients. *J Hepatol* 2022; **77**: S716 [DOI: 10.1016/S0168-8278(22)01750-0]

161 **Kirschberg T**, Jones C, Xu Y, Wang Y, Fenaux M, Klucher K. TERN-501, a potent and selective agonist of thyroid hormone receptor beta, strongly reduces histological features and biomarkers of non-alcoholic steatohepatitis associated pathology in rodent models. *J Hepatol* 2020; **73**: S684

162 **Wiering L**, Tacke F. Treating inflammation to combat non-alcoholic fatty liver disease. *J Endocrinol* 2023; **256** [PMID: 36259984 DOI: 10.1530/JOE-22-0194]

163 **Ortiz-López N**, Fuenzalida C, Dufeu MS, Pinto-León A, Escobar A, Poniachik J, Roblero JP, Valenzuela-Pérez L, Beltrán CJ. The immune response as a therapeutic target in non-alcoholic fatty liver disease. *Front Immunol* 2022; **13**: 954869 [PMID: 36300120 DOI: 10.3389/fimmu.2022.954869]

164 **Ndakotsu A**, Vivekanandan G. The Role of Thiazolidinediones in the Amelioration of Nonalcoholic Fatty Liver Disease: A Systematic Review. *Cureus* 2022; **14**: e25380 [PMID: 35765391 DOI: 10.7759/cureus.25380]

165 **Belfort R**, Harrison SA, Brown K, Darland C, Finch J, Hardies J, Balas B, Gastaldelli A, Tio F, Pulcini J, Berria R, Ma JZ, Dwivedi S, Havranek R, Fincke C, DeFronzo R, Bannayan GA, Schenker S, Cusi K. A placebo-controlled trial of pioglitazone in subjects with nonalcoholic steatohepatitis. *N Engl J Med* 2006; **355**: 2297-2307 [PMID: 17135584 DOI: 10.1056/NEJMoa060326]

166 **Ratziu V**, Harrison SA, Francque S, Bedossa P, Lehert P, Serfaty L, Romero-Gomez M, Boursier J, Abdelmalek M, Caldwell S, Drenth J, Anstee QM, Hum D, Hanf R, Roudot A, Megnien S, Staels B, Sanyal A; GOLDEN-505 Investigator Study Group. Elafibranor, an Agonist of the Peroxisome Proliferator-Activated Receptor-α and -δ, Induces Resolution of Nonalcoholic Steatohepatitis Without Fibrosis Worsening. *Gastroenterology* 2016; **150**: 1147-1159.e5 [PMID: 26874076 DOI: 10.1053/j.gastro.2016.01.038]

167 **Sanyal AJ**, Lopez P, Lawitz EJ, Lucas KJ, Loeffler J, Kim W, Goh GBB, Huang JF, Serra C, Andreone P, Chen YC, Hsia SH, Ratziu V, Aizenberg D, Tobita H, Sheikh AM, Vierling JM, Kim YJ, Hyogo H, Tai D, Goodman Z, Schaefer F, Carbarns IRI, Lamle S, Martic M, Naoumov NV, Brass CA. Tropifexor for nonalcoholic steatohepatitis: an adaptive, randomized, placebo-controlled phase 2a/b trial. *Nat Med* 2023; **29**: 392-400 [PMID: 36797481 DOI: 10.1038/s41591-022-02200-8]

168 **Abenavoli L**, Maurizi V, Rinninella E, Tack J, Di Berardino A, Santori P, Rasetti C, Procopio AC, Boccuto L, Scarpellini E. Fecal Microbiota Transplantation in NAFLD Treatment. *Medicina (Kaunas)* 2022; **58** [PMID: 36363516 DOI: 10.3390/medicina58111559]

169 **Zhou D**, Pan Q, Shen F, Cao HX, Ding WJ, Chen YW, Fan JG. Total fecal microbiota transplantation alleviates high-fat diet-induced steatohepatitis in mice *via* beneficial regulation of gut microbiota. *Sci Rep* 2017; **7**: 1529 [PMID: 28484247 DOI: 10.1038/s41598-017-01751-y]

170 **Kootte RS**, Levin E, Salojärvi J, Smits LP, Hartstra AV, Udayappan SD, Hermes G, Bouter KE, Koopen AM, Holst JJ, Knop FK, Blaak EE, Zhao J, Smidt H, Harms AC, Hankemeijer T, Bergman JJGHM, Romijn HA, Schaap FG, Olde Damink SWM, Ackermans MT, Dallinga-Thie GM, Zoetendal E, de Vos WM, Serlie MJ, Stroes ESG, Groen AK, Nieuwdorp M. Improvement of Insulin Sensitivity after Lean Donor Feces in Metabolic Syndrome Is Driven by Baseline Intestinal Microbiota Composition. *Cell Metab* 2017; **26**: 611-619.e6 [PMID: 28978426 DOI: 10.1016/j.cmet.2017.09.008]

171 **Fujita K**, Nozaki Y, Wada K, Yoneda M, Endo H, Takahashi H, Iwasaki T, Inamori M, Abe Y, Kobayashi N, Kirikoshi H, Kubota K, Saito S, Nagashima Y, Nakajima A. Effectiveness of antiplatelet drugs against experimental non-alcoholic fatty liver disease. *Gut* 2008; **57**: 1583-1591 [PMID: 18596193 DOI: 10.1136/gut.2007.144550]

172 **Thongtan T**, Deb A, Vutthikraivit W, Laoveeravat P, Mingbunjerdsuk T, Islam S, Islam E. Antiplatelet therapy associated with lower prevalence of advanced liver fibrosis in non-alcoholic fatty liver disease: A systematic review and meta-analysis. *Indian J Gastroenterol* 2022; **41**: 119-126 [PMID: 35318571 DOI: 10.1007/s12664-021-01230-3]

173 **Hilscher MB**, Shah VH. Small but Mighty: Platelets in NASH and Other Chronic Liver Diseases. *Hepatology* 2020; **71**: 1501-1504 [PMID: 31903616 DOI: 10.1002/hep.31101]

174 **Malehmir M**, Pfister D, Gallage S, Szydlowska M, Inverso D, Kotsiliti E, Leone V, Peiseler M, Surewaard BGJ, Rath D, Ali A, Wolf MJ, Drescher H, Healy ME, Dauch D, Kroy D, Krenkel O, Kohlhepp M, Engleitner T, Olkus A, Sijmonsma T, Volz J, Deppermann C, Stegner D, Helbling P, Nombela-Arrieta C, Rafiei A, Hinterleitner M, Rall M, Baku F, Borst O, Wilson CL, Leslie J, O'Connor T, Weston CJ, Chauhan A, Adams DH, Sheriff L, Teijeiro A, Prinz M, Bogeska R, Anstee N, Bongers MN, Notohamiprodjo M, Geisler T, Withers DJ, Ware J, Mann DA, Augustin HG, Vegiopoulos A, Milsom MD, Rose AJ, Lalor PF, Llovet JM, Pinyol R, Tacke F, Rad R, Matter M, Djouder N, Kubes P, Knolle PA, Unger K, Zender L, Nieswandt B, Gawaz M, Weber A, Heikenwalder M. Platelet GPIbα is a mediator and potential interventional target for NASH and subsequent liver cancer. *Nat Med* 2019; **25**: 641-655 [PMID: 30936549 DOI: 10.1038/s41591-019-0379-5]

175 **Pfister D**, Núñez NG, Pinyol R, Govaere O, Pinter M, Szydlowska M, Gupta R, Qiu M, Deczkowska A, Weiner A, Müller F, Sinha A, Friebel

E, Engleitner T, Lenggenhager D, Moncsek A, Heide D, Stirm K, Kosla J, Kotsiliti E, Leone V, Dudek M, Yousuf S, Inverso D, Singh I, Teijeiro A, Castet F, Montironi C, Haber PK, Tiniakos D, Bedossa P, Cockell S, Younes R, Vacca M, Marra F, Schattenberg JM, Allison M, Bugianesi E, Ratziu V, Pressiani T, D'Alessio A, Personeni N, Rimassa L, Daly AK, Scheiner B, Pomej K, Kirstein MM, Vogel A, Peck-Radosavljevic M, Hucke F, Finkelmeier F, Waidmann O, Trojan J, Schulze K, Wege H, Koch S, Weinmann A, Bueter M, Rössler F, Siebenhüner A, De Dosso S, Mallm JP, Umansky V, Jugold M, Luedde T, Schietinger A, Schirmacher P, Emu B, Augustin HG, Billeter A, Müller-Stich B, Kikuchi H, Duda DG, Kütting F, Waldschmidt DT, Ebert MP, Rahbari N, Mei HE, Schulz AR, Ringelhan M, Malek N, Spahn S, Bitzer M, Ruiz de Galarreta M, Lujambio A, Dufour JF, Marron TU, Kaseb A, Kudo M, Huang YH, Djouder N, Wolter K, Zender L, Marche PN, Decaens T, Pinato DJ, Rad R, Mertens JC, Weber A, Unger K, Meissner F, Roth S, Jilkova ZM, Claassen M, Anstee QM, Amit I, Knolle P, Becher B, Llovet JM, Heikenwalder M. NASH limits anti-tumour surveillance in immunotherapy-treated HCC. *Nature* 2021; **592**: 450-456 [PMID: 33762733 DOI: 10.1038/s41586-021-03362-0]

176 **Jeong S**, Shin WY, Oh YH. Immunotherapy for NAFLD and NAFLD-related hepatocellular carcinoma. *Front Endocrinol (Lausanne)* 2023; **14**: 1150360 [PMID: 37020584 DOI: 10.3389/fendo.2023.1150360]

177 **Kudo M**. Impaired Response to Immunotherapy in Non-Alcoholic Steatohepatitis-Related Hepatocellular Carcinoma? *Liver Cancer* 2021; **10**: 289-295 [PMID: 34414117 DOI: 10.1159/000517841]

178 T-cell Dysfunction Limits Immunotherapy Efficacy in NASH-Induced Liver Cancer. *Cancer Discov* 2021; **11**: OF31 [PMID: 33811045 DOI: 10.1158/2159-8290.CD-RW2021-047]

World Journal of Gastroenterology

Submit a Manuscript: https://www.f6publishing.com

World J Gastroenterol 2023 August 28; 29(32): 4851-4859

DOI: 10.3748/wjg.v29.i32.4851

ISSN 1007-9327 (print) ISSN 2219-2840 (online)

MINIREVIEWS

Role of non-*Helicobacter pylori* gastric Helicobacters in *helicobacter pylori*-negative gastric mucosa-associated lymphoid tissue lymphoma

Fabian Fellipe Bueno Lemos, Marcel Silva Luz, Samuel Luca Rocha Pinheiro, Kádima Nayara Teixeira, Fabrício Freire de Melo

Specialty type: Gastroenterology and hepatology

Provenance and peer review: Invited article; Externally peer reviewed.

Peer-review model: Single blind

Peer-review report's scientific quality classification

Grade A (Excellent): 0
Grade B (Very good): B, B, B
Grade C (Good): C
Grade D (Fair): 0
Grade E (Poor): 0

P-Reviewer: Liu Q, China; Watanabe T, Japan; Yuan Y, China

Received: May 28, 2023
Peer-review started: May 28, 2023
First decision: July 8, 2023
Revised: July 18, 2023
Accepted: August 2, 2023
Article in press: August 2, 2023
Published online: August 28, 2023

Fabian Fellipe Bueno Lemos, Marcel Silva Luz, Samuel Luca Rocha Pinheiro, Fabrício Freire de Melo, Instituto Multidisciplinar em Saúde, Universidade Federal da Bahia, Vitória da Conquista 45029094, Brazil

Kádima Nayara Teixeira, Campus Toledo, Universidade Federal do Paraná, Toledo 85919899, Brazil

Corresponding author: Fabrício Freire de Melo, PhD, Professor, Instituto Multidisciplinar em Saúde, Universidade Federal da Bahia, Estrada do Bem Querer, No. 3293-3391-Candeias, Vitória da Conquista 45029094, Brazil. freiremeloufba@gmail.com

Abstract

Marginal zone lymphomas rank as the third most prevalent form of non-Hodgkin B-cell lymphoma, trailing behind diffuse large B-cell lymphoma and follicular lymphoma. Gastric mucosa-associated lymphoid tissue lymphoma (GML) is a low-grade B-cell neoplasia frequently correlated with *Helicobacter pylori* (*H. pylori*)-induced chronic gastritis. On the other hand, a specific subset of individuals diagnosed with GML does not exhibit *H. pylori* infection. In contrast to its *H. pylori*-positive counterpart, it was previously believed that *H. pylori*-negative GML was less likely to respond to antimicrobial therapy. Despite this, surprisingly, increasing evidence supports that a considerable proportion of patients with *H. pylori*-negative GML show complete histopathological remission after bacterial eradication therapy. Nonetheless, the precise mechanisms underlying this treatment responsiveness are not yet fully comprehended. In recent years, there has been growing interest in investigating the role of non-*H. pylori* gastric helicobacters (NHPHs) in the pathogenesis of *H. pylori*-negative GML. However, additional research is required to establish the causal relationship between NHPHs and GML. In this minireview, we examined the current understanding and proposed prospects on the involvement of NHPHs in *H. pylori*-negative GML, as well as their potential response to bacterial eradication therapy.

Key Words: Lymphoma; B cell; Marginal zone; Gastric mucosa-associated lymphoid tissue lymphoma; *Helicobacter pylori*; Non-*Helicobacter pylori* gastric helicobacters; *Helicobacter heilmannii*; *Helicobacter suis*

©The Author(s) 2023. Published by Baishideng Publishing Group Inc. All rights reserved.

Core Tip: Gastric mucosa-associated lymphoid tissue lymphoma (GML) is a type of non-hodgkin lymphoma that arises in the stomach. It has been well-established that *Helicobacter pylori* (*H. pylori*) infection plays a crucial role in the development of GML. However, a subset of patients diagnosed with GML are negative for *H. pylori.* In recent years, there has been growing interest in investigating the role of non-*H. pylori* gastric helicobacters (NHPHs) in the pathogenesis of *H. pylori*-negative GML. This minireview aims to explore the current understanding of the involvement of NHPHs in the development of GML and its potential responsiveness to bacterial eradication therapy.

Citation: Lemos FFB, Silva Luz M, Rocha Pinheiro SL, Teixeira KN, Freire de Melo F. Role of non-*Helicobacter pylori* gastric Helicobacters in *helicobacter pylori*-negative gastric mucosa-associated lymphoid tissue lymphoma. *World J Gastroenterol* 2023; 29(32): 4851-4859
URL: https://www.wjgnet.com/1007-9327/full/v29/i32/4851.htm
DOI: https://dx.doi.org/10.3748/wjg.v29.i32.4851

INTRODUCTION

Marginal zone lymphomas (MZLs) rank as the third most prevalent form of non-hodgkin B-cell lymphoma, trailing behind diffuse large B-cell lymphoma and follicular lymphoma[1]. The 5th edition of the World Health Organization Classification of Hematolymphoid Tumors-Lymphoid Neoplasms further categorizes MZL into four subtypes: Extranodal MZL of mucosa-associated lymphoid tissue (MALT), primary cutaneous MZL, nodal MZL, and pediatric MZL[2].

Gastric MALT lymphoma (GML) is a low-grade B-cell neoplasia often correlated with *Helicobacter pylori* (*H. pylori*)-induced chronic gastritis[3]. Although the normal gastric mucosa lacks lymphoid follicles, chronic inflammation can lead to the formation of MALT. Continuous antigenic stimulation fosters the clonal expansion of B cells within the MALT, supported by specific T helper cells, which may lead to malignant transformation[4,5]. As GML progresses, genetic and epigenetic alterations occur in both oncogenes and tumour suppressor genes, resulting in dysregulated cell growth and survival. Common genetic alterations seen in MALT lymphoma include chromosomal translocations involving the *API2-MALT1* gene fusion and mutations in genes such as *TP53* and *MYD88*[5-7].

The current clinical guidelines advocate for the use of *H. pylori* eradication therapy as the primary treatment approach for localized GML[8-10]. In a recent systematic review conducted by our group, including meta-analyses, it was highlighted that bacterial eradication treatment resulted in the disappearance of lymphoma in over 75% of patients with low-grade, *H. pylori*-positive GML[11]. Hence, our results ratified that bacterial eradication is effective as the sole initial therapy for early-stage GML.

On the other hand, a specific subset of individuals diagnosed with GML does not exhibit *H. pylori* infection[12-15]. Consequently, it was assumed that these patients might not respond favorably to bacterial eradication therapy. However, another meta-analysis conducted by Jung *et al*[16] showed that 29.3% (95% confidence interval: 22.2%-37.4%, I^2 = 41.5%) of *H. pylori*-negative GML patients experienced complete histopathological remission after eradication therapy. Nonetheless, the underlying mechanisms for this responsiveness remain unclear[16].

There has been a growing interest in exploring the involvement of species of non-*H. pylori* gastric helicobacters (NHPHs) in the development of *H. pylori*-negative GML and its responsiveness to bacterial eradication therapy[17-20]. NHPHs represent a group of bacterial species that colonize the stomach but differ genetically and phenotypically from *H. pylori*[21-24]. These differences include variances in flagella, urease activity, and other virulence factors[25,26]. While NHPHs have been detected in some patients with gastritis and peptic ulcers, their precise role and contribution to disease progression are not yet fully understood[27].

Some studies have indeed suggested an association between specific NHPH species and the development of GML, particularly in *H. pylori*-negative cases[28]. However, further research is required to establish a definitive causal relationship between NHPHs and GML. This article aims to explore the current understanding and propose prospects on the role of NHPHS in *H. pylori*-negative GML and its potential responsiveness to bacterial eradication therapy.

H. pylori-negative GML

H. pylori-negative GML accounts for around 10% of all GML cases[29-31]. The cause of *H. pylori*-negative GML is not fully understood, and ongoing research aims to uncover the underlying factors contributing to its development. Symptoms of this type of lymphoma, such as abdominal pain, indigestion, bloating, nausea, vomiting, and weight loss, are similar to other gastric lymphomas but are nonspecific and can be caused by various conditions[32]. Diagnosis is made based on morphologic, immunophenotypic, and genetic analysis of biopsy material. Once the diagnosis is confirmed, a staging procedure to evaluate the extent of lymphoma dissemination is imperative[33].

In contrast to its *H. pylori*-positive counterpart, *H. pylori*-negative GML was previously believed to have a reduced likelihood of responding to antimicrobial therapy. In this context, treatment options may involve watchful waiting, radiation therapy (RT), chemotherapy (ChT), and immunotherapy[9]. Watchful waiting is suitable for slow-growing

lymphomas without significant symptoms and with regular monitoring[33]. However, RT is the preferred treatment for localized disease in the management of *H. pylori*-negative GML. Several series have reported excellent disease control using RT alone, highlighting the efficacy of moderate-dose involved-field RT. Typically, a dose of 24-30 Gy is delivered to the stomach and perigastric nodes throughout 3-4 wk. To achieve optimal outcomes in gastric extranodal MZL[34,35]. Systemic treatment with ChT, immunotherapy, or a combination of both (chemoimmunotherapy) is recommended for patients with symptomatic systemic disease, contraindications to RT, treatment failure following antibiotic therapy or local treatments (such as RT or surgery), and those with histological transformation[36].

Despite this, surprisingly, increasing evidence supports that a considerable proportion of patients with *H. pylori*-negative GML show complete histopathological remission after bacterial eradication therapy[16,28,37]. Nonetheless, the precise mechanisms underlying this treatment responsiveness are not yet fully comprehended. Initially, it was attributed to false-negative tests for *H. pylori*[8,37]. However, more recently, the infection with other *Helicobacter* species (NHPHs) is acknowledged as a potential explanation for this phenomenon.

NHPHs

The *Helicobacter* genus includes gram-negative, microaerophilic, spiral, helical, curved, or fusiform rod-shaped bacteria that inhabit the gastrointestinal tract of several animals, such as humans, cats, dogs, pigs, and mice[38,39]. Currently, 53 species with validly published names comprise this genus[40], with *H. pylori* being the most prevalent in humans and well-known to be related to the development of chronic gastritis, peptic ulcer, and gastric cancer[41-43]. However, emerging evidence has highlighted the potential role of NHPHs in the progression of these diseases, including GML[24,44-46].

Among the NHPHs, *H. suis*, *H. heilmannii*, *H. felis*, *H. salomonis* and *H. bizzozeronii* are the most common species associated with human infection[47,48]. According to Yakoob *et al*[49], the prevalence of *H. heilmannii* and *H. felis* among patients with dyspepsia was 6% and 4%, respectively. On the other hand, Øverby *et al*[48] revealed a prevalence of gastric NHPH in Japanese patients of 6.1% and within this group, *H. suis* was the most prevalent, followed by *H. heilmannii*. This latter finding agrees with Nakamura *et al*[50], who found a prevalence of NHPHs of 20.8% in gastric mucosal samples of *H. pylori*-negative gastric disease patients, with *H. suis* and *H. heilmannii* also as the most prevalent species. However, it is important to note that the current diagnostic methods available, such as polymerase chain reaction (PCR) and immunohistochemistry, have limited accuracy in detecting NHPHs infections[26]. In a specific study, researchers faced difficulties in identifying the species associated with the infection in approximately 50% of the cases[50]. This challenge can be attributed to several factors, including the high genetic similarity between different NHPH species, significant genetic variation within a single species, limitations imposed by identification methods, and the concurrent presence of multiple NHPH species[51-53]. As a result, there is a concern that the actual prevalence of NHPHs infections among patients with dyspepsia may be underestimated.

Regarding the association of NHPHs with GML, some studies have evaluated the prevalence of infections by these species and its correlation with the complete remission of *H. pylori*-negative GML through eradication therapy. In this regard, Takigawa *et al*[54] report that the rate of complete remission in NHPH positive group of patients was significantly higher (75%) when compared to the negative cases (23%) of *H. pylori*-negative GML, which suggests a potential role for NHPHs in the pathogenesis of GML and the treatment effectiveness of *H. pylori*-negative GML. Such data are corroborated by Morgner *et al*[17], which advocate that *H. heilmannii* infection might be a causative factor in GML and that the current eradication therapy employed for *H. pylori* (standard antibiotics combined with proton pump inhibitors) is effective and results in complete remission of the lymphoma[17]. Nevertheless, upon confirming the presence of NHPH infection, it is strongly advised to implement a therapeutic approach that is tailored to the susceptibility profile of the individual bacterium.

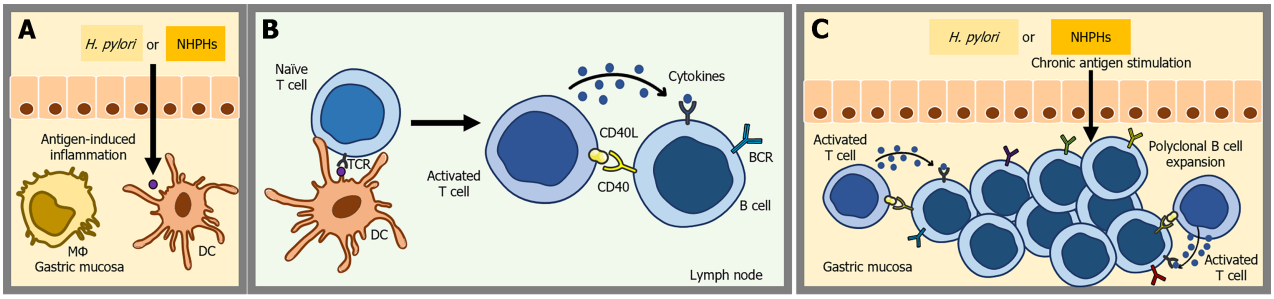
Pathogenesis of GML

The pathogenesis of GML is a complex event that involves antigen-induced transformation of normal marginal-zone B-cells into malignant cells[55]. In contrast to MALT lymphomas observed in various locations, GML is distinguished by its association with specific microbial species: Primarily, *H. pylori*, and to a lesser extent, *Helicobacter heilmannii*[17,54,56]. Under normal physiological conditions, the stomach does not possess MALT. However, in the presence of chronic antigenic stimulation, gastric mucosal cells produce proinflammatory cytokines (such as lymphotoxin beta) and B-cell homing factors (*e.g.*, bicinchoninic acid-1), leading to the infiltration of lymphoid cells into the gastric tissue. This cascade of events leads to the development of MALT[32,57,58] (Figure 1).

Regarding *H. pylori* infection, it is well-established that certain T helper cells target specific epitopes of the bacterium and support polyclonal B cells[59,60]. These B cells possess receptors that are able recognize autoantigens found in the gastric mucosa due to cross-reactivity. Consequently, the polyclonal B cell population undergoes expansion and a selection process, resulting in the emergence of an antigen-dependent MZL clone[61,62].

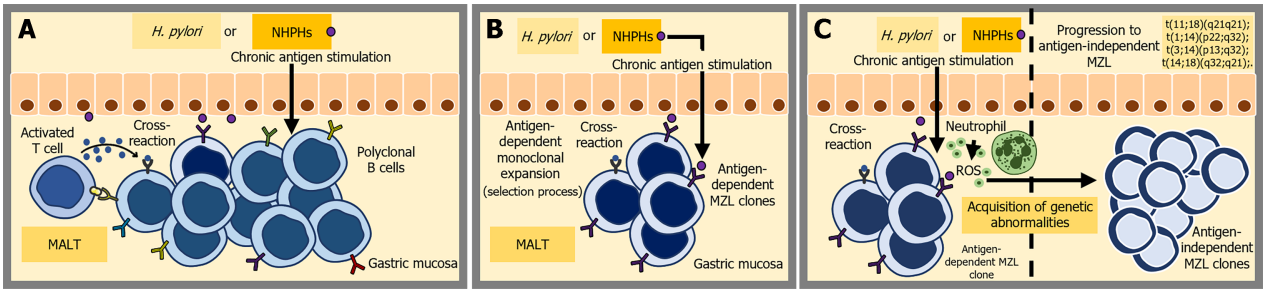
Sustained antigenic exposure not only stimulates the proliferation of a diverse array of B cells but also attracts neutrophils to the site of inflammation. The inflammatory process initiates the release of reactive oxygen species, leading to the occurrence of various genetic abnormalities[55,63,64]. Furthermore, the persistent proliferation of B cells during chronic inflammation increases the risk of double-stranded DNA breaks and translocations[5] (Figure 2).

Likewise, the involvement of NHPHs in *H. pylori*-negative GML could also be attributed to the induction of chronic inflammation, resulting in the local aggregation and proliferation of antigen-dependent B cells and T cells. Indeed, the infection of mice with NHPHs species, including *H. felis*, *H. suis* and *H. heilmannii*, also leads to a similar process of chronic gastritis and GML development with similarities to the human disease[65-69]. Possibly, the inflammatory microenvironment associated with NHPH-induced gastritis also facilitates the acquisition of genetic abnormalities by B cell clones. Nevertheless, further studies are required to construct a more comprehensive pathogenesis model.



DOI: 10.3748/wjg.v29.i32.4851 **Copyright** ©The Author(s) 2023.

Figure 1 Antigen-induced acquisition of gastric mucosa-associated lymphoid tissue. A: Antigen-induced inflammation; B: Clonal expansion of B cells supported by specific T helper cells; C: Acquisition of mucosa-associated lymphoid tissue (MALT). In the presence of chronic antigenic stimulation, gastric mucosal cells undergo activation and produce proinflammatory cytokines. These molecular mediators play a crucial role in initiating and perpetuating an immune response within the gastric tissue. As a consequence, lymphoid cells are recruited and infiltrate the gastric tissue. This cascade of events ultimately culminates in the development of MALT. *H. pylori: Helicobacter pylori*; NHPHs: Non-*Helicobacter pylori* gastric helicobacters; DC: Dendritic cell; MΦ: Macrophage; TCR: T cell receptor; CD40: Cluster of differentiation 40; CD40L: Cluster of differentiation 40 Ligand; BCR: B cell receptor.



DOI: 10.3748/wjg.v29.i32.4851 **Copyright** ©The Author(s) 2023.

Figure 2 Simplified scheme of antigen-induced transformation of normal marginal-zone B-cells into malignant cells. A: Polyclonal B cell expansion and a selection process; B: Antigen-dependent monoclonal expansion; C: Acquisition of genetic abnormalities and antigen-independent lymphomagenesis. The proliferation of B cells is primarily induced by the interaction between CD40 and CD40 Ligand, facilitated by antigen-activated reactive T cells. Additionally, cytokines play a role in driving this B-cell proliferation. The persistent proliferative state of these B cells, along with chronic inflammation, triggers additional oncogenic events. Ultimately, these events lead to the development of antigen-independent lymphoproliferation. NHPHs: Non-*Helicobacter pylori* gastric helicobacters; ROS: Reactive oxygen species; MZL: Marginal zone lymphoma; MALT: Mucosa-associated lymphoid tissue; *H. pylori: Helicobacter pylori*.

Irrespective of etiology, progression towards antigen-independent MZL is associated with genetic events, while the role of direct antigenic stimulation gradually decreases in the development of GML[5,70] (Figure 2). Four recurrent chromosomal translocations have been found in MZL: *t* (1; 14) (p22; q32), *t* (11; 18) (q21; q21), *t* (14; 18) (q32; q21), and *t* (3; 14) (p14.1; q32)[71-73]. In GML, the translocation *t* (11; 18) (q21; q21) is the prominent structural chromosomal abnormality, occurring in approximately 10%-50% of cases[74-76]. This translocation results in the activation of NF-kappaB, which is a downstream target of B-cell receptor (BCR) signaling, independent of BCR signaling itself. The activation is mediated by the disruption of a signalosome complex involving CARD11, BCL10, and MALT1. Within this context, the presence of the MALT1 fusion protein is notably linked to more advanced stages of MALT lymphoma[77-80].

Indeed, numerous studies have demonstrated that GMLs harboring the *t* (11; 18) (q21; q21) translocation are frequently resistant to *H. pylori* eradication treatment compared to tumors that do not possess this specific translocation[11,81,82]. The decrease in the rate of complete histopathological remission following eradication therapy was also observed in *H. pylori*-negative GML cases; however, its influence on the treatment of NHPH-positive GML is still unclear[16].

Clinical implications and research prospects

Given the limited regression observed in *H. pylori*-negative GML after antibiotic treatment, clinical guidelines previously advised prompt initiation of targeted anti-lymphoma treatments[8,83]. Currently, the European Society for Medical Oncology Guidelines Committee suggests that a trial of anti-*Helicobacter* therapy may be worthwhile in *H. pylori*-negative early-stage GML (stages I and II_1)[9]. This recommendation presents new opportunities for research in this field. Specifically, future studies could focus on investigating the mechanisms underlying the response to this therapy and further exploring the involvement of other *Helicobacter* species (NHPHs) in the development of *H. pylori*-negative GML. Additionally, it is crucial to investigate the long-term outcomes and assess the effects of early intervention with targeted anti-lymphoma treatments on patient prognosis.

In this context, accurate detection of NHPHs is vital for precise clinical diagnosis and targeted treatment strategies. However, current diagnostic methods primarily focus on *H. pylori*, leaving a gap in the detection of NHPHs infections. Goji *et al*[26] conducted a review of 26 articles and determined that the sensitivities of diagnostic methods for *H. pylori* infection, such as the rapid urease test, urea breath test, blood antibody analysis, immunohistochemical analysis, and

stool antigen analysis, were low for NHPHs. The calculated sensitivities were only 40.0%, 14.8%, 23.1%, 40.0%, and 0%, respectively[26]. Therefore, at present, the most effective diagnostic tools for identifying NHPH infections are histological techniques and genetic diagnosis based on PCR, which hinders the clinical diagnosis of NHPHs infection, both due to the inflated cost and the dependence on laboratory apparatus. To address this, the development of tests that possess sensitivity, specificity, and the ability to detect different strains of NHPHs is crucial. The availability of reliable diagnostic methods for NHPHs will not only enable timely diagnosis and treatment for *H. pylori*-negative GML, but also contribute to a better understanding of their epidemiology and impact on human health.

When it comes to comprehending the pathogenesis of NHPH-positive GML, the significance of molecular and immunological studies cannot be overstated. These investigations should encompass the analysis of gene expression profiles in affected tissues, identification of pertinent genetic mutations, and study of cellular signaling pathways involved in the development and progression of the lymphoma. Additionally, it would also be interesting to analyze cytokine profiles, characterize immune cells infiltrating the affected gastric tissue, and conduct studies on the interaction between NHPHs and the host immune system. This deeper understanding might open doors to the development of targeted therapeutic strategies and hold promise for improved clinical outcomes in patients with NHPH-positive GML.

CONCLUSION

While *H. pylori* remains the primary pathogenic factor in the development of GML, the role of NHPHs in *H. pylori*-negative cases is an emerging area of research. It is crucial to identify these alternative pathogens and understand their mechanisms of pathogenesis to improve diagnostic accuracy and guide appropriate treatment strategies for patients with *H. pylori*-negative GML. Further research is warranted to elucidate the complex interplay between these bacteria, the host immune system, and the gastric microenvironment, which may lead to the development of novel therapeutic interventions and personalized approaches for this subset of patients.

FOOTNOTES

Author contributions: Lemos FFB, and de Melo FF designed the manuscript; Lemos FFB, Luz MS, Pinheiro SLR, Teixeira KN, and de Melo FF contributed to the investigation; Lemos FFB, Silva Luz M, Pinheiro SLR, Teixeira KN, and de Melo FF contributed to the formal analysis; Lemos FFB, Luz MS, and Pinheiro SLR wrote the original draft; Lemos, FFB, and Luz MS were responsible for manuscript editing; Teixeira KN, and de Melo FF were responsible for manuscript review; and de Melo FF supervised the writing of the original draft.

Supported by Scientific Initiation Scholarship Programme of the Bahia State Research Support Foundation (FAPESB), No. N°BOL1825/2022; Scientific Initiation Scholarship Programme of the National Council for Scientific and Technological Development (CNPq), No. 129894/2022-2; CNPq Research Productivity Fellowship, No. 317005/2021-9.

Conflict-of-interest statement: There is no conflict of interest associated with any of the senior author or other coauthors contributed their efforts in this manuscript.

Open-Access: This article is an open-access article that was selected by an in-house editor and fully peer-reviewed by external reviewers. It is distributed in accordance with the Creative Commons Attribution NonCommercial (CC BY-NC 4.0) license, which permits others to distribute, remix, adapt, build upon this work non-commercially, and license their derivative works on different terms, provided the original work is properly cited and the use is non-commercial. See: https://creativecommons.org/Licenses/by-nc/4.0/

Country/Territory of origin: Brazil

ORCID number: Fabian Fellipe Bueno Lemos 0000-0002-4686-7086; Marcel Silva Luz 0000-0003-1650-5807; Samuel Luca Rocha Pinheiro 0000-0002-8877-892X; Kádima Nayara Teixeira 0000-0002-2928-9181; Fabrício Freire de Melo 0000-0002-5680-2753.

S-Editor: Qu XL
L-Editor: A
P-Editor: Chen YX

REFERENCES

1 **Smith A**, Crouch S, Lax S, Li J, Painter D, Howell D, Patmore R, Jack A, Roman E. Lymphoma incidence, survival and prevalence 2004-2014: sub-type analyses from the UK's Haematological Malignancy Research Network. *Br J Cancer* 2015; **112**: 1575-1584 [PMID: 25867256 DOI: 10.1038/bjc.2015.94]

2 **Alaggio R**, Amador C, Anagnostopoulos I, Attygalle AD, Araujo IBO, Berti E, Bhagat G, Borges AM, Boyer D, Calaminici M, Chadburn A, Chan JKC, Cheuk W, Chng WJ, Choi JK, Chuang SS, Coupland SE, Czader M, Dave SS, de Jong D, Du MQ, Elenitoba-Johnson KS, Ferry J, Geyer J, Gratzinger D, Guitart J, Gujral S, Harris M, Harrison CJ, Hartmann S, Hochhaus A, Jansen PM, Karube K, Kempf W, Khoury J, Kimura H, Klapper W, Kovach AE, Kumar S, Lazar AJ, Lazzi S, Leoncini L, Leung N, Leventaki V, Li XQ, Lim MS, Liu WP, Louissaint A

Jr, Marcogliese A, Medeiros LJ, Michal M, Miranda RN, Mitteldorf C, Montes-Moreno S, Morice W, Nardi V, Naresh KN, Natkunam Y, Ng SB, Oschlies I, Ott G, Parrens M, Pulitzer M, Rajkumar SV, Rawstron AC, Rech K, Rosenwald A, Said J, Sarkozy C, Sayed S, Saygin C, Schuh A, Sewell W, Siebert R, Sohani AR, Tooze R, Traverse-Glehen A, Vega F, Vergier B, Wechalekar AD, Wood B, Xerri L, Xiao W. The 5th edition of the World Health Organization Classification of Haematolymphoid Tumours: Lymphoid Neoplasms. *Leukemia* 2022; **36**: 1720-1748 [PMID: 35732829 DOI: 10.1038/s41375-022-01620-2]

3 **Diaconu S**, Predescu A, Moldoveanu A, Pop CS, Fierbințeanu-Braticevici C. Helicobacter pylori infection: old and new. *J Med Life* 2017; **10**: 112-117 [PMID: 28616085]

4 **Rossi D**, Bertoni F, Zucca E. Marginal-Zone Lymphomas. *N Engl J Med* 2022; **386**: 568-581 [PMID: 35139275 DOI: 10.1056/NEJMra2102568]

5 **Troppan K**, Wenzl K, Neumeister P, Deutsch A. Molecular Pathogenesis of MALT Lymphoma. *Gastroenterol Res Pract* 2015; **2015**: 102656 [PMID: 25922601 DOI: 10.1155/2015/102656]

6 **Liu H**, Ye H, Dogan A, Ranaldi R, Hamoudi RA, Bearzi I, Isaacson PG, Du MQ. T(11;18)(q21;q21) is associated with advanced mucosa-associated lymphoid tissue lymphoma that expresses nuclear BCL10. *Blood* 2001; **98**: 1182-1187 [PMID: 11493468 DOI: 10.1182/blood.v98.4.1182]

7 **Suzuki H**, Saito Y, Hibi T. Helicobacter pylori and Gastric Mucosa-associated Lymphoid Tissue (MALT) Lymphoma: Updated Review of Clinical Outcomes and the Molecular Pathogenesis. *Gut Liver* 2009; **3**: 81-87 [PMID: 20431728 DOI: 10.5009/gnl.2009.3.2.81]

8 **Ruskoné-Fourmestraux A**, Fischbach W, Aleman BM, Boot H, Du MQ, Megraud F, Montalban C, Raderer M, Savio A, Wotherspoon A; EGILS group. EGILS consensus report. Gastric extranodal marginal zone B-cell lymphoma of MALT. *Gut* 2011; **60**: 747-758 [PMID: 21317175 DOI: 10.1136/gut.2010.224949]

9 **Zucca E**, Arcaini L, Buske C, Johnson PW, Ponzoni M, Raderer M, Ricardi U, Salar A, Stamatopoulos K, Thieblemont C, Wotherspoon A, Ladetto M; ESMO Guidelines Committee. Electronic address: clinicalguidelines@esmo.org. Marginal zone lymphomas: ESMO Clinical Practice Guidelines for diagnosis, treatment and follow-up. *Ann Oncol* 2020; **31**: 17-29 [PMID: 31912792 DOI: 10.1016/j.annonc.2019.10.010]

10 **Malfertheiner P**, Megraud F, Rokkas T, Gisbert JP, Liou JM, Schulz C, Gasbarrini A, Hunt RH, Leja M, O'Morain C, Rugge M, Suerbaum S, Tilg H, Sugano K, El-Omar EM; European Helicobacter and Microbiota Study group. Management of Helicobacter pylori infection: the Maastricht VI/Florence consensus report. *Gut* 2022 [PMID: 35944925 DOI: 10.1136/gutjnl-2022-327745]

11 **Lemos FFB**, de Castro CT, Calmon MS, Silva Luz M, Pinheiro SLR, Faria Souza Mendes Dos Santos C, Correa Santos GL, Marques HS, Delgado HA, Teixeira KN, Souza CL, Oliveira MV, Freire de Melo F. Effectiveness of Helicobacter pylori eradication in the treatment of early-stage gastric mucosa-associated lymphoid tissue lymphoma: An up-to-date meta-analysis. *World J Gastroenterol* 2023; **29**: 2202-2221 [PMID: 37122607 DOI: 10.3748/wjg.v29.i14.2202]

12 **Asano N**, Iijima K, Koike T, Imatani A, Shimosegawa T. Helicobacter pylori-negative gastric mucosa-associated lymphoid tissue lymphomas: A review. *World J Gastroenterol* 2015; **21**: 8014-8020 [PMID: 26185372 DOI: 10.3748/wjg.v21.i26.8014]

13 **Matysiak-Budnik T**, Jamet P, Ruskoné-Fourmestraux A, de Mascarel A, Velten M, Maynadié M, Woronoff AS, Trétarre B, Marrer E, Delafosse P, Ligier K, Lapôtre Ledoux B, Daubisse L, Bouzid L, Orazio S, Cowppli-Bony A, Monnereau A. Gastric MALT lymphoma in a population-based study in France: clinical features, treatments and survival. *Aliment Pharmacol Ther* 2019; **50**: 654-663 [PMID: 31347731 DOI: 10.1111/apt.15409]

14 **Strati P**, Lee ST, Teegavarupu P, Karri A, Anireddy S, Hagemeister FB, Romaguera J, Fayad LE, Rodriguez MA, Samaniego F, Fowler N, Westin J, Wang M, Lee HJ, Pinnix C, Gunther JR, Dabaja B, Feng L, Davis RE, Neelapu SS. Frontline antibiotic therapy for early-stage Helicobacter pylori-negative gastric MALT lymphoma. *Am J Hematol* 2019; **94**: E150-E153 [PMID: 30785215 DOI: 10.1002/ajh.25447]

15 **Kuo SH**, Yeh KH, Wu MS, Lin CW, Wei MF, Liou JM, Wang HP, Chen LT, Cheng AL. First-line antibiotic therapy in Helicobacter pylori-negative low-grade gastric mucosa-associated lymphoid tissue lymphoma. *Sci Rep* 2017; **7**: 14333 [PMID: 29084984 DOI: 10.1038/s41598-017-14102-8]

16 **Jung K**, Kim DH, Seo HI, Gong EJ, Bang CS. Efficacy of eradication therapy in Helicobacter pylori-negative gastric mucosa-associated lymphoid tissue lymphoma: A meta-analysis. *Helicobacter* 2021; **26**: e12774 [PMID: 33400830 DOI: 10.1111/hel.12774]

17 **Morgner A**, Lehn N, Andersen LP, Thiede C, Bennedsen M, Trebesius K, Neubauer B, Neubauer A, Stolte M, Bayerdörffer E. Helicobacter heilmannii-associated primary gastric low-grade MALT lymphoma: complete remission after curing the infection. *Gastroenterology* 2000; **118**: 821-828 [PMID: 10784580 DOI: 10.1016/s0016-5085(00)70167-3]

18 **Okamura T**, Iwaya Y, Yokosawa S, Suga T, Arakura N, Matsumoto T, Ogiwara N, Higuchi K, Ota H, Tanaka E. A case of Helicobacter heilmannii-associated primary gastric mucosa-associated lymphoid tissue lymphoma achieving complete remission after eradication. *Clin J Gastroenterol* 2013; **6**: 38-45 [PMID: 26181403 DOI: 10.1007/s12328-012-0355-9]

19 **O'Rourke JL**, Dixon MF, Jack A, Enno A, Lee A. Gastric B-cell mucosa-associated lymphoid tissue (MALT) lymphoma in an animal model of 'Helicobacter heilmannii' infection. *J Pathol* 2004; **203**: 896-903 [PMID: 15258991 DOI: 10.1002/path.1593]

20 **Nakagawa S**, Shimoyama T, Nakamura M, Chiba D, Kikuchi H, Sawaya M, Chinda D, Mikami T, Fukuda S. The Resolution of Helicobacter suis-associated Gastric Lesions after Eradication Therapy. *Intern Med* 2018; **57**: 203-207 [PMID: 29033421 DOI: 10.2169/internalmedicine.8971-17]

21 **Yasuda T**, Lee HS, Nam SY, Katoh H, Ishibashi Y, Yamagata Murayama S, Matsui H, Masuda H, Rimbara E, Sakurazawa N, Suzuki H, Yoshida H, Seto Y, Ishikawa S, Jeon SW, Nakamura M, Nomura S. Non-Helicobacter pylori Helicobacter (NHPH) positive gastric cancer. *Sci Rep* 2022; **12**: 4811 [PMID: 35314746 DOI: 10.1038/s41598-022-08962-y]

22 **Shafaie S**, Kaboosi H, Peyravii Ghadikolaii F. Prevalence of non Helicobacter pylori gastric Helicobacters in Iranian dyspeptic patients. *BMC Gastroenterol* 2020; **20**: 190 [PMID: 32546214 DOI: 10.1186/s12876-020-01331-x]

23 **Bento-Miranda M**, Figueiredo C. Helicobacter heilmannii sensu lato: an overview of the infection in humans. *World J Gastroenterol* 2014; **20**: 17779-17787 [PMID: 25548476 DOI: 10.3748/wjg.v20.i47.17779]

24 **Rimbara E**, Suzuki M, Matsui H, Nakamura M, Morimoto M, Sasakawa C, Masuda H, Nomura S, Osaki T, Nagata N, Shibayama K, Tokunaga K. Isolation and characterization of Helicobacter suis from human stomach. *Proc Natl Acad Sci U S A* 2021; **118** [PMID: 33753513 DOI: 10.1073/pnas.2026337118]

25 **Joosten M**, Lindén S, Rossi M, Tay AC, Skoog E, Padra M, Peters F, Perkins T, Vandamme P, Van Nieuwerburgh F, D'Herde K, Van den Broeck W, Flahou B, Deforce D, Ducatelle R, Marshall B, Haesebrouck F, Smet A. Divergence between the Highly Virulent Zoonotic Pathogen Helicobacter heilmannii and Its Closest Relative, the Low-Virulence "Helicobacter ailurogastricus" sp. nov. *Infect Immun* 2016; **84**: 293-306 [PMID: 26527212 DOI: 10.1128/IAI.01300-15]

26 **Goji S**, Tamura Y, Sasaki M, Nakamura M, Matsui H, Murayama SY, Ebi M, Ogasawara N, Funaki Y, Kasugai K. Helicobacter suis-Infected

Nodular Gastritis and a Review of Diagnostic Sensitivity for Helicobacter heilmannii-Like Organisms. *Case Rep Gastroenterol* 2015; **9**: 179-187 [PMID: 26120299 DOI: 10.1159/000431169]

27 **Keikha M**, Karbalaei M. Clinical aspects of Helicobacter heilmannii-associated gastritis in patients with dyspepsia: A systematic review and meta-analysis. *Microb Pathog* 2022; **166**: 105518 [PMID: 35405277 DOI: 10.1016/j.micpath.2022.105518]

28 **Xie YL**, He CY, Wei SQ, Guan WJ, Jiang Z. Clinical efficacy of the modified Helicobacter pylori eradication therapy for Helicobacter pylori-negative gastric mucosa-associated lymphoid tissue lymphoma: a meta analysis. *Chin Med J (Engl)* 2020; **133**: 1337-1346 [PMID: 32452892 DOI: 10.1097/CM9.0000000000000813]

29 **Nakamura S**, Matsumoto T. Helicobacter pylori and gastric mucosa-associated lymphoid tissue lymphoma: recent progress in pathogenesis and management. *World J Gastroenterol* 2013; **19**: 8181-8187 [PMID: 24363507 DOI: 10.3748/wjg.v19.i45.8181]

30 **Zullo A**, Hassan C, Andriani A, Cristofari F, De Francesco V, Ierardi E, Tomao S, Morini S, Vaira D. Eradication therapy for Helicobacter pylori in patients with gastric MALT lymphoma: a pooled data analysis. *Am J Gastroenterol* 2009; **104**: 1932-7; quiz 1938 [PMID: 19532131 DOI: 10.1038/ajg.2009.314]

31 **Nakamura S**, Sugiyama T, Matsumoto T, Iijima K, Ono S, Tajika M, Tari A, Kitadai Y, Matsumoto H, Nagaya T, Kamoshida T, Watanabe N, Chiba T, Origasa H, Asaka M; JAPAN GAST Study Group. Long-term clinical outcome of gastric MALT lymphoma after eradication of Helicobacter pylori: a multicentre cohort follow-up study of 420 patients in Japan. *Gut* 2012; **61**: 507-513 [PMID: 21890816 DOI: 10.1136/gutjnl-2011-300495]

32 **Violeta Filip P**, Cuciureanu D, Sorina Diaconu L, Maria Vladareanu A, Silvia Pop C. MALT lymphoma: epidemiology, clinical diagnosis and treatment. *J Med Life* 2018; **11**: 187-193 [PMID: 30364585 DOI: 10.25122/jml-2018-0035]

33 **Nakamura S**, Hojo M. Diagnosis and Treatment for Gastric Mucosa-Associated Lymphoid Tissue (MALT) Lymphoma. *J Clin Med* 2022; **12** [PMID: 36614921 DOI: 10.3390/jcm12010120]

34 **Wirth A**, Gospodarowicz M, Aleman BM, Bressel M, Ng A, Chao M, Hoppe RT, Thieblemont C, Tsang R, Moser L, Specht L, Szpytma T, Lennard A, Seymour JF, Zucca E. Long-term outcome for gastric marginal zone lymphoma treated with radiotherapy: a retrospective, multicentre, International Extranodal Lymphoma Study Group study. *Ann Oncol* 2013; **24**: 1344-1351 [PMID: 23293112 DOI: 10.1093/annonc/mds623]

35 **Goda JS**, Gospodarowicz M, Pintilie M, Wells W, Hodgson DC, Sun A, Crump M, Tsang RW. Long-term outcome in localized extranodal mucosa-associated lymphoid tissue lymphomas treated with radiotherapy. *Cancer* 2010; **116**: 3815-3824 [PMID: 20564130 DOI: 10.1002/cncr.25226]

36 **Kuo SH**, Yeh KH, Lin CW, Liou JM, Wu MS, Chen LT, Cheng AL. Current Status of the Spectrum and Therapeutics of Helicobacter pylori-Negative Mucosa-Associated Lymphoid Tissue Lymphoma. *Cancers (Basel)* 2022; **14** [PMID: 35205754 DOI: 10.3390/cancers14041005]

37 **Zullo A**, Hassan C, Ridola L, De Francesco V, Rossi L, Tomao S, Vaira D, Genta RM. Eradication therapy in Helicobacter pylori-negative, gastric low-grade mucosa-associated lymphoid tissue lymphoma patients: a systematic review. *J Clin Gastroenterol* 2013; **47**: 824-827 [PMID: 23442842 DOI: 10.1097/MCG.0b013e318286ff72]

38 **On SLW**, Miller WG, Houf K, Fox JG, Vandamme P. Minimal standards for describing new species belonging to the families Campylobacteraceae and Helicobacteraceae: Campylobacter, Arcobacter, Helicobacter and Wolinella spp. *Int J Syst Evol Microbiol* 2017; **67**: 5296-5311 [PMID: 29034857 DOI: 10.1099/ijsem.0.002255]

39 **Ochoa S**, Collado L. Enterohepatic Helicobacter species - clinical importance, host range, and zoonotic potential. *Crit Rev Microbiol* 2021; **47**: 728-761 [PMID: 34153195 DOI: 10.1080/1040841X.2021.1924117]

40 **Parte AC**, Sardà Carbasse J, Meier-Kolthoff JP, Reimer LC, Göker M. List of Prokaryotic names with Standing in Nomenclature (LPSN) moves to the DSMZ. *Int J Syst Evol Microbiol* 2020; **70**: 5607-5612 [PMID: 32701423 DOI: 10.1099/ijsem.0.004332]

41 **Warren JR**, Marshall B. Unidentified curved bacilli on gastric epithelium in active chronic gastritis. *Lancet* 1983; **1**: 1273-1275 [PMID: 6134060]

42 **Liu J**, He C, Chen M, Wang Z, Xing C, Yuan Y. Association of presence/absence and on/off patterns of Helicobacter pylori oipA gene with peptic ulcer disease and gastric cancer risks: a meta-analysis. *BMC Infect Dis* 2013; **13**: 555 [PMID: 24256489 DOI: 10.1186/1471-2334-13-555]

43 **Alipour M**. Molecular Mechanism of Helicobacter pylori-Induced Gastric Cancer. *J Gastrointest Cancer* 2021; **52**: 23-30 [PMID: 32926335 DOI: 10.1007/s12029-020-00518-5]

44 **Joo M**, Kwak JE, Chang SH, Kim H, Chi JG, Kim KA, Yang JH, Lee JS, Moon YS, Kim KM. Helicobacter heilmannii-associated gastritis: clinicopathologic findings and comparison with Helicobacter pylori-associated gastritis. *J Korean Med Sci* 2007; **22**: 63-69 [PMID: 17297253 DOI: 10.3346/jkms.2007.22.1.63]

45 **Stolte M**, Kroher G, Meining A, Morgner A, Bayerdörffer E, Bethke B. A comparison of Helicobacter pylori and H. heilmannii gastritis. A matched control study involving 404 patients. *Scand J Gastroenterol* 1997; **32**: 28-33 [PMID: 9018763 DOI: 10.3109/00365529709025059]

46 **Takigawa H**, Masaki S, Naito T, Yuge R, Urabe Y, Tanaka S, Sentani K, Matsuo T, Matsuo K, Chayama K, Kitadai Y. Helicobacter suis infection is associated with nodular gastritis-like appearance of gastric mucosa-associated lymphoid tissue lymphoma. *Cancer Med* 2019; **8**: 4370-4379 [PMID: 31210418 DOI: 10.1002/cam4.2314]

47 **Matos R**, Sousa HS, Nogueiro J, Magalhães A, Reis CA, Carneiro F, Amorim I, Haesebrouck F, Gärtner F. Helicobacter species binding to the human gastric mucosa. *Helicobacter* 2022; **27**: e12867 [PMID: 34967491 DOI: 10.1111/hel.12867]

48 **Øverby A**, Murayama SY, Michimae H, Suzuki H, Suzuki M, Serizawa H, Tamura R, Nakamura S, Takahashi S, Nakamura M. Prevalence of Gastric Non-Helicobacter pylori-Helicobacters in Japanese Patients with Gastric Disease. *Digestion* 2017; **95**: 61-66 [PMID: 28052279 DOI: 10.1159/000452400]

49 **Yakoob J**, Abbas Z, Khan R, Naz S, Ahmad Z, Islam M, Awan S, Jafri F, Jafri W. Prevalence of non Helicobacter pylori species in patients presenting with dyspepsia. *BMC Gastroenterol* 2012; **12**: 3 [PMID: 22226326 DOI: 10.1186/1471-230X-12-3]

50 **Nakamura M**, Øverby A, Michimae H, Matsui H, Takahashi S, Mabe K, Shimoyama T, Sasaki M, Terao S, Kamada T, Yanaka A, Iwamoto J, Tanabe S, Tari A, Nasu S, Suzuki H, Yamagata Murayama S. PCR analysis and specific immunohistochemistry revealing a high prevalence of non-Helicobacter pylori Helicobacters in Helicobacter pylori-negative gastric disease patients in Japan: High susceptibility to an Hp eradication regimen. *Helicobacter* 2020; **25**: e12700 [PMID: 32790220 DOI: 10.1111/hel.12700]

51 **Smet A**, Yahara K, Rossi M, Tay A, Backert S, Armin E, Fox JG, Flahou B, Ducatelle R, Haesebrouck F, Corander J. Macroevolution of gastric Helicobacter species unveils interspecies admixture and time of divergence. *ISME J* 2018; **12**: 2518-2531 [PMID: 29942073 DOI: 10.1038/s41396-018-0199-5]

52 **Mannion A**, Shen Z, Fox JG. Comparative genomics analysis to differentiate metabolic and virulence gene potential in gastric versus

enterohepatic Helicobacter species. *BMC Genomics* 2018; **19**: 830 [PMID: 30458713 DOI: 10.1186/s12864-018-5171-2]

53 **Liu J**, He L, Haesebrouck F, Gong Y, Flahou B, Cao Q, Zhang J. Prevalence of Coinfection with Gastric Non-Helicobacter pylori Helicobacter (NHPH) Species in Helicobacter pylori-infected Patients Suffering from Gastric Disease in Beijing, China. *Helicobacter* 2015; **20**: 284-290 [PMID: 25510739 DOI: 10.1111/hel.12201]

54 **Takigawa H**, Yuge R, Masaki S, Otani R, Kadota H, Naito T, Hayashi R, Urabe Y, Oka S, Tanaka S, Chayama K, Kitadai Y. Involvement of non-Helicobacter pylori helicobacter infections in Helicobacter pylori-negative gastric MALT lymphoma pathogenesis and efficacy of eradication therapy. *Gastric Cancer* 2021; **24**: 937-945 [PMID: 33638751 DOI: 10.1007/s10120-021-01172-x]

55 **Sagaert X**, Van Cutsem E, De Hertogh G, Geboes K, Tousseyn T. Gastric MALT lymphoma: a model of chronic inflammation-induced tumor development. *Nat Rev Gastroenterol Hepatol* 2010; **7**: 336-346 [PMID: 20440281 DOI: 10.1038/nrgastro.2010.58]

56 **Di Rocco A**, Petrucci L, Assanto GM, Martelli M, Pulsoni A. Extranodal Marginal Zone Lymphoma: Pathogenesis, Diagnosis and Treatment. *Cancers (Basel)* 2022; **14** [PMID: 35406516 DOI: 10.3390/cancers14071742]

57 **Lenze D**, Berg E, Volkmer-Engert R, Weiser AA, Greiner A, Knörr-Wittmann C, Anagnostopoulos I, Stein H, Hummel M. Influence of antigen on the development of MALT lymphoma. *Blood* 2006; **107**: 1141-1148 [PMID: 16204314 DOI: 10.1182/blood-2005-04-1722]

58 **Mazzucchelli L**, Blaser A, Kappeler A, Schärli P, Laissue JA, Baggiolini M, Uguccioni M. BCA-1 is highly expressed in Helicobacter pylori-induced mucosa-associated lymphoid tissue and gastric lymphoma. *J Clin Invest* 1999; **104**: R49-R54 [PMID: 10562310 DOI: 10.1172/JCI7830]

59 **Guindi M**. Role of activated host T cells in the promotion of MALT lymphoma growth. *Semin Cancer Biol* 2000; **10**: 341-344 [PMID: 11100881 DOI: 10.1006/scbi.2000.0351]

60 **Suarez F**, Lortholary O, Hermine O, Lecuit M. Infection-associated lymphomas derived from marginal zone B cells: a model of antigen-driven lymphoproliferation. *Blood* 2006; **107**: 3034-3044 [PMID: 16397126 DOI: 10.1182/blood-2005-09-3679]

61 **Nakamura S**, Aoyagi K, Furuse M, Suekane H, Matsumoto T, Yao T, Sakai Y, Fuchigami T, Yamamoto I, Tsuneyoshi M, Fujishima M. B-cell monoclonality precedes the development of gastric MALT lymphoma in Helicobacter pylori-associated chronic gastritis. *Am J Pathol* 1998; **152**: 1271-1279 [PMID: 9588895]

62 **Du MQ**, Isaccson PG. Gastric MALT lymphoma: from aetiology to treatment. *Lancet Oncol* 2002; **3**: 97-104 [PMID: 11902529 DOI: 10.1016/s1470-2045(02)00651-4]

63 **Ziech D**, Franco R, Pappa A, Panayiotidis MI. Reactive oxygen species (ROS)--induced genetic and epigenetic alterations in human carcinogenesis. *Mutat Res* 2011; **711**: 167-173 [PMID: 21419141 DOI: 10.1016/j.mrfmmm.2011.02.015]

64 **Rodríguez-Sevilla JJ**, Salar A. Recent Advances in the Genetic of MALT Lymphomas. *Cancers (Basel)* 2021; **14** [PMID: 35008340 DOI: 10.3390/cancers14010176]

65 **Lee A**, O'Rourke J, Enno A. Gastric mucosa-associated lymphoid tissue lymphoma: implications of animal models on pathogenic and therapeutic considerations--mouse models of gastric lymphoma. *Recent Results Cancer Res* 2000; **156**: 42-51 [PMID: 10802862 DOI: 10.1007/978-3-642-57054-4_6]

66 **Zhao Y**, Lu F, Ye J, Ji M, Pang Y, Wang Y, Wang L, Li G, Sun T, Li J, Ma D, Ji C. Myeloid-Derived Suppressor Cells and γδT17 Cells Contribute to the Development of Gastric MALT Lymphoma in H. felis-Infected Mice. *Front Immunol* 2019; **10**: 3104 [PMID: 32063899 DOI: 10.3389/fimmu.2019.03104]

67 **Yamamoto K**, Tanaka H, Nishitani Y, Nishiumi S, Miki I, Takenaka M, Nobutani K, Mimura T, Ben Suleiman Y, Mizuno S, Kawai M, Uchiyama I, Yoshida M, Azuma T. Helicobacter suis KB1 derived from pig gastric lymphoid follicles induces the formation of gastric lymphoid follicles in mice through the activation of B cells and CD4 positive cells. *Microbes Infect* 2011; **13**: 697-708 [PMID: 21397035 DOI: 10.1016/j.micinf.2011.02.007]

68 **Mimura T**, Yoshida M, Nishiumi S, Tanaka H, Nobutani K, Takenaka M, Suleiman YB, Yamamoto K, Ota H, Takahashi S, Matsui H, Nakamura M, Miki I, Azuma T. IFN-γ plays an essential role in the pathogenesis of gastric lymphoid follicles formation caused by Helicobacter suis infection. *FEMS Immunol Med Microbiol* 2011; **63**: 25-34 [PMID: 21631601 DOI: 10.1111/j.1574-695X.2011.00823.x]

69 **Nobutani K**, Yoshida M, Nishiumi S, Nishitani Y, Takagawa T, Tanaka H, Yamamoto K, Mimura T, Bensuleiman Y, Ota H, Takahashi S, Matsui H, Nakamura M, Azuma T. Helicobacter heilmannii can induce gastric lymphoid follicles in mice *via* a Peyer's patch-independent pathway. *FEMS Immunol Med Microbiol* 2010; **60**: 156-164 [PMID: 20846360 DOI: 10.1111/j.1574-695X.2010.00731.x]

70 **Zucca E**, Bertoni F, Vannata B, Cavalli F. Emerging role of infectious etiologies in the pathogenesis of marginal zone B-cell lymphomas. *Clin Cancer Res* 2014; **20**: 5207-5216 [PMID: 25320370 DOI: 10.1158/1078-0432.CCR-14-0496]

71 **Willis TG**, Jadayel DM, Du MQ, Peng H, Perry AR, Abdul-Rauf M, Price H, Karran L, Majekodunmi O, Wlodarska I, Pan L, Crook T, Hamoudi R, Isaacson PG, Dyer MJ. Bcl10 is involved in t(1;14)(p22;q32) of MALT B cell lymphoma and mutated in multiple tumor types. *Cell* 1999; **96**: 35-45 [PMID: 9989495 DOI: 10.1016/s0092-8674(00)80957-5]

72 **Streubel B**, Lamprecht A, Dierlamm J, Cerroni L, Stolte M, Ott G, Raderer M, Chott A. T(14;18)(q32;q21) involving IGH and MALT1 is a frequent chromosomal aberration in MALT lymphoma. *Blood* 2003; **101**: 2335-2339 [PMID: 12406890 DOI: 10.1182/blood-2002-09-2963]

73 **Streubel B**, Vinatzer U, Lamprecht A, Raderer M, Chott A. T(3;14)(p14.1;q32) involving IGH and FOXP1 is a novel recurrent chromosomal aberration in MALT lymphoma. *Leukemia* 2005; **19**: 652-658 [PMID: 15703784 DOI: 10.1038/sj.leu.2403644]

74 **Lima KS**, Albuquerque W, Arantes VN, Drummond-Lage AP, Coelho LG. Helicobacter pylori and t(11;18)(q21;q21) translocation in gastric malt lymphoma. *Arq Gastroenterol* 2014; **51**: 84-89 [PMID: 25003257 DOI: 10.1590/s0004-28032014000200003]

75 **Ye H**, Liu H, Attygalle A, Wotherspoon AC, Nicholson AG, Charlotte F, Leblond V, Speight P, Goodlad J, Lavergne-Slove A, Martin-Subero JI, Siebert R, Dogan A, Isaacson PG, Du MQ. Variable frequencies of t(11;18)(q21;q21) in MALT lymphomas of different sites: significant association with CagA strains of H pylori in gastric MALT lymphoma. *Blood* 2003; **102**: 1012-1018 [PMID: 12676782 DOI: 10.1182/blood-2002-11-3502]

76 **Streubel B**, Simonitsch-Klupp I, Müllauer L, Lamprecht A, Huber D, Siebert R, Stolte M, Trautinger F, Lukas J, Püspök A, Formanek M, Assanasen T, Müller-Hermelink HK, Cerroni L, Raderer M, Chott A. Variable frequencies of MALT lymphoma-associated genetic aberrations in MALT lymphomas of different sites. *Leukemia* 2004; **18**: 1722-1726 [PMID: 15356642 DOI: 10.1038/sj.leu.2403501]

77 **Sagaert X**, Laurent M, Baens M, Wlodarska I, De Wolf-Peeters C. MALT1 and BCL10 aberrations in MALT lymphomas and their effect on the expression of BCL10 in the tumour cells. *Mod Pathol* 2006; **19**: 225-232 [PMID: 16341151 DOI: 10.1038/modpathol.3800523]

78 **Knies N**, Alankus B, Weilemann A, Tzankov A, Brunner K, Ruff T, Kremer M, Keller UB, Lenz G, Ruland J. Lymphomagenic CARD11/BCL10/MALT1 signaling drives malignant B-cell proliferation *via* cooperative NF-κB and JNK activation. *Proc Natl Acad Sci U S A* 2015; **112**: E7230-E7238 [PMID: 26668357 DOI: 10.1073/pnas.1507459112]

79 **Ye H**, Gong L, Liu H, Ruskone-Fourmestraux A, de Jong D, Pileri S, Thiede C, Lavergne A, Boot H, Caletti G, Wündisch T, Molina T, Taal

BG, Elena S, Neubauer A, Maclennan KA, Siebert R, Remstein ED, Dogan A, Du MQ. Strong BCL10 nuclear expression identifies gastric MALT lymphomas that do not respond to H pylori eradication. *Gut* 2006; **55**: 137-138 [PMID: 16344587 DOI: 10.1136/gut.2005.081117]

80 **Rosebeck S**, Rehman AO, Lucas PC, McAllister-Lucas LM. From MALT lymphoma to the CBM signalosome: three decades of discovery. *Cell Cycle* 2011; **10**: 2485-2496 [PMID: 21750409 DOI: 10.4161/cc.10.15.16923]

81 **Zullo A**, Hassan C, Cristofari F, Andriani A, De Francesco V, Ierardi E, Tomao S, Stolte M, Morini S, Vaira D. Effects of Helicobacter pylori eradication on early stage gastric mucosa-associated lymphoid tissue lymphoma. *Clin Gastroenterol Hepatol* 2010; **8**: 105-110 [PMID: 19631287 DOI: 10.1016/j.cgh.2009.07.017]

82 **Liu H**, Ye H, Ruskone-Fourmestraux A, De Jong D, Pileri S, Thiede C, Lavergne A, Boot H, Caletti G, Wündisch T, Molina T, Taal BG, Elena S, Thomas T, Zinzani PL, Neubauer A, Stolte M, Hamoudi RA, Dogan A, Isaacson PG, Du MQ. T(11;18) is a marker for all stage gastric MALT lymphomas that will not respond to H. pylori eradication. *Gastroenterology* 2002; **122**: 1286-1294 [PMID: 11984515 DOI: 10.1053/gast.2002.33047]

83 **Zucca E**, Copie-Bergman C, Ricardi U, Thieblemont C, Raderer M, Ladetto M; ESMO Guidelines Working Group. Gastric marginal zone lymphoma of MALT type: ESMO Clinical Practice Guidelines for diagnosis, treatment and follow-up. *Ann Oncol* 2013; **24** Suppl 6: vi144-vi148 [PMID: 24078657 DOI: 10.1093/annonc/mdt343]

World Journal of Gastroenterology

Submit a Manuscript: https://www.f6publishing.com

World J Gastroenterol 2023 August 28; 29(32): 4860-4872

DOI: 10.3748/wjg.v29.i32.4860

ISSN 1007-9327 (print) ISSN 2219-2840 (online)

ORIGINAL ARTICLE

Basic Study

Linolenic acid-metronidazole inhibits the growth of *Helicobacter pylori* through oxidation

Wen-Ting Zhou, Yuan-Yuan Dai, Li-Juan Liao, Shi-Xian Yang, Hao Chen, Liang Huang, Juan-Li Zhao, Yan-Qiang Huang

Specialty type: Gastroenterology and hepatology

Provenance and peer review: Unsolicited article; Externally peer reviewed.

Peer-review model: Single blind

Peer-review report's scientific quality classification

Grade A (Excellent): 0
Grade B (Very good): B, B
Grade C (Good): 0
Grade D (Fair): 0
Grade E (Poor): 0

P-Reviewer: Krzyzek P, Poland; Maurya DK, India

Received: May 31, 2023
Peer-review started: May 31, 2023
First decision: July 8, 2023
Revised: July 15, 2023
Accepted: July 31, 2023
Article in press: July 31, 2023
Published online: August 28, 2023

Wen-Ting Zhou, Li-Juan Liao, Liang Huang, Juan-Li Zhao, School of Basic Medicine, Youjiang Medical University for Nationalities, Baise 533000, Guangxi Zhuang Autonomous Region, China

Yuan-Yuan Dai, School of Basic Medicine, Youjiang Medical University for Nationalities, Affiliated Hospital of Youjiang Medical University for Nationalities, Baise 533000, Guangxi Zhuang Autonomous Region, China

Shi-Xian Yang, Department of Laboratory, Affiliated Hospital of Youjiang Medical University for Nationalities, Baise 533000, Guangxi Zhuang Autonomous Region, China

Hao Chen, School of Basic Medicine, Department of Pathology, Wannan Medical College, Wuhu 533000, Anhui Province, China

Liang Huang, Key Laboratory of the Prevention and Treatment of Drug Resistant Microbial Infecting, Youjiang Medical University for Nationalities, Baise 533000, Guangxi Zhuang Autonomous Region, China

Yan-Qiang Huang, School of Basic Sciences, Youjiang Medical University for Nationalities, Baise 533000, Guangxi Zhuang Autonomous Region, China

Corresponding author: Liang Huang, Instructor, Key Laboratory of the Prevention and Treatment of Drug Resistant Microbial Infecting, Youjiang Medical University for Nationalities, No. 98 Chengxiang Road, Baise 533000, Guangxi Zhuang Autonomous Region, China. youyihuangl@163.com

Abstract

BACKGROUND

Resistance to antibiotics is one the main factors constraining the treatment and control of *Helicobacter pylori* (*H. pylori*) infections. Therefore, there is an urgent need to develop new antimicrobial agents to replace antibiotics. Our previous study found that linolenic acid-metronidazole (Lla-Met) has a good antibacterial effect against *H. pylori,* both antibiotic-resistant and sensitive *H. pylori*. Also, *H. pylori* does not develop resistance to Lla-Met. Therefore, it could be used for preparing broad-spectrum antibacterial agents. However, since the antibacterial mechanism of Lla-Met is not well understood, we explored this phenomenon in the present study.

AIM
To understand the antimicrobial effect of Lla-Met and how this could be applied in treating corresponding infections.

METHODS
H. pylori cells were treated with the Lla-Met compound, and the effect of the compound on the cell morphology, cell membrane permeability, and oxidation of the bacteria cell was assessed. Meanwhile, the differently expressed genes in *H. pylori* in response to Lla-Met treatment were identified.

RESULTS
Lla-Met treatment induced several changes in *H. pylori* cells, including roughening and swelling. *In vivo* experiments revealed that Lla-Met induced oxidation, DNA fragmentation, and phosphatidylserine ectropionation in *H. pylori* cells. Inhibiting Lla-Met with L-cysteine abrogated the above phenomena. Transcriptome analysis revealed that Lla-Met treatment up-regulated the expression of superoxide dismutase *SodB* and *MdaB* genes, both anti-oxidation-related genes.

CONCLUSION
Lla-Met kills *H. pylori* mainly by inducing oxidative stress, DNA damage, phosphatidylserine ectropionation, and changes on cell morphology.

Key Words: *Helicobacter pylori*; Oxidation; Superoxide dismutase; *SodB* genes; *MdaB* genes

©The Author(s) 2023. Published by Baishideng Publishing Group Inc. All rights reserved.

Core Tip: The clarithromycin resistant *Helicobacter pylori (H. pylori)* is listed by the World Health Organization as the priority bacteria in urgent need of developing new antibiotics. Our previous research found that linolenic acid-metronidazole has a good antibacterial effect on *H. pylori* and is not easy to develop drug resistance. Therefore, we further explored its antibacterial mechanism against *H. pylori*. It was found that it mainly kills *H. pylori* by inducing oxidative stress, DNA damage, phosphatidylserine ectropionation, and changes on cell morphology. This study may provide a theoretical basis for the development and application of new anti *H. pylori* lead compound.

Citation: Zhou WT, Dai YY, Liao LJ, Yang SX, Chen H, Huang L, Zhao JL, Huang YQ. Linolenic acid-metronidazole inhibits the growth of *Helicobacter pylori* through oxidation. *World J Gastroenterol* 2023; 29(32): 4860-4872
URL: https://www.wjgnet.com/1007-9327/full/v29/i32/4860.htm
DOI: https://dx.doi.org/10.3748/wjg.v29.i32.4860

INTRODUCTION

Helicobacter pylori (*H. pylori*) is the main pathogen that causes upper digestive diseases, such as chronic gastritis, peptic ulcer, and gastric cancer[1-4]. At present, the treatment options for *H. pylori* infections include standard triple therapy, bismuth-containing quadruple therapy, and sequential therapy[5,6]. Due to the overuse and misuse of antibiotics, the drug resistance rate of *H. pylori*, including multi-drug resistance, is gradually increasing, negatively impacting the control and treatment of *H. pylori* infections[7-10]. Therefore, there is an urgent need to develop new anti-*H. pylori* agents[11].

Due to the long period and significant investment required for developing new antibiotics, the transformation or modification of the existing drugs is more efficient in shortening the drug research and development cycle. Modifying existing drugs could improve their efficacy while reducing the development of antimicrobial resistance. Zinc linolenic acid and liposome linolenic acid are linolenic acid derivatives effective at increasing the sensitivity of drug-resistant *H. pylori*. Resistance against zinc linolenic acid and liposome linolenic acid is minimal[12,13]. Although metronidazole is a widely used and cost-effective drug, its clinical application for *H. pylori* infection treatment is limited by resistance development.

Our previous study found that the minimum inhibitory concentration (MIC) of linolenic acid-metronidazole (Lla-Met) against six strains of the drug-resistant *H. pylori* was 2-4 μg/mL. Additionally, the *H. pylori* strains did not develop resistance against this compound. Therefore, Lla-Met would serve as promising antibiotics. However, its antibacterial mechanism is poorly understood[14], this study explored this mechanism.

MATERIALS AND METHODS

Materials

H. pylori strain G27 (Courtesy of Prof. Bi Hongkai, Nanjing Medical University), calf serum, a Columbia blood agar base, a brain heart infusion (BHI,OXOID) medium, L-cysteine (L-cys) (AR 99%, MACKLIN), a fluorescence orthomicroscope (OLYMPUS, Tokyo, Japan), reactive oxygen species (ROS) detection kits (Beyotime), cell apoptosis 4',6-diamidino-2-phenylindole (DAPI) detection kits (Beyotime), apoptosis detection kits (Beyotime), reverse transcription kits (Monad), reverse transcription quantitative real-time polymerase chain reaction (RT-qPCR) kits (Monad), a Lightcycler96 fluorescence ration PCR instrument (Roche, Germany), and a scanning electron microscope were used in the present study.

Thawing and culture of H. pylori strain

Standard *H. pylori* strain G27 stored at -80 °C were thawed and centrifuged to remove the preservation solution (Glycerin:BHI:serum = 3:6:1). The bacteria were inoculated on a Columbia agar medium, or a brain heart infusion medium supplemented with 10% calf serum and cultured in a microaerophilic environment.

Cell morphology assay

The effect of the Lla-Met on *H. pylori* morphology was observed by scanning electron microscopy[15-18]. *H. pylori* was treated with 4 and 8 μg/mL of Lla-Met and incubated for 24 h in a three-gas incubator. The bacteria were pelleted by centrifugation and fixed overnight with 2.5% glutaraldehyde. The bacteria suspension was centrifuged to remove glutaraldehyde before dehydration with 30%, 50%, 70%, 90%, and 100% ethanol. The pellet was dried through refrigeration in a vacuum. After that, the *H. pylori* morphology was observed and photographed under a KYKY-EM8100 scanning electron microscope (KYKY, Beijing).

Membrane damage assay

The *H. pylori* cells were stained as previously described by Hwang *et al*[19]. Briefly, the G27 bacterial suspension (1×10^8 CFU/mL) at the logarithmic phase was treated with Lla-Met for 2 h at the rate of 16 μg/mL. The cell suspension was centrifuged at 12000 r/min for 2 min to pellet the cells. The medium was poured out, and the harvested cells were suspended in phosphate buffered saline (PBS). The cells were stained with a propidium iodide solution (PI, 10 μg/mL, Thermo Fisher) at 37 °C protected from light 30 min and thereafter centrifuged at 12000 r for 5 min. The dye unbound to the harvested cells was washed away with sterile PBS. Thereafter, the cells were suspended in PBS and immediately observed under a fluorescence microscope (Olympus Corporation, Tokyo, Japan).

Cell membrane pore size assay

FITC-FD was mainly used to evaluate the degree of *H. pylori* cell membrane damage after treatment with Lla-Met. The process was performed as previously described[20]. Briefly, G27 bacterial suspension (1×10^8 CFU/mL) at the logarithmic phase was incubated with Lla-Met (16 μg/ML) for 2 h, centrifuged, and the pellet was suspended in sterile PBS. The cell suspension was protected from light with FIFC-labeled glucan FD4, about 4.0 kDa, with a diameter of 1.4 nm (Sigma, United States) and FD10, about 10.1 kDa, with a diameter of 2.3 nm (Sigma, United States), both at a final concentration of 100 μg/mL. After 30 min of incubation at 37 °C, the unbound fluorescent dye was washed off with sterile PBS. The cells were suspended in sterile PBS. Finally, the fluorescence influx of FD4 and FD10 was detected at the excitation and emission wavelengths of 495 nm and 520 nm, respectively, by a multimode reader (BioTek, America).

Ion channels assay

The G27 bacterial suspension (1×10^8 CFU/mL) at the logarithmic phase was incubated with Lla-Met (16 μg/mL) for 2 h and centrifuged at 12000 r/min for 2 min. The changes in concentrations of extracellular K^+, Na^+, Cl^-, and Ca^{2+} were determined by ion-selective electrodes. Three biological repeats were performed for each experiment.

Intracellular reactive oxygen assay

The level of intracellular ROS in the *H. pylori* cell was detected by the DC-FDH probe, as described by Akhtar *et al*[21-22]. Briefly, G27 bacterial suspension (1×10^8 CFU/mL) was treated with Lla-Met (8 μg/mL and 16 μg/mL) for 2 h and centrifuged to remove the supernatant. The harvested cells were protected from light DCF-DA (10 μM) for 30 min and centrifuged at 12000 r for 2 min. The excess probe was washed off with sterile PBS. Finally, the cells were resuspended in PBS solution, and the fluorescence intensity was analyzed using a multifunctional microplate reader (BioTek, America) at the excitation and emission wavelengths of 485 nm and 520 nm, respectively. The fluorescence intensity was also analyzed using a fluorescent microscope (OLYMPUS, Tokyo, Japan). PBS and polymyxin were the controls.

Validation of how Lla-Met kills H. pylori

The G27 bacterial suspension was incubated with L-cys, a ROS scavenger, to evaluate the effect of ROS on the viability of G27 bacteria. Briefly, G27 bacterial suspension (1×10^8 CFU/mL) at the logarithmic phase was incubated with or without 40 mmol/L L-cys (which did not affect the viability of G27 cells) for 1 h and thereafter with Lla-Met (16 μg/mL) for 8 h. The optical density values were measured at $OD_{600\ nm}$ using a multifunctional microplate reader (BioTek, America). In addition, the fluorescence intensity was analyzed using fluorescence microscopy (OLYMPUS, Tokyo, Japan). G27 bacterial suspension treated with or without 40 mmol/L L-cys was incubated for 1 h. The suspension was treated with

Lla-Met (16 μg/mL) for 2 h and centrifuged to remove the supernatant. The harvested bacteria were incubated with DCF-DA (10 μM) for 30 min and washed with sterile PBS.

DNA fragmentation assay

When DAPI passes through the intact cell membrane, it binds to bacterial DNA. The bacterial DNA thus stains blue. Damaged DNA appears as dots. Therefore, the fragmentation of *H. pylori* DNA after Lla-Met treatment was detected using the DAPI staining[23]. Briefly, the G27 bacterial suspension (1×10^8 CFU/mL) was incubated with or without 40 mmol/L L-cys for 1 h and thereafter with Lla-Met (16 μg/mL) for 2 h. Thereafter, the suspension was centrifuged to remove the supernatant and treated with DAPI (1 μg/mL) for 30 min. The unbound dye was washed off with PBS, and the cells were resuspended in PBS. Fluorescence intensity was determined at excitation and emission wavelengths of 358 nm and 460 nm, respectively (OLYMPUS, Tokyo, Japan), with PBS as a control.

Phosphatidylserine ectropion assay

Phosphatidylserine (PS) is usually located on the inner side of the cell membrane. At the early stage of apoptosis, PS is translocated to the cell surface. Annexin-V, a $Ca2^+$-dependent phospholipid binding protein, bind to PS with high affinity [24]. The G27 bacterial suspension in the logarithmic phase (1×10^8 CFU/mL) was incubated with or without 40 mmol/L L-cys for 1 h and thereafter with Lla-Met (16 μg/mL) for 2 h. Thereafter, the suspension was centrifuged to remove the supernatant, and the pellet was incubated with Annexin-V and incubated for 30 min. The unbound dye was washed off with PBS, and the cells were resuspended in PBS. The fluorescence intensity was analyzed at excitation and emission wavelengths of 490 nm and 520 nm, respectively, using a multifunctional microplate reader (BioTek, America) and a fluorescence microscope (OLYMPUS, Tokyo, Japan), with PBS as a control.

Transcriptome sequencing

G27 bacterial suspension (1×10^8 CFU/mL) (OD_{600} = 0.3) was incubated with 2, 4, 8, and 10 μg/mL Lla-Met for 0 h, 2 h, and 8 h, and the ODs were measured at 600 nm. Three biological repeats were performed for each experiment. When the OD remained constant (0.3), the bacterial RNA was extracted for transcriptome sequencing, which was performed by Nanjing Fengzi Bio-pharm Technology. Three biological repeats were performed for each experiment.

The sequencing was performed using Illumina PE150 technology. The alignment and transcript assembly were performed using Boetie2 and the Rockhhoper software. All genes were quantitatively analyzed, and the differentially expressed genes (DEGs) were identified. The biological processes and pathways regulated by the DEGs were then identified. Principal component analysis (PCA) demonstrates principal component analysis, analyzing the composition of different samples can respond to the differences and distances between samples, the more similar the sample composition, the closer the distance in the PCA graph.

Validation of differential gene expression

Total bacterial RNA was extracted using a Novizan RNA kit, and the expression of mRNA was analyzed by a real-time fluorescent quantitative PCR instrument (Lightcycler96 fluorescent quantitative PCR instrument, Roche, Germany). The 16s was used as the reference gene. The sequences of primers used in this study are shown Table 1. Three biological repeats were performed for each experiment.

Statistical analysis

Statistical analysis was performed using the SPSS software, Version 26.0. Continuous data were expressed as mean ± SD. Differences between groups were analyzed using the *t*-test, while multiple groups were compared using the single factor variance analysis. $P < 0.05$ was considered statistically significant.

RESULTS

Effect of Lla-Met on H. pylori morphology

The impact of the Lla-Met compound on the morphology of *H. pylori* was observed using scanning electron microscopy. *H. pylori* in the control group was found to have a smooth and homogenous cell surface (Figures 1A and D). The surface of *H. pylori* in the treatment group (4 μg/mL and 8 μg/mL) was rough and swollen, and the cell damage worsened with the Lla-Met concentration (Figures 1B, C, E, and F).

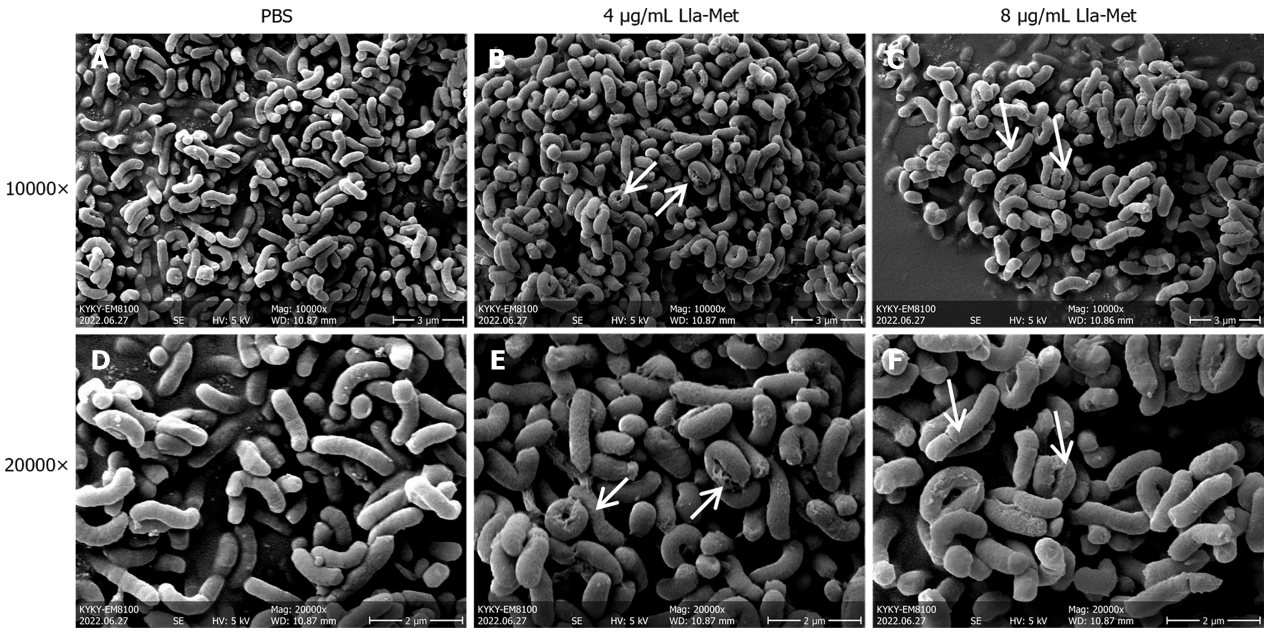
Lla-Met impact of cell membrane integrity

PI penetrates through a damaged cell membrane, where it binds and stains the DNA. Therefore, an influx of intracellular PI represents the integrity of the bacterial cell membrane. The fluorescence intensity of PI in the G27 treatment group (16 μg/mL Lla-Met) was weaker than in the control group, though statistically insignificant (Figure 2A).

FITC-labelled glucans of different pore sizes (FD4 and FD10) were detected using a multifunctional microplate detector to examine damage to the *H. pylori* cell membrane after treatment with Lla-Met. Linolenic acid treatment had no significant effect on the permeability of *H. pylori* cells (Figures 2B and C).

Table 1 List of primers used in this study

Name	Forward primers	Reverse primers
16s	AGGATCAAGGTTTAAGGATT	CTGGAGACTAAGCCCTCC
MdaB	AGGCTATGAACACGCTCAAGAAGTG	TTTCACAATCCAAGGCTCTCCCATC
SodB	AAGCGACTGCCTTAAGCGATGAG	TCCAGCCAGAGCCAAACAAAGTG



DOI: 10.3748/wjg.v29.i32.4860 **Copyright** ©The Author(s) 2023.

Figure 1 The effect of linolenic acid-metronidazole on *Helicobacter pylori* morphology. A: The control group shows the cell morphology at × 10000 magnification; B: The appearance of *Helicobacter pylori* (*H. pylori*) in linolenic acid-metronidazole concentrations of 4 μg/mL shows the cell morphology at × 10000 magnification; C: The appearance of *H. pylori* in linolenic acid-metronidazole concentrations of 8 μg/mL shows the cell morphology at × 10000 magnification; D: The control group shows the cell morphology at × 20000 magnification; E: The appearance of *H. pylori* in linolenic acid-metronidazole concentrations of 4 μg/mL shows the cell morphology at × 20000 magnification; F: The appearance of *H. pylori* in linolenic acid-metronidazole concentrations of 8 μg/mL shows the cell morphology at × 20000 magnification. The arrow points to the cell damage. Roughness, swelling, breakages on the cell surface, *etc.*, are shown. PBS: Phosphate buffered saline; Lla-Met: Linolenic acid-metronidazole.

Lla-Met impact on H. pylori ion channels

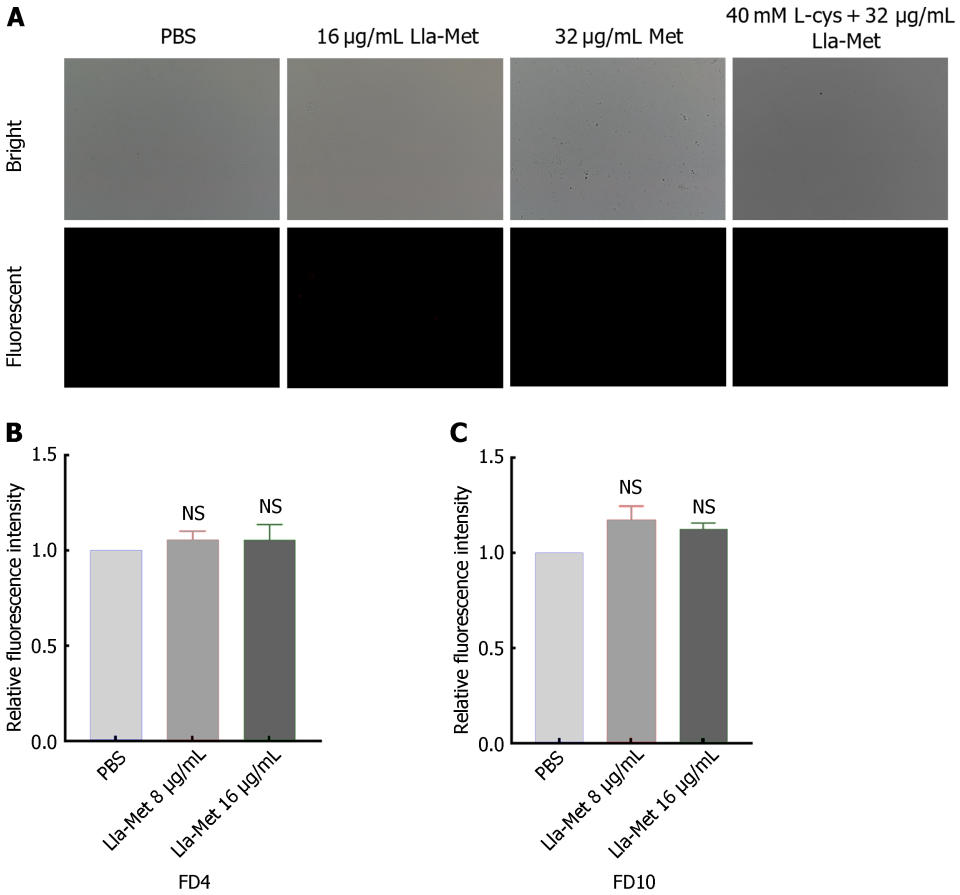
To further investigate whether Lla-Met compound penetrated the cells *via* ion channels, the concentrations of K^+, Na^+, Cl^-, and Ca^{2+} ions in the supernatant were measured after treating *H. pylori* with Lla-Met. There was no statistically significant difference in the concentrations of the aforementioned ions between the treatment and the control group after G27 was applied with 16 μg/mL compound (Figures 3A and B).

Lla-Met impact on the intracellular ROS

DC-FDA fluorescent probes can be used to detect whether Lla-Met compounds can accelerate intracellular oxidation reactions. Compared with the control group, 8 μg/mL and 16 μg/mL Lla-Met compound increased the intracellular oxidation in *H. pylori* cell. Moreover, 8 μg/mL Lla-Met was more potent than 16 μg/mL metronidazole (Figure 4A); The relative fluorescence intensity of *H. pylori* treated with 16 μg/mL Lla-Met was stronger than that treated with 40 μg/mL polymyxin B ($P < 0.01$, Figure 4D). However, L-cys treatment abrogated the effect of Lla-Met (Figures 4B and D, $P < 0.01$), implying that L-cys abolished ROS generated by Lla-Met in *H. pylori*. In addition, L-cys pretreatment increased the cell viability from 20.5% to 57.7% (Figure 4C).

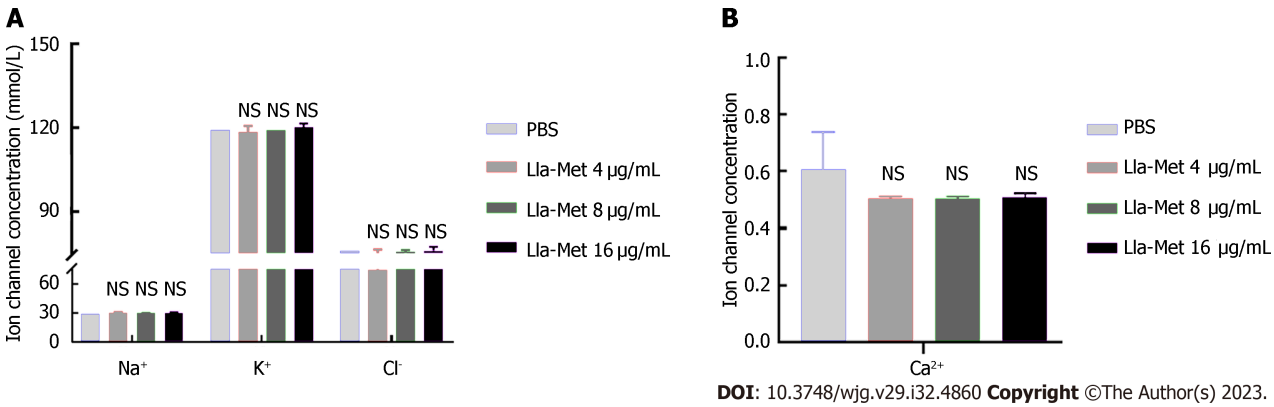
Lla-Met induced DNA fragmentation and apoptosis

In the early stage of apoptosis, PS translocates to the cell surface, where it could be bound by Ca^{2+}-dependent phospholipid-binding protein. Thus, the phospholipid-binding protein could be used for analyzing cell apoptosis in prokaryotes. In the present study, we found that the fluorescence intensity of *H. pylori* treated with 16 μg/mL Lla-Met was higher than that of the untreated group and the L-cys pretreatment group (Figure 5A). The multifunctional microplate labelling instrument results showed that the relative fluorescence intensity of Lla-Met-compound treatment group was significantly stronger than that of the PBS group and L-cys pretreatment group (Figure 5C, $P < 0.0001$). These results indicated that linolenic-acid-metronidazole caused PS eversion, but L-cys pretreatment inhibited this



DOI: 10.3748/wjg.v29.i32.4860 **Copyright** ©The Author(s) 2023.

Figure 2 The effect of linolenic acid-metronidazole on cell membrane permeability. A: Linolenic acid-metronidazole (Lla-met) induced membrane damages of *Helicobacter pylori* (*H. pylori*) using PI staining; B: Lla-met induced membrance pore size damage of *H. pylori* using FD4; C: Lla-met induced membrance pore size damage of *H. pylori* using FD10. PI, FD4 and FD10 can't pass through the intact cell membrane. NS: Not significant; PBS: Phosphate buffered saline; Lla-Met: Linolenic acid-metronidazole.

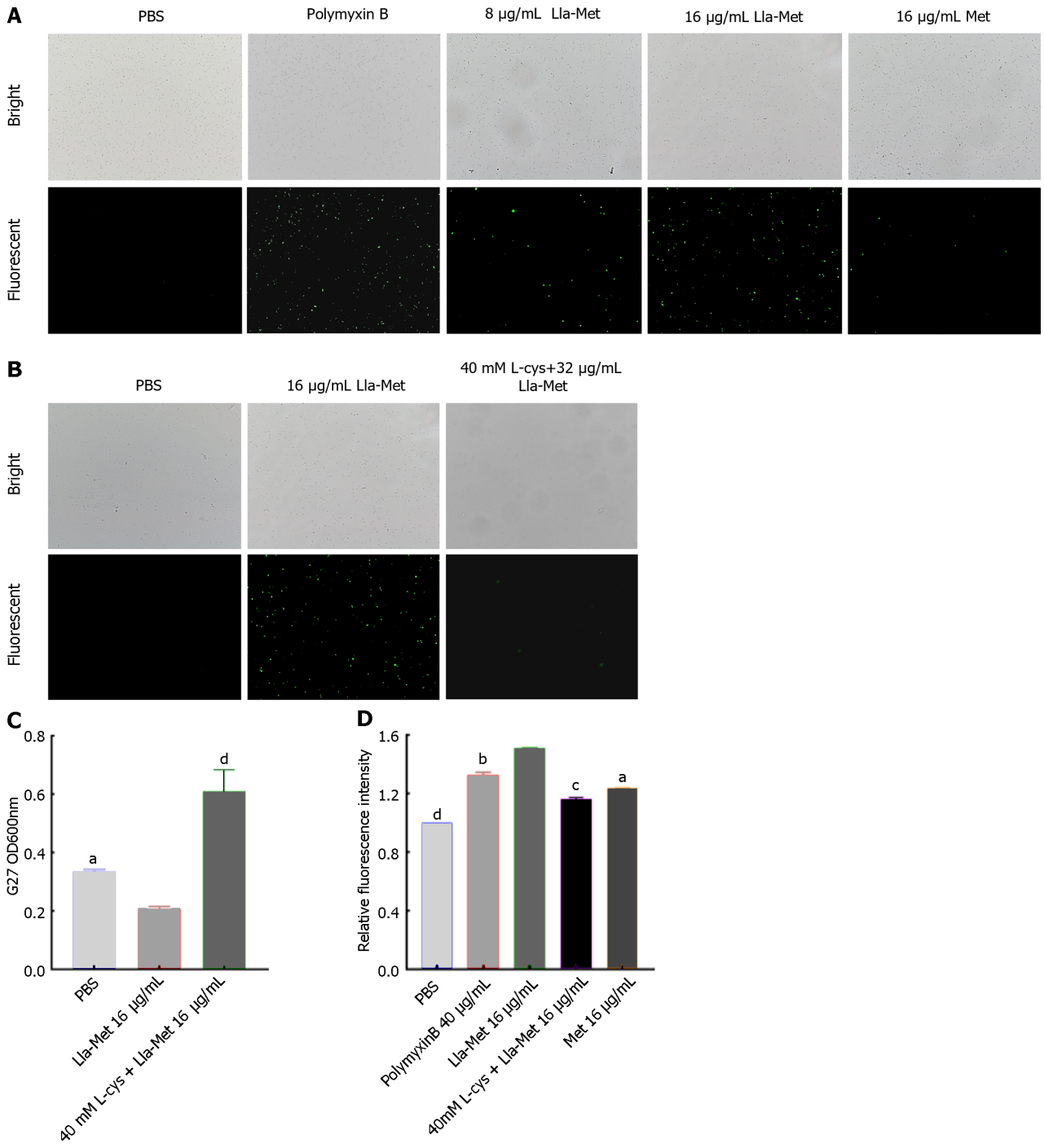


DOI: 10.3748/wjg.v29.i32.4860 **Copyright** ©The Author(s) 2023.

Figure 3 The effect of the linolenic acid-metronidazole compound on *Helicobacter pylori* ion channels. A: K^+, Na^+, Cl^-, and Ca^{2+} ion channels; B: Ca^{2+} ion channels. NS: Not significant; PBS: Phosphate buffered saline; Lla-Met: Linolenic acid-metronidazole.

phenomenon.

Subsequently, cellular DNA fragmentation serves as a marker of late apoptosis. The DAPI staining evaluated whether Lla-Met compound could cause the fragmentation of *H. pylori* DNA. The results showed that 16 μg/mL Lla-Met caused the fragmentation of bacterial *H. pylori* DNA (Figure 5B red circles represent the fragmented DNA). However, DNA fragmentation was inhibited in the L-cys treatment group (Figure 5D, $P < 0.0001$). These findings suggested that Lla-Met caused the fragmentation of *H. pylori* DNA by inducing the accumulation of ROS.

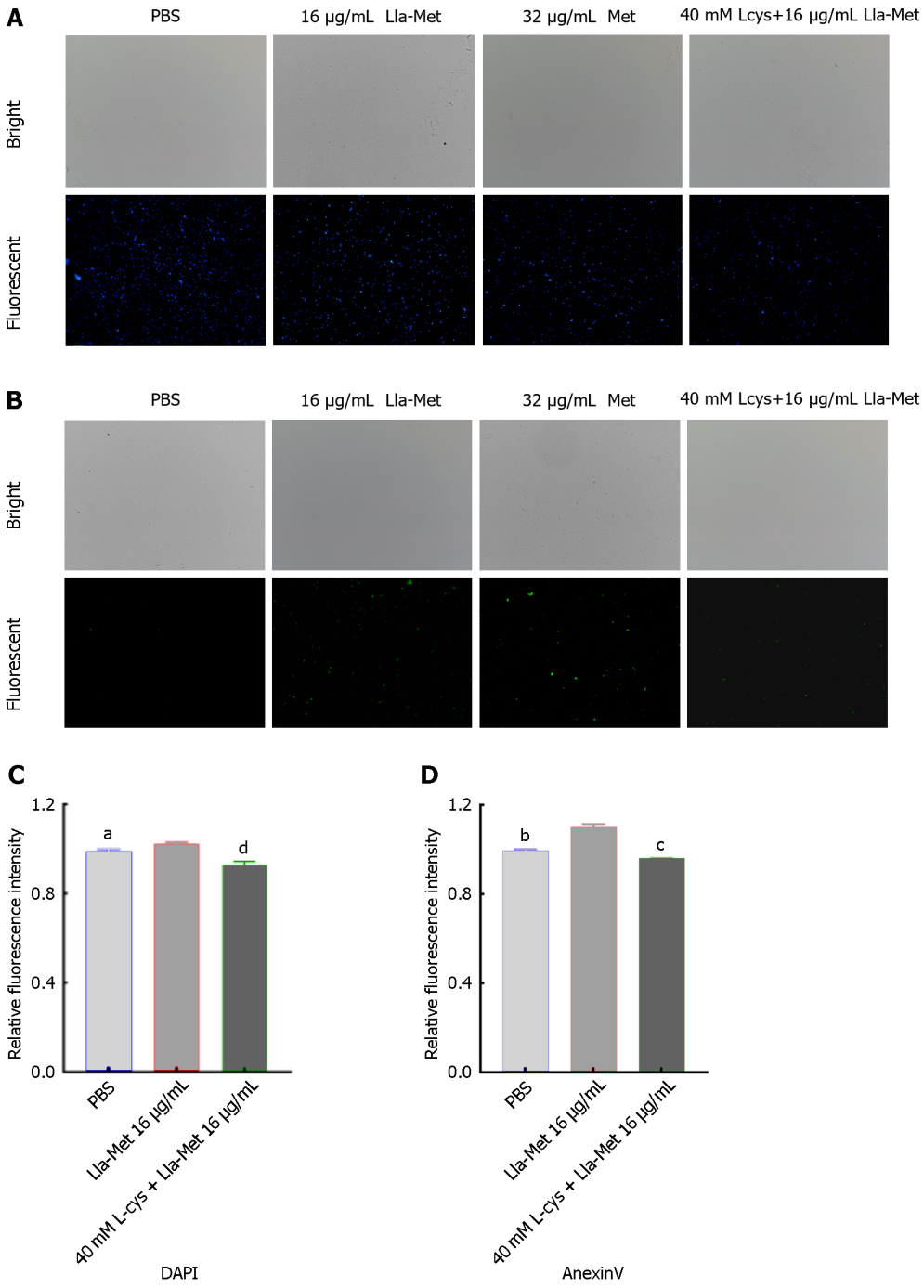


DOI: 10.3748/wjg.v29.i32.4860 **Copyright** ©The Author(s) 2023.

Figure 4 The effect of linolenic acid-metronidazole on the intracellular reactive oxygen species content in *Helicobacter pylori*. A: Fluorescent microscopy for the effect of linolenic acid-metronidazole on the production of reactive oxygen species (ROS); B: The effect of L-cysteine (L-Cys) on intracellular production of ROS; C: The effect of L-cys on cell viability; D: Effect of L-cys on ROS. $^{a}P < 0.05$; $^{b}P < 0.01$; $^{c}P < 0.001$; $^{d}P < 0.0001$. PBS: Phosphate buffered saline; Lla-Met: Linolenic acid-metronidazole; L-Cys: L-cysteine.

Lla-Met upregulates MdaB, SodB expression

The half inhibitory concentration of Lla-Met was used for the oxidation analysis (Figure 6A). The OD values were unchanged after *H. pylori* was dosed with 8 μg/mL Lla-Met compound for 0, 4, and 8 h. The RNA-seq data for *H. pylori* in different treatment groups (Figure 6B). The closer the Pearson correlation coefficient approaches 1, the higher the similarity of events. The PCA is in Figure 6C. The difference and distance between samples are illustrated. The closer the similarity between samples, the closer the distance in the PCA diagram. The Venn diagram, which shows the DEGs in each group. A total of 1130 DEGs were detected between A_M_1 and A_M_2, of which 575 were up-regulated and 555 were down-regulated. A total of 1016 DEGs were detected between A_M_1 and A_M_3, of which 488 were up-regulated, and 528 were down-regulated. A total of 533 DEGs were detected between A_M_2 and A_M_3, including 265 up-regulated genes and 268 down-regulated genes. Among them, 344 genes were co-expressed in A_M_1, A_M_2, and



DOI: 10.3748/wjg.v29.i32.4860 **Copyright** ©The Author(s) 2023.

Figure 5 Detection of phosphatidylserine ectropion and DNA fragmentation of *Helicobacter pylori*. A and C: Fluorescence microscope detection of phosphatidylserine ectropion; B and D: Multifunctional enzyme labeler detection of bacterial DNA fragmentation. $^{a}P < 0.05$; $^{b}P < 0.01$; $^{c}P < 0.001$; $^{d}P < 0.0001$. PBS: Phosphate buffered saline; Lla-Met: Linolenic acid-metronidazole; L-Cys: L-cysteine.

A_M_3 (Figure 6D). The gene set enrichment analysis and Gene Ontology of the DEGs. The DEGs were divided into three main categories: Those that regulate biological processes, secretion of cellular components, and molecular function. The differential genes between the groups are primarily concentrated in tRedox pathways, metabolic processes and other pathways. Gene set enrichment analysis revealed that the DEGs regulated the REDOX and the metabolism pathway (Figure 6E). Lla-Met is inducing production of ROS in *H. pylori*, and therefore an increased expression of MdaB and SodB, both of which are associated with protection against the oxidative stress (Table 2). RT-qPCR and transcriptome sequence analyses revealed comparable findings (Figure 6F).

Table 2 Gene affected by linolenic acid-metronidazole treatment

Gene	Name	Log_2 fold change	Description	Enrichment pathway
MdaB	*HPG27_RS03065*	4.962	Flavodoxin family protein	Oxidoreductase activity
SodB	*HPG27_RS05265*	4.2287	Superoxide dismutase	Oxidoreductase activity

DISCUSSION

Lla-Met compound is synthesized from linolenic acid and metronidazole. Linolenic acid is an essential fatty acid with broad-spectrum antibacterial spectrum and antioxidant activities and capability to overcome *H. pylori* resistance to antibiotic treatment. In addition, with more functional groups, it can react with various substances to form related derivatives, which are widely used in the anti-infection treatment. Obonyo *et al*[25] suggested that the antibacterial mechanism of linolenic acid liposome against *H. pylori* is mainly to cause damage to the bacterial cell membrane. Huang *et al*[26] used linolenic acid and zinc to synthesize zinc linolenic acid with an MIC of 4-8 μg/mL to drug-resistant *H. pylori* strains. Its antibacterial mechanism is mainly to destroy cell membrane and cause accumulation of ROS, which finally leads to the death of bacteria. In this experiment, the damage caused by Lla-Met compound to the cell membrane was detected by PI, FD4, FD10 and lactate dehydrogenase activity determination. There was no change in cell membrane permeability after *H. pylori* was treated with 16 μg/mL Lla-Met compound. This result suggested that Lla-Met compound did not inhibit *H. pylori* by damaging the cell membrane.

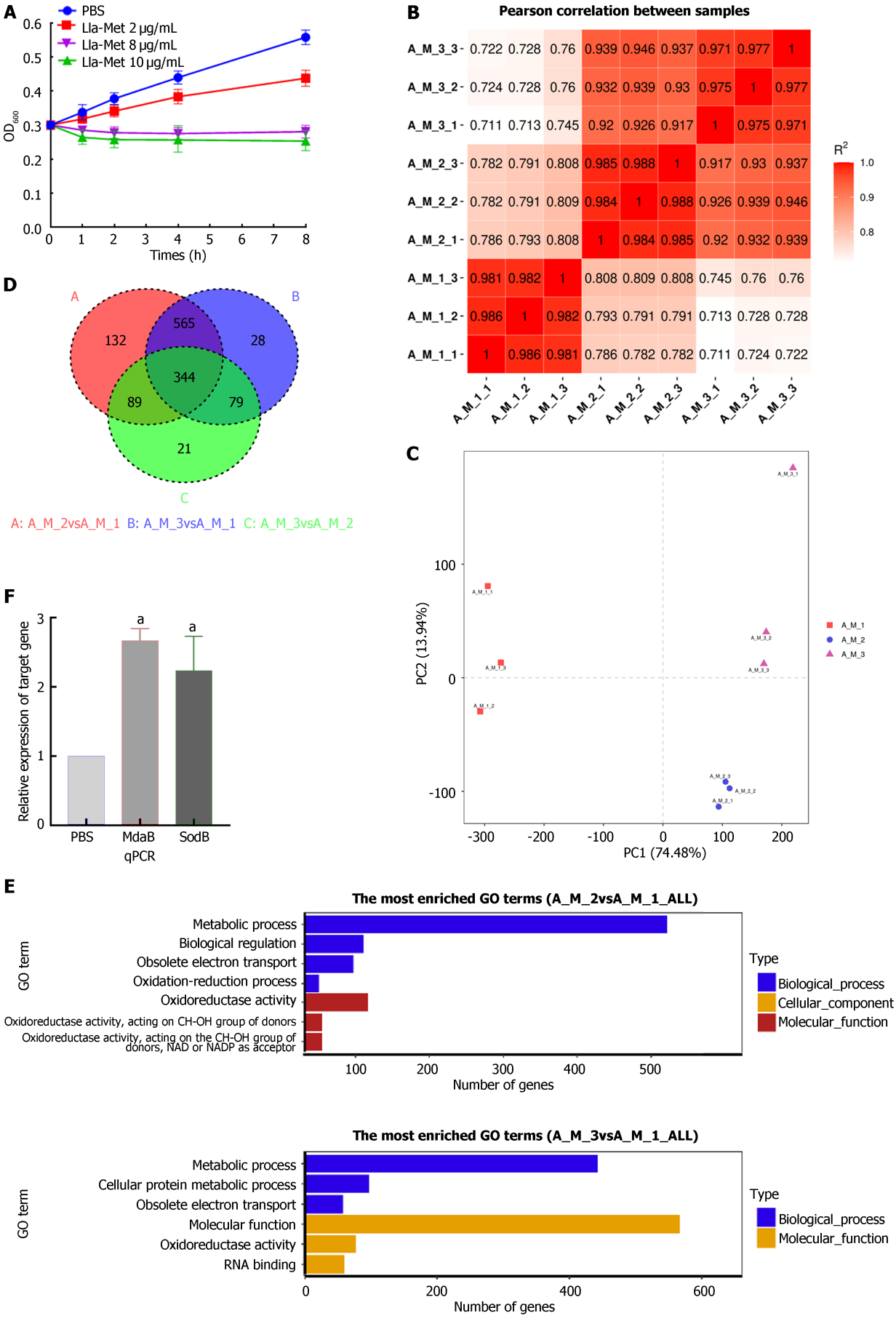
The accumulation of intracellular ROS activates eukaryotic cell apoptosis[27]. This process produces dying cells with typical morphological features, including cell shrinkage, membrane blistering, chromatin condensation, DNA fragmentation, and PS ectropion[28]. Studies have shown that apoptosis also occurs in prokaryotic cells, and is characterized with similar morphological characteristics as those in eukaryotes, such as the destruction of bacterial membrane integrity, DNA fragmentation, and PS ectropion[22,29]. Therefore, in the present study, we investigated whether Lla-Met compound could inhibit *H. pylori* growth by causing oxidative damage. In the experiment, 8 μg/mL Lla-Met compound was found to produce a stronger fluorescence signal compared with the control group. In addition, at a higher dose of 16 μg/mL Lla-Met, *H. pylori* produced a stronger fluorescence signal compared with the positive control group. Indicated that Lla-Met compound could increase accumulation of ROS in *H. pylori* in a dose-and time-dependent manner. This experiment also investigated whether intracellular ROS accumulation could affect *H. pylori* viability. The results showed that excessive accumulation of ROS could affect viability of *H. pylori* by reducing it to 20.5%, which increased to 57.7% when *H. pylori* was treated with 40 mmol/L L-cys. Interestingly, the accumulation of intracellular ROS was also found to significantly decrease after *H. pylori* was treated with L-cys. This result suggested that Lla-Met compound could cause excessive accumulation of intracellular ROS, leading to a decrease in cell viability, and that ROS accumulation could be reversed by L-cys treatment. In addition, after treatment with Lla-Met compound at different concentrations for 24 h, *H. pylori* surface became rough and swollen compared with the control group. As previously demonstrated, Lla-Met compound caused no damage to the cell membrane of *H. pylori*. This suggested that the death of *H. pylori* was due to the accumulation of intracellular ROS caused by Lla-Met compound.

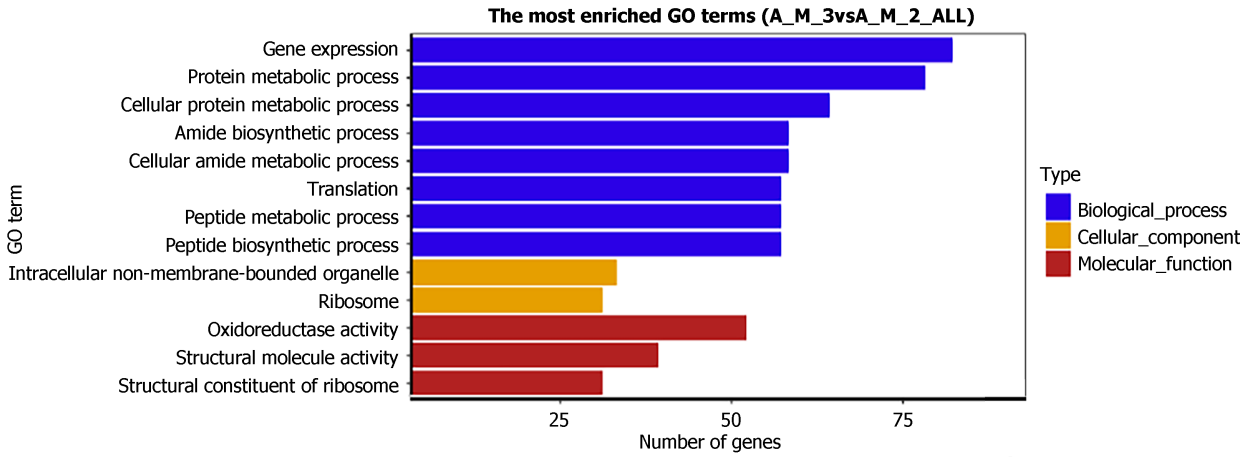
Oxidation can cause both prokaryotic and eukaryotic cell death. In the present study, treatment with 16 μg/mL Lla-Met for 2 h was found to cause *H. pylori* DNA fragmentation and PS ectropion. Meanwhile, these effects were found to be reversed after *H. pylori* was treated with L-cys. DNA damage and membrane depolarization are characteristic changes in eukaryotic cell apoptosis[30]. Our experimental results showed that *H. pylori* cell death is similar to eukaryotic apoptosis, and ROS accumulation could induce prokaryotic cell-like death. However, compared with other studies, significant damage to the cell membrane was not found in the present study. This result indicated that damage to the integrity of the cell membrane might not be as necessary in the apoptosis of prokaryotic cells as slight DNA fragmentation and PS ectropion.

These results indicated that Lla-Met compound can promote intracellular ROS-generation reaction in *H. pylori* and effectively inhibit its growth. However, since several enzymes are involved in ROS-generating reaction, we used RT-qRCR to identify and verify key enzymes involved in this process and detect transcriptome changes. The results revealed that superoxide dismutase *MdaB* and *SodB* genes were found to play an important role. Under normal circumstances, the intracellular oxidative system and antioxidant system are in a dynamic balance. However, after treatment of with linolonic acid-metronidazole compound, superoxide dismutase *MdaB* and *SodB* genes were found to be highly expressed in *H. pylori*, and intracellular ROS was found to accumulate excessively, thereby damaging DNA and causing PS ectropion.

CONCLUSION

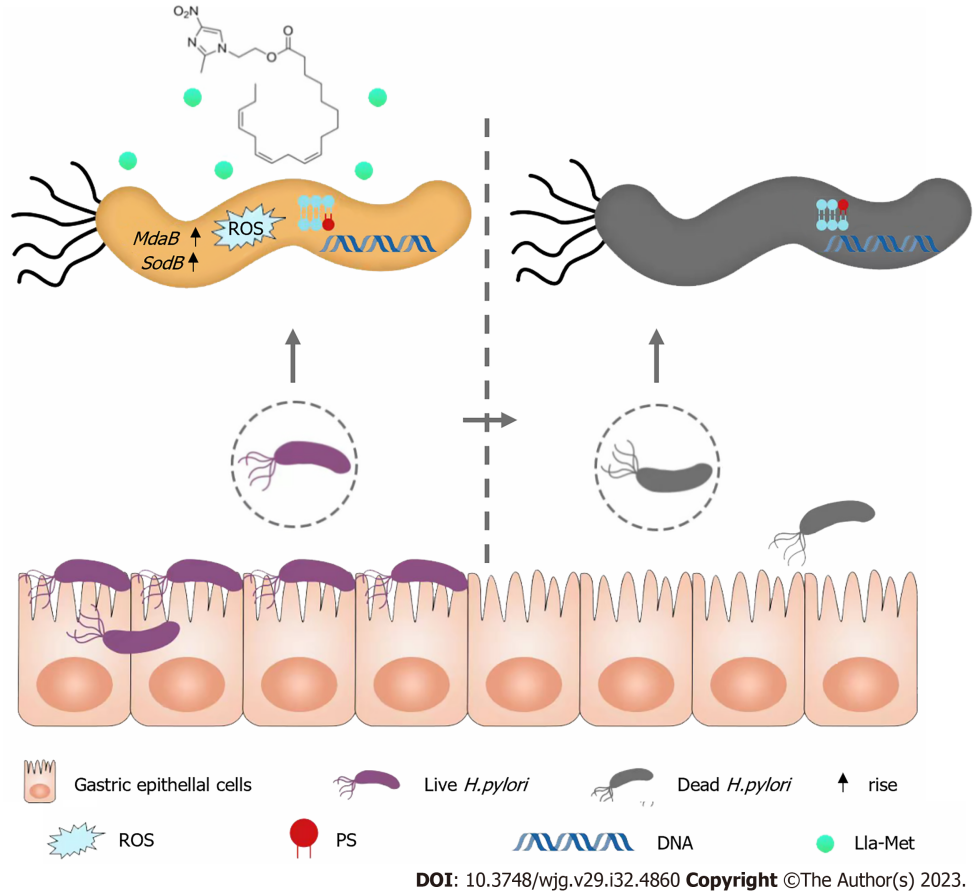
In this paper, the mechanism of linoleic-metronidazole compound was demonstrated to involve inhibiting *H. pylori* growth by inducing excessive ROS accumulation, resulting in excessive superoxide dismutase *MdaB* and *SodB* genes expression (Figure 7). Besides, this study further proves the antibacterial effect of Lla-Met on *H. pylori* at the molecular level, providing theoretical support for further research and development of Lla-Met as an anti-*H. pylori* drug to help overcome *H. pylori* resistance to current antibiotic drugs.


A
PBS
Lla-Met 2 μg/mL
Lla-Met 8 μg/mL
Lla-Met 10 μg/mL
OD600
Times (h)
B
Pearson correlation between samples
A_M_3_3 0.722 0.728 0.76 0.939 0.946 0.937 0.971 0.977 1
A_M_3_2 0.724 0.728 0.76 0.932 0.939 0.93 0.975 1 0.977
A_M_3_1 0.711 0.713 0.745 0.92 0.926 0.917 1 0.975 0.971
A_M_2_3 0.782 0.791 0.808 0.985 0.988 1 0.917 0.93 0.937
A_M_2_2 0.782 0.791 0.809 0.984 1 0.988 0.926 0.939 0.946
A_M_2_1 0.786 0.793 0.808 1 0.984 0.985 0.92 0.932 0.939
A_M_1_3 0.981 0.982 1 0.808 0.809 0.808 0.745 0.76 0.76
A_M_1_2 0.986 1 0.982 0.793 0.791 0.791 0.713 0.728 0.728
A_M_1_1 1 0.986 0.981 0.786 0.782 0.782 0.711 0.724 0.722
R2
D
A
B
C
132
565
28
344
89
79
21
A: A_M_2vsA_M_1 B: A_M_3vsA_M_1 C: A_M_3vsA_M_2
C
PC2 (13.94%)
PC1 (74.48%)
A_M_1
A_M_2
A_M_3
F
Relative expression of target gene
a
a
PBS
MdaB
SodB
qPCR
E
The most enriched GO terms (A_M_2vsA_M_1_ALL)
GO term
Metabolic process
Biological regulation
Obsolete electron transport
Oxidation-reduction process
Oxidoreductase activity
Oxidoreductase activity, acting on CH-OH group of donors
Oxidoreductase activity, acting on the CH-OH group of donors, NAD or NADP as acceptor
Number of genes
Type
Biological_process
Cellular_component
Molecular_function
The most enriched GO terms (A_M_3vsA_M_1_ALL)
GO term
Metabolic process
Cellular protein metabolic process
Obsolete electron transport
Molecular function
Oxidoreductase activity
RNA binding
Number of genes
Type
Biological_process
Molecular_function



DOI: 10.3748/wjg.v29.i32.4860 **Copyright** ©The Author(s) 2023.

Figure 6 Linolenic acid-metronidazole up-regulates the expression of superoxide dismutase. A: The half inhibitory concentration of linolenic acid-metronidazole; B: RNA-seq quality data; C: The principal component analysis; D: Venn diagram; E: Gene set enrichment analysis; F: Up-regulates the expression of genes. $^{a}P < 0.05$. PBS: Phosphate buffered saline; Lla-Met: Linolenic acid-metronidazole; qPCR: Quantitative polymerase chain reaction; GO: Gene Ontology.



DOI: 10.3748/wjg.v29.i32.4860 **Copyright** ©The Author(s) 2023.

Figure 7 Hypothesized model of the mechanism of linolenic acid-metronidazole against *Helicobacter pylori*. ROS: Reactive oxygen species; PS: Phosphatidylserine; Lla-Met: Linolenic acid-metronidazole; *H. pylori*: *Helicobacter pylori*.

ARTICLE HIGHLIGHTS

Research background

Helicobacter pylori (*H. pylori*) is recognized as an important human pathogen associated with superficial gastritis, atrophic gastritis, gastric cancer, *etc.*, each of which has become a serious threat to human health and survival. The rate of drug resistance is increasing due to the wide use of antibiotics and high rates of resistance to clarithromycin, metronidazole, and levofloxacin are associated with the failure of *H. pylori* eradication. At present, the mechanism of antibiotic resistance

of *H. pylori* is not completely understood. It is very difficult to prevent drug resistance and improve the rate of eradication of the target, thus warranting exploration of the mechanism of drug resistance to *H. pylori*, and provision of an experimental basis for the prevention and treatment of drug resistance.

Research motivation

Currently, there is a serious drug resistance situation in *H. pylori* and new antibiotics are urgently needed; however, antibiotic research and development are very difficult. If we can understand the antibacterial mechanism of linolenic acid-metronidazole (Lla-Met), we can better apply it to antimicrobial treatment and solve the problem of antibiotic resistance.

Research objectives

The objectives of this study were to confirm the antibacterial effect of Lla-Met on *H. pylori*, and to provide theoretical support for further research and development of Lla-Met as an anti-*H. pylori* drug, and to help overcome the resistance of *H. pylori* to existing antibiotic drugs.

Research methods

H. pylori cells were treated with the Lla-Met compound, and the effect of the compound on the cell morphology, cell membrane permeability, and oxidation of the bacteria cell was assessed by scanning electron microscope, propidium iodide staining, FIFC-FD, detection of ion channels, detection of intracellular reactive oxygen species, and detection of phosphatidylserine ectropion. Meanwhile, the differently expressed genes in H. pylori in response to Lla-Met treatment were identified by transcriptome sequencing and quantitative real-time polymerase chain reaction.

Research results

The expression of both *SodB* and *MdaB* genes was up-regulated after treatment with Lla-Met, and both genes are associated with antioxidants. Lla-Met inhibits the growth of *H. pylori* through oxidation.

Research conclusions

The mechanism of linoleic-metronidazole compound was demonstrated to involve inhibiting *H. pylori* growth by inducing excessive reactive oxygen species accumulation, resulting in excessive superoxide dismutase *MdaB* and *SodB* genes expression.

Research perspectives

This study proves the antibacterial effect of Lla-Met on *H. pylori* at the molecular level, providing theoretical support for further research and development of Lla-Met as an anti-*H. pylori* drug to help overcome *H. pylori* resistance to current antibiotic drugs.

FOOTNOTES

Author contributions: Zhou WT and Dai YY consulted literature, performed experiments, collected and analyzed data and wrote the first draft, making equal contributions to this work; Liao LJ, Yang SX, and Chen H corrected it; Zhao LJ, Huang YQ, and Huang L designed, checked, modified, and completed the manuscript, making equal contributions to this work as co-corresponding authors; Huang L is the first corresponding author; and all authors approved the final version of the article.

Institutional review board statement: The study was reviewed and approved by the Institutional Review Board at Youjiang Medical University for Nationalities.

Conflict-of-interest statement: All the authors report no relevant conflicts of interest for this article.

Data sharing statement: No additional data are available.

Open-Access: This article is an open-access article that was selected by an in-house editor and fully peer-reviewed by external reviewers. It is distributed in accordance with the Creative Commons Attribution NonCommercial (CC BY-NC 4.0) license, which permits others to distribute, remix, adapt, build upon this work non-commercially, and license their derivative works on different terms, provided the original work is properly cited and the use is non-commercial. See: https://creativecommons.org/Licenses/by-nc/4.0/

Country/Territory of origin: China

ORCID number: Wen-Ting Zhou 0009-0004-0575-1126; Yuan-Yuan Dai 0000-0002-5522-4154; Li-Juan Liao 0000-0003-0547-2026; Shi-Xian Yang 0009-0001-4377-4562; Hao Chen 0000-0003-0760-3552; Juan-Li Zhao 0000-0003-0485-0179; Yan-Qiang Huang 0000-0002-0867-0178; Liang Huang 0000-0001-7937-8150.

S-Editor: Wang JJ
L-Editor: A
P-Editor: Chen YX

REFERENCES

1 **Reshetnyak VI**, Reshetnyak TM. Significance of dormant forms of Helicobacter pylori in ulcerogenesis. *World J Gastroenterol* 2017; **23**: 4867-4878 [PMID: 28785141 DOI: 10.3748/wjg.v23.i27.4867]

2 **Kuipers EJ**. Helicobacter pylori and the risk and management of associated diseases: gastritis, ulcer disease, atrophic gastritis and gastric cancer. *Aliment Pharmacol Ther* 1997; **11** Suppl 1: 71-88 [PMID: 9146793 DOI: 10.1046/j.1365-2036.11.s1.5.x]

3 **Crowe SE**. Helicobacter pylori Infection. *N Engl J Med* 2019; **380**: 1158-1165 [PMID: 30893536 DOI: 10.1056/NEJMcp1710945]

4 **Yamaoka Y**. How to eliminate gastric cancer-related death worldwide? *Nat Rev Clin Oncol* 2018; **15**: 407-408 [PMID: 29700378 DOI: 10.1038/s41571-018-0029-8]

5 **Couturier MR**, Marshall BJ, Goodman KJ, Mégraud F. Helicobacter pylori diagnostics and treatment: could a lack of universal consensus be the best consensus? *Clin Chem* 2014; **60**: 589-594 [PMID: 23908455 DOI: 10.1373/clinchem.2012.201475]

6 **Kanizaj TF**, Kunac N. Helicobacter pylori: future perspectives in therapy reflecting three decades of experience. *World J Gastroenterol* 2014; **20**: 699-705 [PMID: 24574743 DOI: 10.3748/wjg.v20.i3.699]

7 **Thung I**, Aramin H, Vavinskaya V, Gupta S, Park JY, Crowe SE, Valasek MA. Review article: the global emergence of Helicobacter pylori antibiotic resistance. *Aliment Pharmacol Ther* 2016; **43**: 514-533 [PMID: 26694080 DOI: 10.1111/apt.13497]

8 **Hu Y**, Zhu Y, Lu NH. Novel and Effective Therapeutic Regimens for Helicobacter pylori in an Era of Increasing Antibiotic Resistance. *Front Cell Infect Microbiol* 2017; **7**: 168 [PMID: 28529929 DOI: 10.3389/fcimb.2017.00168]

9 **Fallone CA**, Moss SF, Malfertheiner P. Reconciliation of Recent Helicobacter pylori Treatment Guidelines in a Time of Increasing Resistance to Antibiotics. *Gastroenterology* 2019; **157**: 44-53 [PMID: 30998990 DOI: 10.1053/j.gastro.2019.04.011]

10 **Suzuki S**, Esaki M, Kusano C, Ikehara H, Gotoda T. Development of Helicobacter pylori treatment: How do we manage antimicrobial resistance? *World J Gastroenterol* 2019; **25**: 1907-1912 [PMID: 31086459 DOI: 10.3748/wjg.v25.i16.1907]

11 **Tshibangu-Kabamba E**, Yamaoka Y. Helicobacter pylori infection and antibiotic resistance - from biology to clinical implications. *Nat Rev Gastroenterol Hepatol* 2021; **18**: 613-629 [PMID: 34002081 DOI: 10.1038/s41575-021-00449-x]

12 **Desbois AP**, Smith VJ. Antibacterial free fatty acids: activities, mechanisms of action and biotechnological potential. *Appl Microbiol Biotechnol* 2010; **85**: 1629-1642 [PMID: 19956944 DOI: 10.1007/s00253-009-2355-3]

13 **Thamphiwatana S**, Gao W, Obonyo M, Zhang L. In vivo treatment of Helicobacter pylori infection with liposomal linolenic acid reduces colonization and ameliorates inflammation. *Proc Natl Acad Sci U S A* 2014; **111**: 17600-17605 [PMID: 25422427 DOI: 10.1073/pnas.1418230111]

14 **Dai YY**, Qin C, Huang GR, Qin YC, Huang YY, Huang YQ, Zhao LJ. Linolenic Acid-Metronidazole: a Compound Relieving Drug Resistance and Inhibiting Helicobacter pylori. *Antimicrob Agents Chemother* 2022; **66**: e0007322 [PMID: 35758720 DOI: 10.1128/aac.00073-22]

15 **Hakansson AP**, Roche-Hakansson H, Mossberg AK, Svanborg C. Apoptosis-like death in bacteria induced by HAMLET, a human milk lipid-protein complex. *PLoS One* 2011; **6**: e17717 [PMID: 21423701 DOI: 10.1371/journal.pone.0017717]

16 **Nissenkorn I**, Sluzker D, Jaffee A, Servadio C. [Life with an ileal conduit: a long-term follow-up]. *Harefuah* 1986; **111**: 6-8 [PMID: 3781382 DOI: 10.3390/ijms20040850]

17 **Dai G**, Cheng N, Dong L, Muramatsu M, Xiao S, Wang MW, Zhu DX. Bactericidal and morphological effects of NE-2001, a novel synthetic agent directed against Helicobacter pylori. *Antimicrob Agents Chemother* 2005; **49**: 3468-3473 [PMID: 16048962 DOI: 10.1128/AAC.49.8.3468-3473.2005]

18 **Jiamboonsri P**, Pithayanukul P, Bavovada R, Chomnawang MT. The inhibitory potential of Thai mango seed kernel extract against methicillin-resistant Staphylococcus aureus. *Molecules* 2011; **16**: 6255-6270 [PMID: 21788933 DOI: 10.3390/molecules16086255]

19 **Hwang JH**, Jin Q, Woo ER, Lee DG. Antifungal property of hibicuslide C and its membrane-active mechanism in Candida albicans. *Biochimie* 2013; **95**: 1917-1922 [PMID: 23816874 DOI: 10.1016/j.biochi.2013.06.019]

20 **Choi H**, Lee DG. Antifungal activity and pore-forming mechanism of astacidin 1 against Candida albicans. *Biochimie* 2014; **105**: 58-63 [PMID: 24955933 DOI: 10.1016/j.biochi.2014.06.014]

21 **Akhtar F**, Khan AU, Misba L, Akhtar K, Ali A. Antimicrobial and antibiofilm photodynamic therapy against vancomycin resistant Staphylococcus aureus (VRSA) induced infection in vitro and in vivo. *Eur J Pharm Biopharm* 2021; **160**: 65-76 [PMID: 33508436 DOI: 10.1016/j.ejpb.2021.01.012]

22 **Lee H**, Lee DG. Gold nanoparticles induce a reactive oxygen species-independent apoptotic pathway in Escherichia coli. *Colloids Surf B Biointerfaces* 2018; **167**: 1-7 [PMID: 29625418 DOI: 10.1016/j.colsurfb.2018.03.049]

23 **Kim H**, Lee DG. Lupeol-induced nitric oxide elicits apoptosis-like death within Escherichia coli in a DNA fragmentation-independent manner. *Biochem J* 2021; **478**: 855-869 [PMID: 33522568 DOI: 10.1042/BCJ20200925]

24 **Pérez-Lara Á**, Thapa A, Nyenhuis SB, Nyenhuis DA, Halder P, Tietzel M, Tittmann K, Cafiso DS, Jahn R. PtdInsP(2) and PtdSer cooperate to trap synaptotagmin-1 to the plasma membrane in the presence of calcium. *Elife* 2016; **5** [PMID: 27791979 DOI: 10.7554/eLife.15886]

25 **Obonyo M**, Zhang L, Thamphiwatana S, Pornpattananangkul D, Fu V. Antibacterial activities of liposomal linolenic acids against antibiotic-resistant Helicobacter pylori. *Mol Pharm* 2012; **9**: 2677-2685 [PMID: 22827534 DOI: 10.1021/mp300243w]

26 **Huang Y**, Hang X, Jiang X, Zeng L, Jia J, Xie Y, Li F, Bi H. In Vitro and In Vivo Activities of Zinc Linolenate, a Selective Antibacterial Agent against Helicobacter pylori. *Antimicrob Agents Chemother* 2019; **63** [PMID: 30936098 DOI: 10.1128/AAC.00004-19]

27 **Zorov DB**, Juhaszova M, Sollott SJ. Mitochondrial reactive oxygen species (ROS) and ROS-induced ROS release. *Physiol Rev* 2014; **94**: 909-950 [PMID: 24987008 DOI: 10.1152/physrev.00026.2013]

28 **Taylor RC**, Cullen SP, Martin SJ. Apoptosis: controlled demolition at the cellular level. *Nat Rev Mol Cell Biol* 2008; **9**: 231-241 [PMID: 18073771 DOI: 10.1038/nrm2312]

29 **Roche-Hakansson H**, Vansarla G, Marks LR, Hakansson AP. The human milk protein-lipid complex HAMLET disrupts glycolysis and induces death in Streptococcus pneumoniae. *J Biol Chem* 2019; **294**: 19511-19522 [PMID: 31694917 DOI: 10.1074/jbc.RA119.009930]

30 **Erental A**, Kalderon Z, Saada A, Smith Y, Engelberg-Kulka H. Apoptosis-like death, an extreme SOS response in Escherichia coli. *mBio* 2014; **5**: e01426-e01414 [PMID: 25028428 DOI: 10.1128/mBio.01426-14]

World Journal of Gastroenterology

Submit a Manuscript: https://www.f6publishing.com

World J Gastroenterol 2023 August 28; 29(32): 4873-4882

DOI: 10.3748/wjg.v29.i32.4873

ISSN 1007-9327 (print) ISSN 2219-2840 (online)

ORIGINAL ARTICLE

Retrospective Cohort Study

Validation of the albumin-bilirubin score for identifying decompensation risk in patients with compensated cirrhosis

Huttakan Navadurong, Kessarin Thanapirom, Salisa Wejnaruemarn, Thaninee Prasoppokakorn, Roongruedee Chaiteerakij, Piyawat Komolmit, Sombat Treeprasertsuk

Specialty type: Gastroenterology and hepatology

Provenance and peer review: Unsolicited article; Externally peer reviewed.

Peer-review model: Single blind

Peer-review report's scientific quality classification

Grade A (Excellent): 0
Grade B (Very good): B, B
Grade C (Good): C
Grade D (Fair): D
Grade E (Poor): 0

P-Reviewer: Grgurevic I, Croatia; Gupta R, India; Reshetnyak VI, Russia; Yang XR, China

Received: May 21, 2023
Peer-review started: May 21, 2023
First decision: July 10, 2023
Revised: July 20, 2023
Accepted: August 9, 2023
Article in press: August 9, 2023
Published online: August 28, 2023

Huttakan Navadurong, Kessarin Thanapirom, Salisa Wejnaruemarn, Thaninee Prasoppokakorn, Roongruedee Chaiteerakij, Piyawat Komolmit, Sombat Treeprasertsuk, Division of Gastroenterology, Department of Medicine, Faculty of Medicine, Chulalongkorn University and King Chulalongkorn Memorial Hospital, Thai Red Cross Society, Bangkok 10330, Thailand

Thaninee Prasoppokakorn, Department of Medicine, Queen Savang Vadhana Memorial Hospital, Chonburi 20110, Thailand

Corresponding author: Sombat Treeprasertsuk, MD, PhD, Professor, Division of Gastroenterology, Department of Medicine, Faculty of Medicine, Chulalongkorn University and King Chulalongkorn Memorial Hospital, Thai Red Cross Society, 1873 Rama 4 Road, Pathumwan District, Bangkok 10330, Thailand. battan5410@gmail.com

Abstract

BACKGROUND

The albumin-bilirubin (ALBI) score is an index of liver function recently developed to assess prognosis in patients with hepatocellular carcinoma (HCC). It can detect small changes in liver dysfunction and has been successfully applied to the prediction of survival in patients with non-malignant liver diseases of various etiologies.

AIM

To investigate the ALBI score for identifying decompensation risk at the 3-year follow-up in patients with compensated cirrhosis.

METHODS

One-hundred and twenty-three patients with compensated cirrhosis without HCC in King Chulalongkorn Memorial Hospital diagnosed by imaging were retrospectively enrolled from January 2016 to December 2020. A total of 113 patients (91.9%) had Child A cirrhosis with a median model for end-stage liver disease (MELD) score of less than 9. Baseline clinical and laboratory variables and decompensation events were collected. The ALBI score was calculated and validated to classify decompensation risk into low-, middle-, and high-risk groups using three ALBI grade ranges (ALBI grade 1: ≤ -2.60; grade 2: > -2.60 but ≤ -1.39; grade 3: > -1.39). Decompensation events were defined as ascites development, variceal bleeding, or grade 3 or 4 hepatic encephalopathy.

RESULTS

Among 123 cirrhotic patients enrolled, 13.8% (n = 17) developed decompensating events at a median time of 25 [95% confidence interval (CI): 17-31] mo. Median baseline ALBI score in compensated cirrhosis was significantly lower than that of patients who developed decompensation events [-2.768 (-2.956 to -2.453) *vs* -2.007 (-2.533 to -1.537); P = 0.01]. Analysis of decompensation risk at 3 years showed that ALBI score had a time-dependent area under the curve (tAUC) of 0.86 (95%CI: 0.78-0.92), which was significantly better than that of ALBI-Fibrosis-4 (ALBI-FIB4) score (tAUC = 0.77), MELD score (tAUC = 0.66), Child-Pugh score (tAUC = 0.65), and FIB-4 score (tAUC = 0.48) (P < 0.05 for all). The 3-year cumulative incidence of decompensation was 3.1%, 22.6%, and 50% in the low-, middle-, and high-risk groups, respectively (P < 0.001). The odds ratio for decompensation in patients of the high-risk group was 23.33 (95%CI: 3.88-140.12, P = 0.001).

CONCLUSION

The ALBI score accurately identifies decompensation risk at the 3-year follow-up in patients with compensated cirrhosis. Those cirrhotic patients with a high-risk grade of ALBI score showed a 23 times greater odds of decompensation.

Key Words: Albumin-bilirubin score; Compensated cirrhosis; Hepatic decompensation risk

©The Author(s) 2023. Published by Baishideng Publishing Group Inc. All rights reserved.

Core Tip: The albumin-bilirubin (ALBI) score has been successfully applied to the prediction of survival in patients with non-malignant liver diseases of various etiologies. This study demonstrated that the ALBI score can accurately identify decompensation risk at the 3-year follow-up in patients with compensated cirrhosis. The ALBI score is a simple and ready-to-use tool to help clinicians monitor and make appropriate treatment strategies in patients with compensated cirrhosis.

Citation: Navadurong H, Thanapirom K, Wejnaruemarn S, Prasoppokakorn T, Chaiteerakij R, Komolmit P, Treeprasertsuk S. Validation of the albumin-bilirubin score for identifying decompensation risk in patients with compensated cirrhosis. *World J Gastroenterol* 2023; 29(32): 4873-4882

URL: https://www.wjgnet.com/1007-9327/full/v29/i32/4873.htm

DOI: https://dx.doi.org/10.3748/wjg.v29.i32.4873

INTRODUCTION

Cirrhosis is the end stage of chronic liver disease which is currently the 11th leading cause of death and 15th leading cause of morbidity across the world, accounting for 2.2% of deaths and 1.5% of disability-adjusted life years worldwide[1]. The disease evolves from an asymptomatic phase as compensated cirrhosis to a symptomatic phase as decompensated cirrhosis[2]. Decompensated cirrhosis is defined by the presence of variceal bleeding, encephalopathy, ascites, hepatorenal syndrome, and/or jaundice[3]. Transition from a compensated to a decompensated stage occurs at a rate of 5%-7% per year[4]. Median survival of patients with compensated cirrhosis is 12 years, while that of decompensated patients is less than 2 years[5]. Once decompensation has occurred, mortality without transplant is as high as 85% over 5 years[4].

For over 60 years, the best predictor of decompensation in cirrhotic patients has been the hepatic venous pressure gradient (HVPG)[6]. HVPG has a greater discriminative ability to predict clinical decompensation in patients with compensated cirrhosis than either the model for end-stage liver disease (MELD) or Child-Pugh score. Research shows that patients with a HVPG < 10 mmHg have a 90% probability of not developing clinical decompensation in a median follow-up of 4 years[6]. However, HVPG measurement is invasive, requires specialized healthcare personnel, and is often unavailable in many healthcare systems. The appearance of noninvasive tests, most notably, transient elastography, has provided a staging tool for prognostic markers of portal hypertension[7]. Recently, Baveno VII criteria were developed using transient elastography for liver stiffness measurements and platelet counts to define clinically significant portal hypertension and prognosis, risk stratification, and indication to start beta-blocker therapy in compensated advanced chronic liver disease and compensated cirrhosis patients[8]. Within a median follow-up of 40 mo, 7.2% of the 1159 compensated advanced chronic liver disease and compensated cirrhosis patients developed an initial decompensation event[8].

Well-known prognostic scoring systems that are currently used such as the MELD score and Child-Pugh score were primarily established to predict mortality in patients with cirrhosis. The Child-Pugh score was originally developed to assess the survival of cirrhotic patients undergoing shunt surgery to relieve portal hypertension in order to treat variceal bleeding[9,10]. The MELD score was developed to more precisely evaluate 3-mo mortality for patients with cirrhosis in order to prioritize liver donor allocation[11]. The MELD score is considered more reproducible than the Child-Pugh score because it does not include subjective variables such as ascites and encephalopathy. However, the MELD score has not been shown to be superior to the Child-Pugh score in terms of predictive accuracy in different cirrhotic populations[12].

Many studies have attempted to evaluate or develop a prognostic scoring system for predicting the risk of decompensation in a patient with compensated cirrhosis based on clinical and laboratory parameters. Well-known scoring systems such as MELD, Child-Pugh, Fibrosis-4 (FIB-4) scores and newly developed scoring system such as albumin-bilirubin FIB-4 (ALBI-FIB4) score which combine the ALBI score and FIB-4 score were evaluated for predicting the risk of decompensation in a patient with compensated cirrhosis. Prior studies show that the ALBI-FIB4 score can identify a high-risk patient more accurately than MELD, Child-Pugh and FIB-4 scores[13-15].

The ALBI score was recently created and validated to specifically assess hepatocellular carcinoma (HCC) liver functional reserve for predicting survival of HCC patients receiving various treatment modalities[16]. The ALBI grade was calculated using albumin and bilirubin levels. Its application has been increasingly expanded to chronic liver disease in general and has proven remarkably accurate in terms of prognosis[17]. Many publications have shown that the ALBI score is highly prognostic in cirrhotic patients and has shown the ability to correlate to HVPG levels[18], predicting the presence of gastroesophageal varices and stratifying bleeding risk[19], and severe portopulmonary hypertension[20].

Since the utility of ALBI score in predicting decompensation risk in patients with compensated cirrhosis has yet been fully investigated, we aimed to evaluate the ALBI score's ability to identify decompensation risk at 3 years follow-up in patients with compensated cirrhosis.

MATERIALS AND METHODS

Patients with compensated cirrhosis receiving care at King Chulalongkorn Memorial Hospital from January 2016 to December 2020 were enrolled retrospectively. The diagnosis of cirrhosis was made by imaging with ultrasonography, multiphasic contrast-enhanced computed tomography, or gadoxetic acid-enhanced magnetic resonance imaging. Patients with missing data, HCC at baseline, or a history of hepatic decompensation at the time of diagnosis were excluded. Baseline characteristics of patients including age, sex, and etiologies of cirrhosis were obtained from medical records. Laboratory data including serum creatinine, albumin, bilirubin, aspartate transaminase (AST), alanine transaminase (ALT), platelets, and international normalized ratio (INR) were collected.

Decompensation events, defined as ascites development, variceal bleeding, or grade 3 or 4 hepatic encephalopathy, were ascertained by clinicians in charge of their care and supported with either endoscopy reports, abdominal imaging, or medical reports. Time to decompensation was calculated from date of study entry until date of first recorded decompensation.

The ALBI score at baseline was calculated using the equation (log10 bilirubin in μmol/L × 0.66) + [albumin in g/L × (-0.085)][16] and validated to categorize decompensation risk into low-, middle-, and high-risk groups classified by ALBI grades 1, 2, and 3. The cut points of ALBI grades were similar to those in HCC patients: ALBI grade 1: ≤ -2.60; grade 2: > -2.60 but ≤ -1.39; grade 3: > -1.39.

Statistical analysis

For baseline characteristics, continuous variables with a normal distribution are presented as the mean ± SD, while those with a non-normal distribution are presented as median and interquartile range (IQR). The Mann-Whitney *U* test was used to compare differences in continuous variables while Fisher's exact test was used to assess for significant differences in binomial variables. Time to decompensation according to baseline ALBI grade and overall survival following the first decompensation were examined by Kaplan-Meier graphs and compared using the log-rank test. Cox proportional hazards analysis was used to identify ALBI score and other potential factors associated with decompensation. Significant factors identified in the univariate analysis were included in the multivariate analysis. The odds ratio (OR) calculated by logistic regression analysis provided estimates of the change in decompensation odds at each ALBI grade at baseline. The time-dependent area under the curve (tAUC) was estimated to evaluate the ability of each prognostic score to predict decompensation. A *P*-value of < 0.05 was considered statistically significant. All statistical analyses were performed using IBM SPSS Statistics version 22.

RESULTS

A total of 123 compensated cirrhotic patients were enrolled in our study. Table 1 summarizes their baseline characteristics. Mean age was 63.9 years (SD: 12.3), and 72 (58.5%) patients were male. Mean body mass index was 24.5 kg/m^2 (SD: 3.7). Viral hepatitis B was the most common etiology of cirrhosis (n = 43, 35%), followed by viral hepatitis C (n = 30, 24.4%), nonalcoholic steatohepatitis (NASH) (n = 29, 23.6%), alcohol liver disease (n = 19, 15.4%), and autoimmune hepatitis (n = 2, 1.6%). All patients with viral hepatitis B or viral hepatitis C received antiviral treatment with a sustained virological response. For patients with NASH, 17 (58.6%) patients had diabetes mellitus and 15 (51.7%) patients were obese. At baseline, 113 (91.9%) patients had Child-Pugh class A with 91 (80.5%) and 22 (19.5%) patients having a Child-Pugh score of 5 and 6, respectively, and 10 (8.1%) had Child-Pugh class B. For ALBI grade at baseline, 64 (52%) patients had ALBI grade 1, 53 (43.1%) had ALBI grade 2, and 6 (4.9%) had ALBI grade 3. Median prognostic scores predicting first decompensation at baseline were: MELD score (8.7; IQR: 7.8-10.1), ALBI score (-2.63; IQR: -2.91 to -2.06), ALBI-FIB4 score (-2.79; IQR: -3.28 to -1.93), and FIB-4 score (3.2; IQR: 1.8-5.3).

Table 1 Baseline characteristics of patients with compensated cirrhosis, *n* (%)

Variable	*n* = 123
Age, yr, mean (SD)	63.9 (12.3)
Male	72 (58.5)
Body mass index, kg/m^2, mean (SD)	24.5 (3.7)
Obesity	54 (43.9)
Diabetes	33 (26.8)
Etiology of disease	
HBV	43 (35)
HCV	30 (24.4)
NASH	29 (23.6)
Alcohol	19 (15.4)
Autoimmune hepatitis	2 (1.6)
Laboratory data	
Creatinine, mg/dL, median (IQR)	0.8 (0.7-0.9)
Albumin, g/dL, median (IQR)	4 (3.4-4.3)
Bilirubin, mg/dL, median (IQR)	0.9 (0.6-1.5)
AST, U/L, median (IQR)	44 (28-66)
ALT, U/L, median (IQR)	33 (24-58)
Platelets, × 10^9/L, median (IQR)	142 (104-200)
INR, median (IQR)	1.1 (1-1.2)
Child-Pugh grade	
A	113 (91.9)
B	10 (8.1)
Decompensation event	17 (13.8)
Variceal bleeding	8 (47)
Ascites development	5 (29.4)
Grade 3 or 4 hepatic encephalopathy	4 (23.6)
MELD, median (IQR)	8.7 (7.8-10.1)
ALBI score, median (IQR)	-2.63 (-2.91 to -2.06)
ALBI grade	
1	64 (52)
2	53 (43.1)
3	6 (4.9)
ALBI-FIB4 score, median (IQR)	-2.79 (-3.28 to -1.93)
FIB-4 score, median (IQR)	3.2 (1.8-5.3)

NASH: Nonalcoholic steatohepatitis; HBV: Hepatitis B virus; HCV: Hepatitis C virus; AST: Aspartate transaminase; ALT: Alanine transaminase; INR: International normalized ratio; MELD: Model for end-stage liver disease; ALBI: Albumin-bilirubin; FIB-4: Fibrosis-4; SD: Standard deviation; IQR: Interquartile range

Predictors of decompensation in patients with compensated cirrhosis

During a median follow-up of 36 (IQR: 35-36) mo, 17 (13.8%) patients developed an initial decompensation event within 3 years follow-up at a median time of 25 [95% confidence interval (CI): 17-31] mo. Events included variceal bleeding in eight (47%) patients, ascites in five (29.4%), and grade 3 or 4 hepatic encephalopathy in four (23.6%). Among the 17 patients who experienced decompensating events, the most common precipitants of hepatic decompensation were

gastrointestinal bleeding (n = 8, 47%), followed by infection (n = 1, 6%). However, in eight (47%) of the patients who developed decompensating events, no specific cause of decompensation could be identified. The eight patients who experienced variceal bleeding received a combination of endoscopic treatment, intravenous octreotide, and antibiotic prophylaxis. Treatment for ascites in the five affected patients involved a combination of spironolactone and furosemide, with one patient requiring abdominal paracentesis due to tense ascites. All the four patients with grade 3 or 4 hepatic encephalopathy were treated with lactulose. Additionally, the patient who experienced decompensation due to infection received intravenous antibiotic therapy. Overall survival following the first decompensation was 82.4% at 3 years. The median overall survival of patients who developed the first decompensation was 29.9 (95%CI: 23.7-36.0) mo.

In compensated cirrhotic patients who developed an initial decompensation, albumin, bilirubin, ALT, ALBI, MELD, ALBI-FIB4, and Child-Pugh scores were found to be associated with initial decompensation, with an hazard ratio (HR) of 0.10 (95%CI: 0.03-0.26, P < 0.001), 1.21 (95%CI: 1.02-1.43, P = 0.02), 1.01 (95%CI: 1.00-1.02, P = 0.01), 8.31 (95%CI: 3.48-19.85, P < 0.001), 1.11 (95%CI: 1.02-1.21, P = 0.01), 2.30 (95%CI: 1.60-3.31, P < 0.001), and 1.98 (95%CI: 1.15-3.39, P = 0.01), respectively. In the multivariate analysis, ALBI score remained independently associated with initial decompensation with an adjusted HR of 4.18 (95%CI: 1.40-12.53) (P = 0.01) (Table 2).

Performance of each prognostic score for predicting decompensation at 3-year follow-up

An analysis of decompensation risk at the 3-year follow-up demonstrated that ALBI score had an tAUC of 0.86 (95%CI: 0.78-0.92), which performed significantly better than ALBI-FIB4 (tAUC = 0.77), MELD (tAUC = 0.66), Child-Pugh (tAUC = 0.65), or FIB-4 scores (tAUC = 0.48) (P < 0.05 for all) (Table 3 and Figure 1).

Decompensation risk stratification based on ALBI grade

In patients who developed a decompensation event, the majority were in the middle-risk group (n = 12, 70.6%), two in low-risk group (11.8%), and three in high-risk group (17.6%) according to the ALBI grade (Table 4). Median baseline ALBI score in the decompensated cirrhosis group was significantly higher than that of the compensated cirrhosis group [-2.768 (-2.956 to -2.453) *vs* -2.007 (-2.533 to -1.537), P = 0.01]. The cumulative incidence of decompensation at 3 years was 3.1% in the low-risk group, 22.6% in the middle-risk group, and 50% in the high-risk group (P = 0.003 and P < 0.001, respectively) (Table 4). The OR for decompensation in patients in the high-risk and middle-risk groups was 23.33 (95%CI: 3.88-140.12, P = 0.001) and 7.83 (95%CI: 1.75-35.01, P = 0.007), respectively (Table 4). Patients in the high-risk group exhibited a significantly shorter time to the initial decompensation compared to those in both the middle-risk and low-risk groups [26.5 mo (95%CI: 18.5-34.5), 33.2 mo (95%CI: 31.5-35.1), and 35.5 mo (95%CI: 34.7-36.2), respectively (P < 0.001)] (Figure 2).

Regarding the etiology of liver disease within each decompensation risk group, viral hepatitis was found in a significantly higher number of patients within the low-risk group compared to the middle and high-risk groups, with 45 (61%), 24 (32.9%), and 4 (5.5%) patients, respectively (P = 0.02). However, there was no statistically significant difference in the prevalence of NASH, alcohol-related liver disease, or autoimmune hepatitis among the decompensation risk groups.

DISCUSSION

This study validated the ALBI score as an accurate prognostic tool to stratify patients with compensated cirrhosis for the risk of decompensation at the 3-year follow-up. The ALBI grade identified high-risk patients more effectively than either MELD, Child-Pugh, ALBI-FIB4, or FIB-4 score.

Novel scoring systems have been developed for prognostic stratification risk of decompensation among patients with compensated cirrhosis over a medium- or long-term follow-up period. One novel scoring system focusing on liver stiffness and measured by transient elastography, presence of gastroesophageal varices from endoscopic screening, albumin, and platelets, has shown excellent accuracy in predicting risk of decompensation at the 3-year follow-up with a tAUC of 0.89. This performance was significantly higher than that of ALBI-FIB-4, Baveno VII criteria, or MELD score. ALBI grade score maintained a tAUC of over 0.8 throughout the 5-year follow-up period[15]. Other novel scoring systems, which consisted of simple and routinely performed serum marker-based scores such as AST, ALT, albumin, bilirubin, and platelets, have also shown an effective ability to identify high-risk patients for the risk of decompensation. The tAUC ranged from 0.69-0.80 using these scoring systems, which was significantly higher than that of the MELD or Child-Pugh score[14,21].

The ALBI score was recently developed to assess liver functional reserve and prognosis among HCC patients[16]. It offers a simple, evidence-based, objective, and discriminatory method that has been extensively tested with an international cohort and enables more detailed prognostic classification than the Child-Pugh grade[16]. Due to the fact that ALBI is simple to calculate needing only albumin and bilirubin measures, application of ALBI has been increasingly extended to other chronic liver diseases including decompensation for liver cirrhosis[17]. Several studies reported that ALBI might be comparable to MELD for predicting short-term mortality, but better than MELD in predicting longer-term mortality in patients with decompensated cirrhosis[22-25]. Recently, one study that evaluated the correlation between the ALBI score and portal pressure in cirrhotic patients showed that ALBI had a better correlation with HVPG compared to MELD, Child-Pugh, FIB-4, and aminotransferase/platelet ratio index scores with a tAUC of 0.72 (P < 0.001)[18]. This study also showed that ALBI grade 3 was able to predict early mortality in patients with a MELD score lower than 14. Based on the pathophysiology of decompensated cirrhosis, which involves an elevation in portal pressure, it has been observed that when the HVPG surpasses 10 mmHg, it correlates with the occurrence of decompensation[26], Therefore, the ALBI score exhibits potential in predicting decompensation by virtue of its correlation with HVPG. However, this study had a higher

Table 2 Predictors of decompensation in patients with compensated cirrhosis

Variable	Univariate		Multivariate	
	Hazard ratio (95%CI)	*P* value	Adjusted hazard ratio (95%CI)	*P* value
Age	1.01 (0.97-1.05)	0.47	1.01 (0.97-1.06)	0.56
Male	0.58 (0.22-1.50)	0.26	0.55 (0.18-1.69)	0.29
Creatinine	1.20 (0.83-1.74)	0.31		
Albumin	0.10 (0.03-0.26)	< 0.001		
Bilirubin	1.21 (1.02-1.43)	0.02		
AST	1.00 (0.99-1.00)	0.34		
ALT	1.01 (1.00-1.02)	0.01		
Platelets	0.99 (0.98-1.00)	0.27		
INR	1.58 (0.11-22.29)	0.73		
ALBI score	8.31 (3.48-19.85)	< 0.001	4.18 (1.40-12.53)	0.01
MELD score	1.11 (1.02-1.21)	0.01	1.07 (0.92-1.24)	0.34
ALBI-FIB4 score	2.30 (1.60-3.31)	< 0.001	1.73 (0.82-3.64)	0.15
FIB-4 score	1.02 (0.92-1.13)	0.67		
Child-Pugh score	1.98 (1.15-3.39)	0.01	1.26 (0.61-2.58)	0.54

AST: Aspartate transaminase; ALT: Alanine transaminase; INR: International normalized ratio; MELD: Model for end-stage liver disease; ALBI: Albumin-bilirubin; FIB-4: Fibrosis-4; CI: Confidence interval.

Table 3 Comparative performance of each prognostic score for predicting decompensation at 3 years

Prognostic score	tAUC	*P* value *vs* ALBI score
ALBI	0.86 (0.78-0.92)	Reference
MELD	0.66 (0.56-0.75)	< 0.001
ALBI-FIB4	0.77 (0.68-0.86)	0.04
FIB-4	0.48 (0.38-0.58)	< 0.001
Child-Pugh	0.65 (0.55-0.75)	< 0.001

MELD: Model for end-stage liver disease; ALBI: Albumin-bilirubin; FIB-4: Fibrosis-4; tAUC: Time-dependent area under the curve.

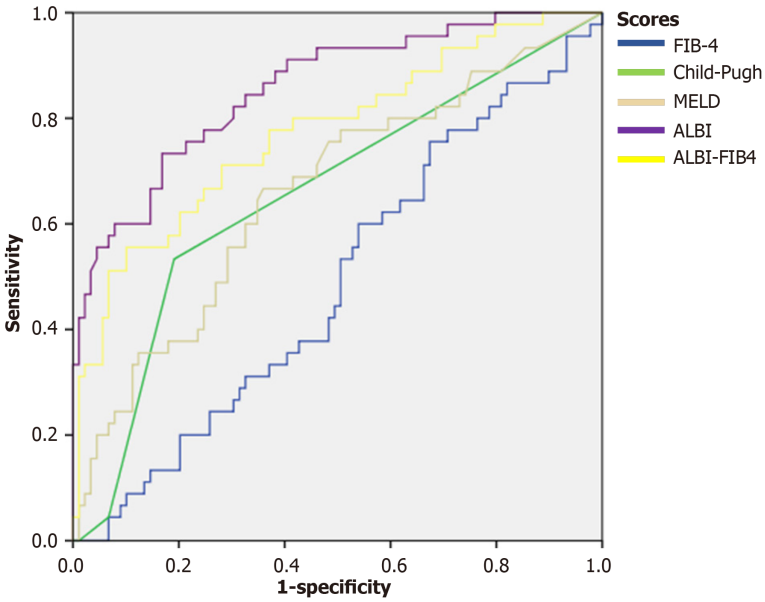
Table 4 Decompensation risk stratification based on albumin-bilirubin grade at baseline

ALBI grade	Decompensation at 3-yr (*n*, %)	*P* value	OR (95%CI)	*P* value
1	2/64 (3.1)	-	1.0 (reference)	-
2	12/53 (22.6)	0.003	7.83 (1.75-35.01)	0.007
3	3/6 (50)	< 0.001	23.33 (3.88-140.12)	0.001

ALBI: Albumin-bilirubin; OR: Odds ratio.

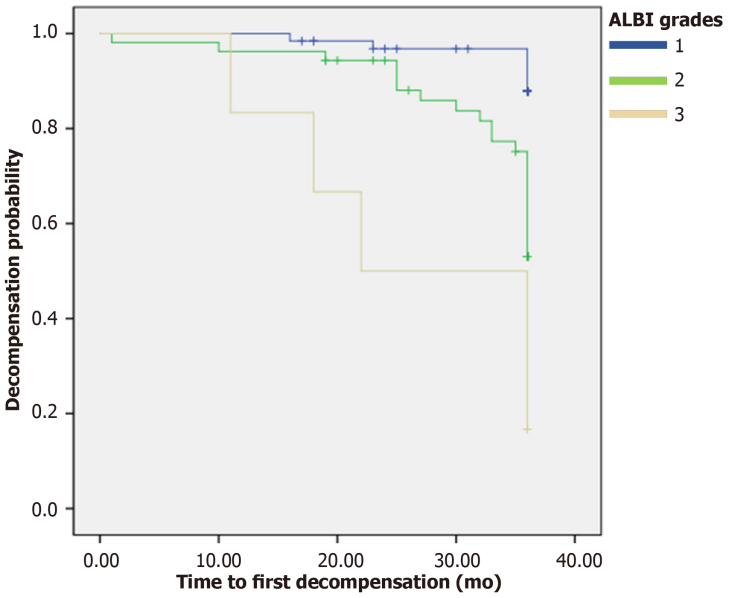
median MELD score at enrollment than our study (13 *vs* 8.7). By using ALBI grade 3 to predict decompensation stemming from increases in portal pressure, our study may need more patients with a higher MELD score at enrollment to evaluate the performance of ALBI to predict decompensation due to an increase in HVPG.

Our study found that the odds of decompensation in patients of the high-risk group was 23.33 times higher compared to patients in the lower risk group. The small sample size of the high-risk group and the high dispersion of ALBI score causes the precision of the OR in our study to be low. Thus, we need a greater number of high-risk patients for quantitative confirmation and to more precisely analyze the predictive performance of the high-risk group.



DOI: 10.3748/wjg.v29.i32.4873 **Copyright** ©The Author(s) 2023.

Figure 1 Comparative performance of each prognostic score for predicting decompensation at 3 years. FIB-4: Fibrosis-4; MELD: Model for end-stage liver disease; ALBI: Albumin-bilirubin.



DOI: 10.3748/wjg.v29.i32.4873 **Copyright** ©The Author(s) 2023.

Figure 2 Time to decompensation using the albumin-bilirubin grade at baseline. ALBI: Albumin-bilirubin.

Although our study cohort was enrolled at a single-centered tertiary care hospital in Thailand, baseline characteristics of our patients were similar to those of cohorts used to validate other newly developed scoring systems in different countries and continents. In a cohort comprised of an Asian population[15], the most common etiology of cirrhosis was viral hepatitis B at 37.1% compared to 35% in our study cohort. Baseline MELD score and Child-Pugh score in our study cohort were similar to those of cohorts used to validate other scoring systems, where 90% of patients had Child-Pugh class A with a median MELD score ranging from 7-9[14,15,21]. The rate of decompensation in our study cohort, at 13.8%, was found to be lower compared to those of other cohorts utilizing different scoring systems, where the decompensation rates ranged between 19.3% and 26.9%[14,15,21]. This discrepancy in decompensation rates could potentially be attributed to a shorter median follow-up time in our cohort, which was 3 years, in contrast to the longer follow-up periods of 4.1 to 4.5 years observed in other cohorts[14,15,21].

Viral hepatitis accounted for 59% of patients in our cohort, all of whom received antiviral treatment resulting in a sustained virological response. Among patients with viral hepatitis, 70.3% were classified as belonging to the low-risk group. We observed a significant increase in the number of patients with viral hepatitis in the low-risk group compared to the middle and high-risk groups (P = 0.02). Consequently, 52% (n = 64) of patients in our cohort were categorized as

belonging to the low-risk group, while only 4.9% (n = 6) were classified as high-risk. This distribution can primarily be attributed to the prevalence of viral hepatitis as the underlying etiology of liver disease in our study population.

The strength of this study was that we provided the first evidence that the ALBI score accurately identified decompensation risk at the 3-year follow-up in patients with compensated cirrhosis. The ALBI score is a useful tool to help select high-risk patients to guide treatment to reduce the risk of decompensation. This study represents the ability of the ALBI score to assess liver function and liver disease progression with the advantage of being simple to calculate using only serum albumin and bilirubin levels.

This study has several limitations. First, the cohort in our study was retrospectively completely only at a single-center tertiary care hospital in Thailand. A large multi-center prospective cohort study is required to validate the ALBI score. Second, most of patients had Child-Pugh class A, suggesting that the number of patients with decompensated cirrhosis is relatively low. Thus, our findings may not be readily applicable to a population predominantly with advanced cirrhosis. Third, comparisons to other novel scoring systems that require predictors besides laboratory variables such as transient elastography and gastroesophageal varices from endoscopic findings, could not be performed due to the lack of this information in our study cohort. Inclusion of patients with prompt predictor variables to validate is required. Finally, additional data of the ALBI score including changes in annual ALBI grading or changing of ALBI grades between compensation and decompensation may give new information for the prediction of a decompensation event.

CONCLUSION

This study has documented the excellent performance of the ALBI score to accurately identify decompensation risk at the 3-year follow-up in patients with compensated cirrhosis. The ALBI score is a simple and ready-to-use tool to help clinicians monitor and make appropriate treatment decisions among patients with compensated cirrhosis.

ARTICLE HIGHLIGHTS

Research background

The albumin-bilirubin (ALBI) score is an index of liver function recently developed to assess prognosis in patients with hepatocellular carcinoma (HCC). It has been successfully applied to the prediction of survival in patients with non-malignant liver diseases of various etiologies.

Research motivation

The utility of ALBI score in predicting decompensation risk in patients with compensated cirrhosis has yet been fully investigated.

Research objectives

The objective of this study was to investigate the ALBI score for identifying decompensation risk at the 3-year follow-up in patients with compensated cirrhosis.

Research methods

One-hundred and twenty-three patients with compensated cirrhosis without HCC in King Chulalongkorn Memorial Hospital diagnosed by imaging were retrospectively enrolled from January 2016 to December 2020. The ALBI score was calculated and validated to classify decompensation risk into low-, middle-, and high-risk groups using three ALBI grade ranges (ALBI grade 1: ≤ -2.60; grade 2: > -2.60 but ≤ -1.39; grade 3: > -1.39). Decompensation events were defined as ascites development, variceal bleeding, or grade 3 or 4 hepatic encephalopathy.

Research results

Among 123 cirrhotic patients enrolled, 13.8% (n = 17) developed decompensating events at a median time of 25 [95% confidence interval (CI): 17-31] mo. Analysis of decompensation risk at 3 years showed that ALBI score had a time-dependent area under the curve (tAUC) of 0.86 (95%CI: 0.78-0.92) which was significantly better than that of ALBI-Fibrosis-4 (ALBI-FIB4) score (tAUC = 0.77), model for end-stage liver disease score (tAUC = 0.66), Child-Pugh score (tAUC = 0.65), or FIB-4 score (tAUC = 0.48) (P < 0.05 for all). The 3-year cumulative incidence of decompensation was 3.1%, 22.6% and 50% in the low-, middle-, and high-risk groups, respectively (P < 0.001). The odds ratio for decompensation in patients of the high-risk group was 23.33 (95%CI: 3.88-140.12, P = 0.001).

Research conclusions

The ALBI score accurately identifies decompensation risk at the 3-year follow-up in patients with compensated cirrhosis. Those patients with a high-risk grade of ALBI score showed a 23 times greater odds of decompensation.

Research perspectives

The ALBI score represents an outstanding non-invasive scoring system, enabling clinicians to make precise decisions regarding the monitoring and guidance of treatment for patients with compensated cirrhosis.

ACKNOWLEDGEMENTS

This work was supported by funding from the Fatty Liver Research Grant, Division of Gastroenterology, Faculty of Medicine Foundation, Chulalongkorn University. We would like to thank all the clinical and research staff from the Division of Gastroenterology, King Chulalongkorn Memorial Hospital.

FOOTNOTES

Author contributions: Navadurong H and Treeprasertsuk S designed the research, analyzed the data, and wrote the manuscript; Thanapirom K, Wejnaruemarn S, Prasoppokakorn T, Chaiteerakij R, and Komolmit P administered support; Navadurong H, Thanapirom K, Wejnaruemarn S, and Treeprasertsuk S provided the study materials; Navadurong H and Wejnaruemarn S collected and assembly the data.

Institutional review board statement: The study protocol was approved by the Institutional Review Board of the Faculty of Medicine, Chulalongkorn University (IRB No. 423/64).

Informed consent statement: The informed consent was waived.

Conflict-of-interest statement: All the authors report no relevant conflicts of interest for this article.

Data sharing statement: No additional data are available.

STROBE statement: The authors have read the STROBE Statement-checklist of items, and the manuscript was prepared and revised according to the STROBE Statement-checklist of items.

Open-Access: This article is an open-access article that was selected by an in-house editor and fully peer-reviewed by external reviewers. It is distributed in accordance with the Creative Commons Attribution NonCommercial (CC BY-NC 4.0) license, which permits others to distribute, remix, adapt, build upon this work non-commercially, and license their derivative works on different terms, provided the original work is properly cited and the use is non-commercial. See: https://creativecommons.org/Licenses/by-nc/4.0/

Country/Territory of origin: Thailand

ORCID number: Salisa Wejnaruemarn 0000-0001-8455-426X; Thaninee Prasoppokakorn 0000-0002-1012-9874; Roongruedee Chaiteerakij 0000-0002-7191-3881; Piyawat Komolmit 0000-0002-1357-9547; Sombat Treeprasertsuk 0000-0001-6459-8329.

S-Editor: Wang JJ
L-Editor: Wang TQ
P-Editor: Wang JJ

REFERENCES

1 **Cheemerla S**, Balakrishnan M. Global Epidemiology of Chronic Liver Disease. *Clin Liver Dis (Hoboken)* 2021; **17**: 365-370 [PMID: 34136143 DOI: 10.1002/cld.1061]
2 **Ginès P**, Krag A, Abraldes JG, Solà E, Fabrellas N, Kamath PS. Liver cirrhosis. *Lancet* 2021; **398**: 1359-1376 [PMID: 34543610 DOI: 10.1016/S0140-6736(21)01374-X]
3 **D'Amico G**, Garcia-Tsao G, Pagliaro L. Natural history and prognostic indicators of survival in cirrhosis: a systematic review of 118 studies. *J Hepatol* 2006; **44**: 217-231 [PMID: 16298014 DOI: 10.1016/j.jhep.2005.10.013]
4 **Schuppan D**, Afdhal NH. Liver cirrhosis. *Lancet* 2008; **371**: 838-851 [PMID: 18328931 DOI: 10.1016/S0140-6736(08)60383-9]
5 **Samonakis DN**, Koulentaki M, Coucoutsi C, Augoustaki A, Baritaki C, Digenakis E, Papiamonis N, Fragaki M, Matrella E, Tzardi M, Kouroumalis EA. Clinical outcomes of compensated and decompensated cirrhosis: A long term study. *World J Hepatol* 2014; **6**: 504-512 [PMID: 25068002 DOI: 10.4254/wjh.v6.i7.504]
6 **Ripoll C**, Groszmann R, Garcia-Tsao G, Grace N, Burroughs A, Planas R, Escorsell A, Garcia-Pagan JC, Makuch R, Patch D, Matloff DS, Bosch J; Portal Hypertension Collaborative Group. Hepatic venous pressure gradient predicts clinical decompensation in patients with compensated cirrhosis. *Gastroenterology* 2007; **133**: 481-488 [PMID: 17681169 DOI: 10.1053/j.gastro.2007.05.024]
7 **Sandrin L**, Fourquet B, Hasquenoph JM, Yon S, Fournier C, Mal F, Christidis C, Ziol M, Poulet B, Kazemi F, Beaugrand M, Palau R. Transient elastography: a new noninvasive method for assessment of hepatic fibrosis. *Ultrasound Med Biol* 2003; **29**: 1705-1713 [PMID: 14698338 DOI: 10.1016/j.ultrasmedbio.2003.07.001]
8 **de Franchis R**, Bosch J, Garcia-Tsao G, Reiberger T, Ripoll C; Baveno VII Faculty. Baveno VII - Renewing consensus in portal hypertension. *J Hepatol* 2022; **76**: 959-974 [PMID: 35120736 DOI: 10.1016/j.jhep.2021.12.022]
9 **Child CG**, Turcotte JG. Surgery and portal hypertension. *Major Probl Clin Surg* 1964; **1**: 1-85 [PMID: 4950264]
10 **Infante-Rivard C**, Esnaola S, Villeneuve JP. Clinical and statistical validity of conventional prognostic factors in predicting short-term survival among cirrhotics. *Hepatology* 1987; **7**: 660-664 [PMID: 3610046 DOI: 10.1002/hep.1840070408]
11 **Kamath PS**, Wiesner RH, Malinchoc M, Kremers W, Therneau TM, Kosberg CL, D'Amico G, Dickson ER, Kim WR. A model to predict survival in patients with end-stage liver disease. *Hepatology* 2001; **33**: 464-470 [PMID: 11172350 DOI: 10.1053/jhep.2001.22172]

12 **Durand F**, Valla D. Assessment of the prognosis of cirrhosis: Child-Pugh versus MELD. *J Hepatol* 2005; **42** Suppl: S100-S107 [PMID: 15777564 DOI: 10.1016/j.jhep.2004.11.015]

13 **Yu Q**, Xu C, Li Q, Ding Z, Lv Y, Liu C, Huang Y, Zhou J, Huang S, Xia C, Meng X, Lu C, Li Y, Tang T, Wang Y, Song Y, Qi X, Ye J, Ju S. Spleen volume-based non-invasive tool for predicting hepatic decompensation in people with compensated cirrhosis (CHESS1701). *JHEP Rep* 2022; **4**: 100575 [PMID: 36204707 DOI: 10.1016/j.jhepr.2022.100575]

14 **Guha IN**, Harris R, Berhane S, Dillon A, Coffey L, James MW, Cucchetti A, Harman DJ, Aithal GP, Elshaarawy O, Waked I, Stewart S, Johnson PJ. Validation of a Model for Identification of Patients With Compensated Cirrhosis at High Risk of Decompensation. *Clin Gastroenterol Hepatol* 2019; **17**: 2330-2338.e1 [PMID: 30716478 DOI: 10.1016/j.cgh.2019.01.042]

15 **Liu C**, Cao Z, Yan H, Wong YJ, Xie Q, Hirooka M, Enomoto H, Kim TH, Hanafy AS, Liu Y, Huang Y, Li X, Kang N, Koizumi Y, Hiasa Y, Nishimura T, Iijima H, Jung YK, Yim HJ, Guo Y, Zhang L, Ma J, Kumar M, Jindal A, Teh KB, Sarin SK, Qi X. A Novel SAVE Score to Stratify Decompensation Risk in Compensated Advanced Chronic Liver Disease (CHESS2102): An International Multicenter Cohort Study. *Am J Gastroenterol* 2022; **117**: 1605-1613 [PMID: 35973168 DOI: 10.14309/ajg.0000000000001873]

16 **Johnson PJ**, Berhane S, Kagebayashi C, Satomura S, Teng M, Reeves HL, O'Beirne J, Fox R, Skowronska A, Palmer D, Yeo W, Mo F, Lai P, Iñarrairaegui M, Chan SL, Sangro B, Miksad R, Tada T, Kumada T, Toyoda H. Assessment of liver function in patients with hepatocellular carcinoma: a new evidence-based approach-the ALBI grade. *J Clin Oncol* 2015; **33**: 550-558 [PMID: 25512453 DOI: 10.1200/JCO.2014.57.9151]

17 **Toyoda H**, Johnson PJ. The ALBI score: From liver function in patients with HCC to a general measure of liver function. *JHEP Rep* 2022; **4**: 100557 [PMID: 36124124 DOI: 10.1016/j.jhepr.2022.100557]

18 **Hsieh YC**, Lee KC, Wang YW, Yang YY, Hou MC, Huo TI, Lin HC. Correlation and prognostic accuracy between noninvasive liver fibrosismarkers and portal pressure in cirrhosis: Role of ALBI score. *PLoS One* 2018; **13**: e0208903 [PMID: 30540824 DOI: 10.1371/journal.pone.0208903]

19 **Miyamoto Y**, Enomoto H, Nishikawa H, Nishimura T, Iwata Y, Nishiguchi S, Iijima H. Association of the Modified ALBI Grade With Endoscopic Findings of Gastroesophageal Varices. *In Vivo* 2021; **35**: 1163-1168 [PMID: 33622916 DOI: 10.21873/invivo.12364]

20 **Kawaguchi T**, Honda A, Sugiyama Y, Nakano D, Tsutsumi T, Tahara N, Torimura T, Fukumoto Y. Association between the albumin-bilirubin (ALBI) score and severity of portopulmonary hypertension (PoPH): A data-mining analysis. *Hepatol Res* 2021; **51**: 1207-1218 [PMID: 34534392 DOI: 10.1111/hepr.13714]

21 **Schneider ARP**, Schneider CV, Schneider KM, Baier V, Schaper S, Diedrich C, Coboeken K, Mayer H, Gu W, Trebicka J, Blank LM, Burghaus R, Lippert J, Rader DJ, Thaiss CA, Schlender JF, Trautwein C, Kuepfer L. Early prediction of decompensation (EPOD) score: Non-invasive determination of cirrhosis decompensation risk. *Liver Int* 2022; **42**: 640-650 [PMID: 35007409 DOI: 10.1111/liv.15161]

22 **Zou D**, Qi X, Zhu C, Ning Z, Hou F, Zhao J, Peng Y, Li J, Deng H, Guo X. Albumin-bilirubin score for predicting the in-hospital mortality of acute upper gastrointestinal bleeding in liver cirrhosis: A retrospective study. *Turk J Gastroenterol* 2016; **27**: 180-186 [PMID: 27015623 DOI: 10.5152/tjg.2016.15502]

23 **Fragaki M**, Sifaki-Pistolla D, Orfanoudaki E, Kouroumalis E. Comparative evaluation of ALBI, MELD, and Child-Pugh scores in prognosis of cirrhosis: is ALBI the new alternative? *Ann Gastroenterol* 2019; **32**: 626-632 [PMID: 31700241 DOI: 10.20524/aog.2019.0417]

24 **Oikonomou T**, Goulis L, Doumtsis P, Tzoumari T, Akriviadis E, Cholongitas E. ALBI and PALBI Grades Are Associated with the Outcome of Patients with Stable Decompensated Cirrhosis. *Ann Hepatol* 2019; **18**: 126-136 [PMID: 31113581 DOI: 10.5604/01.3001.0012.7904]

25 **Wan SZ**, Nie Y, Zhang Y, Liu C, Zhu X. Assessing the Prognostic Performance of the Child-Pugh, Model for End-Stage Liver Disease, and Albumin-Bilirubin Scores in Patients with Decompensated Cirrhosis: A Large Asian Cohort from Gastroenterology Department. *Dis Markers* 2020; **2020**: 5193028 [PMID: 32148566 DOI: 10.1155/2020/5193028]

26 **Engelmann C**, Clària J, Szabo G, Bosch J, Bernardi M. Pathophysiology of decompensated cirrhosis: Portal hypertension, circulatory dysfunction, inflammation, metabolism and mitochondrial dysfunction. *J Hepatol* 2021; **75** Suppl 1: S49-S66 [PMID: 34039492 DOI: 10.1016/j.jhep.2021.01.002]

World Journal of Gastroenterology

Submit a Manuscript: https://www.f6publishing.com

World J Gastroenterol 2023 August 28; 29(32): 4883-4899

DOI: 10.3748/wjg.v29.i32.4883

ISSN 1007-9327 (print) ISSN 2219-2840 (online)

ORIGINAL ARTICLE

Retrospective Cohort Study

Different oncological features of colorectal cancer codon-specific *KRAS* mutations: Not codon 13 but codon 12 have prognostic value

Hong-Min Ahn, Duck-Woo Kim, Hyeon Jeong Oh, Hyung Kyung Kim, Hye Seung Lee, Tae Gyun Lee, Hye-Rim Shin, In Jun Yang, Jeehye Lee, Jung Wook Suh, Heung-Kwon Oh, Sung-Bum Kang

Specialty type: Oncology

Provenance and peer review: Unsolicited article; Externally peer reviewed.

Peer-review model: Single blind

Peer-review report's scientific quality classification

Grade A (Excellent): 0
Grade B (Very good): B
Grade C (Good): C, C
Grade D (Fair): 0
Grade E (Poor): 0

P-Reviewer: Malekpour A, Iran; Wang XL, China; Xie Q, China

Received: May 20, 2023
Peer-review started: May 20, 2023
First decision: June 22, 2023
Revised: July 6, 2023
Accepted: July 31, 2023
Article in press: July 31, 2023
Published online: August 28, 2023

Hong-Min Ahn, Duck-Woo Kim, Tae Gyun Lee, Hye-Rim Shin, In Jun Yang, Jeehye Lee, Jung Wook Suh, Heung-Kwon Oh, Sung-Bum Kang, Department of Surgery, Seoul National University Bundang Hospital, Seongnam 13620, South Korea

Hyeon Jeong Oh, Hyung Kyung Kim, Department of Pathology, Seoul National University Bundang Hospital, Seongnam 13620, South Korea

Hye Seung Lee, Department of Pathology, Seoul National University Hospital, Seoul 03080, South Korea

Corresponding author: Duck-Woo Kim, MD, PhD, Professor, Department of Surgery, Seoul National University Bundang Hospital, 166 Gumi-ro, Bundang-gu, Seongnam 13620, South Korea. kdw@snubh.org

Abstract

BACKGROUND

Approximately 40% of colorectal cancer (CRC) cases are linked to Kirsten rat sarcoma viral oncogene homolog (*KRAS*) mutations. *KRAS* mutations are associated with poor CRC prognosis, especially *KRAS* codon 12 mutation, which is associated with metastasis and poorer survival. However, the clinicopathological characteristics and prognosis of *KRAS* codon 13 mutation in CRC remain unclear.

AIM

To evaluate the clinicopathological characteristics and prognostic value of codon-specific *KRAS* mutations, especially in codon 13.

METHODS

This retrospective, single-center, observational cohort study included patients who underwent surgery for stage I-III CRC between January 2009 and December 2019. Patients with *KRAS* mutation status confirmed by molecular pathology reports were included. The relationships between clinicopathological characteristics and individual codon-specific *KRAS* mutations were analyzed. Survival data were analyzed to identify codon-specific *KRAS* mutations as recurrence-related factors using the Cox proportional hazards regression model.

RESULTS

Among the 2203 patients, the incidence of *KRAS* codons 12, 13, and 61 mutations was 27.7%, 9.1%, and 1.3%, respectively. Both *KARS* codons 12 and 13 mutations showed a tendency to be associated with clinical characteristics, but only codon 12 was associated with pathological features, such as stage of primary tumor (T stage), lymph node involvement (N stage), vascular invasion, perineural invasion, tumor size, and microsatellite instability. *KRAS* codon 13 mutation showed no associations (77.2% *vs* 85.3%, $P = 0.159$), whereas codon 12 was associated with a lower 5-year recurrence-free survival rate (78.9% *vs* 75.5%, $P = 0.025$). In multivariable analysis, along with T and N stages and vascular and perineural invasion, only codon 12 (hazard ratio: 1.399; 95% confidence interval: 1.034-1.894; $P = 0.030$) among *KRAS* mutations was an independent risk factor for recurrence.

CONCLUSION

This study provides evidence that *KRAS* codon 13 mutation is less likely to serve as a prognostic biomarker than codon 12 mutation for CRC in a large-scale cohort.

Key Words: Genes; Ras; Codon; Colonic neoplasms; Rectal neoplasms

©The Author(s) 2023. Published by Baishideng Publishing Group Inc. All rights reserved.

Core Tip: Based on a large-scale cohort of patients with stage I-III colorectal cancer (CRC), Kirsten rat sarcoma viral oncogene homolog (*KRAS*) codon 13 mutation is less pathogenic and recurrent. Moreover, focusing on the biological effects of codon-specific *KRAS* mutations and minimizing interference with various medical therapies, previous *in vivo* studies demonstrating that *KRAS* codon 13 mutation is less aggressive were translated into clinical outcomes in this study. This may influence many oncologists to consult with patients on their prognosis after surgery. We propose that *KRAS* codon 13 mutation is less likely to serve as a prognostic factor of CRC, compared with codon 12.

Citation: Ahn HM, Kim DW, Oh HJ, Kim HK, Lee HS, Lee TG, Shin HR, Yang IJ, Lee J, Suh JW, Oh HK, Kang SB. Different oncological features of colorectal cancer codon-specific *KRAS* mutations: Not codon 13 but codon 12 have prognostic value. *World J Gastroenterol* 2023; 29(32): 4883-4899
URL: https://www.wjgnet.com/1007-9327/full/v29/i32/4883.htm
DOI: https://dx.doi.org/10.3748/wjg.v29.i32.4883

INTRODUCTION

Kirsten rat sarcoma viral oncogene homolog (*KRAS*) is one of the downstream molecules of the epidermal growth factor receptor (EGFR) associated with cell proliferation, anti-apoptosis, and survival[1-3]. Abnormal activation of *KRAS*, a well-known oncogene, triggers uncontrolled tumor cell proliferation regardless of the initiating molecular signal from EGFR [4]. Mutations in *KRAS* promote the development of cancer in a variety of organs including the breast, prostate, lung, pancreas, colon, and rectum[1,2]. According to previous reports, approximately 40% of colorectal cancer (CRC) cases are linked to *KRAS* mutations[5-7], which occur more frequently in the proximal rather than in the distal colon[4,8,9]. Clinically, *KRAS* mutations are associated with resistance to anti-EGFR therapy and poor CRC prognosis[10,11].

CRC-related point mutations in *KRAS* occur at different codon locations. In most cases, *KRAS* mutations are detected in codon 12 or 13, whereas mutations in codon 61 or 146 have been reported only in a minority of patients with CRC[12]. Several clinical studies have indicated that *KRAS* codon 12 mutations are associated with metastasis and poor survival in advanced CRC[8,12-14]. *In-vitro* studies comparing cells with *KRAS* codon 12 and 13 mutations have demonstrated stronger transforming activity and resistance to apoptosis in cells with mutations in *KRAS* codon 12 than codon 13[15,16]. Most reports have concluded that *KRAS* codon 12 mutation is a poor prognostic factor following CRC resection. However, the oncological role of *KRAS* codon 13 mutation is controversial. *KRAS* codon 13 mutation has been linked to advanced-stage or lymph node metastasis and has been considered predictive of a higher likelihood of death in several studies[17,18]. In contrast, other investigators have shown no association between *KRAS* codon 13 mutations and tumor progression or CRC prognosis[4,19].

In addition to the controversial prognostic significance of *KRAS* codon 13 mutations, limited information is available regarding the clinical characteristics of codon-specific *KRAS* mutations in CRC. The incidence of codon-specific *KRAS* mutations other than those involving codon 12 (including codon 13) is low. Owing to the infrequency of *KRAS* abnormalities, the pathological features of codon-specific mutations at sites other than codon 12 remain unclear. Owing to the small cohort sizes of previous studies[4,8,12,14,20], the clinical roles of codon-specific *KRAS* mutations in CRC, including codons 12 and 13, are yet to be validated. Moreover, studies on the oncological effects of codon-specific *KRAS* mutations, particularly regarding abnormalities located within minor codons, are limited.

This study was designed to elucidate the clinicopathological characteristics associated with codon-specific *KRAS* mutations in CRC, including codons 12, 13, and 61. The main objective of this study was to determine whether *KRAS* codon 13 mutation could serve as a prognostic biomarker for CRC in a relatively large cohort of individuals.

MATERIALS AND METHODS

Patients

This retrospective observational cohort study was registered at ClinicalTrials.gov (NCT05657210) and reviewed 3144 patients who underwent surgery for CRC between January 2009 and December 2019, with available clinical data on recurrence and survival. All patients underwent routine colon or rectal resection and lymph node dissection according to the tumor location, with or without diverting ileostomies or colostomies. The surgical specimens were submitted to the laboratory for pathological evaluation. Patients with confirmed molecular pathology reports of *KRAS* mutation status were included, whereas those with incomplete data on *KRAS* mutations (n = 368) or microsatellite instability (MSI) status (n = 232) were excluded. Patients with dual or triple *KRAS* mutations (within more than one codon) from pathology reports (n = 2) were excluded. Additionally, to understand the biological importance and minimize the potential influence of systemic therapeutic factors on the prognosis of codon-specific *KRAS* mutations, we excluded patients with stage IV metastatic CRC (n = 339). Finally, data from 2203 eligible patients were collected separately for statistical analysis. This study was approved by the Institutional Review Board (IRB No. B-2203-742-101) of Seoul National University Bundang Hospital and the requirement for informed consent was waived.

Adjuvant/neoadjuvant therapy and follow-ups

All patients who underwent colorectal surgery for curative purposes were recommended adjuvant therapy according to the pathological stage of the cancer. Patients with pathological stage III and high-risk stage II colon cancer are recommended adjuvant chemotherapy. In rectal cancer, patients with pathological stages II and III are treated with adjuvant chemotherapy after surgery. However, in patients with clinical T4 or positive nodes without distant metastasis, preoperative chemoradiation therapy is recommended with long-course radiotherapy (dose of 5040 cGy of radiation over 5 wk; 28 fractions) combined with chemotherapy with 5-fluorouracil/Leucovorin or capecitabine.

According to the cancer monitoring protocol after curative surgery at our facility, patients were evaluated regularly one month after surgery, then every 3 mo for the first 2 years, every 6 mo for the next 3 years, and every 12 mo thereafter for a total of 5 years. Monitoring included measurements of serum carcinoembryonic antigen (CEA) levels every 3 mo; imaging modalities, including computed tomography (CT) (abdomen, pelvis, and chest) every 6 mo; and annual colonoscopy. Cancer recurrence was confirmed histologically or radiologically. The assigned research nurse constantly updated the data on recurrence and death. Information about deaths was double-checked by comparison with the database of the National Health Insurance Service, Korea, which lists the life and death records of Korean people. The registry data were constantly updated and managed by an assigned research nurse in the colorectal surgery department of our hospital.

Data collection

Basic patient clinical information [age, sex, height, weight, and American Society of Anesthesiologists (ASA) score] was collected. Cancer-related clinical characteristics such as primary tumor location, preoperative CEA level, and diverting stoma were included. Data on pathological features were collected based on pathology reports of surgical specimens. The following variables were statistically analyzed: T and N stages, tumor size, lymphatic invasion, vascular invasion, perineural invasion, number of harvested lymph nodes, number of metastatic lymph nodes, MSI status, and *KRAS* mutation status. Codon-specific *KRAS* mutation status was examined for codons 12, 13, and 61.

KRAS mutations were identified from formalin-fixed, paraffin-embedded cancerous tissue obtained from surgical specimens. After deoxyribonucleic acid (DNA) extraction from the tissue, the exons 2 and 3 of the *KRAS* gene were separately amplified by polymerase chain reaction (PCR) using optimized PCR reagents and primers. Codon-specific *KRAS* mutations were identified by pyrosequencing (PyroMark Q24 Mdx, QIAGEN, Hilden, Germany). MSI status was also evaluated using formalin-fixed tissues during surgery. PCR with five markers (*BAT26, BAT25, D5S346, D17S250,* and *D2S123*) followed by fragmentation assay (ABI-3130xl, Thermo Fisher Scientific, MA, United States) was performed to identify the MSI status.

Statistical analysis

Descriptive statistics were used to identify the basic clinicopathological characteristics of the patients, including MSI status frequency and *KRAS* mutations. The differences between wild-type and mutant *KRAS* as well as the mean values of continuous variables, were compared using either the independent *t*-test or the Mann-Whitney *U* test according to the results of the Kolmogorov-Smirnov test. Chi-squared or Fisher's exact tests were used to compare categorical variables. Overall survival (OS) and recurrence-free survival (RFS) were calculated from the date of surgery and compared using the Kaplan-Meier method and the log-rank test. For the analysis of risk factors for tumor recurrence, the Cox proportional hazards regression model was used, with the covariance input criterion set at $P < 0.1$. Patients were subdivided based on the primary tumor location (colon *vs* rectum) and MSI status [microsatellite stable (MSS)/MSI-low *versus* MSI-high]. Each subgroup was analyzed for recurrence-related factors using a Cox proportional hazards regression model. All statistical analyses were performed using the Statistical Package for the Social Sciences (SPSS), version 25.0, for Windows (SPSS, IBM). Descriptive results of continuous variables are expressed as mean ± SD. P value < 0.05 were considered statistically significant.

RESULTS

The present study included 2203 patients who underwent CRC surgery. The clinicopathological characteristics of the patients are shown in Table 1. In terms of MSI status, 1866 patients (84.7%) were identified as MSS, 153 (6.9%) as MSI-low, and 184 (8.4%) as MSI-high (Figure 1A). *KRAS* mutations were detected in 840 patients (38.1%) patients. The incidence of *KRAS* codons 12, 13, and 61 substitutions was 27.7%, 9.1%, and 1.3%, respectively (Figure 1B).

Among the clinical characteristics, female sex, lower ASA score, right-sided colon cancer, higher preoperative CEA levels, and low rates of diverting stoma formation were associated with *KRAS* mutations in codons 12, 13, and 61. Most pathological features, including T stage, N stage, tumor size, lymphatic invasion, perineural invasion, and number of harvested lymph nodes, were associated with *KRAS* mutations, along with molecular features such as MSI status (Table 2).

Analysis of the codon-specific *KRAS* mutational status revealed significant associations of both clinical and pathological characteristics with *KRAS* codon 12 mutations, including female sex, lower ASA score, right-sided colon cancer, preoperative CEA level above the normal range (≥ 5.0 ng/mL), T stage, N stage, MSI status, tumor size, vascular invasion, and perineural invasion. In contrast, only female sex, right-sided colon cancer, high preoperative CEA levels, diverting stoma formation, and no pathological features were significantly correlated with *KRAS* codon 13 mutations. Other than perineural invasion, no clinical characteristics or pathological features were associated with *KRAS* codon 61 mutations (Table 2).

At a mean ± SD follow-up duration of 29.7 mo ± 14.3 mo, and a median of 29 (0-85) months, recurrence within 5 years of curative surgery was observed in 205 (9.3%) among the 2203 patients. Five-year RFS (78.3% *vs* 77.4%, $P = 0.130$) and OS (89.0% *vs* 89.5%, $P = 0.971$) rates did not differ significantly between the wild-type and *KRAS* mutant CRC groups. Notably, the 5-year RFS for all codon-specific *KRAS* mutations was statistically different (wild-type, codon 12, and codon 13 mutations: 78.4%, 75.5%, and 85.3%, respectively; $P = 0.013$; Figure 2A), but the 5-year OS rates were comparable (wild-type, codon 12, and codon 13 mutations: 89.2%, 89.8%, and 86.9%, respectively; $P = 0.805$; Figure 2B). The 5-year RFS rate of the *KRAS* codon 12 mutation group was significantly lower than that of the patients without codon 12 mutations (78.9% *vs* 75.5%, $P = 0.025$; Figure 3A). The 5-year RFS rate of the *KRAS* codon 13 mutation group was higher than that of the patients without codon 13 mutations; however, the difference was not statistically significant (77.2% *vs* 85.3%, $P = 0.159$; Figure 3B). The RFS of the *KRAS* codon 61 mutation group was significantly lower than that of the patients without codon 61 mutations (78.2% *vs* 60.6%, $P = 0.039$; Figure 3C); however, all cases of recurrence occurred within 2 years of surgery.

In the univariate analysis of recurrence-related factors, cancer location (colon or rectum), preoperative CEA level, diverting stoma, T stage, N stage, MSI status, tumor size, lymphatic invasion, vascular invasion, perineural invasion, number of metastatic lymph nodes, and *KRAS* codon 12 mutations were associated with recurrence. In multivariable analysis, most pathological features, including higher T stage [hazard ratio (HR): 2.620; 95% confidence intervals (CI): 1.479-4.641; $P = 0.001$], higher N stage (HR: 2.001; 95%CI: 1.399-2.861; $P < 0.001$), vascular invasion (HR: 1.578; 95%CI: 1.164-2.139; $P = 0.003$), perineural invasion (HR: 1.684; 95%CI: 1.194-2.376; $P = 0.003$), and mutation of *KRAS* codon 12 (HR: 1.399; 95%CI: 1.034-1.894; $P = 0.030$) were identified as independent risk factors of recurrence in multivariable analysis. Among the clinical characteristics, only the presence of a diverting stoma (HR: 1.874; 95%CI: 1.260-2.787; $P = 0.002$) was independently correlated with recurrence (Table 3).

Tumor size (HR: 1.100; 95%CI: 1.011-1.198; $P = 0.027$), vascular invasion (HR: 1.981; 95%CI: 1.362-2.880; $P < 0.001$), perineural invasion (HR: 1.793; 95%CI: 1.200-2.679; $P = 0.004$), the presence of metastatic lymph nodes (HR: 1.048; 95%CI: 1.014-1.083; $P = 0.006$), and *KRAS* codon 12 mutation (HR: 1.496; 95%CI: 1.019-2.196; $P = 0.040$) were determined as independent risk factors for cancer recurrence when the primary tumor location was in the colon. Perineural invasion (HR: 3.358; 95%CI: 1.885-5.983; $P < 0.001$), and the presence of metastatic lymph nodes (HR: 1.095; 95%CI: 1.017-1.178; $P = 0.016$) were independently associated with cancer recurrence when the primary tumor was in the rectum. No codon-specific *KRAS* mutations were associated with recurrent rectal cancer (Table 4).

Among MSS/MSI-low CRC patients, tumor size (HR: 1.117; 95%CI: 1.038-1.202; $P = 0.003$), vascular invasion (HR: 1.740; 95%CI: 1.282-2.363; $P < 0.001$), perineural invasion (HR: 2.335; 95%CI: 1.663-3.279; $P < 0.001$), number of metastatic lymph nodes (HR: 1.050; 95%CI: 1.020-1.081; $P = 0.001$), and *KRAS* codon 12 mutation (HR: 1.467; 95%CI: 1.077-1.998; $P = 0.015$) were independent risk factors for cancer recurrence. In contrast, only a high preoperative CEA level (HR: 8.321; 95%CI: 1.387-49.920; $P = 0.020$) was associated with recurrence in MSI-high CRC. In cases of MSI-high CRC, the *KRAS* codon 12 mutation was statistically irrelevant regarding cancer recurrence, and there were no cases of recurrence during the study period among patients with *KRAS*-mutant CRC involving codons 13 and 61 (Table 5).

DISCUSSION

Among the 2203 patients who underwent curative surgery for stage I-III CRC, the incidence of codon-specific *KRAS* abnormalities was, respectively, 27.7%, 9.1%, and 1.3% for patients with *KRAS* codon 12, 13, and 61 mutations. Only 9.3% (205/2203) recurrences were observed during the 5-year follow-up period. To our knowledge, this study is based on the largest scaled cohort that has ever analyzed not only the oncological impact but also the clinicopathological characteristics of codon-specific *KRAS* mutations in patients with CRC. Most previous studies have reported similar results for *KRAS* codon 12 mutations, but not codon 13, in CRC as a poor oncological factor[4,8,12,14,20]. Despite the minimal oncological effects of minor *KRAS* mutations, such as in codon 61, the data obtained were sufficient to gain statistical power, supporting previous findings that *KRAS* codon 61 mutation is not associated with the clinicopathological features of CRC

Table 1 Clinicopathologic characteristics of the study patients

Clinical characteristics (*n* = 2203)	Value[1]
Age (yr)	64.7 ± 12.2
Sex	
Male	1264 (57.4)
Female	939 (42.6)
Body mass index (kg/m^2)	23.9 ± 3.3
ASA score	
1	575 (26.1)
2	1412 (64.1)
3	211 (9.6)
4	5 (0.2)
Cancer location	
Cecum	46 (2.1)
Ascending colon	386 (17.5)
Hepatic flexure	88 (4.0)
Transverse colon	115 (5.2)
Splenic flexure	18 (0.8)
Descending colon	79 (3.6)
Sigmoid colon	771 (35.0)
Rectum	700 (31.7)
Preoperative CEA (ng/mL)	7.7 ± 42.3
Diverting stoma	
Ileostomy	435 (19.7)
Colostomy	62 (2.8)
T stage	
0	18 (0.8)
1	275 (12.5)
2	383 (17.4)
3	1282 (58.2)
4	245 (11.1)
N stage	
0	1286 (58.4)
1	639 (29.0)
2	278 (12.6)
Tumor size (cm)	4.4 ± 2.4
Lymphatic invasion	597 (27.1)
Vascular invasion	469 (21.3)
Perineural invasion	934 (42.4)
Harvested lymph nodes	45.3 ± 21.2
Metastatic lymph nodes	1.4 ± 2.9
Adjuvant/Neoadjuvant therapy	
Colon	

Adjuvant therapy-stage II	274 (51.4)
Adjuvant therapy-stage III	575 (90.0)
Rectum	
Neoadjuvant therapy	200 (28.6)
Operative first-Adjuvant therapy	264 (52.8)

[1]Results are reported as mean ± SD or as frequency (percent).
ASA: American Society of Anesthesiologists; CEA: Carcinoembryonic antigen; AJCC: American Joint Committee on Cancer.

[21]. An earlier study in a Japanese cohort also identified *KRAS* codon 12, but not codon 13, as an independent risk factor for tumor recurrence in stage I-III CRC. While their results supported the utility of *KRAS* codon 12 mutation as a poor prognostic factor, the correlation between codon-specific *KRAS* mutations and clinicopathological characteristics could not be validated because of the small sample size[20]. In the present study, we analyzed the largest sample group of patients, which provided not only results complementing earlier studies on *KRAS* mutations in CRC, but also additional information on correlations with clinicopathological characteristics and prognostic factors for individual codon-specific *KRAS* mutations.

In addition to resistance to anti-EGFR therapies, such as cetuximab and panitumumab[22], *KRAS* codon 12 mutation in CRC has been established as a poor prognostic factor of survival associated with aggressive behavior[23]. However, the role of *KRAS* codon 13 mutation in CRC remains unclear. Several studies have suggested that *KRAS* codon 13 mutations are associated with advanced-stage disease and metastasis of CRC and potentially serve as a predictive factor for a higher likelihood of death[17,18]. An earlier meta-analysis reported a lower overall survival in patients with *KRAS* codon 13 mutant CRC with no exposure to anti-EGFR therapy than in those treated with targeted therapy[24]. Other studies have demonstrated that *KRAS* codon 13 mutations are not associated with CRC progression[4,19]. Another meta-analysis of metastatic CRC with mutated *KRAS* codon 13 revealed a more significant response to cetuximab than that in patients with other codon-specific *KRAS* mutations[25]. To ascertain the correlation between codon-specific *KRAS* mutations and clinical oncological outcomes throughout the stages of CRC, therapeutic options such as chemotherapy, radiotherapy, and targeted therapy, along with inevitable resistance mechanisms, should be considered[5,26,27].

The survival analysis showed that CRC recurrence, but not overall survival, was associated with codon-specific *KRAS* mutations. Analysis of individual codons showed that *KRAS* codon 12 mutation is an independent risk factor for recurrence, while *KRAS* codon 13 and 61 mutations appeared to be statistically irrelevant. In earlier *in vivo* molecular biology studies, cells with *KRAS* codon 12 and 13 mutations displayed similar morphological changes, but only codon 12 mutants induced anchorage-independent growth, implying a lower aggressiveness of *KRAS* codon 13 mutations[15]. Another *in vitro* study reported that *KRAS* codon 12 mutant cells were more resistant to apoptosis and exhibited enhanced anti-apoptotic molecular signaling relative to codon 13 mutant cells, consistent with the finding that the codon 13 mutation is less aggressive[16]. These *in vivo* results were translated into the clinical outcomes of our study, demonstrating that *KRAS* codon 13 mutation is less aggressive and less likely to serve as a poor prognostic factor for CRC compared with *KRAS* codon 12 mutation.

Interestingly, the prognosis of *KRAS* codon 12 mutant CRC varied based on the primary tumor location in either the colon or rectum. The majority of experiments on tumor location were stratified into right- or left-sided colorectum based on the splenic flexure[28,29]. Even the definition of 'left-sided' differs among studies according to the involvement of the rectum[30,31]. Thus, in the present study, recurrence-related factors were analyzed by subgrouping the tumors into colon and rectum. In the subgroup of tumors located in the colon, patients with *KRAS* codon 12 mutations were estimated to be at a 1.5-fold higher risk of CRC recurrence than those without codon 12 mutations. In contrast, in the rectum, all codon-specific *KRAS* mutations were not linked to recurrence. To the best of our knowledge, this is the first study to investigate the oncological impact of codon-specific *KRAS* mutations based on tumor location (colon or rectum). Our findings support the theory that *KRAS* codon 12 mutation is a poor prognostic factor for colon cancer, but not for rectal cancer.

Previous studies have shown that the combination of *KRAS* mutations and MSI status is a potential prognostic factor in various stages of CRC [26,32-36]. In addition, since MSI status is associated with chemoresistance[37,38], the MSS/MSI-low and MSI-high subgroups were analyzed separately to eliminate the effect of MSI status on prognosis. Interestingly, in the MSS/MSI-low patient subgroup, only *KRAS* codon 12 mutation was statistically related to recurrence, whereas there was no association between codon-specific *KRAS* mutations and recurrence among MSI-high tumors. It is well known that poor oncological outcomes including disease-free and overall survival were reported within MSS tumors combined with *KRAS* mutation[33-36]. To the best of our knowledge, analysis results of codon-specific *KRAS* mutations in MSS/MSI-low and MSI-high tumors have never been reported. Based on our subgroup analysis, *KRAS* codon 12 mutations may be associated with the location of colon and MSS tumors, and not all CRC patients with *KRAS* codon 12 mutations have poor outcomes.

Clarifying the effects of codon-specific *KRAS* mutations on the prognosis of stage IV CRC is a complex issue[5,26,27,39]. A recent study on *KRAS* mutations in CRC with liver metastasis reported that *KRAS* codon 12 mutations were associated with poorer overall survival, while codon 13 was not; however, they also pointed out the exclusion of perioperative management such as anti-epidermal growth factor receptor agents[12]. Among the patients diagnosed with stage IV CRC who underwent surgery in our hospital during the period of the present study, 48.4% had *KRAS* mutations. However, only about half of them (53.1%) underwent surgery with curative intent, whereas the others underwent

Table 2 Univariable analysis[1] of each codon-specific *KRAS* mutation

	***KRAS* overall[2]**			***KRAS* Codon 12**			***KRAS* Codon 13**			***KRAS* Codon 61**		
	WT (%)	**MT (%)**	***P* value**	**WT (%)**	**MT (%)**	***P* value**	**WT (%)**	**MT (%)**	***P* value**	**WT (%)**	**MT (%)**	***P* value**
Age			0.418			0.734			0.698			0.246
< 65 yr	644 (62.8)	382 (37.2)		745 (72.6)	281 (27.4)		936 (91.1)	91 (8.9)		1016 (99.0)	10 (1.0)	
≥ 65 yr	719 (61.1)	458 (38.9)		847 (72.0)	330 (28.0)		1067 (90.7)	110 (9.3)		1160 (98.5)	18 (1.5)	
Sex			**< 0.001**			**< 0.001**			**0.006**			0.238
Male	851 (67.3)	413 (32.7)		961 (76.0)	303 (24.0)		1167 (92.3)	97 (7.7)		1251 (99.0)	13 (1.0)	
Female	512 (54.5)	427 (45.5)		631 (67.2)	308 (32.8)		836 (88.9)	104 (11.1)		924 (98.4)	15 (1.6)	
BMI			0.098			0.347			0.485			0.104
< 25 kg/m^2	853 (60.6)	555 (39.4)		1008 (71.6)	400 (28.4)		1275 (90.6)	133 (9.4)		1386 (98.4)	22 (1.6)	
≥ 25 kg/m^2	510 (64.2)	285 (35.8)		584 (73.5)	211 (26.5)		727 (91.4)	68 (8.6)		789 (99.2)	6 (0.8)	
ASA score			**0.010**			**0.002**			0.942			0.347
1-2	1212 (61.0)	775 (39.0)		1417 (71.3)	570 (28.7)		1806 (90.9)	181 (9.1)		1963 (98.8)	24 (1.2)	
3-4	151 (69.9)	65 (30.1)		175 (81.0)	41 (19.0)		196 (90.7)	20 (9.3)		212 (98.1)	4 (1.9)	
Cancer location (1)[3]			**< 0.001**			**0.002**			**< 0.001**			0.219
Right-sided	329 (51.8)	306 (48.2)		429 (67.6)	206 (32.4)		546 (86.0)	89 (14.0)		624 (98.3)	11 (1.7)	
Left-sided	1034 (65.9)	534 (34.1)		1163 (74.2)	405 (25.8)		1456 (92.9)	112 (7.1)		1552 (98.9)	17 (1.1)	
Cancer location (2)[4]			0.092			0.405			0.117			0.966
Colon	912 (60.7)	591 (39.3)		1078 (71.7)	425 (28.3)		1356 (90.2)	147 (9.8)		1484 (98.7)	19 (1.3)	
Rectum	451 (64.4)	249 (35.6)		514 (73.4)	186 (26.6)		646 (92.3)	54 (7.7)		691 (98.7)	9 (1.3)	
Preoperative CEA			**< 0.001**			**< 0.001**			**0.037**			0.301
< 5.0 ng/mL	1131 (64.7)	616 (35.3)		1299 (74.4)	448 (25.6)		1599 (91.5)	148 (8.5)		1727 (98.9)	20 (1.1)	
≥ 5.0 ng/mL	232 (50.9)	224 (49.1)		293 (64.3)	163 (35.7)		403 (88.4)	53 (11.6)		448 (98.2)	8 (1.8)	
Diverting stoma			**0.001**			0.071			**0.029**			0.131
No	1024 (60.0)	682 (40.0)		1217 (71.3)	489 (28.7)		1538 (90.2)	168 (9.8)		1681 (98.5)	25 (1.5)	
Yes	339 (68.2)	158 (31.8)		375 (75.5)	122 (24.5)		464 (93.4)	33 (6.6)		494 (99.4)	3 (0.6)	
T stage			**0.008**			**0.003**			0.488			0.139

T0-2	446 (66.0)	230 (34.0)		517 (76.5)	159 (23.5)		610 (90.2)	66 (9.8)		671 (99.3)	5 (0.7)	
T3-4	917 (60.1)	610 (39.9)		1075 (70.4)	452 (29.6)		1392 (91.2)	135 (8.8)		1504 (98.5)	23 (1.5)	
N stage			**0.012**			**0.046**			0.617			0.094
N0	824 (64.1)	462 (35.9)		950 (73.9)	336 (26.1)		1172 (91.1)	114 (8.9)		1274 (99.1)	12 (0.9)	
N1-2	539 (58.8)	378 (41.2)		642 (70.0)	275 (30.0)		830 (90.5)	87 (9.5)		901 (98.3)	16 (1.7)	
MSI status			**0.003**			**0.001**			0.458			0.973
MSS	1138 (61.0)	728 (39.0)		1327 (71.1)	539 (28.9)		1701 (91.2)	165 (8.8)		1842 (98.7)	24 (1.3)	
MSI-low	90 (58.8)	63 (41.2)		110 (71.9)	43 (28.1)		135 (88.2)	18 (11.8)		151 (98.7)	2 (1.3)	
MSI-high	135 (73.4)	49 (26.6)		155 (84.2)	29 (15.8)		166 (90.2)	18 (9.8)		182 (98.9)	2 (1.1)	
Tumor size (cm)	4.3 ± 2.4	4.6 ± 2.3	**0.005**	4.3 ± 2.5	4.6 ± 2.1	**0.001**	4.4 ± 2.3	4.6 ± 2.7	0.837	4.4 ± 2.4	4.5 ± 2.1	0.708
Lymphatic invasion			**0.005**			0.099			0.080			0.302
No	1022 (63.6)	584 (36.4)		1176 (73.2)	430 (26.8)		1470 (91.5)	136 (8.5)		1589 (98.9)	18 (1.1)	
Yes	341 (57.1)	256 (42.9)		416 (69.7)	181 (30.3)		532 (89.1)	65 (10.9)		587 (98.3)	10 (1.7)	
Vascular invasion			0.090			**0.047**			0.614			0.061
No	1057 (61.0)	677 (39.0)		1236 (71.3)	498 (28.7)		1573 (90.7)	161 (9.3)		1716 (99.0)	18 (1.0)	
Yes	306 (65.2)	163 (34.8)		356 (75.9)	113 (24.1)		429 (91.5)	40 (8.5)		459 (97.9)	10 (2.1)	
Perineural invasion			**0.003**			**0.027**			0.387			**0.048**
No	819 (64.5)	450 (35.5)		940 (74.1)	329 (25.9)		1159 (91.3)	110 (8.7)		1258 (99.1)	11 (0.9)	
Yes	544 (58.2)	390 (41.8)		652 (69.8)	282 (30.2)		843 (90.3)	91 (9.7)		917 (98.2)	17 (1.8)	
Harvested LN	44.5 ± 20.6	46.5 ± 22.1	**0.040**	45.0 ± 21.1	45.9 ± 21.6	0.500	45.0 ± 20.9	47.9 ± 24.1	0.079	45.2 ± 21.3	47.7 ± 16.6	0.208
Metastatic LN	1.4 ± 3.1	1.3 ± 2.6	0.420	1.4 ± 3.1	1.3 ± 2.4	0.406	1.4 ± 2.9	1.4 ± 3.1	0.832	1.4 ± 2.9	1.4 ± 1.9	0.149

[1]The continuous variables were compared using either independent *t*-test or Mann-Whitney *U* test; the categorical variables were compared using Chi-square or Fisher's exact test.
[2]Kirsten rat sarcoma viral oncogene homolog overall indicates at least one mutation within codon 12, 13, or 61.
[3]Right-sided: From the cecum to distal 2/3 transverse colon; Left-sided: From the splenic flexure to rectum.
[4]Rectum: Below the pelvic inlet (an imaginary line drawn from the sacral promontory to the pubic symphysis).
KRAS: Kirsten rat sarcoma viral oncogene homolog; WT: Wild-type; MT: Mutation; BMI: Body mass index; ASA: American Society of Anesthesiologists; CEA: Carcinoembryonic antigen; MSI: Microsatellite instability; MSS: Microsatellite stable; LN: Lymph node.

palliative treatment. Additionally, there is a wide range of variations in the metastatic burden and forms of treatment for these patients. Therefore, in the present study, we excluded stage IV disease to focus on the biological importance and prognostic impact of codon-specific *KRAS* mutations in stage I-III CRC.

Table 3 Univariable and Cox regression analyses of *KRAS* mutations for determination of recurrence-related factors

	Recurrence			Multivariable Cox regression analysis[2]			
	Absent[1] (*n* = 1998)	Present[1] (*n* = 205)	*P* value	HR	95%CI		*P* value
					Lower	Upper	
Age (yr)			0.716				
< 65	933 (46.7)	93 (45.4)		-	-	-	-
≥ 65	1065 (53.3)	112 (54.6)		-	-	-	
Sex			0.616				
Male	1143 (57.2)	121 (59.0)		-	-	-	-
Female	855 (42.8)	84 (41.0)		-	-	-	
BMI			0.094				
< 25 kg/m^2	1266 (63.4)	142 (69.3)		-	-	-	-
≥ 25 kg/m^2	732 (36.6)	63 (30.7)		-	-	-	
ASA score			0.980				
1-2	1802 (90.2)	185 (90.2)		-	-	-	-
3-4	196 (9.8)	20 (9.8)		-	-	-	
Cancer location (1)[3]			0.860				
Right-sided	577 (28.9)	58 (28.3)		-	-	-	-
Left-sided	1421 (71.1)	147 (71.7)		-	-	-	
Cancer location (2)[4]							
Colon	1376 (68.9)	127 (62.0)	**0.043**	1.000			
Rectum	622 (31.1)	78 (38.0)		1.053	0.718	1.545	0.791
Preoperative CEA			**< 0.001**				
< 5.0 ng/mL	1607 (80.4)	140 (68.3)		1.000			
≥ 5.0 ng/mL	391 (19.6)	65 (31.7)		1.158	0.849	1.579	0.354
Diverting stoma			**< 0.001**				
No	1568 (78.5)	138 (67.3)		1.000			
Yes	430 (21.5)	67 (32.7)		1.874	1.260	2.787	**0.002**
T stage			**< 0.001**				
T0-2	659 (33.0)	17 (8.3)		1.000			
T3-4	1339 (67.0)	188 (91.7)		2.620	1.479	4.641	**0.001**
N stage			**< 0.001**				
N0	1230 (61.6)	56 (27.3)		1.000			
N1-2	768 (38.4)	149 (72.7)		2.001	1.399	2.861	**< 0.001**
MSI status			**0.037**				
MSS	1680 (84.1)	186 (90.7)		0.855	0.342	2.138	0.738
MSI-low	143 (7.2)	10 (4.9)		1.284	0.643	2.566	0.479
MSI-high	175 (8.8)	9 (4.4)		1.000			
Tumor size (cm)	4.3 ± 2.4	4.9 ± 2.1	**< 0.001**	0.997	0.927	1.074	0.944
Lymphatic invasion			**< 0.001**				
No	1493 (74.7)	113 (55.1)		1.000			
Yes	505 (25.3)	92 (44.9)		1.324	0.977	1.793	0.070
Vascular invasion			**< 0.001**				

No	1615 (80.8)	119 (58.0)		1.000			
Yes	383 (19.2)	86 (42.0)		1.578	1.164	2.139	**0.003**
Perineural invasion			**< 0.001**				
No	1211 (60.6)	58 (28.3)		1.000			
Yes	787 (39.4)	147 (71.7)		1.684	1.194	2.376	**0.003**
Harvested LN	45.3 ± 21.2	44.9 ± 21.4	0.705	-	-	-	-
Metastatic LN	1.2 ± 2.6	3.3 ± 4.5	**< 0.001**	1.028	0.995	1.061	0.095
KRAS Codon 12							
Wild-type	1459 (73.0)	133 (64.9)	**0.013**	1.000			
Mutation	539 (27.0)	72 (35.1)		1.399	1.034	1.894	**0.030**
KRAS Codon 13							
Wild-type	1809 (90.5)	193 (94.1)	0.088	1.000			
Mutation	189 (9.5)	12 (5.9)		0.637	0.350	1.160	0.140
KRAS Codon 61							
Wild-type	1975 (98.8)	200 (97.6)	0.176	1.000			
Mutation	23 (1.2)	5 (2.4)		1.950	0.790	4.812	0.147

[1]Results are reported as mean ± SD or as number (percent).
[2]No values indicated variables do not match the covariance input criterion ($P < 0.1$ in univariable analysis).
[3]Right-sided: From the cecum to distal 2/3 transverse colon; Left-sided: From the splenic flexure to rectum.
[4]Rectum: Below the pelvic inlet (an imaginary line drawn from the sacral promontory to the pubic symphysis).
KRAS: Kirsten rat sarcoma viral oncogene homolog; HR: Hazard ratio; CI: Confidence interval; BMI: Body mass index; ASA: American Society of Anesthesiologists; CEA: Carcinoembryonic antigen; MSI: Microsatellite instability; MSS: Microsatellite stable; LN: Lymph node.

Table 4 Cox regression analyses of recurrence-related factors in subgroups based on tumor location in the colon and rectum

	Colon (*n* = 1503)		Rectum (*n* = 700)	
	HR (95%CI)	*P* value	HR (95%CI)	*P* value
Preoperative CEA ≥ 5.0 ng/mL	1.290 (0.860-1.933)	0.218	1.215 (0.705-2.220)	0.444
Diverting stoma (+)	0.903 (0.394-2.067)	0.809	1.249 (0.755-2.065)	0.386
T3-4 stage (*vs* T0-2)	1.211 (0.737-1.991)	0.450	1.079 (0.601-1.939)	0.799
N1-2 stage (*vs* N0)	1.241 (0.863-1.784)	0.244	1.126 (0.649-1.954)	0.674
Tumor size (cm)	1.100 (1.011-1.198)	**0.027**	1.077 (0.948-1.223)	0.256
Lymphatic invasion	1.342 (0.919-1.960)	0.128	0.971 (0.562-1.676)	0.915
Vascular invasion	1.981 (1.362-2.880)	**< 0.001**	1.401 (0.841-2.334)	0.195
Perineural invasion	1.793 (1.200-2.679)	**0.004**	3.358 (1.885-5.983)	**< 0.001**
Metastatic LN	1.048 (1.014-1.083)	**0.006**	1.095 (1.017-1.178)	**0.016**
KRAS Codon 12 mutation	1.496 (1.019-2.196)	**0.040**	1.492 (0.902-2.466)	0.119
KRAS Codon 13 mutation	0.831 (0.412-1.678)	0.606	0.481 (0.146-1.578)	0.227
KRAS Codon 61 mutation	2.385 (0.730-7.795)	0.150	2.270 (0.511-10.088)	0.282

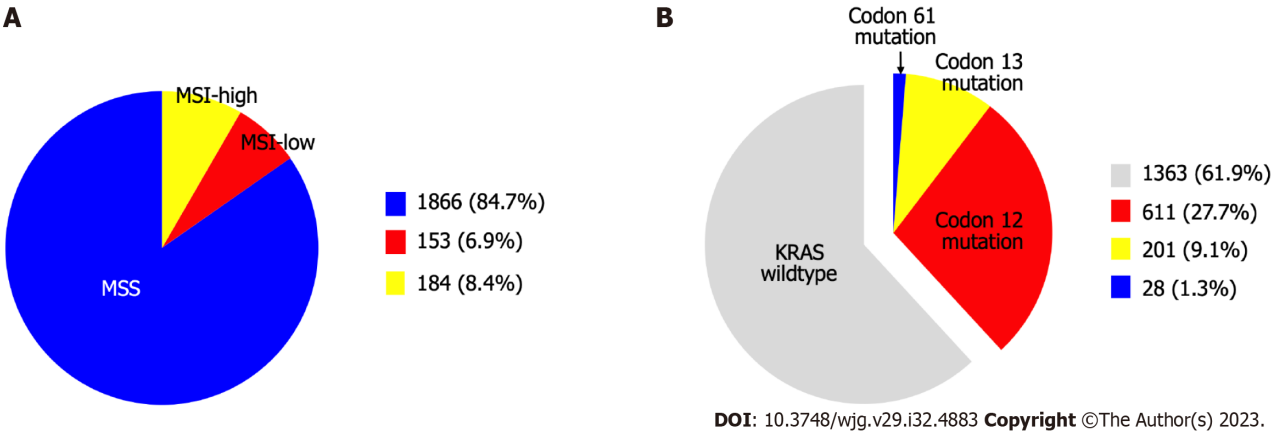
KRAS: Kirsten rat sarcoma viral oncogene homolog; HR: Hazard ratio; CI: Confidence interval; CEA: Carcinoembryonic antigen; MSI: Microsatellite instability; MSS: Microsatellite stable; LN: Lymph node.

In two patients in our cohort, *KRAS* mutations were detected at two or more codon sites. The first patient was a 75-year-old male who underwent surgery for descending colon cancer and was pathologically diagnosed with stage III (pT3N1M0) colon cancer with codon 12 and 13 *KRAS* mutations. The second patient was a 60-year-old female who underwent surgery for sigmoid colon cancer diagnosed as stage I (pT1N0M0) with both codon 12 and 61 *KRAS* mutations. Both patients survived for more than 5 years after surgery with no recurrence or metastasis. In a previous

Table 5 Cox regression analyses of recurrence-related factors in subgroups based on microsatellite instability status: Microsatellite stable/microsatellite instability-low *versus* microsatellite instability-high

	MSS/MSI-low (*n* = 2019)		MSI-high (*n* = 184)[1]	
	HR (95%CI)	*P* value	HR (95%CI)	*P* value
Preoperative CEA ≥ 5.0 ng/mL	1.178 (0.839-1.653)	0.344	8.321 (1.387-49.920)	**0.020**
Rectal cancer (*vs* colon cancer)	1.238 (0.850-1.804)	0.266	-	-
Diverting stoma (+)	1.069 (0.707-1.617)	0.752	2.431 (0.139-42.442)	0.543
T3-4 stage (*vs* T0-2)	1.175 (1.038-1.202)	0.407	0.284 (0.020-4.032)	0.353
N1-2 stage (*vs* N0)	1.190 (0.879-1.610)	0.260	1.000 (0.151-6.643)	1.000
Tumor size (cm)	1.117 (1.038-1.202)	**0.003**	0.991 (0.713-1.379)	0.960
Lymphatic invasion	1.242 (0.909-1.698)	0.174	1.154 (0.149-8.923)	0.891
Vascular invasion	1.740 (1.282-2.363)	**< 0.001**	0.009 (0.000-29.277)	0.255
Perineural invasion	2.335 (1.663-3.279)	**< 0.001**	0.538 (0.049-5.909)	0.613
Metastatic LN	1.050 (1.020-1.081)	**0.001**	1.442 (0.865-2.402)	0.160
KRAS Codon 12 mutation	1.467 (1.077-1.998)	**0.015**	2.508 (0.406-15.510)	0.323
KRAS Codon 13 mutation	0.713 (0.390-1.301)	0.270	-	-
KRAS Codon 61 mutation	2.265 (0.915-5.605)	0.077	-	-

[1]No values: Due to a small sample size, the hazard ratio and confidence interval were not pre.
MSI: Microsatellite instability; MSS: Microsatellite stable; HR: Hazard ratio; CI: Confidence interval; CEA: Carcinoembryonic antigen; MSI: Microsatellite instability; MSS: Microsatellite stable; LN: Lymph node.

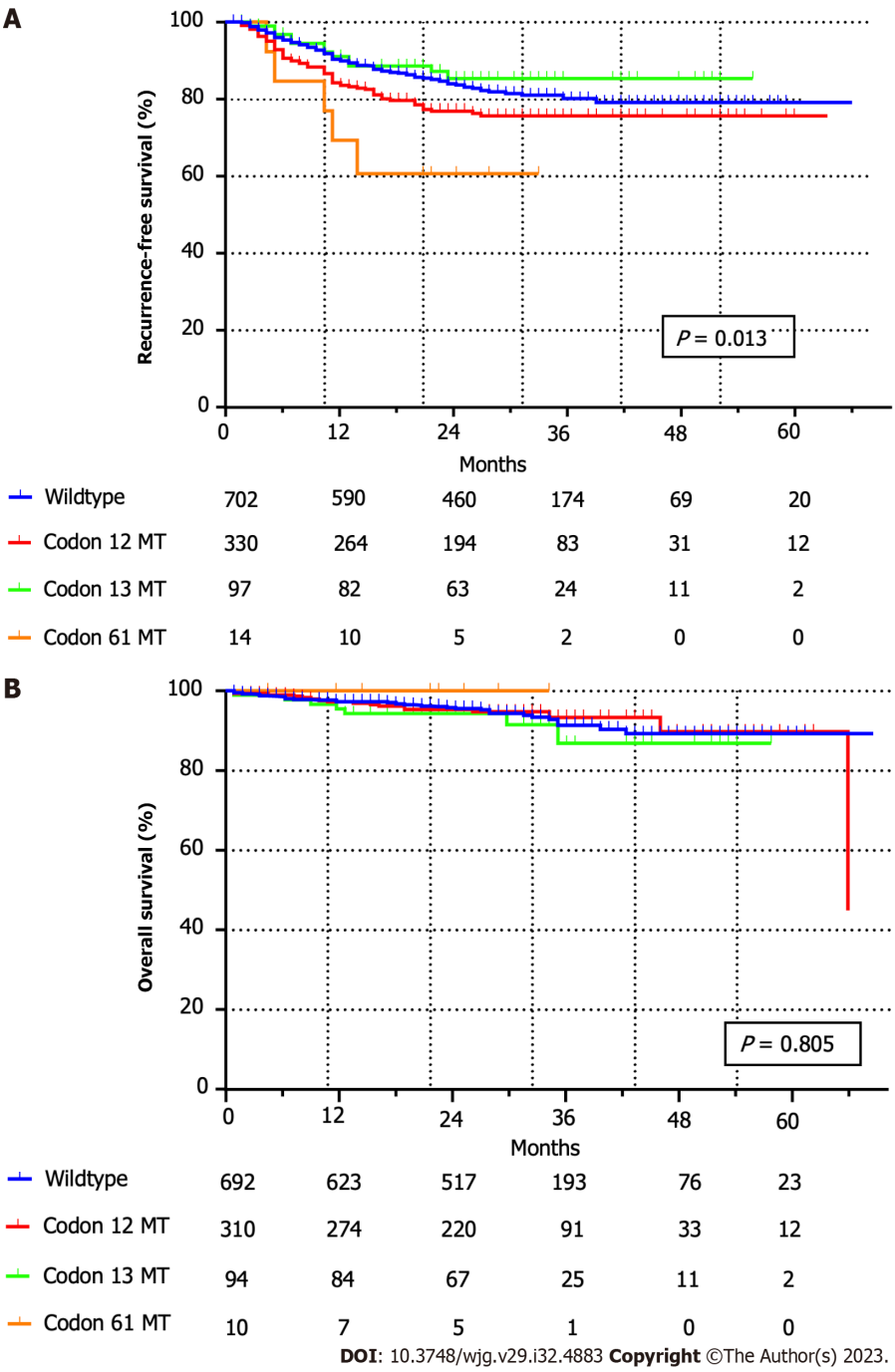


DOI: 10.3748/wjg.v29.i32.4883 **Copyright** ©The Author(s) 2023.

Figure 1 Incidence of microsatellite instability status and Kirsten rat sarcoma viral oncogene homolog mutations. A: Microsatellite instability status; B: Mutations of the Kirsten rat sarcoma viral oncogene homolog (*KRAS*) gene in relation to baseline characteristics. *KRAS*: Kirsten rat sarcoma viral oncogene homolog; MSS: Microsatellite stable; MSI: Microsatellite instability.

study, 12 patients with two or more codon mutations among 505 CRC *KRAS* mutation cases were reported but were eventually excluded from the analysis[21]. For the same reason, these two patients were excluded from the current study despite our intellectual curiosity.

The present study had several limitations. First, *BRAF* mutation, a biomarker related to the prognosis of CRC after surgery, was omitted from our analysis. According to previous studies on CRC biomarkers, both *BRAF* and MSI status have an important prognostic impact on recurrence and survival[34,40]. Unfortunately, a large amount of data was collected without knowledge of the *BRAF* mutation status because of alterations in routine molecular examinations by our facility during the study period. Second, since *KRAS* mutations were evaluated using postoperative specimens for both colon and rectal cancer, it may be audacious to conclude that the *KRAS* codon 12 mutation is a prognostic factor in rectal cancer. In advanced rectal cancer, trimodality therapy comprises chemoradiation followed by surgery, which takes at least 1-2 mo. This delay may affect the oncological outcome; therefore, the prognostic value of codon-specific *KRAS* mutations according to the primary tumor site should be carefully interpreted. Third, uncontacted patients without follow-up could have missing data on recurrence and survival despite constantly updating the clinical data by the



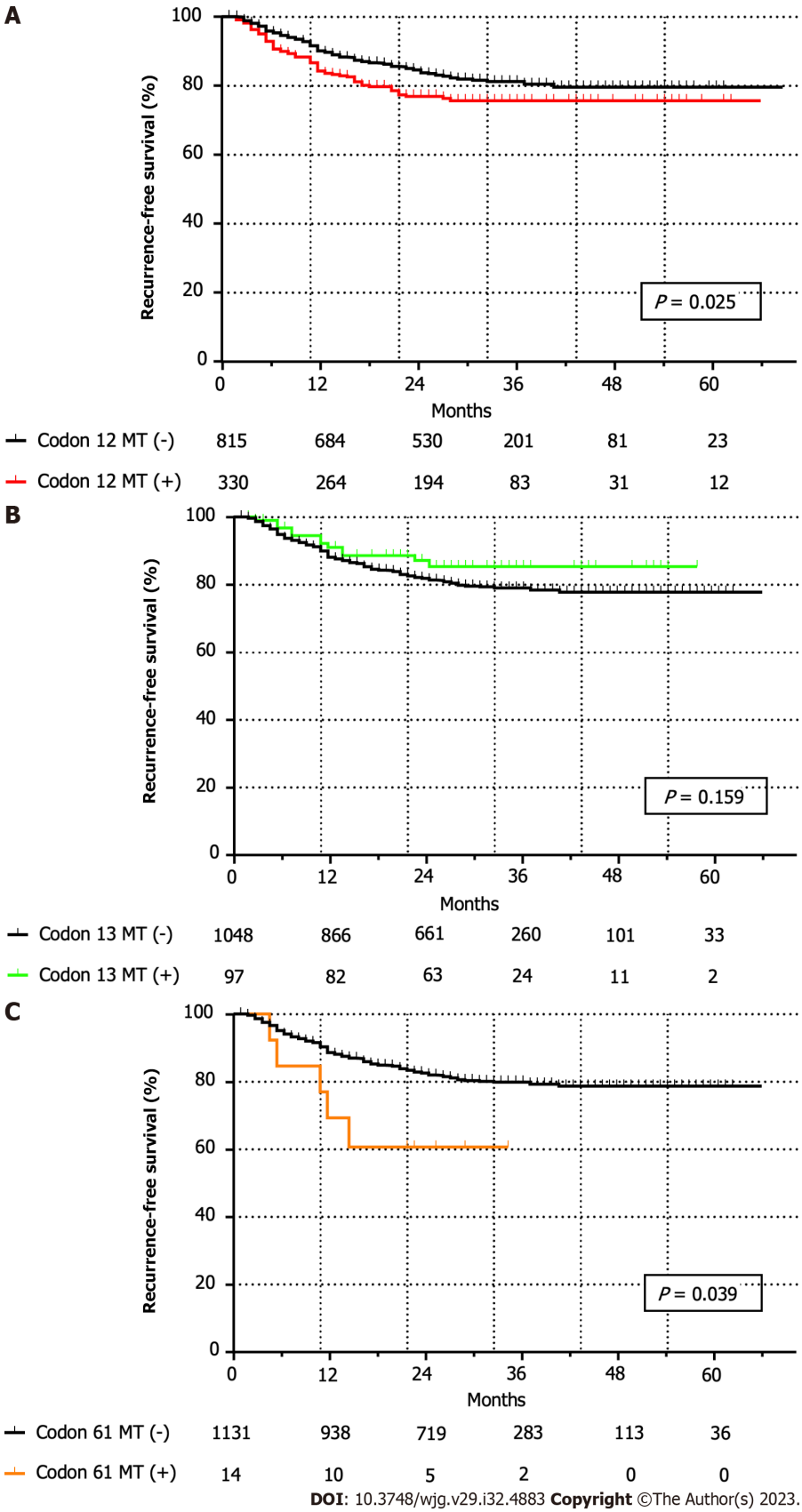
DOI: 10.3748/wjg.v29.i32.4883 **Copyright** ©The Author(s) 2023.

Figure 2 Comparative survival analysis between colorectal cancer samples with wild-type and Kirsten rat sarcoma viral oncogene homolog mutation. Blue lines indicate wild-type Kirsten rat sarcoma viral oncogene homolog (*KRAS*). Other lines represent codon-specific *KRAS* mutations of codon 12 (red), 13 (green), and 61 (orange). A: Recurrence-free survival; B: Overall survival rates were compared using a log-rank test. WT: Wild-type; MT: Mutation.

assigned research nurses in our department. The refusal to revisit after a few follow-ups could have produced missing data in our cohort, and double-checking with the National Health Insurance database might have reduced the error as much as possible. Unfortunately, these efforts could not separate other causes of death from cancer-related ones. Fourth, this study had a retrospective and single-center design, which could have led to selection bias. Despite this, the present study was based on a large-scale cohort with a relatively well-organized CRC registry of patients who underwent surgery, and is the largest cohort study ever that analyzed codon-specific KRAS mutations.

CONCLUSION

Most of the *KRAS* mutations in our study involved *KRAS* codons 12 and 13. Notably, *KRAS* codon 12 mutation was significantly associated with pathological features closely related to cancer recurrence and had a poor prognostic impact



DOI: 10.3748/wjg.v29.i32.4883 **Copyright** ©The Author(s) 2023.

Figure 3 Survival analysis of each codon-specific Kirsten rat sarcoma viral oncogene homolog mutation in colorectal cancer. Colored lines indicate codon-specific Kirsten rat sarcoma viral oncogene homolog (*KRAS*) mutations. A: The red line indicates the recurrence-free survival (RFS) of patients with *KRAS* codon 12 mutations; B: The green line indicates the RFS of patients with *KRAS* codon 13 mutations; C: The orange line indicates the RFS of patients with *KRAS* codon 61 mutations. MT: Mutation.

in patients with MSS tumors, or those located in the colon but not in the rectum. Given its irrelevance to pathological features and recurrence, we propose that *KRAS* codon 13 mutation is less likely to serve as a prognostic factor for CRC.

ARTICLE HIGHLIGHTS

Research background

Abnormal activation of Kirsten rat sarcoma viral oncogene homolog (*KRAS*), a well-known oncogene, triggers uncontrolled tumor cell proliferation. Approximately 40% of colorectal cancer (CRC) are linked to *KRAS* mutations. CRC-related point mutations in *KRAS* occur at different codon locations. *KRAS* codon 12 or 13 mutations are detected in a majority of CRC patients, whereas mutations in codon 61 or 146 have been reported only in a minority.

Research motivation

KRAS mutations are associated with poor CRC prognosis, especially *KRAS* codon 12 mutation, which is associated with metastasis and poorer survival. However, the clinicopathological characteristics and prognosis of *KRAS* codon 13 mutation in CRC remain controversial.

Research objectives

This study aimed to evaluate the clinicopathological characteristics and prognostic value of codon-specific *KRAS* mutations, especially in codon 13.

Research methods

This retrospective, single-center, observational cohort study included patients who underwent surgery for stage I-III CRC. The relationships between clinicopathological characteristics and individual codon-specific *KRAS* mutations were analyzed. By using the Cox proportional hazards regression model, survival analysis were performed to identify codon-specific *KRAS* mutations as recurrence-related factors.

Research results

Both *KARS* codons 12 and 13 mutations showed a tendency to be associated with clinical characteristics, but only codon 12 was associated with pathological features. *KRAS* codon 13 mutation showed no associations, whereas codon 12 was associated with a lower 5-year recurrence-free survival rate. In multivariable analysis, only codon 12 (HR: 1.399; 95% confidence interval: 1.034-1.894; P = 0.030) among *KRAS* mutations was an independent risk factor for recurrence. This may influence many oncologists to consult with patients on their prognosis after surgery.

Research conclusions

KRAS codon 12 mutation was significantly associated with pathological features closely related to cancer recurrence and had a poor prognostic impact in patients with microsatellite stable tumors, or those located in the colon but not in the rectum. On the other hand, *KRAS* codon 13 mutation is irrelevant to pathological features and recurrence, which consider less likely to serve as a prognostic factor for CRC.

Research perspectives

Focusing on the biological effects of codon-specific *KRAS* mutations, *KRAS* codon 13 mutation is less pathogenic and recurrent, Based on a large-scale cohort of patients with stage I-III CRC. This study's results may influence not only the prognosis but also the management of CRC patients individually. Therefore, the therapeutic usage and needs of codon-specific *KRAS* mutation in CRC should be considered in future studies.

ACKNOWLEDGEMENTS

The authors would like to thank the staff involved in the operating room and pathology laboratory of Seoul National University Bundang Hospital. The authors thank the Division of Statistics at the Medical Research Collaborating Center at Seoul National University Bundang Hospital for statistical analyses.

FOOTNOTES

Author contributions: Ahn HM, Kim DW, Oh HJ, Kim HK, Lee HS, Lee TG, Shin HR, Yang IJ, Lee J, Suh JW, Oh HK, and Kang SB solely contributed to this paper; Ahn HM contributed to data curation, formal analysis, investigation, validation, writing-original draft, and writing-editing; Kim DW contributed to conceptualization, investigation, validation, methodology, resources, project administration, writing-review, and editing; Oh HJ contributed to investigation, resources, and methodology; Kim HK contributed to investigation, resources, and methodology; Lee HS contributed to investigation and resources; Lee TG, Shin HR, and Yang IJ contributed to data curation and validation; Lee J and Suh JW contributed to methodology and validation; Oh HK and Kang SB contributed to investigation, validation, methodology, resources, writing, review, and editing.

Institutional review board statement: This study was reviewed and approved by the Institutional Review Board of Seoul National University Bundang Hospital (Approval No. B-2203-742-101).

Informed consent statement: This study was approved by the Institutional Review Board and the requirement for informed consent was waived.

Conflict-of-interest statement: The authors declare no conflicts of interest.

Data sharing statement: The data underlying this article will be shared upon reasonable request to the corresponding author. The data are not publicly available to protect the privacy of the participants.

STROBE statement: The authors have read the STROBE Statement—checklist of items, and the manuscript was prepared and revised according to the STROBE Statement—checklist of items.

Open-Access: This article is an open-access article that was selected by an in-house editor and fully peer-reviewed by external reviewers. It is distributed in accordance with the Creative Commons Attribution NonCommercial (CC BY-NC 4.0) license, which permits others to distribute, remix, adapt, build upon this work non-commercially, and license their derivative works on different terms, provided the original work is properly cited and the use is non-commercial. See: https://creativecommons.org/Licenses/by-nc/4.0/

Country/Territory of origin: South Korea

ORCID number: Hong-Min Ahn 0000-0001-9963-2021; Duck-Woo Kim 0000-0001-9218-4676; Hye Seung Lee 0000-0002-1667-7986; In Jun Yang 0000-0001-9374-353X; Jung Wook Suh 0000-0002-9330-9917; Heung-Kwon Oh 0000-0002-8066-2367; Sung-Bum Kang 0000-0002-9574-5069.

S-Editor: Chen YL
L-Editor: A
P-Editor: Zhang XD

REFERENCES

1 **Cicenas J**, Tamosaitis L, Kvederaviciute K, Tarvydas R, Staniute G, Kalyan K, Meskinyte-Kausiliene E, Stankevicius V, Valius M. KRAS, NRAS and BRAF mutations in colorectal cancer and melanoma. *Med Oncol* 2017; **34**: 26 [PMID: 28074351 DOI: 10.1007/s12032-016-0879-9]

2 **Kerk SA**, Papagiannakopoulos T, Shah YM, Lyssiotis CA. Metabolic networks in mutant KRAS-driven tumours: tissue specificities and the microenvironment. *Nat Rev Cancer* 2021; **21**: 510-525 [PMID: 34244683 DOI: 10.1038/s41568-021-00375-9]

3 **Wan XB**, Wang AQ, Cao J, Dong ZC, Li N, Yang S, Sun MM, Li Z, Luo SX. Relationships among KRAS mutation status, expression of RAS pathway signaling molecules, and clinicopathological features and prognosis of patients with colorectal cancer. *World J Gastroenterol* 2019; **25**: 808-823 [PMID: 30809081 DOI: 10.3748/wjg.v25.i7.808]

4 **Li W**, Liu Y, Cai S, Yang C, Lin Z, Zhou L, Liu L, Cheng X, Zeng W. Not all mutations of KRAS predict poor prognosis in patients with colorectal cancer. *Int J Clin Exp Pathol* 2019; **12**: 957-967 [PMID: 31933906]

5 **Er TK**, Chen CC, Bujanda L, Herreros-Villanueva M. Clinical relevance of KRAS mutations in codon 13: Where are we? *Cancer Lett* 2014; **343**: 1-5 [PMID: 24051306 DOI: 10.1016/j.canlet.2013.09.012]

6 **Kodaz H**, Hacibekiroglu I, Erdogan B, Turkmen E, Tozkir H, Albayrak D, Uzunoglu S, Cicin I. Association between specific KRAS mutations and the clinicopathological characteristics of colorectal tumors. *Mol Clin Oncol* 2015; **3**: 179-184 [PMID: 25469291 DOI: 10.3892/mco.2014.448]

7 **Fan JZ**, Wang GF, Cheng XB, Dong ZH, Chen X, Deng YJ, Song X. Relationship between mismatch repair protein, RAS, BRAF, PIK3CA gene expression and clinicopathological characteristics in elderly colorectal cancer patients. *World J Clin Cases* 2021; **9**: 2458-2468 [PMID: 33889611 DOI: 10.12998/wjcc.v9.i11.2458]

8 **Jones RP**, Sutton PA, Evans JP, Clifford R, McAvoy A, Lewis J, Rousseau A, Mountford R, McWhirter D, Malik HZ. Specific mutations in KRAS codon 12 are associated with worse overall survival in patients with advanced and recurrent colorectal cancer. *Br J Cancer* 2017; **116**: 923-929 [PMID: 28208157 DOI: 10.1038/bjc.2017.37]

9 **Rosty C**, Young JP, Walsh MD, Clendenning M, Walters RJ, Pearson S, Pavluk E, Nagler B, Pakenas D, Jass JR, Jenkins MA, Win AK, Southey MC, Parry S, Hopper JL, Giles GG, Williamson E, English DR, Buchanan DD. Colorectal carcinomas with KRAS mutation are associated with distinctive morphological and molecular features. *Mod Pathol* 2013; **26**: 825-834 [PMID: 23348904 DOI: 10.1038/modpathol.2012.240]

10 **Lièvre A**, Bachet JB, Le Corre D, Boige V, Landi B, Emile JF, Côté JF, Tomasic G, Penna C, Ducreux M, Rougier P, Penault-Llorca F, Laurent-Puig P. KRAS mutation status is predictive of response to cetuximab therapy in colorectal cancer. *Cancer Res* 2006; **66**: 3992-3995 [PMID: 16618717 DOI: 10.1158/0008-5472.CAN-06-0191]

11 **Asawa P**, Bakalov V, Kancharla P, Abel S, Chahine Z, Monga DK, Kirichenko AV, Wegner RE. The prognostic value of KRAS mutation in locally advanced rectal cancer. *Int J Colorectal Dis* 2022; **37**: 1199-1207 [PMID: 35484252 DOI: 10.1007/s00384-022-04167-x]

12 **Margonis GA**, Kim Y, Spolverato G, Ejaz A, Gupta R, Cosgrove D, Anders R, Karagkounis G, Choti MA, Pawlik TM. Association Between Specific Mutations in KRAS Codon 12 and Colorectal Liver Metastasis. *JAMA Surg* 2015; **150**: 722-729 [PMID: 26038887 DOI: 10.1001/jamasurg.2015.0313]

13 **He K**, Wang Y, Zhong Y, Pan X, Si L, Lu J. KRAS Codon 12 Mutation is Associated with More Aggressive Invasiveness in Synchronous Metastatic Colorectal Cancer (mCRC): Retrospective Research. *Onco Targets Ther* 2020; **13**: 12601-12613 [PMID: 33335401 DOI: 10.2147/OTT.S279312]

14 **Li W**, Qiu T, Zhi W, Shi S, Zou S, Ling Y, Shan L, Ying J, Lu N. Colorectal carcinomas with KRAS codon 12 mutation are associated with more advanced tumor stages. *BMC Cancer* 2015; **15**: 340 [PMID: 25929517 DOI: 10.1186/s12885-015-1345-3]

15 **Guerrero S**, Casanova I, Farré L, Mazo A, Capellà G, Mangues R. K-ras codon 12 mutation induces higher level of resistance to apoptosis and predisposition to anchorage-independent growth than codon 13 mutation or proto-oncogene overexpression. *Cancer Res* 2000; **60**: 6750-6756 [PMID: 11118062]

16 **Guerrero S**, Figueras A, Casanova I, Farré L, Lloveras B, Capellà G, Trias M, Mangues R. Codon 12 and codon 13 mutations at the K-ras gene induce different soft tissue sarcoma types in nude mice. *FASEB J* 2002; **16**: 1642-1644 [PMID: 12207005 DOI: 10.1096/fj.02-0050fje]

17 **Samowitz WS**, Curtin K, Schaffer D, Robertson M, Leppert M, Slattery ML. Relationship of Ki-ras mutations in colon cancers to tumor location, stage, and survival: a population-based study. *Cancer Epidemiol Biomarkers Prev* 2000; **9**: 1193-1197 [PMID: 11097226]

18 **Bazan V**, Migliavacca M, Zanna I, Tubiolo C, Grassi N, Latteri MA, La Farina M, Albanese I, Dardanoni G, Salerno S, Tomasino RM, Labianca R, Gebbia N, Russo A. Specific codon 13 K-ras mutations are predictive of clinical outcome in colorectal cancer patients, whereas codon 12 K-ras mutations are associated with mucinous histotype. *Ann Oncol* 2002; **13**: 1438-1446 [PMID: 12196370 DOI: 10.1093/annonc/mdf226]

19 **Imamura Y**, Morikawa T, Liao X, Lochhead P, Kuchiba A, Yamauchi M, Qian ZR, Nishihara R, Meyerhardt JA, Haigis KM, Fuchs CS, Ogino S. Specific mutations in KRAS codons 12 and 13, and patient prognosis in 1075 BRAF wild-type colorectal cancers. *Clin Cancer Res* 2012; **18**: 4753-4763 [PMID: 22753589 DOI: 10.1158/1078-0432.CCR-11-3210]

20 **Hayama T**, Hashiguchi Y, Okamoto K, Okada Y, Ono K, Shimada R, Ozawa T, Toyoda T, Tsuchiya T, Iinuma H, Nozawa K, Matsuda K. G12V and G12C mutations in the gene KRAS are associated with a poorer prognosis in primary colorectal cancer. *Int J Colorectal Dis* 2019; **34**: 1491-1496 [PMID: 31309326 DOI: 10.1007/s00384-019-03344-9]

21 **Imamura Y**, Lochhead P, Yamauchi M, Kuchiba A, Qian ZR, Liao X, Nishihara R, Jung S, Wu K, Nosho K, Wang YE, Peng S, Bass AJ, Haigis KM, Meyerhardt JA, Chan AT, Fuchs CS, Ogino S. Analyses of clinicopathological, molecular, and prognostic associations of KRAS codon 61 and codon 146 mutations in colorectal cancer: cohort study and literature review. *Mol Cancer* 2014; **13**: 135 [PMID: 24885062 DOI: 10.1186/1476-4598-13-135]

22 **Bellio H**, Fumet JD, Ghiringhelli F. Targeting BRAF and RAS in Colorectal Cancer. *Cancers (Basel)* 2021; **13** [PMID: 34063682 DOI: 10.3390/cancers13092201]

23 **Andreyev HJ**, Norman AR, Cunningham D, Oates J, Dix BR, Iacopetta BJ, Young J, Walsh T, Ward R, Hawkins N, Beranek M, Jandik P, Benamouzig R, Jullian E, Laurent-Puig P, Olschwang S, Muller O, Hoffmann I, Rabes HM, Zietz C, Troungos C, Valavanis C, Yuen ST, Ho JW, Croke CT, O'Donoghue DP, Giaretti W, Rapallo A, Russo A, Bazan V, Tanaka M, Omura K, Azuma T, Ohkusa T, Fujimori T, Ono Y, Pauly M, Faber C, Glaesener R, de Goeij AF, Arends JW, Andersen SN, Lövig T, Breivik J, Gaudernack G, Clausen OP, De Angelis PD, Meling GI, Rognum TO, Smith R, Goh HS, Font A, Rosell R, Sun XF, Zhang H, Benhattar J, Losi L, Lee JQ, Wang ST, Clarke PA, Bell S, Quirke P, Bubb VJ, Piris J, Cruickshank NR, Morton D, Fox JC, Al-Mulla F, Lees N, Hall CN, Snary D, Wilkinson K, Dillon D, Costa J, Pricolo VE, Finkelstein SD, Thebo JS, Senagore AJ, Halter SA, Wadler S, Malik S, Krtolica K, Urosevic N. Kirsten ras mutations in patients with colorectal cancer: the 'RASCAL II' study. *Br J Cancer* 2001; **85**: 692-696 [PMID: 11531254 DOI: 10.1054/bjoc.2001.1964]

24 **Kwak MS**, Cha JM, Yoon JY, Jeon JW, Shin HP, Chang HJ, Kim HK, Joo KR, Lee JI. Prognostic value of KRAS codon 13 gene mutation for overall survival in colorectal cancer: Direct and indirect comparison meta-analysis. *Medicine (Baltimore)* 2017; **96**: e7882 [PMID: 28858102 DOI: 10.1097/MD.0000000000007882]

25 **Chen J**, Ye Y, Sun H, Shi G. Association between KRAS codon 13 mutations and clinical response to anti-EGFR treatment in patients with metastatic colorectal cancer: results from a meta-analysis. *Cancer Chemother Pharmacol* 2013; **71**: 265-272 [PMID: 23090619 DOI: 10.1007/s00280-012-2005-9]

26 **Cionca FL**, Dobre M, Dobrea CM, Iosif CI, Comănescu MV, Ardeleanu CM. Mutational status of KRAS and MMR genes in a series of colorectal carcinoma cases. *Rom J Morphol Embryol* 2018; **59**: 121-129 [PMID: 29940619]

27 **Tsilimigras DI**, Ntanasis-Stathopoulos I, Bagante F, Moris D, Cloyd J, Spartalis E, Pawlik TM. Clinical significance and prognostic relevance of KRAS, BRAF, PI3K and TP53 genetic mutation analysis for resectable and unresectable colorectal liver metastases: A systematic review of the current evidence. *Surg Oncol* 2018; **27**: 280-288 [PMID: 29937183 DOI: 10.1016/j.suronc.2018.05.012]

28 **Meguid RA**, Slidell MB, Wolfgang CL, Chang DC, Ahuja N. Is there a difference in survival between right- versus left-sided colon cancers? *Ann Surg Oncol* 2008; **15**: 2388-2394 [PMID: 18622647 DOI: 10.1245/s10434-008-0015-y]

29 **Benedix F**, Kube R, Meyer F, Schmidt U, Gastinger I, Lippert H; Colon/Rectum Carcinomas (Primary Tumor) Study Group. Comparison of 17,641 patients with right- and left-sided colon cancer: differences in epidemiology, perioperative course, histology, and survival. *Dis Colon Rectum* 2010; **53**: 57-64 [PMID: 20010352 DOI: 10.1007/DCR.0b013e3181c703a4]

30 **Brulé SY**, Jonker DJ, Karapetis CS, O'Callaghan CJ, Moore MJ, Wong R, Tebbutt NC, Underhill C, Yip D, Zalcberg JR, Tu D, Goodwin RA. Location of colon cancer (right-sided versus left-sided) as a prognostic factor and a predictor of benefit from cetuximab in NCIC CO.17. *Eur J Cancer* 2015; **51**: 1405-1414 [PMID: 25979833 DOI: 10.1016/j.ejca.2015.03.015]

31 **Elnatan J**, Goh HS, Smith DR. C-KI-RAS activation and the biological behaviour of proximal and distal colonic adenocarcinomas. *Eur J Cancer* 1996; **32A**: 491-497 [PMID: 8814697 DOI: 10.1016/0959-8049(95)00567-6]

32 **Hu J**, Yan WY, Xie L, Cheng L, Yang M, Li L, Shi J, Liu BR, Qian XP. Coexistence of MSI with KRAS mutation is associated with worse prognosis in colorectal cancer. *Medicine (Baltimore)* 2016; **95**: e5649 [PMID: 27977612 DOI: 10.1097/MD.0000000000005649]

33 **Nash GM**, Gimbel M, Cohen AM, Zeng ZS, Ndubuisi MI, Nathanson DR, Ott J, Barany F, Paty PB. KRAS mutation and microsatellite instability: two genetic markers of early tumor development that influence the prognosis of colorectal cancer. *Ann Surg Oncol* 2010; **17**: 416-424 [PMID: 19813061 DOI: 10.1245/s10434-009-0713-0]

34 **Lin CC**, Lin JK, Lin TC, Chen WS, Yang SH, Wang HS, Lan YT, Jiang JK, Yang MH, Chang SC. The prognostic role of microsatellite instability, codon-specific KRAS, and BRAF mutations in colon cancer. *J Surg Oncol* 2014; **110**: 451-457 [PMID: 24964758 DOI: 10.1002/jso.23675]

35 **Taieb J**, Le Malicot K, Shi Q, Penault-Llorca F, Bouché O, Tabernero J, Mini E, Goldberg RM, Folprecht G, Luc Van Laethem J, Sargent DJ, Alberts SR, Emile JF, Laurent Puig P, Sinicrope FA. Prognostic Value of BRAF and KRAS Mutations in MSI and MSS Stage III Colon Cancer. *J Natl Cancer Inst* 2017; **109** [PMID: 28040692 DOI: 10.1093/jnci/djw272]

36 **Nazemalhosseini-Mojarad E**, Kishani Farahani R, Mehrizi M, Baghaei K, Yaghoob Taleghani M, Golmohammadi M, Peyravian N, Ashtari S, Pourhoseingholi MA, Asadzadeh Aghdaei H, Zali MR. Prognostic Value of BRAF and KRAS Mutation in Relation to Colorectal Cancer Survival in Iranian Patients: Correlated to Microsatellite Instability. *J Gastrointest Cancer* 2020; **51**: 53-62 [PMID: 30635874 DOI: 10.1007/s12029-019-00201-4]

37 **Lee SY**, Kim DW, Lee J, Park HM, Kim CH, Lee KH, Oh HK, Kang SB, Kim HR. Association between microsatellite instability and tumor response to neoadjuvant chemoradiotherapy for rectal cancer. *Ann Surg Treat Res* 2022; **103**: 176-182 [PMID: 36128037 DOI: 10.4174/astr.2022.103.3.176]

38 **Lee SY**, Kim DW, Lee HS, Ihn MH, Oh HK, Min BS, Kim WR, Huh JW, Yun JA, Lee KY, Kim NK, Lee WY, Kim HC, Kang SB. Low-Level Microsatellite Instability as a Potential Prognostic Factor in Sporadic Colorectal Cancer. *Medicine (Baltimore)* 2015; **94**: e2260 [PMID: 26683947 DOI: 10.1097/MD.0000000000002260]

39 **Tonello M**, Baratti D, Sammartino P, Di Giorgio A, Robella M, Sassaroli C, Framarini M, Valle M, Macrì A, Graziosi L, Coccolini F, Lippolis PV, Gelmini R, Deraco M, Biacchi D, Santullo F, Vaira M, Di Lauro K, D'Acapito F, Carboni F, Giuffrè G, Donini A, Fugazzola P, Faviana P, Sorrentino L, Scapinello A, Del Bianco P, Sommariva A. Microsatellite and RAS/RAF Mutational Status as Prognostic Factors in Colorectal Peritoneal Metastases Treated with Cytoreductive Surgery and Hyperthermic Intraperitoneal Chemotherapy (HIPEC). *Ann Surg Oncol* 2022; **29**: 3405-3417 [PMID: 34783946 DOI: 10.1245/s10434-021-11045-3]

40 **Formica V**, Sera F, Cremolini C, Riondino S, Morelli C, Arkenau HT, Roselli M. KRAS and BRAF Mutations in Stage II and III Colon Cancer: A Systematic Review and Meta-Analysis. *J Natl Cancer Inst* 2022; **114**: 517-527 [PMID: 34542636 DOI: 10.1093/jnci/djab190]

World Journal of Gastroenterology

Submit a Manuscript: https://www.f6publishing.com

World J Gastroenterol 2023 August 28; 29(32): 4900-4911

DOI: 10.3748/wjg.v29.i32.4900

ISSN 1007-9327 (print) ISSN 2219-2840 (online)

ORIGINAL ARTICLE

Retrospective Cohort Study

Hepatitis B virus infection in patients with Wilson disease: A large retrospective study

Hua-Ying Zhou, Xu Yang, Kai-Zhong Luo, Yong-Fang Jiang, Wen-Long Wang, Jun Liang, Ming-Ming Li, Hong-Yu Luo

Specialty type: Gastroenterology and hepatology

Provenance and peer review: Unsolicited article; Externally peer reviewed.

Peer-review model: Single blind

Peer-review report's scientific quality classification

Grade A (Excellent): A
Grade B (Very good): B
Grade C (Good): 0
Grade D (Fair): 0
Grade E (Poor): 0

P-Reviewer: Elpek GO, Turkey; Shahid M, Pakistan

Received: June 4, 2023
Peer-review started: June 4, 2023
First decision: July 8, 2023
Revised: July 20, 2023
Accepted: July 31, 2023
Article in press: July 31, 2023
Published online: August 28, 2023

Hua-Ying Zhou, Xu Yang, Kai-Zhong Luo, Yong-Fang Jiang, Wen-Long Wang, Jun Liang, Ming-Ming Li, Hong-Yu Luo, Department of Infectious Diseases, Institute of Hepatology, The Second Xiangya Hospital, Central South University, Changsha 410011, Hunan Province, China

Corresponding author: Hong-Yu Luo, MD, Associate Professor, Department of Infectious Diseases, Institute of Hepatology, The Second Xiangya Hospital, Central South University, No. 139 Renming Road, Changsha 410011, Hunan Province, China. luohongyu@csu.edu.cn

Abstract

BACKGROUND

Wilson disease (WD) is the most common genetic metabolic liver disease. Some studies have shown that comorbidities may have important effects on WD. Data on hepatitis B virus (HBV) infection in patients with WD are limited.

AIM

To investigate the prevalence and clinical impact of HBV infection in patients with WD.

METHODS

The clinical data of patients with WD were analyzed retrospectively, and the data of patients with concurrent WD and HBV infection were compared with those of patients with isolated WD.

RESULTS

Among a total of 915 WD patients recruited, the total prevalence of current and previous HBV infection was 2.1% [95% confidence interval (CI): 1.2%-3.0%] and 9.2% (95%CI: 7.3%-11.1%), respectively. The main finding of this study was the identification of 19 patients with concurrent WD and chronic hepatitis B (CHB) infection. The diagnosis of WD was missed in all but two patients with CHB infection. The mean delay in the diagnosis of WD in patients with concurrent WD and CHB infection was 32.5 mo, which was significantly longer than that in patients with isolated WD (10.5 mo). The rates of severe liver disease and mortality in patients with concurrent WD and CHB infection were significantly higher than those in patients with isolated WD (63.1% *vs* 19.3%, $P = 0.000$ and 36.8% *vs* 4.1%, $P < 0.001$, respectively). Binary logistic regression analysis revealed a significantly higher risk of severe liver disease at the diagnosis of WD in patients

with current HBV infection [odds ratio (OR) = 7.748; 95%CI: 2.890-20.774; *P* = 0.000)] or previous HBV infection (OR = 5.525; 95%CI: 3.159-8.739; *P* = 0.000) than in patients with isolated WD.

CONCLUSION

The total prevalence of current HBV infection in patients with WD was 2.1%. The diagnosis of WD in CHB patients is usually missed. HBV infection is an independent risk factor for severe liver disease in WD patients. The diagnosis of WD should be ruled out in some patients with CHB infection.

Key Words: Wilson disease; Hepatitis B virus; Chronic hepatitis B; Kayser-Fleischer ring; Ceruloplasmin; Concurrent Wilson disease and hepatitis B virus infection

©The Author(s) 2023. Published by Baishideng Publishing Group Inc. All rights reserved.

Core Tip: Data on hepatitis B virus (HBV) infection in patients with Wilson disease (WD) are limited. This is the largest investigation of HBV infection in WD patients. The most important finding of this study was the identification of 19 patients with concurrent WD and chronic hepatitis B (CHB) infection. The total prevalence of current HBV infection in patients with WD was 2.1%. The diagnosis of WD in CHB patients is usually missed. HBV infection is an independent risk factor for severe liver disease in WD patients. The diagnosis of WD should be ruled out in some patients with CHB infection.

Citation: Zhou HY, Yang X, Luo KZ, Jiang YF, Wang WL, Liang J, Li MM, Luo HY. Hepatitis B virus infection in patients with Wilson disease: A large retrospective study. *World J Gastroenterol* 2023; 29(32): 4900-4911
URL: https://www.wjgnet.com/1007-9327/full/v29/i32/4900.htm
DOI: https://dx.doi.org/10.3748/wjg.v29.i32.4900

INTRODUCTION

Wilson disease (WD) is an autosomal recessive disorder of copper metabolism caused by a mutation of the gene coding for copper-transporting P-type ATPase (ATP7B). It is characterized by an excessive accumulation of copper in the liver and brain, and occurs in all ethnic groups with an average prevalence of 1:30000[1,2]. The WD gene was cloned in 1993[3-5], and more than 600 gene mutations have been identified[6]. Disease progression in WD may vary, ranging from fulminant WD to an insidious progression to cirrhosis over 20-30 years. Overall, available data in literature strongly suggest that genotypic variability alone does not explain the surprisingly heterogeneous presentation of WD[7]. Some studies have shown that comorbidities may have important effects on WD[8,9].

Currently, hepatitis B virus (HBV) infection is the common cause of liver disease worldwide, affecting 290 million individuals[10,11]. However, data on the prevalence of HBV infection in WD patients are limited and inconsistent. A study from Italy reported that after monitoring 60 WD patients for 20 years, no active HBV infection was found. Accordingly, they hypothesized that the excessive copper levels caused by WD could prevent HBV infection[12]. Contrarily, a study conducted in Taiwan in 1998 reported that the prevalence of HBV infection in 61 patients with WD was 16%, which was similar to that in the general population[13]. However, this finding is different from the previously published observations of Lau *et al*[14] in Hong Kong. Moreover, these studies were conducted many years ago and in small sample size populations; therefore, more studies involving larger sample size populations are needed. Furthermore, the influence of HBV infection on the diagnosis and clinical aspect of WD remains unclear. Given the paucity of studies in this field, this study was undertaken to investigate the prevalence of HBV infection in patients with WD and to explore the impact of HBV infection on the diagnosis, clinical aspect, treatment and prognosis of WD.

MATERIALS AND METHODS

Design overview, setting, and patients

We retrospectively analyzed the data of WD patients diagnosed between May 2003 and December 2020 at the Department of Infectious Diseases/Institute of Hepatology, the Second Xiangya Hospital, Central South University, China, which is the oldest and largest tertiary referral hospital in the Hunan Province. The Institute of Hepatology of this hospital is one of the first centers to carry out research on WD in China, and it offers services to WD patients in the whole province, neighboring provinces, and all over the country.

Patients with suspected WD underwent slit-lamp examination [to identify Kayser-Fleischer (KF) rings], neurological examination, measurement of serum ceruloplasmin levels, and determination of 24 h urinary copper excretion (before and after a penicillamine challenge). In cases where there were no contraindications, a liver biopsy was performed to confirm the presence of copper deposits, and in some other cases, gene analysis was performed. The diagnosis of WD was made based on a combination of clinical symptoms and laboratory tests, and on the WD scoring system published in 2003

[15,16]. WD was confirmed if the WD score was ≥ 4. The WD phenotypes were classified based on previously published criteria[16]. All WD patients were tested for HBV markers, including hepatitis B surface antigen (HBsAg), anti-HBs, hepatitis B e antigen (HBeAg), anti-HBe, and anti-HBc, at the time of diagnosis. Patients positive for HBsAg underwent further analysis to quantify HBV DNA levels. For each patient, all the data obtained at the time of diagnosis and at each follow-up time point were recorded in a medical record specifically designed for the WD study.

All the patients diagnosed with WD during the study period were eligible for inclusion. We excluded WD patients with other types of viral hepatitis (A, C, or E), autoimmune hepatitis, drug-induced liver disease, a history of alcohol intake > 30 g ethanol/day, and patients whose HBV markers were not tested.

Laboratory methods

Routine laboratory data were obtained using standard methods. HBV markers were tested using commercial diagnostic kits (ELISA; Shanghai Kehua Bioengineering Co. Ltd., Shanghai, China). HBV DNA levels were quantified using a commercial hepatitis B DNA quantitative fluorescence diagnostic kit (Sansure Biotech Inc, Changsha, Hunan Province, China). The lower limits of the HBV DNA quantification were 100 and 10 IU/mL before 2011 and after 2012, respectively. The KF rings were examined under a slit-lamp by an experienced ophthalmologist. Serum ceruloplasmin levels were measured using the nephelometric method (normal range, 210-500 mg/L; Beckman Coulter, Image® Immunochemistry System, Brea, CA, United States). Copper levels in serum, urine, and liver were determined as previously described[17]. Moreover, the ATP7B coding region and exon/intron boundaries were amplified and sequenced, as previously described [18].

Study outcomes

The study outcomes included the following: The proportion of patients with WD who had current HBV infection (positive for HBsAg); the proportion of those with previous HBV infection (negative for HBsAg but positive for anti-HBc, with or without anti-HBs); the rate of severe liver disease {defined as the proportion of WD patients who experienced severe decompensated cirrhosis [Child-Turcotte-Pugh (CTP) score ≥ 10] or acute-on-chronic liver failure (ACLF) in WD patients with HBV infection and those without HBV infection}. The CTP score was determined based on a previously described criterion[19,20]. ACLF was diagnosed according to a combination of consensus recommendations published by the Asian Pacific Association for the Study of the Liver (in 2009) and the guidelines for the diagnosis and treatment liver failure published by the Chinese Society of Hepatology in 2006[21,22]. The criteria were as follows: (1) Acute severe exacerbation of liver disease complicated within 4 wk by clinical ascites and/or encephalopathy, with previously diagnosed or undiagnosed chronic liver disease/cirrhosis; (2) Serum bilirubin ≥ 10 mg/d; and (3) Coagulopathy (international normalized ratio ≥ 1.5 or prothrombin activity < 40%).

Statistical analysis

Continuous data were expressed as mean ± SD and compared using the unpaired *t*-test or Mann-Whitney *U* test. Categorical variables were expressed as proportions and compared using the chi-squared test or Fishers exact test. We used a binary logistic regression model to evaluate the association between HBV infection and the risk of severe liver disease at the time of diagnosis of WD, the results were summarized as odds ratio (OR) with 95% confidence intervals (CI). All statistical analyses were performed using the software Statistical Packages for the Social sciences, SPSS version 20.0 Windows (IBM Corp., Armonk, NY, United States). Statistical significance was set at a two-tailed *P* value < 0.05.

RESULTS

During the study period, 973 patients were diagnosed with WD. Among them, 58 patients were excluded because of concurrent hepatitis E infection (*n* = 3), hepatitis C infection (*n* = 3), thalassemia (*n* = 3), and schistosomiasis japonica (*n* = 2), as well as insufficient length of hospital stay to perform the tests (*n* = 47). The remaining 915 patients with WD (532 men, 383 women; mean age, 20.2 ± 13.1 years; age range, 1-68 years) were included in our analysis. The patients resided in 25 provinces and belonged to 825 families. Moreover, 644 (70.4%), 218 (23.8%), 35 (3.8%), and 18 (2.0%) patients presented with only hepatic disease, neuropsychiatric and hepatic disease, only neuropsychiatric disease, and neither hepatic nor neurological disease, respectively. WD diagnosis was confirmed by a liver copper level ≥ 250 μg/g dry weight, the identification of two disease-causing mutations or homozygosity for a single disease-causing mutation, or both criteria in 320, 378, and 102 patients, respectively. All patients met the criteria of the WD scoring system, with 735 (80.3%), 87, and 93 patients having WD scores ≥ 6, 5, and 4, respectively.

Prevalence of HBV infection among patients with WD

Among the 915 patients with WD, 393 tested negative for all HBV markers (43.0%, 95%CI: 39.8%-46.15%) and 419 (45.8%) tested positive for immunization-related anti-HBs alone (45.8%, 95%CI: 42.5%-49.0%). The total prevalence of current and previous HBV infections were 2.1% (95%CI: 1.2%-3.0%) and 9.2% (95%CI: 7.3%-11.1%), respectively. Table 1 summarizes the prevalence of HBV infection stratified by sex and age. The prevalence of both current and previous HBV infections were significantly lower in women than in men and in patients aged ≤ 10 years than in those aged ≥ 11 years. The prevalence of previous HBV infection increased with age; however, the prevalence of current HBV infection remained low irrespective of age (Table 1).

Table 1 Prevalence of hepatitis B infection in patients with Wilson disease stratified by gender and age

	Number of patients	Negative for HBVM (%)	Anti-HBs(+) alone (%)	Prior HBV infection (%)	Current HBV infection (%)
Total group	915	393 (43.0)	419 (45.8)	84 (9.2)	19 (2.1)
Sex					
Male	532	228 (42.9)	239 (44.9)	52 (9.8)	13 (2.4)
Female	383	165 (43.1)	180 (47.0)	32 (8.4)	6 (1.6)
Age group (yr)					
2-10	231	105 (45.5)	119 (51.5)	7 (3.0)	0 (0.0)
11-20	340	156 (45.9)	159 (46.8)	15 (4.4)	10 (2.9)
21-30	153	63 (41.2)	73 (47.7)	13 (8.5)	4 (2.6)
31-40	106	40 (37.7)	42 (39.6)	21 (19.8)	3 (2.8)
41-65	85	29 (34.1)	26 (30.6)	28 (32.9)	2 (2.3)

HBVM: Hepatitis B virus markers; HBV: Hepatitis B virus.

Characteristics of WD patients with current HBV infection

During the study period, 19 WD patients with current HBV infection were consecutively diagnosed (men, 13; women, 6; mean age, 25.1 ± 13.3 years; age range, 11-64 years). Among them, six and ten patients were positive for HBeAg and HBV DNA, respectively. Moreover, 16 patients had a 1- to 30-year history of HBV-related liver disease, among whom there were three patients who had undergone splenectomy 3 years earlier and five patients who had been receiving a treatment based on lamivudine or entecavir for 2-24 mo. All patients met the WD criteria. More specifically, WD diagnosis was based on elevated liver copper levels, identification of two disease-causing mutations or homozygosity for a single disease-causing mutation, or both in 10, 6, and 5 patients, respectively. Furthermore, 16 patients had a WD score ≥ 6 (84.2%). However, among the patients, only two were suspected of having WD; 17 were referred to our hospital because of chronic hepatitis B (CHB) and had never been diagnosed of WD before.

There was a high variability in the clinical manifestations in patients with WD and current HBV infection. Five patients (cases 2, 6, 7, 11, and 19) presented with ACLF, characterized by severe jaundice, markedly decreased albumin levels, and prolonged prothrombin time (except for case 6, the remaining four patients among these patients died within 15-30 d following diagnosis). Two and eight patients presented with evidence of compensated and decompensated cirrhosis, respectively. Two patients presented with symptoms and signs of chronic liver disease, including hepatic enlargement or abnormal serum aminotransferases levels. Two patients were entirely asymptomatic, with normal serum aminotransferase and mild hepatomegaly or splenomegaly (Tables 2-4).

Characteristics of WD patients with previous HBV infection

During the study period, 84 patients with WD and previous HBV infection were consecutively diagnosed (men, 52; women, 32; mean age, 33.3 ± 15.9 years; age range, 3-68 years). Among them, 74 patients were positive for anti-HBs and anti-HBc, 10 patients were positive for anti-HBc only, and none of the patients had detectable levels of HBV DNA. The diagnosis of WD was based on elevated liver copper levels, identification of two disease-causing mutations, or both in 16, 47, and 8 patients, respectively. All patients met the criteria of the WD scoring system, with 70 patients having WD scores ≥ 6 (83.3%).

Comparison between patients with isolated WD and those with concurrent WD and HBV infection

There were no differences in sex, WD phenotype, copper metabolism parameters (such as the positivity rates of KF rings, urinary copper excretion, and hepatic copper content), and mean WD score distribution between patients with isolated WD and those with concurrent WD and current or previous HBV infection. Compared with patients with isolated WD, WD patients having HBV infection were significantly older and had significantly more severe liver function damage (including lower serum albumin levels, higher serum total bilirubin levels, and longer prothrombin time). The ACLF rates in WD patients with current and previous HBV infection were 26.3% and 13.1%, respectively, which were significantly higher than the rate in patients with isolated WD (4.5%, $P = 0.000$). The rates of severe decompensated liver cirrhosis in WD patients with current and previous HBV infection were 40.5% and 36.8%, respectively, and these were significantly higher than the rate in patients with isolated WD (14.8%; $P = 0.000$). The mortality rates during the first 60 d of follow-up following diagnosis were 36.8% and 15.5% in WD patients with current and previous HBV infection, respectively; these values were significantly higher than the rate in patients with isolated WD (4.1%, $P = 0.000$) (Table 5). Based on the binary logistic regression analysis model, after accounting for age, sex, and HBV infection and taking as reference the groups of patients with isolated WD, there was a significantly higher risk of severe liver disease at WD diagnosis in WD patients with current (OR = 7.748; 95%CI: 2.890-20.774; $P = 0.000$) or previous HBV infection (OR = 5.525; 95%CI: 3.159-8.739; $P = 0.000$).

Table 2 Characteristics of patients with Wilson disease and chronic hepatitis B: The demographic characteristics and parameters of hepatitis B virus infection

Case	Sex	Age (yr)	History of HBV (yr)	HBsAg	HBeAg	Anti-HBe	HBV DNA
1	Female	16	2	+	-	+	< 100
2	Male	19	2	+	-	+	9.3e8
3	Female	19	2	+	-	-	< 100
4	Male	26	3	+	+	-	1.9e6
5	Male	43	3	+	-	+	5.6e5
6	Female	37	2	+		+	7.3e3
7	Male	19	3	+	-	+	< 100
8	Male	11	5	+	+	-	3.2e7
9	Male	26	20	+	-	+	1.9e4
10	Female	17	3	+	-	+	< 10
11	Male	20	10	+	+	-	2.3e4
12	Male	11	?	+	-	+	< 10
13	Female	32	?	+	-	+	81
14	Male	27	?	+	+	-	1.3e6
15	Male	24	16	+	+	-	2.1e8
16	Male	15	16	+	-	+	< 10
17	Male	65	30	+	-	+	22.3
18	Female	35	16	+	-	+	< 10
19	Male	15	10	+	+	-	1.8e6

HBV: Hepatitis B virus; HBsAg: Hepatitis B surface antigen; HBeAg: Hepatitis B e antigen.

Treatment and outcomes of WD patients with current HBV infection

Five patients with concurrent WD and current HBV infection diagnosed before 2007 were treated with a chelator alone. The patients refused liver transplantation for financial reasons, rapidly deteriorated, and died from liver failure 2-4 wk after admission. Eight patients with detectable HBV DNA levels, diagnosed after 2008, were treated with a combination of penicillamine and nucleoside. Among them, two patients (cases 11 and 19) with ACLF rapidly deteriorated and died 1 mo after admission. Two patients (cases 6 and 8) were lost to follow-up. The condition of the remaining four patients gradually improved with treatment; however, one patient (case 5) developed hepatocellular carcinoma and died 7 mo after admission. Six patients with undetectable HBV DNA levels, diagnosed after 2008, were initially treated with a chelator only. Their condition gradually improved. However, three among them experienced HBV replication at 7-12 mo after therapy. Among the latter, there was one patient (case 10) with severe hepatitis reactivation and increased serum alanine aminotransferase (ALT; 930 IU/L), aspartate aminotransferase (AST; 790 IU/L), and HBV DNA (9.2×10^4 IU/mL) levels. This patient was treated with entecavir and penicillamine. However, within 2-3 mo after treatment initiation, HBV DNA levels were undetectable, and the AST and ALT levels normalized. The remaining three patients continued treatment with a chelator only. Currently, nine of the 14 patients diagnosed after 2008 have achieved a stable disease status after therapy and have resume their routine living activities (full-time work or study). WD patients with a previous HBV infection were treated using a chelator only. None of the patients experienced HBV reactivation during the study period.

DISCUSSION

To the best of our knowledge, the prevalence of HBV infection in patients with WD has been reported in only two small studies, and only two case studies involving single cases of concurrent WD and CHB infection have been reported in the English literature[23,24]. This is the largest investigation of HBV infection in WD patients, and it is helpful in understanding the true prevalence of HBV infection in WD patients and the impact of HBV infection on WD.

A national survey conducted in 1992 reported that the overall HBsAg prevalence in the Chinese population was 9.8%, declining to 7.2% in 2006[25,26]. In the present study, the total HBsAg prevalence was 2.1% in WD patients, a figure which is far lower than previously reported national HBsAg rates. However, this does not imply that the prevalence of

Table 3 Characteristics of patients with Wilson disease and chronic hepatitis B: Diagnostic parameters of Wilson disease

Case	Neurologic signs	KF rings	Cerulo plasmin (mg/L)	Urinary copper/after PC (μg/24 h)	Hepatic copper (μg/g/dw)	Mutation analysis	WD score
1	No	P	65.0	177/1600	ND	ND	5
2	No	P	50.0	1222/4250	ND	ND	6
3	No	P	95.0	1818/2266	ND	ND	6
4	Yes	P	187.0	434/ND	ND	ND	7
5	No	P	172.0	107/1295	347	ND	6
6	No	P	216.0	431/1436	1165	ND	6
7	No	P	50.0	5171/15398	ND	ND	6
8	No	P	250.0	305/1933	1173	ND	6
9	No	N	74.0	474/1500	926	3532G>T/3532G>T	10
10	No	P	84.0	595/1725	ND	2755C>G/2975C>T	10
11	No	N	135.0	1297/2984	ND	588C>A/2333G>T	7
12	No	P	78.4	160/1773	741	2975C>T/2975C>T	11
13	No	P	129	855/2505	ND	ND	5
14	No	P	31.0	310/1984	1067	3809 >G/	9
15	No	N	104.0	187/1836	896	0	4
16	Yes	P	86.5	237/2374	404	ND	10
17	No	P	83.1	64/714	265	2975C>T/	7
18	No	P	43.0	155/171	906	2804C>T/2810delT	11
19	No	P	63.0	584/2473	ND	2666G>T/2333G>T	10

WD: Wilson disease; KF rings: Kayser-Fleischer rings; ND: Not done; PC: Penicillamine challenge; N: Negative; P: Positive.

HBV infection in patients with WD is lower than that in the general population. First, since the 1990s, the rate of HBV infection in China has been decreasing annually. The data of WD patients today should not be compared with those of the general population many years ago. Second, the age composition of WD patients is different from that of the general population. Among our patients, 41% were aged below 14 years; however, the HBV infection rate is known to be very low in this age group. Therefore, the average HBsAg positivity rate in WD patients should not be directly compared with that in the general population. To find studies with more comparable data, we conducted a literature search and found a large survey on HBV infection conducted in the Henan Province in 2015. This has been the largest survey on HBV infection in China during the recent years, and it involved a total of 13207 children and 16685 adults[27,28]. The Henan Province is located in the middle of China and is adjacent to Hunan. Its economic development level and HBV infection rate are similar to those in Hunan, making the data from Henan comparable with those from our study. We calculate the HBsAg positivity rates among different age groups of the WD patients, according to the age group divisions used in the Henan study (Table 6). The positivity rates of HBsAg in WD patients aged 1-4, 5-9 and 10-14 years were 0.0%, 0.0%, and 1.6%, respectively, which were similar to those in Henan children of the same age groups (0.5%, 0.7%, and 1.2%, respectively). The positivity rates of HBsAg in the 18-34, 35-54, and 55-74 years age groups of WD patients were 3.0%, 2.5%, and 5.3%, respectively, which were similar to those in the general population of the same age group (3.1%, 4.7%, and 5.1%, respectively). Our study indicates that the prevalence of HBV infection in WD patients is similar to that in the general population, and that WD patients are equally susceptible to HBV infection.

The most important finding of this study was the identification of 19 patients with concurrent WD and CHB infection. It is worth noting regarding the 19 patients that 17 were referred for CHB infection and not WD; thus, the WD was diagnosed at our hospital. There was a significant delay in the diagnosis of WD in these patients (mean delay = 32.5 and 10.5 mo in WD patients with concurrent CHB infection and in patients with isolated WD, respectively). Our results suggest that the diagnosis of WD may be missed in patients with CHB infection. Although a missed diagnosis of WD is not uncommon given the rarity of the disease[29-31], it is worth noting that many patients with CHB infection suffer from undiagnosed WD. The clinical manifestations of patients with concurrent CHB infection and WD are nonspecific and difficult to distinguish from those of patients with isolated CHB infection, unless the clinicians deliberately and diligently examine the patients to rule out WD. Therefore, more attention should be paid regarding the coexistence of WD in patients with CHB infection. WD should be considered and ruled out in some patients with CHB infection, especially in those with cirrhosis, hepatic failure, or poor response to antiviral therapies.

Table 4 Characteristics of patients with Wilson disease and chronic hepatitis B: Parameters of liver disease

Case	ALT	AST	ALB	TBIL	GGT	ALP	INR	Severity of liver disease	Outcome
1	29	50	20.3	46.7	46	74	2.61	CTP: 13	Died
2	70	185	26.8	264	84	61	2.8	ACLF	Died
3	86	50	25.1	123	58	85	2.7	CTP: 13	Died
4	41	60	30.4	44.4	90	70	4.5	CTP: 13	Died
5	102	170	35.7	48.0	110	95	1.5	CTP: 10	Died
6	119	291	27.6	417	186	390	2.1	ACLF	Alive
7	79	123	31	456	45	57	4.1	ACLF	Died
8	231	237	37.5	16.5	353	105	1.2	CTP:6	Alive.
9	74	101	29.8	39.0	42	116	1.5	CTP:10	Alive
10	79	105	24.5	42.0	110	130	2.4	CTP:12	Alive
11	223	268	30.0	368	147	252	2.8	ACLF	Died
12	71	83	31.0	23.0	62	357	1.6	CTP:10	Alive
13	70	76	28.0	25.6	35	375	1.63	CTP:10	Alive
14	82	151	37.8	28.7	152	149	1.36	CTP:5	Alive
15	276	102	39.9	25.3	113	93	0.95	Hepatitis	Alive
16	22	47	36.5	16	32	219	1.25	Hepatitis	Alive
17	31	28	47.3	26.3	23	76	1.01	Hepatitis	Alive
18	56	34	42.0	22.0	90	60	1.01	Hepatitis	Alive
19	57	74	28.0	373	268	293	3.01	ACLF	Died

ALT: Alanine aminotransferase; AST: Aspartate aminotransferase; ALB: Albumin; TBIL: Total bilirubin; GGT: Gamma-glutamyl transpeptidase; ALP: Alkaline phosphatase; INR: International normalized ratio; ACLF: Acute-on-chronic liver failure; CTP: Child-Turcotte-Pugh.

Compared to patients with isolated WD, patients with concurrent WD and CHB infection had significantly lower serum albumin levels, higher serum total bilirubin levels, and longer prothrombin time. The mortality rates of WD patients with current and previous HBV infection during the first 60 d of follow-up (following diagnosis) were 36.8% and 15.5%, respectively; these rates were significantly higher than those of patients with isolated WD (4.1%, $P = 0.000$). The ACLF rates in WD patients with current and previous HBV infection were 26.3% and 13.1%, respectively, which were significantly higher than those in patients with isolated WD (4.5%, $P = 0.000$). Binary logistic regression analysis revealed that the risk of severe liver disease in WD patients with current and previous HBV infection was 7.7 and 5.3 times (respectively) higher than that in patients with isolated WD. Our findings indicate that HBV infection substantially affects the severity liver disease in patients with WD (Tables 5 and 7). The mechanism through which CHB causes severe liver injury could involve the induction, by viral hepatitis, of hepatic injury and copper accumulation, which could additively or synergistically aggravate WD-induced liver damage. Many studies have shown that HBsAg clearance usually results in good long-term prognosis[32]. However, an unexpected finding was that previous HBV infection also had a significant impact on the severity of liver disease in patients with WD. The reason for this may be that WD patients with a previous HBV infection usually have severe liver injury and cirrhosis (due to the joint action of HBV and WD) that occurred before the HBsAg clearance. After the HBsAg clearance, the severe liver injury and cirrhosis that had been formed usually persist[33,34]. Considering the serious impact of HBV infection on the clinical aspect of WD patients, current and previous HBV infections must be screened when evaluating the clinical aspect and prognosis of WD patients.

The strengths of this study are: (1) Considering the rarity of the disease, the sample size of the WD patient cohort was very large; (2) All patients were diagnosed in our department and met the diagnostic criteria; among them, 80% were confirmed by genetic examination and/or liver copper level determination; and (3) All data were prospectively collected by the authors and therefore were complete and reliable. The limitation of this study is the relatively small number of WD patients with concurrent CHB infection, as this might impede the detection of more significant differences between patients with isolated WD and those with co-existing CHB infection and WD.

In conclusion, our study indicates that the prevalence of HBV infection stratified by sex and age in patients with WD is similar to that in the general population. There was a significant delay in the diagnosis of WD in CHB patients. Furthermore, our findings suggest that HBV infection significantly affects the severity of liver disease in patients with WD. Therefore, more attention should be paid to patients suffering from concurrent WD and CHB infection. Although we found that previous HBV infection is an independent factor in the exacerbation of WD, its mechanism remains unknown.

Table 5 Factors associated with severe liver disease at the Wilson disease diagnosis

Factors (at diagnosis)	OR	95%CI	*P* value
Gender			
Male	1		
Female	1. 945	1.402-2.698	0.000
Age at diagnosis (yr)			
Group 1 (0-10)	1		
Group 2 (11-20)	1.766	1.145-2.723	0.010
Group 3 (21-30)	0.757	0.423-1.352	0.346
Group 4 (31-40)	1.178	0.646-2.148	0.594
Group 5 (41-65)	1.455	0.777-2.724	0.241
HBV infection			
WD alone	1		
WD with previous HBV	5.255	3.159-8.739	0.000
WD with current HBV	7.748	2.890-20.774	0.000

Severe liver disease is defined as patients with acute-on-chronic liver failure or a Child-Turcotte-Pugh score ≥ 10 at the Wilson disease diagnosis, HBV: Hepatitis B virus; WD: Wilson disease; OR: Odds ratio; CI: Confidence interval.

Table 6 Comparison of hepatitis B surface antigen positivity rates among different age groups between patients with Wilson disease and the general population

Age groups (yr)	Wilson disease		General population (Henan)		*P* value
	Number tested	HBsAg(+) (*n*, %)	Number tested	HBsAg(+) (*n*, %)	
1-4	40	0, 0.0	5474	26, 0.5	0.827
5-9	148	0, 0.0	4407	32, 0.7	0.625
10-14	191	3, 1.6	3376	40, 1.2	0.505
15-17	97	3, 3.1	Not done		
18-34	298	9, 3.0	6764	220, 3.1	0.825
35-54	122	3, 2.5	6777	275, 4.7	0.490
55-74	19	1, 5.3	3144	147, 5.1	0.599
Total	915	19, 2.1	29892	740, 2.5	0.510

HBsAg: Hepatitis B surface antigen.

Further research is needed to confirm this finding and to elucidate the mechanisms underlying the associations between WD progression and previous HBV infection or cryptogenic HBV infection.

CONCLUSION

This is the largest investigation of HBV infection in WD patients, and it is helpful in understanding the true prevalence of HBV infection in WD patients and the impact of HBV infection on WD.

Table 7 Comparison between Wilson disease patients alone and Wilson disease patients with hepatitis B virus infection

	WD alone (*n* = 812)	With previous HBV (*n* = 84)	With current HBV (*n* = 19)	P1	P2
Sex					
Male (*n*, %)	467 (57.5)	46 (61.9)	12 (63.2)	0.509	0.797
Female (*n*, %)	345 (42.5)	32 (38.1)	7 (36.8)	0.509	0.797
Mean age (yr)	18.8 ± 12.0	33. ± 15.9	25.0 ± 13.	0.000	0.031
Diagnosis delay	12.1 ± 21.3	13.7 ± 26.1	34.6 ± 53.5	0.542	0.000
Phenotype					
Pure H (*n*, %)	564 (69.5)	63 (75.0)	17 (89.5)	0.352	0.104
H and N (*n*, %)	195 (24.40)	21 (25.60)	2 (10.5)	0.352	0.104
Pure N (*n*, %)	35 (4.3)	0 (0.0)	0		
Others (*n*, %)	18 (2.2)	0	0		
Copper metabolic					
KF positive	67.6%	84.1%	78.9%	0.102	0.456
Ceruloplasmin	64.1 ± 46.0	97.1 ± 60.3	105.0 ± 61.6	0.000	0.000
Urinary copper	502.4 ± 1030.5	916.3 ± 245.8	767.7 ± 1165.0	0.005	0.323
Urinary Cu after PC	2236.4 ± 1582.1	2283.7 ± 1287.8	2793.8 ± 3157.5	0.842	0.144
Hepatic Cu	832.2 ± 457.7	680.1 ± 407.7	789.0 ± 338.2	0.191	0.767
Mean WD score	7.4 ± 2.3	8.0 ± 2.2	7.8 ± 2.3	0.124	0.412
Biochemical					
ALT (IU/L)	86.2 ± 105.7	63.3 ± 51.0	94.6 ± 71.1	0.0051	0.722
AST (IU/L)	84.25 ± 90.3	90.47 ± 70.4	125.3 ± 80.5	0.0532	0.058
Albumin (g/L)	38.5 ± 8.3	32.5 ± 7.6	32.1 ± 6.8	0.000	0.001
TBIL (μmol/L)	52.1 ± 131.0	104.7 ± 166.7	126.6 ± 158.3	0.001	0.002
GGT (IU/L)	90.9 ± 85.6	138.6 ± 112.3	109 ± 93.3	0000	0.399
ALP (IU/L)	186.7 ± 133.6	137.7 ± 87.7	171.9 ± 123.0	0.001	0.650
INR	1.42 ± 0.81	1.88 ± 0.86	2.09 ± 1.04	0.000	0.000
Liver disease severity					
Hepatitis (*n*, %)	372 (45.8)	7 (8.3)	3 (15.8)	0.000	0.009
CTP5-6 (*n*, %)	189 (23.3)	18 (21.4)	3 (15.8)	0.702	0.444
CTP7-9 (*n*, %)	94 (11.6)	14 (16.7)	1 (5.3)	0.173	0.713
CTP10-14 (*n*, %)	120 (14.8)	34 (40.5)	7 (36.8)	0.000	0.008
ACLF (*n*, %)	37 (4.5)	11 (13.1)	5 (26.3)	0.001	0.000
Mortality (*n*, %),	33 (4.1)	13 (15.5)	7 (36.8)	0.000	0.000

HBV: Hepatitis B virus; WD: Wilson disease; ALT: Alanine aminotransferase; AST: Aspartate aminotransferase; TBIL: Total bilirubin; GGT: Gamma-glutamyl transpeptidase; ALP: Alkaline phosphatase; INR: International normalized ratio; ACLF: Acute-on-chronic liver failure; CTP: Child-Turcotte-Pugh; PC: Penicillamine challenge.

ARTICLE HIGHLIGHTS

Research background

Although hepatitis B virus (HBV) infection is the most common cause of liver disease in China, the occurrence of HBV infection in Wilson disease (WD) patients and the clinical manifestations of concurrent WD and HBV infections have rarely been reported.

Research motivation

Our study suggests that both WD and HBV infections may coexist. The clinical symptoms of concurrent WD and HBV infections are difficult to distinguish from those of simple viral hepatitis. Therefore, the existence of WD may be hidden. The study of concurrent WD and HBV infection deserves careful consideration.

Research objectives

To investigate the incidence of HBV infection in patients with WD and to analyse how HBV infection affects WD.

Research methods

The clinical data of patients with WD were analyzed retrospectively, and the data of patients with concurrent WD and HBV infection were compared with those of patients with isolated WD. Considering the rarity of the disease, the sample size of the WD patient cohort was very large.

Research results

Among a total of 915 WD patients recruited, the total prevalence of current and previous HBV infection was 2.1% and 9.2% respectively. The main finding of this study was the identification of 19 patients with concurrent WD and chronic hepatitis B (CHB) infection. The mean delay in the diagnosis of WD in patients with concurrent WD and CHB infection was 32.5 mo, which was significantly longer than that in patients with isolated WD (10.5 mo). The rates of severe liver disease and mortality in patients with concurrent WD and CHB infection were significantly higher than those in patients with isolated WD (63.1% *vs* 19.3%), respectively. Binary logistic regression analysis revealed a significantly higher risk of severe liver disease at the diagnosis of WD in patients with current HBV infection or previous HBV infection than in patients with isolated WD.

Research conclusions

Our study indicates that the prevalence of HBV infection stratified by sex and age in patients with WD is similar to that in the general population. There was a significant delay in the diagnosis of WD in CHB patients. HBV infection is an independent risk factor for severe liver disease in WD patients. WD should be considered and excluded in some patients with CHB infection.

Research perspectives

As we found that previous HBV infection was an independent factor in the exacerbation of WD, the mechanism of which is speculative, future studies could further explore the mechanism by which WD is exacerbated by previous HBV infection and whether it is related to occult HBV infection.

FOOTNOTES

Author contributions: Zhou HY, Yang X, and Luo HY contributed to study conception, design and writing of the article; Yang X, Luo KZ, Jiang YF, Wang WL, Liang J, Li MM, and Luo HY contributed to data acquisition, data analysis and interpretation; Zhou HY, Yang X, and Luo HY contributed to editing, reviewing, and final approval of the article; and all authors have read and approved the final manuscript.

Institutional review board statement: The study was reviewed and approved by the Ethical Committee of the Second Xiangya Hospital of Central South University, (2022) Lun Shen [Lin Yan] No. (194).

Informed consent statement: Informed consent was waived by the Ethical Committee of the Second Xiangya Hospital of Central South University.

Conflict-of-interest statement: All the authors report no relevant conflicts of interest for this article.

Data sharing statement: The original anonymous dataset is available on request from the corresponding author luohongyu@csu.edu.cn.

STROBE statement: The authors have read the STROBE Statement checklist of items, and the manuscript was prepared according to the STROBE statement checklist of items.

Open-Access: This article is an open-access article that was selected by an in-house editor and fully peer-reviewed by external reviewers. It is distributed in accordance with the Creative Commons Attribution NonCommercial (CC BY-NC 4.0) license, which permits others to distribute, remix, adapt, build upon this work non-commercially, and license their derivative works on different terms, provided the original work is properly cited and the use is non-commercial. See: https://creativecommons.org/Licenses/by-nc/4.0/

Country/Territory of origin: China

ORCID number: Hua-Ying Zhou 0000-0001-5036-1830; Xu Yang 0000-0001-6660-6417; Kai-Zhong Luo 0000-0001-5643-7103; Yong-Fang Jiang 0000-0001-8977-5109; Wen-Long Wang 0000-0003-4095-2770; Jun Liang 0000-0003-0099-1345; Ming-Ming Li 0000-0002-8959-8285; Hong-Yu Luo 0000-0001-8654-4380.

S-Editor: Wang JJ
L-Editor: A
P-Editor: Chen YX

REFERENCES

1 **Walshe JM**. History of Wilson's disease: 1912 to 2000. *Mov Disord* 2006; **21**: 142-147 [PMID: 16229009 DOI: 10.1002/mds.20694]
2 **Frydman M**. Genetic aspects of Wilson's disease. *J Gastroenterol Hepatol* 1990; **5**: 483-490 [PMID: 2129820 DOI: 10.1111/j.1440-1746.1990.tb01427.x]
3 **Bull PC**, Thomas GR, Rommens JM, Forbes JR, Cox DW. The Wilson disease gene is a putative copper transporting P-type ATPase similar to the Menkes gene. *Nat Genet* 1993; **5**: 327-337 [PMID: 8298639 DOI: 10.1038/ng1293-327]
4 **Tanzi RE**, Petrukhin K, Chernov I, Pellequer JL, Wasco W, Ross B, Romano DM, Parano E, Pavone L, Brzustowicz LM. The Wilson disease gene is a copper transporting ATPase with homology to the Menkes disease gene. *Nat Genet* 1993; **5**: 344-350 [PMID: 8298641 DOI: 10.1038/ng1293-344]
5 **Yamaguchi Y**, Heiny ME, Gitlin JD. Isolation and characterization of a human liver cDNA as a candidate gene for Wilson disease. *Biochem Biophys Res Commun* 1993; **197**: 271-277 [PMID: 8250934 DOI: 10.1006/bbrc.1993.2471]
6 **Gao J**, Brackley S, Mann JP. The global prevalence of Wilson disease from next-generation sequencing data. *Genet Med* 2019; **21**: 1155-1163 [PMID: 30254379 DOI: 10.1038/s41436-018-0309-9]
7 **Ferenci P**, Stremmel W, Członkowska A, Szalay F, Viveiros A, Stättermayer AF, Bruha R, Houwen R, Pop TL, Stauber R, Gschwantler M, Pfeiffenberger J, Yurdaydin C, Aigner E, Steindl-Munda P, Dienes HP, Zoller H, Weiss KH. Age and Sex but Not ATP7B Genotype Effectively Influence the Clinical Phenotype of Wilson Disease. *Hepatology* 2019; **69**: 1464-1476 [PMID: 30232804 DOI: 10.1002/hep.30280]
8 **Sallie R**, Chiyende J, Tan KC, Bradley D, Portmann B, Williams R, Mowat AP, Mieli-Vergani G. Fulminant hepatic failure resulting from coexistent Wilson's disease and hepatitis E. *Gut* 1994; **35**: 849-853 [PMID: 8020819 DOI: 10.1136/gut.35.6.849]
9 **Wong RJ**, Gish R, Schilsky M, Frenette C. A clinical assessment of Wilson disease in patients with concurrent liver disease. *J Clin Gastroenterol* 2011; **45**: 267-273 [PMID: 20535024 DOI: 10.1097/MCG.0b013e3181dffaa5]
10 **Chien RN**, Liaw YF. Current Trend in Antiviral Therapy for Chronic Hepatitis B. *Viruses* 2022; **14** [PMID: 35216027 DOI: 10.3390/v14020434]
11 **Polaris Observatory Collaborators**. Global prevalence, treatment, and prevention of hepatitis B virus infection in 2016: a modelling study. *Lancet Gastroenterol Hepatol* 2018; **3**: 383-403 [PMID: 29599078 DOI: 10.1016/S2468-1253(18)30056-6]
12 **Liggi M**, Sini M, Sorbello O, Civolani A, Demelia L. HBV and HCV infections in Wilson's disease patients: copper overload could be protective? *Clin Biochem* 2012; **45**: 1095-1096 [PMID: 22569595 DOI: 10.1016/j.clinbiochem.2012.04.026]
13 **Yu JM**, Chu EC, Chu NC, Huang CC. Wilsons disease with hepatitis B infection: occurrence, clinical presentation, and prognosis. *Acta Neurol Taiwan* 1998; **7**: 262-265
14 **Lau JY**, Lai CL, Wu PC, Pan HY, Lin HJ, Todd D. Wilson's disease: 35 years' experience. *Q J Med* 1990; **75**: 597-605 [PMID: 2217665]
15 **Roberts EA**, Schilsky ML; American Association for Study of Liver Diseases (AASLD). Diagnosis and treatment of Wilson disease: an update. *Hepatology* 2008; **47**: 2089-2111 [PMID: 18506894 DOI: 10.1002/hep.22261]
16 **Ferenci P**, Caca K, Loudianos G, Mieli-Vergani G, Tanner S, Sternlieb I, Schilsky M, Cox D, Berr F. Diagnosis and phenotypic classification of Wilson disease. *Liver Int* 2003; **23**: 139-142 [PMID: 12955875 DOI: 10.1034/j.1600-0676.2003.00824.x]
17 **Yang X**, Tang XP, Zhang YH, Luo KZ, Jiang YF, Luo HY, Lei JH, Wang WL, Li MM, Chen HC, Deng SL, Lai LY, Liang J, Zhang M, Tian Y, Xu Y. Prospective evaluation of the diagnostic accuracy of hepatic copper content, as determined using the entire core of a liver biopsy sample. *Hepatology* 2015; **62**: 1731-1741 [PMID: 26095812 DOI: 10.1002/hep.27932]
18 **Coffey AJ**, Durkie M, Hague S, McLay K, Emmerson J, Lo C, Klaffke S, Joyce CJ, Dhawan A, Hadzic N, Mieli-Vergani G, Kirk R, Elizabeth Allen K, Nicholl D, Wong S, Griffiths W, Smithson S, Giffin N, Taha A, Connolly S, Gillett GT, Tanner S, Bonham J, Sharrack B, Palotie A, Rattray M, Dalton A, Bandmann O. A genetic study of Wilson's disease in the United Kingdom. *Brain* 2013; **136**: 1476-1487 [PMID: 23518715 DOI: 10.1093/brain/awt035]
19 **Child CG**, Turcotte JG. Surgery and portal hypertension. In: Child CG. The liver and portal hypertension. Philadelphia: Saunders, 1964: 50-64
20 **Pugh RN**, Murray-Lyon IM, Dawson JL, Pietroni MC, Williams R. Transection of the oesophagus for bleeding oesophageal varices. *Br J Surg* 1973; **60**: 646-649 [PMID: 4541913 DOI: 10.1002/bjs.1800600817]
21 **Sarin SK**, Kumar A, Almeida JA, Chawla YK, Fan ST, Garg H, de Silva HJ, Hamid SS, Jalan R, Komolmit P, Lau GK, Liu Q, Madan K, Mohamed R, Ning Q, Rahman S, Rastogi A, Riordan SM, Sakhuja P, Samuel D, Shah S, Sharma BC, Sharma P, Takikawa Y, Thapa BR, Wai CT, Yuen MF. Acute-on-chronic liver failure: consensus recommendations of the Asian Pacific Association for the study of the liver (APASL). *Hepatol Int* 2009; **3**: 269-282 [PMID: 19669378 DOI: 10.1007/s12072-008-9106-x]
22 **Liver Failure and Artificial Liver Group**, Chinese Society of Infectious Diseases; Chinese Medical Association; Severe Liver Diseases and Artificial Liver Group, Chinese Society of Hepatology, Chinese Medical Association. [Diagnostic and treatment guidelines for liver failure]. *Zhonghua Gan Zang Bing Za Zhi* 2006; **14**: 643-646 [PMID: 16995974]
23 **Seto WK**, Mak CM, But D, Hung I, Lam CW, Tam S, Yuen MF, Lai CL. Mutational analysis for Wilson's disease. *Lancet* 2009; **374**: 662 [PMID: 19700008 DOI: 10.1016/S0140-6736(09)60915-6]
24 **Lopez Morra HA**, Debes JD, Dickstein G. Wilson's disease: what lies beneath. *Dig Dis Sci* 2007; **52**: 941-942 [PMID: 17333351 DOI: 10.1007/s10620-006-9463-z]
25 **Liang X**, Bi S, Yang W, Wang L, Cui G, Cui F, Zhang Y, Liu J, Gong X, Chen Y, Wang F, Zheng H, Guo J, Jia Z, Ma J, Wang H, Luo H, Li L, Jin S, Hadler SC, Wang Y. Epidemiological serosurvey of hepatitis B in China--declining HBV prevalence due to hepatitis B vaccination. *Vaccine* 2009; **27**: 6550-6557 [PMID: 19729084 DOI: 10.1016/j.vaccine.2009.08.048]
26 **Lu FM**, Li T, Liu S, Zhuang H. Epidemiology and prevention of hepatitis B virus infection in China. *J Viral Hepat* 2010; **17** Suppl 1: 4-9 [PMID: 20586928 DOI: 10.1111/j.1365-2893.2010.01266.x]

27 **Yonghao G**, Jin X, Jun L, Pumei D, Ying Y, Xiuhong F, Yanyang Z, Wanshen G. An epidemiological serosurvey of hepatitis B virus shows evidence of declining prevalence due to hepatitis B vaccination in central China. *Int J Infect Dis* 2015; **40**: 75-80 [PMID: 26456567 DOI: 10.1016/j.ijid.2015.10.002]

28 **Yong Hao G**, Da Xing F, Jin X, Xiu Hong F, Pu Mei D, Jun L, Ying Y, Yan Yang Z, Wan Shen G. The prevalence of hepatitis B infection in central China: An adult population-based serological survey of a large sample size. *J Med Virol* 2017; **89**: 450-457 [PMID: 27504586 DOI: 10.1002/jmv.24649]

29 **Walshe JM**, Yealland M. Wilson's disease: the problem of delayed diagnosis. *J Neurol Neurosurg Psychiatry* 1992; **55**: 692-696 [PMID: 1527540 DOI: 10.1136/jnnp.55.8.692]

30 **Brewer JG**. Wilsons disease: a clinician guide to recognition, diagnosis, and management. 1st ed. Amsterdam: Kluwer Academic Publishers, 2001

31 **Hu J**, Lü D, Wang G. [Study on the clinical misdiagnosis of hepatolenticular degeneration]. *Zhonghua Yi Xue Za Zhi* 2001; **81**: 642-644 [PMID: 11798938]

32 **Yuen MF**, Wong DK, Sablon E, Tse E, Ng IO, Yuan HJ, Siu CW, Sander TJ, Bourne EJ, Hall JG, Condreay LD, Lai CL. HBsAg seroclearance in chronic hepatitis B in the Chinese: virological, histological, and clinical aspects. *Hepatology* 2004; **39**: 1694-1701 [PMID: 15185311 DOI: 10.1002/hep.20240]

33 **Wang H**, Swann R, Thomas E, Innes HA, Valerio H, Hayes PC, Allen S, Barclay ST, Wilks D, Fox R, Bhattacharyya D, Kennedy N, Morris J, Fraser A, Stanley AJ, Gunson R, Mclntyre PG, Hunt A, Hutchinson SJ, Mills PR, Dillon JF. Impact of previous hepatitis B infection on the clinical outcomes from chronic hepatitis C? A population-level analysis. *J Viral Hepat* 2018; **25**: 930-938 [PMID: 29577515 DOI: 10.1111/jvh.12897]

34 **D'Amico G**, Garcia-Tsao G, Pagliaro L. Natural history and prognostic indicators of survival in cirrhosis: a systematic review of 118 studies. *J Hepatol* 2006; **44**: 217-231 [PMID: 16298014 DOI: 10.1016/j.jhep.2005.10.013]

World Journal of Gastroenterology

Submit a Manuscript: https://www.f6publishing.com

World J Gastroenterol 2023 August 28; 29(32): 4912-4919

DOI: 10.3748/wjg.v29.i32.4912

ISSN 1007-9327 (print) ISSN 2219-2840 (online)

CASE REPORT

Drug-induced entero-colitis due to interleukin-17 inhibitor use; capsule endoscopic findings and pathological characteristics: A case report

Keita Saito, Kiichiro Yoza, Shinichiro Takeda, Yoshihiro Shimoyama, Ken Takeuchi

Specialty type: Gastroenterology and hepatology

Provenance and peer review: Unsolicited article; Externally peer reviewed.

Peer-review model: Single blind

Peer-review report's scientific quality classification

Grade A (Excellent): 0
Grade B (Very good): B
Grade C (Good): C, C
Grade D (Fair): 0
Grade E (Poor): 0

P-Reviewer: Dai YC, China; Fries W, Italy; Tang ST, China

Received: May 15, 2023
Peer-review started: May 15, 2023
First decision: July 10, 2023
Revised: July 18, 2023
Accepted: August 1, 2023
Article in press: August 1, 2023
Published online: August 28, 2023

Keita Saito, Kiichiro Yoza, Shinichiro Takeda, Yoshihiro Shimoyama, Ken Takeuchi, Department of Gastroenterology, Tsujinaka Hospital Kashiwano-Ha, Kashiwa 277-0871, Japan

Corresponding author: Keita Saito, MD, Doctor, Department of Gastroenterology, Tsujinaka Hospital Kashiwano-Ha, No. 178-2 Wakashiba, Kashiwa 277-0871, Japan.
keisaitou.ymgt@gmail.com

Abstract

BACKGROUND

Interleukin-17 (IL-17) inhibitors are known to cause exacerbation or new onset of inflammatory bowel disease upon administration. However, few reports have described characteristic endoscopic and histopathologic findings, and no small intestinal lesions have been reported so far.

CASE SUMMARY

A woman in her 60s with psoriasis was administered ixekizumab (IXE), an anti-IL-17A antibody, for the treatment of psoriasis. Twenty months after commencing treatment, the patient visited our hospital because of persistent diarrhea. Blood tests performed at the time of the visit revealed severe inflammation, and colonoscopy revealed multiple round ulcers throughout the colon. A tissue biopsy of the ulcer revealed infiltration of inflammatory cells and granuloma-like findings in the submucosal layer. Capsule endoscopy revealed multiple jejunal erosions. After the withdrawal of IXE, the symptoms gradually improved, and ulcer reduction and scarring of the colon were endoscopically confirmed.

CONCLUSION

To the best of our knowledge, 17 reports have documented IL-17 inhibitor-induced entero-colitis with endoscopic images, endoscopic findings, and pathological characteristics, including the present case. Nine of these cases showed diffuse loss of vascular pattern, coarse mucosa/ulcer formation in the left colon, and endoscopic findings similar to those of ulcerative colitis. In the remaining eight cases, discontinuous erosions and ulcerations from the terminal ileum to the rectum were seen, with endoscopic findings similar to those of Crohn's disease. In this case, the findings were confirmed by capsule endoscopy, which has not been previously reported.

Key Words: Interleukin-17 inhibitor; Ixekizumab; Drug-induced entero-colitis; Capsule endoscopy; Case report

©The Author(s) 2023. Published by Baishideng Publishing Group Inc. All rights reserved.

Core Tip: While Interleukin-17 (IL-17) inhibitors are effectively used in the treatment of psoriasis, psoriatic arthritis, and ankylosing spondylitis, they are ineffective in patients with Crohn's disease (CD) and can worsen their condition. To the best of our knowledge, we present capsule endoscopic images of IL-17 inhibitor-induced entero-colitis for the first time, suggesting that IL-17-induced inflammatory lesions may be distributed in the proximal small bowel, unlike CD lesions. We also compared the endoscopic and pathological features of IL-17 inhibitor-induced entero-colitis with those previously reported.

Citation: Saito K, Yoza K, Takeda S, Shimoyama Y, Takeuchi K. Drug-induced entero-colitis due to interleukin-17 inhibitor use; capsule endoscopic findings and pathological characteristics: A case report. *World J Gastroenterol* 2023; 29(32): 4912-4919
URL: https://www.wjgnet.com/1007-9327/full/v29/i32/4912.htm
DOI: https://dx.doi.org/10.3748/wjg.v29.i32.4912

INTRODUCTION

Interleukin-17 (IL-17) inhibitors, such as ixekizumab (IXE) and secukinumab, are a class of molecular-targeted therapies used to treat psoriasis, psoriatic arthritis, and ankylosing spondylitis. IL-17 is a type of inflammatory cytokine produced by helper T cells and is known not only to induce local inflammation in the human body but also to be involved in host infection defense against pathogens in the skin and intestinal epithelium[1]. In patients with both psoriasis and Crohn's disease (CD), biopsy specimens of lesions express high levels of IL-17[2,3]. Therefore, IL-17 inhibitors were hypothesized to be effective in treating psoriasis and CD. However, IL-17 inhibitors are only effective in psoriasis; in patients with CD, IL-17 inhibitors are ineffective and exacerbate the disease[4]. Furthermore, in clinical trials of IL-17 inhibitors in inflammatory bowel disease (IBD), rheumatic diseases, and dermatological diseases, exacerbations or new-onset IBD have been reported at a frequency of 0.4%[5]. The mechanism underlying this seemingly contradictory adverse reaction remains unclear.

CASE PRESENTATION

Chief complaints

A woman in her 60s with diarrhea and anorexia.

History of present illness

Gastrointestinal symptoms appeared 24 mo after IXE was started for the treatment of psoriasis.

History of past illness

The patient was diagnosed with psoriatic arthritis by her family physician and started on IXE. However, anorexia and diarrhea appeared 20 mo after treatment initiation. After conservative treatment by her family doctor, her symptoms did not improve, and she visited our hospital 24 mo after IXE initiation for a close examination and treatment.

Personal and family history

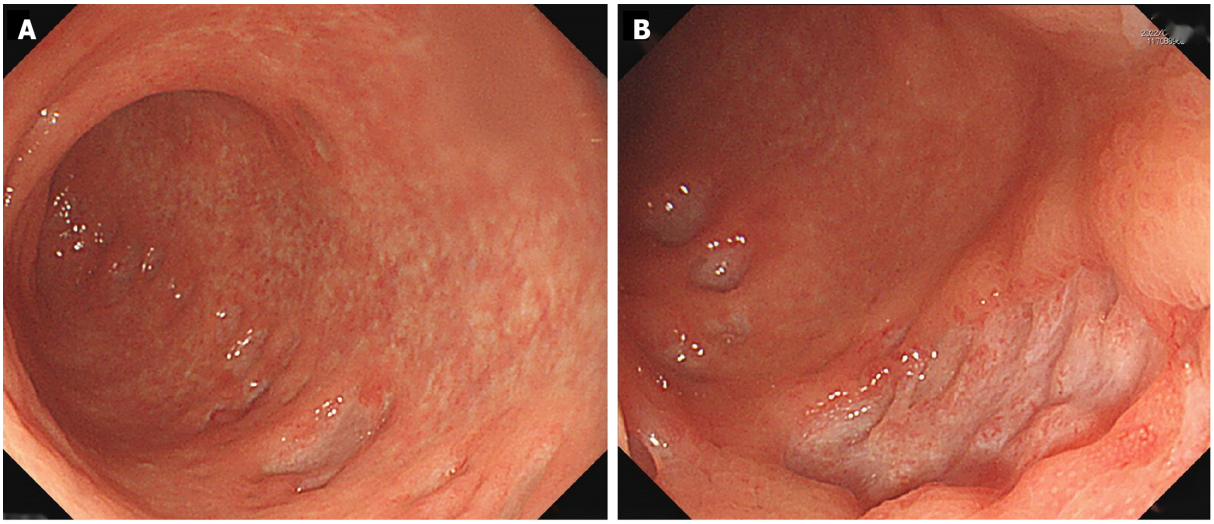
Her medical history included type 1 diabetes at the age of 35 and hypothyroidism at the age of 50 years, each of which was medically managed by her family physician. No family history of IBD was reported; her father had gastric cancer, and her mother had diabetes. The injectable medications used were insulin and IXE for diabetes and psoriasis, respectively.

Physical examination

The patient was conscious but noticeably emaciated, appeared weakened, and walked with a limp. She had a body temperature of 36.0 ℃ and 114/52 mmHg of blood pressure. The skin of the upper extremities was fragile, with epidermal exfoliation of the right forearm. Multiple scars were observed on the upper arm and mild deformities and swelling of the hand joints.

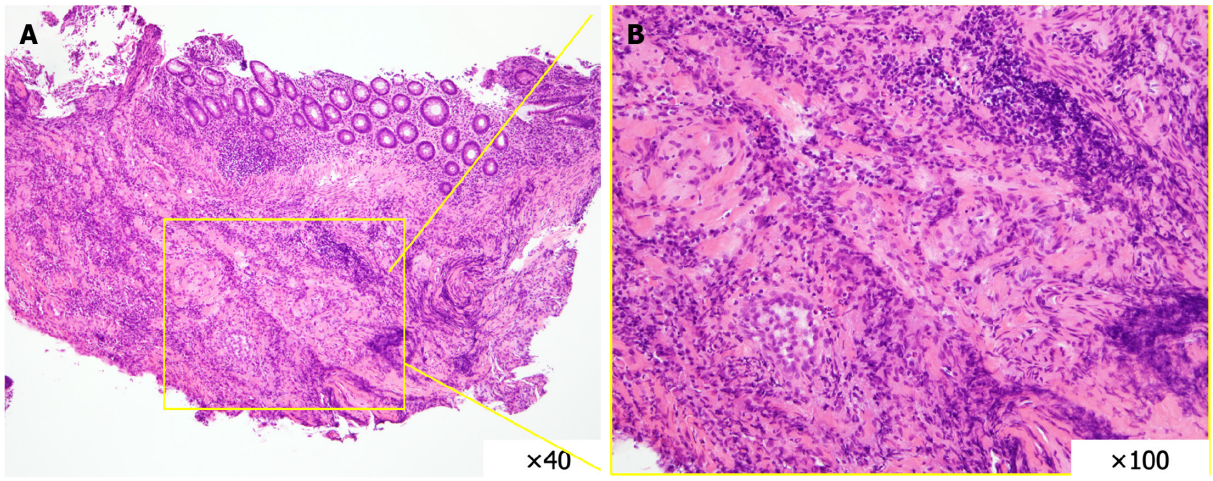
Laboratory examinations

On admission, blood biochemistry tests showed anemia with a hemoglobin level of 10.4 g/dL and hypoalbuminemia with an albumin level of 2.8 g/dL. She was also dehydrated, with a blood urea nitrogen level of 28.2 mg/dL and



DOI: 10.3748/wjg.v29.i32.4912 **Copyright** ©The Author(s) 2023.

Figure 1 Colonoscopy findings at admission. A: Distant view of colon; B: Close-up of ulcer. Multiple round punctate ulcers with a longitudinal trend from the cecum to the rectum are observed. The intervening mucosa of the ulcers is preserved, and the ulcers do not coincide with the mesenteric attachment side.



DOI: 10.3748/wjg.v29.i32.4912 **Copyright** ©The Author(s) 2023.

Figure 2 Pathological findings at admission. A: Hematoxylin-eosin (HE) stained specimen at 40 × magnification; B: HE stained specimen at 100 × magnification. The mucosa is erosive and infiltrated with inflammatory cells, predominantly lymphocytes. The submucosa shows granulomatous collagen fibers and fibroblast proliferation.

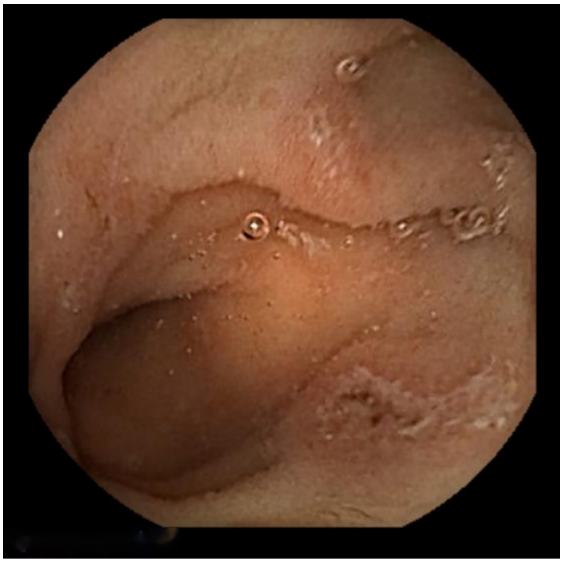
creatinine of 0.8 mg/dL and had high inflammation with a C-reactive protein level of 15.3 mg/dL. Leucine-rich alpha-2 glycoprotein level was 44.1 μg/mL and fecal calprotectin level was also high at 7357 mg/kg, suggesting strong intestinal inflammation.

Imaging examinations

Computed tomography revealed edematous wall thickening of the intestinal tract, continuous from the ascending colon to the rectum.

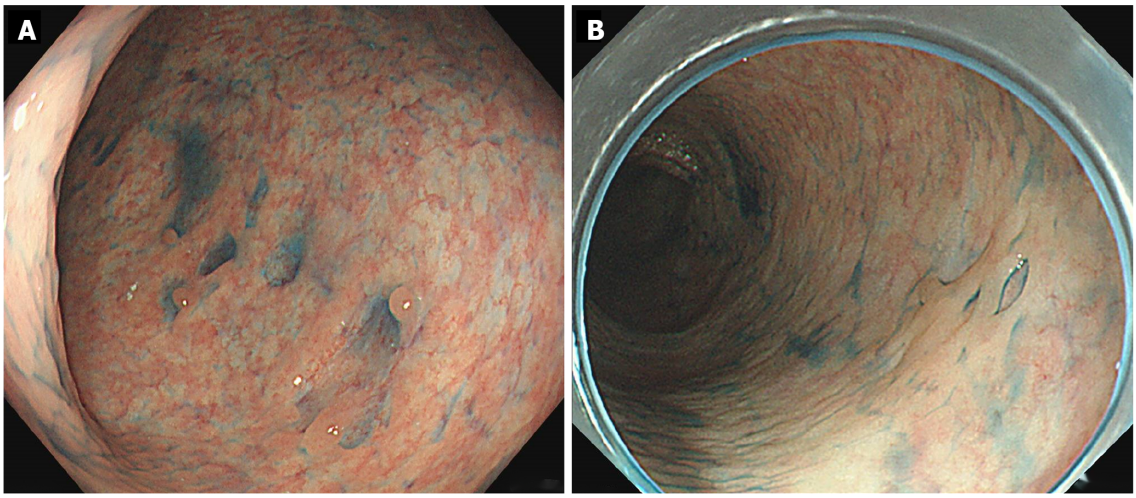
Further diagnosis workup

Colonoscopy revealed multiple round, punched-out ulcers with a longitudinal trend from the cecum to the rectum (Figure 1). The intervening mucosa of the ulcer was nearly normal, and the ulcer did not coincide with the mesenteric attachment. A biopsy of the ulcer showed mucosal erosion, lymphocyte-dominated inflammatory cell infiltration, and regenerative epithelial growth (Figure 2). Submucosal fibroblast and collagen fiber proliferation were also present-a granuloma-like finding similar to that of CD. An upper gastrointestinal endoscopy revealed reflux esophagitis and chronic gastritis. The gastric mucosa exhibited scattered erythema and erosions; however, no specific abnormalities were observed in the duodenum. Capsule endoscopy revealed multiple jejunal erosions (Figure 3). The erosions were scattered on the proximal side of the jejunum; each erosion was shallow and < 1 cm in size, and hematin adhesions were visible on the surface. However, stool culture and *Clostridioides difficile* toxin tests were negative, as were cytomegalovirus antigen



DOI: 10.3748/wjg.v29.i32.4912 **Copyright** ©The Author(s) 2023.

Figure 3 Capsule endoscopy findings. Scattered erosions are seen in the jejunum. The erosions were scattered on the proximal side of the jejunum; each erosion was shallow and < 1 cm in size, and hematin adhesions were visible on the surface.



DOI: 10.3748/wjg.v29.i32.4912 **Copyright** ©The Author(s) 2023.

Figure 4 Colonoscopy findings after drug withdrawal. A: At three weeks, there is shrinkage of ulcers; B: At four months, all ulcers have disappeared and scarring is observed.

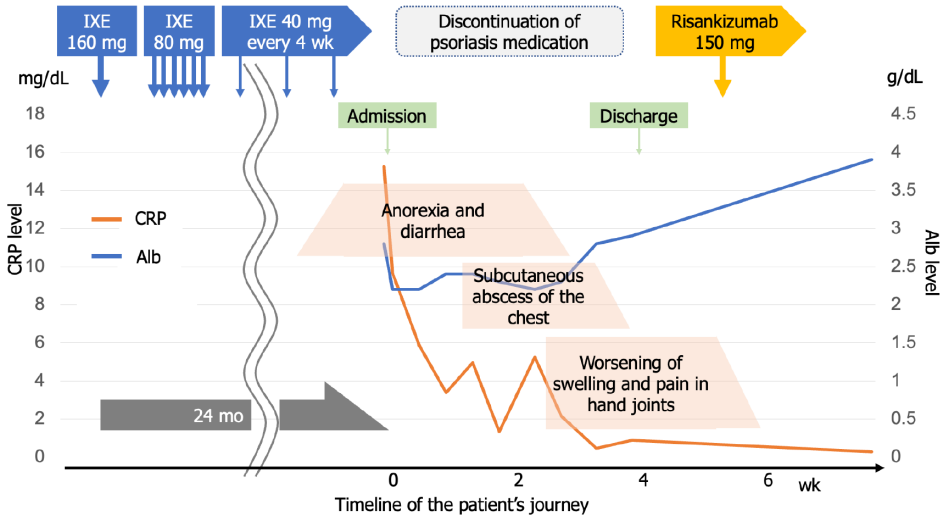
and polymerase chain reaction tests and interferon-gamma release assays.

FINAL DIAGNOSIS

As no episodes of irradiation or introduction of other new drugs occurred, we suspected drug-induced due to IXE.

TREATMENT

First, we monitored the patients' progress during drug withdrawal and intestinal rest after fasting. Multiple erosions in the upper jejunum were also observed; therefore, the patient commenced on bonoprazan fumarate, a potassium-competitive acid blocker. Due to the lack of improvement in symptoms, steroid administration was considered, and a gradual improvement in abdominal symptoms was observed. Three weeks after withdrawal, endoscopy revealed shrinkage of the ulcer and scarring (Figure 4A). Although her abdominal symptoms resolved, her skin and joint symptoms worsened, and she was started on Risankizumab by her family physician for psoriasis treatment.



DOI: 10.3748/wjg.v29.i32.4912 **Copyright** ©The Author(s) 2023.

Figure 5 Albumin (Alb) and C-reactive protein (CRP) levels plotted against the timeline of the patients' journey. The patient visited our hospital 24 mo after the start of the ixekizumab (IXE) administration. In the graph, CRP is shown on the left vertical axis and Alb on the right vertical axis. Abdominal symptoms gradually improved with IXE withdrawal, but skin and joint symptoms tended to worsen. After 4 wk of hospitalization, the patient was discharged home, as the endoscopy showed that the ulcer had healed and the patient was able to eat adequately. After discharge, risankizumab was introduced to control skin and joint symptoms, and the patients' condition stabilized. IXE: Ixekizumab; CRP: C-reactive protein; Alb: Albumin.

OUTCOME AND FOLLOW-UP

The abdominal, skin, and joint symptoms remained stable, and endoscopy performed 4 mo after IXE withdrawal confirmed the disappearance of all ulcers and scarring (Figure 4B). As abdominal symptoms improved, capsule endoscopy was not performed again due to a lack of patient consent, and bonoprazan fumaric acid was also discontinued. The clinical course from IXE initiation to the present is illustrated in Figure 5.

DISCUSSION

Drug-induced entero-colitis caused by IL-17 inhibitors is well known in the field of dermatology; however, very few reports have described all the endoscopic images, endoscopic features, and pathological characteristics of this condition. To the best of our knowledge, only 16 cases have been reported thus far[5-20]; we reviewed 17 cases, including our own (Table 1). Nine reported cases showed ulcerative colitis (UC)-like findings characterized by circumferential loss of vascular pattern and coarse mucosa/ulceration in the left colon, and eight reported cases with CD-like findings characterized by discontinuous erosion/ulceration from the terminal ileum to the rectum. All patients who presented with CD-like endoscopic findings after IXE administration had granulomas. In almost all the reports, the disease prognosis appeared to be good, with improvement in abdominal symptoms after the administration of steroids or molecularly targeted drugs. Only one patient with UC-like endoscopic findings after IXE administration required surgery because of a lack of improvement with drug administration.

Another case similar to CD with multiple ulcers of a similar round shape, as in the present case, has also been reported. However, in the present case, the ulcers tended to be longitudinally arranged and did not coincide with the mesenteric attachment side, which is atypical of CD. Furthermore, no reports have indicated improvement in abdominal symptoms with drug discontinuation alone, as in this case. In the present case, the various test results allowed us to promptly identify IXE as the suspected drug, and we surmised that excessive therapeutic intervention could be avoided. It should be noted that the introduction of a new drug may be necessary to manage the primary disease after drug withdrawal, and close communication with the dermatologist is important.

The association between psoriasis and IBD should be investigated in future studies. It has been reported that 1%-2% of patients with psoriasis have IBD[21]. Coincidentally-timed events during the initiation or administration of IL-17 inhibitors highlighted that IBD cannot be excluded.

CONCLUSION

At the very least, we should always check for IBD-related symptoms and family history before administering IL-17 inhibitors and suggest a screening colonoscopy if possible. Here, we report, for the first time, the capsule endoscopic findings of IL-17 inhibitor-induced entero-colitis. We also compared the endoscopic and pathological features of IL-17 inhibitor-induced entero-colitis with those previously reported. We believe that these findings will be useful for dermato-

Table 1 Patient background and endoscopic and pathological findings of entero-colitis after interleukin-17 administration

Year	Ref.	Age	Sex	Primary disease	Drug	Time to onset	IBD	Endoscopic findings	Pathological findings	Treatment and course
2017	Shiga *et al* [5]	56	M	Psoriasis	SEC	8 wk	CD	Longitudinal ulcer of the ileum and round ulcer of the esophagus	Nonspecific inflammatory cell infiltration	Improved with prednisolone 40 mg/d
2018	Philipose *et al*[6]	31	M	Psoriasis	IXE	3 mo	UC	Loss of vascular permeability throughout the sigmoid colon, erythematous coarse mucosa, ulcer	Lymphoplasmacytic infiltration	Mesalamine and methylprednisolone did not improve, but IFX administration improved
2018	Wang *et al* [7]	41	F	Psoriasis	SEC	1 wk	UC	Coarse mucosa and deep-burrowing ulceration of the entire sigmoid colon	Cryptitis, erosions, lymhoplasmacytic infiltration	Improved with methylprednisolone 40 mg/d and cyclosporine 2 mg/kg
2018	Ehrlich *et al*[8]	42	M	Ankylosing spondylitis	SEC	6 wk	UC	Deep ulcers and fragile mucosa of the transverse and sigmoid colon	Cryptitis, crypt abscess, loss of crypts	No improvement with solumedrol, improved after introduction of IFX
2019	Smith *et al* [9]	42	M	Psoriasis	IXE	12 wk	CD	Deep rounded punctate ulcers of the transverse and descending colon	Pancolitis with rare granuloma	No improvement with solumedrol, improved after introduction of IFX
2019	Uchida *et al*[10]	41	F	Psoriasis	SEC	4 mo	UC	Easy bleeding edematous mucosa of rectum to sigmoid colon, erosions, ulcers	High degree of inflammatory cell infiltration into the stroma and crypt abscess	Improved with mesalazine 2400 mg/d
2019	Achufusi *et al*[11]	39	M	Psoriasis	SEC	6 mo	UC	Ulceration of the splenic flexure, moderate to severe active colitis, ulceration at 30 cm, and active colitis in the rectum	Atrophy of the crypts, decreased goblet cells, cryptitis, crypt abscess	No improvement with steroids, improved after introduction of IFX
2019	Johnston and Veettil [12]	27	M	Ankylosing spondylitis	SEC	4 mo	UC	Multiple ulcers and moderate inflammation, sigmoid colon	Crypt abscess	No improvement with mesalazine and hydrocortisone, improvement with introduction of IFX
2019	Haidari *et al*[13]	69	M	Psoriatic arthritis	SEC	18 mo	CD	Multiple ulcers of the terminal ileum	Neutrophil infiltration of the epithelium of the crypts, no granuloma	Originally asymptomatic
2020	Nazarian *et al*[14]	48	F	Psoriasis	IXE	12 wk	CD	Mild erythema and punctate ulcerations in the terminal ileum	Active inflammation with the presence of granuloma	Improved with budesonide administration
2020	Varga *et al* [15]	52	M	Psoriasis	SEC	2 wk	UC	Loss of vascular permeability of sigmoid colon, ulcer	Lymphocytic infiltration of lamina propria, cryptitis, crypt abscess	Improved with prednisone 60 mg/d and mesalazine 3200 mg
2020	Gallego *et al*[16]	42	M	Psoriasis	IXE	2 wk	CD	Aphthous erosions and patchy ulcers of the rectum to cecum and terminal ileum	Cryptitis, crypt abscess, non-caseating granuloma	Improved with systemic corticosteroid administration
2021	Ali *et al*[20]	70	F	Psoriasis	SEC	1 mo	UC	Ulcerated and edematous mucosa in sigmoid colon	Acutely and chronically inflamed granulation tissue with extensive plasma cell infiltrate	Intravenous methylprednisolone
2022	Kakizoe *et al*[17]	65	M	Psoriasis	SEC	15 mo	CD	Deep ulcers of the cecum and transverse colon	No description	Hematochezia persisted after drug discontinuation and improved after induction of ADA
2022	Morosanu *et al*[19]	42	F	Psoriasis	IXE	1 wk	UC	Continuous congestive, friable rectal and colonic mucosa, spontan-	Neutrophilic inflammatory infiltrate disposed irregularly, edema and congestion, decrease of the crypts mucose-	Total colectomy with ileostoma and rectum preservation

								eously bleeding, deep and large ulcerations	cretion and crypt's abscesses	
2023	Khouri *et al*[18]	38	F	Psoriatic arthritis	SEC	1 mo	CD	Small ulcerations throughout the entire lumen of the terminal ileum and the cecum	Minimal architecture distortion in the large bowel mucosa, along with focal acute colitis	Initiated with prednisone and SEC was switched to IFX
2022	Our case	69	F	Psoriatic arthritis	IXE	21 mo	CD	Multiple round punctate ulcers throughout the colon. Capsule endoscopy shows multiple erosions in the jejunum	Inflammatory cell infiltrate, predominantly lymphocytes. Granulomatous fibroblasts and collagen fibers in the submucosa	Improvement only with drug discontinuation and fasting bowel rest

CD: Crohn's disease; SEC: Secukinumab; M: Male; F: Female; IBD: Inflammatory bowel disease; IXE: Ixekizumab; UC: Ulcerative colitis; ADA: Adalimumab.

logists and gastroenterologists in clinical practice.

ACKNOWLEDGEMENTS

The authors express their profound gratitude to the doctors, nurses, endoscopy staff, and medical personnel involved in the treatment of this patient.

FOOTNOTES

Author contributions: Saito K wrote the first draft of the manuscript; Yoza K and Takeda S were mainly responsible for the endoscopic procedures; Shimoyama Y and Takeuchi K were primarily responsible for the patients' inpatient care.

Informed consent statement: Informed written consent was obtained from the patient and her parents for the publication of this report and any accompanying images.

Conflict-of-interest statement: All the authors report no relevant conflicts of interest for this article.

CARE Checklist (2016) statement: The authors have read the CARE Checklist (2016), and the manuscript was prepared and revised according to the CARE Checklist (2016).

Open-Access: This article is an open-access article that was selected by an in-house editor and fully peer-reviewed by external reviewers. It is distributed in accordance with the Creative Commons Attribution NonCommercial (CC BY-NC 4.0) license, which permits others to distribute, remix, adapt, build upon this work non-commercially, and license their derivative works on different terms, provided the original work is properly cited and the use is non-commercial. See: https://creativecommons.org/Licenses/by-nc/4.0/

Country/Territory of origin: Japan

ORCID number: Keita Saito 0000-0003-2740-4518; Shinichiro Takeda 0000-0002-6302-5073.

S-Editor: Qu XL
L-Editor: A
P-Editor: Zhang XD

REFERENCES

1 **Miossec P**, Kolls JK. Targeting IL-17 and TH17 cells in chronic inflammation. *Nat Rev Drug Discov* 2012; **11**: 763-776 [PMID: 23023676 DOI: 10.1038/nrd3794]

2 **Kobayashi T**, Okamoto S, Hisamatsu T, Kamada N, Chinen H, Saito R, Kitazume MT, Nakazawa A, Sugita A, Koganei K, Isobe K, Hibi T. IL23 differentially regulates the Th1/Th17 balance in ulcerative colitis and Crohn's disease. *Gut* 2008; **57**: 1682-1689 [PMID: 18653729 DOI: 10.1136/gut.2007.135053]

3 **Lowes MA**, Kikuchi T, Fuentes-Duculan J, Cardinale I, Zaba LC, Haider AS, Bowman EP, Krueger JG. Psoriasis vulgaris lesions contain discrete populations of Th1 and Th17 T cells. *J Invest Dermatol* 2008; **128**: 1207-1211 [PMID: 18200064 DOI: 10.1038/sj.jid.5701213]

4 **Hueber W**, Sands BE, Lewitzky S, Vandemeulebroecke M, Reinisch W, Higgins PD, Wehkamp J, Feagan BG, Yao MD, Karczewski M, Karczewski J, Pezous N, Bek S, Bruin G, Mellgard B, Berger C, Londei M, Bertolino AP, Tougas G, Travis SP; Secukinumab in Crohn's Disease Study Group. Secukinumab, a human anti-IL-17A monoclonal antibody, for moderate to severe Crohn's disease: unexpected results of

a randomised, double-blind placebo-controlled trial. *Gut* 2012; **61**: 1693-1700 [PMID: 22595313 DOI: 10.1136/gutjnl-2011-301668]

5 **Shiga H**, Fukuda S, Iijima K. Interleukin-17A Inhibitor-induced Crohn's Disease/Behçet's Disease-like Lesions. *Inflamm Bowel Dis* 2017; **23**: E38-E39 [PMID: 28471836 DOI: 10.1097/MIB.0000000000001142]

6 **Philipose J**, Ahmed M, Idiculla PS, Mulrooney SM, Gumaste VV. Severe de novo Ulcerative Colitis following Ixekizumab Therapy. *Case Rep Gastroenterol* 2018; **12**: 617-621 [PMID: 30483039 DOI: 10.1159/000493922]

7 **Wang J**, Bhatia A, Krugliak Cleveland N, Gupta N, Dalal S, Rubin DT, Sakuraba A. Rapid Onset of Inflammatory Bowel Disease after Receiving Secukinumab Infusion. *ACG Case Rep J* 2018; **5**: e56 [PMID: 30105273 DOI: 10.14309/crj.2018.56]

8 **Ehrlich D**, Jamaluddin N, Pisegna J, Padua D. A Challenging Case of Severe Ulcerative Colitis following the Initiation of Secukinumab for Ankylosing Spondylitis. *Case Rep Gastrointest Med* 2018; **2018**: 9679287 [PMID: 29666723 DOI: 10.1155/2018/9679287]

9 **Smith MK**, Pai J, Panaccione R, Beck P, Ferraz JG, Jijon H. Crohn's-like disease in a patient exposed to anti-Interleukin-17 blockade (Ixekizumab) for the treatment of chronic plaque psoriasis: a case report. *BMC Gastroenterol* 2019; **19**: 162 [PMID: 31488067 DOI: 10.1186/s12876-019-1067-0]

10 **Uchida S**, Oiso N, Komeda Y, Kudo M, Kawada A. Paradoxical ulcerative colitis during treatment with secukinumab for psoriasis. *Eur J Dermatol* 2019; **29**: 444-445 [PMID: 30442634 DOI: 10.1684/ejd.2018.3391]

11 **Achufusi TG**, Harnee PS, Rawlins S. A Rare Case of New-Onset Ulcerative Colitis following Initiation of Secukinumab. *Case Rep Med* 2019; **2019**: 2975631 [PMID: 31467555 DOI: 10.1155/2019/2975631]

12 **Johnston DN**, Veettil R. A case of new onset ulcerative colitis following secukinumab treatment. *Br J Hosp Med (Lond)* 2019; **80**: 544-545 [PMID: 31498681 DOI: 10.12968/hmed.2019.80.9.544]

13 **Haidari W**, Al-Naqshabandi S, Ahn CS, Bloomfeld RS, Feldman SR. Asymptomatic Crohn's disease identified in a patient being treated with secukinumab: A case report. *SAGE Open Med Case Rep* 2019; **7**: 2050313X19893580 [PMID: 31839950 DOI: 10.1177/2050313X19893580]

14 **Nazarian A**, Grin A, Wijeratne DT. Ixekizumab Associated New-Onset Inflammatory Bowel Disease. *ACG Case Rep J* 2020; **7**: e00316 [PMID: 32440523 DOI: 10.14309/crj.0000000000000316]

15 **Fernández-de la Varga M**, Del Pozo-Del Valle P, Béjar-Serrano S, Garrido-Marín A, Bastida Paz G. Secukinumab-induced ulcerative colitis: opening Pandora's box of immunity. *Gastroenterol Hepatol* 2020; **43**: 358-359 [PMID: 32561217 DOI: 10.1016/j.gastrohep]

16 **Merino Gallego E**, Gómez Torres K, Martínez Amate E. Debut Of Inflammatory Bowel Disease Associated To Ixekizumab In Patient With Moderate, Difficult -To-Manage Psoriasis. *Gastroenterol Hepatol* 2020; **43**: 622-623 [PMID: 32674878 DOI: 10.1016/j.gastrohep.2020.04.009]

17 **Kakizoe K**, Fujioka S, Noda M, Torisu T. IBD-like Lesions in a Secukinumab-treated Patient. *Intern Med* 2022; **61**: 2077-2078 [PMID: 34803103 DOI: 10.2169/internalmedicine.8475-21]

18 **Khouri A**, Moreno C, Niland B. New-Onset Crohn's Disease following Initiation of Secukinumab: A Case Report and Review of the Role of IL-17 in the Pathogenesis of Crohn's Disease. *Case Rep Gastrointest Med* 2023; **2023**: 1769290 [PMID: 37260537 DOI: 10.1155/2023/1769290]

19 **Morosanu AM**, Mihai IR, Rezus II, Gavrilescu O, Dranga M, Prelipcean CC, Mihai C. New onset severe ulcerative colitis following Ixekizumab therapy. *Arch Clin Cases* 2022; **9**: 173-176 [PMID: 36628163 DOI: 10.22551/2022.37.090410227]

20 **Ali AK**, Torosian A, Porter C, Bloomfeld RS, Feldman SR. New onset inflammatory bowel disease in patient treated with secukinumab: Case report and review of literature. *Dermatol Ther* 2021; **34**: e15151 [PMID: 34609037 DOI: 10.1111/dth.15151]

21 **Eppinga H**, Poortinga S, Thio HB, Nijsten TEC, Nuij VJAA, van der Woude CJ, Vodegel RM, Fuhler GM, Peppelenbosch MP. Prevalence and Phenotype of Concurrent Psoriasis and Inflammatory Bowel Disease. *Inflamm Bowel Dis* 2017; **23**: 1783-1789 [PMID: 28617755 DOI: 10.1097/MIB.0000000000001169]



Published by **Baishideng Publishing Group Inc**
7041 Koll Center Parkway, Suite 160, Pleasanton, CA 94566, USA
Telephone: +1-925-3991568
E-mail: bpgoffice@wjgnet.com
Help Desk: https://www.f6publishing.com/helpdesk
https://www.wjgnet.com



© 2023 Baishideng Publishing Group Inc. All rights reserved.